André Freiwald

J. Murray Roberts

Editors

Cold-Water Corals and Ecosystems

Erlangen Earth
Conference Series

Springer

Erlangen Earth Conference Series

Series Editor: André Freiwald

André Freiwald
J. Murray Roberts
(Editors)

Cold-Water Corals and Ecosystems

With 361 Figures, 116 in Colour, and 104 Tables

Springer

Professor Dr. André Freiwald
Institute of Paleontology, Erlangen University
Loewenichstr. 28, D-91054 Erlangen, Germany
E-mail: *andre.freiwald@pal.uni-erlangen.de*

Dr. J. Murray Roberts
Scottish Association for Marine Science, Dunstaffnage Marine Laboratory
Oban, Argyll, PA37 1QA, United Kingdom
E-mail: *murray.roberts@sams.ac.uk*

Foreword

Cold-water coral reefs – fascinating, fragile and threatened ecosystems found in deep, dark waters. For centuries, scientists and fishermen knew that these corals live in the colder parts of our oceans, far beneath the sunlit surface. However, only in recent years has technology allowed us to look closer at these cold-water corals – the findings amazed even the experts. Large and complex structures, raised from the seabed and stretching for miles with an abundance of life and harbouring a dazzling array of species: reefs very similar to their well known cousins in shallow tropical waters.

Like the hydrothermal vent communities, cold-water coral reefs took the spotlight very quickly, and are now regularly referred to as one of the key ecosystems in the colder and deeper parts of our oceans. The discovery of this extraordinary ecosystem came with a warning: many reefs showed scars and were partly or completely destroyed by commercial fishing activities, especially from the use of bottom trawls. The evidence was so compelling that national authorities started to adapt regulatory measures to protect reefs in their waters. However, the location of these reefs, their vulnerability and the practical irreversibility of damage highlighted the need for a concerted, international approach to be taken in their protection, conservation and sustainable management. At the 2003 Ministerial Meeting of the OSPAR Convention for the Protection of the Marine Environment of the North East Atlantic, Ministers declared their intention to take immediate steps to protect cold-water coral reefs from the damage inflicted by active fishing gear on the reefs. At the same meeting, the United Nations Environment Programme (UNEP) offered its support for action.

The goal of the 2nd International Symposium on Deep-Sea Corals, held at Erlangen in September 2003, was to prepare an executive report summarizing the current knowledge of cold-water coral reefs and setting out recommendations for further action, primarily for consideration by policy and decision-makers. Sixteen months later, I am pleased that this report (UNEP/WCMC 2004, "Cold-water Coral Reefs") was produced and published, and that cold-water coral reefs have featured in a multitude of international reports and high-level discussions, amongst others the 7th Meeting of the Conference of the Parties to the Convention on Biological Diversity and the 58th and 59th sessions of the UN General Assembly. In July 2004 the International Coral Reef Initiative (ICRI) agreed to include cold-water coral reefs in its remit and programme of work, thereby providing governments, international organisations and experts with a dedicated global forum to exchange views and initiate further activities.

There is still a long way to go until cold-water coral reefs, especially those in international waters and high sea areas, are sufficiently protected and sustainably

managed. Nevertheless, the increased awareness of cold-water coral reefs among stakeholders around the world is encouraging. Thanks to the dedication of scientists, many of them participants at the 2nd International Symposium on Deep-Sea Corals and contributors to this volume, there is every hope that cold-water coral reefs might be out of sight, but will no longer be out of mind.

Dr. Stefan Hain
Head of the UNEP Coral Reef Unit

Preface

Coral ecosystems, especially coral reefs, are usually associated with shallow-water oligotrophic tropical seas. Discoveries of the last few years challenge this widespread belief and show that substantial scleractinian coral reef frameworks and gorgonian coral forests thrive on continental shelves and slopes around the world (Freiwald et al. 2004). Many of these discoveries have been driven by increasing human exploitation of deep-water natural resources, principally hydrocarbon reserves and fish stocks. The papers in this volume reflect the global spread of these discoveries (Fig. 1). They also reflect the range of disciplines, from the physical, chemical, geo- and biological sciences, needed to understand the highly complex nature of coral ecosystems.

This volume contains a series of peer-reviewed papers from the 2nd International Symposium on Deep-Sea Corals held in Erlangen, Germany, 8-12 September 2003. In the three years since the first symposium in Halifax, Canada, research interest in coral ecosystems from deep, cold waters has grown rapidly around the world. Eighteen peer-reviewed papers were published following 42 talks and 22 poster presentations in Halifax (Watling and Risk 2002) with a special volume containing another 17 articles (Willison et al. 2001). In Erlangen, 67 talks and 42 posters were presented and these have produced this collection of 62 peer-reviewed papers on topics as diverse as coral reproduction, biodiversity, paleoclimatic reconstruction and sedimentary geology.

Defining cold-water corals and reefs

Scleractinian corals are found in all the world's oceans from the intertidal zone to abyssal depths. The term reef derives from the Norse seafaring term *rif*, a submerged structure rising from the surrounding seafloor that forms a hazard to shipping. Such structures could be rock ridges, sandbanks or substantial accumulations of limestone formed by a framework of coral skeletons often cemented by coralline algae in shallow-water tropical seas – the classic definition of a coral reef (Wood 1999). Reefs create distinct patches on the seafloor that either trap sediment or otherwise alter its deposition. Over time they develop to form structures rising from the surrounding seafloor that provide habitat for other species. In terms of cold-water coral reefs, this habitat is predominantly composed of the skeletal framework formed by scleractinian corals. These coral frameworks may be considered as true biogenic reefs if they locally alter sediment deposition, provide complex three-dimensional structural habitat and are subject to dynamic processes of growth and (bio)erosion.

The robust anastomosing skeleton formed by *Lophelia pertusa* dominates reef frameworks in the north-east Atlantic where the more fragile *Madrepora oculata* often occurs forming a secondary reef framework (Freiwald 2002). Like *L. pertusa*, *Solenosmilia variabilis* produces tightly-branched reef frameworks which form
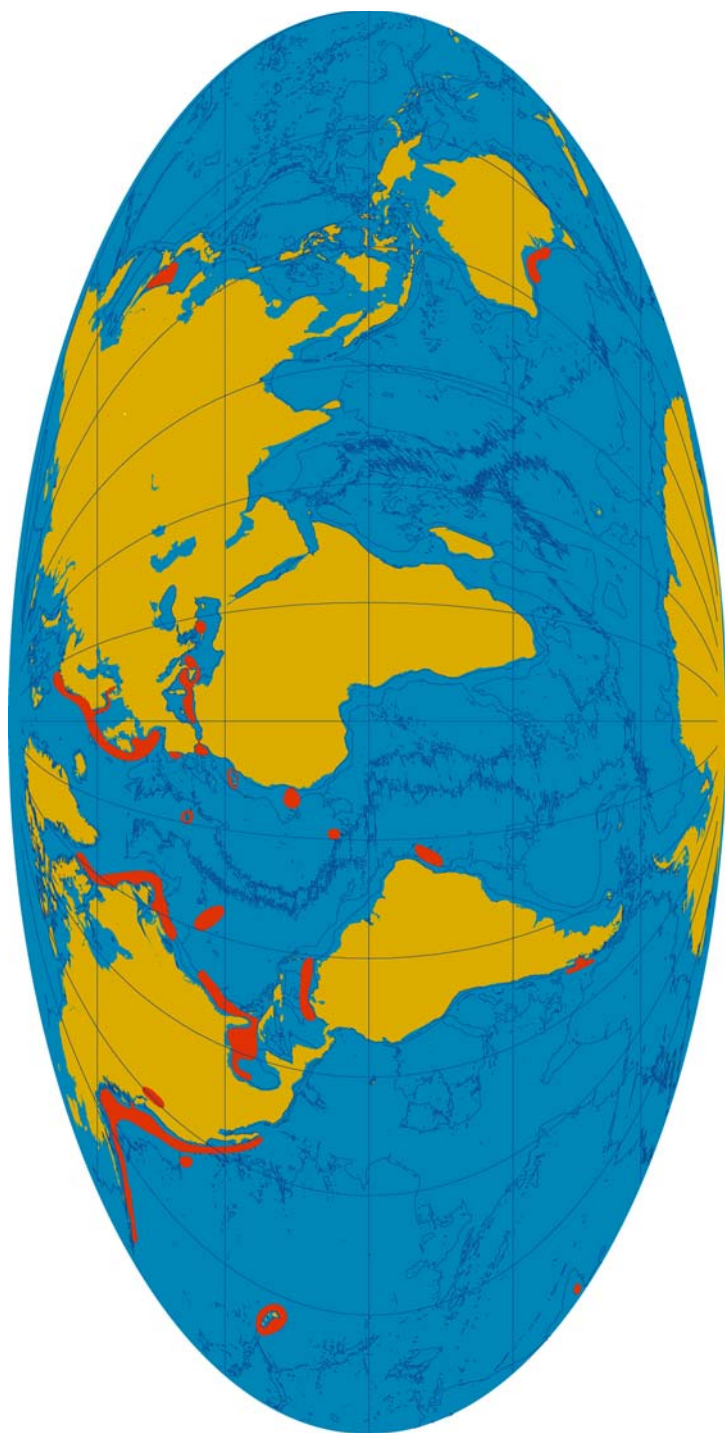
Fig. 1 Overview of cold-water coral ecosystems presented in this volume

dense clusters on Tasmanian seamounts (Koslow et al. 2001), along the Heezen Fracture Zone in the South Pacific (Zibrowius 1974), on the Little Bahama Bank in the Atlantic (Mullins et al. 1981) and south of Iceland on the Reykjanes Ridge (Copley et al. 1996). *Goniocorella dumosa* is restricted to the southern hemisphere and forms reef frameworks best known from waters around New Zealand (Cairns 1995). *Enallopsammia profunda* is often associated with *L. pertusa*, *M. oculata* and *S. variabilis* and forms reef frameworks in the western Atlantic on the Blake Plateau and along the Florida-Hatteras Slope (Reed 2002). *Oculina varicosa* is a scleractinian that crosses the divide from shallow to deeper waters. Zooxanthellate *O. varicosa* is found in shallow waters from the Caribbean, Gulf of Mexico and Atlantic coasts off Florida. Interestingly this species also occurs without endosymbiotic algae and can form substantial deep-water reef frameworks along the eastern Florida Shelf (Reed 2002).

The terms 'cold-water coral', 'deep-water coral' and 'deep-sea coral' have all been used as shorthand to discriminate these scleractinian coral frameworks and gorgonian forests from the coral reefs of shallow, warm-water tropical seas. None of these terms gives a really robust definition. For instance, *Lophelia pertusa* is found at depths of just 40 m in some Norwegian fjords to over 3000 m on the New England seamount chain. Recently the solitary coral *Desmophyllum dianthus,* normally regarded as a deep-water species, was discovered at just 20 m depth in Chilean fjords (see Försterra et al. 2005). In this volume we adopt the term *cold-water coral* to signify that the species, habitats and ecosystems discussed are not associated with tropical coral reefs, but rather are systems associated with colder conditions, often in deep offshore waters.

Research themes

Since the mid-1990s research interest in cold-water corals and the reef structures they form has grown rapidly around the world. Developments in acoustic survey technology and the use of research submersibles led to the discovery of unexpectedly large cold-water coral reef complexes. Much recent research effort has been devoted to understanding the nature of any coupling between cold-water coral reef development and light hydrocarbon seepage. We are now seeing the development of biological and ecological studies on the foundation of an improved geological understanding of how and where reef structures have developed. The driving research questions during the 2nd International Symposium on Deep-Sea Corals are reflected in the contributions to this volume: What controls cold-water coral reef distribution? What factors promote the biodiversity of cold-water coral reefs? How significant are they in the life history of fish? What controls coral growth and development? How do the dominant reef framework species reproduce and disperse? The list goes on.

We have chosen eight themes providing a structure to group the contributions to this volume. The first theme considers cold-water coral reefs in terms of their *Paleoenvironmental Context*. What lessons can paleontology tell us and how can

these help us understand the processes of evolution and change on cold-water coral reefs today? Our ability to generate testable hypotheses regarding cold-water coral reefs must be grounded in a sound understanding of where they occur. We need to know where they occur before we can ask how their distributions are controlled. Thus the **Distribution** of cold-water corals and the approaches we take to **Mapping** this distribution are critical. We have grouped contributions considering factors that control distribution under **Exogenic and Endogenic Controls**. These controlling factors have a strong bearing on the next two themes, **Coral Biology** and **Diversity**. Intriguingly cold-water coral reefs may provide an archive of the environmental variability they have experienced through time. Contributions that discuss the analysis of skeletal remains of reef fauna as an **Environmental Archive** for paleoclimatic reconstruction are grouped together. In addition, many studies have raised the concern that cold-water coral reefs around the globe are threatened by human activities (principally bottom trawl fishing). The final theme section of this volume considers these issues and the urgent need to develop strategies for the **Conservation** of cold-water coral reefs.

Acknowledgements

Nancy Knowlton, La Jolla, USA
Tony Koslow, Hobart, AUS
Manfred Krautter, Stuttgart, GER
Anton Kuijpers, Copenhagen, DEN
Bruce A. Marshall, Wellington, NZ
Douglas G. Masson, Southampton, UK
Mona McCrea, Dublin, IRE
Lance Morgan, Glen Ellen, USA
Pål Mortensen, Bergen, N
Fritz Neuweiler, Montreal, CAN
Martha S. Nizinski, Washington, USA
Jörn Peckmann, Bremen, GER
Olaf Pfannkuche, Kiel, GER
John Reed, Fort Pierce, USA
Götz B. Reinicke, Stralsund, GER
Michael Risk, Hamilton, CAN
Alex Rogers, Cambridge, UK

Andres Rüggeberg, Kiel, GER
Kathryn M. Scanlon, Woods Hole, USA
Joachim Schönfeld, Kiel, GER
William Schroeder, Dauphin Island, USA
Geoff Shester, Juneau, USA
Tracy Shimmield, Oban, UK
Mark Tasker, Aberdeen, UK
Marco Taviani, Bologna, I
Paul Tyler, Southampton, UK
Ann Vanreusel, Gent, BEL
Klaus Vogel, Frankfurt, GER
Andrew J. Wheeler, Cork, IRE
Martin White, Galway, IRE
Martin Willison, Halifax, CAN
John Brodie Wilson, Egham, UK
Max Wisshak, Erlangen, GER
Helmut Zibrowius, Marseille, F

References

Cairns SD (1995) The marine fauna of New Zealand: Scleractinia (Cnidaria: Anthozoa). New Zealand Oceanogr Inst Mem 103: 1-210

Copley JTP, Tyler PA, Sheader M, Murton BJ, German CR (1996) Megafauna from sublittoral to abyssal depths along the Mid-Atlantic Ridge south of Iceland. Oceanol Acta 19: 549-559

Försterra G, Beuck L, Häussermann V, Freiwald A (2005) Shallow-water *Desmophyllum dianthus* (Scleractinia) from Chile: characteristics of the biocoenoses and the bioeroding community, heterotrophic interactions and (paleo)-bathymetric implications. In: Freiwald A, Roberts JM (eds) Cold-water Corals and Ecosystems. Springer, Berlin Heidelberg, pp 937-977

Freiwald A (2002) Reef-forming cold-water corals. In: Wefer G, Billett D, Hebbeln D, Jørgensen BB, Schlüter M, van Weering T (eds) Ocean Margin Systems. Springer, Berlin Heidelberg, pp 365-385

Freiwald A, Fosså JH, Grehan A, Koslow T, Roberts JM (2004) Cold-water coral reefs. UNEP-WCMC, Cambridge, UK, Biodivers Ser 22: 84 pp

Koslow JA, Gowlett-Holmes K, Lowry JK, O'Hara T, Poore GCB, Williams A (2001) Seamount benthic macrofauna off southern Tasmania: community structure and impacts of trawling. Mar Ecol Prog Ser 213: 111-125

Mullins HT, Newton CR, Heath K, Vanburen HM (1981) Modern deep-water coral mounds north of Little Bahama Bank: criteria for recognition of deep-water coral bioherms in the rock record. J Sediment Petrol 51: 999-1013

Reed JK (2002) Deep-water *Oculina* reefs of Florida: biology, impacts, and management. Hydrobiologia 471: 43-55

Watling L, Risk M (2002) Biology of cold water corals. Hydrobiologia 471: 166 pp

Willison JHM, Hall J, Gass SE, Kenchington ELR, Butler M, Doherty P (2001) Proceedings of the First International Symposium on Deep-sea Corals. Ecology Action Centre and Nova Scotia Museum, Halifax, NS, 231 pp

Wood R (1999) Reef evolution. Oxford Univ Press, Oxford, 414 pp

Zibrowius H (1974) Scléractiniaires des iles Saint Paul et Amsterdam (Sud de l'Océan Indien). Téthys 5: 747-778

André Freiwald   **J. Murray Roberts**
andre.freiwald@pal.uni-erlangen.de   murray.roberts@sams.ac.uk

February 2005

Content

III Mapping   357

IV Exogenic and endogenic controls   481

V Coral Biology   651

VII Environmental Archives   1003

VIII Conservation   1127

Contributors

Damian **Allen**
Ecological Consultancy Services Ltd
(EcoServe), B19, K.C.R. Industrial
Estate, Kimmage, Dublin 12, Ireland

David L. **Allison**
Oceana, 2501 M Street NW
#300,Washington DC 20037,USA

German **Álvarez-Pérez**
Departament d'Estratigrafia,
Paleontologia i Geociències Marines,
Universitat de Barcelona, Martí
Franquès s/n., E-08028 Barcelona,
Spain

John **Alvsvåg**
Institute of Marine Research, P.O.
Box 1879 Nordnes, N-5817 Bergen,
Norway

Allen H. **Andrews**
Moss Landing Marine Laboratories,
8272 Moss Landing Road, Moss
Landing, CA 95039, USA

Peter J. **Auster**
National Undersea Research Center,
Department of Marine Sciences,
University of Connecticut, Groton,
CT 06340, USA

Jim **Ayers**
Oceana, Pacific Office, 175 S. Franklin
St., Ste 418, Juneau, AK 99801, USA

Kumiko **Azetsu-Scott**
Bedford Institute of Oceanography,
Dartmouth, Nova Scotia, Canada

Russ C. **Babcock**
Commonwealth Scientific and
Industrial Research Organisation,
Marine Research Private Bag 5,
Wembley, WA 6913, Australia

Amy R. **Baco**
Woods Hole Oceanographic Institution,
Biology Department, MS 33, Woods
Hole, MA 02543, USA

J. Vaughn **Barrie**
Geological Survey of Canada, Pacific
Geoscience Centre, 9860 W Saanich
Rd, Box 6000, Sidney, BC, V8L 4B2,
Canada

Tim **Beck**
Institute of Paleontology, Erlangen
University, Loewenichstr. 28,
D-91054 Erlangen, Germany

Milena **Benavides**
Instituto de Investigaciones Marinas
y Costeras, INVEMAR, Cerro
Punta Betín, AA 1016, Santa Marta,
Colombia

Adriana **Bermúdez**
Instituto de Investigaciones Marinas
y Costeras, INVEMAR, Cerro
Punta Betín, AA 1016, Santa Marta,
Colombia

Michaela **Bernecker**
Institute of Paleontology, Erlangen
University, Loewenichstr. 28,
D-91054 Erlangen, Germany

Miriam **Bertram**
Pacific Marine Environmental
Laboratory, Seattle, WA, USA

Brian J. **Bett**
Southampton Oceanography Centre,
Empress Dock, Southampton,
SO14 3ZH, UK

Lydia **Beuck**
Institute of Paleontology, Erlangen
University, Loewenichstr. 28,
D-91054 Erlangen, Germany

Andreas **Beyer**
Alfred Wegener Institute for Polar and
Marine Research, Columbusstr.,
D-27568 Bremerhaven, Germany

Dominique **Blamart**
Laboratoire des Sciences du Climat
et de l'Environnement (LSCE) Unité
mixte de Recherche CEA-CNRS, Bât.
12, Avenue de la Terrasse, F-91198 Gif-
sur-Yvette Cedex, France

Giomar **Borrero-Pérez**
Instituto de Investigaciones Marinas
y Costeras, INVEMAR, Cerro
Punta Betín, AA 1016, Santa Marta,
Colombia

Robert J. **Brock**
U.S. National Oceanic and
Atmospheric Administration, Silver
Springs, MD 20910, USA

Richard G. **Bromley**
Geological Institute, University of
Copenhagen, Øster Voldgade 10,
DK-1350 Copenhagen K, Denmark

Sandra D. **Brooke**
Oregon Institute of Marine Biology,
University of Oregon, Charleston,
OR 97420, USA

Lene **Buhl-Mortensen**
Benthic Habitat Research Group,
Institute of Marine Research, P.O.
Box 1870 Nordnes, N-5817 Bergen,
Norway

Samantha N. **Burgess**
Research School of Earth Sciences,
Australian National University,
Canberra, ACT 0200, Australia

Erica J. **Burton**
Monterey Bay National Marine
Sanctuary, 299 Foam Street, Monterey,
CA 93940, USA

Pere **Busquets**
Departament d'Estratigrafia,
Paleontologia i Geociències Marines,
Universitat de Barcelona, Martí
Franquès s/n., E-08028 Barcelona,
Spain

Mark **Butler**
Ecology Action Centre, 1568 Argyle
Street, Halifax, Nova Scotia, B3J 2B3,
Canada

Gregor M. **Cailliet**
Moss Landing Marine Laboratories,
8272 Moss Landing Road, Moss
Landing, CA 95039, USA

Miquel **Canals**
Departament d'Estratigrafia,
Paleontologia i Geociències Marines,
Universitat de Barcelona, Martí
Franquès s/n., E-08028 Barcelona,
Spain

José Luis **Casamor**
Departament d'Estratigrafia,
Paleontologia i Geociències Marines,
Universitat de Barcelona, Martí
Franquès s/n., E-08028 Barcelona,
Spain

Ole **Christensen**
Geological Survey of Norway, P.O.
Box 3006 Lade, N-7002 Trondheim,
Norway

David A. **Clague**
Monterey Bay Aquarium Research
Institute, 7700 Sandholdt Road, Moss
Landing, CA 95039, USA

Kenneth H. **Coale**
Moss Landing Marine Laboratories,
8272 Moss Landing Road, Moss
Landing, CA 95039, USA

Jeremy G. **Colman**
Woodside Energy Ltd, Box D188,
GPO Perth, Western Australia 6840,
Australia

Kim W. **Conway**
Geological Survey of Canada, Pacific
Geoscience Centre, 9860 W Saanich
Rd, Box 6000, Sidney, BC, V8L 4B2,
Canada

Mark J. **Costello**
Leigh Marine Laboratory, University of
Auckland, P.O. Box 349, Warkworth,
New Zealand

Jean-Pierre **Cuif**
Université de Paris XI, Faculté des
Sciences, Bat 504 Géologie,
F-91405 Orsay Cédex, France

Henk **de Haas**
Koninklijk Nederlands Instituut voor
Onderzoek der Zee (NIOZ), P.O. Box
59, NL-1790 AB Den Burg, Texel,
The Netherlands

Ben **De Mol**
Departament d'Estratigrafia,
Paleontologia i Geociències Marines,
Universitat de Barcelona, Martí
Franquès s/n., E-08028 Barcelona,
Spain

Henko **de Stigter**
Koninklijk Nederlands Instituut voor
Onderzoek der Zee (NIOZ), P.O. Box
59, NL-1790 AB Den Burg, Texel,
The Netherlands

Karine **Dekindt**
IFREMER, Centre de Brest, BP 70,
F-29280 Plouzané, France

Andrew P. **DeVogelaere**
Monterey Bay National Marine
Sanctuary, 299 Foam Street, Monterey,
CA 93940, USA

Italo **Di Geronimo**
Dipartimento di Scienze Geologiche,
Università di Catania, Corso Italia 55,
I-95129 Catania, Italy

Lyndsey A. **Dodds**
Scottish Association for Marine
Science, Dunstaffnage Marine
Laboratory, Oban, Argyll, PA37 1QA,
UK

Boris **Dorschel**
Department of Geosciences, University
of Bremen, P.O. Box 330 440,
D-28334 Bremen, Germany

William J. **Douros**
Monterey Bay National Marine
Sanctuary, 299 Foam Street, Monterey,
CA 93940, USA

Wolf-Christian **Dullo**
IFM-GEOMAR - Leibniz Institute of
Marine Sciences, Wischhofstr. 1-3,
D-24148 Kiel, Germany

Peter **Etnoyer**
Aquanautix Consulting, 3777 Griffith
View Drive, Los Angeles, CA 90039,
USA

Elizabeth **Fisher**
Department of Earth and Ocean
Sciences, University of Liverpool, 4
Brownlow Street, Liverpool, L69 3GP,
UK

Jeremy J. **Fitzpatrick**
Bowman Bishaw Gorham, P.O. Box
465, Subiaco, Western Australia 6904,
Australia

Günter **Försterra**
Departamento de Biologia Marina,
Universidad Austral de Chile, Avda.
Inés de Haverbeck, casas 9, 11 y 13,
Campus Isla Teja, casilla 567, Valdivia,
Chile

Mike J. **Forde**
Bowman Bishaw Gorham, P.O. Box
465, Subiaco, Western Australia 6904,
Australia

Jan Helge **Fosså**
Institute of Marine Research, P.O.
Box 1879 Nordnes, N-5817 Bergen,
Norway

Anneleen **Foubert**
Renard Centre of Marine Geology,
Gent University, Krijgslaan 281, S8,
B-9000 Gent, Belgium

Norbert **Frank**
Laboratoire des Sciences du Climat
et de l'Environnement (LSCE) Unité
mixte de Recherche CEA-CNRS, Bât.
12, Avenue de la Terrasse, F-91198 Gif-
sur-Yvette Cedex, France

André **Freiwald**
Institute of Paleontology, Erlangen
University, Loewenichstr. 28,
D-91054 Erlangen, Germany

John D. **Gage**
Scottish Association for Marine
Science, Dunstaffnage Marine
Laboratory, Oban, Argyll, PA37 1QA,
UK

Susan E. **Gass**
Scottish Association for Marine
Science, Dunstaffnage Marine
Laboratory, Oban, Argyll, PA37 1QA,
UK

Marcos **Gektidis**
Institute of Paleontology, Erlangen
University, Loewenichstr. 28,
D-91054 Erlangen, Germany

R. Grant **Gilmore** Jr.
Estuarine, Coastal, and Ocean Sciences,
Inc., 5920 1st St. SW, Vero Beach,
FL 32968, USA

James L. **Goedert**
Geology and Paleontology Division,
Burke Museum of Natural History and
Culture, University of Washington,
Seattle, WA 98195, USA

David M. **Gordon**
Woodside Energy Ltd, Box D188,
GPO Perth, Western Australia 6840,
Australia

Adriana **Gracia**
Instituto de Investigaciones Marinas
y Costeras, INVEMAR, Cerro
Punta Betín, AA 1016, Santa Marta,
Colombia

Anthony **Grehan**
Martin Ryan Marine Science Institute,
National University of Ireland, Galway,
Ireland

Vreni **Häussermann**
Departamento de Biologia Marina,
Universidad Austral de Chile, Avda.
Inés de Haverbeck, casas 9, 11 y 13,
Campus Isla Teja, casilla 567, Valdivia,
Chile

Stefan **Hain**
UNEP Coral Reef Unit (CRU), UNEP
World Conservation Monitoring Centre,
219 Huntingdon Road, Cambridge
CB3 0DL, UK

Jason **Hall-Spencer**
Department of Biological Sciences,
University of Plymouth, Plymouth,
PL4 8AA, UK

Lorraine C. **Hamilton**
Fisheries and Oceans Canada, Bedford
Institute of Oceanography, Dartmouth,
Nova Scotia, Canada

Andrea D. **Hawkes**
Sea Level Research Laboratory,
Department of Earth and
Environmental Science, University of
Pennsylvania, Philadelphia,
PA 19104-6313, USA

Dierk **Hebbeln**
Department of Geosciences, University
of Bremen, P.O. Box 330 440,
D-28334 Bremen, Germany

Jeffrey M. **Heikoop**
Los Alamos National Laboratory, EES-
6, MSD462, Los Alamos, NM 87545,
USA

Kari B. **Heinonen**
National Undersea Research Center,
Department of Marine Sciences,
University of Connecticut, Groton,
CT 06340, USA

Jean-Pierre **Henriet**
Renard Centre of Marine Geology,
Gent University, Krijgslaan 281, S8,
B-9000 Gent, Belgium

Claude **Hillaire-Marcel**
GEOTOP, Université du Québec à
Montréal and McGill University,
Québec, Canada

Michael F. **Hirshfield**
Oceana, 2501 M Street NW
#300,Washington DC 20037,USA

Martin **Hovland**
Statoil, N-4035 Stavanger, Norway

Veerle A. I. **Huvenne**
Renard Centre of Marine Geology,
Gent University, Krijgslaan 281, S8,
B-9000 Gent, Belgium

Lisbeth **Jonsson**
Tjärnö Marine Biological Laboratory,
SE-452 96 Strömstad, Sweden

Anne **Juillet-Leclerc**
Laboratoire des Sciences du Climat
et de l'Environnement (LSCE) Unité
mixte de Recherche CEA-CNRS, Bât.
12, Avenue de la Terrasse, F-91198 Gif-
sur-Yvette Cedex, France

Ellen L. **Kenchington**
Fisheries and Oceans Canada, Bedford
Institute of Oceanography, Dartmouth,
Nova Scotia, Canada

Lisa A. **Kerr**
Moss Landing Marine Laboratories,
8272 Moss Landing Road, Moss
Landing, CA 95039, USA

Chad E. **King**
Sanctuary Integrated Monitoring
Network, Monterey Bay National
Marine Sanctuary, 299 Foam Street,
Monterey, CA 93940, USA

Les **Kinsley**
Research School of Earth Sciences,
Australian National University,
Canberra, ACT 0200, Australia

Kostas **Kiriakoulakis**
Department of Earth and Ocean
Sciences, University of Liverpool, 4
Brownlow Street, Liverpool, L69 3GP,
UK

Michael **Klages**
Alfred Wegener Institute for Polar and
Marine Research, Am Handelshafen 12,
D-27570 Bremerhaven, Germany

Randall E. **Kochevar**
Monterey Bay Aquarium, 886 Cannery
Row, Monterey, CA 93940, USA

Christopher C. **Koenig**
Institute for Fishery Resource Ecology
(FSU/NMFS), Florida State University,
Tallahassee, FL 32306-1100, USA

Maxim **Kozachenko**
Coastal and Marine Resources Centre,
Environmental Research Institute,
University College Cork, Ireland

Manfred **Krautter**
Institute of Geology and Palaeontology,
Herdweg 51, D-70174 Stuttgart,
Germany

Laurent **Labeyrie**
Laboratoire des Sciences du Climat
et de l'Environnement (LSCE) Unité
mixte de Recherche CEA-CNRS, Bât.
12, Avenue de la Terrasse, F-91198 Gif-
sur-Yvette Cedex, France

Andy P. **Lane**
Woodside Energy Ltd, Box D188,
GPO Perth, Western Australia 6840,
Australia

Marie C. **Le Goff-Vitry**
School of Ocean and Earth Science,
Southampton Oceanography Centre,
Empress Dock, Southampton,
SO14 3ZH, UK

Helmut **Lehnert**
Eichenstr. 14, D-86507
Oberottmarshausen, Germany

Tanya L. **Leverette**
Department of Oceanography,
Dalhousie University, Halifax, Nova
Scotia, B3H 4J1, Canada

Björn **Lindberg**
Department of Geology, University of Tromsö, Norway, Dramsveien 201, N-9037 Tromsö, Norway

Matthias **López Correa**
Institute of Paleontology, Erlangen University, Loewenichstr. 28, D-91054 Erlangen, Germany

Tomas **Lundälv**
Tjärnö Marine Biological Laboratory, SE-452 96 Strömstad, Sweden

Craig **Lundstrom**
Department of Geology, University of Illinois, Urbana Champaign, 255 Natural History Building, 1301 West Green Street, Urbana, IL 61801, USA

Audrey **Lutringer**
Laboratoire des Sciences du Climat et de l'Environnement (LSCE) Unité mixte de Recherche CEA-CNRS, Bât. 12, Avenue de la Terrasse, F-91198 Gif-sur-Yvette Cedex, France

Augusto **Mangini**
Heidelberg Academy of Sciences, Im Neuenheimer Feld 229, D-69120 Heidelberg, Germany

Douglas G. **Masson**
Southampton Oceanography Centre, Empress Dock, Southampton, SO14 3ZH, UK

Asako K. **Matsumoto**
Department of Earth and Planetary Science, University of Tokyo, 7-3-1, Hongo, Tokyo 113-0033, Japan

Mona **McCrea**
Ecological Consultancy Services Ltd (EcoServe), B19, K.C.R. Industrial Estate, Kimmage, Dublin 12, Ireland

Malcolm **McCulloch**
Research School of Earth Sciences, Australian National University, Canberra, ACT 0200, Australia

John J. **McDonough** III
U.S. National Oceanic and Atmospheric Administration, Silver Springs, MD 20910, USA

Luz Marina **Mejía-Ladino**
Instituto de Investigaciones Marinas y Costeras, INVEMAR, Cerro Punta Betín, AA 1016, Santa Marta, Colombia

David T. **Meldrum**
Scottish Association for Marine Science, Dunstaffnage Marine Laboratory, Oban, Argyll, PA37 1QA, UK

Duncan J. **Mercer**
Scottish Association for Marine Science, Dunstaffnage Marine Laboratory, Oban, Argyll, PA37 1QA, UK

Mike **Mertens**
Ecotrust, 721 NW Ninth Avenue, Portland, OR 97209, USA

Carlo **Messina**
Dipartimento di Scienze Geologiche, Università di Catania, Corso Italia 55, I-95129 Catania, Italy

Anna **Metaxas**
Department of Oceanography,
Dalhousie University, Halifax, Nova
Scotia, B3H 4J1, Canada

Jürgen **Mienert**
Department of Geology, University of
Tromsö, Norway, Dramsveien 201,
N-9037 Tromsö, Norway

Christian **Mohn**
Department of Earth and Ocean
Sciences, National University of
Ireland, Galway, Ireland

Paolo **Montagna**
Department of Mineralogy and
Petrology, University of Padua, Italy

F. Xavier **Monteys**
Geological Survey of Ireland, Beggars
Bush, Haddington Road, Dublin 4,
Ireland

Jon **Moore**
Florida Atlantic University, Honors
College, Jupiter, FL 33458, USA

Lance E. **Morgan**
Marine Conservation Biology Institute,
4878 Warm Springs Rd., Glen Ellen,
CA 95442, USA

Pål B. **Mortensen**
Benthic Habitat Research Group,
Institute of Marine Research, P.O.
Box 1870 Nordnes, N-5817 Bergen,
Norway

Gareth **Mottram**
Remote Sensing Group, Plymouth
Marine Laboratory, Plymouth, UK

George **Mungov**
Institute of Ocean Sciences, Sidney,
BC, Canada

Gabriel **Navas**
Instituto de Investigaciones Marinas
y Costeras, INVEMAR, Cerro
Punta Betín, AA 1016, Santa Marta,
Colombia

Julie B. **Olson**
Department of Biological Sciences,
University of Alabama, Tuscaloosa,
AL 35487, USA

Karine **Olu-Le Roy**
IFREMER, Centre de Brest, BP 70,
F-29280 Plouzané, France

Jan **Opderbecke**
IFREMER - Underwater Robotics,
Navigation and Vision Department
(RNV), Zone Portuaire de Brégaillon,
F-83507 La Seyne-sur-mer, France

Martine **Paterne**
Laboratoire des Sciences du Climat
et de l'Environnement (LSCE) Unité
mixte de Recherche CEA-CNRS, Bât.
12, Avenue de la Terrasse, F-91198 Gif-
sur-Yvette Cedex, France

Jörn **Peckmann**
Research Center for Ocean Margins,
University of Bremen, P.O. Box
330 440, D-28334 Bremen, Germany

Oliver C. **Peppe**
Scottish Association for Marine
Science, Dunstaffnage Marine
Laboratory, Oban, Argyll, PA37 1QA,
UK

Brett **Phaneuf**
Department of Oceanography, Texas A
and M University, College Station,
TX 77845, USA

Mark **Powell**
The Ocean Conservancy, 2479
Soundview Dr. NE, Bainbridge Island,
WA 98110, USA

Kimberly A. **Puglise**
U.S. National Oceanic and
Atmospheric Administration, Silver
Springs, MD 20910, USA

Maarten **Raes**
Marine Biology Section, Gent
University, Krijgslaan 281, S8,
B-9000 Gent, Belgium

John K. **Reed**
Harbor Branch Oceanographic
Institution, 5600 U.S. 1, North, Fort
Pierce, FL 34946, USA

Henry **Reiswig**
Royal British Columbia Museum, 675
Belleville Street, Victoria BC,
V8W 3N5, Canada

Joachim **Reitner**
Geobiology-GZG, Göttingen
University, Goldschmidtstr. 3,
D-37077 Göttingen, Germany

Alessandro **Remia**
ISMAR-Marine Geology Division,
CNR, Via Gobetti 101,
I-40129 Bologna, Italy

Javier **Reyes**
Instituto de Investigaciones Marinas
y Costeras, INVEMAR, Cerro
Punta Betín, AA 1016, Santa Marta,
Colombia

Michael J. **Risk**
School of Geography and Geology,
McMaster University, Hamilton ON,
L8S 4M1, Canada

J. Murray **Roberts**
Scottish Association for Marine
Science, Dunstaffnage Marine
Laboratory, Oban, Argyll, PA37 1QA,
UK

Santi **Roberts**
Oceana, 2501 M Street NW
#300,Washington DC 20037,USA

Alex D. **Rogers**
British Antarctic Survey, High Cross,
Madingley Road, Cambridge,
CB3 0ET, UK

Claire **Rollion-Bard**
CRPG-CNRS, BP 20, 15, rue Notre-
Dame des Pauvres,
F-54500 Vandoeuvre-lès-Nancy, France

Antonietta **Rosso**
Dipartimento di Scienze Geologiche,
Università di Catania, Corso Italia 55,
I-95129 Catania, Italy

Greg **Rouse**
South Australian Museum, Nth Terrace,
Adelaide, Australia

Andres **Rüggeberg**
IFM-GEOMAR - Leibniz Institute of
Marine Sciences, Wischhofstr. 1-3,
D-24148 Kiel, Germany

Nicolás G. **Sandoval**
Compañía SECEGSA (Sociedad
Española de Comunicaciones del
Estrecho de Gibraltar), Estébanez
Calderón, 3 - 1º, E-28020 Madrid,
Spain

Rossana **Sanfilippo**
Dipartimento di Scienze Geologiche, Università di Catania, Corso Italia 55, I-95129 Catania, Italy

Nadiezhda **Santodomingo**
Instituto de Investigaciones Marinas y Costeras, INVEMAR, Cerro Punta Betín, AA 1016, Santa Marta, Colombia

Kathryn M. **Scanlon**
U.S. Geological Survey, 384 Woods Hole Road, Woods Hole, MA 02543, USA

Astrid J. **Scholz**
Ecotrust, 721 NW Ninth Avenue, Portland, OR 97209, USA

William W. **Schroeder**
Marine Science Program, University of Alabama, Dauphin Island Sea Lab, Dauphin Island, AL 36528, USA

Andrea **Schröder-Ritzrau**
Heidelberg Academy of Sciences, Im Neuenheimer Feld 229, D-69120 Heidelberg, Germany

Francesco **Sciuto**
Dipartimento di Scienze Geologiche, Università di Catania, Corso Italia 55, I-95129 Catania, Italy

David B. **Scott**
Department of Earth Science, Dalhousie University, Halifax, Nova Scotia, B3H 3J5, Canada

Timothy M. **Shank**
Woods Hole Oceanographic Institution, Biology Department, MS 33, Woods Hole, MA 02543, USA

Chip **Shearer**
Institute of Meteoritics, University of New Mexico, Albuquerque, NM 87131, USA

Andrew N. **Shepard**
National Undersea Research Center, University of North Carolina, 5600 Marvin K. Moss. Lane, Wilmington, NC 28409, USA

Owen A. **Sherwood**
Centre for Marine Geology, Dalhousie University, Halifax, Nova Scotia, B3H 4J1, Canada

Geoff **Shester**
Interdisciplinary Program in Environment and Resources, Stanford University, USA

Daniel J. **Sinclair**
GEOTOP, Université du Québec à Montréal and McGill University, Québec, Canada

Kevin B. **Strychar**
Department of Earth Science, Dalhousie University, Halifax, Nova Scotia, B3H 3J5, Canada

Ingvald **Svellingen**
Institute of Marine Research, P.O. Box 1879 Nordnes, N-5817 Bergen, Norway

Paul **Sylvester**
Memorial University of Newfoundland, St John's, Newfoundland, Canada

Mario N. **Tamburri**
Chesapeake Biological Laboratory, University of Maryland, P.O. Box 38, Solomons, MD 20688, USA

Marco **Taviani**
ISMAR-Marine Geology Division,
CNR, Via Gobetti 101,
I-40129 Bologna, Italy

Jörn **Thiede**
Alfred Wegener Institute for Polar and
Marine Research, Am Handelshafen 12,
D-27570 Bremerhaven, Germany

Richard E. **Thomson**
Institute of Ocean Sciences, Sidney,
BC, Canada

William T. **Thomson**
Scottish Association for Marine
Science, Dunstaffnage Marine
Laboratory, Oban, Argyll, PA37 1QA,
UK

Jürgen **Titschack**
Institute of Paleontology, Erlangen
University, Loewenichstr. 28,
D-91054 Erlangen, Germany

Tonatiuh **Trejo**
Moss Landing Marine Laboratories,
8272 Moss Landing Road, Moss
Landing, CA 95039, USA

Mike **Tubrett**
Memorial University of Newfoundland,
St John's, Newfoundland, Canada

David **van Rooij**
Renard Centre of Marine Geology,
Gent University, Krijgslaan 281, S8,
B-9000 Gent, Belgium

Tjeerd C. E. **van Weering**
Koninklijk Nederlands Instituut voor
Onderzoek der Zee (NIOZ), P.O. Box
59, NL-1790 AB Den Burg, Texel,
The Netherlands

Ann **Vanreusel**
Marine Biology Section, Gent
University, Krijgslaan 281, S8,
B-9000 Gent, Belgium

Agostina **Vertino**
Institute of Paleontology, Erlangen
University, Loewenichstr. 28,
D-91054 Erlangen, Germany

Rhian G. **Waller**
Woods Hole Oceanographic Institution,
Biology Department, MS 33, Woods
Hole, MA 02543, USA

Les **Watling**
Darling Marine Center, University of
Maine, Walpole, ME 04573, USA

Oliver **Weidlich**
Department of Geology, Royal
Holloway University of London,
Egham, Surrey, TW20 0EX,UK

Andrew J. **Wheeler**
Department of Geology, Environmental
Research Institute, University College
Cork, Ireland

Martin **White**
Department of Earth and Ocean
Sciences, National University of
Ireland, Galway, Ireland

Frank **Whitney**
Institute of Ocean Sciences, Sidney,
BC, Canada

Branwen **Williams**
School of Geography and Geology,
McMaster University, Hamilton ON,
L8S 4M1, Canada

J.H. Martin **Willison**
School for Resource and
Environmental Studies, Dalhousie
University, Halifax, Nova Scotia,
B3H 3J5, Canada

Max **Wisshak**
Institute of Paleontology, Erlangen
University, Loewenichstr. 28,
D-91054 Erlangen, Germany

George A. **Wolff**
Department of Earth and Ocean
Sciences, University of Liverpool, 4
Brownlow Street, Liverpool, L69 3GP,
UK

Helmut **Zibrowius**
Centre d'Océanologie de Marseille,
Station Marine d'Endoume, Rue
Batterie des Lions, F-13007 Marseille,
France

I

The paleoenvironmental context

Chapter content

Azooxanthellate corals in the Late Maastrichtian - Early Paleocene of the Danish basin: bryozoan and coral mounds in a boreal shelf setting

Michaela Bernecker[1], Oliver Weidlich[2]

[1]Institute of Paleontology, Erlangen University, Loewenichstr. 28, D-91054
  Erlangen, Germany
  (bernecker@pal.uni-erlangen.de)
[2] Department of Geology, Royal Holloway University of London, Egham, Surrey,
  TW20 0EX,UK

Abstract. The Late Cretaceous-Danian of the northwest European shelf represents one of the largest and longest-lived cool-water carbonate shelves in the stratigraphic record. The palaeolatitude of the Danish basin was 45°N during that time. The heterozoan faunas are dominated by bryozoans, echinoids, molluscs, brachiopods, serpulids, and, to varying degree, by azooxanthellate corals. During the Late Maastrichtian, rare soft-substrate-dwelling solitary scleractinians occur, including *Parasmilia cylindrica*, *P. excavata*, *Caryophyllia* sp. as well as octocorals, especially *Moltkia minuta*. Contemporaneous bryozoan mound complexes below the photic zone, which provided hard substrates for the settlement of larvae, were not colonized by azooxanthellate corals.

Neither environmental nor faunal changes among the corals across the Cretaceous-Tertiary (K/T) boundary were significant. After the K/T boundary, the first solitary corals (moulds of *Parasmilia biseriata, P. cincta, Trochocyathus hemisphaericus, Caryophyllia* sp.) and octocorals appeared in the Cerithium Limestone, which lies above the Fish Clay. Similar to their Late Maastrichtian counterparts, these corals formed level-bottom communities.

The Early Danian post-Cerithium Limestone represents the peak of bryozoan mound development. Corals are present but rare. The Middle Danian is characterized by reduced bryozoan mound growth and by the mound-forming dendroid scleractinians *Dendrophyllia candelabrum, Oculina becki* and *Faksephyllia faxoensis*, which flourished predominantely in the vicinity of the Ringkøbing-Fyn High. Nine species of solitary scleractinians, stylasterinid hydrocorals, and octocorals contributed to reef building. Important criteria for the interpretation of "cold and deep-water coral bioherms" are (1) absence of algae, (2) low-diverse azooxanthellate coral communities, (3) dominance of dendroid growth forms in the corals, (4) surrounding pelagic sediment adjacent to the coral mounds, (5) occurrence of pelagic organisms (globigerinid foraminifers, coccoliths) in the

lime mud, (6) breakdown of coral colonies predominantly by bioerosion instead of mechanical destruction waves, (7) mound- or bank-like morphology of the buildups and (8) occurrence at a high palaeolatitude.

Mound morphology and growth direction were traced by variations in the abundance of colonial corals. Gross morphology of scleractinian corals, stylasterinid hydrocorals and octocorals suggests an azooxanthellate character of the reefbuilders: the scleractinians developed dendroid growth forms, while stylasterinids and octocorals formed fan-like colonies oriented perpendicular to the nutrient-rich currents. Strong bioerosion was responsible for the breakdown of the skeletons, and the resulting bioclasts formed the substrate for larvae.

Modern azooxanthellate *Oculina* coral reefs along the shelf edge off central eastern Florida, USA show similarities in position, morphology, environment, water depth and current orientation with the coral mounds of the Paleocene and suggest a palaeodepth for the counterparts from the Danish basin of 100-300 m.

Key Words. Azooxanthellate corals, bryozoan mounds, coral mounds, NW European shelf, Cretaceous, Paleocene, coral distribution

Introduction

Schlager (2000) differentiated three carbonate factories comprising the mound, the tropical, and the cool-water carbonate factories. Among these, carbonate-secreting, cool-water communities and their sediments have been the focus of researchers for more than two decades and are the subject of a rapidly growing body of literature (see Nelson 1988 and James 1997 with further references herein). Cool-water carbonates are the product of the heterozoan community (James 1997), which consists of coralline red algae, bivalves, gastropods, brachiopods, crinoids, echinoids, serpulids, and barnacles. Azooxanthellate corals (scleractinians lacking algal symbionts) contribute to a varying degree to the accumulation of carbonate. Coral reefs of modern temperate and boreal environments are also currently being investigated in detail (e.g., Freiwald et al. 1997; Malakoff 2003) although their existence has been known for more than 60 years (e.g., Dons 1944; Teichert 1958). Conversely, the distributional patterns of scleractinians, hydrocorals and octocorals from Cretaceous and Tertiary environments attracted few authors (e.g., Floris 1980; Bernecker and Weidlich 1990; Willumsen 1995), although the first taxonomic data go back to the 19th century. Well-exposed Maastrichtian-Danian cool-water carbonate deposits from northwest Europe yield corals in different environments and, thus, represent one of the most important study areas for the investigation of Mesozoic and Tertiary coral faunas in boreal and temperate realms. The shelf area was situated between palaeolatitudes 35°-50°N and our study area, the Danish basin, had a palaeoposition of about 45°N. The Maastrichtian-Danian of the northwest European shelf represents one of the largest and longest-lived cool-water carbonate accumulations (Surlyk 1997) and is a paradigm for the birth, climax, and demise of cool-water carbonate shelves. The Danish basin, which was situated fully within the mid latitude association of Lees (1975), is characterized by abundant

benthos including molluscs, brachiopods, echinoderms, bryozoans, serpulids, siliceous sponges and corals. The lime mud largely consists of pelagic coccoliths. The chalks of the mid and inner boreal shelf and over structural highs are especially rich in bryozoans, which are mound-forming shoreward and towards tectonic highs. Although azooxanthellate, non-tropical corals occur quite commonly during the Cenomanian-Danian, they are mound- and bank-forming exclusively during the Middle Danian.

The aim of our study is to (1) summarize the distributional patterns of the corals and bryozoans of the Danish basin during the Maastrichtian-Danian, (2) to provide a general picture of the coral faunas before and after the K/T boundary, (3) to summarize the knowledge of the impressive Middle Danian coral mound complexes, and (4) to recognize the main controlling parameters for scleractinians, hydrocorals and octocorals.

Geological setting

A number of major sedimentary basins occurred in northwest Europe during the Maastrichtian-Danian time. Among these, the Danish basin is the most important locality to study the distributional patterns of azooxanthellate corals (Fig. 1). The elongated depression of the Danish basin had a NW-SE orientation and extended from the Central Graben of the North Sea in the northwest, *via* Denmark to Poland in the southeast and was connected from time to time with the Tethys. Tectonic movements complicated the topography of the basin and controlled facies heterogeneity. The southern and south-western margin of the Danish basin is formed by the Ringkøbing-Fyn High, which was a tectonically stable uplift area during the Danian (Thomsen 1995). The village of Fakse in southeastern Sealand is situated at the rim of the Ringkøbing-Fyn High and represents the site of the most prolific coral growth with intense mound development (Fig. 1). Smaller coral mounds have been described from Limhamn, Aggersborggaard, Spjelderup, and Herlufsholm (see Bernecker and Weidlich 1990 and further references herein).

Sea level is an important factor controlling the sedimentary patterns of Mesozoic and Cenozoic basins. From the Late Maastrichtian-Middle Danian, four sequence boundaries were observed in the Danish basin (Surlyk 1997). During this time interval, sea level was highest during the Late Maastrichtian. Prominent lowstands occur at the K/T boundary (Fish Clay), overlying the Cerithium Limestone, at the end of Early and Middle Danian, and within the Middle Danian (Fig. 2). With the exception of the K/T boundary, sea level lowstands are indicated by hardgrounds and caused no significant change in the sedimentologic patterns. During the subsequent transgression, cool-water carbonates were deposited again.

The palaeogeographic maps of Golonka et al. (1994) provide useful information concerning connecting gateways of the Danish basin, which are in turn of major importance for the reconstruction of migration patterns of invertebrates. During the Maastrichtian, the phase of highest sea level, the Danish basin was connected to the polar ocean in the north and to the Tethys in the southeast. This latter connection was most probably lost during the Danian. As a consequence, larval migration patterns
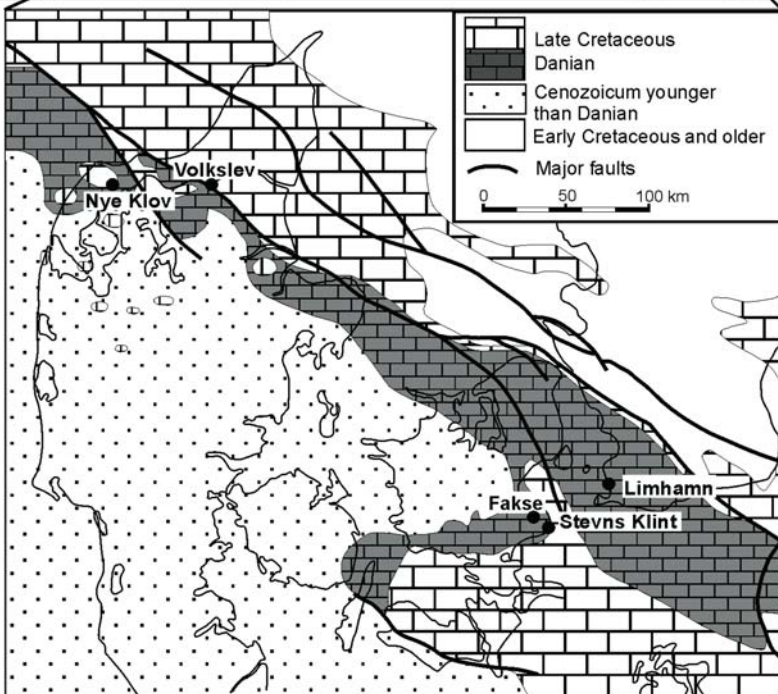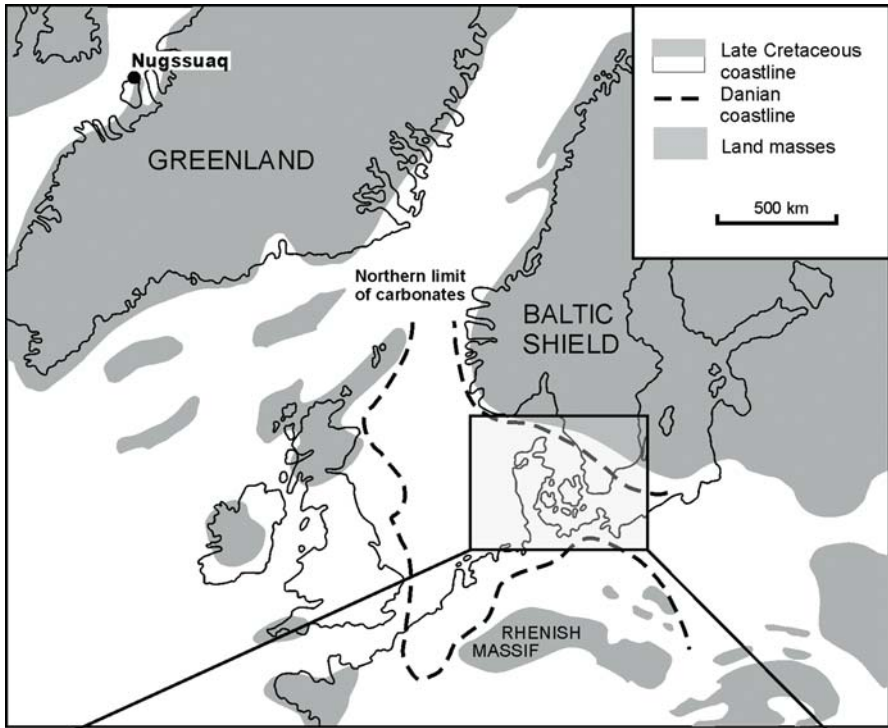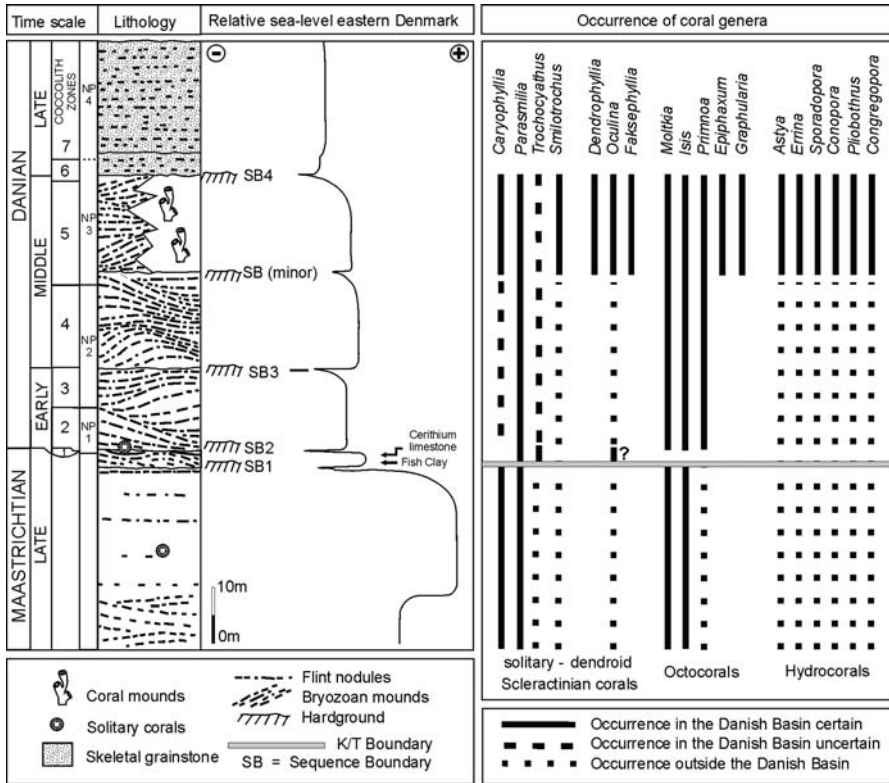
Fig. 2 Schematic section through the Late Maastrichtian-Danian of eastern Denmark based on data from Stevns Klint and Fakse showing stratigraphy (standard nannoplankton zones, local coccolith zones) (Thomsen 1995), relative sea level curve (Surlyk 1997), and coral distribution

from the north are most likely, as demonstrated by the occurrence of Maastrichtian and Danian coral-rich strata in Greenland (Floris 1972).

Maastrichtian-Danian deposits of the Danish basin are almost exclusively carbonates representing a ramp setting (Surlyk 1997). A generalized facies succession from the Baltic shield to the centre of the Danish basin comprises (1) skeletal sandstone, (2) skeletal siltstone, (3) intercalation of bryozoan packstone mounds and coral mounds, (4) small bryozoan wackestone mounds, (5) benthos-rich chalk, and (6) benthos-poor chalk. The change from carbonate to clastic sedimentation commenced with the deposition of the basinal Kerteminde Marl and the marginal Lellinge Green Sand with the beginning of the Selandian.

Fig. 1 Palaeogeography of the North-European-North Atlantic region during Maastrichtian-Danian, based on Ziegler (1990), Thomsen (1995) and Surlyk (1997). Distribution of Maastrichtian-Tertiary strata in the Danish basin follows Håkansson and Thomsen (1999)

Late Maastrichtian level-bottom and mound communities

The Maastrichtian sediments exposed at Stevns Klint reveals the greatest lithologic diversity in comparison to localities of the same age, which record the K/T boundary with higher resolution (e.g., Nye Kløv or Vokslev, see Heinberg 1999; Håkansson and Thomsen 1999) and, thus, are ideal to study the distributional patterns of azooxanthellate corals (Fig. 3). The following vertical lithologic succession occurs from top to base (e.g., Surlyk and Håkansson 1999):

Latest Maastrichtian bryozoan chalk mounds: Just below the K/T boundary, asymmetric bryozoan mounds with a maximum height of 4 m represent the oldest bryozoan buildups in the Danish basin. The southern flanks with silicified *Thalassinoides*-burrows are more prominent than their northern counterparts. The mounds are predominantly composed of lime mud and broken fragments of bryozoans, which reach maximum packing densities of 20 %.

Horizon of hardgrounds: Two very minor hardgrounds and a prominent horizon of flint representing silicified *Thalassinoides*-burrows characterize this unit. According to Surlyk (1997), these hardgrounds are indicative of a fall of relative sea level.

Deep-water Maastrichtian chalk: This interval at the base of the section is a transition from bryozoan-rich chalk with wavy layers (below shoreline in Fig. 3) to horizontal chalk with fewer bryozoans and abundant *Zoophycos*-burrows. The benthos-poor facies represents the facies of greatest water depth in comparison to the other facies types.

In addition to the dominating cheilostome and cyclostome bryozoans, the Late Maastrichtian benthos comprises a diverse assemblage of serpulids, bivalves, brachiopods, echinoderms and siliceous sponges, biased by a calcite preservation taphonomy (e.g., Heinberg 1999). Scleractinian corals are represented by solitary taxa including *Parasmilia excavata, Parasmilia cylindrica,* and *Caryophyllia* sp. (Fig. 2). An uncertain specimen of a dendroid scleractinian that has been mentioned in the literature (Floris 1979) is not considered. Octocorals are represented by *Moltkia minuta* and *Isis* sp. Solitary scleractinians and octocorals are not a dominating group throughout the section and occur subordinately. Thus, it is hardly possible to differentiate between sampling biases and substrate preferences. Field analysis suggests however that both coral groups preferred deep-water chalk facies. The coral occurrences within the bryozoan mounds or on hardgrounds are unknown. Solitary scleractinians and octocorals developed colonization strategies for this soft-bottom environment. Octocoral larvae settled commonly on larger fossils including belemnite rostra or tests of irregular echinoids. Some solitary corals were attached during life to a substrate and developed a broad base (see Surlyk 1974: Fig.1).

Fig. 3 Maastrichtian-Danian section from Stevns Klint showing the position of the K/T boundary. **A** Overview of the Late Maastrichtian (1) and Danian cool-water carbonates (3). Note position of K/T boundary (2). The rectangle refers to the close up view of Fig. 3B. **B** Close-up of the transition from Late Maastrichtian horizontally bedded chalk (1) with
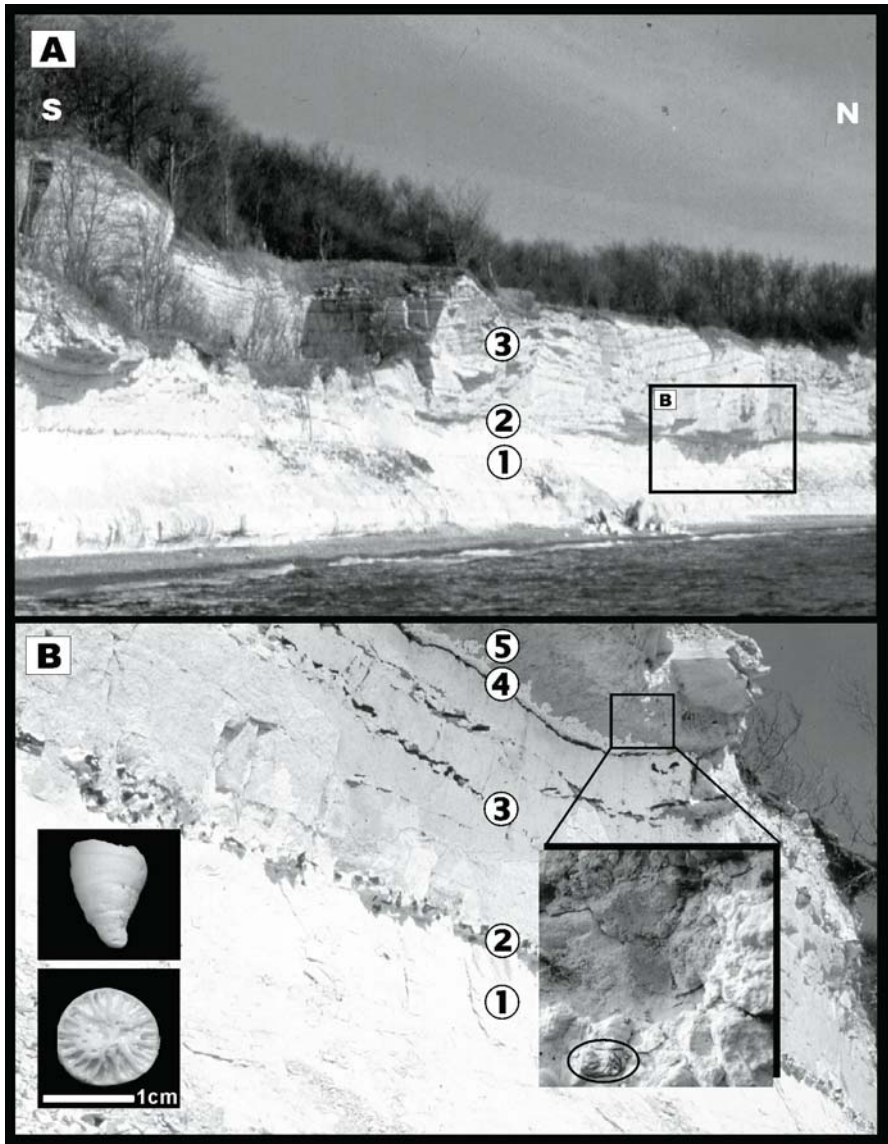
prominent horizon of flint (2) to bryozoan mounds with asymmetrical flanks (3). The Fish Clay (4) representing the K/T boundary reaches the greatest thickness in intermound troughs and pinches out towards the top of Maastrichtian mounds. The Cerithium Limestone (5) marks the onset of prolific boreal carbonate production. Both the tops of the Late Maastrichtian mounds and the Early Danian Cerithium Limestone filling the intermound depressions are capped by a hardground (not visible). The inset pictures (left side) represent an axial and longitudinal view of Maastrichtian *Parasmilia cylindrica* (solitary coral), a typical Maastrichtian soft-bottom dweller. The inset picture (right side) is a close up view of the Cerithium Limestone showing a mould of a solitary coral

Other specimens lived attached to a hard substrate only during an early ontogenic stage. During their lifetime, they broke off and adopted a free-living lifestyle on the sediment. This mode of life is characterized by slightly bent calices and an eroded base (Fig. 3). To conclude, the Maastrichtian solitary corals and octocorals represent a low-diverse level-bottom community that did not develop habitats for new organisms.

Early Danian level-bottom community

The Fish Clay marks the only prominent collapse of the cool-water carbonate factory during the Maastrichtian-Danian. As a consequence of the K/T boundary scenario, the clay contains the famous iridium anomaly and fallout products produced by an asterioid impact (e.g., Alvarez et al. 1980; Kastner et al. 1984; Smit 1999). The dark, probably euxinic sediment reaches a maximum thickness of 35 cm in the center of the troughs between the Maastrichtian bryozoan mounds and pinches out towards their tops (Surlyk and Håkansson 1999). Common fossils are small fish scales and teeth (Christensen et al. 1973) as well as dinoflagellate cysts (Wendler and Willems 2002). No coral occurrences have been reported.

The Fish Clay passes gradually upward into the Cerithium Limestone. This unit is characterized by a dense network of *Thalassinoides*-burrows, which are partly filled with bioclasts from the overlying Lower Danian bryozoan limestone. The top of the Cerithium Limestone, another sequence boundary according to Surlyk (1997), is characterized by a submarine erosion and cementation. Benthic metazoans are fairly abundant and represented by bivalves (Heinberg 1999), echinoids, crinoids and gastropods (Rosenkrantz 1939), as well as siliceous sponges. According to Christensen et al. (1973), the Cerithium Limestone is devoid of bryozoans. Interestingly, the first solitary corals occurring after the K/T boundary in the Cerithium Limestone are *Parasmilia biseriata*, *Parasmilia cincta*, and *Trochocyathus hemisphaericus* (Rosenkrantz 1939). These taxa resemble their ancestors from the Maastrichtian deep-water chalk. Our own field data confirm the occurrence of an undeterminable solitary coral in the Cerithium Limestone (Fig. 3B). The specimen is embedded in the Cerithium Limestone and is not part of an infill of younger bryozoan limestone in a previously open *Thalassinoides*-burrow.

Early Danian bryozoan mound community

Bryozoan mound development was especially characteristic of the Early Danian and subordinately during the Middle Danian. The Early Danian mounds of Stevns Klint are typically stacked into mound complexes, separated by at least two orders of erosional surfaces. They are generally 5-10 m high, 50-75 m long and asymmetric in sections parallel to the migration direction. The steepest flanks dip towards the southeast in the direction of the prevailing current. The asymmetry and growth directions are revealed by flint layers formed by silicification of levels rich in *Thalassinoides* reflecting periods of low sedimentation rates. Differences in current velocities favoured the growth of dense thickets of fairly robust bryozoans in the

areas of relatively strong currents on the summit and up-current flank, whereas less robust bryozoans grew on the down-current flank (Thomsen 1983). The robustness of the bryozoan colonies is positively correlated with relative current velocities, whereas the densities were highest in the areas of relatively moderate velocities. The mounds consist of fragmented bryozoans and lime mud composed of debris of coccoliths, globigerinid foraminiferans and small invertebrate shells. The bryozoan content of the wackestone or packstone is typically between 20-45 % (Thomsen 1977, 1983). In addition to suspension feeding cheilostome and cyclostome bryozoans, echinoids, crinoids, brachiopods, bivalves, gastropods, serpulids and asteroids occur. Although bryozoans dominate in both species number and volume, irregular and regular echinoids occur in extreme abundance at many levels (Thomsen 1977, 1983). Corals are rare dwellers of the mounds and include the solitary coral *Parasmilia danica* and two species of octocorals (*Isis steenstrupi*, *Moltkia isis*).

Middle Danian coral and bryozoan mound communities

The Early(?)-Middle Danian of Fakse is characterized by the greatest variability of Maastrichtian-Danian facies including (1) bedded, flint-rich chalk, (2) bryozoan mounds and banks, (3) coral banks and mounds, (4) transitional coral/bryozoan facies overlying of the coral mounds, and (5) muddy intermound facies (Fig. 4).

The **bedded, flint-rich chalk** occurs at the base of Fakse quarry and is rich in lime mud. The benthos is an impoverished level-bottom community with large octocorals (*Moltkia isis*), bryozoans, molluscs (*Pycnodonte vesicularis*), and brachiopods.

The **bryozoan mounds** are chalky, poorly cemented wacke- and packstone with local chert layers emphasizing the mound shape. Recognition criteria of the bryozoan limestones are high percentages of fragmented cheilostome and cyclostome bryozoans. Colonial scleractinian corals and stylasterinid hydrocorals are obviously absent. The bryozoan/micrite ratio may vary greatly.

The faunal assemblages of the **coral banks and mounds** are dominated by suspension feeding corals including solitary and dendroid scleractinians, stylasterinid hydrocorals, and octocorals. We recognized further faunal zones according to the number of corals. Quantitative criteria are based on point-count analysis of thin-sections as well as on field observations (Bernecker and Weidlich 1990). The coral limestone banks and mounds are subdivided according to the dominance of the three scleractinian coral genera and species *Dendrophyllia candelabrum* Henning, 1899, *Faksephyllia faxoensis* (Beck, 1835) and *Oculina becki* (Nielsen, 1922). Bryozoans, hydro- and octocorals are present everywhere within the coral limestone, but occur in varying frequencies. Characteristic facies fossils are missing. The associated fauna of the coral limestone is more highly diverse than that of the bryozoan limestone. The *Dendrophyllia* zone is dominated by *D. candelabrum*. Octocorals and hydrocorals are abundant and bryozoans are more common than within the *Faksephyllia* zone. The *Faksephyllia* zone is dominated by *F. faxoensis*. Octocorals, hydrocorals and bryozoans are rare. The *Oculina* zone is dominated by *O. becki*. Octocorals and hydrocorals are rare, bryozoans are more common.

The **transitional coral/bryozoan facies overlying the coral mounds** represents the transition between bryozoan and coral bioconstructions and is characterized by a percentage of bryozoans exceeding 50 % and a varying number of scleractinian corals; *Dendrophyllia* and *Oculina* are more common than *Faksephyllia*; the bryozoan
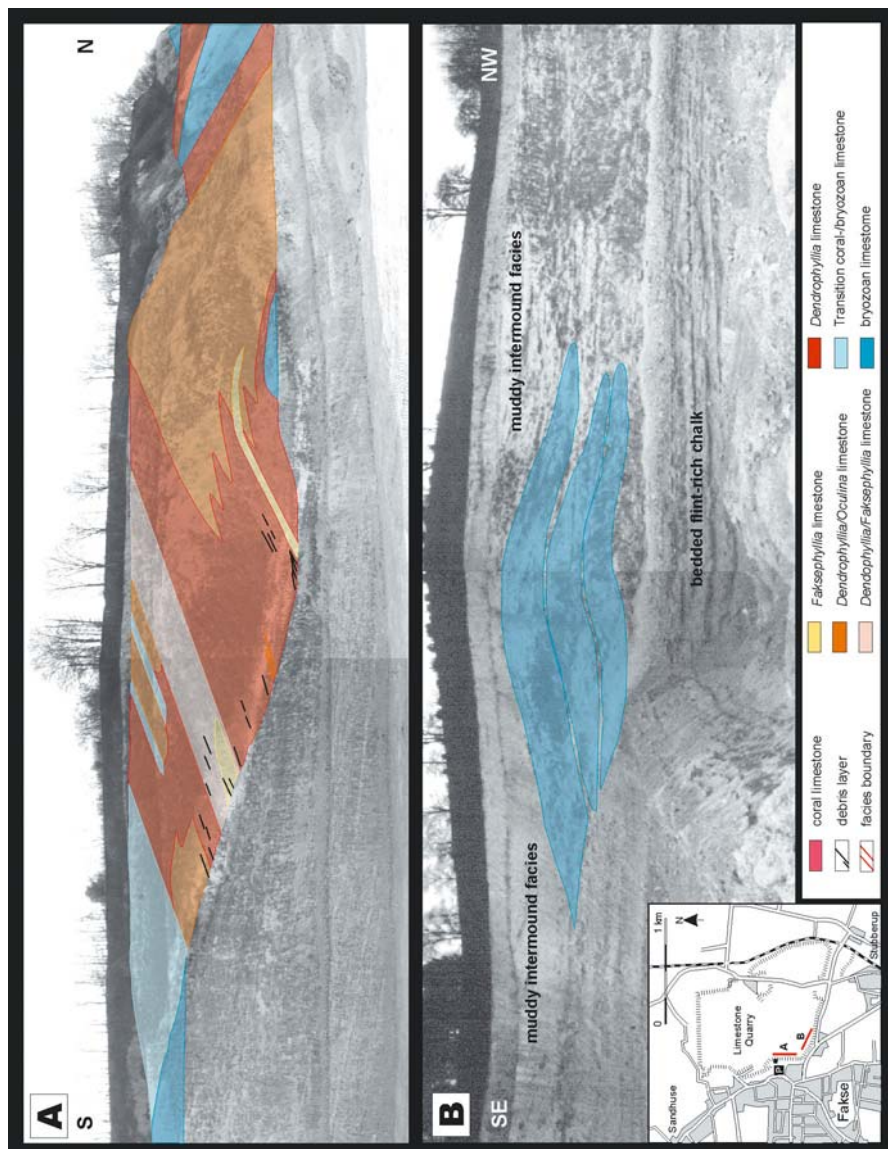
Fig. 4 Mound morphology reconstructed from sections of the Fakse limestone quarry (map). **A** Asymmetrical coral mound with internal growth structure and the dominant growth direction to the south. **B** Bryozoan mound intercalated with flint layers emphasizing the morphology and intermound facies on both sides

encrustations on corals are thicker than within the coral limestone; sponges and sponge spicules occur; octocorals and hydrocorals are rare. Thalassinoid burrows of crustaceans can be found (Bromley 1967). This transition facies is typical for small lenticular shaped bioherms lacking internal zonation patterns.

The **muddy intermound facies** contains octocorals, especially *Moltkia isis* is represented by large colonies.

The Middle Danian **coral banks and mounds** of the Danish basin consist of several ridges, which can be reconstructed from cross- and longitudinal sections. Smaller lenticular-shaped bioherms reach 50 m in length and 15 m in height consisting exclusively of transitional coral/bryozoan facies. The largest coral mounds are 200 m long, 80 m wide and at least 30 m high (Fig. 4A). The exact height cannot be measured, because the top of the mounds is glacially eroded. The large coral mounds exhibit a defined internal zonation according to the dominant coral assemblages. The mound crest is highest near the upcurrent end and falls away gradually (Fig. 4). The growth of corals starts mostly on tops of the preexisting relief. The base of the coral mounds is very distinct. Bioclasts, mostly bryozoans, derived from the underlying bryozoan mounds, decrease towards the base of the coral mounds. This suggests that the pioneer assemblages colonizing the soft sediment required only few skeletal grains for settlement. The corals grew faster on the current-facing side, thereby shaping the coral mound geometry asymmetrically. The sediment is a bioturbated muddy limestone float/rudstone. In addition to the fine sediments produced by bioeroders, the coral rubble is also subject to physical abrasion. Sediments are dominated by mud, gravel-size coral debris and sand particles, which are primarily fragments of corals, bryozoan, molluscs, echinoids, ostracods and foraminifers. Coral fragments comprised the majority of sand-size particles. Much of the mound flanks visible in cross sections is a series of concentrically exposed, lithified crusts with relatively smooth, hard upper surfaces and less consolidated, irregular lower surfaces (Willumsen 1995). Material between successive crusts is poorly cemented or unconsolidated, resulting in eroded and undercut crescentic embayments along the flanks. Most of the sediments occurring within the mounds and surrounding the mounds seem to be of parautochthonous origin. The varying content of broken coral branches is obvious in rock slabs. Modal analysis indicates that the percentage of corals varies between 10-30 %. The size of broken corals ranges between 0.1 mm and 50 cm. Colonial corals in life position are common. Pelagic skeletal grains, such as coccoliths and globigerinids, are important constituents of the lime mud. They are frequent and occur in all subfacies types of the coral limestone. Small southward dipping debris fans of 2-20 cm in thickness and up to 3 m in length can be observed on the current exposed flanks of larger internally differentiated mound structures (Fig. 4). They exhibit an erosional base, consist of grain-supported coral debris with a few limestone lithoclasts and a winnowed micritic fabric.

Faunal inventory of the Middle Danian coral mounds

Although scleractinian diversity of the coral mounds is moderate, new habitats for vertebrates (sharks, fishes, and probably crocodiles, see Floris 1979) and

invertebrates (e.g. *Nautilus* sp.) came into existence. Many of these habitats are unique for Maastrichtian-Danian, contributed to invertebrate diversity and have been found only in Fakse. Of special interest are two types of reef cavities. One type of these crypts resulted from the breakdown of reefbuilders, the other is related to a hardground and housed the enigmatic crinoid *Cyathidium holopus* and siliceous sponges. In addition to the organisms mentioned below, other invertebrates (e.g. molluscs) are represented with many taxa that are not treated here (see Bernecker and Weidlich 1990 for further references).

Dendroid scleractinian corals: The dominant mound-forming corals (Fig. 5) are three genera comprising the species *Dendrophyllia candelabrum* Henning, 1899, *Faksephyllia faxoensis* (Beck, 1835) and *Oculina becki* (Nielsen, 1922). They can be distinguished easily by diameter, wall structure and the mode of budding. *D. candelabrum* (Fig. 6/1, A) is the most common dendroid coral. It is represented
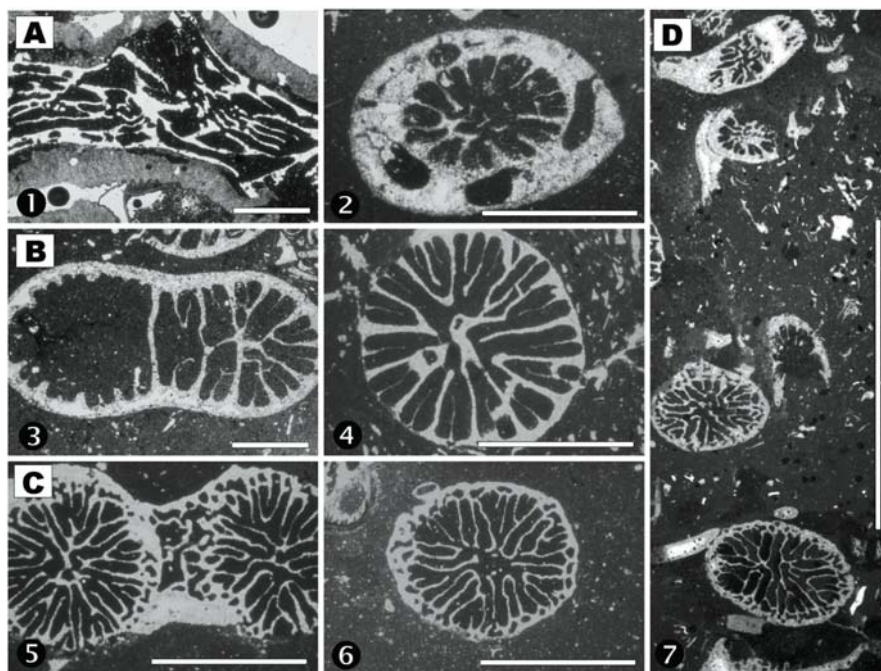
Fig. 5 Photomicrographs of mound-forming scleractinian corals. **A** *Oculina becki* (Nielsen, 1922): (1) longitudinal section with octocoral encrustation; (2) cross section, wall thickened by stereome with sponge boring; all scales are 0.5 cm. **B** *Faksephyllia faxoensis* (Beck, 1835): (3) cross section with intratentacular budding; (4) cross section with septothecal wall, all scales are 0.5 cm. **C** *Dendrophyllia candelabrum* Hennig, 1899: (5) cross section with extratentacular budding; (6) cross section with synapticulothecal wall; all scales are 0.5 cm. **D** *Dendrophyllia candelabrum* and *Oculina becki*: (7) matrix material between *Oculina* (top) and *Dendrophyllia* (base) is carbonate mud with locally derived calcareous skeletal remains (e.g., bryozoan, mollusks, echinoids); scale bar 1 cm
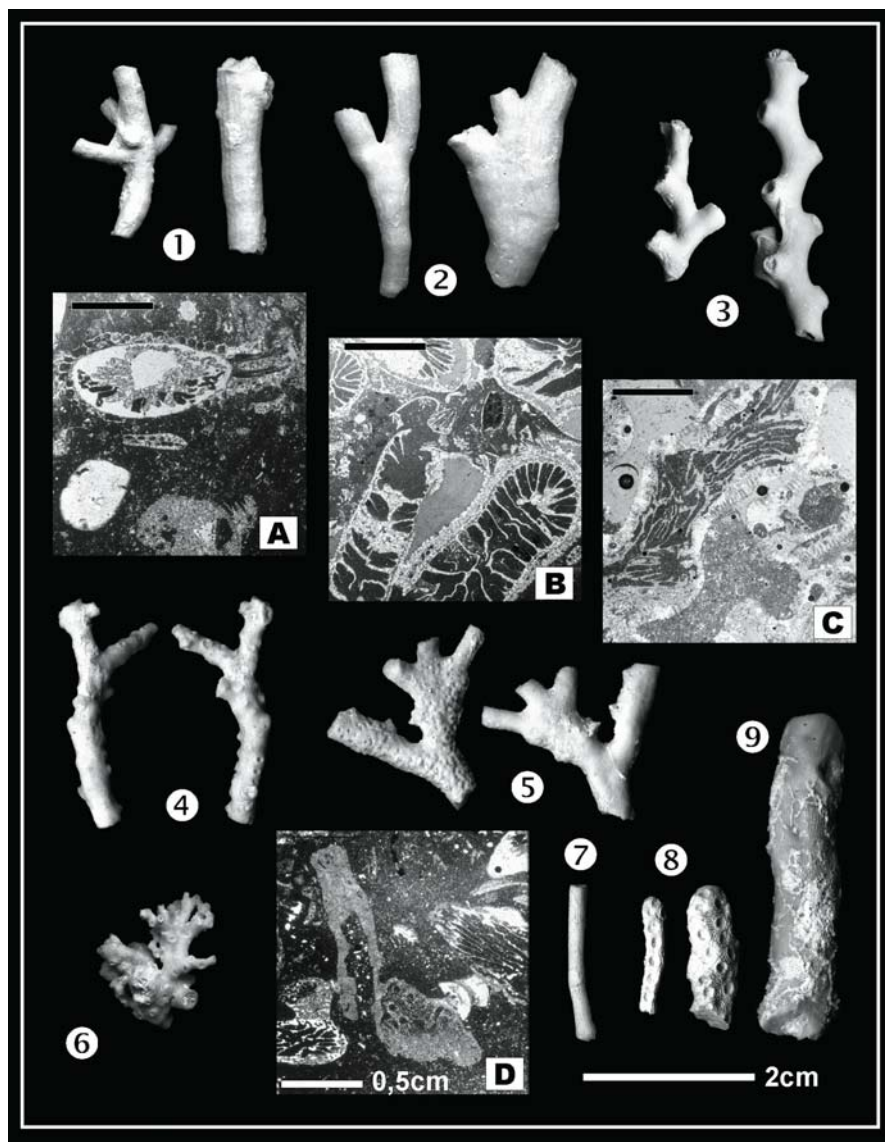
Fig. 6 Colonial scleractinians: 1 *Dendrophyllia candelabrum*, **2** *Faksephyllia faxoensis*, **3** *Oculina becki.*
Stylasterinid hydrocorals: 4 *Conopora arborescens,* **5** *Errina lobata*, **6** *Astya crassus.*
Octocorals: 7 *Isis steenstrupi*, internodium, **8** *Moltkia isis*, juvenile internodia with calices, **9** *Moltkia isis*, adult internodium with postmortal bryozoan encrustations.
Encrustation patterns in thin-sections: A *Dendrophyllia* with serpulid and bryozoan encrustation, **B** *Faksephyllia* with bryozoan encrustation, **C** *Oculina* entirely encrusted by *Moltkia isis*, **D** *Dendrophyllia* with stylasterinid hydrocoral and octocoral

by phaceloid colonies with extratentacular, normal rectangular budding. The wall is synapticulothecal and structured by costae and granules. The diameter of the branches is 0.2-0.4 cm and the size of the colonies is at least 50 cm high. The monospecific taxon *Faksephyllia faxoensis* (Fig. 6/2, B) is known only from the Danian of the Danish basin (Fakse, Limhamn) and Greenland (Nugssuaq), see Fig. 1. The species is characterized by large dendroid colonies, up to 1 m in height, with intratentacular budding. The angle between the buds varies between 20° and 30°. The wall is septothecal and the branch diameter varies between 0.4-0.5 cm. *Oculina becki* (Fig. 6/3,C) formed colonies by extratentacular budding. The buds alternate regularly in two opposite rows and have a constant spacing of 1-1.2 cm. The angle of the buds varies between 50°-55°. The branch diameter is 0.20-0.55 cm. The specimens thicken their wall by stereome and are commonly bored by endolithic sponges.

Solitary scleractinian corals: Solitary scleractinians are attached to dendroid colonies. They can change their growth direction up to 90° and orientate their calices in the direction of nutrient-rich currents. Nielsen (1919, 1922) described 9 species from the Danian, but only *Smilotrochus faxoensis* (Fig. 7A-1, 4, 5); *Caryophyllia danica* (Fig. 7A-2, 3) and *Parasmilia lindstroemi* (Fig. 7A-6) are frequent.

Hydrocorals: Branching and fan-shaped hydrocorals are an important constituent of the coral mounds. All genera collected in the Middle Danian are known from Cretaceous to Recent. Nielsen described 9 stylasterinid taxa from the coral limestone. Among them, *Sporadopora faxensis* (Nielsen, 1919) is a common hydrocoral with the concentration of pores on the anterior side. *Conopora arborescens* Nielsen, 1919 (Fig. 6/4) has irregularly branched colonies. The diameter of the thin juvenile branches measures 0.15 cm, it increases to 0.4 cm, attaining an elliptical shape. The surface of the coenosteum is smooth or slightly sculptured by dots. *Errina lobata* (Nielsen, 1919) (Fig. 6/5) forms fan-like colonies up to 20 cm in height and is also found encrusted on scleractinians. The arrangement of gastropores causes a nodular surface. *Astya crassus* (Nielsen, 1919) (Fig. 6/6) is a hydrocoral with a typical fan-like growth-form and extremely anastomosing branches. The largest colony is 17 cm in height. *Congregopora nasiformis* (Nielsen, 1919), *Errina (Inferiolabiata) irregularis* (Nielsen, 1919) and *Pliobothrus laevis* Nielsen, 1919 are rare.

Octocorals: Octocorals of the Danian limestone belong to 7 genera and include *Moltkia isis* (Steenstrup, 1846), see Fig. 6/8-9, *Moltkia lyelli* Nielsen, 1913, *Isis steenstrupi* Nielsen, 1913, see Fig. 6/7, *Primnoa costata* Nielsen, 1913, *Graphularia groenwalli* Nielsen, 1915, *Gorgonella torta* Nielsen, 1913, *Epiphaxum auloporides* Lonsdale, 1850 and *Heliopora incrustans* Nielsen, 1917. *Moltkia*, the most abundant genus, is illustrated and described by Voigt (1958) in its different species and ontogenetic stages. The calcareous internodes of juvenile specimens have distinct calices and the articulation planes are visible at the proximal and distal side (Fig. 6/8). Adult specimens have overgrown calices and the surface is granulated (Fig. 6/9). Old internodes of *Moltkia isis* can be recognized by an absence
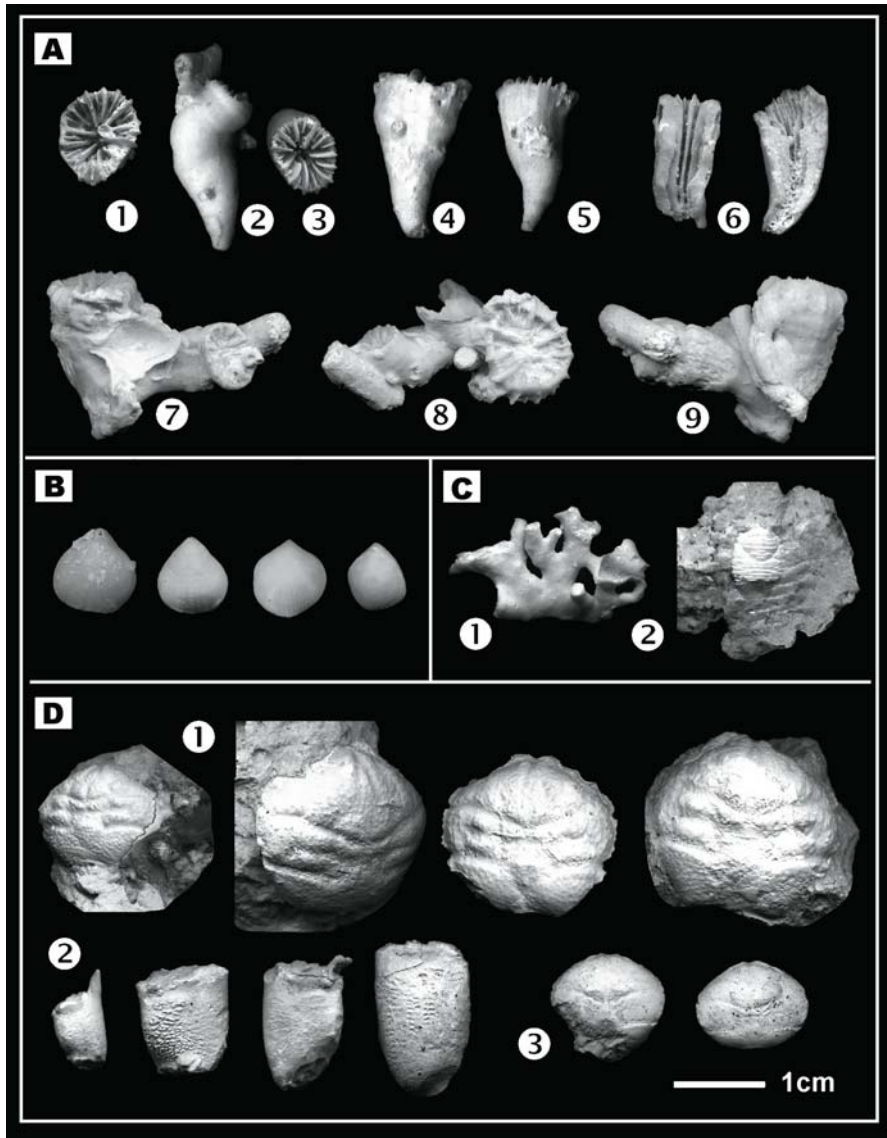
Fig. 7: Associated fauna of the mounds.
A Solitary corals: (1), (4), (5) *Smilotrochus faxoensis*, (2), (3) *Caryophyllia danica*, (6) *Parasmilia lindstroemi*, (7), (8), (9) *Smilotrochus faxoensis* and *Caryophyllia danica* with oyster *Exogyra lateralis* and serpulids on a colony of *Dendrophyllia candelabrum*.
B Brachiopods: *Rhynchonella flustracea* with asymmetric shell as an adaptation for life between the branches in the coral colony.
C Crustaceans: (1) *Astya crassus* with a cyst, probably caused by a parasitic crustacean, (2) *Galathea strigifera*. **D Decapod crabs:** (1) carapace of *Dromiopsis rugosa*, (2) claws of *Dromiopsis*, (3) carapace of *Dromiopsis elegans*

of calices and by large diameters up to 1.8 cm. At this stage, they tend to overgrow the horny nodes by layers of calcite creating a massive corallum, which hindered the internodes in breaking apart during fossilization. Complete, large fan-shaped colonies (about 12 x 7 cm) found in intermound areas of the leeward sedimentation allow a reconstruction of the growth form. Investigations of modern Isididae show that calcification of the primary horny nodes reduces the flexibility of the colony. This has been interpreted as an adaptation to deeper water environments and slower current velocities (Grasshoff and Zibrowius 1983).

Biogenic encrustations and bioerosion: The mound-forming corals were often encrusted in life position, but do not show a defined encrustation pattern (Fig. 6A-D). Affected are colonial and solitary scleractinians, stylasterinids, octocorals (Fig. 6C), bryozoans (Fig. 6B), serpulids (Fig. 6A), brachiopods, and oysters (Fig. 7A-7). Encrustation was an important factor to support and stabilize the mound structure, but also to increase weight on the corals. The stability of the corals was gradually weakened by a network of sponge and bryozoan borings. This resulted in the breakdown of the coral colonies, which formed new substrates for further colonization and encrustation. Most abundant encrusting organisms were bryozoans, serpulids, brachiopods, and bivalves. It is noteworthy that precipitates of microbes are rare to absent in the newly formed habitats.

Brachiopods: *Rhynchonella flustracea* (Fig. 7B) is extremely common in the coral mounds. The specimens are found caught between the coral branches often with their beaks pointing downward. The fold on the frontal commissure of *R. flustracea* is invariably asymmetrical, either left-hand or right-hand and the asymmetry increased with growth. These brachiopods are restricted to the coral limestone. It seems that they had become specialized for attachment to coral branches in a fixed position that rendered a more adequate current system (Asgaard 1968).

Crustaceans: The decapod fauna of the coral mounds has already been described and illustrated by Fischer-Benzon (1866). Most common in the mounds is the crab *Dromiopsis* (Fig. 7D) with two species, *D. rugosa* and *D. elegans*. Carapace (Fig. 7D-1, 3) and claws (Fig. 7D-2) are preserved. *Dromiopsis rugosa* (Schlotheim 1820) is the larger one, the diameter of the subcircular carapace varies from 1-2.5 cm (Fig. 7D-1); *Dromiopsis elegans* (Stenstrup and Forchhammer, 1849) is smaller and compressed in outline (Fig. 7D-3). The small galatheid decapod *Galathea strigifera* Fischer-Benzon, 1866 is restricted to the coral mounds (Fig. 7C-2). Probably parasitic crustaceans may cause cysts found on fossil octocorals and hydrocorals (Fig. 7C-1). Ascothoracids seem to be responsible for cysts on *Moltkia minuta* from the Cretaceous (Voigt 1959). Parasitic copepods in modern *Primnoa resedaeformis* were discovered recently by Buhl-Mortensen and Mortensen (2004).

Fish fauna: Modern azooxanthellate coral reefs are habitats for a diverse fish fauna. It can be assumed that this was similar in the Danian, but most of the fish

skeletons are not preserved. Small broken fish remains are accumulated in the Early Danian fish clay. In the Middle Danian several kinds of shark teeth (*Lamna appendiculata*, *Scaphanorhynchus tenuis*, *Orthacodus lundgreni*) occur in the mounds and point to the existence of sharks in the Danish basin.

Comparison with modern counterparts

Bryozoan reef mounds have not been found in modern oceans. Bryozoan carpets and complex sponge-bryozoan-serpulid-echinoderm biogenic structures are known from many regions including the arctic Vesterisbanken Seamount in the central Greenland Sea (Henrich et al. 1992), where they form bioclastic sediments. Pleistocene bryozoan mounds were found on the upper slope of the Great Australian Bight (James et al. 2000; Holbourn et al. 2002). Interestingly, these reefs grew during phases of low sea level and increased upwelling.

By contrast, azooxanthellate corals form extended biogenic structures along many shelves in the North Atlantic, off Florida and many other regions (see contributions in this volume). Although *Lophelia pertusa* has the greatest distribution in modern oceans, living *Oculina varicosa* has closer taxonomic relationships to *Oculina becki* from the Danish basin and thus has been chosen for comparison. An extensive area of deep-water coral reefs growing along the shelf edge off eastern Florida was described by Reed (1980, 2002a, b). The reef structures consist of numerous pinnacles and ridges, 3-35 m in height and up to 100-300 m in width. Each pinnacle is actually a veneer of living coral, overlying a mound of sand and mud sediment, coral debris, and oolithic limestone at the base, this having formed during the Holocene transgression (Macintyre and Milliman 1970; Reed 1980). These living reefs are composed of *Oculina varicosa* Lesueur, 1820. This species is unusual in that it is facultatively zooxanthellate: in deep water (>60 m) it generally lacks zooxanthellae, but colonies in shallow water possess the algal symbionts. Shallow-water *Oculina varicosa* does not form massive thickets or bank structures like the deep-water form, but grows as sparsely scattered, individual colonies. They are usually <30 cm in diameter and have zooxanthellae in their tissues, which they can expel during periods of cold-water upwelling. Deep-water *Oculina varicosa* lacking zooxanthellae (Teichert 1958) have been found at a depth of 49-152 m (Reed 1980). They occur as large colonies up to 2 m in diameter, some of them broken in half, probably due to their weight and bioerosion. Extensive banks generally have a steep slope of 30-45°, especially on the south side, which faces into the Florida Current. The north slopes are less steep. The growth rate of the deep-water *Oculina* at 80 m averaged 16.1 mm yr^{-1} and was significantly greater compared to the growth at 6 m (11.3 mm yr^{-1}; Reed 1981). Growth rate was positively correlated with water temperature, but paradoxically the coral growth was faster in deep water, where it lacks zooxanthellae (Reed 2002a, b). The associated fauna with *Oculina varicosa* comprise a diverse molluscan community (Reed and Mikkelsen 1987). A predominantly anomuran decapod fauna with hermit, porcellanid and galatheid crabs was described by Reed (1982). The dense invertebrate community helps

support the dense and diverse population of fishes (>70 species). The deep-water *Oculina* reefs form breeding and feeding grounds for a variety of fishes like grouper, snapper, tuna, ray and shark (Koenig et al. 2000).

Control mechanisms

Biological factors, such as larval recruitment strategies, surely influenced the distributional patterns of sessile metazoans in the Danish basin during the Danian-Maastrichtian. However, these factors are too speculative to be used as control factors in the fossil benthic communities of the Danish basin. The complex distributional pattern of Maastrichtian-Danian bryozoans and corals suggests that changing environmental parameters of different magnitude influenced the metazoans. In descending order of their dimension, the following control mechanisms must be considered:

Impact of K/T boundary: In the Danish basin, bryozoan mounds grew prior to and after (with the exception of Fish Clay and Cerithium Limestone) the K/T boundary in the vicinity of the Ringkøbing-Fyn High. This similarity of carbonate factories suggests that the complex mechanisms causing the K/T boundary event did not restructure the carbonate shelf over a larger period of time. The Late Maastrichtian and the Early Danian scleractinian and octocoral soft-bottom communities experienced no major change at the generic level. Their first appearance is in the Cerithium Limestone, while bryozoans recovered much later. Thus, corals of the Danish basin were not affected significantly by the complex K/T boundary events. Flügel and Kiessling (2002: 715) described this phenomenon also from tropical reef ecosystems. They expected a profound diversity decline, but the calculations from their PaleoReefs data base indicate the opposite. Most Maastrichtian reefs are dominated by monospecific or very low-diversity assemblages, but Danian reefs are commonly moderately diverse. Such finding is not surprising for the coral fauna of the Danish basin, because other benthic metazoans including the bivalves (Heinberg 1999) and the brachiopods (Surlyk and Johansen 1984), show similar patterns.

Faults and basin topography: Faults are responsible for the morphology and the internal architecture of the Danish basin. Prolific coral growth is restricted to topographic highs, especially the Ringkøbing-Fyn High. Thus, tectonics played a key role concerning the distributional patterns of the coral mounds and banks in the Middle Danian. The Fakse mounds situated in the vicinity of this high reached the greatest dimension, while counterparts near the Fennoscandian Shield were comparatively small (Fig. 1).

Sea level and sediment composition: Surlyk (1997) recognized during the latest Maastrichtian-Late Danian five depositional sequences in the Danish basin. Among these, the Maastrichtian trangression had the greatest magnitude (Fig. 2). Sequence boundaries SB 2-4 most likely coincide with a temporal decline in bryozoan and

coral development and suggest that sea level was a potential control factor for the distributional pattern and aggradation of the mounds. In contrast to scleractinians inhabiting shallow-water reefs, azooxanthellate metazoans in deeper water are not extraordinarily sensitive to sea-level changes. Thus, base level changes were of subordinate importance for the mounds in the Danish basin.

Currents: The bryozoan and coral mounds of the Danish basin migrated upcurrent by progradation and aggradation towards the southeast, parallel to the coastline and towards nutrient–carrying currents. Water movement was an important factor controlling the morphology and distribution of bryozoans in the mounds (Cheetham 1971). Mound growth and migration are interpreted following the model developed for bryozoan mounds by Thomsen (1977, 1983). This model does not, however, incorporate the nucleation and early phases of mound growth. Current velocities were highest at the summit or crest of the mounds and lowest in the intervening basins according to the model. Flank velocities were intermediate but considerably higher on the up-current flank than on the down-current flank.

Greatest scleractinian growth can be observed on the top and the current-facing side of the Danian coral mounds. The axes of all the fan-shaped hydrocorals and octocorals are orientated perpendicular to the current. Fairly strong currents (>50 cm s^{-1}) undoubtedly contributed to the growth of the corals in providing particle flux for suspension feeding (Teichert 1958; Reed 1981; Messing et al. 1990). Currents must be regarded as one of the prime control mechanisms delivering oxygen and nutrients to the reefbuilders.

Substrate relationship: The skeletal debris of Maastrichtian-Danian mounds provided enough substrate for coral larvae. The soft bottom environments were inhabited and bioturbated by various infaunal organisms including molluscs, irregular echinoids, and crustaceans. Their skeletons provided the substrate for the larvae of the epibenthic communities. Interestingly, the hardgrounds were not colonized by corals. Thus, it can be assumed that substrate was not an important control mechanism.

Light and water depth: The taxonomic composition of the fossil corals in the Danish basin is similar to azooxanthellate genera known from modern deeper and cooler coral banks. Azooxanthellate corals are able to flourish in euphotic to aphotic environments independent of light. Recent and subrecent species of *Dendrophyllia* are cosmopolitan, azooxanthellate and constructional corals. They form mounds in the Eastern Atlantic between Ireland and North Africa (LeDanois 1948: depth 200-450 m; Gruvel 1923: 100 m), Niger Delta (Allan and Wells 1962: 50-120 m) and in the Red Sea (Fricke and Hottinger 1983: 120 m; Dullo et al. 1984: 500 m). *Oculina* occurs with and without zooxanthellae. Large colonies and banks up to 2 m in height of *Oculina varicosa* live in deep waters off Florida, whereas smaller colonies with a diameter of less than 50 cm live in the photic zone (Reed 1980, 1981). The exclusively fossil and endemic *Faksephyllia* belongs to the azooxanthellate

Parasmiliinae. The octocorals and hydrocorals have a slender arborescent or fan-like growth form. Their modern counterparts live preferably in deeper and cooler waters (Cairns 1983). All Danian corals are azooxanthellate and show an optimal adaptation to heterotrophic nourishment in growth form and orientation. The absence of light, which is also a function of depth, is not a limiting factor.

Relevance of biogenic structures and open questions

The distributional patterns of biogenic sediments in the Danish basin are of relevance for our understanding of the role of corals and bryozoans in Mesozoic and Tertiary cool-water environments. Level-bottom solitary scleractinians and octocorals are opportunistic communities, because they lived constantly over 30 million years in the Danish basin and were not affected in the long run by the extrinsic perturbations of the K/T boundary event. By contrast, the Danian coral mounds are unique environments, because they represent the first cool-water coral community that extensively created new habitats for other invertebrates and vertebrates as evidenced by an increase in the diversity of the associated fauna. The restriction of this ecologically diverse community to one distinct time window, the Middle Danian, and one specific locality, indicates very special prerequisites and extreme vulnerability of the ecosystem. Thus, our "state of the art" contribution provokes new questions:

(1)   Most coral taxa existed already during the Late Cretaceous. Why were the mound formation and associated habitat-increase limited only to the Middle Danian?

(2)   The temporal distribution pattern of bryozoan and coral mounds is enigmatic. Which factors including oceanography, sea level changes, and nutrient supply are important?

(3)   Bryozoans occur in coral mounds commonly. By contrast, corals are extraordinarily rare in bryozoan mounds. Is this phenomenon related to substrate preferences?

(4)   Is methane expulsion by cold vent systems a control mechanism of cool-water coral reef distribution in the Danish basin?

(5)   Bryozoan mounds are absent in modern oceans and rare in the Pleistocene. Are the Maastrichtian and Danian bryozoan biogenic structures indeed parautochthonous mounds or migrated megadunes?

These questions show that the distributional pattern of bryozoans and corals in the Danish basin is still far from understood. More research under consideration of their modern equivalents is therefore recommended!

Acknowledgements

Schäfer (University Kiel) for her support and information on the life of modern bryozoans. We acknowledge the constructive comments of the reviewers Richard Bromley and Erik Flügel who helped us to improve our manuscript.

References

Allan JRP, Wells JW (1962) Holocene coral banks and subsidence in the Niger Delta. J Geol 70: 381-397

Alvarez LW, Alvarez W, Asaro F, Michel HV (1980) Extraterrestrial cause for the Cretaceous-Tertiary extinction. Science 208: 4448

Asgaard U (1968) Brachiopod palaeoecology in the Middle Danian limestone at Fakse, Denmark. Lethaia 1: 103-121

Bernecker M, Weidlich O (1990) The Danian (Paleocene) Coral Limestone of Fakse, Denmark: a model for ancient aphotic, azooxanthellate coral mounds. Facies 22: 103-138

Bromley RG (1967) Some observations on burrows of thalassinidean Crustacea in chalk hardgrounds. Quart J Geol Soc London 123: 157-182

Buhl-Mortensen L, Mortensen PB (2004) Symbiosis in deep-water corals. Symbiosis 37: 33-61

Cairns SD (1983) Antarctic and subantarctic *Stylasterina* (Coelenterata: Hydrozoa). Antarct Res Ser 38: 61-64

Cheetham AH (1971) Functional morphology and biofacies distribution of cheilostome Bryozoa in the Danian Stage (Paleocene) of southern Scandinavia. Smithsonian Contr Paleobiol 6: 1-87

Christensen L, Fregerslev S, Simonsen A, Thiede J (1973) Sedimentology and depositional environment of Lower Danian fish clay from Stevns Klint, Denmark. Bull Geol Denmark 22: 193-212

Dons C (1944) Norges korallrev. K norske Vidensk Selsk Forh 16: 37-82

Dullo W-Chr, Süssmeier G, Tietz GF (1984) Diversity and distributional patterns of reef building scleractinians in recent lagoonal patch reefs on the coast of Kenya. Facies 16: 1-10

Fischer-Benzon R (1866) Über das relative Alter des Faxekalkes und die in demselben vorkommenden Anomuren und Brachyuren. Schwer'sche Buchhandlung, Kiel

Floris S (1972) Scleractinian corals from the Upper Cretaceous and Lower Tertiary of Nugssuaq, West Greenland. Medd Gronland, Komm Vidensk unders Gronland 196: 4-132

Floris S (1979) Guide to Fakse Limestone Quarry. In: Birkelund T, Bromley RG (eds) Cretaceous - Tertiary Boundary Events, 1. The Maastrichtian and Danian of Denmark, pp 152-163

Floris S (1980) The coral banks of the Danian of Denmark: Acta Palaeontol Pol 25: 531-540

Flügel E, Kiessling W (2002) Patterns of Phanerozoic reef crisis. In: Kiessling W, Flügel E, Golonka J (eds) Phanerozoic Reef Patterns. SEPM Spec Publ 72: 691-733

Freiwald A, Henrich R, Pätzold J (1997) Anatomy of a deep-water coral reef mound from Stjernsund, West Finnmark, northern Norway. SEPM Spec Publ 56: 141-162

Fricke HW, Hottinger L (1983) Coral bioherms below the euphotic zone in the Red Sea. Mar Ecol Prog Ser 11: 113-117

Golonka J, Ross MI, Scotese CR (1994) Phanerozoic paleogeographic and paleoclimatic maps. In: Embry AF, Beauchamp B, Glass DJ (eds) Pangea: global environments and resources. Canad Soc Petrol Geol Mem 17: 1-47

Grasshoff M, Zibrowius H (1983) Kalkkrusten auf Achsen von Hornkorallen, rezent und fossil. Senckenb marit 15: 111-145

Gruvel M (1923) Quelques gisements de coraux sur la cote occidentale du Maroc: C R Acad Sci 176: 1637

Håkansson E, Thomsen E (1999) Benthic extinction and recovery patterns at the K/T boundary in shallow water carbonates, Denmark. Palaeogeogr Palaeoclimatol Palaeoecol 154: 67-85

Heinberg C (1999) Lower Danian bivalves, Stevns Klint, Denmark: continuity across the K/T boundary. Palaeogeogr Palaeoclimatol Palaeoecol 154: 87-106

Henrich R, Hartmann M, Reitner J, Schäfer P, Freiwald A, Steinmetz S, Dietrich P, Thiede J (1992) Facies belts and communities of the arctic Vesterisbanken Seamount (central Greenland Sea). Facies: 27: 71-104

Holbourn A, Kuhnt W, James NP (2002) Late Pleistocene bryozoan reef mounds of the Great Australian Bight: Isotope stratigraphy and benthic foraminiferal record. Paleoceanography 17: 1-13

James NP (1997) The cool-water carbonate depositional realm. SEPM Spec Publ 56: 1-20

James NP, Feary DA, Surlyk F, Simo JA, Betzler C, Holbourn AE, Li Q, Matsuda H, Machiyama H, Brooks GR, Andres MS, Hine AC, Malone MJ (2000) Quaternary bryozoan reef mounds in cool-water, upper slope environments: Great Australian Bight. Geology 28: 647-650

Kastner M, Asaro F, Michel HV, Alvarez W, Alvarez LW (1984) The precursor of the Cretaceous-Tertiary boundary clays at Stevns Klint, and DSDP hole 465A. Science 226: 137-143

Koenig CC, Coleman FC, Grimes CB, Fitzhugh GR, Scanlon KM, Gledhill CT, Grace M (2000) Protection of fish spawning habitat for the conservation of warm-temperate reef-fish fisheries on shelf-edge reefs of Florida. Bull Mar Sci 66: 593-616

LeDanois E (1948) Le profondeurs de la mer. Payot, Paris

Lees A (1975) Possible influences of salinity and temperature on modern shelf carbonate sedimentation. Mar Geol 19: 159-198

Malakoff D (2003) Cool corals become hot topic. Science 299: 195

Macintyre IG, Milliman JD (1970) Physiographic features on the outer shelf and upper continental slope, Atlantic continental margin, southeastern United States. Bull Amer Geol Soc 81: 2577-2598

Messing CG, Neumann AC, Lang JC (1990) Biozonation of deep-water lithoherms and associated hardgrounds in the northeastern Straits of Florida. Palaios 5: 15-33

Nelson CS (1988) An introductory perspective on non-tropical shelf carbonates. Sediment Geol 60: 3-12

Nielsen BK (1913) Crinoiderne i Danmarks kridtaflejringer. Danmark geol Unders 26: 1-120

Nielsen BK (1917) Cerithiumkalken in Stevns Klint. Medd Dansk geol Foren 5: 3-14

Nielsen BK (1919) En Hydrocoralfauna fra Faxe. Medd Dansk geol Foren 5: 1-65

Nielsen BK (1922) Zoantharia from Senone and Paleocene Deposits in Denmark and Skaane. K Dansk Vidensk Selsk Skr, Natv Math 3: 202-233

Reed JK (1980) Distribution and structure of deep-water *Oculina varicosa* coral reefs off central eastern Florida. Bull Mar Sci 30: 667-677

Reed JK (1981) *In situ* growth rates of the scleractinian coral *Oculina varicosa* occurring with zooxanthellae on 6-m reefs and without on 80-m banks. Proc 4th Int Coral Reef Symp 2: 201-206

Reed JK (1982) Community composition, structure areal and trophic relationship of decapods associated with shallow- and deep-water *Oculina varicosa* coral reefs. Bull Mar Sci 32: 761-786

Reed JK (2002a) Deep-water *Oculina* coral reefs of Florida: biology, impacts, and management. Hydrobiologia 471: 43-55

Reed JK (2002b) Comparison of deep-water coral reefs and lithoherms off southeastern USA. Hydrobiologia 471: 57-69

Reed JK, Mikkelsen PM (1987) The molluscan community associated with the scleractinian coral *Oculina varicosa*. Bull Mar Sci 40: 99-131

Rosenkrantz A (1939) Faunaen i Cerithiumkalken og det haerdnede Skrivekridt i Stevns Klint. Medd Dansk geol Foren 9: 509-514

Schlager W (2000) Sedimentation rates and growth potential of tropical, cool-water and mud-mound carbonate systems. Geol Soc London Spec Publ 178: 217-227

Smit J (1999) The global stratigraphy of the Cretaceous-Tertiary boundary impact ejecta. Annu Rev Earth Planet Sci 27: 75-113

Surlyk F (1974) Life habit, feeding mechanism and population structure of the Cretaceous brachiopod genus *Aemula*. Palaeogeogr Palaeoclimatol Palaeoecol 15: 185-203

Surlyk F (1997) A cool-water carbonate ramp with bryozoan mounds: Late Cretaceous - Danian of the Danish Basin. SEPM Spec Publ 56: 293-307

Surlyk F, Håkansson E (1999) Maastrichtian and Danian strata in the southeastern part of the Danish Basin. In: Pedersen GK, Clemmensen LB (eds) 19th Reg Europ Meet Sediment, Field Trip Guidebook. IAS, Copenhagen, pp 29-58

Surlyk F, Johansen G (1984) End-Cretaceous brachiopod extinctions in the chalk of Denmark. Science 223: 1174-1177

Teichert C (1958) Cold and deep-water coral banks. AAPG Bull 42: 1064-1082

Thomsen E (1977) Phenetic variability and functional morphology of erect cheilostome bryozoans from the Danian (Palaeocene) of Denmark. Paleobiology 3: 360-376

Thomsen E (1983) Relation between currents and growth of Palaeocene reef mounds. Lethaia 16: 165-184

Thomsen E (1995) Kalk og kridt i den danske undergrund. In: Nielsen OB (ed) Danmarks geologi fra Kridt til I dag. Aarhus Geokompend, Geol Inst, Arhus Univ 1, pp 31-67

Voigt E (1958) Untersuchungen an Oktokorallen aus der oberen Kreide. Mitt Geol Staatsinst Hamburg 27: 5-49

Voigt E (1959) *Endosacculus moltkiae*, n.g., n.sp., ein vermutlicher fossiler Ascothoracide (Entomostr.) als Cystenbildner bei der Oktokoralle *Moltkia minuta*. Paläont Z 33: 211-223

Wendler J, Willems H (2002) Distribution pattern of calcareous dinoflagellate cysts across the Cretaceous-Tertiary boundary (Fish Clay, Stevns Klint, Denmark): Implications for our understanding of species-selective extinction. GSA Spec Pap 356: 265-393

Willumsen ME (1995) Early lithification in Danian azooxanthellate scleractinian lithoherms, Faxe Quarry, Denmark. Beitr Paläont Wien 20: 123-131

Ziegler PA (1990) Geological Atlas of Western and Central Europe. Shell, The Hague, 239 pp, 56 maps

Corals from deep-water methane-seep deposits in Paleogene strata of Western Oregon and Washington, U.S.A.

James L. Goedert[1], Jörn Peckmann[2]

[1] Geology and Paleontology Division, Burke Museum of Natural History and Culture, University of Washington, Seattle, WA 98195, USA (jgoedert@u.washington.edu)

[2] Research Center for Ocean Margins, University of Bremen, P.O. Box 330 440, D-28334 Bremen, Germany

Abstract. In general, fossils of corals are rare within Eocene and Oligocene marine strata that accumulated in a deep-water, convergent-margin setting and are now exposed in western Oregon and Washington, northwestern USA. At some localities, however, specimens of a few coral taxa are relatively abundant and associated with authigenic limestone deposits. Recently, these highly-localized limestone deposits were recognized as having precipitated due to the microbial oxidation of methane at seeps, areas where hydrocarbon-rich fluids were vented to the sea floor because of the tectonic compression and faulting of underlying sediments. As at modern methane-seeps, the ancient seeps supported dense invertebrate communities, in most cases dominated by tube-dwelling worms and bivalve mollusks, but they can also include gastropods, polyplacophorans, sponges, and corals. A few methane-seep assemblages in Eocene and Oligocene rocks of the Lincoln Creek Formation include the corals *Caryophyllia wynoocheensis* Durham, and an undescribed *Flabellum* (*Ulocyathus*) species. A new species of *Deltocyathus* appears to be restricted to a single methane-seep site. The corals *Stephanocyathus holcombensis* Durham, and *Flabellum hertleini* Durham have been reported from what may be methane-seeps sites in the Lincoln Creek Formation near Holcomb, Washington, and associated with an unusual crinoid-rich bioherm in the Keasey Formation near Mist, Oregon. Other corals, *Flabellum* (*Ulocyathus*) n. sp., *Archohelia*? sp., *Caryophyllia wynoocheensis*, and *Dendrophyllia hannibali* Nomland, are reported from a Lincoln Creek Formation locality that includes methane-seep related assemblages near Knappton, Washington. Although widespread in the deep sea today, none of the genera found in the ancient seeps in Washington and Oregon have yet been reported from modern seeps, and corals have rarely been reported from pre-Tertiary methane-seep deposits. It is unlikely that any of these corals, like the bivalves and tubeworms found at methane-seeps, hosted and derived nutrients from

endosymbiotic chemotrophic bacteria that were capable of metabolizing some of the reduced compounds in the seeping fluids. More likely, the corals probably were attracted to the greater amount of food at seeps relative to the surrounding deep sea, or to the attachment sites provided by hardgrounds of methane-derived carbonate deposits on the muddy seafloor.

Keywords. Corals, methane, Paleogene, Oregon, Washington

Introduction

Outcrops of Eocene and Oligocene deep-water marine strata are widespread in western Oregon and Washington, in the northwestern USA. Fossil invertebrate assemblages from these rocks have been studied for more than a century (e.g., Conrad 1848; Weaver 1943; Durham 1944; Hickman 1969; Moore 1984). Fossils of corals in these deposits are, however, relatively rare. Other than incidental inclusion in reports on molluscan assemblages, Tertiary corals from Washington and Oregon have been the sole subject of only a few reports (Durham 1942; Blake 1968). At a few localities, deep-water corals increase in abundance and this appears to reflect some highly-localized paleoecological effect such as, for example, methane seepage.

Modern methane-seeps support dense communities of invertebrates that rely on the oxidation of reduced seepage compounds (hydrogen sulfide and methane) by endosymbiotic bacteria hosted in their tissues (Sibuet and Olu 1998, and references therein). Apart from these chemosymbiotic communities, authigenic carbonates with low $\delta^{13}C$ values are another typical feature of methane-seeps. Here, carbonate formation results from the anaerobic oxidation of methane (AOM) by a microbial consortium of methanotrophic archaea and sulfate-reducing bacteria; this consortium was isolated by Boetius et al. (2000) for the first time. Carbonate precipitation at methane-seeps is consequently confined to anoxic environments (Peckmann et al. 2001). Seep carbonates are essentially the product of microbial activity as revealed by their low $\delta^{13}C$ values documenting the incorporation of methane-derived carbon, isotopically-depleted biomarkers of the AOM-performing consortium, and microbial carbonate fabrics (Peckmann et al. 2002).

The fossils from Washington were found in bathyal sediments that accumulated in a convergent-margin, forearc setting (Armentrout 1987). These strata also enclose localized, anomalous, authigenic limestone deposits (Goedert and Squires 1990; Squires and Goedert 1991; Campbell 1992; Campbell and Bottjer 1993; Peckmann et al. 2002). These limestones were recently recognized as being the product of the ancient microbial oxidation of methane in areas where hydrocarbon-rich fluids were vented to the sea floor. This seepage of pore waters occurred due to the compression and faulting of underlying sediments as the Juan de Fuca plate was subducting beneath the North American plate, a continuing process that began in Late Eocene time (Vance et al. 1987; Kulm et al. 1986; Ritger et al. 1987). At some places on the seafloor where seepage of hydrocarbons occurs today, carbonate chimneys, crusts, and other structures can be found (Schroeder et al. 1987; Kulm and Suess 1990). As at modern methane-seeps, many ancient seeps supported dense invertebrate
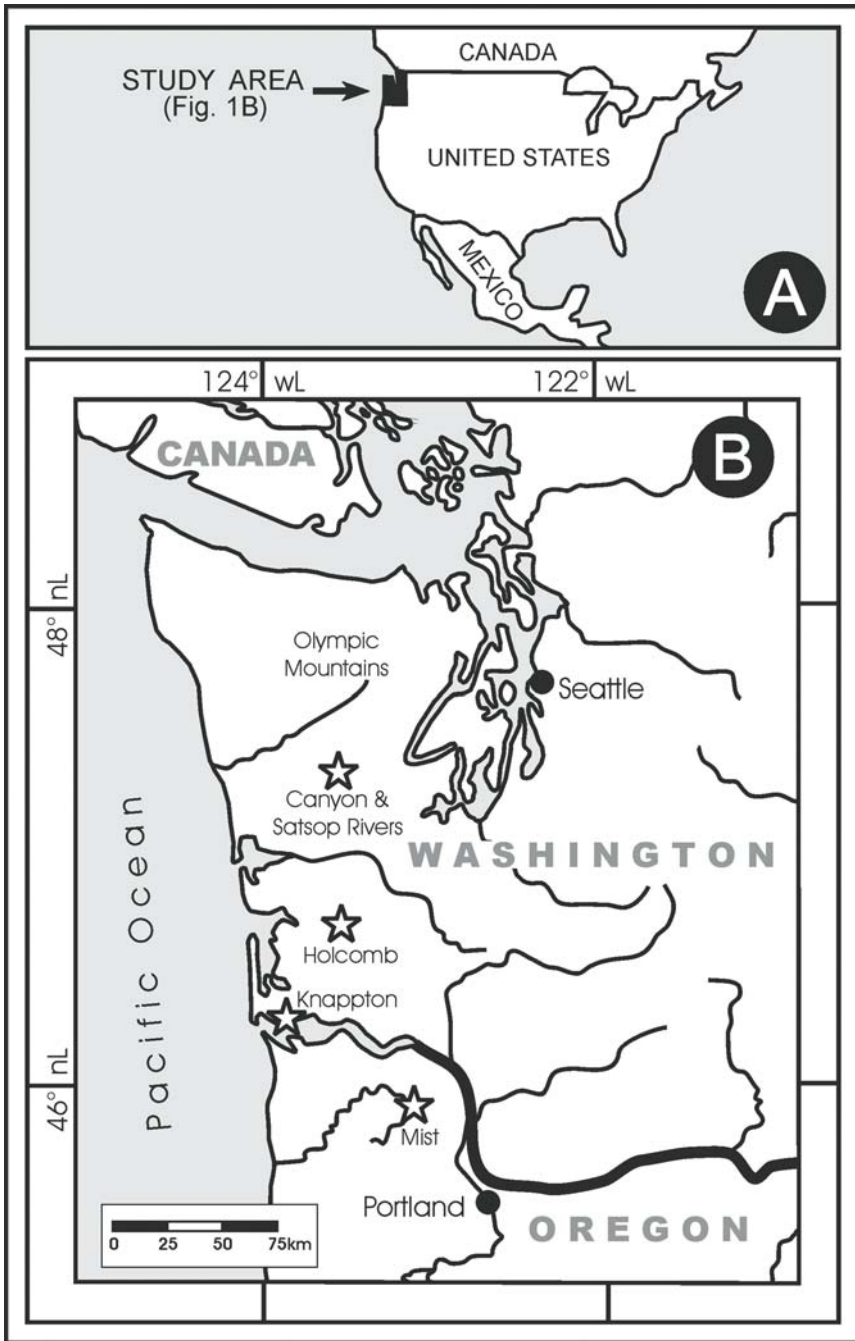
Fig. 1 A Index map of USA showing the study area. **B** Map of western Washington and Oregon showing proven and suspected methane-seep coral localities

communities (e.g., Gaillard et al. 1985; Taviani 1994; Majima 1999; Peckmann et al. 1999; Kelly et al. 2000; Campbell et al. 2002). In most cases, Tertiary seep assemblages were dominated by tube-dwelling worms and bivalve mollusks, on the floor of the relatively nutrient-poor and otherwise nearly barren deep sea. Worm tubes, bivalves, gastropods, polyplacophorans, sponges, and in a few cases, corals (Peckmann et al. 2002) have been found in the Eocene and Oligocene seep deposits in Washington State. Methane-seep deposits have been recognized in several formations in western Washington, ranging in age from middle Eocene to Pliocene (Campbell and Bottjer 1993; Orange and Campbell 1997) but corals have only been found in seep deposits identified within various geographically widespread outcrops (Fig. 1) of the Lincoln Creek Formation.

The primary aim of this paper is to record those corals that have been found in association with both proven and suspected methane-seep deposits in Washington. Institutional abbreviations used for specimen and locality numbers are: UWBM, The Burke Museum of Natural History and Culture, University of Washington, Seattle, Washington 98195; and LACMIP, Natural History Museum of Los Angeles County, Invertebrate Paleontology, 900 Exposition Boulevard, Los Angeles, California 90007.

Lincoln Creek Formation

Southern flank of the Olympic Mountains

South of the Olympic Mountains, in the Satsop and Canyon River valleys, the Lincoln Creek Formation is approximately 3000 m thick (Rau 1966) and provides a nearly continuous depositional record from Late Eocene to latest Oligocene time (Prothero and Armentrout 1985). Deposition occurred at depths of between 400 and 800 m (Rau 1966), but in places, possibly less than 210 m (Peckmann et al. 2002). Methane-seep deposits are relatively common throughout the formation in this area (Campbell and Bottjer 1993; Squires 1995; Peckmann et al. 2002). The corals that have been identified in these methane-seep deposits include at one site a new species of *Deltocyathus* (Figs. 2a, 3a-d; Appendix 1) that has not been found anywhere else, *Caryophyllia wynoocheensis* Durham, 1942 (Figs. 2b-d), and a new species of *Flabellum* (*Ulocyathus*) (Fig. 2e). The *Flabellum* is referred to the subgenus *Ulocyathus* on the basis of the serrate calicular edge, but more complete specimens are needed to formally describe the species. *Caryophyllia wynoocheensis* is also found away from seep deposits (Durham 1942; Armentrout 1973). This is only the second record for *Deltocyathus* for the eastern North Pacific Ocean (Peckmann et al. 2002), and the first fossil record for the subgenus *Ulocyathus* from western North America.

Willapa River

Along the banks of the Willapa River near Holcomb, Washington, in a Late Eocene or Early Oligocene exposure of the Lincoln Creek Formation, is a locality that is suspected to be an ancient methane-seep site (Nesbitt et al. 1994: 1D-8).
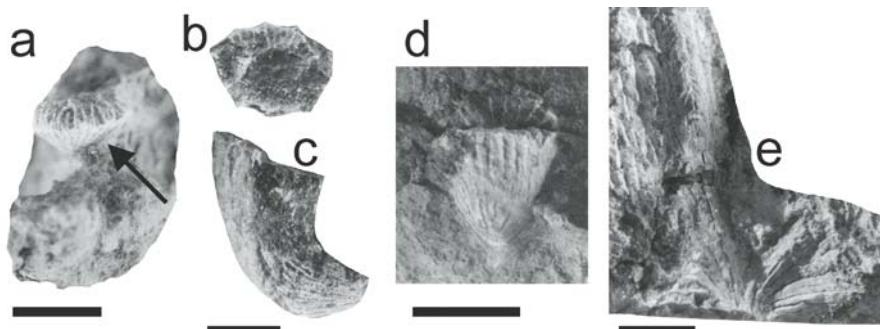
Fig. 2 Fossil methane-seep-associated corals from the Satsop and Canyon River localities. **a** *Deltocyathus insperatus* new species, referred specimen UWBM 97520, lateral view, scale is 5 mm. **b** *Caryophyllia wynoocheensis* Durham, 1942, UWBM 97524, UWBM loc. B6782, calicular view, scale for b and c is 5 mm. **c** Same specimen as **b**, lateral view. **d** *Caryophyllia wynoocheensis*, UWBM 97525, UWBM loc. B6783, lateral view, scale is 10 mm. **e** *Flabellum* (*Ulocyathus*) sp., UWBM 97526, UWBM loc. B6783, lateral view, scale is 10 mm

Very large solemyid and abundant thyasirid bivalves have been reported from this locality (Weaver 1943; Armentrout 1973) along with corals (Durham 1942). Solemyid and thyasirid bivalves are common constituents of modern and ancient methane-seep assemblages (e.g., Campbell and Bottjer 1993; Sibuet and Olu 1998). Two corals, *Stephanocyathus holcombensis* Durham, 1942, and *Flabellum hertleini* Durham, 1942, are fairly abundant at the Holcomb site. The molluscan fossils from this locality were regarded as being a "deep-water" assemblage by Hickman (1984), but estimates of water depth vary from approximately 20 to 100 m (Armentrout 1973), to more than 200 m (Hickman 1980).

Knappton

Corals have been reported (Moore 1984) from the Lincoln Creek Formation near Knappton, Washington, at localities that include methane-seep related assemblages (Goedert and Squires 1993). Fossiliferous concretions from the Lincoln Creek
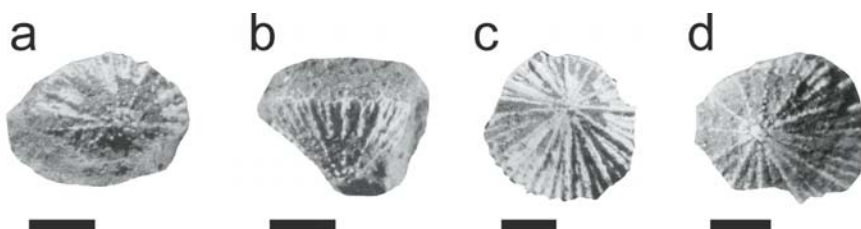
Fig. 3 *Deltocyathus insperatus* new species (see Appendix 1 for description). All from UWBM loc. B6781; all scales are 2 mm. **a** *Deltocyathus insperatus* new species, paratype UWBM 97521, basal view. **b** Same specimen as **a**, lateral view. **c** *Deltocyathus insperatus* new species, paratype UWBM 97522, basal view. **d** *Deltocyathus insperatus* new species, paratype UWBM 97523, basal view

Formation near Knappton are mostly found in modern landslide blocks (Moore 1984), but some methane-seep limestones have recently been found *in situ* (Goedert and Benham 2003). Some of the Knappton limestones are allochthonous ("Type 3" deposits of Conti and Fontana 1998), having been transported from the original seep site and redeposited by debris flows or turbidity currents. Paleobathymetry of the Lincoln Creek Formation at Knappton was estimated to have been 100 to 350 m, based on mollusks, or as deep as 1000 m, based on foraminiferans (Moore 1984). Moore (1984) reported the corals *Flabellum* sp. and *Dendrophyllia hannibali* Nomland, 1916, from the Knappton locality.

The *Flabellum* sp. reported by Moore (1984) is actually a new species, referred to as *Flabellum* (*Ulocyathus*) n. sp. herein. Specimens of *Flabellum* (*Ulocyathus*) n. sp. (Figs. 4a-d) from Knappton are moderately abundant, and are in all cases found in carbonate nodules. They are complete and unabraded, and the few coral-bearing nodules found *in situ* do not appear to have been reworked. They are more expanded than the specimens from the Lincoln Creek Formation south of the Olympic Mountains, but more specimens are needed for a formal description.

One block of carbonate containing abundant echinoid spines and a few "mud pectens" also contained a single specimen of *Caryophyllia wynoocheensis* (Fig. 4e). We also collected a nodule containing numerous branches of *Archohelia*? sp. that had overgrown, or intergrown with, a hexactinellid sponge (Figs. 4f-h). Hexactinellid sponges have been reported from several methane-seep sites in Washington (Rigby and Jenkins 1983; Rigby and Goedert 1996; Peckmann et al. 2002), and in some cases they appear to have been the dominant faunal component. Some of the seep limestone blocks found at Knappton also contain hexactinellid sponges.

The corals from Knappton are not clearly indicative of the past presence of a methane-seep, but their abundance, coupled with the common occurrence of seep limestones in the same strata seem more than coincidental.

Mist, Oregon

The corals *Stephanocyathus holcombensis* and *Flabellum hertleini* have been found associated with an unusual crinoid-rich bioherm in the Early Oligocene Keasey Formation near Mist, Oregon, that is suspected to be yet another seep site (Burns and Mooi 2003). Solemyid bivalves, pogonophoran tubes, asteroids, and ophiuroids were also found in the localized Mist assemblage, while the surrounding strata are nearly barren of megafossils. Based on data from several sources, water depths of approximately 300 to 450 m are likely for this site (Burns and Mooi 2003). Further investigations are underway on this site by C. Burns (Seattle) and K.A. Campbell (Auckland).

Discussion and conclusions

Although corals have been reported from several present-day methane-seeps worldwide (e.g., Sibuet and Olu 1998), none of the genera found in the ancient seeps in Washington have yet been reported from modern seeps. Ancient marine
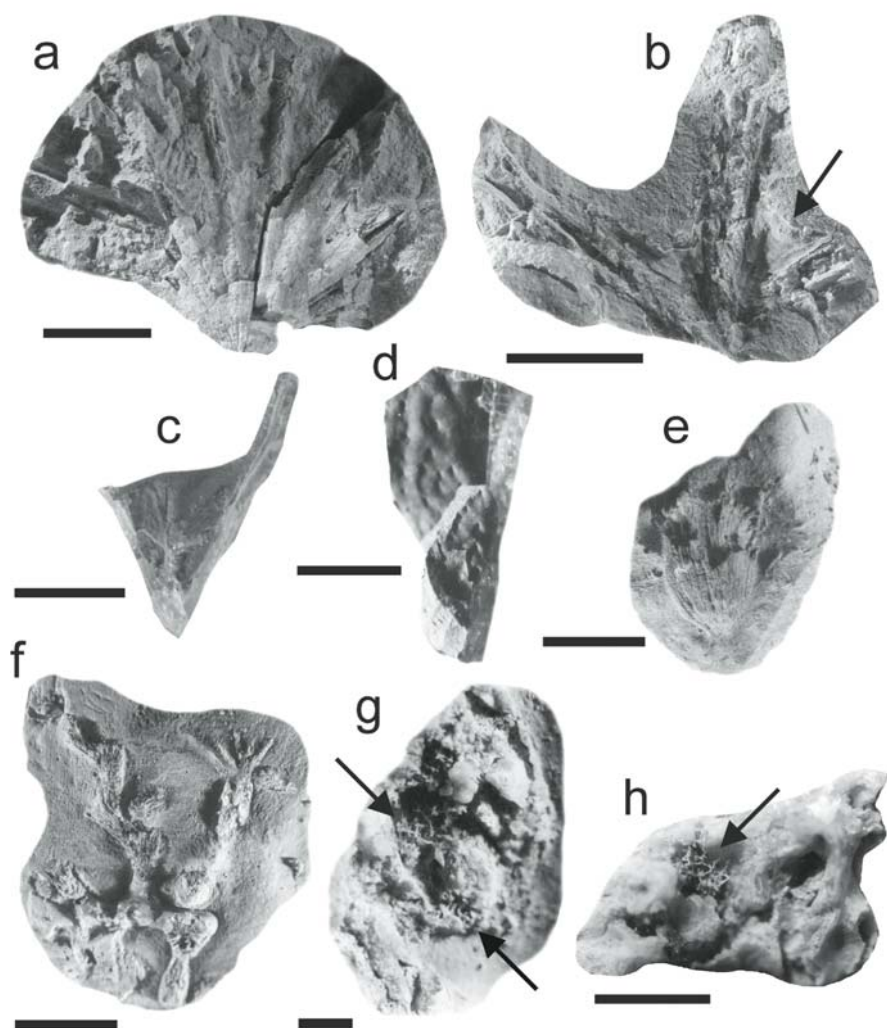
Fig. 4 Corals from the Lincoln Creek Formation near Knappton, Washington. **a** *Flabellum* (*Ulocyathus*) n. sp., UWBM 97529, LACMIP loc. 5842, lateral view, scale is 10 mm. **b** *Flabellum* (*Ulocyathus*) n. sp., UWBM 97530, LACMIP loc. 5842, fragment in lateral view showing growth lines (arrow), scale is 10 mm. **c** Same specimen as **a,** side view of specimen showing calicular expansion, scale is 10 mm. **d** Same specimen as **a**, view of septal faces showing pits, scale is 5 mm. **e** *Caryophyllia wynoocheensis*, UWBM 97527, LACMIP loc. 5843, lateral view, scale is 10 mm. **f** *Archohelia*? sp., UWBM 97528, LACMIP loc. 5843, scale is 10 mm. **g** Same specimen as **f**, view of basal portion of colony intergrown with the basal part of a hexactinellid sponge (arrow), scale is 2 mm. **h** Same specimen as **f** and **g**, note sponge skeletal fragment (arrow) in coral, scale is 5 mm

vent and seep paleocommunities range in age from Silurian to Pliocene and have been reported from many parts of the world (Campbell and Bottjer 1995; Little et al. 1998; Campbell et al. 2002). There are, however, very few reports of corals from methane-seep assemblages older than Late Eocene (Schwartz et al. 2003; Shapiro, in press). Reasons for this are not at all clear, but the near absence of corals from pre-Eocene seeps may be a sampling bias related to the greater abundance of geochronologically younger seep deposits.

The deep-water corals from the Lincoln Creek Formation in Washington may have been attracted to seeps because of the firm substrates offered by methane-derived carbonate deposits, or by the greater production and relative abundance of food near seeps. Some small corals like *Deltocyathus* may be automobile (Gill and Coates 1977; Plusquellec et al. 1999). Automobility would be a useful attribute for a solitary coral living near methane-seeps enabling it to cope with bioturbation by bivalves (e.g., vesicomyids), to avoid toxicity due to concentrations of various seepage compounds (e.g., hydrogen sulfide), and to continuously reposition itself in order to optimize feeding opportunities.

Hovland and Thomsen (1997) and Hovland et al. (1998) originally proposed a link between the occurrence of the reef-forming deep-water coral *Lophelia pertusa* and hydrocarbon seepage. This idea is still put forward by its advocates (Hovland and Risk 2003), but there is no unambiguous evidence to corroborate this scenario. Corals live on seepage-related mounds in the northeastern Atlantic Ocean off Ireland, but are only part of a community of suspension-feeders that apparently find the elevation of the mound to be beneficial (Masson et al. 2003). Likewise, other recent studies on coral-topped carbonate mounds in the Rockall Trough off Ireland found no evidence for a link between hydrocarbon seepage and coral growth (Kenyon et al. 2003; van Weering et al. 2003). The fact that *Lophelia* has been found to be largely dependant on zooplankton and, thus, on the transfer of pelagic particles and food from the productive surface waters (Freiwald et al. 2002) is also not in favor of the postulated link to hydrocarbon seepage.

In some cases, the fossil, seep-associated corals appear to have been only attached to the surface of the carbonate after both seepage and carbonate formation had stopped. For example, the specimen of *Caryophyllia wynoocheensis* in Figures 2b-c was found on the top of a small carbonate deposit, with its base at the contact between the carbonate and the enclosing siltstone. In other cases, however, some corals (Figs. 2a, 2e, 3a-d) appear to have been part of the seep-associated invertebrate assemblage because they are found only in direct association with methane-seep carbonate and not elsewhere in the surrounding strata. For example, the new species of *Deltocyathus* from the Satsop River seep (UWBM loc. 6781) is found throughout the small limestone deposit and in direct association with vesicomyid, nuculanid, solemyid, and thyasirid bivalves. Therefore, the *Deltocyathus* were living at the seep during periods of active methane seepage. It is unlikely that the *Deltocyathus* were only taking advantage of the hard seep carbonate as a substrate, because they have not been found anywhere else (e.g., on whale bones, mollusk shells, other carbonates). The seep-associated invertebrate assemblage from UWBM loc. B6781

is one of the most diverse so far reported and includes some gastropod taxa not reported from any other seep, modern or ancient (Peckmann et al. 2002). Some of the gastropods (and most likely the new species of *Deltocyathus*) were dependent on some food source that was either restricted to or enhanced in some way by this particular seep.

Schwartz et al. (2003) reported specimens of an unidentified species of *Flabellum* associated with ancient methane-seep sites in the Maastrichtian-Danian Moreno Formation in California. It is suspected that *Flabellum* was attracted to the vicinity of the seep sites by the greater amount of food production by the seep paleocommunity (Schwartz et al. 2003).

Some coral species such as *Caryophyllia wynoocheensis* were apparently opportunists better able to take advantage of a variety of bottom conditions because it is also found at localities away from seeps. Living species of *Caryophyllia* commonly have wide geographic distributions (e.g., Cairns 1994).

It cannot be excluded that some of these corals, like the bivalves and tubeworms found at methane-seeps, had the ability to host and derive nutrients from endosymbiotic chemotrophic bacteria. This is, however, unlikely because this trophic strategy has not yet been demonstrated for living corals.

Acknowledgments

References

Armentrout JM (1973) Molluscan paleontology and biostratigraphy of the Lincoln Creek Formation (late Eocene - Oligocene), southwestern Washington. Unpubl PhD Thesis, Univ Washington, pp 1-478

Armentrout JM (1987) Cenozoic stratigraphy, unconformity-bounded sequences, and tectonic history of southwestern Washington. In: Schuster JE (ed) Selected papers on the geology of Washington. Washington Dept Nat Resour, Div Geol Earth Resour Bull 77: 291-320

Blake DB (1968) Two new Eocene corals from Oregon. J Paleontol 42: 201-204

Boetius A, Ravenschlag K, Schubert CJ, Rickert D, Widdel F, Gieseke A, Amann R, Jørgensen BB, Witte U, Pfannkuche O (2000) A marine consortium apparently mediating anaerobic oxidation of methane. Nature 407: 623-626

Burns C, Mooi R (2003) An overview of Eocene-Oligocene echinoderm faunas of the Pacific Northwest. In: Prothero DR, Ivany LC, Nesbitt EA (eds) From Greenhouse to Icehouse, the marine Eocene-Oligocene transition. Columbia Univ Press, New York, pp 88-106

Cairns SD (1994) Scleractinia of the temperate North Pacific. Smithsonian Contr Zool 557: 1-150

Campbell KA (1992) Recognition of a Mio-Pliocene cold seep setting from the northeast Pacific convergent Margin, Washington, U.S.A. Palaios 7: 422-433

Campbell KA, Bottjer DJ (1993) Fossil cold seeps. Nat Geogr Res Explor 9: 326-343

Campbell KA, Bottjer DJ (1995) Brachiopods and chemosymbiotic bivalves in Phanerozoic hydrothermal vent and cold seep environments. Geology 23: 321-324

Campbell KA, Farmer JD, Des Marais D (2002) Ancient hydrocarbon seeps from the Mesozoic convergent margin of California: carbonate geochemistry, fluids and paleoenvironments. Geofluids 2: 63-94

Conti S, Fontana D (1998) Recognition of primary and secondary Miocene lucinid deposits in the Apennine Chain. Mem Sci Geol 50: 101-131

Conrad TA (1848) Fossil shells from Tertiary deposits on the Columbia River, near Astoria. Amer J Sci, ser 2, 5: 432-433

Durham JW (1942) Eocene and Oligocene coral faunas of Washington. J Paleontol 16: 84-104

Durham JW (1943) Pacific Coast Cretaceous and Tertiary corals. J Paleontol 17: 196-202

Durham JW (1944) Megafaunal zones of the Oligocene of northwestern Washington. Univ California, Bull Dept Geol Sci 27: 101-212

Freiwald A, Hühnerbach V, Lindberg B, Wilson JB, Campbell J (2002) The Sula Reef complex, Norwegian shelf. Facies 47: 179-200

Gaillard C, Bourseau J-P, Boudeulle M, Pailleret P, Rio M, Roux M (1985) Les pseudo-bioherms de Beauvoisin (Drome): un site hydrothermal sur la marge téthysienne à l'Oxfordien? Bull Soc Geol France 8: 69-78

Gill GA, Coates AG (1977) Mobility, growth patterns and substrate in some fossil and Recent corals. Lethaia 10: 119-134

Goedert JL, Benham SR (2003) Biogeochemical processes at ancient methane seeps: The Bear River site in southwestern Washington. In: Swanson TW (ed) Western Cordillera and adjacent areas. Geol Soc Amer, Field Guide 4: 201-208

Goedert JL, Squires RL (1990) Eocene deep-sea communities in localized limestones formed by subduction-related methane seeps, southwestern Washington. Geology 18: 1182-1185

Goedert JL, Squires RL (1993) First Oligocene Records of *Calyptogena* (Bivalvia: Vesicomyidae). Veliger 36: 72-77

Hickman CS (1969) The Oligocene marine molluscan fauna of the Eugene Formation in Oregon. Univ Oregon, Nat Hist Mus Bull 16: 1-112

Hickman CS (1980) A remarkable case of coaxial heterostrophy in an Eocene gastropod. J Paleontol 54: 196-199

Hickman CS (1984) Composition, structure, ecology, and evolution of six Cenozoic deep-water mollusk communities. J Paleont 58: 1215-1234

Hovland M, Risk M (2003) Do Norwegian deep-water coral reefs rely on seeping fluids? Mar Geol 198: 83-96

Hovland M, Thomsen E (1997) Cold-water corals - are they hydrocarbon seep related? Mar Geol 137: 159-164

Hovland M, Mortensen PB, Brattegard T, Strass P, Rokoengen K (1998) Ahermatypic coral banks off Mid-Norway: Evidence for a link with seepage of light hydrocarbons. Palaios 13: 189-200

Kelly SRA, Blanc E, Price SP, Whitham AG (2000) Early Cretaceous giant bivalves from seep-related limestone mounds, Wollaston Forland, northeast Greenland. In: Harper EM, Taylor JD and Crame JA (eds) The Evolutionary Biology of the Bivalvia. Geol Soc London, Spec Publ 177: 227-246

Kenyon NH, Akhmetzhanov AM, Wheeler AJ, van Weering TCE, de Haas H, Ivanov MK (2003) Giant carbonate mud mounds in the southern Rockall Trough. Mar Geol 195: 5-30

Kulm LD, Suess E (1990) Relationship between carbonate deposits and fluid venting: Oregon accretionary prism. J Geophys Res 95: 8899-8915

Kulm LD, Suess E, Moore JC, Carson B, Lewis BT, Ritger SD, Kadko DC, Thornburg TM, Embley RW, Rugh WD, Massoth GJ, Langseth MG, Cochrane GR, Scamman RL (1986) Oregon subduction zone: venting fauna and carbonates. Science 231: 561-566

Little CTS, Herrington RJ, Maslennikov VV, Zaykov VV (1998) The fossil record of hydrothermal vent communities. In: Mills RA and Harrison K (eds) Modern Ocean Floor Processes and the Geological Record. Geol Soc London, Spec Publ 148: 259-270

Majima R (1999) Mode of occurrences of the Cenozoic chemosynthetic communities in Japan. Mem Geol Soc Japan 54: 117-129 (In Japanese)

Masson DG, Bett BJ, Billett DSM, Jacobs CL, Wheeler AJ, Wynn RB (2003) The origin of deep-water, coral-topped mounds in the northern Rockall Trough, northeast Atlantic. Mar Geol 194: 159-180

Moore EJ (1984) Molluscan paleontology and biostratigraphy of the lower Miocene upper part of the Lincoln Creek Formation in southwestern Washington. Contr Sci 351: 1-42

Nesbitt EA, Campbell KA, Goedert JL (1994) Paleogene cold seeps and macroinvertebrate faunas in a forearc sequence of Oregon and Washington. In: Swanson DA, Haugerud RA (eds) Geologic field trips in the Pacific Northwest. Geol Soc Amer, Guidebook, 1: 1D1-1D11

Nomland JO (1916) Corals from the Cretaceous and Tertiary of California and Oregon. Univ California, Bull Dept Geol 9: 59-76

Orange DL, Campbell KA (1997) Modern and ancient cold seeps on the Pacific Coast - Monterey Bay, California, and offshore Oregon as modern-day analogs to the Hoh Accretionary Complex and Quinault Formation, Washington. Washington Geol 25: 3-13.

Peckmann J, Walliser OH, Riegel W, Reitner J (1999) Signatures of hydrocarbon venting in a Middle Devonian carbonate mound (Hollard Mound) at the Hamar Laghdad (Antiatlas, Morocco). Facies 40: 281-296

Peckmann J, Reimer A, Luth U, Luth C, Hansen BT, Heinicke C, Hoefs J, Reitner J (2001) Methane-derived carbonates and authigenic pyrite from the northwestern Black Sea. Mar Geol 177: 129-150

Peckmann J, Goedert JL, Thiel V, Michaelis W, Reitner J (2002) A comprehensive approach to the study of methane-seep deposits from the Lincoln Creek Formation, western Washington State, USA. Sedimentology 49: 855-873

Plusquellec Y, Webb GE, Hoeksema BW (1999) Automobility in Tabulata, Rugosa, and extant scleractinian analogues: Stratigraphic and paleogeographic distribution of Paleozoic mobile corals. J Paleont 73: 985-1001

Prothero DR, Armentrout JM (1985) Magnetostratigraphic correlation of the Lincoln Creek Formation, Washington: Implications for the age of the Eocene/Oligocene boundary. Geology 13: 208-211

Rau WW (1966) Stratigraphy and Foraminifera of the Satsop River area, southern Olympic Peninsula, Washington. State Washington Div Mines Geol Bull 53: 1-66

Rigby JK, Goedert JL (1996) Fossil sponges from a localized cold-seep limestone in Oligocene rocks of the Olympic Peninsula, Washington. J Paleont 70: 900-908

Rigby JK, Jenkins DE (1983) The Tertiary sponges *Aphrocallistes* and *Eurete* from western Washington and Oregon. Contr Sci 344: 1-13

Ritger S, Carson B, Suess E (1987) Methane-derived authigenic carbonates formed by subduction-induced pore-water expulsion along the Oregon/Washington margin. Geol Soc Amer Bull 98: 147-156

Schroeder NAM, Kulm LD, Muehlberg GE (1987) Carbonate chimneys on the outer continental shelf: Evidence for fluid venting on the Oregon margin. Oregon Geol 49: 91-96

Schwartz H, Sample J, Weberling KD, Minisini D, Moore JC (2003) An ancient linked fluid migration system: Cold seep deposits and sandstone intrusions in the Panoche Hills, California, USA. Geo-Mar Lett 23: 340-350

Shapiro RS (in press) Recognition of fossil prokaryotes in Cretaceous methane-seep carbonates: Relevance for astrobiology. Astrobiology

Sibuet M, Olu K (1998) Biogeography, biodiversity and fluid dependence of deep-sea cold-seep communities at active and passive margins. Deep-Sea Res Pt II 45: 517-567

Squires RL (1995) First fossil species of the chemosynthetic-community gastropod *Provanna*: Localized cold-seep limestones in upper Eocene and Oligocene rocks, Washington. Veliger 38: 30-36

Squires RL, Goedert JL (1991) New late Eocene mollusks from localized limestone deposits formed by subduction-related methane seeps, southwestern Washington. J Paleont 65: 412-416

Taviani M (1994) The "calcari a *Lucina*" macrofauna reconsidered: Deep-sea faunal oases from Miocene-age cold vents in the Romagna Apennines, Italy. Geo-Mar Lett 14: 185-191

Vance JA, Clayton GA, Mattison JM, Naeser CW (1987) Early and middle Cenozoic stratigraphy of the Mount Rainier-Tieton River area, southern Washington Cascades. Washington State Div Geol Earth Resour Bull 77: 269-290

Van Weering TCE, de Haas H, de Stiger HC, Lykke-Andersen H, Kouvaev I (2003) Structure and development of giant carbonate mounds at the SW and SE Rockall Trough margins, NE Atlantic Ocean. Mar Geol 198: 67-81

Weaver CE (1943) Paleontology of the marine Tertiary formations of Oregon and Washington. Univ Washington Publ Geol 5: 1-789

Appendix 1

SYSTEMATIC PALEONTOLOGY
Order Scleractinia

Superfamily Caryophyllioidea Dana, 1846

Family Caryophylliidae Dana, 1846

Genus *Deltocyathus* Milne Edwards and Haime, 1848

Type species.—*Turbinolia italica* Michelotti, 1838, by monotypy.

Deltocyathus insperatus n. sp.
Figs. 2a, 3a-d

2002   *Deltocyathus* n. sp. – Peckmann, Goedert, Thiel, Michaelis, Reitner, p. 858, Fig. 3G

Description.- A small *Deltocyathus* with septa arranged in four cycles, appearing to have 48 septa in all specimens complete enough to count. Costae of unworn specimens have an uneven, smooth to sharply serrate appearance. Base of unworn specimens with a blunt central granule. Septa exsert, with S_1 being the most highly exsert, S_2 less so, and S_{3-4} least exsert. Lateral septal faces with irregular arrangement of low, pointed to blunt spines.

Material.- Holotype, LACMIP 12981 (Peckmann et al. 2002: Fig. 3G); paratypes UWBM 97521-97523; referred specimen UWBM 97520.

Occurrence.- Found in only one methane-seep deposit on the Middle Fork of the Satsop River, Mason County, Washington, LACMIP loc. 17426 (= UWBM loc. B6781), Lincoln Creek Formation, Late Oligocene.

Etymology.- From Latin, *insperatus*, meaning surprising or unexpected, in reference to the occurrence in a methane-seep deposit.

Remarks.- *Deltocyathus insperatus* new species is similar to *D. conicus* and *D. italicus* in conical form, but the costae are less spinose. The septal faces of *D. insperatus* are also less spinose than those of *D. conicus*. *Deltocyathus insperatus* is a very small species, with the largest specimens all being less than 6 mm in diameter, and only 2.5 to 3.3 mm in height. There is no other fossil coral from western North America that can be confused with the new species. The only other West Coast species is *D. whitei* Durham, 1943, from the Paleocene age Lodo Formation in California, and it is much larger, with a flattened, discoid corallum. There is apparently no living species of *Deltocyathus* found in the eastern North Pacific Ocean (Cairns 1994).

Appendix 2

Locality descriptions

UWBM B6781: (= LACMIP loc. 17426) Lincoln Creek Formation, Late Oligocene
Map: Dry Bed Lakes, WA USGS Quad., 7.5' Ser., Topo., Provisional Edition 1990.
Methane-seep carbonate deposit at water level, east bank of the Middle Fork of the Satsop River, approximately 80 m south and 240 m east of the northwest corner of Sec. 32, T. 21 N., R. 6 W., Mason County, Washington. (= SR4 of Peckmann et al. 2002).

UWBM B6782: Lincoln Creek Formation, Early Oligocene
Map: Dry Bed Lakes, WA USGS Quad., 7.5' Ser., Topo., Provisional Edition 1990.
Very small methane-seep carbonate, less than 50 cm in diameter (as exposed in 2002), south bank of the Middle Fork of the Satsop River, approximately 800 m south and 310 m east of the northwest corner of Sec. 20, T. 21 N., R. 6 W., Mason County, Washington.
(= SR1 of Peckmann et al. 2002).

UWBM B6783: Lincoln Creek Formation, Oligocene? (float)
Map: Grisdale, WA USGS Quad., 7.5' Ser., Topo., Provisional Edition 1990.
Methane-seep carbonate block found as float on a gravel bar in the Canyon River, SW1/4 SW1/4 NW1/4 of Sec. 36, T. 20 N., R. 7 W., Grays Harbor County, Washington.
Collected by J.L. Goedert and K.L. Kaler, 13 August 1994.

UWBM B6784: Lincoln Creek Formation, Late Eocene - Early Oligocene
Map: Dry Bed Lakes, WA USGS Quad., 7.5' Ser., Topo., Provisional Edition 1990.
Solitary coral found in carbonate deposit (methane-seep?), north side of the Middle Fork of the Satsop River, at upstream end of bend in river, approximately 460 m south and 820 m west of the northeast corner of Sec. 20, T. 21 N., R. 6 W., Mason County, Washington.
Collected by J.L. Goedert and F. Gill, 12 July 2003.

LACMIP 5842: Lincoln Creek Formation, Late Oligocene
Map: Knappton, WA USGS Quad., 7.5' Ser., Topo., 1973 Edition.
Fossils found as float on beach northeast of the townsite of Knappton, north shore of the Columbia River, N½ N½ Sec. 9, T. 9 N., R. 9 W., Pacific County, Washington.

LACMIP 5843: Lincoln Creek Formation, Late Oligocene
Map: Knappton, WA USGS Quad., 7.5' Ser., Topo., 1973 Edition.
Fossils found as float on beach northeast of the townsite of Knappton, north shore of the Columbia River, approximately 305 m south and 430 m east of the northwest corner of Sec. 9, T. 9 N., R. 9 W., Pacific County, Washington.

Growth, deposition, and facies of Pleistocene bathyal coral communities from Rhodes, Greece

Jürgen Titschack, André Freiwald

Institute of Paleontology, Erlangen University, Loewenichstr. 28, D-91054
  Erlangen, Germany
  (juergen.titschack@pal.uni-erlangen.de)

Abstract. Modern and widespread deep-water coral ecosystems have become a major target of research during the last decades. So far, only a few fossil counterparts of such carbonate-secreting deep-water communities have been described. This scarcity might be a result of either, a possible miss-identification as a tropical deposit and/or the rare case of tectonic uplift and subsequent access to these deep-water deposits.

The early Pleistocene St. Paul's Bay Limestone on the island of Rhodes (Greece) represents one of the few known examples of the bathyal 'white coral community' dominated by *Lophelia pertusa* which are exposed on land. This occurrence relates to a convergent tectonic setting with large-scale uplifts in the vicinity of the European-African plate boundary that is responsible for the exposure of these early Pleistocene deep-water deposits.

The geometry of the St. Paul's Bay Limestone significantly differs from the mound-forming *Lophelia* occurrences as known, e.g., from the NE-Atlantic or the Florida Strait. Instead, it appears similar to the modern 'white coral community' of the western Mediterranean Sea that is usually associated with submarine cliffs. Much like the latter, the St. Paul's Bay Limestone demonstrates that the growth and final deposition of the 'white coral community' was strongly influenced by the complex relief with steep submarine basement cliffs generated by horst-graben systems. These submarine cliffs not only provided the main habitat for the 'white coral community', they also explain recurrent instability and redeposition by debris falls along the submarine cliffs. Such a debris fall mechanism is strongly suggested by: (1) the steep slope angles (>30°), (2) the short transport distance (<20 m), (3) the wedge-like geometry, (4) the lack of grading, (5) the fabric complexity with incorporated fragments of hardgrounds, intraclasts and slightly consolidated sediment, (6) geopetal structures of various directions, thus indicating multiple resedimentation events, and (7) the variety of fragmentation and bioerosion. This resulted in the final deposition of the 'white coral community' (1) at the foot of submarine cliffs and (2) in neptunian dykes and, to a minor extent (3) in erosional depressions of the basement rock. In conclusion, the basic characters of the St.

Paul's Bay Limestone in terms of the initial facies, fabric and fauna largely match those described for lithoherms (Florida Strait). The enhanced complexity in terms of the final fabric and the wedge-like geometry appear due to multiple resedimentation events *via* debris falls along submarine cliffs.

Keywords. Bathyal corals, Rhodes, Mediterranean Sea, Pleistocene, facies, depositional processes

Introduction and objectives

Modern deep-water coral ecosystems with *Lophelia pertusa* (Linné, 1758) and *Madrepora oculata* Linné, 1758 as the dominant framework builder are the focus of current research on mound-forming processes and bioherm construction in the Northeast Atlantic (De Mol et al. 2002; Freiwald et al. 2002; Van Rooij et al. 2003; Van Weering et al. 2003). Fossil counterparts are rare, e.g., Squires (1964) or Montenat et al. (1991), most probably due to the scarce case of tectonic uplift and preservation of such geologically young deep-water deposits. Beside the occurrence described here on Rhodes (Greece) in vicinity of the Hellenic Arc (which corresponds to the collision zone of the European and African Plates, Fig. 1/A), other fossil *Lophelia* occurrences are found along the uplifted flanks of the Messina Strait (Plio-Pleistocene; Di Geronimo et al. 2005 and further references therein) as well as in Miocene and Pliocene deposits flanking the Cook Strait of
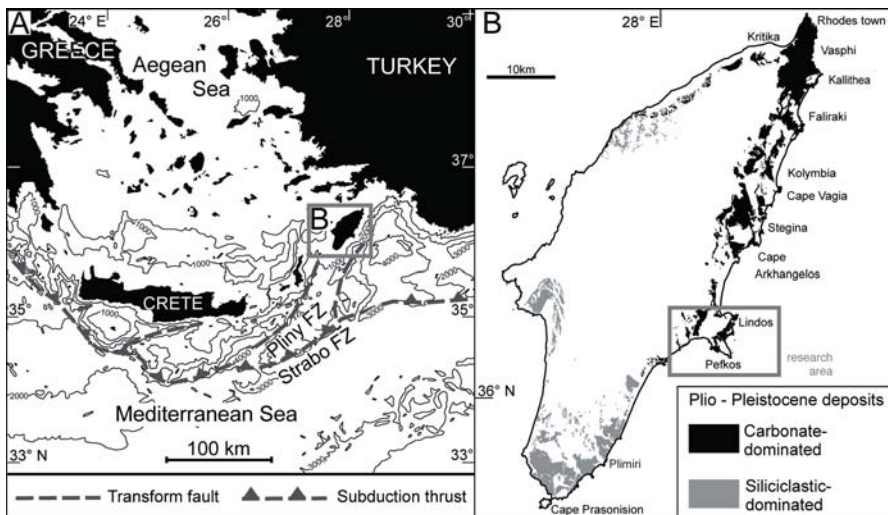
Fig. 1 A Tectonic overview of the eastern Hellenic Arc. FZ: Fault Zone. **B** Map of the island of Rhodes showing the main Plio-Pleistocene outcrops, distinguished as marine- *versus* terrestrial-dominated (after Mutti et al. 1970; Meulenkamp et al. 1972; Hanken et al. 1996). The isolated nature of the marine-dominated Plio-Pleistocene sediments is caused by the deposition in depocentres due to graben systems in NW-SE direction

New Zealand (Squires 1964). Plio-Pleistocene deep-water coral communities along the passive continental margins of the North Atlantic are still located at bathyal depths (De Mol et al. 2002; Van Rooij et al. 2003; Van Weering et al. 2003).

The current research in the NE-Atlantic stimulated the re-investigation of the early Pleistocene *Lophelia pertusa*-bearing St. Paul's Bay Limestone (later referred to as SPBL) of Rhodes, Greece. This occurrence from Rhodes earlier described by Jüssen (1890) and Hanken et al. (1996) offers a promising opportunity to re-examine an ancient deep-water coral ecosystem from outcrops. The objective of this paper is to draw a baseline in terms of the original habitat, the conditions of growth and the depositional environment of the Rhodes deep-water coral community. It includes an assessment of the main sedimentary processes involved in the formation of the Pleistocene SPBL as well as some remarks of comparison with the late Pleistocene to modern *Lophelia pertusa*-bearing lithoherms of the Florida Strait (Wilber and Neumann 1993). The preservation of the primary aragonitic and high-Mg calcite mineralogy provides the possibility of palaeoenvironmental and diagenetic studies with stable isotopes.

Location and geological setting

The research area is located in the vicinity of the town Lindos in the mid-eastern part of Rhodes (Fig. 1/B) where we examined six SPBL outcrops (Fig. 2). The type section of the examined SPBL is located in the south of St. Paul's Bay (Hanken et al. 1996; locality 1 in Fig. 2); reference sections are present in the wider Lindos area (Fig. 2).

The modern morphology of the Lindos area is characterised by a pre Plio-Pleistocene designed series of steeply inclined fault lines dissecting basement rock, i.e., consisting of the Lindos Limestone, a Cretaceous carbonate ramp (Mutti et al. 1970). This morphology is the result of a complex system of small-dimensional halfgrabens, grabens and horsts (Fig. 2). The graben systems, tens of metres to several kilometres wide, are oriented predominantly in a NW-SE direction and acted as the major depocentres for the Plio-Pleistocene sedimentary units (Hanken et al. 1996). On the now elevated, deeply karstified horst-blocks the preservation of Plio-Pleistocene deposits is restricted to neptunian dyke infills that are oriented subparallel to fault zones and cliff faces.

The island of Rhodes in the south-eastern Aegean Sea has been strongly influenced by the convergent active plate boundary between the European and African plates since the Miocene (Mascle et al. 1986; Fig. 1/A). This resulted in large vertical displacements (100s of metres) documented as an extremely high amplitude of relative sea-level changes recorded in the Plio-Pleistocene deposits exceeding greatly the range of glacial-interglacial sea-level changes (Hansen 1999; Nelson et al. 2001).

According to Hanken et al. (1996), the SPBL was deposited during the maximum transgression episode of the Rhodes Formation in the late Pliocene or early Pleistocene (for details of the Plio-Pleistocene stratigraphy on Rhodes see
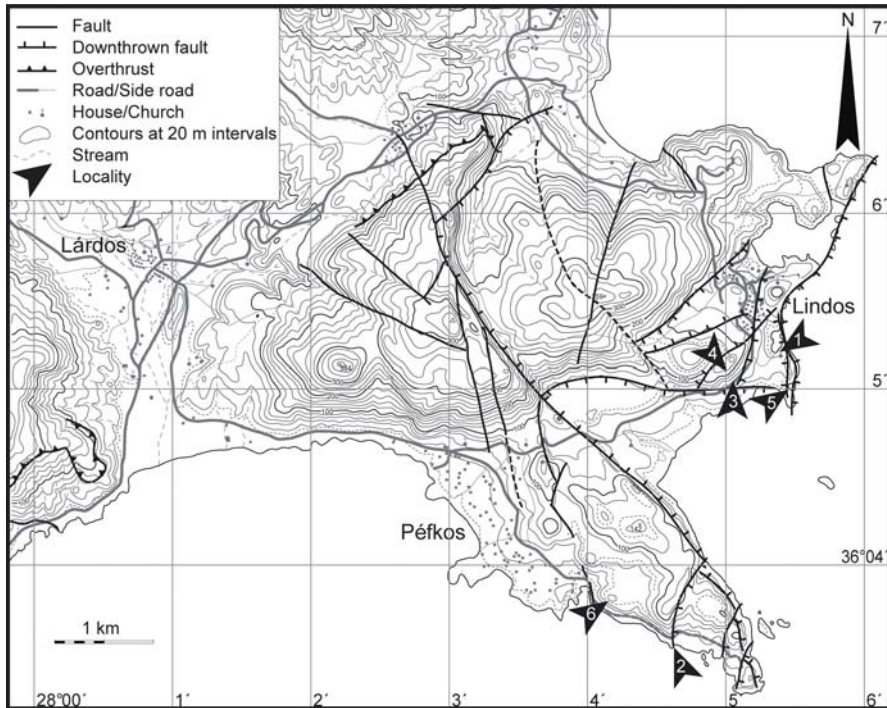
Fig. 2 Research area in the Lindos region (modified after Mutti et al. 1970). Arrowheads show investigated localities with SPBL. **1** St. Paul's Bay (type locality), **2** Gines east, **3** Lindos-Pefkos Road-cutting, **4** Lindos-Pefkos Road-cutting terrace, **5** Soumani Bay, **6** Pefkos east. Note that all localities are in vicinity of faults or steep Lindos Limestone slopes

Hanken et al. 1996). The SPBL developed as relatively proximal deposits bound to submarine cliffs and highs. Simultaneously the shallow-bathyal, marly Lindos Bay clay was deposited further out in the basins. Palaeobathymetric interpretations based on ostracod, bryozoan and scleractinian coral assemblages in the Lindos Bay clay and the SPBL together suggest bathyal conditions of around 300 to 500 m water depth (Moissette and Spjeldnæs 1995). The presence of large burrows of *Zoophycos rhodensis* Bromley and Hanken, 2003 in the lower part of the Lindos Bay clay indicates even greater depths (Bromley and Hanken 2003).

Material and methods

A total of 39 rock samples were taken from six outcrops and were sawn into two to four slices. From each slice, surface acetate peels were prepared (a total of 122 peels). Thin-sections were prepared of 49 selected samples. Peels and thin-sections were examined using a light microscope with and without polarised light.

Results

Outcrop observations

The SPBL outcrops are associated with steep (>30°) Lindos Limestone cliffs and fault planes (Fig. 2). The lateral extent of SPBL outcrops is limited, generally less than 20 m of horizontal extension, with a maximum thickness near the cliff faces or fault planes not exceeding 3 m. In many cases, the SPBL reveals a wedge-like geometry in outcrops, thinning rapidly away from the fault or cliff face (localities 2, 3, 5; Fig. 3/1).

Neptunian dykes within the Lindos Limestone occur subparallel to fault planes or cliff faces. Dyke fillings composed of SPBL are exposed in all localities studied (Fig. 3/2). In some cases the fillings reflect a horizontal deepening trend from the outer pre-SPBL shallow-water deposits (Kolymbia Limestone in Hanken et al. 1996) that are attached to the dyke-walls (Lindos Limestone) to the central part filled with the deep-water SPBL. Typically, the SPBL in neptunian dykes is relatively poor in corals but rich in brachiopods, especially in *Gryphus vitreus* (Born, 1778). SPBL occurrences in Lindos Limestone erosional depressions are rare (locality 4).

In general, the coral fragmentation varies from arborescent, relatively intact colonies of *Lophelia pertusa* (up to 40 cm in height; Fig. 3/3) to coral rubble. The intact colonies show no major bioerosion patterns within the skeletons indicating a rapid burial (Freiwald and Wilson 1998). Instead, the preservational status of the coral rubble shows a wide spectrum from rather pristine, unaltered to intensely altered sponge-excavated corallites (see also Bromley 2005).

In most cases, the SPBL succeeds the Cretaceous Lindos Limestone (localities 1, 4, 5, 6) or discordantly drapes the older shallow-water deposits which documents the transgressive phase of the Rhodes Formation (Kolymbia Limestone; localities 2, 3). Lindos Limestone surfaces covered by SPBL contain the borings *Entobia gigantea* Bromley and D'Alessandro, 1989 and *Entobia ovula* Bromley and D'Alessandro, 1984 (locality 5).

In some places, the SPBL unit includes patchy intraformational hardgrounds (Fig. 3/5), and in rare cases hardground-surrounded intraclasts occur (Fig. 3/4). The top of the SPBL is developed as hardground in localities 3 and 5 (Fig. 3/6). The undulating hardground surfaces of the SPBL are bioeroded by sponges *(Entobia* isp.; Fig. 3/5). The undulations were probably caused by crustacean burrows that were produced when the deposited sediments were already at a firmground stage. At locality 3, undulations of the hardground surface, here succeeded by the shallow-water deposits of the regressive phase of the Rhodes Formation (Cape Arkhangelos calcarenite in Hanken et al. 1996), could be identified as the trace fossil *Thalassinoides paradoxicus* (Woodward, 1830) overprinted by *Entobia ovula*. Such an ichnocommunity replacement during substrate hardening is a common feature of many hardgrounds (e.g., Bromley and Allouc 1992).
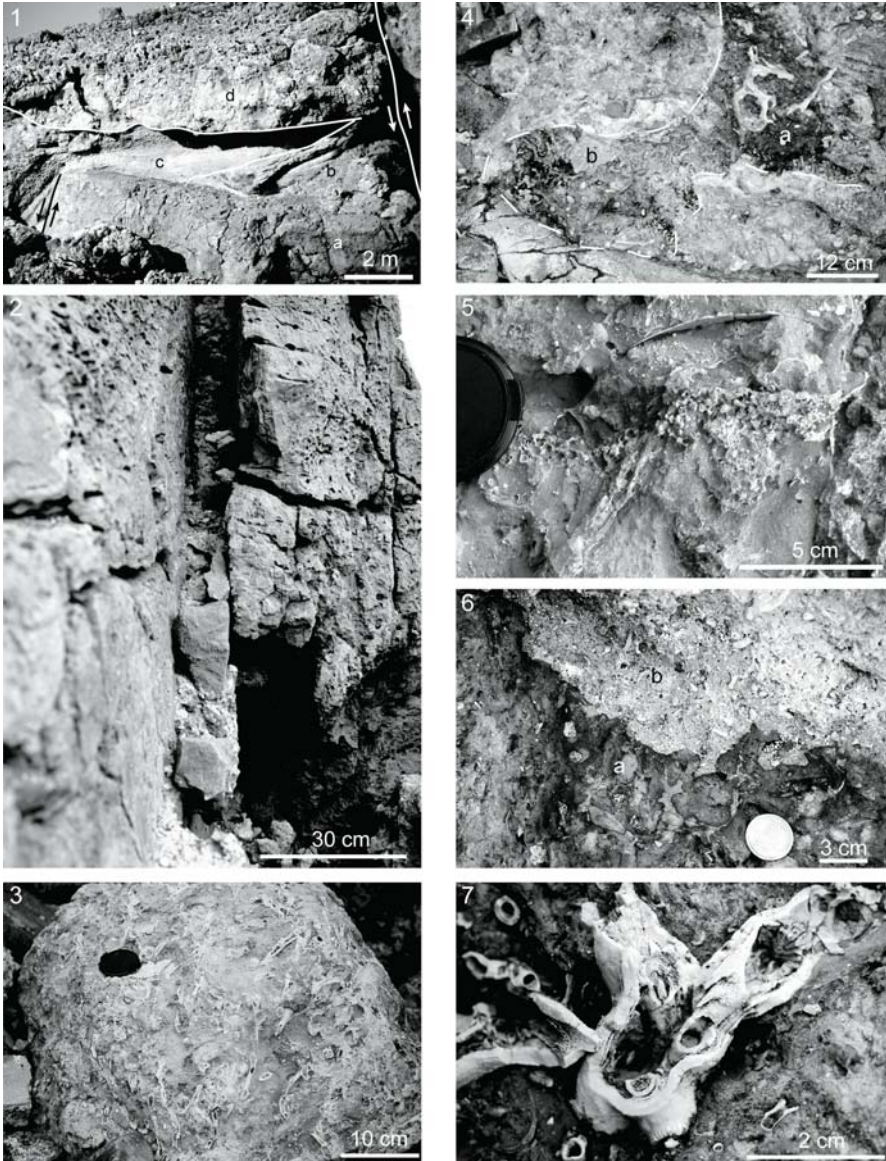
Fig. 3 St. Paul's Bay Limestone outcrops. **1** Locality 5; a: Lindos Limestone, b: St. Paul's Bay Limestone, c: Cape Arkhangelos calcarenite, d: Lindos Acropolis Formation. Note the wedge-like form of St. Paul's Bay Limestone in contact with a fault. **2** Locality 5; Neptunian dyke in Lindos Limestone filled with St. Paul's Bay Limestone. **3** Locality 1; Large colony (~40 cm in height) of *Lophelia pertusa*. **4** Locality 5; a: Aggregate of St. Paul's Bay Limestone with iron-manganese impregnated hardground on the surface in St. Paul's Bay Limestone, b: Incorporated Lindos Limestone clast. **5** Locality 1: Intraformational hardground in St. Paul's Bay Limestone strongly bioeroded with *Entobia* isp. **6** Locality 5; Hardground on top

Sedimentary facies and community

Facies

The SPBL is classified as a float- to rudstone with a mud- to wackestone matrix. The components >2 mm are almost exclusively skeletal in origin and dominated by azooxanthellate corals and complemented by rare Lindos Limestone clasts and intraclasts (Fig. 3/4).

The matrix is dominated by red to beige coloured mud- to wackestones, rich in foraminifers, brachiopods, common crustacean fragments, rare gastropods, bivalves, caryophyllid corals, pteropods, Lindos Limestone clasts and ostracods. Bryozoans, serpulids and sponges occur occasionally as overgrowth upon corals. Locally, especially at localities 2 and 3, minor amounts of coralline red algae as well as higher amounts of bryozoans do occur.

Fabric

The SPBL shows a complex patchwork of different sediment zones separated by discontinuity surfaces and occasionally with different geopetal orientation (Fig. 4). At least five sediment zones could be defined. Zone 1 occurs as intraclasts or areas with a red colour. Its surfaces are developed as an intensely bioeroded iron-manganese impregnated hardground and are rarely encrusted by serpulids (Fig. 5/1). Locally stylolites are observed along this surface (Fig. 5/2). Zone 1 is discordantly overlain by Zones 2 or 3. Zone 2 appears also as intraclasts or areas with a red to beige colour, overlaying or surrounding Zone 3. In contrast to Zone 1, surfaces of Zone 2 are developed as an undulating, slightly iron-manganese impregnated surface lacking bioerosion (Fig. 5/2). Partially, the boundary between Zones 2 and 3 changes from the undulated surface into a gradational transition where no differentiation of the two zones is possible.

While Zones 1 - 3 build up the main rock of SPBL, Zones 4 and 5 are restricted to centimetre-sized vugs in Zones 1 - 3 (Fig. 4). This difference is emphasized in the facies where Zones 4 and 5 are reduced in components >2 mm when compared to Zones 1 - 3. The sediments of Zone 4 are divided into: (1) a lower part that is comparable with the matrix sediment of Zones 1 - 3 showing a grey colour, and (2) an upper part consisting of a nearly fossil-free mudstone grading into a peloid grainstone (Figs. 5/3, 6/3). Locally, multiples of these inversely graded fillings are developed. The peloids provide diameters varying between 20 and 140 μm with a mean of 60 μm. They are of unknown origin, but their angular shape, the occurrence of fecal pellets, rare planktonic foraminiferans and other detrital bioclasts (Fig. 6/4) suggest a detrital origin. Further support is provided by the rare occurrence of sedimentary textures interpreted as flute marks (Fig. 6/5). The interparticle pores of the peloid grainstone are filled with isopachous bladed spar. Where the upper part

of St. Paul's Bay Limestone (a) overlain by Cape Arkhangelos calcarenite (b). **7** Locality 1; *Lophelia pertusa* with thick outer theca in St. Paul's Bay Limestone
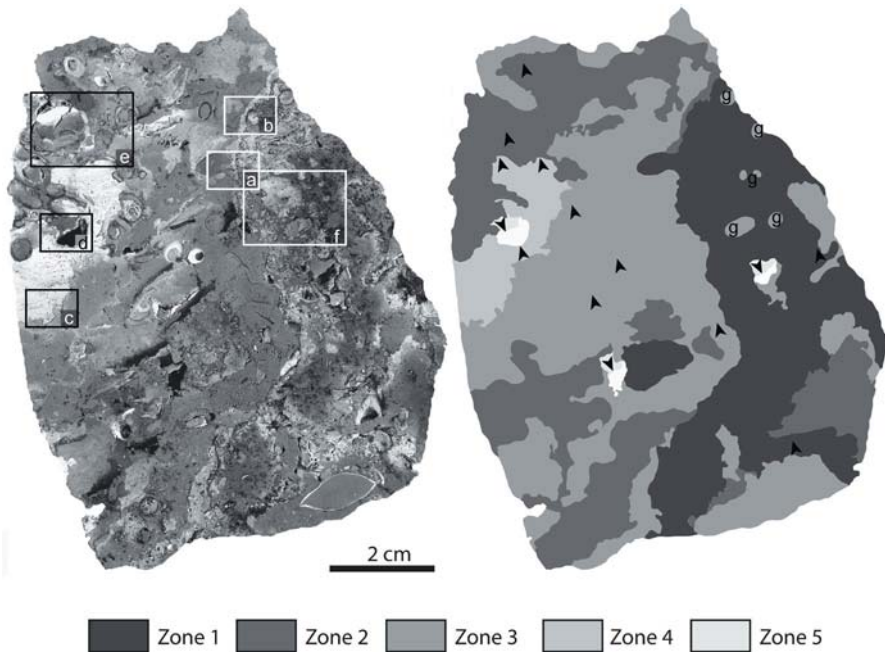
Fig. 4 Polished slab (left) and interpretation (right) of the St. Paul's Bay Limestone showing its fabric complexity (locality 1; arrowheads show up-direction of geopetal structures). Five sedimentary zones could be identified. Frames: a: Fig. 5/1, b:Fig. 5/2, c: Fig. 5/3, d: Fig. 5/4, e: Fig. 5/5, f: Fig. 5/6, g: *Gastrochaenolites* isp.

of Zone 4 is missing, a slight iron-manganese impregnation is developed on the top of the lower part of Zone 4 (Fig. 5/4). Zone 5 is developed in the remaining vugs of Zones 1 - 4 and is characterised by a different geopetal orientation from Zone 4 (Fig. 5/4) and therefore it clearly postdates Zone 4. Its facies is comparable to the lower part of Zone 4.

Fossil content

A characteristic feature of the SPBL, especially in the Zones 1 - 3, is the richness in azooxanthellate scleractinian corals of the so-called 'white coral community' (in the sense of Pérès and Picard 1964). It is dominated by *Lophelia pertusa* (Fig. 3/7) and the less abundant *Madrepora oculata*, *Desmophyllum cristagalli* Milne Edwards and Haime, 1848, *Dendrophyllia cornigera* (Lamarck, 1816), and *Caryophyllia* sp. The outer theca of *Lophelia pertusa* shows characteristic tubes that are indicative for the symbiotic polychaete *Eunice* sp. (Fig. 5/5; Mortensen 2001).

The accompanying macrofauna is dominated by brachiopods, especially *Gryphus vitreus*, and *Terebratulina retusa* (Linné, 1758), trochid gastropods, rare other gastropods, pectinids and other bivalves, regular echinoids and galatheid crustacean fragments. Imprints of the bivalve *Acesta excavata* (Fabricius, 1779) and isolated internodia of the octocoral *Keratoisis* sp. are rarely found. Primary aragonitic skeletons and shells are still preserved as aragonite.

The microfauna consists of planktonic foraminiferans, ostracods and pteropods. Among the foraminiferans the planktonic forms such as *Globorotalia scitula* Brady, 1882, *Globorotalia inflata* (d'Orbigny, 1839), *Globigerinoides ruber* (d'Orbigny, 1839) and *Orbulina universa* d'Orbigny, 1839 are dominant. Miliolid foraminiferans with the genera *Quinqueloculina*, *Triloculina*, *Spiroloculina* and *Pyrgo* are common.
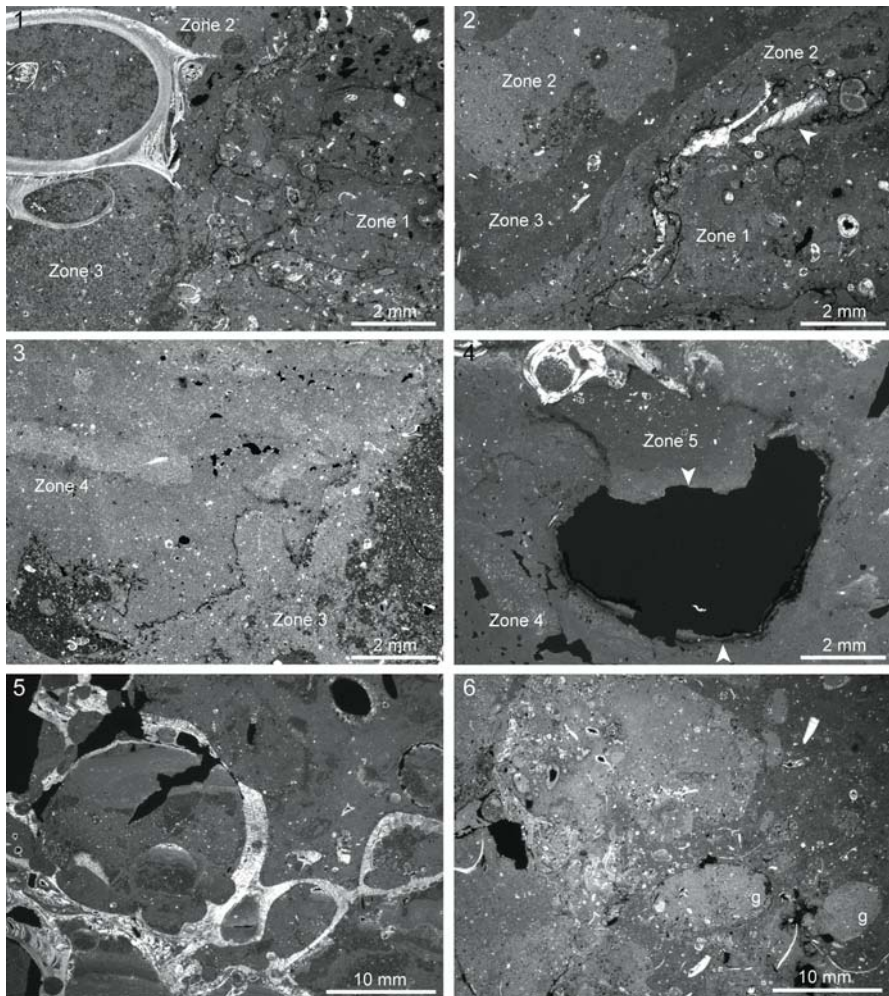
Fig. 5 St. Paul's Bay Limestone thin sections (see overview in Fig. 4). **1** Iron-manganese impregnated and heavily bioeroded surface of Zone 1 encrusted by a serpulid and overlain by Zones 2 and 3. **2** Zone 1 overlain by Zone 2, which is overlain by Zone 3. Zone 2 occurs also as a clast in Zone 3. Note that the surface of Zone 1 is developed as microstylolite (arrow). **3** Contact between Zones 3 and 4. **4** Contact between Zones 4 and 5 showing different orientations of geopetal structures (arrows). Because the upper part of Zone 4 is missing, a slight iron-manganese impregnation is observed. **5** Tube of the polychaete *Eunice* sp. **6** *Gastrochaenolites* isp. (g) in Zone 1

In contrast to these aforementioned benthic foraminiferans, *Hyalinea balthica* (Schröter, 1783), *Hyrrokkin sarcophaga* Cedhagen, 1994 together with *Ammonia* sp., *Melonis* sp., *Lenticulina* sp., *Epistomina* sp., *Cibicides lobatulus* (Walker and Jacob, 1798) and the agglutinated *Textularia* are rare.
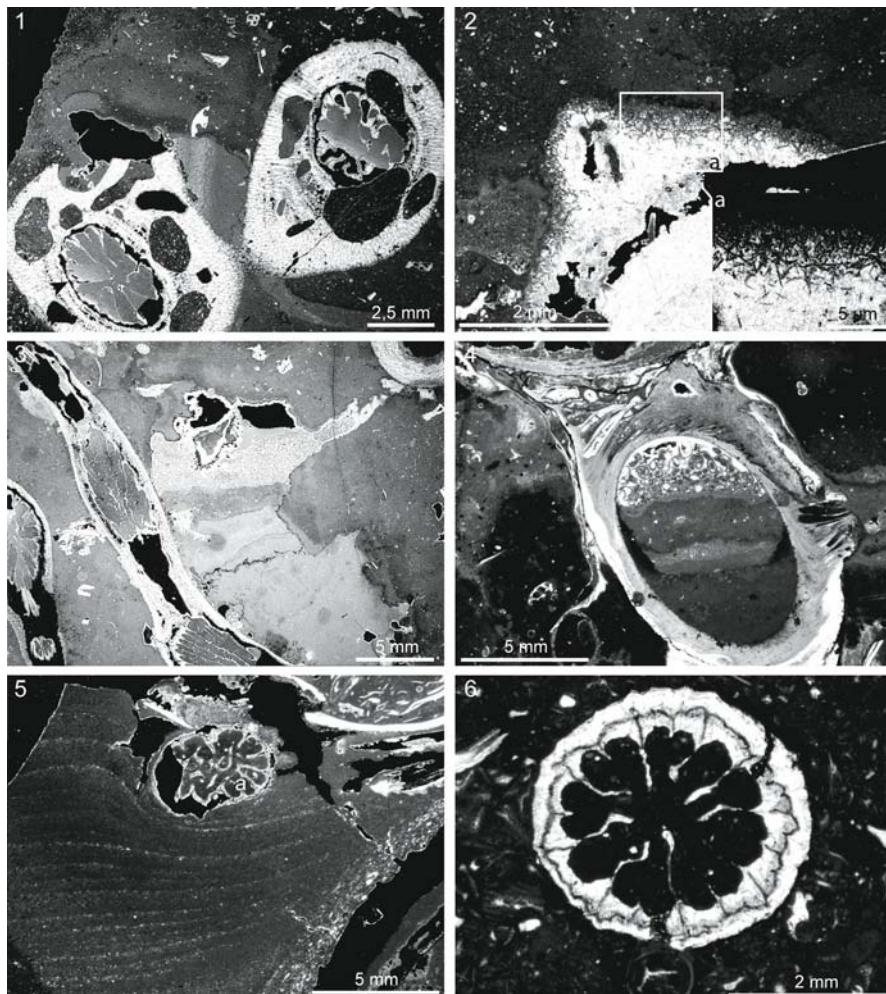
Fig. 6 St. Paul's Bay Limestone thin sections. **1** Locality 1; Strongly bioeroded *Lophelia pertusa* with *Entobia* cf. *ovula* in St. Paul's Bay Limestone. Arrowhead points to the dissolved centre of calcification. **2** Locality 1; Surface of *Lophelia pertusa* with *Orthogonum* isp. **3** Locality 1; Vug associated with *Lophelia pertusa* geopetally filled with internal sediment of Zone 4. The upper part shows alteration of internal sediment with micritic and peloidal texture. **4** Locality 1; Serpulid tube filled with internal sediment of Zone 3. Note the foraminiferan fragments mixed with peloids in the upper part. **5** Locality 1; Internal sediment with multiple inversely graded fillings. The sedimentary texture is interpreted as flute mark related to coral fragment as curvature of the vug wall (a). **6** Locality 1; Pristine *Lophelia pertusa* skeleton with preserved centres of calcification

Bioerosion

Bioerosion is a common feature of bioclasts, intraclasts and Lindos Limestone clasts of the SPBL (Bromley 2005). Lindos Limestone clasts and intraclasts are dominantly bioeroded with *Entobia* isp. Rarely *Gastrochaenolites* isp., borings of bivalves, related to the hardground of Zone 1 are observed (Fig. 5/6). In contrast, coral-fragments, serpulids, and molluscs are commonly infested by *Entobia* isp. (Fig. 6/1), *Saccomorpha clava* Radtke, 1991, and rarely by *Orthogonum* isp. (Fig. 6/2).

Dissolution and alteration of skeletal aragonite

Dissolution in the SPBL is restricted to the centres of calcification (dust line) of corals in aragonitic preservation (Figs. 6/1, 6/2). The degree of dissolution can vary significantly within the same sample from nearly no dissolution (Fig. 6/6) to complete dissolution of the centres of calcification and parts of the outer theca (Fig. 6/1). We observe a typical dissolution pattern starting in the centres of calcification at the junction spots of septa and theca. From there, the dissolution spreads until complete dissolution of the centres of calcification. In contrast, no dissolution is observed in aragonitic molluscs or other skeletal debris.

Lithification

The lithification of SPBL is provided by the combination of: (1) an early lithification of the matrix sediment documented by the different consolidated sediment zones that are separated by discontinuity surfaces, and (2) by isopachous bladed spar. The latter overgrows vug rims, provided by the remaining vugs in the host rock or by intraparticle pores as for example foraminiferans or bryozoan chambers. Furthermore, it fills the interparticle pores of the peloid-grainstones of the upper part of Zone 4.

Discussion

Palaeoenvironment

Present-day *Lophelia pertusa* predominates in eutrophic seas at a temperature range from 4 - 12°C (Freiwald 2002). The present-day Mediterranean Sea is characterised by an oligotrophic regime (<5.5 μmol/l nitrate; Hofrichter 2001), and high temperatures (>13°C) and salinities of the deep-water masses (>38.4 psu; Hofrichter 2001). This underlines the peculiarity of the rare occurrence of *Lophelia pertusa* in the modern Western Mediterranean Basin and the Ionian Sea (Best 1969; Zibrowius 1980; Taviani et al. 2004, 2005). In contrast, Pleistocene fossils of *Lophelia pertusa* are comparably common with a concentration in the western to central Mediterranean Sea (Zibrowius 1980; Delibrias and Taviani 1985; Vafidis et al. 1997; Remia and Taviani 2004; Di Geronimo et al. 2005; Taviani et al. 2005). The easternmost known occurrences are the south slope of the island of Thassos in the Aegean Sea (Vafidis et al. 1997), the SPBL on Rhodes (Jüssen 1890; Hanken et al. 1996), and the south coast of Turkey near Kastellórizo (Zibrowius 1979).

The modern 'white coral community' in the Mediterranean Sea is suggested to represent relics of the Pleistocene period when this community flourished and when, especially during glacial times, the Atlantic deep-water influence was stronger in the Mediterranean Sea than today (Taviani and Colantoni 1979; Delibrias and Taviani 1985; Taviani et al. 2004, 2005). Taking into account the eastern, nowadays oligotrophic, position of Rhodes and, in accordance with Taviani and Colantoni (1979) and Delibrias and Taviani (1985), the flourishing 'white coral community' during glacial times, it is likely that the SPBL was deposited during more eutrophic periods with lower deep-water temperatures, which occurred during glacial periods.

The occurrence of the 'white coral community' in the SPBL suggests a palaeo-water depth between 300 and 600 m (see Zibrowius 1987). The foraminiferal assemblage is dominated by planktonic foraminiferans typical for wackestones of the shallow bathyal environment. Further support is provided by the microborings in bioclasts of the SPBL which are characterised by the aphotic *Saccomorpha clava* / *Orthogonum lineare* ichnocoenosis (Glaub 1999). Therefore we suggest growth and deposition in a shallow bathyal environment. This is in good agreement with Hanken et al. (1996) and Moissette and Spjeldnæs (1995), who for Rhodes suggest a palaeo-water depth range between 300 and 500 m for the maximum transgression during early Pleistocene times based on ostracod and bryozoan analysis, as well as the distribution patterns of *Gryphus vitreus* (>100 m, Logan 1979; 70 - 1050 m, Gaetani and Sacca 1984). The fossil assemblage of the SPBL has characteristic bathyal affinities comparable to the *Lophelia pertusa*-bearing deposits in the Strait of Messina (Di Geronimo et al. 2005).

Similarities with the lithoherms of the Florida Strait (Neumann et al. 1977; Mullins et al. 1980; Messing et al. 1990; Major and Wilber 1991; Wilber and Neumann 1993) exist in terms of the faunal assemblage, the associated hardgrounds and the vug fillings. However, multiple re-sedimentation events recorded in the SPBL (see discussion below) largely mask the larger-scale style of primary skeletal growth and syndepositional lithification.

We interpret the five sediment zones to be produced in the same palaeoenvironment with successive consolidation stages. Zone 1 was considerably lithified as documented by the hardground. In contrast, Zones 2 and 3 were incorporated within a late and early firmground stages, respectively, as evidenced by the slight iron-manganese impregnation and the lack of bioerosion. Zones 4 and 5 were infiltrated as loose sediment into the remaining vugs.

The inversely graded fillings in the upper part of Zone 4 are comparable in texture to the 'paste-to-peloids precipitation' described by Wilber and Neumann (1993) as vug fillings in the lithoherms of the Florida Strait as well as to the 'inverse graded internal sediments' described by Scoffin (1993) from tropical reefs. Based on the following observations, we favour a sedimentary origin for the inversely graded fillings in the upper part of Zone 4 of the SPBL: (1) the vug fillings are always geopetal, (2) the peloids are often angular in shape with a great size range from 20 to 140 µm, (3) rarely the peloids are mixed with planktonic foraminiferans (Fig. 6/4),

bioclasts and fecal pellets and (4) flute marks (Fig. 6/5) rarely occur in relation to curvatures of the vug walls. However, the origin of many peloids is unknown, so that their source is open to speculations.

The inverse gradation of the upper part of Zone 4 may be explained in accordance with Scoffin (1993) by the pumping of seawater through vugs, resulting in the agitation of trapped sediment so that the fine sediment gets sifted to the base. The hypothesis of an active pumping mechanism is supported by the intense cementation of the upper peloid-grainstone part of Zone 4 with isopachous bladed spar that was most likely facilitated by an active pore water flow. Multiple inversely graded fillings are consequently interpreted as repeated sediment input. A high pore-water flow and a shallow bathyal environment are not necessarily a contradiction; bottom or contour currents in the existing Florida Strait reach current speeds exceeding 50 cm/s down to 600 m water depth (Wilber and Neumann 1993) and internal waves or tides observed in modern *Lophelia pertusa* occurrences in the NE Atlantic reach comparable velocities (De Mol et al. 2002; Freiwald 2002; White et al. 2005).

Pattern of growth, displacement and deposition

The SPBL shows similarities of facies and fossil assemblage with the modern NE-Atlantic, where the 'white coral community' builds mounds several kilometres long and hundreds of metres in height (e.g., Mortensen et al. 1995; Freiwald et al. 2002; Huvenne et al. 2005), and also to the lithoherms in the Florida Strait which are hundreds of metres long and up to 50 m high (Neumann et al. 1977). In contrast, however, the SPBL differs in its fabric complexity and depositional geometry (wedges on the foot of Lindos Limestone cliffs *versus* mounds).

Therefore we conclude that the 'white coral community' preserved in the SPBL did not form mounds but lived as coral thickets on the Lindos Limestone cliffs, which served as hard substrate during the late Pliocene to early Pleistocene. This interpretation is in accordance with the modern and late Pleistocene bathyal distribution of the 'white coral community' in the Mediterranean Sea that is dominantly related to steeply-inclined hard substrates and submarine cliffs (Pérès and Picard 1964; Sartori 1980; Zabala et al. 1993; Tunesi and Diviacco 1997; Hofrichter 2003; Remia and Taviani 2004; Taviani et al. 2005). An idealised palaeoenvironmental model for the SPBL is shown in Figure 7.

Frequently, re-sedimentation events occurred whereby living corals, coral rubble, hardgrounds, intraclasts and different consolidated sediment zones were transported downslope and deposited within neptunian dykes or at the foot of submarine cliffs. In some cases the incorporated sediment received input from the photic zone as documented by red algae clasts and shallow-water foraminifers (*Elphidium* sp., *Spiroloculina* sp., *Triloculina* sp., *Quinqueloculina* sp., etc.).

The sedimentary processes in environments related to submarine cliffs depend chiefly on the sediment supplied (material, grain size, grain sorting) and on slope inclination. Following the criteria given by Nemec (1990), Einsele (2000), Mulder and Alexander (2001) and Drzewiecki and Simó (2002), several arguments suggest a deposition of the SPBL *via* multiple debris falls: (1) the steep slope angles (>30°)

Living colonies of the "white coral community"

Debris of the "white coral community" with different grades of fragmentation

20 m

20 m

faults
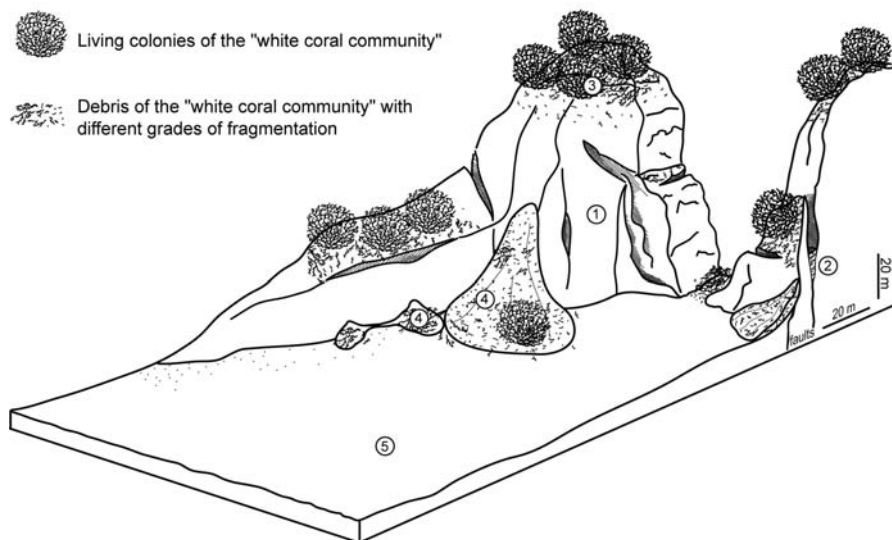
Fig. 7 Reconstruction of the palaeoenvironment during deposition of the St. Paul's Bay Limestone. 1: Submarine cliffs of Lindos Limestone. 2: Neptunian dykes (localities 1-6). 3: living colonies of the 'white coral community'. 4: Debris fall (St. Paul's Bay Limestone, localities 1-6). 5: Lindos Bay clay

of Lindos Limestone-cliffs in vicinity of the outcrops, (2) the short transport distance (<20 m from the Lindos Limestone-cliffs), (3) the wedge-like geometry, (4) the lack of grading, (5) the fabric complexity with incorporated fragments of hardgrounds, intraclasts and slightly consolidated sediment, (6) geopetal structures of various directions, indicating multiple re-sedimentation events, (7) the variety of fragmentation and bioerosion.

A possible deposition *via* gravity flows, as suggested for the *Lophelia pertusa*-bearing deposits of the Messina Strait (Montenat et al. 1991), can be excluded for the SPBL. A fine-grained unconsolidated matrix is needed for a deposition *via* a flow process. This is in contradiction to the fabric of the SPBL that documents a transport of different sediment zones with variable consolidation. Therefore, a fine loose matrix supporting a flow process was not available. Nevertheless, further research is needed in order to discriminate with certainty fall- and flow-like gravitational transport processes in a bathyal environment.

Diagenesis

The early diagenesis of non-tropical deep-water carbonates is generally thought to be destructive, due to an enhanced dissolution, especially of aragonite, caused by lower temperatures and higher pCO_2 (Alexandersson 1979; Lewy 1981; Nelson 1988; James and Clarke 1997). The dissolution pattern of the SPBL is restricted to the centres of calcification of *Lophelia pertusa*. This might be explained by two aspects of selective dissolution: (1) the reduced crystal size and therefore larger reactive surface in the centres of calcification is more sensitive to dissolution by

undersaturated sea water and/or (2) the activities of bacteria or fungi, which utilize the higher amount of intraskeletal organic matter within the centres of calcification, produce a carbonate undersaturated microenvironment. The latter interpretation is supported by Millero et al. (1979), who observed, with respect to calcite and aragonite, highly supersaturated deep-water in the Mediterranean Sea, making abiotic exclusively chemical dissolution unlikely.

The lithification in the SPBL is interpreted to be of early diagenetic origin in the marine realm. The different consolidation of the sediment generation as well as the isopachous bladed spar in the SPBL point to a constructive early diagenesis comparable to the hardground, nodular limestone and IMC cement formation in the bathyal basins of the modern Mediterranean Sea as documented by Milliman and Müller (1973, 1977), Müller and Staesche (1973), Müller and Fabricius (1974), Sartori (1974), Bernoulli and McKenzie (1981), McKenzie and Bernoulli (1982), Allouc (1990) and Aghib et al. (1991). Furthermore, Allouc (1990) suggests efficient lithification due to a supersaturation with respect to calcite also for glacial episodes, so that the deposition of SPBL and its early marine lithification during a glacial period are not necessarily a contradiction.

Conclusions

(1)   The depositional environment of the SPBL differs in geometry (submarine wedges *versus* mounds) from the NE-Atlantic occurrences or the lithoherms in the Florida Strait, respectively. The occurrence of the SPBL are related to the foot of submarine cliffs, to neptunian dykes, and occasionally to erosional depressions formed on Lindos Limestone palaeosurfaces, thus suggesting submarine cliffs as the major growth habitat of its 'white coral community'. A deposition of the SPBL during a glacial period is likely.

(2)   The occurrence of an early marine lithification documented by intraformational hardgrounds, sediment zones with different consolidation as well as the inversely graded fillings in vugs combined with the deep-water 'white coral community' in the SPBL represent similarities to the deep-water coral lithoherms in the Florida Strait in fabric and facies even while the SPBL builds no mounds. The higher fabric complexity and the wedge-like geometry of the SPBL are due to the transport by multiple re-sedimentation events.

(3)   Steep slope angles (>30°), low transport distances, wedge-like geometries, lack of gradation, fabric complexity with incorporated fragments of hardgrounds, intraclasts and slightly consolidated sediment, geopetal structures of various directions and the variety of fragmentation and bioerosion suggest a debris fall mechanism for the deposition of the SPBL.

Acknowledgements

References

Aghib F, Bernoulli D, Weissert H (1991) Hardground formation in the Bannock Basin, eastern Mediterranean. Mar Geol 100: 103-113

Alexandersson ET (1979) Marine maceration of skeletal carbonates in the Skagerrak, North Sea. Sedimentology 26: 845-852

Allouc J (1990) Quaternary crusts on slopes of the Mediterranean Sea: A tentative explanation for their genesis. Mar Geol 94: 205-238

Bernoulli D, McKenzie JA (1981) Hardground formation in the Hellenic Trench: pensaline to hypersaline marine carbonate diagenesis. In: Dercourt J (ed) Programme HEAT, Campagne Submersible. Les Fossés Helléniques. Résult Campagnes Mer Publ CNEXO 23, pp 197-213

Best MB (1969) Étude systématique et écologique des madréporaires de la region de Banyuls-sur-mer (Pyrénées-orientales). Vie Milieu 20: 293-325

Bromley RG (2005) Preliminary study of bioerosion in the deep-water coral *Lophelia*, Pleistocene, Rhodes, Greece. In: Freiwald A, Roberts JM (eds) Cold-water Corals and Ecosystems. Springer, Berlin Heidelberg, pp 895-914

Bromley RG, Allouc J (1992) Trace fossils in bathyal hardgrounds, Mediterranean Sea. Ichnos 2: 43-54

Bromley RG, Hanken N-M (2003) Structure and function of large, lobed *Zoophycos*, Pliocene of Rhodes, Greece. Palaeogeogr Palaeoclimatol Palaeoecol 192: 79-100

De Mol B, van Rensbergen P, Pillen S, van Herreweghe K, van Rooij D, McDonnell A, Huvenne V, Ivanov M, Swennen R, Henriet JP (2002) Large deep-water coral banks in the Porcupine Basin, southwest of Ireland. Mar Geol 188: 193-231

Delibrias G, Taviani M (1985) Dating the death of Mediterranean deep-sea scleractinian corals. Mar Geol 62: 175-180

Di Geronimo I, Messina C, Rosso A, Sanfilippo R, Sciuto F, Vertino A (2005) Enhanced biodiversity on the deep: Early Pleistocene coral communities from southern Italy. In: Freiwald A, Roberts JM (eds) Cold-water Corals and Ecosystems. Springer, Berlin Heidelberg, pp 61-86

Drzewiecki PA, Simó JA (2002) Depositional processes, triggering mechanisms and sediment composition of carbonate gravity flow deposits: examples from the Late Cretaceous of the south-central Pyrenees, Spain. Sediment Geol 146: 155-189

Einsele G (2000) Gravity Mass Flow Deposits and Turbidites. In: Einsele G (ed) Sedimentary Basins. Springer, Berlin Heidelberg, pp 210-234

Freiwald A (2002) Reef-forming cold-water corals. In: Wefer G, Billett D, Hebbeln D, Jørgensen BB, Schlüter M, van Weering T (eds) Ocean Margin Systems. Springer, Berlin Heidelberg, pp 365-385

Freiwald A, Wilson JB (1998) Taphonomy of modern deep, cold-temperate water coral reefs. Hist Biol 13: 37-52

Freiwald A, Hühnerbach V, Lindberg B, Wilson JB, Campbell J (2002) The Sula Reef complex, Norwegian Shelf. Facies 47: 179-200

Gaetani M, Sacca D (1984) Brachiopodi batiali nel Pliocene e Pleistocene di Sicilia e Calabria. Riv ital Paleont Stratigr 90: 407-458

Glaub I (1999) Paleobathymetric reconstructions and fossil microborings. Bull Geol Soc Denmark 45: 143-146

Hanken N-M, Bromley RG, Miller J (1996) Plio-Pleistocene sedimentation in coastal grabens, north-east Rhodes, Greece. Geol J 31: 393-418

Hansen KS (1999) Development of a prograding carbonate wedge during sea level fall: Lower Pleistocene of Rhodes, Greece. Sedimentology 46: 559-576

Hofrichter R (2001) Das Mittelmeer: Fauna, Flora, Ökologie – Teil 1. Spektrum, Heidelberg

Hofrichter R (2003) Das Mittelmeer: Fauna, Flora, Ökologie – Teil 2. Spektrum, Heidelberg

Huvenne VAI, Beyer A, de Haas H, DeKindt K, Henriet JP, Kozachenko M, Olu-Le Roy K, Wheeler AJ, TOBI/Pelagia 197 and CARACOLE cruise participants. In: Freiwald A, Roberts JM (eds) Cold-water Corals and Ecosystems. Springer, Berlin Heidelberg, pp 535-569

James NP, Clarke JAD (1997) Cool-Water Carbonates. SEPM Spec Publ 56, 440 pp

Jüssen E (1890) Über pliocäne Korallen von der Insel Rhodus. Sitzber kais Akad Wiss, math-natw Cl 99: 13-24

Lewy Z (1981) Maceration of calcareous skeletons. Sedimentology 28: 893-895

Logan A (1979) The recent Brachiopoda of the Mediterranean Sea. Bull Inst Océanogr Monaco 72: 7-21

Major RP, Wilber RJ (1991) Crystal habit, geochemistry, and cathodoluminescence of magnesian calcite marine cements from the lower slope of Little Bahama Bank. Bull Geol Soc Amer 103: 461-471

Mascle J, Le Cleac'h A, Jongsma D (1986) The eastern Hellenic margin from Crete to Rhodes: Example of progressive collision. Mar Geol 73: 145-168

McKenzie JA, Bernoulli D (1982) Geochemical variations in Quaternary hardgrounds from the Hellenic Trench region and possible relationship to their tectonic setting. Tectonophysics 86: 149-157

Messing CG, Neumann AC, Lang JC (1990) Biozonation of deep-water lithoherms and associated hardgrounds in the northeastern Strait of Florida. Palaios 5: 15-30

Meulenkamp E, de Mulder EFJ, van der Weerd A (1972) Sedimentary history and paleogeography of the late Cenozoic of the Island of Rhodes. Z dt geol Ges 123: 541-553

Millero FJ, Morse J, Chen C-T (1979) The carbonate system in the western Mediterranean Sea. Deep-Sea Res 26A: 1395-1404

Milliman JD, Müller J (1973) Precipitation and lithification of magnesium calcite in the deep-sea sediments of the eastern Mediterranean Sea. Sedimentology 20: 29-45

Milliman JD, Müller J (1977) Characteristic and genesis of shallow-water and deep-sea limestones. In: Andersen NR, Malahoff A (eds) The fate of fossil fuel CO_2 in the oceans. Plenum, New York, pp 655-672

Moissette P, Spjeldnæs N (1995) Plio-Pleistocene deep-water bryozoans from Rhodes, Greece. Palaeontology 38: 771-799

Montenat C, Barrier P, Ott d'Estevou P (1991) Some aspects of the recent tectonics in the Strait of Messina, Italy. Tectonophysics 194: 203-215

Mortensen PB (2001) Aquarium observations on the deep-water coral *Lophelia pertusa* (L., 1758) (Scleractinia) and selected associated invertebrates. Ophelia 54: 83-104

Mortensen PB, Hovland M, Brattegard T, Farestveit R (1995) Deep water bioherms of the scleractinian coral *Lophelia pertusa* (L.) at 64°N on the Norwegian shelf: structure and associated megafauna. Sarsia 80: 145-158

Müller J, Fabricius F (1974) Magnesian-calcite nodules in the Ionian deep sea: an actualistic model for the formation of some nodular limestones. IAS, Spec Publ 1: 235-247

Müller J, Staesche W (1973) Precipitation and diagenesis of carbonates in the Ionian deep-sea. Bull Geol Soc Greece 10: 145-151

Mulder T, Alexander J (2001) The physical character of subaqueous sedimentary density flows and their deposits. Sedimentology 48: 269-299

Mullins HT, Neumann AC, Wilber RJ, Boardman, MR (1980) Nodular carbonate sediment on Bahamian slopes: possible precursors to nodular limestones. J Sediment Petrol 50: 117-131

Mutti E, Orombelli G, Pozzi R (1970) IX. Geological map of the Island of Rhodes (Greece) explanatory notes. Ann géol Pays hellén 22: 79-241

Nelson CS (1988) An introductory perspective on non-tropical shelf carbonates. Sediment Geol 60: 3-12

Nelson CS, Freiwald A, Titschack J, List S (2001) Lithostratigraphy and sequence architecture of temperate mixed siliciclastic-carbonate facies in the new Plio-Pleistocene section at Plimiri, Rhodes Island (Greece). Dept Earth Sci, Univ Waikato, Occas Rep 25: 1-50

Nemec W (1990) Aspects of sediment movement on steep delta slopes. IAS, Spec Publ 10: 29-73

Neumann AC, Kofoed JW, Keller GH (1977) Lithoherms in the Straits of Florida. Geology 5: 4-10

Pérès JM, Picard J (1964) Nouveau manuel de bionomie benthique de la Mer Méditerranée. Recl Trav Station Mar Endoume, Bull 31, 137 pp

Remia A, Taviani M (2004) Shallow-buried Pleistocene *Madrepora*-dominated coral mounds on a muddy continental slope, Tuscan Archipelago, NE Tyrrhenian Sea. Facies 50, DOI 10.1007/s10347-004-0029-2

Sartori R (1974) Modern deep-sea Magnesian calcite in the central Tyrrhenian Sea. J Sediment Petrol 44: 1313-1322

Sartori R (1980) Factors affecting the distribution of ahermatypic corals on the Mediterranean seafloor: a probabilistic study. Deep-Sea Res 27A: 655-663

Scoffin TP (1993) Microfabrics of carbonate muds in reefs. In: Rezak R, Lavoie DL (eds) Carbonate Microfabrics. Frontiers in Sedimentary Geology. Springer, Berlin Heidelberg, pp 65-74

Squires DF (1964) Fossil coral thickets in Wairarapa, New Zealand. J Paleont 38: 904-915

Taviani M, Colantoni P (1979) Thanatocoenoses Wurmiennes associées aux coraux blancs. Rapp Comm Int Mer Méditerr 25/26: 141-142

Taviani M, Remia A, Corselli C, Freiwald A, Malinverno E, Mastrototaro F, Savini A, Tursi A, CORAL Shipboard Staff (2004): First geo-marine survey of living cold-water *Lophelia* reefs in the Ionian Sea (Mediterranean Basin). Facies 50, DOI 10.1007/s10347-004-0039-0

Taviani M, Freiwald A, Zibrowius H (2005) Deep coral growth in the Mediterranean Sea: an overview. In: Freiwald A, Roberts JM (eds) Cold-water Corals and Ecosystems. Springer, Berlin Heidelberg, pp 137-156

Tunesi L, Diviacco G (1997) Observations by submersible on the bottoms off shore Portefino promontory (Ligurian Sea). Atti 12° Congr Assoc Ital Oceanol Limnol 1: 61-74

Vafidis D, Koukouras A, Voultsiadou-Koukoura E (1997) Actinaria, Corallimorpharia, and Scleractinia (Hexacorallia, Anthozoa) of the Aegean Sea, with a checklist of the Eastern Mediterranean and Black Sea species. Israel J Zool 43: 55-70

Van Rooij D, de Mol B, Huvenne V, Ivanov M, Henriet J-P (2003) Seismic evidence of current-controlled sedimentation in the Belgica mound province, upper Porcupine slope, southwest of Ireland. Mar Geol 195: 31-53

Van Weering TCE, de Haas H, de Stigter HC, Lykke-Andersen H, Kouvaev I (2003) Structure and development of giant carbonate mounds at the SW and SE Rockall Trough margins, NE Atlantic Ocean. Mar Geol 198: 67-81

White M, Mohn C, de Stigter H, Mottram G (2005) Deep-water coral development as a function of hydrodynamics and surface productivity around the submarine banks of the Rockall Trough, NE Atlantic. In: Freiwald A, Roberts JM (eds) Cold-water Corals and Ecosystems. Springer, Berlin Heidelberg, pp 503-514

Wilber RJ, Neumann AC (1993) Effects of submarine cementation on microfabrics and physical properties of carbonate slope deposits, Northern Bahamas. In: Rezak R, Lavoie DL (eds) Carbonate Microfabrics. Frontiers in Sedimentary Geology. Springer, Berlin Heidelberg, pp 79-94

Zabala M, Maluquer P, Harmelin J-G (1993) Epibiotic bryozoans on deep-water scleractinian corals from the Catalonia slope (western Mediterranean, Spain, France). Sci Mar 57: 65-78

Zibrowius H (1979) Campagne de la Calypso en Méditerranée nord-orientale (1955, 1956, 1960, 1964). 7. Scléractiniaires. Ann Inst Océanogr Paris 55, Suppl: 7-28

Zibrowius H (1980) Les Scléractiniaires de la Méditerranée et de l´Atlantique nord-orientale. Mem Inst Océanogr Monaco 11: 227

Zibrowius H (1987) Scléractiniaires et Polychètes Serpulidae des faunes bathyales actuelle et plio-pléistocène de Méditerranée. Doc Trav 11: 255-257

Enhanced biodiversity in the deep: Early Pleistocene coral communities from southern Italy

Italo Di Geronimo[1], Carlo Messina[1], Antonietta Rosso[1], Rossana Sanfilippo[1], Francesco Sciuto[1], Agostina Vertino[2]

[1] Dipartimento di Scienze Geologiche, Università di Catania, Corso Italia 55, I-95129 Catania, Italy
  (rosso@unict.it)
[2] Institute of Paleontology, Erlangen University, Loewenichstr. 28, D-91054 Erlangen, Germany

Abstract. The Early Pleistocene fault plane of Furnari, that outcrops in northeastern Sicily (southern Italy), provided a primary hard substrate for the settling and growth of large coral colonies. Even though the corals did not form frameworks, they influenced the composition and distribution of the benthic communities. Corals and associated fauna produced organogenic debris, which was deposited along the fault scarp, within its fractures or at its base.

Bulk-samples from coarse debris sediments along the palaeoescarpment and from silty sediments at the scarp foot have been studied, with focus on corals, molluscs, serpulids, bryozoans and ostracods. The fossil assemblages examined can be related to original coral and mud-communities from a shallow epibathyal palaeoenvironment, 400 to 500 m deep.

High values in species richness and diversity were recorded, especially for the deep-coral communities. Owing to the inferred elevated biodiversity, the Furnari coral communities show similarities with those flourishing in the present day North Atlantic and appear congruent with the scenario of cold stenothermic Pleistocene deep Mediterranean waters.

Keywords. Deep-water, Mediterranean, corals, molluscs, serpulids, bryozoans, ostracods, palaeodiversity, Pleistocene

Introduction

Deep-water coral assemblages are rather common in the Plio-Pleistocene deposits from the Messina Straits area but they are rare in other eastern sectors of Sicily. The area as a whole is actually affected by strong Quaternary tectonic activity causing remarkable uplift. Sediments originally deposited at bathyal depths, in some

localities crop out hundreds of metres above sea level (Barrier 1984, 1987; Barrier et al. 1986; Di Geronimo 1987; Kezirian 1993).

In this area, fossil assemblages mainly record palaeocommunities referred to as the "bathyal mud biocoenosis" (Pérès and Picard 1964), with corals as subordinate components (see Guadagno et al. 1979; Di Geronimo et al. 1997). Locally, however, cold-water coral assemblages, mainly made up of *Madrepora* and *Lophelia* ("white corals biocoenosis"; Pérès and Picard 1964), are common (Di Geronimo 1987) and even abundant (Vertino 2003). Some occurrences of such assemblages were studied in the second half of 1900's (Seguenza 1864, 1875-1876), but were even mentioned earlier (Scilla 1670).

Some outcrops show original deep-water hard substrates, like steep cliffs, palaeoescarpments or detached boulders. The surfaces of the hard substrates are largely colonised or heavily encrusted by sessile organisms (Barrier 1984; Barrier et al. 1996); in some places, coral rubble deposits - as narrow belts or rims - are also found adjacent to these surfaces (Barrier et al. 1996), both locally covered by muds. Skeletal remains of benthic organisms are usually preserved in sub-primary position on and near the hard surfaces and *in situ* within the adjacent muddy sediments. Therefore, it is possible to study both composition and structure of the different assemblages, and evaluate changes in specific richness, although fossil assemblages are unavoidably biased by diagenesis with respect to the original biocoenoses they belong to. These outcrops are of particular interest as they offer the opportunity to compare deep-water hard and soft bottom communities and to observe the transition between them, often taking place within few decimetres. In the present day deep-water environments this can be observed only by using Remotely Operated Vehicles (ROVs).

The Furnari outcrop, a palaeofault plane colonised by deep-water corals, allows us to evaluate how the rigid elevated substrate provided by corals exerted an active control on the palaeoenvironment. Though the corals did not form true banks or thickets, they influenced the benthic communities and their species richness. These occurrences offer the exceptional opportunity to study *in situ* deep-water coral assemblages in outcrop.

Most of the existing studies of deep-water coral communities refer to bank or mound assemblages, both in the Atlantic (Le Danois 1948; Teichert 1958; Wilson 1979; Jensen and Frederiksen 1992; Mortensen et al. 1995; Freiwald et al. 1997, 1999, 2002) and in the Pleistocene-to-Recent Mediterranean (Seguenza 1879; Delibrias and Taviani 1985; Allouc 1987; Corselli and Bernocchi 1990; Zabala et al. 1993; Mastrototaro et al. 2002). Knowledge of present day analogues of the Furnari situation, i.e. deep-sea rocky slopes and cliffs, are still rare. Although deep decametre-sized bioconstructions can be discovered and investigated by using side-scan-sonar mapping systems, close examination of rocky slope biological covers is difficult or nearly impossible. ROVs or direct observation from submersibles have only been exploited in the last decades (Tyler and Zibrowius 1992; Freiwald et al. 2002; Malakoff 2003).

Geological setting

The area studied is located in the northeastern part of Sicily, southern Italy (Fig. 1A). The sedimentary succession unconformably lies on pre-Quaternary sedimentary units and belongs to the informally called "Barcellona P.G." Basin (Messina 2003). It is a small extensional Quaternary depression formed in a highly tectonically mobile setting experiencing a complex structural evolution associated with the Kabilo-Calabrian Arc (e.g., Amodio Morelli et al. 1976; Boccaletti et al. 1990; Monaco et al. 1996; Lentini et al. 2000; Bonardi et al. 2001). Kezirian (1993) carried out a detailed study focusing on the tectonic control of sedimentation. The stratigraphic architecture records different terrigenous depositional systems developed as a response to phases of local or regional uplift, subsidence and sea level changes. The sedimentary units of the basin are relatively well exposed and reach a thickness of a few hundred metres. Sediments are predominantly mixed siliciclastic-bioclastic and characterized by common unconformities and abrupt vertical facies changes.

In the Furnari area (Messina 2003), sedimentation begins with organogenic sandy silts and interbedded sands deposited in tide-dominated environments overlaid by silts, evolving from inner bay to bay centre (mid-to-outer shelf) recording a transgressive episode (Fig. 1B). A submeridian normal fault system (N-S) dissected these partly consolidated sediments forming a half graben. The fault plane was cemented by early diagenesis and coated by discontinuous goethite crusts. Subsequently, bathyal muds deposited indicating a sea level rise seemingly joined to subsidence of the whole basin, also involving temporary sand-starved conditions. The succession is capped by cross-bedded coarse sands and biocalcarenites forming
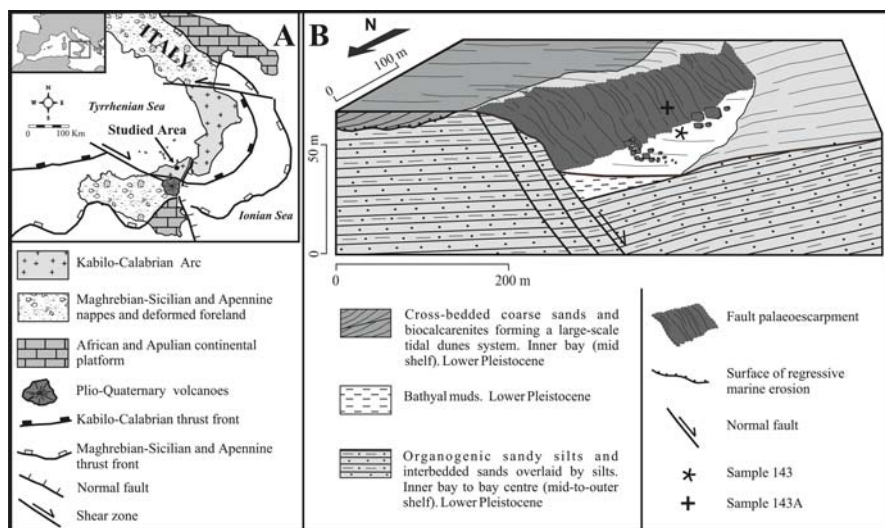
Fig. 1 A Location of the Furnari outcrop and tectono-sedimentary framework of the area (after Lentini et al. 2000). **B** Block-diagram illustrating the Furnari palaeoescarpment and the sedimentary sequence geometry

a large-scale tidal dunes system. They are sharp-based, resting on the surface of regressive marine erosion, and deposited in an inner bay (mid shelf) environment during times of relative falling sea level.

The presence of *Hyalinea balthica* (Schröther) suggested that all these sediments formed during the Early Pleistocene; in particular clay deposition and coeval colonisation of the fault plane apparently happened no earlier than the Emilian.

Materials and methods

Detailed observations have been performed on the fault plane and two bulk-samples have been collected (Fig. 1B): the former from coarse debris sediments along the fault (sample 143A), the latter from muddy sediments, a dozen metres from the scarp foot (sample 143), respectively 6 and 8 dm^3 in volume. Sediments were routinely sieved.

Skeletons of benthic organisms belonging to corals, molluscs, serpulids and bryozoans were picked up from fractions larger than 500 μm, identified at specific level, when possible, and counted; the results were tabulated in order to evaluate biodiversity. Ostracods were studied from 300 cm^3 samples with specimens collected from the 63-500 μm fraction. Abundances were calculated following standard methods; for scleractinians corallites of both colonial and solitary species were scored; for octocorals and stylasterines, skeletal fragments were counted.

The species not congruent with bathyal biocoenoses but restricted to infralittoral and/or circalittoral bottoms, although tabulated as part of the fossil assemblages, were considered as displaced and consequently excluded from biodiversity and richness evaluations. Palaeoecological interpretation follows Pérès and Picard (1964) using all organisms.

According to Vertino (2003) and Vertino and Di Geronimo (2003), the living northeastern Atlantic scleractinian species *Caryophyllia calveri*, *Aulocyathus atlanticus*, *Flabellum alabastrum* and *Enallopsammia rostrata* have been considered respectively synonyms of the Plio-Pleistocene species *Caryophyllia aradasiana*, *Conotrochus typus*, *Flabellum messanense* and *Enallopsammia scillae*.

Palaeoescarpment

The exposed steep palaeoescarpment crops out for about 30 m in height and 600 m in length. It is irregularly shaped showing overhangs, projecting parts, ledges and steps interspaced with large recesses, grooves and cavities. The original fault surface, cutting almost unconsolidated sands, appears cemented by early diagenesis

Fig. 2   1 The exposed fault plane of Furnari (Early Pleistocene), scale bar 1 m. **2** Portion of the fault plane, with the rubble organogenic sediment cemented by early diagenesis to form a thick crust, scale bar 1 m. **3** Detail of the crust with the exposed surface, coated by goethite and encrusted by scleractinians and octocorals, scale bar 5 mm. **4** and **5** Root-like bases of the octocoral *Keratoisis peloritana* (Seguenza), locally coated by oxides, scale bars 1 cm. **6** Massive base of an octocoral on the bathyal crust, scale bar 1 cm. **7** An encrusting valve of *Spondylus gussoni* Costa on an early lithified ledge, scale bar 1 cm. **8** Fractures within the
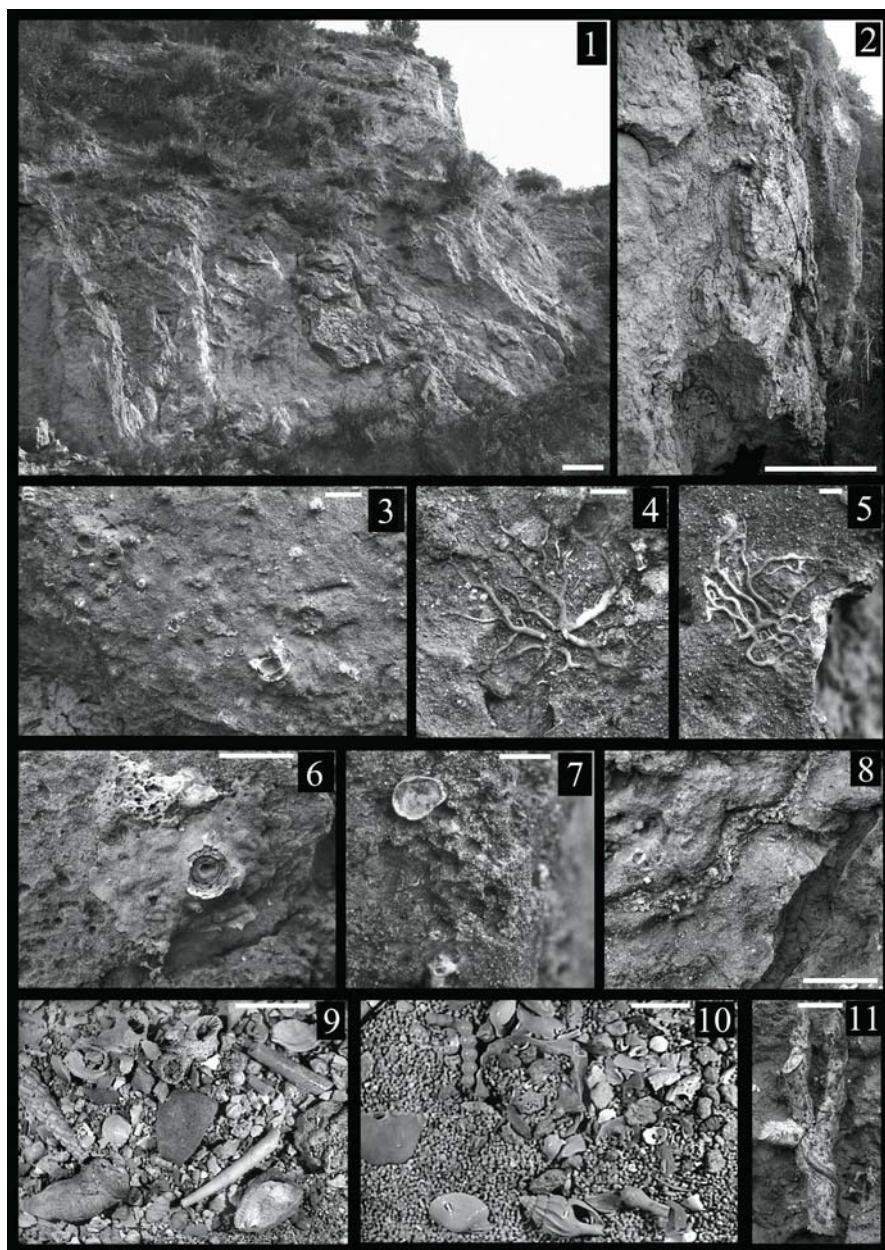
fault wall filled by clays (below) and by coarse sediments containing organogenic debris (above), scale bar 5 cm. **9** Washed residue from the rubble pocket sample (143A); it is mainly organogenic, bioclasts representing about 95 %, scale bar 1 cm. **10** Washed residue from the deep-sea silty sample (143); the organogenic content is scant (ca. 30 %), scale bar 1 cm. **11** A large-sized branch of the coral *Enallopsammia scillae* (Seguenza) encrusted by the serpulid *Placostegus tridentatus* (Fabricius), scale bar 1 cm

and coated by discontinuous goethite crusts (Fig. 2/1). Locally, a 10-15 cm thick, sandy-gravely biodetritic layer is present. It consists of entire or fragmented skeletons of species detached from the palaeoescarpment and, secondarily, of millimetre to centimetre-sized lithic clasts. Skeletal remains mainly belong to corals, although brachiopods, mainly *Gryphus* sp. and *Terebratulina retusa* (Linnaeus), can become locally abundant. Other skeletons from the water column, such as those of the pteropod *Euclio pyramidata* (Linnaeus), and the normal sedimentary inputs are also present. These coarse biodetritic drapes were subjected to early diagenetic cementation, which led to the formation of hard surfaces and steeply inclined walls (up to 70-90°). This sedimentary body is somewhat comparable with the rubble apron as described by Freiwald et al. (1997) for its genesis and meaning, although its extension and geometry (and probably lithic content) are quite different. The term "rubble pocket" is suggested here to indicate these thin, discontinuous bodies of sediment locally draping sub-vertical walls. Muddy and silty sediments are locally preserved on the surfaces and within cavities and fractures, testifying to continuous deposition of fine-grained sediments (Fig. 2/2).

The fault and cavity surfaces and also the diagenised exposed surface of the "rubble pocket" sediments are locally encrusted by deep-sea sessile fauna (Figs. 2/3-6). Scleractinians and gorgonians are the most abundant taxa; on the exposed surfaces their bases show a mean covering rate not exceeding 2-3 %, with local values of about 20 %. Most of the coral bases are badly preserved and rarely determinable at genus or species level; among them dendrophylliids and caryophylliids prevail, but octocoral basal parts are rather common. The occurrence of some well-preserved root-like and massive bases respectively belonging to *Keratoisis melitensis* and *K. peloritana* (Figs. 2/4-5), is particularly interesting. The sessile bivalve *Spondylus gussoni* (Fig. 2/7) is present and locally common. Some barely detectable serpulids and bryozoans sporadically encrust both corals and the substrate directly showing a preference for sheltered small cavities (Figs. 3/10, 14). Close observations on small scale point out to subsequent colonisation phases with well-preserved and fresh-looking skeletons growing near and/or on the older oxidized ones. Furthermore, the fault wall is dissected by an irregular network of fractures some of which are filled with clays and others with coarse sediments mainly constituted by organogenic debris (Fig. 2/8).

Fig. 3   **1** A branch of the scleractinian *Enallopsammia scillae* (Seguenza), sample 143A, scale bar 5 mm. **2** Lateral (a) and calicular (b) view of the scleractinian *Caryophyllia aradasiana* Seguenza, sample 143A, scale bar 3 mm. **3** Valves of *Spondylus gussoni* Costa encrusting on a branch of *Enallopsammia scillae* (Seguenza), sample 143A, scale bar 5 mm. **4** The gastropod *Amphissa acutecostata* (Philippi), sample 143, scale bar 2 mm. **5** The gastropod *Benthomangelia tenuicostata* Seguenza, sample 143A, scale bar 1 mm. **6** The bivalve *Bathyspinula excisa* Philippi, sample 143, scale bar 3 mm. **7** The solitary mud-dwelling coral ?*Fungiacyathus* sp., sample 143, scale bar 1 mm. **8** Left valve of the ostracod *Quasibuntonia radiatopora* (Seguenza), sample 143, scale bar 250 μm. **9** Left valve of the ostracod *Bythocypris obtusata* (Sars), sample 143, scale bar 250 μm. **10** The small-sized tube of the serpulid *Hyalopomatus variorugosus* Ben-Eliahu and Fiege inside a cavity, sample 143A, scale bar 1 mm. **11** Tubes of *Metavermilia multicristata* (Philippi) and *Hyalopomatus*
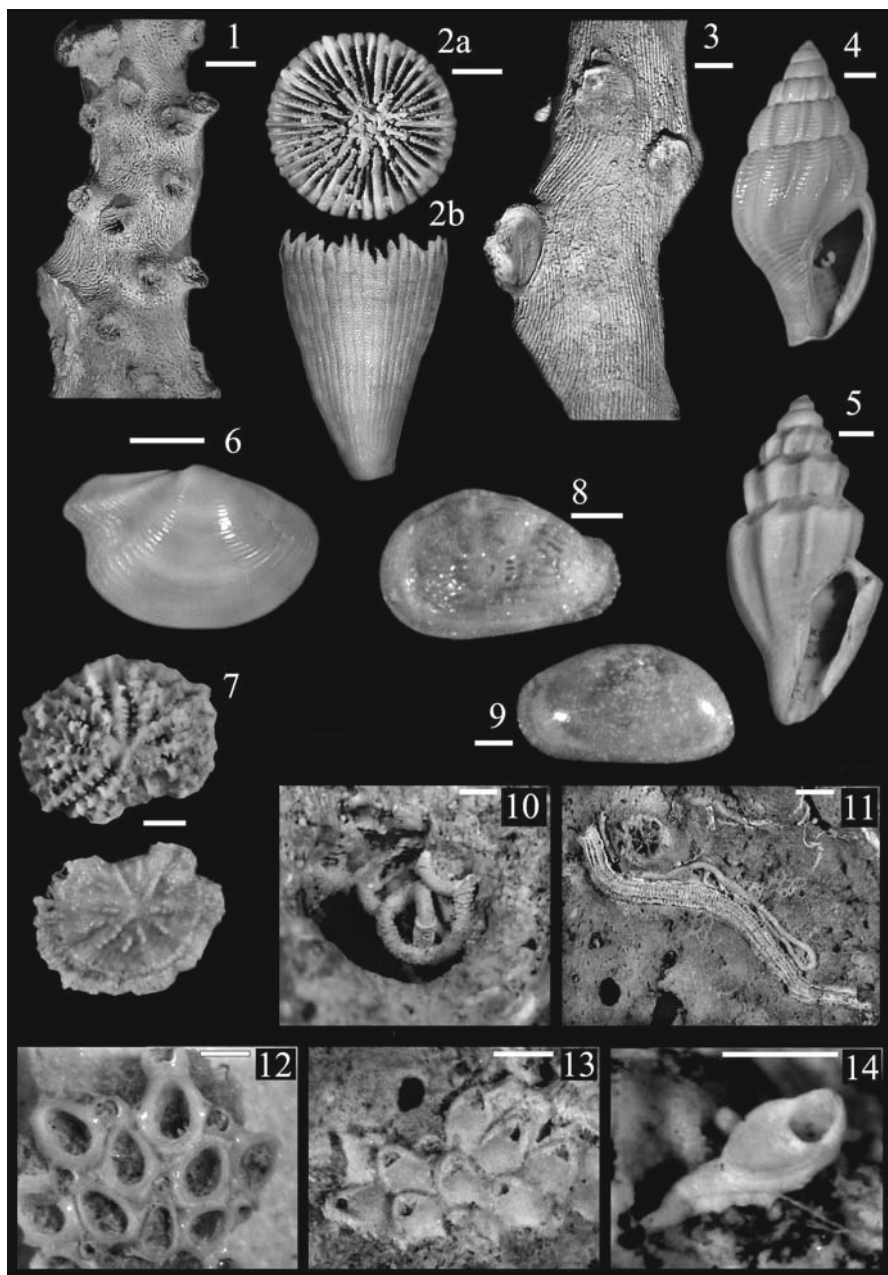
variorugosus Ben-Eliahu and Fiege, sample 143A, scale bar 2 mm. **12** The setoselliniform bryozoan colony *Setosellina roulei* (Calvet), sample 143, scale bar 250 μm. **13** The bryozoan *Steraechmella buski* Lagaaij directly encrusting the fault surface, sample 143A, scale bar 500 μm. **14** A zooid of the uniserial bryozoan *Crepis longipes* Jullien, sample 143A, scale bar 250 μm

Rubble pocket (sample 143A)

The residue is mainly organogenic, bioclasts representing about 95 % (Fig. 2/9). Corals are by far the most abundant group (70 %) followed by molluscs (15 %), serpulids (5 %), bryozoans (1 %) and ostracods (less than 1 %). Brachiopods and crustaceans form the remainder. Large coral colonies are always fragmented; fractures are sharp and elements often close each other; their external surfaces are heavily etched and often bioeroded.

Sixteen coral species have been identified (Table 1): 12 scleractinians, 2 octocorals and 2 stylasterines. Among the scleractinians, solitary taxa prevail over colonial. Nevertheless, the corallites of only two colonial species (*E. scillae* and *M. oculata*) constitute almost 85 % of the total number of the coral specimens. The remaining percentage is mainly represented by the solitary species *Stenocyathus vermiformis* (5.03 %), *Javania cailleti* (3.48 %), *C. aradasiana* (1.61 %) and *C. typus* (1.03 %). Isidid internodes are common, while stylasterid fragments, belonging to the genera *Stenohelia* and *Errina*, are rare.

Table 1 Systematic list of the corals from Furnari. For each taxon the number of specimens (ab.) and the relative abundance (dom.) is given. The abundance of *Keratoisis* species was not evaluated, as only the basal internodes were not distinguishable at specific level. Juveniles in brackets

Samples	143A		143	
Scleractinians	**Ab.**	**Dom.**	**Ab.**	**Dom.**
?*Fungiacyathus* sp.			1	1.23
Madrepora oculata Linnaeus	380	24.58	48	59.26
Caryophyllia aradasiana Seguenza	25(12)	1.62		
Conotrochus typus Seguenza	16	1.03	3	3.70
Desmophyllum cristagalli Milne Edwards and Haime	10	0.65		
Lophelia pertusa (Linnaeus)	14	0.91	4	4.94
Flabellum messanense Seguenza	1	0.06		
Javania cailleti (Duchassaing and Michelotti)	54	3.49	2	2.47
Stenocyathus vermiformis (Pourtalès)	78	5.05	1	1.23
Dendrophyllia cornigera (Lamarck)	7	0.45		
Balanophyllia irregularis Seguenza	2	0.13		
Balanophyllia caryophylloides Seguenza	1	0.06		
Enallopsammia scillae (Seguenza)	930	60.16	6	7.41
undetermined	28	1.81	16	19.75
Number of specimens	**1546**	**100**	**81**	**100**
Number of species	**12**		**7**	
Octocorals				
Keratoisis melitensis (Goldfuss)	internodes not distinguishable at species level			
Keratoisis peloritana (Seguenza)				
Number of specimens	**162**	**100**	**1**	**1**
Number of species	**2**		**1**	

Table 1 continued

Samples		143A		143	
Stylasterines		**Ab.**	**Dom.**	**Ab.**	**Dom.**
Stenohelia sp.		4	66.67	1	100
Errina aspera (Linnaeus)		2	33.33		
	Number of specimens	**6**	**100**	**1**	**100**
	Number of species	**2**		**1**	

Molluscs (Table 2) represent the most diversified systematic group comprising as many as 61 species, with prevailing gastropods (43 species) and subordinate bivalves (14 species) whereas scaphopods, with only four species, scarcely contribute to biodiversity. Molluscs are also numerically important with 748 specimens: gastropods still prevail (more than 57 %), followed by bivalves (29 %) and subordinate scaphopods (15 %). The most abundant species are the gastropods *Alvania cimicoides* (15.1 %), *Amphissa acutecostata* (7.21 %) and *Benthomangelia tenuicostata* (4.63 %), the bivalves *Bathyspinula excisa* (8.98 %), *S. gussoni* (6.53 %), *Limopsis minuta* (3.54 %), *Nucula sulcata* (3.27 %) and *Asperarca nodulosa scabra* (3.27 %) and the scaphopods *Graptacme agilis* (6.80 %) and *Gadila jeffreysi* (5.44 %).

Table 2 Systematic list of the molluscs from Furnari. For each taxon the number of specimens (ab.) and the relative abundance (dom.) is given. Species considered as displaced are marked with an asterisk. Juveniles in brackets

Samples	143A		143	
Molluscs	**Ab.**	**Dom.**	**Ab.**	**Dom.**
Gastropods				
"Gibbula" maurolici Seguenza	3	0.41		
"Gibbula" luciae Seguenza	1	0.14		
Propilidium ancyloide Forbes	1	0.14		
Emarginula compressa (Cantraine)	2(1)	0.27		
?Emarginula multistriata Jeffreys	3	0.41		
Fissurella sp.	1	0.14		
Clelandella miliaris Brocchi	4	0.54		
Cantrainea peloritana (Cantraine)	3(2)	0.41		
?Danilia otaviana (Cantraine)	17	2.31	1	0.25
Putzeysia wiseri (Calcara)	22(18)	2.99	1(1)	0.25
Solariella marginulata (Philippi)	14(12)	1.90	46(28)	11.62
Seguenzia monocingulata Seguenza	1	0.14		
Seguenzia sp.	1	0.14		
Cirsonella romettensis (Granata Grillo)	1	0.14	7(5)	1.77
Moelleriopsis messanensis (Seguenza)	3(1)	0.41		

Table 2 continued

Samples	143A		143	
Molluscs	**Ab.**	**Dom.**	**Ab.**	**Dom.**
Gastropods				
Polinices fusca (Blainville)	5(5)	0.68		
Cerithiopsis sp.	1	0.14		
Alvania cimicoides (Forbes)	111	15.10	9	2.27
Alvania elegantissima Seguenza	29	3.95	42	10.61
Alvania zetlandica (Montagu)	6	0.82		
Eulima sp.	4	0.54		
Strobiligera brychia (Bouchet and Guillemot)	15	2.04		
Eumetula aliceae (Dautzenberg and Fischer)			1	0.25
Graphis gracilis (Monterosato)			8	2.02
Epitonium dallianum (Smith and Verrill*)*	4	0.54		
Aclis attenuans Jeffreys			1	0.25
Opaliopsis atlantis (Clench and Turner)	4	0.54		
Opaliopsis sp.	3	0.41		
Iphitus tenuisculptus (Seguenza)			1	0.25
Claviscala aff. *richardi* (Dautzenberg and De Boury)	12	1.63		
Fusinus rostratus (Olivi)	6	0.82		
Pagodula echinata (Kiener)	5	0.68	11(5)	2.78
Profundinassa spinulosa (Philippi)	7	0.95		
Nassarius lima (Dillwin)	1	0.14		
Amphissa acutecostata (Philippi)	53(30)	7.21	18(17)	4.55
Mitrolumna smithi (Dautzenberg and Fischer)	10	1.36		
Spirotropis modiolus (De Cristofori and Jan)	3	0.41		
Drilliola emendata (Monterosato)	8(4)	1.09		
Aphanitoma bellardii Seguenza	4	0.54		
Benthomangelia tenuicostata (Seguenza)	34(6)	4.63	7(4)	1.77
Taranis borealis Bouchet and Warén	1	0.14		
Heliacus alleryi (Seguenza)	2	0.27		
Heliacus contextus (Seguenza)	1	0.14		
Heliacus zancleus (Seguenza)	1(1)	0.14		
Heliacus sp.	4	0.54		
Odostomia acuta Jeffreys	4	0.54	1	0.25
Bulla pingiugula Jeffreys	1	0.14		
Japonacteon pusillus (McGillivray)	2	0.27		
Chrysallida microscalaria (Seguenza)	2	0.27	2	0.51
Chrysallida brattstroemi Warén			2	0.51

Table 2 continued

Samples	143A		143	
Molluscs	**Ab.**	**Dom.**	**Ab.**	**Dom.**
Gastropods				
Pyrunculus opesiusculus (Brugnone)	1	0.14	12(4)	3.03
Number of specimens	**421**	**57.28**	**170**	**42.93**
Number of species	**43**		**17**	
Scaphopods				
Graptacme agilis (Sars)	50	6.80	18	4.55
Cadulus ovulum (Philippi)	13	1.77	23	5.81
Gadila jefrreysi (Monterosato)	40	5.44	6	1.52
Entalina tetragona (Brocchi)	10	1.36	41	10.35
Number of specimens	**113**	**15.37**	**88**	**22.22**
Number of species	**4**		**4**	
Bivalves				
Nucula sulcata Bronn	24(1)	3.27	22(10)	5.56
Ennucula corbuloides (Seguenza)			3	0.76
Yoldia minima (Seguenza)			1	0.25
Phaseolus ovatus Seguenza	1	0.14		
Thestileda cuspidata (Philippi)	1	0.14	9	2.27
Bathyspinula excisa (Philippi)	66(20)	8.98	43(5)	10.86
Katadesmia confusa (Seguenza)			8	2.02
Ledella messanensis (Jeffreys)	2	0.27	4	1.01
Yoldiella micrometrica (Seguenza)			8	2.02
Yoldiella seguenzae Bonfitto and Sabelli			2	0.51
Asperarca nodulosa scabra (Poli)	24	3.27	4	1.01
Limopsis minuta (Philippi)	26	3.54	3	0.76
Cyclopecten hoskynsi (Forbes)	4	0.54	8	2.02
Delectopecten vitreus (Gmelin)	1	0.14	15	3.79
Karnekampia sulcata (Mueller)	3	0.41		
Spondylus gussonii Costa	48	6.53		
Pododesmus aculeatus (Mueller)	10	1.36	1	0.25
Acesta excavata (Fabricius)			1	0.25
Abra longicallus (Scacchi)	2	0.27	2	0.51
Kelliella abyssicola (Forbes)		0.00	3	0.76
Spinosipella acuticostata (Philippi)	2	0.27		
Cuspidaria sp.			1	0.25
Number of specimens	**214**	**29.12**	**138**	**34.85**
Number of species	**14**		**18**	
Total number of specimens	**748**	**100**	**396**	**100**
Total number of species	**61**		**39**	

Table 2 continued

Samples	143A		143	
Molluscs	**Ab.**	**Dom.**	**Ab.**	**Dom.**
Bivalves				
Bittium reticulatum Da Costa*	5			
Turritella sp.*	3(3)			
Timoclea ovata (Pennant)*	2(2)		1(1)	

Among <u>serpulids</u> (Table 3) a total of 9 species and 249 specimens have been detected. *Placostegus tridentatus* is the dominant species, representing 48.19 % of the total assemblage, whereas *Hyalopomatus variorugosus*, *Metavermilia multicristata*, *Vermiliopsis monodiscus* and *Vitreotubus digeronimoi*, each possessing similar dominances, cover altogether more than 34 %. *Neovermilia falcigera* and *Semivermilia pomatostegoides* are subordinate; only one tube of the deep morphotype of *Serpula concharum* has been found.

Table 3 Systematic list of the serpulids from Furnari. For each taxon the number of specimens (ab.) and the relative abundance (dom.) is given

Samples	143A		143	
Serpulids	**Ab.**	**Dom.**	**Ab.**	**Dom.**
Serpula concharum type B Langerhans	1	0.40		
Vermiliopsis monodiscus Zibrowius	21	8.43	2	5.41
Metavermilia multicristata (Philippi)	22	8.84		
Semivermilia pomatostegoides (Zibrowius)	7	2.81	4	10.81
Filogranula stellata (Southward)			1	2.70
Janita fimbriata (Delle Chiaje)	3	1.20		
Placostegus tridentatus (Fabricius)	120	48.19	14	37.84
Neovermilia falcigera (Roule)	8	3.21	7	18.92
Hyalopomatus variorugosus Ben-Eliahu and Fiege	24	9.64		
Protula sp. 1			5	13.51
Vitreotubus digeronimoi Zibrowius	19	7.63		
Serpulidae spp.	24	9.64	4	10.81
Number of specimens	**249**	**100**	**37**	**100**
Number of species	**9**		**6**	

<u>Bryozoans</u> (Table 4) are subordinate at the specimen level (212) but they noticeably contribute to biodiversity with a total of 35 species, most of which have a rigid erect (18 species) or encrusting (11 species) growth habit. Only five species, i.e. *Tervia irregularis*, *T. barrieri*, *Hornera frondiculata*, *Cellaria sinuosa* and *Tessaradoma boreale* cover more than 54 %. The presence of some other species, i.e. *Hornera lichenoides*, *Copidozoum exiguum*, *Steraechmella buski*, *Bryocryptella koelheri*

together with *Anguisia verrucosa* and *Crepis longipes*, although with dominances lower than 3 %, are noteworthy.

Table 4 Systematic list of the bryozoans from Furnari. For each taxon the number of specimens (ab.) and the relative abundance (dom.) is given. Species considered as displaced are marked with an asterisk

Samples	143A		143	
Bryozoans	**Ab.**	**Dom.**	**Ab.**	**Dom.**
Crisia tenella longinodata Rosso			1	0.94
Anguisia verrucosa Jullien	3	1.42	20	18.87
Annectocyma major (Johnston)	4	1.89		
Annectocyma tubulosa (Busk)	1	0.47		
Entalophoroecia deflexa Couch	3	1.42	2	1.89
Entalophoroecia gracilis Harmelin	1	0.47	2	1.89
Tervia irregularis (Meneghini)	32	15.09	3	2.83
Tervia barrieri Rosso	14	6.60	7	6.60
Tubulipora sp. 1	2	0.94	7	6.60
Eximonea triforis Heller	5	2.36	9	8.49
Exidmonea coerulea Harmelin	3	1.42	1	0.94
Hornera frondiculata Lamouroux	21	9.91	4	3.77
Hornera lichenoides (Linnaeus)	6	2.83	1	0.94
Aetea spp.	1	0.47		
Copidozoum exiguum (Barroso)	1	0.47		
Setosellina roulei (Calvet)	1	0.47	8	7.55
Heliodoma angusta Rosso	2	0.94	4	3.77
Steraechmella buski Lagaaij	4	1.89		
Setosella vulnerata (Busk)	6	2.83	13	12.26
Cellaria fistulosa (Pallas)	6	2.83	12	11.32
Cellaria salicornioides Audouin	2	0.94		
Cellaria sinuosa (Hassall)	13	6.13		
Crepis longipes Jullien	1	0.47		
Cribrimorph sp. 1	1	0.47		
Hippothoa flagellum Manzoni	1	0.47		
Gemellipora eburnea Smitt			1	0.94
Bryocryptella koelheri Calvet	3	1.42		
Escharoides coccinea (Abildgaard)	1	0.47		
Tessaradoma boreale (Busk)	31	14.62	1	0.94
Smittina cervicornis (Pallas)	8	3.77		
Schizomavella sp. 1			2	1.89
Microporella ciliata (Pallas)	1	0.47		
Porinidae sp. 1	1	0.47		
Characodoma sp. 1	1	0.47		

Table 4 continued

Samples	143A		143	
Bryozoans	**Ab.**	**Dom.**	**Ab.**	**Dom.**
Palmicellaria sp.	5	2.36		
Celleporina spp.	3	1.42		
Turbicellepora sp.	1	0.47		
Reteporella sp.	2	0.94		
Undetermined	21	9.91	8	7.55
Number of specimens	212	100	106	100
Number of species	35		18	
Crisia fistulosa Heller *			2	
Crisia ramosa Harmer *			6	
Crisia sigmoidea Waters *			3	
Frondipora verrucosa (Lamouroux) *	1			
Chaperiopsis annulus (Manzoni) *	1			
Adeonella calveti Canù and Bassler *	1			
Celleporina globulosa d'Orbigny *	8			

Ostracods (Table 5) are extremely subordinate with only 15 specimens belonging to 5 species. *Bythocypris obtusata* is the most abundant species (40 %) followed by *Quasibuntonia radiatopora* (20 %). All other species, i.e. *Henryhowella sarsi profunda*, *H. parthenopea* and *Cytherella vulgatella,* are present with 2 specimens, each accounting for 13 % of the total.

Table 5 Systematic list of the ostracods from Furnari. For each taxon the number of specimens (ab.) and the relative abundance (dom.) is given. Crosses indicate the presence of juveniles; bold numbers the presence of only right or left valves; species considered as displaced are marked with an asterisk

Samples	143 A			143		
Ostracods	**Ab.**	**Dom.**	**J**	**Ab.**	**Dom.**	**J**
Cytherella vulgatella Aiello, Barra, Bonaduce and Russo	2	13.33	+	22	5.61	+
Bairdoppilata conformis (Terquem)				40	10.20	+
Bythocypris bosquetiana (Brady)				6	1.53	+
Bythocypris obtusata (Sars)	6	40.00		80	20.41	+
Zabythocypris antemacella (Maddocks)				10	2.55	+
Saida limbata Colalongo and Pasini				2	0.51	
Argilloecia acuminata Mueller				**1**	0.26	
Propontocypris sp.				2	0.51	+
Krithe compressa (Seguenza)				28	7.14	
Krithe monosteracensis (Seguenza)				**1**	0.26	
Krithe sinuosa Ciampo				27	6.89	

Table 5 continued

Samples		143 A			143	
Ostracods	Ab.	Dom.	J	Ab.	Dom.	J
Krithe sp.1				26	6.63	
Krithe spp.				22	5.61	+
Henryhowella parthenopea Bonaduce, Barra and Aiello	2	13.33		3	0.77	
Henryhowella sarsi profunda Bonaduce, Barra and Aiello	2	13.33	+	45	11.48	+
Henryhowella cf. *H. sarsi sarsi* (Mueller)				2	0.51	
Quasibuntonia radiatopora (Seguenza)	3	20.00		56	14.29	+
Rectobuntonia inflata Colalongo and Pasini				4	1.02	
Typhloeucytherura sp.				2	0.51	
Cytheropteron alatum Sars				1	0.26	
Cytheropteron circumactum Colalongo and Pasini				**3**	0.77	
Cytheropteron retrosulcatum Colalongo and Pasini				1	0.26	
Xestoleberis sp.				4	1.02	
Sclerochilus contortus (Normann)				4	1.02	
Number of specimens	15	100		392	100	
Number of species	5			24		
Callistocythere sp.*	1					
Carinocythereis carinata (Roemer) *				1		+
Carinocythereis whitei (Baird) *				1		
Costa edwardsi (Roemer)*	**1**					
Celtia quadridentata (Baird)*	**2**					
Echinocythereis laticarina (Mueller) *				**1**		
Mutilus retiformis Ruggieri *				1		
Aurila gr. *convexa* (Baird) *	3			2		+
Aurila interpretis Uliczny *	4			1		
Aurila nimbosa Ruggieri *	1					
Aurila gr. *punctata* (Muenster) *	2			4		+
Aurila spp.*				3		
Aurilia (Cimbaurila) cimbaeformis (Seguenza)*				**1**		
Aurilia (Cimbaurila) latisolea Ruggieri *				2		+
Tenedocythere prava (Baird) *	**1**		+			
Urocythereis favosa (Roemer) *	**1**					
Urocythereis oblonga (Brady) *				1		
Loxoconcha sp.*	1					
Xestoleberis communis Mueller *				1		
Xestoleberis plana Mueller *				1		

Deep-sea silts (sample 143)

The sediment is silt, containing subordinate fine sands (10 %) and clays (6 %). Organogenic content is scant, representing about 30 % of the washed residue (Fig. 2/10). Molluscs prevail (40 %), followed by corals (20 %) and brachiopods (20 %). Serpulids (5 %), ostracods (2 %) and bryozoans (1 %) are subordinate. Foraminifers, echinoids and decapods are also present. Skeletons of all organisms but corals are usually well preserved.

Corals (Table 1) sharply decrease both in specimen and species number in comparison with the previous sample. Only a few, small scleractinian fragments from the coarse fraction and one stylasterid (*Stenohelia* sp.) specimen from the fine one were identified. Octocorals are present with a single *Keratoisis* internode. Among the seven identified scleractinian species, *M. oculata* (59.26 %) is dominant. Corallites of *E. scillae* (7.41 %) sharply decrease whereas *Lophelia pertusa* (4.94 %) and *C. typus* (3.70 %) are relatively more abundant. The occurrence of a juvenile discoid specimen (?*Fungiacyathus* sp.), typical of mobile substrates, is remarkable (Fig. 3/7).

The number of molluscs also declines. A total of 396 specimens belonging to 39 species have been detected (Table 2). Bivalves prevail at species level with 18 species but represent about 35 % at specimen level. Gastropods and scaphopods behave inversely, accounting for 17 and 4 species and 43 % and 22 % of individuals respectively. Only a few species, i.e. the gastropods *Solariella marginulata* (11.62 %), *Alvania elegantissima* (10.61 %) and *A. acutecostata* (4.55 %), the scaphopods *Entalina tetragona* (10.35 %), *Cadulus ovulum* (5.81 %) and *G. agilis* (4.55 %) and the bivalves *B. excisa* (10.86 %), *N. sulcata* (5.56 %) and *D. vitreus* (3.79 %) constitute the bulk of the assemblage. Among other species *Pagodula echinata* (2.78 %) is noteworthy.

The serpulid assemblage (Table 3) is poorer in comparison to the previous sample (6 species and only 37 specimens). *P. tridentatus* still prevails with 37.84 %, followed by *Neovermilia falcigera* (18.92 %), *S. pomatostegoides* (10.81 %) and *V. monodiscus* (5.41 %). *Protula* sp. 1, a typical soft dweller absent from the previous sample, shows a high dominance (13.51 %). *Filogranula stellata* is present as a single specimen.

Also bryozoans (Table 4) are less abundant and diversified than in the rubble pocket sample, although they still contribute considerably to diversity. As a whole 18 species and 106 specimens have been detected. The erect, both rigid (53 %) and flexible (12 %) growths prevail while encrusters are nearly absent (less than 2 %); setoselliniforms become important reaching 24 %. The bulk is given by only five species, i.e. *A. verrucosa* (18.87 %), *Setosella vulnerata* (12.26 %), *Cellaria fistulosa* (11.32 %), *Setosellina roulei* (7.55 %) and *Heliodoma angusta* (3.77 %). Among other species *Tervia barrieri* and *Tubulipora* sp. 1 deserve a mention.

Unlike all other taxonomic groups studied, ostracods are more diversified than in the previous sample (Table 5) with at least 24 species, without considering the presence of possible additional species belonging to the genus *Krithe*. Only four species cover more than 56 %. They are *Bythocypris obtusata* (20.41 %), *Quasibuntonia*

radiatopora (14.29 %), *H. sarsi profunda* (11.48 %) and *Bairdoppilata conformis* (10.20 %). Also *Krithe* sp. 1, *K. sinuosa*, *K. compressa* and *Cytherella vulgatella* are abundant, each accounting for about 5-7 %. All other species are scant.

Discussion

The palaeocommunity colonising the fault scarp and both the assemblages from the rubble pocket and the deep-sea silty samples testify to bathyal palaeoenvironments.

Most of the species, which directly encrusted the palaeoescarpment and/or whose skeletal remains have been found in the rubble pockets, such as the corals *M. oculata, D. cristagalli* and *L. pertusa* and the bivalves *S. gussoni* and *A. nodulosa scabra,* are already known as constituents of the bathyal "deep coral" community (Pérès and Picard 1964; Zibrowius 1980; Di Geronimo 1987). Other species, such as the serpulids *H. variorugosus* and *V. monodiscus* (Bianchi 1981; Sanfilippo 1998), and the bryozoan *C. exiguum* (Zabala et al. 1993; Rosso 2003), have been found on deep-sea scleractinians.

Similarly, nearly all the species from the silty sample, such as the bivalves *D. vitreus, Abra longicallus* and almost all nuculoids are common representatives of the "bathyal mud" community (e.g., Pérès and Picard 1964; Di Geronimo 1987; La Perna 2003).

Depth

Palaeobathymetrical inferences are difficult to make from deep-water fossil assemblages. Nevertheless, some conclusions can be reached combining results from the communities studied and the vertical distribution of some taxa.

A large number of species, from all the investigated taxonomic groups, shows very wide vertical distributions, usually comprising not only the upper horizon of the bathyal zone but also the transition to the circalittoral one. This is a predictable feature after Pérès and Picard (1964) and Carpine (1970), mainly for the upper horizon of the bathyal zone. This zone is restricted to between about 200 and 500 m depths in the present day Mediterranean. A sharp environmental change occurs at similar depths (500-600 m) also in the Recent northeastern Atlantic (Le Tareau 1977; Van Aken 2000).

Further consistent data could be gained from analysing the upper distribution boundary of some species. Among molluscs, some Atlantic-Mediterranean nuculoids are noteworthy. They are *Ennucula corbuloides* and *Yoldiella seguenzae*, known from below 500 m and *Y. micrometrica* found not shallower than about 400 m (La Perna 2003). The bryozoans *A. verrucosa* and *S. roulei* have been found from about 500 m (Harmelin and d'Hondt 1982; Rosso and Di Geronimo 1998 and references therein) in both the Mediterranean and the Atlantic, although they locally rise towards shallower bottoms, in up-welling sites (Harmelin 1977). The former species has been recorded also from 248 m, in Holocene Mediterranean thanatocoenoses (Di Geronimo et al. 2001). The serpulid *F. stellata* is present in

the Atlantic-Mediterranean region from below 300 m, becoming common at 600 m (Ben-Eliahu and Fiege 1996). The gastropod *A. elegantissima* also thrives in bottoms deeper than about 300-400 m (Oliverio et al. 1992). Similarly, *Strobiligera brychia* and *A. acutecostata* have an upper distributional boundary at 300 m, shallowing at 170 m in Norwegian colder waters for the latter species (Bouchet and Warén 1985).

Comparable upper bathymetrical boundaries are shown by some species extinct in the Mediterranean but living in the Atlantic. The gastropods *Epitonium dallianum*, *Opaliopsis atlantis* and *Mitrolumna smithi*, known from 350-400 m, the former species becoming frequent below 500 m (Bouchet and Warén 1986). The bryozoan *C. longipes,* seemingly absent from the present day Mediterranean being restricted to 500-600 m in the Gibraltar Straits, has an Atlantic upper boundary at about 360 m (Harmelin and d'Hondt 1992). Also the solitary scleractinian *C. typus* is known in northeastern Atlantic below 400 m (Zibrowius 1980).

Some extinct species such as the bryozoans *H. angusta* and *T. barrieri* have been found in bathyal assemblages with inferred palaeodepths respectively not shallower than 300 and 500 m (Rosso 1998). The bivalve *B. excisa* is common, although not dominant in shallow bathyal assemblages whose upper boundary could be placed at 250-300 m (Di Geronimo and La Perna 1996). The Mediterranean palaeoendemic corals *K. melitensis* and *K. peloritana,* belonging to the Atlantic bathyal genus *Keratoisis* have been found in southern Italy Plio-Pleistocene assemblages ascribed to palaeodepths not shallower than 300 m (Di Geronimo 1979; Di Geronimo 1987; Barrier et al. 1989, 1996).

Slightly shallower upper limits are shown by the ostracods *K. sinuosa* and *Bythocypris bosquetiana* and the scleractinian *J. cailleti,* respectively recorded in the Atlantic-Mediterranean area from below 185 m, 150 m and 200 m (Puri and Dickau 1969; Zibrowius 1980; Coles et al. 1994).

Assemblages also consist of very deep species, some of which are known as psychrospheric. They mostly comprise ostracods, such as *Q. radiatopora,* and the coral *F. messanense,* both seemingly extinct in the Mediterranean but known in the northern Atlantic from below 1000 m (Benson 1972) and around 600 m (Zibrowius 1980; Alvarez 1994) respectively.

In addition the Atlantic-Mediterranean ostracod *B. obtusata* is known from below about 1200 m in the Atlantic and 600 m in the Mediterranean (Bonaduce et al. 1983), although a single shallower record from 300 m (Naples Gulf; Bonaduce and Pugliese 1979). Finally, the distribution boundary of the serpulids *N. falcigera* and *V. digeronimoi* is below 600-650 m (Zibrowius 1979; Zibrowius and Ten Hove 1987).

The nuculoid association found in the silty sample, largely made up by *B. excisa*, has a composition somewhat similar to that known from the Mediterranean Pleistocene from about 400 to 1000 m (La Perna 2003). Nevertheless, the low dominance of some species characteristic of the deeper horizons (i.e. *Y. micrometrica, Y. seguenzae, Thestileda cuspidata, E. corbuloides* and *Yoldia minima*) together with the abundance of the circa-bathyal *N. sulcata*, points to the upper part of this interval, probably not below 500 m.

All these data allow a shallow epibathyal palaeoenvironment to be inferred, located in the upper horizon of the bathyal zone seemingly at depths ranging from about 400 to 500 m.

Hydrology

Temperatures were colder than in the Recent Mediterranean at similar depths, i.e. lower than 12.6°C. Several species are cold stenothermic; among them, all the palaeoendemics and the so-called "Atlantic" taxa occur. They are species presently living in deep Atlantic waters but extinct in the warm-homothermic present-day Mediterranean, where they flourished during the colder Pliocene and/or Pleistocene times (Di Geronimo et al. 1996; Di Geronimo and La Perna 1997; Rosso and Di Geronimo 1998). Several molluscs, among which *S. marginulata, Moerellopsis messanensis*, *Eumetula alicae* and *Iphitus tenuisculptus,* are cold stenothermic. The scleractinian *F. messanense* lives in Atlantic waters not warmer than 10°C. Also the serpulid *P. tridentatus*, showing its "Atlantic" form (Sanfilippo 2003), together with *N. falcigera* and *V. digeronimoi,* point to "oceanic" conditions (Barrier et al. 1989), suggesting near bottom temperatures below 8-10°C (Zibrowius 1979; Zibrowius and Ten Hove 1987). *Q. radiatopora*, once considered as psychrospheric by Benson (1972), suggested a similar interpretation is valid. Finally, the scleractinians *L. pertusa* and *D. cristagalli*, although living in the Recent Mediterranean, have been usually recorded from the Atlantic in waters colder than 10°C (Frederiksen et al. 1992; Freiwald et al. 1997).

Near bottom currents swept the deep slope, as suggested by early diagenetic processes evident all along the exposed fault scarp. Goethite coverings together with surface and subsurface cementation of both faulted sediments and organogenic rubble pocket deposits were produced. The presence itself of deep-water scleractinians, together with stylasterids (Zibrowius and Cairns 1992), could be an evidence of hydrodynamism. *Lophelia* usually lives in sites of current speeds ranging from 4-5 cm/s up to 100 cm/s (Freiwald et al. 1997).

Biodiversity

The assemblages from the two samples show different kinds of inputs from shallow (infralittoral and circalittoral) environments. In the rubble pocket sample lithic clasts together with a few mollusc (Table 2), bryozoan (Table 4) and ostracod (Table 5) species occur. In the silty sample, only displaced molluscs decrease. Nevertheless, it is interesting to emphasize that as skeletal inputs in the rubble pocket involve large-sized species, gravity usually displaced these near the bottom. On the contrary, shelf species from the silty sample exclusively consist of small-sized, crisidiid internodes and ostracod carapaces, which seemingly lived on seagrass, and whose skeletons floated and subsequently settled. Finally fallout of pelagic skeletons added to both assemblages.

Fauna from the bathyal fault scarp and from the deep-sea pelitic sediments lived side by side. Moreover, it can be assumed that fossil assemblages, although biased by diagenesis, well represent the original communities. Nearly all the organisms

possessing mineralised parts seemingly fossilised *in situ* or slightly displaced. The small scleractinian specimens and the erect tube fragments of some serpulids could originate respectively from small-sized corals and polychaetes exploiting the biodetritic elements from the silty bottom as substrata. These assumptions allow the composition and structure of both palaeocommunities to be compared confidently.

At first sight, it is obvious that the two assemblages strongly differ in both number of species and specimens (Table 6). The rubble pocket sample contains more numerous (5400 specimens against 1493) and more diverse benthic communities (203 species against 144) than the deep-sea silty sample, although the volume of silty sediment analysed was less (6 compared to 8 dm^3).

Such a trend in species richness (α-diversity) is normal, the number of species usually becoming scarce in soft bottoms. Notwithstanding some variations, this trend

Table 6 Biodiversity and specimen richness; for each systematic group the total number of species and specimens is reported

	143A		143	
	species	specimens	species	specimens
Corals	16	1714	9	83
Scleractinians	12	1546	7	81
Octocorals	2	162	1	1
Stylasterines	2	6	1	1
Molluscs	61	748	39	396
Gastropods	43	421	17	170
Scaphopods	4	113	4	88
Bivalves	14	214	18	138
Serpulids	9	249	6	37
Bryozoans	35	212	18	106
Ostracods	5	15	24	392
	203	**5400**	**144**	**1493**

is shared by all the investigated groups but ostracods. In bathyal environments this taxon comprises vagile, mostly shallow-infaunal deposit-feeding species, mainly thriving in silty bottoms. Also some mollusc groups, namely the scaphopods and the nuculoid bivalves, sharing similar ecological and trophic adaptations, show a comparable trend, increasing in species number and, above all, in specimen abundances in the silty sample, accounting for about one half of the community.

In contrast, corals, bryozoans and serpulids are sessile epibenthic suspension-feeding species, which need suitable hard substrata to settle and live, as do some filter-feeding molluscs, such as *S. gussoni* and *Pododesmus aculeatus*. This implies strongly impoverished species richness for these groups in soft, especially fine-grained bottoms, as in the bathyal zone where only a few species, which evolved peculiar adaptations, can survive. In the silty sample the presence, with high

percentages, of the free-living bryozoans *S. vulnerata, S. roulei* and *H. angusta* is noteworthy. These "setoselliniform" species are common in silty sediments from Pleistocene of southern Italy (see Barrier et al. 1996) being able to encrust single sandy, and even silty particles forming small colonies "floating" on the mud, cleaning themselves using setiform heterozooids. Also the coral ?*Fungiacyathus* sp., having a discoidal shape with a wide basal surface compared to the total volume, shows a similar adaptation. The pelophilic serpulid *Protula* sp.1 lives exclusively or preferentially on soft bottoms. Also the small-sized *F. stellata* and, to a less extent, *P. tridentatus,* can colonise fine-grained sediments, encrusting relatively small substrates initially, later becoming free-growing.

The situation is quite different for the slope palaeocommunity, partly visible on the exposed fault plane and also recorded in the rubble pocket sediment. The hard bottom suitable to be colonised was extremely complex in relation to the bathyal silt homogeneity, offering steps and ledges but also grooves and cavities, submitted to different hydrological conditions, ledges seemingly enhancing current speeds. Several sessile erect species, such as the large *E. scillae* colonies, grew far away from the bottom providing further colonisable surfaces. These colonies became the base for other smaller species, such as some molluscs, serpulids and bryozoans, but also constituted the trophic resource for some gastropods. In such a way large coral colonies contributed to the diversification of both microenvironments and ecological niches, thus enhancing biodiversity (see Zabala et al. 1993). Also several soft-bodied organisms lived in this community, as indirectly indicated by some of the skeleton bearing ones. The presence of unpreservable sea anemones, for instance, could be deduced by Epitoniidae, living and/or feeding on them.

Within grooves and steps at coral bases, large bioclasts from corals themselves and associated faunas, such as most vagile gastropods living and feeding on scleractinians, accumulated at places. Even silts and muds locally coated surfaces and filled small sheltered depressions. This deposition was seemingly enhanced by the baffling activity of large dendroid corals. Both coarse and fine-grained sediment pockets, could be colonised by faunas especially adapted for thriving in such sediments, as well as the free-living solitary coral *F. messanense,* the setoselliniform bryozoans (Fig. 3/12) and all, although scant, ostracods recorded from the rubble pocket sample.

From these data it appears obvious as the deep-sea escarpment offered the primary hard substrate needed for the settlement and the life of large scleractinian corals and other smaller organisms. Corals, in turn, largely contributed to increase colonisable hard surfaces and, at the same time, supplied organogenic debris, thus exerting a control on edaphic conditions of deep-sea near bottoms, forming coarse sediments and/or adding coarse fractions in otherwise fine-grained sediments. The result was a considerable differentiation of microhabitat and niches promoting a palaeocommunity richer and more diversified than those living on deep-sea muds.

Comparable communities are now found on deep-sea slopes in the North Atlantic from where they have been recorded down to about 3000 m by means of submersible observations (Tyler and Zibrowius 1992; Freiwald et al. 2002).

It is worthy of note that the exposed fault plane shows a patchy distribution of sessile organisms, such as corals and *S. gussoni*, often clustered along a ledge's edge or encrusting more jutting out surfaces. The presence of large scleractinians and the flourishing other faunas in themselves indicate the presence of near-bottom currents, whereas the clustered distribution of all organisms seemingly indicates enhanced speed around projecting rocks. The same observations have been made in the Atlantic where organisms mainly flourish within the flux of the "North Eastern Atlantic Deep Water" and prevail on the edges of rocks where, "owing to constrictions of space, water flow may be accelerated thus increasing the supply of food particles" (Tyler and Zibrowius 1992). The near-bottom currents probably acted re-suspending detritus fallen down from the shallow pelagic into the aphotic zone. This also implies high productivity in the euphotic zone, as recorded by Frederiksen et al. (1992) for Recent *Lophelia* assemblages. The fallout of organic matter also influenced the relative proliferation of benthic organisms in silty near-slope bottoms, mainly the abundant detritus-feeders such as ostracods, nuculoids and scaphopods.

Conclusions

The Early Pleistocene deep-sea fault plane offered the primary hard substrate needed for settlement and growth of large scleractinian corals and other organisms.

Colonies, although large-sized, as suggested by some base diameters, seemingly remained isolated and did not coalesce or form frameworks. Nevertheless, corals largely contributed to increase colonisable hard surfaces in an elevated water layer above the bottom, thus allowing life for several epizoans. The presence of skeletal remains of predators feeding on soft-bodied organisms, imply a flourishing cover of sea anemones, sponges and other poorly-preservable benthic faunas. Thus corals created a considerable microhabitat and niche differentiation promoting the life for a palaeocommunity more rich and diversified than those living on neighbouring deep-sea sediments. The result was an increased total biomass.

Corals also supplied organogenic debris, which were partly deposited along the fault scarp and partly fell at and near the base scarp. Thus corals not only largely contributed to carbonate production, but also exerted a control on the edaphic conditions of deep-sea near bottoms, forming coarse sediments and/or adding coarse fractions in otherwise fine-grained sediments.

The inferred elevation in total biomass characterising the rich and diversified Furnari coral communities show similarities with those flourishing in the present day North Atlantic and appears congruent with the scenario of cold stenothermic Pleistocene deep Mediterranean.

Acknowledgements

References

Allouc J (1987) Les paléocommunautés profondes sur fond rocheux du Pléistocène méditerranéen. Description et essai d'interpretation paléoécologique. Géobios 20: 241-263

Alvarez C (1994) Deep-water Scleractinia (Cnidaria: Anthozoa) from southern Biscay Bay. Cah Biol Mar 35: 461-469

Amodio Morelli L, Bonardi G, Colonna V, Dietrich D, Giunta G, Ippolito F, Lorenzoni S, Paglionico A, Piccarreta G, Russo M, Scandone P, Zanettin-Lorenzoni E, Zuppetta A (1976) L'Arco calabro-peloritano nell'orogene appenninico-maghrebide. Mem Soc Geol Ital 17: 1-6

Barrier P (1984) Evolution tectono-sédimentaire pliocène et pléistocène du Détroit de Messine (Italie). Unpublished PhD Thesis, Univ Marseille-Luminy: 270 pp

Barrier P (1987) Stratigraphie des dépôts pliocènes et quaternaires du Détroit de Messine. Doc et Trav IGAL 11: 59-81

Barrier P, Di Geronimo I, Lanzafame G (1986) L'evoluzione recente dell'Aspromonte meridionale (Calabria). Riv Ital Paleont Stratigr 81: 537-556

Barrier P, Di Geronimo I, Montenat C, Roux M, Zibrowius H (1989) Présence de faunes bathyales atlantiques dans le Pliocène et le Pléistocène de la Méditerranée (Detroit de Messine, Italie). Bull Soc Geol France, ser 8, 5: 787-796

Barrier P, Di Geronimo I, La Perna R, Rosso A, Sanfilippo R, Zibrowius H (1996) Taphonomy of deep-sea hard and soft bottom communities: the Pleistocene of Lazzàro (Southern Italy). In: Meléndez G, Blasco F, Pérez I (eds) Tafonomia y fosilización. II Reunion, Zaragoza, pp 39-46

Ben-Eliahu MN, Fiege D (1996) Serpulid tube-worms (Annelida: Polychaeta) of the central and eastern Mediterranean with particular attention to the Levant basin. Senckenb marit 28: 1-51

Benson RH (1972) Ostracodes as indicators of threshold depth in the Mediterranean during the Pliocene. In: Stanley DJ (ed) The Mediterranean Sea: a natural sedimentation laboratory. Dowden, Hutchinson & Ross, Stoudsbourg, pp 63-73

Bianchi CN (1981) Guida per il riconoscimento delle specie animali delle acque lagunari e costiere italiane. AQ/1/96 5, Policheti Serpuloidei, 187 pp

Boccaletti M, Ciaranfi N, Cosentino D, Deiana G, Gelati R, Lentini F, Massari F, Moratti G, Pescatore T, Ricci Lucchi F, Tortorici L (1990) Palinspastic restoration and paleogeographic reconstruction of the peri-Tyrrhenian area during the Neogene. Palaeogeogr Palaeoclimatol Palaeoecol 77: 41-50

Bonaduce G, Pugliese N (1979) Benthic ostracods as depth indicators. Rapp Comm Int Mer Médit 25/26: 167-169

Bonaduce G, Ciliberto B, Masoli M, Minichelli G, Pugliese N (1983) The deep-water benthic ostracodes of the Mediterranean. In: Maddocks RF (ed) Applications of Ostracoda. Univ Houston, pp 459-471

Bonardi G, Cavazza W, Perrone V, Rossi S (2001) Calabria-Peloritani terrane and northern Ionian Sea. In: Vai GB, Martini IB (eds) Anatomy of an Orogen: The Apennines and Adjacent Mediterranean Basins. Kluwer Acad Publ, Dordrecht, pp 287-306

Bouchet P, Warén A (1985) Revision of the northeast Atlantic bathyal and abyssal Neogastropoda excluding Turrida (Mollusca, Gastropoda). Boll Malacol, suppl 1, 121-296

Bouchet P, Warén A (1986) Revision of the northeast Atlantic bathyal and abyssal Aclididae, Eulimidae, Epitoneiidae (Mollusca, Gastropoda). Boll Malacol, suppl 2, 299-576

Carpine C (1970) Ecologie de l'étage bathyal dans le Méditerranée occidentale. Mem Inst Oceanogr Monaco 2: 1-146

Coles GP, Whatley RC, Mouguilevsky A (1994) The ostracod genus *Krithe* from the Tertiary and Quaternary of the North Atlantic. Palaeontology 37: 71-120

Corselli C, Bernocchi A (1990) Palaeocommunities of the last glacial from the Sardinia continental slope: a palaeoceanography problem. Boll Mus Reg Sci Nat Torino, spec vol: 576-595

Delibrias G, Taviani M (1985) Dating the death of Mediterranean deep-sea scleractinian corals. Mar Geol 62: 175-180

Di Geronimo I (1979) Il Pleistocene in facies batiale di Valle Palione (Grammichele, Catania). Boll Malacol 15: 85-156

Di Geronimo I (1987) Bionomie des peuplements benthiques des substrats meubles et rocheux plio-quaternaires du Détroit de Messine. Doc et Trav IGAL 11: 153-170

Di Geronimo I, La Perna R (1996) *Bathyspinula excisa* (Philippi, 1844) (Bivalvia, Protobranchia): a witness of the Plio-Quaternary history of the deep Mediterranean benthos. Riv Ital Paleont Stratigr 102: 105-118

Di Geronimo I, La Perna R (1997) Pleistocene bathyal molluscan assemblages from southern Italy. Riv Ital Paleont Stratigr 103: 389-426

Di Geronimo I, La Perna R, Rosso A (1996) The Plio-Quaternary evolution of the Mediterranean deep-sea benthos: an outline. In: La Méditerranée: variabilitès climatiques, environments et biodiversité. Actes Coll Sci Int Montpellier: 286-291

Di Geronimo I, D'Atri A, La Perna R, Rosso A, Sanfilippo R, Violanti D (1997) The Pleistocene bathyal section of Archi (Southern Italy). Boll Soc Paleont Ital 36: 189-212

Di Geronimo I, Rosso A, La Perna R, Sanfilippo R (2001) Deep-sea (250-1,550) benthic thanatocoenoses from the southern Tyrrhenian Sea. In: Faranda FM, Guglielmo L, Spezie G (eds) Mediterranean Ecosystems. Structures Processes 36: 277-287

Frederiksen R, Jensen A, Westerberg H (1992) The distribution of the scleractinian coral *Lophelia pertusa* around the Faroe Islands and the relation to internal tidal mixing. Sarsia 77: 157-171

Freiwald A, Henrich R, Pätzold J (1997) Anatomy of a deep-water coral reef mound from Stjernsund, West Finnmark, Northern Norway. SEPM Spec Publ 56: 141-162

Freiwald A, Wilson JB, Henrich R (1999) Grounding Pleistocene icebergs shape recent deep-water coral reefs. Sediment Geol 125: 1-8

Freiwald A, Hühnerbach V, Lindberg B, Wilson JB, Campbell J (2002) The Sula Reef Complex, Norwegian shelf. Facies 47: 179-200

Guadagno FM, Taddei Ruggiero E, De Blasio I, Placella B, Sgarrella F (1979) La sezione pleistocenica di Archi (RC). Boll Soc Natur Napoli 88: 1-29

Harmelin J-G (1977) Bryozoaires du banc de la Conception (nord des Canaries) Campagne Cineca I du "Jean Charcot". Bull Mus Natl Hist Nat Paris, sér 3, 493 (Zool. 341): 1057-1076

Harmelin J-G, d'Hondt J-L (1982) Bryozoaires Cyclostomes bathyaux del campagnes océanographiques de l' "Atlantis II", du "Chain" et du "Knorr" (1967-1972). Bull Mus Natl Hist Nat Paris, sér 4, A, 1-2: 3-23

Harmelin J-G, d'Hondt J-L (1992) Bryozoaires des parages de Gibraltar (campagne océanographique BALGIM, 1984) 1 - Cheilostomes. Bull Mus Natl Hist Nat Paris, sér 4, 14, A, 1: 23-67

Jensen A, Frederiksen R (1992) The fauna associated with the bank-forming deepwater coral *Lophelia pertusa* (Scleractinia) on the Faroe shelf. Sarsia 77: 53-69

Kezirian F (1993) Evolution tectono-sédimentaire post-nappes des Monts Péloritains (Sicile Nord-Orientale, Italie). Mém Géol Inst Géol Albert de Lapparent Paris 49: 260 pp

La Perna R (2003) The Quaternary deep-sea protobranch fauna from the Mediterranean: composition, depth related distribution and changes. Boll Malacol 39: 17-34

Le Danois E (1948) Les profondeurs de la mer. Trente ans de recherches sur la faune sous marine au large des côtes de France. Payot, Paris

Le Tareau JY (1977) Contribution à l'étude de l'Océanographie phisique du Proche Atlantique. Problèmes relatifs à l'extension des eaux d'origine méditerranéenne. Univ Bretagne Occid, Lab Océan Phys, Rapp Sci, 125 pp

Lentini F, Carbone S, Catalano S (2000) Carta Geologica della provincia di Messina. Prov Reg Messina Assessorato Territorio, SELCA, Firenze

Malakoff D (2003) Deep-sea mountaineering. Science 301: 1034-1037

Mastrototaro F, Matarrese A, Tursi A (2002) Un mare di coralli nel Mar Ionio. Biol Mar Medit 9: 616-619

Messina C (2003) Il bacino plio-quaternario di Barcellona P.G. (Sicilia nord-orientale): analisi di facies ed evoluzione stratigrafico-sequenziale. Unpublished PhD Thesis, Catania

Monaco C, Tortorici L, Nicolich R, Cernobori L, Costa M (1996) From collisional to rifted basins: an example from the southern Calabrian arc (Italy). Tectonophysics 266: 233-249

Mortensen PB, Hovland M, Brattegard T, Farestveit R (1995) Deep water bioherms of the scleractinian coral *Lophelia pertusa* (L.) at 64° N on the Norwegian shelf: structure and associated megafauna. Sarsia 80: 145-158

Oliverio M, Nofroni I, Amati B (1992) Revision of the *Alvania testae* group of species (Gastropoda, Prosobranchia, Truncatelloidea, Rissoidea). Lav SIM 24: 249-259

Pérès JM, Picard J (1964) Nouveau manuel de bionomie benthique de la Mer Méditerranèe. Rec Trav Stat Mar Endoume 31: 137 pp

Puri HS, Dickau BE (1969) Use of normal pores in taxonomy of Ostracoda. Trans Gulf Coast Assoc Geol Soc 19: 353-367

Rosso A (1998) New bryozoan species from the deep-sea Pleistocene sediments of southern Italy. Riv Ital Paleont Stratigr 104: 423-430

Rosso A (2003) Bryozoans on deep-water scleractinians from the Mediterranean: a first sight. 2nd Int Symp Deep-sea Corals, Erlanger geol Abh, Sonderbd 4: 73

Rosso A, Di Geronimo I (1998) Deep-sea Pleistocene Bryozoa of southern Italy. Géobios 30: 303-317

Sanfilippo R (1998) Tube morphology and structure of the bathyal Mediterranean serpulid *Hyalopomatus variorugosus* Ben-Eliahu & Fiege, 1996 (Annelida Polychaeta). Riv Ital Paleont Stratigr 104: 131-138

Sanfilippo R (2003) Climatic response in the genus *Placostegus* Philippi, 1844 from Plio-Pleistocene to Recent Mediterranean, with description of a new species (Polychaeta, Serpulidae). Boll Soc Paleont Ital 42: 171-178

Scilla A (1670) La vana speculazione disingannata dal senso. Lettera risponsiva circa i corpi marini, che petrificati si trovano in varij luoghi terrestri. Appresso a Colicchia, Napoli, 168 pp

Seguenza G (1864) Disquisizioni paleontologiche intorno ai Coralli fossili delle rocce terziarie del distretto di Messina. Mem Reale Accad Sci Torino, Cl Sci Fis Mat, ser 2, 21: 399-560

Seguenza G (1875-1876) Studi paleontologici sulla fauna malacologica dei sedimenti pliocenici depositatisi a grandi profondità. Boll Soc Malacol Ital 1: 99-124 (1875); 2: 17-49 (1876)

Seguenza G (1879) Le formazioni terziarie della provincia di Reggio (Calabria). Mem R Accad Lincei, Cl Sci Fis Mat Nat, ser 3(6): 1-446

Teichert C (1958) Cold and deep-water coral banks. Bull Amer Assoc Petrol Geol 42: 1064-1082

Tyler PA, Zibrowius H (1992) Submersible observations of the invertebrate fauna on the continental slope southwest of Ireland (NE Atlantic Ocean). Oceanol Acta 15: 211-226

Van Aken HM (2000) The hydrography of the mid-latitude Northeast Atlantic Ocean. II: The intermediate water masses. Deep-Sea Res 47: 789-824

Vertino A (2003) Sclerattiniari plio-pleistocenici ed attuali del Mediterraneo. Unpublished PhD thesis, Messina Univ, 306 pp

Vertino A, Di Geronimo I (2003) How many *Caryophyllia* species lived in the Plio-Pleistocene Mediterranean: Seguenza's taxonomy revised. Abstract 9th Int Symp Fossil Cnidaria and Porifera, 113

Wilson JB (1979) The distribution of the coral *Lophelia pertusa* (Linneus) [*Lophelia prolifera* (Pallas)] in the North-East Atlantic. J Mar biol Ass UK 59: 149-164

Zabala M, Maluquer P, Harmelin J-G (1993) Epibiotic bryozoans on deep-water scleractinian corals from the Catalonia slope (western Mediterranean, Spain, France). Sci Mar 57: 65-78

Zibrowius H (1979) *Viterotubus digeronimoi* n.g., n.sp. (Polychete Serpulidae) du Pléistocène inferieur de la Sicile et de l'étage bathyal des Açores et de l'Océan Indien. Téthys 9: 183-190

Zibrowius H (1980) Les Scléractiniaires de la Mediterranée et de l'Atlantique nord-oriental. Mém Inst Océanogr 11: 1-284

Zibrowius H, Cairns S (1992) Revision of the northeastern Atlantic and Mediterranean Stylasteridae (Cnidaria: Hydrozoa). Mem Mus natl Hist nat 153: 1-136

Zibrowius H, Ten Hove HA (1987) *Neovermilia falcigera* (Roule, 1898) a deep- and cold-water serpulid polychaete common in the Mediterranean Plio-Pleistocene. Bull Biol Soc Washington 7: 259-271

Sedimentary patterns in the vicinity of a carbonate mound in the Hovland Mound Province, northern Porcupine Seabight

Andres Rüggeberg[1], Boris Dorschel[2], Wolf-Christian Dullo[1], Dierk Hebbeln[2]

[1] IFM-GEOMAR - Leibniz Institute of Marine Sciences, Wischhofstr. 1-3, D-24148 Kiel, Germany
(arueggeberg@ifm-geomar.de)

[2] Department of Geosciences, University of Bremen, P.O. Box 330 440, D-28334 Bremen, Germany

Abstract. Large carbonate mound structures have been discovered in the northern Porcupine Seabight (Northeast Atlantic) at depths between 600 and 1000 m. These mounds are associated with the growth of deep-sea corals *Lophelia pertusa* and *Madrepora oculata*. In this study, three sediment cores have been analysed. They are from locations close to Propeller Mound, a 150 m high ridge-like feature covered with a cold-water coral ecosystem at its upper flanks. The investigations are concentrated on grain-size analyses, carbon measurements and on the visual description of the cores and computer tomographic images, to evaluate sediment content and structure.

The cores portray the depositional history of the past ~31 kyr BP, mainly controlled by sea-level fluctuations and the climate regime with the advance and retreat of the Irish Ice Sheet onto the Irish Mainland Shelf. A first advance of glaciers is indicated by a turbiditic release slightly older than 31 kyr BP, coherent with Heinrich event 3 deposition. During Late Marine Isotope Stage 3 (MIS 3) and MIS 2 shelf erosion prevailed with abundant gravity flows and turbidity currents. A change from glaciomarine to hemipelagic contourite sedimentation during the onset of the Holocene indicates the establishment of the strong, present-day hydrodynamic regime at intermediate depths.

The general decrease in accumulation of sediments with decreasing distance towards Propeller Mound suggests that currents (turbidity currents, gravity flows, bottom currents) had a generally stronger impact on the sediment accumulation at the mound base for the past ~31 kyr BP, respectively.

Keywords. Carbonate mound, Porcupine Seabight, grain-size, sediment structure, British-Irish Ice Sheet, paleoenvironment

Introduction

Carbonate mounds along the European continental margin have been the subject of detailed investigation by several campaigns during the past decade (OMARC projects of the 5th Framework Programme, EU). Within the Porcupine Seabight (PSB), several mounds clustered in three distinct provinces have been identified from high-resolution seismic profiles (e.g., De Mol et al. 2002; Van Rooij et al. 2003) and side-scan sonar images (e.g., Huvenne et al. 2002; Kenyon et al. 2003; Masson et al. 2003), and were intensively sampled during cruises between 1997 and 2003 (e.g., Freiwald et al. 2000; Freiwald and Shipboard Party 2002). The Hovland Mound province in the north of the PSB (Fig. 1) is bound by the Magellan Mound province further northwest, which mainly consists of already buried mounds under a Pleistocene sediment cover. The sea-floor protruding Hovland Mounds reach a height of up to 200 m and occur as single, conical features or ridge-like structures with several summits (De Mol et al. 2002). These mound structures are constructed by the framework builder *Lophelia pertusa* and associated fauna (Freiwald 1998; Hovland and Mortensen 1999; Rogers 1999), which baffle fine-grained sediment and form these large topographic features. The occurrence of deep-water carbonate mounds in a distinct depth range of 600 m to 900 m is closely related to oceanographic conditions favourable for azooxanthellate corals, of which high nutrient supply, strong current activity, temperatures between 4-12°C, and slow sedimentation rate seem most important (Teichert 1958; Frederiksen et al. 1992; Freiwald et al. 1999; De Mol et al. 2002).

Intermediate-water circulation along the European continental margin and within the PSB has an important role in sediment distribution and downslope transport of terrigenous and biogenic material (e.g., Joint et al. 2001; McCave et al. 2001). The influence of currents is known to be an important factor in mound initiation, growth and decay (Freiwald and Wilson 1998; De Mol et al. 2002). Sand sheets and sand waves suggest the present-day sea-floor is swept by relatively strong bottom currents at the Belgica Mound province (Akhmetzhanov et al. 2001), which are reduced in the Hovland Mound province (Huvenne et al. 2002) but still exceed 15 cm s^{-1} (White in press). Thus, strong current strength intensities prevent the burial of the carbonate mounds.

High sedimentation rates are one limiting factor of carbonate mound development, as can be seen from the already buried Magellan Mounds (Huvenne et al. 2002). The Holocene sedimentation rate within the PSB is generally low with 1-8 cm/kyr, which is the result of strong benthic currents removing fine-grained material. However, sediment deposition was about 3 to 10 times higher during the last glacial period, comparable to results of other studies from the Celtic margin to the south or the Hebridean continental slope to the north of the PSB (Knutz et al. 2001; Auffret et al. 2002). Generally, Quaternary sediment deposition in near shelf areas is essentially controlled by the climate regime and sea-level variability. Both factors control the weathering of soils, the transport capacity of rivers, ice sheet dynamics, the annual coverage of sea ice, and the prevailing wind and current regimes (Auffret et al. 2002; McCave 2002). Continental margins are preferentially sites of terrigenous
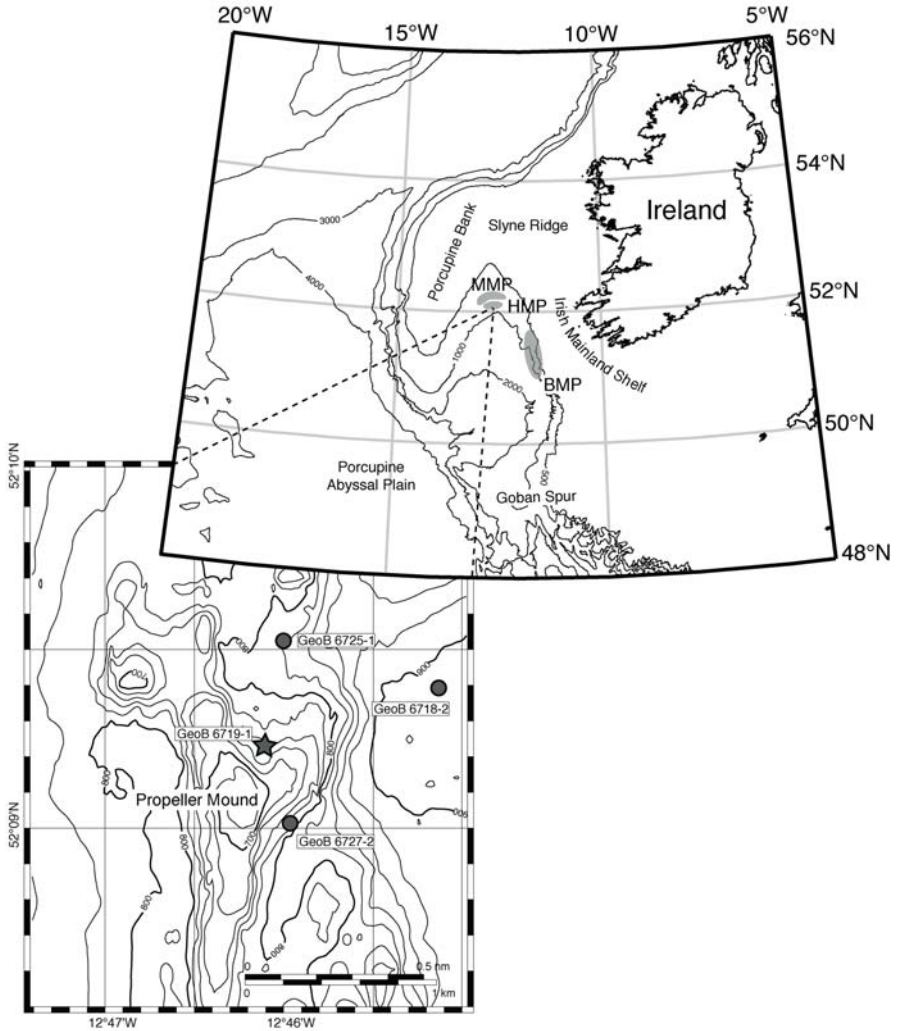
Fig. 1 Bathymetric setting of the Porcupine Seabight west off Ireland. Propeller Mound is located at the southern margin of the Hovland Mound province and was mapped during RV POSEIDON cruise POS 265 in September 2000 (Freiwald et al. 2000). Indicated are the positions of investigated gravity cores (core GeoB 6719-1 (star) was only used for stratigraphic correlation). MMP = Magellan Mound province, HMP = Hovland Mound province, BMP = Belgica Mound province

sediment deposition eroded from land and exported to the ocean essentially through transport by rivers. However, present-day riverine influx of terrigenous sediments into the PSB is low. During peak glacials, the maximum lowering of the sea-level was 120-130 m below present level (Labeyrie et al. 1987; Fairbanks 1989). This degree of lowering uncovers effectively the Irish Mainland shelf and sediments were discharged directly into the Porcupine Basin with much reduced trapping

in coastal plains. Additionally, shelf-protruding glaciers overrode the uncovered shelves leading to strong glacial erosion and high supply of reworked sediments into the basin.

The aim of this study is to describe the sedimentary setting and processes in the northern Porcupine Seabight around a carbonate mound. It is based on the description of sediments in three gravity cores revealed from visual core description and computer tomographic (CT) images, analyses on grain-size distribution, contents, carbon measurements, and stable isotope data. The variability of sediments is influenced by the hydrodynamic setting and the shifting climate regime through the advance and retreat of the British-Irish Ice Sheet (BIIS). The BIIS controls the sediment flux from Ireland and the Irish shelves into the Seabight. Surface morphology of carbonate mounds and adjacent areas have been analysed in detail (e.g., De Mol et al. 2002; Huvenne et al. 2002; Masson et al. 2003). However, here we present a first detailed study on the sedimentary downcore variability within the closer vicinity of a carbonate mound.

Regional setting

The Porcupine Seabight

The Porcupine Seabight is an embayment in the Atlantic Irish shelf, located southwest of Ireland. It has an extension of about 200 km in N-S direction and widens from 65 km in the north to 100 km in the south. The Seabight is surrounded by shallow shelves and ridges to the west, north and east (Porcupine Ridge and Bank, Slyne Ridge and Irish Mainland shelf) and deepens gradually to the south into the Porcupine Abyssal Plain (Fig. 1). The study area is Propeller Mound and its surrounding sea-floor, which was mapped during RV POSEIDON cruise 265 in September 2000 (Freiwald et al. 2000). This mound is part of a cluster of high relief mounds of the Hovland Mound province in a water depth between 650 and 1000 m (52°06'-52°22' N and 11°53'-12°45' W; Hovland et al. 1994; De Mol et al. 2002). The Propeller Mound is elevated up to 150 m above the surrounding sea-floor, possesses a N-S elongation of about 3 km and a maximum extension of 1.5 km in EW direction (Fig. 1). The base of the triangular-shaped mound lies in water depths of around 800 m to the west and 900 m to the east. Smaller mounds appear further NE and NW of Propeller Mound. Its morphology clearly indicates a relation to strong currents running in N-S direction. At the northern, eastern and western flanks of the mound little depressions or moats occur, which are generated by scouring of turbulence currents around the mound (De Mol 2002). Drift bodies further off mound also indicate the erosive hydrodynamic regime.

Recent hydrography

The general hydrography along the East Atlantic Margin is characterised by northward along-slope currents flowing from the Iberian Margin to the Norwegian Sea (Huthnance and Gould 1989; Pingree and LeCann 1989, 1990). Within the PSB, the Eastern North Atlantic Water (ENAW), a winter mode water formed by strong

cooling of waters northwest of Spain, is found to a water depth of about 750 m. It flows along the continental margin of the Bay of Biscay into the Porcupine Seabight (Pollard et al. 1996; van Aken 2000; White in press). Between 150 and 400 m, ENAW can be divided into an upper and lower core of the Shelf Edge Current (SEC), expressed in salinity maxima (Hill and Mitchelson-Jacob 1993; White and Bowyer 1997). SEC plays an important role in physical exchange processes at the shelf break and hence cross-shelf fluxes (Huthnance 1995). Mediterranean Outflow Water (MOW) is underlying ENAW, characterised by a salinity maximum and an oxygen minimum at a depth of about 950 m (Pollard et al. 1996). A mixing between ENAW and MOW occurs between 600 and 700 m water depth.

The general flow pattern in the Porcupine Seabight is characterized by poleward flowing currents at all depth levels along the eastern slope. Direct measurements of benthic currents indicate mean velocities of 5 cm s^{-1}, exceeding 15 cm s^{-1} for 15 % of the measured period (White in press). There is evidence of topographic steering of the mean flow at the northern end of the PSB. Currents become weaker (1-5 cm s^{-1}) and flow cyclonically around the slope leading to a southward flow at the western slope of the Seabight (White in press).

Materials and methods

Sediment cores GeoB 6718-2, GeoB 6719-1, GeoB 6725-1, and GeoB 6727-2 were recovered during RV POSEIDON cruise POS 265 close to Propeller Mound (Freiwald et al. 2000; Table 1). Before sampling and splitting of sediment cores, computer tomographic analysis was performed at the Universitätsklinikum Kiel, Department of Radiology with Dr. Morvain. Still closed core sections were investigated for their content and sedimentary structures using a Phillips Tomoscan LX. The CT radiographs have been scanned and visually described and were compared with core description of split core halves.

Table 1 Sediment core information

Core number	Latitude N	Longitude W	Water depth (m)	Recovery (cm)
GeoB 6718-2	52°09.379'	12°45.158'	900	450
GeoB 6719-1	52°09.233'	12°46.127'	758	580
GeoB 6725-1	52°09.520'	12°46.010'	820	450
GeoB 6727-2	52°08.017'	12°45.970'	794	470

Each core was sampled using 10 cm^3 syringes at 5 cm intervals. All samples were weighed and than freeze-dried at -50°C. With known sediment volume and weight loss during freeze-drying, the dry bulk density, porosity and water content were calculated. One set of samples was wet sieved through a 63 μm sieve and the suspended fine fraction (<63 μm) was collected in 5-litre jars for fine fraction analysis. The coarse fraction (>63 μm) was oven dried at 50°C and weighed afterwards. To separate the sample into grain-size fractions, the coarse fraction was dry sieved through a sieve set with 125 μm, 250 μm, 500 μm and 1000 μm mesh widths. All samples were weighed thereafter.

Stable oxygen isotope analysis was carried out at Isotope Lab, Bremen University. 3 to 5 individuals of benthic foraminifera *Cibicidoides wuellerstorfi* or *Cibicidoides kullenbergi* were selected from fraction 250-500 μm. *C. wuellerstorfi* was rare in most of the samples, especially within the glaciomarine sediments. Therefore, the two species were analysed in some samples, where both occurred, which revealed comparable $\delta^{18}O$ values for both benthic species. The isotopic composition of foraminiferal tests was determined on the CO_2 gas evolved by treatment with phosphoric acid at a constant temperature of 75°C. Working standard (Burgbrohl CO_2 gas) was used for all stable isotope measurements. $\delta^{18}O$ data have been calibrated against PDB by using the NBS 18, 19 and 20 standards and are given here relative to the PDB standard. Analytical standard deviation is about ±0.07 ‰ PDB.

Radiocarbon dating (AMS ^{14}C) using mono-species samples (~10 mg) of planktonic foraminifera *Neogloboquadrina pachyderma* (either dextral or sinistral) from fraction 125-250 μm were analysed at the Leibniz Laboratory for Age Determinations and Isotope Research at the University of Kiel (Nadeau et al. 1997). The data were corrected for ^{13}C and the calibration to calendar years was performed using Calib 4.3 program (Stuiver and Reimer 1993) and the marine data set of Stuiver et al. (1998) with a reservoir age of 400 years. All ages are given in 1000 calendar years before present (kyr BP; Table 2). Ages greater 21 kyr BP were calibrated using the method of Voelker et al. (1998).

Table 2 AMS ^{14}C dates of cores GeoB 6719-1 and GeoB 6725-1

Core number	sample depth (cm)	AMS ^{14}C age (± err.) (kyr BP)	calibrated age (kyr BP)	Remarks
GeoB 6719-1	18	6.2 (0.035)	6.64	KIA 17091[a]
	98	16.1 (0.07)	18.6	KIA 17092[a]
	163	21.7 (0.11)	25.4	KIA 17093[a]
	273	26.8 (0.18)	30.8	KIA 17094[a]
GeoB 6725-1	68	7.1 (0.045)	7.6	KIA 16206[a]
	168	20.4 (0.14)	23.5	KIA 16206[a]

AMS ^{14}C ages were corrected for a reservoir effect of 400 yr and calibrated using the Calib 4.3 software of Stuiver and Reimer (1993). [a]KIA laboratory number, Leibniz Laboratory, University of Kiel, Germany

The collected fine fraction (<63 μm) of cores GeoB 6718-2, GeoB 6725-1 and GeoB 6727-2 was used to determine grain-size distribution of the silt-sized fraction (2-63 μm) and the sortable silt spectrum (10-63 μm; McCave et al. 1995). For this, Micromeritics Sedigraph 5100 was used. It measures the concentration of the suspension by the attenuation of an X-Ray beam. The water of the samples was replaced by Sodium polyphosphate (0.05 %) to avoid hindered settling. The samples were homogenised on a rotating carousel overnight (at least 15 hours) and sonified for 10 seconds before analysis. The grain-size analysis was performed with a density setting of calcite (2.71 g/cm^3) at a constant water temperature of 35°C and

with an analysis range from 1 to 63.1 μm. In a second step, organic material and CaCO$_3$ was removed on samples from off-mound core GeoB 6718-2 using H$_2$O$_2$ (35 %) and and acetic acid (6 %) to evaluate the difference of bulk and carbonate-free grain-size distribution.

Those samples were measured with the density setting of quartz (2.65 g/cm^3). Cumulative and mass frequency data output were used to calculate mean silt and mean sortable silt distribution, as well as size frequency distribution. The data were converted into weight percentages (wt.-%).

Another set of samples was ground in an agate mortar after freeze-drying. About 10 mg was weighed into a tin cup for analysing total carbon (TC) using Carlo Erba NA-1500-CNS at IFM-GEOMAR, Kiel. Calibration standards for TC were Acetanilid (N = 10.36 %, C = 71.09 %) and SOIL Standard BSTD1 (N = 0.216 %, C = 3.5 %). Standard deviation of continuously analysed standards was better than 2 %. Carbonate contents of sediments were finally calculated according to their atomic weight ratios:

$$CaCO_3 \ (\%) = 8.33 \cdot (C_{total} - C_{org}).$$

In addition to the discrete carbonate analysis, high-resolution calcium determinations were performed with CORTEX-XRF scanner (Jansen et al. 1998) at University of Bremen. The resulting data are element intensities in counts per second (cps). Correlation of calcium data and carbonate content of the analysed sediment cores presents a linear regression with $R^2 = 0.77$ (Dorschel et al. in press).

Stratigraphy

The stratigraphic framework of the investigated cores is primarily based on AMS ^{14}C ages and benthic stable oxygen isotopes. Additional evidence is derived from calibrated Ca corescanner data (Dorschel et al. in press), tracing glacial-interglacial fluctuations of calcium carbonate. Core GeoB 6719-1 is used here for stratigraphic correlation to the other cores, as four AMS ^{14}C dates have been performed (Table 2). All cores present a rather continuous record reaching back to Late MIS 3 (Fig. 2). The correlation of the lower core section of GeoB 6727-2 (>280 cm) and GeoB 6719-1 (>420 cm) remains questionable, as very small numbers of benthic and planktonic foraminifera in fraction >125 μm prevent stable isotope and AMS ^{14}C analyses. However, low carbonate content of <20 % suggests comparable conditions as during MIS 2 and/or dilution of sediment by a high supply of terrigenous material.

The records of GeoB 6727-2, GeoB 6719-1 and GeoB 6725-1 are marked by a major horizon of reworked sediment (dark grey area in Fig. 2). This event seems to be slightly older than 31 kyr BP according to an AMS ^{14}C date in core GeoB 6719-1 at 273 cm (Fig. 2; Table 2). The thickness of this horizon varies between 60 cm (GeoB 6725-1) and 130 cm (GeoB 6719-1). Due to higher sedimentation rates in core GeoB 6718-2 the level of reworked sediments is not reached. An additional tie point is indicated by a characteristic double peak in records of XRF Calcium counts (Fig. 2; Dorschel et al. in press). This peak corresponds to an age of around 25 kyr BP, related to Heinrich event 2 (HE 2) and its European precursor event (Grousset
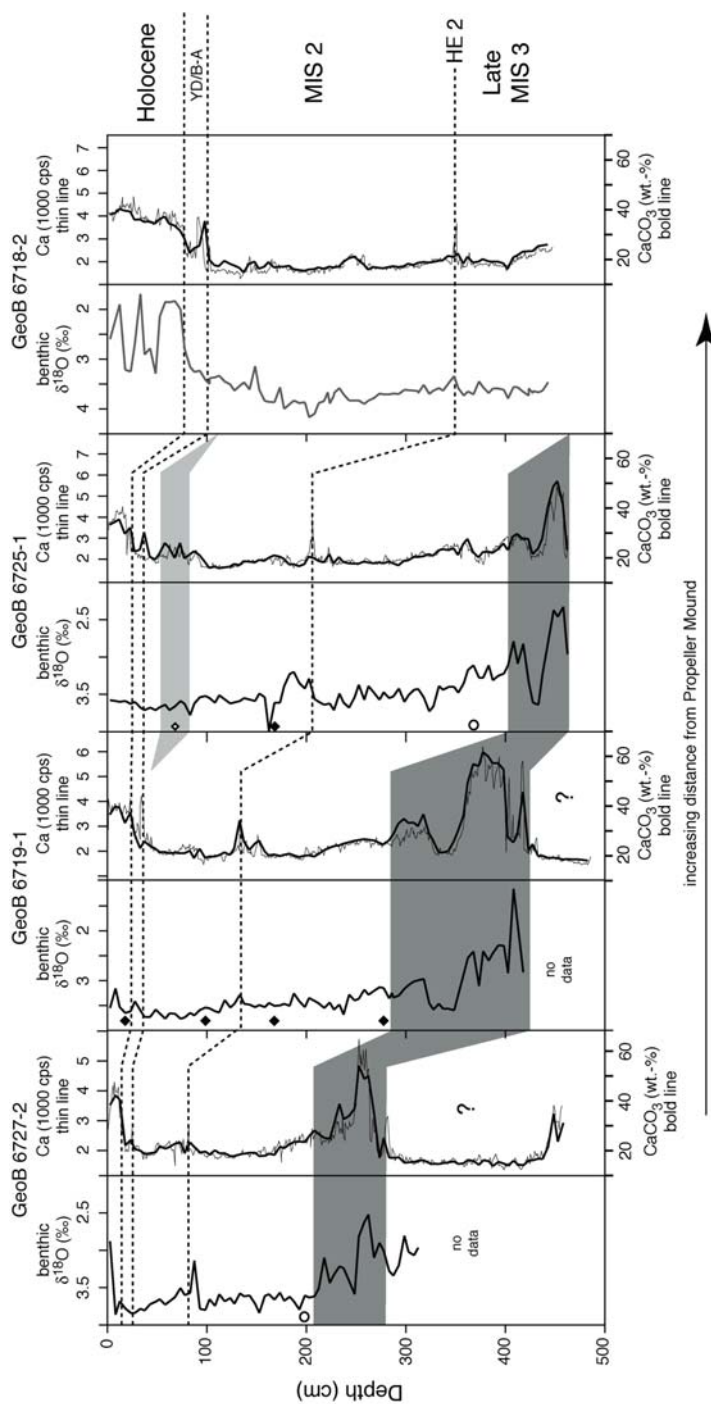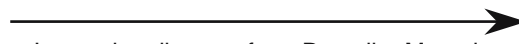
Fig. 2 Benthic stable oxygen isotope data and CaCO₃ content, as well as XRF Ca-counts of sediment cores GeoB 6718-2, GeoB 6719-1, GeoB 6725-1, and GeoB 6727-2. The cores follow the increasing distance from Propeller Mound (from left to right). Stratigraphy is indicated to the right. Dashed lines indicate stratigraphic boundaries between marine isotope stages 1, 2 and 3, based on calibrated scanner data (Dorschel et al. in press), rectangles = AMS ¹⁴C dates, open rectangle = bioturbated AMS ¹⁴C age, open circle = age determination from inter core correlation (Dorschel et al. in press), light grey area = bioturbated sediments, dark grey = reworked sediments (turbidite). Surface of turbidite seems to be slightly older than 31 kyr BP. Below turbidite, no foraminifera were available for stable isotope measurements and AMS ¹⁴C dating

et al. 2000) at the stage boundary of MIS 2 and 3. A significant increase in the carbonate content close to the core top indicates Termination Ia (12 kyr BP) and Ib (10 kyr BP), the onset of the Holocene (Martinson et al. 1987). The latter $CaCO_3$ increase is coherent with a decrease of benthic $\delta^{18}O$ values in cores GeoB 6718-2 and GeoB 6727-2. However, $\delta^{18}O$ values of core GeoB 6725-1 and GeoB 6719-1 remain at high level most certainly due to bioturbation. The resulting sedimentation rate decreases from Late MIS 3 towards the Holocene and increases with increasing distance from Propeller Mound (Table 3).

Table 3 Sedimentation rates of investigated cores

	GeoB 6727-2	GeoB 6719-1	GeoB 6725-1	GeoB 6718-2
	(cm/kyr)	(cm/kyr)	(cm/kyr)	(cm/kyr)
Holocene	1.70	2.50	2.00	7.30
MIS 2	5.50	8.33	15.67	20.42
Late MIS 3	7.86	20.86	27.86	–

Increasing distance from Propeller Mound

Results

Sedimentology of sediment cores around Propeller Mound

The sediments of the three investigated cores GeoB 6718-2, GeoB 6725-1 and GeoB 6727-2 are dominated by dark greyish brown silty clay and olive grey to greyish brown sandy silt (Fig. 3). Greyish brown silty sands occur at the core tops representing Holocene sediments, and at the core base of GeoB 6725-1 and within a section at around 250 cm of core GeoB 6727-2 (Fig. 3). The latter two sections are composed of reworked material with high amounts of coarse lithic grains, drop stones, deep-water coral fragments (mainly *Lophelia pertusa* and *Madrepora oculata*), and shells of molluscs, gastropods, bryozoans, echinoderms, and brachiopods, comprising the associated fauna of the deep-water coral reef ecosystem. The carbonate content of the reworked sediments is much higher reaching 60 %, compared to the Holocene sections (Fig. 2). Between 300-400 cm of core GeoB 6725-1, high numbers of coral fragments indicate a supply of sediments from the nearby mound.

The sedimentary structure revealed from CT images varies from sections dominated by silty and clayey laminae, diffuse structures with no clear lineation, to heavily disorganised sediments. Indications of burrows and bioturbation occur within the coarser sediments of the Holocene, but are also present in the glaciomarine sediments, especially between 50 and 80 cm of core GeoB 6725-1 (Fig. 3). Fining upward cycles describe the turbidite section of core GeoB 6727-2 and GeoB 6725-1.

Legend:

- fining upward sediments
- dropstone, coarse lithic grains (>1000μm)
- coral fragment and associated benthic fauna
- associated benthic fauna
- burrows filled with coarser sediment
- greyish brown silty sand
- olive grey to greyish brown sandy silt
- dark greyish brown silty clay
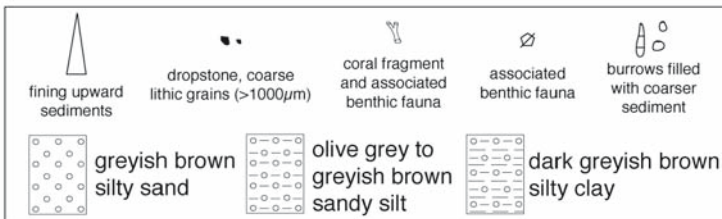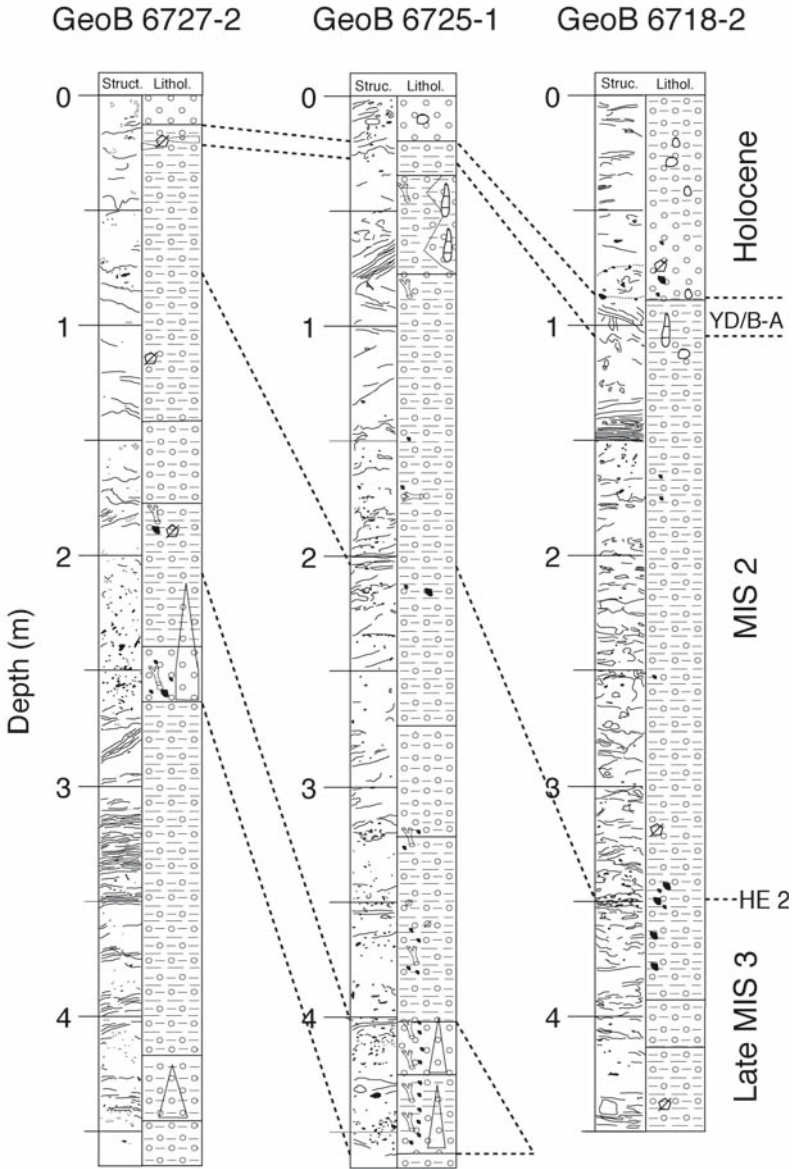
Sediment facies

From the visual examination of cores, computed tomographic imaging, grain-size analysis, and calcium carbonate content, six sediment facies types have been distinguished in the studied cores (Fig. 4). CT images allow identifying different sediment structures and composition. Bright (white) structures occur, when the density is high (e.g., lithic grains, coral fragments), whereas dark sections correspond to lower densities (clayey to silty matrix, higher porosity).
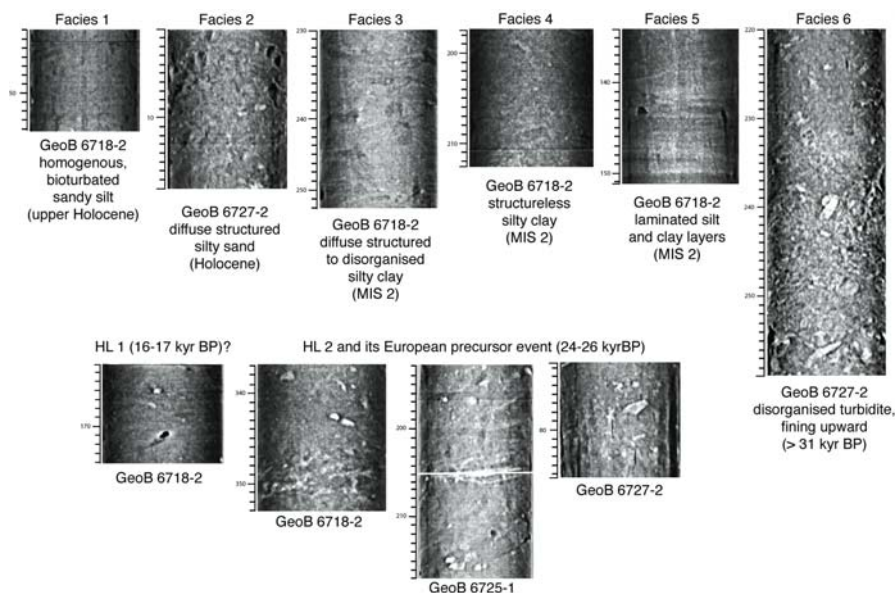
Fig. 4 Sediment facies identified from CT images and visual core description. Within Facies 3 and 4, sections with ice rafted gravel and debris have been identified, corresponding to Heinrich layer 1 and 2 (HL 1 and 2). Scale to the left of CT images is in cm and corresponds to the core depth

Facies 1: homogenous, structureless hemipelagic sandy silt

Facies 1 appears on CT images as homogenous, bioturbated sediment (Fig. 4). It is composed of olive grey to greyish brown sandy silt with relatively high concentrations of foraminiferans. The $CaCO_3$ content is around 40 % (Fig. 2). Silt is the dominating fraction of this sediment (62 wt.-%), while clay and sand have an similar contribution (22 wt.-% and 16 wt.-%). This facies is observed within the late Holocene of core GeoB 6718-2 (top ~70 cm; Fig. 5) and is interpreted as hemipelagic drape sediment, as this sediment has been reported from different sites within the PSB (Coles et al. 1996; De Mol et al. 2002; Huvenne et al. 2002).

Fig. 3 Lithology and sediment structure of cores GeoB 6727-2, GeoB 6725-1 and GeoB 6718-2 from visual core description, CT images, carbonate content and grain-size analyses
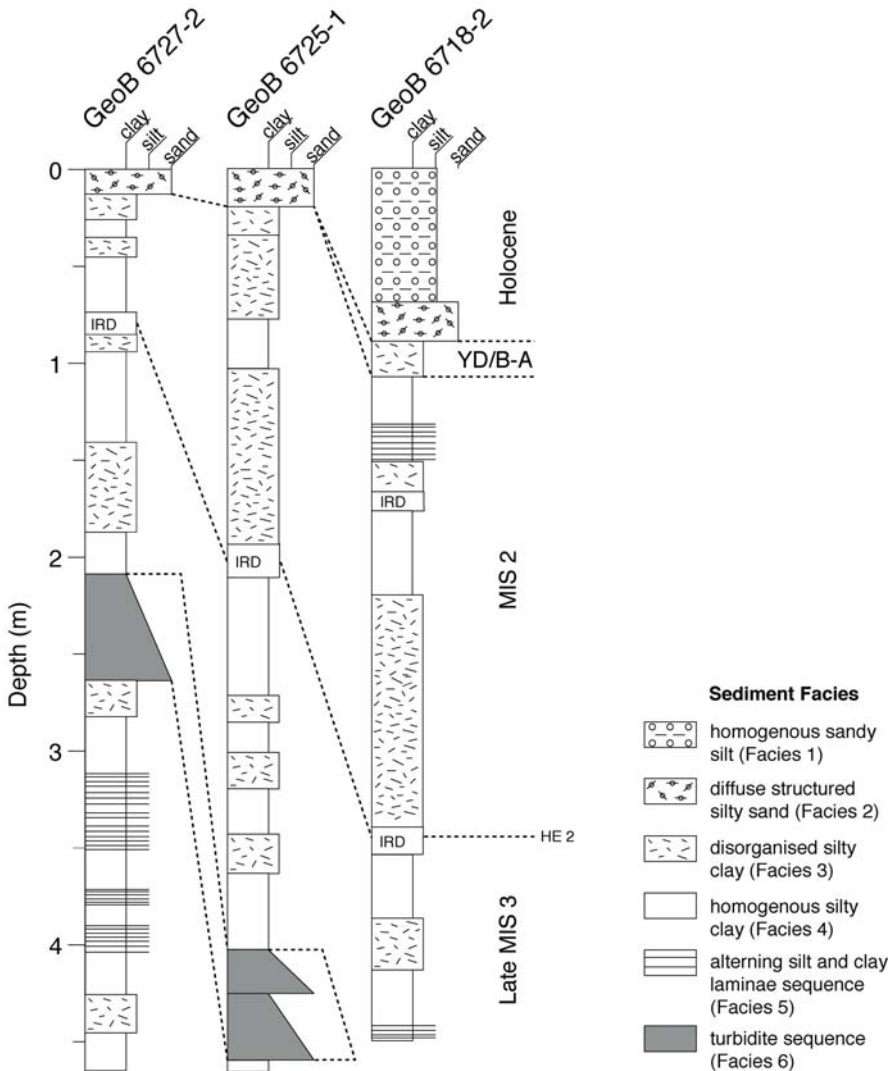
Fig. 5 Downcore record of identified sediment Facies 1-6. The Holocene succession is characterised by Facies 1 and 2. Facies 3 and 4 dominate MIS 2 and Late MIS 3. Alternating silt and clay laminae only occur in core GeoB 6718-2 and below the turbidite (Facies 6) of core GeoB 6727-2

Facies 2: diffuse structured silty sand

Facies 2 describes a diffuse structured silty sand, consisting of strongly bioturbated, hemipelagic silty sand (Fig. 4). The carbonate content varies between 35 % and 45 % (Fig. 2). Sand reaches maximum content of 50 wt.-%, whereas clay is generally below 20 wt.-%. This facies describes the top section of cores GeoB 6727-2 (top 15 cm) and GeoB 6725-1 (top 25 cm), and early Holocene section of

core GeoB 6718-2 (~70-85 cm; Fig. 5). It is interpreted as a hemipelagic contourite sediment, which was probably deposited under a stronger current regime.

Facies 3: diffuse laminated to dis-organised silty clay

Facies 3 consists of intervals with varying thickness (10-120 cm) of diffuse laminated to chaotic, disorganised silty clay (Fig. 4). The carbonate content rarely exceeds 20 % (Fig. 2). The clay content is generally >40 wt.-%, while the sand content lies below 20 wt.-%. Due to its diffuse and disorganised structure, Facies 3 is interpreted as a result from mass transport of fine-grained sediments (slump, debris flow, strong turbidity currents), whether from the shelf or from the mounds. It describes most of MIS 2 and Late MIS 3 (Fig. 5).

Facies 4: structureless silty clay

Facies 4 is a structureless silty clay (Fig. 4), dominated by terrigenous material ($CaCO_3$ content <20 %; Fig. 2). It consists of dark greyish brown clay (40 to 50 wt.-%) with low sand content of <20 wt.-%. In some areas, this facies contains black dots. In deeper environments black coloured bandings occur usually due to the presence of black hydrotroilite (Nelson et al. 1992; Zaragosi et al. 2000) and represent enhanced preservation of organic material due to high sedimentation rate and/or anoxic bottom water conditions (Stow et al. 1996). Facies 4 occurs during MIS 2 and Late MIS 3 and represents the high deposition rate under calm hydrodynamic condition.

Facies 5: laminated silt and clay

At the base of core GeoB 6718-2 and in 150 cm core depth (~14 kyr BP), CT images clearly present laminated sediments (Fig. 4). The carbonate content below 20 % is similar to Facies 3 and 4. These alternating silt and clay laminae have a sharp contact at the base and gradually change into Facies 4. Facies 5 sequences are observed in core GeoB 6718-2 during MIS 2 and 3 and below the turbidite in core GeoB 6727-2. The altering silt and clay laminae have also been reported from the Celtic margin south of the PSB and probably also indicate a fine-grained turbidite facies being deposited by low-density turbidity currents (Zaragosi et al. 2000).

Facies 6: disorganised turbidite sequence

Facies 6 consists of disorganised, coarse-grained sediments (sand content up to 50 wt.-%) with high amounts of coral fragments and shells from bivalves, gastropods and echinoderms, but also of dropstones and coarse lithic grains (Figs. 3, 4). The abundance of fragments and pebbles decreases towards the top of the turbidite, where the sediment gradually turns into Facies 4. The carbonate content is 50 % high at the base and decreases towards the top of the turbidite section to reach similar low values as in Facies 4 (Fig. 2). This facies is interpreted as being deposited by high-density turbidity currents and/or as resulting from mass transport deposits (slump or debris flow). Facies 6 is present in cores GeoB 6727-2 and GeoB 6725-1 (Fig 5). Due to the stratigraphic correlation to other sediment cores, the turbidite is suggested to be slightly older than 31 kyr BP and possibly comprises Ice-Rafted Detritus (IRD) of HE 3 (32.5 to 29.6 kyr BP) as reported from the Celtic margin (Auffret et al. 2002).

Ice-rafted detritus layer

Within Facies 3 and 4, CT images show gravel sized dropstones at the transition from MIS 2 to 3 (24-26 kyr BP; Figs. 3, 5), which most certainly corresponds to HE 2 and the European precursor event (Grousset et al. 2000). High sand content is coherent with the IRD layer of core GeoB 6718-2, but is absent in the other cores. At ~170 cm of core GeoB 6718-2, another horizon containing coarse lithic grains is visible from CT images (Fig 4). Sand content increases slightly from 10 to 20 wt.-%. According to the stratigraphy, this IRD layer may be related to HE 1, but does not occur in the cores located closer to Propeller Mound (Fig. 5).

Silt fraction analysis

Grain-size analysis on fine sediment size (<63 μm) of carbonate-free samples has been proposed to indicate paleocurrent strength intensities (McCave et al. 1995). Sortable silt describes the grain-size range of fraction 10-63 μm, which behaves dominantly noncohesively, whereas grains smaller than 10 μm show a cohesive behavior. Thus, silt coarser than 10 μm displays size sorting in response to hydrodynamic processes and its properties are used to infer current speed.

On samples of core GeoB 6718-2 grain-size analyses were performed on bulk and carbonate-free samples of fraction <63 μm (Fig. 6). The results indicate a similar downcore record for both bulk and lithogenic samples. Differences only occur with respect to their intensity, especially of fraction <10 μm and at the core top in fraction 20-40 μm, which is the result of dissolution of coccoliths and foraminiferan test fragments. However, correlation of both bulk and lithogenic mean sortable silt records present a correlation coefficient of $R^2 = 0.87$ and the records display similar downcore variability (Fig. 6). This pattern is also suggested for cores GeoB 6725-1 and GeoB 6727-2, as they display comparable sediments with similar carbonate contents (Figs. 2, 3). Therefore, all cores will be discussed with respect to their bulk fine fraction distribution, representing sorting of sediment dependent on changes of current strength intensity.

Sedimentary processes may vary from strongly erosive, transport dominated to accumulative, and control the rate of sedimentation. Höppner and Henrich (1999) characterised different sediment types, each related to a different hydrodynamic setting. Type I is characterised by relatively coarse sediments and shows a unimodal distribution within the silt range (Fig. 7). Relatively strong currents remove fine-grained material from the sediment surface and leave behind this sorted, residual sediment. Within the marine milieu, contour currents often produce these sediments. Type II portrays a polymodal distribution, formed under strongly variable bottom current velocities. Decreasing current intensity reduces the ability of water to keep larger particles in suspension, which results into the accumulation of fine material (Type III). Sediment Type III is here divided into Type IIIa and IIIb (Fig. 7). Both show generally fine material of fine-silt spectrum (2-10 μm) and describe accumulated sediments, caused by weak currents. However, Type IIIa has a stronger affinity to slightly coarser sediments, indicating transitional sediments between Type II and Type IIIb. This sediment type is related to in- or decreasing current activity (Fig. 7).
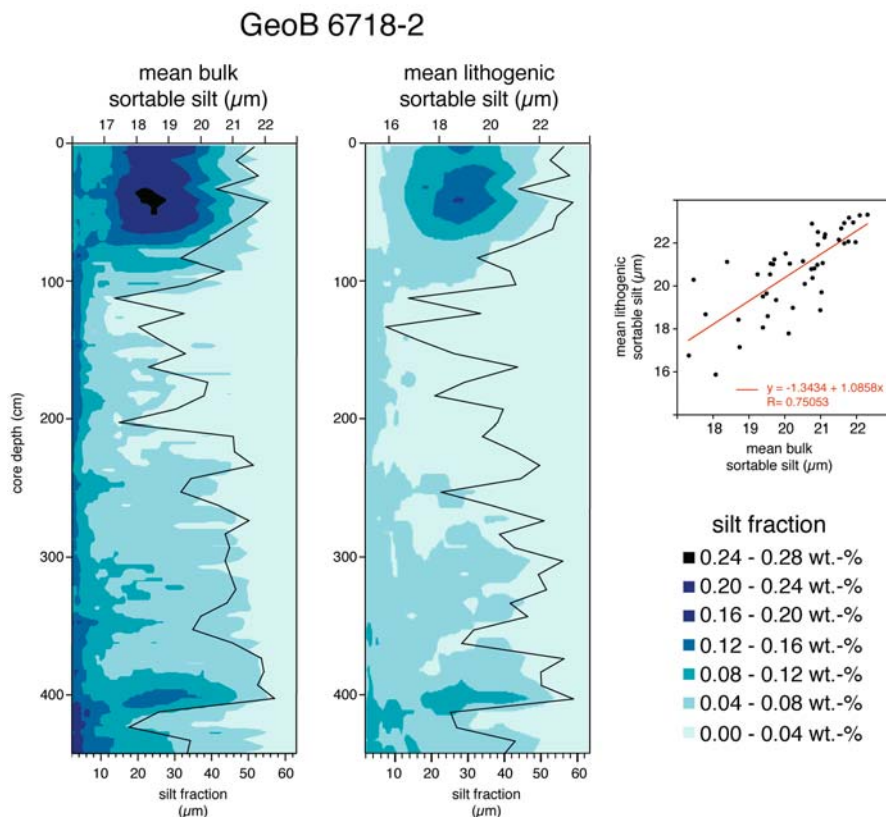
Fig. 6 Comparison of bulk and lithogenic silt fraction analysis of core GeoB 6718-2. Silt spectrum and mean sortable silt present good correlation with $R^2 = 0.87$. Changes in intensity of silt spectrum are the result of removal of $CaCO_3$ (shell fragments of foraminiferans and coccoliths)

The downcore record of the classified sediment Types I to III is illustrated in Figure 8. The base of the turbidite is described by polymodal distributed silt spectrum (Type II), fining upward to accumulated sediments (Type IIIb). The period of Late MIS 3 (31-24 kyr BP) is dominated by accumulation of sediments (Type IIIa and b). An increase towards coarser sediments (sorted and residual, Type I and II) occurs at around 28-29 kyr BP (GeoB 6727-2: 140-180 cm, GeoB 6725-1: 275-315 cm), indicating an increase of the generally weak current regime (Fig. 8). Accumulated sediments dominate MIS 2 implying a weak hydrodynamic regime. A trend to finer sediments occurs at around 18 kyr BP in core GeoB 6718-2 (~220 cm) and GeoB 6725-1 (~130 cm), illustrated by a gradual change from sediment Type IIIa to IIIb. However, this feature is not visible in core GeoB 6727-2 (Fig. 8). A slight increase from Type IIIb to IIIa at around 80 cm in core Geob 6725-1 defines the transition to the bioturbated section. The abrupt change from accumulated sediments to polymodally distributed and residual sediments at Termination Ia is clearly visible
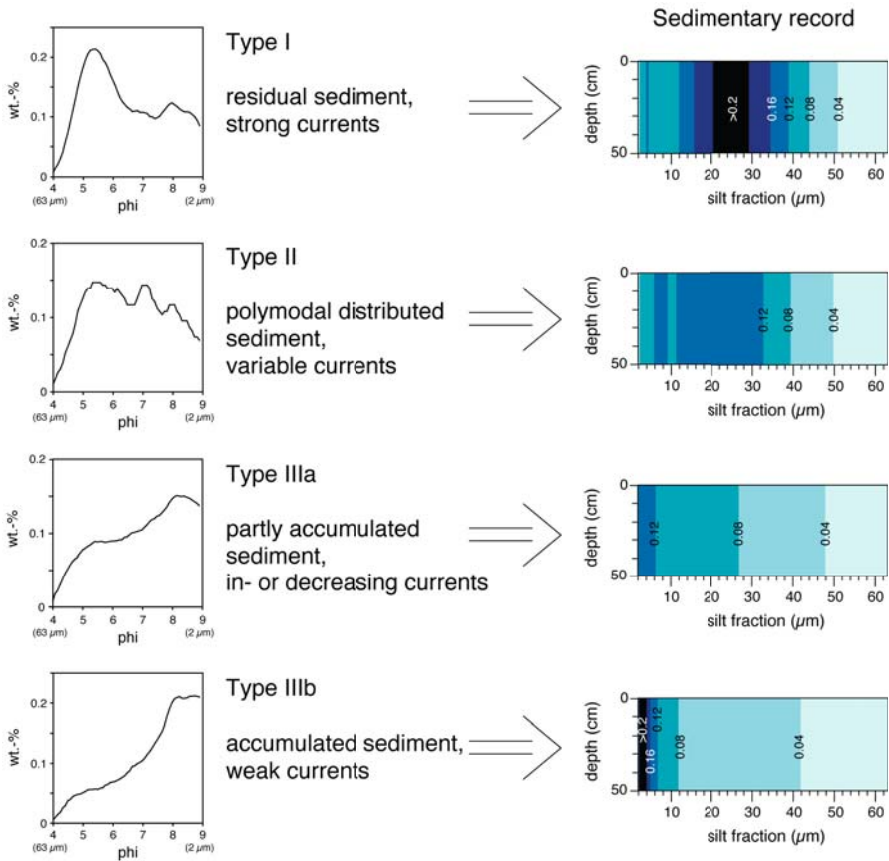
Fig. 7 Characterised sediment types of silt fraction analyses after Höppner and Henrich (1999) and their sedimentary record to the right. The phi-scale corresponds to the negative logarithm to the base 2 of the grain size (in mm). Values in sedimentary record are in wt.-%

in core GeoB 6718-2, indicating an intensified current regime, which persists for the whole Holocene period (Fig. 8).

The mean sortable silt record generally follows the change between accumulated and polymodally distributed to residual sediments with an increasing or decreasing signature between 16 and 25 μm (Fig. 8). In all three cores the mean sortable silt record displays similar variability:

(1)   an increase from the top of the turbidite to maximum values of ~24 μm at 140-180 cm (GeoB 6727-2), and 275 to 305 cm (GeoB 6725-1), corresponding to ~28-29 kyr BP,

(2)   a decrease towards the stage boundary MIS 2/3 (GeoB 6727-1, GeoB 6725-1),

(3)   an increase to a maximum of 24-25 μm at ~18 kyr BP (GeoB 6727-2: ~50 cm, GeoB 6725-1: ~130 cm, GeoB 6718-2: 230 cm),
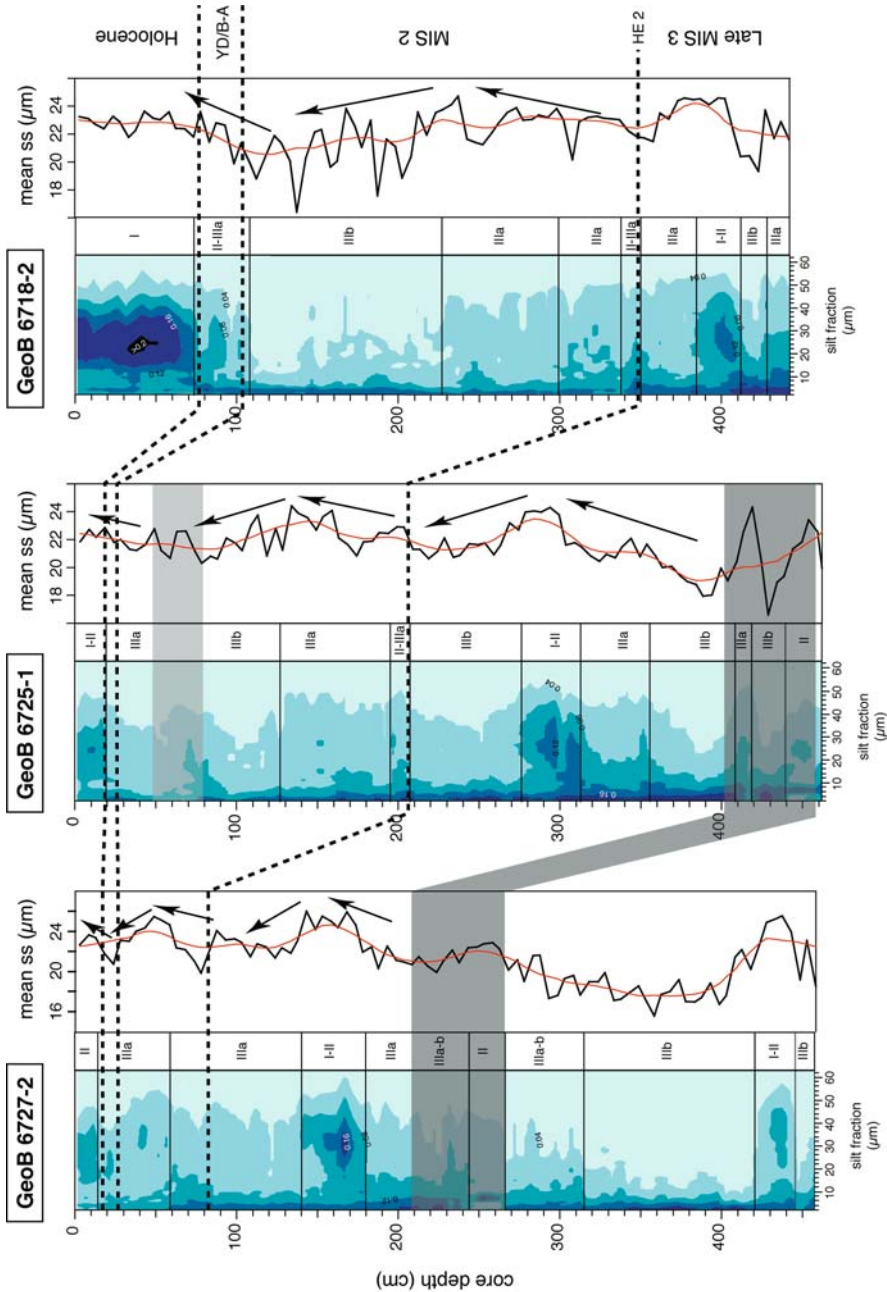
Fig. 8 Downcore record of silt fraction (in wt.-%; see Fig. 7) and the corresponding Types I - III (after Höppner and Henrich 1999). Mean sortable silt (black curve) and the weighted mean (20 %, red curve) indicate an in- or decrease in current strength intensity (arrows). Dark grey area = turbidite, light grey = bioturbation, stratigraphic units are illustrated to the right

(4)   a decrease towards the Younger Dryas/Bølling-Allerød,
(5)   and finally an increase towards the Holocene, where the values remain at one
        level (e.g., GeoB 6718-1: top 80 cm).

Discussion

Irish ice sheet advance and shelf erosion during Late MIS 3

Coarse-grained turbidites have been suggested as being derived from an ice-proximal glaciomarine environment and are possibly associated with high discharges of subglacial meltwater. They are reported from the Hebrides Shelf (Knutz et al. 2001) and from the Celtic margin (Zaragosi et al. 2000; Auffret et al. 2002). Their presence may thus indicate periods when glacial ice was grounded on the shelf margins.

Before 30 kyr BP, Ireland was largely ice-free and interstadial conditions prevailed (Jones and Keen 1993). Glaciers may have existed in western Scotland and Northern Ireland (Bowen 1999) but were probably grounded above the marine limit. However, Knutz et al. (2001) reported variable deposition of quartz-rich IRD between 45 and 30 kyr BP suggesting glaciomarine conditions were intermittently established along the NW British margin. According to McCabe (1987), Irish inland ice was rapidly advancing after 30 ^{14}C kyr BP ($\sim$33.5 kyr BP), coherent with subarctic, tundra-like, open vegetation of the Derryvree cold phase (30-35 ^{14}C kyr; Jones and Keen 1993). A sea-level decrease and worsened climatic conditions are reported for the western margin of Ireland during Late MIS 3 (Auffret et al. 2002).

The turbidite section in core GeoB 6725-1 and GeoB 6727-2 probably indicates a first advance of the BIIS. High carbonate contents (>50 %) of the reworked material implies the deposition of interglacial sediments, which is also suggested by high abundance of benthic foraminifera representing an interglacial assemblage (Rüggeberg et al. in press). These sediments must have been eroded from (a) the exposed shallow shelves due to the low sea-level stand and a first advance of the glaciers onto the shelf, or (b) from the nearby Propeller Mound. The occurrence of coral fragments within the turbidite section accounts for a sediment source from the mound. However, epibenthic foraminifera typical for the deep-water coral ecosystem are scarce and the assemblage is similar to species describing the Holocene section of core GeoB 6725-1 (Rüggeberg et al. subm.).

High abundance of IRD within the turbidite may correspond to HE 3 (32.5 to 29.6 kyr BP). Isotopic analysis of the coarse lithic fraction from the Celtic margin indicates a presumably European origin of HE 3 deposits along the western margin of the British Isles (Auffret et al. 2002). The general ice flow on Ireland accounts for high terrigenous fluxes from Ireland, across Galway Bay and into the PSB (Fig. 9; Eyles and McCabe 1989; Jones and Keen 1993). Hence both IRD and reworked interglacial sediments indicate that glaciers had reached the western margin of the Irish shelf at a time that correlates with HE 3. Therefore, the turbidite represents a release of eroded sediments (mass wasting) by a first advance of glaciers onto the
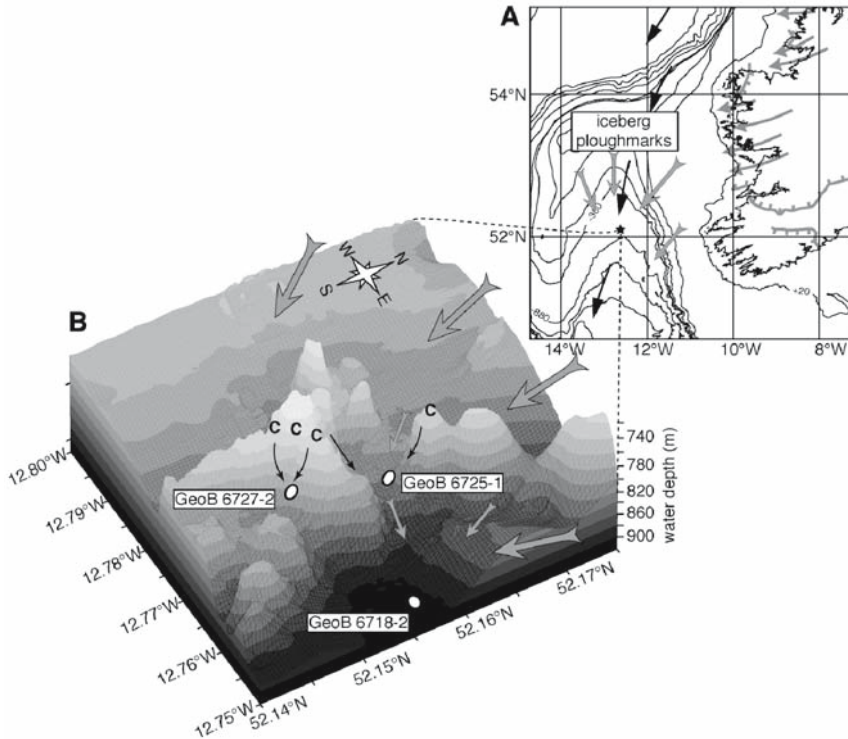
Fig. 9 A Map of the Porcupine Seabight for the last glacial stage. Ice limits on Ireland (grey lines on Ireland) and general ice flow across the Galway Bay (thin grey arrows) are from Eyles and McCabe (1989) and Jones and Keen (1993). The general southward flow of surface waters is indicated with black arrows (Sarnthein et al. 1995). Big grey arrows correspond to sediment transport (shelf erosion, turbidity currents). **B** Propeller Mound, viewed from the SE, with indicated core sites, flow path of turbidity currents and gravity flows (grey arrows) and the erosion paths from the mound contributing coral fragments to the off-mound sites. V.E. ≈ 1:3

shelf. However, the occurrence of coral fragments in the turbidite layer suggests, that strong turbidity currents also had an effect on the elevated mounds with a removal of sediments from them (Fig. 9). It seems, that this turbidite facies is a result of mass waste from both the elevated mounds and the Irish Mainland shelf.

The glaciomarine environment was established after the first advance of the Irish ice sheet onto the Irish shelf. Sediments covering the period of Late MIS 3 (~31-24 kyr BP) are described by homogenous to laminated and disorganised silty clays (Facies 3-5) indicating a weak benthic current regime interrupted by phases of fine-grained debris flow or turbidity currents (Fig. 5). The substantial high sedimentation rate further indicates an enormous sediment supply from the shelf into the PSB. During this period, sea level was decreasing and the climatic conditions worsened (Auffret et al. 2002), while the BIIS propagated to its maximum extent between

24 and 20 ^{14}C kyr BP (McCabe 1987). Additional information supporting strong shelf erosional processes is indicated by displaced benthic foraminiferan species preferably living in an estuarine and near-glacial shelf environment.

Towards the transition between MIS 3 and 2, the double peak in XRF Ca-records (Fig. 2), as well as abundant IRD (Fig. 4) indicate the deposition related to HE 2 and its European precursor event (Grousset et al. 2000; Richter et al. 2001). The abundant IRD is related to the calving of icebergs from Irish glaciers, which started significantly at ~25 kyr BP (Auffret et al. 2002; Siegert and Dowdeswell 2002). Richter et al. (2001) reported an increased supply of detrital carbonates during HE 2 and MIS 2 at Feni Drift in the Rockall Trough and argued that this site was dominantly effected by British-Irish detrital IRD input, eroded from the Carboniferous limestone formations of Ireland. An increased input of detrital carbonates of Irish origin is assumed for the PSB, indicated by peaks in the Ca counts (Fig. 3).

Redistribution of glacial sediments during MIS 2

After HE 2, the sediments around Propeller Mound are dominated by disorganised silty clays (Facies 3; Fig. 5) indicating abundant gravity flows and turbidity currents during early MIS 2. The sedimentation rate decreased from 17 to 28 cm/kyr for Late MIS 3 to 5-20 cm/kyr during MIS 2 (Table 3). According to McCabe (1987), the maximum expansion of the BIIS was reached between 24-20 ^{14}C kyr BP, coherent with the onset of iceberg calving from British glaciers at ~25 kyr BP (Fig. 9; Siegert and Dowdeswell 2002). The final position of the BIIS without any indications of a further advance to the southwest resulted in an abrupt decrease of sediments supplied into the PSB. Sea level was still decreasing to its maximum lowstand of 120 m below present level at ~17-18 kyr BP (Labeyrie et al. 1987; Fairbanks 1989; Auffret et al. 2002), while the Irish ice sheet margin retreated markedly from 21-18 kyr BP (McCabe and Clark 1998).

As a consequence, glacial material had been exposed to erosion, documented in an important phase of shelf sediment erosion at the Celtic margin (Auffret et al. 2002). The sediment cores off Propeller Mound show an increase in mean sortable silt to approx. 18-19 kyr BP, which portrays the increase in abundant turbidity currents (Fig. 8). A change to fine-grained, accumulated sediments (Facies 4, Type IIIb) indicates a decline in sediment erosion from the shelf and/or mound (decreasing currents) at the sea-level lowstand, when the glaciers on SW Ireland were already above the marine limit (Eyles and McCabe 1989).

The period of deglaciation is expressed in decreasing terrigenous fluxes along the Celtic margin (16.7-11 kyr BP; Auffret et al. 2002), whereas Knutz et al. (2001) reported of a re-advance of the western sector of British Ice Sheet further north with renewed gravity flow sedimentation and a clearly defined IRD horizon, corresponding to HE 1 (16-17 kyr BP). Only in core GeoB 6718-2 a layer with IRD occurs at ~170 cm (Fig. 5), indicating a release of terrigenous material by icebergs, probably indicating HE 1 deposits. However, an advance of glaciers onto the Irish shelf is not reported after 19 kyr BP (Eyles and McCabe 1989). The low abundance of *E. excavatum* supports this indication by an absence of a near-glacial

environment along the Irish Mainland shelf (Rüggeberg et al. subm.) Therefore, the IRD layer in core GeoB 6718-2 seems to be a result of the southward transport of IRD by icebergs, as indicated by N-S trending iceberg plough marks on Slyne Ridge (Fig. 9; Games 2001).

Late MIS 2 deposition around Propeller Mound is described by the renewed establishment of turbiditic supply (Facies 3 and 5; Fig. 5), indicating the reworking of shelf sediments by the rising sea level. This sea-level rise started at ~18 kyr BP and reached its highstand at ~6 kyr BP (Clark et al. 1999; Siddall et al. 2003). However, the shelf erosion during late MIS 2 was probably not as high as for Late MIS 3, as shallow shelf dwelling benthic foraminiferans have low abundance during MIS 2 (Rüggeberg et al. subm.).

Holocene and present-day sedimentary setting around Propeller Mound

During Termination I, a change from glaciomarine to hemipelagic deposition is indicated by an increase of the sediment grain-size (Facies 3 (IIIa) to Facies 2 (I-II); Figs. 5, 8), an increase in the carbonate content (Fig. 3), as well as a change towards stronger currents, expressed in an increase of the mean sortable silt record (Fig. 8). The oceanographic setting changed remarkably with the establishment of the present-day hydrodynamic regime. The Polar Front moved northward across the PSB (Jones and Keen 1993) and intermediate water masses with a southern source (ENAW, MOW) entered the PSB. The decrease in sedimentation rate from 5-20 cm/kyr during MIS 2 to 1.7-7.3 cm/kyr for the Holocene (Table 3), portrays the strong current regime at intermediate depths (White in press) with the deposition of polymodally distributed to residual silty sands (Facies 1 and 2; Fig. 5).

In core GeoB 6718-2, Facies 2 probably indicates the reintroduction of ENAW and MOW during the onset of MIS 1 (Fig 5). The top 70 cm of this core is described by Facies 1, which is composed of slightly finer material. Masson et al. (2003) described a similar sediment in areas of depressions in the vicinity of the Darwin Mound, NE Rockall Trough. With sea-floor photographs they confirmed that this sediment accumulates in areas where bottom currents are weak and generally lack bedforms typical in areas of strong current activity. GeoB 6718-2 is situated in a small basin further off the mound (Fig. 9), where the sea-floor is also characterised by heavily bioturbated sediments. Towards the foot of Propeller Mound, the Holocene cover thins out and the sediments become coarser (Figs. 3-5, 8). According to White (in press), the carbonate mounds themselves generate a rough topography that induces localised strong currents. Indeed, observations using the ROV CHEROKEE during RV POSEIDON cruise 292 indicated strongest currents occurring at the foot of the mound, with increased abundance of IRD boulders and outcropping hardgrounds (Freiwald and Shipboard Party 2002). Therefore, the ~20 cm Holocene cover of GeoB 6725-1 and GeoB 6727-2 indicates the influence of generally stronger currents near the mound, generating this contourite sand sheet. A similar Holocene layer is described by Masson et al. (2003) indicating maximum velocities of >25-30 cm s^{-1}.

Conclusions

Sea-level evolution and climatic conditions have been the main controls on the sedimentary system at the northern Porcupine Seabight during the past ~31 kyr BP, which are summarised in Table 4. A first advance of the Irish Ice Sheet onto the Irish Mainland shelf led to the deposition of thick turbidite layer of reworked interglacial sediments. This event also had an erosional impact on the carbonate mounds, as abundant coral fragments are embedded within the turbidite layer. IRD probably indicates the conjunction with HE 3.

Table 4 Summary of the Paleoenvironmental setting in the northern Porcupine Seabight

Period	Age*	"What do we see?"	"Why do we see it?"
Holocene	0-10	Silty sands (Facies 1 and 2), low sedimentation rate (1.7-7.3 cm/kyr)	Present-day oceanographic setting with a strong hydrodynamic regime
Younger Dryas/ Bølling-Allerød	10-12	Change from glaciomarine to hemipelagic deposition, increase in mean sortable silt, grain-size and change from accumulated to current-induced sedimentation	Polar Front moved across PSB, introduction of ENAW and MOW with strong hydrodynamic signature at intermediate depths, sea-level increase
MIS 2	12-17	IRD deposit (GeoB 6718-2, HE 1?), increasing turbidity currents	Increasing sea level during deglaciation of BIIS
	17-18	Quiet sedimentary pattern (Facies 4)	Maximum sea-level lowstand (-120 m)
	18-24	High sedimentation rate (5-20cm/kyr) of abundant gravity flow and turbidity current deposition (Facies 3)	Decreasing sea level, erosion of shelf and/or mound sediments, retreat of Irish Ice Sheet above marine limit
Late MIS 3	24-31	very high sedimentation rates (17 to 28 cm/kyr) with abundant gravity flows and turbidity currents (Facies 3 and 4), establishment of glaciomarine environment	Further advance of Irish Ice Sheet to maximum extent at ~25 kyr BP, coherent with onset of iceberg calving and HE 2 deposition, decreasing sea level, strong shelf erosion
	>31	release of turbidite (Facies 6) with eroded (interglacial) sediments and abundant coral fragments	First advance of the Irish Ice Sheet onto the shelf, turbidity currents remove sediments from mounds

* in kyr BP; references within text

Late MIS 3 and MIS 2 deposition is essentially controlled by sea-level fluctuations and the further advance of the BIIS, inducing shelf erosion and releasing turbidity currents and gravity flows. During the terminations and the onset of the Holocene the sedimentation had a pronounced current induced signature, indicating the introduction of the present-day strong hydrodynamic regime at intermediate depths. The decreasing trend of sedimentation rate towards the Propeller Mound for the last glacial period and the Holocene suggests that currents (turbidity currents, gravity flows, bottom currents) had a generally stronger impact on the sediment accumulation at the mound base.

Acknowledgements

References

Akhmetzhanov AM, Kenyon NH, Nielsen T, Habgood E, Ivanov MK, Henriet J-P, Shashkin P (2001) Deep-sea bottom current depositional systems with active sand transport on the North-Eastern Atlantic Margin. IOC Workshop Rep 175, UNESCO, p 11

Auffret G, Zaragosi S, Dennielou B, Cortijo E, Van Rooij D, Grousset F, Pujol C, Eynaud F, Siegert M (2002) Terrigenous fluxes at the Celtic margin during the last glacial cycle. Mar Geol 188: 79-108

Bowen DQ (1999) Only four major 100-ka glaciations during the Bruhnes Chron? Int J Earth Sci 88: 276-284

Clark PU, Alley RB, Pollard D (1999) Northern Hemisphere ice-sheet influences on global climate change. Science 286: 1104-1111

Coles GP, Ainsworth NR, Whatley RC, Jones RW (1996) Foraminifera and Ostracoda from Quaternary carbonate mounds associated with gas seepage in the Porcupine Basin, offshore western Ireland. Rev Espan Micropaleont 28: 113-151

De Mol B (2002) Development of coral banks in Porcupine Seabight (SW Ireland) - A multidiscipinary approach. PhD Thesis, Univ Gent, 363 pp

De Mol B, Van Rensbergen P, Pillen S, Van Herreweghe K, Van Rooij D, McDonnell A, Huvenne V, Ivanov M, Swennen R, Henriet J-P (2002) Large deep-water coral banks in the Porcupine Basin, southwest of Ireland. Mar Geol 188: 193-231

Dorschel B, Hebbeln D, Rüggeberg A, Dullo W-Chr (in press) Carbonate budget of a deep-water coral mound: Propeller Mound, Porcupine Seabight. Int J Earth Sci

Eyles N, McCabe AM (1989) The Late Devensian (<22,000 BP) Irish Sea Basin: the sedimentary record of a collapsed ice sheet margin. Quaternary Sci Rev 8: 307-351

Fairbanks G (1989) A 17 000-year glacio-eustatic sea level record, influence of glacial melting rates on the Younger Dryas event and deep-ocean circulation. Nature 342: 637-642

Frederiksen R, Jensen A, Westerberg H (1992) The distribution of the scleractinian coral *Lophelia pertusa* around the Faroe islands and the relation to internal tidal mixing. Sarsia 77: 157-171

Freiwald A (1998) Geobiology of *Lophelia pertusa* (Scleractinia) reefs in the North Atlantic. Habilitation thesis, Bremen Univ, 116 pp

Freiwald A, Shipboard Party (2002) Cruise Report RV POSEIDON Cruise 292, Reykjavik - Galway, 15th July - 4th August 2002, 84 pp

Freiwald A, Wilson JB (1998) Taphonomy of modern deep, cold-temperate water coral reefs. Hist Biol 13: 37-52

Freiwald A, Wilson JB, Henrich R (1999) Grounding Pleistocene icebergs shape Recent deep-water coral reefs. Sediment Geol 125: 1-8

Freiwald A, Dullo W-Chr, Shipboard Party (2000) Cruise Report RV POSEIDON Cruise 265, Thorshavn - Galway - Kiel, 13th September - 1st October 2000, 65 pp

Games KP (2001) Evidence of shallow gas above the Connemara oil accumulation, Block 26/28, Porcupine Basin. In: Shannon PM, Haughton PDW, Corcoran DV (eds) The Petroleum Exploration of Ireland's Offshore Basins. Geol Soc Spec Publ 188: 361-373

Grousset FE, Pujol C, Labeyrie L, Auffret G, Boelaert A (2000) Were the North Atlantic Heinrich events triggered by the behavior of the European ice sheets? Geology 28: 123-126

Hill AE, Mitchelson-Jacob EG (1993) Observations of a poleward-flowing saline core on the continental slope west of Scotland. Deep-Sea Res I 40: 1521-1527

Hovland M, Mortensen PB (1999) Norske korallrev og prosesser i havbunnen. John Grieg Forlag

Hovland M, Croker PF, Martin M (1994) Fault-associated seabed mounds (carbonate knolls?) off western Ireland and north-west Australia. Mar Petrol Geol 11: 232-246

Höppner R, Henrich R (1999) Kornsortierungsprozesse am argentinischen Kontinentalhang anhand von Siltkorn-Analysen. Zbl Geol Paläont, I, 1997: 897-905

Huthnance JM (1995) Circulation, exchange and water masses at the ocean margin: the role of physical processes at the shelf edge. Prog Oceanogr 35: 353-431

Huthnance JM, Gould WJ (1989) On the Northeast Atlantic slope current. In: Neshyba SJ (ed) Poleward flows along eastern ocean boundaries. Coastal Estuarine Stud 34: 76-81

Huvenne VAI, Blondel P, Henriet, J-P (2002) Textural analyses of sidescan sonar imagery from two mound provinces in the Porcupine Seabight. Mar Geol 189: 323-341

Jansen JH, Van der Gaast SJ, Koster B, Vaars AJ (1998) CORTEX, a shipboard XRF-scanner for element analyses in split sediment cores. Mar Geol 151: 143-153

Joint I, Wollast R, Chou L, Batten S, Elskens M, Edwards E, Hirst A, Burkill P, Groom S, Gibb S, Miller A, Hydes D, Dehairs F, Antia A, Barlow R, Rees A, Pomroy A, Brockmann U, Cummings D, Lampitt R, Loijens M, Mantoura F, Miller P, Raabe T, Alvarez-Salgado X, Stelfox C, Woolfenden J (2001) Pelagic production at the Celtic Sea shelf break. Deep-Sea Res II 48: 3049-3081

Jones RL, Keen DH (1993) Pleistocene Environments in the British Isles. Chapman & Hall, London, 368 pp

Kenyon NH, Akhmetzhanov AM, Wheeler AJ, Van Weering TCE, De Hass H, Ivanov MK (2003) Giant carbonate mud mounds in the southern Rockall Trough. Mar Geol 195: 5-30

Knutz PC, Austin WEN, Jones EJW (2001) Millennial-scale depositional cycles related to British Ice Sheet variability and North Atlantic paleocirculation since 45 kyr B.P., Barra Fan, U.K. margin. Paleoceanography 16: 53-64

Labeyrie LD, Duplessy J-C, Blanc PL (1987) Variations in mode of formation and temperature of oceanic deep-waters over the past 125 000 years. Nature 327: 477-482

Martinson DG, Pisias NG, Hays JD, Imbrie J, Moore TC, Shackleton NJ (1987) Age dating and the orbital theory of the ice ages: development of a high resolution 0 to 300 000-year chronostratigraphy. Quaternary Res 27: 1-29

Masson DG, Bett BJ, Billett DSM, Jacobs CL, Wheeler AJ, Wynn RB (2003) The origin of deep-water, coral-topped mounds in the northern Rockall Trough, Northeast Atlantic. Mar Geol 194: 159-180

McCabe AM (1987) Quaternary deposits and glacial stratigraphy in Ireland. Quaternary Sci Rev 6: 259-299

McCabe AM, Clark PU (1998) Ice-sheet variability around the North Atlantic Ocean during the last deglaciation. Nature 392: 373-377

McCave IN (2002) Sedimentary settings on continental margins - an overview. In: Wefer G, Billett D, Hebbeln D, Jørgensen BB, Schlüter M, Van Weering T (eds) Ocean Margin Systems. Springer, Berlin Heidelberg, pp 1-14

McCave IN, Manighetti B, Robinson SG (1995) Sortable silt and fine sediment size/composition slicing: Parameters for paleocurrent speed and paleoceanography. Paleoceanography 10: 593-610

McCave IN, Hall IR, Antia AN, Chou L, Dehairs F, Lampitt RS, Thomsen L, van Weering TCE, Wollast R (2001) Distribution, composition and flux of particulate material over the European margin at 47°-50°N. Deep-Sea Res II 48: 3107-3139

Nadeau MJ, Schleicher M, Grootes P, Erlenkeuser H, Gottolong A, Mous DJW, Sarnthein M, Willkomm N (1997) The Leibnitz-Labor AMS Facility at the Christian-Albrechts University, Kiel, Germany. Nucl Instrum Methods Phys Res 123: 22-30

Nelson CH, Twichell DC, Schwab WC, Lee HJ, Kenyon NH (1992) Upper Pleistocene turbidite sand beds and chaotic silt beds in the channelized, distal, outer-fan lobes of the Mississippi fan. Geology 20: 693-696

Pingree RD, LeCann B (1989) Celtic and Amorican slope and shelf residual currents. Prog Oceanogr 23: 303-338

Pingree RD, LeCann B (1990) Structure, strength and seasonality of the slope currents in the Bay of Biscay region. J Mar Biol Assoc UK 70: 857-885

Pollard RT, Griffiths MJ, Cunningham SA, Read JF, Perez FF, Rios AF (1996) Vivaldi 1991 - a study of the formation, circulation and ventilation of Eastern North Atlantic Water. Prog Oceanogr 37: 167-192

Richter TO, Lassen S, Van Weering TCE, De Haas H (2001) Magnetic susceptibility patterns and provenance of ice-rafted material at Feni Drift, Rockall Trough: implications for the history of the British-Irish ice sheet. Mar Geol 173: 37-54

Rogers AD (1999) The biology of *Lophelia pertusa* (Linnaeus 1758) and other deep-water reef forming corals and impact from human activities. Int Rev Hydrobiol 84: 315-406

Rüggeberg A, Dorschel B, Dullo W-Chr, Hebbeln D (subm.) Benthic foraminiferal assemblages from Propeller Mound, northern Porcupine Seabight. Mar Micropaleont

Rüggeberg A, Dorschel B, Dullo W-Chr, Hebbeln D (in press) Environmental changes and growth history of a cold-water carbonate mound (Propeller Mound, Porcupine Seabight). Int J Earth Sci

Sarnthein M, Jansen W, Weinelt M, Arnold M, Duplessy J-C, Erlenkeuser H, Flatøy A, Johannessen G, Johannessen T, Jung S, Koc N, Labeyrie L, Maslin M, Pflaumann U, Schulz H (1995) Variations in Atlantic surface ocean paleoceanography, 50°-80°N: A time-slice record of the last 30,000 years. Paleoceanography 10: 1063-1094

Siddall M, Rohling EJ, Almogi-Labin A, Hemleben C, Meischner D, Schmelzer I, Smeed DA (2003) Sea-level fluctuations during the last glacial cycle. Nature 423: 853-858

Siegert MJ, Dowdeswell JA (2002) Late Weichselian iceberg, surface-melt and sediment production from the Eurasian Ice Sheet: results from numerical ice-sheet modelling. Mar Geol 188: 109-127

Stow DAV, Reading HG, Collinson JD (1996) Deep seas. In: Reading HG (ed) Sedimentary environments: Processes, Facies and Stratigraphy. Blackwell, Oxford, pp 385-453

Stuiver M, Reimer PJ (1993) Extended ^{14}C data base and revised CALIB 3.0 ^{14}C age calibration program. Radiocarbon 35: 215-230

Stuiver M, Reimer PJ, Braziunas TF (1998) (revised dataset). Radiocarbon 40: 1127-1151

Teichert C (1958) Cold- and deep-water coral banks. AAPG Bull 42: 1064-1082

Van Aken HM (2000) The hydrography of the mid-latitude northeast Atlantic Ocean II: The intermediate water masses. Deep-Sea Res I 47: 789-824

Van Rooij D, De Mol B, Huvenne V, Ivanov M, Henriet J-P (2003) Seismic evidence of current-controlled sedimentation in the Belgica mound province, upper Porcupine slope, southwest of Ireland. Mar Geol 195: 31-53

Voelker AHL, Sarnthein M, Grootes PM, Erlenkeuser H, Laj C, Mazaud A, Nadeau M-J, Schleicher M (1998) Correlation of marine ^{14}C ages from the Nordic Seas with the GISP2 isotope record: implications for radiocarbon calibration beyond 25 ka BP. Radiocarbon 40: 517-534

White M (in press) The hydrography of the Porcupine Bank and Sea Bight and associated carbonate mounds. Int J Earth Sci

White M, Bowyer P (1997) The shelf-edge current north-west of Ireland. Ann Geophys 15: 1076-1083

Zaragosi S, Auffret GA, Faugeres J-C, Garlan T, Pujol C, Cortijo E (2000) Physiography and Recent sediment distribution of the Celtic Deep-Sea Fan, Bay of Biscay. Mar Geol 169: 207-237

Deep-water corals of the northeastern Atlantic margin: carbonate mound evolution and upper intermediate water ventilation during the Holocene

Norbert Frank[1], Audrey Lutringer[1], Martine Paterne[1], Dominique Blamart[1], Jean-Pierre Henriet[2], David van Rooij[2], Tjeerd C. E. van Weering[3]

[1] Laboratoire des Sciences du Climat et de l'Environnement (LSCE) Unité mixte de Recherche CEA-CNRS, Bât. 12, Avenue de la Terrasse, F-91198 Gif-sur-Yvette Cedex, France
(Norbert.Frank@lsce.cnrs-gif.fr)
[2] Renard Centre of Marine Geology, Gent University, Krijgslaan 281, S8, B-9000 Gent, Belgium
[3] Koninklijk Nederlands Instituut voor Onderzoek der Zee (NIOZ), P.O. Box 59, NL-1790 AB Den Burg, Texel, The Netherlands

Abstract. We present combined ^{230}Th/U and ^{14}C dating on deep-water corals from the northeastern North Atlantic in order to investigate coral growth and sedimentation on carbonate mounds, as well as past changes of intermediate water ventilation. Within European projects GEOMOUND and ECOMOUND reef forming *Lophelia pertusa* deep-water corals were raised from intermediate depth (~610 to 888 m bsl) from top of carbonate mounds at southeast Rockall Bank and at Porcupine Seabight. XRD analyses, δ^{234}U, and ^{230}Th/^{232}Th indicate negligible alteration of the investigated corals, i.e. open system U-series behavior. ^{230}Th/U ages from coral specimens of the uppermost coral sequence of the investigated mounds range from today to 10,950 CAL yr BP, i.e. coral growth during the Holocene. A modern *Lophelia* gave a ^{230}Th/U age of 1983±6 AD, close to the date of collection in 2001 AD. Deep-water coral growth is the driving process of sediment accumulation on the summit of carbonate mounds, with sediment accumulation rates in the order of ~0.3 mm yr^{-1}. However, coral growth is discontinuous and irregular, and complete coral sequences are frequently altered (dissolved) likely due to organic matter consumption by oxidizing pore fluids. Mound top sediments indicate the presence of corals over several glacial/interglacial cycles, but corals of glacial origin could not be identified on the investigated mounds.

Upper intermediate water Δ^{14}C and reservoir ages (R) were reconstructed on 11 deep-water corals. Δ^{14}C of -13±7 ‰ obtained on the coral dated to 1983 AD shows a significant lower value than the ones previously reported for the late 90's (+27 ‰), but in agreement with seawater measurements performed in the early 80's.

Between 10,950 CAL yr BP and 420 CAL yr BP, R exhibit variations between as low as 240 ± 110 yrs (at 5,440 CAL yr BP) to up to 750 ± 230 yrs (at 10,450 CAL yr BP). However, most of the data (8 out of 10 corals) yield R between 400 and 600 yrs similar to previously reported pre-anthropogenic R values. Thus, the overall hydrographical pattern and surface to intermediate water CO_2 exchange in the eastern North Atlantic was similar to the present day one.

Keywords. Deep-water corals, carbonate mounds, Northeast Atlantic, Rockall-Bank, Porcupine Seabight, ^{230}Th/U dating, ^{14}C Dating, ocean ventilation

Introduction

Extensive deep-water coral ecosystems have been discovered along the northeast Atlantic continental shelves of Ireland, Scotland and Norway (Freiwald et al. 1997; Henriet et al. 1998; De Mol et al. 2002). These intermediate depth coral ecosystems provide a unique archive to investigate environmental changes in the eastern North Atlantic driven by climate and ocean circulation changes. This is because (i) the corals grow under the influence of water masses taking part in North Atlantic overturning, as they are situated in a key area for understanding past ocean circulation changes (Dickson and Brown 1994) and (ii) because their aragonite skeleton can be precisely dated by means of ^{230}Th/U and ^{14}C dating (Smith et al. 1997; Adkins et al. 1998; Lomitschka and Mangini 1999; Cheng et al. 2000a; Goldstein et al. 2001; Frank et al. 2004) providing accurate timescales to investigate the development of coral colonies and carbonate mounds in light of marine environmental and climate changes. Furthermore, the combined use of both dating techniques provides a tool to trace changes of seawater ^{14}C, which depends on atmospheric ^{14}C/^{12}C, ^{14}C decay and degree of CO_2 exchange between carbon reservoirs (biosphere, atmosphere, and surface to deep oceanic water), i.e. changes of the carbon cycle, climate, and ocean ventilation and circulation (Adkins et al. 1998; Mangini et al. 1998; Schröder-Ritzrau et al. 2003).

To express such changes the seawater Δ^{14}C values ($\Delta^{14}C_{SW}$ in ‰) (Stuiver and Polach 1977) can be calculated from corals using the ^{230}Th/U ages, following equation (1):

$$\Delta^{14}C_{SW} \, [\text{‰}] = 1000 \cdot (e^{(-\lambda_L \cdot t_{BP})}/e^{(-\lambda_t \cdot t_0)} - 1) \text{ (Adkins et al. 1998).} \qquad (1)$$

Where λ_L is $1.2449 \, 10^{-4}$ is the Libby decay constant, λ_t is $1.2097 \, 10^{-4}$ the true decay constant, t_L is the ^{14}C age, and t_0 is the true age of the coral (^{230}Th/U age). By using the ^{14}C calibration record (Stuiver et al. 1998) atmospheric Δ^{14}C values ($\Delta^{14}C_{atm}$) can be retrieved for coral growth episodes, and then reservoir ages indicative of the degree of ventilation can be determined (Bard et al. 1994; Stuiver et al. 1998; Siani et al. 2000, 2001; Frank et al. 2004):

$$R \, [\text{yrs}] = t_L - t_0^{14C} = -\lambda_L^{-1} \ln\{(\Delta^{14}C_{SW}+1000)/(\Delta^{14}C_{atm}+1000)\} \qquad (2)$$

For well-ventilated surface waters in the tropical, sub-tropical and northern Atlantic, pre-anthropogenic R values are homogenous in the order of 400 yrs. With increasing depth and decreasing degree of ventilation, R increases due to ^{14}C decay, the lack of CO_2 exchange with the atmosphere, and mixing of ^{14}C-depleted deep-water with surface water. Hence, changes of reservoir ages at a given location can be interpreted in terms of (i) changes of atmospheric ^{14}C and/or (ii) changes of surface to intermediate water ventilation and circulation (Bard et al. 1994; Adkins et al. 1998; Siani et al. 2001). First results from combined ^{14}C and ^{230}Th/U dating of deep-water corals from Rockall and Porcupine Bank were recently obtained, demonstrating that modern *Lophelia pertusa* corals record indeed seawater $\Delta^{14}C_{SW}$ and that pre-anthropogenic $\Delta^{14}C_{SW}$ of upper intermediate water was ~-69 ‰ (Frank et al. 2004), corresponding to reservoir ages between 400 and 600 yrs during the past 700 CAL yrs.

During the European funded projects GEOMOUND and ECOMOUND gravity cores were recovered from the top of carbonate mounds at Rockall Bank and in Porcupine Seabight. These cores provide us with "quasi" continuous coral deposits over several thousand years. Here, we present combined radiocarbon and ^{230}Th/U dating on deep-water corals from these cores to investigate the development of corals on the carbonate mounds and to better constrain the record on $^{14}C/^{12}C$ variability of upper intermediate water and thus intermediate water ventilation during the Holocene.

Samples and methods

Geographical setting and core description

The Northeast Atlantic carbonate mounds covered with deep-water coral colonies are situated at the transition between near-surface waters and North Atlantic Intermediate Water between ~200 m and ~1000 m water depth (Fig. 1) (Freiwald et al. 1997; Henriet et al. 1998; van Weering and shipboard scientific party 1998, 1999; De Mol et al. 2002). Here, surface and sub-surface waters result from mixing of fresh North Atlantic Water of northwestern origin with saline Eastern North Atlantic Water (ENAW) of southern origin (Ellett and Martin 1973; Holliday et al. 2000, see also for a review; New and Smythe-Wright 2001). Below the near-surface layer between 1000 to 1200 m depth, a high salinity body was identified and related either to Mediterranean Outflow Water (MOW) and/or to sinking of the saline near-surface layer northwards the Rockall Trough. The deeper water masses are formed by Labrador Sea Water (LSW) at about 1600 to 1900 and by North East Atlantic Deep Water (NEADW) originating in the Norwegian Sea. The complex topography of the Rockall Bank result in a local cyclonic near bottom water current at ~400 m bsl that seasonally cascades down the slopes (White et al. 2005). These near bottom currents along the shelf edge and along the Rockall and Porcupine Bank can reach more than 15 cm s^{-1} hindering sediment deposition, but providing sediment free hard substrate for coral growth.
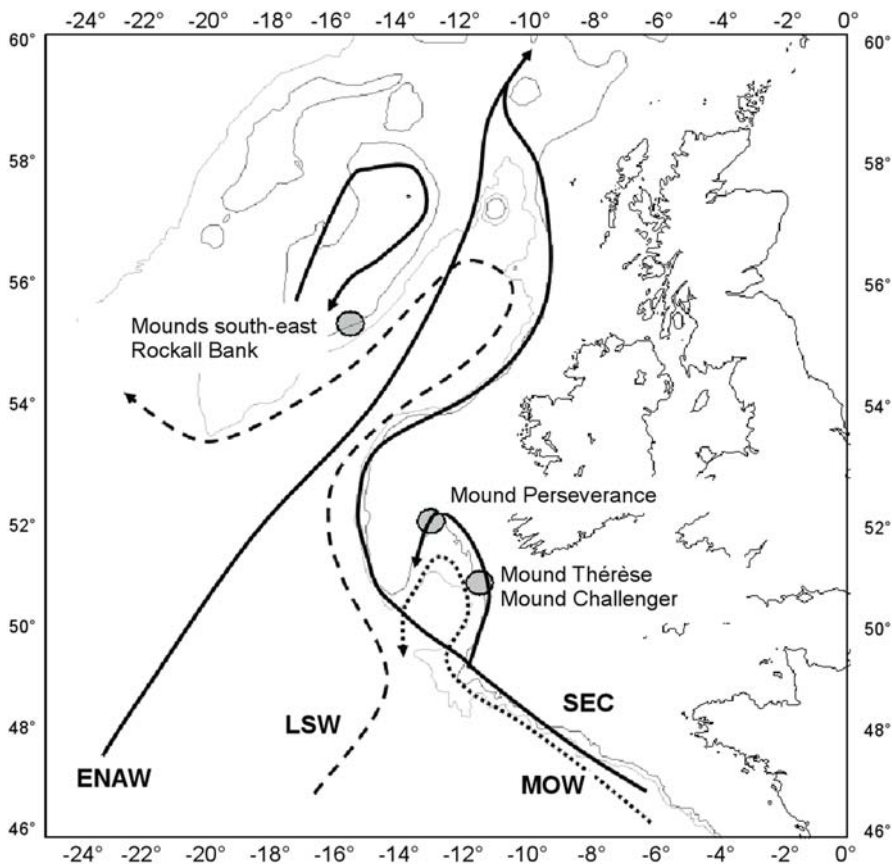
Fig. 1 Topographic map of the 4 areas showing the investigated deep-water coral mounds. Solid lines mark major surface water currents such as the Eastern North Atlantic Water (ENAW) the Shelf Edge Current (SEC) and the anticyclonic circulation along the Rockall Bank. The dashed line mark the major deep-water current (Labrador Sea Water: LSW), and the dotted line the intermediate depth Mediterranean Outflow Water (MOW)

The most abundant coral species found on these mounds is the framework builder *Lophelia pertusa* (Freiwald et al. 1997; Henriet et al. 1998; van Weering and shipboard scientific party 1998, 1999; De Mol et al. 2002). The presence of such mounds along the Rockall and Procupine Bank, and the Porcupine Seabight is considered to be closely related to oceanographic conditions favorable for coral growth, of which nutrient supply, strong current activity, and slow sedimentation seem most important (Freiwald 2002).

During the GEOMOUND/ECOMOUND - Marion Dufresne cruise (2001) a set of gravity cores was obtained from several cold-water coral mound provinces in the Porcupine Basin and Rockall Trough at water depth ranging from 610 m to 888 m (Fig. 1; Table 1) (van Rooji et al. 2001). The investigated deep-water corals were picked from those cores taken on the summit of carbonate mounds. All cores were

Table 1 Location and description of gravity cores from which cold-water corals were sampled

Core	Site	Location	Depth [m]	Length [m]	SCOPIX report
MD01 2454 gravity	Top „unnamed" Mound, Southeast Rockall Bank	55°31'N 15°39'W	747	2.73	Full of big coral chunks, alternating zones of coral density
MD01 2455 gravity	Top „unnamed" Mound, Southeast Rockall Bank	55°33'N 15°40'W	637	1.93	Small coral fragments from 0 to 0.5 m / between 0.75 and 1.15 m coral abundance diminishes / rest large coral chunks
MD01 2459 gravity	Top Mound Perseverance, Northern Porcupine Seabight	52°18'N 13°03'W	610	10.79	Till 5.35 m full of big coral chunks with alternating density. Deeper parts of the core are bioturbated and show solely small coral fragments
MD01 2451 gravity	Top Mound Challenger, Western Porcupine Seabight	51°23'N 11°43'W	773	12.84	Complex sequence of coral abundance and coral free sediment (see Fig. 2 for details)
MD01 2463 gravity	Top Mound Thérèse Western Porcupine Seabight	51°26'N 11°46'W	888	10.75	Variable coral density and coral debris throughout the core

taken in areas, where active cold-water coral growth was identified by sea floor video imaging. MD01 cores were processed through X-ray imaging at University Bordeaux I (DGO UMR5805) providing us constrains on coral abundance. Figure 2 gives a representative example of the X-ray images for a core having significantly different coral abundance. Gravity core MD01-2459G close to the summit of Mound Perseverance (52°23' N, 13°03' W, 610 m bsl) is almost homogenously filled with corals of different size and different species (*Lophelia pertusa*, *Madrepora oculata*, and *Desmophyllum cristagalli*) till 5.35 m core-depth. The first part of the core is richer in organic matter than the second part. This is indicated (0 - 5.35 m core depth) by the dark green colour of the sediment. Below corals seem absent on the X-ray image, but in fact corals are dissolved leaving skeleton footprints, carbonate-rich sediments poor on organic matter behind. At the base of core MD01-2459G several pieces of a carbonate hardground layer were recovered. Hence, this core nicely demonstrates the development of at least the upper most part of a carbonate mound driven by coral growth on a hard substrate and coral alteration.

For ^{230}Th/U and ^{14}C dating solely corals showing almost no physicochemical alteration and bacterial destruction were picked from the unaltered section of the cores. None of the corals reflected a visible coating with manganese and iron oxides/hydroxides frequently observed on dead deep-water corals (Lomitschka and Mangini 1999; Cheng et al. 2000a; Goldstein et al. 2001). However, all investigated corals showed detrital contamination on the outer and inner surface of the skeleton.
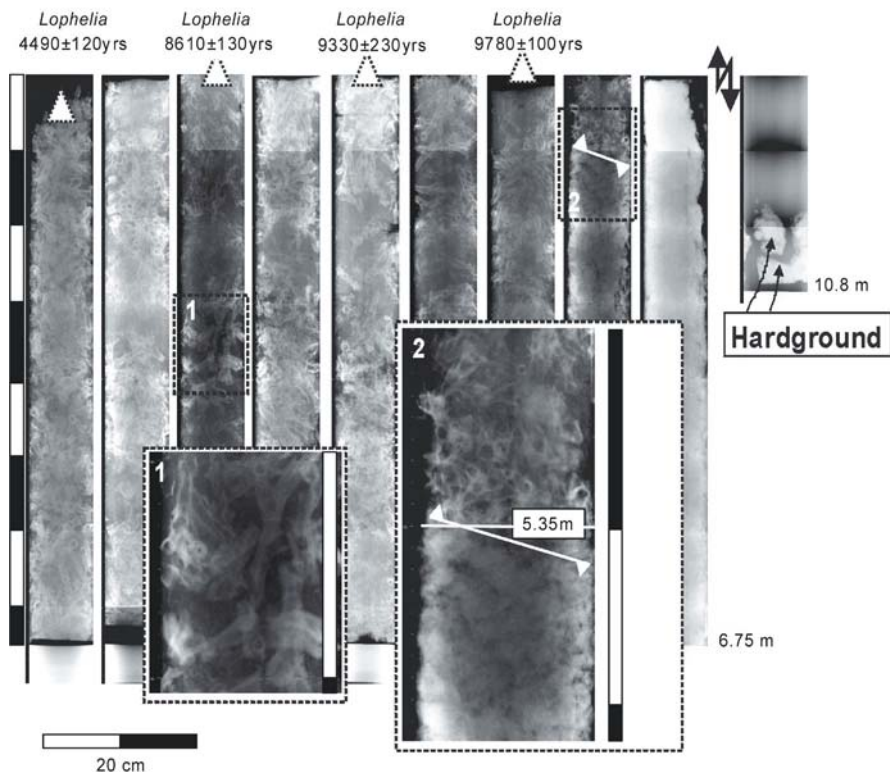
Fig. 2 X-Ray (SCOPIX) image of the sequence 0-6.75 m core depth and base of core MD01-2459G from the top of Mound Perseverance (Porcupine Seabight). The topmost 5.35 m of the core is filled with *Lophelia pertusa* and other coral species with variable density and coral size. Below 5.35 m almost no coral debris is visible in the X-Ray image. At the base of the core several pieces of a carbonate hardground are present. In the lower part of the figure section 1 zooms an area of large pieces of *Lophelia* corals (up to 8 cm length) and section 2 zooms on the transition from high deep-water coral density to sediment layers. Ages of *Lophelia* corals range from 4,500 years at the core top to 9,780 years in 4.5 m depth, indicating a Holocene growth episode for the entire core section. Actively growing corals were not found at the core top but were identified in close vicinity. Between 6.75 and 10.8 m core depth, the SCOPIX image is homogenously grey as for the section 6.0-6.75 m, indicating absent dead corals and coral debris. In fact this section represents a carbonate-rich sediment containing footprints of re-worked corals

In addition, the corals calyx was mostly filled with carbonate and aluminosilicate sediments that needed to be removed prior to further investigation. To do this, we carefully scraped off the outer and inner surface of the corals calyx containing remains of organic tissue, and detritus. Then, the mechanically cleaned *Lophelia* calyxes were cut along their growth axis in three aliquots, of which the first one was powdered and processed through X-ray diffraction (XRD) to insure that samples consist of more than 99 % aragonite, otherwise further analyses was rejected. The remaining two aliquots were used for ^{230}Th/U and ^{14}C dating.

Mass spectrometric ^{230}Th/U dating and AMS ^{14}C dating

^{230}Th/U age determination of 28 samples was carried out (Table 2). Sample weights of average 0.5 g were used. Mechanical cleaning of the corals was followed by a weak acid leach (diluted ascorbic acid + Na$_2$EDTA at 60 °C), ultrasound treatment, and several rinses with quartz distilled (QD) water to remove any remaining U-series

Table 2 Sample description, U series data, and ^{230}Th/U ages

	Depth (cm)	U (ppm)	$\delta^{234}U_m$ (‰)	Th (ppm)	[^{230}Th/^{232}Th]	$\delta^{234}U_0$ (‰)	^{230}Th/U age (years)
MD01-2454 modern P1	0	4.019	145±4	0.0001	28	145±4	18±6
MD01-2454 Top	0	3.445	142±3	0.0031	27	142±3	470±140*
MD01-2454	30	4.811	145±2	0.0042	62	146±2	1450±120
MD01-2454	121	4.452	146±2	0.0014	394	148±2	3820±70
MD01-2454	150	3.378	145±3	0.0007	805	148±3	5090±80
MD01-2454	247	4.986	144±3	0.0318	49	148±3	8300±920*
MD01-2454	273	4.236	145±3	0.0037	339	149±3	9430±190
MD01-2454 cc 1	>273	3.405	144±3	0.0059	203	148±3	11000±380
MD01-2454 cc 2	>273	4.278	144±3	0.0114	130	149±4	10500±440
MD01-2455G top	0	4.043	144±11	0.0006	55	144±11	230±40
MD01-2455G	150	4.136	144±3	0.0077	178	148±3	10350±350
MD01-2455G	193	4.719	149±6	0.0001	5553	151±6	5490±175
MD01-2455G cc 2	>193	4.798	146±3	0.0036	341	149±4	8050±300
MD01-2459G	0	3.145	144±3	0.0004	1071	147±3	4490±120
MD01-2459	150	3.370	148±3	0.0018	515	152±3	8610±130
MD01-2459	300	3.578	143±2	0.0043	245	147±2	9330±230
MD01-2459	450	3.382	144±3	0.0001	12036	148±3	9780±100
MD01-2463G	0	3.909	148±9	0.0008	60	148±9	315±43
MD01-2451G	0	4.052	151±3	0.0210	22	152±3	2070±670*

$\delta^{234}U_m = ([\{^{234}U/^{238}U_{measured}\}/\{^{234}U/^{238}U_{equilibrium}\} - 1] \cdot 1000)$ with $^{234}U/^{238}U_{equilibrium} = 54.89 \pm 0.1 \cdot 10^{-6}$. $\delta^{234}U_0$ and the ^{230}Th/U ages (seawater ^{230}Th corrected) were calculated using ISOPLOT (Ludwig 2001). [^{230}Th/^{232}Th] represent the activity ratio calculated from the measured isotopic ratio. $\Delta\delta^{234}U$ is given as 2σ uncertainty of counting statistics. Assuming that the modern coral of core MD01-2454G (modern Polyp 1) and the modern coral from core ENAM 9915 (0 cm depth) (Frank et al. 2004) have an age of less than 50 yrs one can reconstruct seawater [^{230}Th/^{232}Th] by using the decay equation to calculate the ^{230}Th derived from U decay. Doing this we find [^{230}Th/^{232}Th] ranging between 7±3 and 13±3, in agreement with measured seawater [^{230}Th/^{232}Th] of 10±4 used to correct the ^{230}Th/U ages. * ^{230}Th/U ages are strongly affected by the seawater ^{232}Th correction. cc = core cutter sample

nuclides potentially adsorbed *via* authigenic Mn/Fe precipitation. Next, U and Th was extracted and purified utilizing standard ion exchanges chemistry as described by Frank et al. (2004). U and Th analyses were carried out on the Gif-sur-Yvette thermal ionization mass spectrometer (Finnigan MAT262). Repeated analyses of HU-1 (Ludwig et al. 1992) reference material measured over the course of coral data acquisition yielded an average $[^{234}U/^{238}U]$ activity ratio of 0.9998±0.0011 (2σ, N = 29) and a $[^{230}Th/^{238}U]$ activity ratio of 1.0013±0.0014 (2σ, N = 12), respectively. Activity ratios were calculated from measured atomic ratios using the decay constants of ^{238}U, ^{234}U, and ^{230}Th of $\lambda_{238} = 1.5515 \cdot 10^{-10}$ a^{-1}, $\lambda_{234} = 2.8263 \cdot 10^{-6}$ a^{-1}, $\lambda_{234} = 9.1577 \cdot 10^{-6}$ a^{-1} (Cheng et al. 2000b), respectively. The 1σ standard deviation for U and Th standards processed through chemistry indicative of the reproducibility of measurements is ±3 ‰ and ±3.4 ‰, respectively.

Routinely measured chemical blanks within a set of 6 samples yield less than 100 pg ^{238}U and less than 70 pg ^{232}Th and are negligible.

AMS ^{14}C analyses were performed on 11 of the $^{230}Th/U$ dated corals (Table 3) following the procedure given in Frank et al. (2004). About ~10 mg of coral was

Table 3 ^{14}C ages of deep-sea corals, $\Delta^{14}C$ of corals and atmosphere and reservoir ages

Sample	$^{230}Th/U$ age CAL yr B.P.	^{14}C age (yrs B.P.)	$\Delta^{14}C_{seawater}$ (‰)	$\Delta^{14}C_{atmosphere}$ (‰)	R (yrs)
Mound, southeastern Rockall Bank					
MD01-2454 modern P1	-32±3	70±60	-13±7	126±20	
MD01-2454 Top	420±70	770±50	-44±10	6±6	410±100
MD01-2454 150cm	5050±30	5010±30	-13±5	56±4	540±80
MD01-2454 273cm	9380±80	8920±140	24±20	100±6	570±170
MD01-2454 cc1	10950±180	9880±90	99±26	142±15	310±220
MD01-2454 cc2	10450±210	10030±100	15±28	114±7	750±230
Mound, southeastern Rockall Bank					
MD01-2455 150cm	10300±160	9710 ± 100	38±24	113±7	560±190
MD01-2455 193cm	5440±90	4920±70	46±13	78±5	240±110
Top Mound Perseverance, northern Porcupine Seabight					
MD01-2459 150cm	8560±50	8200±80	15±12	70±3	420±100
MD01-2459 300cm	9280±110	8620±80	51±17	97±5	360±140
MD01-2459 450cm	9730±50	9090±90	46±13	91±3	370±100

The $^{230}Th/U$ ages from Table 2 are given here with 1σ uncertainty and normalized to 1950 AD. The seawater $\Delta^{14}C$ ($\Delta^{14}C_{SW}$) values at 1σ were calculated from coral radiocarbon ages following the equation (1). $\Delta^{14}C_{atmos}$ at t_0 is obtained from the atmospheric radiocarbon calibration record (Stuiver et al. 1998). The R age at 1σ is derived from the $\Delta^{14}C_{SW}$ and $\Delta^{14}C_{atmos}$ values following equation (2)

picked from the cleaned *Lophelia* calyxes and rinsed in an ultrasonic bath, and then crushed into an agate mortar. The fine powder was than further cleaned by rinsing with a 0.01 N solution of HNO_3. AMS ^{14}C dating was performed at the Gif-sur-Yvette Tandetron (Arnold et al. 1989). Blanks were obtained on a *Lophelia* coral dated >100,000 yrs by the [230]Th/U method, and yield a mean ^{14}C activity of 0.20±0.05 pMC (apparent ^{14}C age ~50,000 yr).

Results

U-series data

The U concentrations of cold-water species *Lophelia pertusa* and *Madrepora oculata* vary strongly between 3.1 and 4.8 µg g^{-1}, but similar to U concentrations obtained on other species such as *Desmophyllum cristagalli* (Smith et al. 1997; Lomitschka and Mangini 1999; Cheng et al. 2000a; Goldstein et al. 2001). The U abundance is in average higher than the one of aragonite build up by surface water corals (2 - 3.5 µg g^{-1}) (Shen and Dunbar 1995), most likely representing low ambient seawater temperatures (8-10°C) and low pH for aragonite precipitation within upper intermediate waters.

The initial δ^{234}U measured in cold-water corals range from 152 ‰ to 142 ‰ with analytical errors of average 2-4 ‰ (2 σ) (Table 2). The mean value of all samples is determined at 148.1±2.4 ‰ (1 SD; Table 2), which closely matches recent seawater δ^{234}U values of 149.6 ‰ (Delanghe et al. 2002), and 146.6 ‰ (Robinson et al. 2004). It also cooperates with earlier seawater measurements of 145.1±3.5 ‰ performed by Chen et al. (1986), taking into account systematic differences between laboratories and using the decay constants given by Cheng et al. (2000b). The corals δ^{234}U values are thus mostly within analytical error of modern seawater, indicating no detectable departure from U-series close system behaviour. Taking into account that X-ray diffraction did not show the presence of calcite or magnesium calcite, we conclude that re-crystallization of the corals is unlikely.

Measured [232]Th concentrations are small (<4 ng g^{-1}) for most samples except two, such that a [232]Th and [230]Th contribution from detritus and seawater is small. However, any contribution of [232]Th and [230]Th from detritus and seawater affect the [230]Th/U age and will thus be considered for age estimation.

In the northeastern North Atlantic intermediate water at 500 to 1000 m depth, measured [230]Th/[232]Th activity ratios [[230]Th/[232]Th] vary between 6 (Moran et al. 1995) and 14 (Vogler et al. 1998). These values are close to seawater [[230]Th/[232]Th] of 7±3 and 13±3 reconstructed from two modern corals specimens (see captions of Table 2 for details). Thus, [230]Th/U ages need to be corrected for contamination with excess [230]Th from seawater. We used the average of the measured [[230]Th/[232]Th] of 10±4 (Moran et al. 1995; Vogler et al. 1998), and propagated its uncertainty into the age error (Table 2). This correction is generally small, mostly within uncertainty of the uncorrected age estimates. However, two samples MD01-2454 (247 cm) and MD01-2451G (Top) show exceptional high [232]Th concentrations and age corrections and age errors consequently larger.

Such a correction using seawater [^{230}Th/^{232}Th] for old corals is valid assuming that seawater is the only source of excess ^{230}Th. However, it would not be effective if excess ^{230}Th, without addition of ^{232}Th, is related to open system U-series behavior controlled by α-recoil processes (Thompson et al. 2003; Villemant and Feuillet 2003), as mentioned before. To investigate the accuracy of our age estimate the effect of such processes on the age determination was tested for the older corals, as corals younger than 1000 yrs are not sensitive to such long-term processes.

To do this we applied a correction model proposed by Villemant and Feuillet (2003) that corrects for re-distribution of U-series nuclides following loss or gain of U-series nuclides from recoil processes and that takes excess ^{230}Th into account. For surface water corals, fractionation (re-distribution) factors for ^{234}U (*via* ^{234}Th) and ^{230}Th, implemented in the age equation by Villemant and Feuillet (2003) (equation (5) (Villemant and Feuillet 2003)), range form f_{234}=1.25 to 0.85 following the measured variability of the U-isotopic composition in surface water corals of about 125,000 yrs age (Thompson et al. 2003; Villemant and Feuillet 2003).

By using seawater U isotopic composition of 148 ‰, and re-distribution factors f_{234} ranging from 1.05 to 0.95, we calculated open system U-series evolution curves and compared them to our data in Figure 3. Our data show no departure from close
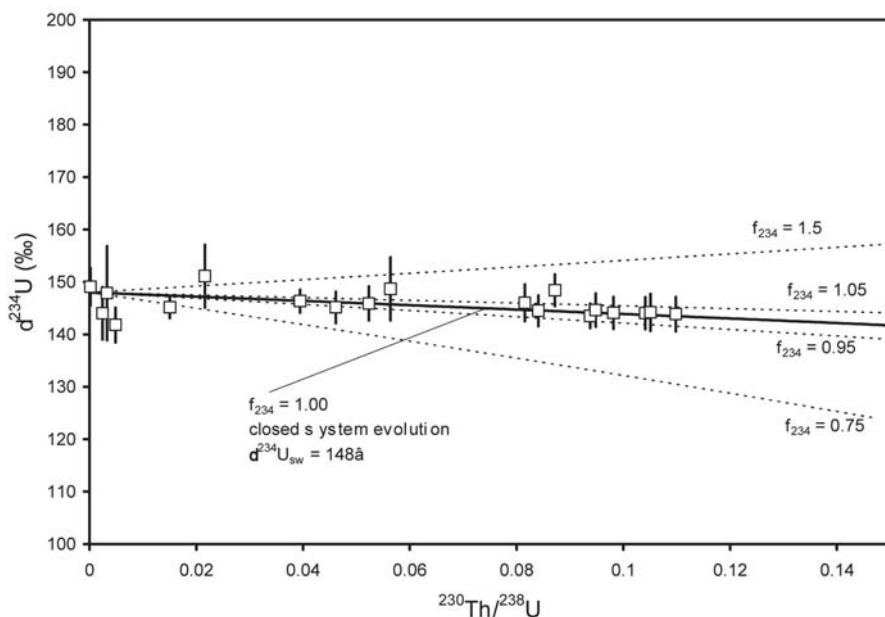
Fig. 3 U isotopic composition and [^{230}Th/^{238}U] activity ratio of deep-water corals. The solid line corresponds to the close system U-series evolution of the U-series system. The dashed line reflects the evolution of the U-series nuclides for an open system taking α-recoil re-distribution of ^{234}U and ^{230}Th into account (Villemant and Feuillet 2003). To calculate the closed system and open system U-series evolution lines we used a seawater δ^{234}U$_{SW}$ of 148 ‰. The mean initial δ^{234}U of all coral samples is 148.1±2.4 ‰ (1σ SD)

system U-series evolution within error of measurements (±3-5 ‰) and f_{234} values of 1.05 to 0.95. Thus, we conclude that α-recoil effects on the U-series behavior of the selected deep-water corals can be ruled out.

^{230}Th/U ages and ^{14}C ages

^{230}Th/U ages determined following the approach to correct for seawater [^{230}Th/^{232}Th] are given in Table 2. In Table 3 ^{230}Th/U ages are referred to 1950 AD, in order to compare them later on to ^{14}C ages.

The deep-water corals yield ^{230}Th/U ages ranging from today to ~11,000 yrs (Table 2). Most of the gravity cores show a progressive increase of coral ages with core depth (Table 2). In contrast, core MD01-2455G shows an age inversion at 150 cm depth and an age range of 3000 yrs between the core base (193 cm depth) and the core cutter indicating at least one gap (Table 2).

From coral growth episodes obtained in gravity cores MD01-2454G on Rockall Bank and MD01-2459G at Porcupine Seabight, the sediment accumulation rate can be estimated to be ~0.34 mm per year or less (Fig. 4). Assuming *Lophelia pertusa*
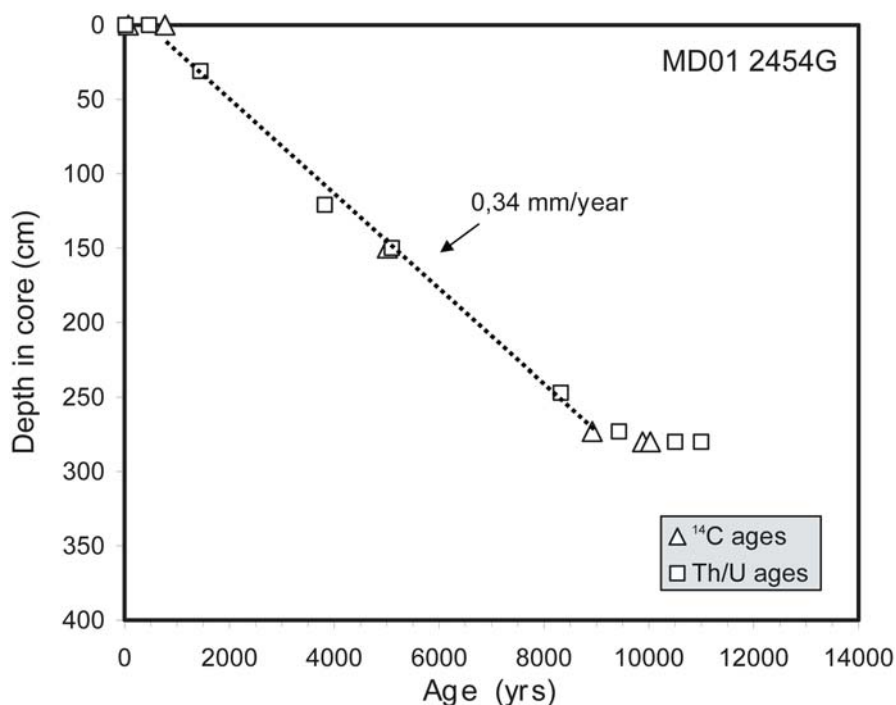
Fig. 4 ^{230}Th/U and ^{14}C ages of corals *versus* core depth for gravity core MD01-2454G from a Mound at southeast Rockall Bank. Coral growth in vertical direction seems relatively regular over the past 9,000 yrs. The core is homogenously filled with large *Lophelia* pieces with a sediment accumulation rate of 0.34 mm per year. Solely the base of the core exhibits a minor vertical extension rate as corals of different age are mixed at similar depth. Apparent ^{14}C ages are different from ^{230}Th/U age, as expected, but yield a similar sedimentation pattern

growth rates in the order of 2 to 7 mm per year (Wilson 1979), the coral development predominantly in horizontal but also in vertical direction seems the driving process for sediment accumulation on the investigated mounds.

The corals sampled at the surface of gravity cores show in general young ages (modern to a few hundred years) in agreement with the fact that cores where taken in areas of active coral growth and at the top of the mounds. Several modern *Lophelia* branches were collected at the surface of core MD01-2454G, of which one coral polyp was dated to 1983±6 AD, close to the date of collection (2001 AD; Table 3). Solely, the top of core MD01-2459G from Mound Perseverance bare corals of ~4500 yrs age. The lack of modern corals from this mound may simply reflect missing accessibility due to erosion, as Mound Perseverance is an 80 m high singular mound with steep flanks, and the core was taken close but slightly off the top.

^{14}C ages obtained on corals from gravity core MD01-2454G, MD01-2455G, and MD01-2459G range from modern to 10,030 yrs and agree with the sediment accumulation pattern deduced from ^{230}Th/U dating (see Fig. 4). One studied deep-water coral present a modern ^{14}C age (Table 3), as expected from the modern ^{230}Th/U age. This indicates that this coral grew after the atmospheric nuclear weapon tests, which led to an atmospheric ^{14}C increase by a factor of ~2 (Levin et al. 1992).

Discussion

The presented ^{230}Th/U and ^{14}C ages can now be used to study coral growth and sedimentation on the investigated carbonate mounds, and combined ^{14}C and ^{230}Th/U dating can be used to study upper intermediate water ventilation and circulation on Rockall Bank and in Porcupine Seabight.

Coral growth and mound formation

Sedimentary processes are complex and result from (1) deep-water coral growth in vertical and predominantly in horizontal direction, (2) degradation of the skeletal framework by various kinds of bioerosion, (3) internal sediment production and (4) the accumulation of allochthonous mud (Freiwald et al. 1997 and references therein). Furthermore, the sedimentary environment is affected by highly variable bottom water currents both in direction and velocity ranging from ~2.5 cm s^{-1} to more than 15 cm s^{-1}, which result in frequent hiatuses and sediment as well as coral debris re-distribution along the mound slope and probably also on the mound top.

The topmost sediments on the investigated 5 mounds clearly reflect the Holocene development of coral colonies, associated fauna, and internal sediment production. From the gravity cores MD01-2454G and MD01-2459G we found continuous but irregular coral growth, with sedimentation rates in the order of 0.3 mm yr^{-1} and less.

High bottom water currents result in frequent coral debris and sediment re-distribution as documented by the hiatus seen in core MD01-2455G on the summit of a mound at southeast Rockall Bank. This hiatus is indicated by an age inversion at 150 cm depth (Table 2).

Underneath the unaltered Holocene coral sequence, several cores indicate the presence of deep-water corals (for example MD01-2459G, depth 5.35 m to 10.9 m), but corals are strongly altered (almost completely dissolved) inhibiting dating of these corals.

A process leading to such coral alteration could be organic matter burn down by oxidizing pore fluids, assuming that the initial organic matter to carbonate ratio was similar in both the altered and unaltered core sections. Organic matter consumption would yield elevated pore fluid CO_2 concentrations, which result in $CaCO_3$ dissolution, by which coral aragonite would be preferentially dissolved, compared to calcite. This core sequence and the coral alteration have to be further investigated, but for the moment timing of coral growth and alteration is not possible. Hence, deep-water corals may have developed during glacial episodes and could have been altered by degradation of organic matter. Alternatively, corals may have developed earlier, for example in previous interglacial periods, and were altered during the glacial, assuming glacial coral development was limited due to changes of ocean circulation and nutrient supply.

The latter hypothesis is supported by sediments from Mound Thérèse (MD01-2463G), of which a *Lophelia* coral yield a ^{230}Th/U age of ~250,000 yrs ($\delta^{234}U_0 = 150 ‰$) at 3 m core depth, while a core top sample yield a Holocene age (Table 1). A potential unconformity in this core is located at 1.8 m depth, probably reflecting erosion of Mound Thérèse. In addition, coral debris recovered from 4.5 m and 9.0 m depth on the summit of Mound Challenger (MD01-2451G) indicated ages larger than 150,000 yrs and a core top age of an unaltered coral of ~2000 yrs (Table 2), but here the coral skeleton fragments at depth were partly dissolved inhibiting precise U-series dating. Several significant changes in sediment properties can be seen in the X-ray image of this core (Fig. 5), indicating discontinuous coral growth and sedimentation. Hence, several metres of sediment on top of carbonate mounds do reflect several hundred thousand years of sedimentation and coral development, due to frequent mound erosion by high bottom currents.

From our dating results we can not rule out the presence of deep-water corals on Rockall Bank and in Porcupine Seabight during glacial episodes. But, it was suggested that ice advance and a weaker thermohaline circulation slows down the surface and upper intermediate water currents of the north-eastern North Atlantic or even inverts the shelf edge flow path (Rüggeberg et al. 2005). This could result in diminishing nutrient supply and would thus inhibit coral growth. Further south on the continental margin or deeper in the Rockall Trough, such effects should be much less profound, hence deep-water corals should be present also during glacial periods. ^{230}Th/U ages obtained on deep-water corals by Schröder-Ritzrau et al. (2005) confirm this hypothesis, as they found corals reflecting growth episodes during glacial stages 2, 3, and 4 further south on the eastern margin of the European shelf. To resolve in more detail the development of carbonate mounds on Rockall Bank and in Porcupine Seabight related to coral growth and diagenesis further geochronological studies and deep drilling of mounds are mandatory.
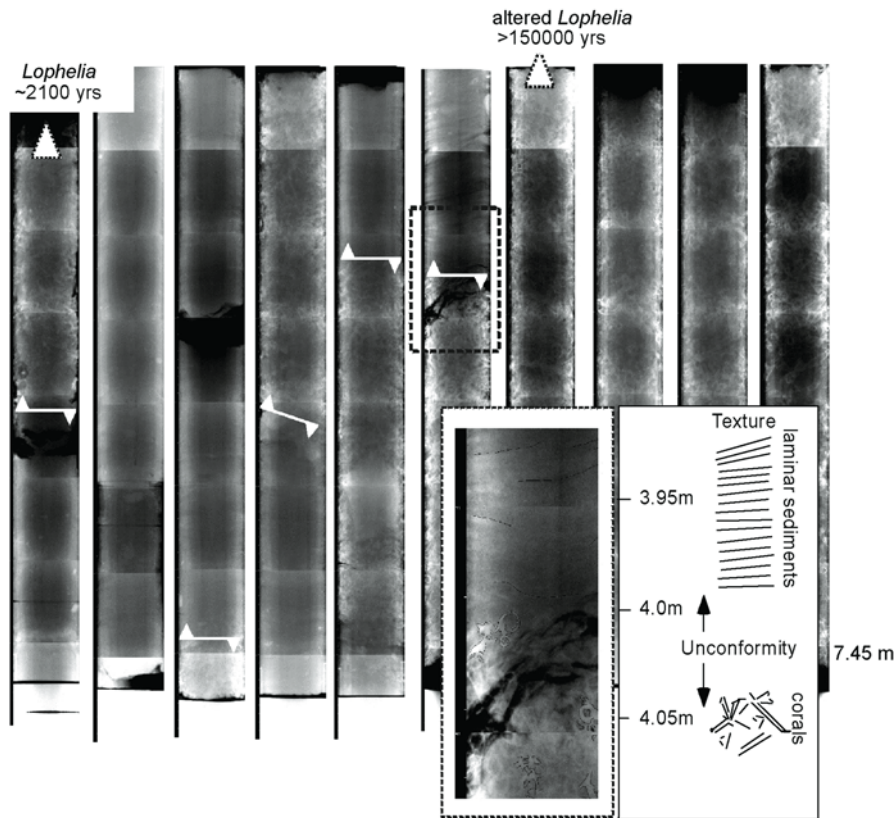
Fig. 5 SCOPIX image of core MD01-2451G from top Mound Challenger and zoom of an unconformity at 4.0 m core depth, with laminar sediments on top of a sequence of high coral abundance. *Lophelia* corals from the deeper core section were not datable due to alteration of the coral skeleton and likely open-system U-series behavior. However, low δ^{234}U of 38 ‰ and [^{230}Th/^{238}U] ratios larger than 0.7, indicate ages most likely older than 150,000 years

Present and past ocean ventilation

To investigate past ocean ventilation we determined Δ^{14}C values and reservoir ages R for upper intermediate waters from the 11 corals having combined ^{14}C and ^{230}Th/U dating (Table 3). Then, upper intermediate water Δ^{14}C of the past 50 yrs is compared to the atmospheric Δ^{14}C (Nydal and Gislefoss 1996) (Table 3) and to surface water Δ^{14}C determined on an annual banded reef-coral from Florida (Druffel and Linick 1978) to demonstrate the sensitivity of deep-water coral Δ^{14}C in light of rapid atmospheric ^{14}C changes, such as ^{14}C injection into the atmosphere by the nuclear weapon tests. To study changes of ocean ventilation and circulation during the past 11,000 yrs we then compare the upper intermediate water Δ^{14}C with the atmospheric calibration record (Stuiver et al. 1998) and surface water Δ^{14}C determined on varved sediments from the Cariaco basin (Hughen et al. 1998, 2000), i.e. the marine ^{14}C calibration.

Figure 6 shows the comparison of $\Delta^{14}C$ of the modern atmosphere, subtropical surface Atlantic, and of upper intermediate water on Rockall Bank. The four $\Delta^{14}C$ values of the upper intermediate water represent $\Delta^{14}C$ from modern coral MD01-2454 P1 (Table 3) and from two corals (LOP.1 and LOP.2 top and base) of box core ENAM-9915 (Frank et al. 2004).

The deep-water corals monitor a rapid ^{14}C increase around 1970 AD as the increase is documented in a single *Lophelia* branch of 20 mm length (Frank et al. 2004), which corresponds to ~3-10 yrs of growth, adopting growth rate estimates of up to 2-7 mm per year by Wilson (1979). But, the ^{14}C increase is strongly buffered at ~730 m depth compared to the surface ocean with $\Delta^{14}C$ equal ~+60±10 ‰ (~1/4 of the surface ocean peak $\Delta\Delta^{14}C_{atm}$ ~210 ‰), reflecting the important contribution of ^{14}C-depleted intermediate water (pre-anthropogenic $\Delta\Delta^{14}C$ ~-69 ‰ (Frank et al. 2004)). Thus, eastern North Atlantic upper intermediate water $\Delta^{14}C$ is not as sensitive as surface water to such strong and rapid atmospheric ^{14}C changes even though strong vertical winter mixing (down to 1000 m depth (Holliday et al. 2000))
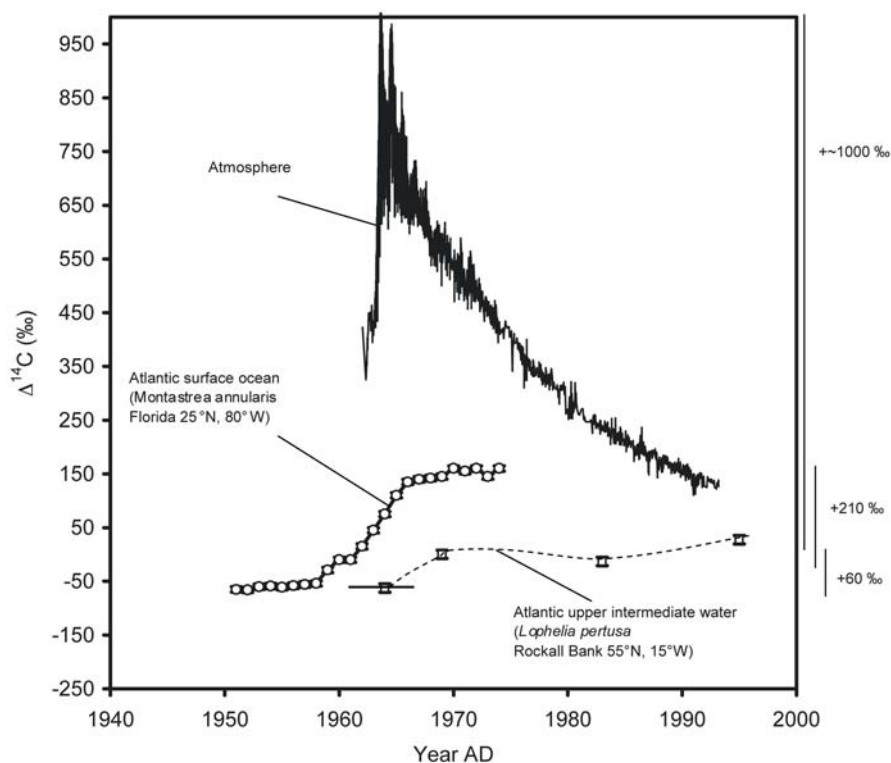
Fig. 6 Comparison of $\Delta^{14}C$ of modern deep-water corals with $\Delta^{14}C$ of a shallow-water coral from Florida (Druffel and Linick 1978) and atmospheric $\Delta^{14}C$ (Nydal and Gislefoss 1996). The bar on the right indicates the overall pattern of $\Delta^{14}C$ in the three reservoirs: atmosphere, surface water, and upper intermediate water

occurs. The $\Delta^{14}C$ value of -13±7 ‰ obtained from the modern coral MD01-2454 P1 living in 1983±6 AD is in agreement with seawater measurements performed in 1981 in the nearby Iceland basin (TTONAS sta142 (Nydal and Gislefoss 1996)) as are the other modern corals (Frank et al. 2004).

Between 5500 CAL yrs BP and 5000 CAL yrs BP, the atmosphere and ocean surface show a long term decrease of $\Delta^{14}C$ by ~20 ‰ (Fig. 7). Two deep-sea corals having ages between 5,440 CAL yrs BP and 5,050 CAL yrs BP exhibit much stronger variations in $\Delta^{14}C$ of almost ~-60 ‰ (Fig. 7), corresponding to reservoir ages of 240±110 yrs at 5440 CAL yr BP and 540±80 yrs at 5050 CAL yr BP (Table 3). A reservoir age of 240 yrs seems too low for upper intermediate water at 640 m depth on southeast Rockall Bank, as it is similar to the range of surface water reservoir ages determined on tropical corals (R ~ 200 to 450 yrs) (Bard et al. 1998). This coral comes from core MD01-2455G situated on a mound close to the slope of southeast Rockall Bank, which has a well-documented hiatus and a disturbed core base. Hence the coral was likely re-distributed from upper depth as the slope of

Fig. 7 Comparison of $\Delta^{14}C$ of deep-sea corals with $\Delta^{14}C$ from the marine (solid line) and atmospheric (dashed line) ^{14}C calibration (Stuiver et al. 1998). 1 is the coral at 150 cm depth in core MD01-2454G at 747 m water depth and 2 is the coral sampled at the core base of core MD01-2455G at 637 m water depth

Rockall Bank is steep rising to up to 400 m water depth. Hence, the low R value of this coral could in fact reflect the R value of the well mixing sub-surface to surface ocean in the Rockall Trough at 5,440 CAL yrs BP. The European climate of this episode is marked by more frequent droughts (Kalis et al. 2003), which indicate a lesser storm activity in the eastern north Atlantic compared to modern and Holocene climate optimum conditions. The low reservoir age of the sub-surface waters could thus result from less deep winter mixing, reducing the influence of ^{14}C depleted intermediate water at less than 640 m depth.

In contrast, the reservoir age of 540 yrs at 750 m depth agrees well with previously reported pre-anthropogenic reservoir ages ranging between 400 and 600 yrs for 725 m depth (Frank et al. 2004). Hence, this second coral clearly reflects modern-like ocean circulation and ventilation patterns. In future, we will further investigate this time interval based on deep-water corals from cores MD01-2454G (740 m depth) and MD01-2459G (610 m depth in Porcupine Seabight) having an undisturbed coral record of this time span.

During the second step of the deglaciation and during the Holocene climate optimum from ~11,000 CAL yr BP to ~8,000 CAL yr BP, atmospheric and marine Δ^{14}C decrease by ~120 ‰ showing frequent secular variations in the order of ±20 ‰ (Fig. 8). Deep-water corals yield Δ^{14}C values for the eastern North Atlantic upper intermediate waters about ~10±10 ‰ lower compared to surface water Δ^{14}C, but having variations of similar amplitude (Fig. 8). Reservoir ages of the upper intermediate water yield an overall average of 490±60 yrs, similar to the one determined for the pre-anthropogenic eastern North Atlantic ((Frank et al. 2004) and sample MD01-2454G Top). According to this, no sea surface ^{14}C gradient existed from the low to high latitudes in the North Atlantic Ocean, reflecting modern like hydrological patterns and surface to sub-surface water ventilation. It is also noteworthy that the 3 R values obtained from sediments of Mound Perseverance at 610 m depth in the Porcupine Seabight (MD01-2459G) are very constant over the Holocene climate optimum with an average of 380±30 yrs, equal to pre-anthropogenic Atlantic surface water (Stuiver et al. 1998), indicative of well-ventilated surface to sub-surface waters.

Conclusions

Coupled ^{230}Th/U and ^{14}C measurements were applied to *Lophelia pertusa* deep-sea corals from mound top sediments at intermediate depth on Rockall Bank and Porcupine Seabight. They provide new constrains on the carbonate mound evolution and further data points for pre-anthropogenic and Holocene Δ^{14}C and R values that contribute to a better knowledge of past changes of the North Atlantic ventilation and oceanic circulation.

None of selected deep-water corals at ~610 m to 888 m depth exhibited open-system behaviour with respect to their U and Th isotopes as they all present initial δ^{234}U values close to that of modern seawater. Moreover, it was possible to apply a reliable correction for "excess" non-radiogenic ^{230}Th based on the seawater
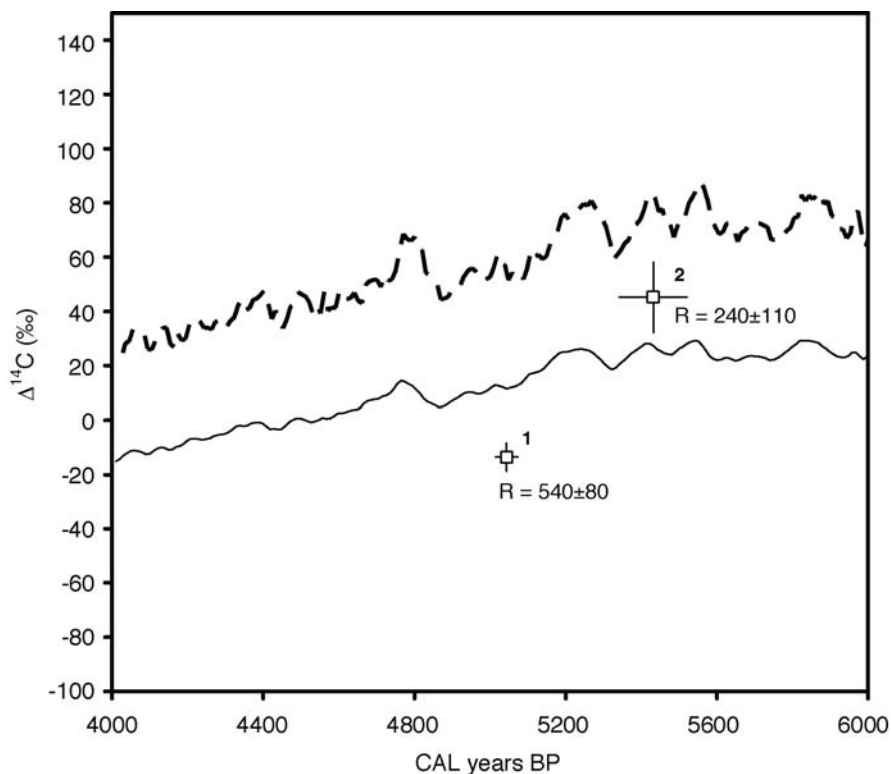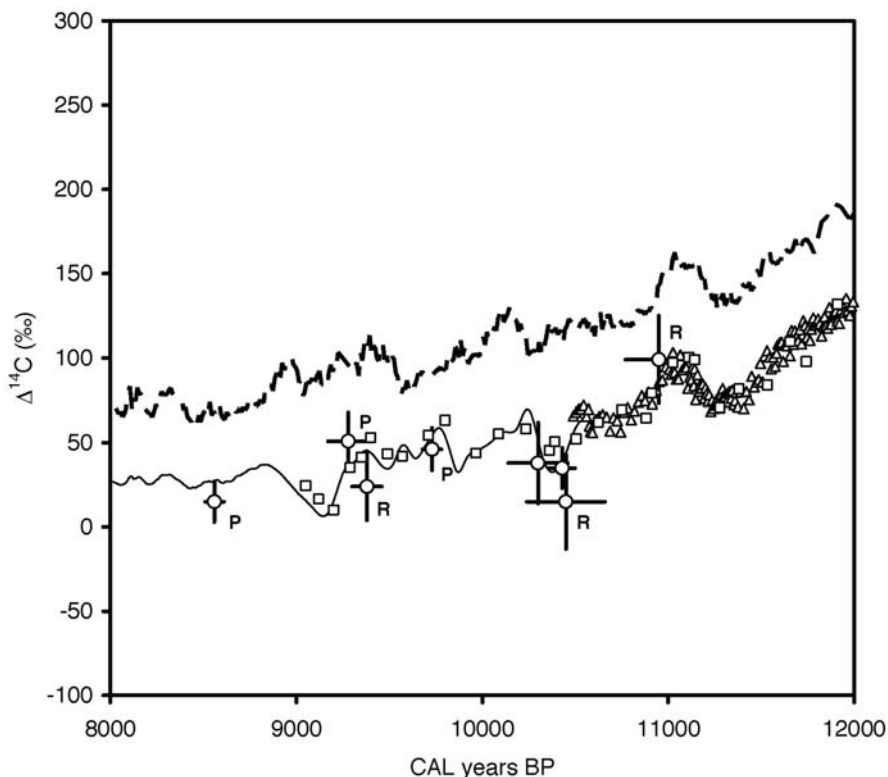
Fig. 8 Comparison of $\Delta^{14}C$ of deep-sea corals with $\Delta^{14}C$ from the marine (solid line) and atmospheric (dashed line) ^{14}C calibration (Stuiver et al. 1998), and $\Delta^{14}C$ from the Cariaco record (triangles and open squares) (Hughen et al. 1998, 2000). P represents corals from Mound Perseverance in the Porcupine Seabight at 610 m depth, while samples R are from two Mounds on Rockall Bank (637 and 747 m water depth)

$^{230}Th/^{232}Th$ providing accurate $^{230}Th/U$ dating for a modern specimen. These deep-sea corals adequately recorded past changes of the $^{14}C/^{12}C$ content of the North Atlantic upper intermediate waters.

Other corals yield ages between 10,950 CAL yr BP and 180 CAL yr BP. The tested model of open system U-series behavior indicated no detectable re-distribution of U-series nuclides due to α-recoil processes, with fractionation factors $1.05 > f_{234} > 0.95$. Thus, the robust skeleton of *Lophelia pertusa* deep-water corals seems less susceptible to such processes compared to surface water coral species.

Sedimentation and coral growth on the carbonate mounds was found to be complex and irregular, with sediment accumulation rates in the order of 0.3 mm yr^{-1}. Coral diagenesis and mound erosion are frequently observed, hence records are discontinuous.

Finally, the investigated corals provided evidence for a modern-like ocean-atmosphere and surface to intermediate $^{14}CO_2$ exchange in the eastern North Atlantic

during the Holocene, despite the fact that deglaciation was not terminated at the beginning of our record.

These results from sediments of the summit of carbonate mounds on the western North Atlantic margin demonstrate their potential for the reconstruction of continues high resolution records on eastern North Atlantic ventilation and circulation related to climate and environmental change.

Acknowledgements

References

Adkins JF, Cheng H, Boyle EA, Druffel ERM, Edwards RL (1998) Deep-sea coral evidence for rapid change in ventilation of the deep North Atlantic 15,400 years ago. Science 280: 725-728

Arnold M, Bard E, Maurice P, Valladas H, Duplessy J-C (1989) ^{14}C dating with the Gif-sur-Yvette tandetron accelerator: status report and study of isotopic fractionation in the sputter ion source. Radiocarbon 31: 284-291

Bard E, Arnold M, Mangerud J, Paterne M, Labeyrie L, Duprat J, Mélières M-A, Sonstegaard E, Duplessy J-C (1994) The North Atlantic atmosphere-sea surface ^{14}C gradient during the Younger Dryas climatic event. Earth Planet Sci Lett 126: 275-287

Bard E, Arnold M, Hamelin B, Tisnerat-Laborde N, Cabioch G (1998) Radiocarbon calibration by means of mass spectrometric ^{230}Th/^{234}U and ^{14}C ages of corals: an updated database including samples from Barbados, Mururoa and Thahiti. Radiocarbon 40: 1085-1092

Chen JH, Edwards RL, Wasserburg GJ (1986) ^{238}U, ^{234}U and ^{232}Th in seawater. Earth Planet Sci Lett 80: 241-251

Cheng H, Adkins JF, Edwards RL, Boyle EA (2000a) U-Th dating of deep-sea corals. Geochim Cosmochim Acta 64: 2401-2416

Cheng H, Edwards RL, Hoff J, Gallup CD, Richards DA, Asmeron Y (2000b) The half-lives of uranium-234 and thorium-230. Chem Geol 169: 17-33

De Mol B, van Rensbergen P, Pillen S, van Herreweghe K, van Rooji D, McDonnell A, Huvenne V, Ivanov M, Swennen R, Henriet JP (2002) Large deep-water coral banks in the Porcupine Basin southeast of Ireland. Mar Geol 188: 193-231

Delanghe D, Bard E, Hamelin B (2002) New TIMS constraints on the uranium-238 and uranium-234 in seawaters from the main ocean basins and the Mediterranean Sea. Mar Chem 80: 79-93

Dickson B, Brown J (1994) The production of North Atlantic deep water: sources, rates, and pathways. J Geophys Res 99: 12319-12341

Druffel ERM, Linick TW (1978) Radiocarbon in annual banded coral rings of Florida. Geophys Res Lett 5: 913-916

Ellett DJ, Martin JHA (1973) The physical and chemical oceanography of the Rockall Channel. Deep-Sea Res 20: 585-625

Frank N, Paterne M, Ayliffe LK, Blamart D, van Weering T, Henriet JP (2004) Eastern North Atlantic deep-sea corals: tracing upper intermediate water Δ^{14}C during the Holocene. Earth Planet Sci Lett 219: 297-309

Freiwald A (2002) Reef-forming cold-water corals. In: Wefer G, Billett D, Hebbeln D, Jørgensen BB, Schlüter M, van Weering T (eds) Ocean Margin Systems. Springer, Berlin Heidelberg, pp 365-385

Freiwald A, Henrich R, Pätzold J (1997) Anatomy of a deep-water coral reef mound from Stjernsund West Finnmark, northern Norway. SEPM Spec Publ 56: 141-162

Goldstein SJ, Lea DW, Charaborty S, Kasharian M, Murrell MT (2001) Uranium-series and radiocarbon geochronology of deep-sea corals: implications for Southern Ocean ventilation rates and oceanic carbon cycle. Earth Planet Sci Lett 193: 167-182

Henriet JP, De Mol B, Pillen S, Vanneste M, van Rooij D, Versteeg W, Croker PF (1998) Gas hydrate crystals may help build reefs. Nature 391: 648-649

Holliday NP, Pollard RT, Read JF, Leach H (2000) Water mass properties and fluxes in the Rockall Trough 1975-1998. Deep-Sea Res I 47: 1303-1332

Hughen KA, Overpeck JT, Lehman JS, Kashgarian M, Southon J, Peterson LC, Alley R, Sigman DM (1998) Deglacial changes in ocean circulation from an extended radiocarbon calibration. Nature 391: 65-68

Hughen KA, Southon J, Lehman S, Overpeck JT (2000) Synchronous radiocarbon and climate shifts during the last deglaciation. Science 290: 1951-1954

Kalis AJ, Merkt J, Wunderlich J (2003) Environmental changes during the Holocene climate optimum in central Europe - human impact and natural causes. Quaternary Sci Rev 22: 33-79

Levin I, Bösinger R, Bonani G, Francey R, Kromer B, Münnich KO, Suter M, Trivett NBA, Wölfli W (1992) Radiocarbon in atmospheric carbon dioxide and methane: global distribution and trends. In: Taylor RE, Long A, Kra R (eds) Radiocarbon after four Decades: an interdiscipilanry Perspective. Springer, New York, pp 503-518

Lomitschka M, Mangini A (1999) Precise Th/U-dating of small and heavily coated samples of deep-sea corals. Earth Planet Sci Lett 170: 391-401

Ludwig KR (2001) ISOPLOT 2.49. Berkeley Geochronolog Cent Spec Publ 1a, 58

Ludwig KR, Simmons KR, Szabo BJ, Winograd IJ, Landwehr JM, Riggs AC, Hoffman RJ (1992) Mass-spectrometric ^{230}Th-^{234}U-^{238}U dating of the Devils Hole calcite vein. Science 258: 284-287

Mangini A, Lomitschka M, Eichstädter R, Frank N, Vogler S, Bonani G, Hajdas I, Pätzold J (1998) Coral provides way to age deep water. Nature 392: 347

Moran SB, Hoff JA, Buesseler KO, Edwards RL (1995) High precision ^{230}Th and ^{232}Th in the Norwegian Sea and Denmark by thermal ionization mass spectrometry. Geophys Res Lett 22: 2589-2592

New AL, Smythe-Wright D (2001) Aspects of the circulation in the Rockall Trough. Cont Shelf Res 21: 777-810

Nydal R, Gislefoss JS (1996) Further application of bomb ^{14}C as a tracer in the atmosphere and ocean. Radiocarbon 38: 389-406

Robinson LF, Belshaw NS, Henderson GM (2004) U and Th concentrations and isotope ratios in modern carbonates and waters from the Bahamas. Geochim Cosmochim Acta 68: 1777-1789

Rüggeberg A, Dorschel B, Dullo W-Chr, Hebbeln D (2005) Sedimentary patterns in the vicinity of a carbonate mounds in the Hovland Mound Province, northern Porcupine Seabight. In: Freiwald A, Roberts JM (eds) Cold-water Corals and Ecosystems. Springer, Berlin Heidelberg, pp 87-112

Schröder-Ritzrau A, Mangini A, Lomitschka M (2003) Deep-sea corals evidence periodic reduced ventilation in the North Atlantic during the LGM/Holocene transition. Earth Planet Sci Lett 216: 399-410

Schröder-Ritzrau A, Mangini A, Freiwald A (2005) U/Th-dating of deep-water corals from the Eastern North Atlantic and the Mediterranean Sea. In: Freiwald A, Roberts JM (eds) Cold-water Corals and Ecosystems. Springer, Berlin Heidelberg, pp 157-172

Shen GT, Dunbar RB (1995) Environmental controls on uranium in reef corals. Geochim Cosmochim Acta 59: 2009-2024

Siani G, Paterne M, Arnold M, Bard E, Métivier B, Tisnerat N, Bassinot F (2000) Radiocarbon reservoir ages in the Mediterranean Sea and Black Sea. Radiocarbon 42: 271-280

Siani G, Paterne M, Michel E, Sulpizio R, Sbrana A, Arnold M, Haddad G (2001) Mediterranean sea surface radiocarbon reservoir age changes since the last glacial maximum. Science 294: 1917-1920

Smith JE, Risk MJ, Schwarcz HP, McConnaughey TA (1997) Rapid climate change in the North Atlantic during the Younger Dryas recorded by deep-sea corals. Nature 386: 818-820

Stuiver M, Polach H (1977) Discussion: Reporting of ^{14}C data. Radiocarbon 19: 355-363

Stuiver M, Reimer PJ, Bard E, Beck JW, Burr GS, Hughen KA, Kromer B, McCormac G, van der Plicht J, Spurk M (1998) Intcal98 radiocarbon age calibration: 24,000-0 cal BP. Radiocarbon 40: 1041-1083

Thompson WG, Spiegelman MW, Goldstein SL, Speed RC (2003) An open-system model for U-series age determinations of fossil corals. Earth Planet Sci Lett 210: 365-381

Van Rooji D, Blamart D, Unnithan V (2001) Cruise-report MD123 Geosciences: Leg 2, part GEOMOUND. Porcupine Basin and Rockall Trough, off western Ireland, pp. 67

Van Weering T, Shipboard Scientific Party (1998) Shipboard report RV Pelagia, Cruise 64/124 Leg 2, A survey of the SE Rockall Trough and Porcupine margin. NIOZ, Texel, 26 pp

Van Weering T, Shipboard Scientific Party (1999) Shipboard cruise report RV Pelagia 64PE143: A survey of carbonate mud mounds of Porcupine Bight and S. Rockall Trough margins. NIOZ, Texel, 82 pp

Villemant B, Feuillet N (2003) Dating open systems by the ^{238}U-^{234}U-^{230}Th method: application to Quaternary reef terraces. Earth Planet Sci Lett 210: 105-118

Vogler S, Scholten J, van der Loeff MR, Mangini A (1998) ^{230}Th in the eastern North Atlantic: the importance of water mass ventilation in the balance of ^{230}Th. Earth Planet Sci Lett 156: 61-74

White M, Mohn C, de Stigter H, Mottram G (2005) Deep-water coral development as a function of hydrodynamics and surface productivity around the submarine banks of the Rockall Trough, NE Atlantic. In: Freiwald A, Roberts JM (eds) Cold-water Corals and Ecosystems. Springer, Berlin Heidelberg, pp 503-514

Wilson JB (1979) 'Patch' development of the deep-water coral *Lophelia pertusa* (L.) on Rockall Bank. J Mar Biol Ass UK 59: 165-177

II

Distribution

Chapter content

Deep coral growth in the Mediterranean Sea: an overview

Marco Taviani[1], André Freiwald[2], Helmut Zibrowius[3]

[1] ISMAR-Marine Geology Division, CNR, Via Gobetti 101, I-40129 Bologna, Italy
(marco.taviani@bo.ismar.cnr.it)
[2] Institute of Paleontology, Erlangen University, Loewenichstr. 28, D-91054 Erlangen, Germany
[3] Centre d'Océanologie de Marseille, Station Marine d'Endoume, Rue Batterie des Lions, F-13007 Marseille, France

Abstract. The Mediterranean basin represents an excellent biological archive of past and modern deep coral growth whose study may help to understand taxonomic, biogeographic, ecological, and evolutionary patterns of modern deep coral bioconstructions, best embodied by the *Lophelia*-reefs and mounds of the Atlantic Ocean. In fact, the occurrence of extant deep coral genera in the Mediterranean basin is documented, although not continuously, since the Miocene. Following the Messinian crisis the re-colonisation of the basin by deep coral is likely to have started with the Pliocene but little is known about deep coral biota linked to hard substrates during this epoch. It is certain that Atlantic-type deep-sea corals including the scleractinian triad *Lophelia-Madrepora-Desmophyllum* have been established in the basin since the latest Pliocene-Early Pleistocene as proven by outcrop evidence in southern Italy, especially Sicily and Calabria, and in Rhodes. Still-submerged dead coral assemblages are widespread in the entire basin between c. 250-2500 m depth; the majority is aged at the last glacial by AMS, C^{14} and U/Th dating. The present situation (post-glacial) is a general decline of such deep corals in the Mediterranean, and this is especially true for *Lophelia* which appears to be more severely affected by local extinctions. To date, the only exception to this general rule is represented by the recent discovery of prosperous *Lophelia* populations in the Eastern Ionian Sea.

Keywords. Mediterranean, deep-water corals, Pleistocene, Pliocene, Miocene

Introduction

In the last decade, the topic of habitat-forming deep-sea corals in the world ocean has become the focus of an unprecedented attention resulting in many often inter-related international and national scientific programmes (Freiwald et al. 2004). The

majority of such interest has been focused on the northeastern Atlantic, a region characterised by the occurrence of many living and subfossil deep-sea coral reefs and mounds (Freiwald 2002; Freiwald et al. 2004, and references therein). This includes the Mediterranean Sea, that, in spite of its being a semi-enclosed marginal sea of the Atlantic Ocean, hosts deep-sea coral habitats, although impoverished with respect to their oceanic counterparts (e.g., Remia and Taviani 2004; Taviani et al. 2004). In addition, the Mediterranean is also a significant location in light of its extensive Upper Cenozoic paleontological documentation of Atlantic-type extant deep-sea coral genera (e.g., Di Geronimo 1979; Placella 1979; Zibrowius 1980, 1987, 1991; Taviani and Colantoni 1984; Corselli 2001; Taviani and Remia 2001; Vertino 2003, 2004).

A profound understanding of Mediterranean deep-sea coral biota evolution through time is thus central to issues of more general interest. First, how and when was the Mediterranean basin colonised by deep-sea corals? Second, with respect to the main frame builders of the present East Atlantic-Mediterranean mounds, i.e. the triad *Lophelia pertusa* (Linné, 1758), *Madrepora oculata* Linné, 1758, *Desmophyllum dianthus* (Esper, 1794) (better known as *D. cristagalli* Milne Edwards and Haime, 1848), which was the function of this basin play in terms of coral origination, dispersal avenues, refuge availability in times of crisis, and colonisation patterns?

This article is an introductory account to deep-sea scleractinian corals of the Mediterranean basin through time with special reference to the main taxa contributing to *Lophelia* coral mounds (Fig. 1). It also intends to provide the basic bibliography concerning various aspects of Mediterranean extant deep-sea taxa.

Frame-building deep-sea corals in the modern Mediterranean Sea

It is not easy to discriminate between subfossil and modern material based only on the external appearance of coral skeletons. Corals of proven Pleistocene age that have been rapidly buried in fine-grained sediment, that efficiently sealed the carbonate skeleton from seawater circulation, could still maintain their original lustre and a strikingly fresh appearance (Remia and Taviani 2004). At places, skeletons exposed to seawater may be easily patinated by Fe-Mn-films. In fact, dead corals exhibiting both situations on different parts of the skeleton may have been mistakenly considered alive (cf. Selli 1970; Sartori 1980). Thus, the status of many old claims of presumed "living" corals is in need of verification (e.g., Duncan 1873; Steindachner 1891; Marenzeller 1893; Lacaze-Duthiers 1897; Cecchini 1917; Brunelli and Bini 1934, etc.). As a precaution, we solely consider as living only those corals that still display polyp tissue. Only a few of the verified records of the triad *Lophelia, Madrepora, Desmophyllum* fulfil this condition. To date, Zibrowius' (1980) monograph on Mediterranean and Northeast Atlantic Scleractinia represents a useful base for investigations devoted to taxonomy and distribution of deep-sea scleractinians in the former area. From that study, it is evident that all three members of the triad are presently in recession in the Mediterranean basin, although

Fig. 1 General map of the Mediterranean Basin showing occurrences of fossil deep-sea scleractinian corals (submerged taphocoenoses excluded) with at least one representative of the triad *Madrepora, Lophelia, Desmophyllum*; black triangle = Miocene s.l.; red triangle = Upper Miocene (Carboneras); black square = Lower-Middle Pliocene; red square = Upper Pliocene; black circle = Early-Middle Pleistocene (many localities); living *Lophelia* banks at Santa Maria di Leuca also shown (red circle)

not at equal rates. Before the discovery of a thriving population off Santa Maria di Leuca (Mastrototaro et al. 2001; Taviani et al. 2004; Tursi et al. 2004), *Lophelia pertusa* was considered close to extinction in the Mediterranean Sea. From his own experience, Zibrowius (1980) reported only two potential occurrences of small live branches (i.e., with polyp tissue), one off Banyuls, Gulf de Lion, and the other from Cabo de Gata, Alboran Sea. These records are based upon old museum specimens from cable ship, so that their origin may be imprecise.

To those, we can now add the record of a small branch dredged from the Nameless Bank in the Strait of Sicily, and which seemed to contain some polyp tissue (Zibrowius and Taviani 2005). Vafidis et al. (1997) mentioned it as alive from the northern Aegean Sea but we are unsure about the presence of living polyps.

Madrepora oculata, originally described by Linné on the basis of samples from Sicily and the Tyrrhenian Sea (Zibrowius 1980), is more widespread in the Mediterranean and live records are not as rare as those of *Lophelia* (Figs. 2a, f). In fact, it has been cited as alive from various regions of the basin, from the Alboran to the Aegean Seas, but not yet from the Adriatic Sea (Reyss 1964; Bourcier and Zibrowius 1973; Zibrowius 1980; Vafidis et al. 1997; Tunesi and Diviacco 1997; Tursi et al. 2004; Orejas et al. 2003; Álvarez-Pérez et al. 2005).

Desmophyllum dianthus is relatively common and widespread in the whole Mediterranean (Figs. 2c, e), with the possible exclusion of the Adriatic (Zibrowius 1979, 1980). It has been reported alive between c. 200-1200 m depth, from the Alboran Sea (Álvarez-Pérez et al. 2005), Balearic Sea (escarpments north of Mallorca and east of Menorca, COBAS Cruise of RV *Urania*, April 2004), Gulf of Lions (Zibrowius 1980; J.-M. Gili, pers. com.), Western Tyrrhenian Sea (Vertino 2003), Ionian Sea off Apulia (Galil and Zibrowius 1998; Tursi et al. 2004; Taviani et al. 2004), Aegean Sea (Zibrowius 1979, 1980), and Eratosthenes Seamount south
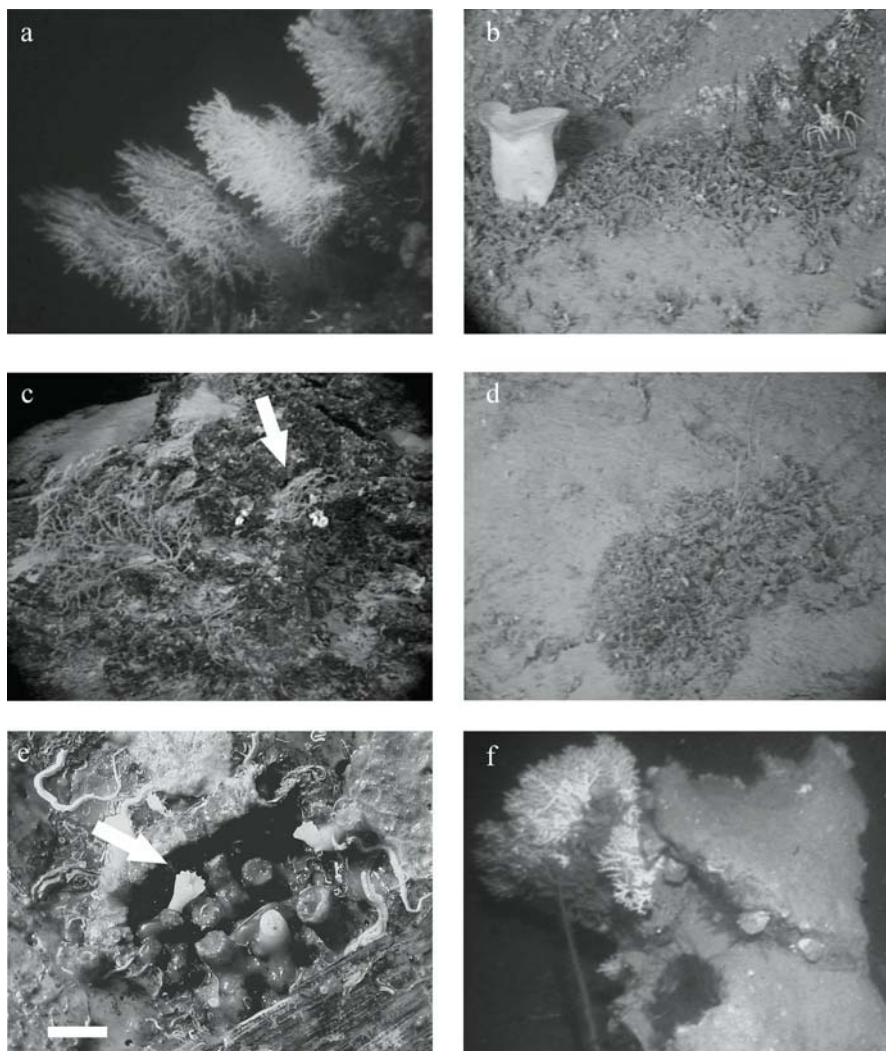
Fig. 2 Examples of living and subrecent deep-sea corals from various Mediterranean localities. **a** Iso-aligned fans of living *Madrepora oculata* photographed at 260 m depth from a manned submersible in the Cassidaigne Canyon, east of Marseille (dive with Cousteau's SP 350). **b** Coral debris (biostromal facies) scattered on muddy bottom in the Alboran Sea at 349 m depth; corals are mostly *Dendrophyllia* and possibly *Madrepora* and *Lophelia*, note a scavenging decapod (right) and a living sponge (left); (photo from the manned submersible *Cyana*, stat. CYALB3-067; © Ifremer). **c** Living *Desmophyllum dianthus* (arrow) together with living gorgoniaceans and dead corals encrusting a rocky bottom on the western margin of Corsica (photo from the manned submersible *Cyana*, stat. CYL19-027; © Ifremer). **d** *Madrepora-Lophelia* coral debris (biostromal facies) on muddy bottom near Alboran Island, Western Mediterranean at 448 m depth (photo from the manned submersible *Cyana*, stat. CYALB3-037; © Ifremer). **e** Living (arrow) and dead juvenile *Desmophyllum dianthus* encrusting the surface of a large deep-sea oyster dredged from the escarpment on the eastern

of Cyprus (Galil and Zibrowius 1998: c. 1200 m, deepest known occurrence in the Mediterranean Sea).

Paleobiological documentation of deep-sea corals in the Upper Cenozoic of the Mediterranean basin

General

Although frame-building deep-sea scleractinians are in principle suitable for easy preservation in the geological record (Teichert 1958), the overall paleontological documentation of extant taxa is, in fact, rather scant (Cairns and Stanley 1981; Stanley and Cairns 1988). For instance, the distribution map provided by Cairns and Stanley (1981: Fig. 2) shows only one Upper Tertiary locality, i.e. the Miocene and Pliocene coral thickets described by Squires (1964) for New Zealand. However, the map does not take into account the abundant paleontological documentation on extant deep-sea coral genera and species in the Mediterranean basin (e.g., Seguenza 1864, 1880; Chevalier 1961, 1962; Placella 1979, and many others). Nevertheless, the paucity of such occurrences in the Earth's geological record seems confirmed. This is not surprising since the subaerial exposure of Recent deep-sea habitats such as those represented by coral banks may only take place under special geodynamic conditions. Considerable uplift can be achieved in terranes subject to significant compression or as a consequence of isostatic rebound; the latter process is responsible for the postglacial (c. Holocene) uplifting of coral banks in Scandinavia (Dons 1944) but has no impact on the Mediterranean region that was deprived of a glacial cap. Here, uplift in response to collisional synsedimentary tectonics was by far the most powerful mechanism driving the raising of formerly submerged escarpments and other deep-sea topographic features, enriched in deep-sea corals which can now be observed in southern Italy (especially northeastern Sicily and Calabria: Barrier 1986; Barrier et al. 1996; Lentini et al. 2000) and in Rhodes (e.g., Titschack and Freiwald 2005). Pre-Modern occurrences of subfossil deep-sea corals are also a common feature of the submerged topography of the present Mediterranean.

What follows is a revision of geological deep coral situations ordered by increasing antiquity.

Submerged taphocoenoses (Late Pleistocene to Early Holocene)

Pre-modern deep-sea scleractinians (no living polyps) occur commonly throughout the basin (Figs. 2b-e, 3a-c) both as still *in situ* assemblages (from single occurrences to well-structured mounds) or as coral-bearing sedimentary deposits (biostromal: Figs. 2b, d), at depths ranging between 250-3000 m (e.g., Gravier 1920; Bourcart 1952; Broch 1953; Rossi 1957, 1958, 1961; Segre 1959; Županovič

---

side of Menorca island, Baleares (RV *Urania* stat. COBAS 96, 40°01.1 N, 04°23.6 E, 572 m depth); bar = 1 cm (photo courtesy of B. Sabelli). **f** Patchy colonies of living *Madrepora oculata* encrusting a rocky seabottom at 120 m depth from Cap Creus Canyon, offshore Catalunya; note entangled fishing line (photo courtesy of J.-M. Gili)
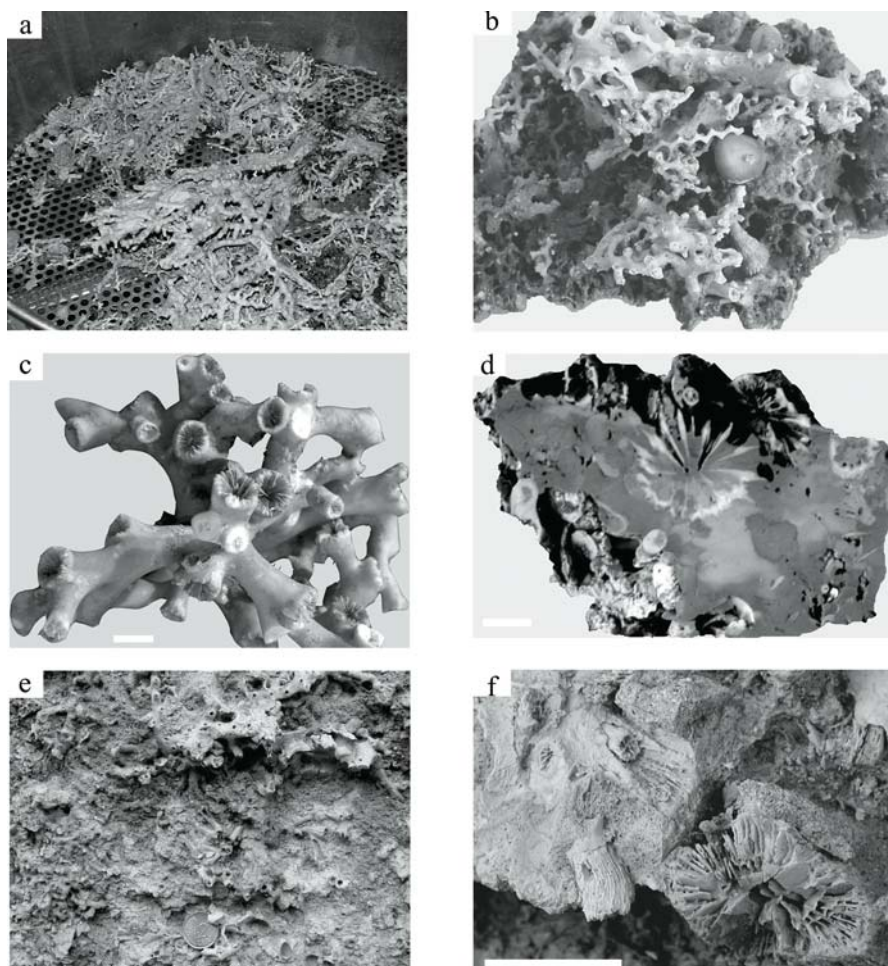
Fig. 3 Examples of Late Pleistocene (submerged taphocoenoses) and Early Pleistocene (outcrop) deep-sea coral deposits from various Mediterranean localities. **a** Coral shell hash after washing the mud of a dredged shallow-buried *Madrepora* mound off the Tuscan Archipelago, Eastern Tyrrhenian Sea (RV *Urania*, cruise CORTI, c. 370 m depth) (photo courtesy of B. Sabelli). **b** Coral framestone formed by loosely cemented branches of *Madrepora oculata* and subordinate *Lophelia pertusa* entrapping skeletonised benthic tests (such as the terebratulid brachiopod *Gryphus vitreus*, centre); Late Pleistocene coral mound, Tuscan Archipelago (RV *Urania*, station CORTI 71, 43°13.7 N, 09°36.3 E, 384 m depth); the striking colour difference reflects the degree of burying within mud; the dark patinated and bioeroded parts are exposed to sea water while white corals are still embedded in mud (photo courtesy of A. Remia). **c** Large and thickened "glacial" morphotype of *Lophelia pertusa* from a Late Pleistocene submerged taphocoenosis, Strait of Sicily; bar = 1 cm (photo courtesy of A. Remia). **d** *Desmophyllum dianthus* coral bafflestone from the Malta escarpment (RV *Jean Charcot*, Escarmed st. DD4, 36°34.5 N, 15°37.0 E, 3200-2500 m; Last Glacial); fresh detachment section (polished) showing pristine *Desmophyllum* corallites embedded in micrite; note that external surface is heavily patinated by Mn-Fe oxides; bar = 1 cm

1969; Best 1970; Bourcier and Zibrowius 1970, 1973; Reyss 1973; Forest and Cals 1977; Zibrowius and Grieshaber 1977; Zibrowius 1979, 1980; Sartori 1980; Pérès 1982, 1989; Rocchini 1983; Di Geronimo and Bellagamba 1986; Pérès 1989; Corselli and Bernocchi 1990; Di Geronimo et al. 1993; Zabala et al. 1993; Bonfitto et al. 1994; Tunesi and Diviacco 1997; Vertino 2003; Taviani and Remia 2001; Remia and Taviani 2004). Occurrences represented by dead, encrusted and/or heavily bioeroded and often patinated (Figs. 3b, d), altogether "old-looking" corals (Segre and Stocchino 1969; Bourcier and Zibrowius 1970; Selli 1970; Taviani and Colantoni 1979, 1984; Cita et al. 1979, 1980; Allouc 1987) were generally considered as belonging to pre-modern Quaternary assemblages (Blanc et al. 1959; Pérès and Picard 1964; Bellaiche et al. 1974). This interpretation was confirmed by radiometric dating that, in most cases, provided a Late Pleistocene age (Hersey 1965; Zibrowius 1980, 1981; Pudsey et al. 1981; Taviani 1981; Taviani and Colantoni 1984; Delibrias and Taviani 1985; Allouc 1987; Remia and Taviani 2004; Schröder-Ritzrau et al. 2005). Deep-sea corals are also often incorporated in limestones at various stages of submarine micritization (e.g., Cita et al. 1980; Zibrowius 1981, 1985; Taviani and Colantoni 1984; Allouc 1987; Remia et al. 2004; Remia and Taviani 2004; Zibrowius and Taviani 2005). However, their general aspect should not induce to overestimate their antiquity (last interglacial as presumed by Blanc et al. 1959). Many such coral hardgrounds are in fact Late Pleistocene in age as proven by C^{14} dating (e.g., Taviani and Colantoni 1984).

Outcrop Pleistocene record

For its areal extension, number and quality of outcrops, variety of facies and richness of fossil fauna, the Early Pleistocene Mediterranean archive of extant Atlantic-type deep-sea scleractinian coral and associated invertebrates is unmatched by any other known Cenozoic occurrence worldwide. The best exposures are found in southern peninsular Italy (Basilicata, Calabria) and Sicily (Figs. 3e, f), especially on both sides of the Strait of Messina (Seguenza 1864, 1880; De Stefano 1900; De Stefani 1955; Sganga 1978; Placella 1979; Guadagno et al. 1979; Ruggieri et al. 1979; Di Geronimo 1979, 1987, 1995; Di Geronimo and Zibrowius 1983; Gaetani and Saccà 1983; Barrier 1984, 1986, 1987; Barrier et al. 1985, 1986, 1989, 1996; Micali and Villari 1989; Colella et al. 1996; Colella and D'Alessandro 1988; Di Geronimo et al. 2005). Elsewhere in the Mediterranean basin, well-preserved extant-type deep coral occurrences containing the *Lophelia-Madrepora-Desmophyllum* triad crop out on the island of Rhodes (Figs. 4b-f), in the Aegean Sea (Jüssen 1890; Hanken et al. 1996; Bromley 2005; Titschack and Freiwald 2005). Conditions at the origin of the spectacular collection of deep coral-bearing facies described from southern Italy can be attributed to the complex geodynamic evolution of this sector of the Mediterranean basin (e.g., Barrier 1986, 1987; Montenat et al. 1987; Barrier

(photo courtesy of A. Remia). **e** Coral framestone-bafflestone with *Lophelia*, *Madrepora* and *Desmophyllum*, Early Pleistocene, near Messina, Sicily (photo courtesy of A. Vertino). **f** Early Pleistocene *Desmophyllum* coral boundstone, uplifted paleoescarpment near Messina, Sicily; coin diameter = 2 cm (photo courtesy of A. Vertino)

et al. 1990, 1996; Lentini et al. 2000). The evolution of the Calabro-Peloritan Arc is marked by strong synsedimentary processes conducive to the uplifting of former paleoescarpments, deep-submarine hydraulic dunes, mass-gravity deposits and other deep coral-bearing settings, including sedimentary dykes in-filled by coarse
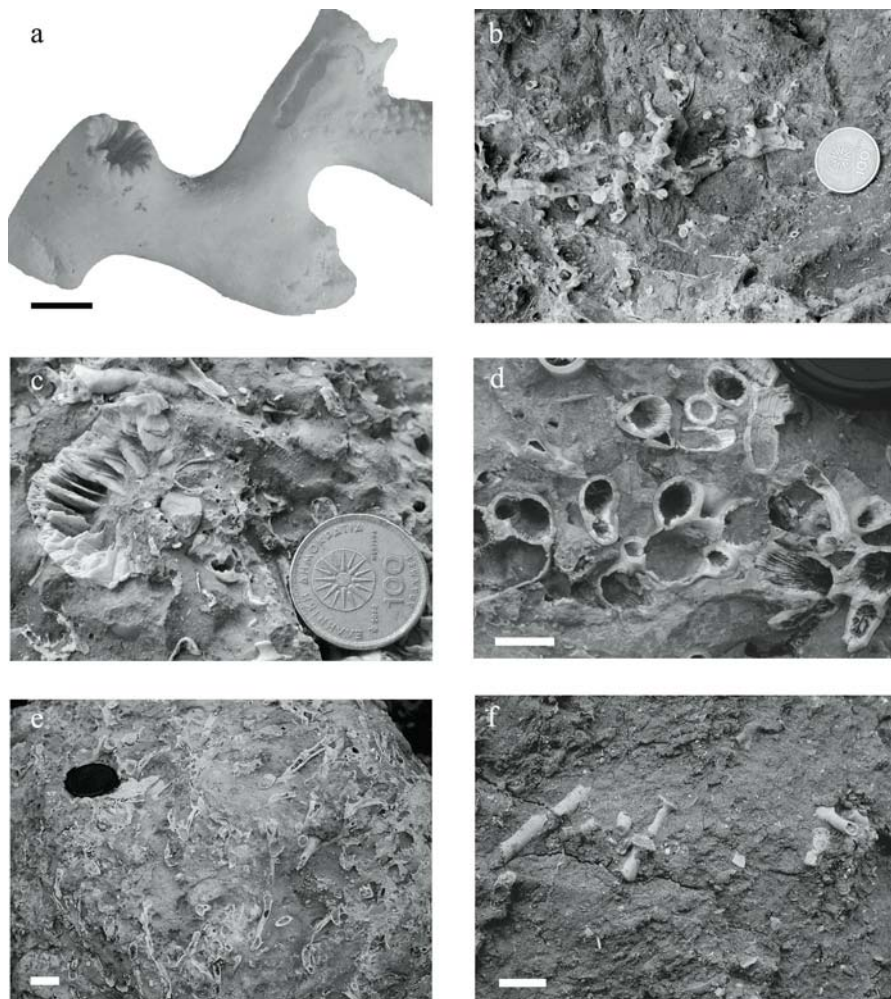
Fig. 4 Examples of Neogene and Early Pleistocene deep-sea coral occurrences from various Mediterranean localities. **a** Specimen of *Madrepora* sp. from the Upper Miocene (Messinian) "Red Breccia" of Carboneras, Spain; bar = 1cm. **b** *Madrepora* sp. branch from the Early Pleistocene of Rhodes, Greece; coin diameter = 2 cm. **c** *Desmophyllum* coral bafflestone from Rhodes; note strong degree of coral recrystallisation; coin diameter = 2 cm. **d** Intensely lithified *Lophelia* limestone from Rhodes; bar = 1 cm. **e** Early Pleistocene *Lophelia* thicket (*sensu* Squires 1964) from Rhodes, diameter of camera cap = 6 cm. **f** Early Pleistocene *Lophelia* coral gravity deposit from Lindos, Rhodes; bar = 1 cm (photo courtesy of A. Vertino)

bioclastic deposits (e.g., Barrier 1986). The rich deep-sea coral fauna from these outcrops was described by the prominent Sicilian paleontologist Giuseppe Seguenza (Seguenza 1864, 1873-77, 1880) who, little aware of variability, introduced various new species to the *Madrepora* (as *Amphihelia* and *Diplohelia*), *Lophelia* (as *Lophoelia*, including *L. pertusa* as *prolifera*) and *Desmophyllum*. His stratigraphy, however, was largely incorrect since he attributed many outcrops to the Pliocene. The modern stratigraphic revisitation of many of these outcrops has proven that their age is in fact Early Pleistocene (e.g., Guadagno et al. 1979; Barrier 1987; Lentini et al. 2000, etc.). The affinity of such faunas with modern counterparts inhabiting the Atlantic and other oceans is obvious and has not gone unnoticed (e.g., Di Geronimo 1979). The taxonomic position of closely similar fossil and modern taxa, and their potential synonymy has been variously interpreted (e.g., Zibrowius 1974, 1980; Corselli 2001; Vertino 2003). The taxonomic status of taxa described by Seguenza with respect to their recent equivalents is at present the subject of a comprehensive critical evaluation based on morphological characters of the skeletons (Vertino 2003, and work in progress). It should be observed, however, that coral skeletal morphology may not always be sufficiently diagnostic to distinguish species, as demonstrated by molecular studies of colonial zooxanthellate scleractinians from Indo-Pacific coral reefs where various morphotypes ascribed to the same taxon revealed instead significant genetic distances (e.g., Knowlton and Jackson 1994). Although deep-sea coral taxonomy is traditionally based on skeleton morphology (e.g., Zibrowius 1980; Cairns 1989), the potential uncertainty related to this approach should be taken into consideration when synonyms are proposed based only on skeletal similarities (e.g., Corselli 2001; Vertino and Di Geronimo 2003). The ongoing genetic studies of geographically-disjunct *Lophelia* populations may serve as a test for understanding the degree of morphological and genetic plasticity within an emblematic deep-sea taxon characterised by an apparent geological longevity and a wide geographic distribution (Le Goff-Vitry et al. 2004; Le Goff-Vitry and Rogers 2005).

Pliocene record

The rarity of deep-sea hard substrates suitable for coral growth preserved in the geologic record of the Mediterranean basin (e.g., Corselli et al. 1985) makes it difficult to ascertain the actual presence or absence of the main taxa under scrutiny (*Lophelia, Madrepora, Desmophyllum*) during this epoch. In fact, scleractinian corals are relatively frequent in deep-sea sequences of Pliocene age but typically records refer to solitary species adapted to muddy outer-shelf and slope environments (e.g., De Angelis d'Ossat 1895; Osasco 1895; Simonelli 1895; Zuffardi-Comerci 1927; Montanaro-Gallitelli 1931; Annoscia 1963, etc.). However, there are a few exceptions that do not conform this impression. One is provided by the coral fauna identified on a cold-seep chemoherm of Early Piacenzian age associated with hemipelagic and sapropel marls in the Stirone river sequence, northern Apennines (Parma province). Here a large limestone block was the substrate of colonial (*Coenocyathus* sp.) and solitary (*Caryophyllia* sp.) corals (Taviani et al. 1997; Monegatti et al. 2001). *Dendrophyllia* spp. are recorded from Pliocene deep-sea

sediments in northern Italy (Osasco 1895; Corselli and Bernocchi 1990). Extant genera and sometimes species, including *Madrepora* (as *Amphihelia* or *Diplohelia*), have also been reported from the Pliocene of Emilia, northern Italy (Simonelli 1895, 1896; Montanaro-Gallitelli 1931). *Desmophyllum* is recorded from the Early Pliocene of Liguria by Osasco (1895). In addition, *Madrepora* cf. *oculata* (a doubtful record as *Amphihelia* cf. *oculata*), *Dendrophyllia cornigera*, and *Caryophyllia* spp., have all been reported from the "Pliocene" of the east coast of Sardinia, near Orosei (Dieni and Omenetto 1960; Chevalier 1962). The real stratigraphic position of those deposits is, however, confusing and in need of revision. For example, Seguenza (1880) attributed to this epoch (his "Astiano") terranes that, as discussed above, are now assigned to the Pleistocene. Thus, the claim by Chevalier (1961) that *Lophelia* (as *Lophohelia*) has been present in the Mediterranean basin since the Lower Pliocene must be judged with caution since this assertion is possibly based on Seguenza's outdated stratigraphy. Most of the fauna from the sequence of Masseria Concarone, near Matera (southern Italy), has also been considered as of Pliocene age (Placella 1980; Zibrowius and Placella 1981), although representatives of the triad have only been recorded from the Pleistocene part of this sequence. Upper Pliocene deep-sea coral-bearing deposits with *Madrepora* and *Desmophyllum* are reported from outcrops in southern Italy (Barrier 1984, 1987; Zibrowius and Ten Hove 1987; Roux et al. 1988; Barrier et al. 1989, 1990; Lentini et al. 2000) and Rhodes (Hanken et al. 1996). The intrinsic complexity of dating deposits representing paleoescarpments, debris flows and biostromal accumulations from steep settings may at times make inequivocal stratigraphic assignment problematic. However, a late Pliocene age for such deep coral bearing deposits seems likely.

Miocene records

At Carboneras, north of Cabo de Gata (southeastern Spain), a deep-sea assemblage containing corals, sponges, stalked crinoids and gastropods has been reported associated with an olistostrome (Barrier et al. 1992). Corals are diverse and comprehend stylasterids, gorgonians (including *Corallium* and *Keratoisis*) and scleractinians (among others, *Desmophyllum* and *Madrepora*; Fig. 4a). This bathyal macrofauna infilled fissures of the "Red Breccia", a re-sedimented volcanic unit, for which a Lower Messinian age has been proposed on the basis of planktonic foraminiferan evidence. So far, the Carboneras fauna represents the most comprehensive and reliable example of this age, in the Mediterranean area, of a hard substrate bathyal coral fauna containing extant Atlantic-type taxa (at least at the generic level).

A historical review of the literature reveals that the three generic taxa forming the triad have been recorded from the Middle Miocene of the Mediterranean basin.

Madrepora (as *Amphihelia* or *Diplohelia*) and *Desmophyllum* (including the species *D. cristagalli*) were recorded from the Miocene (Burdigalian) of the Turin Hill, northern Italy (De Angelis 1894; Osasco 1897; Zuffardi-Comerci 1932; Chevalier 1961) and a single record of *Madrepora* exists from the Upper Miocene (Tortonian), also from northern Italy (Zuffardi-Comerci 1932). *Lophelia* (as *Lophohelia*) is only cited from the Middle Miocene of Sardinia (De Angelis d'Ossat

and Neviani 1897; Zuffardi-Comerci 1932; Comaschi Caria 1963).

In addition, Upper Miocene deep-water coral banks containing *Oculina* and *Dendrophyllia* (*Calcare di Mendocino*) occur in Calabria, southern Italy (Mastandrea et al. 2002).

No taxonomic and ecological work has been done on such Miocene deep-sea coral faunas more recently. However, the interest of this subject in the more general context of *Lophelia* mound evolution and biogeography is self-evident.

Discussion

The large amount of fossil documentation within the Mediterranean region of extant deep-sea scleractinian corals, at present the top frame builders within deep-sea ecosystems (Freiwald et al. 2004), makes this basin a key-area for tracking evolutionary and dispersal patterns of such coral communities.

As previously discussed, the existence of a diversified oceanic-type, bathyal coral fauna in the Miocene of the Mediterranean basin is well supported by various lines of evidence. These include the occurrence of the solitary scleractinian genus *Deltocyathus* (Corselli 2001). *Deltocyathus italicus* (Michelotti, 1838) was described from the Upper Miocene (Tortonian) of northern Italy. This taxon has sometimes been considered conspecific with a modern representative of the Atlantic fauna (Cairns 1981) whereas Zibrowius (1980) described the modern form as a separate taxon, *D. conicus*. The Middle-Upper Miocene coral fauna is coherent with the reconstructed physiography of the Mediterranean basin (Mesogea), at a time that allowed unrestricted hydrological exchanges with the ocean through wide and deep corridors, in addition to the existence of psychrospheric conditions (e.g., Corselli 2001).

The end of the Miocene epoch coincided with the Messinian Salinity Crisis, whose oceanographic signature is thought to have been lethal for stenoecious marine ecosystems inhabiting the Mediterranean basin (see Por and Dimentman 1985; Taviani 2002; Emig and Geistdoerfer 2004, for a critical discussion of this topic).

The restoration of water exchanges with the Atlantic Ocean at the beginning of the Pliocene epoch replenished the basin with marine biota. Ocean-type deep-sea corals once again had the opportunity to colonise suitable regions of the Mediterranean basin, although the documentation for this specific group is rather scant. For part of the Pliocene, at least, the Mediterranean basin enjoyed quasi-oceanic, psychrospheric conditions enhanced by a corridor with the Atlantic deep enough to guarantee the free access of deep-water benthos and nekton from the ocean (e.g., Benson 1972; Russo 1980; Cigala-Fulgosi 1986, 1996; Corselli 2001). The lack of unequivocal documentation of *Lophelia*, *Madrepora,* and *Desmophyllum* in most of the Mediterranean Pliocene may either be an artifact linked to the scarcity of outcropping suitable fossil settings or a real response to unsuitable ecological conditions. In contrast, these extant taxa are fully documented since the late Pliocene and, most of all, Early Pleistocene. Faunal data (e.g., Zibrowius 1987; Roux et al. 1988; Barrier et al. 1989; Di Geronimo and La Perna 1997) support the view

that at that time the oceanographic conditions in the Mediterranean were closer to those of the modern Atlantic Ocean than at present. The result was a Mediterranean scleractinian deep-sea fauna of Atlantic affinity more diverse than during the remaining part of the Quaternary. A similar situation occurred during glacial ages, as supported by data from submerged taphocoenoses presented above, indicating that a deep-sea coral fauna thrived throughout the basin during the Late Pleistocene (c. last glaciation). Many occurrences of fossil *Lophelia* of this age display large and thick skeletal morphotypes, similar to present counterparts in the northeastern Atlantic. With a few exceptions, these vigorous coral communities are now extinct or in recession (Zibrowius 1980; Fredj and Laubier 1985). The Mediterranean, as well as its precursor basins, are colonised by such coral faunas at times when special contour conditions (submarine topography and oceanography) are realised. Times as the present postglacial, are adverse for strong coral growth which, instead, is reduced although not annihilated.

The quasi cosmopolitan distribution of the target taxa in the world ocean (Zibrowius 1980; Cairns and Stanley 1981) implies a considerable longevity of these corals through geological times. The paleontological documentation outlined above provides further arguments that the core of the scleractinian deep-sea fauna was and is found in the open ocean.

Mediterranean deep-sea corals: present research and perspectives

Recent research (e.g., De Mol et al. 2005; Schröder-Ritzrau et al. 2005) documents that *Lophelia* bioconstructions in the NE Atlantic display dynamics similar to those of their Mediterranean counterparts throughout the latest Pleistocene in response to global and local climatic-driven events. A picture now emerges that populations along a theoretical geographic continuum are in fact arranged in a complex mosaic-like web susceptible to rapid modifications, connections and disconnections through time. One fundamental question is how to understand the relationships existing between Late Pleistocene to present coral occurrences in the Mediterranean basin and their Atlantic counterparts. Within this scenario, a first significant step should be to investigate the genetic exchanges among various coral populations within the Mediterranean basin itself. The recently discovered prosperous *Lophelia* sites at Santa Maria di Leuca, in the Ionian Sea (Tursi et al. 2004; Taviani et al. 2004), and possibly in the westernmost Mediterranean (Álvarez-Pérez et al. 2005), offers an opportunity of that type of investigation. It should then be extended to unravelling genetic links between Mediterranean and Atlantic populations. In principle, this approach would help to test the controversial hypothesis of the Mediterranean basin having acted as a refuge for Atlantic deep-sea corals during stresses of the Late Pleistocene (De Mol et al. 2005).

Investigating genetic relationships between coral sites within and outside the Mediterranean during the latest Pleistocene may benefit from discovering undegraded DNA still retained in pre-modern pristine coral material. Samples of *Lophelia, Madrepora* and *Desmophyllum* from submerged coral assemblages in the

Tyrrhenian and the Baleares (RV *Urania* cruises CORTI and COBAS) are presently under investigation.

Ongoing research on Mediterranean living and pre-modern deep-sea coral carbonates is mostly focused on providing a comprehensive overview of their geographic occurrence, biotic organisation, and temporal evolution (e.g., Remia and Taviani 2004; Taviani et al. 2004). The expected result is a comprehensive understanding of the major mechanisms controlling the onset and demise of coral mounds throughout the basin.

Finally, a novel line of coral-based investigation relies on advanced geochemical techniques to extract climatic signals from deep-sea coral and associated carbonates as proxies of intermediate water characteristics through time (e.g., Montagna et al. 2005; López Correa et al. 2005).

Acknowledgments

References

Allouc J (1987) Les paléocommunautés profondes sur fond rocheux du Pléistocène méditerranéen. Description et essai d'interprétation paléoécologique. Géobios 20: 241-263

Álvarez-Pérez G, Busquets P, Sandoval N, Canals M, Casamor JL, De Mol B (2005) Deep-water coral occurrences in the Strait of Gibraltar. In: Freiwald A, Roberts JM (eds) Cold-water Corals and Ecosystems. Springer, Berlin Heidelberg, pp 207-221

Annoscia E (1963) Antozoi e Briozoi nelle argille calabriane di Venosa (Potenza). Geol Romana 2: 215-278

Barrier P (1984) Évolution tectono-sédimentaire pliocène et pléistocène du détroit de Messine (Italie). Unpubl Thesis Univ Marseille-Luminy, 270 pp

Barrier P (1986) Evolution paléogeographique du détroit de Messine au Pliocène et au Pléistocène. Giorn Geol (ser 3) 48: 7-24

Barrier P (1987) Stratigraphie des dépôts pliocènes et quaternaires du Détroit de Messine. Doc Trav IGAL 11: 59-81

Barrier P, Bonfiglio L, Di Geronimo I, Gaudant J, Grasso M, Rosso A, Zibrowius H (1985)

Guida alle escursioni. 3° Simp Ecol Paleoecol Comunità Bentoniche, 32 pp

Barrier P, Di Geronimo I, Lanzafame G (1986) I rapporti tra tettonica e sedimentazione nell'evoluzione recente dell'Aspromonte occidentale (Calabria). Riv Ital Paleont Stratigr 91: 537-556

Barrier P, Di Geronimo I, Montenat C, Roux M, Zibrowius H (1989) Présence de faunes bathyales atlantiques dans le Pliocène et le Pléistocène de Méditerranée (détroit de Messine, Italie). Boll Soc Géol France (8) 5: 787-796

Barrier P, Di Geronimo I, Zibrowius H, Raisson F (1990) Faune Sénégalienne du paléoescarpement du Capo Vaticano (Calabre Meridionale). Implications néotectoniques. Atti IV Simp Ecol Paleoecol Com Bent Sorrento 1-5 Novembre 1988, pp 511-526

Barrier P, Zibrowius H, Lozouet P, Montenat C, Ott D'Estevou P, Serrano F, Soudet HJ (1992) Une faune de fond dur du bathyal supérieur dans le Miocène terminal des Cordillères Bétiques (Carboneras, SE, Espagne). Mésogée 51 (1991): 3-13

Barrier P, Di Geronimo I, La Perna R, Rosso A, Sanfilippo R, Zibrowius H (1996) Taphonomy of deep-sea hard and soft bottom communities: the Pleistocene of Lazzàro (Southern Italy). In: Meléndez Hevia G, Blasco Sancho MF, Pérez Urresti I (eds) Com II Reun Tafon Fosiliz, Zaragoza 13-15 Jun 1996, pp 39-45

Bellaiche C, Gennesseaux M, Mauffret A, Réhault JP (1974) Prélèvements systématiques et caractérisation des réflecteurs acoustiques: nouvelle étape dans la compréhension de la géologie de la Méditerranée occidentale. Mar Geol 16: M47-M56

Benson RH (1972) Ostracodes as indicators of threshold depth in the Mediterranean during the Pliocene. In: Stanley DJ (ed) The Mediterranean Sea: A Natural Sedimentation Laboratory. Dowden, Hutchinson and Ross, Stroudsburg, pp 63-73

Best MB (1970) Etude systématique et écologique des Madréporaires de la région de Banyuls-sur-Mer (Pyrénées-Orientales). Vie Milieu (A) 20: 293-325

Blanc JJ, Pérès JM, Picard J (1959) Coraux profonds et thanatocoenoses quaternaires en Méditerranée. La topographie et la géologie des profondeurs océaniques. Coll Int CNRS 83: 185-192

Bonfitto A, Bigazzi M, Fellegara I, Impiccini R, Gofas S, Oliverio M, Taviani M, Taviani N (1994) Rapporto scientifico sulla crociera DP 91 (Margine orientale della Sardegna, Mar Mediterraneo). Boll Malacol 30: 129-140

Bourcart J (1952) Rapport sur les canons sous-marins da la région de Banyuls-sur-Mer. Vie Milieu Suppl 2: 165-168

Bourcier M, Zibrowius H (1970) Note sur *Lima excavata* (Fabricius), pélécypode associé aux bancs de coraux profonds. Bull Soc Zool Fr 94 (1969): 201-206

Bourcier M, Zibrowius H (1973) Les "boues rouges" déversées dans le Canyon de la Cassidaigne (région de Marseille), Observations en soucoupe plongeante SP 350 (juin 1971) et résultats de dragages. Téthys 4 (1972): 811-842

Broch H (1953) Octocorals and stony corals of the high Adriatic trawling grounds. Izvjesca-Inst Oceanogr Ribar 6: 22 pp

Bromley RG (2005) Preliminary study of bioerosion in the deep-water coral *Lophelia,* Pleistocene, Rhodes, Greece. In: Freiwald A, Roberts JM (eds) Cold-water Corals and Ecosystems. Springer, Berlin Heidelberg, pp 895-914

Brunelli G, Bini G (1934) Ricerche comparative sulle pesche profonde di diversi mari italiani. Boll Pesca Piscicolt Idrobiol 10: 733-744

Cairns SD (1981) Marine flora and fauna of the northeastern United States: Scleractinia. NOAA Tech Rep 438: 1-15

Cairns SD (1989) A revision of the ahermatypic Scleractinia of the Caribbean Sea and adjacent waters, Part 1: Fungiacyathidae, Micrabaciidae, Turbinoliinae, Guyniidae, and Flabellidae. Smithsonian Contr Zool 486: 1-136

Cairns SD, Stanley GD (1981) Ahermatypic coral banks: living and fossil counterparts. Proc Fourth Int Coral Reef Symp Manila 1: 611-618

Cecchini C (1917) Gli Alcionari e i Madreporari raccolti nel Mediterraneo dalla R.N. "Washington" (1881-1883). Arch Zool Ital 9: 123-157

Chevalier JP (1961) Recerces sur les Madréporaires et le formations récifales miocènes de la Méditerranée occidentale. Mém Soc Gèol France 93: 1-562

Chevalier JP (1962) Les Madréporaires du Pliocène d'Orosei (Nuoro, Sardaigne). Bull Soc Géol France 3: 266-270

Cigala-Fulgosi F (1986) A deep-water elasmobranch fauna from a Lower Pliocene outcropping (Northern Italy). In: Uyeno T, Arai R, Taniuchi T, Matsuura K (eds) Indo-Pacific Fish Biology. Proc Second Int Conf Indo-Pacific Fishes, Icht Soc Jap, pp 133-139

Cigala-Fulgosi F (1996) Rare oceanic deep-water squaloid sharks from the Lower Pliocene of the Northern Apennines (Parma Province, Italy). Boll Soc Paleont Ital 34 (1995): 301-322

Cita MB, Fantini Sestini N, Salvatorini G, Mazzei R, Kidd RB (1979) Late Neogene sediments and fossils from the Malta Escarpment and their geodynamic significance. Ann Géol Pays Hellen 1: 273-283

Cita MB, Benelli F, Biggiogero B, Chezar H, Colombo A, Fantini Sestini N, Freeman-Lynde R, Iaccarino S, Jadoul F, Legnani R, Malinverno A, Massiotta P, Paggi L, Premoli-Silva I (1980) Contribution to the geological exploration of the Malta Escarpment (eastern Mediterranean). Riv Ital Paleont 86: 317-356

Colella A, D'Alessandro A (1988) Sand waves, *Echinocardium* traces and their bathyal depositional setting (Monte Torre Palaeostrait, Plio-Pleistocene, southern Italy). Sedimentology 35: 219-237

Colella A, Di Geronimo I, Rosso A (1996) Successione sedimentaria dello Stretto di Messina: la sezione pleistocenica di Lazzàro. In: Colella A (ed) Guida alle escursioni del GIS 1996, pp 23-33

Comaschi Caria I (1963) La fauna miocenica della zona di Funtanazza compresa tra le Marine di Montevecchio ed Arbus in Sardegna. Rend Sem Fac Sci Univ Cagliari 33: 3-70

Corselli C (2001) Change and diversity: the Mediterranean deep corals from the Miocene to the Present. In: Faranda FM, Gugliemo L, Spezie G (eds) Mediterranean Ecosystems: Structures and Processes. Springer Italia, pp 361-366

Corselli C, Bernocchi A (1990) Paleocommunities of the last glacial from the Sardinia continental slope: a paleoceanography problem. Atti 4° Simp Ecol Paleoecol Comun Bent Sorrento, 1-5 Novembre 1988, Mus Nat Sci Nat, Torino, pp 575-595

Corselli C, Cremaschi M, Violanti D (1985) Il canyon messiniano di Malnate (Varese); pedogenesi tardomiocenica ed ingressione marina pliocenica al margine meridionale delle Alpi. Riv Ital Paleont Stratig 91: 259-286

De Angelis G (1894) I Corallari dei terreni terziari dell'Italia settentrionale. Collezione Michelotti. Mus Geol R Univ Roma. Atti R Accad Lincei, Mem Sci Fis Mat Nat 5: 164-280

De Angelis d'Ossat G (1895) Descripción de los Antozoos fósiles pliocénicos de Cataluña. Mem R Accad Cienc Artes Barcelona 3, 25 pp

De Angelis d'Ossat G, Neviani A (1897) Corallari e briozoi neogenici. Boll Soc Geol Ital 15: 571-594

Delibrias G, Taviani M (1985) Dating the death of Mediterranean deep-sea scleractinian corals. Mar Geol 62: 175-180

De Mol B, Henriet J-P, Canals M (2005) Development of coral banks in Porcupine Seabight: do they have Mediterranean ancestors? In: Freiwald A, Roberts JM (eds) Cold-water Corals and Ecosystems. Springer, Berlin Heidelberg, pp 515-533

De Stefani T (1955) Considerazioni geologiche sulla frana di Naso. Riv Min Sicil 4: 14-19

De Stefano G (1900) Le argille a *Coenopsammia scillae* Seguenza e le sabbie marine della contrada Corvo in Reggio di Calabria. Atti Accad Gioenia Sci Nat (ser 4) 12: 1-9

Di Geronimo I (1979) Il Pleistocene in facies batiale di Valle Palione (Grammichele, Catania). Boll Malacol 15: 85-156

Di Geronimo I (1987) Bionomie des peuplements benthiques des substrats meubles et rocheux plio-quaternaires du Détroit de Messine. Doc Trav IGAL 11: 153-169

Di Geronimo I (1995) Benthic assemblage of the Plio-Quaternary soft and hard substrata in the Straits of Messina area. In: Guglielmo L, Manganaro A, De Domenico E (eds) The Straits of Messina Ecosystem. Proc Symp Messina, 4-6 April 1991

Di Geronimo I, Bellagamba M (1986) Malacofaune dei dragaggi BS77/1 e BS77/2 (Sardegna nord-orientale). Boll Soc Paleont Ital 24: 111-129

Di Geronimo I, La Perna R (1997) Pleistocene bathyal molluscan assemblages from southern Italy. Riv Ital Paleont Stratigr 103: 389-426

Di Geronimo I, Zibrowius H (1983) Le scléractiniaire *Fungiacyathus fragilis* et l'octocoralliaire Stolonifère *Scyphopodium ingolfi* dans le Pléistocène de la Méditerranée. Rapp Comm int Mer Médit 28: 303-306

Di Geronimo I, Rosso A, Sanfilippo R (1993) I banchi fossiliferi di *Corallium rubrum* al largo di Sciacca (Canale di Sicilia). In: Cicogna F, Cattaneo-Vietti R (eds) Il corallo rosso in Mediterraneo. Arte, Storia Sci, pp 75-107

Di Geronimo I, Messina C, Rosso A, Sanfilippo R, Sciuto F, Vertino A (2005) Enhanced biodiversity in the deep: Early Pleistocene coral communities from southern Italy. In: Freiwald A, Roberts JM (eds) Cold-water Corals and Ecosystems. Springer, Berlin Heidelberg, pp 61-86

Dieni J, Omenetto P (1960) Studio di una macrofauna del Pliocene inferiore di Orosei. Riv Ital Paleont 66: 605-618

Dons C (1944) Norges koralrev. K Norske Videnensk Selsk Forh 16: 37-82

Duncan PM (1873) A description of the Madreporaria dredged up during the expedition of H.M.S. Porcupine in 1869 and 1870. Part 1. Trans R Soc London 8: 303-344

Emig CC, Geistdoerfer P (2004) The Mediterranean deep-sea fauna: historical evolution, bathymetric variations and geographic changes. Carnets Geol / Notebooks Geology, Art 2004/01 (CG2004_A01_CCE-PG), pp 1-10

Forest J, Cals P (1977) Une deuxième espèce du genre *Bresilia* Calman, *B. corsicana* sp. nov. Comparaison avec *B. atlantica* Calman (Crustacea Decapoda Bresiliidae). Bull Mus Natl Hist Nat (3 ser) 453: 549-565

Fredj G, Laubier L (1985) The deep Mediterranean benthos. In: Moraitou-Apostopulou M, Kiortsis V (eds) Mediterranean Marine Ecosystems. NATO Conf Ser, Plenum Press, New York London, pp 169-188

Freiwald A (2002) Reef-forming cold-water corals. In: Wefer G, Billett D, Hebbeln D, Jørgensen BB, Schlüter M, Van Weering T (eds) Ocean Margin Systems. Springer, Berlin Heidelberg, pp 365-385

Freiwald A, Fosså JH, Grehan AJ, Koslow JA, Roberts JM (2004) Cold-water coral reefs. UNEP-WCMC Rep, Biodivers Ser 22, pp 1-84

Gaetani M, Saccà D (1983) Brachiopodi batiali nel Pliocene e Pleistocene di Sicilia e Calabria. Riv Ital Paleont Stratigr 90: 407-458

Galil B, Zibrowius H (1998) First benthos samples from Eratosthenes Seamount, eastern Mediterranean. Senckenb marit 28: 111-121

Gravier C (1920) Madréporaires provenant des campagnes des yachts Princesse-Alice et Hirondelle II (1893-1913). Résult campag sci Albert I Prince Monaco 55: 123 pp

Guadagno FM, Taddei Ruggiero E, De Blasio I, Placella B, Sgarrella F (1979) La sezione pleistocenica di Archi (RC). Boll Soc Nat Napoli 88: 1-29

Hanken N-M, Bromley RG, Miller J (1996) Plio-Pleistocene sedimentation in coastal grabens, north-east Rhodes, Greece. Geol J 31: 393-418

Hersey JB (1965) Sedimentary basins of the Mediterranean Sea. Colston Pap 17: 75-91

Jüssen E (1890) Über pliocäne Korallen von der Inseln Rhodus. Sitz kais Akad Wiss Wien, math-natw Cl 99: 13-23

Knowlton N, Jackson JBC (1994) New taxonomy and niche partitioning on coral reefs: jack of all trades or master of some? TREE 9: 7-9

Lacaze-Duthiers H de (1897) Fauna du Golfe de Lyon. Coralliaires. Arch Zool expér gén (ser 3) 5: 1-249

Le Goff-Vitry MC, Rogers AD (2005) Molecular ecology of *Lophelia pertusa* in the NE Atlantic. In: Freiwald A, Roberts JM (eds) Cold-water Corals and Ecosystems. Springer, Berlin Heidelberg, pp 653-662

Le Goff-Vitry MC, Pybus OG, Rogers AD (2004) Genetic structure of the deep-sea coral *Lophelia pertusa* in the northeast Atlantic revealed by microsatellites and internal transcribed spacer techniques. Mol Ecol 13: 537-549

Lentini F, Catalano S, Carbone S (2000) Carta geologica della provincia di Messina scala 1:50.000. Prov region Messina (Assessorato territorio-Servizio geologico) SELCA Firenze

López Correa M, Freiwald A, Hall-Spencer J, Taviani M (2005) Distribution and habitats of *Acesta excavata* (Mollusca: Limidae) with new data on its shell ultrastructure. In: Freiwald A, Roberts JM (eds) Cold-water Corals and Ecosystems. Springer, Berlin Heidelberg, pp 173-205

Marenzeller E von (1893) Zoologische Ergebnisse. II. Polychäten des Grundes, gesammelt 1890, 1891 und 1892. Denkschr kais Akad Wiss, Math-natw Cl 60: 25-48

Mastandrea A, Muto F, Neri C, Papazzoni CA, Perri E, Russo F (2002) Deep-water coral banks: an example from the "Calcare di Mendocino" (Upper Miocene, Northern Calabria, Italy). Facies 47: 27-42

Mastrototaro F, Tursi A, Matarrese A (2001) Un mare di coralli in Mar Ionio. 32° Congr SIBM, Numana-Riviera del Conero 4-9/6/2001, Abstr , pp 112

Micali P, Villari A (1989) Il deposito fossilifero di Salìce (Messina) con particolare riguardo alle specie istituite da Giuseppe Seguenza. Contributo I. Boll Malacol 25: 77-84

Monegatti P, Raffi S, Roveri M, Taviani M (2001) One day trip in the outcrops of Castell'Arquato Plio-Pleistocene Basin: from the badland of Monte Giogo to the Stirone River. Int Conf Paleobiogeogr Paleoecol, Piacenza Castell'Arquato (Italy), May 31-June 2, 2001, pp 1-25

Montagna P, McCulloch M, Taviani M, Remia A, Rouse G (2005) High resolution trace and minor element compositions in deep-water scleractinian solitary corals (*Desmophyllum dianthus*) from the Mediterranean Sea and the Great Australian Bight. In: Freiwald A, Roberts JM (eds) Cold-water Corals and Ecosystems. Springer, Berlin Heidelberg, pp 1109-1126

Montanaro-Gallitelli E (1931) Coralli pliocenici dell'Emilia. Paleontogr Ital 31: 63-91

Montenat C, Barrier P, Di Geronimo I (1987) The strait of Messina, past and present: a review. Doc Trav IGAL 11: 7-13

Orejas C, Gili JM, Rossi S, López-Gonzalez PJ (2003) The deep coral banks in the Mediterranean submarine canyons: an unexplored nursery habitat for commercial species. 2nd Int Symp Deep Sea Corals, September 9-12, 2003, Erlangen, Poster

Osasco E (1895) Di alcuni corallari pliocenici del Piemonte e della Liguria. Atti R Accad Sci Torino 31: 225-238

Osasco E (1897) Di alcuni corallari miocenici del Piemonte. Atti R Accad Sci Torino 32: 436-449

Pérès JM (1982) Major benthic assemblages. In: Kinne O (ed) Marine Ecology. Wiley and Sons, Chichester 5: 373-521

Pérès JM (1989) History of the Mediterranean biota and the colonization of the depths. In: Por FD, Dimentman D (eds) The Legacy of Tethys. Monogr Biol 63: 198-232

Pérès JM, Picard J (1964) Nouveau manuel de bionomie benthique de la Mer Méditerranée. Rec Tr Stat Mar Endoume Bull 31: 3-137

Placella B (1979) Nuove osservazioni sulla corallofauna delle argille pleistoceniche di Archi (Reggio Calabria). Boll Soc Nat Napoli 87: 1-31

Placella B (1980) I coralli pliocenici di Masseria Concarone, Pisticci (Mt). Boll Soc Nat Napoli 89: 19-32

Por FD, Dimentman C (1985) Continuity of Messinian biota in the Mediterranean basin. In: Stanley DJ, Wezel F-C (eds) Geologic Evolution of the Mediterranean Basin. Springer, Berlin Heidelberg, pp 545-556

Pudsey CJ, Jenkins DG, Curry D (1981) Sedimentology and paleontology of samples from the Hellenic Trench. Mar Geol 44: 273-288

Remia A, Taviani M (2004) Shallow-buried Pleistocene *Madrepora*-coral mounds on a muddy continental slope, Tuscan Archipelago, NE Tyrrhenian Sea. Facies 50, DOI 10.1007/s10347-004-0029-2

Remia A, Montagna P, Taviani M (2004) Submarine diagenetic products on the sediment-starved Gorgona slope, Tuscan Archipelago (Tyrrhenian Sea). Chem Ecol 20 (Suppl 1): S131-S153

Reyss D (1964) Observation faites en soucoupe plongeante dans deux vallées sous-marines de la Mer Catalane: le rech du Cap et le rech Lacaze-Duthiers. Bull Inst Océanogr Monaco 63: 1-8

Reyss D (1973) Les canyons sous-marins de la mer Catalane, le rech du Cap et le rech Lacaze-Duthiers. III. Les peuplements de macrofaune benthique. Vie Milieu (B) 22 (3): 529-613

Rocchini R (1983) *Acesta excavata* (Fabricius, 1779), nuovo ritrovamento in Mediterraneo. Boll Malacol 19: 83-86

Rossi L (1957) Revisione critica dei Madreporarii del mar Ligure. Doriana 2 (76): 19 pp

Rossi L (1958) Contributo allo studio della fauna di profondità vivente presso la riviera ligure di levante. Ann Mus Civ St Nat "G. Doria" Genova 2: 1-13

Rossi L (1961) Etudes sur le Seuil Siculo-Tunisien. 6. Madréporaires. Campagne de la "Calypso" (août-septembre 1954). Ann Inst Océanogr Paris 39: 33-48

Roux M, Barrier P, Di Geronimo I, Montenat C (1988) Découverte de Crinoïdes pédonculés bathyaux d'origine atlantique dans le Pliocène supérieur et le Pleistocène moyen méditerranéen: conséquences biogéographiques. C R Acad Sci Paris (ser 3) 307: 259-364

Ruggieri G, Sprovieri R, Unti M, Moroni MA (1979) Indagini batimetriche sulle argille pleistoceniche (Siciliano) di Primosole (Siracusa). Nat Sicil (ser 4) 3: 119-129

Russo A (1980) The psychrospheric coral fauna from the lower Pliocene of northern Italy. Acta Palaeont Pol 25: 614-617

Sartori R (1980) Factors affecting the distribution of ahermatypic corals on the Mediterranean seafloor: a probabilistic study. Deep-Sea Res 27A: 655-663

Schröder-Ritzrau A, Freiwald A, Mangini A (2005) U/Th-dating of deep-water corals from the eastern North Atlantic and the western Mediterranean Sea. In: Freiwald A, Roberts JM (eds) Cold-water Corals and Ecosystems. Springer, Berlin Heidelberg, pp 157-172

Segre AG (1959) Observations générales sur l'orographie sous-marine de la Mer Tyrrhénienne. La topographie et la géologie des profondeurs océaniques. Coll Int CNRS 83: 53-59

Segre AG, Stocchino C (1969) Nuove osservazioni sulla geologia e morfologia delle montagne submarine del Mar Tirreno. Ist Idrogr Mar Genova 1037: 11-15

Seguenza G (1864) Disquisizioni paleontologiche intorno ai Corallarii fossili delle rocce terziarie del distretto di Messina. Mem R Acc Sci Torino (ser 2) 21: 399-560

Seguenza G (1873–1877) Studi stratigrafici sulla formazione pliocenica dell'Italia meridionale. Boll Reg Comit Geol Ital 4: 29-45, 84-103, 131-153, 213-230, 280-301, 345-357 (1873); 8: 7-27, 91-99, 359-367 (1877)

Seguenza G (1880) La formazione terziaria nella provincia di Reggio (Calabria). Atti R Accad Lincei, Cl Sci Fis (ser 3) Mem 6: 446 pp

Selli R (1970) Campioni raccolti. Giorn Geol (ser 2) 37: 55-72

Sganga P (1978) La sezione stratigrafica calabriana di Naso (Messina). Riv Min Sicil 15: 3-23

Simonelli V (1895) Gli Antozoi pliocenici del Ponticello di Savena presso Bologna. Paleont Ital 1: 149-168

Simonelli V (1896) Antozoi neogenici del Museo Parmense. Paleont Ital 2: 185-201

Squires DF (1964) Fossil corals thickets in Wairarapa, New Zealand. J Paleont 38: 904-915

Stanley GD, Cairns SD (1988) Constructional azooxanthellate coral communities: an overview with implications for the fossil record. Palaios 3: 233-242

Steindachner F (1891) Veröffentlichungen der Commission für Erforschung des östlichen Mittelmeeres. Vorläufiger Bericht über die zoologischen Arbeiten im Sommer 1891. Sitz kais Akad Wiss, Math-natw Cl 1 (100): 435-447

Taviani M (1981) Discussion. In: Journées d'études sur la systématique évolutive et la biogéographie en Méditerranée. Cagliari, 13 et 14 octobre 1980 CIESM Monaco, pp 136-137

Taviani M (2002) The Mediterranean benthos from late Miocene up to present: ten million years of dramatic and geologic vicissitudes. Biol Mar Medit 9: 445-463

Taviani M, Colantoni P (1979) Thanatocoenoses würmiennes associées aux coraux blancs. Rapp Comm int Mer Médit 25/26: 141-142

Taviani M, Colantoni P (1984) Paléobiocenoses profondes a scléractiniaires sur l'escarpement de Malte-Syracuse (Mer Méditerranée): leur structure, leur âge et leur signification. Rev Inst Fr Pétr 39: 547-552

Taviani M, Remia A (2001) I coralli del buio: archivi climatici degli oceani passati. Ricerca Futuro 18: 28-30

Taviani M, Roveri M, Aharon P, Zibrowius H (1997) A Pliocene deepwater cold seep (Stirone River, N. Italy). COLD-E-VENT International Workshop: Hydrocarbon Seepage and Chemosynthesis in Tethyan Relic Basins: Products, Processes and Causes, pp 20

Taviani M, Remia A, Corselli C, Freiwald A, Malinverno E, Mastrototaro F, Savini A, Tursi A, CORAL Shipboard Staff (2004) First geo-marine survey of living cold-water *Lophelia* reefs in the Ionian Sea (Mediterranean basin). Facies 50, DOI 10.1007/s10347-004-0039-0

Teichert C (1958) Cold- and deep-water coral banks. AAPG Bull 42: 1064-1082

Titschack J, Freiwald A (2005) Growth, deposition, and facies of Pleistocene bathyal coral communities from Rhodes, Greece. In: Freiwald A, Roberts JM (eds) Cold-water Corals and Ecosystems. Springer, Berlin Heidelberg, pp 41-59

Tunesi L, Diviacco G (1997) Observations by submersible on the bottoms off shore Portofino Promontory (Ligurian Sea). In: Piccazzo M (ed) Atti 12° Congr AIOL Isola di Vulcano 18-21 Settembre 1996, Genova 1: 61-74

Tursi A, Mastrototaro F, Matarrese A, Maiorano P, D'Onghia G (2004) Biodiversity of the white coral reefs in the Ionian Sea (Central Mediterranean). Chem Ecol 20 (Suppl 1): S107-S116

Vafidis D, Koukouras A, Voultsiadou-Koukoura E (1997) Actiniaria, Corallimorpharia, and Scleractinia (Hexacorallia, Anthozoa) of the Aegean Sea, with a checklist of the eastern Mediterranean and Black Sea species. Israel J Zool 43: 55-70

Vertino A (2003) Sclerattiniari Plio-Pleistocenici ed attuali del Mediterraneo (Sistematica, Biostratinomia e Paleoecologia). PhD Thesis Univ Messina (unpubl), Messina, 306 pp

Vertino A (2004) Esacoralli plio-pleistocenici del Mediterraneo (Sistematica, Biostratinomia, Paleoecologia). PaleoItalia Modena, 4 pp

Vertino A, Di Geronimo I (2003) How many *Caryophyllia* species lived in the Plio-Pleistocene Mediterranean? Seguenza's taxonomy revised. 9th Int Symp fossil Cnidaria and Porifera, 3-7 August Graz, Abstr

Zabala N, Maluquer P, Harmelin JG (1993) Epibiotic bryozoans on deep-water scleractinian corals from the Catalonia slope (western Mediterranean, Spain, France). Sci Mar 57: 65-78

Zibrowius H (1974) *Caryophyllia sarsiae* n. sp. and other recent deep-water *Caryophyllia* (Scleractinia) previously referred to little-known fossil species (*C. arcuata, C. cylindracea*). J Mar Biol Assoc UK 54: 769-784

Zibrowius H (1979) Campagne de la Calypso en Méditerranée nord-orientale (1955, 1956, 1960, 1964). 7. Scléractiniaires. Ann Inst Océanogr Paris 55 Suppl: 7-28

Zibrowius H (1980) Les Scléractiniaires de la Méditerranée et de l'Atlantique nord-oriental. Mém Inst Océanogr Monaco 11: 284 p 104 pl

Zibrowius H (1981) Thanatocoenose pléistocène profonde à spongiaires et scléractiniaires dans la fosse Hellénique. In: Journées d'études sur la systématique évolutive et la biogéographie en Méditerranée. Cagliari, 13-14 octobre 1980. CIESM Monaco, 133-136

Zibrowius H (1985) Spongiaires hexactinellides vivant en mer Ionienne par 2000 m de profondeur. Rapp Comm int Mer Médit 29: 335-338

Zibrowius H (1987) Scléractiniaires et Polychètes Serpulidae des faunes bathyales actuelle et plio-pléistocène de Méditerranée. Doc Trav IGAL 11: 255-257

Zibrowius H (1991) Les Scléractiniaires du Miocène au Pléistocène de Sicile et de Calabre de Giuseppe Seguenza (1864-1880) (Cnidaria: Anthozoa). Atti Accad Peloritana Pericolanti, Cl Sci Mat Fis Nat 67: 159-179

Zibrowius H, Grieshaber A (1977) Scléractinaires de l'Adriatique. Tethys (4) 1975: 375-384

Zibrowius H, Placella B (1981) First record of the genus *Fungiacyathus* (Cnidaria, Scleractinia) from the Mediterranean area: Pliocene of Masseria Concarone (MT), Southern Italy. Boll Soc Paleont Ital 20: 143-146

Zibrowius H, Taviani M (2005): Remarkable sessile fauna associated with deep coral and other calcareous substrates in the Strait of Sicily, Mediterranean Sea. In: Freiwald A, Roberts JM (eds) Cold-water Corals and Ecosystems. Springer, Berlin Heidelberg, pp 807-819

Zibrowius H, Ten Hove HA (1987) *Neovermilia falcigera* (Roule, 1898) a deep- and cold-water serpulid polychaete common in the Mediterranean Plio-Pleistocene. Biol Soc Washington Bull 7: 259-271

Zuffardi-Comerci R (1927) Faunetta di corallari pliocenici dell'isola di Rodi. Atti R Accad Sci Torino 63: 231-237

Zuffardi-Comerci R (1932) Corallari-Zoantari fossili del Miocene della "Collina di Torino". Paleont Ital 23: 86-132

Županovič S (1969) Prilog izučavanju bentoske faune Jabučke kotline. Thal Jugosl 5: 477-493

U/Th-dating of deep-water corals from the eastern North Atlantic and the western Mediterranean Sea

Andrea Schröder-Ritzrau[1], André Freiwald[2], Augusto Mangini[1]

[1] Heidelberg Academy of Sciences, Im Neuenheimer Feld 229, D-69120 Heidelberg, Germany
 (andrea.schroeder-ritzrau@iup.uni-heidelberg.de)
[2] Institute of Paleontology, Erlangen University, Loewenichstr. 28, D-91054 Erlangen, Germany

Abstract. Deep-water corals are widespread in the North Atlantic. Colonial azooxanthellate scleractinians sustain ecosystems mostly in the bathyal zone down the slopes and oceanic banks off the Iberian Peninsula to as far north as the Scandinavian shelf off northern Norway. Estimates of the geological age of 37 deep-water corals exposed at the seabed from major reef areas in the North Atlantic were based on U/Th datings. In contrast to the purely Holocene ages of deep-water corals in Scandinavian waters, the Faroe area and the Rockall Trough, deep-water corals from lower latitudes like the seamounts off NW-Africa, the Mid-Atlantic Ridge and the western Mediterranean Sea seemed to have grown continuously over the last 50 ka. Overall, deep-water corals showed U/Th ages between 0.09 and 53.5 ka.

Keywords. Uranium-Thorium dating, *Lophelia*, *Madrepora*, North Atlantic, Mediterranean Sea, Pleistocene, Holocene

Introduction

In the NE-Atlantic deep-water coral communities are widely distributed down the slopes and oceanic banks off the Iberian Peninsula to as far north as the Scandinavian shelf (Freiwald and ACES Party 2000). They form small patches but can also build up large reefs of several kilometres in length. The Atlantic Coral Ecosystem Study (ACES) focussed on five key locations (Galicia Bank 43°N, Porcupine Slope 51°N, Rockall Trough 59°N, Kosterfjord 59°N and Sula Ridge 64°N) to study the distribution, the ecological habitats and the water mass properties associated with the deep-water coral reefs. These environmental parameters may be linked to the geological record of these deep-water corals. Therefore an U/Th data base was generated on deep-water corals obtained from surface sediments of all five ACES study sites, complemented with samples from the Penmarc'h Bank (47°N), the area east of the Azores (35°N), off Northwest Africa (30°N) and from the western Mediterranean (35°N). Generally, aragonitic scleractinian corals are suitable

for uranium-series disequilibria dating (e.g., Edwards et al. 2003). However, the problem of post-depositional coating of the deep-water corals with Fe/Mn-oxides, resulting in contamination by ^{230}Th from seawater and the initial incorporation of ^{230}Th into the carbonate, both significantly influencing the U/Th age, has to yet be solved (Lomitschka and Mangini 1999; Cheng et al. 2000a; Schröder-Ritzrau et al. 2003). In this paper we present 27 new and 10 published (Schröder-Ritzrau et al. 2003) uranium-series datings on deep-water corals covering the last 53.5 ka. To separate the radiogenic ^{230}Th from the non-radiogenic ^{230}Th fraction added from the surrounding environment, we used the sample specific Rosholt-II-isochron method for highly contaminated samples to correct for adsorbed or initial thorium (Ludwig and Titterington 1994; Lomitschka and Mangini 1999). For samples with small or moderate non-radiogenic thorium contamination we used modern ^{230}Th/^{232}Th-activity ratios from seawater of the North Atlantic as correction factor (Vogler et al. 1998).

Samples and methods

Twenty-seven deep-water coral individuals from surface sediments (Fig. 1; Table 1) collected with dredge, box or gravity cores were investigated. Ten already published additional U/Th-ages from the North Atlantic (Schröder-Ritzrau et al. 2003) complemented the data set. Seven azooxanthellate coral species including the dominant colonial scleractinian *Lophelia pertusa* but also solitary or pseudosolitary species like *Desmophyllum cristagalli* were sampled (Table 1). Water depths of samples ranged from 77 m to 2306 m. According to the recent oceanographic circulation pattern in the North Atlantic (Schmitz and McCartney 1993; Reid 1994; Paillet et al. 1998; Rhein 2000), 29 of these 37 coral samples lived in intermediate water masses, mainly the Eastern North Atlantic Water (ENAW) and the North Atlantic Central Water (NACW) with varying contributions of Labrador Sea Water (LSW) and Mediterranean Outflow Water (MOW). The northernmost four samples, from the Sula Ridge and the Faroe areas, are from shallower water depths (less than 300 m) and were influenced by the North Atlantic Current (NAC). Two samples are from the shallow western Swedish Skagerrak. Two samples from the Penmarc'h Bank are also from shallow water depths (240 m).

Sample selection and preparation

Almost all deep-water corals analysed showed varying degrees of cortical corrosion (Fig. 2a) and cortical contamination with iron and manganese oxides/hydroxides (Fig. 2b). Depending on the degree of cortical contamination of the samples, which adsorb excess thorium from surrounding seawater two different procedures were applied.

1. Heavily coated deep-water corals (Fig. 2b; Table 3) including the samples #654, #660, #1471, #2629, #2657, #3036, and #3056 were treated according to the following procedure:

Two to four fractions of the sample with different contamination were analysed applying the method by Lomitschka and Mangini (1999). The first fraction was

the coating, forming the most contaminated part of the coral with up to 500 ng ^{232}Th/g carbonate (Table 3). The second fraction was an uncleaned piece of carbonate, while the third fraction was thoroughly mechanically cleaned. The fourth fraction was first thoroughly mechanically cleaned and then either leached with 1 N HNO$_3$ or cleaned with NaEDTA/Vit.C (Lomitschka and Mangini 1999) and
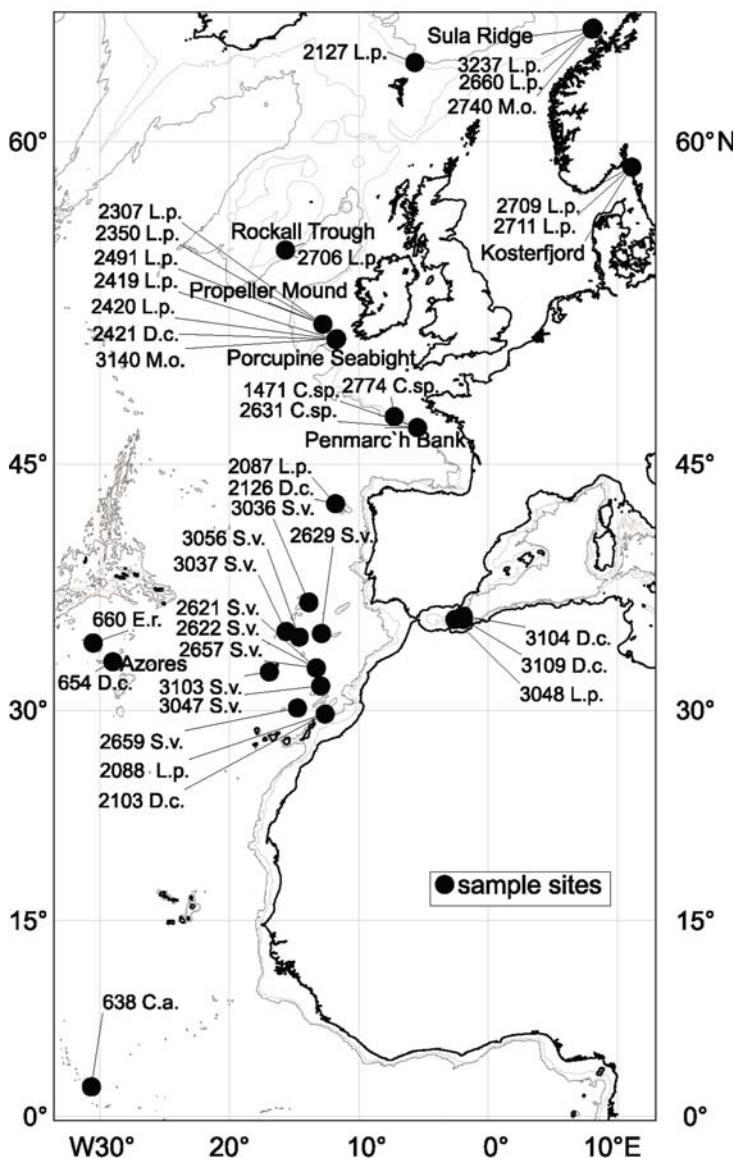
Fig. 1 Location map of deep-water coral samples for U/Th dating. For recognition of abbreviated coral species names see Table 1

Table 1 Deep-water coral sample locations

Sample	Latitude	Longitude	Area	Water depth [m]	Species
638 [1]	02° 18.7 N	30° 38.8 W	St. Paul Seamount	2306	*Caryophyllia ambrosia*
654 [1]	33° 11.9 N	28° 59.3 W	Plato Seamount	695	*Desmophyllum cristagalli*
660 [1]	34° 24.7 N	30° 30.8 W	Atlantis Seamount	795-830	*Enallopsammia rostrata*
1471 [1]	46° 58.1 N	05° 27.6 W	Penmarc'h Bank	240	*Caryophyllia* sp.
2087	42° 46.6 N	11° 46.9 W	Galicia Bank	823	*Lophelia pertusa*
2088 [1]	29° 49.4 N	12° 39.9 W	Conception Seamount	652-986	*Lophelia pertusa*
2103	29° 49.4 N	12° 39.9 W	Conception Seamount	652-986	*Desmophyllum cristagalli*
2126	42° 46.6 N	11° 46.9 W	Galicia Bank	823	*Desmophyllum cristagalli*
2127	62° 56 N	05° 34 W	Faroer	252	*Lophelia pertusa*
2307 [1]	52° 09.1 N	12° 46.2 W	Propeller Mound	686	*Lophelia pertusa*
2350	52° 09.1 N	12° 46.2 W	Propeller Mound	686	*Lophelia pertusa*
2419	51° 24.8 N	11° 45.9 W	Porcupine Seabight	1005	*Lophelia pertusa*
2420	51° 24.8 N	11° 45.9 W	Porcupine Seabight	1005	*Lophelia pertusa*
2421	51° 24.8 N	11° 45.9 W	Porcupine Seabight	1005	*Desmophyllum cristagalli*
2491	52° 09.2 N	12° 46.0 W	Propeller Mound	749	*Lophelia pertusa*
2621	32° 48.2 N	13° 17.2 W	"Lars Seamount"	1284-1350	*Solenosmilia variabilis*
2622	32° 48.2 N	13° 17.2 W	"Lars Seamount"	1284-1350	*Solenosmilia variabilis*
2629	35° 01.2 N	12° 52.3 W	Ampère Seamount	1047-1135	*Solenosmilia variabilis*
2631 [1]	46° 58.1 N	05° 27.6 W	Penmarc'h Bank	240	*Caryophyllia* sp.
2657 [1]	32° 48.2 N	13° 17.2 W	"Lars Seamount"	1284-1350	*Solenosmilia variabilis*
2659	30° 09.7N	14° 44.9 W	"Last Minute Seamount"	1111-1230	*Solenosmilia variabilis*
2660	64°06.5 N	08°06.9 E	Sula Ridge	276	*Lophelia pertusa*
2706 [1]	55° 32.1 N	15° 40.0 W	Rockall Trough	724	*Lophelia pertusa*
2709	59° 00.8 N	11° 06.9 E	Kosterfjord	80	*Lophelia pertusa*
2711	59° 00.8 N	11° 06.9 E	Kosterfjord	77	*Lophelia pertusa*
2740	64°06.5 N	08°06.9 E	Sula Ridge	276	*Madrepora oculata*
2774 [1]	47° 33.8 N	07° 15.1 W	Penmarc'h Bank	490	*Caryophyllia* sp.
3036	36° 57.5 N	13° 51.2 W	Josephine Seamount	1317-1343	*Solenosmilia variabilis*
3037	35° 08.6 N	15° 37.1 W	Lion Seamount	1767-1951	*Solenosmilia variabilis*
3047	31° 37.4 N	12° 56.8 W	"Annika Seamount"	1423-1781	*Solenosmilia variabilis*
3048	35° 53.7 N	02° 34.0 W	NW Cabliers Bank, Alboran Sea	501-744	*Lophelia pertusa*
3056	34° 47.4 N	14° 35.3 W	Unicorn Seamount	1100-1352	*Solenosmilia variabilis*
3103	32° 32.7 N	16° 54.7 W	Filho do Funchal	1387-1773	*Solenosmilia variabilis*
3104	36° 07.4 N	01° 55.7 W	Al Mansour Seamount, Alboran Sea	1478-1630	*Desmophyllum cristagalli*
3109	35° 54.5 N	01° 54.3 W	Yusuf Ridge, Alboran Sea	1578-1777	*Desmophyllum cristagalli*
3140	51° 27.2 N	11° 42.2 W	Poseidon Mound	681	*Madrepora oculata*
3237	64° 04.6 N	08°00.7 E	Sula Ridge	276	*Lophelia pertusa*

[1] samples published in Schröder-Ritzrau et al. 2003

showed remaining contamination with ^{232}Th contents between 3.7 and 40.3 ng per g. Uranium-series measurements were performed for each sample and the Rosholt-II-isochron standard method was applied (Ludwig and Titterington 1994; Lomitschka and Mangini 1999).

2. Samples with varying degrees of cortical corrosion were treated as following: Samples were thoroughly mechanically cleaned scraping off the surface of the
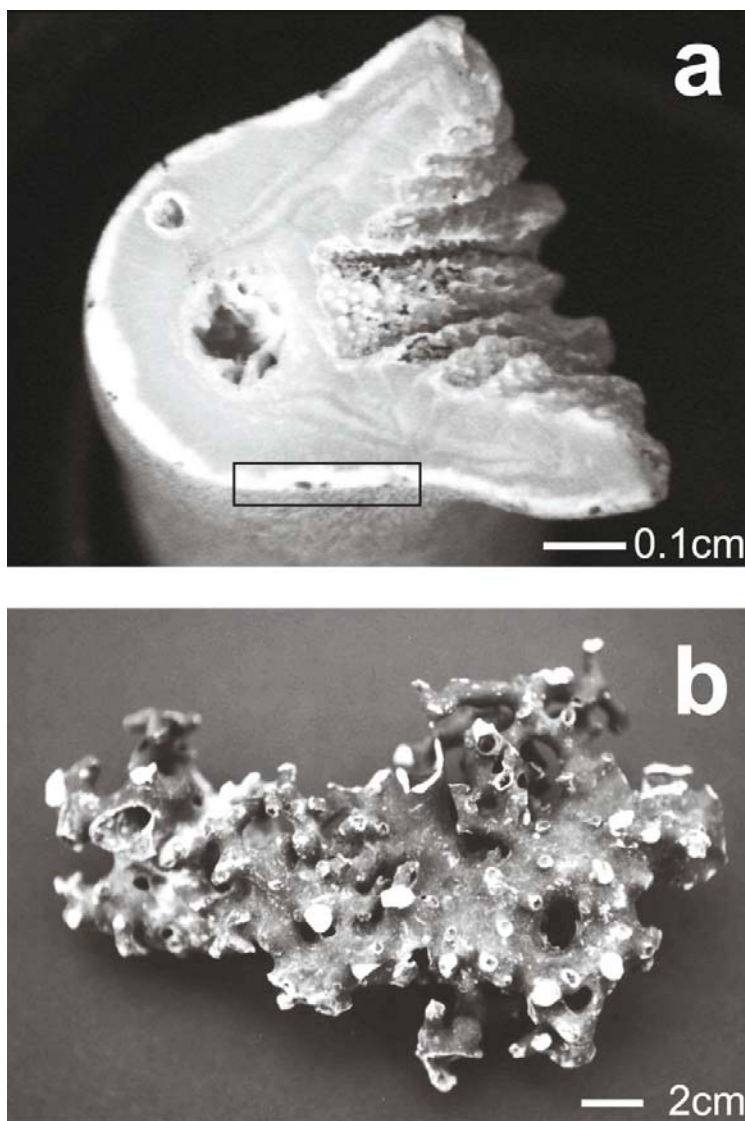
Fig. 2 a *Lophelia pertusa* without coating, outer surface bio-corroded (marked section); **b** *Solenosmilia variabilis* totally covered with brownish black coating

sample. For a few samples up to one to two millimetres of the surface were scraped off in order to remove all corroded carbonate and adhering detritus (Fig. 2a). Subsequently the remainder was leached with nitric acid for several seconds and washed with distilled water. Twenty-three of these thirty samples gave remaining quantities of ^{232}Th of less than 5 ng per g carbonate (Table 2). However, seven samples had multiple ^{232}Th contents between 6 and 21 ng per g (Table 2), which account for higher age uncertainties.

Uranium-series dating and age calculation

Uranium-series nuclides were measured and ages were calculated for each sample. The sample weights of the different fractions ranged from 0.03 to 0.7 g. All samples were dissolved in supra-pure nitric acid. The solutions were spiked with a ^{233}U-^{236}U double spike (atomic ratio of 0.87231) and a ^{229}Th spike. Uranium and thorium were isolated with anion exchange columns (DOWEX 1X8) (Ivanovich et al. 1992). The samples were loaded on a preheated rhenium double filament. Thorium and uranium isotopes were measured with a thermal ionization mass spectrometer (Finnigan MAT 262 RPQ). Mass abundances were measured with Faraday cups or ion counting multiplier (ICM), respectively. For better mass separation a retarding potential quadrupol (RPQ) was used for measurements of Th isotopes. Uranium standard material NBL 112a from Brunswick Laboratories was used to estimate reproducibility and inter-comparability with other laboratories. A total of 203 measurements yielded an isotope ratio ^{234}U/^{238}U of $5.2839 \cdot 10^{-5} \pm 1.26 \cdot 10^{-7}$. This gives a reproducibility of 2 ‰ (1σ). The isotope ratio is in very good agreement with published values as for example $5.2860 \cdot 10^{-5} \pm 0.95 \cdot 10^{-7}$ (Cheng et al. 2000b). The measured mean concentration of ^{230}Th (n = 86) in NBL 112a is 7.351 ± 0.083pg/g (2σ), an internal reproducibility of 5.2 ‰ (1σ). Data were corrected for chemical blanks yielding less than 0.07 ng ^{238}U and 0.05 ng ^{232}Th.

Table 2 Uranium-series data (TIMS) for deep-water coral samples

All errors are ± 2 σ and do not include errors in decay constants.

Decay constant used to convert atom ratios to activity ratios are from Cheng et al. (2000)

[1] Samples published in Schröder-Ritzrau et al. (2003)

[a] ^{230}Th/^{232}Th act. ratio corr. factor; averaged ^{230}Th/^{232}Th ratio from the water column (Vogler et al. 1998) station L2-500 m and 3-500 m; for age calc. the analytical error was applied

[a1] ^{230}Th/^{232}Th act. ratio corr. factor; averaged ^{230}Th/^{232}Th ratio from the water column (Vogler et al. 1998) station L1-950 m and L1-3000 m; for age calc. a 50 % error was applied

[a2] ^{230}Th/^{232}Th act. ratio corr. factor; averaged ^{230}Th/^{232}Th ratio from the water column (Vogler et al. 1998]) station L2-500 m and 3-500 m; for age calc. a 50 % error was applied

[a3] ^{230}Th/^{232}Th act. ratio corr. factor estimated via isochron for sample 2657 from the same location

[a4] ^{230}Th/^{232}Th act. ratio corr. factor estimated via isochron for sample 1471 from the same location

[b] Initial δ^{234}U estimated with Th-corrected Th/U ages

Sample	^{238}U [µg/g]	^{232}Th [ng/g]	$(^{234}U/^{238}U)$ Activity ratio	$(^{230}Th/^{238}U)$ Activity ratio	$^{230}Th/^{232}Th$ corr.[a] Activity ratio	Cal. age Th corr.[a] [years]	$\delta^{234}U_0$[b] Activity ratio
638 [1]	4.186 ± 0.016	0.677 ± 0.004	1.142 ± 0.003	0.1391 ± 0.0012	42.5 ± 21.5[a1]	13950 ± 280	148.2 ± 3.4
2088 [1]	3.680 ± 0.009	1.912 ± 0.006	1.150 ± 0.005	0.1261 ± 0.0015	8.6 ± 4.3[a2]	12520 ± 280	155.3 ± 4.9
2087	4.531 ± 0.005	0.109 ± 0.002	1.146 ± 0.002	0.0012 ± 0.0002	8.6 ± 2	110 ± 25	146.1 ± 2.3
2103	3.541 ± 0.006	7.985 ± 0.051	1.156 ± 0.004	0.1690 ± 0.0014	8.6 ± 2	16530 ± 360	163.9 ± 4.2
2126	2.820 ± 0.010	0.189 ± 0.002	1.160 ± 0.007	0.0011 ± 0.0002	8.6 ± 2	90 ± 20	160.7 ± 7.1
2127	3.702 ± 0.007	1.903 ± 0.012	1.149 ± 0.003	0.0328 ± 0.0005	8.6 ± 2	3010 ± 90	150.4 ± 3.3
2307 [1]	4.364 ± 0.004	2.741 ± 0.012	1.144 ± 0.002	0.0911 ± 0.0006	8.6 ± 4.3[a2]	8890 ± 160	147.3 ± 2.0
2350	3.323 ± 0.007	3.262 ± 0.049	1.144 ± 0.005	0.0889 ± 0.0028	8.6 ± 2	8560 ± 390	147.2 ± 4.9
2419	4.190 ± 0.008	1.547 ± 0.028	1.145 ± 0.003	0.0058 ± 0.0005	8.6 ± 2	460 ± 60	146.6 ± 3.4
2420	4.416 ± 0.008	17.100 ± 0.162	1.148 ± 0.003	0.0217 ± 0.0006	8.6 ± 2	1050 ± 190	148.3 ± 3.5
2421	4.196 ± 0.008	10.111 ± 0.085	1.148 ± 0.003	0.0138 ± 0.0004	8.6 ± 2	680 ± 120	148.7 ± 3.1
2491	4.008 ± 0.004	7.163 ± 0.035	1.146 ± 0.003	0.0210 ± 0.0004	8.6 ± 2	1540 ± 160	146.6 ± 2.8
2621	4.177 ± 0.006	0.429 ± 0.002	1.150 ± 0.003	0.0069 ± 0.0002	20,3 ± 0,8[a3]	600 ± 15	150.2 ± 2,7
2622	4.004 ± 0.006	8.409 ± 0.027	1.151 ± 0.003	0.0258 ± 0.0003	20,3 ± 0,8[a3]	1150 ± 95	152.0 ± 2,8
2631 [1]	4.891 ± 0.004	4.736 ± 0.016	1.140 ± 0.002	0.1384 ± 0.0006	4.8 ± 0.6[a4]	13960 ± 120	145.4 ± 2.1
2659	3.654 ± 0.004	21.43 ± 0.04	1.129 ± 0.002	0.4515 ± 0.002	8.6 ± 2	53500 ± 895	150.6 ± 3.1
2660	3.209 ± 0.004	6.102 ± 0.040	1.149 ± 0.003	0.0164 ± 0.0007	8.6 ± 2	1060 ± 180	149.9 ± 2.6
2706 [1]	3.873 ± 0.015	0.505 ± 0.004	1.147 ± 0.006	0.0061 ± 0.0005	8.6 ± 4.3[a2]	560 ± 70	147.1 ± 6.6
2709	4.582 ± 0.004	1.060 ± 0.004	1.154 ± 0.003	0.0228 ± 0.0005	8.6 ± 2	2110 ± 50	154.9 ± 2.8
2711	3.742 ± 0.007	0.696 ± 0.004	1.150 ± 0.004	0.0314 ± 0.0008	8.6 ± 2	2980 ± 90	151.1 ± 4.4
2740	3.659 ± 0.003	0.355 ± 0.001	1.150 ± 0.002	0.0013 ± 0.0001	8.6 ± 2	100 ± 5	150.0 ± 1.9
2774 [1]	4.727 ± 0.006	1.408 ± 0.007	1.142 ± 0.003	0.1119 ± 0.0011	8.6 ± 4.3[a2]	11170 ± 180	146.4 ± 2.9
3037	4.321 ± 0.005	1.845 ± 0.002	1.142 ± 0.002	0.0074 ± 0.0001	8.6 ± 2	600 ± 30	141.8 ± 2.0
3047	5.510 ± 0.006	3.552 ± 0.008	1.141 ± 0.002	0.0987 ± 0.0004	8.6 ± 2	9700 ± 100	144.8 ± 2.2
3048	3.743 ± 0.004	1.989 ± 0.007	1.149 ± 0.002	0.0876 ± 0.0001	8.6 ± 2	8500 ± 115	153.1 ± 2.4
3103	4.588 ± 0.006	0.036 ± 0.001	1.149 ± 0.003	0.0110 ± 0.0004	8.6 ± 2	1050 ± 40	149.9 ± 2.6
3104	3.361 ± 0.003	2.749 ± 0.011	1.128 ± 0.002	0.3430 ± 0.0028	8.6 ± 2	39090 ± 520	142.9 ± 2.4
3109	3.464 ± 0.004	3.019 ± 0.010	1.131 ± 0.003	0.3403 ± 0.0021	8.6 ± 2	38560 ± 440	146.3 ± 3.0
3140	4.719 ± 0.008	2.181 ± 0.005	1.149 ± 0.004	0.0797 ± 0.0007	8.6 ± 2	7720 ± 100	152.6 ± 4.1
3237	3.524 ± 0.004	4.012 ± 0.008	1.147 ± 0.002	0.0186 ± 0.0002	8.6 ± 2	1480 ± 100	147.7 ± 2.0

Isochron samples: The age relevant activity ratios estimated *via* the slope of the isochrones were filled in the ^{230}Th/^{238}U age equation (Edwards et al. 2003) and ages were determined iteratively (Table 3). Isochrones were calculated with Origin. Usual error estimates for linear fit were used.

Non-isochron samples: The ^{230}Th/^{238}U age equation, including a term for initial ^{230}Th/^{238}U ratio (Cheng et al. 2000a; Edwards et al. 2003), was applied taking account of the initial ^{230}Th/^{232}Th activity ratio (Table 2) (see below).

For all ages, estimated half-lives reported in Cheng et al. (2000b) were used. Errors are given as 2σ values in Table 2 and do not include uncertainties in half-lives.

In order to produce reliable ages for the coral samples, the closed-system assumption must be proved. Several approaches have been used to assess this assumption, summarized in Edwards et al. (2003). Though data on deep-water corals are still few, it is reasonable to assume that deep-water corals incorporate uranium from seawater without fractionation and hence the initial ^{234}U/^{238}U activity ratio must be close to the seawater value. The modern δ^{234}U measured in marine waters, in modern shallow-water corals and in deep-water corals is 140-150 ‰ (Chen et al. 1986), 145.8 ± 1.7 ‰ (Cheng et al. 2000b) and 145.5 ± 2.3 ‰ (Cheng et al. 2000a), respectively. Using a strict range of 145.5 ± 4 ‰, thirty of the samples lie in this range, at least within the level of analytical error recorded. Seven values are slightly higher. We consider all ages as reliable since ^{14}C-analyses processed for the majority of the samples also gave consistent results (Schröder-Ritzrau et al. 2003; Schröder-Ritzrau unpubl. data).

Thorium correction

It is known that deep-water corals to some extent have a ^{230}Th content, which does not originate from decay of ^{234}U embedded in the skeletal carbonate (Adkins and Boyle 1999; Cheng et al. 2000a; Goldstein et al. 2001). Reliable ages need correction for this non-radiogenic thorium component. Two different modes of contaminating ^{230}Th were addressed in the present study. One mode is the external coating with iron and manganese oxides/hydroxides most likely soon after death of the coral, which adsorb thorium from surrounding sea water (Lomitschka and Mangini 1999) (Fig. 2b). Here the Rosholt-II-isochron method establishes sample specific corrections, which enable determination of U/Th ages. The 2σ age errors of the presented heavily coated samples ranged between 0.9 and 3.2 % (Table 3).

Table 3 Isochron-data: Uranium-series data (TIMS) for deep-sea coral samples; samples denoted
 - 1 = coating, - 2 = uncleaned carbonate, - 3 = leached carbonate, - 4 = NaEDTA/Vit.C cleaned

[1] samples published in Schröder-Ritzrau et al. (2003)
[2] Calendar age calculated with ^{234}U/^{238}U and ^{230}Th/^{238}U activity ratios estimated *via* isochron
[3] Initial δ^{234}U estimated with isochron age

Sample	^{238}U [µg/g]	^{232}Th [ng/g]	^{230}Th [pg/g]	(^{234}U/^{238}U) Activity ratio	(^{230}Th/^{232}Th) Activity ratio	(^{230}Th/^{238}U) Activity ratio	Cal. age isochr. [years][2]	(^{230}Th/^{232}Th) Activity ratio	δ^{234}U$_0$ Activity ratio[3]
654 - *1*¹	4.069 ± 0.014	2979.42 ± 21.75	342.12 ± 5.34	1.151 ± 0.010	21.44 ± 0.37	5.1376 ± 0.0821	-	-	-
654 - *2*¹	2.151 ± 0.004	48.78 ± 0.48	10.60 ± 0.26	1.148 ± 0.003	40.58 ± 1.08	0.3013 ± 0.0075	-	-	-
654 - *4*¹	3.702 ± 0.015	15.83 ± 0.07	8.78 ± 0.18	1.158 ± 0.009	103.64 ± 2.12	0.1450 ± 0.0030	-	-	-
654 - *4*¹	3.902 ± 0.018	18.51 ± 0.12	9.33 ± 0.30	1.149 ± 0.010	94.13 ± 3.13	0.1461 ± 0.0048	-	-	-
654 *isochr.*¹	-	-	-	1.152 ± 0.006	-	0.1172 ± 0.0030	11690 ± 380	21.3 ± 0.9	157.1 ± 6.4
660 - *1*¹	5.544 ± 0.018	5023.0 ± 49.7	728.50 ± 11.80	1.140 ± 0.012	27.08 ± 0.51	8.0290 ± 0.1327	-	-	-
660 - *4*¹	3.949 ± 0.017	22.6 ± 0.24	10.58 ± 0.14	1.146 ± 0.008	87.55 ± 1.50	0.1637 ± 0.0023	-	-	-
660 - *isochr.*¹	-	-	-	1.144 ± 0.010	-	0.1138 ± 0.0021	11430 ± 340	26.7 ± 0.8	148.2 ± 10.8
1471 - *1*¹	3.924 ± 0.010	522.64 ± 5.54	21.77 ± 0.98	1.167 ± 0.011	7.78 ± 0.36	0.3389 ± 0.0152	-	-	-
1471 - *4*¹	4.587 ± 0.013	7.40 ± 0.09	10.23 ± 0.17	1.141 ± 0.007	258.01 ± 5.24	0.1363 ± 0.0023	-	-	-
1471 - *4*¹	5.114 ± 0.012	3.67 ± 0.02	10.83 ± 0.15	1.149 ± 0.006	550.08 ± 8.20	0.1293 ± 0.0019	-	-	-
1471 - *isochr.*¹	-	-	-	1.151 ± 0.005	-	0.1300 ± 0.0016	13060 ± 240	4.8 ± 0.6	156.8 ± 5.3
2629 - *3*	3.263 ± 0.011	15.49 ± 0.34	11.54 ± 0.55	1.149 ± 0.007	139.09 ± 7.34	0.2162 ± 0.0104	-	-	-
2629 - *4*	3.704 ± 0.004	5.00 ± 0.02	12.12 ± 0.06	1.134 ± 0.002	452.09 ± 2.70	0.1999 ± 0.0010	-	-	-
2629 - *isochr.*	-	-	-	1.133 ± 0.003	-	0.1934 ± 0.0010	20370 ± 185	14.6 ± 0.8	141.3 ± 3.7
2657 - *3*¹	4.703 ± 0.007	5.26 ± 0.02	8.16 ± 0.07	1.141 ± 0.003	289.92 ± 2.83	0.1060 ± 0.0010	-	-	-
2657 - *4*¹	4.427 ± 0.008	8.56 ± 0.04	8.07 ± 0.08	1.142 ± 0.004	176.20 ± 1.83	0.1115 ± 0.0011	-	-	-
2657 - *isochr.*¹	-	-	-	1.142 ± 0.004	-	0.0986 ± 0.0006	9850 ± 220	20.3 ± 0.8	145.6 ± 4.2
3036 - *3*	4.737 ± 0.009	36.54 ± 0.25	16.92 ± 0.23	1.139 ± 0.003	86.47 ± 1.31	0.2183 ± 0.0030	-	-	-
3036 - *4*	4.441 ± 0.007	11.64 ± 0,09	14.41 ± 0.19	1.137 ± 0.003	231.11 ± 3.53	0.1983 ± 0.0026	-	-	-
3036 - *4*	4.494 ± 0.008	9.66 ± 0.04	15.22 ± 0.12	1.144 ± 0.004	294.08 ± 2.68	0.2069 ± 0.0017	-	-	-
3036 - *isochr.*	-	-	-	1.141 ± 0.004	-	0.1992 ± 0.0027	20870 ± 390	7.3 ± 2.0	149.9 ± 4.6
3056-*3*	4.519 ± 0.009	72.97 ± 0.39	16.91 ± 0.22	1.145 ± 0.005	43.26 ± 0.61	0.2286 ± 0.0030	-	-	-
3056-*4*	4.709 ± 0.009	40.32 ± 0.12	16.33 ± 0.11	1.139 ± 0.004	75.63 ± 0.57	0.2119 ± 0.0015	-	-	-
3056 - *isochr.*	-	-	-	1.141 ± 0.004	-	0.1931 ± 0.0019	20180 ± 290	6.7 ± 0.5	148.7 ± 4.2

Additionally the ^{230}Th/^{232}Th activity ratio of the contaminating phase, i.e., the ^{230}Th/^{232}Th activity ratio of the former seawater can be determined. These ^{230}Th/^{232}Th activity ratios varied between 4.8 ± 0.6 and 26.7 ± 0.8. They are uncorrected for the ^{230}Th decay after incorporation since the exact time of contamination is unknown. The second mode is the incorporation of small amounts of thorium during the lifetime of the coral with a ^{230}Th/^{232}Th initial activity ratio of the seawater the coral lived in (Cheng et al. 2000a).

The fact that the estimated ^{230}Th/^{232}Th activity ratio *via* isochron (Table 3) (Lomitschka 1999; Lomitschka and Mangini 1999), the initial ^{230}Th/^{232}Th activity ratios measured for modern deep-water corals (Cheng et al. 2000a) and the measured ^{230}Th/^{232}Th activity ratios of dissolved and total thorium from seawater of the North Atlantic (Moran et al. 1997; Vogler et al. 1998) are of the same order of magnitude (Fig. 3), supports the use of activity ratios of water samples for thorium correction of deep-water corals.

Thus all U/Th ages of deep-water corals that were not estimated *via* the isochron method (Table 2) were corrected with a ^{230}Th/^{232}Th activity ratio of 8.6 ± 2, the average of different measurements at 500 m water depth (Vogler et al. 1998). However, for deep-water corals from locations where an isochron dating of another individual exists, the correction factor estimated *via* the isochron (#2621, #2622, #2631) was applied (Table 2).

Ten of the U/Th ages published in Schröder-Ritzrau et al. (2003) were corrected with a ^{230}Th/^{232}Th activity ratio of 8.6 ± 4.3. The higher error in the correction factor was used to account for a higher uncertainty, since ages were coupled with ^{14}C-AMS age and were used for estimation of intermediate water ages (Table 2).
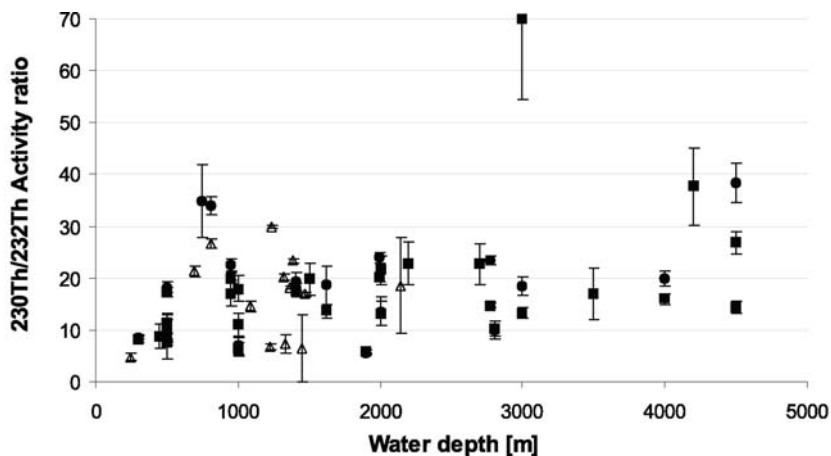
● 230Th/232Th sea water diss.; activity ratio; Moran et al. 1997; Vogler et al. 1998

■ 230Th/232Th sea water total; activity ratio; Moran et al. 1997; Vogler et al. 1998

△ 230Th/232Th initial deep sea corals; isochrone data; Cheng et al. 2000, Lomitschka & Mangini 1999; Lomitschka 1999

Fig. 3 ^{230}Th/^{232}Th activity ratios from water samples and deep-water corals from the North Atlantic plotted *versus* water depth

Effects of Th-correction on ages and their errors

The corrected age of a deep-water coral is dependent on the applied correction factor and its varying errors, the age itself and the ^{232}Th content of the sample. Fig. 4 displays this dependency for three younger samples with ages less than 2 ka and three older samples from 9 ka to 14 ka and ^{232}Th concentrations of 0.03 to 5 ng. Ages of these samples were corrected each with the terrigenous factor of 0.75, 8.6, the water value for 500 m water depth in the North Atlantic and 20, a moderately high value (Fig. 4a). For all factors errors between 0 % and 100 % were calculated. Sample #3237 from very shallow waters (276 m) was not corrected with the moderately high value since such high values are unlikely for very shallow water depths.

For samples younger than 2 ka only a few ng ^{232}Th contamination caused age corrections of several hundred years. Hence, the correction is a multiple of the analytical error when high values for the correction factor and 100 % error (e.g., 20 ± 20) are assumed (Fig. 4a).

In contrast, for older Early Holocene samples few ng were less critical even when high correction factors were applied (Fig. 4b).

Depending on the purpose of these ages for further investigations, such as the determination of intermediate water ages or exact chronologies of climatic variations, the selection of samples with low ^{232}Th content and the use of appropriate caution in correction factor are crucial. Even for shallow-water corals Th-correction can become a problem. In a recent investigation, Cobb et al. (2003) showed that modern shallow-water corals from the Pacific, which were previously corrected with the terrigenous activity ratio of 0.75, may have initial ^{230}Th/^{232}Th activity ratio of 3.74.

Temporal and spatial occurrences of deep-water corals in the North Atlantic

Based on 37 deep-water corals from surface samples of the North East Atlantic, a detailed regional chronology is now available with U/Th ages between 0.09 and 53.5 ka (Fig. 5; Tables 2, 3). While exposed occurrences of deep-water corals studied to date in Scandinavian waters, the Faroe area and the Rockall Trough are solely of Holocene age, deep-water corals from lower latitudes from seamounts off NW-Africa, the Mid-Atlantic Ridge Zone and the Mediterranean Sea show continuous coral growth over the last 53.5 ka (Figs. 5, 6). The Late Holocene U/Th ages (Fig. 5; Table 2) of the northernmost samples, north of the Faroer Ridge system reflect the ongoing present-day reef growth seen at the Sula Ridge complex (Freiwald et al. 2002). The late glacial to early postglacial iceberg scour on the crest and shoulder of the Sula Ridge provided the first settling ground for scleractinian corals (Freiwald et al. 2002). Thus far, no corals in this area from the Late Glacial or the Termination have been documented. The seven ages of the Porcupine Basin area (Fig. 5) are of Holocene age. Investigations of deep-water corals in gravity cores from this area indicate reef growth only during interglacial times, which appears to be strongly related to the environmental forcing of the major oceanic circulation pattern (Dorschel et al. in press; Rüggeberg et al. 2005).

Environmental forcing predominantly by circulation pattern has been discussed as a controlling mechanism for modern occurrences of deep-water communities. Freiwald (2002) provided a substantial summary of the oceanographic conditions
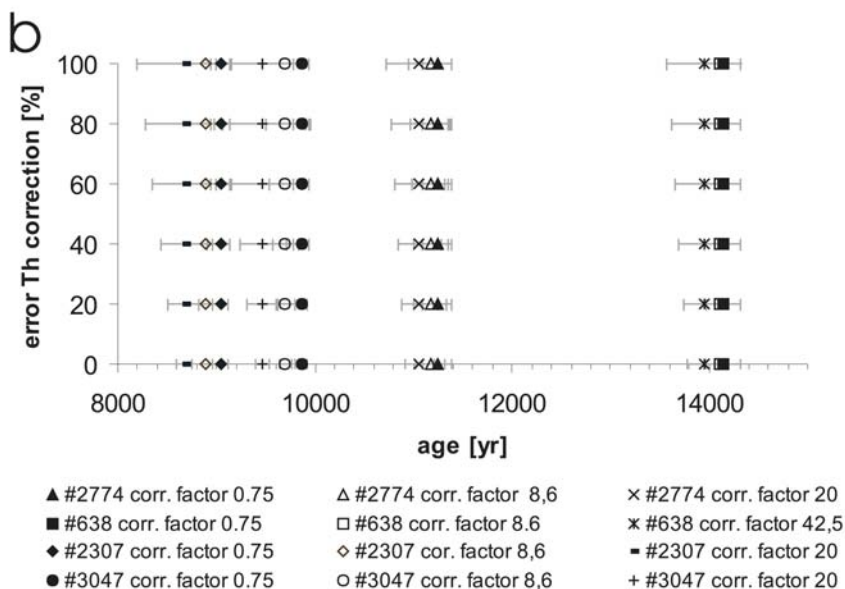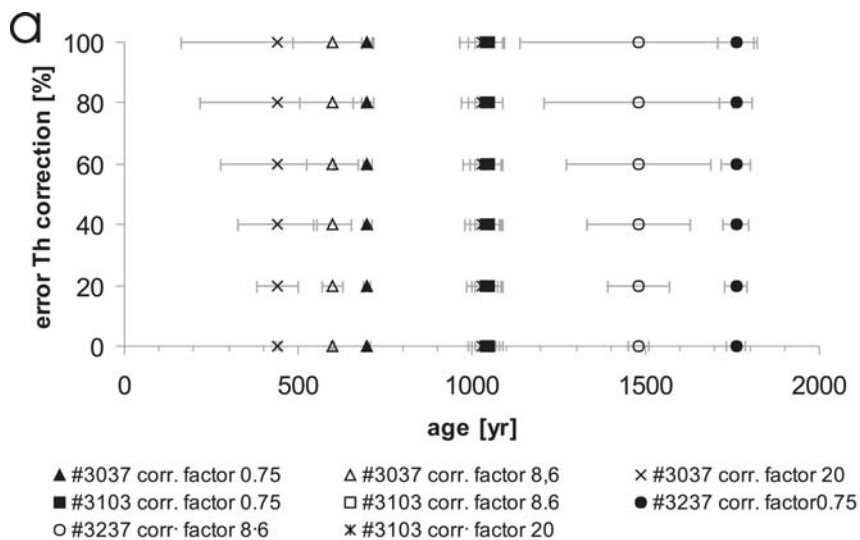
Fig. 4 Ages and age errors of deep-water corals (**a** samples 0-2 ka; **b** samples 8-14 ka) containing different concentration of ^{232}Th (see Table 2). Ages and age errors are plotted in relation to Th-correction factor and its assumed error percentage

favoured by the modern deep-water coral community in the North East Atlantic. He pointed out that the MOW (Mediterranean Outflow Water) has a major impact on the modern distribution. It provides warm and higher salinity water preferred by *Lophelia* or *Lophelia*-dominated coral occurrences (Freiwald 2002). They occur also within the relative oxygen minimum zone caused by the oxygenation of organic matter and oxygen respiration by organisms at these depths. Hence, oceanographic
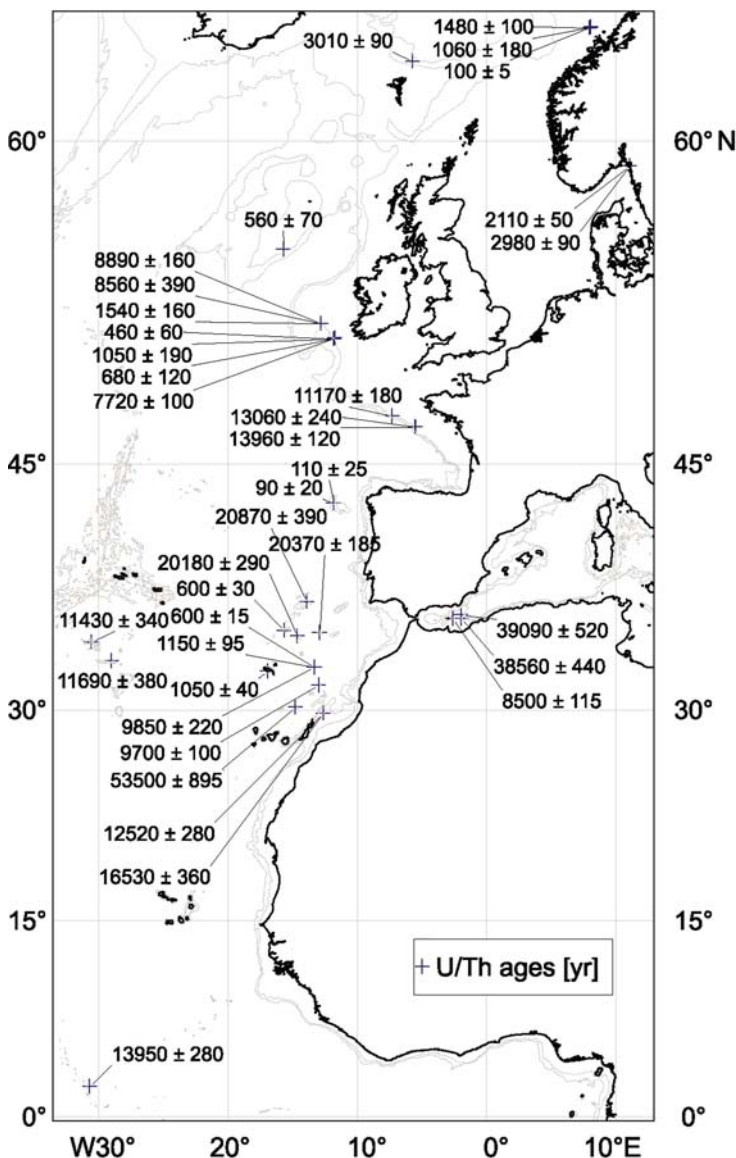
Fig. 5 U/Th ages (error 2σ) of deep-water corals
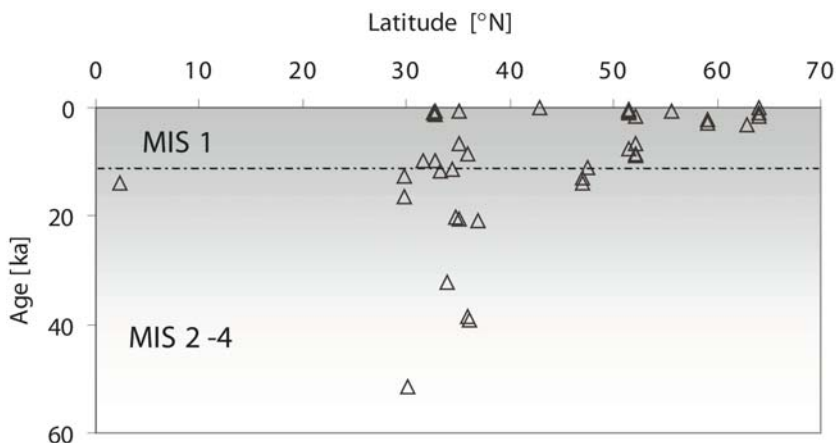
Fig. 6 Deep-water coral ages of surface samples *versus* latitude

conditions have varied during interglacial cycles most probably affecting the distribution of deep-water corals.

In contrast, the deep-water corals from lower latitudes from seamounts of NW-Africa, the Mid-Atlantic Ridge and east of the Azores show that conditions were suitable for deep-water coral growth during glacial times. Sixteen U/Th ages from lower latitudes indicate that deep-water corals occurred at least more or less continuously from 53.5 ka to modern times. Further work to determine the intermediate water ages for selected samples from the present study, especially those from lower latitudes, will give useful information on the water mass properties of the Last Glacial and the Termination.

Conclusions

- The investigated deep-water corals from surface samples of the North East Atlantic depict U/Th ages between 0.09 and 53.5 ka.
- The exposed occurrences of deep-water corals studied to date in Scandinavian waters and the Faroe area are solely of Holocene age. Probably, environmental conditions in that area during glacial times were not favourable for coral growth.
- Seamounts of NW-Africa, the low latitude Mid-Atlantic Ridge and the Azores had conditions suitable for deep-water coral growth during glacial time as well as the interglacial periods.
- Selecting samples with low [232]Th content is crucial for age determination of deep-water corals in order to minimize age uncertainty by correction for seawater and detritus derived excess Th.

Acknowledgements

References

Adkins JF, Boyle EA (1999) Age screening of deep-sea corals and the record of deep North Atlantic circulation change at 15,4 KA. In: Abrantes F., Mix A (eds) Reconstructing Ocean History: a Window into the Future. Kluwer Academic Plenum Publisher, New York, pp 103-120

Chen JH, Edwards RL, Wasserburg GJ (1986) ^{238}U, ^{234}U and ^{232}Th in seawater. Earth Planet Sci Lett 80: 241-251

Cheng H, Adkins J, Edwards RL, Boyle EA (2000a) U-Th dating of deep-sea corals. Geochim Cosmochim Acta 64: 2401-2416

Cheng H, Edwards RL, Hoff J, Gallup CD, Richards DA, Asmerom Y (2000b) The half-lives of uranium-234 and thorium-230. Chem Geol 169: 17-33

Cobb KK, Charles DC, Cheng H, Kastner M, Edwards Rl (2003) U/Th-dating living and young fossil corals from the central tropical Pacific. Earth Planet Sci Lett 210: 91-103

Dorschel B, Hebbeln D, Rüggeberg A, Dullo W-Chr (in press) Carbonate budget of a cold-water coral carbonate mound: Propeller Mound, Porcupine Seabight. Int J Earth Sci

Edwards RL, Gallup CD, Cheng H (2003) Uranium-series dating of marine and lacustrine carbonates. In: Bourdon B, Henderson GM, Lundstrom CC, Turner SP (eds) Uranium-series Geochemistry. Rev Mineral Geochem 52: 363-405

Freiwald A (2002) Reef-forming cold-water corals. In: Wefer G, Billett D, Hebbeln D, Jørgensen BB, Schlüter M, van Weering T (eds) Ocean Margin Systems. Springer, Berlin Heidelberg, pp 365-385

Freiwald A, ACES Party (2000) The Atlantic Coral Ecosystem Study (ACES): a margin-wide assessment of corals and their environmental sensitivities in Europe's deep waters. EurOCEAN 2000 Project Synopses. Marine processes, ecosystems and interactions. 1: 312-317

Freiwald A, Hühnerbach V, Lindberg B, Wilson JB, Campbell J (2002) The Sula Reef Complex, Norwegian Shelf. Facies 47: 179-200

Goldstein SJ, Lea DW, Chakraboty S, Kashgarian M, Murrell MT (2001) Uranium-series and radiocarbon geochronology of deep-sea corals: implications for Southern Ocean ventilation rates and the oceanic carbon cycle. Earth Planet Sci Lett 193: 167-182

Ivanovich M, Latham AG, Ku T-L (1992) Uranium-series disequilibrium applications in geochronology. In: Ivanovich M, Harmon RS (eds) Uranium-series Disequilibrium: Applications to Earth, Marine, and Environmental Sciences. Clarendon Press, Oxford, pp 62-94

Lomitschka M (1999) Untersuchungen zur Th/U - und Pa/U-Datierbarkeit von Tiefseekorallen und Pteropoden. PhD thesis, Univ Heidelberg, 91 pp

Lomitschka M, Mangini A (1999) Precise Th/U-dating of small and heavily coated samples of deep sea corals. Earth Planet Sci Lett 170: 391-401

Ludwig KR, Titterington DM (1994) Calculation of [230]Th/U isochrons, ages and errors. Geochim Cosmochim Acta 58: 5031-5042

Moran SB, Charette MA, Hoff JA, Edwards RL, Landing WM (1997) Distribution of [230]Th in the Labrador Sea and its relation to ventilation. Earth Planet Sci Lett 150: 151-160

Paillet J, Arhan M, McCartney MS (1998) Spreading of Labrador Sea Water in the eastern North Atlantic. J Geophys Res 103: 10223-10239

Reid JR (1994) On the total geostrophic circulation of the North Atlantic Ocean: Flow patterns, tracers, and transports. Progr Oceanogr 33: 1-92

Rhein M (2000) Drifters reveal deep circulation. Nature 407: 30-31

Rüggeberg A, Dorschel B, Dullo W-Chr, Hebbeln D (2005) Sedimentary patterns in the vicinity of a carbonate mound in the Hovland Mound Province, northern Porcupine Seabight. In: Freiwald A, Roberts JM (eds) Cold-water Corals and Ecosystems. Springer, Berlin Heidelberg, pp 87-112

Schmitz WJJ, McCartney MS (1993) On the North Atlantic circulation. Rev Geophys 31: 29-49

Schröder-Ritzrau A, Lomitschka M, Mangini A (2003) Deep-sea corals evidence periodic reduced ventilation in the North Atlantic during LGM/Holocene transition. Earth Planet Sci Lett 216: 399-410

Vogler S, Scholten J, Rutgers van der Loeff M, Mangini A (1998) [230]Th in the eastern North Atlantic: the importance of water mass ventilation in the balance of [230]Th. Earth Planet Sci Lett 156: 61-74

Distribution and habitats of *Acesta excavata* (Bivalvia: Limidae) with new data on its shell ultrastructure

Matthias López Correa[1], André Freiwald[1], Jason Hall-Spencer[2], Marco Taviani[3]

[1] Institute of Paleontology, Erlangen University, Loewenichstr. 28, D-91054 Erlangen, Germany
  (lopez@pal.uni-erlangen.de)
[2] Department of Biological Sciences, University of Plymouth, Plymouth, PL4 8AA, UK
[3] ISMAR-Marine Geology Division, CNR, Via Gobetti 101, I-40129 Bologna, Italy

Abstract. *Acesta excavata* is the largest known bivalve associated with the *Lophelia pertusa* communities along the northeast Atlantic continental margin, but has also been found along steep cliffs, devoid of bathyal corals, and on more subdued topographies. During the Pleistocene, including the last glacial, *A. excavata* was widespread in the Mediterranean, but is in the Recent fauna known only from four Mediterranean sites. A new possible live-record from the Canyon du Var off Nice is presented. Radiocarbon dating (AMS ^{14}C-method) on an *A. excavata* assemblage from the Strait of Sicily yielded a Late Pleistocene age of 39.9 ka. Biometric parameters indicate that Pleistocene Mediterranean shells achieved about the same maximum sizes as their Recent Atlantic counterparts, but individuals have been slightly smaller on average. The subspecies *Acesta excavata sublaevis* Nordsieck, based on a subfossil juvenile Mediterranean shell, is not considered a valid taxon. Mineralogical composition and ultrastructure of *A. excavata* have been analyzed using thin-sections, Feigel staining, x-ray diffractometry (XRD) and SEM-imaging. Its wide distribution, large size (15 cm) and simple shell architecture makes it a prime candidate for palaeoenvironmental studies in cold-water coral settings.

Keywords. *Acesta,* North Atlantic, Mediterranean Sea, biogeography, ultrastructure, ecology

Introduction

Cold-water scleractinians are the focus of a growing interest in the field of palaeoceanography and palaeoclimatology (Adkins et al. 1998; Mangini et al. 1998). Corals secrete an aragonitic exoskeleton whose growth pattern and geochemical

composition is complex, making the extraction of suitable climatic signals often technically difficult and not always easy to decipher (e.g., Mikkelsen et al. 1982; Adkins et al. 2002; Risk et al. 2005). There is, therefore, a strong motivation to test additional calcareous organisms co-occurring with cold-water corals, and thus sharing the same ambient environmental conditions. Bivalvia are particularly useful and reliable tracers to reconstruct past attributes of seawater (e.g., Jones et al. 1983; Richardson 2001; Owen et al. 2002). In this respect, *Acesta excavata* Fabricius, 1779 (Fig. 1) is one of the most prominent bivalves that inhabit bathyal cold-water coral communities along the European continental margin. *A. excavata* is expected to be a more reliable environmental recorder than the corals, with a much simpler growth pattern. The margin-wide occurrence in intermediate water masses could provide us with an *in situ* archive.
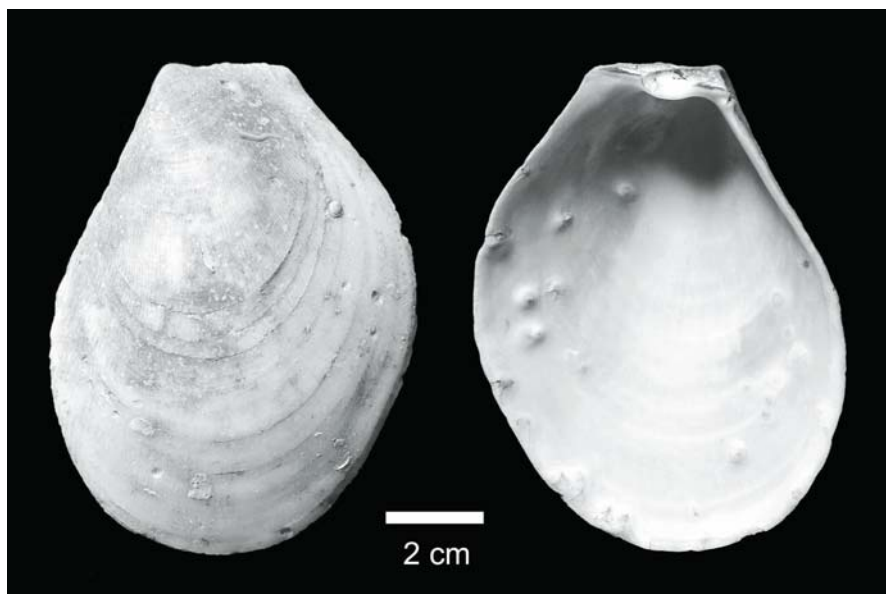
Fig. 1 *Acesta excavata* Fabricius, 1779, from 180 m in Trondheimfjord, Norway. Major growth lines and fine radial ribs sculpture the exterior. Note the attached parasitic foraminifer *Hyrrokkin sarcophaga* and several circular grooves produced by the parasite. The shell interior has a smooth surface. Interior swellings are due to the callus production of *A. excavata*, where *H. sarcophaga* pits had entered the mantle cavity

We propose *A. excavata* as a possible target-species for studies of environmental conditions in cold-water coral settings. This paper summarizes the known distribution of *A. excavata* and its habitats. Herein we provide a biometric analysis and a description of its shell structure, including an examination of its ultrastructure. Our data on shell mineralogy and internal architecture provide a basis for subsequent geochemical examinations.

Taxonomy and biology of *Acesta*

The cosmopolitan genus *Acesta* is represented by more than 30 Recent species, grouped within four subgenera (e.g., Vokes 1963, 1964; Dawson 1995; Coan et al. 2000; Marshall 2001). All of them are epifaunal filter feeders, found in cold-water environments (e.g., Jeffreys 1879; Sowerby 1883; Dall 1902, 1908; Bartsch 1913; Lamy 1930-1931; Madsen 1949; Hertlein 1952; Barnard 1963; Vokes 1963; Kuroda et al. 1971; Coan et al. 2000; Marshall 2001), often associated with bathyal cold-water corals.

The genus *Acesta* comprises larger (~25 cm) species (Lamy 1930-1931), than other genera within the Limidae (*Limaria, Lima, Ctenoides, Limatula* and *Limea*) are smaller and, with exceptions, tend to occur mostly in shallower waters (e.g., Coan et al. 2000; Hall-Spencer and Moore 2001; Mikkelsen and Bieler 2003). Limidae live on the surface of seabed sediments or settle various types of hard substrata. They are similar to the Pectinidae in many respects, for both families have species that are active swimmers and that can attach to hard substrata by a byssus (Yonge 1936).

Acesta excavata (Fig. 1) was first described as *Ostrea excavata* from Norwegian fjords in 1779 by Fabricius, a Danish student of the pioneering Swedish taxonomist Carolus Linnaeus. Its current taxonomic position within the phylum Mollusca is shown below, having been transferred to the genus *Acesta* by H. and A. Adams (1858). *Lima solida* Calcara, 1845, *Radula (Acesta) excavata* H. and A. Adams, 1858 and *Lima excavata* Lamarck, 1819 are synonyms of *Acesta excavata* (for details see Vokes 1963), which is the type species for the genus *Acesta*.

Class BIVALVIA Linnaeus, 1758
Subclass PTERIOMORPHA Beuerlen, 1944
Order LIMOIDA Waller, 1978
Superfamily LIMOIDEA Rafinesque, 1815
Family LIMIDAE Rafinesque, 1815
Genus *Acesta* H. and A. Adams, 1858
Species *excavata* Fabricius, 1779

Acesta excavata is a suspension feeder which lives attached to hard substrata and is distributed along the continental shelf-break of the north-eastern Atlantic Ocean (Fig. 2) and during the Pleistocene to Recent within the Mediterranean basin (e.g., Bourcier and Zibrowius 1969), often co-occurring with *Lophelia pertusa* and *Madrepora oculata*. Most specimens for this study were recovered from cold-water coral sites (Fig. 3). Remotely Operated Vehicle (ROV) investigations showed a direct byssal attachment to dead coral frameworks, just below the active growth zone.

Acesta rathbuni (Dawson, 1995) and *A. bullisi* are capable of releasing themselves from their byssus and swimming to more favourable sites (Kohl and Vokes 1994) yet *A. excavata* seems unable to swim actively. Nevertheless, even adult specimens can move easily using their strong byssus (Järnegren 1999).
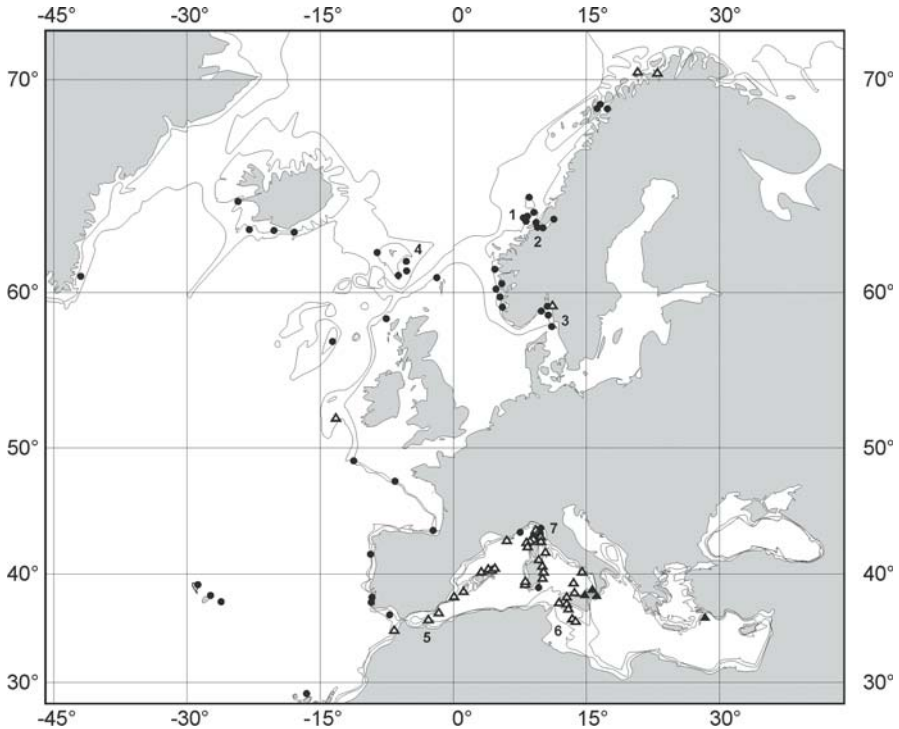
Fig. 2 Distribution of Recent *Acesta excavata* in Europe (black circles). Bathymetry is simplified to the 200 m and the 1000 m depth contour. White triangles indicate submerged sites of subfossil to Late Pleistocene age and black triangles denote uplifted Lower Pleistocene sections on Sicily and Rhodes. Sampling sites covered in detail are: 1 - Sula Ridge, 2 - Trondheimfjord, 3 - Kosterfjord, 4 - Faroe Bank, 5 - Cabliers Bank, 6 - Strait of Sicily, 7 - North Tyrrhenian Sea

Acesta bullisi Vokes, 1963 from the Gulf of Mexico is found attached to large vestimentiferan tubeworms (*Lamellibrachia luymesi*) in chemosymbiotic bottom communities at hydrocarbon seeps (e.g., Boland 1986; MacDonald et al. 1989; Kohl and Vokes 1994). Järnegren et al. (2003) observed an oophagous lifestyle for *A. bullisi*, in addition to its filter feeding habit. This combination is unique in the animal kingdom. *A. bullisi* preys on lipid-rich tubeworm eggs.

Little is known about *Acesta angolensis* Adam and Knudsen 1955, the south-eastern 'neighbour' of *A. excavata*, which inhabits bathyal depths along the west-African continental margin (Boss 1965). *A. angolensis* has its northernmost distribution off north-west Gabon at 439 to 595 m depth, but is more commonly found further south from Pointe-Noire to Moçamedes (pers. comm. R. von Cosel 2003).

Fig. 3 Haltenpipe Reef cluster, 300 m depth, off Mid-Norway. Dense clusters of large (>10 cm) *A. excavata*, byssally attached to dead coral framework, just below the active growth zone (photo courtesy of M. Hovland, Statoil Company; Hovland and Mortensen 1999)

Description of *Acesta excavata*

The thin white shell, often translucent in juvenile specimens, is roughly oval and higher than wide (Fig. 1). The anteroventral margin is oblique, while a prominent auricle marks the posterior. Adult specimens can reach 20 cm in height and are moderately inflated, strongly inequilateral, but equivalved. The lunular field is excavated, sometimes slightly gaping at the byssal notch.

Many fine radial ribs restricted to the exterior originate from the umbo. Each rib can be traced across the entire shell to its margin. On the medial portion they are often subdued and faint, but again more pronounced towards the valve margin. In anteroventral and dorsal portions the ribs are most prominent, especially on either side of the umbo, in the lunular area and on the posterior auricle. Interspaces between ribs are shallow concave grooves, equally wide as the adjacent costae. The posterodorsal margin shows a distinctly ribbed angular auricle behind the small umbones, while the anterior auricle is reduced.

Major growth lines occur on the exterior side in relatively regular increments (Fig. 1). In large adult specimens (>10 cm) these lines get narrower and are increasingly crowded. Earliest growth lines close to the umbo are often indistinct.

The shiny interior side, in contrast, is smooth with a slight opalescence, only interrupted by the imprints of the posterior muscles. The non-sinuate pallial line is situated close to the valve margin.

The hinge is straight, without teeth, slightly indented by an oblique triangular ligament pit in the middle (Fig. 2). Most of the ligament is restricted to the oblique triangular groove, with narrow lateral extensions onto the actively growing hinge zone. Contact with the valves is partly calcified, in contrast to a black elastic exterior part. The extremely thin periostracum is light brown to brown, often abraded during lifetime on the medial shell portion.

The soft body of the living animal is light orange to white and shows a gaping mantle cavity (Fig. 4), without fused margins and without siphon. Long tentacles, some with eyes, extend from the folded mantle margin (Järnegren 1999). Two muscle imprints are visible on the posterior portion of the shell interior. Usually one large approximately circular imprint is accompanied by a field with dense accumulation of smaller pedal muscle holdfast. This patch is made up of several muscle strings, which can be fused in adult shells. In old shells both muscle attachment areas may form a joint imprint, up to 4 cm in length (1.5 cm wide). The strong foot allows the animal to crawl hinge-first, assisted by strong byssus threads originating from the byssus gland. These fibres exit at the lunular field and allow for a firm attachment to hard substrata. Järnegren (1999) has documented a sex change during the lifetime of *A. excavata*; most specimens from Trondheimfjord (Røberg and Hitra) <9.0 cm were male, while shells >11.5 cm were female.
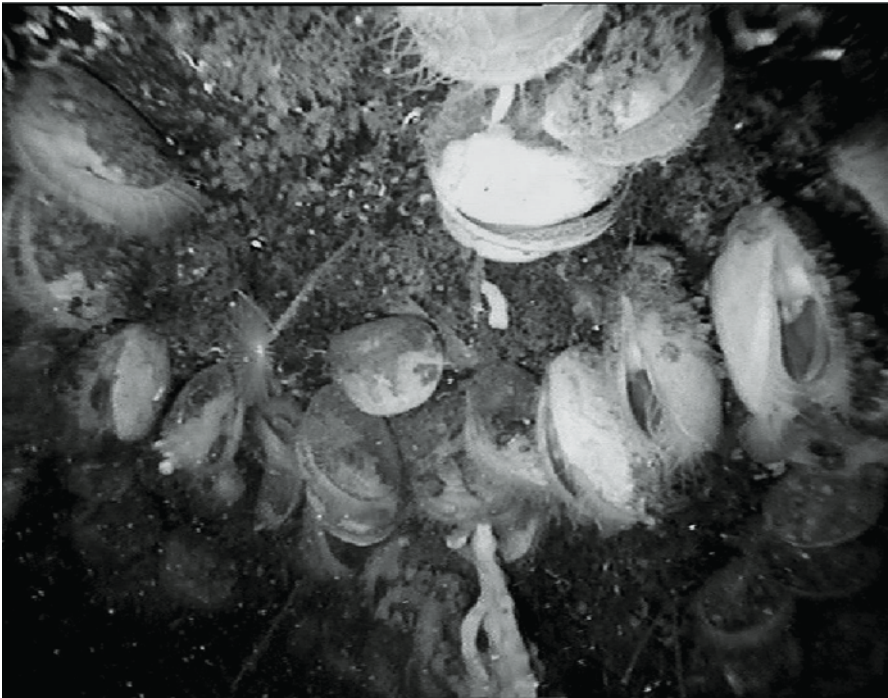

Fig. 4 *A. excavata* byssally attached to a steep bedrock cliff at 85 m in the Kosterfjord, Sweden. Shells reach 13 cm height (photo courtesy of T. Lundälv, TMBL)

Fossil record of the genus *Acesta*

Taxa attributed to the Limidae can be traced back at least to the Carboniferous (e.g., Coan et al. 2000), while the fossil record of the genus *Acesta* spans the Late Mesozoic and Cenozoic era (e.g., Dall 1900; Clark 1925; Yokoyama 1925; Woodring 1938; Otuka 1940; Kanno 1960, 1971; Vokes 1963, 1964; Aoki 1976; Hickman 1984; Beu and Maxwell 1990; Stilwell and Zinsmeister 1992; Palazzi and Villari 1996; Stilwell and Gazdzicki 1998; Coan et al. 2000). Today more than 30 fossil species are attributed to *Acesta*.

All known Mesozoic *Acesta* localities originate from the southern hemisphere supercontinent Gondwana, encompassing its continental margins. The oldest *Acesta* records are reported from Late Jurassic deposits (Kanjilal 1990) of western India. Early Cretaceous sites are known from New Caledonia (Freneix 1980), southern Chile (Dawson 1995) and India (Kanjilal 1990). Latest Cretaceous to Early Tertiary sections on Seymour Island in Antarctica document the continuous record of *Acesta* across the K/T boundary, represented by *Acesta shakletoni*, *A. seymourensis, A. laticostata* and *A. bibbyi* (Stilwell and Zinsmeister 1992; Stilwell and Gazdzicki 1998).

Lower Oligocene deposits of Austria document early occurrences in Europe with *Acesta szabói* and *A. mittereri* (Löffler 1999). During mid-Tertiary times (especially Miocene) the genus has at least 16 species documented (Vokes 1963). This peak in diversity also marks the onset of its cosmopolitan distribution. Most species are reported from Japan (e.g., Matsumoto 1986), but also from New Zealand (Beu and Climo 1974; Marshall 2001) and from the Pacific side of North America (Moore 1984). According to Sacco (1898) the European *Acesta miocenica* Sismonda, found in Miocene deep-water deposits of Italy and Hungary (Sacco 1898; Báldi 1986), represents potentially a mid-Tertiary ancestor of *Acesta excavata*.

The bathyal, neotectonically uplifted Plio-Pleistocene sections of Rhodes (pers. observ. A. Freiwald) and Sicily (Seguenza 1870, 1880) provide the oldest known *A. excavata* sites. Many occurrences are recorded from Early to Mid-Pleistocene deposits from Sicily and the adjacent southern Italian province Calabria (e.g., Seguenza 1873-1879, 1880; De Stefani 1891; Di Geronimo and Li Gioi 1980; Di Geronimo 1987; Barrier et al. 1996; Palazzi and Villari 1996; Vazzana 1996; Di Geronimo and La Perna 1997).

Apart from those emerged sections, *A. excavata* is also recorded from numerous Late Pleistocene submerged deposits in the western part of the Mediterranean Sea (Fig. 2), often associated with subfossil azooxanthellate scleractinian corals (Segre and Stocchino 1969; Taviani and Colantoni 1979; Corselli and Bernocchi 1990; Bonfitto et al. 1994a, b). *A. excavata* has been recorded so far from the Alboran Sea over the Balearic Sea to the Strait of Sicily (Taviani and Colantoni 1979) and from the Adriatic (Ghisotti 1979). These submerged sites document together with the southern Italian outcrops the frequent fossil (Pleistocene) distribution of the bivalve in the western Mediterranean. Recently dredged hardgrounds (CORTI mission) on the flanks of Cialdi Seamount in the Tyrrhenian Sea have yielded the first submerged example of a micritic limestone containing *A. excavata* (Fig. 5).
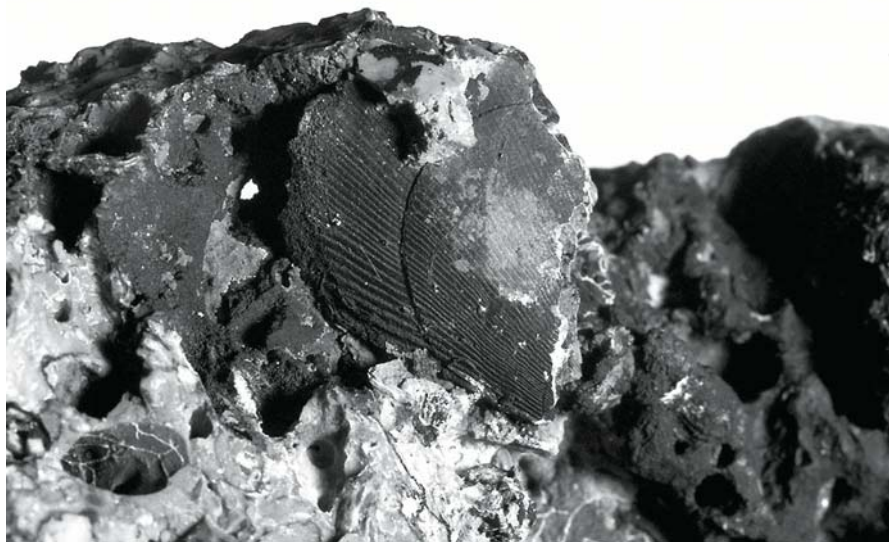
Fig. 5 Pleistocene *A. excavata* from a hardground dredged from Cialdi Seamount (CORTI 86) in the Tyrrhenian Sea (450-1074 m). The pictured fragment is 1.7 cm long, but specimens >10 cm height have been recovered

Emerged Late Glacial to Holocene *A. excavata* have been noted from the glacial isostatically uplifted Norwegian coast (Jeffreys 1879), also together with *L. pertusa* from the Oslofjord (Broch 1922).

Recent distribution of *Acesta excavata*

The Recent distribution (Fig. 2) encompasses the north-eastern Atlantic between Norway and Mauritania (e.g., Sars 1878; Jeffreys 1879; Locard 1898; Friele and Grieg 1901; Kiær and Wollebæk 1913; Madsen 1949; Filatova 1959; Bourcier and Zibrowius 1969; Nordsieck 1969; Poppe and Goto 1991; Mikkelsen and Bieler 2003), including occurrences off southern Iceland (Madsen 1949) and south-western Greenland (Lamy 1930-1931). A record from a fjord setting in south-western Newfoundland (Bay D'Espoir) extends the geographical range to the western Atlantic margin (Haedrich and Gagnon 1991; Gagnon and Haedrich 2003).

At present *Acesta excavata* is a common component of cold-water coral reefs and circalittoral submarine cliffs in Sweden and Norway (Høisæter 1986). The earliest records of *A. excavata* come from Norwegian fjords, which yield the shallowest occurrences at water depths of less than 200 m. Stjernsund in West Finnmark at 70° is the northernmost record for live *A. excavata* (Freiwald et al. 1997). Among the best documented occurrences is the Trondheimfjord, were *A. excavata* is found down to 500 m (Järnegren 1999). Many mid-Norwegian fjords (Grieg 1913; Kiær and Wollebæk 1913; Nordgaard 1929; Dons 1932, 1944; Burdon-Jones and Tambs-Lyche 1960) host the typical deep-water bivalve at relatively shallow depths. The

Swedish Kosterfjord, which is connected to Atlantic waters by an over 500 m deep trough, is inhabited by dense *A. excavata* clusters on steep rock cliffs (Fig. 4) between 65 and 90 m depth (Lundälv 1997).

Apart from the fjord sites, *A. excavata* is distributed all over the relatively deep, glacially influenced Norwegian shelf, between 200 and 350 m (e.g., Sula Ridge; see Freiwald et al. 2002). Further south this species is restricted to the western European shelf-break area. The sites show a rough north-south depth trend, with the shallowest locations at 180 to 380 m on the continental margin off the Faroe Islands (Jensen and Frederiksen 1992; Delongueville and Scaillet 2000) and the deepest sites west of the Strait of Gibraltar (Dautzenberg and Fischer 1897; Hidalgo 1917), off south-western Portugal (1200 m). Southwards *A. excavata* has been scarcely reported from the Moroccan shelf (Reynell 1910; Ghisotti 1979), down to western Sahara (Locard 1898) and Mauritania (Table 1), and from an isolated site off the Ivory Coast (pers. comm. R. von Cosel 2003). Marche-Marchad (1979) reports and figured *A.* cf. *excavata* from 900 m in the Golf of Guinea near Abidjan. Additionally *A. excavata* has also been reported at 3200 m from the Canaries (Dautzenberg and Fischer 1906; Dautzenberg 1927) and between 599 to 1850 m around the Azores archipelago (Dautzenberg 1927).

In the Mediterranean, *A. excavata* was widespread during the last glacial period (Malatesta and Zarlenga 1986) but is currently less successful with only scattered records of live animals (Fig. 2). Early records, like that of Madsen (1949) who was the first to record this species as alive from the Mediterranean, may be questionable since fresh looking shells were often considered as living at that time. Appearances can be deceiving, as fresh-looking shells might be of Pleistocene age. Today there are four reliable reports for live *A. excavata* in the Mediterranean (Ghisotti 1979; Carcassi 1983; Rocchini 1983; Terreni and Voliani 1995), located between 430 and 570 m. Three of those sites are in the northern half of the western Mediterranean, north of Corsica in the Tuscan Archipelago (Fig. 2). The fourth site is located southwest of Sardinia in the Tyrrhenian Sea with a specimen found attached to a thick plastic canvas on a muddy bottom (Terreni and Voliani 1995). Numerous subfossil to fossil sites have been recorded from the western Mediterranean (Table 1) and document the former wide distribution within the basin (e.g., Bourcier and Zibrowius 1969; Taviani 1976; Taviani and Colantoni 1979; Remia and Taviani 2004). Segre and Stocchino (1969) and Colantoni et al. (1970) record fossil *A. excavata* deposits in the Tyrrhenian Sea. Two questionable subfossil sites are recorded from the Adriatic Sea (Ghisotti 1979).

Habitats

The species has an overall depth range report from 40 to 3200 m, but is usually found between 200 and 800 m, bound to intermediate water masses, particularly along the shelf-break area (Fig. 2). Living specimens are reported between 3 and 13°C (e.g., Bourcier and Zibrowius 1969; Ghisotti 1979), while most *A. excavata* sites have a temperature range of 6 to 8°C and salinities of 33.4 to 38.5 ‰ (Malatesta and Zarlenga 1986).

Table 1 Sampling sites of *Acesta excavata* from the North Atlantic and the Mediterranean Sea, which were investigated for this paper. Stations marked with (*) were contributed by H. Zibrowius, indicating further occurrences

Cruise	Station	R/V - ship	Location	Latitude	Longitude	Depth [m]	Preservation
JR-Carbo	JR-111	Johan Ruud	Stjernsund	N 70° 12. 00	E 022° 20. 00	210-280	Recent & subfossil
JH-5-99	4/8	Johan Hjort	Trondheimfjord	N 63° 36. 55	E 009° 23. 13	180-200	Recent & subfossil
POS-228	200-3	Poseidon	Sula Ridge	N 64° 05. 51	E 008° 03. 94	273	Recent
POS-228	215	Poseidon	Sula Ridge	N 64° 06. 53	E 008° 06. 87	250-320	Recent
POS-228	228-JAGO 8	Poseidon	Sula Ridge	N 64° 04. 77	E 008° 01. 71	250-320	Recent
LI-94	162	Littorina	Sula Ridge	N 64° 04. 77	E 008° 01. 71	250-320	Recent
LI-94	163	Littorina	Sula Ridge	N 64° 04. 95	E 008° 01. 63	283-295	Recent
ALK-232	VC-1019	Alkor	Tisler Reef	N 58° 59. 86	E 010° 57. 84	81	Subfossil
ALK-232	GKG-1021-2	Alkor	Tisler Reef	N 58° 59. 86	E 010° 57. 84	81	Subfossil
ALK-232	GKG-1022	Alkor	Tisler Reef	N 58° 59. 88	E 010° 57. 80	91	Subfossil
ALK-232	1051-2	Alkor	Skagerrak	N 59° 05. 85	E 010° 43. 87	120	Subfossil
ALK-232	BG-1053	Alkor	Skagerrak	N 59° 05. 46	E 010° 43. 65	161	Subfossil
ALK-232	BG-1066	Alkor	Skagerrak	N 59° 03. 66	E 010° 44. 25	88	Subfossil
ALK-232	BG-1071-2	Alkor	Skagerrak	N 59° 03. 25	E 010° 44. 56	112	Subfossil
ALK-232	BG-1082-1	Alkor	Djupekrak	N 59° 01. 43	E 010° 52. 01	161	Subfossil
ALK-232	BG-1083-2	Alkor	Djupekrak	N 59° 01. 46	E 010° 51. 98	159	Subfossil
ALK-232	BG-1087	Alkor	Skagerrak	N 59° 05. 02	E 010° 48. 39	130	Subfossil
ALK-232	BG-1092	Alkor	Skagerrak	N 59° 04. 52	E 010° 48. 22	82	Subfossil
ALK-232	BG-1147	Alkor	Skagerrak	N 59° 05. 95	E 010° 48. 34	64	Subfossil
ALK-232	BG-1152	Alkor	Skagerrak	N 59° 05. 83	E 010° 48. 16	91	Subfossil
ALK-232	GKG-1155-2	Alkor	Skagerrak	N 59° 04. 71	E 010° 43. 90	106	Subfossil
TMBL	1	ROV	Kosterfjord	N 58° 88. 00	E 011° 10. 00	85-90	Recent
TMBL	2	ROV	Kosterfjord	N 58° 88. 00	E 011° 10. 00	85-90	Recent
Faroe-1	23-332	(DAFS)	Faroe Bank	N 61° 43. 00	W 005° 54. 00	320	Recent
Procelt 1*	K 220	Thalassa I	S-Irish Margin	N 49° 13. 00	W 011° 46. 00	767-840	Recent
Thalassa*	Y-381	Thalassa I	Portugal	N 41° 28. 50	W 009° 14. 10	420	Recent
CYANA*	CY 86-53	Cyana	Canyon du Var	N 43° 63. 00	W 007° 20. 00	<1548	Recent
LM-99	50	Urania	La Gorgona	N 43° 24. 94	E 009° 44. 63	438-536	? subfossil
LM-99	125	Urania	La Gorgona	N 43° 13. 55	E 009° 36. 31	370-374	Pleistocene
CORTI	29	Urania	N Capraia	N 43° 14. 00	E 009° 36. 33	385-399	Pleistocene
CORTI	70	Urania	N Capraia	N 43° 13. 48	E 009° 36. 34	357-402	Pleistocene
CORTI	86	Urania	Cialdi Seamount	N 41° 44. 92	E 010° 32. 68	450-1074	Pleistocene
CORTI	87	Urania	Cialdi Seamount	N 41° 45. 08	E 010° 33. 78	359-495	Pleistocene

Table 1 continued

Cruise	Station	R/V - ship	Location	Latitude	Longitude	Depth [m]	Preservation
CORTI	88	Urania	Cialdi Seamount	N 41° 45. 19	E 010° 34. 65	391-600	Pleistocene
MARCO*	DR-14	Le Suroit	Corsica Margin	N 42° 32. 00	E 008° 31. 80	1175	Pleistocene
MARCO*	DR-15	Le Suroit	Corsica Margin	N 42° 45. 11	E 008° 58. 12	460	Pleistocene
MARCO*	DR-25	Le Suroit	Corsica Margin	N 42° 59. 40	E 009° 10. 90	1265	Pleistocene
MARCO*	DR-30	Le Suroit	Corsica Margin	N 43° 04. 55	E 009° 07. 45	1900	Pleistocene
MARCO*	DR-31	Le Suroit	Corsica Margin	N 43° 04. 54	E 009° 06. 46	1350	Pleistocene
MARCO*	DR-40	Le Suroit	Corsica Margin	N 43° 34. 90	E 009° 25. 50	450	Pleistocene
MARCO*	DR-52	Le Suroit	Corsica Margin	N 43° 45. 50	E 008° 47. 09	900	Pleistocene
SONNE-41*	148DC	Sonne	Eolo Seamount	N 38° 38. 95	E 013° 58. 78	679	? subfossil
CS-96	240	Urania	Strait of Sicily	N 36° 51. 45	E 013° 08. 26	400-767	Pleistocene
CS-96	243	Urania	Strait of Sicily	N 36° 51. 46	E 013° 08. 30	181-634	Pleistocene
CS-96	245	Urania	Strait of Sicily	N 36° 51. 19	E 013° 07. 40	190-435	Pleistocene
COR2	8	Urania	Strait of Sicily	N 36° 51. 43	E 013° 08. 12	181-631	39.9 ka
COR2	39	Urania	Strait of Sicily	N 36° 23. 48	E 013° 15. 17	523	Pleistocene
COR2	46	Urania	Strait of Sicily	N 36° 23. 49	E 013° 15. 18	505	Pleistocene
COR2	53	Urania	Strait of Sicily	N 36° 51. 53	E 013° 06. 29	178	Pleistocene
M-51-1	476 DR	Meteor	Cabliers Bank	N 35° 50. 19	W 002° 09. 57	790-954	Fossil
M-51-1	493 DR	Meteor	SE Cabo de Gata	N 36° 43. 20	W 001° 42. 15	1041-881	Fossil-subrecent
B-74	3	Bannock	SW-Ibiza Channel	N 37° 38. 90	W 000° 01. 40	260-940	Pleistocene
COBAS	43	Urania	S-Ibiza Channel	N 38° 33. 78	E 000° 40. 59	384-715	Pleistocene
COBAS	107	Urania	NE Menorca	N 40° 01. 16	E 004° 23. 62	299-557	Pleistocene
COBAS	109	Urania	NE Menorca	N 40° 01. 14	E 004° 23. 37	341-367	Recent-subrecent
COBAS	115	Urania	NE Menorca	N 40° 02. 43	E 004° 21. 19	344	Pleistocene
MD-04	2804	MarionDufresne	Larache, Marokko	N 35° 17. 45	W 006° 47. 00	550	Pleistocene
(MNHN)*	2	N'Diago	Mauritania	N 19° 04. 00	W 016° 50. 00	425	Recent
ISMAR	-	-	Mauritania	N 19° 00. 00	W 017° 00. 00	600	Recent
(MNHN)*	-	-	Senegal, Dakar	N 14° 30. 00	W 017° 35. 70	240-320	Recent

The most detailed insights into *A. excavata* habitats come from Scandinavian waters (Figs. 3, 4), based on ROV images and submersible observations from several cruises. *A. excavata* is for example common at the 300 m deep Haltenpipe Reef Cluster, on the shelf off mid-Norway (Hovland et al. 1998). Many *A. excavata* are found byssally attached to steep or overhanging hard substrata, especially to *Lophelia* corals and rocks (Hovland and Mortensen 1999). The shells are attached to dead coral skeletons, just below their soft tissue protected active growth zone (Fig. 3). Most *A. excavata* appear to be large (>10 cm height), orientated with the gape of their shells protruding into the water column. They co-occur with the gorgonacean octocorals *Paragorgia arborea* and *Primnoa resedaeformis,* as well as with the actinarian *Protanthea simplex.*

Surveys on the 200 m deep Nord-Leksa *L. pertusa* reefs off western Norway also revealed dense clusters of large (>10 cm) *A. excavata* on vertical to overhanging *L. pertusa* colonies, accompanied by live *L. pertusa*, *Paragorgia arborea* and *Primnoa resedaeformis* as conspicuous associated species (pers. comm. M. Hovland 2003).

Similar observations were possible from submersible (Jago) photographs taken on R/V Poseidon cruise POS 228 to the *L. pertusa* reef complex on the 250 to 320 m deep Sula Ridge (Freiwald et al. 2002). Here large *A. excavata* (up to 13 cm) were attached to vertical faces of dead coral rubble associated with the demosponge *Pachastrella* sp.

A. excavata has been documented at 40 m depth by SCUBA divers in Trondheimfjord, Tautraryggen, mid-Norway (pers. comm. E. Svensen 2003), and from several other sites down to 500 m at the fjord outlet (Hitra). Tautraryggen is at the same time the shallowest known site for the cold-water coral *L. pertusa* and for the bivalve *A. excavata*. Again, *A. excavata* was found attached to live *Lophelia* corals and to vertical faces of dead coral, associated with *Ascidia mentula* forming conspicuous parts of the sessile community.

Recent *A. excavata* from the Mediterranean have been reported attached to hard substrata and were found in the vicinity of dead cold-water scleractinians (*L. pertusa* and *M. oculata*).

ROV investigations from the Swedish Kosterfjord (Fig. 4) revealed a different picture (Fig. 4). *A. excavata* thrives in dense clusters on steep to overhanging bedrock cliffs, in absence of *L. pertusa*. They occur at 65 to 90 m depth with the actinians *Bolocera tuediae* and *Urticina eques*, the tube-dwelling polychaetes *Serpula vermicularis*, *Hydroides norvegica* and *Sabella pavonina*, as well as with encrusting and erect bryozoans *Alcyonidium diaphanum*, and with the ascidians *Dendrodoa grossularia* and *Ascidia* sp. (Lundälv 1997).

A. excavata also occurs in the adjacent Oslofjord (Table 1) on bouldery glacial deposits, as well as on muddy bottoms where dropstones provide hard substrata.

Di Geronimo (1995) reported *A. excavata* from emerged Plio-Pleistocene deposits (Fig. 2) of the Straits of Messina, in the community of "White Corals". The bivalve occurs together with *L. pertusa* and *M. oculata*, all originating from nearby escarpments, later embedded in bathyal marls (Di Geronimo 1987).

Sampling station COR2-56 in the Strait of Sicily in Late Pleistocene muddy sediments at the base (-505 m) of a steep cliff yielded a similar picture. The grab

sample contained numerous disarticulated *A. excavata* shells (>200), including at least 64 other macrofaunal taxa within the mixed pelagic to benthic death assemblage. Several organisms that live on hard substrata, like *L. pertusa* and *M. oculata*, the brachiopod *Gryphus vitreus* and the bivalves *Spondylus gussoni* and *A. excavata*, originate from the adjacent cliff.

Epibionts, parasites and endolithic organisms

Acesta excavata valves provide a hard substratum for epibionts. Recent shells often show dense overgrowth of serpulids, bryozoans and sponges, but also scleractinians and saddle-oysters (Anomiidae sp.). Fossil Mediterranean shells were often colonized by the brachiopod *Novocrania anomala*, which produces a typical imprint on the shells.

A. excavata is frequently infested by *Hyrrokkin sarcophaga* Cedhagen, 1994. This parasitic foraminifer also settles on the scleractinian *L. pertusa*, on other bivalves (e.g., *Delectopecten vitreus*), and even on sponges, within cold-water coral settings (Freiwald and Schönfeld 1996). *H. sarcophaga* preferentially uses *A. excavata* and *L. pertusa* as host (Cedhagen 1994). In early ontogenetic stages the foraminifer produces a 0.5 to 1 mm deep and up to 3 mm wide circular groove on the shell surface of *A. excavata* (Fig. 1), usually within the outer calcite zone. Adult foraminifer produce a narrow pit, which penetrates the entire valve and enters the inner soft tissue (Freiwald and Schönfeld 1996). *A. excavata* then forms a callus to close the hole, easily recognized as swelling on the shell interior (Fig. 1). Typical swelling diameter is 5 mm, formed by thin aragonite laminae, enriched in organic matter. More than forty pits have been observed on single valves, often with the parasite still attached in life-position.

A similar relationship is reported from *Acesta angolensis*, which is infested by *Rosalina carnivora* (Todd 1965). *A. angolensis* is the southern 'neighbour' of *A. excavata* and at the same time a closely related species. Both limid bivalves can hardly be distinguished by their biometric parameters (e.g., width and height). The two parasitic Foraminifera *Hyrrokkin sarcophaga* and *Rosalina carnivora* (Marche-Marchad 1979) are also closely related (see discussion in Cedhagen 1994).

The foraminiferan *Hyrrokkin sarcophaga* has not yet been documented from the present day Mediterranean (Cedhagen 1994; Freiwald and Schönfeld 1996). Boring traces preserved in Pleistocene *A. excavata* shells instead suggest that the foraminifer must have persisted in the Mediterranean as well. Unfortunately none of the fossil samples had the parasite still attached. Only a detailed investigation of the trace can consolidate this likely possibility.

Cedhagen (1994) noted that *A. excavata* from the Kosterfjord, although some hundred specimens were collected, had not shown an infestation by *H. sarcophaga*. Samples of *A. excavata* collected during the R/V Alkor cruise 232 to the Kosterfjord and the Skagerrak in November 2003 (Table 1), showed instead traces of the foraminifer at most sampled sites, including Kosterfjord. Both, subfossil to Recent shells were infested.

On older shell portions the periostracum tends to disappear, enhancing early bioerosion during the lifetime of the bivalve. Consequently bioerosion lacks in the youngest shell parts, but becomes increasingly frequent towards the umbonal area. The same pattern can be observed on the hinge plate, where only the youngest part is occupied by the ligament, while the older parts are already slightly affected by boring organisms.

The micro-borings *Orthogonum lineare* and *Saccomorpha clava*, produced by fungi (e.g., *Dodgella priscus*) are the most common ichnotaxa observed in *A. excavata* shells. The macro-boring *Entobia*, produced by sponges like *Cliona,* has been observed on many Pleistocene Mediterranean shells. Traces of boring foraminifers, especially of *Hyrrokkin sarcophaga* are highly abundant on Recent Norwegian *A. excavata* and on Pleistocene material from the Mediterranean.

Materials and methods

Live specimens sampled along the European continental margin, e.g. on the mid-Norwegian shelf or in the Swedish Kosterfjord, and dead specimens (subfossil and fossil) from the Mediterranean Sea, were analysed with various methods. Samples were collected over the years on many cruises (Table 1), supported by the following European research vessels: R/V Bannock, R/V Poseidon, R/V Urania, R/V Johan Hjort, R/V Meteor, R/V Littorina, R/V Lophelia, R/V Victor Hensen, R/V Alkor and R/V Marion Dufresne. Most specimens were obtained with an epibenthic dredge device or by grab sampling (Van Veen grab). Sampling at the Sula Reef site off mid-Norway, involved direct collection with the manned submersible Jago (Freiwald et al. 2002) and the Kosterfjord colonies were documented with ROV. Positions were usually fixed with a differential global positioning system (DGPS).

Over 350 single valves were measured for a biometric analysis. Using a digital calliper, length of the straight hinge line, maximum shell width (parallel to the hinge line) and maximum length (height) along the main growth axes from umbo to margin, as well as single valve inflation and hinge height were measured.

Thin sections were prepared along and across the main growth axes, to study internal architecture and layering of the shell with a high resolution light-optical microscope (Zeiss). Single valves were embedded in a two compound epoxy resin (Araldit and Araldur) to ensure sawing stability.

Some polished slabs were immersed in Feigel's solution for 3 to 4 minutes, resulting in dark staining of aragonitic shell portions. This silver coating leaves calcite unaffected and allows for a quick distinction of major mineralogical zones. Homogenous powder samples were prepared of several interior and exterior shell portions to verify this preliminary mineralogical zonation with x-ray diffractometry (XRD).

Shell ultrastructure was investigated using a Scanning Electron Microscope (SEM). Polished shell sections were etched with 0.1 N dilute hydrochloric acid (HCl) for 30 seconds, then rinsed in deionized water, dried, sputter coated with gold, and photographed under the SEM.

A numeric radiocarbon age from a Mediterranean *A. excavata* (COR2-8) was obtained with the AMS-^{14}C method at the Eidgenössische Technische Hochschule (ETH) in Zurich.

Results

Taxonomy

The subspecies *Acesta excavata sublaevis* Nordsieck, 1969 was established on the photo of a juvenile subfossil specimen from Cassidaigne Canyon off Marseille in the Mediterranean (pers. comm. H. Zibrowius 2004). It is actually the same specimen which is described in Bourcier and Zibrowius (1969) and now stored at the Museum of Natural History in Paris (MNHN). This single valve does not differ in any respect from Recent juvenile *Acesta excavata* Fabricius, 1779 from the North Atlantic and, therefore, the taxon is not considered valid.

Possible documentation of living *in situ Acesta excavata* in the Mediterranean

CYANA-submersible dive CY 86-53 (6th November 1986; SAME-cruise) in Canyon du Var, off Nice (France), photographed *Acesta excavata* on steep canyon walls of conglomerate bedrock (Fig. 6). Still articulated shells with gaping valves occurred on slightly overhanging canyon walls next to solitary scleractinian corals – presumably *Desmophyllum cristagalli*. The 10 cm large shells were either alive or recently dead, being open, but the soft body is not visible on the pictures (pers. comm. H. Zibrowius 2004). The exact depth is unknown, but was shallower than 1548 m.

Radiocarbon dating

A large well-preserved *A. excavata* specimen (COR2-8) from a grab sample in the Strait of Sicily (Table 1) has been radiocarbon dated to 39,960 ± 820 cal yr BP, dating back to the latest glacial period of the Pleistocene. This numeric age is close to the upper age limit of the AMS-^{14}C method and has to be judged carefully. If the numeric age of 39.9 kyr does not correspond to the real value, then it provides at least a minimum age.

Tyrrhenian hardgrounds with *Acesta excavata*

Dredge samples (CORTI 86 to 88) from the steep western and eastern slopes of Cialdi Seamount (Table 1) in the Tyrrhenian Basin have yielded calcareous hardgrounds between 1073 and 450 m (CORTI 86) and between 494 and 358 m (CORTI 87). The rocks contained a high number of fossil *A. excavata* and represent the first known submerged occurrence in lithified Pleistocene deposits (Fig. 5) from steep sediment starved seamount flanks. All rock samples showed a black stained irregular surface with dissolution cavities and partly lithified yellowish brown mud. The interior was built up of micrite containing numerous fossils, dominated by *Gryphus vitreus* and *A. excavata* (~8 cm), associated with *Desmophyllum*
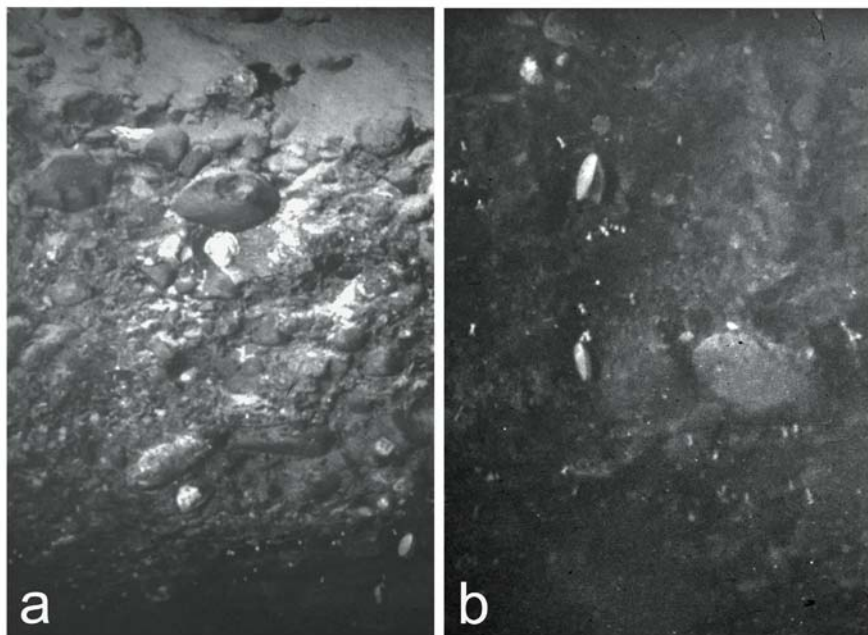
Fig. 6 Pictures from CYANA dive CY86-53 (6th Nov. 1986) in Canyon du Var (<1548 m) off Nice (France) show paired valves of *A. excavata* (**a** - lower right corner, **b** - enlarged), documenting living or recently dead specimens (~10 cm height). The steep conglomeratic bedrock walls are colonized by solitary scleractinians (most likely *Desmophyllum* sp.) (courtesy of H. Zibrowius, modified from IFREMER material)

cristagalli, *Stenocyathus vermiformis*, *Lophelia pertusa* and large oysters. Thin black manganese veneers and irregular seams mark dissolutional horizons. Rock surfaces were densely populated by *Vermiliopsis monodiscus* and *Protula* sp., which occur also as fossils within the rock.

Shell banding and hierarchic growth patterns

Regularly-spaced growth bands on the shell surface are a prominent feature of *A. excavata* (Fig. 1). Growth increments are widest along the main growth axes, and get narrower towards the cardinal area, were they continue as fine ribs on the hinge (Fig. 7). Increments have average widths of 0.3 to 0.5 cm in juvenile shells of around 5 cm height. Older shells, up to 10 cm height, show the widest bands, ranging from 0.4 to 0.9 cm, and measuring 0.6 cm on average. In adult specimens larger than 10 cm, the bands become increasingly narrower (<0.3 cm) and crowded (Fig. 7). The growth band boundaries can be traced as lines across the whole shell. Incomplete and irregular growth bands occur especially where parasitic foraminifers were attached to the valve margins. These 'false' rings cannot be traced across the entire shell. Banding of left and right valve is equal, showing the same cyclic patterns and also the same irregularities and incomplete bands in pathologic specimens.
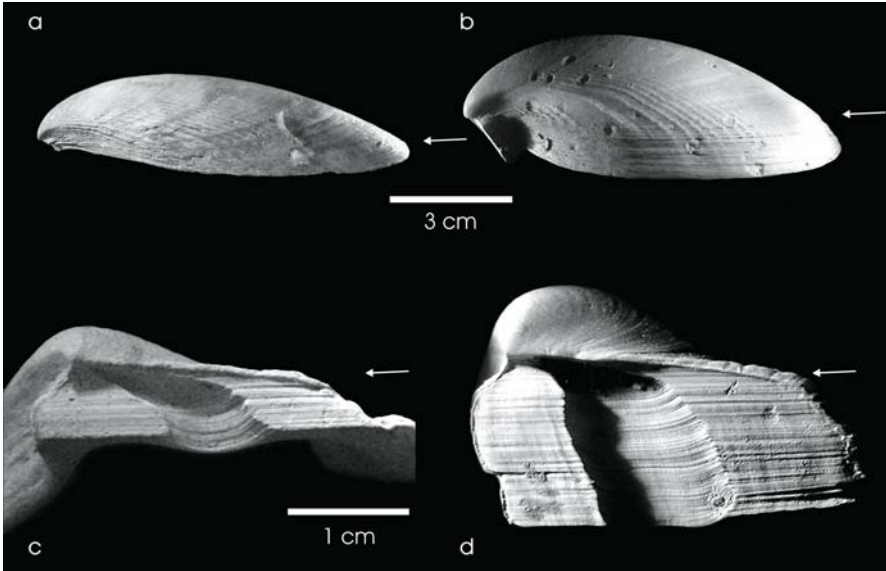
Fig. 7 Shell growth shows two phases. The first phase (**a**), typically up to 10 cm shell height, is marked by a flat shell shape and an oblique ligament pit (**c**). The second phase (arrows) is marked by increased valve inflation and reduced height growth (**b**), while a broad hinge plate is formed (**d**). Samples: JH-5-99 (**a**, **c**) and COR2-39 (**b**, **d**)

Growth increments are clearest on the central portions of large shells (>10 cm). Proximal bands are frequently abraded or faint and hard to recognize, whereas crowded and narrow bands of old shells cannot be accurately counted either. Shells with 10 cm height have typically 18 to 22 bands. These shells, still in their first growth mode, show a raw linear correlation of increment number and height.

Minute banding of parallel, equally wide (<0.4 mm), ribs marks the hinge plate (Fig. 7). Their number corresponds to the number of external growth increments. Shells at the end of the first growth phase, with about 10 cm height, have 18 to 22 hinge lines. The second growth phase produces large arched shells width an extended hinge plate, showing more than 50 hinge lines (e.g., COR2-39). Up to 80 ribs have been counted from Norwegian samples. The maximum number of hinge lines in some Trondheimfjord (Røberg) specimens was in excess of 100 ribs (pers. comm. J. Elvestrand 2003).

Live specimens from one location caught at the same time of the year show a similar degree of growth increment completion. However, exact growth band completion could not be calculated accurately, due to changing band widths during clam ontogeny. Variability of growth ring width, possibly driven by local environmental changes, further prohibited an exact calculation of growth band completion. Relative variation of increment width for the latest 10 growth bands showed a similar pattern for shells from the same location.

Thin-sections revealed hierarchic growth patterns also for the valve interior and especially the hinge shows a rhythmic banding.

Shell growth and allometric changes

Allometric growth shows linear correlations among most biometric parameters (Fig. 8). Shell width correlates linearly especially well with height at an average width/height ratio of 0.77±0.05 (min./max. 0.71-0.90). Older specimens, typically larger than 10 cm (e.g., TMBL 1-4), tend to slightly wider forms with a width/height ratio of 0.83. In these adult shells, the pallial line is retracted a considerable distance (~1 cm) into the shell, resulting in slowed growth ring precipitation. This decrease in growth rate is well depicted by a reduced distance between growth increments on the shell exterior. At this time the valve form changes from a flat cross-section to an increasingly glabrus, arched shape with crowded growth lines (Fig. 7). The onset of the second growth mode is well depicted in the lunular area by the first emplacement of a straight rib. Arched ribs in the excavated lunular area characterize the first growth period. Lunular ribs are parallel in the second growth phase and rapidly increase the valve inflation (Fig. 7).

This changing growth pattern also affects the hinge morphology. In young shells, with sizes of less than 8 to 10 cm the hinge has a strongly oblique ligament groove. At the change of growth modes the hinge reaches a typical width of 3.0 cm and a height of 0.8 cm. Subsequently the shell forms a prominent hinge plate, with the ligament pit approximately centred within the parallel hinge margins (orthogonal to hinge line). Old specimens can reach an inflation of about 3.5 cm and show a prominent hinge plate, with a hinge height of around 1.5 cm and a hinge with of about 3.5 cm.

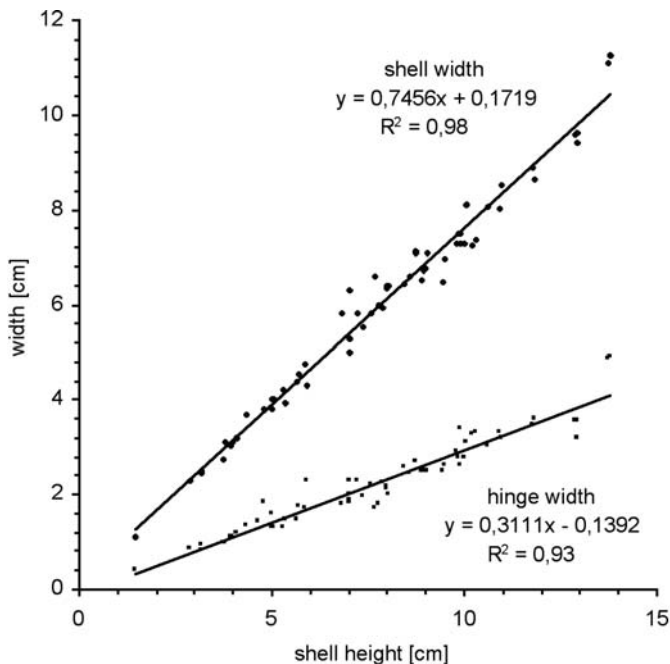

shell width
$y = 0{,}7456x + 0{,}1719$
$R^2 = 0{,}98$

hinge width
$y = 0{,}3111x - 0{,}1392$
$R^2 = 0{,}93$

Fig. 8 Linear correlation of shell width *versus* shell height and also linear correlation of hinge width to shell height

Hinge height *versus* hinge width shows similar plots for Recent Atlantic and Pleistocene Mediterranean shells (Fig. 9). The overlap is considerable, although Mediterranean hinges seem to be slightly narrower and start to produce a hinge plate slightly earlier than their Atlantic counterparts. Atlantic shells switched to the second growth mode at a typical height of 10 cm, while Pleistocene Mediterranean shells switch at heights of 8 to 9 cm. The hinge width shows a linear correlation to shell height for Atlantic samples >10 cm (Fig. 8). This morphological relation can be used to reconstruct shell height estimates of Mediterranean populations where often only the hinges are preserved.

Microstructure and shell mineralogy

Polished or broken shell sections show a general subdivision into two layers visible to the naked eye, corresponding to the bimodal mineralogy of *A. excavata* with an outer calcitic and an inner aragonitic layer (Fig. 10). Staining with Feigel's solution of vertical transects along the main growth axes visualized this differentiation. XRD-investigations of powdered shell material from interior and exterior portions confirmed this first mineralogical zonation.
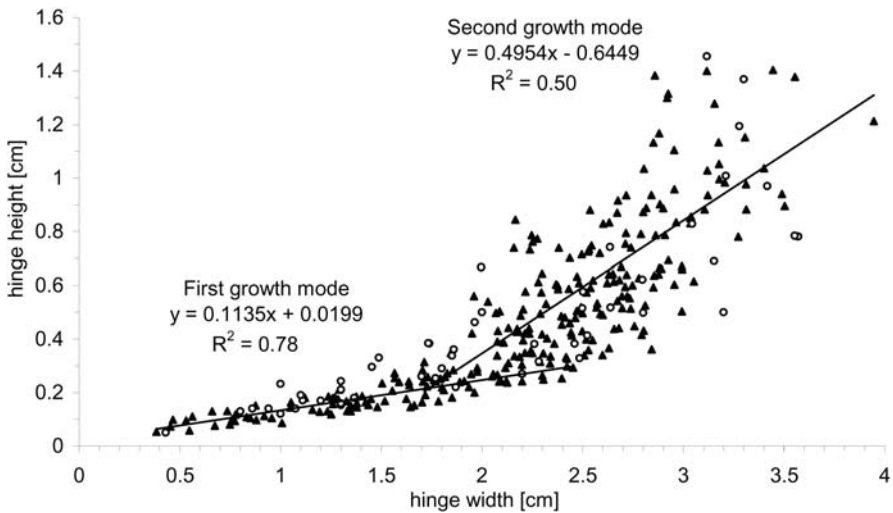
Fig. 9 Hinge width *versus* hinge height for Recent Atlantic *A. excavata* and Pleistocene Mediterranean specimens (triangles) plot in the same field, indicating that fossil Mediterranean shells attained similar sizes as their Recent Atlantic (circles) counterparts. Hinge parameters for shells of the first or second growth mode plot in different fields

Aragonite makes up the entire hinge and the interior valve side (Fig. 10). In the umbonal part of juvenile specimens this aragonitic layer is covered by a thin (<10 %) exterior calcitic veneer, which extends all the way to the valve margins. Along radial transects there is a considerable change in mineralogical proportioning, with the calcitic zone gaining in thickness towards more distal parts. At the pallial line calcite provides about 70 % of the valve over the remaining 30 % of interior

Fig. 10 Shell mineralogy and internal structure. The external calcite is often missing near the umbo

aragonite. The narrow zone (2 to 5 mm) between the pallial line and the margin is entirely formed by calcite. This calcitic z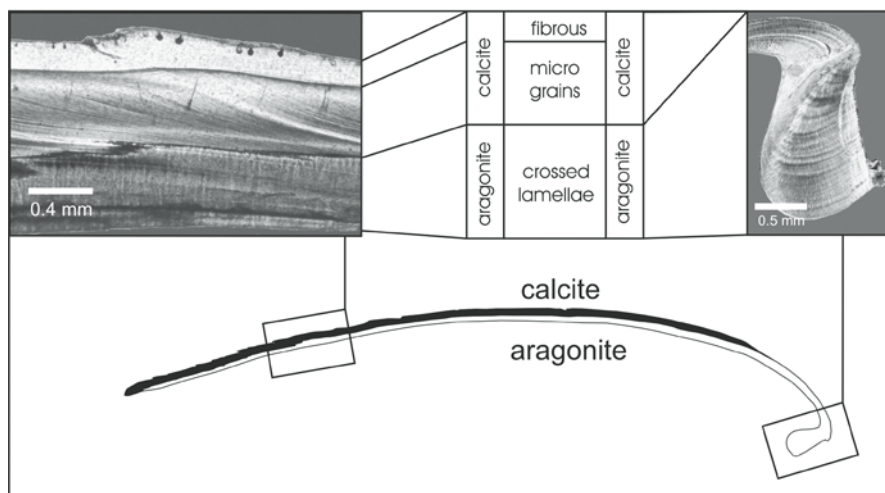one frequently lacks on the umbonal to central shell portion of adult clams (Fig. 10). Instead intense bioerosion, which penetrates also into the aragonite, often marks this part.

Calcitic outer layer

The calcitic layer is responsible for the thin radiating ribs, which weakly sculpture the shell surface and which are regularly interrupted by growth rings (Figs. 1, 7). The ribs are pronounced towards the anterior and posterior margin of the clam and are least developed in the central portion. In juvenile specimens, the entire shell is covered by ribs. A smooth appearance on the central to umbonal portion in adult shells is due to secondary reduction of the calcitic layer (Fig. 10).

Aragonitic inner layer

The shiny shell interior is made of aragonite layers (Fig. 10). The surface of the interior valve side exhibits a characteristic zebra-fur pattern, which is also visible in shell cross-sections along the growth direction. The aragonitic interior layer shows a fine horizontal banding, with numerous bands close to the umbo and just one layer behind the pallial line. In correspondence to the number of external growth lines there is an equal increase in number of aragonite strata towards older and more proximal shell parts. Each stratum is thinnest in the medial shell part and thickest adjacent to the pallial line. Where the parasitic Foraminifera *Hyrrokkin sarcophaga* penetrated the shell and entered the mantle cavity with its pseudopodia, the mollusc formed a several millimetre thick callus (Fig. 1) of multi-layered aragonite to seal the wound.

Ultrastructure

SEM analysis of polished and slightly etched shell sections has revealed five distinct ultrastructural zones. The calcitic layer exhibits an outer fibrous-prismatic zone (Fig. 11) and a microgranular zone (Fig. 12) below. The aragonitic layer shows mainly a crossed-lamellar structure (Fig. 13), which grades into a radiating crossed-lamellar fashion in the hinge. On the inside of the umbones is a spatially restricted complex crossed-lamellar zone.

Fibrous-prismatic calcite

Thin calcite prisms make up the outermost sublayer of the shell (Fig. 11). They lie subparallel to the outer shell surface, but often inclined up to 20°. Mineralogical c-axes have the same orientation and large areas show synchronous extinction under crossed-nichols. This layer is usually 100 to 150 μm wide, with a well defined boundary against the granular sublayer underneath. Individual prisms reach 50 μm in length and 5 to 10 μm width. The calcite fibres show several forms. Most common are flat, lath-type prisms and rod-type fibres. The longest linear prisms occur on the shell exterior (Fig. 11), which grade inwards into thinner and shorter fibres. Larger prisms often form areas with equally oriented crystals. The broad lath-type prisms attain the largest sizes and show a minute internal banding. SEM-studied shell surfaces show fine prisms that are oriented approximately orthogonal to the closest growth line.
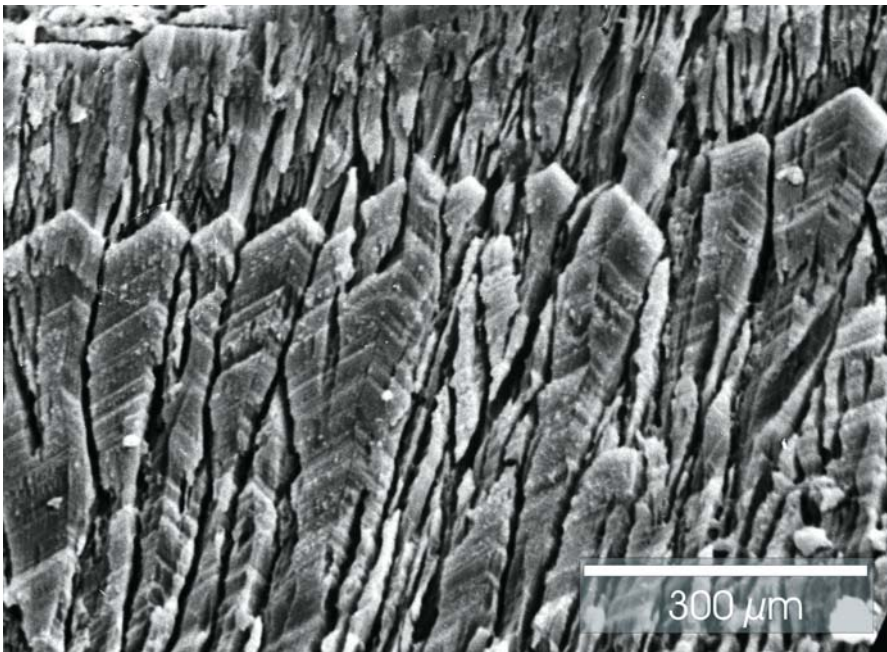
Fig. 11 Surficial SEM image of the exterior fibrous-prismatic calcite layer. The tips of the prisms point in growth direction and mark the boundary of a growth band. The interspaces between the prisms had been filled with intercrystalline organic matrix
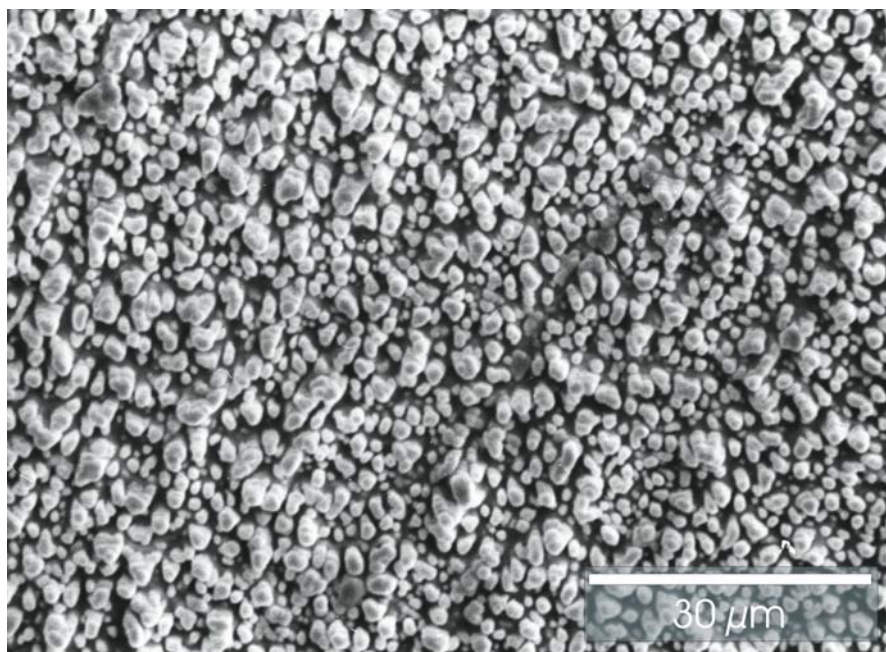
Fig. 12 SEM image of the calcitic microgranular layer, situated below the fibrous-prismatic layer. The shape of the granules varies from near spherical to short fibres. The calcitic granules are often arranged in single-grain layers
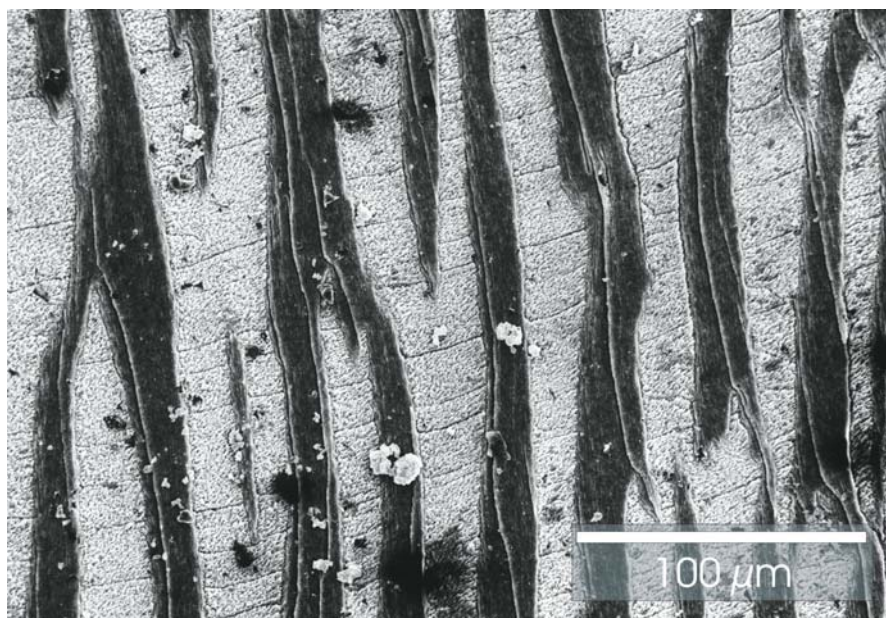
Fig. 13 SEM image of the crossed-lamellar interior aragonite. The first-order lamellae of this ultrastructural and mineralogical unit exhibit a characteristic zebra fur pattern

Microgranular calcite

Light-microscopy on this thickest calcite layer (170 to 250 μm) shows a fine varved appearance. An undulating asynchronous extinction under crossed-nichols is typical for this sublayer. SEM investigations revealed a microgranular ultrastructural zone. Minute calcite granules (Fig. 12), usually less than 1 μm in diameter, comprise 90 % of this sublayer. Irregular globular grains are arranged in monogranular layers, which are inclined against the outer fibrous layer at an angle of 10 to 15°. The lower part shows a shift from almost spherical grains to increasingly elongated particles, which grade inwards into fibrous calcite prisms at the boundary to the aragonitic below. Fibrous calcite is developed closely along the margin towards the aragonitic inner shell material, predominantly in adult specimens. The upper boundary against the outer fibrous-prismatic layer appears very sharp in thin sections, but shows a narrow transition zone under the SEM. This shift of different structure compositions seems to be triggered by the adjacent intercrystalline matrix.

Crossed-lamellar aragonite

Crossed-lamellar aragonite (Fig. 13) builds the interior shell-layer and makes up the entire hinge. Even at thin-section scale crossed-lamellae are visible as repeated vertical zones of extinction under polarized light. Those first-order lamellae (10 to 25 μm wide), which produce a straight to branching zebra fur pattern (Fig. 13), are aligned parallel to the valve outline. The crossed first-order lamellae commence as linear lamellae, but are often branching inward and grade into a radiating pattern in the hinge. SEM images show second-order lamellae within each 'zebra stripe', with equal orientation, responsible for the synchronous extinction of a single stripe under crossed-nichols. The second-order lamellae are inclined at an angle of 30 to 45° against the vertical axes of the first order lamellae, resembling a series of inclined books on a shelf board. The lamellae grow in optical continuity, across all internal growth increment boundaries.

Complex crossed-lamellar aragonite

The innermost shell layer, which occurs only on the inside of the umbo and at the hinge, is formed by complex-crossed aragonite lamellae. This ultrastructure zone is thickest (~100 μm) in large shells and is lacking in smaller specimens. Individual lamellae grow in optical continuity to the adjacent crossed-lamellae, starting from a distinct ultrastructural boundary. The first-order lamellae have widths of 15 to 30 μm and branch inward.

Myostracal aragonite prisms

The adductory muscle scar comprises fine aragonite prisms, with a complex layer-wise intertongueing of crossed-lamellar aragonite layers. The overall distribution of this myostracal aragonite is thickest at the muscle scar and thins gradually towards the valve margins. At the muscle scar this ultrastructure unit has a thickness of 150 μm and shows a banded structure, with individual layers of 5 to 15 μm thickness. Typically 10 μm high and wide pyramid-shaped aragonite prisms form these internal bands.

Discussion

The present-day distribution of *A. excavata* is largely bound to the continental margin at depths of 200 m and more (Fig. 2). The depth trend from deep sites (>1000 m) at the Strait of Gibraltar to increasingly shallower localities northwards to the Faroe Islands is likely to be guided by watermass boundaries. Depth range and spatial distribution of *A. excavata* are restricted by temperature (Bourcier and Zibrowius 1969), while salinity does not seem to play a major role. However, the large depth and temperature range of *A. excavata* sites makes it unlikely that these parameters are the singlemost important for the geographical spread of the species.

Depth is certainly not a limiting factor, while 3 and 13°C are the reported extreme temperatures withstood by this bivalve. The extreme depths (Dautzenberg and Fischer 1906; Dautzenberg 1927) reported around the Azores (>1500 to 3200 m) and the resulting lowest temperatures (~3°C) for *A. excavata* have to be regarded with suspicion. Exact depths of dredge samples could not be precisely measured at that time and the deepest records do certainly not refer to living specimens (pers. comm. H. Zibrowius 2004). The continental margin of western Europe and especially the shelf-break are entirely located within this temperature window. Therefore temperature cannot account for the northward 'climbing' of *A. excavata* sites. Western European shelf-break areas are characterized by strong currents, due to the boundary zone of intermediate watermass against deeper water bodies. Plankton from the water column gets enriched along these density boundaries. High levels of nutrients in combination with enforced water circulation allow for thriving cold-water coral ecosystems (Broch 1922) and occurrence of *A. excavata*, which favours similar conditions.

Temperature is though a possible limiting factor in the present day eurythermal Mediterranean Sea, where *A. excavata* seems close to its ecological boundaries, as does the scleractinian *L. pertusa*.

The deepest sites around the Canaries and off Senegal (Table 1), including the isolated record off Ivory Coast, are located in tropical latitudes. Upwelling on the African west coast (Le Lœuff and von Cosel 1998) provides cold watermasses at the continental rise and along narrow shelf edge, allowing for a spread of non-tropical species. The wide distribution gap south of Senegal, between Guinea Bissau and southern Liberia, might be due to the lack of upwelling and could explain this distribution pattern, which is also typical for other northern Bivalvia (Le Lœuff and von Cosel 1998).

Northern guests and oceanographic change

A. excavata was much more widespread during the Pleistocene in the Mediterranean basin (Fig. 2). Several submerged sites indicate a link to the palaeocommunity of 'White Corals' (*sensu* Pérès and Picard 1964) in general. But *A. excavata* does not only occur within mud-covered mound structures, which resemble their present day counterparts in the North Atlantic. The grab samples from the Strait of Sicily indicate that the bivalve also thrived on steep cliffs in absence of the bathyal azooxanthellate scleractinians. These two substrata observed

in the Recent North Atlantic sites, cold-water corals and steep bedrock outcrops, occur also in the fossil record. Interestingly enough, the single specimen recorded by Terreni and Voliani (1995) was living on a muddy bottom, although attached to an artificial hard substratum (plastic canvas).

The obtained radiocarbon age of 39.9 kyr from a submerged *A. excavata* site from the Strait of Sicily (Table 1) supports the widespread distribution during the colder periods of the Pleistocene. *A. excavata* joins species like *Arctica islandica*, *Pseudoamussium septemradiatum* and *Mya truncata* as an example of a mollusc with a northern distribution pattern in the present day that spread into the Mediterranean during the last Ice Age and prior glacial periods as a so called 'northern guest' (Segre and Stocchino 1969; Colantoni et al. 1970; Colantoni 1973; Taviani and Colantoni 1979; Malatesta and Zarlenga 1986; Bouchet and Taviani 1992). Nevertheless, there is growing evidence that *A. excavata* is not a pure northern guest, as for example stated in Malatesta and Zarlenga (1986). Instead, the scarce Recent finds indicate that *A. excavata* is capable of surviving in the relatively warm basin at present. Extinct *Lophelia* colonies at North Cabliers Bank, between Spain and Morocco, had revealed an Early Holocene age of 8.5 kyr (±365 yr), which have been dated, using the TIMS U/Th-method (for details see Schröder-Ritzrau et al. 2005). Several *A. excavata* specimens from the same dredge sample indicate that the bivalve might have a similar age. Consequently it could have persisted in the basin throughout the Holocene. There is no doubt that Holocene warming radically diminished the distribution of *A. excavata* in the Mediterranean, which is at present a nutrient-poor isothermal sea with temperatures of around 13°C throughout the bathyal zone. *A. excavata* samples (LM-99-50) from the Tuscan archipelago (Remia and Taviani 2004), northeast of Corsica (Fig. 2), contain pristine shells, accompanied by subfossil valves. Comparing the state of shell degradation with known Late Pleistocene sites makes it likely that those are much younger, possibly latest Pleistocene as co-occurring corals (Remia and Taviani 2004). Shell degradation can only provide hints and further radiometric dating is necessary.

CYANA-submersible pictures from Canyon du Var (Fig. 6), document another possible live-record for *A. excavata* in the Mediterranean Sea (pers. comm. H. Zibrowius 2004). The paired valves hanging from an overhang indicate that the shells were alive or died recently.

Habitats

Marshall (2001) noted that the genus *Acesta* has been found associated with rocky or coral bank facies in deep waters worldwide. Isolated *Acesta* valves have been recorded from sedimentary facies (Vokes 1963); Marshall (2001) considered it likely that at least some of these were byssally attached to hard substrata when alive. Our observations for *A. excavata* from the northeast Atlantic and Mediterranean Sea support and extend these general observations. All photographic records from Norwegian waters suggest a strong link between *A. excavata* and the *Lophelia pertusa* coral sites (Fig. 3) in high biomass saxicolous communities indicating high food availability.

Surveys of *Lophelia/Madrepora* coral provinces on the Irish continental margin (Porcupine Seabight) have not recorded *A. excavata* from these habitats, showing that the bivalve is not as strongly linked to the bathyal coral facies as Norwegian surveys would suggest. Instead the smaller *Lima marioni* (Mikkelsen and Bieler 2003) was frequently found byssally attached to *L. pertusa* and *M. oculata* (pers. observ. A. Freiwald). Similarly, living *L. pertusa* and *M. oculata* occurrences in the Tyrrhenian and the Ionian Sea lacked *A. excavata*. This confirms that European cold-water coral facies do not always support populations of *A. excavata*.

Pleistocene submerged sites in the Mediterranean show that steep cliffs have been commonly inhabited by *A. excavata* (COR2-39; Table. 1), similar to the habitats observed in Scandinavian fjords. The steep rugged slopes of Cialdi Seamount in the Tyrrhenian Sea with the recovered *A. excavata* limestone (hardgrounds) provide another example for rock wall habitats (Fig. 5). These rock sites might be in fact more typical for *A. excavata* than the coral sites, where current research is focused. Cialdi Seamount is the first known submerged *A. excavata* occurrence in lithified Pleistocene deposits from a steep sediment starved submarine relief. High number of specimens, often with preserved shell material, document the fossilisation potential of *A. excavata* communities, even in sediment deprived seamount settings. Observations in Canyon du Var provide another record of rock wall habitats (Fig. 6).

Growth rate

Regular spacing of growth increments suggests a rhythmic, possibly annual, control on the shell deposition. Shells collected at different times of the year showed different completions of increments. It cannot be ruled out that increment boundaries are triggered by rhythmic spawning events or changing fluxes in food supply from the water column. First observations though make a seasonal emplacement of growth-increments likely. Thin-sections of the hinge showed a rhythmic internal banding with changing density and different amounts of intercrystalline organic matter. These internal changes were repeated in each ring, making an overriding seasonal control more likely than single events.

Accepting an annual character of the growth increments the shell shows two different modes of growth. The first phase ceases after the deposition of about 18 to 22 increments indicating that the shell reaches a size of about 10 cm within the first 18 to 22 years of its life. The second phase is resolved with possibly annual ribs on the hinge plate, but shows little further size gain (Fig. 7). A typical lifespan of 50 to 80 years, including the first growth phase, is suggested by the number of hinge ribs (pers. comm. J. Elvestrand 2003).

Underwater images from Scandinavia (Figs. 3, 4) all showed that large *A. excavata* live out in the open both on steep rock surfaces (e.g., Kosterfjord and Trondheimfjord) and on cold-water corals of the northeast Atlantic (e.g., Sula Ridge). That smaller *A. excavata* were not visible suggests that they may be cryptic, only moving out onto open areas when they are large enough to be safer from predators. More likely though is a biased size distribution due to the two growth modes (Fig. 7) with an early gain of maximum size during its life time (Fig. 9).

It is possible that the monogranular layers (Fig. 12) of the second calcite layer reflect diurnal deposition of shell calcite, which is also depicted by the banding of individual prisms in the outermost fibrous-prismatic layer.

Biometry

Similar biometric patterns of Pleistocene Mediterranean specimens and Recent Atlantic shells (Fig. 9) indicate that *A. excavata* was thriving under glacial oceanographic conditions in the Mediterranean basin. They show about the same maximum sizes, as their Recent Atlantic counterparts.

Samples from both areas exhibited the abrupt shift between growth modes at around 10 cm height, from flat to more arched valves. The sex change during the lifetime (Järnegren 1999), might account for the abrupt switch between the two observed growth modes. The timing of sex-change from male to female and the change from a flat to a more arched valve seems to take place at the same stage of shell growth.

Ultrastructure

Detailed ultrastructure observations were made in anticipation of isotopic studies that need to be based on a sound understanding of shell structure and composition. The observed structures reflect the characteristics for Limidae, given in Carter (1990), with a fibrous-prismatic outer calcitic layer and a crossed-lamellar interior aragonitic layer. The fine costae on the exterior shell surface (Figs. 1, 7) are exclusively built by the fibrous-prismatic calcitic subzone (Fig. 10). Nevertheless, the sculpture is not guided by the microstructure. The prisms typically run across the costae at an angle, their directions are only equal on the medial shell portion. It is likely that the ribs follow a pattern provided by the precipitating mantle, while the prismatic microstructure follows crystallographic laws. The first-order lamellae of the crossed-lamellar interior aragonitic are oriented commarginal. The exterior fibres and prisms are in every position of the shell orthogonal to the lamellae underneath. This pattern allows for thin shells with a strong architecture, even for large valves.

Aragonitic strata are difficult to count in central portions, since their crossed lamellar ultrastructure shows a syntaxial mineralogical growth across the boundaries of individually deposited layers (Fig. 13). This often makes a distinction of internal growth increments impossible. Therefore the stack of layers cannot be isotopically subsampled for each period precisely, nor would it provide inter-annual resolution.

The calcitic layer has a much simpler growth pattern. Typical growth ring widths on the external surface offer about 0.4 to 1.0 cm of sampling interval per growth increment. The sampling interval in the corresponding aragonitic layer on contrast is usually less than 0.5 mm (best case). It becomes obvious from these growth patterns that only calcitic shell portion with its macroscopic banding is accessible for isotopic sampling with a hand-held drilling device. Based on the observed ultrastructure, we propose an isotopic sampling within the outer calcitic zone of the shell (Fig. 10). The two calcitic zones (fibrous-prismatic and micro-granular) cannot be sampled individually with a hand held drilling device. The resolution of the aragonite is

highest in the hinge, where cyclic banding is visible under the microscope, but is not accessible for manual sampling.

Conclusions

Fast growth rate, compared with other organisms containing calcified structures from the same environment, its widespread distribution and its frequent co-occurrence with cold-water corals, make *A. excavata* an ideal sampling object for palaeoenvironmental studies. Moreover, shell architecture is much simpler than in the associated cold-water corals. Its extensive distribution along the northeast Atlantic continental margin and its widespread subfossil to fossil Mediterranean communities will allow for a margin-wide assessment of environmental changes for cold-water coral environments. Both submerged and emergent, uplifted Quaternary fossil occurrences might allow us to extend datasets into the past. We propose that sclerochronology be applied to large limid bivalves to study intermediate and cold waters, as they are large, clearly banded and occur world-wide in bathyal environments of tropical and boreal settings.

Acknowledgements

References

Adams H, Adams A (1858) The genera of Recent Mollusca. 2 (1854-1858), 661 pp

Adkins JF, Cheng H, Boyle EA, Druffel ERM, Edwards RL (1998) Deep-sea coral evidence for rapid change in ventilation of deep North Atlantic 15,400 years ago. Science 280: 725-728

Adkins JF, Boyle EA, Curry WB, Lutringer A (2002) Stable isotopes in deep-sea corals and a new mechanism for "vital effects". Geochim Cosmochim Acta 67: 1129-1143

Aoki S (1976) On the variations of *Lima (Acesta) goliath* and its allied species, with the descriptions of a new species. Trans Proc Paleont Soc Japan NS 22: 185-190

Báldi T (1986) Mid-Tertiary stratigraphy and paleogeographic evolution of Hungary. Akadémiai Kiadó, Budapest

Barnard KH (1963) Deep-sea Mollusca from the region south of Madagascar. Commerce Industry 4: 485-501

Barrier P, Di Geronimo I, La Perna R, Rosso A, Sanfilippo R, Zibrowius H (1996) Taphonomy of deep-sea hard and soft bottom communities: the Pleistocene of Lazzàro (southern Italy). In: Hevia GM, Sancho FM, Urrest IP (eds) II reuniòn de Tafonomìa y fosilizacion, pp 39-46

Bartsch P (1913) The giant species of the molluscan genus *Lima* obtained in Philippine and adjacent waters. US Natl Mus Proc 45: 235-240

Beu AG, Climo FM (1974) Mollusca from a Recent coral community in Palliser Bay, Cook Strait. New Zealand J Mar Fresh 8: 307-332

Beu AG, Maxwell PA (1990) Cenozoic Mollusca of New Zealand. New Zealand Geol Surv Paleont Bull 58: 1-518

Boland GS (1986) Discovery of co-occurring bivalve *Acesta* sp. and chemosynthetic tube worms *Lamellibrachia* sp. Nature 323: 759

Bonfitto A, Bigazzi M, Fellegara I, Impiccini R, Gofas S, Oliverio M, Taviani M, Taviani N (1994a) Rapporto scientifico sulla crociera DP'91 (margine orientale della Sardegna, Mar Mediterraneo). Boll Malacol 30: 129-140

Bonfitto A, Oliverio M, Sabelli B, Taviani M (1994b) A Quaternary deep-sea marine molluscan assemblage from East Sardinia (Western Tyrrhenian Sea). Boll Malacol 30: 141-157

Boss KJ (1965) Note on *Lima (Acesta) angolensis*. Nautilus 79: 54-58

Bouchet P, Taviani M (1992) The Mediterranean deep-sea fauna: pseudopopulations of Atlantic species? Deep-Sea Res 39: 169-184

Bourcier M, Zibrowius H (1969) Note sur *Lima excavata* (Fabricius) pélécypode associée aux bancs de coraux profonds. Bull Soc Zool France 94: 201-206

Broch H (1922) Riffkorallen im Nordmeer einst und jetzt. Naturwissenschaften 10: 804-806

Burdon-Jones C, Tambs-Lyche H (1960) Observations on the fauna of the North Brattholmen stone-coral reef near Bergen. Arb Univ Bergen, mat naturv Ser 4: 1-24

Carcassi A (1983) Ulteriore ritrovamento di *Acesta excavata* vivente in Mediterraneo. Boll Malacol 19: 264

Carter JG (1990) Skeletal biomineralisation: patterns, processes and evolutionary trends. Van Nostrand Reinhold, New York, 1, 832 pp

Cedhagen T (1994) Taxonomy and biology of *Hyrrokkin sarcophaga* gen. et sp. n., a parasitic foraminiferan (Rosalinidae). Sarsia 79: 65-82

Clark BL (1925) Pelecypoda from the marine Oligocene of western North America. Univ Calif Publ Bull Dept Geol 15: 69-136

Coan EV, Valentich Scott P, Bernard FR (2000) Bivalve seashells of western North America. Santa Barbara Mus Nat Hist Monogr 2, Stud Biodiversity, 2, 764 pp

Colantoni P (1973) A glacial mollusc fauna from Baronie Seamount (off eastern Sardinia). Rapp Comm int Mer Méditerranée 21: 896-900

Colantoni P, Padovani A, Tampieri R (1970) XI. Molluschi. Giorn Geol, Ser 2, 37: 163-188

Corselli C, Bernocchi A (1990) Paleocommunities of the last glacial from the Sardinia continental slope: a paleoceanography problem. Mus Reg Sci Nat Torino. Atti Quarto Simp Ecol Paleoecol Comunità Bentoniche, pp 575-595

Dall WH (1900) A new species of *Lima*. Nautilus 14: 15–16

Dall WH (1902) Notes on the giant Limas. Nautilus 16: 15–17

Dall WH (1908) Reports on the dredging operations off the west coast of Central America to the Galapagos, to the west coast of Mexico, and in the Gulf of California. The Mollusca and the Brachiopoda. Bull Mus Comp Zool 43: 205-487

Dautzenberg P (1927) Mollusques provenant des campagnes scientifiques du Prince Albert Ier de Monaco dans l'Ocean Atlantique et dans le Golfe de Gascogne. Rés Camp Sci Prince Albert Ier 52: 1-400

Dautzenberg P, Fischer H (1897) Campagnes scientifiques de S.A. le Prince Albert Ier de Monaco. Dragages effectués par l'Hirondelle et par la Princesse Alice, 1883-1896. Mém Soc Zool France 10: 139-234

Dautzenberg P, Fischer H (1906) Mollusques provenant des dragages effectués à l'Ouest de l'Afrique pendant les campagnes scientifiques de S.A.S. le Prince de Monaco. Rés Camp Monaco 32: 1-125

Dawson EW (1995) A whopper of a bivalve: the story of *Acesta* (Limidae). Cookia 7: 13-21

De Stefani C (1891) Les terrains tertiares supérieurs du basin de la Mediterranée. Ann Soc Géol Belg 18: 201-403

Di Geronimo I (1987) Bionomie des peuplements benthiques des substrats meubles et rocheux plio-quaternaires du Détroit de Messine. Doc Trav IGAL 11: 153-167

Di Geronimo I (1995) Benthic assemblages of the Plio-Quaternary soft and hard substrata in the Straits of Messina area. In: Guglielmo L, Manganaro A, De Domenico E (eds) The Straits of Messina Ecosystem. Proc Symp Messina, 4-6 April 1991, pp 105-118

Di Geronimo I, La Perna R (1997) Pleistocene bathyal molluscan assemblages from southern Italy. Riv Ital Paleontol Stratigr 103: 389-426

Di Geronimo I, Li Gioi R (1980) La malacofauna würmiana della Staz. 77/4 al largo di Capo Coda di Cavallo (Sardegna nordorient.). Ann Univ Ferrara NS sez 9, 6 (suppl): 123-151

Delongueville C, Scaillet R (2000) Malaco-faune associée aux colonies de *Lophelia pertusa* (Linnaeus, 1758). Récoltes au large des îles Féroé. Novapex 1: 59-69

Dons C (1932) Zoologiske Notiser XV. Om Nord-Norges korallsamfund. Norske Vidensk Selsk Forh 5: 13-16

Dons C (1944) Norges korallrev. Norske Vidensk Selsk Forh 16: 37-82

Fabricius JC (1779) Reise Norwegen. Hamburg

Filatova ZA (1959) Deep-sea bottom fauna communities (complexes) of the northern Pacific. Int Oceanogr Congr Preprints, pp 372-374

Freiwald A, Schönfeld J (1996) Substrate pitting and boring pattern of *Hyrrokkin sarcophaga* Cedhagen, 1994 (Foraminifera) in a modern deep-water coral reef mound. Mar Micropaleont 28: 199-207

Freiwald A, Henrich R, Pätzold J (1997) Anatomy of a deep-water coral reef mound from Stjernsund, West Finnmark, northern Norway. SEPM Spec Publ 56: 141-162

Freiwald A, Hühnerbach V, Lindberg B, Wilson JB, Campbell J (2002) The Sula Reef complex, Norwegian Shelf. Facies 47: 179-200

Freneix S (1980) Bivalves Néocrétacés de Nouvelle-Calédonie, signification biogéographique, biostratigraphique, paléoécologique. Ann Paléont (Invertébrés) 66: 67-134

Friele H, Grieg JA (1901) Den Norske Nordhavs-Expedition, 1876-1878. 28. Zoology, Mollusca III, 7, pp 1-128

Gagnon JM, Haedrich RL (2003) First record of the European giant file clam, *Acesta excavata* (Bivalvia : Pectinoidea : Limidae) in the Northwest Atlantic. Canad Field-Naturalist 117: 440-447

Ghisotti F (1979) Ritrovamento di *Acesta excavata* (Fabricius, 1779) vivente in Mediterraneo. Boll Malacol 15: 57-66

Grieg JA (1913) Marine mollusker fra Indre Sogn. Nyt Mag Naturvidensk 51: 27-42

Haedrich RL, Gagnon JM (1991) Rock wall fauna in a deep Newfoundland fiord. Cont Shelf Res 11: 1199-1207

Hall-Spencer JM, Moore PG (2001) *Limaria hians* (Mollusca: Limacea): a neglected biogenic reef-forming 'keystone' species. Aquat Conserv 10: 267-277

Hertlein LG (1952) Description of a new pelecypod of the genus *Lima* from deep water off central California. Proc Acad Sci 27: 377-381

Hickman CS (1984) Composition, structure, ecology, and evolution of six Cenozoic deep-water mollusk communities. J Paleont 58: 1215-1234

Hidalgo JC (1917) Fauna malacologica de España, Portugal y les Baleares. Moluscos Testaceos marinas. Trab Mus Nac Cienc Nat Zool 30: 1-752

Høisæter T (1986) An annotated check-list of marine molluscs of the Norwegian coast and adjacent waters. Sarsia 71: 73-145

Hovland M, Mortensen PB (1999) Norske korallrev og prosesser i havbunnen. John Grieg Forlag, Bergen

Hovland M, Mortensen PB, Brattegard T, Strass P, Rokoengen K (1998) Ahermatypic coral banks off mid-Norway: evidence for a link with seepage of light hydrocarbons. Palaios 13: 189-200

Järnegren J (1999) Filtration biology and basic morphology of *Acesta excavata* (Fabricius, 1779) (Mollusca: Bivalvia). Unpubli MSc thesis, Trondheim Univ, 20 pp

Järnegren J, Young CM, Tobias CR, Macko SA (2003) Oophagous lifestyle in a bivalve associated with cold-seep tube worms. Abstract. 10th Deep Sea Biology Symp, Oregon

Jeffreys JG (1879) On the Mollusca procured during the Lightning and Porcupine Expeditions, 1868-1870. Proc Zool Soc London 2: 538-588

Jensen A, Frederiksen R (1992) The fauna associated with the bank-forming deepwater coral *Lophelia pertusa* (Scleractinaria) on the Faroe shelf. Sarsia 77: 53-69

Jones DS, Williams DF, Arthur MA (1983) Growth history and ecology of the Atlantic surf clam, *Spisula solidissima* (Dillwyn), as revealed by stable isotopes and annual shell increments. J Exp Biol Mar Ecol 73: 225-242

Kanjilal S (1990) Middle Callovian (Jurassic) *Acesta* Adams & Adams and *Plagiostoma* J. Sowerby (Limidae: Bivalvia) from the Habo Hill, District Kachchh, Gujarat: their taxonomy and paleoecology. Indian J Geol 2: 67-79

Kanno S (1960) Tertiary system of the Chichibu Basin, Saitama Prefecture, Central Japan. Part II. Paleontology. Japan Soc Prom Sci Ueno Tokyo: 123-396

Kanno S (1971) Tertiary molluscan fauna from the Yakataga District and adjacent areas of southern Alaska. Palaeont Soc Japan Spec Pap 16: 154 pp

Kiær H, Wollebæk A (1913) Om dyrelivet i Kristianiafjorden. Nyt Mag Naturvidensk 51: 43-52

Kohl B, Vokes HE (1994) On the living habits of *Acesta bullisi* (Vokes) in the chemosynthetic bottom communities, Gulf of México. Nautilus 108: 9-14

Kuroda T, Habe T, Oyama K (1971) The Sea Shells of Sagami Bay. Maruzen Co., Tokyo

Lamy E (1930-1931) Revision des Limidae vivants du Museum National d'Histoire Naturelle de Paris. J Conchyliol 74: 89-114 (1930); 74: 169-198 (1930); 74: 245-269 (1931)

Le Lœuff P, von Cosel R (1998) Biodiversity patterns of the marine benthic fauna on the Atlantic coast of tropical Africa in relation to hydroclimatic conditions and paleogeographic events. Acta Oecol 19: 309-321

Locard A (1898) Mollusques testacés. Expéditions Scientifiques du Travailleur et du Talisman pendant les Années 1880, 1881, 1882, 1883. Masson et Cie, Paris, 2, 1-515

Löffler S-B (1999) Systematische Neubearbeitung und paläoökologische Aspekte der unteroligozänen Molluskenfauna aus den Zementmergeln von Bad Häring (Unterinntal, Tirol). Tübinger geowiss Arb, A, 54: 1-207

Lundälv T (1997) Koster/Väderörännan - Sveriges rikaste marina miljö. Biodiverse 2: 4-5

Madsen FJ (1949) Marine Bivalvia. Zool Iceland 4: 1-116

Malatesta A, Zarlenga F (1986) Northern guests in the Pleistocene Mediterranean Sea. Geol Rom 25: 91-154

Mangini A, Lomitschka M, Eichstädter R, Frank N, Vogler S, Bonani G, Hajdas I, Pätzold J (1998) Corals provide way to age deep water. Nature 392: 347-348

Marche-Marchad I (1979) Sur le foraminifère *Rosalina carnivora* Todd, 1964 (Discorbidae) parasite d'un Lamellibranche. Bull I.F.A.N. 41 (ser. A, n°1): 103-111

Marshall BA (2001) The genus *Acesta* H & A Adams, 1858 in the south-west Pacific (Bivalvia: Limidae). In: Bouchet P, Marshall BA (eds) Tropical Deep-Sea Benthos, vol 22. Mém Mus natn Hist nat 185: 97-109

MacDonald IR, Boland GS, Baker JS, Brooks JM, Kennicutt MC, Bidigare RR (1989) Gulf of Mexico hydrocarbon seep communities. Mar Biol 101: 235-247

Matsumoto T (1986) Stratigraphical study of the Miocene series in the eastern part of Tottori Prefecture, southwest Japan. J Sci Hiroshima Univ, Ser C, Geol Miner 9: 199-235

Mikkelsen N, Erlenkeuser H, Killingley JS, Berger WH (1982) Norwegian corals: radiocarbon and stable isotopes in *Lophelia pertusa*. Boreas 11: 163-171

Mikkelsen PA, Bieler R (2003) Systematic revision of the western Atlantic file clams, *Lima* and *Ctenoides* (Bivalvia : Limoida : Limidae). Invertebrate System 17: 667-710

Moore EJ (1984): Molluscan paleontology and biostratigraphy of the Lower Miocene upper part of the Lincoln Creek Formation in southwestern Washington. Contr Sci 315: 1-42

Nordgaard O (1929) Faunistic notes on marine evertebrates. VI. On the distribution of some Madreporarian corals in northern Norway. Norske Vidensk Selsk Forh 2: 102-105

Nordsieck F (1969) Die europäischen Meeresmuscheln (Bivalvia) vom Eismeer bis Kapverden, Mittelmeer und Schwarzes Meer. Fischer, Stuttgart

Otuka Y (1940) Miocene Mollusca from the Tesio province, Hokkaido. Japan J Geol Geogr 17: 91-99

Owen R, Kennedy H, Richardson CA (2002) An experimental investigation into partitioning of stable isotopes between scallop (*Pecten maximus*) shell calcite and sea water. *Palaeogeogr Palaeoclimatol Palaeoecol* 185: 163-174

Palazzi S, Villari A (1996) Malacofaune batiali plio-pleistoceniche del messinese. 2: Capo Milazzo. Natur sicil ser 4, 20: 327-279

Pérès JM, Picard J (1964) Nouveau manuel de bionomie benthique de la Mer Méditerranée. Rec Trav Stat Mar d'Endoume 31: 1-137

Poppe GT, Goto Y (1993) European Seashells. 2. Christa Hemmen, Wiesbaden

Remia A, Taviani M (2004): Shallow-buried Pleistocene *Madrepora*-dominated coral mounds on a muddy continental slope, Tuscan Archipelago, NE Tyrrhenian Sea. Facies 50, DOI 10.1007/s10347-004-0029-2

Reynell A (1910) The mollusca collected by the Huxley from the north side of the Bay of Biscay in August 1906. J Mar Biol Ass UK 8: 359-391

Richardson CA (2001) Bivalves as archives of environmental information. Ocean Mar Biol 39: 103-164

Risk MJ, Hall-Spencer J, Williams B (2005) Climate records from the Faroe-Shetland Trough using *Lophelia*: problems and prospects. In: Freiwald A, Roberts JM (eds) Cold-water Corals and Ecosystems. Springer, Berlin Heidelberg, pp 1097-1108

Rocchini R (1983) *Acesta excavata* (Fabricius, 1779) nuovo ritrovamento in Mediterraneo. Boll Malacol 19: 83-84

Sacco F (1898) I molluschi dei terreni terziari del Piemonte e della Liguria. Mem Reg Acad Sci Torino, Clausen, Torino (1890-1904): 1-76

Sars GO (1878) Mollusca regiones Arcticae Norvegiae. Christiania, Norway, 467 pp

Schröder-Ritzrau A, Freiwald A, Mangini A (2005) U/Th-dating of deep-water corals from the Eastern North Atlantic and the western Mediterranean Sea. In: Freiwald A, Roberts JM (eds) Cold-water Corals and Ecosystems. Springer, Berlin Heidelberg, pp 157-172

Segre AG, Stocchino C (1969) Nuove osservazioni sulla geologia e morfologia delle montagne submarine del Mar Tirreno. Ist Idrogr Mar 1037: 11-15

Seguenza G (1870) Sull'antica distribuzione geografica di talune specie malacologiche viventi. Boll Malacol Ital 3: 18 pp

Seguenza G (1873-1879) Studi stratigrafici sulla formazione pliocenica dell'Italia meridionale. Boll Reg Com Geol Ital 4-8: 229 pp

Seguenza G (1880) Le formazioni terziarie della Provincia di Reggio. Atti reg Accad Naz Lincei, Mem Cl Sci Fis, Mat Nat 6: 1-446

Sowerby GB (1883) Descriptions of five new species of shells. Proc Zool Soc London: 30-32

Stilwell JD, Gazdzicki A (1998) New limid bivalve from the La Meseta formation (Eocene) of Seymour Island, Antarctic Peninsula. Acta Geol Pol 48: 149-155

Stilwell JD, Zinsmeister WJ (1992) Molluscan systematics and biostratigraphy. Lower Tertiary La Meseta Formation, Seymour Island, Antarctic Peninsula. Amer Geophys Union Antarctic Res Ser 55: 1-192

Taviani M (1976): Studio di una tanatocenosi pleistocenica dragata nel basso Adriatico. Unpubli MSc thesis, Univ Bologna, 145 pp

Taviani M, Colantoni P (1979) Thanatocoenoses würmiennes associées aux coraux blancs. Rapp Comm int Mer Méditerranée 25/26: 141-142

Terreni G, Voliani A (1995) New finding of *Acesta excavata* (Fabricius, 1779) in the Northern Tyrrhenian Sea. Conchiglia 276: 13-14

Todd R (1965) A new *Rosalina* (Foraminifera) parasitic on a bivalve. Deep-Sea Res 12: 831-837

Vazzana A (1996) Malacofauna batiale del Pleistocene inferiore del vallone Catrica (Reggio Calabria, Italia). Boll Malacol 31: 143-162

Vokes HE (1963) Studies on Tertiary and Recent giant Limidae. Tulane Stud Geol 1: 73-92

Vokes HE (1964) Additions to a catalogue of the described Recent and Tertiary species of *Acesta* and *Plicacesta*. Tulane Stud Geol 2: 18-20

Woodring WP (1938) Lower Pliocene molluscs and echinoids from the Los Angeles Basin, California. US Dept Interior, Geol Surv Prof Pap 190: 67 p

Yokoyama M (1925) Molluscan remains from the uppermost part of the Jo-Ban coal-field. J Coll Sci Imp Univ Tokyo 45: 1-34

Yonge CM (1936) The evolution of the swimming habit in the Lamellibranchia. Mém Mus R Hist Nat Belg 3: 80-100

Deep-water coral occurrences in the Strait of Gibraltar

German Álvarez-Pérez[1], Pere Busquets[1], Ben De Mol[1], Nicolás G. Sandoval[2], Miquel Canals[1], José Luis Casamor[1]

[1] Departament d'Estratigrafia, Paleontologia i Geociències Marines, Universitat de Barcelona, Martí Franquès s/n., E-08028 Barcelona, Spain (german.alvarez@gencat.net)

[2] Compañía SECEGSA (Sociedad Española de Comunicaciones del Estrecho de Gibraltar), Estébanez Calderón, 3 - 1º, E-28020 Madrid, Spain

Abstract. This study reports for the first time on the occurrences of deep-water coral species in the Spanish territorial waters of the Strait of Gibraltar. Based on an extensive dataset of 334 grab samples, 16 species of calcareous corals have been identified in water depths between 13-443 m. Scleractinian corals form the dominant benthic community between 140-330 m water depth. The corals appear on the seabed both as solitary individuals and as patches on small biological topographic build-ups. The most common coral species *Lophelia pertusa* and *Madrepora oculata* are associated with coarse-grained calcareous sediments and mound structures. In the shallowest part of the study area (<150 m) algae and bryozoans are dominant and only a few coral species are observed. This zonation and the occurrence of the azooxanthellate corals in the Strait of Gibraltar relates to light availability and perhaps also to the complex interaction between the outflow of Mediterranean water and surficial inflow of Atlantic water into the Mediterranean Sea.

Keywords. Deep-water corals, benthic distribution, Strait of Gibraltar

Introduction

Deep-water coral distributions are well studied in the NE Atlantic Ocean and in the Mediterranean Sea (Zibrowius 1983, 1988; Rogers 1999; Roberts et al. 2003). Nevertheless, the knowledge of deep-water coral occurrences at the interface between both basins is very limited. SECEGSA (Sociedad Española de Estudios para la Comunicación Fija Europa - Africa a través del Estrecho de Gibraltar) made 334 grab samples available from a sampling survey conducted in 1994 to study the sediment grain size and coral species present. This dense sampling grid includes the Spanish Algeciras shelf and the trough of the Gibraltar Arc up to the outer limit of the Moroccan shelf, between 35º56' and 36º03.4' N, and 5º40' and
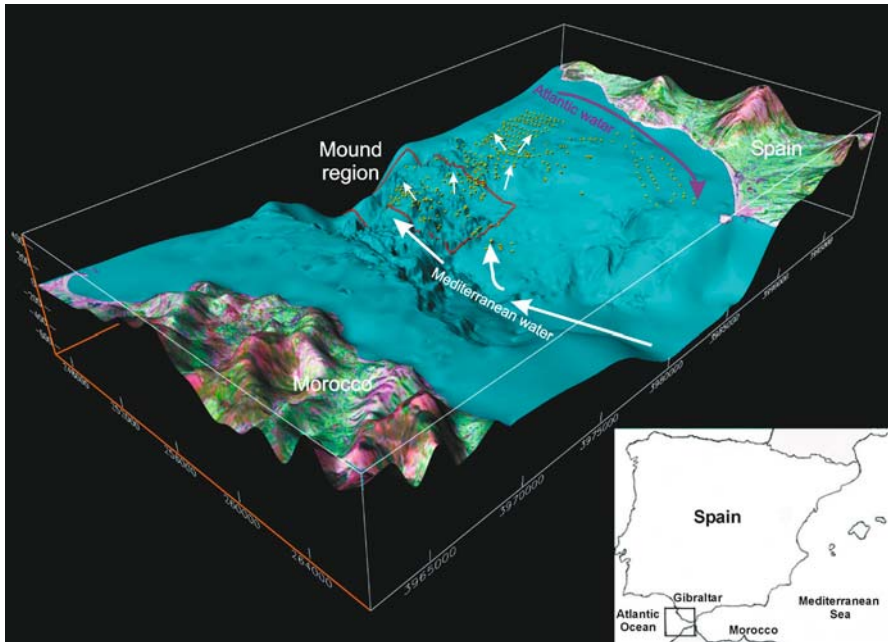
Fig. 1 Location map of the study area indicating the sample grid (yellow), the general oceanography (Atlantic waters = purple, Mediterranean waters = white) and the zone of biological mound build-up = red square)

5º47.5' W (Fig. 1), which allows a detailed study of the general and specific coral species distribution in the study area. The study area includes a zone with mound structures reported between 180-300 m water depths with living *Lophelia pertusa* and *Madrepora oculata* scleractinian corals (Izquierdo et al. 1996; Sandoval et al. 1996). These biological build-ups seem to have similar features to the carbonate mud mounds and deep-sea coral banks reported along the north Atlantic margin (Teichert 1958; Neumann et al. 1977; Mortensen et al. 2001; De Mol et al. 2002; Roberts et al. 2003). The study area is located on the geological structure of the Gibraltar Arc, which is mainly composed of the synorogenic Betic-Rif flysch unit. More detailed geological unit mapping is published by Sandoval et al. (1996). The Strait of Gibraltar is an oceanographic transition area, connecting the Atlantic Ocean and the Mediterranean Sea. The circulation in the Strait is characterised by a two-layer system: a surface eastward Atlantic water inflow and a deep westward outflow of saline Mediterranean water, with variable interface depth at around 100 m (Lacombe and Richez 1982). The aim of this paper is to present the distribution and diversity of deep-water corals species in the Spanish part of the Strait of Gibraltar and their environmental setting.

Material and methods

The study area comprises 65 km² on the Spanish shelf of the Strait of Gibraltar between 35°56' and 36°03' N, and 5°40' and 5°47.5' W. The dense grab sampling grid, with a spatial distribution of about 500 m, was completed between 13 to 501 m water depth. Grain-size analysis has been performed on the recovered sediments to identify the substrates associated with the corals. The sediments were treated with hydrogen peroxide to dissolve organic material. For each sample the dry weight of the 3 major fractions 'fine' (less than 1000 μm), 'medium' (1000-2500 μm), and 'coarse' (more than 2500 μm) was determined.

For each of the three fractions, the coral fragments were separated for subsequent identification. In order to study some of the structural details of the coralline skeletons, a Cambridge Instruments 'Stereoscan S-120' electronic scanning microscope was used. The coral species collected from the samples are classified to species level based on previous systematic deep-water coral work in the Mediterranean Sea (Zibrowius 1980, 1983, 1988; Gili 1982; Zibrowius and Cairns 1992; López-González 1993; Alvarez et al. 1995; Izquierdo et al. 1996; SECEGSA 1997; Cairns 2001). A database was created describing the occurrence of coral per sampling site and the percentage of the coarse grain fraction.

The results of the coral species and grain size analysis were gridded by Earthvision 7.0.1. with a 2-D minimum tension gridding algorithm to calculate a smooth surface that closely fitted the input data values using a bicubic spline technique. The gridcells are 200x200 m. The quantity of coral species obtained in each sample were not taken into account. The contours on the coral distribution maps represent the percentage of probability of the different species in the gridcells. For the most abundant coral species *Lophelia pertusa* and *Madrepora oculata*, specific distribution maps have been gridded (Figs. 2-4). The original report does not indicate if the coral species were live or dead when recovered. Some of the corals were without bioerosion and mechanical erosion, which suggests they were live when sampled.

Results

Systematics and corals distribution

In total, 16 different calcareous coral species were identified in the study area (Table 1). All recognised coral species were previously recorded in the Mediterranean Sea (Alvarez et al. 1995). The coral occurrences are described according to their depth and spatial distribution, without taking into account whether the samples contain contemporary specimens or from Holocene or Pleistocene times. No information is available if the corals were live or dead when sampled.

The identified coral species in the study area include one hydrozoan species (*Errina aspera*), one octocoral species (*Corallium rubrum*) and fourteen scleractinian species (Table 1).

Errina aspera (Fig. 5/1-3) is particularly abundant between 150 and 330 m. The recovered fragments of this species consist of small, poorly developed branches,
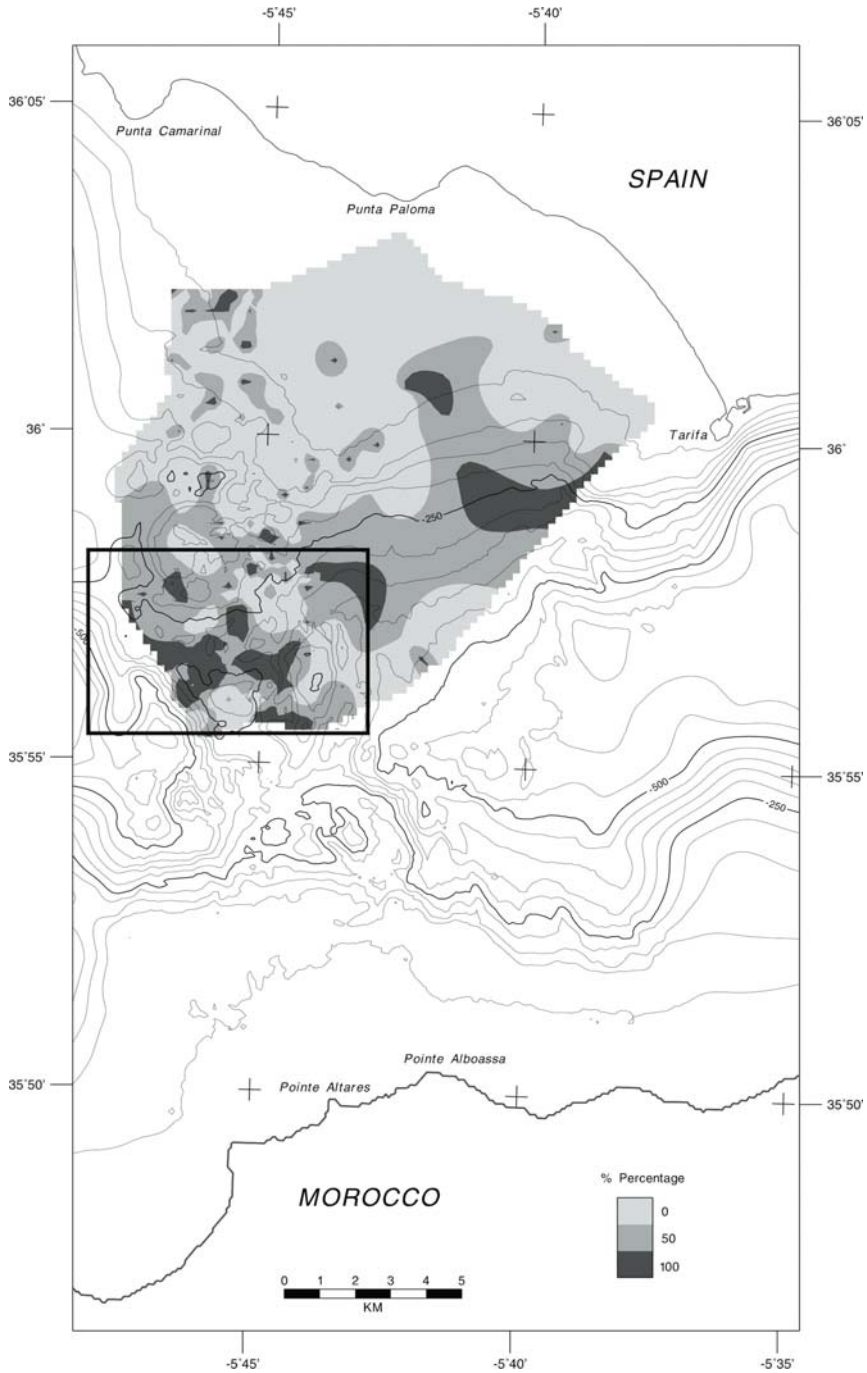
Fig. 2 Map showing the coral distribution, based on presence or absence of corals in the samples
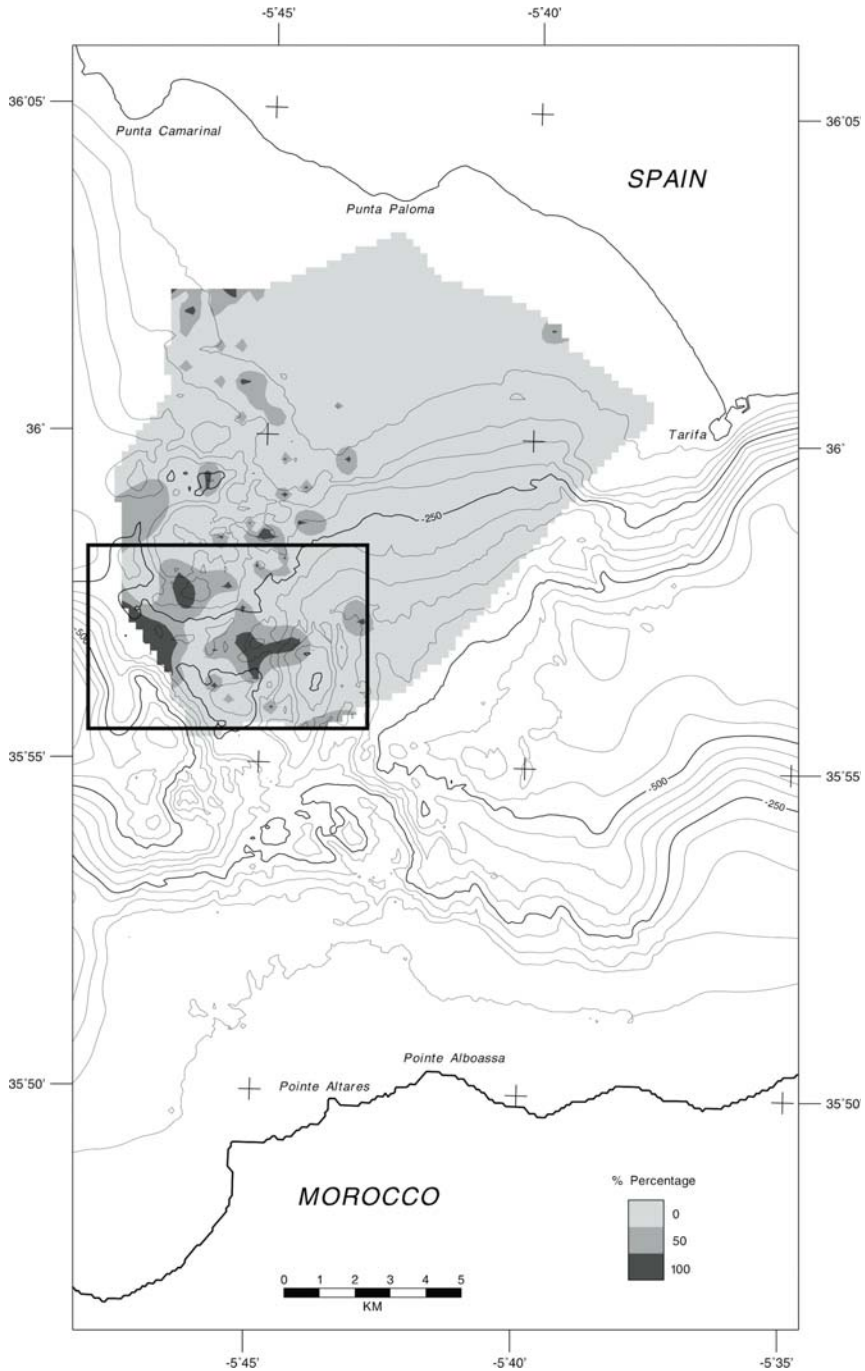
Fig. 3 Areas with highest occurrence of *Madrepora oculata* correlate with the mound area
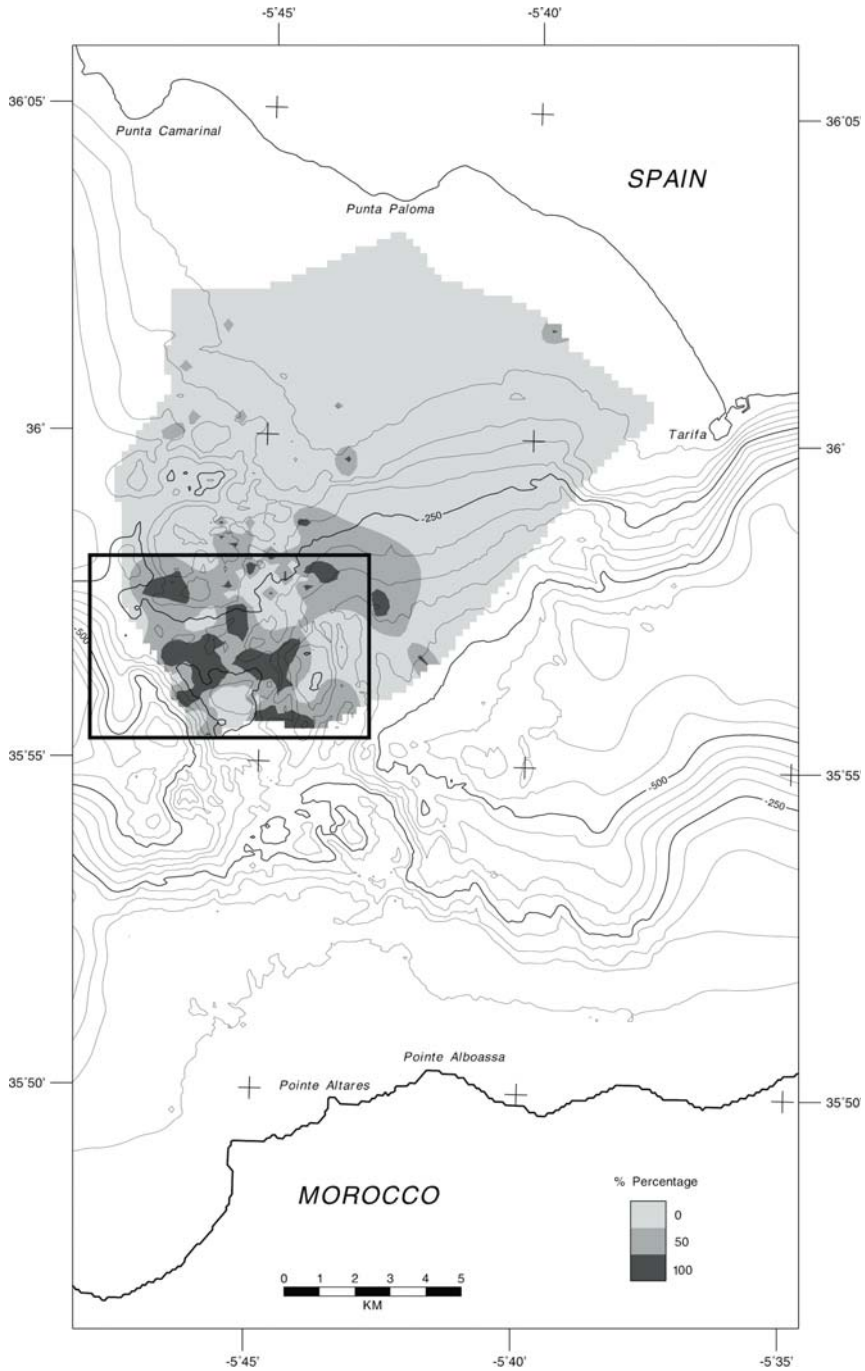
Fig. 4 Map showing the distribution of *Lophelia pertusa*, which follows the distribution of *Madrepora oculata*

Table 1 Listed coral species observed in the study area and their depth range of occurrences

Class	Order	Species	Depth (m)	samples
Hydrozoa	Filifera	*Errina aspera* Linnaeus, 1767	61 – 443	83
Octocorallia	Gorgonacea	*Corallium rubrum* Linnaeus, 1758	73 – 138	4
	Scleractinia	*Cladocora caespitosa* Linnaeus, 1767	23 – 219	5
		Cladocora debilis Edwards and Haime, 1849	24 – 219	6
		Madrepora oculata Linnaeus, 1758	33 – 443	75
		Caryophyllia cyathus (Ellis and Solander, 1786)	66 – 432	56
		Caryophyllia inornata (Duncan, 1878)	13 – 443	31
		Desmophyllum cristagalli Edwards and Haime, 1848	30 – 370	5
		Lophelia pertusa (Linnaeus, 1758)	39 – 463	108
		Dendrophyllia cornigera (Lamarck, 1816)	72 – 432	4
		Stenocyathus vermiformis (Pourtalès, 1868)	43 – 443	40
		Paracyathus pulchellus (Philippi, 1842)	184 – 221	3
		Sphenotrochus andrewianus Edwards and Haime, 1848	66 – 187	9
		Polycyathus muellerae (Abel, 1959)	13 – 65	3
		Astroides calycularis (Pallas, 1766)	27	1
		Monomyces pygmea (Risso, 1826)	58	1

which are highly eroded. On several coral branches the well-preserved gastropod *Pedicularia sicula* Swains (Fig. 6/21-22) was observed, which lives in fixed symbiosis. This symbiosis modifies the coral at the gastropod fixation points.

Corallium rubrum (Fig. 5/4) was very rare in the study area. Only a single short branch was observed besides plenty of highly physically eroded to rounded fragments.

One specimen of *Cladocora caespitosa* (Fig. 5/5-6) was observed at 23 m. Four samples of this coral species were recovered between 114 and 219 m water depth. The distribution of *Cladocora debilis* (Fig. 5/7-8) is geographically limited but appeared in a large depth range between 24 and 219 m. *Madrepora oculata* (Fig. 5/9-11) was abundant in the study area. Nevertheless, the highest abundance is found between 95 and 269 m water depth (Fig. 3). The coral fragments were well-preserved colonial branches. In the deepest water depth range more robust specimens were recovered with a dark patina of manganese dioxide. *Caryophyllia cyathus* (Fig. 5/15-18) was collected in water depths between 143 and 327 m. Some specimens showed regenerated branches with geniculations (Fig. 5/17) and rejuvenation calyces (Fig. 5/18). Physically eroded and manganese dioxide stained fragments occurred in the deepest part of the depth range. *Caryophyllia inornata* (Fig. 5/19-20) was relatively abundant in the study area. *Desmophyllum cristagalli* (Fig. 5/12-14) was rare in the study area. Although this species is known to be a deep-water coral, it was observed in just 30 m water depth. Some specimens were strongly elongated (Fig. 5/12) while others had a more oblate (Fig. 5/13) geometry. *Lophelia pertusa* (Fig. 6/1-6) was the most abundant species in the area, and appeared in a large water depth range but seems to have a preferential depth range of 170 to 332 m (Fig. 4). *Dendrophyllia cornigera* (Fig. 6/7-8) was very uncommon in the area. *Stenocyathus vermiformis* (Fig. 5/21-22) was observed fixed to a hard substratum. One specimen was observed on both sides of the coral fragment calyx
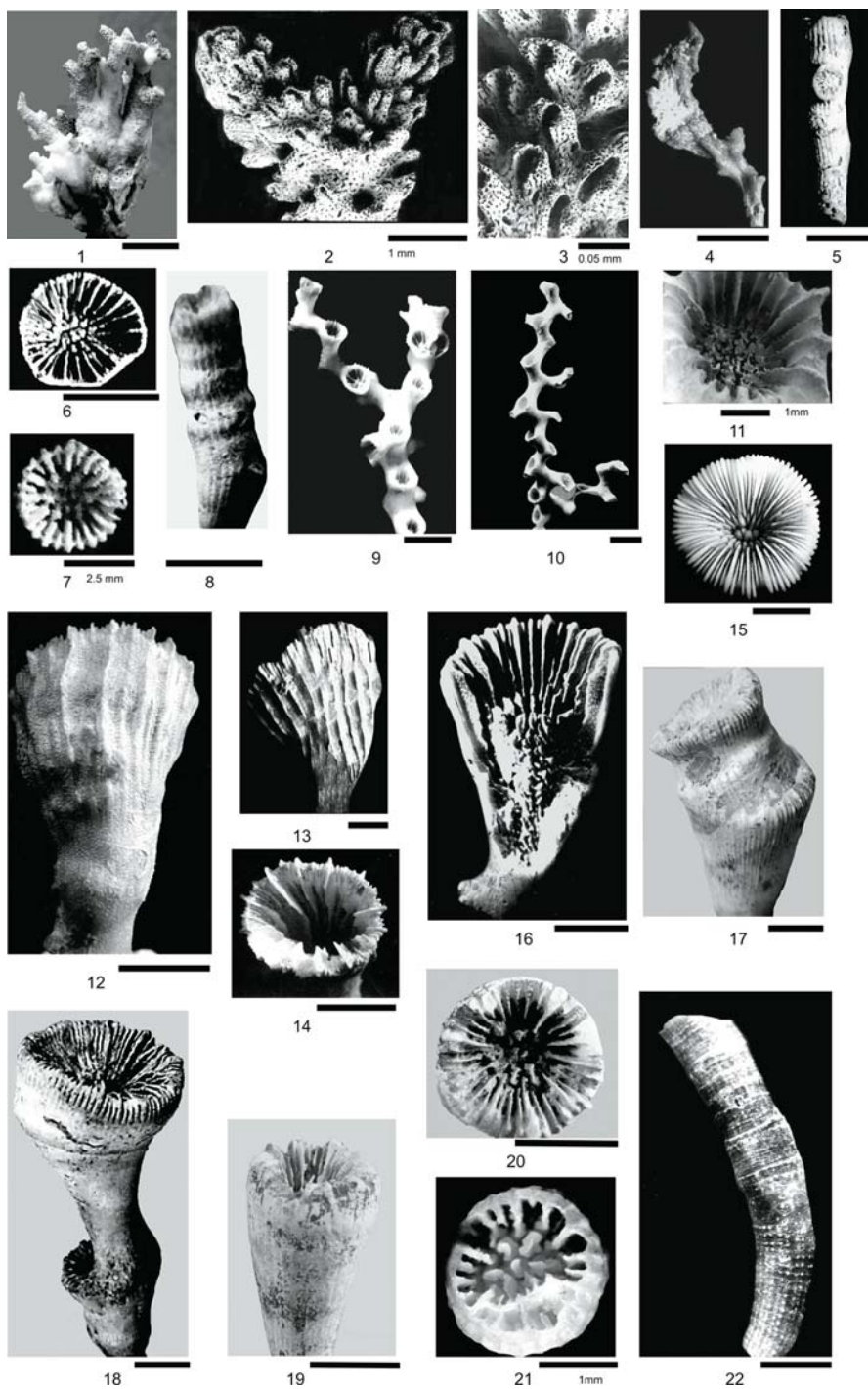
formation. *Paracyathus pulchellus* (Fig. 6/9-10) was rare in the area and appears as solitary fragments. *Sphenotrochus andrewianus* (Fig. 6/14-15) was associated with sandy sediments. *Polycyathus muellerae* (Fig. 6/11-13) was found as solitary corals in a relatively large spatial distribution, fixed on a hard substratum. One colony of *Astroides calycularis* (Fig. 6/16-18) was found at a depth of 27 m. One specimen of *Monomyces pygmea* (Fig. 6/19-12) was collected at 58 m water depth, with the adventitious fixation root.

Corals and sediments

The grain size distribution in the study area is presented in Figure 7 as the percentage of the coarse fraction (>2.5 mm). Two zones with a dominance of coarse grain sediments can be observed: firstly a zone in the shore area on the Algeciras shelf and secondly a zone in the deepest part of the study area (Fig. 7). The grain size distribution shows coarser sediments in the western part than in the eastern part of the study area. High concentrations of coral occurrences, especially of *Lophelia* and *Madrepora,* coincide with coarse-grained sediments in the deepest part of the study area (Figs. 2-4). The sediment in this area is largely composed of residual coral fragments larger than 2.5 mm. The second zone of coarse grained sediments is located closer to the Algeciras shelf which coincides with the occurrences of algae and in some cases bryozoans (Fig. 7).

Discussion and conclusion

This paper reports for the first time on the distribution and occurrences of azoo-xanthellate corals in Spanish territorial water of the Strait of Gibraltar. According to López-González (1993), the Gibraltar Strait forms a distinct zoogeographic area between the Lusitanian zoogeographic area (stretching out from the southern limit of the English Channel to the Strait of Gibraltar), the Mediterranean and the Mauritanian zoogeographic area (which extends from the Gibraltar Strait to Cape Blanc). Following this work, the fauna of the Strait of Gibraltar is similar to the western Mediterranean and to a lesser extent of the Lusitanian zoogeographic zone. All reported species in the study area are also described in the Mediterranean Sea zone, which support this view of a dominance of the Mediterranean above the Lusitanian zoogeographic zone.

Scleractinian corals are by far the most common corals in this area, with rare occurrences of Filifera (hydroids) and Gorgonacea (octocorals). Corals appear throughout the sampling depth range between 13 m and 440 m water depth. The bathymetric ranges of the species in the study area are similar to the depth occurrences of the same species in the Mediterranean Sea (Zibrowius 1980). The shallow occurrences of a few fragments of *Madrepora oculata* at 33 m,

Fig. 5   **1-3** *Errina aspera.* **4** *Corallium rubrum.* **5-6** *Cladocora caespitosa.* **7-8** *Cladocora debilis.* **9-11** *Madrepora oculata.* **12-14** *Desmophyllum cristagalli.* **15-18** *Caryophyllia cyathus* **19-20** *Caryophyllia inornata.* **21-22** *Stenocyathus vermiformis.* Scale bar is 5 mm (if not indicated differently)
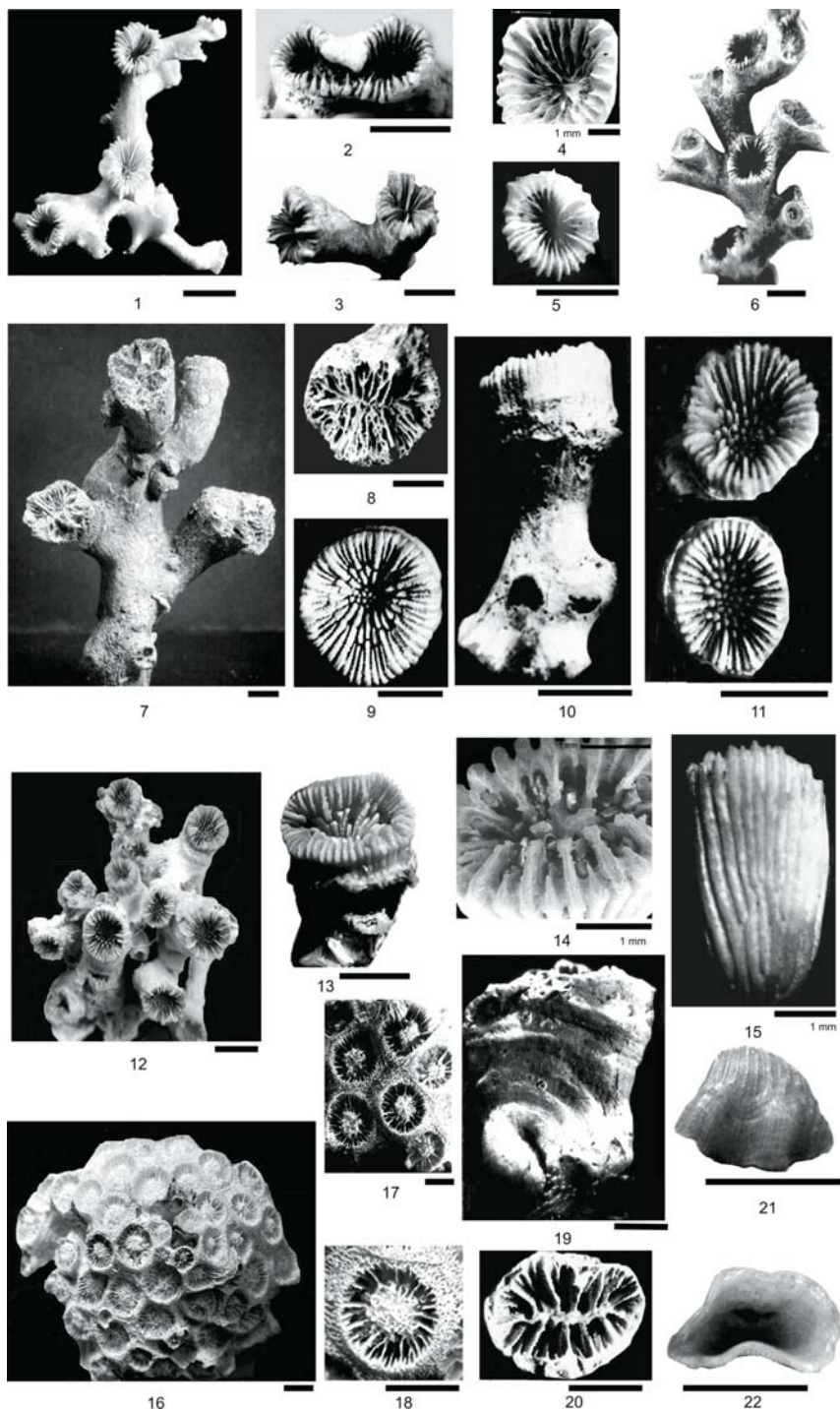
Desmophyllum cristagalli at 30 m, and *Stenocyathus vermiformis* at 43 m are exceptional. Nevertheless these fragments show certain degrees of mechanical abrasion, biological erosion and Mg-staining indicating that the corals were dead when recovered in the shallower parts of the study area. It is not clear if currents or anthropogenic activity has transported the coral fragments to these shallow areas or that the corals were sampled *in situ* and colonised these areas in previous times.

Remarkable quantities of living reef-forming deep-water corals were found at the depth range between 150-330 m of *Lophelia pertusa* and to a lesser extent *Madrepora oculata* associated with large dead coral fragments at the interface between Atlantic and Mediterranean waters. These observations fit with the reports of living corals on top of topographic structures interpreted as a lithoherm in water depths around 300 m (Izquierdo et al. 1996; Sandoval et al. 1996). The highest concentrations of corals appear in the deepest part of the Strait of Gibraltar with complex seabed morphology. The corals seem to settle on hard substratum of outcropping flysch and on locally steep slopes.

The coarse-grained sediment in this depth interval is largely composed of residual coral fragments (Figs. 2-4, 7), flysch fragments, and to a lesser extent the remains of the skeletons of other invertebrates providing the coral with a suitable hard substratum to settle.

In contrast to the deeper part of the study area, corals are sporadically observed on the Algeciras shelf. The coarse sediment fraction here is composed of crust-forming algae and bryozoans, which are common at these depths in the Mediterranean Sea (Fig. 7).

The basic requirements of the deep-water corals are nutrient supply, hard substratum for settlement and low sedimentation rates. Suitable substratum is available in the deeper part of the study area from outcropping Gibraltar flysch and coral rubble. Nutrient supply and low sedimentation rates are directly related to the current regime in the area. The role of the oceanographic conditions and the role of topographic slope breaks are discussed in other deep-water coral settings in the Atlantic (De Mol et al. 2002; Roberts et al. 2003) and in the Mediterranean Sea (Taviani et al. 2005). The Strait of Gibraltar has a peculiar oceanographic setting and acts as the bottleneck between the exchange of Atlantic and Mediterranean water, which is strongly influenced by tidal currents as well as by wind and atmospheric pressure variations (Candela et al. 1989; García Lafuente et al. 2002). The interaction of the different oceanographic processes related to the watermass stratification and the morphology of the basin generates mixing and related processes such as internal waves which contribute to the eventual intrusion of deep water in the productive zone, which makes the Strait of Gibraltar a pulsating upwelling area, and enriches the upper illuminated zone with nutrients (Santana-Casiano et al. 2002). Echevarría et al. (2002) demonstrated a relevant role of interface position and oscillations

Fig. 6   1-6 *Lophelia pertusa*. **7-8** *Dendrophyllia cornigera*. **9-10** *Paracyathus pulchellus*. **11-13** *Polycyathus muellerae*. **14-15** *Sphenotrochus andrewianus*. **16-18** *Astroides calycularis*. **19-20** *Monomyces pygmea*. **21-22** *Pedicularia sicula*. Scale bar is 5 mm (if not indicated differently)
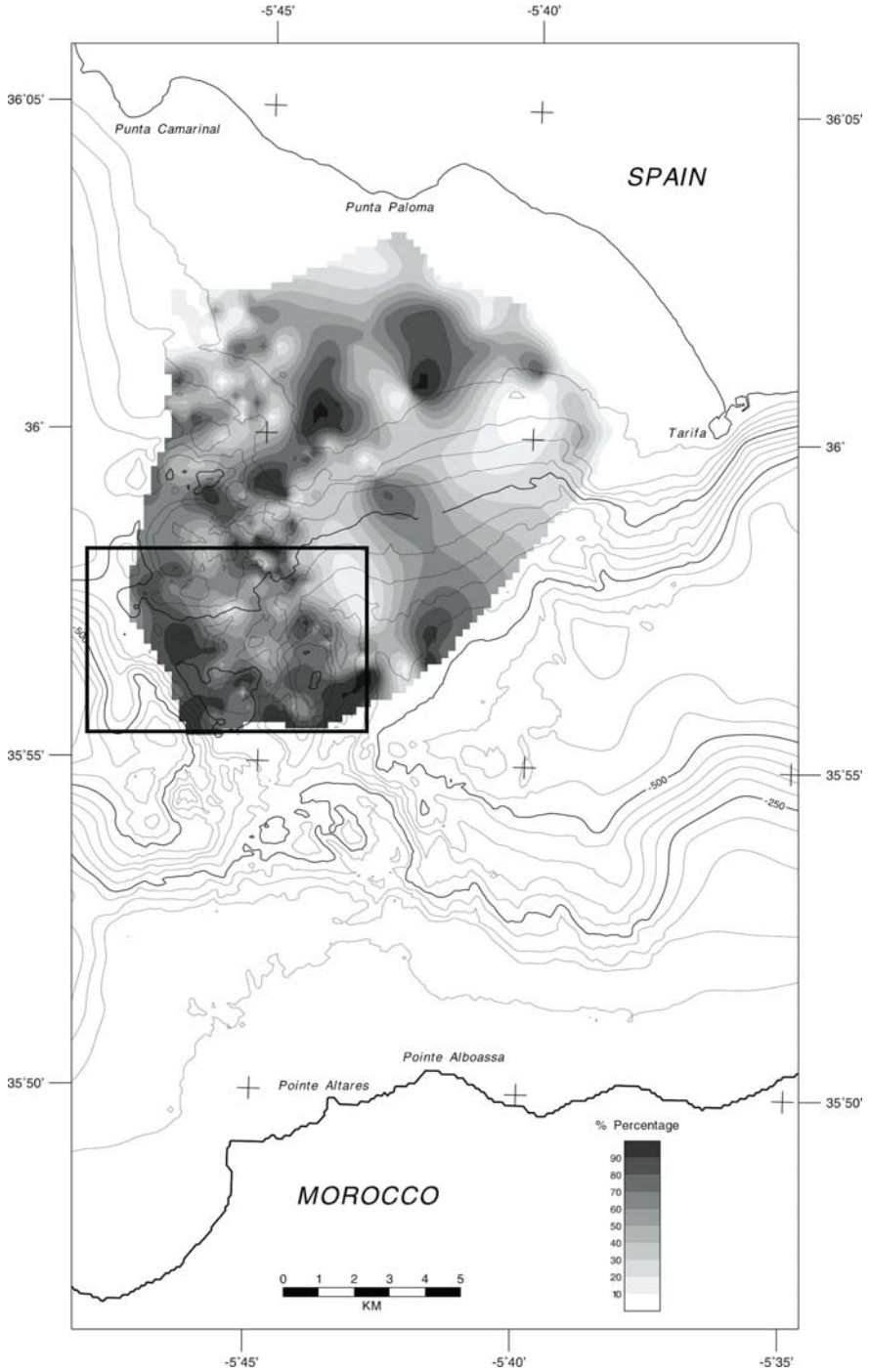
Fig. 7 Distribution map of the coarse grain fraction (>2.5 mm) in the study area

explaining the biomass distribution pattern. A general increase in biomass towards the northwest was observed, which parallels the interface ascent. The depth of the interface affects the distribution of chlorophyll and microphytoplankton, which shows a clear ascent towards the northeast of the Strait of Gibraltar or the zone of coral occurrences. The upwelling and mixing of the watermasses results in a higher nutrient availability to the coral fauna and the combination of the seafloor morphology and the current patterns safeguard the corals against sediment burial. In other deep-water coral settings the association between watermass mixing, internal waves and upwelling has been related to the occurrence of corals in the North Atlantic and Mauritanian margin (Frederiksen et al. 1992; Rogers 1999; Mortensen et al. 2001; Roberts et al. 2003; Colman et al. 2005).

The corals of Gibraltar hold the key to understanding the relation between the Atlantic and Mediterranean coral communities and the relationship to their oceanographic setting and migrations pathways in or from the Mediterranean Sea and Atlantic Ocean. Studies of the distribution and age of these corals might help to understand the general palaeobiogeography and on a wider scale, the deep-water coral environment along European continental margins.

Acknowledgments

References

Alvarez G, Busquets P, Reguant S, Alonso B (1995) Corales y Briozoos de los sedimentos del fondo del Estrecho de Gibraltar: significado paleoambiental. IV Coloquio Internacional sobre el enlace fijo del estrecho de Gibraltar, Sevilla, pp 413-414

Cairns SD (2001) A generic revision and phylogenetic analysis of the Dendrophylliidae (Cnidaria: Scleractinia). Smithsonian Contr Zoology 615: 1-75

Candela J, Winant CD, Bryden HL (1989) Meteorologically forced subinertial flows through the Strait of Gibraltar. J Geophys Res 94: 12667-12674

Colman JG, Gordon DM, Lane AP, Forde MJ, Fitzpatrick JJ (2005) Carbonate mounds off Mauritania, Northwest Africa: Status of deep-water corals and implications for management of fishing and oil exploration activities. In: Freiwald A, Roberts JM (eds) Cold-water Corals and Ecosystems. Springer, Berlin Heidelberg, pp 417-441

De Mol B, Van Rensbergen P, Pillen S, Van Herreweghe K, Van Rooij D, McDonnell A, Huvenne V, Ivanov M, Swennen R, Henriet JP (2002) Large deep water coral banks in the Porcupine Basin, southwest of Ireland. Mar Geol 188: 193-231

Echevarrá F, Garciá Lafuente J, Bruno M, Gorsky G, Goutx M, Gonzálas N, Garciá CM, Gómez F, Vargas JM, Picheral M, Striby L, Varela M, Alonso JJ, Reul A, Cózar A, Prieto L, Sarhan T, Plaza F, Jiménez-Gómez F (2002) Physical-biological coupling in the Strait of Gibraltar. Deep-Sea Res II 49: 4115-4130

Frederiksen R, Jensen A, Westerberg H (1992) The distribution of the scleractinian coral *Lophelia pertusa* around the Faeroe Islands and the relation to internal tidal mixing. Sarsia 77: 157-167

García Lafuente J, Delgado J, Vargas JM, Vargas M, Plaza F, Sarhan T (2002) Low frequency variability of the exchanged flows through the Strait of Gibraltar during CANIGO. Deep-Sea Res II 49: 4051-4067

Gili JM (1982) Fauna dels Cnidaris de les illes Medes. Treballs Inst Catalana Hist Nat, Barcelona 10: 1-175

Izquierdo FJ, Esteras M, Sandoval NG (1996) Depósitos coralinos litificados en el Estrecho de Gibraltar. Geogaceta 20: 401- 404

Lacombe H, Richez C (1982) The regime of the Strait of Gibraltar. In: Nihoul JCJ (ed) Hydrodynamics of Semi-enclosed Seas. Elsevier, Amsterdam, pp 13-73

López-González PJ (1993) Taxonomía y zoogeografía de los antozoos del Estrecho de Gibraltar y áreas próximas. PhD tesis, Univ Granada, pp 1-569

Mortensen PB, Hovland MT, Fosså JH, Furevik DM (2001) Distribution, abundance and size of *Lophelia pertusa* coral reefs in mid-Norway in relation to seabed characteristics. J Mar Biol Assoc UK 81: 581-597

Neumann AC, Kofoed JW, Keller GH (1977) Lithoherms in the Strait of Florida. Geology 5: 4-10

Roberts JM, Long D, Wilson JB, Mortensen PB, Gage JD (2003) The cold-water coral *Lophelia pertusa* (Scleractinia) and enigmatic seabed mounds along the north-east Atlantic margin: are they related? Mar Pollut Bull 46: 7-20

Rogers AD (1999) The biology of *Lophelia pertusa* (Linnaeus 1758) and other deep-water reef-forming corals and impacts from human activities. Int Rev Hydrobiol 84: 315-406

Sandoval NG, Sanz JL, Izquierdo FJ (1996) Fisiografía y Geología del umbral del Estrecho de Gibraltar. Geogaceta 20: 343-346

Santana-Casiano JM, Gonzalez-Davila M, Laglera LM (2002) The carbon dioxide system in the Strait of Gibraltar. Deep-Sea Res II 49: 4145-4161

SECEGSA (Sociedad Española de Estudios para la Comunicación Fija Europa-Africa a través del Estrecho de Gibraltar) (1997) Las formaciones de corales ahermatípicos del Estrecho de Gibraltar. pp 1-20

Taviani M, Freiwald A, Zibrowius H (2005) Deep-coral growth in the Mediterranean Sea: an overview. In: Freiwald A, Roberts JM (eds) Cold-water Corals and Ecosystems. Springer, Berlin Heidelberg, pp 137-156

Teichert C (1958) Cold- and deep-water Coral Banks. AAPG Bull 42: 1064-1082

Zibrowius H (1980) Les Sclèractinaires de la Mèditerranèe et de l'Atlantique nord-oriental. Mém Inst Océanogr Monaco 11: 1-228, 11(2): 1-107, 11(3): 229-284

Zibrowius H (1983) Nouvelles donnèes sur la distribution de quelques Sclèractinaires «mèditerranèens» à l'est et à l'ouest du detroit de Gibraltar. Rapp Comm Int Mer Mèdit 28: 307-309

Zibrowius H (1988) Mise au point sur les Sclèractinaires comme indicateurs de profondeur (Cnidaria: Anthozoa). Gèol Mèditerr 15: 27-47

Zibrowius H, Cairns SD (1992) Revision of the northeast Atlantic and Mediterranean Stylasteridae (Cnidaria: Hydrozoa). Mém Mus Natl Hist Nat 153: 1-136

An assessment of the distribution of deep-sea corals in Atlantic Canada by using both scientific and local forms of knowledge

Susan E. Gass*, J.H. Martin Willison

School for Resource and Environmental Studies, Dalhousie University, Halifax,
  Nova Scotia, B3H 3J5, Canada

*Current address: Scottish Association for Marine Science, Dunstaffnage Marine
  Laboratory, Oban, Argyll, PA37 1QA, UK
  (susan.gass@sams.ac.uk)

Abstract. More than 27 species of deep-sea corals have been identified off Atlantic Canada but their distributions are largely unknown. Bottom trawling is recognized as a threat to deep-sea corals in Atlantic Canada but the degree of damage has not been quantified. It is difficult to assess the level of conservation required for these organisms without basic information about their distribution. This study attempts to improve our knowledge of the distribution of deep-sea corals in Atlantic Canada.

   The study uses three sources of data to map the distribution of deep-sea corals in Atlantic Canada including the Canadian Department of Fisheries and Oceans (DFO) groundfish trawl surveys from 1999-2001, DFO fisheries observer records from 2000 and 2001, and local ecological knowledge of fishermen in northern Nova Scotia and Newfoundland. The results reveal that deep-sea corals are widely distributed along the edge of the continental shelf from the Gulf of Maine to the Davis Strait. The study confirms the presence of eight species including: *Acanella arbuscula*, *Acanthogorgia armata*, *Flabellum* spp., *Keratoisis ornata*, *Lophelia pertusa*, *Paragorgia arborea*, *Paramuricea* spp. and *Primnoa resedaeformis*. Significant findings from the study include: documentation of an antipatharian, an order not previously recorded in Atlantic Canada; documentation of *L. pertusa* from the Stone Fence and reported locations from Jordan Basin and the Gully; and the extension of the known ranges of *P. arborea, K. ornata*, and *Paramuricea* spp. Relatively high abundances of *P. resedaeformis* and *P. arborea* are reported from the Northeast Channel off southwest Nova Scotia and east of Cape Chidley, Labrador. The highest coral species richness is found along the edge of the continental shelf between the Gully and the Laurentian Channel at the edge of the Scotian Shelf. Fishermen reported catching the largest specimens and highest numbers of corals from the Stone Fence and also identified the Gully as an area of high coral abundance. Several fishermen reported significant changes to the seafloor on the

eastern Scotian Shelf and the Stone Fence over the duration of their fishing careers, including a decrease in the size and number of corals they caught.

Introduction

To date at least 27 species of deep-sea corals have been identified in Atlantic Canadian waters, six Alcyonacea, 10 Gorgonacea and 11 Scleractinia (Breeze et al. 1997; Mukhida and Gass 2001). Exact locations for each species were largely unknown until the current study was completed. The majority of pre-existing distribution data were based on specimens and information provided by fishermen, and the majority of the data dates back to the late 19th and early 20th centuries. Much of the early work is based on collections made by Gloucester (Massachusetts) fishermen from the fishing banks of Atlantic Canada (Verrill 1864, 1878, 1922; Collins 1884; Goode 1887; Whiteaves 1901). These collections included specimens of *Paragorgia arborea*, *Acanthogorgia armata*, *Acanella arbuscula*, *Keratoisis ornata*, *Paramuricea grandis*, *Primnoa resedaeformis* and *Flabellum alabastrum*. Subsequently, Deichmann (1936) compiled and published the remainder of work by Verrill after he died in 1927 and included further descriptions of *P. arborea*, *A. armata*, *A. arbuscula* and *P. resedaeformis*. Miner (1950) provided brief descriptions of several species found in Atlantic Canada. Litvin and Rvachev (1963) described the bottom topography of Newfoundland and Labrador's fishing areas including the presence of "lime corals and their fragments" occupying several areas.

Hecker et al. (1980) conducted photographic surveys of three deep-sea canyons on the US side of Georges Bank and provided descriptions of several species of both scleractinians and gorgonians, many of which occur in Atlantic Canada. Tendal (1992) compiled and mapped existing data on the distribution of *P. arborea* including several locations around Atlantic Canada.

In the past decade, concern has been raised about the impacts of fishing activities on deep-sea corals off Atlantic Canada. Bottom trawling has been shown to have deleterious impacts on complex benthic habitats (Watling and Norse 1998; Auster and Langton 1999; ICES 2000). The structural characteristics and long-lived nature of deep-sea corals make them especially vulnerable to such impacts (Probert et al. 1997; Phillipart 1998; ICES 2000). Significant damage to deep-sea corals as a result of bottom trawling has been documented in several parts of the world including damage to *Solenosmilia variabilis* on seamounts off Tasmania (Koslow and Gowlett-Holmes 1998; Koslow et al. 2001), *Lophelia pertusa* reefs off Norway (Fosså et al. 2000) and *Primnoa* spp. off Alaska (Krieger 2001). In Nova Scotia, concerns first brought forward by fishermen (Jones and Willison 2001) were investigated by the Ecology Action Centre (EAC) and the results of a preliminary investigation are found in the report by Breeze et al. (1997) on the distribution and status of deep-sea corals off Nova Scotia. This report was the first comprehensive work that focused

on the distribution of deep-sea corals in Atlantic Canada, and more specifically it focused only on areas near Nova Scotia. The results are based on fishermen's Local Ecological Knowledge (LEK) as well as data from existing museum and scientific collections. The results show a general trend of deep-sea corals being distributed along the edge of the continental shelf at depths of 183-293 m and in deep canyons and channels at depths of 914-1097 m. The findings also confirmed the impressions of several fishermen, and in particular those who had been fishing for long periods of time, that there was a decrease in the abundance of corals in several areas off Nova Scotia where bottom trawling regularly occurred.

The First International Symposium on Deep-sea Corals (Willison et al. 2001) generated, in part, several new coral research and conservation initiatives being conducted by government, academic and non-government organizations. For example, preliminary results from recent investigations of coral habitats on the Scotian Shelf using underwater video found a total of 15 coral species ranging from the Northeast Channel to the northern Labrador Shelf with the highest densities observed at the mouth of the Northeast Channel and highest species diversity observed in the Gully and the Stone Fence (MacIsaac et al. 2001). World Wildlife Fund Canada produced a summary of the current state of knowledge of deep-sea corals in Atlantic Canada together with a review of their conservation objectives (Gass 2003). Mortensen et al. (2004) documented the effects of fishing in the Northeast Channel and 4 % of observed corals were impacted by fishing activities. The distribution of deep-sea corals in the Northeast Channel have been documented by Mortensen and Buhl-Mortensen (2004), and Mortensen and Buhl-Mortensen (2005) describe the distribution of corals in the Gully.

The goal of the present study was to better determine the distribution of deep-sea corals off Atlantic Canada by producing distribution maps based on three sources of information.

Local Ecological Knowledge

"Local Ecological Knowledge" (LEK) as used in this study can be described as knowledge gained by local residents about their environment based on experiences of living and/or working in the environment. This knowledge may have been gained by one person over a period of a few years, or accumulated by a community over several generations. Similar to many of the previous reports of deep-sea corals in Atlantic Canada, the present study relies partially on fishermen's LEK for information about the location and status of deep-sea corals in Atlantic Canada. Interviewing fishermen as a means of obtaining LEK for use in science and management has been practiced previously (Johannes 1981; Hutchings 1996; Breeze et al. 1997; Fuller and Cameron 1998; Neis and Felt 2000). Fishermen, as resource users, develop detailed knowledge of their resources, their environments, and their fishing practices, hence personal interviews with fishermen can elicit large amounts of information about species that are of both commercial and scientific interest (Neis et al. 1999). Some fishermen have fished the same grounds for decades, while some fishing

communities have existed for several hundred years (Neis and Felt 2000). In many cases, fishermen's knowledge of a fishery and the associated marine environments exceeds current scientific knowledge (Neis and Felt 2000). This is apparently the case with the current state of knowledge of the distribution of deep-sea corals in Atlantic Canada. Such continuous observation of one area over a long period of time, and wealth of data that it can yield, would be difficult to replicate given the financial and time constraints of many scientific research projects (Fischer 2000).

Methods

To identify as many locations of deep-sea corals as possible over the large spatial area of Atlantic Canada and within the two-year time frame of the study, three methods of data collection were used. Presence data for scleractinian and gorgonian corals were collected from the Canadian Department of Fisheries and Oceans (DFO) groundfish trawl surveys and from DFO fisheries observer records. These methods are described as *opportunistic* because corals are incidental catches during these activities. The third method of data collection involved interviewing fishermen in Novia Scotia and Newfoundland about their LEK of the distribution of deep-sea corals within their fishing grounds.

DFO groundfish trawl surveys

DFO conducts annual groundfish trawl surveys in the four regions of Atlantic Canada: the Maritimes, Gulf of St. Lawrence, Newfoundland and Labrador, and the Arctic. The general purpose of these surveys is to determine the distribution and abundance of economically important groundfish and shellfish species (DFO 1999), but corals are also incidentally caught during the surveys. All surveys used a stratified random sample design for selecting the trawl locations. Depending on the survey, different types of bottom trawls were used, including shrimp trawls and bottom trawls with and without rockhopper gear. The length of each trawl set was consistent for each survey, varying between 15 and 30 minutes. Specimens of corals were collected during surveys off Nova Scotia, Newfoundland and Labrador, and the Gulf of St. Lawrence between 1999 and 2001, and during the 2001 surveys in the Arctic. All corals caught during the cruises were labelled with the cruise and trawl sample numbers and kept frozen until they were identified.

Fisheries observer records

One of the primary objectives of the fisheries observer program is "to provide scientific data and management information for direct input into the management of Canada's fisheries and the conservation of fishery resources for the benefit of Canadians" (DFO 2001). This includes recording fishery bycatch. Fisheries observer coverage on vessels in Nova Scotia varies depending on the fishery, fishing grounds, gear type and vessel size. For example, foreign vessels and northern shrimp vessels have 100 % observer coverage, longline and bottom trawling vessels under 100 ft in length have a target of 5-10 % coverage, vessels over 100ft have a target of 10 % coverage, and small vessels using gillnets have less than 5 % coverage.

In 1999, coral species were added to the list of bycatch recorded by fisheries observers working on vessels fishing from Nova Scotia. To aid in this process, an identification guide for eight species of deep-sea corals found in Nova Scotian waters was provided to each observer. Observers recorded the species of corals found in the fishing gear and the location of the vessel at the time the specimens were retrieved.

Local Ecological Knowledge

Breeze et al. (1997) successfully interviewed 22 fishermen about their knowledge of coral locations off Nova Scotia. The fishing grounds included in the study ranged from Georges Bank to the Laurentian Channel. The majority of the participants lived in southern Nova Scotia. Two field sites were selected for the present study to supplement the initial interviews: Northern Nova Scotia (particularly Cape Breton Island) and Newfoundland.

Thirty-six interviews were conducted with fishermen in Nova Scotia and Newfoundland between July and November 2001. Participants were chosen using purposive sampling and snowball sampling. Purposive sampling involves choosing participants who are believed to yield the most comprehensive information and snowball sampling involves asking those participants to provide names of future participants (Babbie 1992). Further to the observation made by Maurstad (2000) that snowball sampling can create a bias by accessing participants with similar opinions and status, names of participants were also obtained from the Directory of Fishermen's and Other Organizations in Scotia-Fundy, the Fishermen and Scientist Research Society, and from professional contacts.

The selection of participants focused on vessel masters who had been fishing with bottom gears for at least 10 years (Mailhot 1994). This decision rule was made to obtain information on changes in the abundance of corals over time and therefore targeted fishermen who have been fishing over a long period of time.

The majority of the interviews took place in the fishermen's homes, but in several cases the interview took place on the wharf, and in one case on a fishing vessel. A semi-structured interview technique was used (Mailhot 1994). The interviews were not tape recorded, but rather the interviewers wrote down what was said. The interview started with several short answer questions regarding the fishing history and experience of the participants. For example, the number of years they had been fishing, whether they were captains or crew, and what type of fishing gear they used. These short answer questions were followed by questions about deep-sea corals to determine whether the participants were in fact familiar with these organisms. Next, the participants were asked about their fishing grounds, where they had caught corals, and with what gear type(s). Following this discussion, the appropriate nautical chart was chosen and the participant was asked to mark the locations of coral catches on the chart. To finish the interview the participants were asked about any changes they had observed in the locations and abundance of coral they caught throughout their careers.

Results

Groundfish trawl surveys

From 1999-2001, four research surveys on the Scotian Shelf, five off Newfoundland and Labrador and two in the Arctic region successfully retrieved 57 coral specimens among which seven species were identified. Figure 1 shows several examples of specimens caught during the surveys. Corals were caught at depths between 154 and 1400 m and were located from the Gulf of Maine to the Davis
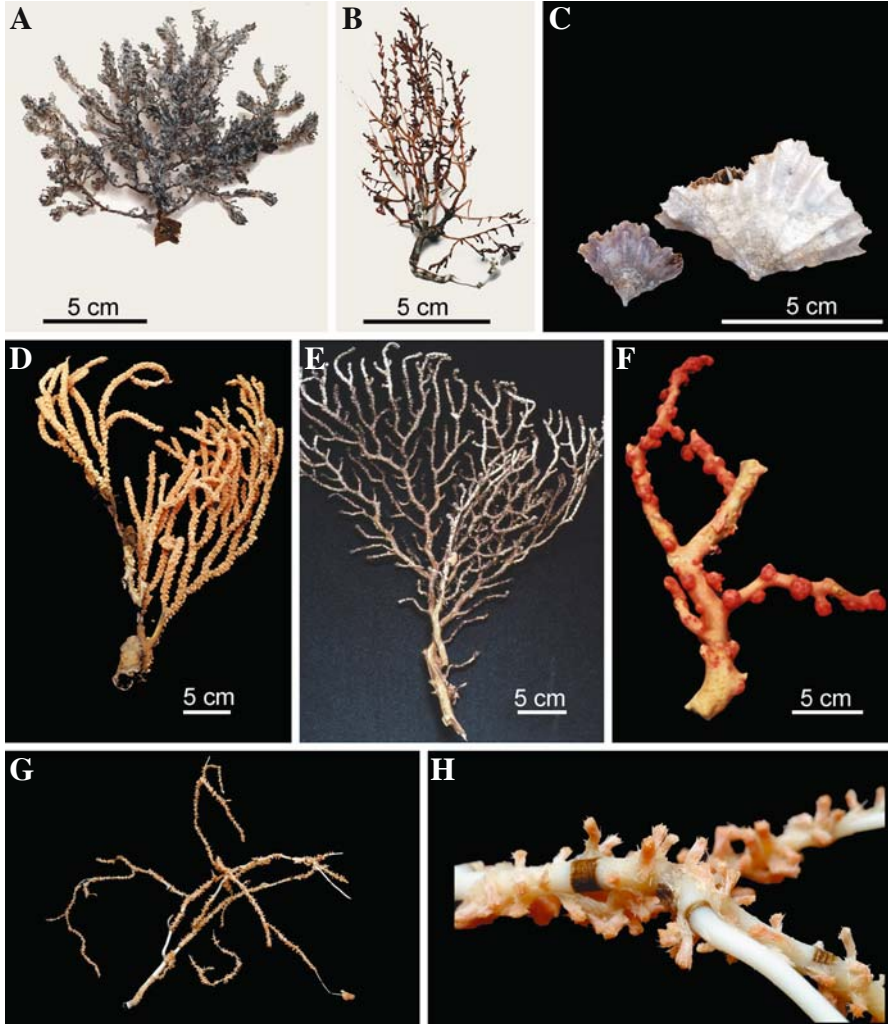
Fig. 1 Specimens collected from DFO groundfish trawl surveys 1999-2001. **A** *Acanthogorgia armata*; **B** *Acanella arbuscula*; **C** *Flabellum alabastrum;* **D** *Primnoa resedaeformis*; **E** *Paramuricea* spp.; **F** *Paragorgia arborea;* **G**, **H** *Keratoisis ornata;* Photos courtesy of Bio Photoshop
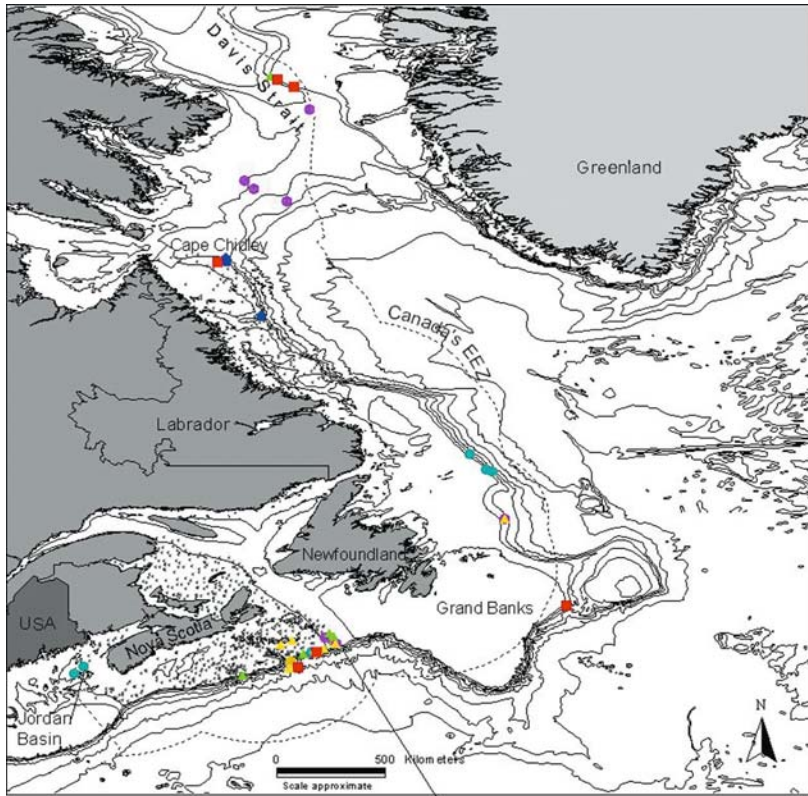
Fig. 2 The distribution of deep-sea corals off Atlantic Canada based on DFO groundfish trawl surveys from 1999-2001. Note: absence data was not available for three DFO southern Newfoundland and two Arctic surveys

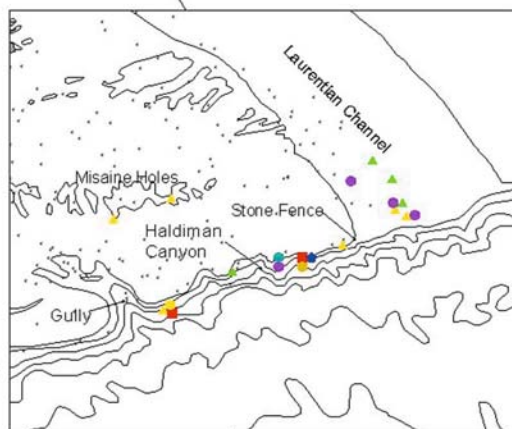| Species	No. of records*	Locations **	Depth range at each location (m)	No. of occurrences with other coral species
Acanella arbuscula	4 – M 1 – NF 5 – A 1 – FO (longline)	Haldiman Canyon (1T) Laurentian Channel (3T) Davis Strait (T5) Newfoundland Slope (1T) Northeast Channel (1FO)	281 400-441 468-1151 1400 283	*Acanthogorgia armata* (3) *Flabellum* spp. (2) *Paragorgia arborea* (2) *Paramuricea* spp. (1)
Acanthogorgia armata	6 – M 1 – NF	Eastern Scotian Shelf (1T) Stone Fence (T1) Laurentian Channel (2T) Misaine Holes (2T) Newfoundland Slope (1T)	439 380 400-419 164-201 1400	*Acanella arbuscula* (3) *Flabellum* spp. (1) *Keratoisis ornata* (1) *Paragorgia arborea* (1)
Flabellum spp.	5 – M 1 – A 1 – FO (otter Trawl)	Laurentian Channel (3T) Eastern Scotian Shelf (1FO; 2T) Davis Strait (1T)	419-453 278-510 516	*Acanella arbuscula* (2) *Acanthogorgia armata* (1) *Paragorgia arborea* (1)
Keratoisis ornata	2 – M	Eastern Scotian Shelf (2T)	393-439	*Acanthogorgia armata* (1) *Primnoa resedaeformis* (1) *Paragorgia arborea* (2)
Paramuricea spp.	3 – M 3 – NF 2 – FO (longline)	Jordan Basin (2T) Eastern Scotian Shelf (1T) Newfoundland Slope (3T) Northeast Channel (2FO)	154-222 281 449-1159 256-375	*Acanella arbuscula* (1) *Paragorgia arborea* (1) *Primnoa resedaeformis* (1)
Primnoa resedaeformis	1 – M 3 – NF 130 – FO (otter trawls, shrimp trawls, longlines and gillnets)	Jordan Basin (5FO) Northeast Channel (82FO) Stone Fence (2FO) Laurentian Channel (5FO) St. Pierre Bank (1FO) Cape Chidley (33FO, 2T) Labrador Shelf (1FO, 1T) Eastern Scotian Shelf (1T)	166-229 172-439 307-333 411-467 426 324-463 280-379 393	*Paragorgia arborea* (20) *Keratoisis ornata* (1) *Lophelia pertusa* (1) *Paramuricea* spp. (1)
Paragorgia arborea	2 – M 2 – NF 2 – A 35 – FO (otter trawls, shrimp trawls, longlines, gillnets)	Northeast Channel (18FO) SW Grand Banks (1FO) Labrador Shelf (2FO) Cape Chidley (13FO, 1T) Eastern Scotian Shelf (2T) NE Grand Banks (1T) Davis Strait (2T)	249-439 720 266-322 353-463 439-393 588 516-556	*Primnoa resedaeformis* (20) *Keratoisis ornata* (2) *Acanella arbuscula* (2) *Flabellum* spp. (1) *Acanthogorgia armata* (1) *Paramuricea* spp. (1)
Lophelia pertusa	1 – FO (otter trawl)	Jordan Basin (1FO)	166	*Primnoa resedaeformis* (1)

Strait, generally along the edge of the continental shelf (Fig. 2; Table 1). The group of records lying on the Scotian Shelf east from the Gully to the Laurentian Channel denotes the highest coral species richness, with records for all seven species.

Fisheries observer reports

During 2000 and 2001, fisheries observers on board vessels fishing from Nova Scotia made 170 bycatch records of six species of corals caught by four different gear types (Table 1). Corals were caught at depths ranging from 166 to 720 m. Similar to the trawl survey results, these records indicate a general trend of deep-sea corals along the edge of the continental shelf off Nova Scotia and Newfoundland, as well as several records from Jordan Basin (Fig. 3). There are two major clusters of records: 1) the southwestern side of the Northeast Channel with 104 coral catches and 2) east of Cape Chidley, Labrador, with 46 coral catches.

Fishermen's Local Ecological Knowledge

Twenty-six successful interviews with fishermen contributed to the information collected for the locations of corals. Ten of the fishermen had not caught corals and are not considered further. Ten of the 26 interviews were conducted in Cape Breton, two on mainland Nova Scotia and 14 in Newfoundland. Twelve (six from Nova Scotia and six from Newfoundland) of the 26 participants were retired from fishing, and at least four fishermen recounted memories from as early as the late 1940s and early 1950s. Seventeen participants were captains of their fishing vessels, three previous captains had recently become managers and were no longer going out to sea, two were crew members, three had identified themselves as both captain and crew members depending on the fishing vessel, and the status of one participant was not identified.

Using photos and sample specimens, the fishermen identified eight species of deep-sea corals and the general locations where they were caught. Table 2 presents the species identified, the locations where they were caught, the years the fishermen fished those locations, and the number of participants who reported coral catches from those locations. Figure 4 presents the map of the coral species and general locations where fishermen reported catching corals. The larger gorgonian species were often referred to as *trees* and were not identified to the species level. Two fishermen presented me with specimens they had kept: one specimen of *L. pertusa* caught on the Stone Fence and one specimen of an Antipatharian coral retrieved from the continental slope off Newfoundland.

In general, the reports of corals from Newfoundland are more recent than those from Nova Scotia. The inshore cod fishery occupied most fishermen until the Atlantic cod moratorium in 1992. Post moratorium, fishermen in Newfoundland have been fishing for crab, shrimp and turbot in offshore areas at depths and locations more suitable for corals.

Table 1 The coral fauna

* Maritimes Trawl Surveys (M); Newfoundland Trawl Surveys (NF); Arctic Trawl Surveys (A); Fisheries Observer (FO)
** T = Record from a Trawl Survey; FO = Record from a Fisheries Observer

Commonalities among the three sources of data

The three sources of data (i.e. the fisheries observer records, the DFO groundfish trawl surveys and LEK) provided data on the distribution of corals in Atlantic Canada. Further, the three sources provided both unique as well as overlapping data. The complete data set from all three sources is plotted in Figure 5.

The DFO fisheries observer records and trawl surveys both revealed corals found in Jordan Basin, but different species were recorded. None of the fishermen interviewed fished as far west as Jordan Basin and the Northeast Channel, thus
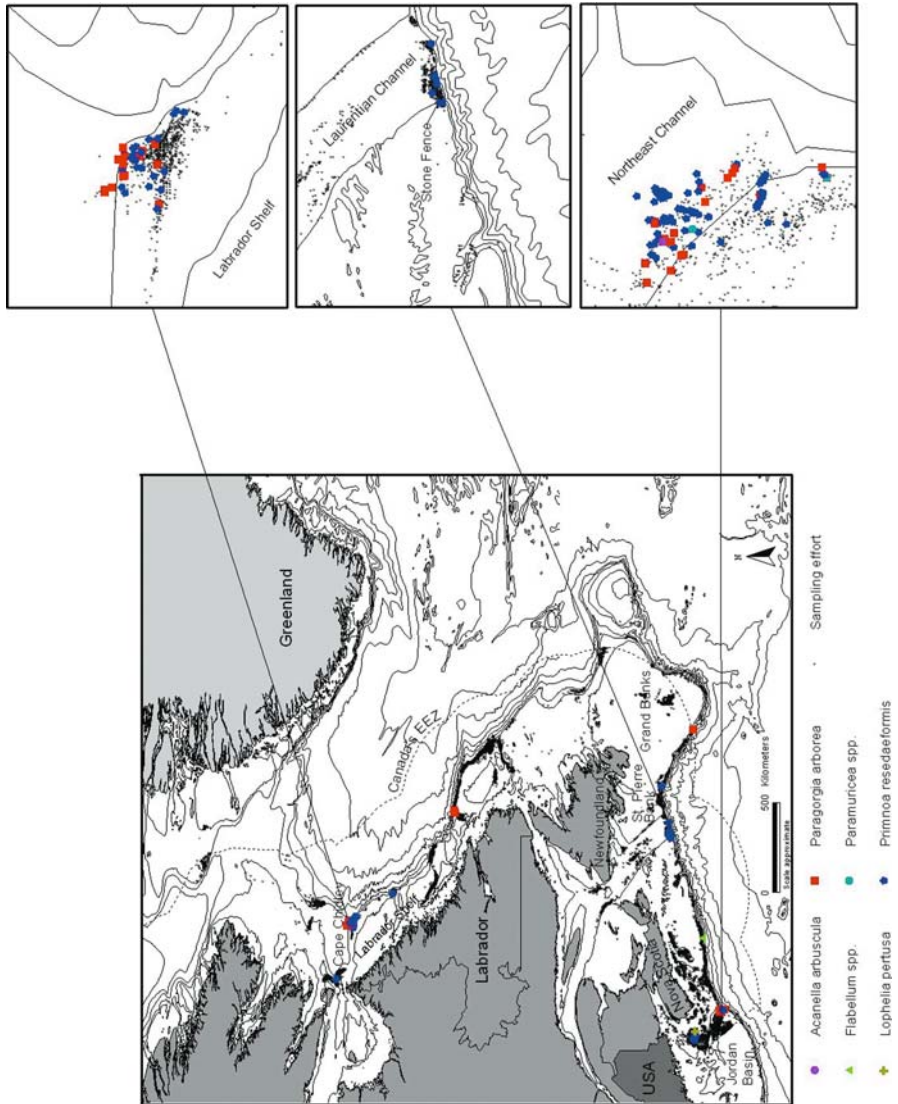

Fig. 3 The distribution of deep-sea corals based on fisheries observer records for 2000-2001

Table 2 Results from fishermen's LEK

Species	Location	Years fished	No. of participant(s)
Acanella arbuscula	Edges of holes on Misaine Bank	1965-1990	1
	Continental Shelf and Slope off Nfld. & Labrador	1976-2001	3
	Funk Islands	1992-2001	1
Keratoisis ornata	Stone Fence	1948-1974	1
	Gulf of Saint Lawrence	1984-1985	1
	North of Grand Banks at EEZ	1992-2001	1
Paragorgia arborea	Emerald Basin		1
	Edge of holes on Misaine Bank	1965-1990	1
	Stone Fence	1948-2001	4
	Gully	1969-2001	2
	Southern Edge of Banquereau Bank	1980-2001	1
	Edge of St. Pierre Bank	1980-2001	1
	North of Grand Banks at EEZ	1952-2001	1
	Continental edge & slope off Nfld.	1987-2001	3
	Funk Islands	1970-1990	1
Paramuricea spp.	On Banks off Cape Breton	1974-1998	1
	Edges of holes on Misaine Bank	1965-1998	2
	Tail of the Bank	1992-2001	1
	North of Grand Banks at EEZ	1992-2001	1
	Continental shelf edge and slope off Nfld.	1992-2001	2
Primnoa resedaeformis	St Ann's Bank	1975-1995	1
	Edges of holes on Misaine Bank	1965-1990	1
	Gully	1948-2001	3
	Stone Fence	1948-2001	3
	Southern edge of Banquereau Bank	1980-2001	1
	Edge of St Pierre Bank	1980-2001	1
	North of Grand Banks at EEZ	1992-2001	1
	Funk Islands	1992-2001	1
	Continental Shelf Slope off Nfld.	1992-2001	1
	Off Cape Spear	1986-2001	1
	North of Labrador	1998	1
Trees	Stone Fence	1934-1992	4
	Edge of Laurentian Channel	1962-1992	1
	Gully	1934-1993	3
	Southern edge of St. Pierre Bank Southeast edge of Grand Banks at EEZ North of Grand Banks at EEZ North edge of shelf	1992-2001	1
Flabellum spp.	Middle of the Scotian Shelf Most westerly location seen on map	1980-present	1
Lophelia pertusa	Edges of holes on Misaine Bank	1965-1990	1
	Stone Fence	1934-2001	3
	Gully	1934-1980	1
Antipatharian	Continental Slope off Nfld	2000-2001	1

the DFO provided a complementary data source. The Northeast Channel was not sampled by the DFO trawl surveys and therefore fisheries observer records were the only source of data for this location.

Further northeast along the edge of the Scotian Shelf, there were two reports of *Flabellum* spp., one from a fisherman and one from a fisheries observer record. Reports of corals in the Gully only came from fishermen. There were five trawl survey stations in this area and five fisheries observer records in this area, none of which reported coral catches. Reports of corals in and around the holes in the

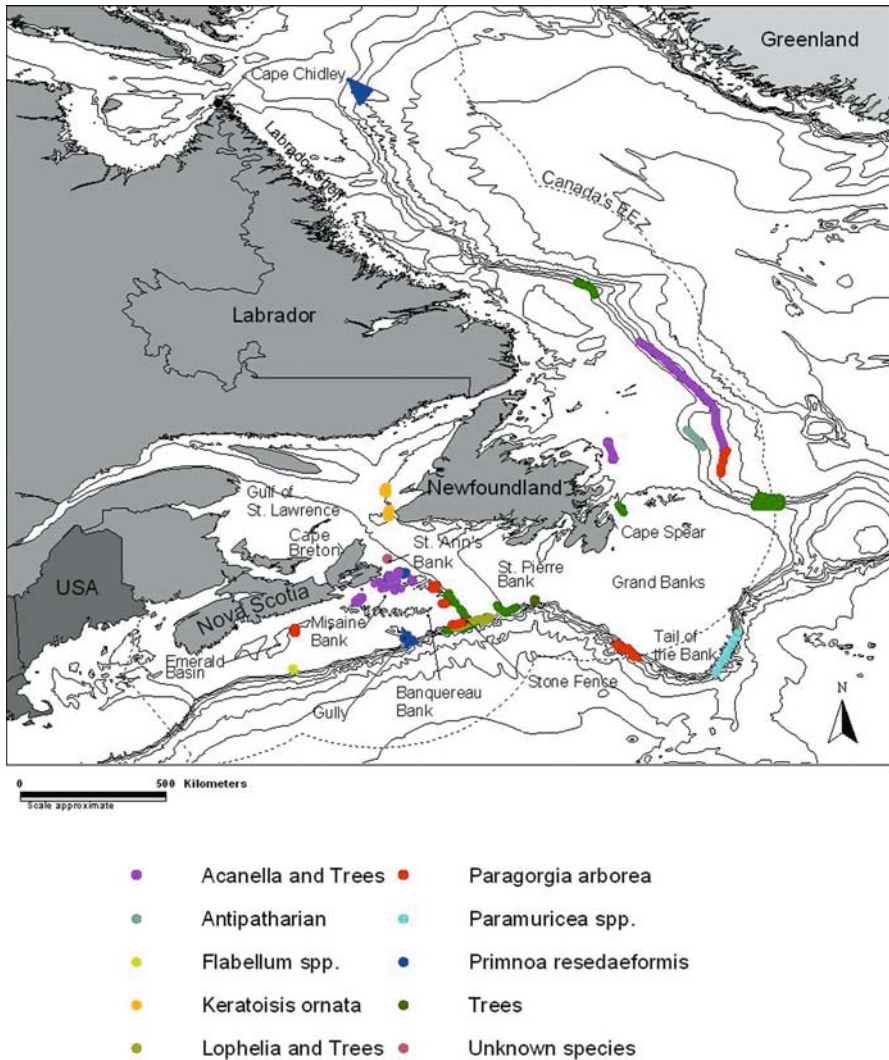|	Acanella and Trees	●	Paragorgia arborea
●	Antipatharian	●	Paramuricea spp.
●	Flabellum spp.	●	Primnoa resedaeformis
●	Keratoisis ornata	●	Trees
●	Lophelia and Trees	●	Unknown species

Fig. 4 The distribution of deep-sea corals as identified by fishermen's local ecological knowledge. Note: in several cases large gorgonian species were referred to as *trees* and were not identified to the species level

inshore areas off Cape Breton primarily came from fishermen. The exception was further offshore, with two reports from trawl surveys of *A. armata* in and on the edges of the Misaine Holes.

All three sources of data identified coral locations on the Stone Fence. Both fisheries observers and fishermen's reports indicated that corals are present on the southern edge of St. Pierre Bank. The fisheries observers reported *P. resedaeformis* and the fishermen reported *trees*. Fisheries observer records and fishermen's reports on the southwest side of the Grand Banks just inside the 200-mile EEZ overlapped, with both sources reporting the presence of *P. arborea*.

Changes in coral abundances observed by fishermen

Seven fishermen said that they had noticed changes in the abundance of deep-sea corals over time. Three fishermen reported decreases in the number of corals seen on the eastern Scotian Shelf. One participant fished from 1970-1990 and commented that in the early 1980s he did not see the large corals that he saw in the 1970s. In particular, he reported that the Stone Fence is now "as level as a table", and "is a desert compared to what it used to be". He attributed these changes to the impacts of bottom trawlers. Another participant also commented on seeing changes on the Stone Fence over a 10-year period starting in 1958. The first six years he fished the Stone Fence, he stated he could fill his dory (a small rowing boat) with corals caught on his fishing lines. By the 10th year of fishing on the Stone Fence he reported that the corals were gone. He attributed the disappearance of corals to the large trawlers that began fishing in the area for redfish and cod in 1964. Another fisherman also commented that from the 1950s to mid 1970s, he noticed a decrease in the number of corals he saw on the Stone Fence and also attributed the changes to the impact of bottom trawling in the area. However, a fisherman who still longlines on the Stone Fence stated that he saw fairly large pieces of coral on the Stone Fence in 2000, indicating there are some existing coral colonies or coral aggregations.

Two fishermen, one who has fished in deep-water since 1987 and another who has been fishing in deep-water since 1992, remarked that they had not seen any changes in the abundance of corals on the continental slope off Newfoundland. Such statements suggest that there may have been lower impacts of fishing in this area during this time period.

Discussion

Using three sources of information, the fishermen's LEK, fisheries observer records, and DFO groundfish trawl surveys, proved to be an effective way to gather data on the location of deep-sea corals. In several cases, coral locations from different sources of data overlapped, enhancing confidence in the reliability of each method. Each method also provided unique locations thereby expanding the results beyond what would have been found by the use of only one or two of these methods. Fishermen were able to identify species and their locations and demonstrated that LEK is valuable and provides historical data largely unavailable from any other source. Cumulatively, the fishermen provided data from a large spatial area.

- • DFO groundfish trawl surveys

- • Fisheries Observer Reports
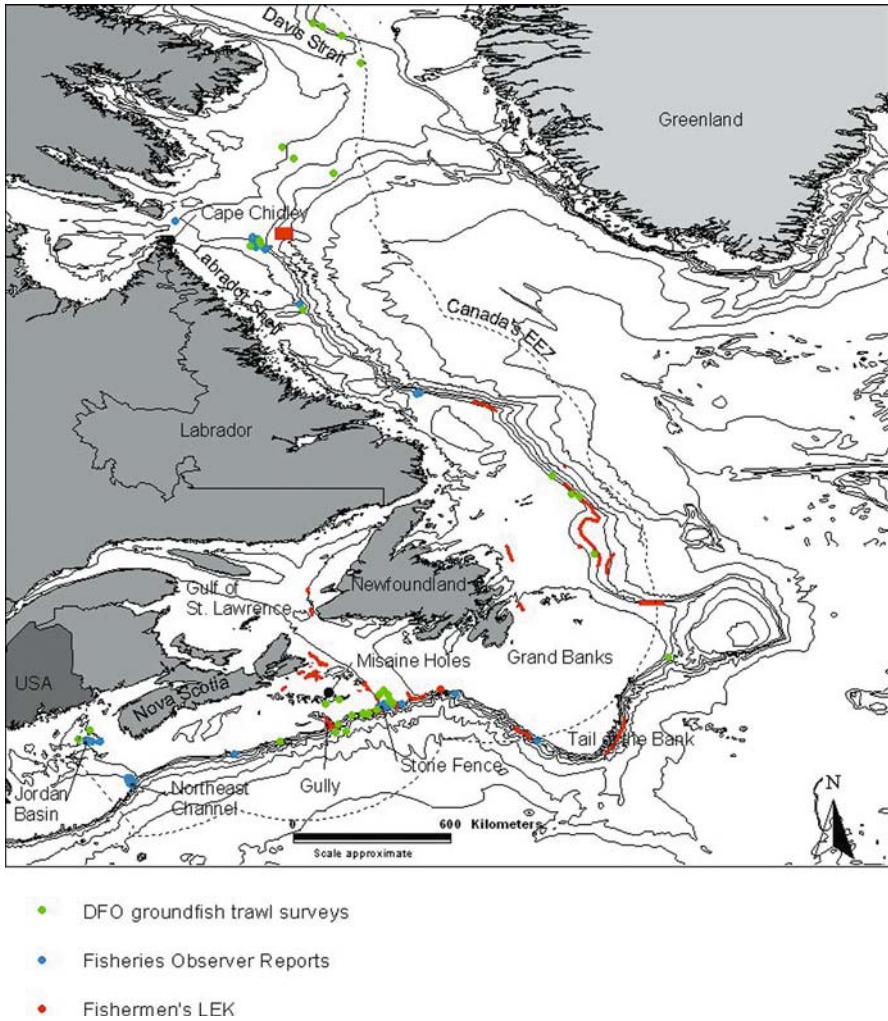
- • Fishermen's LEK

Fig. 5 The distribution of deep-sea corals off Atlantic Canada based on data collected from DFO groundfish trawl surveys, fisheries observer records and fishermen's local ecological knowledge

Locations identified by fishermen, especially those that were identified by more than one participant, can be made available to scientists to assist in planning surveys of deep-sea corals using remotely operated vehicles or submersibles.

The results from this study confirm and add to the existing knowledge about the distribution of deep-sea corals in Atlantic Canada. The distribution of six species of gorgonians and two scleractinian species were further clarified from previous reports (Breeze et al. 1997; Mukhida and Gass 2001). *Paramuricea placomus* and *Paramuricea grandis* are difficult to differentiate and hence were not identified to

the species level. Furthermore, it is difficult for fishermen and fisheries observers to distinguish between the three species of *Flabellum* (*F. alabastrum, F. macandrewi, and F. angulare*). Only *F. alabastrum* was included in the identification guide, creating an obvious bias for this identification. In addition to these species, Breeze et al. (1997) confirmed the presence of *Anthothelia grandiflora*, *Radicipes gracilis* and *Javania cailleti*. It is possible that these species were not confirmed here because they were not included on the identification guide. However, a new species to Atlantic Canada, thought to be *Bathypathes arctica* from the order Antipatharia, was discovered.

The known range of several species was expanded particularly in the case of species identified offshore of Newfoundland and Labrador. New locations were identified for the reef building coral *L. pertusa*. This species is likely rare in Atlantic Canadian waters as this area represents its northern limit in the Northwest Atlantic (Zibrowius 1980).

Areas of special interest off Nova Scotia

Several areas of special interest near Nova Scotia were identified in the study with respect to coral abundance and/or diversity.

Jordan Basin

Jordan Basin was not included in the coral distribution study by Breeze et al. (1997). Tendal (1992) presented records of *P. arborea* from this region and Verrill (1878) presented records of *P. resedaeformis* from the mouth of the Bay of Fundy. Furthermore, records of *P. resedaeformis* and *Paramuricea* spp. from this area have recently been confirmed by researchers at the University of Maine (Watling, unpublished observation). Corals in this area were found at relatively shallow depths for these species. Although *L. pertusa* has been reported to occur off Nova Scotia (Hecker et al. 1980; Zibrowius 1980; Breeze et al. 1997), very few records exist which include specific locations. Therefore the report of a specimen caught in Jordan Basin is valuable and provides more detail about the occurrence of this species.

Northeast Channel

Several maps based on fishermen's LEK highlight the Northeast Channel as an area with particularly high coral abundance (Goode 1887; Breeze et al. 1997; Willison et al. 2002). Data collected by the fisheries observers indicate high concentrations of *P. resedaeformis* and *P. arborea* on the Georges Bank side of the Northeast Channel. In 2000 and 2001, the Northeast Channel was surveyed using a towed camera system that confirmed a high abundance of corals (MacIsaac et al. 2001; Mortensen and Buhl-Mortensen 2004).

Eastern Scotian Shelf

The present study demonstrates that the region along the edge of the continental shelf between the Laurentian Channel and the Gully has relatively high coral species richness. There were records for all gorgonians and scleractinians reported in the

current study, including fishermen's reports of *L. pertusa* in the Gully and along the edge of continental shelf near the Stone Fence. This area also contains the two records of *K. ornata* reported from the DFO groundfish trawl surveys. The small number of reports of *K. ornata* suggests that it may be relatively rare compared to the other coral species identified in this study. Collins (1884) recalled catching the greatest concentration of it along the middle prong on the edge of Banquereau Bank, which is in the centre of this region. The Gully was also identified as a significant coral area by a number of longline fishermen, however, no reports came from the other sources. This could be attributed to a patchy distribution of corals which may exist in the Gully and because the steep nature of the canyon makes it unfavorable for trawling.

Gulf of Saint Lawrence

The report of *K. ornata* from the Gulf of St. Lawrence not only extends the known range of *K. ornata* beyond the Scotian Shelf as described by Collins (1884), Verrill (1878), Verrill (1883), Deichmann (1936), Miner (1950), and Breeze et al. (1997), but also represents the first record of corals from the Gulf of St. Lawrence region. *K. ornata* is also a species of interest because it has only been reported from Atlantic Canada and therefore may be an endemic species.

Stone Fence

Breeze et al. (1997) identified the Gully and the Northeast Channel as two main hotspots of coral abundance near Nova Scotia. The present study confirms a high abundance of corals in the Gully based on reports from fishermen. However, several fishermen, who fished both the Gully and Stone Fence, identified the Stone Fence as hosting the largest specimens and the greatest abundance of corals. Furthermore, there were four reports of *L. pertusa*, a relatively rare species, from the area. Several *L. pertusa* reefs concentrated in one area on the Stone Fence have recently been precisely located (see below). Collins (1884) referred to the region of the Stone Fence as the place of greatest abundance of *P. resedaeformis* and Goode (1887 Explanation of Chart No. 4, XVII) remarked that the Stone Fence "is noted for the great abundance of corals growing on the bottom". Finally, Litvin and Rvachev (1963) also depict corals present on the Stone Fence in their description of bottom deposits in the region.

Newfoundland and Labrador

There are few previous references to corals off Newfoundland and Labrador. Therefore, the records presented here have greatly increased existing knowledge of the distribution of corals in this region. Litvin and Rvachev (1963) described five occurrences of corals in their description of the sediment deposits on the Grand Banks and on the shelf and slope of northern Newfoundland and Labrador. Tendal (1992) described two records of *P. arborea* on the slope of the Grand Banks. The present study identified six gorgonian, one scleractinian, and one antipatharian species off Newfoundland and Labrador. All of these species were also found off Nova Scotia, except for the antipatharian that has not been previously recorded in Atlantic Canada.

Corals from the order Antipatharia are commonly known as the black or thorny corals and are typically organisms found in deeper and abyssal ocean waters (Hyman 1940). They are rare in the Northwest Atlantic north of the southern US (Kramp 1932). The specimen reported here was collected from the continental slope at a depth between 800 and 1000 m. It is likely that this specimen is *Bathypathes arctica* as it is the only species of antipatharian reported this far north in the western Atlantic. The species was first described as *Antipathes arctica* by Lütken in 1871, when it was taken from the stomach of a shark captured off the coast of northern Greenland (Brook 1889). It was later removed from the genus *Antipathes* and referred to *Bathypathes* by Pax in 1932. It has since been reported west of Greenland at depths of 1100-1200 m (Kramp 1932; Pax 1932) and northeast of the Faroe Islands (Pax 1932).

The data presented in this study overlap with several earlier reports of Newfoundland corals. Litvin and Rvachev (1963) reported corals on the northeast side of the Grand Banks, which is at a shallower depth but similar latitude to a DFO groundfish trawl survey record. In addition, their locations of corals off northern Newfoundland overlap with reports from fishermen and DFO groundfish trawl surveys. One discrepancy with previous coral distributions lies with Tendal (1992) who equates the lack of *P. arborea* off the Labrador coast to the low temperatures found in these areas (he reports temperatures of 3.0-3.5°C). Regardless of the cool temperatures, which were recorded during the DFO groundfish trawl surveys to be between 3.4-4.4°C, all three sources of information in the current study provide data for corals, including *P. arborea*, off the Labrador coast.

The depths and location records for *A. arbuscula* from the present study are consistent with previous reports. Miner (1950) described *A. arbuscula* as abundantly distributed in deep-water on the banks off Nova Scotia and Newfoundland. Opresko (1980) also described *A. arbuscula* to occur as far north as Newfoundland. The present study, and especially the information provided by Newfoundland fishermen, confirms this information. It would appear however, based on information collected from the interviews, that *A. arbuscula* is more common off Newfoundland than other coral species. In one instance, roughly a hundred specimens of *A. arbuscula* were seen scattered on a wharf and tangled in a gillnet in a fishing village in Newfoundland. Specimens of *A. arbuscula* collected from this wharf were shown during the following interviews and this may have increased the probability of fishermen reporting it. Moreover, it is possible that *A. arbuscula* is more easily caught by gillnets compared with other species. *A. arbuscula* is one of the few species that does not require hard substrate on which to attach but rather has a root-like structure that is used as a support in soft sediments (Opresko 1980). This may make it more susceptible to being taken in gillnets compared with other species which are more firmly attached to hard substrate such as rocks and boulders.

The data presented here for *Paramuricea* spp. off northern Newfoundland extend its range beyond previous records from off New England, Nova Scotia and on the Grand Banks (Verrill 1883; Deichmann 1936; Miner 1950; Opresko 1980; Breeze et al. 1997).

Conservation concerns and actions

The results from the interviews, in addition to the past reports made by Goode (1887), Whiteaves (1901), Verrill (1922), and Breeze et al. (1997), reveal that fishermen working off Nova Scotia have been catching corals throughout the late 19th and 20th centuries and continue to catch them today. The fisheries observer records and the interviews with fishermen point to three gear types that catch corals: bottom trawls for groundfish and shrimp, bottom longlines, and set gillnets. Results from the interviews with fishermen in Nova Scotia report significant change to bottom habitats on the eastern Scotian Shelf, and in particular the disappearance of hard bottom and decreases in the size and number of the corals on the Stone Fence. They attribute these changes to damage caused by mobile bottom trawls. Although fishermen attribute the major changes to mobile bottom trawls, fishermen fishing with fixed gear also reported coral catches. The proportion of damage caused by mobile *versus* fixed gear remains unclear. The extent of damage to corals as a result of fixed gears has been documented in the Northeast Channel where 4 % of colonies where damaged; there was no evidence that trawling occurred in the area (Mortensen et al. 2004). However, trawling is a mobile fishing gear which covers a greater surface area of the seabed and is accompanied by a greater force resulting in more destructive potential when it comes into contact with the seabed and corals. Also, there is some incentive for fixed gear fishermen to avoid coral areas because their gear can be snagged. As in all cases, the degree of impact will depend on the level of fishing effort in coral areas.

The majority of references to corals on the Stone Fence are based on data collected prior to 1965 (Collins 1884; Goode 1887; Litvin and Rvachev 1963; Breeze et al. 1997). In addition, reports made by fishermen reported here refer to catches made prior to 1992, in several cases prior to 1980, and in one case prior to 1970. Therefore, the present state of coral communities on the Stone Fence remains unclear. There was, however, one fisherman who continues to longline in this area and who reported catching pieces of *P. resedaeformis* in 2000. Furthermore, fisheries observers report several catches of *P. resedaeformis* from the Stone Fence, and the DFO groundfish trawl surveys caught a specimen of *A. armata* in the area. A DFO survey in 2002 using a towed camera has confirmed the presence of one piece of live *L. pertusa* among *Lophelia* rubble on the Stone Fence (personal observation; Auld 2002). A second DFO survey in 2003 returned to the same area and found a one kilometre by 500 m area of *L. pertusa* reefs, 99 percent of which was described as rubble and appeared to have been damaged by bottom trawlers (Mortensen pers. comm. 2003; Sayfy et al. 2003). Although there are indications that corals still exist on the Stone Fence, there does not appear to be the outstanding abundances that were reported at the end of the 19th century and first half of the 20th century. As a result of the recent findings and efforts by local non-government environmental organization, consultations are currently underway regarding the design of a closed area to protect the *L. pertusa* reefs.

Interviews with fishermen in Newfoundland suggest that corals were not caught in the Atlantic cod fishery, which was the major fishery off Newfoundland prior to

the cod fishing moratorium in 1992. Since 1992, Newfoundland fishermen focused more of their fishing efforts on shrimp, snow crab, and offshore groundfish such turbot. It appears that fishermen in the deep-water turbot fishery on the continental slope off Newfoundland are catching corals. The turbot fishermen, however, have not noticed a change in bottom type or coral abundance over the past ten years. This may not reflect the actual situation as it could take some time before coral abundance falls noticeably, by which time the impact may likely be considerable.

The discovery of a specimen of an antipatharian coral, an order not yet recorded in Atlantic Canada and caught in deep-water (800-1200 m), is an indication of how little is known about benthic communities beyond the continental shelf. Therefore, although the fishermen have not noticed a change in the abundance of corals off Newfoundland, caution should be applied when carrying out potentially harmful activities in unfamiliar environments.

The fisheries observer data reveal two areas that have experienced relatively high coral catches in the past two years in Atlantic Canada. These are the Northeast Channel off southwest Nova Scotia and the region east of Cape Chidley, Labrador. In both cases, the majority of the records are of *P. resedaeformis* and to a lesser extent *P. arborea*. The coral catches reported from the Northeast Channel were caught using longline, bottom trawls and gillnets, and therefore the data are derived from only 5-10 % of the total catches from that area assuming that the fisheries observer program reached its observer coverage targets. This contrasts with the reports from the Northern Shrimp fishery east of Cape Chidley which has 100 % observer coverage.

The Northeast Channel has been attracting much attention over the past two years based on the efforts of fishermen (see Willison et al. 2002), earlier reports of corals by Breeze et al. (1997), and the results of two consecutive years of DFO and Dalhousie University surveys of the coral communities in this region (Mortensen and Buhl-Mortensen 2004). As a result of these surveys, and the increased public awareness of the need to protect deep-sea corals in Nova Scotia, a Coral Conservation Area fishery closure was established in the Northeast Channel in 2002 (DFO 2002).

Unlike the Northeast Channel, the region showing high coral catches off Labrador has had no consideration regarding protecting the corals in the area. Fisheries observers started recording coral bycatch data in 2000. Therefore, we do not know the extent of damage prior to this time. This region merits further exploration using video and photographic surveys to assess the status of the coral communities in this region.

The Gully has been identified as an Area of Interest (AOI) under Canada's Oceans Act. The AOI is currently undergoing the process to be designated a permanent marine protected area. The Gully initially attracted attention because it is home to an endangered population of the Northern Bottlenose Whales, however, subsequent information came to light that the Gully also provides habitat for deep-sea corals and is an area of relatively high coral species richness on the Scotian Shelf (Breeze et al. 1997; MacIsaac et al. 2001).

Recent efforts to protect known hotspots of deep-sea corals off Nova Scotia are positive steps towards the long term survival of this group of species, however, the

full extent of damage to coral populations as a result of fishing activities off Atlantic Canada remains unknown. A suggestion for future research is to use predictive models to gain insight into suitable habitats for corals off Atlantic Canada and to overlay this distribution with past and present fishing effort (i.e. longlines, gillnets and bottom trawls). This may elucidate the potential extent of damage which has occurred over the past century and the areas which remain under threat. This will ultimately assist to focus conservation efforts in areas where they will be most effective.

Acknowledgements

References

Auld A (2002) We couldn't believe our eyes: Scientists find reef building coral near Sable Island. September 25, 2002 edition. Halifax Herald Ltd. (Accessed at http://www.herald.ns.ca/stories/2002/09/25/f163.raw.html)

Auster PJ, Langton RW (1999) The effects of fishing on fish habitat. Amer Fish Soc Symp 22: 150-187

Babbie ER (1992) The Practice of Social Research. Wardsworth Publishing Company, Belmont, California

Breeze H, Davis DS, Butler M, Kostylev V (1997) Distribution and status of deep-sea corals off Nova Scotia. Marine Issue Comm Spec Publ 1. Ecology Action Centre, Halifax, NS

Brook G (1889) Report on the Antipatharia. Rep Sci Results Voyage Challenger. Zoology 32: 1-222

Collins JW (1884) On the occurrence of corals on the Grand Banks. Bull US Fish Comm, 237

Deichmann E (1936) The Alcyonaria of the western part of the Atlantic Ocean. Mem Mus Comp Zool 53. Cambridge US, Harvard College

DFO (1999) Teleost Trip No. 85, October 22 – November 5, 1999. NAFO Division 2GH. Department of Fisheries and Oceans, Science, Oceans and Evironment Branch, St. John's Newfoundland

DFO (2001) DFO NF – Fisheries Management - Observer Program. (Accessed at http://nfl.dfo-mpo.gc.ca/FM/cp/observers/)

DFO (2002) Backgrounder: Deep-sea coral research and conservation in offshore Nova Scotia. DFO Communications. (Accessed at http://www.mar.dfo-mpo.gc.ca/communications/maritimes/back02e/B-MAR-02-(5E).html)

Fischer J (2000) Participatory research in ecological fieldwork: a Nicaraguan study. In: Neis B, Felt L (eds) Finding our Sea Legs: Linking Fishery People and their Knowledge with Science and Management. Inst Soc Econ Res, Memorial University, St. John's, Newfoundland, pp 41-54

Fosså JH, Mortensen PB, Furevik DM (2000) *Lophelia* coral reefs in Norway: distribution and effects of fishing. Inst Marine Res, Bergen, 94 pp

Fuller S, Cameron P (1998) Marine Benthic Seascapes: Fishermen's perspective. Ecology Action Centre, Halifax, Nova Scotia, 64 pp

Gass S (2003) Conservation of deep-sea corals in Atlantic Canada. World Wildlife Fund Canada, Toronto, Ontario, 54 pp

Goode GB (1887) The fisheries and fishery industries of the United States. Section III: The fishing grounds of North America. US Comm Fish Fisheries Washington, 238 pp

Hecker B, Blechschmidt G, Gibson P (1980) Final report – Canyon assessment study in the Mid and North Atlantic areas of the U.S. outer continental shelf. US Dept Interior, Bureau Land Manage, Washington, DC

Hutchings JA (1996) Spatial and temporal variation in the density of Northern Cod and a review of hypotheses for the stock's collapse. Canad J Fish Aquat Sci 53: 943-962

Hyman LH (1940) The Invertebrates: Protozoa through Ctenophora. McGraw-Hill, New York, 726 pp

International Council for the Exploration of the Sea (ICES) (2000) Effects of different types of fisheries on North Sea and Irish Sea benthic ecosystems: review of the IMPACT II Report. Int Council Explor Sea, Copenhagen, Denmark

Johannes RE (1981) Words of the Lagoon: fishing and marine lore in the Palau District of Micronesia. Univ California Press, Berkeley, California, 245 pp

Jones DP, Willison JHM (2001) The role of the Canadian Ocean Habitat Protection Society in deep-sea coral education and conservation advocacy in Nova Scotia. In: Willison JHM, Hall J, Gass SE, Kenchington ELR, Butler M, Doherty P (eds) Proceedings of the First International Symposium on Deep-sea Corals. Ecology Action Centre and Nova Scotia Museum, Halifax, NS, pp 166-174

Koslow JA, Gowlett-Holmes K (1998) The seamount fauna off southern Tasmania: benthic communities, their conservation and impacts of trawling. Final Rep Environ Australia Fish Res Dev Corp, Australia, 104 pp

Koslow JA, Gowlett-Holmes K, Lowry JK, O'Hara TO, Poore GC, Williams A (2001) Seamount benthic macrofauna off southern Tasmania: community structure and impacts of trawling. Mar Ecol Prog Ser 213: 11-125

Kramp PL (1932) The Godthaab expedition 1928 Alcyonaria, Antipatharia, and Madreporaria. Medd Gronland 79: 1-20

Krieger KJ (2001) Coral (*Primnoa*) impacted by fishing gear in the Gulf of Alaska. In: Willison JHM, Hall J, Gass SE, Kenchington ELR, Butler M, Doherty P (eds) Proceedings of the First International Symposium on Deep-sea Corals. Ecology Action Centre and Nova Scotia Museum, Halifax, NS, pp 106-116

Litvin VM, Rvachev VD (1963) The bottom topography and sediments of the Labrador and Newfoundland fishing areas. In: Marti YY (ed) United States Department of the Interior and the National Science Foundation (Translated from Russian)

Lutken C (1871) En ny sortkoral fra Polarhavet. Overs. K Danske Vidensk Slesk Forhandl 2: 18-26

MacIsaac K, Bourbonnais C, Kenchington E, Gordon D, Gass S (2001) Observations on the occurrence and habitat preference of corals in Atlantic Canada. In: Willison JHM, Hall J, Gass SE, Kenchington ELR, Butler M, Doherty P (eds) Proceedings of the First International Symposium on Deep-sea Corals. Ecology Action Centre and Nova Scotia Museum, Halifax, NS, pp 58-75

Mailhot J (1994) Traditional ecological knowledge: the diversity of knowledge systems and the study. Great Whale Environ Assess, Montreal, QC, 50 pp

Maurstad A (2000) Trapped in biology: an interdisciplinary attempt to integrate fish harvesters' knowledge into Norwegian fisheries management. In: Neis B, Felt L (eds) Finding our Sea Legs: Linking Fishery People and their Knowledge with Science and Management. Inst Soc Econ Res, Memorial University, St. John's, Newfoundland, pp 135-152

Miner RW (1950) Field Book of Seashore Life. G.P. Putnam's Sons, New York

Mortensen PB, Buhl- Mortensen L, Gordon DC, Fader GBJ, McKeown DL, Fenton DG (2004) Effects of fisheries on deep-water gorgonian corals in the Northeast Channel, Nova Scotia (Canada). In: Thomas J, Barnes P (eds) Proceeding from the Symposium on the Effects of Fishing Activities on Benthic Habitats: Linking Geology, Biology, Socioeconomics and Management. Amer Fish Soc, November 12-14, 2002, Florida, USA

Mortensen PB, Buhl-Mortensen L (2004) Distribution of deep-water gorgonian corals in relation to benthic habitat features in the Northeast Channel (Atlantic Canada). Mar Biol 144: 1223-1238

Mortensen PB, Buhl-Mortensen L (2005) Deep-water corals and their habitats in The Gully, a submarine canyon off Atlantic Canada. In: Freiwald A, Roberts JM (eds) Cold-water Corals and Ecosystems. Springer, Berlin Heidelberg, pp 247-277

Mukhida A, Gass SE (2001) Corals of the Maritime Provinces of Canada: an illustrated guide. Unpubl Doc, School Resource Environ Stud, Dalhousie Univ, Halifax, NS

Neis B, Felt L (2000) Finding our Sea Legs: Linking Fishery People and their Knowledge with Science and Management. Inst Soc Econ Res, Memorial University, St. John's, Newfoundland,

Neis B, Sneider DC, Felt L, Haedrich RL, Fisher J, Hutchings JA (1999) Fisheries assessment: what can be learned from interviewing resource users? Canad J Fish Aquat Sci 56: 1949-1963

Opresko DM (1980) Taxonomic description of some deep-sea octocorals of the Mid and North Atlantic. In: Hecker BG, Blechschmidt G, Gibson P. (eds) Final report – Canyon Assessment Study in the Mid and North Atlantic areas of the U.S. Outer Continental Shelf. Appendix B. US Dept Interior, Bureau Land Manage, Washington, D.C.

Pax F (1932) Die Antipatharien und Madreporarien des arktischen Gebietes. Fauna Arctica 6: 267-280

Philippart CJM (1998) Long-term impacts of bottom fisheries on several by-catch species of demersal fish and benthic invertebrates. ICES J Mar Sci 55: 342-352

Probert PK, McKnight DG, Grove SL (1997) Benthic invertebrate bycatch from a deep-water trawl fishery, Chatham Rise, New Zealand. Aquat Conserv 7: 27-40

Sayfy A, Willison M, Sheppard V, Millar D (2003) Canada's first ever coral reef discovered; conservation measures urgently needed. Newsl CPAW Nova Scotia Issue 3: 7

Tendal OS (1992) The North Atlantic distribution of the octocoral *Paragorgia arborea* (L., 1758) (Cnidaria, Anthozoa). Sarsia 77: 213-217

Verrill AE (1864) List of the polyps and corals sent by the Museum of Comparative Zoology to other institutions in exchange, with annotations. Bull Mus Comp Zoology 1: 29-60

Verrill AE (1878) Canadian Naturalist. Second Ser 8: 476. (Cited in Whiteaves JF Catalogue of the Marine Invertebrata of Eastern Canada. 32. S.E. Dawson, Ottawa.)

Verrill AE (1883) Results of the explorations made by the steamer "Albatross", off the Northern Coast of the United States in 1883. US Comm Fish Fisheries, Comm Rep, 2, Appendix D, Nat Hist Biol Res

Verrill AE (1922) The Alcyonaria of the Canadian Arctic Expedition, 1913-1918, with a revision of some other Canadian genera and species. Rep Canad Arctic Exped 8, Mollusks, Echinoderms, Coelenterates, etc. Part G: Alcyonaria and Actinaria

Watling L, Norse EA (1998) Disturbance of the seabed by mobile fishing gear: a comparison to forest clearcutting. Conserv Biol 12: 1180-1197

Whiteaves JF (1901) Catalogue of the marine Invertebrata of Eastern Canada. Geological Survey of Canada, Ottawa, 271 pp

Willison JHM, Hall J, Gass SE, Kenchington ELR, Butler M, Doherty P (2001) Proceedings of the First International Symposium on Deep-sea Corals. Ecology Action Centre and Nova Scotia Museum, Halifax, NS, 231 pp

Willison JHM, Jones DP, Atwood S (2002) Deep-sea corals and marine protected areas in Nova Scotia. In: Bondrup-Nielsen S, Munro NWP, Nelson G, Willison JHW, Herman TB, Eagles P (eds) Managing Protected Areas in a Changing World. SAMPAA, Wolfville, Canada, pp 1157-1163

Zibrowius H (1980) Les Scleractinaires de la Méditerranée et de l'Atlantique nord-oriental. Mem Inst Oceanogr Found Albert I, Prince de Monaco, 247 pp

Deep-water corals and their habitats in The Gully, a submarine canyon off Atlantic Canada

Pål B. Mortensen, Lene Buhl-Mortensen

Benthic Habitat Research Group, Institute of Marine Research, P.O. Box 1870
 Nordnes, N-5817 Bergen, Norway
 (Paal.Mortensen@IMR.no)

Abstract. Submarine canyons are structurally complex habitats known to support high densities and diversity of megafaunal organisms. This study describes deep-water corals and their habitats in The Gully, the largest submarine canyon in eastern North America, situated at the Canadian margin off Nova Scotia. Video recordings of the seabed were made along 49 transects, at depths between 110 and 544 m, using a tethered video camera system. The Gully has a high diversity of habitats with steep bedrock outcrops, high relief bottom with ledges of semi-consolidated mudstone, as well as level soft bottoms and areas with gravel. In total 95 megafaunal taxa were observed of which 16 species were corals. There was a strong, positive correlation between the total number of megafaunal taxa and number of coral species along transects, suggesting that coral diversity is a good indicator for overall megafaunal diversity. Corals were present in most parts of the canyon, and up to 11 species were observed along a single transect. The distribution patterns of corals were mainly related to distance along the axis from the canyon head and type of seabed substratum. The highest abundance of corals was found on the western side in the outer part of the canyon and is probably related to circulation patterns with a higher load of particulate matter in the out-flowing water. Nephtheid soft corals, mainly *Duva florida*, were most frequent and were found within the whole depth range. Gorgonian corals were observed only deeper than 340 m. Except for *Acanella arbuscula* and *Radicipes gracilis*, which are anchored in mud, the gorgonians were mainly confined to areas with cobble and boulder and in a few cases to semi-consolidated mudstone. Multivariate analyses were applied to identify groups of transects and species, and to indicate which environmental factors control the distribution of corals and other megafauna in The Gully.

Keywords. Deep-water corals, submarine canyon, Atlantic Canada, habitat

Introduction

Submarine canyons are a major feature along the edge of the continental shelf and slope along the northeastern USA and Atlantic Canada. In general, they contain a high diversity of habitats within a relatively small area, and have been recognised as rich coral habitats (Hecker at al. 1980; Breeze and Davis 1998). The Gully, the largest submarine canyon in eastern North America, is located off Nova Scotia just east of Sable Island. The Gully was formally declared as a Marine Protected Area in 2004 (DFO 2004). This designation is largely based on the residency of a small population of the Northern Bottlenose whale (*Hyperoodon ampullatus*) found there (Gowans et al. 2000) but considers other special attributes as well.

Deep-water corals are found around the world at depths most commonly on the order of 200-1500 m (Broch 1912, 1935, 1957; Jungersen 1917; Madsen 1944; Carlgren 1945; Hecker et al. 1980; Zibrowius 1980; Genin et al. 1986; Tendal 1992; Cairns 1994; Rogers 1999), and may be important components of deep-sea ecosystems. They occur off Atlantic Canada, mainly in channels between fishing banks and in submarine canyons (Breeze et al. 1997; MacIsaac et al. 2001; Gass and Willison 2005; Mortensen et al. in press). Until recently, most of the limited information available on the distribution of deep-sea corals in Atlantic Canada was anecdotal, based primarily on observations made by the fishing industry (Breeze et al. 1997). Since 1997 DFO has been collecting video and photographic information of epibenthic communities on an opportunistic basis at prime coral habitat sites in Atlantic Canada including the Northeast Channel, Stone Fence and The Gully. Some of the results have been published by MacIsaac et al. (2001), Buhl-Mortensen and Mortensen (2004), Gass and Willison (2005) and by Mortensen et al. (in press). These studies have improved the understanding of the distribution of corals and controlling environmental factors in Atlantic Canada, and have also documented that bottom fishing can impact corals (Mortensen et al. in press). However, the knowledge of how the presence of corals influences the faunal associations and the general megafauna composition remains rudimentary.

Awareness of deep-sea corals and their ecological importance is growing rapidly. Concern has been expressed about the potential effects of human activities on deep-water coral ecosystems, especially fishing and oil and gas activities (Rogers 1999). While there is considerable debate over the extent of past damage, it is clear that certain fishing activities can affect deep-sea coral ecosystems (Fosså et al. 2002; Mortensen et al. in press). The first offshore hydrocarbon developments in Atlantic Canada have been in shallow water, where only the soft corals (Alcyonacea) *Alcyonium digitatum* and *Gersemia rubiformis* have been recorded. However, exploration activity is now moving into deeper water where black (Antipatharia), horny (Gorgonacea), stony (Scleractinia) and soft corals can occur. Available information indicates that these corals provide important habitat and could play a critical role in the life history of many marine species, including some of commercial interest (Rogers 1999; Buhl-Mortensen and Mortensen 2005; Mortensen et al. in press). The conservation community is calling for the establishment of marine protected

areas (MPAs) to protect important coral habitats (Hall-Spencer et al. 2002). More information about the distribution of deep-sea corals is needed to define relevant coral protection areas.

The main goal of DFO coral studies in recent years has been to expand the knowledge of the distribution and ecology of deep-sea corals and their habitats in Atlantic Canada. The objectives of this paper are to describe the distribution of corals in The Gully and to relate their abundance to environmental factors and megafaunal composition.

The study area

The Gully is a deep and large submarine canyon approximately 40 km east of Sable Island on the edge of the Scotian Shelf (Fig. 1A). It is the largest submarine canyon off Atlantic Canada and eastern North America, being more than 70 km long and 20 km wide (Harrison and Fenton 1998). It consists of a deep (up to 2700 m) main canyon with several side-canyons (termed feeder canyons or channels) branching into the continental shelf. Reviews of the environment and processes of The Gully are provided by Harrison and Fenton (1998) and Gordon and Fenton (2002). It is thought to be an area of high productivity and important marine mammal habitat. Fifteen species of whales and dolphins have been identified in the area.

The Gully was formed from a combination of fluvial, glacial ice and glacial meltwater erosion occurring mainly 150-450 kyrs ago. It is cut into Tertiary bedrock in the deeper sections, and covered with thick quaternary glaciomarine sediments, mainly the Sambro Sand unit (sand and silty mud) in the shallower parts (200-600 m) (Fader et al. 1998). The steep-walled "ridge and valley" core area of The Gully widens seaward until the shelf break (Fig. 1B). Further down the continental slope it narrows again. At depths of about 600 to 3000 m sequences of mud and silts predominate, with sandier channels interspersed. The thalweg (deepest channel floor profile) of The Gully presents a remarkably uniform, sand-covered surface, sloping at approximately 2 degrees seaward from its head (Fader et al. 1998). At 2700 m depth the slope of the thalweg begins to decrease slightly. Nine major feeder canyons and many other smaller associated channels occur on the western flank of The Gully (Fig. 1A).

The physical oceanography of The Gully is described by Petrie et al. (1998). The main current pattern, as indicated by numerical modelling, is a strong south-westward flow along the shelf edge with greatest strength in fall and winter (Han et al. 2002). Some of that flow is steered into The Gully along its eastern side and out along its western side, forming a partial cyclonic gyre. There is an enhanced vertical mixing in The Gully in summer and fall as a result of tidally generated internal waves. This indicates that there is vertical transport of nutrients from below the pycnocline during periods of stratification, and that one might expect to find enhanced phytoplankton production (Mann 2002).
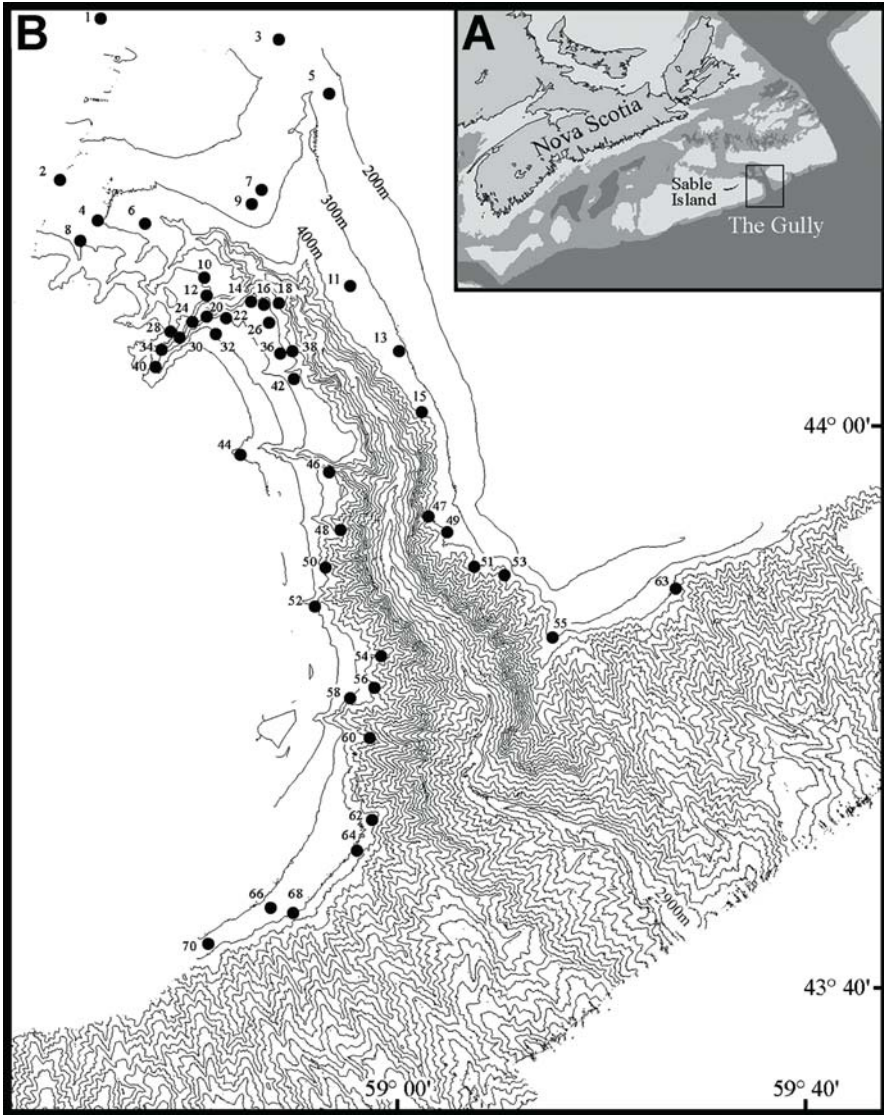
Fig. 1 A Map showing the location of The Gully. **B** The topography of The Gully, based on multibeam bathymetry, and the location of survey sites

Material and methods

Video imagery

The seabed was investigated with the video and still photo camera system Campod. Campod is an observation platform, without propulsion, equipped with a high-resolution video camera for viewing the seabed directly below and an oblique

video camera providing an overview of the seabed ahead. It can also land on the seabed and take photographs. Working depth is limited to ~500 m by cable length. Gordon et al. (2000) provides a more detailed description of this system. Campod was deployed while the ship was slowly (<1 knot) drifting and was kept close (1-2 m) to the seabed for at least 5 min on each transect. Campod was equipped with an Ultra Short Baseline navigation system (ORE Trackpoint II) providing detailed records of the tracks along the seabed. The geographical positions provided by the navigation system were quite noisy with an error in the order of ±5 m. However, after post-processing and filtering of the data, the navigation error was reduced to ±2 m.

Study sites

Video footage was recorded during one cruise on the C.C.G.S. *Parizeau* (8 transects in October 1997) and three cruises on the C.C.G.S. *Hudson* (12 transects in May 1999, 7 transects in June 2000, and 22 transects in September 2001). In total, 49 sites at depths between 110 and 544 m (Fig. 1B; Table 1) were selected for deployment of Campod. The sites were selected based on two criteria: high likelihood of finding coral, and good spatial coverage of the area. The site selection process made use of multibeam bathymetry collected in The Gully by the Canadian Hydrographic Service, the Geological Survey of Canada (Atlantic) and the oil and gas industry (Fader and Strang 2002). Twenty-two sites were selected within areas with rugged seabed topography most likely to support corals (i.e. at noses and ridges along the canyon edge at depths in the range of 300 to 500 m). The rest of the sites were selected to fill in areas poorly represented in order to describe the geographical distribution and the upper depth limits for corals in The Gully. As a reference for later discussions, The Gully was divided into an inner and an outer part, which in turn were divided into a western and an eastern part. Five transects were located outside The Gully just below the shelf break. The maximum depth of the investigated transects increased seaward along the axis of the canyon. The inner transects (<20 km from the innermost transect) covered depths between 110 and 370 m while middle and outer transects were located at depths from 140 to 544 m.

Estimates of megafaunal abundance

Transects varied between 19 and 1327 m in length covering a total distance of 16.6 km along the seabed (Table 1) and an area of approximately 43,940 m^2. The total duration of the video records was 18 h and 34 min. Transects covering a depth range >100 m were divided into two parts at the site of the middle depth. These parts are denoted as 'a' and 'b' in Table 1. The abundance of coral colonies was estimated from subsamples (sequences) of the video transects. These sequences were mainly of 30 s duration but were made shorter when abrupt changes in the habitat occurred. Geographical positions and depth were registered at the start and end of each sequence. In total 1879 video sequences were analysed each covering a distance of between 5 and 100 m (average = 9 m) as estimated from the navigation data. Unfortunately, there was no practical way to continuously estimate the width of the visual field, which varied with the height above bottom and the pitch angle

Table 1 Brief description of video transects in The Gully. Depth range, number of video sequences (Seq), length of transects (Dist). Percentage cover of different bottom substrates: M-st = semi-consolidated mudstone, Bo = boulder, Co = cobble, Pe = pebble, Sa = sand, M = mud. Diversity is given as Shannon-Wiener index (H') and abundance is given as individuals or colonies per 100 m^2

Tr. #	Depth	Seq	Dist	M-st	Bo	Co	Pe	Sa	M	H'	No of taxa		Abundance	
											All	Coral	All	Coral
Inner canyon														
Eastern side														
1	110-111	14	42	0	0	13.2	55	31.8	0	1.3	7	0	22.9	0
3	254-258	18	151	0	0	0.1	0	0	99.9	1.49	7	0	11.5	0
5	223-232	14	26	0	0	0	0.6	99.4	0	1.21	5	0	40.7	0
7	275-276	20	47	0	0	0	0	100	0	0.18	6	1	272.4	0.8
9	274-276	13	176	0	0	0.1	1	0	99	0.47	8	1	119.7	0.4
11	323-325	8	43	0	3.1	5.5	1	90.4	0	1.15	4	1	34.4	10.9
13	321-345	24	398	0	0.4	0.3	0	0	99.3	1.71	11	0	3.2	0
15	374-466	118	1041	2.2	0.3	0.3	0	0	97.2	1.21	29	3	181.1	37.1
Western side														
2	287-290	16	76	0	0	0.3	1.5	98.2	0	1.1	3	0	2.6	0
4	298-300	25	123	0	0.2	1	10.6	88.2	0	1.06	3	0	1.2	0
6	364-367	52	309	0.3	0.1	0.3	3.6	95.7	0	0.96	3	0	0.6	0
8	271-274	13	88	0	0	0	1	99	0	0	1	0	0.8	0
10	322-323	12	31	0	0	0	0.1	99.9	0	0.64	2	0	4.2	0
12	306-308	11	57	0	0	0.1	0	99.9	0	1.33	4	0	4.4	0
14	387-411	34	319	0	1.4	10.6	20.9	67.1	0	2.35	25	6	26.6	13.4

Table 1 continued

Tr. #	Depth	Seq	Dist	M-st	Bo	Co	Pe	Sa	M	H'	No of taxa		Abundance	
											All	Coral	All	Coral
Inner canyon														
Western side														
16	406-411	26	161	0.2	5.2	12.4	10.7	0	71.5	2	19	6	50.9	8.9
18	277-316	6	68	0	0.2	43.3	43.3	0	13.2	2.05	10	1	17.4	0.8
20	400-436	51	393	7.2	0	0	0	0	92.8	1.62	12	2	13.1	2.3
22	316-369	44	556	34.6	0.3	0.2	0	64.9	0	1.24	25	5	126.9	24.9
24	439-460	13	151	0	0	0	0	100	0	1.77	7	0	4.3	0
26	397-446	49	597	9.8	2	15.9	14.4	57.9	0	2.19	30	7	47	6.6
28	274-331	26	136	4.9	0.1	0	1	94	0	1.81	8	1	7.6	0.8
30	396-399	12	72	0	0	0	0	0	100	1.23	6	0	17.5	0
32	233-306	92	1007	3.7	0.4	0.6	0.2	95.1	0	2.73	28	1	6.7	0.1
34	302-306	6	19	0	0	0	0	100	0	0.69	2	0	7	0
36	403-416	15	79	4.4	1.8	10.4	12.1	0	71.3	0.95	11	2	164.8	5
38	441-466	14	202	0	0.2	0.1	0.1	0	99.6	0.33	5	0	19.1	0
40	246-290	10	72	0	0.3	0	0.3	0	99.4	1.06	9	0	29.9	0
42	387-404	22	184	9.9	0.7	1.5	1.5	0	86.5	0.77	12	3	49.1	1.3
44	139-148	40	235	0	0	0	0	0	100	0.7	11	0	202.7	0
46a	368-444	40	440	23	0.02	0	0	0	77		16	2	38.7	12.1
46b	445-519	50	366	72	0	0	0	0	28		23	6	52	40

Table 1 continued

Tr. #	Depth	Seq	Dist	M-st	Bo	Co	Pe	Sa	M	H'	No of taxa		Abundance	
											All	Coral	All	Coral
Outer canyon														
Eastern side														
47	473-527	18	149	31.1	0.6	5.1	0.6	0	62.6	2.52	19	1	22.5	3.2
49	421-433	25	124	0	1.4	16.1	20.2	0	62.3	1.56	8	0	14	0
51	432-506	83	690	10.6	1.2	2.6	2.4	0	83.2	2.43	41	8	32.8	10.1
53	470-541	11	159	0	0	0	0	0	100	0.75	11	1	146.8	14.6
55	395-436	54	415	0	1.7	8.4	12.2	0	77.7	2.77	35	9	50.6	22.1
Western side														
48a	364-434	51	495	0.4	0	0.1	0	0	99.5		18	2	46.4	0.7
48b	439-509	13	117	47.2	0	0	0	0	52.8		16	4	24.7	8.2
50	424-490	14	37	0	0	0	0.1	0	99.9	0.08	2	0	63.8	0
52a	247-339	30	331	31.7	0.4	0.6	0.7	0	66.7		21	3	70.8	9.1
52b	152-244	30	267	29.8	0.6	1.1	0.7	0	67.8		19	2	92.2	13.7
54	395-443	71	604	0	0.6	1	1	0	97.4	2.6	34	6	46.8	8.2
56	399-487	70	1327	0	1.1	5.1	0.2	92.1	0	0.77	30	5	99.8	85.7
58	357-364	54	324	23.6	1.5	1.3	0.2	0	73.4	1.57	23	2	72.1	9.4
60	479-518	58	390	15.5	0.3	0.7	0	0	83.5	2.17	24	3	30.2	8
62a	424-484	32	239	0	0.03	0.1	0	0	99.9		27	6	45.5	7
62b	486-544	40	375	0.2	0.9	3	2.9	0	93		40	9	43.5	5.3

Table 1 continued

Tr. #	Depth	Seq	Dist	M-st	Bo	Co	Pe	Sa	M	H'	No of taxa		Abundance	
											All	Coral	All	Coral
Slope														
63	404-409	41	237	0	0	0	0.2	0	98.5	1.21	25	6	438.1	303.6
64a	389-440	73	553	0.3	1.9	3	28.8	0	66		37	6	56.1	0.9
64b	441-493	20	245	0	2.8	5.1	7.2	0	85	1.87	20	2	35.7	1.3
66	433-487	55	553	0	1.1	1.8	5.7	0	91.4	2.49	25	3	28.1	0.8
68	338-350	101	998	1.3	1.2	4.3	4.9	0	87.4	2.01	37	5	70.3	9.3
70	337-368	27	305	0	0.3	0.9	1.7	0	97.1		23	2	40.4	9.7
Sum	110-544	1879	16599								95	17		
Average				6.7	0.6	3.3	5.0	29.1	55.2	1.47	16.4	2.5	58.4	12.9

of the video camera lens. Most of the time the Campod was kept c. 1.5 m above the bottom, giving a visual field width of 2 and 4 m for the vertical and oblique camera respectively. These values were used for calculation of the approximate area covered by each of the investigated video sequences. Organisms were identified and counted within the sequences and abundances of observed species were calculated by applying the approximate area of the sequences.

Estimates of seabed substratum coverage

The percentage cover of six classes of bottom substrates (mud, sand, pebbles, cobbles, boulders and outcrops including bedrock and semi-consolidated mudstone, following the size classes as defined by the Wentworth scale (Wentworth 1922), was estimated subjectively at a scale of 5 % intervals in the same video sequences In cases where the substrate composition showed clear variation within a video sequence, average values of two or more estimates were used.

Estimates of seabed topography

An index of seabed relief was estimated for each video transect as the actual length of the bottom profile along the transect divided by the horizontal distance. The angle of the seabed inclination was measured as the average and maximum inclination along each transect.

Temperature and salinity

Data on temperature and salinity for the study area were extracted from the hydrographic database assembled at the Bedford Institute of Oceanography, Fisheries and Ocean Canada (Petrie and Dean-Moore 1996; also accessible at http://www.mar.dfo-mpo.gc.ca/science/ocean/home.html). These data, from 1933 to the present, represent 843 unevenly distributed records (single measurements or vertical profiles) from different times of the year. The data set did not have sufficient resolution in time and space to enable detailed maps of the distribution of near-bottom temperature and salinity. To gain information on these variables for the video transects, all temperature and salinity records from the five divisions of the study area were plotted against depth. These plots were used to determine minimum, average and maximum values for temperature and salinity for the depths of each of the video transects.

Statistical analyses

Diversity indices - The Shannon-Wiener index (H') was used as a measure of the diversity of megafaunal taxa using the formula:

$$H' = - \sum_{i=1}^{S} (N_i/N) \cdot \log_2 (N_i/N) \qquad \text{(Shannon and Weaver 1949)}$$

were S = total number of taxa, N = total number of individuals, and N_i = number of individuals of the ith taxa.

Canonical Correspondence Analysis - CCA was applied to group transects and species, based on species composition and environmental conditions, using the software PC-Ord. In total 17 environmental variables were used for this analysis: axis distance (distance from the head of the canyon measured along the thalweg), depth (average, minimum and maximum for the transects), temperature (average, minimum and maximum), salinity (average, minimum and maximum), angle (average and maximum), topographic index (relief), and the percentage cover of the six types of seabed substrates. CCA was performed on two sets of the transect data (all video sequences in a transect pooled): 1) all megafaunal species, and 2) only coral species. Only species occurring on >5 % of the transects (occurrence at >2 transects) were included. These criteria left 72 species and 42 transects for the analysis of the first data set, and 14 species and 36 transects for the second data set. Transect 44, situated on the shelf on the western side of The Gully (Fig. 1B) was omitted from the CCA because it differed markedly in species composition and occurred as an extreme outlier in an initial analysis of all transects. This anomaly resulted from an extreme high abundance of sculpins (Cottidae).

Results

General habitat description

Five types of seabed substrate types were identified: 1) bedrock walls, 2) terraced ledges of semi-consolidated mudstone, 3) gravel (with boulder), 4) sand, and 5) mud. The highest topographic relief was associated with the bedrock walls, and semi-consolidated mudstone. More level or gently sloping bottoms were found in areas with soft bottoms and gravel. Sand and mud were the dominant bottom types covering 29 and 55 % on average, respectively (Table 1). The composition of the seabed changed along the axis of the canyon, and with increasing depth. Sand dominated in the inner part of the canyon while mud dominated the outer part. Boulders occurred on 30 transects with an average cover of only 0.6 % (Table 1). The highest cover of 5.2 % was recorded at Transect 16 (values for transects are average of estimates of video sequences). Smaller stones (cobbles and pebbles) were more common (occurring on 33 and 34 transects respectively) and had higher average % cover than boulder (3.5 and 5.2 % respectively). Semi-consolidated mudstone was observed below 150 m depth, but was most common and abundant below 250 m. On average this bottom type covered 6.7 % of the seabed. Sudden changes in bottom type composition were often related to changes in bottom inclination. The mean bottom inclination for whole transects varied between 0.6 and 26.6°, while the maximum value for video sequences was 74.6°. Even though the steepest transect was found within the inner west division, on average the transects in the outer part of The Gully (average inclination = 11.5°) were about twice as steep as those in the inner part.

Analysis of temperature and salinity data revealed some slight differences between the five divisions of the study area. The estimated bottom temperature varies between 1.9 and 10.3°C, with a mean value of 5.3°C. Largest difference in

mean temperatures was found on the eastern side between the inner (6.2°C) and outer (5.0°C) divisions. The highest mean salinity was found for the outer eastern division (34.86 ‰), and the lowest was found for the inner western division (34.55 ‰).

We were not able to detect any consistent pattern of bathymetric distribution for the megafauna. The general picture of the distribution of coral habitats along the transects can be summarised as follows: The shallower parts inside the shelf break consisted mainly of sandy mud in the inner parts of The Gully. Here, the only corals observed were alcyonarians attached to scattered cobbles. The most common organisms in this habitat were cerianthid anemones. In the other parts of The Gully, the seabed inside the shelf break could be characterised more as clayey mud. In this habitat *Flabellum* spp. were abundant. Below the shelf break the seabed became suddenly coarser with gravelly patches supporting a great diversity of suspension feeders. Of corals, the gorgonian *Acanthogorgia armata* and the alcyonarian *Anthomastus grandiflorus* were observed on cobbles and boulders. On transects in areas with small side canyons a rugged terrain was observed with dense cover of semi-consolidated mudstone. The nephtheid soft corals were situated on the crests of these structures, and along Transect 46 *Paragorgia* and *Primnoa* were observed on the top of ridges were this semi-hard bottom substratum was exposed. Elsewhere, *P. resedaeformis* and *P. arborea* were more commonly found on boulders. The gorgonian *Keratoisis ornata* was often observed on cobbles and boulders in the bottom of small channels.

Distribution and abundance of corals

Colonial corals (Alcyonacea, Gorgonacea and Scleractinia) were represented by 1067 colonies, belonging to 16 taxa (Table 2), whereas solitary scleractinians accounted for 4206 individuals and three species (*Flabellum* cf. *angulare, F. alabastrum* and *F. macandrewi*). *Flabellum* specimens that could not be identified to species were recorded as *Flabellum* spp. but were most likely represented by both *F. angulare* and *F. macandrewi*. The three orders of deep-sea corals were quite evenly represented in terms of number of species (Alcyonacea: 5 spp., Gorgonacea: 6 spp. and Scleractinia: 4 spp.; Table 2). Up to 11 species were observed along a single transect (Transect 62). The corals showed distribution patterns both with depth, and along the axis of the canyon. Corals were present in most parts of the canyon, except for the shallower locations near the canyon head (Figs. 2A-D). The gorgonians *Paragorgia arborea* and *Primnoa resedaeformis* were observed in inner and outer divisions along five and four transects respectively (Fig. 2A). They occurred together on three transects. *Acanella arbuscula* and *Acanthogorgia armata* were observed only on the outer transects on the slope close to the canyon mouth (Fig. 2B). *Flabellum* species were observed along transects mainly in the outer divisions (Fig. 2D). A small fragment or colony of *Lophelia* was spotted on Transect 46b at a depth of 451 m but it was not possible to determine whether this coral was alive. The depth distribution of corals is summarized in Table 2, Figs. 3 and 4. Gorgonians and scleractinians were observed only deeper than about 340 m while some of the alcyonarians (the nephtheids) occurred as shallow as 170 m.
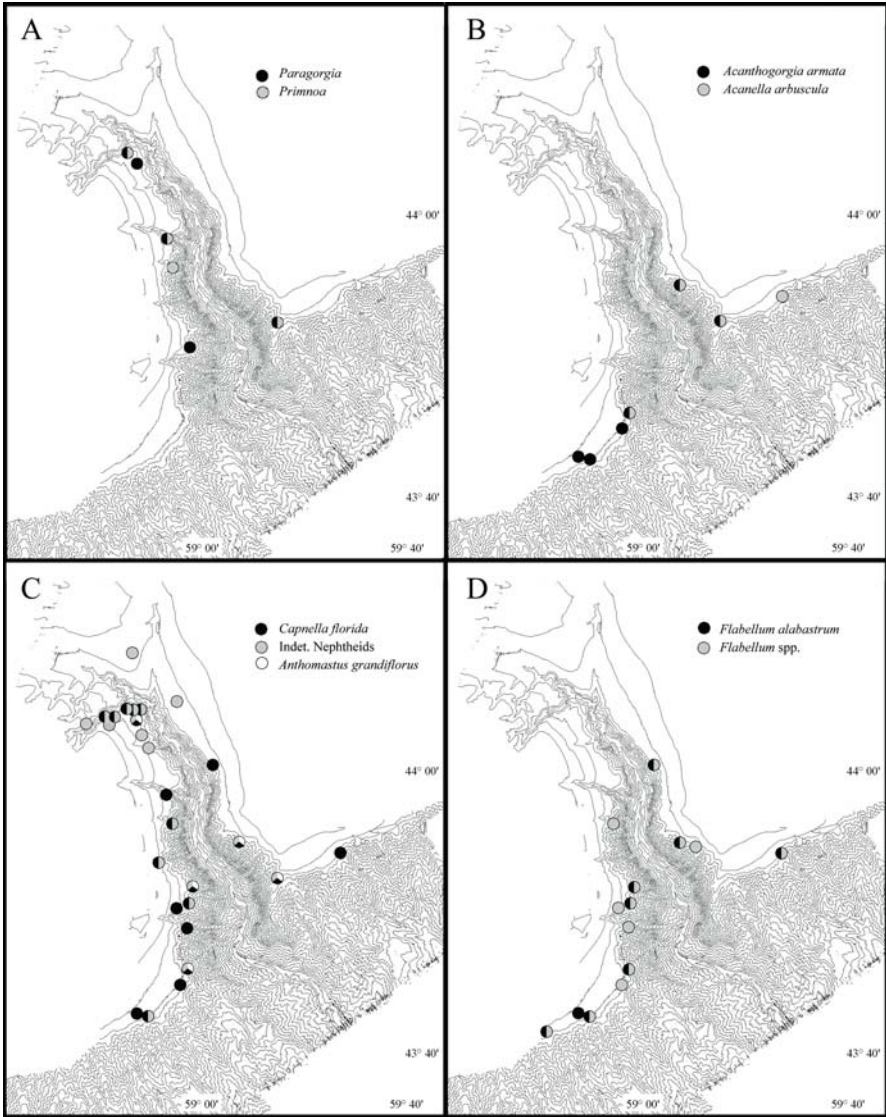
Table 2 Average densities (colonies or individuals per 100 m^2) (Ave), number of specimens observed, transects with occurrence (Tr), and depth distribution for coral species observed during visual surveys in The Gully. Average, Std and Max densities are provided for transects with corals and patches

	All transects			Trans. with presence			Patches			Depth distribution	
	Ave	Specimens	Tr	Ave	Std	Max	Ave	Std	Max	Range	Ave
Alcyonacea											
Anthomastus grandiflorus	0.04	17	6	0.2	0.3	0.9	9.1	5.4	23.1	399-523	440
Duva florida	3.40	1498	21	5.2	6.0	22.6	69.9	140.2	1061	172-537	403
Nephtheidae sp. 1 (White)	0.42	186	15	1.8	3.2	10.9	30.3	55.1	387.6	287-539	412
Nephtheidae sp. 2 (Blue)	0.36	160	10	2.3	2.3	6.5	15.5	14.9	69	270-446	400
Nephtheidae indet.	0.92	403	132	2.1	5.2	19.2	30	40.2	232	237-538	380
Gorgonacea											
Acanella arbuscula	0.17	74	5	3.4	7.2	282	43.2	85.7	471.7	404-540	428
Acanthogorgia armata	0.07	32	4	0.7	0.8	1.8	10.5	9.9	47.6	346-493	430
Keratoisis ornata	0.14	63	8	0.9	1.2	3.2	9.9	10.5	54.6	396-509	461
Paragorgia arborea	0.06	28	8	0.3	0.2	0.5	11.6	14.2	62.5	341-495	435
Primnoa resedaeformis	0.25	108	5	2.0	1.4	3.2	40.1	99.8	530.3	388-516	429
Radicipes gracilis	0.09	40	8	0.7	0.9	2.7	42.4	108.3	443	404-535	441
Scleractinia											
Flabellum alabastrum	0.26	116	11	0.9	1.01	2.8	28.3	83.8	648.9	341-541	425
Flabellum cf. angulare (Small red)	2.55	1124	3	94.1	162.8	282	706.1	810.8	3845	337-541	418
F. macandrewi	0.01	3	1	-	-	-	-	-	-	439	-
Flabellum spp.	7.72	3396	12	12.1	24.1	85	116.9	348.2	4542	404-439	408
Lophelia pertusa	<0.01	1	1	-	-	-	-	-	-	450	-

Fig. 2 The distribution of corals in The Gully. **A** *Paragorgia arborea* and *Primnoa resedaeformis*, **B** *Acanthogorgia armata* and *Acanella arbuscula*, **C** *Duva florida*, unidentified Nephtheidae and *Anthomastus grandiflorus*, **D** *Flabellum alabastrum* and *Flabellum* spp.

Maximum abundance tended to occur between about 350 and 450 m. These data do not identify the full depth range of corals since observations were limited to about 500 m because of cable length.

A summary of the abundance of corals is given in Tables 2 and 3. In general, the larger corals were less abundant than smaller corals. The nephtheid soft coral *Duva*
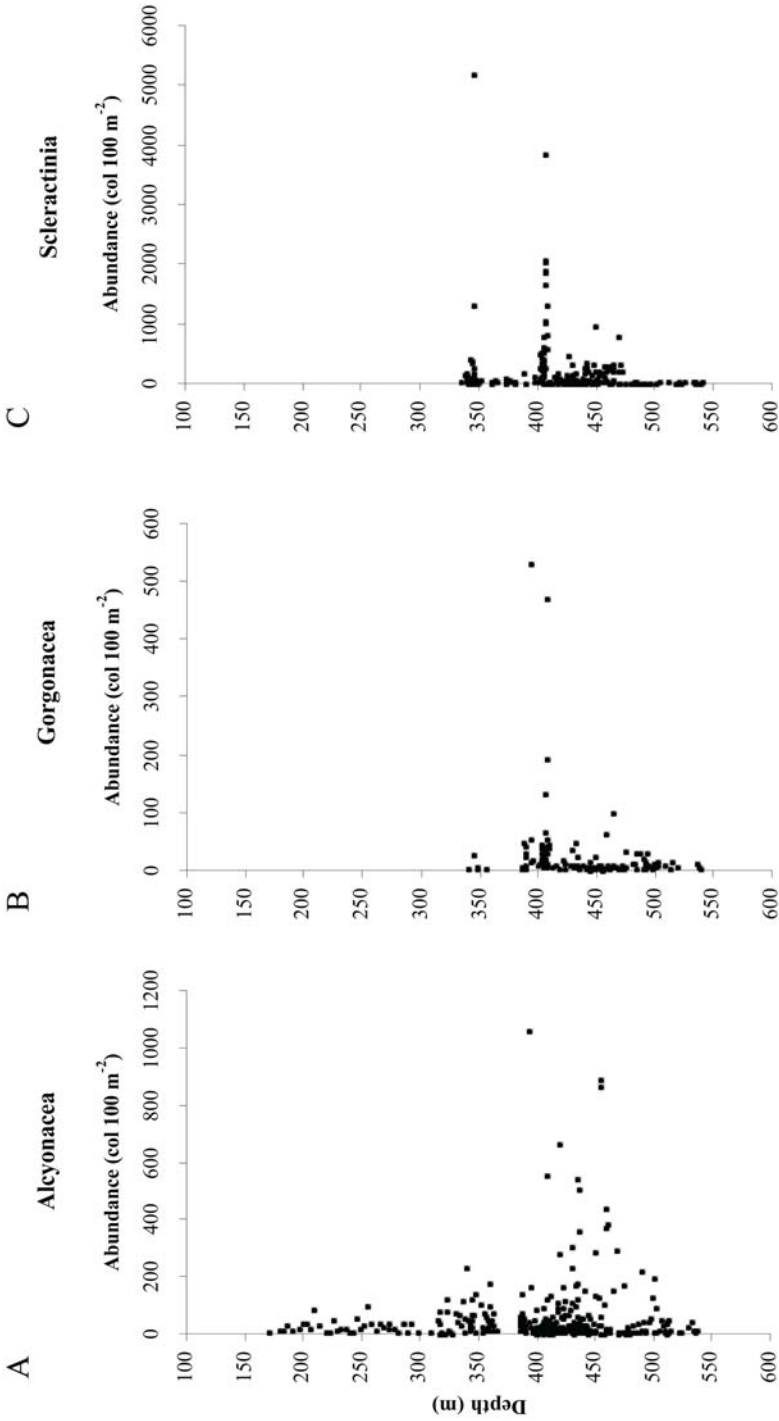
Fig. 3 Abundance of corals *versus* depth. **A** Alcyonacea, **B** Gorgonacea and **C** Scleractinia
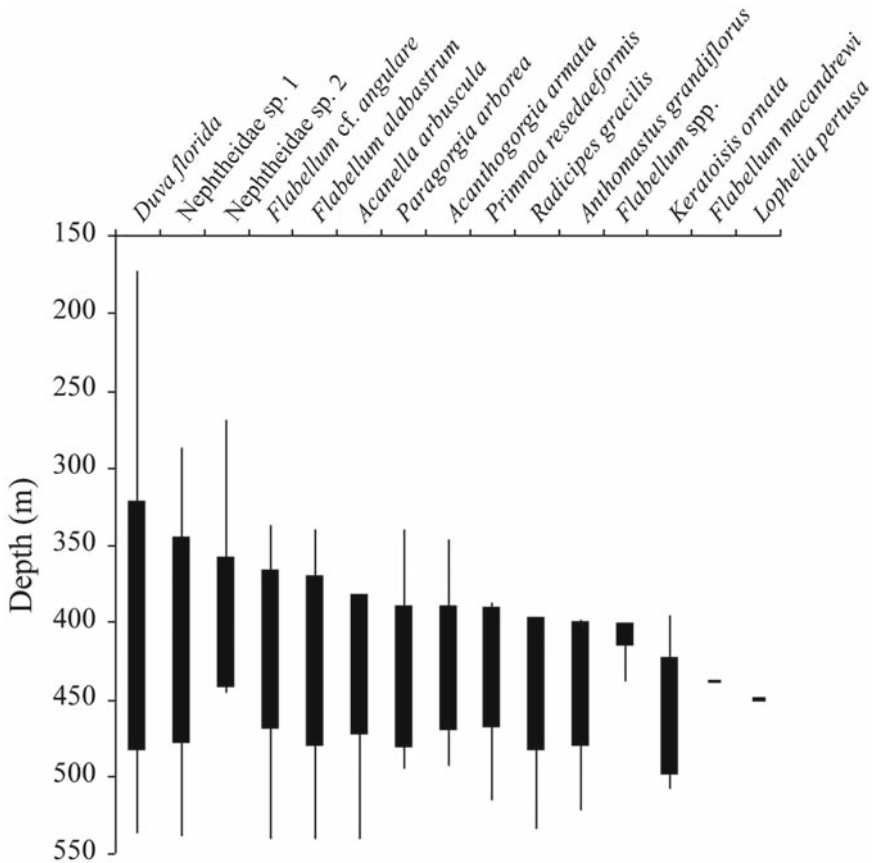
Fig. 4 Bathymetrical distribution of corals. Bars indicate standard depth range expressed as ± standard deviation of depth records. Vertical lines indicate maximum and minimum depth of occurrence

florida was the most abundant coral with a total of 1498 specimens and an average abundance of 3.4 col · 100 m^{-2}. *Flabellum* cf. *angulare* was the most abundant coral locally with an average abundance of 706 ind · 100 m^{-2} within patches (video sequences with presence of the coral; Table 2). The most abundant gorgonians were *Acanella arbuscula*, *Primnoa resedaeformis* and *Radicipes gracilis* which occurred with average patch abundance between 40.1 and 43.2 col · 100 m^{-2}. The abundance of corals was higher in the outer divisions than the inner (Table 3). The highest abundance was found for the transects on the slope with an average abundance of 64.9 specimens · 100 m^{-2}. This was mainly due to high numbers of *Flabellum* spp. Within the canyon, the highest abundance of corals was found for the western outer division with an average abundance of 16.4 col · 100 m^{-2}. The lowest coral abundance was found for the western inner division with 3.9 col · 100 m^{-2}.

Table 3 Diversity (H'), average number of species per transect, and average abundance of individuals and colonies (col·100 m^{-2}) for all megafauna and corals only within the different divisions of the study area in The Gully

	H'	Average no of species/transect		Average abundance (col·100 m^{-2})	
		All	Coral	All	Coral
Inner					
East	1.1	9.6	0.8	85.7	6.2
West	1.3	11.6	1.7	37.0	3.9
Outer					
East	2.0	22.8	3.8	53.3	10.0
West	1.6	25.5	4.4	59.9	16.4
Slope	2.1	29.6	4.4	125.2	64.9
Average	1.5	16.5	2.5	59.3	13.2

Composition and diversity of megafauna

In total 95 megafaunal taxa were recorded, of which 16 species were corals (Table 4). The number of taxa per transect varied between 1 and 41, and the diversity index (H') varied between 0 and 2.77 (Table 1). The highest numbers of taxa (both for all megafauna and for corals only) were found below 400 m depth. The number of taxa was positively correlated with maximum transect depth (r = 0.52, p <0.001), distance along the canyon axis (r = 0.71, p <0.001), and maximum salinity (r = 0.47, p <0.001). There was a strong and positive correlation between the total number of megafaunal taxa and number of coral species along transects (r = 0.87, p <0.001) suggesting that coral diversity is a good indicator for overall species diversity. The most species rich groups were fish (Teleostei, 19 taxa), and octocorals (18 taxa). Fifteen species level taxa occurred on more than 35 % of the transects. The agglutinated foraminifer *Bathysiphon* cf. *filiformis* occurred on 57 % of the transects.

The most common fish species was redfish (*Sebastes* sp.) which occurred on 68 % of the transects. The second most common fish was long-finned hake (*Urophycis chesteri*), which occurred on 51 % of the transects. Fish abundance was strongly correlated with maximum temperature (r = 0.57, p <0.05, N = 54). The correlation between abundance of fish and corals, collectively or as single species, was weak and not significant (p <0.05).

Relationship between species composition and the environment

In total, the 17 environmental variables (listed in Table 5) explained 18.3 % of the variance represented by the three first CCA axes in the analysis of all megafauna. The percentage explained was much higher for the CCA of the coral species alone (43.4 %). Some of the environmental factors were strongly inter-correlated (Table 5): for example depth/maximum temperature (r = -0.87), average temperature/

Table 4 Megafaunal taxa observed along the 54 video transects in The Gully, and the number of transects they were observed on

Taxon name	Descriptive name	No of transects
Foraminifera		
Bathysiphon cf. *filiformis*		32
Porifera		
cf. *Hymedesmia* spp.		11
Clathrididae indet.		1
Farrea occa		5
Geodia sp.		1
Phakellia sp.		6
Polymastia cf. *mammillaris*		24
Porifera indet.		34
Porifera sp. 1	Small white round	34
Porifera sp. 2	Branched	1
Porifera sp. 3	Stalked	13
Vazella pourtalesi		4
Cnidaria		
Hydrozoa		
Hydroidea Thecaphora		10
Actinaria		
Actinaria indet.		14
Actinaria sp. 1	Red-orange	17
Actinaria sp. 2	Small red	19
Actinaria sp. 3	Small dark	9
Actinaria sp. 4	Small orange	14
Actinauge sp.		14
Cerianthidae indet.		18
Cerianthidae sp. 1	White	2
Cerianthidae sp. 2	Small	10
Cerianthidae sp. 3	Pink	9
Cerianthidae sp. 4	Small violet	5
cf. *Bolocera tuediae*		3
Pennatulacea		
Halipteris cf. *finmarchica*		18
Pennatula sp.		5
Pennatulidae indet.		8
Virgularia mirabilis		18
Alcyonacea		
Anthomastus grandiflorus		6
Duva florida		21
Nephtheidae sp. 1	White	15
Nephteheidae sp. 2	Blue	10
Neptheidae indet.		12
Gorgonacea		
Acanella arbuscula		5

Table 4 continued

Taxon name	Descriptive name	No of transects
Acanthogorgia armata		4
Gorgonacea		6
Keratoisis ornata		8
Paragorgia arborea		8
Primnoa resedaeformis		5
Radicipes gracilis		8
Scleractinia		
Flabellum alabastrum		11
Flabellum macandrewi		1
Flabellum cf. *angulare*		3
Flabellum spp.		12
Lophelia pertusa		1
Polychaeta		
Hyalinoecia tubicola		5
Polychaeta indet.		2
Sabellidae indet.		10
Serpulida indet.		7
Mollusca		
cf. *Bathypolypus* sp.		2
cf. *Buccinum* sp.		3
Decapoda indet.		6
Octopoda indet.		1
Echinodermata		
Crinoidea		
Crinoidea indet.		10
Ophiuroidea		
Novodinia sp.		3
Ophiuroidea indet.		11
Asteroidea		
Asteroidae indet.		22
Asteroidae sp. 1	*Porania*-like	1
Astropecten irregularis		2
Ceramaster sp.		4
Henricia sp.		22
Hippasterias cf. *phrygiana*		8
Porania cf. *pulvillus*		4
Solaster endeca		2
Tremaster mirabilis		2
Echinoidea		
Echinarachnius parma		3
Echinoidae indet.		1

Table 4 continued

Taxon name	Descriptive name	No of transects
Pycnogonidae		1
Crustacea		
Brachyura indet.		10
Brachyura sp.1	*Hyas*-like	1
Chionoecetes opilio		20
Chaceon quinquedens		1
Lithodes maja		12
Natantia indet.		1
Aanomura indet.		1
Paguridae indet.		10
Pandalidae indet.		2
Agnatha		
Myxine glutinosa		5
Condrichthyes		
Chimaera sp.		2
Raja sp. 1		10
Raja sp. 2	Small pink	4
Squalus acanthias		5
Teleostei		
Cottidae indet.		3
Gadeidae indet.		3
Gadus morhua		1
Hippoglossus hippoglossus		4
Lophius americanus		15
Macrouridae indet.		28
Molva molva		3
Pleouronectidae indet.		29
Sebastes sp.		37
Teleostei indet.		28
Teleostei sp. 1	Eel-like	17
Urophycis chesteri		27

maximum temperature and (r = 0.85), average salinity/maximum salinity (r = 0.86), average angle/maximum angle (r = 0.84), and sand/clay (r = -0.89). In Figures 5 and 6 only variables with a relatively strong correlation (r >0.34) with axes are shown. CCA identified four environmental factors (% boulder, axis distance, % sand and maximum salinity) that explained most of the variation in the total species data. For the coral-only data the combination of the following variables explained most of the variation: axis distance, average salinity, % sand, % clay, % cobbles, % mudstone and average seabed angle. The percentage of boulder substrate was strongly negatively correlated with Axis 1 in Figures 5A and 5B (Table 6) and the species (Fig. 5B) were distributed widely along this axis. Most coral species occurred to the left in this diagram, reflecting their substratum needs. Much of the

Table 5 Correlation coefficients (r) for the relationship between environmental variables for the video transects. T = temperature, S = salinity, Ang. = seabed angle, Topo = topographic relief, Bo = % boulder, M-st = % mudstone, Co = % cobble, Pe = % pebble, Sa = % sand, M = % mud. Values >0.36 are significant (p <0.01)

	Axis dist.	Depth	T ave	T min	T max	S ave	S min	S max	Angle ave	Angle max	Topo	Bo	M-st	Co	Pe	Sa	M
Axis dist.	1.00																
Depth	0.60	1.00															
T ave	-0.34	-0.70	1.00														
T min	0.18	0.42	-0.01	1.00													
T max	-0.36	-0.87	0.85	-0.45	1.00												
S ave	0.62	0.73	-0.16	0.63	-0.49	1.00											
S min	-0.10	0.09	-0.06	0.08	-0.03	0.03	1.00										
S max	0.63	0.53	-0.02	0.22	-0.17	0.86	0.03	1.00									
Ang. Ave	0.36	0.49	-0.35	0.09	-0.33	0.29	0.25	0.33	1.00								
Ang. Max	0.23	0.37	-0.36	0.13	-0.32	0.16	0.33	0.15	0.84	1.00							
Topo	0.00	0.26	-0.23	0.09	-0.22	0.13	0.30	0.13	0.61	0.77	1.00						
Bo	0.28	0.28	-0.15	0.09	-0.22	0.20	-0.09	0.16	-0.14	-0.21	-0.19	1.00					
M-st	0.11	0.16	-0.07	0.00	-0.06	0.19	0.00	0.28	0.65	0.40	0.47	-0.12	1.00				
Co	-0.09	-0.07	-0.12	-0.20	-0.02	-0.17	-0.07	-0.16	-0.11	-0.16	-0.17	0.31	-0.13	1.00			
Pe	-0.14	-0.25	-0.16	-0.62	0.16	-0.44	-0.07	-0.25	-0.22	-0.23	-0.16	0.20	-0.19	0.77	1.00		
Sa	-0.56	-0.40	0.16	0.02	0.15	-0.41	-0.10	-0.50	-0.39	-0.18	-0.04	-0.17	-0.22	-0.12	-0.09	1.00	
M	0.57	0.42	-0.07	0.17	-0.16	0.48	0.13	0.50	0.25	0.14	-0.04	0.09	-0.04	-0.20	-0.23	-0.89	1.00
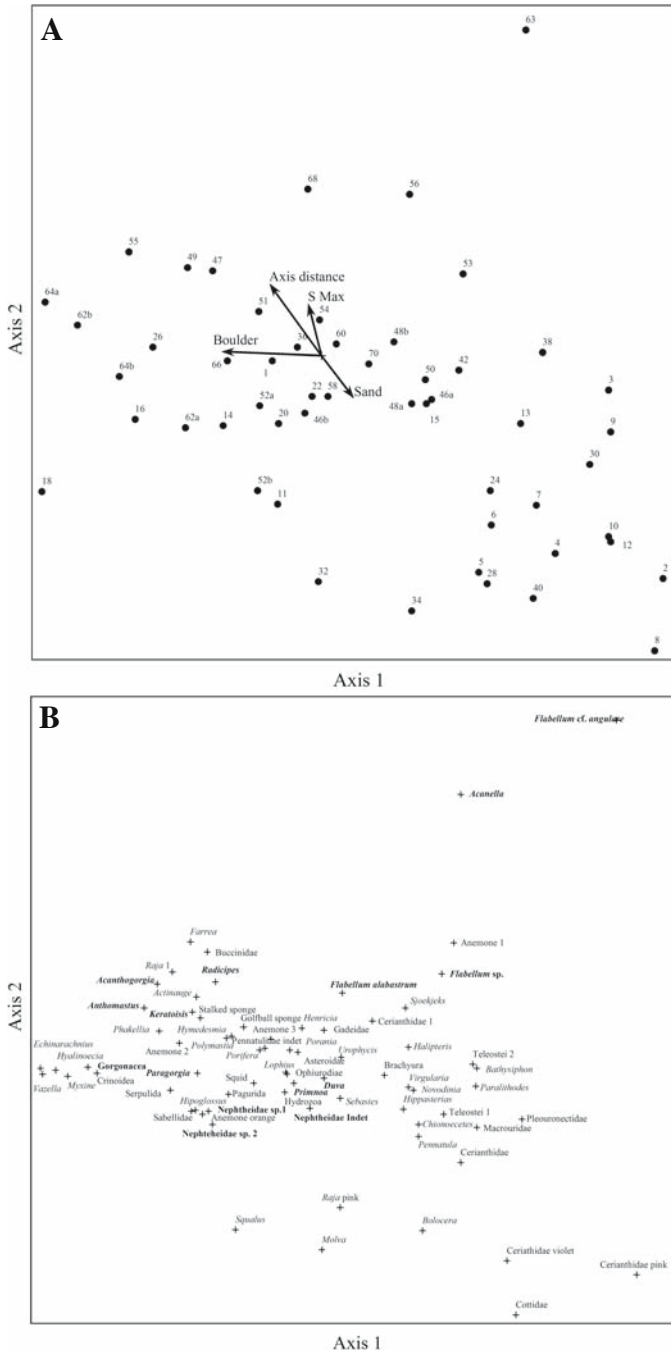
Fig. 5 Ordination plots from Canonical Correspondence Analysis of all species. **A** Plot of transects and environmental vectors. **B** Plot of species
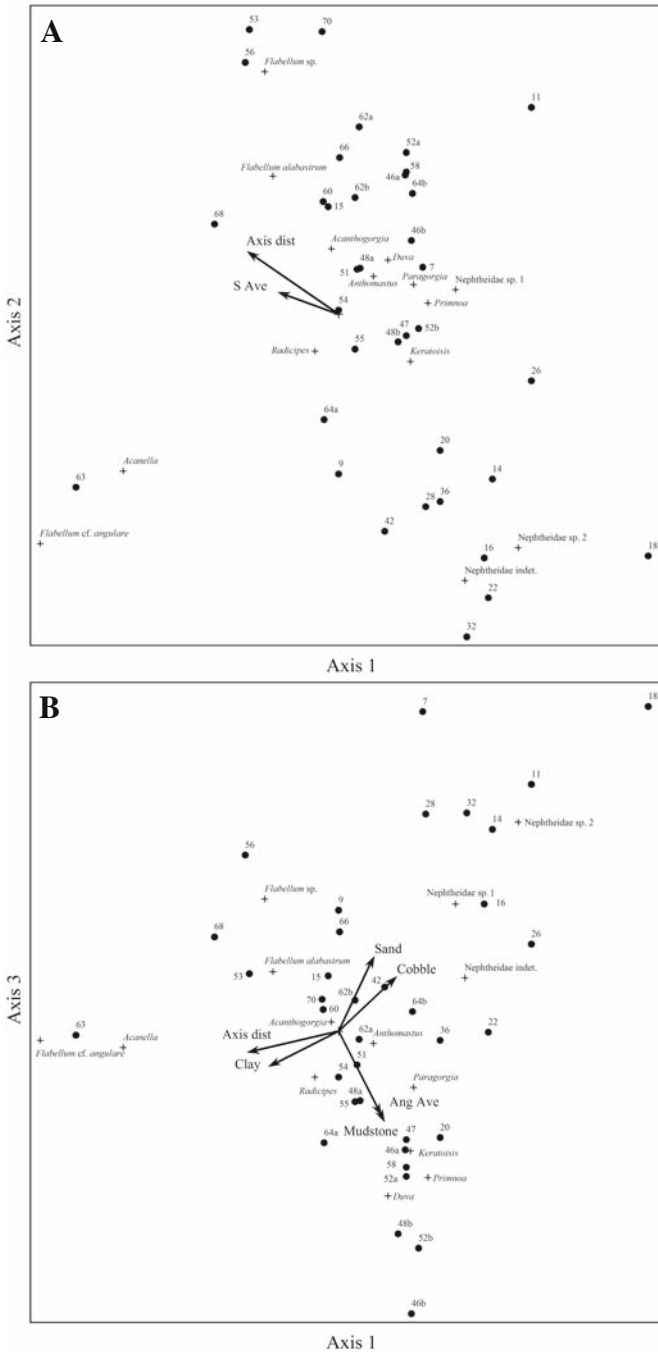
Fig. 6 Ordination plots from Canonical Correspondence Analysis of only the corals. **A** Plot of transects, species and environmental vectors on first and second axis. **B** Plot of transects, species and environmental vectors on first and third axis

Table 6 Correlation coefficients (R^2) for the relationship between environmental variables and CCA axis (inter-set correlation) in analyses of all species and for corals only

Variables	All megafauna			Corals only		
	Axis 1	Axis 2	Axis 3	Axis 1	Axis 2	Axis 3
Axis dist	-0.31	0.53	-0.36	-0.67	0.34	-0.14
Depth	-0.26	0.39	-0.08	-0.17	0.24	-0.05
T Ave	0.34	-0.34	0.04	0.13	0.07	0.06
T Min	0.10	-0.06	-0.03	0.29	0.14	0.25
T Max	0.24	-0.32	0.07	0.10	0.11	-0.05
S Ave	-0.04	0.45	0.03	-0.44	0.12	-0.09
S Min	-0.03	-0.05	0.04	0.08	-0.08	-0.08
S max	-0.08	0.38	0.07	-0.26	0.26	-0.27
Ang Ave	-0.22	-0.18	-0.03	0.32	0.34	-0.56
Ang Max	-0.22	-0.25	-0.18	0.30	0.31	-0.51
Topo	-0.02	-0.18	0.03	0.22	0.16	-0.51
Boulders	-0.61	0.03	-0.01	0.39	-0.07	0.31
Mudstone	-0.05	-0.13	0.38	0.34	0.00	-0.60
Cobbles	-0.46	-0.03	0.30	0.43	-0.19	0.37
Pebbles	-0.50	0.01	0.13	0.38	-0.29	0.25
Sand	0.20	-0.32	-0.07	0.26	0.03	0.51
Clay	0.06	0.33	-0.17	-0.52	0.05	-0.24

variation in the coral-only data was not explained by the environmental variables. This was demonstrated by the few environmental variables selected for the second axis (Fig. 6A).

Except for *Acanella arbuscula* and *Radicipes gracilis*, which occurred on clay bottoms, the gorgonians were confined to areas with cobble and boulder. The nephtheid corals utilised a wider range of substrates including semi-consolidated mudstone. Figure 6b indicated that the nephtheid corals, except *Duva florida*, occurred in areas with a relatively dense cover of sand and cobble close to the head of the canyon. On the other side of the plot *Flabellum* cf. *angulare* and *Acanella arbuscula* was associated with dense cover of clay in the outer part of the canyon (high value of "axis distance"). The figure also demonstrated that *Keratoisis ornata, P. resedaeformis*, and *D. florida* were associated with steep transects and dense cover of semi-consolidated mudstone. All *Flabellum* species were associated with low values for average angle, indicating that they are associated with level seabed. The position of *R. gracilis* in the centre of the plot indicated that this species occurred in areas with mixed seabed.

Discussion

Methods

It is difficult to standardise video recording of habitats in deep-water to enable quantitative data with minimal error. As video-records and photos are not well suited for identification of small epibenthic organisms (<5 cm), only larger forms were taxonomically identified (i.e. megafauna). The diversity and abundance of epibenthos reported here are therefore minimum estimates. The inaccuracy of the estimates of investigated areas leads to errors in abundance estimates for megafauna. There were two sources of error in estimating the area of video sequences: inaccurate geographical positions, and variable width of the visual field. The navigation error of ±2 m induced an error of ~17 % in the abundance of corals. Unfortunately, there was no practical way available to estimate the width of the visual field continuously. However, the height above bottom was quite stable most of the time and the error resulting from this factor is estimated to be <10 %.

The method used for estimating the relative abundance of different bottom types is not as precise as a point-count method. However, the latter method would have been very time-consuming applied to the large amount of video records used in this study. Previously Mortensen and Buhl-Mortensen (2004) compared estimates gained by the visual "subjective" method with estimates made by counting points overlying the different substrate classes in a grid of 20 point. This comparison was based on parallel estimates using the two techniques at three transects with a total of 72 video sequences. Since the correlation between the two estimation techniques was good ($R^2 = 0.86$, p <0.001) the simple and fast visual "subjective" method was chosen for this study.

The seabed below 500 m has been poorly investigated in The Gully, and little is known about the distribution and abundance of corals below this depth. Based on the results from a study of megafauna in canyons off northeastern USA (Hecker et al. 1980) larger gorgonians such as *Paragorgia* and *Primnoa* may occur with higher abundance deeper.

The abundance of corals compared to other regions

The average abundance of corals found in this study was lower than what has been reported from deep-sea coral reefs off Norway (Mortensen et al. 1995) and from gorgonian "forests" in the Northeast Channel off Atlantic Canada (Mortensen and Buhl-Mortensen 2004), but comparable to what Hecker et al. (1980) found for Canyons off the northeast coast of USA. Hecker et al. (1980) provided an early quantitative study of the distribution of corals and megafauna from photographs and submersible observations in three canyons. Averaged for 100-m depth intervals, they estimated a highest abundance for *Acanthogorgia armata* of 3.2 colonies $\cdot 100$ m^{-2} and for *Paragorgia arborea* of 0.3 colonies $\cdot 100$ m^{-2} between 400 and 800 m depth in Oceanographers Canyon. The average abundance of *Primnoa resedaeformis* is 4.8 and 4.3 colonies $\cdot 100$ m^{-2} in the Northeast Channel and on the Sula Reef respectively, compared to 2.0 colonies $\cdot 100$ m^{-2} for transects with presence in The

Gully (Table 2). The same pattern applies for *P. arborea* with 0.6 and 3.1 colonies ·100 m^{-2} in the Northeast Channel and on the Sula Reef respectively, whereas only 0.3 colonies·100 m^{-2} were observed in The Gully, identical to the value reported from Oceanographers Canyon (Hecker et al. 1980). Unfortunately, there are no similar data to provide a similar comparison for the other corals. However, *Keratoisis ornata* seems to be more common in The Gully than other sites in Atlantic Canada.

Distribution of corals and environmental controls

In general, the distribution of deep-water corals is uneven and the importance of different environmental factors may differ between regions. Of physical factors, suitable seabed substratum, water temperature and salinity are obvious requirements that must be met to enable the colonisation and growth of corals. Mortensen and Buhl-Mortensen (2004) found that the distribution of deep-water gorgonians in the Northeast Channel was patchy even within areas with high percentage of cobble and boulder, and within the depth range were the highest abundance was found. This indicated that other factors varying over small spatial scales are also important.

Geographic location

The number of species was significantly (p <0.005) correlated with the distance along the canyon axis, and different species were more common or abundant in certain divisions than others. This is explained by the strong correlation of axis distance with other variables such as depth, substratum types and salinity (Table 5). The two sides of The Gully have some differences in oceanographic conditions (currents, temperature, and salinity). The possible effects of these factors will be discussed below.

Substratum and topography

With the exception of a few species having anchorage structures for soft sediments, deep-water gorgonians are found on hard substrata such as cobbles, boulders or bedrock. In The Gully, the distribution of the gorgonians appears to be controlled by the availability of hard substrata. The average percentage cover of cobble and boulder in The Gully (3.9 % combined) is lower than in the Northeast Channel (25 %) (Mortensen and Buhl-Mortensen 2004) where the abundance of gorgonian corals is higher. The semi-consolidated mudstone was a suitable substrate for nephtheid corals but is probably too loose to serve as a solid substrate for the larger gorgonians.

The topographic index was poorly correlated with diversity and abundance of megafauna. The angle of the seabed was relatively strongly correlated with the fauna patterns revealed by CCA (Figs. 5 and 6). This variable is also a collective variable correlated with the topographic index and the cover of semi-consolidated mudstone. Topography also influences to the strength and pattern of near-bottom currents, and has been suggested as factor modifying the environment to the benefit of corals (Genin et al. 1986; Mortensen et al. 2001). Previous studies have demonstrated that the inclination of the seabed is related to re-suspension of

particulate matter and increased productivity (Rice et al. 1990; Frederiksen et al. 1992).

Depth and hydrography

Many factors that co-vary with depth can be expected to determine vertical distribution patterns. In the Northeast Atlantic different regional maximum depths of deep-water corals in offshore areas generally reflect different maximum depths of water masses with suitable temperatures (Frederiksen et al. 1992; Tendal 1992; Freiwald 1998; Mortensen et al. 2001). Unfortunately, this investigation was limited to depths above 544 m, which prevents discussion of the local maximum depths of corals in The Gully. There are few attempts to study corals below this depth off Nova Scotia. These studies, using dredges or trawls, have found *Paragorgia* and *Primnoa* as deep as 1097 and 457 m, respectively (Verrill 1922; Deichman 1936; Breeze et al. 1997). During previous habitat mapping in The Gully using a deep-sea drop camera *Keratoisis ornata*, *Anthomastus grandiflorus*, and *Radicipes gracilis* were observed at depths between 800 and 1300 m (Kostylev 2000). On the northeast coast of USA, Hecker et al. (1980) found *Paragorgia* down to 800 m depth, and *Primnoa* down to 560 m. These observations indicate that peak abundance for these corals may occur deeper than indicated by our study (Fig. 3).

Depth was not selected as a variable explaining much of the variation in the species data by CCA. This is probably explained by inter-correlation with temperature, which was strongly correlated with the variance in species data. Diversity and abundance of corals was negatively correlated with maximum temperature and positively correlated with maximum salinity. Tendal (1992) and Madsen (1944) describe the distribution of *Paragorgia* and *Primnoa* in the North Atlantic and suggest it is connected to the North Atlantic Current characterised by temperatures generally between 4 and 8°C, and stable salinity around 35 ‰. Our study indicated a shallower upper limit for alcyonacean corals (170 m) than for the rest (340 m; Fig. 3), suggesting that these taxa have different environmental requirements.

The lower abundance and diversity of corals on the eastern side of the canyon (Table 3) may be explained by the hydrographical conditions and currents, but it is hard to draw conclusions because the conditions are not known in a sufficient detail. These differences may also relate to differences in food supply. Food supply is an important biological factor, which may control the distribution of sessile invertebrates at both large and small scales. Unfortunately, the food requirement of deep-water gorgonians is generally unknown.

The significance of canyons as coral habitats

Similar to other submarine canyons, The Gully houses a diverse coral fauna. Nine coral species (one alcyonacean, seven gorgonians and one scleractinian) have previously been reported from The Gully (Breeze et al. 1997; MacIsaac et al. 2001). The new records for the area include *Anthomastus grandiflorus*, *Duva florida*, all three *Flabellum* species, and *Radicipes gracilis*. *Paramuricea placomus* has

previously been recorded from The Gully (Breeze et al. 1997), but was not observed during this study. Other canyons off Nova Scotia, such as Shortland and Halidimand Canyons, have been identified by fishermen as sites where large, colonial corals are found at depths greater than 300 m (Breeze et al. 1997). The reason why canyons are diverse coral habitats is probably primarily due to their great variety of habitats (depth, topography, bottom substrates and hydrographic conditions). Previous studies have shown that the benthic communities are more diverse and have greater abundance in canyons than in nearby slope areas (Hecker et al. 1980; Harrison and Fenton 1998; Vetter and Dayton 1998).

Hargrave et al. (2004) found the highest diversity of epifauna in The Gully on hard substrates of glacial origin along the edges of the channels, where alcyonaceans and gorgonians were common. In contrast with our findings Hargrave et al. (2004) found the maximum species richness of epifauna to be relatively shallow, around 180 m. Within the depth range of our study the species richness was higher below 300 m than above. This difference may occur because of the different scales of imagery processed in these two studies, which could mean that different components of the fauna were studied (photographs *vs*. sequences of video records).

Canyons influence local water properties and zooplankton distribution (Allen et al. 2001). It has been suggested that submarine canyons accumulate organic debris (Vetter 1994), and it is possible that deep-ocean currents, such as the south-westward flowing deep-water in the North Atlantic (Dickson et al. 1990) may bring particulate organic matter (POM) into The Gully. Harding (1998) suggests that there is a greater availability of POM in submarine canyons because of deposition of organic matter on continental slopes and patterns of water circulation in canyons. Storm activity may be an important factor for the high input of benthic detritus from shelf (Harding 1998). High concentration of POM may be important as food for the corals. The high coral abundance on the western outer division fits with an outflow of water that has been trapped from the current following the slope from northeast. Hargrave et al. (2004) conclude that organic matter is transported down the axis of the canyon. This transport is likely to be stronger on the western side because of the general current direction to the west.

There are very few species known to be obligate symbionts on deep-sea corals. The associated fauna of corals generally consists of generalistic commensal species that are able to survive without corals in other habitats. The frequency and abundance of larger corals in The Gully is low, which indicates that these corals play a limited role as habitat for other megafaunal species. The abundance of fish in The Gully was not significantly correlated with abundance of corals. Probably a coral habitat needs to have certain minimum abundance before it serves the function of shelter, and enhanced food availability.

Acknowledgements

References

Allen SE, Vindeirinho C, Thomson RE, Foreman MGG, Mackas DL (2001) Physical and biological processes over a submarine canyon during an upwelling event. Canad J Fish Aquat Sci 58: 671-684

Breeze H, Davis, DS (1998) Deep-sea corals. In: Harrison WG, Fenton DG (eds) The Gully: A scientific Review of its Environment and Ecosystem. Dept Fish Oceans, Canad Stock Assess Secr Res Doc 98/83, Dartmouth, NS, pp 113-120

Breeze H, Davis DS, Butler M, Kostylev V (1997) Distribution and status of deep-sea corals off Nova Scotia. Marine Issue Comm Spec Publ 1, Ecology Action Centre

Broch H (1912) Die Alcyonarien des Trondhjemsfjordes II. Gorgonacea. K Norske Vidensk Selsk Skr 1912: 1-48

Broch H (1935) Oktokorallen des nördlichsten Pazifischen Ozeans. Norske Vidensk Akad Oslo I, Mat-Natv kl 1935: 1-53

Broch H (1957) The northern octocoral, *Paragorgia arborea* (L.), in sub-antarctic waters. Nature 170: 1356

Buhl-Mortensen L, Mortensen PB (2004) Crustaceans associated with the deep-water gorgonian corals *Paragorgia arborea* (L., 1758) and *Primnoa resedaeformis* (Gunnerus 1763). J Nat Hist 38 1233-1248

Buhl-Mortensen L, Mortensen PB (2005) Distribution and diversity of species associated with deep-sea gorgonian corals off Atlantic Canada. In: Freiwald A, Roberts JM (eds) Cold-water Corals and Ecosystems. Springer, Berlin Heidelberg, pp 849-879

Cairns SD (1994) Scleractinia of the temperate North Pacific. Smithsonian Contr Zool 557, 150 pp

Carlgren O (1945) Polyppdyr (Coelenterata) III. Koraldyr. Danmarks Fauna 51, G.E.C. Gads forlag, Copenhagen, 168 pp

Deichman E (1936) The Alcyonaria of the western part of the Atlantic Ocean. Mus Comp Zool Mem 53: 1-317

DFO (2004) The Gully Marine Protected Area Regulations. Canada Gaz I 138 (10) (SOR/2004-112 May, 2004)

Dickson RR, Gmitrowicz EM, Watson AJ (1990) Deep-water renewal in the northern North Atlantic. Nature 344: 848-850

Fader GBJ, Piper DJW, Amos CL (1998) Surficial, bedrock geology and morphology of The Gully. In: Harrison WG, Fenton DG (eds) The Gully: A scientific Review of its Environment and Ecosystem. Dept Fish Oceans, Canad Stock Assess Secr Res Doc 98/83, Dartmouth, NS, pp 7-12

Fader GBJ, Strang J (2002) An interpretation of multibeam bathymetry from The Gully, outer Scotian Shelf: materials, habitats, slopes, features and processes. Canad Tech Rep Fish Aquat Sci 2377

Fosså JH, Mortensen PB, Furevik DM (2002) The deep-water coral *Lophelia pertusa* in Norwegian waters: Distribution and fishery impacts. Hydrobiologia 471: 1-12

Frederiksen R, Jensen A, Westerberg H (1992) The distribution of the scleractinian coral *Lophelia pertusa* around the Faroe islands and the relation to internal mixing. Sarsia 77: 157-171

Freiwald A (1998) Geobiology of *Lophelia pertusa* (Scleractinia) reefs in the north Atlantic. Habilitation thesis, Univ Bremen

Gass SE, Willison JHM (2005) An assessment of the distribution and status of deep sea corals in Atlantic Canada by using both scientific and local forms of knowledge. In: Freiwald A, Roberts JM (eds) Cold-water Corals and Ecosystems. Springer, Berlin Heidelberg, pp 223-245

Genin A, Dayton PK, Lonsdale PF, Speiss FN (1986) Corals on seamount peaks provide evidence of current acceleration over deep-sea topography. Nature 322: 59-61

Gordon DC, Fenton DG (2002) Advances in understanding the Gully ecosystem: a summary of research projects conducted at the Bedford Institute of Oceanography (1999-2001). Canad Tech Rep Fish Aquat Sci 2377

Gordon DC, Kenchington ELR, Gilkinson KD, McKeown DL, Steeves G, Chin-Yee M, Vass WP, Bentham K, Boudreau PR (2000) Canadian imaging and sampling technology for studying marine benthic habitat and biological communities. CM 2000/T:07. ICES 2000 Ann Sci Conf 27-30 September 2000, Bruges, Belgium

Gowans S, Whitehead H, Arch JK, Hooker SK (2000) Population size and residency patterns of northern bottlenose whales (*Hyperoodon ampullatus*) using the Gully, Nova Scotia. J Cetacean Res Manage 2: 201-210

Hall-Spencer J, Allain V, Fosså JH (2002) Trawling damage to Northeast Atlantic ancient coral reefs. Proc R Soc London, B 269: 507-511

Han G, Roussel P, Loder JW (2002) Seasonal-mean circulation and tidal currents in the The Gully. In: Gordon DC, Fenton DG (eds) Advances in understanding the Gully ecosystem: a summary of research projects conducted at the Bedford Institute of Oceanography (1999-2001). Canad Tech Rep Fish Aquat Sci 2377, 87 pp

Harding GC (1998) Submarine canyons: deposition centres for detrital organic matter? In: Harrison WG, Fenton DG (eds) The Gully: A scientific review of its environment and ecosystem. Dept Fish Oceans, Canad Stock Assess Secr Res Doc 98/83, Dartmouth, NS, pp 105-106

Hargrave BT, Kostylev VE, Hawkins CM (2004) Benthic epifauna assemblages, biomass and respiration in the Gully region on the Scotian Shelf, NW Atlantic. Mar Ecol Prog Ser 270: 55-70

Harrison WG, Fenton DG (1998) The Gully: A scientific review of its environment and ecosystem. Dept Fish Oceans, Canad Stock Assess Secr Res Doc 98/83, Dartmouth, NS

Hecker B, Blechschmidt G, Gibson P (1980) Final report-canyon assessment study in the Mid- and North Atlantic area of the U.S. outer continental shelf. U.S Dept Interior, Bur Land Manage, Washington, D.C., Contract No. BLM AA551-CT8-49

Jungersen HFE (1917) Alcyonarian and Madreporarian corals in the museum of Bergen, collected by Fram-Expedition 1898 - 1900 and by the "Michael Sars 1900 - 1906. Bergen museums Aarbok 1915 - 16. Naturvidensk Række 6, 44 pp

Kostylev VE (2000) Database on underwater imagery from the Sable Island Gully. Contract Rep

MacIsaac K, Bourbonnais C, Kenchington E, Gordon D, Gass S (2001) Observations on the occurrence and habitat preference of corals in Atlantic Canada. In: Willison JHM, Hall J, Gass SE, Kenchington ELR, Butler M, Doherty P (eds) Proceedings of the First International Symposium on Deep-Sea Corals. Ecology Action Centre, Nova Scotia Museum, Halifax, Nova Scotia, pp 58-75

Madsen FJ (1944) Octocorallia (Stolonifera - Telestacea - Xeniidea - Alcyonacea - Gorgonacea). Danish Ingolf-Exped 13, 65 pp

Mann, KH (2002) Overview of results. In: Gordon DC, Fenton DG (2002) Advances in understanding the Gully ecosystem: a summary of research projects conducted at the Bedford Institute of Oceanography (1999-2001). Canad Tech Rep Fish Aquat Sci 2377, 87 pp

Mortensen PB, Buhl-Mortensen L (2004) Distribution of deep-water gorgonian corals in relation to benthic habitat features in the Northeast Channel (Atlantic Canada). Mar Biol 144: 1223-1238

Mortensen PB, Hovland MT, Brattegard T, Farestveit R (1995) Deep water bioherms of the scleractinian coral *Lophelia pertusa* (L.) at 64° N on the Norwegian shelf: structure and associated megafauna. Sarsia 80: 145-158

Mortensen PB, Hovland MT, Fosså JH, Furevik DM (2001) Distribution, abundance and size of *Lophelia pertusa* coral reefs in mid-Norway in relation to seabed characteristics. J Mar Biol Ass UK 81: 581-597

Mortensen PB, Buhl-Mortensen L, Gordon DC, Fader GBJ, McKeown DL, Fenton DG (in press) Effects of fisheries on deep-water gorgonian corals in the Northeast Channel, Nova Scotia (Canada). Proceedings of a Symposium on Effects of Fishing on Benthic Habitats, Tampa Florida

Petrie B, Dean-Moore J (1996) Temporal and spatial scales of temperature and salinity on the Scotian Shelf. Canad Tech Rep Hydrogr Ocean Sci 177, 53 pp

Petrie B, Shore J, Hannah C, Loder J (1998) Physical oceanography. In: Harrison WG, Fenton DG (1998) The Gully: A scientific Review of its Environment and Ecosystem. Dept Fish Oceans, Canad Stock Assess Secr Res Doc 98/83, Dartmouth, NS, 20-57

Rice AL, Thurston MH, New AL (1990) Dense aggregation of a hexactinellid sponge, *Pheronema carpenteri*, in the Porcupine Seabight (Northeast Atlantic Ocean) and possible causes. Prog Oceanogr 24: 179-196

Rogers AD (1999) The biology of *Lophelia pertusa* (Linnaeus 1758) and other deep-water reef-forming corals and impacts from human activities. Int Rev Hydrobiol 84: 315-406

Shannon CE, Weaver W (1949) The mathematical theory of communication. Univ Illinois Press, Urbana, 117 pp

Tendal OS (1992) The North Atlantic distribution of the octocoral *Paragorgia arborea* (L., 1758) (Cnidaria, Anthozoa). Sarsia 77: 213-217

Verrill AE (1922) The Alcyonaria of the Canadian Arctic Expedition, 1913-1918, with a revision of some other Canadian genera and species. Rep Canad Arctic Exped 1913-18, 8, Molluscs, Echinoderms, Coelenterates, Etc. G, Alcyonaria and Actinaria

Vetter EW (1994) Hotspots of benthic production. Nature 372: 47

Vetter EW, Dayton PK (1998) Macrofaunal communities within and adjacent to a detritus-rich submarine canyon system. Deep-Sea Res II 45: 25-54

Wentworth C K (1922) A scale of grade and class terms for clastic sediments. J Geol 30: 377-392

Zibrowius H (1980) Les Scléractiniaires de la Méditerranée et de l'Atlantique nord-oriental. Mem Inst Oceanogr 11, 226 pp

Distribution of deep-water Alcyonacea off the Northeast Coast of the United States

Les Watling[1], Peter J. Auster[2]

[1] Darling Marine Center, University of Maine, Walpole, ME 04573, USA
 (watling@maine.edu)
[2] National Undersea Research Center, Department of Marine Sciences, University
 of Connecticut, Groton, CT 06340, USA

Abstract. A database of deep-water alcyonacean records has been assembled using information that reaches back to the work of A.E. Verrill from the 1800s. These database records fall into two time periods, those from 1874 to 1920, and from 1950 to 2001. A total of 25 species in 10 families are so far known from the northeastern U.S. Most of these species are common in deeper waters of the continental shelf, with a few being restricted to the canyons and other slope environments. A comparison of western and eastern North Atlantic records indicates there is little similarity between the regions. In the cold-temperate to boreal part of the region there is about 41 % similarity of the "stoloniferous" and "massive body" soft coral species, but only about 28 % similarity amongst all the "gorgonian" species. In the warm temperate part of the region the similarity for all groups is less than 10 %. Deep-water alcyonaceans are strongly impacted by bottom fishing gear so it is likely that modern distributional records will not be exactly similar to those from deep in the past.

Keywords. Alcyonacea, continental slope, database, distributions, octocorals

Introduction

Deep-water corals have been an increasing focus for marine conservation since about 1998. Attention was brought to bear on deep corals in Europe and Canada, especially in Norway, where large deep reefs, constructed by *Lophelia pertusa* over thousands of years were found to be easily destroyed by mobile fishing gear (Fosså et al. 2000). In Canada, long-line fishermen who had occasionally pulled large corals from the depths were concerned about the possibility that these coral areas would be destroyed in a short time period by the trawl fisheries (Breeze et al. 1997; Gass 2002). Following the First International Symposium on Deep-Sea Corals, held in Halifax in 2000, deep-dwelling corals became the "poster child" of non-governmental organizations, symbolizing all that was wrong with fisheries management, especially in the United States where the record of protection of these

species has been dismal compared to Europe and Canada, both of the latter having recently established no trawling zones in areas where deep corals are known to be abundant.

A significant part of the problem regarding conservation of deep-water corals in the United States is the lack of a comprehensive knowledge about the distribution of deep-water coral taxa in this region. It should be noted, however, that along the American east coast deep-water corals have been known since at least 1862 when Verrill documented the presence of a *Primnoa* "on Georges Bank" (Verrill 1862). Several other deep-water coral species from depths greater than 200 fathoms (365 m) off the coasts of New England and Nova Scotia were documented by Verrill during the latter part of the 19th century (e.g., Verrill 1878a, 1878b, 1879, 1884). Many specimens were captured during dredging programs instituted by the U.S. Fish Commission (as the National Marine Fisheries Service was known in those days), but an equally large number of specimens were brought to Verrill's attention by schooner captains who had pulled the corals from the bottom while tub trawling. While few "reefs" have been found off northeast North America (there is one news report of a *Lophelia* reef about 1 km long off Nova Scotia), the coral fauna is diverse and includes several octocoral species as well as hard corals (Breeze et al. 1997; Gass 2002). Seventeen species of scleractinian corals (hard corals) are known from Cape Hatteras to the Gulf of Maine (Cairns and Chapman 2001). Only one species (*Astrangia poculata*) occurs in shallow water and 71 % of the 17 species occur deeper than 1000 m. Forty-seven percent of the scleractinian corals from the cold-temperate U.S. coast are widespread species and 28 % occur across the Atlantic, with only a single species, *Vaughanella margaritata*, endemic to the NW Atlantic (Cairns and Chapman 2001). Photographic transects of the slope and canyon faunas south of Georges Bank recorded over 25 species of both hard corals and octocorals with several taxa dominant in the overall megafaunal community (Hecker et al. 1980, 1983; Valentine et al. 1980; Cooper et al. 1987; Hecker 1990). However, seven species (two hard corals and five soft corals, respectively) tend to occur in high densities in different areas of the canyon/slope environment: *Desmosmilia lymani*, *Flabellum alabastrum*, *Acanella arbuscula*, *Anthomastus agassizii*, *Eunepthya* (now *Capnella*) *florida*, *Paramuricea borealis* (now *P. grandis*), and *Primnoa resedaeformis* (Valentine et al. 1980; Hecker 1990).

The benthic fauna of the Northeast Peak of Georges Bank was characterized as having two octocorals, *Primnoa resedaeformis* and *Paragorgia arborea*, as common components based on dredge sampling (Theroux and Grosslein 1987). Wigley (1968) described *Paragorgia* as a common component of the gravel fauna of the Gulf of Maine and stated that representative gravel faunas occurred on "Cashes Ledge, parts of Great South Channel, the northeastern part of Georges Bank, western Browns Bank, Jeffreys Ledge, and numerous other smaller banks in the Gulf of Maine region."

The report by Theroux and Wigley (1998) on the distribution of macrobenthic invertebrates off the northeastern United States, while an excellent summary of the distribution of major taxonomic groups, lacked taxonomic specificity for

corals. Stony corals were lumped with all of the Zoantharia (including burrowing anemones, solitary epibenthic anemones, and colonial anemones). However, the distribution of the Alcyonaria (now the Octocorallia), comprising the soft corals (Alcyonacea and Gorgonacea, now combined under the single name Alcyonacea) and sea pens (Pennatulacea), showed patterns useful for predicting the distribution of soft coral taxa (based on 63 samples, 6 % of total). These taxa were patchily distributed primarily along the outer margin of the continental shelf and on the continental slope and rise. They were not collected in samples shallower than 50 m depth (and it is unclear if deeper samples included the shallow soft coral *Gersemia rubiformis,* as there were many samples unidentified to the level of genus in the database). Alcyonaceans and gorgonaceans (soft corals) were collected from gravel and rock outcrop habitats while pennatulids were collected from sand-silt and silt-clay sediments.

As one can see, deep-water corals have been recorded, often sporadically, for the northeastern United States for more than 125 years. Until now, however, these various records have not been pulled together into one database which can be analyzed for distributional patterns. In this paper we present a summary of the known records of deep-water alcyonaceans from the northeastern United States, and compare these records to the alcyonacean fauna of the North Atlantic Ocean as a whole (see Appendix 1).

Methods

We created a GIS database of known occurrences of deep-water corals (soft corals and sea fans of the Order Alcyonacea) off the northeastern United States. The database was first constructed in Microsoft Access, then ported to ArcView for record mapping. The dataset includes records from published accounts of Verrill (as cited above), Deichmann (1936), and the detailed maps of camera tows from Hecker et al. (1980, 1983), as well as the web-accessible records of the Yale Peabody Museum collection, Northeast Fisheries Science Center Benthic Database records (of identified coral taxa), and observations from recent NOAA supported studies in 2001 (NURC, Ocean Exploration projects). This database does not currently include other possible data sources: (1) photographic transect studies in submarine canyons led by Richard Cooper (e.g., Valentine et al. 1980; Cooper et al. 1987), (2) video records from the NURC North Atlantic and Great Lakes (office in Groton, Connecticut) video archive, (3) specimens deposited in museums by the U.S. Northeast Fisheries Science Center and not yet identified, and (4) specimens in museums from this area but whose records are not available electronically.

For the broader geographic comparisons, we used records compiled from the following sources: Madsen (1944), Bayer (1957, 1964a, 1964b, 1979, 2001), Carpine and Grasshoff (1975), Grasshoff (1977, 1981, 1985, 1989), Cairns (2001), and Cairns and Bayer (2002). The classification of alcyonaceans used here is that of Bayer and Grasshoff, as updated and modified by Williams and Cairns and posted on Gary Williams' web site (http://www.calacademy.org/research/izg/OCTOCLASS.htm) where no formal suborder level names are used within the Order Alcyonacea.

Results and discussion

In all, the database currently contains 761 records, from the years 1874 to 2001. Certain locations, such as Oceanographer and Lydonia Canyons, as well as a few other locations examined with a towed camera sled by Hecker et al. (1980, 1983), have a high density of data records, most of which do not show well at the scale of the illustrations used here. That information can be obtained by requesting from the authors a copy of the ArcView database CD (Watling et al. 2003).

The database records fall into two distinct time periods: 1874-1920 (Fig. 1) and 1950-2001 (Fig. 2). The early records come primarily from the expeditions of many U.S. vessels, most of which were involved in mapping of the seabed and various oceanographic features. The corals were obtained incidentally in dredge hauls, and most were identified by Louis de Pourtalès and A.E. Verrill. All of these records are summarized in Deichmann (1936), or are listed on the Yale Peabody Museum web site of specimen records (http://www.peabody.yale.edu/collections/iz/).

The records from 1950 onwards come from a variety of sources, and represent a series of explorations of the continental shelf and slope of the U.S. The earliest represent corals found in sediment samples taken by the U.S. Geological Survey. Many of the canyon and slope records are from early Alvin submersible dives, also made for geological studies as well as baseline studies conducted in anticipation of
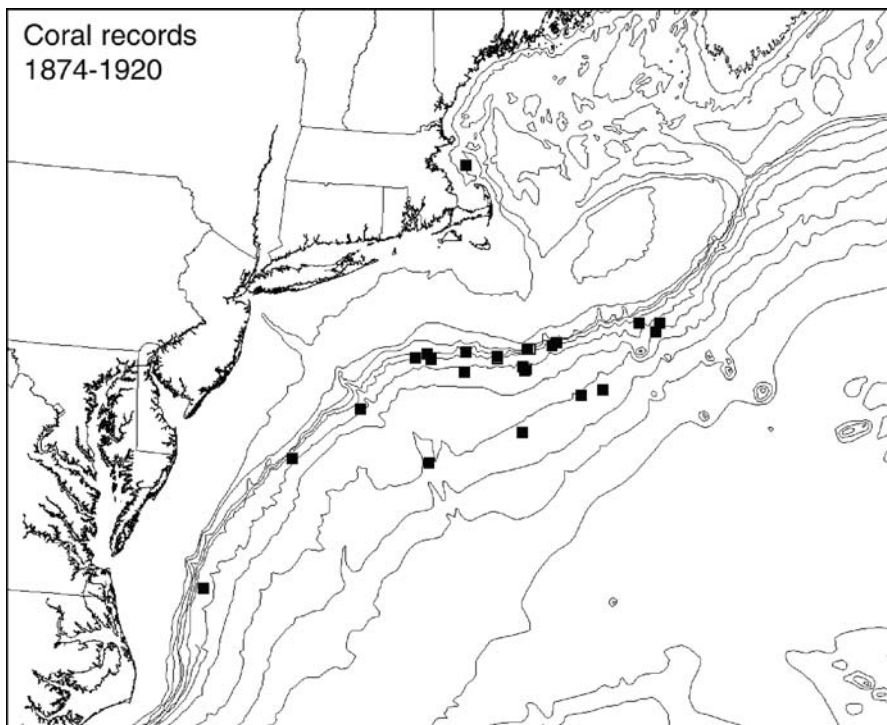
Fig. 1 Coral records for the years 1874-1920. With the exception of the single record off Boston, all are from deep-water along the continental slope and rise
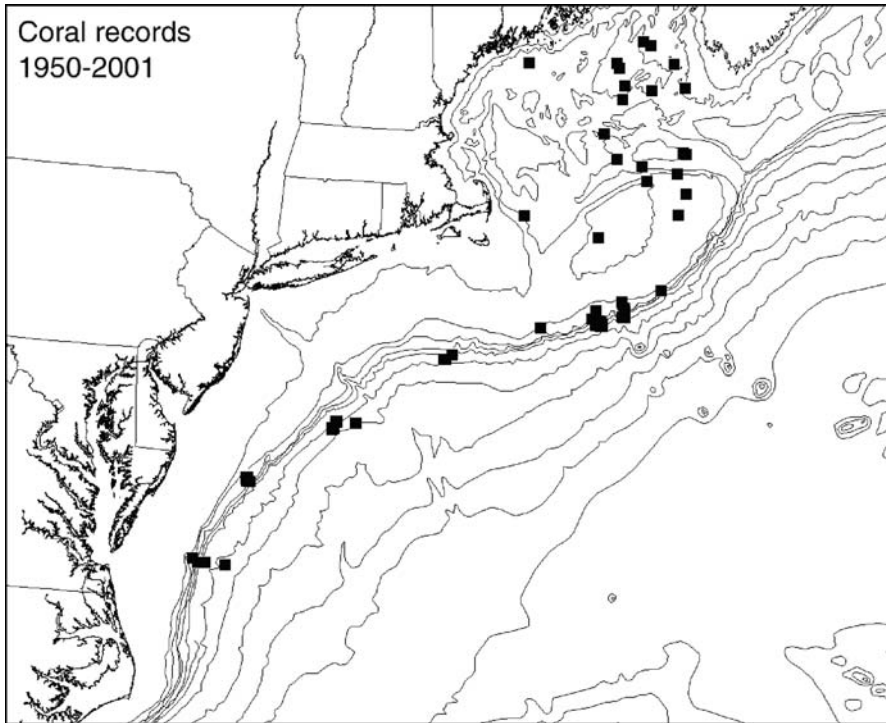
Fig. 2 Coral records for the years 1950-2001. There is a broad distribution of coral records from the Gulf of Maine, reflecting records from the U.S. National Marine Fisheries Service, and clusters of records from various canyons along the continental slope. Most of the latter are attributable to geological surveys of the canyons and baseline environmental surveys preparatory to proposed oil drilling

exploratory oil drilling, with the species identified from 35 mm film images by Dr. Barbara Hecker or her associates and recorded in Hecker et al. (1980, 1983). Other records, especially in Oceanographer, Lydonia, and Baltimore Canyons, as well as sites along the continental slope come from 35 mm film images made by Hecker et al. (1980, 1983) using a towed camera system. As a part of the Hecker et al. (1980) report, Dennis Opresko prepared a guide to the common octocorals, and a limited number of "voucher" specimens were examined to ground truth the identifications made from the film. In fact, Hecker et al. (1980, 1983) acknowledge that it was very difficult to be certain of all identifications in part because "voucher" specimens were often contracted whereas on film a specimen might look quite different, a fact that needs to be kept in mind when examining the distribution patterns in the database. The last of the modern records used here are from trawl samples made for fisheries investigations by the National Marine Fisheries Service. In some cases, these records include a species identification, but many times do not. If species identification was not given, the record was not used when the database was ported over to ArcView. Again there is uncertainty about the accuracy of the identifications.

A total of 25 species in 10 families have been recorded from the northeastern U.S. continental shelf and slope north of Cape Hatteras (Table 1). Species in the "Holaxonia", "Scleraxonia", and "Calcaxonia" are the best documented, primarily because of their larger form, but also because they are most abundant in the deeper waters of the continental slope. The Clavulariidae are most likely under-represented in NW Atlantic waters. Because of their small size they are probably overlooked by biologists unfamiliar with their general morphology.

Records in the database fell into two time periods, 1920 and earlier, and 1950 and later. The early records, beginning with what is now *Clavularia modesta* (Verrill) from Stellwagen Bank in 1874, are all from dredge samples obtained by U.S. Coast Survey vessels. Most of the effort was directed toward sampling in the deep waters off the continental shelf. After a hiatus of three decades or so, exploration of the continental slope began again, this time by geologists and then deep-sea biologists.

Table 1 List of Alcyonacea known to occur on the northeastern U.S. (north of Cape Hatteras) continental shelf and slope

"Stoloniferous forms"	"Scleraxonia"
Clavulariidae	**Anthothelidae**
Clavularia modesta (Verrill, 1874)	*Anthothela grandiflora* (Sars, 1856)
Clavularia rudis (Verrill, 1922)	
	Paragorgiidae
"massive body forms"	*Paragorgia arborea* (Linné, 1758)
Alcyoniidae	
Alcyonium digitatum Linné, 1758	"Calcaxonia"
Anthomastus grandiflorus Verrill, 1878	**Chrysogorgiidae**
Anthomastus agassizii Verrill 1922	*Chrysogorgia agassizii* (Verrill, 1883)
	Iridogorgia pourtalesii Verrill, 1883
Nephtheidae	*Radicipes gracilis* (Verrill, 1884)
Gersemia rubriformis (Ehrenberg, 1834)	
Gersemia fructicosa (Sars, 1860)	**Primnoidae**
Capnella florida (Rathke, 1806)	*Narella laxa* Deichmann, 1936
Capnella glomerata (Verrill, 1869)	*Primnoa resedaeformis* (Gunnerus, 1763)
	Thouarella n. sp.
"Holaxonia"	
Acanthogorgiidae	**Isididae**
Acanthogorgia armata Verrill, 1878	*Acanella arbuscula* (Johnson, 1862)
	Keratoisis ornata Verrill, 1878
Plexauridae	*Keratoisis grayi* Wright, 1869
Paramuricea grandis Verrill, 1883	*Lepidisis caryophyllia* Verrill, 1883
Paramuricea placomus (Linné, 1758)	
Paramuricea **n. sp.**	
Swiftia casta (Verrill, 1883)	

Much of the geological work was directed first to understanding the formation of deep-sea canyons, and then to the search for deep oil deposits. Biologists became a significant part of this work in the 1980s as environmental baseline studies were conducted in case deep-water oil drilling was to commence. Other coral records were produced, especially in the Georges Bank and Gulf of Maine waters, as bycatch from the National Marine Fisheries Service spring and fall groundfish surveys.

For the species in the database, two distinct distributional patterns emerge. Most of the alcyonaceans are species of deep-water, for example, those in the genera *Anthomastus*, *Acanthogorgia*, *Acanella*, *Anthothela*, *Lepidisis*, *Radicipes*, *Clavularia*, and *Swiftia* (Figs. 3 and 4). The records of all these species are for depths greater than 500 m. Other species, such as *Paragorgia arborea*, *Primnoa resedaeformis*, and those in the genus *Paramuricea*, range throughout shelf waters to the upper continental slope (Figs. 3 and 4). *Paragorgia arborea* and *P. resedaeformis* are widespread North Atlantic and North Pacific species (Madsen 1944; Tendal 1992). Not shown in these maps, and not common in the database as it is now constructed, are the numerous nearshore records of *Gersemia rubiformis* and *Alcyonium* species.

Cairns and Chapman (2001) analyzed distributional records of deep-water scleractinian corals. They divided the eastern and western Atlantic into several
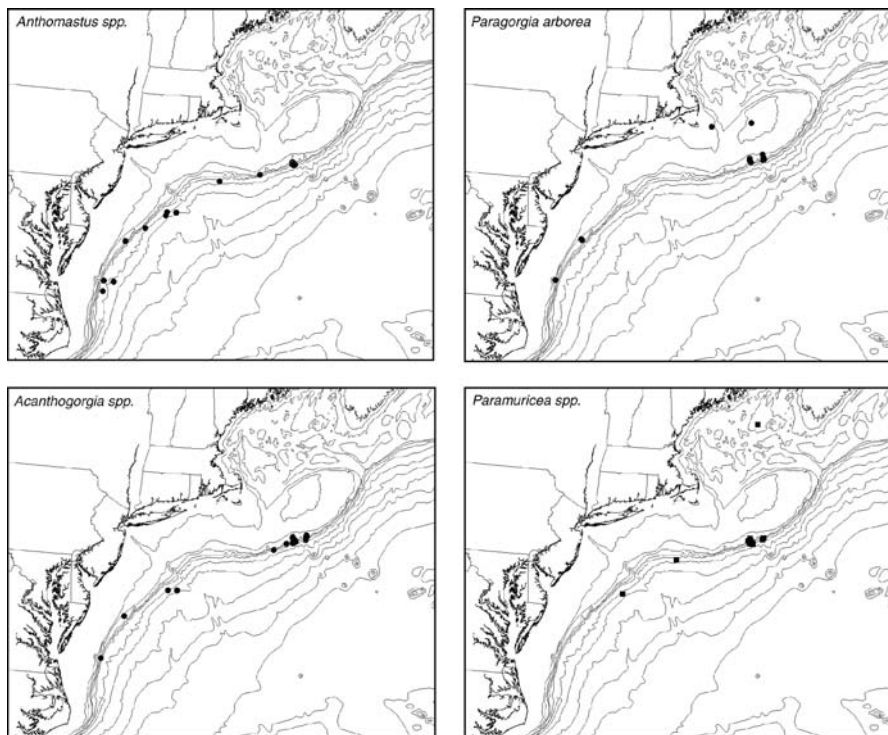
Fig. 3 Distribution of four alcyonacean genera along the east coast of the United States
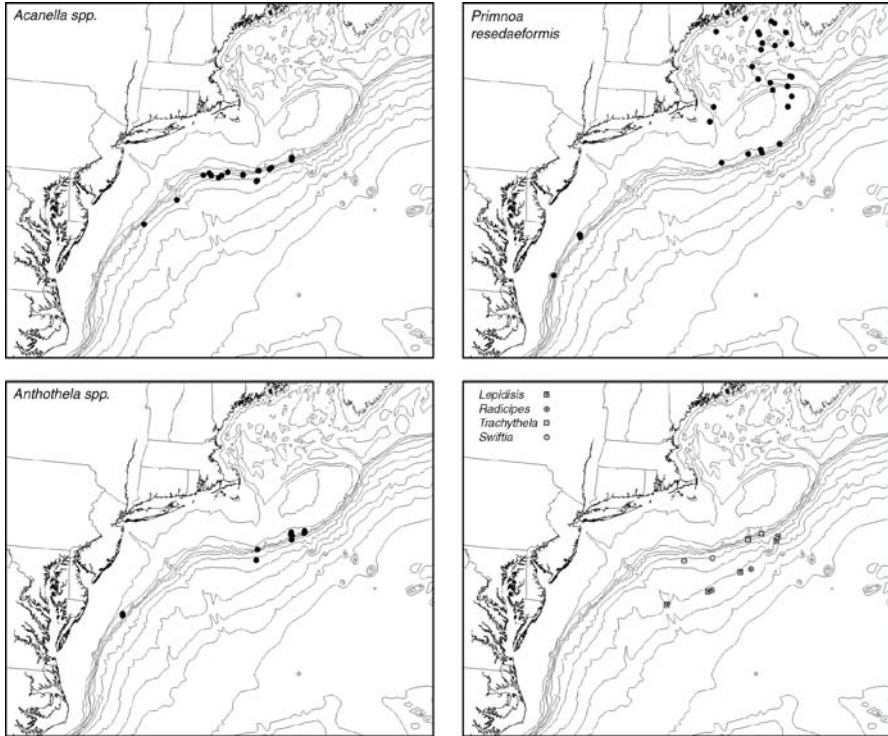
Fig. 4 Distribution of seven genera along the U.S. east coast

regions, four of which are adopted here with slight modifications. The eastern Atlantic includes regions IIB, ranging from the English Channel to northern Scandinavia and Iceland, and IIIA extending from the English Channel south to western Africa, including the Azores and associated seamounts. In the western Atlantic, region IIA extends from the Straits of Belle Isle in northern Newfoundland south to Cape Hatteras, and IA from Cape Hatteras to the Florida Straits (see Appendix 2). In this paper, we extended region IIA northwards to Baffin Island and Davis Straits. Cairns and Chapman had labelled those waters as part of their Arctic region. The extension of region IIA, we believe, is strengthened by an analysis of cumacean distributions, several species of which are seen to track Norwegian-Greenland Sea Overflow Water south of Iceland to the Davis Straits and southward along the northeastern U.S. continental slope in what is usually called the Western Boundary Undercurrent (Watling, unpublished).

A summary of the species distributions for these regions is given in Table 2 and Appendix 1. As a result of extending region IIA into the Davis Straits area, four additional species are included, all in the Family Clavulariidae. The greatest similarity of Regions IIA and IIB is in the "stoloniferous" and "massive body form" soft corals, where 7 of the 17 species (41 %) recorded to date can be found on both sides of the Atlantic. For the remaining alcyonaceans, the "Gorgonacea" of old, only 6 of 21 species (28 %) are common to both regions.

Table 2 Zoogeographic relationships of alcyonaceans of the temperate and cold-water North Atlantic region. Roman numerals and letters in the first line refer to regions as defined by Cairns and Chapman (2001) and used for analysis of deep scleractinian patterns

	IIA E. Canada to Cape Hatteras	IIB Boreal Eastern Atlantic	IIA : IIB in common	IA Cape Hatteras to Florida Straits	IIIA Lusitanian-Mediterranean	IA : IIIA in common
"Stoloniferous forms"						
Clavulariidae	6	7	2	2	8	0
"massive body forms"						
Alcyoniidae	3	2	2	1	6	1
Nephtheidae	3	3	3	0	1	0
"Scleraxonia"						
Anthothelidae	1	1	1	1	1	0
Paragorgiidae	1	1	1	2	2	1
Coralliidae	0	0	0	2	5	1
"Holaxonia"						
Acanthogorgiidae	1	0	0	2	2	0
Plexauridae	4	4	1	4	22	0
Gorgoniidae	0	0	0	4	9	0
"Calcaxonia"						
Chrysogorgiidae	3	0	0	4	8	2
Ellisellidae	0	0	0	1	3	0
Primnoidae	3	1	1	6	10	2
Isididae	4	3	2	4	12	3
Total Species	29	22	13	33	89	10

For the warm-temperate regions IA and IIIA, the picture is vastly different (Table 2). Only 1 of the 17 species (5 %) of soft corals, and 8 of 95 species (8 %) of "gorgonaceans" are common to both regions. This disparity is most likely due to the very different amount of hard substrate area involved. Region IIIA includes the Azores, Madeira, and several seamount groups that increase total habitat area. In Region IA, the deep slope widens along the Blake Plateau, but narrows again quickly off Florida, and seamounts are absent. Our recent work on the New England seamount chain suggests that the diversity of "gorgonaceans" in the western Atlantic might be more similar to that of the eastern Atlantic than we currently have data to support, but this statement will have to await detailed taxonomic work.

Fishing has had significant impacts on deep-water coral populations worldwide. While the effects of fishing on the deep reefs off Norway have been by now well-documented (e.g., Fosså et al. 2000), similar data for alcyonacean communities are sparse. Observations of the impacts of a single trawl tow through *Primnoa* habitat in the Gulf of Alaska, where 1000 kg of coral were landed, showed seven years later that 7 of 31 colonies remaining in the trawl path were missing 80-99 % of their branches and boulders with corals attached were tipped and dragged (Krieger 2001). Damage was restricted to the net path. Approximately 50 colonies were observed within 10 m of the net (where bridles would have swept over the seafloor) and no damaged colonies or disturbed boulders were observed. Long-line gear is also noted to tip and dislodge corals (Krieger 2001). Bycatch data from a long-line survey in the Gulf of Alaska and Aleutian Islands showed *Primnoa* and other coral taxa were caught on 619 of 541,350 hooks fished at 150-900 m depths (Krieger 2001).

Corals are clearly sensitive to fishing gear impacts and recovery rates are extremely slow based on our knowledge of recruitment, growth rates, and age structure. The ability to age deep-water octocorals is relatively new and various

methods are used in different studies. For *Primnoa resedaeformis*, a common outer shelf-upper slope species, Risk et al. (2002) estimates linear growth rates at the distal tips of the colonies at 1.5-2.5 mm yr^{-1} based on comparisons of live specimens with growth rates through the base of a sub-fossil specimen collected from the Northeast Channel at 450 m. Growth rates of this species in the Gulf of Alaska are reported as 1.60-2.32 cm yr^{-1}, although these samples were collected at less than 200 m depth (Andrews et al. 2002). Age estimates for only a few specimens demonstrate this species lives for hundreds of years. The colony collected from the Northeast Channel (Risk et al. 2002) has an estimated age of >300 years, which is in accordance with age estimates of the same species collected in Alaska (>100 years; Andrews et al. 2002).

Data on recruitment patterns is even more limited. A single series of observations in the Gulf of Alaska suggest that recruitment of *Primnoa* sp. is patchy and aperiodic (Krieger 2001). No recruitment of new colonies was observed in an area where *Primnoa* was removed by trawling after seven years. However, six new colonies were observed at a second site one year after trawling. Four of these colonies were attached to the bases of colonies removed by trawling. Recruits of *Primnoa* were also observed on two 7 cm diameter cables (>15 colonies each). On the other hand, our limited observations of corals in the Gulf of Maine and in submarine canyons has revealed abundant new recruits of both *Primnoa resedaeformis* and *Paramuricea* spp. (Watling, Auster, and France, unpublished observations). Whether these young colonies were produced by larval recruitment or branch dropping (as in shallow-water gorgonians) is impossible to say at this time.

In conclusion, our knowledge of the biology of deep-water alcyonaceans in the North Atlantic is still very limited. Unfortunately, because of the widespread use of fishing gear in this region, it may be that many records, especially of the gorgonians, may be simply historical. That is, if recruitment rates away from centers of colony abundance are really low, reestablishment of populations in areas where there has been widespread removal, is likely to take a very long time.

Acknowledgements

References

Andrews AH, Cordes EE, Mahoney MM, Munk K, Coale KH, Cailliet GM, Heifetz J (2002) Age, growth and radiometric age validation of a deep-sea, habitat forming gorgonian (*Primnoa resedaeformis*) from the Gulf of Alaska. Hydrobiologia 471: 101-110

Bayer FM (1957) Additional records of western Atlantic octocorals. J Washington Acad Sci 47: 379-390

Bayer FM (1964a) A new species of the octocorallian genus *Paragorgia* trawled in Florida waters by R.V. "Gerda". Zool Meded 39: 526-532

Bayer FM (1964b) The genus *Corallium* (Gorgonacea: Scleraxonia) in the western North Atlantic Ocean. Bull Marine Sci Gulf Caribbean 14: 465-478

Bayer FM (1979) *Distichogorgia sconsa*, a new genus and species of chrysogorgiid octocoral (Coelenterata: Anthozoa) from the Blake Plateau off northern Florida. Proc Biol Soc Washington 92: 876-882

Bayer FM (2001) New species of *Calyptrophora* (Coelenterata: Octocorallia: Primnoidae) from the western part of the Atlantic Ocean. Proc Biol Soc Washington 114: 367-380

Breeze H, Davis DS, Butler M, Kostylev V (1997) Distribution and status of deep-sea corals off Nova Scotia. Marine Issue Comm Spec Publ 1. Ecology Action Center, Halifax, NS, Canada, 58 pp

Cairns SD (2001) Studies on western Atlantic Octocorallia (Coelenterata: Anthozoa). Part 1. The genus *Chrysogorgia* Duchassaing & Michelotti, 1864. Proc Biol Soc Washington 114: 746-787

Cairns SD, Bayer FM (2002) Studies on western Atlantic Octocorallia (Coelenterata: Anthozoa). Part 2. The genus *Callogorgia* Gray, 1858. Proc Biol Soc Washington 115: 840-867

Cairns SD, Chapman RE (2001) Biogeographic affinities of the North Atlantic deep-water Scleractinia. In: Willison JHM, Hall J, Gass SE, Kenchington ELR, Butler M, Doherty P (eds) Proceedings of the First International Symposium on Deep-Sea Corals. Ecology Action Centre, Halifax, pp 30-57

Carpine C, Grasshoff M (1975) Les gorgonaires de la Méditerrannée. Bull Inst Océanogr Monaco 2: 1-146

Cooper RA, Valentine P, Uzmann JR, Slater RA (1987) Submarine canyons. In: Backus RH (ed) Georges Bank. MIT Press, Cambridge, Massachusetts, pp 52-63

Deichmann E (1936) The Alcyonaria of the western part of the Atlantic Ocean. Mem Mus Comp Zool 53: 1-317

Fosså JH, Mortensen PB, Furevik DM (2000) *Lophelia* korallrev langs norskekysten forekomst og tilstand (*Lophelia* coral reefs in Norway, distribution and effects of fishing). Prosjektrapport Havforskningsinstituttet, Bergen, 94 pp (in Norwegian with English summary and tables)

Gass S (2002) An assessment of the distribution and status of deep-sea corals in Atlantic Canada by using both scientific and local forms of knowledge. M.S. thesis, Environmental Studies, Univ Dalhousie

Grasshoff M (1977) Die Gorgonarien des östlichen Nordatlantik und des Mittelmeeres III. Die Familie Paramuriceidae (Cnidaria, Anthozoa). "Meteor" Forsch-Ergeb Sect D 27: 5-76

Grasshoff M (1981) Die Gorgonaria, Pennatularia, und Antipatharia des Tiefwassers der Biskaya (Cnidaria, Anthozoa). Bull Mus Natl Hist Nat Paris, 4e sér 3: 731-766

Grasshoff M (1985) Die Gorgonaria und Antipatharia der Großen Meteor-Bank und der Josephine-Bank (Cnidaria: Anthozoa). Senckenbergiana marit 17: 65-87

Grasshoff M (1989) Die Meerenge von Gibraltar als Faunenbarriere: die Gorgonaria, Pennatularia und Antipatharia der BALGIM-Expedition (Cnidaria: Anthozoa). Senckenbergiana marit 20: 201-223

Hecker B (1990) Variation in megafaunal assemblages on the continental margin south of New England. Deep-Sea Res 37: 37-57

Hecker B, Blechschmidt G, Gibson P (1980) Final report – Canyon Assessment Study in the Mid- and North Atlantic Areas of the U.S. Outer Continental Shelf. U.S. Dept Interior, Bureau Land Management, Washington, D.C. Contract No. BLM-AA551-CT8-49

Hecker B, Logan DT, Gandarillas FE, Gibson PR (1983) Megafaunal assemblages in Lydonia Canyon, Baltimore Canyon, and selected slope areas. In: Canyon and Slope Processes Study 3. Final Rep, U.S. Dept Interior, Mineral Manage Serv Contract 14-12-001-29178

Krieger KJ (2001) Coral (*Primnoa*) impacted by fishing gear in the Gulf of Alaska. In: Willison JHM, Hall J, Gass SE, Kenchington ELR, Butler M, Doherty P (eds) Proceedings of the First International Symposium on Deep-Sea Corals. Ecology Action Centre, Halifax, pp 106-116

Madsen FJ (1944) Octocorallia (Stolonifera, Telestacea, Xeniidea, Alcyonacea, Gorgonacea). Danish Ingolf-Exped 5: 1-65

Risk MJ, Heikoop JM, Snow MG, Beukens R (2002) Life spans and growth patterns of two deep-sea corals: *Primnoa resedaeformis* and *Desmophyllum cristagalli*. Hydrobiologia 471: 125-131

Tendal OS (1992) The North Atlantic distribution of the octocoral, *Paragorgia arborea* (L., 1758) (Cnidaria, Anthozoa). Sarsia 77: 213-217

Theroux RB, Grosslein MD (1987) Benthic fauna. In: Backus RH (ed) Georges Bank. MIT Press, Cambridge, Massachusetts, pp 283-295

Theroux RB, Wigley RL (1998) Quantitative composition and distribution of the macrobenthic invertebrate fauna of the continental shelf ecosystems of the northeastern United States. U.S. Dept Comm, NOAA Tech Rep NMFS 140

Valentine PC, Uzmann JR, Cooper RA (1980) Geology and biology of Oceanographer submarine canyon. Mar Geol 38: 283-312

Verrill AE (1862) Notice of a *Primnoa* from Georges Bank. Proc Essex Inst Salem MA 3: 127-129

Verrill AE (1878a) Notice of recent additions to the marine fauna of the eastern coast of North America. Amer J Sci Arts, Ser 3, 16: 207-215

Verrill AE (1878b) Notice of recent additions to the marine fauna of the eastern coast of North America, No. 2. Amer J Sci Arts, Ser 3, 16: 371-379

Verrill AE (1879) Notice of recent additions to the marine fauna of the eastern coast of North America, No. 5. Amer J Sci Arts, Ser 3, 17: 472-474

Verrill AE (1884) Notice of the remarkable marine fauna occupying the outer banks of the southern coast of New England. Amer J Sci Arts, Ser 3, 28: 213-220

Watling L, Auster P, Babb I, Skinder C, Hecker B (2003) A geographic database of deepwater alcyonaceans of the Northeastern U.S. continental shelf and slope. Version 1.0 CD-ROM. Natl Undersea Res Cent, Connecticut Univ, Groton

Wigley RL (1968) Benthic invertebrates of the New England fishing banks. Underwater Naturalist 5: 8-13

Appendix 1

Complete list of all alcyonacean species included in the biogeographic comparison (see Table 2) of the eastern and western Atlantic regions, as defined in Cairns and Chapman (2001), that are north of the tropics

	IIA W N Atlantic E. Canada to Cape Hatteras	IIB Boreal Eastern Atlantic	IA W N Atlantic Cape Hatteras to Florida Straits	IIIA Lusitanian-Mediterranean
"Stoloniferous forms"				
Clavulariidae				
Anthelia borealis (Koren and Danielssen, 1883)		X		X
Anthelia fallax Broch, 1912		X		X
Clavularia alba (Grieg, 1888)	X	X		
Clavularia arctica (Sars, 1860)		X		X
Clavularia griegii Madsen, 1944		X		
Clavularia levidensis Madsen, 1944	X			
Clavularia marioni (von Koch, 1891)				X
Clavularia modesta (Verrill, 1874)	X			
Clavularia rudis (Verrill, 1922)	X			
Clavularia venustella Madsen, 1944	X			
Sarcodictyon roseum (Philippi, 1842)		X		X
Scleranthelia rugosa (Pourtalès, 1867)				X
Scyphopodium ingolfi (Madsen, 1944)			X	X
Telesto fructiculosa Dana, 1846			X	
Telestula septentrionalis Madsen, 1944	X	X		X
	6	7	2	**8**
"massive body forms"				
Paralcyoniidae				
Paralcyonium spinulosum Delle Chiaje, 1822				X
	0	0		**1**
Alcyoniidae				
Alcyonium acaule Marion, 1878				X
Alcyonium coralloides (Pallas, 1766)				X
Alcyonium digitatum Linnaeus, 1758	X	X		X
Alcyonium palmatum Pallas, 1766				X
Anthomastus agassizii Verrill 1922	X			
Anthomastus grandiflorus Verrill, 1878	X	X	X	X
Ceratocaulon wandeli Jungersen, 1892				X
	3	2	1	**6**

Appendix 1 continued

	IIA W N Atlantic E. Canada to Cape Hatteras	IIB Boreal Eastern Atlantic	IA W N Atlantic Cape Hatteras to Florida Straits	IIIA Lusitanian-Mediterranean
Nephtheidae				
Gersemia rubiformis (Ehrenberg, 1834)	X	X		
Capnella florida (Rathke, 1806)	X	X		X
Capnella glomerata (Verrill, 1869)	X	X		
	3	3	0	**1**
"Scleraxonia"				
Anthothelidae				
Anthothela grandiflora (M. Sars, 1856)	X	X		X
Titanidium suberosum (Ellis and Solander, 1786)			X	
	1	1	1	**1**
Paragorgiidae				
Paragorgia boschmai Bayer, 1964			X	
Paragorgia arborea (Linnaeus, 1758)	X	X		X
Paragorgia johnsoni Gray, 1862			X	X
	1	1	2	**2**
Coralliidae				
Corallium maderense (Johnson, 1899)				X
Corallium medea Bayer, 1964			X	
Corallium **sp.**				
Corallium johnsoni Gray, 1860				X
Corallium niobe Bayer, 1964			X	X
Corallium rubrum (Linnaeus, 1758)				X
Corallium tricolor (Johnson, 1899)				X
	0	0	2	**5**
"Holaxonia"				
Acanthogorgiidae				
Acanthogorgia armata Verrill, 1878	X			X
Acanthogorgia hirsuta Gray, 1857				X
Acanthogorgia schrammi (Duchassaing and Michelotti, 1864)			X	
Acanthogorgia aspera Pourtalès, 1867			X	
	1	0	2	**2**

Appendix 1 continued

	IIA W N Atlantic E. Canada to Cape Hatteras	IIB Boreal Eastern Atlantic	IA W N Atlantic Cape Hatteras to Florida Straits	IIIA Lusitanian-Mediterranean
Plexauridae				
Bebryce mollis Molippi, 1842				X
Dentomuricea meteor Grasshoff, 1977				X
Echinomuricea klavereni Carpine and Grasshoff, 1975				X
Muricea pendula Verrill, 1868			X	
Muriceides kuekenthali (Broch, 1912)		X		
Muriceides lepida Carpine and Grasshoff, 1975				X
Muriceides paucituberculata (Marion, 1882)				X
Paramuricea clavata (Risso, 1826)				X
Paramuricea grandis (Verrill, 1883)	X			
Paramuricea grayi (Johnson, 1861)				X
Paramuricea macrospina (Koch, 1882)				X
Paramuricea **sp.** GOM	X		X	
Paramuricea biscaya Grasshoff, 1977				X
Paramuricea candida Grasshoff, 1977				X
Paramuricea placomus (Linnaeus, 1758)	X	X		X
Placogorgia massiliensis Carpine and Grasshoff, 1975				X
Placogorgia becena Grasshoff, 1977				X
Placogorgia coronata Carpine and Grasshoff, 1975				X
Placogorgia graciosa (Tixier-Durivault and d'Hond, 1975)				X
Placogorgia intermedia (Thomson, 1927)				X
Placogorgia terceira Grasshoff, 1977				X
Spinimuricea atlantica (Johnson, 1862)				X
Swiftia casta (Verrill, 1883)	X		X	
Swiftia pourtalesii Deichmann, 1936			X	
Swiftia borealis (Kramp, 1930)		X		
Swiftia dubia (Thomson, 1929)				X
Swiftia pallida Madsen, 1970				X
Swiftia rosea (Grieg, 1887)		X		
Thesea talismani Grasshoff, 1986				X
Villogorgia bebrycoides (Koch, 1887)				X
	4	4	4	**22**
Gorgoniidae				
Eunicella filiformis Studer, 1879				X
Eunicella gazella Studer, 1878				X

Appendix 1 continued

	IIA W N Atlantic E. Canada to Cape Hatteras	IIB Boreal Eastern Atlantic	IA W N Atlantic Cape Hatteras to Florida Straits	IIIA Lusitanian-Mediterranean
Eunicella labiata Thomson, 1927				X
(?Eunicella) modesta Verrill, 1883			X	
Eunicella verrucosa (Pallas, 1766)				X
Leptogorgia albipunctata Stiasny, 1936				X
Leptogorgia purpureoviolacea (Stiasny, 1936)				X
Leptogorgia sarmentosa (Esper, 1791)				X
Leptogorgia viminalis (Pallas, 1766)				X
Leptogorgia virgulata (Lamarck, 1815)			X	
Leptogorgia setacea (Pallas, 1766)			X	
Leptogorgia hebes Verrill, 1869			X	
Lophogorgia capeverdiensis Grasshoff, 1986				X
	0	0	4	**9**
"Calcaxonia"				
Chrysogorgiidae				
Chrysogorgia herdendorfi Cairns, 2001			X	
Chrysogorgia agassizii (Verrill, 1883)	X			X
Chrysogorgia campanula Madsen, 1944				X
Chrysogorgia elegans (Verrill, 1883)			X	X
Chrysogorgia quadruplex Thomson, 1927				X
Distichogorgia sconsa Bayer, 1979			X	
Iridogorgia pourtalesii Verrill, 1883	X			X
Metallogorgia melanotrichos (Wright and Studer, 1889)				X
Radicipes challengeri (Wright, 1885)				X
Radicipes gracilis (Verrill, 1884)	X		X	X
	3	0	4	**8**
Ellisellidae				
Ctenocella (Ellisella) paraplexauroides Stiasny, 1936				X
Nicella granifera (Kölliker, 1865)				X
Ctenocella (Viminella) flagellum (Johnson, 1863)				X
Ctenocella (Ellisella) schmitti (Bayer, 1961)			X	
	0	0	1	**3**

Appendix 1 continued

	IIA W N Atlantic E. Canada to Cape Hatteras	IIB Boreal Eastern Atlantic	IA W N Atlantic Cape Hatteras to Florida Straits	IIIA Lusitanian-Mediterranean
Primnoidae				
Callogorgia americana Cairns and Bayer 2002			X	
Callogorgia verticillata (Pallas, 1766)				X
Calyptrophora gerdae Bayer, 2001			X	
Calyptrophora josephinae (Lindstroem, 1877)				X
Calyptrophora trilepis (Pourtalès, 1868)			X	
Candidella (=Stenella) imbricata (Johnson, 1862)			X	X
Narella bellissima (Kükenthal, 1915)				X
Narella laxa Deichmann, 1936	X			X
Narella regularis (Duchassaing and Michelotti, 1860)			X	X
Narella versluysi (Hickson, 1909)				X
Paracalyptrophora josephinae (Lindström, 1877)				X
Plumarella pourtalesii (Verrill, 1883)			X	
Primnoa resedaeformis (Gunnerus, 1763)	X	**X**		X
Primnoella jungerseni Madsen, 1944				X
Thouarella **n. sp.**	X			
Thouarella hilgendorfi (Studer, 1879)				X
	3	1	6	**11**
Isididae				
Acanella arbuscula (Johnson, 1862)	X	X		X
Chelidonisis aurantiaca Studer, 1891				X
Isidella longiflora (Verrill, 1883)				X
Isidella elongata (Esper, 1788)				X
Isidella lofotensis Sars, 1868		X		X
Keratoisis ornata Verrill, 1878	X		X	
Keratoisis flexibilis (Pourtalès, 1868)			X	X
Keratoisis grayi Wright, 1869	X	X	X	X
Lepidisis caryophyllia Verrill, 1883	X			X
Lepidisis cyanae Grasshoff, 1986				X
Lepidisis longiflora Verrill, 1883			X	X
Lepidisis macrospiculata (Kükenthal, 1915)				X
	4	3	4	**12**
Total Alcyonacea	**29**	**22**	**33**	**91**

Appendix 2

Reprint of Figure 3 from Cairns and Chapman (2001) showing regions used in a biogeographic comparison of scleractinian corals of the North Atlantic Ocean
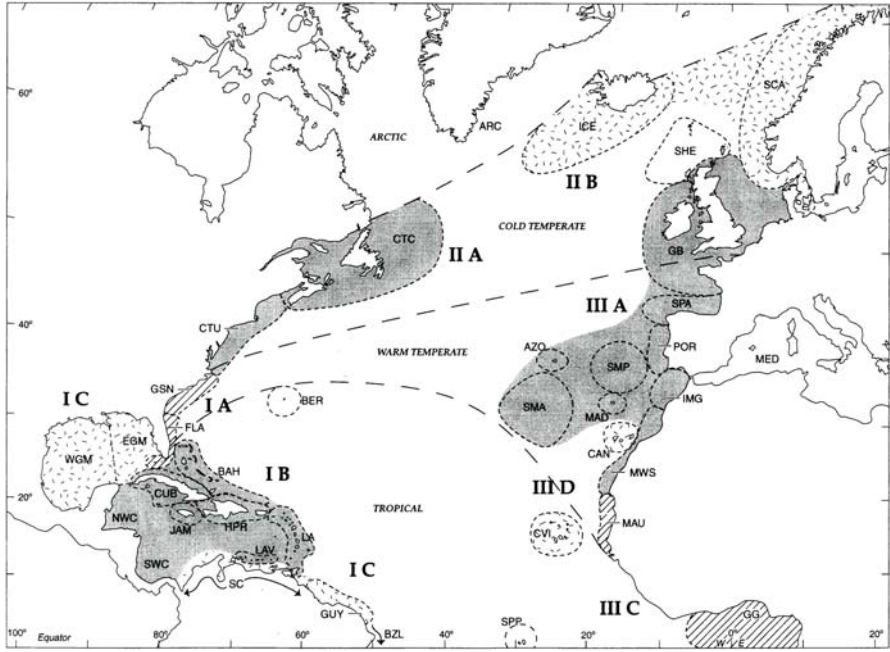
Occurrence of deep-water *Lophelia pertusa* and *Madrepora oculata* in the Gulf of Mexico

William W. Schroeder[1], Sandra D. Brooke[2], Julie B. Olson[3], Brett Phaneuf[4], John J. McDonough III[5], Peter Etnoyer[6]

[1] Marine Science Program, University of Alabama, Dauphin Island Sea Lab, Dauphin Island, AL 36528, USA
(wschroeder@disl.org)
[2] Oregon Institute of Marine Biology, University of Oregon, Charleston, OR 97420, USA
[3] Department of Biological Sciences, University of Alabama, Tuscaloosa, AL 35487, USA
[4] Department of Oceanography, Texas A and M University, College Station, TX 77845, USA
[5] U.S. National Oceanic and Atmospheric Administration, Silver Springs, MD 20910, USA
[6] Aquanautix Consulting, 3777 Griffith View Drive, Los Angeles, CA 90039, USA

Abstract. One of the critical information needs identified at the 2003 Deep-Sea Corals Workshop in Galway, Ireland, was to locate and chart deep-sea corals in order to develop reliable estimates of their distribution and abundance. While reports of deep-sea corals from the Gulf of Mexico date back to the 1860s, relatively little is known about their distribution or abundance. This paper attempts to provide a current assessment of the occurrence of *Lophelia pertusa* and *Madrepora oculata* in water depths greater than 200 m in the Gulf of Mexico by summarizing records from (1) published material, (2) the 2003 National Museum of Natural History Taxonomic Database, (3) findings obtained during the September-October 2003 NOAA-OE *RV Ronald H. Brown* cruise RB-03-07-leg-2 in the northern Gulf, and (4) from various unpublished sources.

Keywords. Gulf of Mexico, *Lophelia, Madrepora*, distribution

Introduction

Assemblages of *Lophelia pertusa* and *Madrepora oculata* often support diverse and abundant communities of associated fauna, including some commercially-important species (Mortensen et al. 1995; Fosså and Mortensen 1998; Sumida and Kennedy 1998; Rogers 1999; Husebø et al. 2002). These deep-water corals are fragile, slow-growing, and long-lived, and their growth patterns are thought to reflect the local

environmental conditions (e.g., current speed, current direction, water temperature) of their habitat. Deep-water coral assemblages are globally threatened, primarily from destructive fishing practices, but also from the exploration for and extraction of fossil fuels (e.g., Rogers 1999; Koenig et al. 2000; Gage 2001; Hall-Spencer et al. 2001; Fosså et al. 2002; Schroeder 2002). One of the fundamental information needs identified at the 2003 Deep-Sea Corals Workshop in Galway, Ireland, was to locate and chart deep-sea corals in order to develop reliable estimates of their distribution and abundance (McDonough and Puglise 2003). This information would then serve as the basis for further ecological studies.

The distribution and ecology of *Lophelia* reefs and banks from the coasts of Europe have been well documented (Joubin 1912; Dons 1944; Ekman 1953; Mortensen et al. 1995, 2000; Freiwald et al. 1997; Mortensen and Rapp 1998; Rogers 1999; De Mol et al. 2002). Conversely, although the earliest records of deep-sea corals in the Gulf of Mexico (GoM) date back to Pourtales's surveys in the Straits of Florida and between the Dry Tortugas and the Campeche Bank in the late 1860s (Smith 1954; Cairns 1979), relatively little is yet known about their distribution, abundance, and ecology. The objective of this paper is to contribute to our understanding of deep-water coral presence in the GoM by compiling and summarizing the reported occurrences of *Lophelia pertusa* and *Madrepora oculata* in water depths greater than 200 m. This information was obtained from a variety of sources, including (1) published material, (2) the 2003 National Museum of Natural History Taxonomic Database, (3) findings obtained during the September-October 2003 NOAA-OE *RV Ronald H. Brown* cruise (RB-03-07-leg-2) in the northern GoM, and (4) various unpublished sources. By providing a review of previous observations and descriptions of deep-water corals in the GoM, we anticipate that future deep-water coral studies will be able to utilize ship time more efficiently and have a higher probability of rapid success in locating coral ecosystems.

Methods

Reports of occurrences of *Lophelia pertusa* and *Madrepora oculata* in the northern GoM were found in 6 publications: Moore and Bullis (1960), Cairns (1979), Viada and Cairns (1987), MacDonald et al. (1989), Cairns (2000), Schroeder (2002). Additional reports of deep-water coral observations within the Straits of Florida (shown in the boxed region on Figure 1) are available but are not addressed in this manuscript. Records from the National Museum of Natural History Taxonomic Database (2003) were reviewed for samples of *Lophelia pertusa* and *Madrepora oculata* collected in the GoM. The accession information available with each sample was used to further document deep-water coral presence in Figure 1.

Observations of coral presence obtained during the September-October 2003 NOAA Office of Ocean Exploration funded cruise on the *RV Ronald H. Brown* (RB-03-07-leg-2) in the northern GoM are also shown in Figure 1. Results from this cruise have been summarized in Olson et al. (2004). A variety of GoM researchers have also generously provided information on unpublished observations of
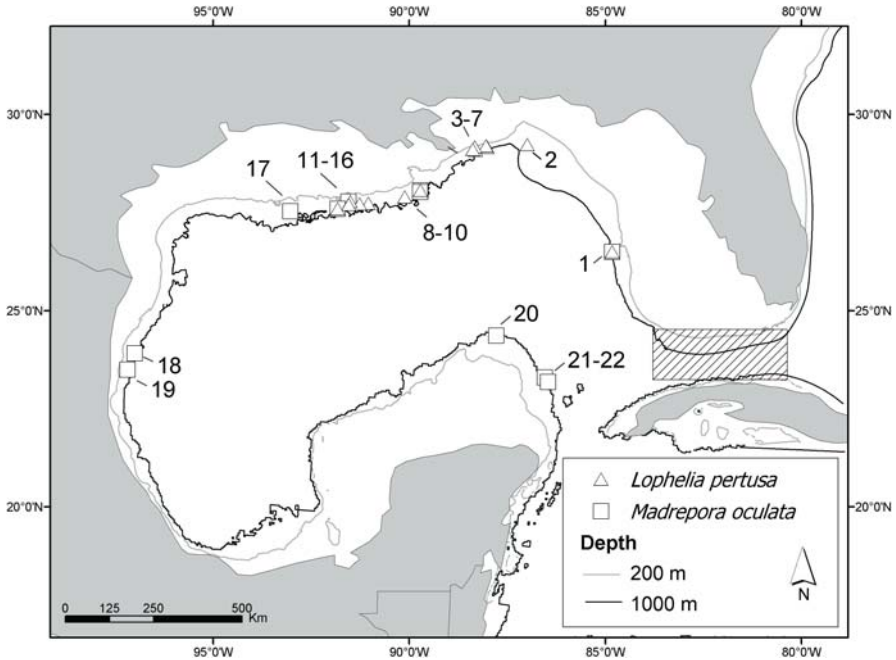
Fig. 1 Occurrence of *Lophelia pertusa* and *Madrepora oculata* in the Gulf of Mexico. See Table 1 for details

Lophelia pertusa and *Madrepora oculata* and these locations are included in Figure 1. Bathymetry lines for 200 m and 1000 m have been added to this figure to provide a reference for deep-water coral distribution.

Results

Occurrences of *Lophelia pertusa* and *Madrepora oculata* in the Gulf of Mexico are presented in Table 1 and depicted in Figure 1. A summary of the available information for each site is presented below. Collected samples are designated by the acronym of institution where the sample is accessed: NMNH = National Museum of Natural History, TAMU = Texas A&M University.

Site 1: *Lophelia pertusa* (USNM 84355) and *Madrepora oculata* (USNM 84354) collected in a trawl at 640 m by the *RV Aleutian Bounty* on 12 November, 1983, at station 83-165 (Cairns 2000). *Note*: This site is at the northern end of a series of Late Pleistocene age *L. pertusa* buildups on the west Florida carbonate ramp slope at depths of 500 m (Newton et al. 1987).

Site 2: *Lophelia pertusa* (TAMU 68A7-12B) collected in a trawl at 878 m by the *RV Alaminos* on 6 August, 1968, at station 68A7-12B (Cairns 1979).

Table 1 Location, depth, and presence of deep-water coral species at sites in the Gulf of Mexico. N.D. = No data

Site	Latitude (N)	Longitude (W)	Depth (m)	*Lophelia pertusa*	*Madrepora oculata*
1	26°30.0	84°50.0	640	X	X
2	29°14.0	87°00.0	878	X	
3	29°09.5	88°01.0	430-520	X	
4	29°12.0	88°03.0	457-549	X	
5	29°05.0	88°19.0	421-512	X	
6	29°10.0	88°20.0	519	X	
7	29°06.4	88°22.9	343	X	
8	28°04.0	89°43.0	616-630	X	X
9	28°01.7	89°43.6	650		X
10	27°53.6	90°07.1	635	X	
11	27°44.0	91°02.7	720		X
12	27°43.0	91°16.0	N.D.	X	
13	27°46.9	91°30.4	540-570	X	
14	27°42.3	91°32.9	543-783	X	
15	27°47.0	91°33.0	300		X
16	27°35.8	91°49.6	524-539	X	X
17	27°32.0	93°02.0	732-823		X
18	23°55.0	97°00.0	937		X
19	23°30.0	97°11.0	732		X
20	24°22.0	87°47.0	549		X
21	23°18.0	86°33.0	914		X
22	23°11.0	86°28.0	914		X

Site 3: *Lophelia pertusa* reported in Schroeder (2002). This site is a low-relief knoll located in approximately 520 m of water on the upper De Soto slope. It rises up to 90 m above the surrounding seafloor to a minimum depth of about 430 m. Authigenic carbonate occurs on the crest and sides of the knoll. The most extensive and highly developed *L. pertusa* assemblages noted in the GoM to date have been observed at this site. Colonies display the typical bushy morphology and range in size up to 2 m in diameter, while aggregations of closely associated colonies with linear orientations have been observed to attain 1.5-2 m in width and 3-4 m in length. Many of the colonies are beginning to coalesce and appear to be in the first phase of the "thicket" building stage (see Fig. 2) described by Squires (1964). Additional manned submersible dives at this site since the first report have provided a *Lophelia pertusa* sample (USNM 1010792), further video documentation, and side-scan sonographs (courtesy of the US Navy submarine NR-1, July 2002; NMNH Taxonomic Database 2003).

Site 4: *Lophelia pertusa* collected in a trawl at 457-549 m by the *MV Oregon* on 25 July, 1962, at station 3651 (Cairns 1979).
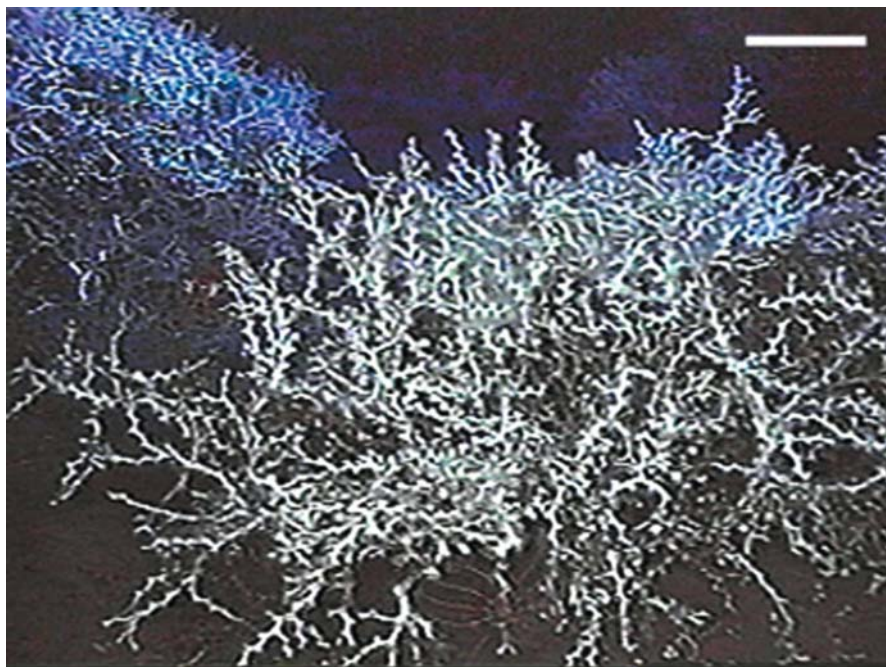
Fig. 2 *Lophelia pertusa* colonies illustrating the thicket building stage at Site 3. Scale bar: 25 cm

Site 5: *Lophelia pertusa* reported in Moore and Bullis (1960). The area sampled is described as a deep-water reef system comprised of several sections up to 300 m long and 55 m thick vertically. The location where the *MV Oregon* (station 1283; 13 March 1955) is reported to have collected the approximately 136 kg of *Lophelia pertusa* (= *L. prolifera*) was investigated by the U.S. Navy submarine NR-1 in July 2002 (unpublished cruise logs). No evidence of coral or hard substrate was observed or imaged on sonar at, or in the vicinity of, this location. This confirmed an earlier finding in the United States Department of Interior's (USDI) Minerals Management Service in-house 3D-seismic surface amplitude and bathymetry data which did not indicate the presence of any geological features similar to those described by Moore and Bullis (1960) or signs of hard substrate. Therefore, this site is considered unreliable because of the apparent error in navigation. *Note*: See description of Site 7 for a possible alternative location for this collection site.

Site 6: *Lophelia pertusa* (USNM 88393) collected by the *MV C Hawk* at 519 m. The date of collection is unknown but the sample was identified in 1990 (Cairns 2000, NMNH Taxonomic Database 2003). The NMNH Taxonomic Database (2003) records indicate that the samples were collected at USDI lease block VK826. The latitude reported for this site crosses the lower region of VK826; however, the reported longitude lies 30 km to the west and runs through lease block VK820. The

MV C Hawk did conduct a series of remotely operated vehicle (ROV) surveys and sampling services at VK826, in the same location as Site 3 above, for Oceaneering International, Inc., Houston, Texas, in August and September, 1990 (unpublished report). Therefore, these specimens were most likely collected at VK826 and the reported longitude is simply incorrect.

Site 7: *Lophelia pertusa* photographed at a depth of 343 m on ROV dive 31 during the NOAA-OE *RV Ronald H. Brown* cruise RB-03-07-leg-2 on 23 September 2003 (unpublished NOAA ROV Data Log and photographs). This site is a low-relief mound located on the northern edge of an exposed carbonate rock complex which extends southward for over 2 km to the eastern rim of a submarine canyon. *Note*: The cross-sectional profile and water depths of the submarine canyon, which is located approximately 7 km due west of Site 5, are similar to the depth recorder tracing presented in Figure 1 of Moore and Bullis (1960). Although no evidence of *Lophelia* was observed during a July 2002 survey in the canyon by the U.S. Navy submarine NR-1 (unpublished cruise logs and video recordings), this location is a possible candidate for the area where Moore and Bullis (1960) found coral in 1955.

Site 8: *Lophelia pertusa* and *Madrepora oculata* photographed and collected between 616-630 m on ROV dive 43 during the NOAA-OE *RV Ronald H. Brown* cruise RB-03-07-leg-2 on 30 September, 2003 (unpublished NOAA ROV Data Log and photographs). It is predominantly a low relief mound-like sea floor feature with mostly single *Lophelia* and *Madrepora* colonies. No large regions of exposed carbonate were noted.

Site 9: A single *Madrepora oculata* colony collected at a depth of 650 m during *Johnson-Sea-Link* dive 3340 on 8 October, 2002 (unpublished data: S. D. Brooke).

Site 10: A single *Lophelia pertusa* colony photographed (see Boland 1986) at a depth of 635 m during a towed camera sled survey conducted by the *MV Citation* on 12 November, 1984 (unpublished data: G. S. Boland).

Site 11: A branch from a single *Madrepora oculata* colony collected at a depth of approximately 720 m during *Johnson-Sea-Link-1* dive 4398 on 5 May, 2002 (unpublished data: H. H. Roberts).

Site 12: *Lophelia pertusa* (USNM 78511) collected in a trawl during *RV Gyre* cruise 87-G-2 on 5 March, 1987. The station number and depth of collection are unknown (Cairns 2000; NMNH Taxonomic Database 2003).

Site 13: *Lophelia* sp. reported in MacDonald et al. (1989). This site, known as Bush Hill, is a low-relief knoll located in approximately 580 m of water. It rises up to 40 m above the surrounding seafloor to a minimum depth of approximately

540 m. In 1986, during four dives with the research submersible *Johnson-Sea-Link-I*, colonies were observed and photographed attached to the larger, exposed boulders along an escarpment on the western side of the site.

Site 14: *Lophelia pertusa* (USNM 75691, 75692, 76838) collected in a trawl at 783 m by the *MV Citation* on 10 June, 1985, at station WC-6 (Viada and Cairns 1987; NMNH Taxonomic Database 2003).

Site 15: *Madrepora oculata* (NMNH 100097) collected at a depth of 300 m during *Johnson-Sea-Link* dive 2064 on 16 June, 1987 (NMNH Taxonomic Database 2003).

Site 16: *Lophelia pertusa* photographed (see Figure 3) and collected between 524-539 m on ROV dive 36 during the NOAA-OE *RV Ronald H. Brown* cruise RB-03-07-leg-2 on 25 September, 2003 (unpublished NOAA ROV Data Log and photographs). Small *Madrepora oculata* colonies were photographed at a depth of 524 m during *Johnson-Sea-Link* dive 4577 on 29 August, 2003 (unpublished data: E. Cordes).

Fig. 3 Small colonies of *Lophelia pertusa* on an isolated carbonate outcrop at Site 16. Other sessile megafauna include large white demosponges in the family Corallistidae and a gorgonian colony (background). Many different species of invertebrates are found in association with deep Gulf of Mexico hardbottom communities, including anomuran crabs such as *Eumunida picta* (large red species) and the smaller galatheid crabs. Scale bar: 25 cm

Site 17: *Madrepora oculata* (USNM 96228) collected in a trawl at 732-823 m by the *MV Oregon* on 11 April, 1952, at station 534 (Cairns 1979).

Site 18: *Madrepora oculata* (TAMU 71A8-29) collected in a trawl at 937 m by the *RV Alaminos* on 4 August, 1971, at station TAMU 71A8-29 (Cairns 1979).

Site 19: *Madrepora oculata* (USNM 96226) collected in a trawl at 732 m by the *MV Oregon* on 10 April, 1964, at station 4807 (NMNH Taxonomic Database 2003).

Site 20: *Madrepora oculata* (USNM 96232) collected in a trawl at 549 m by the *MV Oregon* II on 9 August, 1970, at station 11134 (NMNH Taxonomic Database 2003).

Site 21: *Madrepora oculata* collected in a trawl at 914 m by the *MV Oregon* on 7 December, 1963, at station 4569 (Cairns 1979).

Site 22: *Madrepora oculata* collected in a trawl at 914 m by the *MV Oregon* on 7 December, 1963, at station 4570 (Cairns 1979).

Discussion

This report summarizes the occurrence and distribution of deep-water corals in the GoM at water depths between 200-1000 m. At depths of 200 m or greater, the surficial sediment regime is generally dominated by fine-grained pelagic and hemipelagic material. Notable exceptions include limestone outcrops located on the west Florida and Banco de Campeche slopes and in the Florida Straits, and authigenic carbonate deposits, associated with hydrocarbon and related fluid seepage, on the De Soto, Texas-Louisiana, and Golfo de Campeche slopes. These indurated substrates provide suitable surfaces for the colonization and development of different types of sessile megafauna assemblages. Mapping of exposed hard substrates in the GoM has provided (and will continue to provide) information on potential habitats for deep-sea corals.

Two observations are immediately apparent from this review of deep-water corals in the GoM. First, approximately half of the coral records provide little to no detail about the coral habitat as the samples were recovered by bottom trawls. While we acknowledge that solid substrate must be present for coral growth, these reports provide no information regarding the extent or type of the substrate, bottom topography, coral distribution, abundance, or ecology. Some of the fauna that appear to be associated with deep-water corals in the GoM (e.g., anemones and small crustaceans) are fragile and would be difficult to effectively retrieve and identify from a bottom trawl. Additionally, most trawls are conducted over a relatively large area of benthos before retrieving the equipment, making it difficult to impossible to

precisely identify the site from which the coral was obtained. This lack of precise location will necessitate that future science parties map the potential site using sonar to identify topographical features that might support corals prior to launching their research equipment. While both manned submersibles and remotely operated vehicles permit the scientists to accumulate significantly more data about the coral habitat, neither vehicle can explore large areas of benthos effectively.

Another interesting observation is the relative lack of deep-water corals in the southern GoM. This could be due to a variety of factors. We recognize that records of coral presence are a function of research effort, indicating where sampling has been undertaken. Much research focus has been directed at those environments off of the Gulf Coast states, most notably at sites supporting chemosynthetic communities, resulting in a number of coral observations. If similar focus has not been placed in the southern GoM, then the lack of reports of deep-water corals may reflect this lessened research effort. Additionally, coral distribution is potentially regulated by a number of biological (e.g., recruitment, food availability) and physical (e.g., current regime, temperature) processes and mechanisms. Since our understanding of deep-water coral distribution, abundance, and ecology in the GoM is minimal, it is not yet known which of these processes or mechanisms are most influential.

To date, there have been no records of *Lophelia pertusa* at sites located below 25 degrees latitude (except in the Straits of Florida). While there are far fewer observations of coral presence overall in this region, those that exist document only *Madrepora oculata*. Again, our lack of understanding of ecological processes regulating deep-water corals in the GoM limits our ability to explain this observation. By providing this summation of deep-sea coral presence in the GoM, we hope to stimulate additional research interest that may address the questions raised during this discussion and therefore provide the information required for appropriate resource management decisions.

Acknowledgements

ADDENDUM: Subsequent to the acceptance of this paper, John Reed, Harbor Branch Oceanographic Institution, provided the following information on the occurrence of *Lophelia pertusa* at two additional locations. These observations were obtained during ROV surveys on Leg-1 of NOAA-OE *RV Ronald H. Brown* cruise RB-03-07.

- HBOI/DBMR Site: 12-IX-03-3 [26°20.0115'N, 84°45.0045'W]. *Lophelia pertusa* colonies/thickets, up to one meter in diameter and 0.6 m tall, were observed

on the tops of numerous small, low-relief mounds at depths of 428-466 m. *Note*: This site is within the linear zone of Late Pleistocene age *L. pertusa* buildups on the west Florida carbonate ramp slope described by Newton et al. (1987) and is located approximately 23 km south southeast of site 1 reported in this paper (see Table 1 and Fig. 1).

- HBOI/DBMR Site: 16-IX-03-1 [28° 58.3820'N, 88° 37.5590'W]. Numerous small (15-30 cm) living *Lophelia pertusa* colonies were observed attached to British Petroleum's Pompano Production Platform at 204-292 m in a total water depth of 393 m. This is the first confirmed deep-water record of *Lophelia pertusa* colonizing an artificial hard substrate in the Gulf of Mexico. *Note*: This site is located approximately 28 km west southwest of site 7 reported in this paper (see Table 1 and Fig. 1).

References

Boland GS (1986) Discovery of co-occurring bivalve *Acesta* sp. and chemosynthetic tube worms *Lamellibrachia* sp. Nature 323: 759

Cairns SD (1979) The deep-water Scleractinia of the Caribbean Sea and adjacent waters. Stud Fauna Curaçao 57, 341 pp

Cairns SD 2000 A revision of the shallow-water azooxanthellate Scleractinia of the Western Atlantic. Stud Nat Hist Caribbean Reg 75: 1-231

De Mol B, Van Rensbergen P, Pillen S, Van Herreweghe K, Van Rooij D, McDonnell A, Huvenne V, Ivanov M, Swennen R, Henriet JP (2002) Large deep-water coral banks in the Porcupine Basin, southwest of Ireland. Mar Geol 188: 193-231

Dons C (1944) Norges korallrev. Det Kongl Norsk Vidensk Selsk Forh 16: 37-82

Ekman S (1953) Zoogeography of the sea. Sidgewick and Jackson

Fosså JH, Mortensen PB (1998) Diversity of species associated with *Lophelia* coral reef and methods for mapping and monitoring. Fisken Havet 17, 95 pp

Fosså JH, Mortensen PB, Furevik DM (2002) The deep-water coral *Lophelia pertusa* in Norwegian waters: distribution and fishery impacts. Hydrobiologia 471: 91-99

Freiwald A, Henrich R, Pätzold J (1997) Anatomy of a deep-water coral reef mound from Stjernsund, West Finnmark, northern Norway. SEPM Spec Publ 56: 140-161

Gage JD (2001) Deep-sea benthic community and environmental impact assessment at the Atlantic Frontier. Cont Shelf Res 21: 957-986

Hall-Spencer J, Allain V, Fosså JH (2001) Trawling damage to Northeast Atlantic ancient coral reefs. Proc R Soc London B 269: 507-511

Husebø A, Nøttestad L, Fosså JH, Furevik DM, Jørgensen SB (2002) Distribution and abundance of fish in deep-water coral habitats. Hydrobiologia 471: 91-99

Joubin L (1912) 1. Carte des bancs et recifs de coraux. Ann Inst Oceanogr Monaco 4, pp 7

Koenig CC, Coleman FC, Grimes CB, Fitzhugh GR, Scanlon KM, Gledhill CT, Grace M (2000) Protection of fish spawning habitat for the conservation of warm-temperate reef-fish fisheries of shelf-edge reefs of Florida. Bull Mar Sci 66: 593-616

MacDonald IR, Boland GS, Baker JS, Brooks JM, Kennicutt II MC, Bidigare RR (1989) Gulf of Mexico hydrocarbon seep communities. II. Spatial distribution of seep organisms and hydrocarbons at Bush Hill. Mar Biol 101: 235-247

McDonough JJ, Puglise KA (2003) Summary: Deep-Sea Corals Workshop. International Planning and Collaboration Workshop for the Gulf of Mexico and the North Atlantic Ocean. Galway, Ireland, January 16-17, 2003. U.S. Dep. Commerce, NOAA Tech. Memo, NMFS-F/SPO-60, 51 pp

Moore DR, Bullis HR (1960) A deep-water coral reef in the Gulf of Mexico. Bull Mar Sci 10: 25-128

Mortensen PB, Hovland M, Brattegard T, Farestveit R (1995) Deep-water bioherms of the scleractinian coral *Lophelia pertusa* L. at 64°N on the Norwegian shelf: structure and associated megafauna. Sarsia 80: 145-158

Mortensen PB, Rapp HT (1998) Oxygen and carbon isotope ratios related to growth line patterns in skeletons of *Lophelia pertusa* (L) (Anthozoa, Scleractinia): implications for determinations of linear extension rates. Sarsia 83: 433-446

Mortensen PB, Roberts JM, Sundt RC (2000) Video assisted grabbing: a minimally destructive method of sampling azooxanthellate coral banks. J Mar Biol Ass UK 80: 365-366

National Museum of Natural History (NMNH) Taxonomic Database 2003. Curators for *Lophelia* sp. and *Madrepora* sp. records from the Department of Invertebrate Zoology: Stephen Cairns and Frederick Bayer. Natl Mus Nat Hist, Smithsonian Inst, Washington, DC

Newton CR, Mullins HT, Gardulski AF (1987) Coral mounds on the west Florida slope: unanswered questions regarding the development of deep-water banks. Palaios 2: 59-367

Olson JB, Brooke SD, Phaneuf B, Schroeder WW (2004) An evaluation of the Innovator ROV as a tool for deep-water coral research. Proc 2004 Underwater Intervention Conf, CD-ROM Ref, February 18, E-3 NOAA, E32

Rogers AD (1999) The biology of *Lophelia pertusa* (Linnaeus 1758) and other deep-water reef forming corals and impacts from human activities. Int Rev Hydrobiol 844: 315-406

Schroeder WW (2002) Observations of *Lophelia pertusa* and the surficial geology at a deep-water site in the northeastern Gulf of Mexico. Hydrobiologia 471: 29-33

Smith FGW (1954) Gulf of Mexico Madreporaria. In: Galtsoff PS (ed) Gulf of Mexico - its origins, waters, and marine life. Fish Bull, US Fish Wildlife Serv 55: 291-296

Squires DF (1964) Fossil coral thickets in Wairarapa, New Zealand. J Paleont 38: 905-915

Sumida P, Kennedy R (1998) Porcupine Seabight – biological data. In: Kenyon NH, Ivanov MK, Akhmetzhanov AM (eds) Cold-Water Carbonate Mounds and Sediment Transport on the Northeast Atlantic Margin. Tech Ser 52, UNESCO: 102-106

Viada ST, Cairns SD (1987) Range extensions of the ahermatypic Scleractinia in the Gulf of Mexico. Northeast Gulf Sci 9: 131-134

Southern Caribbean azooxanthellate coral communities off Colombia

Javier Reyes, Nadiezhda Santodomingo, Adriana Gracia, Giomar Borrero-Pérez, Gabriel Navas, Luz Marina Mejía-Ladino, Adriana Bermúdez, Milena Benavides

Instituto de Investigaciones Marinas y Costeras, INVEMAR, Cerro Punta Betín, AA 1016, Santa Marta, Colombia
  (jreyes@invemar.org.co)

Abstract. As a result of the explorations carried out by the Colombian Marine and Coastal Research Institute (INVEMAR) between 1998-2002 along the Colombian Caribbean continental shelf and upper slope, the occurrence of azooxanthellate coral banks was suspected at three sites (from the northern to southern Colombian Caribbean coast): off La Guajira Peninsula, at a water depth of 70 m; off Santa Marta, at 200 m, and nearby the San Bernardo Archipelago, at 150 m). Each site exhibited particular bottom features (relief and substrate), suggestive of reef structures. The analysis of the fauna collected by bottom trawling at these sites showed that many of the fishes, mollusks, echinoderms, crustaceans, antipatharians, soft corals and bryozoans collected are characteristic dwellers of hard substrates or reef bottoms. At the first site (Guajira) the hard coral *Cladocora debilis*, was the most abundant; a total of 156 species of invertebrates and fishes were identified among the material collected at this site. At the second site (Santa Marta), 13 scleractinian species were collected, but *Madracis myriaster*, was the dominant species; another 102 species of invertebrates and fishes were also found. At the third site (San Bernardo) 19 scleractinian species were found, *M. myriaster* being the dominant. A total of 135 species of invertebrates and fishes were collected at this site. It is presumed that deep-sea coral banks have developed in these three settings, since many of the collected species are known to be hard or reef bottom dwellers.

Keywords. Colombian Caribbean, biodiversity, deep-water communities, azooxanthellate corals, mollusks, echinoderms, fishes, crustaceans

Introduction

The most extensive and unknown ecosystems on earth are on the sea floor (Snelgrove et al. 1997). The majority of marine bottoms are sedimentary plains, showing quite homogeneous features and similar oceanographic characteristics and biota, which are considered cosmopolitan in distribution (Snelgrove et al. 1997). However, within those extensive plains there are small areas like seamounts,

deep-sea trenches, reef-forming corals, submarine canyons, and cold seeps, whose characteristics make possible a relative increase of the biodiversity from surrounding soft bottom areas; these ecosystems are remarkable exceptions to the paradigm of the deep sea as one of the most stable, and least productive biospheres on earth (Mortensen et al. 1995; Koslow 1997; Koslow et al. 2001; Korn et al. 2003). They exhibit unique characteristics and support a diverse community of organisms which have been documented in limited biotic inventories and whose ecologic relationships are so far understood (de Forges et al. 2000).

Deep-sea coral communities have been reported throughout the world oceans, and although they seem to be constrained mainly to the North Atlantic and Pacific temperate waters, there are also some other records in tropical waters off the African coast, the Caribbean Antillean, and the Indopacific (Roberts and Hirschfield 2003). Contrasting to shallow-water coral reefs, deep-sea corals do not depend on sunlight to obtain energy, but feed on microscopic organisms from surrounding waters, and their productivity may be related to their association with light hydrocarbon seeps (de Forges et al. 2000). The discovery of these communities has been incidental, and generally made by fishermen (Fosså et al. 2002). Nevertheless, during the last decade the interest in the continental shelf communities has remarkably increased, to the point, that there is current characterization and mapping information available for the North Atlantic and the Pacific (Freiwald et al. 2002).

Although more than one hundred species can be associated with these unique reef habitats, deep-sea coral communities have been classified by the main framework species. Until now four deep-sea coral bank types have been described: *Lophelia pertusa* banks (200-1000 m water depth), *Oculina varicosa* banks (45-150 m water depth), *Primnoa-Paragorgia* forests (35-750 m water depth), and other living habitats colonized not exclusively by corals, but also by sponges, sea anemones, ascidians and bryozoans (Reed and Mikkelsen 1987; Freiwald et al. 2002; Krieger and Wing 2002).

Similar to shallow-water coral reefs, whose high biodiversity is comparable to that of the rain forest (Hubbell 1997), deep-sea corals have demonstrated that coral framework can modify the seabed. Thus, these coral assemblages provide an essential habitat for many species of invertebrates, including sea stars, nudibranchs, octopuses, snails, crinoids, basket stars, sponges, and anemones, by providing shelter, protection from currents and predators, breeding areas, spawning areas, nurseries, food, and resting areas (Krieger 2001; Tunesi et al. 2001). Some of the associated fauna are commercially and recreationally important such as the red porgy, the greater amberjack, the rockfish, the Pacific Ocean perch, the flatfish, the Atka mackerel, many species of snappers and groupers (Robins et al. 1986; Reed and Mikkelsen 1987; Allen and Robertson 1994) and crustaceans like golden king crab and shrimps. In addition, this biodiversity could be a potential source of numerous marine natural products with medical, pharmaceutical and cosmetological value (Bruckner 2002).

The Colombian continental shelf and break areas have been explored through few

expeditions, the most relevant include the R/V Oregon in the 70´s made by BCF, R/V Pillsbury in 1972 made by RSMAS and CIOH-INVEMAR-Smithsonian in 1995 on board at R/V ANCON, from which a systematic survey was done. Based on their results the INVEMAR carried out the 'Macrofauna' cruises (1998-2002) on board at R/V ANCON, whose primary aim was to fill the information gaps in the inventories of the Colombian soft bottom fauna between 20 and 520 m depth. A total of 72400 specimens were collected during the 'Macrofauna' expeditions, of which 50 % of the species were new records for Colombia (Saavedra-Díaz et al. 2000; Lattig and Reyes 2001; Borrero-Pérez et al. 2002a, b; Cruz et al. 2002; Gonzalez et al. 2002; Gracia et al. 2002; Roa-Varón et al. 2003; Borrero-Pérez and Benavides-Serrato 2004; Campos et al. 2004). In total 10 new species have been described (Lattig and Cairns 2000; Lemaitre and Bermúdez 2000; Lemaitre et al. 2001; Saavedra-Díaz et al. 2001; Ardila and Díaz 2002; Saavedra-Díaz et al. 2003).

The principal aim of the present study is to show and discuss the occurrence of azooxanthellate coral banks in three localities of the southwestern Caribbean sampled by the 'Macrofauna' cruises (INVEMAR 1998-2002). The results of this study represent new evidence of coralline banks constructed by different azooxanthellate corals species than those already reported (Freiwald et al. 2002). The associated faunas are quite different in each one of the three coral settings, represented primarily by anthozoans, crustaceans, mollusks, echinoderms and fishes. In this way, these three unique azooxanthellate coral communities sustain one of the highest species diversities found along the Colombian continental shelf. Due to the fact that the sampling performed by the Macrofauna cruises focused on macrobenthic fauna living on soft bottoms, the discovery of these three localities rich in azooxanthellate corals and their associated fauna was an unexpected result.

Abbreviations

AC: Azooxanthellate corals
BCF: Bureau of Commercial Fisheries, U.S. Department of Interior
DSC: Deep-sea corals
INVEMAR: Instituto de investigaciones Marinas y costeras
GIS-SR Lab: Geographic information systems and remote sensors laboratory at INVEMAR
MCZ: Museum of Comparative Zoology, Harvard University, Cambridge, Massachusetts
MHNMC: Museo de Historia Natural Marina de Colombia
NMNH: National Museum of Natural History, Washington
SIBM: Colombian marine biodiversity database
RMNH: Nationaal Natuurhistorische Museum, Leiden, The Netherlands
RSMAS: Rosenstiel School of Marine and Atmospheric Science, Miami
Senckenberg: Senckenberg Museum Frankfurt, Germany

Materials and methods

The sampling was carried out on board the R/V ANCON in two phases: Macrofauna I (October 1998 - April 1999) and Macrofauna II (March - April 2001). In total 80 trawling stations were included between off La Guajira Peninsula (12º 34'N 71º 50' W) and off Gulf of Urabá (09º 02' N 76º 02' W) at five depth ranks (20, 70, 150, 300 and 500 m). A bottom area of about 25000 m^2 was swept at each station by using a semi-balloon trawl net (ca. 9 x 1 m opening) during 20 min, and at a vessel speed of about 3 knots (5.5 km/h). Sea-bottom relief was differentiated using a FURUNO FE 824 echo sounder (200 kHz). On board, the samples were washed through a sieve, sorted and preserved in 70 % and 96 % ethanol (invertebrates) and 10 % formalin (fishes). The locations of the three sites where a significant abundance of azooxanthellate corals and their associated organisms were collected are shown in Table 1 and Figure 1. The specimens were identified to species level by consulting group specific monographs and through direct examination of museum repositories from the NMNH, MCZ, RMNH, RSMAS, Senckenberg, and MHNMC collections. Species relevant information was stored in the SIBM data base, hosted at http://web.invemar.org.co/redcostera1/invemar/sib.jsp.

Results

During the expeditions, three localities with a significant abundance of AC and associated organisms were discovered unexpectedly; however, AC species in other localities have recorded in small amounts. The AC stations were located along the Colombian continental shelf (Fig. 1), off La Guajira Peninsula, off Santa Marta, and off San Bernardo Islands (Table 1). Unlike other sampled bottoms of continental shelves and upper slope, the species richness found for these three AC stations (338 species) was relatively high, with a value representing around 40 % of the species collected throughout the whole study. Species list is shown in Appendix 1. Although the most abundant AC and dwellers found in the three settings belong to different species (in terms of taxonomic identification), the number of species observed in each station was similar, the species common to all sectors remains low (11 species). The most diverse and abundant group sampled corresponds to mollusks (Fig. 2). Some of the echinoderms collected from these three coralline formations constitute

Table 1 Station list, samples collected in each of the coralline communities. Locality (INVEMAR Macrofauna project station name), depth range, and initial (superior coordinates) and final (inferior coordinates) trawl position are shown

Station	Depth (m)	Lat (N)	Long (W)
La Guajira (INV 048)	70-71	11º 23.53'	73º27.78'
		11º24.40'	73º27.62'
Santa Marta (INV 019)	200–220	11º23.25'	74º12.46'
		11º23.61'	74º12.37'
San Bernardo (INV 073)	155-160	9º47.12'	76º13.45'
		9º46.61'	76º13.72'

Fig. 1 Map of the Colombian Caribbean showing the three localities where the coral communities were discovered (stars), and where *Lophelia pertusa* was recorded (triangles)

the first records for the Colombian Caribbean. Many fish species associated with coral reef and rocky bottoms were also collected in the areas mentioned.

Common species

The stony coral *Madracis myriaster* (Fig. 3a), common in Santa Marta and San Bernardo, but rare in La Guajira (the shallowest site), appears to be the main coralline matrix builder in the two first areas. Other species common to all localities were the stony coral *Anomocora fecunda* (Fig. 3c), the black coral *Antipathes lenta*, the alcyonarian *Stereonephthya portorricensis* (Fig. 3k) and the brittle-star *Ophiothrix suensonii*, both of them coralline ground dwellers. *Paracyathus pulchellus* (Scleractinia) was commonly found attached to other stony corals skeletons; crabs belonging to the genera *Mithrax* and *Stenorhyncus*, and the fishes *Synagrops bella* and *Antigonia capros* were also recorded.

Associated biota, general characteristics

La Guajira. Water depth 70 m. *Cladocora debilis* (thin tube coral; Fig. 3b) was the main coral matrix builder, its sympodial budding and recumbent shapes provide more surfaces on which sponges, bryozoans, octocorals and tunicates can settle. Other scleractinian species such as *Madracis myriaster* (Fig. 3a),
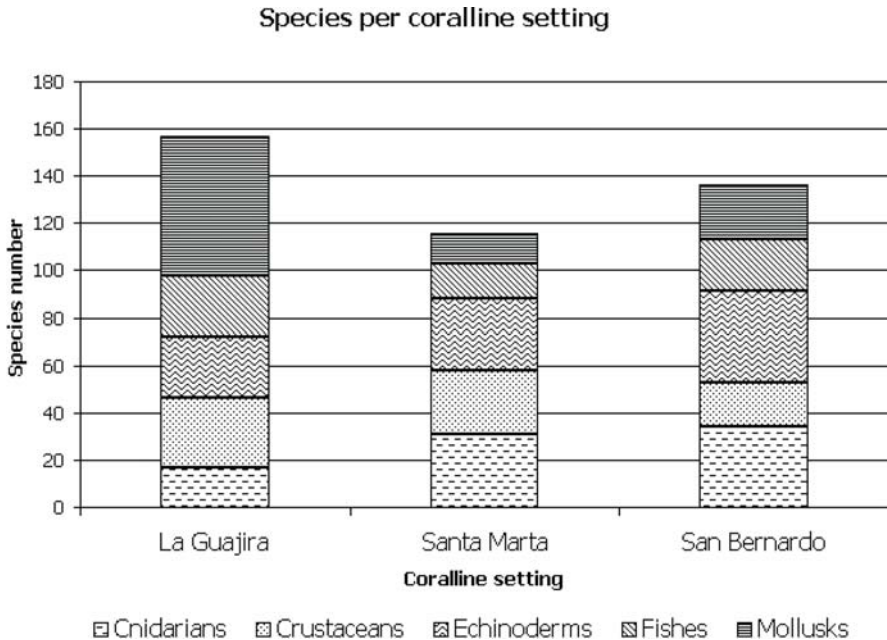
Fig. 2 Species number by major taxa (cnidarians, mollusks, crustaceans, echinoderms and fishes) in each of the coral communities: La Guajira, Santa Marta, and San Bernardo

Anomocora fecunda (Fig. 3c)*, Anomocora prolifera*, and *Paracyathus pulchellus* also occasionally occur.

A total of 156 species were collected in this locality, where mollusks were the most diverse taxon (59 species). Bivalves like *Chlamys munda* and *Arca zebra,* and gastropods like *Petaloconchus erectus*, and *Vermicularia spirata* were the most abundant mollusk species. *V. spirata* was often found attached to sponges and to *C. debilis* in small clusters with bryozoans. *V. spirata* is a facultative coral associate, using it as refuge or preying on it (Reed and Mikkelsen 1987). Echinoderms were the most abundant taxon, with 1367 specimens (Fig. 2). The crinoid *Analcidometra armata* was the dominant echinoderm, it has been reported as a common species attached to the gorgonians in the Caribbean Sea (Meyer 1973; Hendler et al. 1995). *Ophiothrix angulata* (Fig. 3u) was found in several stations along the sampling area,

Fig. 3 Invertebrates and fishes collected in the Southern Caribbean deep-sea coral banks off Colombia. The measures given in parenthesis following the species names correspond to the specimen approximate height (invertebrates) and length (fishes). The species shown in this figure were selected to be hard bottom dwellers or associated to their surrounding areas. Cnidarians: **a** *Madracis myriaster* [10 cm]; **b** *Cladocora debilis* [3 cm]; **c** *Anomocora fecunda* [3 cm]; **d** *Thalamophyllia riisei* [5 cm]; **e** *Caryophyllia berteriana* [5 cm]; **f** *Nicella* cf. *guadalupensis* [4 cm]; **g** *Chrysogorgia desbonni* [8 cm]; **h** *Callogorgia* sp. [11 cm]; **i** *Nidalia rubripunctata* [7 cm]; **j** *Antipathes* n. sp. [4 cm]; **k** *Stereonephthya portorricensis* [11 cm]. Mollusks: **l** *Coralliophila caribaea* [2 cm]; **m** *Coralliophila squamosa* [2 cm];
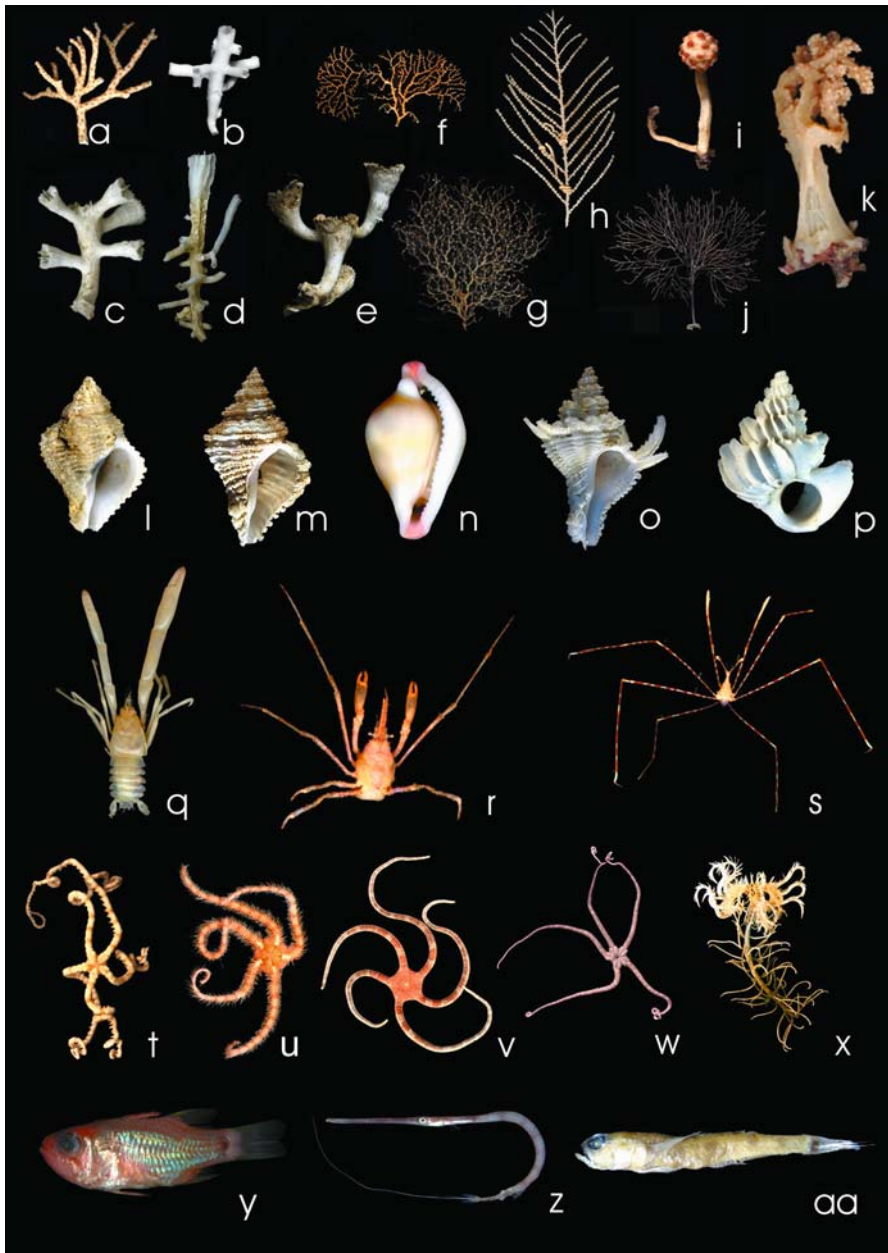
n *Pseudosimnia vanhyningi* [1.3 cm]; **o** *Babelomurex dalli* [2.4 cm]; **p** *Sthenorytis pernobilis* [1.6 cm]. Crustaceans: **q** *Uroptychus uncifer*; **r** *Anomalothir frontalis*; **s** *Latreillia elegans*. Echinoderms: **t** *Asteroschema* cf. *oligactes* [3 cm]; **u** *Ophiothrix angulata* [4 cm]; **v** *Ophioderma rubicundum* [6 cm]; **w** *Astrocnida* cf. *isidis* [10 cm]; **x** *Pentacrinus* sp. [14 cm]. Fishes: **y** *Apogon pseudomaculatus* [3 cm]; **z** *Fistularia petimba* [15 cm]; **aa** *Bollmannia* sp. [2 cm]

but it was especially abundant in the La Guajira community. *O. angulata* has also been reported on *Oculina varicosa* banks off Florida (Reed and Mikkelsen 1987).

In the La Guajira setting, coral reef dweller fishes such as the family Apogonidae (*Apogon affinis*, *A. quadrisquamatus* and *A. pseudomaculatus*) were common (Palacio 1974; Uyeno et al. 1983; Böhlke and Chaplin 1993; Cervigón 1993; Allen and Robertson 1994). Seagrass-inhabitant species like *Paradiplogrammus bairdi*, were also found there.

Santa Marta. Water depth 200 m. 13 scleractinian species were collected. *Madracis myriaster* (Fig. 3a), *Coenosmilia arbuscula, Anomocora fecunda* and the solitary *Polymices fragilis*, were the most abundant species. Here, the stony corals are characterized by bushy shaped colonies (*M. myriaster*, *A. fecunda* and *C. arbuscula*) or individual polyps (*Polymices fragilis* and *Javania cailleti*), both forms have strong bases attached directly to the rock.

Another 102 species of fishes, echinoderms, mollusks, crustaceans, and cnidarians were also found. However, in contrast to La Guajira, other organisms did not significantly encrust the coral skeletons. The species of black corals and octocorals were also numerous, especially *Antipathes columnaris*, *Aphanipates abietina*; and species of the genus *Stichopathes*, and the octocorals *Chrysogorgia desbonni* (Fig. 3g), *Trychogorgia lyra*, *Nidalia* sp. (Fig. 3i) and *Nicella* cf. *guadalupensis* (Fig. 3f). The abundance of mollusks was low; the gastropods found were anthozoan´s dwellers, which usually prey on it; *Sthenorytis pernobilis* (Epitoniidae) (Fig. 3p) on sea anemones; *Pseudosimnia vanhyningi* (Ovulidae) (Fig. 3n) on octocorals; and *Babelomurex dalli* (Fig. 3o), and *Coralliophila squamosa* (Fig. 3m) (Coralliophilidae) on stony corals (Keen 1971; Cate 1972; Reed and Mikkelsen 1987), all of these constitute first records for the Colombian Caribbean (Gracia et al. 2004).

In Santa Marta, *Ophiothrix suensonii*, commonly found on gorgonians, recorded by Hendler et al. (1995) from shallow to deep reef zones and the sea cucumber *Holothuria lentiginosa enodis* previously recorded off Florida from *Oculina varicosa* banks (Pawson et al. 1982), were found (Borrero-Pérez et al. 2003). Another 14 species were found exclusively in this area; three of them, *Stephanasterias* cf. *albula*, *Trigonocidaris albida*, and *Palaeobrissus hilgardi* were the first records for the southern Caribbean.

The crustacean fauna found in the three coralline formations presents no major exclusive coral associations, however, in Santa Marta species of the family Chyrostilidae like *Uroptychus* sp., were recorded as hosted in octocorals of the *Chysogorgia* genus (Pequegnat and Pequegnat 1970). Some crab species collected, like those of the genera *Anomalothir* and *Latreillia*, are known to be common inhabitants of rubble shells and sandy bottoms (Williams 1984). *Palicus affinis, P. alternatus, P. gracilipes* and *P. sicus*, exhibit no particular habitat preferences (Rathbun 1918), but were found associated with coral grounds only in the Santa Marta and San Bernardo areas.

Rocky-bottom fishes like *Gymnothorax poligonius*, *Chlorophthalmus agassizi*, *Bellator egretta*, *Antigonia capros*, *Antigonia combatia*, and *Pontinus nematophthalmus* were the first records for the Colombian Caribbean.

San Bernardo. Water depth: 155-160 m. 19 scleractinian species were found, among which, *Anomocora fecunda*, *Coenosmilia arbuscula*, *Thalamophyllia riisei* (Fig. 3d) and *Madracis myriaster* were dominant. *Eguchipsammia cornucopia*, mostly devoid of living tissue, was also common. Other less abundant scleractinians were also found attached to the four species mentioned above. Three different growth forms of stony corals were present: recumbent (*T. riisei* and *E. cornucopia*); bushy (*M. myriaster* and *A. fecunda*); and solitary (*Caryophyllia berteriana*, Fig. 3e, and *Coenocyathus parvulus*). The San Bernardo site corresponds to an extensive carbonate deposit formed during the Pleistocene epoch over older strata deformed by tectonism and diapiric intrusion (Vernette 1989a).

Beside corals, a total of 115 species of invertebrates and fishes were collected at this site. San Bernardo was the most diverse sector in echinoderms with 38 species (Fig. 2); brittle stars such as *Ophioderma appressum*, *Astrocnida* cf. *isidis* (Fig. 3w), *Asteroporpa* cf. *annulata*, *Asteroschema* cf. *laeve* and *Asteroschema* cf. *oligactes* (Fig. 3t) were found attached to stony corals and gorgonians. Also, rare species, like *Ophiosyzygus disacanthus*, previously recorded as dwelling in hard bottoms (Turner and Heyman 1995; Borrero-Pérez and Benavides-Serrato in press), the pedunculate crinoids *Democrinus conifer* (Macurda and Meyer 1976), and the coral reef crinoid *Nemaster rubiginosus* (Hendler et al. 1995) were also present in San Bernardo. The mollusk fauna here has no restricted coral dwellers, except the gastropod *Coralliophila caribaea*, 10 species of bivalves were found.

In San Bernardo, five fish species associated with coral reefs (Allen and Robertson 1994; Cervigón 1994) were caught. *Fistularia petimba*, *Bollmannia* sp., *Serranus atrobranchus*, *Decodon puellaris* and *Pristigenys alta*, although they were not the most abundant species collected (Fig. 3). While *Citharichthys cornutus*, *Lipogramma evides* and *Neomerinthe beanorum* were the most frequent species caught.

Discussion

The Colombian seabed still remains poorly known. The efforts addressed to the study the shallow-water coral reefs and seagrasses during the last three decades have been increased, and data about characterization and mapping of them are already available (Díaz et al. 2000, 2003), but shallow-coral reefs and seagrasses, represent only less than 1 % of the Colombian marine bottoms (SIG-SR Lab). Recently, other complex ecosystems occurring on the continental shelf and slope around the world are being discovered and studied mainly in North Atlantic and Pacific oceans. DSC banks belong to those recently described ecosystems (Mortensen et al. 1995; Freiwald et al. 2002; Korn et al. 2003). According to the results of this study, three new records of azooxanthellate coral communities occurring on the Colombian continental shelf are documented. The records registered off La Guajira, Santa Marta and San Bernardo were fortuitous, because the Macrofauna expeditions were focused to explore the soft bottoms of the continental shelf and slope between 20 and 500 m. In 77 of the 80 stations sampled no major amounts of corals on hard

substrates were found. Occasionally, in some sampling areas, where rough relief was observed, trawling was avoided to prevent net damage; for that reason, more areas where deep-sea coral communities occur would be expected. Further research aiming to map and study their biodiversity is necessary to assess the value of these deep-sea coral ecosystems and to propose conservation measures.

The results suggest that the deep-sea coral communities observed on the Colombian continental shelf have a similar ecological role (in terms of dwelling and food supply) to those reported in temperate regions. The fauna composition of the stony coral framework here however is different. *Lophelia* spp., *Oculina* spp. and *Madrepora* spp. were uncommon species; *Madracis myriaster* and *Cladocora debilis* seem to be the main frame building species found. *M. myriaster* belongs to the apozooxanthellate coral group defined by Best (2001), which developed adaptive strategies to survive in colder waters; this adaptive response could derive from the facultative presence of zooxanthellae, followed by the migration to deep waters. This kind of adaptation explains the extensive bathymetric range of *M. myriaster* namely 20-700 m in the West Atlantic (Best 2001).

On the other hand, the *Lophelia pertusa* records in the Oceana Report (Roberts and Hirschfield 2003) give some evidence of the possible occurrence of *Lophelia* banks off Venezuela. In addition, some other non-living *Lophelia* records from the R/V Pillsbury (Cairns 1979) and INVEMAR expeditions in Colombian waters at 500 m depth, suggest that *Lophelia* could have occurred there in the recent past, or could be alive there now and forming coral banks in the surrounding waters.

The differences in stony coral species composition found among the surveyed localities indicate some differences in environmental conditions. *Cladocora debilis* is the most important coral established in La Guajira formation. This suggests that the growth of recumbent species is favored of a homogeneous non-consolidated bottom in this locality. In fact, sedimentary data sets indicate that deposited material on the coast off La Guajira comes from upper Tertiary and Quaternary alluviums (Thomas and MacDonald 1969). Metamorphic rocks from the Sierra Nevada de Santa Marta mountain system (Gonzáles and Rodríguez 2003) form a favourable substrate for the corals settled at Santa Marta site. There, the coralline fauna was mainly represented by species with corallums showing an extended base attached to the rock (*Polymices fragilis* and *M. myriaster*). In San Bernardo both corallum shapes were common, suggesting a heterogeneous substrate that probably promoted the variability in the corallum forms settled there. Apparently, the attached species grow on limestone substrate, which is composed mainly of a fossil reef terrace built during the last marine regression about 20 ky ago when the sea level was 120 m below the current one (Vernette 1989b). This fossil reef terrace has developed on diapiric domes or mud vulcanoes which can be related to the active plate tectonics off the Colombian Caribbean continental margin (Vernette 1989c).

Although the hard corals that build framework belonged to different species, they exhibit a similar shape characterized by recumbent growth with secondary corallites located both sides of the principal axis (see Figs. 3a-e). The branching pattern displayed by *Anomocora fecunda* (Fig. 3c) and *Coenosmilia arbuscula*,

was quite similar, and sometimes establishing differences between them was very difficult. Some specimens exhibit a transitional form, which indicates a possible hybridization process, analogous to that described for shallow coral reefs (Vollmer and Palumbi 2002). Other evidence suggests that corallum shape convergence is a common phenomenon; species previously described by Cairns (2000) as reptoid colonies (*Thalamophyllia riisei*; Fig. 3d) or as individual polyps (*Caryophyllia berteriana*; Fig. 3e), showed a branching pattern similar to that of *Cladocora debilis* (Fig. 3b). Such convergence suggests an environmental factor response, analogous to those corallum-shape changes showed by some species in shallow coral reefs, responding to hydrodynamic factors.

The differences among the faunas associated with the three DSC communities give some hints about the environmental conditions of the surrounding waters. At La Guajira site, sponges and ascidians (suspension feeders) were abundant; this fact indicates an environment enriched with suspension material, perhaps produced by the upwelling conditions typical of the area. Epizoic fauna was common in La Guajira coral community; sponges, ascidians, bryozoans, antipatharians, octocorals, and scleractinians were settled on *Cladocora debilis* (Fig. 3b) skeletons. Sponges also provide substrates to other fauna; the scleractinian *Paracyathus pulchellus* which was often observed settled on them. In San Bernardo some epizoites were noticed whereas in Santa Marta the epizoites were rare.

Tropical coral reefs present a fragmented distribution due to their specific ecological requirements to develop complex structures (Birkeland 1997). Some typical shallow reef species were found associated with these deep-sea coral communities. The brittle star *Ophioderma* spp., the gobiid fish *Bollmannia* spp. and *Apogon* spp. increased their bathymetric range to deeper waters, suggesting that there may be an ecological relationship (i.e. breeding areas) between shallow-water reef habitats and their deep-water continental shelf counterparts. This example suggests that distributional patterns of some coral reef species may be characterized by a continuum rather than by isolated populations, using these deep-water environments as stepping stone habitats between shallow reefs in order to disperse.

Different facultative or obligate epizoic interactions within these communities were observed, including stony corals, gorgonians and sponges as substrates for bryozoans, mollusks, echinoderms, other stony corals and sponges. Some studies on invertebrate fauna associated with corals have demonstrated that while corals play an important role in framework building, crinoids, sea anemones, bryozoans, sponges, and other scleractinians, participate in the accumulation of carbonate sediments and the accretion of coralline matrix (Sulak and Ross 2003).

Further investigation will be focused on studying the biological and ecological relationships in these settings. It is necessary to carry out research on habitat characterization and mapping, as well as on the assessment of impacts caused by trawl fishing in order to support arguments for the sustainable use and conservation of these unique biological communities.

Acknowledgements

References

Ardila NE, Díaz JM (2002) *Armina juliana* (Gastropoda: Nudibranchia: Arminidae) a new species from southern Caribbean. Bol Inst Inv Mar Cost 31: 25-32

Best MB (2001) Some notes on the terms "deep-sea ahermatypic" and "azooxanthellate" illustrated by the coral genus *Madracis*. Proc First Int Symp Deep-sea Corals, Halifax: 19-29

Birkeland C (1997) Life and death of coral reefs. Chapman and Hall, New York

Böhlke J, Chaplin C (1993) Fishes of the Bahamas and adjacent tropical waters. Texas, Austin, 771 pp

Borrero-Pérez GH, Benavides-Serrato M (2004) New record of *Ophiosyzygus disacanthus* Clark, 1911 (Echinodermata: Ophiuroidea: Ophiomyxidae) in the Caribbean Sea. Proc Biol Soc Washington 117

Borrero-Pérez GH, Benavides-Serrato M, Solano O, Navas G (2002a) Equinoideos (Echinodermata: Echinoidea) colectados en la franja superior del talud continental del Caribe colombiano. Bol Inst Inv Mar Cost 31: 133-166

Borrero-Pérez GH, Solano OD, Benavides M (2002b) Lista revisada de los erizos (Echinodermata: Echinoidea) del mar Caribe colombiano. Biota Colombiana 3: 137-144

Borrero-Pérez GH, Benavides-Serrato M, Solano O, Navas G (2003) Holothuroideos (Echinodermata: Holothuroidea) recolectados en el talud continental superior del Caribe colombiano. Bol Inst Ocenogr Venezuela Univ Oriente 42: 65-85

Bruckner AW (2002) Life saving products from coral reefs. Issues in Science and Technology online. Spring 2002. http://www.nap.edu/issues/18.3/p_bruckner.html.

Cairns SD (1979) The deep-water Scleractinia of the Caribbean Sea and adjacent waters. Stud Fauna Curaçao and other Caribb Is 180, 341 pp

Cairns SD (2000) A revision of the shallow-water azooxanthellate Scleractinia of the Western Atlantic. Stud Nat Hist Caribb Reg 75: 1-231

Campos NH, Navas G, Bermúdez A, Cruz A (2004) Los crustáceos decápodos de la franja superior del talud continental (300–500 m) del Mar Caribe Colombiano. Monogr Fauna Colombia. 2. Inst Cienc Nat Mus Hist Nat, Univ Nac Colombia, Bogotá, 180 pp

Cate CN (1972) A systematic revision of the recent cypraeid family Ovulidae (Mollusca, Gastropoda). Veliger (supp) 15: 1-116

Cervigón F (1993) Los peces marinos de Venezuela. 2. Fundación Científica Los Roques, Caracas, 423 pp

Cervigón F (1994) Los peces marinos de Venezuela. 3. Fundación Científica Los Roques, Caracas, 354 pp

Cruz N, Bermúdez A, Campos NH, Navas GR (2002) Los camarones de la Familia Crangonidae del talud continental entre 200 y 500 m del Mar Caribe colombiano. Bol Inv Mar Cost 31: 183-203

De Forges BR, Koslow JA, Poore GCB (2000) Diversity and endemism of the benthic seamount fauna in the southwest Pacific. Nature 405: 944-947

Díaz JM, Barrios LM, Cendales MH, Garzon-Ferreira J, Geister J, López-Victoria M, Ospina GH, Parra-Valencia F, Pinzón J, Vargas-Angel B, Zapata FA, Zea S (2000) Áreas coralinas de Colombia. INVEMAR Ser Publ Espec 5, 176 pp

Díaz JM, Barrios LM, Gómez-López DI (2003) Las praderas de pastos marinos en Colombia. Estructura y distribución de un ecosistema estratégico. INVEMAR Ser Publ Espec 10, 159 pp

Fosså JH, Mortensen PB, Furevik DM (2002) The deep-water *Lophelia pertusa* in Norwegian waters: distribution and fisheries impacts. Hydrobiologia 471: 1-12

Freiwald A, Hühnerbach V, Lindberg B, Wilson JB, Campbell J (2002) The Sula reef Complex, Norwegian shelf. Facies 47: 179-200

González DN, Solano OD, Navas GR (2002) Equinodermos colectados por la expedición CIOH-INVEMAR-SMITHSONIAN desde Cartagena hasta el Golfo de Urabá, Caribe Colombiano. Bol Inst Inv Mar Cost 31: 85-132

González H, Rodríguez G (2003) Rocas metamórficas de alto grado en la Sierra Nevada de Santa Marta: Edad y posibles correlaciones. Mem IX Cong Col Geol: 75-76

Gracia A, Ardila NE, Díaz JM (2002) Cefalópodos (Mollusca: Cephalopoda) del talud superior del Caribe colombiano. Bol Inst Inv Mar Cost 31: 219-238

Gracia A, Ardila NE, Díaz JM (2004) Gastropods collected along the continental slope of the Colombian Carribean during the INVEMAR-macrofauna campains (1998-2001). Iberus 22: 43-75

Hendler G, Miller JE, Pawson DL, Kier PM (1995) Sea stars, sea urchis and allies: echinoderms of Florida and the Caribbean. Smithsonian Inst Press, Washington, 390 pp

Hubbell SP (1997) A unified theory of biogeography and relative species abundance and its aplication to tropical rain forest and coral reef. Proc 8th Int Coral Reef Symp 1: 33-42

Keen M (1971) Sea shells of tropical West America. Stanford Univ Press, Stanford, California

Korn H, Friedrich S, Feit U (2003) Deep-sea genetic resources in the context of the Convention on Biological Diversity and the United Nations Convention on the Law of the Sea. Bundesamt Naturschutz (BfN), Bonn, 84 pp

Koslow JA (1997) Seamounts and the ecology of deep-sea fisheries. Amer Sci 85: 168-176

Koslow JA, Gowlett-Holmes K, Lowry J, O'Hara T, Poore G, Williams A. (2001) The seamount benthic macrofauna off southern Tasmania: community structure and impacts of trawling. Mar Ecol Prog Ser 213: 111-125

Krieger KG (2001) Coral (*Primnoa*) impacted by fishing Gear in the Gulf of Alaska. Proc First Int Symp Deep-sea Corals, Halifax, pp 106-116

Krieger KG, Wing BL (2002) Megafauna associations with deepwater corals (*Primnoa* spp.) in the Gulf of Alaska. Hydrobiologia 471: 83-90

Lattig P, Cairns S (2000) A new species of *Tethocyathus* (Cnidaria: Anthozoa: Scleractinia: Caryophyllidae), a trans-isthmian azooxanthellate species. Proc Biol Soc Washington 113: 590-595

Lattig P, Reyes J (2001) Nueve primeros registros de corales azooxanthellados (Anthozoa: Scleractinia) del Caribe colombiano (200-500 m). Bol Inv Mar Cost 30: 19-38

Lemaitre R, Bermúdez A (2000) A new cyclodorippoid crab of the genus *Cymonomoides* Tavares, 1993 (Crustacea: Decapoda: Brachyura: Cymonomidae) from Caribbean coast of Colombia. Proc Biol Soc Washington 113: 974-979

Lemaitre R, Campos NH, Bermudez A (2001) A new species of *Pyromaia* from the Caribbean Sea, with a rediscription of *P. propinqua* Chace, 1940 (Decapoda: Brachyura: Majoidea: Inachoididae). J Crus Biol 2: 760-773

Macurda DB, Meyer DL (1976) The identification and interpretation of stalked crinoids (Echinodermata) from deep-water photographs. Bull Mar Sci 26: 205-215

Meyer, DL (1973) Coral Reef Project-Papers in memory of Dr. Thomas F. Goreau. 10. Distribution and living habits of comatulid crinoids near Discovery Bay, Jamaica. Bull Mar Sci 23: 244-259

Mortensen PB, Hovland M, Brattegard T, Farestveit R (1995) Deep water bioherms of the scleractinian coral *Lophelia pertusa* (L.) at 64°N on the Norwegian shelf: structure and associated megafauna. Sarsia 80: 145-158

Palacio F (1974) Peces colectados en el Caribe Colombiano por la Universidad de Miami. Bol Museo Mar 6: 1-137

Pawson DL, Miller JE, Hoskin CM (1982) Distribution of *Holothuria lentiginosa enodis* Miller and Pawson in relation to a deep-water *Oculina* coral reef Fort Pierce, Florida (Echinodermata: Holothuroidea). In: Lawrence JM (ed) Proceedings of the International Echinoderms Conference, Tampa Bay, 1981. Balkema Press, Rotterdam, pp 321

Pequegnat WE, Pequegnat LH (1970) Deep-sea anomurans of superfamily Galatheoidea with descriptions of three new species. In: Pequegnat WE, Chace FA (eds) Contribution on the Biology of the Gulf of Mexico. Texas A and M, Univ Oceanogr Stud, pp 171-204

Rathbun MJ (1918) The grapsoid crabs of America. Smithsonian Inst Washington Bull 97: 1-461

Reed JK, Mikkelsen PM (1987) The molluscan community associated with the scleractinian coral *Oculina varicosa*. Bull Mar Sci 40: 99-131

Roa-Varón A, Saavedra-Díaz L, Acero A, Mejía LS, Navas G (2003) Nuevos registros de peces óseos para el Caribe colombiano de los órdenes Beryciformes, Zeiformes, Perciformes y Tetraodontiformes. Bol Inst Inv Mar Cost 32: 3-24

Roberts S, Hirshfield M (2003) Deep-sea corals: out of sight, but no longer out of mind. Oceana, Washington DC, pp 16

Robins CR, Ray CG, Douglass J (1986) A field guide to Atlantic coast fishes of North America. Houghton Miflinn Co., Boston, 354 pp

Saavedra-Díaz L, Acero A, Navas A (2000) Lenguados de la familia Paralichthyidae (Pisces: Pleuronectiformes) conocidos del Caribe colombiano. Rev Acad Colomb Cienc Exact, Fís Nat 24: 295-310

Saavedra-Díaz L, Munroe T, Acero A (2003) *Symphurus hernandezi* (Pleuronectiformes: Cynoglossidae), a new deep-water tonguefish from the southern Caribbean Sea off Colombia. Bull Mar Sci 72: 955-970

Saavedra-Díaz LM, Mok H, Acero A (2001) Two new species of hagfishes, *Eptatretus wayuu* and *Paramyxine ancon* (Myxinidae: Myxiniformes) from the Caribbean Coast of Colombia. Copeia 4: 1026-1033

Snelgrove PV, Blackburn TH, Hutchings PA (1997) The importance of marine sediment biodiversity in ecosystem processes. Ambio 26: 578-583

Sulak KJ, Ross SW (2003) A profile of the *Lophelia* Reefs. NOAA, U.S. Department of Commerce. (Internet: http://oceanexplorer.noaa.gov/explorations/islands01/background/islands/sup10_lophelia.html)

Thomas DJ, MacDonald WD (1969) Summary of Tertiary stratigraphy and structure, Guajira Peninsula. 1er Congr Colomb Geol: 207-216

Tunesi L, Diviacco G, Mo G (2001) Observations by submersible on the biocoenosis of the deep-sea corals off Portofino promontory (Northwestern Mediterranean Sea). Proc First Int Symp Deep-sea Corals, Halifax, pp 76-87

Turner RL, Heyman RM (1995) Rediagnosis of the brittlestar genus *Ophiosyzygus* and notes on its type species *O. disacanthus* (Echinodermata: Ophiuroidea: Ophiomyxidae) based on the type specimens from Japanese waters and new material from the Gulf of Mexico. Proc Biol Soc Washington 108: 292-297

Uyeno T, Matsuura K, Fujii E (1983) Fishes trawled off Suriname and French Guiana. Japan Mar Fish Res Res Cent, Nat Sci Mus Tokyo, 519 pp

Vernette G (1989a) Impact du diapirisme argileux sur les récifs de la plate-forme Colombienne des Caraïbes. Bull Inst Geol Bassin Áquitain 45: 97-105

Vernette G (1989b) Les variations du niveau marin exemple de la cote Colombienne de Caraïbes a l'Holocene. Bull Inst Geol Bassin Áquitain 45: 81-95

Vernette G (1989c) Examples of diapiric control on shelf topography and sedimentation patterns on the Colombian Caribbean continental shelf. J South Amer Earth Sci 4: 391-400

Vollmer ST, Palumbi SR (2002) Hybridization and the evolution of reef coral diversity. Science 296: 2023-2025

Williams AB (1984) Shrimps, lobsters and crabs of the Atlantic coast of the eastern United States, Maine to Florida. Smithsonian Inst Press, Washington D.C., 550 pp

Appendix 1

Species list of invertebrates and fishes collected in the coralline settings off Colombia. La Guajira (GUA), Santa Marta (SMA) and San Bernardo (SBE). The new records (NR) for Colombian Caribbean are shown

Group	Species	Coral Setting			NR
		GUA	SMA	SBE	
Cnidarians	*Acanthogorgia schrammi*	×		×	+
	Acryptolaria conferta		×		+
	Amphiantus caribaea		×		+
	Anomocora fecunda	×	×	×	
	Anomocora prolifera	×	×		
	Antipathes atlantica	×			
	Antipathes cf. *salix*		×		+
	Antipathes columnaris		×	×	+
	Antipathes furcata	×			
	Antipathes gracilis	×		×	
	Antipathes lenta	×	×	×	
	Antipathes n. sp.		×		
	Aphanipathes abietina			×	+
	Balanophyllia bayeri		×		+
	Balanophyllia cyathoides		×	×	+
	Balanophyllia palifera		×	×	+
	Balanophyllia pittieri		×		
	Balanophyllia wellsi			×	+
	Bellonella rubistella	×			+
	Callogorgia sp.		×		+
	Caryophyllia ambrossia		×		
	Caryophyllia barbadensis			×	+
	Caryophyllia berteriana		×	×	
	Caryophyllia sp.		×	×	
	Chrysogorgia desbonni			×	+
	Chrysogorgia sp.			×	
	Cladocora debilis	×			
	Coenocyathus parvulus			×	+
	Coenosmilia arbuscula		×	×	
	Deltocyathus calcar			×	
	Diodogorgia sp.			×	
	Eguchipsammia cornucopia			×	+
	Javania cailleti		×	×	
	Leipsiceras pollens		×		
	Madracis asperula	×			
	Madracis myriaster	×	×	×	
	Madracis pharensis			×	
	Madrepora carolina			×	+
	Nicella guadalupensis			×	+
	Nicella sp.1		×		
	Nicella sp.2		×		
	Nidalia cf. *occidentalis*	×			+
	Nidalia dissidens		×	×	+
	Oxysmilia rotundifolia			×	
	Paracyathus pulchellus	×		×	
	Placogorgia tenuis		×		+
	Polycyathus mayae			×	+
	Polymyces fragilis		×		+
	Renilla muelleri	×			
	Riisea sp.		×		
	Stereonephthya portorricensis	×	×	×	+

Appendix 1 continued

Group	Species	GUA	SMA	SBE	NR
...Cnidarians	*Stichopathes* cf. *lutkeni*			×	+
	Stichopathes cf. *occidentalis*			×	
	Stichopathes pourtalessi			×	+
	Stichopathes n. sp.		×		
	Swiftia sp.			×	
	Thalamophyllia riisei			×	+
	Thelogorgia vossi		×		
	Thesea sp.1	×			
	Trichogorgia lyra	×			
	Villogorgia nigrensis		×		+
	Viminella sp.		×		+
Crustaceans	*Aepinus septemspinosus*	×			+
	Agaricochirus alexandri		×		
	Anasimus latus	×			
	Anomalothir frontalis		×	×	+
	Anomalothir furcillatus		×		+
	Anomalothir sp.		×		
	Arachnopsis sp.	×			
	Batrachonotus fragosus	×			
	Calappa sulcata	×	×		
	Callidactylus asper	×			
	Chasmocarcinus cylindricus		×	×	
	Chyrostilidae sp.2			×	
	Chyrostilidae sp.3			×	
	Clythrocerus moreirai		×		+
	Collodes trispinosus			×	+
	Cyclodorippe antenaria		×		+
	Ethusa mascarone	×			
	Euchirograpsus americanus	×		×	
	Eucratopsis crassimanus	×			+
	Euphrognata rastellifera		×		
	Homola barbata	×			+
	Iliacantha subglobosa	×			
	Latreilliia elegans		×		+
	Macrocoeloma eutheca	×			+
	Macrocoeloma septemspinosus	×			+
	Mesorhoea sexspinosa	×			
	Mithrax cornutus	×		×	
	Munida benedicti			×	+
	Munida evermani			×	+
	Munida flinti			×	+
	Munida sp.3	×			
	Munida sp.4	×			
	Munidopsis platirostris		×		+
	Munidopsis sp.1			×	
	Osachila antillensis			×	
	Paguristes sp.1		×		
	Palicus affinis	×			+
	Palicus alternatus	×			
	Palicus gracilipes		×		+
	Palicus sicus		×	×	+
	Panoplax depressa	×			
	Pantomus sp.	×		×	
	Parapontophylus gracilis		×		+
	Parthenope agona	×			
	Parthenope fraterculus	×			
	Parthenope pourtalessi		×		+

Appendix 1 continued

Group	Species	Coral Setting			NR
		GUA	SMA	SBE	
...Crustaceans	*Persephona crinita*			×	+
	Petrochirus diogenes	×			
	Plesionika acanthonotus		×		+
	Plesionika longicauda	×			+
	Plesionika longipes		×		+
	Plesionika miles		×		+
	Plesionika tenuipes		×		+
	Podochela gracilipes	×			
	Pylopaguropsis atlantica		×		+
	Pylopagurus discoidalis		×	×	+
	Pyromaia acanthina		×		
	Pyromaia propinqua			×	+
	Rhodochirus rosaceus		×		
	Stenocionops furcata	×			
	Stenorhynchus seticornis	×		×	
	Stenorhynchus yangii	×	×	×	+
	Uroptychus sp.		×		
	Xylopagus tayrona		×		
Echinoderms	*Agassizia excentrica*	×		×	
	Amphioplus sp.1	×			
	Amphioplus sp.2			×	
	Analcidometra armata	×			
	Asteroporpa cf. *annulata*			×	
	Asteroschema cf. *laeve*			×	
	Asteroschema cf. *oligactes*		×	×	
	Astrocnida cf. *isidis*			×	
	Astropecten alligator		×		
	Bathyplotes natans		×		+
	Brissopsis elongata	×			
	Centrostephanus sp.	×			
	Clypeaster euclastus			×	
	Clypeaster lamprus			×	
	Coccometra sp.			×	
	Coelopleurus floridanus		×	×	
	Comactinia meridionalis	×		×	
	Coronaster sp.		×		
	Crinometra brevipinna			×	
	Democrinus conifer			×	
	Dipsacaster sp.		×		
	Pentacrinus sp.		×	×	
	Eucidaris tribuloides	×			
	Genocidaris maculata	×			
	Histampica cf. *duplicata*		×	×	
	Holothuria lentiginosa enodis		×		+
	Holothuria occidentalis			×	
	Hypalometra defecta	×			
	Leptonemaster venustus	×		×	
	Marginaster cf. *pectinatus*		×		
	Mediaster sp.	×			
	Nemaster discoidea	×			
	Nemaster rubiginosus			×	
	Neocomatella cf. *pulchella*		×		
	Ophiacantha sp.1	×			
	Ophiacantha sp.2			×	
	Ophiacantha sp.3			×	
	Ophiactis algicola	×			
	Ophiactis savignyi	×			

Appendix 1 continued

Group	Species	Coral Setting			NR
		GUA	SMA	SBE	
…Echinoderms	*Ophiochondrus* cf. *convolutus*		×		
	Ophioderma appressum			×	
	Ophioderma rubicundum	×			
	Ophiomitra cf. *valida*		×		
	Ophiomitrella cf. *laevipellis*			×	
	Ophiomyxa cf. *tumida*		×		
	Ophiomusium acuferum	×	×	×	
	Ophiomusium eburneum		×		
	Ophiomusium cf. *testudo*		×	×	
	Ophiomusium validum			×	
	Ophionereis dolabriformis	×			
	Ophiopaepale cf. *goesiana*			×	
	Ophiophragmus riisei			×	
	Ophioplax cf. *ljungmani*		×	×	
	Ophiopristis cf. *hirsuta*		×	×	
	Ophiopsila hartmeyeri	×			
	Ophiostigma isocanthum	×			
	Ophiosyzygus disacanthus			×	+
	Ophiothrix angulata	×			
	Ophiothrix orstedii	×			
	Ophiothyreus cf. *goesi*			×	
	Ophiothrix suensonii	×	×	×	
	Ophiura cf. *acervata*	×	×	×	
	Palaeobrissus hilgardi		×		+
	Paleopneustes cristatus			×	
	Paleopneustes tholoformis			×	
	Persephonaster echinulatus		×		
	Plutonaster agassizi agassizi	×		×	
	Pteraster sp.		×		
	Rosaster cf. *alexandri*		×		
	Stephanasterias cf. *albula*		×		
	Stylocidaris affinis	×	×		
	Stylocydaris lineata		×	×	+
	Stylometra cf. *spinifera*			×	
	Tamaria cf. *halperni*		×		
	Trigonocidaris albida		×		+
Fishes	*Ancylopsetta cycloidea*			×	
	Antigonia capros	×	×	×	+
	Antigonia combatia		×	×	+
	Apogon affinis	×			
	Apogon pseudomaculatus	×			
	Apogon quadrisquamatus	×			
	Bathyanthias mexicana	×			+
	Bellator brachychir			×	
	Bellator egretta		×		+
	Bembrops anatirostris	×	×		
	Bollmannia sp.			×	
	Bregmaceros atlanticus	×		×	
	Chlorophthalmus agassizi		×		+
	Citharichthys cornutus			×	
	Citharichthys gymnorhinus	×			
	Decodon puellaris			×	
	Engyophrys sentus	×			
	Fistularia petimba			×	
	Gymnothorax polygonius		×		+
	Halieutichthys aculeatus		×		
	Holanthias martinicensis	×		×	

Appendix 1 continued

Group	Species	Coral Setting			NR
		GUA	SMA	SBE	
...Fishes	*Kathetostoma cubana*			×	
	Lipogramma evides			×	+
	Lophiodes reticulatus		×		
	Monacanthus ciliatus	×			
	Pontinus nematophthalmus		×	×	+
	Priacanthus arenatus	×			
	Prionotus beani			×	
	Prionotus stearnsi	×			
	Pristigenys alta			×	
	Saurida brasiliensis	×			
	Saurida caribbaea		×		+
	Scorpaena agassizii			×	
	Scorpaena calcarata	×			
	Serranus atrobranchus	×		×	
	Serranus chionaraia	×			
	Serranus sp.1		×		
	Serranus sp.2	×			
	Serranus tortugarum	×			
	Steindachneria argentea		×		
	Syacium micrurum	×			
	Syacium gunteri	×			
	Symphurus piger	×	×	×	
	Synagrops bella	×	×	×	+
	Synagrops spinosus	×			
	Synodus poeyi	×			
	Thalassophryne maculosa			×	
Mollusks	*Abra* sp.		×		
	Abra longicallis			×	
	Acesta colombiana	×			
	Acteon sp.	×			
	Anadara sp.	×			
	Arca zebra	×			
	Arcopsis adamsi	×			
	Arene sp.	×			
	Babelomurex dalli		×		+
	Barbatia candida	×		×	
	Bellaspira pentagonalis	×			
	Calliostoma fernandezi	×			
	Calliostoma sp.			×	
	Capulus sp.1	×			
	Capulus sp.2	×			
	Cardiomya sp.	×			
	Chama congregata	×			
	Chama macerophylla	×			
	Cheilea equestris			×	
	Chlamys munda	×			
	Circomphalus strigillinus	×			
	Cocculina sp.		×		
	Cochlespira radiata			×	+
	Conus cf. *daucus*	×			
	Conus cf. *granarius*	×			
	Coralliophila caribaea			×	
	Coralliophila squamosa		×		+
	Cosmioconcha nitens	×			
	Crucibulum cf. *marense*	×			
	Crucibulum sp.	×			
	Cuspidaria sp.			×	

Appendix 1 continued

Group	Species	Coral Setting			NR
		GUA	SMA	SBE	
…Mollusks	*Cypraea cassis*			×	
	Cypraea cinerea	×			
	Dentalium sp.			×	
	Dentimargo sp.	×			
	Diodora cayennensis	×	×		
	Diodora sp.1			×	
	Diodora sp.2			×	
	Discotectonica discus		×		+
	Distorsio cf. *mcgintyi*			×	
	Douglassia sp.	×			
	Entodesma beana	×			
	Eratoidea hematita	×			
	Eudolium crosseanum			×	
	Eudollium thompsoni		×		
	Fusinus lightbourni		×		
	Glyphostoma gabbi	×			
	Hypselodoris sp.	×			
	Laevicardium sybariticum	×			
	Laevidentalium callipeplum		×		+
	Limaria sp.		×	×	
	Limopsis antillensis	×			
	Loligo sp.	×			
	Macoma tenta	×			
	Mitrolumna biplicata	×			
	Myrtea prystiphora	×			
	Nassarius scissuratus		×		
	Nassarius hotessieri	×			
	Nemocardium sp.			×	
	Nemocardium tinctum	×			
	Notocrater sp.			×	
	Nuculana cestrota	×			
	Octopus sp.	×			
	Olivella cf. *acteocina*	×			
	Parvamussium pourtalesianum			×	
	Pecten chazaliei	×			
	Persicula pulcherrima	×			
	Petaloconchus erectus	×			
	Pitar albida	×			
	Pitar arestus			×	
	Pitar cf. *albida*	×			
	Pleurobranchus sp.	×			
	Plicatula cf. *gibbosa*			×	
	Polystira tellea	×		×	+
	Poromya rostrata	×		×	
	Prunum marginatum	×			
	Pseudosimnia vanhyningi		×		+
	Pyrgospira sp.	×			
	Semirossia tenera			×	+
	Sthenorytis pernobilis		×		+
	Tellina persica	×			
	Trachipollia didyma	×			
	Tucetona pectinata	×			
	Ventricolaria listeroides	×			
	Vermicularia spirata	×			
	Volvarina cf. *avena*	×			
	Volvarina sp.1	×			
	Volvarina sp.2	×			

Appendix 1 continued

| Group | Species | Coral Setting | | | NR |
		GUA	SMA	SBE	
…Mollusks	*Xenophora caribaea*			×	
	Xenophora conchyliophora	×			
TOTAL	**338 species**	**156**	**115**	**134**	**84**

Habitat-forming deep-sea corals in the Northeast Pacific Ocean

Peter Etnoyer[1], Lance E. Morgan[2]

[1] Aquanautix Consulting, 3777 Griffith View Drive, Los Angeles, CA 90039, USA
  (peter@aquanautix.com)
[2] Marine Conservation Biology Institute, 4878 Warm Springs Rd., Glen Ellen, CA
  95442, USA

Abstract. We define habitat-forming deep-sea corals as those families of octocorals, hexacorals, and stylasterids with species that live deeper than 200 m, with a majority of species exhibiting complex branching morphology and a sufficient size to provide substrata or refugia to associated species. We present 2,649 records (name, geoposition, depth, and data quality) from eleven institutions on eight habitat-forming deep-sea coral families, including octocorals in the families Coralliidae, Isididae, Paragorgiidae and Primnoidae, hexacorals in the families Antipathidae, Oculinidae and Caryophylliidae, and stylasterids in the family Stylasteridae. The data are ranked according to record quality. We compare family range and distribution as predicted by historical records to the family extent as informed by recent collections aboard the National Oceanic of Atmospheric Administration (NOAA) Office of Ocean Exploration 2002 Gulf of Alaska Seamount Expedition (GOASEX). We present a map of one of these families, the Primnoidae.

We find that these habitat-forming families are widespread throughout the Northeast Pacific, save Caryophylliidae (*Lophelia* sp.) and Oculinidae (*Madrepora* sp.), which are limited in occurrence. Most coral records fall on the continental shelves, in Alaska, or Hawaii, likely reflecting research effort. The vertical range of these families, based on large samples ($N > 200$), is impressive. Four families have maximum-recorded depths deeper than 1500 m, and minimum depths shallower than 40 m. Isidid, primnoid, and antipatharian records all exceed 2500 m depth. GOASEX collections are made from each of seven seamounts surveyed, extending the known range of Coralliidae 2500 km northward and the known limits of Isididae 450 km seaward, beyond the continental shelf, to seamounts in the Gulf of Alaska.

Keywords. Deep-sea coral, Northeast Pacific, distribution, mapping, data base

Introduction

Deep-sea coral records in the Northeast Pacific date to the late 19th century (Verrill 1869). Dall (1884), Fisher (1938), and Ostarello (1973) described the stylasterids

of California and Alaska. Nutting (1909) documented isidids (Bamboo corals) and primnoids (Red tree corals) in California and Southeast Alaska during the Albatross stations 4766 - 4787 (see Cimberg 1981). Heifetz (2002) described the distribution of several different polypoid Cnidarian orders in Alaskan waters in great detail. However, none of these studies examined the horizontal and vertical ranges of deep-sea coral families over the Northeast Pacific extent. Contemporary concerns about commercial fishery sustainability and the benthic impacts of commercial fishing gear have renewed interest in habitat forming deep-sea corals and their areas of occurrence. In 1996, the United States Congress revised the Magnuson-Stevens Fishery Conservation and Management Act to include new habitat conservation provisions for U.S. marine fisheries. One candidate for a Habitat Area of Particular Concern (HAPC) under these provisions is "coral" areas. The *Oculina* Banks off Florida were destroyed by trawling over 25 years ago and are now designated HAPC. These banks were important habitats and spawning areas for commercially important snappers and groupers (Koenig et al. 2000). Proposals for similar HAPC designations are being developed for corals in the North Pacific.

In the tropics, reef fish species richness is less associated with coral species richness than it is with "rugosity", a measure of three-dimensional complexity (Connell and Jones 1991; Friedlander and Parrish 1998). Complex habitats, such as seagrass beds and branching corals, are known to provide more refuge to prey species than less rugose habitats. Risk (1972) stated for tropical coral reefs, "there exists a striking positive correlation between fish species diversity and degree of substrate topographic complexity." Complex habitats also provide more vertical relief, more surface area for settlement, and more microhabitat variability than simpler habitats. Habitat-forming deep-sea corals are defined here as those families of octocorals, hexacorals and stylasterids that have a majority of species able to grow deeper than 200 m, with a complex branching morphology, and a size sufficient to provide substrate or refuge to associated species. The depth cutoff of 200 m reflects a colloquial definition of deep-sea, deeper than the continental shelf, generally regarded as 200 m. This figure was a loose guideline. Ultimately, we find that all these families prosper deeper than 400 m. In this manuscript, we use the term deep-sea coral to refer to most of the families of hexacorals, octocorals, and stylasterids we know to thrive beyond the traditional sunlit tropical boundaries commonly attributed to zooxanthellate shallow-water tropical scleractinian corals.

Habitat-forming deep-sea corals often occur on rocky habitats in deep-water with strong water currents, similar to habitats preferred by shallow-water gorgonians. These currents may facilitate settlement onto clean swept surfaces, increase food availability and capture and, therefore, growth rate and survivorship (Patterson 1984; Sponaugle and LaBarbera 1991). Octocorals have been used as indicators of flow velocity on seamount peaks (Genin et al. 1986), but small differences in relief (<1 m) also accommodate deep-sea corals. Octocorals can be found in abundance in current swept muddy and mixed substrates of low relief (Lissner 1989; Lissner et al. 1991). Strong currents can benefit suspension feeders but challenge smaller marine life, such as juvenile fish. Deep coral reefs are important habitat for adult

fishes, juvenile fish, crustaceans, sea stars, brittle stars, anemones and sponges because they provide protection from these currents and from predators. Clusters of biodiversity around deep-sea corals were recently documented by submersible craft in missions to the Gulf of Alaska, the Gulf of Maine, in Europe, Japan, and Australia by the National Oceanic and Atmospheric Administration, International Council for Exploration of the Sea, and International Oceanographic Committee. Scientists document 300 reef associated invertebrate species in the Faroe Islands alone (Jensen and Frederiksen 1992). A variety of fishes and sharks also rely on coral areas for food, protection, and a place to lay their eggs. *In situ* evidence of habitat functions for deep-sea corals is currently limited to video and photographic observations (e.g., an egg case attached to a *Paragorgia*, crabs perched atop *Isidella*, snail fish resting in the polyps of *Isidella*). Research is expanding into the deep-sea. More quantifiable results of habitat function are forthcoming from cooperative programs in both Europe and America.

Commercially important fish species are also found in association with these reefs, such as Atka mackerel, *Pleurogrammus monopterygius,* and shortspine thornyhead, *Sebastolobus alascanus,* in Alaska (Heifetz 2002). Krieger and Wing (2002) reported rockfish associated with *Primnoa* octocorals in the Gulf of Alaska. Fosså et al. (2002) showed a dense aggregation of *Sebastes* sp. associated with *Lophelia* corals off the coast of Norway. Elsewhere, Husebø et al. (2002) found that fish in coral habitats tended to be larger than in non-coral habitat. Endangered species are also known to frequent coral beds. Surveys with Hawaii Undersea Research Laboratory (HURL) submersibles found deep-sea coral colonies may aggregate conger eels, and attract foraging monk seals to *Gerardia* sp. and *Corallium* sp. reefs at depths over 500 m (Parrish et al. 2000).

Commercial fishing is the most obvious threat to these complex habitats (Koslow et al. 2001; Hall-Spencer et al. 2002). Deep-sea trawling is expanding globally, with more than 5000 km^2 of the Northeast Pacific seabed trawled more than once annually for Atka mackerel and other species (NRC 2002). Trawl nets and longline gear frequently remove octocoral colonies from the rocks and boulders they grow upon. The benthic impacts of this mobile fishing gear have been likened to clear-cutting techniques in old growth forests (Watling and Norse 1998). Other anthropogenic activities, such as ocean dumping and seafloor mining also threaten deep-sea corals (Rogers 1999).

Based on limited knowledge of deep-sea corals and their growing conservation significance, NOAA's Office of Protected Resources commissioned Marine Conservation Biology Institute to document the known occurrences of habitat-forming deep-sea corals for the Northeast Pacific and the adjacent Bering Sea.

Methods

The goals of this project were to map Northeast Pacific occurrences of selected deep-sea corals suspected of being important formers of biogenic habitat, as well as to construct a ranked database of the accumulated records that informed these maps.

Our definition of deep-sea, habitat-forming coral excludes deep-sea scleractinian solitary corals. Our investigation of the families Caryophylliidae and Oculinidae were limited to *Lophelia* sp. and *Madrepora* sp., but Antipathidae, Coralliidae, Isididae, Paragorgiidae, Primnoidae, and Stylasteridae were not limited to any particular species.

Our initial data gathering efforts focused on records of a few well-documented species, e.g., *Paragorgia arborea* and *Primnoa resedaeformis,* in the Northeast Pacific. However, record reviews of database outputs from participating institutions revealed that species-specific searching often resulted in record loss due to species name changes and spelling changes over time spans sometimes exceeding 100 years. For example, records from the Smithsonian Institution for the family Isididae revealed that the name *Ceratoisis* has been revised to *Keratoisis*. Likewise, in the family Stylasteridae, *Allopora californica* has been revised to *Stylaster californicus* (Cairns 1983). Deep-sea coral systematics are still poorly resolved due to the diversity and scarcity of the material, despite the monumental efforts of a limited number of experts around the world. Unfortunately, few researchers are qualified to make genus level distinctions between octocorals, and even then, this distinction might be revised later (e.g., Cairns 1983; Alderslade 1998).

Drs. Frederick Bayer and Stephen Cairns of the Smithsonian Institution, (leading taxonomic authorities on octocorals and deep-sea scleractinian corals respectively), suggested that searches should be conducted by family name rather than species name to minimize the impacts of taxonomic revision and misidentification at the species level. This approach alleviated issues related to misspelling and synonymy, but also speeded search time, limited institutional effort, incorporated lesser-known species names with similar morphology. This study seeks to take advantage of data that ranges in quality without sacrificing validity. We assume that family level descriptions are likely correct for trained observers, while genus and species levels might be incorrect. Drs. Bayer and Cairns identified 8 families as habitat-formers in the Northeast Pacific Ocean: hexacorals in the families Antipathidae, Oculinidae and Caryophylliidae; octocorals in the families Coralliidae, Isididae, Paragorgiidae and Primnoidae; and stylasterids in the family Stylasteridae.

Based upon this list of families, we contacted deep-sea coral researchers through a series of networked contacts that resulted from the First International Symposium on Deep-sea Corals held in Halifax, Canada, July 30-August 3, 2000. Of these contacts, a limited number maintained deep-sea coral records, and of those, a further reduced number maintained geo-positional records and were willing or able to distribute these records due to staffing constraints or other institutional limitations. A total of eleven different organizations supplied range and distribution records, including the California Academy of Sciences (CAS), Canadian Museum of Nature, Canadian Department of Fisheries and Oceans (combined here to CMN-DFO), the Monterey Bay Aquarium Research Institute (MBARI), the National Museum of Natural History at the Smithsonian Institution (NMNH), National Oceanic and Atmospheric Administration Office of Ocean Exploration (NOAA-OE), NOAA Fisheries Resource Assessment and Conservation Engineering (RACE) Division,

the Santa Barbara Museum of Natural History (SBMNH), the REEF Foundation (REEF), the Scripps Institution of Oceanography (SIO) and a study performed by the late Dr. Robert Cimberg for VTN Oregon (Cimberg 1981).

The record selection methodology varied only slightly between institutions. Generally, we selected only those records that included a field for taxonomic identification. RACEBASE includes many records identified as "coral", but these were not included in this effort. Our NOAA-OE records represent the results of a single expedition to the Gulf of Alaska. Each organization maintained different information, so all database records were subset to five common fields: latitude, longitude, family, species name, and depth in meters. Additional fields were added to these records in order to facilitate potential researcher follow up. These fields include an institution name, an institution specific identification number, a "coordinates code", and a rank. Not all records included depth information.

The "coordinates code" is a measure of accuracy for the latitude and longitude information. If a given record included coordinate information, it was assigned a value of 1, if that record included a place name only it was assigned the value of 2, and we assigned approximate coordinates to that place name. If a record lacked either of these qualities, or if the place name was too general (e.g., Alaska) it was dropped from the database. Most often, these records were duplicated by other more specific records (e.g., Alaska, Aleutian Islands, Unimak Pass).

"Rank" is a relative measure of record quality based upon two factors: 1) whether a physical sample is associated with that record and 2) the identifiers level of expertise. The ranking system is as such:

  1 = sample collected, expert identification
  2 = sample collected, non-expert identification
  3 = no sample collected, expert identification
  4 = no sample collected, non-expert identification

This ranking system is consistent with ongoing efforts at the Hawaiian Undersea Research Laboratory, where a fleet of manned submersibles makes frequent deep-water dives, but takes few samples, relying instead on video and photo identification. This ranking is also consistent with a need to conserve slow growing deep-sea coral resources, and to limit the impact of scientific collections.

Results

The families Isididae, Paragorgiidae and Primnoidae are reported to occur throughout the Northeast Pacific from the Bering Sea south to the Equator and west to the Hawaiian Islands. Antipathidae likewise appear widespread, but are documented only as far south as Baja California. Coralliidae, Caryophylliidae, Oculinidae, and Stylasteridae are not documented north of the Aleutian Islands chain.

Bamboo corals, in the family Isididae, have the deepest coral record, listed as an *Isidella* sp. at 3880 m off the coast of Southern California from Scripps Institution. Cimberg (1981) documents a specimen of *Keratoisis profunda* at 3532 m in the Aleutian Islands. Specimens of Primnoidae and Antipathidae are also documented

at depths nearing 3000 m. Isididae, Antipathidae, Primnoidae, and Paragorgiidae are the deepest occurring deep-sea coral families, respectively. Paragorgiidae and Primnoidae have maximum depths of approximately 2500 m. Each of these families is also represented by species records shallower than 220 m, suggesting a wide vertical distribution. Depth ranges for the families of interest are detailed in Table 1, and the frequency of occurrence is shown in Figure 1.

Table 1 Deep-sea coral families exhibit a range of species richness and depth distributions. Isididae and Antipathidae are documented at the greatest depths

Taxa	Species listed	N	Mean Depth (m)	Min Depth (m)	Max Depth (m)
Isididae	21	335	1262	107	3880
Antipathidae	3	208	924	9	2957
Primnoidae	63	925	324	25.5	2600
Coralliidae	8	130	539	215	2116
Paragorgiidae	4	257	406	19	1925
Stylasteridae	11	7	265	79	823
Oculinidae	2	2	278	40	556
Caryophylliidae	1	10	301	115	486

A total of 2649 records from eleven participating organizations in the United States and Canada documents 105 species of habitat-forming deep-sea corals in Northeast Pacific. The family Primnoidae had the most listed species (63), with 14 species names for Isididae, 9 for Stylasteridae, 10 for Coralliidae, 4 for Paragorgiidae, 3 for Antipathidae, and one each for Caryophylliidae and Oculinidae. The species
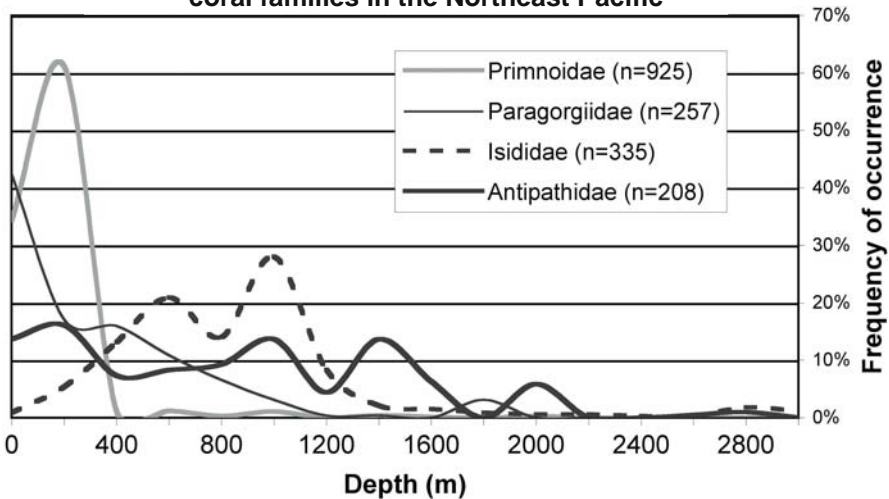
Fig. 1 The majority of records for families Primnoidae and Paragorgiidae are shallower than 500 m, while more than half of all isidid and antipatharian records occur deeper than 800 m

names associated with each family are detailed in Appendix 1. This database is publicly available through Marine Conservation Biology Institute's Baja California to Bering Sea 1.1 (B2B) CD-ROM (Etnoyer et al. 2002). An example map for the family Primnoidae is presented in Figure 2. Maps of all families are available in the NOAA report on this database (Etnoyer and Morgan 2003) available for download at www.mcbi.org.
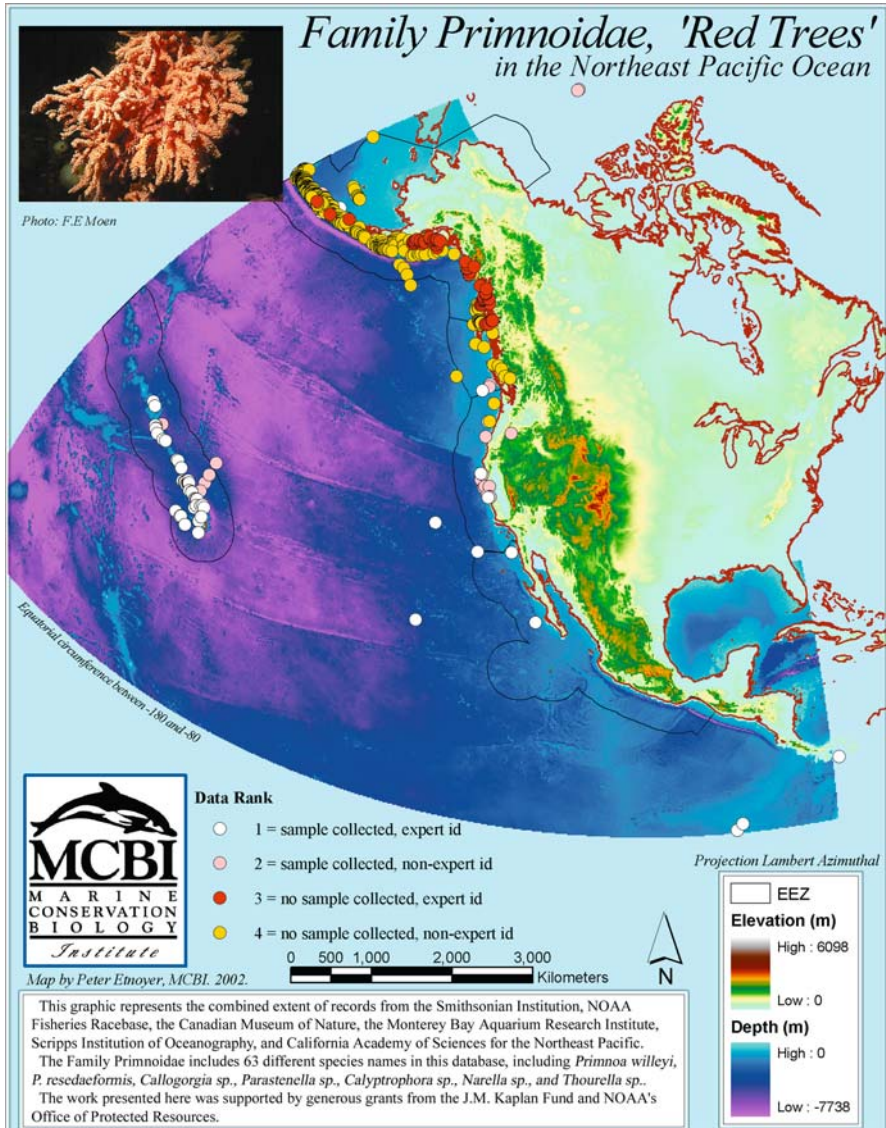
Fig. 2 An example map of Northeast Pacific occurrences for family Primnoidae, symbolized by data rank

The National Marine Fisheries Service's RACEBASE was the largest contributor with 1540 records on five families, followed by the Smithsonian Institution, the most comprehensive contributor, with 423 records in seven of the eight families. MBARI was a substantial contributor for a very specific locale, namely Monterey Bay, where "easy" access to deep-water and remotely operated vehicles (ROVs) facilitates almost daily expeditions to the Monterey Canyon. Video archivists at MBARI meticulously document most of those species familiar to them. Canadian Museum of Nature and Department of Fisheries and Oceans (CMN-DFO) records were restricted to waters around British Columbia. CAS also worked closely with this study to accommodate numerous data requests, and their high quality, very comprehensive information based on Dr. Gary Williams' identification was an important supplement to this study. Records from NOAA-OE are derived from the 2002 Gulf of Alaska Seamount expedition aboard the R/V Atlantis with the Alvin submersible. Though the NOAA-OE contribution was small in number, this remote expedition to seamounts in the Gulf documented several habitat-forming corals where none were known before, extending the known range of Isididae and Coralliidae into the Gulf of Alaska.

Accessing institutional databases by family name (Table 2) resulted in a 13 % increase in data records for Isididae across all institutions. For Paragorgiidae, searching by family increased CAS records from 6 to 18, and NMNH records from 16 to 39. *Primnoa* records increased from 1 record for *Primnoa willeyi* to 53 records for *Primnoa* sp. A review of the taxonomic methods practiced by each of the participating institutions indicated that CAS, NMNH and SIO records ranked "1" (see Table 2). CMN-DFO, NOAA-OE, and SBMNH ranked "2". Each of these institutions maintains physical samples associated with their records. MBARI and Cimberg's Report ranked "3", while REEF and RACE ranked "4", as these records failed to maintain a physical sample. RACE represents data gathered by fisheries observers with minimal training in taxonomic identification, and REEF records are gathered by volunteer scuba divers with a similar cursory training and background. As an example, in order to the identify octocorals to the species level, one often requires a high powered microscope to identify sclerites in the preserved tissue. Thus, even a physical sample of a calcified skeleton may be insufficient to satisfy the highest-level criterion.

The specimen collection dates are not included as a field in the database presented here, but the history of the largest collections may be of some interest to readers. *Paragorgia* and primnoid collections from RACEBASE date from the mid-80's, while isidids date from the mid-90's. This observer based program sets a formidable precedent. Paragorgidae and Isididae records in the Aleutian Islands from NMNH date back to the Albatross expeditions of 1890 and 1906 but Coralliidae records do not appear in the Northeast Pacific until a Scripps Pelagic Area Studies cruise in 1954. The early 1970's produced a dramatic increase in records for many families of deep-sea corals in Hawaii, attributed largely to Dr. Richard Grigg of the Sango Expeditions. Those contributions were not matched until the mid-1990's, when the crew and scientists of manned submersible expeditions aboard ALVIN and PISCES DSR/Vs introduced many new specimens to NMNH collections.

Table 2 Details of 2649 records from eleven institutions are shown here for eight habitat-forming deep-sea coral families in the Northeast Pacific

Taxa	NMNH	CAS	SIO	NOAA-OE	SBMNH	MBARI	Cimberg	CMN-DFO	RACE	REEF	Total
Antipathidae	29	8		3		101			102		243
Oculinidae	2										2
Caryophilliidae	8		1		1						10
Coralliidae	128			2							130
Isididae	60	17	5	4		237	2		19		344
Paragorgiidae	38	12		2		51	9	11	143		266
Primnoidae	158	53		5			73	15	1012		1316
Stylasteridae		58							264	16	338
Total	423	148	6	16	1	389	84	26	1540	16	2649
Data rank		1			2			3		4	

Discussion

While a few deep-sea coral records in the Northeast Pacific are more than a hundred years old, the majority of our understanding about deep-sea coral biogeography is founded in records less than fifty years old, and most of those are less than fifteen years old. Though deep-sea coral occurrences are most abundant on Pacific North American continental shelves in Hawaii, and Alaska's Aleutian Islands, GOASEX shows that all of these habitat forming deep-sea coral families have records on one or more seamounts in the Gulf of Alaska. Deep-sea corals are likely widespread, occurring on all seamounts, shelves, and banks that provide sufficient relief and substrate (Bayer pers. comm.). This database benefited greatly from a groundtruthing exercise that looked for corals where none were known before. The distribution map in Figure 2 would look different without recent manned submersible records (rank 2, central Gulf of Alaska in pink), but even more different without a ranking system to incorporate observer data (in yellow).

The maps generated by the database most likely represent maps of research effort rather than maps of the true extent of deep-sea coral occurrences in the Northeast Pacific. This is evidenced by two GOASEX collections, a Corallid specimen that extends the known range of that family 2500 km north, and an Isidid specimen that extends the known range of that species 500 km seaward, from the continental shelf, onto several seamounts in the Northeast Pacific. A map of historical records of the family Coralliidae would have shown the northernmost extent for this precious ornamental coral as *Corallium imperiale* USNM 85082 from 600 m depth on Fieberling Seamount off Baja California. Recently, GOASEX scientists aboard ALVIN 3802 collected a colony or *Corallium* sp. from 1652 m depth on Patton Seamount, south of the Aleutian Islands. Though we present an unprecedented collection of deep-sea coral records, it is well informed by continued exploration.

Stylasteridae is best documented along the continental shelf on relatively shallow banks within 25 miles of shore. *Stylaster californicus* of the family Stylasteridae has a maximum recorded depth of 823 m (2700 ft), from CAS. Several northeast Pacific seamounts reach beyond that depth, and may provide habitat for stylasteriids. Alternatively, stylasteriids may actually be restricted to the nearshore. They are widely distributed in nearshore habitats of California (Fisher 1931) and most of the records reported here are from SCUBA surveys (REEF). The southern extent of Stylasterid records along the mainland of North America is the northern tip of Baja California. However, since this family is present at lower latitudes in the Hawaiian Islands, its southern range limit along the North America margin might be an artifact of the geographic extent of our national databases.

Similarly, the distribution map for Antipathidae suggests that any apparent geographic limit for deep-sea corals is most likely an artifact of sampling effort and expertise. Antipatharians are best documented in the islands of Hawaii, partly due to collaborations between scientists there and a manned submersible fishery (Grigg and Opresko 1977). Antipatharians are likely to be present in seamounts off western Mexico at latitudes similar to those from Hawaii. Isididae, Paragorgiidae, and Primnoidae occur north and south of Pacific Mexico with an absence of records in Mexico, and west of Baja California (Fig. 2).

Future data gathering might concentrate on building collaborations with Mexican benthic ecologists to test these southern range limits. Future submersible research might focus on the Islas Revillagigedo and the Mathematician Seamounts off the coast of western Mexico to better understand the southern extent of these deep-sea coral species in the Northeast Pacific. The volcanic origin of the Islas Revillagigedo and their proximity to the highly productive Gulf of California make these impressive seamounts prime candidates for abundant coral forests.

Madrepora oculata in the family Oculinidae and *Lophelia* sp. in the family Caryophylliidae are well documented in the Atlantic but poorly documented here. This may be due to some oceanographic conditions that bias against hermatypic scleractinian reefs, or this may be the fault of the authors. Recent findings suggest that some *potentially* hermatypic scleractinians, e.g., *Dendrophyllia* spp., may have been overlooked in the Northeast Pacific. Future investigations of the biogeography of deep hermatypic Scleractinia in North America could alleviate some of the confusion surrounding these deep hermatypic species. Also, the family list used in this study is likely a subset of those that satisfy the habitat forming criteria at this basin scale. Some genera in the family Zooanthidae, and some in the family Gorgoniidae should be considered for future study.

Clear patterns are evident in the frequency distribution chart in Figure 1. Primnoid occurrences appear to be bracketed entirely by the 0-400 m bins. These charts should be appreciated as shadows of reality, biased by the question "where have we looked?". Based upon 900 primnoid records, sixty percent fall within 200-400 m, yet we recorded an unusually dense field of *Parastenella* sp. (ALVIN dive no. 3808) at 2200 m on Warwick Seamount, suggesting primnoids thrive at these extremes. It is evident that reports of *Paragorgia* sp. tail off with increasing depth with relatively

few reports deeper than 1200 m. Again, a small number of the 200+ reports from that family are between 1600 m and 1800 m. Clearly, isidid and antipatharian deep-sea corals are the habitat-formers best adapted to life at these profound depths. More than half of the records from those families are from depths greater than 800 m. Sampling effort can only be partly responsible for this distribution.

It is important to note that this data ranking exercise was a relative one, and that a low data rank does not necessarily indicate poor quality. A low data rank in this case indicates that the researcher failed to preserve an intact sample, and that the researcher lacks scientific expertise in systematics. Neither of these conditions is surprising or rare. Research vessels may have limited human resources available, with few specialists dedicated to benthic invertebrates, limited quantities of ethanol preservative, and/or limited storage facilities. Also, the global number of researchers that can claim systematic expertise with deep-sea stony corals and gorgonians is less than a dozen (S. Cairns pers. comm.). The number of researchers that may claim this expertise in the Northeast Pacific accounts for less than half that number.

The data ranking exercise suggests that the waters around Hawaii and Southern California have the largest numbers of high quality records. This is most likely due to the efforts of particular researchers in those regions to collect samples and submit them to the proper authorities for species level identification. However, Alaskan waters exhibit the greatest number of data points. This can be largely attributed to the RACEBASE program, as evidenced by Table 1. The RACEBASE program is as strong candidate for data quality improvement in the near future. Capacity-building training in deep-sea coral systematics should be a high priority for these observers and record keepers.

The occurrences of the habitat-forming deep-sea coral families presented here suggest they have a large depth range throughout the Northeast Pacific. Frederick Bayer (pers. comm.) supports the conclusion that these families are widespread throughout their depth range (9-3880 m) along the Pacific rim. Too few data points and too little effort have been focused on seamounts in the Gulf of Alaska, and in the Northeast Pacific. Sampling effort in the Gulf of Alaska and the Bering Sea, however, is unfortunately defined as "bycatch" to the commercial bottom trawl industry. While some of these records represent first occurrences, most of these records are dated, and may represent deep-sea coral reefs that are no longer. With the expansion of trawl fleets into deeper waters and seamounts, deep-sea corals are certain to suffer greater risk in the future (Roberts 2002). These animals form habitat for diverse assemblages uniquely adapted to extreme environments, and must be protected from fishing gears which destroy seafloor habitat (Watling and Norse 1998; Koslow et al. 2001; Hall-Spencer et al. 2002; Morgan and Chuen-pagdee 2003).

Acknowledgements

References

Alderslade P (1998) Revisionary systematics in the gorgonian family Isididae, with descriptions of numerous new taxa (Coelenterata : Octocorallia). Rec West Austral Mus (Suppl) 55: 1-359

Cairns SD (1983) A generic revision of the Stylasterina (Coelenterata: Hydrozoa), Part 1. Description of the genera. Bull Mar Sci 33: 427-508

Cimberg RL (1981) Habitat requirements and expected distribution of Alaska Coral. VTN Oregon, Inc. Final Rep Res Unit #601, 54 pp, 4 append

Connell J, Jones GP (1991) The influence of habitat complexity on post-recruitment processes in a temperate reef fish population. J Exp Mar Biol Ecol 151: 271-294

Dall WA (1884) On some Hydrocorallinae from Alaska and California. Proc Biol Soc Washington 2: 111-115

Etnoyer P, Canny D, Morgan LE (2002) B2B 1.0 CDROM, Information for Conservation Planning Baja California to the Bering Sea. Available from MCBI, Redmond, WA, USA: http:// www.mcbi.org

Etnoyer P, Morgan LE (2003) Occurrences of habitat forming deep-sea corals in the Northeast Pacific Ocean. NOAA Office Habitat Protection, Silver Spring, MD

Fisher WK (1931) California hydrocorals. Amer Mag Nat Hist ser 9, 8: 391-399

Fisher WK (1938) Hydrocorals of the North Pacific Ocean. Proc US Nat Mus 84: 493-554

Fosså JH, Mortensen PB, Furevik DM (2002) The deep-water coral *Lophelia pertusa* in Norwegian waters: distribution and fishery impacts. Hydrobiologia 471: 1-12

Friedlander AM, Parrish JD (1998) Habitat characteristics affecting fish assemblages on a Hawaiian coral reef. J Exp Mar Biol Ecol 224: 1-30

Genin A, Dayton PK, Lonsdale PF, Spiess FN (1986) Corals on seamount peaks provide evidence of current acceleration over deep-sea topography. Nature 322: 59-61

Grigg RW, Opresko D (1977) Order Antipatharia. In: Devaney DM, Eldredge LG (eds) Reef and shore fauna of Hawaii. Section 1: Protozoa through Ctenophora. Bishop Mus Press, Honolulu, pp 242-261

Hall-Spencer J, Allain V, Fosså JH (2002) Trawling damage to Northeast Atlantic ancient coral reefs. Proc R Soc London B 269: 507-511

Husebø A, Nøttestad L, Fosså JH, Furevik DM, Jørgensen SB (2002) Distribution and abundance of fish in deep-sea coral habitats. Hydrobiologia 471: 91–99

Heifetz J (2002) Coral in Alaska: distribution, abundance, and species associations. Hydrobiologia 471: 19-28

Jensen A, Frederiksen R (1992) The fauna associated with the bank-forming deepwater coral *Lophelia pertusa* (Scleractinia) on the Faroe shelf. Sarsia 77: 53-69

Koslow JA, Gowlett-Holmes K, Lowry J, O'Hara T, Poore G, Williams A (2001) The seamount benthic macrofauna off southern Tasmania: community structure and impacts of trawling. Mar Ecol Progr Ser 213: 111-125

Koenig CC, Coleman FC, Grimes CB, Fitzhugh GR, Gledhill CT, Scanlon KM, Grace MA (2000) Protection of fish spawning habitat for the conservation of warm temperate reef fish fisheries of shelf-edge reefs of Florida. Bull Mar Sci 66: 593-616

Krieger KJ, Wing BL (2002) Megafauna associations with deepwater corals (*Primnoa* spp.) in the Gulf of Alaska. Hydrobiologia 471: 82-90

Lissner A (1989) Benthic reconnaissance of central and northern California OCS Areas. Final Rep, Sci Appl Int Corp and MEC Analytical Syst, Inc. to the U.S. Dept Interior, Miner Managem Serv, Pacific OCS Reg, Contract No. 14-12-0001-30388

Lissner AL, Taghon GL, Diener RR, Schroeter SC, Dixon JD (1991) Review of recolonization and recovery of deep-water hard substrate communities. Ecol Appl 1: 258-267

Morgan LE, Chuenpagdee R (2003) Shifting Gears: addressing the collateral impacts of fishing methods in US waters. Pew Sci Ser, Washington DC, pp 42

National Research Council (2002) Effects of trawling and dredging on sea floor habitats. Washington, DC

Nutting CC (1909) Alcyonaria of the California Coast. Proc US Nat Mus 35: 681-727

Ostarello GL (1973) Natural history of the hydrocoral *Allopora californica* Verrill (1886). Biol Bull 145: 548-565

Patterson MR (1984) Patterns of whole colony prey capture in the octocoral *Alcyonium siderium*. Biol Bull 167: 613-629

Parrish FA, Craig MP, Ragen TJ, Marshall GJ, Buhleier BM (2000) Identifying diurnal foraging habitat of endangered Hawaiian monk seals using a seal-mounted video camera. Mar Mammal Sci 16: 392-412

Risk MJ (1972) Fish diversity on a coral reef in the Virgin Islands. Atoll Res Bull 153: 1-6

Roberts CM (2002) Deep impact: the rising toll of fishing in the deep-sea. Trends Ecol Evol 17: 242-245

Rogers AD (1999) The biology of *Lophelia pertusa* and other deep-water reef forming corals and impacts from human activities. Int Rev Hydrobiol 84: 315-406

Sponaugle S, LaBarbera M (1991) Drag-induced deformation: a functional feeding strategy in two species of gorgonians. J Exp Mar Biol Ecol 148: 121-134

Verrill AE (1869) Synopsis of the polyps and corals of the North Pacific Exploring Expedition, under Commodore C. Ringgold and Capt. John Rodgers, U.S.N., from 1853-1856. Collected by Dr. Wm. Stimpson, naturalist to the expedition. Additions and corrections. Comm Essex Inst Salem 6: 75-104

Watling L, Norse EA (1998) Disturbance of the seabed by mobile fishing gear: a comparison to forest clearcutting. Conserv Biol 12: 1180-1197

Recent observations on the distribution of deep-sea coral communities on the Shiribeshi Seamount, Sea of Japan

Asako K. Matsumoto

Department of Earth and Planetary Science, University of Tokyo, 7-3-1, Hongo, Tokyo 113-0033, Japan
(amatsu@gorgonian.jp)

Abstract. The benthic deep-water coral fauna of the Shiribeshi Seamount, Japan, was examined using the JAMSTEC video archives of four submersible dives in July 2001. An observational dataset containing n = 2055 records was obtained. The vertical distributions of the deep-water gorgonians Family Primnoidae and Paragorgiidae were determined. Primnoid corals include at least one species, *Primnoa resedaeformis pacifica* (Kinoshita, 1907) and are distributed between 1030 m and 271 m in depth and at a water temperature of 0.24-1.11°C. Paragorgiid corals were observed between 491 m and 178 m in depth and at a water temperature of 0.66-1.69°C, in shallower and warmer areas than primnoid species. It was observed that deep-sea gorgonians on the Shiribeshi Seamount in the North-West Pacific region exhibit family zonation and vertical distribution patterns. The distribution of hydrocorals, unidentified sponges, shrimp, and nudibranchs was also recorded. This is the first report on a deep-sea gorgonian coral community inhabiting Japanese waters.

Keywords. Deep-water gorgonian, Octocorallia, submersible, Shiribeshi Seamount, North-West Pacific, vertical distribution

Introduction

The main species of deep-sea corals in the Pacific Ocean waters are gorgonian corals (Anthozoa, Octocorallia). Gorgonian corals are known to be distributed in all seas from the Arctic to Antarctic and from intertidal to abyssal waters and comprise over 740 nominal species worldwide (Bayer 1981). Since the 19th century, the literature has recorded more than 260 species of gorgonian corals from Japan and adjacent areas, including several species endemic to this district (Imahara 1994, 1996, 2003). They include several deep-water species. All of this evidence indicates that Japanese waters have one of the highest biodiversities of gorgonian corals in the world. However, only precious corals (genus *Corallium*) have been treated as

important commercial species in Japan and there have been no studies conducted on gorgonian corals as important structural habitats for other deep-water organisms.

During the course of JAMSTEC (Japan Agency for Marine-Earth Science and Technology) deep-sea research, gorgonian corals were observed on several submersible dives, but no research or review of the video archives focusing on their importance as habitats for deep-sea communities has been conducted. This paper is thus the first report on the structures of Japanese deep-sea gorgonian communities.

Methods

Study site

The Shiribeshi Seamount (Fig. 1) is a submarine volcano with a relative height of 2,700 m located to the west off the Shakotan peninsula of Hokkaido, the northernmost Japanese island, in the Sea of Japan. This area is located in the cold-temperate zone. Although the Sea of Japan generally has low biodiversity (Nishimura 1992), the Shiribeshi Seamount has been known to be abundant in a variety of organisms and fauna since the first research was conducted there by JAMSTEC in 1989.

Submersible data collection

Data were collected from four dives on the four main points of the compass on the Shiribeshi Seamount in July 2001 for non-deep-sea coral research (Fig. 1B). All dives were made with the remotely operated vehicle Dolphin 3K (Table 1).

The Dolphin 3K was equipped with a three-chip CCD camera, Super Harp camera and four lights: three 400-W SeaArc HMI/MSR metal halide lamps and one 250-W SeaLine SL-120/250 halogen lamp. Video footage was recorded simultaneously on
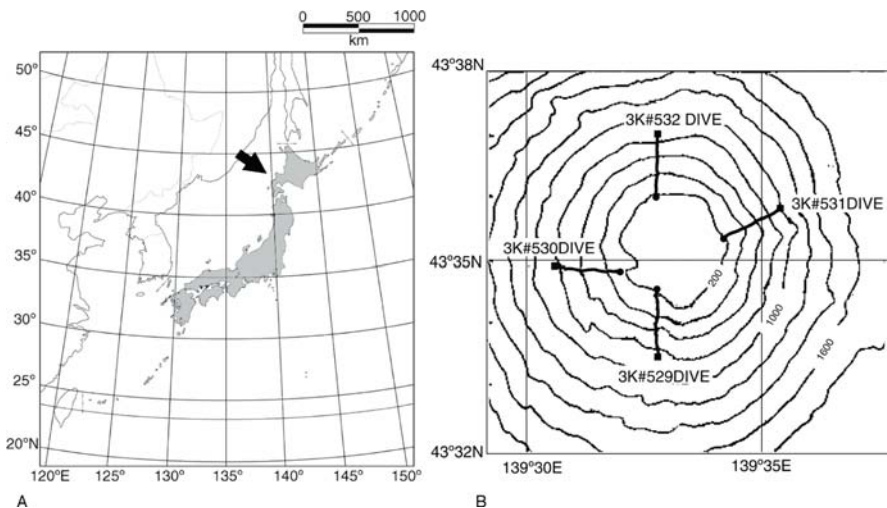
Fig. 1 A Map of the survey area off the western coast of Hokkaido, Japan. **B** Topography of Shiribeshi Seamount and the track lines of the 'Dolphin 3K' dives. ■: Start point, ●: End point. Contour intervals are 200 m

Table 1 Information on dives analysed in the study

Dive No.	Date	Latitude	Longitude	Landing time (GMT+9h)	Take off time (GMT+9h)	Bottom time (h:min)	Bottom Depth Range (m)
3K#529	11 Jul 2001	43°34.000'N	139°33.000'E	9:03	11:27	2:24	821 - 178
3K#530	11 Jul 2001	43°35.000'N	139°31.500'E	13:40	16:12	2:32	779 - 238
3K#531	12 Jul 2001	43°35.500'N	139°35.000'E	9:16	11:24	2:08	1038 - 228
3K#532	13 Jul 2001	43°36.500'N	139°33.000'E	8:47	10:28	1:41	871 - 142

Digital Betacam tapes. These video archives were reviewed in their entirety, and habitat-forming organisms were identified whenever possible. Coral samples were collected during dives 3K#529, 3K#530, and 3K#532. Water temperature data for Dolphin 3K dives #529-532 were collected using a SeaBird SBE19 CTD attached to the vehicle (Fig. 2).
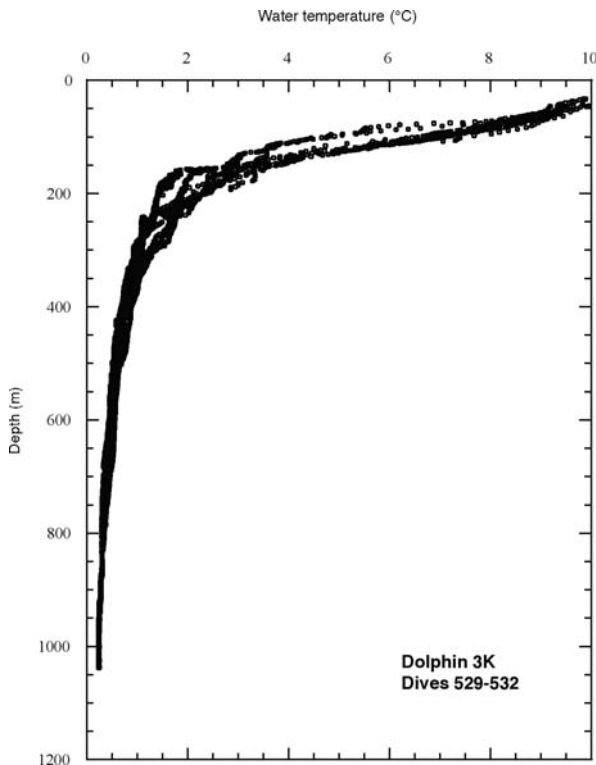
Fig. 2 CTD profiles showing the temperature profile during Dolphin 3K dives #529-532 at the Shiribeshi Seamount, Japan

Video analysis

Video identification of deep-water gorgonian species is very difficult because it is necessary to examine the sclerites microscopically for accurate species identification. It is known that many different gorgonian species in the same habitat often have similar colony morphology. Estimation is still required because we cannot sample all colonies recorded on video. Therefore, the most abundant white primnoid corals were defined as three morphotypes: Single stalk colonies (Fig. 3A), large colonies with more than 100 branches (Fig. 3C) and the other colonies (Figs. 3A-E).

Video identifications (n = 2055) were entered on a spreadsheet along with depth, time of day, and observations of each colony. When numerous species inhabit the same community, as shown in Figure 3B and 3C, to avoid double counting of the colonies, they were traced on the video screen. When the colonies are so abundant and small, as shown in Figure 3F, only the colonies on which the video cameras zoomed in on were counted on the video screen. Figure 4 is not meant to indicate quantitative abundance but rather the overall patterns of depth distribution.

Results and discussion

Table 1 shows the video archive records of Dolphin 3K dives #529-532 from 1038 m to 142 m analysed in this study. The shallowest point was 142 m on dive #532 and this was located at the top of the seamount.

Typical photographs of deep-sea gorgonian corals, other habitat-forming organisms, and associated animals in the video footage are shown in Figure 3. Their vertical distributions in each dive are shown in Fig. 4. Water temperature on this seamount varied between 0.24°C and 2.98°C from landing to taking off from the sea floor during the four dives (Fig. 2).

Gorgonian corals

Primnoid corals

Figure 3 shows that many species of gorgonians are distributed on the Shiribeshi Seamount. The most abundant corals are from the white-coloured family Primnoidae. It is not possible to make an accurate identification without sclerites as described above. The vertical distribution of primnoid corals may include plural species of Primnoidae. It may also contain other families because the colonies observed

Fig. 3 Video graphs of specimens from the Shiribeshi Seamount. **a** White primnoid gorgonians with single stalk (depth 820 m, dive #529). **b** White primnoid coral colonies (depth 623 m, dive #531). **c** Large white primnoid gorgonians (depth 444 m, dive #532). **d** White paragorgiid gorgonians (lower) with white primnoid corals (upper) (228 m, dive #530). **e** White primnoid corals (left), white paragorgiid corals (middle), and stylasterid corals (right) (depth 294 m, dive #531). **f** Unidentified gorgonians or sponges (depth 178 m, dive #532). **g** Decapod shrimps (depth 385 m, dive #530). **h** Nudibranch *Tritonia* on *Primnoa resedaeformis pacifica* (depth 315 m, dive #530)
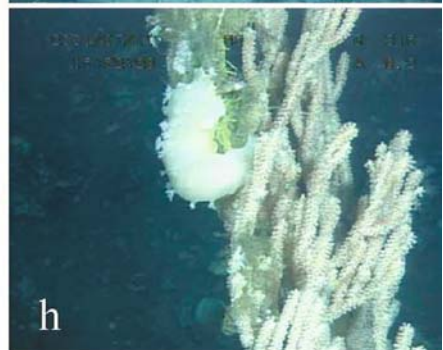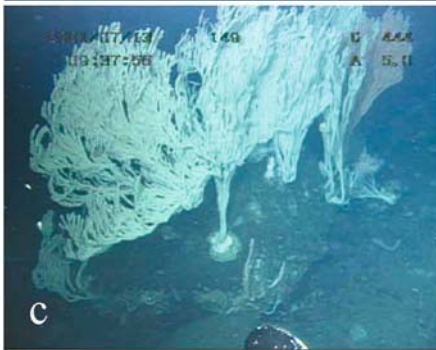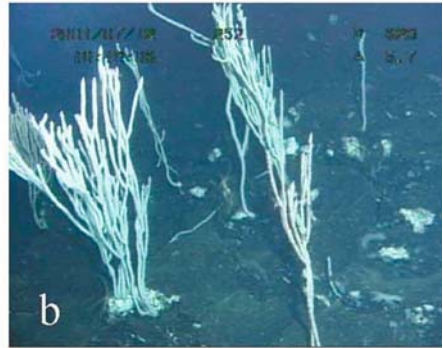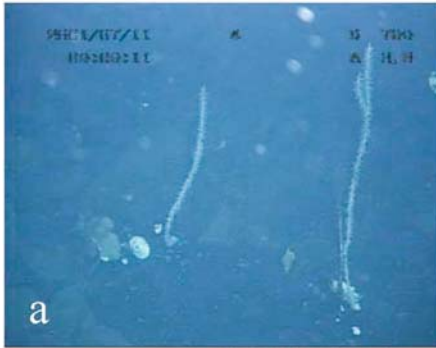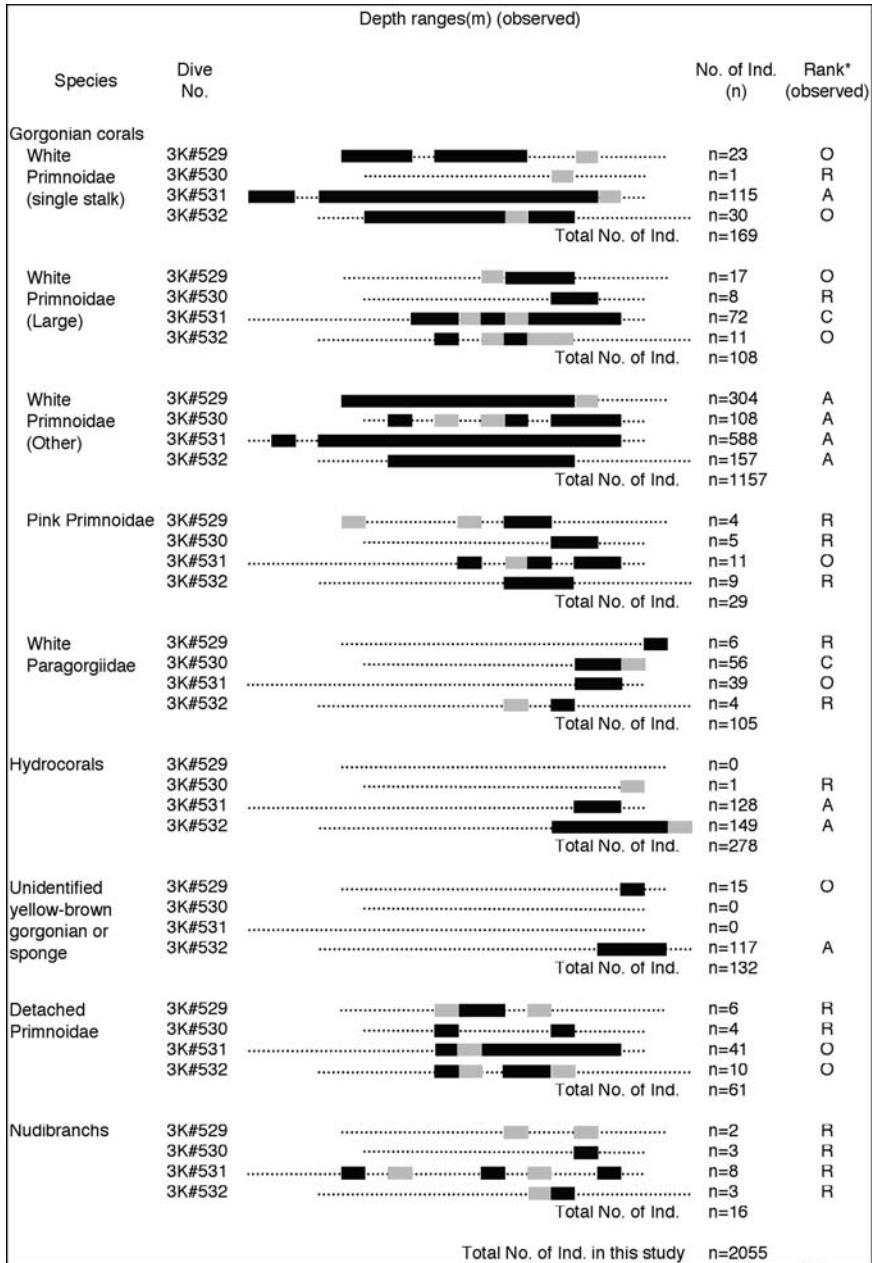
Fig. 4 Depth distribution ranges of Shiribeshi Seamount corals and number of associated organisms.

* Number of photographed animals ranked as follows: A (abundant), greater than 100; C (common), 50-99, O (occasional), 10-49; R (rare), 1-9. ■ shows that n >1 per depth range, ▨ shows that n = 1 per depth range, blank shows that n = 0, dive range are shown as ·········

on this seamount have many variations in branching pattern, thickness, and size (Fig. 3). These communities may include *P. resedaeformis pacifica* (Kinoshita 1907), which was identified in samples collected in the study. One of the *Primnoa* samples collected in dive 3K#532 had eggs in the polyps. The reproduction season of the Primnoidae community in the Shiribeshi Seamount included July in 2001.

White primnoid corals with a single stalk (n = 169) are observed at depths between 1030 m and 292 m and at water temperatures of 0.24 to 1.08°C (Fig. 2 and 1st species listed in Fig. 4). They have slightly deeper distributions compared to the other primnoid corals. Other species of the Family Ellisellidae may be present because they also contain single stalk morphotypes.

White primnoid corals with more than 100 branches (n = 108) are distributed at depths between 671 m and 284 m and at water temperatures of 0.44 to 1.11°C (Fig. 2 and 2nd species listed in Fig. 4). They most likely have a relatively narrow distribution of depth range among the primnoid corals. Also, the greatest number of colonies of all primnoid corals are observed at this depth range.

The other white primnoid corals (n = 1157) were recorded at depths between 968 m and 271 m and at water temperatures of 0.24 to 1.11°C (Fig. 2 and 3rd species listed in Fig. 4). They are observed to be widely distributed and may still contain plumal species of gorgonian corals. All primnoid corals were observed to be most abundant (n = 786) at the eastern area of the seamount (dive #531).

Kinoshita (1907, 1908) described the species *Primnoa pacifica* collected at Misaki, Sagami Bay, at a depth of 600 m as a new species. Kükenthal (1919) redescribed this species as *P. resedaeformis* var. *pacifica* and since then this species has been treated as a variation or forma in the Pacific Ocean. This species had been recorded only at this location until Broch (1935) reported a specimen from the Sea of Okhotsk and the Sea of Japan. The species collected at the Shiribeshi Seamount in this study is very similar to the *P. resedaeformis pacifica* described by Broch in 1935, but occurs very far from Sagami Bay, the first area described in 1907 and 1908, which is near Tokyo. Also the specimen of Broch (1935) had a large variation in polyp form and it is not clear that all samples were the same species as the type specimen of Kinoshita (1907, 1908). *P. resedaeformis* has been reported to be the same species in both the East Pacific Ocean and Atlantic Ocean. But *P. resedaeformis pacifica* reported in the West Pacific Ocean is treated as a variation or forma. It is not entirely improbable from a marine-biogeographic point of view that only the West-Pacific species is a variation though the East Pacific and Atlantic Ocean species are the same. There are two probable hypotheses that they are all same species as a cosmopolitan, or they are all different species. Kükenthal (1919, 1924) insisted that it is a borealcircumpolar species. Therefore, it is necessary to undertake a taxonomic revision of *Primnoa resedaeformis* species and to clarify their actual distribution worldwide. For this purpose, it is also necessary to re-examine unidentified samples collected in Japan.

The distribution of pink primnoid colonies (n = 29) is shown in Figure 4 (listed as 4th species). They were found at the depths between 822 m and 285 m and at water temperatures of 0.30 to 1.10°C. *P. resedaeformis* (red tree coral) observed in

the Atlantic Ocean and eastern Pacific Ocean is red, but most primnoid corals on the Shiribeshi Seamount are white (Fig. 3). There are very few pink colonies among the white ones and it is difficult to estimate their vertical distribution pattern. These pink colonies have not been observed to distribute singly but were always recorded along with white colonies on the video footage.

A pink colour is very common in the Families Primnoidae and Chrysogorgiidae that are distributed widely in deep waters around Japan. Their pinkness is due to the colour of the living polyp tissue and cannot be maintained in fixed samples. In gorgonian corals, the colour of the sclerites is one of the taxonomic characteristics for identification, and their colour does not fade when they are fixed. Therefore, the colour of living tissue has not been used as a taxonomical characteristic and neither Kinoshita (1907, 1908) nor Kükenthal (1919, 1924) described the living colours of *P. pacifica* and *P. resedaeformis pacifica*. Whether or not *P. pacifica* and *P. resedaeformis pacifica* have colours when they are alive has not been reported.

It is not clear what the difference is between the pink and white colonies on the Shiribeshi Seamount. It is important to collect additional pink Primnoidae for accurate identification and taxonomic revision.

Paragorgiid corals

As shown in Figures 3D and 3E and in Figure 4 (listed as 5th species), species of the Family Paragorgiidae (n = 105) are commonly observed on this seamount. They are distributed between 491 m and 175 m and in a water temperature range of 0.66 to 1.74°C. They were found at a narrow depth range, and in shallower and warmer areas compared to primnoid corals (Fig. 4). They were mostly seen in the eastern and western areas of the seamount. The paragorgiid gorgonians on the Shiribeshi Seamount were also all white.

Kinoshita (1913) first recorded *Paragorgia arborea* (Linné) in the North-West Pacific Ocean. Hickson (1915) also reported this species in the North-East Pacific. Thereafter Broch (1935, 1957) suggested that *P. arborea* is an amphi-boreal species and distributed in both the Pacific Ocean and Atlantic Ocean and claimed that this is a very widespread species (Grasshoff 1979). *P. nodosa* and *P. regalis* was also reported in the Pacific Ocean (Nutting 1912). *P. nodosa* is said to be the same species as *P. aborea* (Hickson 1915; Broch 1957). Although it was reported that paragorgiid gorgonians are rare in Japan (Iwase 1992), in the present video analysis, it was found that paragorgiid corals are very common on this northern seamount in the Sea of Japan. It is suggested that the reason why this family was previously thought to be rare in Japanese waters is that the sampling areas of gorgonians in recent years have mainly been around the main islands and that this family is comprised of deep-water species in Japan. Unfortunately, samples of paragorgiid corals were not collected from the Shiribeshi Seamount during the dives on which this study is based. Therefore, additional sampling of this family is needed.

Hydrocorals

The small pink colonies distributed at the base of Primnoidae and *Paragorgia* in Figure 3E are hydrocorals of the Family Stylasteridae (n = 278). They were observed

at the depths between 361 m and 143 m and in a water temperature range of 0.83-2.92°C on dives #530-532 (the 6th species in Fig. 4). Although there are a number of hydrocorals, the distribution area was restricted to the eastern to northern part of the seamount. They were also reported from dives conducted in 1990 (Fujikura et al. 1991). It is not clear whether or not these communities contain a single species.

Unidentified yellow-brown gorgonian corals or sponges

Figure 3F shows unidentified yellow-brown arborescent colonies (n = 132) distributed on the shallow part of the seamount during dives #529 and #532 (the 7th species in Fig. 4) in a water temperature range of 1.40-2.41°C. The phylum of these organisms is unclear because they have not been reported previously and we did not collect samples. They are most likely sponges. They were numerous at depths shallower than 300 m of dive #532, suggesting that these organisms are one of the dominant species on the northern top of the seamount. It is difficult to estimate the population size because individual colonies were too small to distinguish when the camera was too far from these communities. Therefore, the number of colonies is underestimated in Figure 4. Because of their small colony size, it is suggested the total amount of the organisms is smaller than that of primnoid corals.

Detached primnoid colonies

As shown in Figure 4, detached primnoid colonies (n = 61) were observed between depths of 639 m and 284 m and in a water temperature range of 0.44-1.11°C. It is not clear whether their occurrence is correlated with depth. At depths greater than 650 m, the colonies are not very large or highly branching, and therefore it is likely that such colonies are more difficult to detach than large, branching colonies at depths of less than 650 m. They were often observed in the middle of living colonies that were not detached and also usually observed as intact, not collapsed, colonies. There were no observations of dragged boulder or trawl path from a submersible. The cause for these detachments is unknown at this time.

Associated organisms

Shrimps

Figure 3G shows a zoom-in view of shrimp associated with primnoid corals. Their abundance on large colonies is a typical phenomenon in this area. The associated shrimp were previously reported and identified as Decapoda, Pandalidae (Fujikura et al. 1991). In deeper and smaller colonies, these associated shrimps could not be observed.

Nudibranchs

The nudibranch *Tritonia diomedea* Bergh, 1894 (Opisthobranchia: Mollusca) has been observed to attach to primnoid corals, as shown in Figure 3H, and it was reported that they feed on gorgonian corals (Kuramochi et al. 2002). In this study, a total of 16 individuals were observed to be associated with the corals (the last species listed in Fig. 4) between depths of 702 m and 291 m and in a water temperature range of 0.38-1.08°C. It was observed that sometimes the surface of

the corals where nudibranchs were attached was bare due to feeding activity. This species was observed to have a fatal effect on small gorgonian colonies. In shallow water, it is known that nudibranchs are one of the main predators on gorgonian species (Cronin et al. 1995).

Distribution of deep-water corals in Japanese waters

In the past 100 years, about 620 octocoral species of the worldwide total of 2000 known octocorals which include gorgonian corals, have been reported in Japanese territorial seas (Bayer 1981). About 200 endemic species constitute the Japanese octocoral fauna (Imahara 1994). This high biodiversity and high percentage of endemic species is thought to result from the geographic and oceanographic location of Japan. Japan has more than 6,800 islands, which span 20° of latitude from the south (24°02'N) to the north (45°31'N). Japanese territorial waters extend from the tropical zone to the subarctic zone. Therefore, Japanese waters extend through three marine biogeographic regions: the Indo-West Pacific region, East Asia (Japanese-Chinese) region, and North Pacific region (Briggs 1974; Nishimura 1992).

The southern part of Japan is a tropical to subtropical zone in the Indo-West Pacific region. Fishery records and dive video archives show that the deep-sea fauna of this region include precious corals (genus *Corallium*). The results of academic research cruises by the University of Tokyo have revealed rich biodiversity of fauna, including many gorgonian species, below 100 m in depth (personal observation). It is important to take into account the relations between shallow coral reef communities and deep-water coral communities in this region.

The middle part extends through the East Asian region (Japanese-Chinese region) of the warm-temperate zone and has the greatest biodiversity and number of endemic species. Many gorgonian species have been recorded and described in this area, which includes Sagami Bay and the warm Kuroshio current and cold Oyashio current (Aurivillius 1931; Kinoshita 1907, 1913; Kükenthal and Gorzawsky 1908; Kükenthal 1909; Nutting 1912). This region also includes precious coral fishery areas but the species are endemic to this district and different from those in the southern part.

The North Pacific region is in the northern part of Japan and extends from the cold-temperate zone to the subarctic zone. The Shiribeshi Seamount analysed in this study is located west of the northernmost island of Japan in this region. In this study, the species constitution that includes *Primnoa* and *Paragorgia* corals as the dominant species bears a close resemblance to that in the East Pacific or Atlantic. It was previously reported that some organisms including gorgonians are commonly distributed from the Sea of Okhotsk to the Bering Sea (Broch 1935; Nishimura 1981). Therefore, it is probable that some coral fauna in the northern part of Japan are also related to Bering Sea or East Pacific coral fauna.

Although deep-water gorgonian coral communities in Japanese territorial waters are described in this paper, it is possible that other deep-sea hexacoral communities may be found in Japan. Previously, a cold-water colonial hexacoral, *Goniocorella*

dumosa (Alcock, 1992) was collected from Sagami Bay at a depth of approximately 300 m (personal observation). Cold-water hexacoral communities would have different habitats and different biodiversity from deep-water gorgonian coral communities.

Conclusions

In this study, it was observed that deep-sea gorgonians on the Shiribeshi Seamount in the North Pacific region exhibit family zonation and vertical distribution patterns. The horizontal and vertical distributions of other deep-water species in the East Asian and Indo-West Pacific regions are not clear. The first step is to investigate the number of deep-water species and their horizontal distribution in the three marine biogeographical regions in Japan. Because the biodiversity of Japanese gorgonian corals is very high, it is expected that the deep-water coral ecosystems will also have high biodiversity. The population size and distribution of the deep-sea coral communities, including both octocorals and hexacorals, is an important subject in Japan and the West Pacific Ocean. There is a more than 100-year history of coral study in Japan but the taxonomic revision of deep-sea coral communities has just begun.

Acknowledgments

References

Aurivillius M (1931) The gorgonarians from Dr. Sixten Bock's expedition to Japan and Bonin Islands 1914. K Svenska Vetenskapsakad Handl (3) 9:1–337

Bayer FM (1981) Key to the genera of Octocorallia exclusive of Pennatulacea (Coelenterata: Anthozoa), with diagnoses of new taxa. Proc Biol Soc Washington 94: 901-947

Briggs JC (1974) Marine zoogeography. McGraw-Hill, New York

Broch H (1935) Oktokorallen des nördlichsten pazifischen Ozeans und ihre Beziehungen zur atlantischen Fauna. Avh Norske Vidensk Akad Oslo, Math-Nat Kl, 1935: 1-53

Broch H (1957) The northern octocoral, *Paragorgia arborea* (L.), in sub-antarctic waters. Nature 179: 1356

Cronin G, Hay ME, Fenical W, Lindquist N (1995) Distribution, density, and sequestration of host chemical defences by the specialist nudibranch *Tritonia hamnerorum* found at high densities on the sea fan *Gorgonia ventalina*. Mar Ecol Prog Ser 119: 177-189

Fujikura K, Hashimoto J, Tanaka T, Hotta H (1991) Biological community at Shiribeshi Seamount off the west coast of Hokkaido. JAMSTECTR Deep-Sea Res 283-291 (in Japanese)

Grasshoff M (1979) Zur bipolaren Verbreitung der Oktokoralle *Paragorgia arborea* (Cnidaria: Anthozoa: Scleraxonia). Seckenb Marit 11: 115-137

Hickson SJ (1915) Some Alcyonaria and a *Stylaster* from the west coast of North America. Proc Zool Soc London 1915: 541-557

Imahara Y (1994) Octocorals of Japan. Marine Parks J 103: 3-8 (in Japanese)

Imahara Y (1996) Previously recorded octocorals from Japan and adjacent seas. Precious Corals Octocoral Res 4-5: 17-44

Imahara Y (2003) Octocorals of the Doderlein collection. Rep Activ 2000–2002. Grant-in-Aid, Sci Res (B) (No. 12575008), Jap Soc Promot Sci, pp 259-266

Iwase F (1992) Cnidaria, Gorgonacea. In: Nishimura S (ed) Guide to seashore animals of Japan with colour pictures and keys. 1, Hoikusha, Osaka, Japan, pp 100-118

Kinoshita K (1907) Vorläufige Mitteilung über einige neue japanische Primnoid-Korallen. Ann Zool Japan 6: 229-234

Kinoshita K (1908) Primnoidae von Japan. J Coll Sci Univ Tokyo 23: 1-74

Kinoshita K (1913) Beiträge zur Kenntnis der Morphologie und Stammesgeschichte der Gorgoniden. J Coll Sci Univ Tokyo 32: 1-50

Kükenthal W (1909) Japanische Gorgoniden. 2. Teil: Die Familien der Plexauriden, Chrysogorgiiden und Melitodiden. In: Doflein F (ed) Beiträge zur Naturgeschichte Ostasiens. Abh K Bayer Akad Wiss, math-phys Kl, Suppl-Bd 1(5): 1-78

Kükenthal W (1919) Gorgonaria. Wissensch. Ergeb dt Tiefsee-Exped "Valdivia" 13: 1-946

Kükenthal W (1924) Gorgonaria. Das Tierreich 47. De Gruyter, Berlin Leipzig, 478 pp

Kükenthal W, Gorzawsky H (1908) Japanische Gorgoniden. 1. Teil: Die Familien der Primnoiden, Muriceiden und Acanthogorgiiden. In: Doflein F (ed) Beiträge zur Naturgeschichte Ostasiens. Abh K Bayer Akad Wiss, math-phys Kl, Suppl-Bd. 1(3): 1-71

Kuramochi T, Ogawa M, Naganuma T (2002) On *Tritonia diomedea* Bergh 1894 (Opishobranchia: Mollusca) from Shiribeshi Seamount, northern Japan Sea. JAMSTEC J Deep-Sea Res 21: 1-4 (in Japanese)

Nishimura S (1981) Sea and Life on the Earth. Kaimei-sha. Tokyo (in Japanese)

Nishimura S (1992) Guide to seashore animals of Japan with colour pictures and keys. 1, Hoikusha, Osaka, Japan

Nutting CC (1912) Descriptions of the Alcyonaria collected by the U.S. Fisheries steamer "Albatross," mainly in Japanese waters, during 1906. Proc US Nat Mus 43: 1-104

III

Mapping

Chapter content

Mapping of *Lophelia* reefs in Norway: experiences and survey methods

Jan Helge Fosså[1], Björn Lindberg[2], Ole Christensen[3], Tomas Lundälv[4], Ingvald Svellingen[1], Pål B. Mortensen[1], John Alvsvåg[1]

[1] Institute of Marine Research, P.O. Box 1879 Nordnes, N-5817 Bergen, Norway (jhf@imr.no)

[2] Department of Geology, University of Tromsö, Norway, Dramsveien 201, N-9037 Tromsö, Norway

[3] Geological Survey of Norway, P.O. Box 3006 Lade, N-7002 Trondheim, Norway

[4] Tjärnö Marine Biological Laboratory, SE-452 96 Strömstad, Sweden

Abstract. The Institute of Marine Research commenced a program for mapping and assessment of *Lophelia* reefs in 1997. It was initiated by reports from fishermen claiming that bottom trawling damaged deep-water coral reefs. The strategy was to survey coral sites reported in the literature and by the fishermen. This has provided an extensive database of coral occurrences, both damaged and undamaged sites. A number of major coral reefs have been identified, which has provided a better understanding of the morphology of *Lophelia* reefs and where they are likely to occur. We are now able to identify potential coral areas by analysing seafloor topography on maps. Fast and reliable ground-truthing methods using simple and inexpensive systems have been developed. Mapping and quantification of corals demand more advanced instrumentation, such as singlebeam and multibeam echo sounders in combination with data processing software allowing coral reefs to be detected in real time. Systems providing real time presentation of multibeam data are especially useful in combination with Remotely Operated Vehicle (ROV) positioned with acoustic navigation systems. We suggest the following mapping procedure: 1) acoustical reef detection followed by multibeam mapping, preferably along with collection of seismic reflection data. 2) ground-truthing with a tethered video camera platform or an ROV. The position of the observation platform is plotted online and draped on the multibeam maps, either in 2D or 3D mode. Examples from the reefs on Sula, Røst, Træna and Fugløy are given.

Keywords. Deep-water corals, cold-water corals, reefs, *Lophelia*, mapping, detection, ground-truthing, monitoring

Introduction

Deep-water coral reefs formed by *Lophelia pertusa* (Linné, 1758) are widely distributed along the shelf and coast of Norway (Dons 1944; Hovland and Mortensen 1999; Fosså et al. 2000, 2002). Although there has been a number of studies of the distribution of *Lophelia* in the North East Atlantic (e.g., Dons 1944; Wilson 1979a; Mortensen et al. 2001; Fosså et al. 2002), information about the precise location of the reefs and their size and abundance was largely lacking until modern technologies enabled more detailed mapping (Hovland et al. 1997; Freiwald 1998; Mortensen et al. 2001).

The Institute of Marine Research (IMR) in Bergen, Norway, commenced investigations and mapping of deep-water corals in 1997. Information on the presence of corals comes from a number of sources (fishermen, oil companies and older literature). Since then, IMR and other institutions such as the University of Tromsø and the Geological Survey of Norway, have carried out dedicated research cruises to map reef occurrences along the continental shelf and in the fjords (Fig. 1).

Lophelia polyps have a growth rate of about 7 mm a year and are able to form massive reef complexes several km long and up to 30 m high (Wilson 1979b; Mortensen et al. 1995; Fosså et al. 2002; Freiwald et al. 2002). They are generally found on elevated features on the seafloor such as ridges and moraine structures formed since the last glaciation. Coral debris in the Sula area has been dated to be about 9000 years old (Hovland and Mortensen 1999). There are several definitions of what a coral reef is (see references in Mortensen 2000). Here we use the term in the following meaning: a reef is an individual seabed feature consisting of an accumulation of coral skeleton. A reef may consist of a single or several coalesced coral mounds. A reef-complex is an area consisting of closely located coral reefs that are separated by other seabed substrates.

Reefs are fragile structures easily damaged by bottom trawling fishing gear. Based on information from fishermen and other sources, it has been estimated that between 30 and 50 % of the Norwegian reefs have been impacted by bottom trawling (Fosså et al. 2000, 2002). Therefore the Norwegian Ministry of Fisheries passed legislation in March 1999 to protect reefs from fishing activities. This legislation prohibits wilful damage or destruction of coral reefs, and fishermen are required to exert caution when fishing in the vicinity of known reefs. The legislation also provides a means for closing areas with corals to fishing activities. So far five reefs have received this special protection: the Sula Reef, Iverryggen Reef, Røst Reef, Tisler Reef and Fjellknausene Reef. In addition, the Selligrunnen Reef in Trondheimsfjorden has been temporarily conserved by the environmental authorities through the Norwegian Nature Conservation Act (Fig. 1).

Fig. 1 Large-scale distribution of *Lophelia* in Norway. Grey shaded areas indicate major coral areas. The Røst Reef, Iver Ridge, Sula Reef, Selligrunnen, and Hvaler are protected areas (squares = confirmed occurrences; circles = unconfirmed information from fishermen)

The Norwegian Sea

Fugløy

Røst Reef

Træna

Sula Reef

Iver Ridge

Storegga

Selligrunnen

Møredypet

Hvaler
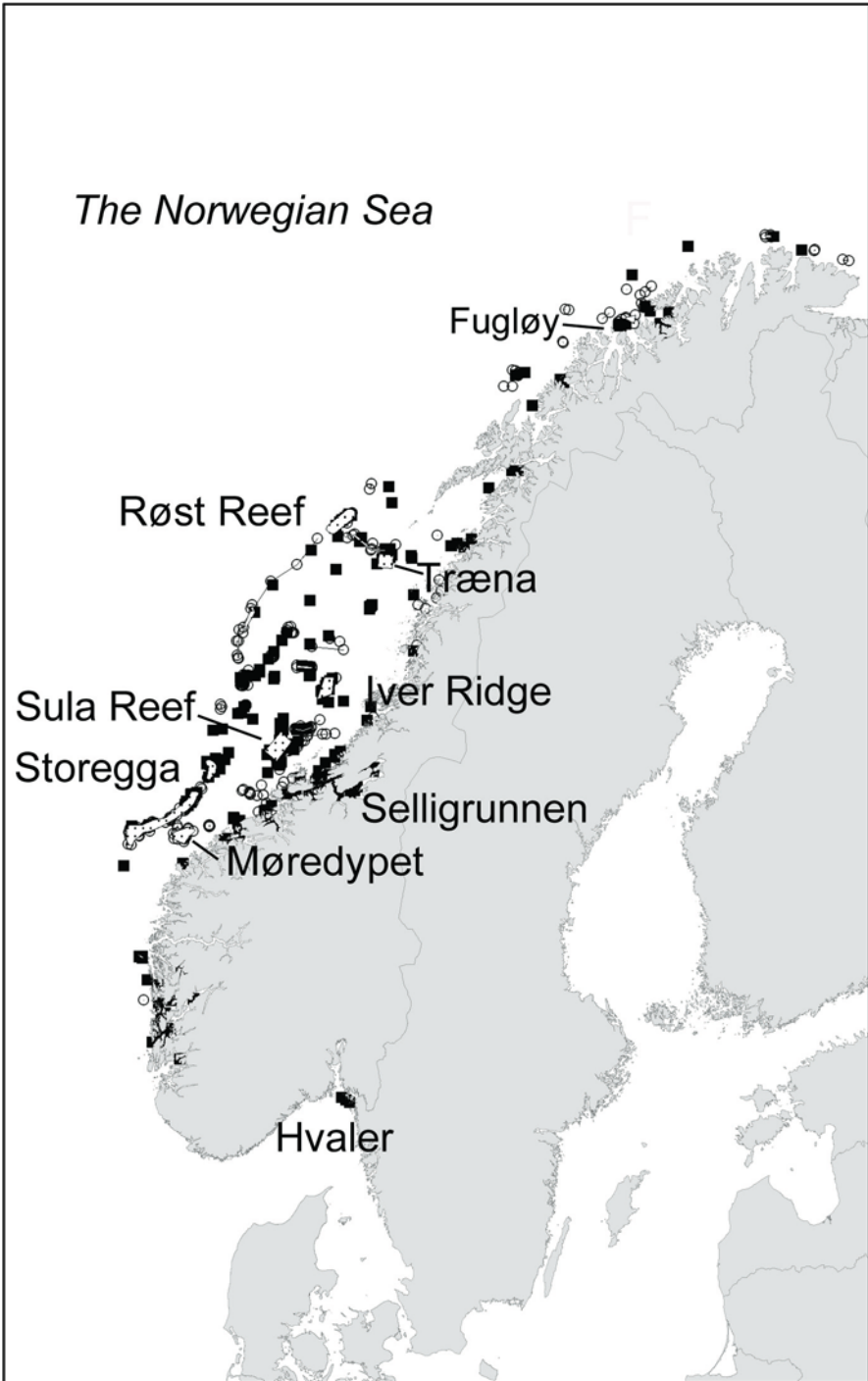
A reef is a complex structure that forms a habitat for a range of other marine organisms (Fig. 2). More than 1300 species of animals have been recorded living on, or in association with, the *Lophelia* reefs in the northeast Atlantic (Roberts et al. 2003). Redfish (*Sebastes* sp.) in particular are found in high abundance in reef areas. Also demersal species such as ling and tusk seem to be more common around corals than on the surrounding seabed (Husebø et al. 2002; Costello et al. 2005). The reefs are therefore important both from a general biodiversity perspective and as a habitat for commercial fish. At present there is a growing understanding of the ecological importance of the deep-water corals and the need for further mapping and research and management plans (Freiwald et al. 2004).

Deep-water coral reefs are difficult to map and sample. However, seabed mapping techniques are rapidly developing and methods based on modern technologies are now available. The majority and the most efficient methods are based on acoustics, while the most accurate and reliable are based on visual observation such as video

Fig. 2 Model of a *Lophelia*-reef. Due to poor light conditions and abundant particles in the water it is difficult to present an overview photo of a *Lophelia*-reef. Therefore we have combined several photos taken from ROVs to illustrate a "representative" reef. On the top of the reef the hemispherical living colonies are found. Below this zone living colonies of varying size are found with dead corals in between. At the base of the reef there is a zone characterised by smaller fragments of coral (rubble) mixed with sand and mud. *Paragorgia arborea* and other gorgonians are common on the reefs. *Sebastes* spp. are often seen in considerable numbers in connection with the reefs. The reef is about 10 m across. From Fosså et al. (2000)

and photograph. The purpose of this paper is to review existing mapping and sampling methods used on *Lophelia*-reefs in Norwegian waters, and to suggest an effective mapping procedure.

Large-scale mapping

Single split-beam echosounder

Acoustic reef recognition

IMR has developed an acoustic method to detect *Lophelia* reefs (Svellingen et al. 2002). The systems used are the Bergen Echo Integrator (BEI) (Foote et al. 1991; Korneliussen 1993) and the RoxAnn bottom classification system (Burns et al. 1989; Anonymous 1995). BEI is connected to a Simrad EK500 multi-frequency echo sounder, equipped with vertical looking split-beam transducers operating at 18, 38, 120 and 200 kHz respectively. The RoxAnn system is connected to one of the pairs of the 38 kHz split-beam transducer cable.

Bergen Echo Integrator

Acoustic sample data are stored in files as volume backscattering coefficients (sv), together with spatial data with a resolution of 500 sv per ping for each frequency. In addition, 150 values are recorded around the automatically detected seabed in order to increase the resolution. Horizontal data resolution varies with water depth and the EK500 processing speed, but a typical value is 1 ping per second (for more details see Knudsen 1990).

Data acquired using an EK500 is processed by the BEI, where the entire duration of the first bottom echo is integrated for all acoustic frequencies. This gives the frequency response r(f), defined in Korneliussen and Ona (2002) as $r(f) \equiv s_v(f)/s_v(38\ kHz) \equiv s_A(f)/s_A(38\ kHz)$, where f is the acoustic frequency. Since different bottom habitats and sediments will return different amounts of acoustic energy at the various frequencies, the frequency response can be used to classify the seafloor based on return energy (for further explanation see Korneliussen and Ona 2002; Svellingen et al. 2002).

RoxAnn

The two parameters used by the RoxAnn are roughness (E1) and hardness (E2). E1 is a measure of the energy in the tail of the first acoustic bottom return and E2 is a measure of the total energy of the complete second acoustic bottom return (Burns et al. 1989). The combination of the two parameters is used to distinguish coral reefs from the surrounding bottom, and the resolution is higher than for the BEI as a result of integration distance. The calculations of E1 and E2 are stored in a database together with time, depth and navigational data every five seconds.

The Leksa Reef – case study

The Leksa Reef is situated in a fjord system outside Trondheimsfjorden (63°36.40'N, 09°22.60'E). *Lophelia* colonies grow on a pronounced high in the
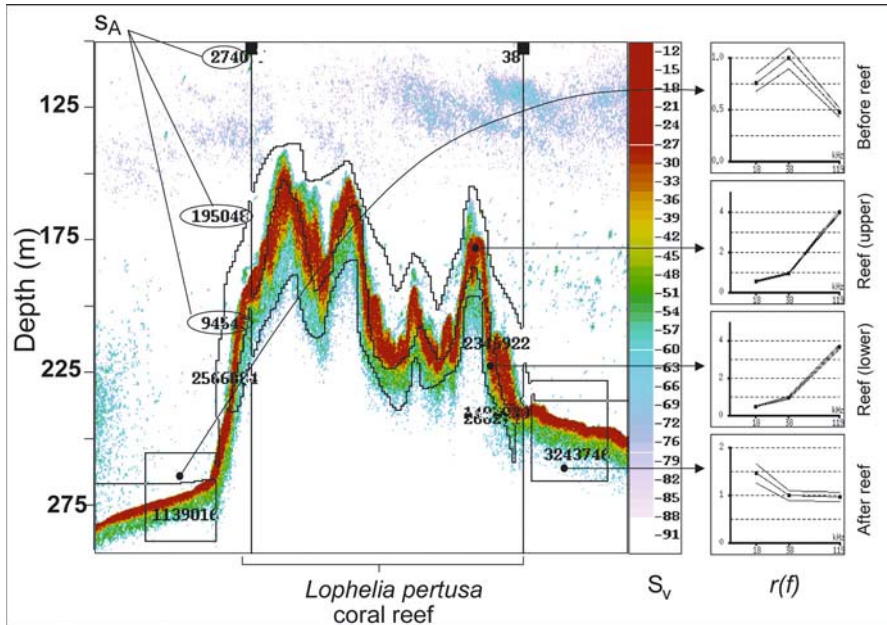
Fig. 3 The Leksa Reef west of Trondheimsfjorden. A 2.0 nautical mile echogram taken at 120 kHz across the reef for about 17 minutes. The panel to the right shows the relative frequency response, $r(f) \equiv s_v(f)/s_v(38 \text{ kHz})$, where f is the acoustic frequency, just before the reef, the first and last received backscatter from the reef, and just after the reef has been passed. From Svellingen et al. (2002)

fjord at water depths between 190 and 140 m with the surrounding bottom mostly deeper than 250 m. The site was studied with four ROV-dives 14-16 May 1999. We found three summits (Fig. 3); two western summits, about 500 m apart, and one eastern summit about 1 km to the east. The westernmost summit is the shallowest one and supports the highest densities of *Lophelia* corals. Between the two western and the eastern summits, the seabed consists mostly of sand. Below the areas with living *Lophelia* colonies, there is a steep hill with a spectacular coral rubble zone with high densities of gorgonians and soft corals.

Figure 3 displays a 120 kHz echogram transect over the Leksa Reef, covering a distance of two nautical miles acquired during cruising for approximately 17 minutes. The panels to the right depict the results of BEI-processing of the echosounder data (relative frequency response, r(f)), and clearly shows that the off-reef r(f) differ from the on-reef r(f). This is related to the different backscatter of energy at the different frequencies from the on- and off-reef areas (for further explanation see Korneliussen and Ona 2002; Svellingen et al. 2002).

Figure 4 shows the processed parameters *vs*. distance for the same transect as in Figure 3. The first profile (Fig. 4A) is the Nautical area backscattering (Nab) coefficient for 38 kHz, and the second profile (Fig. 4B) is the r(f) for 18 and 120 kHz, both calculated using BEI. Both parameters change when passing over an area comprising coral structures, most clearly for the Nab (a) and the r(120) kHz (b).
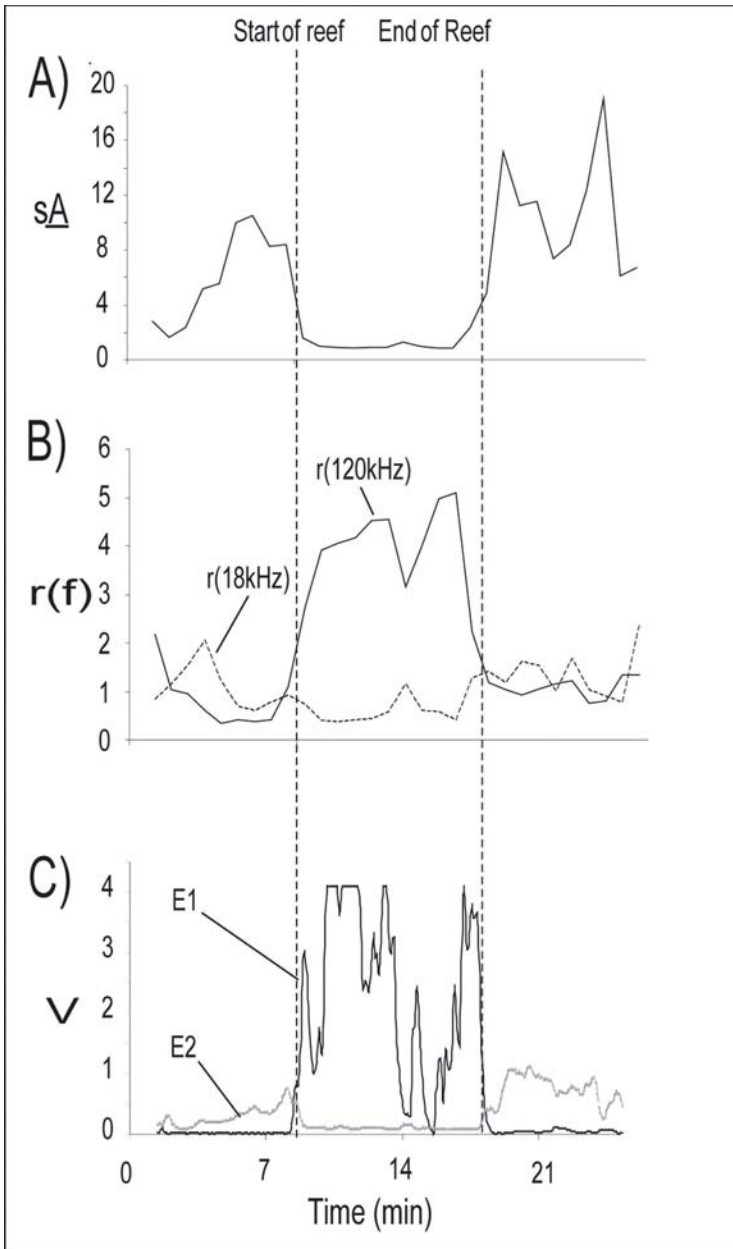
Fig. 4 Acoustic classification of the Leksa Reef west of Trondheimsfjorden. **A** Nautical Area Backscattering Coefficient, s_A, for the first bottom echo at 38 kHz. **B** r(18kHz) and r(120kHz) as functions of sailed distance. **C** Roughness, E1, and hardness, E2, from the RoxAnn system as a function of time. The data in **A** and **B** are averaged over 0.1 nautical miles, which in this case is about 50 pings, while the RoxAnn system averages over five seconds or approximately five pings. From Svellingen et al. (2002)

Figure 4C shows the roughness (E1) and hardness (E2) parameters processed by RoxAnn. RoxAnn also recognises a clear difference in character when entering the zone with living corals; E1 rises sharply and E2 drops to a minimum.

Equally important is that the area between the two western summits and the eastern, having no corals, is recognized, most clearly by the RoxAnn E1 parameter.

The Røst Reef – case study

The RoxAnn system was used when the large Røst Reef-complex was discovered in May 2002. The presence of corals was verified by ground-truthing using tethered camera platform (Fosså and Alvsvåg 2003). Figure 5 shows the cruise tracks where the E1 and E2 combination indicative of corals is shown in green. The reef-complex is 35-40 km long, up to 3 km wide and lies mainly between 300 and 400 m depth in a steep and rugged part of the continental shelf break.

The reef complex was mapped in detail in October 2002 and May 2003 using an EM 1002 multibeam echosounder and was ground-truthed with an ROV. Multibeam data showed that the corals grow along the back wall of a giant submarine slide which took place 4 000 years ago (Laberg and Vorren 2000). The geological setting of this reef complex is spectacular consisting of steep, dissected ridges, which are several tens of metres high occurring within a zone up to 2 km wide seaward from the shelf break. Inspection with the ROV showed that the highest concentrations of
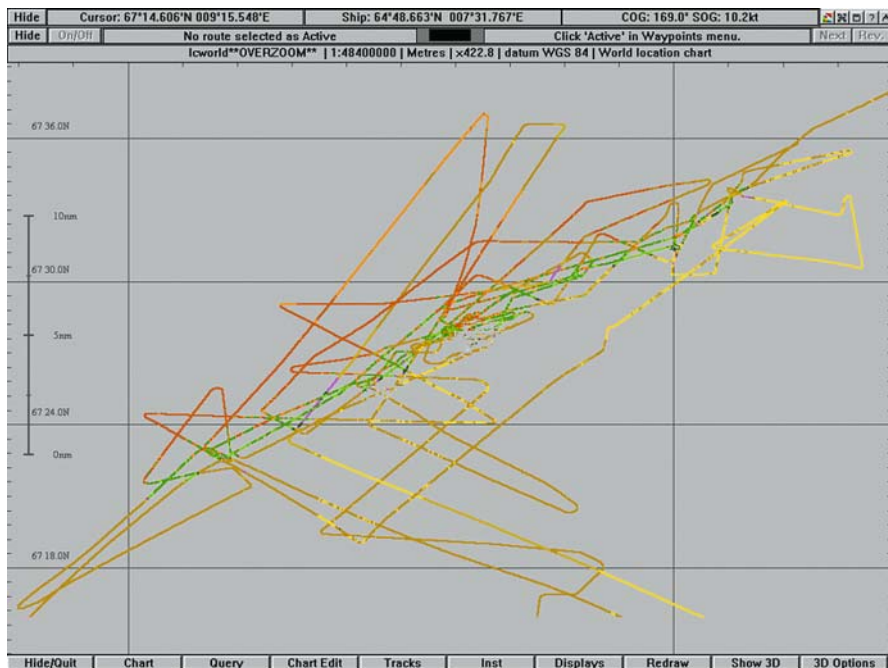
Fig. 5 Monitor screen dump showing the path of RV "Johan Hjort" over the Røst Reef in May 2002. Coral reef echoes are recognized and coloured green by the RoxAnn bottom classification system. The green area is about 35 km long

Lophelia colonies were found on the ridges in the uppermost part of the back wall zone between 300 and 380 m depth. Coral mounds also occurred on the shelf close to the slide area.

Conclusion

It is possible to identify coral reefs using standard hydro-acoustic instrumentation. The Simrad EK500 multi-frequency echo sounder used in combination with the BEI and the RoxAnn bottom classification system provides fairly accurate identification of *Lophelia* reefs. The RoxAnn system uses a single frequency, while the BEI uses multiple frequencies to recognize the reefs. The identification of the r(f) signature for *Lophelia* reefs used by BEI is based on empirical data from only two sites, and therefore needs further validation. There is also a need for a conceptual model to explain why the backscatter from the reefs differs from that of the surrounding seabed. It is currently not possible to decide which of these systems perform best. Furthermore, we have experienced that topographical heights and a steep hilly seafloor may give false indications of coral reefs. In practical use, however, we can confirm the expediancy of this system to support detection of coral reefs.

Seismic

Seismic acquisition is used for investigating the seafloor and sub-seafloor by remote sensing. A source, generating an acoustic signal which can vary from MHz to 10 Hz, and receivers (hydrophones) recording the reflected sound, constitute the basic setup. The configuration can vary greatly, depending on the source signal, distance from source to receivers, and amount of receivers as some of the main parameters that can be adjusted. The settings vary according to the target of the investigation; deeper investigations require lower frequencies and generally give lower resolution.

Industry seismic

Seismic performed by the oil industry in Norway is acquired with the main areas of interest deep below the seafloor. This requires low frequency equipment, and dominating frequencies are usually 10-100 Hz. Processing is performed to optimise the deeper features, thus neglecting surficial features such as the cold-water reefs.

High resolution seismic

One example of a configuration for shallow investigations/high resolution acquisition is two 40 cubic inch sleeve-guns generating a signal with typical frequencies between 80 and 200 Hz, and a single channel digital streamer with 20 hydrophones receiving the signal, resulting in a vertical resolution of ~3 m.

Sub bottom profiler

Collection of sub-bottom profiler (SBP) data ('pinger', penetration echosounder, *TOPAS* etc.) is often done simultaneously with heavier equipment (airguns, 'boomer', 'sparker' etc.). SBP gives better resolution than seismic data, but poorer

penetration. SBP typically consists of a number of transceivers mounted in the keel or hull of the vessel, and typically operates at frequencies from 2-12 kHz, obtaining vertical resolution of less than one metre.

Shooting rate and vessel-speed are two parameters that influence the horizontal resolution (and file-size) of the data, along with the non-adjustable water depth. A shooting rate of 10 seconds and vessel speed of 5 knots results in trace distance of 25.7 m, whereas a shooting rate of 5 seconds and a vessel speed of 3 knots gives a trace distance of 7.7 m.

For modern seismic acquisition systems, signals are recorded digitally, and the signal to noise ratio (S/N) can be improved by post-processing using methods such as bandpass filtering, trace mixing and automatic gain control (AGC), among others.

The Fugløy reefs – case study

The ability to identify cold-water coral reefs using seismic data depends on the acquisition parameters (resolution) of the seismic system, and the size of the reefs. Identifiable reefs typically appear as acoustically semi-transparent cone-shapes, often located on, or forming their own topographic highs (Fig. 6). The reef structure causes high spreading and absorption of acoustic energy, resulting in a weakened, or even absent sub-reef seafloor, also noted on conventional echosounder (Strømgren 1971). The frequency content of high resolution seismic data such as the example in Figure 6A usually allows penetration of the reef structure, so that the sub-reef seafloor is imaged, which is of importance for estimating the size of the coral reefs. SBP sometimes yields internal reflections within and around the reef structure (Fig. 6B), which allows for a tentative, but by no means definitive, classification of the various reef-zones, related to the state of the reefs (open coral structures, sediment-clogging, rubble zone etc.).

As reefs often have an acoustic signature that can be interpreted and discarded as noise, they need to be of a certain size in order to be correctly identified on seismic data. Reefs larger than ~2 times the vertical resolution of the seismic systems are distinguishable on individual traces, but in order for the reefs to be identifiable, they must be of sufficient horizontal extent compared to the spacing of seismic traces to allow for identification of their characteristic acoustic signature. This is further dependant on the water depth and vessel speed, and can thus vary from survey to survey.

The sub-bottom profiler data are usually acquired with higher data density than lower frequency seismic, and is as such a better tool for identifying deep-water

Fig. 6 A Sleeve-gun profile across a reef, showing the acoustically transparent cone-shape characteristic of a reef. The frequency and penetration of this equipment allows us to measure the height of the reef, which in this case is 30 m. **B** Sub-bottom profiler over the same reef (but on a different course) showing the low amplitudes that result from the scattering of energy. Internal reflectors are sometimes visible on sub-bottom profiler, but reefs that exceed 20 m in height are seldom penetrated fully to reveal the sub-reef seafloor. From Lindberg et al. in press
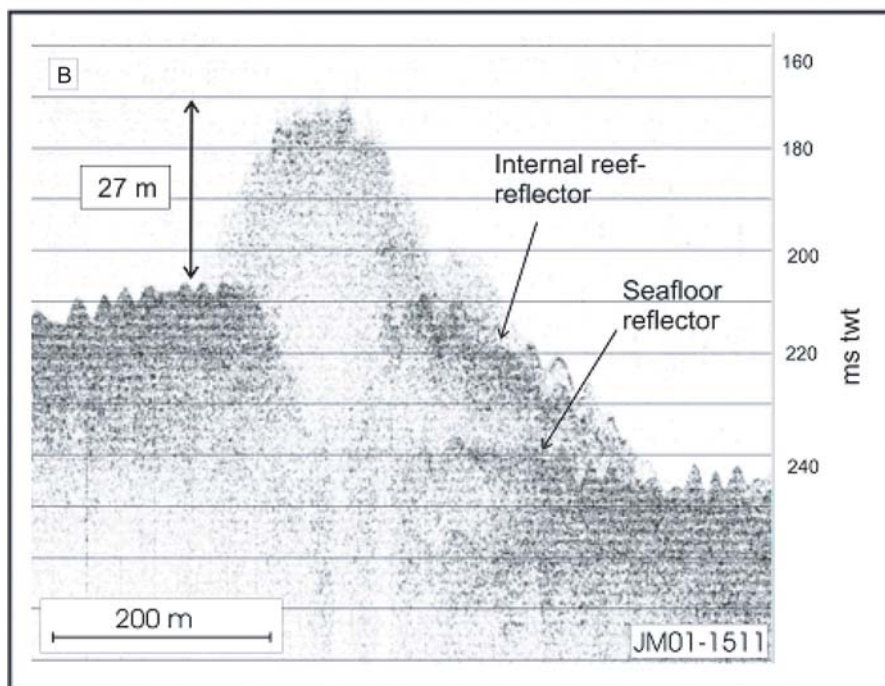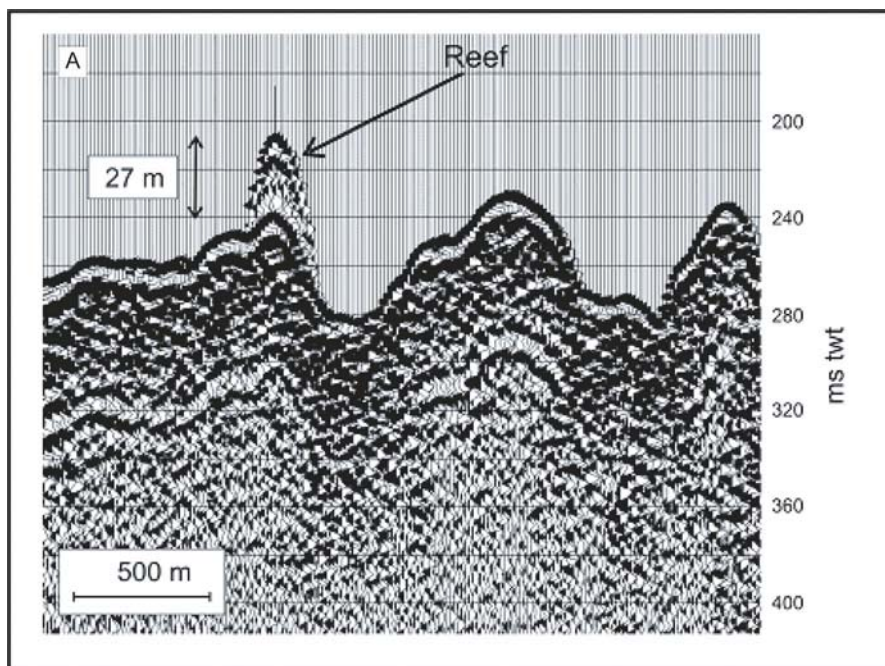
coral reefs, but lower frequency seismic (sleeve-gun data) constitute an important supplement for a complete image of the reefs and their surroundings. Full penetration of the reefs in order to image their true vertical extent, is only achieved by this type of profiling.

Conclusions

Identification of reefs using seismic profiling is possible, but it is not an optimal tool without additional information. Seismic data and sub bottom profiling provides detailed two-dimensional information about the reefs and their surroundings which is not accessible through other sensing systems. It does not, however, provide definite confirmation of reef existence or detailed information on their horizontal extent. On-going research on the use of high-resolution 3D seismic will greatly contribute to the understanding of the reefs in space and time, and will be an important supplement to other mapping techniques. Increased awareness on the characteristic appearance of reefs on seismic records is desirable as there are undoubtedly many reefs profiled on oil drill-site surveys etc. that have not been properly identified.

Side-scan sonar

Method

Side-scan sonar (SSS) is a common tool for mapping features on the seafloor. The system consists of a torpedo-shaped towfish that is towed behind the vessel (although hull-mounted versions exist) and contains transducers transmitting sound waves sideways and receiving the reflected signals. The signals are conveyed to the vessel and recorded digitally and/or printed on paper to produce an image comparable to an aerial photograph of the seafloor (Fig. 7). The SSS exist in a wide range of frequencies, usually ranging from 100 to 500 kHz for high-resolution mapping, but systems down to 30 kHz (TOBI) and 6.5 kHz (GLORIA) exist for larger scale mapping purposes. Higher frequencies result in better resolution, but a reduced coverage area per unit time. Depending on the frequencies used, some penetration can be achieved so that the sonograms do not exclusively represent the seafloor, but also characteristics of the uppermost deposits on the seafloor. This allows for imaging of features that are not identifiable by multibeam bathymetry, as the latter only represents seafloor topography. The swath-widths of SSS-systems vary greatly according to the height above the seafloor the towfish is towed, the applied frequency and beam-width.

Signature of reefs on SSS

Given that the frequency and resolution are sufficient, reefs can be distinguished from the adjacent seafloor using SSS (Fig. 7; Freiwald et al. 2002; Lindberg et al. in press). This is due to a number of factors: the difference in incidence angle caused by the reefs steep sides, the rough surface that the coral colonies form, and finally the comparatively flat and often homogeneous sediments found next to the reefs.

Generally, the coral reefs appear as areas of highly varying backscatter ('rough
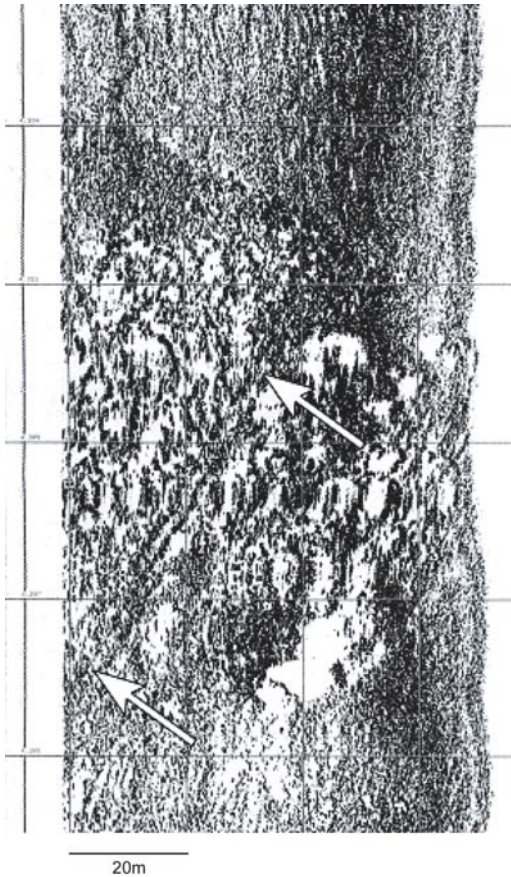
Fig. 7 Side-scan sonar echogram. *Lophelia* colonies and a trawl track (between the arrows) through the coral area as seen by an SSS. The coral mounds are elongated in shape due to the speed of the printer. The area was ground-truthed with ROV. From Fosså et al. (2002)

20m

texture') and sometimes exhibit a 'cauliflower' signature on the sonargraphs (Fosså et al. 1997; Freiwald et al. 2002; Masson et al. 2003; Lindberg et al. submitted). This is caused by the individual colonies which have a hemispheroidal shape and therefore cause widely different backscatter over short distances, resulting in a mottled, or cauliflower texture.

Depending on the height above the seafloor at which the towfish is towed, the reefs often cast an acoustic shadow on their far side, which can also be used to estimate their height (Fosså et al. 1997).

Conclusions

Side-scan sonar provides relatively fast mapping of large areas and can detect features not visible by other instruments, e.g., multibeam bathymetry or seismic. Advanced image and texture analyses significantly increase the data quality and if acquired close enough to the seafloor, sonograms can be of high resolution. Drawbacks are that the systems are often difficult to operate in areas of high relief, which is often the case with reefs, and that the system is susceptible to rough seas.

Multibeam echosounder

Modern multibeam swath systems use frequencies spanning from a few kHz to several hundred kHz and typically comprise more than hundred beams. The beams are transmitted at different angles from the same transducer unit, creating a fan perpendicular to the vessel direction. The angle of the fan is termed swath angle, which along with the water depth determines the width of the corridor mapped.

A wider swath angle and deeper water increases the corridor mapped but reduces the resolution as the distance between the individual beams increases; the so-called footprint (the area covered by a single beam) increases. For the mapping of large coral reefs, such as observed on the continental shelf at Røst, a large swath angle is sufficient (Fig. 8A). The individual mounds are clear and relatively easy to interpret. With a narrow swath angle and thereby increased resolution (Fig. 8B), it does not resolve any new features but makes it possible to study the morphology of individual mounds in larger detail. This is useful when studying individual coral mounds, but not for regional mapping.

Only the depth information is used to produce topographic maps of the seafloor. Echo strength, or backscatter strength, can be extracted from the multibeam data and presented as seabed backscatter maps (Kenny et al. 2000). Echo strength depends on hardness, roughness and the homogeneity of the seabed sediments. Some sediment types can be identified from the backscatter. The analysis of backscatter strength is, however, complicated as this factor is not given only by the seabed properties (Lurton 2002). One of the main problems is the variation due to the incident angle across an individual swath. This causes a characteristic stripe effect through the backscatter mosaic (Fig. 9). A normalization of the backscatter across the swath is therefore an essential part of the backscatter processing, but has been largely unsuccessful until recently (Novarini and Caruther 1998).

At present there is much effort dedicated to improve the processing of backscatter data. Robert Courtney (Geological Survey of Canada, Atlantic) has recently developed a new technique to normalize backscatter. This technique has been used on data from the Røst Reef. The results show high backscatter intensity associated with mounds identified as coral reefs (Fig. 10). To understand backscatter response and enable interpretation of the data, it is necessary to ground-truth an area as shown in Figure 10 and to compare the results with the backscatter. A coral reef is a mosaic of surface morphologies with different reflectivity. There can be living colonies only on parts of a mound, e.g., on the top or on one side, or small colonies. This

Fig. 8 Bathymetry data acquired with a Simrad EM1002 multibeam swath system, which has 111 beams and adjustable swath angle. **A** A 1.07 km^2 wide area from the Røst Reef mapped using a swath width of 68 degrees. At 300 m depth, the distance between the beams is 10 m. **B** The swath angle reduced to obtain a distance of 2 m between the beams. Similar processing methods were used for both data sets and the XYZ files where gridded using a cell size of approximately one-third of the acquisition cell size. Noise seems to be more dominating at the high-resolution data set, but also provide a tool for investigating the morphology of individual mounds, which can be used to differentiate between sediment mounds and coral reefs
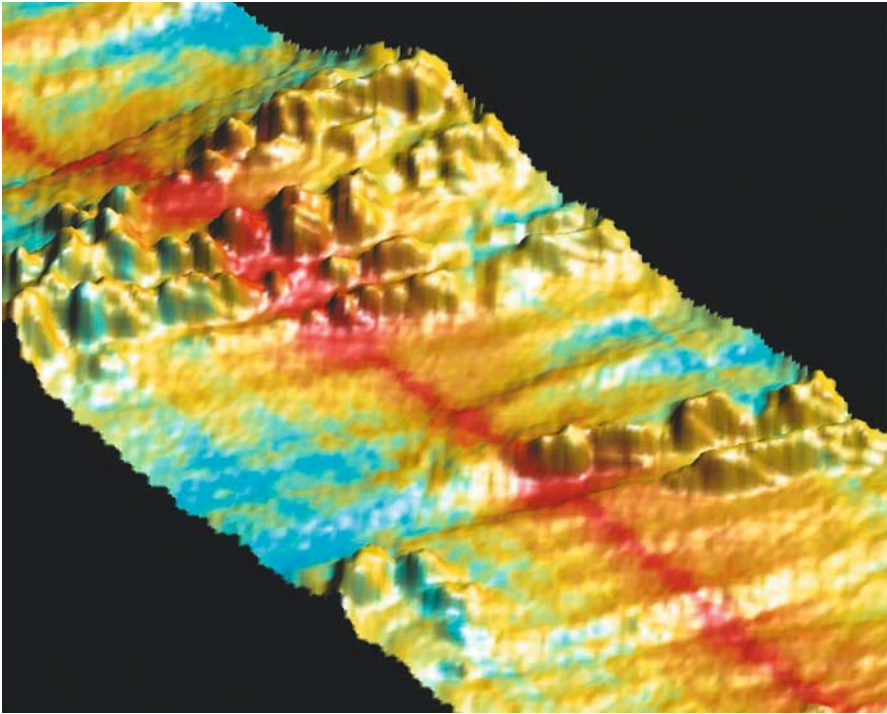
Fig. 9 A 300 m wide transect of multibeam backscatter intensity draped over multibeam bathymetry data over the Sula Reef. The backscatter intensity drops with the distance from the center beam, easily observed with the very high backscatter intensity indicated in red

variation in surface morphology and proportion between live *versus* dead corals complicates the interpretation.

Automatic reef recognition using backscatter

The ideal mapping tool would be automatic recognition of coral reefs from backscatter data, similar to the use of RoxAnn, but with the advantage of covering larger areas. Automatic interpretation and coral recognition has previously failed due to the above-mentioned striping effect. Hopefully, it will be improved with novel normalizing methods.

A first trial of automatic reef classification was performed by transforming backscatter data into a raster format and creating a scatter diagram. A supervised automatic classification over the central part of the Røst Reef was tested for mapping areas with corals. High backscatter strength is believed to represent corals due to the roughness and hardness of the coral mounds (Fig. 11). In the figure the two centerlines of a swath that covers the central area of the figure were processed using the new normalizing technique. The red areas represent high backscatter, which are being classified as coral reefs according to the backscatter strength. The classification seems to be correct in interpreting the coral mounds on the continental
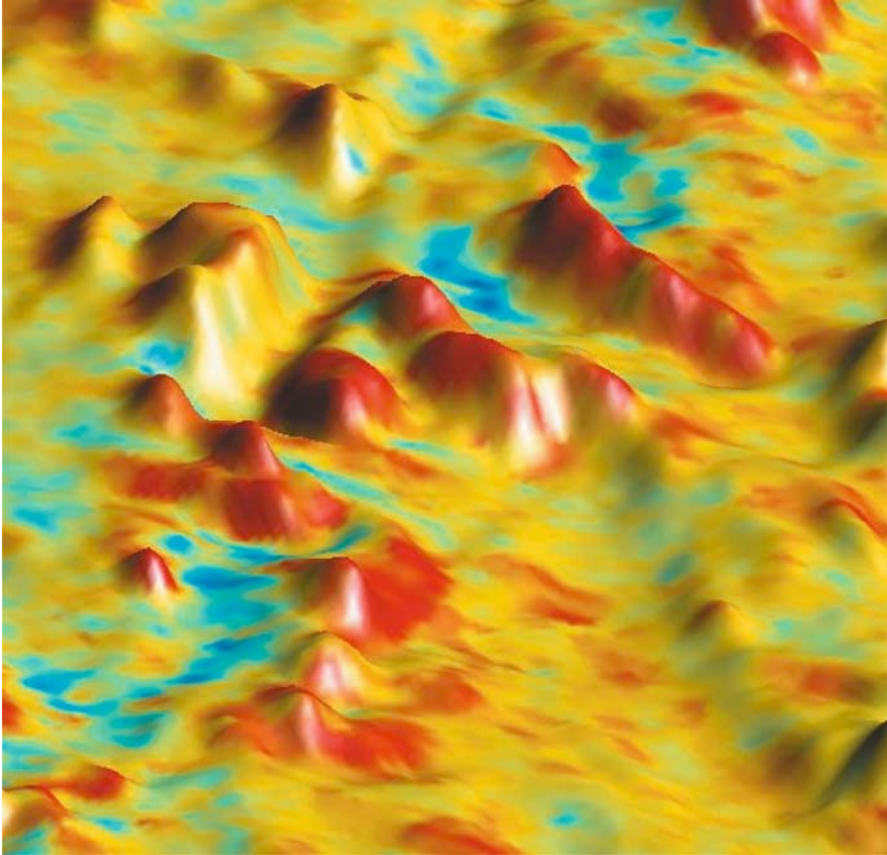
Fig. 10 Multibeam backscatter intensity draped over multibeam bathymetry from a 250 m wide part of the continental shelf at the Røst Reef. The majority of the mounds defined as possible coral reefs are associated with very high backscatter intensity, however a few located in the top left corner area have low backscatter intensity. This can be artificially due to backscatter processing, but so far no evidence is found for this. Speculation regarding this phenomenon has been link to the condition of the reefs

shelf and the corals located on the detached sediment ridges, but also parts of the seabed where we believe there are no corals were classified as such.

Automatic recognition of coral reefs involves automatic processing of backscatter and unsupervised classification. Figure 11 shows the first step, but many problems must be solved before the processing and classification is automatic. Depth dependency of backscatter data is just one of the problems, and the EM1002 multibeam echosounder uses three different pulse lengths according to depth and the pulse duration is also affecting the backscatter strength (Bunchuk and Zhitkovskii 1980). The results are promising, but exact ground-truthing is necessary for further adjustments of the classification parameters.
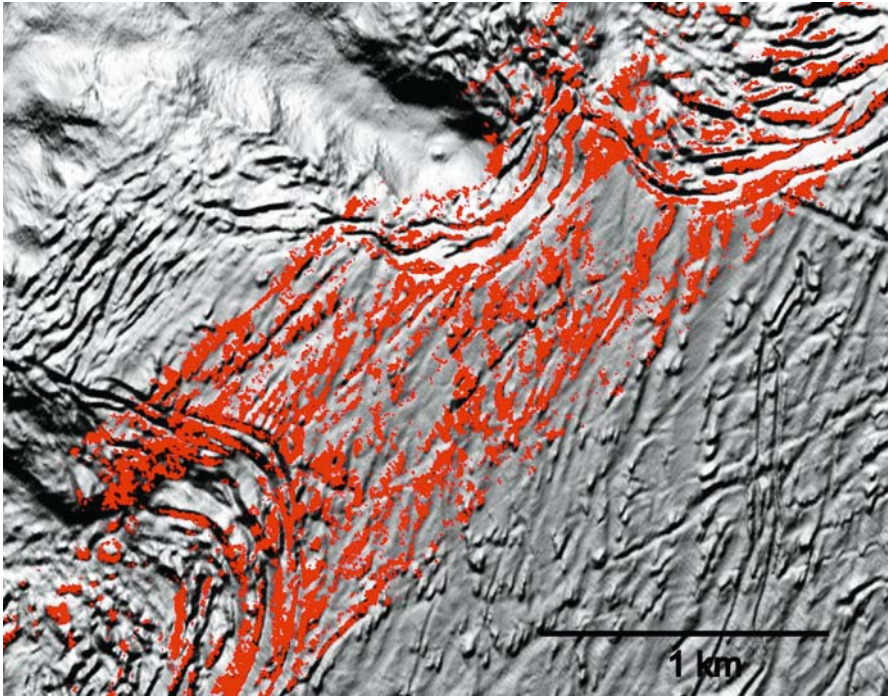
Fig. 11 Automatic reef recognition using backscatter data. Bathymetry from central Røst Reef, draped by the supervised classification of the newly processed backscatter data. Only the two centre lines (corresponding to the red belt) were processed using the new technique, which covers the central area of the figure. The red areas being classified as coral reefs according to the backscatter strength. It is clear that the classification is correct in interpreting all coral mounds on the continental shelf and the corals located on the detached sediment ridges. Further adjustment of the classification parameters is needed, as the interpreted areas seem to extend beyond the known occurrence of corals

Olex and multibeam bathymetry

To handle the large amounts of data obtained during multibeam mapping and to clean the data and produce maps requires an operator dedicated to that work. It can take many hours to obtain the maps. At sea it is, however, a great advantage to be able to display the acquired data in real time for immediate identification of potential coral reefs. An example of software that can be connected directly to a multibeam echosounder and display data continuously is Olex, a mapping and navigational software which also allows for plotting of ROVs or benthic landers during operation given sufficient positioning equipment is used.

Our experience is that Olex, in combination with multibeam echosounders, provides an efficient tool for coral mapping. The most important characteristic to use for detecting *Lophelia* reefs from multibeam data is the characteristic growth forms of the reefs. They form dome-shaped, often elongated structures, which rise

significantly over the surrounding seabed. Further indications can be spotted from the surrounding seabed since the reefs are often associated with irregularities in the seafloor topography, such as iceberg plough-marks, slide ridges or other features that contribute to locally increased current velocities.

Although the procedure described above is effective for large-scale mapping of coral occurrences, representative validation and ground-truthing are essential. However, our experience is that benthic structures of non-coral origin seldom exhibit similar topography to *Lophelia* reefs.

The Træna reefs – case study

In Træna a 23 x 13 km area was mapped in 2003 (Fig. 12). During the last glaciation the ice sheet shaped large ridges parallel to the ice flow direction on this part of the continental shelf (Rokoengen et al. 1995; Ottesen et al. 2002). These lineations are all orientated in a WNW-ESE direction, clearly imaged by the multibeam bathymetry (Fig. 12). The processes that shaped the large circular deep in the mid-eastern part of the mapped area are not known. New data indicate different glacial movement directions or possibly that the structure was generated during several glacial periods (Dag Ottesen, NGU pers. comm.).

Ground-truthing with ROV on five locations confirmed the presence of *Lophelia* on the inspected mounds. Interpretation of the multibeam bathymetry indicates that there are nearly fifteen hundred coral reefs in the mapped area. These were similar in size (approximately 150 m long, 40 m wide) and locally orientated in the same direction. There is no obvious geological explanation to the orientation of the reefs. The most obvious explanation is that the local current regime directs the growth of the corals.

Side-scan sonar *versus* multibeam bathymetry

A site survey with SSS and some ground-truthing with ROV was performed by Fugro Geoteam on behalf of Statoil in 1992 in a part of the Træna area (Figs. 12A, 13). The results indicated numerous coral reefs in the area (Hovland and Mortensen 1999).

Multibeam data were not acquired during this survey so the presence of coral reefs was interpreted using SSS data only (Hovland and Mortensen 1999). The site is therefore suitable for a comparison between two of the methods used for coral mapping.

Figure 13 shows the interpretation of multibeam bathymetry (B) and SSS-data (C) from the same sub-area in Træna. The major topographical features of the area can be found with both methods, such as the large iceberg plough-marks and the larger mounds. However, the interpretation of what is coral mounds and what is not differs in the two studies. The interpretation of the SSS gives much more coral mounds than the multibeam, and occasionally two close, but individual reefs, was merged into one.

Why these differences? Apart from the subjectivity of the interpretation, there are some explanations related to the specifics of the instruments. The grazing angle
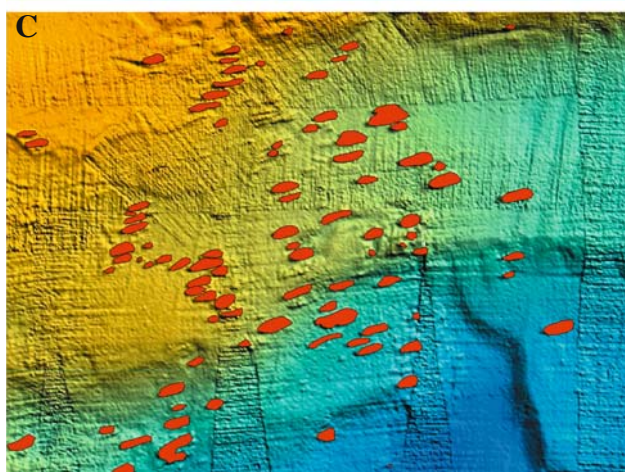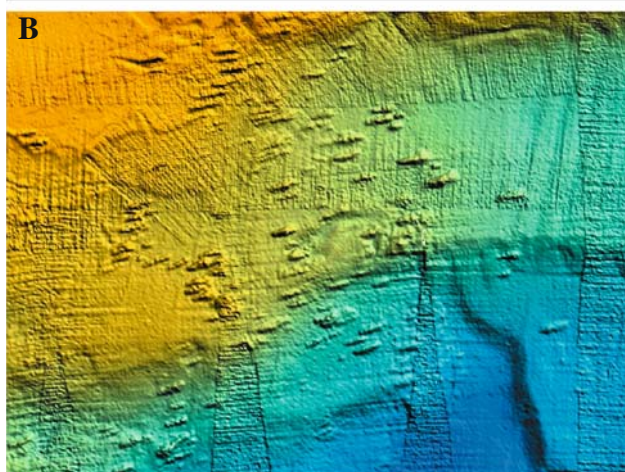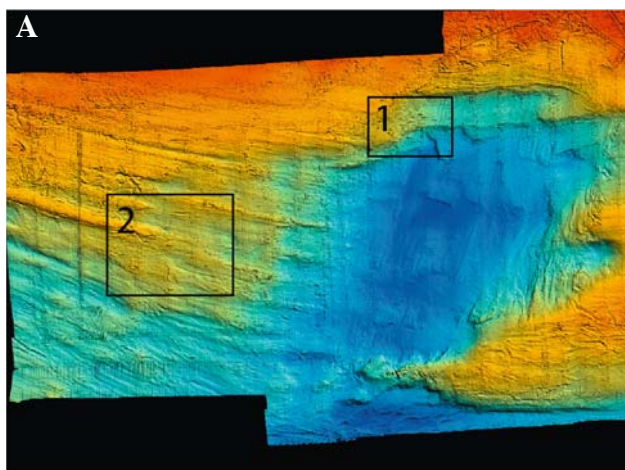
and the acoustic shadows caused by the topography makes it difficult to obtain an overview of the mounds and their morphology with SSS. The morphology is one of the most important characteristics used to distinguish between coral mounds and sediment mounds using multibeam bathymetry. Even with the difficulties associated with SSS-interpretation, the results have many similarities with the multibeam interpretation, both regarding identifying the coral reefs and determining the shape.

The detailed positioning is another problematic issue associated with the SSS. In deep water cable length causes a large layback. Large beacons must be attached on the cable or the side-scan fish for an accurate acoustic positioning, which often cause instability of the towfish and add noise to the data. By only using the layback as used by the Geoteam survey there will be significant error in positioning the towfish due to strong currents often observed in coral reef areas.

Conclusions

Mapping coral reefs using multibeam bathymetry is greatly assisted by visualization tools, such as sun-shaded relief maps where the sun illumination can be altered. Using sun-shaded bathymetry, the pattern of mounds and the general topography are visible, and it often becomes possible to differentiate between coral mounds and sediment mounds, when combining typical reef shapes. High-resolution multibeam bathymetry can resolve morphology of individual mounds and is very useful in differentiating coral reefs from sediment mounds in complex areas. Newly developed processing methods for multibeam backscatter data will be crucial to obtain more confidence regarding mapping of coral reefs. With further development and the use of multibeam echosounders close to the bottom, for example in an Autonomous Underwater Vehicle (AUV), this may also allow for interpretation of the proportion between living and dead coral on a reef.

Ground-truthing, detailed mapping and assessment

Sampling the reef fauna

The most extensive studies of the fauna on *Lophelia* reefs have been performed by Dons (1944), Burdon Jones and Tambs Lyche (1960), Jensen and Frederiksen (1992) and Fosså and Mortensen (1998), based entirely or partially on sampling with triangular dredge. Mortensen et al. (1995) studied the megafauna (>5 cm) using ROV and video.

Fig. 12 A Multibeam map of a coral area in Træna (23 x 13 km). The colours denote depth. Blues about 400 m and yellow about 300 m depth. (Area 2 is described in Fig. 13). **B** Magnified picture of framed area 1 (2 x 3 km). *Lophelia* build characteristic mounds on the sea bottom that are easily recognised on the multibeam map. However, mounds of stones and till can be misinterpreted as coral mounds, so ground-truthing is necessary. **C** Interpretation of B. Red areas is interpreted as being coral mounds
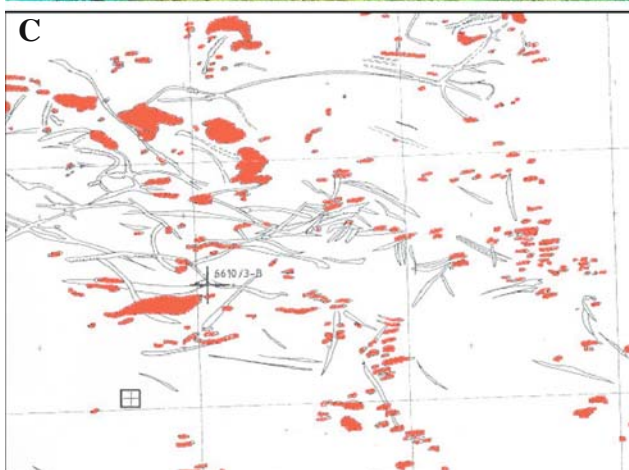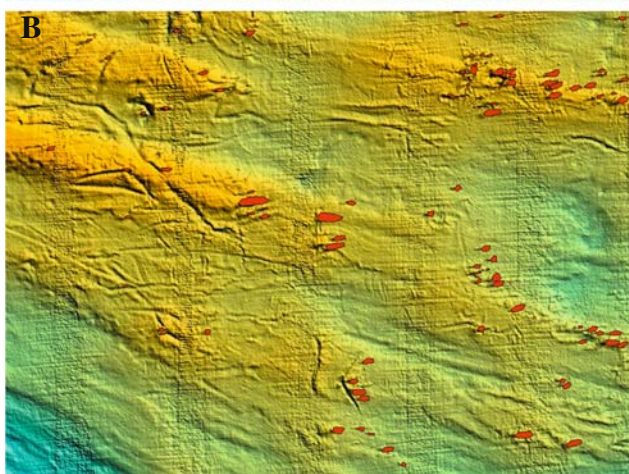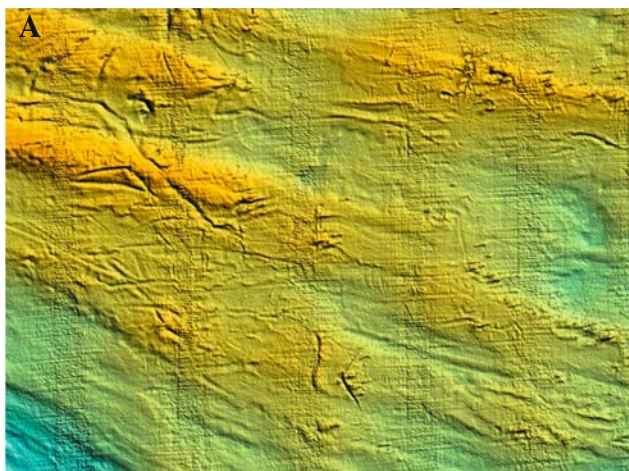
Fosså and Mortensen (1998) compared the number species from their own study with four earlier studies in the northeast Atlantic and found that only 15 species of a total of 744 were in common for all studies. This reflects that the studies were undertaken in regions with fauna differences. However, it also indicates that the number of species associated with the reefs is much higher than recorded so far. The number of studies of the fauna is too low, which partly reflects the inherent difficulties with sampling this habitat.

Fosså and Mortensen (1998) compared the sampling characteristics of van Veen grab, triangular dredge, ROV and gravity corer in the study of reef biodiversity and concluded that grab and dredge are the two most effective gears with respect to number of species. Suction sampling using ROV (e.g., Buhl-Mortensen and Mortensen 2004) samples a part of the fauna that is very poorly collected with other gear.

Grab

Fosså and Mortensen (1998) recommend using a grab for description of the macrofauna because it effectively samples both coral and associated fauna and damages less corals than dredge sampling. It is also recommended to equip the grab with a video camera to improve sampling precision. Mortensen et al. (2000) describe a video-assisted grab which was used to locate and sample *Lophelia*. They conclude that a video-assisted grab can replace the use of traditional, more destructive dredging and trawling techniques. In Canada, Schwinghamer et al. (1996) developed a hydraulically-actuated video-grab. It was designed to minimize disturbance to the sampling area and to provide the scientific operator with the ability to visually select the precise sampling area on the seabed, close and open the grab remotely, and verify that it closed properly prior to recovery. This grab has also been used to sample corals and associated fauna (Buhl-Mortensen and Mortensen 2005).

Because a *Lophelia* reef represents a habitat with several sub habitats (Fosså and Mortensen 1998; Freiwald et al. 2002), many samples are needed to provide a representative picture of the associated fauna, qualitatively as well as quantitatively. The only way to know exactly which part of a reef that has been sampled is to simultaneously use video recording of the bottom, e.g., video-assisted grab or ROV-sampling.

Dredge

A triangular dredge provides large samples with a corresponding large area being impacted. Dredges are not suitable for sampling mobile fauna, e.g., crustaceans, because they are easily washed out of the sample on the way to the surface and it is

Fig. 13 Interpretation of the seafloor using multibeam bathymetry and Side-Scan Sonar (SSS). **A** Framed area 2 (3.5 x 4.5 km) from Figure 12a without any interpretation. **B** Possible coral mounds (red). Interpretation based on multibeam map. **C** Interpretation of seabed features in the same area based on SSS

not known from which part of a reef, or perhaps the surrounding seabed, they were caught. Grab sampling actually catch small mobile animals better then a dredge, but the larger and scattered animals will usually not be represented (Fosså and Mortensen 1998). During the 1990's it became clear that any form of trawling or dredging has a devastating effect on the *Lophelia* colonies and should be avoided (Fosså et al. 2002).

Gravity and vibro corers

Vertical sampling of reefs and the surrounding seabed is important in order to understand the recent geological history of the area. As most of the reefs along the Norwegian continental shelf are still growing, and the areas experience continuous sedimentation, one must sample coral skeleton below the seafloor in order to unravel the development of the reefs through time. Information about the sediment, paleo-oceanography, age-determination (^{14}C and U/Th), geochemistry (stable isotopes, gas-content), and bio-erosion are some examples of useful application of gravity and vibro cores (Hovland et al. 1997; Lindberg and Mienert 2005; Dorschel et al. in press; Rüggeberg et al. in press).

Coring is not suitable for investigation of macrofauna, but can give a good description of the temporal changes of a specific location rather than allowing for mapping of the seafloor in the area. Both gravity and vibro corer may cause physical damage to the reefs if used among living colonies. The vibro corer is probably the most damaging.

Tethered video platform

IMR has used a very simple camera system developed in-house for ground-truthing. The system is connected to the vessel with a cable supplying camera and lights with electrical power and transmitting video signal to a monitor in real time. The inspection of the seabed is performed as the vessel drifts with the current and the wind. Lowering and lifting the camera control the distance to the seabed. The video platform is cheap, lightweight, and easy to operate and repair at sea. A dive takes very little time and it can be operated from relatively small vessels. It has been used extensively in the coral mapping project in Norway, especially when ROV-systems were not available.

The drawback of the system is that it is drifting with the vessel, meaning that one cannot stop or turn. Coral mounds may consist of only small patches of living corals that are easily missed during a drift leading to wrong conclusions about the status of a reef. However, in major coral areas this equipment is very useful for ground-truthing giving presence-absence information.

Remotely Operated Vehicle (ROV)

When detailed observations, high quality imagery or selective samples are required, ROVs often offer the best solution. While considerably more costly, technically complicated and demanding for the basic organisation of an investigation than the techniques described above, ROVs are very useful tools for the characterisation

of habitats, targeted sampling and operational tasks such as installation of *in situ* experiments. Videos and photographs obtained during ROV-surveys provide the best documentation of both biological values and current threats to a broader public. Very precise and well-controlled ground-truthing and mapping operations can also be performed with ROVs.

The success of ROV-operations is largely dependent on the support systems available, such as for precise navigation. A good procedure is to obtain high-resolution multibeam maps prior to ROV-operations, and then use this information for ROV-navigation. Operations of this type were successfully performed on board the R/V "G.O. Sars" in 2003. Advanced software (e.g., Olex) and hardware (positioning equipment) allowed the ROV to be directed to specific sites for close inspection and targeted sampling (Fig. 14).

Conclusions

Description of the biological diversity of *Lophelia*-reefs requires many samples because of the highly variable habitat architecture. A summary of advantages and disadvantages of different sampling gear is given in Table 1.

The triangular dredge is an effective gear to sample both dead and live corals and to study epifauna. However, it is destructive and should under all circumstances be avoided in areas with living corals. A dredge is still useful in the coral rubble zone if one can assure that living corals will not be impacted. However, also here one should be careful because this zone has a rich fauna and is part of the complete coral habitat. The grab is a more precise and a more considerate gear. The most effective is a video-assisted grab where one sees the seabed and can release the grab precisely. This method is also well fitted to sample live corals with a minimum of damage. The gravity corer is not adequate for studying the living *Lophelia* community. The only way to know exactly which part of a reef that has been sampled is the simultaneous use of video, e.g., video-assisted grab or ROV-sampling. The combination of these methods provides the best picture on both fine and broad scales.

Mapping procedure by the oil industry

Oil companies operating in Norway are obliged to map corals in connection with laying of pipelines and drilling operations. A typical mapping procedure has four phases as described by the Norwegian Directorate of Fisheries (2004):

1. A corridor 150-300 m wide is mapped with multibeam echosounder, side-scan sonar and ultra high resolution 2D seismic (250-1500 Hz) in order to obtain a rapid and inexpensive overview of the regional seabed conditions and the possibility for coral reefs to occur in the area.
2. Processing and interpretation to identify potential reefs and other obstacles. Planned pipeline transects and drill-sites are then adjusted accordingly.
3. In the third phase, ROV with video camera and optional side-scan sonar (1000 Hz) are used for ground-truthing.
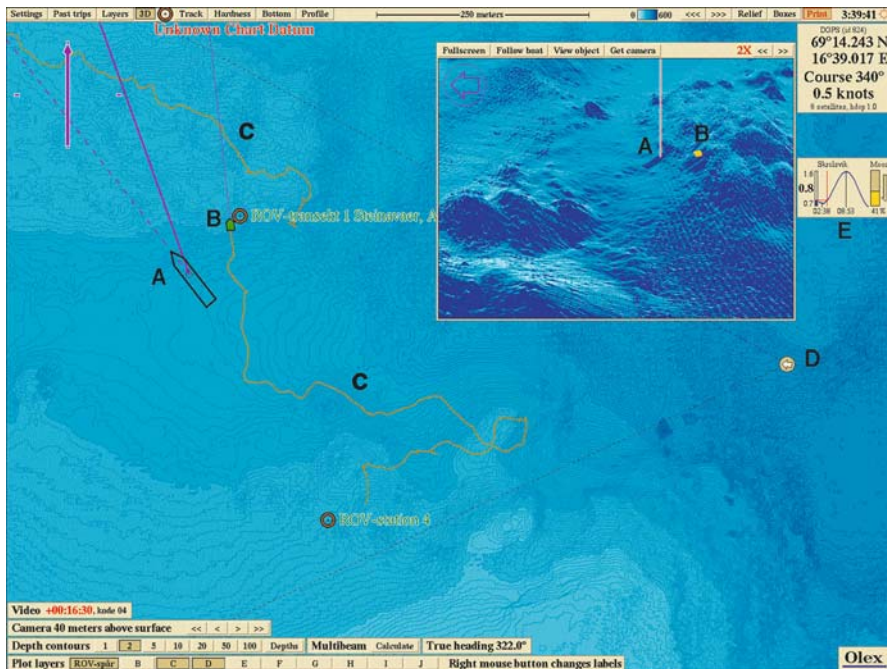
Fig. 14 Monitor screen dump from the Olex navigational software during work with an ROV survey in the Steinavær area, Andfjord, Northern Norway from the R/V "G.O. Sars", July 2003. The bathymetry of the area was surveyed immediately prior to the ROV work, and is illustrated by shaded depth contours (2 m isobaths) and a 3D view (2x vertical exaggeration). **A** Position of the research vessel. **B** Position of the ROV. **C** Recorded ROV tracks (individual parts of the tracks are time-coded, permitting synchronisation with recorded video). **D** Origin of 3D view. **E** Position in the tidal cycle at the closest recording station

4.   The final pipeline track or drill site is decided upon based on all the information.

Monitoring

Monitoring is an increasingly urgent issue as more reefs and deep-water coral habitats are discovered in areas with human activities. In Norwegian waters and elsewhere, deep-water reefs have become protected against trawling and some have received status as Marine Protected Areas (Fosså and Alvsvåg 2003; Freiwald et al. 2004). Programmes should be initiated to monitor important biological factors and the implementation of regulations. At present there is no coral monitoring in Norway, nor is there any experience. The issue, however, is very important and therefore we present some of the methods and possibilities regarding monitoring of reefs at great depths.

Due to the complexity of *Lophelia* reefs, traditional methods such as grab and dredge for sampling the seabed are probably not suitable for monitoring temporal

Table 1 Pros and cons of different gear used for sampling the *Lophelia* coral habitat (modified from Fosså and Mortensen (1998))

	Pros	Cons
Triangular dredge	Covers large area Large samples Inexpensive	Destructive Poor spatial resolution Not quantitative
Grab	Approximately quantitative Good spatial resolution Small impacted area Inexpensive Video-assisted grab increases spatial information	Somewhat destructive Often difficult to obtain successful samples
ROV	Covers large areas Documents damage to corals and other fauna from human activity Maps megabenthos Documents fish behaviour Describes macro-structure of *Lophelia* colonies and reef Precise sampling with manipulator	Expensive to very expensive Complicated
Gravity corer	Samples the sediment stratification Sample micro- and meiofauna	Covers small area Not suitable for studies of living macrofaunal community

changes of reef fauna. Video and photographic sampling of fixed areas will probably give better indications on changes in the megafauna and the condition of the reefs. To obtain high-resolution data from deep-water benthic habitats platforms equipped with electronic sensors and electro/hydraulic engines are needed. For monitoring there are two different types of platforms: (i) mobile, e.g., ROVs, AUVs and towed gear, and (ii) stationary, e.g., landers and cabled systems. Below we deal in short with the possibilities of landers and cabled systems for monitoring.

Landers

Benthic landers are instrumented platforms that are left on the seafloor for measuring physical and biological variables over a period of time. The employment of landers in deep-water coral habitats has a recent history and few results have been published (Duineveld et al. 2004; Roberts et al. 2005). Landers have proven very useful for process studies and detailed description of the near seafloor environment (Parker et al. 2003; Duineveld et al. 2004; Roberts et al. 2005). Roberts et al. (2005) used a so-called photolander with still cameras and a set of optical instruments at two reef sites (the Sula Reef off mid-Norway and the Galway carbonate mound in the Porcupine Seabight). The cameras provided time-lapse photographs from the seabed, while other instruments recorded particles in the water close to the seafloor.

A drawback of landers is the limited power supply. They are not connected to power lines from land and therefore rely on battery power.

Cabled systems

Cabled seafloor observatories have many attributes in common with benthic landers, but an important difference is that they are supplied with electric power from land. Several cabled ocean observatories are being planned around the world (Momma 2000; Heath 2003) such as The Monterey Accelerated Research System (MARS) and The European Sea Floor Observatory Network (ESONET). A few successful attempts have previously been made to observe isolated deep-sea phenomena using out-of-service analogue cables (Petitt et al. 2002).

Cabled seafloor observatories enable long time-series of data from benthic environments, but because they rely on expensive fibre optic cable networks this technology is dependent on major economical support, e.g., large institutions and industry.

By linking visual monitoring with environmental recording, we can begin to understand the effect of long-term environmental dynamics on deep-water reef communities. Approaches like this have tremendous potential to help us understand not just the natural history of this ecosystem, but also offers a unique opportunity to evaluate and calibrate climatic proxies that potentially can be extracted from deep-water coral skeletons.

Conclusions and recommendations

In order to fully understand the reef habitat, its structure and ecological function, it is necessary to have a good understanding of the biology, geology, hydrography and geochemistry of coral ecosystems achieved by systematic research. Mapping, sampling and monitoring of deep-water coral reefs in Norwegian waters and elsewhere are essential tasks for which we have presented methods and strategies summarised in Tables 2 and 3. Not surprisingly, the best methods are often linked to the highest cost, but there are also viable low-cost alternatives that can be performed from small vessels.

Below we describe a procedure for mapping of deep-water coral reefs that we have found useful. It can be accomplished during one single cruise or following several successive ones. Site selection is based on existing information (e.g., from fishermen) or by studying the general seabed topography. The first search in a new area is performed following a grid of survey lines and with the RoxAnn activated. Usually in an area with well developed reefs, RoxAnn will give positive signals. Having received strong indications that corals are present, we perform a multibeam mapping of the area. The multibeam data are then interpreted and potential structures for ground-truthing are chosen.

Mapping procedure

Prior to the cruise

1. Background information about coral fields from fishermen, oil companies etc.
2. Selection of study area

Table 2 Overview of mapping tools for *Lophelia* reefs

Method	Purpose	Type of sample	Horizontal resolution	Vertical resolution	Resolution and time span	Size of vessel	Costs	Comments
			Large scale mapping					
Single (split-) beam	Identification, mapping,	Single track acoustic data	Effort dependent	cm		All sizes	Low/ high	Efficient and low-cost
Seismic	Identification (mapping)	Single track acoustic data	N/A	N/A		Large/ medium	High	Useful supplement for geological understanding
Side-Scan Sonar	Identification, mapping,	Area coverage, and reflection strength of bottom	Down to dm	N/A		All sizes	Low	
Multibeam	Identification, mapping,	Area coverage, bathymetry and backscatter	Down to 2x2m	cm		Medium/ Large	Very high	Highly recommended
			Ground-truthing & detailed mapping					
Dredge	Biodiversity, (mapping)	Epi(coral)fauna and corals	Depends on distance travelled on bottom	N/A	Poor	Small	Low	Destructive to reefs Not recommended
Grab	Ground-truthing, biodiversity, substrate	Fauna and corals, sediment	Equals grab size	N/A	Poor	Small	Low	Recommended with video
Corer	Sub bottom investigation	Coral skeleton, sediment	Equals corer size	mm	Potentially thousands of years	Medium	Low	Useful for paleo studies
Tethered camera platform	Ground-truthing	Video footage, photo	Down to dm	N/A		Small	Low	
ROV	Ground-truthing, fauna, deployment and retrieval of instruments *in situ*	Multiple	Down to cm	N/A		Small/ medium	High	Highly recommended
Manned submersible		Multiple	Down to cm	N/A		Large	Very high	Highly recommended

During cruise
3. Initial survey using RoxAnn as a coral detection method
4. Confining the area subject to multibeam mapping using indications from RoxAnn and coarse topographical clues
5. Multibeam mapping

Table 3 Monitoring of deep-water coral reefs

Platform	Mobility	Tasks	Range	Temporal resolution	Comments
ROV	Moving (stationary)	Visual inspections	Small to medium. Depends on instrumentation: e.g., video, acoustics	Short-term	Highly recommended
AUV	Moving	Acoustics, (visual)	Large; miles	Short-term	Recommended
Lander	Stationary	Visual	Local to medium	Short- and long term. Non permanent	Highly recommended
Cabled system	Stationary	Visual, Multiple sensors	Short to long. Depends on instrumentation and cable network	Long term, almost permanent	Authors have no experience, but the method has a great potential

6. Interpretation of seafloor features and identification of possible coral mounds
7. Ground-truthing using ROV or tethered video platform. ROV can be navigated on topographical maps obtained in 5
8. Optional biological sampling of the coral ecosystem and environmental factors

Post cruise
9. Analyses of multibeam backscatter and production of maps.

Acknowledgements

References

Anonymous (1995) Seatech International Ltd. Aberdeen, Scotland 1995. RoxMap, RoxAnn Information Display. Manual for RoxMap Scientific Version 1.00

Bodholt H, Nes H, Solli H (1989) A new echo-sounder system. Proc UK Inst Acoust 11: 123-30

Bunchuk AV, Zhitkovskii YY (1980) Sound scattering by the ocean bottom in shallow-water regions. Sov Phys Acoust 26: 363-370

Buhl-Mortensen L, Mortensen PB (2004) Crustaceans associated with the deep-water gorgonian corals *Paragorgia arborea* (L., 1758) and *Primnoa resedaeformis* (Gunnerus 1763)**.** J Nat Hist 38: 1233-1247

Buhl-Mortensen L, Mortensen PB (2005) Distribution and diversity of species associated with deep-sea gorgonian corals off Atlantic Canada. In: Freiwald A, Roberts JM (eds) Cold-water Corals and Ecosystems. Springer, Berlin Heidelberg, pp 849-879

Burdon-Jones C, Tambs-Lyche H (1960) Observations on the fauna of the North Brattholmen stone-coral reef near Bergen. Årb Univ Bergen, Mat-Naturvitensk Ser 1960: 1-24

Burns DR, Queen CB, Sisk H, Mullarkey W, Chivers RC (1989) Rapid and convenient acoustic seabed discrimination. Proc UK Inst Acoust 11: 169-178

Costello MJ, McCrea M, Freiwald A, Lundälv T, Jonsson L, Bett BJ, van Weering T, de Haas H, Roberts JM, Allen D (2005) Role of cold-water *Lophelia pertusa* coral reefs as fish habitat in the NE Atlantic. In: Freiwald A, Roberts JM (eds) Cold-water Corals and Ecosystems. Springer, Berlin Heidelberg, pp 771-805

Dons C (1944) Norges korallrev. K Norske Vidensk Selsk Forh 16: 37-82

Dorschel B, Hebbeln D, Rüggeberg A, Dullo W-Chr (in press) Carbonate budget of a deep-water coral mound: Propeller Mound, Porcupine Seabight. Int J Earth Sci

Duineveld G, Lavaleye M, Berghuis E (2004) Particle flux and food supply to a seamount cold-water coral community (Galicia Bank, NW Spain). Mar Ecol Prog Ser 277: 13-23

Foote KG, Knudsen HP, Korneliussen RJ, Nordbø PE, Røang K (1991) Postprocessing system for echo sounder data. J Acoust Soc Amer 90: 37-47

Fosså JH, Alvsvåg J (2003) Kartlegging og overvåkning av korallrev. In: Asplin L, Dahl E (eds) Havets Miljø 2003. Fisken Havet Spec Issue 2: 62-67

Fosså JH, Furevik D, Mortensen PB (1997) Methods for detecting and mapping of *Lophelia* coral banks: preliminary results. ICES Benthos Ecology Working Group, Gdynia, Poland, 23 - 26 Apr. 1997, 17 pp

Fosså JH, Mortensen PB (1998) Artsmangfoldet på *Lophelia*-korallrev og metoder for kartlegging og overvåkning. Fisken Havet 17: 95 pp

Fosså JH, Mortensen PB, Furevik D (2000) *Lophelia* korallrev langs norskekysten. Forekomst og tilstand. Fisken Havet 2: 94 pp

Fosså JH, Mortensen PB, Furevik D (2002) The deep-water coral *Lophelia pertusa* in Norwegian waters; distribution and fishery impacts. Hydrobiologia 471: 1-12

Freiwald, A (1998) Geobiology of *Lophelia pertusa* (Scleractinia) reefs in the North Atlantic. Habilitation thesis, Univ Bremen

Freiwald A (2002) Reef-forming cold-water corals. In: Wefer G, Billett D, Hebbeln D, Jørgensen BB, Schlüter M, van Weering T (eds.) Ocean Margin Systems. Springer, Berlin, pp 365-385

Freiwald A, Hühnerbach V, Lindberg B, Wilson JB, Campbell J (2002) The Sula reef complex, Norwegian shelf. Facies 47: 179-200

Freiwald A, Fosså JH, Grehan A, Koslow T, Roberts JM (2004) Cold-water coral reefs. UNEP-WCMC, Cambridge, UK, Biodivers Ser 22: 84 pp

Heath R (2003) Cabled seafloor observatories - potential and challenges. Geophys Res Abstr 5: 04645

Hovland M, Mortensen PB, Thomsen E, Brattegard T (1997) Substratum-related ahermatypic corals on the Norwegian continental shelf. Proc 8th Int Coral Reef Symp, Panama 1996, 2: 1203-1206

Hovland M, Mortensen PB (1999) Norske korallrev og prosesser i havbunnen. John Grieg, Bergen

Husebø Å, Nøttestad L, Fosså JH, Furevik DM, Jørgensen SB (2002) Distribution and abundance of fish in deep-sea coral habitats. Hydrobiologia 471: 91-99

Jensen A, Frederiksen R (1992) The fauna associated with the bank-forming deepwater coral *Lophelia pertusa* (Scleractinia) on the Faroe shelf. Sarsia 77: 53-69

Kenny AJ, Andrulewich H, Bokuniewicz, Boyd SE, Breslin J, Brown C, Cato I, Costelloe J, Desprez M, Dijkshoorn C, Fader G, Courtney R, Freeman S, de Groot B, Galtier L, Helmig S, Hillewaert H, Krause JC, Lauwaert B, Leuchs H, Markwell G, Mastowske M, Murray AJ, Nielsen PE, Ottesen D, Pearson R, Rendas MJ, Rogers S, Schuttenhelm R, Stolk A, Side J, Simpson T, Uscinowicz S, Zeiler M (2000) An overview of seabed mapping technologies in the context of marine habitat classification. ICES ASC September 2000: Theme session on classification and mapping of marine habitats

Knudsen HP (1990) The Bergen Echo Integrator: an introduction. J Cons Int Explor Mer 47: 167-174

Kongsberg Simrad (2001) Operator manual for Triton. Horten, Norway, 116 pp

Korneliussen R (1993) Advances in Bergen Echo Integrator. ICES C.M.1993/B: 28 (mimeo)

Korneliussen RJ, Ona E (2002) An operational system for processing and visualising multi-frequency acoustic data. ICES J Mar Sci 59: 293-313

Laberg JS, Vorren TO (2000) The Trænadjupet Slide, offshore Norway - morphology, evacuation and triggering mechanisms. Mar Geol 171: 95-114

Lindberg B, Berndt C, Mienert J (in press) The Fugløy Reefs on the Norwegian-Barents continental margin: cold-water corals at 70°N, their acoustic signature, geologic, geomorphologic and oceanographic setting. Int J Earth Sci

Lindberg B, Mienert J (2005). Sedimentological and geochemical environment of the Fugløy Reefs off northern Norway. In: Freiwald A, Roberts JM (eds) Cold-water Corals and Ecosystems. Springer, Berlin Heidelberg, pp 633-650

Lurton X (2002) An introduction to underwater acoustics; principles and applications. Springer, London

Lyall G (2000) Minimum standards for submarine cable route surveys. ICPC Plenary, May 2000, Copenhagen, pp 1-7

Masson DG, Bett BJ, Billett DSM, Jacobs CL, Wheeler AJ, Wynn RB (2003) The origin of deep-water, coral-topped mounds in the northern Rockall Trough, Northeast Atlantic. Mar Geol 194: 159-180

Momma H (2000) Deep ocean technology at JAMSTEC. Mar Technol Soc J 33: 49-64

Mortensen PB (2000) *Lophelia pertusa* (Scleractinia) in Norwegian waters. Distribution, growth, and associated fauna. PhD thesis, Dept Fish Marine Biol, Univ Bergen, Norway

Mortensen PB (2001) Aquarium observations on the deep-water coral *Lophelia pertusa* (L., 1758) (Scleractinia) and selected associated invertebrates. Ophelia 54: 83-104

Mortensen PB, Rapp HT (1998) Oxygen- and carbon isotope ratios related to growth line patterns in skeletons of *Lophelia pertusa* (L) (Anthozoa: Scleractinia): Implications for determination of linear extension rates. Sarsia 83: 433-446

Mortensen PB, Hovland MT, Fosså JH, Furevik DM (2001) Distribution, abundance and size of *Lophelia pertusa* coral reefs in mid-Norway in relation to seabed characteristics. J Mar Biol Ass UK 81: 581-597

Mortensen PB, Hovland M, Brattegard T, Farestveit R (1995) Deep water bioherms of the scleractinian coral *Lophelia pertusa* (L.) at 64°N on the Norwegian shelf: structure and associated megafauna. Sarsia 80: 145-158

Mortensen PB, Roberts JM, Sundt RC (2000) Video-assisted grabbing: a minimally destructive method of sampling azooxanthellate coral banks. J Mar Biol Ass UK 80: 365-366

Norwegian Directorate of Fisheries (2004) Rapport fra arbeidsgruppen for vern av koraller (Report from the working group for the protection of coral reefs). Norw Directorate Fish, Bergen, 54 pp

Novarini JC, Caruther JW (1998) A simplified approach to backscattering from a rough seafloor with sediment inhomogeneities. J Ocean Engin 23: 157-166

Ottesen D, Dowdeswell JA, Rise L, Rokoengen K, Henriksen S (2002) Large-scale morphological evidence for past ice-stream flow on the mid-Norwegian continental margin. In: Dowdeswell JA, Ocofaigh C (eds) Glacier-influenced sedimentation in high-latitude continental margins. Geol Soc London Spec Publ 203, pp 245-258

Parker WR, Doyle K, Parker ER, Kershaw PJ, Malcolm SJ, Lomas P (2003) Benthic interface studies with landers. Consideration of lander/interface interactions and their design implications. J Exper Mar Biol Ecol 285: 179-190

Petitt, RA Jr, Harris DW, Wooding B, Bailey J, Jolly J, Hobart E, Chave AD, Duennebier F, Butler R, Bowen A, Yoerger D (2002) The Hawaii-2 Observatory. J Ocean Engin 27: 245-253

Roberts JM, Gage JD, ACES party (2003) Assessing biodiversity associated with cold-water coral reefs: pleasures and pitfalls. Erlanger Geol Abh Sonderbd 4: 73

Roberts JM, Peppe OC, Dodds LA, Mercer DJ, Thomson WT, Gage JD, Meldrum DT (2005) Monitoring environmental variability around cold-water coral reefs: the use of a benthic photolander and the potential of seafloor observatories. In: Freiwald A, Roberts JM (eds) Cold-water Corals and Ecosystems. Springer, Berlin Heidelberg, pp 483-502

Rokoengen K, Rise L, Bryn P, Frengstad B, Gustavsen B, Nygaard E, Sættem J (1995) Upper Cenozoic stratigraphy on the Mid-Norwegian continental shelf. Norsk Geol Tidsskr 75: 88-104

Rüggeberg A, Dorschel B, Dullo W-Chr (in press) The record of past oceans locked in a carbonate mound in the Porcupine Basin: benthic forams and grain-size clues. Int J Earth Sci

Schwinghamer P, Guigné JY, Siu WC (1996) Quantifying the impact of trawling on benthic habitat structure using high-resolution acoustics and chaos theory. Can J Fish Aquat Sci 53: 288-296

Strømgren T (1971) Vertical and Horizontal Distribution of *Lophelia pertusa* (Linné) in Trondheimsfjorden on the West Coast of Norway. K Norske Vidensk Selsk Skr 6: 1-19

Svellingen IK, Korneliussen RJ, Furevik D (2002) Acoustic discrimination of deep-sea coral reefs from the sea-bed. Poster. 6th ICES Symp Acoust Fish Aqua Ecol, Montpellier, France, June 2002

Wilson JB (1979a) The distribution of the coral *Lophelia pertusa* (L.) (*L. prolifera* (Pallas)) in the north-east Atlantic. J Mar Biol Ass UK 59: 149-164

Wilson JB (1979b) 'Patch' development of the deep-water coral *Lophelia pertusa* (L.) on Rockall Bank. J Mar Biol Ass UK 59:165-177

Deep-water coral mounds on the Porcupine Bank, Irish Margin: preliminary results from the Polarstern ARK-XIX/3a ROV cruise

Andrew J. Wheeler[1], Tim Beck[2], Jörn Thiede[3], Michael Klages[3], Anthony Grehan[4], F. Xavier Monteys[5] and Polarstern ARK XIX/3a Shipboard Party

[1] Department of Geology, Environmental Research Institute, University College Cork, Ireland
  (a.wheeler@ucc.ie)
[2] Institute of Paleontology, Erlangen University, Loewenichstr. 28, D-91054 Erlangen, Germany
[3] Alfred Wegener Institute for Polar and Marine Research, Am Handelshafen 12, D-27570 Bremerhaven, Germany
[4] Martin Ryan Marine Science Institute, National University of Ireland, Galway, Ireland
[5] Geological Survey of Ireland, Beggars Bush, Haddington Road, Dublin 4, Ireland

Abstract. An overview of preliminary results from a series of recent Remotely Operated Vehicle (ROV) dives on the deep-water coral provinces of the Porcupine Bank, Irish continental margin, NE Atlantic is presented. The Porcupine Bank exhibits numerous giant carbonate mounds (up to 100s of metres in height) that occur predominantly, although not exclusively, on topographic ridges. The results revealed that, although these ridges have a tectonic origin, contemporaneous activity is typified by erosion due to strong hydrodynamic controls. The carbonate mounds are colonized by a variety of suspension feeders and associated fauna including framework-building corals (e.g., *Lophelia pertusa* and *Madrepora oculata*) although dense coral reef-like fauna coverage is not evident at present. The ecology of the carbonate mounds varied widely. Sessile megafauna, such as sponges, gorgonians and framework-building corals (e.g., *Lophelia pertusa*), were abundant on some of the carbonate mounds. Other mounds were relatively barren and appeared to be undergoing a natural senescence, with a much lower biomass of megafauna than is typical of shallow-water coral reefs. Some mounds had been damaged by demersal trawls, with smashed coral and lost gear common, whereas others appeared relatively pristine with occasional evidence of man-made litter.

Keywords. Carbonate mounds, cold-water coral, Irish margin, ROV, biodiversity, trawling impact, hydrodynamics

Introduction

Deep-water corals are widespread along the European continental margin where they are often associated with carbonate mounds. These elevated features are composed of carbonate mud, the skeletal remains of framework-forming corals (particularly *Lophelia pertusa* and *Madrepora oculata*) and material derived from associated fauna together with allochthonous sediment. Carbonate mound growth benefits from positive feedback whereby the corals grow preferentially in elevated positions where they can take advantage of faster flowing waters delivering organic particulate food supply, and avoid the higher concentration of inorganic sediment closer to the benthic boundary layer (Frederiksen et al. 1992; Freiwald 2002). The coral framework traps sediment and also, upon death, provides suitable substrata for renewed growth. This increases mound elevation which enhances environmental conditions and thus stimulates further coral colonisation and growth (see Genin et al. 1986; Freiwald et al. 1999).

Along the Irish margin, these carbonate mounds are massive features being 10s to 100s of metres high and often several kilometres across the base. Seismic investigations suggest that this may in part be due to the longevity of the carbonate mounds in this region with examples on the Porcupine Bank initiated on common erosion surfaces tentatively dated as Late-Early Pliocene (Kenyon et al. 2003; van Weering et al. 2003a, b). Previous studies (Kenyon et al. 1998; de Haas et al. 2002; Akhmetzhanov et al. 2003; Kenyon et al. 2003; van Weering et al. 2003a, b) also note that the Porcupine Bank carbonate mounds (Pelagia Mounds) are relatively isolated, discrete mounds existing in a strong current regime with intermediate nepheloid layers (Dickson and McCave 1986; Kenyon et al. 2003) providing an abundant food supply.

The influence of hydrodynamic processes peculiar to banks and seamounts seem to have an important role in carbonate mound growth. White et al. (2005) and White (in press) point out that circulation around banks along the Irish margin causes the accumulation of nutrient rich waters on the top of banks. This leads to high surface productivity values that in turn provide important enriched food sources to carbonate mound ecosystems. Furthermore, the presence of the banks causes an acceleration of contourite currents as they flow along the margin. Bank topography may also enhance internal wave dynamics (Frederiksen et al. 1992) and a strong (if not dominant) tidal current signal is evident. As these carbonate mounds exist at the boundary between two water masses, rigorous hydrodynamics may allow corals to take advantage of characteristics of both water masses.

The Porcupine Bank (Fig. 1A for location of study area) is an upstanding block between the Rockall Trough (to the west) and Porcupine Seabight (to the east) formed during Mesozoic rifting associated with the opening of the proto-Atlantic (Naylor and Mounteney 1975). The northeastern bank is connected to the continental landmass by onlapping western Irish continental shelf sediments. The bank's north-western flank overlies the Macdára Basin and basin boundary faults. Lower slopes (>1000 m water depth) on the margin are typified by submarine canyon systems
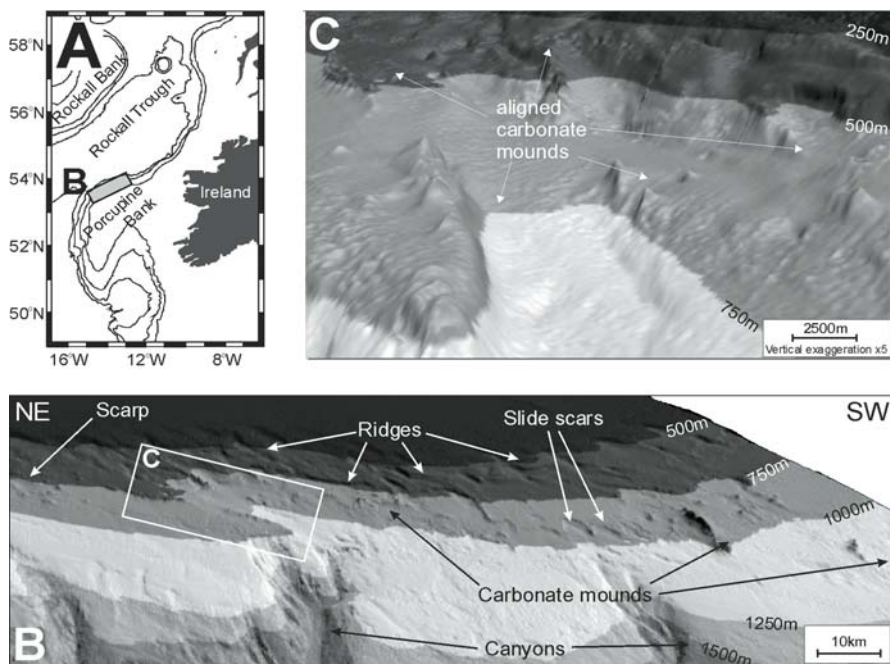
Fig. 1 Morphological setting of features discussed in the text. **A** Location map showing the Porcupine Bank and study area on the Irish continental margin. **B** Digital terrain model of the bank derived from multibeam echosounder data showing ridges, carbonate mounds, scarp and slide scars upslope of submarine canyons. **C** Detail showing carbonate mounds aligned along the crest of topographic ridges

and feeder systems (Fig. 1B). Carbonate mounds exist between 500-1200 m water depth. These occur predominantly on bank sub-parallel topographic ridges (Figs. 1B-C) that overlie boundary faults (Croker et al. 2003) and are interpreted as fault scarps (de Haas et al. 2002). Croker et al. (2003) suggested that a spatial relationship between boundary faults, fault scarps and carbonate mound occurrence might imply a cold seep origin to these mounds due to thermogenic hydrocarbon seepage (*sensu* Hovland et al. 1994) from underlying hydrocarbon reservoirs in the underlying Macdára Basin. Headwall scars due to submarine slides are also evident (Fig. 1B). Upslope areas (<500 m water depth) are dominated by iceberg ploughmarks (de Haas et al. 2002).

This paper presents *preliminary* results from the Remotely Operated Vehicle VICTOR6000 (ROV) deployments from the RV Polarstern in June 2003 that were performed to assess the following research questions.

- To what extent are carbonate mound growth processes influenced by hydrodynamic processes?
- What is the extent of biotic heterogeneity between carbonate mounds?

- Do we find evidence of deep-water trawling activity damaging the coral ecosystem?
- Are the ridges on which carbonate mounds are located a focus for thermogenic hydrocarbon seepage?

Results

Influence of hydrodynamic processes

Abundant evidence is found of a strong benthic current regime in the study area. The seabed between carbonate mounds is typified by sands and exposed dropstones (deposited by melting icebergs) implying strong currents (Fig. 2A). These dropstones provide suitable attachments for sessile organisms including sponges, stylasterids, corals, gorgonians, antipatharians, anemones and barnacles (see Fig. 2A). The strong hydrodynamic regime and the exposed nature of carbonate mounds result in
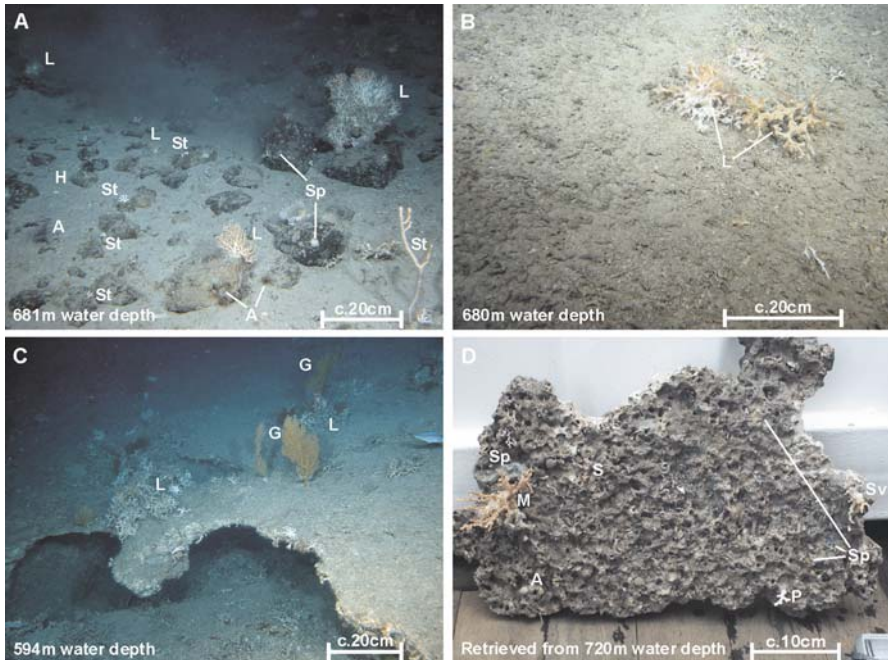
Fig. 2 Visible evidence of a strong hydrodynamic regime on the Porcupine Bank. **A** Typical seabed with sand sediment and exposed dropstones supporting communities of sponges (Sp), stylasterids (St), *Lophelia pertusa* (L) and anemones (A). **B** A typical carbonate mound surface showing exposed dead coral framework providing a firm substrate for attachment of *Lophelia pertusa* (L). **C** Seabed erosion exposing lithified sediments and providing a hardground for colonisation by *Lophelia pertusa* (L), other scleractinians and gorgonians (G). **D** Retrieved hardground showing extensive borings and colonisation by scleractinians including *Madrepora oculata* (M) and *Stenocyathus vermiformis* (Sv), stylasterids (*Pliobothrus* sp.) (P), serpulids (S), sponges (Sp) and anemones (A)

very little sedimentary cover on the carbonate mounds themselves with sub-fossil coral frameworks often exposed. Figure 2B shows a typical view with sporadic colonisation of the carbonate mounds by cold-water corals by attachment directly onto dead skeletal material.

In many areas, intense current activity also resulted in physical erosion of the seabed and the carbonate mounds exposing lithified sediment which act as hard substrates (Fig. 2C). These provide firm substrata for colonisation and support a diverse fauna (e.g., *Lophelia pertusa*, *Madrepora oculata*, stylasterids, gorgonians, byssate bivalves (*Asperarca nodulosa* and *Chlamys sulcata*), serpulids and clionid sponges; Figs. 2C-D).

Examination of a 21 km ridge (680 m water depth) revealed carbonate mounds on top of the ridge provided its topographic expression although between mound areas were typified by a vertical escarpment (Fig. 1B). The exposure of soft sediment between hardgrounds exposed on the escarpment (Fig. 3A) suggests that the structure post-dates the last tectonic activity probably occurring as extensional fault reactivation in the Tertiary (e.g., Shannon et al. 2001) and was probably formed by seabed erosion. The alternation of hard and softer sediment may represent Quaternary climatic forcing of sedimentation patterns on the banks with glacial periods typified by sluggish current and high sediment rates and interglacial periods typified by fast currents causing seabed erosion. Preferential cementation of hardgrounds may be due to increased carbonate contents and biological productivity. Some hardgrounds are covered in a thin layer of black metallic oxides suggesting exposure at the seabed.

Biotic heterogeneity between carbonate mounds

A limited number of carbonate mounds in the study area were studied on a previous survey using the VICTOR6000 robotic submersible (CARACOLE cruise; Olu-Le Roy et al. 2002). The survey presented here purposely covered a greater variety of mounds in order to assess whether a typical faunal assemblage can be defined as truly representative of all the mounds on the Bank. Some observations are in accordance with CARACOLE findings, for example sessile megafauna covered only an average of about >5 % the coral facies. Most ROV observations were made a few metres from the seabed, to cover a wide area quickly, but macro- and microfauna (evidence based on box-coring) were present in abundance on coral facies wherever close-up observations were made.

Preliminary observations (Fig. 4) suggest that the dominant sessile megafauna documented in the study area included corals (*Lophelia pertusa*, *Madrepora oculata*, *Desmophyllum cristagalli*, antipatharians, gorgonians (*Acanthogorgia* sp.) and others), and sponges. Mobile megafauna included conspicuous numbers of echinoderms, fish and crabs. The important habitat complexity provided even by sparse coral coverage showed an enhancement of faunal diversity. While some of the mounds surveyed had relatively low coral cover, there was clear visual evidence that the density and diversity of megafauna was greater on the mounds than on the surrounding seabed (Figs. 4A-C, E; see Olu-Le Roy et al. 2002; Foubert et al. 2005).
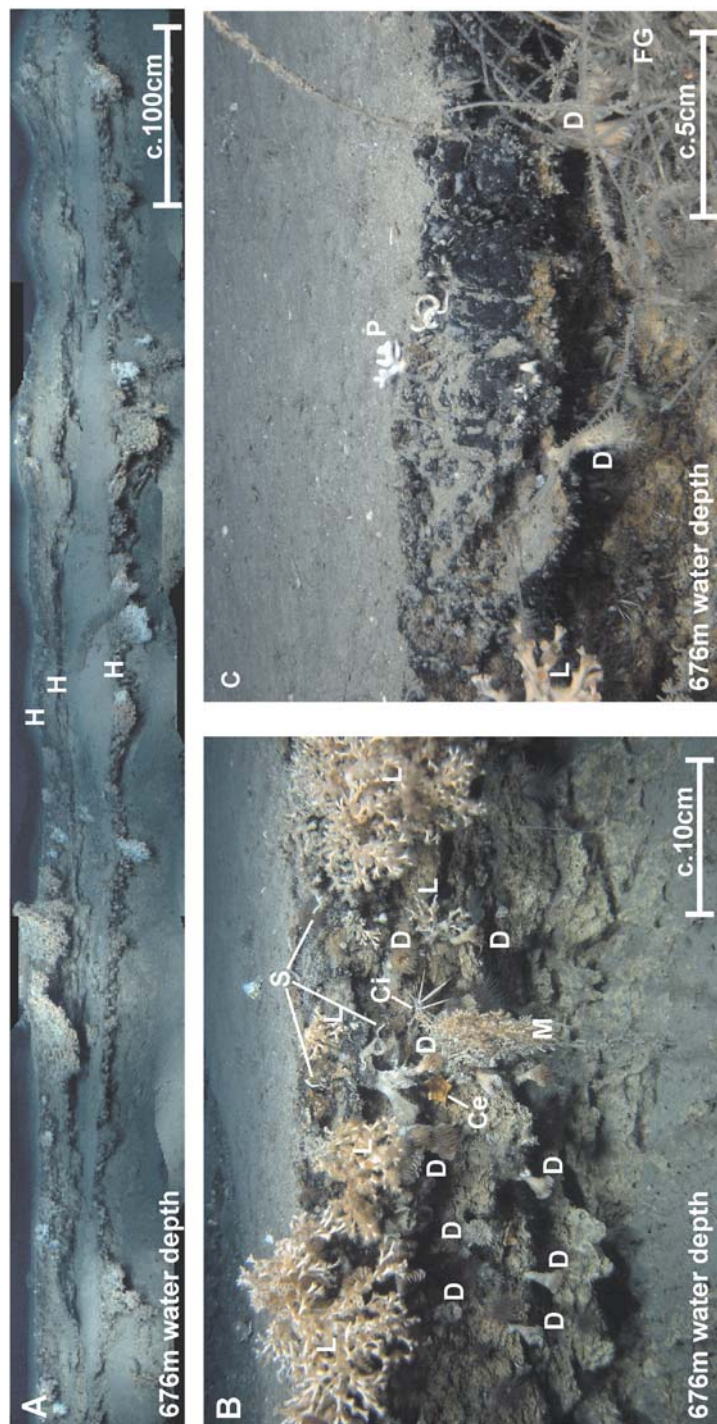
Fig. 3 Eroded seabed scarp colonised by cold-water coral: **A** Photo montage showing the face of the scarp. Several prominent resistant layers (?palaeo-hardgrounds) (H) are evident to which sessile organisms are attached. These prominent layers are separated by softer sediment. **B** Detail of colonisation on the upper hardground showing *Lophelia pertusa* (L), *Desmophyllum cristagalli* (D), *Madrepora oculata* (M), *Cidaris cidaris* (Ci), starfish (*Ceramaster* sp.) (Ce) and serpulids (S). **C** Closer detail of the hardground showing a thin black metallic oxide coating suggesting persistent exposure at the seabed. Some lost fishing gear (FG), *Lophelia pertusa* (L), *Desmophyllum cristagalli* (D) and *Pliobothrus* sp. (P) are also present
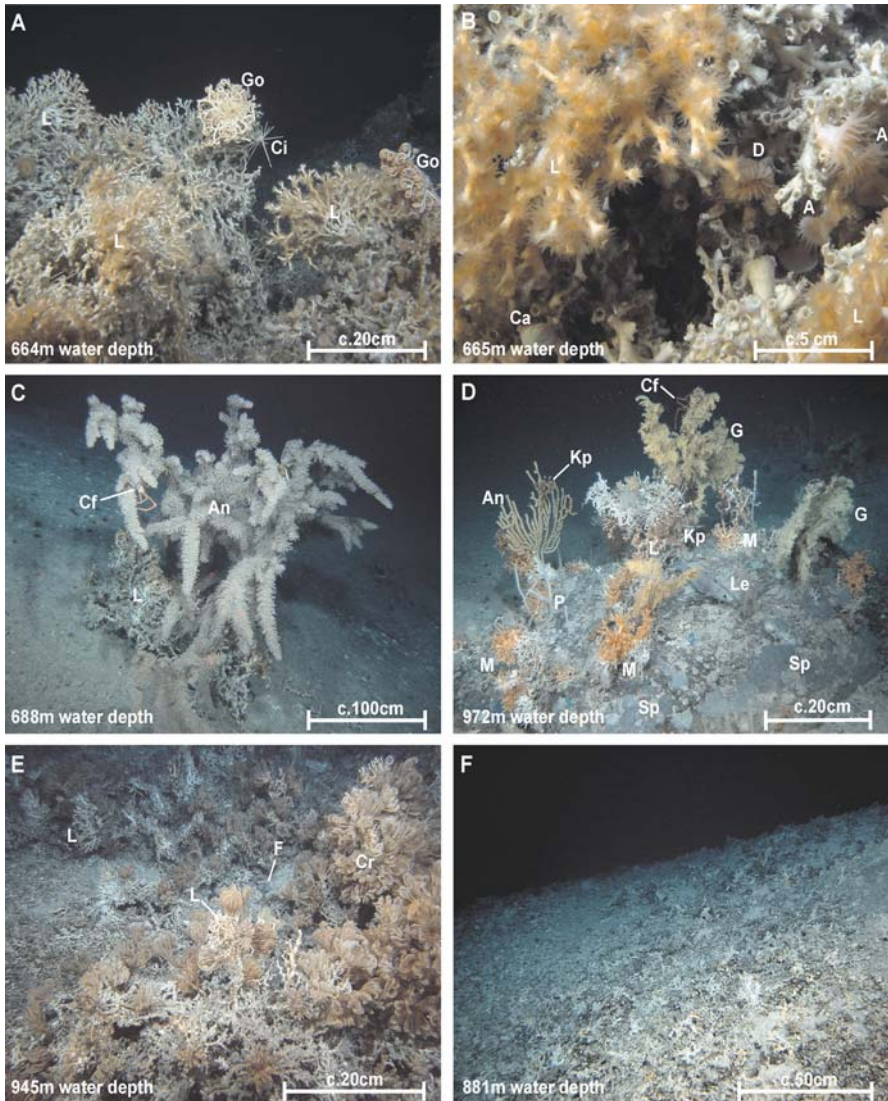
Fig. 4 Selected images showing the variety of organisms and their association encountered on the northwest Porcupine Bank. **A** *Lophelia pertusa* colonies (L) with *Gorgonocephalus* sp. (Go) and *Cidaris cidaris* (Ci). **B** Close up of *Lophelia pertusa* colonies (L) with polyps extended. An anemone (A), a gastropod (*Calliostoma* sp.) (Ca) and *Desmopyllum cristagalli* (solitary coral) (D) are also present. **C** An antipatharian (An) with spider crabs (*Chirostylus formosus*) (Cf) attached to a *Lophelia pertusa* colony (L). **D** Heavily colonised dropstone with several sponge-species (Sp), *Lophelia pertusa* (L), *Madrepora oculata* (M), antipatharians (An), sylasterids (*Pliobothrus* sp.) (P), crinoids (*Koehlerometra porrecta*)(Kp) and spider crabs (*Chirostylus formosus*) (Cf) attached to gorgonians (*Acanthogorgia* sp. and others) (G) as well as a fish (*Lepidion eques*) (Le) **E** Crinoids (Cr) attached to *Lophelia pertusa* colonies (L) with a fish (F) **F** Coral rubble field as a result of demersal trawling activity

Colonised dropstones represent an important habitat on the lower mound flanks and in off-mound areas (Fig. 4D), where they form oasis-like habitats providing hard substrate for many sessile organisms (see Oschmann 1990).

Certain fauna are found on all mounds (including most scleractinian coral species, e.g., *Lophelia pertusa*, *Madrepora oculata* and *Desmophyllum cristagalli*) whereas others seem only to be specific to or dominant on individual mounds (e.g., stylasterids with *Stylaster* sp., crinoids, gorgonocephalids; Figs. 4A, E).

Evidence of deep-water trawling activity

Destruction of the coral habitat by demersal trawling was noted (Fig. 4F; see also Grehan et al. 2003), clearly an even greater concern if certain mounds do harbour specific faunal assemblages. Trawled mounds are characterised by extensive coral rubble fields suggesting that coral cover may have been formerly more extensive here than on the other mounds surveyed in the area. This also suggests that demersal trawling activity (Hall-Spencer et al. 2002) may be targeting mounds with the most prolific coral growth (therefore of the highest conservation value) due to related high fish populations.

Thermogenic hydrocarbon seepage

Despite 88 hours of dedicated dive time on carbonate mounds, no gas bubbles, authogenic carbonate crusts, bacterial mats, chemosynthetic fauna (e.g., tube worms, pogonophorans or distinct molluscs species), pockmarks or any other evidence of cold seepage were found (see Dando and Hovland 1992; Sibuet and Olu 1998).

Preliminary conclusions

Fast-flowing currents along the Porcupine Bank at depths where cold-water corals and resultant carbonate mounds occur induces seabed erosion thereby providing hard substrata, in the form of exposed dropstones and hardgrounds, suitable for the colonisation by sessile megafauna. Paradoxically, at present seabed erosion seems to be the dominant process stimulating renewed colonisation of carbonate mounds by framework building corals and therefore mound growth. This mechanism may also explain the stratigraphy exposed on escarpments with climate controlled alternations in sediment and hydrodynamic regimes producing a repetition of soft sediment overlain by hardgrounds (see Fig. 3A).

Surveys of a variety of mounds showed that although megafaunal species cover was reduced in comparison with some other mound provinces (e.g., the Galway Mound; Foubert et al. 2005), biodiversity remained high with mounds offering an important habitat to corals, gorgonians, antipatharians, sponges, crustacea and fish. Demersal trawling has produced drastic alterations to the ecology of impacted carbonate mounds.

Previous studies have identified a number of ridges and scarps on the Porcupine Bank where carbonate mounds were preferentially located (de Haas et al. 2002). The coincidence of boundary faults overlying hydrocarbon reserves led to speculation

that the carbonate mounds may be associated with cold seeps (Croker et al. 2003). After 88 hours of ROV observation where this was suspected, we conclude that as no evidence of hydrocarbon seepage was found, thermogenic hydrocarbon seepage does not account for mound growth. Furthermore, the strong influence of fast currents on the benthic environment, coupled with probable high surface productivity, implies that hydrodynamic influence on food supply is probably a major factor contributing to coral growth. However, it is also noted that present conditions are not optimal for the prolific growth of cold-water coral which may be due to high present day current speeds as suggested by Kenyon et al. (2003).

Acknowledgements

References

Akhmetzhanov AM, Kenyon NH, Ivanov MK, Wheeler A, Shashkin PV, van Weering TCE (2003) Giant carbonate mounds and current swept seafloors on the slopes of the southern Rockall Trough. In: Mienert J, Weaver P (eds) European Margin Sediment Dynamics: Side-scan Sonar and Seismic Images. Springer, Berlin Heidelberg, pp 203-210

Croker PF, de Haas H, Huvenne VAI, Wheeler AJ (2003) The 2002 TOBI sidescan survey of carbonate mounds in the Rockall and Porcupine basins. 46th Annu Irish Geol Res Meet, Ulster Mus, Belfast, 21st-23rd February 2003

Dando PR, Hovland M (1992) Environmental effects of submarine seeping natural gas. Cont Shelf Res 12: 1197-1207

Dickson RR, McCave IN (1986) Nepheloid layers on the continental slope west of Porcupine Bank. Deep-Sea Res 33: 791-818

Foubert A, Beck T, Wheeler AJ, Opderbecke J, Grehan A, Klages M, Thiede J, Henriet J-P, the Polarstern ARK-XIX/3a Shipboard Party (2005) New view of the Belgica Mounds, Porcupine Seabight, NE Atlantic: Preliminary results from the Polarstern ARK-XIX/3a ROV cruise. In: Freiwald A, Roberts JM (eds) Cold-water Corals and Ecosystems. Springer, Berlin Heidelberg, pp 403-415

Frederiksen R, Jensen A, Westerberg H (1992) The distribution of scleractinian coral *Lophelia pertusa* around the Faeroe islands and the relation to internal tidal mixing. Sarsia 77: 157-171

Freiwald A (2002) Reef-forming cold-water corals. In: Wefer G, Billett D, Hebbeln D, Jørgensen BB, Schlüter M, van Weering T (eds) Ocean Margin Systems. Springer, Berlin Heidelberg, pp 365-385

Freiwald A, Wilson JB, Henrich R (1999) Grounding Pleistocene icebergs shape recent deep-water coral reefs. Sediment Geol 125: 1-8

Genin A, Dayton PK, Lonsdale PF, Spiess FN (1986) Corals on seamount peaks provide evidence of current acceleration over deep-sea topography. Nature 322: 59-61

Grehan AJ, Unnithan V, Wheeler AJ, Monteys FX, Beck T, Wilson M, Guinan J, Hall-Spencer JH, Foubert A, Klages M, Thiede J (2003) Evidence of major fisheries impact on cold-water corals off the Porcupine Bank, west coast of Ireland: implications for offshore coral conservation within the European Union. Erlanger Geol Abh Sonderbd 4: 42

De Haas H, Huvenne V, Wheeler A, Unnithan V, shipboard scientific crew (2002) M2002 Cruise report (R.V. Pelagia Cruise 64PE197): A TOBI Side Scan Sonar Survey of Cold Water Coral Carbonate Mounds in the Rockall Trough and Porcupine Sea Bight - Texel-Southampton-Galway, 21 June – 14 July 2002. R Netherl Sea Res, Texel, The Netherlands, 2002

Hall-Spencer J, Allain V, Fosså JH (2002) Trawling damage to Northeast Atlantic ancient coral reefs. Proc R Soc London B 269: 507-511

Hovland M, Croker PF, Martin M (1994) Fault associated seabed mounds (carbonate knolls?) off western Ireland and North-west Australia. Mar Petrol Geol 11: 232-246

Kenyon NH, Akhmetzhanov AM, Wheeler AJ, van Weering TCE, de Haas H, Ivanov MK (2003) Giant carbonate mud mounds in the southern Rockall Trough. Mar Geol 195: 5-30

Kenyon NH, Ivanov MK, Akhmetzhanov AM (1998) Cold-water carbonate mounds and sediment transport on the Northeast Atlantic Margin. IOC Tech Ser 52, UNESCO, Paris, pp 178

Naylor D, Mounteney SN (1975) Geology of the North-West European continental shelf. 1. Graham Trotman Dudley Publ, London, 162 pp

Olu-Le Roy K, Caprais J-C, Crassous P, Dejonghe E, Eardley D, Freiwald A, Galeron J, Grehan A, Henriet J-P, Huvenne V, Lorance P, Noel P, Opderbecke J, Pitout C, Sibuet M, Unnithan V, Vacelet J, van Weering T, Wheeler A, Zibrowius H (2002) CARACOLE Cruise Report. 30/07/2001 (Cobh) – 15/08/2001 (Foynes) N/O L'Atalante & ROV VICTOR. 1 and 2. Unpubl Rep, IFREMER, Brest

Oschmann W (1990) Dropstones-rocky mini-islands in high-latitude pelagic soft substrate environments. Senckenb Marit 21: 55-75

Shannon PM, Haughton PDW, Corcoran DV (2001) The petroleum exploration of Ireland's offshore basins. Geol Soc London Spec Publ 188, 473 pp

Sibuet M, Olu K (1998) Biogeography, biodiversity and fluid dependence of deep-sea cold-seep communities at active and passive margins. Deep-Sea Res 45: 517-567

Van Weering TCE, de Haas H, Akhmetzhanov AM, Kenyon NH (2003a) Giant carbonate mounds along the Porcupine and SW Rockall Trough margins. In: Mienert J, Weaver P (eds) European Margin Sediment Dynamics: Side-scan Sonar and Seismic Images. Springer, Berlin Heidelberg, pp 211-216

Van Weering TCE, de Haas H, de Stigter HC, Lykke-Andersen H, Kouvaev I (2003b) Structure and development of giant carbonate mounds at the SW and SE Rockall Trough margins, NE Atlantic Ocean. Mar Geol 198: 67-81

White M (in press) The hydrographic setting for the carbonate mounds of the Porcupine Bank and Seabight. Int J Earth Sci

White M, Mohn C, de Stigter H, Mottram G (2005) Deep-water coral development as a function of hydrodynamics and surface productivity around the submarine banks of the Rockall Trough, NE Atlantic. In: Freiwald A, Roberts JM (eds) Cold-water Corals and Ecosystems. Springer, Berlin-Heidelberg, pp 503-514

New view of the Belgica Mounds, Porcupine Seabight, NE Atlantic: preliminary results from the Polarstern ARK-XIX/3a ROV cruise

Anneleen Foubert[1], Tim Beck[2], Andrew J. Wheeler[3], Jan Opderbecke[4], Anthony Grehan[5], Michael Klages[6], Jörn Thiede[6], Jean-Pierre Henriet[1] and the Polarstern ARK-XIX/3a Shipboard Party

[1] Renard Centre of Marine Geology, Gent University, Krijgslaan 281, S8, B-9000 Gent, Belgium
(anneleen.foubert@UGent.be)
[2] Institute of Paleontology, Erlangen University, Loewenichstr. 28, D-91054 Erlangen, Germany
[3] Department of Geology, Environmental Research Institute, University College Cork, Ireland
[4] IFREMER - Underwater Robotics, Navigation and Vision Department (RNV), Zone Portuaire de Brégaillon, F-83507 La Seyne-sur-mer, France
[5] Martin Ryan Marine Science Institute, National University of Ireland, Galway, Ireland
[6] Alfred Wegener Institute for Polar and Marine Research, Am Handelshafen 12, D-27570 Bremerhaven, Germany

Abstract. The Belgica Mound province is one of three provinces where carbonate mounds are associated with cold-water coral species in Porcupine Seabight, west of Ireland. Building upon extensive existing datasets, the Polarstern ARK XIX/3a cruise, deploying the robotic submersible VICTOR6000 (ROV), was undertaken in June 2003. This paper presents an overview of preliminary results from a reconnaissance video survey over and between several steep-flanked Belgica Mounds (giant mounds) and from a microbathymetric survey over some smaller mounds (Moira Mounds). Visual evidence for a strong hydrodynamic regime in the vicinity of the carbonate mounds is found with the interaction between currents and sedimentation having an important role in mound growth and development. Only some mounds show a high percentage of live coral coverage although there is a clear increase of megafaunal concentrations and species on mounds. One area of the province (the eastern ridge of aligned mounds) revealed very little live coral cover, asymmetrical drift accumulations burying the eastern sides and sediment-clogged dead coral frameworks at the western sides. This is in contrast to other areas (e.g., the western alignment of mounds) that

show abundant live coral cover at present. In nearly all parts of the survey area the impact of fisheries, especially demersal trawling, is noted.

Keywords. Carbonate mounds, cold-water coral, Porcupine Seabight, ROV, microbathymetry

Introduction

Porcupine Seabight, a deep embayment in the Atlantic shelf west of Ireland (Fig. 1A), is one of the locations where cold-water corals, associated with carbonate mounds are recognised along the European continental margin (Henriet et al. 1998, 2003; Wheeler et al. 2000; De Mol et al. 2002; Huvenne et al. 2002). Three well-delineated mound provinces are noted: the Belgica Mounds (Fig. 1B) on the eastern flank (De Mol et al. 2002; Van Rooij et al. 2003), the Hovland Mounds in the north (Hovland et al. 1994; De Mol et al. 2002) and a large number of buried Magellan Mounds further to the northwest (Huvenne et al. 2002, 2003). The mounds have been defined as deep-water coral banks where colonies of dead and living corals
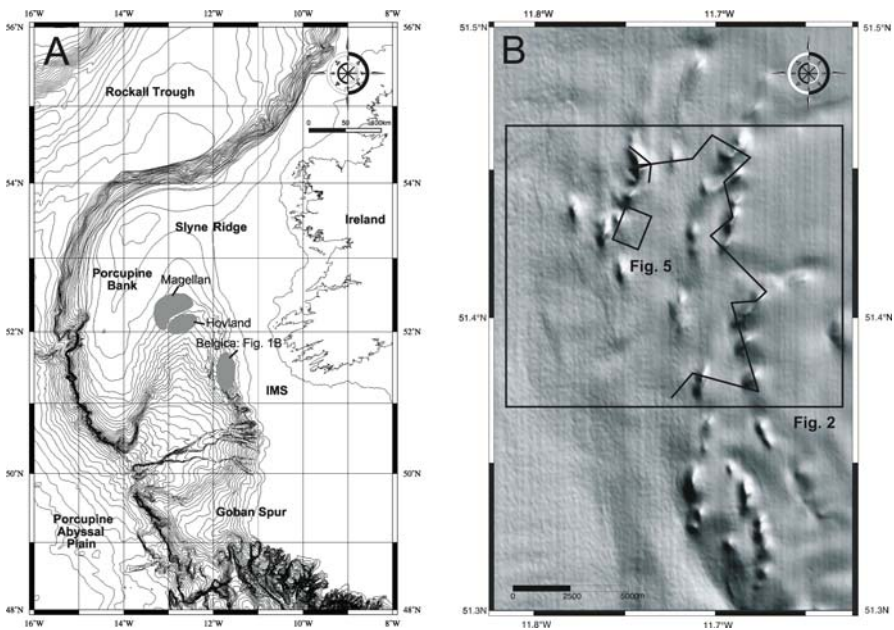
Fig. 1 Localisation of the study areas. **A** Location map showing Porcupine Seabight, his surroundings (Porcupine Bank, Slyne Ridge, Goban Spur and IMS = Irish Mainland Shelf) and the three mound provinces (Magellan, Hovland and Belgica Mound province). Contour interval is 100 m. **B** Shaded relief map of the Belgica Mound province showing morphological features (carbonate mounds, channels). Locations of the ROV track over and in between different Belgica Mounds (black line) and of the microbathymetric dive (black rectangle Fig. 5) are shown

(namely *Lophelia pertusa* and *Madrepora oculata*) interact with sediment drifts in a dynamic environment (De Mol et al. 2002).

The Porcupine Seabight is enclosed by four shallow platforms, consisting of Precambrian and Paleozoic rocks: the Porcupine Bank on the western side, the Slyne Ridge to the north, the Irish continental shelf to the east and the Goban Spur to the south (Fig. 1A). Only a relatively small opening towards the deeper North Atlantic basin is present to the southeast. The underlying structure of the Porcupine Basin is a Middle to Late Jurassic failed rift of the proto-North Atlantic (Naylor and Shannon 1982; Moore and Shannon 1992). The centre of the basin is infilled with 10 km of sediment deposited during the Cenozoic post-rift period. Mound growth probably started during Pliocene times after periods of erosion or non-deposition (De Mol et al. 2002; Van Rooij et al. 2003). Recent basin sedimentation is pelagic to hemi-pelagic, although (probably reworked) foraminiferal sands can be found on the upper slope of the eastern continental margin (Rice et al. 1991).

The present-day hydrographic setting in Porcupine Seabight, which has been extensively reviewed by White (2001), is principally dominated by the Mediterranean Outflow Water (MOW). The water masses of the MOW are characterised by a salinity maximum between 600 m and 1100 m in the Belgica Mound province. Shallow Eastern North Atlantic Water (ENAW) is present down to a depth of about 500 m and North East Atlantic Deep Water (NEADW) below 1500 m (Rice et al. 1991; White 2001). Modelling and current measurements suggest the presence of a general thermohaline northerly-flowing current along the eastern slope of Porcupine Seabight, although the influence of tidal currents sometimes exceeds the influence of the net poleward flow (White 2001). Rice et al. (1990) and De Mol et al. (2002) suggested that reflecting internal waves cause enhanced currents along the eastern margin of the Seabight. The combined effects of a northerly North-Atlantic slope current, superimposed internal waves and tides exert a strong hydrodynamic control on the Belgica Mound province (Huvenne et al. 2002).

Building on extensive datasets already acquired in Porcupine Seabight (e.g., multibeam echosounder and sidescan sonar coverage, box-, piston- and gravity coring, detailed high resolution and industrial seismic surveys) the CARACOLE cruise with the robotic submersible VICTOR6000 (ROV) was undertaken (R/V L'Atalante) in June 2001 (Olu-Le Roy et al. 2002). This cruise gave new insights into the faunal, coral and coral debris distribution as well as mound dynamics and sediment interaction of the area, beyond that could have been achieved using towed video systems. Based on these experiences, a further deployment of the ROV VICTOR6000 was undertaken (RV Polarstern ARKXIX/3a) to further extend our understanding. In this cruise, focus was placed on mound formation processes, mound dynamics and sediment interactions and biodiversity differences between mounds in the Belgica Mound province. Two dives were carried out (Fig. 1B):

-       A reconnaissance video survey over numerous steep-flanked Belgica Mounds.
-       A microbathymetric survey with the multibeam system SIMRAD EM 2000 mounted on the ROV, over the Moira Mounds.

Environmental setting of the Belgica Mounds

The Belgica Mound province is characterised by conical mounds asymmetrically buried along the eastern continental margin in the Porcupine Seabight (De Mol et al. 2002; Van Rooij et al. 2003). Multibeam imagery (Beyer et al. 2003) (Fig. 1B) revealed that this part of the basin is dominated by surface mounds and some buried mounds, aligned in north-south directions at depths of 500-1000 m. These mounds can rise up to 300 m above the seabed and can measure up to a few km across. Some mounds are characterised by depressions at the steep downslope side of the mounds that are probably the result of strong bottom currents around the mounds (Van Rooij et al. 2003).

De Mol et al. (2002) and Van Rooij et al. (2003) attributed the net south-north alignment of the coral banks to the presence of eroded ridges of an acoustically transparent unit of probable Miocene origin. Since corals grow preferential in elevated locations (Frederiksen et al. 1992; Freiwald 2002), the local morphological characteristics made this site attractive for deep-sea coral settlement and growth. In the vicinity of these large coral mounds, small mounds (Moira Mounds) exist (Wheeler et al. 2000; 2005b).

As well as these mound structures, a multitude of channels are also observed in the area. A large, along-slope, north-south to northeast-southwest channel forms the western limit of the Belgica Mound province. Shallow south-west trending down-slope gullies feed into the north-south channel (Van Rooij et al. 2003). Contourite drift systems dominate the sedimentological processes in the Belgica Mound area, shaped by the presence of giant carbonate mounds and channels (Van Rooij et al. 2003). Moreover, high resolution side-scan sonar imagery in inter-mound areas revealed the presence of extensive sand sheets with numerous bedforms (sediment waves, barchan dunes, gravel ridges, seabed striations) indicative of high benthic current strengths and active sediment transport (Wheeler et al. 1998; 2000; Huvenne et al. 2002; Wheeler et al. 2005a, b).

Sedimentary facies distribution and faunal presence

The reconnaissance video survey with the ROV VICTOR6000 over and in between several mounds in the Belgica Mound province visualised different facies reflecting changes in the distribution of coral populations on mounds and mound flanks and characterising the seabed in off-mound regions. On the basis of these video observations, a number of facies characteristic of the study area are derived (Table 1; see also Wheeler et al. 2005b). Each facies is given a colour-code and integrated within a GIS (ArcView 3.2a), resulting in a facies-interpretation map (Fig. 2).

The lack of live coral on the eastern ridge of mounds is obvious. From the Challenger Mound to Poseidon Mound (see also Freiwald and Shipboard Party 2002), the most common coral facies is the presence of sediment clogged dead corals and/or coral rubble (Fig. 3A). This lack of live coral is probably due to the exposed nature of carbonate mounds existing in an excessive hydrodynamic regime.

Table 1 Seabed facies classification used for the ROV Victor6000 dive over the Belgica Mounds (see also Wheeler et al. 2005b)

Facies No	Facies name
1	Dense coral coverage (mostly live)
2	Dense coral coverage (mostly dead)
3	Sediment clogged dead coral framework and/or coral rubble
4	Patchy mostly live corals on rippled seabed
5	Patchy mostly dead corals on rippled seabed
6	Patchy mostly dead corals on unrippled seabed
7	Dropstones (gravel and/or boulders) dominated seabed
8	Dropstones (gravel and/or boulders) - patchy distribution on unrippled seabed
9	Dropstones (gravel and/or boulders) - patchy distribution on rippled seabed
10	Rippled seabed with occasional dropstones
11	Unrippled seabed with occasional dropstones
12	Rock outcrops (?)

Moreover, the exposed dead coral facies seems to be confined to the western side of the mounds whereas the eastern flank of the mounds are characterised by the presence of sandy material. This corresponds with the observations of De Mol et al. (2002) and Van Rooij et al. (2003) on seismic profiles of a well-exposed western side and a buried eastern side of mounds. In several places, the coral rubble is colonised by large anemones (*Phelliactis* sp.) and large alcyonarians (*Anthomastus* sp.) (Fig. 3A). Patches of finer sediment between the dead coral frameworks are frequently inhabited by tube anemones (*Cerianthus* sp.).

Dense coral coverage with a large percentage of live coral species (Figs. 3B-C) was only encountered on Galway Mound and on the little mound (BEL 44) between Galway Mound and Poseidon Mound (see also Freiwald and Shipboard Party 2002). The coral facies distribution pattern of the Galway Mound is similar to the Thérèse Mound (also aligned in this western ridge of mounds), where a transition of dead coral and coral rubble at the base of the mounds gives way to denser live coral coverage progressing up the mound (Olu-Le Roy et al. 2002; Huvenne et al. 2005). The seabed immediately east of Galway Mound is characterised by a patchy distribution of corals on rippled sand (Fig. 3D), where the presence of stylasterids (*Pliobothrus* sp.) growing on the coral framework indicates stronger currents.

A clear increase of megafaunal concentrations and species on mounds with live coral coverage is noted (Figs. 3B-C), especially for the hexactinellid sponge *Aphrocallistes* sp. and the gorgonian *Acanthogorgia* sp. Several species of antipatharians are also represented by many colonies. Spider crabs (*Paromola cuvieri*) frequently occur in and over the coral framework.

The presence of dropstones (gravels and/or boulders) is very common in areas between the mounds and in the channels flanking the mounds. At some locations, the seabed is dominated by dropstones (gravel and boulders) barnacle plates and broken coral fragments (Figs. 4A-B). In this dropstone facies, larger boulders are abundantly covered by barnacles (*Bathylasma* sp.). Beside some serpulids, encrusting sponges and bryozoans, the epifauna of these boulders is very poor. Very

Fig. 2 Facies interpretation map over the Belgica Mounds plotted against bathymetric map. Contour interval is 10 m. Black arrows correspond with the deduced current orientations. The location of the ROV images are shown (stars, e.g. 4A refers to Figure 4A)
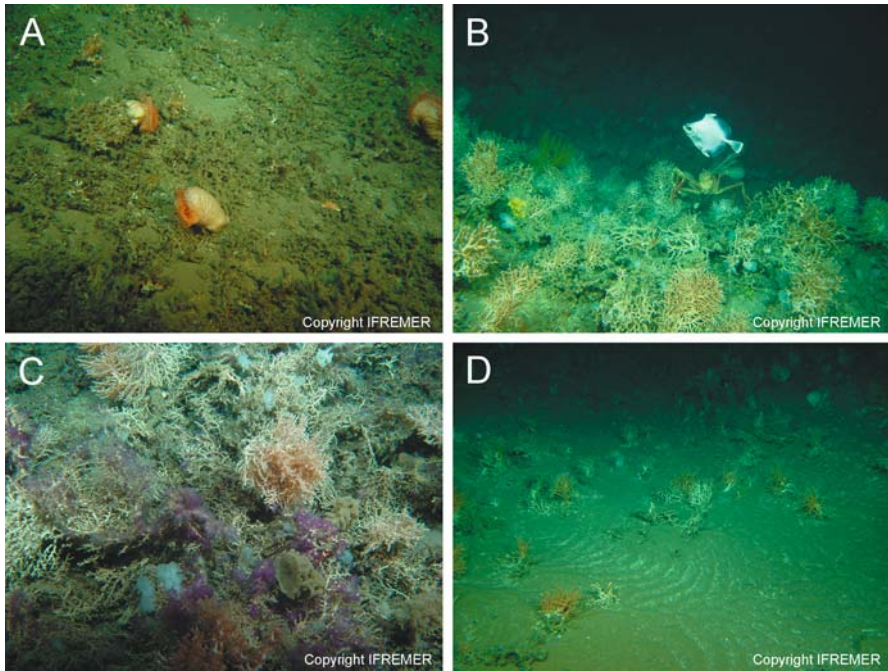
Fig. 3 A Coral rubble providing a firm substrate for the anemones (*Phelliactis* sp.). **B-C** Dense coral coverage on top of Galway Mound with a huge amount of live coral colonies of *Madrepora oculata* and *Lophelia pertusa*. **B** *Lophelia* and *Madrepora* thickets with some gorgonians (*Acanthogorgia* sp.). In between the corals a hexactinellid sponge (*Aphrocallistes* sp.) is very frequent. Common fish in Belgica Mound province (*Neocyttus helgae*) together with a spider crab (*Paromola cuvieri*). **C** Living coral thicket (*Lophelia pertusa* and *Madrepora oculata*) with several *Aphrocallistes* and larger alcyonarians (*Anthothelia* sp.). **D** Patchy distribution of live coral (*Madrepora oculata* and *Lophelia pertusa*) on rippled sand. Several stylasterids (*Pliobothrus* sp.) are growing on the coral framework, indicating high currents

few boulders show prolific growth of larger sessile animals such as gorgonians, antipatharians or corals (*Madrepora oculata* or *Lophelia pertusa*). This may be due to excessive current speeds that are also responsible for the creation of the exposed dropstones. The presence of *Bathylasma* sp. and some stylasterids (*Pliobothrus* sp.) also indicates strong currents.

Other areas are characterised by a patchy distribution of dropstones on an unrippled or rippled seabed (Figs. 4C-D) with scouring in front of boulders and typical a gravel patch behind (Fig. 4D). In this facies, the isolated dropstones are frequently colonised by encrusting sponges, barnacles (*Bathylasma* sp.) and stylasterids (*Pliobothrus* sp.). Rippled sand sheets tend to dominate the remaining seabed (Fig. 4E).

These observations confirm the presence of strong benthic currents in this part of the Belgica Mound province which are at present conditions probably too strong for the settling and growth of cold-water coral in many places. However, a few small

patches of unrippled fine silty sand represent areas of quiescence within this region of strong bottom currents. The silty sand patches are localised on the eastern side of the mounds where sediment drift is accumulating.

The orientation of current marks, scouring marks and sand ripples made it possible to deduce the orientation of the currents in some places (Fig. 2). The overall image of
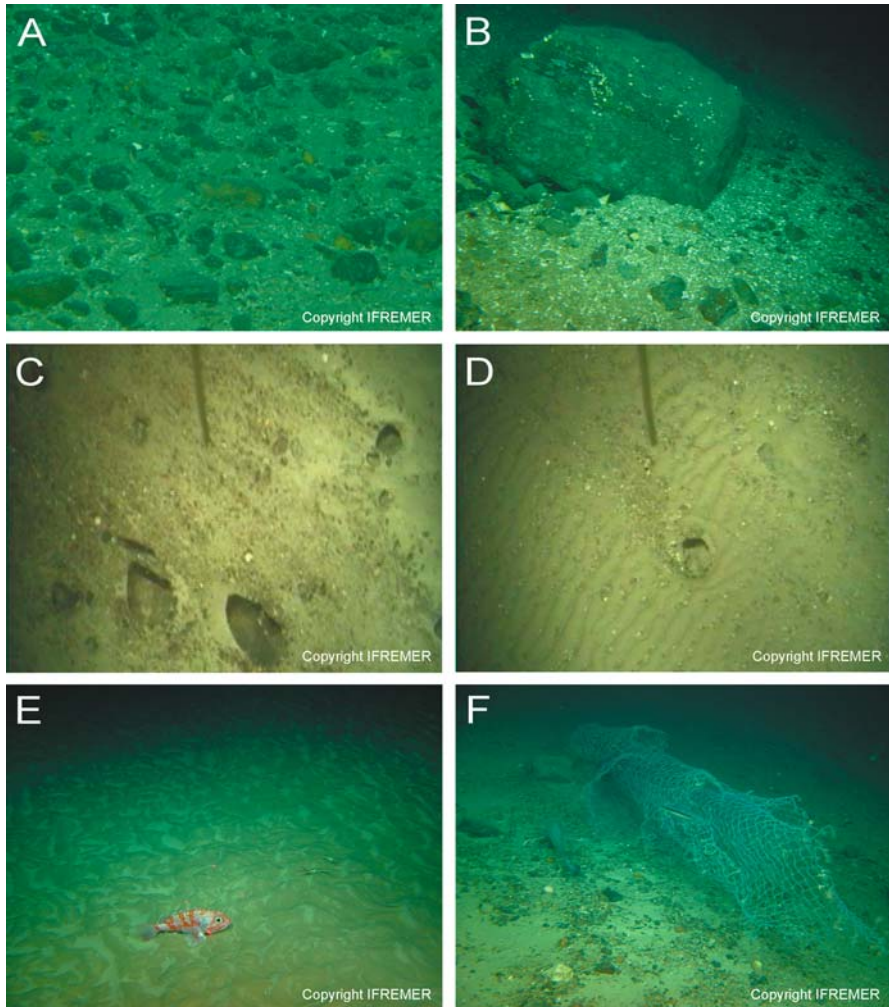
Fig. 4 Seabed in between coral-dominated areas **A** Seabed dominated by dropstones. Stylasterids (*Pliobothrus* sp.) settling on dropstones. **B** Dropstone colonized by barnacles (*Bathylasma* sp.) on a seabed characterized by barnacle plates, dropstones and broken coral fragments. **C** Patchy distribution of dropstones on an unrippled seabed. Current marks visible in the neighbourhood of dropstones with scouring and gravel patches. **D** Patchy distribution of dropstones on a rippled seabed. **E** Rippled seabed and Redfish. **F** Lost fishing net and *Phycis blennoides*

the sedimentary patterns, bedform occurrences and the deduced current orientations fits very well with the general idea of a northward directed slope current.

The impact of trawl marks and even the presence of stranded fishing nets were also noted (Fig. 4F; Grehan et al. 2003).

Morphology of the Moira Mounds

The Moira Mounds are identified in the Belgica Mound province (Fig. 1B) and were first imaged on 100 and 410 kHz sidescan sonar (Wheeler et al. 2000, 2005b). These are small mounds up to 5-10 m high and 15 to 40 m across. The mounds include isolated examples although most occur in swarms or clusters (Wheeler et al. 2005b). The Moira Mounds located to the east of Thérèse Mound were investigated using ROV Victor (Olu-Le Roy et al. 2002). These video dives and sidescan sonar images showed that the Moira Mounds occur in areas of active sediment transport on rippled sand sheets in areas of sediment wave development (Wheeler et al. 2005b). A rippled sand facies with occasional dropstones and isolated coral patches is present in between the mounds. The flanks of the mounds are characterised by patches of live coral coverage in a rippled sand facies. Towards the centre of the mounds the coral framework becomes denser (Huvenne et al. 2005; Wheeler et al. 2005b). The Moira Mounds are confined to the present-day seabed surface with no seismic evidence for buried components (Huvenne et al. 2005). This implies that the Moira Mounds are probably a recent feature (?Holocene).

The use of the multibeam echosounder SIMRAD EM2000 mounted on the ROV VICTOR6000 made it possible to map the Moira Mounds by producing a very high-resolution microbathymetric grid with a pixel size corresponding to 20 cm. All the data were recorded and processed in Qinsy. Based on the microbathymetric grid three different areas can be delineated (Fig. 5).

The first area reveals some structures at the eastern flank of the little mound (BEL 36) in between the Thérèse Mound and the Galway Mound (Fig. 5, area 1). Video imagery shows that these structures correspond with dead patchy coral cover (Huvenne et al. 2005). Moreover, the patches of dead coral seem to be aligned E-W, comparable with the structures seen on the microbathymetric grid at the flank of Thérèse Mound (Olu-Le Roy et al. 2002). Probably these structures are stabilised sediment structures or overgrown sand waves caused by a northward-directed current.

The second area corresponds to rippled sand sheets (Fig. 5, area 2). Video imagery reveals two kinds of bedforms, sandwaves and superimposed ripples respectively. Only the sandwaves are visible on the microbathymetry and are up to 50 cm high, with a wavelength of 15 to 20 m and are aligned E-W. They demonstrate the presence of strong northerly-directed benthic bottom currents up to 65 cm/s (Belderson et al. 1982). The superimposed ripples have different orientations that may be caused by the influence of tidal currents.

The Moira Mounds themselves are clustered in front of and on some lineated features (Fig. 5, area 3). These lineated features are palaeo-features, aligned N-S
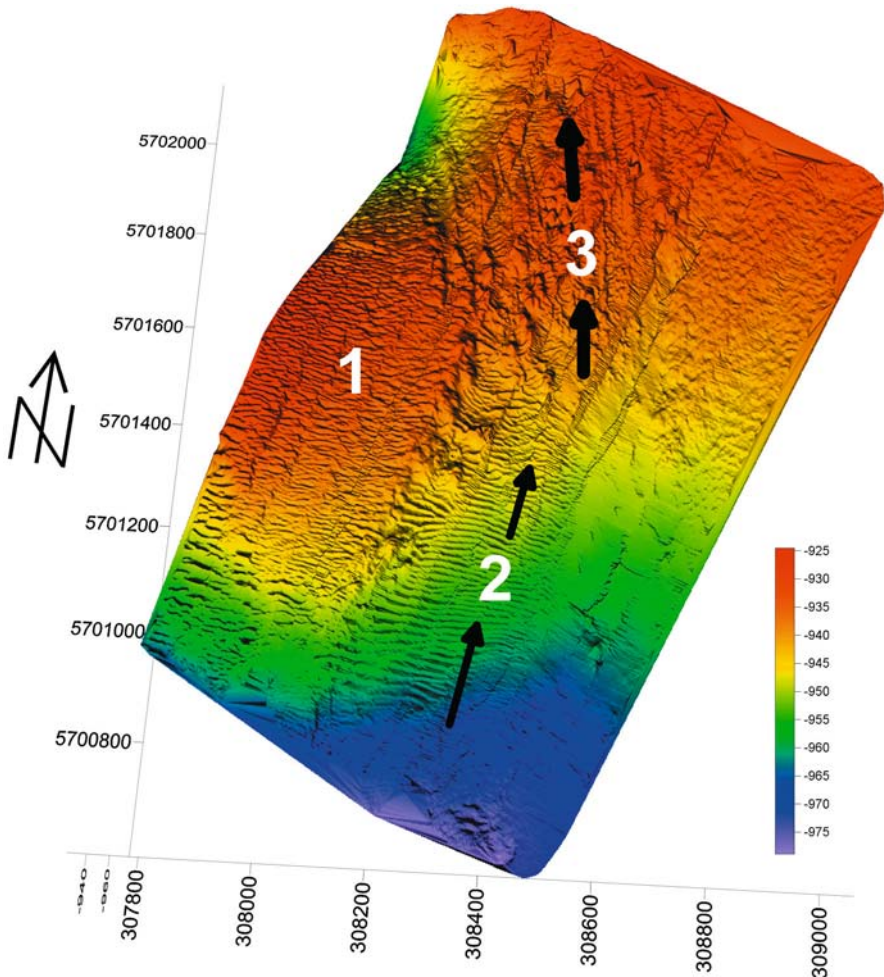
Fig. 5 Microbathymetric map over the Moira Mounds. White numbers correspond with described structures in the text. Black arrows correspond with deduced current orientations

and have a length about 200 to 250 m possibly formed by (helicoidally) strong currents up to 100-150 cm/s (Belderson et al. 1982) and may have offered a hard surface suitable for coral settlement and attachment.

A positive feedback mechanism controlling mound growth is proposed. The lineations were formed by very strong currents above the tolerance of deep-water corals. However, once these currents waned they provided suitable substrates and corals started to settle on the bedforms. Under this new current regime, active bedload sand transport dominates with coral frameworks trapping sediment. This coral sediment entrapment process provides support for coral colonies encouraging new coral growth.

Preliminary conclusions

The reconnaissance video survey over and between several mounds in the Belgica Mound province visualised different sedimentary seabed facies. All the mounds along the transect from Challenger Mound up to Poseidon Mound are covered with sediment clogged dead coral and coral rubble at the western sides and sandy sediments at the eastern sides and are inactive with respect to coral occurrence and coral-stimulated growth at present. Only the Galway Mound and the little mound (BEL 44) in between the Galway Mound and the Poseidon Mound are covered with a high percentage of living coral. These mounds as well as the Thérèse Mound and Moira Mounds occur in the western area of the Belgica Mounds that now provides adequate conditions for rigorous coral growth. A clear increase of megafaunal concentrations and species on mounds with live coral coverage is noted.

A range of local current effects and local current intensifications are recognised between the mounds on the eastern ridge, expressed by the presence of dropstone and associated current marks. However, very few boulders show prolific growth of larger sessile animals such as gorgonians, antipatharians or corals (*Madrepora oculata* or *Lophelia pertusa*), which may be due to excessive current speeds. The overall image of the sedimentary patterns and bedforms fits very well with the general idea of a northerly directed slope current, probably centred, and most erosive, at the western side of the eastern ridge of aligned mounds. However, the buried eastern sides of these mounds also show that downslope orientated transport plays an important role in the interaction between mounds and alongslope sediment transport.

The microbathymetric survey shed a new light on the environmental and sedimentological setting of the Moira Mounds that occurs within an area influenced by strong currents with large fields of ripples and sandwaves. The mounds occur on the tops of features formed under extreme currents that probably provided suitable substrates for colonisation. Contemporary currents facilitate sediment entrapment with coral frameworks as a driven mechanism for mound growth.

Acknowledgements

References

Belderson RH, Johnson MA, Kenyon NH (1982) Bedforms. In: Stride AH (ed) Offshore Tidal Sands: Processes and Deposits. Chapman and Hall, London, pp 27-57

Beyer A, Schenke HW, Klenke M, Niederjasper F (2003) High resolution bathymetry of the eastern slope of the Porcupine Seabight. Mar Geol 198: 27-54

De Mol B, Van Rensbergen P, Pillen S, Van Herreweghe K, Van Rooij D, MacDonnell A, Huvenne V, Ivanov M, Swennen R, Henriet JP (2002) Large deep-water coral banks in the Porcupine Basin, southwest of Ireland. Mar Geol 188: 193-231

Frederiksen R, Jensen A, Westerberg H (1992) The distribution of scleractinian coral *Lophelia pertusa* around the Faeroe Islands and the relation to internal tidal mixing. Sarsia 77: 157-171

Freiwald A (2002) Reef-forming cold-water corals. In: Wefer G, Billett D, Hebbeln D, Jørgensen BB, Schlüter M, Van Weering T (eds) Ocean Margin Systems. Springer, Berlin Heidelberg, pp 365-385

Freiwald A, Shipboard Party (2002) Cruise report RV Poseidon Cruise 292, Reykjavik-Galway, 15 July - 4 August 2002

Freiwald A, Wilson JB, Henrich R (1999) Grounding Pleistocene icebergs shape recent deep-water coral reefs. Sediment Geol 125: 1-8

Grehan AJ, Unnithan V, Wheeler AJ, Monteys FX, Beck T, Wilson M, Guinan J, Hall-Spencer JH, Foubert A, Klages M, Thiede J (2003) Evidence of major fisheries impact on cold-water corals off the Porcupine Bank, west coast of Ireland: implications for offshore coral conservation within the European Union. Erlanger Geol. Abh. Sonderbd 4: 42

Henriet JP, De Mol B, Pillen S, Vanneste M, Van Rooij D, Versteeg W, Croker PF, Shannon PM, Unnithan V, Bouriak S, Chachkine P (1998) Gas hydrate crystals may help build reefs. Nature 391: 648-649

Henriet JP, Van Rooij D, Huvenne V, De Mol B, Guidard S (2003) Mounds and sediment drifts in the Porcupine Basin, west of Ireland. In: Mienert J, Weaver P (eds) European margin sediment dynamics, side-scan sonar and seismic images. Springer, Berlin Heidelberg, pp 217-220

Hovland M, Croker PF, Martin M (1994) Fault-associated seabed mounds (carbonate knolls?) off western Ireland and north-west Australia. Mar Petrol Geol 11: 232-246

Huvenne VAI, Blondel Ph, Henriet JP (2002) Textural analyses of sidescan sonar imagery from two mound provinces in the Porcupine Seabight. Mar Geol 188: 323-341

Huvenne VAI, De Mol B, Henriet JP (2003) A 3D seismic study of the morphology and spatial distribution of buried coral banks in the Porcupine Basin, SW of Ireland. Mar Geol 198: 5-25

Huvenne VAI, Beyer A, de Haas H, Dekindt K, Henriet JP, Kozachenko M, Olu-Le Roy K, Wheeler AJ, TOBI/Pelagia 197 and CARACOLE cruise participants (2005) The seabed appearance of different coral bank provinces in the Porcupine Seabight, NE Atlantic: results from sidescan sonar and ROV seabed mapping. In: Freiwald A, Roberts JM (eds) Cold-water Corals and Ecosystems. Springer, Berlin Heidelberg, pp 535-569

Moore JG, Shannon PM (1992) Paleocene-Eocene deltaic sedimentation, Porcupine Basin, offshore Ireland – a sequence stratigraphic approach. First Break 10: 461-469

Olu-Le Roy K, Caprais J-C, Crassous P, Dejonghe E, Eardley D, Freiwald A, Galeron J, Grehan A, Henriet JP, Huvenne V, Lorance P, Noel P, Opderbecke J, Pitout C, Sibuet M, Unnithan V, Vacelet J, van Weering T, Wheeler A, Zibrowius H (2002) CARACOLE Cruise Report 30/07/2001 (Cobh) – 15/08/2001 (Foynes) N/O L'Atalante & ROV VICTOR. 1 and 2, unpubl Rep, IFREMER, Brest

Naylor D, Shannon PM (1982) The Geology of Offshore Ireland and West Britain. Graham and Trotman, London

Rice AL, Billet DSM, Thurston MH, Lampitt RS (1991) The institute of Oceanographic Sciences Biology Programme in the Porcupine Seabight: background and general introduction. J Mar Biol Ass UK 71: 281-310

Van Rooij D, De Mol B, Huvenne V, Ivanov M, Henriet JP (2003) Seismic evidence of current-controlled sedimentation in the Belgica mound province, southwest of Ireland. Mar Geol 195: 31-53

Wheeler AJ, Bett B, Billett DSM, Masson DG and Scientific Party, Officers and Crew of RRS Discovery 248 (2000) High resolution side-scan sonar mapping of deep-water coral mounds: surface morphology and processes affecting growth. Eos, Transactions, American Geophysical Union 81: F638

Wheeler AJ, Beck T, Thiede J, Klages M, Grehan A, Monteys FX, Polarstern ARK XIX/ 3a Shipboard Party (2005a) Deep-water coral mounds on the Porcupine Bank, Irish Margin: preliminary results from the Polarstern ARK-XIX/3a ROV cruise. In: Freiwald A, Roberts JM (eds) Cold-water Corals and Ecosystems. Springer, Berlin Heidelberg, pp 393-402

Wheeler A, Kozachenko M, Beyer A, Foubert A, Huvenne VAI, Klages M, Masson DG, Thiede J, Olu-Le Roy K. (2005b) Sedimentary processes and carbonate mound morphology in the Belgica Mound province, Porcupine Seabight, NE Atlantic. In: Freiwald A, Roberts JM (eds) Cold-water Corals and Ecosystems. Springer, Berlin Heidelberg, pp 571-603

White M (2001) Hydrography and physical dynamics at the NE Atlantic margin that influence the deep water coral reef ecosystem. EU ACES-ECOMOUND Internal Rep, Dept Oceanogr, NUI Galway, Galway, 31 pp

Carbonate mounds off Mauritania, Northwest Africa: status of deep-water corals and implications for management of fishing and oil exploration activities

Jeremy G. Colman[1], David M. Gordon[1], Andy P. Lane[1], Mike J. Forde[2], Jeremy J. Fitzpatrick[2]

[1] Woodside Energy Ltd, Box D188, GPO Perth, Western Australia 6840, Australia
  (JEREMY.COLMAN@woodside.com.au)
[2] Bowman Bishaw Gorham, P.O. Box 465, Subiaco, Western Australia 6904,
  Australia

Abstract. Since 1998, Woodside Mauritania Pty Ltd has been exploring for hydrocarbon deposits offshore from the Islamic Republic of Mauritania, in Northwest Africa. A 3-D seismic survey, undertaken in 1999-2000, revealed the presence of buried and seabed carbonate mounds at approximately 450-550 m water depth on the continental slope. These mounds are approximately 100 m in height, 500 m wide at the base, and cover a linear extent of at least 190 km. Core samples from the mounds were found to contain dead fragments of four species of cold-water corals: *Lophelia pertusa*, *Madrepora oculata*, *Solenosmilia variabilis* and *Desmophyllum* sp. In 2002, a preliminary towed camera survey revealed large areas of coral rubble at two mound sites suggesting that corals were previously a dominant component of the benthic community. A second video survey, in 2003, recorded some live hard coral polyps and a single live coral colony, probably *L. pertusa*, at one of the mound sites. Coral rubble at all sites surveyed was found to support epibenthic invertebrate and fish assemblages. The mound areas surveyed may have been exposed to physical impacts that have resulted in damage of coral colonies previously inhabiting these features. Based on the nature of the damage and past and present demersal fishing activity in the region, bottom trawling could have caused these impacts. The discovery of a significant deep-water reefal system offshore Mauritania has implications for future management of trawling and oil exploration activities. These issues are discussed in the context of the potential biodiversity significance and conservation importance of the carbonate mud mounds and their associated biological communities.

Keywords. Carbonate mounds, Mauritania, deep-water corals, trawling impacts, oil exploration

Introduction

Carbonate mound occurrence in the Northeast Atlantic margin

Carbonate mud mounds and coral banks have been discovered in several areas of the continental shelf and slope of the Northeast Atlantic margin (Hovland et al. 1994; Mortensen et al. 1995; Henriet et al. 1998; Hovland et al. 1998; Freiwald et al. 1999; Rogers 1999; Mortensen et al. 2001; De Mol et al. 2002; Huvenne et al. 2003; Kenyon et al. 2003; Masson et al. 2003; O'Reilly et al. 2003; Roberts et al. 2003; van Weering et al. 2003; Wheeler et al. submitted). Oil exploration activities, involving systematic acoustic surveys of the seabed, with side scan sonar and geophysical seismic equipment, have led to the discovery of localised occurrences of carbonate mud mound features, particularly in the Porcupine Seabight and the "Atlantic Frontier" waters west of the Shetlands (Croker and O'Loughlin 1998; AFEN 2000). These mound features have been shown to be associated with deep-water, azooxanthellate scleractinian corals, particularly *Lophelia pertusa* (Linné, 1758). *L. pertusa* has a widespread distribution along the Northeast Atlantic margin, from the Faeroe Islands and Norway to Senegal and the Cape Verde Islands in Northwest Africa (Wilson 1979; Frederiksen et al. 1992; Rogers 1999; Mortensen et al. 1995; Mortensen et al. 2001; Fosså et al. 2002).

Recent hydrocarbon exploration offshore Mauritania

Since 1998, Woodside Energy Ltd, Australia's largest independent oil exploration and production company, has been exploring for hydrocarbon deposits offshore from the Islamic Republic of Mauritania, in Northwest Africa. A wholly-owned subsidiary company, Woodside Mauritania Pty Ltd, has been conducting exploration and appraisal activities in five hydrocarbon exploration permit areas, or blocks, situated off the central coastal region of Mauritania. Blocks 2, 3, 4, 5 and 6 (Fig. 1) are operated by Woodside Mauritania Pty Ltd under Production Sharing Contracts (PSC) with the Government of Mauritania. On the basis of two-dimensional (2-D) and three-dimensional (3-D) seismic data, two exploration wells were drilled in 2001, which resulted in the discovery of the Chinguetti oil field. The field is located in ~800 m water depth, approximately 80 km due west of the Mauritanian coastline (Fig. 1). Four wells were drilled in 2002, which resulted in the Banda gas discovery 25 km east of the Chinguetti field (Fig. 1). Examination of seismic profiles from 3-D data across the upper continental slope (Fig. 2) revealed the presence of a regionally continuous linear feature, comprised of a series of large seabed mounds, located at approximately 450-550 m water depth.

Seabed images (Figs. 3, 4), derived from data collected during a large 3-D seismic survey undertaken between November 1999 and March 2000, confirmed the presence of these features, which are aligned at the same water depth range (450-550 m) across the continental slope, parallel to Mauritania's central coastline (Fig. 5). It is now recognised, as a result of further examination of seismic data, and from coring studies and seabed video surveys, that these features are probably carbonate mud mounds, previously inhabited by dense communities of cold-water corals, including the reef-forming species *Lophelia pertusa*.
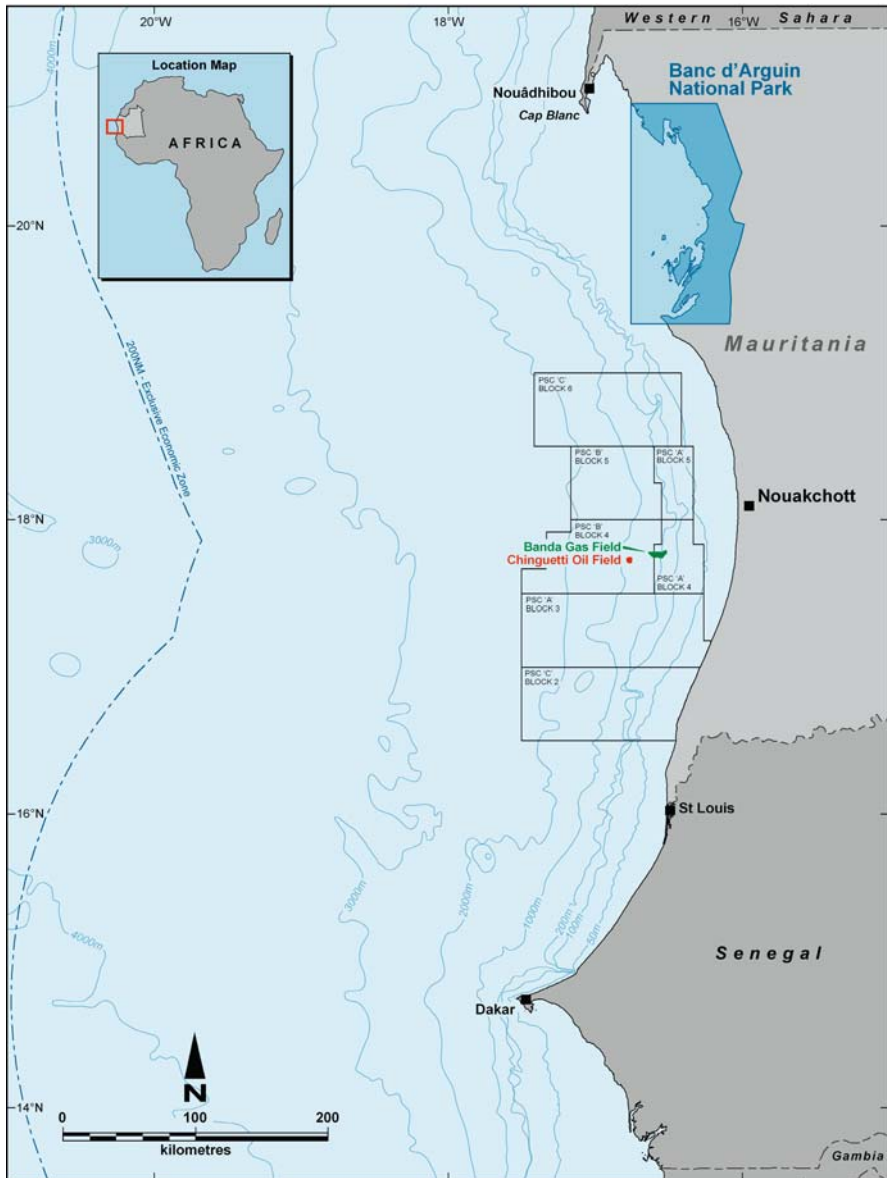
Fig. 1 The location of PSC Blocks 2, 3, 4, 5 and 6, and the Chinguetti and Banda oil and gas fields, offshore Mauritania, Northwest Africa. PSC Blocks 2, 3, 4, 5 and 6 comprise the outer extent of the study area
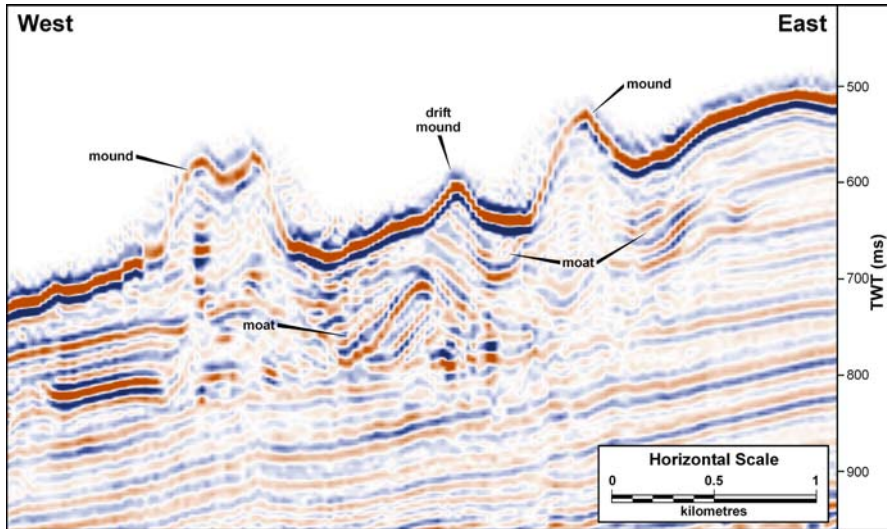
Fig. 2 Representative seismic profile through carbonate mound structures offshore Mauritania, from 3-D seismic data. The location of this profile is shown on Figures 3 and 5

Environmental setting

Physical setting and bathymetry

The study area is located within PSC Blocks 2, 3, 4, 5 and 6, which are situated off the central coastline of Mauritania (Fig. 1). The blocks cover an area of approximately 35,000 km^2, from 16°30'N to 19°00'N and 16°00'W to 17°30'W, in water depths of 0 - >2,000 m. East of the blocks, the coastline forms a gigantic arc opening towards the west, and the width of the continental shelf does not exceed 50 km in this area. The 200 m isobath, which constitutes the shelf-break across most of the Mauritanian margin, is orientated north-west to south-east in its northern part, curves gradually toward the south, following the shape of the coastline and follows a NNE-SSW direction from the latitude of Nouakchott (Fig. 1).

Beyond the shelf-break, the continental slope has a width of 50-250 km, and displays slope angles of 1-6° (Wynn et al. 2000). General slope gradient across the study area is approximately 3-4°. The study area includes a deeply-incised submarine canyon to the north, and a large area of landslides in the southwest of the area (Fig. 3). The Chinguetti field location lies upslope of the main slide and north of a series of smaller slides in an area of relatively flat seabed (Fig. 3). The landslides in the study area produce sediment flows that transport sediment downslope towards the Gambia Abyssal Plain and adjacent fracture zone valleys (Wynn et al. 2000).

The discontinuous carbonate mud mound system is located parallel to the coast in the eastern part of the study area, at a distance of approximately 60 km offshore (Fig. 5).

Oceanography

The oceanography of this region is thought to be dominated by the interaction of medium-to-large scale geostrophic currents (CNROP 1991; Mittelstaedt 1991). Eddies and areas of ocean upwelling are persistent features. The principal wind-
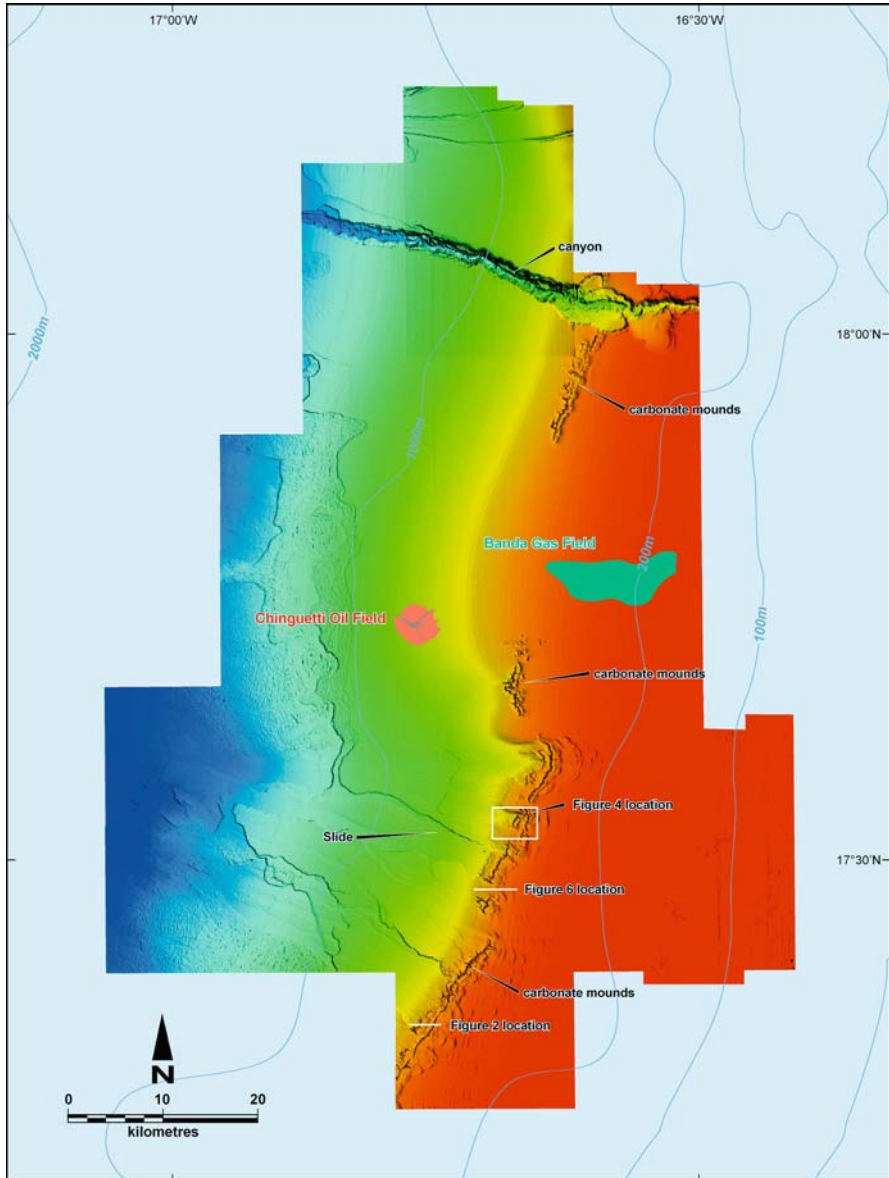
Fig. 3 Bathymetric map, based on 3-D seismic data, showing carbonate mound structures, canyon system and slope slide features. The location of Figures 2, 4 and 6 are shown
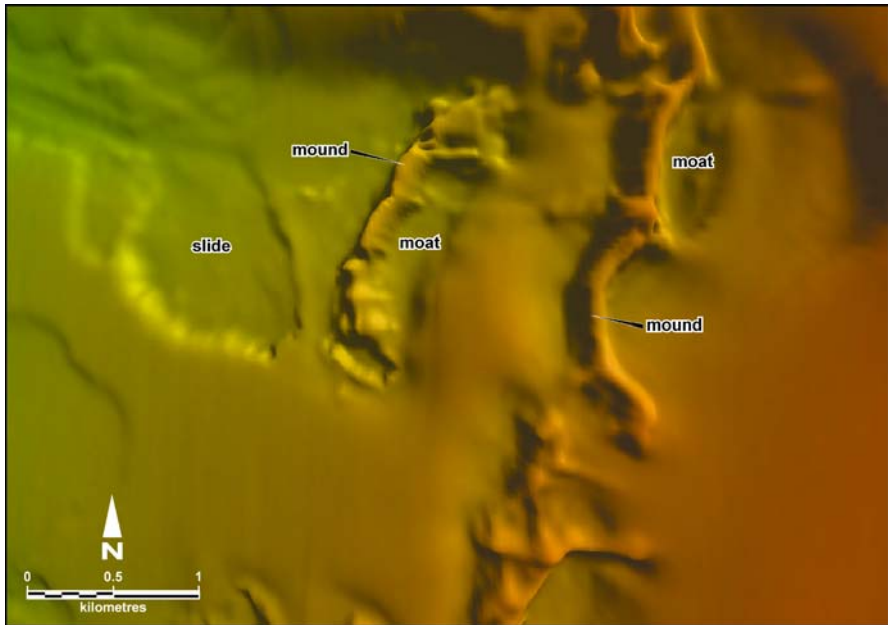
Fig. 4 Bathymetric map, based on 3-D seismic data, showing arcuate form of mounds, associated moats, and slide feature. The location of this figure is shown on Figures 3 and 5

driven currents affecting coastal waters off Mauritania are the Canary Current, the North Equatorial Current and the Equatorial Counter Current. The Canary Current transports cool, nutrient-rich water to the southwest. It is strongest near the continental coast, becoming progressively weaker offshore. This current, in combination with coastal and continental shelf topography, is a major influence on oceanic upwelling. The effect of tidal currents on general circulation in offshore waters is small. Over the entire Northwest African upwelling area the mean amplitude of semi-diurnal tidal currents is small. Mixing by tidal currents is therefore hardly noticeable, even in shallow waters (Fugro GEOS 1999; WNI 2002).

Subsurface currents in the study area are not well studied, but are generally thought to flow northwards. Between about 100-400 m water depth a north-flowing undercurrent occurs, with reported current velocities of 5 to 10 cm s^{-1} (Fugro GEOS 1999). This pattern is seen in the OCCAM global circulation model (GeoSed 2002). The water mass at 100-400 m water depth forms an oxygen minimum layer and is the nutrient-rich source of upwelling water in the region. At greater water depths data are patchy, but North Atlantic Deep Water (NADW) is thought to occur below 2,000-3,800 m water depth and flow southwards, while Antarctic Bottom Water (AABW) is found below 3,800 m and flows in a north-easterly direction (Wynn et al. 2000). Generally, the deep currents below 500 m water depth are thought to be fairly weak at the present day, with velocities in the order 1-6 cm s^{-1}. However, local factors such as internal waves between water masses can lead to locally-enhanced near-bottom flow. The OCCAM model predicts current velocities near

seabed that are generally less than 18 cm s^{-1} (GeoSed 2002). This is consistent with the sedimentary features at the seabed in the study area, which show only limited evidence of current activity.
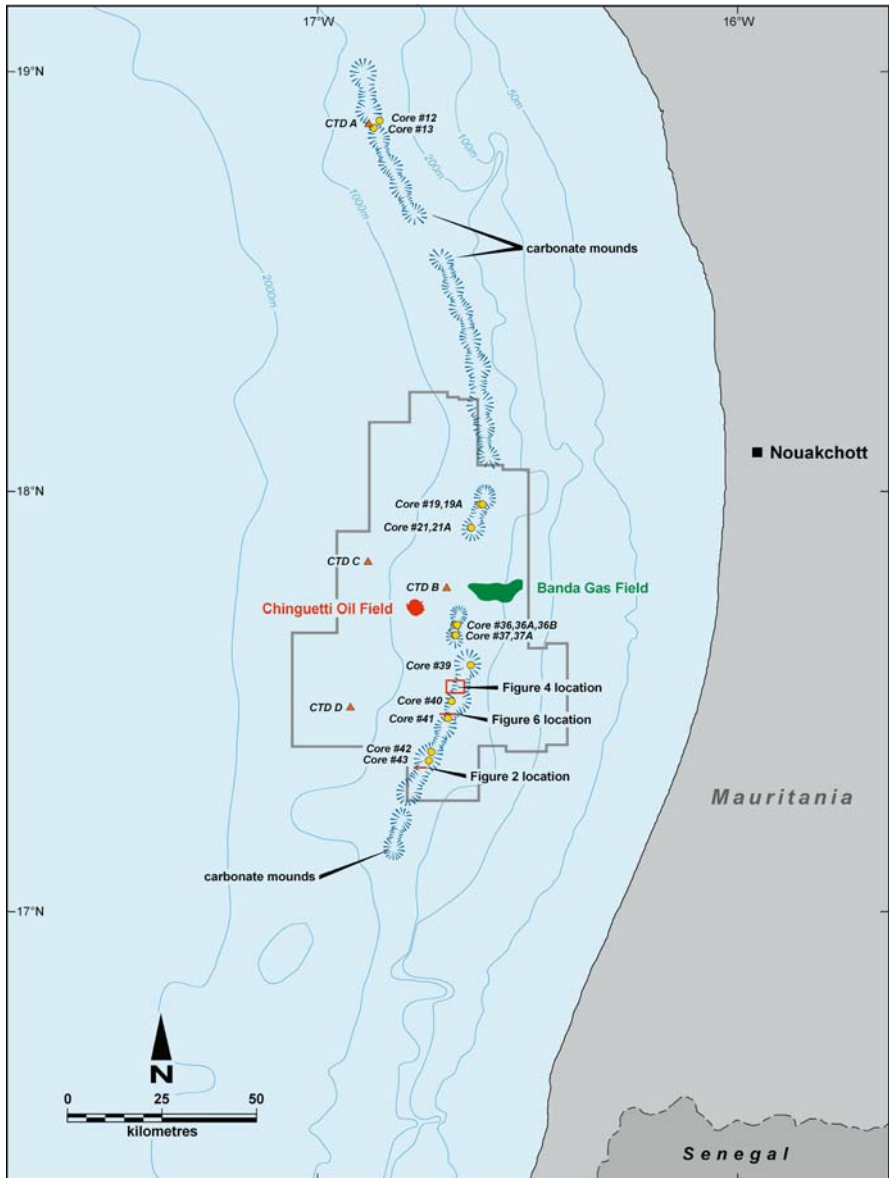
Fig. 5 Representation of the known extent of carbonate mound structures off Mauritania, from 2-D and 3-D seismic data. This figure shows the outline of 3-D seismic data coverage (Fig. 3). It also shows the location of on-mound core locations, and on-mound and off-mound CTD dips

Oceanographic upwelling involves the movement of cold, nutrient-rich water from the continental slope into shallower coastal waters, driven by prevailing winds, mainly subtropical anticyclonic wind systems, which result in the displacement offshore of warmer, coastal waters. The timing and intensity of upwelling off the coast of Mauritania varies, depending on location and time of year. Upwelling is effectively permanent off the Banc d'Arguin (~20ºN) and is seasonal further south (Mittlesteadt 1983; Roy 1992). At the regional scale, it is most conspicuous off Mauritania from October to June. At the local scale, at least two distinct upwelling features occur, the most productive around Cap Blanc (~21ºN). The upwelling season near, and south of Cap Blanc, is short (December-March) (Minas et al. 1982; Mittelstaedt 1991). The upwelling zone is located in a narrow belt parallel to the coast, centred on the outer shelf/upper slope area.

Methods

3-D seismic

Information on the locations and morphology of the carbonate mound system was obtained from exploration 3-D seismic data (Fig. 3), acquired by Woodside between November 1999 and March 2000. During this survey, approximately 10,000 km^2 of 3-D data was acquired, with a vertical resolution of 10 m (at seabed), and a 25 m bin size. The seismic source had a volume of 3,000 cui and operating pressure of 2,000 psi for the total air-gun array. Processing of the 3-D data included pre-stacked depth migration.

Side scan sonar

Mapping of the sea floor in the study area was carried out during a hydrographic survey in July 2003 using an Edgetech FS-DW/FS-IU side scan sonar system. The side scan sonar was operated at a frequency of 120 kHz, and the transducers produced a pulse with a 1º horizontal beam and a 50º vertical beam width, depressed 20º from the horizontal. A sonar range of 300 m per channel was used throughout the survey, and the towfish height above the seabed was maintained at approximately 10 % of the range.

Only three lines of side scan sonar data were acquired during this survey, and none of these covered the carbonate mound areas.

Coring

Physical and geochemical characteristics of surface sediments from the carbonate mounds were derived from analyses of 16 piston core samples taken at on-mound locations during a seabed survey in November 2000 (Fig. 5). During this survey, an additional 37 core samples were taken at off-mound locations in the study area. The results of analyses of these off-mound cores are not presented in this paper.

The purpose of this survey was the identification of hydrocarbon seepage, and core analyses included a suite of geochemical testing - total scanning fluorescence; $C_{15}+$ hydrocarbon gas chromatographic analysis; and C_1 to C_5 headspace gas analysis

- to evaluate each core section for the presence of migrated mature hydrocarbons (Woodside 2002). Samples believed to contain migrated hydrocarbons were also analysed for stable carbon isotopes. Full results from these analyses are not presented in this paper.

Conductivity, temperature, depth profiles

During the November 2000 seabed survey, four conductivity, temperature, depth (CTD) dips were conducted at one on-mound (CTD A) and three off-mound (CTD B, C and D) coring locations (Fig. 5), in water depths of 588 m, 516 m, 1,231 m and 1,378 m respectively. Additional measurements of water column temperatures and currents were obtained from the deployment of a current meter string in ~750 m water depth adjacent to the Chinguetti field location.

Video surveys

Two separate carbonate mound areas, located approximately 133 km apart, were surveyed during two surveys in 2002 and 2003, using a towed deep-water camera system deployed from an anchor handling vessel. Both surveys covered the flanks and summits of the mounds.

2002 survey

In July 2002, a preliminary seabed survey of two areas of mounds, one at the northern extremity of Block 6 (Core #12 location, Fig. 5; UTM coordinates 304000E 2087750N Zone 28N) and the other adjacent to the Chinguetti oil field in Block 4 (Core #36 location, Fig. 5; UTM coordinates 323000E 1954400N Zone 28N), was undertaken. The camera and lens were mounted in a one atmosphere stainless steel housing, which was mounted on a modular aluminium tow frame, fitted with a stabilising wing and two variable intensity lights (BBG 2002). Control of the height of the tow frame above the seabed, and its lateral position on the mounds, were constrained by the manoeuvring capabilities of the vessel, winch performance and the steep-sided topography of the mounds.

2003 survey

In July 2003, a second survey was conducted over the same area of mounds adjacent to the Chinguetti field location that was surveyed in the 2002 survey (see Section 2.5.1; Fig. 5). Improvements were made to the towed camera system prior to the survey in order to obtain better quality video imagery. Additional lighting was installed on the tow frame and live-to-surface transfer of images was *via* a 1,500 m armoured optical fibre umbilical cable deployed and retrieved using a high speed electric winch (BBG 2004).

Grab and sledge sampling

During the July 2003 survey, three replicate sediment samples were collected at each of two sites on the mounds using a stainless steel Van Veen grab. These sediment samples were analysed for particle size distribution, organic content, heavy metal and total petroleum hydrocarbon content, and sediment infauna composition.

Samples of macrofauna were collected along transects over the mounds using a modified Ockelmann sledge, fitted with a 1.5 cm mesh size primary collection net, mounted inside a 2.5 cm mesh size heavy protective net (BBG 2004). Sediment grab samples and sledge samples were preserved immediately after collection, either by freezing, or by storage in 10 % buffered formaldehyde. A summary of preliminary results from the grab and sledge sampling are presented here.

Results

Seismic data

Interpretation of 3-D exploration seismic data indicated regionally continuous seabed (Fig. 3) and buried features (Fig. 6) across the upper continental slope at approximately 450-550 m water depth, parallel to the central coastline of Mauritania (Fig. 5). The seabed features, the largest of which measure ~500 m across the base and ~100 m in height (Fig. 2) (topographic width and height measured from the seabed rather than from the buried base of the mound), are believed to be carbonate mud mounds, based on seismic characteristics that are similar to other mound systems elsewhere in the Northeast Atlantic margin (Hovland et al. 1994; Henriet et al. 1998; De Mol et al. 2002; Huvenne et al. 2003; Kenyon et al. 2003; van Weering et al. 2003). Seabed and buried mounds were found to occur throughout Blocks 2, 3, 4, 5 and 6 (Fig. 5). Seabed images from 3-D seismic data acquired in 1999-2000 (Fig. 3) showed the mounds extending as linear features with remarkable lateral continuity. The mounds have a localised curved or arcuate form and distinct scour features, or moats, at the base on either side (Fig. 4). From 3-D seismic profiles the
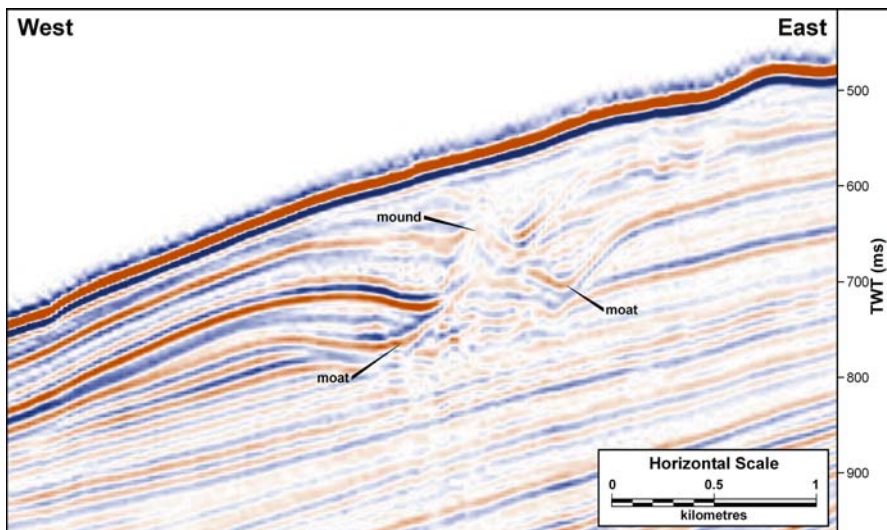
Fig. 6 Seismic profile showing buried carbonate mound structures. The location of this profile is shown on Figures 3 and 5

mounds appear to have average slopes in the order of 10-15º (Fig. 2), and maximum slope angles up to 30º on the mound flanks. In several areas, mound ridges occur parallel to each other (Fig. 4).

Known linear extent of the mound system is ~190 km (Fig. 5). At a local scale, the system is not continuous, with large gaps evident from seabed images generated from 3-D seismic data (Fig. 3). Buried mounds are evident in the seismic data, extending in an easterly, or inshore, direction from the present day mounds (Fig. 6). In some areas, buried mounds also appear to extend in a north-south direction beneath the gaps in the present day system.

The 3-D seismic data revealed the presence of a series of low amplitude sediment waves extending in a northwesterly direction; between ~2 to ~10 km distance from the carbonate mound system closest to the Chinguetti field location (Fig. 3). These sediment waves have wavelengths of approximately 500 m and amplitudes of less than 2 m. They appear to be temporally persistent, suggesting that the process of formation was operating for a long time period. It is difficult to determine whether these waves are a product of bottom currents or turbidity currents. However, their 'fixed' morphology through several stratigraphic intervals suggests bottom currents are the cause (GeoSed 2002). The seismic data also indicates a series of retrogressive slides in the area south of the Chinguetti field location (Fig. 3). In this area, the slides have progressively cut back into the slope by headwall erosion until they have reached the base of the mound system (GeoSed 2002).

Cores

Maximum core depth was 4.6 m with an average recovery of 3.2 m. All 16 cores were recovered from on-mound locations (Fig. 5), and were comprised of carbonate-rich clay or clayey silt with abundant dead coral fragments. Taxonomic analysis of coral fragments indicated the presence of four species of deep-water corals - *Lophelia pertusa*, *Madrepora oculata* Linné, 1758, *Solenosmilia variabilis* (Duncan, 1873) and *Desmophyllum* sp. (D. Billett, Southampton Oceanographic Centre, pers. comm. 2002). Identification of some of the more heavily decayed material was uncertain, and an additional two species were present in the samples - *Pourtalosmilia anthophyllites* (Ellis and Solander, 1786) and *Enallopsammia rostrata* (Pourtalès, 1878). All cores taken at off-mound locations during the survey were comprised of silty clay/clayey silt sediments and were free of coral fragments. Overall, cores from the mound areas had higher clay content than cores taken from other areas. Coral fragments were most numerous in the upper 2 m of the cores. Fragments from the upper 10 cm of the cores included material that was relatively un-eroded, with sharp edges where it had been broken, and material that was heavily decayed.

Geochemical analysis of cores from the mounds consistently indicated very low hydrocarbon levels from total scanning fluorescence, C_{15}+ hydrocarbon gas chromatographic analysis; and C_1 to C_5 headspace gas analysis, in comparison to cores taken at off mound locations (Woodside 2002). These results suggest that the present mound building process does not depend on gas seepage.

Hydrographic data

The CTD data indicated a moderate thermocline at ~100 m, and a minor thermocline at ~450 m water depth (Fig. 7a). A marked halocline occurred at ~450 m water depth (Fig. 7b). Seawater temperature at ~500 m water depth is indicated as ~10.5°C from CTD data (taken in November). Data from a current meter at 500 m water depth (in the string deployed at ~750 m water depth adjacent to the Chinguetti field location) indicated a mean temperature range of 9.6 to 10.5°C in a five-month period between August and December 2002 (WNI 2002). No data was available
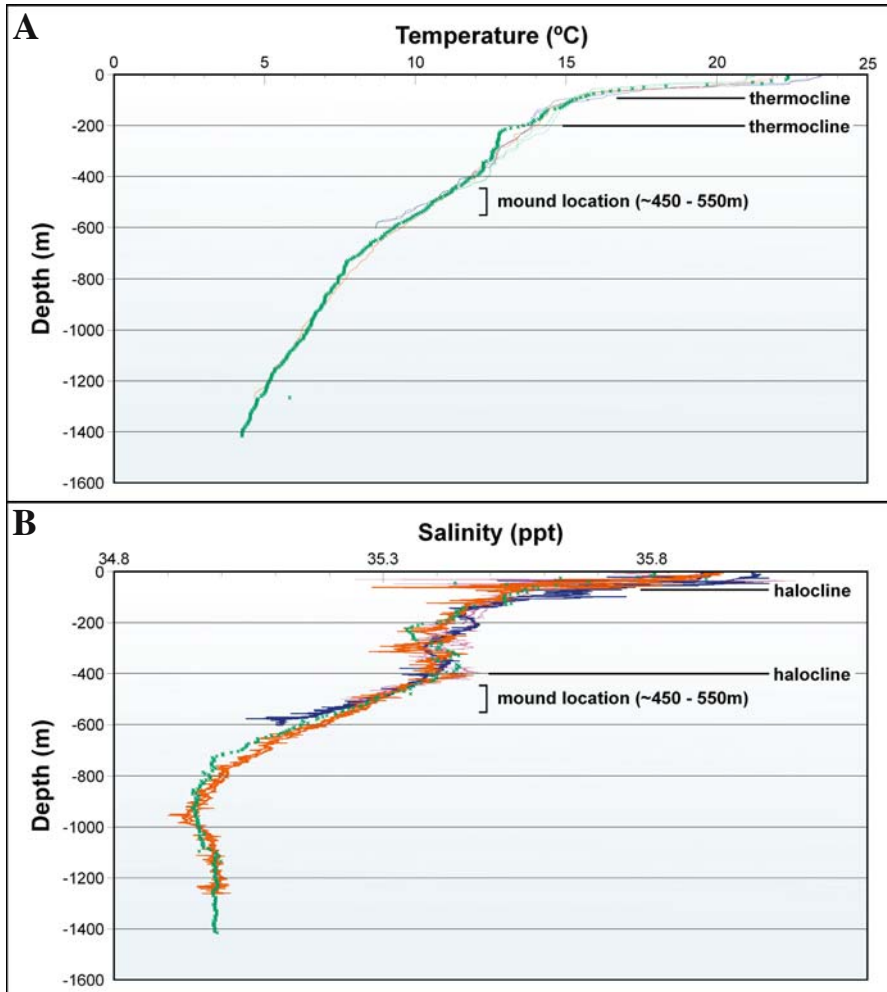
Fig. 7 A Temperature / depth profiles from the four CTD dips conducted in November 2000. An interpretation of the position of primary and secondary thermoclines, and the depth range of carbonate mound occurrence, are shown. **B** Salinity / depth profiles from the four CTD dips conducted in November 2000. An interpretation of the position of primary and secondary haloclines, and the depth range of carbonate mound occurrence, are shown

for other periods of the year. Mean current velocities, measured over the same period with the same meter, ranged from 8.2 cm s^{-2} to 10.0 cm s^{-2}, with a maximum recorded velocity of 27.3 cm s^{-2}. Current directions were mainly along a north-south axis. No current data were available for the mound areas.

Video surveys

The mound area in Block 6, surveyed during the July 2002 survey, is located in 480-550 m water depth (Fig. 5). The tops of the mounds appeared to be comprised of fine silt and clay sediments with scattered dead coral fragments and other biogenic carbonate rubble. Dense aggregations of coral fragments formed rubble zones on the upper flanks and tops of the mounds. The rubble habitat appeared to support sparse epibenthic faunal assemblages, comprised of very small sponges and gorgonians, galatheid and other crabs, sea stars, sea cucumbers (possibly *Stichopus regalis*), gastropods and teleost fishes, including small rattails. The extensive areas of fine sediments and scattered coral fragments observed between the rubble zones were dominated by tube worms. The seabed in deeper areas on the sides of the mounds, and in moats surrounding the base, comprised soft muds without visible coral fragments. Epibenthic assemblages were limited to scattered sea pens (possibly *Funiculina quadrangularis*). No organisms positively identified as live corals were observed during the survey (BBG 2002).

The July 2002 and July 2003 surveys of the area of mounds closest to the Chinguetti field location (Fig. 8) indicated a water depth range of 420-550 m. Seabed substrates and epibenthic communities varied in relation to their position on the mounds. Preliminary analysis of video imagery indicates that the seabed of the deep areas around the base of the mounds comprised bioturbated fine sands/muds. The epibenthic community in these areas comprised sea pens and occasional hydroids. Motile species observed included large numbers of a deep-water red prawn, rattail and scorpaenid fishes, crabs and small sharks. The sides and tops of the mounds comprised sand/rubble substrates with a more diverse assemblage of epibenthic organisms, including small gorgonians, ascidians, bryozoans, sponges, sea stars and brittle stars. Some live polyps, believed to be isolated hard coral polyps, were observed during the July 2003 survey, along with a single live coral colony that appears to be *L. pertusa* (Fig. 9). Patches of tube worms and aggregations of pencil urchins (probably *Cidaris cidaris*) were observed, generally on the tops of the mounds. Crustaceans were common, particularly portunid and galatheid crabs. The rubble zones appeared to be comprised of dead fragments of hard corals, which occurred in sufficient density in some areas to indicate that the past level of live coral cover was greatly in excess of the level observed during these surveys. The observation of a single, small, live colony of *L. pertusa* (Fig. 9) and what could have been some individual live coral polyps, suggests that the present condition of the benthic community on the mounds is greatly degraded from a pristine condition (BBG 2004). Detailed analysis of the digital video imagery has not been undertaken to date.

There was no indication from any of the video imagery taken of present day, small-scale, seabed bedforms or erosion patterns (such as rippled sand or sand waves) that would indicate high current speeds near the seabed.
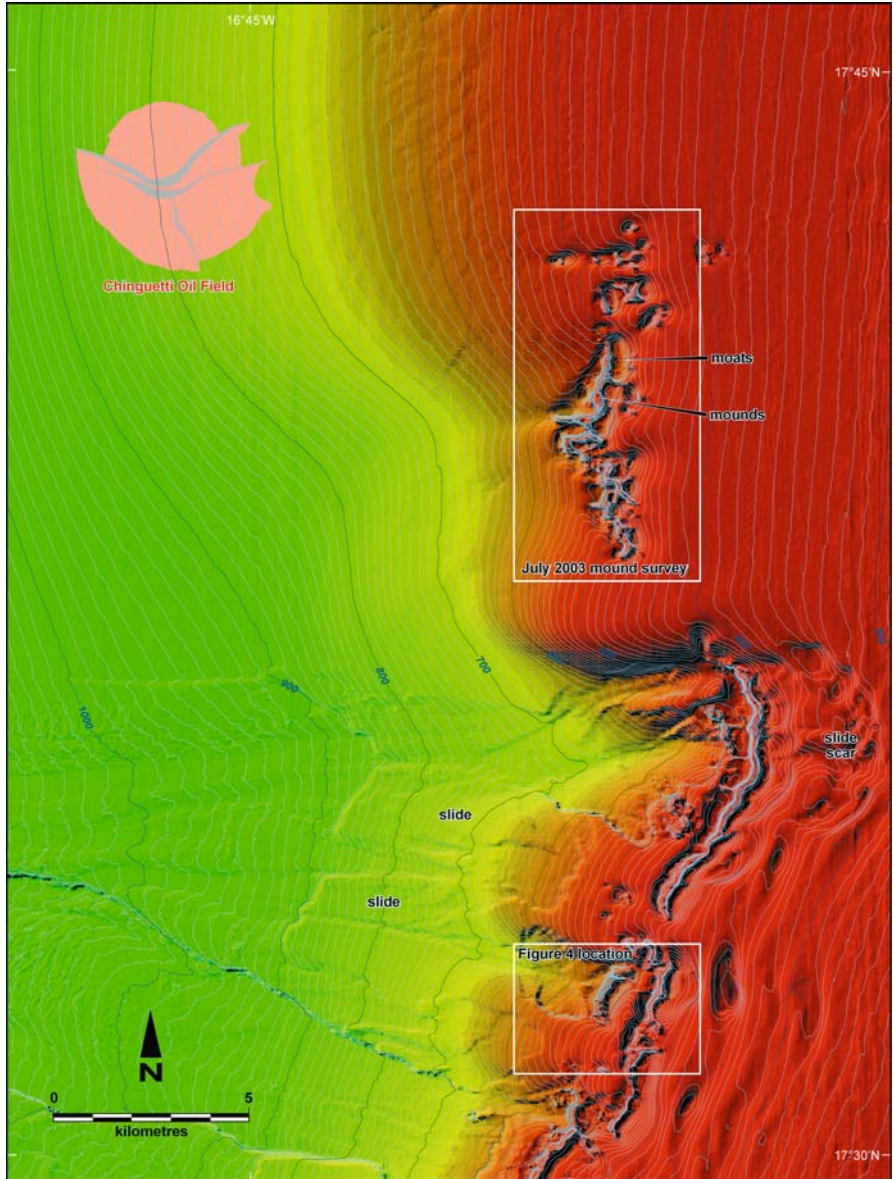
Fig. 8 Carbonate mound structures in the vicinity of the Chinguetti oil field location. The box indicates the area surveyed during the July 2002 and July 2003 video surveys. The location of Figure 4 is also shown

Fig. 9 Single, small, live *L. pertusa* colony observed during the July 2003 video survey of the carbonate mounds closest to the Chinguetti field location (see Fig. 8)

Grab sampling

Six grab samples were collected from the carbonate mounds during the July 2003 survey of the mound area closest to the Chinguetti field location (Fig. 8). These samples were comprised of three replicate samples from two separate mounds. Each of the grabs had only moderate returns of material, mainly comprised of dead coral fragments. Sufficient fine material was present in the samples to collect sub-samples for physical and chemical analysis. Preliminary analysis of the grab samples indicated a diverse range of macrofauna, including sponges, hydroids, ascidians, gorgonians, polychaetes, ophiuroids, molluscs and various crustaceans, generally in low abundance (BBG 2004). Detailed analysis of sediment physical and chemical characteristics, quantitative analysis of sediment microfauna and taxonomic identification of preserved macrofauna is currently in progress.

Sledge sampling

Sledge samples were collected from three of the carbonate mounds adjacent to the Chinguetti field location (Fig. 8). Each of the samples recovered from the nets were relatively small, and very little dead coral material was found (BBG 2004). Preliminary analysis indicated that sea pens were common in all the samples, suggesting that the sledge samples had probably been taken on the sand/mud

sediments around the base of the mounds, rather than on the tops or flanks of the mounds. The absence from the sledge samples of some of the organisms recorded from rubble zones during the video surveys, such as gorgonians, sponges and sea stars, tends to supports this. The deep-water red prawn observed during the video surveys was collected in low numbers, with 30 individuals from one sample being the largest number found. Teleost fishes were represented by a small number of species, including blackbelly rosefish (*Helicolenus dactylopterus dactylopterus*) (Fig. 10), roughsnout grenadier (*Trachyrincus scabrus*) (Fig. 10), Mediterranean slimehead (*Hoplostethus mediterraneus mediterraneus*) (Fig. 10), and legless cuskeel (*Lamprogrammus exutus*) (Fig. 10). Detailed taxonomic identification of preserved macrofauna is currently in progress.

Discussion

Mound extent

The seabed surveys carried out in July 2002 and July 2003 covered an area that represents less than 10 % of the known extent of the carbonate mound system

Fig. 10 A Epibenthic sledge samples from the base of the mounds closest to the Chinguetti field location (see Fig. 8), including the fish species *Helicolenus dactylopterus dactylopterus, Trachyrincus scabrus, Hoplostethus mediterraneus mediterraneus* and *Lamprogrammus exutus*. **B** Epibenthic sledge samples from the base of the mounds closest to the Chinguetti field location (see Fig. 8), including the fish species *Trachyrincus scabrus, Hoplostethus mediterraneus mediterraneus* and *Lamprogrammus exutus*, and the deep-water red crab *Chaceon maritae*

in Mauritanian waters (Fig. 5). Existing seismic coverage in 500 m water depth indicates that the system has a linear extent of at least 190 km, stretching from the southern area of Block 2 to the northern area of Block 6 (Figs. 1, 5). Assuming an average width across the base of 500 m, and not taking into account the area covered by the moat features, this represents an area of ~95 km^2. This system may be one of the largest areas of carbonate mud mounds so far discovered in the Northeast Atlantic margin. It is expected that the system extends north and south of the mounds recorded in Blocks 2-6. However, outside this area there is either no 3-D seismic coverage in 500 m depth, or the data is held by companies who are not part of the joint venture partnerships covering Blocks 2-6.

Corals associated with the mounds

From the core samples and video surveys it is evident that live coral coverage at the two mound sites surveyed is much less than was previously present. The presence of a small live colony of *L. pertusa*, and perhaps isolated single live polyps, in rubble zones comprised almost entirely of dead coral fragments, suggests that previous conditions were more suitable for the growth of corals on the tops of the mounds. The present current regime, water temperature or food supply may be less suitable for sustained growth and development of deep-water scleractinian corals. Alternatively, it is possible that fishing activity in the area has previously impacted the coral communities, and that intermittent trawling pressure does not allow time for continual long-term growth (Fosså et al. 2002). It may be that the coral communities on this mound system were in natural decline due to changes in oceanographic conditions prior to the advent of sustained trawling activity in Mauritanian waters.

Of the four species of scleractinian corals identified from dead coral fragments recovered from core samples, *S. variabilis* and *Desmophyllum* sp. may represent new records for this region. In a review of the biogeographic affinities of North Atlantic deep-water Scleractinia, Cairns and Chapman (2001) listed 14 species that had been recorded for the Mauritania region (coasts of Mauritania and Senegal: 22°-13°N). Of these, five species were reported to have depth ranges that spanned 500 m - *L. pertusa, M. oculata, Dendrophyllia cornigera* (Lamarck, 1816), *Coenocyathus cylindricus* (Milne Edwards and Haime, 1848) and *Flabellum macandrewi* (Gray, 1849). The depth ranges of the other nine species fall outside the water depth range of the carbonate mound system in Mauritanian waters. Positive taxonomic identification of coral species is problematic in this instance, given the heavily degraded nature of some of the fragments recovered for analysis from the core samples.

Are mounds hydrocarbon-related?

There is some evidence, from seismic data and geochemical analysis of core samples, of active hydrocarbon seepage down-slope of the mounds in the area of the Chinguetti field location (Woodside 2002). The zone that appears most preferential for upward migrating hydrocarbons has a water depth range of 650-700 m, and

water temperatures in this zone are appropriate for the formation of gas hydrates. To date, there is no indication, from seismic data or geochemical studies, of present day hydrocarbon seepage in the vicinity of the carbonate mound system. No chemosynthetic species have been identified so far from the sampling of epibenthic or infaunal communities inhabiting the mounds.

Are they linked to oceanographic conditions?

The water depth range (450-550 m) for the mound system coincides with a weak thermocline (Fig. 7a) and a well-developed halocline feature (Fig. 7b). The marked halocline is believed to result from saline Canary Current water overlying fresher Atlantic Antarctic Intermediate Water (AAIW). The hypothesis is that this interface may have promoted and sustained the development of deep-water corals and other carbonate-producing, suspension-feeding organisms in this region. Internal waves moving along this boundary layer, and breaking once they reach the seabed, may cause a redistribution of suspended particles in the bottom mixed layer. This causal factor has been indicated from other studies of other deep-water coral ecosystems in the Northeast Atlantic (Frederiksen et al. 1992). As reported by Rogers (1999), there are many observations that indicate that *L. pertusa* is found in areas where current-seabed topography interactions generate accelerated flow close to the seabed. No physical indicators of high bottom current speeds, such as sand waves or ripples, were observed for the Mauritanian mound locations during the video surveys. Data from 500 m water depth west of the mound system indicates low current speeds, in the order of 10 cm s^{-2}. The low amplitude sediment waves observed between the carbonate mounds and the Chinguetti field location may be indicative of a previous period of higher current speeds close to the seabed.

The presence of buried mounds (Fig. 6) that formed at a similar water depth to the present day system suggests that oceanographic conditions may have promoted their formation. The oldest of the buried mounds are estimated to be of Pleistocene age (1-2 million years ago). Whilst the evidence suggests that the corals on the present day mound system may be reliant on hydrographic conditions for their survival, this does not discount the possibility that hydrocarbon seepage was an initial factor in promoting the formation of carbonate mounds in the first place, as suggested for other mound systems in the Northeast Atlantic margin (Hovland et al. 1994; Henriet et al. 1998; Hovland et al. 1998). The presence of chemosynthetic communities, utilising hydrocarbons as an energy source, may have formed a carbonate crust upon which corals and other organisms could settle and grow. It is well established that *Lophelia* requires hard substrate on which to attach (Wilson 1979; Rogers 1999).

Fishing activity

Both pelagic and demersal trawling fleets operate in Mauritania's Exclusive Economic Zone (EEZ) (Fig. 1). The intensity of fishing operations in the sector covering the Chinguetti field location indicates that it is situated within a major fishing zone for demersal trawlers, targeting cephalopods, hake, shrimp and crab

on or just above the seabed, and also for large pelagic trawlers, targeting schools of small pelagic species (e.g., sardines, sardinella and mackerel) (Oceanic Development 2002). The smaller demersal trawlers are believed to operate to ~600 m water depth in vicinity of the Chinguetti field location, and deploy smaller and lighter trawling gear than the pelagic trawlers. Observations indicate that the frequency of demersal trawlers increases to the east, in shallower waters further up the slope and onto the continental shelf (Oceanic Development 2002).

The upper continental slope along the entire Northwest African margin has been targeted by demersal trawling fleets targeting crustaceans and fish. Target species include *Palinurus mauritanicus* (southern spiny lobster), *Parpenaeus longirostris* (deep-water rose shrimp), *Aristeus varidens* (striped red shrimp), *Chaceon maritae* (deep-water red crab) and *Merluccius* spp. (Senegalese hake, Benguela hake, and black hake) (Cervantes and Goni 1985; Sobrino and Garcia 1991; Sobrino and Garcia 1997; Ramos et al. 1998). The southern spiny lobster *P. mauritanicus* occurs between 60 and 600 m water depth and has been reported to be particularly common near coral formations off the Northwest African coast (Maigret 1985). Coral species recorded as bycatch from fisheries for *P. mauritanicus* included *Dendrophyllia ramea, Dendrophyllia cornigera* and *Lophelia pertusa* (cited as *Lophohelia prolifera*).

The crustacean fishery off Northwest Africa started in the early 1960s when some 3,595 tonnes were taken annually. By 1970, the catches had fallen dramatically to only 200 tonnes per annum. The catches have made a small recovery through management of the fishery, but are still much lower than the original catches (Maigret 1985). The black hake fishery occurs principally between 200 m and 600 m water depth. Until the mid 1970s, eastern European fleets landed more than 10,000 tonnes of hake annually. At present, the Spanish fishing fleet is apparently the only one actively targeting hake, catching about 12,000 tonnes annually (Ramos et al. 1998). There was a clear cycle of boom and bust of this fishery over a period of only a few years.

The deep-water red crab *C. maritae*, observed on video imagery from both of the survey sites and also found in epibenthic sledge samples taken in July 2003 (Fig. 10b), occurs between 300 m and 700 m water depth (Sobrino and Garcia 1991). Demersal trawl fisheries for this species, and for *P. longirostris* and *A. varidens*, leads to a large bycatch - about 89 % of the catch (by weight) is discarded. Of some 147 species collected by trawls, only two species are targeted, about 2 % of the catch (Sobrino and Garcia 1997).

Given the level of demersal trawling activity that has occurred on the Northwest African continental shelf and upper slope, including the waters of Mauritania's EEZ, since the 1960s and particularly in the 1970s, it is highly likely that seabed habitats have been significantly modified. This may particularly be the case for coral communities associated with carbonate mounds, as fish and crustacean species would have probably used these areas for shelter, and as feeding and perhaps nursery grounds. Whilst it is not known whether the coral ecosystems in Mauritania's waters functioned as critical habitat for commercially important

fish and crustaceans, major physical impacts on them from trawling activities may well have had a significant effect on the sustainability of some of these deep-water fisheries (Fosså et al. 2002).

Trawl scars, which are linear scour features in soft sediments on the seabed, are evident from side-scan sonar and video images of the seabed in water depths of at least ~700-750 m in the vicinity of the Chinguetti field. The frequency of trawl scars increases up the continental slope in shallower waters (Fig. 11), which probably reflects increased activity, particularly by demersal trawlers targeting crustaceans on the seabed. No side scan sonar data has been acquired over the mound areas to date, and no signs of recent trawling impacts were seen in video imagery of the seabed at either of the two mound areas surveyed.

Trawling damage to *Lophelia* reefs and other corals has been reported for a number of locations in the Northeast Atlantic, including waters off the Norwegian coast (Fosså et al. 2002), the continental slope area west of Ireland (Hall-Spencer et al. 2002) and the northern Rockall Trough (Wheeler et al. in press; Wheeler et al. submitted).
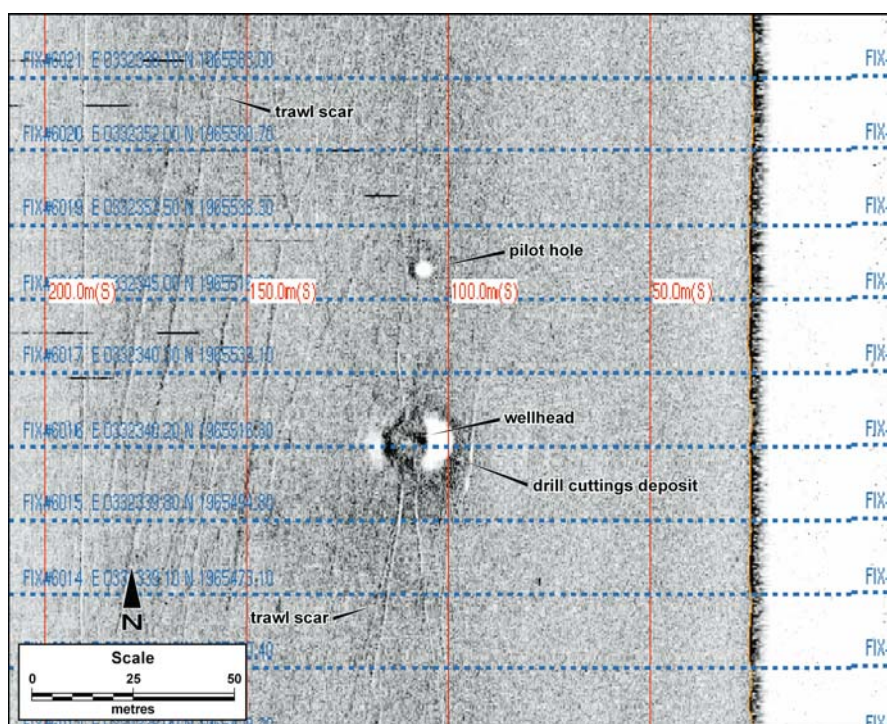
Fig 11 Trawl scars identified in 120 kHz side scan sonar data collected over the Chinguetti-4-3 well site (270 m water depth)

Threats from hydrocarbon exploration and exploitation activities

The activities of the offshore oil and gas industry present another potential threat to deep-water coral communities. In some areas of the Northeast Atlantic, discharges of drill cuttings and drilling mud from the drilling of exploration, appraisal and production wells has been identified as a significant threat to *Lophelia* and other deep-water coral species (Rogers 1999). Corals are generally sensitive to the effects of sedimentation and several studies have examined the effects of drill cuttings and drilling muds on shallow-water, reef-forming corals (cited in Rogers 1999). Reviews of these studies have indicated that there is no clear-cut separation between the effects on corals resulting from sedimentation alone, against those caused by the chemical constituents of drilling muds, or as a result of synergistic effects between the two (Rogers 1999).

These studies have established that exposure of corals to drill cuttings and drilling muds can result in: death of the coral colony *via* smothering; alteration of feeding behaviour; disruption of the normal pattern of polyp expansion and retraction; alteration of coral physiology; morphological changes; and disruption of coral calcification (Rogers 1999). A concentration of 100 mg L (drilling mud-in-water) appears to be critical in causing noticeable effects on coral function. However, it is evident that the tolerance of individual species to the effects of drill cuttings and drilling muds is highly variable, and these results cannot be extrapolated directly from one species to another, or from shallow to deep-water coral habitats - particularly given the lack of information for deep-water species (Rogers 1999).

Deep-water corals tend to be found in areas with low rates of sedimentation (Mortensen et al. 2001), and they have lower growth rates than the majority of shallow water corals - consequently they are relatively long-lived. Given that *Lophelia* - and other reef-forming, deep-water corals - are suspension feeders, increases in sediment load in the water may affect the feeding apparatus of these animals, and consequently impact on growth rates. At worst, *Lophelia* may be killed by sedimentation and recolonisation may be prevented. Sedimentation resulting from drill cuttings and drilling mud discharge is also likely to have a significant impact on associated faunal communities, particularly those that are also suspension feeders (Rogers 1999).

At present, drilling activity in the vicinity of the mound system in Blocks 2-6 in Mauritanian waters is limited, as the focus of interest is on the potential development of the Chinguetti oil field, which is located in ~800 m water depth some 12 km WNW of the closest area of mounds. However, exploration wells have been drilled in close proximity of the mounds in the past, and further ones could be drilled in these areas in the future. Localised effects from the discharge of drill cuttings and associated drilling mud could be significant if the benthic communities are already widely impacted by trawling activities over a wide area. Effects could also be more significant if there are wells drilled in locations where adjacent carbonate mounds have a much higher coverage of live coral than that observed at the two sites surveyed to date.

Conclusions

The main observations from this study are:

- Deep-water carbonate mounds occur in Mauritanian waters;
- This is the first recorded observation of mounds in this area of the Northeast Atlantic margin;
- Both seabed and buried mounds have been observed;
- This could constitute one of the largest mound occurrences so far discovered;
- The mounds occur in a hydrocarbon basin but do not appear to be seepage-related;
- The mounds could be related to oceanographic conditions;
- Live coral cover on the mounds appears to be much less than was previously present; and
- It is unclear whether the decline in coral communities has occurred as a result of demersal trawling activity, or from past changes in oceanographic conditions, or from a combination of these two factors.

A key aspect in managing threats to benthic communities inhabiting the carbonate mound system in Mauritanian waters is the acquisition of further information. Studies carried out to date, as reported here, are preliminary in nature. Future research effort should be targeted to address a number of critical information needs. As identified by McDonough and Puglise (2003) and Puglise et al. (2005), three categories of research studies are necessary to address these needs:

1. Mapping - determination of the location of carbonate mounds outside the area already studied.
2. Biology and ecology - detailed assessment of the status of deep-water corals and associated biological communities on the mounds.
3. Palaeoclimate analysis - investigation of the physical characteristics of the mound structures, and determination of the processes that led to their formation, and maintain them to the present day.

Without this detailed information, it is going to be difficult to determine, and subsequently manage, potential anthropogenic impacts on these deep-water reefal systems, whether from commercial trawl fisheries or from the offshore oil and gas industry. If further studies establish that previous trawling effort has severely reduced the levels of live coral cover on these mounds, what are the chances of recovery and over what time frame? Detailed knowledge of the location and status of coral communities will assist in the process of determining the best management approach to conserve what remains of these systems, and to promote recovery. Options could include exclusion zones for demersal trawlers, or perhaps deep-water marine protected areas.

Engagement of all stakeholders will be a key aspect in conservation efforts, whether it will be the fishing industry, the Government of Mauritania, the scientific community or non-governmental environmental and conservation organisations. Management of interactions between the fishing industry and the offshore oil and gas industry will be central to future conservation of this resource. Collaboration between the scientific community, government regulators and oil companies will also be beneficial, as demonstrated by the constructive partnerships between these stakeholders in other areas of the Northeast Atlantic.

Acknowledgements

References

AFEN (2000) Atlantic margin environmental surveys of the seabed 1996 and 1998. UK Offshore Operators Assoc, CD-ROM ISBN 0-9538399-0-7

BBG (2002) Video surveys of carbonate mounds in offshore Mauritania, July 2002. Bowman Bishaw Gorham, Rep R02084, Woodside Energy Ltd, Perth, Australia (unpublished)

BBG (2004) Benthic surveys of the Chinguetti oil field and adjacent carbonate mounds, offshore Mauritania, July 2003. Rep R03005FR, Woodside Energy Ltd, Perth, Australia (unpublished)

Cairns SD, Chapman RE (2001) Biogeographic affinities of the North Atlantic deep-water Scleractinia. In: Willison JHM, Hall J, Gass SE, Kenchington ELR, Butler M, Doherty P (eds) Proceedings of the First International Symposium on Deep-Sea Corals. Ecology Action Centre and Nova Scotia Museum, Halifax, Nova Scotia, pp 30-57

Cervantes A, Goni R (1985) Descripcion de las pesquerias espanolas de merluzas y crustaceos de Africa Occidental al norte de cabo Blanco. Int Symp Upwelling off West Africa. Invest Pesqueras Barcelona 2: 825-850

CNROP (1991) L'environnement, les resources et les pecheries de la Zee Mauritanienne. In: Chavance P, Girardin M (eds) Bull Centre Nat Rech Oceanogr Peches 23/1991. Ministere des Peches et de l'Economie Maritime, Nouâdhibou

Croker PF, O'Loughlin O (1998) A catalogue of Irish offshore carbonate mud mounds. In: De Mol B (ed) Geosphere-biosphere coupling: carbonate mud mounds and cold-water reefs. Int Conf Sixth Post-Cruise Meet Training Through Res Programme. Gent, Belgium, 7-11 February 1998. Intergov Oceanogr Comm Workshop Rep 143, UNESCO

De Mol B, Van Rensbergen P, Pillen S, Van Herreweghe K, Van Rooij D, McDonnell A, Huvenne V, Ivanov M, Swennen R, Henriet JP (2002) Large deep-water coral banks in the Porcupine Basin, southwest of Ireland. Mar Geol 188: 193-231

Fosså JH, Mortensen PB, Furevik DM (2002) The deep-water coral *Lophelia pertusa* in Norwegian waters: distribution and fishery impacts. Hydrobiologia 471: 1-12

Frederiksen R, Jensen A, Westerberg H (1992) The distribution of the scleractinian coral *Lophelia pertusa* around the Faroe Islands and the relation to internal tidal mixing. Sarsia 77: 157-171

Freiwald A, Wilson JB, Henrich R (1999) Grounding Pleistocene icebergs shape recent deep-water reefs. Sediment Geol 125: 1-8

Fugro GEOS (1999) Current Regime Offshore Mauritania. Fugro GEOS Rep C50075, Woodside Energy Ltd, Perth, Australia (unpublished)

GeoSed (2002) Preliminary geohazards study Chinguetti Cluster Development, Mauritania. GeoSed Ltd, Rep 2002/03, Woodside Energy Ltd, Perth, Australia (unpublished)

Hall-Spencer J, Allain V, Fosså JH (2002) Trawling damage to Northeast Atlantic ancient coral reefs. Proc R Soc London B 269: 507-511

Henriet JP, De Mol B, Pillen S, Vanneste M, Van Rooij D, Versteeg W, Croker PF, Shannon PM, Unnithan V, Bouriak S, Chachkine P (1998) Gas hydrate crystals may help build reefs. Nature 391: 648-649

Hovland M, Croker PF, Martin M (1994) Fault-associated seabed mounds (carbonate knolls?) off western Ireland and North-west Australia. Mar Petrol Geol 11: 232-246

Hovland M, Mortensen PB, Brattegard T, Strass P, Rokoengen K (1998) Ahermatypic coral banks off mid-Norway: evidence for a link with seepage of light hydrocarbons. Palaios 13: 189-200

Huvenne VAI, De Mol B, Henriet JP (2003) A 3D seismic study of the morphology and spatial distribution of buried mounds in the Porcupine Basin. Mar Geol 198: 5-25

Kenyon N, Akhmetzhanov AM, Wheeler AJ, van Weering TCE, de Haas H, Ivanov MK (2003) Giant carbonate mounds in the southern Rockall Trough. Mar Geol 195: 5-30

Maigret C (1985) Les stocks de Palinuridae de la cote nord-ouest africaine. Int Symp Upwelling off West Africa. Invest Pesqueras Barcelona 2: 977-987

Masson DG, Bett BJ, Billett DSM, Jacobs CL, Wheeler AJ, Wynn RB (2003) The origin of deep-water, coral-topped mounds in the northern Rockall Trough, Northeast Atlantic. Mar Geol 194: 159-180

McDonough JJ, Puglise KA (2003) Summary: Deep-Sea Corals Workshop. International Planning and Collaboration Workshop for the Gulf of Mexico and the North Atlantic Ocean. Galway, Ireland, January 16-17, 2003. US Dept Commerce, NOAA Tech Memo NFMS-F/SPO-60, 51 pp

Minas HJ, Codispoti LA, Dugdale RC (1982) Nutrients and primary production in the upwelling region off Northwest Africa. Rapp P-v Réun Cons Int Explor Mer 180: 148-183

Mittlesteadt E (1983) The upwelling area off Northwest Africa - a description of phenomena related to coastal upwelling. Progr Oceanogr 12: 307-331

Mittlesteadt E (1991) The ocean boundary along the northwest Africa coast: circulation and oceanographic properties at the sea surface. Progr Oceanogr 26: 307-355

Mortensen PB, Hovland M, Brattegard T, Farestveit R (1995) Deep water bioherms of the scleractinian coral *Lophelia pertusa* (L.) at 64ºN on the Norwegian Shelf: structure and associated megafauna. Sarsia 80: 145-158

Mortensen PB, Hovland M, Fosså JH, Furevik D (2001) Distribution, abundance and size of *Lophelia pertusa* coral reefs in mid-Norway in relation to seabed characteristics. J Mar Biol Ass UK 84: 581-597

Oceanic Development (2002) Fisheries Assessment Study Mauritania. Final Report by Oceanic Development in association with Promoconsult, with the support of IMROP, for Woodside Australian Energy, October 2002 (unpublished)

O'Reilly BM, Readman PW, Shannon PM, Jacob AWB (2003) A model for the development of a carbonate mound population in the Rockall Trough based on deep-towed sidescan sonar. Mar Geol 198: 55-66

Puglise KA, Brock RJ, McDonough JJ (2005) Identifying critical information needs and developing institutional partnerships to further the understanding of Atlantic deep-sea coral ecosystems. In: Freiwald A, Roberts JM (eds) Cold-water Corals and Ecosystems. Springer, Berlin Heidelberg, pp 1129-1140

Ramos A, Fernandez L, Gonzalez R (1998) The black hake fishery in the Mauritanian EEZ: analysis of the possible application of a 30 cm minimum. Informes Tecnicos. Inst Espan Oceanogr 173, 40 pp

Roberts JM, Long D, Wilson JB, Mortensen PB, Gage JD (2003) The cold-water coral *Lophelia pertusa* (Scleractinia) and enigmatic seabed mounds along the north-east Atlantic margin: are they related? Mar Pollut Bull 46: 7-20

Rogers AD (1999) The biology of *Lophelia pertusa* (Linnaeus, 1758) and other deep-water reef-forming corals and impacts from human activities. Int Rev Hydrobiol 84: 315-406

Roy C (1992) Réponses des stocks de poissons pélagiques à la dynamique des upwellings en Afrique de l'ouest: analyse et modélisation. ORSTOM, Paris, 146 pp

Sobrino I, Garcia T (1991) Analisis y descripcion de las pesquerias de crustaceos decapodos en agues de la republica islamica de Mauritania durante el periodo 1987-1990. Informes Tecnicos. Inst Espan Oceanogr 112, 18 pp

Sobrino I and Garcia, T (1997) Analisis de los Descartes producidos por la flota Espanola en la pesqueria de crustaceos decapodos en agues de la republica islamica de Mauritania. Informes Tecnicos. Inst Espan Oceanogr 166, 24 pp

Van Weering TCE, de Haas H, De Stigter HC, Lykke-Andersen H, Kouvaev I (2003) Structure and development of giant carbonate mounds at the SW and SE Rockall Trough margins, NE Atlantic Ocean. Mar Geol 198: 67-81

Wheeler AJ, Bett, BJ, Billett DSM, Masson DG, Mayor D (in press) The impact of demersal trawling on NE Atlantic deep-water coral habitats: the case of the Darwin Mounds, UK. In: Thomas J, Barnes P (eds) Benthic Habitats and the Effects of Fishing. Amer Fish Soc, Bethesda, Maryland, USA

Wheeler AJ, Kozachenko M, de Haas H, Henriet JP, Huvenne V, Masson DG, Olu-Le Roy K (submitted) Hydrodynamically influenced small deep-water reefs (Moira Mounds) in the Porcupine Seabight, NE Atlantic. Int J Earth Sci

Wilson JB (1979) The distribution of the coral *Lophelia pertusa* (L.) [*L. prolifera* (Pallas)] in the north-east Atlantic. J Mar Biol Soc UK 59: 149-164

WNI (2002) Mauritania Development metocean measurements, August to December 2002. Rep R1152, Woodside Energy Ltd, WNI Oceanographers & Meteorologists, Australia (unpublished)

Woodside (2002) Mauritania integrated remote sensing and seabed studies. Rep VT00092, Woodside Energy Ltd, Perth, Australia (unpublished)

Wynn RB, Masson DG, Stow DAV, Weaver PE (2000) The Northwest African slope apron: a modern analogue for deep-water systems with complex seafloor topography. Mar Petrol Geol 17: 253-265

Mapping, habitat characterization, and fish surveys of the deep-water *Oculina* coral reef Marine Protected Area: a review of historical and current research

John K. Reed[1], Andrew N. Shepard[2], Christopher C. Koenig[3],
Kathryn M. Scanlon[4], R. Grant Gilmore Jr.[5]

[1] Harbor Branch Oceanographic Institution, 5600 U.S. 1, North, Fort Pierce, FL
   34946, USA
   (jreed@hboi.edu)
[2] National Undersea Research Center, University of North Carolina, 5600 Marvin
   K. Moss. Lane, Wilmington, NC 28409, USA
[3] Institute for Fishery Resource Ecology (FSU/NMFS), Florida State University,
   Tallahassee, FL 32306-1100, USA
[4] U.S. Geological Survey, 384 Woods Hole Road, Woods Hole, MA 02543, USA
[5] Estuarine, Coastal, and Ocean Sciences, Inc., 5920 1st St. SW, Vero Beach, FL
   32968, USA

Abstract. Deep-water *Oculina* coral reefs, which are similar in structure and development to deep-water *Lophelia* reefs, stretch 167 km (90 nm) at depths of 60-100 m along the eastern Florida shelf of the United States. These consist of numerous pinnacles and ridges, 3-35 m in height, that are capped with thickets of living and dead coral, *Oculina varicosa*. Extensive areas of dead *Oculina* rubble are due in part to human impacts (e.g., fish and shrimp trawling, scallop dredging, anchoring, bottom longlines, and depth charges) but also may be due in part to natural processes such as bioerosion, disease, or global warming. In the 1970s, the reefs were teeming with fish. By the early 1990s, both commercial and recreational fisheries had taken a toll on the reefs, especially on the coral habitat and populations of grouper and snapper. In 1984, 315 km^2 (92 nm^2) was designated the *Oculina* Habitat of Particular Concern (OHAPC), prohibiting trawling, dredging, bottom longlines and anchoring, and establishing the first deep-sea coral marine protected area in the world. In 2000, the *Oculina* Marine Protected Area (MPA) was expanded to 1029 km^2 (300 nm^2). Despite these protective measures, manned submersible and ROV observations in the *Oculina* MPA between 1995 and 2003 suggest that portions of the coral habitat have been reduced to rubble since the 1970s, grouper spawning aggregations may be absent, and illegal trawling continues. This paper

is a review of the results of the mapping, habitat characterization, and fish surveys from the early historical studies (1960-1980s) to the more recent surveys (1995-2003).

Keywords. *Oculina*, *Lophelia*, deep-water, coral reef, Marine Protected Area

Introduction

Two types of deep-water coral reefs, formed principally by the framework constructing species of scleractinian corals, *Oculina varicosa* and *Lophelia pertusa*, occur off the southeastern United States. Deep-water *Oculina* reefs grow at depths of 60-100 m and are only known off central eastern Florida, whereas *Lophelia* reefs in this region occur at depths of 490-870 m from North Carolina to Florida. Both types, however, consist primarily of a single species of azooxanthellate coral, occur in areas of strong currents or zones of upwelling, and form high-relief mounds and pinnacles. Both provide essential habitat for diverse communities of fish and invertebrates (Reed 2002a, b). Deep-water coral reefs have recently gained considerable attention as fisheries expand to deeper habitats. Unfortunately few deep-water reefs have been mapped and little is known regarding the ecology of these diverse and fragile ecosystems.

The *Oculina* reefs are the first deep-water coral reefs in the world to be designated as a marine protected area. The first management plan for these reefs, enacted in 1984 by the South Atlantic Fishery Management Council, banned bottom trawling, bottom longlines, and anchoring in a 315 km^2 (92 nm^2) portion of the *Oculina* reef system (NOAA 1982). The *Oculina* Marine Protected Area (MPA) was expanded in 2000 and now encompasses 1029 km^2 (300 nm^2; Fig. 1).

The deep-water *Oculina* reefs were first described in the 1960s (Moe 1963; Macintyre and Milliman 1970) from dredge and camera drops and from surveys of commercial fisheries. The first detailed submersible surveys describing the reefs began in the 1970s (Avent et al. 1976, 1977; Avent and Stanton 1979; Reed 1980). These were followed by a sidescan sonar survey on a small portion of the bank system (Thompson et al. 1978; Thompson and Gulliland 1980). From 1975 to 1985, various studies followed: coral growth rates, biodiversity of associated invertebrates and fish, and geology (Reed 2002a). Unfortunately over the following years, poaching by illegal shrimp trawlers and fishing pressure resulted in the collapse of the grouper and snapper fish populations as well as considerable damage to the coral habitat (G. Gilmore, J. Reed, personal observations; Koenig 2001; Koenig et al. 2004).

Recent surveys (1995 to present) of the *Oculina* MPA characterized the condition of the coral habitat and fish populations in the only MPA on the U.S. east coast. These surveys have been sponsored largely by the National Oceanic and Atmospheric Administration (NOAA). This paper reviews the results of the mapping, habitat characterization, and fish surveys from the historical studies (1960-1980s) to the more recent surveys (1995-2003).
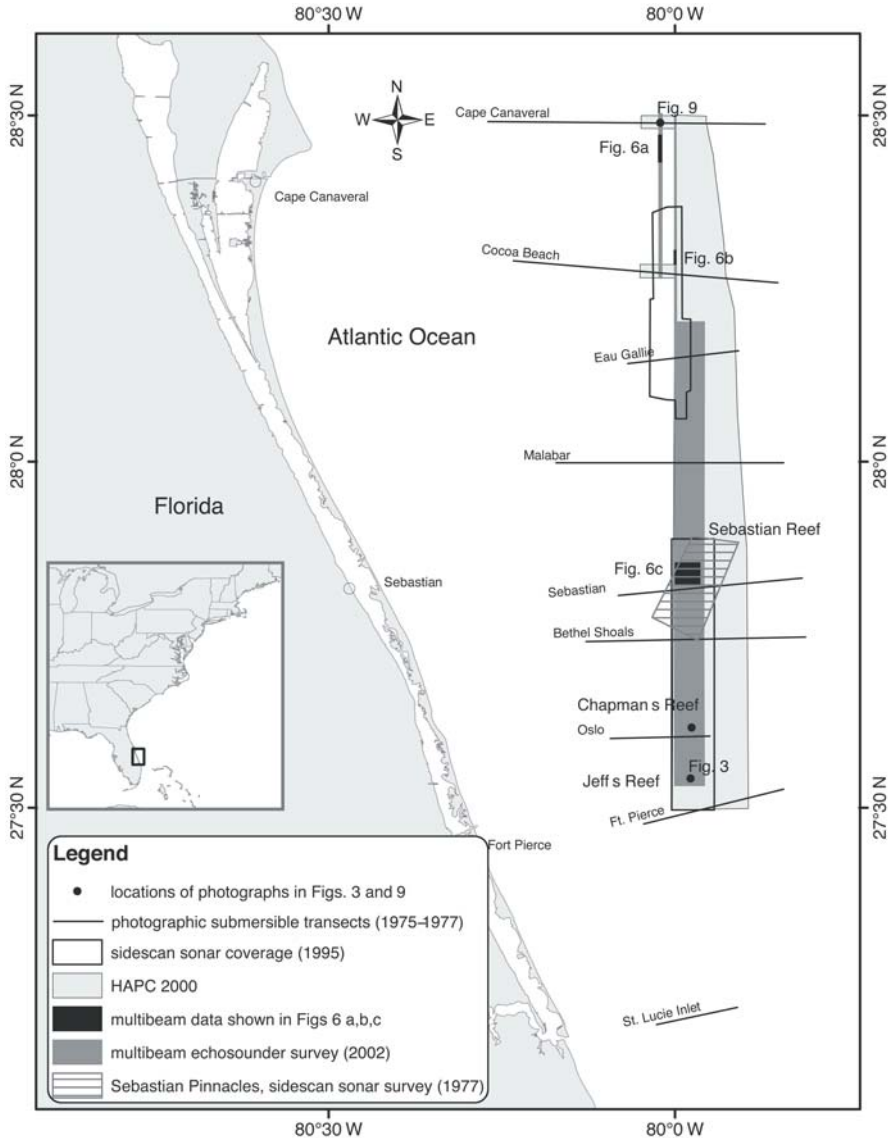
Fig. 1 Light shaded area: 1029 km^2 (300 nm^2) deep-water *Oculina* Marine Protected Area (MPA) off eastern Florida. The original 315 km^2 (92 nm^2) *Oculina* Habitat of Particular Concern (OHAPC) that was designated in 1984 (also known as the Experimental *Oculina* Research Reserve) is indicated by the boxed area (1995 sidescan sonar coverage) that extends from the Sebastian Reef area to the south at the Ft. Pierce transect line

Methods

Historical surveys

1960s dredge and commercial fish surveys

Moe (1963) first described some of the shelf-edge features off eastern Florida based on interviews with commercial fishermen. Macintyre and Milliman (1970) surveyed the physiographic features of the shelf-edge break (80-110 m) from Cape Hatteras, North Carolina (35°N) to Ft. Lauderdale, Florida (26°N) using echosounder profiles, rock dredge, sediment samples, and bottom photographs. Information on coral distribution was also summarized from 57 dredge and trawl records from the R/V *Gosnold* and R/V *Aquarius* between 1973 and 1977 (Reed 1980).

1977 sidescan sonar survey

The Sebastian Pinnacle site (110 km^2), within the region now designated as the *Oculina* MPA, was mapped in 1977-78 using a Klein Series 400 sidescan sonar and echosounder (fathometer) tracings (Fig. 1; Thompson et al. 1978; Thompson and Gulliland 1980). LORAN C was used for positioning which had navigational accuracy in this region of ±36 m in the east-west direction and ±850 m north-south. The fathometer had a vertical resolution of 0.25-1.0 m. Bathymetric maps were plotted with 1 m isobath contours.

1975-1983 submersible and ROV surveys

Between 1975 and 1983, data were compiled in the region of the deep-water *Oculina* banks using Harbor Branch Oceanographic Institution's (HBOI, Harbor Branch Foundation) *Johnson-Sea-Link* (*JSL*) I and II submersibles and *CORD* Remotely Operated Vehicle (ROV). These data included photographs, videotapes, cruise reports, logs, dive transcripts, hydrographic data, and collections by lockout dives from the submersibles.

From 1975 to 1977, a benthic survey consisting of 12 east-west photographic transects was made with the *JSL* submersibles at the shelf-edge break within the region that is now designated as the *Oculina* MPA (Fig. 1; Avent et al. 1976; Avent and Stanton 1979). The transects were spaced approximately 19 km apart, extended to 300 m depth, and consisted of 55 submersible dives covering 298 km. It was during this survey that the live deep-water *Oculina* banks were first observed and described in detail (Avent et al. 1977). Navigation used LORAN-A which in this region had an accuracy of ±150-300 m. Photographs were taken every 1-2 minutes during each transect and analyzed using a microfilm reader with a grid overlay for estimating percent cover. Photographic data along with hydrographic and navigation information were entered into a computer database (unfortunately the computer tapes are obsolete, but hard copies and photos are archived at HBOI).

JSL dives and echosounder recordings were also conducted from 1979 to 1983 for biological and geological studies within the area of the *Oculina* MPA (C. Hoskin, J. Reed pers. observations; see Reed 2002a). In addition, a time-lapse camera was deployed to document the reef community over several 48-hour periods. Extensive

surveys of the fish populations and fish behavior were made concurrently between 1975 and 1983 (G. Gilmore pers. comm.; Gilmore and Jones 1992).

Tethered, mixed-gas dives (lockout) were made with the *JSL* submersibles from 1976 to 1983 on the deep-water *Oculina* banks for studies on biodiversity of animals associated with the coral, coral growth rates, and geology (Fig. 2; Reed 2002a). The scientist-lockout diver used a Kirby-Morgan band mask attached to a 30 m umbilical hose which supplied the gas mix (10 % oxygen / 90 % helium) and voice communications from the submersible.
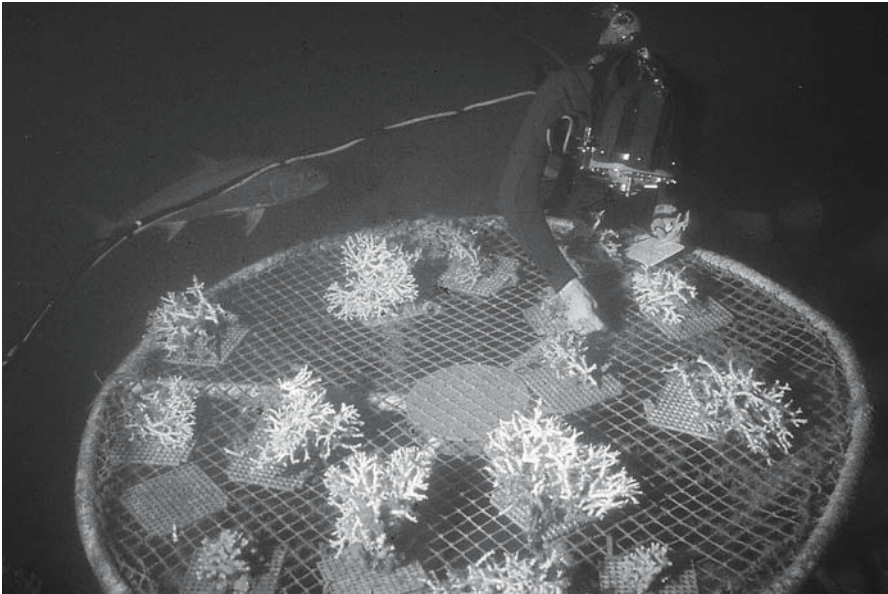
Fig. 2 Tethered, mixed-gas dives (lockout) were made with the *Johnson-Sea-Link* submersibles from 1976 to 1983 on the deep-water *Oculina* reefs for studies on biodiversity of animals associated with the coral, coral growth rates, and geology (Jeff's Reef, 80 m depth)

Videotape and photographic archives

Some of the original videotapes (3/4" and 1/2" open reel) and 30 m rolls of 35 mm Ektachrome film are currently in the process of being restored and archived. Unfortunately videotapes of that age are prone to hydrolysis problems. The restoration process stabilizes the polymers of the tape coating. Once stabilized the tapes will be restored and archived onto Beta SP videotapes and copied to digital video disk (DVD) for analyses. The 35 mm photographs will be digitized with a Nikon LS-2000 scanner and copied to DVD. Plans are to analyze these historical tapes and images for comparison with recent mapping and habitat characterization surveys.

Recent surveys

Most of the recent surveys (1995 to present) of the *Oculina* MPA are a series of continuing research projects to characterize the condition of the coral habitat and fish populations. These surveys have been sponsored largely by NOAA's National Marine Fisheries Service (NMFS), NOAA's National Undersea Research Center at the University of North Carolina at Wilmington (NURC/UNCW), and NOAA's Ocean Service (NOS).

1995 sidescan sonar survey

In 1995, the U.S. Geological Survey, using the NOAA ship *R/V Chapman*, conducted a 100-kHz sidescan sonar survey covering 206 km^2, and approximately 20 % of the *Oculina* MPA (Fig. 1; Scanlon et al. 1999). The goal was to provide reconnaissance geologic maps of the Experimental *Oculina* Research Reserve (EORR; equivalent to the original 315 km^2 *Oculina* MPA) and an unprotected Control Area north of the reserve (now part of the current 1029 km^2 *Oculina* MPA) to support NMFS studies of grouper populations.

2002 multi-beam echosounder survey

In 2002, a multi-beam echosounder survey from NASA's *M/V Liberty Star*, provided the first high-resolution (1.5-3.0 m) bathymetric map of the coral habitat in the *Oculina* MPA and covered 295 km^2, approximately 29 % of the MPA (Fig. 1). Seafloor Systems Inc., Oregon, performed the survey using a 240-kHz RESON 8101 multi-beam echosounder system integrated with the ship's Differential Global Positioning System (GPS) unit, a DMSO 5 TSS motion sensor (quantifies heave, pitch, and roll), a SG Brown gyrocompass (yaw), and HYPACK navigation. All data were compiled in real-time using an ISIS Shipboard Data Acquisition and Image Processing System. Conductivity, temperature and density (CTD) casts were made every six hours. Raw data were post-processed in CARIS software to remove outliers and correct for sound velocity and tidal stage.

1995-2003 ROV and submersible surveys

NOAA/NURC's *Phantom S4* ROV and *Spectrum II* ROV, and HBOI's *Clelia* submersible were used for habitat and fish surveys in 1995, 2001, and 2003. These surveys covered approximately 1.13 km^2, or 0.11 % of the *Oculina* MPA. The ROVs and submersible were equipped with digital still cameras and color video cameras with parallel lasers to indicate scale in the images. Objectives included: (1) survey high-, moderate- and low-relief areas to document the various habitats including live coral thickets, dead coral rubble, and hard bottom, and (2) revisit historical sites identified in the 1970s to document any changes in habitat. In 2003, the position of the ship and ROV were overlaid on the 2002 multi-beam map which allowed precise targeting of specific features for exploration during the dives.

Oculina geographic information system (OGIS)

A multi-media geographic information system (GIS) has been developed to allow access and comparison of past and present data in the *Oculina* MPA. Portions of

OGIS are available *via* the Internet for use by resource managers and stakeholders (http://www.uncw.edu/oculina). Georeferenced digital photographs and logs from submersible dives complete the multi-media component of OGIS.

Results and discussion

Historical surveys

1960s dredge and commercial fish surveys

Moe (1963) first described the shelf-edge region of Cape Canaveral to Fort Pierce, Florida from interviews with commercial fishermen. "The Peaks" at depths of 35 to 65 fathoms (64-119 m) were described as highly irregular coral rock with many peaks and ledges up to 50 fathoms (91 m) high in places and a fishery composed of red and vermilion snapper, red grouper, and trigger fish.

Macintyre and Milliman (1970) described the shelf-edge features from north Florida to north Palm Beach as relict oolitic ridges or dunes formed during the Holocene transgression and covered by modern *Oculina* sp. coral debris. Radiocarbon ages of two samples of oolitic limestone were 13,730 years and 9,620 years B.P. Macintyre and Milliman (1970) stated that the oolitic sediments were apparently deposited and built into mounds during the Holocene transgression and that the 80 m deep oolitic ridge corresponded to the depth of submerged terraces elsewhere in the Caribbean and may indicate a still stand in the rising post-Pleistocene sea level (Fairbanks 1989).

1977 sidescan sonar survey

Sidescan sonar surveys from 1977 to 1978 produced three high-definition contour maps of a 110 km^2 portion of the Sebastian Pinnacles which is a small subset of the region now designated as the *Oculina* MPA (Fig. 1; Thompson et al. 1978; Thompson and Gulliland 1980). They described the region as topographically consisting of bifurcating ridge complexes, irregular knolls, cones, multi-peaked hills, and crater-like depressions. The maps also showed a series of 15 prominences along the 79°59'W meridian from 27°32'N to 28°02'N; many had ridges oriented E-W to SE-NW.

1975-1983 submersible surveys

Reed (1980) described the *Oculina* banks from a compilation of a total of 157 submersible dives (including the Avent dives) and 57 dredge and trawl records. This study described the extensive area of unique deep-water *Oculina* coral reefs which stretches over 167 km (90 nm) along the shelf edge off eastern Florida, at depths of 60-100 m, and ranges from 32 to 68 km offshore (Reed 1980; Thompson and Gilliland 1980). These extend from 27°32'N to 28°59'N latitude, along the western edge of the Gulf Stream (Florida Current).

Deep-water *Oculina* banks are found exclusively here and are not known to exist anywhere else on earth. A single species of azooxanthellate scleractinian coral,

Oculina varicosa Lesueur, 1820, forms these reefs. Individual colonies, up to 2 m in diameter, grow as discrete, branched, spherical heads that coalesce into thickets. The reef system consists of numerous individual coral pinnacles, mounds, and ridges that are low- to high-relief structures, ranging from 3 to 35 m in height and 100-300 m in width (Reed 1980).

High-relief Oculina banks and thickets

In general, the high-relief banks and larger thickets of *Oculina* coral occur in a zone ~6 km wide, paralleling the 80° meridian. In addition to the high-relief pinnacles, coral thickets which consist of 3-4 m linear colonies or groups of 1-2 m diameter colonies are also common on flat sandy bottom or on low-relief limestone outcrops (Reed 1980).

Reed (1980) described the southernmost *Oculina* bank discovered to date at 27°32'N, known as Jeff's Reef and named after the *JSL* submersible pilot Jeff Prentice (Fig. 1). This is an isolated *Oculina* bank, ~300 m in width and somewhat rectangular in shape, that consists of three parallel ridges running approximately E-W, with a minimum depth of 64 m at the crest and 81 m at the base. The south face generally has a steep 30-45° slope and is covered with massive contiguous *Oculina* 1-2 m in height (Fig. 3). In places, the coral colonies form linear E-W oriented rows, 2-3 m in width, that form step-like terraces up the slope. The three ridge crests are covered with live coral 1-2 m in height. The north slope is less steep (<25°) and
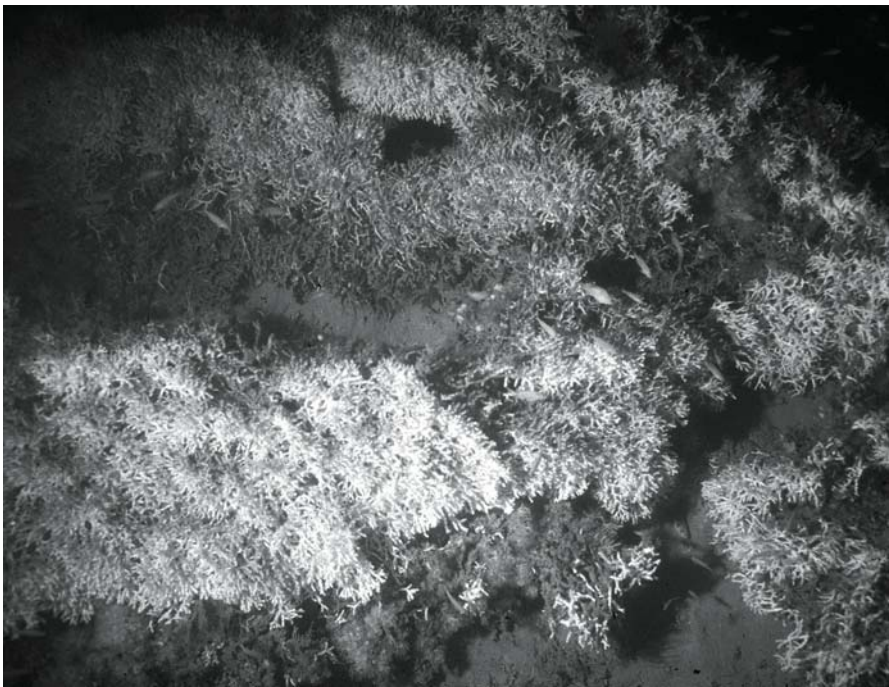
Fig. 3 South slope of Jeff's Reef, a 17 m high *Oculina* coral reef (80 m depth)

has scattered 0.5-2.0 m diameter colonies and more extensive coral rubble. This site appears relatively intact in recent surveys. In 1982, Reed discovered 14-20 m high pinnacles as far north as 28°59.2'N, 80°06.6'W at depths of 79-84 m. These are the northernmost *Oculina* pinnacles discovered to date, and appear to have more exposed rock than the pinnacles south of Cape Canaveral, but also have scattered thickets of live *Oculina*.

During a lockout dive from the *Johnson-Sea-Link* submersible, a 22-cm long, 6-cm diameter core taken from about half way up the flank of the bank sampled a piece of coral rubble with a radiocarbon age of 480 ±70 yr B.P. (Reed 1981; Hoskin et al. 1987). The age of the mound, extrapolated from this and from coral growth rates (1.6 cm yr^{-1}; Reed 1981), was estimated to be 1000 to 1500 years old. It is postulated that the base of these reefs would have been exposed ~18,000 years ago during the last glacial maximum when sea level was 100-125 m below present (Fairbanks 1989).

Isolated colonies and rubble areas

In addition to the high-relief *Oculina* banks and low-relief coral thickets, Reed (1980) further described over 50 sites within the area now designated as the *Oculina* MPA that had sparsely scattered live *Oculina varicosa* colonies from 0.25 to 2.0 m diameter. These were found in areas ranging from low to high relief, including flat sand bottom, limestone pavement, and limestone knolls with 1-2 m relief. Some of the high-relief *Oculina* banks that were mostly dead coral rubble also contained sparse live coral.

Between 27°45'N and 27°52'N, the majority of coral banks in the zone of dense high-relief pinnacles were covered with dead *Oculina* rubble (Fig. 4). This Sebastian Pinnacle site is the same area mapped in part by the 1977 sidescan sonar survey (Thompson et al. 1978). The submersible surveys found that some of these prominences had scattered, live coral colonies, less than 1 m diameter, covering up to 10 % of the bottom while other banks in this region appeared to be 100 % dead coral rubble. The dead coral fragments were less than 10 cm in length, but in some places standing dead colonies less than 0.5 m in diameter were present (Reed 1980; Hoskin et al. 1987).

Fish populations

Surveys of fish populations and grouper behavior were conducted concurrently with the above submersible habitat and coral studies from 1976 to 1983 (G. Gilmore, R. Jones pers. observations). The deep-water *Oculina* reefs formed impressive breeding grounds for commercially important populations of snapper (*Lutjanus* spp.) and grouper (Serranidae), and dense populations of gag (*Mycteroperca microlepis*) and scamp (*M. phenax*) grouper were common (Fig. 5A; G. Gilmore pers. observations; NOAA 1982; Reed 1985; Reed and Hoskin 1987; Gilmore and Jones 1992; Reed 2002a). Scamp were seasonally abundant, forming dense spawning aggregations of several hundred individuals per hectare (Gilmore and Jones 1992).

Fig. 4 Peak of *Oculina* reef covered with dead coral rubble (Sebastian Pinnacles, 60 m depth)

Recent surveys

1995 sidescan sonar survey

A sidescan sonar survey by Scanlon et al. (1999) characterized habitat for portions of the *Oculina* MPA into three principal types. 1) High-relief/high-backscatter (HR/HB) areas constitute very rough terrain that is concentrated along the 80 meter isobath and comprises about 3 % of the total area enclosed in the EORR (the original 315 km^2 *Oculina* HAPC). Portions are isolated peaks with relief up to 30 m. Two large, elongate areas of multiple peaks, ledges, and outcrops occur in the northern portion of the EORR and the northern portion of the Control Area. 2) Low-relief/high-backscatter (LR/HB) areas generally surround HR/HB areas, in 70-90 m depth, but with less than 1 m relief. 3) Low-relief/low-backscatter (LR/LB) areas are generally seaward and landward of the high-relief areas and between the isolated peaks where the seafloor appears to be smooth and is covered by sand and muddy sand. The habitat map derived from these data is included in OGIS.

2001 ROV and submersible-habitat surveys

Seven ROV line transects were made over 7.6 km of high-relief pinnacles and ridges (habitat types 1 and 2, described above) in the EORR. Koenig et al. (2004) reported that 464 m (6 %) of the transects contained dense coral cover, 302 m (4 %)
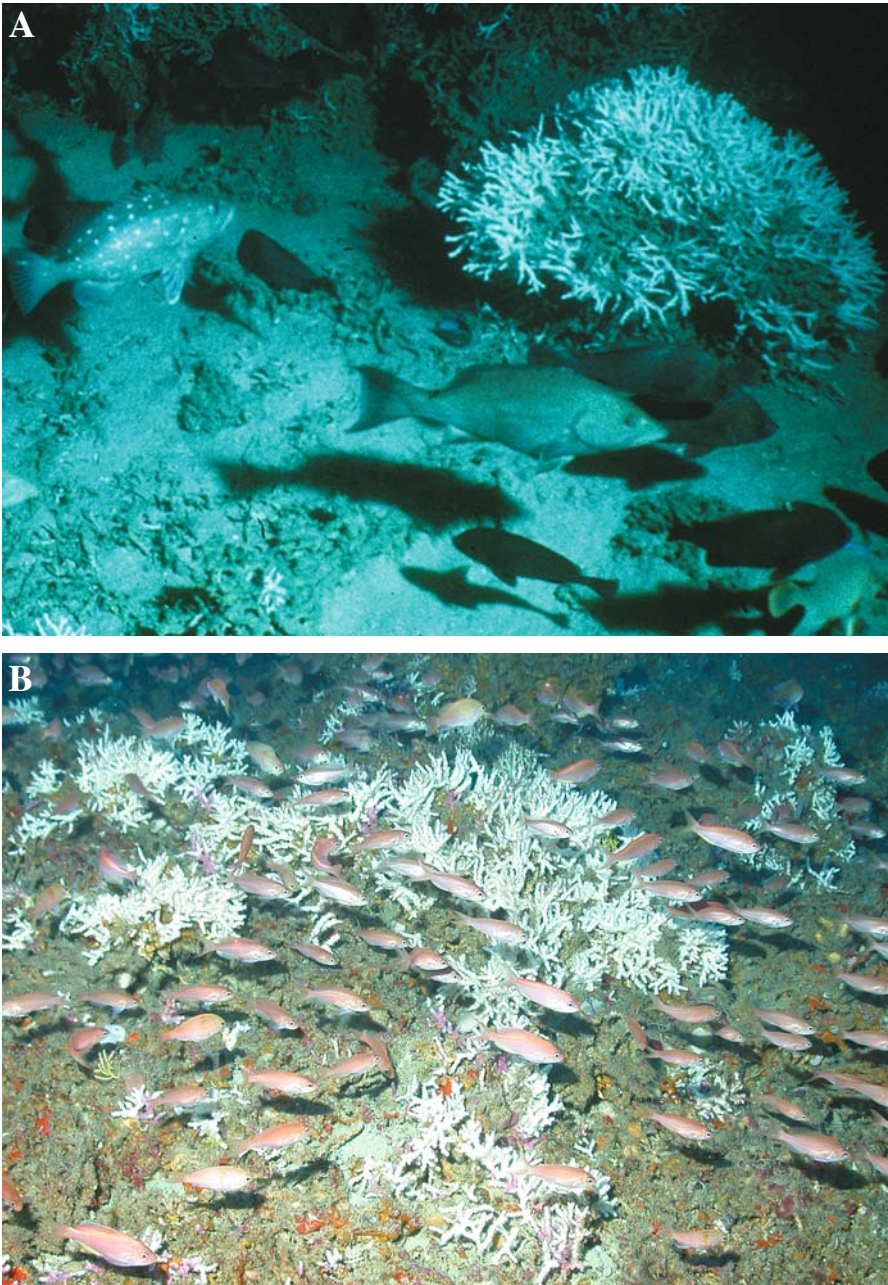
Fig. 5 A Schools of scamp and gag grouper were abundant on deep-water *Oculina* reefs in 1970s and 1980s (Jeff's Reef, 70 m depth); **B** Healthy *Oculina varicosa* coral colony with associated schools of anthiid fish in 2003 (Sebastian Pinnacles, 80 m depth)

contained sparse cover, and 6,877 m (90 %) contained primarily rubble which provides little to no fish habitat.

Koenig et al. (2004) also conducted 16 submersible transects within the EORR at three high-relief *Oculina* coral bank sites (Jeff's Reef, Chapman's Reef West, and Sebastian Reef), and described four habitat types: intact live coral, intact dead coral, coral rubble, and bare rock and sand. Intact live coral thickets occurred on Jeff's Reef and Chapman's Reef West within this survey. Mean live coral coverage ranged from 7 % to 22 %. Coral colony diameter ranged from 8 to 143 cm, with a mean of 47.4 cm (SE = 4.75 cm, n = 43).

Results from the 2001 expedition suggest that within the limited area surveyed (about 0.002 % of the *Oculina* MPA) considerable portions of the *Oculina* habitat consist of unconsolidated coral rubble. Only about 8 hectares (20 acres) of fully intact *Oculina* thicket habitat were documented within this survey. Unconsolidated rubble is the major habitat type on the high-relief features within the Sebastian Pinnacle region.

2002 multi-beam echosounder survey

During eight survey days in 2002, approximately 1704 km of multi-beam echosounder system (MBES) surveys were completed, covering 295 km^2 (~29 % of the total *Oculina* MPA; Fig. 6). The resulting bathymetric map, included in OGIS, was instrumental in dive site selection and in directing the ROV tracks during the 2003 ROV mission described below.

2003 ROV-habitat survey

During this survey, ROV dives were conducted throughout the *Oculina* MPA (Shepard and Reed 2003). Prior to the mission, 30 dive areas were overlaid on the 2002 multi-beam chart targeting the following sites: 1) new sites within and outside the *Oculina* MPA that were never explored previously; 2) sites that had not been explored since submersible dives from 1975-1983; 3) artificial reef and restoration experiments; and 4) a variety of habitats and features based on the multi-beam chart, e.g., high-relief pinnacles and associated scours, moderate-relief ledges and plateaus, and low-relief bottom.

Overall, 23 ROV transects at 20 dive stations produced 40 hr of videotape, 2200 digital still photos (Fig. 5B), and covered approximately 65 km (35 nm) of bottom. Areal coverage was ~0.194 km^2 (65 km x 3 m width transects), or ~0.02 % of the entire 1029 km^2 *Oculina* MPA. The videotapes and still photographs will be analyzed for habitat type and condition, and fish populations; these data will be added to OGIS. Dive results support conclusions from the 2001 expedition that much has changed during the past two decades, including habitat destruction and significantly reduced populations of commercially and recreationally important fish since the 1970s.

Qualitative observations of note from this survey include:

- Several isolated live *Oculina* thickets within the newly expanded *Oculina* MPA were discovered in previously unexplored regions of low to moderate relief (<2-3 m).
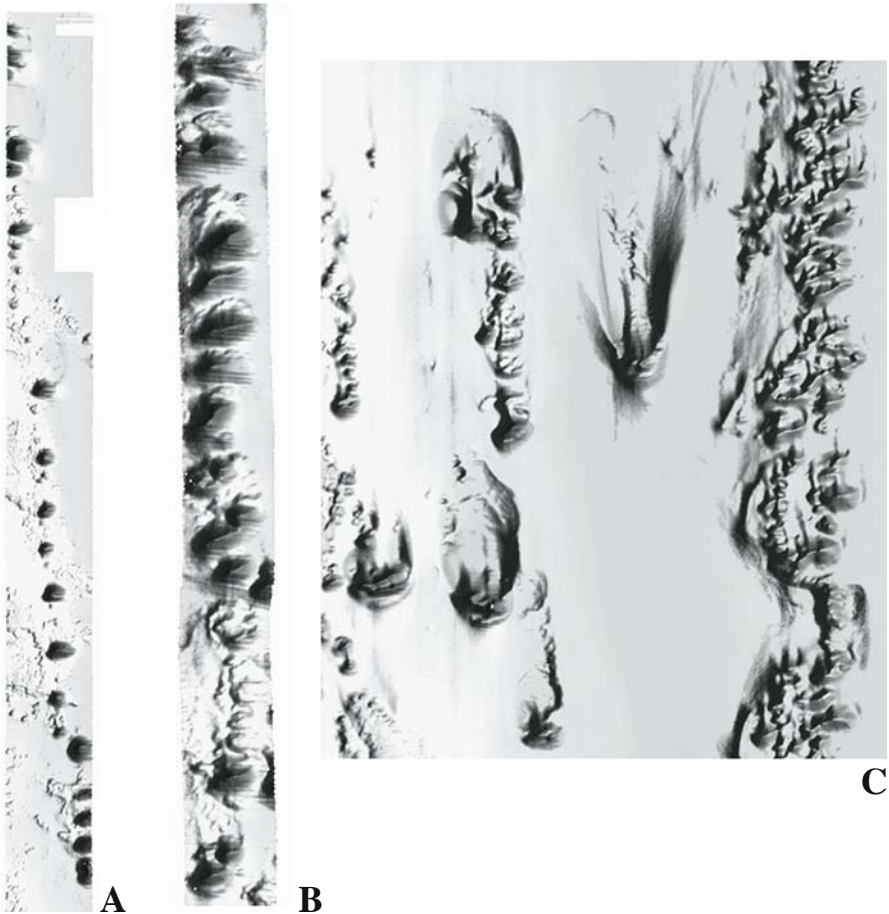
Fig. 6 Multi-beam images of deep-water *Oculina* reefs from 2002 survey: **A, B** series of high-relief pinnacles recently discovered outside the *Oculina* MPA; **C** high-relief pinnacles within the MPA. Scale- length of maps N-S, **A** = 4.3 km (28°28.32'N to 28°25.95'N and 80°01.46'W to 80°01.15'W), **B** = 2.3 km (28°18.33'N to 28°17.08'N and 80°00.10'W to 79°59.92'W), **C** = 3.5 km (27°51.24'N to 27°49.28'N and 80°00'W to 79°57.83'W)

- Extensive live-bottom areas (primarily hard-bottom, limestone pavement and ledges with live benthos and fish) were documented, including considerable portions of the *Oculina* MPA that appeared relatively flat in the multi-beam survey. This supports the need to combine depth and backscatter data not completed in the 2002 multi-beam survey due to technical issues.
- Twenty-three high-relief *Oculina* pinnacles were discovered adjacent to but outside of the current boundaries of the *Oculina* MPA (Figs. 6A, B).
- Evidence during both the 2002 and 2003 surveys indicate that rock-shrimp fishers continue to trawl illegally within the *Oculina* MPA and some bottom fishing continues. This included visual sightings of trawlers during the

surveys; evidence of recent fishing lines and bottom longlines wrapped around coral colonies and remnants of bottom trawl nets; damaged artificial reef modules; and apparent trawl tracks in the rubble noted near the damaged modules (Figs. 7A-C).

- Many of the high-relief pinnacles are primarily coral rubble of unknown age, but many have small (10-50 cm) colonies of live *Oculina* on their slopes. Many also have live bottom at the base of their flanks where rock pavement, boulders and ledges also provide habitat for fish and epifauna.

- Areas of standing dead coral colonies (10-50 cm diameter) are fairly common on high-relief pinnacles, on low- and moderate-relief pavement and rubble areas, and along the rims of depressions that are probable scour areas at the northern bases of the high pinnacles (Fig. 6C). Historical data from the 1970s and 1980s suggest that many of these corals were alive then, but are now dead from unknown cause(s). Since these corals are standing, the cause of death may be other than trawl-related. However, continued trawling in the area may cause resuspension of sediments and smothering of coral polyps.

- Two types of coral rubble habitat are evident: 1) extensive areas of coral rubble/sediment matrix that provide little apparent habitat for epifaunal growth, relative to standing live or dead coral; 2) structured coral rubble habitat, but without the sediment matrix, which provides some habitat *lebensraum* for epifauna, and is often associated with the flanks and peaks of the high-relief pinnacles.

- Most of the pinnacles that have been explored to date, including the newly discovered pinnacles outside the *Oculina* MPA, are *Oculina* bioherms or mud mounds that may be made entirely of unconsolidated coral rubble and sediment, with varying amounts of live coral capping the slopes and peaks. In general, no rock is observed on the upper slopes or peaks on most of these bioherms; but rock pavement and ledges are present near the bases of some of these pinnacles. This suggests the presence of an underlying rock structure on which these bioherms developed several thousands of years ago.

1995-2003 ROV and submersible-fish surveys

Population densities for the dominant fish species correlated highly with habitat type (Koenig et al. 2000; Koenig 2001; Shepard and Reed 2003; Koenig et al. 2004). Gag (*Mycteroperca microlepis*) and scamp (*M. phenax*), grouper and juvenile speckled hind (*Epinephelus drummondhayi*) were predominately associated with the intact coral habitat. In 1994, a 10-year moratorium on bottom hook-and-line fishing was enacted within the *Oculina* MPA. Although fish populations observed in 2001 and 2003 were not directly comparable to previous surveys in 1995 or 1970s,

---

Fig. 7 Damage from fishing gear within *Oculina* MPA: **A** longline fishing gear wrapped around colony of *Oculina varicosa* (Sebastian Pinnacles, 80 m depth); **B** discarded shrimp trawl net (Sebastian Pinnacles, 80 m depth); **C** apparent trawl track at Cape Canaveral Pinnacle site (67 m depth)
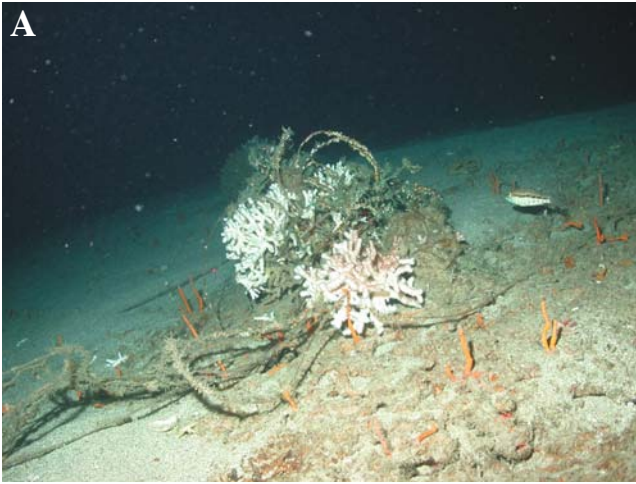
there was a noted increase in grouper numbers and size. There was also an increase in the abundance of males of gag and scamp since the 1995 survey, suggesting the possible reoccurrence of spawning aggregations of both species.

Still, very few commercial reef fish (snapper and grouper) were observed in 2003, even after a 10-year moratorium on bottom fishing. The most common fish encountered included: tattler (*Serranus phoebe*), yellow-tail reef fish (*Chromis enchrysurus*), bigeye (*Priacanthus arenatus*), short-bigeye (*Pristigenys alta*), flounder (*Paralichthys* sp.), bank butterfly fish (*Chaetodon aya*), blue angelfish (*Holocanthus bermudensis*), red barbier (*Hemanthias vivanus*), roughtongue bass (*Holanthias martinicensis*), and greater amberjack (*Seriola dumerili*) (Shepard and Reed 2003). The most common larger grouper observed were red grouper (*Epinephelus morio*) and scamp, although a few snowy (*E. niveatus*) and gag grouper were also present. In the 1970s and 1980s, red grouper were not common on the reefs whereas black sea bass (*Centropristis striata*) were abundant and large (50-100 kg) warsaw grouper (*Epinephelus nigritus*) were common (G. Gilmore, J. Reed pers. observations; Reed 2002a). However, neither black sea bass nor warsaw grouper were observed on any of the recent ROV or submersible dives.

Artificial reef restoration experiments

Surveys also included artificial reef restoration experiments that consist of clusters of 1 m diameter, hollow, concrete domes which were placed in rubble areas of the *Oculina* MPA in 2000 and 2001 (Figs. 8A, B; Koenig 2001; Koenig et al. 2004). The reefballs were constructed to simulate the size and aspect of *Oculina* coral colonies and serve as coral larval recruitment surfaces and structure for reef fish. Gag, scamp and snowy grouper were observed to associate with the reefball clusters. Several artificial reef blocks (~1 m x 1 m aggregates of concrete blocks) that were deployed in 1998 were also revisited in 2003 (Shepard and Reed 2003). Numerous small colonies (1-10 cm) of *Oculina* were photographed growing on the blocks providing additional data on growth rates and evidence of settlement by planula larvae (Brooke and Young 2003). Estimates of the minimum growth rate for the larger corals on the reef blocks was 1.6 to 2.0 cm yr^{-1}, which is similar to previous studies by Reed (1981, 2002a).

Summary and conclusions

Since these deep-water *Oculina* reefs were first discovered and described, irreparable habitat damage and decimated fish populations have occurred (Koenig 2001; Koenig et al. 2004). Recent ROV and submersible surveys have confirmed the evidence of continued poaching by shrimp trawlers and fishers within the *Oculina* MPA. Bottom trawl nets, bottom longlines, and fishing lines are evident on the bottom.

Although the *Oculina* reefs were the first deep-water coral reefs in the world to be designated as a marine protected area, the protection given in 1984 only extended to <30 % of the reef system. Since then, shrimp bottom trawlers were allowed to continue trawling in the northern sector of the reefs until 2000 when the boundary
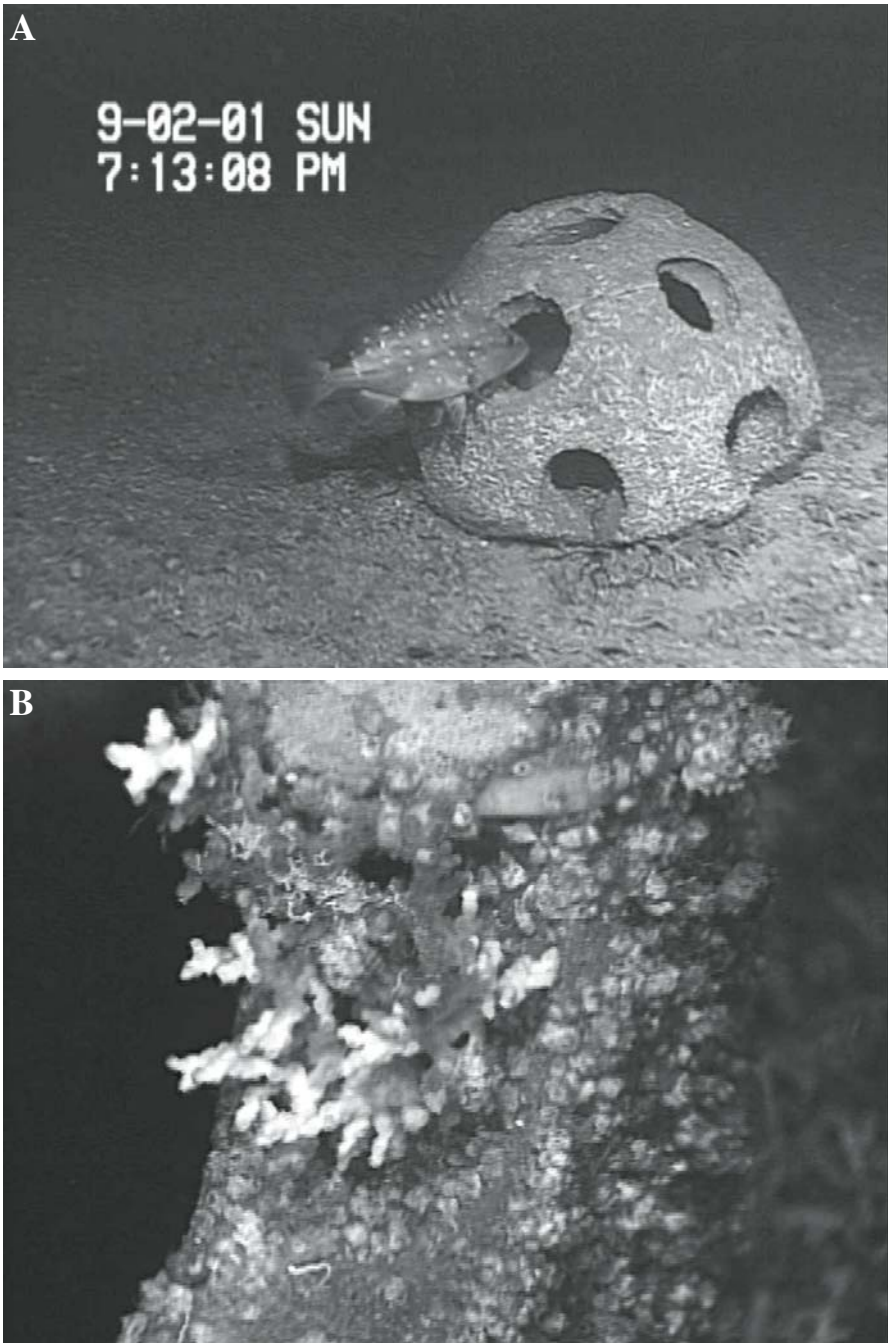
Fig. 8 Reefballs deployed within Sebastian Pinnacles of *Oculina* MPA: **A** reefball with snowy grouper (80 m depth); **B** close-up of *Oculina varicosa* coral growing on reefball (80 m depth)

of the *Oculina* MPA was extended to Cape Canaveral. Even this does not cover the extent of the known deep-water *Oculina* habitat. The 2002 multi-beam survey and the 2003 ROV video transects revealed a series of high-relief *Oculina* bioherms that extend over a linear distance of 22 km just outside the western boundary of the current *Oculina* MPA. Over 23 high-relief *Oculina* mounds were mapped with the multi-beam echosounder outside the reserve, and it is estimated that over 100 bioherms may exist in this unprotected zone. In addition, based on a few submersible dives in 1982, *Oculina* pinnacles extend at least 55 km north of the current *Oculina* MPA, but no recent studies have been made in this region.

Since 1995, surveys have only covered a portion of the *Oculina* MPA and very little of the potential *Oculina* habitat outside the reserve. Areal coverage of all surveys since 1995 (excluding the new sites discovered outside the MPA), includes:

- Submersible dives, 0.45 km^2 (0.13 nm^2) (0.04 % of MPA);
- ROV dives, 0.69 km^2 (0.2 nm^2) (0.07 % of MPA);
- Sidescan sonar survey, 206 km^2 (60 nm^2) (20 % of MPA);
- Multi-beam survey, 295 km^2 (86 nm^2) (29 % of MPA).

Therefore, all ROV and submersible dives combined since 1995 cover less than 0.11 % of the *Oculina* MPA. Only a few of the sites that were described from the surveys of the 1970s have been directly compared to the present. This is, in part, due to the difficulty of precisely pinpointing sites recorded historically with LORAN-A or -C relative to modern GPS as well as due to the limited areal coverage of the recent submersible surveys.

The sidescan and multi-beam maps have been especially helpful in providing high precision details of the bottom topography. Even with these, however, it is not possible to determine the bottom habitat without video or direct visual observation. From the remote geophysical surveys, for example, it is impossible to differentiate intact live coral from standing dead coral, or coral rubble fields from coarse shell hash bottom. From the current multi-beam map, one can only differentiate features of 2-3 m, therefore low- to moderate-relief features can not be ascertained. The recent ROV ground-truthing of the multi-beam map provided new information, including: 1) discoveries of isolated thickets of live *Oculina* that exist within the newly expanded *Oculina* MPA; 2) numerous high-relief *Oculina* bioherms that were previously unknown exist outside the *Oculina* MPA; and 3) extensive areas of live-bottom habitat (primarily hard-bottom, rock pavement and ledges) and *Oculina* thickets occur within the low-relief areas. However, ROV surveys are extremely difficult to conduct on these high-current, high-relief reefs and are limited to drifting with the current in most cases. Human-occupied submersibles have consistently proved to be of greater value in surveying the fish populations and mapping the deep-water *Oculina* reefs.

Recent surveys (1995 to present) documented that the *Oculina* coral habitat on some of the reefs initially described in the 1970s is still thriving and apparently healthy. Most of these healthy reefs that we have surveyed recently occur within the southern portion of the *Oculina* MPA where trawl damage is apparently less than the northern portion.

Evidence of habitat damage, during the interval between the discovery of the *Oculina* reefs and the present, was especially evident from a submersible dive made in 2001 on a 20 m high *Oculina* pinnacle off Cape Canaveral. In 1976, this reef had been described from a submersible dive (*JSL* II-63) as having an estimated 25 to 100 % cover of live *Oculina* coral thickets on the slopes and crest of the reef (Fig. 9A; J. Reed, unpub. dive notes). This region, however, had been open to trawling until 2000 when the *Oculina* MPA was expanded. The 2001 submersible survey (*Clelia* 616), however, found that the coral thickets on the mound had been reduced to rubble (Fig. 9B). Except for a few scattered intact coral colonies at the base, all the coral on the crest and the flanks of the reef had been demolished.

Fish populations have yet to recover from overfishing in the 1980s and 1990s. Population densities of the dominant fish species correlate highly with habitat type (Koenig 2001; Koenig et al. 2004). Speckled hind, which may be designated in the near future as a threatened species, and gag and scamp grouper are predominately associated with the intact coral habitat. Twenty years ago the deep-water *Oculina* reefs formed impressive breeding and feeding grounds for commercially important populations of grouper and snapper. Large spawning aggregations of scamp and gag grouper commonly schooled above individual *Oculina* reefs. Unfortunately these large aggregations made perfect targets for both commercial and recreational fishermen and were decimated by the early 1990s (G. Gilmore pers. observations; Koenig et al. 2000). Even after a 10-year moratorium on hook-and-line fishing for grouper and snapper, which was extended indefinitely in 2003 by the South Atlantic Fishery Management Council, our recent ROV and submersible surveys show limited improvement in fish stocks.

Protection and management

In 1984, the uniqueness, productivity, and vulnerability of the *Oculina* habitat prompted the South Atlantic Fishery Management Council (SAFMC) to declare a 315 km^2 (92 nm^2) portion of the banks a Habitat Area of Particular Concern (HAPC), in order to protect the coral from bottom trawling, dredging, and other mechanically disruptive activities. Impacts of overfishing on grouper spawning aggregations further stimulated the SAFMC in 1994 to close the original HAPC for a period of 10 years to bottom hook-and-line fishing as a test of the effectiveness of a fishery reserve in protecting the reproductive capacity of groupers. The area was called the Experimental *Oculina* Research Reserve (EORR; Fig. 1). In 2000, the *Oculina* HAPC was further expanded to 1029 km^2 (300 nm^2). In 2003, the EORR closure to bottom fishing was extended indefinitely to protect the overfished deep-water species of grouper and snapper. In addition, the SAFMC has mandated that the rock shrimp industry develop and implement a vessel monitoring system (VMS) for the fishery to aid in enforcement of the closed *Oculina* MPA areas. Bottom trawling for rock shrimp and brown shrimp has been the primary threat to these reefs.
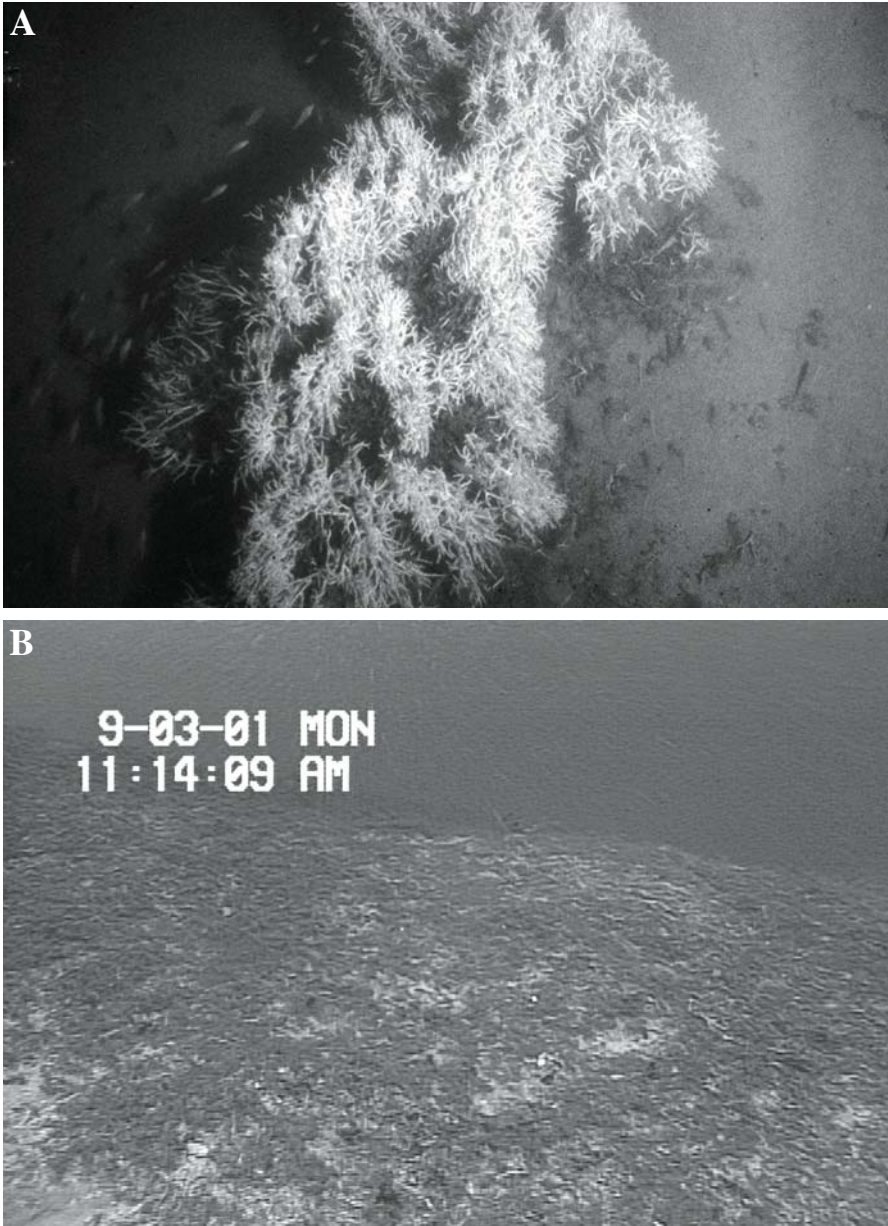
Fig. 9 Peak of 20 m high *Oculina* reef at Cape Canaveral Pinnacle site (67 m depth; 28°29.8'N, 80°01.27'W): **A** historical photo (*JSL* II-63) from June 8, 1976; **B** same site (*Clelia* 616) on Sept. 3, 2001, reduced to rubble from apparent trawling

Future of the *Oculina* MPA

Large gaps still exist in our knowledge of these deep-water *Oculina* reefs. Priorities for habitat mapping and characterization include: 1) complete multi-beam maps of the *Oculina* MPA and adjacent areas that may contain *Oculina* bioherms; 2) ground-truth these maps with submersible and ROV dives to characterize and document the extent and distribution of the *Oculina* reefs and other habitats; 3) document the extent of damage from recent trawling, both by direct mechanical damage and by indirect damage from resuspension of sediments and smothering of coral; 4) document other potential causes of coral death such as possible temperature changes from global warming, increased nutrient loading, or disease; 5) document the recovery of the fish populations and relationships with artificial reefball structures.

We have little data on when or how the coral rubble was formed, especially the vast areas that were rubble in the 1970s. It is important to know how much of this is from natural causes and how much is man-made. For example, during World War II the Sebastian Pinnacle and Bethel Shoals region (Fig. 1) was bombed extensively with depth charges by the U.S. military in search of German U-boat submarines (Cremer 1986). However, the age of dead coral, whether due to trawling *versus* depth charges, is too young for radiocarbon dating. Also little is known about the rubble ecosystem. For example, what role does it play as habitat for shrimp and other benthic fauna? Characterization should continue and experimental research is needed to quantify the value of coral thicket habitat (live and dead of various sizes) *versus* the alternate rubble state.

Certainly, trawling continues to be the primary threat to the ecosystem as evident from recent photographs of trawl nets found on the bottom (Fig. 7), destroyed reefball modules, and the documented destruction of the Cape Canaveral Pinnacle reef in the past 25 years (Fig. 9). Since 2000, illegal trawling has been documented within the *Oculina* MPA, and several poachers have been intercepted by the U.S. Coast Guard. Surveillance and enforcement remain the greatest tasks in protecting the *Oculina* MPA, as well as any deep-water coral reserve. We remain hopeful that the recently mandated use of a vessel monitoring system for the shrimp fishery in this region along with additional enforcement vessels will aid in the long-term protection of the *Oculina* MPA. In addition, proposed projects are envisioned to use surface buoys with satellite relay to monitor the reefs with acoustic devices which could relay real-time data on sounds of boat traffic and illegal trawlers. These could also be used by scientists studying the fish population patterns, and perhaps include arrays of thermographs, current meters, cameras, and other equipment to help understand this remote yet valuable resource.

Acknowledgments

References

Avent RM, King ME, Gore RH (1977) Topographic and faunal studies of shelf-edge prominences off the central eastern Florida coast. Int Rev Ges Hydrobiol 62: 185-208

Avent RM, Stanton FG (1979) Observations from research submersible of megafaunal distribution on the continental margin off central eastern Florida. Harbor Branch Found Tech Rep 25, 40 pp

Avent RM, Stanton FG, Reed JK (1976) Submersible reconnaissance and research program. Harbor Branch Found, Inc, Fort Pierce, Florida, Annu Rep, 52 pp

Brooke S, Young CM (2003) Reproductive ecology of a deep-water scleractinian coral, *Oculina varicosa*, from the southeast Florida shelf. Cont Shelf Res 23: 847-858

Cremer P (1986) U-boat commander. Berkley Books, New York, 244 pp

Gilmore RG, Jones RS (1992) Color variation and associated behavior in the epinepheline groupers, *Mycteroperca microlepis* (Goode and Bean) and *M. phenax* Jordan and Swain. Bull Mar Sci 51: 83-103

Fairbanks RG (1989) A 17,000 year glacialeustatic sea level record: influence of glacial melting rates on younger Dryas event and deep-ocean circulation. Nature 342: 637-642

Hoskin CM, Reed JK, Mook DH (1987) Sediments from a living shelf-edge reef and adjacent area off central eastern Florida. In: Maurrasse F (ed) Symposium on South Florida Geology. Miami Geol Soc Mem 3: 42-57

Koenig CC (2001) *Oculina* banks: habitat, fish populations, restoration, and enforcement. Rep South Atlantic Fish Managem Counc, Charleston, South Carolina, December 1, 2001, 24 pp

Koenig CC, Coleman FC, Grimes C, Fitzhugh G, Scanlon K, Gledhill C, Grace M (2000) Protection of fish spawning habitat for the conservation of warm-temperate reef-fish fisheries of shelf-edge reefs of Florida. Bull Mar Sci 66: 593-616

Koenig CC, Shepard AN, Reed JK, Coleman FC, Brooke SD, Brusher J, Scanlon K (2004, in press) Habitat and fish populations in the deep-sea *Oculina* coral ecosystem of the Western Atlantic. Proc Benthic Habitat Meet, Amer Fish Soc, Spec Publ, Tampa, Florida

Macintyre IG, Milliman GD (1970) Physiographic features on the outer shelf and upper continental slope, Atlantic continental margin, southeastern United States. Bull Amer Geol Soc 81: 2577-2598

Moe MA (1963) A survey of offshore fishing in Florida. Prof Pap Ser 4, Florida State Bd Conserv Marine Lab, St. Petersburg, Florida

National Oceanic and Atmospheric Administration (1982) Fishery Management Plan for Coral and Coral Reefs of the Gulf of Mexico and South Atlantic. Gulf Mexico and South Atlantic Fish Managem Counc, Tampa, Florida, 342 pp

Reed JK (1980) Distribution and structure of deep-water *Oculina varicosa* coral reefs off central eastern Florida. Bull Mar Sci 30: 667-677

Reed JK (1981) *In situ* growth rates of the scleractinian coral *Oculina varicosa* occurring with zooxanthellae on 6-m reefs and without on 80-m banks. Proc 4th Int Coral Reef Symp, Manila 2, pp 201-206

Reed JK (1985) Shelf edge *Oculina* reefs. In: Seaman W (ed) Florida Aquatic Habitat and Fishery Resources. Florida Chapter Amer Fish Soc, Kissimmee, Florida, pp 466-468

Reed JK (2002a) Deep-water *Oculina* coral reefs of Florida: biology, impacts, and management. Hydrobiologia 471: 43-55

Reed JK (2002b) Comparison of deep-water coral reefs and lithoherms off southeastern U.S.A. Hydrobiologia 471: 57-69

Reed JK, Hoskin CM (1987) Biological and geological processes at the shelf edge investigated with submersibles. In: Scientific Applications of Current Diving Technology on the U.S. Continental Shelf. NOAA Symp Ser Undersea Res 2: 191-199

Scanlon KM, Briere P, Koenig C (1999) *Oculina* Bank: sidescan sonar and sediment data from a deep-water coral reef habitat off east-central Florida. U.S. Geol Surv Open File Rep 99-10, CD ROM

Shepard A., Reed JK (2003) *Oculina* Banks 2003: characterization of benthic habitat and fish populations in the *Oculina* Habitat Area of Particular Concern (OHAPC), Mission Summary Report. NOAA/ NURC and South Atlantic Fish Managem Counc, 14 pp

Thompson MJ, Gulliland LE (1980) Topographic mapping of shelf edge prominences off southeastern Florida. Southeast Geol 21: 155-164

Thompson MJ, Gulliland LE, Mendlein GE (1978) Bathymetric mapping of three selected areas on the southeastern Florida continental shelf. Harbor Branch Found, Inc, Fort Pierce, Florida, Tech Rep 27, 54 pp

Predicting habitat for two species of deep-water coral on the Canadian Atlantic continental shelf and slope

Tanya L. Leverette, Anna Metaxas

Department of Oceanography, Dalhousie University, Halifax, Nova Scotia,
  B3H 4J1, Canada
  (tleveret@dal.ca)

Abstract. Documentation of hundreds of locations for Canadian deep-water corals has been obtained through scientific initiatives and local fishermen's knowledge. Using these locations, as well as relevant oceanographic data, this study determined areas of suitable habitat for *Paragorgia arborea* and *Primnoa resedaeformis* along the Canadian Atlantic continental shelf and shelf break using predictive models. The study area included a band approximately 800 km long x 200 km wide from Cape Breton to the Gulf of Maine, and was chosen based on density of coral sites. Several environmental factors including slope, temperature, chlorophyll *a*, current speed and substrate may be important in determining suitable coral habitat and were included in the analysis. There are many different techniques used to model habitats, but frequently they are limited by the type of data available. Comparatively, few techniques using presence-only data are available. We utilized BioMapper, a program which uses Ecological Niche Factor Analysis (ENFA), to generate habitat suitability maps by relating data on species presence with background environmental data to determine the species' niche. We found that habitat requirements differed between the two species of coral. For *Paragorgia arborea*, the niche was highly specialized, and characterized by steeply sloped environments and rocky substrate. In contrast, for *Primnoa resedaeformis*, suitable habitat was more broadly distributed in the study area, and located in areas with high current speed, rocky substrates and an approximate temperature range between 5 and 10°C. This is the first study to use predictive modelling to identify suitable habitat for deep-water coral, which may prove an important tool for the conservation of these organisms.

Keywords. Deep-water corals, mapping, *Paragorgia arborea*, *Primnoa resedaeformis*, predictive modelling, BioMapper

Introduction

Over the past decade, research on deep-water corals has intensified globally. In the Canadian northwest Atlantic continental margin, *Paragorgia arborea* (Linnaeus, 1758) and *Primnoa resedaeformis* (Gunnerus, 1763), both Order Gorgonacea, are the most abundant corals (Willison et al. 2000). *Paragorgia* occurs in the northeast and northwest Atlantic Ocean, off the Norwegian coast and from Newfoundland to Maine (Tendal 1992). Also termed "bubble gum" coral, this species is often bright pink in colour with a spongy outer layer and colonies that can grow to 2.5-3 m tall (Breeze et al. 1997). *Primnoa*, also called "popcorn coral", is smaller, lighter in colour and more densely branched than *Paragorgia*. The two species occupy similar habitats and often, but not always, co-occur. Most often found along shelf edges and in deeper channels, these corals colonize areas with hard substrate and strong bottom currents ($\sim$60 cm s^{-1}) (Tendal 1992). Local fishermen have reported that corals are found at water depths from 200 m to 650 m, although this may reflect gear restrictions rather than an accurate measurement of the range of the species. Specimens have also been reported in much shallower water (128 m) off the coast of Maine (Breeze et al. 1997). Estimated temperature range for both species is between 4°C and 8vC (Tendal 1992). Recent research on the ecology of deep-water corals in Atlantic Canada has mainly focused on the Northeast Channel, because of high abundance, and on the Sable Island Gully, because of high species diversity.

Although advancements in surveying technologies have increased the number and accuracy of large-scale mapping projects in shallow-water marine systems, data collection from deep-water environments is considerably more difficult. Consequently, data on the spatial distribution of most deep-water species, including deep-water corals, are also sparse. Species distribution maps can be generated by habitat modelling, a method which examines relationships between the presence and/or absence of species and relevant environmental parameters. There are many different techniques to generate habitat maps, but frequently they are limited by the type of available data. Because of the remoteness and low accessibility of deep-water marine environments, only information on species presence is most frequently available, constraining the range of suitable habitat models. One suitable modelling program is BioMapper. This program uses the statistical technique Ecological Niche Factor Analysis (ENFA), which generates habitat suitability (HS) maps by relating species presence data with background environmental data (ecogeographical variables (EGVs)) to determine the species' niche (Hirzel et al. 2001). BioMapper has been utilized to generate HS maps for several terrestrial floral and fauna, such as ferns in New Zealand and ibex and alpine mice in Switzerland (Hirzel 2001; Sachot 2002; Zaniewski et al. 2002; Reutter et al. 2003). This type of modelling approach is highly recommended when absence data are not available (e.g., most deep-water data sets), unreliable (e.g., cryptic or rare species), or ecologically meaningless (e.g., invading species) (Reutter et al. 2003). Ours is the first study to use ENFA in the marine environment.

We used ENFA to generate habitat suitability maps for the two species, belonging to two different families (Paragorgiidae and Primnoidae), of deep-water

coral that are most abundant in the NW Atlantic, *Paragorgia arborea* and *Primnoa resedaeformis*. We also compared the relative importance of several environmental factors (temperature, slope, current, chlorophyll *a* and substrate) in determining suitable habitat for each species. These factors were selected based on available data in locations where coral have been recorded (MacIsaac et al. 2001; Del Mol et al. 2002; Freiwald 2002).

Methods

Study area

The study area encompassed approximately a band 800 km long x 200 km wide along the continental shelf and shelf break, from Cape Breton to the Gulf of Maine (58°N to 67°N and 42°W to 46°W) (Fig. 1). This is an area of current active research on deep-water corals.
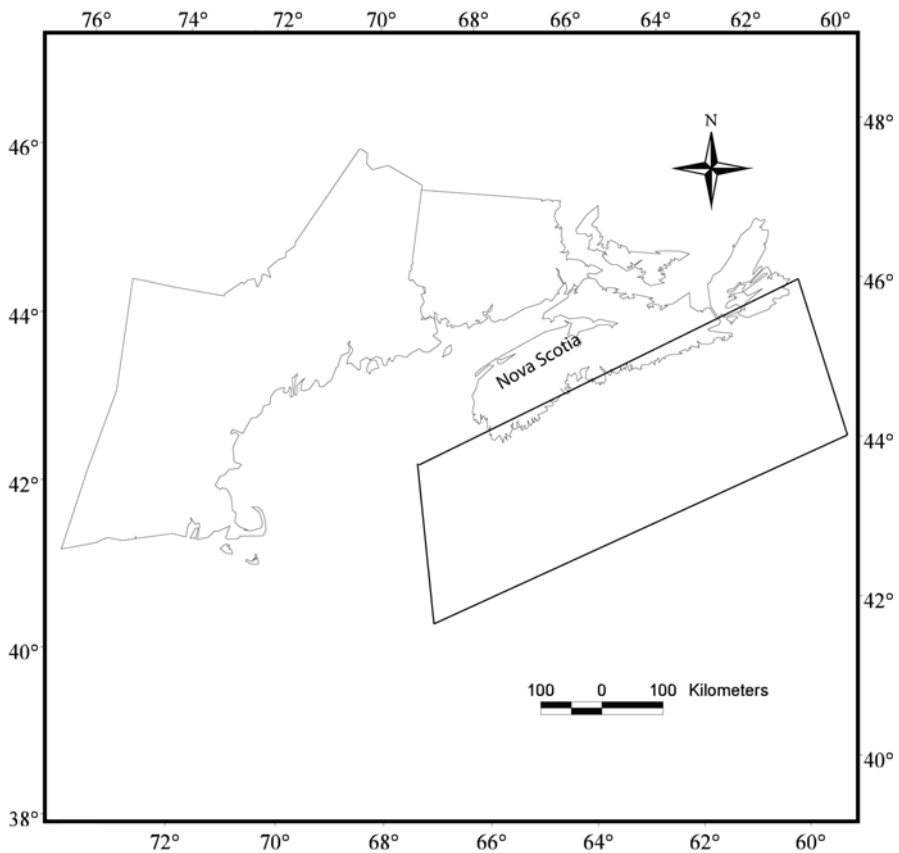
Fig. 1 The study area from Cape Breton to the Gulf of Maine (see box)

Data collection

Locations of *Paragorgia arborea* (n = 72) and *Primnoa resedaeformis* (n = 270) were obtained from scientific cruise reports and literature sources, including Breeze et al. (1997), Gass (2002) and Watling (unpublished data, University of Maine). The literature sources included data mainly acquired from interviews with local fishermen. Environmental data on bathymetry, bottom temperature, surface chlorophyll *a*, substrate and bottom current speed were obtained from several oceanographic sources. Minimum, maximum, and average values were calculated from the temperature, chlorophyll *a*, and current speed datasets. Slope was calculated from the bathymetry data, using ARCView 3.2. Although data were available, salinity was not included as an environmental variable in the analysis because the variation within the study area was small. Sources of empirical data were used whenever possible, although current velocity was obtained through oceanographic models representing 3D seasonal circulation (Hannah et al. 2001). There is little temporal variation in temperature at depths >100 m (typical of coral occurrence), and thus bottom temperature data were averaged over one-year periods (Alidina and Roff 2003). Chlorophyll *a* data were obtained from SeaWIFS data and averaged over 5-year periods, as corals are sessile. Substrate was categorized into classes based on the Lidden-Wentworth size classification for sediment grains and assigned increasing phi values (-12 to +14) to decreasing grain size (boulder to clay) (Pettijohn et al. 1972). This classification produces continuous data for substrate (Kostylev pers. comm). Current data were annual averages calculated from the seasonal (winter, spring, summer, fall) model outputs.

Model generation

ENFA was used to generate habitat suitability maps for *Paragorgia arborea* and *Primnoa resedaeformis* with the software program BioMapper 2.1. ENFA is similar to principal component analysis (PCA) in that it determines relationships between variables and finds combinations of these variables to produce uncorrelated indices or axes (Manly 1986). These axes represent composite factors that explain variability in the data, with the first axis displaying the largest amount of variation. Unlike PCA, however, in ENFA, the axes have direct ecological meaning. The first axis is defined as the "marginality" of the species' niche, which describes the mean of the species distribution in relation to the mean of the global (study) distribution. It is defined as "the absolute difference between the global mean and the species mean" for each environmental variable (Hirzel et al. 2002) and is calculated as:

$$M = \frac{|m_G - m_S|}{1.96 \cdot \sigma_G}$$

where M is the marginality for a particular environmental variable, m_G is the global mean of the variable, m_S is the species mean of the variable and σ_G is the standard deviation of the global distribution for the variable. Unlike PCA, the first axis in ENFA is chosen to account for 100 % of the marginality of the species as well as some proportion of specialization, with the remaining axes maximizing the

remaining amount of specialization of the species. Thus, eigenvalues associated with specialization axes can be larger than the values associated with the marginality values (Hirzel 2001).

The remaining axes explain progressively decreasing amounts of the "niche specialization" of the species. Specialization indicates how restricted the species' niche is in relation to the study area and is defined as "the ratio of variance in the global distribution to that in the species distribution" of the environmental variable (Hirzel et al. 2002; Reutter et al. 2003):

$$S = \frac{\sigma_G}{\sigma_S}$$

where S is the specialization for a particular environmental variable and σ_S is the standard deviation of the species distribution for the variable.

Combining the marginality and specialization of individual environmental factors, ENFA then computes an overall global marginality (Hirzel et al. 2002; Reutter et al. 2003):

$$M = \frac{\sqrt{\sum_{i=1}^{V} m_i^2}}{1.96}$$

where V is the number of EGVs and m_i indicates the marginality value for each EGV, and a global specialization coefficient:

$$S = \frac{\sqrt{\sum_{i=1}^{V} \lambda_i^2}}{1.96}$$

where σ indicates the specialization value for each EGV (Hirzel et al. 2002). The marginality coefficient M generally ranges between 0 and 1, with large values indicating that the species inhabits a narrow range of the globally available environment. The specialization coefficient S ranges from 1 to ∞, and tolerance, which is the inverse of specialization, from 0 to 1. The greater the tolerance coefficient, the wider the niche of a particular species (Reutter et al. 2003).

An HS map was constructed to visually represent the ENFA results. Firstly, for each environmental factor, the values at each location of species occurrence were determined. A frequency histogram was generated with these values, and scores were assigned to each class in the histogram. Assuming a normal distribution, these scores are maximal at the median of the distribution and decrease towards

either tail (Hirzel et al. 2002). Secondly, the class of each cell in the study area was determined and a suitability value ("partial suitability") assigned based on the score of that class in the histogram. The further the class of the cell is from the median, the lower the habitat suitability of the cell. A global suitability map was then generated by computing a weighted mean of the partial suitabilities, producing a habitat suitability (HS) index which ranged from 0 to 100, with zero being completely unsuitable (Hirzel et al. 2004). Model validation and confidence limits for the HS maps were calculated using a built-in jackknifing method in which the presence data were partitioned into ten subsets of equal size. Nine of these subsets were used to calibrate the HS map and the remaining subset was used for validation (Boyce et al. 2002). This procedure was repeated ten times, with a new subset being used for validation each time. Two statistics generated from the jackknifing procedure are useful for evaluating model validity. The Absolute Validation Index (AVI) provides an overall assessment of the model and is determined by calculating the number of validation points which have an HS index greater than 50 %. Higher values indicate a more accurate model. The Contrast Validation Index (CVI) is the difference between the AVI of the model and an AVI generated for a completely randomly-distributed species. This number should also be large if the data fit the model well. In BioMapper 2.1, the most accurate model is one that maximizes both the AVI and CVI.

Coral location data for the species and environmental data were imported into BioMapper as a raster-based grid file with a 9-km cell size. ENFA was used to obtain marginality and specialization values, which indicated those environmental parameters with the greatest influence (weight) on the distribution of each coral species. A total of 11 ecogeographical variables (EGVs) (Table 1) were used to generate 27 possible model combinations (which contained all five environmental factors: temperature, slope, current speed, chlorophyll *a* and substrate).

Table 1 List of the eleven ecogeographical variables (EGV) used to generate the 27 models included in the Ecological Niche Factor Analysis (ENFA) for *Primnoa resedaeformis* and *Paragorgia arborea* in the NW Atlantic Ocean

Code	EGV
Sl	Slope
Tn	Temperature (minimum)
Tv	Temperature (average)
Tx	Temperature (maximum)
Cn	Current (minimum)
Cv	Current (average)
Cx	Current (maximum)
Chn	Chlorophyll *a* (minimum)
Chv	Chlorophyll *a* (average)
Chx	Chlorophyll *a* (maximum)
Sb	Substrate

Results

Paragorgia arborea

For this species, the model that included slope, average temperature (1.2-10.2°C), average current speed (0.02-0.21 m s⁻¹), maximum chlorophyll *a* concentration (0.9-6.9 mg m⁻³) and substrate, resulted in the best combination of AVI (82.7 %, SD = 18 %) and CVI (0.63, SD = 0.19) (Table 2). Global marginality was 0.61 and

Table 2 Validation indices for the three best models (those with the highest AVI and CVI) run to evaluate habitat suitability for each coral species

Species	Factors included in the model	AVI %	CVI
P. arborea	Sl,Tv,Cv,Chx,Sb	83	0.63
	Sl,Tv,Cn,Chn,Sb	77	0.58
	Sl,Tx,Cn,Chn,Sb	75	0.40
P. resedaeformis	Sl,Tv,Cn,Chn,Sb	82	0.33
	Sl,Tn,Cv,Chv,Sb	81	0.25
	Sl,Tn,Cv,Chx,Sb	80	0.19

global tolerance was 0.16, indicating that the conditions in the preferred habitat of this coral species are notably different from average for the study area. The three retained factors (of the five computed) accounted for 100 % of marginality and 98 % of total specialization. Marginality coefficients showed that suitable habitat for this species is most strongly associated with steep slope (0.72) and rocky substrate (-0.40) (Table 3). Current speed, chlorophyll *a* concentration and average temperature are less important in determining suitable habitat (Table 3). As the first factor accounts for 100 % of the marginality, the large eigenvalue (40 %) associated with this indicates that a large portion of the specialization of *Paragorgia arborea* is strongly influenced by changes in topography. The next two factors account for the remaining specialization in response to chlorophyll *a* concentration (factor 2) and

Table 3 Coefficients of each ecogeographical variables (EGV) in the best model generated by ENFA for *Paragorgia arborea*. The first axis explains 100 % of the marginality, as well as a proportion of the specialization. The specialization explained by the first three (of five) factors is shown in brackets. Positive values on the marginality factor indicate that the species prefers locations with higher values on the corresponding EGV than the global (study area) average

EGV	Marginality (40 %)	Specialization1 (55 %)	Specialization2 (4 %)
Sl	0.72	0.33	0.14
Tv	0.26	0.07	0.89
Cv	0.38	0.07	0.16
Chx	-0.31	0.91	0.14
Sb	-0.40	0.23	0.38

average temperature (factor 3). A habitat suitability map illustrated that relatively suitable habitat for this species occupies a very narrow band along the shelf break (Fig. 2).

Primnoa resedaeformis

For this species, the model that included slope, average temperature (0-8.6°C), minimum current speed (0-0.16 m s^{-1}), minimum chlorophyll *a* concentration (0.5-5.7 mg m^{-3}), and substrate resulted in the best combination of AVI (75.5 %, SD = 23 %) and CVI (0.34, SD = 0.21) (Table 2). Global marginality was 0.50 and global tolerance was 0.53, indicating that the preferred habitat of *P. resedaeformis* is more similar to the average conditions in the study area than that of *P. arborea*. The three retained factors (of the five computed) accounted for 100 % of marginality and 90 % of total specialization. Marginality coefficients show that suitable habitat for this species is most strongly associated with average temperature (0.53), minimum
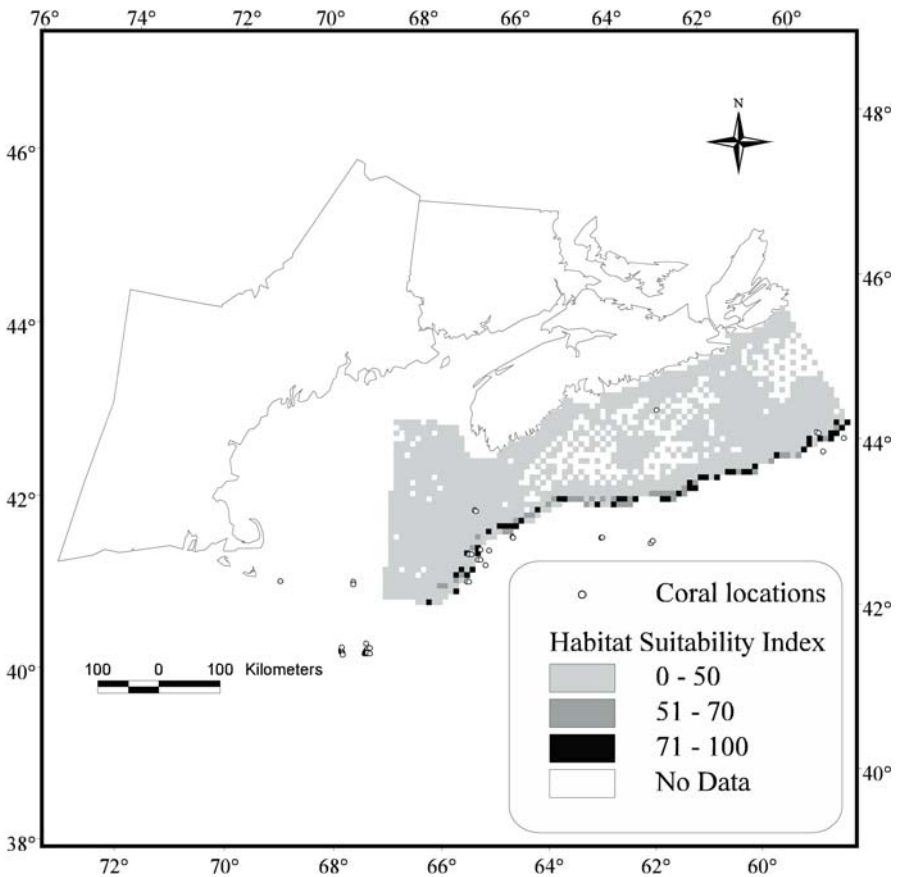
Fig. 2 Habitat suitability map for *Paragorgia arborea* on the Atlantic Canadian continental shelf and shelf break, as computed by the Ecological Niche Factor Analysis. The scale indicates habitat suitability values

current speed (0.54) and rocky substrates (-0.56) (Table 4). Slope and chlorophyll *a* concentrations are less important in determining suitable habitat (Table 4). A small eigenvalue (15 %) associated with the first factor, indicates that *P. resedaeformis* is not particularly sensitive to changes in the environmental factors included in this axis. The next two factors account for more specialization, mainly in response to chlorophyll *a* concentration (factor 2) and substrate (factor 3). The eigenvalues for the specialization factors are relatively large, indicating that they have a strong effect in restricting the range of *P. resedaeformis*. A habitat suitability map generated from these variables illustrates areas with suitable habitat for this species are scattered throughout the continental shelf and shelf break (Fig. 3).

Table 4 Coefficients of each ecogeographical variables (EGV) in the best model generated by ENFA for *Primnoa resedaeformis*. The first axis explains 100 % of the marginality, as well as a proportion of the specialization. The specialization explained by the first three (of five) factors is shown in brackets. Positive values on the marginality factor indicate that the species prefers locations with higher values on the corresponding EGV than the global (study area) average

EGV	Marginality (15 %)	Specialization1 (64 %)	Specialization2 (11 %)
Sl	0.30	0.25	0.08
Tv	0.53	0.02	0.63
Cn	0.54	0.10	0.15
Chn	-0.16	0.93	0.13
Sb	-0.56	0.25	0.75

Discussion

Fisheries and Oceans Canada have been collecting qualitative and quantitative data on deep-water coral habitat on the Scotian Margin since 1997. These observations have revealed that, in general, the highest densities of corals are found in elevated areas, such as iceberg scours, with strong currents (MacIsaac et al. 2001). Our results also indicated a strong relationship between habitat suitability and current speed, particularly for *P. resedaeformis*. As deep-water corals are sessile, filter-feeding organisms that rely on near-bottom currents for nutrient supply in order to obtain adequate nutrients, they must exist in habitats with strong currents (Mortensen 2001).

The results of our study also indicate that distributions for both species were strongly influenced by temperature. Previous observations indicated that most deep-water corals inhabit areas with minimum temperatures >3°C, with some species present in locations with temperatures as low as -1°C (Cimberg et al. 1981). Our study showed that although these species can tolerate colder waters, the majority of the locations were found in warmer waters, ranging between 4-8°C (Tendal 1992; Krieger 2001).
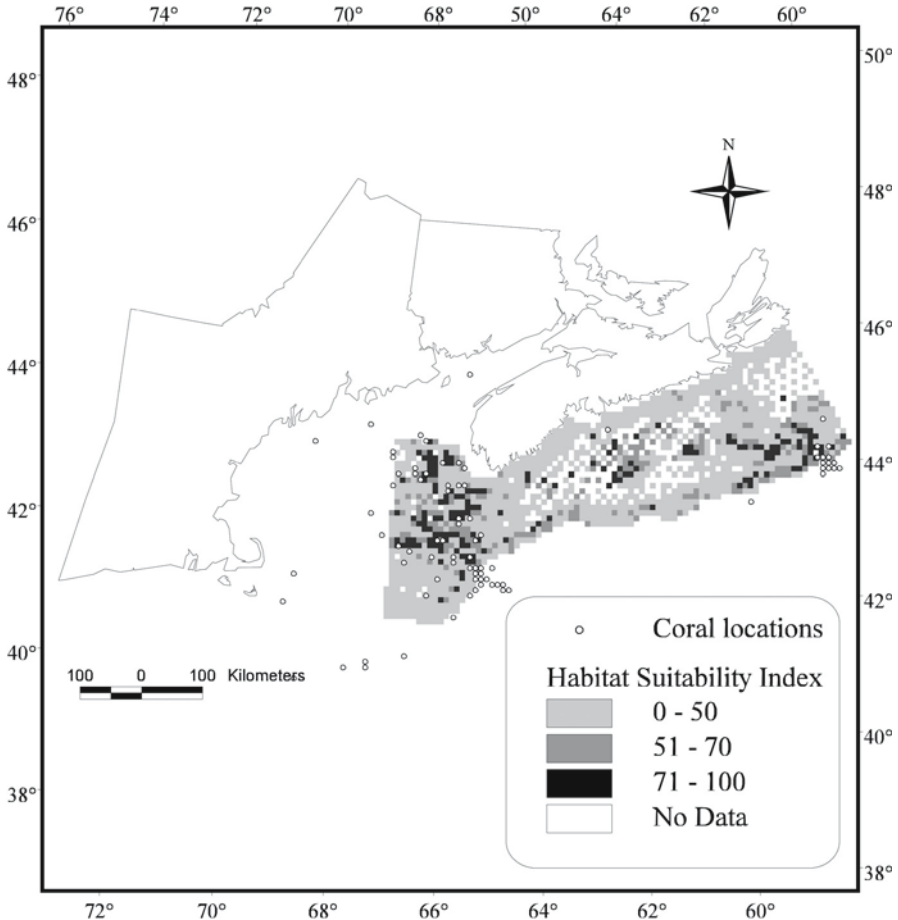
Fig. 3 Habitat suitability map for *Primnoa resedaeformis* on the Atlantic Canadian continental shelf and shelf break, as computed by the Ecological Niche Factor Analysis. The scale indicates habitat suitability values

Corals are abundant on slopes, in and around submarine canyons, gullies and the edge of the continental shelf (MacIsaac et al. 2001). These sloping areas are normally associated with hard substrate, such as cobble and boulders, making then ideal for coral attachment (Freiwald et al. 1999). Suitable habitats for *P. arborea* were associated most strongly with slope values that were above average for the study area. Steeply sloping areas can be a highly suitable habitat for these large corals, as current velocities are often high there. *P. arborea* is a large gorgonian species, reaching 2.5-3 m in height (Breeze et al. 1997), and their branches form large fan-like structures, often convex and facing into the main direction of current (Reed 2002). This adaptation likely maximizes the surface area exposed to the current flow and, thus, the filter feeding effectiveness of the organism, as well as reducing torsion in the basal stem (Tunnicliffe 1983). In contrast, suitable habitat

for *P. resedaeformis* was defined by a combination of ranges for substrate, current speed and temperature. The differences in niche breadth between the two coral species were clearly illustrated in the ENFA results. Although *P. resedaeformis* and *P. arborea* have similar global marginality coefficients (0.5 and 0.6 respectively), their tolerance coefficients differ markedly (0.53 and 0.15 respectively). These values indicate that although these two species of coral are expected to co-exist often, *P. resedaeformis* is considerably more tolerant of inhabiting a wider range of habitats.

This study increased our understanding of the relative importance of different environmental factors in determining suitable habitat for deep-water corals. In turn, the habitat suitability maps generated from the results of ENFA can allow for clear identification of target areas for exploration. Data collected as presence-only, and previously unusable data, such as those from museum collections, can be successfully processed with ENFA. Several recent international fora (e.g., the NOAA funded Symposium on the Effects of Fishing Activities on Benthic Habitats (McDonough and Puglise 2003)), have recommended that mapping of coral locations is an immediate priority (see also Puglise et al. 2005). We have used ENFA to extend these recommendations by attempting to predict potential coral locations presently unknown, based on suitability of the habitat. To our knowledge, this is the first study that attempts to predict deep-water coral habitat. Our study is also the first to use ENFA for marine species. This analysis may prove particularly useful for the remote and relatively inaccessible deep-water environment.

Acknowledgements

References

Alidina H, Roff JC (2003) Classifying and mapping physical habitat types (seascapes) in the Gulf of Maine and the Scotian Shelf: seascape version to May 2003. Rep World Wildlife Fund Canada and Conservation Law Foundation, Halifax, Nova Scotia

Boyce MS, Vernier PR, Nielson SE, Schmiegelow FKA (2002) Evaluating resource selection functions. Ecol Model 157: 281-300

Breeze H, Davis DS, Butler M, Kostylev V (1997) Distribution and status of deep-sea corals off Nova Scotia. Marine Issue Comm Spec Publ 1, Ecology Action Centre, Halifax, Nova Scotia

Cimberg RL, Gerrodette T, Muzik K (1981) Habitat requirements and expected distribution of Alaska coral. Final Rep, VTN Oregon, Inc. Rep Office Marine Pollut Assess, Alaska Off, US Dept Commerce, NOAA, OCSEAP Final Rep 54: 207-308

De Mol B, Van Rensbergen P, Pillen S, Van Herreweghe K, Van Rooij D, McDonnell A, Huvenne V, Ivanov M, Swennen R, Henriet JP (2002) Large deep-water coral banks in the Porcupine Basin, southwest of Ireland. Mar Geol 188: 193-231

Freiwald A (2002) Reef-forming cold-water corals. In: Wefer G, Billett D, Hebbeln D, Jørgensen BB, Schlüter M, Van Weering T (eds) Ocean Margin Systems. Springer, Berlin Heidelberg, pp 365-385

Freiwald A, Wilson JB, Henrich R (1999) Grounding Pleistocene iceberg shape recent deep-water coral reefs. Sediment Geol 125: 1-8

Gass SE (2002) An assessment of the distribution and status of deep-sea corals in Atlantic Canada by using both scientific and local forms of knowledge. MES thesis, Dalhousie Univ, Halifax, Canada

Hannah CG, Shore JA, Loder JW (2001) Seasonal circulation on the western and central Scotian Shelf. J Phys Oceanogr 31: 591-615

Hirzel A (2001) When GIS comes to life. Linking landscape- and population ecology for large population management modelling: the case of Ibex (*Capra ibex*) in Switzerland. PhD thesis. Inst Ecol, Lab Conserv Biol. Univ Lausanne, Switzerland

Hirzel A, Helfer V, Métral F (2001) Assessing habitat-suitability models with a virtual species. Ecol Model 145: 111-121

Hirzel A, Hausser J, Chessel D, Perrin N (2002) Ecological-niche factor analysis: how to compute habitat-suitability maps without absence data? Ecology 83: 2027-2036

Hirzel A, Hausser J, Perrin N (2004) Biomapper 3.0. Laboratory for Conservation Biology, Inst Ecol, Univ Lausanne. URL: http://www.unil.ch/biomapper

Krieger KJ (2001) Coral (*Primnoa*) impacted by fishing gear in the Gulf of Alaska. In: Willison JHM, Hall J, Gass SE, Kenchington ELR, Butler M, Doherty P (eds) Proceedings of the First International Symposium on Deep-sea Corals, July 30 - August 3, 2000. Ecology Action Center and Nova Scotia Museum, Halifax, Nova Scotia, Canada, pp 106-116

MacIsaac K, Bourbonnais C, Kenchington E, Gordon D, Gass S (2001) Observations on the occurrence and habitat preference of corals in Atlantic Canada. In: Willison JHM, Hall J, Gass SE, Kenchington ELR, Butler M, Doherty P (eds) Proceedings of the First International Symposium on Deep-sea Corals, July 30 - August 3, 2000. Ecology Action Center and Nova Scotia Museum, Halifax, Nova Scotia, Canada, pp 58-75

Manly BFJ (1986) Multivariate statistical methods: a primer. Chapman and Hall, New York, pp 59-71

McDonough JJ, Puglise KA (2003) Summary: deep-sea coral workshop, international planning and collaboration workshop for the Gulf of Mexico and the North Atlantic, Galway, Ireland, January 16-17, 2003. NOAA Tech Mem NMFS-SPO-60

Mortensen PB (2001) Aquarium observations on the deep-water coral *Lophelia pertusa* (L., 1758) (Scleractinia) and selected associated invertebrates. Ophelia 54: 83-104

Pettijohn FJ, Potter PE, Siever R (1972) Sand and Sandstone. Springer, New York

Puglise KA, Brock RJ, McDonough JJ (2005) Identifying critical information needs and developing institutional partnerships to further the understanding of Atlantic deep-sea coral ecosystems. In: Freiwald A, Roberts JM (eds) Cold-water Corals and Ecosystems. Springer, Berlin Heidelberg, pp 1129-1140

Reed JK (2002) Comparison of deep-water coral reefs and lithoherms off southeastern USA. Hydrobiologia 471: 57-69

Reutter BA, Helfer V, Hirzel A, Vogel P (2003) Modelling habitat-suitability on the base of museum collections: an example with three sympatric *Apodemus* species from the Alps. J Biogeogr 30: 581-590

Sachot S (2002) Viability and management of an endangered capercaillie (*Tetrao urogallus*) metapopulation. PhD thesis. Inst Ecol, Lab Conserv Biol. Univ Lausanne, Switzerland

Tendal OS (1992) The North Atlantic distribution of the octocoral *Paragorgia arborea* (L. 1758) (Cnidaria, Anthozoa). Sarsia 77: 213-217

Tunnicliffe V (1983) Corals move boulders: an unusual mechanism of sediment transport. Limnol Oceanogr 28: 564-568

Willison JHM, Jones DKP, Atwood S (2000) Deep-sea corals and marine protected areas in Nova Scotia. In: Bondrup-Nielsen S, Munro NWP, Nelson G, Willison JHM, Herman TB, Eagles P (eds) Managing Protected Areas in a Changing World. Proceedings of the Fourth International Conference on Science and Management of Protected Areas, 14-19 May 2000. Sci Manage Protected Areas Assoc, Wolfville, Nova Scotia, Canada, pp 1157-1163

Zaniewski AE, Lehmann A, Overton JM (2002) Predicting species spatial distributions using presence-only data: a case study of native New Zealand ferns. Ecol Model 157: 261-280

IV

Exogenic and endogenic controls

Chapter content

Monitoring environmental variability around cold-water coral reefs: the use of a benthic photolander and the potential of seafloor observatories

J. Murray Roberts, Oliver C. Peppe, Lyndsey A. Dodds, Duncan J. Mercer, William T. Thomson, John D. Gage, David T. Meldrum

Scottish Association for Marine Science, Dunstaffnage Marine Laboratory, Oban, Argyll, PA37 1QA, UK
(murray.roberts@sams.ac.uk)

Abstract. The environmental sensitivies of cold-water corals and their associated biota are likely to be determined by the natural variability of the cold-water coral reef environment. The sensitivity of reef biota to sedimentation and resuspension events is largely unknown and the influence of seasonal phytodetrital deposition is poorly understood. Here we describe the use of a benthic photolander to monitor this variability by the Sula Ridge reef complex on the mid-Norwegian continental shelf and from the Galway carbonate mound in the Porcupine Seabight. The photolander provides a platform for time-lapse digital and film cameras to image the seabed while recording the current regime and optical characteristics (light transmission, backscatter and fluorescence) of the seawater. In its first two deployments carried out in 2001 and 2002 by the Sula Ridge the lander recorded a dynamic environment around the reef site with a tidal current regime and periods of sediment resuspension. Current speeds by the Sula Ridge reef complex reached a maximum of 28 cm s^{-1} and 70 cm s^{-1} on the Galway carbonate mound, reinforcing much speculation about the dependence of these communities on current-swept conditions. Seabed photographs show intense feeding activity of echiuran worms (*Bonellia viridis*) near the Sula Ridge reef complex pointing to rapid bioturbation of the sediment. Fish were recorded sheltering near sponges that had colonised glacial dropstones. Longer term monitoring *in situ* is needed for study of seasonal change, to identify functional roles of associated fauna and to monitor potential coral spawning events. Benthic landers and seafloor observatories have great potential in these areas. Only with a better understanding of the natural variability of the cold-water coral environment can informed decisions about the environmental sensitivity of cold-water coral reefs and their management be made.

Keywords. *Lophelia pertusa,* Sula Ridge, carbonate mound, benthic lander

Cold-water corals

Corals such as *Lophelia pertusa* and *Madrepora oculata*, both of which have widespread distributions in the northeast Atlantic are commonly referred to as deep-water or cold-water corals. These terms distinguish them from warm-water corals that are in large part restricted to shallow, well-lit waters and can develop to form the coral reefs characteristic of nutrient-poor tropical seas. To date, the vast majority of scientific research has concentrated on the shallow-water tropical corals that often contain algal symbionts (zooxanthellae). The inaccessibility of deep-water azooxanthellate species means that little is known about their basic biology and inferences about their environmental sensitivity are often drawn from studies of warm-water zooxanthellate species. Historically, the greatest research effort on cold-water corals has been in the northeast Atlantic where one species, *Lophelia pertusa*, appears to be the most significant in terms of its occurrence in some areas as sizeable reef-like structures. Most records of this species are from the northeast Atlantic, probably reflecting the intensity of research work in this area (Rogers 1999; Roberts et al. 2003). The work described in the present study has taken place in the northeast Atlantic and so discussion will largely focus on the cold-water coral reefs found in this region, in particular those dominated by *L. pertusa*.

In the last ten to fifteen years, hydrocarbon exploration and production in deeper shelf edge waters have driven discoveries of cold-water coral provinces. For example, in Norway, Statoil's Haltenpipe development project laid a pipeline on the seabed beside cold-water coral reefs. These were mapped (Hovland et al. 1994) and several remotely operated vehicle (ROV) surveys of the reefs and their megafaunal communities completed while pipeline inspection work was carried out (Mortensen et al. 1995). In the UK, a large-scale oil and gas industry environmental survey of the Atlantic Margin discovered an area of seabed mounds and tails colonised by corals, named the Darwin Mounds (Masson et al. 2003). Between 1997 and 2000, a UK partnership of scientific research councils and oil companies commissioned a series of projects under a Managing Impacts on the Marine Environment (MIME) initiative. One of these projects focussed on the distribution and potential environmental sensitivity of cold-water corals (Roberts 1997). In the south Atlantic, sidescan and ROV surveys in the Brazilian Campos Basin have revealed apparently high densities of cold-water coral reefs (Gardline 2002). However, in parallel with this work great concern has been expressed over the environmental impacts of oil exploration and production in deep-water, especially with respect to the potentially smothering effects of drill cutting release in the vicinity of cold-water coral ecosystems (Rogers 1999).

A second major driver for research into cold-water coral provinces has been growing evidence of damage by deep-water trawl gear. Recent surveys have shown that 30-50 % of Norway's cold-water coral reefs show signs of damage (Fosså et al. 2002), although new discoveries of many more reefs in this region may reduce this initial estimate (Fosså et al. 2005). There is also historical evidence for trawl damage to coral areas west of Scotland (Roberts et al. 2003) as well as direct evidence for deep-water trawl impacts along the Hebridean continental margin (Roberts

et al. 2000), to the Darwin Mounds in the northern Rockall Trough (Wheeler et al. in press) and to coral areas west of Ireland (Hall-Spencer et al. 2002). Around Tasmania, corals and other sessile suspension feeding organisms have been removed by trawlers from seamounts (Koslow et al. 2001). The growing evidence for damage has provoked debate on whether such areas should be protected. Indeed, in both Norway and Tasmania several areas have now been designated as marine protected areas and are closed to any trawl gear. In August 2003, the UK government secured an emergency measure through the European Union Common Fisheries Policy to close the Darwin Mounds to bottom fishing. Following this, agreement to prohibit bottom fishing within an area of 1,300 km^2 around the mounds was reached and came into force a year later. The UK now intends to designate the Darwin Mounds as a Special Area of Conservation or SAC through the European Union Habitats Directive (Freiwald et al. 2004).

Benthic landers and cold-water coral ecology

Historically, research on the benthic animal communities inhabiting continental shelf, slope and abyssal depths has relied on samples gathered by trawls, dredges and cores and to a lesser extent on visual surveys using photography, video and submersible observations. Cold-water coral ecosystems are patchily distributed making locating them difficult, while dredge or trawl sampling is extremely destructive. Detailed observations of cold-water coral ecosystems have been carried out using manned submersibles including PISCES observations of *Lophelia* patches on Rockall Bank (Wilson 1979), JAGO observations of the Sula Ridge reef complex (Freiwald et al. 1999, 2002) and Johnson-Sea-Link study of *Oculina* banks off Florida (Reed 2002). In recent years, there have been great advances in the development of ROVs allowing researchers to observe deep-water species and perform experiments *in situ*. The use of ROVs has greatly facilitated research on cold-water coral reefs with demonstrative examples from Norway (Mortensen et al. 1995; Fosså et al. 2002) and Sweden (Lundälv and Jonsson 2003) among others. However, all such techniques rely on the presence of a research ship to provide a surface platform as well as favourable weather for the safe launch and recovery of submersibles. They are therefore costly and suffer the disadvantage of only being able to operate for short periods of time, in the order of hours or a few days at maximum and at times of year that provide suitable weather conditions. For longer-term studies to observe fauna that may be disturbed by the presence a submersible and to collect seasonal information, an alternative approach is needed. Benthic landers fill this role by allowing unobtrusive observations and measurements to be made *in situ* while the research vessel either continues with other operations or even leaves the area altogether. Long duration systems can also operate over winter during times of the year when vessel operations are restricted.

A benthic lander consists of a framework on which are mounted various sensors and instruments, releasable ballast to keep the system negatively buoyant and buoyancy so that the lander floats back to the surface when the ballast is released.

Frameworks and buoyancy configurations vary depending on the scientific payload to be deployed and the environment in which the lander will operate. Many lander systems have been developed to deploy time-lapse cameras from the long-term bathysnap system (Lampitt and Burnham 1983) that has been used to study seasonal input of phytodetritus to the deep-sea floor (Lampitt 1985), to short-term systems designed to record the behaviour and movement patterns of deep-sea scavenging fish species when attracted to bait (Priede and Bagley 2000). As well as long-term visual monitoring of the seafloor, benthic landers have proved versatile platforms from which to study sedimentary and hydrodynamic processes in the benthic boundary layer and through the sediment-water interface. For example, systems have been developed to measure benthic respiration rates *in situ* using chambers to seal an area of seafloor sediment and record the consumption of oxygen by the benthic faunal community. Others record consumption of oxygen or production of sulphide within the upper few centimetres of sediment by inserting micro-electrodes in carefully controlled steps through the sediment-water interface and recording a profile with depth. The erosion characteristics of sediment have been assessed using stirred chambers to create controlled flow regimes across the sediment (see review by Tengberg et al. 1995 for details on these various approaches).

However, deploying and successfully recovering benthic landers from cold-water coral reef environments presents a number of challenges. Although some reefs may have developed to form relatively large features, they are patchily distributed and consequently landers allowed to free-fall from the surface may simply miss their targets. Unlike the relatively uniform topography presented by deep-sea sediment, cold-water coral reefs form structurally complex features and in some cases, such as the Sula Ridge, can rise tens of metres in height from the surrounding seafloor. Within these reef structures hollows and crevices provide a wealth of opportunities for a lander framework to become entangled and lost. Given this, visually-guided launching systems and ROVs capable of moving landers to the required deployment area become especially relevant. As well as the difficulties of the rough substratum, the current-swept nature of reef areas presents further problems. Virtually all studies of the distribution of suspension feeding communities of deep-water corals and sponges refer to their correlation with areas of seabed where currents are strong or locally accelerated by the seafloor topography. Thus near-bed currents can reach well over a knot in some areas (see below) and lander platforms must be designed to remain stable when exposed to the lateral forces of these strong currents. A final consideration, especially in terms of landers designed for long-term deployment, is the risk that they may be hit, damaged, or even carried away by fishing gear.

Photolander development and objectives

The overall objectives of the lander development described here were to produce a simple, robust and adaptable platform to deploy a variety of cameras and other sensors to record the environmental dynamics on and around cold-water coral reefs and to monitor the behaviour of the benthic biological communities. It was

of particular interest to attempt to estimate particle resuspension by cold-water coral reefs, especially given the foregoing discussion of their potential sensitivity to smothering impacts and to develop a novel mass-storage digital camera capable of operating autonomously. To date this photolander has completed three offshore deployments in the northeast Atlantic, two by the Sula Ridge reef complex on the mid-Norwegian shelf at 280 m water depth and one on the Galway carbonate mound in the Porcupine Seabight at 824 m water depth.

An existing benthic lander design from Oceanlab at Aberdeen University (described for the deployment of an ISIT camera by Battle et al. 2002) was adapted to provide a tripod frame giving a stable platform for time-lapse photography on the rough substrata found in and around cold-water coral reef areas. The aluminium lander frame stands 3 m high with 3.5 m between each of the three feet. To-date the photolander has been deployed with the following cameras and sensors:

- Benthos 5010 digital stills camera, adapted for mass picture storage (see below)
- CI 251 Camel Camera Alive film camera
- Mk 5 film camera (Institute of Oceanographic Sciences)
- UMI data logger controlling a transmissometer, light scattering sensor and fluorometer
- Recording current meter (Interocean S4 or Falmouth Scientific Inc. 3D-ACM with conductivity, temperature and depth sensors)
- Temperature loggers (Minilog VEMCO Ltd.)

The framework has proved a versatile platform on which to secure a variety of cameras, sensors and data-loggers. This versatility is a great bonus since it allows the lander to be easily adapted to perform a variety of scientific tasks. Steel ballast giving an 80 kg hold-down weight is attached at each of the three legs while a single buoyancy sphere is held above the tripod frame forming a single module mooring. For deployments of up to 400 m depth, a steel sphere has been used while for deployments of up to 1200 m a syntactic foam sphere has been used. A recording current meter is placed in this mooring line and three optical instruments are secured 0.5 m above the bed. Central to the design requirements was the need to allow unrestricted water and particle flow beneath the frame where these instruments were suspended. To help achieve this, the ballast was attached at each leg by a hook. These are opened by one of two acoustic release mechanisms (Oceano Instruments Ltd.) attached at the top of the lander frame. Depending on the nature of the syntactic buoyancy an Acoustic Doppler Current Profiler (ADCP) can also be deployed within the buoyancy module. The lander and single module mooring configuration is illustrated in Figure 1.
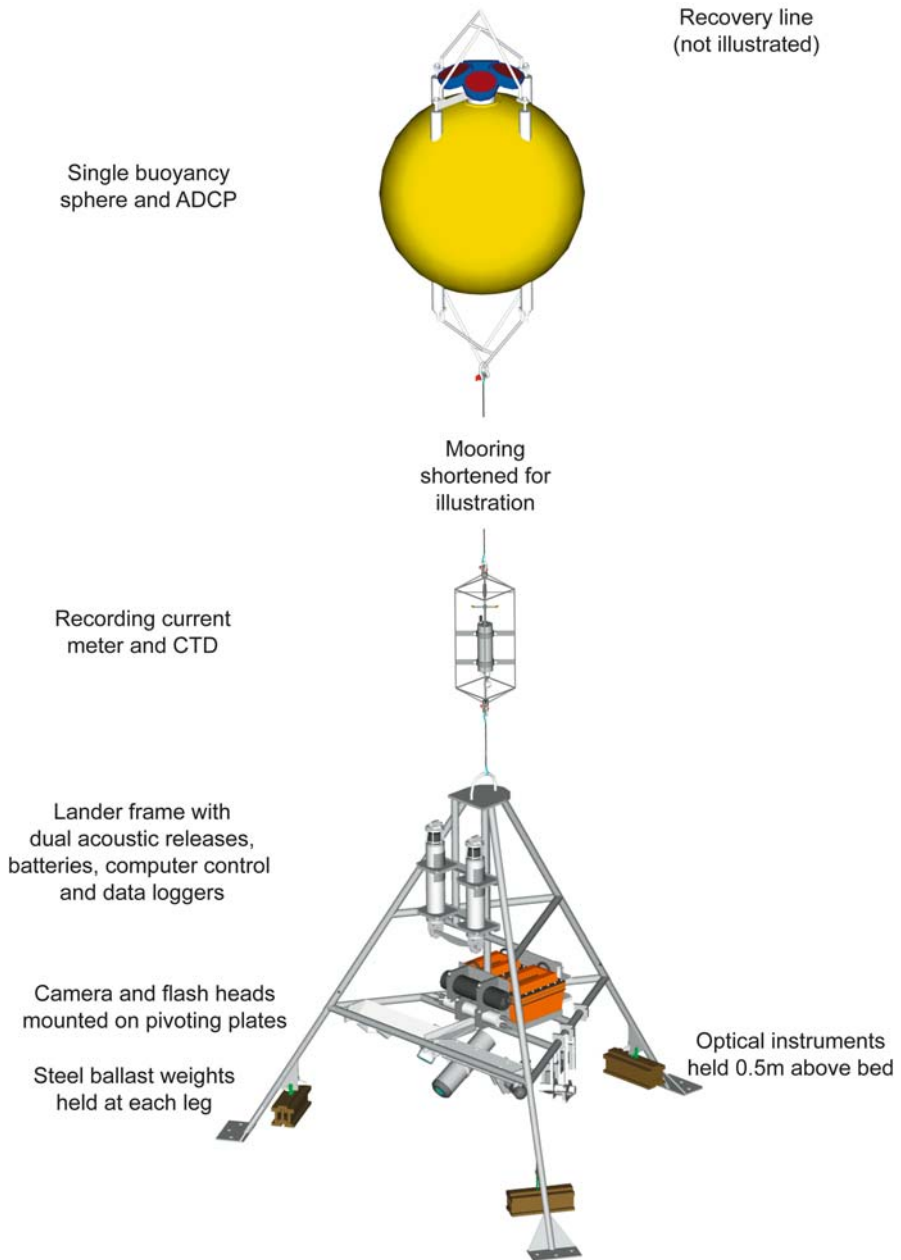
Fig. 1 Simplified diagram of the Scottish Association for Marine Science photolander illustrating the major components of the system and the single module mooring design

Adaptation of a digital stills camera for autonomous operation

To date, studies of seabed processes using time-lapse photography have relied on film cameras (e.g., Lampitt and Burnham 1983; Bett et al. 2001). With improvements in digital camera resolution in the last ten years it has become increasingly feasible to use these cameras in their place. Digital photography offers a number of advantages over traditional film; it removes the need to scan bulk film before digital analysis, there is less danger of damaging delicate film stocks, the cameras do not need to store large rolls of film and there is no danger of losing information from jammed film. The camera system adapted for use on the photolander was developed using a Benthos 5010 digital stills camera. This had been primarily intended for ROV use and therefore relied on power and control from the surface *via* an umbilical connection. The photolander was designed to carry two 12V 84Ah batteries (Deep-Sea Power & Light Ltd.) providing enough power for over 1000 photographs. To control the system and process images, the existing PC-104 computer module was upgraded to a TB486 board (DSP Designs) with on-board ethernet controller and an add-on compact flash adapter. This adapter allowed a miniature hard drive to be used to store images within the confined space available in the camera control pressure housing. A 1 GByte microdrive (IBM) was used that can store 400 images in the uncompressed file format produced by the camera (flat file format, 2.3 Mbyte per image). The same adapter can be used with solid-state compact flash cards. To control the camera to take a series of time-lapse photographs while not consuming too much power over extended deployments, a wake-up control circuit was used. This very low power circuit incorporated a real-time clock set by the TB486 computer. The system can be programmed for an initial delay of up to 1 day and the picture interval can be set for between 5 minutes and 1 day. The original C source code for system control, image processing and storage was supplied by the manufacturer and adapted for the TB486 board and for autonomous operation. To communicate with this system a 'host mode' protocol using Procomm Plus interface software and an RS232 serial link is used. This allows configuration files, deployment logs and images to be transferred. All these adaptations were carried out within the existing control pressure housing and to give the system additional flexibility, an external trigger switch was included to allow pictures to be taken in response to an external event (such as a bottom switch or the output from a sensor).

When first connected to the batteries, the system performs a self-test and looks for user intervention. If there is none, it goes by default into autonomous mode. *Via* the control mode, the user can set up the drive configuration, perform manual tests and transfer files to and from the on-board computer. When in autonomous mode, the system sleeps until the time for the next picture at which time it wakes up, turns on the camera and flash, waits for the flash to charge, takes a picture, writes it to disc, sets the next wake-up time and turns off both the camera and flash. All status information and operations completed are written to a log file. After deployment, the images and log file can be transferred over the RS232 link at 115200 baud but to transfer the bulk of the images, the microdrive is removed and they are downloaded

directly to a computer. It is hoped that future developments will use recent advances in memory availability and image compression technology to allow more images to be stored.

Environmental parameters

Current speed and direction were recorded 4.5 m above the bed above using electromagnetic (Interocean S4) or 3D acoustic (Falmouth Scientific, Inc.) recording current meters. By deploying the current meter above the lander in the mooring line, current direction and velocity could be measured without interference from the lander framework. Three optical instruments were secured 0.5 m above the bed: light transmission was measured using a 25 cm path length, 660 nm wavelength transmissometer (WET Labs C-Star), the backscatter produced by particles in the water was measured with a light back-scattering sensor (LBSS, WET Labs, 880 nm) and a fluorometer centred at 455 nm and designed to detect fluoresced light emitted at 685 nm (WET Labs ECO AFLD) was used to monitor the presence of fluorescent material indicative of photosynthetic pigments of phytoplankton. The instruments were controlled and their outputs processed by a data logger (WS Ocean Systems Marine Monitor, UMI-2SB7). Details of instrument preparation, calibration and interpretation of results will be given in a later paper.

Study sites

Following inshore trials from the RV Calanus in Scottish waters (56º29.68N and 05º39.4W), the photolander was deployed for a short offshore trial from the F/F Johan Hjort by the Sula Ridge reef complex on the mid-Norwegian shelf (64º05.03N and 08º02.34E) from 9-13 July 2001. This led to a longer-term deployment from the RRS James Clark Ross at the same site from 18 June - 8 July 2002. These deployment sites are illustrated in Figure 2. Subsequently the buoyancy was upgraded to syntactic foam allowing a deeper deployment at 824 m on the Galway carbonate mound from RV Polarstern in the Porcupine Seabight (51º27.09N and 11º45.24W) from 8 June - 9 July 2003. At each of the sites the photolander was deployed by lowering the entire single module mooring illustrated in Figure 1 from an acoustic release on a ship's wire. After lowering the system to within 20 m of the seabed and when in position the lander was released by triggering the acoustic release. Since there were no means of visually guiding the first two deployments on the Sula Ridge, the lander was deployed on the flat topography to the northern side of the reef complex. This was intended to provide a relatively flat substrate close to the reef and within the zone of dead coral rubble known to support a high diversity of associated fauna (Jensen and Frederiksen 1992). Following the 2002 deployment by the Sula Ridge reef complex, both the lander site and adjacent reef area were characterised using a 'bed-hop' camera system that takes detailed photographs of 1 m² of the seabed (see Roberts et al. 2000 for description of the camera system). These images illustrate the uneven substrate at the lander site (Figs. 3A, B) as well as the coral and sponge rich habitats of the reef itself (Figs. 3C, D). For the Galway
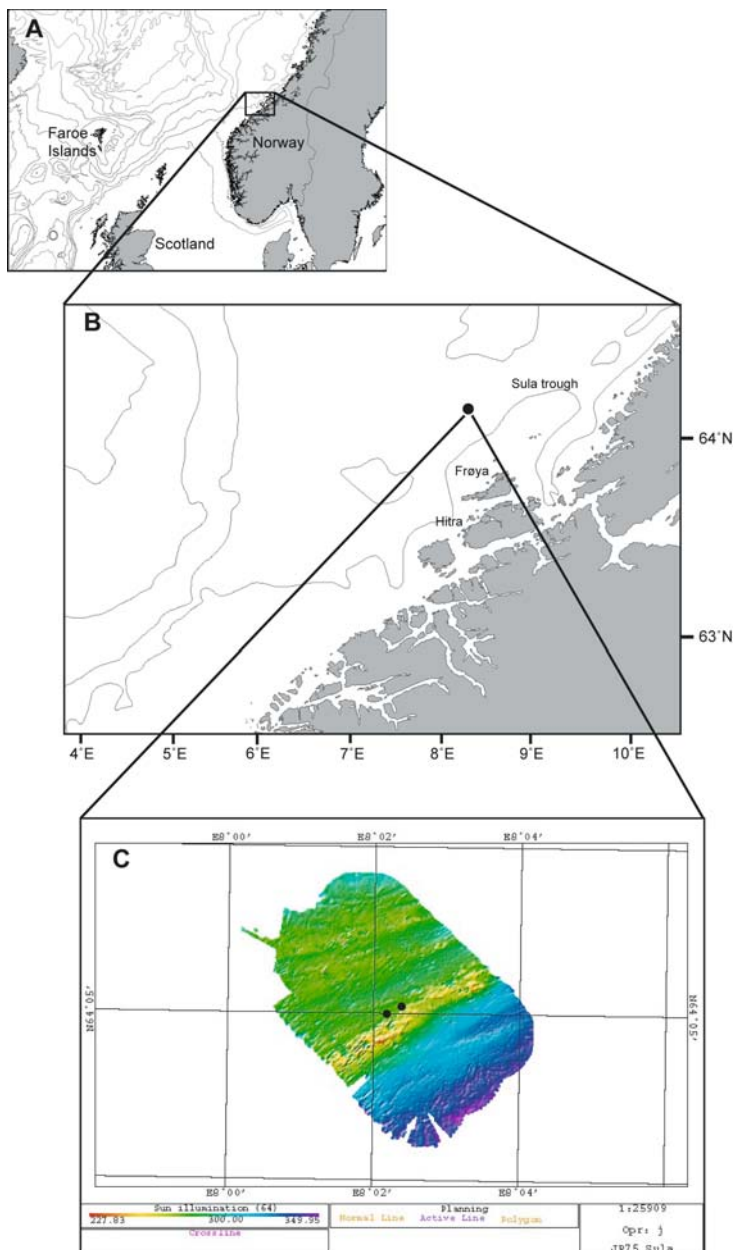
Fig. 2 The location of the photolander deployment sites by the Sula Ridge reef complex on the mid-Norwegian continental shelf. **A** Chart showing regional area, **B** Position of the Sula Ridge, **C** Lander sites illustrated on an EM120 multibeam bathymetric image showing a portion of the Sula Ridge reef. Using this swath survey it is possible to estimate the photolanders position relative to the reef complex; in 2001 it was 44 m from the edge of the reef complex and in 2002 it was 90 m away
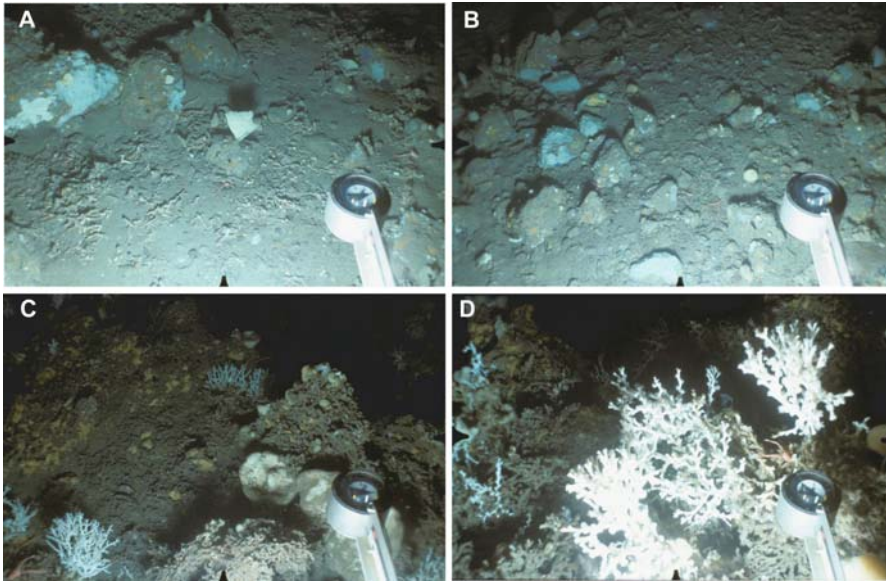
Fig. 3 Drop camera images ('bed-hop' camera system). **A** and **B** Glacial dropstones were abundant to the side of the Sula Ridge reef complex, giving a rough substratum for lander deployment. The dropstones were frequently colonised by both encrusting and erect sponges. Some coral rubble could be seen across the bed as could several galatheid Crustacea (*Munida sarsi*). **C** and **D** Photographs taken on the reef complex showed both live *L. pertusa* and gorgonian coral colonies with the underlying dead coral framework. Many sponges, sabellid polychaetes, a cephalopod mollusc and the ubiquitous *Munida sarsi* were also seen

Mound deployment, the deep-water ROV VICTOR (IFREMER, France) was used to identify a suitable deployment site and inspect the photolander *in situ*. However, it was not possible to adjust the lander's position after deployment. Both ROV-guided placement (Breuer et al. 2002) and video-guided launchers have great potential to accurately place landers, an obviously valuable technique in context of working among cold-water coral reef areas.

The dynamic environment of cold-water coral reefs

The Sula reef complex (SRC) has developed on the Sula Ridge, a northeast plunging spur from the Frøyabanken at between 250 and 320 m water depth, which crosses the southern end of the Haltenbank Deep. The SRC has been the focus of detailed studies to map its extent, describe its morphology and to elucidate the environmental factors controlling its development (see Freiwald et al. 2002 for detailed discussion). This area of the Norwegian shelf was subjected to iceberg scouring as the Fennoscandian icesheet retreated 12,000 years before present. The SRC is believed to have grown upon iceberg ploughmark-derived boulder levees which explain the slight offset in the orientation of the reef chain from the underlying
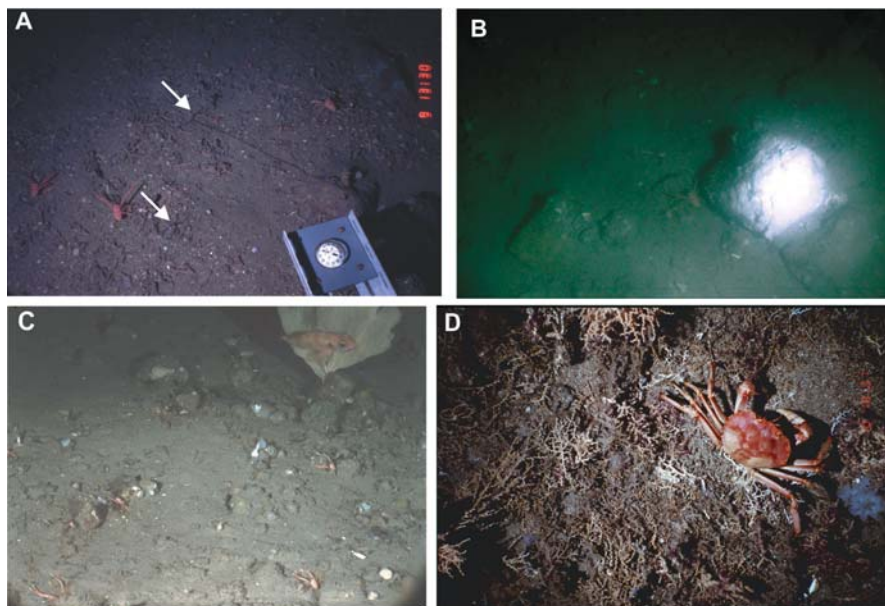
Fig. 4 Photolander images. **A** Oblique image of *Lophelia pertusa* rubble-strewn seabed taken in 2001, 44 m from the Sula Ridge reef complex. The feeding proboscides of two echiuran worms (*Bonellia viridis*, arrowed) can be seen extended from their burrows. One of these is next to a glacial dropstone colonised by encrusting sponges. *Munida sarsi* were abundant (Camera Alive film camera). **B** Oblique image of seabed from the 2002 deployment, 90 m from the reef complex. Here far less coral rubble was seen, glacial dropstones were scattered across the bed and *Munida sarsi* were abundant (Benthos 5010 digital stills camera). **C** Oblique image of seabed from the 2002 deployment again showing abundant *Munida sarsi* and glacial dropstones. An erect sponge can be seen towards the top of the image, and was frequently seen to be refuge for a solitary redfish (*Sebastes* sp.). A cephalopod mollusc can be seen just beneath this sponge (Mk 5 IOS film camera). **D** Vertical image of the *Madrepora oculata* rubble-strewn seabed on the Galway giant carbonate mound in the Porcupine Seabight taken in 2003. Purple octocorals (probably *Anthothelia grandiflora*) and glass sponges (*Aphrocallistes* sp.) can be seen as were several megafauna including this crab (probably *Geryon (Chaceon) affinis*) (Camera Alive film camera)

Sula Ridge structure (Freiwald et al. 1999). Dropstones supporting a rich epifaunal community of erect and encrusting sponges as well as other suspension-feeding organisms were seen in the images from both lander deployments (Fig. 4).

Sula Ridge, 9-13 July 2001

Seabed photographs from this deployment showed that the lander was successfully deployed as intended on a flat seabed covered in dead coral rubble (Fig. 4A) with occasional dropstones. The lander was deployed 44 m from the summit of the reef complex. All counts and measurements were made on digitised images using personal computer-based digitising software. The angles of camera view, inclination and height from seabed were used to scale objects according to the equations

described by Wakefield and Genin (1987). The feeding proboscides of echiuran worms, subsequently identified from samples as *Bonellia viridis*, and the galatheid crustacean *Munida sarsi* were conspicuous in these photographs. Of the 77 frames analysed, *B. viridis* were seen in 89 % at a mean density of 0.52 m^{-2} (SE 0.33) and *M. sarsi* were seen in all the frames at a mean density of 2.37 m^{-2} (SE 0.09). A fish was observed once (*Sebastes* sp.) and an unidentified nemertean worm was seen in

Table 1 Mean densities of conspicuous fauna (m^{-2}, ±SE) seen during the two Sula Ridge photolander deployments. (-, not observed)

Deployment dates: Camera type:	9-13 July 2001 Camera Alive	18 June - 8 July 2002 Benthos DSC	18 June - 8 July 2002 IOS Mk5
Nemertea	-	0.01 (0.004)	0.19 (0.01)
Munida sarsi	2.37 (0.09)	6.65 (0.08)	4.88 (0.03)
Natantia	-	0.1 (0.02)	0.001 (0.001)
Bonellia viridis	0.52 (0.33)	0.42 (0.03)	0.01 (0.003)
Asteroidae	-	0.38 (0.02)	0.16 (0.01)
Sepiolidae	-	-	0.05 (0.01)
Sebastes spp.	0.004 (0.004)	-	0.03 (0.005)
Unidentified teleost	-	-	0.01 (0.01)

two of the frames (Table 1). The positions of the echiuran proboscides are illustrated in Figure 5. The presence of large burrowing echiuran worms suggests rapid rates of bioturbation of the sediments by the Sula Ridge reef complex. A detailed spatial and temporal description of the fauna present can be found in Dodds (2003).

The current regime recorded 4.5 m above the bed showed a maximum velocity of 8.8 cm s^{-1}, a mean of 3.3 cm s^{-1} (Fig. 6A) and predominant directions of 150° to 350° True (Fig. 6B). To investigate this further, the N-S and E-W current vectors were calculated and a cumulative vector diagram produced (Fig. 6C), the latter illustrating a residual current towards the southwest (255° at 0.8 cm s^{-1}). The calculated current speed at 0.5 m above the bed where the optical instruments were positioned had a maximum velocity of 6.9 cm s^{-1} and a mean velocity of 2.6 cm s^{-1}. The maximum estimated sediment resuspension at 0.5 m above the bed at the lander site was 474 μg l^{-1} with a mean level of 133 μg l^{-1}.

Sula Ridge, 18 June - 8 July 2002

Seabed photographs show that in 2002 the photolander was situated on a flat area of seabed with frequent glacial dropstones (Fig. 4). Far less coral rubble was visible in the field of view of the cameras than during the previous deployment, probably because the lander was further from the summit of the reef complex (see Fig. 2). *M. sarsi* remained abundant and the feeding proboscides of *B. viridis* were seen. In this longer deployment, a greater variety of fauna was observed including asteroids, sepiolids and fish (see Table 1). Of the latter, a solitary redfish (*Sebastes* sp.) was often seen apparently sheltering next to an erect sponge growing on a dropstone (see Fig. 4C) pointing to the importance of structural habitat to these species. Over the course of the deployment, the current speeds recorded 4.5 m above the bed reached
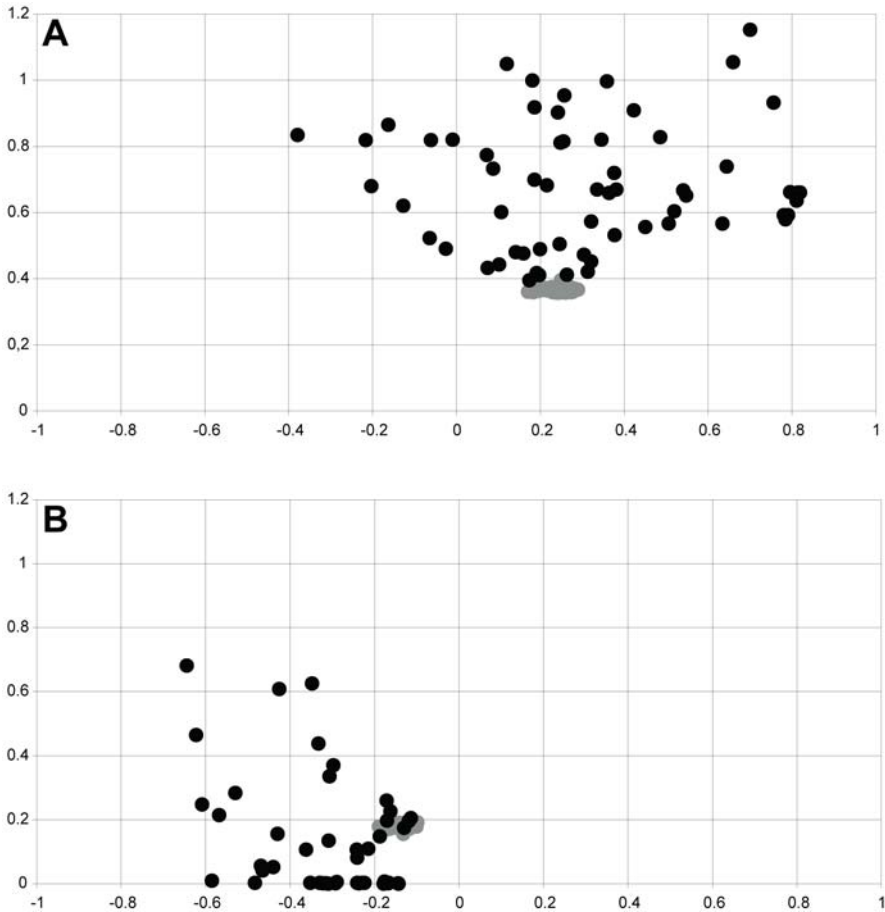
Fig. 5 Echiuran proboscis activity. Diagrams showing the maximum proboscis extension measured in metres on each of the photographs. Images were taken every half hour and a total of 85 photographs from the 2001 deployment were analysed. Both proboscides can be seen in Fig 4A. Interestingly, although the excursion areas of seabed available to the two worms could have overlapped, this was not recorded over the time 1.8 d time period available

a maximum of 27.5 cm s⁻¹ with a mean velocity of 6.2 cm s⁻¹. Unfortunately a failure within the compass unit of the current meter prevented the direction of flow of being recorded. Temperature varied between 7.33 and 8.35 with a mean of 7.35°C.

The hydrography of the mid-Norwegian shelf is described by Sætre (1999). The water mass at the depth of the Sula Ridge reef complex is dominated by Atlantic Water at around 8°C at 35.1 to 35.3 ppt salinity. Beneath this the Arctic Intermediate Water (AIW) mass described by Blindheim (1990), typically at water depths of 500 to 600 m, is slightly less saline (34.87 to 34.91 ppt) and colder than Atlantic Water (-0.5 and 1.0°C). Deeper still is the densest and coldest water mass, Norwegian Sea Deep Water (NSDW). There have been few near-bed current measurements from
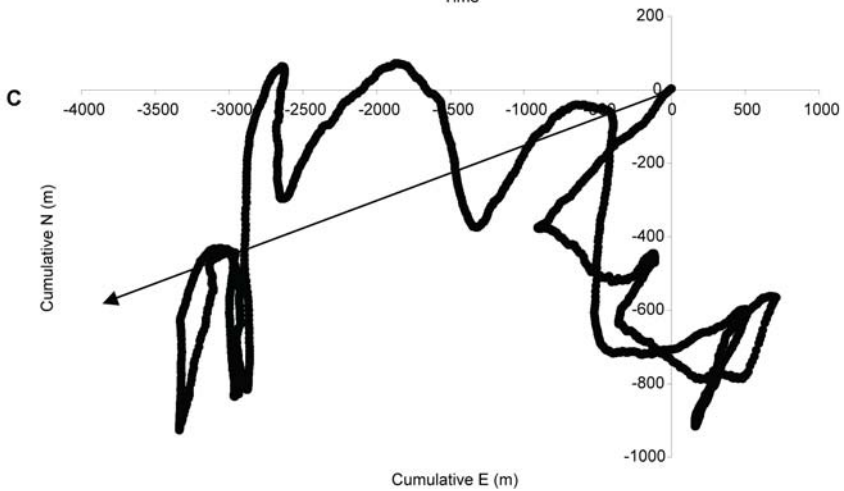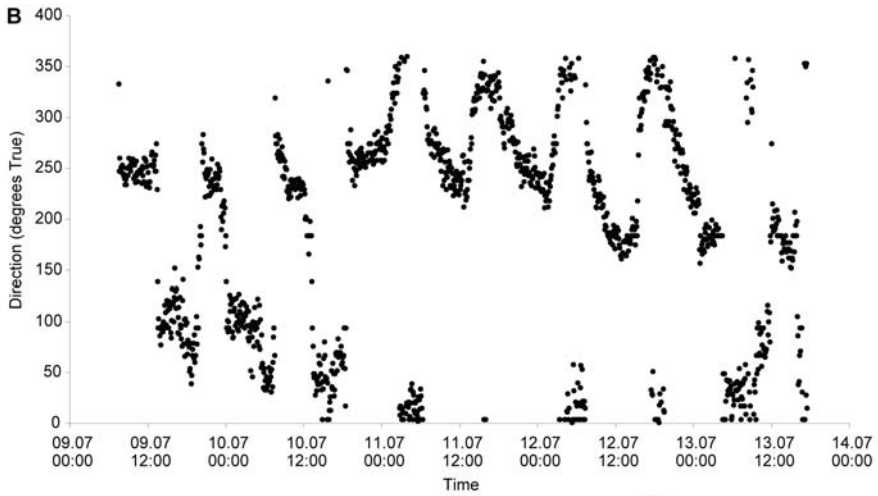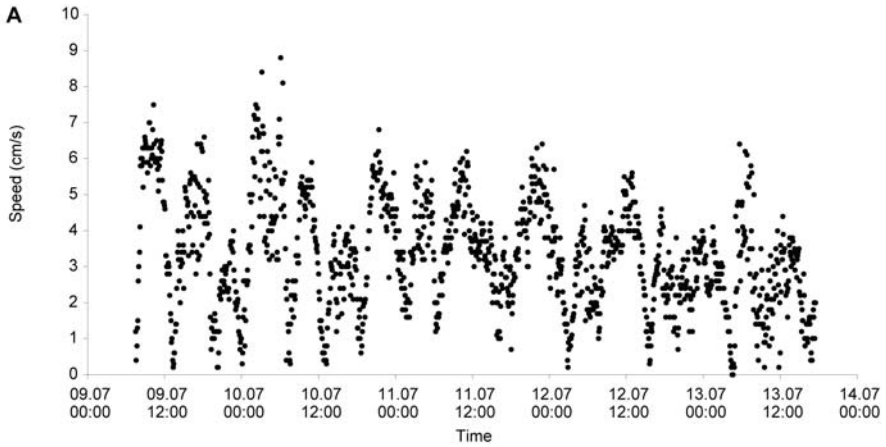
the Sula Ridge area. Mortensen et al. (2001) refer to commercial records from the Norwegian state oil company Statoil that describe the current regime to the north of the Sula Ridge as having a main current direction to the southeast and a maximum velocity of 38 cm s^{-1}. To the south of the ridge current flows were equally strong to the south and north and had a maximum velocity of 20 cm s^{-1}. As reiterated by Blindheim (1990) and Sætre (1999), current flows on the Norwegian shelf are strongly affected by seafloor topography. The current regimes recorded both by Statoil and the photolander are likely to be even more prone to local topographic influences since they were taken near the seabed and, in the case of the photolander, very close to the topographically complex Sula Ridge. Such local differences might explain the fact that Statoil reported a residual current flow north of the Sula Ridge to the southeast whereas the photolander record from close to the reef complex suggests a residual flow to the southwest. In terms of current velocities, the maximum velocity recorded by Statoil, 38 cm s^{-1}, is of a similar order to that recorded by the second photolander deployment of 28 cm s^{-1}.

Galway carbonate mound, 8 June - 9 July 2003

The Galway Mound in the Porcupine Seabight is a 100 m tall double peaked, ridge-shaped mound orientated to the NNW. It is 1.6 km long and 0.8 km across rising from 920 m water depth to 820 m at the summit (pers. comm. A Wheeler). Early analysis of results from the third deployment of the photolander on the Galway Mound showed an even more intense current regime with a maximum recorded velocity of 70 cm s^{-1}. Here the residual current flow of 13.6 cm s^{-1} was to the north west and speeds exceeded 50 cm s^{-1} on all diurnal tidal cycles 2-3 days either side of spring tides (pers. comm. M White). The maximum mean daily currents occurred at diurnal spring tides and the minimum at neap tides. Similar observations have been recorded to the north of the Galway Mound by Pingree and LeCann (1989, 1990).

These near-bed photolander current records reinforce the well-known, but rarely measured, association of cold-water coral communities with areas of high current flow and emphasise the importance of drag assessment in the design of benthic landers for these environments. However, while information on the hydrographic regime around cold-water coral reefs is growing, the role of these high current flows in supplying food particles to the suspension feeding communities is less well known. White et al. (submitted) propose that coral reefs colonising carbonate mounds in the Porcupine Seabight, including the Galway Mound, benefit from the retention of dense, nutrient-rich domes of water on the bank summit that slowly drain towards the carbonate mounds around the flanks of the bank. Particulate material is maintained in suspension by the dynamic current flows recorded downslope, such as that shown by the photolander record from the Galway Mound. Despite

---

Fig. 6 Current records from the Sula Ridge, 9-13 July 2001. **A** Current speed and **B** direction (True) over the duration of the photolander deployment showing the Sula Ridge reef complex is subjected to a tidal current regime. **C** A cumulative vector diagram illustrating that at the lander deployment site to the north of the Sula Ridge the residual current flow is towards the south west (arrowed)

these indications of the origin of a food supply, information on the food particles and especially on plankton communities near cold-water reefs is almost entirely lacking, perhaps because of the difficulties associated with traditional net sampling of zooplankton near large and topographically complex reef structures. Once again *in situ* lander approaches to record and quantify plankton communities amongst live reef areas hold great potential to fill this gap in our understanding. Approaches using optical particle counter technologies (e.g., Herman et al. 1993) and bulk assessments using ADCP instruments to assess plankton migration by recording the movement of scattering layers (e.g., Tarling et al. 2002) should be considered. Similarly the role of reef areas as refuges for fish species (Husebø et al. 2002) and their importance as essential fish habitat (Auster 2005) could be assessed *in situ* both visually and using acoustic tagging techniques (Priede and Bagley 2000). Early assessments of the lander datasets point to the importance of flow regime as a key environmental determinant of cold-water coral occurrence. The results also suggest that reef areas are subject to noticeable periods of sediment resuspension. Longer-term deployments covering periods of seasonal change are now needed to investigate these factors in more detail.

Lander refinements and seafloor observatories

In situ observations have great potential to enhance our understanding of poorly studied cold-water coral reef ecosystems in a number of different ways. Firstly, the physiology and behaviour of framework-constructing coral species can only be studied in the laboratory in relation to a sound understanding of the environment from which they have been collected and how naturally variable that environment is. Laboratory studies of live coral directed by *in situ* observations will advance our understanding of the basic biology and ecology of these systems. Secondly, since benthic landers can be left on the bottom for extended periods of time they provide a means of monitoring and recording the environment and the activity of the biota at times of the year when it is hard or impossible to work from a surface vessel. It is becoming increasingly clear that many aspects of the biology of cold-water corals are seasonally driven yet there is little or no information on how major seasonal influences, such as plankton blooms, influence them. We have yet to unravel the precise timing of cold-water coral reproduction in the northeast Atlantic but early indications suggest that both *Lophelia pertusa* and *Madrepora oculata* spawn in the first few months of the year (Waller 2005, Waller and Tyler in press). As shown here, cold-water coral reef areas along the northeast Atlantic margin are subject to distinct tidal cycles. Could the tidal regime provide the signal to synchronise spawning time, as in some warm-water corals? While we know that cold-water coral reefs support diverse associated communities, our knowledge of the functional roles of the fauna remains poor. Aquarium studies provide intriguing glimpses into the role of commensal species such as the polychaete *Eunice norvegica* that has been seen to clean coral polyps, steal food from the tentacles (Mortensen 2001) and even aid the reef-building process by joining adjacent coral colonies (Roberts

in press). Time-lapse video recording using infra-red illumination has proved useful to monitor cold-water coral polyp behaviour in the laboratory (Roberts and Anderson 2002). Lander-based time-lapse video systems illuminated with low power infra-red diodes could be used to record the activity of white-light sensitive animals such as the commensal polychaetes and other associated fauna *in situ*. Such measurements would benefit from 'intelligent' system controls capable of responding to periods of change rather than blindly logging at pre-set intervals. For example the movement of fauna or the output of specific sensors could be used to alter the rate of photography or to initialise a video system for a short period of time. This approach becomes particularly relevant to help conserve power during extending autonomous deployments.

A long-term benthic observatory capable of recording an area of live reef would allow us to observe the behaviour of coral polyps and associated fauna and could provide a first glimpse of coral spawning in deep-water. Plans for long-term seafloor observatories permanently connected to sophisticated information networks are now well-advanced (Copley 2004). For example the North American NEPTUNE project proposes to establish a 3000 km network of communications and power cables across the the Juan de Fuca tectonic plate in the northeast Pacific Ocean to monitor an area of approximately 1000 by 500 km. Within this area, between 30 and 50 nodes will be established to monitor a range of physical, chemical, biological and tectonic processes (Delaney et al. 2001). Similar proposals in the northeast Atlantic may allow us to install a seafloor observatory within a cold-water coral reef to observe and record seasonal variability and relate this to the behaviour and reproduction of the dominant framework-forming coral species. While technically challenging and costly in terms of initial capital outlay, seafloor observatories have vast potential to allow researchers of all disciplines real-time continuous access to the deep-water environment. Our understanding of the natural world and our predictions of future change depend on our ability to measure its current state and inherent variability. Industrial and technological developments in deep water now open the opportunity to reduce our reliance as marine scientists on surface vessels and move towards long-term *in situ* observations. These observatories have great potential to advance our understanding of otherwise inaccessible 'hot-spot' environments in deep water, including cold-water coral reefs.

Acknowledgements

References

Auster PJ (2005) Are deep-water corals essential habitats for fishes? In: Freiwald A, Roberts JM (eds) Cold-water Corals and Ecosystems. Springer, Berlin Heidelberg, pp 747-760

Battle EJV, Priede IG, Collins MA, Bagley PM (2002) Seasonal variation in bioluminescence in the Porcupine Seabight, NE Atlantic, to 4800 m depth. Bioluminescence and chemiluminescence: progress and current applications. In: Stanley PE, Kricka LJ (eds) World Scientific, Singapore, pp 379-382

Bett BJ, Malzone MG, Narayanswamy BE, Wigham BD (2001) Temporal variability in phytodetritus and megabenthic activity at the seabed in the deep northeast Atlantic. Progr Oceanogr 50: 349-368

Blindheim J (1990) Arctic Intermediate Water in the Norwegian Sea. Deep-Sea Res 37: 1475-1489

Breuer E, Peppe OC, Shimmield GB (2002) A novel approach for the study of North Sea drill cuttings accumulations: the combined use of an ROV and benthic lander for *in situ* measurements. Underwater Technol 25: 77-82

Copley J (2004) All wired up. Nature 427: 10-12

Delaney J, Heath G, Chave A, Kirkham H, Howe B, Wilcock W, Beauchamp P, Maffei A (2001) NEPTUNE. Real-time, long-term ocean and earth studies at the scale of a tectonic plate. OCEANS 2001 Conf, Honolulu, Hawaii, 8 pp

Dodds LA (2003) Spatial and temporal analysis of the megafauna and environment near the Sula Ridge reef, Norway, using time-lapse photography. MSc thesis, Univ Aberdeen, 48 pp

Fosså JH, Mortensen PB, Furevik DM (2002). The deep-water coral *Lophelia pertusa* in Norwegian waters: distribution and fishery impacts. Hydrobiologia 471: 1-12

Fosså JH, Lindberg B, Christensen O, Lundälv T, Svellingen I, Mortensen PB, Alvsvåg J (2005) Mapping of *Lophelia* reefs in Norway, experiences and survey methods. In: Freiwald A, Roberts JM (eds) Cold-water Corals and Ecosystems. Springer, Berlin Heidelberg, pp 359-391

Freiwald A, Wilson JB, Henrich R (1999) Grounding Pleistocene icebergs shape recent deep-water coral reefs. Sediment Geol 125: 1-8

Freiwald A, Hühnerbach V, Lindberg B, Wilson JB, Campbell J (2002) The Sula Reef Complex, Norwegian Shelf. Facies 47: 179-200

Freiwald A, Fosså JH, Grehan A, Koslow T, Roberts JM (2004) Cold-water coral reefs. UNEP-WCMC, Cambridge, UK, 84 pp

Gardline Ltd (2002) Environmental assessment of deep-water carbonate structures in the vicinity of the Salema & Bijupira development. Rep 5771, 28 pp

Hall-Spencer J, Allain V, Fosså JH (2002) Trawling damage to Northeast Atlantic ancient coral reefs. Proc R Soc London B 269: 507-511

Herman AW, Cochrane NA, Sameoto DD (1993) Detection and abundance estimation of euphausiids using an optical plankton counter. Mar Ecol Progr Ser 94: 165-173

Hovland M, Farestveit R, Mortensen PB (1994). Large cold-water coral reefs off mid-Norway - a problem for pipe-laying. Proc Oceanol Int (3), 8-11 March 1994, Brighton, UK

Husebø A, Nøttestad L, Fosså J, Furevik D, Jørgensen S (2002) Distribution and abundance of fish in deep-sea coral habitats. Hydrobiologia 471: 91-99

Jensen A, Frederiksen R (1992) The fauna associated with the bank-forming deepwater coral *Lophelia pertusa* (Scleractinaria) on the Faroe shelf. Sarsia 77: 53-69

Koslow JA, Gowlett-Holmes K, Lowry JK, O'Hara T, Poore GCB, Williams A (2001) Seamount benthic macrofauna off southern Tasmania: community structure and impacts of trawling. Mar Ecol Progr Ser 213: 111-125

Lampitt RS (1985) Evidence for the seasonal deposition of detritus to the deep-sea floor and its subsequent resuspension. Deep-Sea Res 23: 885-897

Lampitt RS, Burnham MP (1983) A free-fall time-lapse camera and current meter system "Bathysnap" with notes on the foraging behaviour of a bathyal decapod shrimp. Deep-Sea Res 30A: 1009-1017

Lundälv T, Jonsson L (2003) Cold-water corals in the Skagerrak – more significant than expected but in deep peril. Erlanger Geol Abh Sonderbd 4: 58

Masson DG, Bett BJ, Billett DSM, Jacobs CL, Wheeler AJ, Wynn RB (2003) The origin of deep-water, coral-topped mounds in the northern Rockall Trough, Northeast Atlantic. Mar Geol 194: 159-180

Mortensen PB (2001) Aquarium observations on the deep-water coral *Lophelia pertusa* (L., 1758) (Scleractinia) and selected associated invertebrates. Ophelia 54: 83-104

Mortensen PB, Hovland M, Brattegard T, Farestveit R (1995) Deep water bioherms of the scleractinian coral *Lophelia pertusa* (L.) at 64° N on the Norwegian shelf: Structure and associated megafauna. Sarsia 80: 145-158

Mortensen PB, Hovland MT, Fosså JH, Furevik DM (2001) Distribution, abundance and size of *Lophelia pertusa* coral-reefs in mid-Norway in relation to seabed characteristics. J Mar Biol Ass UK 81: 581-597

Pingree R, Le Cann B (1989) Celtic and Armorican slope and shelf residual currents. Progr Oceanogr 23: 303-338

Pingree R, Le Cann B (1990) Structure, strength and seasonality of the slope currents in the Bay of Biscay region. J Mar Biol Ass UK 70: 857-885

Priede IG, Bagley PM (2000) *In situ* studies on deep-sea demersal fishes using autonomous unmanned lander platforms. Oceanogr Mar Biol 38: 357-392

Reed JK (2002) Deep-water *Oculina* coral reefs of Florida: biology, impacts, and management. Hydrobiologia 471: 43-55

Roberts M (1997) Coral in deep water. New Scientist 2100: 40-43

Roberts JM (in press) Reef-aggregating behaviour by eunicid polychaete symbionts of cold-water corals: do worms assemble reefs? J Mar Biol Ass UK

Roberts JM, Anderson RM (2002) A new laboratory method for monitoring deep-water coral polyp behaviour. Hydrobiologia 471: 143-148

Roberts JM, Harvey SM, Lamont PA Gage JD, Humphery JD (2000) Seabed photography, environmental assessment and evidence for deep-water trawling on the continental margin west of the Hebrides. Hydrobiologia 441: 173-183

Roberts JM, D Long, JB Wilson, PB Mortensen, JD Gage (2003) The cold-water coral *Lophelia pertusa* (Scleractinia) and enigmatic seabed mounds along the north-east Atlantic margin: are they related? Mar Pollut Bull 46: 7-20

Rogers AD (1999) The biology of *Lophelia pertusa* (Linnaeus 1758) and other deep-water reef-forming corals and impacts from human activities. Int Rev Hydrobiol 84: 315-406

Sætre R (1999) Features of the central Norwegian shelf circulation. Cont Shelf Res 19: 1809-1831

Tarling G, Jarvis T, Emsley S, Matthews J (2002) Midnight sinking behaviour in *Calanus finmarchicus*: a response to satiation or krill predation? Mar Ecol Progr Ser 240: 183-194

Tengberg A, De Bovee F, Hall P, Berelson W, Chadwick D, Ciceri G, Crassous P, Devol A, Emerson S, Gage J, Glud R, Gratiottini F, Gunderson J, Hammond D, Helder W, Hinga K, Holby O, Jahnke R, Khripounoff A, Lieberman S, Nuppenau V, Pfannkuche O, Reimers C, Rowe G, Sahami A, Sayles F, Schurter M, Smallman D, Wehrli B, De Wilde P (1995) Benthic chamber and profiling landers in oceanography - A review of design, technical solutions and functioning. Progr Oceanogr 35: 253-294

Wakefield WW, Genin A (1987) The use of a Canadian (perspective) grid in deep-sea photography. Deep-Sea Res 34: 469-478

Waller RG (2005) Deep-water scleractinians - current knowledge of reproductive processes. In: Freiwald A, Roberts JM (eds) Cold-water Corals and Ecosystems. Springer, Berlin Heidelberg, pp 697-700

Waller RG, Tyler PA (in press) The reproductive ecology of two deep water reef building scleractinians in the NE Atlantic Ocean. Coral Reefs

Wheeler AJ, Bett BJ, Billett DSM, Masson DG, Mayor D (in press) The impact of demersal trawling on NE Atlantic deep-water coral habitats: the Darwin Mounds, UK. Amer Fish Soc Spec Vol

White M, de Stigter H, de Haas H, van Weering T (submitted) Physical dynamics at the Rockall Trough margin that influence the carbonate mound and cold coral reef ecosystem. Progr Oceanogr

Wilson JB (1979) 'Patch' development of the deep-water coral *Lophelia pertusa* (L.) on Rockall Bank. J Mar Biol Ass UK 59: 165-177

Deep-water coral development as a function of hydrodynamics and surface productivity around the submarine banks of the Rockall Trough, NE Atlantic

Martin White[1], Christian Mohn[1], Henko de Stigter[2], Gareth Mottram[3]

[1] Department of Earth and Ocean Sciences, National University of Ireland, Galway, Ireland
(Martin.White@nuigalway.ie)
[2] Koninklijk Nederlands Instituut voor Onderzoek der Zee (NIOZ), P.O. Box 59, NL-1790 AB Den Burg, Texel, The Netherlands
[3] Remote Sensing Group, Plymouth Marine Laboratory, Plymouth, UK

Abstract. The dynamics that occur at the Porcupine Bank, Rockall Trough, are described in relation to the role the bank, and others like it, may play in the development of deep-water corals, such as *Lophelia pertusa* (L.), which occurs widely in the NE Atlantic. High productivity has been measured over the bank, and it appears that this productivity may be fuelled by an increase in nutrients available over the bank through winter convection which leaves dense, nutrient rich water on the bank. This dense water drains away slowly through the benthic boundary layer (BBL) providing a mechanism for downslope transport of organic material in the boundary layer. Processes such as rectification of diurnal tides and Taylor column formation generate closed circulation patterns around the bank and promote the retention of organic matter over the bank. Similar processes have been observed over other Rockall Trough banks, and the combination of these processes appear to promote the availability of food to the corals that inhabit the lower flanks of the banks, particularly on the coral-dominated carbonate mounds that also occur there.

Keywords. Physical oceanography, benthic dynamics, submarine banks, cold-water corals

Introduction

The continental margin of the NE Atlantic is characterised by a high abundance of deep cold-water corals, particularly *Lophelia pertusa*, and *Madrepora oculata* (Fig. 1A; Rogers 1999; Freiwald 2002; Roberts et al. 2003). The majority of the corals are found in water depths ranging between 150-1200 m. Living *Lophelia pertusa* is most abundant between 600-800 m in the southern Rockall Trough. This
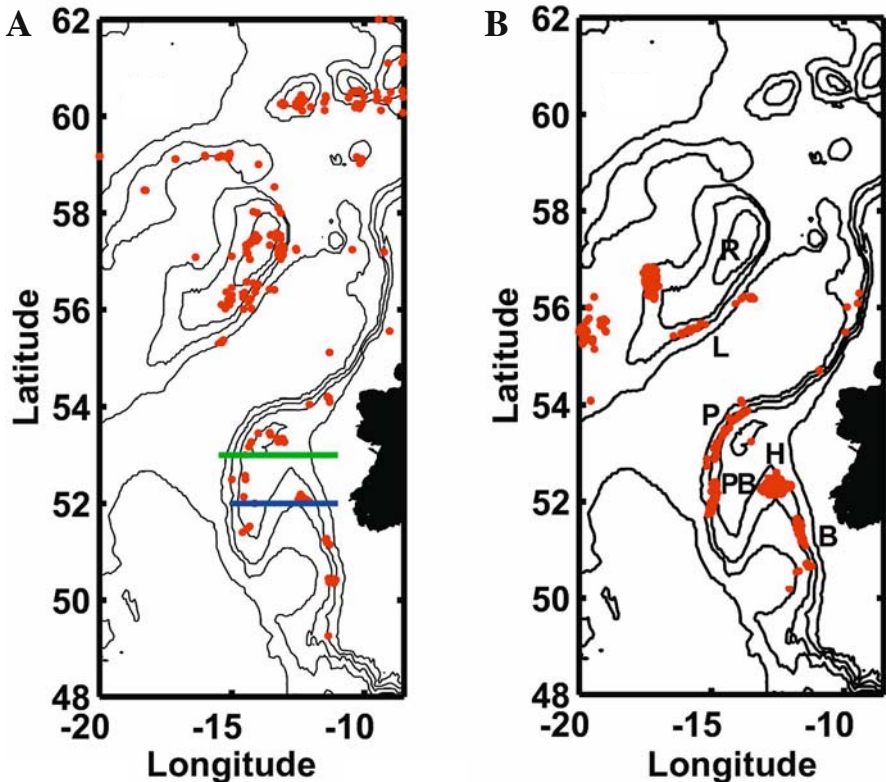
Fig. 1 A Locations of live sampled *Lophelia pertusa* (data from Freiwald et al. 2004). The blue line denotes the longitudinal extent of the chlorophyll measurements shown in Figure 2 and the green line the CTD section in Figure 3. **B** Locations of carbonate mounds in the Rockall Trough (courtesy of V. Unnithan and GEOMOUND project team (unpublished data)). Mound regions are labelled L-Logachev, B-Belgica, P-Pelagia and H- Hovland/Magellan respectively and the Rockall and Porcupine Banks are labelled R and PB

depth zone of peak abundance shifts to shallower water towards the north (Roberts et al. 2003). The number of recorded coral specimens are particularly high around the many submarine banks and seamounts of the Rockall Trough, such as Porcupine and Rockall Bank in the south (Kenyon et al. 2003; van Weering et al. 2003) and seamounts/banks such as Lousy, Bill Bailey Banks and Rosemary Seamount to the north (e.g., Frederiksen et al. 1992; Roberts et al. 2003). The corals in the depth zone between 600-800 m in the southern Rockall Trough are mostly associated with the carbonate mounds located along the flanks of Rockall and Porcupine Bank (van Weering et al. 2003). These mounds, several km in diameter and up to 200 m high, are composed of a carbonate sediment-filled dead coral framework, often topped by live coral (Fig. 1B; Kenyon et al. 2003).

The dynamical aspects that influence the deep-water coral ecosystem are becoming well known (e.g., Frederiksen et al. 1992; Freiwald 2002, White et al.

submitted). *Lophelia pertusa* requires a hard substrate on which to settle, with sufficient near-seabed currents to keep organic matter in suspension and prevent sediment from settling and smothering the developing corals. Frederiksen et al. (1992) has discussed the influence of internal waves in controlling depth range for *Lophelia pertusa*, both from the view of enhanced near seabed physical dynamics and on the influence of the waves on food availability through generating conditions to promote surface productivity. Other benthic dynamical processes, such as bottom intensified subtidal wave motions, have also been found to generate the large near-seabed currents favoured by the corals (White et al. submitted).

Seamounts and other isolated submarine banks have a unique aspect to their dynamics, such as the rectification of tidal motions and enclosed residual circulation patterns (e.g., Kunze et al. 1997; Mohn and Beckmann 2002). For example, Kunze et al. (1997) have demonstrated that a variety of intensified baroclinic motions of diurnal period may exist over a seamount in the Pacific. Goldner and Chapman (1997) have shown, through modelling studies, that an enclosed mean anti-cyclonic circulation can be generated around isolated seamounts through forcing by diurnal tides or by Taylor column circulation. A Taylor column is a region of enclosed anti-cyclonic circulation over an obstacle, formed as a result of a slow steady flow impinging on the obstacle under certain topographic and stratification scaling conditions. A Taylor column will cause isopycnal doming over the obstacle (White et al. 1998; Mohn and Beckmann 2002).

This paper is focused on the role of the hydrodynamics around, and the productivity over, the submarine banks in promoting the deep-water coral ecosystem in the Rockall Trough, using the Porcupine Bank as a case study. Porcupine Bank is a submarine shelf break bank, partly attached to the Irish continental shelf (Fig. 1B). Its main axis covers a length of approximately 200 km and is oriented essentially north-south, rising to a water depth of 180 m to the north. To the southeast, the bank is separated from the Irish Shelf by the Porcupine Seabight (of depth 2000 m), whereas to the west it is marked by a steep flank sloping down rapidly to water depths of 4000 m into the Porcupine Abyssal Plain. There are numerous carbonate mounds around the flanks of the bank (Fig. 1B). These mounds and associated corals lie within the depth range associated with the warm upper Eastern North Atlantic Water (ENAW) and intermediate Mediterranean Outflow Water (MOW) masses (van Aken and Becker 1996).

The paper uses both established and new results for the dynamics and productivity around the Porcupine Bank. The results are synthesised to highlight processes that are likely to occur around the Porcupine Bank, and other submarine banks of the Rockall Trough, and a conceptual model for the coral development around these features is presented. The presence of, and the reasons for, enhanced productivity over the bank is shown in this study. The principal flow dynamics around the Porcupine Bank and its impact on the dispersion of passive tracers, based on an idealised process study, are described. A conceptual model is presented and discussed below.

Methodology

In this study, we present a combined observational and modelling approach. SeaWiFS (Sea-viewing Wide Field-of-view Sensor) imagery measured between October 1997 and May 2003 has been routinely collected and processed at the NERC Remote Sensing Services, Plymouth Marine Laboratory. Mean monthly sea-surface chlorophyll across the Porcupine Bank was derived from the 1 km data set. Conductivity Temperature and Depth (CTD) measurements throughout the Porcupine Bank area have been used to illustrate hydrographic characteristics. To investigate the effect of the flow dynamics on the dispersion of biological material at the Porcupine Bank, the 3-D S-coordinate Primitive Equation Model (SPEM) was employed, described in detail by Mohn and Beckmann (2002). An idealised topography was used with the main focus on a realistic representation of the topographic east-west asymmetry of the bank near its summit. The model grid contained 128 x 128 grid points covering a model domain of 640 x 640 km with 20 vertical levels. The initialisation of the model was prescribed for a typical early summer situation assuming high biological productivity and strong background stratification of the oceanic far field. The model forcing was extended to the dominant semidiurnal (M_2, S_2) and diurnal (K_1, O_1) tides to give a more realistic representation of the tidal activity. Additionally, a mean background flow was introduced representing the poleward flowing slope current found at the southern Rockall Trough margin (White et al. submitted).

Productivity and water masses over the Porcupine Bank

Figure 2 shows a time series of SeaWiFS mean monthly measured surface chlorophyll between 11-15°W at the latitude of 52°N (see Fig. 1A). An increase in
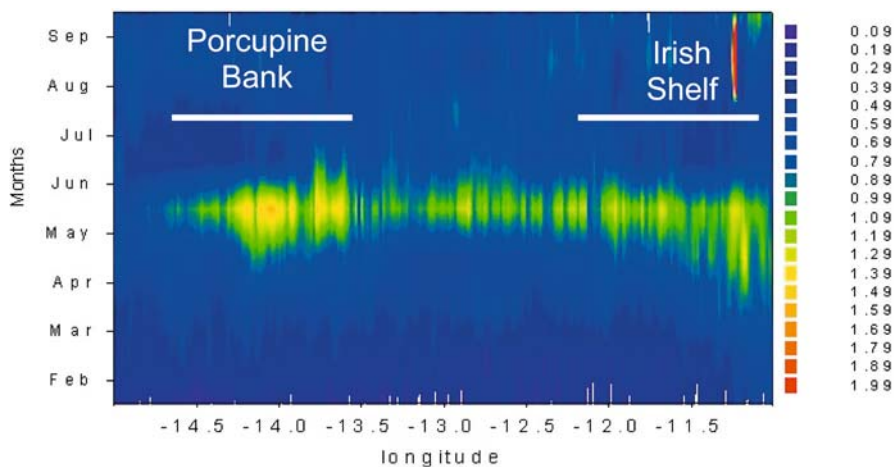
Fig. 2 Mean monthly chlorophyll at 52°N against Longitude, based on 1 km SeaWiFS imagery from Oct 1997 – May 2003. The Longitude range corresponding to the Porcupine Bank and Irish Shelf are indicated. A scale, in mg l^{-1}, is indicated

chlorophyll on the Irish Shelf, from low winter values (<0.3 mg l^{-1}) up to 2 mg l^{-1}, commences in early April signifying the spring bloom. Over the bank itself, chlorophyll values start to rise somewhat later, in May. The highest values in the chlorophyll occur in the surface waters over the bank region, separated from the high shelf values by low values over deep water. A similar transect across the bank and shelf at 53.25°N show similar characteristics, but relatively high chlorophyll values are found along most of the section, perhaps due to the relatively shallow water depths associated with the col between the summit of the bank and the Irish Shelf. Mixed diatom and coccolithophorid blooms are common at this time of the year west of Ireland (Robin Raine, NUI, Galway pers. comm.). Similar plankton types have been observed in a benthic nepheloid layer sampled on the northern flanks of the Porcupine Bank (de Stigter et al. submitted). Whilst the organic content of such plankton is small, other material with high, and more importantly fresh, chlorophyll content, have been observed in material sampled in the BBL. This would suggest that plankton production in the vicinity of the bank has sunk out to the seabed and dynamical processes acting there are keeping organic material in suspension.

Elevated chlorophyll levels over the Porcupine Bank suggest that enhanced productivity may be occurring there and presumably requiring sufficient nutrients to fuel such production. White et al. (1998) have shown that cold, nutrient rich water, of higher density than water at the corresponding depth adjacent to the bank forms in the spring. Figure 3 shows an April temperature and density transect across the Porcupine Bank along 53°N. The transect shows that temperatures on the Irish Shelf and Porcupine Bank are up to 0.5°C colder and 0.1 kg m^{-3} denser than water at the same depth in the deep Rockall Trough. White et al. (1998) presented several hydrographic and nutrient sections from 51.5°-53.5°N which indicated that the dense water mass forms across the whole north-south extent of the bank between those latitudes, and remained on the bank at least until July and probably longer. The dense dome was observed to extend from 100 m above the seabed over the shallow portion of the bank, but was deeper, >250 m in height, further south. The entire dense dome becomes capped in the summer by the seasonal thermocline, and its formation was initially attributed to the isopycnal doming caused by Taylor column formation.

An alternative explanation for the dense water masses, however, is that they may be formed through winter convection processes. The depth of winter mixing due to oceanic heat loss at these latitudes has the potential to reach between 600-900 m depth (van Aken and Becker 1996), and will reach a maximum by March. Shallow water, such as that over the continental shelf and the Porcupine Bank, may therefore become vertically mixed throughout the whole water column and cool faster than the adjacent deeper water. It might seem that this water would cascade off-slope, as observed off the NW Irish Shelf (Hill et al. 1998). Shapiro and Hill (1997) have shown, however, that under certain conditions of density stratification and particularly bottom slope, a dense water lens will not cascade off the bank, but instead slowly drains off-slope through the BBL. This has been termed 'Ekman drainage'. The process may be thought of as the slow flow of the dense water from
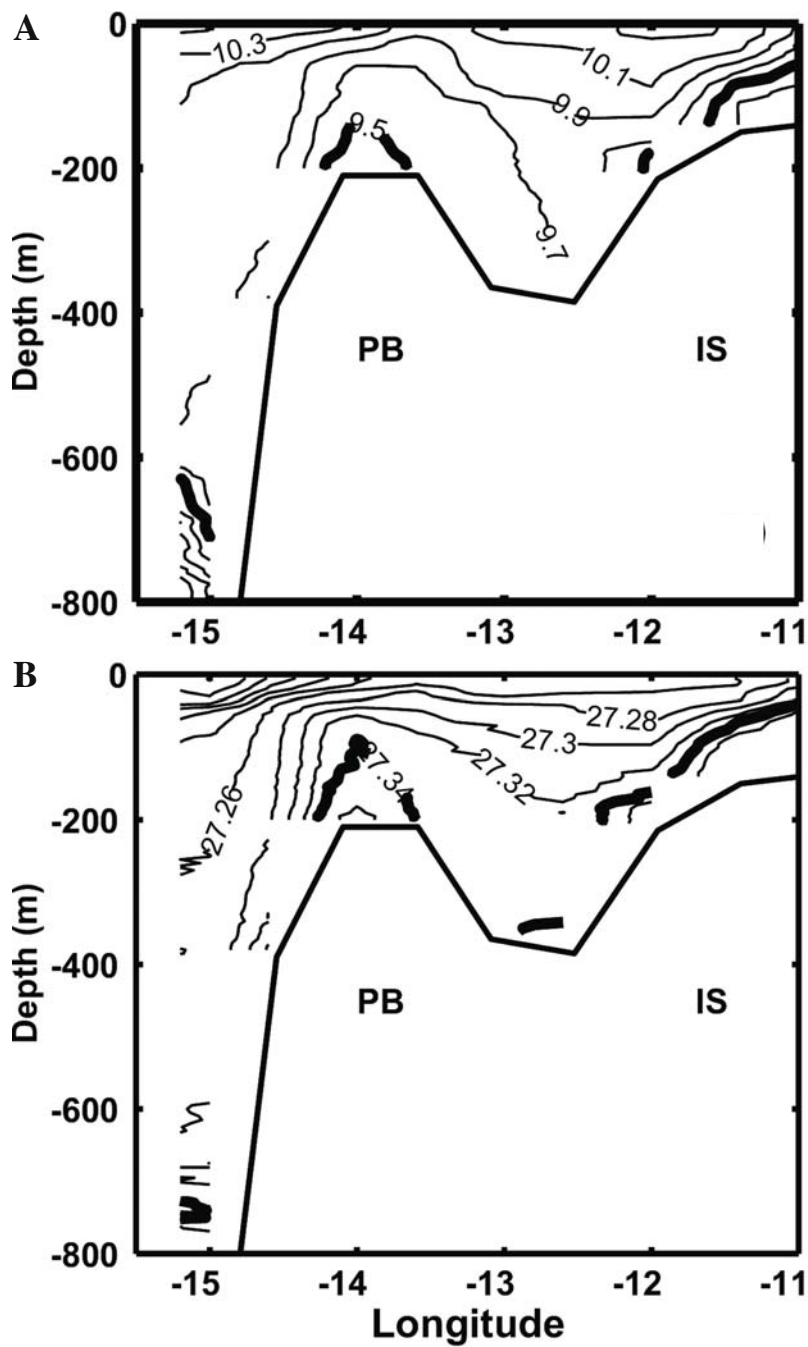
Fig. 3 Zonal section at 53°N of temperature (**A**) and density (**B**), April 1995. Contour intervals are (**A**) 0.2°C and (**B**) 0.02 kg m^{-3} respectively. The 9.5°C isotherm and 27.34 kg m^{-3} isopycnal are highlighted with a thicker line to show the cold, dense water mass on the bank

the summit, which initially tries to flow downslope under gravity. Rotational forces, however, cause the water to flow principally along the isobaths, but with near-seabed friction causing in a downslope component to the transport. It would appear that this process is the dominant off-slope transport mechanism for the Porcupine Bank. In addition, it should be noted that Ekman drainage acts only near the seabed as opposed to the overlying residual circulation driven by a Taylor column, or tidal forcing mechanism.

The time-scale for this drainage may be approximated as the initial water volume formed over the bank divided by the volume flux through the BBL driven by the Ekman drainage, i.e.

$$T = L \cdot W \cdot H / 2 \cdot (W+L) \cdot h \cdot Ve \qquad (1)$$

Here for simplicity one assumes a rectangular dome of dense water formed over the bank, with L the length of the bank, W the width, and H the height of the dense dome. The BBL height is h and Ve the downslope Ekman drainage velocity through the BBL. For the Porcupine Bank, an initial volume of dense water formed on the bank may be estimated from the data of White et al. (1998), which gives a mean height for the dense water dome of H = 150 m over a length L = 200 km and width (W = 50 km) of the bank. The BBL height and drainage velocity may be estimated using the equations presented by Shapiro and Hill (1997) and typical values for the vertical density stratification and overlying flow velocity (White et al. 1998). For a BBL of height h = 10 m and Ekman velocity Ve = 2 cm s^{-1}, the time-scale would be T = 5.5 months. Given that the dome formation mechanism will cease around March, this time-scale would imply that the dense domes will last until August.

This estimation is a first order approximation based on knowledge of the measured physical parameters at the Porcupine Bank. This time-scale, however, is comparable to the period over which White et al. (1998) observed the dense water dome and high nutrients over the Porcupine Bank, even if overestimated. It should be noted that the Ekman drainage velocity has to date not been measured directly, although the up/downslope veering of currents in the BBL due to the bottom friction has been measured (e.g., White et al. submitted). It would seem however, that the process of winter mixing would generate conditions which allow water with elevated nutrient levels to be present over the bank for long time periods. This water, whilst capped by the seasonal thermocline in summer, is present at a relatively shallow depth with a potential to be mixed up to the surface layers (e.g., Mohn et al. 2002), resulting in increased nutrient availability for surface production.

Dynamics around Porcupine Bank: modelling results

The model experiments simulate the effects of the 3-D circulation on the dispersion of passive particles representing organic material such as phytoplankton. The starting point of our simulations assumes a late spring/early summer situation when the primary productivity has fully developed over the bank. To achieve this,

the model was spun up for 20 days to allow the flow field to fully establish to a steady state before tracers were released into a volume over the summit of the bank within a circular area with waters shallower than 1000 m. After the initial release, the dispersion of the tracers was mainly driven using the advective/diffusive scheme of the circulation model and observed over time.

The results are shown in Figure 4 which shows the residual flow (Fig. 4A), and the tracer distribution (Fig. 4B) at 150 m depth, averaged over 5 days, after another 120 days of model integration from the time of tracer release. The flow field is dominated by a slope current of mean velocity 6 cm s^{-1} flowing poleward along the continental margin. Above the summit of the bank, the flow is deflected along the isobaths forming an anticyclonic recirculation around the bank. The distribution of tracers at 150 m shows significant retention of particles within the initial release area over the bank. A fraction of those particles, however, had been advected downstream with the background boundary current, interacting with the anticyclonic vortex and stripping off the tracers. When all tracers in the release volume are accounted for, it is found that 30 percent of the tracers are retained over the bank after 120 days (4 months), a significant proportion. This result would suggest that planktonic material present over the bank can be retained over a relatively long time assuming that the physical environment remains unchanged (or does not encounter significant changes like wind, winter convection, or seasonal variations in the strength of the slope current) for this period.

Discussion

The requirement for the development of deep-water coral is a combination of a suitable hard substrate on which to settle, a dynamical environment to keep such substrates clear of sediment, and sufficient food availability. In terms of food availability, the results in section 3 indicate that the submarine banks of the Rockall Trough, such as Porcupine Bank, are regions of high productivity. The interaction of these processes may well be beneficial to the development of deep-water coral, as indicated in a conceptual model (Fig. 5). Winter convection in the NE Atlantic results in conditions that generate water masses high in nutrients over the bank. Whilst this water mass is located below the seasonal thermocline, which develops later in time, the water mass is shallow enough that it can be mixed up into the surface layers by wind mixing events, as observed by Mohn et al. (2002), to support enhanced surface productivity over the banks (Fig. 2). Furthermore, the dynamics around the bank can act in two ways – the residual circulation acts to retain this material in the upper and mid water depths, and the Ekman drainage flows in the BBL may deliver the material downslope. The interaction of these processes, particularly the interaction between mid-water retention processes and near-bottom downslope dynamics, would appear complicated and, as yet, not fully quantified.

Further down the flanks of the Porcupine Bank, other dynamical processes like internal reflection or bottom intensified trapped waves, such as diurnal wave motions, act to keep the transported organic material available. In fact, the bottom
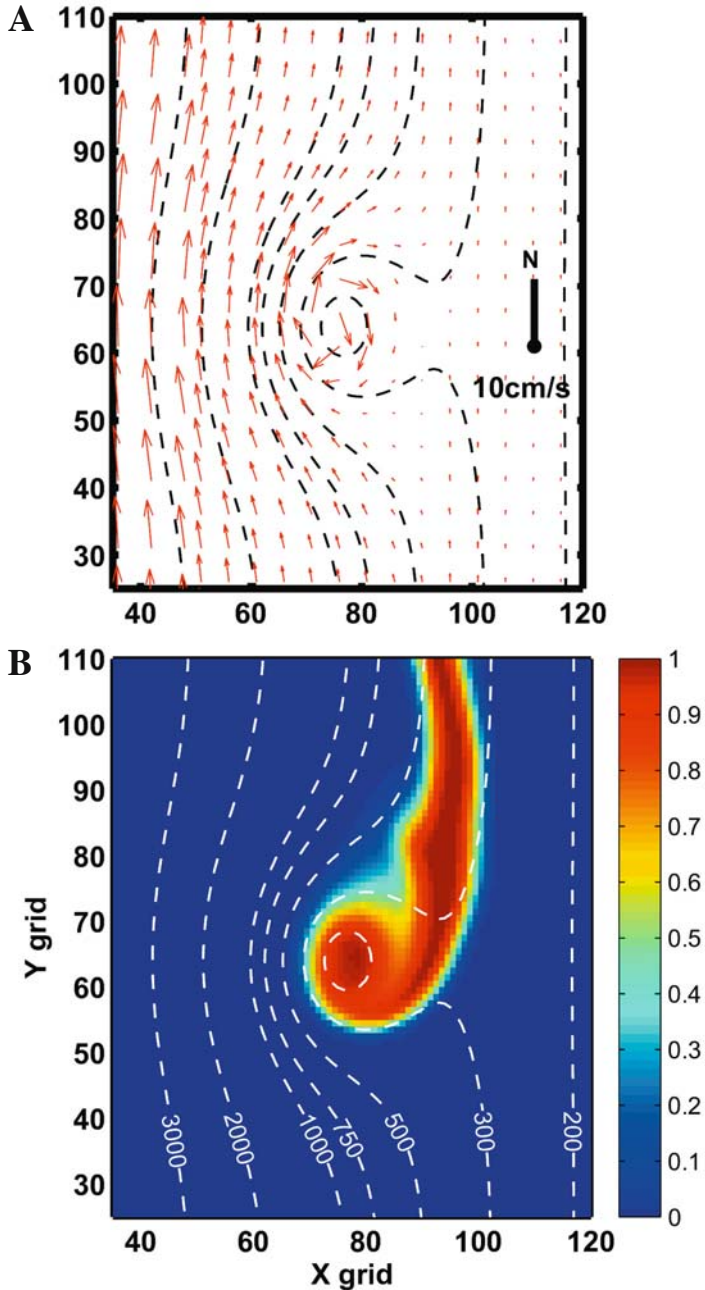
Fig. 4 Vectors of 5-day average simulated mean flow at 150 m depth for idealised topography representing Porcupine Bank after 120 days of model integration. The associated distribution of tracers, 120 days after release over the bank, is shown in **B**. In **A**, a velocity scale is shown by the black line, with 'N' denoting the north direction

A

B
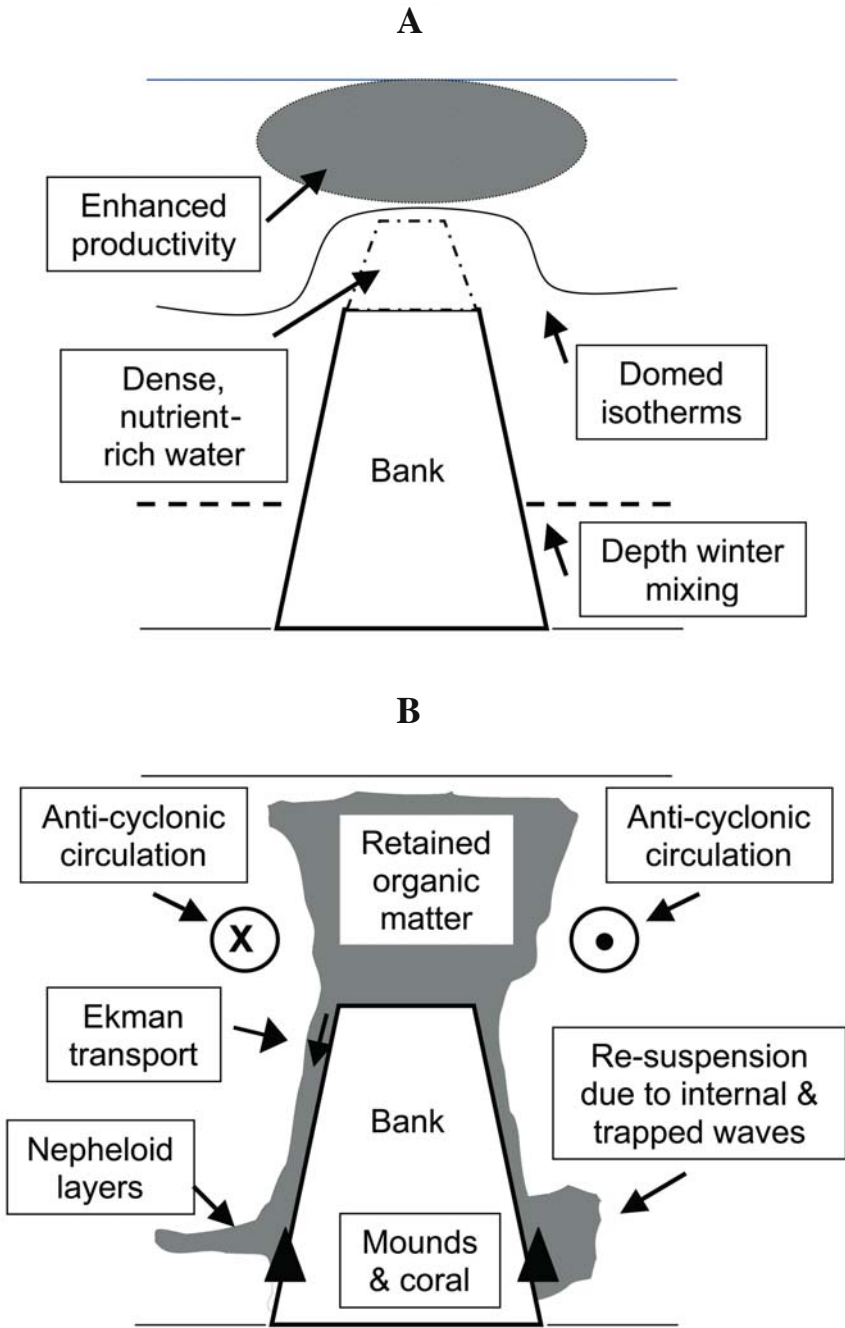
Fig. 5 Conceptual model of processes acting at submarine banks of the Rockall Trough: **A** formation of cold nutrient-rich water and enhanced productivity over bank, and **B** sinking and transport of organic matter downslope to coral communities

intensified diurnal motions are a result of the (weak) diurnal tidal forcing over the bank. These bottom currents tend to be amplified at much greater depths than the upper slope, due to the increased bottom slope and also the vertical stratification due to the permanent thermocline (White submitted). Similar conditions would be expected for the Rockall Bank where many of the dynamics identified with the Porcupine Bank have been measured at the Rockall Bank, e.g., rectification of tidal currents (de Stigter et al. submitted), and the Taylor column process (Dooley 1984).

The highest abundance of corals is found below the summit depths and not at the top of the bank. Reasons for this are unclear but may be due to several factors, including (i) entrainment of the organic material into the stronger residual currents found at the edge of the bank, (ii) the exposure of the relatively shallow summit to winter storm activity providing hostile conditions for coral development (e.g., Frederiksen et al. 1992), or (iii) geological control of the initial carbonate mound development, which may provide the initial topographic high and favourable local currents for initial coral development. These mounds are generally found further down the continental slope. A further uncertainty is the relationship between the trophic levels as they relate to the deep-water corals. The supply and availability of relatively fresh organic material in the BBL to the lower continental slopes, however, would appear be important in initiating a food chain that is of direct importance to the corals and other benthic organisms. As a result, it appears that if the larvae of deep-water corals, such as *Lophelia pertusa,* can find a hard substrate on which to settle on the flanks of the submarine banks, then food availability will not likely be a limiting factor to the development of the coral.

In summary, whilst there are many locations where deep-water corals are found along the NE Atlantic margin, e.g., the Norwegian Shelf, the submarine banks do appear particularly important for the distribution of corals in the Rockall Trough region. It may also be a reason for the high number of carbonate mounds that are found on the flanks of the larger submarine banks like Rockall and Porcupine Bank, as a high export of organic matter from the surface waters above the bank to the deeper flanks may be expected. If other dynamical conditions are favourable to initial coral growth, then there is potential to build large aggregates of carbonate/ organic material below the banks. The nature of the organic matter transport and utilization around these banks requires further study, particularly in regard to the complex physical – bio-geochemical interaction.

Acknowledgements

References

De Stigter H, White M, van Weering TCE, de Haas H (submitted) Hydrodynamics of carbonate mounds on the south Rockall Trough margins, NE Atlantic Ocean. Mar Geol

Dooley HD (1984) Aspects of oceanographic variability on Scottish fishing grounds. PhD thesis, Aberdeen Univ

Frederiksen R, Jensen A, Westerberg H (1992) The distribution of the scleractinian coral *Lophelia pertusa* around the Faeroe Islands and the relation to internal tidal mixing. Sarsia 77: 157-171

Freiwald A (2002) Reef-forming cold-water corals. In: Wefer G, Billett D, Hebbeln D, Jørgensen BB, Schlüter M, van Weering T (eds) Ocean Margin Systems. Springer, Berlin Heidelberg, pp 365-385

Freiwald A, Fosså JH, Grehan AJ, Koslow JA, Roberts JM (2004) Cold-water coral reefs. UNEP-WCMC Rep, Biodiversity Ser 22, 84 pp

Hill AE, Souza AJ, Jones K, Simpson JH, Shapiro G, McCandliss R, Wilson H, Leftley J (1998) The Malin cascade in winter 1996. J Mar Res 56: 87-106

Goldner DR, Chapman DC (1997) Flow and particle motion induced above a tall seamount by steady and tidal background currents. Deep-Sea Res 44: 719-744

Kenyon NH, Akhmetzhanov AM, Wheeler AJ, van Weering TCE, de Haas H, Ivanov MI (2003) Giant carbonate mounds in the southern Rockall Trough. Mar Geol 195: 5-30

Kunze E, Toole JM (1997) Tidally driven vorticity, diurnal shear, and turbulence atop Fieberling Seamount. J Phys Oceanogr 27: 2663-2693

Mohn C, Beckmann A (2002) Numerical studies on flow amplification at an isolated shelf break bank, with application to Porcupine Bank. Cont Shelf Res 22: 1325-1338

Mohn C, Bartsch J, Meincke J (2002) Observations of the mass and flow field at Porcupine Bank. ICES J Mar Sci 59: 380-392

Roberts JM, Long D, Wilson JB, Mortensen PB, Gage JD (2003) The cold-water coral *Lophelia pertusa* (Scleractinia) and enigmatic seabed mounds along the north-east Atlantic margin; are they related? Mar Pollut Bull 46: 7-20

Rogers AD (1999) The biology of *Lophelia pertusa* (Linnaeus 1758). Int Rev Hydrobiol 84: 315-406

Shapiro GI, Hill AE (1997) Dynamics of dense water cascades at the shelf edge. J Phys Oceanogr 27: 2381-2394

Van Aken HM, Becker G (1996) Hydrography and through-flow in the north-eastern North Atlantic; the NANSEN project. Progr Oceanogr 38: 297-346

Van Weering TCE, de Haas H, de Stigter H, Lykke-Anderson H, Kouvaev I (2003) Structure and development of giant carbonate mounds at the SW and SE Rockall Trough margins, NE Atlantic Ocean. Mar Geol 198: 67-81

White M (submitted) The hydrography of the Porcupine Bank and Sea Bight and associated carbonate mounds. Int J Earth Sci

White M, Mohn C, Orren MJ (1998) Nutrient distributions across the Porcupine Bank. ICES J Mar Sci 55: 1082-1094

White M, de Stigter H, de Haas H, van Weering T (submitted) Physical dynamics at the Rockall Trough margin that influence the carbonate mound and cold coral reef ecosystem. Progr Oceanogr

Development of coral banks in Porcupine Seabight: do they have Mediterranean ancestors?

Ben De Mol[1], Jean-Pierre Henriet[2], Miquel Canals[1]

[1] Departament d'Estratigrafia, Paleontologia i Geociències Marines, Universitat de Barcelona, Martí Franquès s/n., E-08028 Barcelona, Spain
(bmol@geo.ub.es)
[2] Renard Centre of Marine Geology, Gent University, Krijgslaan 281, S8, B-9000 Gent, Belgium

Abstract. This paper presents an overview of the spatial distribution and morphology of coral banks in the Porcupine Seabight in relation to their environmental settings. The study area is characterised by well-delimited clusters of coral banks, each featuring typical bank morphology and environmental setting. In the central part of the basin, two mound provinces can be identified: a set of complex flat topped seafloor mounds in the Hovland Mound province is flanked to the north by a crescent of numerous north-south elongated buried coral banks in the Magellan Mound province, along the eastern margin of the basin partly buried and seabed coral banks represent the Belgica Mound province. The banks are mound-shaped elevations, many of them hosting living deep-water corals (*Lophelia pertusa, Madrepora oculata, Desmophyllum cristagalli, Dendrophyllia* sp.) and associated fauna. This active biological layer covers a dead assemblage of corals clogged with mud. All coral banks, buried or seabed, occur in association with current-induced features (e.g., scouring features, dunes) and steep palaeo- and present-seabed slopes. Only a few banks have a present-day seabed expression, which suggests that environmental conditions have been more favourable for bank development in the past. The depth range of the seabed coral banks coincides with the Mediterranean Outflow Water which may control indirectly the coral distribution. The distribution of corals in the southern part of the North Atlantic and the actual link with Mediterranean water suggest a possible migration of corals within the Mediterranean water along the NE Atlantic margin. The start-up phase of the coral bank development in the basin has taken place simultaneously for all provinces, and tentatively framed in times subsequent to a Late Pliocene period of erosion and non-deposition. It is considered that the sedimentary load of the currents plays an important role in the bank development. Coral banks accrete by the active baffling of sediment by the biological framework and growth of the biological cap. When sedimentation and biological growth get out of balance, the framework will progressively be clogged

with sediment. Once sediment dominates the structure the coral banks get buried and draped by sediment.

Introduction

The presence of deep-water corals in the Northeast Atlantic is considered to be closely related to certain oceanographic conditions favourable for the azooxanthellate corals, for which nutrient supply, current activity, and slow sedimentation rates are the most important controlling parameter, besides a hard substratum to settle on (Stetson et al. 1962; Cairns and Stanley 1981; Mullins et al. 1981; Frederiksen et al. 1992; Mortensen et al. 1995; Freiwald et al. 1999). Coral banks are less common than coral patches and appear in clusters along the Atlantic margins (Henriet et al. 1998; De Mol 2002; Freiwald 2002; Huvenne et al. 2003; Kenyon et al. 2003; O'Reilly et al. 2003; van Weering et al. 2003).

The Porcupine Seabight is known for its unique set of seabed and buried mound provinces associated with deep-water scleractinian corals. The patchy distribution of these large biological build-ups had intrigued scientists since their discovery and has led to several genetic models (Hovland et al. 1994; Henriet et al. 2001; De Mol 2002). The paper of Hovland et al. (1994) has brought deep-water coral banks in the Porcupine Seabight, southwest of Ireland, in the spotlights of deep-water ecosystem research. These authors had identified some 33 dome-like seabed mounds on conventional 2D exploration seismic profiles, in the central part of the Porcupine Basin. Sediment samples on the mounds yielded the deep-sea coral *Lophelia pertusa,* besides mud.

Later seismic surveys in the same basin have revealed three well-delineated mound provinces along the central and eastern margin of the Porcupine Basin (Fig. 1), each characterised by their geometry and environmental setting (Henriet et al. 1998; De Mol et al. 2002; Huvenne et al. 2003; Van Rooij et al. 2003).

The central part of the basin is characterised by complex flat-topped seafloor mounds in the Hovland Mound province surrounded to the north by numerous buried mounds in the Magellan Mound province. Along the steep eastern margin of the basin partly conical, both buried and seabed mounds represent the Belgica Mound province (Henriet et al. 1998; De Mol et al. 2002, Huvenne et al. 2003; Van Rooij et al. 2003). The banks are mound-shaped elevations, hosting living deep-water scleractinian coral (*Lophelia pertusa, Madrepora oculata, Desmophyllum cristagalli, Dendrophyllia* sp.) and associated fauna. This active biological layer covers a dead assemblage of corals clogged with mud (De Mol et al. 2002). In the Belgica Mound province the live coral is more disseminated than in the Hovland Mound province (e.g., Thérèse Mound; De Mol et al. submitted) and also corals seem to stabilise sand dunes in between the large Belgica Mounds, forming smaller structures known as the Moira Mounds (Wheeler et al. 2005).
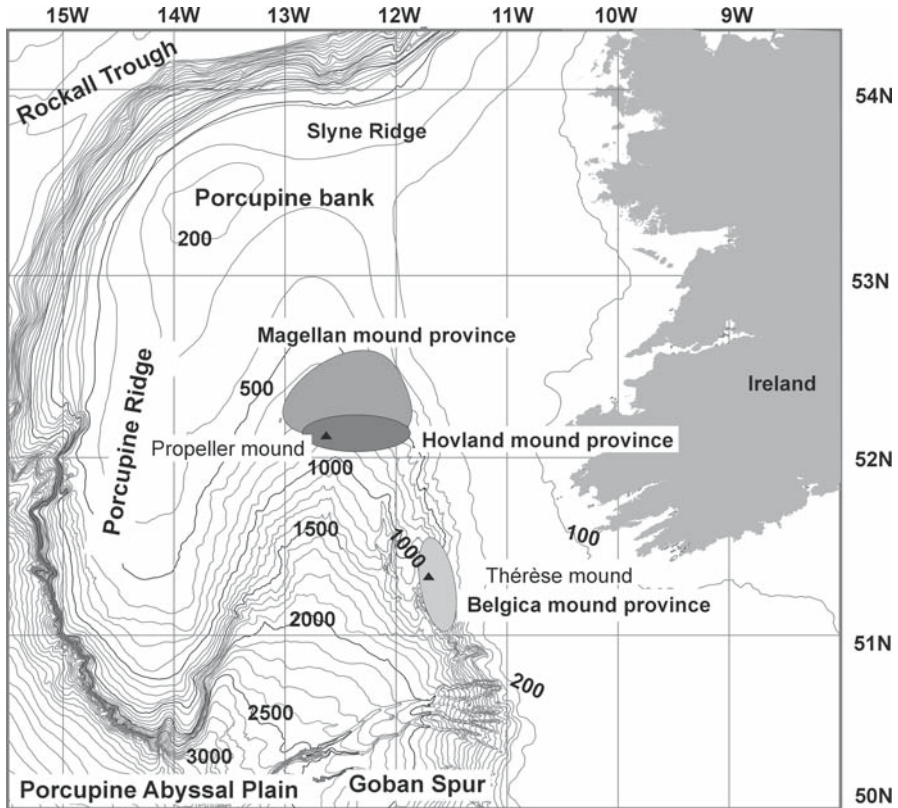
Fig. 1 Location map of the mound provinces in the Porcupine Seabight

Due to the close relation between the mounds and the deep-water corals, the spatial distribution of the mounds have been related to oceanographic boundary conditions, such as salinity and temperature (Freiwald 2002), internal tides (Frederiksen et al. 1992), oceanographic currents and food supply (Mortensen et al. 2001; De Mol et al. 2002; Kenyon et al. 2003). Nevertheless several papers (e.g., Hovland et al. 1994; Hovland and Thomsen 1997; Henriet et al. 1998; Hovland et al. 1998; Henriet et al. 2001; Hovland and Risk 2003) suggest that some deep-water coral mounds may have initially formed in areas of methane or fluid seepage. These models explain the distribution of the mounds by past events of localised or regional seepage of fluids, which may have created hard substratum of authigenic carbonates providing at least the settling ground (Henriet et al. 1998, 2001; Masson et al. 2003) and favours direct or indirect food supply for the coral community (Hovland and Thomsen 1997; Hovland and Risk 2003).

All models try to explain the spatial distribution of the mounds in the basin and relate this to local environmental circumstances. The key question in this research is which environmental change leads to the development of a coral bank in a coral-rich environment, and how the coral may support the coral bank development. The

variety in dimension and the occurrences of buried and exposed deep-water coral build-ups in well-delineated provinces makes the Porcupine Seabight a unique site to study the development and the environmental parameters influencing these deep-water coral mounds. This paper presents the spatial distribution and the geometry of the different mound structures and the general external environmental factors during their present-setting and start-up phase.

Methods and data

This paper summarises results from about 2600 km of high-resolution sparker seismic profiles with a frequency range between 200-3000 Hz, collected with research vessel R/V *Belgica* in the period between 1997 to 2001 (*Belgica* 1997/12, 1998/11, 1999/13, 2000/16-17 and 2001/12 cruises).

The description of the data is subdivided according to the expected environmental significance and the possible role in the initiation of the coral banks.

Seismic facies: clues for the internal structure of the mounds

In this study we consider the mound morphology as limited by the apex of the top diffraction and the seismic mound facies (Fig. 2). Mounds appear on the seismic profiles as almost transparent dome shape structures (Hovland et al. 1994; Henriet et al. 1998; De Mol et al. 2002). This seismic facies indicates no abrupt internal variations of seismic impedance in the mounds and argues for an almost uniform lithology. Still, where detailed velocity analyses are available, a core with higher velocity may suggest early diagenesis (Henriet et al. 2003). The shallow cores taken in the different mound areas (De Mol 2002; De Mol et al. 2002; Van Rooij et al. 2003; Dorschel et al. submitted; Rüggeberg et al. submitted) suggest carbonate-rich sediment with intermixing of siliciclastic sediments, clogged in a deep-sea coral framework.

Mound spatial distribution

The mound spatial distribution is based on the mapping of the seismic mound facies along high-resolution seismic profiles. In addition, for the Belgica Mound province the location of the seabed mounds has been verified by swath bathymetry (Beyer et al. 2003). The coral banks are subdivided into seabed and buried mounds, by geographic area. Seabed mounds are defined as mounds reaching the seafloor and having a topographic expression. Buried mounds are defined as those covered by the enclosing sediments. The inferred top, apex of the diffraction, of the mounds are plotted on bathymetric maps based on the available bathymetric data (GEBCO data; IOC et al. 1997) refined with the seismic data and swath bathymetry (Beyer et al. 2003; Figs. 3-4).

In total, 64 mounds have been mapped in the Belgica Mound province of which 20 are buried mounds (Fig. 3). In the Hovland Mound province, 14 seabed mounds

and 27 large buried mounds, in the eastern part of this province have been recognised (Fig. 4). The latter forms together with the buried Magellan Mound province a
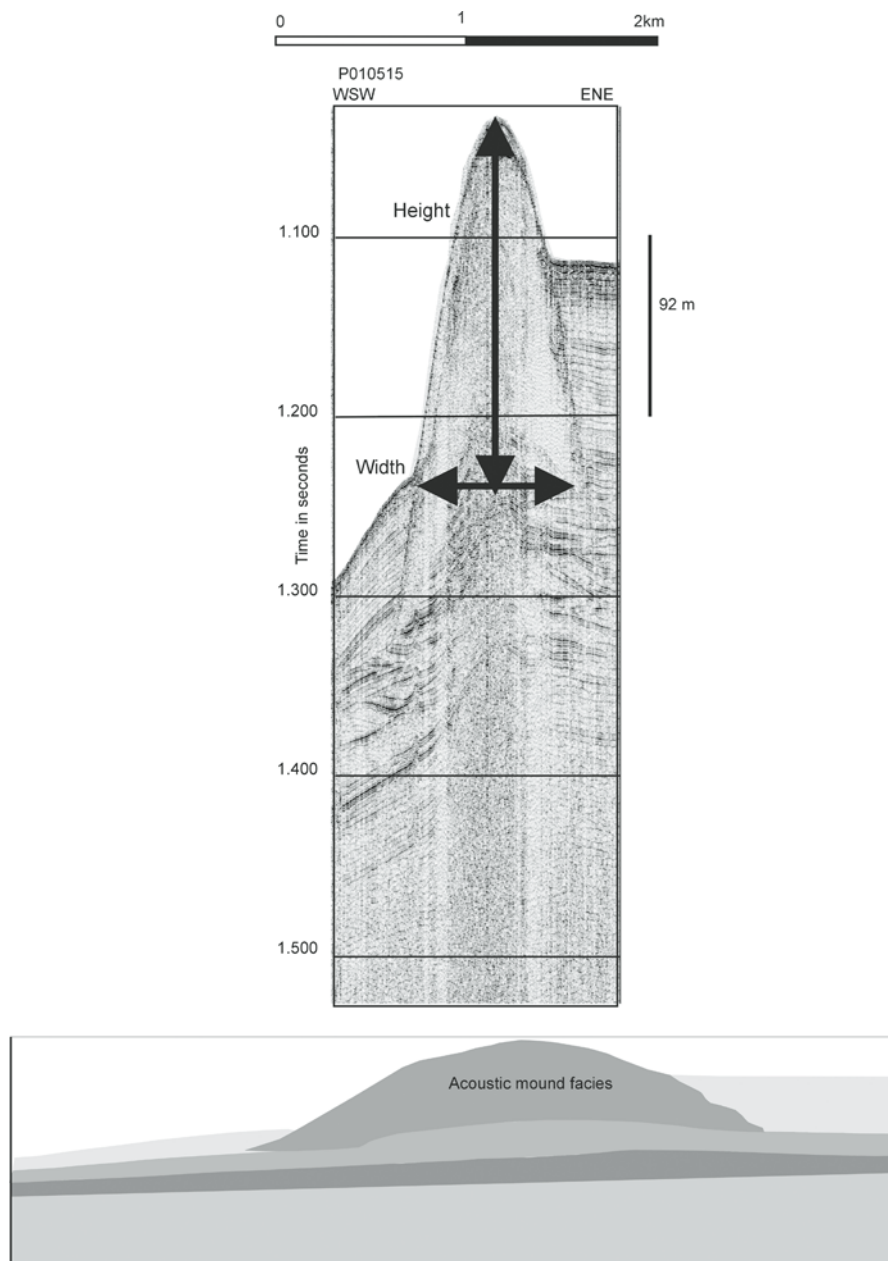
Fig. 2 High-resolution seismic profile in the Belgica Mound province demostrates the mound geometry and acoustic character. The lower drawing illustrates the mound geometry without vertical exaggeration
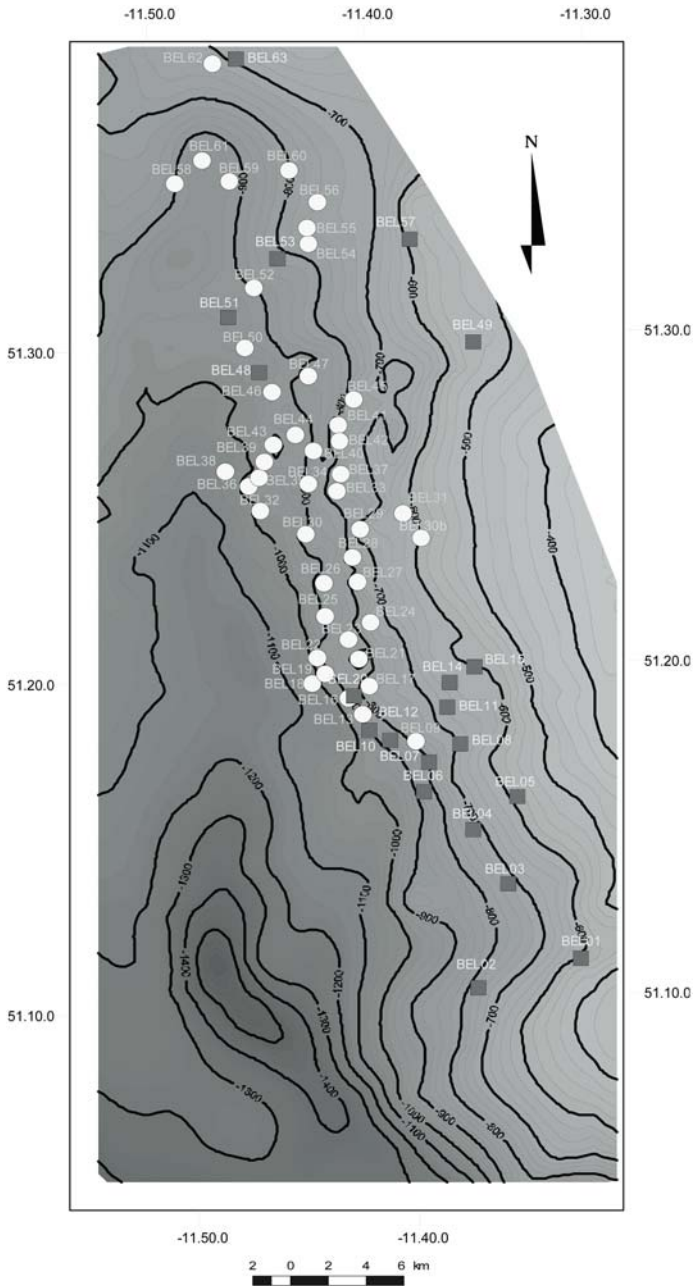
Fig. 3 Mound distribution in the Belgica Mound province (circles = exposed mounds, squares = buried mounds)
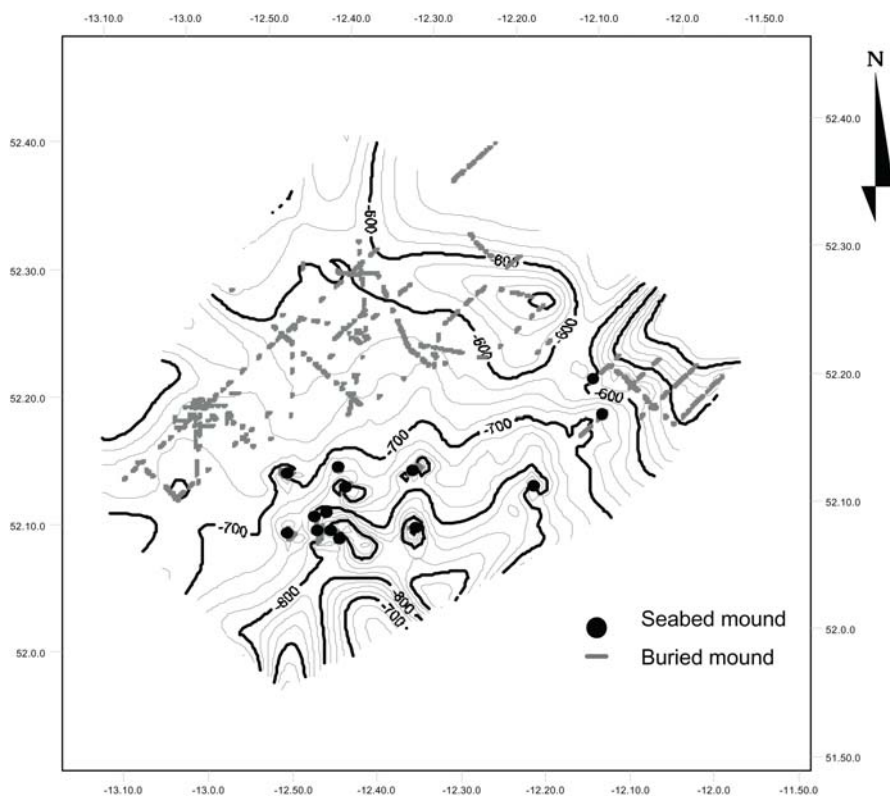
Fig. 4 Mound distribution in the Hovland-Magellan Mound province

crescent around the central part of the Hovland Mound province on the northern and northwestern flanks of the province. A mound-free zone between 6 and 10 km is observed between the seabed and the buried Hovland Mounds.

The mounds in the Magellan Mound province occur in a much denser cluster than in the Hovland Mounds. In total 255 Magellan Mounds have been observed on a 2D high-resolution seismic grid covering an area of 1080 km^2, 306 on a 350 km^2 3D seismic block (Huvenne et al. 2003) northwest of the 2D grid and about 80 on an industrial 2D data set of 72 km^2 (Britsurvey 1997). The density of the Magellan Mounds is rated to approximately 1 mound per km^2 (Britsurvey 1997; Huvenne et al. 2003). Extrapolation over the known limits of the Magellan province yields a total number of 1500 mounds.

The total number of observed mounds in the Porcupine Seabight is 58 seabed and 688 buried mounds, but a realistic estimation of the total occurrence of individual mounds is between 1500 and 2000.

Depth of the mounds

In the Belgica Mound province, buried mounds are found in the shallowest and most southern and northern outliers of the province between the bathymetric contours 600 m and 800 m. In these areas, the seafloor has a normal slope gradient without any large anomalies (Fig. 3).

The seabed mounds cluster in two ridges at 700 and 900 m water depth on the steep western flank of the main contourite channel of a confined drift (Van Rooij et al. 2003). The channel fades out to the north and has its strongest seafloor expression in the central mound province between 1500-1000 m water depth. The origin of the channel is related to an N-S directed contour current (Van Rooij et al. 2003).

The buried Magellan and Hovland Mounds are located in the present bathymetric zone around 600 m. The seafloor at this location is gently dipping to the south (0.5-1°) interrupted by a relatively steep amphitheatre shaped depression in the central Hovland Mound province. This depression consists of four N-S oriented branches, which merge in a local depression in the south of the province (Fig. 4). All seabed mounds are located on the most northern and steepest margins of the depressions. The observed seafloor depressions have their strongest expression between 840-1000 m. These features have the same trend as the slope-parallel marginal channel in the Belgica Mound province and are interpreted as results of scouring by N-S trending currents.

In general, the seabed mounds appear in both geographic mound areas between 800-1000 m water depth with relatively steep seabed topography as channel flanks and heads. The buried mounds appear in shallower water depths around 600 m where no major seafloor features are observed.

Mound morphology

The tallest Belgica Mounds, with heights up to 166 m (or 188 ms with an average internal velocity of 1850 m/s) are observed along the 900 m contour on the steep flank of the N-S oriented contour channel. Mounds further inshore are generally smaller (100 ms or 90 m high) than the mound cluster located near the centre of the contour channel. In general, mound heights decrease toward the outliers of the province.

The seabed mounds have a mean width of 1100 m measured along the seismic profiles and an average height of about 139 m. The buried mounds reach a height of 50 m. The mean width measured along the seismic profiles of the buried Belgica Mounds is 710 m.

The mound morphology varies locally and follows the general seabed topography such as turbidite and contour channels.

The height of the mound is clearly a function of the thickness of the enclosing sediments (De Mol et al. 2002; Van Rooij et al. 2003). The tallest mounds appear in zones with reduced sediment thickness of enclosing sediments. Where the deposition of sediment is limited, such as near the central part of the contour channel, mounds have an almost circular geometry (De Mol et al. submitted).

It can be stated that the Hovland Mounds are larger and have a more complex geometry than the Belgica Mounds. The average width measured along the seismic profiles is 1315 m for the seabed mounds and 600 m for the buried Hovland Mound. The elongation of the Hovland Mounds follows the trend of the channel flank on which the mound is seated. The average height of the seabed mounds is 200 m. The highest mounds are observed on the flank of the deep depression around 900 m water depth. In the Belgica and the Hovland Mound provinces the complex mounds are interpreted as an amalgamation of several smaller mounds connected by sediment (e.g., Propeller Mound, Thérèse Mound; De Mol 2002).

The Magellan Mounds are more vertical stock-like features and have a clearly different geometry. The buried Magellan Mounds have an average width of 250 m and a height of about 70 m (Huvenne et al. 2003). The mounds display a clear N-S elongated trend, which is suggested to be due to their development in a N-S directed current regime (Huvenne et al. 2003).

Mound base

The last major erosional event in the basin formed the unconformity of the mound base, corresponding to a great instability and/or to a drastic change in the current regime. After this erosional event, a new depositional phase started, which did not significantly change till recent times. This seismic facies is characterised by an alternation of parallel low and high amplitude packages following the local contours and interpreted as drift deposits (Van Rooij et al. 2003). The underlying sediment are characterised by drift deposits with erosional episodes but under different current regime (De Mol 2002; Huvenne et al. 2003; Van Rooij et al. 2003; Van Rooij et al. submitted). The largest seabed mounds are located on slope breaks in the mound base reflector (e.g., the steepest slopes of local channels). In the Magellan Mound province the mound base is gently dipping without any major submerged topography, but the largest Magellan Mounds are located in local breaks in the moundbase (Fig. 5).
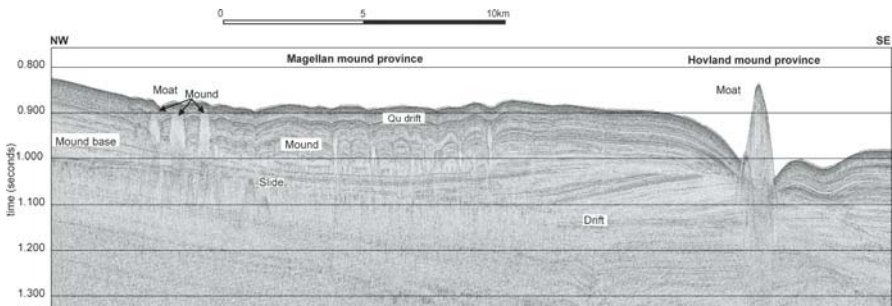
Fig. 5 High-resolution seismic profile crossing the Magellan and Hovland Mound provinces. The tallest mounds occur on local slope breaks and are associated with current induced seabed features. Qu drift: Quarternary drift

Dating

The moundbase or the uppermost erosional reflector in the basin corresponds with the C10 reflector (McDonnell 2001) defined by Stoker et al. (2002) for the Rockall Trough. McDonnell (2001) assigns an intra-Early Pliocene age to this reflector, supporting an intra-Neogene major regional unconformity (Stoker et al. 2002). The dating of the sequences is based on a seismic stratigraphic interpretation within the basin and on the correlation of the seismic facies with Rockall Trough sequences.

Still, the facies correlation from the Rockall to the Hovland-Magellan Mound province mounds is not clear. Many more erosional events appear in the upper section between C20 and C10 than in the Rockall Trough. On the other hand, two industrial seismic studies have been carried out in the region, which place the mound base at a near Quaternary age, based on the extrapolation of deep wells (Britsurvey 1997; Games 2001).

The onset of the drift sedimentation, followed after a period of erosion and non-deposition, is estimated by extrapolation of sediment rates of shallow cores. The drift sedimentation had probably started at 1.2 Ma (Van Rooij et al. submitted), after a period of non-deposition. In the Hovland Mound province the age of the mound base has been extrapolated from ages of on-mound sediments and has been estimated to be Late Pliocene-Quaternary for both provinces (Saoutkin 1998). Furthermore, the infill of the mounds and the occurrence of the moat flanking the mounds, suggest that the mounds already attained a certain height before the drift sedimentation commenced (De Mol et al. 2002). For these reasons the start-up phase of the mounds is estimated to be of Late Pliocene - Early Pleistocene age.

Discussion

The mound structures in the basin are interpreted as coral banks due to their lithological and seismic appearance (De Mol et al. 2002; Huvenne et al. 2003). The coral bank distribution and geometry illustrates that in the recent past the conditions for coral bank development or preservation were more favourable in the Belgica Mound province than in the Hovland-Magellan Mound province. Nevertheless, the high number of coral banks in the Hovland-Magellan Mound province argues that during the start-up phase hundreds of small coral banks started to develop but only a few of them could develop to large present day seabed mounds. In the Belgica Mound province the coral banks are not as numerous as in the Hovland-Magellan Mound province but the majority of the coral banks are exposed on the seafloor.

Seabed coral banks

The largest coral banks in the basin are located on the steepest part of present channels of N-S directed contour current (De Mol et al. 2002; Van Rooij et al. 2003). These zones are characterised by the reduced sediment thickness of the enclosing sequences, which is a combined effect of bottom currents and the coral banks creating turbulence.

The depth range of the large exposed coral banks indicates that the coral banks have a preferable depth range between 700-900 m throughout the basin. This depth range in the present setting fits with water masses largely influenced by the Mediterranean Water, bringing warm and saline water in the basin (White 2003).

Buried coral banks

The buried coral banks, the Magellan Mounds and buried Belgica Mounds, appear in zones with a gently dipping seafloor. These coral banks are located in zones with higher sediment accumulations of Quaternary age. Most of the buried coral banks occur in water depths around 600 m at the extremities of the coral bank provinces.

Coral bank morphology

Circular coral banks are located in 'protected' areas surrounded by other coral banks in the Belgica Mound province. At the present seafloor, these circular coral banks appear often as N-S elongated mounds due to the deposition of sediments on the flanks. Circular mounds developed in the most ideal conditions.

The elongated coral banks are mostly located at the edge of channels and follow the channel geometry. The Magellan Mounds are characterised by the high density of vertical, stock-like coral banks with a N-S elongation, which suggests that they have been shaped by N-S currents (Huvenne et al. 2003).

Sediment pressure-development

The development direction of the coral banks is inferred from the height/width ratio of the seabed and buried coral banks, measured on the seismic profiles. We consider the buried coral banks as a frozen earlier development stage of the seabed coral banks, which have continued to develop to the present.

The seabed coral banks are about 3.5 times higher, and the width of the base of the mounds is only 1.5 times longer, than that of the buried coral banks. This suggests that the coral banks formed initially a broad base and later started to develop in a vertical direction.

Oceanographic environment

Several geophysical observations suggest that the exposed coral banks are closely related to high current regimes during certain periods in mound development (De Mol et al. 2002; Huvenne et al. 2003; Van Rooij et al. 2003). This is suggested by the observations of N-S trending contourite channels (Van Rooij et al. 2003), the presence of sand ripples, sand sheets, ribbons in the Belgica Mound province (Wheeler et al. 2005; De Mol et al. submitted), the moat formation around the coral banks and the reduced sedimentation thickness in the mound areas (De Mol et al. 2002; Huvenne et al. 2003). Present-day oceanographic surveys confirm that the near-bed currents in the mound provinces are stronger than the mean northward cyclonic flow driven by the south-north decrease in sealevel. In the present circumstances the bottom currents are much more intensive in the Belgica Mound province than in

the northern mound provinces, which might explains the higher biological activity in this province (Huvenne et al. 2002). Bottom current intensifications in the region are largely generated by the stratification of the watermasses in combination with the seabed topography and physical processes such as tides and baroclinic motions (White 2003). The stratification in the mound region is due to the interaction of the Eastern North Atlantic Water (ENAW) and watermasses influenced by the Mediterranean Outflow Water (MOW) and winter mixing creating a permanent thermocline approximately at the coral bank level (van Aken and Becker 1996). The combined effect of the water stratification of the sites is responsible for the formation of trapped and internal waves against the continental slope due to baroclinic diurnal tidal modulation (White 2003).

Most of the benthic life consists of suspension feeders, which prefer locations with moderate to high current speeds transporting nutrients. Deep-sea corals prefer sites in current-enhanced regions, which are characterised by reduced sedimentation, relatively high nutrient content and the availability of hard substrates. Nevertheless, too strong currents can topple or break the corals. This effect explains the localized living cap on the mounds but implies that the system is very sensitive to changes in oceanographic conditions. For instance changes in the MOW flow, bringing warm and saline water in the basin, will effect the coral distribution and coral bank development due to the change in physical dynamics.

Offshore the Faeroe Islands (Frederiksen et al. 1992) and in the Rockall Trough (Kenyon et al. 2003), the link between enhanced localised currents with a tidal signature, and the occurrence of deep-water corals has also proposed.

Origin of the mound base

The origin of the regional moundbase erosional event is linked to the oceanographic changes in the Late Pliocene (De Mol et al. 2002; Van Rooij et al. 2003). A regional Late Pliocene hiatus is found in the Rockall-Goban Spur transect and is interpreted in terms of the reintroduction of MOW in the NE Atlantic (Pearson and Jenkins 1986). Based on microfaunal associations in deep cores of the North Atlantic (west of Rockall Bank and at the Western Approaches), Schnitker (1986) suggested that the present-day water stratification in the North Atlantic Deep Water only established at the onset of modern glacial conditions about 2-2.5 Ma ago. The onset of the drift sedimentation is estimated to be at 1.2 Ma (Van Rooij et al. 2003), which leaves a significant time gap of non-deposition and erosion in the basin. This is regarded as the time at which the mounds could develop to a certain extent as suggested by several authors (Henriet et al. 1998; De Mol et al. 2002; Van Rooij et al. 2003).

The introduction of the MOW in the NE Atlantic is recorded in terrigenous drift in the Gulf of Cadiz (Maldonado and Nelson 1999). Sedimentological and biostratigraphic studies of the drift of Late Pliocene and Quaternary age in the Gulf of Cadiz (Nelson et al. 1999; Sierro et al. 1999) revealed a periodic intensification of the MOW related to periods of sea level rise. Van Rooij et al. (submitted) observed a change in faunal assemblages during the intensification of the current regime with occurrence of the benthic foraminifer *Uvigerina mediterranea* in the

drift sediments of the Belgica Mound province. This suggests that intensification of currents occurred during the introduction of MOW in the Holocene and in the Eemian period. In the Hovland Mound province similar analysis of shallow on-mound cores suggest an intensification of currents in relation to Mediterranean-related faunal assemblages (Rüggeberg et al. submitted). During these periods the mound development was more intense than in the glacial periods (Dorschel et al. submitted; Rüggeberg et al. submitted).

Coral bank triggering

Lophelia and *Madrepora* corals require a hard substratum, an adequate nutrient supply and a protection against burial to grow. Concentrations of *Lophelia* corals are found where strong currents (upwelling, Ekman dynamics, internal and trapped waves, etc.) prevent deposition of fine-grained sediment and supply large quantities of food (Cairns and Stanley 1981; Freiwald 1998). In these favourable areas, azooxanthellate corals might form patches or banks on top of topographic elevations, for example on moraine ridges (Freiwald et al. 1999), on seamounts (Zibrowius and Gili 1990), on carbonate-cemented rocks (Messing et al. 1990), in hydrocarbon seep areas (Hovland et al. 1994; Hovland and Risk 2003), on outcropping hardrock (Stetson et al. 1962) or even on submarine pipelines and oil rigs (Roberts et al. 2003) or sand dunes (Wheeler et al. 2005). Topographic irregularities and water stratification are the driving forces for local oceanographic dynamic processes that create favourable settlement sites for deep-sea coral by increasing food supply and protecting against burial by sediment. When these environmental requirements are fulfilled for an extensive period, the corals can produce extensive frameworks providing niches for other benthic life (see Rogers 1999).

Deep-water corals, banks or patches occur all along the European shelf margin from Gibraltar up to Norway (Rogers 1999; Freiwald 2002). It is therefore possible that larvae of azooxanthellate corals got introduced in the southern NE Atlantic together with the MOW, and took advantage of the dynamic processes related to this watermasses in the North Atlantic to colonize the continental slopes (Fig. 6). The MOW, however, only extends north up to the Porcupine Bank or the Rockall Basin (van Aken 2000; New et al. 2001). Larvae may have been carried further northwards by other polewards flowing currents (Freiwald 2002). This provoking hypothesis, that the Mediterranean Sea might act as a refuge for deep-water corals is not yet proven by the palaeobiography for the Mediterranean deep-sea corals. Further research of the Mediterranean deep-sea coral communities and deep drilling of the Porcupine coral banks might prove or disprove this hypothesis.

Conclusion: development of coral banks

In Figure 7, a hypothetical model is proposed of the coral bank development based on the results discussed above in the Procupine Seabight.

Coral bank development stages can be related to general oceanographic events related to the MOW input in the Porcupine Seabight. Deep-water coral larvae
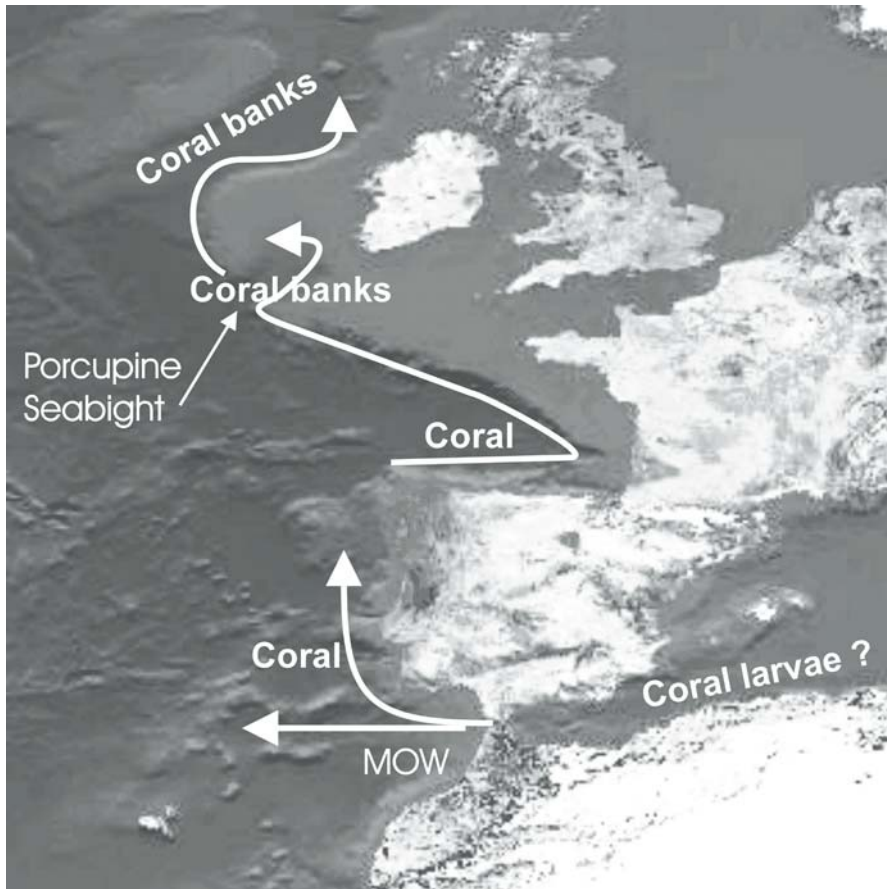
Fig. 6 It is possible that the deep-water coral larvae are introduced together with the MOW flow in the southern part of the NE Atlantic. Deep-water corals occur all along the pathway of the MOW, but only in the Porcupine Seabight and in the Rockall Trough have coral banks been formed

may have been transported along the pathway of the MOW along the northeast continental margin from a southern source, potentially the Mediterranean Basin. The dynamic processes related to the MOW watermass and the marginal morphology in the Porcupine Seabight are the driving force for several dynamic processes in the mound provinces which promote local current intensification (White 2003).

These dynamic processes can provide the framework builders with nutrients at locations where the current balance is most favourable to transport the nutrients and to safeguard the framework constructors from sedimentation, without breaking the corals. These conditions were widespread in the Porcupine Seabight during the start-up phases of the coral banks after a period of significant erosion. These conditions will allow large coral fields to develop, creating patches of circular coral accumulations as described by Wilson (1979) in the Rockall (Fig. 7A). After this

start-up phase, the initial coral build-ups continued growing and coalesced with adjacent clusters into multiple structures. Continuous growth of closely-spaced coral banks may have caused lateral amalgamation along channels in any phase of the development (Fig. 7B). From this stage onwards, the banks could modify the bottom currents by acting as a structural high. In this way the coral banks protected themselves against burial and moats were created in environments with a high sedimentation rate. During periods in the development of the coral banks, the currents decreased resulting in a higher lateral sediment stress, which may have forced the banks to grow in a vertical direction (Fig. 7C). In the final stage the slow infill of the coral framework and progressive onlap of the embedding sediment on the mound flanks terminated coral growth (Fig. 7D).
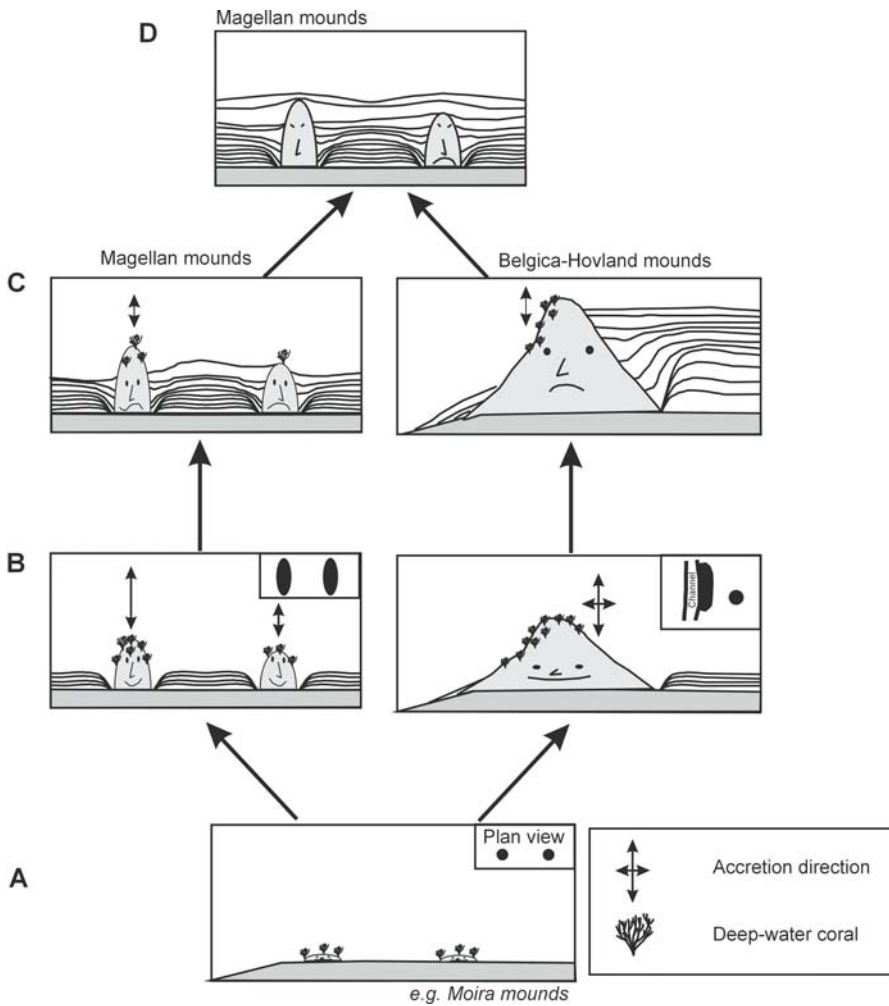
Fig. 7 Model for mound development in the Porcupine Seabight steered by sediment supply. See text for explanation

Acknowledgements

References

Beyer A, Schenke HW, Klenke M, Niederjasper F (2003) High resolution bathymetry of the eastern slope of the Porcupine Seabight. Mar Geol 198: 27-54

Britsurvey (1997) Total Oil Marine plc, site survey Irish Block 35/17-1, 14/11/96-13/12/96, final report. Rep Petrol Affair Div, Dublin

Cairns SD, Stanley GD (1981) Ahermatypic coral banks: living and fossil counterparts. Proc 4th Int Coral Reef Symp, Manila, pp 611-618

De Mol B (2002) Development of coral banks in Porcupine Seabight (SW Ireland) A multidisciplinary approach. PhD thesis, Ghent Univ

De Mol B, Kozachenko M, Wheeler A, Hugo-Alvares H, Henriet J-P, Olu-Le-Roy K (submitted) Thérèse Mound: a case study of coral bank development in the Belgica Mound Province, Porcupine Seabight. Int J Earth Sci

De Mol B, Van Rensbergen P, Pillen S, Van Herreweghe K, Van Rooij D, McDonnell A, Huvenne V, Ivanov M, Swennen R, Henriet JP (2002) Large deep-water coral banks in the Porcupine Basin, southwest of Ireland. Mar Geol 188: 193-231

Dorschel B, Hebbeln D, Rüggeberg A, Dullo W-Chr (submitted) Carbonate budget of a cold-water coral carbonate mound: Propeller mound. Int J Earth Sci

Frederiksen R, Jensen A, Westerberg H (1992) The distribution of the scleractinian coral *Lophelia pertusa* around the Faeroe Islands and the relation to internal tidal mixing. Sarsia 77: 157-167

Freiwald A (1998) Geobiology of *Lophelia pertusa* (Scleractinina) reefs in the North Atlantic. Habilation thesis, Bremen Univ

Freiwald A (2002) Reef-forming cold-water corals. In: Wefer G, Billett D, Hebbeln D, Jørgensen BB, Schlüter M, Van Weering T (eds) Ocean Margin Systems. Springer, Berlin-Heidelberg, pp 365-385

Freiwald A, Wilson JB, Henrich R (1999) Grounding Pleistocene icebergs shape recent deep-water coral reefs. Sediment Geol 125: 1-8

Games KP (2001) Evidence of shallow gas above the Connemara oil accumulation, Block 26/28, Porcupine Basin. In: Shannon PM, Haughton PDW, Corcoran DV (eds) The Petroleum Exploration of Ireland's Offshore Basins. Geol Soc London Spec Publ 188: 361-373

Henriet JP, De Mol B, Pillen S, Vanneste M, Van Rooij D, Versteeg W, Croker PF, Shannon PM, Unnithan V, Bouriak S, Chachkine P (1998) Gas hydrate crystals may help build reefs. Nature 391: 648-649

Henriet JP, De Mol B, Vanneste M, Huvenne V, Van Rooij D (2001) Carbonate mounds and slope failures in the Porcupine Basin: a development model involving past fluid venting. In: Shannon PM, Haughton PDW, Corcoran DV (eds) The Petroleum Exploration of Ireland's Offshore Basins. Geol Soc London Spec Publ 188: 375-383

Henriet JP, Van Rooij D, Huvenne V, De Mol B, Guidard S (2003) Mounds and sediment drift in the Porcupine Basin, west of Ireland. In: Mienert J, Weaver P (eds) European Continental Margin Sedimentary Processes: an atlas of side-scan sonar and seismic images. Springer, Berlin Heidelberg, pp 217-220

Hovland M, Risk M (2003) Do Norwegian deep-water coral reefs rely on seeping fluids? Mar Geol 198: 83-96

Hovland M, Thomsen E (1997) Cold-water corals - are they hydrocarbon seep related? Mar Geol 137: 159-164

Hovland M, Croker PF, Martin M (1994) Fault-associated seabed mounds (carbonate knolls?) off western Ireland and north-west Australia. Mar Petrol Geol 11: 232-246

Hovland M, Mortensen PB, Brattegard T, Strass P, Rokoengen K (1998) Ahermatypic coral banks off Mid-Norway: evidence for a link with seepage of light hydrocarbons. Palaios 13: 189-200

Huvenne V, Blondel P, Henriet JP (2002) Textural analyses of sidescan sonar imagery from two mound provinces in the Porcupine Seabight. Mar Geol 189: 323-341

Huvenne VAI, De Mol B, Henriet JP (2003) A 3D seismic study of the morphology and spatial distribution of buried mounds in the Porcupine Basin. Mar Geol 198: 5-25

IOC, IHO, BODC (1997) GEBCO-1997: The 1997 Edition of the GEBCO Digital Atlas. Brit Oceanogr Data Cent, Birkenhead

Kenyon N, Akhmetzhanov AM, Wheeler AJ, van Weering TCE, de Haas H, Ivanov MK (2003) Giant carbonate mud mound in the southern Rockall Trough. Mar Geol 195: 5-30

Maldonado A, Nelson CH (1999) Interaction of tectonic and depositional processes that control the evolution of the Iberian Gulf of Cadiz margin. Mar Geol 155: 217-242

Masson DG, Bett BJ, Billett DSM, Jacobs CL, Wheeler AJ, Wynn RB (2003) The origin of deep-water, coral-topped mounds in the northern Rockall Trough, Northeast Atlantic. Mar Geol 194: 159-180

McDonnell A (2001) Comparative Tertiary basin development in the Porcupine and Rockall basins. PhD thesis, Natl Univ Ireland, Dublin

Messing CG, Neumann CA, Lang JC (1990) Biozonation of deep-water lithoherms and associated hardgrounds in the northeastern Straits of Florida. Palaios 5: 15-33

Mortensen PB, Hovland M, Brattegard T. Farestveit R (1995) Deep-water bioherms of the scleractinian coral *Lophelia pertusa* (L.) at 64°N on the Norwegian Shelf: structure and associated megafauna. Sarsia 80: 145-158

Mortensen PB, Hovland M, Fosså JH, Furevik D (2001) Distribution, abundance and size of *Lophelia pertusa* coral reefs in mid-Norway in relation to seabed characteristics. J Mar Biol Ass UK 84: 581-597

Mullins HT, Newton CR, Kathryn H, Van Buren HM (1981) Modern deep-water coral mounds north of Little Bahama Bank: criteria for recognition of deep-water coral bioherms in the rock record. J Sediment Petrol 51: 999-1013

Nelson CH, Baraza J, Maldonado A, Rodero J, Escutia C, Barber JH (1999) Influence of the Atlantic inflow and Mediterranean outflow currents on Late Quaternary sedimentary facies of the Gulf of Cadiz continental margin. Mar Geol 155: 99-129

New AL, Barnard S, Herrmann P, Molines J-M (2001) On the origin and pathway of the saline inflow to the Nordic Seas: insight from models. Progr Oceanogr 48: 255-287

O'Reilly BM, Readman PW, Shannon PM, Jacob AWB (2003) A model for the development of a carbonate mound population in the Rockall Trough based on deep-towed sidescan sonar data. Mar Geol 198: 55-66

Pearson I, Jenkins DG (1986) Unconformities in the Cenozoic of the North-East Atlantic. In: Summerhayes CP, Shackleton NJ (eds) North Atlantic Palaeoceanography. Geol Soc London Spec Publ 21: 79-86

Roberts JM, Long D, Wilson JB, Mortensen PB, Gage JD (2003) The cold-water coral *Lophelia pertusa* (Scleractinia) and enigmatic seabed mounds along the north-east Atlantic margin: are they related? Mar Pollut Bull 46: 7-20

Rogers AD (1999) The biology of *Lophelia pertusa* (Linnaeus 1758) and other deep-water reef-forming corals and impacts from human activities. Int Rev Hydrobiol 84: 315-406

Rüggeberg A, Dullo W-Chr, Dorschel B, Hebbeln D (submitted) Environmental changes and growth history of Propeller Mound, Porcupine Seabight: evidence from benthic foraminiferal assemblages. Int J Earth Sci

Saoutkin A (1998) Calcareous nannoplankton from upper Quaternary deep-water coral banks in Porcupine Basin (North Atlantic) implications to environmental growth conditions of the coral banks. MSc thesis, Moscow State Univ

Schnitker D (1986) North-east Atlantic Neogene benthic foraminiferal faunas: tracers of deep-water palaeoceanography. In: Summerhayes CP, Shackleton NJ (eds) North Atlantic Palaeoceanography. Geol Soc London Spec Publ 21: 191-203

Sierro FJ, Flores JA, Baraza J (1999) Late Glacial to Recent paleoenvironmental changes in the Gulf of Cadiz and formation of sandy contourite layers. Mar Geol 155: 157-172

Stetson TR, Squires DF, Pratt RM (1962) Coral banks occurring in deep water on the Blake Plateau. Amer Mus Nov 2114: 1-39

Stoker MS, van Weering TCE, Svaerdborg T (2002) A Mid- to Late Cenozoic tectonostratigraphic framework for the Rockall Trough. In: Shannon PM, Haughton PDW, Corcoran DV (eds) The Petroleum Exploration of Ireland's Offshore Basins. Geol Soc London Spec Publ 188: 411-438

Van Aken HM (2000) The hydrography of the mid-latitude Northeast Atlantic Ocean II: The intermediate water masses. Deep-Sea Res I 47: 789-824

Van Aken HM, Becker G (1996) Hydrography and through-flow in the north-eastern North Atlantic Ocean: the NANSEN project. Progr Oceanogr 38: 297-346

Van Rooij D, Blamart D, Richter T, Wheeler AJ, Kozachenko M, Henriet J-P (submitted) Quaternary drift sediment dynamics in the Belgica mound province, Porcupine Seabight: a multidisciplinary approach. Int J Earth Sci

Van Rooij D, De Mol B, Huvenne V, Ivanov M, Henriet JP (2003) Seismic evidence of current-controlled sedimentation in the Belgica mound province, southwest of Ireland. Mar Geol 195: 31-53

Van Weering TCE, de Haas H, De Stigter HC, Lykke-Andersen H, Kouvaev I (2003) Structure and development of giant carbonate mounds at the SW and SE Rockall Trough margins, NE Atlantic Ocean. Mar Geol 198: 67-81

Wheeler AJ, Kozachenko M, Beyer A, Foubert A, Huvenne VAI, Klages M, Masson DG, Olu-Le Roy K, Thiede J (2005) Sedimentary processes and carbonate mounds in the Belgica Mound province, Porcupine Seabight, NE Atlantic. In: Freiwald A, Roberts JM (eds) Cold-water Corals and Ecosystems. Springer, Berlin Heidelberg, pp 571-603

White M (2003) Comparison of near seabed currents at two locations in the Porcupine Sea Bight - implications for benthic fauna. J Mar Biol Ass UK 83: 683-686

Wilson JB (1979) "Patch" development of the deep-water coral *Lophelia pertusa* (L.) on Rockall Bank. J Mar Biol Ass UK 59: 165-177

Zibrowius H, Gili J-M (1990) Deep-water Scleractinia (Cnidaria: Anthozoa) from Namibia, South Africa, and Walvis Ridge, southeastern Atlantic. Sci Mar 54: 19-46

The seabed appearance of different coral bank provinces in the Porcupine Seabight, NE Atlantic: results from sidescan sonar and ROV seabed mapping

Veerle A. I. Huvenne[1,2], Andreas Beyer[3], Henk de Haas[4], Karine Dekindt[5], Jean-Pierre Henriet[1], Maxim Kozachenko[6], Karine Olu-Le Roy[5], Andrew J. Wheeler[6] and the TOBI/Pelagia 197 and CARACOLE cruise participants

[1] Renard Centre of Marine Geology, Gent University, Krijgslaan 281, S8, B-9000 Gent, Belgium

[2] Present address: Challenger Division for Seafloor Processes, Southampton Oceanography Centre, Empress Dock, Southampton, SO14 3ZH, UK (vaih@soc.soton.ac.uk)

[3] Alfred Wegener Institute for Polar and Marine Research, Columbusstr., D-27568 Bremerhaven, Germany

[4] Koninklijk Nederlands Instituut voor Onderzoek der Zee (NIOZ), P.O. Box 59, NL-1790 AB Den Burg, Texel, The Netherlands

[5] IFREMER, Centre de Brest, BP 70, F-29280 Plouzané, France

[6] Department of Geology, Environmental Research Institute, University College Cork, Ireland

Abstract. Carbonate mounds, identified as deep-water coral banks, have been reported recently from three provinces in the Porcupine Seabight, SW of Ireland. As yet, the mechanisms behind their formation and development are only partly understood. This contribution discusses their seabed appearance and present-day sedimentary environment, based on a large-scale TOBI sidescan sonar mapping carried out in 2002, and on detailed ROV video records from specific sites within the three mound provinces, collected in 2001. The study of the present-day characteristics and variability of these mounds can help to understand their development history in the past.

The imagery clearly shows that the sedimentary environment in the Magellan and Hovland Mound provinces in the northern Porcupine Seabight is much quieter than in the current-swept Belgica Mound province on the eastern flank of the basin. In the latter area, for example, gravel lags and coarse sediments are found, together with patches of sorted sands, striations, barchan dunes and sediment waves. The difference in environment results in different mound appearances. The richest coral communities with the most abundant live coral occurrences are found in the Belgica

province, while for example on the Magellan Mounds only a few live coral colonies are left. The present-day situation of the coral banks in the Porcupine Seabight thus illustrates the influence of the interplay between current and sediment dynamics on coral growth and mound development.

Keywords. Deep-water corals, seabed facies mapping, sedimentary bedforms, Porcupine Seabight, ROV, sidescan sonar

Introduction and background

Over the last decennia, large mound structures were discovered along the NE Atlantic continental margin, W of Ireland (Hovland et al. 1994; Henriet et al. 1998; De Mol et al. 2002; Kenyon et al. 2003). In the Porcupine Seabight they occur in 3 provinces, indicated on the location map in Figure 1: the Magellan, Hovland and Belgica Mound provinces. Deep-water corals and coral fragments were encountered on the summits, flanks and in the upper metres of several of them, prompting De Mol et al. (2002) to classify these mounds as 'coral banks'. The main species found are *Lophelia pertusa* (Linné, 1758) and *Madrepora oculata* Linné, 1758 (Kenyon et al. 1998), but also other corals such as *Desmophyllum cristagalli* have been reported (Olu-Le Roy et al. 2002; H. Zibrowius and A. Freiwald pers. comm.). The occurrence of deep-water corals in this area is known since at least the historical cruise of the HMS Porcupine (Thomson 1873), and both Pratje (1924) and Le Danois (1948) incorporated the Porcupine Seabight in their early maps of the coral distribution along the European margin. But only when the offshore industry, moving into deeper waters, re-discovered the corals and mounds some decades ago, did scientific interest for these enigmatic structures rise again.

Major questions concerning the origin and formation controls of the coral banks have been posed. It has been suggested that they are caused and controlled by the seepage of hydrocarbons from depth (e.g., Hovland et al. 1994; Henriet et al. 1998, 2001), by the establishment of specific oceanographic conditions (e.g., Kenyon et al. 1998; De Mol et al. 2002) or by a combination of the two (Henriet et al. 2002). In order to gain more insight, the banks were studied with a variety of techniques, partly within the EU 5th Framework projects GEOMOUND, ECOMOUND and ACES. 2D and 3D seismic data showed the geological context and embedding sediment packages (De Mol et al. 2002; Huvenne et al. 2003). Cores and video observations supplied local information of the seabed and the shallow subsurface on and around the mounds (Kenyon et al. 1998), and were recently complemented with ROV video observations acquired during the CARACOLE cruise on board of the R/V L'Atalante (Olu-Le Roy et al. 2002). A limited sidescan sonar survey carried out during the Training-Through-Research cruises 7 and 8 (Kenyon et al. 1998, 1999), together with a high-resolution sidescan sonar survey over part of the Belgica Mound province (Wheeler et al. 2000; Wheeler et al. 2005) illustrated the power of this technique in mapping the seabed characteristics. Partly based on these results, a large-scale 30 kHz TOBI (Towed Ocean Bottom Instrument) sidescan sonar survey was planned and carried out in summer 2002 over the various mound provinces in order to map them in full, in a consistent manner.
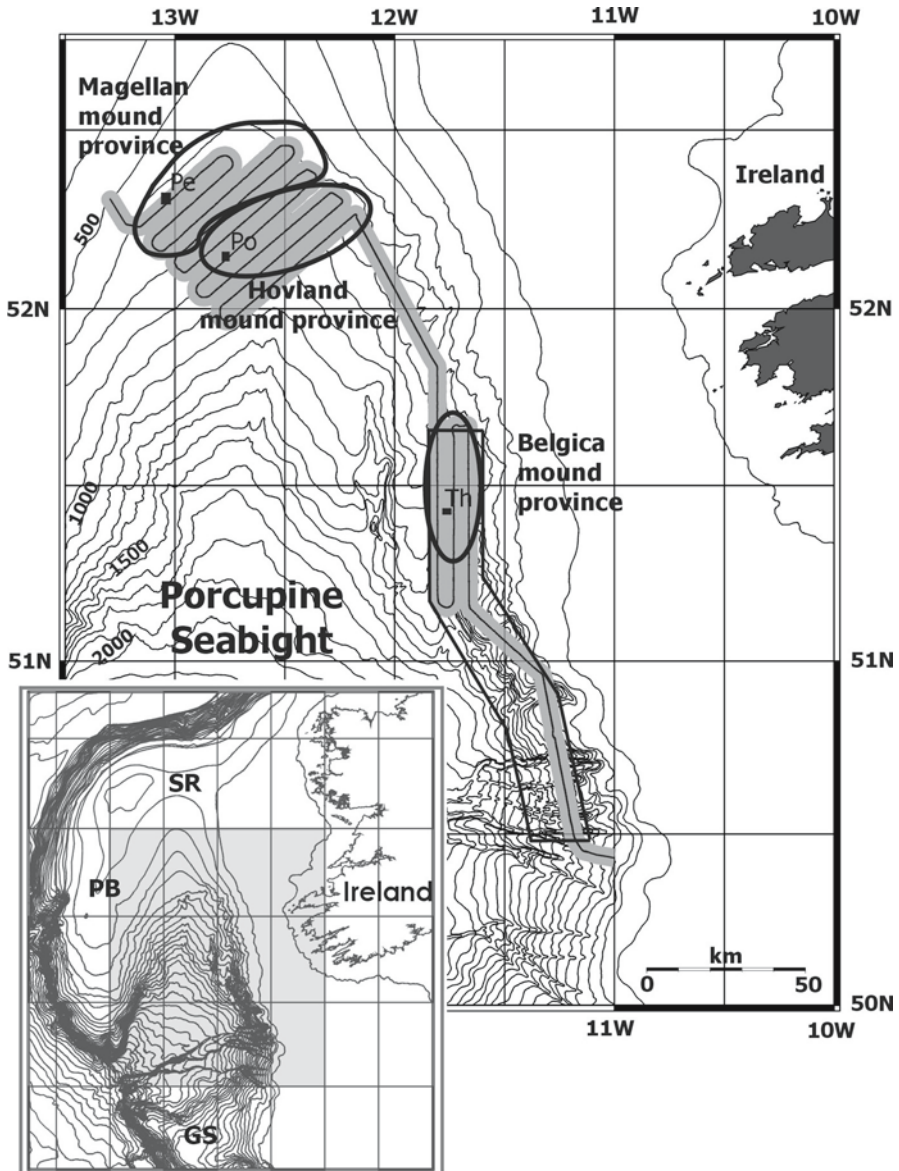
Fig. 1 Overview map of the Porcupine Seabight, its mound provinces and the data sets used in this study. The coverage of the 2002 TOBI sidescan sonar survey is indicated in grey; the locations of the 3 dive sites of the 2001 CARACOLE cruise ROV dives are marked with small black boxes (Pe: Mound Perseverance, dive 127; Po: Propeller Mound, dive 126; Th: Thérèse Mound, dives 123 to 125; see Table 1). The area delineated along the eastern flank of the Seabight was covered during the 2000 multibeam survey with the R/V Polarstern. The inset to the left situates the Seabight along the Irish continental margin, the coverage of the main map is marked with a grey box (PB: Porcupine Bank, SR: Slyne Ridge, GS: Goban Spur)

This paper presents the results of the seabed mapping in the Porcupine Mound provinces. An accurate knowledge of the present morphology and characteristics of the different types of mounds in the area, together with the sedimentary processes affecting them, will help in the understanding of the past formation and development of the mounds. Furthermore, based on the ROV video footage collected during the CARACOLE cruise, together with the information from sidescan sonar mapping, one mound from each province is discussed in detail as an illustration of the specific conditions around mounds in that province.

Setting

Geology

The Porcupine Seabight forms an embayment in the continental margin, bound by the Porcupine Bank, the Slyne Ridge, the Irish shelf and the Goban Spur (Fig. 1). It overlies the Porcupine Basin, a deep sedimentary basin that formed as a failed rift during the opening of the North Atlantic Ocean. The major rifting phases occurred during the Permo-Triassic, Late Jurassic and Middle Cretaceous (Sinclair et al. 1994), and were followed by basin subsidence and sedimentation. Locally the Cretaceous and Tertiary sequences can be more than 9 km thick. The most recent sedimentation in the area consists mainly of (hemi) pelagic and locally reworked sediments which appear to become finer towards greater depth (Rice et al. 1991). At depths of ca. 500 to 1000 m, where the mounds occur, the general succession in cores consists of an upper layer of Holocene, foraminiferal sands, representative of the interglacial sedimentary environment, overlying several metres of silty clays or marls with dropstones, deposited during the last glacial event (Swennen et al. 1998; De Mol 2002; Foubert 2002). On the eastern flank of the Porcupine Seabight, in the Belgica Mound area, Van Rooij et al. (2003) found seismic evidence for the existence of two types of sediment drift. An elongated and a confined drift of presumably Quaternary age occur in the sedimentary sequences within which also the mounds are embedded.

Hydrography

Water depths in the Porcupine Seabight range from less than 400 m in the north to more than 3000 m in the southwest, where the embayment opens onto the Porcupine Abyssal Plain (Fig. 1). The water mass structure in the Seabight was described by Rice et al. (1991), Mohn (2000) and White (2001), and consists of an upper layer of 750 m of Eastern North Atlantic Water (ENAW), overlying a core of Mediterranean Outflow Water (MOW), reaching down to ca. 1500 m, marked by a salinity maximum and oxygen minimum. A fresher and more oxygen-rich layer of Labrador Sea Water is located between ca. 1500 and 1800 m, and is underlain by Norwegian Sea Water. In general, a poleward (northward) boundary or slope current is described along the NE Atlantic continental margin (e.g., Huthnance et al. 1986; Kenyon 1986). The existence of a general northward flow along the slope in the Porcupine Seabight has indeed been confirmed by several sets of current

measurements, e.g. as reported by Pingree and Le Cann (1989, 1990). White (2001) found a mean northward bottom current of 2-5 cm/s, however steered cyclonically by the topography in the north of the Porcupine Seabight. In that area currents appeared the weakest and most variable ones. In addition to these average residual currents, strong tidal influences were reported by Pingree and Le Cann (1989) from the eastern flank of the Seabight (both semi-diurnal and diurnal tides) and by Mohn et al. (2002) from the flanks of the Porcupine Bank (diurnal tide). Some of these tidal signals, for example on the eastern flank of the Seabight, appear to be caused by internal tides (Pingree and Le Cann 1989). Rice et al. (1990) mapped the zones where semi-diurnal internal tides could be created or enhanced, and part of these coincide with the Belgica Mound province.

Mounds and corals

In total 3 mound provinces were discovered in the Porcupine Seabight during the last decennia (De Mol et al. 2002; Fig. 1). The Hovland Mound province is located in the north, and was originally described by Hovland et al. (1994). The mounds are conical to elongated, ridge-like structures, reaching up to 150 m above the seabed. The Magellan Mound province is located just north and west of the Hovland province. A very large number of mainly smaller mounds have been found in this area, they are nowadays mostly buried under semi-parallel stratified sediments (Huvenne et al. 2003). Along the eastern flank of the Seabight lies the Belgica Mound province, comprising a set of mostly conical mounds, partly buried by sediments at their upslope flank (Henriet et al. 1998). Most of these mounds are still visible at the present-day seafloor, and they can reach a height of up to 100 m above the seabed. Some, however, are already buried. The main coral species found on the banks, *Lophelia pertusa* and *Madrepora oculata*, are known to prefer locations with enhanced current regimes (such as local elevations) and need a hard substrate for their initial settlement (e.g., rock, hardground, a dropstone or piece of coral; Freiwald 1998; Rogers 1999; Mortensen et al. 2001). Furthermore, they tend to live in waters of 4 to 12°C, with a salinity varying between 34 and 37‰ and with a sufficient food supply.

Material and methods

The main data used for this study are TOBI sidescan sonar mosaics and ROV Victor 6000 video footage. The TOBI sidescan sonar data were recorded in July 2002, during a cruise of the R/V Pelagia in the Porcupine Seabight and Rockall Trough (de Haas et al. 2002). TOBI stands for Towed Ocean Bottom Instrument, a deep-towed vehicle developed at the Southampton Oceanography Centre (UK). The main instrument is a 30 kHz sidescan sonar with a swath width of 2 x 3000 m. During the survey, the vehicle was towed at a constant speed of 2.5 kn and was kept at a height of about 300 to 400 m above the seabed. The survey track plot is shown in Figure 1: ca. 2300 km^2 of seafloor were mapped in the Hovland/Magellan area and 1000 km^2 over the Belgica province. For data processing, the software package PRISM ('Processing Remotely sensed Imagery for Seafloor Mapping';

LeBas 2002) and the image processing software ERDAS were used, resulting in mosaics with a pixel resolution of 6 x 6 m. The data interpretation was carried out partly on paper, but mostly within the GIS software ArcView v3.2. Ground-truthing was based on existing data sets. In particular, core descriptions from various types of coring operations, carried out during different cruises were used (Swennen et al. 1998; De Mol et al. 1999; de Haas et al. 2000, 2002; Freiwald et al. 2000; Freiwald and Shipboard Party 2002; Van Rooij et al. 2001; De Mol 2002). Furthermore, the interpretation of video transects collected during the TTR7 cruise (Kenyon et al. 1998; De Bergé 2000), the 3.5 kHz shipboard subbottom profiler records acquired during the sidescan survey and the ROV Victor 6000 video footage (see below) were also used for ground-truthing. Bathymetric information, kindly provided by the Geological Survey of Ireland (GSI Dublin) was used to aid in the interpretation of the sidescan imagery of the Hovland/Magellan area. Bathymetry data of the Belgica Mound province was collected during the 2000 R/V Polarstern cruise ANT XVII/4, using a Hydrosweep DS2 system. Processing of these data occurred at the Alfred-Wegener-Institute (Bremerhaven) and resulted in a digital terrain model of the area with horizontal resolution of 50 x 50 m.

Several dives of IFREMER's Remotely Operated Vehicle (ROV) Victor 6000 were carried out in the Porcupine Seabight during the 2001 CARACOLE cruise of the R/V L'Atalante (Olu-Le Roy et al. 2002). The specifications of the dives are given in Table 1 and the dive sites are indicated on Figure 1. The first dive on Thérèse Mound was used to acquire a high-resolution multibeam grid (Opderbecke and Pitout 2002; Hinsinger 2002). The other dives were targeted at video observations, together with the sampling of sediment and biota and the collection of digital photographs. Post-processing of the dive data was based on the software 'Adélie' (a set of ArcView-based routines developed at IFREMER for the analysis of ROV and submersible data) and included the correction of the navigation data and the

Table 1 Specifications of the CARACOLE ROV dives targeted towards different mounds in the Porcupine Seabight

dive number	123	124	125	126	127
location	Thérèse Mound	Thérèse Mound	Thérèse Mound	Propeller Mound	Mound Perseverance
start latitude	51° 25.42'	51° 25.88'	51° 25.05'	52° 13.94'	53° 18.12'
start longitude	-11° 46.54'	-11° 45.21'	-11° 47.58'	-12° 45.46'	-13° 02.15'
min depth	847 m	807 m	860 m	670 m	598 m
max depth	1016 m	1016 m	961 m	869 m	671 m
total time on seabed	14h20	14h43	17h36	12h04	14h36
total length	14 km	6 km	3 km	6.2 km	8 km
main aim	high-res. multibeam bathymetry & video survey	sampling and video surveying	sampling and video surveying	video surveying and sampling	video surveying and sampling

linking of video (snapshots) and photographs to these. Based on the dive reports and the video data, different seabed facies were recognised and mapped. It has to be noted that this facies mapping was mainly carried out from a geological and sedimentological point of view, hence that differences in faunal assemblages and ecological communities have not been recognised. All video data and photos, taken with the ROV and presented here, are under copyright of IFREMER. Finally, all the information was collected in the GIS projects (ArcView v3.2), which allowed a multidisciplinary interpretation.

Results

Magellan and Hovland provinces

TOBI sidescan sonar mosaic

In general, the Magellan/Hovland region appears on the TOBI sidescan sonar imagery as an area with a homogeneous acoustic facies of medium backscatter strength (Fig. 2). The intensity seems to decrease slightly from the north to the south, while the backscatter texture becomes smoother in that direction. This facies could be identified as bioturbated muddy or silty hemipelagic sediments, often with a watery or 'soupy' upper layer of a few cm, containing a high concentration of foraminifera. The gradual change from north to south is probably due to a gradual change in grain-size, sorting and compaction of the sediments. In the Hovland province, the seafloor is cut by 6 elongated depressions or blind channels, generally running N-S (except for one which changes direction towards the NW; Fig. 2). They were also reported by Hovland et al. (1994) who attributed them to bottom current erosion or to the escape of pore water or gases through the seafloor. De Mol (2002) suggested they were caused by current scouring, and interpreted their elongation direction as the result of a northward-directed current. Apart from these channels and the obvious mounds with their associated, scoured moats, the seafloor appears relatively featureless. Evidence of recent erosion or sedimentation patterns, such as bedforms, is absent between these structures. A few pockmarks were found around 52°15'N, 12°30'W and around 52°04'N, 12°55'W, but the overall environment of the Magellan and Hovland Mounds seems relatively quiet.

Against this background the coral banks are clear features: they have a strong backscatter on the flank facing the sidescan, reflecting their topography and their composition of (live) coral framework and coral debris (see below). An acoustic shadow can be seen behind the features. The Magellan Mounds are relatively small (some 300 to 800 m across, and up to some 50 m above the present-day seabed), and some of them are less easily recognisable (Fig. 3). These latter mounds are smoother, have a less strong backscatter and do not create a strong shadow. They are interpreted as being buried already under a thin drape of sediments. In total, 19 covered mounds could be found, while 14 mounds still seemed to be active at the present-day seafloor. Seismic studies however, have shown that the Magellan province contains many more mounds (possibly more than 1000 structures; Huvenne et al. 2003), but that most of these are buried already.
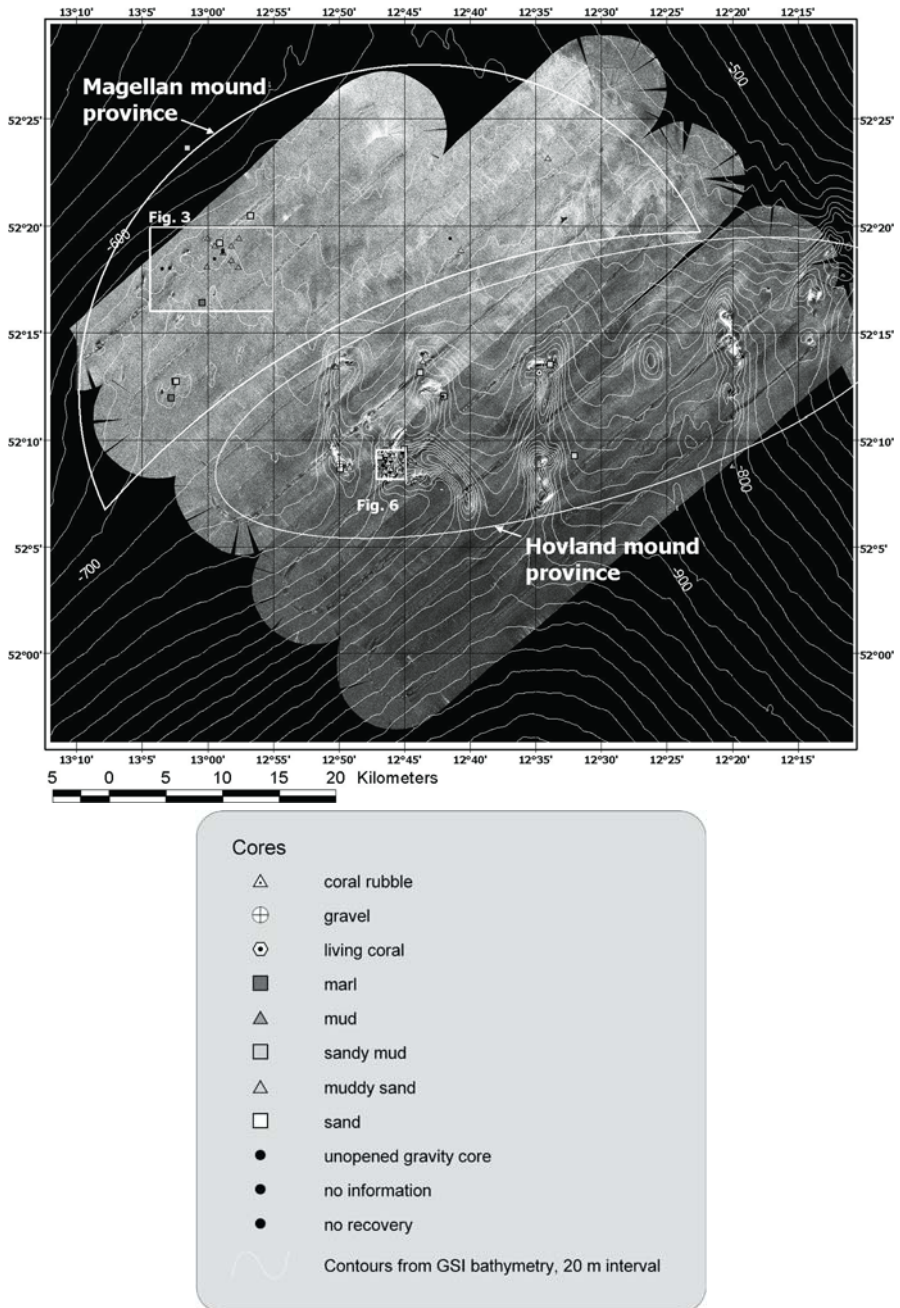
Fig. 2 TOBI sidescan sonar mosaic of the Magellan and Hovland Mound provinces. The bathymetric contours are derived from GSI data, and the core information was obtained from existing data sets, mentioned in the text. The rectangles indicate the positions of Figs. 3 and 6
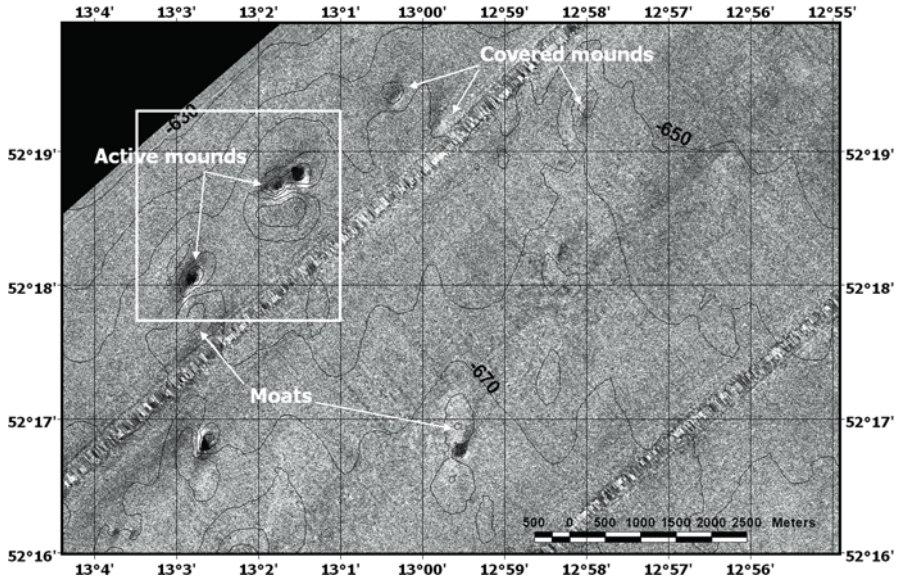
Fig. 3 Detail of the TOBI sidescan sonar mosaic over the Magellan Mound province, illustrating the seabed appearance of mounds and moats. Some of these are already covered by a drape of hemipelagic sediments. The bathymetry information is derived from the time-depth converted seafloor reflection mapped from 3D seismic data in the Magellan province (Huvenne et al. 2003). The box indicates the position of Fig. 4

The Hovland Mounds on the other hand appear to be much larger, and in several cases they form elongated ridges. Their length can vary between 1700 and 3200 or even 5000 m, and their width ranges from 450 to 1200 m. The ridges have different orientations and may be forked, with spurs extending in different directions. Still, often there is a north-south directed component (spurs, or the ridge itself). Eleven large and 15 smaller mounds could be recognised on the sidescan sonar mosaics. De Mol (2002) studied seismic profiles from the province which indicate that some of the mounds may have a common, subsurface base. He also found several buried Hovland Mounds. Most of the mounds are located at the flanks or at the heads of the elongated depressions in the area. They can be grouped in 2 clusters: one on the northeastern flank of the province and one more to the centre.

Depressions, described as 'moats' can be found around most of the mounds. They were previously recognised from seismic data already (De Mol et al. 2002; Huvenne et al. 2003), and were attributed to the scouring action of currents. Especially around the Magellan Mounds, the moats appear to be elongated in a N/S direction, possibly due to the action of a reversing current (Huvenne et al. 2003). And although most of these depressions are largely filled in nowadays, which indicates they might not be very active any more, with the help of the bathymetry data they still can be recognised in the sidescan images as subtle variations in backscatter (Fig. 3). Also some of the Hovland Mounds have associated moats to their south and north, which often merge with the N-S trending depressions. The most western depression even seems to be formed through the merging of several moats (Fig. 2).

Mound Perseverance: a case study in the Magellan province

Mound Perseverance, one of the few Magellan Mounds that actually reach the present-day seabed, is located at 52°18'3"N and 13°2'48"W (Fig. 4), at a depth of about 650 m on the western edge of the province. It is ca. 820 m long and 310 m wide and is elongated in a NNE-SSW-ly direction, towering some 50 m above the seabed. Seismic data indicate that its total height above its base is ca. 160 m (Huvenne et al. subm.). It was visited with the ROV together with another seabed protruding mound slightly to the northeast (Fig. 4). This second mound measures about 1000 x 440 m, and is directed in an ENE/WSW-ly direction. It is a double structure, with two summits at 33 and 55 m above the surrounding seabed. Its total height above its base is estimated as 145 m (Huvenne 2003).

Seven sedimentary facies were recognised on the video data of both mounds (Fig. 5):

Facies Perseverance

- heavily bioturbated
- lightly bioturbated
- non-bioturbated
- scattered debris
- abundant debris
- dead coral
- live coral
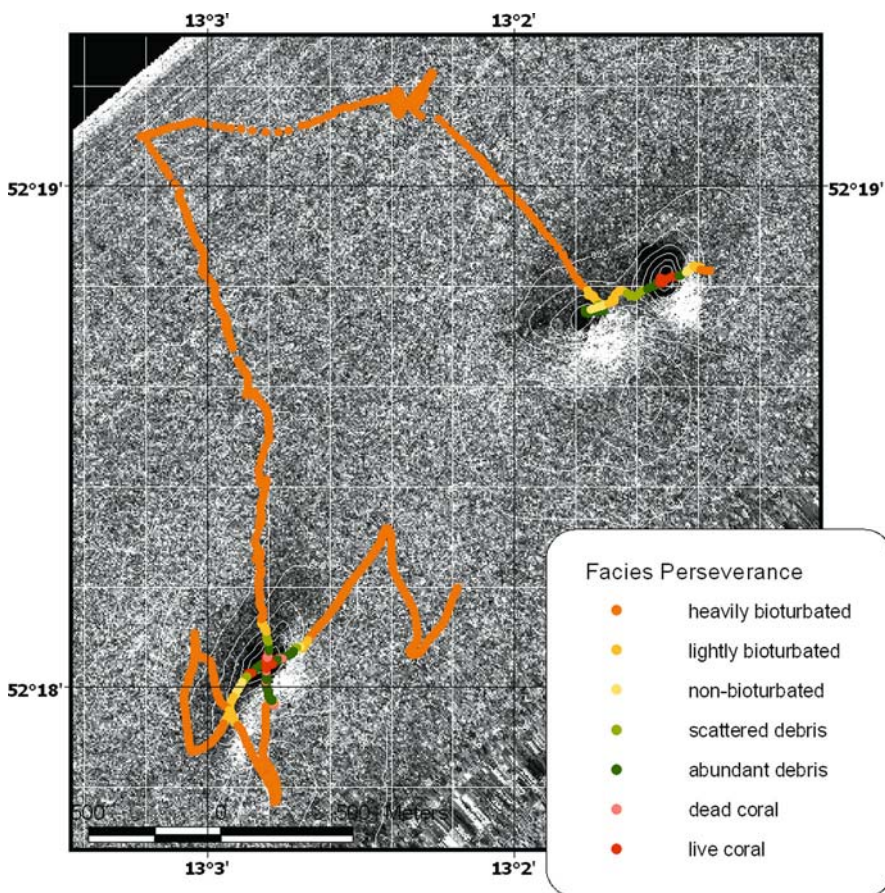
Fig. 4 Overview map and seabed facies interpretation of CARACOLE dive 127 on Mound Perseverance and a nearby Magellan Mound, overlaid on the TOBI sidescan sonar imagery. The bathymetric information is again derived from 3D seismic data (Huvenne et al. 2003)

1.   heavily bioturbated sediment (high concentration of burrows)
2.   lightly bioturbated sediment (low concentration of burrows)
3.   non-bioturbated sediment
4.   scattered coral debris
5.   abundant coral debris
6.   dead coral (containing an open framework structure, devoid of sediment)
7.   live coral
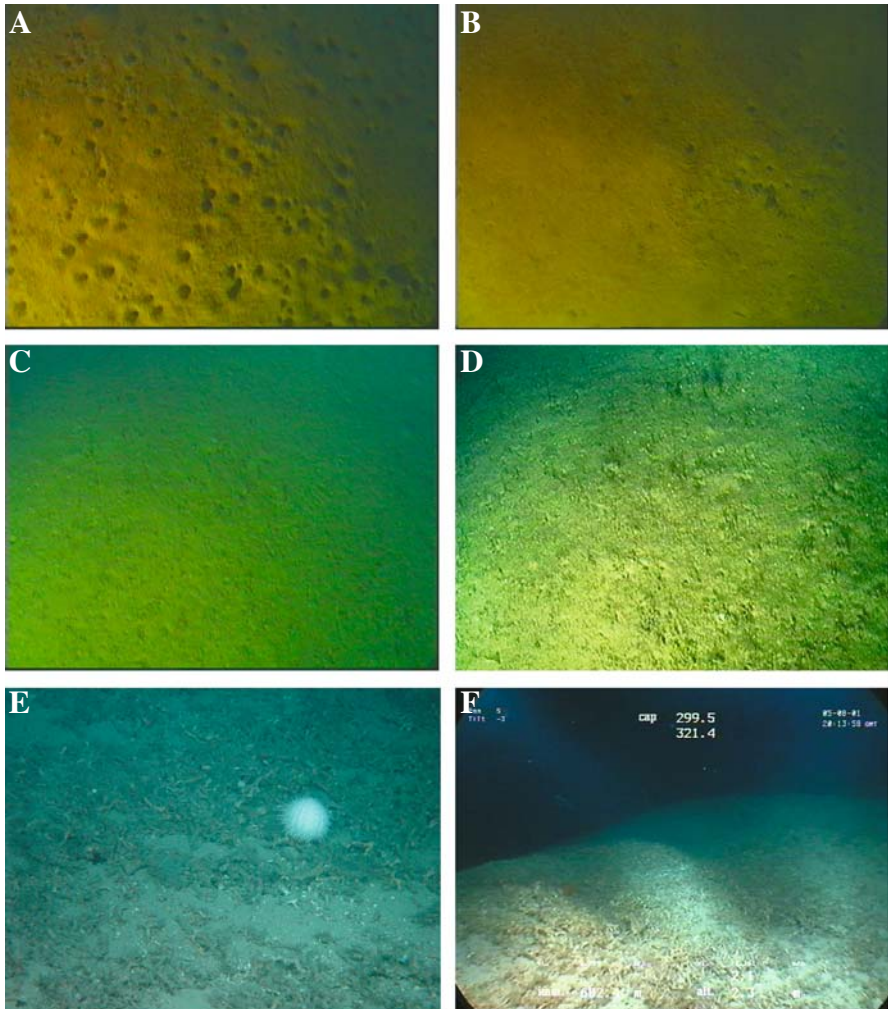
Fig. 5 Different seabed facies recognised on Mound Perseverance (Magellan province) and Propeller Mound (Hovland province): **A** heavily bioturbated sediment, **B** lightly bioturbated sediment, **C** non-bioturbated sediment, **D** scattered coral debris, **E** abundant coral debris, **F** dead coral
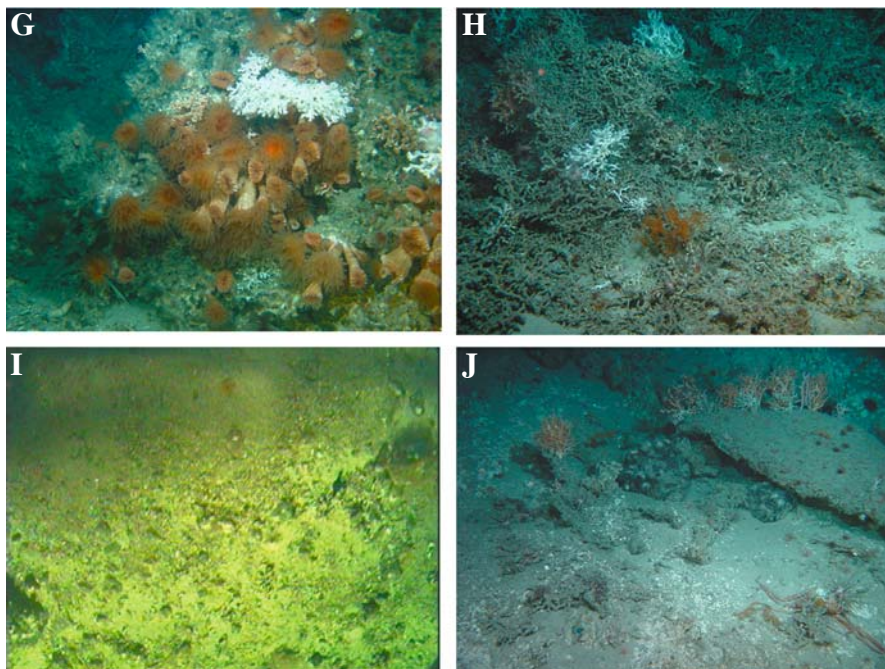
Fig 5 continued Different seabed facies recognised on Mound Perseverance (Magellan province) and Propeller Mound (Hovland province): **G** live coral colony on Mound Perseverance, containing *Lophelia* and *Desmophyllum*, **H** live coral on Propeller Mound, placed between dead coral framework, **I** gravel and pebble lag found on Propeller Mound, **J** part of outcropping crust and nanoplankton ooze found at the tip of the NE spur of Propeller Mound. All photographs with courtesy to IFREMER

The facies map (Fig. 4) shows that the largest part of the area is covered with bioturbated fine sediments. Only on the mounds themselves, coral debris, dead and live coral are encountered, causing part of the high-backscatter response on the TOBI imagery. Live corals are only found on the highest mound tops, or on a shoulder of Mound Perseverance. *Lophelia pertusa* and *Desmophyllum cristagalli* are the most abundant species, occurring in bushy colonies of some 1 to 1.5 m across and 0.75 to 1 m high (Fig. 5G). These are built of a framework of older (dead) material with live polyps at the outer shell, often facing the downslope direction (especially the *Lophelia*). The colonies occur in groups of 5 to 10, generally situated in areas of coral debris with patches of plain sediment. They are not necessarily located between large amounts of dead coral as is the case, for example, in the Haltenbanken-Frøyabanken area or on the Sula Ridge off Norway (Mortensen et al. 1995; Freiwald et al. 2002). On most of the mound flanks, the transition from bioturbated sediments to the debris facies occurs at a depth of ca. 635 m. Only on one of the flanks of Mound Perseverance this is not true (southern flank). The slope of the mound here makes a slight inward curve, and the seafloor comes closer to the 'core' of the mound. It seems that this flank has received less sedimentation.

Another possibility could be that part of the coral debris was transported down along this flank as a small slope failure.

Propeller Mound, an example of a Hovland Mound

Propeller Mound is located in the central Hovland Mound province, at 52°09'48"N and 12°46'24"W, and is so-called due to its shape in plan view (Freiwald et al. 2000). The mound has 3 spurs, and hence resembles the letter Y, or a propeller (Fig. 6). The recent TOBI survey revealed that the NW spur is connected to another long, NNE-SSW tending ridge (Fig. 2). This way it is the largest mound in the area, and in the whole of the Porcupine Seabight, with a total length of more than 5 km. The width of the individual spurs is about 500 m, and the top is located at a water depth of ca. 660 m, while the mound towers about 140 m above the surrounding seafloor. More precisely the seafloor is dipping in the area, which causes the mound flanks to be considerably higher on the eastern than on the western side. From seismic profiles it is known that Propeller Mound reaches a height of about 280 m above its base (De Mol 2002). Furthermore, the mound is located at the head of one of the deepest depression in the province, being the blind channel that bends towards the northwest. This setting may well have influenced the mound development.

Towards the southeast of Propeller Mound, an extra complex of 3 irregular, smaller mound structures can be seen. They are probably linked at their base to the main mound, and reach ca. 90 m above the seabed.

Compared to the study of Mound Perseverance, one more facies was distinguished on the video images of Propeller Mound (Fig. 5):

8.   gravel, most probably a pebble lag of ice-rafted debris and dropstones

On the whole, Propeller Mound shows a more complex scenario than Mound Perseverance. Bioturbated fine sediment again is the typical facies of the off-mound seafloor. It is only encountered along a few stretches of the dive track, as most of the dive was targeted on the mound top and flanks. Its occurrence however is less depth-related than on Mound Perseverance.

Live coral is found far more often than on Mound Perseverance. Again it is mainly concentrated on the tops of Propeller Mound and the smaller mounds to the SE, but also on the upper flanks (especially the western one) and on the ridge of the NW spur. Also on the tip of the NE spur some live coral is seen, related to an outcropping hardground and the exposure of some nanoplankton ooze (A. Freiwald pers. comm.) (Figs. 5J, 6). The top of Propeller Mound on the other hand is not fully covered with live corals, large patches of dead coral and coral debris are encountered as well. Live coral seems to occur in a similar way as on Mound Perseverance: forming bushy colonies, often with the live polyps all on one side. On the contrary, these colonies here are set between bunches of dead coral and coral debris (Fig. 5H). The most prolific occurrences of live coral are actually found on the tops of the smaller mounds to the SE. *Lophelia pertusa* and *Madrepora oculata* are the dominant coral species again, but *Desmophyllum cristagalli* and *Stenocyathus vermiformis* are found as well (Olu-Le Roy et al. 2002).
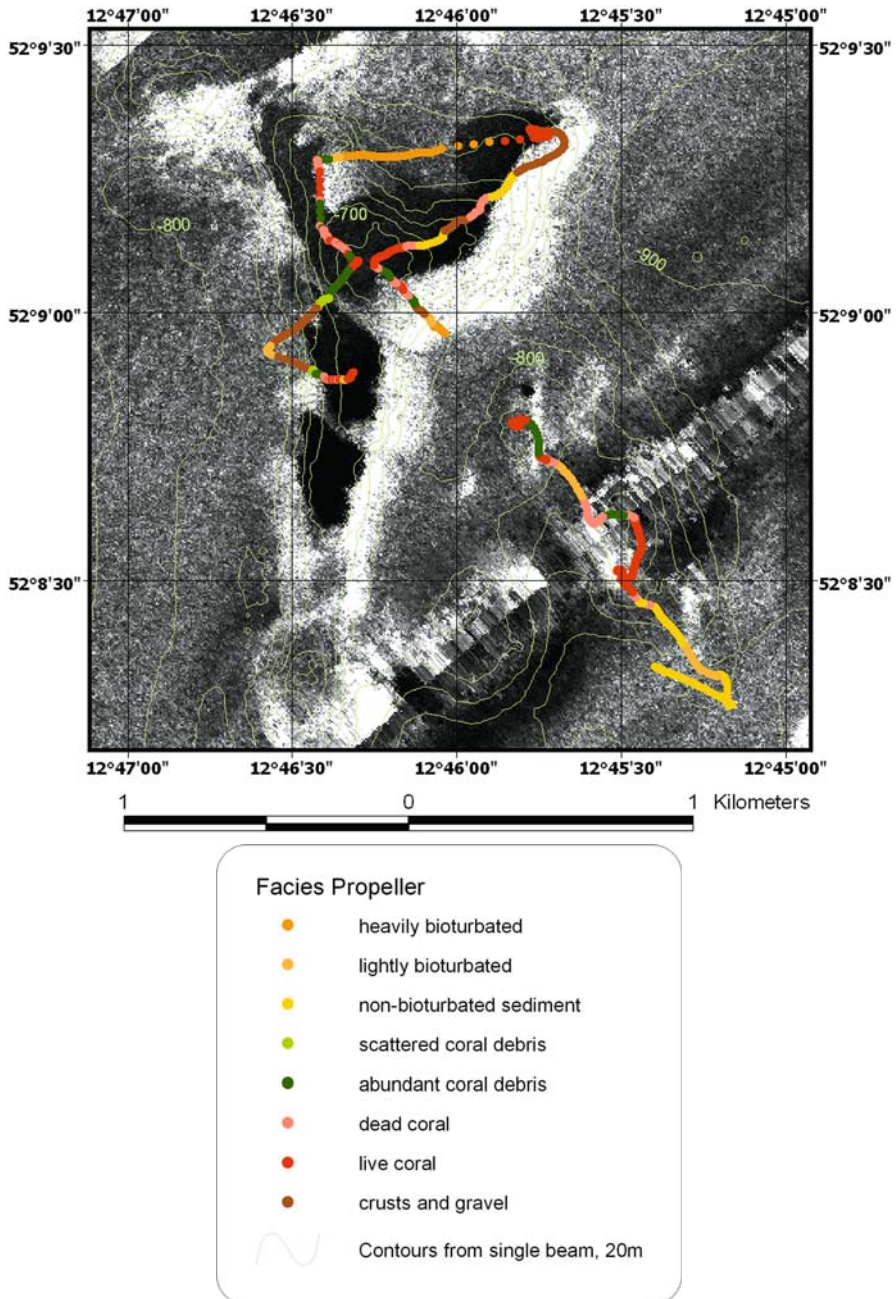
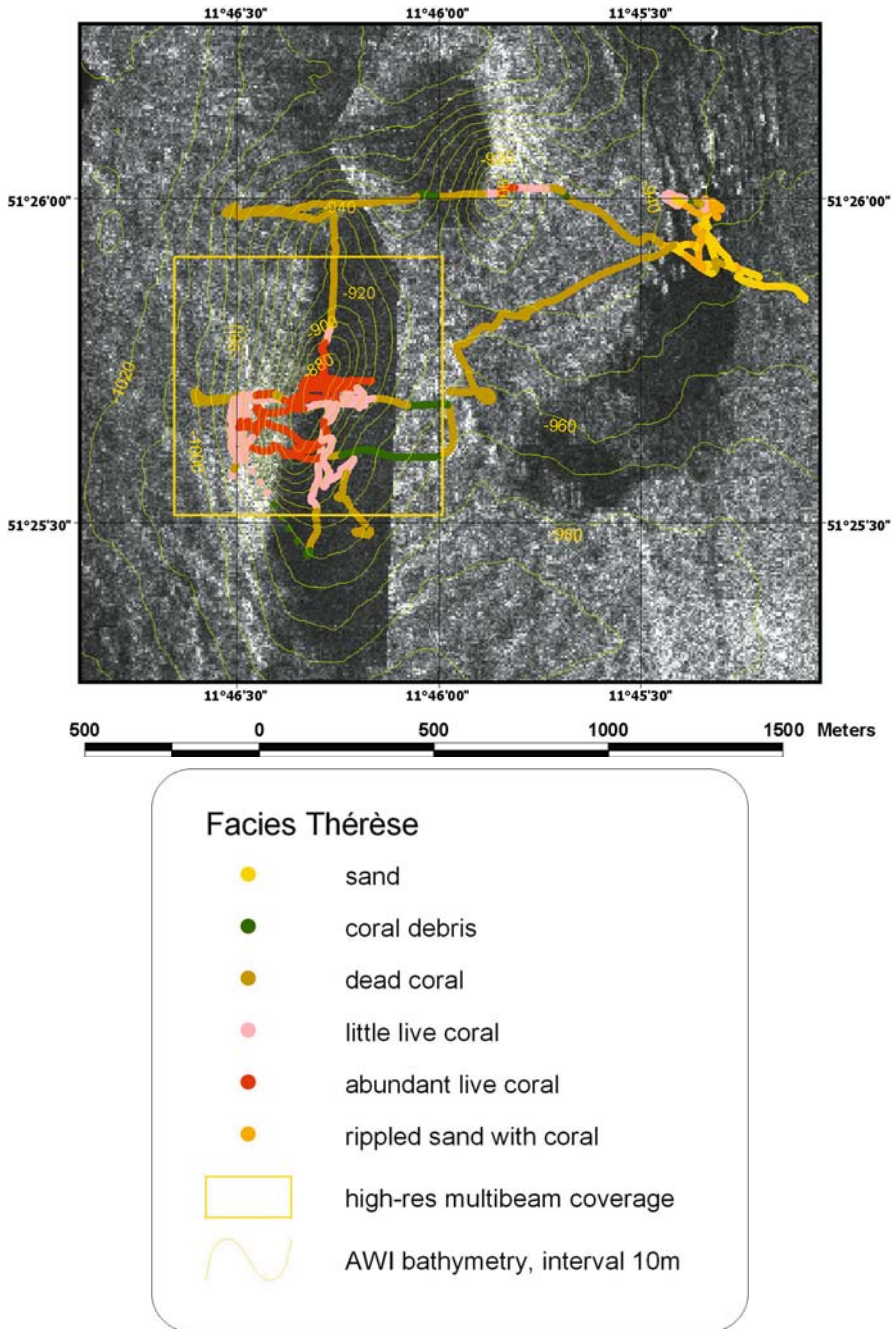**Fig. 6** Overview map and seabed facies interpretation of CARACOLE dive 126 on Propeller Mound, overlaid on the TOBI sidescan sonar imagery. The bathymetry information is derived from single beam data, obtained during a cruise with the R/V Poseidon in 2000 (Freiwald et al. 2000)

Two remarkable observations were made: the occurrence of the hardground and nanoplankton ooze on the tip of the NE spur, and the fact that large parts of the dive were crossing grounds with facies 8 material: gravel and pebble lag, interspersed with sandy deposits. These facies seem to indicate erosion, and are mainly found on the middle flanks of Propeller Mound, especially on the eastern and western flank.

Belgica province

TOBI sidescan sonar data

The sidescan sonar mosaic of the Belgica Mound province shows an entirely different pattern compared to the Magellan and Hovland provinces (Fig. 7). The image is less smooth, which is partly due to the more irregular bathymetry of the area. First of all, the eastern slope of the Porcupine Seabight is steeper (2 to 3° *versus* 0.2 to 0.5° in the Magellan/Hovland area). Furthermore, the province is bound to the west by a blind channel that runs approximately north-south, bending towards the SE in the southern part of the TOBI mosaic. Between the mounds, the slope is cut by several small, downslope directed channels or gullies. Van Rooij et al. (2003) attributed the large channel to the action of a northward-directed bottom current, and interpreted the smaller gullies as minor turbiditic channels. The Belgica Mounds on their turn are often arranged 'en echelon', generally in north-south trending ridges, more or less parallel to the depth contours (especially to the south of the province). This way they create some sort of terrace-like morphology along the slope, as they tend to pile up sediments on their upslope flank (Wheeler et al. subm.). Their asymmetrical shape causes a lack of shadow formation when they are ensonified from the downslope direction. This, together with the fact that there are also other features with the same high-backscatter signature as the mound flanks facing the instrument, makes the mounds less easily recognisable than in the Magellan and Hovland province. In total 43 mounds were recognised in the combined sidescan sonar/bathymetry data set. This is similar to what is reported by De Mol (2002), who also found 20 more buried mounds on seismic profiles in the area. The mounds are between 300 and 2000 m wide, up to 100 m high above the present-day seabed and often have a slight NNE-SSW elongation (Wheeler et al. subm.).

Overall, three types of backscatter pattern were recognised in the Belgica province, besides a range of specific features and bedforms (Figs. 7-8):

❋   A **low backscatter facies** of **smooth texture** (1) occurs mainly in the southern part of the TOBI mosaic. It also includes part of the large blind channel, and becomes darker (less backscatter) towards the south-east. On the echosounder profiles, a parallel-stratified sediment was found, with an acoustic penetration of locally up to 50 m. The facies is interpreted as a package of hemipelagic sediments.

❋   A **high-backscatter facies** of **irregular texture** (2) is found mainly in the central and northern part of the image, between the mounds and around the gullies. On echosounder profiles of these areas the penetration
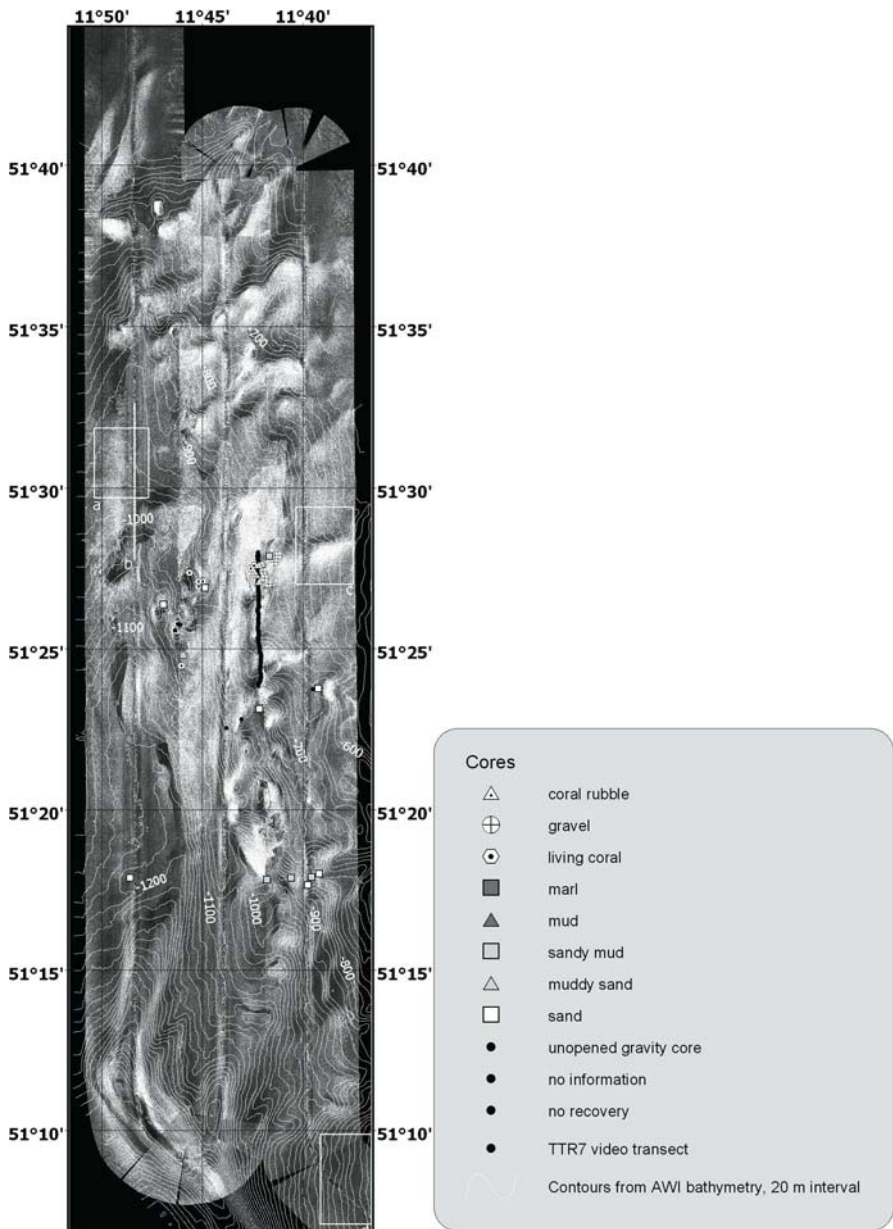
Fig. 7 TOBI sidescan sonar mosaic of the Belgica Mound province, with bathymetry data from the R/V Polarstern cruise (Beyer et al. 2003). Core information from different sources mentioned in the text. The TTR7 video transect was described by De Bergé (2000). The rectangles and line indicate the locations of the details presented in Figs. 9A-D
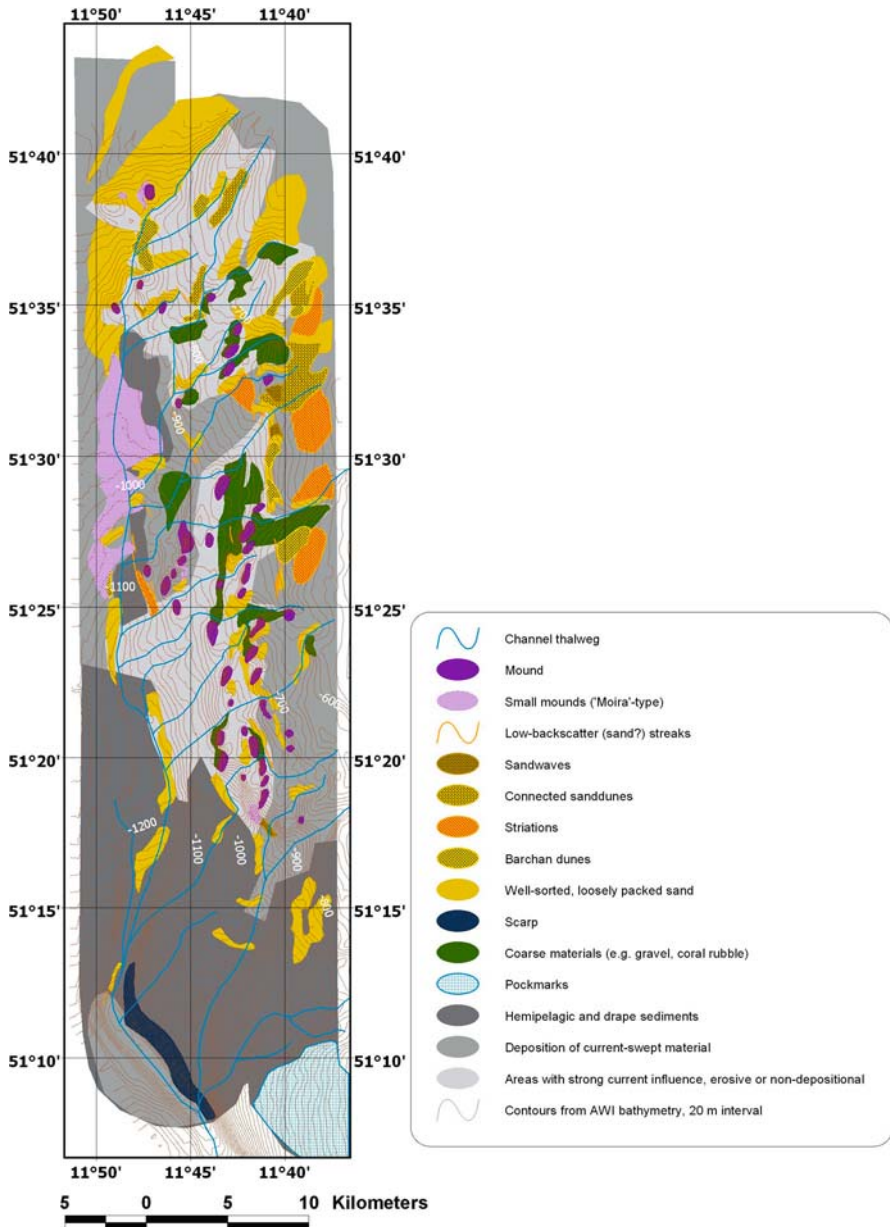
Fig. 8 Interpretation of the TOBI sidescan sonar and bathymetry data in the Belgica Mound province

decreases a little to ca. 30 m, and the amplitude of the seafloor and upper reflections is much higher, masking any underlying reflections. This facies is interpreted as indicative for current-swept areas, where the finest fractions are winnowed from the sediment and in some cases even non-deposition or erosion can occur. This results in a coarser, sometimes purely lag deposit. Core information describes foraminiferal sands and in some locations gravel or coral rubble.

❋ A **medium backscatter facies** with **irregular texture** (3) occurs in the northern half of the TOBI image, more specifically east and west of the previous facies. It shows intermediate characteristics both on sidescan sonar and echosounder images. It is, however, also related to the area with irregular bathymetry, caused by the mounds and gullies. Therefore this facies is interpreted as an area with a higher sedimentation rate than estimated for facies 2, but no drape sedimentation such as seen in facies 1. It probably also exhibits some kind of sorting or winnowing effect, although less strong than seen in facies 2.

It has to be noted that the boundaries between these facies are indicated more or less arbitrarily on the map, as in most places the facies change rather gradually.

Besides the overall backscatter pattern, some specific features have been recognised on the sidescan sonar records:

❋ **Mounds**: the Belgica Mounds were described above.
❋ **Small positive, high-backscatter features**: in some locations, especially in the northern part of the blind channel, slightly elongated (N-S) positive features of some 30 to 50 m wide can be seen (Fig. 9A). In these areas small (up to 10 m), positive features can be identified on the echosounder data as well (Fig. 9B). Based on their similarity with a set of small mounds further to the east, these structures are interpreted as Moira-type mounds (Wheeler et al. 2000; Wheeler et al. 2005).
❋ Towards the southeastern corner of the mosaic, a whole set of **depressions** is found, with an average diameter of 140 m. Although no trace of them was seen on the echosounder profiles, they are interpreted as shallow pockmarks (Fig. 9C).
❋ **Patches with very high backscatter** (apart from facies 2) were found between the mounds and along the north-facing slopes of the gullies on the upper slope (Fig. 9D). They are also interpreted as areas with a very coarse seafloor, consisting of gravel lags or coral fragments. The echosounder profiles crossing the gullies show that the north-facing flanks are rather eroded, which may have caused the higher backscatter in these areas.
❋ **Patches of very low backscatter** occur at several locations, especially on the south-facing slopes of gullies, the large channel, mounds etc. (Fig. 9D). In some cases they are sharply bound, in other locations their boundaries are rather fuzzy. On some of the patches zones with a wavy pattern of higher backscatter can be recognised.
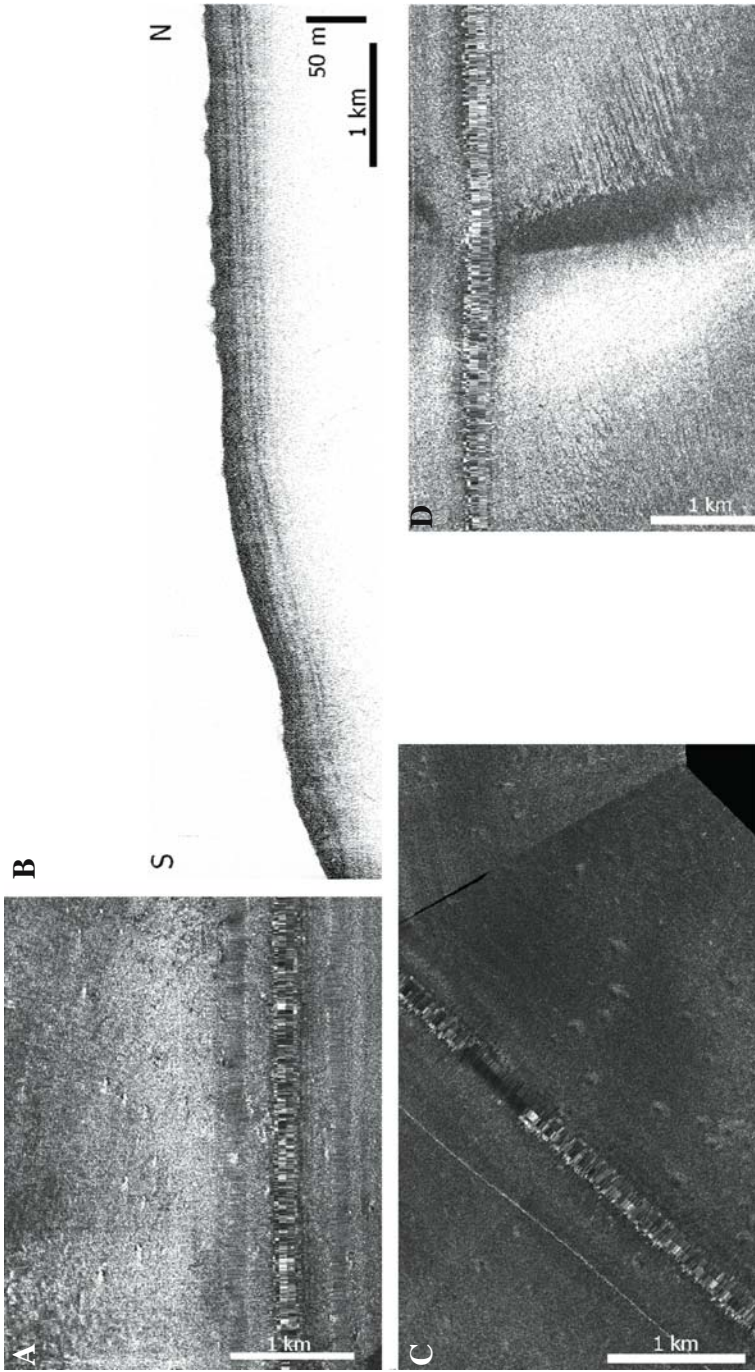
Fig. 9 Details of the TOBI sidescan sonar and shipboard 3.5 kHz profiler data in the Belgica Mound province (locations indicated on Fig. 7). Small positive structures (**A, B**), interpreted as small mounds; pockmarks (**C**); and a detail of a downslope gully (**D**) with high backscatter on the northward facing flank, and very low backscatter on the southward facing flank, interpreted as well-sorted sands. Striations depart from this patch of low backscatter, and to the south of the gully, some barchan dunes can be seen, associated with the sand patch of a second gully further to the south

✳   **Striations**: lines of very low backscatter placed on a high backscatter background are found at several locations, especially along the higher slope between the gullies (Fig. 9D). The lines are often directed in a NNW-SSE direction, and are mostly connected with/starting from a patch of very low backscatter. They can be up to 1500 or 2200 m long and up to 40 m wide.

✳   Irregular patches of low backscatter on a high backscatter background exhibit different shapes, ranging from **crescent-shaped** to **geometric patterns** and spots of higher backscatter surrounded by lower backscatter lines. Some of these features occur directly besides a patch of very low backscatter, and gradually fade towards that signature.

✳   **Single low-backscatter streaks** occur especially in the central part of the TOBI mosaic. They are up to 1500 m long and between 30 and 60 m wide. Overall, they are directed more or less N-S, and often they are linked to one of the patches of very low backscatter.

Based on ROV video observations and core descriptions of one very low backscatter zone east of Thérèse Mound (see below), this type of acoustic facies is interpreted as well-sorted, loosely packed sands. A similar interpretation was described by Masson (2001), who found a large area with very low backscatter on TOBI imagery from the Faeroe-Shetland Channel. Through ground-truthing with boxcores and photographs, they concluded that this facies was caused by a thin sheet of very well sorted sand or muddy sand, about 10 to 15 cm thick, covered with sand ripples. This interpretation can explain the other low-backscatter features in the Belgica province as well. Probably all of these bedforms are caused by sands, shaped by the currents and deposited on a coarser or a more compacted, higher reflective underlying seafloor. Both the striations and the individual streaks are current-parallel ribbons of sand. The crescent-shaped patterns can be interpreted as barchan dunes, up to 90 m wide, while the geometric patterns probably are caused by a dense pattern of barchan dunes, located closely enough to each other to be linked. The fact that all of these features occur very close to the deposits of sorted sands, supports the interpretation that these deposits acted as sediment sources for the bedforms to develop under the current action.

The overall pattern of bedforms and sedimentary features relates quite well with the descriptions of single sidescan sonar lines in the area (TTR7 and TTR8-records; Wheeler et al. 1998; De Mol et al. 1999; Huvenne et al. 2002). A more detailed description of the sedimentary environment in the Belgica province, based on high-resolution sidescan sonar records, is given by Wheeler et al. (2005).

Thérèse Mound as case study of a Belgica Mound

The third case study, visited by ROV, is located at 51°25'44"N and 11°46'15"W. Thérèse Mound is one of the most westerly mounds in the province, and hence also one of the deepest ones (Fig. 7). Its top is located in a water depth of 860 m, while its flanks run down to about 950 m (eastern flank) resp. 1000 m (western, steeper flank). Hence the mound shows the typical asymmetrical shape of the Belgica Mounds, and reaches a height of ca. 100 to 140 m above the present-day seafloor. The mound is

elongated in N-S direction, and measures 1250 by 650 m. Seismic profiles indicate that it reaches a total height of ca. 190 m above its base (De Mol 2002).

Thérèse Mound is part of a small cluster of mounds (Figs. 7, 10), and another, smaller mound to the NE of Thérèse was included in the ROV investigations during the CARACOLE cruise. It is about 550 by 350 m wide and reaches a height of about 50 to 70 m above the surrounding seafloor, with its top at 900 m water depth. It has its steepest (and longest) slope to the north. Apart from these 2 mounds, the ROV dives were extended even further to the east, in order to investigate a few small structures recognised on high-resolution sidescan sonar imagery, and interpreted to be small mounds as well ('Moira Mounds'; Wheeler et al. 2000). They are discussed in detail in Wheeler et al. (2005).

In total 3 ROV dives were carried out on Thérèse Mound and its surroundings (Table 1). Opderbecke and Pitout (2001) and Hinsinger (2002) processed the high-resolution multibeam data collected during the first dive, and integrated this data set in a 3D model of the mound. From their results it appears that the elongated mound has a fairly sharp ridge crest over its southern half, while the northern part of the mound appears a little lower and more rounded or concave. The flanks are covered with waveforms, with a general E-W strike direction and sinuous, bifurcating crests. They have an average wavelength of some 10 to 12 m, and are 0.5 to 1.5 m high. They can be interpreted as sediment waves and could indicate the influence of a northward or southward current. Virtually the whole mound is covered with them, except for the steepest part of the western upper flank, just beneath the mound crest. It must be noted that the waveforms on top of the mound are mostly covered, and hence now stabilised, by coral.

The facies definitions and mapping of Thérèse Mound were partly based on the work of Dekindt (2001). A more extensive description of the video data is also given in Wheeler et al. (2005), as part of the detailed analysis of local sedimentary processes in the Belgica Mound province. In total, 6 different facies were recognised in the video data here. They differ a little from the facies definitions used in the previous two case studies, as the environment around Thérèse Mound differs so much from the Hovland and Magellan Mound provinces (Fig. 11). The following facies types were found:

1.   sandy sediment (without faunal occurrence)
2.   coral debris
3.   dead coral
4.   limited amount of live coral (on average 25 to 30 % of the video coverage)
5.   abundant live coral (on average 65 to 70 % of the video coverage)
6.   live coral sitting between rippled sand

The resulting facies map (Fig. 10) shows a very large abundance of coral (live, dead or debris). Only in the eastern part of the dives, rippled sands are found. The richest coral areas, with the highest amount of live coral (and its associated fauna) are found on the highest parts of Thérèse Mound and the smaller mound to the

Fig. 10 Overview map and seabed facies interpretation of CARACOLE dives 124 and 125 on Thérèse Mound, overlaid on TOBI sidescan sonar imagery. The bathymetry information is extracted from the data collected during the R/V Polarstern cruise

northeast. Especially on the western upper flank of Thérèse Mound, a large field of abundant live coral is located. It has to be noted that this is the area where no sediment waves were encountered on the multibeam map (Hinsinger 2002). These areas of abundant live coral occurrence (facies 5) are very rich. Corals occur in thick bunches, and no patches of sediment can be seen between them. The main coral species on Thérèse Mound are *Lophelia pertusa* and *Madrepora oculata* again,
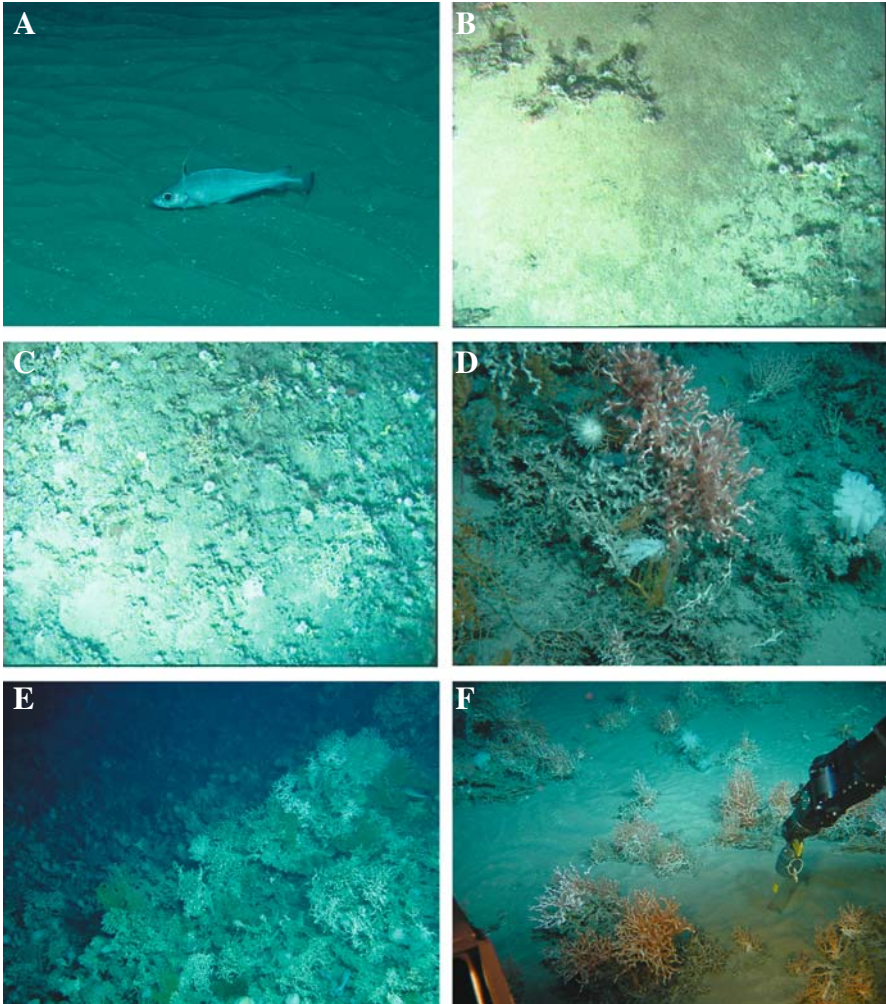
Fig. 11 Different seabed facies recognised on Thérèse Mound and its surroundings: **A** rippled sand, **B** coral debris, **C** dead coral, with a high abundance of sponges, **D** limited amount of live coral, **E** abundant live coral, **F** live coral sitting between rippled sand. The abundant live coral (**E**) is sitting on a steep flank, and the morphology of large-scale waveforms can be seen underneath the coral framework. Note also that the direction of the ripples between the corals (**F**) is variable, showing how the bottom currents are deflected by the coral colonies. All photographs with courtesy to IFREMER

but also large amounts of cnidaria and sponges were found (H. Zibrowius and A. Freiwald pers. comm.). Several cables and lost fishing nets were hooked between the corals, and in some locations the framework was damaged. Evidence of trawling activities between the Belgica Mounds is also given by Wheeler et al. (2001). It indicates the importance of the rich faunal community, associated with the mounds, attracting fishing activity in the area.

The areas of dead coral framework are very extensive. The northern, more rounded part of Thérèse Mound shows a large area of dead coral, and towards the east a vast plain of dead coral is located as well. Remarkable is the high abundance of sponges (*Aphrocallistes* sp.; J. Vacelet pers. comm.) in these areas, which seem to have colonised the dead coral frameworks. However, in many cases only the sponge skeleton is left, indicating that also for them the environments are not optimal any more (Dekindt 2001). Between the coral frameworks patches of (non-rippled) sediment can be seen.

On the eastern flank of Thérèse Mound, large sediment waves were seen on the video records, which correspond to the waveforms identified on the multibeam bathymetry data (Hinsinger 2002). On the upper slope they are fully covered with (live) coral, but further down the slope the corals seem to prefer the wave crests or the south-facing flanks of the waves. The troughs and the north-facing flanks contain coral rubble and patches of sandy sediment. Further towards the east, the less and less live coral can be seen, and the patches of sediment show some ripple marks. Some of these sediment waves are quite steep, as their slope is supported by the coral framework. They are interpreted as relict features, as they are overgrown by corals.

The sandy sediment of facies 1 consists of well-sorted, loosely packed sands, causing the patches of very low backscatter on the TOBI sidescan sonar images. The nature of the sand is not known, but it probably contains a large amount of foraminifera, as is reported for the upper sediment layer elsewhere in the area. Generally these sands are rippled, with ripples having a wavelength in the order of 10 cm and a height in the order of 1 cm (Wheeler et al. 2005). Besides the ripples, sandwaves of larger scale can be recognised on the video data of the same area. Their size (estimated roughly from the video images) seems to match the size of the sediment waves revealed by the high-resolution multibeam image further to the west. Most of them also have an E-W strike, indicating again a northward or southward current. Recent additional observations with a multibeam system mounted on the ROV Victor 6000 have confirmed the presence and pattern of these sandwaves (Foubert et al. 2005).

The zone with facies 1 and 6 takes a particular position in these ROV dives. The small structures seen on high-resolution sidescan sonar data (Wheeler et al. 2000) and described as small positive structures from the TOBI sidescan records indeed proved to be small mounds, called 'Moira Mounds'. As stated above, these are described in detail by Wheeler et al. (2005).

Discussion

Different environments

The sidescan sonar and ROV data presented here clearly show the very different seabed environments in the Belgica and Magellan/Hovland Mound provinces. Similar results were also reported by Huvenne et al. (2002), who found that image texture analysis of selected OreTech sidescan sonar details in the Hovland and Belgica provinces revealed considerable differences in terms of textural homogeneity and entropy. This points to actual differences in the nature of the sedimentary environment between the two provinces, which affect the present-day development of the mounds in these areas.

The Belgica Mound province appears to be a much more dynamic environment than the Magellan and Hovland provinces. Many different types of bedforms are encountered in this area, sediments are coarser, the bathymetry is more irregular and the province is located on a steeper slope. All this indicates a stronger influence of local bottom currents. The highest residual currents at the seabed in the Porcupine Seabight were indeed measured along the eastern slope (11 cm/s, at 8 m above the seabed, in a NNW-ward direction; Pingree and Le Cann, 1989), while mean values for the northern Porcupine Seabight do not exceed 5 cm/s (White 2001). Additionally, Pingree and Le Cann (1989, 1990) found evidence for strong diurnal tides on the eastern slope of the Porcupine Seabight with maximum instantaneous current speeds of 54 cm/s in a northerly direction. Rice et al. (1990) indicated that the seabed slope in this area is also close to the characteristic slope of the M_2 internal tide, and hence that local enhancement of bottom currents, associated with increased turbulence in the water column, is likely. De Mol (2002) also mentioned the role of the interface between the ENAW and MOW, possibly contributing to this effect. These tidal effects may influence the creation of the bedforms, or may play a role in the formation of the ripple patterns in the sandy areas, such as the Moira Mound area. In any case they add to the overall turbulence and dynamics of the Belgica Mound province.

Moreover, the overall image of the sedimentary pattern and bedform occurrence in the Belgica province, as it is described above, fits very well with the observations of a northward directed slope- or bottom current. As suggested by Van Rooij et al. (2003), this current is probably focused along the blind channel in the southern part of the area, creating deep scouring there, and allowing hemipelagic sedimentation in the adjacent areas. Further to the north, where the channel becomes shallower, the current might spread over a wider area. This results in local current intensifications between the mounds and the creation of coarser lag sediments. The finer fractions are winnowed out, and are partly deposited besides or towards the north of the source areas, in locations with a facies-3 backscatter pattern. Where the northward current meets an obstacle (such as a southward facing flank), the heaviest particles of the bedload cannot be transported any further, and are deposited in patches of well-sorted sediments (sands). On the opposite flank of the downslope gullies, erosion occurs. A similar process was suggested by Flood (1988) and by Masson et

al. (2002) to explain the formation and migration of sediment waves of mixed grain size composition under contour currents. Hence the very low backscatter patches are witnesses of a fairly continuous, long-term process.

The other features, for which the sand deposits are the sediment source, such as the striations or the sediment waves around Thérèse Mound, also point to a N/ S-directed current influence. The morphology of the barchan dunes specifically indicates a northward current. However, these bedforms might be created by more instantaneous events. For example, on tidally influenced shelves, a mean peak spring near-surface current of ca. 100 cm/s would be necessary to create the striations (sand ribbons), while for the barchan dunes some 75 cm/s would be sufficient (Stride 1982). The necessary currents at the seabed seem to be a little lower; Wynn and Stow (2002), for example, suggest that values of 40 cm/s would be sufficient to create barchan dunes on the continental slope. Still, this value is much higher than the average residual current speed in the Belgica province, which indicates that the barchan dunes and striations are not formed during a continuous process, but are rather related to the episodic peak current speeds caused by the tidal processes.

Some of the bedforms could also be fossil features, created by a higher current speed some time ago. The overgrown sediment waves on Thérèse Mound are a possible example of this. However, they are probably still of post-glacial origin, because the current speeds in the area were strongly reduced during glacial times, as is indicated by the much finer glacial deposits found in gravity and piston cores (Foubert 2002; Van Rooij et al. subm.). The other features linked to the patches of well-sorted sands, seem to be more recent.

Compared to this current-influenced area, the Magellan and Hovland provinces are much more quiet. No bedforms are found, the sediment is finer, is bioturbated and watery, related to the lower overall current speeds. However, higher current speeds must have affected the area before, as is seen from the moat formation around both Magellan and Hovland Mounds and from the scouring of the blind channels/elongated depressions in the Hovland province. Probably tidal currents may have played a role in some of the scouring processes: due to the circulation around the Porcupine Bank, the present-day diurnal tidal currents in the area are enhanced, especially at the seabed, in a N-S direction, the elongation direction of the moats (Mohn et al. 2002). However, they are not strong enough any more to create any reasonable amount of scouring around the mounds: the moats are slowly filled in. This is illustrated by seismic profiles (Huvenne et al. 2003), by the smooth backscatter pattern on the sidescan sonar images and by the facies mapping: the moats contain the same type of bioturbated fine sediment as encountered elsewhere in the sedimentary areas of these two mound provinces. It appears that since the initiation of the mounds, probably in (Late) Pliocene times (De Mol et al. 2002; Van Rooij et al. 2003), the northern Porcupine Seabight gradually became quieter, and that, in general, the amount of current influence during the development of the mounds decreased.

Overall, it may be clear that throughout the development history of the mounds, the water mass structure and associated current regimes in the Porcupine Seabight,

together with the sedimentation patterns, have changed considerably. For example, one of the most prominent factors influencing the oceanographic and sedimentary conditions in the North Atlantic during that time interval, is the climatic variability associated with the glacial and interglacial cycles. Schönfeld and Zahn (2000), for example, argue that during the last glaciation, the pattern of the MOW along the European margin was seriously different compared to the present situation, and that this water mass did not occur north of Spain. Such a switch-on and switch-off of the MOW in the Porcupine Seabight region must have had severe consequences for the development of internal tides, for example, or for the circulation along the Porcupine Bank, due to a change or disappearance of the ENAW/MOW interface and a change in the density structure of the water column. Also the characteristics of the ENAW itself will have changed under the different climatic conditions. Hall and McCave (1998) and Foubert (2002) report a current reduction and higher sediment input during glacial times in the area, witnessed by a higher sedimentation rate and finer deposits. Other changes in sea level or in density structure may also have affected the seabed environment in the area since the Late Pliocene. A complete understanding of the paleoceanography and of the reason why the mound environment in the northern Porcupine Seabight became quieter, will require much more research effort.

The only place in the Magellan/Hovland provinces where some non-deposition can be found on the present-day seabed, is along one of the channel flanks in the Hovland province. This is the only serious difference observed in the present-day sedimentary environment between the Magellan and Hovland provinces: the presence of the channels, which probably still focus the limited bottom currents in the Hovland area. De Mol (2002) showed from seismic profiles that channels and erosional depressions have been present in this area for a long time, and therefore are a key feature distinguishing both provinces in general. The Hovland Mounds are specifically located along these channels and depressions, and could benefit from the enhanced currents. Scouring in the Magellan province only happened as a result of the presence of the mounds, and it appears that current enhancement in this area never reached the same levels as in the depressions/channels in the Hovland province. This may have been an important factor explaining why the Hovland Mounds could develop to much larger structures, and could escape early burial as happened with the Magellan Mounds.

Stages of mound development

Because the Porcupine Seabight has such different environments, also mounds with a very different appearance can be found. They can be interpreted tentatively as different stages of mound development:

Possible incipient mounds: the Moira-type mounds could be considered as an example of incipient mound structures, or at least as an example of coral expansion or (re)colonisation of a new area. The small mounds, only a few metres high, seem to have initiated fairly recently: the 3.5 kHz profiles through small mounds show parallel stratification directly under the structures at the seabed (Fig. 9B).

Therefore it appears that these mounds are very shallow, and not rooted deeper in the sedimentary sequences. Possible processes behind their formation are outlined by Wheeler et al. (2005).

It has to be noted, however, that the finding of these mounds of presumed initial stage is a remarkable fact, as no other examples of mound initiation have been recognised on seismic records of the area (De Mol et al. 2002). It is possible that other Moira-type mounds were formed in previous times, but became buried quickly, before they could reach a considerable height. It is also possible that a specific sediment/current environment is necessary. Other coral colonies do not expand vertically into initial mounds, and even do not survive for a very long time (e.g., the extended area of dead coral east and north of Thérèse Mound).

A fully 'active' mound: once small mounds have survived the initial stages, they might develop further, and expand until they reach a stage in which they form large structures on the seabed, carrying a healthy, rich faunal community, based on coral species such as *Lophelia* and *Madrepora*. Thérèse Mound is an example of such a 'grown-up' individual. On the western upper flank of this mound large amounts of live coral and associated fauna were found. However, the vast areas of dead coral on the northern part of the mound indicate that also Thérèse Mound has known even more prolific times. The position of the live corals again is closely related to the current pattern around the mound: the western upper flank is the steepest part of the mound, and may therefore have the highest current speeds. This was confirmed during the ROV dives: the southern part of the mound, and especially the western flank, was the area where the instrument had the highest difficulties to stay on track, as a result of the currents (Olu-Le Roy et al. 2002).

The coverage of nearly the entire mound with sediment waves is an enigmatic observation. As stated above, most of these bedforms are relict features, because they are overgrown with corals and coral framework material. They imply that there was a period, before the present-day coral growth, when mobile sediment was reworked and/or deposited on the flanks and the northern ridge of Thérèse Mound. It is possible that the process of sediment dynamics reached as far to the east as the area of the Moira Mounds, and even beyond, as sediment waves have been found there too. It is however also possible that these waves were formed in a similar, but later process, because they are not yet overgrown. To what extent these processes of sediment wave formation were the result of changing environments at, for example, glacial/interglacial boundaries, related to the reintroduction of the MOW in the area and the establishment or shift in the interface between the MOW and ENAW, is as yet unknown, and asks for more detailed sedimentological studies. After the deposition of the sediment waves, corals have colonised the flanks of Thérèse Mound again, first choosing the most favourable places: the ridge crests of the waves, and their upcurrent flanks. Higher up the slope the corals and fauna could even spread over the entire waveforms. However, they preserved the morphology, and in some places maybe even enhanced it, by growing preferentially on the ridge crests, and reinforcing these with their framework structure.

It is remarkable that in the area where no sediment waves were mapped, on the upper western flank of Thérèse Mound, the coral life seems to be most abundant. It

is possible that this area was too steep, and hence currents were different, resulting in no formation of sediment waves. It is also possible that the prolific life in the meantime has smoothed out all traces of bedforms. One could also wonder if there was a similar pattern of coral growth on Thérèse Mound before the deposition of the bedforms. If that was the case, the rich communities on the upper western flank probably inhibited the deposition of well-shaped sediment waves, and baffled most of the sediment between the coral framework. From that point of view it is then tempting to see this area as the origin from where the recolonisation of the sediment waves could start, under a process similar to that seen nowadays around the Moira Mounds.

It has to be noted that similar waveforms were observed during two ROV dives (CARACOLE cruise) on a mound in the Logachev province, Rockall Trough (Olu-Le Roy et al. 2002). In that area the mounds and waveforms are fully covered with corals and coral framework. Wheeler et al. (subm.) suggest that the waveforms could also be built by the coral colonies, arranging themselves in a lined-up pattern that could be beneficial for their food supply. The waveforms in the Belgica province however seem to be rather related with the sedimentary processes in the area, as sediment waves of similar dimensions and with similar E-W strike have been found in large parts of the province (e.g., De Mol et al. 1999).

A mound 'on retirement': an example of a mound that is not at its full strength any more, and that slowly might 'give up', is Propeller Mound. There is still some live coral, but it is rather scattered over single colonies or thickets, set between bunches of dead coral. There seems to be, by far, a poorer biological community in comparison with the upper flanks of Thérèse Mound. The live corals again have chosen the more elevated or exposed positions, trying to profit from an enhanced current at the mound ridges or the tops of the spurs.

The outcropping crust and nanoplankton ooze at one of these spurs seems to indicate some amount of erosion within the (recent) past. Also the gravel and dropstone facies originated from winnowing of the fine sediments, and points to a certain amount of erosion. This is confirmed by recent datings of corals in gravity cores on Propeller Mound (Dorschel et al. subm.). Large hiatuses are found in the stratigraphy of the on-mound cores, while in off-mound cores (from the moats or from even further away), these hiatuses were not present. Both the fully glacial and the peak interglacial sediments appear to be removed from the mound, leaving only interstadial strata (Rüggeberg et al. subm.). In some places on the mound slope, the coral rubble at the surface of Propeller Mound has ages of 140 ka and more (Dorschel et al. subm.). Most probably these coral fragments have been exposed due to erosion, or were exposed higher up the mound, and have moved down along the steep slopes.

On the whole, many of the Hovland Mounds appear very similar to Propeller Mound. Several of them have spurs, probably due to the current action shaping them. The largest mounds are located close to the channels, indicating that these probably were substantial in the focusing of enhanced currents. It appears as if most of the Hovland Mounds, although not at their full strength any more, have managed to avoid complete burial thanks to their size. They reach high enough above the

seabed to create some extra current enhancement, and in this way to preserve some coral cover.

A mound about to die: the fate of Mound Perseverance (despite its fierce name) seems to be quite clear. If there are no changes in the sedimentation or current patterns in the Magellan province, this mound will end up in the same situation as the other Magellan Mounds: buried by the hemipelagic sediment. Most of the material encountered is debris or dead coral, often covered already with a thin veneer of sediments. The live coral which is present can only be found at the mound top or on a spur, and consists of a few meagre thickets. However it is striking that these thickets are placed on a surface of coral debris, and not amidst bunches of dead coral. They could be the last few bits of coral surviving on the mound, or may have just recolonised the coral debris, on which they could find a hard substrate to start growing. Again one can wonder if part of the debris is older material, exposed by a phase of erosion. However, the present-day process clearly is one of sedimentation, shown by the bioturbated sediment covering the lower flanks of the mound and the moats. It probably causes the clear depth-dependence of the different facies on the mound, a characteristic absent on Propeller Mound for example, because of its complex shape, its position at the head of a channel, and its interaction with the limited bottom currents.

The different stages of mound activity presented above, illustrate that both phases of erosion (such as on Propeller Mound) and deposition (such as on Thérèse Mound, creating the sediment wave patterns) can occur on mounds. Dorschel (2003), for example, presents a model of phased mound growth for Propeller Mound, explaining the hiatuses found on that coral bank by periods of erosion. From that point of view, one could expect that, if the oceanographic and environmental conditions became more favourable again for abundant coral growth in the Hovland province, the mounds would soon be recolonised, as there are many hard substrates available for the corals to settle. However, outside the mounds, in the homogeneous fine sediment areas, coral settlement would be less easy, and the Hovland Mounds would form islands surrounded by hemipelagic sediments. A similar conclusion can be drawn for the Magellan Mounds, which are even smaller and hence would experience more difficulties for recolonisation. The Belgica province on the other hand offers plenty of settling grounds (coarse lag deposits, coral rubble), and the irregular bathymetry provides many local highs where currents can be enhanced.

Conclusions

The first analysis of the TOBI sidescan sonar mosaics and ROV Victor 6000 video imagery of the Porcupine Seabight reveals that the present-day environment is markedly different in the three provinces of coral banks in the area. Especially between the north and the east of the Seabight there is a clear difference, with more quiet, hemipelagic conditions in the Magellan and Hovland provinces and a more dynamic environment in the Belgica province, which is affected by a northward (episodically strong) current regime and sediment transport. This results in mound

structures with a different seabed appearance: the most 'active' mounds were found in the Belgica province, together with small structures that possibly could be interpreted as initial mounds. The Magellan Mounds on the other hand are clearly becoming buried, while the Hovland Mounds take an intermediate position. Partly due to their size, the latter are not buried like the Magellan Mounds, but they do not show the same abundance of live coral as the Belgica Mounds.

Overall, the Porcupine Seabight forms a unique study laboratory, containing large numbers of mounds at different stages of development, displaying both conditions of erosion and sedimentation. These different appearances and environmental regimes illustrate the importance of local current and sedimentation regimes influencing mound development.

Acknowledgements

References

Beyer A, Schenke HW, Klenke M, Niederjasper F (2003) High resolution bathymetry of the eastern slope of the Porcupine Seabight. Mar Geol 198: 27-54

De Bergé B (2000) Epi- en endofauna geassocieerd met koudwaterkoralen in de NO Atlantische Oceaan. MSc thesis, Marine Biol Dept, Univ Gent, 133 pp

De Haas H, Grehan A, White M, shipboard scientific crew (2000) Cold-water corals in the Porcupine Bight and along the Porcupine and Rockall Bank margins, RV Pelagia cruise M2000 (64PE165). Den Helder, R Netherland Inst Sea Res (NIOZ), 25 pp

De Haas H, Huvenne V, Wheeler A, Unnithan V, shipboard scientific crew (2002) A TOBI side scan sonar survey of cold-water coral carbonate mounds in the Rockall Trough and Porcupine Sea Bight, RV Pelagia cruise M2002 (64PE197). Den Helder, R Netherland Inst Sea Res (NIOZ), 44 pp

De Mol B (2002) Development of coral banks in Porcupine Seabight (SW Ireland). A multidisciplinary approach. PhD thesis, Fac Sci, Dept Geol Soil Sci, Univ Ghent, 363 pp

De Mol B, Friend P, Akhmetzhanov A, Ivanov M, de Haas H, Belenkaya I, Stadnitskaya A (1999) Porcupine Seabight: short visit. In: Kenyon NH, Ivanov MK, Akhmetzhanov AM (eds) Geological processes on the Northeast Atlantic Margin, UNESCO, Paris, IOC Tech Ser 54: 34-47

De Mol B, Van Rensbergen P, Pillen S, Van Herreweghe K, Van Rooij D, McDonnell A, Huvenne V, Ivanov M, Swennen R, Henriet JP (2002) Large deep-water coral banks in the Porcupine Basin, southwest of Ireland. Mar Geol 188: 193-231

Dekindt K (2001) Contribution a l'étude de la distribution spatiale des coraux, caractérisation des differents facies et de la faune associée sur le site du Mont Thérèse. Brest, IFREMER, Dépt Environ Profond, 32 pp

Dorschel B (2003) Late Quaternary development of a deep-water carbonate mound in the northeast Atlantic. PhD thesis, Univ Bremen, 90 pp

Dorschel B, Hebbeln D, Rüggeberg A, Dullo W-Chr (submitted) Carbonate budget of a cold-water coral carbonate mound: Propeller Mound, Porcupine Seabight. Int J Earth Sci

Flood RD (1988) A lee wave model for deep-sea mudwave activity. Deep-Sea Res 35: 973-983

Foubert A (2002) Een paleomagnetische studie met zeer hoge resolutie op Calypso-kernen in Porcupine Seabight, ten zuidwesten van Ierland. MSc thesis, Dept Geol Soil Sci, Univ Gent, 151 pp

Foubert A, Beck T, Wheeler AJ, Opderbecke J, Grehan A, Klages M, Thiede J, Henriet JP, Polarstern ARK-XIX/3a Shipboard Party (2005) New view of the Belgica Mounds, Porcupine Seabight, NE Atlantic: preliminary results from the Polarstern ARK-XIX/3a ROV cruise. In: Freiwald A, Roberts JM (eds) Cold-water Corals and Ecosystems. Springer, Berlin Heidelberg, pp 403-415

Freiwald A (1998) Geobiology of *Lophelia pertusa* (Scleractinia) reefs in the North Atlantic. Habilitation thesis, Bremen Univ, 116 pp

Freiwald A, Shipboard Party (2002) RV Poseidon Cruise 292. 86 pp

Freiwald A, Dullo W-Chr, Shipboard Party (2000) RV Poseidon cruise 265, Thorshavn - Galway – Kiel. 50 pp

Freiwald A, Hühnerbach V, Lindberg B, Wilson JB, Campbell J (2002) The Sula reef complex, Norwegian shelf. Facies 47: 179-200

Hall IR, McCave IN (1998) Late glacial to recent accumulation fluxes of sediments at the shelf edge and slope of NW Europe, 48-50°N. In: Stoker MS, Evans D, Cramp A (eds) Geological processes on continental margins: sedimentation, mass-wasting and stability. Geol Soc London Spec Publ 129: 339-350

Henriet JP, De Mol B, Pillen S, Vanneste M, Van Rooij D, Versteeg W, Croker PF, Shannon PM, Unnithan V, Bouriak S, Chachkine P (1998) Gas hydrate crystals may help build reefs. Nature 391: 648-649

Henriet JP, De Mol B, Vanneste M, Huvenne V, Van Rooij D, 'Porcupine-Belgica' 97, 98 and 99 shipboard parties (2001) Carbonate mounds and slope failures in the Porcupine Basin: a development model involving fluid venting. Geol Soc London Spec Publ 188: 375-383

Henriet JP, Guidard S, ODP "Proposal 573" Team (2002) Carbonate mounds as a possible example for microbial activity in geological processes. In: Wefer G, Billet D, Hebbeln D, Jørgensen BB, Schlüter M, van Weering T (eds) Ocean Margin Systems. Springer, Berlin Heidelberg, pp 439-455

Hinsinger V (2002) Analyse et définition d'un module d'investigation sous-marine proche du fond. MSc thesis, Brest, Ensieta, 49 pp

Hovland M, Croker PF, Martin M (1994) Fault-associated seabed mounds (carbonate knolls?) off western Ireland and north-west Australia. Mar Petrol Geol 11: 232-246

Huthnance JM (1986) The Rockall slope current and shelf-edge processes. Proc R Soc Edinburgh 88B: 83-101

Huvenne V (2003) Spatial geophysical analysis of the Magellan carbonate build-ups and the interaction with sedimentary processes: key to a genetic interpretation? PhD thesis, Fac Sci, Dept Geol Soil Sci, Univ Ghent, 285 pp

Huvenne VAI, Blondel Ph, Henriet JP (2002) Textural analyses of sidescan sonar imagery from two mound provinces in the Porcupine Seabight. Mar Geol 188: 323-341

Huvenne VAI, De Mol B, Henriet JP (2003) A 3D seismic study of the morphology and spatial distribution of buried coral banks in the Porcupine Basin, SW of Ireland. Mar Geol 198: 5-25

Huvenne VAI, Bailey WR, Shannon P, Naeth J, Di Primio R, Henriet JP, Horsfield B, de Haas H, Wheeler A, Olu-Le Roy K (submitted) The Magellan mound province in the Porcupine Basin. Int J Earth Sci

Kenyon NH (1986) Evidence from bedforms for a strong poleward current along the upper continental slope of northwest Europe. Mar Geol 72: 187-198

Kenyon NH, Ivanov MK, Akhmetzhanov AM (1998) Cold-water carbonate mounds and sediment transport on the Northeast Atlantic Margin. IOC Tech Ser, Paris, UNESCO 52, 178 pp

Kenyon NH, Ivanov MK, Akhmetzhanov AM (1999) Geological processes on the Northeast Atlantic Margin. IOC Tech Ser, Paris, UNESCO 54, 141 pp

Kenyon NH, Akhmetzhanov AM, Wheeler AJ, van Weering TCE, de Haas H, Ivanov MK (2003) Giant carbonate mud mounds in the Southern Rockall Trough. Mar Geol 195: 5-30

Le Danois E (1948) Les profondeurs de la mer. Payot, Paris, 303 pp

LeBas T (2002) PRISM - Processing of Remotely-sensed Imagery for Seafloor Mapping. Version 4. Southampton, Southampton Oceanogr Cent, 196 pp

Masson DG (2001) Sedimentary processes shaping the eastern slope of the Faeroe-Shetland Channel. Cont Shelf Res 21: 825-857

Masson DG, Howe JA, Stoker MS (2002) Bottom-current sediment waves, sediment drifts and contourites in the northern Rockall Trough. Mar Geol 192: 215-237

Mohn C (2000) Über Wassermassen und Strömungen im Bereich des europäischen Kontinentalrandes westlich von Irland. PhD thesis, FB Geowiss Hamburg, Univ Hamburg, 122 pp

Mohn C, Bartsch J, Meinke J (2002) Observations of the mass and flow field at Porcupine Bank. J Mar Sci 59: 380-392

Mortensen PB, Hovland M, Brattegard T, Farestveit R (1995) Deep-water bioherms of the scleractinian coral *Lophelia pertusa* (L.) at 64°N on the Norwegian shelf: structure and associated megafauna. Sarsia 80: 145-158

Mortensen PB, Hovland MT, Fosså JH, Furevik DM (2001) Distribution, abundance and size of *Lophelia pertusa* coral reefs in mid-Norway in relation to seabed characteristics. J Mar Biol Ass UK 81: 581-597

Olu-Le Roy K, Caprais J-C, Crassous P, Dejonghe E, Eardley D, Freiwald A, Galeron J, Grehan A, Henriet JP, Huvenne V, Lorance P, Noel P, Opderbecke J, Pitout C, Sibuet M, Unnithan V, Vacelet J, van Weering T, Wheeler A, Zibrowius H (2002) CARACOLE cruise N/O L'Atalante & ROV Victor. 1 + 2, Brest, IFREMER

Opderbecke J, Pitout C (2001) Cartographie acoustique et optique avec Victor. Brest, IFREMER, 27 pp

Pingree RD, Le Cann B (1989) Celtic and Armorican slope and shelf residual currents. Progr Oceanogr 23: 303-338

Pingree RD, Le Cann B (1990) Structure, strength and seasonality of the slope currents in the Bay of Biscay region. J Mar Biol Ass UK 70: 857-885

Pratje O (1924) Korallenbänke in tiefem und kühlem Wasser. Zbl Mineral Geol Paläont 1924: 410-415

Rice AL, Thurston MH, New AL (1990) Dense aggregations of a hexactinellid sponge, *Pheronema carpenteri,* in the Porcupine Seabight (northeast Atlantic Ocean) and possible causes. Progr Oceanogr 24: 179-196

Rice AL, Billet DSM, Thurston MH, Lampitt RS (1991) The Institute of Oceanographic Sciences biology programme in the Porcupine Seabight: background and general introduction. J Mar Biol Ass UK 71: 281-310

Rogers AD (1999) The biology of *Lophelia pertusa* (LINNAEUS 1758) and other deep-water reef-forming corals and impacts from human activities. Int Rev Hydrobiol 84: 315-406

Rüggeberg A, Dullo W-Chr, Dorschel B, Hebbeln D (submitted) Environmental changes and growth history of Propeller Mound, Porcupine Seabight: evidence from benthic foraminiferal assemblages. Int J Earth Sci

Schönfeld J, Zahn R (2000) Late Glacial to Holocene history of the Mediterranean Outflow. Evidence from benthic foraminiferal assemblages and stable istotopes at the Portuguese margin. Palaeogeogr Palaeoclimatol Palaeoecol 159: 85-111

Sinclair IK, Shannon PM, Williams BPJ, Harker SD, Moore JG (1994) Tectonic control on sedimentary evolution of three North Atlantic borderland Mesozoic basins. Basin Res 6: 193-218

Stride AH (1982) Offshore tidal sands. Chapman and Hall, London, 222 pp

Swennen R, Cronin B, Ivanov M, Kozlova E, Wheeler AJ, Akhmetzhanov A, Sautkin A, Van Rooij D, Zaragosi S, Mazurenko L, Degryse C, Sumida P, Satur N, Kennedy R, Akhmanov G, Belen'kaya I, Pillen S, Naumov Y, Stadnitskaya A, De Mol B, Balashova A, Saprykina A (1998) Bottom sampling results. In: Kenyon NH, Ivanov MK, Akhmetzhanov AM (eds.) Cold-water carbonate mounds and sediment transport on the Northeast Atlantic margin. UNESCO, Paris, IOC Tech Ser 52: 59-97

Thomson CW (1873) The depths of the Sea. MacMillan, London, 527 pp

Van Rooij D, Blamart D, Unnithan V (2001) Cruise Report MD 123 - Géosciences: Leg 2, part GEOMOUND. 67 pp

Van Rooij D, De Mol B, Huvenne V, Ivanov M, Henriet JP (2003) Seismic evidence of current-controlled sedimentation in the Belgica mound province, upper Porcupine slope, southwest of Ireland. Mar Geol 195: 31-53

Van Rooij D, Blamart D, Wheeler A, Kozachenko M, Richter T, Henriet JP (submitted) Quaternary drift sediment dynamics in the Belgica mound province, Porcupine Seabight: a multidisciplinary approach. Int J Earth Sci

Wheeler A, Degryse C, Limonov A, Kenyon N (1998) The northern Porcupine Seabight. In: Kenyon NH, Ivanov MK, Akhmetzhanov AM (eds) Cold-water carbonate mounds and sediment transport on the Northeast Atlantic margin. UNESCO, Paris, IOC Tech Ser 52: 40-54

Wheeler AJ, Bett B, Billett DSM, Masson DG, Scientific Party, Officers and Crew of RRS Discovery 248 (2000) High resolution side-scan sonar mapping of deep-water coral mounds: surface morphology and processes affecting growth. Eos, Trans, Amer Geophys Union 81: F638

Wheeler AJ, Billet DSM, Masson DG, Grehan A (2001) The impact of demersal trawling on NE Atlantic coral ecosystems with particular reference to the northern Rockall Trough. ICES Ann Sci Conf, Oslo

Wheeler AJ, Kozachenko M, Beyer A, Foubert A, Huvenne VAI, Klages M, Masson DG, Olu-Le Roy K, Thiede J (2005) Sedimentary processes and carbonate mounds in the Belgica Mound province, Porcupine Seabight, NE Atlantic. In: Freiwald A, Roberts JM (eds) Cold-water Corals and Ecosystems. Springer, Berlin Heidelberg, pp 571-603

Wheeler AJ, Beyer A, Freiwald A, de Haas H, Huvenne VAI, Kozachenko M, Olu-Le Roy K (submitted). Morphology and environment of deep-water coral mounds on the NW European Margin. Int J Earth Sci

White M (2001) Hydrography and physical dynamics at the NE Atlantic margin that influence the deep-water cold coral reef ecosystem. Dept Oceanogr, NUI Galway, Ireland, 31 pp

Wynn RB, Stow DAV (2002) Classification and characterisation of deep-water sediment waves. Mar Geol 192: 7-22

Sedimentary processes and carbonate mounds in the Belgica Mound province, Porcupine Seabight, NE Atlantic

Andrew J. Wheeler[1], Maxim Kozachenko[2], Andreas Beyer[3], Anneleen Foubert[4], Veerle A. I. Huvenne[4,5], Michael Klages[3], Douglas G. Masson[5], Karine Olu-Le Roy[6], Jörn Thiede[3]

[1] Department of Geology, Environmental Research Institute, University College Cork, Ireland
  (a.wheeler@ucc.ie)
[2] Coastal and Marine Resources Centre, Environmental Research Institute, University College Cork, Ireland
[3] Alfred Wegener Institute for Polar and Marine Research, Columbusstr., D-27568 Bremerhaven, Germany
[4] Renard Centre of Marine Geology, Gent University, Krijgslaan 281, S8, B-9000 Gent, Belgium
[5] Southampton Oceanography Centre, Empress Dock, Southampton, SO14 3ZH, UK
[6] IFREMER, Centre de Brest, BP 70, F-29280 Plouzané, France

Abstract. Carbonate mounds (up to 200 m high) formed from the accumulated remains of cold-water corals (principally *Lophelia pertusa* and *Madrepora oculata*), associated calcareous fauna and interstitial sediment are present at 500-1000 m water depths west of Ireland. Seabed mapping datasets (side-scan sonar, multibeam echosounder, sub-bottom profiler and underwater video imagery) are presented here from the Belgica Mound province on the eastern Porcupine Seabight margin. The data, integrated within a Geographic Information System (GIS), provide an environmental context to mound development. Analysis of this multidisciplinary dataset and resultant facies map highlight differing sedimentary processes (e.g., sediment wave, barchan dune, gravel lag and sand ribbon development) operating under strong northward flowing bottom currents with sandy sediment supply where the influence of mound topography on benthic currents and sediment pathways is evident. Correspondingly, benthic current pathways and associated sediment transport also exert an influence on carbonate mound surface morphology and growth. Giant mounds show a transition from sediment waves that, with increasing coral colonisation, give way to banks of coral towards the mound summits. Smaller

mound features (Moira Mounds) show sand entrapment as an important mound-forming process.

Keywords. Northeast Atlantic, Porcupine Seabight, carbonate mounds, sedimentary facies, side-scan sonar, sub-bottom profiler, deep-water corals

Introduction

Deep-water corals are common along the European continental margin (e.g., Wilson 1979a; Freiwald 1998, 2002; Rogers 1999; Freiwald et al. 2002; Wheeler et al. submitted) where they are often found in close association with other organisms as part of a diverse ecosystem (Olu-Le Roy et al. 2002). In some cases the corals form reef communities (Freiwald 2002). Over time their accumulated remains, the remains of associated organisms and interstitial sediment have formed carbonate mounds (referred to as coral banks by De Mol et al. 2002). These vary in dimensions from a few metres high and tens of metres across (e.g., the Darwin Mounds; Masson et al. 2003) to giant features often greater than 100 metres tall and several kilometres across (e.g., De Mol et al. 2002; Kenyon et al. 2003; van Weering et al. 2003). The mounds take a variety of morphological forms dictated by environmental controls on growth and the morphology of the underlying substrate (Wheeler et al. submitted).

Deep-water corals and associated carbonate mounds occur in dynamic hydrological settings with high current speeds, enhanced organic particulate food delivery and reduced fine-grained sedimentation seen as important to coral vitality (Freiwald 1998). Conditions generating enhanced surface productivity, hence supplying food to underlying communities, are also important. Seabed mapping exercises have located mounds and also revealed sedimentary processes in the environs of the mounds. These exercises show evidence of strong benthic currents including evidence of seabed erosion (e.g., Porcupine Bank: Wheeler et al. 2005) and sediment transport (e.g., Wheeler et al. 2000; Kozachenko et al. 2003a, b). In some cases, the lack of a rigorous benthic environment is coincident with poor to sporadic coral cover (e.g., the Hovland Mounds: Huvenne et al. 2005). Results and an interpretation of seabed mapping surveys of the Belgica Mound province in the Porcupine Seabight are presented here.

The Porcupine Seabight is a north-south trending basin on the continental margin of the west coast of Ireland (Fig. 1A). Two distinct clusters of carbonate mounds (provinces) are found on the margins of this basin: the Hovland-Magellan province on the northern margin (De Mol et al. 2002; Huvenne et al. 2005; Wheeler et al. submitted) and the Belgica Mound province on the eastern margin from approximately 51.17°N to 51.60°N and from 11.60°W to 11.80°W (De Mol et al. 2002; Fig. 1A). This province is c. 45 km in length and c. 10 km wide. Mounds are distributed between the 500 and 1100 m isobaths on a part of the continental slope with an average slope angle of 2.7°. Some of the mounds within the Belgica province have been specifically named (e.g., the Challenger Mound, Galway Mound,
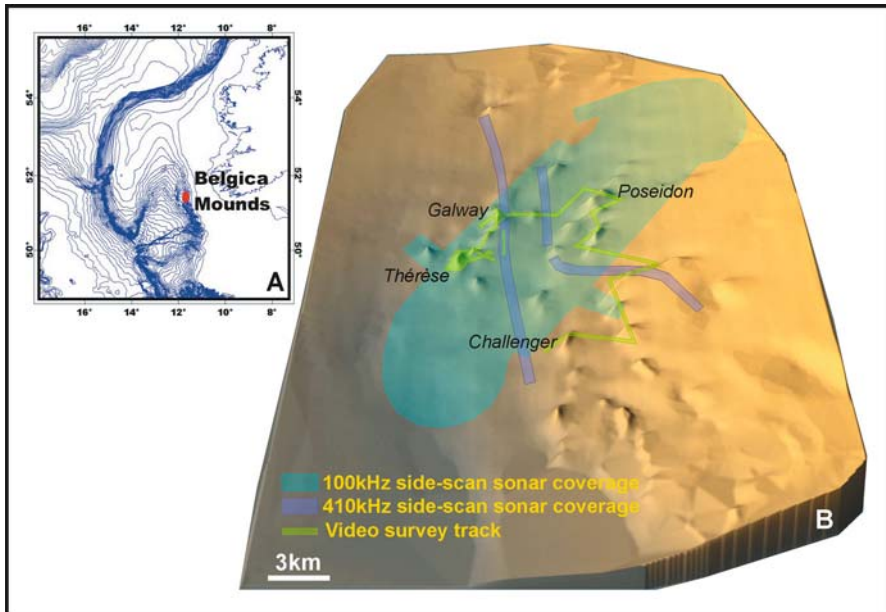
Fig. 1 A Location map showing the location of the Belgica Mounds study area on the regional scale, eastern Porcupine Seabight, NE Atlantic (contours from GEBCO 97); **B** Terrain model of the central part of the Belgica Mound province based on multibeam bathymetry (AWI). Transparent layers show 100 kHz and 410 kHz side-scan sonar coverage and underwater video survey track. Names of individual mounds within the province are shown

Poseidon Mound, Thérèse Mound), with others ascribed a code (e.g., BEL32) and catalogued by De Mol (2002).

Seismic data from the Belgica Mounds are presented by De Mol et al. (2002) and Van Rooij et al. (2003a) who note that the initiation of mound growth was simultaneous upon a Miocene or Late Pliocene unconformity (erosional surface) respectively. The geology of contourite drifts within the province was interpreted by Van Rooij et al. (2000), Kozachenko et al. (2002) and Van Rooij et al. (2003a). Comparison of the Belgica Mound province with other mound provinces is presented by Wheeler et al. (submitted) and Huvenne et al. (2005). Foubert et al. (2005) present an overview of ROV data collected from the province onboard RV Polarstern ARK XIX/3a cruise. This publication presents a detailed interpretation of sedimentary processes operating in the Belgica Mound province based on multidisciplinary datasets.

Materials and methods

Detailed bathymetry of the Belgica Mound province was obtained using the Hydrosweep DS-2 multibeam echosounder system operated at 15.5 kHz during

RV Polarstern ANT XVII/4 cruise June 2000 (see Beyer et al. 2003 for a detailed description of the multibeam data collection and processing).

The central part of the Belgica Mound province was surveyed using a dual frequency GeoAcoustic (100 and 410 kHz) side-scan sonar in conjunction with a 3.5 kHz sub-bottom profiler onboard RRS Discovery 248 (Bett et al. 2000; Wheeler et al. 2000). Approximately 80 km^2 was mapped with the 100 kHz resolution and 6.6 km^2 with the 410 kHz resolution. Side-scan sonar swath width was 800 m at 100 kHz and 220 m at 410 kHz. The height of the side-scan fish above the seabed was controlled *via* a remotely operated electro-hydraulic winch and flown at 25 m off the seabed at 100 kHz and 10 m off the seabed at 410 kHz. To obtain optimum results, the speed of the vessel was kept at 3.5 knots. A hytech cable counter was used to calculate cable layback. The signal to the towfish was supplied by a GeoAcoustics transceiver (SS941) that was externally triggered from a CODA DA100 sonar processing system that supplied a real-time image recorded to DAT tapes. A hardcopy output of the side-scan record was also obtained directly from the GeoAcoustics transceiver using an Ultraelectronics Wideline 200 series 12 thermographic recorder with manual fixes. Navigation was supplied by the NaviPac survey software running on PC, providing the coordinate fix points and heading for the vessel from which the side-scan sonar image location was extrapolated using a layback calculation. The distance of the towfish behind the vessel was calculated using trigonometry (based on water depth, towfish height above the seabed and wire out) with error correction for inertia movements around corners and wire catenation effects. Based on this method, accuracy of image navigation is +/- 50 m.

Acquired digital side-scan sonar data were processed at the Southampton Oceanography Centre using the *PRISM* sonar software system (Le Bas and Hühnerbach 1999) and integrated within a GIS (ArcView 3.2a). Obtained side-scan sonar imagery was draped over a digital terrain model (DTM) derived from the multibeam bathymetry. Sub-bottom profiler data were unprocessed and recorded on a thermographic paper.

Geophysical imagery was ground-truthed with video imagery during RV Discovery 248 (2000) using the Seabed High Resolution Imaging Platform (SHRIMP) using a CCD colour video camera, and on RV L'Atalante (CARACOLE 2001) and RV Polarstern XIX3a (2003) (see also Foubert et al. 2005) cruises using IFREMER's VICTOR 6000 ROV. Underwater video surveys of the study area resulted in collection of ~103 hours of video imagery.

A number of seabed facies were defined based on the video imagery emphasising changes in the coral population (live or dead; total or patchy coverage) on mounds and sedimentary character in off-mound areas (Table 1).

A more generalised interpretative facies map for the Belgica Mound province has been constructed based on geophysical mapping and video ground-truthing datasets. Each dataset was analysed and correlated with other relevant datasets, therefore supporting and extending the final interpretation. Multibeam bathymetry was overlaid with the 100 and 410 kHz side-scan sonar mosaic, and analysed in conjunction with 3.5 kHz sub-bottom profiler records. Sub-bottom profiler lines

Table 1 Seabed facies classification used for the ROV VICTOR 6000 and SHRIMP video observations in the Belgica Mounds area (see also the less detailed facies scheme adopted by Huvenne et al. (2005) based on ROV video data only)

Facies Code	Facies description
1	Dense coral coverage (live and dead)
2	Dense coral coverage (mostly dead)
3	Sediment-clogged dead corals/rubble
4	Patchy mostly live corals on rippled seabed
5	Patchy mostly dead corals on rippled seabed
6	Patchy mostly dead corals on unrippled seabed
7	Dropstone (gravel and/or boulders) dominated seabed
8	Dropstones (gravel and/or boulders) – patchy distribution on unrippled seabed
9	Dropstones (gravel and/or boulders) – patchy distribution on rippled seabed
10	Rippled seabed with occasional dropstones
11	Unrippled seabed with occasional dropstones
12	Rock outcrops (?)

show the surface geomorphological features of the seabed directly underneath the side-scan sonar vehicle, hence making it easier to relate bedform distribution to the local topography. This allowed complex analysis of the side-scan sonar backscatter from a three-dimensional prospective that gave insight into the ongoing and past sedimentary processes on and near the coral mounds. Interpretation of the remotely sensed dataset was then updated in the light of ground-truthing information, which was represented by underwater video imagery. Orientation of bedforms imaged on the side-scan sonar and video imagery was interpreted in terms of current/ palaeocurrent directions, which are indicated by white arrows on the facies map in Figure 2. Seven main seabed facies/types are defined: background uniform backscatter facies, sediment wave facies, barchan dune facies, gravel ridge facies, sand ribbon facies, Moira Mound facies and Belgica Mound facies. Each of these facies is described in detail.

General description of the Belgica Mounds

Multibeam echosounder data (Beyer et al. 2003) reveal that carbonate mounds in the Belgica Mound province are aligned along the slope in two parallel ridges. Some mounds rise above the seabed whereas others are buried or half buried within drift sediment. Mounds from the eastern ridge occur between water depths from 550 to 900 m. The eastern flanks of these mounds are covered by the contourite drift deposits, and therefore possess a half or, in some cases, near-total buried morphology. Mounds located at a deeper water setting, from 870 to 1030 m water depth, form the western ridge and possess an outcropping morphology with a subtle difference in slope angles between their eastern and western flanks. Slope angles of individual mounds vary from 7 to 23°, with western flanks of the mounds being generally steeper then their eastern flanks. Individual mounds are also elongated in a general north-south direction parallel to the dominant current direction implying
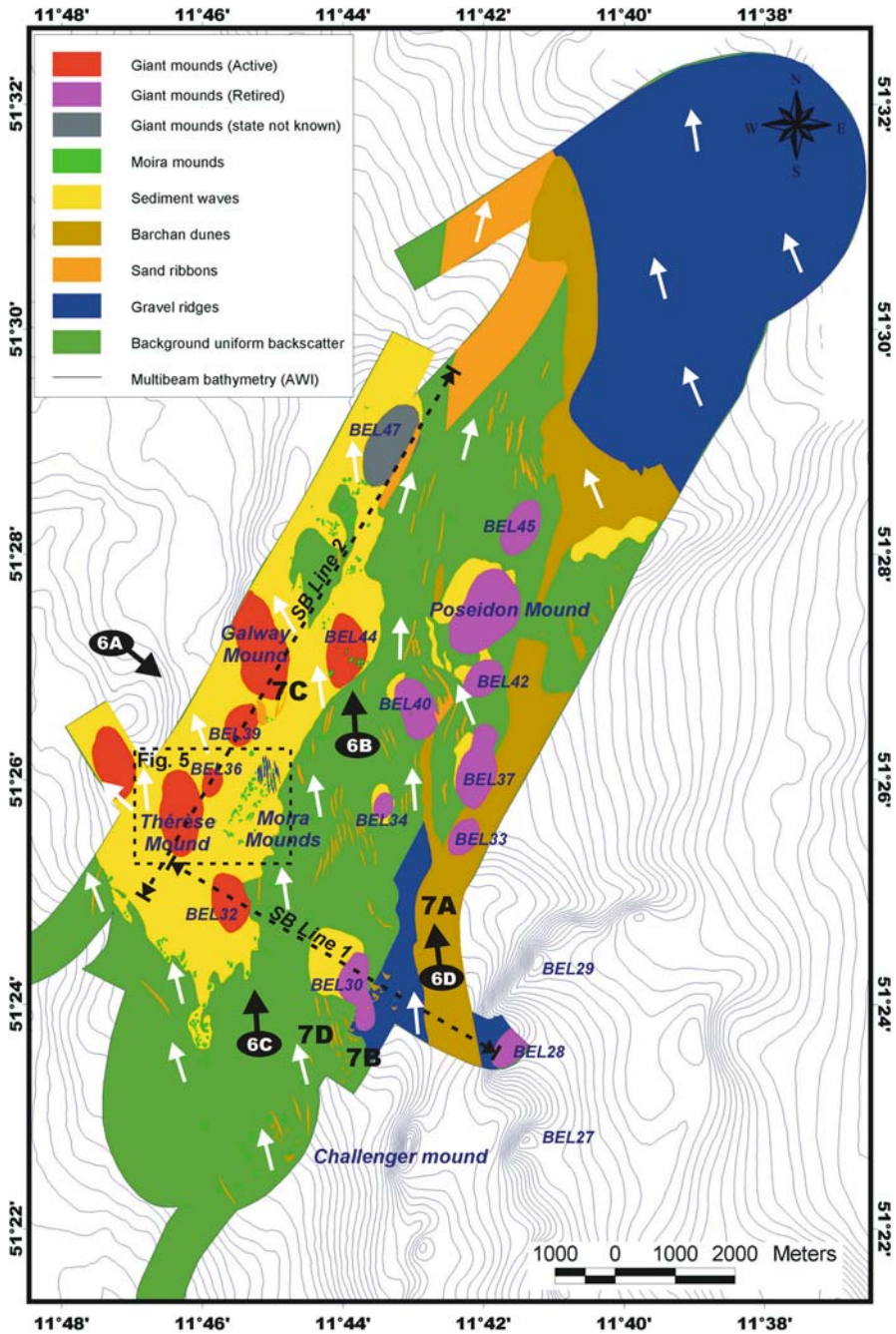
Fig. 2 Interpretation (facies) map of the Belgica Mounds area based on side-scan sonar, sub-bottom profiler and video data. Dashed lines indicate the location of selected 3.5 kHz sub-bottom profiler lines (SB Line 1 and 2; see Fig. 10 for detail). A number of 3D views

a hydrodynamic control on preferential coral growth and interstitial sediment accumulation.

Seabed facies within the Belgica Mound province

Several interpretative facies are defined for the Belgica Mounds area and are described below. An interpretative facies map is presented in Figure 2.

Background uniform backscatter facies

Inter-mound areas, especially in the eastern part of the province, reveal a homogenous uniform background backscatter pattern on the side-scan sonar imagery. This seabed facies occurs in relatively flat or gently sloping areas of the seabed, although in some cases may also characterise the flanks of carbonate mounds (e.g., the eastern flank of Poseidon Mound). Video truthing (Fig. 3) suggests that this facies is represented by a smooth current swept seabed surface with a patchy to dense distribution of dropstones, or, in some places, by rippled sand sheets (Fig. 8A). This facies possesses sharp boundaries with areas of sediment wave or barchan dune development and accommodates a number of sand ribbons and solitary Moira Mounds. This facies exists between the eastern and western mound areas.

Sediment wave facies

Side-scan sonar imagery shows that sediment waves are distributed throughout the mapped area, although more frequent in the western part of the province. Sediment waves shape the seabed in between mound areas and also develop on mound's flanks, indicating that mound surface morphology is strongly dictated by prevailing basal current activity. Sediment waves can be grouped in fields that possess sharp boundaries with the surrounding seabed. Boundaries between sediment wave fields are defined by differences in wave dimensions.

The orientation and size of sediment waves is dependent on hydrodynamic conditions and particle-size. Sediment wave bedforms vary in shape and size with a wavelength of 5 to 60 m and a wave height of 1 to 10 m, whilst on mound flanks they range between 10 to 15 m wavelength and 1 to 3 m height and show larger dimensions on the stoss slopes of the mounds then on their lee sides.

Most of the waves within the sediment wave fields at the lower and upper flanks of the giant mounds have been stabilised by corals and associated biocommunities, with corals growing preferentially on wave crests (Fig. 5B).

BEL44 shows a good example of a rapid transition from uniform backscatter representing rippled or current swept sand sheets to a sediment wave field at the lower flanks of the mound (Figs. 3, 6B). Due to the low topography of this mound (c. 40 m) sediment waves migrate over the mound's summit. Moira Mounds can be observed on the lower southeastern flank of this mound.

---

of the 100 kHz side-scan sonar imagery draped over the multibeam bathymetry are located (e.g., 6A; see Fig. 6). Location of 410 kHz side-scan sonar highlight images is shown (7A, 7B, 7C, 7D; see Fig. 7). Dashed box outlines the area of Thérèse and Moira Mounds that was extensively video-truthed (see Figs. 5, 8, 9 for detail). White arrows indicate directions of benthic currents derived from bedforms orientation on side-scan sonar and video imagery
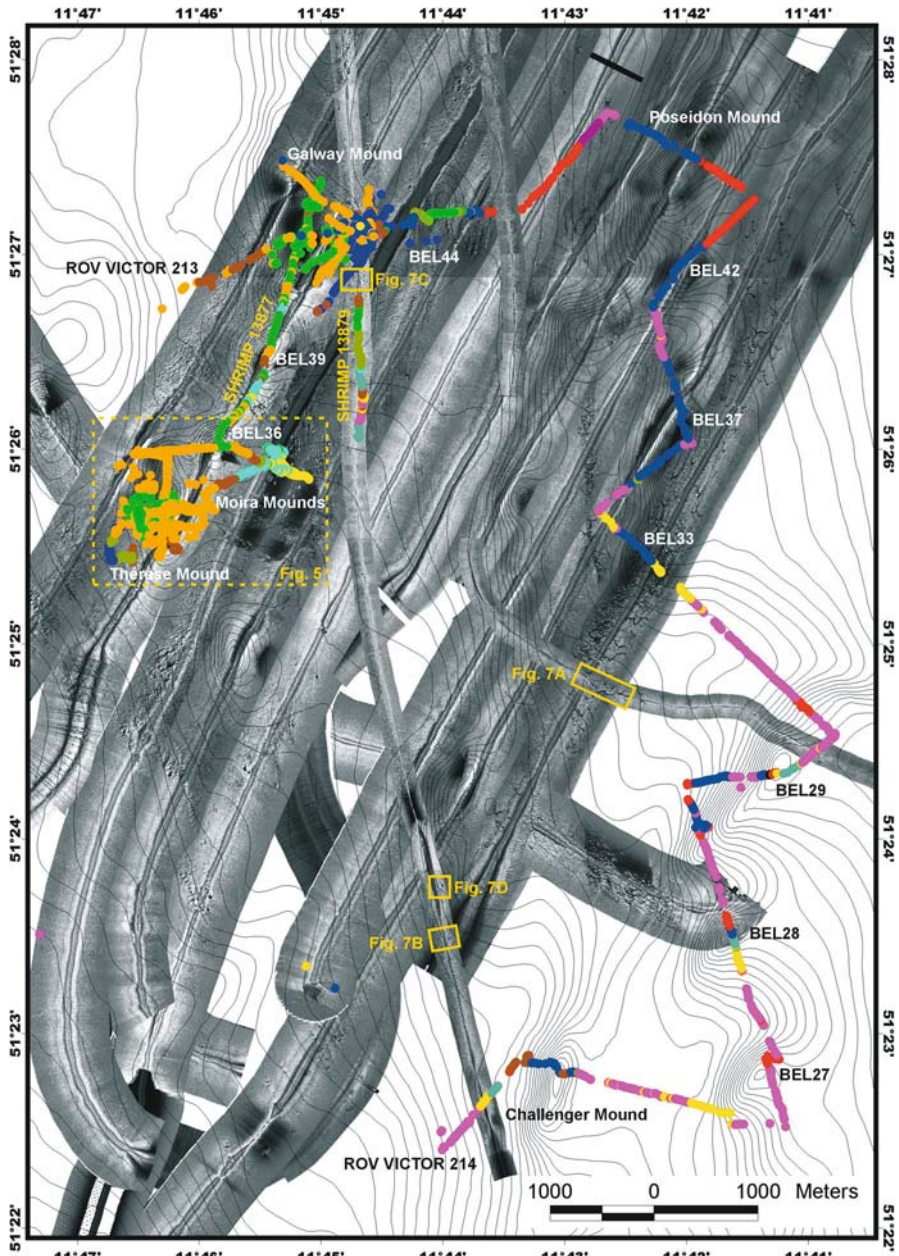
Fig. 3 This map presents a facies interpretation of the video survey tracks overlying remotely sensed imagery (100/410 kHz side-scan sonar and multibeam bathymetry contours). Video data include all video surveys undertaken in the study area with ROV VICTOR 6000 and SHRIMP video systems (see Table 1 for details). Legend provided on the next page

Legend - video facies interpretation

- Dense coral coverage (live & dead)
- Dense coral coverage (mostly dead)
- Sediment clogged dead corals/rubble
- Patchy mostly live corals on rippled seabed
- Patchy mostly dead corals on rippled seabed
- Patchy mostly dead corals on unrippled seabed
- Dropstone (gravel and/or boulders) dominated seabed
- Dropstones (gravel and/or boulders) - patchy distribution on unrippled seabed
- Dropstones (gravel and/or boulders) - patchy distribution on rippled seabed
- Rippled seabed with occasional dropstones
- Unrippled seabed with occasional dropstones
- Rock outcrops(?)

Fig. 3 Legend for the facies interpretation of the underwater video survey tracks presented

Barchan dune facies

The distribution of barchan dune forms is limited to the eastern part of the Belgica Mound province. Side-scan sonar imagery reveals an extensive barchan dune field stretched in a SSW-NNE direction along the eastern edge of the mosaiced area. This implies active sediment transport over the eastern flanks of the half buried mounds. If these features were relic (palaeofeatures) reflecting former palaeocurrent speeds, one might expect the preserved palaeomorphology for the entire area, including the gravel ridges, to be covered by rippled sands. This is not implied by the side-scan sonar backscatter characteristics suggesting the peak current speeds implied by the larger scale bedforms are contemporaneous. Bedforms orientation provides evidence for strong northward flowing bottom currents. Dunes show larger dimensions at the lower stoss flanks of the mounds and decrease in sizes while migrating over the upper flanks and mound's crests (e.g., BEL33). Therefore wavelengths of observed dune forms vary from 10 to 70 m. Dunes show a denser distribution in the proximity of BEL33 and become sparser to the northeast of BEL33. The main barchan dune field goes over the top of BEL33, covers the eastern flank of BEL37 and continues as far north as the southern edge of the Poseidon Mound, followed by a sharp transition to the light toned uniform backscatter. Smaller areas of barchan dunes development are observed further to the north.

A relatively narrow zone (c. 150 m) of barchan dunes runs in a south-north direction following the isobaths west of BEL33 and BEL37 to the base of BEL40 (Fig. 2). The orientation of dunes in the upper field (over BEL33 and BEL37) show a NNE sediment transport direction while in the field west of BEL37 it indicates a northern sediment transport.

A 410 kHz side-scan sonar highlight (Fig. 7A; see Fig. 2 for location) shows a zone of barchan dune development. Solitary forms are evident at the eastern edge of the field (bottom of image) whereas the centre of the field shows the bedforms combining into wavy ridges. Note that the tails of the dunes feed the centre of the dunes behind. This pattern is still evident when the dunes have coalesced into ridges. In the centre of the image, dunes migrate over a gravel ridge-dominated seabed. Gravel ridges are imaged as thinner wavy areas of dark toned backscatter (Fig. 7).
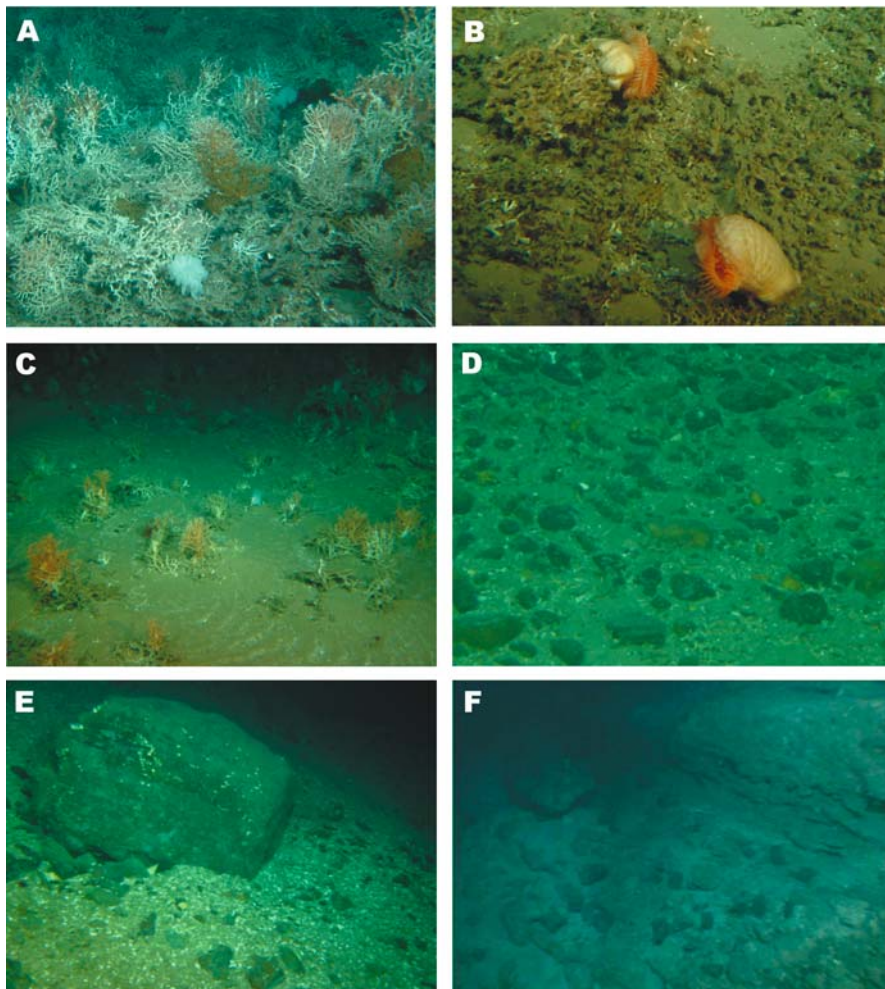
Fig. 4 Video highlights of different facies characteristic for the Belgica Mounds study area. **A** Dense coral coverage (live and dead); **B** Sediment-clogged dead corals/rubble; **C** Patchy mostly live corals on rippled seabed; **D, E** Dropstone (gravel and/or boulders) dominated seabed; **F** Hardground outcrops (All images © IFREMER)
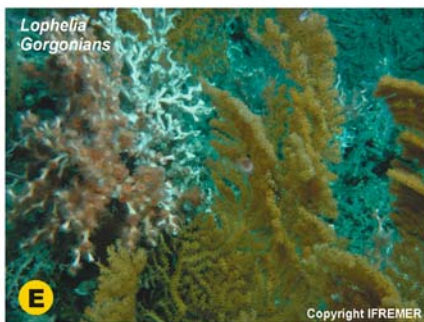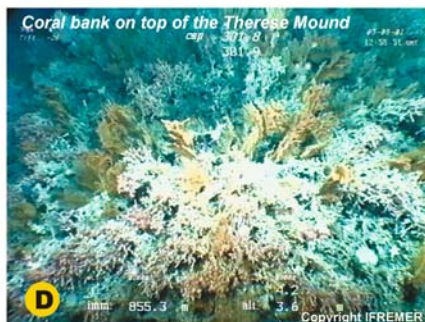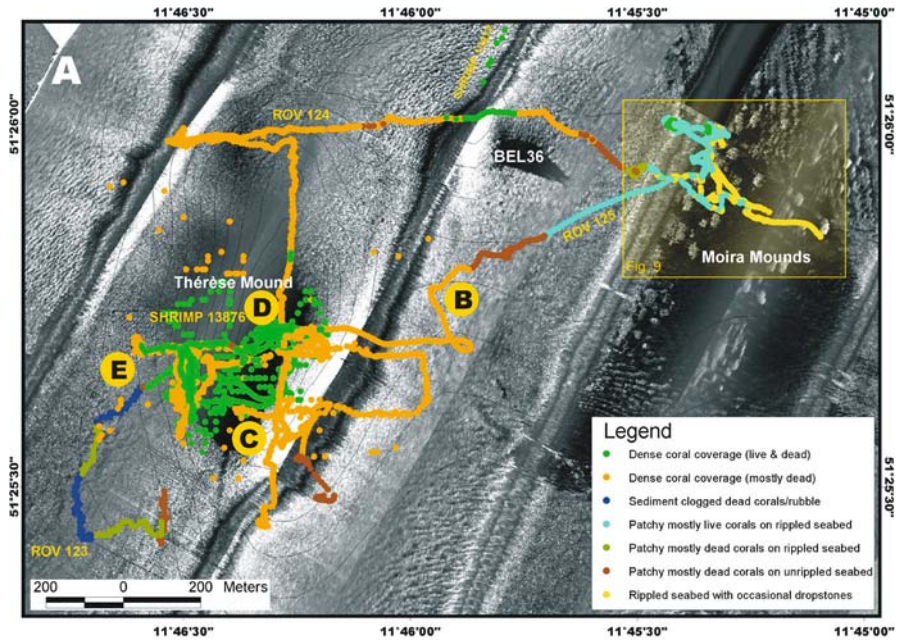
Fig. 5 A Thérèse Mound and Moira Mounds video facies interpretation overlaid over 100 kHz GeoAcoustic side-scan sonar mosaic. Analysed video data include: ROV VICTOR dives 123, 124 and 125, and SHRIMP dives 13876, 13977. See also video highlight images (**B** to **E** © IFREMER)
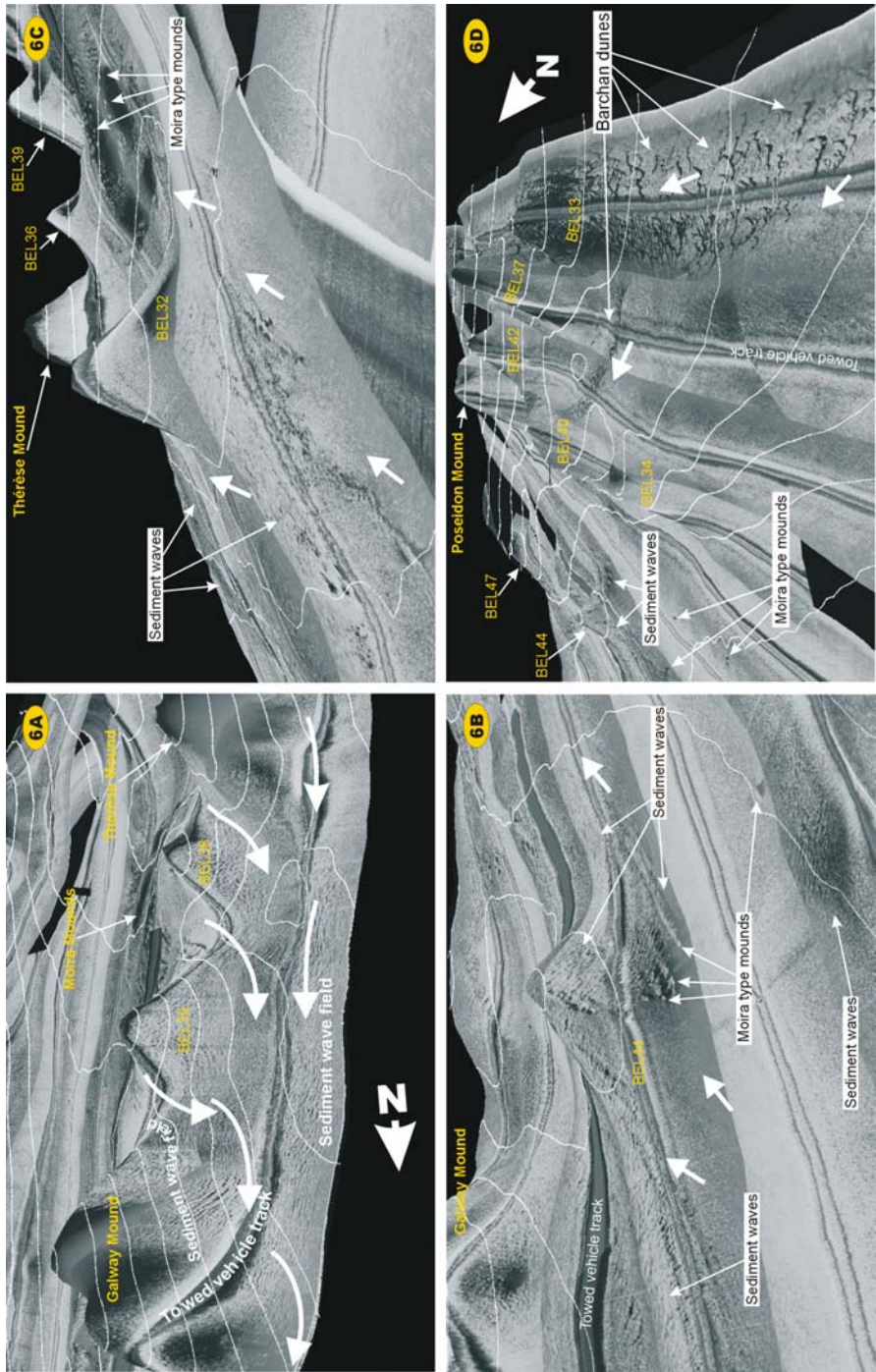
About 16 barchan dune forms migrate over the seabed directly to the east of BEL30. Wavelength varies between 30 and 70 m, with wave height reaching only a few metres. More to the east and northeast barchan dunes develop into more aggregated fields as described above (Fig. 7B).

Gravel ridge facies

Two types of gravel ridges were observed within the mosaiced area: ridges with lunate and linear crest alignment. Ridges with lunate crest alignments develop in the eastern part of the province, and in most cases coexist with superimposed barchan dune forms composed of sandy material (white backscatter on Fig. 7). Gravel ridges are represented here by sinuous crested lines. They show a predominantly sinuous out of phase plan pattern with some bifurcation and have a wavelength varying between 10 and 40 m. The 410 kHz imagery implies that some sandy sediment (white backscatter) is deposited on the leeward sides of the ridges.

Ridges with linear crest alignment were observed at the northern and northwestern ends of the Belgica Mound province. The northern part of the mosaic area shows an extensive field of sand and gravel ridges (ribbons). These ridges possess a SE-NW elongation therefore indicating currents flowing from SSE to the NNW. In parts of this zone, sand ridges are replaced by barchan or transverse dune forms indicating fluctuations in the benthic current strength. An area of apparently buried linear gravel ridges also exists in the Moira Mounds area to the east of the Thérèse Mound (Figs. 2, 5A), where a series of SSE-NNW oriented features can be observed. These features are c. 10-20 m wide and distributed with an average spacing of 30 m.

Sand ribbon facies

Sand ribbons are distributed throughout the mapped area. These are relatively narrow features with straight to wavy crest alignment. They are normally elongated in the SSE-NNW direction indicating a northern sediment transport direction and possess lengths from c. 150 to 900 m. Sand ribbons in the vicinity of mounds show basal currents directional change depending on the local topography. Most of the sand ribbons tend to occur in groups, although 100 kHz side-scan sonar shows that solitary examples may also take place. Video truthing shows that in some places current induced sand ripples are superimposed on the body of the sand ribbons. Ripple crests show orientation perpendicular to the elongation of the sand ribbon, therefore indicating the same direction of basal current that was responsibly for formation of bedforms of both scales.

Moira Mound facies

Moira Mounds are relatively small (tens of metres across and a few metres high) coral mounds that occur in the areas between giant carbonate mounds (Fig. 6C),

Fig. 6 A-D These images show a three-dimensional prospective of 100 kHz GeoAcoustic side-scan sonar mosaic of the Belgica Mounds draped over multibeam bathymetry. Location and viewpoint for each of the 3D images is shown on Fig. 2 (marked as 6A to 6D). Notice distribution and variation in bedform type and dimensions on mound flanks and between mound areas. White arrows indicate benthic current directions derived from bedforms interpretation. Thin white curves show multibeam bathymetrical contours
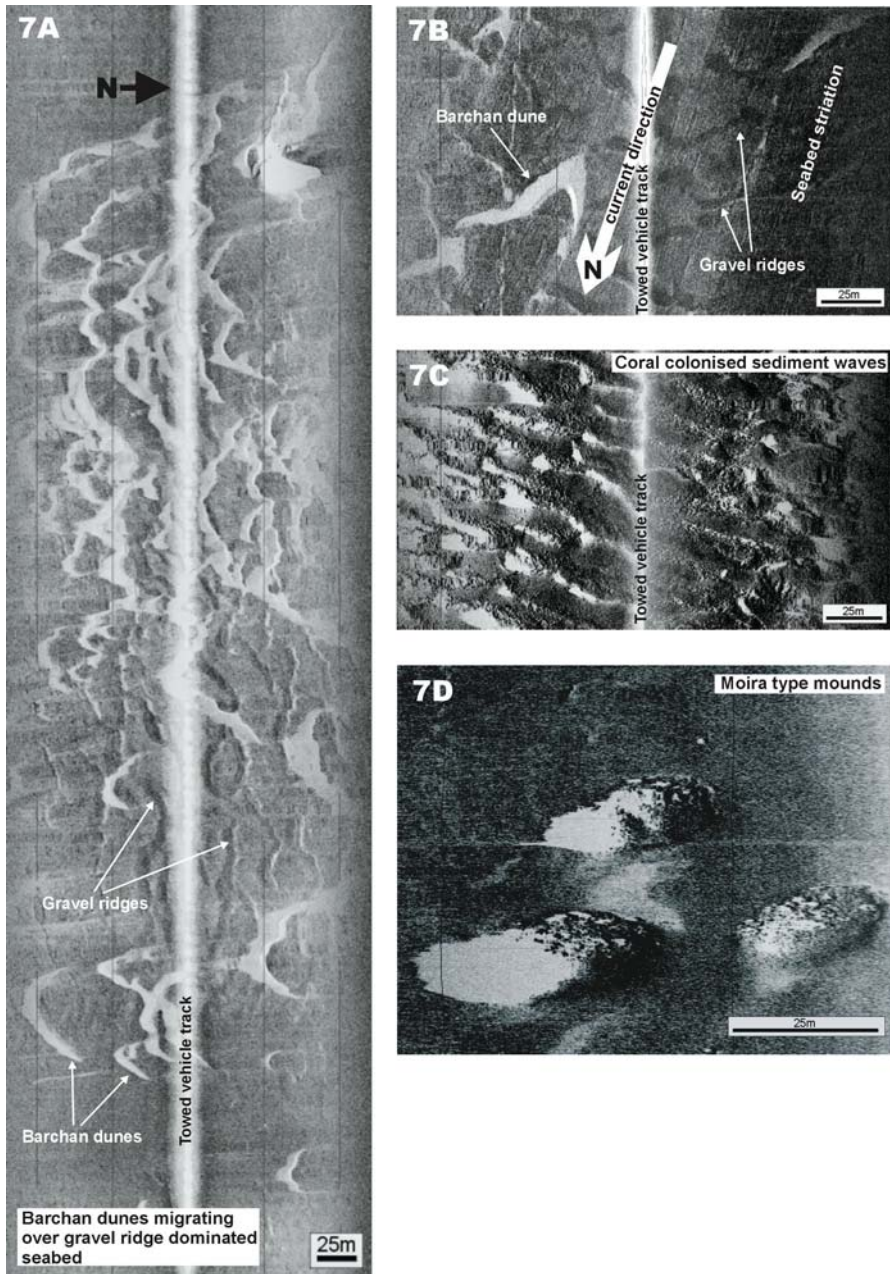
Fig. 7   410 kHz side-scan sonar highlight images. Location of images is shown on Fig. 2.
7A This image shows a zone of barchan dune (white backscatter) development migrating over gravel ridge (black backscatter) dominated seafloor in the area between carbonate mounds.
7B Image shows barchan dune forms composed of sandy material (white backscatter) migrating across gravel ridges (black backscatter), as well as seabed striation caused by intense current

with some apparent examples located near BEL44 on Figure 2 and 6B. Side-scan sonar imagery indicates that the Moira Mounds preferentially occur in areas with active hydrodynamics: on the upstream margins of sediment wave fields, and the far end of gravel ridge or barchan dune dominated seabed. The facies map of the study area (Fig. 2) indicates that the majority of the Moira Mounds are located within the area of the western mounds where environmental conditions seems to be optimal for dense coral colonisation and contemporary coral growth. Most of the Moira Mounds are sub-circular in shape, showing elongation in the direction of the dominant current flow. Some Moira Mounds (Figs. 3, 6B) possess long (c. 150-500 m) tail-like structures aligned in a south-north direction representing down-current sediment wave trains. Moira Mounds tend to occur in groups, although solitary examples were also documented (Fig. 2). Although only a limited number of Moira Mounds was mapped with 100 and 410 kHz side-scan sonar, the survey with 30 kHz TOBI side-scan sonar (de Haas et al. 2002; Huvenne et al. 2005) showed that hundreds of Moira Mounds exist in the study area.

By using high-resolution 410 kHz side-scan sonar imagery, the acoustic signature for coral accumulations on top of the Moira Mounds was detected. Figure 7D shows three closely spaced Moira Mounds, which possess a lumpy structure with spots of high backscatter indicative of coral colonies. The mounds are sub-circular with the uppermost mound showing bimodality in form suggesting that it may have formed as a result of intergrowth between two mounds. This example exists on a gravelly substrate at the edge of a gravel ridge field (Fig. 7D; see Fig. 2 for location). Video imagery shows that mounds have a slope gradient of about c. 15° (Fig. 8D).

The most studied Moira Mounds are located to the east of the Thérèse Mound (see Figs. 2, 5). This area was mapped with 100 kHz side-scan sonar and truthed with detailed ROV VICTOR 6000 video observations (Olu-Le Roy et al. 2002). These Moira Mounds occur within an area of sediment wave development that covers longitudinal gravel ridges. It is speculated here that the gravel ridges probably formed the original substrate for coral colonisation that has been subsequently buried. Wave crests within this field have an east-west orientation indicating that Moira Mound development occurs under a northerly flowing current regime. Most of the mounds show elongation with the regional current flow in the south-north direction.

Between mound areas are represented by rippled sand sheets with occasional small dropstones and, in places, patchy live coral cover. In some areas, current

velocities. **7C** This image shows that the surface morphology of the lower flanks of the carbonate mounds is strongly controlled by sediment waves. High backscatter spots on the surface of the waves are caused by coral and associated bioaccumulations. White backscatter represents acoustic shadows cast by wave crests. This image is from the southeastern flank of the Galway Mound. **7D** Three closely spaced Moira type mounds are imaged in the area between giant carbonate mounds. Moira Mounds possess a lumpy structure with spots of high backscatter indicative of coral colonisation. This example exists on a gravely substrate at the edge of a gravel ridge field. Areas of white backscatter represent acoustic shadows, implying that mounds are sufficiently elevated above the surrounding seabed

ripples are superimposed on larger scale current-induced bedforms (low angle sand waves). Current ripples also shape the surface morphology of the sediment infilling coral framework on mound flanks and summits. Occurrence of the Moira Mounds in the areas of rippled sand sheets development within the sediment wave
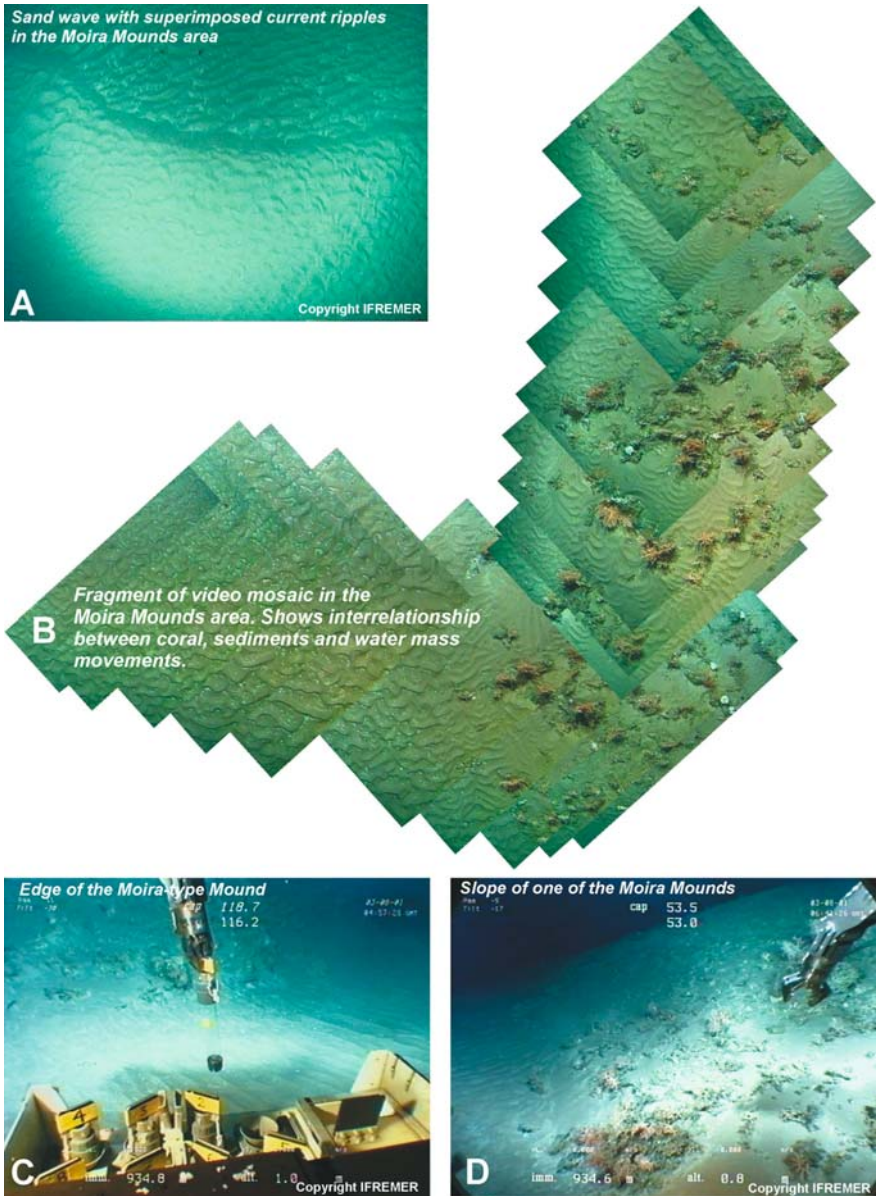
Fig. 8A-D Fragment of video mosaic in the Moira Mounds area and video highlights. (All images © IFREMER)
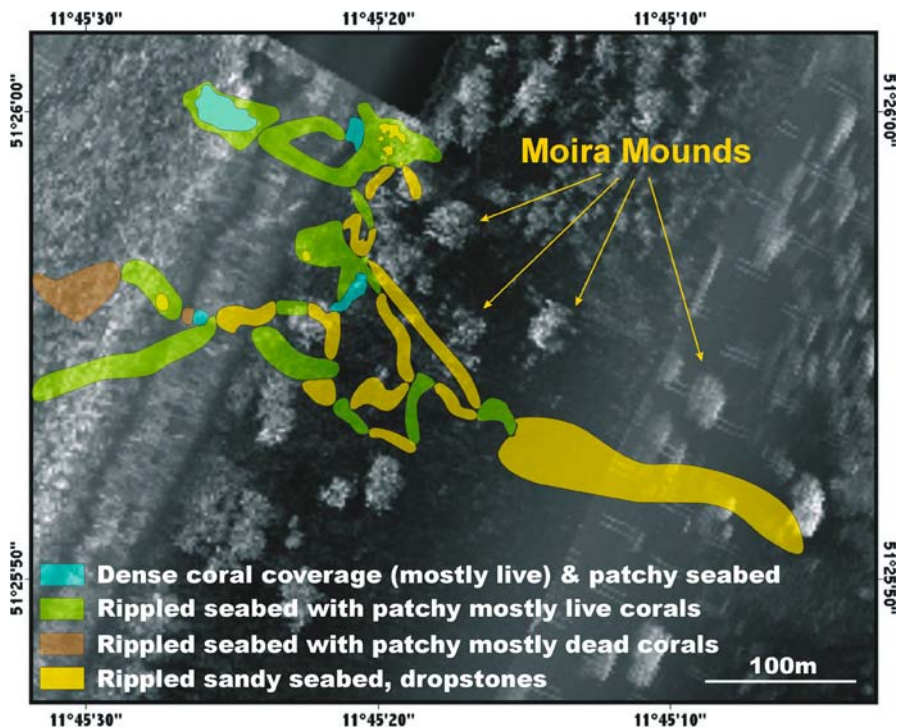
Fig. 9 Moira Mounds video facies interpretation (ROV VICTOR 6000 dives 124 and 125) overlaid over 100 kHz GeoAcoustic side-scan sonar mosaic

fields implies benthic current strength of approximately 60 cm s^{-1} (Southard and Boguchwal 1990).

Belgica Mound facies

Geophysical observations

The location of the giant mounds (and hence the giant mound seabed facies) is best documented from the multibeam and sub-bottom profiler data. Furthermore, sub-bottom profiler records interpreted together with the available ground-truthing information allows a distinction between active and retired mounds to be made (see also ROV-based conclusions in Foubert et al. 2005). This interpretation was based on the nature of the seabed reflector. Sub-bottom profiler records show two types of seabed reflectors of the mound's surface: a solid seabed reflector with the same characteristics as the surrounding seabed and a diffuse reflector. Video and sampling surveys of several mounds suggest that a diffuse reflector occurs where mounds are topped with exposed coral framework (see below). In most cases this will imply the coexistence of both dead and live coral populations. Mounds possessing a solid seabed reflector normally show no evidence of coral life and are dominated by coral rubble or sediment clogged dead coral framework. In this

Table 2 Summary of ground-truthing information for Belgica Mounds imaged on 3.5 kHz sub-bottom profiler lines

List of mounds imaged on 3.5 kHz sub-bottom profiler lines	Seabed reflector type on 3.5 kHz profiler	Ground-truthing information	Mound type (active/retired)
Thérèse Mound (BEL35)	Diffuse	Dense coral coverage (live and dead) *Video data*: ROV VICTOR dives 123, 124, 125; SHRIMP 13876#1; *Box core samples*: PS64/271-2, PS64/271-1, PS64/271-3, 13881#1, 13881#2, 13881#3, 13874#1, 13874#2, 13874#3	Active
Galway Mound (BEL43)	Diffuse	Dense coral coverage (live and dead) *Video data*: ROV VICTOR dives 213, 214 *Box core samples*: PS64/254-1, PS64/254-2, PS64/254-3, PS64/257-2	Active
BEL36	Diffuse	Dense (live and dead) coral coverage on the mound's summit *Video data*: ROV VICTOR dive 124, SRIMP13877#1	Active
BEL39	Diffuse	Dense (live and dead) coral coverage on the mound's summit *Video data*: SRIMP13877#1	Active
BEL32	Diffuse	Coral framework *Box core samples*: see Van Rooij et al. 2003b	Active
BEL38	Diffuse	n/a	Active (?)
BEL44	Not crossed at the summit, but shows diffuse reflector on the western flank	Dense (live and dead) coral coverage on the mound's summit *Video data*: ROV VICTOR dive 214	Active

Table 2 continued

List of mounds imaged on 3.5 kHz sub-bottom profiler lines	Seabed reflector type on 3.5 kHz profiler	Ground-truthing information	Mound type (active/retired)
BEL29	Solid	Mound's summit is dominated by unrippled seabed with patchy dropstones; with sediment clogged dead corals/coral rubble on the western flank of the mound *Video data*: ROV VICTOR dive 214	Retired
BEL33	Solid	Sediment clogged dead corals/coral rubble *Video data*: ROV VICTOR dive 214	Retired
BEL37	Solid	Sediment clogged dead corals/coral rubble *Video data*: ROV VICTOR dive 214	Retired
Poseidon Mound (BEL41)	Solid	Sediment clogged dead corals/coral rubble on the western flank, and dropstones dominated seabed on the eastern flank *Video data*: ROV VICTOR dive 214 *Box core samples*: PS64/276-2, PS64/276-3	Retired
BEL30	Solid	n/a	Retired (?)
BEL34	Solid	n/a	Retired (?)
BEL40	Solid	n/a	Retired (?)
BEL42	Solid	n/a	Retired (?)
BEL45	Solid	n/a	Retired (?)

way, the 3.5 kHz sub-bottom profiler record provides a rough estimate of mound cover and coral ecosystem "health". Table 2 lists all mounds imaged on the 3.5 kHz sub-bottom profiler in the central Belgica Mound province, and summarises, where available, ground-truthing information on particular mounds. Ground-truthing information has been collected for 9 mounds imaged on the sub-bottom profiler that has been extrapolated to mounds that were imaged on the sub-bottom profiler only (Table 2).

Side-scan sonar data provide details of the surface morphology of the upper and lower flanks of the mounds. Side-scan sonar imagery reveals that mound morphology is strongly dictated by prevailing basal current activity. Most of the outcropping mounds of the western mound belt are largely covered in sediment waves. The type and size of bedforms changes depending on the local topography related to mound proximity and position up the flanks of the mounds (Fig. 6). 410 kHz side-scan sonar data revealed sediment waves with coral accumulations (Fig. 7C). Mounds of the eastern mound belt possess a half buried morphology due to onlap of the contourite drift deposits. Drifting sediments are superimposed on the eastern flanks of the mounds in the form of barchan dunes, which in some cases (e.g., BEL33 on Fig. 6D) migrate over the mound summits.
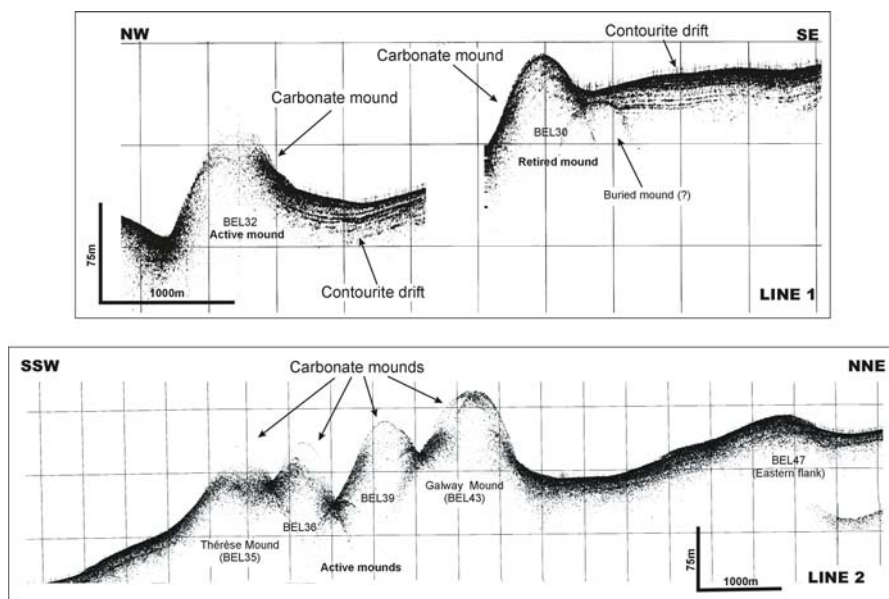
Fig. 10   3.5 kHz sub-bottom profiler lines. Location of profiles is shown on Fig. 2. LINE 1: images two carbonate mounds (BEL30 and BEL32) and contourite drift sequences that are characteristic for the study area. Solid seabed reflector of BEL30 suggests that this mound is retired at present, while diffuse reflector of BEL32 suggests that this mound is active. LINE 2 shows few active mounds of the western mound belt including Thérèse and Galway Mounds

Table 2 and the facies map of the study area (Fig. 2) clearly show that at present mounds of the eastern belt of the province are retired (purple facies) and mounds of the western belt are active (red facies) in terms of the vitality of the coral cover and hence mound growth. The two most representative 3.5 kHz sub-bottom profiles are indicated by the dashed lines on the facies map (Fig. 2) and presented with some interpretations on Figure 10.

Line 1 (Figs. 2, 10) images two carbonate mounds (BEL30 and BEL32) and contourite drift, which, on the sub-bottom profiler data, appear as a well-stratified sediment succession. The south-eastern flank of BEL30 is partly covered by this drift, another carbonate mound immediately to the east of BEL30 has been totally buried by this drift and the area between BEL30 and BEL32 is filled with contourite drift deposits with sediments onlapping on the south-eastern slope of BEL32. This mound is bounded from the northwest by a seabed depression (gully) between BEL32 and Thérèse Mound. The first mound on this line (BEL30) possesses a solid seabed reflector, while BEL32 shows a diffuse seabed reflector, which implies that BEL30 is retired, and BEL32 is active at present (see Table 2).

Line 2 (Figs. 2, 10) images the westernmost mounds of the Belgica province including the eastern flank of BEL47, an interval of gently sloping seabed and four outcropping carbonate mounds: Galway Mound, BEL39, BEL36 and Thérèse Mound. Each mound is nearly symmetrical in a NNE-SSW direction, showing highly diffuse seabed reflectors especially at their summits. Groundtruthing reveals these mounds are heavily colonised by corals (see Table 2) and represent the best examples of active mounds within the province.

Video observations

Eight mounds were video ground-truthed within the eastern area of the province, which can be characterised as a "retired" mound belt, as all mounds here show a lack of live coral cover. The mounds' flanks and summits are mostly composed of sediment-clogged dead coral frameworks or coral rubble. A general description of video transects across these mounds is presented below paying particular attention to evidence for sediment transport (see Figs. 3, 4). Video facies descriptions are also summarised by Foubert et al. (2005).

The Challenger Mound is characterised by sediment clogged dead coral and coral rubble facies. No living framework-building corals were observed on this mound although gorgonians and sponges were found growing on dead corals on the flanks and summit of the mound. At the lower eastern flank, patchy dead corals and coral rubble clogged within a rippled sand sheet were encountered. The orientation of ripples indicates active sediment transport to the NNW, which implies that currents follow the contours of the lower flank of the mound.

The lower southwestern flank of BEL27 also showed rippled sands. The orientation of ripple crests indicates that currents are flowing to the NNE, following the topographical contours of the lower western flank of the mound. The orientation of comet and scour marks at the lower southern flank of the mound shows westerly-directed currents implying that regional northerly flowing contour currents are being deflected and intensified to the west by the mound's topography. The northern

upper flank of BEL27 shows a dense dropstones distribution, implying further active seabed erosion on this side of the mound also.

The southern flank of BEL28 also shows rippled sands migrating in the form of low relief sediment waves over a current swept seafloor typified by a coarser gravel lag. The orientation of the current-induced ripples superimposed on sediment waves and the orientation of comet marks behind dropstones in between wave areas indicates south-westerly flowing currents. The summit and flanks of this mound are represented by background uniform backscatter on 100 kHz side-scan sonar. Video truthing suggests that the upper southern flank of BEL28 is represented by muddy bioturbated seabed, with the summit of this mound (c. 690 m water depth) possessing sediment-clogged dead coral cover. No live framework-building corals were observed on this mound although gorgonians and antipatharians growing on dead coral framework and dropstones were present. Video imagery shows the presence of dropstones on the mound's summit embedded within sediment-clogged coral cover implying strong seabed erosion by bottom currents. This may be one of the reasons for the mound's retirement.

The lower southwestern flank of BEL29 shows a dropstone dominated seabed. Areas between dropstones are filled with carbonate-rich sediment probably composed of broken shells and coral rubble. The western flank of BEL29 shows sediment-clogged dead coral cover. Mid-slope areas contain a c. 200 m area with patchy dropstones that are embedded within coarse-grained carbonate rich sediment suggesting erosion and reworking of a pre-existed coral cover. Extensive hardgrounds are exposed on the upper western flank of BEL29 suggesting strong seabed erosion and exposure of the lithified internal mound sediment. Erosive currents may account for an absence of coral settlement in this area. The possible hardground outcrop is followed for c. 40 m to the east by a very dense distribution of boulder size dropstones. Rippled sands drape dropstone-dominated seabed at the summit of the mound. Orientation of the ripple crests and current induced features surrounding exposed dropstones suggests northerly currents flowing over the mound's summit. A similar situation develops at the upper eastern flank of the mound.

To the northeast of the BEL29 summit, the dive track crosses the 410 kHz side-scan sonar line. The light toned uniform backscatter on the side-scan sonar imagery with apparent boulder and ridge-like structures is represented on the video imagery with relatively flat muddy bioturbated seabed with a patchy distribution of boulder size material.

Video imagery of the lower southeastern flank of BEL33 shows active sediment transport in the form of transverse and barchan sand dunes in accordance with 100 kHz side-scan sonar data. The summit and western flank of the mound demonstrate dead sediment clogged corals and coral rubble cover. This mound does not reveal any framework-building corals and only shows epifauna (e.g., actinians) that uses dead coral framework as an attachment substrate.

The flanks of BEL37 also show dead sediment-clogged coral coverage. The southern flank of BEL37 shows no evidences of live corals or epifauna. The northern upper and mid flank of the mound demonstrates the abundance of soft corals (e.g.,

gorgonians). BEL42 at its flanks and summit shows patchy to dense dead coral cover, which corresponds to background uniform backscatter on 100 kHz side-scan sonar (Fig. 3). In some areas this is more reminiscent of the coral rubble facies. Both corals and coral rubble are sediment clogged and show patchy growth of gorgonians.

The Poseidon Mound is the biggest mound of the eastern mound belt, the eastern flank of which is covered in coarse gravel lag. The summit and the western flank of the mound show dense, mostly dead, coral cover. However, very sparse live *Madrepora oculata* is found growing on the mound's summit. Mostly dead coral framework supports the growth of epifauna (e.g., antipatharians, sponges, anemones). Video imagery of the lower western flank of Poseidon Mound confirms the 100 kHz side-scan sonar interpretation that sediment waves are colonised by corals although corals are mostly dead at present. Coral preferentially grow on the sediment wave crests with very limited growth in wave troughs. It is plausible to assume that these sediment waves are not active at present, as they have been stabilised by coral growth.

In contrast to the eastern mounds, western mounds in the Belgica Mound province show dense coral coverage with a large percentage of live colonies of *Lophelia pertusa* and *Madrepora oculata* on their summits. The lower flanks of the mounds show mostly dead coral cover with sediment clogged corals and coral rubble at mound's basements (see also Foubert et al. 2005).

Mapping of the Thérèse Mound (Figs. 3, 5) suggests that the surface morphological details of this mound show distinct relationships to sediment waves that have become colonised and stabilised by coral and associated communities (Fig. 5B). On the lower flanks of the mounds, corals colonise the crests of sediment waves with limited growth in the troughs, therefore taking advantage of stronger current and nutrient flux. Coral density increases up the mounds (Fig. 5C) until sediment waves become fully stabilised and corals continue to grow into coral banks (Fig. 5D). Coral population is mainly represented by *Lophelia pertusa* and *Madrepora oculata*. Coral growth supports extensive epifauna (e.g., sponges, gorgonians; Fig. 5E), and a wide range of benthic organisms, as well as deep-sea fishes (Olu-Le Roy et al. 2000).

The observations from the Thérèse Mound are also typical for most active mounds of the western mounds in the Belgica Mound province (including BEL36, BEL39, BEL44 and the Galway Mound). BEL36 shows dense live and dead coral coverage with patchy unrippled seabed at its lower and mid flanks. Live coral are documented on the summit of the mound. The northern slope of BEL39 shows dense live and dead coral coverage. On the top of the mound a well-developed but predominantly dead coral framework is observed that may suggest limited erosion. The southern slope is characterised by a smooth seabed with patchy dead and living coral cover.

Video imagery of the Galway Mound shows that the sediment waves imaged on 410 kHz side-scan sonar at the eastern lower flank of the mound are stabilised by coral growth (Fig. 7C). Corals are mostly dead at present, but in places show rather dense coverage. Corals show a preference for colonisation on wave crests, and are

very sparse in the wave troughs and coexist with abundant populations of sponges and soft corals (e.g., gorgonians and antipatharians). The seabed between the coral-colonised sediment waves show unrippled sand. The lower northeastern flank of this mound also shows dense but mostly dead coral cover whilst the upper flanks and the mound's summit show dense, mostly live coral cover. The dominant coral species on this mound are *Madrepora oculata* and *Lophelia pertusa*. Live corals grow on dead coral skeletons that also form a substrate for sponges, gorgonians and other epifaunal growth. The lower eastern flank of the mound is dominated by sediment-clogged corals and coral rubble facies. In some places, areas of sediment-clogged corals are surrounded by rippled sands whereas further a field active sand transport is in the form of rippled sand sheets and low relief sand waves.

BEL44 is the most easterly located mound of the western "active" mound belt (Fig. 2). The lower eastern flank of BEL44 shows sediment-clogged coral rubble facies with occasional dropstones (Fig. 3). This facies dominates the flank of the mound from c. 910 m to c. 900 m water depth. In places it is apparent that corals colonise previously mobile sediment wave structures. Further upslope from c. 900 to c. 860 m water depth, mound's upper flanks and summit show dense mostly live coral coverage. Live corals coexist with dead corals and support epifauna of sponges, gorgonians and antipatharians. Live coral population is dominated by *Madrepora oculata*, although *Lophelia pertusa* was also observed. Rippled sands infilling the space between corals implies active sediment transport over the flanks of the mound and possibly in parts of the summit where coral coverage is not too dense.

Discussion

Seabed mapping data have been presented at varying scales of resolution. The multibeam data provide a general geomorphological prospective of the area whereas side-scan sonar and sub-bottom profiler data provide a higher resolution view on the scale of major bedforms. The interpretation of these bedforms provides information on sediment mobility, current directions and current speeds. These bedforms record peak flow events that may only be representative of extremes in the contemporary benthic environment and may, in some cases, be relict features representative of past conditions (although probably post-glacial in nature). Video data provide information on smaller bedforms often superimposed on the larger bedforms that are representative of general contemporary conditions and allow a qualification of the above premise, e.g., current ripples and sediment waves showing correspondence in current directions reveal information on current speeds during steady-state and extreme conditions. Sub-bottom profiler and video data also allow an assessment of mound "health" in relation to the vitality of the coral ecosystem and whether mounds are "active" or "retired" (*sensu* De Mol 2002; Huvenne 2003; Foubert et al. 2005). Studying all these data together allows us to draw conclusions regarding the topographic influence of mound presence on benthic sedimentary processes and the influence of benthic sedimentary processes on mound "health". Furthermore, we can also appraise the role of sediment supply and bedform-scale mound morphology on mound growth processes.

The influence of mound topography on regional sedimentation patterns

The "background uniform backscatter facies" is dominant in areas between the two main ridges of mounds and represents sedimentation unaffected by the mound presence. This is supported by the observation that on 30 kHz TOBI side-scan sonar data this seabed facies extends to the south upstream of mounds (Huvenne 2003; Huvenne et al. 2005). This facies contains rippled sands suggesting the currents are more sluggish than near the mounds and flow to the north and northwest. Active sediment transport by currents at speeds of between 0.15 and 50 cm s^{-1} (Lonsdale and Speiss 1977; Howe and Humphery 1995) is implied. Occasional dropstones are also present in this facies suggesting low, long-term sedimentation rates with periodic erosion events causing re-exposure and winnowing of the underlying glacial deposits.

The facies map also reveals a general increase in current speeds (as confirmed by resultant bedforms) related to water depth with an upslope (and southwest to northeast) transition from rippled sand (background uniform backscatter facies) to sediment waves to gravel ridges. This suggests that the eastern province (typified by retired mounds) occurs within the main area of drift sedimentation where contour currents are strongest and the western province (typified by active mounds) occurs on the margins of this contourite drift field. The implications of this are discussed below.

Set against this background trend are more localized, but in some cases extreme, variations in current speeds that can be explained as accelerations due to flow over and around the carbonate mounds that represent an obstacle to current flow. Multibeam bathymetric data reveal that these obstacles are significant being c. 1km across at their base and rising to 100 m above the seabed on average (Wheeler et al. submitted). Areas in the vicinity of carbonate mounds are generally typified by sediment wave fields (extra-local effects) suggesting that extra-local current speeds have increased from 20-50 cm s^{-1} to c. 60 cm s^{-1} (Southard and Boguchwal 1990) representing significant obstacle-related current speed accelerations. These sediment waves also possess differing morphologies reflecting subtler responses to localised hydrodynamic conditions and follow the contours of the local topography indicating that the currents both accelerate and change their directions in the proximity of giant carbonate mounds as an obstacle response. These bedforms are found at the base of carbonate mounds as well as, in some cases, across their summits suggesting that sediment wave-carbonate mound associations are not solely related to the altitude of the carbonate mounds elevating their summits into faster flowing waters causing the higher energy bedforms found upslope.

Furthermore, the presence of barchan dune trains shows more energetic spatially restricted current accelerations passing around the carbonate mounds, e.g., Figure 6B. These bedforms suggest that locally, the topographic obstacle of the carbonate mounds cause local accelerations from c. 60 cm s^{-1} (forming sediment waves) to c. 80 cm s^{-1} (forming barchan dunes) and in excess of 150 cm s^{-1} (forming gravel ridges) (Belderson et al. 1982; Southard and Boguchwal 1990). However, it is noted

that the ridges may represent either high palaeocurrent speeds (relic features) or the contemporary peak flow regime with normal lesser flow regimes characterised by non-deposition or barchan dune formation. In other areas sand ribbons are present which implies that currents with speeds up to 100 cm s^{-1} (Belderson et al. 1982). The presence of ripples superimposed on sand ribbons formed by currents flowing in the same direction as those that formed the sand ribbons suggests that sediment transport in the form of sand ribbons is an active process. Video evidence reveals ripples covering the sediment waves and barchan dunes implying that more quiescent conditions occur between these peak flow events although similar crest alignments suggest both type of bedforms are contemporaneous as they are formed by currents flowing in the same current direction.

Video evidence also shows the western flanks of "retired" carbonate mounds are typified by the presence of exposed dropstones, dead coral frameworks or hardgrounds suggesting accelerating currents inhibit sand grade sedimentation, common in off-mound areas, and may even result in a predominately erosive current regime in these exposed mounds (see also Foubert et al. 2005).

Environmental influences on mound biogeological processes

As well as mound topography having an influence on regional sedimentation patterns, sedimentary processes also have a profound influence on mound biogeological processes and may partly explain the distinction between the eastern "retired" mounds and western "active" mounds. Most of the eastern "retired" mounds are partially buried on their eastern flanks by the contourite drift sequences. As mentioned above, these mounds exist at water depths within the main zone of contourite drift sedimentation where along-slope northerly-flowing geostrophic currents are most active. Sub-bottom profiler and seismic data (De Mol et al. 2002; Van Rooij et al. 2003a) also reveal that these drifts have affected this area since Miocene times and throughout mound growth. Contourite deposition in the area is variable reflecting changes in climate-related ocean circulation dynamics (Van Rooij et al. 2003a; Van Rooij et al. submitted) and the precise long-term relationships between mound growth and contourite accumulation is as yet unknown. Nevertheless, particle size data presented by Van Rooij et al. (submitted) shows that late Holocene contourite deposition reflects relatively high current speeds (in relation to sedimentation over the last 100 ka) although sedimentation rates may be reduced (1 cm ka^{-1}). The side-scan sonar data presented confirms this through the imaging of associated high-energy bedforms.

These strong contour currents have a dual impact on coral mounds by burying their eastern flanks through the deposition of thick sediment sequences and eroding their western flanks and summits. The burial of their eastern flanks is a long-term geological process whereby mound growth rates are comparable with contourite sedimentation rates. The Holocene sedimentation rates calculated by Van Rooij et al. (2003a) are orders of magnitude lower than estimated deep-water coral growth rates (e.g., 0.4-2.5 cm yr^{-1}; Wilson 1979b; Mikkelsen et al. 1982; Freiwald et al. 1997; Mortensen and Rapp 1998) suggesting that deep-water corals, were they

present, would be able to compete with contemporary contourite sedimentation. However, in some cases on geological timescales contourite sedimentation rates outstrip mound growth rates and mounds become buried (De Mol et al. 2002). In the late stages of this burial processes, sediment waves may migrate across the summits of these mounds and, in such scenarios, sedimentation rates may prove excessive for coral colonies which may become buried. In most cases, however, it appears that excessive sedimentation by contourite drifts cannot be taken as a reason for forcing mounds into retirement. In fact, there are numerous examples (see below) where active sand encroachment is tolerated by coral colonies and may even encourage mound growth.

The reasons that eastern mounds are "retired" may simply be that current speeds are too excessive to facilitate abundant growth. The exposed dead coral frameworks and dropstones suggest that excessive currents inhibit sand grade sedimentation and, it is speculated here, may also inhibit the settlement of coral larvae preventing renewed colonisation. Additionally, the high current speeds may also break rigid coral exoskeletons once, and if, corals start to grow. Frederiksen et al. (1992) suggest that current speeds >100 m s^{-1} probably cause coral colonies to topple over.

The western part of the province shows a different scenario where most of the mounds possess a dense live coral cover. The western off-mound areas are characterised by extensive areas of rippled sands and sediment wave fields and lack the higher energy bedforms present in the eastern area (barchan dunes and gravel ridges). The deeper water location of western mounds on the margins of the main contourite drift area means that these mounds have not had to compete with high drift sedimentation rates throughout their geological history which have been outstrip by both mound and coral growth rates. Infact, currents in conjunction with moderate sediment supply and transport may play a positive role in the development of the carbonate mounds by providing basal support to coral colonies, stimulating mound growth by preventing coral colonies from toppling over (see below).

Another important factor probably influencing the observed zonation within the province is the relationship to water masses properties (see White 2001, submitted). The depth interval where the western "active" mound summits occur coincides with the core of Mediterranean Outflow Water, which appears favourable to deep-water coral growth along the European continental margin (De Mol 2002; De Mol et al. 2005). The eastern "retired" mounds summits occur in shallower water, thus probably under less favourable circumstances with respect to contemporary water masses (but may also reveal tantalising insights in possible palaeo-watermass structures).

Biogeological processes, mechanisms for mound growth and mound micromorphology

Hydrodynamics and sediment transport exert a strong control on carbonate mound growth and resultant surface morphology. From a biological perspective, currents are an essential prerequisite for suspension feeders such as deep-water corals. Currents deliver organic particulate material on which the coral polyps

feed: the stronger the currents, the higher the flux of food. Currents also prevent fine-grained clastic sedimentation that has a smothering effect on coral. From a biogeological perspective, excessive currents can erode the seabed and hinder coral colonisation as discussed above with respect to the eastern retired mounds. Of more interest is the role of bedload sand transport in the western active mounds where this process has a positive effect on mound growth. Two examples are discussed below to illustrate this mechanism.

Moira Mounds

The Moira Mounds are small, relatively young, deep-water coral mounds. It is speculated here that they may have initiated as late as the start of the Holocene with the rejuvenation of ocean circulation reaching comparable statures as the Holocene reefs from the Norwegian shelf. These are the only small-scale carbonate mound features found in the Porcupine Seabight and southern Rockall Trough. The Darwin Mounds in the northern Rockall Trough are comparable in size only because, unlike the Moira Mounds, they are coral-colonised fluid escape structures (Bett et al. 2000; Masson et al. 2003). Furthermore, there is no evidence of buried examples imaged on seismic data suggesting that these are probably not transient features that grow during interglacials when conditions are optimal only to become buried during glacials when conditions for coral growth deteriorate. In fact, it would appear that we are witnessing a new phase in carbonate mound development at its early stage, a phase which may eventually lead to the formation of further giant mounds after tens of thousands of years or perhaps develop into a new form of deep-water coral bioherm.

Moira Mounds represent accumulations of living and dead coral frameworks filled with sediment and show patchy to dense mostly live coral coverage on their summits. Once coral colonies gained a "footing" in these areas, coral colonies trap sand and build positive features for further coral development on the seafloor. In doing so, corals become elevated above the benthic-boundary layer gaining access to fast flowing waters (with increased nutrient flux and lower bedload sediment transport) thus stimulating further biological growth, sand entrapment and increases in mound elevation.

Side-scan sonar data reveal that the Moira Mounds occur in areas of active sand transport and often occur at the head of sediment wave trains. For instance, an interpretation-facies map of ROV video ground-truthing presented on Figure 9 shows that Moira Mounds occur in areas of active sand transport on rippled sand sheets and the upstream margins of sediment wave fields. This would suggest that not only are deep-water corals capable of tolerating sand encroachment but active sand transport may actually provide a benefit to the colonies by encouraging vertical mound growth. Video data reveal that the Moira Mounds are composed of coral frameworks and interstitial sands. Figure 8 shows a change in bedforms from off-mound lunate rippled sand to linear ripple and unrippled sand within the mounds demonstrating that currents slow down as they flow over the mounds. Coral colonies and the mounds themselves therefore form obstacles to basal currents thereby

retarding bedload transport, which becomes eventually trapped at the base of the coral colonies. Sand entrapment within the coral framework strengthens the coral colonies preventing them from toppling over and allowing them to grow taller.

The side-scan sonar also reveals the importance of a suitable substrate for initial coral colonisation as a common prerequisite for Moira Mound development. The Moira Mounds to the east of the Thérèse Mound (Figs. 8, 9) occur on longitudinal gravel ridges (also imaged on multibeam data; Foubert et al. 2005) formed under previous, more energetic seabed conditions provided a suitable attachment substrate for coral growth that was also in an elevated position. Figure 7B shows another example of three Moira Mounds in an area of gravel ridges that provide a suitable substrate for colonisation.

Belgica Mound micromorphology

Active sand transport is also a consistent observation in the vicinity of the western active Belgica Mounds and it is reasonable to assume that this factor also makes a positive contribution to mound growth. The facies map (Fig. 2) shows that sediments are active in the vicinity of these mounds due to obstacle-related acceleration in benthic currents (see above). Figure 6a and 6c show that these sediment waves or comparable modified forms transgress from the off-mound areas, over mound flanks and even mound summits. Figure 7C shows a side-scan sonar image of the flank of one of the mounds showing the micromorphology of the mound is strongly reminiscent of off-mound sediment waves. However, the image also shows irregular bright backscatter spots representative of coral colonises growing on the surface of the sediment waves. Video ground-truthing confirms this hypothesis and shows a transition from off-mound mobile sediment waves, to coral colonised sediment waves to coral banks near mound summits.

In this way, it is envisaged that coral colonies on the flanks of mounds are encroached upon by sediment waves whose progress is retarded by the coral colonies that also trap the sand. In a similar way as on the Moira Mounds, the trapped sands provides support to the coral colonies allowing them to grow higher without he risk of toppling. This enhanced growth facilitates further sand entrapment thereby encouraging more grow. Overtime the sediment waves become larger and steeper, as seen in Figure 6C, with rigorous coral growth on their crests and restricted or absence coral growth in the sheltered troughs between sediment waves. This is an example of a positive feedback relationship between geological and biological growth processes. Towards mound summits the supply of sand sediment through a highly colonised mound is restricted whilst the conditions for coral growth are enhanced. We therefore see a transition from sediment waves to coral banks whereby growth is pure biological although a similar mound surface morphology is retained with corals growing preferentially in positions of higher elevation. This is an example of an inherited micromorphology (Wheeler et al. submitted).

Conclusions

Multidisciplinary seabed mapping studies based on geophysical (multibeam, 100/410 kHz side-scan sonar and 3.5 kHz sub-bottom profiler) and video surveys reveal the complexity of the environmental setting of the Belgica Mound province affected by strong northerly current flows and associated drift sedimentation. The creation of an interpretation-facies map provides information on sediment pathways and benthic current patterns that are influenced by mound topography and also influence mounds growth and morphology. Seven main seabed facies are identified and described: background uniform backscatter facies, sediment wave facies, barchan dune facies, gravel ridge facies, sand ribbon facies, Moira Mound facies and Belgica Mound facies. The data also identified "active" and "retired" mounds subdividing the mound province into two mound belts. "Retired" mounds of the eastern mound belt possess buried or a half buried morphologies due to onlap of the contourite drift deposits that migrate over the mound flanks in the form of barchan dunes, and show a lack of contemporary coral life. "Active" mounds of the western mound belt show outcropping morphology with dense mostly live coral cover, with mound bases dominated by coral colonised sediment waves that, with increasing coral colonisation, give way to coral banks towards the mound summits. Small mound features (Moira Mounds) exist in areas between the giant (Belgica) mounds, and possibly represent an early stage of mound development. The growth and development of Moira Mounds is strongly affected by hydrodynamics and active sand transport.

Acknowledgements

References

Belderson RH, Johnson MA, Kenyon NH (1982) Bedforms. In: Stride AH (ed) Offshore Tidal Sands. Processes and Deposits. Chapman and Hall, London

Bett BJ, Billett DSM, Masson DG, Tyler PA (2000) RRS Discovery Cruise 248, 07 Jul – 10 Aug 2000. A multidisciplinary study of the environment and ecology of deep-water coral ecosystems and associated seabed facies and features (the Darwin Mounds, Porcupine Bank and Porcupine Seabight). Southampton Oceanogr Cruise Rep 36

Beyer A, Schenke HW, Klenke M, Niederjasper N (2003) High resolution bathymetry of the eastern slope of the Porcupine Seabight. Mar Geol 198: 27-54

De Haas H, Huvenne V, Wheeler A, Unnithan V and shipboard scientific crew (2002) M2002 Cruise report (R.V. Pelagia Cruise 64PE197): A TOBI side scan sonar survey of cold-

water coral carbonate mounds in the Rockall Trough and Porcupine Sea Bight - Texel-Southampton-Galway, 21 June – 14 July 2002. R Netherl Sea Res (NIOZ), Texel, The Netherlands, 2002

De Mol B (2002) Development of coral banks in Porcupine Seabight (SW Ireland). A multidisciplinary approach. PhD thesis, Fac Sci, Dept Geol Soil Sci, Univ Ghent, 363 pp

De Mol B, Henriet JP, Canals M (2005) Development of coral banks in Porcupine Seabight: do they have Mediterranean ancestors? In: Freiwald A, Roberts JM (eds) Cold-water Corals and Ecosystems. Springer, Berlin Heidelberg, pp 515-533

De Mol B, Van Rensbergen P, Pillen S, Van Rooij D, McDonnell A, Ivanov M, Swennen R, Henriet JP (2002) Larger deep-water coral banks in the Porcupine Basin, southwest of Ireland. Mar Geol 188: 193-231

Foubert A, Beck T, Wheeler AJ, Opderbecke J, Grehan A, Klages M, Thiede J, Henriet JP and the Polarstern ARK-XIX/3a shipboard party (2005) New view of the Belgica Mounds, Porcupine Seabight, NE Atlantic: preliminary results from the Polarstern ARK-XIX/3a ROV cruise. In: Freiwald A, Roberts JM (eds) Cold-water Corals and Ecosystems. Springer, Berlin Heidelberg, pp 403-415

Frederiksen R, Jensen A, Westerberg H (1992) The distribution of the scleractinian coral *Lophelia pertusa* around the Faroe Islands and the relation to internal tidal mixing. Sarsia 77: 157-171

Freiwald A (1998) Geobiology of *Lophelia pertusa* (Scleractinia) reefs in the North Atlantic. Habilitation thesis, Univ Bremen, 116 pp

Freiwald A (2002) Reef-forming cold-water corals. In: Wefer G, Billett D, Hebbeln D, Jørgensen BB, Schlüter M, Van Weering T (eds) Ocean Margin Systems. Springer, Berlin Heidelberg, pp 365-385

Freiwald A, Henrich R, Pätzold J (1997) Anatomy of a deep-water coral reef mound from Stjernsund, west Finnmark, north Norway. SEPM Spec Publ 56: 142-162

Freiwald A, Hühnerbach V, Lindberg B, Wilson JB, Campbell J (2002) The Sula Ridge Complex, Norwegian Shelf. Facies 47: 179-200

Howe JA, Humphery JD (1995) Photographic evidence for slope-current activity, Hebrides Slope, NE Atlantic Ocean. Scot J Geol 30: 107-115

Huvenne VAI (2003) Spatial geophysical analysis of the Magellan carbonate build-ups and the interaction with sedimentary processes: key to a genetic interpretation? PhD thesis, Fac Sci, Dept Geol Soil Sci, Univ Ghent

Huvenne VAI, Beyer A, de Haas H, DeKindt K, Henriet JP, Kozachenko M, Olu-Le Roy K, Wheeler A. (2005) The seabed appearance of coral bank provinces in the Porcupine Seabight, NE Atlantic: results from side-scan sonar and ROV seabed mapping. In: Freiwald A, Roberts JM (eds) Cold-water Corals and Ecosystems. Springer, Berlin Heidelberg, pp 535-569

Kenyon NH, Akhmetzhanov AM, Wheeler AJ, van Weering TCE, de Haas H, Ivanov MK (2003) Giant carbonate mud mounds in the southern Rockall Trough. Mar Geol 195: 5-30

Kozachenko M, Wheeler A, Beyer A, Blamart D, Masson D, Olu-Le Roy K (2002) A four dimensional prospective of the sedimentary processes and their interactions with Ireland's deep-water coral carbonate mound ecosystems: Belgica carbonate mound province, Eastern Porcupine Seabight, NE Atlantic. Geophys Res Abstr 4, Abstr EGS02-A-02529, 27th Gen Assem Europ Geophys Soc, Nice, 21-26 April 2002

Kozachenko M, Wheeler AJ, Beyer A, Blamart D, Masson D, Olu-Le Roy K (2003a) Ireland's deep-water coral carbonate mounds: multidisciplinary research results. Abstr, EGS - AGU - EUG Joint Assem, Nice, France, April 2003

Kozachenko M, Wheeler A, Beyer A, Huvenne VAI, Masson D, Olu-Le Roy K (2003b) Sedimentary processes and carbonate mound morphology: the Belgica Mounds, Porcupine Seabight. Erlanger Geol Abh Sonderbd 4: 53-54

Le Bas T, Hühnerbach V (1999) P.R.I.S.M. Processing of remotely-sensed imagery for seafloor mapping operators manual version 3.1. Southampton Oceanogr Cent, UK

Lonsdale P, Speiss FN (1977) Abyssal bedforms explored with a deeply-towed instrument package. Mar Geol 23: 57-75

Masson DG, Bett BJ, Billett DSM, Jacobs CL, Wheeler AJ, Wynn RB (2003) The origin of deep-water, coral-topped mounds in the northern Rockall Trough, Northeast Atlantic. Mar Geol 194: 159-180

Mikkelsen N, Erlenkeuser H, Killingley JS, Berger WH (1982) Norwegian corals: radiocarbon and stable isotopes in *Lophelia pertusa*. Boreas 11: 163-171

Mortensen PB, Rapp HT (1998) Oxygen and carbon isotope ratios related to growth line patterns in skeletons of *Lophelia pertusa* (L.) (Anthozoa, Scleractinia): implications for determination of linear extension rates. Sarsia 83: 433-446

Olu-Le Roy K, Caprais JC, Crassous P, Dejonghe E, Eardley D, Freiwald A, Galeron J, Grehan A, Henriet JP, Huvenne V, Lorance P, Noel P, Opderbecke J, Pitout C, Sibuet M, Unnithan V, Vacelet J, Van Weering T, Wheeler A, Zibrowius H (2002) CARACOLE Cruise Report. 30/07/2001 (Cobh) – 15/08/2001 (Foynes) N/O L'Atalante and ROV VICTOR. 1 and 2, Unpubl Rep, IFREMER, Brest

Rogers AD (1999) The biology of *Lophelia pertusa* (Linnaeus 1758) and other deep-water reef-forming corals and impacts from human activities. Int Rev Hydrobiol 84: 15-406

Southard JB, Boguchwal LA (1990) Bed configurations in steady state unidirectional water flows. Part 2. Synthesis of flume data. J Sediment Petrol 60: 658-679

Van Rooij D, Kozachenko M, Blamart D, Lekens W, Wheeler A, Henriet JP (2000) The acoustic and sedimentological face of the sediments surrounding the Belgica mound province. EOS 81(48): F638

Van Rooij D, De Mol B, Huvenne V, Ivanov M, Henriet JP (2003a) Seismic evidence of current-controlled sedimentation in the Belgica mound province, upper Porcupine slope, southwest of Ireland**.** Mar Geol 195: 31-53

Van Rooij D, Raes M, Tseu G, Henriet JP (2003b) RV Belgica 03/13 cruise report, 18-28 May 2003, Porcupine Seabight. Unpubl Rep, Univ Ghent

Van Rooij D, Blamart D, Wheeler A, Kozachenko M, Richter T, Henriet JP (submitted) Quaternary drift sediment dynamics in the Belgica mound province, Porcupine Seabight: a multidisciplinary approach. Int J Earth Sci

Van Weering TCE, de Haas H, de Stigter HC, Lykke-Andersen H, Kouvaev I (2003) Structure and development of giant carbonate mounds at the SW and SE Rockall Trough margins, NE Atlantic Ocean. Mar Geol 198: 67-81

Wheeler AJ, Bett BJ, Billett DSM, Masson DG and Scientific Party, Officers and Crew of Discovery 248 (2000) Very high resolution side-scan mapping of deep-water coral mounds: surface morphology and processes affecting growth. EOS 81(48): F638

Wheeler AJ, Beck T, Thiede J, Klages M, Grehan A, Monteys FX, Polarstern ARK XIX/3a Shipboard Party (2005) Deep-water coral mounds on the Porcupine Bank, Irish Margin: preliminary results from the Polarstern ARK-XIX/3a ROV cruise. In: Freiwald A, Roberts JM (eds) Cold-water Corals and Ecosystems. Springer, Berlin Heidelberg, pp 393-402

Wheeler AJ, Beyer A, Freiwald A, de Haas H, Huvenne VAI, Kozachenko M, Olu-Le Roy K (submitted) Morphology and environment of deep-water coral mounds on the NW European margin. Int J Earth Sci

White M (2001) Hydrography and physical dynamics at the NE Atlantic margin that influence the deep-water cold coral reef ecosystem. Dept Oceanogr, NUI Galway, Ireland, 31 pp

White M (submitted) The hydrographic setting for the carbonate mounds of the Porcupine Bank and Sea Bight. Int J Earth Sci

Wilson JB (1979a) The distribution of the coral *Lophelia pertusa* (L.) [*L. prolifera* (Pallas)] in the North East Atlantic. J Mar Biol Ass UK 59: 149-164

Wilson JB (1979b) 'Patch' development of the deep-water coral *Lophelia pertusa* (L.) on Rockall Bank. J Mar Biol Ass UK 59: 165-177

Sponge reefs in the Queen Charlotte Basin, Canada: controls on distribution, growth and development

Kim W. Conway[1], Manfred Krautter[2], J. Vaughn Barrie[1], Frank Whitney[3], Richard E. Thomson[3], Henry Reiswig[4], Helmut Lehnert[5], George Mungov[3], Miriam Bertram[6]

[1] Geological Survey of Canada, Pacific Geoscience Centre, 9860 W Saanich Rd, Box 6000, Sidney, BC, V8L 4B2, Canada
   (KConway@NRCan.gc.ca)
[2] Institute of Geology and Palaeontology, Herdweg 51, D-70174 Stuttgart, Germany
[3] Institute of Ocean Sciences, Sidney, BC, Canada
[4] Royal British Columbia Museum, 675 Belleville Street, Victoria BC, V8W 3N5, Canada
[5] Eichenstr. 14, D-86507 Oberottmarshausen, Germany
[6] Pacific Marine Environmental Laboratory, Seattle, WA, USA

Abstract. Sponge reefs in the Queen Charlotte Basin exist at 165-240 m depth within tidally influenced shelf troughs subject to near bottom current velocities of 25-50 cm s^{-1} where nutrient supply from coastal runoff is augmented by wind-induced upwelling of nutrient rich water from the adjacent continental slope. Large reef mounds to 21 m in elevation affect tidally driven bottom currents by deflecting water flows through extensive reef complexes that are up to 300 km^2 in area. Three hexactinellid species construct reefs by building a siliceous skeletal framework through several frame-building processes. These sponge reefs exist in waters with 90 to 150 μM dissolved oxygen, a temperature range of 5.9 to 7.3°C and salinity of 33.2 to 33.9 ‰. Relatively high nutrient levels occur at the reef sites, including silica, which in bottom waters are typically >40 μM and may be up to 80 μM. A high dissolved silica level is potentially an important control on occurrence of these and other dense siliceous sponge populations. The sponge reefs are mainly confined to seafloor areas where exposed iceberg plough marks are common. Sediment accumulation rates are negligible on the relict, glacial surface where the reefs grow, and trapping of flocculated suspended particulate matter by hexactinosidan or framework skeleton hexactinellid sponges accounts for a large proportion of the reef matrix. Suspended sediment concentration is reduced within the nepheloid layer over reef sites suggesting efficient particle trapping by the sponges. The reef matrix sediments are enriched in organic carbon, nitrogen and

---

carbonate, relative to surrounding and underlying sediments. The sponges baffle and trap suspended sediments from water masses, which in one trough have a residence time of approximately 6 days, ensuring a close association of the sponges with the bottom waters. The location of the reef complexes at the heads of canyons provide a means of regionally funnelling particulate material that sponges can trap to enrich their environment with organic carbon and biogenic silica. Like deep-sea coral reefs, the sponge reefs are a remote and poorly known ecosystem that can present logistical challenges and survey costs. Also like deep-sea coral reefs, many of the hexactinosidan sponge reefs have been damaged or destroyed by the groundfish trawl fishery.

Introduction

Hexactinellid sponge reefs, formed by framework skeleton sponges of the Order Hexactinosida, have developed in three glacial troughs that cross the continental shelf of northwestern Canada (Conway et al. 1991; Krautter et al. 2001). These reefs form extensive complexes, with bioherms up to 21 m in height and flat lying, biostromal areas that can cover many square kilometres of seabed (Fig. 1), and they have existed at some sites for up to 9000 years (Conway et al. 2001). The four main reef complexes are found in 165-240 m water depth, separated by up to 80 kilometres, but all share a common late Quaternary geologic history (Barrie and Conway 2002). The reefs are constructed through several processes of frame building by three hexactinosidan species (Fig. 2) and baffling and trapping of suspended sediments by these sponges (Krautter et al. 2001). The reefs are thought to provide habitat for many species of fishes, including rockfish, and a wide variety of invertebrates (Jamieson and Chew 2002). On the Alaskan and Washington State continental shelves this habitat association is also indicated by a large sponge bycatch coupled with the rockfish catches in the trawl fishery (Malecha et al. in press; Lowry written communication). Geological and palaeontological scientific interest in the reefs is stimulated by their similarity to widespread Mesozoic Era reefs that formed a discontinuous belt 7,000 km long during the Late Jurassic along the northern margin of the Tethys Ocean. This was the largest reef belt ever to exist on earth (Krautter et al. 2001).

Database – geological, oceanographic and biological data sets

Multiparameter scientific surveys to examine the sponge reefs in detail were mounted in 1999 (PGC99001) with Canadian Coast Guard Ship (CCGS) *John P. Tully*, 2001 (PGC01004) with CCGS *Vector*, and in 2002 (PGC02002) with CCGS *John P. Tully*. In addition CCGS *Vector* collected multibeam swath bathymetric data in summer 2003 in two of the four reef complexes. These extensive data sets

include grab and water samples, piston and gravity cores, high-resolution seismic and sidescan sonar underway geophysical surveys (Krautter et al. 2001) as well as oceanographic moorings deployed as part of the 2002 program which included current meters and sediment traps. In addition, in February 2000 and September 2002, detailed oceanographic surveys were completed in the vicinity of the northern sponge reef collecting nutrient, transmissivity and conductivity, temperature and

Fig. 1 Distribution of sponge reefs in the Queen Charlotte Basin. The basin includes the seafloor of Dixon Entrance, Hecate Strait, Queen Charlotte Sound and much of the subaerial Queen Charlotte Islands

depth (CTD) data. Other samplings of opportunity collected small data sets in the vicinity of the reefs.

Extensive diving operations by the manned submersible *Delta* (1999) and a HD2+2 DeepOcean Engineering Remote Operated Vehicle (2002) provided a library of seabed video and still imagery (http://www.pgc.nrcan.gc.ca/marine/sponge/index_e.htm and http://www.porifera.org; see Krautter 2000 and Geological Survey of Canada 2002. In addition, archived geophysical and sample data housed at the Pacific Geoscience Centre of the Geological Survey of Canada provided data compiled from many previous regional geophysical surveys (Conway et al. 1991; Barrie and Conway 2002).
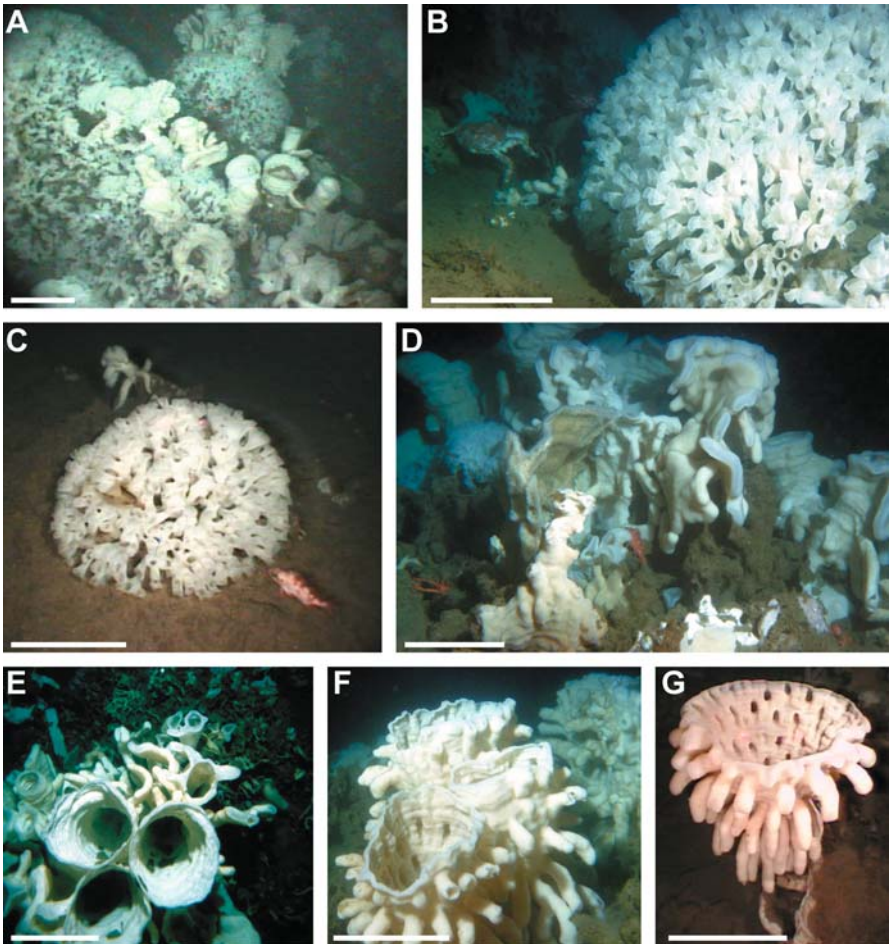
Fig. 2 A Surface of sponge reef in Hecate Strait. Scale bar is 60 cm. **B-C** *Farrea occa*. Note Puget Sound King crab to left of sponge in **B** and juvenile rockfish at lower left in **C**; **D-E** *Aphrocallistes vastus*. Note squat lobster (*Munida* sp.) at lower left and juvenile rockfish partially hidden at centre in **D**. **F-G** *Heterochone calyx*. Scale bar is 20 cm in **B-G**

Geological and physiographic controls on reef development

The physiography of the north-western continental shelf has been shaped by successive glaciations, resulting in the formation of glacial troughs to 450 m deep, with intervening banks rising to 40 m water depth (Luternauer and Murray 1983). The most recent Late Quaternary glaciation, when ice advanced to the shelf edge in all the major shelf troughs (Josenhans et al. 1995), combined with post-glacial sea-level changes, established the surficial sediment distribution of seafloor substrates on much of the continental shelf (Barrie and Bornhold 1989; Luternauer et al. 1989a, b; Barrie and Conway 2002). The surficial geological units are similar in all three major toughs (Fig. 1) where the sponge reefs are found; with a relatively thick (up to 50 m) late Quaternary diamicton overlying the Neogene aged Skonun Formation that forms much of the sedimentary infill of the Queen Charlotte Basin (Barrie et al. 1991; Woodsworth 1991). Glaciomarine sediments of variable thickness rest conformably on this diamicton, with a total thickness of Quaternary sediments of up to 100 m in some areas (Barrie and Conway 1999).

Sea-levels in the Queen Charlotte Basin were as low as 150 m below present on the continental shelf (Josenhans et al. 1995; Barrie and Conway 2002) and this led to a widespread distribution of coastal deposits and thick sublittoral sediments in some areas and erosion and intensive sediment transport across much of the shelf. Where sublittoral sands and silts were deposited during the lowstand, the antecedent coarse glacial substrates were buried and sealed off from access by epibenthic organisms requiring hard substrate. Holocene terrestrial sediments are largely trapped in the deep fjords and channels that border the continental shelf on the British Columbia mainland (Luternauer and Murray 1983). On the inner to mid shelf, the seabed remained relict and iceberg furrowed glaciomarine sediments were preserved at the seabed (Fig. 3; Luternauer and Murray 1983; Barrie and Bornhold 1989) as sea-level rose. Iceberg furrows form suitable attachment sites for benthic epifauna as the berms of the furrows tend to be more coarse as boulders are cast up by the ploughing action of the iceberg (Woodward-Lynas et al. 1991). Fines are winnowed from the berms of the furrow by bottom currents further concentrating coarse debris (Conway et al. 1991).

Sponge bioherms are preferentially initiated on the coarse debris on the shoulders of the furrows (Fig. 3). After establishment of the bioherm, subsequent lateral and vertical growth is dependent on the capture of suspended sediments by trapping and baffling, and the biological processes of reef growth that include several related ways of frame building by the sponges (Krautter et al. 2002). This relationship is similar to that described for the *Lophelia pertusa* reefs found on the Sula Ridge, on the Norwegian continental shelf, where coral reefs are clustered along relict iceberg ploughmarks (Freiwald et al. 1999, 2002). Ultimately the small sponge bioherms grow vertically as well as laterally over less favourable seafloor substrates and coalesce to form very large continuous structures covering kilometres of seafloor (Fig. 4). The mechanisms of reef growth are further described below.
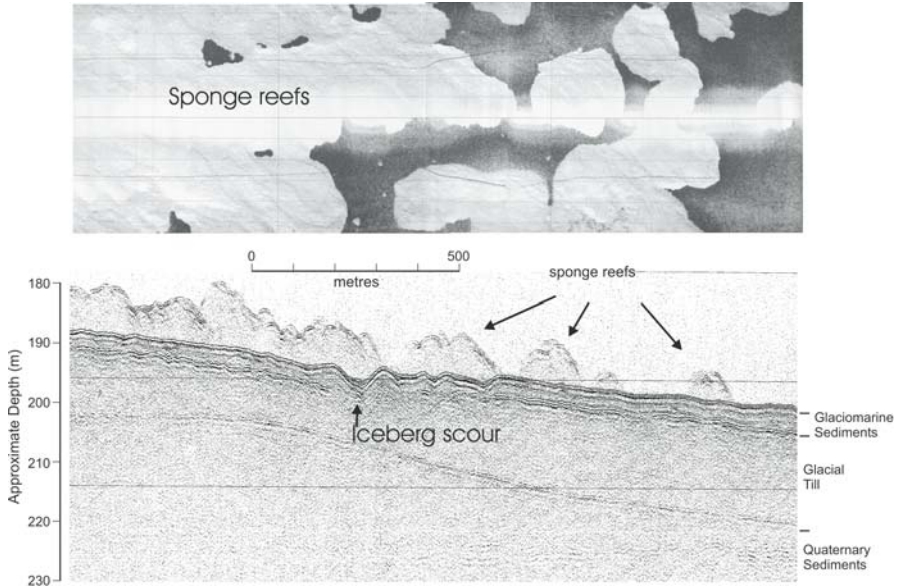
Fig. 3 Coincident sidescan sonar and high-resolution seismic record of sponge reefs in Hecate Strait showing relationship to underlying geological units. Dark grey tones indicate areas of higher reflectivity. Sponge reefs are clay rich so much less reflective than the underlying sandy and gravelly glacial sediments. The reefs coalesce to form larger continuous structures

Modern tractive transport of fine sands occurs along bank margins in water depths to 140 m (Barrie et al. 1988) and oscillation (wave) ripples can develop in depths to at least 110 m (Yorath et al. 1979). Hexactinosidan sponges, with their glass frame skeletons, are fragile and require quiescent conditions and so are precluded from colonizing such energetic areas. The glacially and sea-level derived sediment distribution pattern coupled with present day shelf bathymetry thus control distribution of potential reef sites. The sponge reefs are found in dense clusters of various shapes at four locations in the troughs (Fig. 1). These clusters consist of steep sided bioherms or reef mounds, and also as elongate irregularly shaped and variably sloping ridges, where bioherms have coalesced and grown together over time. In addition, flat lying sponge meadows, or biostromal reefs are found at these sites. We refer to each of these four geographically separate groupings of diverse reef forms, as reef complexes (Conway et al. 2001).

Oceanographic controls on development

The oceanography of the northern British Columbia continental shelf is a mixed semi-diurnal, meso to macrotidal regime where circulation is affected by winds, runoff, and shore configuration (Thomson 1981). Bathymetric constraints are prevalent in focussing of currents within and along the axes of the shelf troughs. Shelf waters within British Columbia are noted to have a high ambient relative
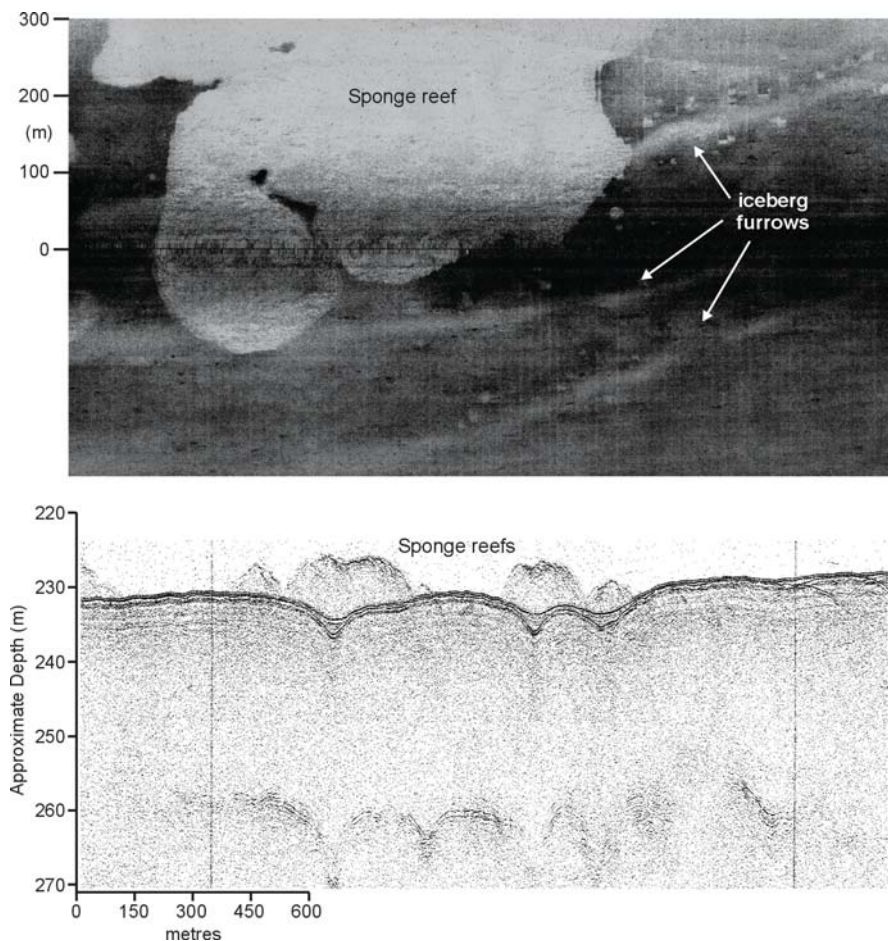
Fig. 4 Sidescan sonogram and high-resolution seismic record of sponge reef in southern Queen Charlotte Sound. Note the small bioherms concentrated along the trace of the relict iceberg furrow. Bioherms are up to 10 m in height at this site

silica concentration and this has been suggested to be an important control on shallow populations of hexactinellid sponges (Austin 1998). Seasonal wind induced upwelling is an important process whereby nutrient rich slope waters are brought to the surface through the shelf troughs (Crawford 2001). This area is at the northern extreme of coastal upwelling, according to upwelling indices provided by the National Atmospheric and Oceanic Administration (NOAA). Upwelling is wind-driven and restricted to the summer months when the appropriate northwest wind and water density conditions exist. Because higher salinity waters are brought onto shelf regions during summer (Dodimead et al. 1963; Herman et al. 1989), salinity and nutrient concentrations are considerably higher in summer, compared with winter. Measured near-bottom nitrate increased from 27 to 35 µM as salinity

increased from 33.2 to 33.7 ‰. Likewise, silicate increased from 49 to 70 μM and oxygen decreased from 152 to 101 μM from winter to summer. Measurements of conductivity, temperature and depth show the effects of winter downwelling and summer upwelling clearly. Summer bottom waters are thus cooler, more saline, nutrient rich and oxygen poor (Whitney et al. 2005).

Using results from the World Ocean Circulation Experiment (WOCE), concentrations of silicate and oxygen are shown for the 200 m depth strata (Fig. 5) along a section that starts in the North Atlantic, extends into the Southern Ocean (WOCE section A16), then runs northward through the Pacific Ocean to the Aleutian Islands (WOCE section P15). The x-axis on this plot is an along-track measure of the distance from the first station, located at 63°20'N, 20°0'W. The final station is in the North Pacific, near the coast of Alaska (53°55'N, 164°59'W). A section at 200 m matches the depth of the sponge reefs and also is representative of the source of upwelled nutrients in the Northeast Pacific (Freeland and Denman 1982; Wheeler et al. 2003). The two regions with highest silicate levels are in the Southern Ocean, south of the Polar Front, and in the North Pacific, north of the Subarctic Front. Silicate concentrations range from <1 μM in subtropical regions of the Atlantic and Pacific Oceans to 91 μM in the Southern Ocean and 87 μM in the subarctic Pacific. Oxygen levels at 200 m range from >300 μM in the Southern Ocean and ~270 μM in the North Atlantic and Pacific, to as little as 56 μM in the subarctic Pacific and 16 μM in the Equatorial Pacific.

The trough head location of the sponge reefs provides a means of funnelling these enriched bottom waters to the reefs. Detrital material, derived from both onshore coastal sources and the resuspension of offshore particles, is suspended in a bottom nepheloid layer and effectively trapped by dense populations of sponges (Whitney et al. 2005). Trapping of these materials results in the observed enrichment of
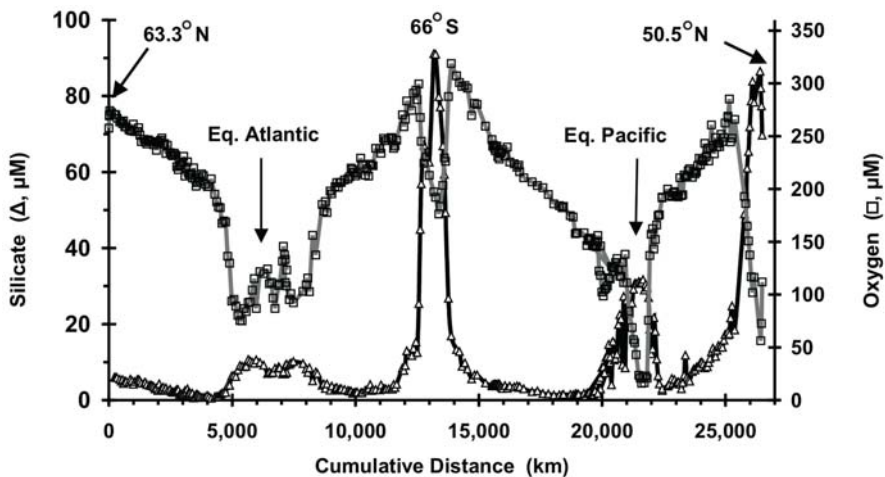
Fig. 5 Silicate (dark curve) and oxygen concentrations at 200 m along a section starting at 63°N in the North Atlantic, extending to the Southern Ocean in the Atlantic and Pacific, then heading northward through the Pacific to 54°N
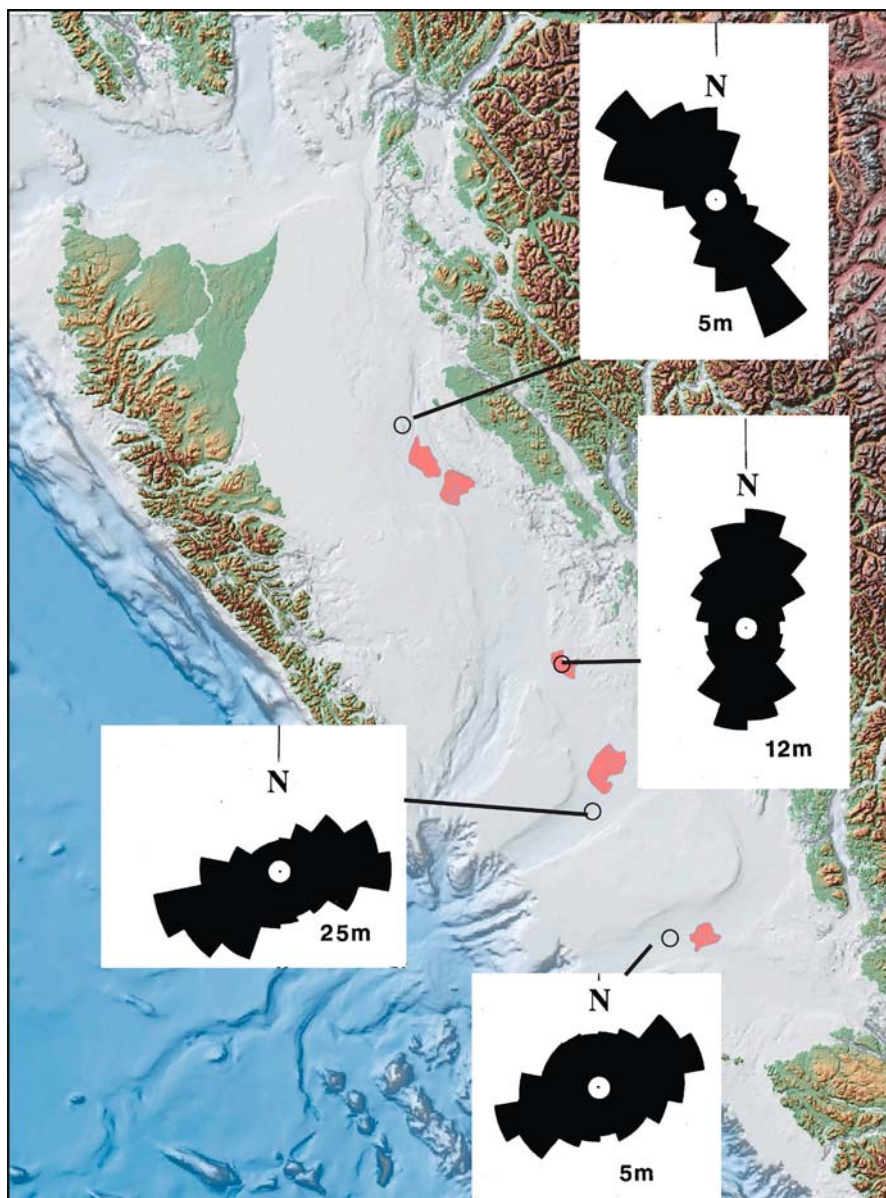
Fig. 6 Near bottom current directions at sponge reef complexes (stippled areas) are strongly constrained by bathymetry. Current roses show distribution of all measured current directions. Current velocities are discussed in text. The value below the current rose refers to height of current meter above seabed. Data courtesy of Department of Fisheries and Oceans (DFO), Canada

organic carbon, nitrogen and opal as measured in core, relative to surrounding and underlying sediments (Conway et al. 2001). Near bottom currents are constrained and focused by bathymetry at all sponge reef complexes (Fig. 6). The sponges thus exist in relatively enriched zones where several oceanographic processes ensure an optimal delivery of dissolved nutrients and potential food particles. Furthermore, the reefs are situated within a current regime where seabed currents reach a maximum of 50 cm/sec. This both provides access to required nutrients and keeps fine sediments in suspension, preventing smothering by sediment deposition.

Tidal currents repeatedly cycle bottom waters across the reefs. In Hecate Strait, where the northernmost sponge reef is located, such bottom water has a residence time over the reef within the trough of approximately six days, calculated from the net transport by currents measured at mooring sites. This water residence time ensures a close association of the reefs with the bottom water. The sponges are
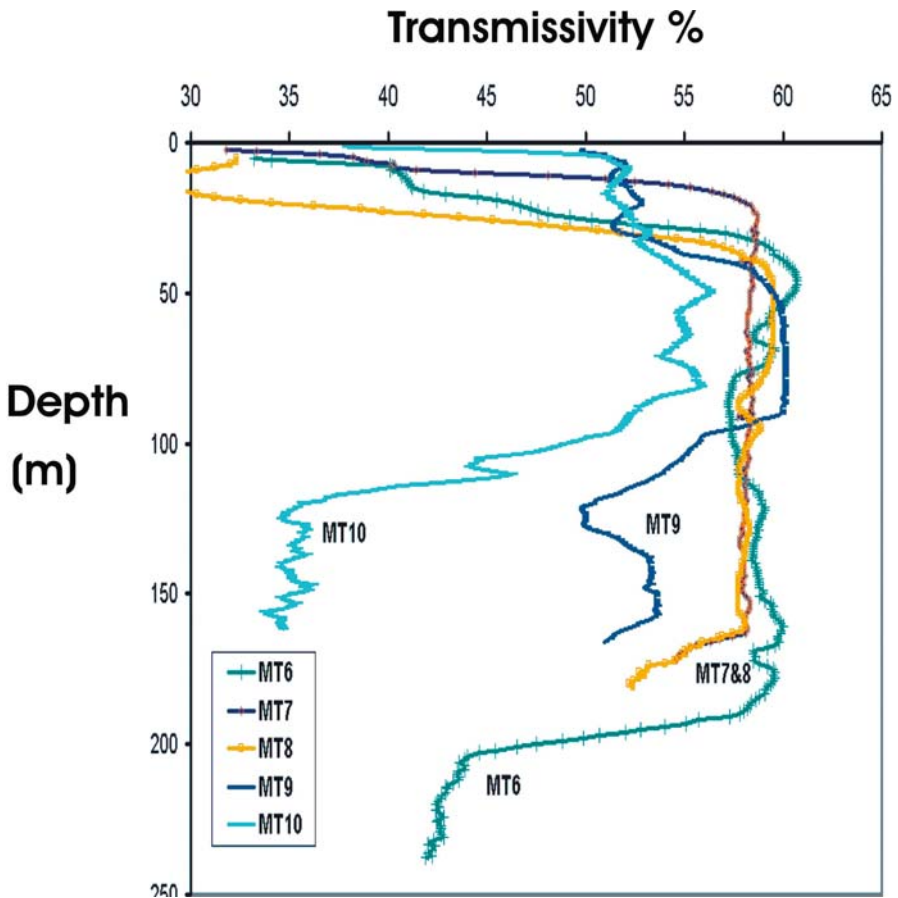
Fig. 7 Light transmission (%) *vs.* depth at stations at North Hecate Strait reef complex (MT 7, 8 and 9) and 28 km south (MT6) and 30 km north (MT10) of reef. Particle density is reduced in the vicinity of the reefs

exposed to suspended sediment in a nepheloid layer that is up to 30 m thick above the seabed. In transmissivity profiles obtained at reef sites, particle concentrations are reduced in the nepheloid layer relative to profiles obtained nearby; suggesting particle trapping by sponges is efficient (Fig. 7). Construction of large mounds is probably favoured by a positive feedback by increased access to nutrients by sponges living on high points of the reef (Conway et al. 1991). The large obstructing mounds on the seabed appear to deflect the tidal currents, creating flow conditions that are more locally complex than outside of the reef areas.

Biological controls on development

The sponges that form the framework of the reefs are all members of the Hexactinosida, and possess a mainframe skeleton composed of fused spicules of hydrated amorphous silica. The three sponges that build the reef framework (*Farrea occa* (Figs. 2B, C), *Heterochone calyx* (Figs. 2D, E) and *Aphrocallistes vastus* (Figs. 2F, G)) all require firm substrate for attachment of larvae (Conway et al. 1991). The sponges variably cover the surface of the reef mounds, and may completely cover the seafloor (Fig. 2A). The framework is created through three related processes that include 1) stabilizing, accessory outgrowths (Figs. 8A-C, E), 2) skeletal welding, where a living sponge overgrows or incorporates the skeleton of a neighbouring sponge, and 3) larval attachment (Fig. 8D) (Neuweiler 2001; Krautter et al. 2002). These processes all require the availability of a bare hexactinosidan skeleton (Neuweiler 2001). The surface of the bioherm is only successfully colonised by larvae where unburied skeletons project from the seabed. The development of a bioherm is also dependent on the natural selection for larvae that preferentially attach to the reef surface rather than available adjacent hard substrates (gravel). Hexactinosidan sponges are, in general, less common in the Atlantic than in the Pacific Ocean, and the genus *Heterochone*, which has the most robust and durable skeleton of the three reef framework builders, is entirely Pacific in distribution (Reiswig 2002). Sponge morphology includes broad forms including dish, basket and shield shapes (Fig. 8A), (Krautter et al. 2001; Conway et al. 2004). In such cases the site of growth of one of these broad forms may initially be a small clast or, in later stages of development, a fragment of projecting skeleton on the bioherm surface. The surface area eventually covered by such a sponge may be several square metres (Fig. 2A) resulting in a greatly expanded surface area for attachment of subsequent sponge generations when this sponge dies and becomes partially buried. In this way sponge morphology may contribute to the lateral expansion of the bioherm over adjacent seafloor.

The sediment trapping and baffling capacity of the sponges is an important control on reef growth in that sponges control the sedimentation at reef sites through these processes (Conway et al. 2004). The biological controls on development are perhaps the least known factors, as this group of sponges have not been extensively studied. Aspects that are very poorly known include such subjects as sponge larval production and motility as well as life span and growth rates. In addition, mechanisms of sediment capture and particle removal and surface cleaning by the
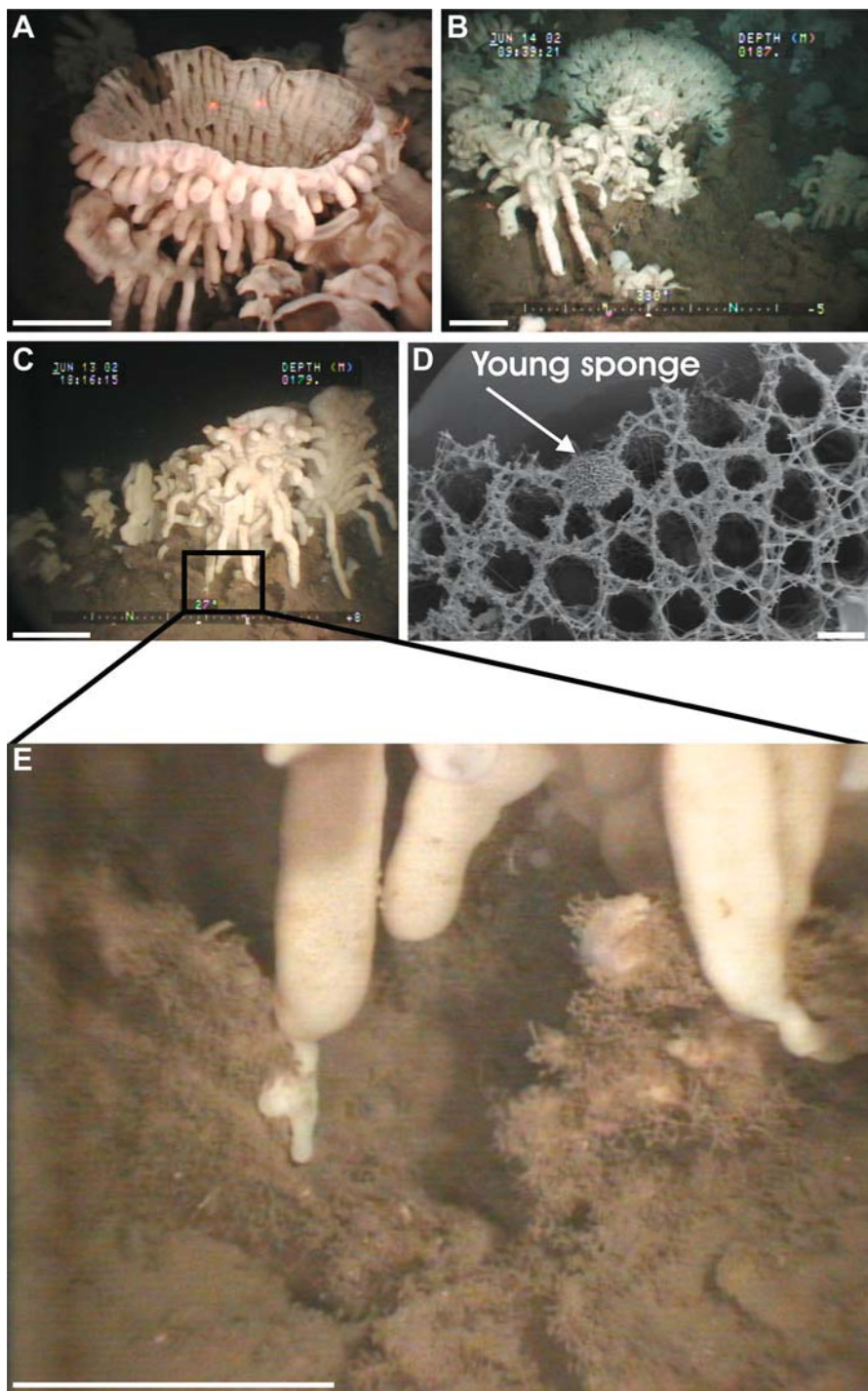
sponge are not understood. Seasonal aspects of sponge growth and reproduction are probably important, given the seasonal oceanographic changes in nutrient and sediment flux. Other sponges are evident on the reef surface though they are not involved in forming the reef framework. These include the rossellid hexactinellid species *Rhabdocalyptus dawsoni*, *Staurocalyptus dowlingi*, *Acanthascus platei*, *Acanthascus cactus*. Demosponges are present in abundance, both on the reefs as individuals such as *Poecillastra tenuilaminaris* and *Geodia mesotriaena,* and also as cryptic commensal, epizootic or possibly parasitic sponges that grow on and within hexactinosan skeletons including *Halichondria disparilis*, *Desmacella* sp., *Poecillastra rickettsi*, *Asbestopluma lycopodium*, and *Antho* (*Plocamia*) *illgi*. It is most likely that hexactinosidan sponges have no natural predators. Reef accompanying benthic organisms are echinoderms, crustaceans, bryozoans, Foraminifera, brachiopods and bivalves to a minor degree. Frequently immature rockfish are seen in the complex surface of the reef, suggesting a refugium function for the reef. Reef destroying organisms are absent. Due to the dysaerobic conditions in the sediment infaunal organisms are rare except terebellid worms. Organic carbon content of the sediments is typically greater than 3 %, which leads to this hypoxic subsurface condition (Conway et al. 2001).

Ocean management and trawl impacts

Sponge reefs have sustained extensive and well-documented damage by groundfish trawling (Conway et al. 2001; Jamieson and Chew 2002) at all four reef complexes. The reefs were presumably subject to large-scale damage during the years of unrestricted fishing by foreign trawling fleets fishing Pacific Ocean Perch and other rockfish in Queen Charlotte Sound 1956-1971 (DFO 1999). Between 1971 and 1977 foreign fleets continued to operate, but at a somewhat reduced level. This fishery was largely located within the troughs that form the known sponge reef habitat (Conway et al. 2001). Reefs in central Hecate Strait, which were outside of the areas targeted by the foreign fishery (DFO 1999), remain the most pristine and undamaged. Closure of the sponge reef areas to groundfish trawling was instituted in July 2002 as a control measure to reduce trawl fishery impacts on the reefs. Recovery from trawl impacts may be very slow as the sponges grow to a large size relatively slowly. A 1 m tall hexactinellid sponge may be up to 220 years old, based on work by Leys and Lauzon (1998) focused on the volumetric relationship of sponge lengths to measured growth rates and recovery of a destroyed reef surface may thus take 100-200 years (Conway 1999). Uncertainty of recovery from trawl impacts also

Fig. 8 A *Heterochone calyx* at centre with *A. vastus* at lower right; **B** *H. calyx* is at left above scale bar; **C** Cluster of *H. calyx* displays elongate accessory stabilizing supports or holdfasts that attach to the bioherm surface. Scale bar is 20 cm. **D** Scanning electron microscope micrograph of a young hexactinosidan sponge of uncertain species, 1 mm in diameter, growing on the surface of the skeleton of *A. vastus*. Scale bar is 1 mm (after Neuweiler 2001). **E** Close up view of attachment points of secondary holdfasts of *H. calyx*. Note moss or spider web-like covering of bioherm surface. Scale bar is 10 cm

stems from the almost complete lack of knowledge of the reproductive strategies of hexactinosidan sponges. Recovery from the widespread trawl fishery impacts may depend on the longevity, motility and transport of the, as yet undiscovered, larval stages of the reef forming hexactinosidan sponges. Analysis of the groundfish trawl fishery bycatch indicates that close to 95 % of the sponge bycatch in the Queen
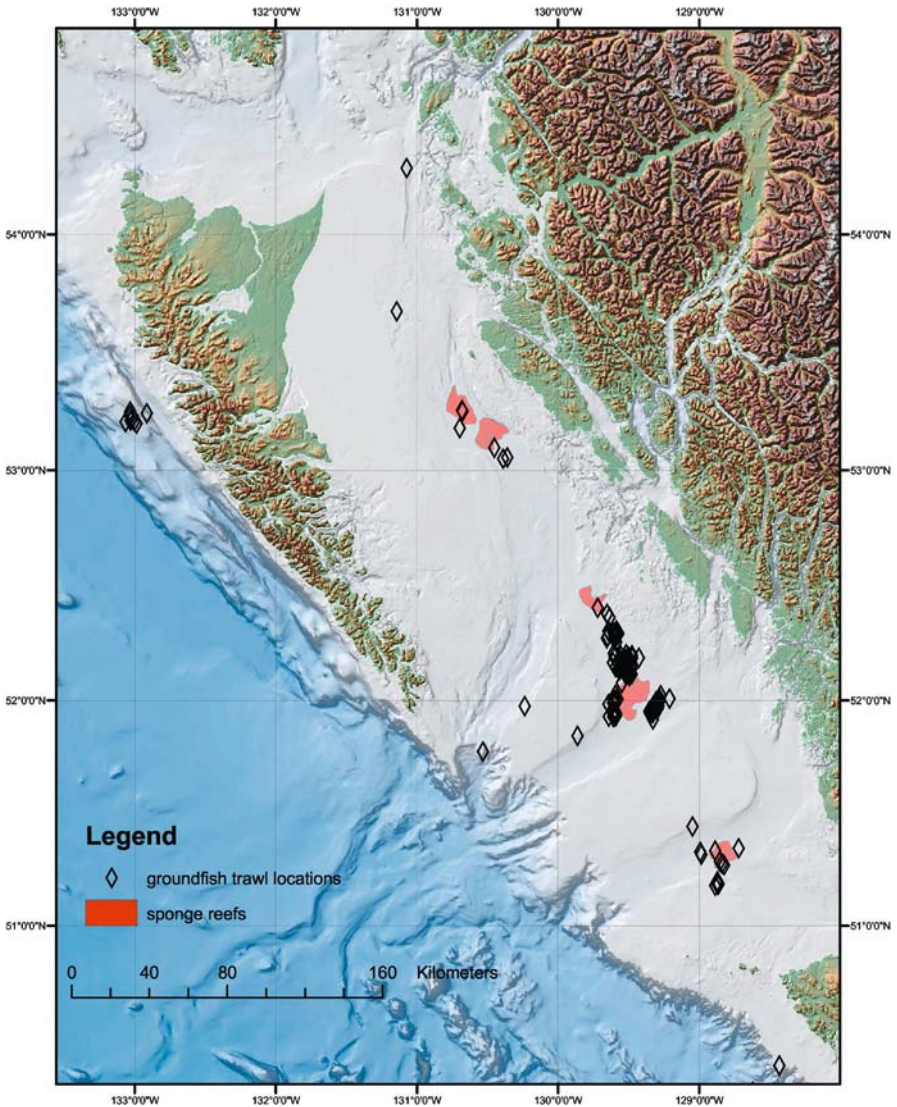
Fig. 9 Distribution of groundfish trawl sets where 95 % of the total sponge bycatch was reported in the fishery between 1996 and 2002. Most sponge bycatch, regionally, is captured in or near the reef complexes (red tone). Data provided courtesy of Alan Sinclair (Pacific Biological Station, DFO, Canada)

Charlotte Sound/Hecate Strait area was caught close to the reef complexes between 1996 and 2002 (Fig. 9). Fish and crab trap and longline fisheries continue to operate in, and presumably have some impact on, sponge reefs in all areas.

Summary and conclusions

Physical environmental conditions favourable to the formation of large siliceous sponge reefs include a relict, environmentally stable shelf, in quiescent water that is below wave base, which in much of the Queen Charlotte Basin is below 140 m. A seafloor of low slope angle with the availability of coarse (gravel) substrate is required. Oceanographic conditions include the delivery of suspended sediments and appropriate nutrient levels including a relatively high concentration of dissolved silicate (>40 μM). Moderate currents, directed and focussed by tidal processes within the shelf troughs, enriched by a combination of seasonal upwelling and coastal runoff and surface water productivity are also critical conditions for development. These oceanographic and geological conditions provide an enriched, yet non-depositional, benthic environment that is very favourable to dense hexactinellid sponge populations. Development of hexactinosidan sponge reefs also requires the appropriate frame-building sponge fauna be present. The frame-building capability of the three species of hexactinosidan sponges includes three related mechanisms for framework formation that include skeletal "welding", or intergrowth, secondary holdfast development seen especially in *Heterochone calyx* and attachment of larvae to the reef framework. The Atlantic Ocean is less well endowed with such a hexactinosidan sponge fauna than is the Pacific Ocean, with the important reef-forming genus, *Heterochone*, restricted entirely to the Pacific. Although the sponge reefs found on the western Canadian continental shelf appear to be unique to this region, many continental margin areas of the Pacific remain to be surveyed, so that their occurrence elsewhere cannot be precluded. However, in view of the critical oceanographic, geological and biological processes that in combination control reef development on the western Canadian continental shelf, it is apparent that conditions favourable to the formation of extensive hexactinellid sponge reefs are not commonly found in the present world ocean.

Acknowledgements

References

Austin WC (1998) The relationship of silicate levels to the shallow water distribution of Hexactinellids in British Columbia. Mem Queensland Mus 44: 44

Barrie JV, Bornhold BD (1989) Surficial geology of Hecate Strait, British Columbia continental shelf. Can J Earth Sci 26: 1241-1254

Barrie JV, Conway KW (1999) Late Quaternary glaciation and postglacial stratigraphy of the northern Pacific margin of Canada. Quatern Res 51: 113-123

Barrie JV, Conway KW (2002) Contrasting glacial sedimentation processes and sea-level changes in two adjacent basins on the pacific margin of Canada. Geol Soc London Spec Publ 203: 181-194

Barrie JV, Emory-Moore M, Luternauer JL, Bornhold BD (1988) Origin of modern heavy mineral deposits, northern British Columbia continental shelf. Mar Geol 84: 43-51

Barrie JV, Bornhold BD, Conway KW, Luternauer JL (1991) Surficial geology of the northwestern Canadian continental shelf. Cont Shelf Res 11: 701-715

Conway KW (1999) Hexactinellid sponge reefs on the British Columbia continental shelf: geological and biological structure with a perspective on their role in the shelf ecosystem. Canad Stock Assess Secr Res Doc 99/192, 21 pp

Conway KW, Barrie JV, Austin WC, Luternauer JL (1991) Holocene sponge bioherms on the western Canadian continental shelf. Cont Shelf Res 11: 771-790

Conway KW, Krautter M, Barrie JV, Neuweiler M (2001) Hexactinellid sponge reefs on the Canadian continental shelf: a unique "living fossil". Geosci Canada 28: 71-78

Conway KW, Barrie JV, Krautter M (2004) Modern siliceous sponge reefs in a turbid, siliciclastic setting: Fraser River delta, British Columbia, Canada. N Jb Geol Paläont Mh 6: 335-350

Crawford WR (2001) Oceans of the Queen Charlotte Islands. Can Tech Rep Fish Aqua Sci 2383

Department of Fisheries and Oceans Canada (DFO) (1999) Pacific Ocean Perch, British Columbia Coast. DFO Stock Status Report A6-11

Dodimead AJ, Favorite F, Hirano T (1963) Salmon of the North Pacific Ocean, Part II. Review of Oceanography of the Subarctic Pacific region. Int North Pacific Fish Comm Bull 13, 195 pp

Freeland HJ, Denman KL (1982) A topographically controlled upwelling center off southern Vancouver Island. J Mar Res 40: 1069-1093

Freiwald A, Wilson JB, Henrich R (1999) Grounding Pleistocene icebergs shape recent deep-water coral reefs. Sediment Geol 125: 1-8

Freiwald A, Hühnerbach V, Lindberg B, Wilson JB, Campbell J (2002) The Sula reef complex, Norwegian shelf. Facies 47: 179-200

Geological Survey of Canada (2002) Marine/sponge reef project website. http://www.pgc. nrcan.gc.ca/marine/sponge/index_e.htm

Hermann AJ, Hickey BM, Landry MR, Winter DF (1989) Coastal upwelling dynamics. In: Landry MR, Hickey BM (eds) Coastal Oceanography of Washington and Oregon. Elsevier, Amsterdam, pp 211-253

Jamieson GS, Chew L (2002) Hexactinellid sponge reefs: areas of interest as marine protected areas in the north and central coast areas. Canad Sci Adv Secr, Res Doc 2002/12

Josenhans HW, Fedje DW, Conway KW, Barrie JV (1995) Post glacial sea levels on the western Canadian continental shelf: evidence for rapid change, extensive subaerial exposure and early human habitation. Mar Geol 125: 73-94

Krautter M (2000) Sponge reef website.http://www.porifera.org

Krautter M, Conway KW, Barrie JV, Neuweiler M (2001) Discovery of a "living Dinosaur": globally unique modern hexactinellid sponge reefs off British Columbia, Canada. Facies 44: 265-282

Krautter M, Conway KW, Barrie JV, Neuweiler M (2002) Hexactinosan sponges: larval attachment mechanism and related reef framebuilding processes. Boll Mus Inst Biol Genova: 66-67

Leys SP, Lauzon NRJ (1998) Hexactinellid sponge ecology: growth rates and seasonality in deep water sponges. J Exp Mar Biol 230: 111-129

Luternauer JL, Murray JW (1983) Late Quaternary morphologic development and sedimentation, central British Columbia continental shelf. Geol Surv Canad Pap 83-21, 38 pp

Luternauer JL, Clague JJ, Conway KW, Barrie JV, Blaise B, Mathewes RW (1989a) Late Pleistocene terrestrial deposits on the continental shelf of western Canada: evidence for rapid sea-level change at the end of the last glaciation. Geology 17: 357-360

Luternauer JL, Conway KW, Clague JJ, Blaise B (1989b) Late Quaternary geology and geochronology of the central continental shelf of western Canada. Mar Geol 89: 57-68

Malecha PW, Stone RP, Heifetz J (in press) Living substrate in Alaska: distribution, abundance and species associations. In: Barnes P, Thomas J (eds) Benthic habitats and the effects of fishing. Amer Fish Soc Proc, Bethesda, MD

Neuweiler M (2001) Untersuchungen an Kieselnadeln rezenter hexactinellider Schwämme. Unpubl MSc thesis, Univ Stuttgart, 166 pp

Reiswig HM (2002) Family Aphrocallistidae. In: Hooper JNA, Van Soest RWM (eds) Systema Porifera: A Guide to the Classification of Sponges. 2, Kluwer/Plenum, New York, pp 1282-1286

Thomson RE (1981) Oceanography of the British Columbia Coast. Canad Spec Publ Fish Aqua Sci 56, 291 pp

Wheeler PA, Huyer A, Fleischbein J (2003) Cold halocline, increased nutrients and higher chlorophyll off Oregon in 2002. Geophys Res Lett 30: 8021

Whitney F, Conway KW, Thomson RE, Barrie JV, Krautter M, Mungov G (2005) Oceanographic habitat of sponge reefs on the western Canadian Continental Shelf. Cont Shelf Res 25: 211-226

Woodsworth GJ (1991) Evolution and hydrocarbon potential of the Queen Charlotte Basin, British Columbia. GSC Pap 90-10, 569 pp

Woodworth-Lynas CMT, Josenhans HW, Barrie JV, Lewis CFM, Parrot DR (1991) The physical process of seabed disturbance during iceberg grounding and scouring. Cont Shelf Res 11: 939-961

Yorath CJ, Bornhold BD, Thomson RE (1979) Oscillation ripples on the northeast Pacific continental shelf. Mar Geol 31: 45-58

Pockmark-associated coral reefs at the Kristin field off Mid-Norway

Martin Hovland

Statoil, N-4035 Stavanger, Norway
 (mhovland@statoil.com)

Abstract. Topographic and geophysical seafloor mapping has shown that in some areas there apparently is a close relationship between pockmarks and coral reefs. Off Norway there are three such occurrences: The Haltenpipe Reef Cluster (HRC), the Fugløy Reefs, and reefs in the Kristin hydrocarbon field. In the Porcupine area off Ireland, there is also a close relationship between large pockmark-like depressions and carbonate mounds with corals. Such is also the case with the Darwin Mounds, at 1000 m depth, where pockmarks occur close to the mounds containing *Lophelia* corals. In the Gulf of Mexico and off Brazil there are similar associations.

At the Kristin hydrocarbon field off Mid-Norway (located 130 km NW of the HRC and the Sula Ridge Reefs), pockmarks and coral reefs occur in abundance. Out of 120 reefs mapped within an area of 14 km^2, there are 33 reefs that occur inside or along the inside rim of pockmarks. Most of the other 87 reefs are located within 200 m of a pockmark. The largest reefs at Kristin are up to 3.5 m high and 90 m in length.

The observed co-occurrence between corals and pockmarks suggests that gas and porewater emanating from pockmarks stimulates coral growth, probably through the provision into the water column of a stable food (nutrient) supply, in the form of bacteria and micro-organisms. This theory has previously been called the "hydraulic theory" for coral reefs. Both of the new (Kristin and Fugløy) reef/ pockmark cases strengthen the validity of this theory. Furthermore, this close association also indicates that the sessile animals living in these reefs (*Lophelia*, *Paragorgia*, *Primnoa*, *Acesta*, etc.) may be more robust and tolerant to episodes of silting than previously suspected.

Keywords. Norwegian shelf, *Lophelia,* pockmark, hydrocarbon, hydraulic theory

Introduction

It may be fair to say that modern geophysical and visual documentation of deep-water coral reefs, with side scan sonars, sub bottom profilers, and remotely operated vehicles (ROVs) started in Norway in 1982, when Statoil unexpectedly encountered a large coral reef in the Fugløy Reef complex, while surveying a potential pipeline

route in northern Norway (Hovland 1990; Hovland et al. 1994b; Hovland and Mortensen 1999). Even at this "first" location, pockmarks - the most common seabed fluid expulsion feature (King and MacLean 1970; Hovland and Judd 1988) - were found, less than one kilometre from the reef location. During subsequent reconnaissance pipeline route surveys off Mid-Norway (1984-1990), numerous relatively isolated (individual) large coral reefs were mapped, some of which were clearly associated with small (<30 m wide) pockmarks (Fig. 1).

Although, the possibility of deep-water coral reefs actually depending on fluid expulsion was discussed by Hovland in 1990, "the hydraulic theory" was launched later (Hovland et al. 1998; Hovland and Mortensen 1999). There are many indications pointing to a dependency between Norwegian deep-water coral reefs and seepage, but there is still no undisputable proof of such a link (Hovland and Risk 2003). However further evidence is presented here, with survey data showing an intimate relationship between fluid expulsion features, large (>30 m wide) pockmarks, and Norwegian coral reefs in the Kristin field.

The Kristin field

The Kristin hydrocarbon field is located on the "shoulder" of the continental shelf off Mid-Norway, at water depths ranging between 310 and 385 m (location: 65°N, 06°30'E). The field is currently undergoing development and will contain
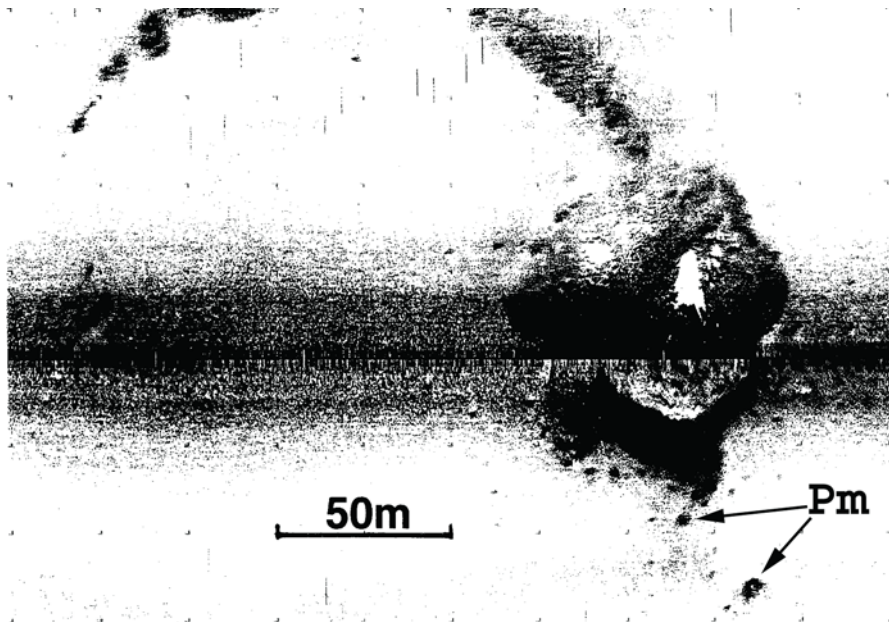
Fig. 1 Image from a side scan sonar record showing a pattern of small (~10 m diameter) pockmarks occurring in association with a *Lophelia* reef off Mid-Norway. The reef is seen here as the large circular mass of about 60 m diameter to the right

several sub-sea and one floating production units (Storvoll et al. 2002). During the detailed mapping with hull-mounted and ROV-mounted multi-beam echosounders and side scan sonars, it became evident that this location contains numerous large pockmarks and also coral reefs.

Within the 14 km^2 area mapped there is a medium density of pockmarks (approximately 6 per km^2), of typically 130 m width and 10-12 m depth. A total of 120 reefs were mapped within the same 14 km^2 area. About a quarter of these (33 reefs) occur inside or along the inside rim of pockmarks. Most of the other 87 reefs, are located within 200 m of a pockmark. The largest reefs at Kristin are up to 3.5 m high and 90 m in length.

As part of the seafloor documentation prior to field development, three of the pockmark-occupying coral reefs were surveyed visually in July 2003. It should be mentioned that none of the reefs will be damaged during the field development and production phase, as anchor patterns and flowline routes have been chosen such that they avoid the reefs. The three visually documented reefs are designated KP1, KA1, and KA2. The size of the reefs, their depth span, and size of the pockmark they occupy are given in Table 1.

Because the seafloor detailed mapping has been performed with ROV-mounted multibeam echosounder and side scan sonar, the exact location and extent of the coral reefs are well documented. From the bathymetric profile, shown in Figure 2, the location of two reefs is seen to be inside two distinct pockmark craters, one of these reefs (KA2) having been surveyed visually. Figure 3A is a video-grabbed image from the coral reef KA2, located inside pockmark PmA2, at Kristin. It shows a healthy *Lophelia* colony which seems to have grown around a large *Paragorgia arborea* and a suspected *Primnoa* sp. colony. For comparison, Figure 3B is a rare photograph, showing a small *Lophelia* colony, located adjacent to a *Paragorgia arborea*, and a small bacterial mat (arrowed) located between them. This photograph was acquired in 1991 from another location off Mid-Norway (concession block: 6407/4) above a hydrocarbon reservoir of no commercial potential. Normally, a bacterial mat suggests strong chemical concentration gradients and/or limited bottom water oxygen. When found on the general seafloor as small patches, we interpet them as indicators of seepage of anoxic fluids from the subsurface (Hovland 2002).

Table 1 Characteristic size and depth spans of coral reefs and their associated pockmarks at three locations in the Kristin field. The reef height is measured from the sloping pockmark bottom

	REEFS			**POCKMARKS**		
Depth span (m)	319-327	323-329	316-326	316-328	317-329	316-327
Height / depth (m)	3.0	3.5	3.0	12	12	11
Length (m)	90	60	85	150	180	130
Width (m)	30	50	40	120	75	120
Reef or pockmark id	KP1	KA1	KA2	PmP1	PmA1	PmA2
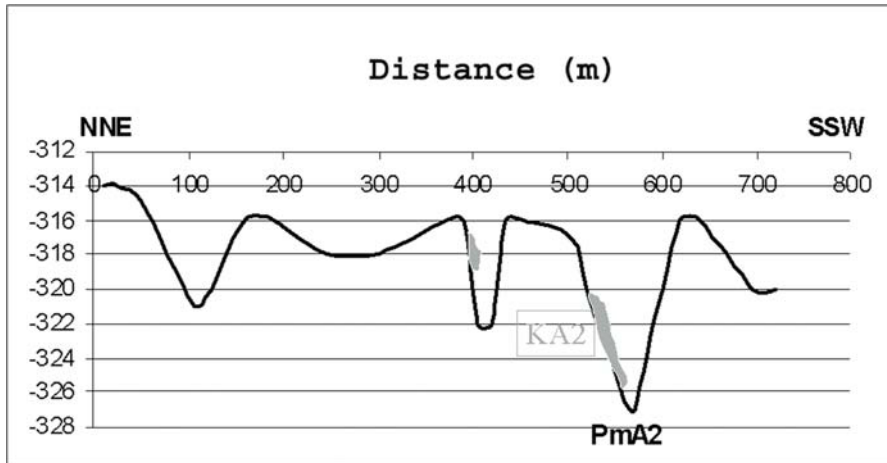
Fig. 2 A bathymetric transect through three pockmarks in the Kristin hydrocarbon field. Pockmark-occupying coral reefs are seen in two of these, including KA2, which was visually investigated (see Table 1 and Fig. 4). Note that the reefs occur below the rim of the two more-or-less circular pockmark depressions. Water depth is shown in m below mean sea level (-312 to -328 m)

From a preliminary analysis of the video footage, it can be determined that the dominant sessile macro-organisms and reef builders on these three reefs are (in order of apparent abundance): the stony coral *Lophelia pertusa*, various types of large sponges (including *Geodia* sp.), the octocorals *Paragorgia arborea* and *Primnoa resedaeformis*, and the mussel *Acesta excavata* (Fig. 3C). The most common fish living in these pockmarks are: *Sebastes* sp. and *Brosme brosme*.

Besides the Kristin coral reefs, there are only a handful of other known occurrences where reefs are directly associated with large pockmarks. These are: at the Haltenpipe Reef Cluster (HRC; Hovland and Risk 2003); the Fugløy Reef complex (Lindberg and Mienert 2005; Lindberg et al. submitted); off Brazil, where pockmark craters of several hundred metres width contain coral reefs (Sumida et

Fig. 3 A Video-grabbed image of a pockmark-dwelling *Lophelia* colony on reef KA2, inside pockmark PmA2, at the Kristin field. The water depth is 317 m. Here, the *Lophelia* is clearly growing on the proximal current side of large *Paragorgia arborea* and *Primnoa* sp. colonies. Is it just by chance that these three species combine in this manner, or may it have to do with a fierce competition for the same local nutrient source? The previous photograph (Fig. 2) suggests that such competition may develop over time. **B** A rare photograph, showing a small *Lophelia* colony, located adjacent to a *Paragorgia arborea*, and a small bacterial mat (arrowed) located between them. Normally, a bacterial mat suggests seepage of anoxic fluids from the subsurface (Hovland 2002). This photograph was acquired during a seabed survey in 1991, on the seabed above a hydrocarbon reservoir of no commercial potential, off mid-Norway (concession block: 6407/5). **C** Clusters of *Acesta excavata* also occur on reef KA2, as seen in this video-grabbed image. They are located inside coral colonies. The water depth is 313 m. On other reefs off Mid-Norway, growing on the general seafloor away from pockmarks, it is rare to find this bivalve growing in clusters. See text for further discussion
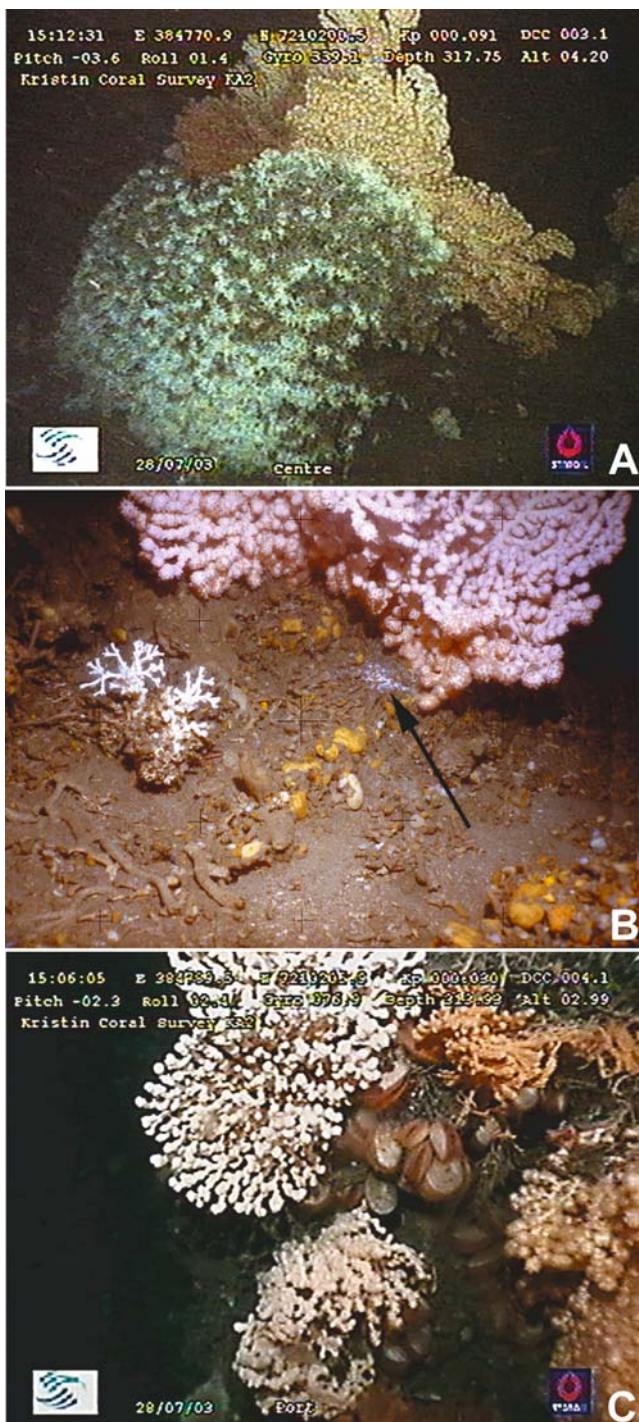
al. 2004); Gulf of Mexico (Moore and Bullis 1960); occurrences in the Porcupine Basin off Ireland (Hovland et al. 1994a; De Mol et al. 2002); occurrences in deep-water off Angola (Myriam Sibuet, pers. communication 2001); and large mound reefs with pockmarks in the vicinity off Mauritania (Colman et al. 2005). In addition, the Darwin Mounds, found at 1000 m water depth in the Rockall Trough (Masson et al. 2003), where *Lophelia pertusa* occurs, are themselves interpreted as representing likely fluid escape features. But although these build mounds instead of depressions, they occur just north of a large field of normal pockmarks. At other Norwegian occurrences (other than at Kristin), the large associated pockmarks are normally located less than one km distance from the reefs.

Discussion

Since 1977, Statoil has performed numerous modern pipeline route seafloor surveys, from the Barents Sea, in the north, to Dunkerque in the south. For the construction of trunkline gas pipelines, up to 3 km wide linear seabed transects have been mapped, over hundreds of kilometres at a time, with modern survey systems, enabling the detection of metre-size features (Hovland and Indreeide 1980; Hovland et al. 1998; Hovland et al. 2002). It should be noted, that these long transects are randomly located, relative to small-size natural seabed features, such as pockmarks and coral reefs. From Statoil's seabed features database, it is possible to say that the "normal" (dominating) seafloor in northern European waters is "uneventful", i.e. there are very few significant features (larger than 10 m width). In order of occurrence, the most common significant natural seabed features are:

-     relict iceberg ploughmarks (Lien 1983), typically 50 m wide, 5 m deep and over 10 km long
-     normal sized (>30 m wide, up to 15 m deep) pockmarks (Hovland and Judd 1988)
-     coral reefs (>20 m diameter, up to 30 m high) (Dons 1944; Hovland and Mortensen 1999; Freiwald et al. 2002)
-     sandwaves, normally 1-2 m high, but up to 15 m high and 300 m long, in areas of strong tidal currents, such as in the southern North Sea.

Relict iceberg ploughmarks tend to occur within large regions, i.e. off Mid-Norway and in large parts of the Barents Sea. Pockmarks are also regionally abundantly, such as in the Barents Sea and the Norwegian Trench (Hovland 1981; Hovland and Judd 1988). But, coral reefs occur only patchily, and their whereabouts are impossible to predict before the detailed surveys have been conducted (Mortensen et al. 2001). Although the exact formation mechanism for pockmarks is still unknown (there is a lack of long-term detailed and dedicated instrumented measurements) it is known that they are generally dependent upon two factors: 1) sub-bottom hydrology (hydraulically active conditions, due to the presence of shallow gas, or pressurized porewaters), 2) a seabed that consists of fine-grained

sand, silt and/or clays. Similar statements can also be made for Norwegian coral reefs: although their mechanism of formation is still unknown (again there is a lack of long-term detailed and dedicated [current, nutrient, microbial, and hydraulic] measurements) it is believed that they are generally dependent on two factors: 1) relatively hard and stable seabed sediments, and 2) a stable supply of nutrients, i.e. probably originating locally from the primary and secondary trophic level.

Because pockmarks tend to destabilize fine-grained sediments, it is a paradox to find reefs inside and along the inside rims of pockmarks, like at Kristin. However, some large pockmarks are known to erode the fine-grained sediments right down to a firm substratum (Hovland and Judd 1988; Judd and Hovland 1992), and on rare occasions, exhume sediment-embedded rocks, subsequently found inside the pockmarks. Also, authigenic methane-related carbonate slabs and nodules occur inside some pockmarks (Hovland et al. 1987). However, at Kristin, no such hard substrates have been found so far.

Based on the Statoil database of seabed conditions, it is fair to say that pockmarks only occur in specific areas, and that large (more than 2.5 m high) coral reefs are relatively rare seabed features. Even small coral reefs only occur in certain regions of the Norwegian continental shelf. This means that the two seabed features, pockmarks and coral reefs, would probably not occur together without some connecting factor.

Whereas pockmarks are most common in the deep portions of the northern North Sea and in the Barents Sea, coral reefs mainly occur on the continental shelf and on the shelf break off Mid-Norway. Previously, no pockmarks have been found with coral reefs inside them in the North Sea or in the Barents Sea. The only known occurrence in Norwegian waters is that of the Kristin field. The previous findings of such co-occurrence, has been close proximity of coral reefs to pockmarks, as mentioned previously (Haltenpipe Reefs and Fugløy Reefs).

Because pockmarks are generally found in areas with soft, fine grained sediments, and in areas where occasionally strong currents cause very turbid waters (noticed during ROV operations inside these pockmarks), filter-feeding organisms are neither expected to be found or are normally found inside pockmarks. The only organisms thus far found inside pockmarks of the North Sea, have been rare occasions of numerous sea anemones, centrally in pockmarks, one occurrence of bivalves (*Arctica islandica*), and the "eyed pockmarks" at Tommeliten, associated with bubbling methane seeps, authigenic carbonate formation, and bacterial mats (Hovland and Judd 1988).

From numerous submarine seep-sites, worldwide, including pockmarks in the Tommeliten area of the North Sea and areas of the Gulf of Mexico, we know that seeps stimulate the growth of primary producers (Bacteria and Archaea), which rely on the chemical gradients always present at seep locations (Hovland 2002; MacDonald et al. 2003). The only reasonable unifying connecting factor expected to exist, therefore, between pockmarks and reefs is that gas and porewater emanating from pockmarks stimulates primary organic production and provides a stable nutrient source to the reefs (Hovland and Risk 2003). Thus, the Kristin pockmark-

associated reefs described here, strengthens the validity of the "hydraulic theory" (Hovland et al. 1998).

Because pockmarks are formed by suspected episodic removal of fine-grained sediments by focused gas and porewater expulsion (Hovland and Judd 1988), the pockmark-dwelling reef-building animals (i.e. *Lophelia*, *Paragorgia*, *Primnoa*, and *Acesta* species) must be able to tolerate periods, probably lasting for several hours at a time, of very turbid water ("silting episodes"). Thus, it is believed that coral reefs, in general, are more robust to silting episodes than previously suspected. The conspicuous finding of dense aggregates of the giant limid bivalve *Acesta excavata*, inside and at the base of *Lophelia* corals in the Kristin pockmark-associated reefs suggests that the bivalve is especially "seep-prone". This means that it not only tolerates silting episodes, but that it perhaps is dependent in some way on chemicals dissolved in the water, such as methane. To follow this reasoning through, it may mean that the *Acesta excavata* may host endosymbiont bacteria or archaea, as is known to be the case with giant bivalves living in similar seep-prone settings in the Gulf of Mexico (MacDonald et al. 2003).

If there is a specific reason why coral reefs develop inside the Kristin pockmarks despite the apparently negative factors of occasionally turbid waters (silting) and occasionally (mechanically) unstable sediments, the reason may be expected to be the provision of a stable nutrient supply. Most pelagic and benthic organisms in the North Atlantic rely on and depend on a seasonally varying nutrient supply. However, according to the previously discussed "hydraulic theory" for coral reefs (Hovland et al. 1998; Hovland and Risk 2003), such a seasonally varying nutrient supply may not be adequately stable for prolonged subsistence and development. The factor that alleviates annual nutrient sparse periods may be nutrients added to the water column from a local source, which is independent of seasonal variations. Because seepage depends on ambient pressure on the seafloor (MacDonald et al. 2003), the only variations that would be expected from such a seepage-associated source would be those induced by tidal forces. Thus, if monthly and spring tide variations are found in skeleton building of the coral reefs at Kristin, this could be a strong indicator of a local, tide-associated and seep-associated nutrient source.

Over the last 25 years, Statoil and other companies have developed numerous hydrocarbon fields where pockmarks occur on the seafloor. There are also two other hydrocarbon fields (Aasgard and Heidrun) where small coral reefs occur within the development boundary of the fields. However, Kristin is the only field where relatively large pockmarks are found with relatively large coral reefs found within them. In order to find out if this rare co-occurrence is by chance or if there could be a relationship between the corals and pockmarks, further biological and geochemical studies could be done. Over the operational time span of the Kristin field, it is therefore hoped that careful monitoring and sampling of sediments, water, and corals can provide material for chemical, organic, and isotopic analyses that will determine what the relationship may be.

Acknowledgements

References

Colman JG, Gordon, DM, Lane AP, Forde MJ, Fitzpatrick JJ (2005) Carbonate mounds off Mauritania, Northwest Africa: status of deep-water corals and implications for management of fishing and oil exploration activities. In: Freiwald A, Roberts JM (eds) Cold-water Corals and Ecosystems. Springer, Berlin Heidelberg, pp 417-441

De Mol B, Van Rensbergen P, Pillen S, Van Herreweghe K, Van Rooij D, McDonnell A, Huvenne V, Ivanov M, Swennen R, Henriet JP (2002) Large deep-water coral banks in the Porcupine Basin, southwest of Ireland. Mar Geol 188: 192-231

Dons C (1944) Norges korallrev. Norsk Vidensk Selsk Forh 16A: 37-82

Freiwald A, Hühnerbach V, Lindberg B, Wilson JB Campbell J (2002) The Sula Reef complex, Norwegian Shelf. Facies 47: 179-200

Hovland M (1981) Characteristics of pockmarks in the Norwegian Trench. Mar Geol 39: 103-117

Hovland M (1990) Do carbonate reefs form due to fluid seepage? Terra Nova 2: 8-18

Hovland M (2002) On the self-sealing nature of marine seeps. Cont Shelf Res 22: 2387-2394

Hovland M, Indreeide A (1980) Detailed sea-bed mapping for a pipeline across the Norwegian Trench. Int Hydrogr Rev 57: 101-117

Hovland M, Judd AG (1988) Seabed pockmarks and seepages. Graham and Trotman, London, 293 pp

Hovland M, Mortensen PB (1999) Norske korallrev og prosesser i havbunnen. John Grieg, Bergen, Norway, 160 pp

Hovland M, Risk M (2003) Do Norwegian deep-water coral reefs rely on seeping fluids? Mar Geol 198: 83-96

Hovland M, Croker P, Martin M (1994a) Fault-associated seabed mounds (carbonate knolls?) off western Ireland and north-west Australia. Mar Petrol Geol 11: 232-246

Hovland M, Farestveit R, Mortensen PB (1994b) Large cold-water coral reefs off mid-Norway - a problem for pipelaying? Proc Oceanol Int, Brighton 3: 35-40

Hovland M, Talbot M, Qvale H, Olaussen S, Aasberg L (1987) Methane-related carbonate cements in pockmarks of the North Sea. J Sed Petrol 57: 881-892

Hovland M, Mortensen PB, Brattegard T, Strass P, Rokoengen K (1998) Ahermatypic coral banks off mid-Norway: evidence for a link with seepage of light hydrocarbons. Palaios 13: 189-200

Hovland M, Vasshus S, Indreeide A, Austdal L, Nilsen Ø (2002) Mapping and imaging deep-sea coral reefs off Norway, 1982-2000. Hydrobiologia 471: 13-17

Judd AG, Hovland M (1992) The evidence of shallow gas in marine sediments. Cont Shelf Res 12: 1081-1096

King LH, MacLean B (1970) Pockmarks on the Scotian Shelf. Geol Soc Amer Bull 81: 3142-3148

Lien R (1983) Iceberg scouring on the Norwegian continental shelf. Proc Ann Offsh Tech Conf, Houston, Texas 15: 41-45

Lindberg B, Mienert J (2005) Sedimentological and geochemical environment of the Fugløy reefs off northern Norway. In: Freiwald A, Roberts JM (eds) Cold-water Corals and Ecosystems. Springer, Berlin Heidelberg, pp 633-650

Lindberg B, Berndt C, Mienert J (submitted) The Fugløy Reefs on the Norwegian-Barents continental margin: Cold-water corals at 70°N, their acoustic signature, geologic, geomorphologic and oceanographic setting. Int J Earth Sci

MacDonald IR, Sager WW, Peccini MB (2003) Gas hydrate and chemosynthetic biota in mounded bathymetry at mid-slope hydrocarbon seeps: Northern Gulf of Mexico. Mar Geol 198: 133-158

Masson DG, Bett BJ, Billett DSM, Jacobs CL, Wheeler AJ, Wynn RB (2003) The origin of deep-water, coral-topped mounds in the northern Rockall Trough, Northeast Atlantic. Mar Geol 194: 159-180

Moore DR, Bullis HR (1960) A deep-water coral reef in the Gulf of Mexico. Bull Mar Sci 10: 125-128

Mortensen PB, Hovland MT, Fosså JH, Furevik DM (2001) Distribution, abundance and size of *Lophelia pertusa* coral reefs in mid-Norway in relation to seabed characteristics. J Mar Biol Assoc UK 81: 581-597

Storvoll V, Bjørlykke K, Karlsen D, Saigal G (2002) Porosity preservation in reservoir sandstones due to grain-coating illite; a study of the Jurassic Garn Formation from the Kristin and Lavrans fields, offshore mid-Norway. Mar Petrol Geol 19: 767-781

Sumida PYG, Yoshinaga MY, Saint-Pastous Madureira LA, Hovland M (2004) Seabed pockmarks associated with deep-water corals off SE Brazilian continental slope, Santos basin. Mar Geol 207: 159-167

Sedimentological and geochemical environment of the Fugløy Reef off northern Norway

Björn Lindberg, Jürgen Mienert

Department of Geology, University of Tromsö, Norway, Dramsveien 201, N-9037
  Tromsö, Norway
  (Bjorn.Lindberg@ig.uit.no)

Abstract. A number of reefs are found along the coast of northern Norway, and a cluster of particularly high reefs off Troms County at 70°N are known collectively as the Fugløy Reef. The reefs, up to 40 m high and more than 200 m wide, consist mainly of the reef-building *Lophelia pertusa*. Most of the reefs identified in the study area are located on moraine ridges in water depths of 140-190 m, and in water masses dominated by the relatively warm and saline Norwegian Current. Several of the reefs are located on the flanks of channels incising the moraine highs, where currents are tidally dominated and periodically reach velocities of 30 cm/s. Gravity cores were acquired from the reefs and their surroundings, and thorough analyses of the sampled sediments provide valuable information about three (paleo-) sedimentary environments surrounding the reefs. The immediate vicinity of the reefs consists of coarse and unsorted deposits that are interpreted to be moraine material deposited by the retreating inland ice. Elevated current velocities have prevented fine sediments from settling since the ice retreated. The second province is a pockmarked basin at water depths down to ~300 m. Gravity cores from the basin reveal silty sand deposits of more than 4 m thickness representing post-glacial sedimentation in the area. Gas analyses reveal that the hydrocarbons found in the sediments clearly are of biogenic origin, although it is somewhat enigmatic whether biogenic gas is the sole driving force behind the pockmarks in the area. No direct link between the reefs and the pockmarks is found. The third sedimentary province is characterised by resedimentation of coral debris, clearly illustrated by sorted deposits and U/Th-datings from the allochthonous deposits. Remobilisation of coral debris is modest in areal extent, but an important mechanism linked to the occurrence of the coral reefs.

Keywords. Cold-water corals, *Lophelia*, geochemistry, sedimentology, dating

Introduction

Cold-water corals along the coast of Norway have been known for several decades, but thorough scientific studies were first conducted in the 1920's and

1930's. The introduction of manned and unmanned submersibles in the 1980's led to an increased scientific and societal interest, and several hundred areas of reef growth have now been identified on the Norwegian shelf and in fjords (Fosså et al. 2000). Among the largest and best-known reefs is the Sula Reef Complex off mid-Norway which encompasses several hundred individual reefs en echelon over a distance of 14 km (e.g., Hovland et al. 1994; Mortensen et al. 1995; Freiwald et al. 2002). The Røst Reef is reported to be even larger, stretching for 35 km along the shelf edge, and is the subject of ongoing studies (Fosså et al. 2005). The role of hydrocarbons through (micro-) seepage in relation to reef growth is a subject of recurring discussion, and a theory has been formulated linking the reefs to increased nourishment supply due to the chemical front created by introduction of 'foreign' elements in the water column ('the hydraulic theory'; Hovland 1990; Hovland and Mortensen 1999). This theory is disputed by other authors (e.g., Frederiksen et al. 1992; Freiwald et al.1997), who claim oceanographic factors determine the distribution of the reefs.

New data presented in this paper illuminate several processes linked to the Fugløy Reef and the adjacent pockmarked basin discussed in Lindberg et al. (submitted). The sedimentary environment surrounding the reefs is described based on analyses of gravity cores. Geochemical analyses of the gas in the sediments as well as dating of coral fragments provide additional information about the geological development of the area.

The paper is based on further analyses of existing geophysical data presented in Lindberg et al. (submitted), as well as new data from gravity cores, additional very-high-resolution acoustic data and oceanographic measurements.

Physiographic setting

The Fugløy Reef is located at 70°N at the mouth of prominent fjords up to 300 m deep incising the Norwegian mainland (Fig. 1). The basement consists of metamorphosised bedrock of Cambro-Silurian age, with sedimentary Mesozoic bedrock found less than 20 km to the north (Sigmond 1992). The area has repeatedly been glaciated during the last 600 ka (Henrich and Baumann 1994), thereby scouring most of the sediments off the shelf and into the deep-sea, leaving mostly moraine ridges and sub- and pro-glacial tills after the ice-sheet retreated. Post-glacial sediments consist of glaciomarine deposits with dropstones, and Holocene marine sedimentation, constituting >20 m in thickness in local basins (Rokoengen et al. 1979; Vorren and Kristoffersen 1986; Lindberg et al. submitted).

The large-scale oceanography is dominated by the northwards flowing warm North Atlantic Current (typically T: 6-9°C and S: >35 ‰), overlain by the Norwegian Coastal Current, usually constituting a colder and less saline water mass (Blindheim 1990; Loeng 1991; Poulain et al. 1996). Detailed oceanographic measurements have proven the influx of Atlantic Water at the reef sites with a strong tidal signal, periodically yielding current velocities of more than 30 cm/s (Lindberg et al. submitted). Measurements performed over several years at a nearby hydrographic
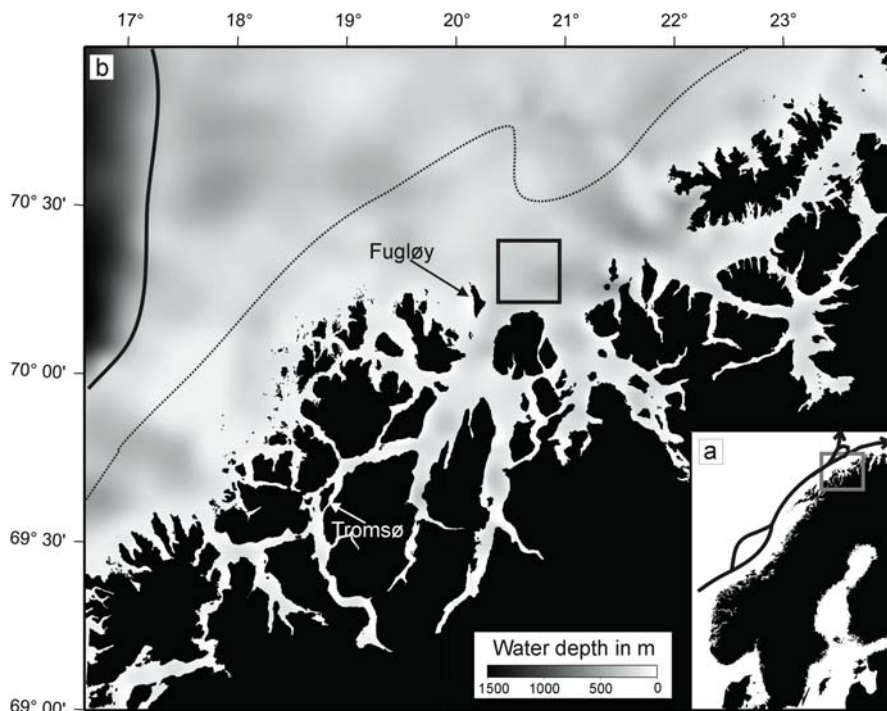
Fig. 1 Location map of the study area relative to Scandinavia (**a**) and a regional map of the Fugløy area (**b**) with location of Figure 2 indicated by a black square. The study area is at the confluence point of several glacially eroded troughs and has been ice-free since ~12 ka. The solid black line indicates the ice-front position at ~20 ka and the dotted line is the approximate boundary between the sedimentary bedrock towards northwest, and metamorphic bedrock towards southeast

station (NFH Norwegian Fishery College, http://lupus.nfh.uit.no) demonstrate that long-term (decadal scale) temperatures below 100 m depth are stable between 5 and 9°C, with salinities between 34 and 35 ‰.

The individual reefs off Fugløy have been documented to be among the highest on the Norwegian shelf, reaching 40 m in height and more than 200 m in diameter. The reefs are found at water depths between 140 and 190 m, mostly on morainic highs (Fig. 2). A basin with abundant pockmarks is identified on the geophysical data, and the seeping fluid is tentatively proposed to be biogenic gas generated from decaying organic material. A possible link between the reefs and the adjacent pockmarks has been proposed, but this has not yet been confirmed or rejected based on the available data (Hovland and Risk 2003; Lindberg et al. submitted).

Material and methods

As a part of the EU-funded program ECOMOUND (Environmental Control on Mound Formation along the European Margin), a multi-disciplinary data set
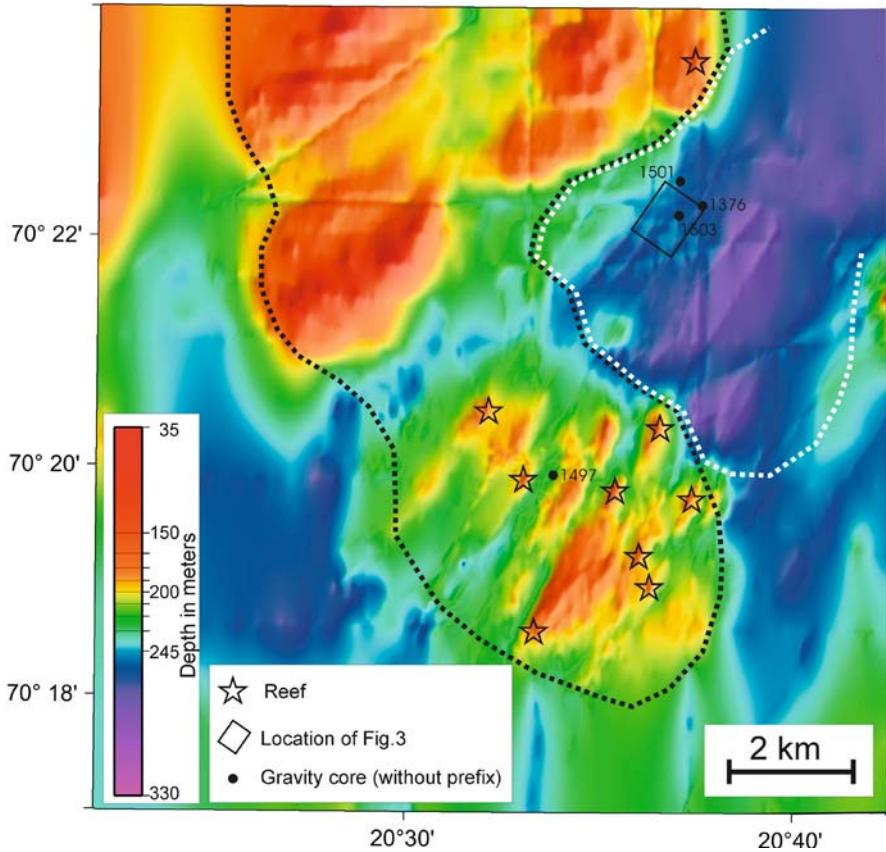
Fig. 2 Detailed bathymetric map of the study-area based on echo-soundings and seismic lines (some of the tracklines are visible). The black stars indicate identified reefs and the presence of living corals (*Lophelia pertusa*) some of which have been verified by video-imaging and sampling. The black dotted line circumscribes the morainic high where reefs are found, and the white dotted line delineates the pockmarked basin

was acquired using the R/V Jan Mayen (University of Tromsö) during cruises in 2000, 2001, and 2002. Geophysical data comprising ~350 km of simultaneously recorded mini sleeve-gun and 3.5 kHz seismic data, and 35 km^2 of side-scan sonar was acquired, as well as gravity cores (Table 1).

Gravity cores

The gravity cores presented in Table 1 were collected using a 6 m long steel-pipe with plastic liner, core-catcher, and a weight of ~1.5 t. The cores were cut in pieces of 1 m length for practical handling and then sealed and stored at 4°C. Onshore, the magnetic susceptibility, P-wave velocity and density of the sediments were measured using a Geotek multi-sensor core logger, and the cores were subsequently split longitudinally. Due to difficulties with calibrations, the values of magnetic

Table 1 Sediment cores used in this study

Core no.	Position	Water depth (m)	Core length (cm)
JM00-1376	70°22.3'N 20°37.6'E	231	430
JM01-1501	70°22.5'N 20°37.0'E	223	50
JM01-1497	70°19.9'N 20°33.8'E	185	168
JM01-1503	70°22.2'N 20°37.0'E	228	467

susceptibility obtained are considered only as relative down-core values, and not absolute values. One half of the core was X-rayed and used for further investigations, and the other half was stored for archive purposes. The working half was described visually with regards to lithology, structures and colour variations (Munsell soil colour chart). We measured undrained shear-strength on two of the cores using a drop-cone penetrometer (Hansbo 1957). Samples of representative lithology were taken and grain-size analysed using wet-sieve for the >63 μm fraction and a Micromeritics SediGraph for the <63 μm fraction.

Dates

Four fragments of *Lophelia pertusa* (Tables 2, 3) were dated by the U/Th-method using a Finnigan MAT 262 mass spectrometer, and uranium reference material (HU1 standard in radioactive equilibrium) reproduced certified values. Ages were calculated from measured uranium and thorium isotopes using the program Isoplot (Ludwig 2001) using a Monte Carlo simulation of 4000 steps for error estimates.

Table 2 U/Th dating of coral fragments *Lophelia pertusa*, measured values. Uncertainties are given with 2σ. U-activity ratio is given in DELTA notation $\{([^{234}U/^{238}U]measured - 1) \cdot 1000\}$

Sample no. and depth	Lab. Nr	^{238}U (ppm)	^{232}Th (ppm)	$\delta^{234}U_{meas}$ (‰)
JM01-1501-10 cm	184	3.4112±0.0038	0.08189±0.00020	149.5±3.9
JM01-1501-28 cm	185	3.2453±0.0029	0.00189±0.00001	147.5±1.8
JM01-1501-41 cm	186	3.1989±0.0035	0.00815±0.00005	144.9±2.6
JM01-1501-47 cm	187	2.7118±0.0024	0.00352±0.00003	147.1±2.5

Table 3 U/Th dating of coral fragments *Lophelia pertusa*, calculated values. Uncertainties are given with 2σ

Sample no. and depth	Lab. Nr	$^{230}Th/^{238}U$	$^{230}Th/^{232}Th$	Age and Δ (years)
JM01-1501-10 cm	184	0.01792±0.00023	2.281±0.006	1150±210
JM01-1501-28 cm	185	0.01395±0.00008	72.86±0.22	1321±12
JM01-1501-41 cm	186	0.00612±0.00019	16.30±0.10	1244±38
JM01-1501-47 cm	187	0.01360±0.00019	14.37±0.11	554±25

Gas analyses

Samples for gas analyses were taken from the cores immediately after retrieval, put in airtight cans and frozen on board. The gas content was analysed in Trondheim, Norway by GeolabNor. Analyses of occluded hydrocarbon and non-hydrocarbon

gas were performed using a Varian 3500 gas-chromatograph, and $\delta^{13}C$ gas-isotopes (CO_2, CH_4 and C_4H_8) were measured with VG Isochrom II (mass spectrometer) with HP 5890 gas chromatograph.

Sedimentary provinces

Based on sedimentological analysis, geochemical analyses and datings of the sediment cores, the study area can be divided into three distinct provinces surrounding the reefs. Here, we present the details of the specific provinces.

Pockmarked basin

A basin from 200 to 300 m water depth is found north of the main reef cluster (Fig. 2). The basin contains up to 20 m thick post-glacial deposits, and displays prominent pockmarks that are interpreted to be active based on the lack of overlying sediments and their morphologically fresh appearance (Lindberg et al. submitted; Fig. 3). Four gravity cores from water depths of 228 to 231 m were examined. Since
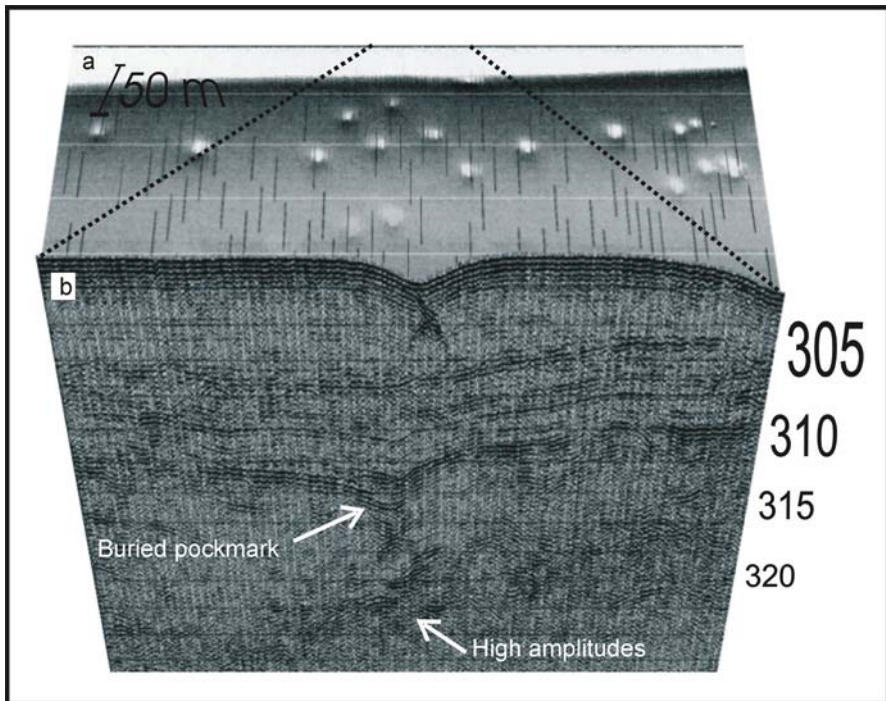
Fig. 3 Side scan sonar record (**a**) and seismic record (**b**) with vertical scale in ms of the pockmarks (see Fig. 2 for location). The pockmarks are ~5 m deep and up to 100 m wide, appearing in an area with otherwise very low relief. Little or no overlying sedimentation is found on the pockmarks. A buried pockmark appears at ~312 ms on the seismic profile below which higher amplitudes are found, possibly indicating the presence of gas (from Lindberg et al. submitted)

their stratigraphy was found to be consistent, only the two longest cores (of 467 and 430 cm length) are presented and discussed here (JM00-1376 and JM01-1503; Table 1; Figs. 2, 4).

Unit A

This layer constitutes all (430 cm) of core JM00-1376 and most (430 cm) of core JM01-1503 and consists of silty sand with few structures visible (Fig. 4). X-ray pictures reveal abundant shell fragments in the layer, and possible faint cross-
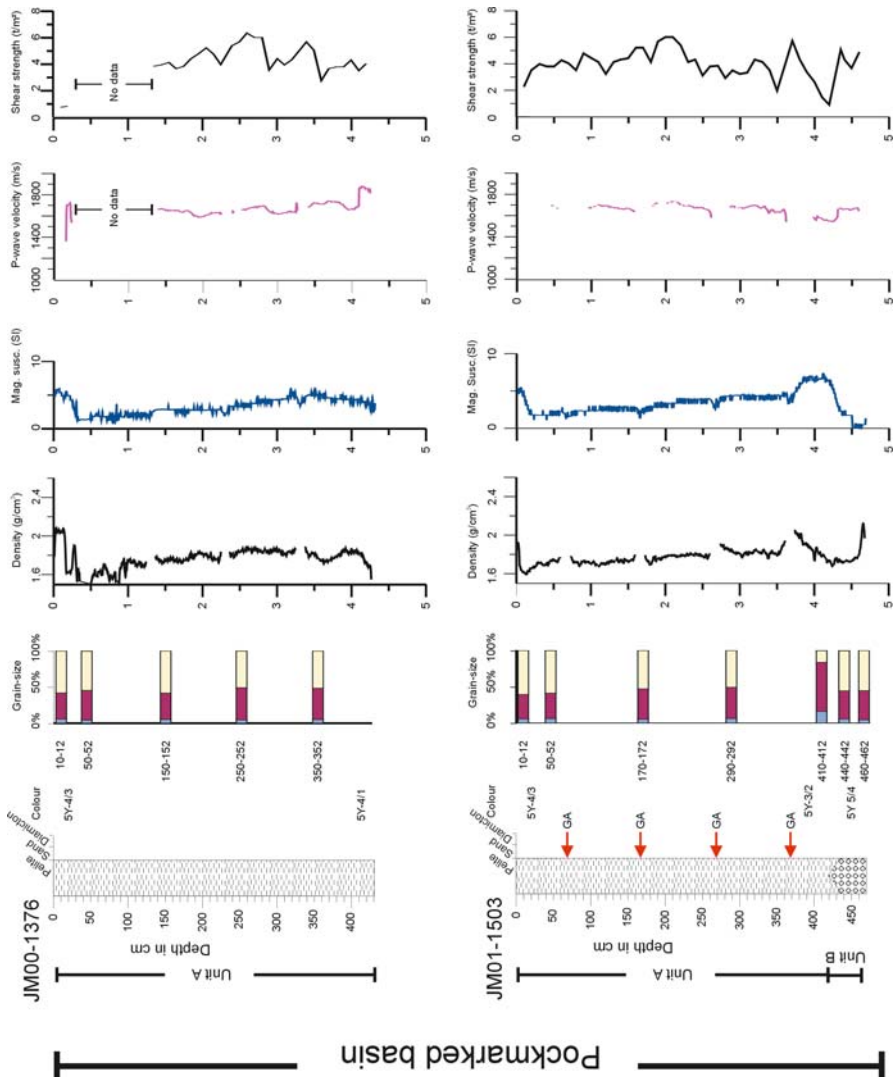
Fig. 4 Core logs of the gravity cores representing the pockmarked basin. Units described in the text (A-E) are indicated on the logs, as well as locations of sampling for gas analyses (GA) and U/Th dating (U/Th). See text for further discussion
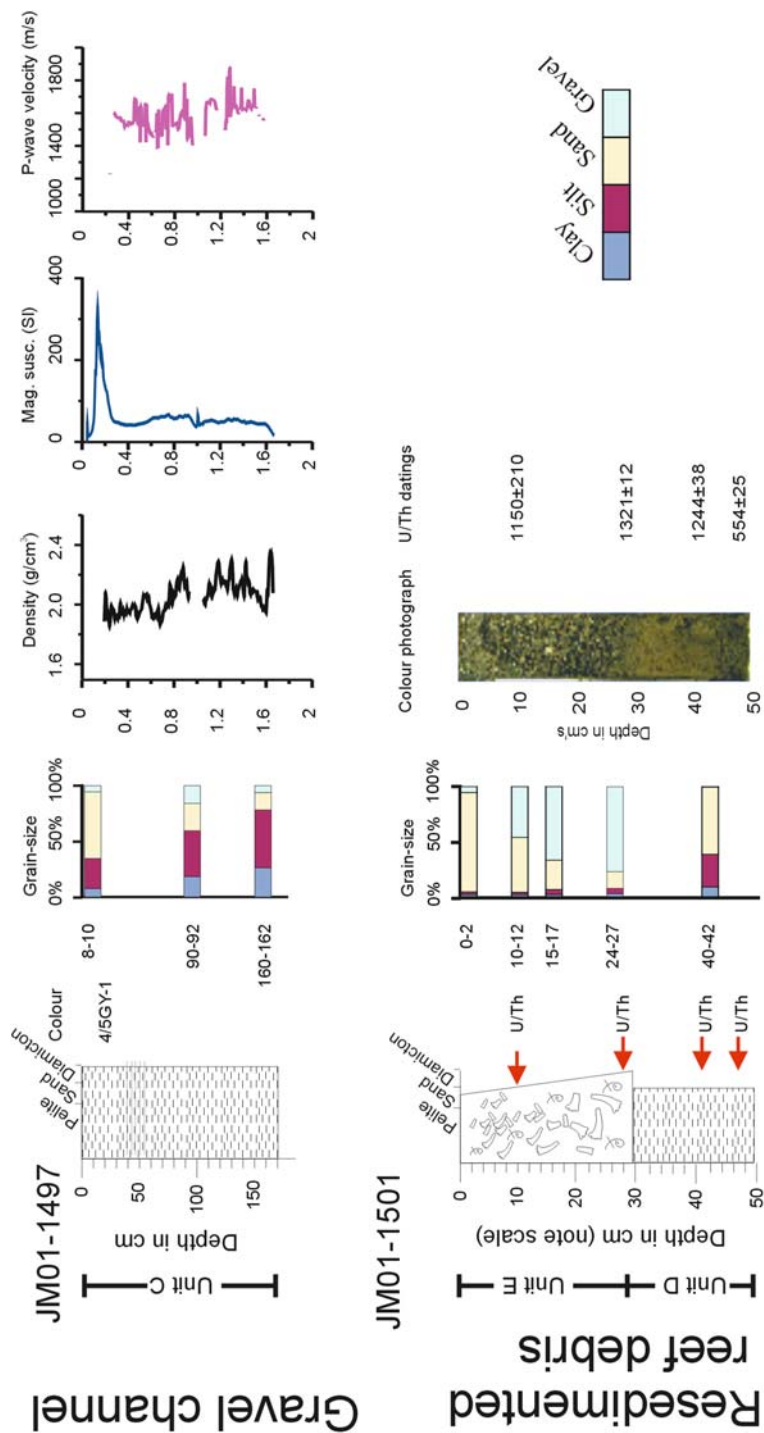
Fig. 5 Core-logs of the gravity cores representing the gravel channel and resedimented reef debris. Units described in the text (A-E) are indicated on the logs, as well as locations of sampling for gas analyses (GA) and U/Th dating (U/Th). See text for further discussion

bedding is seen. The layer is light olive grey (5Y 4/3) in colour, changing to somewhat darker olive grey (5Y 3/2) down-core. The sand and silt fractions constitute >90 % of the total dry-weight for all but the lowermost sample in core JM00-1503, which contains less sand and more clay. The density and magnetic susceptibility values steadily increase down-core. The P-wave velocity is relatively constant down-core with values between 1600 and 1700 m/s. As one of the sections of core JM00-1376 had been opened while in storage, the core was dry and no reliable P-wave velocity- or shear strength values were obtained from 30-130 cm.

Unit B

In core JM00-1503, there is a basal layer below 430 cm displaying a somewhat different lithology and physical properties compared to the upper layer (Fig. 4). The boundary between units A and B is undulating and distinct with regards to grain size and colour (from 5Y 3/2 to 5Y 5/4), and Unit B is also distinguished by lower magnetic susceptibility, higher P-wave velocity and higher shear strength. The grain-size distribution is similar to that of the upper part of Unit A, with sand and silt constituting more than 90 % of the total dry-weight.

Gravel channel

A morainic high is found in the southern part of the study area, where water depths range from 130 to 220 m. Several attempts to core the near-reef sediments with both a box-corer and a gravity corer were unsuccessful, indicating a hard seafloor and/or presence of large clasts. One gravity core (JM01-1497) penetrated 185 cm of the sea bed and yielded a sedimentary sequence of 168 cm (Fig. 5). The core site is located in a NNE-SSW trending channel, and has been monitored with a current meter registering both tidally-driven currents reaching more than 30 cm/s and a clear influx of relatively warm (6-9°C) and saline (~35) Atlantic Water (Lindberg et al. submitted).

Unit C

The core JM01-1497 was taken at 185 m water depths, is 168 cm long, and contains a homogeneous diamicton with faint lamination present in one interval (Fig. 5). Clasts up to 10 cm (the plastic liner diameter) are found in the core, and the dominating grain-size decreases down-core. It is noteworthy that large clasts were avoided when sampling for grain-size analyses. A down-core increase in density (from 1.95 g/cm^3 to 2.1 g/cm^3) and P-wave velocity (from 1550 m/s to 1620 m/s) is observed, whereas the magnetic susceptibility decreases down-core after reaching peak values exceeding 300 as a result of a large clast in the core.

Resedimented reef debris

One core (JM01-1501) retrieved from the pockmark area contained a significantly different lithology from the adjacent cores (JM00-1376 and JM01-1503, ~550 m away; see above), and is thought to reflect different depositional processes. The core was acquired from 223 m water depth, and contained 50 cm sediments (Fig. 5). No density, magnetic susceptibility, or shear strength logs exist for this core.

Unit D

The lowermost 20 cm in core JM01-1501 consists mainly of silty sand sediments similar to Unit A, but contains coral fragments (*Lophelia*) of up to 4 cm in length. No depositional structures are present in the layer, which has a clear boundary to the overlying unit E, defined by lithology, grain size and colour.

Unit E

This unit is 30 cm thick, and consists mostly of fragments of *Lophelia* and other organic debris. The unit displays a clear fining upward throughout, grading from predominantly gravel-size at the base to almost exclusively sand-size at the top (from >65 % to <5 % gravel). As the dominating grain size decreases towards the top of the unit, the relative terrigenous content seems to increase but this has not been quantified. By visual inspection, the coral fragments are highly varying in degree of degradation with regards to bio-erosion and physical erosion.

Gas analyses

Gas analyses were performed on samples from four levels at one-meter intervals in core JM01-1503 (Figs. 4, 6). Occluded gas analyses yield values of less than 30 ppb (ng/g) sediment methane gas, and much lower levels of the heavier hydrocarbons. Down-core variations in occluded gas content are most markedly shown by the consistently higher content of all hydrocarbons in the deepest sample (367 cm). The δ^{13}C-isotope content (*vs.* PDB-standard) for the CH_4 (methane), C_4H_8 (butene), and CO_2 (carbon dioxide) gases was also determined, and the values are relatively constant down-core at -60 ‰, -30 ‰ and -10 ‰, respectively (Fig. 6).
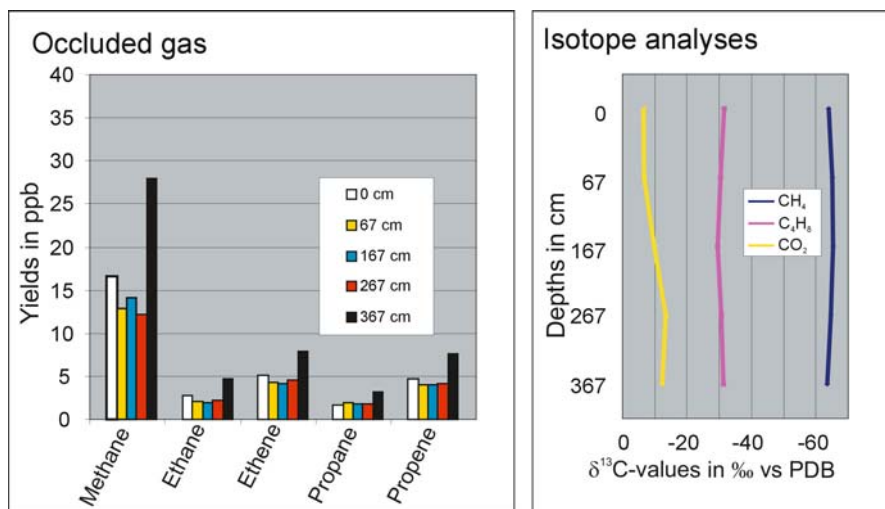
Fig. 6 Occluded gas and δ^{13}C-isotope-analyses from core JM00-1503 (Fig. 4). Hydrocarbons are found in low amounts compared to other seepage sites, and the levels are highest for the deepest sample (367 cm) and for the lightest hydrocarbons (methane). The isotopic signature of the methane clearly points to a biogenic origin of the gas

Dating

Four fragments of *Lophelia* were dated using the U/Th-method, two from each of the units (E and D) described in core JM01-1501. The results yielded ages from 554±25 to 1321±12 years (Tables 2, 3). The dates are inverted with respect to the stratigraphical levels that the samples are from, and without any apparent chronology.

Discussion

Depositional environments

Pockmarked basin

The acoustic signature and development of the pockmarked basin north of the main reef locations have been described recently (Lindberg et al. submitted), but the deposits found in the basin have not previously been investigated or discussed. Unit A constitutes the uppermost ~430 cm and is thought to represent present-day sedimentological conditions that have prevailed for some period of time (during the present oceanographic conditions). The homogenous nature of these sediments, including their physical parameters, indicates a continuous sediment deposition history with no prolonged halts in sediment supply. The relatively large grain-sizes are attributed to the elevated current, as evidenced from sea bed monitoring nearby (Lindberg et al. submitted), which shows tidally-driven currents capable of transporting up to coarse sand size according to the Hjulström diagram (Sundborg 1956). A decrease in current velocities would halt the deposition of sandy sediment and result in a draping of the basin with more typical marine clays found in fjord basins and at the mouth of fjords (e.g., Aarseth 1980; Plassen and Vorren 2002). The source of the sandy sediments is thought to be the surrounding morainic highs consisting of diamictons deposited in connection with the last inland ice sheet at ~12 ka.

Unit A is comparable to the Fugløybank sand found further out on the shelf. The Fugløybank sand is described as up to 88 cm thick, rich in foraminifera, and interpreted to be of Holocene age. It is the product of combined winnowing of glacial deposits and contemporaneous deposition of skeletal material, and is described as having a gravel lag base, thought to be formed by intense winnowing of glaciomarine sediment at the onset of the Holocene (Vorren et al. 1978). Apart from the gravel lag, not found in conjunction with the sand in any cores in this study, the major difference is the thickness of the Fugløybank sand compared with Unit A, which is much thicker. This difference could be explained by the core-locations. Vorren et al. (1978) studied cores from banks further out on the continental shelf whereas our Unit A is found in cores from a semi-confined basin closer to shore, providing conditions more suitable for a high sedimentation rate.

Unit B does not differ much from the overlying Unit A, but displays somewhat deviating physical characteristics. Unit B is also deposited during post-glacial

marine conditions not influenced by glaciers since there is no indication of IRD. The clear decrease in magnetic susceptibility could indicate a different source of sediments due to for instance a shift in current regime.

Unit D is thought to be equivalent of Unit A, only differing in the input of occasional coral fragments that are transported by gravity from the reefs found on surrounding highs (see *Mass-movement* below)

Pro-glacial moraine, Unit C

The only core from the immediate vicinity of the reefs which yielded sediment contained an unstratified diamicton. Failed coring attempts are attributed to coarse sediments in the area, also evident from the low penetration seen on the seismic data (Lindberg et al. submitted). The sample location confirms this. Clasts up to 10 cm in diameter are found in the core, and the only feasibly transport agent in this area is ice, either directly from the ice-sheet or as ice-rafted detritus (IRD). The unit is thought to be pro-glacial sediments derived from a still-stand in the ice-sheet retreat rather than glaciomarine sediments with IRD, since the latter usually results in greater sorting and stratified deposits over larger areas (e.g., Edwards 1986; Syvitski et al. 1987; Plassen and Vorren 2002). There is a possibility that the unit is a gravel lag resulting from erosion and transport of the finer material, and that it could originally have contained significantly more fine-grained sediments, thus being an analogue to the basal gravel layer (Vorren et al. 1978) created by winnowing of the diamicton at the onset of the Holocene. The local morphology of the high, stretching in a crescent shape opening towards the east (Fig. 2), also points to a pro-glacial origin for the highs, representing a still-stand in ice-retreat of an ice-tongue coming from the fjord-system (cf. Vorren and Kristoffersen 1986). The morainic high does not, however, coincide with any of the identified regional moraines.

Due to current activity, the morainic highs have not been buried in post-glacial sediment, but rather have provided an ample supply of sediment which has been eroded and transported by the prevailing tidal currents in the area, and subsequently deposited in the pockmarked basin to the north. Morphologically dominating ploughmarks are seen and taken as further indication that sedimentation since the last collapse of the inland ice-sheet has been sparse, as the ploughmarks would otherwise have been covered by Holocene sedimentation.

As such, the surface of core JM01-1497 is thought to represent a hiatus since the last deglaciation of the area, but this has not been confirmed by dating.

Mass-movement, Unit E

The third depositional environment identified in this study lies within the pockmark basin, and is characterised by abundant coral fragments at a distance of ~2 km from the nearest known living reefs. The distinct grading along with the inverted dates in Unit E in core JM01-1501 are indications that reworking and rapid deposition has taken place. We interpret the deposit to represent a turbidity flow or a grain flow from one of the reefs on the nearby morainic highs. The lateral extension of the deposit is not well known, as its acoustic signature does not differ significantly from that of Unit A, and hence cannot be traced on seismic data or

side-scan sonar. The unit is likely to have limited lateral extent, probably following an existing depression or trough in the seabed. Nevertheless, redistributition of coral debris by mass-movement can be a significant process in the area as the reefs are all located on, or constitute, topographic highs.

The coral fragments found in Unit D are not interpreted to be related to mass-movement, but simply explained as sporadic, singular and rather large fragments that are transported down to the basin separately. But they confirm that the remobilisation of reef debris is not uncommon.

Although no quantitative analyses has been performed on the relative content of terrigenous and biogenic sediment in Unit E, a preliminary impression is that the terrigenous material is consistently of smaller size than the biogenic material at the same stratigraphically level. The differences in particle density and grain shapes (roundness and sphericity) between the terrigenous sediments and organic (mostly aragonitic coral) fragments are believed to be responsible for different transport characteristics, in accordance with studies performed on foraminifera of sand size and terrigenous grains of silt size (Oehmig 1993).

Relative age of the turbidity current

The age of the turbidity current is not accurately known. However, the complete lack of overlying sediments indicates that the event occurred recently, as the present-day sedimentation consisting of the sandy sediments seen in JM01-1503 and JM00-1376 would otherwise be expected to be overlying Unit E as well. Based on the youngest date from Unit D, we can say that the mass movement must be less than 554 years old.

Possible triggering causes for the mass transport include collapse of parts of the reef due to earthquake activity and fishing activity in more recent years.

Resedimentation of coral debris

The nearest coral reef location to the core site of JM01-1501, based on seismic interpretation, is ~2 km from the core site at ~120 m water depth (Fig. 2). This gives an average slope of 3° over which the coral fragments must have been transported by gravity force alone, but the slope is significantly steeper close to the initiation point. Such distances and angles are not unusual for marine mass-movements, including various turbidity currents, debris flows and slides (Bugge 1983; Syvitski et al. 1987; Laberg and Vorren 1995, 2000).

Origin of the pockmarks

Sample location and stratigraphic origin of gas

The gas content of the sediments from the pockmarked basin yield values of light hydrocarbons of maximum 28 ppb, decreasing rapidly for the heavier hydrocarbons. The levels are consistently higher for the deepest sample (367 cm) than for the shallower ones, pointing to a buried source of the gas (Fig. 6). The absolute values of occluded gas in our study area are relatively low in comparison with reported values along the Norwegian Shelf. For example, the average methane-content of 350 cores from the North Sea is reported to be ~140 ppb (Faber and Stahl 1984).

Values of >1400 ppb methane have been measured from within active pockmarks, but methane content rapidly decreased away from the pockmark, and at distances of less than 100 m from the centre of the pockmark, values of only 9-27 ppb were reported (Hovland and Sommerville 1985). We are left with three possibilities regarding the origin of the Fugløy pockmarks:

a)   The seepage of gas has receded or is no longer active,
b)   the gravity corer did not sample the pockmark, but rather the flank, thus explaining the relatively low methane values,
c)   the low seep values indicate that a driving force other than gas is responsible for the fluid expulsion.

Re. a): The appearance of the pockmarks on seismic and side-scan sonar data indicate that they are still active, as they are morphologically fresh, without any overlying sediments. A draping of sediments would be expected if the pockmarks had been inactive for a longer period.

Re. b): Unfortunately it is not possible to confirm or reject sampling within the pockmark. This is due to the lack of differential global positioning (DGPS) of the ship, which may have drifted slightly during the time the cores were on their way down to the seafloor. Also, current activity is high in the area and causes additional difficulties in exact positioning.

Re. c): This is a possibility also addressed in Lindberg et al. (submitted). Hovland and Risk (2003) propose that the driving force could be groundwater, which would require water under artesian pressure and existing pathways in the sub-seafloor. As the distribution of the pockmarks seems to be random (Lindberg et al. submitted), it is difficult to envisage underlying fault patterns as pathways for migrating fluids. The surface expressions of fault-related seep is often linear, following the fault structures (e.g., Henry et al. 2002; Kobayashi 2003), and it is therefore suggested that the seeping fluid in the Fugløy pockmark field has a shallower origin than the bedrock.

Isotopic signature of the occluded gas

Isotopic analyses of the methane gas show a clear biogenic δ^{13}C-signature, with values stable at approximately -64 ‰, taken to be positive evidence of biogenic origin rather than thermogenic (e.g., Shoell 1983; Faber and Stahl 1984; Aharon et al. 1997). This is also supported by the fact that the surrounding bedrock consists of metamorphic rocks (Sigmond 1992; Lindberg et al. submitted) and is therefore not likely to produce thermogenic hydrocarbons. Biogenic gas is produced by microbial decomposition of organic matter and in order for sufficient amounts of gas to be produced, organic matter must be transported to the dysphotic basin where the pockmarks are found. A possible source for organic matter is the annual and synchronous shedding of brown algae colonies found along the coast of Norway (A. Freiwald pers. comm.; Freitag 1997). Large amounts of organic matter can be supplied by shedding of these algae and subsequent current-controlled transportation

to local basins, thus creating organically-rich horizons that may generate gas.

As of now, the main fluid creating the pockmarks can not be determined positively, but in our view the most plausible candidate for driving forces is biogenic gas.

Pockmark influence on reefs

The so-called hydraulic theory states that a chemical front created by introduction of a foreign fluid (biogenic gas, groundwater, mantle gases) into the water column will initiate bacterial activity that will be beneficial for the reefs (Hovland 1990; Hovland and Mortensen 1999; Hovland and Risk 2003). However, many authors disagree with the hydraulic theory, and there are several published papers where oceanographic agents rather than hydrocarbon seep are considered pivotal for reef growth (e.g., Freiwald et al. 1997; Frederiksen et al. 1992; Masson et al. 2003). There is little doubt that fluid expulsion has existed and may still exist in the vicinity of the Fugløy Reef, as exemplified by the pockmarks, but the possible influence of the venting fluid on the reefs is as of now undisclosed. There is a possibility that the seeping fluids influence reef growth in the area, as the prominent tidal activity will periodically transport potentially 'nutrient-rich' water from the pockmark basin to the reefs. However, no direct signal of seeping fluids has been proven in the coral skeleton in form of extremely low C-isotope values or other (Freiwald et al. 1997; unpublished data from Fugløy). So far, only circumstantial evidence supports the hydraulic theory for the Fugløy Reef, whereas other models sufficiently can explain the distribution of the reefs as well. Ultimately, direct proof in the coral skeleton or tissue will be the only way to confirm or reject the validity of the hydraulic theory.

Summary

- Three distinct sedimentary provinces (Fig. 7) have been identified in the vicinity of the Fugløy Reef, apart from the reefs themselves:
  a) A sandy basin from 200 m to 300 m water depth with abundant pockmarks due to fluid expulsion, possibly biogenic gas.
  b) An area with diamicton deposits thought to represent a hiatus surface going back to the retreat of the last ice-sheet from the area, and providing the reefs with hard substrate to settle on and the surroundings with ample sediment eroded by the relatively strong currents in the area.
  c) Allochthonous coral debris from the reefs which has been re-mobilised by gravity, sorted and deposited.
- The gas identified in cores from the pockmarked area has a clear biogenic signal, and the small amounts compared to other sites are interpreted to be a result of sampling outside the pockmark due to poor positioning possibilities.
- No direct link between pockmarks and reefs has been found, only circumstantial evidence. For verification, traces of seeping fluids must be identified in coral skeleton or tissue.
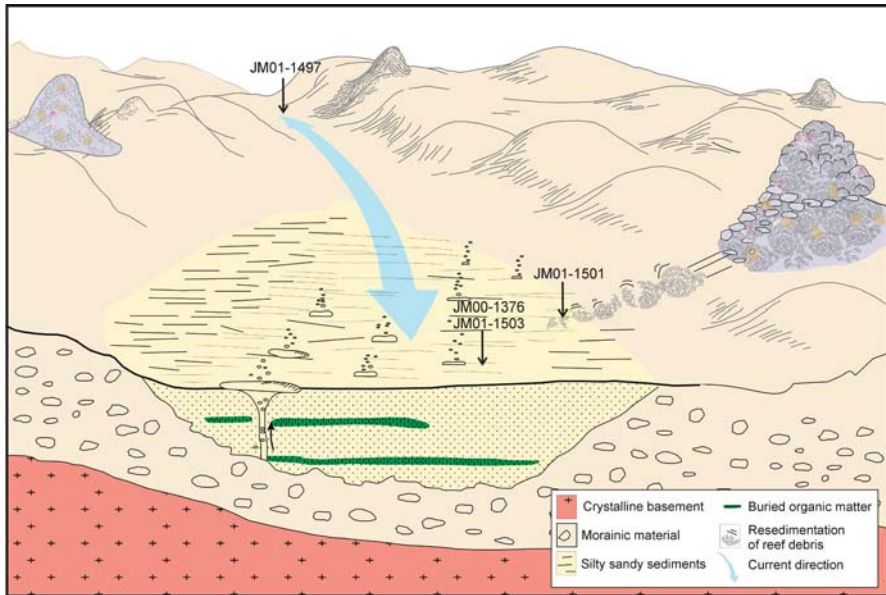
Fig. 7 Synthesized model of the area illustrating the three identified sedimentary provinces and approximate core locations: I (JM01-1497): morainic high where living reefs are found. This consists of unsorted coarse material deposited by the inland ice during retreat. II (JM00-1376 and JM01-1501): a silty sandy basin with abundant pockmarks proposed to be fuelled by biogenic gas derived from decaying organic matter. III (JM01-1501): coral debris redistributed and transported to the silty sandy basin by mass movement

Acknowledgements

References

Aarseth I (1980) Glaciomarine sedimentation in a fjord environment: example from Sognefjord. In: Orheim O (ed) Glaciation and Deglaciation in Central Norway. Field Guide, Norv Polarinst Oslo, pp 16-21

Aharon P, Schwarcz HP, Roberts HH (1997) Radiometric dating of submarine hydrocarbon seeps in the Gulf of Mexico. Geol Soc Amer Bull 109: 568-579

Blindheim J (1990) Arctic Intermediate Water in the Norwegian Sea. Deep-Sea Res 35: 1475-1489

Bugge T (1983) Submarine slides on the Norwegian continental margin, with special emphasis on the Storegga area. IKU Rep 110, Trondheim, 152 pp

Edwards M (1986) Glacial environments. In: Reading HG (ed) Sedimentary Environments and Facies. Blackwell Science, Oxford

Faber E, Stahl W (1984) Geochemical surface exploration for hydrocarbons in North Sea. AAPG Bull 68: 363-386

Fosså JH, Mortensen PB, Furevik DM (2000) *Lophelia*-korallrev langs norskekysten. Forekomst og tillstand. Fisken Havet 2, 94 pp

Fosså JH, Lindberg B, Christensen O, Lundälv T, Svellingen I, Mortensen PB, Alvsvåg J (2005) Mapping of *Lophelia* reefs in Norway – experiences and survey methods. In: Freiwald A, Roberts JM (eds) Cold-water Corals and Ecosystems. Springer, Berlin Heidelberg, pp 359-391

Frederiksen R, Jensen A, Westerberg H (1992) The distribution of the scleractinian coral *Lophelia pertusa* around the Faroe Islands and the relation to internal tidal mixing. Sarsia 77: 157-167

Freitag T (1997) Sedimentologische und palökologischen Studien an holozänen Fjordtrog-Sedimentkernen Nordnorwegens (Sandøyfjord). MSc thesis, Bremen Univ, unpublished

Freiwald A, Henrich R, Pätzold J (1997) Anatomy of a deep-water coral reef mound from Stjernsund, West Finnmark, northern Norway. SEPM Spec Publ 56: 141-161

Freiwald A, Hühnerbach V, Lindberg B, Wilson JB, Campbell J (2002) The Sula Reef Complex, Norwegian Shelf. Facies 47: 179-200

Hansbo S (1957) A new approach to the determination of the shear strength of clay by the fall-cone test. Proc R Swed Geotech Inst 14, 47 pp

Henrich R, Baumann K-H (1994) Evolution of the Norwegian Current and the Scandinavian ice sheets during the past 2.6 m.y.: evidence from ODP Leg 104 biogenic carbonate and terrigenous records. Palaeogeogr Palaeoclimatol Palaeoecol 108: 75-94

Henry P, Lallemant S, Nakamura K, Tsunogai U, Mazzotti S, Kobayashi K (2002) Surface expression of fluid venting at the toe of the Nankai wedge and implications for flow paths. Mar Geol 187: 119-143

Hovland M (1990) Do carbonate reefs form due to fluid seepage? Terra Nova 2: 8-18

Hovland M, Mortensen PB (1999) Norske korallrev og prosesser i havbunnen. John Grieg, Bergen

Hovland M, Risk MJ (2003) Do Norwegian deep-water coral reefs rely on seeping fluids? Mar Geol 198: 83-97

Hovland M, Sommerville JH (1985) Characteristics of two natural gas seepages in the North Sea. Mar Petrol Geol 2: 319-326

Hovland M, Farestveit R, Mortensen PB (1994) Large cold-water coral reefs off mid-Norway - a problem for pipe-laying? Conf Proc, Oceanol Int, 8-11 March, 1994, Brighton

Kobayashi K (2002) Tectonic significance of the cold seepage zones in the eastern Nankai accretionary wedge – an outcome of the 15 years' KAIKO projects. Mar Geol 187: 3-30

Laberg JS, Vorren TO (1995) Late Weichselian submarine debris flow deposits on the Bear Island Trough mouth fan. Mar Geol 127: 45-72

Laberg JS, Vorren TO (2000) The Trænadjupet Slide, offshore Norway – morphology, evacuation and triggering mechanisms. Mar Geol 171: 95-114

Lindberg B, Berndt C, Mienert J (submitted) The Fugløy Reef on the Norwegian-Barents continental margin: cold-water corals at 70°N, their acoustic signature, geologic, geomorphologic and oceanographic setting. Int J Earth Sci

Loeng H (1991) Features of the physical oceanographic conditions of the Barents Sea. Polar Res 10: 5-18

Ludwig KR (2001) ISOPLOT 2.49. Berkeley Geochronolog Cent Spec Publ 1a, 58 pp

Masson DG, Bett BJ, Billett DSM, Jacobs CL, Wheeler AJ, Wynn RB (2003) The origin of deep-water, coral-topped mounds in the northern Rockall Trough, Northeast Atlantic. Mar Geol 194: 159-180

Mortensen PB, Hovland M, Brattegard T, Farestveit R (1995) Deep-water bioherms of the scleractinian coral *Lophelia pertusa* (L.) at 64°N on the Norwegian Shelf: structure and associated megafauna. Sarsia: 145-158

Oehmig R (1993) Entrainment of planktonic foraminifera: effect of bulk density. Sedimentology 40: 869-877

Plassen L, Vorren TO (2002) Deglaciation and palaeoclimate of the Andfjord-Vågsfjord area, North Norway. Boreas 31: 97-125

Poulain P-M, Warn-Varnas A, Niiler PP (1996) Near-surface circulation of the Nordic seas as measured by Lagrangian drifters. J Geophys Res 101: 18237-18258

Rokoengen K, Bugge T, Løfaldli M (1979) Quaternary geology and deglaciation of the continental shelf off Troms, north Norway. Boreas 8: 271-227

Shoell M (1983) Genetic characterization of natural gases. AAPG Bull 67: 225-2238

Sigmond EMO (1992) Bedrock map of Norway and adjacent ocean areas. Scale 1:3 Million. Geol Surv Norway

Sundborg Å (1956) The river Klarälven. A study of fluvial processes. Geogr Ann 38: 127-316

Syvitski JPM, Burell DC, Skei JM (1987) Fjords – Processes and Products. Springer, New York

Vorren TO, Strass IF, Lind-Hansen OW (1978) Late Quaternary sediments and stratigraphy on the continental shelf off Troms and West Finnmark, northern Norway. Quatern Res 10: 340-365

Vorren TO, Kristoffersen Y (1986) Late Quaternary glaciation in the south-western Barents Sea. Boreas 15: 51-59

Wessel P, Smith WHF (1998) New, improved version of the Generic Mapping Tools released. EOS Trans AGU 79: 579

V

Coral Biology

Chapter content

Molecular ecology of *Lophelia pertusa* in the NE Atlantic

Marie C. Le Goff-Vitry[1], Alex D. Rogers[2]

[1] School of Ocean and Earth Science, Southampton Oceanography Centre, Empress Dock, Southampton, SO14 3ZH, UK
(mclgv@yahoo.co.uk)
[2] British Antarctic Survey, High Cross, Madingley Road, Cambridge, CB3 0ET, UK

Abstract. During the ACES (Atlantic Coral Ecosystem Study) European Programme, various molecular methods were used to assess the genetic diversity of deep-water corals, by focusing on *Lophelia pertusa*, the main reef-building species in the northeast Atlantic. Investigations at a high taxonomic level aimed at understanding the evolutionary history of azooxanthellate corals by placing them in the phylogenetic tree of scleractinian corals, using partial sequences of the mitochondrial 16S region. The taxonomy of *L. pertusa* was consistent with morphological studies at the family level. However, eastern and western Atlantic specimens were genetically highly differentiated. *Madrepora oculata* was found to be incorrectly classified by morphological analysis. Intraspecific analyses were undertaken for *L. pertusa*, using specific microsatellite markers, to screen individuals collected at 10 different sampling sites, distributed along the European margin and in Scandinavian fjords. Sequencing of the ribosomal Internal Transcribed Spacer (ITS) 1 and 2 nuclear DNA regions was used as a complementary method. Both microsatellite and gene sequence data showed that *L. pertusa* is not constituted by one panmictic population in the northeast Atlantic, but instead forms distinct, offshore and fjord populations. Along the continental slope, the subpopulations are moderately differentiated. Although larvae might be dispersed along the European margin, the gene flow occurring among these subpopulations is likely to be sporadic, and must be considered in the light of the age of these coral communities, the prevalence of asexual reproduction in the development of the reefs and the longevity of individual clones. Inbreeding was shown at several sites, suggesting a high degree of self-recruitment. The level of genetic diversity and the contribution of asexual reproduction to the maintenance of the subpopulations were highly variable from site to site. These results are of major importance in the generation of a sustainable management strategy for these diversity-rich deep-sea ecosystems.

Keywords. *Lophelia*, *Madrepora*, molecular phylogeny, northeast Atlantic, genetic population structure, microsatellites, ITS sequencing

Introduction

The development of molecular genetic approaches has proved very useful to tackle many aspects of conservation biology (reviewed in Frankham et al. 2002; Pullin 2002; Beebee and Rowe 2004). Molecular markers can be used to estimate the genetic diversity among populations that reflect the long-term evolutionary potential of a species. By investigating the genetic structure of a species in a certain area, it is possible to estimate if it is constituted by one or several populations, and if so, how much gene flow is occurring among them. When all populations are genetically uniform, the loss of a population is recoverable over time because the gene pool of the species has not been affected and gene flow will eventually permit natural recolonisation. In the case of genetically distinct populations, such an event will have much more serious consequences because of the lack of gene flow occurring across populations. It is especially important to monitor and preserve the genetic diversity of small and isolated populations because they are more prone to losing genetic diversity and to suffering from significant genetic problems that will make them vulnerable to extinction. Genetic studies can also be helpful to clarify the taxonomic status of a species or a subspecies, and hence to define conservation priorities. Finally, using molecular genetic techniques to understand the past history of extant populations can be useful to design conservation strategies. In the context of the multidisciplinary European programme ACES, which objective was to formulate recommendations for a future sustainable use of Europe's deep-water coral margin, it was important to include the basic level of biodiversity and evolution, the genetic variability of deep-water coral ecosystems in the northeast Atlantic.

The knowledge of evolutionary relationships among taxa is a prerequisite for targeting conservation units. Until now, evolutionary relationships of deep-sea corals with other scleractinians were poorly understood. A phylogenetic analysis, based on a partial region of the mitochondrial 16S ribosomal RNA encoding gene, was undertaken to place several azooxanthellate coral species within the evolutionary tree of the Order Scleractinia. The main objective was to resolve the phylogenetic relationships of the two main framework-building coral species in the northeast Atlantic: *L. pertusa* and *M. oculata*. Samples of *L. pertusa* from the northeastern and southwestern Atlantic were used in this analysis in order to assess the global intraspecific genetic diversity of *L. pertusa* and to assign a global conservation value to European populations.

The population genetic structure of *L. pertusa* was also examined at the scale of the European margin, in order to understand whether there is a genetic cohesiveness among the European populations, or whether some populations are genetically isolated, and if so, to what extent. Two molecular methods were used: sequencing of two non-coding nuclear regions (ITS 1 and 2) and the screening of high-resolution molecular markers, namely microsatellites that were developed for this species (Le Goff and Rogers 2002).

Material and methods

Sample collection and DNA extraction

For the phylogenetic analysis, fifteen coral species were sampled, comprising six deep-sea coral species: *Dendrophyllia alternata*, *Madrepora oculata*, *Fungiacyathus marenzelleri*, *Caryophyllia ambrosia*, *Flabellum angulare* and *Lophelia pertusa* from the northeastern and southwestern Atlantic (Brazilian slope), and nine tropical, shallow-water coral species, collected in Réunion Island (Indian Ocean): *Pocillopora meandriana*, *Montipora circumvallata*, *Acropora danai*, *A. hemprichii*, *A. humilis*, *A. muricata*, *Psammocora contigua*, *Pavona cactus*, *Porites lobata*.

For the analysis of population structure, *L. pertusa* samples were collected from ten sampling sites distributed along the European margin and in Scandinavian fjords (see Fig. 2).

For each individual sample, one to three coral polyps per colony were either placed into 95 % ethanol or frozen.

Two methods were used for extracting DNA: a high salt extraction protocol and the Qiagen QIAquick (Qiagen Ltd., Crawley, West Sussex, U.K.) DNA extraction kits (Le Goff-Vitry et al. 2004b).

Sequencing

16S region

The universal primers 16Sar and 16Sbr (Palumbi et al. 1991) were used to identify useful primers for *L. pertusa*. The newly designed primers LP16SF and LP16SR were then used to amplify and sequence a part of the 16S region for deep-sea and tropical corals (Le Goff-Vitry et al. 2004b). The obtained sequences, which varied in length between 227 and 465 bp, were aligned with 69 previously published scleractinian homologous sequences (France et al. 1996; Romano and Palumbi 1996; Romano and Cairns 2000). *Hydra vulgaris* (Cunningham and Buss 1993) was used as an out-group. The data were analysed using maximum parsimony and minimum evolution criteria with the program PAUP* Version 4.0b10 (Swofford 2002) and a Bayesian approach with the program MrBayes Version 3 (Huelsenbeck and Ronquist 2001); pairwise genetic distances were calculated with the program DNADIST Version 3.6a2.1 (Felsenstein 1990; Le Goff-Vitry et al. 2004b).

ITS region

Polymerase Chain Reaction (PCR) amplification of the ITS 1 and part of the 5.8s region was performed using the primers 1S and A4 from Chen et al. (1996). The primers ITS2FA and ITS2RA were designed for the amplification of the ITS 2 region for *L. pertusa*, using sequences obtained with the primers A7 and 2SS (Chen et al. 1996; Le Goff-Vitry et al. 2004a). For each individual, the two regions were joined to form a single sequence. The length of these sequences, obtained for a total of 77 individuals over the 10 sampled sites, varied between 834 and 1004 bp. They were aligned and the intraspecific genetic diversity was analysed using maximum likelihood criterion with the program PAUP* Version 4.0b10 (Swofford 2002; Le Goff-Vitry et al. 2004a).

Microsatellites

The ten specific microsatellite markers developed for *L. pertusa* (Le Goff and Rogers 2002) were genotyped for a total of 334 individuals across the 10 sampling sites. Analyses were performed at different levels, from the individual level to local geographic areas, and at scale of the whole European margin, allowing notably the estimation of the proportion of asexual reproduction at each site, the distribution of genetic diversity over the studied area and the assessment of genetic differentiation between geographic areas (Le Goff-Vitry et al. 2004a).

Results and discussion

Phylogenetic analysis

The phylogenetic tree resulting from Bayesian analysis is shown in Figure 1. *L. pertusa* is placed, according to morphological characters, into the family Caryophylliidae (Wells 1956). Representatives of this family are found throughout the scleractinian phylogenetic tree, which suggests it is not monophyletic. This is consistent with the molecular topology published by Romano and Cairns (2000), and supports the idea that the combination of shared ancestral characters used to define this family in morphological taxonomy has led to a poor resolution of the evolutionary relationships of its constituent genera and species. The two specimens of *L. pertusa* form a sister clade to the group consisting of the genera *Caryophyllia* and *Crispatotrochus*, which was described as forming a well-supported clade by Romano and Cairns (2000). Both these genera are from the family Caryophylliidae, which suggests that the classification of *L. pertusa* is consistent with morphological studies at the family level. The tree branches separating *L. pertusa* specimens collected in the northeast Atlantic and off Brazil are extremely long and the calculated genetic distance separating them was high (6.96 %). This indicates a high level of genetic differentiation and suggests that eastern and western Atlantic populations have been reproductively isolated for a considerable time, and may even represent separate species.

This phylogenetic analysis does not support the current classification of *Madrepora oculata* in family Oculinidae (Wells 1956). This family has a poor fossil record (Veron 1995) and its monophyletic status was debated by Romano and Cairns (2000). *M. oculata* occurs in a monotypic grouping lying between the Caryophylliinae and the Pocilloporiidae. As such, this species may form a new family or even higher systematic grouping.

Population structure analysis

The 10 microsatellites developed for *L. pertusa* (Le Goff and Rogers 2002) are the most comprehensive for any species of scleractinian and have proved to be excellent high-resolution markers at the individual level.

Through the assignment of multilocus genotypes (MLGs), and by identifying the MLGs observed more than once that were unlikely to be the result of sexual reproduction (Stenberg et al. 2003), it was possible to discriminate sexually *versus*
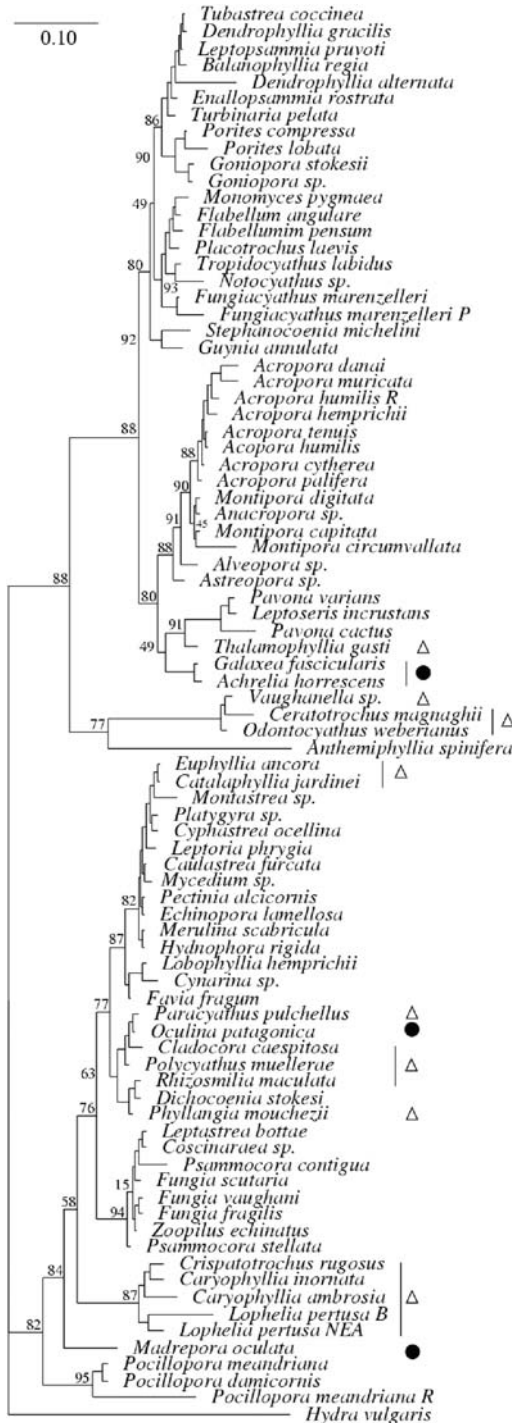
Fig. 1 Phylogram resulting from the Bayesian analysis showing the evolutionary relationships among scleractinians, including *Lophelia pertusa*. Probabilities of the partitions, expressed in percentages, are shown at node labels. The scale unit is the mean of the posterior probability density. A capital letter by the species indicates the origin of the sample (R - Réunion Island; B - off Brazil; NEA - North East Atlantic; P - Porcupine Seabight). Symbols show representatives of the families

Δ = Caryophylliidae,
● = Oculinidae

asexually produced individuals. The proportion of clonemates varied dramatically from site to site (see Fig. 2). The highest proportion of clonemates was reported in the Darwin Mounds area. The low number of distinct MLGs and the prevalence of asexual reproduction in this area could be explained by its particular ecological conditions. In contrast to other sites, *L. pertusa* does not form large reefs at the Darwin Mounds, but small colonies, aggregated on the top of these small mounds, where the coral benefits from enhanced current velocities (Masson et al. 2003). Low recruitment rates of sexually produced larvae could be caused by the patchiness of suitable habitat in this area, and the high number of clones could be explained by the subsequent colonization of the available space through asexual reproduction. The gene diversity indices (Nei 1987), calculated on the basis of sexually produced individuals only, revealed a spatially heterogeneous distribution of genetic
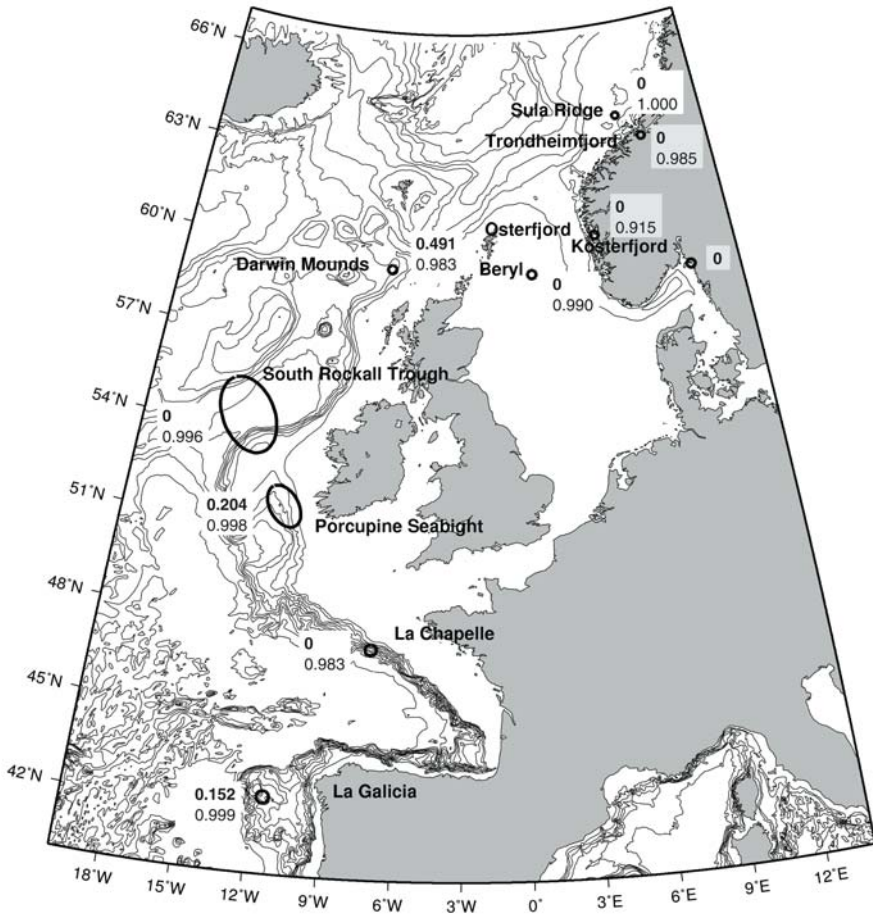
Fig. 2 For each sampling site for *Lophelia pertusa* in the Northeast Atlantic, indicated as a circle, proportion of clonemates (in bold) and gene diversity (mean value), obtained with microsatellite data

variability (see Fig. 2); the lowest values were found at Osterfjord and in the Darwin Mounds area. In Osterfjord, several identical MLGs were encountered more than once, although the sample size was very small. However, the hypothesis that these were the result of sexual reproduction could not be rejected and they could be the result of genetic recombination. This could reflect a bottleneck, arising during the founding of the population.

Strong deviations from Hardy-Weinberg equilibrium (a reference model for detecting the occurrence of evolutionary processes at the population level) were found for all sub-populations, for a majority of loci. Such departures could result from inbreeding. Inbreeding indices have proved statistically significant for many sites in this study (Sula Ridge, Beryl, South Rockall Trough, Porcupine Seabight and Galicia Bank) and could be caused by a spatially restricted effective gene flow and a predominance of self-recruitment of sexually produced larvae within subpopulations (see examples in shallow-water corals, e.g., Ayre and Hughes 2000). Genetic bottlenecks were detected for two subpopulations: Osterfjord, and Darwin Mounds. In the case of deep-sea populations, potential bottlenecks could result from historical events (e.g., changes in sedimentation resulting from alterations in the near seabed current flow, changes in surface productivity patterns), or natural catastrophic events (e.g., slope failures).

The calculation of pairwise fixation indices (an estimate of genetic differentiation among the sampled locations) revealed a high genetic differentiation between the fjord subpopulations and the continental margin subpopulations and between the fjord subpopulations themselves. Among the continental margin subpopulations, a globally moderate, but significant, genetic differentiation was found, which suggests that a certain genetic cohesion is maintained over the open slope over long periods of time, through larval dispersal. This is consistent with the reports of colonisation of man-made structures by *L. pertusa* in the northeast Atlantic (Roberts 2002). However, because of asexual proliferation and the longevity of the clones, even a low-level and sporadic recruitment of sexually produced larvae from outside a given subpopulation might be sufficient to maintain such cohesion.

The correlation between genetic differentiation and geographic distance over the continental margin could not be shown statistically. This result could be explained by the combination of a moderate gene flow and temporal fluctuations in the magnitude of gene flow, caused by historical changes, such as regional extinctions (see Slatkin 1993).

The high genetic differentiation between fjord subpopulations and offshore ones is consistent with studies performed on other marine species (e.g., Drengstig et al. 2000). Local geological and hydrological characteristics (Farmer and Freeland 1983) can explain the limited gene flow between the fjords and offshore waters.

The results obtained with the ITS sequences support the genetic distinctiveness of the fjords between one another and suggests their initial colonisation, after the last glaciation period, through migrants originating from more closely related, continental margin populations. They also suggest a low genetic variability in the Osterfjord. However, some inconsistencies were found, suggesting that a bias might be introduced by intra-individual variability (see Harris and Crandall 2000). The

microsatellites offered a more reliable approach, and a higher resolution at the scale of this study.

Conservation implications

Recent studies have shown the key importance of *L. pertusa*, as the main reef-building species in the Northeast Atlantic, sustaining a rich biodiversity (e.g., Fosså et al. 2002). Understanding the population structure, dispersal capacities, and development pattern of *L. pertusa* along the European margin is fundamental to the generation of a sustainable management strategy for these ecosystems, threatened by the increasing intensity of deep-water fisheries (e.g., Hall Spencer et al. 2002). The results of the studies reported here have important consequences in terms of management strategies.

Lophelia pertusa, distributed from off the Iberian margin to the Scandinavian fjords, cannot be considered as one panmictic population, but instead forms genetically distinct, offshore and fjord, subpopulations. The moderate genetic differentiation observed along the continental margin suggests the occurrence of a sporadic gene flow, indicating that the recolonisation of any destroyed coral area along the continental margin could occur, through larval dispersal from adjacent subpopulations, over long periods of time. However, this must be considered in the light of the age of these coral communities, the prevalence of asexual reproduction in the development of the reefs and the longevity of individual clones. Moreover, inbreeding was shown at several sites, suggesting that there is a high degree of self-recruitment in these subpopulations, which is supported by data arising on the biological features of the coral. The seasonal broadcast of gametes around January/February, when little food support is available in the Northeast Atlantic, and the relatively small size of oocytes, compared to other deep-sea coral species, suggests that the dispersal of the lecithotrophic larvae might be spatially restricted (Waller and Tyler in press). Finally, such a recolonisation implies that the initial impacts have not altered the nature of the seabed substrates or local current regimes and the settlement of larvae is still possible.

A high variation of the genetic diversity amongst the subpopulations was shown. The Darwin Mounds subpopulation revealed a high proportion of clones and a low gene diversity, which is consistent with biological data, as no reproductive coral has been found in this area (Waller and Tyler in press). The particular ecological conditions of this area could explain the patchiness of the coral colonies, and the predominance of asexual reproduction to the maintenance of the subpopulation. However, intense bottom-trawling occurring in this area is also likely to influence the genetic structure of this subpopulation as it could, through mechanical destruction, impede sexual reproduction by fragmentation to below the minimum size for reproduction (see Waller and Tyler in press). Effective conservation measures, such as the designation of a protected area where bottom trawling would be banned, would be necessary to preserve this vulnerable subpopulation. The Darwin Mounds have recently been protected by an emergency measure (European Commission Regulation No 1475/2003), which prohibits the use of bottom trawl; and might

be designated as a Special Area of Conservation, under the European Habitats Directive (92/43/EEC).

The fjord subpopulations are highly differentiated genetically. The Osterfjord subpopulation showed very low gene diversity. A careful monitoring of the fjord subpopulations should be undertaken, as they are particularly sensitive to genetic drift, due to their small sizes, and are vulnerable to coastal pollution. Trondheimfjord and Osterfjord subpopulations are protected from trawling, but this is not the case for Kosterfjord, where sample size was too small for analyses to be performed.

Acknowledgements

References

Ayre DJ, Hughes T (2000) Genotypic diversity and gene flow in brooding and spawning corals along the Great Barrier Reef, Australia. Evolution 54: 1590-1605

Beebee TJC, Rowe G (2004) An introduction to molecular ecology. Oxford Univ Press, Oxford

Chen CA, Willis BL, Miller DJ (1996) Systematic relationships between tropical corallimorpharians (Cnidaria: Anthozoa: Corallimorpharia): Utility of the 5.8s and internal transcribed spacer (ITS) regions of the rRNA transcription unit. Bull Mar Sci 59: 196-208

Cunningham CW, Buss LW (1993) Molecular evidence for multiple episodes of paedomorphosis in the family Hydractiniidae. Biochem Syst Ecol 21: 57-69

Drengstig A, Fevolden S-E, Galand PE, Aschan MM (2000) Population structure of the deep-sea shrimp (*Pandalus borealis*) in the north-east Atlantic based on allozyme variation. Aquat Living Resour 13: 121-128

Farmer DM, Freeland HJ (1983) The physical oceanography of the fjords. Prog Oceanogr 12: 147-220

Felsenstein J (1990) Phylogeny Inference Package (PHYLIP). Univ Washington, Seattle

Fosså JH, Mortensen PB, Furevik DM (2002) The deep water coral *Lophelia pertusa* in Norwegian waters: distribution and fishery impacts. Hydrobiologia 471: 1-12

France SC, Rosel PE, Agenbroad JE Mullineaux LS, Kocher TD (1996) DNA sequence variation of mitochondrial large-subunit rRNA provides support for a two subclass organization of the Anthozoa (Cnidaria). Mol Mar Biol Biotech 5: 15-28

Frankham R, Ballou JD, Briscoe DA (2002) Introduction to conservation genetics. Cambridge Univ Press, Cambridge

Hall-Spencer J, Allain V, Fosså JH (2002) Trawling damage to Northeast Atlantic ancient coral reefs. Proc R Soc London Bull Biol Sci 269: 507-511

Harris DJ, Crandall KA (2000) Intragenomic variation within ITS1 and ITS2 of crayfish (Decapoda: Cambaridae): implications for phylogenetic and microsatellite studies. Mol Biol Evol 17: 284-291

Huelsenbeck JP, Ronquist FR (2001) MRBAYES: Bayesian inference of phylogeny. Bioinformatics 17: 754-755

Le Goff MC, Rogers AD (2002) Characterisation of 10 microsatellite loci for the deep-sea coral *Lophelia pertusa* (Linnaeus 1758). Mol Ecol Notes 2: 164-166

Le Goff-Vitry MC, Pybus, OG, Rogers AD (2004a) Genetic structure of the deep-sea coral *Lophelia pertusa* in the North East Atlantic revealed by microsatellites and ITS sequences. Mol Ecol 13: 537-549

Le Goff-Vitry MC, Rogers AD, Baglow D (2004b) A deep-sea slant on the molecular phylogeny of the Scleractinia. Mol Phylogenet Evol 30: 167-177

Masson DG, Bett BJ, Billet DSM, Jacobs CL, Wheeler AJ, Wynn RB (2003) The origin of deep-water, coral-topped mounds in the northern Rockall Trough, Northeast Atlantic. Mar Geol 194: 159-180

Nei M (1987) Molecular Evolutionary Genetics. Columbia Univ Press, New York

Palumbi SR, Martin RA, Romano S, McMillan WO, Stice L, Gabrowski G (1991) The simple fool's guide to PCR. Hawaii Univ, Honolulu

Pullin AS (2002) Conservation biology. Cambridge Univ Press, Cambridge, UK

Roberts JM (2002) The occurrence of the coral *Lophelia pertusa* and other conspicuous epifauna around an oil platform in the North Sea. J Soc Underwater Tech London 25: 83-91

Romano SL, Palumbi SR (1996) Evolution of scleractinian corals inferred from molecular systematics. Science 271: 640-642

Romano SL, Cairns SD (2000) Molecular phylogenetic hypotheses for the evolution of scleractinian corals. Bull Mar Sci 67: 1043-1068

Slatkin M (1993) Isolation by distance in equilibrium and nonequilibrium populations. Evolution 47: 264-279

Stenberg P, Lundmark M, Saura A (2003) MLGsim: a program for detecting clones using a simulation approach. Mol Ecol Notes 3: 329-331

Swofford DL (2002) PAUP* 4.0: Phylogenetic analysis using parsimony (and other methods). Sinauer Associates, Sunderland

Veron JEN (1995) Corals in Space and Time: the Biogeography and Evolution of the Scleractinia. Univ New South Wales Press, Sydney

Waller RG, Tyler PA (in press) The reproductive ecology of two deep-sea reef building scleractinians from the NE Atlantic Ocean. Coral Reefs

Wells JW (1956) Scleractinia. In: Moore RC (ed) Treatise on Invertebrate Paleontology. F, Coelenterata. Geol Soc Amer Univ Kansas Press, Lawrence, pp F328-F443

Population genetic structure of the Hawaiian precious coral *Corallium lauuense* (Octocorallia: Coralliidae) using microsatellites

Amy R. Baco, Timothy M. Shank

Woods Hole Oceanographic Institution, Biology Department, MS 33, Woods Hole, MA 02543, USA
   (abaco@whoi.edu)

Abstract. Seamount fauna are threatened by destructive fisheries practices, yet little is known about the physical and biological processes (e.g., dispersal and connectivity) that maintain species on seamounts. Gorgonian octocorals are among the dominant epifaunal taxa of many seamounts and represent a model taxon with which to understand processes of dispersal and gene flow in seamount fauna. One of the more common deep-sea octocorals on the seamounts and islands of the Hawaiian Archipelago is the precious coral *Corallium lauuense*. Here, we present results of a preliminary study to examine the population genetic structure of widely-distributed populations of *C. lauuense* within and among eight Hawaiian seamounts using three highly polymorphic microsatellite loci. Genic diversity and population differentiation estimated from the number of alleles, heterozygosity, and a hierarchical analysis of molecular variance revealed relatively high levels of genetic diversity as well as low yet significant levels of population differentiation among several of the seamounts and islands (predominantly among population comparisons with any site and the Kauai and Makapu'u coral beds). Despite these genetic differences between sites, population differentiation based on F_{ST} and R_{ST} for all sites was not significant at any locus. No linkage disequilibrium or pattern of isolation by distance was observed, and heterozygote deficiency was found in every population within at least one locus. The low heterozygosity throughout the Hawaiian Archipelago raises the concern that this species may be suffering from inbreeding depression. Further investigation of precious coral population demographic structure is needed to assess the risk of habitat loss and fisheries activities on these seamounts.

Keywords. Deep-sea corals, seamounts, precious corals, microsatellites, gene flow, Hawaii

Introduction

   The benthic fauna of seamounts are often isolated from other seamount fauna and from continental shelf and slope fauna at similar depths. Distance is not the only

factor contributing to the isolation of seamount biota; physical oceanography and life history strategies of seamount fauna may add to the isolation (Parker and Tunnicliffe 1994, and reviewed in Rogers 1994). Because of their isolation, seamounts are often cited as potential locations for high rates of speciation (Hubbs 1959; Wilson and Kaufmann 1987; Parker and Tunnicliffe 1994; Rogers 1994; DeForges et al. 2000). Not surprisingly, a large percentage of the seamount fauna has been found to be endemic, as high as 34 % on some south Pacific seamounts (Rogers 1994; DeForges et al. 2000). In many parts of the Pacific Ocean, seamounts are being impacted and in some cases scraped clean of most of the epifauna during destructive trawl and long-line fishing (Rogers 1994; DeForges et al. 2000). Because of the threats to seamount fauna, it is crucial to understand the biological processes of dispersal and gene flow occurring between populations of species in these important deep-sea habitats.

The benthic environment of seamounts, compared to other deep-sea habitats, have a high occurrence of hard substrates dominated by suspension feeders, including many types of gorgonian corals (Genin et al. 1992; Rogers 1994; DeForges et al. 2000). For this reason, gorgonian corals make an ideal target group to understand the ecology of seamount fauna. The seamounts and islands of the Hawaiian Archipelago include some of the most isolated benthic marine habitats in the world. Therefore, they represent an ideal location to study evolutionary processes of speciation and gene flow of benthic organisms.

The deep-sea hard-bottom communities of many of the Hawaiian seamounts and islands are dominated by diverse coral assemblages, including gorgonian octocorals. There are three species of deep-water corals in Hawaii that are particularly abundant and widely distributed. They are also harvested for the jewelry industry. These so-called "precious corals" include two octocorals in the Family Coralliidae; *Corallium secundum* and *Corallium lauuense* (*C. lauuense* was previously misidentified and referred to as *C. regale* in Grigg (2002) and other publications as well as in the Fisheries Management Plan), and a hexacoral in the Family Gerardiidae; *Gerardia* sp. These three precious coral species occur at depths ranging from 300-600 m throughout the Hawaiian Archipelago, with the highest abundances found in the Northwestern Hawaiian Islands (NWHI) and along the Emperor Seamount chain. Of these three species, *C. lauuense* or "red coral" is the most valuable and may sell for as much as $880/kg (Grigg 2002). Precious coral fisheries worldwide have followed boom-bust cycles, emphasizing the need for management of the fishery (Grigg 1994). Despite the value and past fishing pressures on *C. lauuense*, fundamental questions remain regarding the biology or ecology of this species (see Grigg 2002 for a review of coral collection in the Hawaiian Archipelago and Emperor Seamount chain).

To ensure a viable coral fishery and provide guidelines for managing seamount fauna affected by fish fisheries in other parts of the world's oceans, one must understand the "stock structure" of seamount fauna. As with any heavily-harvested or potentially threatened species, population viability will depend on the "stock structure", defined as dispersal between populations, rates and patterns of re-establishment, and basic life-history pattern. Understanding these factors is critical

to both management and conservation (Lande 1988; Avise 1996). This information can be used to define minimal stocks or management units that can be incorporated into management models. Molecular genetic methods have been used to understand stock structure in a variety of marine organisms (e.g., Graves 1996; Palumbi 1996; Palumbi and Baker 1996; Smith and Wayne 1996).

Several studies of shallow-water corals have provided evidence of significant genetic structure between populations. Evidence for genetic isolation of populations was found in both hard and soft corals, including several species capable of long distance dispersal (Ayre and Duffy 1994; Hellberg 1994, 1995; Benzie et al. 1995; Burnett et al. 1995; McFadden 1997). While these shallow-water corals are not closely related to the deeper corals of this study, they do exhibit similar life history characteristics (e.g., presence of both sexual and asexual reproduction). If significant genetic structure exists in populations of Hawaiian precious corals, this would support the idea of isolation between seamount populations and would suggest that the elimination (through overharvesting) of a bed of precious corals would result in loss of overall genetic diversity in the species. Significant genetic structure between populations would also suggest that propagules from unharvested populations might not restock harvested coral beds.

In fact, recent genetic studies of a species closely related to *C. lauuense*, *Corallium rubrum,* in the Mediterranean have shown that populations exhibited significant genetic structure (Abbiati et al. 1993). The mean F_{ST} value for two *C. rubrum* populations separated by about 80 km in the Mediterranean was 0.1, indicating moderate but significant isolation between the two populations. Based on these results, the authors suggest that rotational harvesting will significantly alter the genetic stability of *C. rubrum* populations. Along the same lines, the ultimate objectives of this study are to define the genetic units of Hawaiian precious corals and to determine if beds represent genetically isolated units as found in the Mediterranean.

Corals have been difficult to use for both phylogenetic and population genetic studies because they tend to have very low levels of variation in mitochondrial DNA (reviewed in Shearer et al. 2002). Therefore until recently, coral population genetic studies have had to rely on allozyme markers. Allozyme studies of shallow-water corals have provided evidence of significant genetic structure between populations as discussed above. Recently, amplified fragment length polymorphisms (AFLP's) and microsatellites have shown some promise for coral population genetic studies (Barki et al. 2000; Maier et al. 2001; Le Goff and Rogers 2002; Le Goff et al. 2004; Miller and Howard 2004). Here we discuss the results of population genetic studies for *C. lauuense* based on three microsatellite loci.

Materials and methods

Study sites

Precious coral samples were collected during 5 cruises using the Pisces IV and Pisces V submersibles in 1998-2002. A total of 134 individuals of *Corallium*

lauuense were collected from 8 sites in the Hawaiian Archipelago (Fig. 1, Table 1). Collection depths ranged from 385 to 535 m, with the single individual from French Frigate Shoals collected at 575 m. Individual coral trees were sampled by clipping a small piece of the coral tree using the submersible manipulator (and leaving the remainder of the tree intact on the bottom). The pieces were then placed in numbered jars in the submersible basket. For each tree sampled, size and depth were noted. Upon return to the surface, each individual was placed in both liquid nitrogen and in 95 % ethanol.

In addition to the sites shown in Figure 1 and listed in Table 1, we also visited the "refuge" bed between Nihoa and Necker Islands, and a precious coral bed east of French Frigate Shoals. *C. lauuense* was not observed during 5 dives at the "refuge" bed and only 1 individual was observed during 2 dives at the French Frigate Shoals bed.
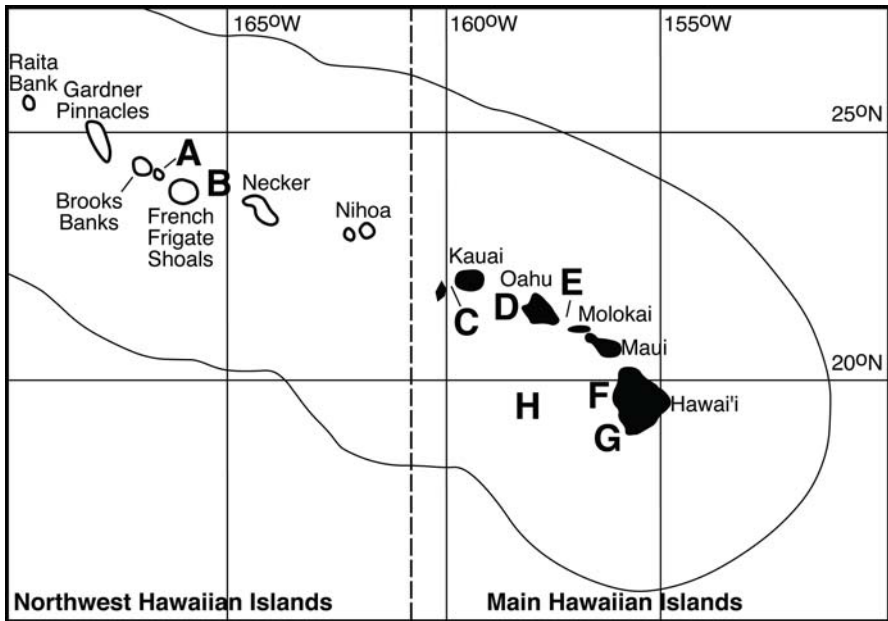
Fig. 1 Map of precious coral bed sampling locations for *Corallium lauuense*. A – Brooks Banks, B – East French Frigate Shoals, C – Kauai, D – Ka'ena Point, E – Makapu'u, F – Keahole Point, G – Pohue, H – Cross Seamount

Laboratory methods

DNA was extracted from tissue scraped from the coral skeletons following a standard CTAB extraction (Doyle and Dickson 1987) or using DNeasy kits (Qiagen). Genomic DNA libraries from 2 individuals of *C. lauuense* were enriched for CA/GT microsatellite repeats using biotin probes bonded to streptavidin-coated beads following protocols in *Tools for Developing Molecular Markers* (ICBR 2001, modified from Kandpal et al. 1994). Clones were screened using a biotin-labeled $(CA)_{15}$ probe. Plasmids from positive colonies were sequenced on an ABI 3730. For all microsatellite loci with sufficient flanking sequence, primers were designed

Table 1 Collection information for *Corallium lauuense*.
Site Abbreviations: BB = Brooks Banks; EFFS = East French Frigate Shoals, KP = Keahole Point, MK = Makapu'u

	BB NW	BB SW	BB SE	All BB	Cross	EFFS	Kaena Pt.	Kauai	KP 15	KP 19	KP All	MK 358	MK 359	All MK	Pohue	All Pops.
Number Collected	9	12	11	32	17	1	6	20	11	14	25	10	12	22	11	134
Average depth (m)	432.2	463.2	458.1	452.7	416.6	575	432.6	500.2	395	395.8	395.7	422.1	426.7	424.6	462.8	444.3
Range (m)	427-442	448-503	454-462	427-503	409-427	-	417-450	480-531	395	385-410	385-410	415-431	400-439	400-439	420-525	385-575

Table 2 Summary of microsatellite loci used for this study

Microsatellite locus	Repeat type	Sequence length (bp)	Repeat number range	Total number of observed alleles	Annealing temperature (°C)
CR3A-B1	$(CA)_n$	145-203	8-37	28	48
CR5-C12	$(CA)_n$	77-197	7-67	37	44
CR3A-O3	$(CAT)_n$	160-217	18-37	16	52

using Primer 3 (Rozen and Skaletsky 1998, 2000). Of the many microsatellite loci tested, only the three loci discussed here amplified in every individual. These three loci are listed in Table 2.

The genotypes of each coral were assayed for all three loci, CR3A-B1, CR5-C12, and CR3A-O3. One primer per pair for each locus was labeled at the 5' end with the fluorescent label FAM (MWG Biotech). Polymerase chain reaction (PCR) conditions were 94°C for 2 min followed by 35 cycles of 94°C for 45 sec, X°C for 30 sec, where X is the allele-specific annealing temperature listed in Table 1, and 72°C for 45 sec, followed by a 5 min extension at 72°C. One µl of PCR product was combined with ROX 500 size standard (Applied Biosystems) and electrophoresed on an ABI 377 DNA sequencer running GeneScan (ver. 3.1; Applied Biosystems). Alleles were scored directly using GeneScan.

Data analyses

To test for hierarchical genetic structure, submersible dives on which at least 10 individuals were collected were analyzed as separate subpopulations within sites. Observed (H_o) and expected (H_e) heterozygosities, and number of alleles were calculated in ARLEQUIN 2.0 (Schneider et al. 1997). Genotypic departures from Hardy-Weinberg expectations were calculated using Fisher's exact test with a Markov chain randomization method (Guo and Thompson 1992) in GENEPOP version 3.1c (Raymond and Rousset 1995) set up for online access by E. Morgan (http://wbiomed.curtin.edu.au). When conducting these tests, we selected the option that allowed for the alternate hypothesis of heterozygote deficiency (Rousset and Raymond 1995). The Markov chain parameters for this test were dememorization number, 10,000; number of batches, 200; number of iterations per batch, 1000. For the test of linkage disequilibrium in GENEPOP, Markov chain parameters were increased to 1000 for the number of batches and 10,000 for the number of iterations per batch. F_{IS} values were also calculated in GENEPOP following Weir and Cockerham (1984).

To test the null hypotheses of identical allelic distribution across populations, an unbiased estimate of P-values was calculated for each locus and for each pair of populations in GENEPOP as in Raymond and Rousset (1995). The null hypothesis of identical genotypic distributions across populations was also tested in GENEPOP using an unbiased estimate of the P-value of a G-based exact test as in Goudet et al. (1996).

To test for population differentiation, pairwise F_{ST} values were calculated as in Weir and Cockerham (1984). F_{ST} is a measure based on variance in allele frequencies. R_{ST} is a form of F_{ST} designed specifically for microsatellites and based on allele sizes (Slatkin 1995). It assumes the loci follow a generalized stepwise mutation model (Slatkin 1995). A hierarchical analysis of molecular variance (AMOVA; Excoffier et al. 1992) was performed with dives within sites analyzed as separate subpopulations. Finally, the regression of $F_{ST}/(1-F_{ST})$ to the natural log of geographic distance between sites was tested for isolation by distance using a Mantel Test with 2000 permutations. F- and R-statistics, their P-values, AMOVA and the Mantel test were conducted in ARLEQUIN.

Results

Estimates of genetic diversity for all collections of *Corallium lauuense* are shown in Table 3. All three loci were highly polymorphic with 16-37 alleles observed per locus. Gene diversities (H_e) were high for most site/locus combinations (range 0.86-0.98). No linkage disequilibrium was detected.

Significant heterozygote deficiencies ($P<0.05$) were observed at 27 of the 45 site/locus combinations and for all individuals combined. F_{IS} values ranged from 0.05 to 0.49 for populations that had significant heterozygote deficiencies. These values indicate that some level of inbreeding may be occurring.

Genic differentiation, or the difference in distribution of allele frequencies across sites, was highly significant ($P<0.01$) for each locus and for the combination of the three loci (data not shown). Genotypic differentiation was significant only for locus B1 ($P<0.05$) (data not shown).

Pairwise comparisons of F_{ST} and R_{ST} for populations are given in Table 4. Only 6 pairwise comparisons had F_{ST} values statistically different from 0. These values ranged from 0.02 to 0.05, generally considered as low levels of genetic differentiation between populations. The 14 significant R_{ST} values ranged from 0.05 to 0.21. One of the highest R_{ST} values was for a comparison from two dives in the Makapu'u coral bed ($R_{ST}=0.17$). These two dives sites were separated by <1.6 km distance in what is a well-surveyed, continuous coral bed, suggesting there may be some genetic subdivision even within what appear to be continuous coral populations. However, dives on the northwest and southwest side of Brooks Banks (3 km apart) and both dives on the Keahole Bed also were within continuous coral beds, but did not show any significant pairwise comparisons between dives.

Several islands/seamounts had multiple beds that were not connected. These included the southeastern slope coral bed of Brooks Banks relative to the western bed; the Kaena Point Bed and Makapu'u Bed are on the northwest and southeast slopes, respectively, of Oahu; and the Keahole Bed and the Pohue bed are both on the western slope of the island of Hawaii. The only significant F_{ST} or R_{ST} value for pairwise comparisons between beds on the same island/seamount was between the southern side of the Makapu'u bed (Mak 359) and the Kaena Point Bed ($R_{ST}=0.16$), both on the island of Oahu.

Except for the pairwise comparisons within the Makapu'u bed, all of the significant F_{ST} and R_{ST} values occurred for comparisons between islands/seamounts. The Kauai bed in particular showed significant genetic differentiation from the Brooks Banks Bed, the Cross Seamount Bed, the northern side of the Makapu'u Bed (Mak 358), and one dive at the Keahole Bed (Kea 19). The Mak 358 site also showed genetic differentiation from the total for all Brooks Banks dives and the individual dives on the SW and SE slopes of Brooks. The Mak 359 site (southern portion of bed) showed significant F_{ST} or R_{ST} values for comparisons to Cross Seamount and to the bed on the SE side of Brooks Banks.

Despite these genetic differences between islands/seamounts, the overall AMOVA based on F_{ST} and R_{ST} for all sites was not significant at any locus. The highest level of genetic variability was found within subpopulations. There was also not a significant pattern of isolation by distance (Fig. 2).

Table 3 *Corallium lauuense*. Genetic variability at 3 microsatellite loci for all collection locations. Number of coral trees (N), number of alleles (A), observed (H_o) and expected (H_e) heterozygosities, as well as F_{IS} values for each locus. Asterisks at H_o estimates indicate the significance of test for departure from Hardy-Weinberg expectations in the form of heterozygote deficiency (* - $P<0.05$, ** - $P<0.01$, [a] - heterozygote excess). Sites are in order from northwest to southeast plus Cross Seamount. Site Abbreviations: BB = Brooks Banks; EFFS = East French Frigate Shoals; KA = Kaena Point; KI = Kauai; KP = Keahole Point, Mk = Makapu'u; PO = Pohue; CS = Cross Seamount

		BB NW	BB SW	BB SE	BB All	EFFS	KA	KI	KP 15	KP 19	KP All	MK 358	MK 359	MK All	PO	CS	All Pops
B1	N	9	12	11	32	1	6	20	11	14	25	10	12	22	11	17	134
	A	6	14	12	18	2	10	17	16	12	20	11	14	19	16	16	28
	H_o	0.56*	0.75	0.73**	0.69**	1	1.0	1.0	1.0	1.0[a]	1.0[a]	0.70**	0.83*	0.77**	0.82*	0.82*	0.85**
	H_e	0.88	0.95	0.94	0.93	1	0.97	0.93	0.97	0.93	0.95	0.95	0.97	0.96	0.98	0.94	0.95
	F_{IS}	0.37	0.21	0.23	0.26	-	-0.03	-0.08	-0.03	-0.08	-0.06	0.26	0.13	0.20	0.16	0.12	0.10
C12	A	10	11	15	24	2	8	18	14	13	20	15	9	19	18	18	37
	H_o	0.56**	0.50**	0.82*	0.63**	1	0.50**	0.85*	0.82*	0.50**	0.64**	0.90	0.50**	0.68**	0.91	0.82*	0.72**
	H_e	0.95	0.93	0.96	0.95	1	0.99	0.96	0.95	0.96	0.96	0.98	0.87	0.94	0.98	0.96	0.95
	F_{IS}	0.42	0.46	0.15	0.34	-	0.48	0.11	0.14	0.46	0.33	0.07	0.42	0.27	0.07	0.14	0.25
O3	A	6	8	7	11	2	7	9	7	7	9	9	9	10	9	9	16
	H_o	0.44**	0.58*	0.82	0.63**	1	0.83	0.80*	0.27**	0.64*	0.48**	0.70	0.83	0.77	0.82	0.73	0.69**
	H_e	0.92	0.86	0.86	0.86	1	0.92	0.84	0.91	0.84	0.88	0.89	0.88	0.88	0.91	0.89	0.87
	F_{IS}	0.49	0.28	0.04	0.26	-	0.07	0.05	0.69	0.24	0.44	0.19	0.06	0.12	0.10	0.15	0.20

Table 4 Pairwise F_{ST} (above the diagonal) and R_{ST} (below diagonal) for for populations of *Corallium lauuense* from the Hawaiian Archipelago based on three microsatellite loci (* P<0.05). Site Abbreviations: BB = Brooks Banks; EFFS = East French Frigate Shoals; KA = Kaena Point; KI = Kauai; KP = Keahole Point, Mk = Makapu'u; PO = Pohue; CS = Cross Seamount

	BB NW	BB SW	BB SE	BB All	CS	EFFS	KA	KI	KP 15	KP 19	KP All	MK 358	MK 359	MK All	PO
BB NW		0.0407	0.0013	-0.0065	0.0126	0.0273	0.0084	0.0236	0.0069	0.0204	0.0085	0.0264	0.0272	0.0192	0.0216
BB SW	-0.0065		0.0165	-0.0050	0.0198	0.0159	0.0352	0.0492*	0.0224	0.0261	0.0187	0.0219	0.0326	0.0203	0.0137
BB SE	-0.0030	0.0411		-0.0160	-0.0101	-0.0024	-0.0032	0.0121	0.0041	0.0110	0.0025	0.0134	0.0132	0.0063	-0.0108
BB All	-0.0189	-0.0119	-0.0097		-0.0002	0.0038	0.0082	0.0232*	0.0055	0.0125	0.0041	0.0139	0.0176	0.0091	0.0018
CS	-0.0234	0.0237	-0.0101	-0.0061		0.0095	0.0071	0.0089	-0.0047	0.0164	0.0009	-0.0014	0.0230*	0.0040	-0.0038
EFFS	-0.0719	0.2009	0.0823	0.0454	-0.0564		-0.0046	0.0241	-0.0202	0.0393	0.0062	-0.0559	0.0446	-0.0089	-0.0087
KA	-0.0064	0.2081*	0.1551*	0.1016	0.0309	0.0715		0.0038	0.0081	0.0139	0.0059	0.0054	0.0310	0.0125	-0.0196
KI	-0.0239	0.1426*	0.1416*	0.0619*	0.0461*	0.3535*	0.0316		0.0125	0.0178*	0.0101	0.0195*	0.0101	0.0075	-0.0024
KP 15	-0.0446	0.0202	0.0480	0.0070	-0.0104	0.0087	-0.0024	-0.0106		0.0211	-0.0137	-0.0011	0.0035	-0.0055	-0.0072
KP 19	-0.0475	0.0406	0.0426	-0.0027	-0.0078	0.2283	0.0562	-0.0041	-0.0298		-0.0161	0.0200	0.0198	0.0127	0.0023
KP All	-0.0366	0.0330	0.0474	0.0098	-0.0013	0.1200	0.0313	-0.0027	-0.0303	-0.0260		0.0054	0.0070	-0.0005	-0.0069
MK 358	0.0245	0.1816*	0.1277*	0.1075*	0.0297	-0.0721	-0.0575	0.0807*	0.0202	0.0751	0.0558		0.0269	-0.0150	-0.0045
MK 359	-0.0371	0.0387	0.1113*	0.0155	0.0504	0.3936	0.1566*	0.0278	-0.0087	-0.0069	-0.0033	0.1700*		-0.0174	0.0051
MK All	-0.0311	0.0655	0.0622	0.0256	-0.0017	0.1121	-0.0006	-0.0085	-0.0299	-0.0199	-0.0174	0.0260	0.0212		-0.0058
PO	-0.0511	0.0362	0.0152	-0.0096	-0.0177	0.1531	0.0419	-0.0056	-0.0254	-0.0392	-0.0242	0.0647	-0.0080	-0.0185	
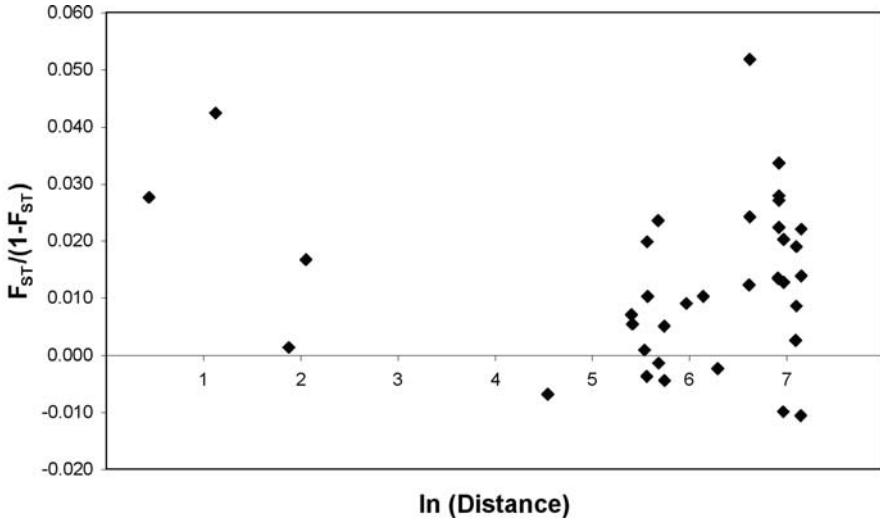
Fig. 2 Relationship between transformed pairwise values of $F_{ST}/(1-F_{ST})$ and natural log of geographic distance between sites

Discussion

The primary goal of this study was to determine levels of gene flow and connectedness between precious coral beds in the Hawaiian Archipelago to obtain a better understanding of the ecological and evolutionary processes that maintain coral species through seamount dispersal processes. In addition, assessing the degree of inbreeding, the amount of genetic variation, and partitioning of this variation into within- and among-population components are essential for understanding how potentially isolated species can evolve in response to environmental changes and for evaluating management strategies.

Heterozygote deficiency

Deviations from Hardy-Weinberg expectations in the form of heterozygote deficiency were found in most samples across loci. Previous allozyme studies of scleractinian corals have often revealed significant departures from Hardy-Weinberg expectations (e.g., Stoddart 1984). Recent studies have also shown departures at 9 of 10 microsatellite loci in the deep-sea scleractinian *Lophelia pertusa* (Le Goff and Rogers 2002; Le Goff et al. 2004) and at most loci in three shallow-water scleractinians (Maier et al. 2001; Miller and Howard 2004). Allozymes have also shown heterozygote deficiencies in individual populations of the octocorals *Briareum asbestinum* (Brazeau and Harvell 1994) and *Corallium rubrum* (Abbiati et al. 1993).

Heterozygote deficiency may result from several possibilities including the presence of null alleles, isolation and genetic drift, the Wahlund Effect (sampling individuals from more than one population) or inbreeding. Null alleles occur when mutations in the primer region prevent primer binding (Callen et al. 1993). We feel

null alleles are unlikely to be the cause of heterozygote deficiency in this species. Every locus amplified for every individual. If there were individuals in which one locus did not amplify and the other two did as has been found in other microsatellite studies (e.g., Ball and Chapman 2003), null alleles would be a more likely suspect.

Isolation and genetic drift may contribute to heterozygote deficiency. This possibility is also less likely for most populations. The relatively low values of F_{ST} and R_{ST} suggest sufficiently high levels of migration between sites to offset drift for most of these populations.

The Wahlund Effect is a more likely possibility since little is known about population boundaries or ranges in these species. In at least one of the coral beds, the Makapu'u Bed, there was an R_{ST} value of 0.17 for pairwise comparison between collection dives. These dives were separated by <1.6 km, indicating there may be dispersal barriers within continuous beds. If samples at other beds were collected across these barriers, the Wahlund Effect could result. Increased sampling within sites would help resolve this issue.

Another possibility is that inbreeding may be occurring in these populations. F_{IS} values were relatively high for all site/locus combinations that had significant heterozygote deficiencies. Several factors could potentially contribute to inbreeding at these sites. Several of these sites, particularly Makapu'u and Keahole were subject to intensive fishing pressure before fishing regulations were implemented in the late 1970s (fishing pressure at other sites is not well documented). This could lead to a temporary bottleneck effect if new recruits to these sites were from local populations. It is also possible that only episodic events provide recruits from outside the populations and these have not occurred since fishing ceased.

Population genetic structure

The allele frequency distribution differed significantly across populations, but these differences were not reflected in overall AMOVA or isolation by distance comparisons. Rather, genetic differentiation occurred in pairwise comparisons of individual sites. Differentiation was found at three different levels, within a continuous coral bed, between beds on the same island and between islands. Geographic scales of differentiation were not consistent across sites however.

At the scale of a continuous coral bed, two dives at the Makapu'u site had R_{ST} values that suggested moderate isolation between the northern part of the bed and the southern part of the bed. Statistically significant F_{ST} values have been found for other soft corals on smaller spatial scales, for example, the soft coral *Alcyonium rudyi* showed moderate F_{ST} values on scales of hundreds of meters (McFadden 1997). The solitary cup coral, *Balanophyllia elegans*, also shows significant genetic structure between patches on even smaller spatial scales (Hellberg 1994, 1995). More intensive sampling within the Makapu'u Bed would allow for better resolution of population structure within this site and the smaller scales at which genetic differentiation may be occurring in this species.

The genetic differentiation found between sites on the same island was low compared to that found in *Corallium rubrum*, a species in the same genus found in

the Mediterranean (Abbiati et al. 1983). *C. rubrum* populations were found to have significant F_{ST} values ($F_{ST} = 0.11$) for populations separated by only 80 km.

The differentiation observed between populations does not appear to follow a pattern of isolation by distance. This is surprising because the islands/seamounts of the Archipelago are arranged in a pattern befitting a classic stepping-stone model, which should lead to isolation by distance. Instead, the Kauai coral bed, which is towards the center of the sampled geographic range, shows the most isolation of any of the populations. Little is known of deep-sea currents around the Hawaiian Archipelago, but it seems unlikely that a current capable of sustaining gene flow between the northwestern islands/seamounts and the southeastern end of the chain would skip the island of Kauai. Many studies of general deep-sea fauna have shown depth to substantially influence species composition and genetic diversity (e.g., Carney et al. 1983; Bucklin et al. 1987; Gage and Tyler 1991; France and Kocher 1996; Chase et al. 1998). Additionally, some species have been shown to have higher rates of gene flow horizontally than vertically with depth (France and Kocher 1996; Bucklin et al. 1987). While the samples collected at the Kauai Bed came from an average of 50 m deeper than at any other bed, additional collections are necessary to determine the influences of possible stratification of water masses with depth on genetic diversity.

Nothing is known about the reproductive biology or life histories of *Corallium lauuense*. It is difficult to infer reproductive mode from other species of *Corallium*. Aspects of reproductive biology have been studied for *Corallium secundum* (Grigg 1976). This species has separate sexes, an annual reproductive cycle and is a spawner. In contrast, the Mediterranean *Corallium rubrum* is a brooder with short-lived passive larvae (Weinberg 1979; Grillo and Chessa 1992). Reproductive data and growth rates for *C. secundum* were used as a basis to determine the fisheries management for both *C. secundum* and *C. lauuense* (Department of Commerce 1980). Management of *C. lauuense* would undoubtedly benefit from a greater understanding of it reproductive biology.

Management implications

This is the first study of seamount populations using microsatellite markers. Little population differentiation was found between seamount/island populations, yet significant levels of inbreeding were detected. These results and the lack of hierarchical genetic structure between populations suggest that populations of *C. lauuense* are primarily self-recruiting with occasional long-distance dispersal events maintaining genetic connectivity between sites. This pattern of dispersal has also been found in shallow-water coral populations (e.g., Ayre and Hughes 2000). The longevity of gorgonian corals (e.g., Andrews et al. 2002) may lead to the accumulation of genotypes from recruitment events over long time periods, complicating the genetic signal (McFadden 1997).

These populations may also be in a state of rebound from high fishing pressures 25 years ago. In addition, the low heterozygosity in most populations raises the

concern that this species may be suffering from inbreeding depression. Of all the populations, the Kauai population was clearly the most isolated from the other populations. Based on these results, we suggest the Kauai population be considered and managed as a separate "stock".

Further investigation regarding population demographic structure will be needed to obtain a more accurate estimation of the effects of inbreeding. We are developing additional microsatellite loci for this species and for the other 2 precious coral species. Greater numbers of microsatellite loci may increase our ability to detect variation and isolation among seamount populations (Hellberg 1994).

Acknowledgments

References

Abbiati M, Santangelo G, Novelli S (1993) Genetic variation within and between two Tyrrhenian populations of the Mediterranean alcyonarian *Corallium rubrum*. Mar Ecol Progr Ser 95: 245-250

Andrews AH, Cordes EE, Mahoney MM, Munk K, Coale KH, Cailliet GM, Heifetz J (2002) Age, growth and radiometric age validation of a deep-sea habitat-forming gorgonian (*Primnoa resedaeformis*) from the Gulf of Alaska. Hydrobiologia 471: 101-110

Avise JC (1996) The scope of conservation genetics. In: Avise JC, Hamrick JL (eds) Conservation Genetics. Chapman and Hall, New York, pp 1-9

Ayre DJ, Duffy S (1994) Evidence for restricted gene flow in the viviparous coral, *Seriatopora histrix* on Australia's Great Barrier Reef. Evolution 48:1183-1201

Ayre DJ, Hughes TP (2000) Genotypic diversity and gene flow in brooding and spawning corals along the Great Barrier Reef, Australia. Evolution 54: 1590-1605

Ball AO, Chapman RW (2003) Population genetic analysis of white shrimp, *Litopenaeus setiferus*, using microsatellite genetic markers. Mol Ecol 12: 2319-2330

Barki Y, Douek J, Graur D, Gateno D, Rinkevich B (2000) Polymorphism in soft coral larvae revealed by amplified fragment-length polymorphism (AFLP) markers. Mar Biol 136: 37-41

Benzie JAH, Haskell A, Lehman H (1995) Variation in the genetic composition of coral (*Pocillopora damicornis* and *Acropora palifera*) populations from different reef habitats. Mar Biol 121: 731-739

Brazeau DA, Harvell CD (1994) Genetic structure of local populations and divergence between growth forms in a clonal invertebrate, the Caribbean octocoral *Briareum abstineum*. Mar Biol 119: 53-60

Bucklin A, Wilson RR, Smith KL (1987) Genetic differentiation of seamount and basin populations of the deep-sea amphipod *Eurythenes gryllus*. Deep-Sea Res 34: 1795-1810

Burnett WJ, Benzie JAH, Beardmore JA, Ryland JS (1995) Patterns of genetic subdivision in populations of a clonal cnidarian, *Zoanthus coppingeri*, from the Great Barrier Reef. Mar Biol 122: 665-673

Callen DF, Thompson AD, Shen Y, Phillips HA, Richards RI, Mulley JC, Sutherland GR (1993) Incidence and origin of 'null' alleles in the $(AC)_n$ microsatellite markers. Amer J Hum Gen 52: 922-927

Carney RS, Haedrich RL, Rowe GT (1983) Zonation of fauna in the deep-sea. In: Rowe GT (ed) Deep-Sea Biology, The Sea. 8, Wiley, New York, pp 371-398

Chase MR, Etter RJ, Rex MA, Quattro JM (1998) Bathymetric patterns of genetic variation in a deep-sea protobranch bivalve, *Deminucula atacellana*. Mar Biol 131: 301-308

DeForges BR, Koslow JA, Poore GCB (2000) Diversity and endemism of the benthic seamount fauna in the southwest Pacific. Nature 405: 944-946

Department of Commerce (1980) FMP for the precious coral fishery of the Western Pacific Region. Fed Reg 45(180): 60957-60981

Doyle JJ, Dickson E (1987) Preservation of plant samples for DNA restriction endonuclease analysis. Taxon 36: 715-722

Excoffier L, Smouse PE, Quattro JM (1992) Analysis of molecular variance inferred from metric distances among DNA haplotypes: application to human mitochondrial DNA restriction data. Genetics 131: 479-491

France SC, Kocher TD (1996) Geographic and bathymetric patterns of mitochondrial 16SrRNA sequence divergence among deep-sea amphipods, *Eurythenes gryllus*. Mar Biol 126: 633-643

Gage JD, Tyler PA (1991) Deep-Sea Biology: A Natural History of Organisms at the Deep-Sea Floor. Cambridge Univ Press, Cambridge, UK

Genin A, Paull CK, Dillon WP (1992) Anomalous abundances of deep-sea fauna on a rocky bottom exposed to strong currents. Deep-Sea Res 39: 293-302

Goudet J, Raymond M, DeMeeues T, Rousset F (1996) Testing differentiation in diploid populations. Genetics 144: 1933-1940

Graves JE (1996) Conservation genetics of fishes in the pelagic marine realm. In: Avise JC, Hamrick JL (eds) Conservation Genetics. Chapman and Hall, New York, pp 335-366

Grigg RW (1976) Fishery management of precious and stony corals in Hawaii. Univ Hawaii Sea Grant Progr, UNIHI-SEAGRANT-TR-77-03: pp 1-48

Grigg RW (1994) History of the precious coral fishery in Hawaii. Precious Corals Octocoral Res 3: 1-18

Grigg RW (2002) Precious corals in Hawaii: discovery of a new bed and revised management measures for existing beds. Mar Fish Rev 64: 13-20

Grillo MC, Chessa LA (1992) Developpement larvaire de *Corallium rubrum*: etude. Rapp P-v Comm Int Explor Sci Mer Mediterr 33: 40

Guo SW, Thompson EA (1992) Performing the exact test of Hardy-Weinberg proportions for multiple alleles. Biometrics 48: 361-372

Hellberg ME (1994) Relationships between inferred levels of gene flow and geographic distance in a philopatric coral, *Balanophyllia elegans*. Evolution 48: 1829-1854

Hellberg ME (1995) Stepping-stone gene flow in the solitary coral *Balanophyllia elegans*: equilibrium and nonequilibrium at different spatial scales. Mar Biol 123: 573-581

Hubbs CL (1959) Initial discoveries of the fish faunas on the seamounts and offshore banks of the eastern Pacific. Pac Sci 13: 311-316

Interdisciplinary Center for Biotechnology Research (2001) (ICBR) Tools for Developing Molecular Markers. Manual

Kandpal RP, Kandpal G, Weissman SM (1994) Construction of libraries enriched for sequence repeats and jumping clones, and hybridization selection for region-specific markers. Proc Natl Acad Sci USA 91: 88-92

Lande R (1988) Genetics and demography in biological conservation. Science 24: 1455-1460

Le Goff MC, Rogers AD (2002) Characterization of 10 microsatellite loci for the deep-sea coral *Lophelia pertusa* (Linnaeus 1758). Mol Ecol Notes 2: 164-166

Le Goff M, Pybus O, Rogers AD (2004) Genetic structure of the deep-sea coral *Lophelia pertusa* in the North East Atlantic revealed by microsatellites and ITS sequences. Mol Ecol 13: 537-549

Maier E, Tollrian R, Nurnberger B (2001) Development of species-specific markers in an organism with endosymbionts: microsatellites in the scleractinian coral *Seriatopora hystrix*. Mol Ecol Notes 1: 157-159

McFadden CS (1997) Contributions of sexual and asexual reproduction to population structure in the clonal soft coral, *Alcyonium rudyi*. Evolution 51: 112-126

Miller KJ, Howard CG (2004) Isolation of microsatellites from two species of scleractinian coral. Mol Ecol Notes 4: 11-13

Palumbi SR (1996) Macrospatial genetic structure and speciation in taxa with high dispersal abilities. In: Ferraris J, Palumbi SR (eds) Molecular Zoology: Advances, Strategies, and Protocols. Wiley, New York, pp 101-117

Palumbi SR, Baker CS (1996) Nuclear genetic analysis of population structure and genetic variation using intron primers. In: Smith TB, Wayne RK (eds) Molecular Genetic Approaches in Conservation. Oxford Univ Press, pp 25-37

Parker T, Tunnicliffe V (1994) Dispersal strategies of the biota on an oceanic seamount: implications for ecology and biogeography. Biol Bull 187: 336-345

Raymond M, Rousset F (1995) GENEPOP version 1.2: population genetics software for exact tests and ecumenicism. J Hered 86: 248-249

Rogers AD (1994) The biology of seamounts. Adv Mar Biol 30: 305-351

Rousset F, Raymond M (1995) Testing heterozygote deficiency and excess. Genetics 140: 1413-1419

Rozen S, Skaletsky HJ (1998) Primer 3. Code available at: http://frodo.wi.mit.edu/cgi-bin/primer3/primer3_www.cgi

Rozen S, Skaletsky HJ (2000) Primer3 on the WWW for general users and for biologist programmers. In: Krawetz S, Misener S (eds) Bioinformatics Methods and Protocols: Methods in Molecular Biology. Humana Press, Totowa, NJ, pp 365-386

Schneider S, Kueffer JM, Roessli D, Excoffier L (1997) Arlequin version 1.1: a software programme for population genetic data analysis. Genet Biometry Lab, Univ Geneva

Shearer TL, Van Oppen MJH, Romano SL, Wörheide G (2002) Slow mitochondrial DNA sequence evolution in the Anthozoa (Cnidaria). Mol Ecol 11: 2475-2487

Slatkin M (1995) A measure of population subdivision based on microsatellite allele frequencies. Genetics 139: 457-462

Smith TB, Wayne RK (1996) Molecular Genetic Approaches in Conservation. Oxford Univ Press

Stoddart JA (1984) Genetical structure within populations of the coral *Pocillopora damicornis*. Mar Biol 81: 19-30

Weinberg S (1979) The light-dependent behavior of planulae larvae of *Eunicella singularis* and *Corallium rubrum* and its implications for octocorallian ecology. Bijd Dierkd 49: 16-30

Weir BS, Cockerham CC (1984) Estimating F-statistics for the analysis of population structure. Evolution 38: 1358-1370

Wilson RR, Kaufmann RS (1987) Seamount biota and biogeography. In: Keating BH, Fryer P, Batiza R, Backland GW (eds) Seamounts, Islands and Atolls. Geophys Monogr 43, pp 355-377

Genetic circumscription of deep-water coral species in Canada using 18S rRNA

Kevin B. Strychar[1,2], Lorraine C. Hamilton[2], Ellen L. Kenchington[2], David B. Scott[1]

[1] Department of Earth Science, Dalhousie University, Halifax, Nova Scotia, B3H 3J5, Canada
  (strychar@dal.ca)
[2] Fisheries and Oceans Canada, Bedford Institute of Oceanography, Dartmouth, Nova Scotia, Canada

Abstract. Many deep-water coral species have very broad global distributions and are eurybathic from depths of meters to kilometers. Such ecological breadth may be confounded by the presence of cryptic species. We are currently comparing the genetic distances between *Paragorgia* sp. and *Primnoa* sp. across their distribution and depth range in Canada using 18S ribosomal DNA (rDNA) sequences. Initial results show a confusing picture amongst the geographically distant *Paragorgia* taxa. Specimens of *P. arborea* from the Canadian Atlantic are very divergent from the specimen from the Canadian Pacific. The placement of *Pennatula* and *Anthomastus* relative to these taxa is also unexpected. We expect this topology to alter with the addition of more taxa and further testing.

Keywords. *Paragorgia*, *Antipatharian*, *Anthomastus*, *Pennatula*, molecular genetics, 18S rDNA, Atlantic Canada

Introduction

   Globally, five major taxonomic groups of deep-water corals (DWCs) have been identified (Cimberg et al. 1981), including: Alcyonacea (soft corals), Gorgonacea (sea fans, bamboo corals, and tree corals), Scleractinia (cup corals, stony corals, or true corals), Stylasterina (hydrocorals), and Antipatharia (black corals), many which appear to be concentrated in the northern latitudes. Along the eastern coast of North America, 35 species of DWCs are believed to exist (Breeze et al. 1997) at depths ranging between 100 and 1,300 m but have been observed at depths greater than 4,000 m (Tendal 1992; Cairns and Chapman 2001; Gass 2002), and include seven soft corals (alcyonaceans), ten horny corals (gorgonians), eight sea pens (pennatulaceans), and ~ten stony corals (scleractinians). Approximately ten species of gorgonian corals are known to occur off the coast of Nova Scotia in the Northwest Atlantic (Breeze et al. 1997). Of these, *Paragorgia arborea* (Linnaeus, 1758) is the largest, attaining heights of greater than 2 m. It is eurybathic, with a global depth range of between 50 and 3000 m (Horridge 1956; Broch and Horridge

1957; Tendal 1992). *P. arborea* is frequently found with a second gorgonian coral, *Primnoa resedaeformis* (Gunnerus, 1763). It is known that *P. resedaeformis* (the red tree coral) appears to occur in "forests/thickets", but little more is known about these corals (Riley 2001). In Atlantic Canada, this species has a broad distribution and depth range. Given the apparently patchy distribution of these corals and their broad depth range, their taxonomic and reproductive biology is of great interest.

Molecular analyses of tropical corals have revealed substantial genetic differences between otherwise taxonomically cryptic species (Knowlton 1993). We speculate that *P. arborea* and *P. resedaeformis* harbour cryptic taxa. These could occur geographically between oceanic boundaries, and/or vertically with depth.

Our goal is to build a comparative data set of *Paragorgia* and *Primnoa* from different localities and depth ranges, based initially on 18S rDNA gene sequences for comparison with published coral sequences (Berntson et al. 1999, 2001; Le Goff-Vitry et al. 2004).

Methods

Specimens of DWCs and associated fauna used for this study were primarily collected from Stone Fence, an area located east of Sable Island along Canada's eastern coast (~44°47'N and 57°17'W). Samples from distant locations (e.g., the Bahamas - *Paragorgia johnsoni*) were provided by the Smithsonian Institute. All samples used were specimens preserved in ethanol.

DNA extraction from corals

To eliminate ethanol and surface contaminants, each sample was thoroughly washed in phosphate buffered saline solution (PBS; Fischer Scientific, USA). DNA was obtained by dissecting approximately 100 mg of tissue and extracting the DNA using a DNeasy tissue kit (Qiagen, Canada) according to the manufacturer's protocol.

Polymerase chain reaction (PCR) amplification

Coral 18S rDNA was amplified by PCR using a modified method following Berntson et al. (1999, 2001). The 18S region was amplified using two overlapping PCR products (primers A_1 and B_1; Table 1). PCR reactions consisted of 1 nmole of A_1 or B_1 primers and a corresponding internal oligonucleotide primer (primers A_{2-5}, B_{2-5}; see Table 1), 200 nmoles of each dNTP, 1 unit of Taq DNA polymerase (MBI Fermentas, Canada), and approximately 50 to 100 ng of DNA template, in a final volume of 50 μl.

Thermal cycling was as follows: denaturation at 94°C for 60 s, annealing at 57°C for 30 s, and extension at 72°C for 60 s, repeated 39 times, followed by one cycle with a 10 min extension at 72°C. The instrument used was a MJ Dyad (MJ Research, USA). PCR products were purified using a QIAquick PCR Purification (Qiagen) kit according to the manufacturer's protocol. To determine the molecular size of the PCR products, all samples were run on 1.0 % agarose gels. For samples that did not amplify or for aged archival specimens, 1 μl of an initial PCR reaction

Table 1 Primers used to amplify and sequence 18S rDNA from deep-water fauna. Primers are listed as: "A_1-A_5" representing forward primers and "B_1-B_5" representing reverse primers. Primers A_1 and B_1 were located according to the DNA sequence of the 18S rRNA gene from *Paragorgia* sp. (AF052917; Berntson et al. 2001); the remaining primers were constructed. Primer locations (PL) are given with respect to the sequence given in AF052917

Primers			
Forward (A_1 – A_5)	PL^1	Reverse Compliment (B_1 – B_5)	PL^1
A_1 AACCTGGTTGATCCTGCCAGT	2-22	B_1 TGATCCTTCTGCAGGTTCACCTAC	1776-1799
A_2 TGAAACTGCGAATGGCTCAT	81-100	B_2 TTTGACCAACTTCTCGGCGG	1715-1734
A_3 TAATTCCAGCTCCAATAGCG	582-601	B_3 CTGGACCTGGTAAGGTTTCC	1202-1221
A_4 ACGATGCCGACTAGGGATGA	1031-1050	B_4 CCTGCTTTGAACACTCTAATTTCT	759-782
A_5 CGTCGTGATGGGAATAGATC	1531-1550	B_5 GGGACTTTTCGCATGTATTAGC	163-184

using universal eukaryotic coral primers A_1 and B_1 (see methods of Elwood et al. 1985; Lane et al. 1985; Weekers et al. 1994; Takabayashi 2000; Berntson et al. 2001) was purified and used as template for the reactions using our constructed internal primers (A_2-A_5, B_2-B_5; Table 1).

Sequencing of amplified 18S rDNAs

PCR amplicons (~40-80 ng) were sequenced using the BigDye Terminator Cycling Sequencing Ready Reaction Kit v 3.1 (Applied Biosystems, CA, USA) following the manufacturer's recommendations. Eight to ten 18S rDNA-specific primers were used in the sequencing reactions (Table 1). Sequencing reactions were analyzed using an MJ Base Station (MJ Research, USA) automated DNA sequencer and Cartographer software (MJ Research, USA). The sequence of the amplicons was assembled using Contig Express from Vector NTI Advance (Informax, USA).

Evolutionary analyses were done using GeneStudio Pro©. A blast search using GeneStudio Pro© was performed in the National Centre for Biotechnology Information (NCBI) GenBank site and matching homologous 18S rDNA sequences were retained for multiple alignment using CLUSTAL W (Thompson et al. 1994). A data set of 46 sequences was constructed using aligned nucleotides based on sequences with a minimum length of 1700 nucleotides. Two out-groups, *Anemonia sulcata* and Hormathiidae gen. sp. (Table 2), were used following Berntson et al. (1999, 2001).

To reduce the likelihood of poor tree representation given the fact that different tree methods are designed on the basis of different evolutionary theories (Steel and Penny 2000), and therefore different algorithms, we chose 3 commonly used tree-building criteria to compare our data. Data were analysed using maximum likelihood (ML), minimum evolution (ME), and Bayesian likelihood analysis (BL). In ML methods, a search for the topology that maximizes the chance of observing a given probabilistic model of nucleotide substitutions was used (Felsenstein 1981). Data sets comprised of more than 7 sequences, however, are computationally demanding and time-consuming (DeBry and Abele 1995) and as a result, we chose to use the quartet-puzzling algorithm (PHYLIP; Felsenstein 1990), setting the bootstrap function to 1,000. MEGA (Molecular Evolutionary Genetics Analysis V2.1;

Table 2 List of 18S rDNA gene sequences of deep-water taxa used in this study consisting of >1700 nucleotides. Accession numbers are related to National Centre for Biotechnology Information (NCBI) coding. Corals analysed in this study are given in bold. Some authors (*) listed under 'Citation' submitted gene sequences to NCBI which may not be published; controls used for tree formation are denoted using the symbol "†"

Scientific name	Accession #	Nucleotides (bp)	Citation
Junceella racemosa	AF052937	1800	Berntson et al. 2001
Acalycigorgia inermis	AJ133545	1822	Won et al. 2001
Acalycigorgia irregularis	AJ133546	1821	Won et al. 2001
Acanthogorgia sp.	AF052907	1852	Berntson et al. 1999
Acanthoptilum sp.	AF052910	1802	Berntson et al. 1999
Anthomastus sp.	AF052881	1798	Berntson et al. 2001
Anthothela nuttingi	AF052922	1822	Berntson et al. 2001
Antipathes fiordensis	AF052900	1798	Berntson et al. 1999
Antipathes lata	Z92908	1798	Song and Won 1997
Bathypathes sp.	AF052901	1798	Berntson et al. 1999
Ceratotrochus magnaghii	F052886	1814	Berntson et al. 1999
Calcigorgia spiculifera	AF052925	1852	Berntson et al. 2001
Chrysogorgia chryseis	AF052913	1811	Berntson et al. 2001
Cirripathes lutkeni	AF052902	1798	Berntson et al. 1999
Corallium cf. *ducale*	AF052919	1801	Berntson et al. 2001
Corallium kishinouyei	AF052918	1801	Berntson et al. 2001
Dendrobrachia paucispina	AF052903	1803	Berntson et al. 1999
Enallopsammia rostrata	AF052885	1797	Berntson et al. 1999
Eunicea laciniata	AF052926	1851	Berntson et al. 2001
Javania insignis	AJ133555	1805	Won et al. 2001
Virgularia gustaviana	Z86106	1805	Kim et al.*
Lepidisis sp.	AF052906	1825	Berntson et al. 1999
Leptogorgia chilensis	AF052928	1823	Berntson et al. 2001
Narella bowersi	AF052905	1799	Berntson et al. 1999
Orstomisis crosnieri	AF052916	1828	Berntson et al. 2001
Paramuricea sp.	AF052920	1850	Berntson et al. 2001
Protodendron sp.	AF052921	1823	Berntson et al. 2001
Protoptilum sp.	AF052911	1799	Berntson et al. 1999
Renilla reniformis	AF052581	1800	Berntson et al. 1999
Rhizopsammia minuta	Z92907	1799	Song and Won 1997
Siphonogorgia sp.	AF052927	1823	Berntson et al. 2001
Stylatula sp.	AF052934	1798	Berntson et al. 2001
Tubastraea aurea	Z92906	1797	Song and Won 1997
Tubipora musica	AF052909	1837	Berntson et al. 2001
Umbellula sp.	AF052904	1802	Berntson et al. 1999
Virgularia juncea	AJ133551	1800	Won et al. 2001
Virgularia sp.	AF052935	1804	Berntson et al. 2001
***Paragorgia arborea* (CP)**	AY838559	1800	Seq7-2
***Antipatharian* sp. (CA)**	AY838560	1763	SeqF-2
***Pennatula* sp. (CA)**	AY838561	1806	SeqK-2
***Paragorgia johnsoni* (B)**	AY838562	1734	Seq9-2
***Paragorgia arborea* (CA)**	AY838563	1802	SeqJ-2
***Anthomastus* sp. (CA)**	AY838564	1792	SeqM-2
Anemonia sulcata†	X53498	1799	Hendriks et al. 1990
Hormathiidae gen. sp.†	AF052890	1800	Berntson et al. 1999
Paragorgia sp.	AF052917	1799	Berntson et al. 2001

Kumar et al. 2001) was used to determine a best-fit ME model using p-distance sequence divergence. ME analysis, unlike ML, 'assumes' the shortest evolutionary route. Bootstrap replication (1,000) was used to test relative nodal support in the topology (Felsenstein 1985). Bayesian analysis was implemented using Mr Bayes Version 3.0b4 (Huelsenbeck and Ronquist 2001) utilizing the gamma function, "4-by-4" model, sampling 1,000,000 generations, with Markov chains sampled every 100 iterations. The analysis was conducted three times using identical settings to ensure convergence on the same l nL values (Huelsenbeck and Bollback 2001; Leaché and Reeder 2002). Approximately 33,000 random iterations generated prior to stationarity (call "burn-in generations"; Huelsenbeck and Ronquist 2001) were discarded and the subsequent generations used to establish the posterior probabilities. Trees were displayed using TreeView Version 1.6.0 (Page 1996).

Preliminary results and discussion

Initial results comparing tree topologies of ME (Fig. 1), ML (Fig. 2) and BL (Fig. 3) show an interesting picture amongst the geographically distant *Paragorgia* taxa. Specimens of *P. arborea* from the North Atlantic (Nova Scotia, Canada) are very similar to *Paragorgia* sp. from the South Pacific (California, USA; >99 % nodal support among all three trees). *P. arborea* from the North Pacific (British Columbia, Canada) however, appear more closely related *P. johnsoni* from Bermuda (Fig. 3; 100 % support). The placement of *Anthomastus* sp. relative to these taxa is also unexpected (Figs. 1-3). Berntson et al. (2001) suggest that *Anthomastus* relative to *Paragorgia, Corallium* and *Umbellula* share many morphological features and are dimorphic, however, resemblances are superficial and further comparisons are needed.

There are several possible reasons which may explain the disparities between the topology of *Anthomastus, Corallium* and *Umbellula* relative to *Paragorgia*. All target genes may not amplify with the same efficiency expected using octocoral-specific designed primers. Such biases inherent to natural mixes of rRNA genes are in the early stages of being investigated (see von Wintzingerode et al. 1997). Gene templates with high G+C content, for example, are not as efficiently amplified as are those with low G+C content (Reysenbach et al. 1992). In contrast, Moon-van der Staay et al. (2000) suggest that templates with G/C content, when amplified with degenerated primers, amplify better than those with A/T content (Polz and Cavanaugh 1998). Moon-van der Staay et al. (2000) also suggest that non-complementarity of either PCR primer may decrease PCR yield through inhibition of binding targets during high annealing temperatures. Hansen et al. (1998) further suggest that some amplified sequences may be inhibited by DNA flanking the template region. Further, the presence of excess templates during reannealing may reduce amplification of templates initially present in high abundance (Suzuki and Giovannoni 1996). As a result primer specificity for some copies of the 18S rDNA may be responsible for the unusual results of such phylogenetic analyses. We expect this topology to alter with the addition of more taxa.
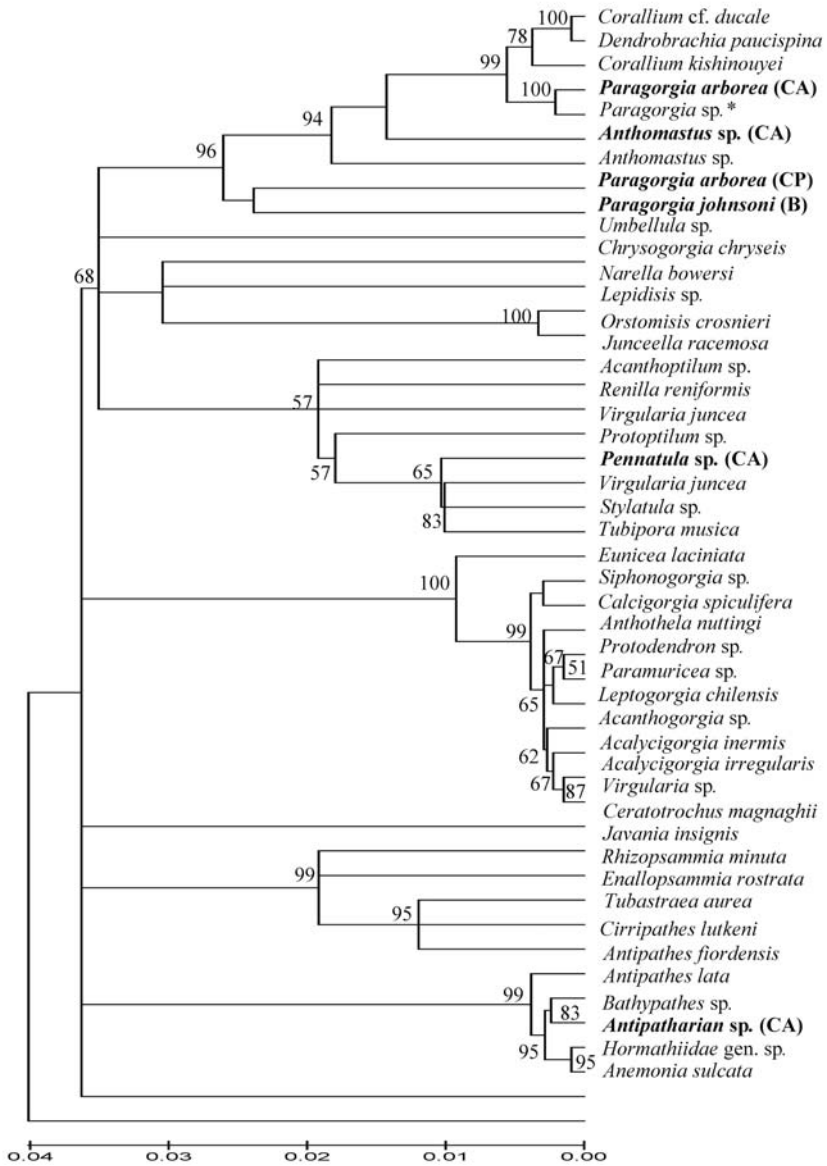
Fig. 1 Phylogenetic tree from minimum-evolution (ME) analysis. Bootstrap analysis (n = 1,000 replicates) provided an estimate of support for internal nodes ranging from 50 to 100 %. The scale bar indicates 0.05 substitutions per nucleotide position. *Paragorgia* sp.* represents "control" gene from Berntson et al. (1999, 2001); outgroups used for tree construction were Hormathiidae gen. sp. (AF052890; Berntson et al. 1999) and *Anemonia sulcata* (X53498; Hendriks et al. 1990). Symbols CA = Canadian Atlantic; CP = Canadian Pacific; B = Bermuda

Placement of *Antipatharian* sp. (Canadian Atlantic (CA)) with *Bathypathes, Antipathes fiordensis* and *A. lata* was not unexpected since these taxa have similar morphological characteristics (Figs. 1-3). However, given that the *Antipatharian*
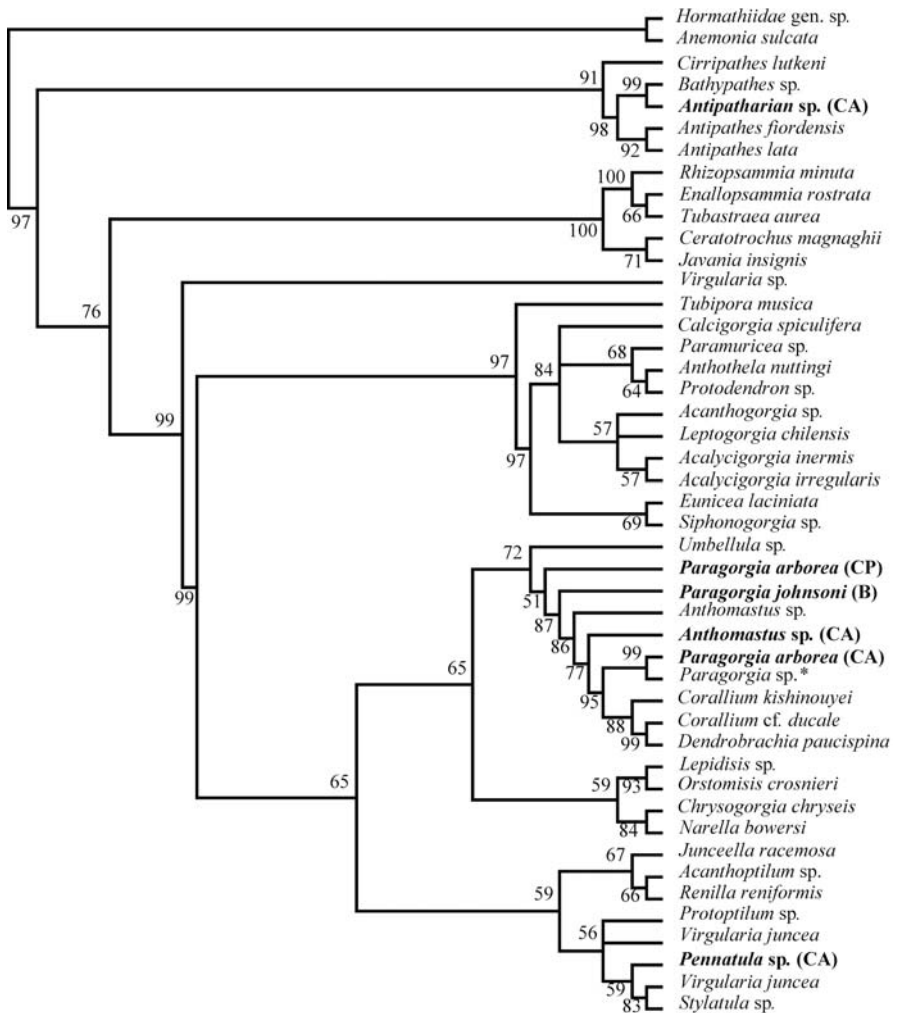
Fig. 2 Phylogenetic tree from maximum likelihood (ML) quartet-puzzling analysis. Bootstrap analysis (n = 1,000 puzzling steps) provided an estimate of support for internal nodes ranging from 50 to 100 %. Note that branch lengths are arbitrary and only the pattern is important. *Paragorgia* sp.* represents "control" gene from Berntson et al. (1999, 2001); outgroups used for tree construction were Hormathiidae gen. sp. (AF052890; Berntson et al. 1999) and *Anemonia sulcata* (X53498; Hendriks et al. 1990). Symbols CA = Canadian Atlantic; CP = Canadian Pacific; B = Bermuda

sp. (CA), *Bathypathes* sp. (Hawaii - Pacific), *Antipathes fiordensis* (New Zealand) and *A. lata* (South Korea) are from geographically distant regions, we question the level of genetic similarity (ME = 99 %, ML = 56 %, BL = 81 %). Similarly,
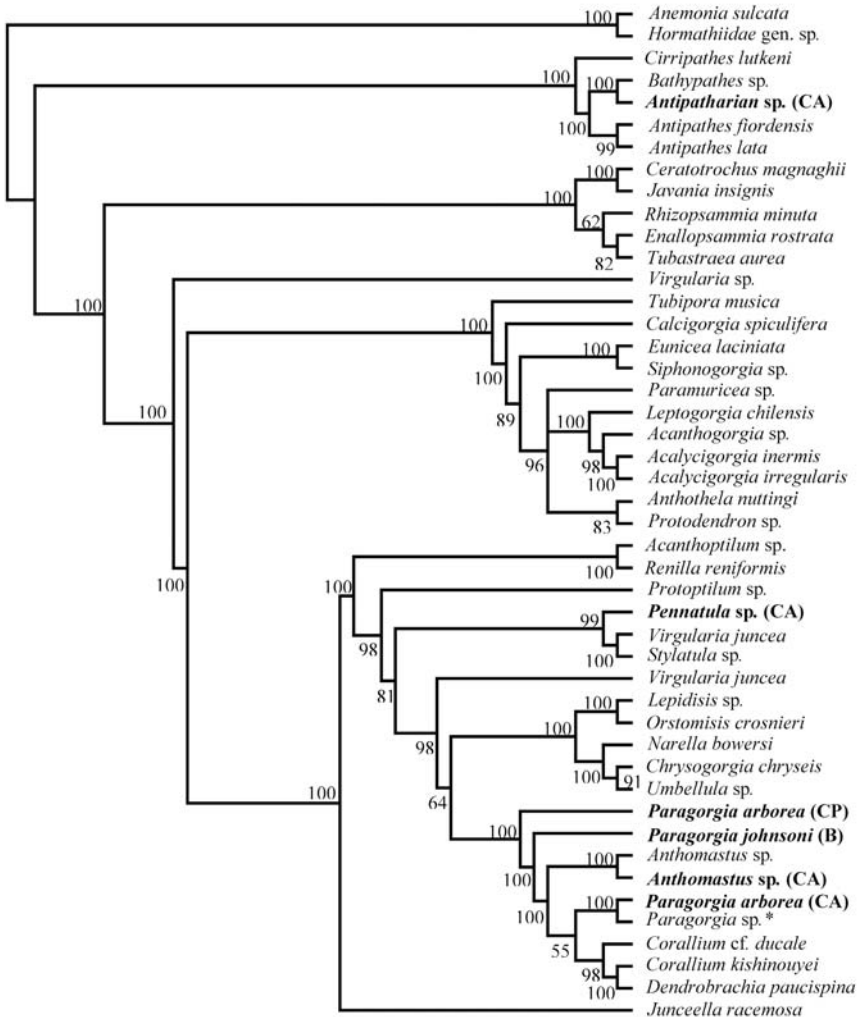
Fig. 3 Phylogenetic tree from bayesian-likelihood (BL) analysis using the gamma function, 4-by-4 model, sampling 1,000,000 generations, with Markov chains sampled every 100 iterations. Above node support is the 50 %-majority-rule consensus from the sampled trees. Values <50 % are not displayed. Note that branch lengths are arbitrary and only the pattern is important. *Paragorgia* sp.* represents "control" gene from Berntson et al. (1999, 2001); outgroups used for tree construction were Hormathiidae gen. sp. (AF052890; Berntson et al. 1999) and *Anemonia sulcata* (X53498; Hendriks et al. 1990). Symbols CA = Canadian Atlantic; CP = Canadian Pacific; B = Bermuda

the topology of our *Pennatula* sp. (CA) amongst *Virgularia* sp., *Stylatula* sp. and *Protoptilum* sp. was consistent between our tested methodologies (ME, ML and BL; Figs. 1-3 respectively). These species, however, are geographically scattered amongst the Pacific and Atlantic Oceans, and Yellow Sea (South Korea). As with previous molecular phylogenetic analyses (e.g., Berntson et al. 1999, 2001; Won et al. 2001), our present trees indicate problematic areas in the current classification of corals.

Attempts to explain why deep-water coral isolates from geographically different regions appear closely related have been hampered by a lack of knowledge of transmission of larvae from one host to another. We propose, although speculative, that the isolation of distinct DWC genes, and different clades and subclades as described by Berntson et al. (2001), is the result of shifting oceanic circulation (Benzie 1999) and global warming and cooling trends (Bluemle et al. 1999), where larval transmission is related to changing environments and host-specific signals. During periods of low sea levels and colder water temperatures, geographical barriers may have promoted coevolution of various DWCs to produce one or more dominant clades per geographical location. As sea levels rose due to global warming and polar ice cap melting (Chappell 1983; Digerfeldt and Hendry 1987; Barnett 1988; Jones and Wigley 1990; Monastersky 1994), changing current patterns and environmental stimuli has probably resulted in limited reproductive events, decreasing diversity and increasing the number of hybridization events (and thus the significant similarity observed between geographically distant populations). Under stressful environmental conditions, Lamb and Avise (1986), Lehman et al. (1991) and Wayne et al. (1992) indicate the likelihood of hybridization increases as species become rare. Further testing using polymorphic nuclear markers, such as microsatellites and allozymes, are techniques that could be used to test our speculation.

No information is available yet for *Primnoa*, or from depth-stratified samples from the Scotian Shelf.

In conclusion, the present study demonstrates for the first time that *Paragorgia* sp. from Eastern and Western Canada, although appearing similar in morphology, are genetically dissimilar. Further, other genera appear more closely related to *Paragorgia* then previously speculated. Such new light potentially provides a new assessment of the relative taxonomic distribution and abundance of the various groups of deep-water corals, associated fauna, and cryptic taxa and to their morphologies. It may also reveal new lineages that may have considerable ecological and/or taxonomic importance. It is clear, however, that more molecular analyses are required to reveal such taxonomic implications.

Acknowledgments

References

Barnett TP (1988) Global sea level change. Climate variations over the past century and the greenhouse effect: First climate trends workshop. NOAA Natl Clim Program Off, Rockville, MD

Benzie JAH (1999) Genetic structure of coral reef organisms: ghosts of dispersal past. Amer Zool 39: 131-145

Berntson EA, France SC, Mullineaux LS (1999) Phylogenetic relationships within the class Anthozoa (Phylum Cnidaria) based on nuclear 18S rDNA sequences. Mol Phylogenet Evol 13: 417-433

Berntson EA, Bayer FM, McArthur AG, France SC (2001) Phylogenetic relationships within the Octocorallia (Cnidaria: Anthozoa) based on nuclear 18S rRNA sequences. Mar Biol 138: 235-246

Bluemle JP, Sabel JM, Karlén W (1999) Rate and magnitude of past global climate changes. Environ Geosci 6: 63-75

Breeze H, Davis DS, Butler M, Kostylev V (1997) Distribution and status of deep-sea corals off Nova Scotia. Mar Iss Comm Spec Publ 1, Ecology Action Centre. Halifax, Canada

Broch H, Horridge A (1957) A new species of *Solenopodium* (Stolonifera: Octocorallia) from the Red Sea. Proc Zool Soc London 128: 149-160

Cairns SD, Chapman RE (2001) Biogeographic affinities of the North Atlantic deep-water Scleractinia. In: Willison JHM, Hall J, Gass SE, Kenchington ELR, Butler M, Doherty P (eds) Proceedings of the First International Symposium on Deep-sea Corals. Ecology Action Centre and Nova Scotia Museum, Halifax, NS, pp 30-57

Chappell J (1983) Evidence for smoothly falling sea level relative to north Queensland, Australia, during the past 6000 years. Nature 302: 406-408

Cimberg RL, Gerrodette T, Muzik K (1981) Habitat requirements and expected distribution of Alaska coral. Final Rep, Res Unit 601, VTN Oregon, Inc. Rep Off Marine Poll Assess, Alaska Off, US Dept Commerce, NOAA, OCSEAP Final Rep 54: 207-308

DeBry RW, Abele LG (1995) The relationship between parsimony and maximum likelihood analyses: tree scores and confidence estimates for three real data sets. Mol Biol Evol 12: 291-297

Digerfeldt G, Hendry MD (1987) An 8000 year Holocene sea level record from Jamaica: implications for interpretation of Caribbean reef and coastal history. Coral Reefs 5: 165-169

Elwood HJ, Olsen GJ, Sogin ML (1985) The small-subunit ribosomal RNA gene sequences from the hypotrichus ciliates *Oxytricha nova* and *Stylonychia pustulata*. Mol Biol Evol 2: 399-410

Felsenstein J (1981) Evolutionary trees from DNA sequences: a maximum likelihood approach. J Mol Evol 17: 368-376

Felsenstein J (1985) Confidence limits on phylogenies: an approach using the bootstrap. Evolution 39: 783-791

Felsenstein J (1990) Phylogeny Inference Package (PHYLIP), Version 3.6a2.1. Univ Washington, Seattle

Gass SE (2002) An assessment of the distribution and status of deep-sea corals in Atlantic Canada by using both scientific and local forms of knowledge. MSc thesis, Dalhousie Univ, Halifax, Canada

Gunnerus JE (1763) Om en Søevext, allevegne ligesom besat med Frøehuse, *Gorgonia resedæformis*. K Norske Vidensk Selsk Skr 2: 321-329

Hansen MC, Tolker-Nielsen T, Givskov M, Molin S (1998) Biased 16S rDNA PCR amplification caused by interference from DNA flanking the template region. FEMS Microbiol Ecol 26: 141-149

Hendricks L, van de Peer Y, van Herck M, Neefs JM, de Wachter R (1990) The 18S ribosomal RNA sequences of the sea anemone *Anemonia sulcata* and its evolutionary position among other eukaryotes. FEBS Lett 269: 445-449

Horridge GA (1956) The responses of *Heteroxenia* (Alcyonaria) to stimulation and to some inorganic ions. J Exper Biol 33: 604-614

Huelsenbeck JP, Bollback JP (2001) Empirical and hierarchical Bayesian estimation of ancestral states. Syst Bio 50: 351-366

Huelsenbeck JP, Ronquist FR (2001) Mr. Bayes: Bayesian inference of phylogenic trees. Bioinformatics 17: 754-755

Jones PD, Wigley TML (1990) Global warming trends. Sci Amer 263: 84-91

Knowlton N (1993) Sibling species in the sea. Ann Rev Ecol Sys 24: 189-216

Kumar S, Tamura K, Jakobsen IB, Nei M (2001) MEGA2. Tempe, Arizona, USA

Lamb T, Avise JC (1986) Directional introgression of mitochondrial DNA in a hybrid population of tree frogs: the influence of mating behavior. Proc Nat Acad Sci USA 83: 2526-2530

Lane DJ, Pace B, Olsen GJ, Stahl DA, Sogin ML, Pace NR (1985) Rapid determination of 16S ribosomal RNA sequences for phylogenetic analyses. Proc Natl Acad Sci USA 82: 6955-6959

Leaché AD, Reeder TW (2002) Molecular systematics of the eastern fence lizard (*Sceloporus undulatus*): a comparison of parsimony, likelihood and bayesian approaches. Sys Biol 51: 44-68

Le Goff-Vitry MC, Rogers AD, Baglow D (2004) A deep-sea slant on the molecular phylogeny of the Scleractinia. Mol Phylogenet Evol 30: 167-177

Lehman N, Eisenhawer A, Hansen K, Mech LD, Petersen RO, Gogan PJP, Wayne RK (1991) Introgression of coyote mitochondrial DNA into sympatric North American gray wolf populations. Evolution 45: 104-119

Linnaeus C (1758) Systema naturae per regna tria naturae, secundum classes, ordines, genera, species, cum characteribus, differentiis, synonymis, locis. I. Ed decima, reformata. Holmiae, 824 pp

Monastersky R (1994) Coral's chilling tale. Ancient reefs may resolve an ice-age paradox. Science News 145: 124-125

Moon-van der Staay SY, van der Staay GWM, Guillou L, Vaulot D, Claustre H, Medlin LK (2000) Abundance and diversity of prymnesiophytes in the picoplankton community from the equatorial Pacific Ocean inferred from 18S rDNA sequences. Limnol Oceanogr 45: 98-109

Page RDM (1996) TREEVIEW: an application to display phylogenetic trees on personal computers. Comput Appl Biosci 12: 357-358

Polz MF, Cavanaugh CM (1998) Bias in template-product ratios in multitemplate PCR. Appl Environ Microbiol 64: 3724-3730

Riley L (2001) Hidden forest. The Halifax Herald Ltd, Sunday, July 15, 2001

Reysenbach AL, Giver LJ, Wickham GS, Pace NR (1992) Differential amplification of rRNA genes by polymerase chain reaction. Appl Environ Microbiol 58: 3417-3418

Song J-I, Won JH (1997) Systematic relationship of the anthozoan orders based on the partial nuclear 18S rRNA sequences. Korean J Biol Sci 1: 43-52.

Steel M, Penny D (2000) Parsimony, likelihood and the role of models in molecular phylogenetics. Mol Biol Evol 17: 839-850

Suzuki MT, Giovannoni SJ (1996) Bias caused by template annealing in the amplification of mixtures of 16S rRNA genes by PCR. Appl Environ Microbiol 62: 625-630

Takabayashi M (2000) Intraspecific genetic variability in scleractinian corals. PhD thesis, Univ Queensland (Australia), 180 pp

Tendal OS (1992) The North Atlantic distribution of the octocroal *Paragorgia arborea* (L., 1758) (Cnidaria: Anthozoa). Sarsia 77: 213-217

Thompson JD, Higgins DG, Gibson TJ (1994) CLUSTAL W: Improving the sensitivity of progressive multiple sequence alignment through sequence weighting, position specific gap penalties and weight matrix choice. Nucleic Acids Res 22: 4673-4680

Von Wintzingerode F, Gobel UB, Stackebrandt E (1997) Determinaiton of microbial diversity in environmental samples: pitfalls of PCR-based rRNA analysis. FEMS Microbiol Rev 21: 213-229

Wayne RK, Lehman N, Allard MW, Honeycutt RL (1992) Mitochondrial DNA variability of the gray wolf: Genetic consequences of population decline and habitat fragmentation. Conserv Biol 6: 559-569

Weekers PHH, Gast RJ, Fuerst PA, Byem TJ (1994) Sequence variations in small-subunit ribosomal RNAs of *Hartmannella vermiformis* and their phylogenetic implications. Mol Biol Evol 11: 684-690

Won JH, Rho BJ, Song JL (2001) A phylogenetic study of the Anthozoa (Phylum Cnidaria) based on morphological and molecular characters. Coral Reefs 20: 39-50

Deep-water Scleractinia (Cnidaria: Anthozoa): current knowledge of reproductive processes

Rhian G. Waller

Woods Hole Oceanographic Institution, Biology Department, MS 33, Woods Hole,
  MA 02543, USA
  (rwaller@whoi.edu)

Abstract. Little is known of the basic biology and ecology of the numerous species of deep-water scleractinians found in all the world's oceans. Of all the biological processes, reproduction is the most fundamental. Without knowledge of a species' reproduction, we know little about how they survive both the environment that is the deep-sea, and the increasing anthropogenic effects of man's exploration for new fisheries and energy reserves.

This review collates current knowledge of the reproductive processes of deep-water scleractinians. Only fifteen deep-water species as yet have had their reproduction described in the literature. Gametogenesis, reproductive seasonality and larval ecology are summarised and compared briefly to shallow-water counterparts.

A summary table of all deep-water scleractinian species, for which the reproductive strategy is known, and their sample locations, is presented here. It is hoped this knowledge will be used as a basis for further understanding of how the deep-sea species of this order survive and disperse. These data are also directly applicable to the conservation and management of these deep-sea ecosystems.

Keywords. Azooxanthellate Scleractinia, deep-sea, gametogenesis, larval ecology

Introduction

The presence of scleractinian corals living at depths beyond 100 m has been known for many decades, and yet there is still a paucity of information on their basic biology and ecology. In recent years the ecological value of deep-water scleractinians has become more apparent. Reef building species, similar to those found in shallow-water systems, form important habitats, creating oases on continental shelves and slopes, seamounts and ridges. These habitats support a wide diversity of life. Koslow and Gowlett-Jones (1998) observed 242 species of invertebrates and 37 species of fish associated with *Solenosmilia variabilis* reefs on the Tasmanian Seamounts, whilst *Lophelia pertusa* reefs in the NE Atlantic have been shown to support over 1300 species of associated fauna (ACES 2003). In

addition, over 350 species of invertebrates were collected from *Oculina varicosa* bioherms off the Florida continental shelf (Reed 1992; Koenig et al. 2000).

Of more economic importance to man, many commercial species of fish have been found using these reefs for feeding, protection and reproduction (Koslow and Gowlett-Jones 1998; Rogers 1999; Mortensen 2000). Of particular importance are Orange Roughy, Roundnose Grenadier (Rogers 1999; Mortensen 2000), Gag and Scamp grouper (Brooke and Young 2003) whist many other fisheries species have also been observed using these reefs (Koenig et al. 2000; Reed 2002).

As traditional pelagic and shallow-water fisheries decline, more fishermen are using deep-water benthic trawls to maintain catches. Large deep-water demersal trawlers now operate in areas of high fish densities, which are often related to coral structures (Wheeler et al. in press). Deep-water reefs were avoided in the past by fishermen because of the damage they caused to expensive nets. However, with developments in equipment, such as rockhoppers and stronger nets, more fishermen are realising the potential of these areas as lucrative fisheries (Koslow et al. 2000; Hall-Spencer et al. 2003). The damage to deep-water coral ecosystems from trawls has been recently observed in many areas around the globe (Probert et al. 1997; Koslow and Gowlett-Jones 1998; Bett 2001; Brooke 2002; Hall-Spencer et al. 2003; Wheeler et al. in press). The Orange Roughy fishery is a classic example. This fish species is found in close association with Tasmanian seamount coral communities, and exploitation has already caused the mass destruction of large reef areas (Koslow and Gowlett-Jones 1998). Within the European margin there has also been active destruction by trawlers occurring within the Darwin Mounds (Wheeler et al. in press). These authors report 28 trawl scars observed in a 5 km^2 area of seabed, and many damaged coral mounds.

As well as fishing pressures, deep-water reefs are also potentially under threat from oil and mineral exploration (Rogers 1999; Bett 2001). Such activities have the potential to cause excessive sedimentation from drilling mud, as well as the production of poisonous chemicals, although no active extraction is occurring at present (Rogers 1999). Only recently have studies targeted the potential impacts of man's various activities on deep-water fauna (Olsgard and Gray 1995; Probert et al. 1997; Jennings and Kaiser 1998; Rogers 1999; Hall-Spencer et al. 2003).

Understanding reproductive processes is essential to aiding conservation and management practices. Reproductive seasonality, gamete quality, fecundity and larval supply of habitat-forming organisms are vital to understanding both ecosystem function and recovery potential following a damaging event. This review presents a summary of the limited information on these basic biological processes in both reef-building and solitary deep-water scleractinians.

Methods

This review is a synthesis of known research on the reproductive processes of deep-water scleractinians. Information was gathered from both published literature and personal communication from colleagues, and is summarised in Table 1.

Sexuality

It is generally not possible to distinguish the sex of individual scleractinian polyps or colonies from external morphology. In a few shallow-water hermatypic species, eggs and sperm are different colours, and so may be distinguished in the polyps just prior to spawning (Fadlallah 1983). After fixation and decalcification, ripe oocytes may be observed within the mesenteries if they are large in size (Brooke 2002; Waller 2003).

The majority of shallow-water scleractinians are hermaphroditic (Fadlallah 1983; Richmond and Hunter 1990). Of the deep-water scleractinians studied to date, only three species were observed to be hermaphroditic. These are solitary corals, all species of the genus *Caryophyllia* (Waller et al. in press). All three species show a novel form of hermaphroditism, cyclical sexuality. Here the spermacysts and oocytes develop within the same mesentery, in a continuous cycle, but not synchronously between individuals. Only sperm or eggs are released at any one time, thus preventing self-fertilisation. Both sperm and eggs would therefore be present near-continually in the water column, whereas gonochorism would require ripe males and females to spawn synchronously to ensure fertilisation.

Twelve of the fifteen species of deep-water scleractinian examined to date are gonochoric (Table 1) compared to 75 % of the shallow species known being hermaphroditic (Fadlallah 1983). Gonochorism has been proposed as a more primitive adaptation than hermaphroditism (Goffredo et al. 2000), and may be more important for maintaining genetic diversity (Szmant 1986).

Gametogenesis

Scleractinians do not have 'gonads' in the traditional metazoan sense of the term. Sperm develop in cysts held together by a mesogleal envelope, hence the term spermacysts. Oocytes develop singularly, but are often found in groups or 'pockets', though there is no direct connection between them.

In shallow-water species, several authors have noted that germ cells are most likely to originate from interstitial cells near the septal filaments (lamellae) (Rinkevich and Loya 1979; Szmant-Froelich 1980; Delvoye 1982; Fadlallah 1983), but there are no data as yet for deep-water species. Gametes of many deep-water species reported appear to develop in the lamellae of the mesentery, eventually migrating into the mesoglea (Brooke 2002; Waller et al. 2002, in press; Waller 2003). Oogonia in *Lophelia pertusa* and *Madrepora oculata* have been observed still attached to the lamellae (Waller and Tyler in press), and even some larger vitellogenic oocytes appear to have a form of attachment (Waller 2003).

Stages of oogenesis in deep-water species studied appear to follow those of shallow-water species (*sensu* Fadlallah 1983). The first stage consists of oogonia attached to the lamellae. These grow into previtellogenic oocytes and migrate into the mesoglea of the mesentery. Previtellogenic oocytes then accumulate large quantities of lipid-rich yolk and form vitellogenic oocytes. The final stage is late vitellogenesis, where a thick cortical granular layer is formed on the outside of the oocyte, prior to release.

Table 1 Reproductive data known for deep-water scleractinian species

Species	Area	Depth [m]	Sex	Max Oocyte	Fecundity
Fungiacyathus marenzelleri (Vaughan, 1906)	Rockall Trough	2000	Gonochoric	750 µm	2900 opp
F. marenzelleri	California	4100	Gonochoric	750 µm	1290 opp
Lophelia pertusa (Linnaeus, 1758)	Porcupine Seabight	900	Gonochoric	140 µm	3146 opp / 3327 ocm^2
L. pertusa	Trondheim Fjord	147	Gonochoric	60 µm (mean)	
Madrepora oculata Linnaeus, 1758	Porcupine Seabight	900	Gonochoric	350 µm	10 opp / 256 ocm^2
M. oculata	Chatham Rise	800-1000	Gonochoric		
Caryophyllia cornuformis Pourtales, 1868	Porcupine Seabight	435-2000	Hermaphrodite (cyclical)	340 µm	-
Caryophyllia ambrosia Alcock 1898	Porcupine Seabight	1100-3000	Hermaphrodite (cyclical)	630 µm	2900 opp
Caryophyllia seguenzae Duncan, 1873	Porcupine Seabight	960-1900	Hermaphrodite (cyclical)	450 µm	940 opp
Oculina varicosa Lesueur, 1821	Florida	3-100	Gonochoric	100 µm	2115-4693 ocm^2
Flabellum alabastrum Moseley, 1876	Porcupine Seabight	1800-2250	Gonochoric	1010 µm	~550 opp
Flabellum angulare Moseley, 1876	Porcupine Seabight	1647-2875	Gonochoric	814 µm	~2800 opp
Enallopsammia rostrata (De Pourtales, 1878)	Chatham Rise	800-1000	Gonochoric	400 µm	144 opp
Solenosmilia variabilis Duncan, 1873	Chatham Rise	800-1000	Gonochoric	165 µm	290 opp
Goniocorella dumosa (Alcock, 1902)	Chatham Rise	800-1000	Gonochoric	135 µm	480 opp
Flabellum thouarsii Milne-Edwards and Haime, 1848	W Antarctic Peninsula	500	Gonochoric	4800 µm	2412 opp
Flabellum curvatum Moseley, 1881	W Antarctic Peninsula	500	Gonochoric	5120 µm	1618 opp
Flabellum impensum Squires, 1962	W Antarctic Peninsula	500	Gonochoric	5167 µm	1270 opp

Key – (I) Inferred: opp = oocytes per polyp; ocm^2 = oocytes per cm^2 of skeletal material
References: 1 Waller et al. 2002; 2 Flint 2003; 3 Waller and Tyler in press; 4 Brooke pers com; 5 Waller et al. in press; 6 Brooke and Young 2003; 7 Waller 2003; 8 Burgess and Babcock 2005

Table 1 continued

Method	Production	Release	Larvae	Notes	Ref
Spawner	Continuous		(I) Lecithotrophic		1
Spawner	Continuous		(I) Lecithotrophic		2
(I) Spawner	June/Aug	Jan/Feb	(I) Lecithotrophic		3
				Nov. only	4
Spawner	Periodic		(I) Lecithotrophic	Female Only	3
				Male Only	8
Spawner	Continuous		(I) Lecithotrophic		5
Spawner	Continuous (sequential)		(I) Lecithotrophic		5
Spawner	Continuous (sequential)		Planktotrophic		5
Spawner	early summer	late summer/fall	Lecithotrophic?		6
Spawner	Continuous		(I) Lecithotrophic		7
Spawner	Continuous		(I) Lecithotrophic		7
Spawner	Continuous		(I) Lecithotrophic	One sample	8
Spawner	Seasonal			One sample	8
Spawner	Seasonal			One sample	8
Broods	Seasonal?		Brooded		7
Broods	Continuous?		Brooded		7
Broods	?		Brooded		7

Gamete release

There are just three records of brooding in deep-water scleractinians from the Antarctic deep continental shelf. Waller (2003) observed brooded planulae in the mesenteries of *Flabellum impensum*, *F. curvatum* and *F. thouarsii*. All other species reported, both reef building and solitary, appear to spawn their gametes into the water column for external fertilisation (Table 1). Waller (2003) however suggests that these three Antarctic species, though found at 500 m, follow reproductive patterns more common amongst shallow Antarctic fauna than deep-water. Broadcast spawning is also more prevalent than brooding in shallow-water species of scleractinian (Richmond and Hunter 1990). Indeed, Stimson (1978) suggested deeper-living corals should spawn gametes rather than brood, to aid wide dispersal needed to find suitable substratum.

Gametogenesis can either be quasi-continuous (Waller et al. 2002; Flint 2003; Burgess and Babcock 2005; Waller et al. in press), periodic (Waller and Tyler in press) or seasonally-controlled (Brooke 2003; Waller and Tyler in press). The majority of shallow-water scleractinians have some form of seasonality, usually controlled by temperature or lunar periodicity (Fadlallah 1983; Harrison and Wallace 1990; Richmond and Hunter 1990). Seasonality in the deep-sea environment has been debated for a number of years (see Gage and Tyler 1991). In most areas, these deep-sea species live below the permanent thermocline, so there is little seasonal fluctuation in temperature. However, there is a seasonal fluctuation in phytodetritus to depth that has been associated with seasonal reproduction in several species of echinoderms and bivalves (Billett et al. 1983; Tyler et al. 1992, 1993; Rice and Lambshead 1994). Waller and Tyler (in press) also suggest the seasonal reproduction found in *Lophelia pertusa*, and the periodic reproduction found in *Madrepora oculata* from the NE Atlantic may also be related to the phytodetrital fall.

Larval development

There have been numerous studies concerning the larval biology and development of shallow-water scleractinians (Rinkevich and Loya 1979; Szmant-Froelich et al. 1980; Fadlallah and Pearse 1982; Tranter et al. 1982). These corals have proved to be ideal candidates for larval ecology, spawning freely when cued by either heat shock (Szmant-Froelich 1980; Fadlallah 1983) or the addition of gametes from the opposing sex (Szmant-Froelich 1980; Tranter et al. 1982).

Deep-water scleractinians, as yet, have proved more difficult to spawn. Trials of heat and cold shock were applied to numerous colonies of *Lophelia pertusa* and *Madrepora oculata* during three cruises in the NE Atlantic (RRS *Discovery* cruises 248, 260 and 266) with no success (Waller 2003).

Brooke (2002) had more success with *Oculina varicosa*, with deep-water colonies observed broadcast spawning after collection. Brooke and Young (2003) is the only detailed study to date on the larval ecology of a deep-water scleractinian. *O. varicosa* produced ciliated planula larvae and patterns of embryogenesis were observed to be similar to those of shallow-water species. These planulae were small

(~100 µm) when compared to the maximum oocyte sizes of other species studied (Table 1), and thus likely to be planktotrophic (Brooke and Young 2003).

Settlement

Brooke (2002) found deep-water *O. varicosa* larvae to remain active for over a month, but the larvae also probed the bottom after 10-14 days, suggesting they are ready to metamorphose. The wide dispersal of many species of deep-water scleractinian would suggest the competency periods of larvae to be long (Rogers 1999), but there are as yet no data to support this.

Brooded planulae tend to have shorter competency times, settling immediately after one or two days (Fadlallah and Pearse 1982; Szmant-Froelich et al. 1985). Broadcasting species tend to settle after 4-6 days (Schlesinger and Loya 1985; Babcock and Heyward 1986; Sakai 1997). Some brooded planulae have a longer larval life. Richmond (1997) estimated larval competency to be over 100 days in *Pocillopora damicornis*. It is possible that this extended period is likely to be due to the zooxanthellae found in these brooded planulae providing extra energy reserves (Richmond 1997). Deep-water species are, however without zooxanthellae, therefore the larval planktonic phase may be shorter, though there is as yet no data.

It is thought that the larvae of deep-water scleractinians require a hard substratum, such as a rock outcrop, or shell or worm tube in sandy areas, for settlement to occur (Wilson 1979; Rogers 1999). Many colonies of *Lophelia pertusa, Desmophyllum cristagalli, Enallopsammia rostrata* have been observed attached to rocky outcrops or dead gorgonian and scleractinian skeletons in the northern Atlantic (Adkins and Schierer 2003).

Discussion

In shallow waters the pattern of reproduction is highly variable both between and within species (Fadlallah 1983; Richmond and Hunter 1990).These interspecific differences are thought to be due to environmental adaptations, and so are also likely to occur within deep-water species. Within the genus *Caryophyllia*, *C. clavus* and *C. smithii* are gonochoric species (Tranter et al. 1982; Fadlallah 1983), however three species of deep water *Caryophyllia* have all been shown to be hermaphroditic (Waller et al. in press). Of the five species of *Flabellum* studied, three brood their young, and two broadcast (Waller 2003).

In the western Atlantic, Brooke (2002) found shallow-water colonies of *O. varicosa* to have the same seasonal pattern of reproduction as the deeper-living colonies suggesting little environmental control in this case. Flint (2003) observed *Fungiacyathus marenzelleri* from 4000 m in the NE Pacific to have similar seasonal cycle as that described by Waller et al. (2002) at 2000 m in the NE Atlantic. However, fecundity was significantly different, with the deeper individuals producing fewer oocytes, possibly a result of reduced food availability at these greater depths.

While there is evidence for both phylogenetically and environmentally constrained reproduction, reproductive studies in definitive areas are required to

allow an adequate assessment of conservation potential. Understanding reproductive processes of a species in a single area, though providing a baseline, cannot be guaranteed to be the pattern observed in other areas.

The main aim of this review is to demonstrate the paucity of biological information that is available on deep-sea corals. Reproduction is one of the most fundamental biological processes and an understanding of it must be attained to complete any conservation or management effort. The intense trawling damage now observed globally (Probert et al. 1997; Koslow and Gowlett-Jones 1998; Bett 2001; Brooke 2002; Hall-Spencer et al. 2003; Wheeler et al. in press) has highlighted the need to attain ecological and biological data quickly, before these areas are damaged beyond repair. Without this information we would have no insight as to this habitats ability, and speed, of re-colonisation after a damaging event.

Acknowledgments

References

ACES (2003) The Atlantic Coral Ecosystem Study Final Report. Compiled by Freiwald A, 250pp

Adkins J, Schierer D (2003) The MEDUSA cruise to the New England Seamounts. Cruise Rep, RV Atlantis 7 leg 13, 200pp

Babcock RC, Heyward AJ (1986) Population biology of reef flat corals of the family Faviidae *(Goniastrea annularis)*. James Cook Univ, North Queensland

Bett BJ (2001) UK Atlantic Margin Environmental Survey: introduction and overview of bathyal benthic ecology. Cont Shelf Res 21: 8-10

Billett DSM, Lampitt RS, Rice AL, Mantoura RFC (1983) Seasonal sedimentation of phytoplankton to the deep-sea benthos. Nature 302: 520-522

Brooke S, Young CM (2003) Reproductive ecology of a deep-water scleractinian coral, *Oculina varicosa*, from the southeast Florida shelf. Cont Shelf Res 23: 847-858

Brooke SD (2002) Reproductive ecology of a deep-water scleractinian coral, *Oculina varicosa* from the South East Florida Shelf. PhD Thesis, School of Ocean and Earth Science, Southampton Oceanogr Cent, 160pp

Burgess S, Babcock RC (2005) Reproductive ecology of three reef-forming, deep-sea corals in the New Zealand region. In: Freiwald A, Roberts JM (eds) Cold-water Corals and Ecosystems. Springer, Berlin Heidelberg, pp 701-713

Delvoye L (1982) Aspects of sexual reproduction in some Scleractinia. Caribbean Mar Biol Inst, Curacao, 93pp

Fadlallah YH (1983) Sexual reproduction, development and larval biology in scleractinian corals: A review. Coral Reefs 2: 129-150

Fadlallah YH, Pearse JS (1982) Sexual reproduction in solitary corals: overlapping oogenic and brooding cycle, and benthic planulas in *Balanophyllia elegans*. Mar Biol 71: 233-231

Flint H (2003) Reproductive biology of the deep-water solitary scleractinian *Fungiacyathus marenzelleri* from the NE Pacific. MSc Thesis, School of Ocean and Earth Science, Southampton Oceanogr Cent, 50pp

Gage JD, Tyler PA (1991) Deep-Sea Biology: A Natural History of Organisms at the Deep-Sea Floor. Cambridge University Press, Cambridge

Goffredo S, Arnone S, Zaccanti F (2002) Sexual reproduction in the Mediterranean solitary coral *Balanophyllia europaea* (Scleractinia, Dendrophylliidae). Mar Ecol Prog Ser 229: 83-94

Hall-Spencer J, Allain V, Fosså JH (2003) Trawling damage to Northeast Atlantic ancient coral reefs. Proc R Soc London 269: 507-511

Harrison PL, Wallace CC (1990) Reproduction, dispersal and recruitment of scleractinian corals. In: Dubinsky Z (ed) Ecosystems of the World: Coral Reefs. Elsevier, New York, pp 133-207

Jennings S, Kaiser MJ (1998) The effects of fishing on marine ecosystems. Advanc Mar Biol 34: 201-352

Koenig CC, Coleman FC, Grimes CB, Fitzhugh GR, Scanlon KM, Gledhill CT, Grace M (2000) Protection of fish spawning habitat for the conservation of warm-temperate reef-fish fisheries of shelf edge reefs of Florida. Bull Mar Sci 66: 593-616

Koslow JA, Boehlert GW, Gordon JD, Haedrich RL, Lorance P, Parin N (2000) Continental slope and deep-sea fisheries: implications for a fragile ecosystem. ICES, J Mar Sci 57: 548-557

Koslow JA, Gowlett-Jones K (1998) The seamount fauna off southern Tasmania: benthic communities, their conservation and impacts of trawling. Final report to Environment Australia and Fisheries Research Development Coorporation. Australia, 104pp

Mortensen PB (2000) *Lophelia pertusa* (Scleractinia) in Norwegian waters: Distribution, growth and associated fauna. PhD Thesis, Univ Bergen, Norway, 31pp

Olsgard F, Gray JS (1995) A comprehensive analysis of the effects of offshore oil and gas exploration and production on benthic communities of the Norwegian continental shelf. Mar Ecol Prog Ser 122: 277-306

Probert PK, McKnight DG, Grover SL (1997) Benthic invertebrate bycatch from a deep-water trawl fishery, Chatham Rise, New Zealand. Aquat Conserv Mar Freshwater Ecosyst 7: 27-40

Reed JK (1992) Submersible studies of deep-water *Oculina* and *Lophelia* coral banks off Southeastern USA. Proc Amer Acad Underwater Sci. 12th Annual Sci Diving Symp, pp 143-151

Reed JK (2002) Comparison of deep-water coral reefs and lithoherms off southeastern Florida. Hydrobiologia 471: 57-69

Rice AL, Lambshead PJD (1994) Patch dynamics in the deep-sea benthos: the role of heterogenous supply of organic matter. In: Giller PS, Hildrew AG, Rafaelli DG (eds) Aquatic ecology: scale, pattern and processes. Blackwell, Oxford, pp 469-497

Richmond RH (1997) Reproduction and recruitment in corals: critical links in the persistence of reefs. In: Birkeland C (ed) Life and Death of Coral Reefs. Chapman and Hall, New York, pp 175-197

Richmond RH, Hunter CL (1990) Reproduction and recruitment of corals: comparisons among the Caribbean, the Tropical Pacific and the Red Sea. Mar Ecol Prog Ser 60: 185-203

Rinkevich B, Loya Y (1979) The reproduction of the Red Sea coral *Stylophora pistillata*. I Gonads and Planulae. Mar Ecol Prog Ser 1: 133-144

Rogers AD (1999) The biology of *Lophelia pertusa* (Linnaeus 1758) and other deep-water reef-forming corals and impacts from human activities. Int Rev Hydrobiol 84: 315-406

Sakai K (1997) Gametogenesis, spawning, and planula brooding by the reef coral *Goniastrea aspera* (Scleractinia) in Okinawa, Japan. Mar Ecol Prog Ser 151: 67-72

Schlesinger Y, Loya Y (1985) Coral community reproductive patterns: Red Sea *versus* the Great Barrier Reef. Science 28: 1333-1335

Stimson JS (1978) Mode and timing of reproduction in some common hermatypic corals of Hawaii and Enewetak. Mar Biol 48: 173-184

Szmant AM (1986) Reproductive ecology of Caribbean reef corals. Coral Reefs 5: 43-54

Szmant-Froelich A (1985) The effect of colony size on the reproductive ability of the Caribbean coral *Montastrea annularis* (Ellis and Solander). Proc Fifth Int Coral Reef Congr 4: 295-300

Szmant-Froelich A, Vevich P, Pilson MEQ (1980) Gametogenesis and early development of the temperate coral *Astrangia danae* (Anthozoa: Scleractinia). Biol Bull 158: 257-269

Tranter PRG, Nicholson DN, Kinchington D (1982) A description of spawning and post-gastrula development of the cool temperate coral *Caryophyllia smithii* (Stokes and Boderip). J Mar Biol Assoc UK 62: 845-854

Tyler PA, Gage JD, Paterson GJL, Rice AL (1993) Dietary constraints on reproductive periodicity in two sympatric deep-sea astropectinid seastars. Mar Biol 115: 267-277

Tyler PA, Harvey R, Giles LA, Gage JD (1992) Reproductive strategies and diet in deep-sea nuculanid protobranchs (Bivalvia: Nuculoidea) from the Rockall Trough. Mar Biol 114: 571-580

Waller RG (2003) The reproductive ecology of deep-water scleractinians. PhD Thesis, School of Ocean and Earth Science, Southampton Oceanogr Cent, 351pp

Waller RG, Tyler PA (in press) The reproductive biology of two deep-water reef building scleractinians from the NE Atlantic Ocean. Coral Reefs

Waller RG, Tyler PA, Gage JD (2002) Reproductive ecology of the deep-water scleractinian coral *Fungiacyathus marenzelleri* (Vaughan, 1906) in the northeast Atlantic Ocean. Coral Reefs 21: 325-331

Waller RG, Tyler, PA, Gage JD (in press) Sexual reproduction in three hermaphroditic deep-sea *Caryophyllia* species (Anthozoa: Scleractinia) from the NE Atlantic Ocean. Coral Reefs

Wheeler AJ, Bett BJ, Billett DSM, Masson D, Mayor D (in press) The impact of demersal trawling on NE Atlantic deep-water coral habitats: the case of the Darwin Mounds, U.K. In: Thomas J and Barnes P (eds) Benthic Habitats and the Effects of Fishing. Amer Fisheries Soc, Bethesda, Maryland, USA

Wilson JB (1979) The distribution of the coral *Lophelia pertusa* in the North East Atlantic. J Mar Biol Ass UK 59: 149-164

Reproductive ecology of three reef-forming, deep-sea corals in the New Zealand region

Samantha N. Burgess[1,2], Russ C. Babcock[3]

[1] Research School of Earth Sciences, Australian National University, Canberra, ACT 0200, Australia
(sam.burgess@anu.edu.au)

[2] South Australian Research and Development Institute: Aquatic Science, P.O. Box 120, Henley Beach, SA 5022, Australia

[3] Commonwealth Scientific and Industrial Research Organisation, Marine Research Private Bag 5, Wembley, WA 6913, Australia

Abstract. Reproductive ecology was examined in three deep-sea, reef-forming corals, *Goniocorella dumosa*, *Solenosmilia variabilis* and *Enallopsammia rostrata* from the 'Graveyard' seamount complex on the Chatham Rise, New Zealand. Samples were collected from 890-1130 m depth in April 2001 using an epibenthic sled from the research vessel *Tangaroa*. *S. variabilis* was found to be gonochoric and this sexual trait was also suggested for *E. rostrata* and *G. dumosa,* although only colonies of one sex were collected. The likely mode of reproduction is broadcast spawning and fertilisation is likely to occur in late April or May coinciding with pelagic biomass accumulations at the end of summer. Reproductive development displayed a high level of synchrony among species and between seamount localities. *E. rostrata* was observed to contain both stage III and stage IV oocytes, indicating overlapping cohorts of oocyte growth, possibly related to food resources available. High fecundities were estimated for *E. rostrata* (>144 oocytes polyp^{-1})*, G. dumosa* (>480 oocytes polyp^{-1}) and *S. variabilis* (>290 oocytes polyp^{-1})*,* with a negative correlation between oocyte size and number observed for all three species.

Keywords. Deep-sea coral, Scleractinia, gametogenesis, fecundity, New Zealand

Introduction

Scleractinian corals have been recorded on seamounts and hard-bottom structures throughout the New Zealand exclusive economic zone since the 1960s (Squires 1964a, b, 1965). New Zealand has a relatively diverse fauna of 105 scleractinian species (Cairns 1995), and colonial species collected from seamount features include *Madrepora oculata* (Linnaeus, 1758), *Solenosmilia variabilis* (Duncan, 1873), *Enallopsammia rostrata* (Pourtalès, 1878), *Goniocorella dumosa* (Alcock, 1902), *Dendrophyllia alcocki* (Wells, 1954), *Oculina virgosa* (Squires, 1958) and *E.*

marenzelleri (Zibrowius, 1973). Of these species the most frequently encountered are *E. rostrata*, *G. dumosa*, *M. oculata* and *S. variabilis* that all form local, massive colonies providing a framework for deep-water structures referred to as 'banks' by Squires (1964b). Hollow spaces within the interlocking branches provide numerous niches for diverse associated invertebrate fauna (e.g., solitary scleractinians, gorgonians, stylasterids, anemones, antipatharians, bryozoans, sponges, echinoids, ophiuroids, crinoids, asteroids, brachiopods, gastropods, bivalves, polychaetes and crustaceans; Cairns 1995).

One of New Zealand's primary deep-water fishing areas is the Chatham Rise, with active commercial fishing since the late 1970s. The Chatham Rise is a relatively broad topographical high (200-400 m) extending over 800 km to the east of central New Zealand. The Subtropical Convergence overlies the Chatham Rise producing a zone of enhanced productivity (Heath 1985). High densities of *Goniocorella* and *Madrepora* provide an important structuring element to the benthos, creating areas of enhanced biodiversity on the Chatham Rise (Probert et al. 1997). The 'Graveyard' complex is a cluster of seamounts on the northwest zone of the Chatham Rise situated around 180º longitude (Fig. 1). These seamounts are small with some steep sides and were formed from inter-plate volcanic activity with approximate ages of 110-40 Ma (Clark et al. 2000). The seamount bases are at approximately 1200 m depth and vary in height rising up to 400 m from the seafloor.

Information available on the proximate causes and cues of scleractinian coral reproduction is often conflicting and in general, processes are poorly understood. In terms of life history patterns the influence of habitat (Stimson 1978; Kojis and Quinn 1981), morphology (Rinkevich and Loya 1979), and environmental conditions (Tomascik and Sander 1987) in determining the mode of reproduction in corals have been the subject of intensive research. Studies to date indicate that scleractinian sexuality (hermaphroditic *versus* gonochoric) is consistent within families, but reproductive mode (brooding *versus* broadcast spawning) is not necessarily consistent at the species level (Harrison and Wallace 1990). Conservation of reproductive mode within a species despite large variations in polyp size suggests a complex link between polyp architecture and reproduction (Fadlallah and Pearse 1982; Szmant 1986; Rinkevich and Loya 1987; Sier and Olive 1994).

Environmental factors that affect deep-sea coral reproduction have been linked to terrestrial magnetism and availability of food (Wilson 1979). Although deep-sea scleractinians are considered opportunistic organisms (observed eating dead material; Mortensen 2001), there is likely to be more food available in warmer months because of phytoplankton blooms and associated biomass increases at different trophic levels. Temperature can also fluctuate seasonally with depth indicating variations in the contributing water masses (Wyrtki 1962). Timing of reproductive maturity may be linked to maximum resource availability coinciding with the end of summer. The level of synchrony displayed in populations of deep-sea scleractinians over varying spatial scales is currently unknown. However, if reproductive effort were directly related to food resources, which are likely to fluctuate yearly and on differing spatial scales, synchrony would appear to be unlikely.

Most research conducted on deep-sea corals has focused on biogeographic and taxonomic observations. Two deep-sea reef-forming species, *Lophelia pertusa* and *Oculina varicosa* have been the subject of several studies (e.g., Hessler and Sanders 1967; Wilson 1979; Reed 1980; Mikkelsen et al. 1982; Frederiksen et al. 1992; Mortensen et al. 1995; Freiwald and Wilson 1998; Rogers 1999; Waller et al. 2002 (on *Fungiacyathus*); Brooke and Young 2003 (on *Oculina*)). Little is known about
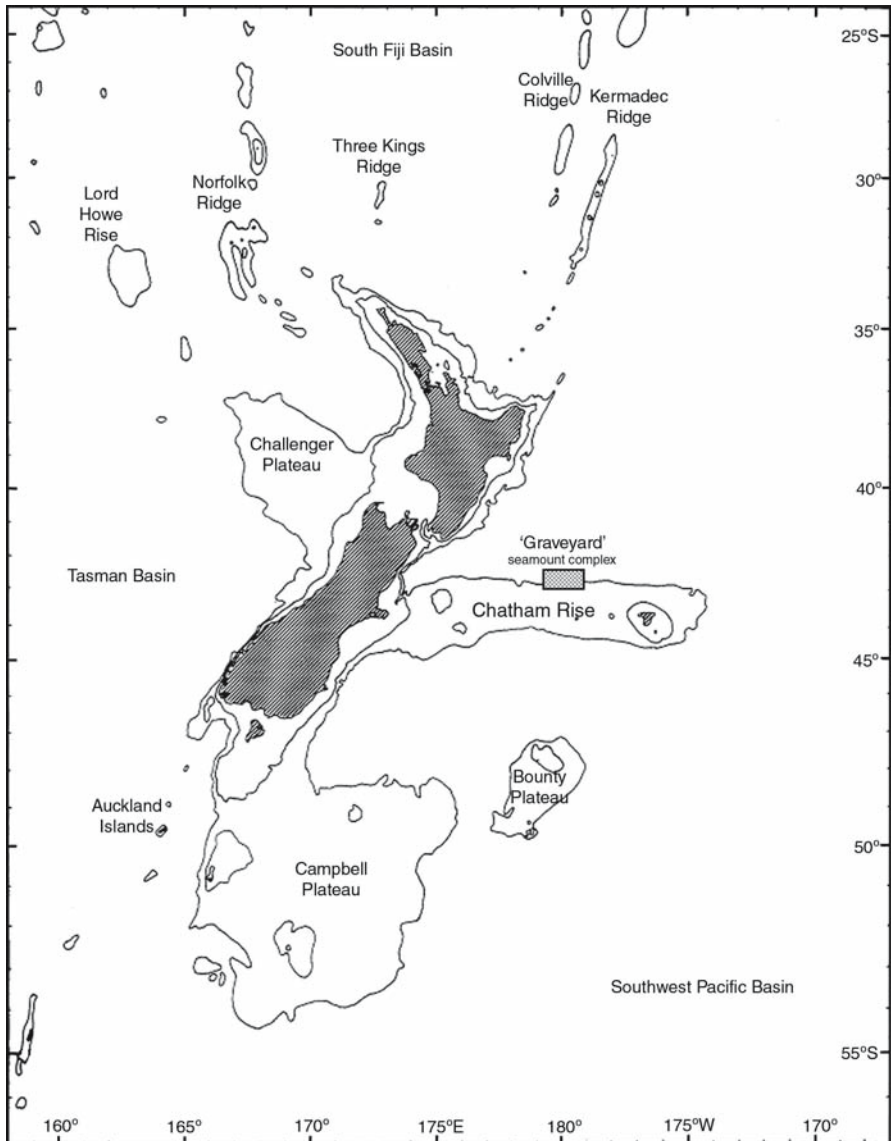
Fig. 1 Map of New Zealand indicating regional bathymetry (500 and 1000 m contour lines), in particular the Chatham Rise and the 'Graveyard' Seamount complex

the ecology of seamounts in the New Zealand region, and the impacts of heavy bottom trawl gear used in fisheries such as orange roughy and oreosomatids on the biological and physical integrity of benthic fauna (Probert et al. 1997; Koslow and Gowlett-Holmes 1998; Clark 1999; Clark et al. 2000; Koslow et al. 2001).

In this study, data were available from only one sampling date; however, this provides a 'snapshot' of part of the scleractinian community present on Chatham Rise. Because the species sampled were at a mature stage of development, inferences can be made about the reproductive potential of the New Zealand deep-sea coral community from the basis of this study, the level of fecundity, when colonies are likely to spawn and optimal times of the year to sample. The main objectives of this study were to determine the sexuality and mode of reproduction of *E. rostrata*, *G. dumosa*, *M. oculata* and *S. variabilis*, assess how much of the coral fragment is gravid and infer the reproductive potential of the colony. A secondary aim was to determine whether deep-sea corals display similar reproductive characteristics (sexual mode and periodicity) to shallow-water species.

Methods

Sample collection

The samples used in this study were collected in April 2001 on the National Institute of Water and Atmospheric Research (NIWA) *RV Tangaroa*. All corals were collected from the Graveyard complex of seamounts on the Chatham Rise. Samples were collected between the depths of 890-1130 m from the Gothic, Graveyard, Ghoul, Pyre, Diabolical and Zombie seamounts. The method of retrieval was an epibenthic sled with approximate dimensions of 1 m wide by 1.5 m long. The sled was constructed of steel and attached to a tow cable with two quick-release links; two nets were used inside the steel frame to optimise the biological catch. Trawl shots were carried out in various parts of the seamounts with tow duration dependent on the amount of catch and a tow speed of 1-1.5 knots up the slope of the seamount. The catch from each trawl was sorted by species, identified, counted and preserved in 10 % formalin.

Histological preparation

Upon collection, all coral specimens were decalcified with 10 % hydrochloric acid. The acid solution was replaced until no aragonite remained in the samples. The decalcified polyps were placed in plastic cassettes for embedding and stored in 70 % ethanol. The polyps then underwent vacuum infiltration with paraffin wax using a Tissue Tek V.I.P. 2000 on a 16-hour cycle. This process involved dehydration with increasing concentrations of ethanol, clearing of tissue with xylol, followed by paraffin wax impregnation. Histological sections were cut to a thickness of 7-8 μm using a rotary microtome. Between 5-11 sections were made of each specimen (depending on the thickness of the polyp). The staining process involved wax removal with xylol followed by hydration. A Mallory Heidenhain stain was used to differentiate nuclear material.

Determination of gametogenic cycle

The coral polyps were first examined for gonads at their maximal diameter, then digital photographs were taken using a Nikon Coolpix 990. The photographs were downloaded, and measured using Sigma Scan Pro version 5 software. Gametocytes were scored, when present, according to the developmental stage described by Giese and Pearse (1974) and Wourms (1987). In the absence of quantitative measurements, fecundity (defined as the number of oocytes per polyp for the purpose of this study) was used as an estimate of reproductive effort. Oocyte diameter was obtained by measuring the maximum axis that dissected an emarginate nuclear vacuole and the axis perpendicular to it, then working out the mean of the two axes. Up to 80 oocytes were measured as oocyte size varied considerably. Polyp diameter and oocyte diameter were compared statistically using the software SAS; Proc GLM regression models were tested to determine if oocyte diameter was dependent on or independent of polyp diameter.

Results

Spermacysts of *Madrepora oculata* and *Solenosmilia variabilis* and were situated inside mesenterial tissue. Oocytes of *Goniocorella dumosa* and *Solenosmilia variabilis* were also situated inside the mesenteries and those of *Enallopsammia rostrata* were closely associated with mesenterial filament. All specimens except one sample of *Solenosmilia* contained gonads. Owing to the nature of the collection method, the samples analysed were quite small and ranged in size from 6 polyps (*M. oculata*) per fragment to >50 polyps (*S. variabilis*) per fragment. Multiple fragments were obtained from most of the collection sites and all fragments from the same site were the same sex. However, fragments were treated as if they were from different colonies because there was no way of determining colony size based on the collection methodology employed.

The fragments of *E. rostrata*, *G. dumosa* and *S. variabilis* that contained >20 polyps, consisted of both live and dead polyps. Dead polyp proportions ranged (35 ± 15 %) between fragments, and were mainly found in the internal structure of the three-dimensional lattice, some were also observed on the external tips. In the larger fragments of *S. variabilis* and *G. dumosa*, there was evidence of asexual reproduction in the form of intratentacular budding for *S. variabilis* and extratentacular budding for *G. dumosa*. The samples of *M. oculata* (3-15 polyps) were very small and no evidence for asexual reproduction was observed. *E. rostrata* was the largest of the branching species studied but no evidence of budding was observed.

Oogenesis and spermatogenesis

Oocytes observed in *E. rostrata*, *G. dumosa* and *S. variabilis* showed signs of maturity, namely condensed nuclear chromatin in a nucleus often located at the periphery of the oocyte. Gonad morphology is described below for each species.

Goniocorella dumosa

Goniocorella dumosa contained up to 22 oocytes per gonad, and 24 gonads were observed per polyp. Fecundity for this species was estimated to be approximately

480 ± 216 oocytes gonad[-1]. Oocytes were located at the base of the polyp, surrounded by mesogleal lining ranging in shape from spherical to elliptical due to compression against the septa. Large nuclear vacuoles were present, with a dense nucleolus (Fig. 2A). Oocytes were all observed to be stage IV development and contained large yolk granules. Maximum oocyte diameter was 135 μm.

Solenosmilia variabilis

In *Solenosmilia variabilis,* spherical to irregular shaped oocytes were surrounded by mesogleal lining. Numbers of oocytes per gonad ranged from 8-16, with 24 gonads located in the mesentery on either side of the septa. Large nuclear vacuoles and condensed nuclei were present. All oocytes were stage IV with large yolk granules (Fig. 2B). Maximum oocyte diameter was 165 μm and gonads were located near the base of the polyp. Fecundity was estimated as 290 ± 144 oocytes polyp[-1].

Spermatogenesis was considered to be stage III development; spermatocytes were not as tightly packed as in the *M. oculata* specimens. Spermatocytes formed small dense clusters inside testicular clusters (Fig. 3A). Gonads contained up to 20 small testicular clusters, surrounded by mesogleal lining.

Enallopsammia rostrata

Oocytes were arranged on approximately 24 long gonads that descended from the base of the oral cavity to the base of the polyp. Oocytes were large but development was not synchronous with ~60 % of oocytes at stage IV (Fig. 2C), the remaining oocytes were located closer to the oral cavity and were in varying stages of development (Fig. 2D). Maximum oocyte diameter was 400 μm. Oocytes were attached to each other by a thin mesogleal layer. Gonads contained between 4-10 mature oocytes with stage III oocytes present in the same gonad. Fecundity was estimated at approximately 144 ± 96 oocytes polyp[-1].

Madrepora oculata

Clusters of spermatocytes and spermatozoa were surrounded by mesogleal lining (Fig. 3B) observed from below the tentacles through to the base of the polyp. The clusters were irregular and there was a mean of 8 ± 4 per gonad, and more than 10 gonads present in polyps. The lumen was tightly packed with mature spermatozoa with peripheral heads and conspicuous nuclei, flagellae were orientated towards the centre of clusters. Clusters were surrounded by groups of large nematocysts. Spermatogenesis was synchronous within and among clusters, although there was variation in the size of the cluster.

Fecundity

Fecundity estimates (Table 1) were taken from both longitudinal and transverse sections. *G. dumosa* was observed to have the highest fecundity per polyp but oocyte and polyp sizes were the smallest out of the three deep-sea species. *E. rostrata* was at the other end of the spectrum with lowest estimated fecundity but largest polyp and oocyte sizes. Regression analysis (Fig. 4) showed fecundity had a positive relationship with polyp diameter for *S. variabilis* ($F = 324$, $p = <0.0001$, $r^2 = 0.7$) and *E. rostrata* ($F = 14.86$, $p = 0.0003$, $r^2 = 0.19$). There was a non-significant size-

dependent relationship for *G. dumosa* ($F = 0.69$, $p = 0.411$, $r^2 = 0.017$).

Comparison of polyp diameter to oocyte diameter indicated large oocyte ranges
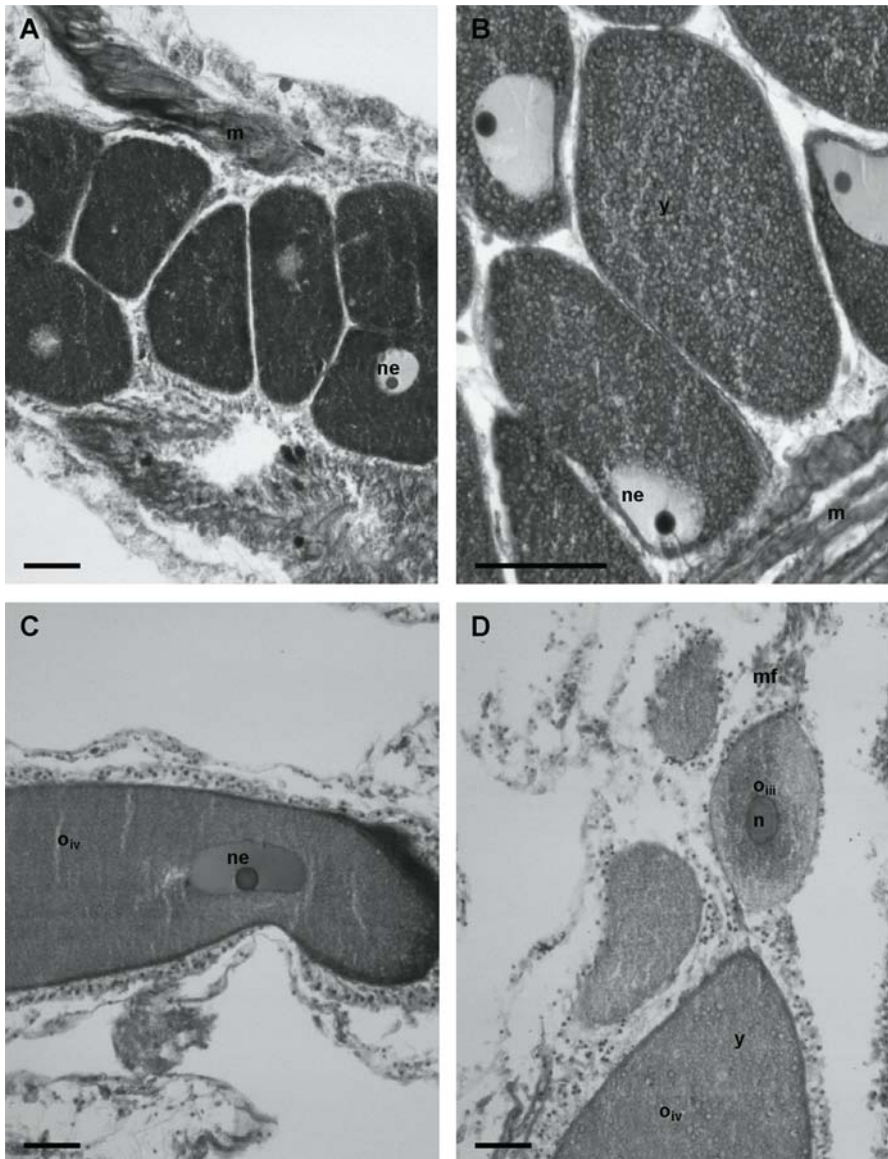
Fig. 2 A *G. dumosa* oocytes surrounded by mesogleal lining (m), displaying nucleolus (ne); **B** *S. variabilis* oocytes containing yolk granules (y), surrounded by mesogleal lining (m), displaying nucleolus (ne); **C** and **D** *E. rostrata* both mature (o_{iv}) and developing (o_{iii}) oocytes attached by mesogleal filament (mf), displaying nucleoli (ne) and yolk granules (y) in mature oocytes and condensed nuclear material (n) in developing oocyte. All scale bars equal 10 μm
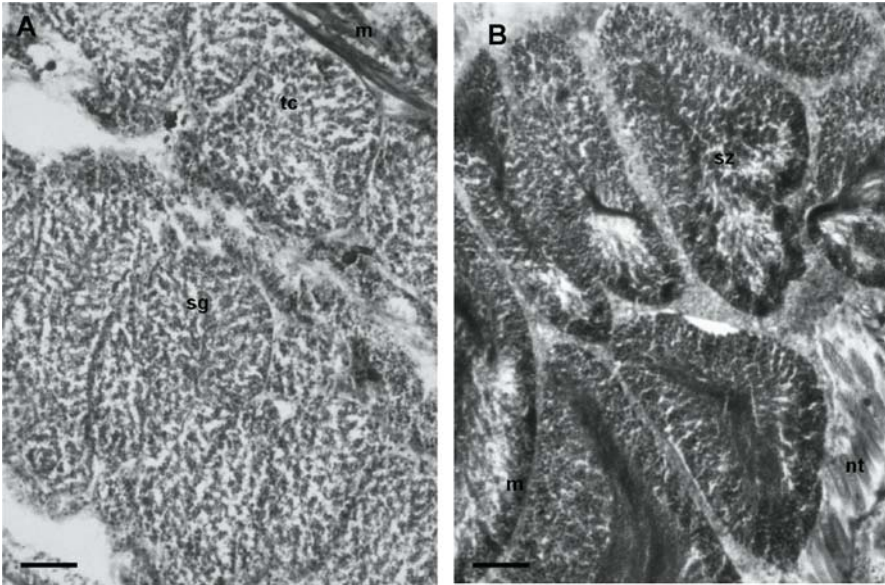
Fig. 3 A *S. variabilis* stage III of spermatogenesis, spermatogonia (sg) were arranged in spherical testicular cysts (tc) surrounded by mesogleal tissue (m) and; **B** *M. oculata* in stage IV of spermatogenesis. Testicular clusters were situated in mesogleal tissue, cysts contained spermatozoa (sz) and were surrounded by large nematocysts (nt), flagellae were orientated towards centre of cyst, and condensed nuclear material was conspicuous. All scale bars equal 10 μm

for each species, with an inverse relationship of oocyte size to polyp size within species. *S. variabilis* oocytes range between 125 and 175 μm, with a large range in polyp sizes. The sample sizes for *E. rostrata* and *G. dumosa* were smaller but a narrow oocyte diameter range was also observed in *G. dumosa. E. rostrata* displayed a broader range in both polyp size and oocyte size. Reproductive allocation between spermary and oocyte area was observed to be similar in *S. variabilis*. However, the average polyp size for *S. variabilis* was larger in male colonies. Polyp volumes of *G. dumosa* and *M. oculata* were similar but *M. oculata* displayed a greater area allocated to spermaries.

Table 1 Measure of fecundity of *E. rostrata, G. dumosa* and *S. variabilis*. Mean polyp and oocyte sizes (expressed as diameters) correlate to Figure 2

Species	Polyp size ± SD (mm)	Oocyte size ± SD (μm)	No. of gonads/polyp	Mean ± SD oocytes/gonad	Polyp Fecundity
Enallopsammia rostrata	5.35 ± 0.9	323 ± 86	24	6 ± 4	144
Goniocorella dumosa	2.75 ± 0.4	121 ± 10	24	20 ± 4	480
Solenosmilia variabilis	3.3 ± 0.7	148 ± 14	24	12 ± 4	290
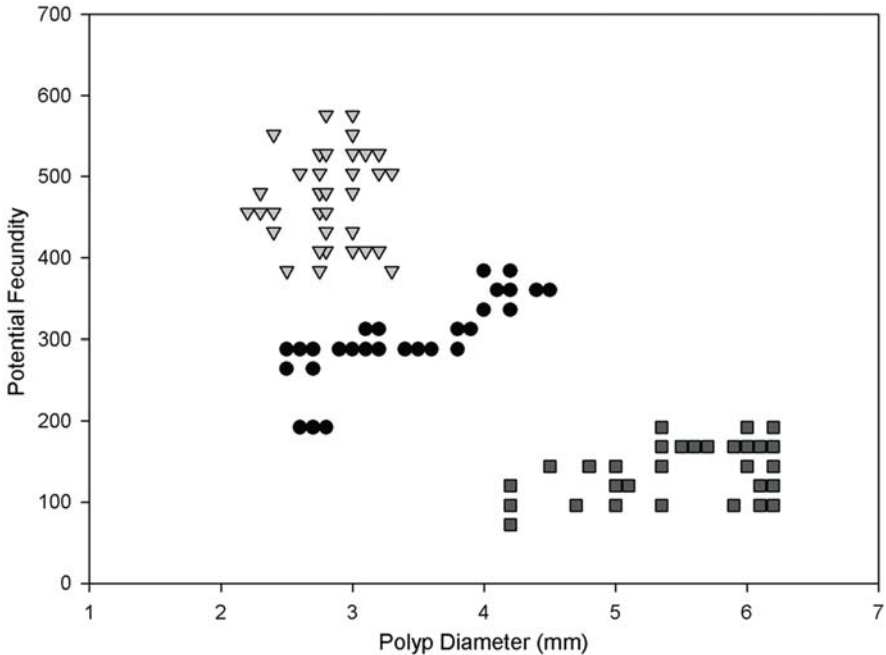
Fig. 4 Polyp diameter of *G. dumosa* (▽), *S. variabilis* (●) and *E. rostrata* (■) plotted against potential fecundity. Regression analysis yielded *G. dumosa* $r^2 = 0.017, p = 0.411$; *S. variabilis* $r^2 = 0.7, p = <0.0001$; and *E. rostrata* $r^2 = 0.19\ p = 0.0003$

Discussion

This is one of the first investigations into fundamental aspects of the reproductive ecology of deep-sea scleractinians in the south Pacific region. Although the extent of this study was limited to one sampling period in April 2001, sampling was conducted on reefs located on different seamounts. Therefore, regional inferences can be made from the results presented, as gametes in each of the species studied were mature or almost mature at the time of collection.

Solenosmilia variabilis is a gonochoric coral, indicated by the synchronous presence of both male and female gametes. Although only oocytes were observed in the samples of *Goniocorella dumosa* and *Enallopsammia rostrata*, and male gonads in *Madrepora oculata*, these species are also considered to be gonochoric, because gametes scored were mature in all colonies containing gonads. A recent study conducted in the northeast Atlantic collected female *M. oculata* with large oocyte diameters and high fecundities (Waller and Tyler in press). There was no evidence of spent spermaries in *E. rostrata* or *G. dumosa* and sections were made from complete polyps, supporting the gonochoric hypothesis. Ninety percent of the colonies sampled contained gametes. These findings correlate with data from shallow-water members of the Oculinidae, Caryophylliidae and Dendrophylliidae,

which have all been found to be gonochoric (Harrison and Wallace 1990).

The mode of reproduction for the scleractinians studied here is believed to be broadcast spawning. Previous research has indicated that species in the families *Oculinidae* and *Caryophylliidae* broadcast gametes (Harrison and Wallace 1990). Spawning is likely to occur in late April or May, based on the maturity of gametes present in colonies studied. This period coincides with late summer and the potential for maximum food resources. *E. rostrata* contained both stage III and stage IV gonads indicating continuous development to some degree. Continuous development in *E. rostrata* could be related to more than one reproductive season per year, although the presence of stage III oocytes at the same time as stage IV, suggests this is unlikely. The observed delayed oocyte development in *E. rostrata* may be related to the level of nutritional resources available for the parent polyp as the main environmental trigger for onset of gametogenesis. *E. rostrata* may display exponential growth rate in oocyte development, producing all oocytes at the start of the reproductive season and continuing development when nutritional resources become available. Continuous development would explain the presence of stage III and stage IV gametes towards the end of the gametogenic cycle. Post-April samples are required to confirm the absence of brooded larvae in *E. rostrata,* because the predominant sexual mode in the family *Dendrophylliidae* is brooding (Harrison and Wallace 1990).

Shlesinger et al. (1998) compared the evolution of sexual reproduction in actinians (sea anemones) and suggested that broadcasting was the ancestral mode of reproduction, and brooding was a derived trait. This suggests that most scleractinian corals retain the ancestral mode of reproduction, i.e., broadcasting of gametes. The advantages of this reproductive mode vary from long distance dispersal to an increased planktonic larval period; however, low settlement rates are one disadvantage of spawning gametes. Little is known about the anatomical constraints imposed on reproduction in corals or the developmental level polyps require before becoming reproductively active. Understanding this relationship may be of particular importance in scleractinians because the aragonite skeleton plays a role in the functional anatomy of the living coral (Fadlallah and Pearse 1982).

Although it is difficult to test environmental factors in the deep-sea, some of the proximate factors that are important in shallow-water communities are not believed to play a role in determining reproduction in deeper communities. However, a recent study by Brooke and Young (2003) linked changes in day length as an environmental cue effecting the gametogenic cycle of *Oculina varicosa*. The trigger for gamete release in *Caryophyllia smithii*, a solitary, cosmopolitan coral was linked to a rise in seawater temperature, and interaction of sperm with female polyps caused the release of ova chemical receptor cells in the oral epidermis (Tranter et al. 1982). It is not known if there are chemoreceptors in deep-sea corals but this hypothesis is plausible as synchrony in fertilization would be essential to justify the energetics of sexual reproduction.

Fecundity can provide a useful index of reproductive effort in corals where the egg size and the number of reproductive cycles each year are consistent (Babcock et al. 1994). Coral fecundity and timing may be synchronous or asynchronous within

a colony, reef, or latitudinal location. Oocyte diameter can vary widely within individual species at different locations (Harriott 1983) or within genera (Babcock et al. 1986; Richmond and Hunter 1990) indicating the need for more extensive comparative studies. The wide distribution of oocyte sizes within species may be due to real differences between sites, or to divergence in technical procedures, i.e., measurements by histological sections *versus* direct tissue measurements (Shlesinger et al. 1998). Polyp fecundity in *E. rostrata, G. dumosa* and *S. variabilis* was high (values summarised in Table 1). An inverse relationship between fecundity and oocyte diameter/polyp diameter was observed between species, consistent with shallow-water scleractinians. A positive relationship was observed within species with potential fecundity increasing for larger polyp diameters of the different species. Environmental cues for the onset of reproduction are not known but the availability of nutrients is thought to be a key factor with gamete release in late autumn.

Physical disturbance in deep-sea corals may be minimised by constructing strong, hydrodynamic skeletons that are resistant to all but severe degrees of disturbance. However, dredges from fishing trawls are certain to have an adverse affect. Another unknown factor is the survival rate of fragments, after colony breakages. Increased physical and physiological stress from deep-sea trawling is anticipated to reduce colony fecundity for a given gametogenic cycle. The importance of sexual reproduction for these deep-water species is not known, but is likely to be a major factor in growth of the reef owing to observed high fecundities. Prolific vegetative growth through branch formation was observed on *G. dumosa* and *S. variabilis* fragments, but this may be disproportionate to the whole colony as it is assumed that the fragments studied were from the outer edges of the colony.

Acknowledgements

References

Babcock RC, Bull G, Harrison PL, Heyward AJ, Oliver JK, Wallace CC, Willis BL (1986) Synchronous spawnings of 105 scleractinian coral species on the Great Barrier Reef. Mar Biol 90: 379-394

Babcock RC, Willis BL, Simpson CJ (1994) Mass spawning of corals on a high latitude coral reef. Coral Reefs 13: 161-169

Brooke S, Young CM (2003) Reproductive ecology of a deep-water scleractinian coral, *Oculina varicosa* from the southeast Florida shelf. Cont Shelf Res 23: 847-858

Cairns SD (1995) The marine fauna of New Zealand: Scleractinia (Cnidaria: Anthozoa). New Zealand Oceanogr Mem 103, 210 pp

Clark M (1999) Fisheries for orange roughy (*Hoplostethus atlantictus*) on seamounts in New Zealand. Oceanol Acta 22: 593-602

Clark M, O'Shea S, Wood B, Wright I (2000) Seamount management: a report on seamounts potentially suitable for consideration under the Ministry of Fisheries seamount management strategy. NIWA Client Rep 00-33, 79 pp

Fadlallah YH, Pearse JS (1982) Sexual reproduction in solitary corals: overlapping oogenic and brooding cycles, and benthic planulas in *Balanophyllia elegans*. Mar Biol 71: 223-231

Frederiksen R, Jensen A, Westerberg H (1992) The distribution of the scleractinian coral *Lophelia pertusa* around the Faroe Islands and the relation to intertidal mixing. Sarsia 77: 157-171

Freiwald A, Wilson JB (1998) Taphonomy of modern deep, cold-temperate water coral reefs. Hist Biol 13: 37-52

Giese AC, Pearse JS (1974) Introduction: General principles. In: Giese AC, Pearse JS (eds) Reproduction of marine invertebrates. 1, Academic Press, New York, pp 1-49

Harriott VJ (1983) Reproductive ecology of four scleractinian species at Lizard Island, Great Barrier Reef. Coral Reefs 2: 9-18

Harrison PL, Wallace CC (1990) Reproduction, dispersal and recruitment of scleractinian corals. In: Dubinsky Z (ed) Coral Reefs. Elsevier, Amsterdam, pp 133-207

Heath RA (1985) A review of the physical oceanography of the seas around New Zealand. New Zealand J Mar Fresh Res 19: 79-124

Hessler RR, Sanders HL (1967) Faunal diversity in the deep-sea. Deep-Sea Res 14: 65-78

Kojis BL, Quinn NJ (1981) Aspects of sexual reproduction and larval development in the shallow water hermatypic coral, *Goniastrea australensis* (Edwards and Haime, 1857). Bull Mar Sci 31: 558-573

Koslow JA, Gowlett-Holmes K (1998) The seamount fauna off southern Tasmania: benthic communities, their conservation and impacts of trawling. Final Rep Environ Australia Fish Res Dev Corp, Australia

Koslow JA, Gowlett-Holmes K, Lowry JK, O'Hara T, Poore GCB, Williams A (2001) Seamount benthic macrofauna off southern Tasmania: community structure and impacts of trawling. Mar Ecol Progr Ser 213: 111-125

Mikkelsen N, Erlenkeuser H, Killingley JS, Berger WH (1982) Norwegian corals: radiocarbon and stable isotopes in *Lophelia pertusa*. Boreas 11: 163-171

Mortensen PB (2001) Aquarium observations on the deep-water coral *Lophelia pertusa* (L. 1758) (Scleractinia) and selected associated invertebrates. Ophelia 54: 83-104

Mortensen PB, Hovland M, Brattegard T, Farestveit R (1995) Deep-water bioherms of the scleractinian coral *Lophelia pertusa* (L.) at 64° N on the Norwegian shelf: structure and associated megafauna. Sarsia 80: 145-158

Probert PK, McKnight DG, Grove SL (1997) Benthic invertebrate bycatch from a deep-water trawl fishery, Chatham Rise, New Zealand. Aquatic Conservation. Mar Fresh Ecosyst 7: 27-40

Reed JK (1980) Distribution and structure of deep-water *Oculina varicosa* coral reefs off central eastern Florida. Bull Mar Sci 30: 667-677

Richmond RH, Hunter CL (1990) Reproduction and recruitment of corals: comparisons among the Caribbean, the Tropical Pacific and the Red Sea. Mar Ecol Progr Ser 60: 185-203

Rinkevich B, Loya Y (1979) The reproduction of the Red Sea Coral *Stylophora pistillata*. I. Gonads and Planulae. Mar Ecol Progr Ser 1: 133-144

Rinkevich B, Loya Y (1987) Variability in the pattern of sexual reproduction of the coral *Stylophora pistillata* at Eilat, Red Sea: a long-term study. Biol Bull 173: 335-344

Rogers AD (1999) The biology of *Lophelia pertusa* (L. 1758) and other deep-water reef-forming corals and impacts from human activities. Int Rev Hydrobiol 84: 315-406

Shlesinger Y, Goulet TL, Loya Y (1998) Reproductive patterns of scleractinian corals in the northern Red Sea. Mar Biol 132: 691-701

Sier CJS, Olive PW (1994) Reproduction and reproductive variability in the coral *Pocillopora verrucosa* from the Republic of Maldives. Mar Biol 118: 713-722

Squires DF (1964a) Biological results of the Chatham Islands 1954 expedition: Part 6: Scleractinia. New Zeal Dep Sci Indus Res Bull 139, 29 pp

Squires DF (1964b) Fossil coral thickets in Wairarapa, New Zealand. J Paleont 38: 904-915

Squires DF (1965) Deep-water coral structure on the Campbell Plateau, New Zealand. Deep-Sea Res 12: 785-788

Stimson JS (1978) Mode and timing of reproduction in some common hermatypic corals of Hawaii and Enewetak. Mar Biol 48: 173-184

Szmant AM (1986) Reproductive ecology of Caribbean reef corals. Coral Reefs 5: 43-54

Tomascik T, Sander F (1987) Effects of eutrophication on reef-building corals II. Structure of scleractinian coral communities on fringing reefs, Barbados, West Indies. Mar Biol 94: 53-75

Tranter PRG, Nicholson DN, Kinchington D (1982) A description of spawning and post-gastrula development of the cool temperate coral, *Caryophyllia smithii*. J Mar Biol Ass UK 62: 845-854

Waller RG, Tyler PA (in press) The reproductive ecology of two deep water, reef building scleractinians from the northeast Atlantic Ocean. Coral Reefs

Waller RG, Tyler PA, Gage JD (2002) Reproductive ecology of the deep-sea scleractinian coral *Fungiacyathus marenzelleri* (Vaughan, 1906) in the northeast Atlantic Ocean. Coral Reefs 21: 325-331

Wilson JB (1979) The distribution of the coral *Lophelia pertusa* (L.) [*L. prolifera* (Pallas)] in the northeast Atlantic. J Mar Biol Ass UK 59:149-164

Wourms JP (1987) Oogenesis. In: Giese AC, Pearse JS (eds) Reproduction of marine invertebrates. 9. Blackwell, California, pp 49-178

Wyrtki K (1962) The subsurface water masses in the Western South Pacific Ocean. Austral J Mar Fresh Res 13: 18-47

Lipids and nitrogen isotopes of two deep-water corals from the North-East Atlantic: initial results and implications for their nutrition

Kostas Kiriakoulakis[1], Elizabeth Fisher[1], George A. Wolff[1], André Freiwald[2], Anthony Grehan[3], J. Murray Roberts[4]

[1] Department of Earth and Ocean Sciences, University of Liverpool, 4 Brownlow Street, Liverpool, L69 3GP, UK
(kos@liverpool.ac.uk)
[2] Institute of Paleontology, Erlangen University, Loewenichstr. 28, D-91054 Erlangen, Germany
[3] Martin Ryan Marine Science Institute, National University of Ireland, Galway, Ireland
[4] Scottish Association for Marine Science, Dunstaffnage Marine Laboratory, Oban, Argyll, PA37 1QA, UK

Abstract. The lipid and organic nitrogen isotopic ($\delta^{15}N$) compositions of two common deep-water corals (*Lophelia pertusa* and *Madrepora oculata*) collected from selected locations of the NE Atlantic are compared to the composition of suspended particulate organic matter, in order to determine their principle food source. Initial results suggest that they may feed primarily on zooplankton. This is based on the increased abundances of mono-unsaturated fatty acids and alcohols and the different ratios of the polyunsaturated fatty acids, 22:6/20:5 of the corals when compared to those of the suspended particulate organic matter. There is enrichment in *L. pertusa* of mono-unsaturated fatty acids and of $\delta^{15}N$ relative to *M. oculata*. It is unclear whether this reflects different feeding strategies or assimilation/storage efficiencies of zooplankton tissue or different metabolism in the two coral species.

Keywords. Deep-water corals, suspended particulate organic matter, nitrogen isotopes, lipids, fatty acids, PUFA, MUFA

Introduction

Cold-water azooxanthellate corals (most commonly *Lophelia pertusa* and *Madrepora oculata*) are widespread at the western European continental margin, where their framework and structure support diverse ecosystems (e.g., Freiwald et al. 2002). The deep-water corals (DWCs) often grow on carbonate mounds (e.g., Hovland et al. 1994; Henriet et al. 1998; Freiwald et al. 1999, 2002; De Mol et al. 2002; Huvenne et al. 2002 amongst others). They normally occur between 50 and

2000 m depth, typically at temperatures of 4-12ºC (Wilson 1979; Kenyon et al. 1998, 2003; Rogers 1999; De Mol et al. 2002, 2005), although they can tolerate sub-zero water temperatures for short periods of time (Bett 2000). *L. pertusa*, the dominant DWC, sometimes forms extensive reefs (e.g., Sula Ridge - Norwegian Shelf; Freiwald et al. 1999, 2002), but more often occurs as small colonies of a few centimetres to a few metres across (e.g., Darwin Mounds - Northern Rockall Trough; Masson et al. 2003).

Despite their widespread distribution, very little is known regarding the nutrition of DWCs and their role in the biogeochemistry of carbon and nitrogen. Observations of corals in aquaria and *in situ* provide evidence that *L. pertusa* can selectively feed on live zooplankton of up to 2 cm, although it also ingests sediment particles (Mortensen 2001; Freiwald 2002). It has also been suggested that DWCs may acquire their nutrients from bacteria associated with seafloor hydrocarbon seeps, which in turn promote carbonate mound formation (Hovland and Thomsen 1997; Henriet et al. 1998). However, coral-colonised mounds occur in areas where such seeps are absent and it seems that ambient current strength, the availability of hard substrata and elevated locations are key factors influencing the distributions of DWCs (Rogers 1999; Masson et al. 2003; van Rooij et al. 2003; Kiriakoulakis et al. 2004).

The principal objective of this study was to assess the preferred food source of the DWCs. Our approach was to investigate the biochemical (lipid) and isotopic ($\delta^{15}N$) compositions of the two most common species in the NW European margin, *L. pertusa* and *M. oculata* and to compare these with suspended particulate organic matter (sPOM) in overlying waters. Lipids are essential in the storage and mobilisation of energy, in reproduction and metabolism and are key components in cell membranes (e.g., Brassell and Eglinton 1986). The distributions of fatty acids can be used to determine the diet of biogenic material of marine organisms (e.g., Parrish et al. 2000). To date, there have been few studies of lipids in DWCs (e.g., Mancini et al. 1999), in contrast to their shallow-water counterparts (e.g., Meyers 1979; Latyshev et al. 1991; Harland et al. 1993; Yamashiro et al. 1999 amongst others).

The stable isotopes of nitrogen ($^{15}N/^{14}N$) also have value in ecosystem studies (Owens 1987; Peterson and Fry 1987; Hesslein et al. 1991; Kling et al. 1992; Kidd et al. 1995), although their application to deep-water settings has been limited (e.g., Iken et al. 2001; Heikoop et al. 2002a, b).

Sampling

Lophelia pertusa and *Madrepora oculata* samples were obtained from selected sites along the western European margin (n = 11, 3 respectively Fig. 1) between the years 1998-2000 (Table 1). Samples were collected from a wide range of depths (Table 1) using a variety of gear (boxcores, grabs, dredges, trawls and remotely operated vehicle (ROV)). When possible, sPOM was collected by *in situ* filtration of large volume (~1000 l) water samples from the same locations (Darwin, Logachev,
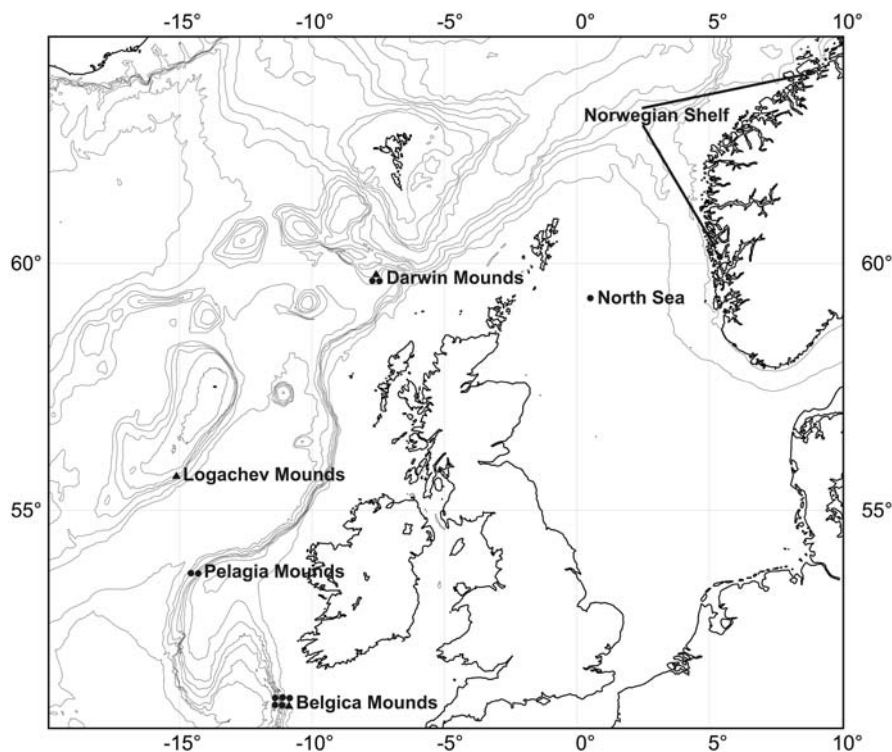
Fig. 1 Bathymetric map of the locations sampled for corals. Contours are every 200 m down to 1000 m, every 500 m down to 2000 m and every 1000 m down to 4000 m. Black circles denote *Lophelia pertusa* and triangles *Madrepora oculata*

Hovland and Belgica Mounds only; Table 2; 293 mm GF/F; stand alone pumping system - Challenger Oceanic; Kiriakoulakis et al. 2004). In all cases the coral and filter samples were immediately frozen (-20°C) and then freeze-dried before analysis.

Methodology

Methods for analysis of lipids have been described in detail elsewhere (Kiriakoulakis et al. 2001). No separation of lipid classes (e.g., phospholipids, glycolipids, etc.) was attempted.

Briefly, separate aliquots of freeze-dried filter and coral tissue material (0.5-1 g) were spiked with internal standard (cholestane), Soxhlet extracted (24 h; dichloromethane:methanol 9:1) and methylated (methanolic acetyl chloride; Christie 1982). GC-MS analyses were carried out on the silylated (bis-trimethyl silyltrifluoroacetamide; BSFTA, 1 % TMS; 30-50 μl; 40°C; 0.5-1 h), methylated total extracts using a Trace 2000 Series gas chromatograph (on-column injector; fused silica high temperature column, 60 m × 0.25 mm i.d.; 0.1 μm film thickness,

Table 1 Sampling and $\delta^{15}N$ values of DWCs collected from the Rockall Trough, Porcupine Bank, North Sea and offshore Norway. WTR is Wyville Thomson Ridge

Station	Coordinates	Gear	Depth	Location	Date	$\delta^{15}N$
Lophelia pertusa						
Dredge 4	63° 36.55N 09° 23.13E	Triangular dredge	200 m	Norwegian shelf	01 May 99	11.01
Osterfjord	60° 39.26N 05° 43.95E	Video-assisted grab	80 m	Norwegian fjord	01 Oct 98	11.72
13831#1	59° 48.88N 07° 17.99W	Trawl	989 m	Darwin Mounds	17 July 00	8.38
S98-467	59° 38.00N 07° 50.00W	Scraper trawl	870 m	South of WTR	01 Oct 98	8.32
Beryl Alpha	59° 32.78N 01° 32.23E	ROV	100 m	North Sea	01 Oct 99	9.58
M2000 BX11#3	53° 46.87N 13° 56.76W	Box core	655 m	Pelagia Mounds	30 July 00	8.16
M2000 BX13#34	53° 46.84N 13° 56.63W	Box core	646	Pelagia Mounds	30 July 00	8.40
13874#2	51° 25.68N 11° 46.40W	Box core	865 m	Belgica Mounds	06 Aug 00	7.37
13881#3	51° 25.66N 11° 46.32W	Box core	859 m	Belgica Mounds	08 Aug 00	7.97
M2000 BX02#50	51° 25.75N 11° 46.29W	Box core	~900 m	Belgica Mounds	28 July 00	7.80
M2000 BX 01#32	51° 25.48N 11° 46.05W	Box core	963 m	Belgica Mounds	28 July 00	7.59
Mean						**8.75**
sd						**1.42**
Madrepora oculata						
13831#1	59° 48.88N 07° 17.99W	Trawl	989 m	Darwin Mounds	17 July 00	7.72
M2000 BX21#51	55° 32.07N 15° 40.12W	Box core	733 m	Logachev Mounds	02 Aug 00	8.62
13874#2	51° 25.68N 11° 46.40W	Box core	865 m	Belgica Mounds	06 Aug 00	6.79
Mean						**7.71**
sd						**0.91**

Table 2 Sampling and δ^{15}N values for sPOM collected from the Rockall Trough and Porcupine Bank. In most cases sPOM was collected from 10-30 m above bottom, i.e., at or close to the benthic boundary layer (BBL). *Water collected at 150 m above bottom (mab)

Station	Location	Date	Depth	δ^{15}N
13823#12*	Darwin Mounds	14-Jul-00	943 m	5.37
13825#1*	Darwin Mounds	15-Jul-00	948 m	5.09
13828#1*	Darwin Mounds	16-Jul-00	938 m	3.03
13832#2*	Darwin Mounds	17-Jul-00	938 m	5.02
13841#1*	Darwin Mounds	19-Jul-00	948 m	6.27
13823#8	Darwin Mounds	14-Jul-00		5.98
13823#12	Darwin Mounds	14-Jul-00	943 m	5.78
13825#1	Darwin Mounds	15-Jul-00	948 m	4.75
13828#1	Darwin Mounds	16-Jul-00	938 m	5.53
13832#2	Darwin Mounds	17-Jul-00	938 m	5.73
13841#1	Darwin Mounds	19-Jul-00	948 m	4.91
SAPS4	Logachev Mounds	12-Aug-01	666 m	
GeoB 8029/1	Logachev Mounds	23-Jul-02	700 m	
GeoB 8036/1	Logachev Mounds	24-Jul-02	700-730m	
SAPS3	Pelagia Mounds	9-Aug-01	635 m	
GeoB 8050/1	Porcupine Bank	27-Jul-02	153 m	
GeoB 6710	Hovland Mounds	17-Sep-00	691 m	
GeoB 6713	Hovland Mounds	18-Sep-00	670 m	
GeoB 6732/1	Hovland Mounds	24-Sep-00	700 m	
GeoB 8042/1	Hovland Mounds	25-Jul-02	710 m	
GeoB 8076/1	Hovland Mounds	29-Jul-02	850 m	
GeoB 8048/1	Hovland Mounds	26-Jul-02	875 m	
GeoB 8068/1	Hovland Mounds	29-Jul-02	655-700m	5.08
GeoB 8044/1	Hovland Mounds	26-Jul-02	805 m	
GeoB 8078/1	Hovland Mounds	30-Jul-02	735-740m	4.67
SAPS2	Hovland Mounds	6-Aug-01	605 m	
GeoB 8081/1	Belgica Mounds	31-Jul-02	916 m	4.48
GeoB 8103/1	Belgica Mounds	2-Aug-02	680 m	4.25
GeoB 8106/1	Belgica Mounds	2-Aug-02	880 m	4.31
GeoB 6742/1	Belgica Mounds	26-Sep-00	830 m	
SAPS1	Belgica Mounds	1-Aug-01	865 m	7.33
GeoB 8107/1	Belgica Mounds	3-Aug-02	785-800m	4.16

5 % phenyl/95 % methyl polysiloxane equivalent phase, DB5-HT, J&W; carrier gas helium at 1.6 ml min^{-1}), coupled with a Thermoquest Finnigan TSQ7000 mass spectrometer (ionisation potential 70 eV; source temperature 215°C; trap current 300 µA) and processed using Xcalibur software. Compounds were identified using authentic standards or relative retention indices, and quantified using cholestane as an internal standard (Kiriakoulakis et al. 2004).

Nitrogen isotopic analyses were carried out on aliquots of sPOM using a PDZ Europa Scientific Geo 20/20 running in continuous flow mode coupled to a Carlo-

Erba Instruments EA1108 elemental analyser. Data were calibrated to atmospheric nitrogen by replicate analyses of the international standards NBS18, NBS19 and IAEACO1 as well as in-house nylon and alanine standards.

Results

Suspended POM

$\delta^{15}N$ of particulate organic nitrogen in selected samples collected at three sites (Darwin, Hovland and Belgica Mounds) ranged from +3.03 to +7.33 ‰ (mean 5.01 ± 0.92 ‰) and were not significantly different between sites and/or depths (Table 2). One sample from the Belgica Mounds collected in summer 2001 (SAPS1) was heavier (+7.33 ‰) than those collected a year later (+4.16 to +4.68 ‰; Table 2). There are no sPOM data from the North Sea and Norwegian fjord and shelf. Detailed lipid results for sPOM are presented elsewhere (Kiriakoulakis et al. 2004, submitted), but to allow easy comparison with the coral lipids, the lipid compositions of POM from four sites (i.e., Darwin, Logachev, Hovland and Belgica Mounds) are presented in Table 3. They show significant regional differences in their distributions, but fatty acids and sterols dominate (mean for all sites 67.6 ± 19.5 % and 24.3 ± 16.6 %, respectively; see Table 3), whereas alcohols are less abundant constituents of the POM (mean of all sites 6.5 % ±3.9 %). Polyunsaturated fatty acids (PUFAs) comprise ~20 % (±13.7 %) of fatty acids and are dominated by $C_{20:4}$, $C_{20:5}$ and $C_{22:6}$ compounds with lesser amounts of $C_{18:4}$ at all sites. Bacterial fatty acids which include C_{15}, C_{17}, all branched and $C_{18:1}$ Δ-7 fatty acids are also abundant (mean ~14 ± 4.14 %), while the mono-unsaturated fatty acids (MUFAs), $C_{20:1}$ and $C_{22:1}$ fatty acids comprise 3 ±3.8 % of fatty acids.

Corals

The $\delta^{15}N$ composition of *L. pertusa* tissue is variable, but this seems to be site-related. Corals from the Belgica Mounds (4) have rather constant composition (mean 7.68 ±0.3 ‰) and this is also true for the two samples from the Pelagia Mounds site (mean 8.28 ‰) and the Northern Rockall Trough (i.e., Darwin Mounds and south of the Wyville Thomson Ridge, see Table 1). There are no seasonal or interannual data for the Pelagia and Belgica Mounds, but samples from the Northern Rockall Trough that were collected in 1998 and 2000 (Table 1) have similar isotopic values. The sample of *L. pertusa* from the North Sea is ~1.3-1.8 ‰ heavier, whereas samples from Norwegian waters are significantly heavier than all other samples (Table 1).

The $\delta^{15}N$ composition of *M. oculata* tissue from three sites is also variable (up to ~2 ‰, Table 1). When comparing the isotopic composition of species collected from the same site *L. pertusa* seems consistently enriched in ^{15}N (up to 1.2 ‰ at Belgica Mounds, Table 1) relative to *M. oculata*.

Lipids in *L. pertusa* are dominated by fatty acids (mean of all sites 67 ±7.8 %) and alcohols (mean of all sites 28.8 ±9.1 %). Sterol abundances are much lower (4.2 ±4.3 %). Fatty acids and alcohols also dominate the lipids of *M. oculata*, with lower proportions of sterols (Table 4). The two species have significantly different PUFA/

Table 3 Lipid composition of sPOM at selected sites. *Water was collected 150 m above bottom (mab). [1]relative to total lipids, [2]relative to total fatty acids. FA is fatty acids, PUFAs, MUFAs and BactFA are poly-unsaturated, mono-unsaturated and bacterial fatty acids respectively. 22:6/20:5 is the ratio of the concentration of $C_{22:6}$ *vs.* $C_{20:5}$ PUFAs

Station	FA	alcohols	sterols	PUFAs	MUFAs	bactFA	22:6/20:5	PUFAs/ MUFAs
	[1] %	[1] %	[1] %	[2] %	[2] %	[2] %		
13823#12*	88.99	1.98	8.97	22.37	0.00	19.20	1.03	
13825#1*	77.75	10.03	11.55	46.38	13.87	10.52	6.49	68.10
13828#1*	21.40	12.81	65.70	11.23	2.06	9.51	0.55	5.46
13832#2*	85.97	4.74	9.10	37.70	14.11	12.24	1.33	16.60
13841#1*	92.49	1.21	5.63	41.63	13.66	13.35	1.18	23.00
13823#8	70.65	2.99	26.01	28.19	1.69	11.27	1.14	16.73
13823#12	86.88	10.02	3.07	29.60	2.93	11.29	0.69	10.11
13825#1	92.00	2.39	5.49	29.94	1.12	19.47	1.11	60.13
13828#1	90.75	2.90	6.11	41.51	2.17	11.24	1.37	19.14
13832#2	90.72	2.28	6.85	22.70	1.50	20.27	0.80	15.11
13841#1	86.43	9.10	4.40	37.56	3.03	17.40	1.16	162.23
mean Darwin	**89.36**	**5.34**	**5.18**	**32.26**	**2.15**	**15.93**	**1.03**	**53.34**
sd (±)	**2.52**	**3.88**	**1.48**	**7.37**	**0.84**	**4.39**	**0.28**	**64.03**
SAPS4	30.69	16.43	46.56	16.32	0.00	5.40		
GeoB8029/1	64.43	2.19	27.00	23.80	0.00	10.52	1.32	
GeoB8036/1	75.71	6.40	17.59	7.39	0.32	12.44	1.41	23.36
mean Logachev	**56.94**	**8.34**	**30.38**	**15.84**	**0.11**	**9.45**	**0.91**	**23.36**
sd (±)	**23.43**	**7.31**	**14.78**	**8.22**	**0.18**	**3.64**	**0.79**	
GeoB 6710	53.38	4.54	41.07	7.85	0.73	19.11	3.40	10.75
GeoB 6713	56.09	5.79	31.14	0.00	0.00	12.89		
GeoB 6732/1	52.59	4.96	38.65	4.42	1.18	16.72		3.75
GeoB 8042/1	71.32	4.05	23.85	22.22	1.01	13.66		0.64
GeoB 8076/1	79.32	3.19	17.49	25.49	4.37	15.04	1.50	5.83
GeoB 8048/1	65.43	5.37	29.20	18.79	2.99	14.06	1.10	6.28
GeoB 8068/1	73.87	12.11	14.02	38.21	2.34	9.74	1.90	16.30
GeoB 8044/1	80.07	10.48	9.36	3.15	1.65	18.75	0.61	1.90
GeoB 8078/1	67.65	7.49	23.69	3.42	1.20	20.50		2.85
SAPS2	31.89	7.50	60.61	0.00	0.00	22.68		
mean Hovland	**63.16**	**6.55**	**28.91**	**12.35**	**1.55**	**16.32**	**1.70**	**6.04**
sd (±)	**14.87**	**2.87**	**15.06**	**13.05**	**1.36**	**3.95**	**1.06**	**5.20**
GeoB 8081/1	59.64	4.47	35.89	31.58	2.50	9.98	1.46	
GeoB 8103/1	52.42	9.22	37.60	21.70	1.92	8.25	1.39	11.30
GeoB 8106/1	64.05	5.84	28.70	17.78	1.97	15.97	1.45	9.04
GeoB 6742/1	52.26	4.05	27.89	2.45	4.12	18.26		0.59
SAPS1	31.86	14.78	51.13	4.41	1.24	16.09		3.56
GeoB 8107/1	61.83	8.31	29.86	7.19	0.00	15.07	0.18	
Mean Belgica	**53.68**	**7.78**	**35.18**	**14.19**	**1.96**	**13.94**	**1.12**	**6.12**
sd (±)	**11.74**	**4.00**	**8.76**	**11.44**	**1.37**	**3.92**	**0.63**	**4.91**
mean total	**67.60**	**6.50**	**24.28**	**20.10**	**2.70**	**14.22**	**1.46**	**20.86**

MUFA ratios (ANOVA; $p<0.05$); in *M. oculata* this ratio is three times higher than in *L. pertusa*. The proportions of bacterial fatty acids and the 22:6/20:5 ratio are similar in both species (Table 4). $C_{20:1}$ and $C_{22:1}$ alcohols constitute >90 % of total alcohols in both species.

Mean lipid compositions of both coral species are also significantly different (ANOVA; $p<0.05$) to those of the sPOM at all sites (Tables 3 and 4). In particular, mean fatty alcohol and MUFA proportions are significantly higher in the DWCs (26.1 ± 10.2 % and 19.7 ± 10.4 %, respectively) than in the sPOM (6.5 ± 3.9 % and 2.7 ± 3.8 %, respectively), whereas the reverse is true for sterols (4.5 ± 4 % for the corals and 24.3 ± 16.6 % for sPOM) and bacterial fatty acids (5.6 ± 1.5 % for the corals and 14.2 ± 4.1 % for sPOM). On the other hand, total fatty acids and PUFAs are not significantly different between the corals (69.5 ± 8.7 % and 25.8 ± 11.1 % respectively) and sPOM (67.6 ± 19.5 % and 20.1 ± 13.7 % respectively). Mean 22:6/20:5 ratios do however differ between the corals (0.6 ± 0.1) and sPOM (1.5 ± 1.2).

Table 4 Lipid composition of collected coral samples. [1]relative to lipids, [2]relative to total fatty acids. FA is fatty acids, PUFAs, MUFAs and BactFA are poly-unsaturated, mono-unsaturated and bacterial fatty acids respectively. 22:6/20:5 is the ratio of the concentration of $C_{22:6}$ *vs.* $C_{20:5}$ PUFAs

Station	FA	alcohols	sterols	PUFAs	MUFAs	bactFA%	22:6/20:5	PUFA/MUFA
	[1]%	[1]%	[1]%	[2]%	[2]%	[2]%		
Lophelia pertusa								
Dredge 4	64.07	35.30	0.63	21.56	38.44	4.95	0.61	0.56
Osterfjord	69.61	28.19	2.20	23.37	12.18	5.92	0.67	1.92
13831#1	62.41	31.41	6.18	24.60	28.32	5.95	0.30	0.87
S98-467	77.56	21.32	1.11	24.80	28.10	5.59	0.52	0.88
Beryl Alpha	63.07	36.62	0.31	27.78	31.46	4.03	0.68	0.88
M2000 BX11#3	64.48	23.08	12.44	9.63	12.27	8.02	0.44	0.78
13874#2	53.72	45.06	1.22	10.17	9.34	5.45	0.76	1.09
13881#3	78.47	16.61	4.91	16.33	28.47	6.81	0.69	0.57
M2000 BX02#50	69.07	21.89	9.04	31.49	12.23	5.26	0.74	2.57
Mean *Lophelia*	**66.94**	**28.83**	**4.23**	**21.08**	**22.31**	**5.77**	**0.60**	**1.13**
sd (±)	**7.76**	**9.08**	**4.27**	**7.56**	**10.75**	**1.13**	**0.15**	**0.68**
Madrepora oculata								
13831#1	68.33	27.12	4.55	27.28	16.40	7.31	0.46	1.66
M2000 BX21#51	84.19	6.79	9.01	45.97	8.53	5.63	0.61	5.39
13874#2	78.69	19.41	1.90	42.69	11.10	2.41	0.66	3.85
Mean *Madrepora*	**77.07**	**17.78**	**5.15**	**38.65**	**12.01**	**5.12**	**0.58**	**3.63**
sd (±)	**8.05**	**10.26**	**3.60**	**9.98**	**4.01**	**2.49**	**0.10**	**1.87**
Mean both species	**69.47**	**26.07**	**4.46**	**25.47**	**19.74**	**5.61**	**0.60**	**1.75**
sd (±)	**8.75**	**10.21**	**3.98**	**11.08**	**10.43**	**1.47**	**0.14**	**1.50**

Discussion

Nitrogen isotopes

Nitrogen isotopes can provide information on food webs, based on the stepwise enrichment of $^{15}N/^{14}N$ ratios with increasing trophic level. This is caused by the preferential elimination of ^{14}N in urine and excretion products and the resulting enrichment of ^{15}N in tissues and faeces (Miyake and Wada 1967; Steele and Daniel 1978; Checkley and Entzeroth 1985). The absolute values ultimately depend on the isotopic composition of the trophic base of the ecosystem. Here, we assume that this is sPOM, since no evidence has been found for hydrocarbon seepage at the sampled sites (Masson et al. 2003; Kiriakoulakis et al. 2004 submitted). $\delta^{15}N$ of sPOM from the three deep-water sites studied here (Darwin, Hovland and Belgica Mounds) shows some variability, but the sites are not significantly different. Interannual variability at the Belgica Mounds area (see Table 2) probably reflects differing nitrogen fractionation during phytoplankton production in the overlying waters (see below). The mean isotopic composition of nitrogen in both coral species studied here is about 2.5-3.5 ‰ heavier than that in sPOM. Many studies have shown that higher trophic levels of an ecosystem show a nitrogen isotopic enrichment of about 3-3.5 ‰, (e.g., DeNiro and Epstein 1981; Miniwaga and Wada 1984; Schoeninger and DeNiro 1984; Toda and Wada 1990; Cabana and Rasmussen 1994). Thus a simplistic view would be that the DWCs feed on sPOM. However, in deep-sea benthic ecosystems, which are usually food limited, the paucity of nitrogen is likely to lead to rather limited isotopic fractionation through benthic respiration. Indeed, Iken et al. (2001) showed that in a deep-sea benthic setting in the NE Atlantic Ocean (Porcupine Abyssal Plain), there is significant overlap in nitrogen isotopic values between trophic levels, reducing the "typical" 3 ‰ stepwise enrichment and indicating overlap in food sources. Therefore, additional information is needed for more secure conclusions regarding the trophic position of the corals (see below).

$\delta^{15}N$ values in *L. pertusa* showed variability between the sites, being heavier in the Norwegian fjord and shelf (see Table 1). Between-reef isotopic variability in $\delta^{15}N$ and $\delta^{13}C$ has been shown before in shallow-water coral tissue (Heikoop et al. 2000a) and this was attributed to varying environmental factors such as temperature, light intensity, eutrophication, and terrestrial inputs, which affect nitrogen fractionation during photosynthesis. Subsequent incorporation of photosynthetic nitrogen into the coral tissue, either *via* autotrophy or heterotrophy, could then reflect or even enhance this variability. Similar "coupling" of regional variation in $\delta^{15}N$ values of phytoplankton with that in DWCs may also occur, if phytoplankton detritus, which forms an important part of sPOM (Kiriakoulakis et al. 2004), stays relatively unaltered (i.e., "fresh") during transport to the sea bed. The regional variation in $\delta^{15}N$ values of the corals may therefore ultimately reflect the nitrogen dynamics of the surface waters. Anthropogenic inputs have also been shown to shift the nitrogen isotopic values of shallow-water coral reefs towards heavier values (Heikoop et al. 2000b; Risk and Erdmann 2000). This could also be a plausible explanation of heavier values in Norwegian corals in this study because they are located very close to land (Fig. 1) and in relatively shallow waters (Table 1).

δ^{15}N values in *M. oculata* also show some variability (see Table 1), but they are lighter than those of *L. pertusa* by about 0.6-0.8 ‰ at the Darwin and Belgica Mounds. These results are preliminary, but could indicate an overlap in feeding, perhaps with a different degree of selection. Iken et al. (2001) showed that suspension feeders (cnidarians) at the Porcupine Abyssal Plain exhibited a wide trophic spectrum, feeding both on particulate material and live prey.

Total lipids

A recent study of sPOM at the benthic boundary layer (BBL) of British and Irish waters revealed that there is fresh (i.e., lipid-rich) sPOM supply at all sites considered here. Nevertheless, there is some variability which may be related to the distinct oceanographic regime of each site (Kiriakoulakis et al. submitted).

The total lipid composition in both coral species is dominated by fatty acids, of which PUFAs and MUFAs comprise significant, although different and variable, proportions (see Table 4). PUFAs in the marine environment are usually thought to derive mainly from phytoplankton (e.g., Parrish et al. 2000), although they are often found in other marine organisms, including herbivorous zooplankton (Corner et al. 1986 and references therein) and deep-sea bacteria (DeLong and Yayanos 1985; Jøstensen and Landfald 1997; Fang et al. 2000). The main source of PUFAs in the phytoplankton are diatoms which biosynthesise mostly $C_{20:5}$ (Volkman et al. 1989), and dinoflagellates which produce more $C_{22:6}$ (Sargent et al. 1987; Harvey et al. 1988).

The 22:6/20:5 PUFA ratios of both coral species are similar, but significantly different to those of the sPOM samples. This implies that coral PUFAs may have a similar source and that this may not be sPOM. Zooplankton are a potential food source for the corals (see also below), but were not collected at the study sites.

Differences in the biochemistry of the two species may also be important. Recently, Mancini et al. (1999) isolated novel 10-hydroxydocosapolyenoic acids in *M. oculata* and *L. pertusa* from Galicia Bank and the Indian Ocean (*M. oculata* only). These authors pointed out that these fatty acids are considered to be intermediates of the $C_{20:4}$ fatty acid cascade in mammals, but rarely are found in marine invertebrates and little is known about their biosynthetic pathways in the marine environment. Such fatty acids were not detected in this study, but the variability in proportions of PUFAs (and MUFAs) of both corals may also be related to environmental, physiological and/or biochemical factors. For example, Oku et al. (2002) showed that the polyps of the shallow-water branching coral *Montipora digitata* have different lipid distributions according to their position in the branch. Clearly much more detailed work is required (see also Mancini et al. 1999).

Herbivorous and omnivorous mesozooplankton feeding predominantly on phytoplankton contain elevated amounts of MUFAs within the wax ester lipid fraction (Ratnayake and Ackman 1979; Graeve et al. 1994; Albers et al. 1996). Moreover, calanoid copepods, which overwinter at depth and constitute a large proportion of the mesozooplankton community in the N.E. Atlantic (e.g., Heath and Jónasdóttir 1999; Planque and Batten 2000), are currently the only organisms

known to biosynthesize de novo $C_{20:1}$ and $C_{22:1}$ fatty acids (MUFAs identified in this study) and alcohols (for a review see Dalsgaard et al. 2003). Thus, MUFAs and their corresponding alcohols are commonly used as mesozooplankton markers. It should be noted that the mean proportion of MUFAs and alcohols (of which $C_{20:1}$ and $C_{22:1}$ alcohols are dominant) in both DWCs are significantly higher than that in sPOM. This suggests that the corals may acquire these fatty acids from mesozooplankton, supporting the indication from 22:6/20:5 ratio. Similarly, enrichment of MUFAs in *L. pertusa* (indicated by the lower PUFA/MUFA ratio), relative to *M. oculata* could be attributed to strategies that assimilate more zooplankton tissue, consistent with the heavier $\delta^{15}N$ values of *L. pertusa*. Alternatively, metabolism of these compound classes could be different in the two species.

Proportions of microbial fatty acids were similar in both coral species but lower than those in sPOM. Microbial biomarkers are commonly found in sPOM (e.g., Kiriakoulakis et al. 2001), therefore their presence in the coral tissue is unsurprising, although it is not clear from whether they are dietary or symbiotic. Even so, their usefulness as biomarkers is currently disputed (see discussion in Parrish et al. 2000) and they should be used with caution and in a qualitative rather than quantitative sense in estimating microbial contributions.

Conclusions

1. Increased abundances of MUFAs and alcohols and different ratios of 22:6/20:5 in DWCs when compared with sPOM implies that they may largely feed on mesozooplankton.
2. The enrichment of MUFAs and ^{15}N in *L. pertusa* relative to *M. oculata* could be attributed to different feeding and/or assimilation/storage strategies of mesozooplankton tissue or to different metabolism in the two coral species.

Acknowledgements

References

Albers CS, Kattner G, Hagen W (1996) The compositions of wax esters, triacylglycerols and phospholipids in Arctic and Antarctic copepods: evidence of energetic adaptations. Mar Chem 55: 347-358

Bett BJ (2000) Benthic ecology of the Faeroe-Shetland Channel, Section 4.3.1 in Environmental Surveys of the Seafloor of the UK Atlantic Margin, Atlantic Frontier Environmental Network [CD-ROM, 53 pp, Geotek Limited, Daventry, Northants NN11 5EA, UK]

Brassell SC, Eglinton G (1986) Molecular geochemical indicators in sediments. In: Sohn M (ed) Organic Marine Geochemistry, 305. Amer Chem Soc, Washington, DC, pp 10-31

Cabana G, Rasmussen JB (1994) Modelling food chain structure and contaminant bioaccumulation using stable nitrogen isotopes. Nature 372: 255-257

Christie WW (1982) Esterification of fatty-acids in adipose-tissue. J Sci Food Agricult 33: 809-809

Checkley DM, Entzeroth LC (1985) Elemental and isotopic fractionation of carbon and nitrogen by marine, planktonic copepods and implications to the marine nitrogen cycle. J Plankton Res 7: 553-568

Corner EDS, O'Hara SCM, Neal AC, Eglinton G (1986) Copepod faecal pellets and the vertical flux of biolipids. In: Corner EDS, O'Hara SCM (eds) The Biological Chemistry of Marine Copepods. Oxford Sci Publ, pp 260-321

Dalsgaard J, St John M, Kattner G, Muller-Navarra D, Hagen W (2003) Fatty acid trophic markers in the pelagic marine environment. Adv Mar Biol 46: 225-340

DeLong EF, Yayanos AA (1985) Adaptation of the membrane lipids of a deep-sea bacterium to changes in hydrostatic pressure. Science 228: 1101-1103

De Mol B, Van Rensbergen P, Pillen S, Van Herreweghe K, Van Rooij D, McDonnell A, Huvenne V, Ivanov M, Swennen R, Henriet JP (2002) Large deep-water coral banks in the Porcupine Basin, southwest of Ireland. Mar Geol 188: 193-231

De Mol B, Henriet JP, Canals M (2005) Development of coral banks in Porcupine Seabight: do they have Mediterranean ancestors? In: Freiwald A, Roberts JM (eds) Cold-water Corals and Ecosystems. Springer, Berlin Heidelberg, pp 515-533

DeNiro MJ, Epstein S (1981) Influence of diet on the distribution of nitrogen isotopes in animals. Geochim Cosmochim Acta 45: 341-351

Fang J, Barcelona MJ, Nogi Y, Kato K (2000) Biochemical implications and geochemical significance of novel phospholipids of the extremely barophilic bacteria from the Marianas Trench at 11,000 m. Deep-Sea Res I 47: 1173-1182

Freiwald A (2002) Reef-forming cold-water corals. In: Wefer G, Billett D, Hebbeln D, Jørgensen BB, Schlüter M, van Weering T (eds) Ocean Margin Systems. Springer, Berlin Heidelberg, pp 365-385

Freiwald A, Wilson JB. Henrich R (1999) Grounding Pleistocene icebergs shape recent deep-water coral reefs. Sediment Geol 125: 1-8

Freiwald A, Hühnerbach V, Lindberg B, Wilson JB, Campbell J (2002) The Sula Reef Complex, Norwegian shelf. Facies 47: 179-200

Graeve M, Hagen W, Kattner G (1994) Herbivorous or omnivorous - on the significance of lipid compositions as trophic markers in Antarctic copepods. Deep-Sea Res 41: 915-924

Harland AD, Navarro JC, Spencer Davies P, Fixter LM (1993) Lipids of some Caribbean and Red Sea corals: total lipid, wax esters, triglycerides and fatty acids. Mar Biol 117: 113-7

Harvey HR, Bradshaw SA, Ohara SCM, Eglinton G, Corner (1988) Lipid composition of the marine dinoflagellate *Scrippsiella trochoidea*. Phytochem 27: 1723-1729

Heath MR, Jónasdóttir SH (1999) Distribution and abundance of overwintering *Calanus finmarchicus* in the Faeroe-Shetland channel. Fish Oceanogr 8 (Suppl 1): 40-60

Heikoop JM, Dunn JJ, Risk MJ, Tomascik T, Schwarcz HP, Sandeman IM, Sammarco PW (2000a) $\delta^{15}N$ and $\delta^{13}C$ of coral tissue show significant inter-reef variation. Coral Reefs 19: 189-193

Heikoop JM, Risk MJ, Lazier AV, Edinger EN, Jompa J, Limmon GV, Dunn JJ, Browne DR, Schwarcz HP (2000b) Nitrogen-15 signals of anthropogenic nutrient loading in reef corals. Mar Pollut Bull 40: 628-636

Heikoop JM, Hickmott DD, Risk MJ, Shearer CK, Atudorei V (2002) Potential climate signals from the deep-sea gorgonian coral *Primnoa resedaeformis*. Hydrobiologia 471: 117-124

Henriet JP, De Mol B, Pillen S, Vanneste M, Van Rooij D, Versteeg W, Croker PF, Shannon PM, Unnithan V, Bouriak S, Chachkine P (1998) Gas hydrate crystals may help build reefs. Nature 391: 648-649

Hesslein RH, Capel MJ, Fox DE, Hallard KA (1991) Stable isotopes of sulphur, carbon, and nitrogen as indicators o trophic level and fish migration in the Lower Mackenzie Rive Basin, Canada. Canad J Fish Aquat Sci 4: 2258-2265

Hovland M, Croker PF, Martin M (1994) Fault-associated seabed mounds (carbonate knolls) off western Ireland and North-West Australia. Mar Petrol Geol 11: 232-246

Hovland M, Thomsen E (1997) Cold-water corals - are they hydrocarbon seep related? Mar Geol 137: 159-164

Huvenne VA, Blondel IP, Henriet JP (2002) Textural analyses of sidescan sonar imagery from two mound provinces in the Porcupine Seabight. Mar Geol 189: 323-341

Iken K, Brey T, Wand U, Voigt J, Junghans P (2001) Food web structure of the benthic community at the Porcupine Abyssal Plain (NE Atlantic): a stable isotope analysis. Progr Oceanogr 50: 383-405

Jøstensen J, Landfald B (1997) High prevalence of polyunsaturated fatty acid producing bacteria in Arctic invertebrates. FEMS Microbiol Lett 151: 95-101

Kenyon NH, Ivanov MK, Akmetzhanov AM (1998) Cold-water carbonate mounds and sediment transport on the Northeast Atlantic margin. IOC Tech Ser Paris UNESCO 52, 179 pp

Kenyon NH, Akmetzhanov AM, Wheeler AJ, van Weering TCE, de Haas H, Ivanov, MK (2003) Giant carbonate mud mounds in the southern Rockall Trough. Mar Geol 195: 5-30

Kidd KA, Schindler DW, Hesslein RH, Muir DCG (1995) Correlation between stable isotope ratios and concentrations of organochlorines in biota from a freshwater food web. Sci Total Environ 161: 381-390

Kiriakoulakis K, Stutt E, Rowland SJ, Vangriesheim A, Lampitt RS, Wolff GA (2001) Controls on the organic chemical composition of settling particles in the Northeast Atlantic Ocean. Progr Oceanogr 50: 65-87

Kiriakoulakis K, White M, Bett BJ, Wolff GA (2004) Organic biogeochemistry of the Darwin Mounds, a deep-water coral ecosystem, of the NE Atlantic. Deep-Sea Res I 51: 1937-1954

Kiriakoulakis K, Fisher E, Freiwald A, White M, Wolff GA (submitted) Biogeochemistry of deep-water coral/mound systems at the NW European Continental Margin. Int J Earth Sci

Kling GW, Fry B, O'Brien WJ (1992) Stable isotopes and planktonic trophic structure in arctic lakes. Ecology 73: 561-566

Latyshev NA, Naumenko NV, Svetashev VI, Latypov YY (1991) Fatty acids of reef-building corals. Mar Ecol Progr Ser 76: 295-301

Mancini I, Guerriero A, Guella G, Bakken T, Zibrowius H, Pietra F (1999) Novel 10-hydroxydocosapolyenoic acids from deep-water scleractinian corals. Helvet Chim Acta 82: 677-684

Masson DG, Bett BJ, Billett DSM, Jacobs CL, Wheeler AJ, Wynn RB (2003) The origin of deep-water, coral-topped mounds in the northern Rockall Trough, Northeast Atlantic. Mar Geol 194: 159-180

Meyers PA (1979) Polyunsaturated fatty acids in coral: indicators of nutritional sources. Mar Biol Lett 1979 1: 69-75

Miniwaga M, Wada E (1984) Stepwise enrichment of N along food chains: further evidence and the relation between $\delta^{15}N$ and animal age. Geochim Cosmochim Acta 48: 1135-1140

Miyake Y, Wada E (1967) The abundance ratio of $^{15}N/^{14}N$ in marine environments. Records of Ocean Works of Japan 9: 32-53

Mortensen PB (2001) Aquarium observations on the deep-water coral *Lophelia pertusa* (L., 1758) (Scleractinia) and selected associated invertebrates. Ophelia 54: 83-104

Oku H, Yamashiro H, Onaga K, Iwasaki H, Takara K (2002) Lipid distribution in branching coral *Montipora digitata*. Fish Sci 68: 517-522

Owens NJP (1987) Natural variations in ^{15}N in the marine environment. Adv Mar Biol 24: 389-451

Parrish CC, Abrajano TA, Budge SM, Helleur RJ, Hudson ED, Pulchan K, Ramos C (2000) Lipid and phenolic biomarkers in marine ecosystems: analysis and applications. In: Wangersky P (ed) The Handbook of Environmental Chemistry. Part D. Marine Chemistry. Springer, Berlin Heidelberg, pp 193-223

Peterson BJ, Fry B (1987) Stable isotopes in ecosystem studies. Ann Rev Ecol Systems 18: 293-320

Planque B, Batten SD (2000) *Calanus finmarchicus* in the North Atlantic: the year of *Calanus* in the context of interdecadal change. ICES J Mar Sci 57: 1528-1535

Ratnayake WM, Ackman RG (1979) Fatty alcohols in capelin, herring and mackerel oils and muscle lipids. I Fatty alcohol details linking dietary copepod fat with certain fish depot fats. Lipids 14: 795-803

Risk MJ, Erdmann MV (2000) Isotopic composition of nitrogen in stomatopod (Crustacea) tissues as an indicator of human sewage impacts on Indonesian coral reefs. Mar Pollut Bull 40: 50-58

Rogers AD (1999) The biology of *Lophelia pertusa* (LINNAEUS 1758) and other deep-water reef-forming corals and impacts from human activities. Int Rev Hydrobiol 84: 315-406

Sargent JR, Parkes RJ, Mueller-Harvey I, Henderson RJ (1987) Lipid biomarkers in marine ecology. In: Sleigh MA (ed) Microbes in the Sea. Wiley and Sons, New York, pp 119-138

Schoeninger MJ, DeNiro MJ (1984) Nitrogen and carbon isotopic composition of bone collagen from marine and terrestrial animals. Geochim Cosmochim Acta 48: 625-639

Steele KW, Daniel RM (1978) Fractionation of nitrogen isotopes by animals: a further complication to the use of variations in the natural abundance of ^{15}N for tracer studies. J Agricult Sci 90: 7-9

Toda H, Wada E (1990) Use of $^{15}N/^{14}N$ ratios to evaluate the food source of the mysid, *Neomysis intermedia* Czerniawsky, in a eutrophic lake in Japan. Hydrobiologia 194: 85-90

Wilson JB (1979). The distribution of the coral *Lophelia pertusa* (L) [*L. prolifera* (Pallas)] in the north-east Altantic. J Mar Biol Ass UK 59: 149-164

Van Rooij D, De Mol B, Huvenne V, Ivanov M, Henriet JP (2003) Seismic evidence of current-controlled sedimentation in the Belgica mound province, upper Porcupine slope, southwest of Ireland. Mar Geol 195: 31-53

Volkman, JK, Jeffrey SW, Nichols PD, Rogers GI, Garland CD (1989) Fatty-acid and lipid-composition of 10 species of microalgae used in mariculture. J Exp Mar Biol Ecol 128: 219-240

Yamashiro HH, Oku H, Higa H, Chinen I, Sakai K (1999) Composition of lipids, fatty acids and sterols in Okinawan corals. Comp Biochem Phys B 122: 397-407

Calcifying extracellular mucus substances (EMS) of *Madrepora oculata* – a first geobiological approach

Joachim Reitner

Geobiology-GZG, Göttingen University, Goldschmidtstr. 3, D-37077 Göttingen, Germany
  (jreitne@gwdg.de)

Abstract. Colonial non-zooxanthellate corals from deep-water coral reefs, *Lophelia pertusa* and *Madrepora oculata,* produce large amounts of extracellular mucus (EMS). This mucus has various functions, e.g., an antifouling capability protecting the coral skeleton from attacks of endolithic and boring organisms. Both corals show thick epithecal and exothecal skeletal parts with a clear lamellar growth pattern. The formation of the epitheca is unclear. It is supposed that the EMS play a central role during the calcification process of the epithecal skeletal parts. Staining with the fluorochrome tetracycline has shown an enrichment of Ca^{2+} ions in the mucus. In order to investigate this hypothesis, the protein content of the mucus and the intracrystalline organic matter from newly formed epithecal aragonite of *Madrepora oculata* was determined *via* sodium dodecyl sulfate (SDS) gel electrophoresis. Identical band patterns within both substances could be detected, one around 45 kDa molecular weight and a cluster around 30-35 kDa molecular weight. The occurrence of identical protein patterns within the mucus and in the newly formed aragonite confirms the idea that the mucus plays an important role during the organomineralization of the coral epitheca.

Keywords. Biomineralisation, extracellular mucus, martix proteins, *Madrepora*, SDS gel electrophoresis

Introduction

Many aspects of the biomineralization of scleractinian skeletons are still unclear. Various authors have described in detail the microstructure of the aragonitic skeleton (Bryan and Hill 1941; Johnston 1980; Gladfelter 1984; Constantz 1986; Constantz and Meike 1989; Cuif et al. 1996; Cuif and Dauphin 1998; Stolarski 2003; and many others). Only some of them have studied the interaction of organic matter and skeletal formation. The hypothesis that acidic organic macromolecules control the nucleation of calcium carbonate minerals developed by Wilbur and Simkiss (1979),

Weiner et al. (1983) and Addadi and Weiner (1985, 1992) provides a fundamentally new view of the calcium carbonate formation and entire architecture of the coral skeleton. The basic idea is that COO^--rich (acidic) proteins form peptides with ß-sheet structures. These ß-sheets or flat-monolayer proteins have highly organized COO^- groups with distinct distances. Divalent cations bond to this COO^- and form an interface which is characterized by a crystal base plane (001 plane). Few authors have used this idea and have started to extract intracrystalline organic matter and to analyse it (Young 1971; Mitterer 1978; Constantz and Weiner 1988; Cuif and Gautret 1995; Cuif et al. 1996; Dauphin and Cuif 1997; Gautret et al. 1997; Allemand et al. 2001).

The focus of the present paper is to show that the proteins of extracellular mucus substances (EMS) mediate the growth of the epitheca of the skeleton of *Madrepora oculata*. The EMS is a complex mixture of weakly acidic proteins and carbohydrates and has some similarities with microbial exopolymeric substances (EPS). Formation of calcium carbonate minerals *via* EPS is not an enzymatically controlled biomineralization. This process is mediated by macromolecules forming the EPS and is called EPS-controlled organomineralization (Reitner 1993; Defarge and Trichet 1995; Reitner et al. 1995, 2001; Trichet and Defarge 1995; Arp et al. 2003).

Freiwald and Wilson (1998) discussed the role and importance of the mucus of *Lophelia* in the formation of deep cold-water coral reefs. They observed that the mucus has a strong antifouling capability including development of biofilms, stops boring attacks, and cleans the tissue from extraneous particles. The most intriguing observation was the reaction of the coral by the settlement of Foraminifera (e.g., *Hyrrokkin sarcophaga*) and the tube-forming polychaete *Eunice norvegica* on the coral branches. Due to the settlement stress, the coral produces large amounts of mucus entrapping the upward growing organisms and *via* this process thickens the epitheca. The organic tubes of *Eunice norvegica* are completely calcified in this way which additionally stabilizes the coral colony. Comparable mucus-controlled process was observed in cementing freshly broken coral branches. This organomineralizing process *via* stress mucus stabilizes the entire reef of azooxanthellate colonial corals. This is a crucial process in the growth of deep-water coral reefs.

Material and methods

The corals were collected during an expedition with the RV "Poseidon" in 1999 (POS 254) near the Sula Ridge (64°N/8°E) 80 km east of Trondheim (Norway). The cold-water *Lophelia* reefs occur in water depth around 250-350 m (Freiwald et al. 1997, 2002; Reitner and Hoffmann 2003). The specimens were collected using the manned German submersible "Jago".

The specimens were immediately fixed with 2 % buffered formol and later stored in 70 % ethanol. Some specimens were fixed with 2 % glutardialdehyde and post fixed with 2 % osmium tetroxide. For biochemical analyses the corals were immediately frozen at -20°C. The coral mucus was extracted from living

specimens by stressing them with freshwater (Fig. 1). This shock-stress induces the organism to produce an enormous amount of mucus. More than 100 ml mucus was produced by a 20 cm-sized *Madrepora* dendroid colony. 50 ml of the mucus were sterilized using $HgCl_2$ and immediately frozen. The non-sterilized mucus was also immediately frozen. The *Madrepora* colony was treated three times with fresh water after a recovery period of 15 minutes. The first mucus was slightly pink in colour, the others were clear.

The formalin-fixed specimens were embedded in resin and then cut with a hard part microtome and stained with various histochemical dyes. The Ca^{2+} load was

Fig. 1 Living *Madrepora* specimen stressed with freshwater. This shock-stress induces the organism to produce an enormous amount of mucus. Picture was taken during the RV "Poseidon" expedition POS 254 in 1999

qualitatively determined using the fluorochrome tetracycline in living colonies of *Madrepora* and *Lophelia*. The mucus was enriched in Ca^{2+} exhibiting a strong yellow-green fluorescence when a narrow band UV-filter linked with an epifluorescence microscope Axioplan/Zeiss (Fig. 2) was applied. For description of the detailed procedure see Reitner (1993).
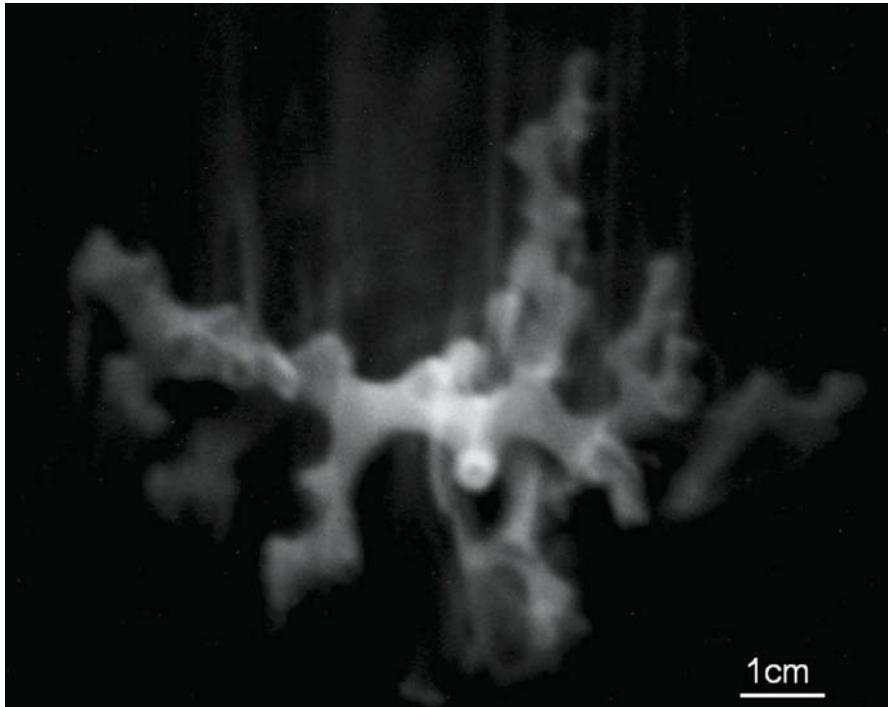
Fig. 2 Living *Madrepora* specimen stained with the Ca^{2+} detecting fluorochrome tetracycline. Ca^{2+}-rich mucus substances fluoresce bright yellow using a narrow band UV-filter. The EMS exhibits a strong yellow fluorescence

The samples for biochemical analyses using High Pressure Liquid Chromatography-HPLC and electrophoresis were frozen. For decalcification, 100 mg of the sample were dissolved in pH 4-controlled acetic acid for 10 hours on a shake table. The insoluble fraction was removed by centrifugation. The insoluble pellet was removed and frozen again. The supernatant was concentrated using Omega-Microsept 3-10 kDa concentrators. The concentrate was carefully desalted using 3-4x HPLC-H_2O (ultrafiltered MilliQ water) with a minimum of 90 minutes centrifugation. After this procedure the concentrate was hydrolyzed with 6N HCl. The hydrolyzed extract was derivatised with the Waters AccQ Flour Kit and analysed using a Waters HPLC. Further detailed descriptions of the analytical procedure see Gautret et al. (1997) and Reitner et al. (1995). For electrophoresis the samples were decalcified with EDTA. Protein concentrations were determined

by the protein quantification assay Bradford (1976) (bovine serum albumin (BSA) BIO-RAD). Samples were electrophoresed on a 14 % sodium dodecyl sulfate (SDS) gel and silver stained. Isoelectrical focussing of proteins was done with precast gels (pH-range 3-10, SERVA). Molecular weights were determined using SDS-page electrophoresis (SDS-polyacrylamid) (further detailed descriptions of the analytical procedure see Lange et al. (2001)).

In vitro mineralization-"inhibition" assay

This experiment is crucial to the understanding of the role of organic molecules during the calcium carbonate crystal formation. *In vitro* mineralization inhibition experiments were carried out based on the procedures described by Wheeler et al. (1981), Gunthorpe et al. (1990) and Lange et al. (2001) using bulk intracrystalline native organic matter that has not been treated with SDS. It is possible to control the molecular weights using SDS-page electrophoresis cutting the stained bands and extraction of the organic matter from the gel. Inhibition experiments give indications of the Ca^{2+}-binding capability of the organic matter and consequently the importance for skeletal and organomineral formation. Mineralization was studied in a reaction tube containing 400 μl $NaHCO_3$ (1 M), 19 ml aqua bidest., and 200 μl sample or 200 μl aqua bidest. in the control assay, respectiveley. The solution contains total proteins or Ca^{2+}-binding proteins. Protein concentration was 0.5 μg ml^{-1} if not indicated otherwise. In order to start the reaction, 400 μl $CaCl_2$ (1 M) were added. Inhibition of mineralization was determined by measuring the pH over a certain period. The extremely acidic artificial peptide polyasparagine 30 kDa and bidest H_2O were used as standard reaction molecules. The mineralization event could be observed through the occurrence of the turbidity of the solution and the drop of the pH to 7 (CP-calcification point). During this process protons were released from $NaHCO_3$ according to the following reaction:

$$NaHCO_3 + CaCl_2 \longrightarrow CaCO_3 + H^+ + 2\ Cl^- + Na^+ \qquad \text{(Fig. 8).}$$

Results

Sections through the dendroid stems of a *Madrepora* colony exhibit two types of mineralization pattern of the aragonite (Fig. 3). The inner corallite area including septa is formed by a microcrystalline fabric, whereas the outer and superficial areas are formed of fibre bundles of elongated aragonite crystals (sclerodermites) which are modified spherulites starting in the so-called "centre of calcification". These centres ("seeds") are small spherulites and clearly distinct from the sclerodermites (Constantz and Meike 1989; Cuif et al. 1999). These seed areas show an enrichment of organic remains and are areas of initial calcification. The microcrystalline fabric is also part of this initial growth process. However, this process is not the goal of this investigation. The outer epitheca demonstrates a clear lamellar skeletal growth pattern. The epitheca is covered by an epidermal cell layer. Between the epidermal
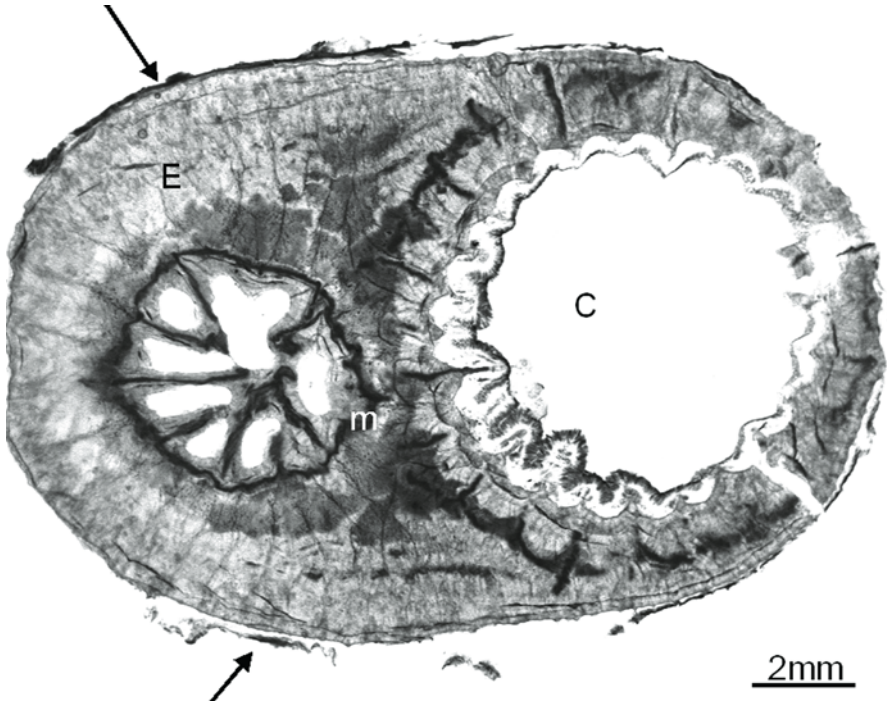
Fig. 3 Cross section through a coral stem of *Madrepora*. Dark areas are microcrystalline aragonite crystals. Bright areas are fibrous aragonite aggregates forming coral-typical clusters. Within the epithecal area a lamellar growth pattern is visible. The epitheca is covered with an epidermal cell layer. Arrows: epithecal tissue, epidermal cell-layer, E: epithecal fibrous aragonite, m: microcrystalline aragonite, c: corallite

cell layer and the calcified skeleton a thin mucus layer (50-100 μm) is formed. The mucus is enriched in small pits between protruding crystal bundles (Fig. 4). Using the fluorochrome tetracycline the mucus exhibits a very strong yellow-green fluorescence when UV-light is applied, indicating an enrichment of Ca^{2+} within the mucus (Fig. 4). Obviously the epitheca grows in certain phases. The lamellae have an average thickness of 50-200 μm. It is assumed that the growth of the epitheca is controlled by the amount of mucus during certain times, possibly during environmental stress phases.

The first crucial question is: Is the epithecal mucus identical with the stress-mucus? In order to test this, living *Madrepora* specimens were stressed with freshwater. This shock-stress induces the organism to produce an enormous amount of mucus (Fig. 1). The different mucus types were analysed *via* 14 % SDS gel electrophoresis in order to check the protein composition (Fig. 5). From the stress-mucus three samples were analysed. The first extract had a slightly pink colour and the remaining samples were clear. The observed protein band patterns were similar in all gel electrophoresis runs. Three-band-patterns of the gel are significant with respect to the following considerations. It was possible to distinguish a single band
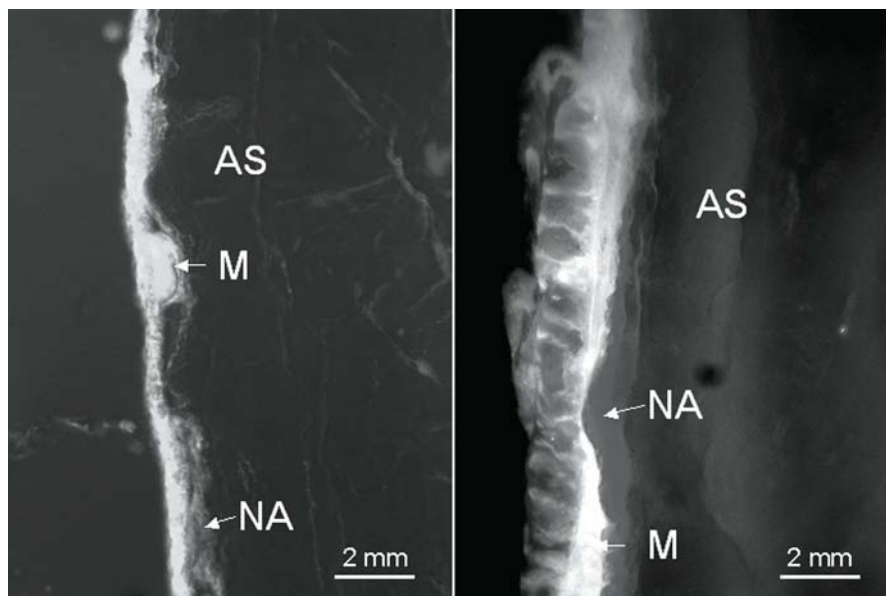
Fig. 4 Hard part microtome section. The specimen was stained with tetracycline. Underneath the epidermal cell layer the calcifying mucus layer exhibits a strong bright yellow fluorescence. The newly formed aragonite also has a weak yellow fluorescence. This fluorescence is caused by mucus remains within the aragonite crystals. The mature portions of the epitheca is non-fluorescent. M: Ca^{2+}-binding mucus, NA: newly formed aragonite, AS: mature aragonitic skeleton

with a molecular weight of ca. 18 kDa, a four-band-pattern with approximately 30-35 kDa and a further single band with ca. 45 kDa. Very characteristic is the four-band-cluster with a strong 30 kDa band. Within control measurements, this band was sometimes divided into two tight-distant bands. In order to investigate the mucus beneath the epidermal cell layer, the superficial organic matter including the mucus layer was treated with SDS in order to remove the proteins. The band pattern of this extract is more diverse due to the protein content of the epidermal cell layer. However, the same band pattern which was detected in the stress mucus was also present. This result is an excellent indication that both mucus types exhibit biochemical similarities. However, the carbohydrate composition has not yet been analysed.

The second crucial question is: Does the mucus play any role during the calcification of the epitheca? In order to investigate this question the outer surface of a *Madrepora* coral stem was cleaned with sodium hypochloride in order to remove all superficial organic matter. The young superficial aragonite layer (ca. 1 mm) and a deeper mature layer in ca. 3 mm depth of the epitheca were sampled. The cleaned aragonite was powdered and intracrystalline organic matter was extracted using EDTA/NaN$_3$ and formic acid. The protein content was much lower than observed in the mucus and the amount decreased significantly within the older inner layer (Fig. 8). Only within the young portion of the epitheca were intracrystalline proteins

detected. Within the mature older portion no clear band pattern was detected. Intriguingly the 30 kDa band pattern was clearly detectable as well as the 45 kDa
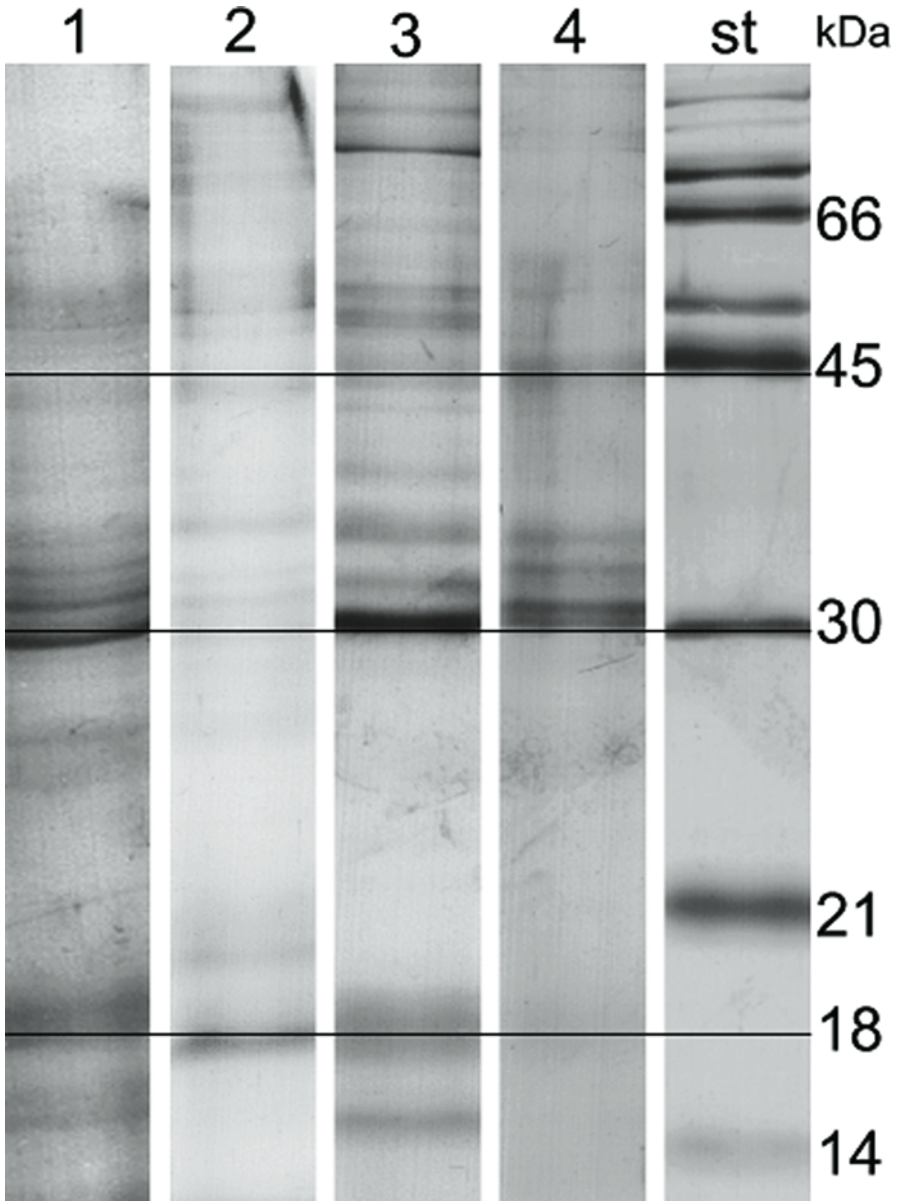
Fig. 5 Silver-stained 14 % SDS gel electrophoresis runs of the stress-EMS (run #1 and #2), epidermal cell-layer including the mucus below the cell-layer (run #3), and the newly formed carbonate (run #4). The stress mucus demonstrates three characteristic band patterns which are also detected in run #3. In run #4 only the 45 kDa and the 30 kDa-cluster is present; st: molecular weight standard

band within the newly formed aragonite. The 30 kDa band cluster consists of three bands, of which the 30 kDa band is the most prominent one and in some electrophoresis runs it is divided into two tight-distant bands as seen in the two mucus types. The 30 kDa band pattern and the 45 kDa band within the skeletal carbonate are identical with the pattern seen in the stress mucus and within the epithecal mucus. This is a clear indication that the EMS is part of the mineralizing system of the epitheca (Fig. 5).

From all three EMS extracts, young, and mature portion of the *Madrepora* epitheca, bulk amino acid analyses (fraction <10 kDa) were carried out (Figs. 6, 7). Amino acid analyses from native proteins separated *via* electrophoresis unfortunately did not give good data sets which was due to the extremely small amount of sampled proteins. With ca. 13 mol% asparagine (asp) and glutamine (glu) the overall EMS is only moderately acidic (Fig. 6). Isoelectric focusing of the mucus proteins demonstrates weakly acidic protein band pattern which corresponds with the measured amounts of asp and glu. More important is the observation that the ratio of asp and glu within the EMS is roughly identical.

In contrast to the extracts from the carbonate, the amount of the amino-sugar D-glucosamine is relativley high. It is assumed that the mucus contains high amounts of glycoproteins, however, the glucidic compounds have not yet been analysed. Histological staining with Alcian blue supports this assumption, because the mucus is strongly stained blue. Goreau (1956) has described a mucopolysaccharid layer located outside the basal ectodermal cell-layer and it was supposed that this layer may play a role as a template during the skeleton growth (Milliman 1974).
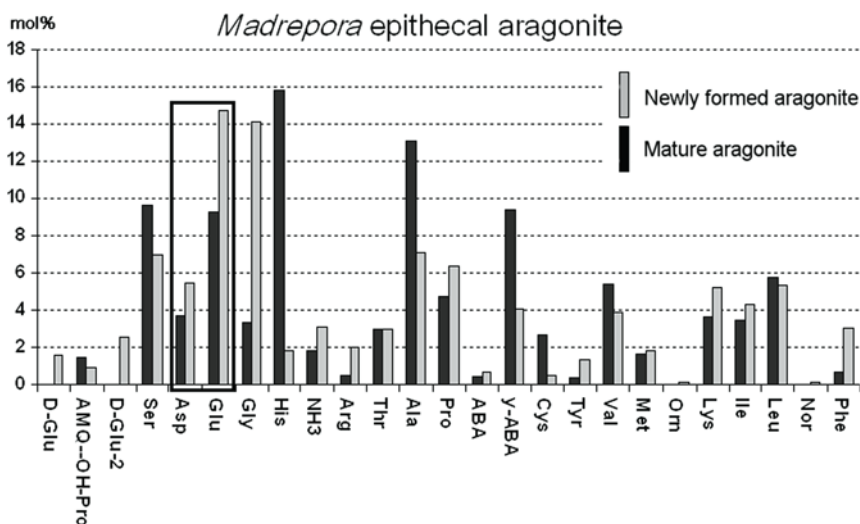
Fig. 6 Bulk amino acid analyses of the stress-EMS. The three extracts are more or less identical, except the excursion of glycine in the 3rd extraction. The acidic amino acids are weakly represented. The ratio of asp/glu (0.79) is more or less similar in all three extracts. All extracts have moderate amounts of amino sugars

However, different results have been gained from the aragonitic carbonate (Fig. 7). Within the newly formed epithecal aragonite, asp and glu represent ca. 20 % of the amino acids. Glutamic acid dominates with 14.6 %. D-glucosamine is significantly reduced. The amino acid content of the mature skeleton part differs in some way in comparison with the young portion. Comparable with the young skeletal portion is the asp/glu ratio with 0.39 and the high amount of ser. High amounts of ala and γ-amino butyric acid (γ-aba) differ in contrast to EMS. Comparable ratios are to be seen in the young portion as well. The extreme excursion of the histidine peak remains unexplained. No amino-sugars were detected. The differences in the bulk analyses are explained by the different bulk protein composition of the EMS and organic remains within the aragonite crystals. The mature portion of the aragonitic skeleton does not show any protein band pattern in gel electrophoresis runs and therefore the analysed amino acid composition is already a diagentic/taphonomic product. We have seen comparable data within an old basal skeleton of *Astrosclera willeyana*, a coralline sponge (Wörheide et al. 1997). The results from the inhibition
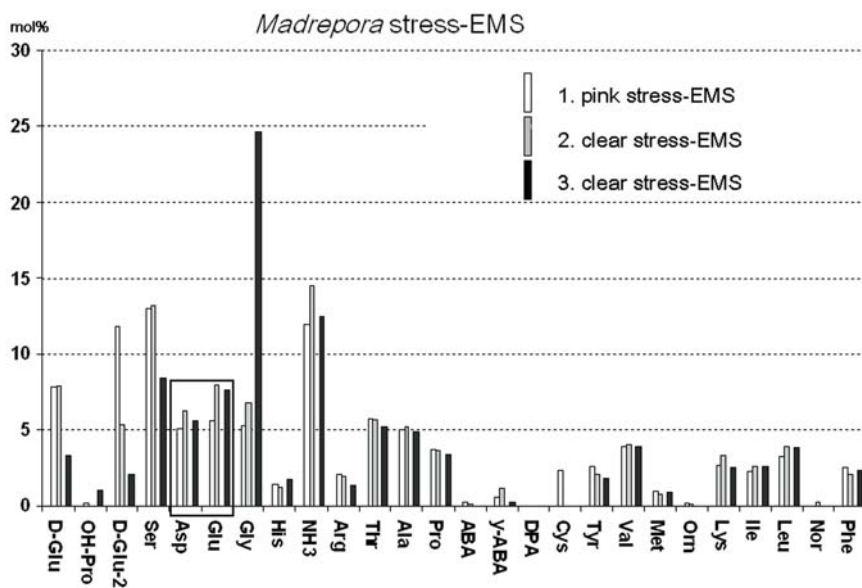
Fig. 7 Bulk amino acid analysis of the newly formed and mature aragonite. The analysed organic matter of the newly formed aragonite is significantly more acidic (ca. 20 mol% asp and glu). The glycine content is also very high as seen in the 3rd extraction of stress EMS. The amino sugar content is significantly decreased, however, still present. The data correspond well with observed weak fluorescence of the aragonite. The organic matter of the mature aragonite is less acidic. However, the ratio of asp/glu is more or less similar as observed within the newly formed aragonite. No amino sugars were detected. Glycine value is significantly lower. In contrast to all other amino acid analyses, the amino acid distribution pattern differs significantly possibly as a result of beginning diagenesis. Within the mature skeleton no distinct electrophoretic band pattern was visible

experiments with the various extracts are intriguing (Fig. 8). In order to carry out this experiment, the EDTA-extract was performed. The EMS, the young skeletal portion and the mature ones exhibit more or less the same weak inhibition character compared with a 30 kDa polyasparagine peptide. The crystallisation point of all extracts is the same! The probably calcifying mucus does not exhibit a strong inhibition character. This observation corresponds well with the amino acid analyses which have shown only moderate amounts of asp and glu.

The observed weak acidic composition of the soluble matrices are in contrast to the data from Gautret et al. (1997). They have detected much higher asp values with up to 40 % of the entire amino acid composition. The glu values are extremely low at around 5 %. A possible reason to explain this difference is the bulk protein composition of the entire skeleton. In contrast to Gautret et al. (1997), who used the entire calcified coral skeleton for analyses, only the EMS and the outermost portion of the coral skeleton were analysed. In any case bulk amino acid analyses are quite problematic to interpret. It is difficult to verify the gel electrophoresis data with the bulk amino acid data. Experiments in which the protein bands are cut from the gel and the single proteins are extracted from the acrylamide gels were successful. However, the amount of extracted protein was too low for biochemical analyses and additional inhibition experiments. The quantity of proper material available was too small to enrich certain molecular weight fractions for biochemical experiments.
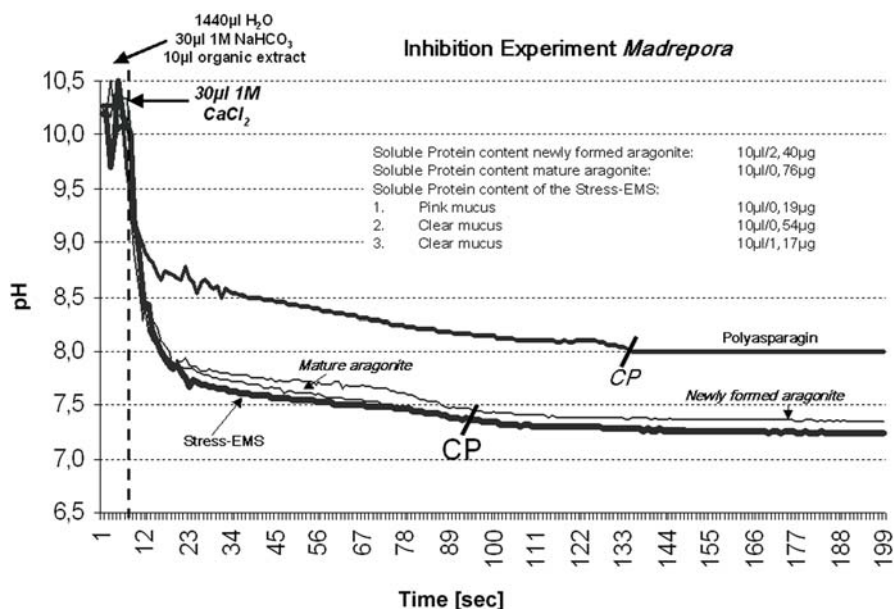
Fig. 8 Calcifying experiment of the stress EMS and organic matter from the aragonitic coral skeleton does not exhibit a strong inhibition of the organic matter until calcification. Intriguingly is that the onset of calcification (CP) happened more or less for all three organic extracts in the same time

Conclusions

1. It was possible to distinguish two anatomical sites with protein-rich mucus substances. *Madrepora* produces an extracellular stress mucus which covers the outer epidermal cell layer of the epitheca. The second mucus is located between the epidermal cell layer and the aragonitic skeleton. Both mucus types bear a comparable protein composition analysed *via* SDS gel electrophoresis. It is possible to distinguish a single protein with a molecular weight of ca. 18 kDa, a four-protein-cluster with approximately 30-35 kDa and a further single protein with ca. 45 kDa.

2. It was possible to extract a soluble protein composition from the newly formed aragonite crystals. Two band patterns are identical with the results obtained from both mucus types. A single protein band with a molecular weight fraction of ca. 45 kDa and the 30-35 kDa protein cluster was detectable. In some electrophoresis runs the very prominent 30 kDa band is divided into two. The IEF-gel analyses show that the mucus proteins and matrix proteins from the epitheca are weakly acidic (pH 5).

3. These data correspond with the bulk amino acids from the mucus and the skeleton. The inhibition experiment shows an intriguing result. The crystallisation point, which stops the inhibition potential of the macromolecules, was the same as in all extracts. This means that only a certain group of molecules inhibit a rapid calcification. However, in contrast to polyasparagine and other very acidic macromolecules, the measured inhibition is only weak.

4. Based on the electrophoresis data, the EMS obviously play an important role in the formation of the thick epithecal skeletal parts of *Madrepora oculata* and obviously plays a crucial role in the formation of extended deep-water azooxanthellate coral reefs.

Acknowledgements

References

Addadi L, Weiner S (1985) Interactions between acidic proteins and crystals: stereochemical requirements in biomineralisation. Proc Natl Acad Sci USA 82: 4110-4114

Addadi L, Weiner S (1992) Kontroll- und Designprinzipien bei der Biomineralisation. Angew Chem 104: 159-176

Allemand D, Tambutté È, Girard J-P, Jaubert J (2001) Organic matrix synthesis in the scleractinian coral *Stylophora pistillata:* role in biomineralization and potential target of the organotin tributyltin. J Exp Biol: 201: 2001-2009

Arp G, Reimer A, Reitner J (2003) Microbialite formation in seawater of increased alkalinity, Satonda Crater Lake, Indonesia. J Sediment Res 73: 105-127

Bradford M (1976) A rapid and sensitive method for the quantitation of microgram quantities of protein utilizing the principle of protein-dye binding. Anal Biochem 72: 248-254

Bryan W, Hill D (1941) Spherulitic crystallization as a mechanism of skeletal growth in the Hexacorals. Proc R Soc Queensland 52: 78-91

Constantz BR (1986) Coral skeleton construction: a physiochemically dominated process. Palaios 1: 152-157

Constantz BR, Meike A (1989) Calcite centres of calcification in *Mussa angulosa* (Scleractinia). In: Crick RE (ed) Origin, Evolution and modern Aspects of Biomineralization in Plants and Animals. Plenum Press, New York, pp 201-207

Constantz BR, Weiner S (1988) Acidic macromolecules associated with the mineral phase of scleractinian coral skeletons. J Exp Zool 248: 253-258

Cuif J-P, Dauphin Y (1998) Microstructural and physico-chemical characterization of "centers of calcification" in septa of some Recent scleractinian corals. Paläont Z 72: 257-270

Cuif J-P, Dauphin Y, Denis A, Gautret P (1996) The organomineral structure of coral skeletons: a potential source of new criteria for scleractinian taxonomy. Bull Inst Océanogr Monaco Spec Issue 14: 359-367

Cuif J-P, Dauphin Y, Gautret P (1999) Compositional diversity of soluble mineralizing matrices in some recent coral skeletons compared to fine-scale growth structures of fibres: discussion of consequences for biomineralization and diagenesis. Int J Earth Sci 88: 582-592

Cuif J-P, Gautret P (1995) Gluides et proteins de la matrice soluble des biocristaux de scleractiniaires acroporides. CR Acad Sci Paris 320 Ser IIa: 273-278

Dauphin Y, Cuif J-P (1997) Isoelectric properties of the soluble matrices in relation to the chemical composition of some scleractinian skeletons. Electrophoresis 18: 1180-1183

Defarge C, Trichet J (1995) From biominerals to "organominerals": the example of the modern lacustrine calcareous stromatolites from Polynesian atolls. Bull Inst Océanogr Monaco Spec Issue 14: 265-271

Freiwald A, Wilson JB (1998) Taphonomy of modern deep, cold-temperate water coral reefs. Hist Biol 13: 37-52

Freiwald A, Henrich R, Pätzold J (1997) Anatomy of a deep-water coral reef mound from Stjernsund. SEPM Spec Publ 56: 141-161

Freiwald A, Hühnerbach V, Lindberg B, Wilson JB, Campbell J (2002) The Sula Reef Complex, Norwegian Shelf. Facies 47: 179-200

Gautret P, Cuif, J-P, Freiwald A (1997) Composition of soluble mineralizing matrices in zooxanthellate and non-zooxanthellate scleractinian corals: biochemical assessment of photosynthetic metabolism through the study of a skeletal feature. Facies 36: 189-194

Gladfelter EH (1984) Skeletal development in *Acropora cervicornis*. A comparison of monthly rates of linear extension and calcium carbonate accretion measured over a year. Coral Reefs 3: 51-57

Goreau T (1956) Histochemistry of mucopolysaccharide-like substances and alkaline phosphatase in Madreporaria. Nature 177: 1029-1030

Gunthorpe ME, Sikes CS, Wheeler AP (1990) Promotion and inhibition of calcium carbonate crystallization in vitro by matrix protein from blue crab exoskeleton. Biol Bull 179: 191-200

Johnston I (1980) The ultrastructure of skeletogenesis in hermatypic corals. Int Rev Cyt 67: 171-214

Lange R, Bergbauer M, Szewzyk U, Reitner J (2001) Soluble proteins control growth of skeleton crystals in three coralline demosponges. Facies 45: 195-202

Milliman JD (1974) Marine carbonates. In: Milliman JD, Müller G, Förstner U (eds) Recent sedimentary Carbonates. Springer, Berlin

Mitterer RM (1978) Amino acid composition and metal binding capability of the skeletal protein of corals. Bull Mar Sci 28: 173-180

Reitner J (1993) Modern cryptic microbialite/metazoan facies from Lizard Island (Great Barrier Reef, Australia). Formation and concepts. Facies 29: 3-39

Reitner J, Hoffmann F (2003) Schwämme in Kaltwasser-Korallenriffen. Kleine Senckenberg-Reihe 45: 75-87

Reitner J, Gautret P, Marin F, Neuweiler F (1995) Automicrites in a modern marine microbialite. Formation model via organic matrices (Lizard Island, Great Barrier Reef, Australia). Bull Inst Océanogr Monaco Spec Issue 14: 237-263

Reitner J, Wörheide G, Lange R, Schumann-Kindel G (2001) Coralline demosponges – a geobiological portait. Bull Tohoku Univ Mus 1: 219-235

Stolarski J (2003) Three-dimensional micro- and nanostructural characteristics of the scleractinian coral skeleton: a biocalcification proxy. Acta Palaeontol Pol 48: 497-530

Trichet J, Defarge C (1995) Non-biologically supported organomineralisation. Bull Inst Océanogr Monaco Spec Issue 14: 203-236

Weiner S, Traub W, Lowenstam HA (1983) Organic matrix in calcified exoskeletons. In: Westbroek P, de Jong EW (eds) Biomineralization and Biological Metal Accumulation. Reidel, Amsterdam, pp 205-224

Wheeler AP, George JW, Evans CA (1981) Control of calcium carbonate nucleation and crystal growth by soluble matrix of oyster shell. Science 212: 1397-1398

Wilbur KM, Simkiss K (1979) Carbonate turnover and depostion by Metazoa. In: Trudinger PA, Swaine DJ (eds) Studies in Environmental Sciences. Biochemical Cycling of Mineral-forming Elements. Elsevier, Amsterdam, pp 69-106

Wörheide G, Gautret P, Reitner J, Böhm F, Joachimski MM, Thiel V, Michaelis W, Massault M (1997) Basal skeletal formation, role and preservation of intracrystalline organic matrices, and isotopic record in the coralline sponge *Astrosclera willeyana* Lister, 1900. Bol R Soc Esp Hist Nat (Sec Geol) 91: 355-374

Young SD (1971) Organic material from scleractinian coral skeleton. 1. Variation in composition between several species. Cop Biochem Physiol 40B: 113-120

VI

Diversity

Chapter content

Are deep-water corals important habitats for fishes?

Peter J. Auster

National Undersea Research Center, Department of Marine Sciences, University
   of Connecticut, Groton, CT 06340, USA
   (auster@uconn.edu)

Abstract. High densities of fishes in aggregations of deep-water corals (e.g., of the genera *Primnoa*, *Paragorgia, Paramuricea*) do not necessarily indicate that corals are important habitats in terms of population processes. Frequency dependent distribution models provide a basis for assessing the role of deep-water corals. It is necessary to understand the overall habitat-related distributions of fish species, at particular life history stages, in order to assess the particular role of corals. Examining the landscape for ecologically equivalent habitats is one approach for assessing the importance of coral habitats. Measures of the functional equivalence of habitats are demonstrated, as an example, for sites from the Gulf of Maine on the northeast United States continental shelf. Fish census data based on surveys with a remotely operated vehicle in 2003 showed that communities in habitats dominated by dense corals and dense epifauna were functionally equivalent when compared with five other less complex habitats (e.g., boulder with sparse coral cover). Comparison of species-individual curves showed that sites with dense coral and dense epifauna habitats supported only moderate levels of fish diversity when compared with other sites. Further, density of Acadian redfish (*Sebastes fasciatus*) in dense coral and dense epifauna habitats, where this species was dominant, was not statistically different but was higher than an outcrop-boulder habitat with sparse epifauna (the only other site where this species was abundant). Such data suggest that coral habitats are not necessarily unique but have attributes similar to other important habitats. However, the level of their importance in the demography of fish populations and communities remains to be demonstrated. Focusing conservation efforts for deep-water corals on their perceived value to exploited species, without good demographic information on fish populations, may ultimately leave corals open to destructive fishing practices if new and contrary information emerges. Conservation efforts for corals, in the absence of explicit ties to managed fish species, might do better emphasizing the intrinsic value of corals, their slow growth, high sensitivity to disturbance, and the questionable potential for recovery.

Keywords. Frequency-dependant models, species-individual relationships, video, functionally equivalent habitat

Introduction

The role of shallow coral reefs as important habitat for fishes has been widely appreciated in both scientific and popular literature for many decades. Studies of coral reef fishes have focused on developing a mechanistic understanding of the role that reef habitats play in mediating survivorship (Sale (2002) provides an extensive review). In contrast to shallow-water systems, the ecological role of deep-water corals as fish habitat has only recently emerged as an area of academic interest as well as an issue related to the conservation and sustainable use of deep-sea fishes and related biological diversity.

The role of deep-water corals as habitats for fishes has focused primarily on the coral genera *Primnoa*, *Lophelia*, and *Oculina*. Corals may provide structure for shelter seeking fishes as well as enhance rates of prey capture. In the Gulf of Alaska, Krieger and Wing (2002) noted that "less than 1 % of the boulders contained coral, but 85 % of the large rockfish [*Sebastes* spp.] were next to boulders with corals" (i.e., *Primnoa* sp.). Data from research survey trawls off Alaska showed rockfish (*Sebastes* spp. and *Sebastolobus alascanus*) and Atka mackerel (*Pleurogrammus monopterygius*) were the most common species of economic importance collected with gorgonian, cup, and hydrocorals, while flounders and gadids were the most common species associated with *Gersemia* sp., a soft coral (Heifetz 2002). Off the coast of Norway, *Lophelia pertusa* reefs (300-500 m water depth) support high densities of gravid deep-water redfish, *Sebastes viviparus* (Fosså et al. 2000). The authors hypothesized that juveniles are released in the corals for protection from predators, as well as for protection of females when escape from predators during development of young and during release is limited. Experimental fishing comparisons inside and outside of *Lophelia* reefs off Norway, using longlines and gillnets, confirmed patterns of increased catch and larger size of redfish (*Sebastes marinus*), ling (*Molva molva*), and tusk (*Brosme brosme*) in coral habitats (Husebø et al. 2002). Diets of these species were composed of the same prey groups regardless of habitat although some prey species were associated with particular habitats. Finally, data demonstrate significant numbers of gag grouper (*Mycteroperca microlepis*) and scamp (*M. phenax*) aggregate on and use the coral *Oculina varicosa* for spawning habitat and juvenile speckled hind (*Epinephelus drummondhayi*) use *Oculina* for shelter (Gilmore and Jones 1992; Koenig et al. 2000, in press). While such studies provide evidence in support of the importance of corals, they do not demonstrate a mechanistic link to population or community variability.

Frequency dependent distribution models provide a basis for assessing the role of deep-water coral habitats (reviewed in Kramer et al. 1997). Such models suggest it is necessary to understand the habitat-related distribution of a species, at particular life history stages, in order to assess the particular role of corals. Understanding the proportion of a population or community occupying coral habitat, and examining the landscape for ecologically equivalent habitats, is one approach for assessing the importance of corals. In this paper, I present a conceptual framework for considering the role corals play in mediating fish populations and communities, provide an example of approaches for measuring the functional equivalence of

habitats based on community and population characteristics, and discuss a rationale for coral conservation that does not depend on the role that corals play as habitat for fishes of economic importance.

A conceptual demographic framework

Defining important habitats of fishes based on empirical observations of high-density patches is consistent with a variety of frequency-dependent habitat selection models (Kramer et al. 1997). One such model, the ideal free distribution model (first described by Fretwell and Lucas 1970) predicts that a range of habitats will have variable fitness benefits and that animals will move to habitats with the highest fitness benefit, hence density will be positively correlated with habitat value. MacCall (1990) described a conceptual "basin" model for a population distributed across a range of habitats, based on ideal free distribution theory. However, the model can be applied to other constructs that are based on differential survivorship, rather than habitat selectivity, and result in similar spatial patterns of density. For this model populations are viewed as filling a basin, with the most important habitats being occupied (or filled) first, with density-dependent processes causing expansion of the spatial distribution of the population (Fig. 1A). The deepest parts of the basin are the preferred or important habitats. From the perspective of the role of deep-water corals, the question remains whether corals are the type of habitat that represents the whole, or only part of the basin.

Functionally equivalent habitats can be defined as those that provide similar levels of shelter from predators and provide similar prey resources. In practice, functionally equivalent habitats can be identified as those supporting a similar density of fishes and similar growth rates. Patterns of immigration, emigration, settlement and survivorship can also provide insight into the role that particular habitats play in the life history of a species. Finally, comparisons of community composition may also elucidate the role of particular habitats, especially when recruitment and predation patterns are patchy and member species are long-lived.

The importance of particular habitats to fish populations and communities can be viewed as a function of both fish density in specific habitats and the area of each habitat. Important habitats can then be defined as those that support a significant percentage of the population at comparatively high densities. This definition is purposely ambiguous because we know little about the demographics of most fish populations and communities at the scale of habitat or landscape features.

The basin model can be used to illustrate several scenarios that should be considered when investigating the nature of corals as habitat for fishes (Fig. 1). Deep-water corals (habitat A) may be the only habitat which supports a high density of species x but it may have different aerial coverage in different systems, thus containing varying percentages of a population (Figs. 1A-B). However, there may be functionally equivalent habitats that have equal or much greater spatial coverage than corals (Figs. 1C-D). In these cases understanding the role that corals play in terms of mediating population variability is key to assessing their role. For example,
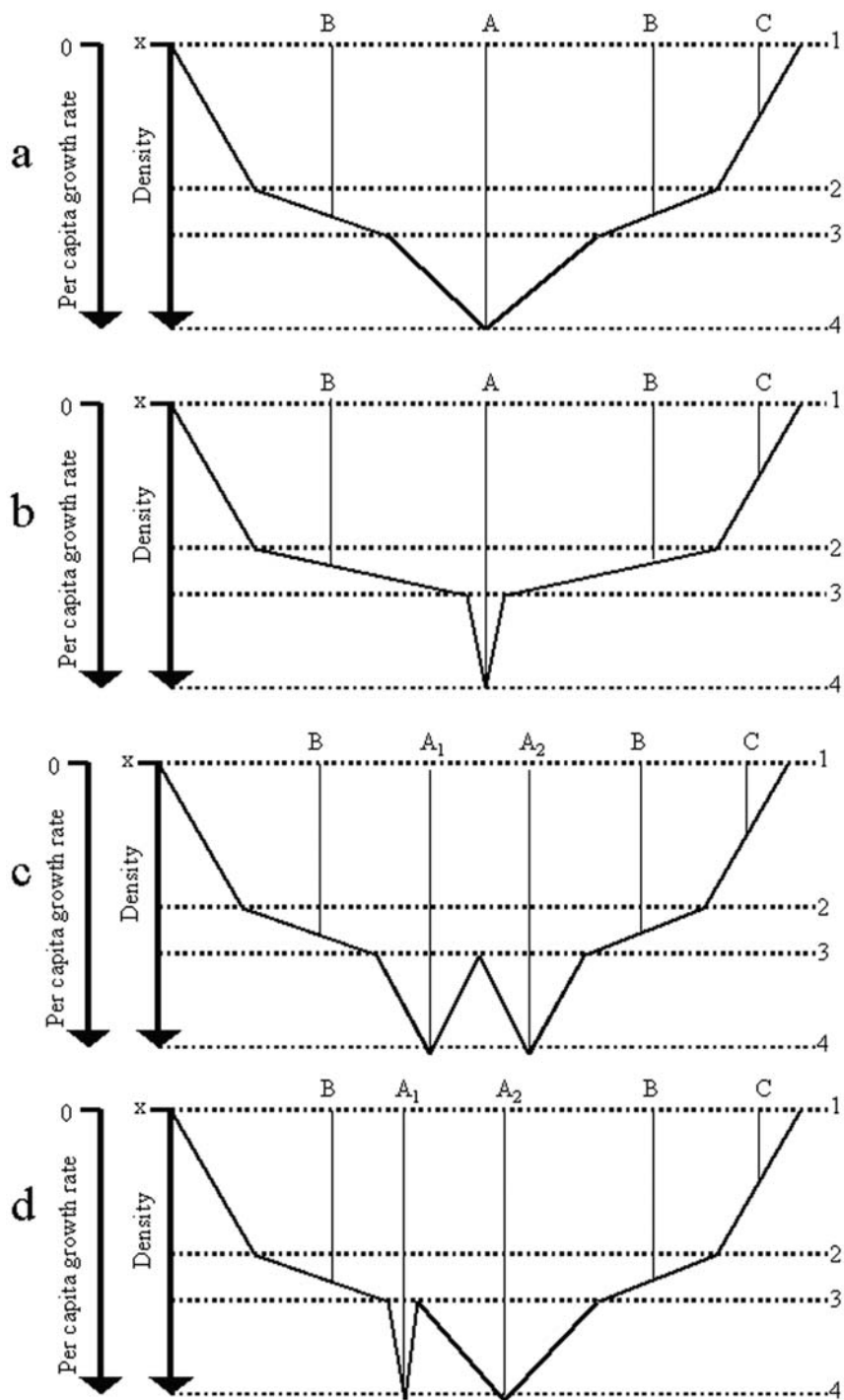
if corals occupy only 1 % of the area of habitats that support the highest densities of a species, are they arguably "important" given annual variations in overall carrying capacity based on environmental variability (e.g., Fig. 1D)?

Clearly, observations of high densities of fishes in coral habitats are consistent with predictions for identifying important habitats from frequency-dependent habitat use models. However, comparisons of fish densities throughout a range of habitat types and habitat patch sizes (e.g., identifying functionally equivalent habitats based on landscape and patch size variations), as well as quantifying the segment of a population using corals *versus* other habitats, will refine our understanding of the importance of corals to populations of fishes.

Identification of functionally equivalent habitats - an example from the Gulf of Maine

Direct observations of fishes and the landscape elements in which they reside can produce data that are useful for quantifying the role of particular habitats. The Kraken ROV was used to survey seven sites for the presence of deep-water corals and census associated fishes in the Jordan Basin region of the Gulf of Maine during August 2003. Kraken carried a 3-chip video camera and images were recorded in DVCam NTSC format. A combination of HMI and quartz-halogen lights was used for illumination. Linear transects of variable length (ca. 0.3 - 1.0 km) were conducted to collect habitat and fish distribution data. Table 1 summarizes the habitat characteristics of each site. Here I treat corals as one type of structural attribute of fish habitat. Only one site supported a dense coral assemblage (primarily *Paragorgia, Paramuricea, Primnoa,* Plexaurid sp.; Figs. 2A-C) while another supported only sparse corals (primarily *Paramuricea* and a Plexaurid sp.). Dense epifauna consisting of a diversity of erect and globose sponge taxa on small boulders and cobble, with burrowing anemones (*Cerianthus borealis*) interspersed in sand covered gravel, was characteristic of another site (Figs. 2D-E). Structure at the remaining sites was primarily boulders and gravel over coarse sand with low-erect or patchily distributed epifauna playing a minor role (Fig. 2F).

Fig. 1 Variation in the abundance of individuals in a population, that occupies a landscape with variable habitat attributes, can be viewed as filling a basin (after MacCall 1990). Per capita growth rate and/or density are highest in the most preferred or suitable habitats. Here habitat A supports the highest density and growth rates of species x. Habitats B and C support lower densities and growth rates respectively. Here various scenarios show the variable role deep-water corals might play in the demography of a species. In **model a**, deep-water corals (habitat A) may be the only habitat which supports a high density of species x. **Model b** shows deep-water coral supporting a small percentage of the population. **Model c** illustrates how two habitats may be functionally equivalent in their role as fish habitat. Note both habitats A_1 and A_2 occupy the same area here. In **model d**, habitat A_1 is significantly smaller in size than habitat A_2. If deep-water corals were distributed as habitat A_1 in the two scenarios, their role in mediating fish populations would be very different

Table 1 Habitat characteristics from Gulf of Maine sites surveyed by ROV in August 2003

Site Abbreviation	Depth Range (m)	Description
OBC	88-51	Outcrop, boulder, and cobble with sparse epifana.
OBDCo	240-238	Outcrop and boulder with dense coral cover (*Paragorgia, Primnoa, Paramuricea*, Plexaurid sp.).
OBSCo	215-197	Outcrop and boulder with sparse coral cover (primarily *Paramuricea* and a Plexaurid sp.).
BG1	233-230	Boulder and gravel with patches of sand and mud. Small erect epifauna (hydroids, bryozoans, brachiopods) on rock surfaces.
BG2	191-153	Boulder and gravel with patches of sand. Small erect epifauna (hydroids, bryozoans, brachiopods) on rock surfaces.
G	176-160	Gravel (no boulders) with sand and silt. *Iophon* sp. sponge patchy on gravel. Sparse cerianthids and sea pens in soft sediments.
BCDEp	189-121	Boulder and cobble with dense epifaunal cover. Diverse and dense erect and globose sponges. Cerianthids in sand covered gravel interspersed.

Fish assemblage composition in coral and non-coral habitats (species x numbers for each site; Table 2) was compared in several ways. Bray-Curtis similarity coefficients were calculated for pairs of sites and hierarchical cluster analysis and non-metric multidimensional scaling (MDS) was used to evaluate the level of similarity in assemblage composition (using PRIMER software; Clarke and Gorley 2001). Abundance data were standardized to percent relative abundance as sample effort between sites was unequal. Both cluster analysis, using complete linkage, and MDS (10 restarts) showed that fish assemblages in the dense coral and dense epifaunal habitats were most similar (Fig. 3). The assemblage in outcrop-boulder-cobble habitat was next closest in distance. Assemblages at the other sites were most distant. Differences could primarily be attributed to the large numbers of Acadian redfish (*Sebastes fasciatus*) that occurred in the dense coral, dense epifaunal, and outcrop-boulder sites.

Another method of comparison is based on the relationship of species and individuals encountered sequentially along video transects. Such relationships are density-independent and provide a quantitative approach for visualizing the composition of communities in particular habitats based on encounters of new species as numbers of individual fishes increase. Figure 4 illustrates semi-log regressions of species richness on number of individuals. Note that the dense coral and dense epifaunal habitats are in the middle of the group of regressions indicating that they support only a moderate level of diversity when compared to other habitats.

The dense coral, dense epibenthos, and outcrop-boulder habitats supported an abundance of Acadian redfish. Comparison of redfish density between habitat types is another method to contrast the functional role of coral as habitat for particular

species. Density of redfish was estimated at each of the three sites from counts of fish from non-overlapping sequential video quadrats (number of fish m^{-2}; paired parallel lasers with 20 cm spacing were used to calibrate the field-of-view to 1 m^2). Data were not normally distributed (Ryan-Joiner test) but paired t-tests (Hochberg correction
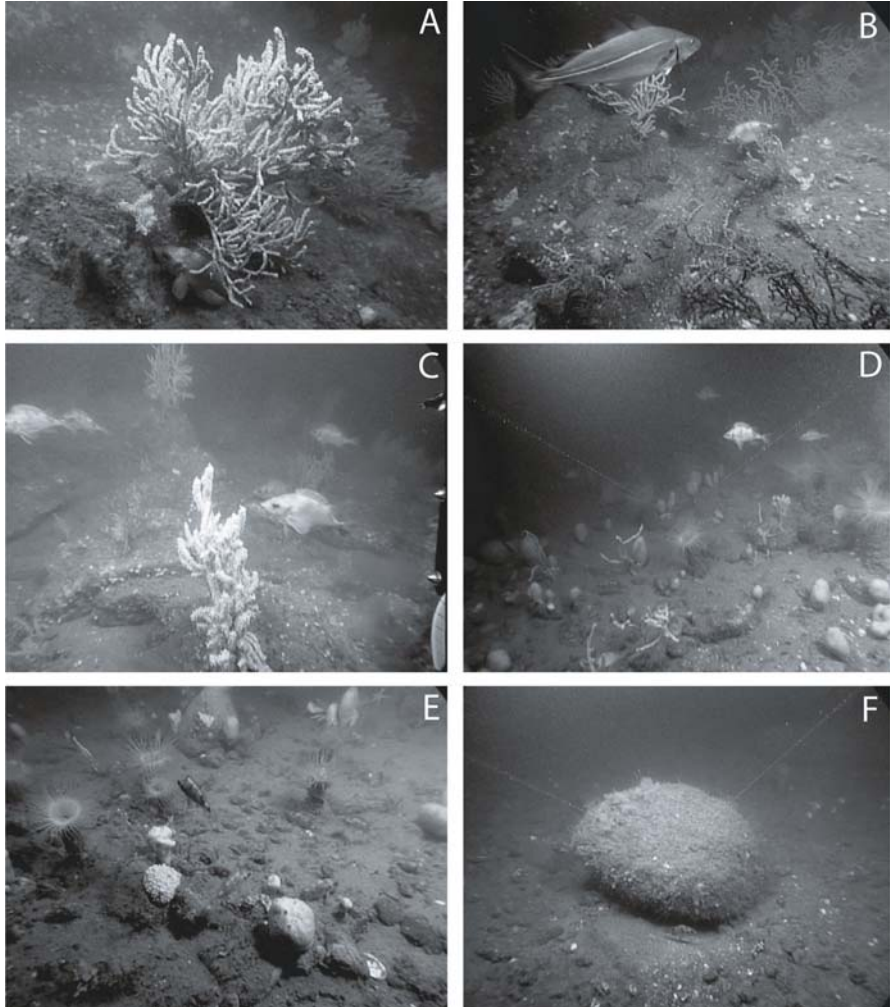
Fig. 2 Examples of seafloor habitat types in the Gulf of Maine. **A-C** Outcrop-boulder with dense corals. For size reference, Acadian redfish are approximately 30 cm total length. **D-E** Boulder-cobble with dense epifauna and cerianthid anemones interspersed in sand covered gravel. Redfish are approximately 15 cm total length. **F** Boulder with crevice along boulder-sediment margin. Redfish at base of boulder is approximately 10 cm total length. In all settings, Acadian redfish are the most abundant fish. Note this species using seafloor structures (i.e., coral, other epifauna) for cover (**A, B, E, F**), as well as a focal site for searching the near-bottom water column for zooplankton prey and as a refuge from flow (**C, D, E**). Images are digital still frames from DVCam format NTSC video

Table 2 Species composition and percent relative abundance of fishes from ROV video transects. Site abbreviations correspond to descriptions in Table 1

Common name	Scientific name	OBC	OBDCo	OBSCo	BG1	BG2	G	BCDEp
Acadian redfish	*Sebastes fasciatus*	78.57	87.60	2.22	6.67	42.28	57.69	92.00
Alligatorfish	*Aspidophoroides monopterygius*	1.79	0.00	0.00	0.00	0.00	0.00	0.00
Atlantic cod	*Gadus morhua*	1.79	0.39	20.00	0.00	0.00	0.00	0.00
Atlantic herring	*Clupea harengus*	0.00	0.00	0.00	0.00	0.00	2.44	0.00
Cusk	*Brosme brosme*	0.00	0.78	11.11	0.00	7.32	0.00	0.00
Flounder sp. A	Pleuronectiformes	0.00	0.00	0.00	0.00	0.00	1.92	0.00
Goosefish	*Lophius americanus*	0.00	0.00	0.00	0.00	2.44	0.00	0.00
Haddock	*Melanogrammus aeglefinus*	0.00	0.00	0.00	0.00	0.81	1.92	0.00
Longhorn sculpin	*Myoxocephalus octodecemspinosus*	7.14	0.00	0.00	0.00	0.00	0.00	0.00
Lumpfish	*Cyclopterus lumpus*	0.00	0.00	0.00	0.00	0.00	0.00	1.60
Myctophid	Myctophidae	0.00	0.39	0.00	0.00	0.00	1.92	0.00
Ocean pout	*Macrozoarces americanus*	0.00	0.00	0.00	0.00	0.00	5.77	0.40
Pollock	*Pollachius virens*	1.79	9.69	51.11	62.22	1.63	11.54	1.60
Red hake	*Urophycis chuss*	5.36	0.78	4.44	11.11	5.69	3.85	0.40
Rock gunnel	*Pholis gunnellus*	1.79	0.00	0.00	0.00	0.00	0.00	0.00
Shorthorn sculpin	*Myoxocephalus scorpius*	1.79	0.00	0.00	0.00	0.00	0.00	0.00
Silver hake	*Merluccius bilinearis*	0.00	0.39	11.11	15.56	30.08	15.38	2.40
Skate sp. A	Rajid sp.	0.00	0.00	0.00	0.00	3.25	0.00	0.80
Smooth skate	*Malacoraja senta*	0.00	0.00	0.00	0.00	0.81	0.00	0.00
Snake blenny	*Lumpenus lumpretaeformis*	0.00	0.00	0.00	0.00	0.00	0.00	0.40
Thorny skate	*Amblyraja radiata*	0.00	0.00	0.00	2.22	0.81	0.00	0.00
White hake	*Urophycis tenuis*	0.00	0.00	0.00	2.22	0.00	0.00	0.00
Witch flounder	*Glyptocephalus cynoglossus*	0.00	0.00	0.00	0.00	2.44	0.00	0.40
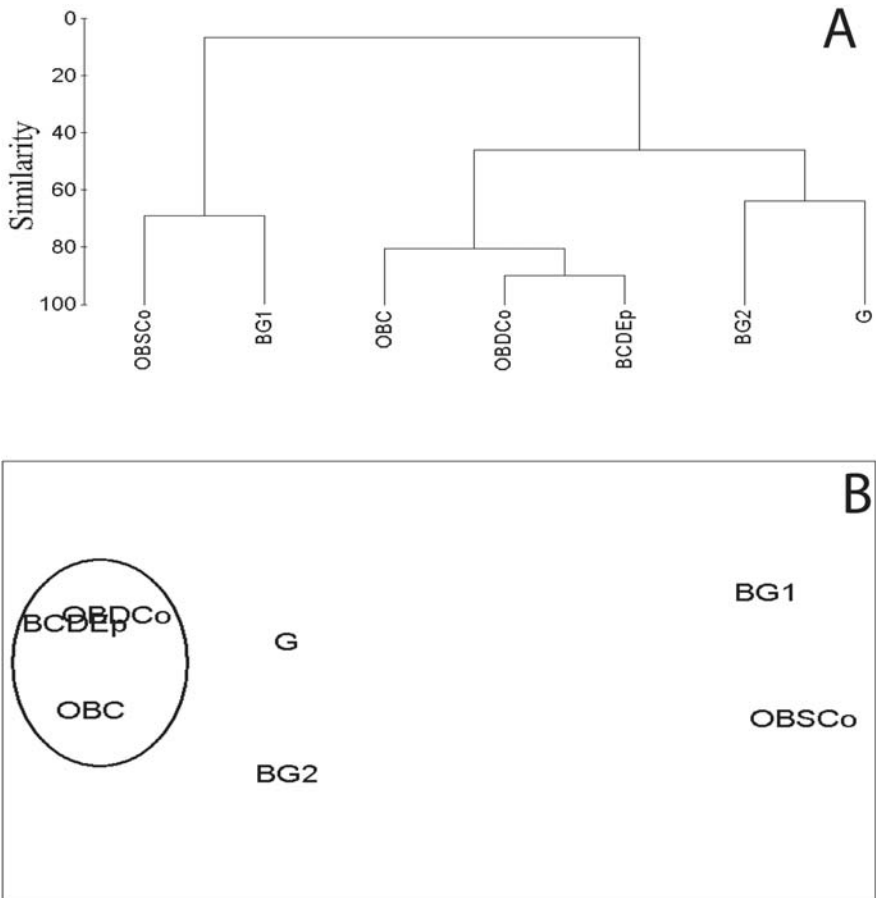
Fig. 3 Dendrogram of hierarchical cluster analysis (top) and MDS plot (below) based on species composition at each survey site (MDS stress level 0.01). Refer to Table 1 for site abbreviations

for multiple comparisons) were used due to unequal sample variances (Table 3). While the density of redfish was not significantly different in dense coral and dense epifauna habitats ($p = 0.12$), density in both habitats was significantly different from the outcrop-boulder-cobble site ($p<0.001$ in both paired sample tests). This analysis demonstrates that a non-coral habitat can support similar densities of fishes. However, it is the actual distribution of each habitat type throughout the region that will ultimately determine the role such habitats play in the demography of particular species and communities. Coral habitats are rare in the Gulf of Maine based on trawl, dredge and grab samples collected throughout the last century (Watling et al. 2003), as well as video records from 20 years of submersible dives in this region (based on the NURC video archive; Auster unpublished observations). However, boulder-cobble habitat with dense epifauna is considerably more common, despite impacts from fishing that have reduced the distribution of both habitat types.
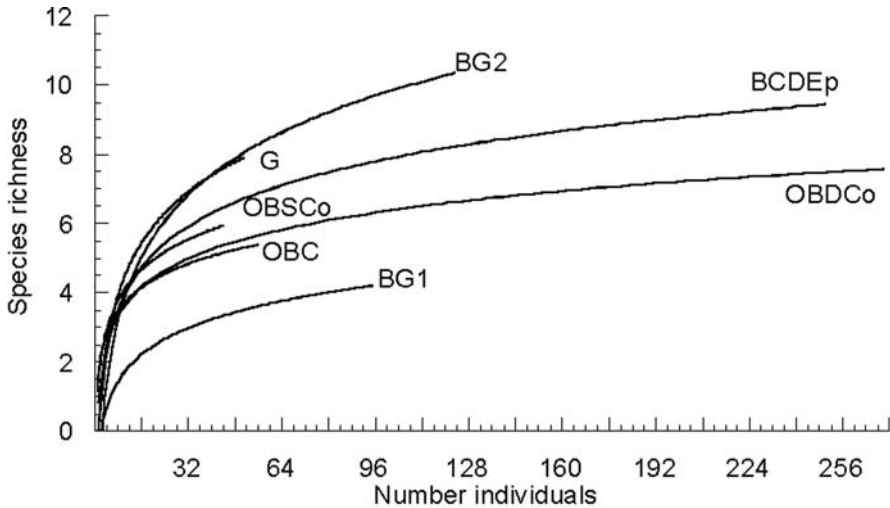
Fig. 4 Semi-log species-individual plots from seven survey sites in the Gulf of Maine (model $y = a + b \cdot \log x$; OBC, $r = 0.7403$; OBDCo, $r = 0.9297$; OBSCo, $r = 0.9413$; BG1, $r = 0.6118$; BG2, $r = 0.9618$; G, $r = 0.9689$; BCDEp, $r = 0.9496$). Refer to Table 1 for site abbreviations

This analysis, albeit based on a limited number of sites, suggests that deepwater corals play a role in mediating the distribution and abundance of fishes but do not singularly support high density, unique, or high diversity fish communities. One unique characteristic of the dense coral site was that the underlying geologic framework provided few small-scale shelter resources for fishes. Except for corals, there were few crevice structures that could be used by fishes. While Acadian redfish, red hake and cusk were observed using areas with sharp changes in the angle of faces on outcrops as cover, these occurrences were uncommon and most individuals were associated with coral structures. Corals provided important structural attributes of habitat but they may not be functionally different than structures provided by other dense epibenthos (e.g., sponges).

Discussion

While many tropical coral reef fishes exhibit obligate habitat requirements, many temperate outer continental shelf fishes exhibit facultative habitat use (Auster et al.

Table 3 Comparisons of Acadian redfish density (number m^2) at three sites. Density estimates are based on fish counts from video transects (i.e, sequential non-overlapping video quadrats of 1 m^2 area)

Site	N	Mean	Std. Dev.	Maximum Density
OBDCo	147	1.54	1.58	7
BCDEp	185	1.25	1.71	12
OBC	83	0.53	0.77	3

1995). Facultative habitat use may be defined as fishes using particular or multiple habitat features or landscape attributes as shelter from predators and currents, focal sites for prey capture, and focal sites for reproduction, but populations do not reach extinction in the absence of such features. That is, use of particular habitat features increases the fitness of individuals but survivorship rates are sufficient for persistence of populations. However, the resilience of populations to disturbance may be reduced in the absence of such habitats (e.g., Lindholm et al. 2001).

Fishes may exhibit associations with deep-water corals as coral colonies provide general types of topographic structures, rather than due to species-specific physical composition or biochemical attributes. Data in this and previous studies (e.g., Auster et al. 1995, 1997, 1998, 2003) suggest that any structure (e.g., coral, exposed cobble, erect sponge, cerianthid anemone) may represent an ecologically equivalent habitat for fishes seeking cover. Geographically comprehensive studies are needed to better understand the role that coral habitats play in the demographics of fishes. At the very least, surveys of particular taxa or communities in a range of habitats are needed to contrast the site-specific data (e.g., species composition, density) that can be acquired when using visual census techniques.

Rationale for the conservation of coral habitats

Fishing has had significant impacts on deep-water coral populations worldwide. Between 30-50 % of *Lophelia* reefs off Norway have been impacted or destroyed by trawling (Fosså et al. 2002). More than 90 % of *Oculina* habitat in a reserve off the east coast of Florida has been reduced to unconsolidated rubble (Koenig et al. in press). The authors present evidence of recent trawling activities as one likely and major cause of the damage but temperature extremes, excess nutrients, disease, strong currents, and other types of ship operations are also potential sources of historic mortalities. Comparisons of fished and unfished communities on seamounts off Tasmania showed that heavy trawling essentially removed the coral aggregate and significantly reduced the number of species and biomass (Koslow et al. 2001). There is a high degree of endemism of seamount fauna (de Forges et al. 2000) making these habitats particularly sensitive to fishing disturbances.

Observations of the impacts of a single trawl tow through *Primnoa* habitat in the Gulf of Alaska, where 1000 kg of coral were landed, showed seven years later that 7 of 31 colonies remaining in the trawl path were missing 80-99 % of their branches and boulders with corals attached were tipped and dragged (Krieger 2001). Damage was restricted to the net path. Approximately 50 colonies were observed within 10 m of the net (where bridles would have swept over the seafloor) and no damaged colonies or disturbed boulders were observed. Longline gear is also noted to tip and dislodge corals (Krieger 2001). Bycatch data from a longline survey in the Gulf of Alaska and Aleutian Islands showed *Primnoa* and other coral taxa were caught on 619 of 541,350 hooks fished at 150-900 m depths (Krieger 2001).

Corals are clearly sensitive to fishing gear impacts and recovery rates are extremely slow based on our knowledge of recruitment, growth rates, and age

structure. The ability to age deep-water scleractinians and octocorals is relatively new and different methods are used in different studies. For *Primnoa resedaeformis*, a common outer shelf-upper slope species, Risk et al. (2002) estimates linear growth rates at the distal tips of the colonies at 1.5-2.5 mm yr^{-1} based on comparisons of live specimens with growth rates through the base of a sub-fossil specimen collected from the Northeast Channel at 450 m. Growth rates of this same species in the Gulf of Alaska are reported as 1.60-2.32 cm yr^{-1}, although these samples were collected at less than 200 m depth (Andrews et al. 2002). Age estimates for only a few specimens demonstrate this species lives for hundreds of years. The colony collected from the Northeast Channel (Risk et al. 2002) has an estimated age of >300 years, which is in accordance with age estimates of the same species collected in Alaska (>100 years; Andrews et al. 2002). *Desmophyllum cristagalli*, a deep-water scleractinian, grows at 0.5-1.0 mm yr^{-1} and lives >200 years, with this growth rate verified by a specimen collected from an aircraft sunk in Baltimore Canyon in 1944 (Lazier et al. 1999; Risk et al. 2002). A 1.5 m high colony of the deep-water scleractinian coral *Lophelia pertusa* may be up to 366 years of age (Breeze et al. 1997). Deep-water reefs of *Oculina varicosa* form pinnacles and ridges 3-35 m in height off the east coast of Florida and have an average growth rate of 16.1 mm yr^{-1} (Reed 2002). Based simply on age and growth information, recovery of impacted colonies and thickets may take hundreds of years.

Data on recruitment patterns are even more limited. A single series of observations in the Gulf of Alaska suggest that recruitment of *Primnoa* sp. is patchy and aperiodic (Krieger 2001). No recruitment of new colonies was observed in an area where *Primnoa* was removed by trawling after seven years. However, six new colonies were observed at a second site one year after trawling. Four of these colonies were attached to the bases of colonies removed by trawling. Recruits of *Primnoa* were also observed on two 7 cm diameter cables (>15 colonies each). Limited observations in the Gulf of Maine region have revealed locally abundant recruits around aggregations of corals (Watling, Auster, France, unpublished observations).

Due to our rudimentary understanding of the functional role of deep-water corals, precautionary approaches (e.g., Auster 2001) will be required if these species are to persist in many parts of the world oceans. If convincing data about the use of coral habitats by fishes of economic importance are lacking, there are clear directions for conserving corals based on bycatch reduction goals, or to reduce the potential for coral taxa being listed as an endangered or threatened species (with concomitant draconian management measures to ensure their survival). For species with extremely long population recovery times, precautionary management strategies are a clear benefit.

Acknowledgements

those of the author and do not necessarily represent the views of NOAA, the National Geographic Society or their sub-agencies.

References

Andrews AH, Cordes EE, Mahoney MM, Munk K, Coale KH, Cailliet GM, Heifetz J (2002) Age, growth and radiometric age validation of a deep-sea, habitat forming gorgonian *(Primnoa resedaeformis)* from the Gulf of Alaska. Hydrobiologia 471: 101-110

Auster PJ (2001) Defining thresholds for precautionary habitat management actions in a fisheries context. North Amer J Fish Managem 21: 1-9

Auster PJ, Malatesta RJ, LaRosa SC (1995) Patterns of microhabitat utilization by mobile megafauna on the southern New England (USA) continental shelf and slope. Mar Ecol Progr Ser 127: 77-85

Auster PJ, Malatesta RJ, Donaldson CLS (1997) Distributional responses to small-scale habitat variability by early juvenile silver hake, *Merluccius bilinearis*. Environ Biol Fish 50: 195-200

Auster PJ, Michalopoulos C, Valentine PC, Malatesta RJ (1998) Delineating and monitoring habitat management units in a temperate deep-water marine protected area. In: Munro NWP, Willison JHM (eds) Linking Protected Areas with Working Landscapes, Conserving Biodiversity. Sci Managem Protected Areas Assoc, Wolfville, Nova Scotia, pp 169-185

Auster PJ, Lindholm J, Valentine PC (2003) Variation in habitat use by juvenile Acadian redfish, *Sebastes fasciatus*. Environ Biol Fish 68: 381-389

Breeze H, Davis DS, Butler M, Kostylev V (1997) Distribution and status of deep-sea corals off Nova Scotia. Marine Issue Comm Spec Publ 1, Ecology Action Center, Halifax, NS, Canada, 58 pp

Clarke KR, Gorley RN (2001) PRIMER v5: User Manual/Tutorial. PRIMER-E Ltd, Plymouth

De Forges BR, Koslow JA, Poore GCP (2000) Diversity and endemism of the benthic seamount fauna in the southwest Pacific. Nature 405: 944-947

Fosså JH, Mortensen PB, Furevik DM (2000) *Lophelia* korallrev langs norskekysten forekomst og tilstand. Prosjektrapp Havforskningsinst, Bergen, 94 pp

Fosså JH, Mortensen PB, Furevik DM (2002) The deep-water coral *Lophelia pertusa* in Norwegian waters: distribution and fishery impacts. Hydrobiologia 471: 1-12

Fretwell SD, Lucas HL (1970) On territorial behavior and other factors influencing habitat distribution in birds. I. Theoretical development. Acta Biotheoret 19: 16-36

Gilmore RG, Jones RS (1992) Color variation and associated behavior in the epihepheline groupers, *Mycteroperca microlepis* (Goode and Bean) and *M. phenax* Jordan Swain. Bull Mar Sci 51: 83-103

Heifetz J (2002) Coral in Alaska: distribution, abundance, and species associations. Hydrobiologia 471: 19-28

Husebø A, Nøttestad L, Fosså JH, Furevik DM, Jørgensen SB (2002) Distribution and abundance of fish in deep-sea coral habitats. Hydrobiologia 471: 91-99

Koenig CC, Coleman FC, Grimes CB, Fizhugh GR, Scanlon KM, Gledhill CT, Grace M (2000) Protection of fish spawning habitat for the conservation of warm-temperate reef fish fisheries of shelf-edge reefs of Florida. Bull Mar Sci 66: 593-616

Koenig CC, Shepard AN, Reed JK, Coleman FC, Brooke SD, Brusher J, Scanlon KM (in press) Habitat and fish populations in the deep-sea *Oculina* coral ecosystem of the western Atlantic. Amer Fish Soc Symp Ser

Koslow JA, Gowlett-Holmes K, Lowry JK, O'Hara T, Poore GCB, Williams A (2001) Seamount benthic macrofauna off southern Tasmania: community structure and impacts of trawling. Mar Ecol Progr Ser 213: 111-125

Kramer DL, Rangeley RW, Chapman LJ (1997) Habitat selection: patterns of spatial distribution from behavioural decisions. In: Godin J (ed) Behavioural Ecology of Teleost Fishes. Oxford Univ Press, New York, pp 37-80

Krieger KJ (2001) Coral (*Primnoa*) impacted by fishing gear in the Gulf of Alaska. In: Willison JHM, Hall J, Gass SE, Kenchington ELR, Butler M, Doherty P (eds) Proceedings of the First International Symposium on Deep-Sea Corals. Ecology Action Centre, Halifax, pp 106-116

Krieger KJ, Wing BL (2002) Megafauna associations with deepwater corals (*Primnoa* spp.) in the Gulf of Alaska. Hydrobiologia 471: 83-90

Lazier A, Smith JE, Risk MJ, Schwarcz HP (1999) The skeletal structure of *Desmophyllum cristagalli*: the use of deep-water corals in sclerochronology. Lethaia 32: 119-130

Lindholm JB, Auster PJ, Ruth M, Kaufman L (2001) Juvenile fish responses to variations in seafloor habitats: modeling the effects of fishing and implications for the design of marine protected areas. Conserv Biol 15: 424-437

MacCall AD (1990) Dynamic Geography of Marine Fish Populations. Univ Washington Press, Seattle, 153 pp

Reed JK (2002) Comparison of deep-water coral reefs and lithotherms off southeastern USA. Hydrobiologia 471: 57-69

Risk MJ, Heikoop JM, Snow MG, Beukens R (2002) Lifespans and growth patterns of two deep-sea corals: *Primnoa resedaeformis* and *Desmophyllum cristagalli*. Hydrobiologia 471: 125-131

Sale PF (2002) Coral Reef Fishes, Dynamics and Diversity in a Complex Ecosystem. Academic Press, San Diego, California, 549 pp

Watling L, Auster PJ, Babb I, Skinder C, Hecker B (2003) A geographic database of deep-water Alcyonaceans of the Northeastern U.S. Continental Shelf and Slope. Version 1.0 CD-ROM. Natl Undersea Res Cent, Univ Connecticut, Groton

A habitat classification scheme for seamount landscapes: assessing the functional role of deep-water corals as fish habitat

Peter J. Auster[1], Jon Moore[2], Kari B. Heinonen[1], Les Watling[3]

[1] National Undersea Research Center, Department of Marine Sciences, University of Connecticut, Groton, CT 06340, USA
  (auster@uconn.edu)
[2] Florida Atlantic University, Honors College, Jupiter, FL 33458, USA
[3] Darling Marine Center, University of Maine, Walpole, ME 04573, USA

Abstract. Seamounts are drowned volcanoes rising from abyssal depths. Fishes on seamounts exploit a range of landscape features that likely enhance probabilities of prey capture and reduce predator success. The epifaunal community on seamounts is dominated by suspension-feeders of which deep-water corals are a dominant element. Such taxa are widespread components of seamount landscapes but their functional role in mediating the distribution and abundance of fishes remains unknown. Here we propose a hierarchical habitat classification matrix, which includes deep-water corals, as a foundation for partitioning seamount landscapes in which fishes are observed. This scheme is based on our observations of fish distributions from the New England Seamounts, as well as literature review. Features of an idealized seamount landscape were divided at multiple spatial scales and included features at habitat class, subclass and microhabitat levels. Habitat classes were divided by major sediment types (i.e., basalt, fine grained sediments). Habitat subclasses included pavement, ridges, walls, ledges and tubes for basalt substrates and flat sediment, ripples and waves for fine-grained sediments. Microhabitat features were classified as flow related features, emergent structures (i.e., geologic and biologic including deep-water corals), and other biogenic structures (e.g., coral debris, depressions, burrows). Variations in the distribution of structures at multiple spatial scales can influence boundary flows and the ability of fishes to search for prey (e.g., where active searching by swimming can occur, where pelagic prey delivery is sufficient when station-keeping) and avoid predators (e.g., the ability to efficiently exhibit various avoidance behaviors such as shelter seeking). Placing fish abundance data in such a matrix of habitat types enables a variety of statistical approaches for testing for non-random distributions of fishes on seamounts and quantifying the functional role of corals as fish habitat.

Keywords. Topographically induced flows, seafloor, microhabitat, slope, habitat classification

Introduction

Seamounts are extinct volcanoes that rise from the abyssal plain and occur in all ocean basins. These major geologic features cross wide depth ranges, predominantly consist of hard substrata, exhibit complex topography, create topographically induced flow patterns, are bathed in clear oceanic waters, and are geographically isolated (Boehlert and Genin 1987; Rogers 1994). The invertebrate fauna of seamounts is dominated by suspension feeders (e.g., corals, sponges) and limited studies have shown variable degrees of endemism (Wilson and Kaufman 1987; de Forges et al. 2000) of the invertebrate fauna. Seamount corals, and deep-water corals in general, have been the focus of a renewed interest by both the scientific and conservation communities. Corals have been found to be of extreme age, have low recruitment rates, and are sensitive to human-mediated disturbances such as fishing (Willison et al. 2001). One of the rationales articulated for conserving deep-water corals is their role in supporting exploited populations of fishes. However, the functional role of deep-water corals in mediating the distribution and abundance of fishes is not well understood (Auster 2005). For seamount fishes, it is important to understand the role that variations in seamount landscape attributes, in which corals are nested, play in mediating their distribution and abundance. In this paper we present a hierarchical habitat classification scheme for partitioning seamount landscapes at multiple spatial scales. This classification scheme includes corals as structural attributes of the landscape and enables assessing the functional role of the full range of landscape attributes as habitat for fishes.

Our classification scheme is based on the direct observation of fishes and their surrounding habitat on Muir Seamount and the New England Seamount chain (i.e., Bear, Retriever, Balanus, Kelvin, and Manning seamounts) during 3 cruises in 2003-2004. The New England Seamounts rise from the Sohm Abyssal Plain and have summit depths that range from 900-3750 m. Our observations were primarily in the range of 2500-1100 m although we made limited observations as deep as 3900 m. Observations were made from DSV Alvin (18 dives), ROV Hercules (12 dives), the AUV Autonomous Benthic Explorer (7 dives), and a towed camera sled (3 deployments).

Seamount landscapes

Seamount landscapes and habitat features, with modifiers specific to the New England Seamounts, were defined along a gradient of spatial scales (Table 1) based on a hierarchical classification system described by Greene et al. (1999). Here seamounts are the landscape unit, given that most deep-water fishes generally have wider distributions and occur across a range of landscape types (Auster et al. 1995; Moore et al. 2003; unpublished observations). Two broad classes of habitat occur on seamounts (i.e., basalt and fine-grained sediments) and are a function of the volcanic origin of seamounts and the accumulation of oceanic sediments. Habitat subclasses include pavement, ridges, walls, ledges and tubes for basalt substrates and flat sediment, sand ripples and sand waves for fine-grained sediments. Microhabitat

Table 1 Habitat classification scheme for seamount landscapes
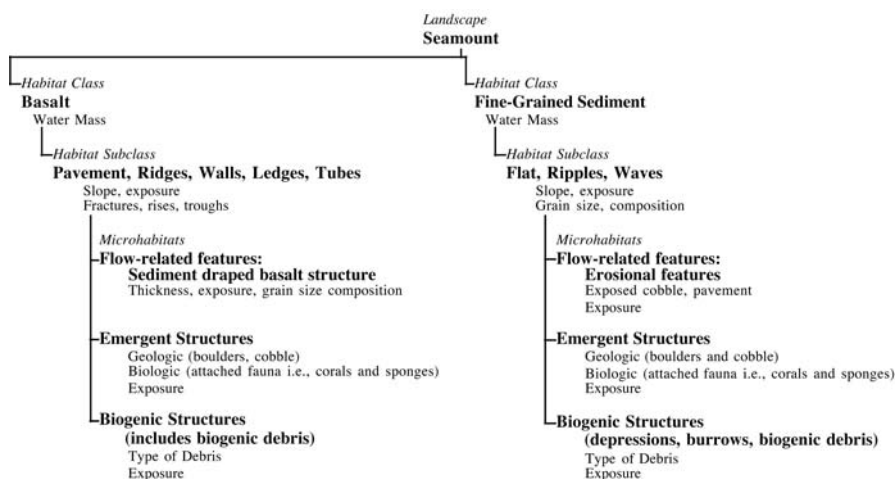
features were classified as flow related features (e.g., exposed patches of cobble or pavement in a predominantly sedimentary substrate), emergent structures (i.e., geologic and biologic including sponges, corals, other attached or emergent fauna), and other biogenic structures (e.g., coral debris, depressions, burrows). Figure 1 provides examples of a range of microhabitat types found within each habitat class.

Geologic attributes that are correlated with the distribution of fishes in other regions include sediment grain size, surface morphology or roughness, and slope (see Auster and Langton 1999 for a review). Grain size and roughness, from a fish habitat perspective, not only include the underlying geology but the biologic attributes of habitats that are composed of emergent fauna such a sponges and corals. These are grouped into a single microhabitat category in our classification scheme but can be divided where appropriate for classifying habitat use by fishes (e.g., boulders, boulders with attached corals). Coral debris, depressions, and burrows are grouped in a separate category (i.e., other biogenic structures) as they are neither static in size nor growing. In fact, coral debris degrades in complexity over time due to burial (and encrustation by manganese deposition). Depressions and burrows are physical alterations of sediment deposits created by individual organisms and are ephemeral habitats on the scale of days to years.

Applying this classification scheme in mixed basalt and sedimentary habitats will require decision rules for classifying habitats under threshold conditions. For example, a threshold is needed to decide if a habitat should be classified as ripples with exposed basalt pavement *versus* basalt pavement with a rippled sediment drape. Threshold values for sediment thickness and percent cover would be most easily applied in such cases. Here we suggest sediment thickness in excess 1 cm and greater than 50 % cover for classification as fine-grained sediment habitat. Less than either of these threshold values, at the scale of habitat class, subclass or microhabitat would require a classification of basalt habitat and associated sub-classes.

Similarly, the suspension feeders, in particular the gorgonians, present variable habitat aspects that could be used by different fish species. For example, deep on the seamount flanks the gorgonian assemblage is a mix of tall and whip-like species and short fans with low density branching (e.g., Fig. 1A). Here, the taller species can form moderately dense stands. In contrast, near and on the seamount summit, the gorgonians are more often large (~1 m wide) robust fans with high density
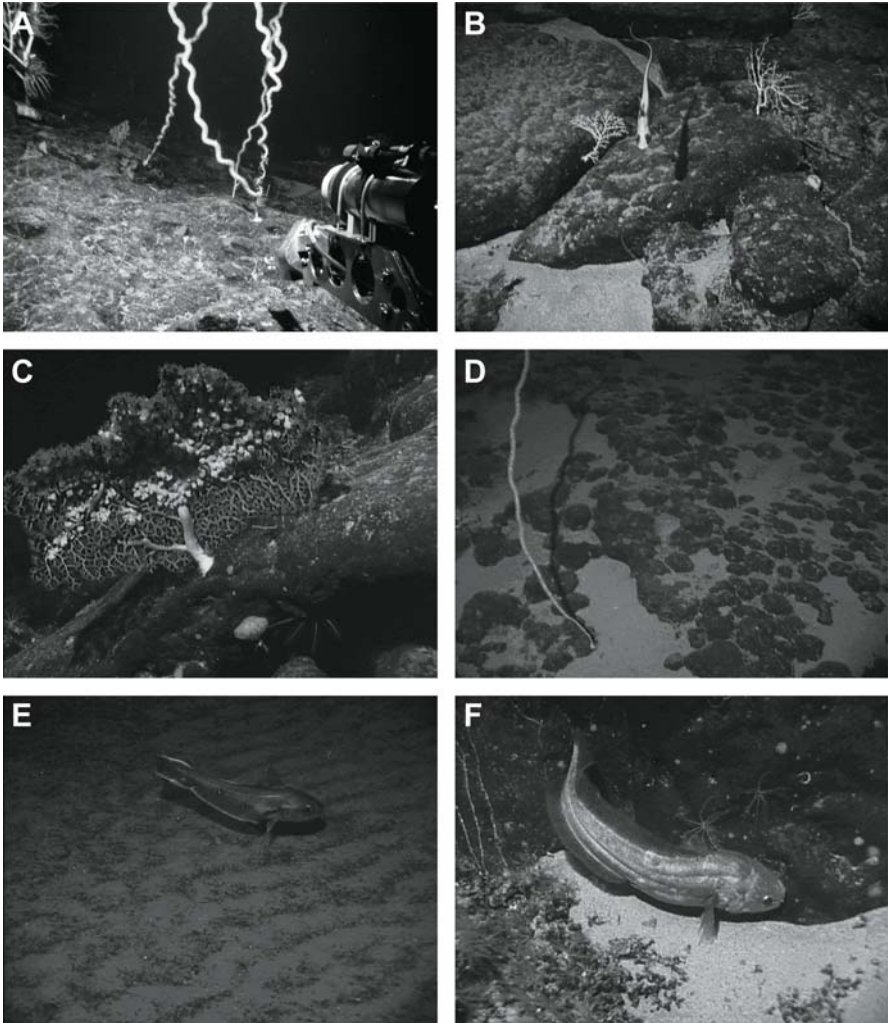
Fig. 1 Examples of microhabitat types found within each habitat class: **A** basalt pavement with tall, whip-like bamboo corals, **B** fractured basalt pavement with shelter sites and flow refuges in sediment-filled depressions between segments, **C** pavement with gorgonian fan with high density branching (i.e., *Paragorgia* sp.) as a shelter and flow refuge, **D** sediment draped basalt pavement, **E** rippled sediment, and **F** basalt-sediment ecotone. For scale, laser dots in images have 10 cm spacing

branching (Fig. 1C). These fans are spread much more widely across the landscape, and their form and density may have a different habitat value in terms of shelter or flow refuge.

Topographically induced flows occur at landscape, habitat class, habitat subclass and microhabitat levels. Water masses (with particular temperature and salinity characteristics) and currents impinging on seamounts produce different conditions despite similar substrate types and therefore are important attributes defining seamount landscape features as habitat for fishes. One or more water masses impinge on seamounts at different depth intervals with the consequence that physiological tolerances (as well as prey and shelter requirements) may determine how fishes are distributed at large spatial scales (ca. 100s - 1000s m). Flow characteristics around seamounts can be divided in a coarse fashion into regions of impingement, flow refuge and columnar flows (Figs. 2A-C). Variations in the distribution of structures at the scales of habitat subclasses (Fig. 2D) and microhabitats (Fig. 3) influence boundary flows and the ability of fishes to search for prey (e.g., where active searching by swimming can occur, where pelagic prey delivery is sufficient when station-keeping) and to avoid predators (e.g., the ability to exhibit efficiently various avoidance behaviors such as shelter seeking).

This habitat classification system was developed for initial application at the spatial scale of where individual organisms are located. The higher-level
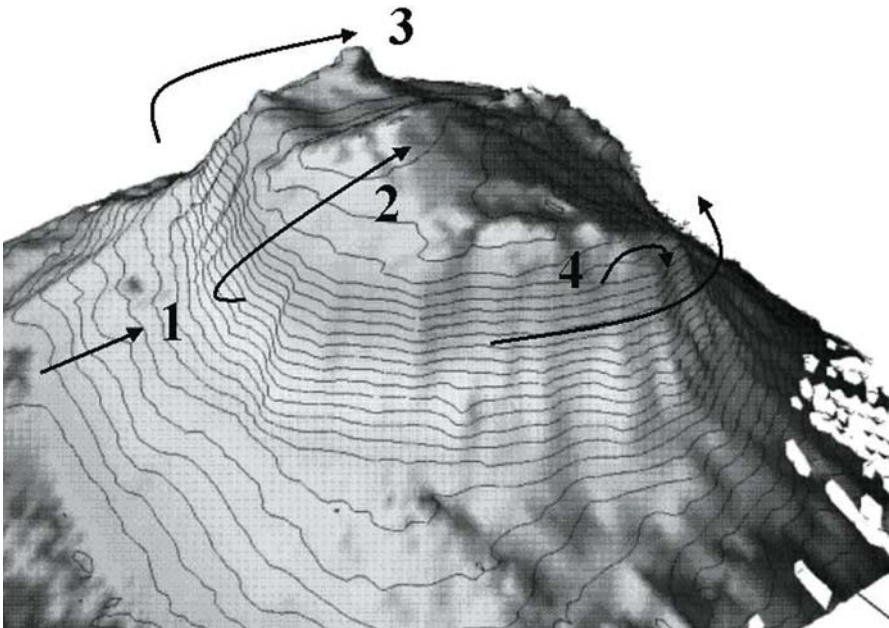
Fig. 2 Examples of variable flow regimes at the spatial scale of habitat classes include regions of (1) impinging flows, (2) flow induced upwellings, and (3) flow refuge or back-eddy. At the spatial scale of habitat subclasses, flows are influenced by features such as ridges and walls (4). (Figure is based on a preliminary multibeam sonar map of Bear Seamount)
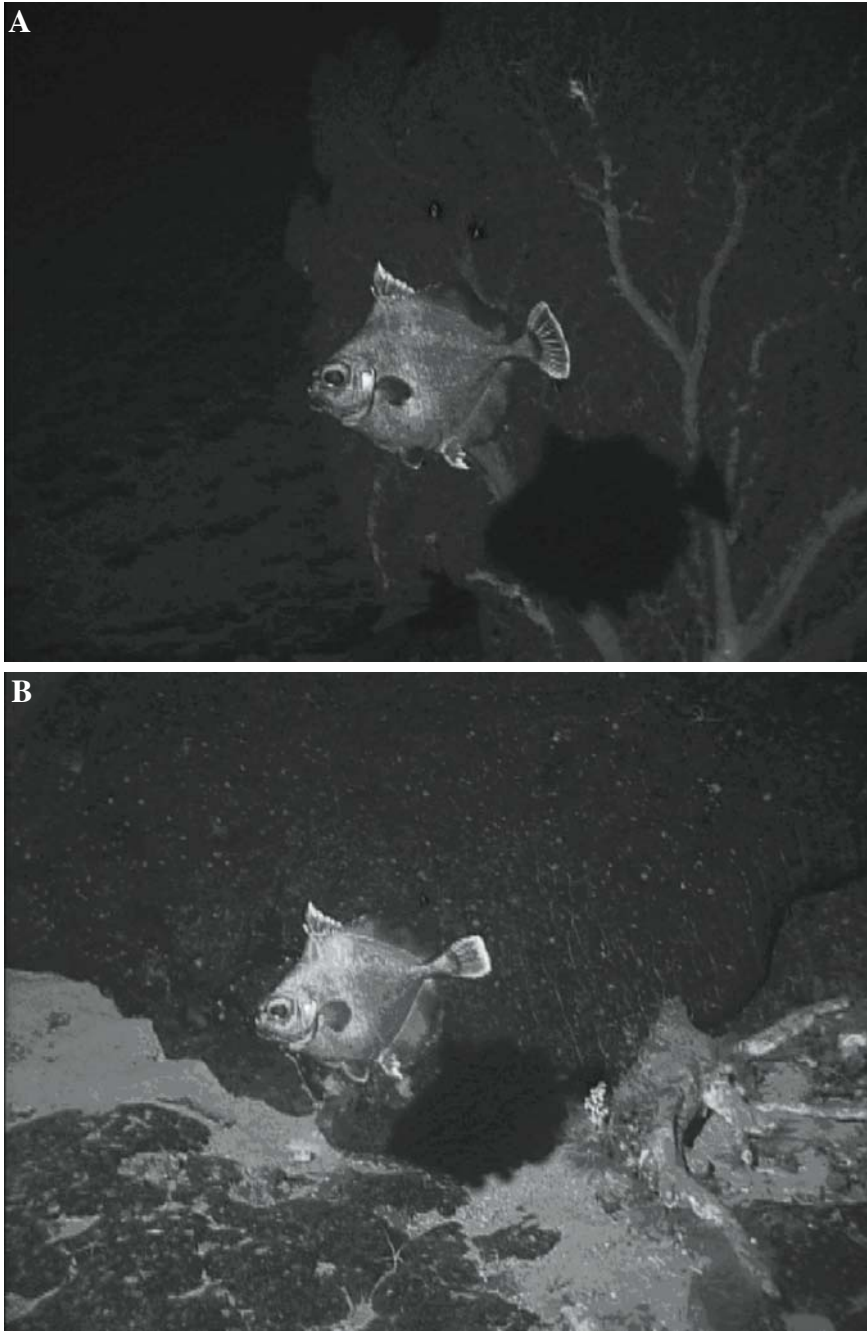
Fig. 3 *Neocyttus helgae* were observed to use (**A**) *Paragorgia* sp. coral and (**B**) depressions in the fractures of basalt pavements as shelter and flow refuge. For scale: fish length approximately 25 cm

classifications were therefore applied in a bottom up fashion. Our approach to delineating categorical habitat types was not designed to produce maps of seamount landscapes *per se* (although it is possible with this approach) but will be used to aid in quantification of the patterns of habitat use by fishes. Placing abundance data for individual species of fish within two different types of data matrices will allow quantitative approaches for assessing the role of particular landscape features in general, and corals in particular. A matrix composed of habitat subclasses *versus* microhabitat type will allow use of a chi-square test of homogeneity of distribution. Here expected values for each cell must be weighted based on the overall occurrence of each cell type along a transect or set of transects (e.g., Auster et al. 1995). A second matrix of sample (or species) abundances *versus* habitat subclass/microhabitat types (e.g., basalt pavement-coral, fine-grained sediment ripples-scattered boulders) can be analyzed using multi-dimensional scaling to ascertain relationships of groups of samples or species with particular microhabitat types.

Preliminary observations suggest that seamount fishes can be divided into four groups. The members of the first group are generalists and occur in all habitat types. These include halosaurids (i.e., *Aldrovandia* spp.), macrourids (i.e., *Caelorinchus* spp., *Nezumia* spp.) and *Synaphobranchus kaupii*. The second group, which occurs primarily in basalt habitats, includes an oreosomatid. Taxa that make up the third group occur in fine-grained sediment habitats, including macrourids (*Coryphaenoides* spp.), chimaerids (*Hydrolagus* spp.), rajids, alepocephalids, ipnopids (*Bathypterois* spp.), and synodontids (*Bathysaurus* spp.). One final group appears to be specialized in living along the ecotone of ledges and sediment and includes morids (*Antimora rostrata* and *Laemonema* spp.), ophidiid cusk-eels and other synaphobranchids besides *S. kaupii*.

Small-scale geologic and biotic components of the landscape include the organisms that are attached to or emerge from different substrate types as well as crests and depressions that influence flow patterns at local scales. Flow refuging by fishes, using depressions below the seafloor horizon and the down-current sides of epi- and emergent fauna can reduce the physiological requirements of station-keeping while enhancing the delivery of prey such as macrozooplankton and small nekton (Hobson 1991). The density of fishes on the New England Seamounts is low when compared to shelf and upper slope habitats (unpublished observations) and predation pressure may be widely dispersed, a hypothesis supported by the lack of most species to exhibit shelter-seeking behaviors (Auster et al. 1995). The exception to this observation is the behavior of *Neocyttus helgae* (family Oreosomatidae) that appears to be associated with *Paragorgia* sp., depressions within fractured basalt, and along depressed edges of pavements (Fig. 3). Their behavior appears to be related to some form of central place foraging and flow refuging. Individuals were observed holding station in the near-bottom water column behind or slightly above corals and small-scale topographic rises, apparently to encounter drifting zooplankton. Additional observations showed individuals picking at coral and sponge surfaces, apparently exploiting prey species associated with coral colonies or the polyps themselves.

It is important to note that co-occurrence does not imply a mechanistic relationship between particular habitat types and demographic processes mediating fish populations. Furthermore, many shelf and slope species exhibit facultative *versus* obligate habitat use patterns (Auster et al. 1995; Auster and Langton 1999). However, precautionary management paradigms suggest that pattern data be interpreted in a conservative manner and decision-making to conserve habitat attributes includes such features.

From a conservation science perspective, we need to evaluate the ecological role of deep-water corals as habitat for fishes within the context of the overall seamount landscape. This does not negate the need to focus first on conservation of corals based on their intrinsic long life spans and sensitivity to human caused disturbance (Koslow et al. 2001; Auster 2005).

Our objective here is to describe a system for classifying habitats in relation to the distribution of fishes. A future paper will provide a quantitative analysis relating the distribution and abundance of fishes to the range of landscape attributes on the New England Seamounts. Moreover, there remains an interest by some nations in expanding deep-water fisheries as well as designating seamounts and other deep-water features as marine reserves. This classification system can be used by those involved in mapping and monitoring to determine the spatial extent of particular habitats and quantify the dynamics of habitat based on natural and antropogenic induced chances.

Acknowledgements

References

Auster PJ (2005) Are deep-water corals important habitats for fishes? In: Freiwald A, Roberts JM (eds) Cold-water Corals and Ecosystems. Springer, Berlin Heidelberg, pp 747-760
Auster PJ, Langton RW (1999) The effects of fishing on fish habitat. In: Benaka L (ed) Fish Habitat: Essential Fish Habitat and Rehabilitation. Amer Fish Soc, Bethesda, Maryland, pp 150-187

Auster PJ, Malatesta RJ, LaRosa SC (1995) Patterns of microhabitat utilization by mobile megafauna on the southern New England (USA) continental shelf and slope. Mar Ecol Progr Ser 127: 77-85

Boehlert GW, Genin A (1987) A review of the effects of seamounts on biological processes. In: Keating BH, Fryer P, Batiza R, Boehlert G (eds) Seamounts, Islands, and Atolls. Amer Geophys Union, Geophys Monogr 43: 319-334

De Forges BR, Koslow JA, Poore GCB (2000) Diversity and endemism of the benthic seamount fauna in the southwest Pacific. Nature 405: 944-947

Greene HG, Yoklavich MM, Starr RM, O'Connell VM, Wakefield WW, Sullivan DE, McRea JE, Cailliet GM (1999) A classification scheme for deep seafloor habitats. Oceanol Acta 22: 663-678

Hobson ES (1991) Trophic relationships of fishes specialized to feed on zooplankters above coral reefs. In: Sale PF (ed) The Ecology of Fishes on Coral Reefs. Academic Press, New York, pp 69-74

Koslow JA, Gowlett-Holmes K, Lowry JK, O'Hara T, Poore GCB, Williams A (2001) Seamount benthic macrofauna off southern Tasmania: community structure and impacts of trawling. Mar Ecol Progr Ser 213: 111-125

Moore JA, Hartel KE, Craddock JE, Galbraith JK (2003) An annotated list of deepwater fishes from the New England region, with new area records. Northeast Natural 10: 159-248

Rogers AD (1994) The biology of seamounts. Adv Mar Biol 30: 305-350

Willison JHM, Hall J, Gass SE, Kenchington ELR, Butler M, Doherty P (2001) Proceedings of the First International Symposium on Deep-Sea Corals. Ecology Action Centre and Nova Scotia Museum Natural History, Halifax, 231 pp

Wilson RR, Kaufmann RS (1987) Seamount biota and biogeography. In: Keating BH, Fryer P, Batiza R, Boehlert G (eds) Seamounts, Islands, and Atolls. Amer Geophys Union, Geophys Monogr 43: 355-378

Role of cold-water *Lophelia pertusa* coral reefs as fish habitat in the NE Atlantic

Mark J. Costello[1,2], Mona McCrea[2], André Freiwald[3], Tomas Lundälv[4],
Lisbeth Jonsson[4], Brian J. Bett[5], Tjeerd C. E. van Weering[6], Henk de Haas[6],
J. Murray Roberts[7], Damian Allen[2]

[1] Leigh Marine Laboratory, University of Auckland, P.O. Box 349, Warkworth,
  New Zealand
  (m.costello@auckland.ac.nz)
[2] Ecological Consultancy Services Ltd (EcoServe), B19, K.C.R. Industrial Estate,
  Kimmage, Dublin 12, Ireland
[3] Institute of Paleontology, Erlangen University, Loewenichstr. 28, D-91054
  Erlangen, Germany
[4] Tjärnö Marine Biological Laboratory, SE-452 96 Strömstad, Sweden
[5] Southampton Oceanography Centre, Empress Dock, Southampton, SO14 3ZH,
  UK
[6] Koninklijk Nederlands Instituut voor Onderzoek der Zee (NIOZ), P.O. Box 59,
  NL-1790 AB Den Burg, Texel, The Netherlands
[7] Scottish Association for Marine Science, Dunstaffnage Marine Laboratory, Oban,
  Argyll, PA37 1QA, UK

Abstract. The rate of discovery of reefs of the cold-water coral *Lophelia pertusa* (Linnaeus, 1758) has been remarkable, and attributable to the increased use of underwater video. These reefs form a major three-dimensional habitat in deeper waters where little other 'cover' for fish is available. They are common in the eastern North Atlantic, and occur at least in the western North Atlantic and off central Africa. There are also other non-reef records of *Lophelia* in the Atlantic, and in Indian and Pacific oceans. Thus, not only are these reefs a significant habitat on a local scale, but they may also provide an important habitat over a very wide geographic scale.

The present study examined the association of fish species with *Lophelia* in the Northeast Atlantic, including the Trondheimsfjord and Sula Ridge in Norway, Kosterfjord in Sweden, Darwin Mounds west of Scotland, and Rockall Bank, Rockall Trough and Porcupine Seabight off Ireland. The fish fauna associated with a shipwreck west of Shetland was also studied. Data were collected from 11 study sites at 8 locations, using 52 hours of video and 15 reels of still photographs. Video and still photographs were collected from (1) manned submersible, (2) surface controlled remotely operated vehicle (ROV), (3) a towed "hopper" camera, (4) wide

angle survey photography (WASP), (5) seabed high resolution imaging platform (SHRIMP), and (6) an *in situ* time-lapse camera "Bathysnap". It was possible to identify 90 % of fish observed to species level and 6.5 % to genus or family level. Only 3.5 % of the fish were not identifiable. A guide to the fishes is given at http://www.ecoserve.ie/projects/aces/. Twenty-five species of fishes from 17 families were recorded over all the sites, of which 17 were of commercial importance and comprised 82 % of fish individuals observed. These commercial fish species contribute 90 % of commercial fish tonnage in the North Atlantic.

The habitats sampled were comprised of 19 % reef, 20 % transitional zone (i.e. between living coral and debris zone), 25 % coral debris and 36 % off-reef seabed. Depth was the most significant parameter in influencing the fish associated with the reefs, both at the species and family level. There was a complete separation of sites above and below 400-600 m depth by multi-dimensional scaling (MDS) analysis. Less distinct assemblages of fish species were associated with each habitat. Fish species richness and abundance was greater on the reef than surrounding seabed. In fact, 92 % of species, and 80 % of individual fish were associated with the reef. The present data indicates that these reefs have a very important functional role in deep-water ecosystems as fish habitat.

Keywords. Methods, video, census, habitat, ROV, ecosystem function, underwater photography, video

Introduction

Reefs of the cold-water coral *Lophelia pertusa* (Linnaeus, 1758) (hereinafter called *Lophelia*) form a major three-dimensional habitat in deeper waters where little other 'cover' for fish is available. *Lophelia* reefs are recorded along the European Atlantic continental margin from Norway to south-west Ireland (Rogers 1999; Roberts et al. 2003; Freiwald et al. 2004), Gibraltar Straits (Álvarez-Pérez et al. 2005), off west Africa (Colman et al. 2005), and in the western North and South Atlantic (Viana et al. 1998; Paull et al. 2000; Reed 2002; Schroeder 2002). There are also records of *Lophelia* from the Mediterranean (Taviani et al. 2004), as well as from the Indian and Pacific oceans (Rogers 1999; Reyes Bonilla and Piñón 2002; Freiwald et al. 2004; Etnoyer and Morgan 2005). The largest known *Lophelia* reef is the Røst reef southwest of Lofoten Archipelago, northern Norway, at 43 x 7 km in area (Fosså et al. 2005). It is about 10 times larger than the previously largest known reef on the Sula Ridge, off the Norwegian west coast (Freiwald et al. 2002).

The rate of discovery of *Lophelia* reefs in the Northeast Atlantic has been remarkable, almost entirely as a result of the increased use of underwater video in deep-sea surveys. It is thus likely that new video surveys will find deep-sea reefs to be more widespread than previously believed. Thus, not only is this a significant habitat on a local scale, but it may have global significance. There is an urgent need for more knowledge of these deep-water coral reefs and their associated fauna due to the increasing anthropogenic activities in these areas. Trawl damage has already occurred to reefs in all studied areas in Europe; namely in Norway (one

third damaged), (Fosså et al. 2002; Hall-Spencer et al. 2002), Sweden (Lundälv and Jonsson 2000, 2003), Scotland (Roberts et al. 2000; Gubbay et al. 2002; Wheeler et al. in press), Ireland (Grehan et al. in press), and off the Iberian peninsula (M. Lavaleye, pers. obs.); and elsewhere, including Alaska (Krieger 2001; Witherell and Coon 2001; Stone and Malecha 2003), Atlantic Canada (Mortensen and Buhl-Mortensen 2005) and off Florida (Reed et al. 2005). The destruction of these reefs may significantly reduce available habitat for fishes in deep waters. Experimental studies on tropical coastal coral reefs show local fish extinctions and emigration following loss of coral habitat (Lewis 1998). Similarly, it is logical to expect that a loss of coral habitat in deep water will result in reduced fish abundance and diversity.

The larger reefs have grown over thousands of years. The Sula Ridge reef is over 8,000 years old (Hovland et al. 1998), and reefs off the west of Ireland are at least 1.8 to 2 million years old (Van Rooij et al. 2003). *Lophelia* may grow from 1 to 25 mm per year (reviewed by J.M. Roberts 2002; Hall-Spencer et al. 2002), so the re-growth of damaged reefs will take tens to hundreds of years.

Deep-water corals provide habitat for a variety of fish species and invertebrates. For example, using underwater video, Krieger and Wing (2002) found 85 % of the larger rockfish (*Sebastes* spp.) were associated with gorgonian corals (*Primnoa* spp.) at 161-365 m depth off Alaska. From underwater video observations of *Lophelia* reefs from the Sula Ridge off Norway, (a) Mortensen et al. (1995) recorded *Sebastes* sp., *Molva molva, Brosme brosme* and *Pollachius virens*, (b) Fosså et al. (2002) observed pregnant *Sebastes viviparus,* and (c) Freiwald et al. (2002) observed that the rabbitfish *Chimaera monstrosa* inhabits the off-reef areas, *B. brosme* and *Anarhichas lupus* occur in fissures amongst the dead coral framework, and the highest concentrations of *Sebastes* sp. were on top of the reef. In the same area but using long-lines and gillnets, Husebø et al. (2002) recorded fishes from three areas, namely over coral, off coral and "uncertain". Those caught over coral were identified as such when coral was brought up on hooks. They captured (a) most abundantly *Sebastes* sp., *B. brosme, M. molva,* in coral habitats; (b) also *Melanogrammus aeglefinus, Anarhichas minor,* and *Phycis blennoides* in coral habitats; (c) *Gadus morhua, P. virens* and *Hippoglossus hippoglossus* equally in both coral and non-coral habitats; and (d) *Squalus acanthias,* Rajidae, and Torpedinidae in non-coral habitats. Commercial fish trawls in deeper waters (800-1300 m) to the west of Ireland that contained extensive amounts of coral material captured at least 13 species of fish: roundnose grenadier *Coryphaenoides ruprestris*, orange roughy *Hoplostethus atlanticus*, leafscale gulper shark *Centrophorus squamosus*, Portuguese dogfish *Centroscymnus coelolepis*, Baird's smooth-head *Alepocephalus bairdii*, North Atlantic codling *Lepidion eques*, small-eyed rabbitfish *Hydrolagus affinis*, spear-nose chimaera *Rhinochimaera atlantica*, rough-nose grenadier *Trachyrincus murrayi*, spear-snouted grenadier *Caelorinchus labiatus*, dogfish sharks Squalidae, Risso's smooth-head *Alepocephalus rostratus*, pallid sculpin *Cottunculus thomsonii*, and pudgy cuskeel *Spectrunculus grandis* (Hall-Spencer et al. 2002). These studies suggested that the *Lophelia* reefs might be an important habitat for commercial fishes. However, the published findings on fishes associated with *Lophelia* are

qualitative, and whether they can be generalised to other *Lophelia* reefs is unknown. Thus, the aim of the present study was to compare, as quantitatively as possible, the fish associated with *Lophelia* at different locations.

The methodology for fish census surveys in shallow waters with rock or coral reefs is well established, and is mainly conducted by scuba diving surveys (e.g., Costello et al. 1995). Because of the difficulty in sampling structurally complex reef habitats remotely, scuba diving is the most accurate method of quantifying the abundance and biomass of fishes. However, scuba and surface-demand diving are not possible at the depths *Lophelia* reefs typically occur, with the exception of the Trondheimsfjord reef in Norway. This reef is at depths that can be dived (39 m; Svensen et al. 1998), but these depths significantly limit observation time. There are few alternatives to surveying at these depths, and most are destructive of the fish, and sometimes the habitat. Trawling will destroy the reefs, long-lines and gillnets are difficult to accurately locate over the reefs, and baited traps would be selective for certain species and sizes. We propose that video photography is the best method for surveying the mobile fauna associated with deep-sea corals.

Several factors may influence the accuracy of visual censuses underwater, notably fish conspicuousness, activity, attraction or avoidance behaviour, water clarity, and observer speed and skill (Costello et al. 1995). The relative importance of these sources of error will vary with the survey method, the species under study, and the local environment. For deep-sea observation, moving (towed or on a Remotely Operated Vehicle) video, manned submersibles, fixed location video, and still photographs, are all options with strengths and weaknesses for different species of fishes. An advantage of video over scuba diver observations is that the video can be re-examined and studied by different persons to check for misidentifications and omissions. Costello et al. (unpublished data) compared scuba diving and video data gathered by ROV for fish census surveys. Results showed that ROV video and scuba diving surveys recorded similar diversities and abundances of fish. Differences did occur at shallow sites (<7 m) where the light came from above and cryptic fishes were difficult to see. However, in deeper water the ROV video was as effective as scuba diving. Thus, scuba diving and ROV video surveys were shown to provide comparable estimates of fish diversity and abundance. The present study used underwater video and photography, by remote and manned submersibles, to study fish abundance, behaviour and ecology in relation to *Lophelia* reefs.

Study area

Data were gathered from eight different areas, the Sula and Tautra reefs in Norway, the Kosterfjord Säcken reefs in Sweden, the Hurtside wreck in the Faroe-Shetland Channel, the Darwin Mounds in the northern Rockall Trough, and sites on the southeast of Rockall Bank, the northwest of Porcupine Bank, and within the Porcupine Seabight (Fig. 1). These areas were where existing research was in progress. No surveys were conducted especially for the present project. Depths ranged from 39 m at the Tautra Reef to 1,015 m in the Porcupine Seabight. Sampling occurred from 1996 to 2001, and during May to September at most sites (Appendix).
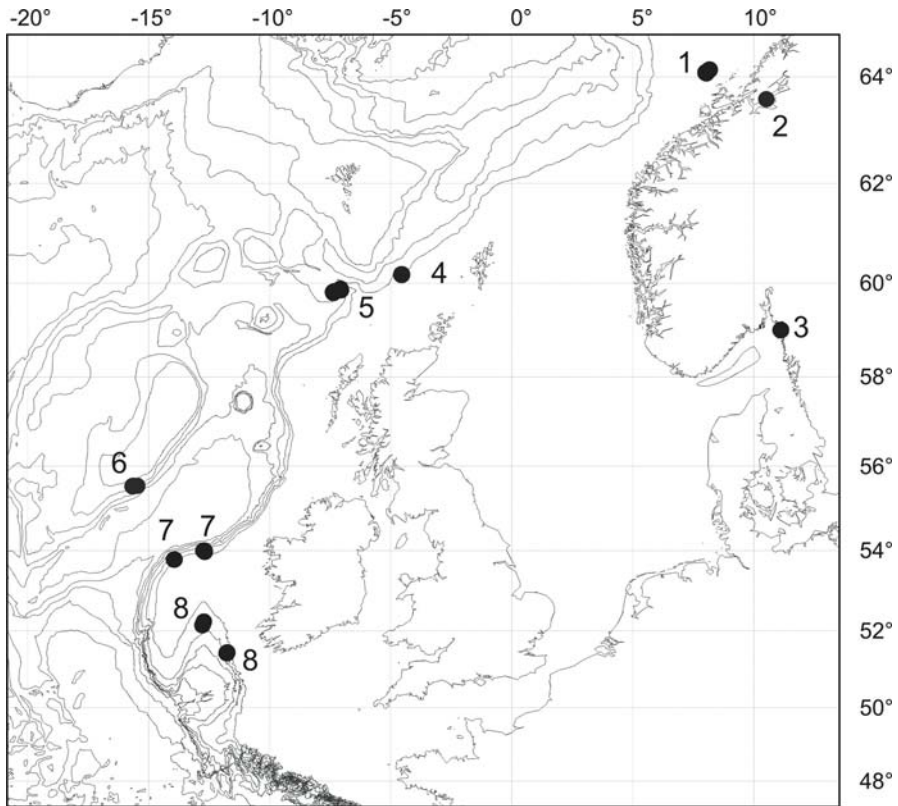
Fig. 1 Location of the study sites: 1 = Sula Ridge; 2 = Tautra Reef, Trondheimsfjord; 3 = Säcken Reef, Kosterfjord; 4 = Hurtside wreck; 5 = Darwin Mounds; 6 = Rockall Bank; 7 = Porcupine Bank; 8 = Porcupine Seabight

The more inshore Kosterfjord site was sampled on 12 occasions over four years and allows a comparison of annual variation.

1. The Sula Reef exists on a spur – the Sula Ridge – northeast of the Froyabank in water depths between 230 and 320 m. The lateral extension was mapped as 15 km (Fosså et al. 2002; Freiwald et al. 2002). Average coral framework thickness is 10-15 m but can exceed 35 m in places. The ambient seawater temperature varies between 6 to 8°C with salinities above 35 ppt. In 2000, the Norwegian Government took legal measures to ban any trawling activities on the Sula Reef (Fosså et al. 2002).

2. The Tautra Reef in the Trondheimsfjord consists of several discrete reefs (Mortensen and Fosså 2001) situated on a shallow sill (c. 35-80 m), traversing the central parts of the fjord, and separating deep basins (>400 m) to either side. Strong tidal currents, combined with compensatory currents resulting from local run-off in the inner parts of the fjord, result in a near-constant flow of deep-water over the sill, thereby creating the physical setting for the most shallow (39 m) *Lophelia* reef known to date. According to Strømgren (1971), *Lophelia* reefs in Norwegian fjord

locations are occasionally exposed to salinities as low as 32 ‰ and temperatures up to 10°C, but to our knowledge no detailed studies have been made of the environmental conditions on the Tautra Reef. Part of the reef was protected as a marine reserve in the year 2000.

3. The Säcken Reef is situated in the northern part of the Kosterfjord, close to the border between Swedish and Norwegian territorial waters. Two small patches (c. 400 m²) of live *Lophelia* occur at a depth of 80-90 m on the south-western sides of two mound structures (c. 80 x 40 x 10 m in length, width and height, respectively) that originated from coral growth (Lundälv and Jonsson 2003). The entire reef system is situated on a morainic sill (c. 85 m deep), separating deep basins (>170 m) to the north and south. The ambient seawater temperature varies between 4.2-10.9°C and the salinity between 33.5-35 ‰. The reef is exposed to semidiurnal tidal currents with a maximum velocity of 0.25 m/s and an average velocity of 0.06 m/s. The Säcken Reef area was protected from trawling in 2001, through additions to the fishery regulations in both Sweden (Norling and Sköld 2002) and Norway.

4. The Hurtside shipwreck is located in the Faroe-Shetland Channel to the west of the Shetland Islands. It was sunk in 1917 and lies at 400 m in water dominated by the North Atlantic Water and Modified North Atlantic Water masses. These surface water masses are significantly warmer (>8 and 5-8°C) than the Arctic water masses found below 500 m (Turrell et al. 1999) where *Lophelia* has not been reported (Roberts et al. 2003). Since 1917 the shipwreck has been colonized by *Lophelia* and appears to have provided a deep-water artificial reef structure that has attracted large numbers of redfish, probably *Sebastes* sp. (Roberts pers. obs.).

5. The Darwin Mounds are a recently discovered coral site in the northern Rockall Trough (Bett 2001). There are hundreds of small (50-100 m diameter, 5 m elevations) sandy seabed mounds spread over an area of some 100 km² at a depth of c. 1,000 m (Masson et al. 2003). Coral (*Lophelia* and *Madrepora oculata*) is more-or-less restricted to the mounds in this area. These mounds and the surrounding area were studied using Bathysnap, WASP and SHRIMP systems (see below).

6-8. Recently, a great many giant carbonate mounds in the Rockall and Porcupine areas have been discovered. They are typically located at upper slope depths (500-1200 m water depth). Single mounds may be up to 2 km in diameter at the base and have an elevation of up to 350 m. Some mounds appear to have coalesced to form more elongate structures. A number of these mounds support extensive coral growth, although coral is not uniformly present. Detailed geological investigations of these mounds are provided by Kenyon et al. (1998) and Huvenne et al. (2002) for the Porcupine Seabight, and Kenyon et al. (2003) for the Rockall and Porcupine Banks.

Methods

Underwater video recordings from five different sampling platforms, and still photographs from three, were studied (Appendix):

1. The manned submersible JAGO, which also collected samples for laboratory study.

2.   Remotely Operated Vehicles (ROV) were submerged on site and operated remotely *via* a connecting cable.

3.   The "Hopper camera" is designed to take digital video and still photography of the seabed. It is suspended below the survey ship as it drifts, and is equipped with two interchangeable cameras.

4.   The Wide Angle Survey Photography (WASP) platform (Huggett 1987) is suspended below the survey ship and towed at c. 0.5 knots. It is designed to take both digital video and 35 mm still photographs of the seabed from a height of about 2-4 m above the seabed. An altimeter automatically initiates recording when less than 10 m from the seabed, with video running continuously and the stills' camera taking pictures every 12 s.

5.   The Seabed High Resolution Imaging Platform (SHRIMP) is designed to transmit real time visual observations from the deep-sea floor. As with the WASP it is suspended below the survey ship as it drifts and is adjusted to keep it at the required height above the seabed. Its cameras provide long-range Hi-8 video recordings, high quality close up inspection videos and high quality still images.

6.   The "Bathysnap" platform is deployed on the seabed from the survey ship using a freefall method (Bett 2003). It can be left *in situ* for over one year. The system, housed in a tripod frame, is designed to take 35 mm still photographs of a 2 m^2 area of seabed at fixed intervals during the deployment period. It also records current speed and temperature.

The data collected included: (a) survey details such as location, dive, site, position, depth, date, duration of video, and source (Appendix); (b) survey effort as the amount of time the video spent on the different habitats of a coral reef (reef, transitional zone, coral debris zones and seabed), and (c) fish species, numbers, and behaviour, including response to the camera and the habitat they were observed in.

Definitions of coral reef habitats were based on Mortensen et al. (1995) and Freiwald et al. (2002), such that the "transition zone" is the seabed adjacent to the reef but with patches of live coral, the "coral debris zone" is dominated by dead coral (some erect, but most fragments on the seabed), and the "seabed zone" has no living or dead coral material. Only the latter can be considered non-coral associated habitat.

Fish behaviour and reaction to the video was recorded in seven categories, namely 'actively swimming', 'hovering' (swimming but stationary), 'hiding' (sitting within the reef), 'feeding', 'resting on seabed', 'no reaction' (no movement), 'avoidance' (move away from the camera), and 'attraction' (move towards camera).

It should be noted that the videos used in this study were not specifically taken for fish census surveys, but for a variety of purposes. Due to the high costs of obtaining information from these deep-water reefs, we used available video data rather than carried out specific fish census surveys. Because of this, only 'actual survey time' was included in this analysis. This excluded the time used when the video zoomed in on a species of interest, took a sample or was in the water column.

This also minimised the likelihood of repeat counting of fish. From a total of 80 h 18 min of video, 52 h 25 min was used for data analysis. The remaining time was spent in the water column, sample collection, or taking close up photographs of items of interest. Out of the 'actual survey time' the times spent over the reef, transitional zone, coral debris zone and seabed substrata were calculated. For data analysis, species abundances were adjusted for effort by dividing counts by the minutes surveyed.

Fish community structure was described by univariate measures and multivariate analysis. Species richness (number of species, the commonest index of diversity), and dominance (percent of the most abundant species comprised of all species in the site), express the two components of diversity more clearly than more compound 'heterogeneity' indices (Costello and Myers 1987; Magurran 2004). Dominance is the inverse of evenness and so calculation of evenness indices was not considered necessary.

The two extremes of data transformation for non-parametric multivariate analysis are to weight the analysis according to either (a) species abundance so the dominant (most abundant) species has most influence on the results, or (b) species presence and absence, so the rare species have equal weight with the common species (Clark and Gorley 2001). There is no statistical reason to transform the data (Clark and Gorley 2001). In the present study both approaches were taken because agreement between them provides greater confidence in the ecological reality of the findings. Analyses were thus conducted on (a) abundance as numbers of all species observed divided by survey time, and (b) all species as presence only. Using PRIMER (Clark and Gorley 2001), data was clustered using the Bray-Curtis similarity index and presented as multi-dimensional scaling (MDS) plots.

Results

Most of the video time was spent over the seabed sediment adjacent to the reef (18 h : 07 m), followed by the coral debris zone (12:52), transitional zone (10:14) and reef zone (9:39) (Fig. 2). Thus survey effort was greater for the seabed (36 %), than the coral debris (25 %), transitional zone (20 %) and living reef (19 %). Survey effort was not equal across sites and habitats, with greater effort and proportionally more reef in Kosterfjord and Sula Ridge (Fig. 2), the two sites where most species were recorded.

It was possible to identify 90 % of fishes to species level, 6.5 % to genus or family level. Only 3.5 % of observations were unidentifiable. A photographic guide to the fishes from the present study is available (McCrea et al. 2003a, b).

Comparison of sampling methods

Different photographic techniques were used at the study sites. At some sites more than one technique was used, but never at the same time (Appendix). It is notable that the still cameras recorded almost as many species as the video images at the same sites (Table 1). The video data gathered from the submersible and ROV were the most useful for fish identification purposes because they showed fish from
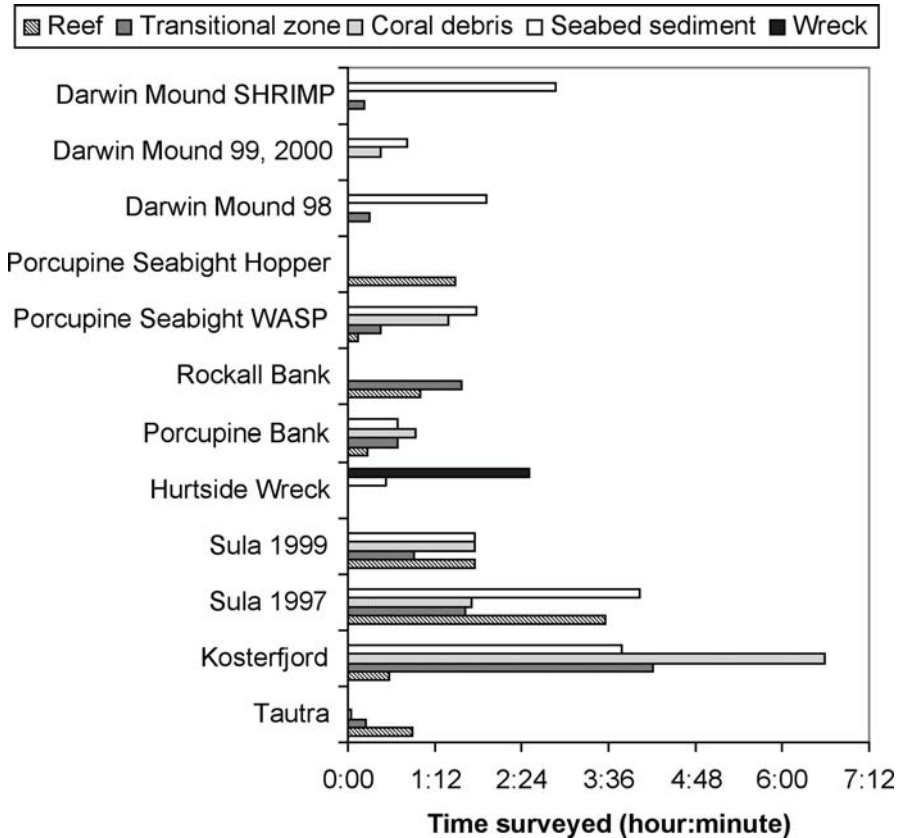
Fig. 2 The amount of time each habitat was surveyed at each study site

different perspectives. The hopper camera only gives a view of the fish from above, making identification difficult.

Fish behaviour

Sula Ridge

Sebastes sp. (redfish) were the most abundant fish on top of the reef, hovering in shoals almost motionless facing into the current (Table 2). They also occurred in the transition zone and more rarely individuals were observed resting on the seabed next to a large boulder or hiding in the reef. When the submersible and ROV approached, they either swam off or hid in the reef. All redfish recorded on the Sula Reef appeared to be *Sebastes viviparus*. At least two size-groups of redfish were observed but it was difficult to estimate size from the videos.

Obviously pregnant redfish were observed at Sula Ridge on 29 May 2001. *Pollachius virens* (saithe) and *Chimaera monstrosa* (rabbitfish) were attracted to the video lights, and were seen to feed on crustaceans swarming in front of lights (Table 2).

Table 1 Fish recorded in association with *Lophelia pertusa* from WASP, Bathysnap and SHRIMP still photographs. Species are in taxonomic order according to Costello et al. (2001). Abundance scored as + = 1-10. ++ = >10

Study site Photography platform	Darwin Mounds WASP	Darwin Mounds Bathysnap	Darwin Mounds SHRIMP	Porcupine Seabight WASP	Porcupine Seabight Bathysnap
Chimaeridae					
Chimaera monstrosa	+	-	+	-	-
Noatocanthidae					
Notocanthus sp.	-	-	+	+	-
Synaphobranchidae					
Synaphobracnhus kaupii	+	++	++	+	-
Macrouridae					
Macrouridae indet.	+	-	+	+	+
Coryphaenoides rupestris	+	-	-	+	+
Moridae					
Moridae indet.	+	-	+	++	-
Lepidion eques	-	+	+	-	++
Lotidae					
Molva molva	-	+	+	-	-
Phycidae					
Phycis/Urophycis	-		-	-	+
Oreosomatidae					
Neocyttus helgae	-	-	-	-	+
Unidentified fish					
Unidentified (black fish)	-	-	-	+	+
Total species	**4**	**3**	**6**	**4**	**3**
Total species from stills		**6**		**7**	
Total species from video		**7**		**9**	

There appeared to be an abundance of planktonic and benthic life at the Sula Ridge, including high densities of squat lobsters, *Munida sarsi*, and seabed features indicating sediment feeding infauna. Such abundance was not observed at other sites.

Tautra Reef

Pollachius virens were the dominant fish at the Tautra Reef, with the majority of individuals occurring over the reef area and fewer over the coral debris zone. Most individuals were actively swimming or hovering and seemed to avoid, or were disturbed by, the submersible. *Sebastes* sp. were abundant hovering over the reef and were apparently undisturbed by the submersible. *Trisopterus minutus* (poor cod) was only recorded from the Tautra Reef and was observed hiding in the reef, apparently avoiding the submersible (Table 2).

Table 2 The behaviour, response to the camera, and habitat observations for each fish species combined for all sites

Family	Species	Fish behaviour					Fish response			Habitat			
		Actively swimming	Hovering	Hiding	Resting on seabed	Feeding	No reaction	Avoidance - disturbed	Attraction	Reef	Transitional zone	Coral debris	Seabed sediment
Scyliorhinidae	Scyliorhinidae indet.	√	-	-	-	-	√	-	-	-	-	√	√
	Scyliorhinus stellaris	√	-	-	√	-	-	√	-	-	√	-	√
Rajidae	*Raja* sp.	-	-	-	-	-	-	-	-	-	-	-	-
	Raja fyllae	-	-	-	√	-	√	-	-	-	-	-	√
Chimaeridae	*Chimaera monstrosa*	√	√	-	-	√	√	-	√	-	-	√	√
Notocanthidae	*Notocanthus* sp.	-	-	-	-	-	-	√	-	-	-	-	-
Synaphobranchidae	*Synaphobranchus kaupii*	√	√	-	-	-	√	√	-	-	√	√	√
Macrouridae	Macrouridae indet.	-	-	-	√	-	√	-	-	-	-	-	-
	Coryphaenoides rupestris	-	-	-	√	-	√	-	-	-	-	-	-
Moridae	Moridae	-	√	-	√	-	√	-	-	-	√	√	-
	Lepidion eques	√	√	-	-	-	√	-	-	-	√	-	-
Gadidae	*Gadus morhua*	√	-	-	-	-	-	√	√	√	√	√	-
	Melanogrammus aeglefinus	√	-	-	-	-	√	-	-	-	-	√	√
	Pollachius virens	√	-	-	-	√	-	√	√	√	-	√	-
	Trisopterus luscus	√	√	√	√	-	√	√	√	√	√	√	√
	Trisopterus minutus	-	-	√	-	-	-	√	-	√	-	-	-
Lotidae	*Brosme brosme*	-	-	-	√	√	√	-	-	√	-	-	√
	Molva molva	√	√	√	√	-	-	√	√	√	√	√	-
Phycidae	*Phycis/Urophycis*	-	√	-	√	-	√	-	-	-	√	-	√
Lophiidae	*Lophius piscatorius*	-	-	-	√	-	-	√	-	-	-	-	√
Oreosomatidae	*Neocyttus helgae*	-	√	-	-	-	√	-	-	-	-	-	-
Sebastidae	*Helicolenus dactylopterus*	-	-	-	-	-	-	-	-	-	-	-	-
	Sebastes viviparus	-	√	√	√	√	√	√	-	√	√	-	√
Cottidae	*Icelus bicornis*	-	-	-	√	-	√	-	-	-	√	-	-
	Micrenophrys lilljeborgi	-	-	√	-	-	-	√	-	-	-	√	-
Zoarcidae	*Lycodes vahlii*	-	-	-	√	-	√	-	-	-	-	-	√
Anarhichadidae	*Anarhichas lupus*	-	-	-	√	-	√	√	-	-	-	-	-
Pleuronectidae	*Hippoglossus hippoglossus*	-	-	-	√	-	-	-	-	-	-	-	√
	Microstomus kitt	-	-	-	√	-	√	-	-	-	-	-	√

Säcken Reef, Kosterfjord

Gadus morhua (cod) were the dominant species occurring in the Kosterfjord, actively swimming over the transitional and coral debris zones, displaying a mixed reaction to the ROV (Table 2). The only observations of *Micrenophrys lilljeborgi* (Norway bullhead), *Icelus bicornis* (two horn sculpin), and *Trisopterus luscus* (bib)
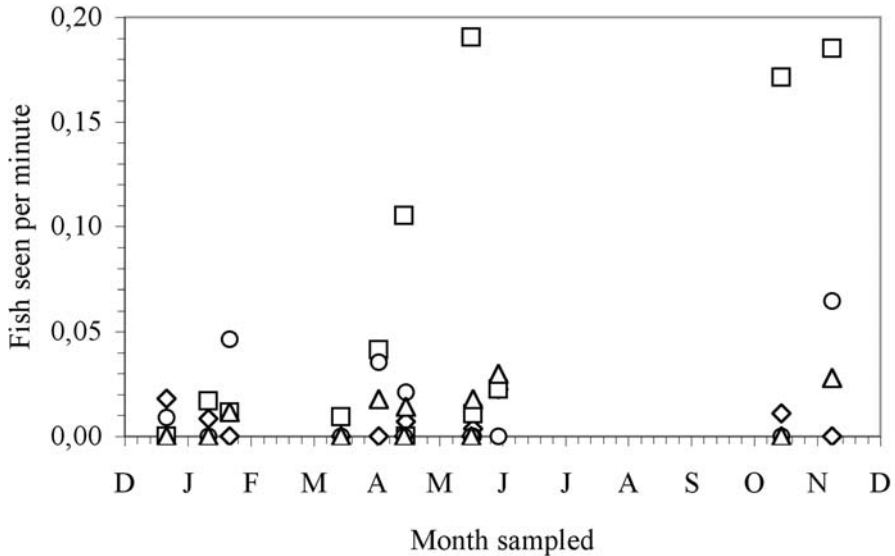
Fig. 3 Numbers of *Gadus morhua* (squares), *Pollachius virens* (circles), *Trisopterus luscus* (diamonds) and *Sebastes* sp. (triangles) observed per minute of survey time on each sampling occasion at the Kosterfjord. Samples were collected from 1998 to 2001 but have been plotted over one calendar year to facilitate examination of possible seasonal variation

occurred at this site. The bullhead was hiding on the coral debris zone avoiding the ROV, while the sculpin was resting on the seabed in the transitional zone with no reaction to the ROV (Table 2). *Trisopterus luscus* displayed the range of behaviours over all the zones (Table 2). High abundances of *Munida rugosa* and planktonic life (e.g., *Meganyctiphanes norvegica* and *Sagitta* spp.) were also noted at Säcken Reef.

Darwin Mounds

Synaphobranchus kaupii and Moridae were the dominant fishes recorded around the Darwin Mounds, and were observed hovering or sometimes swimming over the seabed. The former, *S. kaupii,* either avoided the camera or were not disturbed by it (Table 2).

Porcupine Seabight

Moridae were the dominant fishes recorded from the Porcupine Seabight, and were observed resting or hovering on transitional, coral debris and seabed zones (Table 2). They showed no reaction to the camera.

Porcupine and Rockall Banks

Synaptobranchus kaupii and Moridae were the dominant species on the Porcupine and Rockall Banks. The former were swimming or hovering mainly over coral debris and seabed zones (Table 2). The Moridae were resting on the seabed, often beside coral debris, and showed no reaction to the camera (Table 2).

Hurtside wreck

Sebastes sp. and *Molva molva* (ling) dominated the fish fauna at the Hurtside wreck. *Sebastes* sp. were observed hovering over the wreck and did not react to the ROV. Similarly, ling were actively swimming or hovering over the wreck with no reaction to the ROV (Table 2).

Seasonal variation

Kosterfjord was the only study site with sufficient sampling to examine possible seasonal variation. While data was collected from January to November, there was no data from July to October, and it was spread over four years. Thus the apparent absence of seasonal patterns must be considered with caution (Fig. 3).

Species diversity

From the study sites, 25 species and 17 families of fish were recorded (Table 3). The sites were dominated by different species in relation to depth, namely *P. virens* at Tautra Reef (40 m depth), *G. morhua* at Kosterfjord (77-118 m), *Sebastes* sp. at Sula Reef and Hurtside wreck (300-400 m) and *S. kaupii* and Moridae at sites over 600 m depth (Table 3).

More species were recorded with greater sampling time across all sites (Fig. 4a). However, there was no increase in fish abundance with sampling time (Fig. 4b). These patterns suggest the data are an accurate representation of the overall fish abundance at the time of sampling, because the additional species recorded over time have lower abundance (i.e. they were rare).

The shallowest sites, namely at Tautra and the Hurtside wreck, had few species with high abundance (Fig. 5a). The shallower reef areas of Kosterfjord and Sula Ridge in Norway had more species but similar abundance to the Porcupine, Darwin and Rockall areas off Ireland. Species richness ranged from 5 to 12 species per site, and dominance from 34 % to 85 % (Fig. 5b). There were no differences in dominance that may be attributed to depth or sampling effort.

Depth was a highly significant factor in influencing the occurrence of fish assemblages at family and species levels. Multivariate analysis clearly distinguished shallow and deeper sites (Fig. 6). The Gadidae, Lotidae and *Sebastes* sp. occurred in shallower waters (<400 m depth), the Notocanthidae, Synaphobranchidae, Macrouridae, Moridae, and Oreosomatidae in deeper, and Chimaeridae at all depths (Table 3). Although less abundant, species of the families Cottidae, Zoarcidae, Anarhichadidae, and Pleuronectidae were limited to the shallower areas.

Habitat associations

The greatest richness of species was recorded in the transitional (19 species) habitat (Table 4). The *Lophelia* associated habitats, namely the reef, transition and coral debris zones, contained 92 % (23 of 25) of the species, and 80 % of the abundance of fish at the study sites (excluding the Hurtside wreck data). The species could be grouped according to their frequency of occurrence in these habitats (Table 4):

Table 3 Fish recorded in association with *Lophelia pertusa* from manned submersible (sub), ROV, hopper cameras, WASP and SHRIMP video cameras. Sites are arranged according to depth. Species nomenclature and taxonomic order follow Costello et al. (2001). The total number of sites where fish were recorded combines the (a) Sula 1997 and 1999, (b) Porcupine Seabight WASP and hopper camera, (c) Darwin Mounds WASP and SHRIMP, and (d) excludes the Hurtside Wreck data. * species of commercial importance as defined by occurrence in landings data (ICES 2003), and ** additionally noted as the focus of a deep-water fishery by Gordon (2001). The number of the most abundant species at a site is underlined and in bold text, and this proportion of the total number of fish at the site is used to calculate % dominance index

Site name		Tautra	Kosterfjord	Sula Ridge'97	Sula Ridge'99	Hurtside wreck	Porcupine Bank	Rockall Bank	Porcupine Seabight	Porcupine Seabight	Darwin Mounds	Darwin Mounds'98	Darwin Mounds	Total no. individuals	Total sites
Depth (m)		40	77-118	312-329	300-311	400	600-957	727-858	640-984	866-1015	962-1082	930-983	941-954		
Video type		ROV	ROV	Sub	Sub	ROV	Hopper	Hopper	WASP	Hopper	WASP	WASP	SHRIMP		
Scyliorhinidae															
Scyliorhinidae indet.	*	0	0	0	0	0	0	0	1	0	1	0	0	2	2
Scyliorhinus stellaris	*	0	0	1	2	0	0	0	0	0	0	0	0	3	1
Rajidae															
Raja sp.		0	0	0	0	0	0	0	0	0	0	1	0	1	1
Raja fyllae		0	0	1	1	0	0	0	0	0	0	0	0	1	1
Chimaeridae															
Chimaera monstrosa	*	2	0	13	6	0	3	0	3	1	6	6	12	52	5
Noatocanthidae															
Notocanthus sp.		0	0	0	0	0	5	0	3	0	4	0	16	28	3
Synaphobranchidae															
Synaphobranchus kaupii		0	1?	0	0	0	**113**	25	19	9	24	**61**	**150**	402	5
Macrouridae															
Macrouridae	*	0	0	0	0	0	0	5	0	2	9	0	1	17	3
Coryphaenoides rupestris	**	0	0	0	0	0	0	0	0	0	4	0	6	10	1

Table 3 continued

Site name		Tautra	Kosterfjord	Sula Ridge'97	Sula Ridge'99	Hurtside wreck	Porcupine Bank	Rockall Bank	Porcupine Seabight	Porcupine Seabight	Darwin Mounds	Darwin Mounds'98	Darwin Mounds	Total no. individuals	Total sites
Depth (m)		40	77-118	312-329	300-311	400	600-957	727-858	640-984	866-1015	962-1082	930-983	941-954		
Video type		ROV	ROV	Sub	Sub	ROV	Hopper	Hopper	WASP	Hopper	WASP	WASP	SHRIMP		
Moridae	*														
Moridae	*	0	0	0	0	0	38	27	110	16	20	0	16	227	4
Lepidion eques		0	0	0	0	0	8	7	0	6	0	0	0	21	3
Gadidae															
Gadus morhua	*	0	75	0	6	0	0	0	0	0	0	0	0	81	2
Melanogrammus aeglefinus	*	1	1	0	0	0	0	0	0	0	0	0	0	2	2
Pollachius virens	*	872	18	0	35	0	0	0	0	0	0	0	0	925	3
Trisopterus luscus	*	0	10	0	0	0	0	0	0	0	0	0	0	10	1
Trisopterus minutus	*	27	0	0	0	0	0	0	0	0	0	0	0	27	1
Lotidae															
Brosme brosme	**	0	0	19	12	17	3	0	0	0	0	0	0	49	2
Molva molva	**	0	0	8	4	249	0	3	0	2	0	0	0	266	3
Phycidae															
Phycis/Urophycis	*	0	0	0	0	0	1	0	0	0	0	0	0	1	1
Lophiidae															
Lophius piscatorius	**	0	0	0	4	5	0	0	0	0	0	0	0	9	1
Oreosomatidae															
Neocyttus helgae		0	0	0	0	0	0	0	4	1	0	0	0	5	1
Sebastidae															
Helicolenus dactylopterus		0	0	0	0	0	0	0	2	0	0	0	0	2	1
Sebastes viviparus	*	154	18	270	409	466	0	0	0	0	0	0	0	1317	3

Table 3 continued

Site name	Tautra	Kosterfjord	Sula Ridge'97	Sula Ridge'99	Hurtside wreck	Porcupine Bank	Rockall Bank	Porcupine Seabight	Porcupine Seabight	Darwin Mounds	Darwin Mounds'98	Darwin Mounds	Total no. individuals	Total sites
Depth (m)	40	77-118	312-329	300-311	400	600-957	727-858	640-984	866-1015	962-1082	930-983	941-954		
Video type	ROV	ROV	Sub	Sub	ROV	Hopper	Hopper	WASP	Hopper	WASP	WASP	SHRIMP		
Cottidae														
Icelus bicornis	0	1	0	0	0	0	0	0	0	0	0	0	1	1
Micrenophrys lilljeborgi	0	1	0	0	0	0	0	0	0	0	0	0	1	1
Zoarcidae														
Lycodes vahli	0	3	0	0	0	0	0	0	0	0	0	0	3	1
Anarhichadidae														
Anarhichas lupus *	0	2	0	1	0	0	0	0	0	0	0	0	3	2
Pleuronectidae														
Hippoglossus hippoglossus *	0	0	0	1	0	0	0	0	0	0	0	0	1	1
Microstomus kitt *	0	5	1	1	0	0	0	0	0	0	0	0	7	2
Unidentified fish														
Unidentified	0	15	9	7	2	57	11	0	9	0	0	0	110	
Unidentified (black fish)	0	0	0	0	0	0	0	6	0	3	3	0	12	
Unidentified (eel)	0	0	0	0	0	0	0	5	0	0	0	0	5	
Shark?	0	0	0	0	0	0	0	0	0	0	1	0	1	
Total individuals	1056	149	323	487	737	228	78	153	46	71	72	201	3602	
Total No. species	5	12	9	11	5	8	6	9	8	8	5	6	25	
Dominance (%)	83	50	84	84	63	50	44	72	35	34	85	75		
Total minutes	01:47:00	28:19:20	17:07:51	11:47:17	03:48:45	02:34:03	02:34:23	03:55:19	01:37:02	01:17:35	02:23:38	03:06:20		
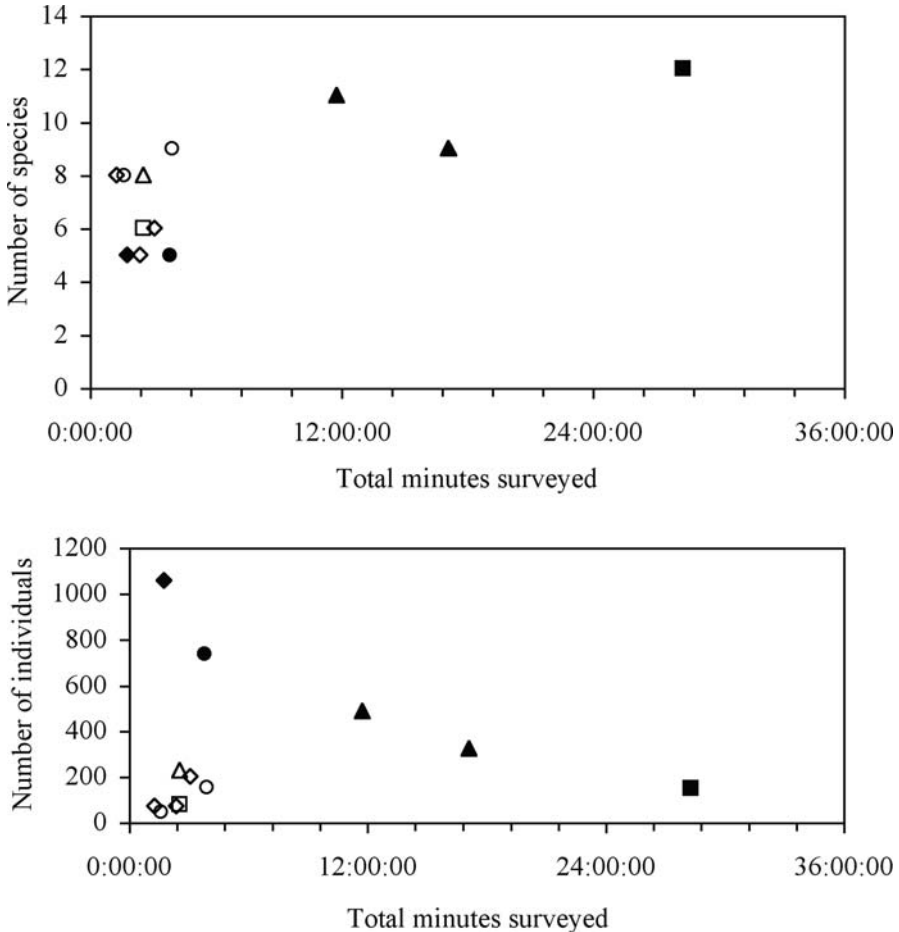
Fig. 4 The relationships of species richness and abundance with sampling time across the study sites: Tautra (solid diamond), Sula (solid triangle), Kosterfjord (solid square), Hurtside wreck (solid circle), Rockall (square), Porcupine (circles), Darwin Mounds (diamonds). Sites less than 400 m depth have solid symbols

(1)   the gadoids *P. virens* and *T. minutus,* wolffish *Anarhichas lupus, Sebastes* sp., and lotid *Brosme brosme* were most frequently recorded in association with the coral reef habitat. Although the lotid *Molva molva* was most frequent on the Hurtside wreck, otherwise they were most often associated with the coral reef and the seabed.

(2)   Coryphaenoides ruprestris, G. morhua, Macrouridae, *T. luscus,* and Moridae including *Lepidion eques,* were more frequently observed in the transitional zone and coral debris habitat.

(3)   Chimaera monstrosa, Notocanthus sp., *S. kaupii,* and *Microstomus kitt* were more closely associated with sedimentary seabed habitat.

Multivariate analysis across sites showed separation of habitats, with a gradient from reef to debris to seabed for the deeper sites when analysed as either abundance (Fig. 7a) or presence-absence (Fig. 7b). The transitional zone habitat, which is a mix of patches of coral over coral debris and seabed, overlapped the other habitats. The habitats were not so clearly distinguished for the shallower sites (Fig. 7). The wreck habitats, namely wreck itself and adjacent seabed, were grouped within the shallow-water habitats.
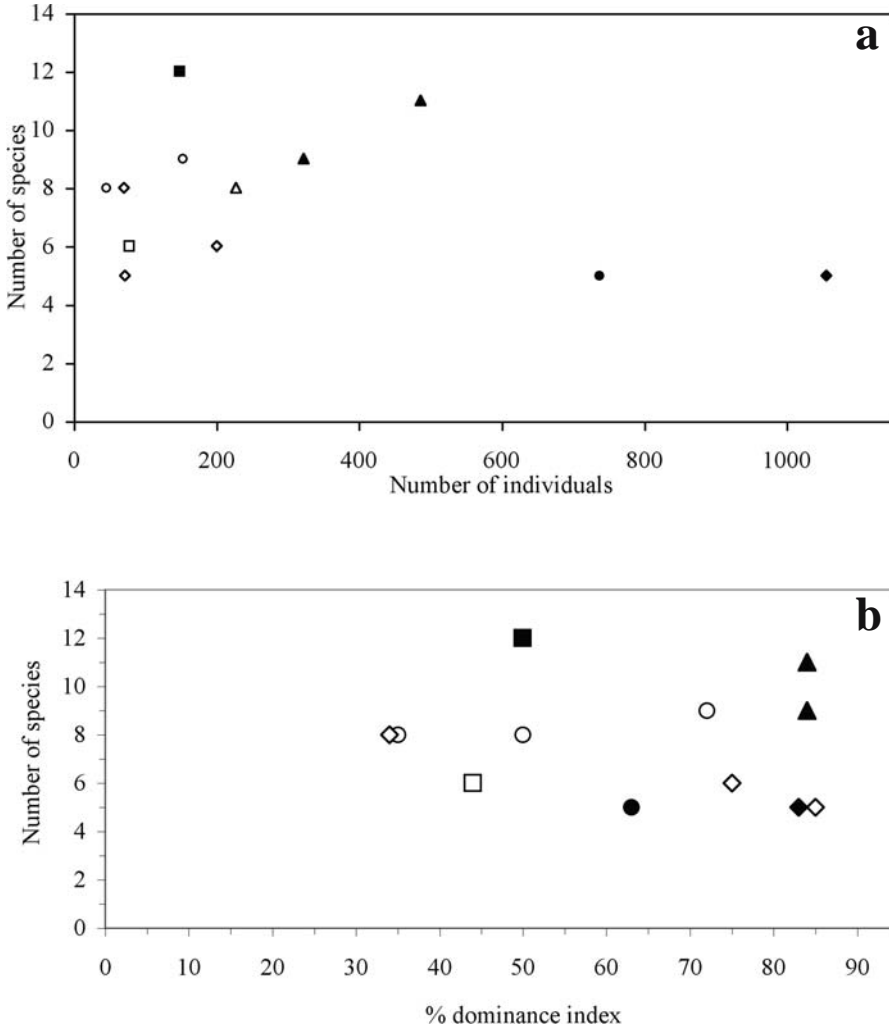
Fig. 5 The relationships of (**a**) species richness and abundance and (**b**) dominance index (%), across the study sites; Tautra (solid diamond), Sula (solid triangle), Kosterfjord (solid square), Hurtside wreck (solid circle), Rockall (square), Porcupine (circles), Darwin Mounds (diamonds). Sites less than 400 m depth have solid symbols
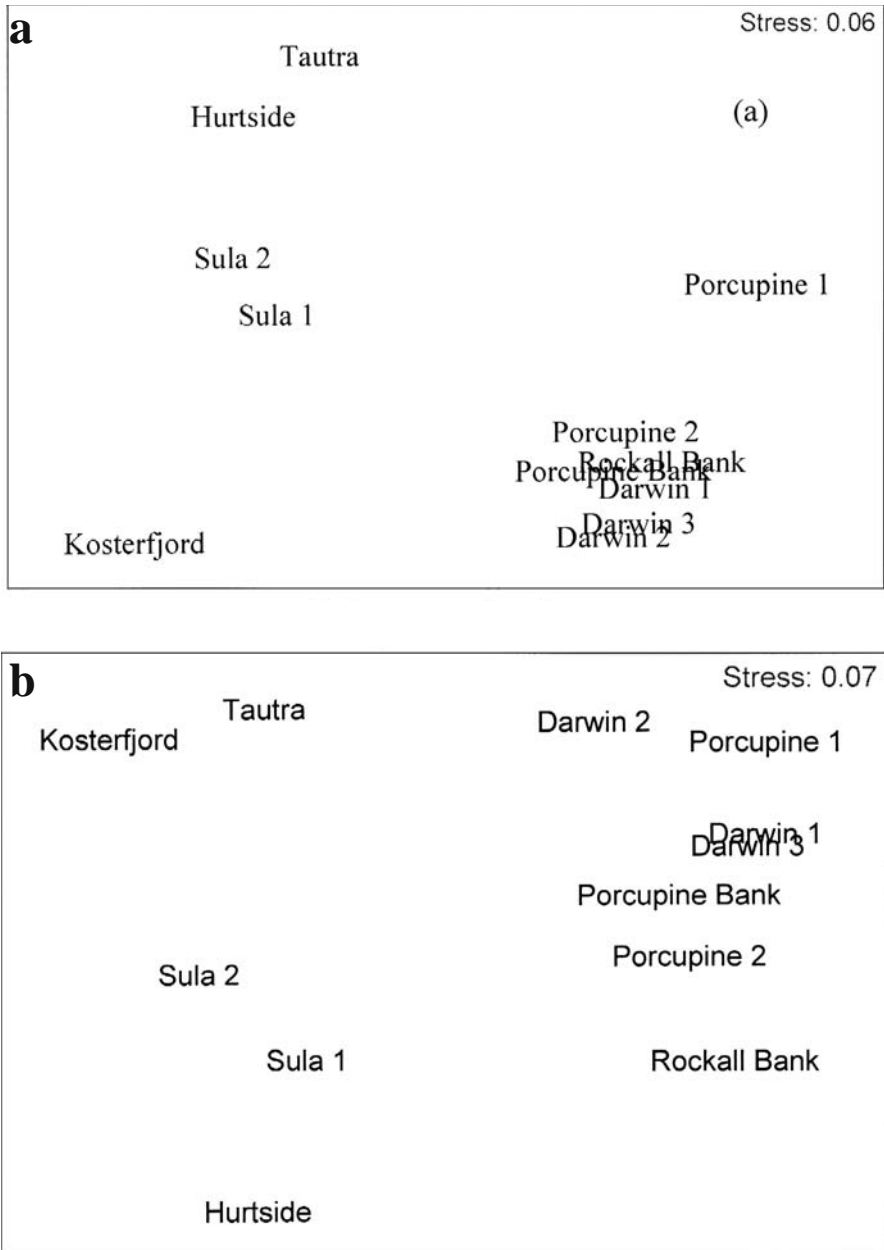
Fig. 6 MDS plots of the similarity between sites based on the (**a**) abundance of each fish species standardised by time surveyed, and (**b**) presence/absence of species. Stress values <0.1 indicate significance

Table 4 The percent occurrence of species in each habitat summer for all sites, and total number of species recorded for each habitat. Potential duplicate counts are excluded, so *Raja* sp. and *Raja fyllae* are counted as one species. Shading indicates the habitats taxa were more frequent in

Species	Reef	Wreck	Transitional	Coral debris	Seabed	Total records
Neocyttus helgae	100	0	0	0	0	2
Trisopterus minutus	85	0	15	0	0	27
Pollachius virens	72	0	25	1	1	925
Anarhichas lupus	67	0	0	33	0	3
Sebastes viviparus	57	33	5	2	3	1317
Helicolenus dactylopterus	50	0	50	0	0	2
Brosme brosme	35	33	10	6	16	49
Molva molva	5	84	3	1	4	266
Lophius piscatorius	13	50	25	0	13	9
Lepidion eques	33	0	57	5	5	21
Gadus morhua	9	0	46	33	12	81
Moridae	16	0	37	19	28	227
Coryphaenoides rupestris	0	0	50	40	10	10
Macrouridae indet.	18	0	29	47	6	17
Trisopterus luscus	10	0	30	50	10	10
Scyliorhinus stellaris	0	0	33	0	67	3
Scyliorhinidae indet.	0	0	0	50	50	2
Lycodes vahlii	0	0	33	0	67	3
Synaphobranchus kaupii	4	0	8	6	81	401
Chimaera monstrosa	2	0	12	12	75	52
Notocanthus sp.	0	0	11	11	79	28
Microstomus kitt	0	0	29	14	57	7
Melanogrammus aeglefinus	0	0	0	100	0	2
Phycis/Urophycis	0	0	100	0	0	1
Icelus bicornis	0	0	100	0	0	1
Micrenophrys lilljeborgi	0	0	0	100	0	1
Raja sp.	0	0	0	0	100	1
Raja fyllae	0	0	0	0	100	1
Hippoglossus hippoglossus	0	0	0	0	100	1
Total no. of species per habitat	**15**	**4**	**19**	**16**	**17**	**25**

Discussion

Methods for fish census on *Lophelia*

The localised occurrence and frequently complex topography of deep-water coral reefs poses significant practical problems to their study. The use of submersibles and ROV offers an ideal method by which to link biological observations with precise knowledge of the habitat under study. However, scientific access to deep-water
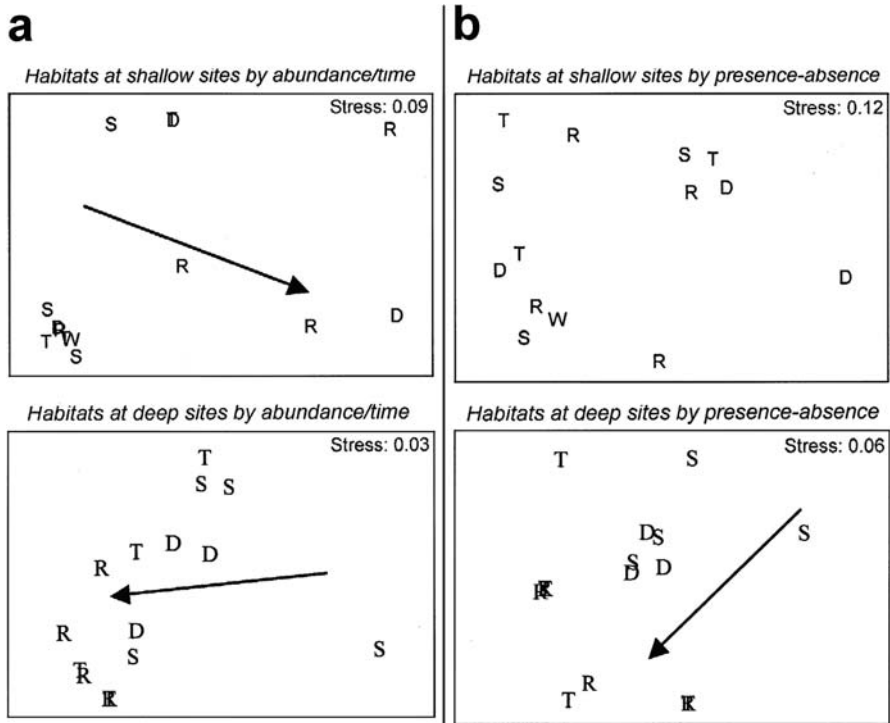
Fig. 7 MDS plots of the similarity between habitats at the sites based on the (a) abundance of each fish species standardised by time surveyed, and (b) presence/absence of species. Habitat abbreviations are R = reef, T = transition zone, D = coral debris zone, S = seabed, W = wreck. Arrows have been drawn to indicate a direction of increasing habitat complexity from seabed to reef

submersibles and ROV is limited and other techniques, including those employed in the present study, remain necessary.

The recording of similar species by the different underwater photographic methods, and with other studies using trawls, long-lines and gill-nets (Mortensen et al. 1995; Fosså et al. 2002; Hall-Spencer et al. 2002; Husebø et al. 2002), suggests that these techniques provide a representative qualitative sample of fish biodiversity in deep waters. Furthermore, the results of the present study indicate that underwater video can be used to quantify fish abundance.

Fish associated with *Lophelia*

Studies using video (Mortensen et al. 1995; Fosså et al. 2002), and long-lining and gillnet (Husebø et al. 2002), recorded fish species in association with *Lophelia* reefs. The present study expands on these by providing more quantitative data that show more species and numbers of fishes associated with the coral reef and transitional reef habitats than with the surrounding seabed.

Three-dimensional (3-D) habitats are known to attract certain fishes. For example, in inshore areas, rocky coasts provide habitats for the gadoids and lotids recorded in this study. Artificial reef habitats, such as shipwrecks, may create localized increases in species richness, and Husebø et al. (2002) cite several sources that found *Sebastes* to be more common on shipwrecks, large sponges and amongst stones. Roberts et al. (2005) reported *Sebastes* sheltering by erect sponges during a month-long lander observation period by the Sula Ridge reef complex. *Sebastes* are also abundant amongst oil industry installations west of Shetland (Bett pers. obs.). Rocky habitat (probably glacial debris) and large sponges are widespread on the upper slope of the Northeast Atlantic continental margin (Klitgaard et al. 1997; Bett 2001; Masson 2001). However, 3-D habitat appears to be less frequent in deeper waters. Furthermore, the present study did not find the fish assemblage of the shipwreck to cluster more closely with the coral reef, as preliminary analysis suggested. This reflects the facts that (a) few (up to five) species of fish were associated with the wreck whereas at least five species occurred in association with the *Lophelia* reefs (Table 3), and (b) that the ship wreck is different from the reef in providing flat surfaces more similar to the seabed. For example, the fourth most abundant species on the wreck was the anglerfish *Lophius piscatorius* which sits on the seabed, or on the deck of the ship wreck. Although species such as *Sebastes* may find a shipwreck and coral reef to be similar for their purposes, this is not necessarily the case with other fish species. Therefore, *Lophelia* reefs provide a significant and unique contribution to biodiversity by providing 3-D habitat, a habitat that is otherwise uncommon in deep-sea areas.

Commercial fish associated with *Lophelia*

It has previously been noted that many of the species associated with *Lophelia* reefs are commercially fished (Hall-Spencer et al. 2002; Husebø et al. 2002). Of the species recorded in the present paper, 17 of the 25 (68 %) are of commercial interest (Table 3). These species comprised 82 % of the abundance of fish associated with the *Lophelia* reefs. The same 17 species make up 90 % of the total tonnage of fish landed in the North Atlantic (ICES 2003). Additional fish species have been captured by commercial trawls in other *Lophelia* reef areas (Hall-Spencer et al. 2002). It is evident that *Lophelia* reefs are an important habitat for commercial fish in these deep-sea areas. Further quantification of the contribution of this habitat to European commercial fish stocks requires a comparative assessment of the area occupied by different habitats, and the relative abundance of fish species in each habitat.

Fish assemblages

The depth of the study sites was the most important factor related to the composition of the fish assemblages in this study. In a review of deep-sea fish, Gordon (2001) found that depth was the most important factor determining the fisheries catches. Trawl surveys of fish on the Faroe Bank from 1988 to 1996, similarly found *G. morhua, M. aeglefinus, T. minutus, M. molva, S. viviparus, A.*

lupus, H. hippoglossus, and *M. kitt* in shallower (<210 m) depths, and *L. eques* at >430 m (Magnussen 2003). This study found *P. virens* to occur at <400 m, and *B. brosme* at <500 m depths, similar to our results. The study noted the occurrence of *Lophelia* below 200 m but did not relate it to fish distribution.

Functional role of *Lophelia* reefs as fish habitat

Analysis of the stomach contents of fish captured around the Sula Ridge found *Sebastes* to be eating crustacean zooplankton, *Molva molva* fish and crustaceans, and *Brosme brosme* benthic decapod crustaceans (also some fish and polychaetes) (Husebø et al. 2002). In a review paper, Gordon (2001) reports that most demersal fish on the European continental slopes feed on demersal (benthopelagic) prey. The reefs may coincide with and provide increased food availability. We and others (e.g., Hovland et al. 2002) have observed abundant zooplankton on video that could be prey for both *Lophelia* and other species, including zooplanktivorous fish such as *Sebastes* species. The reefs may also provide a refuge from predators, and habitat from which to ambush prey. Although food supply generally decreases with depth in the ocean, it can be concentrated by topographic features such as seamounts (Koslow 1997), and, we suggest, along the edges of continental margins where *Lophelia* reefs seem most common.

Fosså et al. (2002), Husebø et al. (2002), and this study, have observed swollen, presumably pregnant female *Sebastes* on the reefs at Sula Ridge. The eggcases of rays (*Raja* sp.) have been observed on *Lophelia* at the Sula Reef. Thus the reefs are spawning habitat for some fish species.

It can be extraordinarily difficult to see juvenile fish in rocky and coral reefs environments, and indeed in reefs within aquaria when larger fish are present (M.J. Costello personal observation). Although no small fish have been found associated with the *Lophelia* reefs in this and previous studies, it is likely that they conceal juveniles and thus these reefs may act as a nursery habitat. More research is needed to test this hypothesis.

The data available in this study did not indicate seasonal variation, and was too limited for more than a preliminary assessment of seasonal variation at one site. Fish at the Great Meteor Seamount at 300-500 m depth showed no seasonal variation (Foch et al. 2002). Whether that also reflected the limitations of their survey, or deep-sea fish show little seasonal variation in abundance, remains to be determined. A consequence of the limited temperature variation in the deep-sea may be less variation in fish activity. Scuba diver estimates of the abundance of four species of coastal wrasse (Labridae) in the Northeast Atlantic varied significantly with sea temperature in the range 8-19°C (Costello et al. 1995). Because temperature variation is considerably less in deeper waters, apparent fish abundance may vary less, unless there is seasonal migration driven by food supply or other factors.

The fish recorded in this study are widespread in the Northeast Atlantic, and not peculiar to coral reefs. However, the results suggest that the reefs act as centres of at least fish species richness and abundance. The importance of the corals as fish habitat will thus be of greater significance the more widespread and developed the

reefs are found to be. Considering that (a) large (over 40 km long) deep-sea coral reefs are still being discovered, (b) that most reefs have only been discovered in the past decade with underwater video, and (c) that *Lophelia pertusa* is widespread in at least the Atlantic ocean, it seems that deep-water coral reefs may be of much greater importance in the functioning of marine ecosystems than hitherto realised. Our observations of abundant zooplankton and benthic communities at several sites suggest the coral may occur at, and/or contribute to, the availability of rich food resources and trophic dynamics. The potential role of *Lophelia* reefs in providing habitat structure for fish and other marine life, and as centres of ecological activity, demands further research.

Management implications

Based on the increased rate of discovery of *Lophelia* reef habitat in the northeastern Atlantic over the past five years, primarily from the use of underwater video, we predict more such reefs will be found. However, these discoveries have simultaneously detected damage and fragmentation of coral reef habitat as a result of deep-water commercial trawling (see references in the Introduction to this paper), including in the deepest areas reefs are known to occur (Wheeler et al. in press). Not only is this habitat being flattened, but recent reviews consider that deep-sea fisheries are inherently unsustainable because of the slow recruitment of deep-sea fish (e.g., Roberts C.M. 2002). Furthermore, persistent contaminants released into shallow seas have contaminated deep-sea fish (Mormede and Davies 2003). Thus, deep-sea fish are threatened by over fishing, loss of habitat, and pollution.

The data presented here show that cold-water reefs are an important habitat for many species of fishes (including many commercially important species), which are more abundant around the reefs than on the surrounding seabed. The reefs may function as feeding, breeding, and nursery habitats. There is no evidence of any alternative habitat at depths where *Lophelia* is commonly found. Thus the loss of reefs would result in a reduced abundance and biodiversity of fish due to habitat loss. Most of the fish associated with the reefs are of commercial importance. The protection of *Lophelia* reefs is thus of both ecological and economic importance, and has resulted in conservation measures being implemented in Norway (Fosså et al. 2002), Sweden (Norling and Sköld 2002; Lundälv and Jonsson 2003), and the Darwin Mounds by a seabed trawling ban at the request of the UK government under a temporary instrument of the European Common Fisheries Policy in anticipation of permanent protection under the EU Habitat's Directive (European Commission 2003). In addition, conservation measures have been proposed elsewhere in the Northeast Atlantic (World Wide Fund 2001), including French, Spanish, Portugese, British (Gubbay et al. 2002), and Irish (Grehan et al. in press), waters. Cold-water corals are also being protected in Atlantic Canada (Fisheries and Oceans 2002). A more comprehensive and quantitative investigation of the role of *Lophelia* reefs in European ecosystems, especially with regard to fish populations, is critical for the wise management of fisheries and biodiversity (Freiwald et al. 2004).

Summary

1.   Underwater video can be used to quantify fish abundance in deep waters, including *Lophelia* habitats.
2.   Far more fishes (80 % abundance) and more fish species (92 %) are associated with *Lophelia* reefs than the adjacent seabed.
3.   *Lophelia* may provide significant three-dimensional habitat in deep-sea areas, in at least the Northeast Atlantic.
4.   Most of the fish species (68 %) and abundance (82 %) associated with *Lophelia* reefs are of commercial importance.
5.   Depth was the most important environmental variable influencing the families and species of fish associated with *Lophelia* across the sites studied.
6.   *Lophelia* reefs may function as feeding, predator refuge, breeding, and/or nursery habitats for fishes.
7.   Whether there is seasonal variation in fish community structure or abundance at *Lophelia* reefs remains to be determined.
8.   Considering the widespread distribution and large size of some *Lophelia* reefs, at least in the Northeast Atlantic, they may provide a hitherto unrecognised role in the functioning of marine ecosystems.
9.   The sensitivity of *Lophelia* to fishing impacts, especially bottom trawling, makes further research into the importance of this habitat to biodiversity (including fisheries and ecosystem functioning) especially urgent.

Acknowledgements

References

Álvarez-Pérez G, Busquets P, De Mol B, Sandoval NG, Canals M, Casamor JL (2005) Deep-water coral occurrences in the Strait of Gibraltar. In: Freiwald A, Roberts JM (eds) Cold-water Corals and Ecosystems. Springer, Berlin Heidelberg, pp 207-221

Bett BJ (2001) UK Atlantic Margin Environmental Survey: introduction and overview of bathyal benthic ecology. Cont Shelf Res 21: 917-956

Bett BJ (2003) Time-lapse photography in the deep sea. Underwater Tech 25: 121-127

Clarke KR, Gorley RN (2001) PRIMER v5: User Manual/Tutorial. PRIMER-E, Plymouth

Colman JG, Gordon DM, Lane AP, Forde MJ, Fitzpatrick JJ (2005) Carbonate mounds off Mauritania, Northwest Africa: status of deep-water corals and implications for management of fishing and oil exploration activities. In: Freiwald A, Roberts JM (eds) Cold-water Corals and Ecosystems. Springer, Berlin Heidelberg, pp 417-441

Costello MJ, Myers AA (1987) Amphipod fauna of the sponges *Halichondria panicea* and *Hymeniacidon perleve* in Lough Hyne, Ireland. Mar Ecol Progr Ser 41: 115-121

Costello MJ, Darwall WR, Lysaght S (1995) Activity patterns of north European wrasse (Pisces, Labridae) and precision of diver survey techniques. In: Eleftheriou A, Ansell AD, Smith CJ (eds) Biology and Ecology of Shallow Coastal Waters. Proc 28th Europ Marine Biol Symp, IMBC, Hersonissos, Crete 1993, pp 343-350

Costello MJ, Emblow CS, White R (2001) European Register of Marine Species. A check-list of the marine species in Europe and a bibliography of guides to their identification. Patrimoines naturels 50: 463 pp

Etnoyer P, Morgan L (2005) Habitat-forming deep-sea corals in the Northeast Pacific Ocean. In: Freiwald A, Roberts JM (eds) Cold-water Corals and Ecosystems. Springer, Berlin Heidelberg, pp 331-343

European Commission (2003) Commission Regulation (EC) No 1475/2003 of 20 August 2003 on the protection of deep-water coral reefs from the effects of trawling in an area north west of Scotland. Official Journal L 211, 21/08/2003: 14-15

Fisheries and Oceans (2002) Deep-sea coral research and conservation in offshore Nova Scotia. http://www.mar.dfo-mpo.gc.ca/communications/maritimes/back02e/B-MAR-02-(5E).html, accessed 4th September 2003

Foch H, Uiblein F, Köster F, von Westerhagen H (2002) Biodiversity and species-environment relationships of the demersal fish assemblage at the Great Meteor Seamount (subtropical North East Atlantic) sampled by different trawls. Mar Biol 141: 185-199

Fosså JH, Mortensen PB, Furevik DM (2002) The deep-water coral *Lophelia pertusa* in Norwegian waters: distribution and fisheries impacts. Hydrobiologia 471: 1-12

Fosså JH, Lindberg B, Christensen O, Lundälv T, Svellingen I, Mortensen PB, Alvsvåg J (2005) Mapping *Lophelia* reefs in Norway: experiences and survey methods. In: Freiwald A, Roberts JM (eds) Cold-water Corals and Ecosystems. Springer, Berlin Heidelberg, pp 359-391

Freiwald A, Hühnerbach V, Lindberg B, Wilson JB, Campbell J (2002) The Sula Reef complex, Norwegian Shelf. Facies 47: 179-200

Freiwald A, Fosså JH, Grehan A, Koslow T, Roberts JM (2004) Cold-water coral reefs. UNEP-WCMC, Cambridge, UK, Biodiversity Series 22, 84 pp

Gordon JDM (2001) Deep-water fisheries at the Atlantic Frontier. Cont Shelf Res 21: 987-1003

Grehan AJ, Unnithan V, Olu-Le Roy K, Opderbecke J (in press) Fishing impacts on Irish deep-water coral reefs: making the case for coral conservation. In: Thomas J, Barnes P (eds) Proceedings from the Symposium on the Effects of Fishing Activities on Benthic

Habitats: Linking Geology, Biology, Socioeconomics and Management. Amer Fish Soc, Bethesda, Maryland, USA

Gubbay S, Baker MC, Bett BJ (2002) The Darwin Mounds and Dogger Bank. Case studies of the management of two potential Special Areas of Conservation in the offshore environment. World Wide Fund for Nature, UK, Godalming, 63 pp

Hall-Spencer J, Allain V, Fosså JH (2002) Trawling damage to northeast Atlantic ancient coral reefs. Proc R Soc London B 269: 507-511

Hovland M, Mortensen PB, Brattegard T, Strass P, Rokoengen K (1998) Ahermatypic coral banks off mid-Norway: evidence for a link with seepage of light hydrocarbons. Palaios 13: 189-200

Hovland M, Vasshus S, Indreeide A, Austdal L, Nilsen Ø (2002) Mapping and imaging deep-sea corals off Norway 1982-2000. Hydrobiologia 471: 13-17

Huggett QJ (1987) Mapping of hemipelagic *versus* turbiditic muds by feeding traces observed in deep-sea photographs. In: Weaver PPE, Thomson J (eds) Geology and Geochemistry of Abyssal Plains. Blackwell, Oxford, pp 105-112

Husebø A, Nøttestad L, Furevik DM, Fosså JH, Jørgensen SB (2002) Distribution and concentration of fish in deep-sea coral habitats. Hydrobiologia 471: 91-99

Huvenne VAI, Blondel Ph, Henriet J-P (2002) Textural analyses of sidescan sonar imagery from two mound provinces in the Porcupine Seabight. Mar Geol 189: 323-341

International Council for the Exploration of the Sea (2003) ICES catch data for 1973-2000. http://www.ices.dk/fish/statlant.asp, accessed 16 June 2003

Kenyon NH, Ivanov MK, Akhmetzhanov AM (1998) Cold-water carbonate mounds and sediment transport on the Northeast Atlantic margin. Preliminary results of the geological and geophysical investigations during TTR-7 cruise of R/V Professor Logachev in co-operation with the CORSAIRES and ENAM 2 programmes. IOC Rep, Tech Ser 52, UNESCO, 178 pp

Kenyon NH, Akhmetzhanov AM, Wheeler AJ, van Weering TCE, de Hass H, Ivanov MK (2003) Giant carbonate mud mounds in the southern Rockall Trough. Mar Geol 195: 5-30

Klitgaard AB, Tendal OS, Westerberg H (1997) Mass occurrences of large-sized sponges (Porifera) in Faroe islands (NE Atlantic) shelf and slope areas: characteristics, distribution and possible causes. In: Hawkins LE, Hutchinson S, Jensen AC, Sheader M, Williams KA (eds) The Response of marine Organsims to their Environments. Proc 30th Europ Marine Biol Symp, pp 129-142

Koslow JA (1997) Seamounts and the ecology of deep-sea fisheries. Amer Sci 85: 168-176

Krieger KJ (2001) Coral (*Primnoa*) impacted by fishing gear in the Gulf of Alaska. In: Willison JHM, Hull J, Gass SE, Kenchington ELR, Butler M, Doherty P (eds) Proceedings of the first international symposium on deep-sea corals. Ecology Action Centre and Nova Scotia Museum, Halifax, Nova Scotia, pp 106-116

Krieger KJ, Wing BL (2002) Megafauna associations with deepwater corals (*Primnoa* spp.) in the Gulf of Alaska. Hydrobiologia 471: 83-90

Lewis AR (1998) Effects of experimental coral disturbance on the population dynamics of fishes on large patch reefs. J Exper Mar Biol Ecol 230: 91-110

Lundälv T, Jonsson L (2000) Inventering av Koster-Väderöområdet med ROV-teknik. En pilotstudie. Naturvårdsverket, Stockholm, 70 pp

Lundälv T, Jonsson L (2003) Mapping of deep-water corals and fishery impacts in the north-east Skagerrak, using acoustical and ROV survey techniques. Proc 6th Underwater Sci Symp, Aberdeen, April 2003

Magnussen E (2003) Demersal fish assemblages of Faroe Banks: species composition, distribution, biomass spectrum and diversity. Mar Ecol Progr Ser 238: 211-225

Magurran AE (2004) Measuring Biological Diversity. Blackwell, Oxford, 256 pp

Masson DG (2001) Sedimentary processes shaping the eastern slope of the Faeroe – Shetland Channel. Cont Shelf Res 21: 825-857

Masson DG, Bett BJ, Billett DSM, Jacobs CL, Wheeler AJ, Wynn RB (2003) The origin of deep-water, coral-topped mounds in the northern Rockall Trough, Northeast Atlantic. Mar Geol 194: 159-180

McCrea M, Costello MJ, Freiwald A, Lundälv T, Jonsson L (2003a) A guide to the fish associated with deep-water coral reefs. http://www.ecoserve.ie/projects/aces, accessed 25 May 2004

McCrea M, Costello MJ, Freiwald A, Lundälv T, Jonsson L (2003b) A guide to the fish associated with deep-water coral reefs. Erlanger Geol Abh Sonderbd 4, pp 60

Mormede S, Davies IM (2003) Horizontal and vertical distribution of organic contaminants in deep-sea fish species. Chemosphere 50: 563-574

Mortensen PB, Buhl-Mortensen L (2005) Deep-water corals and their habitats in The Gully, a submarine canyon off Atlantic Canada. In: Freiwald A, Roberts JM (eds) Cold-water Corals and Ecosystems. Springer, Berlin Heidelberg, pp 247-277

Mortensen PB, Fosså JH (2001) Korallrev og andre bunnhabitater på Tautraryggen i Trondheimsfjorden. Fisken Havet 7, 34 pp

Mortensen PB, Hovland M, Brattegard T, Farestveit R (1995) Deep water bioherms of the scleractinian coral *Lophelia pertusa* (L.) at 64°N on the Norwegian Shelf: structure and associated megafauna. Sarsia 80: 145-158

Norling K, Sköld M (2002) Biologisk mångfald och fiske I Västra Götaland. Rep County Reg Authority Västra Götaland No. 2002:27, 81 pp

Paull CK, Neumann AC, am Ende BA, Ussler W, Rodriguez NM (2000) Lithoherms on the Florida-Hatteras slope. Mar Geol 166: 83-101

Reed JK (2002) Comparison of deep-water coral reefs and lithoherms off eastern USA. Hydrobiologia 471: 57-69

Reed JK, Shephard AN, Koenig CC, Scanlon KM, Gilmore RG (2005) Mapping, habitat characterization, and fish surveys of the deep-water *Oculina* coral reef Marine Protected Area: a review of historical and current research. In: Freiwald A, Roberts JM (eds) Cold-water Corals and Ecosystems. Springer, Berlin Heidelberg, pp 443-465

Reyes-Bonilla H, Pinon GC (2002) Influence of temperature and nutrients on species richness of deep water corals from the western coast of the Americas. Hydrobiologia 471: 35-41

Roberts CM (2002) Deep impact: the rising toll of fishing in the deep sea. Trends Ecol Evol 17: 242-245

Roberts JM (2002) The occurrence of the coral *Lophelia pertusa* and other conspicuous epifauna around an oil platform in the North Sea. J Soc Underwater Tech 25: 83-91

Roberts JM, Harvey SM, Lamont PA, Gage JD, Humphery JD (2000) Seabed photography, environmental assessment and evidence for deep-water trawling on the continental margin west of the Hebrides. Hydrobiologia 441: 173-183

Roberts JM, Long D, Wilson JB, Mortensen PB, Gage JD (2003) The cold-water coral *Lophelia pertusa* (Scleractinia) and enigmatic seabed mounds along the north-east Atlantic margin: are they related? Mar Pollut Bull 46: 7-20

Roberts JM, Peppe OC, Dodds LA, Mercer DJ, Thomson WT, Gage JD, Meldrum DT (2005) Monitoring environmental variability around cold-water coral reefs: the use of a benthic photolander and the potential of seafloor observatories. In: Freiwald A, Roberts JM (eds) Cold-water Corals and Ecosystems. Springer, Berlin Heidelberg, pp 483-502

Rogers AD (1999) The biology of *Lophelia pertusa* (Linnaeus 1758) and other deep-water reef-forming corals and impacts from human activities. Int Rev Hydrobiol 84: 315-406

Schroeder WW (2002) Observations of *Lophelia pertusa* and the surficial geology at a deep-water site in the northeastern Gulf of Mexico. Hydrobiologia 471: 83-90

Strømgren T (1971) Vertical and horizontal distribution of *Lophelia pertusa* (Linné) in Trondheimsfjorden on the west coast of Norway. K Norsk Vidensk Selsk Skr 6: 1-9

Stone RP, Malecha PW (2003) Deep-sea coral habitats in the Aleutian Islands of Alaska. Erlanger Geol Abh Sonderbd 4: pp 81

Svensen R, Svensen R, Emil Moen F (1998) The sea trees of Trondheim. Diver, April 1998: 96-99

Taviani M, Remia A, Corselli C, Freiwald A, Malinverno E, Mastrototaro F, Savini A, Tursi A, CORAL Shipboard Staff (2004) First geo-marine survey of living cold-water *Lophelia* reefs in the Ionian Sea (Mediterranean basin). Facies 50, DOI 10.1007/s10347-004-0039-0

Turrell WR, Slesser G, Adams RD, Payne R, Gillibrand PA (1999) Decadal variability in the composition of Faroe – Shetland Channel bottom water. Deep-Sea Res I 46: 1-25

Van Rooij D, De Mol B, Huvenne V, Ivanov M, Henriet J-P (2003) Seismic evidence of current-controlled sedimentation in the Belgica mound province, upper Porcupine slope, southwest of Ireland. Mar Geol 195: 31-53

Viana AR, Faugères JC, Kowsmann RO, Lima JAM, Caddah LFG, Rizzo JG (1998) Hydrology, morphology and sedimentology of the Campos continental margin, offshore Brazil. Sediment Geol 115: 133-157

Wheeler AJ, Bett BJ, Billett DSM, Masson DG, Mayor D (in press) The impact of demersal trawling on NE Atlantic deep-water coral habitats: the case of the Darwin Mounds, UK. In: Barnes P (ed) Benthic Habitats and the Effects of Fishing. Amer Fish Soc, Bethesda, Maryland, USA

Witherell D, Coon C (2001) Protecting gorgonian corals off Alaska from fishing impacts. In: Willison JHM, Hull J, Gass SE, Kenchington ELR, Butler M, Doherty P (eds) Proceedings of the first international symposium on deep-sea corals. Ecology Action Centre and Nova Scotia Museum, Halifax, Nova Scotia, 117-125 pp

World Wide Fund (2001) Implementation of the EU Habitats Directive offshore: Natura 2000 sites for reefs and submerged banks. WWF, UK, Godalming

Appendix Details of the sources of the data used in this paper

N	Location	Dive or cruise	Site	Tape No.	Latitude	Longitude	Depth [m]	Date-d/m/y	Video format	Sampling platform	Duration h:m:s	Source
1.	Hurtside Wreck	A	-	1	60° 10.48N	4° 32.99W	400	14/12/1996	Analogue	ROV	0:59:30	M. Roberts
2.	Hurtside Wreck	B	-	2	60° 10.48N	4° 32.97W	400	14/12/1996	Analogue	ROV	2:49:15	M. Roberts
3.	Sula Ridge	POS 228/203	-	1/1	64°04.63 N	8°00.95 E	312	11/05/1997	Digital	Submersible	1:02:34	A. Freiwald
4.	Sula Ridge	POS 228/203	-	1/2	64°04.65 N	8°00.73 E	313	11/05/1997	Digital	Submersible	1:02:34	A. Freiwald
5.	Sula Ridge	POS 228/203	-	1/3	64°04.69 N	8°00.69 E	314	11/05/1997	Digital	Submersible	0:51:14	A. Freiwald
6.	Sula Ridge	POS 228/205	-	2/1	64°05.58 N	8°02.80 E	315	12/05/1997	Digital	Submersible	1:01:06	A. Freiwald
7.	Sula Ridge	POS 228/205	-	2/2	64°05.48 N	8°02.75 E	316	12/05/1997	Digital	Submersible	1:02:34	A. Freiwald
8.	Sula Ridge	POS 228/212	-	3/1	64°04.94 N	8°01.77 E	317	12/05/1997	Digital	Submersible	1:02:36	A. Freiwald
9.	Sula Ridge	POS 228/212	-	3/2	64°04.75 N	8°01.92 E	318	12/05/1997	Digital	Submersible	0:30:16	A. Freiwald
10.	Sula Ridge	POS 228/214	-	4/1	64°04.59 N	8°00.70 E	319	13/05/1997	Digital	Submersible	1:02:33	A. Freiwald
11.	Sula Ridge	POS 228/214	-	4/2	64°04.85 N	8°00.45 E	320	13/05/1997	Digital	Submersible	1:02:32	A. Freiwald
12.	Sula Ridge	POS 228/214	-	4/3	64°04.95 N	8°00.43 E	321	13/05/1997	Digital	Submersible	0:27:58	A. Freiwald
13.	Sula Ridge	POS 228/217	-	5/1	64^05.40 N	8°03.48 E	322	13/05/1997	Digital	Submersible	1:02:32	A. Freiwald
14.	Sula Ridge	POS 228/217	-	5/2	64°05.39 N	8°03.48 E	323	13/05/1997	Digital	Submersible	0:55:32	A. Freiwald
15.	Sula Ridge	POS 228/219	-	6/1	64°04.10 N	8°02.52 E	324	14/05/1997	Digital	Submersible	1:02:34	A. Freiwald
16.	Sula Ridge	POS 228/219	-	6/2	64°04.15 N	8°02.47 E	325	14/05/1997	Digital	Submersible	1:02:32	A. Freiwald
17.	Sula Ridge	POS 228/219	-	6/3	64°04.54 N	8°01.31 E	326	14/05/1997	Digital	Submersible	1:02:36	A. Freiwald
18.	Sula Ridge	POS 228/220	-	7/1	64°04.71 N	8°02.52 E	327	14/05/1997	Digital	Submersible	0:51:34	A. Freiwald
19.	Sula Ridge	POS 228/220	-	7/2	64°04.72 N	8°02.53 E	328	14/05/1997	Digital	Submersible	1:02:34	A. Freiwald
20.	Sula Ridge	POS 228/220	-	7/3	64°04.97 N	8°02.83 E	329	14/05/1997	Digital	Submersible	1:02:00	A. Freiwald
21.	Sula Ridge	POS 254/18	-	1	64°05.90 N	8°05.60 E	300	30/07/1999	Digital	Submersible	1:02:50	A. Freiwald
22.	Sula Ridge	POS 254/18	-	2	64°05.90 N	8°05.50 E	301	30/07/1999	Digital	Submersible	1:02:34	A. Freiwald
23.	Sula Ridge	POS 254/20	-	3	64°05.87 N	8°05.43 E	302	30/07/1999	Digital	Submersible	0:41:49	A. Freiwald
24.	Sula Ridge	POS 254/22	-	4	64°04.50 N	8°01.40 E	303	31/07/1999	Digital	Submersible	0:58:07	A. Freiwald
25.	Sula Ridge	POS 254/24	-	5	64°04.67 N	8°01.42 E	304	31/07/1999	Digital	Submersible	0:58:20	A. Freiwald

Appendix continued

N	Location	Dive or cruise	Site	Tape No.	Latitude	Longitude	Depth [m]	Date-d/m/y	Video format	Sampling platform	Duration h:m:s	Source
26.	Sula Ridge	POS 254/24	–	6	64°04.80 N	8°01.30 E	305	31/07/1999	Digital	Submersible	1:02:33	A. Freiwald
27.	Sula Ridge	POS 254/26	–	7	64°05.80 N	8°04.40 E	306	01/08/1999	Digital	Submersible	1:02:38	A. Freiwald
28.	Sula Ridge	POS 254/28	–	8	64°06.80 N	8°07.26 E	307	01/08/1999	Digital	Submersible	1:02:23	A. Freiwald
29.	Sula Ridge	POS 254/28	–	9	64°06.60 N	8°07.50 E	308	01/08/1999	Digital	Submersible	1:02:29	A. Freiwald
30.	Sula Ridge	POS 254/30	–	10	64°07.80 N	8°09.80 E	309	02/08/1999	Digital	Submersible	1:02:46	A. Freiwald
31.	Sula Ridge	POS 254/32	–	11	64°08.10 N	8°10.52 E	310	02/08/1999	Digital	Submersible	0:57:51	A. Freiwald
32.	Sula Ridge	POS 254/32	–	12	64°07.80 N	8°10.80 E	311	02/08/1999	Digital	Submersible	0:52:57	A. Freiwald
33.	Kosterfjord	Nereus, Phantom XTL	alpha	32	59°00.837N	11°06.998E	77-85	02/11/1998	Analogue	ROV	3:01:57	T. Lundälv, L. Jonsson
34.	Kosterfjord	Nereus, Phantom XTL	alpha	34	59°00.837N	11°06.998E	84-87	26/11/1998	Analogue	ROV	1:48:46	T. Lundälv, L. Jonsson
35.	Kosterfjord	Nereus, Phantom XTL	beta	43	59°00.807N	11°06.922E	76-82	06/05/1999	Analogue	ROV	0:19:32	T. Lundälv, L. Jonsson
36.	Kosterfjord	Nereus, Phantom XTL	beta	55	59°00.807N	11°06.922E	84-87	14/01/2000	Analogue	ROV	1:51:10	T. Lundälv, L. Jonsson
37.	Kosterfjord	Nereus, Phantom XTL	alpha	56	59°00.837N	11°06.998E	83-89	03/02/2000	Analogue	ROV	1:58:49	T. Lundälv, L. Jonsson
38.	Kosterfjord	Nereus, Phantom XTL	alpha	59	59°00.837N	11°06.998E	91	06/04/2000	Analogue	ROV	3:00:20	T. Lundälv, L. Jonsson
39.	Kosterfjord	Nereus, Phantom XTL	alpha +beta	60	2 POS	2 POS	83-85	08/06/2000	Analogue	ROV	3:49:00	T. Lundälv, L. Jonsson
40.	Kosterfjord	Nereus, Phantom XTL	alpha +beta	61	2 POS	2 POS	83	20/06/2000	Analogue	ROV	3:03:45	T. Lundälv, L. Jonsson
41.	Kosterfjord	Nereus, Phantom XTL	alpha +beta	62	2 POS	2 POS	84-118	20/06/2000	Analogue	ROV	1:26:13	T. Lundälv, L. Jonsson

Appendix continued

N	Location	Dive or cruise	Site	Tape No.	Latitude	Longitude	Depth [m]	Date-d/m/y	Video format	Sampling platform	Duration h:m:s	Source
42.	Kosterfjord	Nereus, Phantom XTL	alpha	73	59°00.837N	11°06.998E	81-87	30/1/01, 13 &22/02/01	Analogue	ROV	2:25:40	T. Lundälv, L. Jonsson
43.	Kosterfjord	Nereus, Phantom XTL	alpha +beta	74	2 POS	2 POS	80-85	24/04/2001	Analogue	ROV	2:49:50	T. Lundälv, L. Jonsson
44.	Kosterfjord	Nereus, Phantom XTL	alpha	75	59°00.837N	11°06.998E	84-87	07/05/2001	Analogue	ROV	2:23:18	T. Lundälv, L. Jonsson
45.	Kosterfjord	Nereus, Phantom XTL	alpha	80	59°00.837N	11°06.998E	84	07/06/2001	Analogue	ROV	0:21:00	T. Lundälv, L. Jonsson
46.	Trondheimsfjord	Harriborth PhantomXTL	Tautra	1	63°35.577N	10°31.043E	39-40	29/05/2001	Analogue	ROV	1:47:00	T. Lundälv, L. Jonsson
47.	Porcupine Seabight	Pelagia M2000	1	1	51°25.49N	11°46.04W	963	28/07/2000	Analogue	Hopper Camera	0:17:33	T.v.Weering, H.d.Haas
48.	Porcupine Seabight	Pelagia M2000	2	1	51°25.78N	11°46.26W	866?	28/07/2000	Analogue	Hopper Camera	0:14:10	T.v.Weering, H.d.Haas
49.	Porcupine Seabight	Pelagia M2000	3	1	51°26.17N	11°46.57W	1015	28/07/2000	Analogue	Hopper Camera	0:21:25	T.v.Weering, H.d.Haas
50.	Porcupine Seabight	Pelagia M2000	4	2	51°25.76N	11°46.00W	925	28/07/2000	Analogue	Hopper Camera	0:20:54	T.v.Weering, H.d.Haas
51.	Porcupine Seabight	Pelagia M2000	5	2	51°25.52N	11°46.54W	981	28/07/2000	Analogue	Hopper Camera	0:23:00	T.v.Weering, H.d.Haas
52.	Porcupine Bank	Pelagia M2000	8	2	53°46.81N	13°56.13W	796	29/07/2000	Analogue	Hopper Camera	0:17:41	T.v.Weering, H.d.Haas
53.	Porcupine Bank	Pelagia M2000	10	3	53°46.80N	13°55.91W	792	30/07/2000	Analogue	Hopper Camera	0:19:06	T.v.Weering, H.d.Haas
54.	Porcupine Bank	Pelagia M2000	12	3	53°46.86N	13°57.02W	777	30/07/2000	Analogue	Hopper Camera	0:19:32	T.v.Weering, H.d.Haas

Appendix continued

N	Location	Dive or cruise	Site	Tape No.	Latitude	Longitude	Depth [m]	Date-d/m/y	Video format	Sampling platform	Duration h:m:s	Source
55.	Porcupine Bank	Pelagia M2000	13	3	53°46.86N	13°57.02W	778	30/07/2000	Analogue	Hopper Camera	0:16:02	T.v.Weering, H.d.Haas
56.	Porcupine Bank	Pelagia M2000	13A	4	53°46.79N	13°56.65W	646	31/07/2000	Analogue	Hopper Camera	0:20:00	T.v.Weering, H.d.Haas
57.	Porcupine Bank	Pelagia M2000	13B	4	53°46.79N	13°56.61W	693	31/07/2000	Analogue	Hopper Camera	0:20:53	T.v.Weering, H.d.Haas
58.	Porcupine Bank	Pelagia M2000	41	4	53°59.97N	12°41.18W	957	07/08/2000	Analogue	Hopper Camera	0:18:22	T.v.Weering, H.d.Haas
59.	Porcupine Bank	Pelagia M2000	42	4	53°57.89N	12°41.09W	600	31/07/2000	Analogue	Hopper Camera	0:18:30	T.v.Weering, H.d.Haas
60.	Porcupine Bank	Pelagia M2000	43	4	53°59.73N	12°44.49W	826	31/07/2000	Analogue	Hopper Camera	0:03:57	T.v.Weering, H.d.Haas
61.	Rockall Bank	Pelagia M2000	21	4	55°32.09N	15°40.07W	727	02/08/2000	Analogue	Hopper Camera	0:19:31	T.v.Weering, H.d.Haas
62.	Rockall Bank	Pelagia M2000	23	4	55°32.26N	15°39.57W	778	02/08/2000	Analogue	Hopper Camera	0:18:42	T.v.Weering, H.d.Haas
63.	Rockall Bank	Pelagia M2000	24	5	55°32.44N	15°39.08W	751	03/08/2000	Analogue	Hopper Camera	0:18:11	T.v.Weering, H.d.Haas
64.	Rockall Bank	Pelagia M2000	25	5	55°32.55N	15°38.72W	809	03/08/2000	Analogue	Hopper Camera	0:18:23	T.v.Weering, H.d.Haas
65.	Rockall Bank	Pelagia M2000	26	5	55°32.61N	15°28.51W	843	03/08/2000	Analogue	Hopper Camera	0:21:11	T.v.Weering, H.d.Haas
66.	Rockall Bank	Pelagia M2000	27	5	55°32.84N	15°37.71W	858	03/08/2000	Analogue	Hopper Camera	0:18:04	T.v.Weering, H.d.Haas
67.	Rockall Bank	Pelagia M2000	28	5	55°32.08N	15°40.01W	731	04/08/2000	Analogue	Hopper Camera	0:19:58	T.v.Weering, H.d.Haas

Appendix continued

N	Location	Dive or cruise	Site	Tape No.	Latitude	Longitude	Depth [m]	Date-d/m/y	Video format	Sampling platform	Duration h:m:s	Source
68.	Rockall Bank	Pelagia M2000	28A	5	55°32.08N	15°40.01W	729	05/08/2000	Analogue	Hopper Camera	0:20:23	T.v.Weering, H.d.Haas
69.	Porcupine Seabight	Challenger cruise 142	Belgica Mounds	54918#1	51°25.45N	11°46.30W	860 -984	16/05/1999	Digital	WASP	1:05:00	B. Bett
70.	Porcupine Seabight	Challenger cruise 142	Hovland Mounds	54920#1	52°08.60N	12°46.65W	725 -800	16/05/1999	Digital	WASP	1:05:27	B. Bett
71.	Porcupine Seabight	Challenger cruise 142	Hovland Mounds	54921#1	52°10.20N	12°45.65W	700 -845	17/05/1999	Digital	WASP	1:05:20	B. Bett
72.	Porcupine Seabight	Challenger cruise 142	Hovland Mounds	54922#1	52°14.10N	12°43.20W	640 -750	17/05/1999	Digital	WASP	0:39:32	B. Bett
73.	Darwin Mounds	C. Darwin cruise 112	HALOPOC	54557#1	59°48.82N	7°23.31W	930 -937	03/06/1998	Digital	WASP	1:04:00	B. Bett
74.	Darwin Mounds	C. Darwin cruise 112	Mound 1	54565#1	59°47.73N	7°22.34W	957 -966	04/06/1998	Digital	WASP	1:03:13	B. Bett
75.	Darwin Mounds	C. Darwin cruise 112	Mound 2	54569#1	59°48.92N	7°20.12W	967 -983	06/06/1998	Digital	WASP	0:16:25	B. Bett
76.	Darwin Mounds	C. Darwin cruise 119	Site A	55002#1	59°51.21N	7°03.22W	1035 -1082	15/08/1999	Digital	WASP	0:12:15	B. Bett
77.	Darwin Mounds	C. Darwin cruise 123	WTS8	55254#1	59°52.93N	7°04.6W	962	31/07/2000	Digital	WASP	1:05:20	B. Bett
78.	Darwin Mounds	Discovery Cruise 248		13823/7	59°48.90N	7°22.42W	941 -954	13/07/2000	Analogue	SHRIMP	3:06:20	B. Bett
79.	Darwin Mounds	Discovery Cruise 248		13812/1	59°43.12N	07°52.19W	798	09/07/2000	Analogue	SHRIMP	--	B. Bett
80.	Darwin Mounds	Discovery Cruise 248		13814/1	59°49.88N	07°20.34W	968	10-11/7/2000	Analogue	SHRIMP	--	B. Bett

Appendix continued

N	Location	Dive or cruise	Site	Tape No.	Latitude	Longitude	Depth [m]	Date-d/ m/y	Video format	Sampling platform	Duration h:m:s	Source
81.	Darwin Mounds	Discovery Cruise 248		13815/1	59 °37.78N	07°43.55W	890	11/07/2000	Analogue	SHRIMP	--	B. Bett
82.	Darwin Mounds	Discovery Cruise 248		13823/10	59°48.80N	7°22.63W	949	13/07/2000	Analogue	SHRIMP	--	B. Bett
83.	Darwin Mounds	Discovery Cruise 248		13822#2	59°49.71N	7°20.38W	957	12-31/07/00	Analogue	Bathysnap	--	B. Bett
84.	Porcupine Seabight	Discovery Cruise 250	Therese Mound	13880#1	51°26.77N	11°45.22W	894	08/08/00 -01/09/00	Analogue	Bathysnap	--	B. Bett
85.	Porcupine Seabight	Discovery Cruise 250	Therese Mound	13921#1	51°26.77N	11°45.13W	950	27/09/00 -07/06/01	Analogue	Bathysnap	--	B. Bett

Remarkable sessile fauna associated with deep coral and other calcareous substrates in the Strait of Sicily, Mediterranean Sea

Helmut Zibrowius[1], Marco Taviani[2]

[1] Centre d'Océanologie de Marseille, Station Marine d'Endoume, Rue Batterie des Lions, F-13007 Marseille, France
 (hzibrowi@com.univ-mrs.fr)
[2] ISMAR-Marine Geology Division, CNR, Via Gobetti 101, I-40129 Bologna, Italy

Abstract. Deep-sea dredging of sediment-starved steep reliefs in the Strait of Sicily (cruise CS96 of RV *Urania*) recovered various benthic organisms previously unknown or poorly documented in the Mediterranean basin. This Mediterranean case-study refers to deep coral substrates represented by loose or cemented skeletal remains of *Desmophyllum*, *Lophelia* and *Madrepora,* subfossil giant oyster shells, micriticised sponges, from c. 250-1000 m depth. Here we present some of the more remarkable species: one foraminiferan (*Planogypsina*?); the sponges *Stylocordyla pellita*, *Sphinctrella gracilis* and *Siphonidium ramosum*; a bioluminescent zoantharian (still unidentified); the boring actinian *Fagesia loveni;* the stoloniferous octocoral *Scleranthelia musiva;* the gorgonian *Dendrobrachia fallax*; and the holothurian *Psolidium complanatum*.

Keywords. Mediterranean Sea, Strait of Sicily, deep-sea, hard substrate fauna

Introduction

Some modern and fossil deep-water scleractinian corals are typical of soft bottoms whereas others are commonly associated with hard substrates and, although not exclusively, rather precipitous topographies (e.g., Neumann et al. 1977; Mullins et al. 1981; Taviani and Colantoni 1984; Di Geronimo 1987; Newton et al. 1987; Messing et al. 1990; Barrier et al. 1996; Freiwald 2002; Remia and Taviani 2004). In general, the evaluation of fauna living on steep hard bottoms at bathyal depths (overhangs, canyon walls, seamount flanks) is technically constrained by the intrinsic difficulty of sampling such settings. Nevertheless, conventional biological sampling operated from the surface (such as dredges, grabs, trawls) provides basic information about fauna on deep-sea hard substrates (e.g., Zibrowius 1974, 1979; Arnaud 1990; Freiwald et al. 2002). On the other hand such devices are often unsuitable for sampling from very steep submarine reliefs. Significant information

from these habitats has been obtained by visual inspection and, when possible, sampling by means of bottom cameras, ROV and manned submersibles (e.g., Pratt 1967; Picard 1968; Bourcier and Zibrowius 1973; Neumann et al. 1977; Mullins et al. 1981; Zibrowius 1981, 1985; Messing et al. 1990; Tunesi and Diviacco 1997; Freiwald et al. 2002). In addition and with chance helping, deep-sea vertical reliefs can also be efficiently sampled with heavy iron dredges. In fact, this gear is generally used more within geologically-oriented research programs, but it has also provided diversified biological data, including deep coral occurrences from a number of sites throughout the Mediterranean, (e.g., Segre and Stocchino 1969; Bourcier and Zibrowius 1970; Selli 1970; Cita et al. 1980; Taviani and Colantoni 1984; Allouc 1987; Bonfitto et al. 1994).

The Strait of Sicily is a rift zone, characterized by complex topography including deep troughs, banks, and seamounts (e.g., Borsetti et al. 1974; Calanchi et al. 1989; Agate and D'Argenio 1998). The RV *Urania* Cruise CS96 (December 1996 - January 1997) was designed to systematically sample banks, seamounts and troughs throughout the Strait of Sicily, resulting in the collection of various types of deep-sea carbonate sediments and rocks (Taviani and Remia 2001). Sampling by means of a heavy geologic dredge from these rarely sampled substrates recovered many benthic organisms previously unknown or poorly documented in the Mediterranean basin and associated with various carbonate substrates, including subfossil coral.

The presence of deep-sea coral and other calcium carbonates from the Strait of Sicily is known from previous geo-biological surveys. For instance, Borsetti et al. (1974) report the occurrence of Pleistocene hardgrounds (*crostoni calcarei*) embedding foraminifers, corals, serpulids, and molluscs from the sediment-starved flanks of the troughs. Deep-sea scleractinians (including *Dendrophyllia, Desmophyllum, Lophelia, Madrepora* etc.) are recorded from this area by Pérès and Picard (1956), Rossi (1961), Taviani and Colantoni (1979), Zibrowius (1980), Delibrias and Taviani (1985), Di Geronimo et al. (1993), and Taviani and Remia (2001).

In this paper we discuss some remarkable findings from sediment-starved submarine highs in the Strait of Sicily.

Material and methods

Positioning during Cruise CS96 was provided by GPS navigational system installed on RV *Urania*. Potential dredging sites were first imaged by means of high-resolution seismic surveys using Chirp-Sonar (frequency 2-7 kHz). Sampling was then undertaken by using a heavy-chained iron dredge (Bonfitto et al. 1994). Sampling stations and dredging tracks are reported in Figure 1 and Table 1. Depending upon the presence or absence of mud, the recovered material (skeletal hash, calcareous slabs) was first gently washed over two sieves (diameter 75 cm) of 2 cm and 2 mm mesh respectively. The fraction >2 cm was immediately inspected under the binocular for a preliminary identification of benthic organisms. Living organisms were then stored either in ethanol or formalin for a further more precise taxonomic assessment.
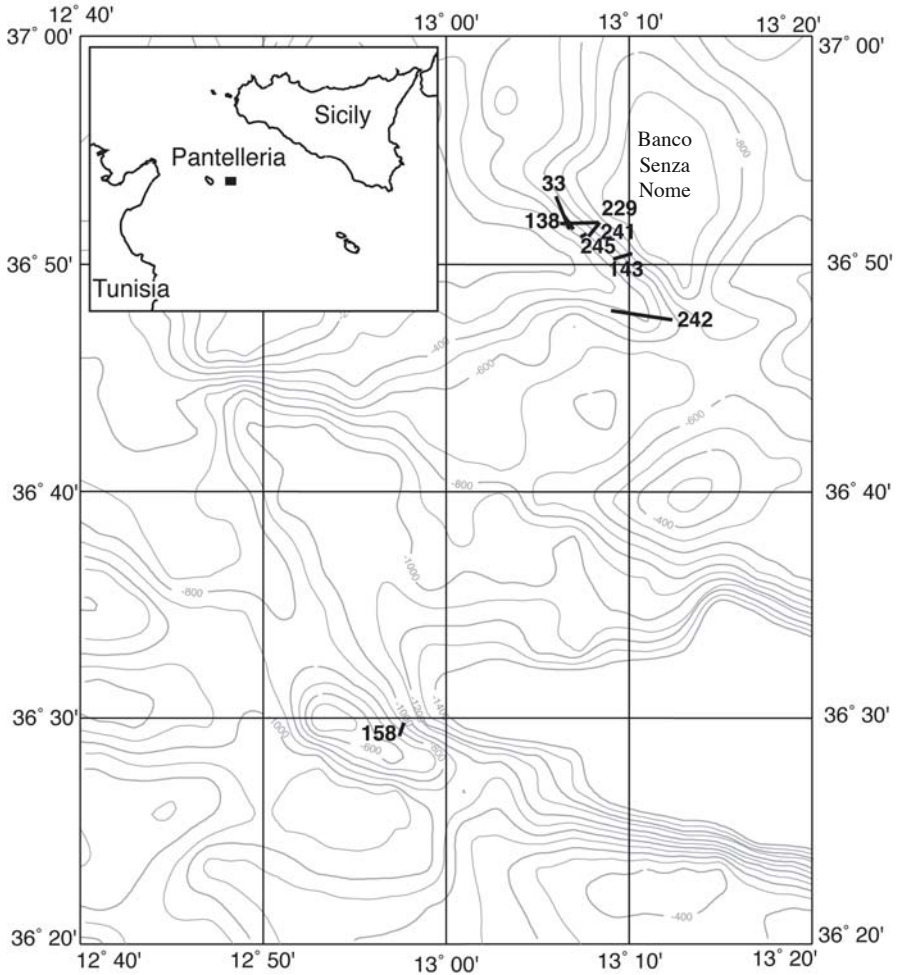
Fig. 1 Bathymetric map of the Strait of Sicily showing position of dredging stations discussed in the text

Data

Location and geology. Samples discussed here originated from steep escarpments eastward of Pantelleria Island. Dredging stations were located on the eastern side of a complex and wide topographic region culminating in the Nameless Bank (*Banco Senza Nome*); with the single exception of one located on the sill separating the Pantelleria and Malta troughs (st. CS96-158) (Fig. 1). The Nameless Bank is a fault-bounded seamount exposing sedimentary rocks (Eocene – Lower Oligocene? limestones) as well as basaltic rocks on its eastern sector (Colantoni 1975; Calanchi et al. 1989).

Table 1 Coordinates (start and end of haul positions) and depths of dredging stations from the Strait of Sicily presented in the text (RV *Urania* cruise CS96)

Station	Lat N	Long E	Depth (m)
33	36°52.96	13°06.00	710
	36°51.53	13°06.73	267
138	36°52.15	13°06.42	580
	36°51.53	13°06.95	224
143	36°50.46	13°10.18	786
	36°50.22	13°09.12	274
158	36°29.80	12°57.68	398
	36°29.20	12°57.45	375
193	35°46.82	13°01.63	690
	35°46.88	13°01.50	674
229	36°51.83	13°08.40	588
	36°51.22	13°07.78	403
241	36°51.81	13°08.35	714
	36°51.76	13°06.22	300
242	36°47.53	13°12.37	558
	36°47.95	13°09.02	322
245	36°51.32	13°07.67	403
	36°51.18	13°07.37	191

Substrates. We recovered a variety of hardgrounds, mostly abundant coral, oyster and sponge framestones, together with skeletal hash. Deep coral substrates were largely represented by loose or cemented skeletal remains of *Desmophyllum dianthus* (solitary), *Lophelia pertusa* and *Madrepora oculata* (both colonial) at times embedded in packstones and framestones. Here, as also observed in Recent Atlantic *Lophelia* mounds, dying and dead coral substrates offer a suitable environment for various sessile organisms (Jensen and Frederiksen 1992; Freiwald and Wilson 1998; Freiwald et al. 2002). A very special substrate was provided by single valves and clusters of a subfossil giant oyster (length >20 cm; Taviani et al. 2005). This deep-sea oyster seems to be of an undescribed deep-sea taxon; it has been regularly dredged below 200 m in the western Mediterranean and Strait of Sicily and long known to scientists although never studied in detail (Vacelet 1969; Selli 1970; Zibrowius 1980; Taviani et al. 2002). Another peculiar substrate is offered by micriticised sponges and spongal hardgrounds as large lamellar and non-lamellar diagenised sponges (probably Lithistidae: stations CS96-33, 193, 229, 241, 242, 245). These sponges are subfossil and were living during the late Pleistocene both in the Western and Eastern Mediterranean (see also Zibrowius 1981, 1985; Brachert et al. 1987).

Macrofauna associated with hard substrates. These carbonate substrates were colonised by various organisms of which only a fraction was found alive at the time of sampling, such as some Actiniaria (e.g., *Protanthea simplex:* st. CS96-138) and Antipatharia (st. CS96-138). Most taxa, however, were represented only with their

skeletal parts (from fresh to highly degraded) and only a fraction was found alive at the time of the sampling. Therefore, our inventory includes both fossil (probably latest Pleistocene) and Recent organisms which settled this peculiar environment. Major benthic macrofauna producing consistent skeletons are represented by Scleractinia, Octocorallia, Brachiopoda, Polychaeta Serpulidae ("calcareous tubeworms") and are listed in Table 2. Among scleractinian corals, only *Stenocyathus vermiformis* and *Thalamophyllia gasti* were found alive and possibly a few small branches of *Lophelia pertusa* from st. CS96-33. Mollusca include among others, subfossil valves of the large limid *Acesta excavata* (st. CS96-33, 193, 245).

Table 2 Major skeletonised macrobenthic invertebrates recovered from hard substrates during cruise CS96

Taxonomic group/Station	33	138	143	158	193	229	241	242	245
Scleractinia									
Caryophyllia calveri	x							x	x
Caryophyllia sarsiae					x				
Caryophyllia smithii								x	x
Ceratotrochus magnaghii				x					x
Coenocyathus cylindricus			x						
Dendrophyllia cornigera	x	x			x				x
Desmophyllum dianthus	x		x		x	x	x		x
Guynia annulata	x								
Javania sp.								x	x
Lophelia pertusa	x	x	x		x			x	
Madrepora oculata	x	x	x			x			x
Paracyathus pulchellus		x	x						x
Stenocyathus vermiformis	x	x	x	x		x	x	x	x
Thalamophyllia gasti	x		x						x
Octocorallia									
Corallium rubrum									x
Funiculina quadrangularis									x
Isidella elongata	x							x	
Brachiopoda									
Novocrania sp.		x	x						
Gryphus vitreus	x								x
Megathyris detruncata									x
Megerlia truncata		x							x
Platidia sp.		x							x
Polychaeta (Serpulidae)									
Filogranula cf. *gracilis*	x	x	x	x	x	x			x
Filograna sp.	x								
Hyalopomatus variorugosus	x	x	x	x	x		x		
Janita fimbriata	x	x	x					x	x
Metavermilia multicristata	x	x	x	x	x	x	x	x	x
Placostegus tridentatus	x	x	x	x	x	x	x	x	x
?*Protis* sp.	x	x	x						

Table 2 continued

Taxonomic group/Station	33	138	143	158	193	229	241	242	245
Protula sp.	x	x	x	x	x	x	x	x	x
Semivermilia agglutinata	x	x	x	x	x	x	x	x	x
Serpula vermicularis	x	x	x	x	x	x	x	x	x
Vermiliopsis monodiscus	x	x	x	x	x	x	x	x	x
Vermiliopsis sp.	x	x	x	x	x	x	x	x	x

The more remarkable species identified from deep-water coral and related calcareous hardgrounds

Protozoa

A particular foraminiferan (*Planogypsina*?) forming shiny bright white "beaded" branched stolons on the substrate was found in CS96-229 (403-588 m depth). It is also known from the Eratosthenes Seamount (south of Cyprus) at 800 m depth (Galil and Zibrowius 1998) and from Enarete Seamount (Tyrrhenian Sea) at 679 m depth (*Sonne* cruise 41 in 1986, st. 148DC; Zibrowius unpublished).

Porifera

The sponges recovered included some species rarely recorded in the Mediterranean Sea. As shown elsewhere, sponges in general are an essential component of fauna from deep-water coral mounds, typically settling dying coral substrates (Freiwald and Wilson 1998).

The pedunculate hadromerid *Stylocordyla pellita* (Topsent, 1904), in the Mediterranean was first reported from the Aegean Sea (360 m depth) and at present known from a few other sites, was found attached to subfossil giant oyster shells (CS96-229: 403-588 m depth).

The astrophorid *Sphinctrella gracilis* (Sollas, 1888), found in CS96-229 (403-588 m depth), has previously been obtained in other areas from similar hard substrates: in the Ligurian Sea (south of Portofino Promontory, 766 m depth; Sarà 1958), and on dead *Lophelia*, near Marseille in the Cassidaigne Canyon (500 m depth; Vacelet 1969) on subfossil giant oyster shells.

The "lithistid" *Siphonidium ramosum* Schmidt, 1868, seems to be a more common or, being remarkably robust like other "lithistids", at least an easily detectable species. There are currently five records from the Straits of Sicily: CS96-138 (223-580 m depth), CS96-143 (274-786 m depth), CS96-193 (673-690 m depth), CS96-229 (403-588 m depth) and CS96-245 (190-402 m depth). In the Cassidaigne Canyon near Marseille (500 m depth; Vacelet 1969) its substrate was subfossil giant oyster shells as in part of the Strait of Sicily sites.

Cnidaria

Bioluminescence in zoantharians has occasionally been mentioned in the literature (Widder et al. 1983; Herring 1987), but not yet for the Mediterranean. The *Urania* records include the first ascertained Mediterranean example of deep-water bioluminescent zoantharian (CS96-229, 403-588 m depth). Unfortunately this species remains unidentified, Zoantharia being a group that presently is infrequently

studied by taxonomists. Two small groups of about ten polyps each, connected by yellowish-white stolons, were observed encrusting a fossilised lamellar sponge, and one polyp was found on a dead small solitary scleractinian (*Stenocyathus vermiformis*) that was attached to the larger previous substrate. Bioluminescence of this zoantharian was accidentally discovered when the substrate bearing the colonies had been taken out of the dredge and was manipulated, moist, in a lowlight environmemt on board. When touched, the live polyps and stolons emitted a greenish-blue light. Once preserved in ethanol the tissues stayed whitish, whereas preserved in formalin they turned red, a feature known also from other zoantharians, such as *Savalia savaglia* (more commonly known as *Gerardia savaglia*; Zibrowius unpublished).

Thanks to the RV *Urania* cruises it is now possible to duly document the occurrence in the Mediterranean of the boring actinian *Fagesia loveni* (Carlgren, 1893). Specimens have been extracted from their burrows in subfossil giant oyster shells (CS96-229, 403-588 m depth) and in dead *Lophelia* branches (CS96-138, 223-580 m depth). Furthermore, in December 2003 during *Urania* cruise CORTI in the Tyrrhenian Sea, we found it in the Tuscan Archipelago, NW of Capraia, in dead *Madrepora* (st. CORTI-57: 43°13 N and 09°36.23 E; 406-447 m depth; Fig. 2). When observed on board in the aquarium, this cylindrical vermiform actinian proved to be of a slightly pinkish colour and, when disturbed, was fast to retract into its burrow.

Previous to our records, there had been an early, imprecise, and generally overlooked record of *F. loveni*, in the Mediterranean. In fact, Rossi (1958: 4, 10-11: *Milne-Edwardsia loveni*) mentioned an actinian boring inside dead *Lophelia* from the Ligurian Sea. This discovery credited to Jacques Picard dates back to a *Calypso* cruise in November 1957. An entry in the corresponding notebook preserved at Station Marine d'Endoume, Marseille, indicates that this record was from south of Portofino Promontory, depth 766 m (stat. 1260, c. 44°12.00 N and 9°13.00 E).

Fagesia loveni had originally been described (as *Milne-Edwardsia loveni*) from inside *Lophelia* branches from off the west coast of Sweden (Carlgren 1893). Recent submersible investigation of the *Lophelia*-mound complex on Sula Ridge revealed an intense infestation of the coral frame at this Norwegian site (Freiwald et al. 2002). Judging from its habit in association with dead skeletal substrate, *F. loveni* seems to be typically "skeletozoan" (*sensu* Taylor and Wilson 2002).

The stoloniferous octocoral *Scleranthelia musiva* Studer, 1878, is a rarely reported deep-sea species previously known from the Cape Verde Islands, Azores and three stations west of Corsica at 200-300 m (Carpine 1964). In the Strait of Sicily it was found to be relatively abundant on subfossil giant oyster shells (CS96-241, 300-714 m).

The unusual gorgonian *Dendrobrachia fallax* Brook, 1889, from CS96-193 (673-690 m) and CS96-229 (403-588 m) is the first record in the Mediterranean. More recently, we have recovered this species also from coral hardgrounds in the Alboran Sea (station COBAS-7; 36°31.27 N, 02°55.56 W, 408-475 m depth; RV *Urania*; Fig. 3). Previously it was known only from Ascension Island (Central South
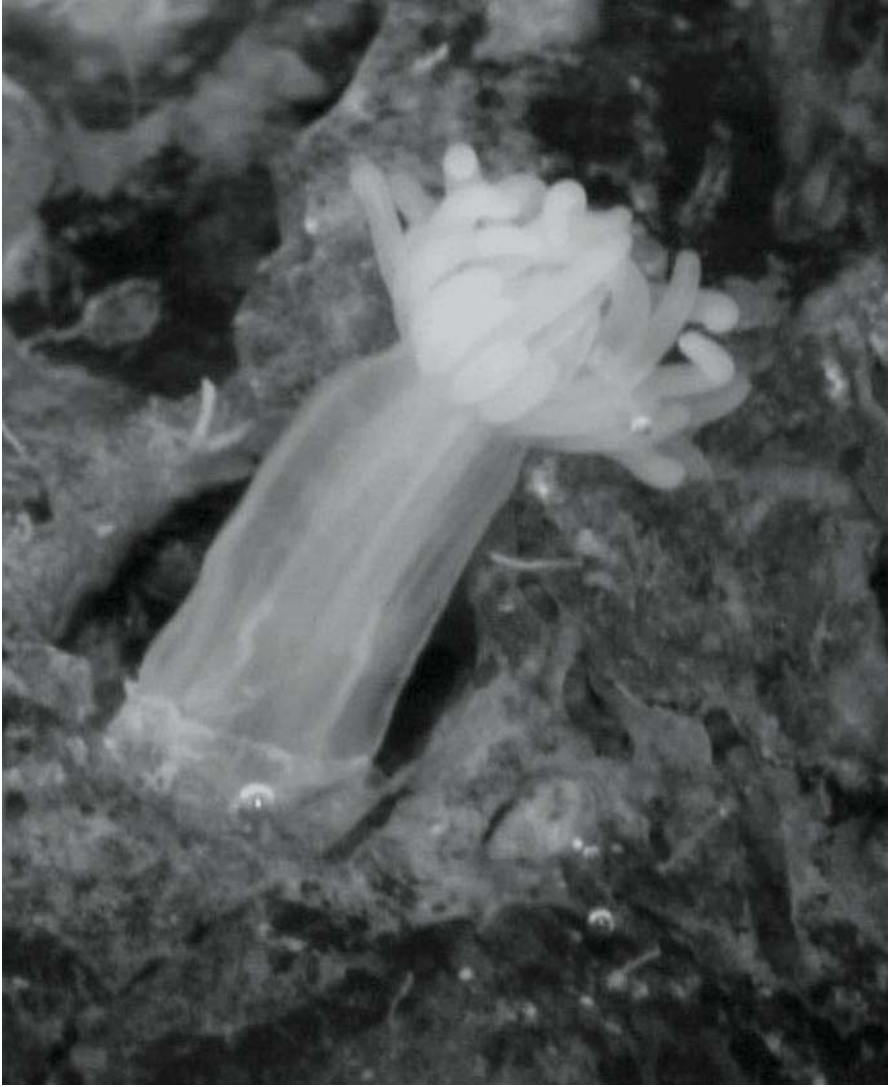
Fig. 2 Close-up of a full-expanded specimen of the boring actinian *Fagesia loveni* infesting a deep coral substrate (st. CORTI 57, Tuscan Archipelago, Mediterranean Sea; photo by B. Sabelli, magnification x 10)

Atlantic; *Challenger* expedition) and the Cape Verde Islands (*Prince of Monaco* expeditions), related forms having been reported from the Florida Straits and from off southern Australia (Opresko and Bayer 1991). Representatives of *Dendrobrachia* are remarkable for their horny axis with ridges and spines and for being devoid of sclerites, an exceptional situation among gorgonians and the reason why previously *D. fallax* had mistakenly been placed among the Anthipatharia.
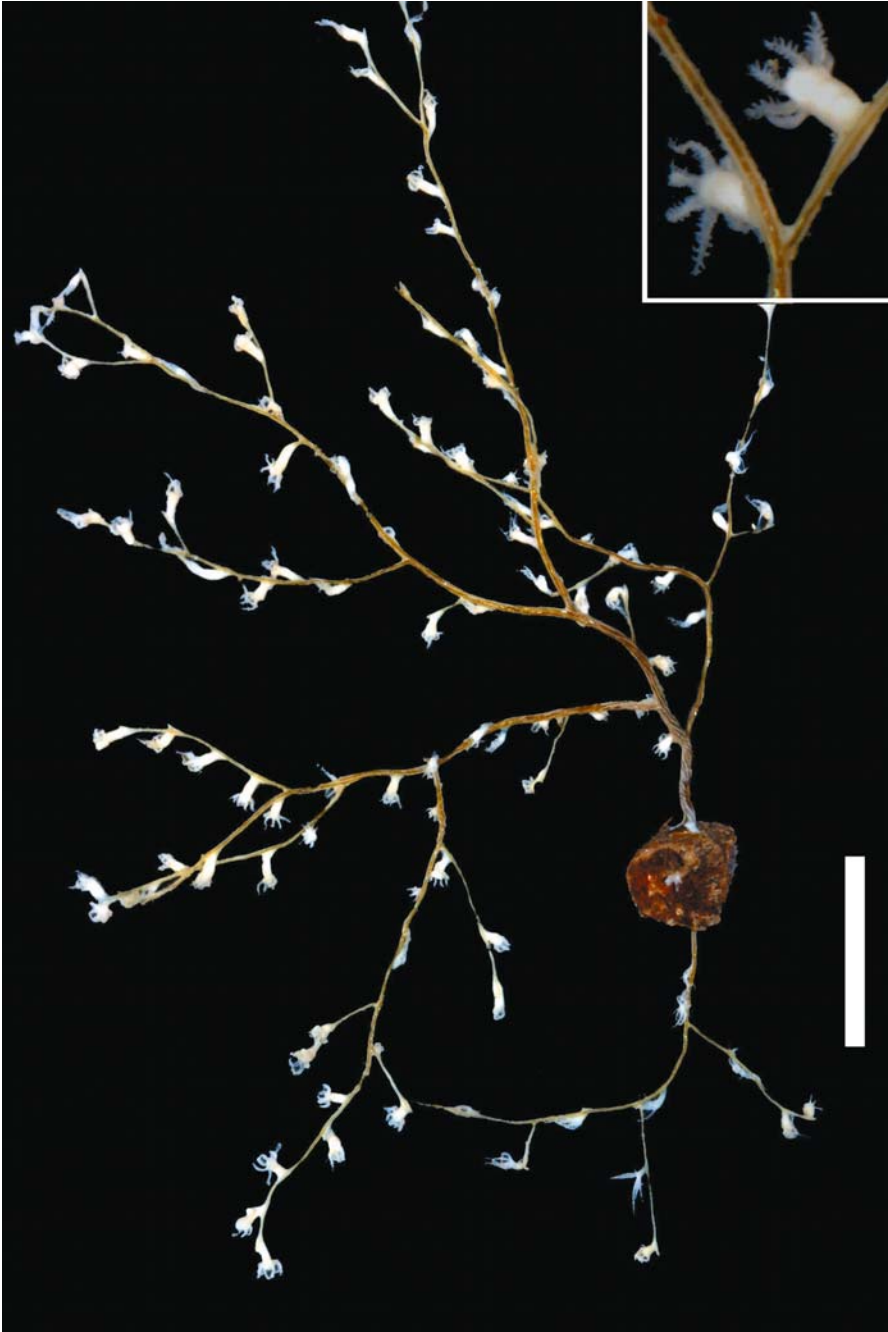
Fig. 3 The gorgonian *Dendrobrachia fallax* Brook, 1889 fixed on a calcareous hardground (st. COBAS-7, Seco de los Olivos, Alboran Sea, photo by B. Sabelli, April 2004: bar = 1.5 cm); inset: magnification of an expanded polyp

Echinodermata

The sessile suspension feeding holothurian *Psolidium complanatum* Cherbonnier, 1969, was recorded in 3 stations (CS96-143, 274-786 m depth; CS96-158, 375-397 m depth; CS96-229, 403-588 m depth). The *Urania* material was published by Massin (1997). This small, flattened species looks like some kind of crust and is firmly attached to the substrate surface (carbonate hardground). This species as well as the family Psolidae were previously unknown in the Mediterranean. Originally, *P. complanatum* had been described from a few bathyal stations off Galicia, northwestern Spain (Cherbonnier 1969).

Conclusions

Sampling by means of heavy dredges in the Strait of Sicily supplied significant information about previously little-known biota represented by sessile organisms exploiting deep-sea calcareous skeletal-hardground substrates (e.g., Messing et al. 1990). Our case study refers to pre-Recent deep coral, associated giant oyster and sponge substrates occurring on very steep settings in the silicoclastic-starved region of the Strait of Sicily. Based on our vast, mostly unpublished dataset, however, it can be observed that such substrates are widespread at many suitable places throughout the Mediterranean basin. The explored submerged settings are similar, at least partly, to fossil equivalents found on the ?Plio-Pleistocene paleo-escarpments of southern Italy and Rhodes (e.g., Montenat et al. 1991; Barrier et al. 1996; Taviani et al. 2005; Titschack and Freiwald 2005).

Acknowledgments

References

Agate M, D'Argenio A (1998) A review of NW Sicily offshore and Sicily Channel bedrock geology. Giorn Geol, Ser 3, 60: 205-218

Allouc J (1987) Les palócommunautés profondes sur fond rocheux du Pléistocène méditerraneén. Description et essai d'interprétation paléoécologique. Géobios 20: 241-263.

Arnaud PM (1990) La campagne MD50/JASUS aux îles Saint-Paul et Amsterdam à bord du "Marion Dufresne" 3 juillet-1er août 1986, Terres Australes et Antarctiques Françaises. Rapp Campagne Mer 86-04, 131 pp

Barrier P, Di Geronimo I, La Perna R, Rosso A, Sanfilippo R, Zibrowius H (1996) Taphonomy of deep-sea hard and soft bottom communities: the Pleistocene of Lazzàro (Southern Italy). In: Meléndez Hevia G, Blasco Sancho MF, Pérez Urresti I (eds) II Reunión de Tafonomía y Fosilización. Zaragoza, 13-15 de Junio de 1996, pp 39-45

Bonfitto A, Bigazzi M, Fellegara I, Impiccini R, Gofas S, Oliverio M, Taviani M, Taviani N (1994) Rapporto scientifico sulla crociera DP 91 (Margine orientale della Sardegna, Mar Mediterraneo). Boll Malac 30: 129-140

Borsetti AM, Colantoni P, Zarudzki EFK (1974) Note strutturali e stratigrafiche sul Canale di Sicilia. Mem Soc Geol Ital 2: 221-232

Bourcier M, Zibrowius H (1970) Note sur *Lima excavata* (Fabricius), pélécypode associé aux bancs de coraux profonds. Bull Soc Zool France 94 (1969): 201-206

Bourcier M, Zibrowius H (1973) Les "boues rouges" déversées dans le Canyon de la Cassidaigne (region de Marseille), Observations en soucoupe plongeante SP 350 (juin 1971) et resultats de dragages. Téthys 4 (1972): 811-842

Brachert T, Dullo W-Chr, Stoffers P (1987) Diagenesis of siliceous sponge limestone from the Pleistocene of the Tyrrenanian Sea (Mediterranean Sea). Facies 17: 41-50

Calanchi N, Colantoni P, Rossi PL, Saitta M, Serri G (1989) The Strait of Sicily continental rift systems: physiography and petrochemistry of the submarine volcanic centres. Mar Geol 87: 55-83

Carlgren O (1893) Studien über nordische Actinien. K Svensk Vetensk Akad Handl 25: 1-148

Carpine C (1964) Un octocoralliaire nouveau pour la Mediterranée *Scleranthelia musiva* Studer, 1878. Bull Inst Oceanogr Monaco 64 (1327): 1-10

Cherbonnier G (1969) Echinodermes récoltés par la «Thalassa» au large des côtes ouest de Bretagne et du Golfe de Gascogne (3-12 août 1967). Bull Mus Natl Hist Nat Paris, Ser 2, 41: 343-361

Cita MB, Benelli F, Biggiogero B, Chezar H, Colombo A, Fantini Sestini N, Freeman-Lynde R, Iaccarino S, Jadoul F, Legnani R, Malinverno A, Massiotta P, Paggi L, Premoli-Silva I (1980) Contribution to the geological exploration of the Malta Escarpment (eastern Mediterranean). Riv Ital Paleont 86: 317-356

Colantoni P (1975) Note di geologia marina sul Canale di Sicilia. Gior Geol, Ser 2, 40: 181-207

Delibrias G, Taviani M (1985) Dating the death of Mediterranean deep-sea scleractinian corals. Mar Geol 62: 175-180

Di Geronimo I (1987) Bionomie des peuplements benthiques des substrats meubles et rocheux plio-quaternaires du Détroit de Messine. Doc Trav Inst Geol Albert-de-Lapparent Paris 11: 153-169

Di Geronimo I, Rosso A, Sanfilippo R (1993) I banchi fossiliferi di *Corallium rubrum* al largo di Sciacca (Canale di Sicilia). In: Cicogna F, Cattaneo-Vietti R (eds) Il corallo rosso in Mediterraneo. Arte, Storia Scienza, pp 75-107

Freiwald A (2002) Reef-forming cold-water corals. In: Wefer G, Billett D, Hebbeln D, Jørgensen BB, Schlüter M, van Weering T (eds) Ocean Margin Systems. Springer, Berlin Heidelberg, pp 365-385

Freiwald A, Wilson JB (1998) Taphonomy of modern deep, cold-temperate water coral reefs. Hist Biol 13: 37-52

Freiwald A, Hühnerbach V, Lindberg B, Wilson JB, Campbell J (2002) The Sula Reef complex, Norwegian shelf. Facies 47: 179-200

Galil BS, Zibrowius H (1998) First benthos samples from Eratosthenes Seamount, eastern Mediterranean. Senckenb marit 28: 111-121

Herring PJ (1987) Systematic distribution of bioluminescence in living organisms. J Biolum Chemilumin 1: 147-163

Jensen A, Frederiksen R (1992) The fauna associated with the bank-forming deep-water coral *Lophelia pertusa* (Scleractinia) on the Faroe shelf. Sarsia 77: 53-69

Massin C (1997) First record of a Psolidae (Holothuroidea, Echinodermata) in the Mediterranean Sea (Sicilian Channel). Bull Inst R Sci Nat Belgique 67: 101-106

Messing CG, Neumann AC, Lang JC (1990) Biozonation of deep-water lithoherms and associated hardgrounds in the northeastern Straits of Florida. Palaios 5: 15-33

Montenat C, Barrier P, Ott d'Estevou P (1991) Some aspects of the recent tectonics in the Strait of Messina, Italy. Tectonophysics 194: 203-215

Mullins HT, Newton CR, Heath K, Vanburen HM (1981) Modern deep-water coral mounds north of Little Bahama Bank: criteria for recognition of deep-water coral bioherms in the rock record. J Sediment Petrol 51: 999-1013

Neumann AC, Kofoed JW, Keller GH (1977) Lithoherms in the Straits of Florida. Geology 5: 4-10

Newton CR, Mullins HT, Gardulski AF, Hine AC, Dix GR (1987) Coral mounds on the West Florida Slope: unanswered questions regarding the development of deep-water banks. Palaios 2: 359-367

Opresko DM, Bayer FM (1991) Rediscovery of the enigmatic coelenterate *Dendrobrachia* (Octocorallia: Gorgonacea) with description of two new species. Trans R Soc South Austral 115: 1-19

Pérès JM, Picard J (1956) Recherches sur les peuplements benthiques du seuil siculo-tunisien. Ann Inst Oceanogr Paris 32: 233-264

Picard J (1968) Observations biologiques effectuées, a bord du bathyscaphe Archimède dans l'une des fosses situées dans le sud du Cap Matapan. Ann Inst Oceanogr Paris 46: 47-51

Pratt RM (1967) Photography of seamounts. In: Hersey JB (ed) Deep-sea Photography. Johns Hopkins Press, Baltimore, pp 145-158

Remia A, Taviani M (2004) Shallow-buried Pleistocene *Madrepora*-coral mounds on a muddy continental slope, Tuscan Archipelago, NE Tyrrhenian Sea. Facies 50, DOI 10.1007/s10347-004-0029-2

Rossi L (1958) Contributo allo studio della fauna di profondità vivente presso la riviera ligure di levante. Doriana 2: 1-13

Rossi L (1961) Etudes sur le Seuil Siculo-Tunisien. 6. Madréporaires. Campagne de la "Calypso" (août-septembre 1954). Ann Inst Oceanogr Paris 39: 33-48

Sarà M (1958) Contributo alla conoscenza dei poriferi del mar Ligure. Ann Mus Civ Storia Nat Genova 70: 207-244

Segre AG, Stocchino C (1969) Nuove osservazioni sulla geologia e morfologia delle montagne submarine del Mar Tirreno. Ist Idrogr Mar Genova, FC 1037: 11-15

Selli R (1970) Campioni raccolti. Giorn Geol, Ser 2, 37: 55-72

Taviani M, Colantoni P (1979) Thanatocoenoses wurmiennes associées aux coraux blancs. Rapp Comm Int Mer Médit 25/26: 141-142

Taviani M, Colantoni P (1984) Paléobiocenoses profondes a scléractiniaires sur l'escarpement de Malte-Syracuse (Mer Méditerranée): leur structure, leur âge et leur signification. Rev Inst Franç Pétrol 39: 547-552

Taviani M, Remia A (2001) I coralli del buio: archivi climatici degli oceani passati. Ricerca & Futuro 18: 28-30

Taviani M, Remia A, Freiwald A (2002) Post-glacial deep-sea banks of giant oysters from the Strait of Sicily: addressing the problem of the mosaic-like temporal demise of Quaternary deep-sea carbonate factories in the Mediterranean basin. Abstr, 2nd Natl Conf SINAPSI, Portonovo-Ancona May 13-15 2002

Taviani M, Freiwald A, Zibrowius H (2005): Deep coral growth in the Mediterranean Sea: an overview. In: Freiwald A, Roberts JM (eds) Cold-water Corals and Ecosystems. Springer, Berlin Heidelberg, pp 137-156

Taylor PD, Wilson MA (2002) A new terminology for marine organisms inhabiting hard substrates. Palaios 17: 522-525

Titschack J, Freiwald A (2005) Growth, deposition, and facies of Pleistocene bathyal coral communities from Rhodes, Greece. In: Freiwald A, Roberts JM (eds) Cold-water Corals and Ecosystems. Springer, Berlin Heidelberg, pp 41-59

Tunesi L, Diviacco G (1997) Observations by submersible on the bottoms off shore Portofino Promontory (Ligurian Sea). In: Piccazzo M (ed) Atti del 12° Congresso dell'A.I.O.L. Isola di Vulcano, 18-21 Settembre 1996, Genova 1: 61-74

Vacelet J (1969) Eponges de la roche du large et de l'étage bathyal de Méditerranée (récoltes de la soucoupe plongeante Cousteau et dragages). Mém Mus Natl Hist Nat Paris, Ser A, Zool 59: 145-219

Widder EA, Latz MI, Case JF (1983) Marine bioluminescence spectra measured with an optical multichannel detection system. Biol Bull 165: 791-810

Zibrowius H (1974) Scléractiniaires des îles Saint Paul et Amsterdam (Sud de l'Océan Indien). Téthys 5: 747-778

Zibrowius H (1979) Campagne de la Calypso en Méditerranée nord-orientale (1955, 1956, 1960, 1964). 7. Scléractiniaires. Ann Inst Oceanogr Paris 55 Suppl: 7-28

Zibrowius H (1980) Les Scléractiniaires de la Méditerranée et de l'Atlantique nord-oriental. Mém Inst Oceanogr Monaco 11: 284 pp

Zibrowius H (1981) Thanatocoenose pléistocène profonde à spongiaires et scléractiniaires dans la fosse Hellénique. In: Journées d'études sur la systèmatique évolutive et la biogéographie en Méditerranée. Cagliari, 13 et 14 octobre 1980. Comm Int Expl Mer Médit Monaco, pp 133-136

Zibrowius H (1985) Spongiaires hexactinellides vivant en mer Ionienne par 2000 m de profondeur. Rapp Comm Int Mer Médit 29: 335-338

The metazoan meiofauna associated with a cold-water coral degradation zone in the Porcupine Seabight (NE Atlantic)

Maarten Raes, Ann Vanreusel

Marine Biology Section, Gent University, Krijgslaan 281, S8, B-9000 Gent, Belgium
  (maarten.raes@UGent.be)

Abstract. The metazoan meiofauna associated with *Lophelia pertusa* reef degradation zones in the Belgica Mound province (Porcupine Seabight, North-East Atlantic) was studied in the framework of the Atlantic Coral Ecosystem Study (ACES; EC Fifth Framework Research Program). Attention was focused on the influence of and differences between different microhabitat types: dead coral fragments, glass sponge skeletons and the underlying sediment. This study demonstrates the importance of dead *Lophelia pertusa* framework and associated substrates for meiofauna along the European continental margins. The presence of these large biogenic structures on the seafloor of the continental margin (1) enables more taxa to be present and (2) particularly favours harpacticoid copepods, naupliar larvae and polychaetes. The meio-epifaunal community on these substrates significantly differs from the meio-infaunal community in the underlying sediment. This is mainly due to a much lower dominance of nematodes and a higher relative abundance of most other taxa, especially harpacticoids, naupliar larvae and polychaetes, in the latter habitat. This situation is comparable to that of epiphytic assemblages. Dominance of nematodes is low. The meio-infaunal assemblage in the underlying sediment is characterized by low densities. There are clear indications that cold-water coral degradation zones are biologically very diverse, in terms of species richness as well as equitability. Of all microhabitat types, coral fragments support the most diverse communities, whereas the underlying sediment is the least diverse.

Keywords. Cold-water corals, dead coral framework, meiofauna, community structure, microhabitats, biodiversity

Introduction

Meio-epifauna: a new chapter in cold-water coral research

Although the existence of cold-water corals was known to science since the 18th century (Pontoppidan 1755), the associated fauna has by no means been studied as

intensely as for tropical corals. Most preceding studies dealing with real epifauna on either living or dead *Lophelia pertusa* (Linnaeus, 1758) have focused on the macrofauna; some studies dealt with the associated fauna in a broader sense and examined the animals that could be identified on live images or photographs from ROV, defined as megafauna (Dons 1944; Le Danois 1948; Burdon-Jones and Tambs-Lyche 1960; Jensen and Frederiksen 1992; Mortensen et al. 1995; Fosså and Mortensen 1998; Rogers 1999; Van Gaever 2001; De Backer 2002). Until the present-day, there is almost no knowledge on the composition and diversity of the smaller fraction, known as meiofauna, associated with *Lophelia pertusa* reefs (except for the study of Jensen and Frederiksen 1992). Obviously, this is an important hiatus in our understanding of cold-water coral associated fauna. Meiofauna is known to play an important role in the marine benthic ecosystem (Heip et al. 1985; Coull 1988) and it serves as food for other organisms (Thiel 1983; Coull 1988). Furthermore, as meiofaunal organisms occur in high abundances and because they are characterized by high species richness (Heip et al. 1985; Lambshead 1993), they are very suitable for biodiversity studies.

For the first time, the meiofauna associated with cold-water corals has been intensively studied. Three years of study on this topic will be presented here, highlighting the most important and striking aspects of this formerly unknown fauna and underlining its particular nature and relevance.

The present study deals only with metazoan meiofauna. In this paper, meiofauna is defined as the fauna that passes through a 1 mm mesh sieve but that is retained on a 32 μm mesh sieve. The 32 μm limit is used primarily in deep-sea studies because of the smaller size of deep-sea meiofauna (Thiel 1975; Thiel 1983; Pfannkuche 1985; Soetaert and Heip 1989). Next to the interstitial and mud-dwelling meiofauna (here referred to as meio-infauna), there is a large group of meiofauna living epifaunally on well-defined surfaces from diverse origin, ranging from large biogenic debris to seagrasses, macro-algae, larger coral fragments, sponge skeletons, manganese nodules and pebbles, to name a few. The term *meio-epifauna* will be used here to cover this unit of the meiofauna. For meiofauna living on seagrasses and macro-algae, the terms "epiphytic" and "foliicolous" have already been used in literature. A suitable substrate for meio-epifauna (1) should be a discrete and well-defined structure of at least about 5 mm in diameter and (2) should not be completely covered with sediment, implying that at least a part of the surface area remains in contact with the water column. Although it is expected that these surfaces will provide higher numbers of typical epifaunal taxa than any other habitat, there is of course no exclusive relationship in either way. This is because the surfaces are always in close contact with the sediment to a certain extent (physical contact with sediment surface, infill from sedimentation and resuspension), and because several typical epifaunal taxa (e.g., representatives from the epifaunal nematode families Epsilonematidae and Draconematidae: Fig. 4) are also found in coarse and poorly sorted sediments. Recently, a representative of the family Epsilonematidae (*Glochinema bathyperuvensis* Neira, Gad, Arroyo and Decraemer, 2001) has even been found living in fluffy, muddy sediments (Neira et al. 2001). In the present

study suitable surfaces for meio-epifauna are found on dead coral fragments of the framework builder *Lophelia pertusa* (Linnaeus, 1758) and skeletons of the glass sponge *Aphrocallistes bocagei* Schultze, 1886, both abundantly present in the cold-water coral degradation zones.

Most preceding studies on marine meiofauna have focused on the meio-infauna. The few studies that dealt with meio-epifauna focused on the fauna associated with macro-algae and seagrasses (e.g., Lewis and Hollingworth 1982; Coull et al. 1983; Bell et al. 1984; Hall and Bell 1993; Jarvis and Seed 1996; De Troch et al. 2001). The present study focuses on dead coral fragments and the dead glass sponge skeletons that are associated with them. Living coral is assumed not to be a suitable substrate for meiofauna, although the absence of meiofauna has not yet been verified. It was observed that the healthy coral responds to the settlement of sessile organisms by (1) an increase in mucus production and (2) selective sclerenchyme precipitation (Freiwald and Wilson 1998). These protective properties have proven to be rather successful antifouling measures against macrofauna (Mortensen 2000).

Location and environmental conditions

The information compiled in this study is based on three box core samples. The box cores were taken on the top and slope of a single seabed mound at depths between 972 and 1005 m (Table 1; Fig. 1). This mound is located in the Belgica Mound province of the Porcupine Seabight. The Porcupine Seabight is a large embayment of the European continental slope, located in the North-East Atlantic Ocean, southwest of Ireland. It is bordered by the Slyne Ridge in the north, the Goban Spur in the south, the Porcupine Bank in the west and the Irish Mainland shelf in the east. In this area numerous seabed mounds occur, grouped in three so called "mound provinces": the Hovland Mound province, the Magellan Mound province and the Belgica Mound province (Fig. 1). The Belgica Mound province is the most southern of all seabed mound provinces. It is characterized by large outcropping or buried, conical (sometimes composite) mounds with well-exposed downslope sides (De Mol et al. 2002), aligned in four along-slope-trending ridges (Van Rooij et al. 2003). In total, 21 outcropping mouds are present. These mounds are known to be associated with deep-water coral banks, mainly constructed by the framework builder *Lophelia pertusa* (Linnaeus, 1758) and associated fauna such as the glass sponge *Aphrocallistes bocagei* Schultze, 1886. These cold-water corals are present only on the basinward flanks of the mounds (De Mol et al. 2002). The presence of these mounds as well as the reefs that are associated with them alters the local hydrodynamic and sedimentary regime.

The presence of transversal sand dunes in the Belgica Mound region indicates very high current velocities, up to 100 cm/s (De Mol 2002). These very high velocities are probably exceptional but normal current speeds are still rather high (about 10-25 cm/s (White submitted) or even 40-50 cm/s (V. Huvenne pers. comm.)). High current speeds are attributed to the combination of strong, northward along-slope bottom currents, internal tides and waves, and the presence of mounds (Rice et al. 1991; Van Rooij et al. 2003; Wheeler et al. submitted; White submitted). Strong current activity is known to affect meiofaunal abundance and community structure

Table 1 An overview of the exact sampling location and depth, as well as the observed and calculated densities of the sediment-dwelling meiofauna found in the underlying sediment of the present study and in sediments from nearby localities at a comparable depth. Artificial values for the respective depths were calculated using the function $Y= 2241-227 \cdot \ln$ depth (Vincx et al. 1994: Fig. 4)

	Area	Coordinates		Depth [m]	Observed density [ind/10cm^2]	Calculated density [ind/10cm^2]
		Latitude	Longitude			
Box IV 2000	Porcupine Seabight	51°24'48.2"N	11°45'55.4"W	1005	376 ± 54	672
Box V 2000	Porcupine Seabight	51°24'49.4"N	11°45'55.9"W	1000	328 ± 178	673
Box IV 2001	Porcupine Seabight	51°25'7.7"N	11°46'9.3"W	972	291	679
Station 511-03 (Pfannkuche 1985)	Porcupine Seabight	51°47'0"N	13°08'36"W	960	1593 ± 143	682
Station 511-04 (Pfannkuche 1985)	Porcupine Seabight	51°21'24"N	13°03'18"W	1492	943 ± 127	582
Vanreusel et al. (1995)	Porcupine Seabight	51°46'12.8"N	13°13'2.4"W	900	1523 ± 267	697
Vanreusel et al. (1995)	Porcupine Seabight	51°39'2.4"N	12°59'1.8"W	1200	1500 ± 270	632
Station I (Vanaverbeke et al. 1997)	Goban Spur	49°24'43.2"N	11°31'51.6"W	670	612 ± 76	764
Station B (Vanaverbeke et al. 1997)	Goban Spur	49°21'59.4"N	11°48'5.4"W	1034	619 ± 47	665
Station II (Vanaverbeke et al. 1997)	Goban Spur	49°11'12.0"N	12°49'10.8"W	1425	509 ± 72	593

(Aller 1989; Aller 1997; Thistle and Levin 1998; Thistle et al. 1999). Currents are less vigorous upslope, to the east of the mounds (Van Rooij et al. 2003).

According to De Mol et al. (2002) and Van Rooij et al. (submitted) the upper 10 cm of the sediment in the Belgica Mound region can be defined as Foraminifera-rich silty sand or soupy, foraminiferal sand, with a high sand content decreasing towards a depth of 10 cm. Below this, the sediment becomes more clayey (pers. obs.), defined as olive grey silty clay by Van Rooij et al. (submitted). In the vicinity of the mounds, the sediment becomes littered with coral fragments and other biogenic debris (see below).
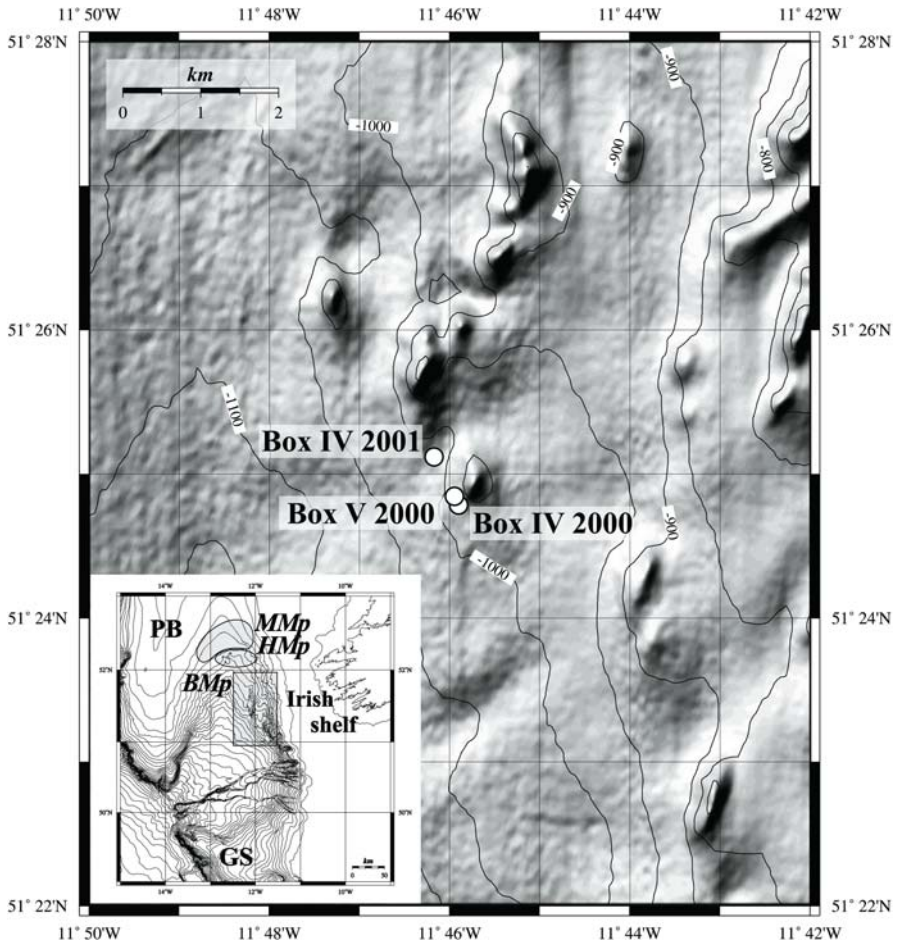
Fig. 1 Map of the Porcupine Seabight area, with a detail showing the ridge of mounds in the Belgica Mound province where the analysed samples originate from (bathymetry after Beyer et al. 2003). Boxcore locations are indicated. (PB = Porcupine Bank; *MMp* = Magellan Mound province; *HMp* = Hovland Mound province; *BMp* = Belgica Mound province; GS = Goban Spur)

The Porcupine Seabight is known to be subject to substantial phytodetrital deposition (Billett et al. 1983; Lampitt 1985; Gooday et al. 1996). The detritus itself as well as the Bacteria and Protozoa that rapidly colonize it are the main food source for deep-sea meiofauna. Taking into account both timing of surface blooms in 2000 and 2001, as well as sinking rates, it was calculated that phytodetritus should have been present on the bottom at both sampling occasions. It is however difficult to judge whether this material already had a relevant impact on the meiobenthos as response speed by benthic organisms may be taxon-specific, or even guild-specific: smaller species that utilize the organic matter directly show a more rapid response than larger species on a higher trophic level (Graf et al. 1982; Gooday et al. 1996).

Next to this, it is not even clear if this deposited material was available for the benthic fauna in the Belgica Mound region, an area subject to strong bottom currents. These currents will certainly cause resuspension and relocation of the material. Downslope and along-slope variability of phytodetrital deposition in this region makes generalizations even more difficult (D. Billett pers. comm.).

Food supply is known to influence meiofaunal abundance and biomass (Graf et al. 1982; Pfannkuche and Thiel 1987; Gooday and Lambshead 1989; Thiel et al. 1990; Pfannkuche 1993; Vanreusel et al. 1995a; Gooday 2002), metabolic activity (Graf et al. 1982; Pfannkuche 1993; Gooday 2002), community structure (Gooday 1988), reproductive cycles (Gooday et al. 1996; Gooday 2002) and size spectra (Thiel 1975; Soetaert and Heip 1989; Vanreusel et al. 1995a; Soltwedel et al. 1996) in the deep-sea. Our samples did not show any evidence of a detrital layer covering the sediment or the large biogenic substrates (pers. obs.).

Cold-water coral degradation zones

As already mentioned above, this study deals mainly with dead coral skeletons. These structures are the result of a bioerosion process that starts with the death of *Lophelia pertusa* colonies due to persistent attack by fouling organisms. The progress of this bioerosion process is visible in the zonation of the deep-water reef mound environment. Although each reef has its own characteristic zonation pattern with its own succession of typical facies (Freiwald et al. 1997; Freiwald et al. 2002), the two zones described by Mortensen et al. (1995) can be distinguished in most cases: according to these authors, a cold-water bioherm can be divided into two zones of approximately equal height: (1) a living coral zone on the summit and the upper flanks, and (2) a lower zone of dead corals. The centre of a deep-water bioherm indeed consists of living coral framework. According to Freiwald and Wilson (1998), the *Lophelia pertusa* bioerosion process starts with the formation of a microbial biofilm and endolithic fungal infestation, followed by colonisation of the coral skeleton by sessile invertebrates such as sponges and octocorals. The microbial biofilm might serve as a food source for small microvores including some meiofauna. As already mentioned above, this meiofauna is a food source for higher trophic levels (macrofauna and megafauna). Thus, the development of such a biofilm might enable an entirely new food web to be established, although there is still no evidence for this. In the reef's zonation pattern the living coral framework is flanked by the dead coral framework.

In a next stage, locally intense sponge excavation results in skeletal loss, and the *in situ* collapse of the dead *Lophelia pertusa* framework. Conversely, the encrusting sponge communities also speed up the closure of the gaps in the open coral framework and catalyse sediment-trapping, resulting in the strengthening of the framework architecture and the origin of large topographic features (De Mol et al. 2002). The dead coral framework gradually changes into a zone composed of smaller and more biodegraded coral skeletons with a rich associated fauna. The gaps between the skeletons and their branches are filled up with sediment (Freiwald et al. 2002). Our samples were taken in this type of habitat (sediment-clogged coral

framework). However, the sediment infill in our samples seemed rather limited, probably due to the high current velocities and the resulting resuspension of the sediment (see above). Because of the dynamic origin of this habitat, it is more generally referred to as a "coral degradation zone" in the present study.

In a final stage, intensified bioerosion will result in accumulations of centimetre-sized coral debris. This so-called coral rubble pavement (Freiwald et al. 1997) then grades into the soft bottom background. The diversity of megafauna living in this *Lophelia pertusa* rubble zone has been found to be lower than that of the zones with living or dead coral colonies (Mortensen et al. 1995). Dead coral colonies accommodate the most diverse macro- and megafauna (Jensen and Frederiksen 1992; Mortensen et al. 1995). This can be attributed to the sheltering function and higher habitat diversity of branched dead coral skeletons (framework) in contrast to the very small fragments in the *Lophelia pertusa* rubble zone.

In the immediate vicinity of the seabed mound examined in this study, every stage between dead coral framework and the coral rubble pavement is present. The dead framework however occurs only in small patches. Live coral framework in this region is present on the ridge directly to the north of the examined mound, from the nearby Thérèse Mound to Galway Mound farther north (A. Foubert pers. comm.). As the seabed mound in question is considered to be the most southern mound of this ridge, it is expected that this structure also contains live coral patches.

The present paper aims to describe the metazoan meiofaunal community structure associated with cold-water coral degradation zones for the first time, investigate the importance of different microhabitats for meiofauna in this area by checking for habitat preferences and compare the observed community structure with the composition of epiphytic assemblages. In addition, densities of the meio-infauna in the underlying sediment will be compared with available data from preceding studies on meiofauna in the northeast Atlantic and the biodiversity of this formerly unknown fauna will be extensively discussed.

Methods used to study the meiofauna

Sampling procedure

Material was obtained by means of a NIOZ (Netherlands Institute for Sea Research) box corer (ø 32 cm). In total, three box cores were examined. Two box cores were taken during the 9-19 June 2000 sampling campaign on the RV Belgica. A third box core was taken on the same location and brought to the surface during the 2-11 May 2001 sampling campaign on the same vessel (Fig. 1). In all cases, the surface of the sediment was partly or entirely covered with several fragments of dead corals (*Lophelia pertusa* (Linnaeus, 1758)) and dead sponge skeletons (*Aphrocallistes bocagei* Schultze, 1886). Only a very small amount of living coral was present. The larger sponge and coral fragments were collected separately. After removal of the large biogenic substrates three sediment cores (10 cm^2) were pushed into the underlying sediment of each box core. All material was fixed with 4 % neutralised formalin.

Microhabitats

The main aim of this study is to examine the differences in community structure due to the presence of different microhabitat types. Obviously, for meiofaunal organisms the conditions within the sediment are clearly different from those on a complex elevated structure on the seafloor, and this in terms of food supply and food quality as well as in terms of the physical influence of strong bottom currents. These differences should have their effect on the presence and abundance of meiofaunal taxa. Next to this obvious distinction between large biogenic substrates and the underlying sediment as a habitat, small differences in microhabitat structure should also influence meiofaunal community composition as meiofauna is known to respond acutely to minor environmental changes. In this respect the rough surface of the branches of *Lophelia pertusa* (Linnaeus, 1758), sometimes covered with a thin layer of bryozoan colonies, is quite dissimilar from the complex three-dimensional build-up of spicules in the glass sponge *Aphrocallistes bocagei* Schultze, 1886 (Fig. 2).

In total, 28 subsamples were examined: 18 subsamples were collected in the first box core (2000), six subsamples in the second box core (2000) and another four subsamples in the box core from 2001. After thorough examination of their contents, the subsamples were classified into one of the following groups, each of them representing a microhabitat type (Fig. 2): (1) coral fragments, (2) sponge skeletons (i.e., the two large biogenic substrates), (3) the underlying sediment and (4) a mixed substrate. Subsamples belonging to the *mixed substrate* group contained coral fragments as well as sponge skeletons. The underlying sediment consisted of fine to medium sand (median 194.9 μm) with a small fine silt fraction and a high amount of globigerine forams. It was observed that this was a poorly-sorted sediment, also containing small fragments of both large biogenic substrates, as well as some small mollusc shells and echinoid radiolas (Fig. 2E). The second sample
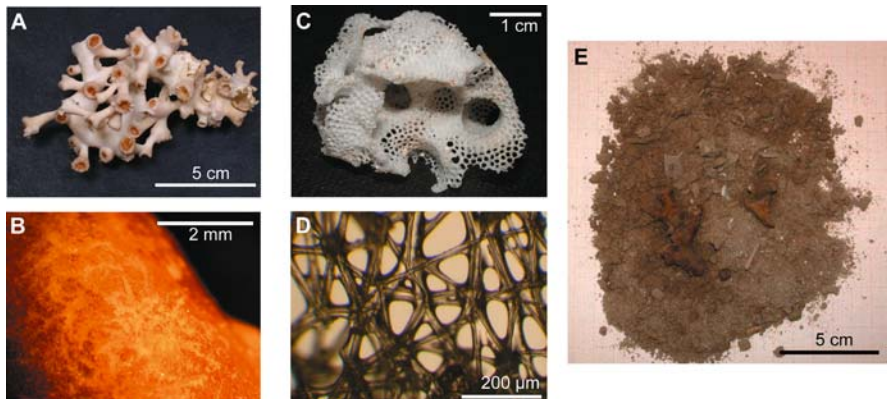
Fig. 2 An overview of the three major microhabitat types: **A** a dead *Lophelia pertusa*-fragment; **B** detail of the fragment's surface; **C** a dead *Aphrocallistes bocagei*-skeleton; **D** detail of the complex three-dimensional sponge spicule framework; **E** the underlying sediment. Note that small coral and sponge debris is present in the underlying sediment, as well as small bivalve and gastropod shells and echinoid radiolas

from 2000 did not yield any "sponge skeletons" subsamples and the sample from the 2001-campaign did not yield any "mixed substrate" subsamples.

Laboratory analyses

Each *Lophelia* and *Aphrocallistes* fragment was rinsed thoroughly over a 1 mm and a 32 μm sieve to separate the macrofauna from the meiofauna fraction. Meiofauna extraction from the underlying or remaining sediment was done by density gradient centrifugation, using Ludox (a colloidal silica polymer; specific gravity 1.18) as a flotation medium (Heip et al. 1985; Vincx 1996). All metazoan meiofauna was stained with Rose Bengal, counted in small counting trays and identified up to higher taxonomic level under a stereomicroscope. Meiofauna was classified into several taxonomic groups, ranging from orders to phyla. Most larvae however were difficult to associate with a single taxon and therefore they were referred to by using the name of their larval stage: nauplii (Crustacea), zoea (Crustacea), metazoea (Crustacea) and trochophora larvae (Polychaeta).

Volumes of all examined large biogenic substrates were measured by immersion. This method only provides a value for the volume of each substrate and not its surface area, but volume can be used as a proxy for surface area: only an extra mathematical factor describing branching complexity of corals or three-dimensional structure of sponge skeletons is needed. The use of volume estimates results from the absence of such a factor and the lack of other good alternatives. Each sediment subsample represented 10 cm^2 of sediment.

Statistical analyses

The PRIMER5 software package was used for most statistical analyses. With this software Bray-Curtis (dis)similarities between all subsamples are calculated, ultimately resulting in a test statistic reflecting within-microhabitat as well as between-microhabitat similarities. The resulting similarity matrix was applied to perform a non-metric multidimensional scaling analysis (MDS; stress 0.11). The stress value gives a measurement of goodness-of-fit of the MDS ordination. A low stress value (<0.2) indicates a good ordination with no real prospect for a misleading interpretation (Clarke 1993). ANalysis Of SIMilarities (ANOSIM) was used to test the statistic for significant differences (p <0.05) between meiofaunal community structure in the different microhabitats and to investigate which taxa were responsible for these differences (SIMilarity of PERcentages: SIMPER). In this study all absolute data were square root transformed prior to the analysis.

Indicator species analysis (ISA; Dufrêne and Legendre 1997) was performed using the PC-ORD4 software. For this type of analysis absolute data were used without any transformation. Calculated indicator values were tested for statistical significance using the Monte Carlo test.

Parametric (one-way ANOVA) and non-parametric (Kruskal-Wallis) analysis of variance were performed using the STATISTICA6 software. Bartlett's and Cochran's test were used to verify the homogeneity of variances prior to the analysis.

Several biodiversity indices were calculated to obtain an extensive overview of taxon diversity of the analysed samples. The Shannon-Wiener index *H'* and Pielou's

evenness *J* (Pielou 1975) are mainly included for reasons of comparability with other studies. Hill's diversity numbers (Hill 1973) gradually change from indices of species richness to indices of dominance with increasing number: N_0 is identical to the number of species, $N_1 = \exp(H')$ and N_∞ reflects evenness. The *expected number of taxa* for a theoretical sample of 100 individuals ET (100) was derived from the *expected number of species* (Hurlbert 1971).

Associated meiofauna: community structure, densities and the influence of suitable substrates

As mentioned above, only the metazoan meiofauna was considered in this study. It is however relevant to mention that intact ciliates and foraminiferans were encountered in our samples.

In this study a total of 16547 metazoan meiofaunal organisms was counted, divided into 16 phyla and 33 groups (i.e., taxonomic groups as well as larval stages). The number of phyla represented here is quite high, especially taking into account that only 22 metazoan phyla (in the traditional sense) have representatives in the meiobenthos (Coull 1988). Because a full taxon list is seldom given in literature, it is difficult to compare the number of taxa. In total, only 31 of the 33 groups were included in the analysis: Hydrozoa and Calanoida were excluded for different reasons. A large number of hydrozoans was found: either individual polyps or branched pieces of hydrocaulus with several polyps still attached. It was reasoned that large branched colonies of Hydrozoa would be withheld on a 1 mm sieve and that therefore the number of individual polyps counted as meiofauna was not an accurate reflection of the natural situation. Calanoida on the other hand are pelagic copepods that have an aggregated spatial distribution in the water column. Therefore, their occurrence in the overlying water of a box core is highly coincidental. As a result, the presence of 29 Calanoida in two subsamples from the same box core and their absence in all the other subsamples indicates that these 29 individuals originated from a swarm of calanoids in the overlying water of this box core and can therefore be considered as contamination. It should be remarked here that a large number of other taxa found in our samples is also capable of permanent or temporary residence in the overlying water (e.g., Chaetognatha, Cladocera, and most larvae), especially when the high current velocities in the region (see above) are taken into account.

A considerable number of larvae or juveniles were encountered. Next to the crustacean and polychaete larvae already mentioned above, an unknown juvenile arthropod, which is probably a recently hatched juvenile amphipod, was encountered. It should be mentioned here that direct development resulting in hatching as a juvenile, i.e., without a nauplius larva, is a feature of all Peracarida (e.g., Amphipoda, Isopoda, Tanaidacea, and Cumacea) and of Cladocera (Williamson 1982). This means that the nauplii encountered in our samples are either from harpacticoid copepods, ostracods or from crustaceans that belong to the macrofauna. Therefore, unlike most other studies, nauplii will be considered separately from harpacticoid copepods here. Judging by their size, the zoea and metazoea are larvae from crustaceans of macrofaunal size and in this respect they are regarded as temporary

meiofauna. Loricifera, Tantulocarida and Bivalvia were only represented by their larvae (Loricifera: "Higgins-larvae"; Tantulocarida: "Tantulus-larvae") or juveniles (Bivalvia).

An overview of the relative abundances and overall average densities of the meiofaunal taxa and larvae associated with cold-water coral degradation zones is given in Table 2A. Overall, the meiofaunal population was dominated by nematodes which made up 67.0 % of the total metazoan meiofaunal community on average. Harpacticoida constituted the second most abundant taxon, comprising 12.6 % of all meiofauna on average. Nauplii were the third most abundant group: they accounted for 7.1 % of the total meiofauna. These results correspond relatively well with the available information on deep-sea meio-infaunal community composition (compiled by Vincx et al. 1994 and Soltwedel 2000), although the observed relative abundance of nematodes is lower than for the meio-infauna in the Porcupine Seabight (Pfannkuche 1985). This relative abundance varies strongly, between 32.7 and 94.7 %, which is due to differences in the type and amount of large biogenic substrates present in the subsamples. These substrates accommodate a community characterized by a significantly lower dominance of nematodes (see below) and higher relative abundances of most other taxa. When only the underlying sediment is considered, nematodes comprise between 71.6 and 94.7 % of the total meiofaunal community, a situation more similar to that of the deep-sea meiobenthos not associated with large biogenic structures on the seafloor (Vincx et al. 1994). Moreover, there are no relevant differences between the meiofaunal community composition on higher taxon level in the underlying sediment of this study and in other deep-sea soft sediments not covered by dead coral framework, at least not for the most abundant taxa.

Next to the three taxa already mentioned, only polychaetes, tardigrades and gastrotrichs have a relative importance of more than 1 %. According to Vincx et al. (1994), polychaetes are indeed the third most abundant taxon in the northeast Atlantic deep-sea meio-infauna (after nematodes and the combined harpacticoids-nauplii).

Only the densities of the meio-infauna in the underlying sediment could be compared with existing data, because no comparable density measurements (ind/l) were made for meio-epifauna in preceding studies and because the accumulation of sedimented material on the substrates obscures the concept of total available surface area for meio-epifaunal organisms. The overall meio-infaunal density of 346 ind/ $10\ cm^2$ found in the present study is below that expected for a depth of 1000 m as indicated by the 'best regression' in Vincx et al. (1994: Fig. 4). This is even more obvious when applying the function given by the same authors, describing the relationship between metazoan meio-infaunal density and depth in the northeast Atlantic, and given as Y = 2241-227 · ln depth. The mean densities (and standard deviations) of the meio-infauna for each examined box core, compared with calculated values for the respective depths, are given in Table 1. It is clear that the observed values are consistently far below the calculated values. Moreover, the mean densities in the Porcupine Seabight area (given as areas 1 and 2 in the considered

Table 2 Relative abundances and overall average densities of the meiofauna associated with cold-water coral degradation zones. **A** Entire community; **B** separate microhabitats. Taxa found exclusively on a certain substrate are underlined. *: for 1 substrate the volume is not known, average densities were measured using only the samples with known volumes

A

Entire community (28)	
taxon	%
Nematoda	67.04
Harpacticoida	12.57
Nauplii	7.14
Polychaeta	5.19
Tardigrada	2.67
Gastrotricha	1.51
Ostracoda	0.81
Turbellaria	0.79
Aplacophora	0.62
Trochophora-larvae	0.56
Acari	0.45
Isopoda	0.21
Oligochaeta	0.10
Sipuncula	0.07
Bivalvia	0.04
Unknown juvenile arthropod	0.04
Cumacea	0.02
Kinorhyncha	0.02
Loricifera	0.02
Pycnogonida	0.02
Tantulocarida	0.02
Chaetognatha	0.01
Priapulida	0.01
Tanaidacea	0.01
Amphipoda	0.01
Cladocera	0.01
Echiura	0.01
Holothuroidea	0.01
Metazoea	0.01
Rotifera	0.01
Zoea	0.01
# of individuals	16392
Average density meio-epifauna	35932 ind/l
Average density meio-endofauna	346 ind/10 cm^2

B

Coral fragments (10)		Sponge skeletons (8)		Mixed substrate (4)		Underlying sediment (6)	
taxon	%	taxon	%	taxon	%	%	taxon
Nematoda	56.59	Nematoda	77.18	Nematoda	78.89	85.83	Nematoda
Harpacticoida	17.85	Harpacticoida	10.59	Harpacticoida	8.30	5.48	Harpacticoida
Nauplii	8.72	Polychaeta	6.07	Polychaeta	4.86	2.96	Polychaeta
Polychaeta	8.09	Tardigrada	2.30	Tardigrada	2.46	2.53	Nauplii
Tardigrada	2.47	Nauplii	1.60	Nauplii	1.35	0.72	Tardigrada
Gastrotricha	2.00	Aplacophora	0.55	Turbellaria	1.20	0.62	Gastrotricha
Ostracoda	0.99	Gastrotricha	0.53	Ostracoda	0.54	0.59	Ostracoda
Aplacophora	0.72	Ostracoda	0.39	Acari	0.53	0.30	Aplacophora
Turbellaria	0.67	Acari	0.32	Gastrotricha	0.47	0.23	Acari
Acari	0.66	Isopoda	0.18	Unknown juv. arthropod	0.28	0.19	Turbellaria
Trochophora-larvae	0.64	Oligochaeta	0.11	Aplacophora	0.21	0.14	Kinorhyncha
Isopoda	0.25	Turbellaria	0.10	Isopoda	0.17	0.08	Cumacea
Oligochaeta	0.07	Sipuncula	0.06	Oligochaeta	0.17	0.08	Oligochaeta
Sipuncula	0.07	Pycnogonida	0.02	Pycnogonida	0.15	0.06	Trochophora-larvae
Tanaidacea	0.07	Kinorhyncha	0.01	Loricifera	0.14	0.05	Metazoea
Bivalvia	0.05			Sipuncula	0.09	0.04	Zoea
Tantulocarida	0.04			Bivalvia	0.05	0.04	Loricifera
Holothuroidea	0.02			Cladocera	0.05	0.04	Rotifera
Priapulida	0.02			Priapulida	0.05	0.02	Isopoda
Chaetognatha	0.02			Tantulocarida	0.05		
Amphipoda	0.01						
Echiura	0.01						
Cumacea	0.01						
# of individuals	7226		4695		1815		2656
Average density	15919 ind/l*		63192 ind/l		26443 ind/l		346 ind/10cm^2

graph) appear to have a position far above the 'best regression' trendline depicted in Vincx et al. (1994: Fig. 4), indicating that this area is normally characterized by very high densities. In a final attempt to confirm that the densities found in the present study are exceptionally low, they are compared with data from three studies dealing with samples from the Porcupine Seabight and nearby Goban Spur at a similar depth (Pfannkuche 1985; Vanreusel et al. 1995b; Vanaverbeke et al. 1997). For optimal comparison, it was attempted each time to select the stations from each study that are most comparable in depth with the samples from the present study, i.e., around 1000 m. The average densities, standard deviations and the corresponding calculated values are given in Table 1. The highest mean density in our samples (376 ind/10 cm^2: Box IV 2000) is still markedly lower than the lowest value found in literature (509 ind/10 cm^2: station II in Vanaverbeke et al. 1997). Moreover, station II in Vanaverbeke et al. (1997) is situated much deeper (1425 m) than Box IV 2000 (1005 m) and therefore the low observed densities in the former are probably due to an effect of depth-related density decrease. Vanaverbeke et al. (1997) attributed their lower density values compared to sites in the Porcupine Seabight to (1) a difference in deposited amount of phytodetritus and (2) differences in sampling gear. Indeed, the Porcupine Seabight is considered an area with exceptionally high organic food input (Billett et al. 1983; Lampitt 1985; Gooday et al. 1996), resulting in very high meiofaunal densities. This contrasts sharply with the low densities observed in our study. Without taking in consideration the current uncertainty about the extent of phytodetrital deposition in the Belgica Mound region, there are several potential explanations for this discrepancy.

Differences in sampling gear and the low efficiency of box corers in collecting meiobenthos may be of importance here, as the studies of Pfannkuche (1985) and Vanreusel et al. (1995b) are based on multiple corer samples. On the other hand, the coral and sponge fragments present at the sample site might act as a sediment trap, preventing resuspension of the sediment and therefore limiting the bow-wave effect generated by box corers. The relative limpidity of the overlying water seems to confirm this last hypothesis. In this case, the presence of large biogenic structures on the seafloor affects the meio-infaunal densities on the sampling site in a positive way. However, their presence may also cause a decline in meiofaunal densities in the underlying sediment as it is thought that the collapsed coral framework and associated substrates act as a kind of 'net', successfully trapping most of the seasonally supplied phytodetritus and in this way limiting the amount of food supplied to the underlying sediment. The high amount of food trapped by the biogenic structures is made unavailable for the fauna in the underlying sediment. It has already been mentioned that meiobenthic densities decrease with decreasing food availability.

Although these large biogenic structures are thought to protect the underlying meio-infauna from physical erosion and removal by strong currents and enable other taxa to dwell among the coral branches, it is not clear to what extent they are able to reduce the impact of strong currents on the underlying sediment. Strong bottom flow may not be adequately decreased under the sediment-clogged cold-

water coral framework. Lower meio-infaunal abundances may therefore be an effect of physical removal of the meiofauna in the upper sediment layers (keeping the fauna in suspension until a time of decreased flow) or an effect of lower microbial biomass due to decreased deposition of food. The relative limpidity of the overlying water as argued above, as well as the presence of a well-established meio-epifaunal community associated with the *Lophelia pertusa* framework as proven by the present study, are however inconsistent with this idea. One should always keep in mind that because of the diurnal and semi-diurnal nature of tidal currents (Rice et al. 1991) the impact on meiobenthos will fluctuate on a short time-scale. This is because the frequently changing current speeds will result in periodic cycles of erosion and deposition. During the latter periods, sediment, food and organisms are redeposited on the seabed and meiofaunal abundances will increase (Aller 1989, 1997).

The presence of small biogenic structures (coral fragments, sponge skeletons, sponge spicules, echinoid radiolas, gastropod and bivalve shells) in the sediment may also have its effect on meiofaunal density. The coarsening of the sediment might particularly affect typical interstitial taxa, such as the dominant nematodes and gastrotrichs, because of its influence on the dimensions of interstitial free space and because the biogenic structures are probably obstacles for organisms crawling between the sand grains. A decrease in nematode density will then directly affect total meiofaunal density. Decreased meiobenthic densities in the underlying sediment can also be explained by high predation pressure by the abundant and diverse macrofaunal community found in association with the sediment-clogged coral framework (Jensen and Frederiksen 1992). A more intense comparison with background sediments is needed to confirm or falsify these and other hypotheses.

In contrast with the underlying sediment, the sediment-clogged coral framework itself is thought to be more densely populated. Because this framework is able to trap sedimented organic food, it can be regarded as a hotspot of abundant food in a generally food-limited environment. Limitation of food is not proven here: on the contrary, fast flows should provide a constant supply of food. It is argued however that fast flows may also interfere with deposition of food and that sediment resuspension due to strong currents makes deposited food less accessible for meiobenthos (see also: Lampitt 1985). This is based on the observed decrease in microbial biomass due to faster flow (Thistle and Levin 1998). As complex biogenic structures may also provide shelter against predation, conditions should be ideal for the development of a rich meio-epifaunal community: low disturbance, low predation pressure and abundant food enable a specific community to be established on and in between the coral branches and sponge skeletons.

Habitat preferences

Within this relatively protected habitat significant differences in meiofaunal community structure were found between the different microhabitats that were distinguished. Only twelve taxa occurred in all four microhabitats (Table 2B). Moreover, on a total of 31 taxa, five taxa were found exclusively on coral fragments, although not in all subsamples. In contrast, only three were found exclusively in the sediment, two on the mixed substrate and not a single taxon was restricted to

sponge skeletons. There were no taxa showing an obligate association with a certain microhabitat in the sense that when a taxon occurred in only one microhabitat it was never found in all subsamples.

The MDS graph given in Figure 3 plots all subsamples relative to each other. There is a high degree of overlap between the different microhabitats in terms of community composition, although on the MDS plot a trend from the upper left corner to the lower right corner (coral fragments - sponge skeletons - underlying sediment) is present. Overall, the image seems however rather complex.
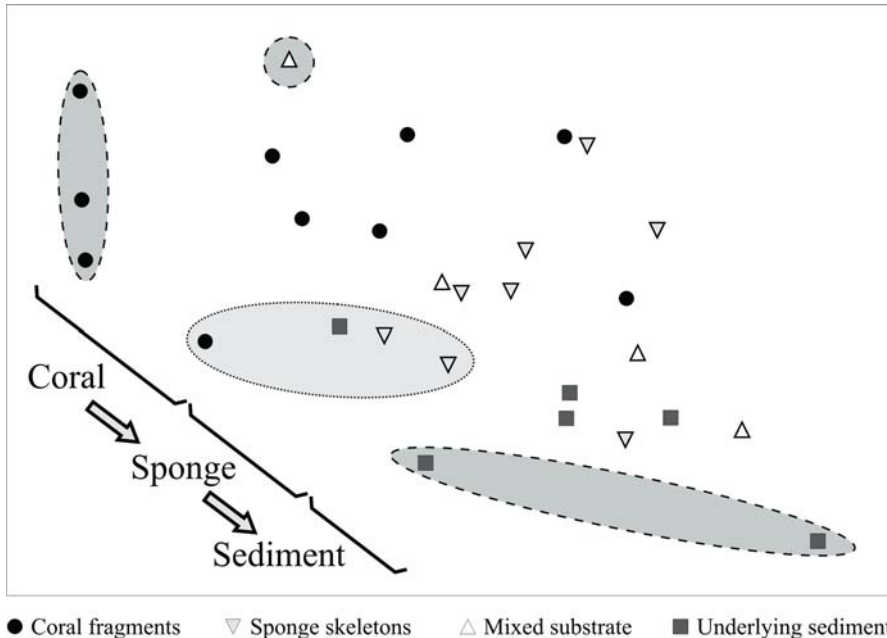
Fig. 3 Multidimensional Scaling (MDS) two-dimensional plot (stress: 0.11) of all subsamples. The subsamples in a pale field surrounded by a dotted line are from the 2001-box core. The subsamples in a darker field surrounded by a dashed line are from the second box core taken in 2000. The trend mentioned in the text is visualized in the lower left corner

ANOSIM showed highly significant ($p = 0.005$) overall differences between the microhabitats. Pairwise tests were carried out and revealed significant differences between the coral microhabitat and all other microhabitats in terms of community composition. It can therefore be concluded that the coral microhabitat houses a very typical and rather unique meiofaunal community. Very highly significant differences ($p = 0.001$) were found between the coral microhabitat and the underlying sediment. This result is in good agreement with the number of taxa found exclusively in each of these microhabitats and the image given by the MDS analysis: the coral fragment subsamples can be clearly separated from the sediment subsamples on the ordination graph.

At this point attention will be focused only on these two extremes. Average dissimilarity (29.7 %) is low, probably because of the large differences between the subsamples within one microhabitat type. More than 50 % of this dissimilarity is caused by four taxa: Harpacticoida (16 %), Nematoda (14 %), nauplii (13.5 %) and Polychaeta (8.5 %). Only nematodes had a significantly higher average relative abundance ($p = 0.0007$) in the sediment subsamples compared to the coral subsamples; all other taxa were relatively more abundant on coral fragments. An indicator species analysis was carried out on all subsamples (including the sponge and mixed subsamples) to elucidate habitat preferences. This yielded three taxa with significant indicator values for coral fragments: nauplii (IV = 74); Harpacticoida (IV = 53) and Polychaeta (IV = 47). Kinorhyncha was the only significant indicator for the sediment subsamples (IV = 40). Nematodes were not identified as indicators for the sediment, although this was put forward by SIMPER and the observed significantly lower relative abundance of this taxon on coral fragments. This is due to the fact that nematodes were still the dominant group on this substrate.

Although nematodes are the dominant group in all microhabitats, they are relatively more important in sedimentary habitats. Because most nematodes are long and slender organisms, they are morphologically more adapted to move between the sand grains than to crawl over a large surface (Giere 1993). Moreover, the presence of interstitial microniches is essential for nematode colonization (Danovaro and Fraschetti 2002). So the presence of sediment is probably essential to ensure a well-developed nematode community. Only those nematodes belonging to the epifaunal families Epsilonematidae and Draconematidae are morphologically adapted to "walk" over hard substrates. These nematodes are known to have a looper caterpillar-like locomotion using ventral setae (*ambulatory setae*: Epsilonematidae) or tubes (*posterior adhesion tubes*: Draconematidae) on their posterior body region, sometimes together with tubes on or near the head capsule (*cephalic adhesion tubes*: Draconematidae) (Fig. 4). A predominance of representatives of these two families on dead *Lophelia pertusa* fragments has been observed (Raes and Vanreusel pers. obs.). The lower dominance of nematodes on coral fragments results in a higher relative abundance of all other taxa. Although some of these taxa are known to be typically interstitial (e.g., Gastrotricha and Tardigrada), only kinorhynchs were found to have a clear habitat preference for the underlying sediment. According to Higgins (1988), kinorhynchs are frequently found in the interstitia of medium to coarse sand or gravel. On the other hand, Coull (1988) stated that Kinorhyncha, being for the most part burrowing organisms in muddy sediments, are excluded from interstitial habitats.

The fact that nematodes are still the dominant group on the coral substrate is mainly attributed to the sediment infill between the fragments and coral branches, these substrates are still in close association with the underlying sediment. The community composition of meio-epifauna on cold-water coral fragments is therefore in a broad sense somewhat comparable to the composition of the infauna, however with some important differences as already argued above. On higher taxon level, a meio-epifaunal community is composed of a sediment-dwelling

background community (predominantly nematodes) but with several groups that are more adapted to a life on large biogenic surfaces than nematodes (evidently Harpacticoida, naupliar larvae and Polychaeta from our Indicator Species Analysis),
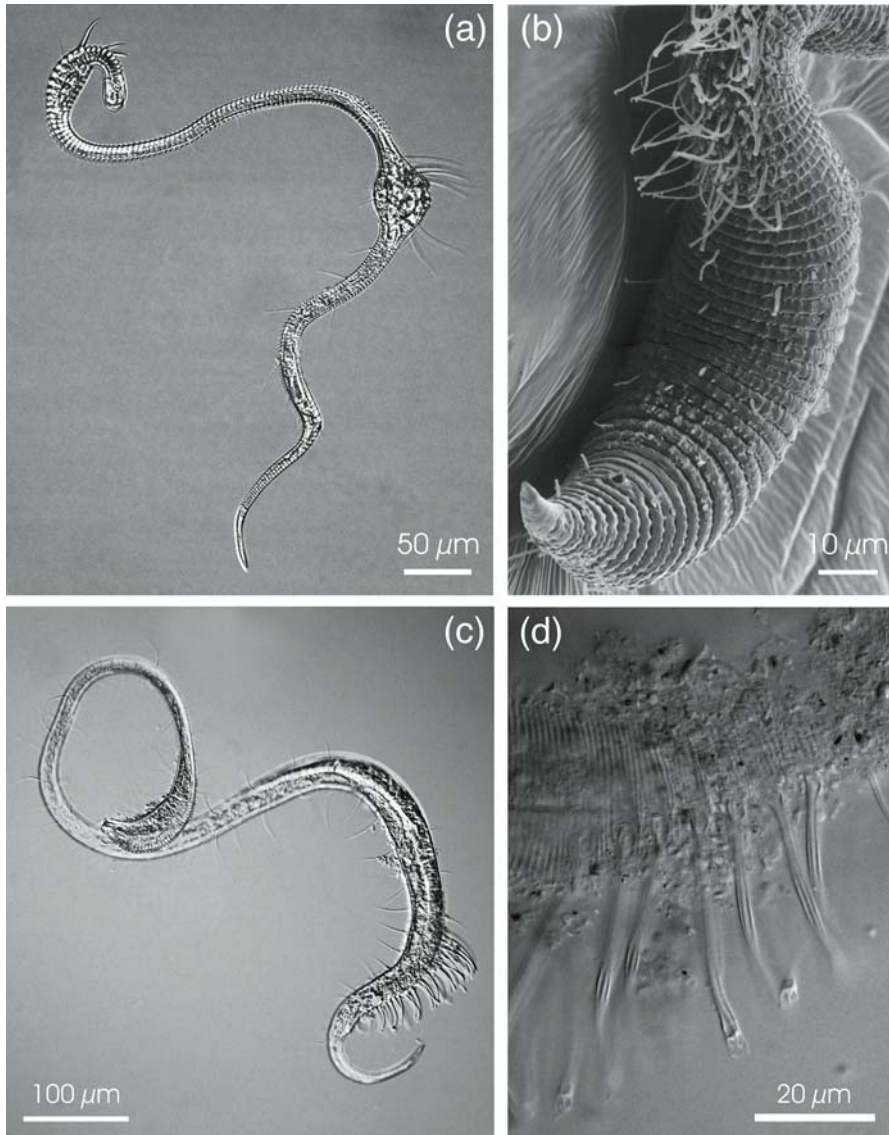
Fig. 4 Some representatives of the nematode families Epsilonematidae and Draconematidae found in the Porcupine Seabight area, and their morphological adaptations to an epifaunal life strategy. **(a)** *Glochinema trispinatum* Raes, Vanreusel and Decraemer, 2003: habitus; **(b)** *Bathyepsilonema lopheliae* Raes, Vanreusel and Decraemer, 2003: ambulatory setae; **(c)** *Tenuidraconema* sp. n.: habitus; **(d)** *Cygnonema* sp. n.: posterior adhesion tubes

showing a significantly increased importance. Although communities found in the sediment are significantly different from those on cold-water coral fragments (see above), it is almost impossible to distinguish between "typical interstitial" and "typical epifaunal" taxa on a higher taxonomic level.

Some dead coral structures may be partly covered with a felty layer of bryozoan colonies that very effectively traps sedimented material. It can be stated that the coral substrate provides a complex habitat for meiofauna because it can possibly be subdivided into even smaller microhabitats: the felty bryozoan encrustation probably combines sediment-dwelling and substrate-crawling taxa; the sediment infill between branches harbours an interstitial fauna; the coral surface is covered with a microbial biofilm and will therefore mainly attract obligate microbial-feeding meio-epifauna, and the cavities within the coral fragments (e.g., those constructed by *Eunice norvegica* (Linné, 1767)) are maybe home to still other communities. These differences within one microhabitat type (dead coral fragments) could then explain the scattered distribution of the coral subsamples in the MDS ordination graph. Analysis of all these very specific microhabitats should be a subject for future research. In the present study, relatively fine-tuned habitat preferences on family-level have been found for nematodes (families Epsilonematidae, Draconematidae) and harpacticoid copepods (families Tegastidae and Laophontidae (H. Gheerardyn pers. comm.)).

Several studies dealing with epiphytic meio-epifauna revealed that this fauna was often dominated by nematodes. In those cases, their relative abundances were rather low, especially compared to infaunal communities (Lewis and Hollingworth 1982; De Troch et al. 2001). Harpacticoida and naupliar larvae are always abundant in epiphytic communities (Lewis and Hollingworth 1982; Jarvis and Seed 1996; De Troch et al. 2001) and several authors reported a shift to a predominance of these two groups in epiphytic samples, especially on seagrass leaves and on macro-algae (Coull et al. 1983; Bell et al. 1984; Hall and Bell 1993 and authors cited herein). These results confirm the observed importance of these two groups as indicator epifauna. The high abundance of naupliar larvae (and copepodites) in seagrass beds has also been attributed to a potential nurseries function (Lewis and Hollingworth 1982; Hall and Bell 1993). It is difficult to say whether this is also the case for cold-water coral degradation zones, although the assumed low disturbance, low predation pressure and abundant food might provide a suitable habitat for larvae and juveniles. Most meiofaunal taxa, and especially nematodes, turned out to be associated with the filamentous epiphytic flora covering the macro-algae and seagrasses (Lewis and Hollingworth 1982; Bell et al. 1984; Hall and Bell 1993; Jarvis and Seed 1996). Algae that accumulate sediment and detritus have a richer nematode community because the sediment provides the interstitial microniches that are crucial for nematodes (Heip et al. 1985). This is an interesting idea, especially when applied to cold-water coral fragments were the coral surface is sometimes covered with a felty layer of bryozoans.

Finally, a comparison between soft-bottom and hard-bottom meiofauna carried out in a shallow environment on the Mediterranean coast (Danovaro and Fraschetti 2002) produced SIMPER-results that are comparable with ours: harpacticoid

copepods were identified as the taxon characterising hard-bottom assemblages and nematodes were identified as responsible for the differences between hard- and soft-bottom community composition.

From the MDS graph given in Figure 3 it is clear that the community structure on sponge skeletons is intermediary between that from coral fragments and that from the sediment, indicating the presence of both infaunal and epifaunal organisms. Because of their intricate structure, these sponge skeletons are able to trap a lot of sediment, in this way stimulating the presence of interstitial taxa. On the other hand, the sponge spicules may act as a substrate for epifaunal forms or as a three-dimensional maze for crawling taxa.

The high number of taxa encountered in this study is attributed to the presence of a large number of different microhabitats that were extensively discussed above. It is hypothesized here that each of these microhabitats favours a community with a different life style and a different composition. The sum of all these separate communities results in a high number of taxa.

Biodiversity

The statement by Jensen and Frederiksen (1992) that the associated fauna of *Lophelia pertusa* is as rich and diverse as that of hermatypic branching species of coral has led to increased efforts to describe the biological diversity of cold-water coral reefs. Although the correctness of this idea is not yet fully proven, for example because tropical coral reefs are much older than cold-water coral reefs and because their diversity is increased by the presence of a higher number of coral species, the presence of coralline algae and a higher diversity in food sources, cold-water coral reefs are without doubt diversity hotspots in the deep-sea. Mortensen et al. (1995) found that diversity is three times higher on the reefs than in the surrounding soft-bottom. In the present study attention is only focused on the dead *Lophelia pertusa* and associated substrates. According to both Jensen and Frederiksen (1992) and Mortensen et al. (1995), the diversity of fauna associated with living *Lophelia* colonies is generally lower than that on dead colonies.

In the foregoing, some strong indications for high taxon diversity, as well as a number of favourable conditions promoting high biodiversity have already been put forward:

1.   A total number of 33 groups (taxa and larvae) was identified. This high taxon richness is attributed to the cumulative effect of different communities associated with a large number of different microhabitats due to the process of niche segregation, and due to the lower dominance of nematodes. A possible effect on an even smaller scale (microhabitats within microhabitats) opens up even more perspectives on this subject.

2.   Low dominance of the most abundant taxon, Nematoda, and the resulting higher relative abundances of all other taxa was observed. This is thought to be due to the preference of nematodes for interstitial habitats resulting from their morphological (slender body shape) and ecological (feeding strategy, locomotion) adaptations to a life between the sandgrains.

3. It is hypothesized that cold-water coral degradation zones are characterized by high habitat complexity for meiofauna, and that each of the large number of microhabitats favours a certain lifestyle among meiofauna. As each of these lifestyles requires some highly specialized morphological adaptations, several habitat-specific taxa were found, at least on the family level (Nematoda: Epsilonematidae, Draconematidae; Harpacticoida: Tegastidae, Laophontidae).

4. The Porcupine Seabight is an area known to be subject to exceptionally high organic food input (Billett et al. 1983; Lampitt 1985; Gooday et al. 1996). Abundant food might support a higher number of individuals as well as a higher number of taxa. It is however still not clear whether this is also the case for the Belgica Mound region.

5. Large biogenic structures might also act as an efficient food trap. This leads to the idea that cold-water coral degradation zones are possible food hotspots, but associated with an impoverished underlying sediment. Although high food concentrations may support enriched, diverse communities, they can also have a negative effect on biodiversity by creating intensified competitive exclusion of species. According to Lambshead (1993), the occurrence of a spatiotemporal mosaic of small-scale patches, low disturbance and a low amount of nutrients keeps evenness high and prevents competitive exclusion of species, thus resulting in a high regional species pool. In the underlying sediment these three conditions are fulfilled, implying that this sediment may be home to a very diverse meiobenthic community.

6. Moreover, the food deposited in cold-water coral degradation zones will become patchily distributed between the substrate fragments, in this way adding to the process of niche segregation.

7. These biogenic structures are also thought to provide a low-disturbance environment in which the meiofauna is protected against physical erosion (currents) and predation from higher trophic levels. Frequent large-scale disturbances resulting from strong bottom currents might lead to (1) a high-dominance community or (2) destruction of life and/or habitats. High predation intensity will result in competitive exclusion and therefore a community characterized by high dominance.

8. Turnover is known to be very high in meiofauna, especially in nematodes. High turnover rates are attributed to the limited mobility and conservative reproductive method (i.e., lack of larvae with dispersive capacities) in nematodes, characterizing them as biogeographically localized organisms with high speciation rates (Castillo-Fernandez and Lambshead 1990). Combined with the presence of a whole spectrum of small-scale patches within and in between coral and sponge fragments, this could ultimately lead to a high number of species on a small or medium spatial scale.

In conclusion, there is a lot of evidence indicating that cold-water coral degradation zones constitute a highly diverse habitat for deep-sea meiofauna.

Diversity values for the entire meiofauna community associated with this habitat (on higher taxon level) are given in Table 3. At present, no diversity measurements on higher taxonomic level are present for comparison.

Another interesting question is which microhabitat type harbours the most diverse meiofaunal community. A whole spectrum of biodiversity indices, ranging from indices of taxon richness (N_0) to indices of evenness (N_∞ and J), is given in Table 3. An obvious difference in taxon richness between the different microhabitats can also be seen on Table 2B. The exact number of taxa per microhabitat type is given by the overall (b) N_0 in Table 3. Although there are of course differences in microhabitat volume, N_0 gives a good first impression of differences in terms of taxon richness. Clearly, coral fragments house the highest number of taxa ($N_0 = 23$) whereas sponge skeletons are characterized by the lowest number of taxa ($N_0 = 15$). The expected number of taxa for 100 individuals ET (100), an index not influenced by differences in sample size, is also highest on coral fragments. The same is true for H'. Differences between microhabitats are visualized by Box and Whisker plots for H' and J in Fig. 5. As expected, equitability (J) is highest on coral fragments and lowest in the underlying sediment, where nematodes exhibit a high dominance. Except for N_0, all indices indicate that the sediments are the least diverse and that coral fragments support the most diverse communities. All differences were statistically highly or very highly significant, with the exception of N_0 and ET (100).

It is also very conspicuous that the entire community has much more taxa than either of the separate microhabitats. This result confirms the statement that

Table 3 Biodiversity indices: Hill's diversity numbers N_0, N_1, N_2 and N_∞, the expected number of taxa for 100 individuals ET (100), the Shannon-Wiener diversity index H' and Pielou's evenness J. Under (a) the average value over all subsamples with its standard deviation is given. Under (b) the value for the total community associated with the respective microhabitat is given. (NS): not significant; (**): highly significant; (***): very highly significant

		N_0	ET (100)	N_1	H'	N_2	J	N_∞
Coral fragments	(a)	11.30 ± 3.65	7.96 ± 1.58	3.97 ± 1.28	1.33 ± 0.34	2.82 ± 1.00	0.55 ± 0.10	1.90 ± 0.57
	(b)	23	9.65	4.89	1.59	3.24	0.51	2.00
Sponge skeletons	(a)	8.75 ± 2.05	6.25 ± 1.23	2.32 ± 0.33	0.83 ± 0.15	1.63 ± 0.17	0.39 ± 0.06	1.30 ± 0.08
	(b)	15	7.06	2.40	0.88	1.58	0.32	1.27
Mixed substrate	(a)	10.50 ± 6.46	6.81 ± 3.55	2.56 ± 1.36	0.84 ± 0.52	1.68 ± 0.60	0.36 ± 0.14	1.30 ± 0.25
	(b)	20	8.04	2.46	0.90	1.56	0.30	1.26
Underlying sediment	(a)	10.00 ± 2.37	5.93 ± 1.65	1.92 ± 0.60	0.61 ± 0.29	1.37 ± 0.28	0.26 ± 0.11	1.17 ± 0.12
	(b)	19	6.76	2.10	0.74	1.42	0.25	1.20
Entire community		31	8.70	3.46	1.24	2.11	0.36	1.49
p-level		0.52 (NS)	0.16 (NS)	0.0057 (**)	0.0011 (**)	0.0015 (**)	0.000051 (***)	0.0018 (**)
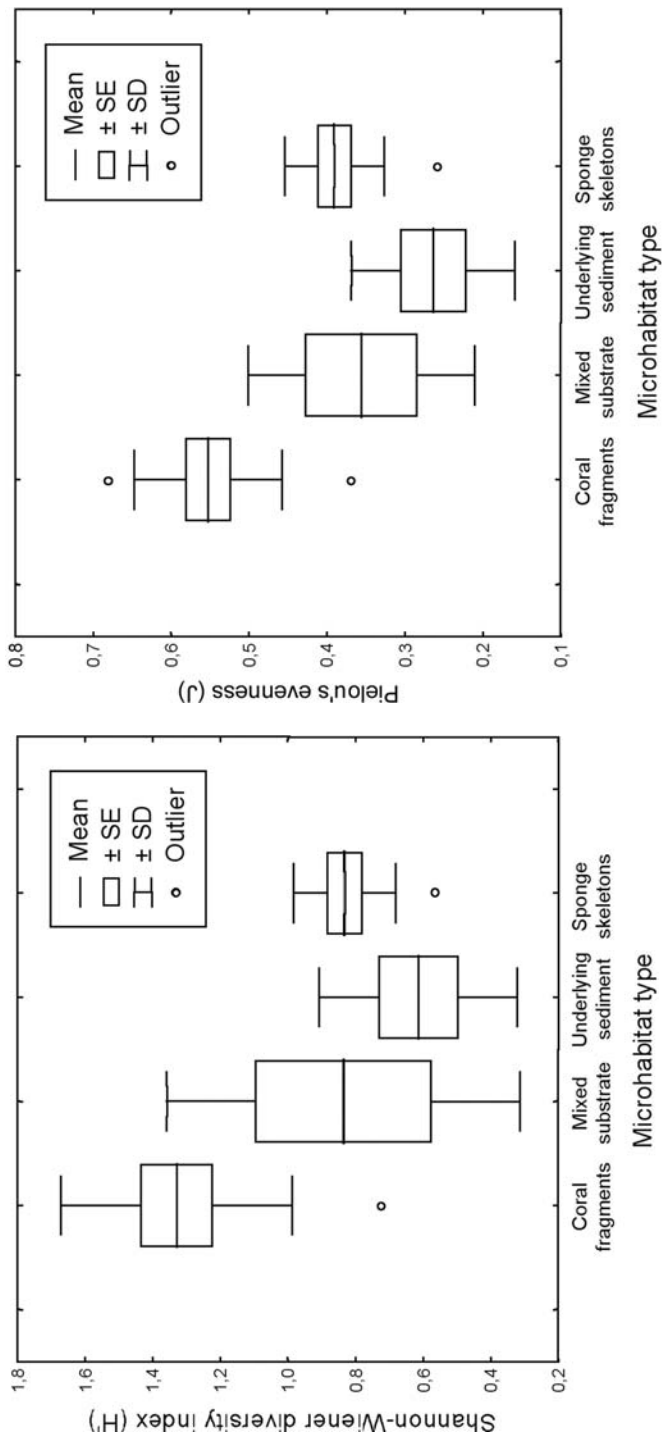
Fig. 5 Box and Whisker plots comparing the microhabitats for the Shannon-Wiener diversity index (*H'*) and Pielou's evenness *J*, a typical equitability index

the combination of all separate communities results in a high number of taxa (see above).

Conclusions

1. The presence of large biogenic structures on the seafloor of the continental margin (1) enables more taxa to be present and (2) particularly favours harpacticoid copepods, naupliar larvae and polychaetes. The nematode community responds by a shift to a predominance of typical epifaunal nematodes on the coral fragments.

2. The large biogenic substrates are characterized by a meio-epifaunal community that is significantly dissimilar from the meio-infaunal community in the underlying sediment.

3. The meio-epifaunal community is composed of a sediment-dwelling background community (predominantly nematodes); however with several groups that are more adapted to a life on large biogenic surfaces showing a significantly increased importance.

4. The meio-infaunal community in the underlying sediment is characterized by low densities.

5. Cold-water coral degradation zones are assumed to be biologically diverse. This high biodiversity is attributed to:

    a) lower physical disturbance by strong bottom currents and lower predation pressure by higher trophic guilds.

    b) a high microhabitat diversity resulting in a high degree of niche segregation. Combined, the communities associated with each microhabitat type give rise to high taxon richness.

    c) low dominance of nematodes.

    d) assumed abundant food from seasonally deposited phytodetritus, partly resulting from the suggested efficient food trapping function of the biogenic substrates.

6. Of all four microhabitat types, coral fragments support the most diverse communities, whereas the underlying sediments are the least diverse.

Acknowledgements

Study (ACES) (EC Fifth Framework Research Program) and the national FWO research project G.0199.03.

References

Aller JY (1989) Quantifying sediment disturbance by bottom currents and its effect on benthic communities in a deep-sea western boundary zone. Deep-Sea Res 36: 901-934

Aller JY (1997) Benthic community response to temporal and spatial gradients in physical disturbance within a deep-sea western boundary region. Deep-Sea Res I 44: 39-69

Bell SS, Walters K, Kern JC (1984) Meiofauna from seagrass habitats: a review and prospectus for future research. Estuaries 7 (4a): 331-338

Beyer A, Schenke HW, Klenke M, Niederjasper F (2003) High resolution bathymetry of the eastern slope of the Porcupine Seabight. Mar Geol 198: 27-54

Billett DSM, Lampitt RS, Rice AL (1983) Seasonal sedimentation of phytoplankton to the deep-sea benthos. Nature 302: 520-522

Burdon-Jones C, Tambs-Lyche H (1960) Observations on the fauna of the North Brattholmen stone-coral reef near Bergen. Årb Univ Bergen, Mat-Naturv Ser 4: 1-24

Castillo-Fernandez D, Lambshead PJD (1990) Revision of the genus *Elzalia* Gerlach, 1957 (Nematoda: Xyalidae) including three new species from an oil producing zone in the Gulf of Mexico, with a discussion of the sibling species problem. Bull Brit Mus Nat Hist 56: 63-71

Clarke KR (1993) Non-parametric multivariate analyses of changes in community structure. Austral J Ecol 18: 117-143

Coull BC (1988) Ecology of the marine meiofauna. In: Higgins RP, Thiel H (eds) Introduction to the Study of Meiofauna. Smithsonian Institution Press, Washington, pp 18-38

Coull BC, Creed EL, Eskin RA, Montagna PA, Palmer MA, Wells JBJ (1983) Phytal meiofauna from the rocky intertidal at Murrells Inlet, South Carolina. Trans Amer Microsc Soc 102: 380-389

Danovaro R, Fraschetti S (2002) Meiofaunal vertical zonation on hard-bottoms: comparison with soft-bottom meiofauna. Mar Ecol Progr Ser 230: 159-169

De Backer A (2002) The biodiversity of the macrofauna associated with the cold water coral *Lophelia* in the Porcupine Seabight. Unpubl MSc thesis, Ghent Univ

De Mol B (2002) Development of coral banks in Porcupine Seabight (SW Ireland): a multidisciplinary approach. Unpubl PhD thesis, Ghent Univ

De Mol B, Van Rensbergen P, Pillen S, Van Herreweghe K, Van Rooij D, McDonnell A, Huvenne V, Ivanov M, Swennen R, Henriet JP (2002) Large deep-water coral banks in the Porcupine Basin, southwest of Ireland. Mar Geol 188: 193-231

De Troch M, Gurdebeke S, Fiers F, Vincx M (2001) Zonation and structuring factors of meiofauna communities in a tropical seagrass bed (Gazi Bay, Kenya). J Sea Res 45: 45-61

Dons C (1944) Norges korallrev. K Norske Vidensk Selsk Forhandl 16: 37-82

Dufrêne M, Legendre P (1997) Species assemblages and indicator species: the need for a flexible asymmetrical approach. Ecol Monogr 67: 356-366

Fosså JH, Mortensen PB (1998) Artsmangfoldet på *Lophelia*-korallrev og metoder for overvåkning. Fisken Havet 17: 1-95

Freiwald A, Wilson JB (1998) Taphonomy of modern deep, cold-temperate water coral reefs. Hist Biol 13: 37-52

Freiwald A, Henrich R, Pätzold J (1997) Anatomy of a deep-water coral reef mound from Stjernsund, West Finnmark, Northern Norway. SEPM Spec Publ 56: 141-162

Freiwald A, Hühnerbach V, Lindberg B, Wilson JB, Campbell J (2002) The Sula Reef Complex, Norwegian Shelf. Facies 47: 179-200

Giere O (1993) Meiobenthology: the microscopic fauna in aquatic sediments. Springer, Berlin Heidelberg

Gooday AJ (1988) A response by benthic Foraminifera to the deposition of phytodetritus in the deep sea. Nature 332: 70-73

Gooday AJ (2002) Biological responses to seasonally varying fluxes of organic matter to the ocean floor: a review. J Oceanogr 58: 305-332

Gooday AJ, Lambshead PJD (1989) Influence of seasonally deposited phytodetritus on benthic foraminiferal populations in the bathyal northeast Atlantic: the species response. Mar Ecol Progr Ser 58: 53-67

Gooday AJ, Pfannkuche O, Lambshead PJD (1996) An apparent lack of response by metazoan meiofauna to phytodetrital deposition in the bathyal North-Eastern Atlantic. J Mar Biol Ass UK 76: 297-310

Graf G, Bengtson W, Diesner U, Schultz R, Theede H (1982) Benthic response to sedimentation of a spring phytoplankton bloom: process and budget. Mar Biol 67: 201-208

Hall MO, Bell SS (1993) Meiofauna on the seagrass *Thalassia testudinum*: population characteristics of harpacticoid copepods and associations with algal epiphytes. Mar Biol 116: 137-146

Heip C, Vincx M, Vranken G (1985) The ecology of marine nematodes. Oceanogr Mar Biol Ann Rev 23: 399-489

Higgins RP (1988) Kinorhyncha. In: Higgins RP, Thiel H (eds) Introduction to the Study of Meiofauna. Smithsonian Institution Press, Washington, pp 328-331

Hill MO (1973) Diversity and evenness: a unifying notation and its consequences. Ecology 54: 427-432

Hurlbert SH (1971) The non-concept of species diversity: a critique and alternative parameters. Ecology 52: 577-586

Jarvis SC, Seed R (1996) The meiofauna of *Ascophyllum nodosum* (L.) Le Jolis: characterization of the assemblages associated with two common epiphytes. J Exp Mar Biol Ecol 199: 249-267

Jensen A, Frederiksen R (1992) The fauna associated with the bank-forming deepwater coral *Lophelia pertusa* (Scleractinaria) on the Faroe shelf. Sarsia 77: 53-69

Lambshead PJD (1993) Recent developments in marine benthic biodiversity research. Océanis 19: 5-24

Lampitt RS (1985) Evidence for the seasonal deposition of detritus to the deep-sea floor and its subsequent resuspension. Deep-Sea Res 32: 885-897

Le Danois E (1948) Les profondeurs de la mer. Payot, Paris

Lewis JB, Hollingworth CE (1982) Leaf epifauna of the seagrass *Thalassia testudinum*. Mar Biol 71: 41-49

Mortensen PB, Hovland M, Brattegard T, Farestveit R (1995) Deep water bioherms of the scleractinian coral *Lophelia pertusa* (L.) at 64° N on the Norwegian shelf: structure and associated megafauna. Sarsia 80: 145-158

Mortensen PB (2000) *Lophelia pertusa* (Scleractinia) in Norwegian waters: distribution, growth, and associated fauna. Thesis submitted in partial fulfillment of the requirements for the degree of Dr. scient. Depart Fish Marine Biol, Univ Bergen

Neira C, Gad G, Arroyo NL, Decraemer W (2001) *Glochinema bathyperuvensis* sp. n. (Nematoda, Epsilonematidae): A new species from Peruvian bathyal sediments, SE Pacific Ocean. Contrib Zool 70: 147-159

Pielou EC (1975) Ecological diversity. Wiley, New York

Pfannkuche O (1985) The deep-sea meiofauna of the Porcupine Seabight and abyssal plain (NE Atlantic): population structure, distribution, standing stocks. Oceanol Acta 8: 343-353

Pfannkuche O (1993) Benthic response to the sedimentation of particulate organic matter at the BIOTRANS station, 47°N, 20°W. Deep-Sea Res II 40: 135-149

Pfannkuche O, Thiel H (1987) Meiobenthic stocks and benthic activity on the NE-Svalbard Shelf and in the Nansen Basin. Polar Biol 7: 253-266

Pontoppidan E (1755) The Natural history of Norway. A Linde, London

Rice AL, Billett DSM, Thurston MH, Lampitt RS (1991) The Institute of Oceanographic Sciences Biology Programme in the Porcupine Seabight: background and general introduction. J Mar Biol Ass UK 71: 281-310

Rogers AD (1999) The biology of *Lophelia pertusa* (Linnaeus 1758) and other deep-water reef-forming corals and impacts from human activities. Int Rev Hydrobiol 84: 315-406

Soetaert K, Heip C (1989) The size structure of nematode assemblages along a Mediterranean deep-sea transect. Deep-Sea Res 36: 93-102

Soltwedel T (2000) Metazoan meiobenthos along continental margins: a review. Progr Oceanogr 46: 59-84

Soltwedel T, Pfannkuche O, Thiel H (1996) The size structure of deep-sea meiobenthos in the North-Eastern Atlantic: nematode size spectra in relation to environmental variables. J Mar Biol Ass UK 76: 327-344

Thiel H (1975) The size structure of the deep-sea benthos. Int Rev Ges Hydrobiol 60: 575-606

Thiel H (1983) Meiobenthos and nanobenthos of the deep sea. In: Rowe GT (ed) Deep Sea Biology. The Sea. 8. John Wiley and Sons, New York, pp 167-230

Thiel H, Pfannkuche O, Shriever G, Lochte K, Gooday AJ, Hemleben C, Mantoura RFG, Turley CM, Patching JW, Riemann F (1990) Phytodetritus on the deep-sea floor in a central oceanic region of the Northeast Atlantic. Biol Oceanogr 6: 203-239

Thistle D, Levin LA (1998) The effect of experimentally increased near-bottom flow on metazoan meiofauna at a deep-sea site, with comparison data on macrofauna. Deep-Sea Res 45: 625-638

Thistle D, Levin LA, Gooday AJ, Pfannkuche O, Lambshead PJD (1999) Physical reworking by near-bottom flow alters the metazoan meiofauna of Fieberling Guyot (northeast Pacific). Deep-Sea Res 46: 2041-2052

Vanaverbeke J, Soetaert K, Heip C, Vanreusel A (1997) The metazoan meiobenthos along the continental slope of the Goban Spur (NE Atlantic). J Sea Res 38: 93-107

Van Gaever S (2001) Gemeenschapsanalyse van macrofauna geassocieerd met koudwaterkoraalriffen in de NO Atlantische Oceaan. Unpubl undergraduate thesis, Ghent Univ

Vanreusel A, Vincx M, Bett BJ, Rice AL (1995a) Nematode biomass spectra at two abyssal sites in the NE Atlantic with a contrasting food supply. Int Rev Ges Hydrobiol 80: 287-296

Vanreusel A, Vincx M, Schram D, Van Gansbeke D (1995b) On the vertical distribution of the metazoan meiofauna in shelf break and upper slope habitats of the NE Atlantic. Int Rev Ges Hydrobiol 80: 1-14

Van Rooij D, De Mol B, Huvenne V, Ivanov M, Henriet JP (2003) Seismic evidence of current-controlled sedimentation in the Belgica mound province, upper Porcupine slope, southwest of Ireland. Mar Geol 195: 31-53

Van Rooij D, Blamart D, Richter T, Wheeler A, Kozachenko M, Henriet J-P (submitted) Quaternary drift sediment dynamics in the Belgica mound province, Porcupine Seabight: a multidisciplinary approach. Int J Earth Sci

Vincx M (1996) Meiofauna in marine and freshwater sediments. In: Hall GS (ed) Methods for the examination of organismal diversity in soils and sediments. Cab Int, pp 187-195

Vincx M, Bett BJ, Dinet A, Ferrero T, Gooday AJ, Lambshead PJD, Pfannkuche O, Soltwedel T, Vanreusel A (1994) Meiobenthos of the deep northeast Atlantic. Adv Mar Biol 30: 2-88

Wheeler AJ, Beyer A, Freiwald A, de Haas H, Huvenne VAI, Kozachenko M, Olu-Le Roy K (submitted) Morphology and environment of deep-water coral mounds on the NW European Margin. Int J Earth Sci

White M (submitted) The hydrography of the Porcupine Bank and Sea Bight and associated carbonate mounds. Int J Earth Sci

Williamson DI (1982) Larval morphology and diversity. In: Abele LG (ed) The Biology of Crustacea. 2. Embryology, Morphology, and Genetics. Academic Press, New York, pp 43-110

Distribution and diversity of species associated with deep-sea gorgonian corals off Atlantic Canada

Lene Buhl-Mortensen, Pål B. Mortensen

Benthic Habitat Research Group, Institute of Marine Research, P.O. Box 1870
  Nordnes, N-5817 Bergen, Norway
  (Lenebu@IMR.no)

Abstract. This paper describes the associated fauna of the deep-sea gorgonian corals *Paragorgia arborea* and *Primnoa resedaeformis*. Composition and distribution of this fauna is described based on material from the continental shelf and slope off Atlantic Canada (300-600 m depth). Samples were collected from five areas with Remotely Operated Vehicle, video grab, and bottom trawl. The collected material consists of 25 samples, 13 from *P. arborea* and 12 from *P. resedaeformis*.

A total of 114 species and 3915 individuals were recorded. The *P. resedaeformis* fauna was more abundant and diverse than the fauna of *P. arborea,* with 2651 specimens and 97 species found on the former and 1264 specimens and 47 species on the latter. Rarefaction analysis indicated that many more associated species are still to be found. Species richness and abundance was significantly correlated with coral morphology (e.g., number of branches, wet weight, and % exposed skeleton). Crustaceans dominated the fauna, contributing 46 % to the total number of individuals and 26 % to the total number of species. Two coral microhabitats were identified: 1) young and live parts of colonies and, 2) old parts with deposits and exposed skeleton. Most of the associated fauna was found in the latter habitat. There was a clear difference in fauna composition of the two coral species. Sessile hydroids, anemones, and molluscs were more abundant on *P. resedaeformis*. These organisms occurred attached to the hard substratum provided by the exposed skeleton. Parasitic copepods and polychaetes were more common on *P. arborea*. Two copepods, a lichomolgid ecto-parasite and a lamippid gall-forming endo-parasite, were associated with *P. arborea*. The echinoderm *Gorgonocephalus lamarckii* was found in the high current environment on the outer branches of *P. arborea*. The shrimp *Pandalus propinquus* was hiding and resting on colonies of both coral species.

Many of the associated taxa are also found on tropical gorgonians but the deep-sea gorgonians lack the diverse decapod and gastropod-fauna of their tropical counterparts. The species richness of the deep-sea gorgonian coral fauna was higher than what has been observed for tropical gorgonians. In contrast to the tropical

associates very few are obligate symbionts. Nevertheless, several of the species are rare in other habitats and have been recorded on the same and other gorgonian species in early studies from the eastern North Atlantic. The sampling gear collected the fauna differently. Corals from bottom trawls had a poorer associated fauna that differed in composition with material collected by ROV or video assisted grab.

Keywords. Deep-water corals, associated fauna, Gorgonacea, *Paragorgia arborea, Primnoa resedaeformis,* Atlantic Canada

Introduction

Primnoa resedaeformis and *Paragorgia arborea* are the most abundant large gorgonians in Atlantic Canada (Mortensen and Buhl-Mortensen 2004; Mortensen et al. in press). The two species are widely distributed in the north Atlantic (Madsen 1944; Tendal 1992). In certain areas (e.g., the Northeast Channel) they can form forest or thicket-like habitats. However, little is known about the role of these deep-water corals as habitat for other species. Research is necessary also to help develop sound scientific advice on habitat and fisheries management issues related to these corals.

The arborescent morphology of most corals allows their polyps to be elevated from the relatively still boundary layer close to the substratum (Wainwright and Koehl 1976) into the faster flowing water above. In addition, the orientation of colonies perpendicular to prevailing currents, which is common for many species, maximizes the volume of water passing the polyps (Wainwright and Dillon 1969). This enables the polyps in the colony to have maximum food access. This advantage is also passed on to any rheophilic, filter-feeding epizoic animal associated with the colony. By the term *associated* we mean any animal found on or in a coral colony.

Corals offer a great variety of microhabitats for other organisms. They have a complex architecture, and provide substrata of different age. Sheltered cavities within a colony often contain organic rich sediments, while the outer parts provide a high water flow with little sedimentation. In contrast to tropical shallow-water corals there are very few examples of obligate relationships between deep-water corals and their associated fauna (Mortensen 2001). From previous studies it is known, more or less anecdotally that deep-water gorgonians often house a large assemblage of mobile crustaceans and attached ophiuroids (Storm 1901; Strømgren 1970). The fauna of deep-water corals, however, is difficult to sample and until recently (Buhl-Mortensen and Mortensen 2004a) no study had quantitatively analysed the invertebrate fauna associated with any deep-water gorgonian. The relation of diversity and abundance of coral associates with colony morphology has been studied for tropical corals (e.g., Abele 1984; Tsuchiya et al. 1986). This paper provides an analysis of the invertebrate fauna associated with *Paragorgia arborea* and *Primnoa resedaeformis* off Atlantic Canada. We examine the fauna composition and how it relates to age and morphology of the host coral. We discuss the richness of this fauna compared to other cold-water corals and tropical gorgonians, and discuss how differences in coral sampling methodology affect the results.

Material and methods

Sampling of corals and associated fauna

The distribution, abundance and habitat of species associated with deep-water corals off Atlantic Canada were studied from material collected in three different ways: 1) incidentally in bottom-trawl during DFO groundfish surveys or commercial fisheries, 2) with the Remotely Operated Vehicle (ROV) "Ropos" and, 3) with a video-assisted grab (VAG; Table 1). Corals were collected from five areas (Fig. 1) during cruises in 2001 in the period between August and October and in September 2002. Ropos is a specialised ROV designed for scientific purposes. It is equipped with a claw and a suction sampler. Colonies or fragments of colonies collected with the claw were stored during transit to surface in a two-chambered box with a lid that could be opened and closed by the ROV pilot. Four samples of *Paragorgia* and three samples of *Primnoa* were collected with this gear. Three samples of *Primnoa* were collected using VAG. The VAG is a large benthic grab (0.5 m^2) equipped with video and can work to a maximum depth of about 450 m (Gordon et al. 2000). Fifteen samples, nine *Paragorgia* and six *Primnoa*, were provided from groundfish trawl surveys by DFO or commercial fisheries.

Processing of samples

Coral were frozen in plastic bags on board immediately after sampling. Some large by-catches containing several colonies were divided into two bags, which were studied as separate samples (i.e. PaB4 and PaB5; PaB6 and PaB7; and PrB2 and PrB3). Before inspection the corals were thawed in seawater. Large organisms adhering to the coral were removed and transferred to 4 % formaldehyde. The seawater used for thawing was filtered through 250 μm sieve and the fraction held back was transferred to 70 % alcohol prior to identification. The two coral species differ markedly in morphology (Fig. 2). The corals were weighed and colony length and width and base diameter was measured and number of branches longer than 3 cm were counted (Table 1). For *Primnoa* the proportion of colony with exposed skeleton was estimated and rings in skeleton counted as an estimate of age (Grigg 1974; Andrews et al. 2002). All organisms were identified to lowest possible taxonomic level and counted. Only colonies were counted for hydroids while for octocorals the polyps were counted and the individuals for colonial anemones. Specialists were consulted for the identification of some polychaetes, molluscs and hydroids.

Numerical methods

Diversity

The number of species associated with the two coral species were compared using Rarefaction Analysis (RA; Hurlbert 1971; Simberloff 1978). RA is a statistical method for estimating the expected number of species, E[S], in a random sample of individuals taken from a collection. Rarefaction curves were calculated for the pooled material from all samples of each coral species.

Table 1 Information on sampled material of *Paragorgia arborea* (Pa) and *Primnoa resedaeformis* (Pr). C: corals collected using a remotely operated vehicle (ROV) or videoassisted-grab (VAG), B: by-catches of corals from bottom-trawl (BT) provided by DFO ground-fish survey or fishermen. Amount of coral sampled is given as: number of colonies/fragments and sample total of: wet weight, width, length, and number of branches >3 cm. Range are given in parenthesis for samples containing more than one colony or fragment. Base width and number of rings (for *Primnoa* only) is given for the largest base in samples with more than one colony/fragment as an indicator of coral age (range in parenthesis). Total percentage of colony with exposed skeleton is estimated for *Primnoa*

Sample ID	Gear	Cruise	SET	Depth [m]	Position Lat	Long	No. Col.	Wet weight [g]	Width [cm]	Height [cm]	No. branches	Base width [cm]	No. rings	% exp. skeleton
Paragorgia														
PaC1	ROV	Ropos 2001	R640	476	42°02.80'	65°34.47'	1	2532	72	160	57	5.7	-	-
PaC2	ROV	Ropos 2001	R637	446	41°59.84'	65°38.88'	1	229	11.5	39	7	2.4	-	-
PaC3	ROV	Ropos 2001	R639	426	41°59.90'	65°38.95'	1	738	26	31	21	2.5	-	-
PaC4	ROV	Ropos 2001	R641	332	41°54.30'	65°42.84'	1	3175	13	27	9	2.9	-	-
PaB1	BT	OA 2001	TOW 13	556	67°34.02'	58°29.03'	1	3571	34	83	70	7.1	-	-
PaB2	BT	OA 2001	TOW 13	556	67°34.02'	58°29.03'	1	3981	42	54	36	6.5	-	-
PaB3	BT	Teleost trip 342	SET 11	630	46°12.55'	46°17.15'	1	1401	42	53.5	24	5.1	-	-
PaB4	BT	WT 369	SET 55	588	46°26.17'	47°26.67'	1	6047	83	157	69	6	-	-
PaB5	BT	WT 369	SET 55	588	46°26.17'	47°26.67'	5	-	74.5	196	56	3.0	-	-
PaB6	BT	NED 2001-037	SET 77	502	43°58.29'	58°35.01'	1	2594	-	65	18	6	-	-
PaB7	BT	NED 2001-037	SET 77	502	43°58.29'	58°35.01'	1	862	-	45	14	2.2	-	-
PaB8	BT	NED 2002-037	SET 46	277	42°03.40'	65°38.12'	1	10400	74.5	102.5	168	13.5	-	-
PaB9	BT	Fisherman 2001		~400	Northeast Channel		1	180	32	46	26	2.3	-	-
SUM	13						13	>32850	504.5	1059	575	-	-	-
Primnoa														
PrC1	VAG	Hudson 2002	VG 1	430	43°52.44'	58°51.04'	3	870 (98-350)	78.4	177 (49-67)	164	1.4	28	41
PrC2	VAG	Hudson 2001	VG 13	337	42°00.53'	65°41.69'	1	858	22	41	120	1	23	10
PrC3	VAG	Hudson 2001	VG 15	321	42°01.25'	65°40.67'	1	171	28	53	94	1.6	42	80
PrC4	ROV	Ropos 2001	R637	476	42°02.80'	65°34.47'	5	291 (21-170)	98 (13-32)	137 (25-32)	125	0.7 (0.4-0.7)	19 (13-19)	18
PrC5	ROV	Ropos 2001	R636	498	42°02.83'	65°34.45'	2	224 (105-108)	44 (21-23)	79 (38-41)	44	1 (0.6-1.0)	24 (15-24)	15
PrC6	ROV	Ropos 2001	R640	446	41°59.84'	65°38.88'	9	1456 (40-580)	203 (13-46)	347 (18-62)	307	1.4 (0.7-1.4)	30 (17-30)	32
PrB1	BT	Fisherman 2001		~400	Northeast Channel		1	79	13.5	22	20	0.3	10	0
PrB2	BT	NED 2001-037	Set 77	502	43°58.29'	58°35.01'	1	1410	43	86	147	1.2	22	0
PrB3	BT	NED 2001-037	Set 77	502	43°58.29'	58°35.01'	1	546	48	76	66	1.5	25	0
PrB4	BT	NED 2002-037	Set 46	277	42° 03.40'	65°38.12'	10	5664 (97-1170)	346 (18-53)	589 (45-75)	878	3.4 (0.7-3.4)	70 (16-70)	30
PrB5	BT	Fisherman 2002		246	41°55.99'	65°43.50'	6	3323 (242-372)	146 (19-30)	335 (49-65)	358	1.9 (0.8-1.9)	30 (25-30)	0
PrB6	BT	Fisherman 2002		246	41°55.99'	65°43.50'	5	4032 (142-1622)	154 (12-54)	244 (36-86)	410	3.9 (0.8-3.9)	60 (17-60)	23
SUM	12						45	18923	1132	2186	2733	-	-	-
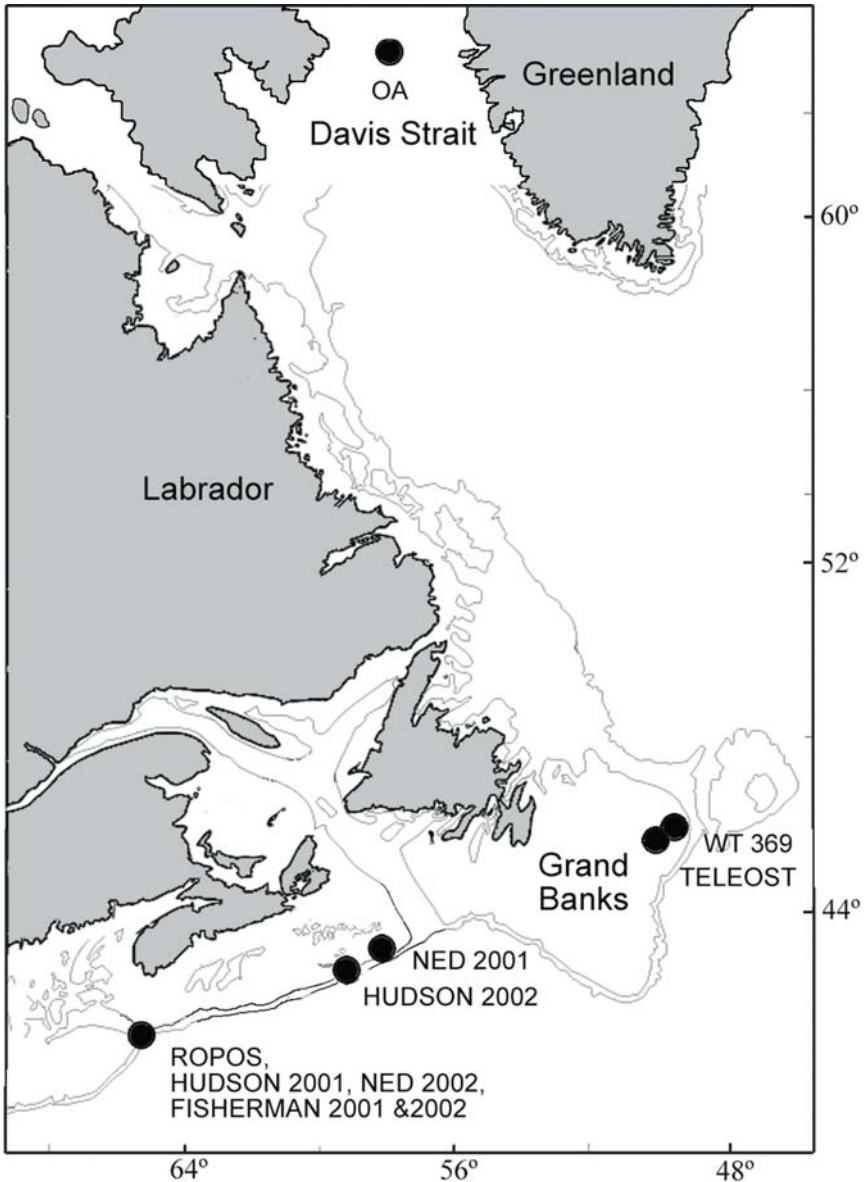
Fig. 1 Map showing the five main areas from which coral material was collected

Species diversity (H') was calculated for each sample using the formula

$$H' = -\sum_{i=1}^{S}(N_i/N) \log_2 (N_i/N) \quad \text{(Shannon and Weaver 1949)}$$

where S = total number of species, N = total number of individuals and N_i = number of individuals of the ith species.
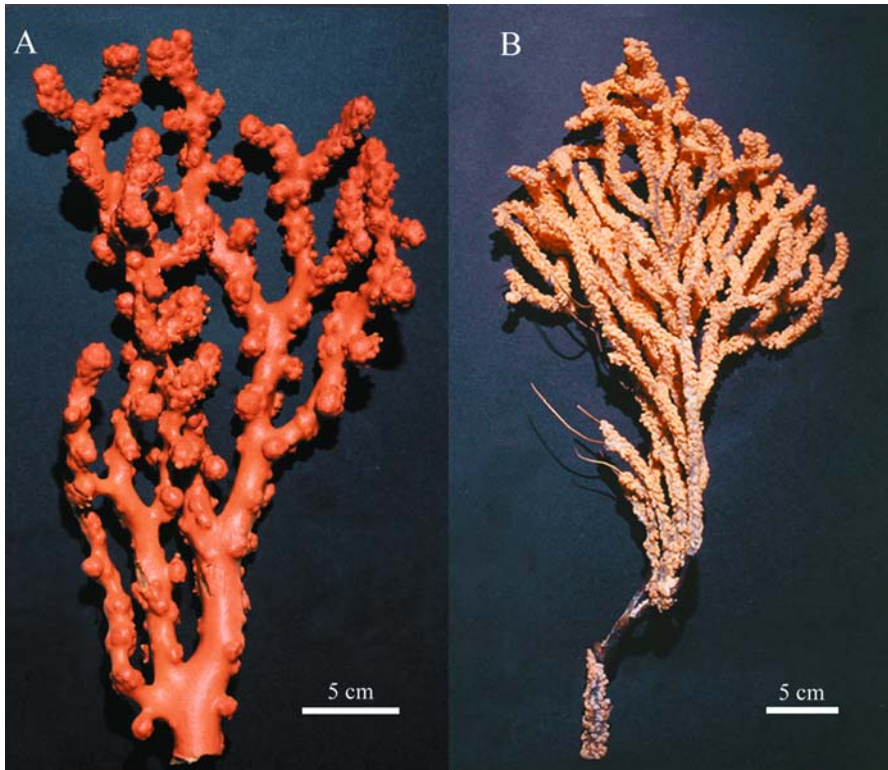
Fig. 2 Photo of a branch of *Paragorgia arborea* (**A**), and a colony of *Primnoa resedaeformis* (**B**)

Faunal patterns

To investigate the similarity in associated fauna between and within the two coral species Detrended Correspondence Analysis (DCA) was performed using the program PCOrd. Only the 55 species occurring at least in two samples were included in the analyses. The underlying theory of this method is presented in Ter Braak (1987). The data were standardised by square root transformation to prevent abundant species from swamping the results.

Results

Diversity patterns

The examined coral material consisted of 33 kg (wet weight) of *Paragorgia arborea* and 19 kg of *Primnoa resedaeformis*. The average weight and height per colony or fraction, ranges in parentheses, was 2.7 kg (0.18-10.4) and 81.5 cm (27-196) and, 0.4 kg (0.02-1.62) and 49 cm (25-86) respectively. A total of 3915 individuals and 114 species was found in the 25 coral samples representing ~58 colonies or fragments (Table 2). The associated fauna of *Primnoa* was more

abundant and diverse than the fauna associated with *Paragorgia*. This is shown both by the species numbers, diversity index (H'), and rarefaction analysis (Table 2 and Fig. 3). 1264 specimens and 47 species were from *Paragorgia* and 2651 specimens and 97 species from *Primnoa* with a diversity (H') of 2.17 and 3.54 respectively. More than twice the amount of *Paragorgia* is needed (on average) to encounter one associated species in comparison to *Primnoa*, 608 g and 233 g coral respectively. In general more specimens of associates were found in material collected by ROV and VAG than by bottom trawl. Average per sample for *Paragorgia* was 254 *versus* 28 specimens and for *Primnoa* 317 *versus* 125. Diversity was also higher in ROV and VAG samples with the largest difference in the *Primnoa* material. The average of species and diversity (H') per sample was 26 and 2.21 respectively while for trawl by-catches the figures were 11 and 1.14. The rarefaction curves clearly differed showing a richer fauna housed by *Primnoa*. There was no sign of the curves levelling out, indicating that many more species of associates would be expected as more material is examined.

Table 2 Abundance, species richness, diversity H' and weight of coral (g) per species for associated fauna of *Paragorgia arborea,*13 samples (total of 33 kg coral), and *Primnoa resedaeformis,*12 samples (total of 19 kg coral). Figures for corals sampled with remotely operated vehicle (ROV) or video assisted grab (VAG) is given separate from trawl by-catches. TOTAL indicates figures based on all material of the coral species (for sampling information see Table 1)

Sample ID	No. ind.	No. species	H'	Weight (g) / species
Paragorgia				
ROV samples				
PaC1	628	3	0.71	844
PaC2	229	9	1.84	25
PaC3	102	11	1.82	67
PaC4	57	4	0.49	79
Average	**254**	**7**	**1.22**	**254**
SUM	**1016**	**20**	**1.54**	
Trawl samples				
PaB1	46	4	1.15	893
PaB2	24	3	0.86	1327
PaB3	9	5	1.15	280
PaB4	29	7	1.55	864
PaB5	33	11	1.82	-
PaB6	2	2	0.69	1297
PaB7	0	0	0	>862
PaB8	104	18	2.16	578
PaB9	1	1	0	180
Average	**28**	**6**	**1.04**	**785**
SUM	**248**	**41**	**2.76**	
TOTAL	**1264**	**47**	**2.17**	**608**

Table 2 continued

Sample ID	No. ind.	No. species	H'	Weight (g) / species
Primnoa				
ROV and VAG samples				
PrC1	722	61	3.4	14
PrC2	263	17	1.44	50
PrC3	209	16	1.86	11
PrC4	176	16	1.82	18
PrC5	134	18	2.02	12
PrC6	399	27	2.69	54
Average	**317**	**26**	**2.21**	**27**
SUM	**1903**	**85**	**3.51**	
Trawl samples				
PrB1	1	1	0	79
PrB2	0	0	0	>1410
PrB3	0	0	0	>546
PrB4	490	26	2.39	218
PrB5	71	16	2.07	208
PrB6	186	23	2.4	175
Average	**125**	**11**	**1.14**	**439**
SUM	**748**	**45**	**2.84**	
TOTAL	**2651**	**97**	**3.54**	**233**
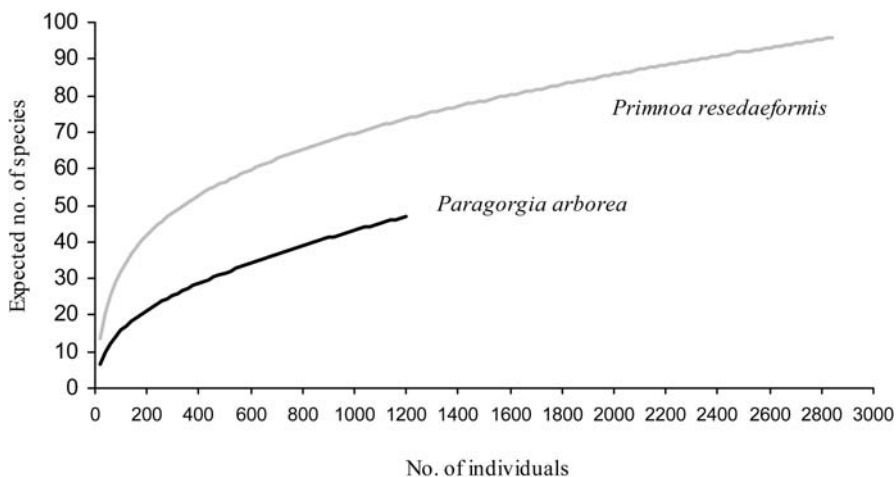
Fig. 3 Rarefaction curves for the associated fauna of *Paragorgia arborea* (13 colonies) and *Primnoa resedaeformis* (45 colonies). Samples from each species were pooled before rarefaction

Coral morphology and associated fauna

The diversity and abundance of associates were significantly correlated with coral morphology (Table 3 and Figs. 4A, B). For *Paragorgia* the strongest correlation was found between species richness and host size measured as number of branches and wet weight (r = 0.66 and 0.62 respectively, p <0.05) (Fig. 4A). Diversity (H') was also most correlated with number of branches and wet weight. This suggests that for *Paragorgia* the large and old colonies with many branches host a richer associated fauna. For *Primnoa* the correlation was strongest between diversity (H') and % exposed skeleton (r = 0.56, p <0.1; Fig. 4B) and abundance was also most correlated with % exposed skeleton. This suggests that for *Primnoa*, colonies with exposed skeleton (these are often old colonies) have the highest number of associates and diversity (H'). The relation between morphology and associated fauna differs between corals from bottom trawl and corals collected with ROV or VAG (Fig. 4).

Table 3 The correlation coefficients (r) between abundance (N), species richness (S) and diversity (H') of associated fauna of *Paragorgia arborea* and *Primnoa resedaeformis* and 7 measurments of host morphology. *: p <0.1, **: p <0.05

Coral measurments	*Paragorgia*			*Primnoa*		
	N	S	H'	N	S	H'
Wet weight (g)	-0.02	0.62**	0.53*	0.26	0.19	0.35
Width of fragment/colony (cm)	0.19	0.32	0.31	0.42	0.3	0.46
Length of fragment/colony (cm)	0.34	0.28	0.35	0.48	0.37	0.54*
No. branches (>3cm)	0.11	0.66**	0.51*	0.43	0.28	0.44
Base width (cm)	0.07	0.48*	0.4	0.27	0.26	0.41
% exposed skeleton	-	-	-	0.54*	0.5	0.56*
Number of rings in base	-	-	-	0.39	0.3	0.48

Fauna patterns

The relative composition of taxonomic groups in the material of associated fauna from both corals is shown in Figure 5. Crustaceans dominated the overall coral fauna, contributing 46 % to the total number of individuals and 26 % to the total in numbers of species. Foraminifers and hydroids were also abundant and species rich group of associates. There are clear differences in the fauna composition of the two coral species (Table 4). Foraminifers and amphipods are amongst the most species rich in the material of both coral species. On *Paragorgia* the parasitic copepods dominated in abundance while hydroids, amphipods and actinarians were more important on *Primnoa*.

Detrended correspondence analysis shows that the associated fauna on *Primnoa* forms a distinct group with higher similarity in composition than fauna from *Paragorgia* (Fig. 6A). The *Paragorgia* colonies sampled in bottom trawl form a sub group of their own (upper right corner). The parasitic copepods together with *Gorgonocephalus lamarckii* are connected to *Paragorgia* while the hydroids (e.g., *Stegopoma plicatile* and *Lafoea dumosa*), the anemone *Epizoanthus* sp. and several amphipod species (e.g., *Aeginella spinosa*, *Metopa bruzelii* and *Stenopleustes*

malmgreni) are related to *Primnoa* samples (Fig. 6B). Table 5 presents a list of all recorded species ranked by abundance together with information on the functional group and presumed relation to the host. Most of the species associated with the

A

B
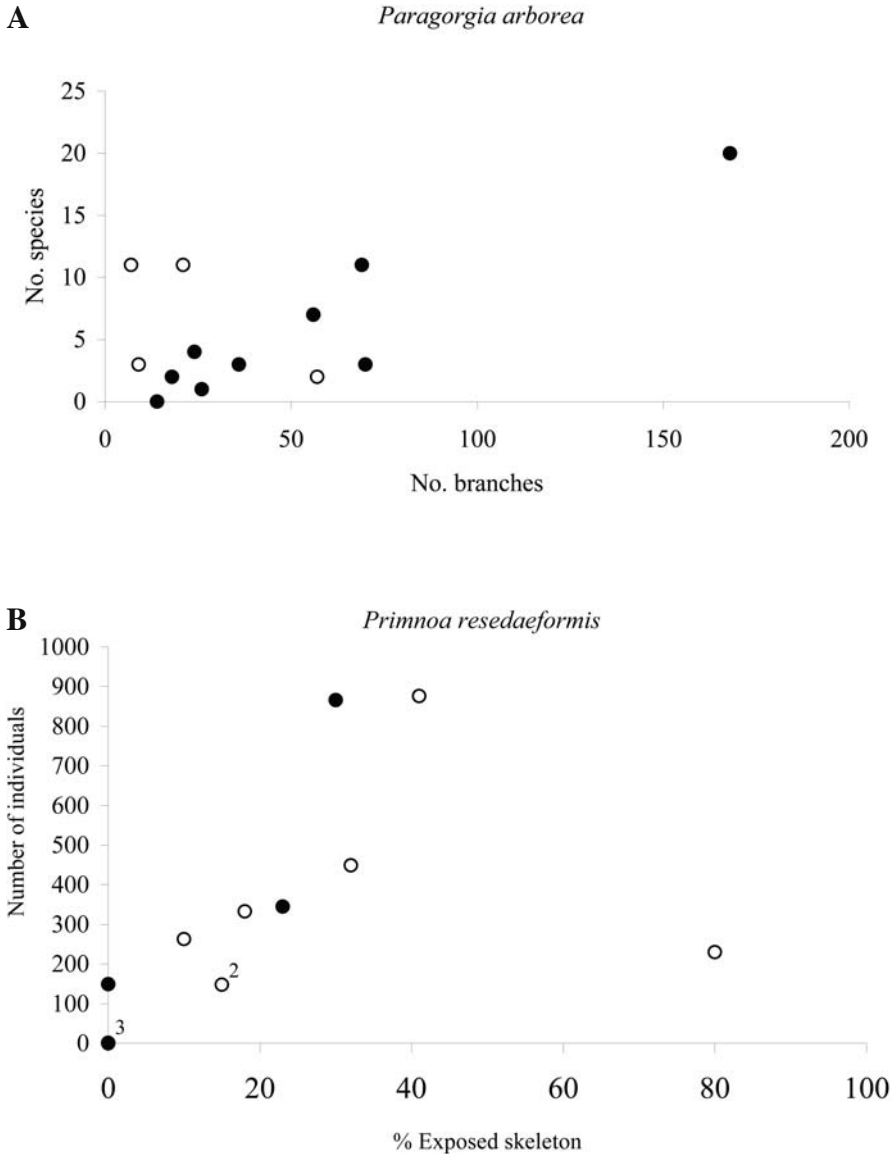
Fig. 4 Associated fauna in relation to coral morphology. **A** Species number of associates *versus* number of branches longer than 3 cm in samples of *Paragorgia arborea*. **B** Abundance of associated species *versus* percentage of exposed skeleton in samples of *Primnoa resedaeformis*. Material collected with ROV or VAG (open circles) and with bottom trawl (closed circles). Number of circles at the same position is indicated by numbers
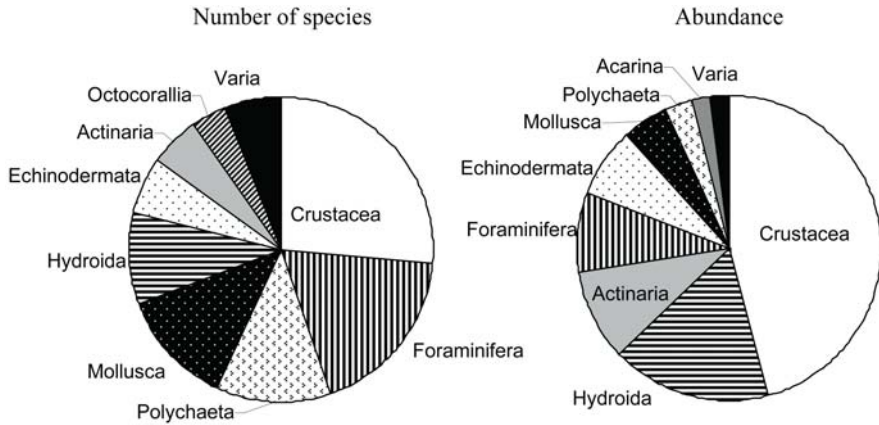
Fig. 5 The relative species richness and abundance of different taxonomic groups associated with 19 kg *Primnoa resedaeformis* and 33 kg *Paragorgia arborea* from off Atlantic Canada

corals were suspension feeders. Typical representatives are hydroids, actinarians, cirripeds and molluscs (bivalves). These are sessile and dominated in numbers on *Primnoa* (Table 5). On this coral the most common species were: *Epizoanthus* sp., *Ornatoscalpellum stroemii*, *Ophiacantha abyssicola* and *Stegopoma plicatile*. Most associated species use the corals as substratum or refuge and very few utilise the coral as a food source. On *Paragorgia*, however, amongst the most abundant associates were two parasitic copepods. Two other abundant species were *Ornatoscalpellum stroemii* and *Gorgonocephalus lamarckii* (Table 5 and Fig. 6).

Microhabitats of the coral species

The deep-water gorgonians offer different microhabitats for both sessile and mobile invertebrates. We identified two microhabitats on the colonies: "Habitat 1", young parts of the colony covered with live tissue and, "Habitat 2", old or dead parts of the colony with exposed skeleton. In what follows the main inhabitants of these habitats of the two corals is presented.

Paragorgia arborea

Habitat 1: Organisms were found both living on the surface of the colony and inside. In general few species were associated with Habitat 1 (Figs. 7A-E). The most common organisms were parasitic copepods. On the surface a parasitic lichomolgid copepod occurred in hundreds on single colonies (Fig. 7A). Inside galls on the outer parts of branches a new lamippid copepod, *Gorgonophilus canadensis* was found (Buhl-Mortensen and Mortensen 2004b). The polyps of the gall area were transformed into chimney-like structures (Figs. 7B and C). Galls were found on 4 colonies and altogether 14 galls were observed. They typically contained many egg-sacks and two large females and several smaller males (Fig. 7D). The echinoderm *Gorgonocephalus lamarckii* seemed to be strongly connected to the high current environment provided by the branches of *Paragorgia* (Fig. 7E). The *G. lamarckii* specimens were mainly large individuals with a disc diameter of 1.5-6 cm. We

Table 4 The number of species and individuals within different faunagroups found to be associated with the deep-water corals *Paragorgia arborea* and *Primnoa resedaeformis*

Species		Individuals	
Paragorgia arborea	*Primnoa resedaeformis*	*Paragorgia arborea*	*Primnoa resedaeformis*
Foraminifera 11	Foraminifera 17	Copepoda 814	Hydroida 578
Polychaeta 7	Amphipoda 14	Foraminifera 113	Amphipoda 406
Amphipoda 6	Mollusca 13	Cirripedia 102	Actinaria 352
Echinodermata 4	Hydroida 12	Echinodermata 88	Cirripedia 274
Porifera 1	Polychaeta 10	Polychaeta 37	Echinodermata 216
Mollusca 3	Echinodermata 7	Actinaria 31	Foraminifera 206
Hydroida 3	Actinaria 5	Hydroida 28	Mollusca 190
Copepoda 3	Octocorallia 4	Amphipoda 20	Isopoda 126
Actinaria 2	Cirripedia 3	Mollusca 15	Polychaeta 84
Tanaidacea 1	Bryozoa 2	Acaria 4	Acarina 68
Ostracoda 1	Copepoda 2	Ostracoda 3	Copepoda 41
Isopoda 1	Decapoda 2	Decapoda 3	Ostracoda 37
Decapoda 1	Porifera 2	Bryozoa 1	Octocorallia 29
Cirripedia 1	Isopoda 1	Isopoda 1	Bryozoa 27
Bryozoa 1	Ostracoda 1	Tanaidacea 1	Pycnogonida 9
Acaria 1	Acarina 1	Porifera 3	Decapoda 4
	Pycnogonida 1		Porifera 4
SUM 47	SUM 97	SUM 1264	SUM 2651

Fig. 6 The detrended correspondence ordination along the first and second principal axes of **A** 22 samples of associated fauna of *Paragorgia arborea* and *Primnoa resedaeformis* (PrB2, PrB3, and PaB7 are omitted) and **B** 55 species associated with the corals

Table 5 Associated species of *Paragorgia arborea* and *Primnoa resedaeformis* with information on taxonomic and functional group and use of host. Species are sorted in three groups based on abundance. Number of individuals and numbers of observations are listed. Taxonomic group: Actinaria (A), Acarina (Aca), Bryozoa (B), Crustacea (C), Echinodermata (E), Foraminifera (F), Mollusca (M), Polychaeta (P), Porifera (Po) and Pycnogonida (Py). Functional group: parasite (Pa), suspension feeder (Su), deposit feeder (De) and uncertain (?). Use of host: food source (F), refuge (R), substratum (S), and uncertain (?)

Paragorgia arborea

Ta. Gr.	Func. Gr.	Use Host	Species	No. ind.	No. obs.
			Common species occurring with >20 ind. in material		
C	Pa	F	Lichomolgidae indet.	743	5
C	Su	S	*Ornatoscalpellum stroemii* M. Sars	94	2
C	Pa	F	*Gorgonophilus canadensis* Buhl-Mortensen and Mortensen	69	4
E	Su	S	*Gorgonocephalus lamarckii* (J. Müller and Troschel)	48	6
E	Su	?	*Ophiacantha abyssicola* G. O. Sars	38	1
F	Su	S	*Discanomalina vermiculata* (d´Orbigny)	30	1
A	Su	S	*Actinaria* sp. C colonial	30	1
F	De	S	*Discanomalina coronata* (Parker and Jones)	27	2
H	Su	S	Hydroids indet.	25	1
P	?	?F	Polynoid indet.	23	2
			Species with 3-19 ind. in material		
F	De	S	*Cibicides lobatulus* (Walker and Jacob)	19	4
F	De	S	*Globigerina* sp.	14	4
F	De	S	*Astronionion tumidum* Cushman and Edwards	11	2
M	Su	S	Anomiidae indet.	11	1
C	Su	R	*Ischyrocerus megacheir* (Boeck)	9	2
C	Su	R	*Jassa pusilla* (G. O. Sars)	7	1
P	Su	S	*Chone* sp. B	6	2
Aca	?Pa	?F	Halacarinae	4	1
C	De	R	*Pandalus propinquus* (G. O. Sars)	3	2
F	De	S	Forams. indet.	3	1
P	Su	S	*Chone* sp. A	3	1
C	De	R	*Polycope punctata* G. O. Sars	3	1
M	?	S	*Lepeta caeca* (Müller)	3	1
Po	Su	S	*Sycon* sp.	3	1
			Rare species with 1-2 ind. in material		
F	De	S	*Cibicides refulgens* de Montfort	2	2
C	Pa	F	*Enalcyonium* cf. *olssoni* (De Zulueta)	2	2
F	De	S	*Robulus* sp.	2	1
F	De	S	*Globorotalia* sp.	2	1
F	De	S	*Planulina bradii* Tormachoff	1	1
F	De	S	*Cribroelphidium incertum* Williamson	1	1
F	De	S	*Dendrophrya* sp.	1	1

Table 5 continued

Paragorgia arborea

Ta. Gr.	Func. Gr.	Use Host	Species	No. ind.	No. obs.
			Rare species with 1-2 ind. in material		
B	Su	S	*Scrupocellaria scrupea* Busk	1	1
H	Su	S	*Acryptolaria conferta* (Allman)	1	1
H	Su	S	*Eudendrium ramosum* (L.)	1	1
H	Su	S	*Lafoea dumosa* (Fleming)	1	1
A	?	S	*Actinaria* sp. D solitary	1	1
P	?	?	*Arctone* sp.	1	1
P	De	?F	Harmathoin polynoid sp. A	1	1
P	De	?F	Harmathoin polynoid sp. B	1	1
P	Pr	S	*Nereis* sp A.	1	1
P	Pr	S	*Nereis* sp B.	1	1
C	Su	R	*Aristias megalops* G. O. Sars	1	1
C	Su	R	*Metopa bruzeli* (Goës)	1	1
C	Su	R	Caprellidae indet.	1	1
C	Su	R	*Proaeginina norvegica* (Stephensen)	1	1
C	Su	R	*Munna boecki* Krøyer	1	1
C	De	R	Tanaid sp.	1	1
E	Su	S	*Ophiacantha anomala* G. O. Sars	1	1
E	Su	S	*Ophiopholis aculeata* (L.)	1	1
M	Pr	R	*Bathypolypus bairdii* (Verrill)	1	1
	Su/De	S/R/F			
	23/16	25/11/7			

Primnoa resedaeformis

Ta. Gr.	Func. Gr.	Use Host	Species	No. ind.	No. obs.
			Common species occurring with >20 ind. in material		
A	Su (Pa)	S,F	*Epizoanthus* sp.	261	3
C	Su	S	*Ornatoscalpellum stroemii* M. Sars	259	8
E	Su	S	*Ophiacantha abyssicola* G. O. Sars	182	4
H	Su	S	*Stegopoma plicatile* (M. Sars)	146	4
C	Su	R	*Munna boecki* Krøyer	126	6
C	Su	R	*Metopa bruzelii* (Goës)	121	6
H	Su	S	*Lafoea dumosa* (Fleming)	117	3
C	Su	R	*Stenopleustes malmgreni* (Boeck)	105	4
H	Su	S	Small athecate Hydr.	87	3
M	Su	S	Anomidae indet.	85	4
A	Su	S	*Actinaria* sp. B colonial	81	3
H	Su	S	Hydroids indet.	70	2
Aca	?Pa	?F	Halacarinae indet.	68	4
H	Su	S	*Sertularella tenella* (Alder)	67	4
F	De	S	*Discanomalina coronata* (Parker and Jones)	66	7

Table 5 continued

Primnoa resedaeformis

Ta. Gr.	Func. Gr.	Use Host	Species	No. ind.	No. obs.
			Common species occurring with >20 ind. in material		
P	Su	S	Spirorbidae indet.	58	1
F	De	S	*Cibicides refulgens* de Montfort	51	5
H	Su	S	*Eudendrium* sp.	41	6
M	?De	S	*Trochaclis* sp.	41	1
C	Pa	F	*Enalcyonium* cf. *olssoni* (De Zulueta)	40	6
C	Su	R	Amphipoda indet.	40	5
C	Su	R	*Proboloides calcarata* (G. O. Sars)	38	5
C	De	S	*Paradoxostoma* sp.	37	5
F	De	S	*Cibicides lobatulus* (Walker and Jacob)	32	7
C	Su	S	*Aeginella spinosa* Boeck	32	2
B	Su	S	*Idmidronea atlantica* (Forbes)	26	1
C	Su	S	*Amphithopsis longicaudata* Boeck	20	1
M	De	S	*Buccinum finmarchianum* Verkrützen	20	1
			Species with 3-19 ind. in material		
H	Su	S	*Eudendrium ramosum* (L.)	19	2
C	Su	S	*Gitana abyssicola* G. O. Sars	18	2
M	Su	S	*Pododesmus* cf. *squama* (Gmelin)	17	2
E	Su	S	*Ophiacantha anomala* G. O. Sars	16	3
F	De	S	*Discanomalina semipunctata* (Bailey)	15	3
O	Su	S	*Clavularia* cf. *griegii* F. J. Madsen	15	1
H	Su	S	*Sertularella* cf. *polyzonias* (L.)	13	2
H	Su	S	Athecate hydroid	11	2
O	Su	S	*Primnoa resedaeformis* (Gunn.) juv.	11	2
C	Su	R	*Stenopleustes nodifer* (G. O. Sars)	11	1
Py	?Pa	F?	Nymphonidae, juvenile	9	2
C	Su	R	*Neopleustes pulchellus* (Kroyer)	9	1
F	De	S	Forams indet.	8	4
A	Su	S	*Actinaria* sp. A solitary	8	3
M	Su	S	*Delectopecten vitreus* (Gmelin)	8	3
E	Su	S	*Hathrometra tenella* (Carpenter)	7	2
M	Su	S	*Heteranomia squamula* (L.)	7	2
F	De	S	*Robulus* sp.	6	2
F	De	S	*Discanomalina vermiculata* (d´Orbigny)	6	2
M	De	S	*Amphissa acutecostata* (Philippi)	6	2
P	Su	S	*Serpulidae* indet.	6	1
P	De	S	*Syllidae* spp.	5	5
P	Su	S	Sabellidae indet.	5	1
C	Su	R	*Jassa pusilla* (G. O. Sars)	5	1
E	Su	S	Ophiuroidea, juvenile	5	1
F	?	?	*Globigerina bulloides* d´Orbigny	4	2

Table 5 continued

Primnoa resedaeformis

Ta. Gr.	Func. Gr.	Use Host	Species	No. ind.	No. obs.
			Species with 3-19 ind. in material (cont.)		
H	Su	S	Big athecate hydroid	4	2
P	Pa?De?	F?S	*Eunice pennata* (O. F. Müller)	4	2
F	De	S	*Planulina ariminensis* d´Orbigny	4	1
F	De	S	*Saccammina sphaerica* M. Sars	4	1
Po	Su	S	*Sycon* sp.	3	2
F	De	S	*Trochammina nana* (Brady)	3	1
			Rare species with 1-2 ind. in material		
P	Pa?De?	F?S	Polynoid indet.	2	2
C	De	R	*Pandalus propinquus* (G. O. Sars)	2	2
E	Su	S	*Ophiopholis aculeata* (L.)	2	2
E	Su	S	Asteridae indet.	2	2
O	Su	S	*Trachytela rudis* Verrill	2	1
C	Su	R	*Aegina echinata* G. O. Sars	2	1
C	Su	R	*Stenothoe marina* (Bate)	2	1
C	Sc	R	*Dorhynchus thomsoni* (Thomson)	2	1
C	Su	S	*Chirona hammeri* (Ascanius)	2	1
F	De	S	*Conglophragmium coronatum* (Brady)	1	1
F	De	S	*Astrononion* sp.	1	1
F	De	S	*Discorbis* sp.	1	1
F	De	S	*Discospirina* sp.	1	1
F	Su	S	*Cyclammina cancellata* Brady	1	1
F	Su	S	*Sphaeroidina bulloides* (d´Orbigny)	1	1
F	De	S	*Eponides* sp.	1	1
B	Su	S	*Tessaradoma boreale* (Busk)	1	1
H	Su	S	*Rhizocaulus verticillatus* (L.)	1	1
H	Su	S	*Cladocarpus integer* (Sars)	1	1
H	Su	S	*Filellum serpens* (Hassall)	1	1
A	Su	S	*Actinaria* sp. D solitary	1	1
A	Su	S	*Actinaria* sp. E solitary	1	1
O	Su	S	*Dova* cf. *florida* (Rathke)	1	1
P	Pa?De?	F?S	*Eunice* sp., juvenile	1	1
P	Su	S	*Chone* sp. B	1	1
P	De	S	*Typosyllidae* sp.	1	1
P	Su	S	*Rodine* sp.	1	1
C	De	R	Harpacticoidea indet.	1	1
C	Su	R	*Caprella* sp.	1	1
C	Su	R	*Ischyrocerus megacheir* (Boeck)	1	1
C	Sc	R	*Lysianassidae* indet.	1	1
C	Su	S	*Heteralepas cantelli* Buhl-Mortensen and Newman	1	1
E	Su	S	*Gorgonocephalus lamarckii* (J. Müller and Troschel)	1	1

Table 5 continued

Primnoa resedaeformis

Ta. Gr.	Func. Gr.	Use Host	Species	No. ind.	No. obs.
			Rare species with 1-2 ind. in material		
E	Su	S	*Ophiacantha spectabilis* G. O. Sars	1	1
M	Su	S	Pectinidae indet.	1	1
M	P?	F?	*Cuthona* sp.	1	1
M	Pa?De?	F?S	*Hanleya mendicaria* Mighels and Adams	1	1
M	Pa?De?	F?S	*Leptochiton* sp.	1	1
M	De	S	*Alvania syngenes* (Verrill)	1	1
M	Pa?De?	F?S	Aplacophora indet.	1	1
Po	Su	S	*Farrea occa* Bowerbank	1	1
	Su/De	S/R/F			
	64/31	81/14/10			

observed 15 individuals on one large *Paragorgia* (sample PaB4). A few unidentified anemones were also found attached to the branches. Polynoid polychaetes were occasionally observed clinging firmly to the surface of the coral.

Habitat 2: Here one typically finds particulate deposits between the branches. In these parts of the colony, with thick branches, the red coenenchyme that entirely covers the outer and younger parts of the branches, gives way to a pale yellow surface with less structure. Organisms were found both on the surface and inside the spongy skeleton of the coral (Figs. 8A-D). In the pale areas we observed polychaete burrows and tubes protruding from inside the coral skeleton (Figs. 8A-C). At least four polychaete species belonging to the families Sabellidae, Nereidae, and Polynoidae were found in burrows in the skeleton. One *Nereis* sp. specimen, probably a predator, had its head protruding from a tube between two branches (Fig. 8A). A harmothoine polynoid was found in a ~15 cm long and 0.5 cm wide burrow (Fig. 8B). Sabellid polychaetes belonging to the genus *Chone* occurred in groups of 2 and 3 individuals with tubes arranged as intricate labyrinths inside the skeleton (Fig. 8C). In detritus laden areas the amphipod *Ischyrocerus megacheir* was found inside detritus pockets that probably are nests built by the amphipod (Fig. 8D). Hydroids were sometimes found close to the centre of the fan formed by the branches of the colony often with the cirriped *Ornatoscalpellum stroemii* attached to them. The hydroids were also the main substratum for most of the foraminifers (e.g., *Discanomalina vermiculata* and *D. coronata*), amphipods, ostracods, isopods and mites.

Primnoa resedaeformis

Habitat 1: In this habitat species are found both living on the surface of the colony and inside. In general few species are found in this habitat (Figs. 9A-C). The shrimp *Pandalus propinquus* is found on the branches (Fig. 9A) and mites were
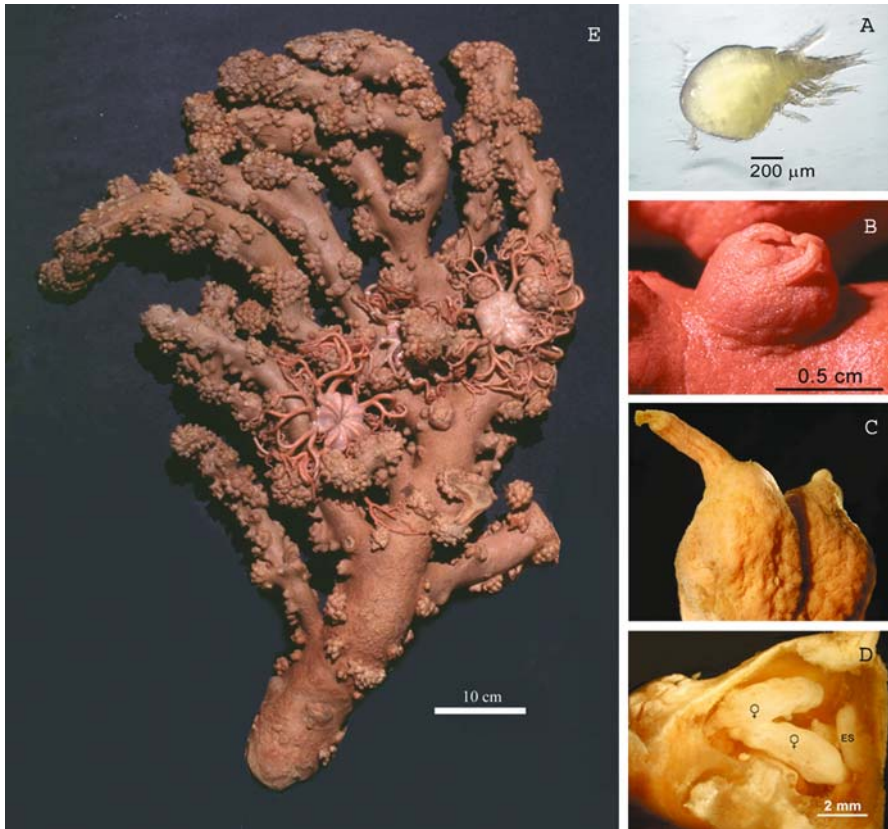
Fig. 7 Organisms inhabiting "Habitat 1" on *Paragorgia arborea*. **A** Lichomolgid parasitic copepod living on the surface of the coral. **B** and **C** Galls formed by the copepod *Gorgonophilus canadensis*. The coral polyps are transformed to chimney-like structures. **D** The interior of a gall is showing two females and an egg-sack. **E** The ophiuroid *Gorgonocephalus lamarckii* on a branch of the coral

observed on the surface (Fig. 9B). The parasitic lamippid copepod *Enalcyonium* cf. *olssoni* probably living inside the polyps was frequently encountered (Fig. 9C). A pair, male and female of the decapod *Dorhynchus thomsoni* was also found in this habitat.

Habitat 2: This habitat is represented by the hard exposed skeleton of the coral and is the substratum of many sessile epizoans (Figs. 10A-E). The skeleton was often occupied by hydroids, molluscs, bryozoans, foraminifers and cirripeds (Figs. 10B and C). The hydroids *Stegopoma plicatile*, *Lafoea dumosa* and *Sertularella tenella* were common and a parasitic anemone *Epizoanthus* sp. sometimes covered large parts of the skeleton (Fig. 10A). The amphipods (e.g., *Metopa bruzelii*, *Stenopleustes malmgreni*, *Aeginella spinosa*) and isopod (*Munna boecki*) were found mainly amongst the hydroids often together with the cirriped *Ornatoscalpellum stroemii*. A rich fauna of foraminifers occurred in this habitat (e.g., *Discanomalina*

vermiculata, *D. coronata* and *Cibicides refulgens*) some of these were attached to the hydroids (Fig. 10D). Several bivalves (e.g., Anomidae species, *Pododesmus* cf. *squama*, and *Delectopecten vitreus*), the cirriped *Chirona hammeri* and bryozoans were attached directly to the coral skeleton. Three octocoral species were also found on the skeleton: young new polyps of *Primnoa resedaeformis*, *Trachytela rudis* and *Clavularia* cf. *griegii* (Fig. 10E).
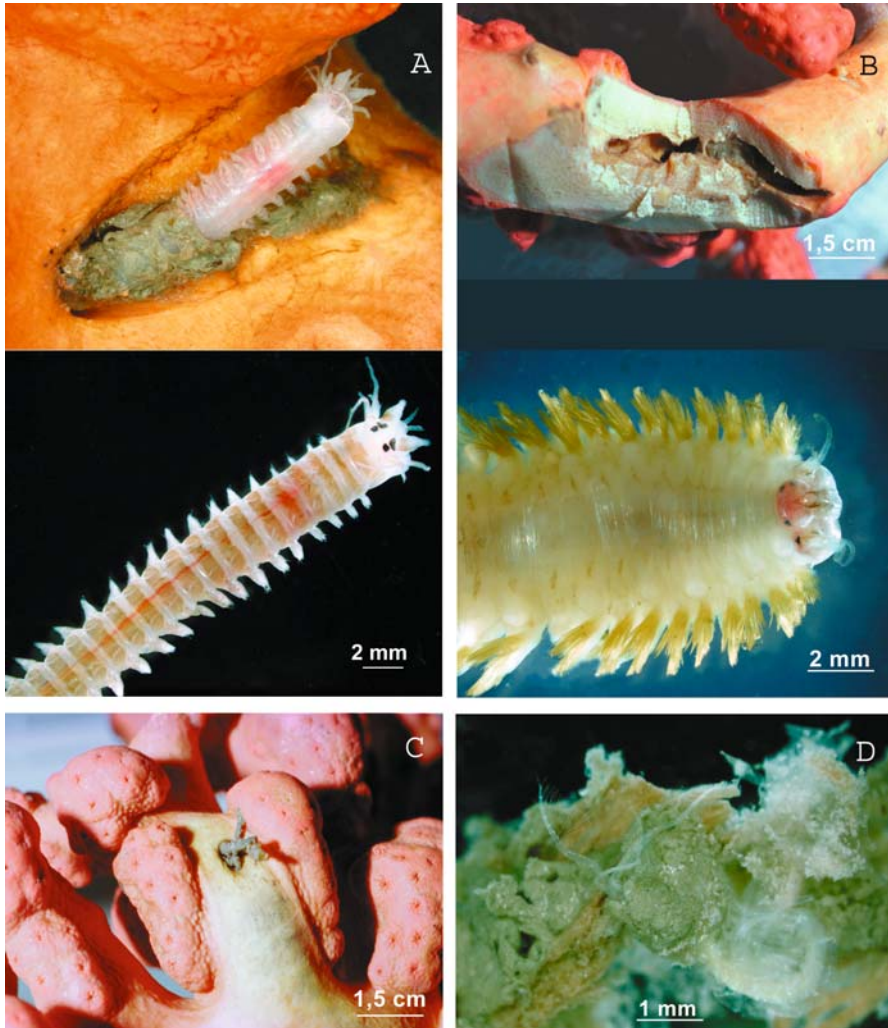
Fig. 8 Organisms inhabiting "Habitat 2" on *Paragorgia arborea*. **A** *Nereis* sp. in a tube protruding from the interior of the coral. **B** Burrow of harmothoin polynoid sp. A and the polychaete, scales are lacking. **C** Tubes of *Chone* sp. A, a sabellid polychaete protruding from the coral skeleton. Note the lighter areas with this coenchyme. **D** The amphipod *Ischyrocerus megacheir* in a detritus pocket, probably a nest it has made. Parts of the detritus layer have been taken away
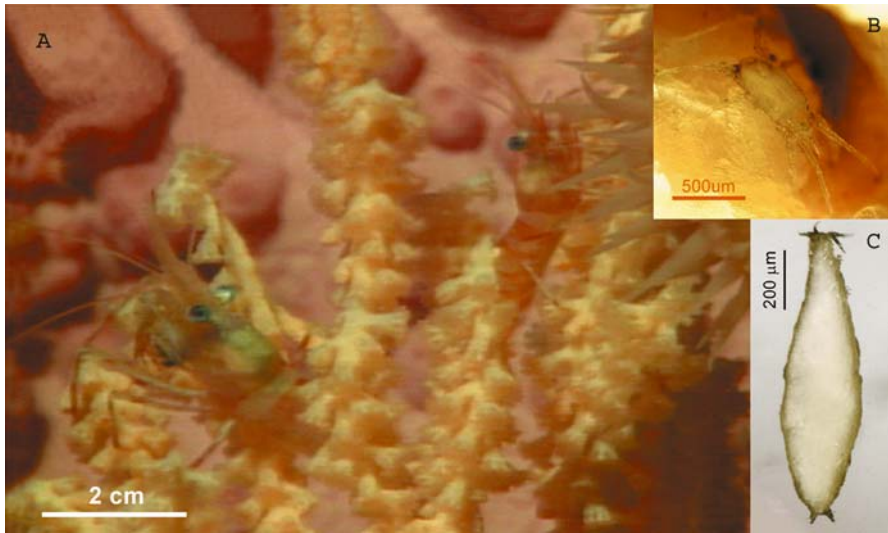
Fig. 9 Organisms inhabiting "Habitat 1" of *Primnoa resedaeformis*. **A** A video frame grab of the shrimp *Pandalus propinquus* climbing on the branches of the coral (recorded with ROPOS on cruise in 2001). **B** Mite living on the surface of the host. **C** The parasitic copepod *Enalcyonium* cf. *olssoni* living inside the coral

Discussion

Comparison of sampling gear

The material used for documentation of associated fauna differed in the terms of quality of information. The abundance of different fauna groups per coral colony in material from different sources is shown in Figure 11. For comparison we have included information from an earlier study using an ROV with suction sampler for documentation of mobile crustaceans associated with the same coral species in the same area (Buhl-Mortensen and Mortensen 2004a). The suction samples contained a rich fauna of mobile crustaceans while the sessile fauna (e.g., molluscs and cirripeds) was less well documented. The corals collected with ROV or VAG revealed a rich and varied fauna while the material collected with bottom trawl in fisheries surveys was very poor in general. Many associated organisms have probably been dislodged or shaken off the coral colonies when they were carried along in the trawl. However, the difference in species diversity between gear types was less for *Paragorgia* than for *Primnoa*. The *Paragorgia* colonies collected by trawl were in general larger with a mean weight three times higher than those sampled by ROV or video-grab. Thus, the associates connected to large colonies and older parts of colonies, e.g., polychaetes living inside the skeleton and the echinoderm *Gorgonocephalus lamarckii*, were better represented in this material.

Diversity patterns

Primnoa clearly had a more diverse fauna than *Paragorgia*. The reason for this difference is mainly that the hard substratum of exposed skeleton often found on old *Primnoa* colonies provides an opportunity for colonisation of sessile organisms that will not find suitable substratum on *Paragorgia*. The more porous skeleton of *Paragorgia* is probably less persistent when exposed, and naked areas at the base of old colonies are not common. This was supported by the correlation between the abundance and diversity (H') of associates of *Primnoa* with percentage exposed
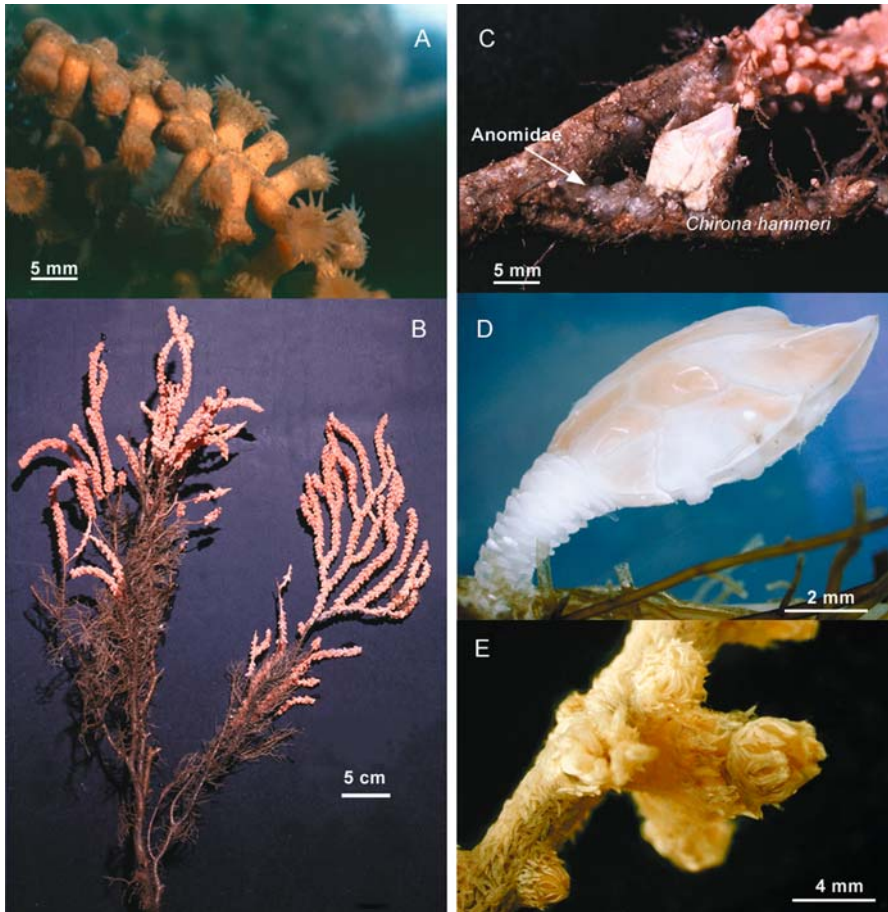
Fig. 10 Organisms inhabiting the exposed skeleton "Habitat 2" of *Primnoa resedaeformis*. **A** The anemone *Epizoanthus* sp. overgrowing the skeleton. **B** A colony with dense growths of the hydroid *Stegopoma plicatile*. **C** and **D** show organisms attached to the skeleton. **C** Anomidae bivalves and the cirriped *Chirona hammeri*. **D** The cirriped *Ornatoscalpellum stroemii* (photo: D. Jackson). **E** A colony of the octocoral *Trachytela rudis* overgrowing the skeleton
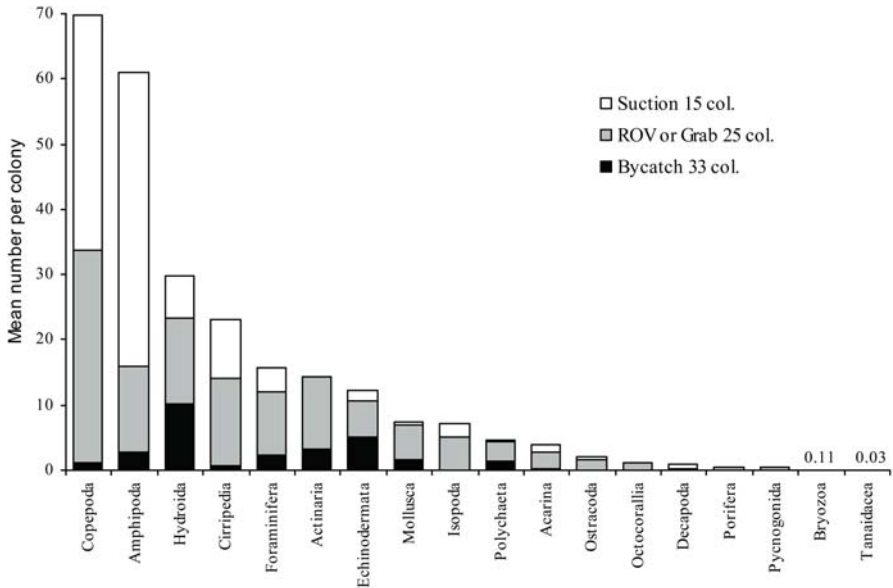
Fig. 11 Mean abundance of associated fauna per colony in material sampled with different gears

skeleton. A parallel to this habitat is found on the deep-water scleractinian *Lophelia pertusa* represented by the dead and old parts of colonies. For *Lophelia* this is the most species rich microhabitat (Jensen and Frederiksen 1992; Fosså and Mortensen 1998; Table 6). The high species diversity on dead exposed coral surfaces is in agreement with observations from warm-water and tropical corals (Patton 1976; Reed et al. 1982) and seems to be a general pattern.

Species richness of associates was related to the size of *Paragorgia* (number of branches and wet weight) and diversity (H') and abundance of associates to percentage of exposed skeleton of *Primnoa*. The relation between size of the host coral habitat and richness of associated fauna has previously been demonstrated for tropical corals (Abele and Patton 1976; Abele 1984). For *Paragorgia* this is probably related to the increased surface available for clinging ophiuroids and parasitic copepods. On *Primnoa* the exposed skeleton hosts a rich sessile fauna and as this area increases, so does the available surface for colonisation. The chance of colonisation by associated fauna will increase with time and since size of host or percentage exposed skeleton is also related to time (age of host) it is not possible to be conclusive about the decisive factor of this correlation.

Microhabitats on the host coral

The deep-water gorgonians offer two different microhabitats for symbionts. Habitat 1: the clean and living surface of coral tissue, in young parts of the colony and, Habitat 2: pockets of detritus and exposed skeleton in old parts of the colonies.

Table 6 Gram coral per associated species and linear correlation (r) between weight of coral and number of associated species. Observations on *Paragorgia arborea* and *Primnoa resedaeformis* are compared with data compiled from literature for the deep-water scleractinian *Lophelia pertusa* and the tropical scleractinian *Oculina arbuscula*. *: p <0.1, ** p <0.05, ***: p <0.01

No. samples	Coral material and source	Weight (g) ass. species	Weight/species r
4	*Paragorgia* bycatch	254	0.54
8	*Paragorgia* collected	785	0.93***
12	*Paragorgia* total	608	0.62**
6	*Primnoa* collected	27	0.41
6	*Primnoa* bycatch	439	0.96***
12	*Primnoa* total	233	0.19
12	*Lophelia* live (Jensen and Frederiksen 1992)	24	0.48
13	*Lophelia* dead (Jensen and Frederiksen 1992)	9	0.48*
25	*Lophelia* total (Jensen and Frederiksen 1992)	16	0.21
5	*Lophelia* live (Fosså and Mortensen 1998)	5.6	0.83*
20	*Lophelia* dead (Fosså and Mortensen 1998)	13.8	0.70***
25	*Lophelia* total (Fosså and Mortensen 1998)	12.2	0.66***
2	*Oculina arbuscula* A (McCloskey 1970)	58	-
2	*Oculina arbuscula* B (McCloskey 1970)	20	-
2	*Oculina arbuscula* C (McCloskey 1970)	14	-
2	*Oculina arbuscula* D (McCloskey 1970)	24	-
8	*Oculina arbuscula* total (McCloskey 1970)	29	0.6

Habitat 1

In general relatively few species are connected to the live parts of tropical corals and it is here one finds the highly specialised and obligate symbionts (Patton 1976; Reed et al. 1982). This agrees with our observations. Three species of highly specialised parasitic copepods were amongst the few organisms found in this habitat. *Enalcyonium* cf. *olssoni* that occurred on *Primnoa* has been found parasitically in the octocoral *Alcyonium digitatum* L. (Stock 1988). It belongs to the family Lamippidae that is exclusively endoparasitic in octocorals (Grygier 1983; Stock 1988). A new lamippid copepod species was found inside galls on the outer parts of the branches of *Paragorgia*. Copepods of the family Lichomolgidae was very common on *P. arborea* (a mean of 57 individuals per colony). This taxonomically difficult group of copepods is mainly associated with invertebrates and many species are known to be parasites on gorgonians in tropical waters (Humes and Stock 1973; Humes 1993). The copepod was not identified to species level and may be a new species. The parasitic copepods are presumed to feed on the coenenchyme of their hosts (Patton 1976). As this is the first study focusing on the associated fauna of deep-water gorgonians we expect that with more studies many more parasitic copepod species will be found.

The shrimp *Pandalus propinquus* is found amongst the branches of both coral species. This relation is probably not obligate. This shrimp has been suggested to be associated with other anthozoans by Jonsson et al. (2001), however, in that study the video-recorded *Pandalus* specimens could not be identified to species level. *P. propinquus* has been found clinging to branches of *P. arborea* collected with triangular dredge (Storm 1901). It is also common on the scleractinian deep-water coral *Lophelia pertusa* (L.), (Dons 1944; Burdon-Jones and Tambs-Lyche 1960; Jensen and Frederiksen 1992; Fosså and Mortensen 1998). Hiding amongst the branches of corals probably offers the shrimp shelter from predators. The shrimp may be beneficial to the coral by cleaning its surface from sedimenting particles. The cleaning function of shrimps is well known from shallow-water coral reefs (Bruce 1970). Sediment removal from corals has been suggested for shrimps (Hickson 1906) and for ophiuroids (Sneli 1985; Grange 1991), however, since we have no detailed observation of this behaviour by *P. propinquus* on the corals, this can only be speculation.

The echinoderm *Gorgonocephalus lamarckii* was often found on *Paragorgia*. In shallow waters in the Bay of Fundy detailed studies on the feeding ecology of *Gorgonocephalus arcticus* have been carried out (Emson et al. 1991). *G. arcticus* sits on rocks in high current environment using its arms to form a feeding fan and is a fortuitous predatory suspension feeder. Since knowledge of *G. lamarkii* is sparse, we presume that the host *Paragorgia* is mainly used as a feeding platform for capturing live or dead particles from the water current. It is suggested that young stages of *Gorgonocephalus* species may live parasitically on the polyps of alcyonarians and that at the stage when branching of the arms begins they leave the alcyonarian and seek the adult specimens (Mortensen 1927). We observed only larger individuals (disk size of 1.5 cm or more) on *Paragorgia* indicating that juveniles are living in another habitat. We have also found younger individuals amongst the branches of the soft coral *Duva florida* from the same area (observations on museum material).

Habitat 2

The corals are in many ways comparable to trees on *terra firma*. It is the old trees, or old parts of the trees (dead and/or without bark), that have most epiflora and -fauna. In *Paragorgia* there are pale areas in these parts that might be analogous to areas without bark on old trees. Like bark, the red coenenchyme seems to protect the coral from damage and colonisation. Another explanation might be that epizoans change their host in a way that leads to a change in structure and coloration of the coral surface. Here we find most of the attached and burrowing epizoans. Several polychaete species were able to build tubes or tunnels inside *Paragorgia*. The relation between polynoid polychaetes and gorgonian corals is well known (Pettibone 1991). In addition to a large tunnel made by a harmotoinae polynoid we also observed a *Nereis* sp. and sabellid polychates protruding from the interior of the coral. Sabellid polychaetes have to our knowledge not been observed in relation to corals earlier.

In *Primnoa* the firm exposed skeleton offers a surface for sessile epifauna. For most scleractinian corals, both tropical and cold water, the older parts with exposed

skeleton hosts the richest associated fauna (Patton 1976; McCloskey 1970; Reed et al. 1982; Jensen and Frederiksen 1992; Mortensen 2001). The hydroids, actinarians and molluscs living on *Primnoa* are sitting on old parts of the colonies having exposed skeleton. A similar habitat is not available on *Paragorgia*. There was a rich fauna of foraminifers living attached to the exposed skeleton of *Primnoa* or on hydroids attached to the corals. These species are not obligate symbionts and many of them (e.g., *D. coronata*, *C. lobatulus* and *C. refulgens*) are common on dead parts of organisms rising above the seabed, such as corals (Jensen and Frederiksen 1992; Fosså and Mortensen 1998) and sponges (Klitgaard 1995; Beaulieu 2001).

Of the most common amphipods three species have earlier been reported from coral habitats, *Stenopleustes malmgreni* on *Paragorgia arborea* (Sars 1890-95; Vader 1969), *Aeginella spinosa* on *Paramuricea placomus*, (Strømgren 1970), and *Proboloides calcarata* has together with the former two been found in habitats with corals, hydroids, and sponges (Storm 1901). *Metopa bruzelii* has to our knowledge not been reported previously as associated with corals. The isopod *Munna boecki* found amongst the hydroids has been documented from deep-water *Lophelia* reefs in several studies (Fosså and Mortensen 1998). The amphipods and isopod are facultative symbionts and the corals together with the hydroids attached to it probably provide shelter against predators and a suitable substratum both for capturing and filtering particles from the water passing the coral.

Several hydroid species created a bushy habitat on the exposed skeleton, e.g., *Stegopoma plicatile*, *Lafoea dumosa*, *Sertularella tenella*, and *Eudendrium* sp. The first three species have been observed on *Primnoa* skeleton from the area before (Henry 2001) and all four species are frequently found on dead *Lophelia* off Norway (Fosså and Mortensen 1998).

Table 7 sums up the main groups of organisms in the two habitats of the corals and their relation with the host coral.

Comparison with other coral habitats

Diversity

Most associated species of *Paragorgia* and *Primnoa* were rare (1-3 individuals in total). In a study of the warm-water gorgonian *Leptogorgia virgulata* Patton (1972) notes that with the exception of the copepods most associated species occur in the low numbers of 0-5 individuals. This fits well with the fauna of *Paragorgia* with the strong domination in numbers of the parasitic copepods. Few studies are available of the associates of warm-water gorgonians (see Goh et al. 1999 for a review). In a study of fauna associated with gorgonians in Singapore only 50 % of the coral species had associates (Goh et al. 1999). A total of 30 species and 729 individuals of associates were collected from the corals by scuba divers, (number of coral colonies is not given). This indicates a much poorer fauna of associates than we found on *Paragorgia* and *Primnoa* in this study (>100 species and ~3600 individuals). Thus the deep-water gorgonians appear to host a richer fauna than their tropical counterparts. However, in comparison with some scleractinian corals both the deep-water reef forming *Lophelia pertusa* and the warm-water *Oculina arbuscula* host a richer fauna than *Primnoa* and *Paragorgia* (Table 6).

Taxonomic composition

The domination by crustaceans, in particular amphipods is in agreement with findings on tropical gorgonians (Goh et al. 1999). Tropical coral habitats also host very specialised parasitic copepods. However, decapods (crabs and shrimps) and gastropods are represented with more species on warm-water corals (Patton 1976; Goh et al. 1999) while the echinoderm fauna seem to be richer on deep-water corals. Several ophiuroids are specialised to capturing particles in the high current environment provided by deep-water corals (Emson and Woodley 1987; Fujita and Ohta 1988).

Functional groups

In general very few species rely on live coral tissue for food. The parasitic copepods and presumably some polynoid polychaetes are the exceptions (Table 7). When the coral tissue is damaged the parasitic anemone *Epizoanthus* sp. seems to be able to overtake larger parts of the coral skeleton by killing and ingesting the coral tissue and the anemone often has coral sclerites incorporated into its tissue. The main food of the anemone, once established on the coral skeleton, is captured from the water current. On warm-water gorgonians there are more species feeding on coral tissue such as gastropods (Goh et al. 1999). Suspension feeders, using the host as a platform for filtering particles from the passing water current, dominate the associated fauna of *Primnoa* and *Paragorgia*. This agrees with observations of associates of the cold-water scleractinian coral *Lophelia pertusa* (Jensen and Frederiksen 1992; Fosså and Mortensen 1998). This is in contrast to the associates of warm-water and tropical corals which are dominated by deposit feeders utilising the mucus and detritus deposited in old parts of the coral-heads as food source (McCloskey 1970; Patton 1976; Reed et al. 1982). Deep-water corals are typically situated in high current habitats rich in organic particles. The corals depend on this import of organic matter as their main food source. Thus they are ideal substratum for other suspension feeding organisms. In tropical waters the corals are surrounded by relatively low-productivity water and rely mainly on autotrophic production through symbiotic algae. Thus the food sources available for associates on tropical corals are produced within the reef, e.g., deposited detritus and mucus. The deposit feeding associates of tropical corals will hardly find a comparable habitat outside the coral reef or colony. In the deep-water coral habitat, however, any structure rising above the seabed (e.g., polychaete tubes, glass sponges) into a high current environment will provide the food source needed for most of the associates of deep-water corals. This difference between the two coral habitats may explain why there are relatively few obligate symbionts connected to deep-water corals compared to tropical corals.

Conclusions

Paragorgia arborea and *Primnoa resedaeformis* host a rich associated fauna dominated by suspension feeders using the coral as substratum or refuge against predators. The fauna is considerably richer than what has been found on tropical gorgonians.

Table 7 Relation between associated taxa and host coral for habitat 1 (young parts of colony) and 2 (old parts) of *Paragorgia arborea* and *Primnoa resedaeformis*

Habitat	Refuge	Feeding site	Food
		Paragorgia	
1	*Pandalus*	*Gorgonocephalus*	Parasitic copepods
		Pandalus	Polynoid polychaetes
		Anemones	?Anemones
2	*Pandalus*	Hydroids	Polynoid polychaetes
	Amphipods	Foraminifers	
	Ostracods	Amphipods	
	Polychaetes	Polychaets	
		Ornatoscalpellum	
		Primnoa	
1	*Pandalus*	*Pandalus*	Parasitic copepods
			?Acarina
2	*Pandalus*	*Pandalus*	*Epizoanthus* sp.
	Amphipods	*Ornatoscalpellum*	
	Isopoda	Hydroida	
	Ostracoda	Amphipods	
		Foraminifers	
		Epizoanthus sp.	
		Bivalves	
		Balanids	

The fauna composition differs for the two gorgonians but consists mainly of species also occurring in other habitats. A few highly specialised parasites are identified for both species.

The abundance and diversity of associated fauna is significantly correlated with host morphology.

The coral sampling methodology clearly affects the material of associated fauna, both in abundance and composition. Sampling using ROV or video-assisted grab is clearly preferable to by-catches from fisheries.

Acknowledgements

References

Abele LG (1984) Biogeography, colonization, and experimental community structure of coral-associated crustaceans. In: Strong RDD, Simberloff LG, Abele A, Thile B (eds) Ecological communities, conceptual issues and the evidence. Princeton Univ Press, Princeton, New Jersey, pp 123-137

Abele LG, Patton WG (1976) The size of coral heads and the community biology of associated decapod crustaceans. J Biogeogr 3: 35-47

Andrews AH, Cordes E, Mahoney MM, Munk K, Coale KH, Cailliet GM, Heifetz J (2002) Age, growth and radiometric age validation of a deep-sea, habitat-forming gorgonian (*Primnoa resedaeformis*) from the Gulf of Alaska. Hydrobiologia 471: 101-110

Beaulieu SE (2001) Life on glass houses: sponge stalk communities in the deep sea. Mar Biol 138: 803-817

Buhl-Mortensen L, Mortensen PB (2004a) Crustaceans associated with the deep-water gorgonian corals *Paragorgia arborea* (L., 1758) and *Primnoa resedaeformis* (Gunnerus 1763). J Nat Hist 38: 1233-1247

Buhl-Mortensen L, Mortensen PB (2004b) *Gorgonophilus canadensis* n. gen., n. sp. (Copepoda: Lamippidae), a gall forming endoparasite in the octocoral *Paragorgia arborea* (L., 1758) from the Northwest Atlantic. Symbiosis 37: 155-268

Burdon-Jones C, Tambs-Lyche H (1960) Observations on the fauna of the North Brattholmen stone-coral reef near Bergen. Årb Univ Bergen, Mat-Naturv Ser 4: 1-24

Bruce AJ (1970) Report on some commensal shrimps (Crustacea: Palaemonidae) associated with an indo-pacific gorgonian host (Coelenterata: Gorgonacea). J Zool 160: 537-44

Dons C (1944) Norges korallrev. K Norske Vidensk Selsk Forhandl 16: 37-82

Emson RH, Woodley JD (1987) Submersible and laboratory observations on *Asterochema tenue*, a long-armed euryaline brittle star epizoic on gorgonians. Mar Biol 96: 31-45

Emson RH, Mladenov PV, Barrow K (1991) The feeding mechanism of the basket star *Gorgonocephalus arcticus*. Canad J Zool 69: 449-455

Fosså JH, Mortensen PB (1998) Artsmangfoldet på *Lophelia*-korallrev og metoder for overvåkning. Fisken Havet 17, 95 pp

Fujita T, Ohta S (1988) Photographic observations of the life style of a deep sea ophiuroid *Asteronyx loveni* (Echinodermata). Deep-Sea Res 35: 2029-2044

Goh NKC, Ng PKL, Chou LM (1999) Notes on the shallow water gorgonian-associated fauna on coral reefs in Singapore. Bull Mar Sci 65: 259-282

Gordon DC, Kenchington ELR, Gilkinson KD, McKeown DL, Steeves G, Chin-Yee M, Vass WP, Bentham K, Boudreau PR (2000) Canadian imaging and sampling technology for studying marine benthic habitat and biological communities. ICES 2000 Ann Sci Conf 27-30 September 2000, Bruges, Belgium

Grange KR (1991) Mutualism between antipatarian *Antipathes fiordensis* and the ophiuroid *Astrobrachion constrictus* in New Zealand fjords. Hydrobiologia 216/217: 297-304

Grigg RW (1974) Growth rings: annual periodicity in two gorgonian corals. Ecology 55: 876-881

Grygier MJ (1983) An endoparasitic lamippid copepod in *Acanella* from the North Atlantic. Crustaceana 45: 178-182

Henry L-A (2001) Hydroids associated with deep-sea corals in the boreal north-west Atlantic. J Mar Biol Ass UK 81: 163-163

Hickson SJ (1906) The Alcyonaria of the Maldives. Part I. The genera *Xenia*, *Telesto*, *Spongodes*, *Nephthya*, *Paraspongodes*, *Chironephthya*, *Siphonogorgia*, *Solenocaulon*, and *Melitodes*. In: Gardiner JS (ed) The Fauna and Geography of the Maldive and Laccadive Archipelagoes. Cambridge Univ Press, pp 473-502

Humes AG (1993) Copepoda associated with gorgonaceans (Cnidaria) in the Indo-Pacific. Bull Mar Sci 53: 1078-1098

Humes AG, Stock HJ (1973) A revision of the family Lichomolgidae Kossman, 1877, cyclopoid copepods mainly associated with marine invertebrates. Smithsonian Contr Zool 127: 1-368

Hurlbert SH (1971) The nonconcept of species diversity: a critique and alternative parameters. Ecology 52: 577-586

Jensen A, Frederiksen R (1992) The fauna associated with the bank-forming deepwater coral *Lophelia pertusa* (Scleractinia) on the Faroe shelf. Sarsia 77: 53-69

Jonsson LG, Lundälv T, Johannesson K (2001) Symbiotic associations between anthozoans and crustaceans in temperate coastal area. Mar Ecol Progr Ser 209: 189-195

Klitgaard AB (1995) The fauna associated with outer shelf and upper slope sponges (Porifera, Demospongiae) at the Faroe Islands, north-eastern Atlantic. Sarsia 80: 1-22

Madsen JF (1944) Octocorallia (Stolonifera - Telestacea - Xeniidea - Alcyonacea - Gorgonacea). Danish Ingolf-Exped V(13), 65 pp

McCloskey LR (1970) The dynamics of the community associated with a marine scleractinian coral. Int Rev Ges Hydrobiol 55: 13-81

Mortensen T (1927) Handbook of the Echinoderms of the British Isles. Humphrey Milford, Oxford UnivPress, London

Mortensen PB (2001) Aquarium observations on the deep-water coral *Lophelia pertusa* (L., 1758) (Scleractinia) and selected associated invertebrates. Ophelia 54: 83-104

Mortensen PB, Buhl-Mortensen L (2004) Distribution of deep-water gorgonian corals in relation to benthic habitat features in the Northeast Channel (Atlantic Canada). Mar Biol 144: 1223-1228

Mortensen PB, Buhl-Mortensen L, Gordon DC, Fader GBJ, McKeown DL, Fenton DG (in press) Effects of fisheries on deep-water gorgonian corals in the Northeast Channel, Nova Scotia (Canada). Proc Symp Effects Fish Benthic Habitats, Tampa Florida

Patton WK (1972) Studies on the animal symbionts of the gorgonian coral, *Leptogorgia virgulata* (Lamarck). Bull Mar Sci 22: 419-431

Patton WK (1976). Animal associates of living reef corals. In: Jones OJ, Endean R (eds) Biology and Geology of Coral Reefs. 3. Academic Press, New York, pp 1-36

Pettibone MH (1991) Polynoids commensal with gorgonian and stylasterid corals, with a new genus, new combinations, and new species (Polychaeta: Polynoidae: Polynoinae). Proc Biol Soc Washington 104: 688-713

Reed JK, Gore RH, Scotto LE, Wilson KA (1982) Community composition, structure, areal and trophic relationships of decapods associated with shallow- and deep-water *Oculina varicosa* coral reefs: studies on decapod Crustacea from the Indian River region of Florida, XXIV. Bull Mar Sci 32: 761-786

Sars GO (1890-1895) Amphipoda. An account of the Crustacea of Norway with short description and figures of all the species I Abs. Cammermeyer, Christiania, 711 pp

Shannon C E, Weaver W (1949) The mathematical theory of communication. Urbana, Univ Illinois Press, 117 pp

Simberloff D (1978) Use of rarefaction and related methods in ecology. In: Dickson KL, Carins J, Livingstion RJ (eds) Biological data in water pollution assessment: quantitative and statistical analyses. ASTM STP 652, Philadelphia. Amer Soc Testing Mater, pp 150-165

Sneli JA (1985) *Paramuricea placomus* in Trondheimfjord, Norway. Fauna (Oslo) 38: 117-119

Stock JH (1988) Lamippidae (Copepoda: Siphonostomatidae) parasitic in *Alcyonium*. J Mar Biol Ass UK 68: 351-359

Storm V (1901) Oversigt over Throndheimsfjordens fauna (med et kort). Trondhjems Biologiske Station, Meddelelser fra stationsanleggets arbeidskomite. H Moe's Bog and Accidentstrykkeri, Trondhjem, 20 pp

Strømgren T (1970) Emergence of *Paramuricea placomus* (L.) and *Primnoa resedaeformis* (Gunn.) in the inner part of Trondheimsfjorden (Western coast of Norway). K Norske Vidensk Selsk Skrift 4: 1-6

Tendal OS (1992) The North Atlantic distribution of the octocoral *Paragorgia arborea* (L., 1758) (Cnidaria, Anthozoa). Sarsia 77: 213-217

Ter Braak CJF (1987) Ordination. In: Jongman RHG, ter Braak CJF, van Tongeren OFR (eds) Data analysis in community and landscape ecology. Pudoc, Wageningen, pp 91-173

Tsuchiya M, Nakasone Y, Nishihira M (1986) Community structure of coral associated invertebrates of the hermatypic coral, *Pavona frondifera*, in the gulf of Thailand. Galaxea 5: 129-140

Vader W (1969) Notes on a collection of Amphipoda from the Trondheimsfjord area. K Norske Vidensk Selsk Skrift 3: 1-20

Wainwright SA, Dillon JR (1969) On the orientation of sea fans (genus *Gorgonia*). Biol Bull 136: 130-139

Wainwright SA, Koehl MAR (1976) The nature of flow and reaction of benthic Cnidaria to it. In: Mackie GO (ed) Coelenterate ecology and behavior. Plenum Press, New York, pp 5-21

Attached benthic Foraminifera as indicators of past and present distribution of the coral *Primnoa resedaeformis* on the Scotian Margin

Andrea D. Hawkes[1], David B. Scott[2]

[1] Sea Level Research Laboratory, Department of Earth and Environmental Science, University of Pennsylvania, Philadelphia, PA 19104-6313, USA (hawkesa@sas.upenn.edu)

[2] Department of Earth Science, Dalhousie University, Halifax, Nova Scotia, B3H 3J5, Canada

Abstract. Benthic Foraminifera found attached to the deep-sea coral *Primnoa resedaeformis* may be used to establish paleo-coral locations long after the coral has disappeared. Recent coral research cruises have revealed that the coral on the Scotian Margin is in peril and in many cases no longer exists. Sea floor video footage suggests various fishing methods have destroyed much of the coral as it has in coastal areas off Norway and Alaska. To date deep-sea corals are sparse on the Scotian Margin; therefore evidence preserved in the sediment may establish whether corals were present and more abundant in the past. A representative assemblage of benthic foraminiferans found attached to the deep-sea coral *Primnoa resedaeformis* may be the evidence necessary to provide presence/absence indicators long after the coral has disappeared. Both foraminiferal species are known to be only associated with the coral, and distortion of the ventral side (attached) of common foraminiferal species found in the sediment, may provide a clue to past coral habitat. Identifying a deep-sea coral paleo-habitat indicator provides insight into the extent to which it existed. Video footage from coral cruises over the last three years indicates that coral and fish go hand in hand, an important observation for a region where fishing comprises 23 % of the local economy.

Twenty-eight foraminiferal species were found in a range of abundances on nine deep-sea coral specimens of *Primnoa resedaeformis*. Attached foraminiferans are found on the basal sections of the coral where they colonize onto the hard calcite substrate. One of the more common and consistent foraminiferal species found attached to the coral, *Discanomalina semipunctata,* is not found commonly on the continental margin in non-coral areas and may provide *in situ* evidence of past coral habitat.

Keywords. Foraminifera, deep-sea coral, coral habitat, indicator species, attached species, epifauna

Introduction

Deep-sea coral on the Scotian Margin is vulnerable and will continue to be as long as hasty and destructive fishing methods are practiced. The quantity of coral that may once have blanketed the margin floor no longer exists. Conservation efforts to protect deep-sea coral patches are constrained by present distribution patterns. Foraminiferal species uniquely coral related may provide present day indicators of past coral habitat. This enables us to identify how much coral has been lost and re-evaluate our conservation tactics. A 424 km² area of Georges Bank was closed to bottom-impact gear, including an area closure to specifically protect deep-sea corals. This is a very small area of a margin that had and has unknown quantities of coral and thereby may not be adequate for habitat sustainability.

Nine deep-sea coral specimens of the species *Primnoa resedaeformis* and seventeen sediment suction samples were collected from the Northeast Channel from water depths between 300-500 m (Fig. 1). The Northeast Channel separates Browns from Georges Bank and acts as the primary conduit by which warm north flowing Atlantic Temperate Slope Water (ATSW) and cold south flowing Labrador Subarctic Slope Water (LSSW) enter the Gulf of Maine and subsequently the Bay of Fundy, creating a complex hydrodynamic setting (Shore et al. 2000; Pershing 2001).
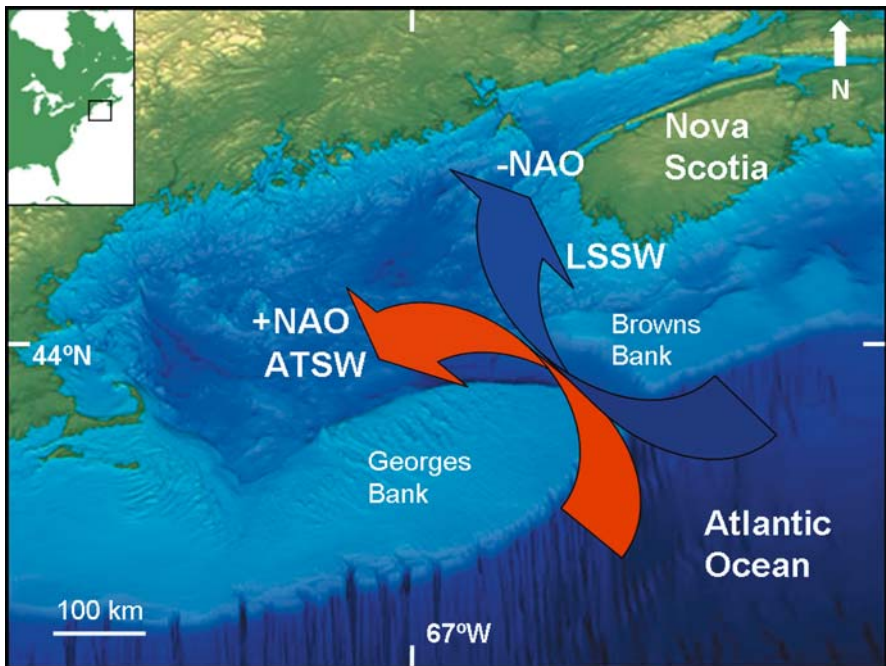
Fig. 1 Mouth of the Northeast Channel where warm (red) ATSW and cold (black) LSSW enter the Gulf of Maine. A 220 m sill rises 30 km from the channel mouth (Shore et al. 2000). Well-sorted sand, lag gravel and boulders characterize the channel floor near its opening onto the continental slope (Petrie et al. 1996)

The North Atlantic Oscillation (NAO), a large scale unbalance in atmospheric mass between the subtropical Atlantic high and Iceland low that creates a 'Coupled Slope Water System' throughout this area between a cold state following a negative NAO and a warm state following a positive NAO. The shift between these two states occurs as the front that separates the ATSW and LSSW shifts northeast toward the Tail of the Grand Bank during the warm state or southwest toward the Mid-Atlantic Bight during the cold state (Pershing 2001; Drinkwater et al. in press).

Deep-sea coral

The strong current, bouldered substrate and downward flux of particulate matter from the surface provide an ideal location for deep-sea coral development. The present study focuses on a type of gorgonian coral common to the Scotian Margin, *Primnoa resedaeformis* (Gunnerus, 1763). This species consists of polyps that are crowded onto arborescent or fan-shaped branches of a heavily calcified tree-like skeleton (Breeze et al. 1997). At depths of 300-500 m, below the euphotic zone, azooxanthellate coral do not form a symbiotic relationship with photosynthetic algae like those of tropical shallow water. Instead, polyps feed by filtering particles out of the passing current (Breeze et al. 1997).

Primnoa resedaeformis on the Scotian Margin are more commonly found in patches at the Northeast Channel, The Gully, and The Stone Fence (see Mortensen and Buhl-Mortensen 2004). The corals range in height from one to two metres and a metre or so wide to smaller than ten centimetres and are often co-habiting the same substrate with *Paragorgia arborea* (personal observation 2002). *Primnoa resedaeformis* grow much slower than *Paragorgia arborea,* at about 2-3 mm/year but are more robust than the readily injured soft tissue of *Paragorgia arborea* (Sherwood et al. 2005).

Foraminifera

Benthic foraminiferans are single celled organisms that inhabit almost every marine environment. They are found living from a few centimetres below (infaunal) and up to the sediment-water interface. There are also attached forms of many benthic foraminiferal species that have been found living on seagrass, scallop shells, hydroids, sponge spicules and boulders up to metres above the sea floor. Such upward (epithrophic) movement of benthic species is associated with opportunistic feeding practices (e.g., Haward and Haynes 1976; Lutze and Thiel 1989; Semeniuk 2000; Schönfeld 2002).

Benthic foraminiferans also have pelagic counterparts (planktonic foramini-ferans) which dominate the oceans surface to intermediate water column. Both benthic and planktonic types of Foraminifera are used to study water mass characteristics. Initially, water depth was once believed to be the primary factor controlling the distribution of Foraminifera. Several studies (e.g., Streeter 1973; Lohman 1978), and including that of Williamson (1983) on the Scotian Margin found that benthic foraminiferal assemblage distributions are dominantly controlled

by water mass parameters. In more recent studies, however, it has been found that other environmental factors such as substrate, food availability, and bottom-water oxygen concentrations may play a more important role (Mackensen et al. 1985; Linke and Lutze 1993; Gooday 1994; Schönfeld 1997; Schönfeld 2002).

A study of the fauna associated with the bank-forming deep-water scleractinian coral, *Lophelia pertusa,* on the Faroe shelf found the foraminifer *Hyrrokkin sarcophaga* (Jensen and Frederiksen 1992). A study of a modern deep-water coral reef mound from the mid-Norwegian continental shelf, north of the Sula Ridge, analyzed the substrate pitting and boring patterns of the *Hyrrokkin sarcophaga* (Cedhagen, 1994), and found that this parasitic foraminifer was the only epibiont capable of attaching itself to the soft tissue protecting the coral skeleton (Freiwald and Schönfeld 1996).

The present study examines the foraminiferal assemblage found attached to the deep-sea coral *Primnoa resedaeformis*. The presence of coral on the Scotian Margin has only been identified in the last decade and therefore questions have been raised as to what extent corals may have existed here in the past. What information exists suggests that coral coverage is sparse. Observations from the 2001 ROPOS cruise suggest that often coral skeletons are not present where they once grew; either being dragged off by bottom fishing gear, broken, eroded and displaced by currents, or buried (personal observation by D.B. Scott 2001). In some locations all that remains are sand and gravel sized *Lophelia* remnants, in areas where *Primnoa* likely did co-exist (personal observation, Hudson coral cruise 2002). To know how much coral may have been present we must identify an indicator that is preserved in the sediment record long after the coral skeletons have disappeared.

Foraminifera are not the only meiofauna present on the coral but they do have certain characteristics that make them a suitable indicator. While other species may biodegrade foraminiferans remain on the coral or are well preserved in the sediment record. The purpose of this study is to evaluate whether there are any foraminiferal species present on the coral that are not readily found living in non-coral areas. In other words, a species that may be identified in the sediment long after the coral has disappeared and provide an idea of paleo-coral habitat.

Methods

Nine deep-sea coral *Primnoa resedaeformis* specimens were used in the present study. Six specimens were retrieved from the ROPOS cruise in the summer of 2001 (~Lat 42° 00 N, Long 65° 36 W, between 410-474 m). The other three specimens were donated by a Cape Sable fisherman in 2000, who caught them in fishing gear. The donated coral lack exact position and water depth but all nine specimens were retrieved from the Northeast Channel in approximately 300-500 m water depth (Fig. 2). The height of the sampled coral specimens varied from 20-45 cm. Seventeen sediment suction samples from the 2001 ROPOS cruise where taken from in and around areas where coral was present and also in location away from coral, these ranged in volume from 5-10 cc. These samples were stained with rose
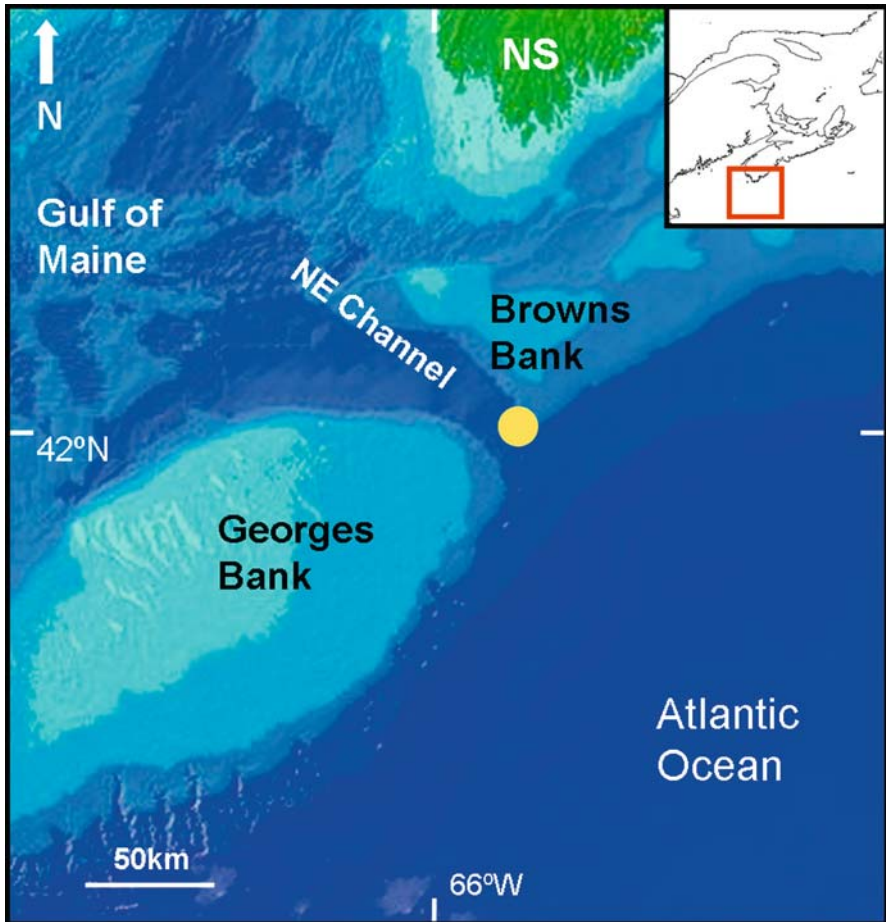
Fig. 2 Yellow dot indicates location of *Primnoa resedaeformis* specimens collected for this study between 300-500 m water near the channel mouth

Bengal and preserved in alcohol then sieved through 500 μm and 63 μm sieves and counted for foraminiferal live and dead abundances. Each *Primnoa* specimen was initially examined under a binocular microscope to see general abundance then washed off in a sink and the residual water sieved through a 45 μm sieve to retain foraminiferans that detached during this process. The foraminiferans were picked off of each coral specimen under a binocular microscope. Species were picked off from the base up and placed on slides to be counted and identified. The approximate size of each species was also considered to determine whether certain species attachment was a process of a life cycle stage. The coral specimens were received dried and therefore staining the protoplasm with rose Bengal was no longer an option. Instead close attention was paid to the mode of attachment and individual deformities of each foraminifer picked. Approximately 90 % of the species were attached aperture

down and had deformities consistent with *in situ* growth; we assumed that these species were at one time living on the coral. Benthic foraminiferal species have been identified to the genus and species level using several papers published on the Scotian Margin foraminifera, including Medioli and Scott (1978), Williamson (1983), Scott et al. (1984, 1989), and for general reference, Jones (1994). Scanning Light Micrographs (SLM) plates of foraminiferal species were provided by the Centre for Environmental and Marine Geology's micropaleontology laboratory at Dalhousie University.

A count of 300 individual foraminiferans in sediment samples is standard (Murray 1973); some allow a minimum of 100 individuals (Murray 1991). Counts from each coral specimen were between 300-2300 except one specimen with only 44 individuals. Here it must be noted that the inclusion of this specimen does not alter the present data. Species percentages and assemblages were determined from raw results and plotted to identify foraminifer-coral assemblage association (Fig. 3). Coral specimen size did not influence the results because percentages were used and not raw counts. The 17 sediment sample counts were entered into a spreadsheet in excel and percentages of each species per sample were calculated.

Results

A total of 29 foraminiferal species have been identified in association with the *Primnoa resedaeformis* specimens (Table 1, Fig. 4). From the abundance results, background species were eliminated from further scrutiny. Background species
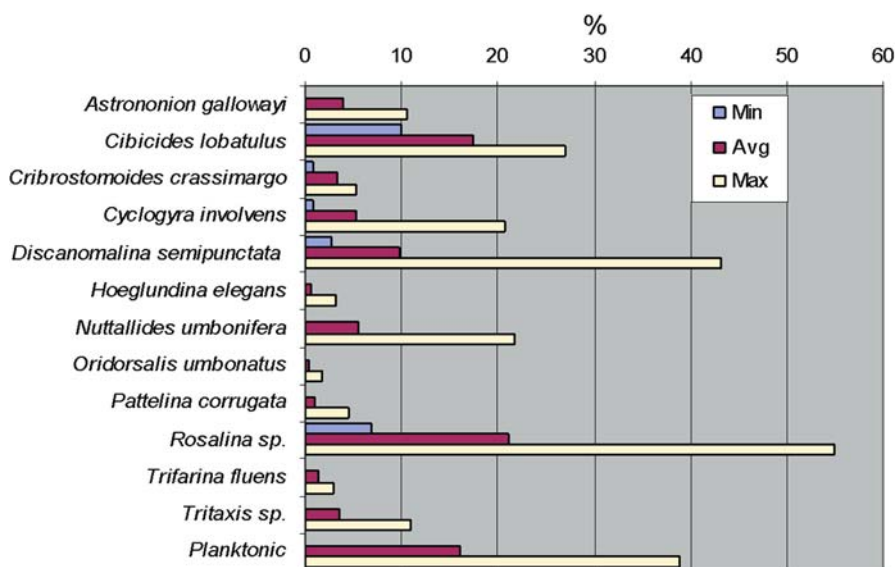
Fig. 3 Bar graph displaying 13 more common foraminiferal species found on *Primnoa resedaeformis*. Top blue bar defines the minimum, red the average, and yellow the maximum abundance

Table 1 Alphabetical taxonomic list of Foraminifera found in association with the *Primnoa resedaeformis* specimens

Astrononion gallowayi (Loeblich and Tappan, 1953)
Brizalina subaenariensis (Brady, 1884)
Buccella frigida (Cushman, 1921)
Bulimina marginata (Brady, 1884)
Cassidulina laevigata (d'Orbigny, 1826)
Cassidulina reniforme (Brady, 1881)
Cibicides lobatulus (Walker and Jacob, 1798)
Cribrostomoides crassimargo (Cushman, 1910)
Cyclogyra involvens (Reuss, 1850)
Discanomalina semipunctata (Bailey, 1851)
Elphidium excavatum (Terquem, 1876)
Fursenkoina fusiformis (Williamson, 1858)
Hoeglundina elegans (d'Orbigny, 1826)
Islandiella teretis (Tappan, 1951)
Lagena sp. (Brady, 1884)
Nuttallides umbonifera (Cushman, 1933)
Oolina apiculata (Colom, 1956)
Oridorsalis umbonatus (Reuss, 1851)
Paromalina coronata (Loeblich and Tappan, 1957)
Pattelina corrugata (Williamson, 1858)
Pullenia bulloides (d'Orbigny, 1846)
Pullenia subcarinata (d'Orbigny, 1846)
Pyrgo williamsoni (Silvestri, 1923)
Quinqueloculina seminulum (Linné, 1758)
Reophax nana (Bradry, 1884)
Rosalina sp. (d'Orbigny, 1846)
Textularia sp. (Brady, 1884)
Trifarina fluens (Cushman, 1923)
Tritaxis sp. (Brady, 1884)
Planktonic sp.

were defined as those species whose abundance was less than 1 % on two of the nine coral specimens. A total of 16 species were eliminated at this stage: *Brizalina subaenariensis, Buccella frigida, Bulimina marginata, Cassidulina laevigata, Cassidulina reniforme, Elphidium excavatum, Fursenkoina fusiformis, Islandiella teretis, Lagena* sp., *Oolina* sp., *Pullenia bulloides, Pullenia subcarinata, Pyrgo williamsoni, Quinqueloculina seminulum, Reophax nana*, and *Textularia* sp.

A basic bar graph was plotted to depict the minimum, average, and maximum percentage of the 13 remaining candidates (Fig. 3). The bar graph shows that 5 of the species occur on all 9 coral specimens; they are *Cibicides lobatulus, Cribrostomoides crassimargo, Cyclogyra involvens, Discanomalina semipunctata,* and *Rosalina* sp. (Fig. 4).

There are some implications that outliers are playing a role in skewing some of the averages. This is evident where a zero or extremely high percentage value occurs once in a species throughout the nine coral. The number of coral specimens in this case is too low to exclude any information. However, caution will be used when discussing validity of the results presented here.
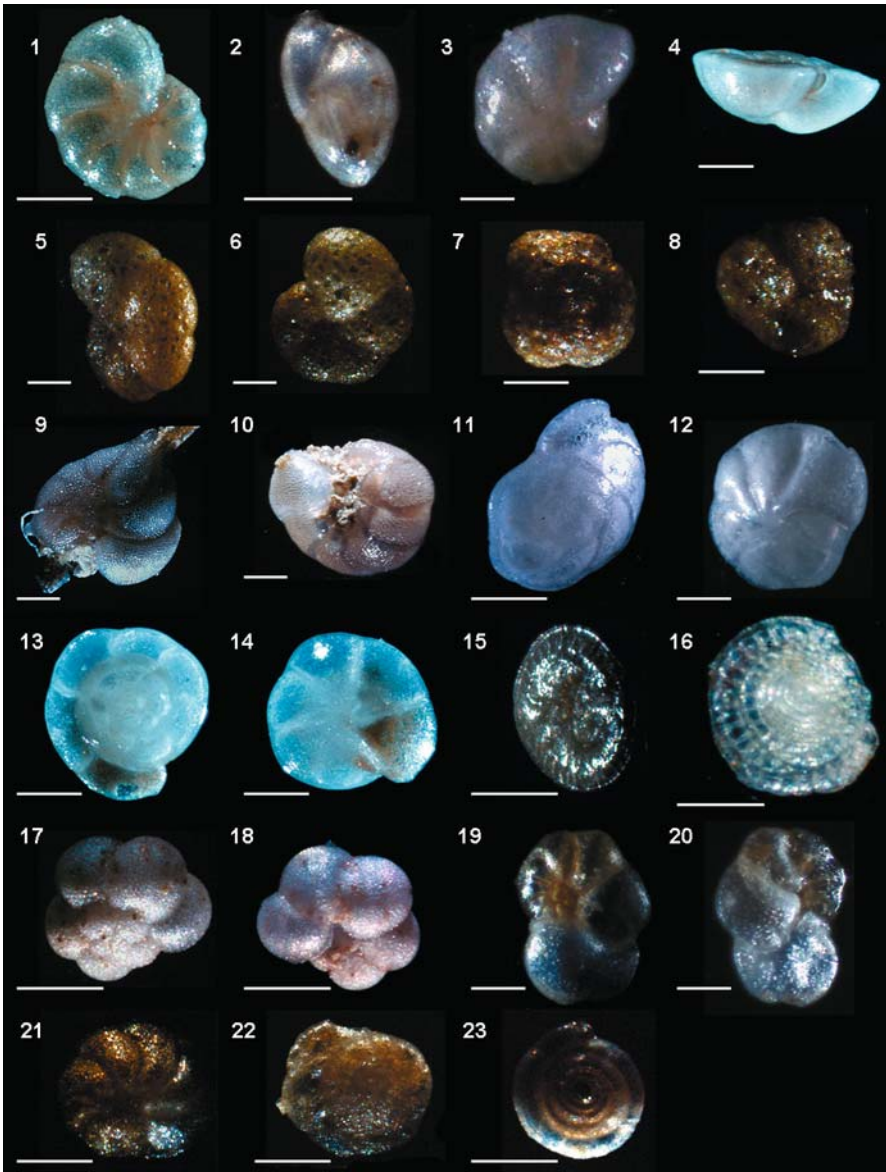
Fig. 4 All white lines are equal to 50 μm, scale reflects average size of specimens in this study. **1** *Astroninion gallowayi*, dorsal or ventral view. **2** *Trifarina fluens*, lateral view. **3** *Cibicides lobatulus* dorsal view. **4** *C. lobatulus*, lateral view. **5** *Cribrostomoides crassimargo*, lateral view. **6** *C. crassimargo*, dorsal or ventral view. **7** *Tritaxis* sp., dorsal view. **8** *Tritaxis* sp., ventral view. **9** *Discanomalina semipunctata*, dorsal view. **10** *D. semipunctata*, clamped ventral view. **11** *Hoeglundina elegans*, dorsal view. **12** *H. elegans*, ventral view. **13** *Oridorsalis umbonatus*, dorsal view. **14** *O. umbonatus*, ventral view. **15** *Pattelina corrugata*, ventral view. **16** *P. corrugata*, dorsal view. **17** Planktonic sp., dorsal view. **18** Planktonic sp., ventral view.

The counting procedure also suggested some interesting patterns concerning the size of the species. Certain species of foraminiferans dominated specific size fractions; *D. semipunctata* the dominant species in the size fraction larger than 125 μm, *Rosalina* and *Cibicides lobatulus* were most abundant in the middle size fraction (63-125 μm), and *Nuttallides umbonifera* and the planktonic species tended to dominate the smaller size fraction (between 45-100 μm). Counting foraminiferans from the base of the coral upward did not reveal any evidence for trends in species or size zonation and therefore colonization seems random. Foraminifera were present on all exposed hard calcite surfaces devoid of polyps. This was not restricted to the upper or lower part of the coral but was often patchy and sporadically distributed, although basal sections were almost always polyp barren.

Of the seventeen sediment samples, eight were proximal to coral and nine were taken away from coral areas. Of the eight samples proximal to the coral, *D. semipunctata* made up on average 20 % of each sample total abundance. Of the nine distal samples, only two samples had *D. semipunctata* in its assemblage. Planktonics generally made up over half the abundance of each of the seventeen samples and *Nuttalides umbonifera* was not found. The following species were present in almost all the samples in relatively high abundances: *Cibicides lobatulus, Trifarina fluens, Elphidium* exc. *clavatum, Cassidulina reniforme, Islandiella teretis, Cibicides pseudogerianus,* and *Rosalina* sp.

Discussion

We classify the foraminiferal assemblage associated with *Primnoa resedaeformis* on the Scotian Margin as those species with average an abundance exceeding 5 %. This includes: *Cibicides lobatulus, Cyclogyra involvens, Discanomalina semipunctata, Nuttallides umbonifera, Rosalina* sp., and Planktonic sp. Although present on the coral, these foraminiferal species are not necessarily confined to its habitat.

Williamson et al. (1984) associated foraminiferal assemblages with five Scotian Margin water masses, where each assemblage includes one or more indicator species. For example *Cibicides lobatulus* is the dominant species inside the 100 m bathymetric line between Halifax and Cape Sable where Cabot Strait and St. Lawrence water masses mix. Attached and unattached specimens of *Cibicides, Rosalina and Cyclogyra* are abundant on this and many other margins (e.g., Williamson 1983; Murray 1991) they are therefore inadequate indicators of *Primnoa* habitat.

Drapeau (1971) found that the foraminifer *D. semipunctata* proved to be responsible for the high concentrations of calcium carbonate on the southwestern Scotian shelf. He, and later Medioli and Scott (1978), identified several elongate bulls-eye patterns where *D. semipunctata* proliferates in lag-like sediment deposits (Fig. 5). Drapeau noted that the ecological factors responsible for the proliferation

---

19 *Rosalina* sp., dorsal view. **20** *Rosalina* sp., ventral view. **21** *Nuttallides umbonifera*, dorsal view. **22** *N. umbonifera*, ventral view. **23** *Cyclogyra involvens*, dorsal or ventral view
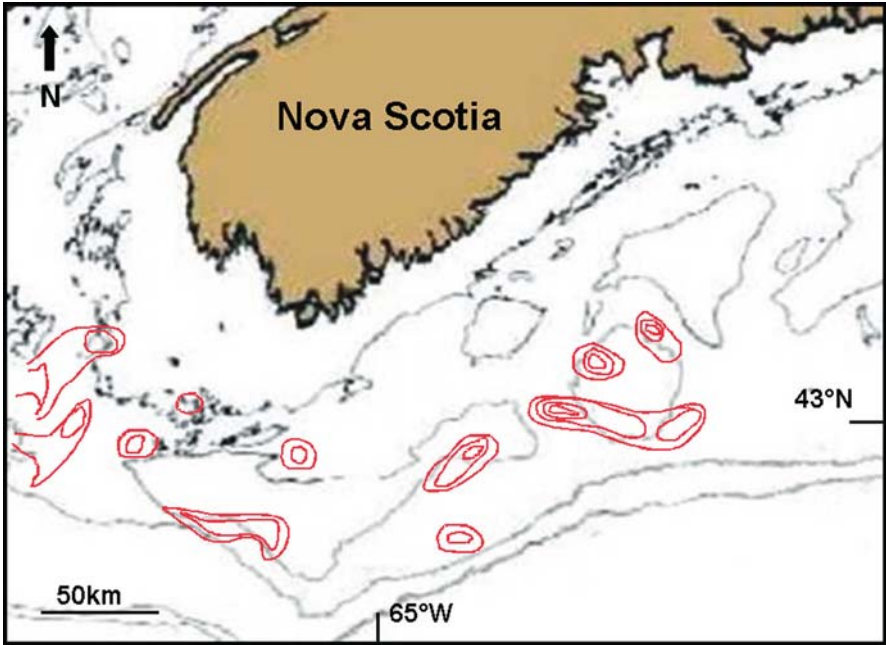
Fig. 5 Southwestern Scotian Shelf with bulls-eye like patterns indicating 20 % by weight concentrations of *D. semipunctata* (modified from Medioli and Scott 1978)

of *D. semipunctata* in these areas are unknown. Although, samples from Drapeau's study were before the time of identifying live *versus* dead abundances, many of the *D. semipunctata* specimens in his samples display deformities related to attached *in situ* growth characteristic of the same species attached to the coral specimens. Although, we cannot exclude that these deformities may be caused by attachment to other substratum.

   Discanomalina semipunctata has a long and complicated taxonomic history, and has often been split into numerous species and subspecies. Spines, engulfed septa, stunted ventral sides, and other deformities may have lead to its over-classification (Medioli and Scott 1978). Deformities of species found in sediment may be due to the previous attachment of *Discanomalina* to hard substrates and may now be resolvable as they are commonly found on deep-sea coral. *Discanomalina* has been previously classified as an epifaunal species (e.g., Mackensen et al. 1985; Schönfeld 1997, 2002). A paper by Klitgaard (1995) studied the associated fauna on sponges from the outer shelf and upper slope of the Faroe Islands. She found 12 associated foraminiferans, including *Paramolina coronata* (Parker and Jones, 1857), a synonym of *Discanomalina semipunctata* (Bailey, 1851) on the sclerites (calcite spicules), of the sponge *Isops phlegraei*. Although present, they were not counted (Klitgaard 1995). This is also later noted by Schönfeld on sponge spicules (1997) and free standing hydroid stocks (2002) on the southern Portuguese continental margin.

   Our results indicate that *D. semipunctata* may have a tendency to preferentially

colonize coral substrate over other available substratum. This affinity may be coincident with substrate elevation, substrate type or a number of other parameters such as; food availability, current speed, species competition, the list goes on. We do know from previous work (e.g., Klitgaard 1995; Schönfeld 1997, 2002) that *D. semipunctata* is often found exclusively on sponge spicules and may be an effect of deep-sea coral being absent. Withstanding all the above parameters the similarity between *D. semipunctata* two preferred substrates (coral and sclerites) is calcite and therefore may be a function of what substrate is of benefit in terms of calcite availability or ease of attachment. We suggest that past *P. resedaeformis* habitat sites may be the ecological factor responsible for such a proliferation of *D. semipunctata* at specific locations (Fig. 5). This raises the question of the origin of *D. semipunctata* on coral, as it is rarely found elsewhere on the Scotian Margin except those areas on Figure 4. The sizes of *Discanomalina* species in the lag-like deposits also coincide with the dominant size fraction of the same species on the coral. Evidence indicating that deep-sea coral was much more abundant and widespread in the past may help to substantiate the severity of the present situation and promote the implementation of fast and efficient conservation practices.

The occurrence of *Nuttallides umbonifera,* a species generally found below 3000 m in Antarctic Bottom Water (Streeter and Lavery 1982; Thomas et al. 1990), is a notable conundrum. It is not solely a question of how can it survive out of its normally cold and very saline bottom water, but that it would have had to migrate from 3000 m to ~500 m into the mouth of the Northeast Channel. This species is commonly found as a background species on this margin and other margins below ~2000 m depth (Murray 1991). Only found on 55 % of the coral specimens its presence may indicate past coral habitat; however, it is an inconclusive indicator in its absence.

Planktonic foraminiferans make up on average 16 % of the total abundance of Foraminifera found on *P. resedaeformis* specimens. This does not solely involve the adaptation of a species of foraminiferans to different environmental parameters like that of *Nutallides umbonifera* discussed above, but the alteration of pelagic species, distributed throughout the water column, to a sessile form attached to deep-sea coral. Although, the staining of protoplasm could not be conducted to determine live/dead assemblages we did find that most species were attached aperture down and had *in situ* growth associated deformities such as; stunted septa, pinching tests at the attachment site, and concave septa due to growth against coral. We assumed that those planktonic species who displayed the deformities above were likely alive on the coral at some time. Further discussion of this topic will be presented in a future paper. However, planktonic species for the purpose of this study do not make adequate indicators as they are commonly found in the margin sediment (Scott et al. 1984, 1989).

A *Primnoa resedaeformis* foraminiferal indicator preserved in the sediment could be used to identify present and ancient *Primnoa* habitat. Only a small area of the margin is covered on each cruise leaving many areas unexplored. Hundreds of thousands of sediment grabs and core samples have been taken over the last century,

all potentially containing information on past and present coral distribution. Due to expense, still cameras and grab samples are often used in lieu of remotely operated equipment or mini-subs. In this light the foraminiferal record contained in sediment samples may prove useful in investigating the present and past distribution of Scotian Margin corals.

Conclusions

Initially 29 foraminiferal species were found attached to the deep-sea coral *Primnoa resedaeformis*. Potential indicator species, defined as those whose averages were above 5 %, reduced the number of possible indicator species to six (Fig. 3). We eliminated four of the species due to their frequent occurrence on this and other margins. These were: *Cibicides, Cyclogyra, Rosalina,* and planktonics (Table 2).

Table 2 In the abundance column c = common and u = uncommon. Highlighted row indicates the species that is common to the coral but not to the margin itself and is consistently present over 5 % abundance on the coral specimens

Attached foraminifera	Abundance margin/coral	Consistency
Cibicides	c/c	yes
Cyclogyra	c/c	yes
Discanomalina	u/c	yes
Nuttallides	u/c	no
Rosalina	c/c	yes
Planktonic	c/c	yes

Nuttallides umbonifera, when present in the margin sediment may reflect past *P. resedaeformis* habitat; however, in its absence it provides inconclusive evidence neither supporting nor denying the former existence *P. resedaeformis. Nuttallides umbonifera* lacks consistency and only occurred on 55 % of the coral specimens analyzed.

Discanomalina semipunctata is consistently abundant on the coral but uncommon on the margin itself making it an ideal indicator of past *P. resedaeformis* habitat. The proliferation of *D. semipunctata* in bulls-eye like lag deposits on the southwestern margin may provide evidence of past coral mounds or ridges. Therefore, this may indicate the existence of a more widely distributed coral habitat, evidence necessary for more stringent conservation methods to be applied to the present deep-sea coral.

We encourage scientists to salvage sediment or retrieve sediment samples when coral specimen sampling does not work or alternate sampling methods are not available. The Foraminifera within these samples may still provide useful coral related evidence.

Further work and many more specimens are required to achieve a good statistical understanding of those foraminiferal species found on the coral and their role as

potential indicators. Due to the low number of coral specimens we were able to obtain these are preliminary results but they do show promise even though their statistical validity is lacking.

References

Breeze H, Derek S, Butler M, Kostylev V (1997) Distribution and status of deep-sea corals off Nova Scotia. Marine Issues Comm Spec Publ 1. Ecology Action Centre, Halifax

Drapeau G (1971) Sedimentology of the surficial sediments of the western portion of the Scotian shelf. PhD thesis, Dalhousie Univ

Drinkwater KF, Mountain DB, Herman A (in press) Variability in the slope water properties off eastern North America and their effects on the adjacent seas. J Geophys Res

Freiwald A, Schönfeld, J (1996) Substrate pitting and boring patterns of *Hyrrokkin sarcophaga* Cedhagen, 1994 (Foraminifera) in a modern deep-water coral reef mound. Mar Micropaleont 28: 199-207

Gooday AJ (1994) The biology of deep-sea Foraminifera: a review of some advances and their applications in paleoceanography. Palaios 9: 14-31

Haward NJB, Haynes JR (1976) *Chlamys opercularis* (Linnaeus) as a mobile substrate for Foraminifera. J Foram Res 6: 30-38

Jensen A, Frederiksen R (1992) The fauna associated with the bank-forming deepwater coral *Lophelia pertusa* (Scleractinia) on the Faroe shelf. Sarsia 77: 53-69

Jones RW (1994) The Challenger Foraminifera. Oxford Univ Press, Oxford, 149 pp

Klitgaard A (1995) The fauna associated with outer shelf and upper slope sponges (Porifera, Demospongiae) at the Faroe Islands, northeastern Atlantic. Sarsia 80: 1-22

Linke P, Lutze GF (1993) Microhabitat preferences of benthic Foraminifera: a static concept or a dynamic adaptation to optimize food acquisition? Mar Micropaleont 20: 215-234

Lohman GP (1978) Abyssal benthonic Foraminifera as hydrographic indicators in the western South Atlantic Ocean. J Foram Res 8: 6-34

Lutze CF, Thiel H (1989) Epibenthic Foraminifera from elevated microhabitats: *Cibicides wuellerstorfi* and *Planulina ariminensis*. J Foram Res 19: 153-158

Mackensen A, Sejrup HP, Jansen E (1985) The distribution of living benthic Foraminifera on the continental slope and rise off southwest Norway. Mar Micropaleont 9: 275-306

Medioli FS, Scott DB (1978) Emendation of the genus *Discanomalina* Asano and its implications on the taxonomy of some of the attached foraminiferal forms. Micropaleont 24: 291-302

Mortensen PB, Buhl-Mortensen L (2004) Distribution of deep-water gorgonian corals in relation to benthic habitat features in the Northeast Channel (Atlantic Canada). Mar Biol 144: 1223-1238

Murray JW (1973) Distribution and Ecology of living benthic Foraminiferids. Heinemann, London

Murray JW (1991) Ecology and palaeoecology of benthic Foraminifera. Longman, London

Pershing AJ (2001) Response of large marine ecosystems to climate variability: patterns, processes, concepts, and methods. PhD thesis, Cornell Univ

Petrie B, Drinkwater K, Gregory D, Pettipas R and Sandstrom A (1996) Temperature and salinity atlas for the Scotian Shelf and Gulf of Maine. Canad Tech Rep Fish Aquat Sci 171, 398 pp

Schönfeld J (1997) The impact of the Mediterranean Outflow Water (MOW) on benthic foraminiferal assemblages and surface sediments at the southern Portuguese continental margin. Mar Micropaleont 29: 211-236

Schönfeld J (2002) A new benthic foraminiferal proxy for near-bottom current velocities in the Gulf of Cadiz, northeastern Atlantic Ocean. Deep-Sea Res I 49: 1853-1875

Scott DB, Mudie PJ, Vilks G, Younger DC (1984) Latest Pleistocene-Holocene paleoceanography trends on the continental margin of eastern Canada: foraminiferal, dinoflagellate and pollen evidence. Mar Micropaleont 9: 181-218

Scott DB, Baki V, Younger CD (1989) Late Pleistocene-Holocene paleoceanographic changes on the eastern Canadian margin: stable isotopic evidence. Paleogeogr Paleoclimatol Paleoecol 74: 279-295

Semeniuk TA (2000) Spatial variability in epiphytic Foraminifera from micro- to regional scale. J Foram Res 30: 99-109

Sherwood OA, Heikoop JM, Sinclair DJ, Scott DB, Risk MJ, Shearer C, Azetsu-Scott K (2005) Skeletal Mg/Ca in *Primnoa resedaeformis:* relationship to temperature. In: Freiwald A, Roberts JM (eds) Cold-water Corals and Ecosystems. Springer, Berlin Heidelberg, pp 1061-1079

Shore JA, Hannah CG, Loder JW (2000) Drift pathways on the western Scotian Shelf and its environs. Canad J Fish Aquat Sci 57: 2488-2505

Streeter SS (1973) Bottom water and benthonic Foraminifera in the North Atlantic Glacial-Interglacial contrast. Quatern Res 3: 131-141

Streeter SS, Lavery SA (1982) Holocene and latest glacial benthic Foraminifera from the slope and rise off eastern North America. Geol Soc Amer Bull 93: 190-199

Thomas FC, Medioli FS, Scott DB (1990) Holocene and latest Wisconsinan benthic foraminiferal assemblages and paleocirculation history, lower Scotian Slope and Rise. J Foram Res 20: 212-245

Williamson MA (1983) Benthic foraminiferal assemblages on the continental margin off Nova Scotia: a multivariate analysis. PhD thesis, Dalhousie Univ

Williamson MA, Keen CE, Mudie PJ (1984) Foraminiferal distribution on the continental margin off Nova Scotia. Mar Micropaleont 9: 219-239

Preliminary study of bioerosion in the deep-water coral *Lophelia*, Pleistocene, Rhodes, Greece

Richard G. Bromley

Geological Institute, University of Copenhagen, Øster Voldgade 10, DK-1350
 Copenhagen K, Denmark
 (rullard@geo.geol.ku.dk)

Abstract. Samples of *Lophelia* were taken at two localities in the Lindos Bay Clay (Lower Pleistocene) of the Rhodes Formation on the Dodecanese Island of Rhodes. At a coastal exposure at Vasphi, northeast Rhodes, about 200 fragments of *Lophelia* were collected *in situ* from the clay and surface preservation of these is consequently particularly fine. The second collection of material was made at an exposure south of Lardos, about 35 km further south. This material comprised some 800 fragments of *Lophelia* collected both *in situ* and loose; preservation quality of the surfaces of these is variable. Both collections derive from single flat beds of coral fragments.

Bioerosion of the corals shows a good diversity, comprising about 18 ichnotaxa, five in open nomenclature, including: *Orthogonum lineare*, *Saccomorpha clava* and other microborings (probably exclusively of endolithic fungi), *Oichnus* isp. (pits and holes of various forms, probably all deriving from foraminifers), dish-shaped etchings possibly produced by the foraminifer *Hyrrokkin sarcophaga*, *Palaeosabella prisca* (polychaete worm borings), *Caulostrepsis* isp. (polychaete borings), probable *Maeandropolydora* isp. (polychaete borings), *Talpina* isp. (phoronid borings), *Podichnus centrifugalis* (attachment scars of brachiopods), *Centrichnus eccentricus* (attachment scars of anomiid bivalves), *Gnathichnus pentax* (tooth scratches by regular echinoids), and *Entobia* ispp. (borings of endolithic sponges).

Three small, radiating forms around a millimetre in size are difficult to attribute to particular tracemaking organisms. They are retained in open nomenclature as *Semidendrina*-form (possibly foraminifera borings), a non-camerate radiating form and a hirsute camerate form. No ctenostome bryozoan borings were observed. *Talpina* isp. is abundant at Vasphi but scarce at Lardos. Otherwise the relative abundance of the trace fossils is comparable at the two localities.

The total amount of bioerosion varies considerably in different parts of the coral skeleton. On the basis of SEM imagery, three categories of bioerosional intensity are introduced: 1, slight bioerosion; 2, medium bioerosion, and 3, heavy bioerosion. The distribution of *Gnathichnus pentax* and the absence of *Radulichnus inopinatus* indicates an aphotic environment. The microbioerosional assemblage correlates

with the *Saccomorpha clava / Orthogonum lineare* Ichnocoenosis, which also indicates an aphotic seafloor.

Introduction

The study of marine bioerosion in lithic substrates has received much attention in recent decades (e.g., Ekdale et al. 1984; Bromley 1994, 2004; Taylor and Wilson 2003). The bulk of this work has concentrated on shallow- and warm-water settings (e.g., Bromley 1978; Günther 1990; Vogel 1993; Perry and Bertling 2000; Macdonald and Perry 2003) and relatively little is known of deeper- and colder-water bioerosion. Nevertheless, bioerosion of high-latitude algal reefs shows a high diversity of elements including borings of endolithic sponges, algae, fungi, gnawing traces by regular echinoids and radulation by chitons and limpets (Bromley and Hanken 1981; Freiwald and Henrich 1994). In addition, Freiwald (1998a) demonstrated a bacterial bioerosion of the test of foraminifers and other carbonate substrates in high-latitude algal reefs.

Bioerosion in deeper, non-tropical water has a considerably different aspect from that of shallow, euphotic environments (e.g., Schmidt and Freiwald 1993; Glaub et al. 2002). Bioeroders of bathyal *Lophelia* mound frameworks have been reported to include the fungus *Dodgella*, the foraminifer *Hyrrokkin sarcophaga* (Cedhagen 1994; Freiwald and Schönfeld 1996), the sponges *Alectona millari* and *Aka labyrinthica* (Freiwald and Schönfeld 1996; Freiwald and Wilson 1998) and the sabellid worm *Perkinsiana socialis* (Freiwald et al. 1997; Freiwald 1998b). Most recently, close study of bioerosion in *Lophelia* skeleton has been done by Beuck and Freiwald (2005) and Wisshak et al. (2005, see further references therein).

In order to compliment that work, it was decided to examine the bioerosion of the Pleistocene deep-water *Lophelia pertusa* using similar techniques, i.e., scanning electron microscopy of epoxy casts. The preliminary results of this study are presented in this paper.

Material and setting

On the Greek island of Rhodes in the southern Aegean Sea, the Plio-Pleistocene sediments of the Rhodes Formation document an extensive transgressive-regressive cycle (Hanken et al. 1996; Hansen 2001). In association with the transgression, bathyal coral assemblages are developed in the Lower Pleistocene Lindos Bay Clay and Saint Paul's Bay Limestone (Hanken et al. 1996; Titschack and Freiwald 2005). These coral assemblages are dominated by *Lophelia pertusa*, with small amounts of *Madrepora oculata* and, more rarely, other corals.

For this study, corals were collected from two localities, both in the Lindos Bay Clay facies. At the coast at the village of Vasphi (Fig. 1C) on the NE coast of the island north of Phaliraki, three horizons of *Lophelia* were recorded (in 1975) in the clay, and some 200 coral fragments were collected from the lowest and middle of
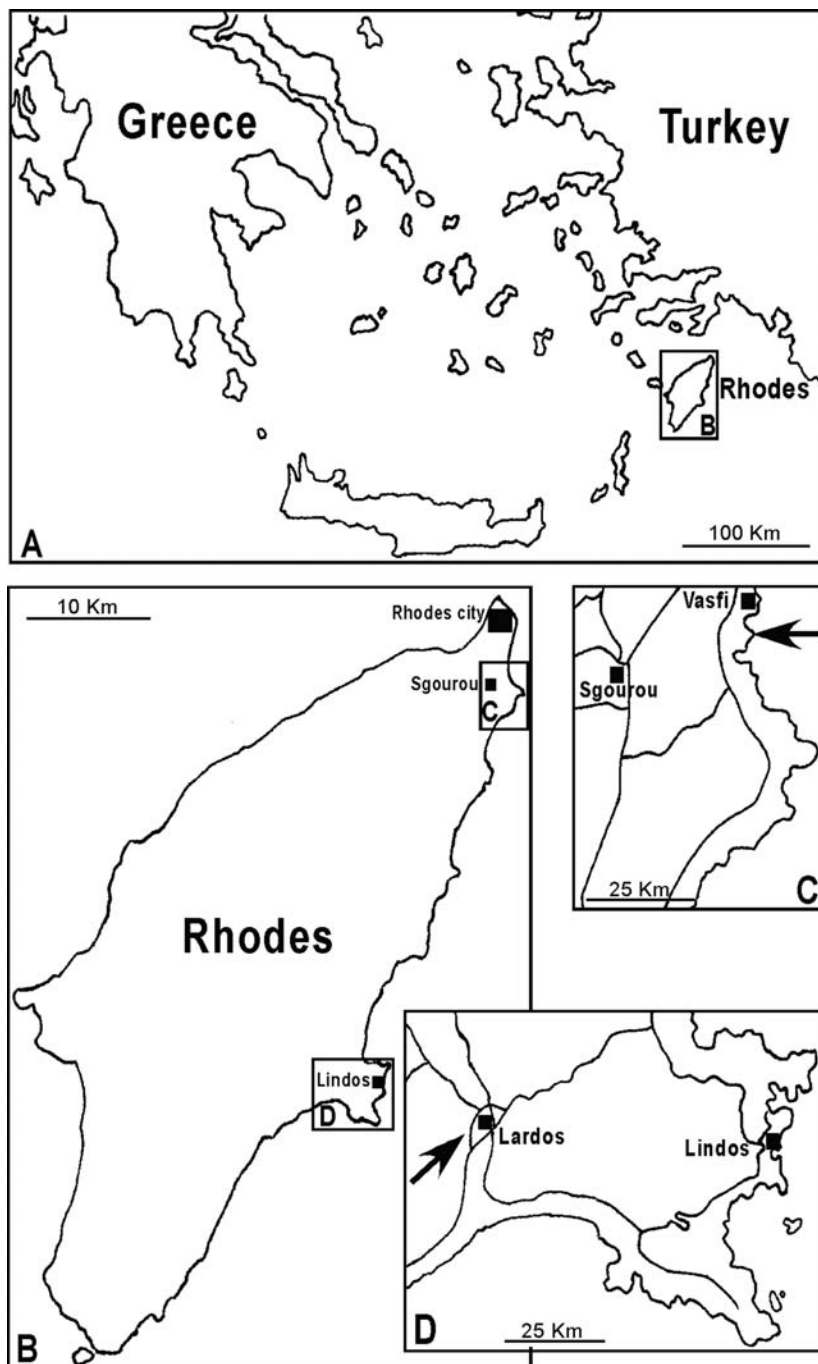
Fig. 1 Map of the Dodecanese island of Rhodes, indicating the location of the *Lophelia*-bearing localities (A-D)

these. Before careful logging of the locality could be attempted in the next season, however, the Sunwing Hotel was built on the site, destroying the outcrop.

The second locality is an isolated hill exposing Lindos Bay Clay, southwest of Lardos village (Fig. 1D), at the start of the road to the Ipsensis monastery. This contains a similar occurrence of a single bed of *Lophelia* and *Madrepora* fragments. Some 800 fragments were collected (in 2003), both loose and *in situ*.

At both localities, the corals are not in life position but have undergone some transport. The transport distance is probably short and, as expected on the muddy seafloor, has incurred no visible wear of the skeletal surfaces. Rather large pieces of coral have survived unbroken, but to a large degree these have been fractured in place by sediment compaction.

Assessing the water depth of *Lophelia* occurrences in the Lindos Bay Clay is not easy. The corals are associated with other faunal elements indicative of the lower bathyal zone, such as the brachiopods *Gryphus vitreus* and *Terebratulina retusa*. However, there are variable amounts of admixture of shallow-water species, especially among the microfossils. This reflects the occurrence, in this tectonically active region, of steep to very steep, fault-controlled seafloor topography and the proximity of shallow-water environments. Such settings may induce the formation of upwelling cells that encourage the development of bathyal-type faunas in unusually shallow-water depths (Wisshak et al. 2005).

Methods

The coral fragments were cleaned briefly in water in an ultrasonic tank. Inspection under a light microscope allowed selection of "promising" specimens for casting. Several trace fossils are, in fact, more easily identified directly on the coral surface by extremely low-angle illumination than cast in resin using scanning electron microscopy (SEM), e.g., *Gnathichnus pentax* and *Centrichnus eccentricus*.

The selected material was thoroughly cleaned of clay matrix filling the borings using hydrogen peroxide and ultrasonics in water, and was then cast in epoxy resin using the methods outlined by Beuck and Freiwald (2005) and Wisshak et al. (2005). The specimens were then sectioned to expose the desired surface for SEM viewing and the aragonite was dissolved using 5 % hydrochloric acid.

The trace fossils

In the following account, trace fossil (ichnotaxonomic) names are used, including some in open nomenclature, as the tracemakers generally are not preserved in this fossil material. However, intelligent guesses as to the nature of the tracemaker are possible in a number of cases. All illustrations are of material from the Lardos locality.

Orthogonum Radtke, 1991 (Figs. 2A, B, D, E)

The producing organisms of this ichnogenus are not clearly defined. Probably more than one ichnospecies is represented in the material but the majority of

specimens are *Orthogonum lineare* Glaub, 1994. The ichnogenus is present almost ubiquitously. The tubes have a diameter ranging from 8 to 12 μm. Some tubes have linearly oriented stumpy spines on their surface.
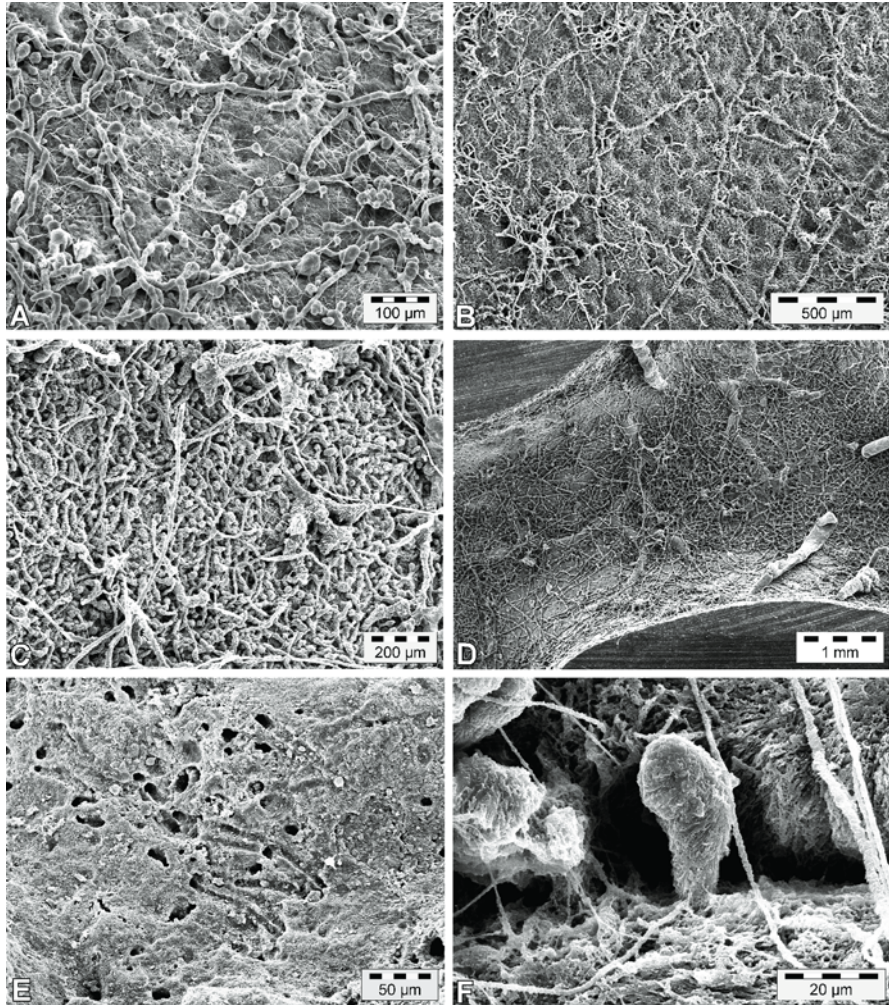
Fig. 2 Fungal microborings seen in resin casts. This and all following Figures are SEM images. **A** Slight bioerosion density including *Orthogonum lineare* and *Saccomorpha clava*. **B** *Orthogonum lineare* showing classic regular rectangular branching pattern. **C** Medium bioerosion density dominated by *Saccomorpha clava*. **D** Medium to heavy bioerosion density showing *Talpina* isp. systems covered by deeper-tier *Orthogonum* isp. **E** External surface of the coral showing parallel-running *Orthogonum lineare* exposed by slight erosion. **F** Close view of a *Saccomorpha clava* sack-shaped body and connecting fine hyphal canals

Saccomorpha clava Radtke, 1991 (Figs. 2A, C, F)

Also occurring in nearly every sample is this striking microboring comprising very slender canals connecting with sack-shaped bodies. The producers are fungi (Radtke 1991), the trace fossils bearing a close resemblance to the borings of *Dodgella priscus*. The tubes are approximately 0.5 to 2 μm in diameter and the sack-like bodies have a maximum diameter of about 30 μm.

Oichnus Bromley, 1981 (Fig. 3)

This ichnogenus in its present diagnostic emendation (e.g., Pickerill and Donovan 1998; Nielsen and Nielsen 2001) may cover small pits in the surfaces of bathyal corals. These are common and occur patchily. They extend to different depths in the substrate, some being but shallow dishes (Figs. 3A, B) while others exceed the hemispherical (Fig. 3C). The roughly circular diameter ranges from 0.35 to 0.6 mm. Three foraminifers were seen fitting the pits exactly and are regarded as the tracemakers (Fig. 3D). Preservation was insufficiently good to allow generic identification of the foraminifers.

Several descriptions of similar pit formation by foraminifers have been published. Both agglutinating as well as calcareous species are reported to produce pits roughly fitting the test size (e.g., Delaca and Lipps 1972; Vénec-Peyré 1987). Banner (1971) described hemispherical borings closely similar to these in the tests of shallow-water
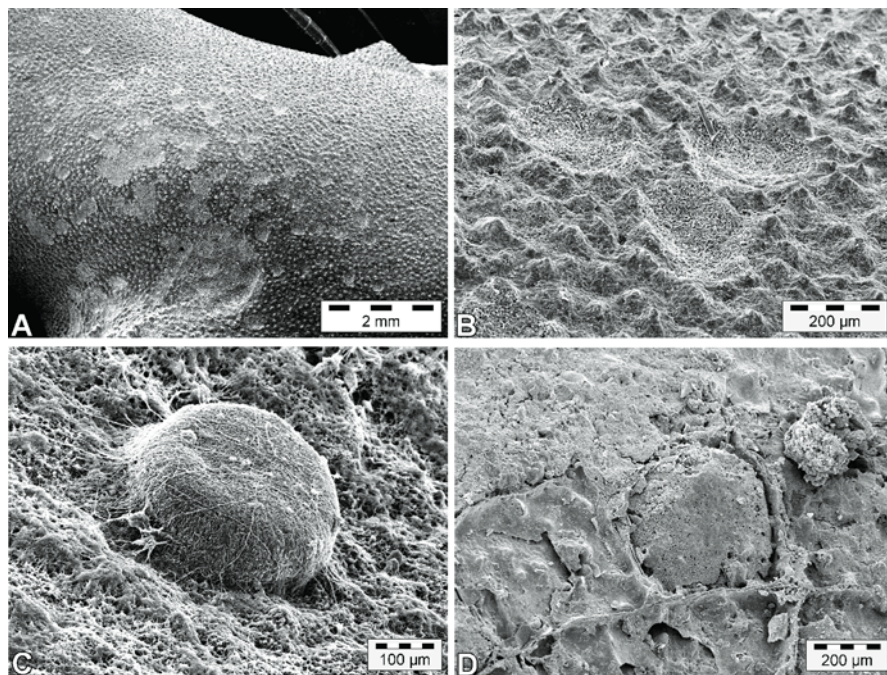
Fig. 3 Small foraminiferal pits, *Oichnus* isp. **A, B** and **D** are external views of the coral. **A** A crowd of pits on the coral surface. **B** Close view of three shallow pits. **C** Resin cast of a deep pit. **D** Poorly preserved foraminifer within its pit

foraminifers and interpreted them as the work of small parasitizing foraminifers. Plewes et al. (1993) and Vénec-Peyré (1996) reviewed foraminiferal pit borings.

Larger dish-shaped etchings (Fig. 4)

Dish-shaped depressions etched into the coral surface close to corallite apertures resemble in shape and location the traces produced in Recent material by the large, parasitic, rosalinid foraminifer *Hyrrokkin sarcophaga* Cedhagen, 1994. In adults a slender canal is bored through the wall of the corallite (Cedhagen 1994; Freiwald and Schönfeld 1996). However, other foraminifers may make shallow dish structures (Plewes et al. 1993).
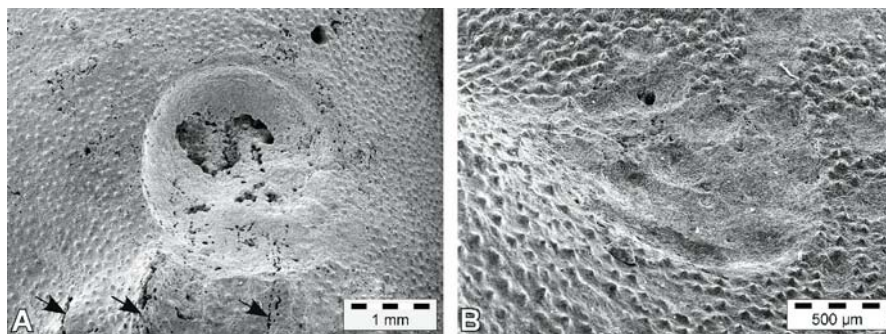
Fig. 4 Outer views of the coral showing large dish-shaped depressions etched by foraminifers. **A** in characteristic position close to the corallite, septa arrowed. **B** A smaller dish. The single boring aperture at the far edge was probably not produced by the foraminifer

Palaeosabella Clarke, 1921 (Figs. 5A, B)

Palaeosabella prisca (McCoy, 1855) covers elongated clavate borings that slightly expand in diameter distally. They are common in the material and are probably attributable to polychaete worms. The largest has a length of 10 mm and a maximum diameter of 0.5 mm. The surface of the tube is smooth. The expanding diameter of this form distinguishes it from *Trypanites* Mägdefrau, 1932, which has a constant diameter (Palmer et al. 1997). Undoubted *Trypanites* was not seen in this study.

Caulostrepsis Clarke, 1908 (Fig. 5C)

These are small, flattened hairpin-like borings, the tube being folded back on itself as a tight U-boring. The vane between the legs of the U is the same thickness as the tube, which suggests attribution to *C. cretacea* (Voigt, 1971). However, the individuals in the corals under study are relatively small for this ichnospecies, being seen for lengths of 2.5 mm or a little more, expanding distally to a width of about 1.5 mm. The borings in some cases are roofless, ploughing along the surface of the substrate. Annelid worms produce such traces today, although they are normally bored well beneath the substrate surface.
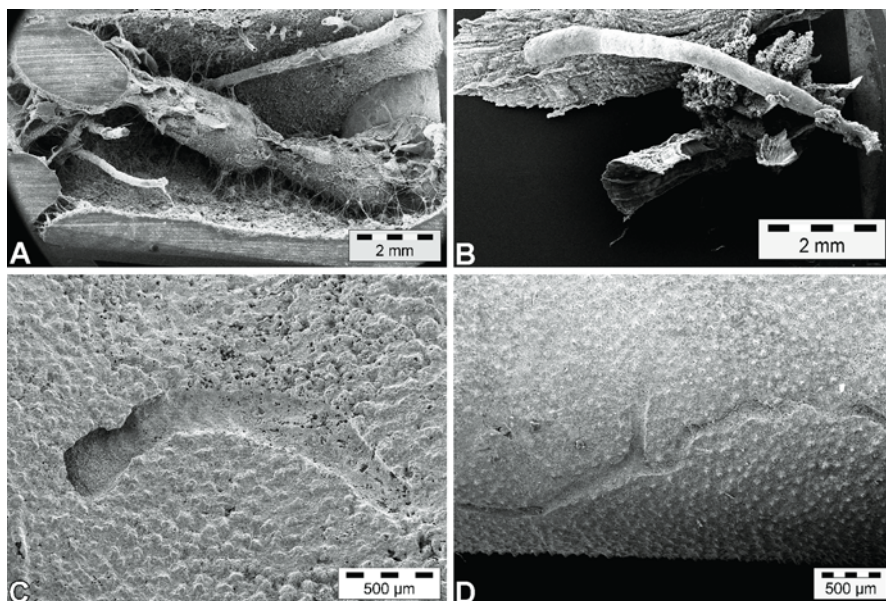
Fig. 5 Polychaete borings. **A, B** are resin casts, **C, D** external views. **A** *Palaeosabella* isp. beside a sponge boring *Entobia* cf. *paradoxa* (Fischer, 1868). **B** A broken example of *Palaeosabella* isp. **C** A small *Caulostrepsis* cf. *cretacea*, apparently originally roofless to the right but plunging into the coral skeleton to the left. **D** A probable *Maeandropolydora* isp.

Maeandropolydora Voigt, 1965 (Fig. 5D)

A single possible example of this ichnogenus was found, an unroofed groove. The meandering course and true branching suggest *M. sulcans* Voigt, 1965. The width of the groove varies from 0.10 to 0.15 mm.

Talpina von Hagenov, 1840 (Figs. 2D, 6A)

Talpina isp. is fairly common at Vasphi, less so at Lardos. The work of Voigt (1972, 1975, 1978) demonstrated that these systems of branched borings are produced by phoronid worm pseudocolonies. The tubes have widths around 0.3 to 0.5 mm and the tube surfaces are smooth.

Podichnus centrifugalis Bromley & Surlyk, 1972 (Figs. 6B-D)

The easily recognizable groups of deep pits or tubes comprising this ichnospecies are produced by the pedicles of brachiopods. The compactness of the cluster of holes indicates whether the brachiopod had a divided pedicle (as in *Terebratulina retusa*) or a massive pedicle (e.g., *Gryphus vitreus*).

The annulations on the tubes seen in epoxy casts have not been described before. Similar annulation was illustrated in *P. centrifugalis* by Hofmann (1996) but not commented upon. The orientation of the ornament is independent of the orientation of the tube within the substrate and thus is not an expression of the laminated
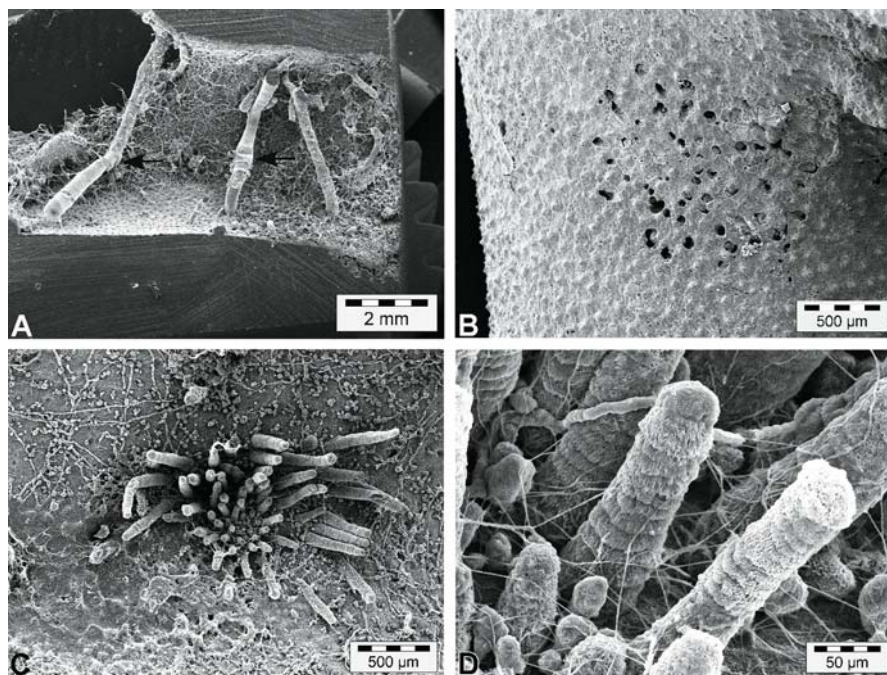
Fig. 6 Phoronid and brachiopod bioerosion. **A** *Talpina* isp., small fragments of the boring of a phoronid pseudocolony. The branching places are not easily seen but an aperture is obscured at the point where the tube changes direction (arrowed). **B-D**, the brachiopod etching scars, *Podichnus centrifugalis*. **B** External view of a scattered individual, indicating a divided pedicle and probably etched by *Terebratulina retusa*. **C** Internal view (resin cast) of a rather compact individual, probably the work of *Gryphus vitreus*. **D** Close view of C showing annular ornamentation

ultrastructure of the coral skeleton (Fremdskulptur of Voigt 1971; xenoglyph of Bromley et al. 1984). The ornament must therefore be produced by the brachiopod as part of the trace fossil, i.e., a bioglyph.

The presence of *P. centrifugalis* marks the spot where a brachiopod has been attached for some years.

Centrichnus Bromley and Martinell, 1991 (Fig. 8A, B)

The coral surfaces are commonly etched to produce shallow scars having a curved form. In most cases several curved grooves lie conformably together, somewhat resembling a spreite. Typically, the depth of etching is so negligible that the trace fossil can only be observed by very low-angle illumination and SEM imagery is difficult.

These scars are referable to *C. eccentricus* Bromley and Martinell, and are etched by the byssal plug of the encrusting bivalve *Anomia* sp. The successive etched arcs represent growth lines. The bivalve is commonly preserved *in situ* above its trace (cf. Bromley 1999) where the coral has extended its coenosarc over the *Anomia* and covered it with skeletal material.

Gnathichnus Bromley, 1975

Another extremely shallow trace fossil is the mechanical scratching by the teeth of regular echinoids. This was not photographed or SEM-imaged satisfactorily in the present study. *G. pentax* Bromley is restricted to small patches on the coral skeleton,
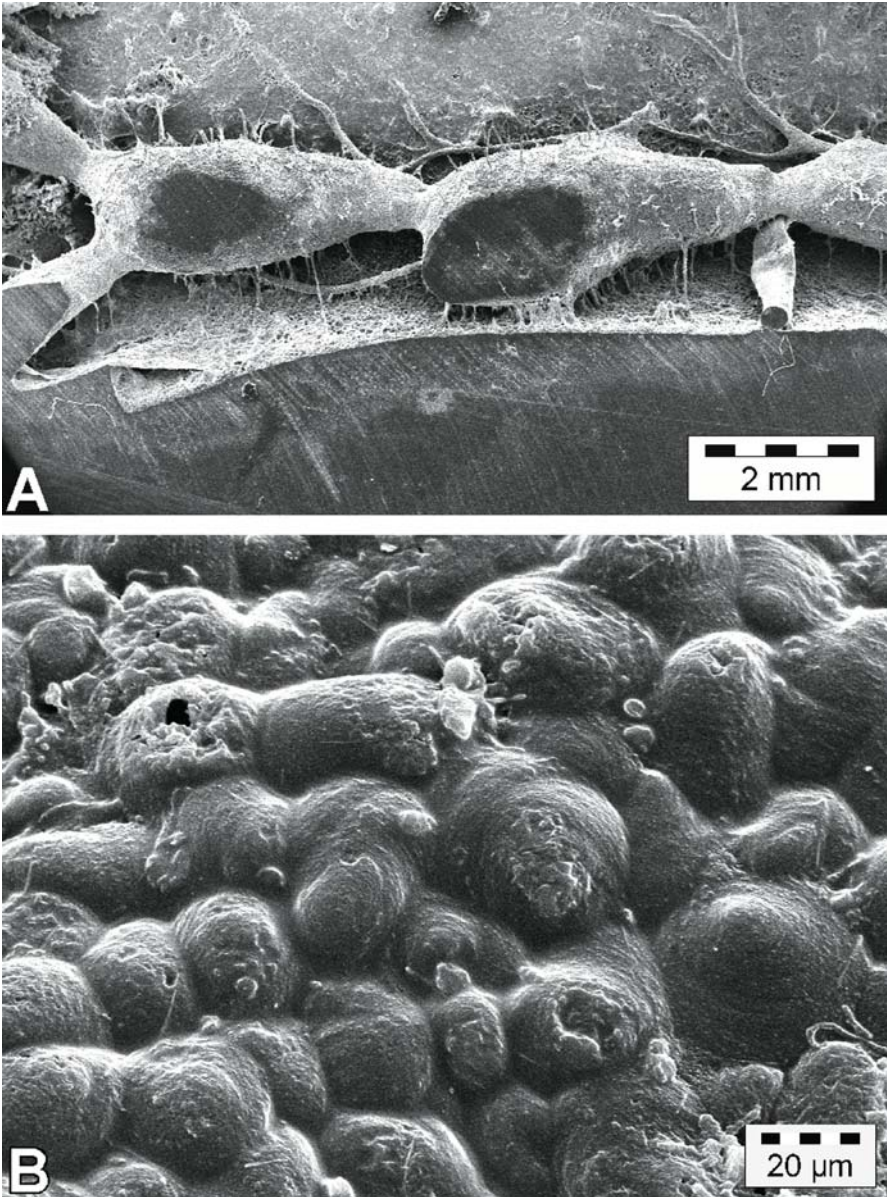
Fig. 7 A *Entobia* cf. *paradoxa* in resin cast. **B** Close view of the resin cast of wall ornamentation on the entobian in Fig. 5A
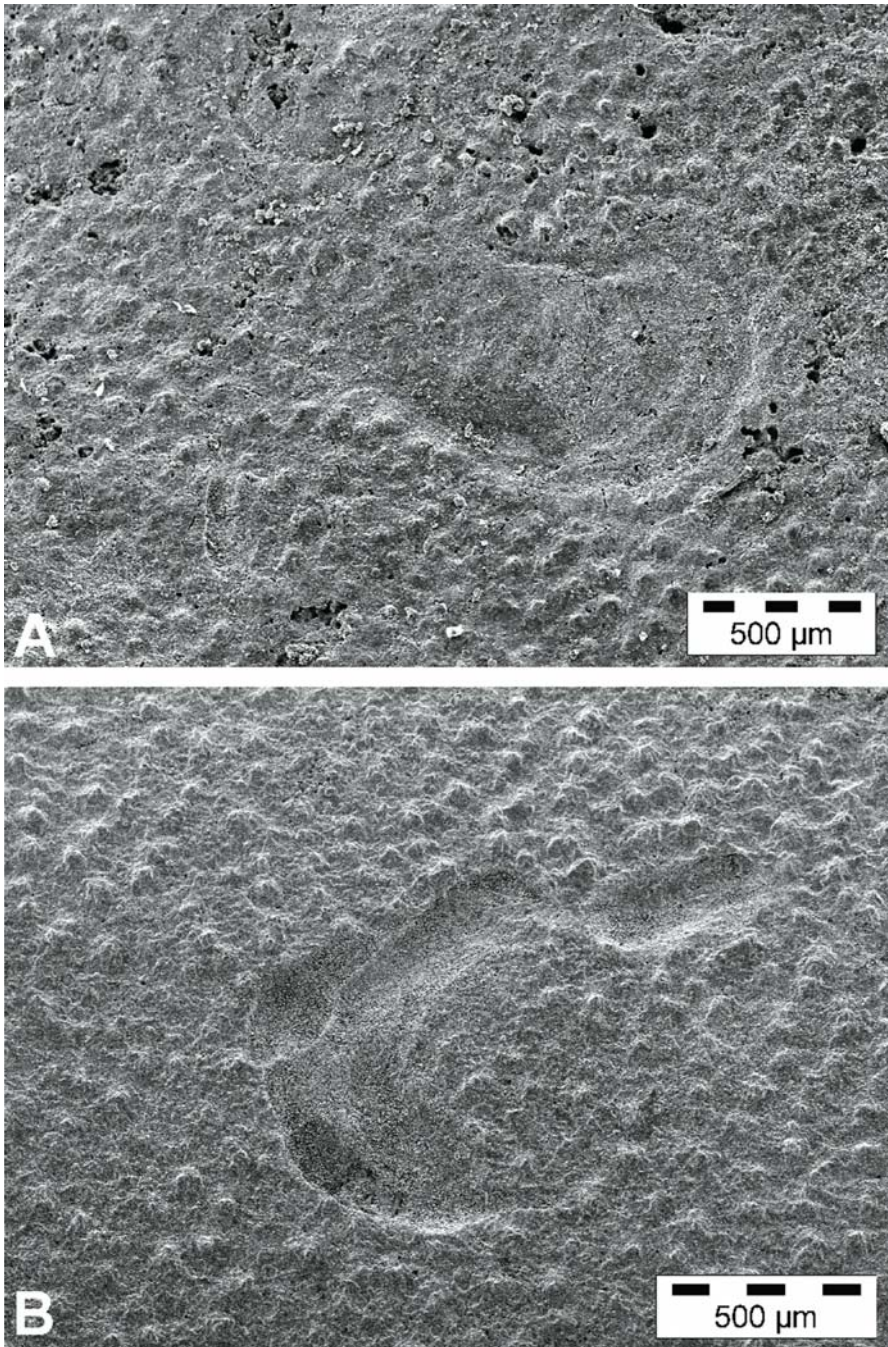
Fig. 8 A, B *Centrichnus eccentricus*, external views of the very shallow etching scars of *Anomia* sp. in the coral surface

commonly around borings, especially *Entobia*. It was observed very rarely on the Pleistocene material, in contrast to the case in Recent material from Sula Bank, Norway, where it occurs in larger patches.

Entobia Bronn, 1837 (Figs. 5A, 7A, B)

This ichnogenus comprises chambered branched systems bored by endolithic sponges and the wall of the boring is ornamented with a characteristic cusped sculpture (Fig. 6A). Details of this ornament are showing themselves to be diagnostic of the genus of the tracemaking sponge (Calcinai et al. 2003); the spicules have been dissolved in this Pleistocene material.

A number of ichnospecies of *Entobia* have been established (e.g., Bromley and D'Alessandro 1984) but these are only distinguishable satisfactorily where the sponge has developed in an extensive substrate in which it can produce an idiomorphic boring. In the slender skeletons of *Lophelia*, there is insufficient space for a large sponge to develop idiomorphically, and the crowded, stenomorphic boring commonly remains ichnospecifically anonymous. Two or three large ichnospecies of *Entobia* were recorded (Figs. 5A, 6A, B).

Small, radiating borings

Using SEM imaging, a number of radiating microborings are coming to light (e.g., Glaub 1994; Beuck and Freiwald 2005; Wisshak et al. 2005). Owing to their small size, these can develop idiomorphically in restricted substrate and further study of these minute borings is recommended.

There is great confusion over the taxonomy of these borings. In general they comprise three similar groups of trace fossils but these have morphological overlap. The three groups are (1) small entobians, including *Clionolithes* Clarke, 1908; (2) the *Dendrina* group of borings (e.g., Hofmann 1996), commonly attributed to foraminifers; and, at a smaller scale, the rosette-shaped cyanobacterial microborings such as *Hyellomorpha* (e.g., Vogel et al. 1987; Schnick 1992). Three such small radiating borings occur in the Rhodes material.

Semidendrina-form Glaub, 1994 (Fig. 9)

This name was given to a camerate, somewhat *Entobia*-like boring spanning about 0.5 to 0.7 mm in diameter. Branches radiate from a point near the periphery of the boring in a tier close beneath the substrate surface. From the point of radiation, a single, large chamber somewhat elongated as a cylinder, extends obliquely or, in some cases, more or less perpendicularly from this tier, reaching a deeper level within the substrate. (The oblique stance seems to be a collapse artifact.) This chamber has short, spiny outgrowths and irregularities over its surface, and measures about 80 μm wide and 180 μm in length. The large chamber does not appear to have a direct contact with the substrate surface.

The remaining chambers are irregularly rounded and of irregular size, ranging in diameter from about 40 to 80 μm. The largest of these may represent fusion of adjacent chambers. Chambers and canal walls have a weakly developed, small-scale cuspate ornament, reminiscent of sponge borings but at a much smaller scale

(Fig. 9E).

Hair-like apophyses connect the system to the substrate surface. Their width is about 1 or 2 μm. Size and distribution of any larger apertures to the substrate surface remain unknown.

A trace described as "*Cliona* sp. 1" illustrated by Schmidt and Freiwald (1993: Fig. 10) somewhat resembles *Semidendrina*-form 1. The form described by Schnick (1992) as *Hyellomorpha microdendritica* Vogel, Golubic and Brett, 1987 is very similar. It has likewise an anomalous large chamber, but this is rounded and not
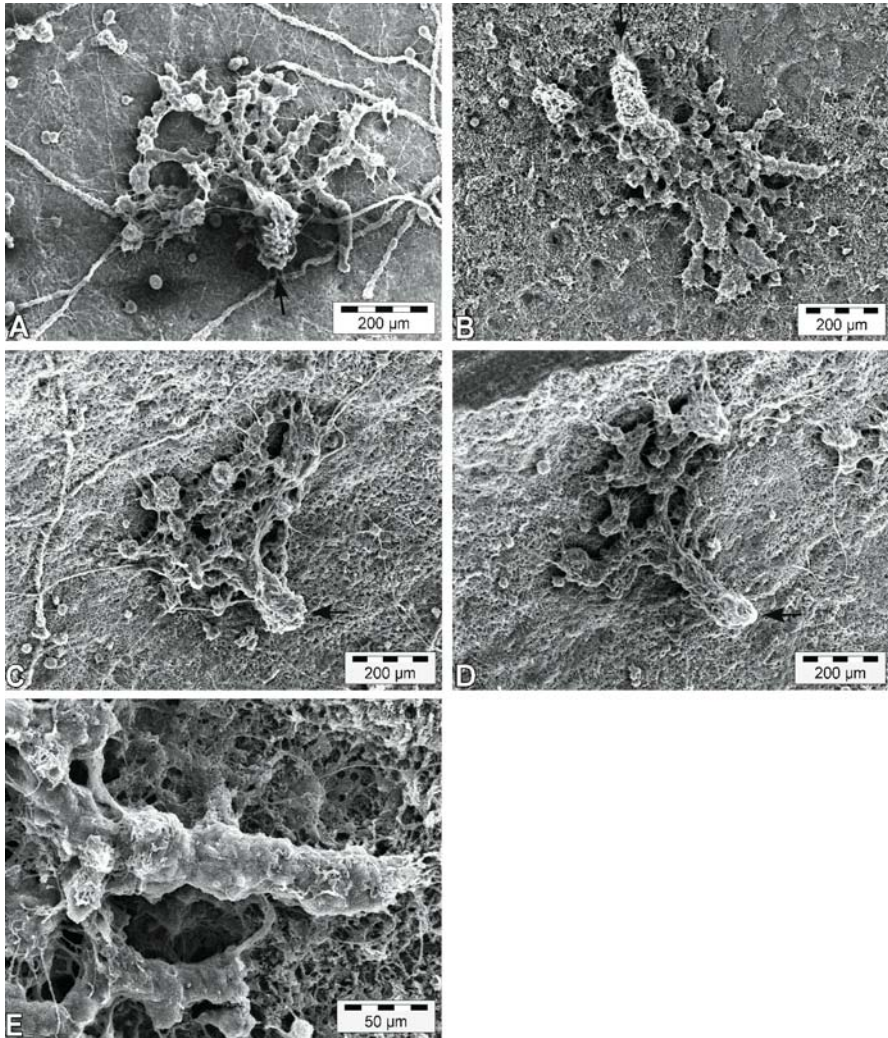
Fig. 9 *Semidendrina*-form. **A-D** Four individuals, the anomalous chamber arrowed. In **A** and **B** this chamber is oblique and the resin casts may have collapsed somewhat. In **C** and **D** it stands perpendicularly to the substrate surface. **E** Close view of part of **B** showing the slight pustular ornamentation

spiny, and the branches are short and stumpy. However, not all microborings identified as *Hyellomorpha* have an anomalously large chamber (e.g., Vogel et al. 1987; Bundschuh et al. 1989).

Most closely the trace fossil resembles the Recent traces described as borings of foraminifers by Cherchi and Schroeder (1991), in shells from Scotland. In three specimens in that material, the large chamber contained the test of a single calcareous foraminifer (revealed by radiography) and the whole, branched system was identified as a foraminiferal boring.

A closely similar, Jurassic trace fossil was named *Globodendrina monile* by Plewes et al. (1993). These authors described a conical "collar" of cemented sediment grains surrounding an aperture from the large chamber, a feature not seen in other occurrences. This agglutinated collar was claimed to represent the reduced test of an agglutinating foraminifer. Plewes et al. (1993) suggested that the calcareous foraminifers seen by Cherchi and Schroeder (1991) were nestlers, and therefore not the tracemakers, but this seems unlikely to be the case.

The anomalous chamber in all these cases from the literature has a spiny surface, but has an overall rounded form. They have all been reported in shallow-water. The present, deep-water boring differs from all these in the markedly elongated shape, powerful surface ornament, and perpendicular attitude of this chamber. *Semidendrina*-form is rather common in the Rhodes material.

Non-camerate radiating form (Fig. 10)

This is a non-camerate boring, having a somewhat *Entobia*-like morphology, but spanning only about 2 to 3 mm. Unlike the *Semidendrina*-form, this boring is commonly visible as an open gutter on external surfaces of the coral, suggesting that the borer could exist in a roofless boring (Figs. 10A-C). However, SEM images of casts suggest that in many individuals a very thin roof is present (Fig. 10D).

Branches radiate from a poorly defined central point, but this pattern is not clear in all individuals. Branches have a width of about 80 μm, but expand smoothly to about 200 μm at branching points, a morphology resembling that of non-camerate *Entobia*. However, unlike *Entobia*, the distal terminations of the branches commonly are expanded and connected to the substrate surface by a number of slender apophyses about 1 to 2 μm wide. In general, apophyses are little developed in this boring. The walls of the boring have a very faint cuspate ornament reminiscent of sponge-chip ornament, but the very small size suggests that this is not a sponge boring. Larger apertures to the surface have not been observed.

Hirsute camerate form (Fig. 11)

This boring spans 1 to 5 mm in diameter. It is remarkable in structure, consisting of one to several irregularly shaped chambers around 0.5 mm in size, and an extraordinarily abundant development of hair-like apophyses 1 to 10 μm thick and maybe over 2 mm long. These canals constitute a hirsute zone around the boring, commonly obscuring the view of the chambers themselves. The canals may by straight or loop in circles. The boring has only been seen in resin casts and it is likely that the very slender hairlike canals have collapsed to some degree after release
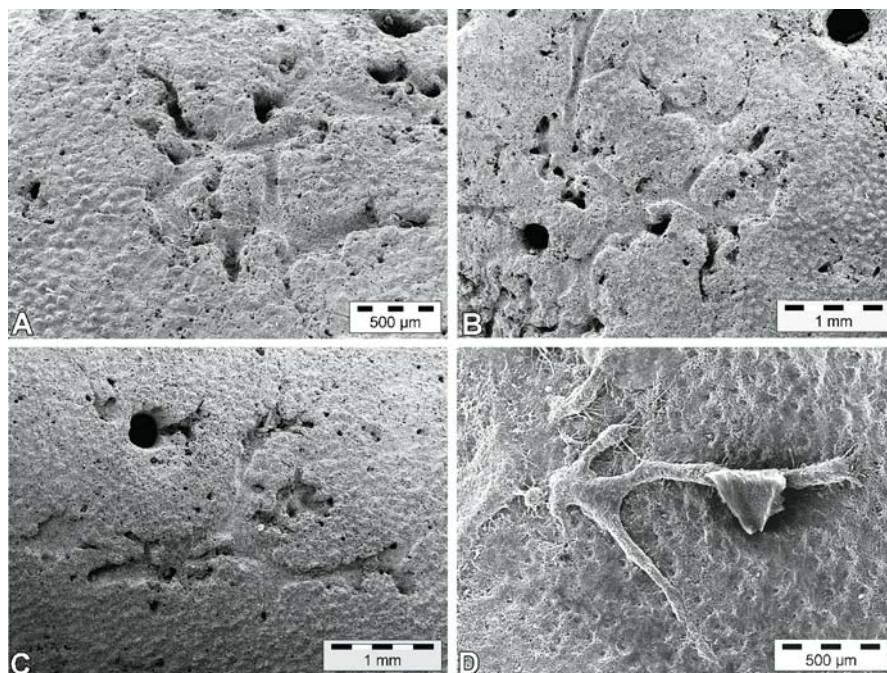
Fig. 10 Four specimens of the non-camerate radiating form. **A-C** are roofless specimens viewed externally. **D** is a resin-cast individual

from the aragonitic substrate; thus the looping of the canals may be an artifact. If surface apertures occur, they are hidden from view.

Discussion

Quantification of bioerosion in *Lophelia* is not possible with any degree of precision. Periodic growth phases of the substrate coral in some cases may cause
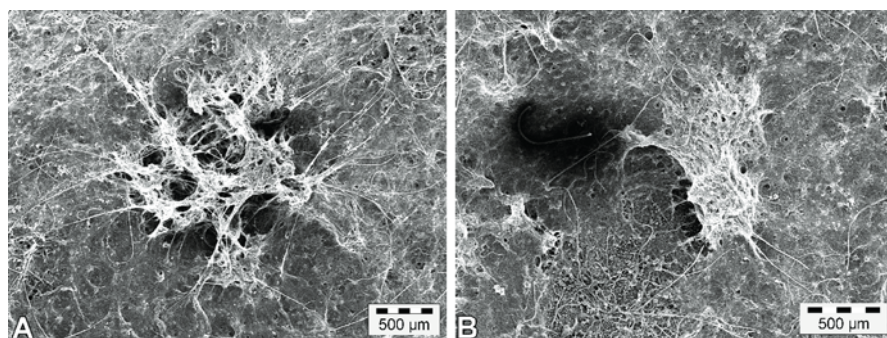
Fig. 11 Two examples of the hirsute camerate form showing extremes of the range of morphology. **A** A highly hirsute individual. **B** A specimen bearing few apophyses and exploratory canals

encrusting and bioeroding organisms to be covered over with new layers of skeleton. This is commonly the case with living (two-valved) *Anomia* sp. Bioerosion structures buried in this way cannot be seen or cast, and are largely lost to the record.

In SEM images, abundance of borings can only be estimated in places where there is little bioerosion. Excessive bioerosion confuses the evidence by deeper-tier bioerosion obscuring shallow-tier forms (Fig. 2D).

Degree of bioerosion may be classified in three categories, based on SEM imagery (see also Beuck and Freiwald 2005). (1) Slight bioerosion, where the original substrate surface is clearly visible (Fig. 12A). (2) Medium bioerosion, in which the position of the substrate surface is clear even though little or none of it may be seen (Fig. 12B). (3) Heavy bioerosion, where the substrate surface is entirely hidden under a thick layer of entangled and matted borings (Fig. 12C). The last category may correspond loosely to the (ichnologically unfortunate) sedimentological description of bathyal coral rubble as "heavily degraded".

Cross-cutting and avoidance relationships between different ichnotaxa theoretically might provide a chronological coding that will reveal the sequence of colonization of the endolithic community. This should be attempted only in short-term bioerosion zones of category 1, close to the active polyps of the coral colony. Heavily bioeroded zones clearly show repeated colonization where borings of early colonists (fungi) circumvent and avoid borings of late colonists (sponges).

Empty borings provide extensions of the outer surface of the substrate available for colonization. In euphotic seafloors, the dark interiors of abandoned borings offer a locally aphotic and restricted environment for colonization by specialized cryptic organisms. Evidence from SEM imagery of bathyal corals, however, indicates no clear difference in colonists using *Palaeosabella* and *Entobia* walls as opposed to the external substrate surface.

In this preliminary study, no *Trypanites* and no bryozoan borings were detected. *Gnathichnus pentax* was seen to be local and patchy and *Radulichnus inopinatus* Voigt, 1977 appeared to be absent. The lack of widespread echinoid gnawing and gastropod and chiton radulation, which dominate photic hard substrates, must be related to the aphotic environment (Bromley 1994). The rapidly growing and renewable food-source of endolithic photoautotrophic algae and cyanobacteria are missing and the slowly growing endolithic fungi are no substitute. The microborings of this community of heterotrophs correspond to the aphotic *Saccomorpha clava* / *Orthogonum lineare* Ichnocoenosis (Glaub 1994; Glaub et al. 2002).

Conclusions

1. Pleistocene bathyal corals were studied by light microscopy and scanning electron microscopy with a view to comparing bioerosion trace fossils with bioerosion of Recent bathyal corals.
2. The following ichnotaxa (and supposed, tracemaking organisms) were observed. *Orthogonum lineare* (fungus?), *Saccomorpha clava* (fungus), *Oichnus* (foraminifers), dish-shaped etching (possibly by the foraminifer
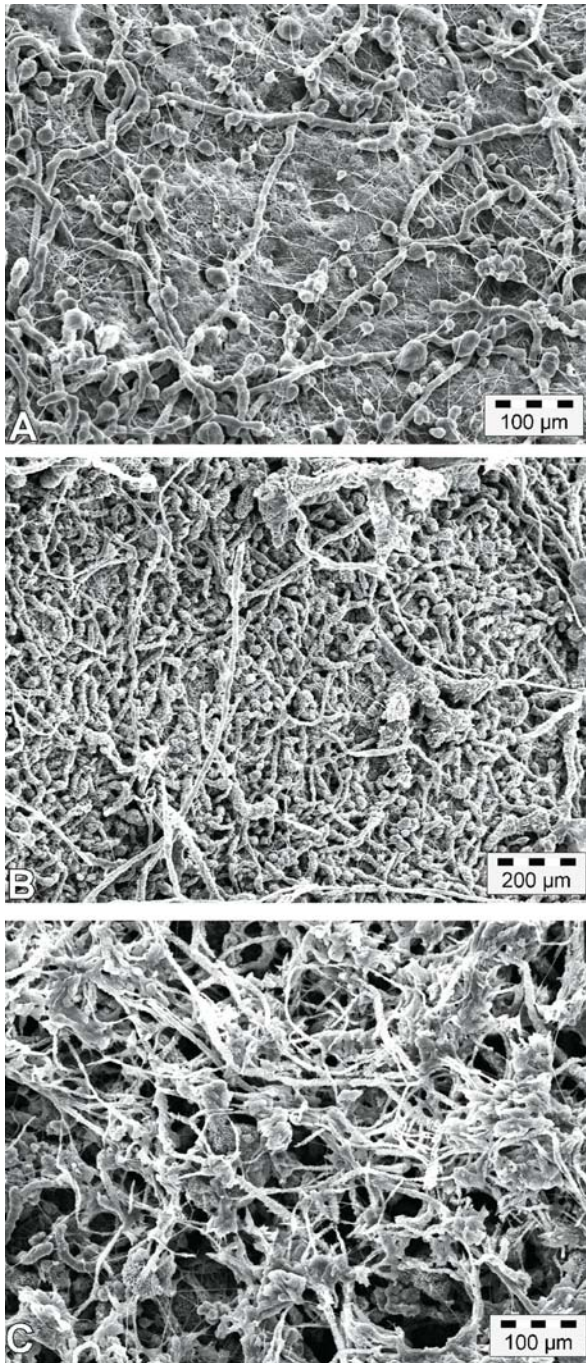
Fig. 12 Three categories of bioerosional density. **A** Slight bioerosion. **B** Medium bioerosion. **C** Heavy bioerosion

Hyrrokkin sarcophaga), *Palaeosabella* isp. (polychaete?), *Caulostrepsis cretacea* (polychaete), *Maeandropolydora* isp. (polychaete), *Talpina* isp. (phoronid), *Centrichnus eccentricus* (anomiid), *Podichnus centrifugalis* (brachiopods), *Gnathichnus pentax* (regular echinoids) and *Entobia* ispp. (sponges). In addition, very small, radiating trace fossils somewhat resembling entobians are described as *Semidendrina*-form (possibly foraminifers), non-camerate radiating form and hirsute camerate form.

3. Some trace fossils offer such low relief that they are easily overlooked and are difficult to image. These include *G. pentax* and *C. eccentricus*.

4. *G. pentax* is patchily distributed and not common and *Radulichnus* (mollusc rasping traces) was not found. These trace fossils dominate photic hard substrates, and their failure to do this indicates an aphotic environment. The slowly growing heterotrophic endoliths do not constitute a reliable food-source for these scraping molluscs and echinoids.

5. Density of bioerosion varies from zero and extremely slight to very heavy infestation. In the latter case, deep-tier structures entirely obscure shallow-tier structures, and this renders attempts at counting abundance of individuals fruitless.

6. The microborings of this community of heterotrophs correspond to the aphotic *Saccomorpha clava / Orthogonum lineare* Ichnocoenosis.

Acknowledgements

References

Banner FT (1971) A new genus of the Planorbulinidae an endoparasite of another foraminifer. Rev Espan Micropaleont 3: 113-128

Beuck L, Freiwald A (2005) Bioerosion patterns in a deep-water *Lophelia pertusa* (Scleractinia) thicket on the Propeller Mound (northern Porcupine Seabight). In: Freiwald A, Roberts JM (eds) Cold-water Corals and Ecosystems. Springer, Berlin Heidelberg, pp 915-936

Bromley RG (1978) Bioerosion of Bermuda reefs. Palaeogeogr Palaeoclimatol Palaeoecol 23: 169-197

Bromley RG (1994) The palaeoecology of bioerosion. In: Donovan SK (ed) The Palaeobiology of Trace Fossils. Belhaven Press, London, pp 134-154

Bromley RG (1999) Anomiid (bivalve) bioerosion on Pleistocene pectinid (bivalve) shells, Rhodes, Greece. Geol Mijnb 78: 175-177

Bromley RG (2004) A stratigraphy of marine bioerosion. In: McIlroy D (ed) The Application of Ichnology to Palaeoenvironmental and Stratigraphic Analysis. Geol Soc London, Spec Publ 228: 455-479

Bromley RG, D'Alessandro A (1984) The ichnogenus *Entobia* from the Miocene, Pliocene and Pleistocene of southern Italy. Riv Ital Paleont Stratigr 90: 227-296

Bromley RG, Hanken N-M (1981) Shallow marine bioerosion at Vardø, arctic Norway. Bull Geol Soc Denm 29: 103-109

Bromley RG, Pemberton SG, Rahmani RA (1984) A Cretaceous woodground: the *Teredolites* ichnofacies. J Paleont 58: 488-498

Bundschuh M, Glaub I, Hofmann K, Radtke G, Vogel K (1989) Bohrorganismen helfen, fossile Meeresbecken zu rekonstruieren. Forschung Frankfurt 1989: 56-64

Calcinai B, Arillo A, Cerrano C, Bavestrello G (2003) Taxonomy-related differences in the excavating micro-patterns of boring sponges. J Mar Biol Ass UK 83: 37-39

Cedhagen T (1994) Taxonomy and biology of *Hyrrokkin sarcophaga* gen. et sp. n., a parasitic foraminiferan (Rosalinidae). Sarsia 79: 65-82

Cherchi A, Schroeder R (1991) Perforations branchues dues à des Foraminifères crypto-biotiques dans des coquilles actuelles et fossiles. CR Acad Sci Paris (2) 312: 111-115

Delaca TE, Lipps JH (1972) The mechanism and adaptation significance of attachment and substrate pitting in the Foraminifera *Rosalina globularis* d'Orbigny. J Foram Res 2: 68-72

Ekdale AA, Bromley RG, Pemberton SG (1984) Ichnology - trace fossils in sedimentology and stratigraphy. SEPM Short Courses 15, 317 pp

Freiwald A (1998a) Microbial maceration and carbonate dissolution on cold-temperate shelves. Hist Biol 13: 27-35

Freiwald A (1998b) Geobiology of *Lophelia pertusa* (Scleractinia) reefs in the North Atlantic. Habilitation thesis, Univ Bremen

Freiwald A, Henrich R (1994) Reefal algal coralline build-ups within the Arctic Circle: morphology and sedimentary dynamics under extreme environmental seasonality. Sedimentology 41: 963-984

Freiwald A, Schönfeld J (1996) Substrate pitting and boring pattern of *Hyrrokkin sarcophaga* Cedhagen, 1994 (Foraminifera) in a modern deep-water coral reef mound. Mar Micropaleont 28: 199-207

Freiwald A, Wilson JB (1998) Taphonomy of modern deep, cold-temperate water coral reefs. Hist Biol 13: 37-52

Freiwald A, Reitner J, Krutschinna J (1997) Microbial alteration of the deep-water coral *Lophelia pertusa*: early postmortem processes. Facies 36: 223-226

Glaub I (1994) Mikrobohrspuren in ausgewählten Ablagerungsräumen des europäischen Jura und der Unterkreide (Klassifikation und Palökologie). Cour Forschinst Senckenb 174: 1-324

Glaub I, Gektidis M, Vogel K (2002) Microborings from different North Atlantic shelf areas - variability of the euphotic zone extension and implications for paleodepth reconstructions. Cour Forschinst Senckenb 237: 25-37

Günther A (1990) Distribution and bathymetric zonation of shell-boring endoliths in Recent reef and shelf environments: Cozumel, Yucatan (Mexico). Facies 22: 233-262

Hansen KS (2001) Sedimentology of Pliocene-Pleistocene temperate water carbonates from northeast Rhodes, Greece. Unpublished PhD thesis, Univ Copenhagen, Denmark

Hanken N-M, Bromley RG, Miller J (1996) Plio-Pleistocene sedimentation in coastal grabens, north-east Rhodes, Greece. Geol J 31: 271-296

Hofmann K (1996) Die mikro-endolithischen Spurenfossilien der borealen Oberkreide Nordwest-Europas und ihre Faziesbeziehungen. Geol Jb A 136: 1-151

Macdonald IA, Perry CT (2003) Biological degradation of coral framework in a turbid lagoon environment, Discovery Bay, north Jamaica. Coral Reefs 22: 523-535

Nielsen KSS, Nielsen JK (2001) Bioerosion in Pliocene to Late Holocene tests of benthic and planktonic foraminiferans, with a revision of the ichnogenera *Oichnus* and *Tremichnus*. Ichnos 8: 99-116

Palmer TJ, Plewes CR, Cole A (1997) The simple and long-ranging worm-boring *Trypanites*: not so simple and long-ranging after all. Geol Soc Amer, Abstr Progr 29: A 107

Perry CT, Bertling M (2000) Spatial and temporal patterns of macroboring within Mesozoic and Cenozoic coral reef systems. In: Insalaco E, Skelton PW, Palmer TJ (eds) Carbonate Platform Systems; Components and Interactions. Geol Soc London Spec Publ 178: 33-50

Pickerill RK, Donovan SK 1998. Ichnology of the Pliocene Bowden shell bed, southeast Jamaica. In: Donovan SK (ed) The Pliocene Bowden Shell Bed, Southeast Jamaica. Contr Tertiary Quatern Geol 35: 161-175

Plewes CR, Palmer TJ, Haynes JR (1993) A boring foraminiferan from the Upper Jurassic of England and northern France. J Micropalaeont 12: 83-89

Radtke G (1991) Die mikroendolithischen Spurenfossilien im Alt-Tertiär West-Europas und ihre palökologische Bedeutung. Cour Forschinst Senckenb 138: 1-185

Schmidt H, Freiwald A (1993) Rezente gesteinsbohrende Kleinorganismen des norwegischen Schelfs. Natur Museum 123: 149-155

Schnick H (1992) Zum Vorkommen der Bohrspur *Hyellomorpha microdendritica* Vogel, Golubic & Brett im oberen Obermaastricht Mittelpolens. Z Geol Wiss 20: 109-124

Taylor PD, Wilson MA (2003) Palaeoecology and evolution of marine hard substrate communities. Earth Sci Rev 62: 1-103

Titschack J, Freiwald A (2005) Growth, deposition, and facies of Pleistocene bathyal coral communities from Rhodes, Greece. In: Freiwald A, Roberts JM (eds) Cold-water Corals and Ecosystems. Springer, Berlin Heidelberg, pp 41-59

Vénec-Peyré M-T (1987) Boring Foraminifera in French Polynesian coral reefs. Coral Reefs 5: 205-212

Vénec-Peyré M-T (1996) Bioeroding foraminifera: a review. Mar Micropaleont 28: 19-30

Vogel K (1993) Bioerosion in fossil reefs. Facies 28: 109-114

Vogel K, Golubic S, Brett CE (1987) Endolith associations and their relation to facies distribution in the Middle Devonian of New York State, U.S.A. Lethaia 20: 263-290

Voigt E (1971) Fremdskulpturen an Steinkernen von Polychaeten-Bohrgängen aus der Maastrichter Tuffkreide. Paläont Z 45: 144-153

Voigt E (1972) Über *Talpina ramosa* v. Hagenow 1840, ein wahrscheinlich zu den Phoroniden gehöriger Bohrorganismus aus der Oberen Kreide, nebst Bemerkungen zu den übrigen bisher beschriebenen kretazischen „*Talpina*"-Arten. Nachr Akad Wissensch Göttingen 2. Mathemat-physik Kl 1972: 93-126

Voigt E (1975) Tunnelbaue rezenter und fossiler Phoronidea. Paläont Z 49: 135-167

Voigt E (1978) Phoronidenbaue (*Talpina ramosa* v. Hagenow) aus der Maastrichter Tuffkreide. Nathist Genoot Limburg 28: 3-6

Wisshak M, Freiwald A, Gektidis M, Lundälv T (2005) The physical niche of the bathyal *Lophelia pertusa* in a non-bathyal setting: environmental controls and palaeoecological implications. In: Freiwald A, Roberts JM (eds) Cold-water Corals and Ecosystems. Springer, Berlin Heidelberg, pp 979-1001

Bioerosion patterns in a deep-water *Lophelia pertusa* (Scleractinia) thicket (Propeller Mound, northern Porcupine Seabight)

Lydia Beuck, André Freiwald

Institute of Paleontology, Erlangen University, Loewenichstr. 28, D-91054
  Erlangen, Germany
  (lydia.beuck@pal.uni-erlangen.de)

Abstract. This study focuses on bioerosion of an aphotic deep-water coral mound, the Propeller Mound, in the northern Porcupine Seabight. The predominant framework builder is the cosmopolitan cold-water coral *Lophelia pertusa*. We demonstrate bioerosion patterns within the skeleton of *L. pertusa* using a new embedding method under vacuum conditions with subsequent scanning electron microscope analysis. Following this method, 23 ichnospecies are documented and related to heterotrophic organism groups such as Bacteria (1), Fungi (12), Bryozoa (1), Foraminifera (3), and Porifera (6). Predominant endolithic sponges in the framework of *L. pertusa* are *Alectona millari* and *Spiroxya heteroclita*. Owing to its characteristic growth and surface ornamentation, trace casts of *Spiroxya heteroclita* are correlated to the well-known trace fossil *Entobia laquea*.

  Investigations of thin sections of *post-mortem* skeletons show a clearly pronounced endolithic tiering of three penetration depths. The analysed samples are divided into three macroscopic preservational stages differing in *post-mortem* age, and exposure of the framework. Bioerosion affects bare parts of the coral skeleton. Bioeroders preferably settle on one side of an upright growing colony. A succession usually starts with the infestation by bacteria and fungi. Contact zones of epiliths are preferred areas for penetration by endoliths. Sponges and foraminifers appear 10 cm below the zone of living polyps, followed by boring bryozoans 15 cm below. However, in one case the sponge *Spiroxya heteroclita* is documented in the skeleton of living polyps. Frameworks exposed to water host 19 ichnospecies, thus forming the most diverse ichnocoenosis, whereas nine ichnospecies are documented in coral specimens buried by sediment. Mapping of epi- and endoliths in living and freshly necrotic colonies represents a useful tool for monitoring environmental conditions and define ecological "health" of deep-water corals in a rapid large-scale assessment of the state of coral reefs.

Keywords. Bioerosion, *Lophelia*, Porcupine Seabight, carbonate mound, ichnocoenosis

Introduction

Biodegradation or bioerosion (Neumann 1966) comprises disintegration processes of hard substrates such as carbonate limestones and calcareous skeletons through the activity of organisms. This includes mechanical removal of carbonates (bioabrasion), chemical dissolution (biocorrosion), or a combination of both (Golubic and Schneider 1979). The different bioerosion processes result in the breakdown of calcareous skeletons to smaller-sized grains, in the collapse of reefal frameworks, and in the modification of carbonate limestone coasts into a deeply eroded biokarst (Schneider and Torunski 1983; MacIntyre 1984; Günther 1990; Wood 1995). The study of bioerosion features is of utmost importance for palaeontologists and biologists in order to reconstruct palaeoenvironments, because the different bioeroding organisms leave characteristic traces such as grazing- and bite-traces, or borings in the calcareous skeleton of their hosts. The latter are the focus of this study. These boring or endolithic trace communities (ichnocoenoses) show a very high fossilisation potential.

Deep-water bioerosion

The majority of studies dealing with modern biologically-driven carbonate alterations concentrate on shallow-water settings (Wilson 2003). In contrast, few investigations have been dedicated to the deep and aphotic environment (Zeff and Perkins 1979; Budd and Perkins 1980; Hook et al. 1984; Hook and Golubic 1988, 1990, 1992, 1993).

In the aphotic zone, endolithic assemblages are dominated by heterotrophic organisms, such as bacteria, fungi, bryozoans, foraminiferans and sponges. Thorough investigations of macro- and microbioerosion in deep-water corals were carried out on *Lophelia pertusa* (Linné, 1758) thickets on the Rockall Bank in 200-400 m water depth (Scoffin et al. 1980). The coral fragments analysed show an "etched" skeletal surface with exposed aragonite needles and granules that are considered the result of maceration or carbonate dissolution. Endolithic sponges have been documented from deep-water coral assemblages on the West Florida slope at a water depth of 500 m (Newton et al. 1987), from the northern Little Bahama Bank between 1000 m and 1300 m water depth (Mullins et al. 1981), and from the Cobb Seamount, northeast Pacific, in 310 m to 360 m water depth (Farrow and Durant 1985).

From his studies, Scoffin (1981) concluded that the regime is destructive for *L. pertusa*, because the rate of bioerosion will surpass that of the background ooze sedimentation. The anticipated fossilisation potential for deep-water coral frameworks is low and will result in the formation of low-relief lenses consisting of bioeroded coral rubble layers. Scoffin (1981) argued that a high sedimentation rate will halt both framework growth and *post-mortem* biodegradation.

Boerboom et al. (1998) analysed the bioerosion of *Desmophyllum cristagalli* Milne-Edwards and Haime, 1848 from Orphan Knoll, northeast off Newfoundland, at 1700 m water depth.

Here, sponges and fungi belong to the most prominent skeletal excavators. The most striking observation of his study, however, is the presence of external

micritisation of the coral skeleton due to the fine-tuned fungal infestation. This micritisation leads to the formation of micritic envelopes within the near-surface perimeter of the coral fragments. Micritic envelopes had previously been considered reliable shallow-water indicators in modern and past environments (<20 m; e.g., Swinchatt 1969; Gunatilaka 1976; Flügel 1982). They are thought to form in warm-water supersaturated with respect to calcium carbonate. Although micritic rims are also described from deeper water (Zeff and Perkins 1979; Hook et al. 1984), they are significantly more abundant in shallow marine environments (Bathurst 1966).

The most prominent difference between the photic shallow-water and the aphotic deep-water ichnocoenoses is that phototrophic boring algae and cyanobacteria and their highly adapted grazers are absent in the latter. The observation of depth-related changes in the endolithic community has led to the recognition of palaeobathymetric depth zonations of neritic environmental settings throughout the Phanerozoic (Perry and MacDonald 2002; Vogel and Glaub 2004).

Mineralisation

The taphonomy, or fossilisation path, of the reef-forming deep-water coral (thereafter refererred to as DWC) *L. pertusa* was studied by Freiwald et al. (1997) and Freiwald and Wilson (1998), who investigated external and internal skeletal alterations from living to post-mortal areas of *L. pertusa* colonies. Based on underwater camera documentation and sampled corals, a characteristic transition from pristine white aragonitic coral skeletons in living zones to increasingly brownish and blackish-stained dead parts was observed in individual colonies. While coral-associated epibenthic organisms are sparse in the pristine whitish zone, intense and diverse colonisation of the coral skeleton drastically increased in the dead, stained, skeletal portions (Freiwald 1998).

Elemental analysis of the dark stain by EDX-SEM methods revealed a thin ferromanganese coating that completely covers exposed external parts of the skeleton, including the surface of hollows, pits and borings into the skeleton. Several lines of evidence pointed towards a microbial trigger for the selective precipitation of the coating. The initial precipitation products form accumulations of individual 3 to 8 μm-large rings, or "doughnuts" that are associated with a microbial consortium of epilithic fungi and bacteria (Allouc et al. 1999). At a later stage, probably without the influence of microbes, the cryptocrystalline metal seed crystals formed larger plates, thus forming a coherent thin coating. Through microbial catalysis, dissolved Mn^{2+} will be converted into solid MnO_2 preferably under dysoxic conditions (Ghiorse and Ehrlich 1992; Konhauser 1998).

Scope of this study

This study focuses on biodegradation of *Lophelia pertusa* thickets sampled on the summit of the Propeller Mound. Therefore, a vacuum embedding method was developed, which allows analysis of ichnofabrics within a carbonate skeleton. We attempt a characterisation of the trace community. This includes a classification of prominent traces and correlation to their producers, and the distribution of traces within a colony framework. On the basis of the borings and their distribution

patterns within a colony, we aimed to reconstruct past ecological conditions. In addition, comprehensive knowledge of composition of the endolithic communities (ichnodiversity) is a key for understanding longevity and fossilisation potential, and can lead to the definition of ecological "health" of DWC for a rapid large-scale assessment of the state of such coral reefs.

Setting

The Propeller Mound (PM) is located in the northern Porcupine Seabight off the western coast of Ireland near the transition between the Porcupine Bank and Slyne Trough, and belongs to the Hovland Mound Province (Fig. 1; De Mol et al. 2002). The summit of the mound lies at 52°09.80N and 12°46.40W in 653 m water depth. The PM forms a freely exposed 140 m high structure emerging from the lower slope of the Porcupine Bank. The vicinity of the mound is dominated by an extended north-west to south-east sloping drift sediment wedge with 740 m water depth in the western section, and 920 m water depth in the eastern section of the surveyed grid. The mound is bathed in a mixture of Eastern North Atlantic (ENAW) and Mediterranean Outflow Water (MOW). Both are northward flowing intermediate water masses that are entrapped in the embayment of the Porcupine Seabight. The temperature varies from 9-10°C, and salinity is generally >35.4 ‰ depending on the proportion of the warmer and more saline MOW. The dredged samples studied here were derived from RV Poseidon Cruise 265 to PM at the station GeoB 6739-1 (52°08.71N, 12°46.33W, 780 m water depth).
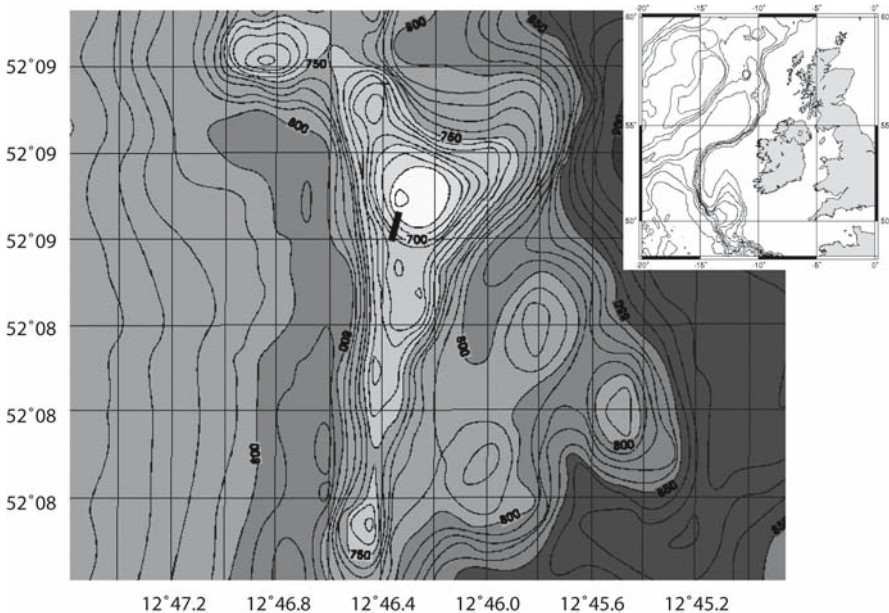
Fig. 1 Bathymetric map of the Propeller Mound, Hovland Mound Province, Porcupine Seabight. The line indicates the dredge site. Bathymetry was obtained during POS-265

Material

Samples from three different, macroscopically defined framework preservational stages were studied:

1) Colony with ochre coloured tissue covering the upper 10 cm of the framework, and with basally exposed skeleton. Tubes of the polychaete *Eunice norvegica* (Linné, 1767) are located in the upper parts. The dead and exposed skeletal framework is encrusted by sessile bryozoans, serpulids and bivalves. Bioerosion patterns are difficult to detect. Three colonies were investigated.

2) Dead colonies coated with a brownish faint Fe-Mn layer and settled by a multitude of epizoans. Bioerosion pattern is clearly visible in form of multiple borings. 12 coral pieces were attributed to this stage.

3) Buried pale to white *L. pertusa* colonies. Bioerosion patterns are clearly visible in the form of "comma"-formed notches and some circular borings. Ten samples were studied.

Laboratory methods

Vacuum cast-embedding technique

For trace studies, methods by Golubic et al. (1970) and Golubic (1983) are widely used. The methods are based on an infiltration phase of acetone into the substratum, and a time-consuming gradual replacement of acetone with the epoxy resin Araldite. Other methods require a boiling of the specimen within the embedding medium under vacuum conditions, generating bubbles (Nielsen and Maiboe 2000).

For this study, we developed a timesaving vacuum cast-embedding technique. This new method excludes gradual infiltration, boiling and a long standby time. The vacuum cast embedding technique was developed to fill the often blind-ending cavities within the massive carbonate of the skeletons. Air-dried samples were cut in pieces of 1.5 cm in length. Organic remains were dissolved either with a solution of hydrogen peroxide (35 %) or sodium hypochlorite (12.5 %) applied to the samples for 24 hours. After cleaning in an ultrasonic bath, the specimens were rinsed in distilled water and dried at 50°C. The coral specimens were then placed in a small silicon cup (r = 12.5 mm) into an exsiccator (see Fig. 2). One of the two exits was connected to a vacuum pump, the other one led *via* a small plastic duct (Ø 4-6 mm) from the cup to the prepared epoxy resin mixture (SpeziFix-20; Struers GmbH). Instructions for preparation of the mixture are included in the resin kit. A hose clamp, positioned at the latter duct, prevented an immediate intake of resin when the vacuum pump was turned on. At vacuum pressures of 100 mbar, the two-component epoxy resin was dosed into the cup *via* the hose clamp by drops until the sample was completely immersed. The subsequent aeration of the exsiccator took place using a valve at the side of the vacuum pump. This set-up is an analogue construction of the Vacuum Impregnation Chamber Epovac (Struers GmbH). The hardening of the epoxy resin lasts for up to eight hours at room temperatures with additional
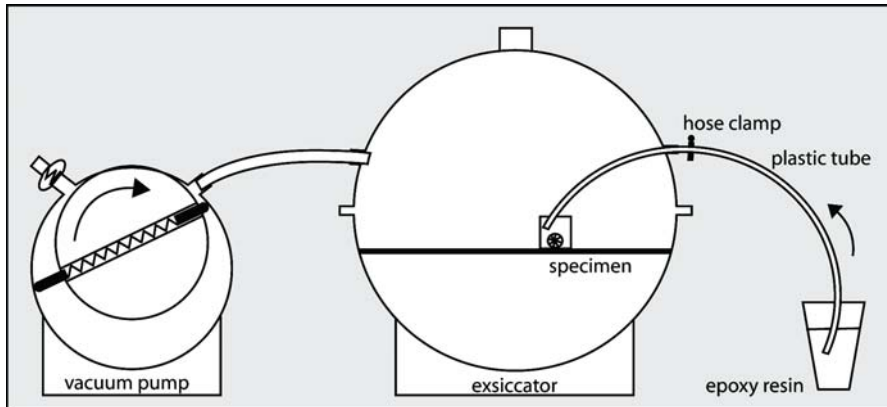
Fig. 2 Experimental set-up for the cast-embedding technique under vacuum conditions

induration in a cabinet drier (50°C) for two hours. SpeziFix-20 is a transparent epoxy, thus the subsequent cutting was monitored visually. Embedded coral pieces were sawn along their longitudinal axes and put in a solution of hydrochloric acid (5 %) so that a total elimination of the carbonate was achieved and the trace casts lay exposed. Subsequently, the epoxy resin pieces were washed in Millipore filtered water to prevent a possible chemical precipitation, and dried at 50°C. Finally, the preparations were glued onto aluminium object holders, sputter-coated with a 20 nm thin gold layer and analysed with a scanning electron microscope (SEM). Digital SEM pictures of resin casts were measured and coloured with the Adobe Photoshop® software to accentuate different boring organism traces.

Due to the preparation, tubular traces with diameters less than 1.5 μm often collapsed during the dissolving process of the carbonate. In addition to traces of endoliths, a multitude of calcified epiliths produced casts, which were restricted to the outer perimeter of the skeleton (Fig. 4H). In contrast, sessile or boring organisms that infested the skeleton during lifetime of the colony were completely encalcified by the coral and therefore could not be documented.

Thin sections

Transverse thin sections of embedded coral pieces were prepared and documented with the light microscope Olympus SZX-ILLD. Digital pictures were edited with Adobe Photoshop® software.

Results and interpretation

Characterisation of aphotic bioeroders

Within the three investigated preservational stages of *Lophelia pertusa* frameworks, 23 different trace types were observed. They exclusively belong to the heterotrophic organism groups Bacteria, Fungi, Bryozoa, Foraminifera and Porifera (see Fig. 3). In this paper, the most prevalent traces and their producers are
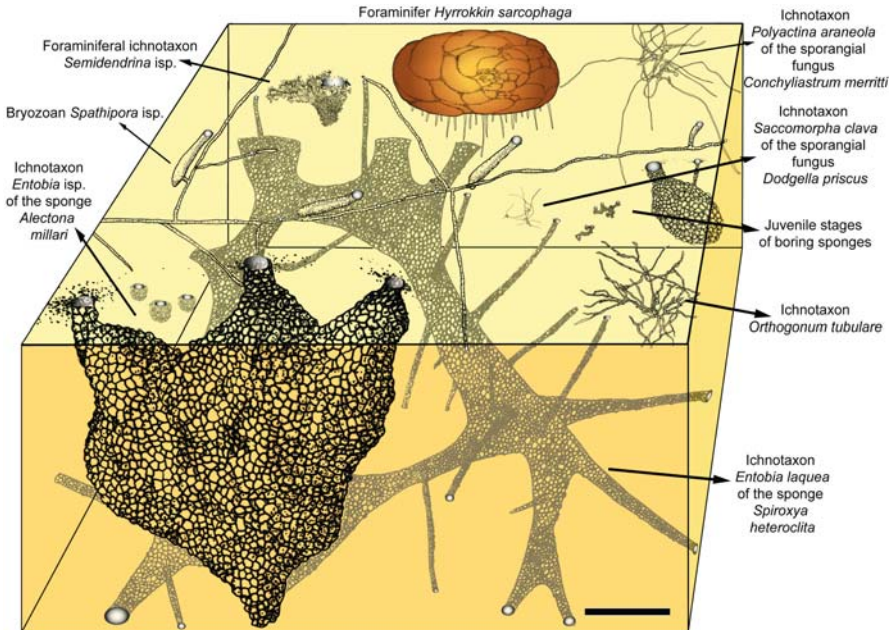
Fig. 3 Schematic overview of the common endolithic ichnocoenoses within the framework of *Lophelia pertusa* at the Propeller Mound; scale bar 1 mm

described and divided according to their size into microborings, which need a SEM for documentation, and macroborings, which are visible by naked eye (Taylor 1999; Bromley 2004).

Microborings

Bacteria

Corroding bacteria are found in chemoorganotrophic groups (Fritsche 1999). They secrete organic acids (e.g., oxalic, gluconic, citric, acetic), which etch the substratum. In this study, a "Coccoidal Form" with diameters of 0.4-0.6 µm forming chains or agglutinated compounds is interpreted as bacteria (Fig. 5B). The dimensions of these spherical traces are reminiscent of coccoidal bacteria that are ubiquitously distributed in different taxonomic groups and habitats (Madigan et al. 2000).

Fungi

Endolithic fungi are known from the orders Saprolegniales, Peronosporales (Oomycota) and Cytridiomycetes (Eumycota) (Glaub 1994). They nourish themselves on organic matter and produce, like bacteria, several acids (e.g., sulfuric or nitric acid), which are mainly secreted from their hyphae apically, and allow them to penetrate the carbonate (Sand 1995). Due to the difficulties in laboratory cultivation of endolithic fungi, taxonomic classifications are usually complicated. Focused on morphology, boring fungi can be divided into two main categories: 1) vegetative, undetermined, branched filaments (hyphae), and 2) homogeneous hyphae which are either locally or centrally enlarged. These swellings function
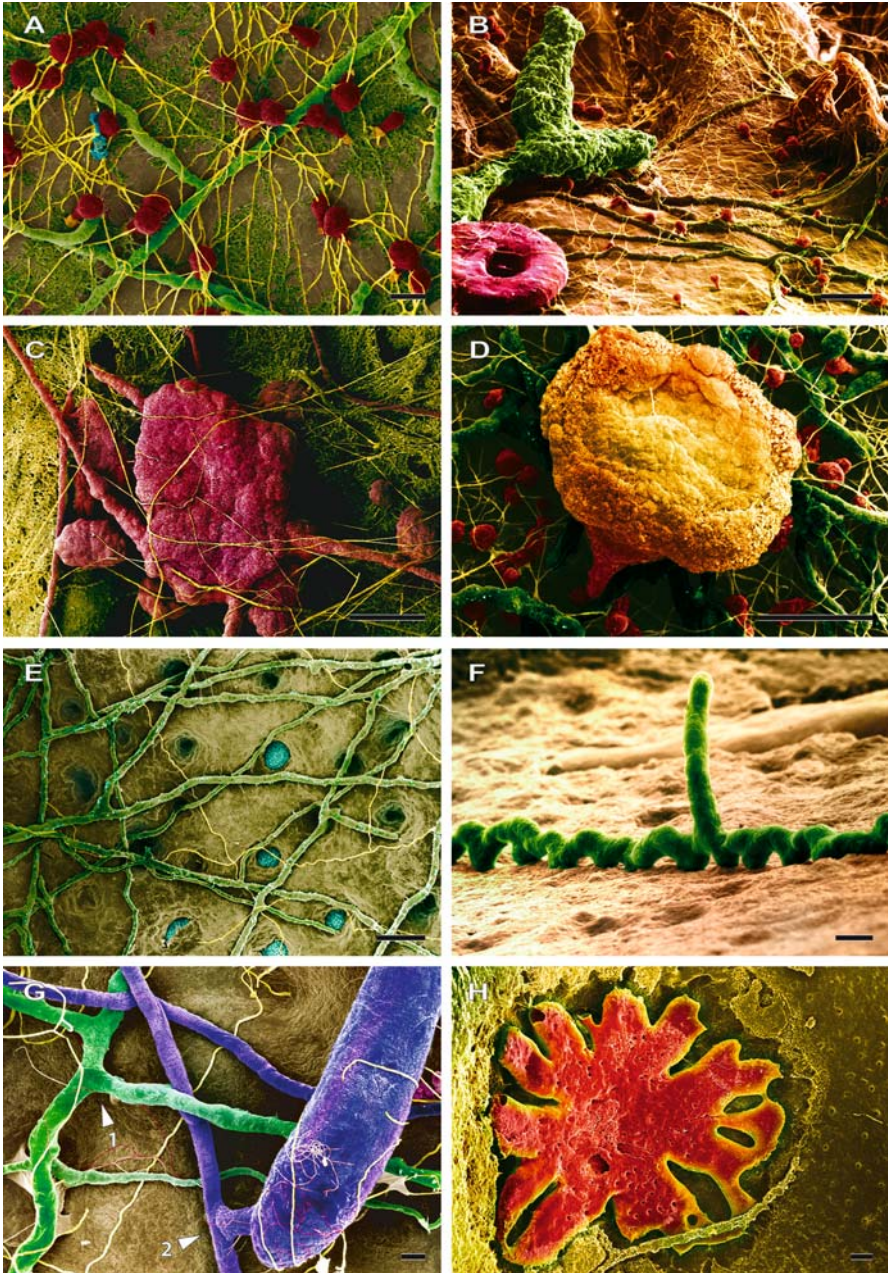
Fig. 4 Coloured SEM images of resin casts. **A** Characteristic ichnocoenosis of the aphotic zone with microboring Sponge Type 1 (blue), associated with tubes of the ichnospecies *Orthogonum lineare* Glaub, 1994 (green), *Scolecia serrata* Radtke, 1991 network (dark green), and ichnospecies *Saccomorpha clava* Radtke, 1991; filaments (yellow) of the latter connect single "bulb"-shaped swellings (red) with each other; scale bar 30 μm. **B** Coloured in pink a

as reproductive chambers (sporangia). The sporangia harbour a high numbers of zoospores and their surfaces become increasingly bumpy as boring progresses (Zebrowski 1936).

At the Propeller Mound six tubular traces were observed. A prevalent trace consists of elongated, filigree tubes of 0.4-0.5 µm in diameter creating wide-meshed networks by ramifying at rare intervals (in the following referred to as "Filigree Form"). The circular tubes terminate by splitting into two to three dichotomous ramifications at short distances. In addition, the network can be found immediately on the cast surface (Fig. 4G). Owing to the small diameter of the tubes, their resin casts can collapse after dissolution of the carbonate. Comparable traces were not found in the literature.

Another common tubular ichnospecies is *Scolecia serrata* Radtke, 1991 (Figs. 4A, C, 5F). In strongly bioeroded specimens this trace often creates dense, partly multi-layered networks, which are able to camouflage other traces. Zeff and Perkins (1979) assume Bacteria or Fungi to be the producer.

The tubular ichnogenus *Orthogonum* is present with two ichnospecies (Figs. 4B, D-G): *Orthogonum tubulare* Radtke, 1991 and *Orthogonum lineare* Glaub, 1994. Both consist of smooth textured tubes, from which up to 4.5 µm-long hairs originate sporadically. At small distances of about 40 µm the ducts of both ichnospecies connect with the exterior. Every trace varies strongly in its tube diameter, termination, its mode of ramification, and the presence of hairs. In the literature, *Orthogonum tubulare* is also mentioned with its synonym "tubular form" by several authors (e.g., Zeff and Perkins 1979; Budd and Perkins 1980).

Six ichnospecies could be related to the group of sporangial Fungi. The prominent trace *Saccomorpha clava* Radtke, 1991 dominates the ichnocoenosis with three morphotypes, considering the sack-like swellings (Figs. 4A-B, D). Its filaments of about 1.5 µm in diameter connect single swellings with each other. This trace is mentioned by several authors, e.g., Zeff and Perkins (1979), and interpreted as borings of the fungi *Dodgella priscus* Zebrowski, 1936 and *Dodgella inconstans*

---

cast of a semi-encalcified epizoan *Spirorbis spirorbis* Linné, 1758, behind which in green a trace of a juvenile sponge; brownish coloured a trace of a foraminiferal boring, ichnospecies *S. clava* (red/yellow), and *O. lineare* filaments (green); scale bar 100 µm. **C** Mature stage of the trace *Polyactina araneola* Radtke, 1991 (red) of the fungus *Conchyliastrum merritti* Zebrowski, 1936, partly covered by *Scolecia serrata* (green); scale bar 100 µm. **D** In the centre a swelling chamber of a currently undescribed fungus, *S. clava* (red/yellow) and *Orthogonum lineare* (green); scale bar 100 µm. **E** Ichnospecies *Orthogonum lineare* (green), coloured in turquoise the attached base of an epilithic organism; scale bar 100 µm. **F** *Orthogonum tubulare* (green); scale bar 20 µm. **G** Filaments of a "Filigree Form" (purple), casts of hyphens of *S. clava* (yellow), microboring Sponge Type 1 (purple), ducts of the ichnospecies *Orthogonum lineare* (green), sporadically covered with small hairs; bryozoan stolons (blue) with identical tube diameter to the fungal trace *O. lineare* (green), but in contrast to the latter always smooth and with a characteristic mode of ramification (see arrows 1 and 2); scale bar 20 µm. **H** Base of a calcareous coral (red), which uses the skeleton of *Lophelia pertusa* as its substrate, scale bar 100 µm
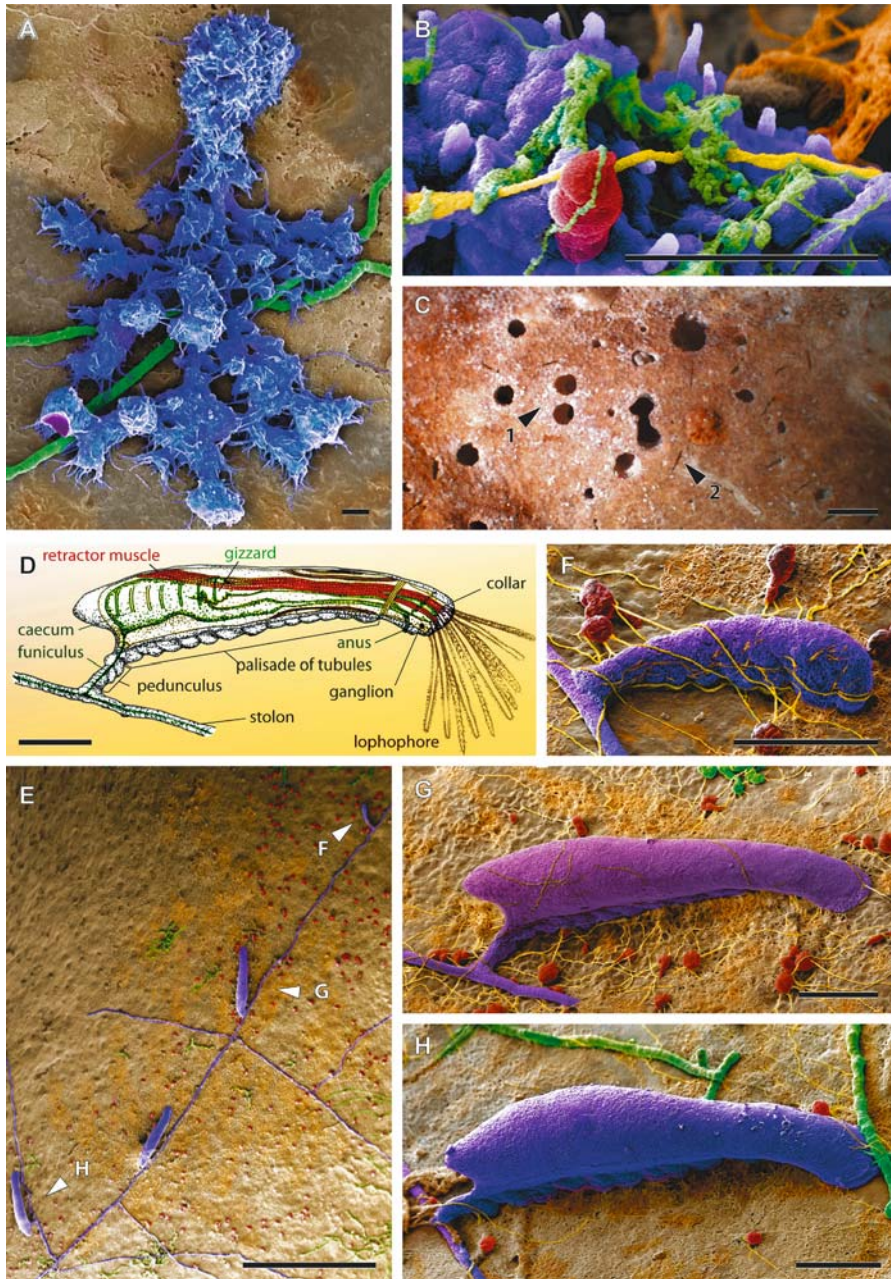
Fig. 5 A-B, E-H Coloured SEM images of resin casts (coloured by Christian Schulbert, IPAL Erlangen), **C** light microscope image, **D** schematic drawing. **A** *Semidendrina* Form (blue) and *Orthogonum tubulare* Radtke, 1991 (green); scale bar 30 μm. **B** Detail of **A** with *Semidendrina* Form (blue), "Coccoidal Form" (green), filaments (yellow) of the fungal trace *Saccomorpha clava* Radtke, 1991 with a swelling (red) as a secondary settler; scale bar

Zebrowski, 1936 (family Cladochytriaceae). Glaub (1994) documents and dates it back to the Jurassic. This cosmopolitan trace is located in the micritic envelope of the coral, which was thus regarded as a *Dodgella*-layer by Freiwald and Wilson (1998). In combination with *O. lineare,* this ichnocoenosis typically indicates aphotic conditions (Glaub 1994).

Another prominent sporangial trace has been correlated to the ichnospecies *Polyactina araneola* Radtke, 1991 (Figs. 4C, 7C-D). Its centrally arranged swellings can reach penetration depths of up to 350 μm. In contrast, its filaments penetrate the entire skeleton. The trace morphology is similar to the boring of the fungus *Conchyliastrum merritti* Zebrowski, 1936. According to Schmidt (1992) it is recognised since the Triassic.

Ectoprocta

In the group of boring Bryozoa (order Ctenostomata), 13 genera including 48 species have been described, mostly from shallow-water environments (Pohowsky 1978). Individual species are distinguished, according to Pohowsky (1978), by such characters as size, shape and spatial orientation of zooids, in ramification angles of the stolons, and in the existence of a connection between stolon and zooid (pedunculus).

In this study, macroscopic "comma-shaped" notches are common on the surfaces of old coral pieces indicating the presence of boring bryozoans with zooid chambers immediately below the surface. When exposed to mechanical forces, the roof above the excavated boring can collapse, exposing the zooid cavities. Within the protective substratum the zooids are connected by an aperture with the exterior. For feeding they extend their lophophore into the water column (Fig. 5D). Associated with *Lophelia pertusa*, traces of the ichnogenus *Spathipora* Fischer, 1866 are found. The trace consists of smooth textured tubes having a homogeneous diameter of about 14 μm. These tubes harbour the stolons. The tubes preferably ramify with an extended insertion (Fig. 4G) at a perpendicular angle from the main tube and end hemispherically. To the left of the growth direction, several zooid cavities up to 510 μm-long are connected by a 50 μm-long interconnection (pedunculus) to the tube (stolon). At the zooid cavity, the pedunculus originates at 25 μm behind the distal end of the aperture. Between the aperture (diameter 72 μm) of the zooid cavity and the pedunculus, a "palisade of tubules" stretches up to 400 μm-long; its tubules end at the surface. Diameters of the zooid cavities increase slightly towards

30 μm. **C** Surface of a Fe/Mn-incrusted, dead colony of preservational stage 2 with in- and exhalant apertures of boring sponges (arrow 1), and "comma"-shaped notches of bryozoan zooid apertures (arrow 2); scale bar 1 mm. **D** Reconstruction of an adult zooid within its trace (modified after Anderson 1998); scale bar 100 μm. **E** Overview of a *Spathipora* isp. colony, single individuals (zooids) are connected by ducts (stolons) with each other (purple), red spots are sporangia of the trace *S. clava*, associated with *O. tubulare* (green); scale bar 1 mm. **F** Juvenile zooid chamber with an incremental growth (purple), *Saccomorpha clava* (yellow/red), *Scolecia serrata* Radtke, 1991 (brownish); scale bar 100 μm. **G** Longitudinal growth stage of a zooid cavity (purple); scale bar 100 μm. **H** In purple, cast of a full-grown zooid (lateral growth stage); scale bar 100 μm

the distal, bluntly rounded cup from 60 μm to 95 μm. The trace can invade the substratum to a depth of 135 μm.

Derived from trace morphology, the ontogeny of a zooid can be divided into three stages:

1) Incremental growth (Fig. 5F)

Perpendicular to the stolon, a pedunculus extends, and expands by lining up 17 μm-long tubules. The consecutive, incremental growth of tubules with increasing diameters result in a linear expansion to a "palisade of tubules" of 400 μm in length. Presumably, the lophophore of the zooid could extend temporary to the outside through the youngest tubulus.

2) Longitudinal growth (Fig. 5G)

The zooid expands into the substrate from the "palisade of tubules" in a sack-like form. At the same time, the part of the "sack" that is at the growing zone of the "palisade of tubes" overgrows the "palisade" and builds a full-sized aperture at its distal tip.

3) Lateral growth (Fig. 5H)

Finally, the aperture's distal end grows hemispherically and, in addition, the rear part of the zooid cavity expands laterally.

The trace is morphologically similar to the ichnogenus *Spathipora*. Its smooth tubes can be mistaken for filaments of the fungus *Orthogonum*, but they have a different ramification patterns. The observed *Orthogonum* traces are lacking in segmentation, in contrast, the bryozoan tubes always bear suture-like junctions between different tube orders (Fig. 4G).

Foraminifera

In this study, a spinous tube relief is considered characteristic for boring traces produced by Foraminifera. The most frequent trace of the three documented foraminiferal ichnospecies is characterised by morphologically variable "juvenile" stages and a conservative end stage. Thus, the trace comprises two morphological parts (Fig. 5A). The first part is a plain basal system of slightly ellipsomorphical tubes of about 35 μm in diameter, which diverge at only small distances from the substrate surface into fan-like chambers. The plain basal system can be up to 660 μm in diameter. The surface of the tubes is densely covered by thin rhizoidal filaments with diameters of 2-4.5 μm, decreasing towards their ends. Older traces show elongated "whip"-like filaments up to 220 μm in length. The second part is located laterally to the basal system, and comprises an exposed tower-like structure penetrating up to 350 μm into the substratum. It is composed of flattened spheres with finger-shaped branches, up to 17 μm-long (see Fig. 5B).

Juvenile stages are usually smaller sized basal systems with short rhizoidal filaments, but also small versions of the mature growth manner could be observed.

The foraminifer *Globodendrina monile* Plewes, Palmer and Haynes, 1993 produces a similar trace, however, surficially attached agglutinating chimneys are not observed in the present material (Plewes et al. 1993). This trace with its characteristic "spinous tube relief" is described in Radtke (1991) as a *Semidendrina* form and as Radiating Form 1 (Bromley 2005). This morphology is believed to be an adaptation

of high-energy environments (Cherchi and Schröder 1991). In addition, a common producer of foraminiferal traces is the surficially attached *Hyrrokkin sarcophaga* Cedhagen, 1994. This species produces a multitude of "whip"-like canals, which penetrate perpendicularly the skeletal wall of *Lophelia* up to 1.5 mm. Basally, the individual canals measure up to 40 μm in diameter, but rejuvenate distally (see also Freiwald and Schönfeld 1996; López Correa et al. 2005).

Macroborings

Porifera

Boring sponges are assigned to the order Hadromerida (Hooper and Soest 2002) and the order Haplosclerida (Soest and Hooper 2002) in the group Demospongiae. Using further determination categories described by Bromley and D'Alessandro (1984), sponge traces vary in aperture size, abundance, morphology and connection of chambers, ontogenetic development and penetration depth. In addition, they are also distinguished by variation in their etching process (Calcinai et al. 2003).

On the surface of dead *L. pertusa* colonies, macroscopic etching holes of up to 1 mm are abundant (Fig. 5C). These openings contain the in- and exhalant papillae of endolithic sponges. In SEM images of resin casts, sponge traces can be easily distinguished from those of other boring organisms by their characteristic verrucous, botryoidal surface within the protective substrate. In this study, the zoological classification is based on the documentation of sponge spicules.

At the Propeller Mound four macroscopic sponges dominate the ichnocoenoses. A common endolithic sponge is *Spiroxya heteroclita* Topsent, 1896. Creating extensive galleries it excavates the entire skeleton (Figs. 6E-F). The single chambers are divided by characteristic constrictions. Perpendicular to the chambers, and having similar diameters, in- and exhalant channels project and exit to the surface. The texture of the chamber walls is composed of slightly flattened etching cells with an average diameter of 40 μm. In contrast, the etching cells of the apertural canals are smaller in size, between 10-15 μm in diameter, and have an extremely conical shape. The ornament of the etching cells is smooth.

A somewhat similar trace is described from the Plio-Pleistocene of the Mediterranean area as *Entobia laquea* Bromley and D'Alessandro, 1984 in the skeleton of *Lophelia pertusa* (Bromley and Asgaard 1993a).

In addition to *S. heteroclita*, another endolithic sponge *Alectona millari* Carter, 1879 is also common in the skeleton of *L. pertusa*. *A. millari* is easily identified by its brownish tissue and its characteristic micro- and megascleres (Fig. 7A). It forms massive central chambers with etching cell diameters between 50-100 μm (Fig. 6D), from which exploratory threads with smaller-sized etching cells can extend. In comparison to *S. heteroclita*, the trace casts differ paradigmatically in the morphology of the chambers, apertural canals, and ornamental sculpture of the etching cells. In *A. millari* the latter are not smooth but bear incremental growth lines (Figs. 6B-E, 7B; see also Vacelet 1999).

In the phylum Porifera, two other morphological types were identified with tube dimensions of microborings. For example, microboring Sponge Type 1 consists of up to 250 μm-long branches, which are between 18-24 μm in diameter. Some of

the preferably perpendicularly projecting tubes fuse after ramifying. The surface of the trace is composed of corroding cells, which are 4 to 4.5 µm in diameter each, and show a strong relief texture. Active etching cell stages are observed. The trace penetrates the skeleton to a depth of 35 µm (Figs. 4A, G, 6A). However, the absence of spicules prevented a zoological classification. This trace is considered to be a
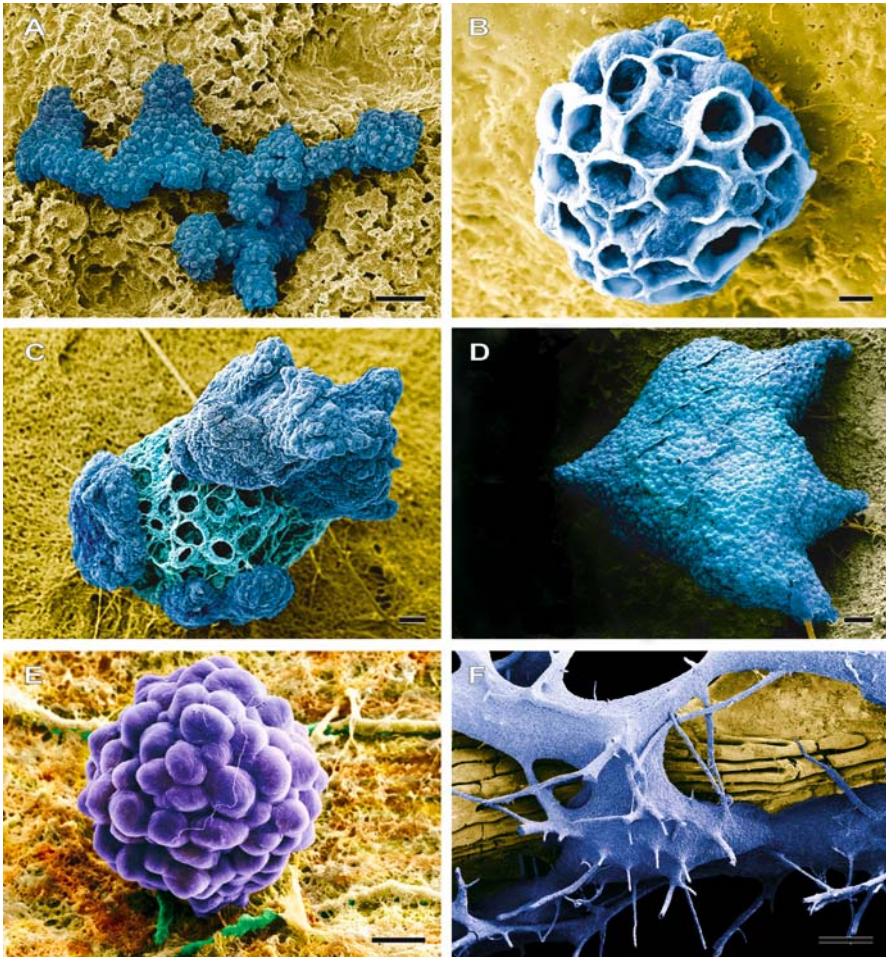
Fig. 6 Coloured SEM images. **A** Juvenile stage of microboring Sponge Type 1 (blue); scale bar 30 µm. **B** Juvenile stage of *Alectona millari* Carter, 1879 (blue) showing the work of specialised archaeocytes, the etching cells; documented are different growth stages of active etching cells with their characteristic incremental growth; scale bar 20 µm. **C** Secondary settlement of an *Alectona millari* cavity (turquoise) by a microboring sponge (blue); scale bar 30 µm. **D** *A. millari* cavity with three apertures (blue); scale bar 300 µm. **E** "Blackberry"-shaped cast chamber of an early juvenile *Spiroxya heteroclita* Topsent, 1896 (purple); scale bar 20 µm. **F** Vast sponge galleries of *S. heteroclita* that infest the skeleton of a living polyp; it produces the trace *Entobia laquea* Bromley and D'Alessandro, 1984 (blue); scale bar 1 mm
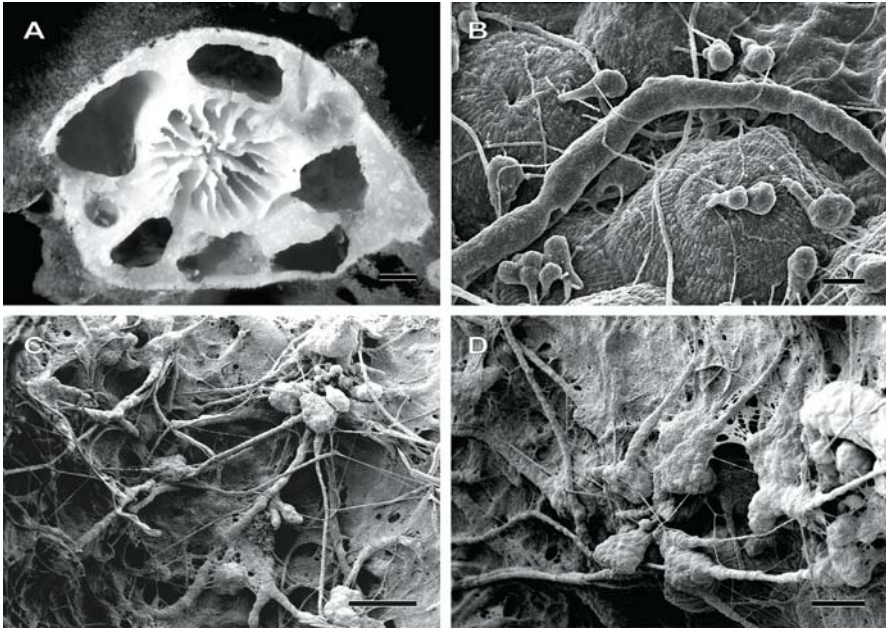
Fig. 7 A Light microscope image, **B-D** SEM images of resin casts. **A** Large endolithic galleries of *Alectona millari* Carter, 1879 within the skeleton of *Lophelia pertusa* (Linné, 1758); scale bar 1000 μm. **B** Cast surface of a sponge chamber of *Alectona millari*, which is settled by the fungus *Dodgella priscus* Zebrowski, 1936; scale bar 20 μm. **C** Ichnocoenosis of preservational stage 3 dominated by traces of non-filtering organisms, e.g., *Polyactina araneola* Radtke, 1991; scale bar 300 μm. **D** Close-up of a mature stage of the trace *P. araneola*; scale bar 100 μm

juvenile stage of a bioeroding sponge (Soest et al. 2000). A similar trace has also been reported within the skeleton of *Lophelia pertusa* from the Swedish Kosterfjord area (Wisshak et al. 2005).

Characterisation of preservational stages

The investigated preservational stages differ in (1) abundance and (2) development of boring traces, (3) age and (4) mode of exposure of the framework, all of these being major factors that determine the population density of the bioeroding biota and the secondary porosity of the host skeletons. Thus, the documented ichnospecies are snapshots along a progressive time gradient. Ichnocenoses are also influenced by geographically or seasonally limited distribution of spores and larvae, or to the specific substratum property of the bioeroding species.

Preservational stage 1: Living colony with basal dead coral framework

In this stage 15 traces have been found. Due to the absence of protecting coenosarc of the living polyps, several organisms colonized the exposed dead skeleton, usually in a patchy pattern. Contact zones of epiliths are preferred areas for penetration by

endoliths, in which the "Coccoidal Form", "Filigree Form", and *Scolecia serrata* were mostly present. A continuous increase of boring invaders occurs by a multitude of excavating fungi. In general, sponge infestation (Figs. 6A-B) begins 10 cm below living polyps, first bryozoan traces (Figs. 5 E-H) are found 15 cm below. However, in one case the endolithic sponge *Spiroxya heteroclita* creates extensive galleries inside the living corallites by growing from bordering dead parts of the colony (see Fig. 6F).

The spatial boring preference on one side of an upright growing colony can be caused by unilateral prevailing currents, which corrode the unprotected skeleton and facilitate a penetration. Consequently, in areas facing the current, the succession stages might be much more compact than in areas on the protected, leeward side, but a preferred settlement on the latter is also possible. Moreover, an early infestation of *Spiroxya heteroclita* within the framework of living polyps might be an indication of stress factors. Thus, a mapping of epi- and endoliths in living and freshly necrotic colonies can be a useful tool for monitoring environmental conditions. But further studies should be conducted for detailed knowledge.

Preservational stage 2: Fe/Mn-incrusted specimen

A strong micritisation in the outer perimeter of the skeleton complicates the identification of traces. However, the most flourishing ichnocoenoses with 19 different ichnospecies are found in this stage of preservation. Among the sponges, *Alectona millari* and *Spiroxya heteroclita* are the most common, causing a high secondary porosity of the carbonate skeletons (see Fig. 7A). However, these sponges create discrete chambers, and the substratum is not completely destroyed. The death of the endolithic sponges exposes new surfaces for settlement. Thus, the majority of observed microborings are secondary settlers of these sponge cavities (Figs. 6C, 7B). The high porosity which is caused by the filtering sponges, in addition to the Fe/Mn-crusts, indicates that this preservational stage is a late succession stage of biodegradation in the course of time exposed to the water column.

Preservational stage 3: Pale to white buried specimen

Sediment-filled colony branches accommodate nine different traces. A strong micritisation of the perimeter prevented a documentation of sub-expanding traces. In contrast to the Fe/Mn-incrusted specimens of preservational stage 2, only small cast chambers of *Alectona millari* and *Spiroxya heteroclita* are abundant, and thus the porosity is lower. Due to the dominance of non-filtering organisms, we concider a short exposure of dead colonies to the water column. Concerning the fungi, *Polyactina araneola* Radtke, 1991 dominates the ichnocoenosis and was easy to identify on account of its characteristic swellings (Figs. 7C-D). On the one hand, the low diversity ichnocoenosis arose from the sediment-carbonate interaction at the outer perimeter of the skeleton, which is not conducive for trace preservation; on the other hand, sediment burial halted the *post-mortem* biodegradation (Scoffin 1981). Thus, the samples document an interrupted biodegradation. The absence of a Fe/Mn crust can be caused either by dissolution or by lack of precipitation.

The morphology of traces, the abundance and association of ichnospecies, and their spatial distribution can be used as a tool for monitoring environmental conditions.

Characterisation of endolithic tierings

Correlation of penetration depths within all samples led to the division into three sub-ichnocoenoses according to Bromley and Asgaard (1993a, b): Shallow boring organisms lived in the upper 100 μm of the skeleton, such as derivates of *Saccomorpha clava*, "Coccoidal Form", *Scolecia serrata*, and some microboring sponges. With ten traces, the upper 100 μm contain the highest density of organisms (see Figs. 8C-D). Dwellers of the second stage reached penetration depths up to 300 μm, e.g., approached by boring bryozoans (*Spathipora* isp.), and most filaments of the ichnogenus *Orthogonum* are restricted to this level. The group of deeply boring organisms is composed of the "Filigree Form", filaments of the trace *Polyactina araneola,* the *Semidendrina* Form, and mainly sponges. In this
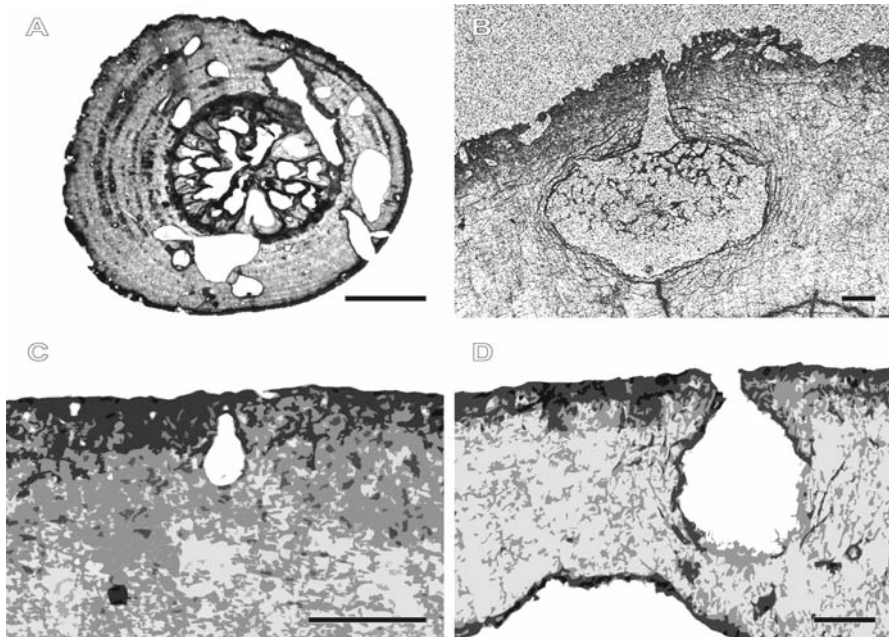
Fig. 8 A-D transmission microscope images of Fe/Mn-incrusted specimens of preservational stage 2. **A** Transversal section of *Lophelia pertusa* corallite with strongly eroded micrite envelope (left) and sponge cavities; scale bar 2 mm. **B** Highly porous perimeter (micrite envelope), and a sponge cavity connected by an apertural canal with the exterior; scale bar 200 μm. **C** Five-colour scheme of the perimeter; the micrite percentage is correlated to the grey intensity. The largest amount of microborings was restricted either to the upper 100 μm (dark grey), or 300 μm (grey); scale bar 200 μm. **D** Five-colour scheme of the perimeter; three grey intensities highlight the penetration levels of the ichnocoenosis. Sponges expose a new surface for settlement after death (dark rim); scale bar 200 μm

investigation, the maximum penetration depth is defined with 2.3 mm, the average thickness of the coral theca.

The grey-level of the black and white images of documented thin sections is proportional to the micrite percentage, due to the small-sized crystals that have a high reflection index and the voids of the crystal matrix of the coral (Figs. 8A-D). The latter is, e.g., caused by the dissolution of crystal lamellae (Boerboom et al. 1998). Most of the microborings are confined to the depth boundary of up to 300 μm. In contrast, endolithic sponges explore the entire carbonate skeleton, and provide a new surface for settlement after their death (Fig. 8D).

The grey-level intensity can reflect the composition and distribution of an ichnocoenosis and rises with the density of microborings.

Conclusions

- The vacuum embedding method is a fast and powerful tool for the study of ichnocoenoses within calcareous substrates.
- In total, 23 forms of traces have been documented and related to the heterotrophic organism groups Bacteria (1), Fungi (12), Bryozoa (1), Foraminifera (3), and Porifera (6).
- Zooid casts of the bryozoan *Spathipora* sp. show three ontogenetic stages: incremental, longitudinal, and lateral growth.
- The predominant macroborings in the framework of *L. pertusa* are the endolithic sponges *Alectona millari* and *Spiroxya heteroclita*. Their traces differ paradigmatically in the morphology of the chambers, apertural canals, and ornamental sculpture of the etching cells.
- Due to its characteristic growth and surface ornamentation the trace of *Spiroxya heteroclita* is correlated to the well-known trace fossil *Entobia laquea*.
- Two microboring sponge types were observed. The etching process of these so far unknown producers is similar to that of one of the macroboring sponges. However, the etching cell size of microboring Sponge Type 1 for example, is more than 10 times smaller than the etching cells from the chambers of *Alectona millari*.
- Thin sections of post-mortal skeletons show an endolithic tiering of three penetration depths in a transmission microscope, varying in grey-level intensities. These intensities correspond with the micrite percentages, which are caused by microboring organisms. Thus, the density of traces is proportional to the grey-level intensity.
- The investigated samples were divided into three preservational stages. They differ in (1) abundance, (2) development of boring traces, (3) age, and (4) mode of exposure of the framework.
- The bioerosion patterns predominantly affect dead parts of the coral skeleton. A succession generally starts with the infestation of Bacteria and Fungi. Contact zones of encrusting epiliths were preferred areas for penetration by

endoliths. Sponges and foraminifers first appeared 10 cm below the zone of living polyps, followed by boring bryozoans 15 cm below.

- Water-exposed frameworks host the most diverse ichnocoenoses, and have the highest secondary porosity, which is caused by endolithic sponges.
- The observation of ichnospecies in a sediment-buried specimens are hampered due to the sediment carbonate interaction in the outer perimeter. The bioerosion level was reduced owing to the inhibition of bioeroding processes of filtrating organisms caused by burial of the framework.
- Bioeroders preferably settle on one side of an upright growing colony. We suppose a positive feedback to facilitate the penetration of boring organisms along the current-exposed parts of the coral framework.
- An early infestation by the sponge *Spiroxya heteroclita* within the framework of living polyps might be an indication of stress factors.
- A mapping of epi- and endoliths in living and freshly necrotic colonies with focus on morphology, abundance, and association of ichnospecies can be a useful tool for monitoring environmental conditions and can lead to the definition of ecological "health" of deep-water corals for a rapid large-scale assessment of the state of coral reefs.

Acknowledgements

References

Allouc J, Hilly J, Ghanbaja J, Villemin G (1999) Phénomèmes biosédimentaires et genèse des croutes et enduits polymétalliques. L'exemple des dépots hydrogénétiques de la marge Oest Africaine et de la Méditerranée. Geobios 32: 769-790

Anderson DT (1998) Invertebrate Zoology. Oxford Univ Press, Australia

Bathurst RGC (1966) Boring algae, micrite envelopes and lithification of molluscan biosparites. J Geol 5: 15-32

Boerboom CM, Smith JE, Risk, MJ (1998) Bioerosion and micritization in the deep sea coral *Desmophyllum cristagalli*. Hist Biol 13: 53-60

Bromley RG (1970) Borings as trace fossils and *Entobia cretacea* Portlock, as an example. In: Crémes TP, Harper JC (eds) Trace fossils. Geol J Spec Issue 3: 49-90

Bromley RG (2004) A stratigraphy of bioerosion. In: McIlroy D (ed) The Application of Ichnology in Palaeoenvironmental and Stratigraphic Analysis. Spec Publ Geol Soc London 228: 455-481

Bromley RG (2005) Preliminary study of bioerosion in the deep-water coral *Lophelia*, Pleistocene, Rhodes, Greece. In: Freiwald A, Roberts JM (eds) Cold-water Corals and Ecosystems. Springer, Berlin Heidelberg, pp 895-914

Bromley RG, Asgaard U (1993a) Endolithic community replacement on a Pliocene rocky coast. Ichnos 2: 93-116

Bromley RG, Asgaard U (1993b) Two bioerosional ichnofacies produced by early and late burial associated with sea-level change. Geol Rdsch 82: 276-280

Bromley RG, D'Alessandro A (1984) The ichnogenus *Entobia* from the Miocene, Pliocene and Pleistocene of Southern Italy. Riv Ital Paleont Stratigr 90: 227-296

Budd DA, Perkins RD (1980) Bathymetric zonation and paleoecological significance of microborings in Puerto Rican shelf and slope sediments. J Sediment Petrol 50: 881-904

Calcinai B, Arillo A, Cerrano C, Bavestrello G (2003) Taxonomy-related differences in the excavating micro-patterns of boring sponges. J Mar Biol Ass UK 83: 37-39

Cedhagen T (1994) Taxonomy and biology of *Hyrrokkin sarcophaga* gen. et sp. n., a parasitic foraminiferan (Rosalinidae). Sarsia 79: 65-82

Cherchi A, Schroeder R (1991) Perforations branchues dues à des Foraminifères cryptobiontiques dans des coquilles actuelles et fossiles. CR Acad Sci Paris, Ser II, 312: 111-115

De Mol B, Rensbergen P van, Pillen S, Van Herreweghe K, Van Rooij D, McDonnell A, Huvenne V, Ivanov M, Swennen R, Henriet JP (2002) Large deep-water coral banks in the Porcupine Basin, southwest of Ireland. Mar Geol 188: 193-231

Farrow GE, Durant GP (1985) Carbonate-basaltic sediments from Cobb Seamount, northeast Pacific: zonation, bioerosion and petrology. Mar Geol 65: 73-102

Flügel E (1982) Microfacies Analysis of Limestones. Springer, Berlin Heidelberg

Freiwald A (1998) Geobiology of *Lophelia pertusa* (Scleractinia) reefs in the North Atlantic. Habilitation thesis, Bremen Univ

Freiwald A, Schönfeld J (1996) Substrate pitting and boring pattern of *Hyrrokkin sarcophaga* Cedhagen, 1994 (Foraminifera) in a modern deep-water coral reef mound. Mar Micropaleont 28: 199-207

Freiwald A, Wilson JB (1998) Taphonomy of modern deep, cold-temperate water coral reefs. Hist Biol 13: 37-52

Freiwald A, Reitner J, Krutschinna J (1997) Microbial alteration of the deep-water coral *Lophelia pertusa*: early postmortem processes. Facies 36: 223-226

Fritsche W (1999) Mikrobiologie. Spektrum, Heidelberg

Ghiorse WC, Ehrlich HL (1992) Microbial biomineralization of Iron and Manganese. Catena, Suppl 21: 75-99

Glaub I (1994) Mikrobohrspuren in ausgewählten Ablagerungsräumen des europäischen Jura und der Unterkreide (Klassifikation und Palökologie). Cour Forschinst Senckenb 174: 1-324

Golubic S (1983) Kunstharzausgüsse fossiler Mikroben-Bohrgänge. Präparator 29: 197-200

Golubic S, Schneider J (1979) Carbonate dissolution. In: Trudinger PA, Swaine DJ (eds) Biogeochemical cycling of mineral-forming elements. Elsevier, Amsterdam, pp 107-129

Golubic S, Brent G, Le Campion T (1970) Scanning electron microscopy of endolithic algae and fungi using a multipurpose casting-embedding technique. Lethaia 3: 203-209

Günther A (1990) Distribution and bathymetric zonation of shell-boring endoliths in recent reef and shelf environments: Cozumel, Yucatan (Mexico). Facies 22: 233-262

Gunatilaka A (1976) Thallophyte boring and micritization within skeletal sands from Connemara, Western Ireland. J Sediment Petrol 46: 548-554

Hook JE, Golubic S (1988) Mussel periostracum from deep-sea redox communities as a microbial habitat: the scalloping periostracum borer. PSZNI: Mar Ecol 9: 347-364

Hook JE, Golubic S (1990) Mussel periostracum from deep-sea redox communities as a microbial habitat: 2. The pit borers. PSZNI: Mar Ecol 11: 239-254

Hook JE, Golubic S (1992) Mussel periostracum from deep-sea redox communities as a microhabitat: 3. Secondary inhabitants. PSZNI: Mar Ecol 13: 119-131

Hook JE, Golubic S (1993) Microbial shell destruction in deep-sea mussels, Florida Escarpment. PSZNI: Mar Ecol 14: 81-89

Hook JE, Golubic S, Milliman JD (1984) Micritic cement in microborings is not necessarily a shallow-water indicator. J Sediment Petrol 54: 425-431

Hooper JNA, Soest RWM van (2002) Order Hadromerida Topsent, 1894. In: Hooper JNA, Soest RWM van (eds) Systema Porifera: a guide to the classification of sponges. Kluwer Acad/Plenum Publ, New York, pp 169-290

Konhauser KO (1998) Diversity of bacterial iron mineralization. Earth Sci Rev 43: 91-121

López Correa M, Freiwald A, Hall-Spencer J, Taviani M (2005) Distribution and habitats of *Acesta excavata* (Bivalvia: Limidae), with new data on its shell ultrastructure. In: Freiwald A, Roberts JM (eds) Cold-water Corals and Ecosystems. Springer, Berlin Heidelberg, pp 173-205

Macintyre IG (1984) Preburial and shallow-subsurface alteration of modern scleractinian corals. Palaeont Amer 54: 229-243

Madigan T, Martinko JM, Parker J (2000) Brock-Mikrobiologie. Spektrum, Berlin, 1175 pp

Mullins HT, Newton CR, Heath K, Vanburen HM (1981) Modern deepwater coral mounds north of Little Bahama Bank: criteria for recognition of deepwater coral bioherms in the rock record. J Sediment Petrol 51: 999-1013

Neumann AC (1966) Observations on coastal erosion in Bermuda and measurements of the boring rate of the sponge, *Cliona lampa*. Limnol Oceanogr 54: 92-108

Newton CR, Mullins HT, Gardulski AF, Hine AC, Dix GR (1987) Coral mounds on the West Florida slope: unanswered questions regarding the development of deep-water banks. Palaios 2: 359-367

Nielsen JK, Maiboe J (2000) Epofix and vacuum: an easy method to make casts of hard substrates. Palaeont Electron 3: 1-10

Perry CT, MacDonald IA (2002) Impacts of light penetration on the bathymetry of reef microboring communities: implications for the development of microendolithic trace assemblages. Palaeogeogr Palaeoclimatol Palaeoecol 186: 101-113

Plewes CR, Palmer TJ, Haynes JR (1993) A boring foraminiferan from the Upper Jurassic of England and Northern France. J Micropalaeont 12: 83-89

Pohowsky RA (1978) The boring ctenostomate Bryozoa: taxonomy and paleobiology based on cavities in calcareous substrata. Bull Amer Paleont 73: 1-192

Radtke G (1991) Die mikroendolithischen Spurenfossilien im Alt-Tertiär West-Europas und ihre palökologische Bedeutung. Cour Forschinst Senckenb 138: 1-185

Sand W (1995) Mineralische Werkstoffe. In: Brill H (ed) Mikrobielle Materialzerstörung und Materialschutz. Fischer, Jena, pp 78-110

Schmidt H (1992) Mikrobohrspuren ausgewählter Faziesbereiche der tethyalen und germanischen Trias (Beschreibung, Vergleich und bathymetrische Interpretation). Frankfurter Geowiss Arb A 12: 228 pp

Schneider J, Torunski H (1983) Biokarst on limestone coasts, morphogenesis and sediment production. Mar Ecol 4: 45-63

Scoffin TP (1981) Aspects of the preservation of deep and shallow water reefs. Proc 4th Int Coral Reef Symp, Manila 1: 499-501

Scoffin TP, Alexandersson ET, Bowes GE, Clokie JJ, Farrow GE, Milliman JD (1980) Recent, temperate, sub-photic, carbonate sedimentation: Rockall Bank, northeast Atlantic. J Sediment Petrol 50: 331-356

Swinchatt JP (1969) Algal boring: a possible depth indicator in carbonate rocks and sediments. Geol Soc Amer Bull 80: 1391-1396

Soest RWM van, Hooper JNA (2002) Order Haplosclerida Topsent, 1928. In: Hooper JNA, Soest RWM van (eds) Systema Porifera: a guide to the classification of sponges. Kluwer Acad/Plenum Publ, New York, pp 831-1019

Soest RWM van, Picton B, Morrow C (2000) Sponges of the North East Atlantic. World Biodiversity Database, Biodiversity Center of ETI, CD-ROM Series. Springer, Berlin Heidelberg

Taylor PD, Wilson MA, Bromley RG (1999) A new ichnogenus for etchings made by cheilostome bryozoans into calcareous substrates. Palaeontology 42: 595-604

Vacelet J (1999) Planctonic armoured propagules of the excavating sponge *Alectona* (Porifera: Demospongiae) are larvae: evidence from *Alectona wallichii* and *A. mesatlantica* sp. nov. Mem Queensl Mus 44: 627-642

Vogel K, Glaub I (2004) 450 Millionen Jahre Beständigkeit in der Evolution endolithischer Mikroorganismen? Franz Steiner, Stuttgart, 42 pp

Wilson MA (2003) Marine Bioerosion Bibliography. http://www.wooster.edu/geology/Bioerosion/BioerosionBiblio.doc

Wisshak M, Freiwald A, Gektidis M, Lundälv T (2005) The physical niche of the bathyal *Lophelia pertusa* in a non-bathyal setting: environmental controls and palaeoecological implications. In: Freiwald A, Roberts JM (eds) Cold-water Corals and Ecosystems. Springer, Berlin Heidelberg, pp 979-1001

Wood R (1995) The changing biology of reef-building. Palaios 10: 517-529

Zebrowski G (1936) New genera of Cladochytriaceae. Ann Missouri Bot Garden 23: 553-564

Zeff ML, Perkins RD (1979) Microbial alteration of Bahamian deep-sea carbonates. Sedimentology 26: 175-201

Shallow-water *Desmophyllum dianthus* (Scleractinia) from Chile: characteristics of the biocoenoses, the bioeroding community, heterotrophic interactions and (paleo)-bathymetric implications

Günter Försterra[1,2], Lydia Beuck[3], Vreni Häussermann[1,2], André Freiwald[3]

[1] Departamento de Biologia Marina, Universidad Austral de Chile, Avda. Inés de Haverbeck, casas 9, 11 y 13, Campus Isla Teja, casilla 567, Valdivia, Chile (gunter_forsterra@yahoo.com)
[2] Department Biologie II, Ludwig-Maximilians-Universität München, Karlstr. 23-25, D-80333 München, Germany
[3] Institute of Paleontology, Erlangen University, Loewenichstr. 28, D-91054 Erlangen, Germany

Abstract. We report an unusually shallow-water occurrence of habitat-forming *Desmophyllum dianthus* (Esper, 1794) from the Chilean fjord region. Most occurrences of the cosmopolitan *D. dianthus* are known from the bathyal zone. In the northern Chilean fjord region, however, this coral is reported within the euphotic zone. The upper limit of distribution was found at 7 m water depth and is confined to the lower boundary of the low salinity layer. Large accumulations both as living aggregations and as sediment-formers typically occur from 20 m water depth and beyond. The corals prefer to colonise the undersides of rock ledges with downward-facing corallites. The motivation of this study is to analyse and discuss the existence of an azooxanthellate coral that generally thrives in aphotic environment but here extends into the photic zone by means of screening of bioerosion patterns. Based on the detailed analysis of scratching and boring traces, we compare the ichnocoenosis found within the Chilean *D. dianthus* with the established bathymetrically indicative ichnocoenoses from other areas around the world. These indicator ichnocoenoses are widely used to reconstruct relative water depths of depositional settings in the geological past. The study of the bioeroding assemblage from two living *D. dianthus* collected at 28 m water depth in the Reñihue Fjord, Chile, shows some remarkable patterns that shed light on the complex way in which the coral's soft tissue expands and retracts at the apical zone of the corallum in response to *in vivo* infestation of endolithic algae. The role of this heterotypic interaction is discussed.

To visualise the endolithic ichnocoenoses, we applied several methodologies such as the vacuum cast embedding technique combined with scanning electron

microscopy, fluorescence microscopy and x-ray analyses. In total, 20 different trace makers are identified. Based on the analysis of the indicator ichnospecies, the endolithic community is indicative for the dysphotic zone. This result is compatible with the sciaphile environment of *D. dianthus*, living under rock ledges in the photic zone.

Introduction

Bathyal coral communities thrive in the absence of light in the aphotic zone. The lack of phototrophic organisms represents a major difference to shallow-water coral communities, where the herbivore food-web plays an important part in ecosystem functioning. Moreover, analysing the presence or absence of phototrophic organisms is a major tool in paleontology for reconstructing the relative paleobathymetry of ancient communities. Here we document the case of the cosmopolitan, azooxanthellate scleractinian *Desmophyllum dianthus* (Esper, 1794) that typically occurs in bathyal depths. In the northern Chilean fjord region, however, this species occurs in the photic zone and forms extended coral banks in water depths as shallow as 20 m (Försterra and Häussermann 2003).

Overview of the Chilean fjord region

The Chilean fjord region extends over more than 1500 km (straight line). With its numerous archipelagos, channels and fjords it is one of the morphologically most structured coastal areas in the world, and is also one of the least studied regions. Hydrographic, taxonomic and ecologic information is fragmentary and substantial portions of the marine environment in this region must be regarded as *terra incognita* (Arntz 1999; Fernández et al. 2000). Data on the benthic life on rocky substrates, which dominate in the shallow water of the channels and fjords, are especially scarce. A biogeographic barrier for shallow-water organisms, separating the southern from the northern Chilean fjord province, seems to be located at the Taitao Peninsula at approximately 46°S (Fig. 1; Brattström and Johanssen 1983; Lancellotti and Vásquez 1999; Häussermann 2004; Häussermann and Försterra accepted).

Overall precipitation in the fjord region is extremely high, and varies locally between 1040 mm/year (Isla Guafo; Pickard 1971), and 6700 mm/year (Isla Guarello). This results in an enormous freshwater influx into the fjords (Pickard 1971; Castilla et al. 1993). Furthermore, large amounts of organic and inorganic matter are imported through the rivers into the fjord system. Many fjords of the southern fjord region are under the influence of glaciers that extend to sea level (Pickard 1971). The constant high freshwater flow produces a superficial low salinity layer that decreases in thickness from the head of the fjord towards the mouth (Pickard 1971), but below 20 m depth salinities are generally more stable, and reach higher values. In the past, most sampling in the fjord region has been carried
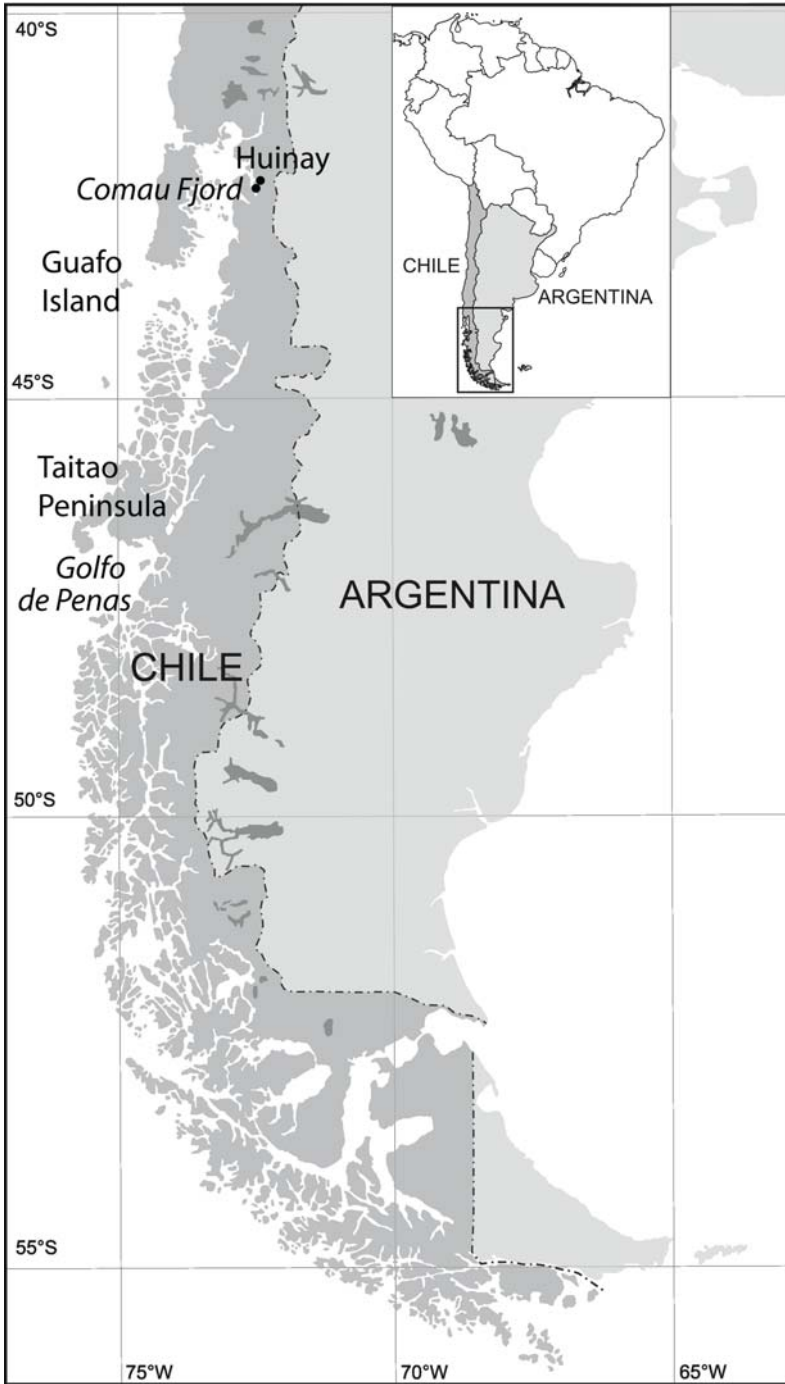
Fig. 1. Geographical setting of the Chilean fjord region

out from boats, equipped with dredges and grabs (e.g., Challenger Expedition 1872-1876, Joint Magellan "Victor Hensen" Campaign 1994, CIMAR Fiordo expeditions 1995-2004), or in the intertidal which excluded rocky subtidal substrates. Therefore, it is not surprising that there are still many undiscovered species in the shallow water of Chilean Patagonia. What is more surprising is the existence of entire benthic communities that have not been documented in this form before, especially the discovery of benthic biocoenoses on the steep rock walls of the inner fjords (Försterra and Häussermann 2003).

The incredibly fast economic development in the Chilean fjord region, led by the booming salmon farming industry, is in contrast to the poor understanding of the affected marine systems. The biocoenoses in the fjords and channels may be very sensitive to the impacts of human activities. As a consequence, the unique benthic communities, such as the coral banks in shallow-water, could sustain lasting damage or could even disappear before they can be studied (Försterra and Häussermann 2003).

Distribution of shallow-water *Desmophyllum dianthus*

A striking feature is undoubtedly the large accumulation of azooxanthellate Scleractinia in shallow water in the euphotic zone (Försterra and Häussermann 2003). The dominant species in these communities is *D. dianthus*. According to Cairns and Zibrowius (1997), *Desmophyllum cristagalli* is a junior synonym of *Desmophyllum dianthus*. This coral is a cosmopolitan species found in a large depth interval from 35 to 2460 m. Moreover, the majority of occurrences are typically located at bathyal depths. In the North Atlantic *Desmophyllum dianthus* is often associated with the prevalent framework builder *Lophelia pertusa* (Linné, 1758), and with *Madrepora oculata* Linné, 1758 (see compilation in Freiwald et al. 2004). Off the Chilean coast, *D. dianthus* exists between 300 and 800 m water-depth, where it was already known to reach high densities (Cairns 1982). New findings of *D. dianthus* in shallow water of the northern Chilean fjord region encounter completely different ecological conditions, including co-existence with photosynthetically active organisms, such as coralline algae. As a characteristic element of the bathyal zone both recent and in the geological record, a co-occurrence of *D. dianthus* with crustose coralline algae

Fig. 2. A *Desmophyllum dianthus* settling hard substrates on the undersides of rock ledges and associated with the red rockfish *Sebastes capensis*; width 2 m. **B** The skeleton of living *D. dianthus* infested by red algae (r), green algae (g), and endolithic sabellids (s); scale bar 5 cm. **C** Top of the boulder incrusted by corallinaceans; on its flanks various organisms settle, amongst them are solitary corals (*Caryophyllia* sp. and *D. dianthus*); scale bar 50 cm. **D** Red rockfish *Sebastes capensis* resting on corallinaceans, *D. dianthus* and *Caryophyllia* sp.; scale bar 10 cm. **E** Bryozoans, sponges and the producer of the Sabellid Trace 1; scale bar 1 cm. **F** Overview of 'Corallum 1'. Apical part (right side) is covered by dried tissue. Its surface shows a multitude of epilithic organisms, e.g., (s) sabellid worm tube, (c) *Caryophyllia* sp., (d) *D. dianthus*; scale bar 3 cm. **G** X-ray image of 'Corallum 1' with 26 (+1) tabulae. The dashed line separates the upper green-coloured side from the whitish side (below the line). The basal 5.5 cm are heavily infested by endolithic sponges; (s) bore hole of a boring sabellid, (d) *D. dianthus*; scale bar 3 cm
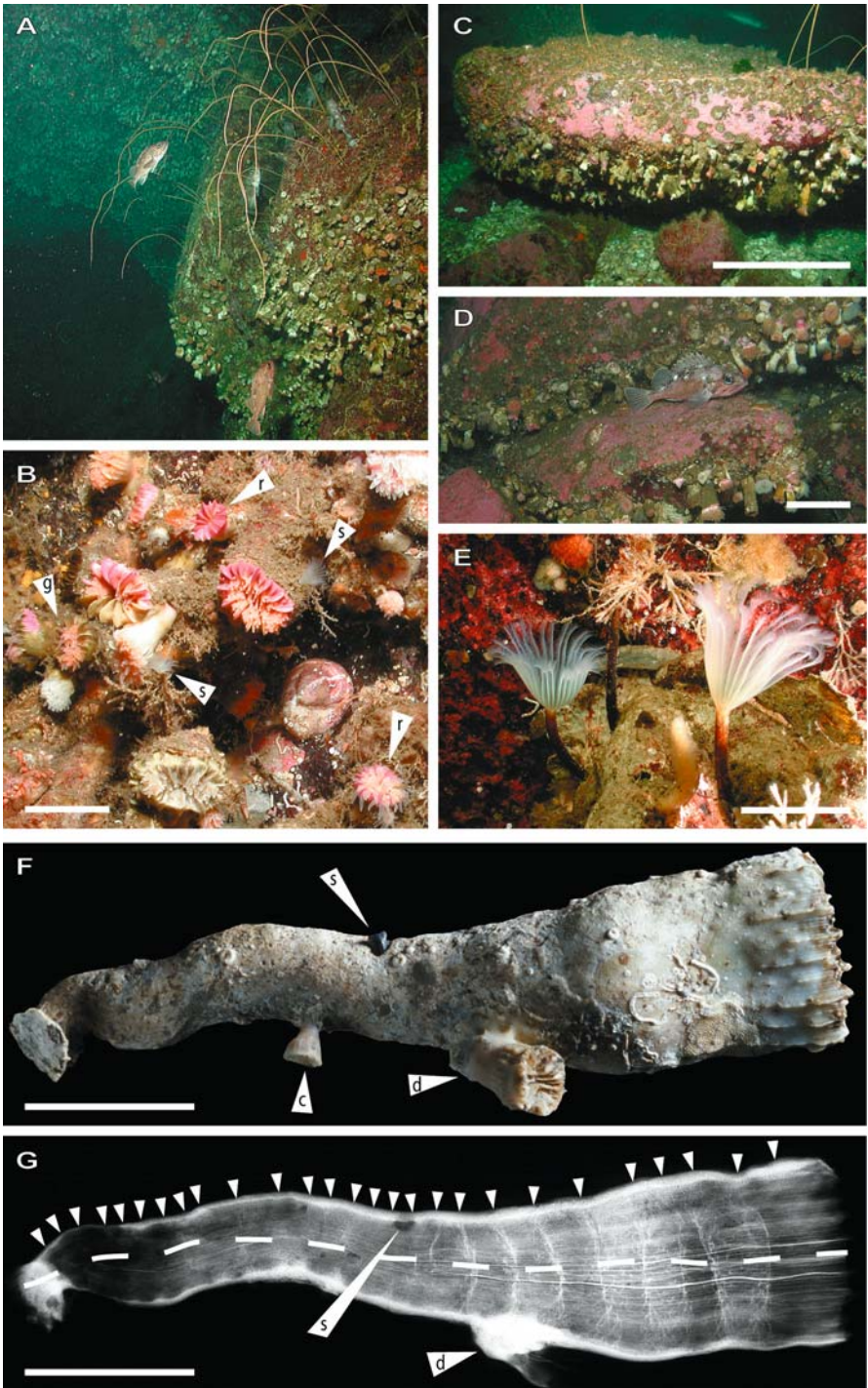
has been considered as unlikely so far (see Figs. 2C, D). Single individuals were found as shallow as 7 m, but larger accumulations are generally found at depths around 20 m and deeper (Försterra and Häussermann 2003). In the northern fjord region, the presence of coral communities in shallow water seems to diminish from North to South. Vast coral populations occur in the Comau and Reñihue Fjords, but single and small corals can also be found outside the fjords in the shallow water of the channels such as Cailín Island (43°09'02.1"S; 73°35'30.9"W), Bahía Santa Domingo (43°58'18.4"S; 73°07'0.6"W) and Archipelago de las Guaitecas (43°53'S; 73°44'W). South of 46° - 47°S (Taitao Peninsula) no scleractinians have yet been reported from shallow water. This might be due to deeper extensions of the low salinity layer, a higher input of sediments of glacial origin, a zoogeographic isolation, or may be a factor of the limited sampling in this region. Salinities measured in habitats of *D. dianthus* generally vary between 28.5 ‰ and 34 ‰, temperatures range from approximately 8°C to 13.5°C. The upper bathymetrical distribution limit of coral banks seems to coincide with the maximum extension of the low salinity surface layer.

Scope of this study

An important observation from *D. dianthus* is the temporary expansion, and subsequent retraction of the soft tissue at the 'edge zone' of the polyp (Stolarski 1996). Once this 'edge zone' is retracted, the bare skeleton is exposed and prone to colonisation by larvae and spores of other organisms. Amongst these benthic organisms, some of them can actively bore into the coral skeleton, and are referred to as euendoliths (Golubic et al. 1975). The infested carbonate substrate provides protection for endolithic organisms against abiotic fluctuations such as salinity, temperature, and water movements. Furthermore, it opens a third dimension to reduce competition for space, and protects from grazing organisms (Vogel and Glaub 2004). Endolithic dwellers play a well-known role of destruction and sediment production consequently (Ekdale et al. 1984; Acker and Risk 1985; Bromley 1992; Schumacher et al. 1995; Schönberg and Wilkinson 2001). Moreover, grazing organisms live on exposed surfaces and feed directly upon sessile invertebrates, or endolithic organisms by etching, rasping or scraping, causing incidental skeletal or substrate damage (Bromley 1975; Voigt 1977). This skeletal degradation by living organisms is called bioerosion (Neumann 1966). The association of ichnospecies, their abundance, spatial distribution, as well as their morphological habit can be used as a bathymetric indicator, and represents a powerful tool for paleoenvironmental reconstructions (Vogel and Glaub 2004).

The focus of this study is the biologically-driven skeletal alteration processes of *D. dianthus* caused by various groups of benthic organisms. Using the vacuum embedding technique as outlined in Beuck and Freiwald (2005; modified after Golubic 1972), we attempt to characterise endolithic traces (ichnocoenoses), their spatial distribution within the skeletons, and identification of their correlated producers. Furthermore, we compare the ichnocoenoses of the Chilean shallow-water *D. dianthus* with those from non-bathyal, and bathyal coral-infesting ichnocoenoses

from various locations in the North Atlantic (Kosterfjord, Sweden), Orphan Knoll (550 km northeast of Newfoundland, north of Flemish Cap), Propeller Mound (Porcupine Seabight), and from the Early Pleistocene of Rhodes (Mediterranean Sea; Boerboom 1996; Beuck and Freiwald 2005, Bromley 2005, Wisshak et al. 2005). These data are completed and compared with *in situ* data and observations on associated organisms and on habitat and dynamics.

Material and methodology

During three major expeditions between 1998 and 2001, we have observed and sampled cold-water corals by means of SCUBA diving in the northern part of the Chilean fjord region between Puerto Montt and Puerto Chacabuco. Since 2003, continuous studies are carried out at the Huinay Scientific Field Station (42°23'S, 72°21'W) and focus on coral assemblages in the Fjords Comau and Quintupeu (Försterra and Häussermann 2003; Cairns et al. submitted).

Habitat and population parameters (such as depth, substrate inclination and population densities) in shallow water were extracted from scaled transect photos showing an inclination and a depth gauge. Deeper coral banks were recorded in the Fjord Comau down to 255 m with a ROV of the model "Spy" in November 2004. The macrobenthic organisms associated with the corals in shallow water were sampled, identified with primary literature or sent to specialists for identification. The specimens of *Desmophyllum dianthus* were from Caleta Gonzalo (42°32'46.6"S, 72°37'00.2"W), Reñihue Fjord, in the northern part of Chilean Patagonia. The corals were sampled by means of SCUBA diving in depths of 28 m, in February 2001. The living individuals of *D. dianthus* were in parts chiselled off the rocky substratum, and subsequently dried for preservation. In this study, two trumpet- to cylindrically-shaped coralla of *D. dianthus* were analysed. During the lifetime of the corals, the outer zone of the coralla ('edge zone' *sensu* Stolarski 1996), was covered by living polyp tissue (see Table 1). Underwater photos were made with a Nikonos V amphibian camera and with a Canon EOS 5 and a Coolpix 990 digital camera in underwater housings and amphibic flashes as light source. Colour slides were digitised with a Nikon Coolscan slight scanner and quantitative analysis of the digital images were made with the software Wega Image Viewer and Adobe Photoshop®. From one specimen, thereafter referred as 'Corallum 1', a radiograph was taken using x-ray radioscopic equipment of Siemens® (94 cm distance; 45 kV; 5 mAs) to study the distribution of macroborings within the skeleton. Longitudinal thin sections were made of apical green-coloured and whitish-coloured corallum parts and these were used to analyse the spatial distribution of boring organism remains using fluorescence microscopy. In addition, the vacuum embedding technique of Beuck and Freiwald (2005) was used to provide a three-dimensional view of traces for ichnotaxonomic analyses. Trace casts were documented *via* a scanning electron microscope (SEM), and individual trace measurements were made using the software Adobe Photoshop®.

Results and interpretation

Underwater field observations

Any hard substratum and even shells of living bivalves, barnacle plates, or synthetic material, like a fibre-glass ship hull, were observed to be accepted as settling ground, where it exceeds inclinations of 80° (e.g., rock walls, overhangs and caves). The largest individuals of *Desmophyllum dianthus* (40 cm length) and highest population densities (>1500 individuals/m^2) are found on well-ventilated overhanging walls having inclinations exceeding 110° at depth greater than 25 m. Here, *D. dianthus* often dominates the benthic communities, shows downward facing coralla and generally forms pseudo-colonies, consisting of up to 20 individuals (Figs. 2A, 3A-B). Its restricted distribution to vertical and overhanging walls indicates sensitivity to sedimentation (Försterra and Häussermann 2003). In addition, the red rockfish *Sebastes capensis* (Valenciennes, 1833) is closely associated with *Desmophyllum dianthus*, taking shelter within the protective coral meadows (Figs. 2A, D). On more gently inclined slopes, the substratum that is left between the basal plates of *D. dianthus* in shallow water is mainly covered with barnacles such as *Austromegabalanus psittacus* (Molina, 1782), sponges (mainly encrusting) such as *Cliona chilensis* Thiele, 1905, *Geodia magellani* (Sollas, 1886), *Mycale thielei* Hajdu and Desqueyroux-Faundez, 1994, *Iophon* sp., bryozoans (*Cellaria malvinensis* (Busk, 1852)), brachiopods (*Magellania venosa* (Dixon, 1789)), tube-forming polychaetes (e.g., *Apomatus* sp.), and corals (*Caryophyllia* sp., *Tethocyathus* sp.). Further associated fauna of *D. dianthus* consists of other anthozoans, such as actinarians (e.g., *Actinostola chilensis* McMurrich, 1904, *Bolocera* aff. *occidua* and *Hormathia* aff. *pectinata;* Häussermann in press), stoloniferans and zoanthids; bryozoans (*Adeonella* aff. *patagonica*); corallinaceans (Figs. 2C-D); gastropods (e.g., *Crepidula* sp.), and mytilids (*Aulacomya atra* Molina, 1782). The sea anemones *Actinostola chilensis*, *Bolocera* aff. *occidua* and *Hormathia* aff. *pectinata* and the sponge *Geodia magellani* are typical deep-

---

Fig. 3 A *Desmophyllum dianthus* meadows growing from overhangs; width 2 m. **B** Cylindrical growth habit of *D. dianthus* (after Försterra and Häussermann 2003); scale bar 5 cm. **C** Coral rubble deposit used as substrate by various organisms, among others the sea urchin *Pseudechinus magellanicus* and the brachiopod *Magellania venosa*; scale bar 2 cm. **D** Tissue of *D. dianthus* (*in situ*) restricted to the upper part of the corallum that is infested by endolithic algae (r, g). In contrast, the 'edge zone' of the neighbouring polyp is much further progressed (e); scale bar 2 cm. **E** Endolithic algae are able to grow from exposed corallum areas into the zone that is covered by polyp tissue; scale bar 2 cm. **F** The echinoid *Arbacia dufresnei*, a common grazer in the coral habitat and the presumed producer of *Gnathichnus pentax*; scale bar 1 cm. **G** Overview of 'Corallum 2'. Attached are several barnacles whose plates again provide new space for epibenthic organisms; scale bar 1 cm. **1** Endolithic green alga *Ostreobium quekettii* infesting septa of living tissue; scale bar 2 mm. **2** 'Edge zone' of the polyp; scale bar 2 mm. **3** Basally the polyp's 'edge zone', the skeleton is settled by encrusting organisms, and already heavily grazed by echinoids (gnawing trace *Gnathichnus pentax*); scale bar 2 mm
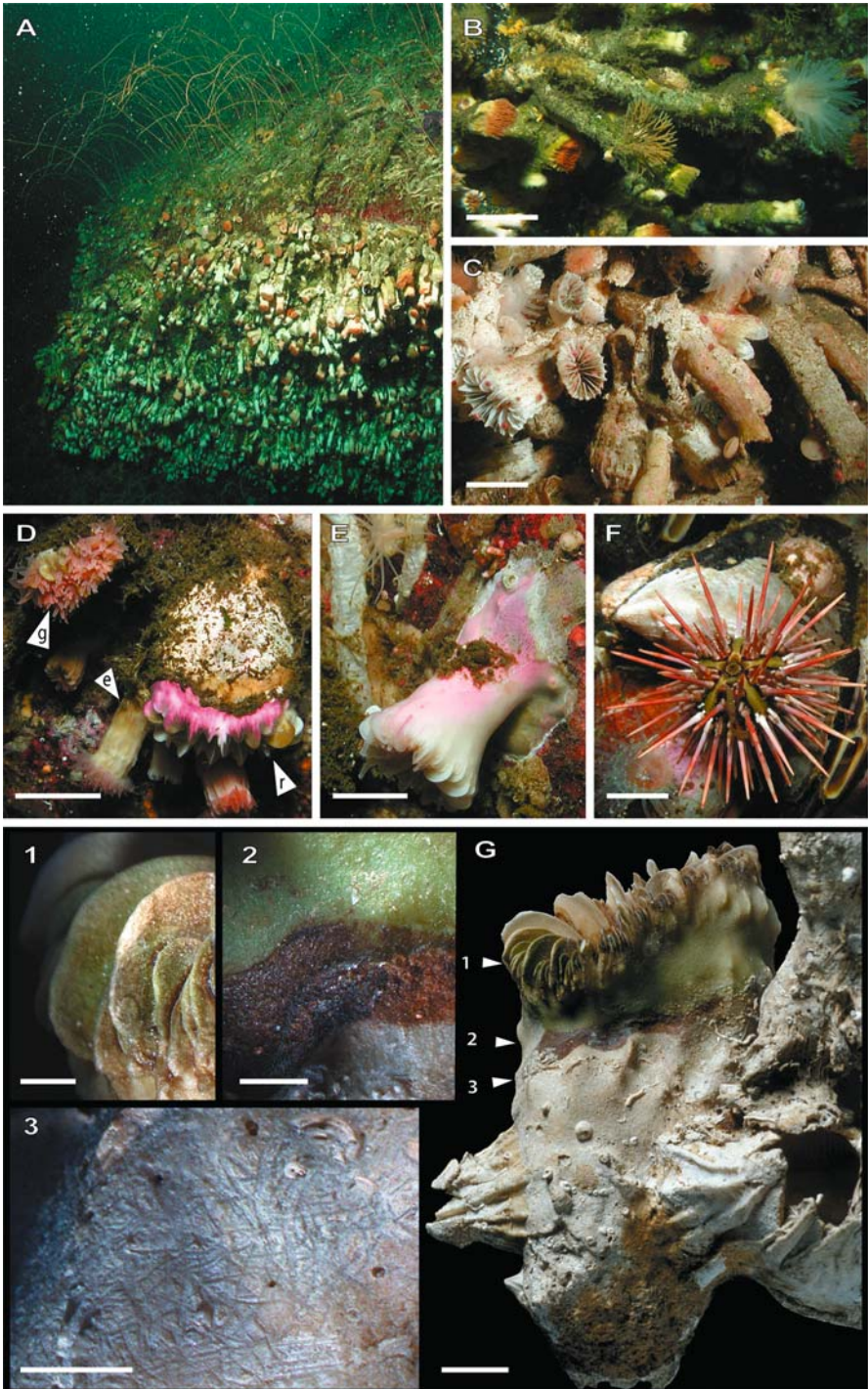
water species. With increasing depth, lesser macroinvertebrates are associated with the corals. Below 100 m depth, corals are strongly associated with bivalves of the species *Acesta patagonica* (Dall, 1902). Other accompanying macrofauna are, e.g., anthozoans, such as the sea anemone *Hormathia* aff. *pectinata, Actinostola chilensis* and *Bolocera* aff. *occidua.* Considering the shape of individual coralla from dense coral aggregations, a pronounced cylindrical growth-form of the coralla is developed. In addition, these corals have thinly calcified theca. This peculiar shape is considered to be indicative of fast growth rates with strong intra-specific competition for space between neighbouring individuals, and exposure to currents (Cairns et al. submitted). In contrast, where coral densities are low, *D. dianthus* remains short in length, and tends to grow trumpet-shaped with thicker theca.

The basal portion of larger coralla, which is not covered by polyp tissue, is generally intensively colonised by epibiontic organisms such as foraminiferans, sponges, bryozoans, hydroids, chitons, polychaetes, gastropods (mainly *Crepidula*)*,* or even mytilids (Table 1; see also Figs. 2B-E, 3B-F, 4). The apical portion of the coralla, which is covered by polyp tissue, is often stained pink, brown or green due to the presence of endolithic algae. In particular, the pink colour is always confined to the most strongly illuminated side of the corallum, whereas the greenish colour is often distributed non-specifically (Figs. 2B, 3B, D-E, G).

Interseptal spaces of dead corals or cavities in corallites that have been perforated by bioeroding organisms are often inhabited by polychaetes, ophiuroids, crustaceans and other cryptic organisms (see Fig. 3C).

Skeletal features of the analysed specimens

The two specimens of *Desmophyllum dianthus* to some extend show on one side a greenish-coloured corallum wall that highly contrasts with the remaining whitish-coloured parts of the corallum (Fig. 2F). The entire length of the specimen 'Corallum 1' is 14 cm (see Table 1). One centimetre below the apical part, its theca measures 0.7 mm in thickness on the whitish side, and 1.5 mm on the green side in thickness. Within the coralla, 27 tabulae are found, of which 26 are completely developed. Distances between single tabulae of 'Corallum 1' enlarge apically from about 0.3 to 0.9 cm in length (Fig. 2G). Minimum growth rates, calculated from specimens found on a sunken boat, could be estimated approximately with 2.3 mm/year linear skeletal extension and approximately 1.6 mm/year increase of diameter (Försterra and Häussermann 2003). First datings of 20 cm long *Desmophyllum dianthus* from the Chilean fjords show a lifespan of approximately 60 years (personal communication Malcom McCulloch, Canberra, Australia). Assuming a linear skeletal extension rate, the annual growth advance may reach 3 mm. Consequently, 'Corallum 1' should have an age less than 50 years (Fig. 2F).

The base of 'Corallum 2' is not preserved, and the inner thecal part is completely hollowed out as far as six centimetres below the apical part of the corallum. However, three barnacles settled on the skeleton, and again provide settlement space for a multitude of organisms (Fig. 3G). On the green-coloured side of 'Corallum 2', the polyp's tissue extends further basal ward than on the whitish side (see Table 1). In

Table 1 Description of specimens. Shown are physical dimensions, substrate, and epilithic organisms of studied coralla

	Corallum 1	**Corallum 2**
Physical Dimensions		
total length (along axis)	14 (14.7) cm	9 cm
attachment base	1.5 - 1.4 cm	not preserved
basal constriction average	0.8 - 1 cm	not preserved
diameter	*0 - 8 cm*: 1.3 - 1.7 cm	*0 - 3 cm*: 1.5 - 2 cm
	8 - 14 cm: 1.5 - 3 cm	*3 - 9 cm*: 2.5 - 4 cm
distal diameter	1.5 - 3.5 cm	2.5 - 4.5 cm
coverage by tissue		
green-coloured side	0.7 cm	2.2 cm
whitish side	0.3 cm	0.9 cm
tabulae		
number	26 (+1)	5
length	0.4 - 0.9 cm	0.3 - 0.7 cm
thickness of theca		
1 cm below apical part	0.7 (whitish) - 1.5 mm (green)	0.5 (whitish) - 2 mm (green)
2.5 cm below apical part	0.9 (whitish) - 1.6 mm (green)	0.7 (whitish) - 3.5 mm (green)
Substrate	corallum	remaining attached to corallum
Epiliths	cheilostome bryozoans (*Fenestrulina* sp.); *Caryophyllia* sp.; polyps of *Desmophyllum dianthus*; cirriped *Austromegabalanus psittacus* (Molina, 1782); ctenostome bryozoan colonies; several foraminiferans amongst *Cibicides lobatulus* (Walker and Jacob, 1798), and *Placopsilina confusa* Cushman, 1920; serpulid *Helicosiphon platyspira* Knight-Jones, 1978; spirorbids (e.g., *Paralaeospira levinseni* Caullery and Mesnil, 1897); sponges	foraminiferans (e.g., *Cibicides lobatulus*, *Placopsilina confusa*); several serpulids; cirriped *Austromegabalanus psittacus*

addition, compared to the whitish side, the theca on the green side is about four times thicker.

Trace analysis

In the investigated ichnocoenoses, epilithic grazers as well as endolithic organisms contribute synergistically to the process of erosion. We documented 20 traces, taxonomically correlated to Cyanobacteria (1), Chlorophyta (1), Rhodophyta (1), Porifera (2), Fungi (1), Foraminifera (1), Bryozoa (2), Polychaeta (5), Echinoida (1), Brachiopoda (1), and four traces of uncertain producer. In the following, bioeroders are distinguished by their taxonomic classification, and are described by their morphology, and abundance (see Table 2; Fig. 5A).

Echinoids

Regular echinoids graze by using their jaw apparatus (Aristotle's lantern). They remove and ingest calcareous material, small invertebrates, and boring organisms.
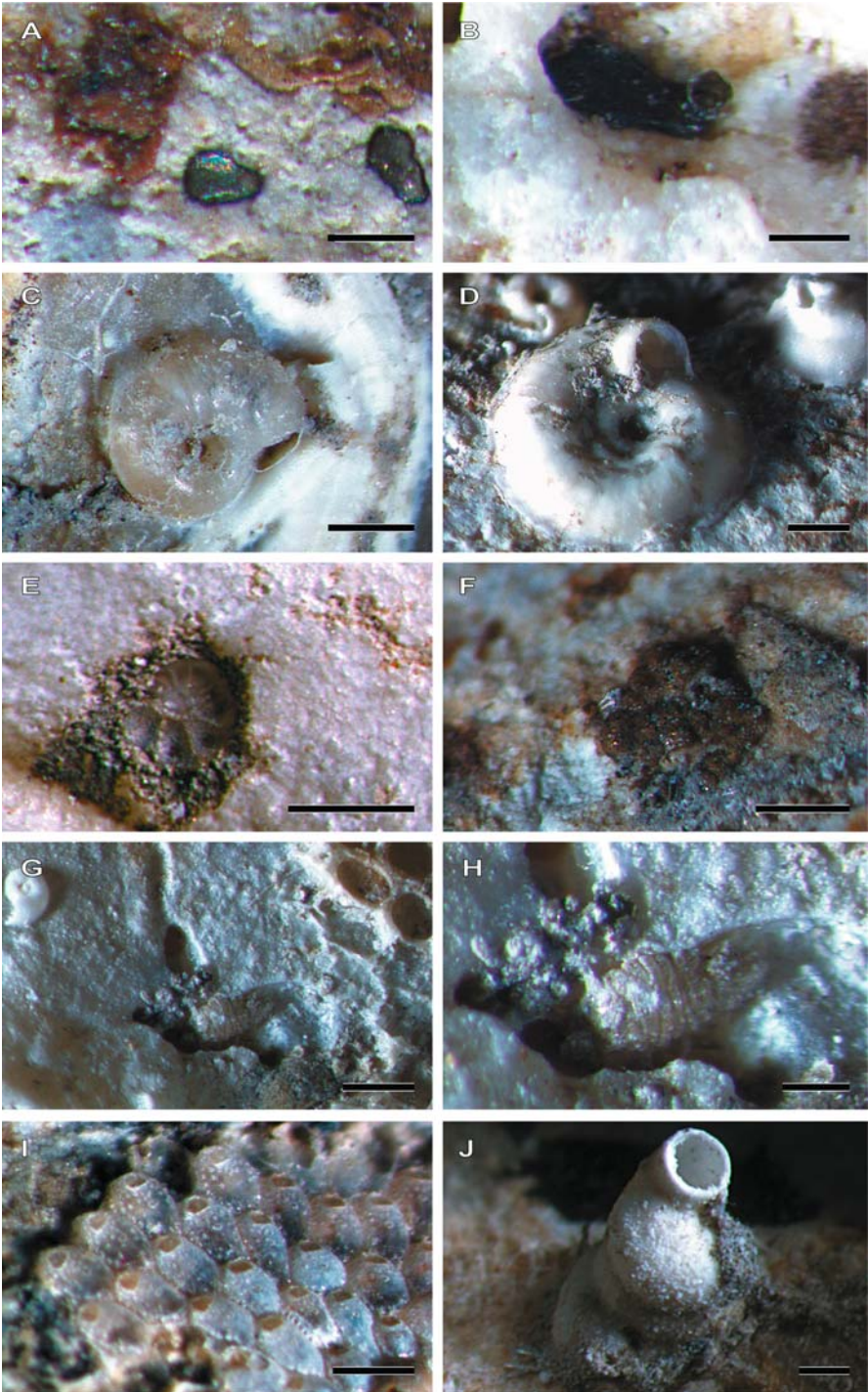
Table 2 Occurrence and abundance of traces within the samples analysed (1: Corallum 1; 2: Corallum 2; g: green-coloured side; w: whitish-coloured side; relative abundance: x rare; xx moderate; xxx dominant; A) Wisshak et al. (2005); B) Beuck and Freiwald (2005); C) Boerboom (1996); D) Bromley (2005); • reported from the studied samples)

	1g	1w	2g	2w	A	B	C	D
Depth [m]			28		85	780	1800	?
Gnathichnus pentax Bromley, 1975	xx	xx	xx	x				•
Scolecia filosa Radtke, 1991	xx	x	x	x				
Reticulina elegans Radtke, 1991	xxx	xx	xxx	xx				
Conchocelis Trace	xx	x	xx	x				
Orthogonum isp.	x	xx		xx	•	•	•	•
Foraminiferan Trace	xxx	xx	xx	xx	•	•		•
Entobia isp. 1	x				•	•		•
Entobia isp. 2	xx	xx					•	
Bryozoan Trace	xx							
Spathipora isp.				xxx	•	•		
Sabellid Trace		x						
Caulostrepsis isp.	xx	x	x	xx				•
C. contorta Bromley and D'Alessandro, 1983		x						
Maeandropolydora sulcans Voigt, 1965			x					
M. elegans Bromley and D'Alessandro, 1983	xx	x	x					
Podichnus centrifugalis Bromley and Surlyk, 1973	x					•		•
Problematical Trace 1	x							
Problematical Trace 2	x					•		
Problematical Trace 3			x					
Problematical Trace 4			x	xx				
Total number of observed traces			20		17	23	5	18

The gnawing traces are regular, stellate modules consisting of five radiating grooves. The pentaradiate symmetry can vary in spacing between the scratches, the curvature of the substrate, and the presence of borings in the substrate. Thus, compound stellate bioerosion sculptures can become increasingly complex by repetition of overlapping stars (Bromley 1975). First echinoid bioeroders having keeled teeth (stirodont lantern) appeared in the Triassic, as does *Gnathichnus pentax* Bromley, 1975. Echinoids started to become important bioeroders since the Jurassic (Vogel 1993).

Fig. 4 Epilithic organisms. **A-B** Shallow-boring ctenostomate bryozoans on the surface of 'Corallum 1'; scale bar 0.2 mm. **C** Probably a juvenile spirorbid (*in situ*) as the tube is not complete; scale bar 0.5 mm. **D** Because of the absence of soft tissue, this spirorbid could not be identified to species level; scale bar 0.5 mm. **E** *Cibicides lobatulus*; scale bar 0.5 mm. **F** *Placopsilina confusa*; scale bar 0.5 mm. **G** Unknown producer of the trace *Maeandropolydora sulcans*; scale bar 0.5 mm. **H** Close-up of **G**; scale bar 0.2 mm. **I** *Fenestrulina* sp. (*in situ*); scale bar 0.5 mm. **J** *Helicosiphon platyspira* (*in situ*); scale bar 0.5 mm

Gnathichnus pentax **Bromley, 1975** (Figs. 3F, 3G)

Trace morphology

Diameters of stellate modules vary between 0.8 cm and 1.1 cm. The rays have a uniform depth and a diameter of about 0.05 mm.
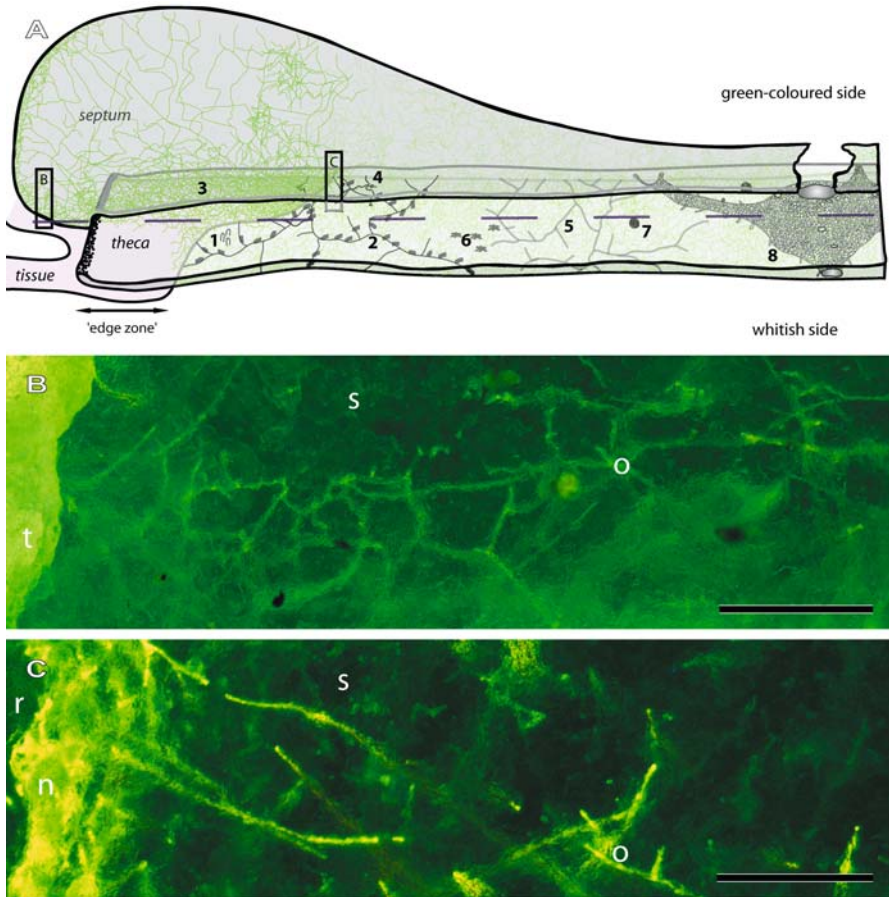
Fig. 5 A Semitransparent three-dimensional sketch of the bioeroder assemblage within shallow-water *Desmophyllum dianthus* from the northern Chilean fjords. The dashed line divides the corallum into an upper green-coloured zone and a lower whitish zone. 1) *Caulostrepsis* isp.; 2) *Spathipora elegans*; 3) *Scolecia filosa* and *Ostreobium quekettii*; 4) Conchocelis Trace; 5) *Orthogonum spinosum*; 6) Foraminiferan Trace; 7) *Podichnus centrifugalis*; 8) *Entobia* isp. **B** Thin section of the septum with tissue (t), coral skeleton (s), and the endolithic green algae *Ostreobium quekettii* (o); scale bar 0.2 mm (fluorescent image; 'Corallum 2'). **C** Thin section of corallum below the 'edge zone': Coral skeleton (s), *Ostreobium quekettii* (o), epoxy resin (r), and concentration of *O. quekettii* filaments directly below the surface (n); scale bar 0.2 mm (fluorescent image; 'Corallum 2')

Producer

In the habitat studied, common grazers are the echinoids *Arbacia dufresnei* Blainville, 1872 and *Pseudechinus magellanicus* (Philippi, 1857), which are most likely the producer of the bite traces.

Remarks

Directly below the polyp's tissue a complex cluster of stellate trace sculptures is present in 'Corallum 2'. The surface of 'Corallum 1' exposes a multitude of scratches. A clear identification to their browsing producer is not given. Thus, we consider synergistic degradation effects caused by a variety of specialised grazers, e.g., gastropods, sea urchins and chitons.

Cyanobacteria

Endolithic Cyanobacteria are restricted to the photic zone, owing to their autotrophic metabolism, and have their highest abundance in shallow water (LeCampion-Alsumard 1979; LeCampion-Alsumard and Golubic 1985; Schuhmacher et al. 1995; Gektidis 1999; Kaehler 1999). Amongst the group of endolithic Cyanobacteria, the correlated ichnospecies *Fasciculus acinosus* Glaub, 1994, and *F. dactylus* Radtke, 1991 are the most dominant traces in the marine intertidal zone, which led to the definition of a microboring index ichnocoenosis, characterised by these two ichnospecies (Glaub 1999). In zones of high light penetration, Cyanobacteria tend to grow perpendicularly to the surface (Golubic et al. 1975), whereas in deeper photic zones, they predominantly grow parallel to the surface (Budd and Perkins 1980; Ekdale et al. 1984). The oldest microborers with cyanobacterial affinities are known since the Precambrian (Zhang and Golubic 1987; Golubic et al. 1999).

Scolecia filosa Radtke, 1991 (Figs. 6A-B)

Trace morphology

Elongated filigree filaments of 1.4-2.2 μm in diameter with a partially rough surface texture form interwoven networks that can penetrate the entire theca. The trace is sparsely branched in rectangular angles (T-branches).

Producer

Plectonema terebrans Bornet and Flahault, 1889 is regarded as the producer of the ichnospecies *S. filosa* (Radtke 1991).

Remarks

P. terebrans is cosmopolitan, and characterised by a wide bathymetric range (Radtke 1991; Gektidis 1997). Günther (1990) describes a bathymetric distribution of *P. terebrans* from 1 m to 42 m at Cozumel, Mexico. Studies at Lee Stocking Island show *P. terebrans* occurrences down to 100 m depth (Vogel et al. 2000). Budd and Perkins (1980) document six endolithic Cyanobacteria from the Puerto Rican Shelf, of which *P. terebrans* was the most abundant down to 85 m depth.
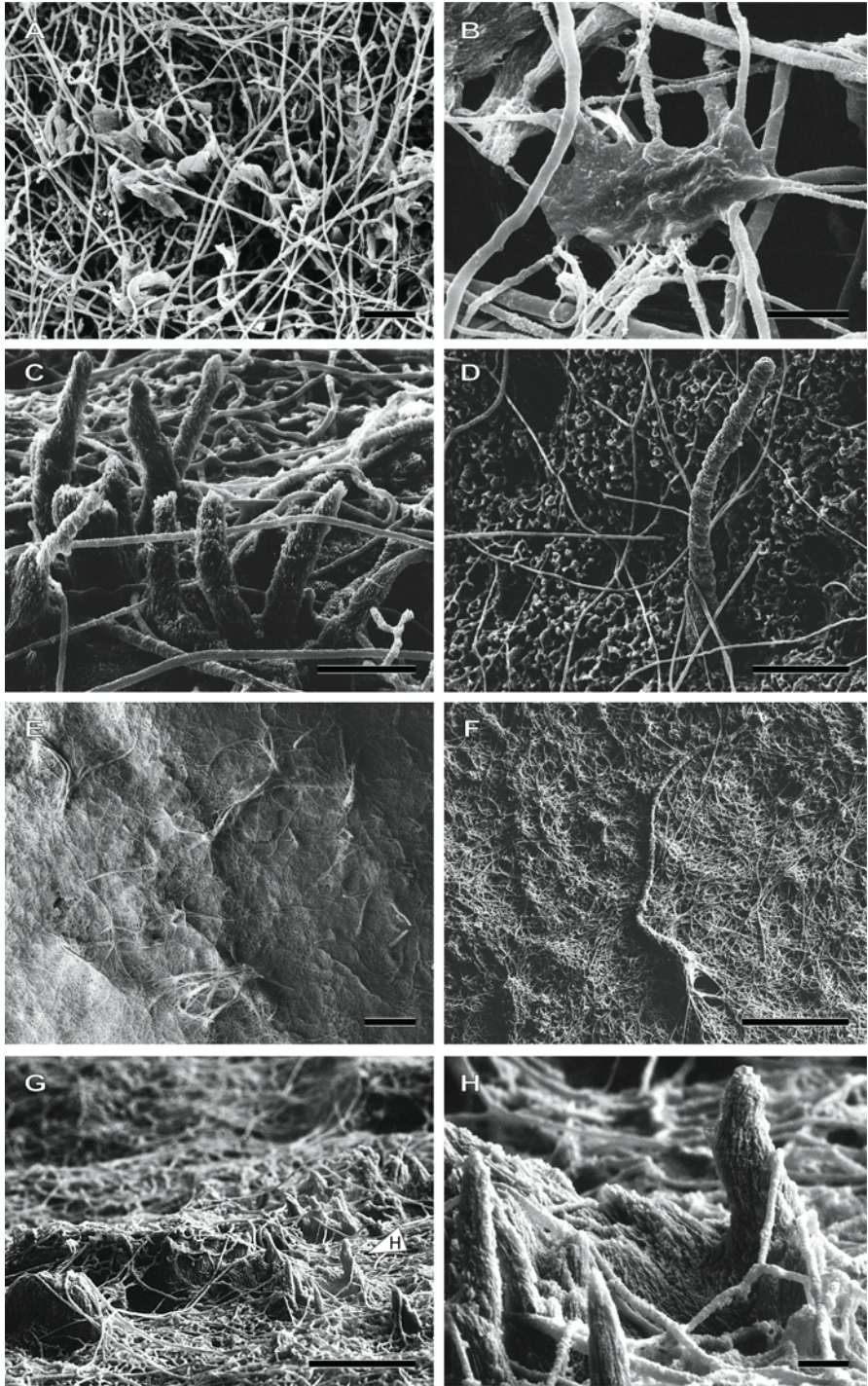
Chlorophyta

A multitude of boring algae are known from tropical shallow-water environments (LeCampion-Alsumard et al. 1995; Gektidis 1997). However, several endolithic algae are also reported from the cold-temperate, upwelling area off Mauritania (Glaub 2004). Endolithic species are restricted to different water depths appropriate to the wavelengths absorbed by their photosynthetically active pigments. Apart from the physical factors, such as irradiance or temperature, the distribution of endolithic algae is also influenced by the grazing activity of herbivores (Highsmith 1981; Fork and Larkum 1989; Schlichter et al. 1997). First borings of endolithic green algae are recorded from the Early Paleozoic (Podhalanska 1984; Vogel 1993).

Reticulina elegans Radtke, 1991 (Figs. 5B, C, 7)

Trace morphology

Spherical to flattened filaments measure between 1.85-3.15 µm in diameter. These filaments can ramify at distances of 3.4 µm and up to several 100 µm in preferred angles of 90° or 120° (morphological structure 1). Directly below the surface, the trace is highly branched, creating a reticulated network. Distances between successive ramifications increase proportionally with penetration depth, producing wide-meshed networks. The smooth-textured filaments can penetrate the entire skeleton. Directly below the surface, the filamentous tubes may enlarge to diameters of about 15 µm (morphological structure 2). This tube peculiarity is located terminally and features slight constrictions at distances of about 10 µm. Morphological structure 2 has a granular surface texture of about 1 µm small units. Its blind-ending tubes end hemispherically and can penetrate the carbonate up to 75 µm deep. In addition, up to ten filaments of morphological structure 1 may coalesce in a polygonal, flattened structure (morphological structure 3) that is about 2.7 µm thick and can measure 18-25 µm in diameter. The surface texture of these flattened structures consists of spherical to 'vermiculate' granules.

Morphological structure 1 is interpreted to be ichnospecies *Reticulina elegans*. This trace is known since the Silurian (Vogel et al. 1995). However, morphological structure 2 is similar to *Fasciculus* isp. Traces resembling morphological structure 3 have not been found in the literature.

Producer

The trace morphology correlates with the shape of the green alga *Ostreobium quekettii* (Bornet and Flahault, 1889) (Chlorophyta, Bryopsidales, Ostreobiaceae). The filigree tubes harbour the siphonal, unpartitioned thallus. Tube enlargements

---

Fig. 6 SEM images of resin casts. **A** *Scolecia filosa* boring of the producer *Plectonema terebrans* associated with tube casts of *Ostreobium quekettii*; scale bar 30 µm. **B** *Scolecia filosa*; scale bar 10 µm. **C** Brachiopod trace *Podichnus centrifugalis*; scale bar 30 µm. **D** Conchocelis Trace; scale bar 100 µm. **E** Spatial distribution of elongated linear filaments of Conchocelis Trace; scale bar 300 µm. **F** Older stage of Conchocelis Trace; scale bar 300 µm. **G** Problematical Trace 2; scale bar 100 µm. **H** Detail of **G** showing a xenoglyphic surface texture; scale bar 10 µm
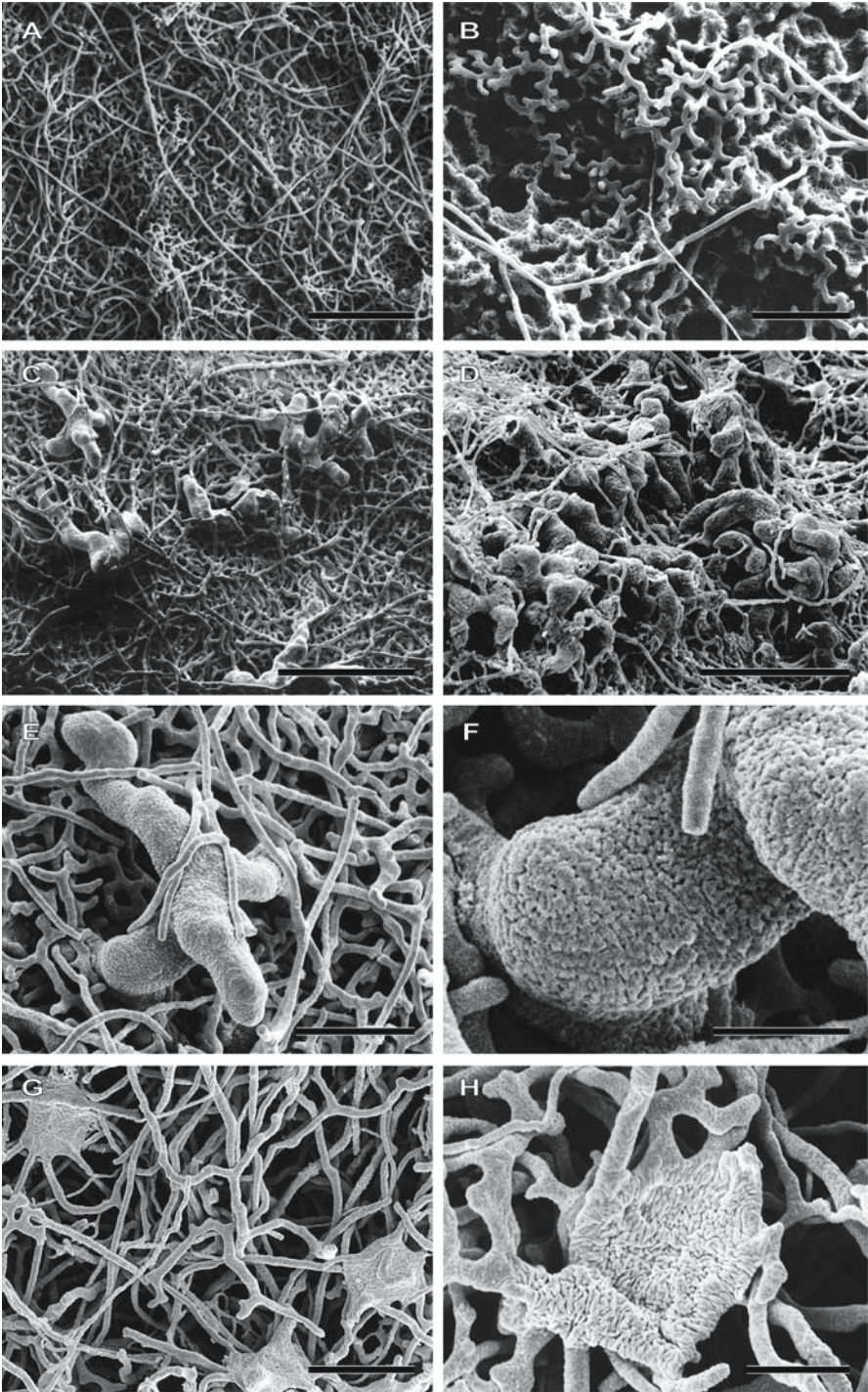
(morphological structure 2) are interpreted to be sporangia, bearing quadriflagellate, vegetative zoospores (Kornmann and Sahling 1980). Lukas (1974) describes intercalar tube enlargements of *O. quekettii* that measure up to 25 μm in width, and are especially located at sites of branching. The description corresponds to the morphology of morphological structure 3. However, observations of spores, or rather gametes are lacking so the function of morphological structure 3 remains uncertain.

Remarks

The trace occurs within the entire coralla of both specimens, but has a higher intra-skeletal density on the green-coloured sides (see Fig. 5B). However, the apical first centimetre of the whitish side ('Corallum 2') has not been infested by the green alga. Living thalli of *O. quekettii* are restricted to septal and thecal walls, which are at least temporarily covered by the 'edge zone' of the polyp (*sensu* Stolarski 1996). Their siphonal thalli seem to infest the skeleton at exposed areas, growing into the apical live zone of *D. dianthus*. Lukas (1974) notes that after infesting living scleractinians, the direction and rate of algal growth follows the host's outer circumference. This growth habit of *O. quekettii* has also been reported from tropical shallow-water corals, such as from *Porites lobata* Dana, 1846 at Moorea, French Polynesia (LeCampion-Alsumard et al. 1995), from *Porites compressa* Dana, 1846 at Kaneohe Bay, Hawaii (Shashar and Stambler 1992), and from *Mycedium elephantotus* (Oken, 1815) in the Gulf of Aqaba, Red Sea (Schlichter et al. 1997). Highsmith (1981) reports annual growth rates of 9.5 mm for *O. quekettii* in *Porites lutea* Quoy and Gaimard, 1833.

Ostreobium quekettii becomes abundant under low light levels, and is also found in sediments of the deep euphotic zone, suggesting a low rate of respiration (Budd and Perkins 1980). Vogel et al. (2000) reported *O. quekettii* occurrences in tropical environments down to 300 m depth. Halldal (1968) showed that photosynthetic activities of different *Ostreobium* species in the scleractinian coral *Favia* sp. are restricted to the peripheral 'green-bands'. Thus short ramification distances creating dense networks directly below the surface can be linked to improvement of photosynthetic productivity (see also Fig. 5C).

Fig. 7 SEM images of resin casts. Morphological structures of the green algal trace *Reticulina elegans* that are produced by *Ostreobium quekettii*. **A** Dense network of morphological structure 1. The spatial arrangement of the overlying linear resin tubes is an artefact caused by the dissolution of the carbonate: long wide meshed filaments originally penetrated the entire carbonate; scale bar 100 μm. **B** Young growth stage with its characteristic reticulated network directly below the surface; scale bar 30 μm. **C** Cluster of young stages of morphological structure 2; scale bar 100 μm. **D** Dense cluster of morphological structure 2 partially covered by morphological structure 1; scale bar 100 μm. **E** Tube enlargements of about 15 μm in diameter with slight constrictions every 10 μm (morphological structure 2); scale bar 30 μm. **F** Close-up of **E**. Tubes of morphological structure 2 have a granular surface texture and end hemispherically; scale bar 10 μm. **G** Polygonal structures (morphological structure 3) with a surface texture of 'vermiculate' granules; scale bar 30 μm. **H** Morphological structure 3; scale bar 10 μm

Rhodophyta

Endolithic red algae appear to be cosmopolitan on rocky shorelines. The greatest diversity is found in cold-temperate and boreal regions. They are present in the order Bangiales that contains currently a single family (Bangiaceae Engler, 1892). Amongst the order Bangiales, some species have a heteromorphic life history as documented from *Porphyra*. Its carpospores germinate to a trichous phase (Conchocelis phase), where filaments in nature are always found boring into a calcium carbonate substrate, and are interpreted to be the diploid sporophyte generation (Sitte et al. 2002). Its conchospore formation is a photoperiodic response, induced by reducing daylengths. Meiosis takes place during germination of the conchospores to a blade-like haploid gametophytic phase that requires cooler seasons (Maggs and Callow 2002). Fossils related to *Porphyra* are dated to 500 million years ago (Campbell 1980). Moreover, borings resembling the Conchocelis stage of *Porphyra*'s sibling genus, *Bangia*, have been discovered in Proterozoic (1.2 billion years) deposits in Arctic Canada, thus displaying on of the oldest taxonomically resolved eukaryotes in the fossil record (Butterfield et al. 1990; Butterfield 2000).

Conchocelis Trace (Figs. 6D-F)

Trace morphology

Unbranched linear tubes intrude perpendicularly from the surface as much as 1100 μm into the substrate. The whip-shaped tubes are distributed irregularly. Tube diameters taper slightly towards their ends from basally 33-45 μm to terminally 22 μm and show slight constrictions at intervals of about 13.5 μm.

Producer

Simply constructed trichous algae with an intercalary growth are present in the order Bangiales (Rhodophyta). However, a lack of observations of the endolithic thallus denies a clear phylogenetic relationship.

Remarks

Similarly sized whip-shaped tubes are produced by the boring foraminifer *Hyrrokkin sarcophaga* Cedhagen, 1994. Here, however the spatial arrangement of single filaments lacks any visible pattern.

Fungi

Endolithic fungi are attributed to the orders Saprolegniales, Peronosporales (Oomycota), and Cytridiomycetes (Eumycota). They are distinguished by their size, shape, mode of ramification, and sporangia (Glaub 1994). Fungal filaments (hyphae) secrete acids mainly apically, which enable them to grow into the substrate (Sand 1995; Sitte et al. 2002). The filamentous morphology of their mycelia facilitates absorption of nutrients.

Orthogonum spinosum **Radtke, 1991** (Figs. 8A-D)

Trace morphology

Homogeneous tubes of about 24 μm ramify preferably rectangularly and end hemisherically. Infrequently, a multitude of small hair-like filaments of about

1.7 μm in diameter protrude from the smooth-textured surface, having an average length of 25 μm. In the ichnogenus *Orthogonum* right-angular branching traces with homogeneous tube diameters are present (Radtke 1991). *Orthogonum spinosum* is characterised by tube diameters of 25-50 μm, similar sized hair diameters, as described above, but maximal hair lengths of only 12 μm.

Producer

Due to difficulties in laboratory cultivation, the taxonomic relationship of endolithic fungi is complicated, and the producer of *Orthogonum spinosum* has still not been identified.

Remarks

However, the ichnogenus *Orthogonum* has already been described from various recent habitats (Budd and Perkins 1980; Beuck and Freiwald 2005; Wisshak et al. 2005) and is known since the Silurian (Bundschuh 2000).

Foraminifera

Boring foraminiferans are known from different families, such as Astrorhizidae Brady, 1881, and Rosalinidae Reiss, 1963. Amongst these some parasitic forms are described, such as *Hyrrokkin sarcophaga* Cedhagen, 1994, recorded from the northern Atlantic on various substrates, e.g., *Acesta excavata* (Fabricius, 1779), sponges of the family Geodiidae, and scleractinians, such as *Lophelia pertusa*, *Caryophyllia* sp. and *Madrepora oculata* (see Cedhagen 1994; Freiwald and Schönfeld 1996; Beuck and Freiwald 2005; López Correa et al. 2005).

Foraminiferan Trace (Figs. 9C-H)

Trace morphology

This dendroid boring system branches in a fan-like pattern, and mature trace stages measure up to 1000 μm across. Its tubes are of variable diameters, however, and in mature stages they can measure up to 80 μm. Tubes ramify at different angles, and are rounded apically. The texture is slightly verrucous. The average base diameter of the single hemispherical warts is 10 μm. From the trace surface a multitude of homogeneous hair-like filaments protrude and taper distally from basal diameters of 3.2 μm to about 1 μm. They have a rough surface texture. Mature stages are characterised by long hairs (up to 500 μm). Individual traces can occur in compounds of three up to five and can have penetration depths up to 300 μm. Glaub (1994) described small rosette borings having a spinous tube relief as *Semidendrina*-Form.

Producer

The dendroid trace bears similarities to traces of the foraminiferan *Globodendrina monile* Plewes, Palmer and Haynes, 1993 that is phylogenetically related to the family Astrorhizidae Brady, 1881. The morphology is believed to be an adaptation to high energy environments (Cherchi and Schröder 1991). However, in the analysed specimen, only the plane dendroid boring system is observed, and not the spherical part that is looming into the substrate.
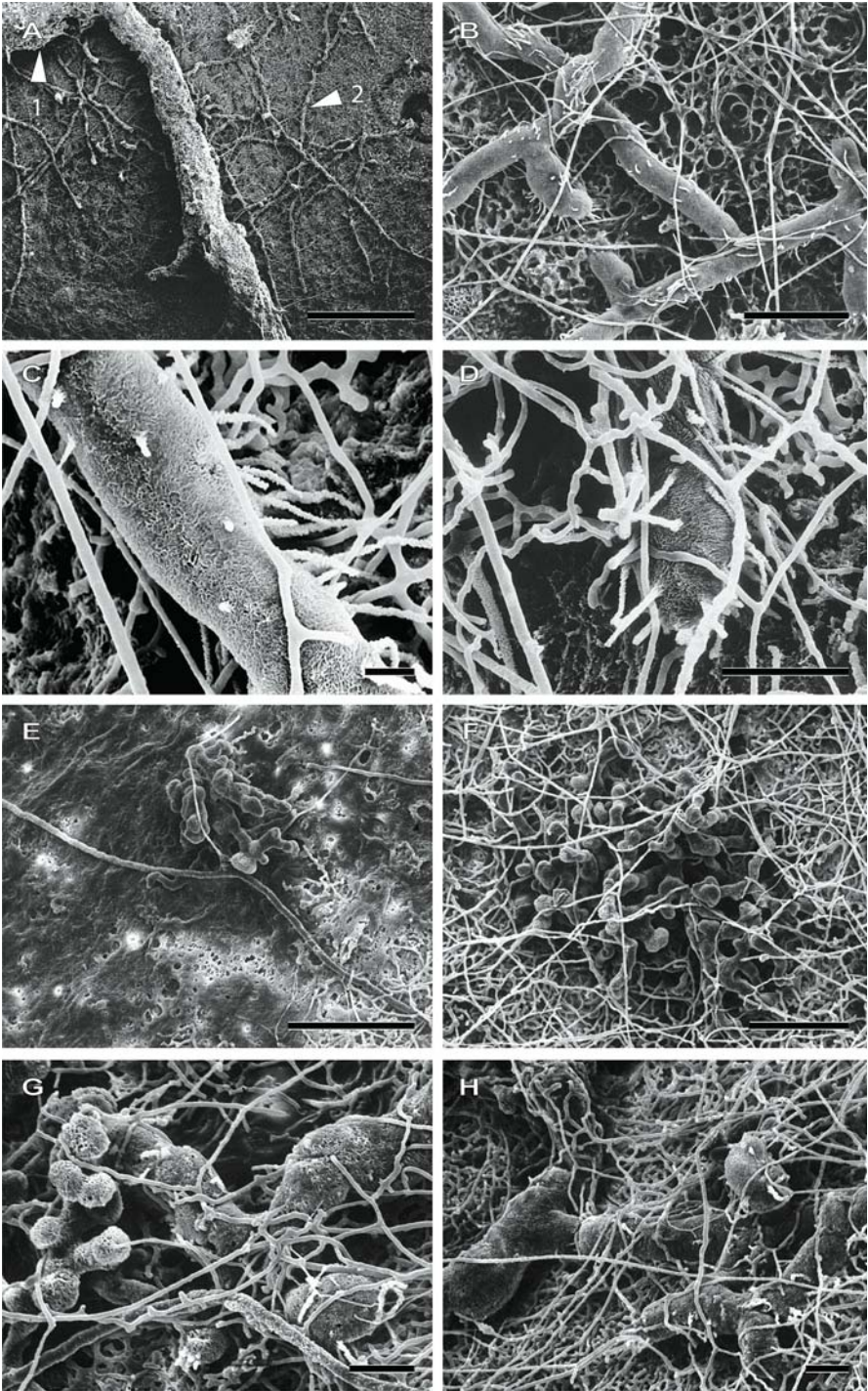
Remarks

Similar traces are also reported in the skeleton of *Lophelia pertusa* from the North Atlantic (Beuck and Freiwald 2005; Wisshak et al. 2005), and as 'hirsute camerate form' from Early Pleistocene coral limestones on Rhodes (Bromley 2005).

Porifera

Endolithic sponges are phylogenetically related to the order Hadromerida (Hooper and Soest 2002) and the order Haplosclerida (Soest and Hooper 2002), belonging to the group Demospongiae. By excavating the protective carbonate, they create vast galleries of chambers, which are connected with the exterior *via* aperture canals. Sponge trace casts are usually visible to the naked eye, and thus belong to the group of macroborings (Bromley 2005). Traces of different ichnospecies can vary, e.g., in morphology, construction of inter-chamber canals, aperture size, and surface ornamentation (see Bromley and D'Alessandro 1984; Calcinai et al. 2003). Sponges play a central role in the destruction of reefal ecosystems (Acker and Risk 1985), but only 2-3 % of the substrate is dissolved by etching cells (Rützler and Rieger 1973; Pomponi 1980), while the rest is removed as characteristical-shaped chips. They are expelled through the oscula, and can accumulate to form sediments (Rützler 1975; Freiwald and Wilson 1998).

Entobia **isp. 1** (Figs. 9A-B)

Trace morphology

The spherical trace is 77 μm in diameter. Its surface is sculptured by hemispherical, smooth textured units which are between 25-31 μm in diameter. It penetrates the carbonate to about 85 μm.

Producer

The spherical trace is a juvenile endolithic sponge chamber, formed by specialised archaeocytes, the etching cells (Rützler and Rieger 1973; Pomponi 1976, 1979). The absence of sponge spicules prevented closer identification of its producer.

Remarks

The trace morphology as well as the surface ornamentation is similar to the blackberry-shaped juvenile stage of *Spiroxya heteroclita* Topsent, 1896, which was found in the skeleton of *Lophelia pertusa* at the Propeller Mound (Beuck and Freiwald 2005). However, a common bioeroding sponge in this fjord habitat is *Cliona chilensis*, which is the most harmful eroder. Most coralla that are broken

---

Fig. 8 SEM images of resin casts. **A-D** Ichnospecies *Orthogonum spinosum*. **A** Ichnocoenosis of *Entobia* isp. (arrow 1) and *O. spinosum* (arrow 2); scale bar 1000 μm. **B** The homogenous tubes often branch in a rectangular angle; scale bar 100 μm. **C** Filigree hairs; scale bar 10 μm. **D** The tubes end hemispherical; scale bar 30 μm. **E-H** Problematic Trace 4. **E** Young trace stages show homogeneous tubes, on which sporangia insert; scale bar 100 μm. **F** Filaments of the sporangia are highly branched, and feature slight constrictions; scale bar 100 μm. **G** Two different distinctive features of the sporangia; scale bar 30 μm. **H** In mature stages sporangia can enlarge to tubes of diameters of up to 55 μm; scale bar 30 μm
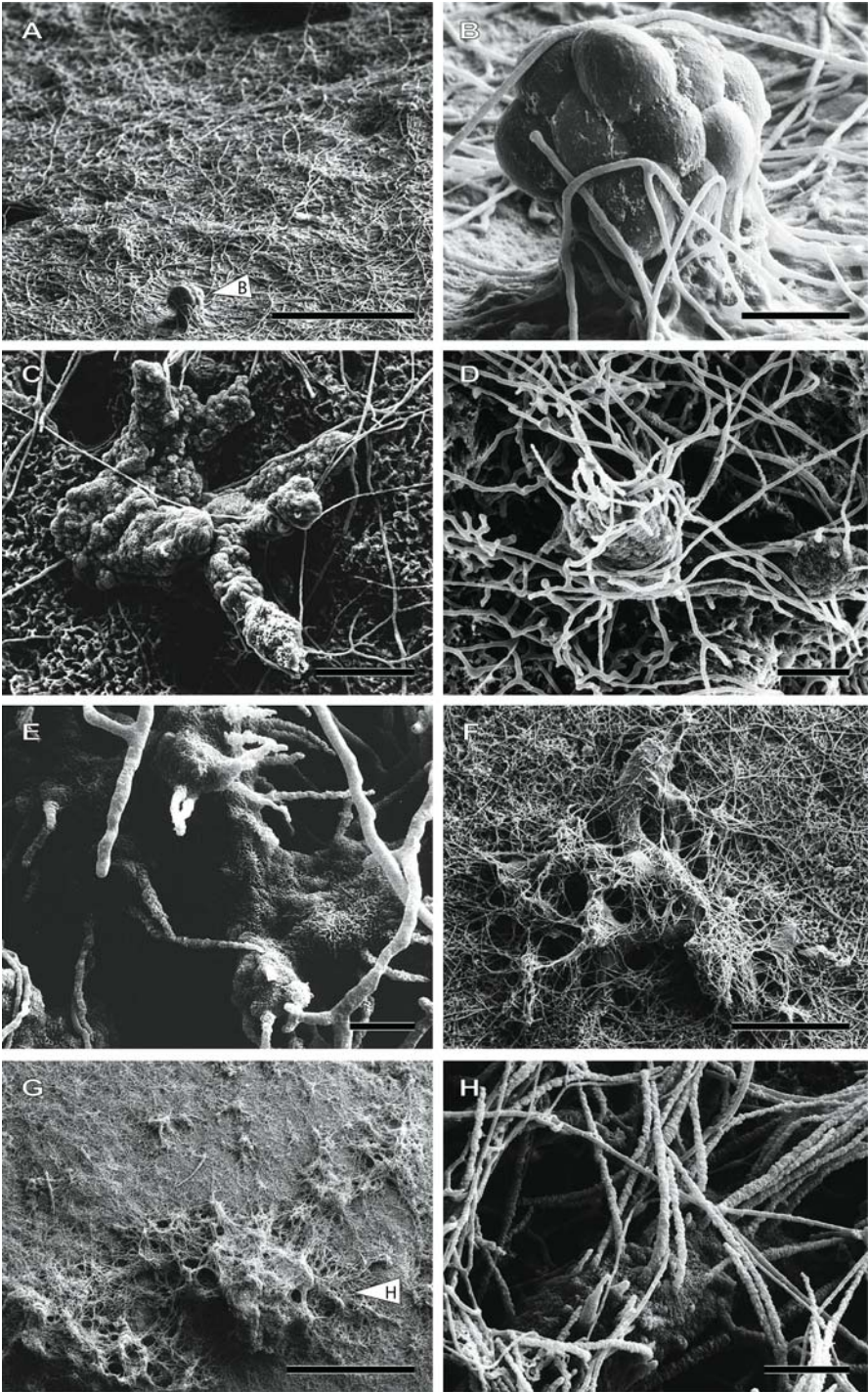
off show strong infestation by and degradation from this sponge which might have been the main cause for the breaking.

Entobia isp. 2 (Fig. 2G)

Trace morphology

The trace consists of spherical chambers, which are between 1.75-2 mm in diameter. They are interconnected by intercameral canals, which are up to 350 μm in diameter. The surface texture of its etching cells eluded documentation, due to a high abundance of the green algal trace *Reticulina elegans*.

Producer

The spicules have not been documented. Thus, identification to its producer is not possible.

Remarks

Owing to the relatively thick intercameral canals, as well as the size of their chambers, the trace is morphologically similar to *Entobia retiformis* (Stephenson, 1952) (see also Bromley and D'Alessandro 1987). X-ray radiographs of 'Corallum 1' document in the basal 5.5 cm a conspicuous infestation by this sponge. The largest part of the vast sponge chamber galleries was constructed within septa. Due to the lack of massive carbonate within the non-thecal coral parts, as well as the presence of high amounts of sponge aperture canals, detailed analysis of non-thecal coral casts is not applicable in thinly calcified coral septa.

Bryozoa

Taxonomically, endolithic bryozoans are attributed to the order Ctenostomata. Single individuals (zooids) of a colony are interconnected by stolons, which underlie the surface. In the deep-water environments of the northern Atlantic, the most common bryozoan trace within the skeleton of cold-water corals is *Spathipora* isp. Its incremental growth stages in the substrate are documented from trace casts by Beuck and Freiwald (2005).

Bryozoan Trace 1 (Figs. 10A-B)

Trace morphology

Bilaterally symmetrical shallow cast elevations of about 350 μm x 120-186 μm are horizontally disposed to tube casts throughout their entire length. Lateral tubes

---

Fig. 9 SEM images of resin casts. **A-B** *Entobia* isp. **A** Three centimetres below the 'edge zone' a juvenile sponge chamber (**B**) is located within dense networks of *Reticulina elegans*; scale bar: 300 μm. **B** Close-up of **A**. The surface texture of the individual etching-cell imprints is smooth; scale bar 30 μm. **C** Probably a young stage of a foraminiferan boring, but the lack of hairs also advocate a juvenile sponge boring; scale bar 100 μm. **D-H** Foraminiferan trace 1. **D** Young stage of a foraminiferan boring; scale bar 30 μm. **E** Young stages are characterised by short filaments, emanating from the surface; scale bar 10 μm. **F** Dendroid tube system with a multitude of long whip-like filaments scale bar 300 μm. **G** Overview of aggregates of Foraminiferan Trace 1; scale bar 1000 μm. **H** Close-up of dendroid tube filaments of **G**; scale bar 30 μm
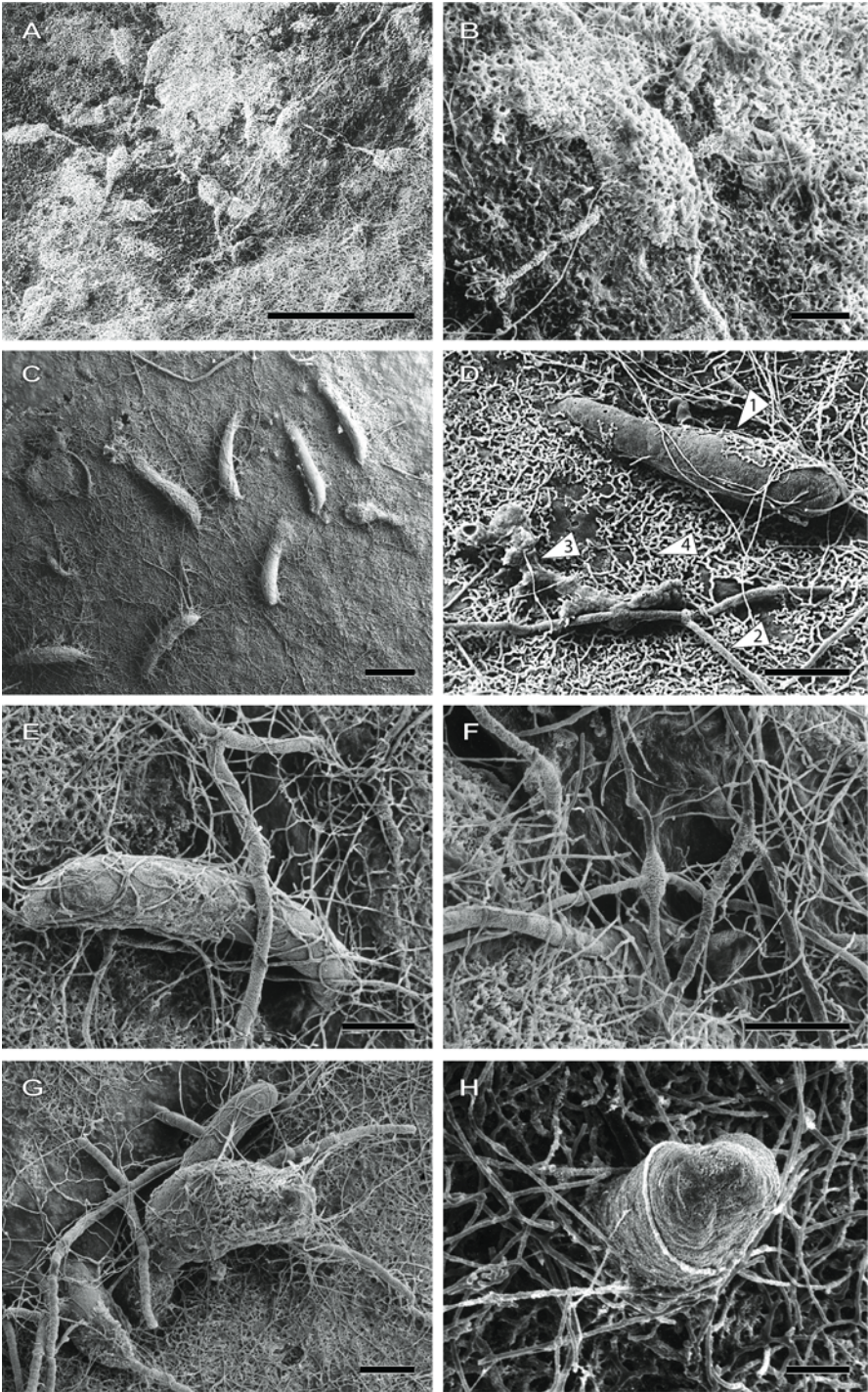
emanate opposite one another near middle length of the shallow cast elevations. The interconnecting tubes measure 12 μm in diameter. Distances between single cast elevations vary between 415 μm to 505 μm. The trace penetrates the carbonate to a depth of up to 67 μm.

Producer

Non-pedunculate growth types are present in the family Orbignyoporidae Pohowsky, 1978, and Immergentiidae Silén, 1946. The morphological diagnosis of the family Orbignyoporidae corresponds to the growth morphology of Bryozoan Trace 1. The family Immergentiidae is characterised by zooids that protrude essentially vertically into the substratum. However, *Immergentia patagoniana* Pohowsky, 1978, described from Argentina, is characterised by location of zooids and stolons at the bottom of relatively broad depressions in the surface of the substratum, which is apparently a unique feature in the family Immergentiidae (see Pohowsky 1978).

Remarks

One colony with about 12 zooids is present 7.5 cm below the apical part of 'Corallum 1'. In addition, a ctenostomate colony on the corallum's surface is located in the corresponding area. However, its exposed zooid lengths are smaller in size than the total lengths of the trace cast elevations.

Spathipora elegans Fischer, 1866 (Figs. 10C-H)

Trace morphology

Directly below the surface, a network of homogeneous tubes of about 11 μm in diameter connects elongated chambers, which are fully grown between 500 and 600 μm in length and about 75 μm in diameter. Casts of the chambers are oriented dextrally to the tube casts and are connected with the tubes *via* a tubular pedunculus that measures about 9 μm in diameter. The surface texture of the trace elements is smooth. Unilateral ramifications usually have an expanded junction to the main stolon, in contrast, the connection of bilateral ramifications is slightly thickened. One chamber with a diameter of 190 μm is tilted nearly vertically, and gives rise to three tubes that are, with respect to the peripheral ones, thicker in diameter. In addition, an ovoid chamber of 30 μm in diameter and 75 μm in height is connected to tubes that insert opposite one another.

Fig. 10 SEM images of resin casts. **A-B** Bryozoan Trace 1. **A** Casts of shallow-boring bryozoans; scale bar 1000 μm. **B** Bilaterally symmetrical shallow cast elevation, which is interconnected by tubes that contain stolons; scale bar 100 μm. **C-H** Bryozoan ichnogenus *Spathipora elegans*. **C** Nine chambers that harboured the autozooids are interconnected by tubes that contained the stolons; scale bar 300 μm. **D** (1) adult autozooid chamber; (2) stolon tube; (3) juvenile foraminiferal trace; (4) the green algal trace *Reticulina elegans* Radtke, 1991; scale bar 100 μm. **E** Chamber of an autozooid that is connected *via* pedunculus to the stolon tube; scale bar 100 μm. **F** Bilateral ramification slightly thickened; scale bar 100 μm. **G** Vertical chamber (ancestrula); scale bar 100 μm. **H** Ovoid chamber (gonozooid); scale bar 30 μm

Producer

Characteristic for endolithic Bryozoa of the suborder Stolonifera are tube casts bearing the stolons, which interconnect the single individuals (zooids). The vertical chamber is interpreted to be the ancestrula. The stolons interconnect the specialised zooids with each other that can be distinguished between autozooids, dwelling in elongated chambers, and gonozooids, which are contained in ovicell-shaped chambers. Similar trace features are described for the bryozoan trace *Spathipora elegans* Fischer, 1866 from the coast of Chile (Pohowsky 1978).

Remarks

First traces of the sinistral bryozoan colony appear on the light-averted side of the 'Corallum 2' directly below the area, which was frequently covered by the polyp. One colony is found with more than 100 zooids. Since individuals have a filtering lifestyle, they are restricted to coral skeletons that are exposed to water. The ichnogenus *Spathipora* is common in aphotic trace communities (ichnocoenoses) from the North Atlantic (Beuck and Freiwald 2005), where the cold-water coral *Desmophyllum dianthus* is associated with the main framework builder *Lophelia pertusa* and *Madrepora oculata*.

Polychaeta

48 species of polychaetes, belonging to the families Spionidae, Sabellidae, and Cirratulidae have been reported as borers of other living marine organisms (Martin and Britayev 1998). Amongst the parasitic boring polychaetes, more than 53 % are additionally considered to be facultative symbionts, boring also into non-living substrates. The boring habit is interpreted to be a protective advantage as well as the easiest way to contact with the water column just above the sediment surface (Martin and Britayev 1998). Boring worms have inhabited in reefs since the Lower Cambrian (Vogel 1993).

Sabellid Trace (Figs. 2E-G)

Trace morphology

A circular tube of 2.8 mm in diameter exits to the surface. Only the region from the surface and in to 1.7 mm is preserved as trace cast, which was originally located in the massive carbonate of the theca. Thus, the penetration depth has not been measured. In addition, its surface texture eluded documentation, owing to attached filaments of the trace *Reticulina elegans*.

Producer

The hole contains remains of a dark coloured tube that is thick-walled and gelatinous, belonging to a euendolithic sabellid worm. The endolithic sabellid *Perkinsiana corcovadensis* (Hartmann-Schröder, 1965) is described from southern Chile at a depth of 190 m (see also Knight-Jones 1983).

Remarks

The cavity is located about 7 cm above the base of 'Corallum 1' on the green side. The boring mechanism seems to be chemical. This euendolithic sabellid worm

is a common bioeroder in the habitat studied mainly in coral substrates, but also often found in shells of the gastropod *Crepidula* sp.

Caulostrepsis contorta Bromley and D'Alessandro, 1983

Trace morphology

The boring is curved and circular in shape. Its limbs are 290 μm in diameter and are interconnected by a well-developed vane. One millimetre below the surface, the limb is constructed in a surface-parallel plane that has a hemispherical course (diameter 1 mm). The trace exits to the surface by an aperture that is 270 μm in diameter.

Producer

A putative producer of the trace is discussed within the genus *Polydora* Bosc, 1802 (see Bromley and D'Alessandro 1983). The boring spionids *Polydora* cf. *ricksettsi* Woodwick, 1961, *Dipolydora huelma* Sato-Okoshi and Takatsuka, 2001 and *Dipolydora giardi* Mesnil, 1896, are known from this region to bore on *Crepidula* sp. (Sato-Okoshi and Takatsuka 2001). The spionid worm *Polydora websteri* Hartman, 1943 forms similar-shaped traces. However, their trace shape varies strongly with different host substrates (Blake and Evans 1973).

Remarks

In contrast to *Maeandropolydora elegans* Voigt, 1970, limbs of this trace do not parallel each other, but have a well-developed vane of varying shape.

Caulostrepsis isp. (Figs. 11B-D)

Trace morphology

Pouches are bent in a narrow U-form, and in cast tower up to 2.3 mm perpendicular to slightly tilt into the substrate. The inward-facing walls of the limbs are fused by complete removal of the intervening substrate (open pocket structure; Bromley and D'Alessandro 1983), and show a slight axial depression in between limbs. Transverse sections of the trace are flattened-elliptically (250 μm x 425 μm), and increase slightly in width towards their aperture. However, the aperture of one trace enlarges up to diameters of 430 μm x 573 μm. The transverse surface ornamentation seems to derive from the structural heterogeneity of the substrate (xenoglyph; Kelly and Bromley 1984), and reflects growth increments which vary between 125 μm and 145 μm. The trace is morphologically similar to the ichnospecies *Caulostrepsis cretacea* (Voigt, 1971). However, *Caulostrepsis cretacea* decreases in size towards its aperture (Bromley and D'Alessandro 1983).

Producer

U-shaped burrows are described from boring activities within spionid polydorids. Blake and Evans (1973) display morphologically similar traces produced by *Polydora ciliata* (Johnston, 1838). However, Bromley (1978) published similar borings produced by the eunicid *Lysidice ninetta*. Thus, it seems that we shall not come closer to the producer of *Caulostrepsis* than polychaete annelids.
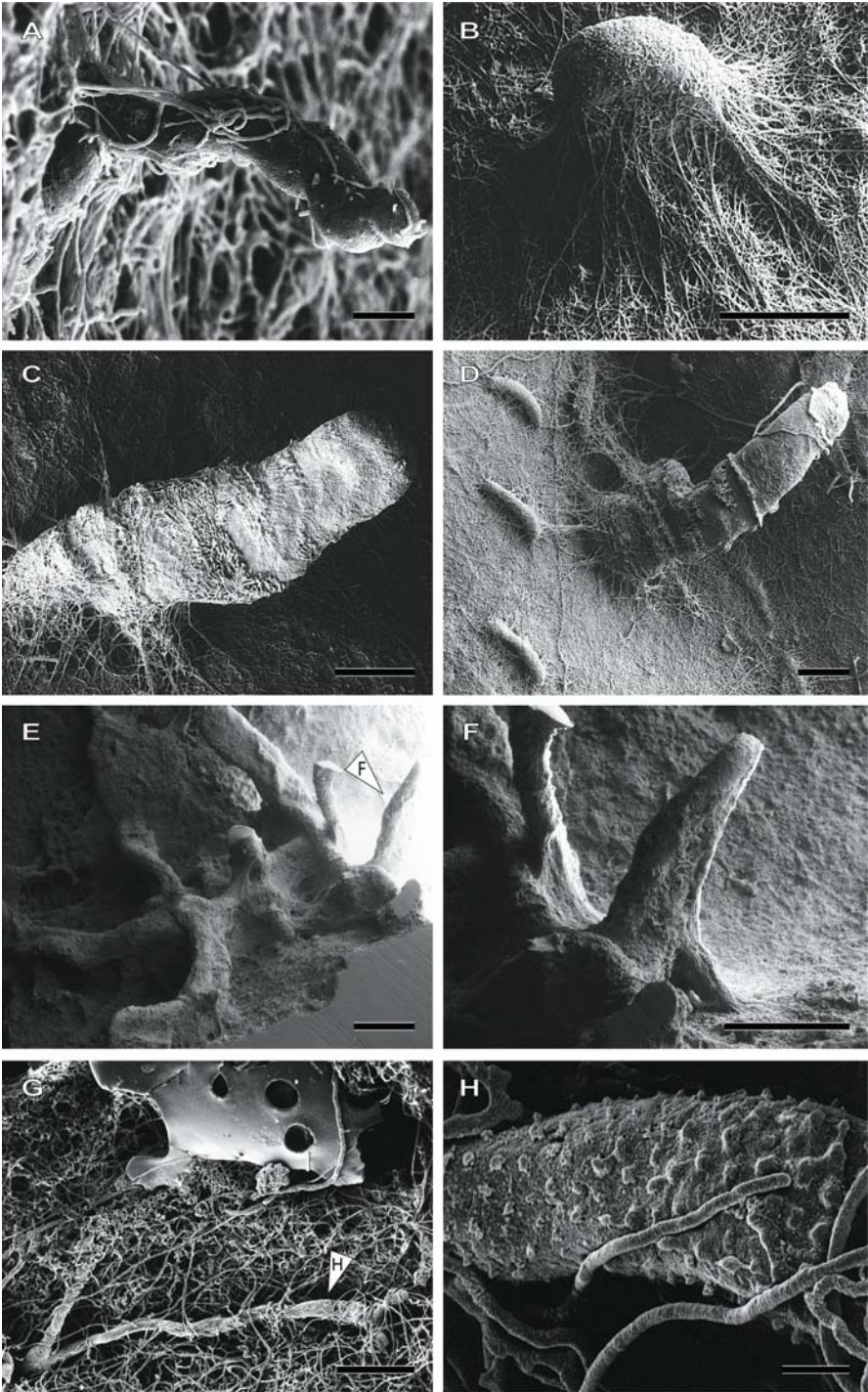
Remarks

Three individuals are present in 'Corallum 2' from the whitish side, 2.8 cm below the 'edge zone', having a gregarious habit. The trace-producing polychaete communicates with the exterior *via* pairs of tubes at the periphery of the corallum. *Caulostrepsis* isp. advances at the vertex (lateral boring; Bromley and D'Alessandro 1983). The excavating mechanism seems to be chemical-mediated.

However, one trace is basally enlarged, which suggests a possible young growth stage of the trace *Maeandropolydora elegans*. Similarly sized traces are also encountered in fossil skeletons of *Lophelia pertusa* from Rhodes (Bromley 2005).

Maeandropolydora elegans **Voigt, 1970** (Figs. 11E-F)

Trace morphology

In total, dimensions of the meandered tube system are 1.1 x 1.3 cm. The trace is composed of cylindrical galleries of constant diameter (700 x 350 μm), running irregularly sinuously in all directions. The cylindrical galleries have one or more apertures. The pair of limbs may show axial torsion, tending to run in a paired fashion. Cross-sectional areas of tubes are 'dumbbell'-shaped (*sensu* Bromley and D'Alessandro 1983), due to the inner edges of U-shaped lobes, which are connected by a vane.

Producer

Based on the morphological similarity to *Caulostrepsis*, the trace *Maeandropolydora* may also be attributed to spionid polychaetes (Voigt 1965; Bromley and D'Alessandro 1987). A similar trace is described from the spionid worm *Polydora concharum* Verrill, 1880 in the shells of the scallop *Placopecten magellanicus* (Gmelin, 1791) (see Evans 1969).

Remarks

The trace is located 5.5 cm below the apical part on the green side of 'Corallum 1'. After Bromley and D'Alessandro (1983), galleries of *Maeandropolydora elegans* extend from the end of one limb (axial boring).

Maeandropolydora sulcans **Voigt, 1965** (Figs. 4G-H)

Trace morphology

This trace consists of long cylindrical galleries that have diameters of 200 to 300 μm. They are irregularly contorted, bent in loops, and always lacking in vane or pouch. The trace can branch at various angles. Several circular apertures of about 200 μm in diameter are developed. Partially, the galleries are exposed at the surface, forming slight etching trenches.

Fig. 11 SEM images of resin casts. **A** Problematical Form 1; scale bar 30 μm. **B-D** *Caulostrepsis* isp. **B** Young growth stage; scale bar 30 μm. **C** *Caulostrepsis* isp.; scale bar 300 μm. **D** *Caulostrepsis* isp. Basally enlarged, and associated with *Spathipora elegans* and *Ostreobium quekettii*; scale bar 300 μm. **E-F** *Maeandropolydora elegans*. **E** Overview; scale bar 1000 μm. **F** Detail of **E**; scale bar 1000 μm. **G-H** Problematic Trace 3. **G** Overview; scale bar 100 μm. **H** Detail of **G**; scale bar 10 μm

Producer

Chughtai and Knight-Jones (1988) describe similar traces etched by sabellid worms. However, its taxonomical relationship has not been ascertained.

Remarks

A similar shaped trace but larger-sized is described from the Pleistocene of Italy by Bromley and D'Alessandro (1983).

Brachiopoda

Attached pedicle of brachiopods produce groups of finger-shaped borings. The spatial arrangement of the single tubes to each other, as well as their surface texture, is indicative of different producers (see Bromley and Surlyk 1973). First brachiopod borings are reported from the Silurian (Bundschuh 2000).

Podichnus centrifugalis Bromley and Surlyk, 1973 (Fig. 6C)

Trace morphology

About a dozen finger-shaped tubes of similar size tower up (in cast) to 55 μm perpendicularly into the substrate, and are grouped without visible pattern. Directly below the surface, they are 10.5 μm in diameter, however, their diameters taper off slightly towards their ends. The trace measures about 200 μm across.

Producer

In the habitat, *Magellania venosa* was regularly observed to grow on *D. dianthus*.

Remarks

Podichnus centrifugalis has been found in Swedish Kosterfjord (Wisshak et al. 2005), as well as from Early Pleistocene coral limestones on Rhodes (Bromley 2005). The trace has a rich fossil record back to the Silurian (Bromley 2004).

Problematical Trace 1 (Fig. 11A)

Trace morphology

The tubular trace is 28 μm in diameter, and penetrates the substrate perpendicularly to a depth of 195 μm. The trace surface shows light constrictions, creating 27-40 μm long ovoid segments. Its surface texture is smooth, but bears hair-like filaments, which are expanded up to 35 μm into the substrate with diameters of about 2 μm. A comparable trace has not been found in the literature.

Problematical Trace 2 (Figs. 6G-H)

Trace morphology

From a group of slight elevations (in cast) that are up to 72 μm high, conical tubes arise perpendicularly. The diameter of the base of the tube is up to 23 μm. However, the trace narrows, and ends after about 65 μm at a spiky, or rounded termination. The surface texture of the trace is a xenoglyph. An individual trace measures about 450 μm across. A similar trace that exhibits a large cluster of straight intrusions and that penetrates from shallow depressions is described as 'Problematic Form 2' from Wisshak et al. (2005). The authors discuss the trace as a possible

attachment scar produced by a heterotrophic epilithic organism, such as brachiopod, or foraminiferan.

Problematical Trace 3 (Figs. 11G-H)

Trace morphology

The cylindrical tube system lies directly below the surface and has an entire length of about 620 μm. It exits to the surface by a circular aperture that is 30 μm in diameter. The tube enlarges after 15 μm to 46 μm and bifurcates with an angle of 40° into two tubes of each 25 μm in diameter. After about 490 μm, one of the two tubes splits again with a similar angle, as mentioned above, into two tubes that are each 21 μm in diameter. The surface texture of the tubes is characterised by a multitude of small, hemispherical-shaped knobs that are each 2.4 μm in diameter.

Problematical Trace 4 (Figs. 8E-H)

Trace morphology

Branched tubes ramify at different angles and are, owing to local constrictions, of inconstant diameters between 7-17 μm. To this local agglomeration, a homogeneous tube of 6.5-7.5 μm in diameter can be connected. The surface texture of the trace is xenoglyphic. In older stages, the constricted tubes are enlarged and irregular-shaped, becoming less branched and measuring up to 55 μm in diameter. This distinctive trace can cover, directly below the surface, an area of up to 600 μm in diameter.

The irregular-shaped part is interpreted to be a sporangium. However, this trace can be distinguished from the morphological structure 2 of *Reticulina elegans* by its thicker and irregular-shaped tube diameters, as well as the different surface texture. In contrast to *Orthogonum spinosum*, the tubes lack hairs.

Discussion

Biocoenotic interactions

Contractions of the scleractinian polyp's 'edge zone', exposing the skeleton to direct contact with the water column, are reported by several authors, e.g., Harmelin (1990), Stolarski (1996), Lazier et al. (1999). Consequently, epi- and endolithic organisms can settle on the skeleton, competing for space (Fig. 5A). Their distribution and abundance is mainly influenced by abiotic factors, such as hydrodynamics, seasons, sedimentation rates, as well as biotic ones, such as grazing activity. Epi- and endolithic organisms can be pests stressing the host polyp to keep them away from the interior (LeCampion-Alsumard et al. 1995; Martin and Britayev 1998). Although, the migrating 'edge zone' can consecutively repress growth of adjacent filtering endoliths and attached epiliths (see Harmelin 1990), living thalli of the endolithic green alga *Ostreobium quekettii* are reported in skeletal areas frequently covered by the polyp's 'edge zone' (LeCampion-Alsumard et al. 1995; Schlichter et al. 1997). Beneath the polyp's tissue, endolithic algae can take shelter from sedimentation and grazers, as well as from epilithic organisms that shade the skeleton (LeCampion-Alsumard et al. 1995). Adjacent to the polyp

'edge zone', the coralla of the *Desmophyllum dianthus* specimens analysed are sculptured by dense patterns of grazing traces, fostering the hypothesis that endolithic algae benefit from the protection by the tissue of their host organisms. Owing to their photoautotrophic nutrition, green algae are restricted to above the light compensatory depth. Schlichter et al. (1997) calculated that their bathymetric distribution is limited to a minimum surface light intensity of 0.0009 %. Reductions of irradiance are caused by water depth, 'edge zone', coral tissue thickness, light-transmissivity of the skeleton, and self-shading of algal filaments. But light-yield can be improved by chromatic adaptation, showing variable photosynthetic-active pigment compositions (Schlichter et al. 1997). Most notable are studies on the green alga *Ostreobium quekettii* in the tropical azooxanthellate coral *Tubastrea micranthus* Ehrenberg, 1834 that show transport of photoassimilates released from the algal filaments to the coral tissue *via* the uptake mechanisms for dissolved organic substances of cnidarians (Schlichter et al. 1995). This interaction raises the polyp's fitness by increasing productivity and biomass. In return, metabolic end products can be used by the endolithic alga. But productivity of endolithic algae reaches a maximum of just 10 % of that of zooxanthellae (Schlichter et al. 1997).

Up to now, no examples for mutualistic symbiotic relationships with deep-water corals are known (Buhl-Mortensen and Mortensen 2004). Nevertheless, the unilateral progression of the polyp's 'edge zone' on the green-coloured side, in contrast to the whitish side, where *Q. quekettii* is absent in the zone of living tissue, can indicate an interaction between the green algal thallus of *Ostreobium quekettii* and its host *Desmophyllum dianthus* (see Table 1). Additionally, we observed a thicker theca on the green-coloured side of both of the investigated coralla, which could be linked with the photosynthetic activity of the endolithic green algae, strengthening the coral individual by stimulating its skeletal mineralisation (see Macintyre and Towe 1976). Both factors can indicate a putative facultative mutualistic ectosymbiosis between endolithic algae and their coral host, but further studies are required to enlighten potential beneficial interactions.

Ichnocoenoses as environmental indicators

The lifespan of *Desmophyllum dianthus* is mainly ruled by skeletal growth *versus* the infestation intensity of macro-borers, such as sponges and polychaetes, which increase the intraskeletal porosity considerably, thus weakening the architectural stability of the coral (Försterra and Häussermann 2003). Eventually corals become detached from the substrate and are piled up in deeper depositional environments (Boerboom 1996; Försterra and Häussermann 2003). Thus, the investigation of trace communities (ichnocoenoses) within coral skeletons and its comparison to growth rates of corals provides a powerful tool to define ecological health conditions for cold-water corals.

The analysed ichnocoenoses are dominated by traces of heterotrophic organisms, which are accompanied by *Scolecia filosa* and *Reticulina elegans*. After Glaub (2004), the present assemblage is a characteristic feature of the dysphotic zone that extends from 1 % level to about 0.01 % or 0.001 % of surface light. This quite shallow occurrence of a dysphotic zone ichnoassemblage can be attributed

to the growth of *Desmophyllum dianthus* on the undersides of rock ledges, where the light intensity is strongly reduced. Therefore, trace assemblages in fossil *Desmophyllum* communities from near coast and cliff-bound environmental settings have to be regarded carefully, since the ichnocoenosis index could indicate much deeper paleodepths than those that actually prevailed at the time of formation. For bathymetrical reconstructions, the past relief and possible environmental conditions have to be evaluated carefully.

True deep-water ichnocoenoses (Table 2) have been reported by Wisshak et al. (2005) from the Kosterfjord off Sweden (-85 m), by Beuck and Freiwald (2005) from the Porcupine Seabight in the Northeast Atlantic (-780 m), and by Boerboom et al. (1998) from Orphan Knoll, off Newfoundland (-1800 m).

In this study, the investigated shallow-water ichnocoenoses have typical deep-water characteristics, but also contain shallow-water elements, due to their occurrence within the photic zone. A general similarity to the deep-water situation is depicted by the common endolithic traces of fungi (*Orthogonum*), foraminiferans (*Semidendrina*), bryozoans (*Spathipora*), and brachiopods (*Podichnus*), as well as by associated epilithic organisms (*Cibicides lobatulus*). The influence of light is shown by the presence of boring algae. Additionally, the non-light-dependant polychaete ichnogenera *Caulostrepsis* and *Maeandropolydora* indicate shallow marine conditions (Bromley and D'Alessandro 1983).

A similar ichnocoenosis, which appears contradictory at first glance, has been reported from Bromley (2005) from Early Pleistocene deposits of Rhodes. Here the trace community and the general fauna assemblage clearly indicate deep-water conditions, while the presence of the ichnogenus *Caulostrepsis* isp. provides the only hint to actually shallower conditions. Despite first studies in the deep Mediterranean, another curiosity is that traces of the bryozoan ichnogenus *Spathipora* have not yet been recorded (Bromley 2005; own observation; personal comm. Max Wisshak).

Deep-water fauna has already been recorded from shallow cryptic habitats from the Mediterranean Basin, especially from caves (Bromley and Asgaard 1993; Vacelet et al. 1994; Vacelet 1996; Harmelin 1997). However, the studied occurrence of deep-water biocoenoses (Försterra and Häussermann 2003) and ichnocoenoses in shallow-waters is strongly linked to the hydrographic conditions of the fjord region with strong freshwater run off, which forces an internal circulation system, allowing marine deep-waters to enter the troughs. These conditions with shallow deep-water fauna and also shallow deep-water ichnocoenosis are also known from other fjord areas, as in Scandinavia and New Zealand's Fjordland (South Island's west coast) (Grange et al. 1981; Wisshak et al. 2005). Within the Chilean fjord system, the upper limit of *Desmophyllum dianthus* is only limited by the lower boundary of the low salinity layer.

Conclusions

- In the Chilean fjords, *Desmophyllum dianthus* has been observed to exist over a wide bathymetrical range under different environmental conditions. Although the structure of the coral banks in different depths may look

similar on first sight, the composition of the associated biocoenoses differ with depth.

- The actinarians and sponges associated with *D. dianthus* in shallow water contain typical shallow-water as well as deep-water species.
- An inventory of 20 traces is given for the ichnocoenosis within the skeleton of *D. dianthus*. They are taxonomically correlated to Cyanobacteria (1), Chlorophyta (1), Rhodophyta (1), Porifera (2), Fungi (1), Foraminifera (1), Bryozoa (2), Polychaeta (5), Echinoida (1), Brachiopoda (1), and four traces of uncertain producer.
- The investigated shallow-water ichnocoenosis comprises typical shallow-water endoliths, as well as deep-water elements.
- The ichnocoenoses are dominated by heterotrophic organisms which are accompanied by *Scolecia filosa*, and *Reticulina elegans*, indicating dysphotic conditions at 28 m depth.
- *D. dianthus* settles on near vertical walls and, preferably, on the undersides of rock ledges with downward facing polyps. This pattern can be observed down to at least 255 m and is probably due to its sensitivity to sedimentation.
- Thus, in photic environments, ichnoassemblages within the skeleton of *D. dianthus* can only be used as a tool for (paleo-) bathymetrical reconstructions with caution.

Acknowledgements

References

Acker KL, Risk MJ (1985) Substrate destruction and sediment production by the boring sponge *Cliona caribbaea* on Grand Cayman Island. J Sediment Petrol 55: 705-711

Arntz WE (1999) Magellanic-Antarctic: Ecosystems that drifted apart. Summary review. In: Arntz WE, Ríos C (eds) Magellanic-Antarctic: Ecosystems that drifted apart. Inst Ciènc Mar, C.S.I.C., Barcelona, pp 503-511

Beuck L, Freiwald A (2005) Bioerosion patterns in a deep-water *Lophelia pertusa* (Scleractinia) thicket (Propeller Mound, northern Porcupine Seabight). In: Freiwald A, Roberts JM (eds) Cold-water Corals and Ecosystems. Springer, Berlin Heidelberg, pp 915-936

Blake JA, Evans JW (1973) *Polydora* and related genera as borers in mollusk shells and other calcareous substrates. Veliger 15: 235-249

Boerboom CM (1996) Bioerosion and micritization in the deep sea. MSc thesis, McMaster Univ

Boerboom CM, Smith JE, Risk, MJ (1998) Bioerosion and micritization in the deep sea coral *Desmophyllum cristagalli*. Hist Biol 13: 53-60

Brattström H, Johanssen A (1983) Ecological and regional zoogeography of the marine benthic fauna of Chile. Sarsia 68: 289-339

Bromley RG (1975) Comparative analysis of fossil and recent echinoid bioerosion. Palaeontology 18: 725-739

Bromley RG (1978) Bioerosion of Bermuda reefs. Palaeogeogr Palaeoclimatol Palaeoecology 23: 169-197

Bromley RG (1992) Bioerosion: eating rock for fun and profit. In: Maples CG, West RR (eds) Short Courses in Paleontology. 5. Trace Fossils. Paleont Soc, Knoxville, pp 121-129

Bromley RG (2004) A stratigraphy of marine bioerosion. In: McIlroy D (ed) The Application of Ichnology to Palaeoenvironmental and Stratigraphic Analysis. Geol Soc London, Spec Publ 228: 455-479

Bromley RG (2005) Preliminary study of bioerosion in the deep-water coral *Lophelia*, Pleistocene, Rhodes, Greece. In: Freiwald A, Roberts JM (eds) Cold-water Corals and Ecosystems. Springer, Berlin Heidelberg, pp 895-914

Bromley RG, Asgaard U (1993) Endolithic community replacement on a Pliocene rocky coast. Ichnos 2: 93-116

Bromley RG, D'Alessandro A (1983) Bioerosion in the Pleistocene of southern Italy: Ichnogenera *Caulostrepsis* and *Maeandropolydora*. Riv Ital Paleont Stratigr 89: 283-309

Bromley RG, D'Alessandro A (1984) The ichnogenus *Entobia* from the Miocene, Pliocene and Pleistocene of southern Italy. Riv Ital Paleont Stratigr 90: 227-296

Bromley RG, D'Alessandro A (1987) Bioerosion of the Plio-Pleistocene transgression of Southern Italy. Riv Ital Paleont Stratigr 93: 379-442

Bromley RG, Surlyk F (1973) Borings produced by brachiopod pedicels, fossil and Recent. Lethaia 6: 349-365

Budd DA, Perkins RD (1980) Bathymetric zonation and paleoecological significance of microborings in Puerto Rican shelf and slope sediments. J Sediment Petrol 50: 881-904

Buhl-Mortensen L, Mortensen PB (2004) Symbiosis in deep-water corals. Symbiosis 37: 33-61

Bundschuh M (2000) Silurische Mikrobohrspuren – Ihre Beschreibung und Verteilung in verschiedenen Faziesräumen (Schweden, Litauen, Großbritannien und U.S.A.). Unpubl PhD thesis, Johann Wolfgang Goethe Univ, Frankfurt am Main

Butterfield NJ (2000) *Bangiomorpha pubescens* n. gen., n. sp.: implications for the evolution of sex, multicellularity, and the Mesoproterozoic/Neoproterozoic radiation of eukaryotes. Paleobiology 26: 386-404

Butterfield NJ, Knoll AH, Swett K (1990) A bangiophyte red alga from the Proterozoic of Arctic Canada. Science 250: 104-107

Cairns SD (1982) Antarctic and Subantarctic Scleractinia. Antarct Res Ser 34: 1-74

Cairns SD, Zibrowius H (1997) Cnidaria Anthozoa: Azooxanthellate Scleractinia from the Philippine and Indonesian Regions. Mém Mus Natl Hist Nat Paris 172: 27-243

Cairns SD, Häussermann V, Försterra G (submitted): A review of the Scleractinia (Cnidaria: Anthozoa) of Chile, with the description of two new species. Zootaxa

Calcinai B, Arillo A, Cerrano C, Bavestrello G (2003) Taxonomy-related differences in the excavating micro-patterns of boring sponges. J Mar Biol Assoc UK 83: 37-39

Campbell SE (1980) *Palaeoconchocelis starmachii*, a carbonate boring microfossil from the Upper Silurian of Poland (425 million years old): implications for the evolution of the Bangiaceae (Rhodophyta). Phycologia 19: 25-36

Castilla JC, Navarrete SA, Lubchenco J (1993) Southeastern Pacific coastal environments: main features, large-scale perturbations, and global climate change. In: Mooney HA, Fuentes ER, Kronberg BI (eds) Earth System Responses to Global Change: Contrasts between North and South America. Academic Press, pp 167-188

Cedhagen T (1994) Taxonomy and biology of *Hyrrokkin sarcophaga* gen. et sp. n., a parasitic foraminiferan (Rosalinidae). Sarsia 79: 65-82

Cherchi A, Schroeder R (1991) Perforations branchues dues à des Foraminifères cryptobiontiques dans des coquilles actuelles et fossiles. C R Acad Sci Paris, Ser II, 312: 111-115

Chugthai I, Knight-Jones EW (1988) Burrowing into limestone by sabellid polychaetes. Zool Scr 17: 231-238

Ekdale AA, Bromley RG, Pemberton SG (1984) Ichnology - trace fossils in sedimentology and stratigraphy. SEPM Short Courses 15, 317 pp

Evans JW (1969) Borers in the shell of the sea scallop, *Placopecten magellanicus*. Amer Zool 9: 775-782

Fernández M, Jaramillo E, Marquet PA, Moreno CA, Navarrete SA, Ojeda FP, Valdovinos, CR, Vásquez, JA (2000) Diversity, dynamics and biogeography of Chilean benthic nearshore ecosystems: an overview and guidelines for conservation. Rev Chil Hist Nat 73: 797-830

Försterra G, Häussermann V (2003) First report on large scleractinian (Cnidaria: Anthozoa) accumulations in cold-temperate shallow water of south Chilean fjords. Zool Verh Leiden 345: 117-128

Fork DC, Larkum WD (1989) Light harvesting in the green algae *Ostreobium* sp., a coral symbiont adapted to extreme shade. Mar Biol 103: 381-385

Freiwald A, Schönfeld J (1996) Substrate pitting and boring pattern of *Hyrrokkin sarcophaga* Cedhagen, 1994 (Foraminifera) in a modern deep-water coral reef mound. Mar Micropaleont 28: 199-207

Freiwald A, Wilson JB (1998) Taphonomy of modern deep, cold-temperate water coral reefs. Hist Biol 13: 37-52

Freiwald A, Fosså JH, Grehan, A, Koslow T, Roberts JM (2004) Cold-water coral reefs. UNEP-WCMC Biodiv Ser 22, 84 pp

Gektidis M (1997) Vorkommen, Ökologie und Taxonomie von Mikrobohrorganismen in ausgewählten Riffbereichen um die Inseln Lee Stocking Island (Bahamas) und One Tree Island (Australien). Unpubl PhD thesis, Johann Wolfgang Goethe Univ, Frankfurt am Main

Gektidis M (1999) Cyanobacteria and associated microorganisms characterize coarse shoreline carbonates of One Tree Island, Australia. Bull Inst Oceanogr Monaco 19: 137-133

Glaub I (1994) Mikrobohrspuren in ausgewählten Ablagerungsräumen des europäischen Jura und der Unterkreide (Klassifikation und Palökologie). Cour Forschinst Senckenberg 174: 1-324

Glaub I (1999) Paleobathymetric reconstructions and fossil microborings. Bull Geol Soc Denmark 45: 143-146

Glaub I (2004) Recent and sub-recent microborings from the upwelling area off Mauritania (West Africa) and their implications for palaeoecology. Geol Soc London, Spec Publ 228: 63-76

Golubic S (1972) Scanning electron microscopy of recent boring cyanophyta and its possible paleontological application. In: Desikachary TV (ed) Proceedings of the Symposium on taxonomy and Biology of blue-green algae. Conf Proc, Madras, pp 167-170

Golubic S, Perkins RD, Lukas KJ (1975) Boring microorganisms and microborings in carbonate substrates. In: Frey RW (ed) The Study of Trace Fossils - A Synthesis of Principles, Problems and Procedures in Ichnology. Springer, New York, pp 229-259

Golubic S, Le Campion-Alsumard T, Campbell SE (1999) Diversity of marine Cyanobacteria. In: Charpy L, Larkum AWD (eds) Marine Cyanobacteria. Bull Inst Océanogr Monaco, Spec Issues 19: 53-76

Grange KR, Singleton RJ, Richardson JR, Hill PJ, Main de LM (1981) Shallow rock-wall biological associations of some southern fjords of New Zealand. New Zealand J Zool 8: 209-227

Günther A (1990) Distribution and bathymetric zonation of shell-boring endoliths in Recent reef and shelf environments: Cozumel, Yucatan (Mexico). Facies 22: 233-262

Häussermann V (2004) Neue integrative Ansätze für das Sammeln, Bearbeiten und Beschreiben skelettloser Hexacorallia am Beispiel chilenischer Seeanemonen. PhD thesis, Ludwig-Maximilians-Univ, Munich

Häussermann V (in press) The sea anemone genus *Actinostola* Verrill, 1883: variability and utility of traditional taxonomic features, and a re-description of *Actinostola chilensis* McMurrich, 1904. Pol Biol

Häussermann V, Försterra G (accepted) Distribution patterns of Chilean shallow-water sea anemones (Cnidaria: Anthozoa: Actiniaria, Corallimorpharia); with a discussion of the taxonomic and zoogeographic relationships between the actinofauna of the South East Pacific, the South West Atlantic and Antarctica. Sci Mar, Spec Vol

Halldal P (1968) Photosynthetic capacities and photosynthetic action spectra of endozoic algae of the massive coral *Favia*. Biol Bull 134: 411-424

Harmelin JG (1990) Interactions between small sciaphilous scleractinians and epizoans in the northern Mediterranean, with particular reference to bryozoans. Mar Ecol 11: 351-364

Harmelin JG (1997) Diversity of bryozoans in a Mediterranean sublittoral cave with bathyal-like conditions: role of dispersal processes and local factors. Mar Ecol Progr Ser 153: 139-152

Highsmith RC (1981) Lime-boring algae in hermatypic coral skeletons. J Exp Mar Biol Ecol 55: 267-281

Hooper JNA, Soest RWM van (2002) Order Hadromerida Topsent, 1894. In: Hooper JNA, Soest RWM van (eds) Systema Porifera: a guide to the classification of sponges. Kluwer Academic/Plenum Publ, New York, pp 169-290

Kaehler S (1999) Incidence and distribution of phototrophic shell degrading endoliths of the brown mussel *Perna perna* (L.). Mar Biol 135: 505-514

Kelly SRA, Bromley RG (1984) Ichnological nomenclature of clavate borings. Paleontology 27: 793-807

Knight-Jones P (1983) Contributions to the taxonomy of Sabellidae (Polychaeta). Zool J Linn Soc 79: 245-295

Kornmann P, Sahling PH (1980) *Ostreobium quekettii* (Codiales, Chlorophyta). Helgol Meeresunt 34: 115-122

Lancellotti DA, Vásquez JA (1999) Biogeographical patterns of benthic macroinvertebrates in the southeastern Pacific littoral. J Biogeogr 26: 1001-1006

Lazier AV, Smith JE, Risk MJ, Schwarcz HP (1999) The skeletal structure of *Desmophyllum cristagalli*: the use of deep-water corals in sclerochronology. Lethaia 32: 119-130

LeCampion-Alsumard T (1979) Les Cyanophycées endoliths marines. Systèmatique, ultrastructure, écologie et biodestruction. Oceanol Acta 2: 143-156

LeCampion-Alsumard T, Golubic S (1985) *Hyella caespitosa* Bornet et Flahault and *Hyella balani* Lehman (Pleurocapsales, Cyanophyta): a comparative study. Arch Hydrobiol Suppl 71: 119-148

LeCampion-Alsumard T, Golubic S, Priess K (1995) Fungi in corals: symbiosis or disease? Interaction between polyps and fungi causes pearl-like skeleton biomineralization. Mar Ecol Progr Ser 117: 137-147

López Correa M, Freiwald A, Hall-Spencer J, Taviani M (2005) Distribution and habitats of *Acesta excavata* (Bivalvia: Limidae), with new data on its shell ultrastructure. In: Freiwald A, Roberts JM (eds) Cold-water Corals and Ecosystems. Springer, Berlin Heidelberg, pp 173-205

Lukas KJ (1974) Two species of the chlorophyte genus *Ostreobium* from skeletons of atlantic and caribbean reef corals. J Phycol 10: 331-335

Macintyre IG, Towe KM (1976) Skeletal calcite in living scleractinia corals: Microboring fillings, not primary skeletal deposits. Science 193: 701-702

Maggs CA, Callow ME (2002) Algal Spores. Encycl Life Sci, Macmillian Publ Ltd, pp 1-6

Martin D, Britayev TA (1998) Symbiotic polychaetes: review of known species. Oceanogr Mar Biol Ann 36: 217-340

Neumann AC (1966) Observations on coastal erosion in Bermuda and measurements of the boring rate of the sponge, *Cliona lampa*. Limnol Oceanogr 54: 92-108

Pickard GL (1971) Some physical oceanographic features of inlets of Chile. J Fish Res Board Canad 28: 1077-1106

Podhalanska T (1984) Microboring assemblage in Lower/Middle Ordovician limestones from northern Poland. N Jb Geol Paläont Mh 1984: 497-511

Pohowsky RA (1978) The boring ctenostomate Bryozoa: taxonomy and paleobiology based on cavities in calcareous substrata. Bull Amer Paleont 73: 1-192

Pomponi SA (1976) An ultrastructural study of boring sponge cells and excavated substrata. Scan Electr Microsc 2: 569-575

Pomponi SA (1979) Ultrastructure of cells associated with excavation of calcium carbonate substrates by boring sponges. J Mar Biol Assoc UK 59: 777-784

Pomponi SA (1980) Cytological mechanisms of calcium carbonate excavation by boring sponges. Int Rev Cytol 65: 301-319

Radtke G (1991) Die mikroendolithischen Spurenfossilien im Alt-Tertiär West-Europas und ihre palökologische Bedeutung. Cour Forschinst Senckenberg 138: 1-185

Rützler K (1975) The role of burrowing sponges in bioerosion. Oecologia 19: 203-216

Rützler K, Rieger G (1973) Sponge burrowing: Fine structure of *Cliona lampa* penetrating calcareous substrata. Mar Biol 21: 144-162

Sand W (1995) Mineralische Werkstoffe. In: Brill H (ed) Mikrobielle Materialzerstörung und Materialschutz. Fischer, Jena, pp 78-110

Sato-Okoshi W, Takatsuka M (2001) *Polydora* and related genera (Polychaeta, Spionidae) around Puerto Montt and Chiloé Island (Chile), with description of a new species of *Dipolydora*. Bull Mar Sci 68: 485-503

Schlichter D, Zscharnack B, Krisch H (1995) Transfer of photoassimilates from endolithic algae to coral tissue. Naturwiss 82: 561-564

Schlichter D, Kampmann H, Conrady S (1997) Trophic and photoecology of endolithic algae living within coral skeletons. Mar Ecol 18: 299-317

Schönberg CHL, Wilkinson CR (2001) Induced colonization of corals by a clionid bioeroding sponge. Coral Reefs 20: 69-76

Schumacher H, Kiene W, Dullo W-Chr, Gektidis, M, Golubic S, Heiss GA, Kampmann H, Kroll DK, Kuhraus ML, Radtke G, Reijmer JG, Reinicke GB, Schlichter D, Vogel K (1995) Factors controlling Holocene reef growth: an interdisciplinary approach. Facies 32: 145-188

Shashar N, Stambler N (1992) Endolithic algae within corals- life in an extreme environment. J Exp Mar Biol Ecol 163: 277-286

Sitte P, Weiler EW, Kadereit JW, Bresinsky A, Körner C (2002) Strasburger - Lehrbuch der Botanik. Spektrum, Heidelberg Berlin, 1123 pp

Soest RWM van, Hooper JNA (2002) Order Haplosclerida Topsent, 1928. In: Hooper JNA, Soest RWM van (eds) Systema Porifera: a guide to the classification of sponges. Kluwer Academic/Plenum Publ, New York, pp 831-1019

Stolarski J (1996) *Gardineria-* a scleractinian living fossil. Acta Palaeont Pol 41: 339-367

Vacelet J (1996) Deep-sea sponges in a Mediterranean cave. In: Uiblein F, Ott J, Stachowistch M (eds) Deep-sea and extreme shallow-water habitats: affinities and adaptions. Vienna, pp 299-312

Vacelet J, Boury-Esnault N, Harmelin JG (1994) Hexactinellid cave, a unique deep-sea habitat in the scuba zone. Deep-Sea Res 41: 965-851

Vogel K (1993) Bioeroders in fossil reefs. Facies 28: 109-114

Vogel K, Glaub I (2004) 450 Millionen Jahre Beständigkeit in der Evolution endolithischer Mikroorganismen? Steiner, Stuttgart, 42 pp

Vogel K, Bundschuh M, Glaub I, Hofmann K, Radtke G, Schmidt H (1995) Hard substrate ichnocoenoses and their relations to light intensity and marine bathymetry. N Jb Geol Paläont Abh 195: 49-61

Vogel K, Gektidis M, Golubic S, Kiene WE, Radtke G (2000) Experimental studies on microbial bioerosion at Lee Stocking Island, Bahamas and One Tree Island, Great Barrier Reef, Australia: implications for paleoecological reconstructions. Lethaia 33: 190-204

Voigt E (1965) Über parasitische Polychaeten in Kreide-Austern sowie einige andere in Muschelschalen bohrende Würmer. Paläont Z 39: 193-221

Voigt E (1977) On grazing traces produced by the radula of fossil and Recent gastropods and chitons. In: Crimes TP, Harper JC (eds) Trace fossils 2. Geol J Spec Issue 9: 335-346

Wisshak M, Freiwald A, Lundälv T, Gektidis M (2005) The physical niche of the bathyal *Lophelia pertusa* in a non-bathyal setting: environmental controls and palaeoecological implications. In: Freiwald A, Roberts JM (eds) Cold-water Corals and Ecosystems. Springer, Berlin Heidelberg, pp 979-1001

Zhang Y, Golubic, S (1987) Endolithic microfossils (Cyanophyta) from early Proterozoic stromatolites, Hebei, China. Acta Micropaleont Sinica 4: 1-12

The physical niche of the bathyal *Lophelia pertusa* in a non-bathyal setting: environmental controls and palaeoecological implications

Max Wisshak[1], André Freiwald[1], Tomas Lundälv[2], Marcos Gektidis[1]

[1] Institute of Paleontology, Erlangen University, Loewenichstr. 28, D-91054
  Erlangen, Germany
  (wisshak@pal.uni-erlangen.de)
[2] Tjärnö Marine Biological Laboratory, SE-452 96 Strömstad, Sweden

Abstract. The habitat-forming scleractinian coral *Lophelia pertusa* supports an ecosystem that is widely known to occur in the bathyal marine ecologic realm along deep shelves, oceanic banks, seamounts and continental margins. Therefore, *L. pertusa* is generally considered a 'deep-water' or 'deep-sea' coral. In contrast, this study analyses the environmental controls of this bathyal ecosystem where it is thriving well in the non-bathyal shallow-water setting of the Swedish Kosterfjord area (NE Skagerrak). This is one of several shallow-water *L. pertusa* occurrences in Scandinavian waters where saline and temperature stable oceanic waters intrude as topographically-guided underflows onto the inner shelf and adjacent fjords, driven by an estuarine circulation.

The *L. pertusa* occurrence of the Säcken site in the northern Kosterfjord exists at 80-90 m water depth and only a few tens of metres beneath a permanently brackish surface water layer. At the depth of the coral patches, however, the hydrographic data reveal fully marine conditions, which are ensured by a deeper inflow of Atlantic water through the Norwegian Trench into the Skagerrak. SEM analyses of resin casts taken from dead *L. pertusa* skeletons yield an endolith assemblage dominated by boring sponges such as *Cliona* spp. (trace: *Entobia* ispp.), the boring bryozoan *Spathipora*, the fungus *Dodgella priscus* (trace *Saccomorpha clava*) and an unknown fungus (trace: *Orthogonum lineare*). Such a composition exclusively of heterotroph organisms resembles the *Saccomorpha clava* / *Orthogonum lineare* ichnocoenosis which is regarded as indicative for fossil and Recent, open marine, aphotic environments. This interpretation is supported by direct light measurements at the Säcken site, which indicate aphotic conditions for at least most of the year.

The finding of bathyal communities in comparatively shallow waters is linked to factors that force deeper oceanic water masses to surface. Such situations are likely to be expected where an estuarine circulation prevails, or in deep-sea basins bordered by narrow shelves and with local upwelling cells driven by the wind regime, facilitating the intrusion of eutrophic deeper waters to shallow depths – including the benthic communities.

This circumstance reveals a major potential pitfall in the palaeobathymetric interpretation of fossil *L. pertusa* occurrences, which tend to be interpreted as bathyal palaeoenvironments. Strikingly, almost all known exposed ancient *L. pertusa* locations (e.g. Rhodes and Messina Strait in the Mediterranean Sea or the Cook Strait, New Zealand) derive from tectonically active regions with steep bathymetric gradients and a specific confined topography which could have forced deep water to the near surface.

Keywords. Deep-water corals, *Lophelia pertusa*, hydrography, bathymetry, palaeobathymetry, bioerosion, palaeoecology, Kosterfjord, Skagerrak

Introduction

For geologists the reconstruction of ancient water depths, or palaeobathymetry, for a depositional setting or palaeocommunity is fundamental to reconstruct palaeoenvironments – but is probably the hardest parameter to measure. Such a heavily disputed example that fits well to the topic addressed in this study is the palaeobathymetric interpretation of the Danian coral mounds at Faxe, Denmark (see Bernecker and Weidlich 2005). Based upon various arguments, the interpretations for the environmental setting of the coral mounds encompass all water depths between wave exposure to 300 m (compiled by Bernecker and Weidlich 1990).

The colonial and azooxanthellate scleractinian coral *Lophelia pertusa* is regarded as a typical member of the bathyal zone community. This zone as a marine ecologic realm extends from the edge of the continental shelf to the depth at which the water temperature drops below 4°C. Both of these limits are variable, but the bathyal zone is generally described as lying between 200 and 2000 m below sea level, or as the aphotic zone where only heterotrophic and chemotrophic organisms can exist. This broad environmental definition matches well with the majority of the known occurrences of *L. pertusa* (Zibrowius 1980) and based on this knowledge, ancient *L. pertusa*-bearing deposits are regarded by palaeontologists as deep-water or as bathyal (Squires 1964; Barrier et al. 1989; Hanken et al. 1996).

This study focuses on non-bathyal *L. pertusa* occurrences from the Swedish Kosterfjord area, thriving at only 80-90 m water depth. Such a finding is not unique for *L. pertusa*, as even shallower locations are known from Norwegian inshore and fjord environments (Dons 1944; Strømgren 1971; Fosså et al. 2000, 2002). Are these shallow-water *L. pertusa* occurrences "extreme", or have scientists underestimated the ecological capacity of this coral species? To answer these striking questions, the presentation of hydrographic data will show that the environmental conditions in the Kosterfjord are not "extreme" and existing knowledge about the ecological limits of *L. pertusa* is still valid.

The investigation of the borer community has been shown to be a strong tool to establish a relative bathymetric gradient in both modern and ancient environmental settings. Extensive calibration studies of the endolithic micro-borer community consisting of bacteria, fungi, algae and several metazoan groups from modern tropical to high latitudinal settings showed a remarkably consistent depth/light-

related zonation pattern which allowed the definition of index ichnocoenoses that are characteristic for the euphotic, dysphotic and aphotic zones (Glaub 1994, 1999; Vogel et al. 1995, 1999; Glaub et al. 2002). The euphotic zone ends at depths where the surface light between 350 and 700 nm wavelength is reduced to 1 %. The dysphotic zone extends from the 1 % to the 0.05-0.001 % level of surface light and below which the aphotic zone starts (Liebau 1984; Lüning 1985). As bioeroding organisms leave boring traces in calcareous skeletons they are very useful for palaeobathymetric reconstructions (Glaub 1994; Glaub and Bundschuh 1997; Glaub et al. 2002). Therefore, we have studied the endolithic community that infested the skeletons of *L. pertusa* and associated bivalves from the non-bathyal Säcken site and discuss the data in relation to the ichnocoenosis found in *L. pertusa* from bathyal water depths.

The Kosterfjord study site

The Kosterfjord is a NNE oriented submarine trench that parallels the coastline of SW-Sweden to the east and is sheltered by numerous islands to the west but deviates to NW, south of the Söstre Islands where it transits into the deep Norwegian Channel (Fig. 1A). The northern Kosterfjord is separated by the Säcken-sill from the Singlefjord (Fig. 1B). From the Säcken area *L. pertusa* was sampled for the first time in Swedish waters (Wahrberg and Eliason 1926). With only around 85 m water depth, the Säcken site is one of the shallowest deep-water coral sites known to date.

In the wider Kosterfjord area seven major and two minor *L. pertusa* patches or mature reefs are known. The recently discovered Tisler Reef (Lundälv and Jonsson 2003), in neighbouring Norwegian waters, probably is the largest structure being
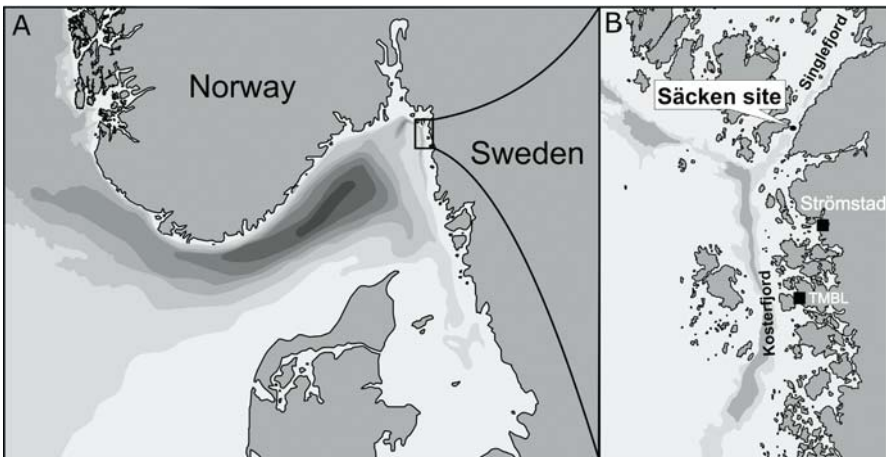
Fig. 1 A The geographic setting of the Kosterfjord in the NE Skagerrak and its relationship to the deep Norwegian Trench. **B** Map of the northern Kosterfjord area with the location of the Tjärnö Marine Biological Laboratory (TMBL), the Säcken Reef site, and further known dead and living *L. pertusa* reef structures

approx. 20 km in length. The entire area was glaciated until the Late Pleistocene. To date it is not known exactly when the evolution of the Kosterfjord reefs commenced. The oldest radiocarbon dates obtained from *L. pertusa* skeletons from various sites off mid and southern Norway cluster around 8700 to 8600 years BP for the Early Holocene coral colonisation (Mikkelsen et al. 1982; Rokoengen and Østmo 1985).

Oceanography and hydrography

The Kosterfjord lies in the northeastern part of the Skagerrak which is the major gateway between the North Atlantic and the Baltic Sea. The overall oceanographic regime is driven by an estuarine circulation pattern. Dense, saline (30-35 ‰ salinity) and oxygenated oceanic water underflows the more brackish (8-30 ‰ salinity) surface water (Svansson 1975). Off the northern Swedish west coast, in the Kosterfjord area, the surface water circulates with a predominating northern heading consisting of the Northern Jutland Current, which continues as the Norwegian Coastal Current along the Norwegian coastline. In addition, more brackish water is added from the Baltic Current, entering the Skagerrak through the Kattegat and the Sound to the south (Svansson 1975). This surface circulation is compensated by a deep counter current that brings the saline Atlantic water from the 700 m deep Norwegian Trench (Fig. 1A) up into the Skagerrak and the Kattegat (Dahl 1978).

The general oceanographic watermass stratification of the Skagerrak is also clearly expressed in the Kosterfjord area. The Tjärnö Marine Biological Laboratory (TMBL) provided an extensive hydrographic dataset consisting of about 700 measurements of temperature, salinity and oxygen, taken near the Säcken Reef site in the northern Kosterfjord between 1967 and 1990 (courtesy of the Swedish Fishery Board).

The temperature of the surface water is subject to strong seasonal fluctuations, ranging from below freezing (sea ice) in the two coldest months February and March to 17-20°C in the warmest months July and August (Fig. 2A-B). This annual fluctuation is also present in deeper waters, but with lower amplitude and a certain time delay – in 100 m water depth for instance – temperatures vary between 4 and 10°C and the amplitudes are delayed by about three to four months (Fig. 2A). The salinity plots draw a similar picture (Fig. 2C-D): the strongest variations, due to varying degrees of freshwater input, are exhibited by the surface waters where they range from a minimum of as low as 8.0 ‰ to 30.9 ‰. The lowest salinities are present between May and August. In 100 m water depth there is only a low annual salinity variation between 33.6 ‰ and 35.0 ‰ with a mean of 34.5 ‰. Temperature and salinity depth plots (Fig. 2B and D) indicate a thermocline and halocline, respectively, at around 20 to 30 m water depth, separating the open marine Atlantic waters from the brackish outflow of the Baltic Sea for most of the year. Another boundary layer is encountered in only a few decimetres to metres water depth, where a brackish to near-freshwater layer is added by the local river runoff. This stratification is most prominent in the coldest (February and March) and warmest (July and August) months in respect to the surface water temperature. The
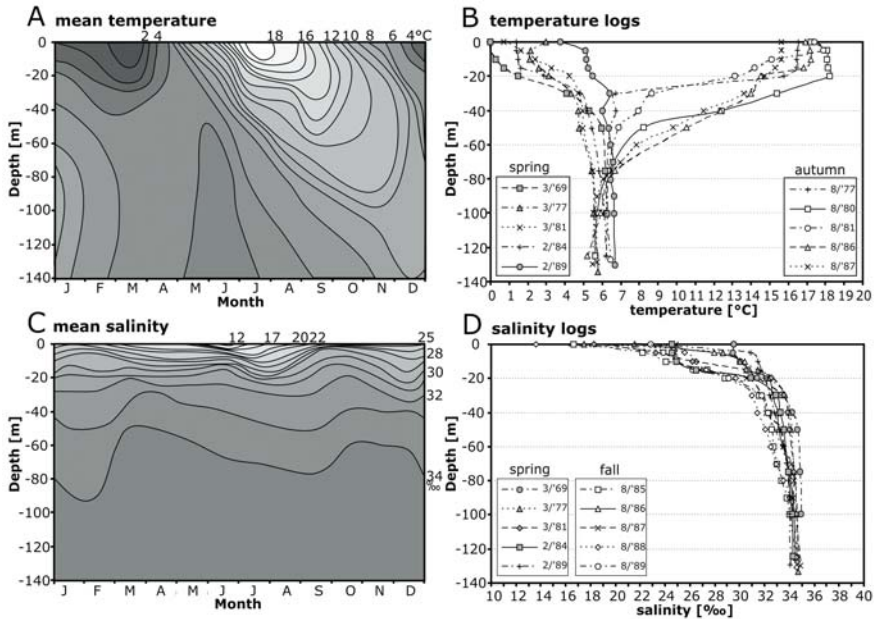
Fig. 2 Temperature and salinity variations in the northern Kosterfjord area compiled from over 700 measurements logged just south of the sample sites (59°00'40" N / 11°06'80" E) between 1967 and 1990 (Data accessible in a database of the Swedish Fishery Board; URL: www.bvvf.com). **A** Annual temperature fluctuation (based on monthly means) with a declining amplitude and typical time delay towards deeper waters. **B** Five representative temperature logs for the springtime and autumn, respectively, exhibiting a main thermocline in 20 to 40 m water depth. **C** Annual salinity fluctuation (based on monthly means) indicating a major freshwater influence in the shallow waters. **D** Five representative salinity logs for the springtime and autumn, respectively, showing a main halocline around 20 m water depth

reduced salinity of the surface water facilitates the formation of sea ice during harsh winters. The oxygen level of the surface water ranges from 4.2 to 9.5 ml/l with the highest values in the springtime and the lowest in the autumn (reverse proportional to the water temperature). Analogously to temperature and salinity, the fluctuation is smaller at 100 m water depth, where the values plot at 4.8 to 6.7 ml/l.

To conclude, *L. pertusa* in the wider Kosterfjord area from at least 150 m to 80 m water depth thrives under fully marine conditions, with temperature fluctuations between 4°C and 10°C (mean: 6°C), salinity fluctuations between 33.6 ‰ and 35.0 ‰ (mean: 34.5 ‰) and oxygen fluctuations between 4.8 and 6.7 ml/l. This physical oceanographic spectrum matches well the conditions found at *L. pertusa* sites along the northwestern European continental margin (Freiwald 2002).

Materials and methods

The *L. pertusa* habitats at the Säcken site in the northern Kosterfjord were visually inspected and mapped from the TMBL with Phantom XTL and Phantom S4

ROVs (Deep Ocean Engineering), equipped with headlights, video camera, sonar, navigation system, depth gauge and a laser scaling device.

The site specific hydrographic conditions at the Säcken site were obtained through two lander deployments (Aanderaa RCM 9) of more than one month each. The first deployment covered part of the warmer seawater conditions in September-October 2000, whereas part of the colder period was covered by a second deployment in February-April 2001. The lander logged temperature, salinity, current direction, current speed, and turbidity at one hour intervals.

Light measurements were carried out using a LICOR™ Spherical Quantum Sensor (LI-193SA) in combination with a Data Logger (LI-1400) which measures within a wavelength range of 400-700 nm the Photosynthetically Active Radiation (PAR; unit: μmol m^{-2} s^{-1}), which was later translated to percentages with respect to surface illumination. The measurements were taken at noon under a wide range of weather conditions from cloudless calm weather to overcast and windy conditions.

The skeletal material for the investigation of the bioeroder community was collected with the ROV at the Säcken site in a water depth of 85 m. The dead portions of *L. pertusa* skeletons and additionally associated bivalve shells of *Timoclea ovata* and *Acesta excavata* were chosen for the analysis. In order to reveal the endolithic boring traces, the following cast-embedding technique was applied. After removing the organic matter *via* treatment with hydrogen peroxide and cleaning in an ultrasonic bath, the samples were put in a vacuum chamber especially designed for the cast embedding method (Struers: Epovac). This vacuum chamber allows the infiltration of several samples with a high viscosity epoxy resin (Struers: SpeciFix-20) while the samples are held under vacuum. This procedure assures that most of the air is removed from the borings prior to the infilling with resin, thus replacing the time-consuming treatment with a sequence of different resin/acetone mixtures as applied by the established method after Golubic et al. (1970, 1983). After curing at 50°C, the samples were formatted and decalcified *via* the treatment with diluted HCl ($\sim$5 %). The sample casts, now exhibiting the positive borings, were then gold-coated and finally analysed and photographed using scanning electron microscopy (SEM).

To date, the International Code of Zoological Nomenclature (International Commission on Zoological Nomenclature 1999) permits the use of ichnotaxa only for fossil borings. This definition is a matter of ongoing debate, since this limitation is not sensible in case of lithic borings for a number of reasons, such as the lack of an applicable definition regarding a boundary between fossil and Recent, or the fact that a Recent boring morphologically resembles its fossil counterpart in all aspects.

In the present paper, we thus apply the dual nomenclature of (1) the biological nomenclature for classifying the potential trace makers, and (2) the ichnotaxonomy as a morphological classification of the traces independent of the potential trace maker (as it has practically been done by a number of workers before, e.g. Tavanier et al. 1992; Radtke 1993; Vogel et al. 2000; Perry and MacDonald 2002). We, however, desist from describing new ichnotaxa based on this Recent material, in favour of an open nomenclature (e.g. 'Sponge form I').

Results

Lophelia pertusa habitat characteristics at the Säcken site, northern Kosterfjord

The benthic substrate in the sound consists mostly of an end moraine with gravel and scattered stones and locally some rocky outcrops. Two small mounds, in a NNE-SSW relationship, are situated on the sill. They are composed mostly of *L. pertusa* rubble and densely packed silty clay. The live *L. pertusa* occurrence forms two major patches, which are found on the SSW flanks of the two mounds (Fig. 3). The patches are situated near the base of the mounds. The northern and southern patches cover areas of about 250 m² and 50 m², respectively. Most of the colonies are small and grow as discrete often spherical colonies with lumps of dead coral, coral rubble, gravel, cobble and sediment in between. At the present time, a total of 307 species have been identified associated with *L. pertusa* at the Säcken site.
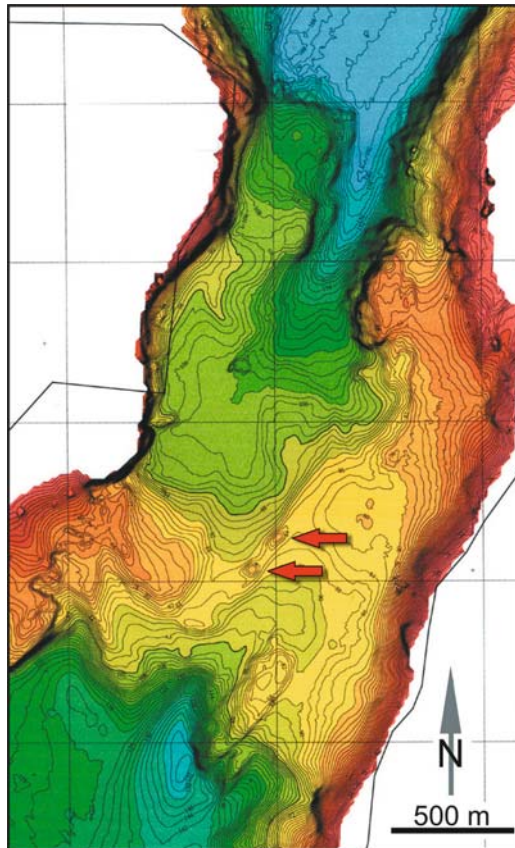
Fig. 3 Detailed map of the Säcken sill (generated from multibeam sonar data) highlighting the two *L. pertusa* mound structures (arrows)

In situ hydrographic data obtained from lander deployments

Two lander deployments lasting more than one month each were carried out near the *L. pertusa* patches on the Säcken site at ca. 85 m water depth. The first deployment covered part of the warmest seawater conditions in September-October 2000 whereas part of the coldest period was covered by a second deployment in February-April 2001. The lander logged temperature, salinity, current direction, current speed, and turbidity at one hour intervals (Table 1).

Table 1 Hydrographic proxies at the Säcken coral site in 85 m water depth recorded in one hour intervals by a lander during September-October 2000 and February-April 2001

	Autumn 2000 (06.09.-05.10.2000)				Spring 2001 (22.02.-24.04.2001)			
	mean	min.	max.	st. dev.	mean	min.	max.	st. dev.
Temperature [°C]	7.9	7.2	8.7	0.2	6.2	5.6	7.1	0.4
Salinity [‰]	34.8	34.4	35.1	0.2	34.6	34.3	34.8	0.2
Turbidity [NTU]	0.5	0.3	1.0	0.1	0.6	0.3	4.6	0.2
Current velocity [cm/s]	6.0	0	24.0	4.4	4.5	0	21.0	2.9
Current direction [°]	203				229			

The temperature at this depth is subject to only minor short-term fluctuations of less than one degree Celsius. The mean autumn temperature plots at 7.9°C while the springtime mean was about two degrees lower at 6.2°C. The autumn salinities ranged from 34.4-35.1 ‰ with a mean of 34.8 ‰ and short-term fluctuations in the range of 0.4 ‰. The mean spring salinity was a little lower (34.6 ‰), with maximum values of around 34.8 ‰. The turbidity was relatively constant at around 0.5 NTU. Short-term fluctuation of all parameters except turbidity was lower in the springtime than in the autumn. The current speed occasionally reached close to 25 cm/s, with a mean of 6 cm/s in the autumn and 4.5 cm/s in the spring. The current direction measurements are influenced by the small- to medium-scale morphology of the reef mounds and are thus not representative for the whole reef site. Nevertheless, it is worth noting that the direction shifted in a cyclic pattern between two main directions. This was especially pronounced in the springtime, where the direction shifted between 100° and 330° heading, the directions which exhibited the highest velocities.

Defining the illumination status of the *Lophelia pertusa* habitat

In order to directly quantify the reduction of the photon flux with depth, a number of light measurements were carried out in March and October 2003. The surface illumination varied between ~600 and 2400 µmol m^{-2} s^{-1} above, and ~200 and 1400 µmol m^{-2} s^{-1} just below the water surface with light levels exponentially decreasing toward deeper waters (A). The boundary to the dysphotic zone (1 % surface illumination) was directly measured in 10 to 25 m water depth while the upper limit of the aphotic zone (~0.01 % surface illumination) was determined by plotting the data and a regression line on a logarithmic scale (Fig. 4), which yields a
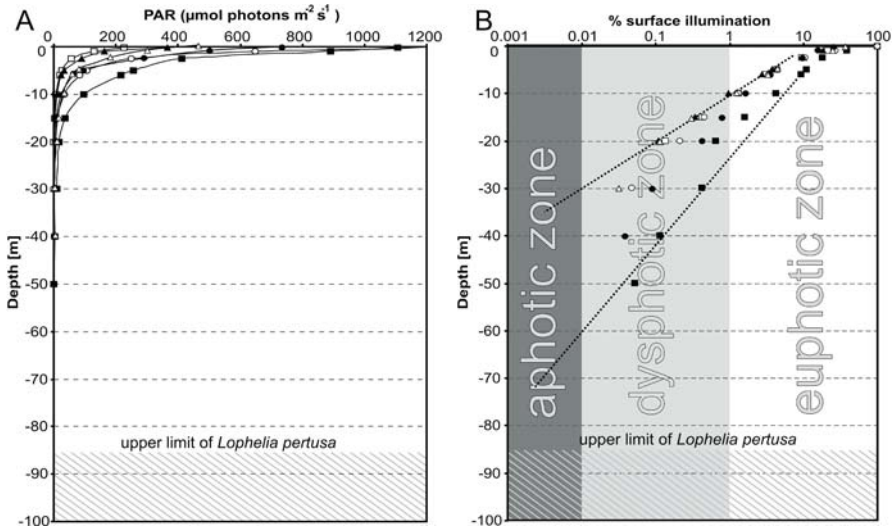
Fig. 4 Measurements of the Photosynthetically Active Radiation (PAR; unit: μmol m^{-2}s^{-1}) with depth, carried out in March and October 2003. **A** The illumination exponentially decreases toward deeper waters. **B** Logarithmic plot with regression lines indicating a boundary to the dysphotic zone (1 % surface illumination) in 10 to 25 m water depth and the upper limit of the aphotic zone (~0.01 % surface illumination) in a range of 30 to 60 m water depth

range of 30 to 60 m water depth (for the calculation of the regression line, the upper 10 m water column was excluded, because of its significantly higher turbidity).

Bioerosion patterns detected in *Lophelia pertusa* skeletons and associated bivalve shells

Skeletons of *L. pertusa*, *Acesta excavata* and *Timoclea ovata* collected from the Säcken site were analysed for endolithic traces. In total 17 different traces produced by fungi (5), sponges (6), bryozoans (2), foraminifers (1) and brachiopods (1) were found. In addition, two traces of unknown affinities are recorded (Table 2).

Fungi – A ubiquitous and important component of Recent and fossil photic and aphotic ichnocoenosis are the traces of the fungus *Dodgella priscus* and its trace *Saccomorpha clava* (Fig. 5A-D), respectively. Their characteristic features are club-shaped sacks, measuring 10-30 μm in size, which host the sporangia. These sacks open to the surface of the infested skeleton through narrow, 4-6 μm-wide necks. The sacks are interconnected by evenly thin (ø 2 μm) tubular galleries (hyphae) protruding from the necks or sacks. Four different morphotypes could be distinguished, three of which most likely represent different ontogenetic stages of the fungal colony: (1) scattered straight (Fig. 5A) or curved (Fig. 5B) individual sacks, 10 to 20 μm in size, interconnected by few thin galleries, (2) ~30 μm-large

Table 2 List of ichnotaxa and their known or assumed producers as well as their relative abundance (++ abundant, + common, - rare, -- very rare)

Ichnotaxa	Producer	Abund.
Saccomorpha clava Radtke, 1991	*Dodgella priscus* Zebrowski, 1936 (fungus)	+ +
Orthogonum lineare Glaub, 1994	? (fungus)	+ +
Orthogonum fusiferum Radtke, 1991	*Ostracoblabe implexa* Bornet and Flahault, 1889 (fungus)	-
Orthogonum isp. I	? (fungus)	+
Orthogonum isp. II	? (fungus)	-
Entobia ispp.	*Cliona* spp. and other Hadromerida (sponges)	+ +
Sponge form I	? (micro-sponge)	- -
Sponge form II	? (micro-sponge)	- -
Sponge form III	? (micro-sponge)	- -
Sponge form IV	? (micro-sponge)	- -
Sponge form V	? (micro-sponge)	- -
-	*Spathipora* (bryozoan)	+ +
-	*Immergentia* Silén 1946; (bryozoan)	-
Semidendrina form Glaub 1994	cf. *Globodendrina monile* Plewes et al. 1993 (foraminiferan)	- -
Podichnus centrifugalis Bromley and Surlyk 1973	*Macandrevia cranium* (Müller 1776); (brachiopod)	- -
Problematic form I	?	-
Problematic form II	?	-

branched sacks (Fig. 5C) and (3) dense layers of multiple sacks and sack clusters (Fig. 5D) interconnected by a network of galleries.

The second type of an abundant fungal trace are mostly rectangular branching networks of galleries close to the substrate surface, summarized under the ichnogenus *Orthogonum* (Fig. 5E-H). The producer of the most important ichnospecies *Orthogonum lineare* is still unknown, but it is certainly a heterotrophic organism (most likely a fungus), since this trace has been recorded from water depths deeper

Fig. 5 SEM images of traces produced by boring fungi. **A-D** Different morphotypes of *Saccomorpha clava*, produced by *Dodgella priscus*. **A** Two characteristic sporangia-bearing sacks connected by thin tubular galleries (hyphae). **B** Curved variation. **C** Branched
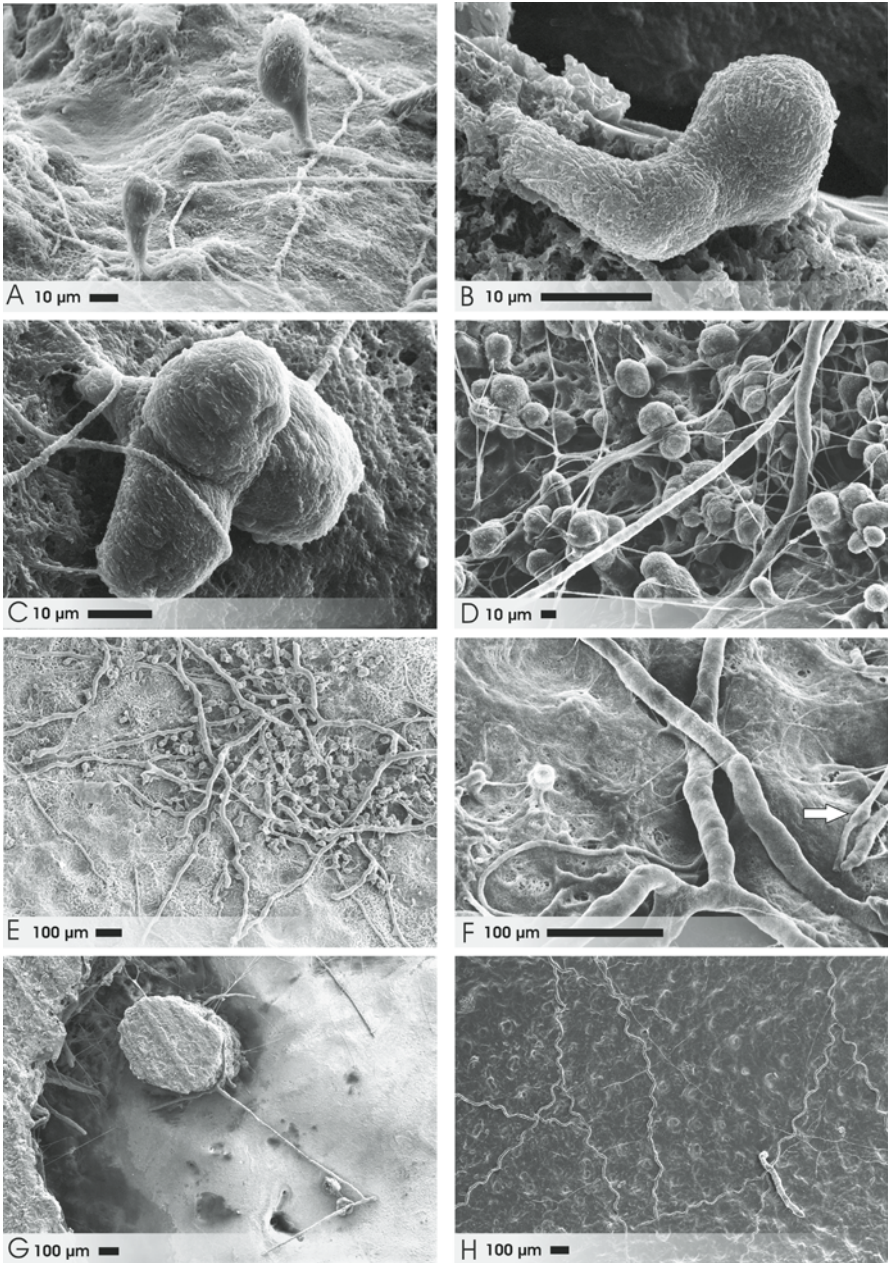
sacks. **D** Dense clusters of sacks. **E-F** Different ichnospecies of the genus *Orthogonum* (producer unknown). **E** *Orthogonum lineare* in typical association with *Saccomorpha clava*. **F** Thick tubes of *Orthogonum lineare* and thin galleries of *Orthogonum fusiferum* exhibiting characteristic swellings (arrow). **G** Deeply penetrating *Orthogonum* isp. I in a partially etched cross section. **H** Long galleries of *Orthogonum* isp. II describing a diagnostic wavy line

than 500 m (Glaub 1994). Its traces are characterised by smooth tubular galleries of near-constant diameter (10-15 µm) without swellings oriented parallel to the substrate surface and exhibiting predominantly perpendicular branchings (Fig. 5E-F). However, the distinction between *Orthogonum tubulare*, *Orthogonum lineare* and *Orthogonum spinosum*, is somewhat arbitrary and indistinct in the original diagnoses and corresponding specimens even merge laterally into each other quite commonly. Spines as a feature for instance, which are regarded as diagnostic for *Orthogonum spinosum*, may as well appear on many other ichnospecies, and thus question the validity of this ichnospecies. The majority of specimens encountered at the Säcken site are closest to the diagnosis for *Orthogonum lineare* as given by Glaub (1994) and are distinguished from *Orthogonum tubulare* by more constant tube diameters, the absence of swellings at branchings, and blunt instead of tapering gallery endings.

The fungus *Ostracoblabe implexa*, responsible for the ichnospecies *Orthogonum fusiferum*, is easily distinguishable by its thin gallery diameters (1–2 µm) and characteristic swellings (Fig. 5F) between or at perpendicular junctions. This ichnospecies was found, however, only very sporadically.

In addition, two unknown forms of fungal traces related to the ichnogenus *Orthogonum* were encountered: The uniformly thick (~10 µm) tubes of *Orthogonum* isp. I (Fig. 5G) do not run parallel to the substrate surface, but expand straight into the substrate, reaching penetration depths of more than one millimetre. The surface is smooth and may exhibit small spiny appendages. Branchings are rather rare and always perpendicular. The deeply penetrating nature of this fungal form becomes obvious in partially etched cross-section casts, where the delicate tubes are not collapsed and thus not feigning an orientation parallel to the substrate surface. The traces of *Orthogonum* isp. II (Fig. 5H) are tubes of near constant diameter (~10 µm) that run parallel to the substrate surface and describe a diagnostic wavy line with a wavelength of 100 to 150 µm. Individual tubes can be traced for several millimetres. Bifurcations are often perpendicular. The tubular galleries exhibit a smooth surface or may show short spiny protrusions.

Sponges – The distinct boring systems produced predominantly by the demosponge family Clionaidae and a number of other sponges of the order Hadromerida (trace: *Entobia*), are easily recognised in the resin casts by their large cavities exhibiting a characteristic verrucose texture (Fig. 6) (Bromley and D'Alessandro 1984 and literature cited therein). The traces comprise different ontogenetic stages as well as species variability from solitary small chambers, ~200-300 µm in size (Fig. 6A) to large networks of chambers (Fig. 6C), galleries, apophyses and exploratory threads. The networks are connected to the surface by several apertures (exhalent canals). For an assignation down to species level, complete mature boring systems (in case of ichnospecies) and additionally *in situ* spicules (in case of sponge species) would be required. There are, however, principally two different types of microsculpture distinguishable: (1) round to oval cells exhibiting a rough surface and concentric 'growth lines' (Fig. 6B). In this type,
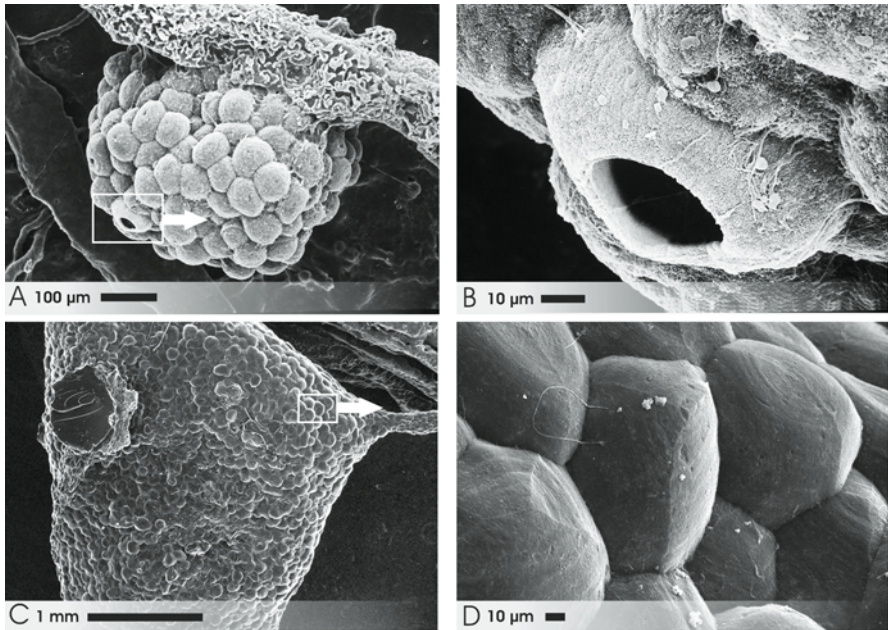
Fig. 6 SEM images of traces produced by a boring clionaid sponge. **A** Small spherical cavity of *Entobia* isp. **B** Close-up of microsculpture exhibiting a boring cell 'caught in action'. **C** Large chamber of *Entobia* isp. exhibiting characteristic verrucose microsculpture. **D** Close up of the microsculpture with individual cells showing distinct ridges and faint growth 'lines' in between

different stages (resembling the construction of a tiny igloo) record the progressive etching activity by the pseudopodia of the boring cells, and (2) cells with a rather smooth surface exhibiting 3-5 distinct radial ridges and only faint 'growth lines' in between (Fig. 6D).

The boring systems of clionaid sponges are especially ubiquitous in advanced taphonomic stages of the coral skeletons, where they may remove more than two thirds of the skeletal material (Freiwald and Wilson 1998). Abandoned sponge cavities are often subject to subsequent infestation of various microendoliths.

Besides *Entobia* a number of further micro-sponge borings were encountered as well as traces only tentatively assignable to this group based on their large size and/or microsculpture: 'Sponge form I' (Fig. 7A) is developing irregular cavities, several hundred micrometres in size, exhibiting a verrucose microsculpture with individual cells measuring only 5 to 10 μm. 'Sponge form II' (Fig. 7B) shows a central cavity, few tens to 100 micrometres in diameter, from which radial thin (~5 μm), bifurcating tunnels emerge and resembles 'Sponge form 3' (Günther 1990). 'Sponge form III' (Fig. 7C) exhibits large sack-shaped traces with diameters of 100 to 200 μm and penetration depths of 150 to 200 μm, connected to the surface by few, thick rhizoidal appendages and thus shows many typical features described for the ichnospecies *Cavernula pediculata*, but can be distinguished from the latter

by its relatively large size. 'Sponge form IV' (Fig. 7D) is highly variable in its morphological appearance and forms irregularly shaped, branching to dendritic borings, 100 to 1000 µm in size, that exhibit characteristic whip-shaped appendages up to 100 µm in length. This form shows close similarities to '*Entobia* form 3' (Glaub 1994), 'Sponge form 1' (Günther 1990), 'Echinoid form' (Radtke 1993), 'Sponge form B' (Budd and Perkins 1980) and possibly 'Spinate boring form'
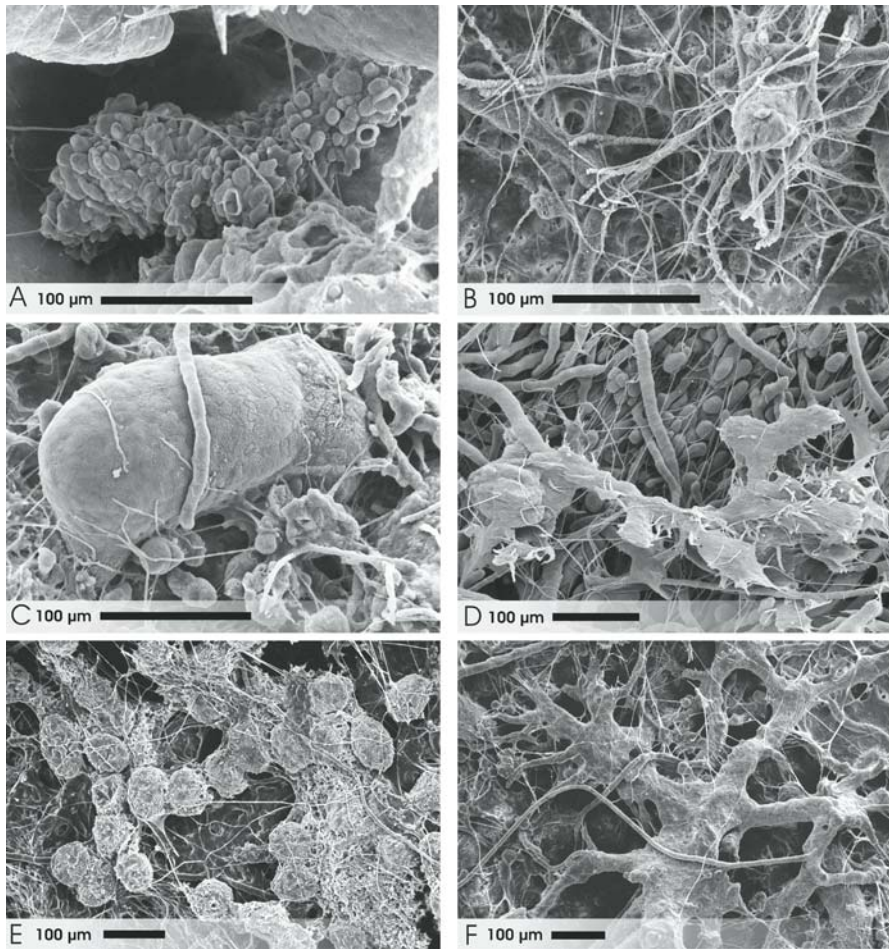
Fig. 7 SEM images of traces tentatively assigned to the activity of boring sponges based on their size and/or microsculpture. **A** 'Sponge form I' exhibiting very small and irregularly shaped boring cells. **B** Central cavity and radiating plus bifurcating galleries of 'Sponge form II'. **C** Main cavity of 'Sponge form III' connected to the surface by thick rhizoidal appendages. **D** Irregularly-shaped boring of 'Sponge form IV' covered with bristle-like protrusions. **E** Spherical (left) to irregularly flat (right) aggregates of 'Sponge form V'. **F** Dendritic boring pattern of 'Sponge form VI'

(Zeff and Perkins 1979). The bristle-like processes, however, also show affinities to the foraminiferan boring '*Semidendrina* form' (Glaub 1994; see below). 'Sponge form V' (Fig. 7E) exhibits a morphological variability, ranging from 40 to 60 µm large isolated or linked spherical aggregates to dendritic irregularly shaped boring systems close to the substrate surface that reach more than 1 mm in size. They exhibit a verrucose to 'granular' microsculpture. Budd and Perkins (1980; p. 899, Fig. 9F) depict similar aggregates, 40 to 50 µm in size, but tentatively interpret them as fungal sporangia. 'Sponge form VI' (Fig. 7F) is a shallow dendritic boring system, in places more than 1 mm in diameter, characterised by a central, irregularly shaped flat area, from which many bifurcating branches radiate and rapidly decrease in width. The form exhibits similarities to the fossil ichnogenus *Platydendrina*.

Bryozoans – Boring bryozoans are represented by two genera. The very common and important *Spathipora* (Fig. 8A), is characterised by tube-shaped zooids, ~300-500 µm long at a width of 80-100 µm, proximally connected by a short (~50 µm) pedunculus to a network of evenly thick (10-15 µm) stolons and distally attached to the surface with a wide aperture (70-90 µm). The second genus, *Immergentia* (Fig. 8B), is only rarely encountered and is characterised by zooids, that penetrate the substrate about perpendicularly with a penetration depth of ~150-250 µm at a width of ~75-125 µm and exhibits thin flags. They are also connected to a network of evenly thick (10-15 µm) stolons. The zooids are locally found in association with spherical cavities, ~100 µm in diameter of unknown function.
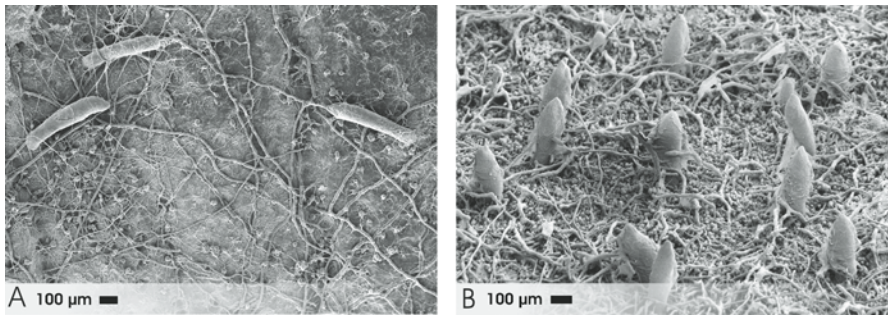
Fig. 8 SEM images of traces produced by boring bryozoans. **A** Substrate parallel zooids of *Spathipora* interconnected by a network of evenly thick stolons (in association with *Saccomorpha clava*). **B** Perpendicular penetrating zooids of *Immergentia* towering a dense layer of *Saccomorpha clava* and *Orthogonum lineare*

Foraminiferans – Only rarely, the presumed foraminiferan boring '*Semidendrina* Form' (Glaub 1994) was encountered. It is a large (~1.5 mm), complex, dendritic boring system, composed of branching cavities, densely covered with bristle-like to whip-shaped appendages up to 100 µm in length (Fig. 9). Corresponding traces have also been reported under the informal name 'Morfotipo B-5' by Mayoral (1988), and as body fossil of the foraminiferan *Globodendrina* by Plewes et al. (1993).
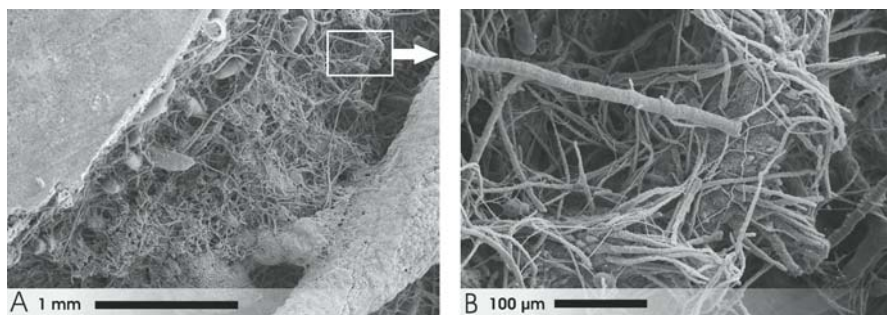
Fig. 9 SEM images of a dendritic trace produced by boring foraminifer. **A** Dendritic 'Semidendrina Form', partly hidden behind a large *Entobia* cavity. **B** Close up showing characteristic wip-shaped appendages

Brachiopods – Two attachment scars etched by brachiopod pedicles were encountered (ichnotaxon: *Podichnus centrifugalis*), the first one of which (Fig. 10A) exhibits a cluster (ø 0.5 mm) of about 20 tapering intrusions. The central ones are shorter (~50 μm) and approximately perpendicular to the surface while the more peripheral ones are longer (~150 μm) and enter the substrate obliquely. The second one (Fig. 10B) is larger (ø 1.5 mm) and more symmetrical and exhibits a shallower pattern of about 25 tapering intrusions. The central ones are again shorter and approximately perpendicular to the surface while the more peripheral ones are longer and enter the substrate obliquely and centrifugally. *Macandrevia cranium* (which is the second-most common brachiopod species that was recorded in the sampled material) was held responsible for corresponding traces by Bromley and Surlyk (1973).
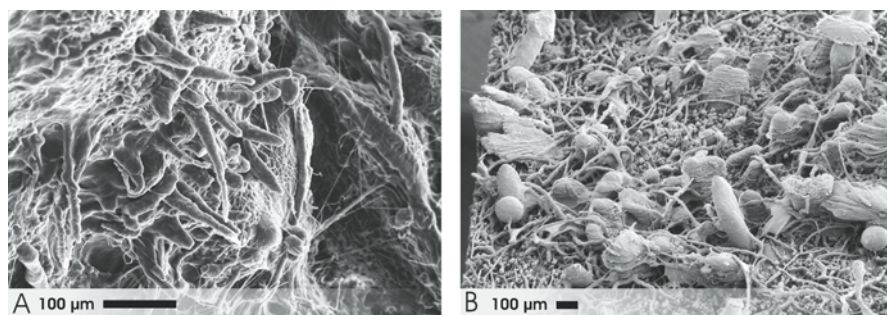
Fig. 10 SEM images of attachment scars etched by brachiopod pedicles. **A** Boring pattern of *Podichnus centrifugalis* with radial tapering, scattered protrusions. **B** A larger and more symmetrical *Podichnus centrifugalis* presumably produced by the brachiopod *Macandrevia cranium*

Traces of unknown affinity – Two traces of unknown affinity were encountered, the first one of which ('Problematic form I', Fig. 11A) comprises very thin (less than 1 μm) fibers, that extend deeply into the substrate and bifurcate
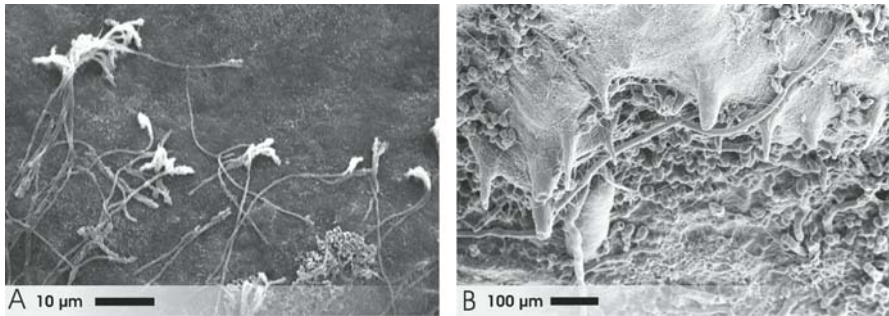
Fig. 11 SEM images of traces of unknown affinity. **A** Deeply penetrating thin and thus collapsed fibres of 'Problematic form I'. **B** 'Problematic form II' exhibiting a large cluster of straight intrusions, penetrating from a shallow depression

towards the surface. In the casts, they are commonly found collapsed due to the delicate nature of this trace and their true spatial shape is hard to estimate even in partially etched cross-sectioned casts. In terms of penetration depth and fibrous nature the trace exhibits affinities to *Scolecia filosa*, produced by the cyanobacterium *Plectonema terebrans*, which is, however, characterised by larger diameters, and a differing branching pattern.

'Problematic form II' (Fig. 11B) is a relatively large trace (up to 600 µm in size), comprising clusters of several straight intrusions (20 to 150 µm), penetrating the substrate perpendicularly from a shallow depression. No corresponding trace was found in the literature, but were also encountered in skeletons of *Desmophyllum dianthus* from the Renihuefjord, southern Chile (Försterra et al. 2005). The trace possibly represents an attachment scar of a heterotrophic epilithic organism, such as a brachiopod or foraminiferan.

Discussion

The deep-water coral *Lophelia pertusa* in shallow-water settings

The habitat-forming *L. pertusa* ecosystem is widely known to occur in the bathyal marine ecologic realm especially in the Atlantic Ocean and Mediterranean Sea along deep shelves, oceanic banks, seamounts and continental margins. Therefore, *L. pertusa* is generally recognized as a 'deep-water' but also as a 'deep-sea' coral (e.g. by Hovland et al. 2002). In contrast, this study analyses the environmental controls of this bathyal ecosystem where it thrives well in a non-bathyal shallow-water setting, thereby addressing the fundamental question of establishing palaeobathymetric reconstructions based on benthic communities.

The *L. pertusa* occurrence of the Säcken site in the Swedish Kosterfjord exists at 80-90 m water depth and only a few tens of metres beneath a permanently brackish surface water layer. However, at the depth of the coral patches, the hydrographic data reveal fully marine conditions, which are ensured by a deeper inflow of Atlantic water through the more than 700 m deep Norwegian Trench into the Skagerrak

to compensate the surface water net outflow. Similar situations are met in some Norwegian fjords where live *L. pertusa* reefs are known to exist at much shallower depths compared to the open shelf off Norway (Freiwald et al. 1997). To conclude, non-bathyal, shallow-water *L. pertusa* occurrences in Scandinavian waters are confined to areas where saline oceanic waters can intrude as topographically-guided underflows onto the inner shelf and adjacent fjords, driven by an estuarine circulation combined with tidal currents.

The light regime at the Säcken site

Another common attribute to describe *L. pertusa* ecosystems is 'aphotic'. Therefore, we measured the photon flux to calculate the depth-related reduction of the surface illumination at the Säcken site. Our dataset only shows results from light measurements carried out in March and October 2003 and not from a summer period where we can expect a somewhat deeper light penetration through the water column. These measurements indicate that *L. pertusa* at 85 m depth in the Kosterfjord thrives under aphotic conditions, which are due to the high geographic latitude combined with eutrophic conditions and outflow of turbid surface water from local river runoff. Even if light penetrates deeper during the summer period it may only reach the level of dysphotic illumination. However, multi-year cultivation of *L. pertusa* in aquaria under daylight exposure did not show any negative impact on the vigour of the coral (Mortensen 2001).

The ichnocoenosis as related to the light regime

Geologists have developed a strong tool to distinguish between different light regimes within the euphotic, dysphotic and aphotic conditions by the definition of index ichnocoenoses, which apparently turned out to represent a stable and conservative element as has been proven from numerous Phanerozoic examples (Vogel et al. 1995). The absence of phototrophic borers is the major character to define the aphotic zone. The endolithic assemblage and ichnocoenosis, respectively, encountered in *L. pertusa* skeletons from the Säcken site, is dominated by boring sponges (trace: *Entobia* ispp.), the bryozoan *Spathipora*, the fungus *Dodgella priscus* (trace: *Saccomorpha clava*) and an unknown fungus (trace: *Orthogonum lineare*). The relative abundance of all further traces, most of which are here tentatively assigned to the boring activity of micro-sponges or unknown fungi, is low. This ichnocoenosis composed solely of traces produced by heterotrophs resembles the *Saccomorpha clava / Orthogonum lineare* ichnocoenosis, which is regarded as indicative for fossil and Recent, open marine, aphotic environments (Glaub 1994; Glaub et al. 2002). The aphotic nature of the ichnocoenosis is furthermore indicated by the absence of the two photoautotrophs with the largest known depth range, the cyanobacterium *Plectonema terebrans* (trace: *Scolecia filosa*) and the chlorophyte alga *Ostreobium quekettii* (trace: *Reticulina elegans*).

These results are in good accordance with the work of Zeff and Perkins (1979) and Budd and Perkins (1980), who investigated endolithic communities in aphotic carbonates from the tropical Bahamas Bank and Puerto Rico Shelf, respectively. In addition, these authors recorded three endolithic traces reminiscent of the ichnotaxa

Scolecia serrata (producer: unknown fungus or bacterium), *Polyactina araneola* (producer: the fungus *Conchyliastrum*) and *Orthogonum sphaerula* (unknown fungus), that were absent in the present material. From other North Atlantic cold-temperate settings, corresponding endolith assemblages were reported by Schmidt and Freiwald (1993) from shell material off northern Norway (170 m water depth), Boerboom et al. (1998) in skeletons of the deep-sea coral *Desmophyllum cristagalli* from Orphan Knoll (>1700 m water depth) and Beuck and Freiwald (2005) in *L. pertusa* skeletons from the Propeller Mound (Porcupine Seabight, >680 m water depth).

To conclude, the typical *Saccomorpha clava* / *Orthogonum lineare* ichnocoenosis encountered at the Säcken site resembles aphotic and real bathyal occurrences in both tropical as well as cold-temperate marine settings and confirms the aphotic conditions in only 85 m water depth at the Säcken site.

Palaeoecological implications

The result of the ichnocoenosis analysis supports the conclusion on the prevailing aphotic conditions derived from the light measurements and bears some important palaeoecological implications. Provided that the non-bathyal coral community will become fossilised, geologists would encounter difficulties finding convincing arguments for a non-bathyal environment. These difficulties arise from the fact that the conclusions were drawn from real bathyal *L. pertusa* communites of the open marine deep-water realm. The finding of bathyal communities in comparatively shallow waters is linked to factors that force deeper oceanic water masses to surface. Such situations are likely to be expected where an estuarine circulation prevails. Other scenarios are deep-sea basins bordered by narrow shelves and with local upwelling cells driven by the wind regime, facilitating the intrusion of eutrophic deeper waters to shallow depths – together with the benthic communities. Areas of interest where such a combination of factors may occur are island arcs with a steep bathymetric gradient towards the subduction zone and narrow straits. Strikingly, almost all known exposed ancient *L. pertusa* locations derive from tectonically active regions with steep bathymetric gradients and a specific confined topography which could have forced deep water to the near surface. Corresponding candidates are Rhodes as part of the Hellenic Arc in the eastern Mediterranean Sea (Hanken et al. 1996; Bromley 2005), occurrences in the Messina Strait (Barrier et al. 1989) and the Cook Strait, New Zealand (Squires 1964).

Summary and conclusions

(1)   The deep-water coral *Lophelia pertusa* in the Kosterfjord area thrives at depths as shallow as 80-90 m under fully marine conditions, with temperature fluctuations between 4°C and 10°C (mean: 6°C), salinity fluctuation between 33.6 ‰ and 35.0 ‰ (mean: 34.5 ‰) and oxygen fluctuation between 4.8 and 6.7 ml/l. This physical oceanographic spectrum matches well the conditions found at *L. pertusa* sites along the northwestern European continental margin.

(2)   The Säcken site located on a sill in the northern Kosterfjord area comprises two major patches with living *L. pertusa*, 250 m^2 and 50 m^2 in size, situated on the flanks of two small mounds in around 85 m water depth. Most of the colonies are small and grow as discrete often spherical colonies with lumps of dead coral, coral rubble, gravel, cobble and sediment in between.

(3)   The fully marine conditions at the Säcken site, only a few tens of metres beneath a permanently brackish surface water layer, are ensured by an inflow of Atlantic water through the more than 700 m deep Norwegian Trench into the Skagerrak to compensate the surface water net outflow.

(4)   Similar situations are met with elsewhere in Scandinavian waters in confined areas where saline oceanic waters can intrude as topographically-guided underflows onto the inner shelf and adjacent fjords driven by an estuarine circulation, combined with tidal currents. There, live shallow-water *L. pertusa* occurrences are known to exist much shallower compared to the open shelf off Norway.

(5)   In general, such situations are likely to be expected where an estuarine circulation prevails, or in deep-sea basins bordered by narrow shelves and with local upwelling cells driven by the wind regime, facilitating the intrusion of eutrophic deeper waters to shallow depths.

(6)   Light measurements carried out in March and October 2003 indicate that *L. pertusa* at 85 m depth in the Kosterfjord thrives under aphotic conditions, which are due to the high geographic latitude combined with eutrophic conditions. Even if light penetrates deeper during the summer period it may only reach the level of dysphotic illumination.

(7)   SEM Analysis of resin casts taken from dead skeletons of *L. pertusa* and associated bivalves collected from the Säcken site yield an endolithic assemblage and ichnocoenosis, respectively, of in total 17 different traces produced by fungi (5), sponges (6), bryozoans (2), foraminifers (1) and brachiopods (1). It is dominated by boring sponges (trace: *Entobia* ispp.), the bryozoan *Spathipora*, the fungus *Dodgella priscus* (trace: *Saccomorpha clava*) and an unknown fungus (trace: *Orthogonum lineare*).

(8)   The ichnocoenosis composed solely of traces produced by heterotrophs resembles the *Saccomorpha clava / Orthogonum lineare* ichnocoenosis, which is typically encountered in fossil and Recent aphotic environments in both tropical as well as cold-temperate marine settings and thus confirms the aphotic conditions in only 85 m water depth at the Säcken site for at least most of the year.

(9)   The finding of bathyal communities in comparatively shallow waters linked to factors that force deeper oceanic water masses to surface, reveals a major potential pitfall in the palaeobathymetric interpretation of fossil *L. pertusa* occurrences, which tend to be interpreted as bathyal palaeoenvironments. Strikingly, almost all known exposed ancient *L. pertusa* locations derive from tectonically active regions with steep bathymetric gradients and a specific confined topography which could have forced deep water to the near surface.

Acknowledgements

References

Barrier P, Di Geronimo I, Montenat C, Roux M, Zibrowius H (1989) Présence de faunes bathyales atlantiques dans le Pliocène et le Pleistocène de Méditerranée (Détroit de Messine, Italie). Bull Soc Géol France 8: 787-796

Bernecker M, Weidlich O (1990) The Danian (Paleocene) coral limestone of Fakse, Denmark: a model for ancient aphotic, azooxanthellate coral mounds. Facies 22: 103-13

Bernecker M, Weidlich O (2005) Azooxanthellate corals in the Late Maastrichtian - Early Paleocene of the Danish basin: bryozoan and coral mounds in a boreal shelf setting. In: Freiwald A, Roberts JM (eds) Cold-water Corals and Ecosystems. Springer, Berlin Heidelberg, pp 3-25

Beuck L, Freiwald A (2005) Bioerosion patterns in a deep-water *Lophelia pertusa* (Scleractinia) thicket (Propeller Mound, northern Porcupine Seabight) In: Freiwald A, Roberts JM (eds) Cold-water Corals and Ecosystems. Springer, Berlin Heidelberg, pp 915-936

Boerboom CM, Smith JE, Risk MJ (1998) Bioerosion and micritization in the deep sea coral *Desmophyllum cristagalli*. Hist Biol 13: 53-60

Bromley RG (2005) Preliminary study of bioerosion in the deep-water coral *Lophelia*, Pleistocene, Rhodes, Greece. In: Freiwald A, Roberts JM (eds) Cold-water Corals and Ecosystems. Springer, Berlin Heidelberg, pp 895-914

Bromley RG, Surlyk F (1973) Borings produced by brachiopod pedicles fossil and recent. Lethaia 6: 349-365

Bromley RG, D'Alessandro A (1984) The ichnogenus *Entobia* from the Miocene, Pliocene and Pleistocene of southern Italy. Riv Ital Paleont Stratigr 90: 227-296

Budd DA, Perkins RD (1980) Bathymetric zonation and paleoecological significance of microborings in Puerto Rican shelf and slope sediments. J Sediment Petrol 50: 881-904

Dahl GE (1978) On the existence of a deep countercurrent to the Norwegian Coastal Current in the Skagerrak. Tellus 30: 552-556

Dons C (1944) Norges korallrev. Det Kongl Norsk Vidensk Selsk Forh 16: 37-82

Försterra G, Beuck L, Häussermann V, Freiwald A (2005) Shallow-water *Desmophyllum dianthus* (Scleractinia) from Chile: characteristics of the biocoenoses and the bioeroding community, heterotrophic interactions and (paleo)-bathymetric implications. In: Freiwald A, Roberts JM (eds) Cold-water Corals and Ecosystems. Springer, Berlin Heidelberg, pp 937-977

Fosså JH, Mortensen PB, Furevik DM (2000) *Lophelia*-korallrev langs norskekysten forekomst og tilstand. Fisken og Havet 2: 1-94

Fosså JH, Mortensen, PB Furevik DM (2002) The deep-water coral *Lophelia pertusa* in Norwegian waters: distribution and fishery impacts. Hydrobiologia 471: 1-12

Freiwald A (2002) Reef-forming cold-water corals. In: Wefer G, Billett D, Hebbeln D, Jørgensen BB, Schlüter M, van Weering T (eds) Ocean Margin Systems. Springer, Berlin Heidelberg, pp 365-385

Freiwald A, Henrich R, Pätzold J (1997) Anatomy of a deep-water coral reef mound from Stjernsund, West-Finnmark, northern Norway. SEPM Spec Publ 56: 141-161

Freiwald A, Wilson JB (1998) Taphonomy of modern deep, cold-temperate water coral reefs. Hist Biol 13: 37-52

Glaub I (1994) Mikrobohrspuren in ausgewählten Ablagerungsräumen des europäischen Jura und der Unterkreide (Klassifikation und Palökologie). Cour Forschinst Senckenberg 174: 1-324

Glaub I (1999) Paleobathymetric reconstructions and fossil microborings. Bull Geol Soc Den 45: 143-146

Glaub I, Bundschuh M (1997) Comparative study on Silurian and Jurassic/Lower Cretaceous microborings. Cour Forschinst Senckenberg 201: 123-135

Glaub I, Gektidis M, Vogel K (2002) Microborings from different North Atlantic shelf areas - Variability of the euphotic zone extension and implications for paleodepth reconstructions. Cour Forschinst Senckenberg 237: 25-37

Golubic S, Brent G, LeCampion T (1970) Scanning electron microscopy of endolithic algae and fungi using a multipurpose casting-embedding technique. Lethaia 3: 203-209

Golubic S, Campell S, Spaeth C (1983) Kunstharzausgüsse fossiler Mikroben-Bohrgänge. Präparator 29: 197-200

Günther A (1990) Distribution and bathymetric zonation of shell-boring endoliths in recent reef and shelf environments: Cozumel, Yucatan (Mexico). Facies 22: 233-262

Hanken N-M, Bromley RG, Miller J (1996) Plio-Pleistocene sedimentation in coastal grabens, north-east Rhodes, Greece. Geol J 31: 393-418

Hovland MT, Vasshus S, Indreeide A, Austdal L, Nilsen Ø (2002) Mapping and imaging deep-sea coral reefs off Norway, 1982-2000. Hydrobiologia 471: 13-17

International Commission on Zoological Nomenclature (1999) International Code of Zoological Nomenclature. Int Trust Zool Nomencl, London

Liebau A (1984) Grundlagen der Ökobathymetrie. In: Luterbacher H (ed) Paläobathymetrie. Paläont Kursb 2: 149-184

Lundälv T, Jonsson L (2003) Mapping of deep-water corals and fishery impacts in the north-east Skagerrak, using acoustical and ROV survey techniques. Proc 6th Underwater Sci Symp, Aberdeen, 2003

Lüning K (1985) Meeresbotanik - Verbreitung, Ökophysiologie und Nutzung der marinen Makroalgen. Thieme, Stuttgart

Mayoral E (1988) Microperforaciones (Tallophyta) sobre bivalvia del Plioceno del Bajo Guadalquivir. Estud Geol 44: 301-316

Mikkelsen N, Erlenkeuser H, Killingley JS, Berger WH (1982) Norwegian corals: radiocarbon and stable isotopes in *Lophelia pertusa*. Boreas 11: 163-171

Mortensen PB (2001) Aquarium observations on the deep-water coral *Lophelia pertusa* (L., 1758) (Scleractinia) and selected associated invertebrates. Ophelia 54: 83-104

Perry CT, MacDonald IA (2002) Impacts of light penetration on the bathymetry of reef microboring communities: implications for the development of microendolithic trace assemblages. Palaeogeogr Palaeoclimatol Palaeoecol 189: 101-113

Plewes CR, Palmer TJ, Haynes, JR (1993) A boring foraminiferan from the Upper Jurassic of England and Northern France. J Micropaleont 12: 83-89

Radtke G (1993) The distribution of microborings in molluscan shells from Recent reef environments at Lee Stocking Island, Bahamas. Facies 29: 81-92

Rokoengen K, Østmo SR (1985) Shallow geology off Fedje, western Norway. IKU-Rep 24.1459/01/25, 20 pp

Schmidt H, Freiwald A (1993) Rezente gesteinsbohrende Kleinorganismen des norwegischen Schelfs. Natur Museum 123: 149-155

Squires DF (1964) Fossil coral thickets in Wairarapa, New Zealand. J Paleont 38: 904-915

Strømgren T (1971) Vertical and horizontal distribution of *Lophelia pertusa* (Linné) in Trondheimsfjorden on the west coast of Norway. K norske Vidensk Selsk Skr 6: 1-9

Svansson A (1975) Physical and chemical oceanography of the Skagerrak and the Kattegat, I. Open sea conditions. Rep Fish Board Swed Inst Mar Res 1: 1-88

Tavanier A, Campbell SE, Golubic S (1992) A complex marine shallow-water boring trace: *Dendrorete balani* n. ichnogen. et ichnospec. Lethaia 25: 303-310

Vogel K, Bundschuh M, Glaub I, Hofmann K, Radtke G, Schmidt H (1995) Hard substrate ichnocoenoses and their relations to light intensity and marine bathymetry. N Jb Geol Paläont, Abh 195: 49-61

Vogel K, Balog S-J, Bundschuh M, Gektidis M, Glaub I, Krutschinna J, Radtke G (1999) Bathymetrical studies in fossil reefs, with microendoliths as paleoecological indicators. Profil 16: 181-191

Vogel K, Gektidis M, Golubic S, Kiene WE, Radtke G (2000) Experimental studies on microbial bioerosion at Lee Stocking Island, Bahamas and One Tree Island, Great Barrier Reef, Australia: implications for paleoecological reconstructions. Lethaia 33: 190-204

Wahrberg R, Eliason A (1926) Ny local för levande *Lophelia prolifera* (PALLAS) vid svensk kust. Fauna och Flora 1926: 256-260

Zeff ML, Perkins RD (1979) Microbial alteration of Bahamian deep-sea carbonates. Sedimentology 26: 175-201

Zibrowius H (1980) Les Scléractiniaires de la Méditerranée et de l'Atlantique nord-oriental. Mem Inst Oceanogr Monaco 11: 1-227

VII

Environmental archive

Chapter content

C and O isotopes in a deep-sea coral *(Lophelia pertusa)* related to skeletal microstructure

Dominique Blamart[1], Claire Rollion-Bard[2], Jean-Pierre Cuif[3], Anne Juillet-Leclerc[1], Audrey Lutringer[1], Tjeerd C. E. van Weering[4], Jean-Pierre Henriet[5]

[1] Laboratoire des Sciences du Climat et de l'Environnement (LSCE) Unité mixte de Recherche CEA-CNRS, Bât. 12, Avenue de la Terrasse, F-91198 Gif-sur-Yvette Cedex, France
   (dominique.blamart@lsce.cnrs-gif.fr)
[2] CRPG-CNRS, BP 20, 15, rue Notre-Dame des Pauvres, F-54500 Vandoeuvre-lès-Nancy, France
[3] Université de Paris XI, Faculté des Sciences, Bat 504 Géologie, F-91405 Orsay Cédex, France
[4] Koninklijk Nederlands Instituut voor Onderzoek der Zee (NIOZ), P.O. Box 59, NL-1790 AB Den Burg, Texel, The Netherlands
[5] Renard Centre of Marine Geology, Gent University, Krijgslaan 281, S8, B-9000 Gent, Belgium

Abstract. *Lophelia pertusa* is a deep-sea scleractinian coral (azooxanthellate) found on the continental margins of the major world oceans. Built of aragonite it can be precisely dated and measured for stable isotope composition (C-O) to reconstruct past oceanic conditions. However, the relation between stable isotope and skeleton microstructures, i.e. centres of calcification and surrounding fibres, is crucial for understanding the isotopic patterns. Values for $\delta^{18}O$ and $\delta^{13}C$ in *Lophelia pertusa* were determined at a micrometer scale using an ion microprobe (SIMS - Secondary Ion Mass Spectrometry). In this coral species, centres of calcification are large (50 µm) and arranged in lines. The centres of calcification have a restricted range of variation in $\delta^{18}O$ (-2.8 ± 0.3 ‰ (V-PDB)), and a larger range in $\delta^{13}C$ (14.3 to 10.9 ‰ (V-PDB)). Surrounding skeletal fibres exhibit large isotopic variation both for C and O (up to 12 ‰) and $\delta^{13}C$ and $\delta^{18}O$ are positively correlated. The C and O isotopic composition of the centres of calcification deviate from this linear trend at the lightest $\delta^{18}O$ values of the surrounding fibres. The fine-scaled variation of $\delta^{18}O$ is probably the result of two processes: (1) isotopic equilibrium calcification with at least 1 pH unit variation in the calcification fluid and (2) kinetic fractionation. The apparent $\delta^{13}C$ disequilibrium in *Lophelia pertusa* may be the result of mixing between depleted $\delta^{13}C$ metabolic CO_2 (respiration) and DIC coming directly from seawater. This study underlines the close relationship between microstructure and

stable isotopes in corals. This relationship must also be taken into consideration for major elements like Mg and trace elements (U-Sr-Ba) increasing the reliability of the geochemical tools used in paleoceanography.

Keywords. Deep-sea corals, SIMS stable isotopes, isotopic disequilibrium, *Lophelia pertusa*

Introduction

Deep-sea scleractinian corals (DSC) have been known for two centuries (see Wilson 1979 for a review). Recently, DSC and their associated ecosystems became a worldwide subject of research of general interest and a cause of concern (Freiwald 2002; Malakoff 2003; Grehan et al., in press). DSC have numerous interesting properties that can provide useful tools in academic research and specially in the fields of biology, ecology and paleoceanography.

Recent submersible explorations have revealed a wide distribution of these ecosystems all around the oceans. Solitary DSC and/or DSC reefs are found from the sublittoral to more than 5000 m water depth. In NE Atlantic DSC are often found in association with carbonate mounds on the continental slope, at a water depth of 500 to 1200 m. DSC are able to live in cold water (about 1°C) (Wilson 1979; Bett 2001) as well as in warm water (about 28°C) (Emiliani et al. 1978 and see Freiwald 2002 for an extensive review).

DSC have an aragonitic skeleton which can be precisely dated by means of ^{230}Th/U and ^{14}C dating (Smith et al. 1997; Adkins et al. 1998; Cheng et al. 2000; Frank et al. 2004; Frank et al. 2005), and analysed for their C-O stable isotope compositions for paleoceanographic purposes as can many other biogenic carbonates (e.g., Wefer and Berger 1991).

The first isotopic studies on *Lophelia pertusa* were performed by Norwegian teams with the idea of using this species to reconstruct environmental parameters such as sea-water temperature (Mortensen and Rapp 1998) and water mass proxy (Mikkelsen et al. 1982). Other isotopic studies have been conducted (Newton et al. 1987; Freiwald et al. 1997; Spiro et al. 2000; Lutringer 2002) and all the data obtained display three main isotopic patterns that complicate the use of DSC in paleoceanography. First, C and O isotopes display large variations (~10 ‰ for carbon and 4-6 ‰ for oxygen) (Fig. 1). Second, δ^{13}C and δ^{18}O values are depleted relative to values of isotopic equilibrium for aragonite with ambient seawater. These characteristics, and particularly the departures from the isotopic equilibriums, have been referred as "vital effect" (Urey et al. 1951). Third, there is a clear linear relationship between the C and O isotopes. Generally, the slope of the regression line is between 0.3 and 0.6. Using the relationship between C and O, a method to calculate past seawater temperature has been proposed by Smith et al. (2000).

However, the mechanisms involved in the calcification processes are still under debate and two sets of explanations have been advocated for the vital effect. The first, developed by McConnaughey (1989, 2003), attributes the isotopic disequilibrium to the combined effect of kinetic fractionation and metabolism. Kinetic fractionation is
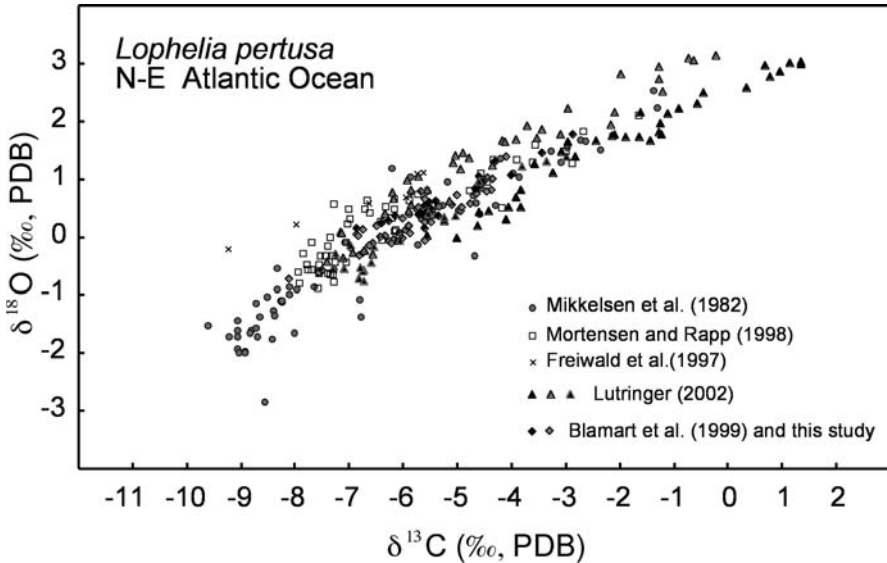
Fig. 1 Relationship between $\delta^{13}C$ and $\delta^{18}O$ in *Lophelia pertusa* using classical sampling (dental drill). The samples are from different areas of the NE Atlantic with: triangle and diamond Porcupine-Rockall area, circle-square and cross: Norwegian offshore

associated with CO_2 hydration and hydroxylation and results in depletion of about 10-15 ‰ for $\delta^{13}C$ and about 4 ‰ for ^{18}O in carbonate with respect to the isotopic equilibrium. The metabolic effects in DSC include respiration, which lowers the $\delta^{13}C$ of the DIC pool.

The second explanation is derived from McCrea's isotopic equilibrium experiment (McCrea 1950) showing a relation between the carbonate depletion in ^{18}O and the $[CO_3^{2-}]$ or pH variations (Spero et al. 1997; Zeebe 1999). Usdowski and Hoefs (1993) showed that the $\delta^{18}O$ of carbonates is a function of the solution pH through the different $\delta^{18}O$ of the dissolved carbonate species (H_2CO_3, HCO_3^- and CO_3^{2-}). The carbon isotopic disequilibrium relative to DIC seawater is caused by the incorporation of ^{13}C-depleted metabolic CO_2 from the respiration. Recently, Adkins et al. (2003) proposed a fractionation model for DSC including a pH variation in the calcifying fluid between 7.9 and more than 10.3.

Regarding the chemical (stable isotopes, not the trace elements) aspect related to the calcification processes, few studies have looked into the distribution of stable isotopes with respect of the microstructure of the skeleton. It has long been recognized that, although entirely aragonitic, coral skeletons are not made only by fibres.

Ogilvie (1896) coined the term of *centres of calcification* (CC) as specific components of septal microstructures. This concept was refined by Wells (1956), and specific structural patterns of CC were introduced by Wainwright (1963). The observations of Wainwright (1963), confirmed later by others studies (e.g., Le Tissier 1988; Hidaka 1991), made it clear that there is a crystallographic difference

between these microstructural units and the surrounding fibres. More recently, it was shown that CC also exhibit chemical and biochemical differences (Cuif and Dauphin 1998; Cohen et al. 2001; Cuif et al. 2003).

Considering this consistent set of data, the question arises whether the biological processes, that lead to specific chemical and crystallographic patterns that are visible in centres of calcification, are portrayed by the measured stable isotopes. Moreover, Land et al. (1975) observed a strong variability in isotopic fractionation depending on coral architecture. Rollion-Bard (2001) and Rollion-Bard et al. (2003b) also found a high diversity in isotopic measurement, exceeding by far the level that can be expected from the zooxanthellate coral *Porites* sp. Therefore a hypothesis can be made that these unexpected isotopic measurements could be related to particular properties of centres of calcification, irregularity in measurements being caused by the irregular fine-scale partition (taxonomy dependant) of the centres within the skeleton.

To test the hypothesis of a strong relationship between stable isotopes and microstructure in DSC, we have made a series of isotopic measurements on coral skeleton where the microstructure was previously studied, taking advantage of the technical performance of ion microprobe (SIMS). The *in situ* stable isotopic ion microprobe measurements have been carried out on a specimen of *Lophelia pertusa*, collected where ambient parameters ($\delta^{18}O$ of seawater and temperature) are known, allowing calculation of the isotopic equilibrium values.

Materials and methods

Samples description and preparation

The skeleton sample came from the Rockall Bank (55°32' N, 15°40' W, 725 m water depth), west of Ireland (van Weering and shipboard scientific party 1999). A branch of the specimen was cut perpendicularly to the growth axis at the upper part of the calyx. The surface was polished, and microstructure was revealed by UV fluorescence and SEM observations before SIMS analyses were run. *Lophelia pertusa* has a well-expressed microstructure. The line of centres of calcification (LCC) is produced at the upper part of each septum (Fig. 2), resulting in a quasi-linear, or sometimes weakly undulating early mineralization zone (EMZ) in the median region of the section of the septum. More details are provided by Rollion-Bard et al. (2003a).

Samples for stable isotopic (C-O) composition were obtained using a conventional sampling method (dental drill, 0.8 mm O.D.). The isotopic analyses were performed on a VG Optima mass spectrometer equipped with an automatic carbonate device. The uncertainties in the isotopic measurements were 0.08 and 0.05 ‰ respectively for oxygen and carbon. The data are given relative to the V-PDB (Table 1).

SIMS Instrumental setting

Ion microprobe permit *in situ* isotopic measurements with high spatial resolution (see Ireland 1995 for a review). Analyses were performed using a Caméca
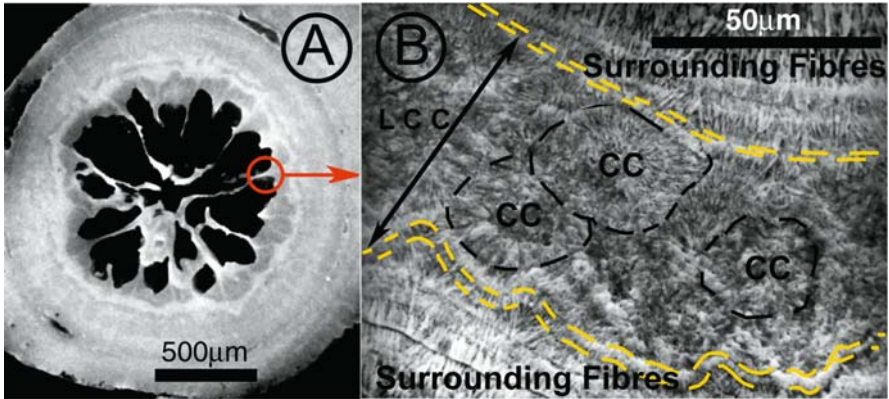
Fig. 2 A SEM (Scanning Electron Microscope) photograph of the general structure of *Lophelia pertusa* in cross section. **B** Detail from area shown in **A** photographed in natural light where the centres of calcification (CC) produce the LCC. The two dashed lines represent the limit between LCC and the surrounding fibres

IMS 1270 ion microprobe at Nancy, France. The sample was sputtered with a 10 kV Cs$^+$ primary beam of 5 nA for oxygen and 30 nA for carbon, focused to 30-50 × 15 μm spots. Detailed descriptions of the instrumental setting are given by Slodzian et al. (1987), De Chambost (1997), Rollion-Bard (2001) and Rollion-Bard et al. (2003a). The measurements were performed with ion intensities of about 5 × 10^6 counts/s on the ^{18}O$^-$ peak and 3 × 10^5 counts/s on the ^{13}C$^-$ peak. The typical acquisition times were 2 s for oxygen analysis and 3 s for carbon analysis during 15 cycles. The instrumental mass fractionation (IMF) was monitored and determined using various carbonate standards analysed conventionally for O and C isotopes: two calcite standards ($\delta^{18}O_{PDB}$ = -19.00 ± 0.04 ‰ and $\delta^{13}C$ = -5.39 ± 0.01 ‰; $\delta^{18}O_{PDB}$ = -7.05 ± 0.02 ‰ and $\delta^{13}C$ = -6.37 ± 0.04 ‰), and one aragonite ($\delta^{18}O_{PDB}$ = -7.18 ± 0.11 ‰, $\delta^{13}C$ = 8.17 ± 0.04 ‰). The homogeneity of the standards for oxygen and carbon isotopes was tested by multiple ion probe measurements along different profiles. The total analytical uncertainty of C and O isotopic measurements resulted from uncertainties introduced by the internal precision of a single measurement and the external reproducibility, i.e. the reproducibility of the measurements performed on the same homogeneous material.

The internal precision of a single measurement was ± 0.1-0.2 ‰ for ^{13}C/^{12}C and ^{18}O/^{16}O ratios. Reproducibility based on the repeated standard measurements was ± 0.4 ‰ for oxygen and ± 0.65 ‰ for carbon. These reproducibilities are better than previous ion microprobe results on carbonate standards (about 0.5 ‰ in internal precision and 0.8 ‰ in external reproducibility) (Mahon et al. 1998).

Validation of ion microprobe measurements

Coral skeletons comprise less than 3 % weight of non-mineral components (organic matter and water associated with the aragonite matrix) (Gladfelter 1982; Gaffey 1988; Cuif et al. 2003). In order to check whether a small amount of organic

Table 1 Stable isotope composition (‰ *vs*. PDB) in skeleton of *Lophelia pertusa* from the Rockall bank. The same samples have been used for the SIMS analysis. * indicates a second measurement on the same powder obtained using the classical dental drill sampling. S: septa, T: theca. On the theca, different aliquots of powder have been obtained by drilling at the same location to different depths

Sample no	δ¹³C (‰, PDB)	δ¹⁸O (‰, PDB)	Sample no	δ¹³C (‰, PDB)	δ¹⁸O (‰, PDB)
S1	-6.83	-0.31	S18	-5.62	0.67
S1*	-6.77	-0.27	S19	-4.93	0.53
S2	-4.65	0.76	S20	-6.24	-0.09
S2*	-5.90	0.08	S21	-6.85	0.03
S3	-6.34	0.03	S22	-5.69	0.80
S3*	-6.18	-0.02	S23	-5.57	0.80
S4	-6.57	-0.09	T1	-6.17	0.37
S4*	-5.49	0.28	T1*	-5.86	0.79
S5	-4.46	1.04	T2	-4.31	1.30
S5*	-4.38	0.83	T2*	-4.60	1.06
S6	-6.03	-0.01	T3	-5.62	0.54
S6 *	-4.78	0.59	T3*	-5.59	0.41
S7	-6.98	-0.18	T4	-2.88	1.77
S7*	-4.95	0.45	T4*	-3.46	1.47
S8	-8.13	-0.72	T5-1	-4.69	0.84
S8*	-7.57	-0.60	T5-2	-5.41	0.62
S9	-6.65	-0.13	T5-3	-5.38	0.38
S9*	-7.50	-0.57	T5-4	-5.48	0.48
S10	-4.47	0.80	T5-5	-6.41	0.24
S10*	-5.61	0.26	T5-6	-6.86	0.15
S11	-6.87	0.05	T5-7	-6.27	0.28
S11*	-5.61	-0.05	T5-8	-5.68	0.42
S12	-5.12	0.56	T6-1	-5.72	0.39
S13	-6.50	0.21	T6-2	-5.52	0.62
S13*	-5.72	0.52	T6-3	-5.67	0.41
S14	-5.53	0.50	T6-4	-5.61	0.16
S14*	-5.03	0.73	T6-5	-4.54	0.96
S15	-6.03	0.33	T6-6	-4.59	0.90
S16	-4.10	1.39	T6-7	-4.02	1.07
S17	-6.43	0.00			
S17*	-6.75	0.15			

matter could affect the δ¹⁸O and δ¹³C SIMS data, measurements from organic matter were made using the same analytical settings as for carbonates. First, the data indicated that the secondary ions intensities are lower for oxygen ions and more important for carbon ions. Secondly, the coral O and C isotopic values are not correlated with the intensities of the secondary ions intensities (Rollion-Bard et al. 2003a). The data obtained on the organic matter are characterised by very negative values (not corrected for by the instrumental mass fractionation) in both carbon

and oxygen isotopes. Therefore, if the measurements were influenced by organic matter contamination, the $\delta^{18}O$ and $\delta^{13}C$ would be correlated to the secondary ions intensities, which was not the case.

Orientation of the aragonite crystals

Previous work has shown that δD (D/H ratio) values are influenced by the crystallographic orientation of the OH-bearing mineral (Deloule et al. 1992). The influence of the orientation could be also a problem in measurements of coral, because of the random orientation of the aragonite fibres in the sample mounts. This effect was tested and was not observed for aragonite and calcite crystals.

Isotopic results

Oxygen isotopes

The variation in isotopic composition measured by the "classic" method is about 2.5 ‰ (+1.7 to -0.7 ‰) (Fig. 1, Table 1). The results from ion microprobe analyses of oxygen isotopes in *Lophelia pertusa* are given in Table 2 and illustrated in Figs. 3 and 4. The two profiles from the upper part of the calyx (P1 and P2) (Table 2) showed a $\delta^{18}O$ variation of about 9 ‰ (Figs. 3 and 4), a range similar to that found for *Porites* sp. (Rollion-Bard 2001; Rollion-Bard et al. 2003a). P1 is located outside of the LCC, while P2 within the LCC. Outside of LCC (P1), the $\delta^{18}O$ values showed a large variation, from about -4.5 ‰ to +4.4 ‰. From the inner part towards the wall, $\delta^{18}O$ values increased by 9 ‰ in a distance of 500 μm (points 1 to 8) and then decreased of about 7 ‰ (points 8 to 13) to reach a value of -3 ‰. Over the last 450 μm $\delta^{18}O$ values increased by about 3 ‰ to reach a value of about 0 ‰.

The 800 μm-long profile P2 within the LCC (Fig. 4) showed little variation in the $\delta^{18}O$ values. All the data fell within the range of -3.2 ‰ to -2.1 ‰, with a mean value of -2.8 ± 0.3 ‰. Only two measurements had higher values at +1.1 ‰ and +3.1 ‰. The first value corresponded to a measurement performed in the external part of the wall (point 20), while the second was located in the septum, outside of the LCC (point 33, not shown in the figure, see Table 2 for data). This point was symmetric to point 7. The $\delta^{18}O$ values of these two points were consistent with those found previously at a similar microstructural level. These two profiles clearly showed that the $\delta^{18}O$ values in and outside of the LCC differ strongly.

Carbon isotopes

The range of $\delta^{13}C$ data measured by the "classic" method is 5.5 ‰, between -2.8 to -8.2 ‰ (Table 1). $\delta^{13}C$ ion microprobe analyses were in the range of -0.7 to -15.3 ‰, with most of the data between -3 to -15 ‰. The amplitude is twice that observed using the conventional method (Table 2). P1 measurements ranged from -0.7 to -15.3 ‰. The general isotopic trend was similar to the trend recorded for oxygen isotopes. In P1, from the inner part towards the wall, the $\delta^{13}C$ values increased from -15.3 to about -4 ‰ over a distance of 300 μm (points 1 to 4), reached a plateau (points 4 to 8) and then decreased to -11 ‰ (point 13). Over the

Table 2 Stable isotope composition (‰ *vs*. PDB) measured by using ion microprobe technique along two profiles in *Lophelia pertusa* skeleton. Pt: point; sd: standard deviation

Lophelia pertusa (September 2001)	Profile number	$\delta^{18}O$ (‰, V-PDB)	1sd	$\delta^{13}C$ (‰, V-PDB)	1sd
Pt 1	1	-4.5	0.2	-15.3	0.2
Pt 2	1	-3.1	0.2	-12.8	0.2
Pt 3	1	-1.4	0.1	-11.9	0.1
Pt 4	1	2.1	0.1	-4.2	0.1
Pt 5	1	2.5	0.2	-4.2	0.2
Pt 6	1	3.4	0.1	-3.5	0.1
Pt 7	1	3.5	0.2	-4.2	0.2
Pt 8	1	4.4	0.1	-6.7	0.1
Pt 9	1	0.9	0.2	-5.9	0.2
Pt 10	1	0.6	0.2	-5.9	0.2
Pt 11	1	-0.5	0.1	-6.7	0.1
Pt 12	1	-1.7	0.1	-10.4	0.1
Pt 13	1	-3.0	0.1	-10.9	0.1
Pt 14	1	-1.2	0.1	-9.7	0.1
Pt 15	1	-1.6	0.1	-7.6	0.1
Pt 16	1	-1.0	0.2	-9.7	0.2
Pt 17	1	0.4	0.1	-6.7	0.1
Pt 18	1	-0.5	0.1	-8.4	0.1
Pt 19	1	0.9	0.1	-0.7	0.1
Pt 20	2	1.1	0.1	-7.5	0.1
Pt 21	2	-2.5	0.1	-14.3	0.1
Pt 22	2	-3.2	0.1	-11.0	0.1
Pt 23	2	-2.8	0.1	-13.8	0.1
Pt 24	2	-2.8	0.1	-11.9	0.1
Pt 25	2	-2.8	0.1	-13.7	0.1
Pt 26	2	-2.1	0.2	-11.9	0.2
Pt 27	2	-2.8	0.1	-13.9	0.1
Pt 28	2	-2.8	0.1	-10.4	0.1
Pt 29	2	-2.9	0.2	-13.7	0.2
Pt 30	2	-3.2	0.1	-10.9	0.1
Pt 31	2	-2.9	0.1	-12.3	0.1
Pt 32	2	-2.9	0.2	-11.2	0.2
Pt 33	2	3.1	0.1	-9.0	0.1

last 450 μm, the $\delta^{13}C$ values increased by about 3-4 ‰. Point 19 was characterised by a higher value at -0.7 ‰. Cross plotting revealed a positive correlation between the C and O isotopic compositions (Fig. 4) where $\delta^{18}O = 0.54\,\delta^{13}C + 4.17$ ($R^2 = 0.67$). The highest $\delta^{13}C$ values were depleted by several 3 to 4 ‰ from the equilibrium point as commonly observed for this species (Mikkelsen et al. 1982; Freiwald et al. 1997; Mortensen and Rapp 1998; Spiro et al. 2000; Adkins et al. 2003).
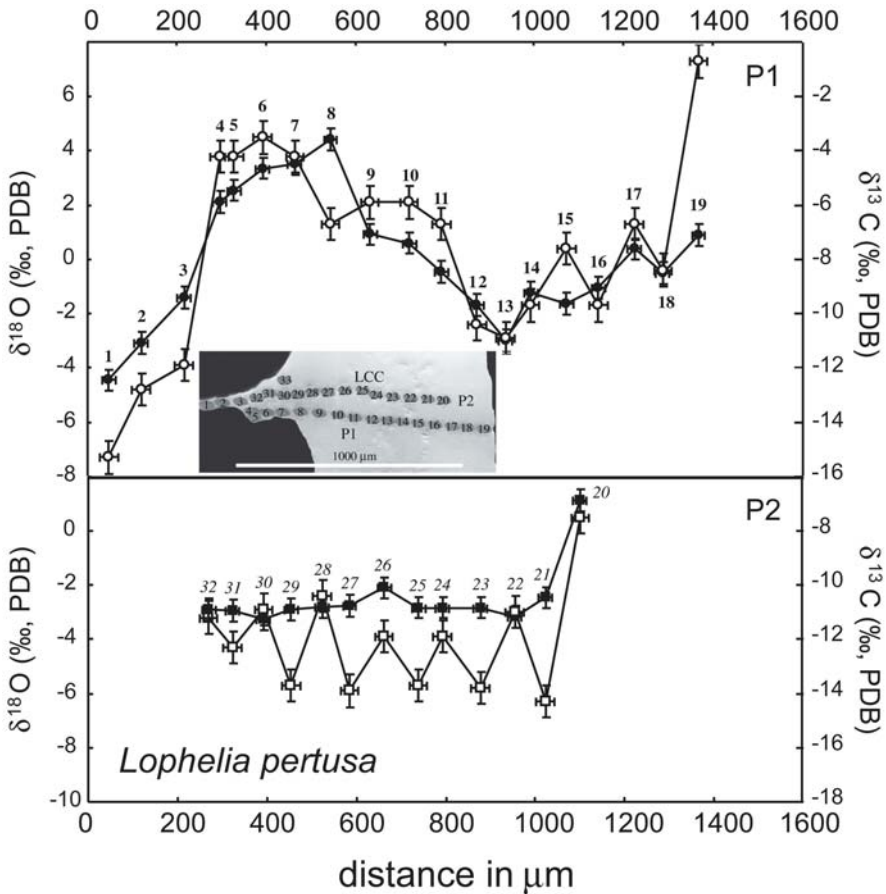
Fig. 3 $\delta^{18}O$ and $\delta^{13}C$ along profile P1 and profile P2 (open and black squares) performed in the upper part of the calyx. Black square and circle correspond to the $\delta^{18}O$ values and open square and circle to $\delta^{13}C$ values. Note the homogeneity of the isotopic values corresponding to the LCC (P2) and the large range of isotopic variation for the surrounding aragonitic fibres (P1)

Profile P2 on the LCC (Fig. 3) showed less variation (about 4 ‰). With the exception of point 20, all the $\delta^{13}C$ values were in the range of -14.3 to -10.9 ‰ and were remarkably ^{13}C-depleted compared to the $\delta^{13}C$ values of P1. In figure 4, the points corresponding to P2 (open squares) deviated from the linear trend described for P1 (black circles) at the lightest $\delta^{18}O$ values. As with O-isotopes, $\delta^{13}C$ profiles performed inside and outside of the LCC showed a clear relationship with the microstructure.
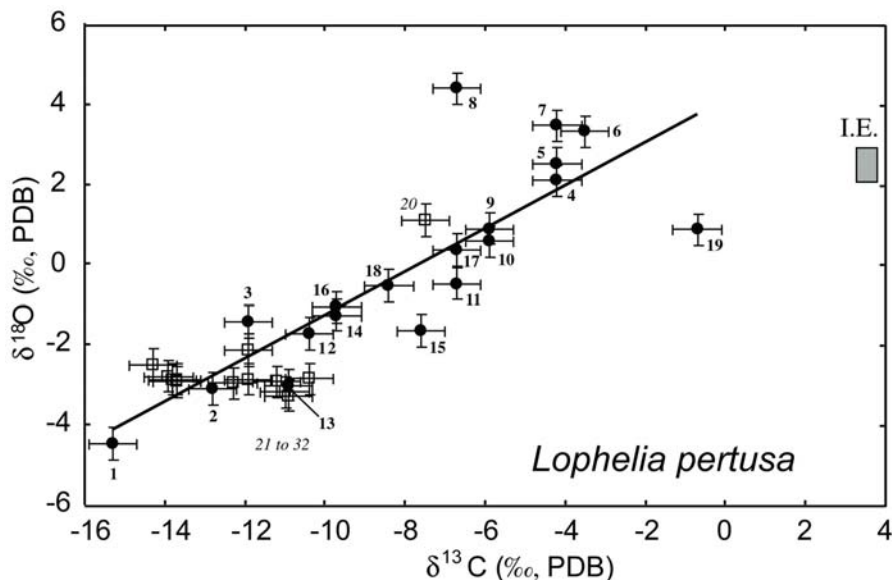
Fig. 4 Relationship between $\delta^{13}C$ and $\delta^{18}O$ in *Lophelia pertusa* measured in the same spots using ion microprobe. Open squares correspond to measurements performed on the LCC and black circles to measurements on the surrounding fibres. I.E. stands for isotopic equilibrium

Discussion

Chemical mechanisms influencing the oxygen isotopic record of fibres

As already noted, environmental parameters (e.g. temperature and salinity) cannot explain the oxygen isotopic range observed in *Lophelia pertusa*. However, the isotopic range could be explained by a variation of pH as observed in Foraminifera (Spero et al. 1997; Zeebe 1999). The variation of carbonate $\delta^{18}O$ with pH was first observed by McCrea (1950) and was calculated by Usdowski and Hoefs (1993). They found that the different dissolved species of carbonate have different fractionation factors with water displaying values of 1.0184 for CO_3^{2-}, 1.0343 for HCO_3^- and 1.0395 for H_2CO_3 (Usdowski et al. 1991). The $\delta^{18}O$ of the carbonate precipitated from a solution reflects the different proportions of the carbonate species present in this solution. If we apply the Usdowski and Hoefs (1993) equation to our range of $\delta^{18}O$ in *Lophelia pertusa,* a pH variation between 7 and 11.3 is derived, (excluding the $\delta^{18}O$ value at 4.4 ‰). However, the more striking feature is the contrast between the homogenous $\delta^{18}O$ values of the LCC and the variable $\delta^{18}O$ values found for the surrounding fibres. Combining the equations of Usdowski and Hoefs (1993) and the $\delta^{18}O$ values of the LCC, a pH of about 10.5 is found. Even if this pH seems a little high, it is not in profound contradiction to measurements performed with microelectrode (Vengosh et al. 1991) or by microsensor on calicoblastic layers

(8.13 and 9.29; Al-Moghrabi et al. 2001) and in the coelenteron (7.93 and 8.74; Al-Horani et al. 2003) of zooxanthellate corals. This range of pH variation can explain only a part of $\delta^{18}O$ values. Indeed, a pH variation of 1 unit corresponds to a variation in $\delta^{18}O$ of about 1 ‰ using the equation of Usdowski and Hoefs (1993). The $\delta^{18}O$ values, which are very depleted in ^{18}O, are probably due to a kinetic fractionation.

Adkins et al. (2003) proposed a new model to explain O and C isotopic patterns in DSC. The model considers two major pools (CO_2 (aq) and seawater DIC) for the mineralization process. The first one results from a passive diffusion of CO_2 (aq) through the wall of the calicoblastic cells at the site of calcification activated by an enzymatic pump (Ca-ATPase). The other reflects diffusion in variable proportions of seawater DIC. The alkalinity pump establishes a pH gradient between the calicoblastic cells and the calcifying fluid. High metabolic activity corresponds to a high pH gradient leading to ^{18}O-depleted isotopic values of the carbonate. This model implies that at that step, CO_2 (aq) is the main reservoir for the mineralization process. If this is true, then the LCC corresponds to a high Ca-ATPase activity and is a result of rapid calcification. For the surrounding fibres, pH variation with two different sources of oxygen (CO_2 (aq) and seawater DIC) can be one of the main mechanisms involved during calcification. At low growth rate, the carbonate species could re-equilibrate totally or partially leading to kinetic effects. As proposed for *Porites lutea*, we suggest that both pH variations and kinetic processes can take place in the calcifying fluid.

However, problems still remain. It is difficult to explain several per mil variations in a few microns between the LCC and surrounding fibres, both growing from the same fluid at the same time. A possible explanation could be a specialisation of the calicoblastic cell at the site of calcification. However, recent histological studies on zooxanthellate corals, do not support this hypothesis (D. Allemand, pers. com.).

Factors influencing the carbon isotopic composition

Stable carbon isotopic results of *Lophelia pertusa* differ from those observed for *Porites lutea* by a large isotopic range and by ^{13}C-depleted values. Figure 4 shows an offset of about 3-4 ‰ from equilibrium. This offset is typical for this species and has been previously reported in the literature (Weber 1973; Land et al. 1975; Emiliani et al. 1978; Swart 1983; Freiwald et al. 1997; Mortensen and Rapp 1998; Blamart et al. 2000; Adkins et al. 2003). It probably corresponds to an isotopic shift associated with respiration. The most interesting feature is the ^{13}C-depleted values found for the LCC. These depleted values are not in contradiction with the model of Adkins et al. (2003) and would correspond to a high alkalinity pump activity. The experimental studies by Furla et al. (2000) indicate that the main source for DIC is metabolic CO_2 modulated by minor input of seawater DIC. A major contribution of metabolic CO_2 implies ^{13}C-depleted values in the calcifying fluid. Seawater DIC at Porcupine Seabight is about 0 ‰ (PDB). A mass balance calculation using a mean value of -13 ‰ for the LCC implies a $\delta^{13}C$ calculated value for the metabolic CO_2 in the range of -25 to -26 ‰. In this case, the metabolic CO_2 represents, between 75 and 100 % of the carbon used for calcification for the LCC (about -10 to -14 ‰). The ^{13}C-depleted value found for the metabolic CO_2 is similar to $\delta^{13}C$ values of

particulate organic carbon (POC). The LCC appears to preferentially consume from the light isotopic reservoir (own unpublished results). The $\delta^{13}C$ values of the surrounding fibres are systematically enriched compared to the LCC. This can be explained by an enrichment of the DIC pool either by light C uptake associated with LCC mineralization or by a higher proportion of seawater DIC.

Biomineralization, coralline microstructure and stable isotopic fractionations

The simple microstructure of *Lophelia pertusa*, with wide and continuous early calcification zones leads to well-located measurements either on the LCC or in the surrounding fibres. The results obtained clearly show that LCC and surrounding fibres have their own isotopic characteristics for O and C (Fig. 4).

Zooxanthellate (*Porites lutea*) or not (*Lophelia pertusa*), the similar amplitude in $\delta^{18}O$ values suggests that a mechanism involved in the calcification process is able to separate the two domains of skeletal secretion during the biomineralization process. Clearly, the outer epithelial mineralizing space cannot be considered as a fluid volume in which chemical properties are uniform.

These remarks are supported by two recent studies. The first one, based on SIMS Sr/Ca measurements in symbiotic coral, demonstrated a strong relationship between this ratio and the microstructure leading to a re-examination of the sea surface temperature using the Sr/Ca paleothermometer (Meibom et al. 2003). The second one using the XANES mapping technique has shown in three coral species (including *Lophelia pertusa*), an exact correspondence between concentration of sulphated polysaccharides and centres of calcification (Cuif et al. 2003). These results suggest that heterogeneity in isotopic fractionations could be due to the influence of specifically secreted organic mineralising matrices, that are already known to control both crystallisation patterns and minor element concentrations (Cuif and Dauphin 1998).

Conclusions

In situ oxygen isotopic composition measurements performed in *Lophelia pertusa* using SIMS techniques, showed 10 ‰ variation in the coral skeleton. The species exhibits pronounced isotopic disequilibrium for oxygen. This feature cannot be explained by variations of environmental parameters like seawater salinity or temperature. Isotopic data indicated a strong correlation with the microstructure of the coral leading to a great heterogeneity in oxygen isotopic composition at a micrometre scale. Selected profiles demonstrated that the line of centres of calcification have a restricted range of oxygen isotopic variation compared to the large amplitude found for the surrounding fibres. The carbon isotopes showed ^{13}C-depleted values and also large amplitudes of variation (up to 10 ‰) related to the microstructures. The LCC were characterised by ^{13}C-depleted values, between -10 and -14 ‰. C and O isotopic compositions were positively correlated.

$\delta^{18}O$ variations in the coral skeleton could be due to a combination of two different processes: (1) isotopic equilibrium calcification with a pH variation of at least one

unit in the calcifying fluid as revealed also by microsensor measurements in living corals and (2) kinetic fractionation. The combination of these two processes could be a pH dependent kinetic fractionation as proposed for Foraminifera.

For carbon isotopes, the isotopic disequilibrium observed between inorganic aragonite and coral skeleton results from the mixing of two DIC sources, seawater DIC and metabolic CO_2. In *Lophelia pertusa*, the calculated $\delta^{13}C$ value for metabolic CO_2 is about -25 ‰ and represents probably the main source of carbon associated with the LCC. $\delta^{13}C$ values of surrounding fibres result from an enrichment in ^{13}C of the DIC pool either by light C uptake associated with LCC mineralization or a higher proportion of seawater DIC.

This study underlines the role of microstructural differences in biogenic carbonates. A better understanding of the spatial relations between the elements (majors, traces and isotopes) is required to use the geochemical characteristics of biogenic carbonates in ocean and paleoclimatic sciences.

Acknowledgements

References

Adkins JF, Cheng H, Boyle EA, Druffel ERM, Edwards RL (1998) Deep-sea coral evidence for rapid change in ventilation of the deep North Atlantic 15,400 years ago. Science 280: 725-728

Adkins JF, Boyle EA, Curry WB, Lutringer A (2003) Stable isotopes in deep-sea corals and a new mechanism for "vital effects". Geochim Cosmochim Acta 67: 1129-1143

Al-Horani FA, Al-Moghrabi SM, de Beer D (2003) Microsensor study of photosynthesis and calcification in the scleractinian coral, *Galaxea fascicularis*: active internal carbon cycle. J Exper Mar Biol Ecol 288: 1-15

Al-Moghrabi SM, Al-Horani FA, de Beer D (2001) Calcification by the scleractinian coral *Galaxea fascicularis*: direct measurements on calicoblastic layer using microsensors. Proc 8th Int Symp Biomineralization, p 45

Bett B (2001) UK Atlantic margin environmental survey: introduction and overview of bathyal benthic ecology. Cont Shelf Res 21: 917-956

Blamart D, van Weering TCE, Ayliffe L, Labeyrie L, Lutringer, A, Vonhof HB, Ganssen G (2000) Modern NE Atlantic Ocean cold water coral characteristics. EOS Trans AGU, 81: 640

Cheng H, Adkins JF, Edwards RL, Boyle EA (2000) U-Th dating of deep-sea corals. Geochim Cosmochim Acta 64: 2401-2416

Cohen A, Layne GD, Hart SR, Lobel PS (2001) Kinetic control of skeletal Sr/Ca in a symbiotic coral: implications for the paleotemperature proxy. Paleoceanography 16: 20-26

Cuif JP, Dauphin Y (1998) Microstructural and physico-chemical characterisation of centres of calcification in septa of some scleractinian corals. Paläont Z 72: 257-270

Cuif JP, Dauphin Y, Doucet J, Salome M, Susini J (2003) XANES mapping of organic sulphate in three scleractinian coral skeletons. Geochim Cosmochim Acta 67: 75-83

De Chambost E (1997) User's Guide for Multicollector Caméca IMS 1270. Caméca, Courbevoie, France

Deloule E, Chaussidon M, Allé P (1992) Instrumental limitations for isotope measurements with a Caméca IMS-3f ion microprobe: Example of H, B, S and Sr. Chem Geol 101: 187-192

Emiliani C, Hudson JH, Shinn EA, George RY (1978) Oxygen and carbon isotopic growth record in a reef coral from the Florida Keys and a deep-sea coral from Blake Plateau. Science 202: 627-629

Frank N, Paterne M, Ayliffe LK, van Weering T, Henriet J P, Blamart D (2004) Eastern North Atlantic deep-sea corals: Tracing upper intermediate water $\Delta^{14}C$ during the Holocene. Earth Planet Sci Lett 219: 297-309

Frank N, Lutringer A, Paterne M, Blamart D, Henriet JP, van Rooij D, van Weering T (2005) Deep-water corals of the northeastern Atlantic margin: carbonate mound evolution and upper intermediate water ventilation during the Holocene. In: Freiwald A, Roberts JM (eds) Cold-water Corals and Ecosystems. Springer, Berlin Heidelberg, pp 113-133

Freiwald A (2002). Reef-forming cold-water corals. In: Wefer G, Billett D, Hebbeln D, Jørgensen BB, Schlüter M, van Weering T (eds) Ocean Margin Systems. Springer, Berlin Heidelberg, pp. 365-385

Freiwald A, Henrich R, Pätzold J (1997) Anatomy of a deep-water coral reef mound from Stjernsund, West Finnmark, northern Norway. SEPM Spec Publ 56: 141-161

Furla P, Galgani I, Durand I, Allemand D (2000) Sources and mechanisms of inorganic carbon transport for coral calcification and photosynthesis. J Exper Biol 203: 3445-3457

Gaffey S (1988) Water in skeletal carbonates. J Sediment Petrol 58: 397-414

Gladfelter EH (1982) Skeletal development in *Acropora cervicornis*: I. Patterns of calcium carbonate accretion in the axial corallite. Coral Reefs 1: 45-51

Grehan AJ, Unnithan V, Olu-Le Roy K, Opderbecke J (in press) Fishing impacts on Irish deep-water coral reefs: making the case for coral conservation. In: Barnes P, Thomas J (eds) Proceedings of the Symposium on Effects of Fishing Activities on Benthic Habitats: Linking Geology, Biology, Socioeconomics and Management. Amer Fish Soc

Hidaka M (1991) Fusiform and needle-shaped crystals found on the skeleton of a coral, *Galaxea fascicularis*. In: Sugo S, Nakaharo H (eds) Mechanism and physiology of biomineralization in biological systems. Springer, Berlin Heidelberg, pp 139-143

Ireland T (1995) Ion microprobe mass spectrometry: techniques and applications in cosmochemistry, geochemistry, and geochronology. Adv Anal Geochem 2: 1-118

Land LS, Lang JC, Barnes DJ (1975) Extension rate: a primary control on the isotopic composition of West Indian (Jamaican) scleractinian reef coral skeletons. Mar Biol 33: 221-233

Le Tissier M d'A (1988) Diurnal pattern of skeleton formation in *Pocillopora damicornis* (Linnaeus). Coral Reefs 7: 81-88

Lutringer A (2002) Validation d'un nouvel outil pour le traçage de la variabilité des eaux intermediaries. Les coraux profonds. Master Univ Paris XI, 33 pp

Mahon KI, Harrison TM, McKeegan KD (1998) The thermal and cementation histories of a sandstone petroleum reservoir, Elk Hills, California. Part 2: *In situ* oxygen and carbon isotopic results. Chem Geol 152: 257-271

Malakoff D (2003) Cool corals become a hot topic. Science 299: 195

McConnaughey T (1989) ^{13}C and ^{18}O isotopic disequilibrium in biological carbonates: II. In vitro simulation of kinetic isotope effects. Geochim Cosmochim Acta 53: 163-171

McConnaughey T (2003) Sub-equilibrium oxygen-18 and carbon-13 levels in biological carbonates: carbonate and kinetic models. Coral Reefs 22: 316-327

McCrea JM (1950) On the isotopic chemistry of carbonates and a paleotemperature scale. J Chem Phys 18: 849-857

Meibom A, Stage M, Wooden J, Constantz BR, Dunbar RB, Owen A, Grumet N, Bacon CR, Chamberlain CP (2003) Monthly Strontium/Calcium oscillations in symbiotic coral aragonite: biological effects limiting the precision of the paleotemperature proxy. Geophys Res Lett 33: 1418. DOI 1029/2002GL016864

Mikkelsen N, Erlenkeuser H, Killingley JS, Berger WH (1982) Norwegian corals: radiocarbon and stable isotopes in *Lophelia pertusa*. Boreas 11: 163-171

Mortensen PB, Rapp HT (1998) Oxygen and carbon isotope ratios related to growth line pattern in skeletons of *Lophelia pertusa* (L) (Anthozoa, Scleractinia): implications for determination of linear extension rates. Sarsia 83: 433-446

Newton CR, Mullins HT, Gardulski AF, Hine AC, Dix GR (1987) Coral mounds on the West Florida slope: unanswered questions regarding the development of deep-water banks. Palaios 2: 359-367

Ogilvie M (1896) Microscopic and systematic study of madreporarian types of corals. Phil Trans R Soc London 187(B): 83-345

Rollion-Bard C (2001) Variabilité des isotopes de l'oxygène dans les coraux *Porites*: développement et implications des microanalyses d'isotopes stables (B, C et O) par sonde ionique. PhD Thesis, Inst Polytech Lorraine, Nancy, France, 165pp

Rollion-Bard C, Blamart D, Cuif JP, Juillet-Leclerc A (2003a) Microanalysis of C and O isotopes of azooxanthellate and zooxanthellate corals by ion microprobe. Coral Reefs 22: 405-415

Rollion-Bard C, Chaussidon M, France-Lanord C (2003b) pH control on oxygen isotopic composition of symbiotic corals. Earth Planet Sci Lett 215: 275-218

Slodzian G, Daigne B, Girard F, Boust F (1987) High sensitivity and high spatial resolution ion probe instrument. In: Benninghoven A, Huber AM, Werner HW (eds) Secondary Ion Mass Spectrometry SIMSVI. Wiley & Sons, Chichester, pp 189-192

Smith JE, Risk MJ, Schwarcz HP, McConnaughey TA (1997) Rapid climate change in the North Atlantic during the Younger Dryas recorded by deep-sea corals. Nature 386: 818-820

Smith JE, Schwarcz HP, Risk MJ, McConnaughey TE, Keller N (2000) Paleotemperatures from deep-sea corals: overcoming "vital effects". Palaios 15: 25-32

Spero HJ, Bijma J, Lea DW, Bemis BE (1997) Effect of seawater carbonate concentration on foraminiferal carbon and oxygen isotopes. Nature 390: 497-500

Spiro B, Roberts M, Gage J, Chenery S (2000) ^{18}O/^{16}O and ^{13}C/^{12}C in ahermatypic deep-sea water coral *Lophelia pertusa* from the North Atlantic: a case of disequilibrium isotope fractionation. Rapid Commun Mass Spectrom 14: 1332-1336

Swart PK (1983) Carbon and oxygen isotope fractionation in scleractinian corals: a review. Earth Sci Rev 19: 51-80

Urey HC, Lowenstam HA, Epstein S, McKinney CR (1951) Measurements of paleotemperatures and temperatures of the Upper Cretaceous of England, Denmark, and the southeastern United States. Bull Geol Soc Am 62: 399-416

Usdowski E, Hoefs J (1993) Oxygen isotope exchange between carbonic acid, bicarbonate, carbonate, and water: a re-examination of the data of McCrea (1950) and an expression for the overall partitioning of oxygen isotopes between the carbonate species and water. Geochim Cosmochim Acta 57: 3815-3818.

Usdowski E, Michaelis J, Böttcher ME, Hoefs J (1991) Factors for the oxygen isotope equilibrium between aqueous and gaseous CO_2, carbonic acid, bicarbonate, carbonate, and water (19°C). Z Phys Chem 170: 237-249

Vengosh A, Kolodny Y, Starinsky A, Chivas AR, McCulloch MT (1991) Coprecipitation and isotopic fractionation of boron in modern biogenic carbonates. Geochim Cosmochim Acta 55: 2901-2910

Van Weering T, shipboard scientific party (1999) Shipboard cruise report R.V. Pelagia 64PE143: A survey of carbonate mud mounds of Porcupine Bight and S. Rockall Trough margins. NIOZ, Texel, 82 pp

Wainwright SA (1963) Skeletal organization in the coral *Pocillopora damicornis*. Quart J Microscop Sci 104:169-183

Weber JN (1973) Deep-sea scleractinian coral: isotopic composition of skeleton. Deep-Sea Res 20: 901-909

Wefer G, Berger WH (1991) Isotope paleontology: growth and composition of extant calcareous species. Mar Geol 100: 207-248

Wells JW (1956) Scleractinia. In: Moore RC (ed) Treatise on Invertebrate Paleontology. F. Coelenterata. Geol Soc Amer, Univ Kansas Press, Lawrence, pp 353-367

Wilson JB (1979) The distribution of the coral *Lophelia pertusa* (L.) [*L. prolifera* (Pallas)] in the North East Atlantic. J Mar Biol Assoc UK 59: 149-164

Zeebe RE (1999) An explanation of the effect of seawater carbonate concentration on foraminiferal oxygen isotopes. Geochim Cosmochim Acta 63: 2001-2007

Investigations of age and growth for three deep-sea corals from the Davidson Seamount off central California

Allen H. Andrews[1], Gregor M. Cailliet[1], Lisa A. Kerr[1], Kenneth H. Coale[1], Craig Lundstrom[2], Andrew P. DeVogelaere[3]

[1] Moss Landing Marine Laboratories, 8272 Moss Landing Road, Moss Landing, CA 95039, USA
(andrews@mlml.calstate.edu)
[2] Department of Geology, University of Illinois, Urbana Champaign, 255 Natural History Building, 1301 West Green Street, Urbana, IL 61801, USA
[3] Monterey Bay National Marine Sanctuary, 299 Foam Street, Monterey, CA 93940, USA

Abstract. A recent biological characterization of the Davidson Seamount off central California using a remotely operated vehicle revealed communities rich with deep-sea corals. During this characterization several corals were collected and three colonies were made available for an age and growth study. The colonies examined were identified as bubblegum coral (*Paragorgia* sp.), bamboo coral (*Keratoisis* sp.), and precious coral (*Corallium* sp.). Age was estimated from growth zone counts made in skeletal cross sections. These age estimates were used to estimate growth rates and colony age. Estimated growth rates determined for each species were quite different. The bubblegum coral had a relatively high estimated growth rate, with the precious and bamboo coral estimated as slow growing. These age and growth observations were evaluated relative to published studies on related species and an attempt was made to validate the age and growth estimates with an independent radiometric ageing technique (i.e., lead-210 dating). This approach was not successful for the bubblegum coral, and was successful for the bamboo and precious corals to differing degrees. For the bamboo coral, a minimum colony age of over 200 years was determined. For the precious coral, a linear growth rate of approximately 0.25 cm/yr led to a colony age of about 115 years; however, based on the radial growth rate, an age of up to 200 year is possible.

Keywords. Octocoral, *Paragorgia*, *Corallium*, *Keratoisis*, Davidson Seamount, age, growth, radiometry, lead-210, radium-226

Introduction

Deep-sea corals can provide high relief habitat that is ecologically diverse and intrinsically valuable. The coral habitats are inhabited by assemblages of species of invertebrates and fishes that are often unique, many of which have yet to be discovered and described (Fosså et al. 2002; Krieger and Wing 2002). The value of the deep-sea environment created by corals is often related to some form of benefit to humans, like essential fish habitat, but it should also be considered important from a perspective of world heritage because these living habitats are very fragile. Once these communities are disturbed or removed, many of the corals and the habitat they create may not recover within our lifetime (Andrews et al. 2002b). With many fish stocks on the decline, there is increasing utilization of deep-water habitat for fishing purposes. The impact to corals by fishing activity is increasing worldwide and has been devastating in some cases (Auster and Langton 1999; Koslow et al. 2000). It is essential that these habitats, especially those that have not been impacted, be identified, conserved, and studied in more detail before irreversible damage occurs. This requirement has been recognized internationally with conservation efforts, such as the preservation of the Darwin Mounds off the United Kingdom and the efforts of nongovernmental agencies like the Ecology Action Center, the Marine Conservation Biology Institute, and Oceana (Breeze et al. 1997; Roberts and Hirshfield 2003; Morgan et al. 2005).

Information about the life history of habitat forming corals, such as age, growth, and longevity, is necessary before their sensitivity and their importance as fisheries habitat can be fully understood. Age determination studies to date have found that deep-sea corals, as well as some of the associated fishes, can attain ages that are on the order of a hundred to perhaps thousands of years (Druffel et al. 1990; Rogers 1999; Cheng et al. 2000; Andrews et al. 2002a, b). Age and growth of deep-sea corals is typically determined from outgrowth studies in the field, growth zone counts in the skeletal structure, a radiometric technique (e.g., lead-210 dating), or a combination of these methodologies.

Lead-210 dating is a radiometric technique that utilizes the radioactive decay of lead-210 that has been isolated from the environment (i.e., incorporated into the skeletal structure of coral) as a natural chronometer (Dodge and Thomson 1974). The approach is analogous to sedimentation rate studies (Lewis et al. 2002). Because the rate of decay for lead-210 is well known (half-life of 22.26 yr), measurements of radioactivity throughout a skeletal structure (young to old) can be used as a natural chronometer. Lead-210 is incorporated into the skeletal matrix at the time of formation; younger growth accretes over the oldest portion of the skeleton and the activity of lead-210 decreases to a point where it is supported by radium-226, a naturally occurring calcium analog. Note that this system is dependent upon the incorporation of lead-210 that is in excess of supported levels from radium-226, this is easily established by measuring lead-210 in the youngest material (i.e., skeleton near the actively growing margin). By taking a series of measurements from near the actively growing margin to parts of the skeleton that are buried deeper by layers of growth, the decrease of lead-210 activity can be used as an independent indicator

of age and growth. This approach is useful to about 100 years of age at which time the activity of lead-210 decreases to a level approaching the activity of radium-226, nearing an equilibrium activity ratio.

The focus of this study was to investigate the age and growth of corals collected from biological characterization surveys of the Davidson Seamount. This seamount is located in the northeastern Pacific Ocean, 120 kilometers to the southwest of Monterey, California. At 42 kilometers in length it is one of the largest seamounts along the western coast of the United States. The Davidson Seamount is 2400 m from base to crest and 1250 m below the sea surface. It has an atypical seamount shape, having northeast-trending ridges created by a type of volcanism only recently described (Davis et al. 2002). At least 20 different corals were identified at this location (DeVogelaere et al. 2005). Three coral colonies typical of the faunal diversity of the surveyed region were collected, the bubblegum coral (*Paragorgia* sp.), bamboo coral (*Keratoisis* sp.), and precious coral (*Corallium* sp.). The first goal was to verify the initial taxonomic identifications of the specimens and determine if specific identifications could be made. The second goal was to investigate age estimation using quantification of growth zones visible in skeletal cross sections from each species. These age and growth observations were evaluated relative to other studies on similar species and an attempt was made to validate the age and growth estimates with an independent radiometric ageing technique (i.e., lead-210 dating).

Materials and methods

Specimen habitat, collection and identification

Coral specimens were collected from the Davidson Seamount during a collaborative survey led by the Monterey Bay National Marine Sanctuary on May 17-24, 2002. Three of the coral species collected were made available for age and growth analyses: 1) bubblegum coral (*Paragorgia* sp.) collected from 1313 m, 2) bamboo coral (*Keratoisis* sp.) collected from 1425 m, and 3) precious coral (*Corallium* sp.) collected from 1482 m. Each coral resided on rocky outcrops and were collected using the Monterey Bay Aquarium Research Institute ROV *Tiburon* from the Davidson Seamount (near 35º45'N/122º42'W) in water that was about 2.5ºC with a salinity of about 34.5 ppt. Specimens were stored frozen until used in the age determinations. The bubblegum coral was a fully intact colony that measured 80 cm from base to the furthest tip along the main axis. The bamboo coral was very fragmented and only sections of the colony were intact. The precious coral was very brittle and in excellent condition, measuring 29 cm in length along the primary axis to the furthest point on the colony from the base. Coral specimens were identified to genus, with a qualified identification to species, by three cnidarian taxonomists.

Age estimation

Each skeletal structure was sectioned with a hacksaw, razor blade, or Dremel® tool. The bubblegum coral had a soft axial skeleton that was cut initially with

either a hacksaw (thick sections of the trunk) or a utility razor blade. Sections from the bamboo and precious coral were extracted with a Dremel® tool or hacksaw (thick base on bamboo coral) and were smoothed with a lapidary wheel. Sections were air dried and mounted to glass with Cytoseal® for viewing with a dissecting microscope. Sections were taken from several locations along the axial skeleton ranging from near the base to near the tip of each colony. To investigate internal structure and growth zones in the bamboo coral, the organic nodes were also thinned and mounted to glass slides. Magnification was varied from low to high to cover all possibilities of growth zone size and resolution for each species. Estimates of age were made from any quantifiable growth zones seen in the sections and an estimated growth rate and colony age was made based on this information. Magnification ranged from the unaided eye to 40 times, depending on the specimen, using an Olympus dissecting microscope.

Lead-210 dating

Adjacent to each section, a small core (center of the skeletal structure) was removed for lead-210 and radium-226 analyses. The decay of exogenous (unsupported) lead-210 over the length of the skeletal structures was used in an attempt to determine an independent growth rate with the possibility of validating age estimation from growth zone counts. For samples with age estimates that exceeded the utility of this method (about 100 years), the use of lead-210:radium-226 equilibrium was used to establish a minimum colony age. This process involved the measurement of lead-210 *via* alpha-spectrometry and radium-226 *via* thermal ionization mass spectrometry (TIMS). For each species, the first assay involved analyzing two sections for growth zone counts and two core samples to evaluate lead-210 and radium-226 levels. Based on the findings for each species, additional sections and core samples were taken to better establish possible trends. The determination of lead-210 and radium-226 were based on previously established protocol (Andrews et al. 1999; Andrews et al. 2002b).

Bubblegum coral

Six segments, 2 cm in length, were extracted adjacent to each location where aged sections were taken (Fig. 1). These segments were cored with a razor blade to a 4-5 mm center portion. These cores were cleaned, dried, weighed, and dissolved for radiochemical analyses.

Bamboo coral

The core material of two segments, adjacent to the first two aged sections near the base of the colony was extracted using a milling machine. The powdered sample was dried, weighed, and dissolved for radiochemical analyses. In a younger section, toward the upper part of the colony (Fig. 2), three additional segments were analyzed whole (not cored); coring was not possible in these thin, tubular segments. Because of these constraints a general pattern of decreasing overall lead-210 was targeted to determine if lead-210 dating would be possible and if a method could be developed to extract core material. The youngest sample consisted of two

skeletal tips that were separated from the colony. These segments were measured in diameter, cleaned, dried, weighed, and dissolved for radiochemical analyses.
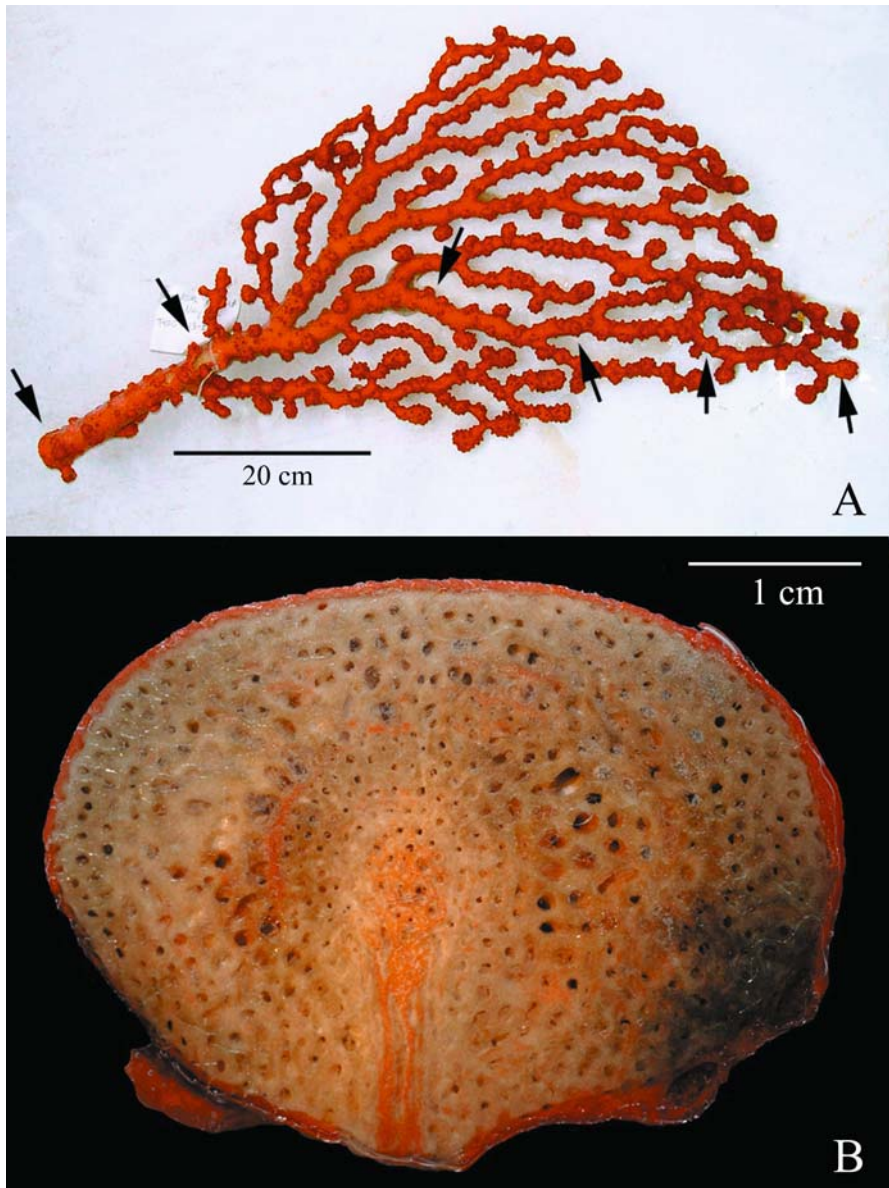
Fig. 1 Photograph of the bubblegum coral (*Paragorgia* sp.) used in this study with the locations of the six segments (used for radiochemical analyses) and sections (used to estimate age from growth zones) marked with arrows (**A**). The length of the colony on its longest axis was 80 cm. The section taken at the colony base (**B**) was estimated for age from what appears to be a concentric orientation of the pores radiating from the center

Precious coral

Five segments of the precious coral colony were analyzed; two from older and thicker parts of the skeleton, two from a thin branch (Fig. 3), and one sample consisting of a collection of tips from all over the colony. All were cored to a 1-2 mm diameter segment, except for the tips, which remained whole. Tips, the most recent growth of the skeletal structure, were collected from various branches in the colony to obtain enough material for the analysis. Because new branches can
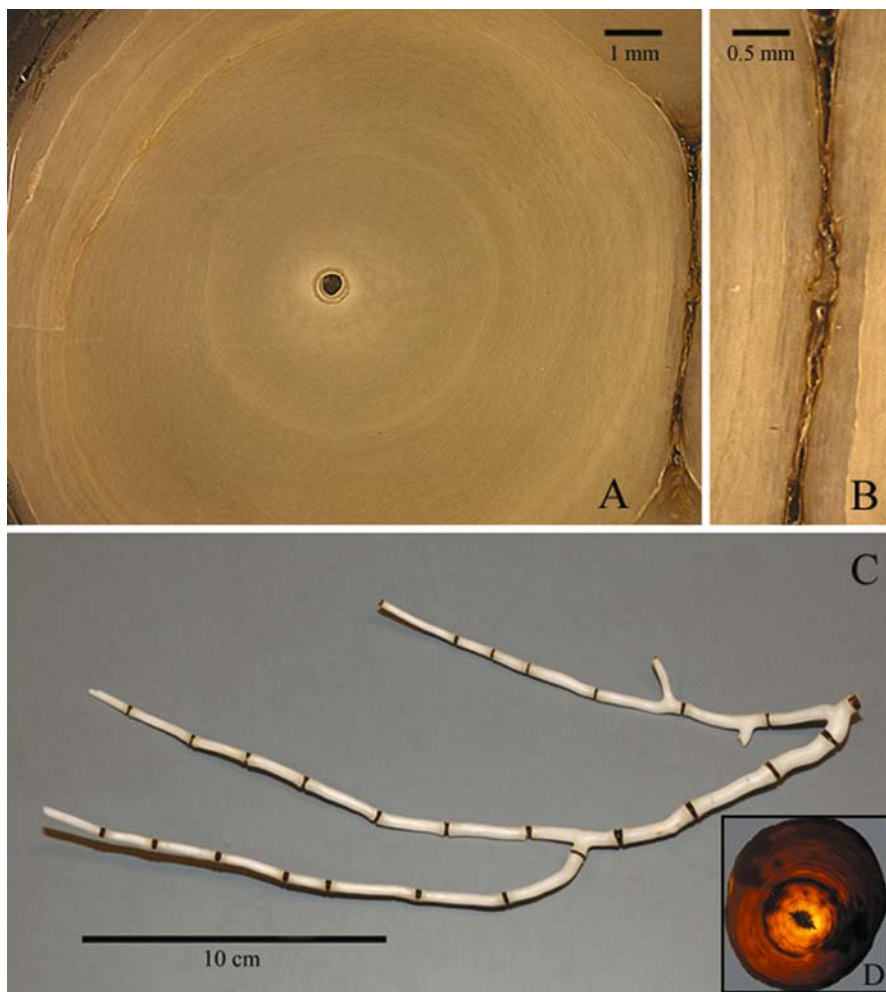
Fig. 2 A composite of images for the bamboo coral (*Keratoisis* sp.) used in this study. A section near the base of the colony (**A**) was very difficult to interpret, having a woven or braided appearance to most of the visible zones. Small regions of this section (**B**) that were clearer than most were used to estimate age. The upper portion of the colony (**C**) was used to investigate other approaches to age estimation and validation. The organic node (**D**) seemed to show the most promise for age estimation from growth zone counts. The diameter of this section was 3 mm
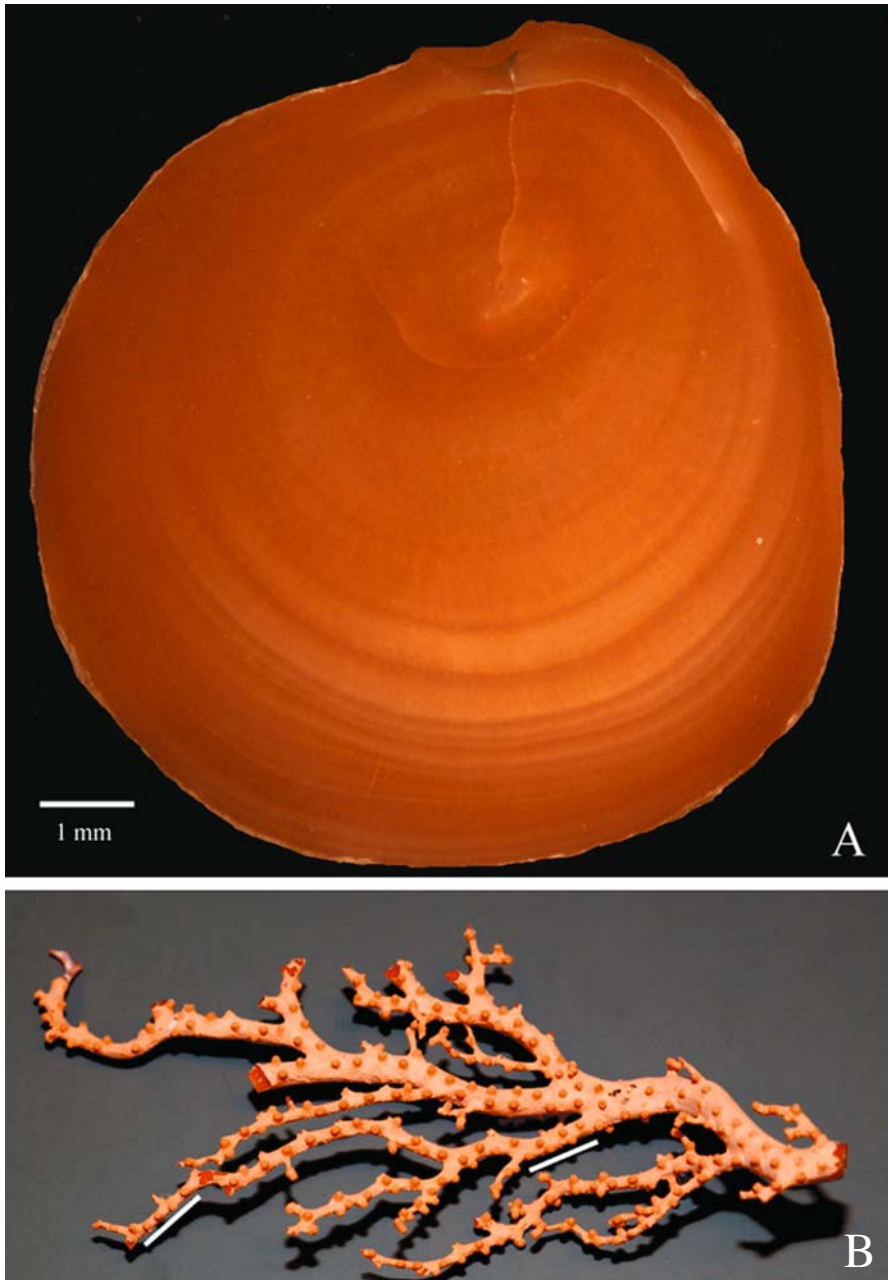
Fig. 3 The growth zones visible in cross sections of the precious coral (*Corallium* sp.) were variable in thickness and counts were subjective (**A**). Based on the radiometric results for the segments near the base (samples 4 and 5), a thinner branch was selected (**B**) from part of the colony for further analyses and age validation with lead-210 dating. Samples 2 and 3 are delineated with a white bar

start on older segments, a relationship between segment diameter and colony length between the segments (slope = 5.97) was used to determine the approximate distance the tips would have been from the younger of the two older segments (~8.9 cm). This necessitated the assumption that once a segment begins growing it continues to grow and that there is a linear relationship between skeletal diameter and colony length (analogous to tree growth). These samples were cleaned, dried, weighed, and dissolved for radiochemical analyses.

Results

Species identification

Coral specimens were identified to genus, with a qualified identification to species, by three cnidarian taxonomists. The determination of deep-water corals to species is not well defined and is a work-in-progress for all experts in the field. Initial identification of each species at the time of collection was 1) gorgonian coral (*Paragorgia* sp.), 2) bamboo coral and, 3) precious coral. Taxonomists confirmed the genus of the gorgonian coral as *Paragorgia*, and indicated that it might be *Paragorgia pacifica* based on branch size (Bruce Wing, Curator at Auke Bay Laboratory, NMFS, Juneau, AK, pers. comm.), but could be a smaller colony of *P. arborea*. In general, the literature is poor for the west coast fauna and revisions in coral taxonomy are required (Gary Williams, Curator at the California Academy of Sciences, San Francisco, CA, pers. comm.). The bamboo coral was identified as a *Keratoisis* sp., possibly *Keratoisis profunda*, the only species listed for the northeastern Pacific Ocean (Bruce Wing and Dr. Gary Williams, pers. comms.). The precious coral was identified as a member of the genus *Corallium* (Stephen Cairns, Curator at Smithsonian Institution, Washington D.C., pers. comm.). Several species have been identified from the Pacific Ocean (Bayer 1996) and this specimen might be *C. regale*; however, the taxonomy of this genus is a work-in-progress and needs a re-evaluation considering two additional species, *C. imperiale* and *C. sulcatum* (Frederick Bayer, Smithsonian Institution, Washington D.C., pers. comm.). Most *Corallium* sp. have been described from latitudes further south than the location on the Davidson Seamount (35º45'N); however, recent collection of a *Corallium imperiale* was made at the Patton Seamount (54ºN, 1750-1850 m; Amy Baco-Taylor, Biology Department, Wood's Hole Oceanographic Institution, Wood's Hole, MA, pers. comm.). Samples from each colony have been accessioned to the California Academy of Sciences, Department of Invertebrate Zoology and Geology, Golden Gate Park, San Francisco, CA 94118 and the Smithsonian Institution, National Museum of Natural History, Department of Systematic Biology - Invertebrate Zoology, Washington D.C. 20013.

Age estimation

Bubblegum coral

Of the six skeletal cross sections taken along the main axis, spanning the tip to the base of the 80 cm colony (Fig. 1A), growth zones were visible at low or

no magnification. The porous nature of the skeleton made what appeared to be concentric zones of pores. Age was estimated from these concentric zones, which were more visible when viewed slightly out of focus. Estimated age at the base of the colony was 9 to 14 years (Fig. 1B). Based on these age estimates and the distance along the axis to the tip, a growth rate of 6 to 9 cm/year was estimated. Additional sections taken between the base and tip supported this finding; however, the counting of these growth zones was very subjective and should be interpreted with caution.

Bamboo coral

The growth zones visible throughout the bamboo coral section were too complex and low in contrast to be enumerated, typically having a woven or braided appearance (Fig. 2A). Therefore, growth zones visible in parts of the section near the base of the colony were used to extrapolate an age for the section and colony. Better-defined portions of the skeleton at the joint between two branches and in another location were used to determine a growth zone width of 0.05-0.11 mm/zone (Fig. 2B). The measured radius of the basal section was 8 to 11 mm, leading to an estimated age for the section of 80 to 220 years, assuming the zones are formed annually and that the pattern or rate is similar throughout. The other portion of the basal section was near the edge of the colony where 16 zones were visible in 1 mm of radius. Based on the calculated radial growth, the estimated age of the second section taken in the colony (5.6-6.5 mm radius) was 56 to 131 years. With a distance of 24.5 cm between sections, a linear growth rate of 0.19 to 0.44 cm/year was estimated.

Additional sections were taken toward the tip of the colony because of the high estimated age of the older sections and the radiometric findings, which are discussed later (Fig. 2C). Estimating age at the nodes looked the most promising. Growth zones were clearly visible, but variable in width. Age estimates from the cleanest section were about 60 years; however, age estimates varied considerably and depended on magnification and growth zone interpretation (Fig. 2D). Based on the calculated radial growth rate from the basal section, the age for these sections would be between 30 and 60 years old. The findings from the node supported the slower growth rate.

Precious coral

Two skeletal cross sections were extracted from the precious coral colony, separated by 15.7 cm. Each section was aged, but growth zones were poorly defined and variable in width. Age was subjectively assigned to both sections. The thickest section was aged at 20 to 21 years (Fig. 3A). The smaller section was aged at 3 to 7 years. Based on the separation between these sections and the extremes of age the estimated growth rate was 0.9 to 1.1 cm/yr. Given this estimate is accurate and we assume a constant growth rate for the 29 cm colony, the overall age of the colony age would be about 30 yr.

Lead-210 dating

For each species the radiochemical analyses and results varied considerably (Table 1). In most cases a small core (center of the skeletal structure) was removed

for lead-210 and radium-226 analyses, with the intent of using either exogenous (unsupported) lead-210 over the length of the skeletal structures to determine a growth rate or the use of lead-210:radium-226 equilibrium as an indicator of a minimum colony or segment age (approximately 100 years).

Bubblegum coral

The activity of lead-210 tended to increase slightly from near the tip to the base for the six segments (range of 1.12 ± 6.5 % to 1.61 ± 3.9 % dpm/g; Table 1). Radium-226, however, was not consistent between the base and tip and differed by a factor of about two (0.649 ± 1.7 % to 1.33 ± 1.4 % dpm/g). The resultant lead-210: radium-226 ratios ranged from 1.2 to 1.9, hence exogenous lead-210 was present in the skeletal system of this species. Because of the inconsistent pattern of lead-210 and radium-226 activity, however, it was not possible to determine a growth rate from the decay of exogenous lead-210.

Bamboo coral

Measurement of lead-210 and radium-226 in the first two aged sections, near the base of the colony (sample numbers 4 and 5), resulted in activity ratios that were near equilibrium (Table 1). Lead-210 levels were similar (0.248 ± 6.3 % and

Table 1 Radiometric data for three corals organized by sample number from the tip to near the base of each colony. Activity for lead-210 and radium-226 was expressed as disintegrations per minute per gram of sample material

Coral	Sample number	Lead-210 (dpm/g) activity ± % error[1]	Radium-226 (dpm/g) activity ± % error[1]	210/226 ratio (error range)
Bubblegum	1 (tip)	1.26 ± 4.1	0.649 ± 1.7	1.9 (1.8-2.1)
(*Paragorgia* sp.)	2	1.12 ± 6.5	n/m[2]	n/a
	3	1.27 ± 6.9	n/m[2]	n/a
	4	1.57 ± 6.7	n/m[2]	n/a
	5	1.51 ± 7.1	n/m[2]	n/a
	6 (basal)	1.61 ± 3.9	1.33 ± 1.4	1.2 (1.1-1.3)
Bamboo	1 (tip)	0.560 ± 10.4	0.228[3]	2.5
(*Keratoisis* sp.)	2	0.533 ± 6.1	0.228[3]	2.3
	3	0.517 ± 5.2	0.228[3]	2.3
	4	0.248 ± 6.3	0.266 ± 8.0	0.9 (0.8-1.1)
	5 (basal)	0.267 ± 10.4	0.190 ± 20[4]	1.4 (1.0-1.9)
Precious	1 (tip)	0.566 ± 5.6	0.273[3]	2.1
(*Corallium* sp.)	2	0.429 ± 11.4	0.273[3]	1.6
	3	0.361 ± 7.7	0.273[3]	1.3
	4	0.248 ± 4.5	0.278 ± 8.8	0.9 (0.8-1.0)
	5 (basal)	0.288 ± 4.2	0.268 ± 7.2	1.1 (1.0-1.2)

[1] Sigma (SD) expressed as a percentage.
[2] Not measured or calculated.
[3] Average of samples 4 and 5 for each respective species.
[4] High error associated with low radium recovery; may be an unreliable run.

0.267 ± 10.4 % dpm/g), with radium-226 differing slightly (0.190 ± 20 % and 0.266 ± 8 % dpm/g). The resultant lead-210:radium-226 ratios ranged from 0.9 to 1.4 with a margin of error that encompassed a ratio of one (equilibrium). Hence, these segments were in or near equilibrium. For sample number 5, low recovery of radium-226 made the assumption of equilibrium more subjective (1.0 to 1.9). Presumably the value of radium-226 was closer to the measured value of sample number 4 (0.266 ± 8.0 %). This is supported by the position of the sample in an older portion of the colony, constrained by the finding of equilibrium for sample 4. Hence, we subjectively conclude that this section of the colony was more than 100 years old. Based on this finding, the decision was made to sample in a thinner, presumably younger, limb of the colony (Fig. 2C).

In the younger limb (sample numbers 1-3), the measured lead-210 activity was highest in the tip segment and decreased in the older segments (0.560 ± 10.4 %, 0.533 ± 6.1 %, 0.517 ± 5.2 % dpm/g; Table 1). These levels were considerably higher than the core material in the basal segments (sample numbers 4 and 5) and the calculated activity ratios (average radium-226 = 0.228 ± 0.054 dpm/g) exceeded 2.0. Hence, exogenous lead-210 was present in the skeletal system of this species. These results indicate lead-210 dating could work for this species, given a method to extract cores from the fragile, tubular segments could be developed. No growth rate was determined for these samples because the samples were whole sections (not cores) and it would require the development of a mass growth rate model with circular reasoning with respect to age.

Precious coral

Results for the two segments near the base of the colony (sample numbers 4 and 5) were similar to that of the basal segments of the bamboo coral (Table 1). Measurement of lead-210 and radium-226 in the core material of these segments resulted in activity ratios that were near equilibrium. Lead-210 levels were similar (0.248 ± 4.5 % and 0.288 ± 4.2 % dpm/g), with radium-226 being very similar (0.268 ± 7.2 % and 0.278 ± 8.8 % dpm/g). The resultant lead-210:radium-226 ratios were 0.9 to 1.1 with a narrow margin of error that encompassed a ratio of one (equilibrium). Hence, these segments were more than 100 years old and the decision was made to collect three samples from thinner, presumably younger, segments of the colony. Two segments were extracted from a thinner limb, and one sample was a collection of the thinnest tips from all over the colony.

For the thinner segments and the tips (sample numbers 1-3), the measured lead-210 activity was highest in the tips and decreased for the segments (0.566 ± 4.6 %, 0.429 ± 11.4 %, 0.361 ± 7.7 % dpm/g; Table 1). These levels were considerably higher than the core material in the basal segments and the calculated activity ratios (average radium-226 = 0.273 ± 0.008 dpm/g) were 2.1, 1.6, and 1.3. Hence, exogenous lead-210 was present in the skeletal system of this species and lead-210 dating was possible and a linear growth model could be applied. Given the distances between samples (measured between the segments and calculated for the tips) relative to the decay of exogenous lead-210, the growth rate of the colony was approximately 0.43 cm/yr (95 % range = 0.25-1.7 cm/yr; Fig. 4). Given this
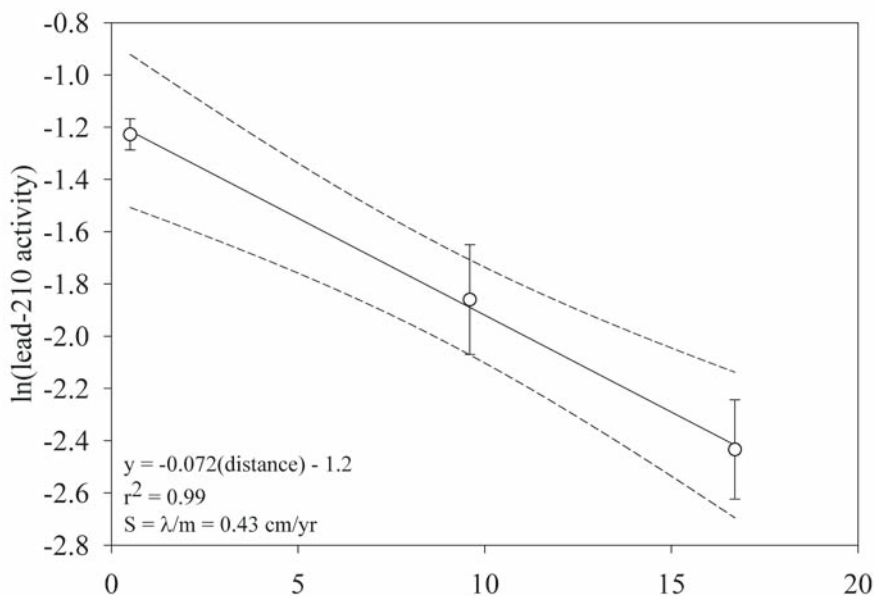
Fig. 4 Plot of exogenous lead-210 activities (total lead-210 activity minus average radium-226 activity) that have been natural log transformed to provide a linear relationship. This relationship was used to determine a growth rate based on the decay of lead-210 over the length on the precious coral colony. Three data points are all that can be plotted because the activities measured in the two segments toward the base (samples 4 and 5) were in equilibrium (lead-210:radium-226 = 1.0)

estimate, and we assume a constant growth rate along the main axis for the 29 cm colony, the overall age of the colony age was about 67 yr (95 % range = 17-116 yr). This presents a possible contradiction relative to the findings in the two older segments because an age of more than 100 years is required to attain lead-210:radium-226 equilibrium. For the oldest of the three thin limb segments (sample number 3), the highest age estimate for the growth rate range (0.25-1.7 cm/yr) from the linear growth model was 63 yr.

To approach the problem from a different perspective, segment diameter was used as an indicator of age. Assuming the second segment from the base was 100 years old (sample number 3), age was related to diameter (4.27 mm) as 23 times the diameter; hence, age was determined for each segment using this relationship and the decay of lead-210 was plotted with these data (Fig. 5). This relationship indicated the colony might have been more than 200 years old.
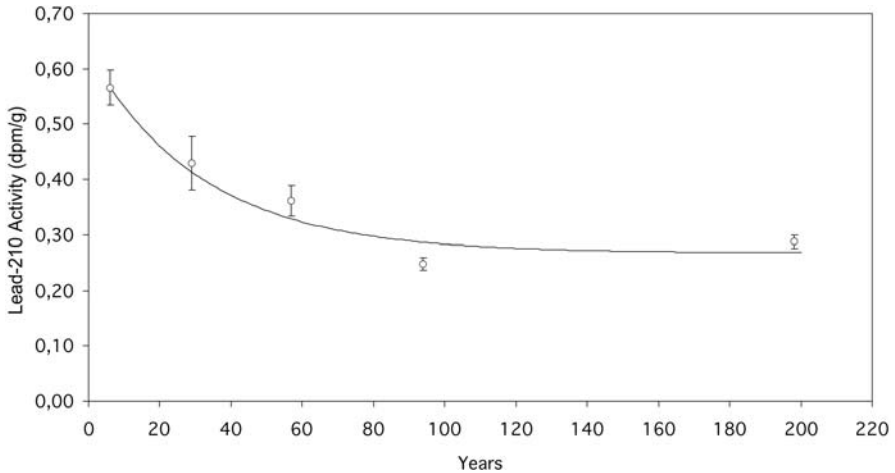
Fig. 5 Plot of age estimated from segment diameter (minus estimated average age of the core material = 6 yr; based on average diameter of 0.5 mm) *versus* the measured total lead-210 activity from all precious coral samples, tips on the right to base on the left. The decay function was driven by initial activity measured in the tips (0.566 dpm/g) with an asymptotic approach to the average lead-210 activity in the two basal segments (samples 4 and 5). The progression of lead-210 decay follows the expected trend, but based on segment diameter the estimated age of the colony could be closer to 200 yr

Discussion

Bubblegum coral

The estimation of age from the growth zones seen in the sections of the bubble gum coral was dubious at best. The pattern of growth used to define growth zones, a series of pores forming concentric arcs, was very different relative to the usual ring pattern identified in calcified structures. When quantified and translated to a linear growth rate, the estimate is relatively high (6-9 cm/yr) compared to other gorgonian species (Andrews et al. 2002b). In some cases, growth rates can be estimated from outgrowth of colonies that settled on a structure of known age. An observation was made for bubblegum coral colonies up to 20 cm in length attached to a telegraph cable known to be 44 years at depth (Davis et al. 2000). Assuming the colony settled shortly after the structure appeared, the growth rate could have been about 0.5 cm/yr, but the rate could be much higher if the timing of settlement occurred later. According to preliminary ^{14}C-dating results, massive colonies collected off New Zealand may have grown at a rate comparable to that calculated here (Dianne Tracy, National Institute of Water and Atmospheric Research Ltd., Wellington, New Zealand, pers. comm.).

The skeletal structure of bubblegum coral is a spongy matrix that is highly organic and may have a cellular component. The presence of tissue throughout the skeleton, and concentrated in the core, that was the same color of the exterior tissue could

mean that the skeleton is not a conserved structure with time. It is possible that the skeletal matrix is regularly reworked, like the cancellous bone of most animals, making the system open to the migration of elements (e.g., lead-210 and radium-226). This is evidenced by the observation that the radiochemical results had no systematic pattern that could be related to growth. Hence, the approach used here did not work for this species and may not work for this kind of skeletal matrix in general. These findings are similar to the results found for the cancellous fin rays of Atlantic sturgeon (*Acipenser oxyrinchus*; Burton et al. 1999) and shark cartilage (Welden et al. 1987).

   One avenue that could be pursued to estimate age and growth is the use of the time specific marker produced by bomb radiocarbon (Kalish 1995). Studies have indicated that shark vertebrae are an open system to lead-210 (Welden et al. 1987); however, the organic matrix is evidently conserved in some species. In a study of porbeagle and mako sharks, the determination of bomb radiocarbon in vertebrae successfully validated the annual formation of growth zones in vertebrae of the porbeagle shark and showed promise of validating age estimates for the mako (Campana et al. 2002). It is possible that the organic portion of the bubblegum coral matrix is conserved in the same manner and that the time specific bomb radiocarbon marker could be used to estimate age, given there are no problems with depth and a phase shift in the timing of bomb radiocarbon signal to the deep-water environment (Kalish 2001).

Bamboo coral

   Initial growth estimates from growth zone counts in the sections taken near the base revealed a possible age range of 80 to 220 years. This estimate, however, was based on an extrapolation of a radial growth rate (0.05-0.11 mm/zone) to the full radius of the section. Because the lead-210:radium-226 activities of the two core samples near the base were in equilibrium, the age of the colony likely exceeded 100 years. This supports the lower growth rate (approximately 0.05 mm/zone) and higher estimated age (131 years) of the second section up from the base. Therefore, the section near the base would be closer to the estimate of 220 years based on the lower growth rate, giving the colony an age of over 200 years. This is similar to the findings of a study on a similar bamboo coral (*Acanella* sp.) collected off San Francisco, California. In that study, the activity of lead-210 was linear (assuming lead-210 and radium-226 were in equilibrium), suggesting the age of the colony was over 100 years (Howard Spero, Department of Geology, University of California, Davis, pers. comm.). In addition, recent carbon-14 work on a coral specimen in the same family (Isididae), collected from the Gulf of Alaska at about 800 m, indicated the age of the colony was about 50 yr. This observation was based on the detection of bomb-produced carbon-14 and its use as a time specific marker. The extrapolated radial growth rate of 0.1 mm/yr was similar to the rate estimated in this study (Roark et al. 2003). In a recent study of *Keratoisis* sp. specimens taken from 1000 m water off southern Australia, the growth rate was 0.05 mm/yr and in agreement with our conclusions, where lead-210 excess and equilibrium values were about half that

recorded in our study (Ron Thresher, CSIRO Marine Research, GPO Box 1538, Hobart, Tasmania 7001 Australia, pers. comm.).

Although age validation of this species using lead-210 dating was not entirely conclusive, this study provides guidance for future studies. Further examination of growth zones in the nodes of this species is necessary. This region seems promising for growth zone counts because zonation patterns were clearly visible and estimated ages were close to expected ages, if the age estimate exceeding 200 years for the colony is correct. It is also apparent that a full study using extracted core material from younger sections (estimated to be less that 100 years old) could prove successful based on the regular decay of total lead-210 in the youngest segments. Because sampling core material proved difficult in this study, an alternative would be to sample along a radial path, as was the case with the precious coral, *Corallium niobe* (Druffel et al. 1990), and *Keratoisis* sp. from off Australia (Ron Thresher, CSIRO Marine Research, GPO Box 1538, Hobart, Tasmania 7001 Australia, pers. comm.).

Precious coral

The estimated linear growth rate from growth zone counts (0.9-1.1 cm/yr), making the colony about 30 years old, falls within the uncertainty associated with the lead-210 dating estimate (0.25-1.7 cm/yr). The existence of segments for which measured lead-210:radium-226 was in equilibrium, however, indicated the age of the colony was over 100 years. In the middle of these estimations was the lead-210 dating results making the colony age approximately 67 years with a range of uncertainty from 17 to 115 yr. These results indicated no conclusion could be made about growth; however, these observations can be explained by discontinuous growth manifested as either halted growth, delayed branching, or both. In this case we assumed that the segments from the younger branch were from a branch that had a delayed start and continuous growth between segments. In addition, we had to assume that the tips collected represented actively growing portions of the colony and that the extrapolated distance to the missing tip for that branch was accurate. The decay of lead-210 in this series of three samples seems to support these assumptions, but age and growth estimates can be further constrained by interrelating the segments in equilibrium with the segments coming into equilibrium *via* cross sectional diameter.

If delayed branching is a problem for the linear growth assumption, then branch diameter should be a better predictor of age. An age of 39 years (range of 9 to 63 years) can be assigned to the younger branch based on the growth rate of 0.43 cm/yr (range of 0.25 to 1.7 cm/yr). Given the younger of the two segments in equilibrium was 4.3 mm in diameter and was at least 100 years old, the age of the younger branch (2.7 mm diameter at its thickest) would necessarily be 64 years old, within the range predicted from the decay of lead-210 (growth rate of 0.25 cm/yr). This implies that delayed branching, as opposed to halted growth, is the explanation for the discrepancy between the two findings (decay *vs*. equilibrium). Note that it is the convergence of 1) a minimum age of about 100 years for equilibrium to

be attained for a given diameter and 2) a maximum age that explains the decay of lead-210 that constrains the calculated growth rates. In conclusion for the precious coral, the findings of this study indicate that 1) the growth zones identified in the cross sections were not formed annually and should not be used as an indicator of age, 2) the linear growth rate of this colony was approximately 0.25 cm/yr with delayed branching, and 3) a diameter growth rate of 0.043 mm/yr. Given constant linear growth along the longest axis, this colony was approximately 115 years old; if however, the growth based on diameter is used to determine age, the age of the colony was in excess of 200 years old.

In further support of the lower growth rate is the potential problem of coring accuracy. Because lead-210 results indicate that the age of the colony is much greater than initially estimated from growth zone counts, the target core of the first few years of growth may have included more recent growth, on the order of a decade or more. Incorporation of younger material would raise the apparent lead-210 activity in segments of the young branch, effectively decreasing the measured decay of lead-210 and artificially increasing the estimated growth rate. Therefore, the lower growth rate estimate would be more accurate. This finding is reflected in the plot of estimated age from branch diameter relative to lead-210 activity where the predicted pattern of lead-210 decay is observed (Fig. 5).

These findings are similar to other studies on precious corals (*Corallium* sp.). In an outgrowth study of *Corallium japonicum* the linear growth rate was measured at about 0.3 cm/yr (Grigg 1974). A more recent age and growth study of the much larger growing *Corallium niobe* was validated using lead-210 dating with a calculated radial growth rate of 0.11 mm/yr (Druffel et al. 1990), higher than the radial growth rate determined in this study (0.043 mm/yr). A calculated linear growth rate for *C. niobe* was 0.45-0.71 cm/yr based on the 1 m height of the colony and its estimated age of 180 ± 40 yr, slightly higher than the linear growth rate estimated here (0.25 cm/yr). In a recent carbon-14 study on a *Corallium* sp. collected from Hawaiian waters at a depth of about 400 m, the radial growth rate was approximately 0.15 mm/yr, leading to an estimated age of about 80 yr for the colony (Roark et al. 2003).

It is apparent from the literature, and this study, that deep-sea corals are typically slow growing with a longevity potential on the order of 100s of years, and that one of the most fundamental and pressing requirements in this field is the development of accurate deep-sea coral taxonomy. The determination of age and growth for bubblegum corals (*Paragorgia* spp.) is inconclusive in this study, as well as in the literature. This group of corals may be one of the fastest growing deep-sea corals, but this is based on subjective observations. Bamboo coral has a unique jointed growth structure that has promising attributes for a full age and growth investigation. The well-calcified segments appear to be conserved with time and contain exogenous lead-210. In addition, the organic nodes appear to have well developed growth zones that may be an accurate indicator of age. The findings for the bamboo coral provide a strong basis for concluding that this species is slow growing and that the colony studied here was over 200 years old. The precious coral provided the most successful results for the lead-210 dating technique in this study. Based of the decay

of lead-210, the colony was about 115 yr (linear growth), but may be as old as 200 yr (radial growth). However, before information in this and any other study can be applied to other deep-sea corals, species identification is necessary. Those working to develop future deep-sea research projects should be mindful of this necessity by incorporating funding for taxonomy as part of the project.

Acknowledgements

References

Andrews AH, Coale KH, Nowicki JL, Lundstrom C, Palacz Z, Burton EJ, Cailliet GM (1999) Application of an ion-exchange separation technique and thermal ionization mass spectrometry to ^{226}Ra determination in otoliths for radiometric age determination of long-lived fishes. Canad J Fish Aquat Sci 56: 1329-1338

Andrews AH, Cailliet GM, Coale KH, Munk KM, Mahoney MM, O'Connell VM (2002a) Radiometric age validation of the yelloweye rockfish (*Sebastes ruberrimus*) from southeastern Alaska. Mar Freshwater Res 53: 139-146

Andrews AH, Cordes E, Mahoney MM, Munk K, Coale KH, Cailliet GM, Heifetz J (2002b) Age and growth and radiometric age validation of a deep-sea, habitat-forming gorgonian (*Primnoa resedaeformis*) from the Gulf of Alaska. Hydrobiologia 471: 101-110

Auster PJ, Langton RW (1999) The effects of fishing on fish habitat. Amer Fish Soc Symp 22: 150-187

Breeze H, Derek DS, Butler M, Kostylev V (1997) Distribution and status of deep-sea corals off Nova Scotia. Marine Issues Comm Spec Publ 1. Ecology Action Center, 58 pp

Burton EJ, Andrews AH, Coale KH, Cailliet GM (1999) Application of radiometric age determination to three long-lived fishes using ^{210}Pb:^{226}Ra disequilibria in calcified structures: a review. Amer Fish Soc Symp, pp 77-87

Campana SE, Natanson LJ, Myklevoll S (2002) Bomb dating and age determination of large pelagic sharks. Canad J Fish Aquat Sci 59: 450-455

Cheng H, Adkins J, Edwards RL, Boyle EA (2000) U-Th dating of deep-sea corals. Geochim Cosmochim Acta 64: 2401-2416

Davis RE, Clague DA, Bohrson WA, Dalrymple GB, Greene HG (2002) Seamounts at the continental margin of California: a different kind of ocean intraplate volcanism. Geol Soc Amer Bulletin 114: 316-333

Davis DS, Hebda A, Pezzack L (2000) Early records of deep sea corals from submarine telegraph cables recovered off Nova Scotia. *Abstract*: First Int Symp Deep Sea Corals. July 30-August 3. Halifax, Nova Scotia, Canada

DeVogelaere AP, Burton EJ, Tonatiuh T, Clague DA, Tamburri MN, Cailliet GM, Kochevar RE, Douros WJ (2005) Deep-sea corals and resource protection at the Davidson Seamount, California, U.S.A. In: Freiwald A, Roberts JM (eds) Cold-water Corals and Ecosystems. Springer, Berlin Heidelberg, pp 1189-1198

Dodge RE, Thomson J (1974) The natural radiochemical and growth records in contemporary hermatypic corals from the Atlantic and Caribbean. Earth Planet Sci Lett 23: 313-322

Druffel ERM, King LL, Belastock RA, Buesseler KO (1990): Growth rate of a deep-sea coral using ^{210}Pb and other isotopes. Geochim Cosmochim Acta 54: 1493-1500

Fosså JH, Mortensen PB, Furevik DM (2002) The deep-water coral *Lophelia pertusa* in Norwegian waters: distribution and fishery impacts. Hydrobiologia 471: 1-12

Grigg RW (1974) Growth rings: annual peridocity in two gorgonian corals. Ecology 55: 876-881

Kalish JM (1995) Radiocarbon and fish biology. In: Secor DH, Dean JM, Campana SE (eds) Recent Developments in Fish Otolith Research. Columbia, South Carolina, Univ South Carolina Press, pp 637-653

Kalish JM (2001) Use of the bomb radiocarbon chronometer to validate fish age. Final Rep FRDC Project 93/109, Fish Res Dev Corp, Canberra, Australia, 384 pp

Koslow JA, Boehlert GW, Gordon JDM, Haedrich RL, Lorance P, Parin N (2000) Continental slope and deep-sea fisheries: implications for a fragile ecosystem. ICES J Mar Sci 57: 548-557

Krieger KJ, Wing B (2002) Megafauna associations with deepwater corals (*Primnoa* spp.) in the Gulf of Alaska. Hydrobiologia 471: 83-90

Lewis RC, Coale KH, Edwards BD, Marot M, Douglas JN, Burton EJ (2002) Accumulation rate and mixing of the shelf sediments in the Monterey Bay National Marine Sanctuary. Mar Geol 181: 157-169

Morgan LE, Etnoyer P, Scholz AJ, Mertens M, Powell M (2005) Conservation and management implications of deep-sea coral and fishing effort distributions in the northeast Pacific Ocean. In: Freiwald A, Roberts JM (eds) Cold-water Corals and Ecosystems. Springer, Berlin Heidelberg, pp 1171-1187

Roark B, Guilderson T, Flood-Page S, Dunbar RB, Ingram BL (2003) Radiocarbon based age and growth rates estimates on deep-sea corals from the Pacific. Erlanger Geol Abh Sonderbd 4: 71

Roberts S, Hirshfield M (2003) Deep sea corals: out of sight, but no longer out of mind. Oceana, 2501 M Street NW, Washington, DC 20037, 16 pp

Rogers AD (1999) The biology of *Lophelia pertusa* (Linnaeus 1758) and other deep-water reef-forming corals and impacts from human activities. Int Rev Hydrobiol 84: 315-406

Welden BA, Cailliet GM, Flegal AR (1987) Comparison of radiometric vertebral band age estimates in four California elasmobranchs. In: Summerfelt RC, Hall GE (eds) The age and growth of fish. Iowa State Univ Press, Ames, pp 301-315

Testing the reproducibility of Mg/Ca profiles in the deep-water coral *Primnoa resedaeformis*: putting the proxy through its paces

Daniel J. Sinclair[1], Owen A. Sherwood[2], Michael J. Risk[3], Claude Hillaire-Marcel[1], Mike Tubrett[4], Paul Sylvester[4], Malcolm McCulloch[5], Les Kinsley[5]

[1] GEOTOP, Université du Québec à Montréal and McGill University, Québec, Canada
 (djsweb1971@yahoo.com.au)
[2] Centre for Marine Geology, Dalhousie University, Halifax, Nova Scotia, B3H 4J1, Canada
[3] School of Geography and Geology, McMaster University, Hamilton ON, L8S 4M1, Canada
[4] Memorial University of Newfoundland, St John's, Newfoundland, Canada
[5] Research School of Earth Sciences, Australian National University, Canberra, ACT 0200, Australia

Abstract. Two samples of the calcitic deep-sea coral *Primnoa resedaeformis* have been analysed for Mg/Ca ratios by micro-beam methods (laser-ablation ICP-MS and electron microprobe). Continuous profiles of Mg/Ca have been studied with the aim of establishing the reproducibility of the variations in different parts of the coral, and therefore the potential use of Mg/Ca as a paleoceanographic or paleoclimatic tracer.

A method of spectral decomposition based on box-filter smoothing has been developed for analysing the signals. This method shows that all profiles measured contain some degree of irreproducibility. Much of this irreproducibility appears to be white-noise added by the analytical methods. The amplitude of this noise is around 15 % of the signal average for the Nd-YAG laser-ablation system at Memorial University of Newfoundland, 5-6 % for the electron microprobe at Dalhousie University, and 4-4.5 % for the ArF Excimer laser-ablation system at the Australian National University.

In the case of the LA-ICP-MS analyses, this noise may relate to uneven ablation of material from the coral and/or an uneven size distribution of particles entering the ICP-MS plasma. For the most stable system (ANU's LA-ICP-MS), features on distance scales smaller than 150-200 μm will be obscured by the noise, and features smaller than 500 μm should be interpreted with caution.

There is some evidence that the coral itself contains compositional heterogeneity, although reproducibility is mostly limited by instrumental noise. We recommend

that several analytical profiles be compared before any attempt is made to interpret Mg/Ca variations in terms of paleoceanographic changes.

Keywords. Deep-sea coral, *Primnoa*, magnesium thermometry, reproducibility, laser-ablation, ICP-MS

Introduction

Deep-sea corals are attracting interest as potential paleoceanographic archives, with their carbonaceous skeletons incorporating trace elements and isotopes in amounts that reflect the physical and chemical conditions of the coral's immediate environment. The long life of these corals (Druffel et al. 1990, 1995; Smith 1997; Risk et al. 2002) and broad depth and geographic range (Stanley and Cairns 1988; Cairns 1994) means that they can contain information about the variation in important major ocean currents over millennial timescales.

Previous paleoclimatic studies of deep-sea corals have focused on corals of the genera *Lophelia* and *Desmophyllum* (Smith et al. 1997; Adkins et al. 1998; Smith et al. 1999, 2000; Goldstein et al. 2001). Both of these corals have a complex calyx architecture that makes extracting unambiguous time-series difficult (Lazier et al. 1999; Risk et al. 2002). Recently, another genera of deep-sea coral has been attracting interest because of its relatively simple growth architecture (Heikoop et al. 2002). Corals of the genus *Primnoa* have a tall branching (arborescent) form, with trunk cross-sections that display a radial growth form, much like tree-rings (Andrews et al. 2002, 2005; Risk et al. 2002; Sherwood 2002).

Primnoa corals have calcitic skeletons which contain high concentrations of magnesium. In other calcitic organisms, for example foraminifera, Mg/Ca ratios have shown potential as a temperature proxy (Rosenthal et al. 1997; Hastings et al. 1998). Research presented in a companion paper shows that Mg/Ca ratios in *Primnoa resedaeformis* skeletons are also sensitive to temperature, varying by approximately 4 % per degree Celsius (Sherwood et al. 2005).

The use of these corals, however, presupposes that meaningful Mg/Ca profiles can be extracted from a coral. This means that corals must contain reproducible Mg/Ca variations, and that these variations must be larger than any noise that might be introduced by measurement.

The aim of this research is to investigate 3 potential methods (2 different laser-ablation systems, and electron microprobe imaging) for measuring Mg/Ca in sections of the deep-sea coral *Primnoa resedaeformis*. These are 'micro-beam' methods, characterized by their ability to provide information on extremely high spatial resolutions. Given the slow growth of *Primnoa* corals (growth rates in the order of 50-350 μm per year (Andrews et al. 2002; Risk et al. 2002), high spatial resolution analyses are necessary if high fidelity ocean temperature records are to be resolved.

Our goals are to quantify the contribution of noise by each analytical method, to determine which Mg/Ca variations represent 'real' compositional fluctuations

within a coral, to study the reproducibility of these real variations, and to assess the confidence with which any particular variation in a profile can be interpreted.

Methods

Samples

Two different *Primnoa* corals were analyzed. Details of these samples are given in Table 1. Coral PR#6 was a sub-fossil specimen with poor constraints on age and location; however, of the samples available, it had the longest section of uninterrupted calcite, and clear radial banding in the crystal fabric, making it ideal for testing reproducibility in parallel profiles. The second specimen, NED 2002-37-2, was collected live in 2002 and details of its location, age and depth are better constrained (Table 1). This specimen was analyzed as part of a temperature calibration study (Sherwood et al. 2005).

Table 1 Details of samples

Sample	Method of Analysis	Description
PR#6	LA-ICP-MS (MUN) + LA-ICP-MS (RSES)	This is a sub-fossil *Primnoa resedaeformis* collected dead from the general area of the Grand Banks. The precise location and depth of the specimen is unknown. Th/U dating puts the sample at around 1600-1800 years old. At the point of sampling, the diameter of the branch was approximately 4 cm radius, representing several hundred years growth. A section of the slab was prepared as a 100 μm polished thick-section, and 2 pairs of profiles were taken during each analysis. The closely spaced pairs were 0.38 mm apart, and the distantly spaced pairs were approximately 4.7 mm apart.
NED2002-37-2	Electron Microprobe (Dalhousie University, Nova Scotia)	Specimen of *Primnoa resedaeformis* trawled accidentally from the NE channel near Romney's Peak (-65.655 - 65.648 W, 42.046 - 42.068 N) in July 2002. The depth is estimated to be between 260 and 290 m. The sample was alive when collected, and has a radius around 1.5 cm. Estimates of the growth rate put the sample at about 40 years old. The Mg/Ca ratio in a polished thin-section was mapped by electron microprobe over an area of approximately 2.5 x 7 cm.

LA-ICP-MS = Laser ablation ICP-MS
MUN = Memorial University of Newfoundland, St John's, Canada
RSES = Research School of Earth Sciences, the Australian National University, Canberra, Australia

Laser ablation analysis

The PR#6 coral was analyzed using two different laser-ablation systems: one at the Memorial University of Newfoundland, and one at the Research School of Earth Sciences of the Australian National University. The LA-ICP-MS methodology for both systems was similar to that described in Sinclair et al. (1998, with the details noted in Table 2).

Table 2: Laser ablation parameters

Parameter	MUN System	ANU System
Scan Speed (coral)	25 μm/s	20 μm/s
Laser	Quadrupled ND YAG 266 nm	ArF Excimer 193 nm
Spot Size	50 μm diameter	50 μm diameter
Energy Density	3-7 J/cm^2	20 J/cm^2
Pulse Rate	10 hz	5 hz
Points per Peak	1	3
Dwell Time	8.3 ms	10.5 ms
Time Slice	0.38-0.47 s	0.498 s
No. Masses Monitored	35	12
Effective Resolution	9.5-11.8 μm/data point	9.96 μm/data point
S Option	on	off
Counts per Point: mass 25 (Mg)	3300	47000
Counts per Point: mass 43 (Ca)	5000	14000
Counting Statistics Error Mg/Ca	2.24 %	0.96 %

A polished thick-section of coral PR#6 was mounted in a sample cell which was purged in helium prior to analysis. Ablation was conducted in a helium atmosphere, and ablated material was entrained in argon for transport to the ICP-MS. The sample cell was mounted on a computer controlled XY stage, and moved (rastered) slowly beneath the laser. Data was collected in time-resolved mode, providing a continuous profile of variation with distance.

Samples were pre-ablated to clean the surface, and to pre-condition the ICP-MS to carbonate material. The position was then re-set and the sample analyzed over the pre-ablated track. After most analyses, a part or the whole of the profile was replicated to check for drift and to study the reproducibility of the profile.

Four profiles were taken on coral PR#6 using each LA-ICP-MS system. These were arranged in 2 pairs of closely spaced parallel profiles (see Fig. 1). The closely spaced profiles were separated by approximately 0.38 mm, while the pairs were separated by approximately 4.7 mm. The spatial resolution of both methods was approximately 1 data point per 10 μm.

Memorial University (MUN) LA-ICP-MS system

Details of the MUN system can be found in Jackson et al. (1992) and Sylvester (2001). The mass spectrometer is a VG Fisons Plasmaquad PQ2, with S option enabled. The laser system is a custom designed quadrupled Nd YAG with a wavelength of 266 nm.

Australian National University (ANU) LA-ICP-MS system

The ANU system is similar to that published in Eggins et al. (1998). It also uses a VG Fisons Plasmaquad PQ2 ICP-MS, but does not use the S option. This results in a higher sensitivity for light mass elements at the expense of higher mass elements. The laser is a Lambda Physik Compex 110 ArF Excimer with a wavelength of 193 nm. The focal optics are custom-designed with a long focal length giving a
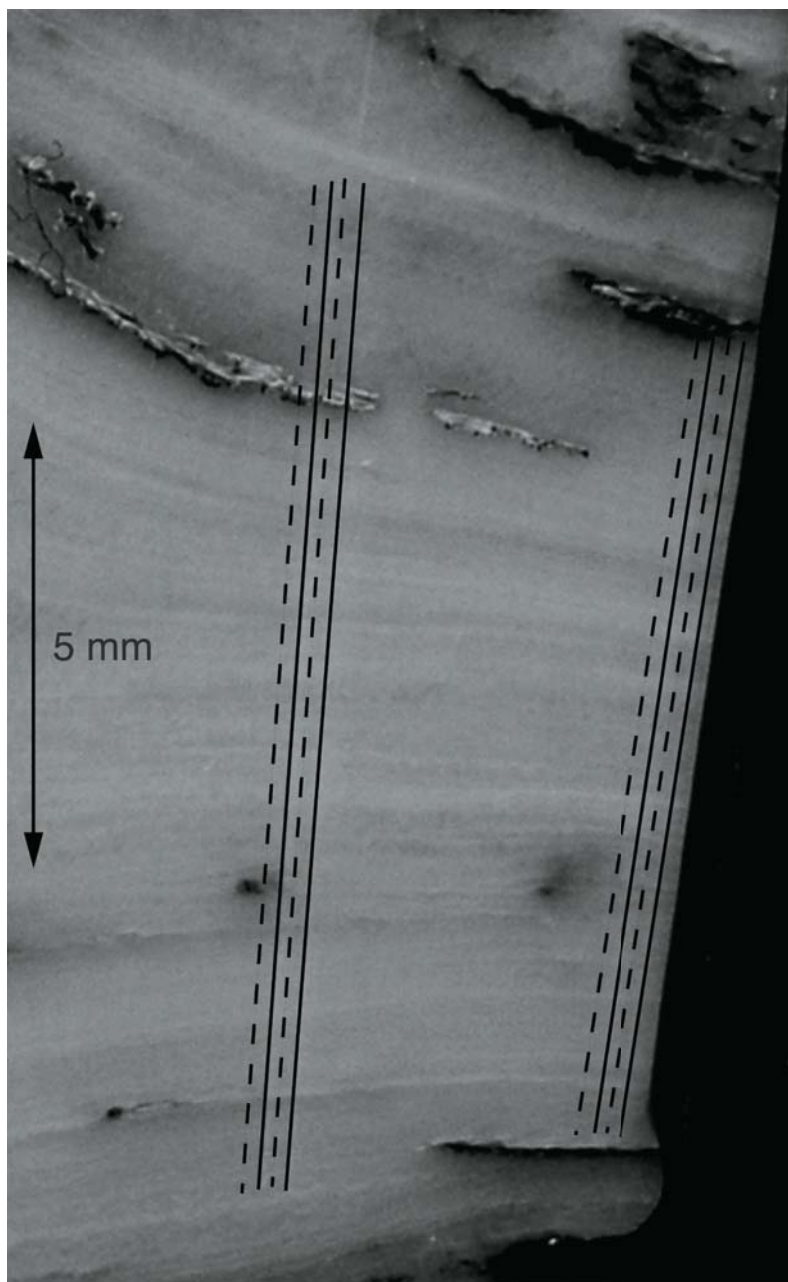
Fig. 1 Laser tracks on PR#6 coral: The contrast has been enhanced to highlight the subtle banding present in the coral. The rough regions of very dark and very light material are bands of organic material. Solid lines represent laser profiles measured at Memorial University of Newfoundland. Dashed lines represent laser profiles measured at the Australian National University

working distance of 10 cm making this less sensitive to variations in surface topography than the MUN system.

Electron microprobe

Details of the ion microprobe methodology are presented fully in the companion paper (Sherwood et al. 2005). In brief: a carbon coated polished thin section was analyzed using a JEOL 8200X Superprobe at Dalhousie University, Halifax, Canada. Analysis was in wavelength dispersive mode. The accelerating voltage was set to 15 kv and current to 80 nA. A 10 micron diameter beam was stepped across the coral surface at 10 micron increments, and data was collected for 100 ms each step. Mg/Ca variations were mapped in 2 dimensions over an area of approximately 2.5 x 7 mm (see Fig. 2).

Data processing

For the laser profiles, the raw Mg and Ca data were background subtracted and the Mg/Ca ratios for each data point were then computed.

The two-dimensional electron microprobe Mg/Ca maps were converted into a greyscale image, with the Mg/Ca ratio linearly correlated to the 8 bit greyscale (0 to 255). Using analytical software (Igor Pro), line profiles of the image were extracted from 7 parallel tracks (5 profiles were evenly spaced across the image, and the 4th profile had two further profiles taken from very close on either side; see Fig. 2).

Parallel laser profiles were spatially aligned by matching between 5 and 10 bands (representing subtle variations in crystal fabric) in high magnification photographs of the corals. All distance scales were then interpolated to match one chosen distance scale, and all Mg/Ca profiles were then re-sampled at the same distance scale. The greyscale intensity profiles from the EM map were aligned by matching Mg/Ca bands in a similar manner.

Occasionally the laser ran over organic layers with higher Mg/Ca ratios than the surrounding calcite. This data was removed from the profiles since it can interfere with spectral analysis (see below). All data profiles were normalized to their average, and the average was subtracted. The signals therefore represent proportional deviations from the mean, allowing profiles from different analytical methods to be directly compared.

Signal analysis

The box-filter spectral deconvolution

Analytical systems like LA-ICP-MS can collect data on a range of spatial resolutions, controlled by the size of the laser beam, the rate at which the beam is

Fig. 2 Electron microprobe image showing a 2D spatial map of Mg/Ca variations in the NED2002-37-2 coral measured by electron microprobe at Dalhousie University. Light grays represent high Mg/Ca ratios, dark grays represent low Mg/Ca ratios. The vertical lines represent locations of greyscale intensity profiles. Dark patches represent gaps in the coral which are filled with epoxy resin, while light patches represent organic material (which has high Mg concentrations)
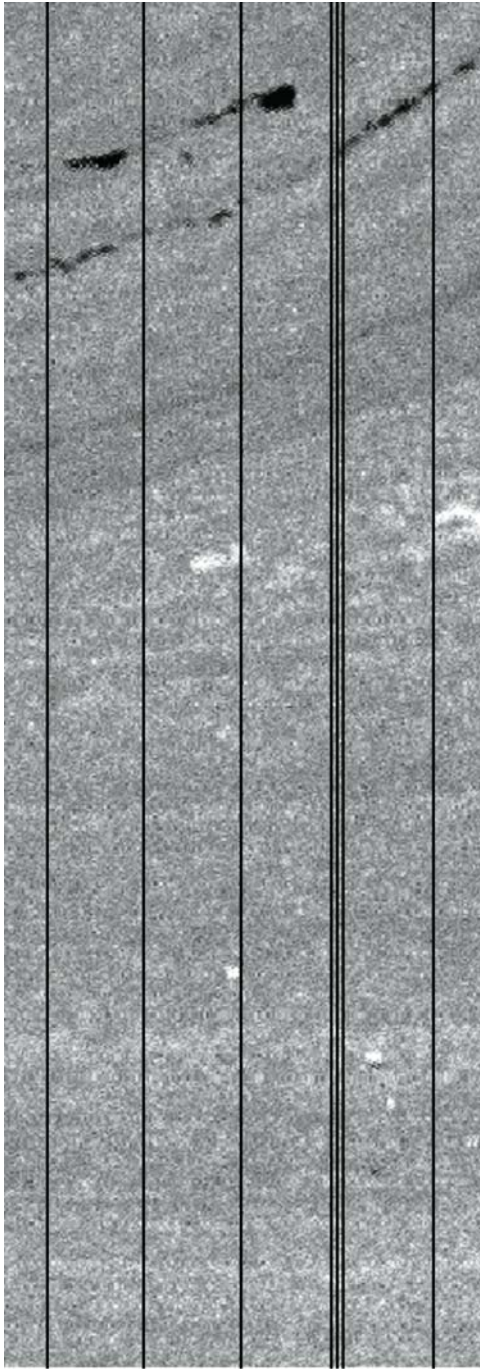
1.0 mm

rastered, and the integration time per data point. Post-collection data processing (decimation, filtering and/or smoothing) can also reduce the resolution as part of noise-reduction strategies. The choice of final resolution is often a subjective judgement by the analyst, who balances spatial resolution against signal to noise ratios. One of our aims is to objectively establish the optimum resolution based on spectral analysis of the data. We also wish to examine variations on different spatial scales, since different processes may add Mg/Ca variations over characteristic times and/or distances.

Both of the analytical methods were set to generate data at a resolution of 1 data point for every 10-13 μm on a coral. A typical analysis (8-15 mm) therefore generates more than 800 data points. This spatial resolution was chosen to be deliberately higher than necessary, to allow us some flexibility in processing and to study the distribution of signal variation over a range of frequencies.

The signals from laser and image profiles were analyzed using a spectral deconvolution based on a box-filter (windowed running average). This was chosen over other techniques like Fourier analysis and Wavelet analysis because of its simplicity and because an evenly weighted (square) window makes interpreting resolution significantly easier. Statistically, there are similarities between decimating (averaging n consecutive points to generate a data signal that is 1/n the original size), box smoothing (replacing each point with the average of the n adjacent points) and simply collecting data at a lower resolution by integrating for n times as long. In each case, the new time series will have statistical properties that can be easily predicted based on rules of error propagation and counting statistics (Poission Distribution).

The box-filter spectral analysis allows us to study a signal by isolating variations over a particular range of frequencies (distance scales). A signal is reduced to a number of 'spectral components' by subtracting the signal smoothed with a window of n from a signal smoothed with a window of 2n. For a signal that is 800 data points long, this results in 9 independent time series (spectral components) corresponding to the differences between signals smoothed with windows of 1, 2, 4, 8, 16, 32, 64, 128, 256 and ∞ points (see Table 3 and Fig. 3).

The average amplitude of each spectral component is quantified by taking the interquartile range. A 'box-filter spectrum' is therefore the interquartile range of the spectral component graphed against the $\log_2$ of the smaller of the two smoothing windows. For example, the first point (x = 0) represents the spectral component extracted by subtracting the unfiltered data (window size = $2^0 = 1$) from next largest window (window size = $2^1 = 2$).

Random noise

The basic statistical properties of the box-filter spectrum of a white-noise signal are demonstrated in Figure 4. This figure was generated by averaging the box-filter spectra of 1000 white noise signals (each comprising 800 data points selected randomly from a Gaussian distribution with an average of 0.0 and a standard deviation of 0.1). These properties have been derived formally and can be requested directly from the senior author.

Table 3 Spectral components in box-filter spectrum

Spectral Component	Contains:	Description:	Approximate spatial scale represented by variations
0	Difference between unsmoothed signal and signal smoothed with 2 point window.	High frequencies, small distance scales.	10 μm
1	Difference between signal smoothed with 2 point window and 4 point window.		20 μm
2	Difference between signal smoothed with 4 point window and 8 point window.		40 μm
3	Difference between signal smoothed with 8 point window and 16 point window.		80 μm
4	Difference between signal smoothed with 16 point window and 32 point window.		160 μm
5	Difference between signal smoothed with 32 point window and 64 point window.		320 μm
6	Difference between signal smoothed with 64 point window and 128 point window.		640 μm
7[1]	Difference between signal smoothed with 128 point window and 256 point window.		1280 μm
8[1]	Contains all variations not included in previous components.	Low frequencies, large distance scales.	> 2560 μm

[1] The highest spectral component corresponds to the largest power of two that is smaller than half the width of the data. Some replicate profiles were shorter than the full data length, and therefore do not have components 7 and 8.

To summarise these properties:

1. The first spectral component (c0) has an amplitude that is $^1/_{\sqrt{2}}$ of the amplitude of the original signal. Since the interquartile range spans $\pm$ 0.675 standard deviations, $c0 = 0.95 \cdot \sigma$, where σ = the standard deviation of the noise in the original signal.

2. Each spectral component has an amplitude that is $^1/_{\sqrt{2}}$ the previous component. In other words:
    $$A_x = A_0 \cdot (^1/_{\sqrt{2}})^x$$
    where:
    x = spectral component (= $\log_2$ of the smaller of the two smoothing windows)
    A_x = amplitude of noise in spectral component x
    A_0 = amplitude of noise in spectral component 0 (highest frequency component)
    Therefore, if amplitude is graphed on a log scale, the result is a straight line with a slope of $-\sqrt{2}$.
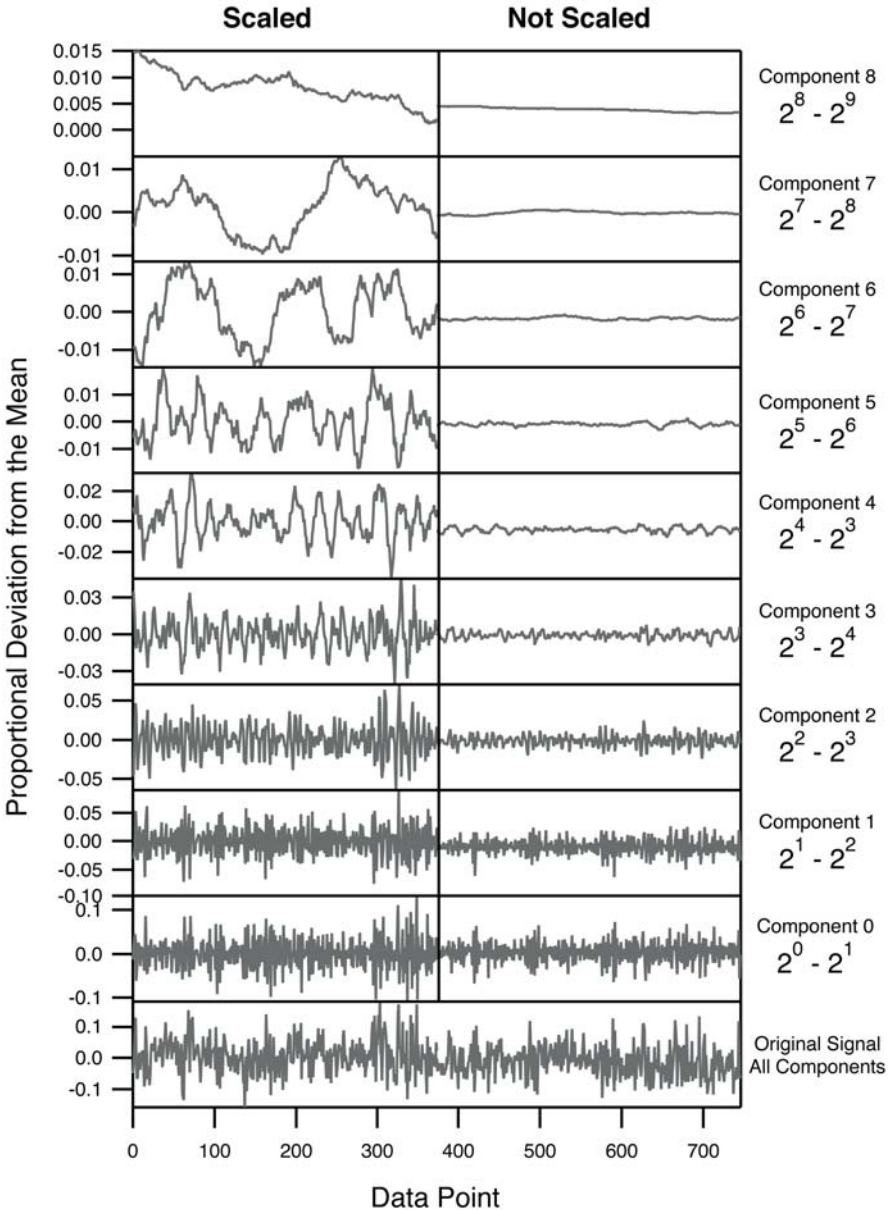
Fig. 3 This figure demonstrates the decomposition of a signal into components by subtracting a signal smoothed with a box filter of size n, from the signal smoothed with a box filter of size 2n. The components have been divided into two: on the left, the scale has been adjusted to show the shape of the component. On the right, the scale has been kept the same as the original signal

3.   The original signal is the sum of all the spectral components. Theoretically, there are an infinite number of these, but in practice we stop calculating components at the largest smoothing window that is $\leq 1/2$ of the length of the time series. The last spectral component therefore contains all the power of the other lower frequency components, and has an amplitude that is equal to the penultimate component.

It is important to note that while white noise can be generated by adding a random fluctuation at the highest frequency (each individual data point), it results in variations which are distributed across all time/space scales. Thus, high frequency noise can result in interferences to real low-frequency signals if they are of sufficiently small amplitude.
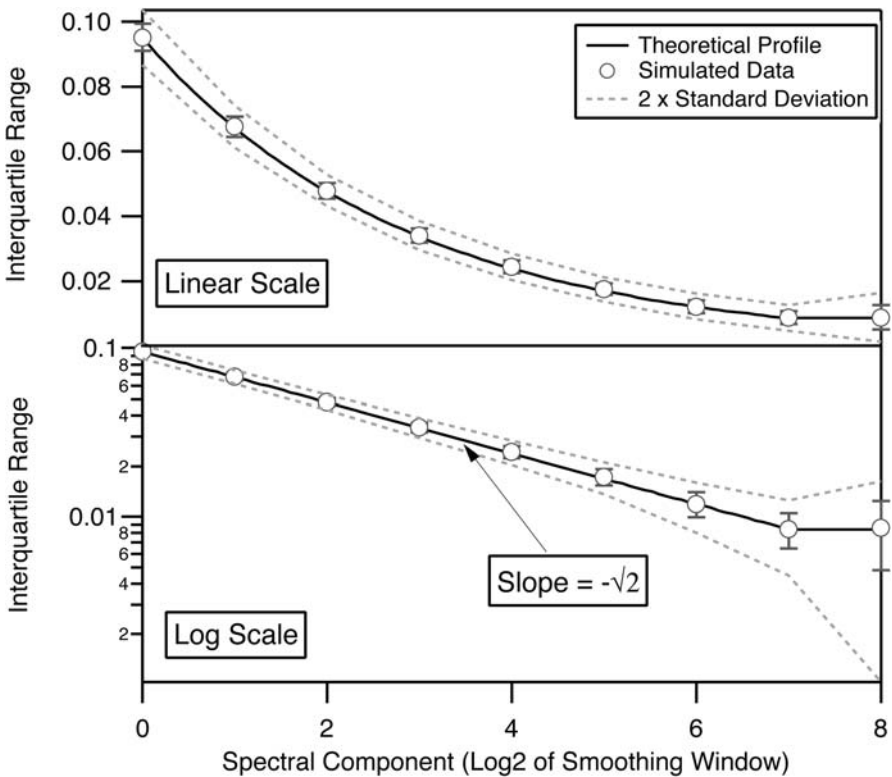
Fig. 4 Box-filter spectrum for simulated noise. The behavior of Gaussian noise in the box-filter decomposition was simulated by generating 1000 profiles containing random noise taken from a normal population with a standard deviation of 0.1. The scale on the left axis is the interquartile range of the spectral component. For a normal distribution, the interquartile range of the first spectral component corresponds to approximately 95 % of the standard deviation of the original signal. Theoretically, Gaussian noise decays with the amplitude of each higher component being $1/\sqrt{2}$ the previous component. The exception is the last component, which contains all the variation that is not accounted for in previous components; the theoretical amplitude of this component is the same as the previous component

Reproducibility and difference spectra

The criterion that distinguishes a real signal from random fluctuation is reproducibility. Reproducibility can be measured by subtracting one profile from another. Variations that are reproduced in two profiles will disappear. In contrast, the laws of error propagation predict that the amplitude of irreproducible (random) variations will increase by a factor of $\sqrt{2}$ under subtraction. Reproducibility is therefore identified by using a box-filter spectral decomposition on the *difference* between two signals, dividing by $\sqrt{2}$, and comparing the 'difference spectrum' to the original spectra. Where variations are reproducible, the difference spectrum will fall below the original spectra. Where the signals are not reproducible, the difference-spectrum will have the same amplitude as the originals.

A 'replicate difference spectrum' is calculated from the difference between two replicate profiles (measured over the same track). A replicate difference spectrum should therefore contain only instrumental noise. A 'parallel difference spectrum' is calculated from two parallel profiles (measured side by side), and will include any real compositional variation in the coral that is not replicated in adjacent profiles ('compositional noise').

Characterizing noise

Non-reproducible fluctuations can have 2 sources: they can be inherent to the coral – i.e. compositional noise, or they can be artefacts of the analytical method – i.e. instrumental noise. Machine noise will tend to be white noise and therefore follow a $(^1/_{\sqrt{2}})^x$ decay. Compositional noise may be distributed unevenly across spatial scales if it is related to skeletal deposition processes which operate on specific time/distance scales.

Compositional noise will also be irreproducible in parallel profiles but reproducible in replicate profiles. Parallel difference spectra should therefore be larger (contain more irreproducibility) than replicate difference spectra. This is summarized in Table 4.

Table 4: Properties used to characterize noise

Property	Instrumental Noise	Compositional Noise
Reproducible in 'replicate difference spectrum'?	No	Yes
Reproducible in 'parallel difference spectrum'?	No	No[1]
Anticipated spectral characteristics.	Probably has a $(^1/_{\sqrt{2}})^x$ profile[2].	May be unevenly distributed on spatial / frequency scales.

[1] Reproducibility expected to decrease as the separation between parallel profiles increases.
[2] x = spectral component.

Growth rate variations and data misalignment

Misalignment between two parallel profiles, resulting from differences in growth rate, will result in some of the high-frequency variations being offset, and therefore appearing irreproducible. A conservative estimate of the uncertainty in alignment is

70-100 μm, or around 7 data points, at each point where profiles were matched. The effect of this misalignment was simulated by distorting the x-axis of a profile by an average of 7 points at 8 locations (the average number of points where profiles were matched).

Misalignment has the effect of making the 2 highest frequency spectral components appear to be irreproducible. Lower frequencies are affected less by the misalignment, and show greater reproducibility. The difference spectrum for these lower frequency components drops quickly, falling *below* the theoretical $(^1/_{\sqrt{2}})^x$ decay profile for white noise.

The uncertainty in spatial calibration therefore means that we cannot expect to identify reproducibility in the first 2-3 spectral components (distance scales of 10-50 μm) of the signal, and significant irreproducibility could also be present in the next 1-2 spectral components. However, misalignment between two perfectly reproducible signals could be identified by a difference spectrum falling significantly below the theoretical white-noise profile.

Results

PR#6 coral measured with the MUN LA-ICP-MS system

The box-filter spectra for the MUN data are presented in Figure 5A. The spectra are similar in shape to that predicted for pure Gaussian noise with a standard deviation of 15 % (see Section on Random noise). At the very lowest frequencies (components 6, 7 and 8), the amplitudes tend to increase in some spectra.

The difference spectra for replicate profiles of the MUN data are almost identical to the normal spectra at most frequencies (Fig. 5A) indicating that there are few or no reproducible variations in the profiles. Since the spectra follow the shape of Gaussian noise, it is concluded that the signal is almost completely white noise with an amplitude of around 15 %. This is likely to be analytical noise since analyses of the same coral by the ANU LA-ICP-MS system (see below) reveal much lower amplitudes of variation in the high frequency components.

The slight increase in the last few components of the normal spectra may indicate that there is a low amplitude real signal being masked by high frequency noise. It is difficult to determine whether these variations are reproducible because only short sections of each profile were replicated, and the difference spectra do not therefore contain the last few components.

Parallel and replicate difference spectra are relatively variable (Fig. 5B) – possibly because the magnitude of machine noise varies with time. There is no consistent trend towards increasing reproducibility in close and distant parallel profiles, and therefore no evidence to show that compositional noise is present in the coral.

PR#6 coral measured with the ANU LA-ICP-MS system

The replicate difference spectra follow white noise with an amplitude of about 4-4.5 % (Fig. 6). The normal spectra match this noise trend, but begin to deviate from it above spectral components 3-4. The ANU data therefore represents compositional

variations in the coral of around 1-1.5 % above the 150-200 μm distance scale, which are obscured at smaller scales by random noise, presumably instrumental.

The difference spectra for replicate, closely spaced parallel, and distantly spaced parallel profiles are roughly similar for the higher frequency components (Fig. 6B). At lower frequencies the amplitudes of the difference spectra for replicate profiles are slightly lower than parallel profiles. This general trend suggests that there
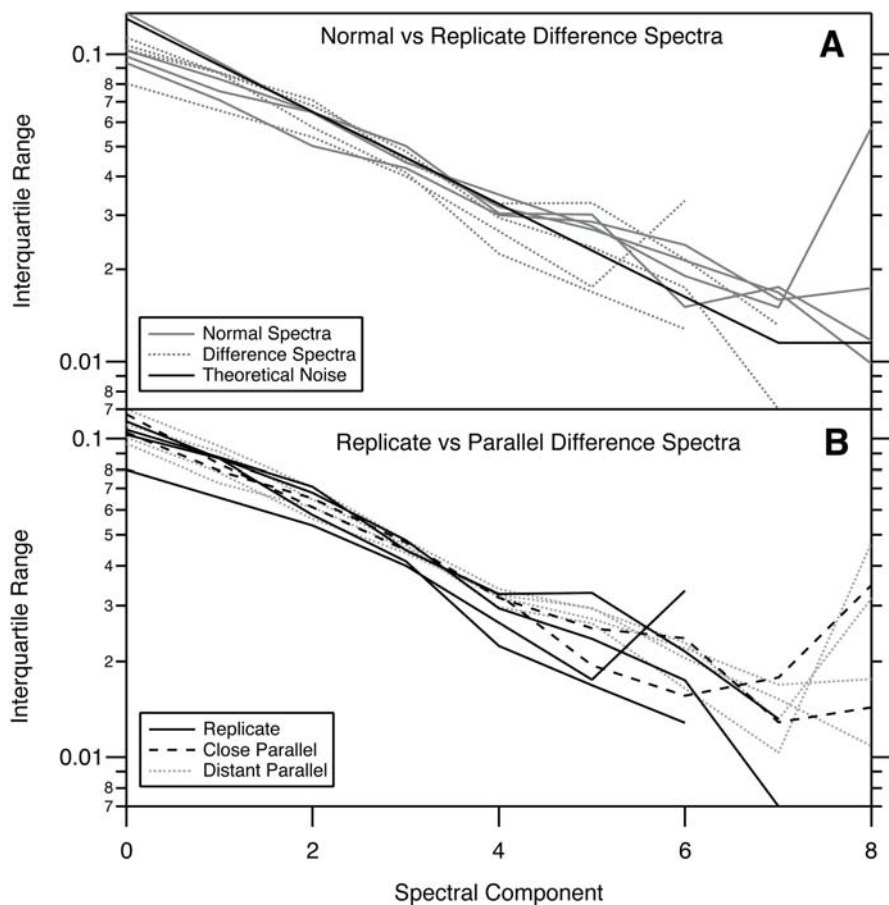
Fig. 5 Box-filter spectra for the PR#6 coral analyzed using the MUN Nd YAG LA-ICP-MS system. **A** comparison between normal spectra and replicate difference spectra. The replicate difference spectra contain fewer components because the replicate profiles were shorter than the original profiles. Note that the signals are relatively variable, but are close to the shape predicted by pure Gaussian noise. The difference spectra are similar to the normal spectra, indicating that there is little reproducibility in these profiles at any frequencies. **B** Difference spectra for replicates, closely spaced parallel profiles, and distantly spaced parallel profiles. There does not appear to be any consistent trend for replicates to be more reproducible than close or distantly spaced parallel profiles

may be some compositional noise in the coral which adds some irreproducible component to the profiles. In fact, it is only for the last 3 spectral components that the parallel profile difference spectra are significantly lower than the normal spectra. This implies that only over distance scales greater than about 500 μm (smoothing windows of about $2^{5.6}$ points) would you expect to be able to confidently resolve reproducible variations in parallel profiles.
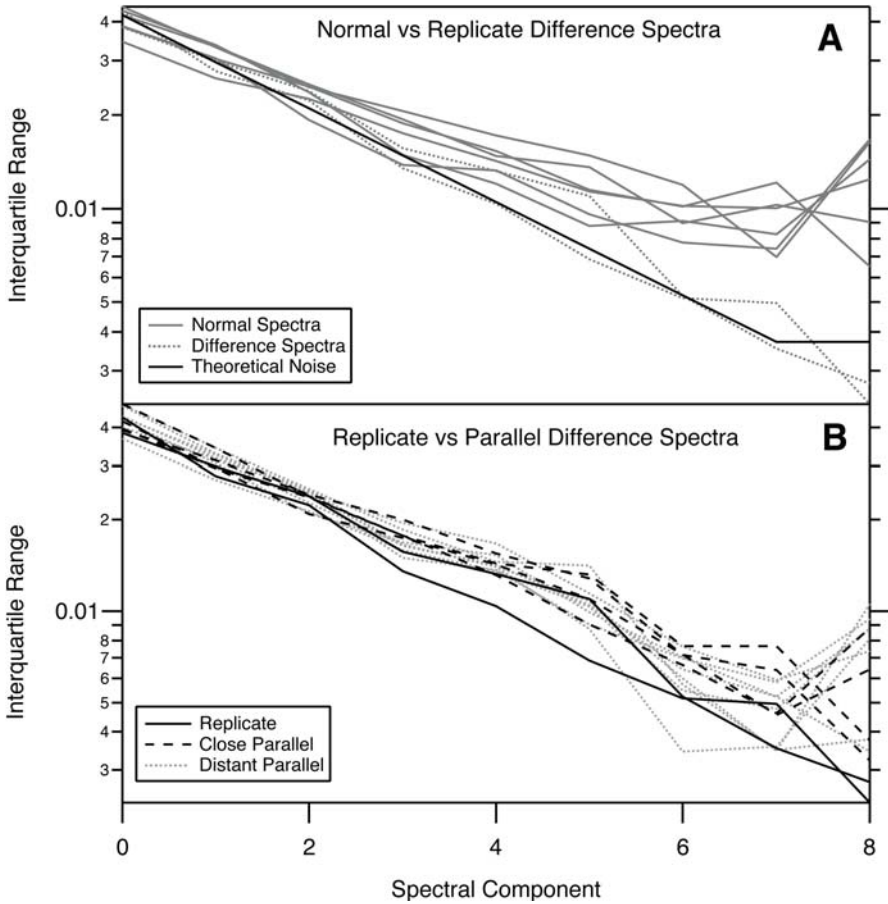
Fig. 6 Box-filter spectra for the PR#6 coral analyzed using the ANU Excimer LA-ICP-MS system. **A** Comparison between normal spectra and replicate difference spectra. Note that the difference spectra dip below the normal spectra between spectral components 3 and 4, indicating reproducibility above these scales. The difference spectra have a similar shape to that predicted by pure Gaussian noise. **B** Difference spectra for replicates, closely spaced parallel profiles, and distantly spaced parallel profiles. Note that the signals are fairly variable, but in general the difference spectra for parallel profiles sit above the replicate spectra for the last 5 or 6 components indicating that they are less reproducible than the replicate profiles. There is no indication that the closely spaced parallel profiles are any more reproducible than the distantly spaced profiles

NED2002-37-2 coral measured by electron microprobe

The greyscale profiles taken from the 2D Mg/Ca images appear to have a lower amplitude of fine-scale variation than the ANU LA-ICP-MS system (Fig. 7), varying by around 3.5 % in the highest frequency component. These profiles do not match
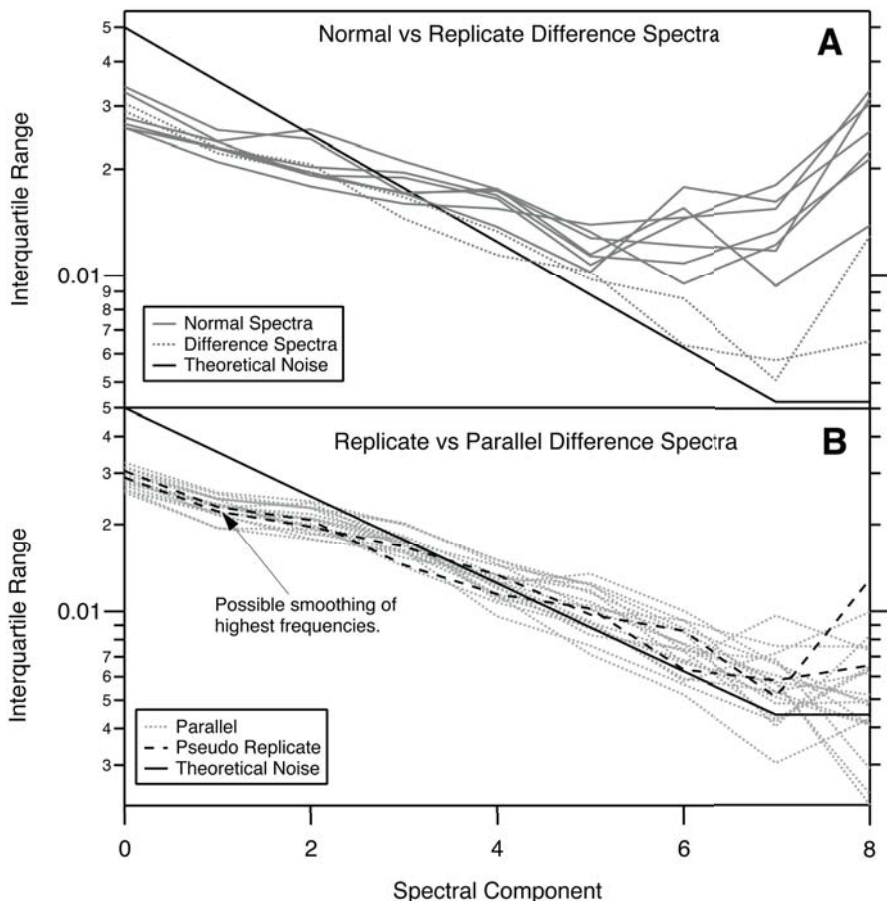
Fig. 7 Box-filter spectra for the line-profiles taken from the electron microprobe image of the NED2002-37-2 coral. **A** Comparison between normal spectra and replicate difference spectra. Note that the difference spectra dip below the normal spectra between spectral components 3 and 4, indicating reproducibility above these scales. The difference spectra have a similar shape to that predicted by pure Gaussian noise with the exception of the last spectral component. This could represent a systematic sensitivity trend in the electron microprobe. **B** Difference spectra for replicates and parallel profiles. The different parallel profiles are examined in greater detail in Figure 8. Note that the difference spectra follow the general shape for theoretical noise with a standard deviation of around 5.5 %, but that the high-frequency signals (spectral components 0 and 1) have a significantly lower amplitude than that predicted by Gaussian noise. This shape is similar to the profile for noise which has been smoothed by a 2 point box-filter, suggesting that the data collection or processing has smoothed the data

the spectrum predicted for white noise, and actually curve upwards above spectral component 6, indicating that this coral has large amplitude variations above 600-1000 μm, in contrast to the PR#6 coral.

Closely spaced parallel profiles were used as pseudo-replicates (Figs. 7 and 8). As with the ANU data, the replicate difference spectra drop below the normal spectra above spectral component 4, indicating that reproducible variations on the 150-200 μm scales can be resolved above the signal noise.

The shape of the difference spectra does not match that of a white-noise spectrum with a 3.5 % variation. In fact, the data more closely matches a white noise spectrum with an amplitude of 5 % which has been smoothed with a 2 point running average filter (Fig. 7B). Some aspect of data collection or processing may be responsible.

The replicate difference spectra are compared with parallel difference spectra in Figures 7B and 8. The spectra are relatively variable, and it is not possible to distinguish any difference between replicate and parallel difference spectra.

Discussion

Source of noise

All profiles clearly contain some degree of irreproducibility (noise), most of which seems to be introduced by the analytical methods. The noise in the laser-ablation
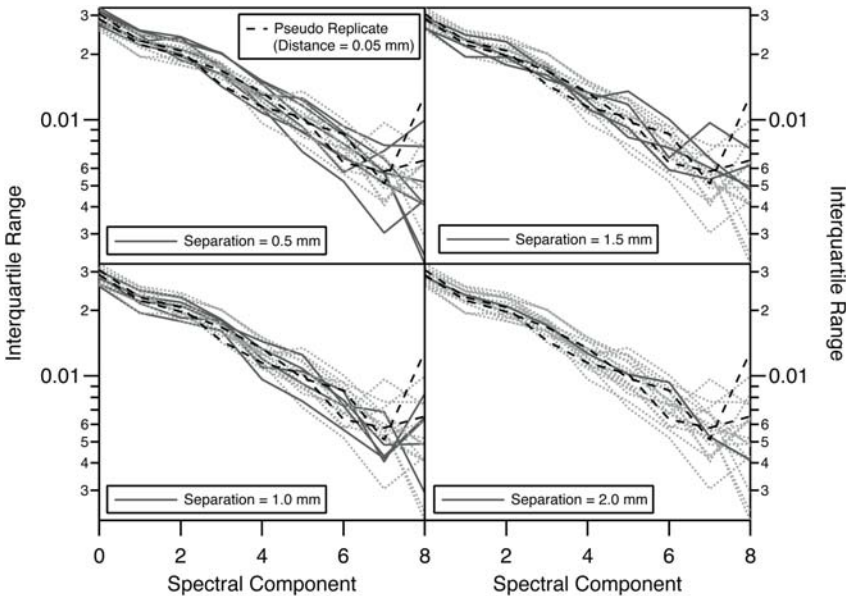
Fig. 8 Details of the difference spectra for parallel EM profiles in the NED2002-37-2 coral. The difference spectra for differing degrees of separation are presented. There does not appear to be any consistent pattern of increasing amplitude with greater separation, as would be predicted if there existed a compositional irreproducibility in the coral. Note, however, that the scatter in the profiles may be masking such a trend

profiles is significantly larger than predicted by counting statistics (Table 2). This is also the case for the electron microprobe, where counting statistics have been estimated at ~2.8 %.

The amplitude of noise is quite different between the profiles obtained from the MUN and the ANU laser-ablation systems. Since the major differences between these two systems are the laser and focusing optics, it seems likely that the noise originates at the ablation stage. Both systems use a UV laser; however, the MUN system uses a quadrupled Nd-YAG, with a wavelength of 266 nm whereas the ANU system uses an ArF Excimer laser which has a wavelength of 193 nm. In previous studies it has been shown that for materials that are partially transparent to ultraviolet lasers (such as $CaCO_3$), 266 nm lasers are adsorbed less efficiently than 193 nm lasers (Horn et al. 2001; Russo et al. 2002) resulting in poorer ablation. The result can be thermal fracturing of the sample, generating an uneven distribution of particles reaching the ICP-MS plasma. This in turn could result in a more unstable signal due to uneven and incomplete vaporization and ionization.

Characterizing variations in the coral

The general pattern within the coral is demonstrated schematically in Figure 9. We can only characterize the variation down to about spectral component number 4. Below that (higher frequencies), the coral signal is swamped by the random noise introduced by the analytical method. Spectral components 4-6 appear to have a relatively constant (interquartile) amplitude of around 1 %, with amplitudes increasing up to 3.5 % for spectral component 8.

Uncertainty in the profiles

For the ANU LA-ICP-MS system, the real and noise components cross over at about spectral component 4. This means that irreproducible variations introduced by the analytical method have a similar amplitude to real, reproducible variations the at distance scales of around 160 μm. As smoothing becomes greater, the noise variations decrease in amplitude, until by spectral component 6 the real variations are twice as large as the noise. At spectral component 8 the noise variations would be about $^1/_{10}$ the real signal. For the larger amplitude noise, such as is the case for the MUN LA-ICP-MS system, the noise component of the signal remains larger than the actual signal right up until spectral component 7 (spatial scales of 1.280 mm).

The ratios of signal to noise are dependent on the amplitude of the coral signal, and of the noise component. The Mg/Ca variations present in the PR#6 coral appear be unusually low (compared with other *Primnoa* samples), and signal/noise could therefore be expected to be better in other cases.

Compositional irreproducibility

For most of the analyses, the variability of the difference spectra makes it difficult to assess whether there is any compositional noise. Only in the ANU laser data is there some suggestion that replicate profiles are more reproducible than parallel profiles. This additional irreproducibility shows up in the mid to high frequencies. It is a subtle effect, and is not obvious when studying the profiles by eye (Fig. 10). However, it does add enough irreproducibility to obscure variations up to 500 μm.

The source of any heterogeneity in the skeletal Mg composition can only be speculated upon. The Mg/Ca ratios in the *Primnoa* calcite average around 100 mol/mol (Sherwood et al. 2005), which is higher than inorganic calcite grown from seawater (Mucci and Morse 1990). The organic material which makes up the horny regions of *Primnoa* skeletons is enriched in Mg relative to the calcite (Sherwood et al. 2005; Sinclair, unpublished data). Traces of organic material in the calcite could therefore result in a patchy heterogeneity. Alternatively, the high Mg/Ca might represent a deliberate concentration of Mg by the coral, and variations in this vital effect from one part of the coral to another would also result in Mg heterogeneity.
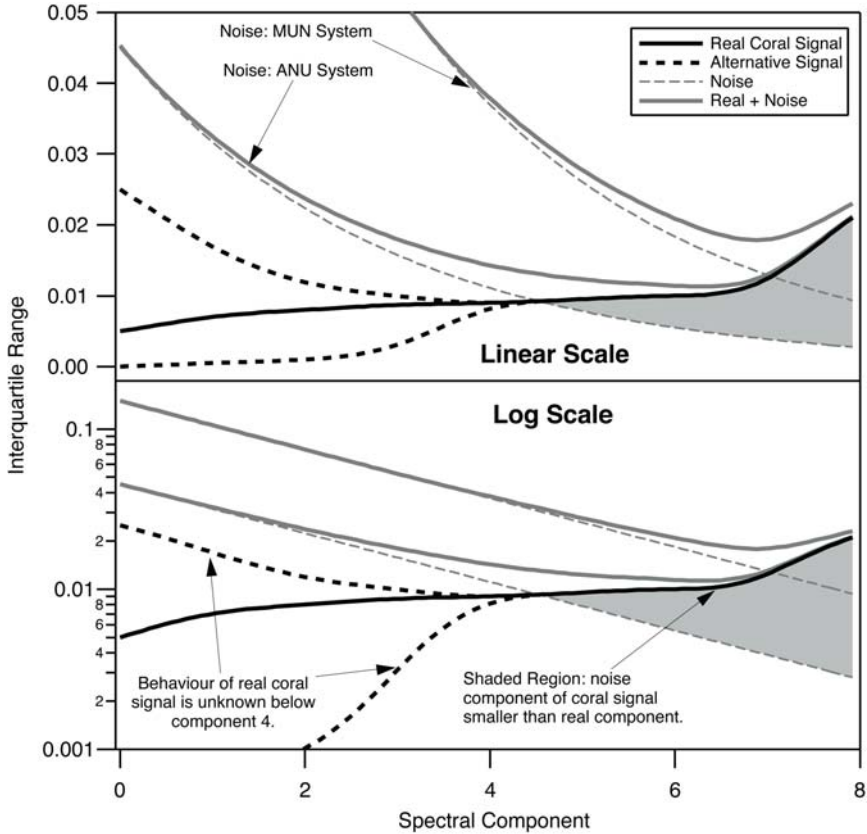
Fig. 9 This is a sketch of the box-filter spectra for a real coral signal and its combination with two levels of noise corresponding approximately to the instrumental noise in the ANU and MUN laser-ablation systems. The top graph and bottom graph are identical except that the left axis is linear in the top graph, and logarithmic in the bottom. Because the real coral signal is dominated by noise below spectral component 4, the shape is unknown. 3 possibilities are presented corresponding to high medium and low amplitudes of fine-scale variation. The shaded region indicates the difference between the real signal and the noise-component for the lower of the two noise levels, and can be used to approximately estimate the ratio of signal to noise in a typical coral analysis

Regardless of the cause, however, compositional heterogeneity is only a minor contributor to the overall irreproducibility; instrumental noise is much more significant in restricting the interpretation of coral Mg/Ca signals.

Conclusions

All of the coral profiles are affected by noise introduced by the analytical methods employed. This noise ranges from greater than 15 % for the Memorial University of Newfoundland LA-ICP-MS system down to around 4-4.5 % for the Australian National University LA-ICP-MS system. The electron microprobe at Dalhousie University seems to add noise equivalent to around 5-6 %, although the method also seems to have some inherent smoothing which lowers the noise amplitude at higher frequencies.

The inherent variations within the coral appear to average around 1-1.5 % over most spatial scales, increasing in amplitude a little for the lower frequency components. For data collected at a spatial resolution of 10-13 µm per data point,
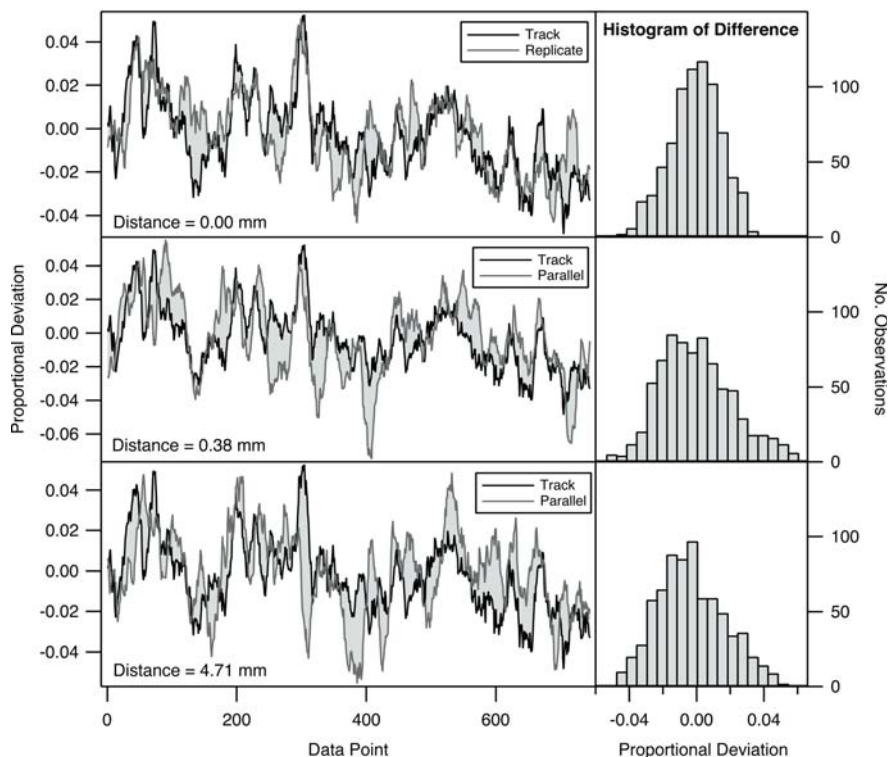
Fig. 10 These figures demonstrate the differences between replicate and parallel tracks in the PR#6 coral, as analyzed by the ANU LA-ICP-MS system. All profiles have been smoothed with a 16 point window. To the right are graphed the histograms of the differences between the original track and the replicate or parallel track to which it is compared. Note that the histogram for the replicate difference is narrower than for the parallel differences

the machine noise for the most precise analytical method dominates the signal for spatial scales less than about 160 μm, and can significantly affect features up to 600 μm. For the least precise analytical method, the signal obtained is almost entirely noise, and only the longest amplitude variations (> several mm) could be resolved.

There is some evidence that there may be irreproducible variations in the composition of the coral, further restricting the resolution. In most cases trying to interpret individual variations within a profile on distance scales less than 500 μm is not justified unless they can be reproduced in one or more parallel profiles. Since the corals grow at between 50-350 μm per year, it should be possible to resolve 5-year to decadal variations in Mg/Ca.

Acknowledgements

References

Adkins JF, Cheng H, Boyle EA, Druffel ERM, Edwards RL (1998) Deep-sea coral evidence for rapid change in ventilation of the deep North Atlantic 15,400 years ago. Science 280: 725-728

Andrews AH, Cordes EE, Mahoney MM, Munk K, Coale KH, Cailliet GM, Heifetz J (2002) Age, growth and radiometric age validation of a deep-sea habitat-forming gorgonian (*Primnoa resedaeformis*) from the Gulf of Alaska. Hydrobiologia 471: 101-110

Andrews AH, Cailliet GM, Kerr Ferry LA, Coale KH, Lundstrom C, DeVogelaere A (2005) Investigations of age and growth for three deep-sea corals from the Davidson Seamount off central California. In: Freiwald A, Roberts JM (eds) Cold-water Corals and Ecosystems. Springer, Berlin Heidelberg, pp 1021-1038

Cairns SD (1994) Scleractinia of the temperate North Pacific. Smithson Contr Zool 557: 1-150

Druffel ERM, King LL, Belastock RA, Buesseler KO (1990) Growth rate of a deep-sea coral using 210Pb and other isotopes. Geochim Cosmochim Acta 54: 1493-1500

Druffel ERM, Griffin S, Witter A, Nelson E, Suthon J, Kashagarian M, Vogel J (1995) *Gerardia:* Bristlecone pine of the deep sea? Geochim Cosmochim Acta 59: 5031-5036

Eggins SM, Kinsley LPJ, Shelley JM (1998) Deposition and fractionation processes during atmospheric pressure laser sampling for analysis by ICP-MS. Appl Surf Sci 127-129:

278-286

Goldstein SJ, Lea DW, Chakraborty S, Kashgarian M, Murrella T (2001) Uranium-series and radiocarbon geochronology of deep-sea corals: implications for Southern Ocean ventilation rates and the oceanic carbon cycle. Earth Planet Sci Lett 193: 167-182

Hastings DW, Russell AD, Emerson SR (1998) Foraminiferal magnesium in *Globeriginoides sacculifer* as a paleotemperature proxy. Paleoceanography 13: 161-169

Heikoop JM, Hickmott DD, Risk MJ, Shearer CK, Atudorei V (2002) Potential climate signals from the deep-sea gorgonian coral *Primnoa resedaeformis*. Hydrobiologia 471: 117-124

Horn I, Guillong M, Günter D (2001) Wavelength dependent ablation rates for metals and silicate glasses using homogenized laser-beam profiles – implications for LA-ICP-MS. Appl Surf Sci 182: 91-102

Jackson SE, Longerich HP, Dunning GR, Fryer BJ (1992) The application of laser ablation microprobe-inductively coupled plasma-mass spectrometry (LAM-ICP-MS) to *in situ* trace element determinations in minerals. Canad Mineral 30: 1049-1064

Lazier AV, Smith JE, Risk MJ, Schwarcz HP (1999) The skeletal structure of *Desmophyllum cristagalli:* the use of deep-water corals in sclerochronology. Lethaia 32: 119-130

Mucci A, Morse JW (1990) Chemistry of low-temperature abiotic calcites: experimental studies on coprecipitation, stability, and fractionation. Rev Aquat Sci 3: 217-254

Risk MJ, Heikoop JM, Snow MG, Beukens R (2002) Lifespans and growth patterns of two deep-sea corals: *Primnoa resedaeformis* and *Desmophyllum cristagalli*. Hydrobiologia 471: 125-131

Rosenthal Y, Boyle EA, Slowley N (1997) Temperature control on the incorporation of magnesium, strontium, fluorine, and cadmium into benthic foraminiferal shells from Little Bahama Bank: prospects for thermocline paleoceanography. Geochim Cosmochim Acta 61: 3633-3643

Russo RE, Mao X, Liu H, Gonzales J, Mao SS (2002) Laser ablation in analytical chemistry – a review. Talanta 57: 425-451

Sherwood O (2002) The deep sea gorgonian coral *Primnoa resedaeformis* as an oceanographic monitor. MSc thesis, McMaster Univ, Hamilton, Ontario, Canada

Sherwood OA, Heikoop JM, Sinclair DJ, Scott DB, Risk MJ, Shearer C, Azetsu-Scott K (2005) Skeletal Mg/Ca in *Primnoa resedaeformis:* relationship to temperature? In: Freiwald A, Roberts JM (eds) Cold-water Corals and Ecosystems. Springer, Berlin Heidelberg, pp 1061-1079

Sinclair DJ, Kinsley LPJ, McCulloch MT (1998) High resolution analysis of trace elements in corals by laser ablation ICP-MS. Geochim Cosmochim Acta 62: 1889-1901

Smith JE (1997) Climate reconstructions using deep-sea corals. PhD thesis, McMaster Univ, Hamilton, Ontario, Canada

Smith JE, Risk MJ, Schwarcz HP, McConnaughey TA (1997) Rapid climate change in the North Atlantic during the Younger Dryas recorded by deep-sea corals. Nature 386: 818-820

Smith JE, Brand U, Risk MJ, Schwarcz H (1999) Mid-Atlantic Ridge hydrothermal events recorded by deep-sea corals. Canad J Earth Sci 36: 511-517

Smith JE, Schwarcz HP, Risk MJ (2000) Paleotemperatures from deep-sea corals: overcoming 'vital effects'. Palaios 15: 25-32

Stanley GD, Cairns SD (1988) Constructional azooxanthellate coral communities: an overview with implications for the fossil record. Palaios 3: 233-242

Sylvester P (2001) Principles and applications of laser ablation ICP mass spectrometry in the earth sciences. Mineral Ass Canad Short Course 29: 203-211

Skeletal Mg/Ca in *Primnoa resedaeformis*: relationship to temperature?

Owen A. Sherwood[1], Jeffrey M. Heikoop[2], Daniel J. Sinclair[3], David B. Scott[1], Michael J. Risk[4], Chip Shearer[5], Kumiko Azetsu-Scott[6]

[1] Centre for Marine Geology, Dalhousie University, Halifax, Nova Scotia, B3H 4J1, Canada
 (osherwoo@dal.ca)
[2] Los Alamos National Laboratory, EES-6, MSD462, Los Alamos, NM 87545, USA
[3] GEOTOP, Université du Québec à Montréal and McGill University, Québec, Canada
[4] School of Geography and Geology, McMaster University, Hamilton ON, L8S 4M1, Canada
[5] Institute of Meteoritics, University of New Mexico, Albuquerque, NM 87131, USA
[6] Bedford Institute of Oceanography, Dartmouth, Nova Scotia, Canada

Abstract. It has been suggested that the deep-sea gorgonian coral *Primnoa resedaeformis* may be an important paleoceanographic archive. Seventeen colonies collected from the upper slope of the NW Atlantic margin (229 - 447 m) were analyzed to see if skeletal Mg/Ca is related to temperature. Analyses were focused on the calcite cortex region of skeletal sections to avoid interference from organic Mg in the horny layers found closer to the center of sections. Comparison of bulk skeletal Mg/Ca with hydrographic temperature yielded the relationship Mg/Ca (mmol/mol) = 5 (+/- 1.4) T (°C) + 64 (+/- 10). This relationship was used to calibrate profiles of Mg/Ca measured across the annual rings of one large, well-dated colony, over the period 1950-2002. Mg/Ca profiles were broadly consistent among three sections spaced 10 cm apart along the main trunk of the colony. These profiles were in general agreement with the local instrumental record of temperature at 375 – 450 m. Some discrepancies between the coral and instrumental records of temperature may be a result of chronological error, poor sampling density, or additional factors influencing Mg partitioning in the coral. Overall, these preliminary results support the hypothesis that temperature drives Mg/Ca in the skeletal calcite of this species. It appears that environmentally meaningful records from *Primnoa resedaeformis* will be found at decadal scales or longer.

Keywords. Deep-sea corals, *Primnoa resedaeformis*, Mg/Ca, paleotemperature, Northwest Atlantic

Introduction

Climate records from the carbonate skeletons of reef corals have proven unrivalled among paleoceanographic archives (Druffel 1997; Hendy et al. 2002; Tudhope et al. 2001; Cobb et al. 2003). These reconstructions are limited, however, to the tropical surface waters. Deep-sea corals have been the focus of increasing attention because they inhabit a wide range of latitudes and depths, and appear to live for several hundreds of years or longer (Griffin and Druffel 1989; Druffel et al. 1990, 1995; Smith 1997; Risk et al. 2002). Previous studies have demonstrated the use of deep-sea corals in monitoring past variations in thermohaline circulation (Smith et al. 1997; Adkins et al. 1998; Mangini et al. 1998; Goldstein et al. 2001). The potential to extract useful data on episodic events has also been demonstrated (Smith et al. 1999).

There has been increasing awareness over the last decade of the deep-sea corals inhabiting the Maritimes region of Atlantic Canada, particularly in the Northeast Channel, situated between Georges and Browns Banks, SE of Halifax (Breeze et al. 1997; Gass and Willison 2005). One of the dominant gorgonian species found there, *Primnoa resedaeformis,* has 5 characteristics making it attractive as a potential marine archive.

1) *Two part skeleton*. The axial skeleton is composed of both calcite and horny protein called gorgonin. The calcite is derived from dissolved inorganic carbon at depth, whereas the gorgonin is derived from sinking particulate organic matter (Griffin and Druffel 1989; Heikoop et al. 1998). Geochemical analyses of both components, therefore, could be used to monitor past variations in both surface and deep-water processes (Heikoop et al. 2002).

2) *Preservation potential*. Calcite resists dissolution above the lysocline and gorgonin is an extremely tough and resistant protein.

3) *Longevity*. Risk et al. (2002) measured a lifespan of 320 years in a sub-fossil fragment collected from the NE Channel. The calculated thickening rate around the trunk was 0.044 mm a^{-1}; applying this growth rate to larger specimens collected from the same area suggests that life-spans of up to one thousand years are possible.

4) *Annual layers*. Tree-like rings are visible both in the younger 'horny axis', made of gorgonin and calcite, and, to a lesser extent, in the older calcite 'cortex' (Sherwood 2002). Andrews et al. (2002) validated the annual timing of these rings in Alaskan specimens.

5) *Distribution*. From samples in the Smithsonian archives, it appears that *Primnoa* inhabits broad geographic (Atlantic and Pacific oceans) and depth ranges (50 m - 3.5 km; Heikoop et al. 2002).

Although deep-sea corals appear promising as paleoceanographic archives, their development has been limited by sample availability and additional factors. The convoluted growth forms of many deep-sea Scleractinia (e.g., *Desmophyllum cristagalli*; Lazier et al. 1999) make it difficult to assign chronological significance to skeletal growth layers. The partitioning of various isotopic and elemental tracers into the coral skeleton is often controlled by growth-related kinetic effects, masking any environmental significance (Emiliani et al. 1978; Smith et al. 2000, 2002; Spiro

et al. 2000; Heikoop et al. 2002; Risk et al. 2005). Smith et al. (2000) developed a way to extract temperatures from patterns of $\delta^{13}C$ and $\delta^{18}O$ disequilibria in *Desmophyllum*, the "lines technique", but it is analytically difficult. Lack of long term hydrographic data from the depths inhabited by deep-sea corals presents a further challenge since the fidelity of coral-based reconstructions cannot be tested if these data do not exist.

In an earlier paper, Heikoop et al. (2002) measured $\delta^{18}O$ and Sr/Ca in the skeletal calcite of *Primnoa resedaeformis*. They concluded that both of these properties appear to be influenced by growth-related kinetic effects, likely masking any environmental significance. Here we examine skeletal Mg/Ca in the same suite of specimens, plus several more that were collected alive in 2000-2002. The temperature dependence of Mg/Ca in calcite is supported both theoretically (e.g., Koziol and Newton 1995; Lea et al. 1999) and by experiments on inorganic calcites (Katz 1973; Mucci 1987; Oomori et al. 1987). Temperature controls Mg/Ca in biological calcites as well, as first noted by Chave (1954) and later confirmed in calibration experiments, notably those involving foraminiferans (Nürnberg et al. 1996; Rosenthal et al. 1997; Lea et al. 1999; Elderfield and Ganssen 2000; Lear et al. 2002; Martin et al. 2002). These calibrations form the basis for the recent application of Mg/Ca paleothermometry to problems of Quaternary climate change (e.g., Mashiotta et al. 1999; Elderfield and Ganssen 2000; Martin et al. 2002; Lea et al. 2003). Concerning gorgonian corals, Weinbauer and Velimirov (1995) and Weinbauer et al. (2000) reported increases in skeletal Mg/Ca with temperature on the order of 5 mmol/mol per °C.

If Mg/Ca in the skeletal calcite of *Primnoa* is controlled by temperature, then profiles across the preserved calcite growth rings could provide continuous records of deep and intermediate water temperatures over hundreds of years. Magnesium is relatively abundant in *Primnoa* calcite (about 10 mol %; preliminary work), and should therefore be easy to measure by any number of solution or microbeam techniques. In a companion paper, Sinclair et al. (2005) compared the reproducibility of microbeam Mg/Ca profiles along the same and parallel traverses of the calcite cortex. Here, we report on preliminary measurements of Mg/Ca in 17 different colonies collected from the slope waters of the Eastern North American margin. We examine the relationship between Mg/Ca and temperature and compare Mg/Ca profiles with the instrumental records of temperature available for the last 50 years.

Methods

Coral collection

Specimens used in this study came from a variety of sources (Table 1 and Fig. 1). Eleven specimens were obtained from the Smithsonian Institution, Washington (Heikoop et al. 2002). Many of these originated from expeditions of the Gloucester Fisheries Company in the 1880's, others were dredged during oceanographic surveys in the mid 1900's. Unfortunately, five of the Gloucester Fisheries samples were

Table 1 Sample collection details

Cruise/Expedition (method, year)	Sample Name	Location	Latitude/Longitude (decimal degr.)	Depth [m]	Bottom Temp. [°C]
	Smithsonian-4258	NE edge of Georges Bank	42.067N/ 65.600W[b]	229	7.6
	Smithsonian-4524	S of Browns Bank	42.133N/ 65.583W	338	6.9
Gloucester Fisheries (fishing, 1879–1880)	Smithsonian-4544	NE edge of Georges Bank	42.067N/ 65.600W[b]	229	7.6
	Smithsonian-4589	Banquereau Bank	44.533N/ 57.167W[c]	274	6.2
	Smithsonian-4591	S of Halifax	42.750N/ 63.250W[c]	366	7.1
	Smithsonian-33576	Banquereau Bank	44.533N/ 57.167W[c]	411	5.5
R/V Albatross (dredge, 1883)	Smithsonian-33577	Georges Bank	42.050N/ 65.800W	240	7.5
R/V Gilliss (dredge, 1974)	Smithsonian-54269	E of Virginia Beach	37.050N/ 74.400W	237–385	11.5
S&B Fisheries (fishing, 2000)	HH2000-6	NE Channel	42.059N/ 65.584W	457	6.0
	HH2000-11	NE Channel	42.046N/ 65.802W	280	6.4
CCGS Hudson 020 (video grab, 2000)	HUD2002-20-VG2	NE Channel	42.047N/ 65.610W	331	7.0
	ROPOS-637.0007	NE Channel	42.047N/ 65.575W	475	6.0
ROPOS (R.O.V., 2001)	ROPOS-637.052	NE Channel	42.048N/ 65.577W	475	5.9
	ROPOS-639.009	NE Channel	41.998N/ 65.648W	410	6.1
	ROPOS-639.0010	NE Channel	41.903N/ 65.717W	376	6.6
CCGS Needler 037 (trawl, 2002)	NED2002-037.46-2	NE Channel	start: 42.0463N/ 65.622W end: 42.068N/ 65.6483W	250–290	7.2
CCGS Needler 037 (trawl, 2002)	NED2002-037.46-3	NE Channel	start: 42.0463N/ 65.622W end: 42.068N/ 65.6483W	250–290	7.2
CCGS Hudson 055 (video grab, 2002)	HUD2002-055-VG15	NE Channel	42.021N/ 65.682W	321	6.9
Confiscated[a] (trawl, 2002)	DFO2002-con5	NE Channel	Approx. 41.83–42.12N/ 65.75–65.43W	~400	n/a

[a] Sample confiscated in the NE Channel Marine Protected Area, exact depth unknown
[b] Co-ordinates estimated from known occurrences in the area
[c] Original co-ordinates incorrect; corrected for known occurrences in the area
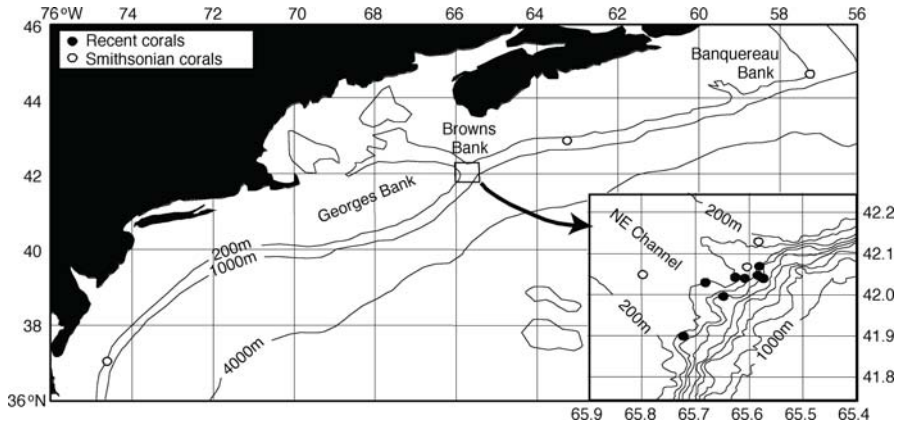
Fig. 1 Map of *P. resedaeformis* collection sites in the NW Atlantic Ocean. 'Smithsonian' corals obtained from archives; 'Recent corals' collected in 2000-2002. Square is close-up of NE Channel

associated with suspect or missing co-ordinates. Positions of these were estimated or corrected by comparison to other samples in the Smithsonian archives collected by the same captain and vessel in the same area. The second suite of specimens was collected more recently by: 1) local fishermen, who caught the corals in their long-lines, 2) benthic surveys conducted by the Bedford Institute of Oceanography, 3) an expedition of the remotely operated submersible *ROPOS* in August, 2001.

Retrieval of instrumental data

Temperature data for Scotian Shelf specimens were obtained from the Oceanographic Database at the Bedford Institute of Oceanography (B.I.O.; available online at: http://www.mar.dfo-mpo.gc.ca/science/ocean.database/data_query.html). Data were retrieved from 0.4° grid boxes centered over each of: 1) the NE Channel (42.00°N / 65.65°W), 2) the shelf break south of Halifax (42.75°N / 63.25°W), and 3) the Eastern edge of Banquereau Bank, in an area known as the Stone Fence (44.53°N / 57.17°W). For each coral, temperature picks were made from the best linear fit of temperature *vs.* depth in the corresponding grid. Data for Smithsonian #54269, collected off East Virginia, were obtained from the World Ocean Atlas 2001 (Conkright et al. 2002). Timeseries temperature data were retrieved for the NE Channel (Area "SS30" in the B.I.O. Oceanographic Database). Sampling density was highest in the 1970s and early 1980s and lowest in the 1950s and early 1990s. In light of the uneven sampling density, we opted to smooth the records by binning the data by year, and taking yearly averages.

Measurement of bulk skeletal Mg/Ca

Measurements of Mg/Ca were carried out independently on the Smithsonian and recent collections. In both cases, sections were cut from the basal parts of the colonies, and made into polished thin and/or thick sections. Analysis focused on the calcite cortex region of the sections. Smithsonian samples were analyzed by

secondary ion mass spectrometry (SIMS) at the University of New Mexico (see Heikoop et al. 2002 for analytical details). Analyses of each sample were replicated 10 times. External reproducibility was 1.4 % (1 sd). Recent specimens were analyzed by inductively coupled plasma mass spectrometry (ICPMS) at McMaster University, Hamilton, Canada. Approx. 2 mg powder samples were drilled from the surfaces of thick sections using a computerized micromill (Merchantek). The powders were dissolved in 0.1 % HNO_3 and diluted following standard procedures. The isotopes ^{24}Mg and ^{44}Ca were measured. Time and financial constraints permitted only three replicates per sample. Standardization used volumetric standards. Reproducibility of Mg/Ca, based on repeat measurements of standards, was approximately 2 % (1 sd).

Measurement of Mg/Ca profiles

Profiles of Mg/Ca across the sections of corals were performed by electron microprobe (EM) at Dalhousie University, Halifax, Canada, using a JEOL JXA 8200 Superprobe. Polished thin sections were carbon coated and analyzed in wavelength dispersive mode. Accelerating voltage was set to 15 kV and current to 80 nA. A 10 μm diameter beam was stepped across the coral surface at 10 μm increments along radial traverses. Traverses were done in triplicate, offset by 50 μm in the direction normal to the traverse. This approach averages out compositional heterogeneity along the direction of a growth layer. Dwell time was 100 ms, and magnification was 2500 x. A dolomite standard of known Mg and Ca composition was used for standardization. Reproducibility of Mg/Ca, based on measurements of the dolomite standard, was approximately 2.5 % (1 sd).

Results and discussion

Bulk Mg/Ca

Bulk skeletal Mg/Ca among all the samples averaged 100 mmol/mol (Fig. 2a). Values of Mg/Ca produced by SIMS (Smithsonian corals) and ICPMS (recent corals) overlapped, attesting to the accuracy of both techniques. Values were closely correlated to temperature by the equation:

$$Mg/Ca \text{ (mmol/mol)} = 5.2 \text{ (+/- 1.4) T (}^{\circ}\text{C)} + 64 \text{ (+/- 10)} \qquad \textbf{(1)}$$

(values in parentheses are the 95 % confidence intervals). The very low value of Mg/Ca (86 mmol/mol) corresponding to Smithsonian #4544 fell much lower from the main trend of values and was excluded from the regression. This specimen was collected by Gloucester Fisheries in 1880 and its exact geographic and depth coordinates were not recorded in the Smithsonian catalogue. Therefore, it probably lived in deeper and/or colder water than we have estimated. It may be argued that the highest value of Mg/Ca (118 mmol/mol), corresponding to Smithsonian #54269, accounts disproportionately for the strength of the correlation ($r^2 = 0.80$). If this
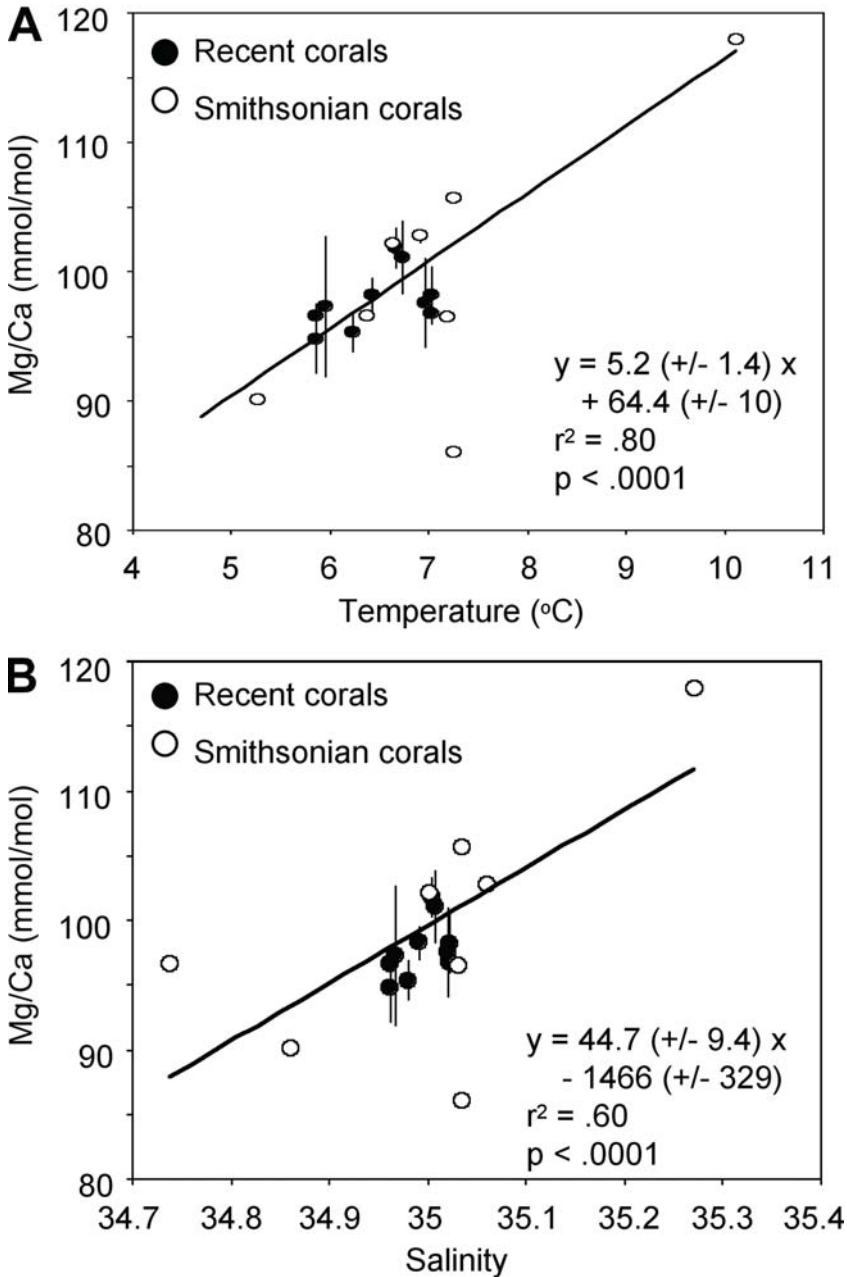
Fig. 2 Plots of bulk Mg/Ca *vs.* temperature **A** and salinity **B** in specimens of *P. resedaeformis*. Recent corals were analyzed by ICPMS, Smithsonian corals by SIMS. Lines of best fit drawn through all values, except lowermost Mg/Ca value, corresponding to Smithsonian sample 4544 (see text for explanation). Vertical bars are 1 standard error. SIMS errors are smaller than symbols. Errors in equations are the 95 % confidence intervals

value is excluded, r^2 drops to 0.47, yet the slope and intercept remain unchanged (within error) and the correlation remains significant at p <0.05. Since this specimen was collected during a research expedition in 1974, and the co-ordinates and temperature estimate are reliable, there are no grounds for excluding it from the regression.

Equation 1 has approximately the same slope, but much higher intercept, compared with two Mg/Ca *vs*. temperature curves recently measured in shallow water gorgonians (Table 2). This suggests that among different gorgonian species, temperature has a similar effect on the rate of Mg partitioning in the skeletal calcite, but factors controlling the amount of Mg available at calcification differ. Species differences in Mg/Ca are well documented from studies on foraminifera (e.g., Rosenthal et al. 1997; Lea et al. 1999). Furthermore, Mg/Ca is an order of magnitude higher in *Primnoa* than in inorganic calcites precipitated at similar temperatures (Mucci 1987; Oomori et al. 1987) and 2 orders higher than in foraminiferans. Therefore, the calcite in *Primnoa* is similar to other biological calcites in that temperature appears to drive both the thermodynamics of Mg partitioning and physiological processes regulating the transport of Ca and Mg to the site of calcification (Rosenthal et al. 1997). We also note that a linear regression gives the best fit to our data, whereas inorganic (Mucci et al. 1987; Oomori et al. 1987) and foraminiferal calcites (Nürnberg et al. 1996; Rosenthal et al. 1997; Lea et al. 1999) exhibit an exponential increase of Mg/Ca with temperature. Clearly, more analyses from *Primnoa* specimens inhabiting a broader range of temperatures are necessary; but these preliminary results are an adequate starting point for calibrating Mg/Ca profiles.

Table 2 Relationship between Mg/Ca (mmol/mol) and temperature in gorgonian calcites reported in this and other studies

Slope	Intercept	Temp. Range [°C]	Species	Reference
4.4	8	16.2 – 20.4	*Paramuricea clavata* *Eunicella cavoliini* *Eunicella singularis* *Lophogorgia ceratophyta*	Weinbauer and Velimirov 1995
5	40	13-18	*Corallium rubrum*	Weinbauer et al. 2000
5.2 +/- 1.4[a]	64 +/- 10[a]	5.2 – 10.1	*Primnoa resedaeformis*	This study

[a] errors are 95 % confidence intervals

Mg/Ca was also significantly correlated to salinity (Fig. 2b). With the available data it is impossible to control for one parameter, temperature or salinity, independent of the other. However, the correlation of Mg/Ca with salinity is most likely accounted for by the tight correspondence between salinity and temperature in the slope waters of the Scotian margin (Houghton and Fairbanks 2001). Waters further to the north along the margin are fresher and cooler, while those from the south are warmer and more saline. In other words, given the strong correlation between Mg/Ca and temperature, we would expect a correlation between Mg/Ca

and salinity in this region. Salinity is known to influence Mg/Ca in foraminiferans, but the effect is secondary to that of temperature (Nürnberg et al. 1996; Lea et al. 1999). Additional factors which are known to affect Mg/Ca in foraminiferal calcites include pH (Lea et al. 1999), the presence of gametogenic calcite (Nürnberg et al. 1996) and preferential diagenesis of Mg/Ca enriched phases (Brown and Elderfield 1996). Future experiments on laboratory grown *Primnoa* colonies may resolve some of these issues.

Chronology

For the purpose of comparing Mg/Ca profiles, we focused on one large colony that was obtained from the Canadian Department of Fisheries and Oceans from the NE Channel (DFO-2002-con5; this specimen was caught in bottom trawl gear, exact depth and hence temperature is unknown). Three sections were cut from the lower and middle part of the main trunk, each separated by a distance of approx. 10 cm (Fig. 3). In all three sections, both horny axis, the darker part toward the middle, and calcite cortex, the white outer part, were present (Fig. 4). Since live tissue was present along the entire 70 cm colony length, calcite deposition would have carried on until the summer of 2002 when it was collected.

Chronology was established by counting the annual rings back from the margin. This proved rather straightforward in the horny axis, since rings there are easily visible as alternating dark brown - light brown couplets (Fig. 4). In the cortex, however, rings are visible as slight differences in translucence but are difficult to trace laterally or count. There were plenty of discontinuous horny rings within the cortex that could be identified more unambiguously, providing greater chronological constraint in this region (Fig. 5). Separate radiocarbon measurements of the horny rings in section A (Sherwood, Guilderson, Scott and Risk, unpublished data) allowed us to locate 1972, the peak in bomb radiocarbon in surface ocean particulate organic matter, from which skeletal gorgonin is derived (Griffin and Druffel 1989; Heikoop et al. 1998). A complete chronology was then established using 1972 and 2002 as control points. Prominent, dark horny rings extending upwards from section A, along the length of the trunk, were used as chronological benchmarks in the other two sections. Chronologies of EM profiles were resolved to the nearest year; but in some cases, an average linear growth rate was interpolated across several consecutive years (Fig. 5). In comparing Mg/Ca profiles among different sections, the estimated chronological error is +/- 2 years.

Filtering and smoothing

A drawback to the EM is sensitivity to surface irregularities. Relief, presence of cracks, detrital surfaces and horny layers were associated with very high or low values of Mg/Ca compared to clean cortex (typically 85-115 mmol/mol). A filtering procedure was applied by converting values of Mg/Ca into corresponding temperatures (T-calc) using equation 1, and comparing the distribution with the observed temperature data (T-obs). The best match with T-calc occurred when T-obs were retrieved from a depth of 375 - 450 m (Fig. 6). Since the bulk of T-obs fell within 4 - 9.5°C, values of T-calc outside this range (Mg/Ca equivalent to 85 –
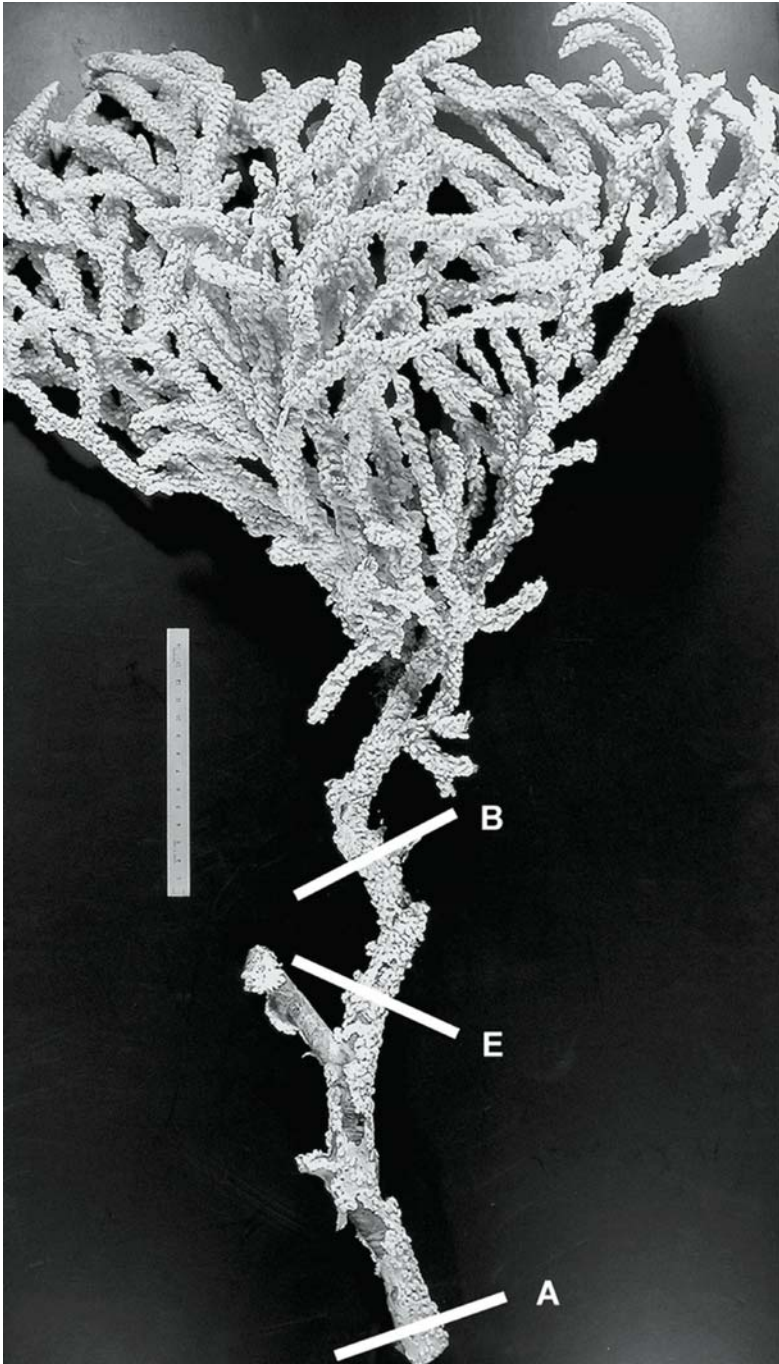
Fig. 3 Picture of *P. resedaeformis* specimen DFO2002-con5, with tissue layer intact. Sections cut for EM probe analysis are indicated by white lines and letters. Ruler for scale is 15 cm
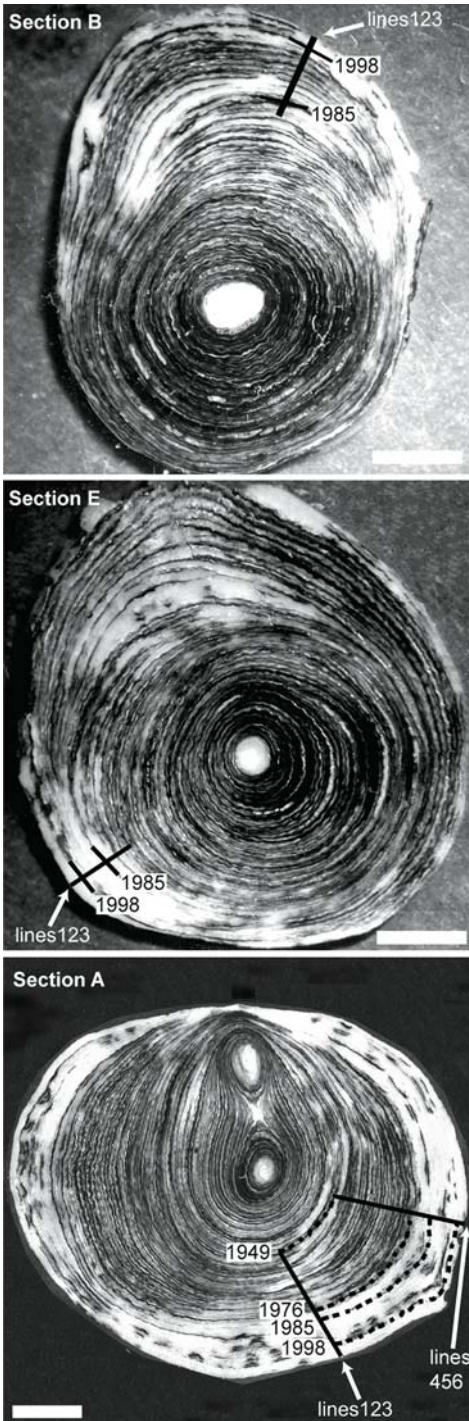
Fig. 4 Photomicrographs of sections indicated in Figure 3. Darker region towards center is horny axis, white region to the outside is calcite cortex. Black lines show positions of radial traverses by EM probe and some of the annual layers used as chronological benchmarks between the different sections and profiles. Each profile of Mg/Ca is the average of three separate lines. Scale bars are 4 mm
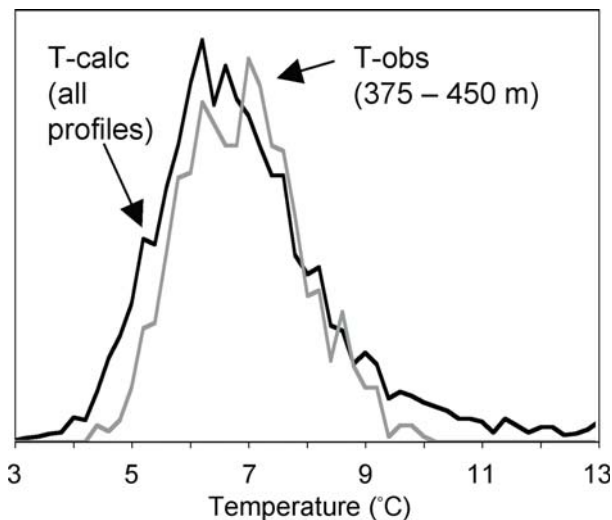
Fig. 5 Histogram showing the distribution of instrumental temperature (T-obs), and calculated temperature (T-calc) from all profiles of coral Mg/Ca. T-calc has a second mode (not shown) centered over 22°C. Values of T-calc falling outside the range 4 – 9.5°C were excluded in filtering. T-obs data are from area SS-30 in the B.I.O. database

113 mmol/mol) were excluded. Any years having less than 3 separate measurements of T-calc or T-obs were also excluded. After filtering, the distributions of T-calc and T-obs were statistically indistinguishable (Fig. 6).

In looking at Mg/Ca profiles (Fig. 7a), it is clear that large variability exists along and among the parallel, triplicate traverses – about 25 % in amplitude. This variability can be attributed to 1) analytical noise, 2) misalignment of the parallel profiles along the same growth surface, and 3) true compositional heterogeneity. Sinclair et al. (2005) estimated an analytical error of around 6 % / ($\sqrt{n}$) with the Dalhousie EM, where n = the number of point measurements. In taking yearly averages, the *estimated analytical error* reduces to 2 %, since there were approximately 10 point measurements in every year's worth of calcite. The *measured error* of 1-year averaged profiles was about 2.5 %, while the amplitude of these profiles was >12 % (Fig. 8). Therefore, most (about 10 %) of the variability seen in the 1-year averaged curves represents a real signal. This amplitude is comparable to that of the 1-year averaged records of T-calc (Fig. 7b).

Profiles

Many features of the 1-year averaged curves were broadly consistent among the different sections (Fig. 8). Highs, where T-calc = 7°C, were centered over 2000, 1995, 1986, and a high of up to 8°C was consistent through much of the 1970s. Likewise, lows of <6°C were centered over 1998, 1989, 1984, and much of the 1960's. Among the different profiles, the amplitude of these highs and lows were the same within the measured error. Values from around 2001 to the time of collection
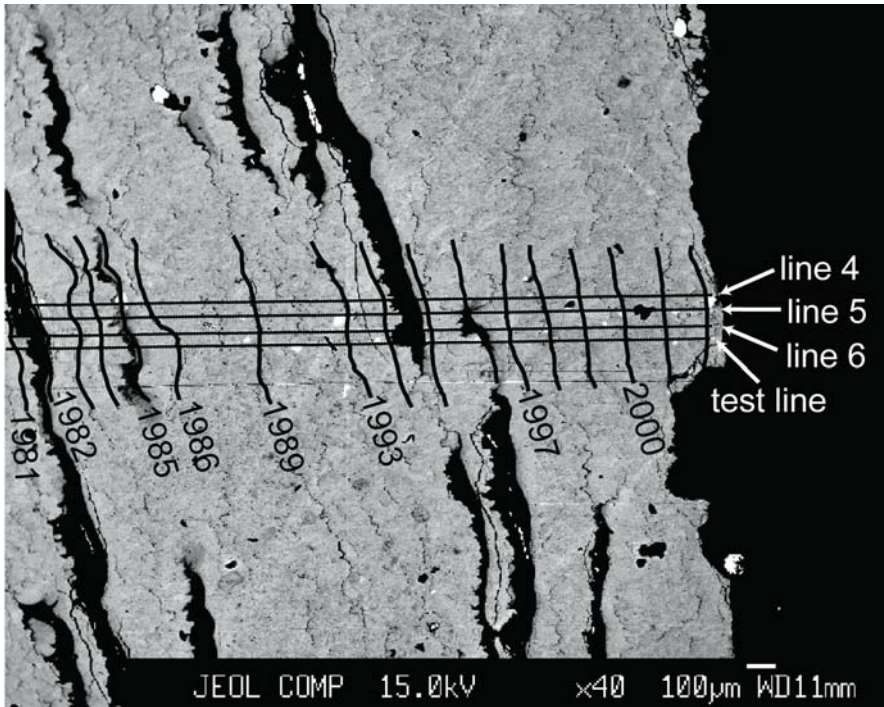
Fig. 6 SEM (backscatter mode) across the most recent part of section A, showing lines 4-5-6, each offset by 50 microns in the vertical direction, and the position of annual layers used to assign chronology. Horizontal line beneath "test line" is a scratch. Note the presence of discontinuous horny layers (dark) inter-layered with the calcite cortex (lighter grey). Also note that some years could not be identified unambiguously, e.g., between 1986 and 1993. In this instance, an average growth rate was interpolated across the time interval

were poorly reproduced; difficulty in positioning the start of the traverse on the most recent skeleton possibly accounts for the discrepancy. Other discrepancies among the different profiles may be accounted for by chronological error.

In comparing profiles of T-calc to the record of T-obs, the best correspondence occurred from 1995 onwards (Fig. 9). Before this time, it seems that highs in T-obs were poorly captured in profiles of T-calc. Linear regression of the two records yielded a weak ($r^2 = 0.21$) but significant ($p < 0.01$) correlation (Fig. 10). Regression of the data from 1995 onwards approached a 1:1 relationship with a higher value of r^2 (0.50). It is not clear why the warmest periods are poorly captured in the record of T-calc, but it may be that these periods favour the synthesis of gorgonin over calcite. Prominent horny rings were associated with 1985 and 1994 in all three sections (Fig. 5). Because of the presence of horny rings in the cortex, the range of climate variability may not be fully expressed in this particular coral. Also, averaging the profiles of T-calc (Fig. 9) tends to dampen out the amplitude of the final curve, especially if the chronology is imperfect. On the other hand, there were gaps in
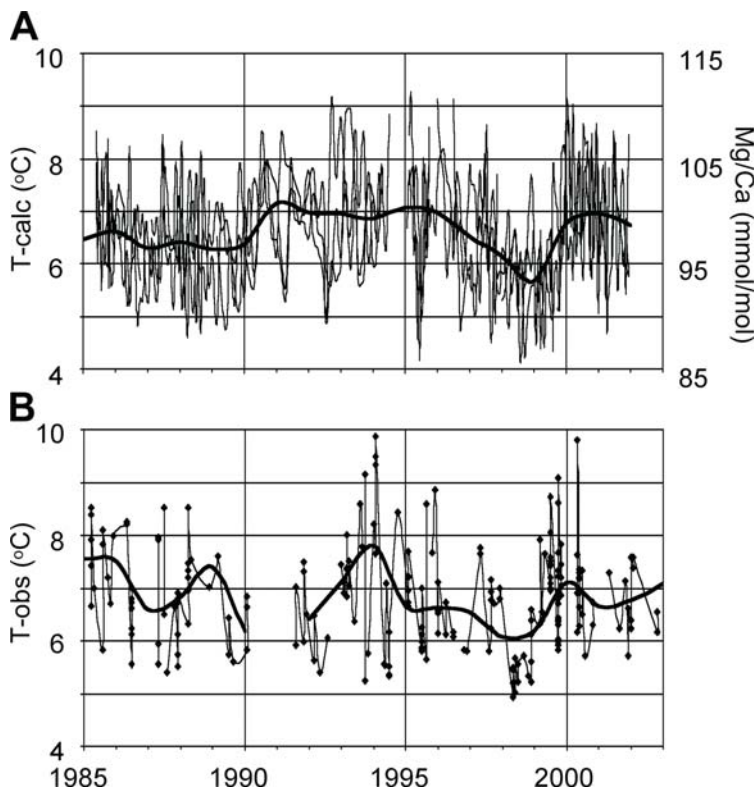
Fig. 7 Example of unsmoothed Mg/Ca **A** and T-obs **B** data, superimposed with one year average curve (bold line). Mg/Ca data are three lines (lines 4-5-6) from section A, as shown in Figure 6. T-calc scaled to Mg/Ca using equation 1 (see text). T-obs data are from area SS-30 in the B.I.O. database
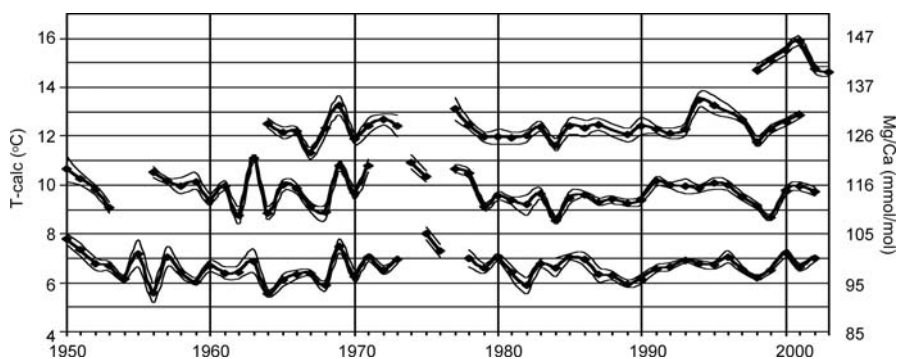
Fig. 8 Mg/Ca profiles across all three sections. Data are the filtered averages of three parallel lines offset by 50 microns in the direction parallel to growth layers. Bold curves are one year averages, enveloped by one standard error. Y-axis scaled to lowermost curve, other curves offset by +3°C to facilitate comparison. T-calc scaled to Mg/Ca using equation 1 (see text). Chronology was established on the basis of ring counts viewed in thin section, and 1972 radiocarbon control point
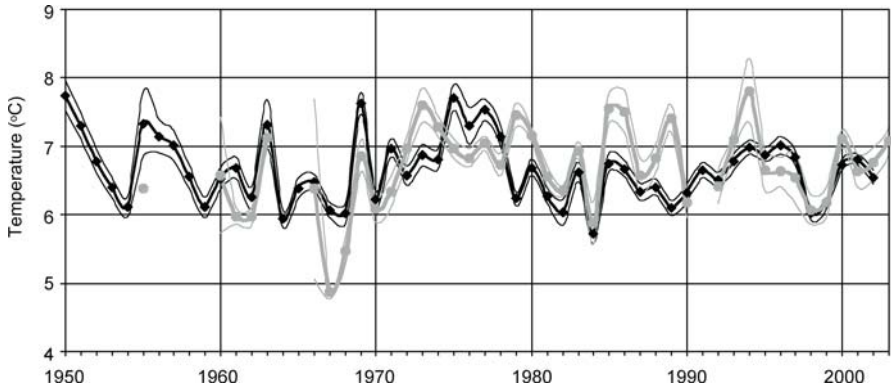
Fig. 9 Average of all four profiles of T-calc across the three sections of DFO2002-con5 (black) compared with the 375 – 450 m temperature record for area SS-30 in the B.I.O database (grey). Lines are enveloped by 1 standard error
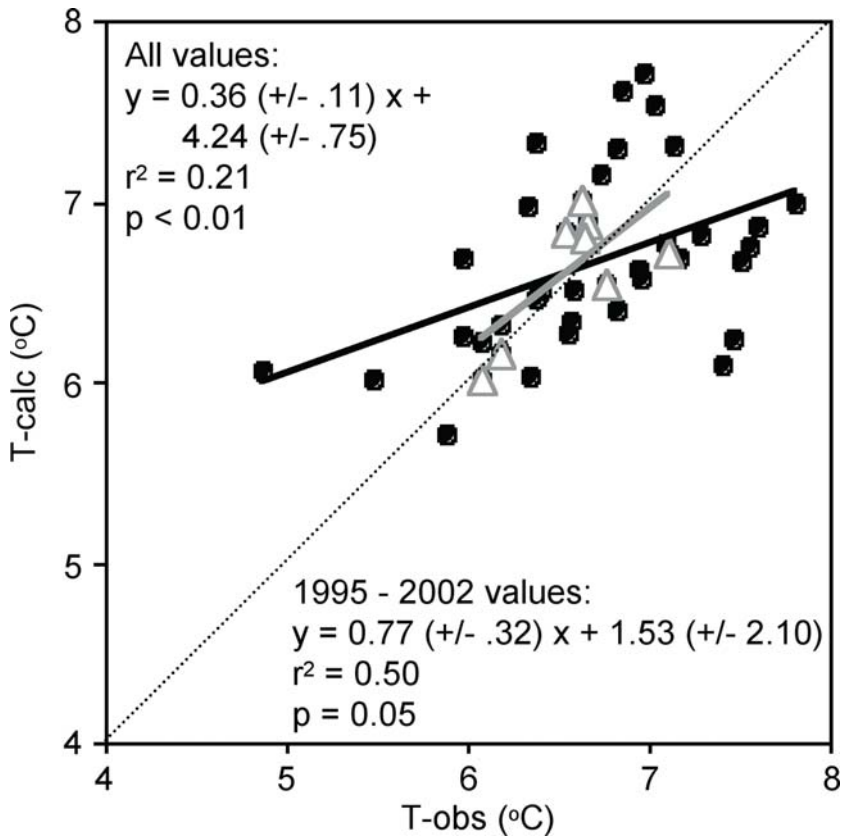
Fig. 10 Regression of T-calc *vs.* T-obs time-series data (from Fig. 9) for all years (black circles) and 1995 – 2002 (open triangles). Errors in equations are the 95 % confidence intervals. Dashed line is the 1:1 relationship, for reference

the record of T-obs where some years were sampled poorly or not at all (Fig. 7). In addition, T-obs data were retrieved from a relatively large geographic area in order to have enough data for a reasonably continuous curve. The climate of this larger area may differ somewhat from that experienced at the mouth of the NE Channel, where the coral was collected.

Conclusions

Though preliminary, our results support the hypothesis that temperature controls Mg/Ca in the calcite cortex region of *Primnoa* skeletons. Bulk values of Mg/Ca from 17 different specimens collected along the NW Atlantic margin were positively correlated to temperature. Values of Mg/Ca were also correlated to salinity, but this is likely a result of the positive correlation between temperature and salinity in the slope waters of this region, more so than an effect of salinity on the partitioning of Mg/Ca. Qualitatively speaking, profiles of Mg/Ca in three different sections of one colony were reproducible. The correlation of these profiles with the instrumental record of temperature was good in some cases, and poor in others. Reasons for the discrepancies include chronological error and poor sampling density of both the coral and instrumental records. Additional factors may also influence Mg/Ca partitioning in these skeletons, including biology.

Inter-colony reproducibility will be the next test of Mg/Ca reliability. We have analyzed many more colonies with the EM probe having many features of Figure 9 in common, but chronological hurdles are presently the most significant impediment in ground-truthing these records. Though meaningful temperature records at sub-annual scales could possibly be attainable, the most reliable and useful records will be found at decadal scales. Ultimately, Mg/Ca from *Primnoa* may prove a potentially valuable archive of deep and intermediate water mass paleotemperatures.

Acknowledgements

References

Adkins JF, Cheng H, Boyle EA, Druffel ERM, Edwards RL (1998) Deep-sea coral evidence for rapid change in ventilation of the deep North Atlantic 15,400 years ago. Science 280: 725-728

Andrews AH, Cordes E, Heifetz J, Cailliet GM, Coale KH, Somerton D, Munk K, Mahoney M (2002) Age and growth of a deep sea, habitat-forming octocorallian (*Primnoa* sp.) from the Gulf of Alaska, with radiometric age validation. Hydrobiologia 471: 101-111

Breeze H, Davis DS, Butler M, Kostylev V (1997) Distribution and status of deep-sea corals off Nova Scotia. Marine Issues Committee Special Publication Number 1, Ecology Action Centre, Halifax

Brown S, Elderfield H (1996) Variations in Mg/Ca and Sr/Ca ratios of planktonic foraminifera caused by postdepositional dissolution - evidence of shallow Mg-dependent dissolution. Paleoceanography 11: 543-551

Chave KE (1954) Aspects of the biogeochemistry of magnesium. 1. Calcareous marine organisms. J Geology 62: 266-283

Cobb KM, Charles CD, Cheng H, Edwards RL (2003) El Nino/Southern Oscillation and tropical Pacific climate during the last millenium. Nature 424: 271-276

Conkright ME, Locarnini RA, Garcia HE, O'Brien TD, Boyer TP, Stephens C, Antonov JI (2002) World Ocean Atlas 2001: Objective Analyses, Data Statistics, and Figures, CD-ROM Documentation. National Oceanographic Data Centre, Silver Springs MD, 17 pp (data available online at http://iridl.ldeo.columbia.edu/SOURCES/.NOAA/.NODC/.WOA01/)

Druffel ERM (1997) Geochemistry of corals: proxies of past ocean chemistry, ocean circulation, and climate. Proc Nat Acad Sci USA 94: 8354-8361

Druffel ERM, King LL, Belastock RA, Buesseler KO (1990) Growth rate of a deep-sea coral using ^{210}Pb and other isotopes. Geochim Cosmochim Acta 54: 1493-1500

Druffel ERM, Griffin S, Witter A, Nelson E, Suthon J, Kashagarian M, Vogel J (1995) *Gerardia*: Bristlecone pine of the deep sea? Geochim Cosmochim Acta 59: 5031-5036

Elderfield H, Ganssen G (2000) Past temperature and δ^{18}O of surface ocean waters inferred from foraminiferal Mg/Ca ratios. Nature 405: 442-445

Emiliani C, Hudson JH, Shinn ES, George RY (1978) Oxygen and carbon isotopic growth record in a reef coral from the Florida Keys and a deep-sea coral from the Blake Plateau. Science 202: 627-629

Gass SE, Willison JHM (2005) An assessment of the distribution of deep-sea corals in Atlantic Canada by using both scientific and local forms of knowledge. In: Freiwald A, Roberts JM (eds) Cold-water Corals and Ecosystems. Springer, Berlin Heidelberg, pp 223-245

Goldstein SJ, Lea DW, Chakraborty S, Kashgarian M, Murrella T (2001) Uranium-series and radiocarbon geochronology of deep-sea corals: implications for Southern Ocean ventilation rates and the oceanic carbon cycle. Earth Plan Sci Lett 193: 167-182

Griffin S, Druffel ERM (1989) Sources of carbon to deep-sea corals. Radiocarbon 31: 533-543

Heikoop JM, Risk MJ, Schwarcz HP (1998) Stable isotopes of C and N in tissue and skeletal organics of a deep-sea gorgonian coral from the Atlantic coast of Canada: dietary and potential climate signals. Abstracts with Programs, Geol Soc Am Ann Meet 30: A317

Heikoop JM, Hickmott DD, Risk MJ, Shearer CK, Atudorei V (2002) Potential climate signals from the deep-sea gorgonian coral *Primnoa resedaeformis*. Hydrobiologia 471: 117-124

Hendy EJ, Gagan MK, Alibert CA, McCulloch MT, Lough JM, Isdale PJ (2002) Abrupt decrease in tropical Pacific Sea surface salinity at end of Little Ice Age. Science 295: 1511-1514

Houghton RW, Fairbanks RG (2001) Water sources for Georges Bank. Deep-Sea Res 48: 95-114

Katz A (1973) The interaction of magnesium with calcite during crystal growth at 25-90°C and one atmosphere. Geochim Cosmochim Acta 37: 1563-1586

Koziol AM, Newton RC (1995) Experimental determination of the reactions magnesite + quartz = periclase + CO_2 and the enthalpies of formation of enstatite and magnesite. Am Mineral 80: 1252-1260

Lazier AV, Smith JE, Risk MJ, Schwarcz HP (1999) The skeletal structure of *Desmophyllum cristigalli* - the use of deep-water corals in sclerochronology. Lethaia 32: 119-130

Lea DW, Mashiotta TA, Spero HJ (1999) Controls on magnesium and strontium uptake in planktonic foraminifera determined by live culturing. Geochim Cosmochim Acta 63: 2369-2379

Lea DW, Pak DK, Peterson LC, Hughen KA (2003) Synchroneity of tropical and high-latitude Atlantic temperatures over the last glacial termination. Science 301: 1361-1364

Lear CH, Rosenthal Y, Slowey N (2002) Benthic foraminiferal Mg/Ca-paleothermometry; a revised core-top calibration. Geochim Cosmochim Acta 66: 3375-3387

Mangini A, Lomitschka M, Eichstädter R, Frank N, Vogler S, Bonani G, Hajdas I, Pätzold J (1998) Coral provides way to age deep water. Nature 392: 347-348

Martin PA, Lea DW, Rosenthal Y, Shackleton NJ, Sarnthein M, Papenfuss T (2002) Quaternary deep-sea temperature histories derived from benthic foraminiferal Mg/Ca. Earth Planet Sci Lett 198: 193-209

Mashiotta TA, Lea DW, Spero HJ (1999) Glacial-interglacial changes in Subantarctic sea surface temperature and δ^{18}O-water using foraminiferal Mg. Earth Planet Sci Lett 170: 417-432

Mucci A (1987) Influence of temperature on the composition of magnesian calcite overgrowths precipitated from seawater. Geochim Cosmochim Acta 51: 1977-1984

Nürnberg D, Bijma J, Hemleben C (1996) Assessing the reliability of magnesium in foraminiferal calcite as a proxy for water mass temperatures. Geochim Cosmochim Acta 60: 803-814

Oomori T, Kaneshima H, Maetzato Y (1987) Distribution coefficient of Mg2+ ions between calcite and solution at 10-50°C. Mar Chem 20: 327-336

Risk MJ, Heikoop JM, Snow MG, Beukens R (2002) Lifespans and growth patterns of two deep-sea corals: *Primnoa resedaeformis* and *Desmophyllum cristagalli*. Hydrobiologia 471: 125-131

Risk MJ, Hall-Spencer J, Williams B (2005) Climate records from the Faroe-Shetland trough using *Lophelia*: Problems and prospects. In: Freiwald A, Roberts JM (eds) Cold-water Corals and Ecosystems. Springer, Berlin Heidelberg, pp 1097-1108

Rosenthal Y, Boyle EA, Slowey N (1997) Temperature control on the incorporation of magnesium, strontium, fluorine, and cadmium into benthic foraminiferal shells from Little Bahama Bank: prospects for thermocline paleoceanography. Geochim Cosmochim Acta 61: 3633-3643

Sherwood OA (2002) The deep-sea gorgonin coral *Primnoa resedaeformis* as an oceanographic monitor. MSc. Thesis, McMaster University, Hamilton, Canada

Sinclair DJ, Sherwood OA, Risk MJ, Hillaire-Marcel C, Tubrett M, Sylvester P, McCulloch M, Kinsley L. (2005) Testing the reproducibility of Mg/Ca profiles in the deep-water coral *Primnoa resedaeformis:* putting the proxy through its paces. In: Freiwald A, Roberts JM (eds) Cold-water Corals and Ecosystems. Springer, Berlin Heidelberg, pp 1039-1060

Smith JE (1997) The use of deep-sea corals as paleoceanographic monitors. PhD Thesis, McMaster University, Hamilton, Canada

Smith JE, Risk MJ, Schwarcz HP, McConnaughey TA (1997) Rapid climate change in the North Atlantic during the Younger Dryas recorded by deep-sea corals. Nature 386: 818-820

Smith JE, Brand U, Risk MJ, Schwarcz HP (1999) Mid-Atlantic ridge hydrothermal events recorded by deep-sea corals. Can J Earth Sci 36: 511-517

Smith JE, Schwarcz HP, Risk MJ, McConnaughey TA, Keller N (2000) Paleotemperatures from deep-sea corals: Overcoming 'vital effects'. Palaios 15: 25-32

Smith JE, Schwarcz HP, Risk MJ (2002) Patterns of isotopic disequilibria in azooxanthellate coral skeletons. Hydrobiologia 471: 111-115

Spiro B, Roberts M, Gage J, Chenery S (2000) $^{18}O/^{16}O$ and $^{13}C/^{12}C$ in an ahermatypic deep-water coral *Lophelia pertusa* from the North Atlantic: a case of disequilibrium isotope fractionation. Rapid Commun Mass Spec 14: 1332-1336

Tudhope AW, Chilcott CP, McCulloch MT, Cook ER, Chappell J, Ellam RM, Lea DW, Lough JM, Shimmield GB (2001) Variability in the El Nino-Southern oscillation through a glacial-interglacial cycle. Science 291: 1511-1517

Weinbauer MG, Velimirov B (1995) Calcium, magnesium and strontium in the calcite sclerites of Mediterranean gorgonians (Coelenterata : Octocorallia). Estuar Coast Shelf Sci 40: 87-104

Weinbauer MG, Brandstatter F, Velimirov B (2000) On the potential use of magnesium and strontium concentrations as ecological indicators in the calcite skeleton of the red coral (*Corallium rubrum*). Mar Biol 137: 801-809

Paleotemperatures from deep-sea corals: scale effects

Audrey Lutringer, Dominique Blamart, Norbert Frank, Laurent Labeyrie

Laboratoire des Sciences du Climat et de l'Environnement (LSCE) Unité mixte de
Recherche CEA-CNRS, Bât. 12, Avenue de la Terrasse, F-91198 Gif-sur-Yvette
Cedex, France
(Audrey.Lutringer@lsce.cnrs-gif.fr)

Abstract. Like other biogenic carbonate that can be dated, aragonite skeleton of
deep-sea corals is a potential archive of oceanographic changes over time. Stable
isotope analysis is commonly used in paleoceanographic reconstruction of past
seawater temperatures, however, offset from isotopic equilibrium as well as recent
observations about isotope distribution with the micro-structure of deep-water
corals implies non direct paleoclimate reconstructions. Here we test the influence of
the sampling scale on oceanographic interpretations.

The stable isotope composition for different modern calyxes of *Lophelia pertusa*
has been analyzed at different scales using either a macro or a micro-sampling
technique. The comparison of the obtained results from the two sampling techniques
shows that the isotopic variability observed with the micro-sampling is twice the
one with macro-sampling. Moreover the macro-sampling is not an average of what
happens at a more precise scale.

Nevertheless a realistic seawater temperature estimate can be retrieved using the
equation of Smith et al. (2000) for both the macro and the micro-sampled corals.
However, a test of the reproducibility on a single calyx reveals important isotopic
inhomogenities at a very fine scale (~μm), yielding an external reproducibility of
the seawater temperature estimates of about ±0.7°C for micro sampled corals.

Keywords. Stable isotopes, deep-sea corals, *Lophelia pertusa*, past seawater
temperature, skeletal structure

Introduction

Deep-water corals are potential archives recording intermediate to sub-surface
water temperatures and salinity. As they grow rapidly, with growth rates in the order
of several mm to centimetres per year (Moore and Krishnaswami 1972; Moore et
al. 1973; Druffel et al. 1990), a branch of a coral of 2 to 20 cm size can represent a
few years to several decades. Moreover, coral aragonite can be precisely dated by
^{230}Th/U and/-or ^{14}C dating (Adkins and Boyle 1997; Smith et al. 1997; Adkins et al.

1998; Mangini et al. 1998; Cheng et al. 2000; Frank et al. 2004; Schröder-Ritzrau et al. 2005).

The oxygen isotopic composition of biogenic carbonates is commonly used to determine paleo-seawater temperatures (McCrea 1950; Urey et al. 1951; Epstein et al. 1953; Shackleton 1974; Aharon 1991; Böhm et al. 2000). Therefore aragonite skeletons of deep-water corals are potential archives recording intermediate to sub-surface water temperatures and salinity. However, this aragonite skeleton is not precipitated in isotopic equilibrium with ambient seawater and consequently the stable oxygen isotope values (expressed in $\delta^{18}O$) are not directly linked to seawater $\delta^{18}O$ and temperature (Weber and Woodhead 1970; Mikkelsen et al. 1982; Freiwald et al. 1997; Mortensen and Rapp 1998; Spiro et al. 2000). Large variations in $\delta^{18}O$ (~5 ‰) and $\delta^{13}C$ (~10 ‰) are observed in coralline aragonite (Weber 1973; Mikkelsen et al. 1982; Swart 1983; Wefer and Berger 1991). Moreover, deep-water corals show a linear relationship between $\delta^{18}O$ and $\delta^{13}C$ values (Weber and Woodhead 1970; Mikkelsen et al. 1982; Swart 1983; Swart et al. 1996; Leder et al. 1996), which has been interpreted in terms of kinetic isotope fractionation (Emiliani et al. 1978; McConnaughey 1989a, b, 2003). However, the linear correlation of C and O isotopes is expected to depend on the metabolism of the coral species as well on environmental controls such as temperature (Furla et al. 2000; Heikoop et al. 2000; Spiro et al. 2000).

Smith et al. (2000) have attempted to establish a first empirical temperature calibration for deep-water corals despite the constraints of the origin of isotopic fractionation. On 18 different modern deep-water coral species from various depth and locations, reflecting a ambient seawater temperature range of 1° to 28°C, the stable oxygen and carbon isotopic composition was determined on macro coral aliquots. All samples yielded a strong linear correlation between the oxygen and carbon isotopic composition. From such a $\delta^{13}C$ *vs.* $\delta^{18}O$ regression line for an individual coral, the $\delta^{18}O$ value corresponding with $\delta^{13}C$ aragonite equal to $\delta^{13}C$ seawater DIC, corrected by $\delta^{18}O$ seawater seems to be a function of temperature (Fig. 1). Knowing seawater $\delta^{18}O$, the temperature dependence of $\delta^{18}O$ aragonite follows then:

$$\delta^{18}O_{aragonite} = \delta^{18}O_{water} - 0.25\ T\ (°C) + 4.97$$

Based on this equation, Smith et al. (2000) demonstrated that paleotemperatures can be retrieved to a precision of ±0.36 to ±1°C. Smith et al. (2000) further proposed that coeval benthic Foraminifera may be used for calibration if the isotopic composition of seawater is unknown, such as in the study of fossil corals.

The sampling procedure chosen by Smith et al. (2000) using macro coral sub-samples does, however, not take different crystal types (Ogilvie 1896; Hidaka 1991; Cuif and Dauphin 1998; Cuif et al. 2003), and thus variable isotope fractionation mechanisms into account. Recently Mortensen and Rapp (1998), Rollion-Bard (2001), Adkins et al. (2003), Rollion-Bard et al. (2003a, b) and Blamart et al. (2005) have demonstrated that the correlation of the coral carbon and oxygen isotope
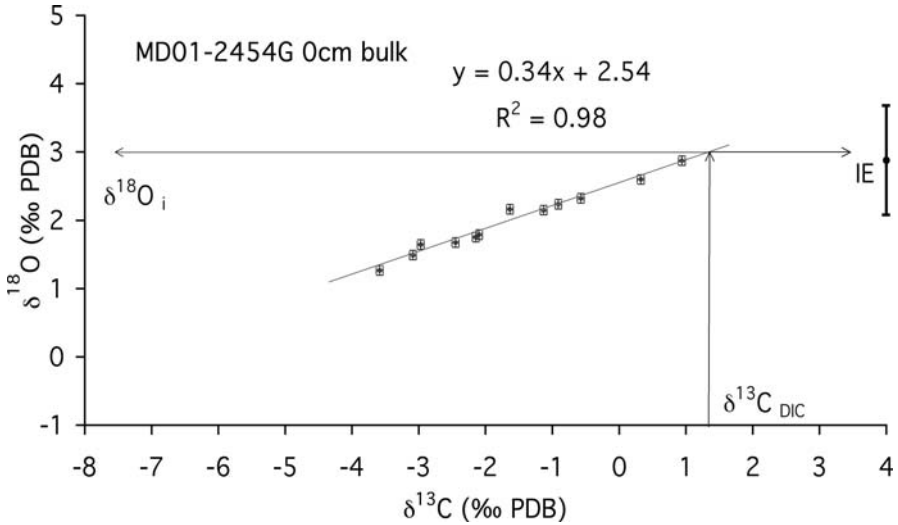
Fig. 1 Principal of the method proposed in Smith et al. (2000). The $\delta^{18}O$ value retrieved from the regression line for $\delta^{13}C = \delta^{13}C_{DIC}$ is assumed to be equal to the $\delta^{18}O$ value of isotopic equilibrium (IE) with seawater, i.e. $\delta^{18}O_i$

composition can be strongly biased if centres of calcification (thin white bands) and fibres are sampled together. Adkins et al. (2003) demonstrated that isotopic data from the region of calcification may even fall off the linear trend between $\delta^{18}O$ and $\delta^{13}C$ in *Desmophyllum cristagalli* corals. This deviation, where $\delta^{13}C$ may remain constant and $\delta^{18}O$ further decreases, does not support "vital-effects" that call upon kinetic fractionation to explain the offset from isotopic equilibrium. Such fractionation processes are more likely to be related to biologically induced pH gradients in the calcifying region (Adkins et al. 2003; Rollion-Bard et al. 2003a, b).

In this contribution, we tested the validity and the reproducibility of the temperature calibration established by Smith et al. (2000) by comparing a macro-sampling strategy with a micro-sampling strategy to account for different crystal types in modern *Lophelia pertusa* corals from a site on Rockall Bank.

Material and methods

The corals used in this study were collected from a marine core MD 01-2454G (55°31'17"N, 15°39'08"W, 747 m depth.)

This core has been taken on the south western slope of the Rockall Trough where carbonate mounds, colonized by an abundant fauna (deep-water corals, sponges, fishes, and crabs) has been identified at water depths between 600 and 1000 m (Hovland et al. 1994, 1998; Henriet et al. 1998; van Weering 1999; Bett 2001; De Mol et al. 2002; see also Freiwald 2002 for details on this site). The annual average $\delta^{18}O$ value of seawater, as well as the ambient seawater temperature can be retrieved

from the eWOCE oceanographic atlas. $\delta^{13}C_{DIC}$ can be retrieved from $\delta^{13}C$ values of benthic Foraminifera (*Planulina ariminensis*). Oceanographic data are reported in Table 1.

Table 1 The annual ambient seawater temperature is taken from the eWOCE oceanographic atlas. $\delta^{18}O$ of seawater ($\delta^{18}Ow$) is estimated based on the relationship of $\delta^{18}O$ and salinity in the North Atlantic (see GEOSECS data). $\delta^{13}C$ of seawater ($\delta^{13}Cw$) is estimated from benthic Foraminifera data of the core

Core	Latitude	Longitude	Depth (m)	$\delta^{18}Ow$ (‰-PDB)	$\delta^{13}C_{DIC}$ (‰-PDB)	$T_{annual\ mean}$ (°C)
MD01-2454G	55°31'17"N	15°39'08"W	747	0.28	1.3	8.5

The deep-water corals of this core have been identified as predominantly *Lophelia pertusa*, but *Madrepora oculata*, and *Desmophyllum cristagalli* are also present.

In this study we focus on the top core MD 01-2454G and particularly on a large branch (10 cm length) where stood living polyps. These corals did not show any visible coating of Fe and Mn oxide/hydroxides and did not have major visible alteration (bioerosion). Corals were then cleaned using double distilled water and ultrasound to efficiently remove sediment particles. They were dried in an oven at 50°C for 12 hours. Prior to further investigation we performed XRD analyses in order to investigate for any secondary crystallisation into calcite. Samples composed of aragonite with no traces of calcite were investigated for their isotopic composition. ^{230}Th/U dating on one calyx of the modern coral branch gives an age of 18±6 years, close to the date of collection (Frank et al. 2005).

On these samples two different subsampling strategies were applied. We first applied macro-sampling to compare the stable isotope composition of our samples to those previously published applying a similar subsampling technique (Emiliani et al. 1978; Mikkelsen et al. 1982; McConnaughey 1989a, b, 2003; Smith et al. 2000). For one coral 10 to 20 sub-samples from random locations have been obtained using a dental drill (0.8 mm diameter) providing about 200 µg of carbonate, largely enough to duplicate the isotopic measurements.

The second sampling strategy is based on recent studies taking into consideration the micro-structure of deep-water corals (Lazier et al. 1999; Adkins et al. 2003; Cuif et al. 2003; Rollion-Bard et al. 2003a, b). Therefore, we used a micro-sampling technique to allow for selective sampling of skeleton micro-structures. A slab of coral was cut perpendicular to its growth axis and mounted with epoxy on a glass slide. The sample was ground to about 300 µm thickness with abrasive paper. Each slide was first digitalized and then milled using a micro-sampler (Micromill) kindly provided by LODYC at Jussieu Paris VI (C. Pierre). The methodology is described in detail by Adkins et al. (2003). A total of 8 corals from top core MD01-2454G have been investigated using this sampling strategy.

The aragonite powder (either from micro-drilling or classical drilling) was roasted under vacuum at 350°C for 45 min to eliminate organic matter, following the procedure by Duplessy et al. (1986). About 100 µg of aragonite were reacted

with 100 % phosphoric acid at 90°C in an automated line coupled to an OPTIMA VG mass spectrometer. Results are reported in delta notation expressed in per mil relative to V-PDB (Vienna Pee Dee Belemnite). The reproducibility (1 SD) is ±0.07 ‰ for $\delta^{18}O$ and ±0.05 ‰ for $\delta^{13}C$.

Results

Results from both macro and micro-sampling of the coral are given in Table 2 and presented in Figure 2. The isotopic variability for macro-sampled corals is 1.33 ‰ for $\delta^{18}O$ (ranging from 0.45 ‰ to 1.78 ‰) and 3.18 ‰ for $\delta^{13}C$ (ranging from -4.42 ‰ to -1.23 ‰) and $\delta^{18}O$ *versus* $\delta^{13}C$ presents a strong linear relationship ($R2 = 0.98$; Fig. 1) similar to previous observations (Mikkelsen et al. 1982; McConnaughey 1989a, b, 1997; Aharon 1991; Leder et al. 1996; Swart et al. 1996; Freiwald et al. 1997; Mortensen and Rapp 1998; Blamart et al. 2001). The slope and the intercept is equal to 0.34 ±0.04 and 2.54 ±0.12 according to the least squares method.

Table 2 Results of stable isotopes analysis with macro (first line) and micro-sampling. Corals are from the same branch from top core MD01-2454G. They are identified by a calyx number. For each calyx the slope and the intercept of the regression line has been calculated with the least square method as well as the correlation coefficient. N is the number of data available to calculate the slope and the intercept. Temperature has been estimated with equation from Smith et al. (2000)

Calyx	N	Slope±2σ	Intercept±2σ	R^2	$\delta^{18}O_i$	T°C Smith
bulk	9	0.34±0.04	2.54±0.12	0.98	2.98±0.05	9.0±0.2
c1(a)	16	0.42±0.02	2.58±0.28	0.98	3.13±0.11	8.5±0.4
c1(b)	7	0.44±0.08	2.51±0.18	0.95	3.08±0.13	8.6±0.5
C3b	18	0.40±0.04	2.80±0.12	0.96	3.32±0.14	7.7±0.6
C7b(a)	6	0.38±0.04	3.15±0.10	0.99	3.64±0.07	6.4±0.3
C7b(b)	10	0.40±0.04	3.00±0.14	0.97	3.52±0.13	6.9±0.5
C7b(c)	9	0.42±0.02	2.91±0.06	0.99	3.46±0.08	7.1±0.3
C7b(c)'	9	0.42±0.04	2.73±0.12	0.98	3.28±0.14	7.9±0.6
c2a	7	0.43±0.04	2.81±0.10	0.99	3.37±0.08	7.5±0.3

For micro-sampled corals $\delta^{18}O$ values range from -0.14 ‰ to 3.71 ‰ and $\delta^{13}C$ values range from -6.24 ‰ to 1.68 ‰. This variability is twice that observed for the macro-sampled coral (2.97 ‰ and 7.21 ‰ respectively) which is about the variability observed in the literature (Mikkelsen et al. 1982; Freiwald et al. 1997; Mortensen and Rapp 1998; Blamart et al. 2001) but half the variability observed by Adkins et al. (2003) working on the much larger coral septa of *Desmophyllum cristagalli* or the one given by Blamart et al. (2005) using a SIMS technique to investigate *Lophelia pertusa* at an even higher spatial resolution.

Along with the coral's microstructures, two examples of $\delta^{18}O$ values from micro-sampling are presented in Figure 3. For each analysed thin section a picture showing the distribution of the different crystal types is superposed to the oxygen isotopic values (Fig. 3). Centres of calcification in the theca appear in white colour with
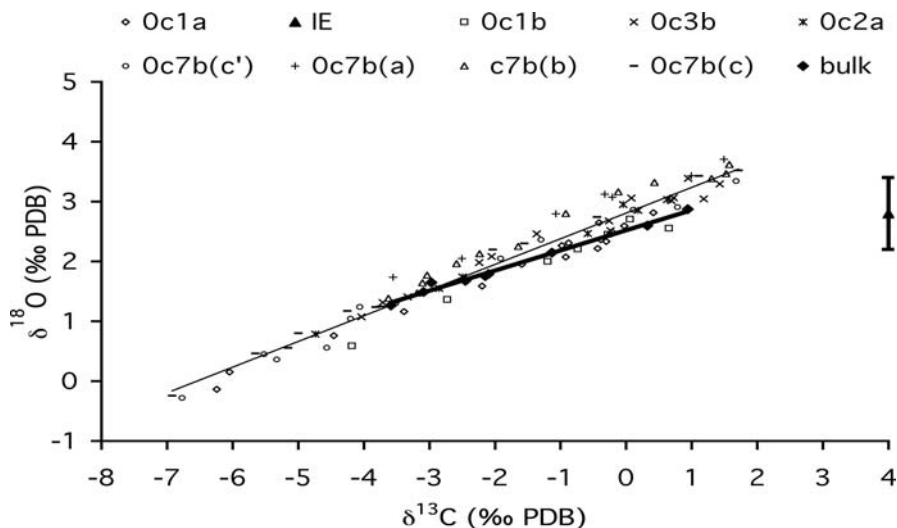
Fig. 2 Results both from macro and micro-sampling. A regression line is drawn for the macro-sampling in bold. Analytical error bars are included in the size of dots. All data are compared to isotopic equilibrium (IE)

reflected light, whereas surrounding aragonite fibers look darker. On the graph, the bar given for each $\delta^{18}O$ value is equal to the required sampling distance to have enough carbonate for the analysis. There is a relationship between the optical density and the isotopic signal in *Lophelia pertusa* similar to the one found by Adkins et al. (2003) for a single septa of *Desmophyllum cristagalli*. Centres of calcification
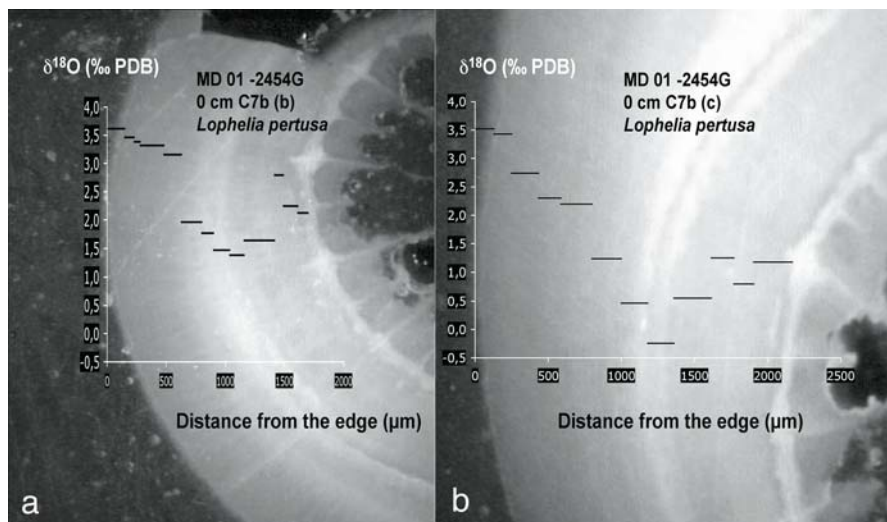
Fig. 3 Two profiles of $\delta^{18}O$ along transversal thin-sections of modern coral calyx C7b (sector b and c). The length of each $\delta^{18}O$ stick is equal to the distance required to have enough carbonate for the analysis

are clearly depleted in ^{18}O by 1 to several permil compared to surrounding fibers (Fig. 3). One striking aspect of these profiles is the decreasing trend of $\delta^{18}O$ values from the most exterior part of the calyx to the line of centre of calcification.

Excluding centres of calcification, $\delta^{18}O$ and $\delta^{13}C$ values follow a clear linear trend like the ones shown for the macro-samples (Fig. 2). The slopes ($\delta^{13}C$ *vs.* $\delta^{18}O$) determined on different polyps of this coral range from 0.38 ±0.04 to 0.44 ±0.08 and are identical within uncertainties. The average slope is 0.41. The intercept values however vary between individual samples from 2.51 ±0.18 to 3.15 ±0.1. Correlation coefficients R are all significant (all above 0.9).

We investigated the reproducibility of our micro-sampling by sampling different sectors on the same thin section. This exercise was performed on two calyxes of the living specimen C1 and C7b (Fig. 4).

The two sectors taken from calyx C1 yield identical regression lines with slope values of 0.42 ±0.02 (sector a) and 0.44 ±0.08 (sector b), and intercept values of 2.58 ±0.28 (sector a) and 2.51 ±0.18 (sector b) (Table 2).

Three sectors analysed on calyx C7b, also yield reproducible slopes and intercepts within uncertainty. Slope values range from 0.38 ±0.04 to 0.42 ±0.04 and intercepts values from 2.73 ±0.12 to 3.15 ±0.1. In addition, we duplicated the isotopic analyses on aliquotes of samples from sector C7(c), i.e. C7(c'), to investigate whether or not the powder obtained was homogeneous. In fact, repeated analyses of aliquotes from individually micro-drilled samples can be as different as 0.35 ‰ $\delta^{18}O$ and 0.7 ‰ $\delta^{13}C$.
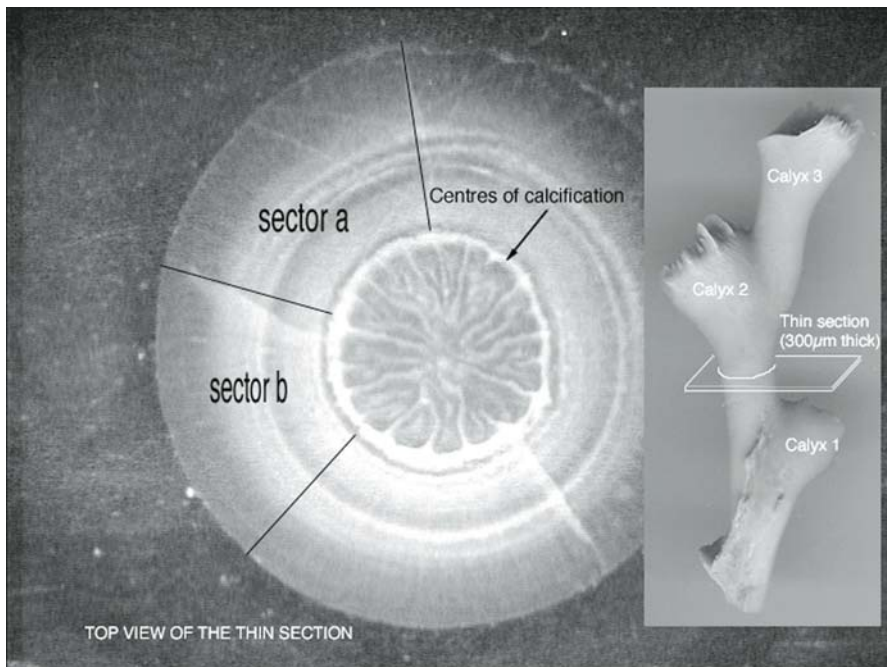
Fig. 4 A thin-section 300 μm thick is cut in a calyx. From this thin section several sectors can be sampled. This has been done for calyx C1 and C7b

Overall, all data collected on calyx C7b plot on a common regression line. The mean slope is 0.45 and intercept is 2.9. But individual sectors show different degrees of O and C isotope fractionation and sample powders are inhomogeneous resulting in an external reproducibility of ~0.25 ‰ for $\delta^{18}O$ and $\delta^{13}C$, three times as high as the analytical precision (Fig. 5).
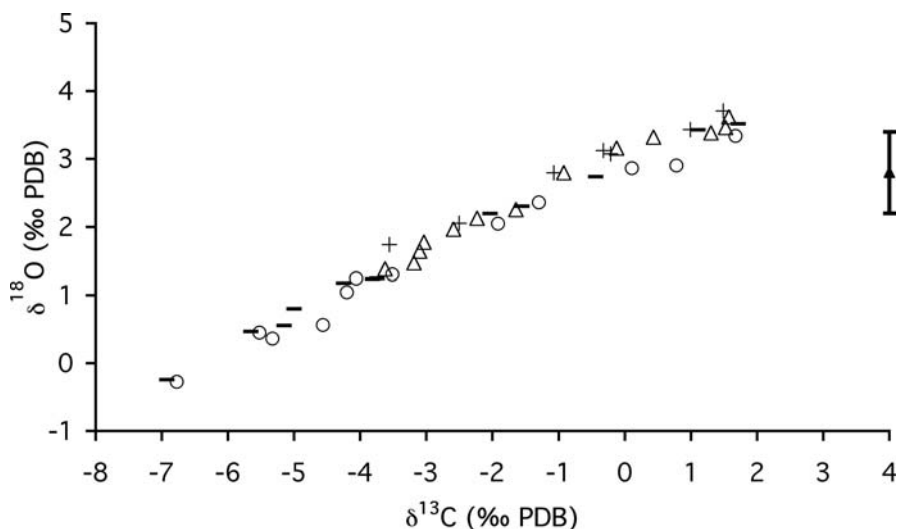
Fig. 5 Stable isotopic results for calyx C7b, sectors a, b, c and c'. The legend is the same as in Figure 2: crosses are sector a, triangles sector b, dashes sector c and circles its duplicate c'. Analytical error bars are included in the size of dots

The deviation of the coral isotopic values from isotopic equilibrium with modern seawater (IE) can be determined using the eWOCE data base and the NASA Global Seawater Oxygen-18 Database to retrieve temperature and seawater $\delta^{18}O$ at the coral site, and using Böhm et al. (2000) and Romanek et al. (1992) equations given below:

$$\delta^{18}O_{aragonite} = \frac{20 - T\ (°C)}{4.42} + \delta^{18}O_{seawater}$$

$$\delta^{13}C_{eq.} = \delta^{13}C_{DIC} + 2.7$$

IE is estimated as:
$\delta^{18}O_{IE} = 2.8 \pm 0.8$ ‰ PDB and
$\delta^{13}C_{IE} = 4$ ‰ PDB.

The large error bar of IE is calculated according to the temperature variability recorded over the last 20 years (up to 3.6°C (ARGO database)) as a result of strong seasonal mixing.

In order to estimate the deviation from isotopic equilibrium, IE has been plotted on δ¹⁸O *vs.* δ¹³C diagrams for the modern corals (Figs. 2, 5, 6). In no case does IE falls on the regression line. There is a strong offset in δ¹³C of about 2 ‰.
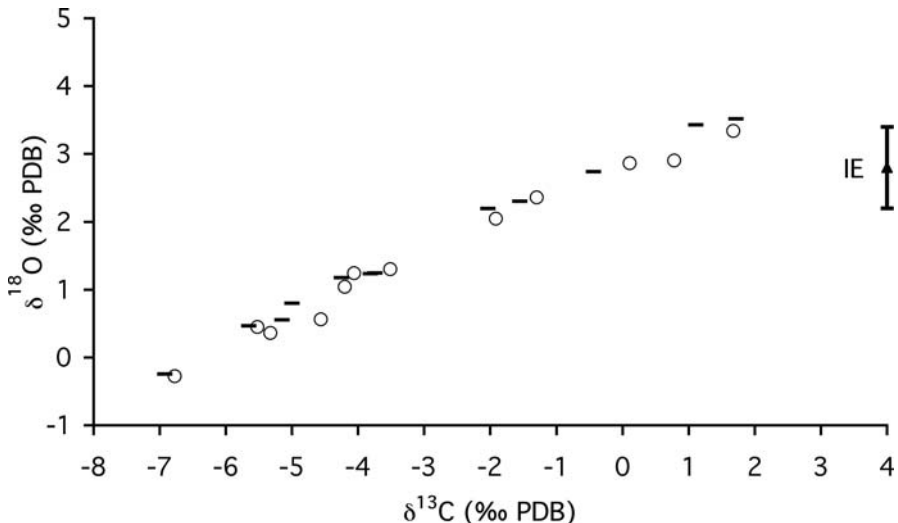
Fig. 6 Comparison of duplicate data from calyx C7b sector c. The 200 µg of powder collected from calyx C7b sector c was separated in two aliquots and analysed, given as C7b (c) and (c'). Analytical error bars are included in the size of dots. The difference between the duplicates exceeds by far the analytical precision

Discussion

Oxygen and carbon isotopic variability in deep-sea corals has been explored at different scales (Emiliani et al. 1978; Mikkelsen et al. 1982; McConnaughey 1989a, b, 1997; Mortensen 1998; Heikoop et al. 2000; Adkins et al. 2003; Rollion-Bard et al. 2003a, b; Blamart et al. 2005) and yielded different interpretations with regard to the contribution of environmental controls. The fractionation of oxygen and carbon isotopes driven by both environmental control and the coral metabolism is not homogeneous. Thus the choice of a specific sampling method likely points out different aspects of the diverse fractionation mechanism.

The comparison of macro-sampling with micro-sampling shows that data from macro-sampling are not representative of the overall isotopic variability. From the macroscopic to the microscopic scale, the isotopic signal is different and a single regression line is no more sufficient to fit the data (Adkins et al. 2003; Rollion-Bard et al. 2003a, b; Blamart et al. 2005). Macro-sampling integrates all fractionation processes and all structural differences (from aragonite fibers and centres of calcification) with respect to the volume of the different sampled aragonite types, which hides the complexity of the isotopic signal. That is why the variability observed is about half the one for micro-sampled corals.

The distribution of stable isotope with regard to the micro-structure of the coral shows that there is a general decreasing trend from the exterior to the interior of the calyx (Fig. 3). The simpliest model for coral growth is an initiation from the centres of calcification and an enlargement from it, which means that the heaviest isotopes (i.e., the less fractionated ones) are in the most recent part of the coral. This theory agrees with Emiliani et al.'s (1978) hypothesis of kinetic fractionation, yielding a linear relationship between $\delta^{18}O$ and $\delta^{13}C$. This linear regression line is supposed to be driven by two end-members: with highest $\delta^{18}O$ and $\delta^{13}C$ values the closest to the isotopic equilibrium with seawater and the lowest $\delta^{18}O$ and $\delta^{13}C$ closest to the centres of calcification (i.e., metabolic fractionation).

In no case does IE falls on the regression line, which is characteristic of *Lophelia* (McConnaughey 1997; Adkins et al. 2003; Blamart et al. 2005). As observed in the literature (Mikkelsen et al. 1982; Freiwald et al. 1997; Mortensen and Rapp 1998; Spiro et al. 2000; Adkins et al. 2003) there is an offset both in $\delta^{18}O$ and $\delta^{13}C$. This offset is commonly attributed to the contribution of respired CO_2 during calcification (Griffin and Druffel 1989; McConnaughey 1997; Adkins et al. 2003). Surprisingly, the observed $\delta^{13}C$ offset between IE and coral data is not constant for all the corals analyzed (shifted from 2.2 to 3.5 ‰) whereas it is expected to be constant and characteristic for a single species (about 3 ‰ in *Lophelia pertusa*) (Adkins et al. 2003; Blamart et al. 2005). However, the total stable isotope variability for a calyx will not always be seen either with the macro or with the micro-sampling and the heaviest end-member of the regression line is unlikely to be reached (Blamart et al. 2005).

The slope of the regression line $\delta^{18}O$ *versus* $\delta^{13}C$ is lower for the macro than for the micro sampled corals. However, centres of calcification are more depleted in ^{18}O than in ^{13}C for the lowest $\delta^{13}C$ values of corals (Adkins et al. 2003). This means that the micro-sampling shows more variability, and is also more likely influenced by the lowest end member of the regression line (i.e., strongest metabolic fractionation).

In terms of temperature, the consequences of the two different sampling techniques can be assesed.

For the modern coral, a temperature can be retrieved using the Smith et al. (2000) approach from the slope and intercept of the regression lines ($\delta^{18}/\delta^{13}C$). $\delta^{13}C$ values of *Planulina ariminensis* (benthic Foraminifera) give a measure of $\delta^{13}C_{DIC}$ (Duplessy et al. 1988) and $\delta^{18}O_w$ is assumed to be constant over time (equal to the modern value).

A confidence interval for the temperature has been calculated based on the standard deviation of the $\delta^{18}O_i$ reconstructed from the regression line intercepts; $\delta^{18}O_i$ is the projection of $\delta^{13}C$ seawater on the regression line $\delta^{18}O$ *versus* $\delta^{13}C$. Its standard deviation follows:

$$S_{\delta^{18}O_i} = \text{var}\,(\delta^{18}O)\,\frac{1 - r^2}{2}$$

$S_{\delta^{18}O_i}$ = *standard deviation of the $\delta^{18}O$ estimated for $\delta^{13}C = \delta^{18}C_{DIC}$, var($\delta^{18}O$) = $\delta^{18}O$ variance, r = correlation coefficient.*

According to the standard deviations for $\delta^{18}O_i$ the mean error on temperature calculation should be about 0.6°C.

Using this approach (Smith et al. 2000) calculated temperatures for the different modern calices vary from 6.4°C to 8.6°C with a mean value equal to 7.6°C for micro-sampling, while macro-sampling gives a temperature of 9°C. The mean annual temperature at the coral site is equal to 8.5°C with an overall variability up to 3.6°C due to strong seasonal mixing (ARGO database). Hence all the temperatures calculated from the coral isotopic composition agree with the range of temperatures at the coral site over the last 20 years. It is thus not possible to discriminate whether the macro or micro-sampling technique gives a more realistic temperature estimate. But both approaches yield temperatures close to the ambient seawater.

The macro-sampling, likely integrates a larger time period than data collected using micro-sampling. But for this coral, the calculated temperature from macro-sampling is about 0.5°C higher than the mean annual temperature estimate (8.5°C) and it is 1.4° higher than the average temperature value calculated with the micro-sampling (7.6°C). This result underlines the fact that macro-sampling is offset from the results taking the microstructure into account and does not represent an average of what happens at a more precise scale.

Nevertheless the temperatures calculated from different micro-sampled calices are significantly different. According to growth rate estimates (from few mm to few cm/year), temperature variations observed between those distinct thin sections of one coral may correspond to real temperature differences. The thin sections in this study are about 300 μm thick and the mean diameter of a polyp being 75 mm. That is to say each section integrates from few months to few decades taking into consideration the above mentioned growth rate estimates. For calices C1 and C7b several sectors have been sampled from the same section and each sector is expected to integrate the same time period within a section. However, the reproducibility of the temperature signal from a single section is very poor. The likelihood of the different $\delta^{18}O_i$ has been calculated; and within a 95 % confidence level only samples C1(a) and C1(b), C7b (b) and (c), are alike. Besides the temperatures calculated with sections C7b (a, b, c and c') are different by up to 1.5°C, which is three times the error due to the $\delta^{18}O_i$ estimate, i.e., 0.6°C. Hence, the temperature calculation seems to amplify little differences in the isotopic data.

The analysis of duplicate samples C7b (c and c') has shown that even if data comes from the same set of powder it may be significantly different. This experiment highlights the heterogeneity within a set of about 200 μg of aragonite. This heterogeneity is likely to cause the observed difference in the intercept value obtained for 0C7b (c) and 0C7b (c'). If pairs of data are assumed to be equal, analytical errors are not large enough to explain the data. A comparison of the two datasets gives ±0.16 ‰ mean confidence interval for $\delta^{18}O$ and ±0.25 ‰ for $\delta^{13}C$. The application of these new confidence intervals shows that all the data from calyx C7b are in good agreement and follow the same trend (Fig. 7). This deviation implies a ±0,7°C mean error for temperature calculation with isotopic data from micro-sampled corals.
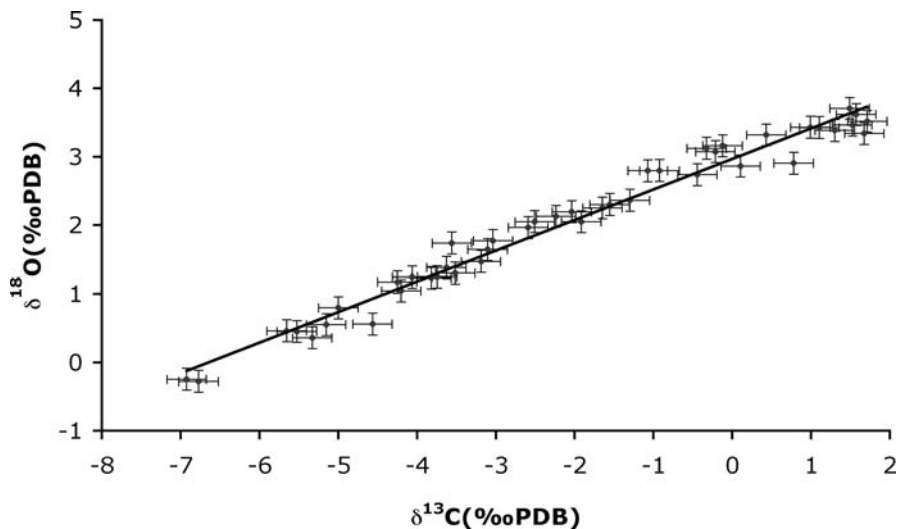
Fig. 7 Summary of stable isotopic results for calyx C7b. Error bars have been calculated assuming data from C7b (c and c') were equal. Within the new error bars all the data follow a common linear trend

The results presented herein, by Smith et al. (2000) and Adkins et al. (2003) demonstrate that, although the oxygen isotope signal from an individual coral or a single coral calyx is a mixture of near equilibrium and biologically-fractionated components, environmental control such as the ambient seawater temperature is extractable and may be used for climatic reconstructions.

The sampling technique, however, influences the results of such reconstructions. For macro-sampling a large portion of the isotopic variability inherent to the coral is lost, but the dependence of the isotopic signal on environmental controls remains extractable. However, the external reproducibility of such an approach has to be reassessed to ~1.5°C taking the micro-structure and heterogeneities of a coral into account.

In contrast, micro-sampling probably yields most of the stable isotope variability inherent to a coral and thus gives a more precise estimate of the ambient seawater temperature, with an external reproducibility of ~0.7°C.

In the future it is necessary to repeat the temperature calibration of Smith et al. (2000) based on a micro-sampling technique to test whether the two sampling techniques yield systematic differences in the calibration and to improve our knowledge in the stable isotope variability in deep-sea corals.

Conclusions

The strong kinetic fractionation of O and C isotopes in deep-water corals and their offset from seawater equilibrium was the major obstacle in using such data to trace environmental controls, such as ambient seawater temperatures.

Micro-sampling of growth layers of *Lophelia pertusa* corals reveals a huge isotopic variability of C and O inherent to the microstructure of this species, while this variability is mostly hidden by using a macro-sampling technique. However, realistic ambient seawater temperature estimates can be retrieved from a temperature calibration proposed by Smith et al. (2000), with either a macro or a micro-sampling technique. But, inhomogenities of the coralline aragonite introduce much larger errors than the ones expected from stable isotope measurements and the temperature calibration of Smith et al. (2000). The more precise the sampling method, the smaller the errors on the temperature estimate; for the macro-sampling the external reproducibility could be reassessed to about ±1.5°C. As micro-sampling captures most of the isotopic variability inherent to the coral aragonite, temperature estimates are found to be more precise by a factor 2, i.e. ±0.7°C.

Acknowledgements

References

Adkins JF, Boyle EA (1997) Changing atmospheric $\Delta^{14}C$ and the record of deep water paleoventilation ages. Paleoceanography 12: 337-344

Adkins JF, Cheng H, Boyle EA, Druffel ERM, Edwards RL (1998) Deep-sea coral evidence for rapid change in ventilation of the deep north Atlantic 15,400 years ago. Nature 280: 725-728

Adkins JF, Boyle EA, Curry WB, Lutringer A (2003) Stable isotopes in deep-sea corals and a new mechanism for "vital effects". Geochim Cosmochim Acta 67: 1129-1143

Aharon P (1991) Recorders of reef environment histories: stable isotopes in corals, giant clams, and calcareous algae. Coral Reefs 10: 71-90

ARGOdatabase: http://db.aoml.noaa.gov/cgi-bin/db/Bin/init_applet.x?argo+ARGOGUI.class

Bett B (2001) UK Atlantic margin environmental survey: introduction and overview of bathyal benthic ecology. Cont Shelf Res 21: 917-956

Blamart D, van Weering TCE, Ayliffe L, Labeyrie L, Lutringer A, Vonhof HB, Ganssen G (2001) Modern NE Atlantic Ocean cold water coral characteristics. EOS Trans, AGU 81, pp 640

Blamart D, Rollion-Bard C, Cuif JP, Juillet-Leclerc A, Lutringer A, van Weering TCE, Henriet JP (2005) C and O isotopes in a deep-sea coral (*Lophelia pertusa*) related to skeletal microstructure. In: Freiwald A, Roberts JM (eds) Cold-water Corals and Ecosystems. Springer, Berlin Heidelberg, pp 1005-1020

Böhm F, Joachimski MM, Dullo W-Chr, Eisenhauer A, Lehnert H, Reitner J, Wörheide G (2000) Oxygen isotope fractionation, in marine aragonite of coralline sponges. Geochim Cosmochim Acta 64: 1695-1703

Cheng H, Adkins JF, Edwards RL, Boyle EA (2000) U-Th dating of deep-sea corals. Geochim Cosmochim Acta 64: 2401-2416

Cuif JP, Dauphin Y (1998) Microstructural and physico-chemical characterisation of centres of calcification in septa of some scleractinian corals. Paläont Z 72: 257-270

Cuif JP, Dauphin Y, Doucet J, Salome M, Susini J (2003) XANES mapping of organic sulphate in three scleractinian coral skeletons. Geochim Cosmochim Acta 67: 75-83

De Mol B, van Rensbergen P, Pillen S, van Herreweghe K, van Rooij D, McDonnell A, Huvenne V, Ivanov M, Swennen R, Henriet JP (2002) Large deep-water coral banks in the Porcupine Basin, southeast of Ireland. Mar Geol 188: 648-231

Druffel ERM, King LL, Belastock RA, Buesseler KO (1990) Growth rate of a deep-sea coral using ^{210}Pb and other isotopes. Geochim Cosmochim Acta 54: 1493-1500

Duplessy JC, Arnold M, Maurice P, Bard E, Duprat J, Moyes J (1986) Direct dating of the oxygen-isotope record of the last deglaciation by ^{14}C accelerator mass spectrometry. Nature 320: 350-352

Duplessy JC, Shackleton NJ, Fairbanks RG, Labeyrie L, Oppo D, Kallel N (1988) Deepwater source variations during the last climatic cycle and their impact on the global deepwater circulation. Paleoceanography 3: 343-360

Emiliani C, Hudson JH, Shinn EA, George RY (1978) Oxygen and carbon isotopic growth record in a reef coral from the Florida Keys and a deep-sea coral from Blake Plateau. Science 202: 627-629

Epstein S, Buchsbaum R, Lowenstam HA, Urey HC (1953) Revised carbonate-water isotope temperature scale. Bull Geol Soc Amer 64: 1315-1326

Frank N, Paterne M, Ayliffe LK, van Weering T, Henriet JP, Blamart D (2004) Eastern North Atlantic deep-sea corals: tracing upper intermediate water δ^{14}C during the Holocene. Earth Planet Sci Lett 219: 297-309

Frank N, Lutringer A, Paterne M, Blamart D, Henriet JP, van Rooij D, van Weering T (2005) Deep-water corals of the northeastern Atlantic margin: carbonate mound evolution and upper intermediate water ventilation during the Holocene. In: Freiwald A, Roberts JM (eds) Cold-water Corals and Ecosystems. Springer, Berlin Heidelberg, pp 113-133

Freiwald A (2002) Reef-forming cold-water corals. In: Wefer G, Billett D, Hebbeln D, Jørgensen BB, Schlüter M, van Weering T (eds) Ocean Margin Systems. Springer, Berlin Heidelberg, pp 365-385

Freiwald A, Henrich R, Pätzold J (1997) Anatomy of a deep-water coral reef mound from Stjernsund, West Finnmark, Northern Norway. SEPM Spec Publ 56: 141-161

Furla P, Galgani I, Durand I, Allemand D (2000) Sources and mechanisms of inorganic carbon transport for coral calcification and photosynthesis. J Exp Biol 203: 3445-3457

GEOSECS: http://ingrid.ldgo.columbia.edu/SOURCES/GEOSECS/

Griffin S, Druffel ERM (1989) Sources of carbon to deep-sea corals. Radiocarbon 31: 533-543

Heikoop JM, Dunn JJ, Risk MJ, Schwarcz HP, McConnaughey T, Sandeman IM (2000) Separation of kinetic and metabolic isotope effects in carbon-13 records preserved in reef coral skeletons. Geochim Cosmochim Acta 64: 975-987

Henriet JP, De Mol B, Pillen S, Vanneste M, van Rooij D, Versteeg W, Croker PF, Shannon PM, Unnithan V, Bouriak S, Chachkine P (1998) Gas hydrate crystals may help build reefs. Nature 391: 648-649

Hidaka M (1991) Fusiform and needle-shaped crystals found on the skeleton of a coral, *Galaxea fascicularis*. In: Sugo S, Nakaharo H (eds) Mechanism and Physiology of Biomineralization in Biological Systems. Springer, Berlin Heidelberg New York, pp 139-143

Hovland M, Croker PF, Martin M (1994) Fault associated seabed mounds (carbonate knolls?) off western Ireland and north-west Australia. Mar Petrol Geol 11: 232-246

Hovland M, Mortensen PB, Brattegard T, Strass P, Rokoengen K (1998) Ahermatypic coral banks off mid-Norway: evidence for a link with seepage of light hydrocarbons. Palaios 13: 189-200

Lazier EV, Smith JE, Risk MJ, Schwarcz JP (1999) The skeletal structure of *Desmophyllum cristagalli:* the use of deep-water corals in sclerochronology. Lethaia 32: 119-130

Leder JJ, Swart PK, Szmant AM, Dodge RE (1996) The origin of variations in the isotopic record of scleractinian corals: I. Oxygen. Geochim Cosmochim Acta 60: 2857-2870

Mangini A, Lomitschka M, Eichstädter R, Frank N, Vogler S, Bonani G, Hajdas I, Pätzold J (1998) Corals provide way to age deep water. Nature 392: 347-348

McConnaughey T (1989a) ^{13}C and ^{18}O isotopic disequilibrium in biological carbonates: I. Patterns. Geochim Cosmochim Acta 53: 151-162

McConnaughey T (1989b) ^{13}C and ^{18}O isotopic disequilibrium in biological carbonates: II. In vitro simulation of kinetic isotope effects. Geochim Cosmochim Acta 53: 163-171

McConnaughey T (1997) Carbon isotopes in biological carbonates: respiration and photosynthesis. Geochim Cosmochim Acta 61: 611-622

McConnaughey T (2003) Sub-equilibrium oxygen-18 and carbon-13 levels in biological carbonates: carbonate and kinetic models. Coral Reefs 22: 316-327

McCrea JM (1950) On the isotopic chemistry of carbonates and a paleotemperature scale. J Chem Phys 18: 849-857

Mikkelsen N, Erlenkeuser H, Killingley JS, Berger WH (1982) Norwegian corals: radiocarbon and stable isotopes in *Lophelia pertusa*. Boreas 11: 163-171

Moore WS, Krishnaswami S (1972) Coral growth rates using ^{228}Ra and ^{210}Pb. Earth Planet Sci Lett 15: 187-190

Moore WS, Krishnaswami S, Bhat SG (1973) Radiometric determinations of coral growth rate. Bull Mar Sci 23: 157-176

Mortensen PB, Rapp HT (1998) Oxygen and carbon isotope ratios related to growth line pattern in skeletons of *Lophelia pertusa* (L) (Anthozoa, Scleractinia): implications for determination of linear extension rates. Sarsia 83: 433-446

Ogilvie M (1896) Microscopic and systematic study of madreporarian types of corals. Phil Trans R Soc London 187(B): 83-345

Rollion-Bard C (2001) Variabilité des isotopes de l'oxygène dans les coraux *Porites*: développement et implications des microanalyses d'isotopes stables (B, C et O) par sonde ionique. PhD thesis, 165 pp

Rollion-Bard C, Blamart D, Cuif JP, Juillet-Leclerc A (2003a) Microanalysis of C and O isotopes of azooxanthellate and zooxanthellate corals by ion microprobe. Coral Reefs 4: 405-415

Rollion-Bard C, Chaussidon M, France-Lanord C (2003b) pH control on oxygen isotopic composition of symbiotic corals. Earth Planet Sci Lett 215: 275-218

Romanek CS, Grossman EL, Morse JW (1992) Carbon isotopic fractionation in synthetic aragonite and calcite: effects of temperature and precipitation rate. Geochim Cosmochim Acta 56: 419-430

Schröder-Ritzrau A, Freiwald A, Mangini A (2005) U/Th-dating of deep-water corals from the eastern North Atlantic and the western Mediterranean Sea. In: Freiwald A, Roberts JM (eds) Cold-water Corals and Ecosystems. Springer, Berlin Heidelberg, pp 157-172

Shackleton NJ (1974) Attainment of isotopic equilibrium between ocean water and benthonic foraminifera genus *Uvigerina*: isotopic changes in the ocean during the last glacial. Les Méth Quant Étude Variation Climat Au Cours Du Pleistocène, Coll Int CNRS 219: 203-209

Smith JE, Risk MJ, Schwarcz HP, McConnaughey TA (1997) Rapid climate change in the North Atlantic during the Younger Dryas recorded by deep-sea corals. Nature 386: 818-820

Smith JE, Schwarcz HP, Risk MJ, McConnaughey T, Keller N (2000) Paleotemperatures from deep-sea corals: overcoming 'vital effects'. Palaios 15: 25-32

Spiro B, Roberts M, Gage J, Chenery S (2000) $^{18}O/^{16}C$ and $^{13}C/^{12}C$ in an ahermatypic deep-water coral *Lophelia pertusa* from the North Atlantic: a case of disequilibrium isotope fractionation. Rapid Comm Mass Spec 14: 1332-1336

Swart PK (1983) Carbon and oxygen isotope fractionation in scleractinian corals: a review. Earth Sci Rev 19: 51-80

Swart PK, Leder JJ, Szmant AM, Dodge RE (1996) The origin of variations in the isotopic record of scleractinian corals: II. Carbon. Geochim Cosmochim Acta 60: 2871-2885

Urey HC, Lowenstam HA, Epstein S, McKinney CR (1951) Measurements of paleotemperatures and temperatures of the Upper Cretaceous of England, Denmark, and the southeastern United States. Bull Geol Soc Amer 62: 399-416

Van Weering T, Shipboard Scientific Party (1999) Shipboard cruise report R.V. Pelagia 64PE143: a survey of carbonate mud mounds of Porcupine Bight and S. Rockall Trough margins. NIOZ, Texel, 82 pp

Weber JN (1973) Deep-sea ahermatypic scleractinian corals: isotopic composition of the skeleton. Deep-Sea Res 20: 901-909

Weber JN, Woodhead MJ (1970) Carbon and oxygen isotope fractionation in the skeletal carbonate of reef building corals. Chem Geol 6: 93-117

Wefer G, Berger WH (1991) Isotope paleontology: growth and composition of extant calcareous species. Mar Geol 100: 207-248

Climate records from the Faroe-Shetland Channel using *Lophelia pertusa* (Linnaeus, 1758)

Michael J. Risk[1], Jason Hall-Spencer[2], Branwen Williams[1,3]

[1] School of Geography and Geology, McMaster University, Hamilton ON, L8S 4M1, Canada
  (riskmj@univmail.cis.mcmaster.ca)
[2] Department of Biological Sciences, University of Plymouth, Plymouth, PL4 8AA, UK
[3] GEOTOP, Université du Québec à Montréal and McGill University, Québec, Canada

Abstract. The longest available time series on ocean currents indicates that the southward flow of water from the Greenland Sea is weakening, and that correlative large-amplitude changes have occurred in the rate of formation of intermediate Labrador Sea water. These have been linked to changes in regional climate which, if trends continue, could within 30 years alter the flow of the North Atlantic Drift and possibly interrupt the formation of Labrador Sea water, profoundly affecting regional climates, marine ecosystems and fisheries. We are attempting to use the carbonate skeletons of cold-water corals to find out how rapidly and how often the thermohaline circulation of the NE *vs*. NW Atlantic has changed in the past, just as tree rings and ice cores are used to investigate climate change on land.

We have focussed on the NE Atlantic for our preliminary work, notably the Faroe-Shetland Channel: a major gateway between the Atlantic Ocean and the Norwegian Sea. Warm North Atlantic Drift water passes north through this channel on the surface, warming northern Europe. Cold Norwegian Sea Overflow Water returns at depth, contributing to the formation of North Atlantic Deep Water. Existing records are too short to allow conclusions regarding recent temporal changes in this inflow, so proxies are sought. We have analysed live-collected *Lophelia pertusa* skeletons collected in October 2001 using a ring dredge from RV Scotia along the worlds longest-running hydrographic transect (from 1893). Corals were sectioned using a slow-speed Isomet saw, and sampled for isotopic analysis using a Merchantek micromill. Observation of sectioned corals revealed dense-less dense couplets, as in every coral studied to date from tropical to deep cold-water environments worldwide. We sampled circumferentially, in the centres of individual bands, so as to produce temperature estimates using the "lines" technique of Smith et al. (2000). The results were simultaneously encouraging and confusing.

Each of the coral samples generated lines from which temperatures could be estimated. Dense skeletal bands had lower temperatures than the less-dense bands,

hence we conclude these were winter and summer bands, respectively. The mean annual temperature (MAT) range determined from one of the corals was 3.8°C. Pooling results from several corals yielded a lower estimate for MAT range: 2.3°C. The absolute temperatures from the corals, however, were somewhat lower than the instrumental record with "winter" records being more depleted than the "summer values". This was unexpected and shows that determining detailed climate records from *L. pertusa* may be more difficult than hoped.

Keywords. *Lophelia pertusa*, Faroe-Shetland Channel, climate records, stable isotopes, corals

Introduction

Obtaining climate records from coral skeletons is proving to be an invaluable aid to climatology (Druffel et al. 2001; Tudhope et al. 2001) in a time of what could possibly be massive and fundamental climate change (Jones et al. 1999; Mann et al. 1999). Most of this research has focussed on tropical reef corals, which have been shown to be archives of past water temperature, large-scale climate events, and sediment stress. These corals produce annual dense/less dense skeletal banding couplets, allowing precise stratigraphic resolution. Massive tropical reef corals may live several centuries allowing long proxy records of ocean climate to be obtained. The major drawbacks to the use of reef corals are restrictions in their depth and geographic range: large colonies of massive corals suitable for climate work tend to be restricted to the eastern fringes of tropical coastlines.

In recent years, however, research in coral paleoclimatology has discovered the enormous potential of climate records in the skeletons of cold-water corals: the "New Archive" (pers. comm. W. Broecker 1995). Families of hexacorals, octocorals and hydrocorals are distributed in all oceans, at virtually all depths from sea level to at least 4 km.

Early use of cold-water corals in paleoclimate research was that of Smith et al. (1997) using *Desmophyllum cristagalli* (Milne-Edwards and Haime, 1848) from Orphan Knoll, located 500 km off the SE coast of Newfoundland. This was followed by work on the skeletal structure of deep-water corals (Lazier et al. 1999), how "vital effects" could be overcome (Smith et al. 2000), and on ocean ventilation (Goldstein et al. 2001). Deep-water scleractinians are proving to be more difficult to work with than the massive forms used in the sclerochronology of tropical coral heads such as *Porites* spp. Many are small in comparison with tropical reef corals, usually less than 10 cm, and slow-growing so although they may be faithful recorders with several decades' information on ocean temperatures the tight spacing of the growth bands makes stratigraphic control extremely difficult. For example, recent work on the gorgonian *Primnoa resedaeformis* (Gunnerus, 1763) has shown that it has beautifully-defined growth bands with climate records spanning almost a century, but the bands are extremely tightly spaced (Sherwood et al. 2003; Sherwood and Risk in press).

Lophelia pertusa may be the most widely-distributed scleractinian on the globe; in the north Atlantic it constructs deep reefs from the Gulf of Mexico to Nova Scotia in the west and from Mauritania to northern Norway in the east with scattered records from locations worldwide (Wilson 1979; Rogers 1999). There is great interest in *L. pertusa*, because of the importance of these reefs as fish habitat coupled with increasing threats from trawling (Hall-Spencer et al. 2002). In addition to the value of this coral in creating fish habitat, it is possible that it may also contain a priceless archive of climate data. We report herein preliminary attempts to read that record.

The Faroe-Shetland Channel is one of the key regions in the thermohaline circulation of the North Atlantic. This channel, only 25 km wide at its narrowest point, forms the main gateway between the Atlantic Ocean and the Norwegian Sea. Warm, saline water of the North Atlantic Drift (the northern extension of the Gulf Stream) flows from the Atlantic into the Norwegian Sea, delivering a significant amount of heat to the climate of northwestern Europe. This water then cools and sinks, and flows south through the Denmark Strait, across the Iceland-Scotland Ridge, and back through the Faroe-Shetland Channel at depth, contributing to North Atlantic Deep Water (NADW) (Crease 1964). This then completes the northern loop of the thermohaline conveyer-belt circulation in the Atlantic. In short, an oceanographic phenomenon which controls much of the distribution and history of civilization in western Europe may be monitored at one site. Another place where both the Gulf Stream and the Gulf Stream Return Flow has been investigated using cold-water corals is Orphan Knoll, some 500 km NE of Newfoundland (Smith et al. 1997).

Recent concerns about climate change due to an increase in greenhouse gases have emphasized the need for long-term proxies of climate change in the oceans. At present, we are unable accurately to predict weather far into the future as a complete understanding of global climate will require much better understanding of ocean circulation. Because long-term oceanographic records at depth in the oceans are so rare, we will have to depend on climate proxies. At the moment, cold-water corals show great promise of being able to provide long, accurate records of ocean conditions (Smith et al. 1997; Adkins et al. 2003; Frank et al. 2003; Sherwood et al. 2003).

Recently, there have been reports of decreases in the intensity and density of overflow through the Faroe-Shetland Channel (Hansen et al. 2001), resulting in a decrease in the water supply to the NADW. When NADW flow is strong, a strong northward flux of warm surface waters in the North Atlantic maintains mass balance, warming northern Europe. An interruption or decrease in NADW flow could plunge much of north-western Europe into frigid conditions (Keigwin and Boyle 2000). There have been recent suggestions that the circulation of this part of the Atlantic has indeed been changing over the past 30 years (Turrell et al. 1999). Increases in meltwater fluxes 12-14 ka BP caused extreme climatic cooling, and the exchange of waters between the Nordic Seas and the Atlantic was essentially reversed (Rasmussen et al. 2002). Increased meltwater flows from polar ice caps might result in similar conditions in the future, a change that could occur with shocking

rapidity (Smith et al. 1997). Proxy records are essential, especially ones that could span several centuries - *L. pertusa* reefs are known to be thousands of years old (Freiwald et al. 2002; Hall-Spencer et al. 2002), hence are excellent candidates for long climate records (Frank et al. 2003).

Because *L. pertusa* is so widespread in regions of critical interest with regard to oceanic change, climate records obtained from their skeletons could prove to be invaluable. In this paper, we report preliminary analyses of *L. pertusa* taken from the Faroe-Shetland Channel. Our hypothesis was that the internal banding observed in the skeletons *L. pertusa* represented annual couplets, similar to those observed in tropical reef corals (Knutson et al. 1972). These couplets might then record variations in annual temperature range.

Methods and materials

Fisheries Research Services, Marine Laboratory Aberdeen run regular (usually triannual) surveys of the Faroe-Shetland Channel using RV Scotia to characterise the water masses below two historic hydrographic transects (Fig. 1). We joined one of these cruises (1501S) on 5-19 Oct 2001 to take ring dredge (1 m wide, 50 mm mesh) samples targeting the calcareous macrobenthos between sampling standard CTD stations. Nine ring dredge samples were taken from four stations on the Fair Isle - Munken transect, amended for the presence of Foinaven oil platform (Fig. 1). The stations were FIM-05 (995 m, 60°29.00' N, 04°26.00' W, two dredge samples taken), FIM-04 (655 m, 60°25.00' N, 04°19.00' W, one dredge sample), SEFOS (330 m, 60°18.00' N, 04°04.50' W, four dredge samples) and FIM-01 (150 m, 60°10.00' N, 03°44.00' W, two dredge samples). Living and dead *Lophelia pertusa* colonies were encountered in two of the dredge samples taken at 330 m, close to the Foinaven oil platform. These samples were washed in freshwater, air dried and transported to the laboratory. The British Oceanographic Data Centre (http://www.bodc.ac.uk) database was accessed for data relating to the site where our *L. pertusa* samples were taken (Table 1).

Coral samples were bleached for one week with sodium hypochlorite before sample preparation. Individual polyps were cut from the mass of coral with a small hand-held circular saw. These polyps were cleaned three times for 10 minutes each time in an ultrasonic bath and dried overnight in an oven at 40 degrees C. In order to ensure the utility of the "lines" technique of Smith et al. (2000), one of the polyps was intensively sampled that was alive when collected. Samples for isotopic analysis were carefully scraped from the outer edges of septa and from the uppermost edge of the septathecal wall. These samples should have been coeval, and hence should record the water temperature at the time of sampling.

In order to investigate isotopic values associated with banding within the coral skeletons, a slow-speed Isomet™ saw was used to cut transverse sections through individual coral polyps, which were then polished flat. Samples for isotopic analysis were milled from these sections using a Merchantek™ microsampler.
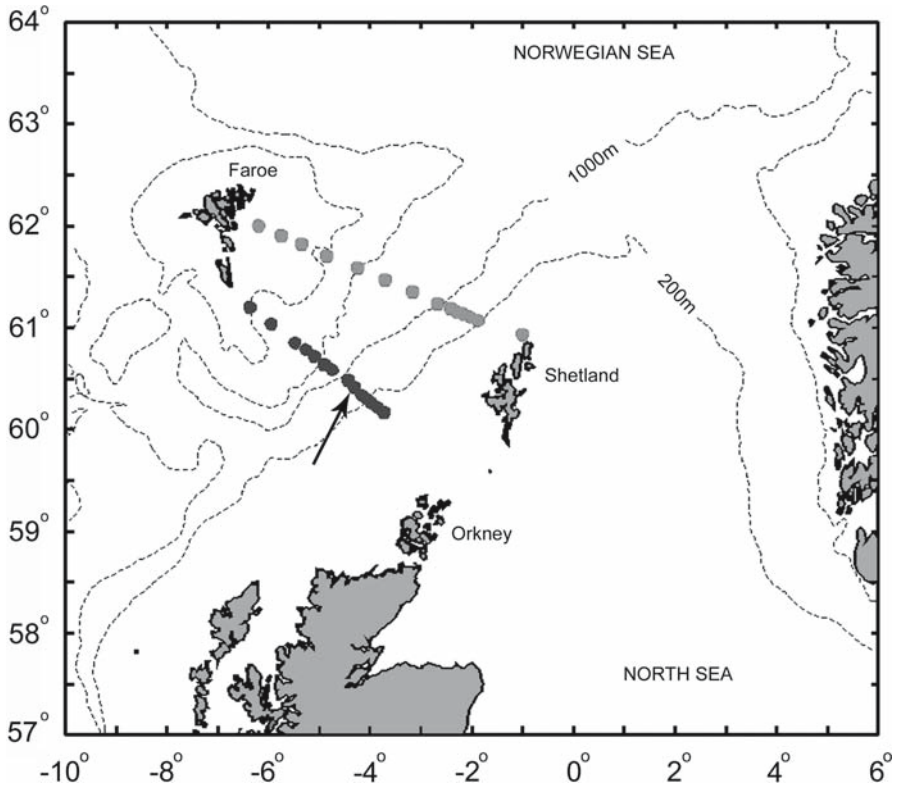
Fig. 1 Two standard hydrographic transects started in 1893. Benthos was sampled in a ring dredge aboard RV Scotia (cruise 1501S) along the southern Fair Isle - Munken transect in October 2001, the arrow shows where *Lophelia pertusa* samples were obtained (source Fisheries Research Services, Aberdeen)

Table 1 Recent hydrographic data for the Faroe-Shetland Channel site where *Lophelia pertusa* was sampled for isotopic analyses (source BODC)

Date	Time	Position	Water depth	Sample depth	Salinity [‰]	Temp [°C]
4.6.96	12.32	60°18.1'N 4°4.3'W	328 m	292 m	35.3326	9.037
20.10.96	19.12	60°18.1'N 4°4.3'W	325 m	311 m	35.2856	9.091
5.10.98	11.19	60°17.7'N 4°4.7'W	324 m	314 m	35.4294	10.062
4.12.98	02.56	60°17.9'N 4°4.6'W	322 m	300 m	35.3960	9.904
9.5.00	23.33	60°18.2'N 4°4.2'W	330 m	324 m	35.3482	8.697

Results

All isotopic data are presented in Table 2. Representative specimens of the corals used in this study are archived at McMaster University.

The results from the sampling of supposedly coeval skeleton are given in Figure 2. Plotted in C-O space, the data form a tight straight line. Using the formula in Smith et al. 2000, we calculate a temperature at time of collection (October) of 5.73°C. Figure 3 shows the measured temperature profile for the Fair Isle - Munken transect of the Faroe-Shetland Channel at the time of collection. The bottom temperature where the *L. pertusa* sample was taken was c. 10°C with other recent measured values ranging from 8.697°C (May 2000) to 10.062°C (Oct 1998) (Table 1).

Table 2 Data from *Lophelia pertusa* collected in the Faroe-Shetland Channel

	$\delta^{13}C$	$\delta^{18}O$		$\delta^{13}C$	$\delta^{18}O$		$\delta^{13}C$	$\delta^{18}O$
Inner	-4.390	0.867	Dense	-6.812	0.197	Less dense	-4.959	0.914
Inner	-6.594	-0.282	Dense	-6.565	0.283	Less dense	-4.085	1.421
Inner	-7.743	-1.118	Dense	-7.858	-0.260	Less dense	-3.881	1.419
Inner	-7.023	-0.553	Dense	-7.977	-0.497	Less dense	-2.228	2.058
Inner	-6.321	-0.063	Dense	-7.564	-0.370	Less dense	-3.163	1.578
Inner	-7.564	-0.968	Dense	-7.844	-0.532	Less dense	-4.884	0.977
Inner	-7.171	-0.831	Dense	-7.383	-0.583	Less dense	-2.961	1.775
Inner	-7.528	-1.006	Dense	-6.206	0.272	Less dense	-2.901	1.830
Inner	-7.132	-0.676	Dense	-6.769	-0.180	Less dense	-4.789	1.066
Inner	-6.805	-0.499	Dense	-7.929	-0.834	Less dense	-3.908	1.463
			Dense	-7.817	-0.807	Less dense	-4.468	1.206
Septa	-3.699	0.908	Dense	-7.914	-0.730	Less dense	-4.562	1.175
Septa	-5.377	0.480	Dense	-7.473	-0.134	Less dense	-4.129	1.368
Septa	-3.134	1.512	Dense	-7.135	0.096	Less dense	-6.225	0.305
Septa	-3.644	1.420	Dense	-8.360	-1.013	Less dense	-5.376	0.793
Septa	-3.559	1.392	Dense	-8.121	-0.607	Less dense	-4.673	0.826
Septa	-2.404	1.741	Dense	-7.585	-0.696	Less dense	-5.622	0.353
Septa	-3.026	1.665	Dense	-4.761	1.001	Less dense	-3.968	1.244
Septa	-3.966	1.125	Dense	-7.955	-0.983	Less dense	-3.595	1.340
Septa	-3.084	1.611	Dense	-8.126	-1.105	Less dense	-5.325	0.622
Septa	-3.304	1.582	Dense	-7.173	-0.423	Less dense	-4.190	1.052
			Dense	-7.784	-0.812	Less dense	-5.583	0.343
			Dense	-8.252	-0.673	Less dense	-5.004	0.722
			Dense	-7.214	-0.124	Less dense	-5.987	0.151
			Dense	-7.721	-0.488	Less dense	-6.130	0.037
			Dense	-8.169	-0.641	Less dense	-5.760	0.470
			Dense	-6.292	0.297	Less dense	-5.188	0.651
			Dense	-8.352	-0.906	Less dense	-6.657	-0.018
			Dense	-8.532	-1.006	Less dense	-3.914	1.624
			Dense	-7.732	-0.658	Less dense	-5.353	0.908
			Dense	-8.043	-0.473			
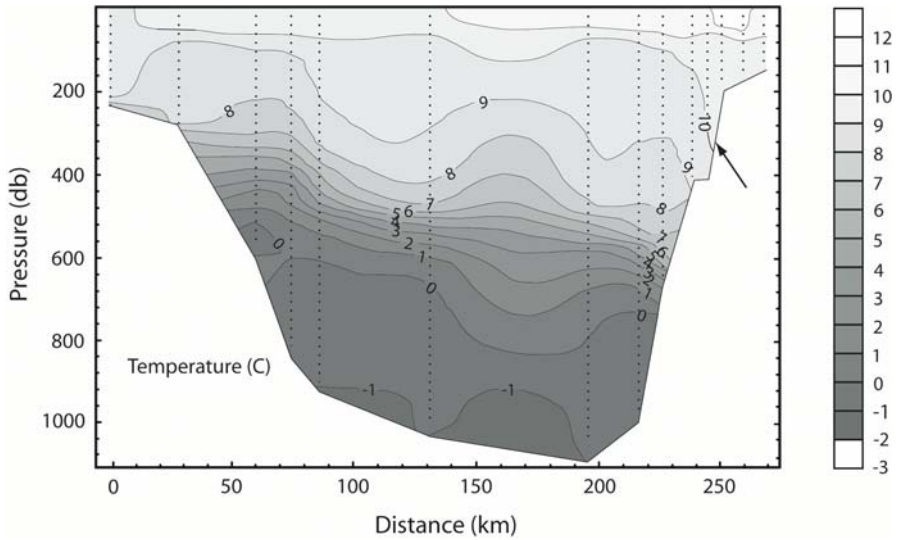
Fig. 2 Temperature profile of the Fair Isle - Munken transect recorded on 12-13 October 2001, dotted vertical lines show positions of the standard hydrographic stations. Note the sub-zero bottom-water and the arrow showing where *Lophelia pertusa* colonies were sampled at 330 m on the eastern side of the Faroe-Shetland channel on 7 October 2001 in 10°C water (source FRS Aberdeen)
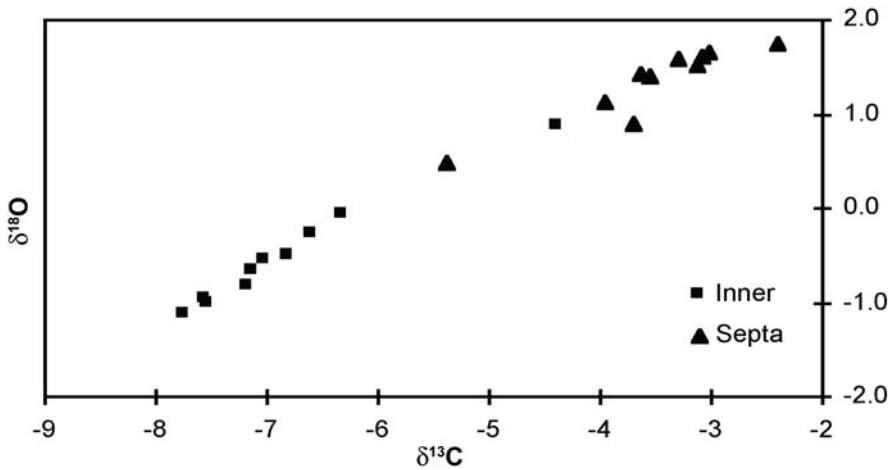
Fig. 3 $\delta^{13}C/\delta^{18}O$ plot of coeval samples taken from one polyp. The line is highly significant, and the calculated temperature for Oct. 2001 is 5.73°C

Results from independently sampling dense and less-dense bands of the skeleton are presented in Figure 4. Results from four polyps are pooled. The calculated temperatures are 3.47°C (dense) and 5.82°C, yielding a mean annual temperature (MAT) range of 2.3°C. Results from one individual polyp returned a MAT range of 3.8°C. Less-dense bands were on the outside of the skeletons, and we assume these represent summer growth. This assumption is reinforced by the higher temperature calculated from isotopic values in these bands. Dense bands were consistently further from equilibrium than less-dense bands.
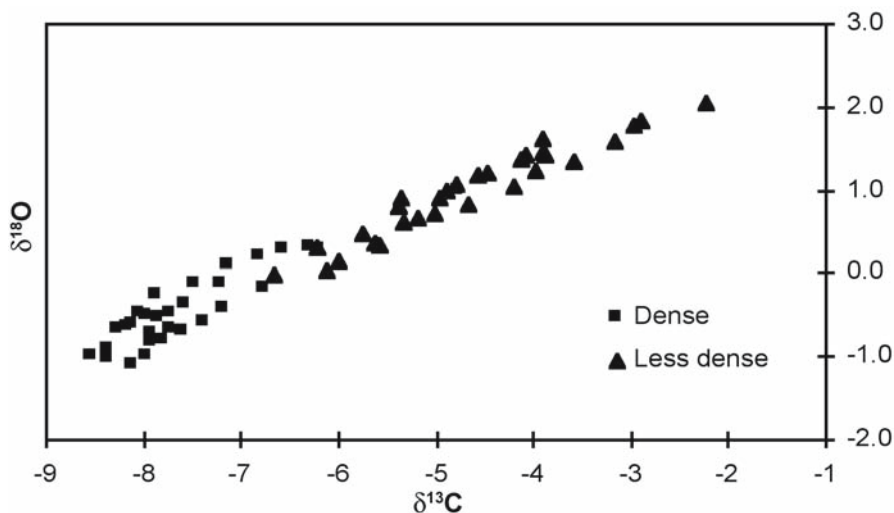
Fig. 4 $\delta^{13}C/\delta^{18}O$ plot of samples from dense and less-dense areas micromilled out of four polyps

Discussion

The lines in C-O space generated by the coral samples are consistent with the results of Smith et al. (2000). In general, isotopic records from deep-sea corals are dominated by scattered departures from equilibrium (so-called "vital effects", or kinetic isotopic equilibrium effects) to such an extent that paleoclimate determinations from these corals by traditional means are impossible (Smith et al. 2002).

From analogy with banding in tropical reef corals, and from the external location of the less-dense bands at time of collection, we assume that less-dense bands are laid down in summer months, and the dense bands in winter. The October temperature determination is very close to those determined from the less-dense "summer" bands, which follows - the warmest months of the year will be August - September. Even with the use of a microsampler, it was extremely difficult to sample precisely along coeval growth lines. Any errors in location will translate into smaller differences between summer and winter determinations: thus, while one polyp returned a temperature range of 3.8°C, the other sampled polyps gave lower

ranges. While these values seem low by comparison with those reported by Hansen and Osterhus (2000) this region of the ocean can experience extreme fluctuations in time and space. Temperatures around 330 m depth on the eastern flank of the Faroe-Shetland Channel typically have a mean annual range of around 4°C (George Slesser, Fisheries Research Services Aberdeen, pers. comm.). However, recent records of temperature from the site where the coral was sampled have a recorded range of just 1.365°C although these are point samples and unlikely to encompass the full range of temperature fluctuations in an area as dynamic as the Faroe-Shetland Channel (see Bett 2001).

Our lowest calculated temperature, 2.3°C, is considerably lower than the 4°C reported by Rogers (1999) from other sources as being a lower limit to the distribution of live *L. pertusa*. On the other hand, Bett (2001) reports on results from a moored CTD that recorded live *L. pertusa* in an area at 550 m on the eastern flank of the Faroe-Shetland Channel that regularly experienced lower temperatures than 4°C, and even reports their ability to survive brief periods of subzero temperatures.

The origin of the kinetic isotope effects in these corals continues to elude us. Adkins et al. (2003) suggest a mechanism to explain "vital effects" that involves pH gradients in the calcifying region. Much of their explanation hinges on data from *Desmophyllum cristagalli* that deviate from straight lines - for some points far from equilibrium, $\delta^{13}C$ remains constant while $\delta^{18}O$ continues to increase. The largest data set for *Desmophyllum cristagalli* may be found in Smith (1997), which includes bulk- and microsampled data points. She was unable to find the same deviations reported by Adkins et al. (2003). Pursuing this line of research may prove to be very fruitful, however, as French colleagues have also suggested involvement of pH in isotopic values in corals (Blamart et al. 2003). There are indeed large fluctuations in pH in coral skeletons: Risk and Kramer (1981) report elevated pH's (over 9, in some cases) from regions immediately under the calicoblastic epithelium, where water chemistry of these tiny compartments is dominated by the activities of boring algae. Further down in the skeleton, nutrient regeneration takes over, and metabolic CO_2 drives the pH down to values well below ambient (Risk and Muller 1983).

Variations in the amount of metabolic CO_2 incorporated into the skeleton may also profoundly impact isotopic values. Here, we suggest that a hard look at the biology of *L. pertusa* is in order. *Lophelia pertusa* is not a filter-feeder (cf. Adkins et al. 2003) and can feed voraciously on copepods in the laboratory and when observed by manned submersible, although submersible lights attract swarms of small Crustacea (Roberts pers. comm. 2002). Like many coelenterates, their nutrition probably is a combination of microcarnivory combined with dissolved organic matter (DOM) absorption. Values of $\delta^{15}N$ in coral tissue reported by Grehan et al. (2003), combined with very high values of free fatty acids in the bottom waters near *L. pertusa* reefs (Kiriakoulakis et al. 2003) support this assumption. Skeletal formation in *L. pertusa*, and indeed many cold-water corals, may therefore be an episodic process controlled fundamentally by feeding rate. Skeletal growth in these corals may be extremely slow for much of the time, as the coral survives on DOM, punctuated by rapid growth when food stocks become available. This would go a

long way to explaining the spread in isotopic values seen by us and others.

The distribution of values along the C/O lines remains one of the most intriguing aspects of our results. In the preliminary investigation, samples from the inner part of the polyps, although coeval with the septa, were consistently further from equilibrium than were the septa (Table 2). Similarly, dense bands were further from equilibrium than less-dense bands. Presumably, the dense bands result from slower growth, and hence might be expected to be closer to equilibrium. This aspect of our results deserves further investigation and may shed light aspects of coral skeletogenesis.

The largest mean annual temperature range of 3.8°C calculated from one of the corals closely agrees with the known temperature variation for this depth. Fluctuation in the annual temperature range can be valuable in providing records of past climate variability. For example, oscillation in the MAT recorded in tropical corals has been used by Tudhope et al. (2001) to show the existence of ENSO over the past 130,000 years by demonstrating interannual variation in temperature from fossil coral records. Climate proxies from the Faroe-Shetland Channel could similarly demonstrate long-term fluctuations over time, allowing us to put present changes in perspective and to help constrain predictions of future changes in thermohaline circulation

Conclusions

1. Temperature values extracted from *Lophelia pertusa* samples, using the "lines" technique of Smith et al. (2000), were consistently lower than instrumental records for the site.
2. The range of temperature values obtained from the corals accurately reflected the mean annual temperature range at 330 m in the Faroe-Shetland Channel.
3. Distribution of values along the lines in C/O space shows systematic fractionation, the nature of which is unexplained.

Acknowledgements

References

Adkins JF, Boyle EA, Curry WB, Lutringer A (2003) Stable isotopes in deep-sea corals and a new mechanisms for "vital effects". Geochim Cosmochim Acta 67: 1129-1143

Bett B (2001) Benthic ecology of the Faeroe-Shetland Channel. In: Atlantic margin environmental surveys of the seafloor 1996 and 1998. CD-ROM Geotek Ltd

Blamart D, Rollion-Bard TC, Cuif J-P, Juillet-Leclerc A, Lutringer A, van Weering T, Henriet J-P (2003) C and O isotopes in deep-sea corals (*Lophelia pertusa*) measured by ion microprobe. Erlanger Geol Abh Sonderbd 4: 22

Crease J (1964) The flow of Norwegian Sea water through the Faroe Bank Channel. Deep-Sea Res 12: 143-150

Druffel ERM, Griffin S, Guilderson T, Kashgarian M, Schrag D (2001) Changes of subtropical North Pacific radiocarbon and correlation with climate variability. Radiocarbon 43: 15-25

Frank N, Paterne M, Ayliffe L, Lutringer A, Blamart D, van Weering T (2003) Cold-water corals of the northeast Atlantic margin: archives of intermediate water circulation during the Holocene. Geophys Res Abstr, 5, Europ Geophys Soc

Freiwald A, Hühnerbach V, Lindberg B, Wilson J, Campbell J (2002) The Sula Reef Complex, Norwegian Shelf. Facies 47: 179-200

Goldstein SJ, Lea DW, Chakraborty S, Kashgarian M, Murrell MT (2001) Uranium-series and radiocarbon geochronology of deep-sea corals: implications for Southern Ocean ventilation rates and the ocean carbon cycle. Earth Planet Sci Lett 193: 167-182

Grehan AJ, Kiriakoulakis K, Mahaffey C, Wolff GA (2003) Food web relationships in deep-water corals from the Porcupine Sea Bight and Rockall Trough, west coast of Ireland. Erlanger Geol Abh Sonderbd 4: 40

Hall-Spencer J, Allain V, Fosså JH (2002) Trawling damage to Northeast Atlantic ancient coral reefs. Proc R Soc London B 269: 507-511

Hansen B, Osterhus S (2000) North Atlantic-Norwegian Sea exchanges. Progr Oceanogr 45: 109-208

Hansen B, Turrell WR, Osterhus S (2001) Decreasing overflow from the Nordic Seas in the Atlantic Ocean through the Faroe Bank channel in 1950. Nature 411: 927-930

Jones PD, New M, Parker DE, Martin S, Rigor IG (1999) Surface air temperature and its changes over the past 150 years. Rev Geophys 37: 173-199

Keigwin LD, Boyle EA (2000) Detecting Holocene changes in thermohaline circulation. Proc Nat Acad Sci 97: 1343-1346

Kiriakoulakis K, White M, Freiwald A, Wolff GA (2003) Biogeochemistry of deep-water coral systems at the NW European Continental Margin. Erlanger Geol Abh Sonderbd 4: 52

Knutson SW, Buddemeier RW, Smith S (1972) Coral chronometers: seasonal growth bands in reef corals. Science 177: 270-272

Lazier AV, Smith JE, Risk MJ, Schwarcz HP (1999) The skeletal structure of *Desmophyllum cristagalli*: the use of deep-water corals in sclerochronology. Lethaia 32: 119-130

Mann ME, Bradley RS, Hughes MK (1999) Northern hemisphere temperatures during the past millennium: interferences, uncertainties, and limitations. Geophys Res Lett 26: 759-762

Rasmussen TL, Bäckström D, Heinemeier J, Klitgaard-Kristensen D, Knutz PC, Kuijpers A, Lassen S, Thomsen E, Troelstra SR, van Weering TCE (2002) The Faroe-Shetland Gateway: Late Quaternary water mass exchange between the Nordic Seas and the northeastern Atlantic. Mar Geol 188: 165-192

Risk MJ, Kramer JR (1981) Water chemistry inside coral heads: determination of pH, Ca and Mg. 4th Int Coral Reef Symp, Manila, pp 54

Risk MJ, Muller HR (1983) Porewater in coral heads: evidence for nutrient regeneration. Limnol Oceanogr 28: 1004-1008

Rogers AD (1999) The biology of *Lophelia pertusa* (Linnaeus 1758) and other deep-water reef-forming corals and impacts from human activities. Int Rev Hydrobiol 84: 315-406

Sherwood OA, Sinclair DJ, Risk MJ, Scott DB (2003) Testing the fidelity of Mg/Ca as a temperature proxy in the deep-sea coral *Primnoa resedaeformis*: Records since 1950. Erlanger Geol Abh Sonderbd 4: 79

Sherwood OA, Risk MJ (in press) Climate significance of growth patterns in the deep-sea coral *Primnoa resedaeforms*. Mar Ecol Progr Ser

Smith JE (1997) The use of deep-sea corals as paleoceanographic monitors. PhD thesis, McMaster Univ, Hamilton, Ontario, Canada

Smith JE, Risk MJ, Schwarz HP, McConnaughey TA (1997) Rapid climate change in the North Atlantic during the younger Dryas recorded by deep-sea corals. Nature 386: 818-820

Smith JE, Risk MJ, Schwarcz HP, McConnaughey TA, Keller NB (2000) Deep-sea corals as paleotemperature indicators: overcoming "vital effects". Palaios 15: 25-32

Smith JE, Schwarcz HP, Risk MJ (2002) Patterns of isotopic equilibrium in azooxanthellate coral skeletons. Hydrobiologia 471: 111-115

Tudhope AW, Chilcott CP, McCulloch MT, Cook ER, Chappell J, Ellam RM, Lea DW, Lough JM, Shimmield GB (2001) Variability in the El Niño-Southern Oscillation through a glacial-interglacial cycle. Science 291: 1511-1517

Turrell WR, Slesser G, Adams RD, Payne R, Gillibrand PA (1999) Decadal variability in the composition of Faroe Shetland Channel bottom water. Deep-Sea Res I 46: 1-25

Wilson JB (1979) The distribution of the coral *Lophelia pertusa* (L.) [*L. prolifera* (Pallas)] in the north-east Atlantic. J Mar Biol Ass UK 59: 149-164

High-resolution trace and minor element compositions in deep-water scleractinian corals (*Desmophyllum dianthus*) from the Mediterranean Sea and the Great Australian Bight

Paolo Montagna[1,2], Malcolm McCulloch[2], Marco Taviani[3], Alessandro Remia[3], Greg Rouse[4]

[1] Department of Mineralogy and Petrology, University of Padua, Italy
 (paolo.montagna@unipd.it)
[2] Research School of Earth Sciences, Australian National University, Canberra, ACT 0200, Australia
[3] ISMAR-Marine Geology Division, CNR, Via Gobetti 101, I-40129 Bologna, Italy
[4] South Australian Museum, Nth Terrace, Adelaide, Australia

Abstract. Zooxanthellate scleractinian corals have been shown to preserve important archives of seasonal variations of climate variables, such as sea surface temperature, salinity, and productivity. By analogy, the recognition of correlated chemical signals in azooxanthellate deep-water corals may provide an important new approach to help unravel the role of intermediate and deep waters in determining climate variability. A first step to determine the suitability of deep-water scleractinian corals as potential paleoceanographic-paleoclimatic tools requires the demonstration of coherent geochemical signals in their skeletons. With this in mind, trace and minor element ratios Sr/Ca, Mg/Ca, U/Ca, B/Ca, P/Ca, Ba/Ca and Mn/Ca have been measured in two deep-water solitary scleractinian corals (*Desmophyllum dianthus*) collected from Last Glacial submerged banks in the Mediterranean basin and in the Great Australian Bight. Most elements show distinct, highly correlated patterns of variation. Although preliminary, these results illustrate the potential use of trace and minor element concentrations in the deep-water scleractinian corals to provide new constraints on the composition and evolution of intermediate and deep waters and thus introduce new perspectives in paleoceanography, such as the assessment of changes in both deep-sea nutrient chemistry and ocean circulation.

Keywords. *Desmophyllum dianthus*, deep-water corals, trace element systematics, laser ablation, Mediterranean Sea, Great Australian Bight, paleoproductivity

Introduction

Scleractinian corals secrete an aragonite exoskeleton, which incorporates chemical signatures from surrounding ambient waters during the calcification process (e.g., Amiel et al. 1973; Weber 1973; Linn et al. 1990; Marshall 1996; Grottoli 1999). The paleoceanographic significance of using shallow-water zooxanthellate (symbiont-bearing) scleractinian corals to decipher oceanographic (climatic) signals preserved within their banded calcareous exoskeletons is well established through a number of stable isotope and trace element studies (e.g., Dunbar and Wellington 1981; Aharon and Chappell 1983; Aharon 1985; Cole et al. 1993; Dunbar and Cole 1993; Carriquiry et al. 1994; Cole 1994; McCulloch et al. 1994; Wellington and Dunbar 1995; Dunbar et al.1996; Beck et al. 1997; Heiss et al. 1997). However, the distribution of symbiont-bearing corals is limited by light penetration and mean seawater temperature, so that their paleoclimatic utility is restricted to the shallow tropical oceans (Veron 1995).

By contrast, deep-water scleractinian corals display an almost cosmopolitan geographic distribution, a wide depth range from the intertidal to 6000 m, and a thermal tolerance between -1°C to 28°C (e.g., Stanley and Cairns 1988). Deep-water scleractinian corals are therefore potentially excellent archives of past oceanographic conditions with their wide depth range providing climate proxies for intermediate and deep waters. The few paleoclimatic studies published so far on deep-water corals consist mostly of ^{14}C-U/Th dating and δ^{18}O signatures (e.g., Newton et al. 1997; Smith et al. 1997, 2000; Adkins et al. 2003; Rollion-Bard et al. 2003a, b), the latter paralleling similar analyses carried out on zooxanthellate shallow-water tropical counterparts (e.g., Dunbar and Wellington 1981; Cole et al. 1993; Dunbar et al. 1996; McCulloch et al. 1996).

Trace and minor element ratios have continued to be explored as an independent means to evaluate water properties and their changes through time. In particular, Sr/Ca and Mg/Ca ratios have been utilised as a proxy for seawater temperatures in shallow-water corals (e.g., Smith et al. 1979; Beck et al. 1992; McCulloch et al. 1994, 1996; Mitsuguchi et al. 1996; Alibert and McCulloch 1997; Heiss et al. 1997; Marshall and McCulloch 2002). In addition Ba/Ca ratios have been shown to provide important paleoceanographic signatures of upwelling (e.g., Shen and Dunbar 1995; Fallon et al. 1999) and river runoff (McCulloch et al. 2003). Although all these studies were performed on shallow-water, tropical corals, their application has been recently expanded to include shallow-temperate corals (Montagna et al. 2004a). The authors demonstrated the feasibility of using high-resolution geochemical records from the non-tropical coral *Cladocora caespitosa* for the high fidelity reconstruction of sea-surface temperatures (SST) records in the Mediterranean Sea.

Until now there has been little information on the trace element characteristics of deep-water scleractinian corals, apart from few measurements of bulk Cd (Adkins et al. 1998) and B, F, Mg, Ca, Sr and Ba variations (Hart and Cohen 1996), because their internal structure are delicate and difficult to study by conventional means. Hart and Cohen (1996) examined the geochemical pattern of a septum from *Desmophyllum*

dianthus and a branch from *Lophelia pertusa*, using an ion microprobe, concluding that the incorporation of the trace elements may be dependent on vital effects, and only indirectly on temperature.

To the best of our knowledge, nutrient sensitive elements, such as P and Mn, along with Ba have not been previously investigated in deep-water scleractinian corals using laser ablation ICP-MS. In order to assess the potential use of azooxanthellate deep-water corals as paleoceanographic proxies, we present the preliminary results of high-resolution, laser ablation ICP-MS, trace and minor element compositions in two *Desmophyllum dianthus* specimens from the Mediterranean Sea and the Great Australian Bight (Fig. 1)
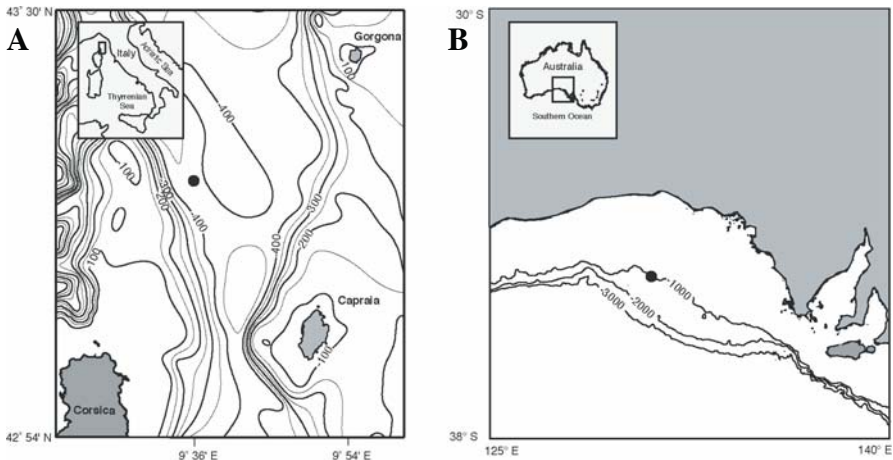
Fig. 1 A Map of the Mediterranean basin (with 100, 200, 300 and 400 m isobaths) and **B** the Great Australian Bight (with 1000, 2000 and 3000 m isobaths), showing locations of late Pleistocene corals discussed in the text (black dots)

Material

Samples consist of two fossil 'pristine' solitary scleractinian corals (Fig. 2) from submerged skeletal assemblages. Both of the studied corals are 100 % aragonite and do not contain discernible traces of secondary aragonite needles and/or micrite cement. In addition, they were not covered with the manganese and iron oxide/hydroxide coatings which are often seen on fossil deep-water corals (Cheng et al. 2000; Goldstein et al. 2001; Schröder-Ritzrau et al. 2003; Taviani et al. 2005). The Mediterranean and the Australian specimens yield ^{230}Th/U ages of 11.1± 0.1 ka and of 29.1± 0.2 ka, respectively and the dating was obtained following methods of Esat et al. (1999), but with analyses undertaken using the multicollector ICP-MS (NEPTUNE).

The taxon selected for this experiment is in both cases *Desmophyllum dianthus* (Esper, 1794). This species, better known in the literature under its younger synonym *D. cristagalli* Milne-Edwards and Haime, 1848, is variable in its morphology (Zibrowius 1977). The choice of this species was dictated by three main factors: first,
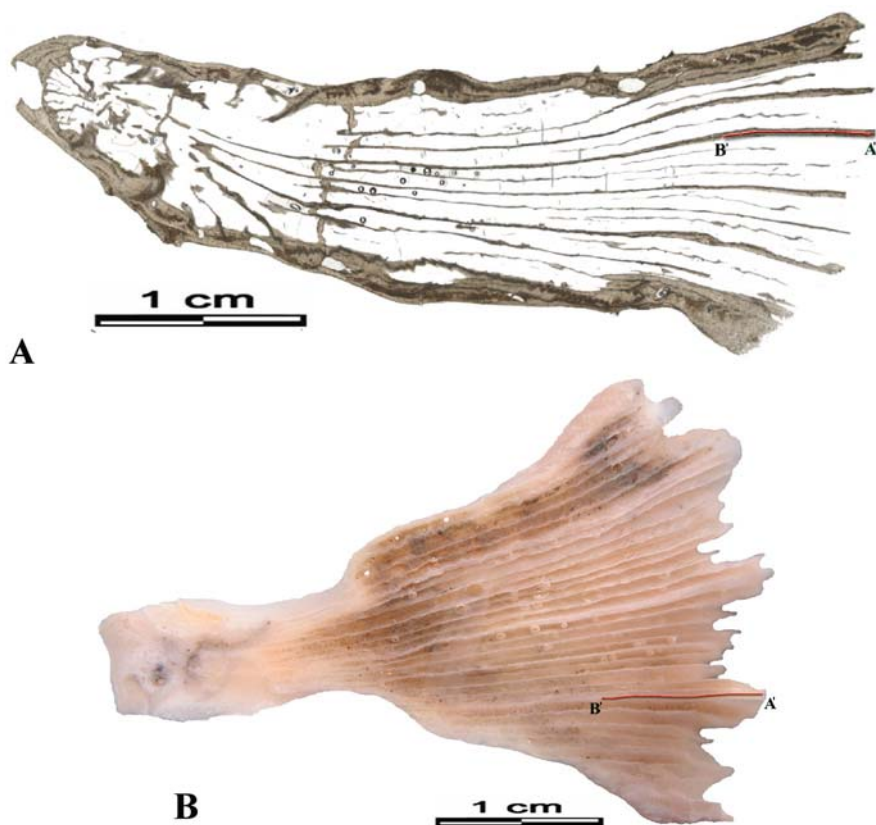
Fig. 2 *D. dianthus*: **A** Mediterranean Sea and **B** Great Australian Bight; both samples were cut parallel to the growth axis showing the typical skeletal structure of *D. dianthus*, consisting of radially symmetric septa, and thin dissepiments, without pali and columella. The high-resolution laser ablation tracks (A'-B') were carried out within the mid-plane of S1 septum, the largest septa in *D. dianthus*

D. dianthus represents a remarkably wide geographic distribution and geological longevity (see below); second, among deep-water scleractinian corals, this solitary 'pseudocolonial' (Cairns and Stanley 1981) species has been widely used for sclerochronological and stable isotope studies (Sorauf and Jell 1977; Adkins et al. 1995, 2003; Smith et al. 1997, 2000; Lazier et al. 1999); and thirdly, as for most scleractinian corals, its skeletal aragonite contains high U (3-4 ppm) and in its more pristine form negligible ^{232}Th and is therefore generally suitable for both accurate and high precision U/Th dating (e.g., Cheng et al. 1995, 2000; Esat et al. 1999; Cobb et al. 2003), which in combination with ^{14}C dating enables the ventilation age of deep waters to be determined (e.g., Adkins and Boyle 1999; Adkins et al. 1995, 1998; Goldstein et al. 2001; Schröder-Ritzrau et al. 2003).

D. dianthus is quasi-cosmopolitan in distribution (Squires 1965; Zibrowius 1977, 1980; Cairns and Stanley 1981; Mullins et al. 1981; Cairns and Parker1992; Fosshagen and Høisæter 1992; Freiwald 2002; Freiwald et al. 2004; Tursi et al. 2004; Taviani et al. 2005). Furthermore, *D. dianthus* has a substantial fossil record having been widely described (mainly as *D. cristagalli* and allied synomyms: see Seguenza 1864) from Early-Middle Pleistocene outcrops in southern Italy (e.g., Zibrowius 1987; Di Geronimo 1995; Vertino 2003; Taviani et al. 2005) and at many Late Pleistocene submerged deposits mainly representing the last glacial epoch (e.g., Taviani and Colantoni 1979, 1984; Cita et al. 1980; Zibrowius 1980; Delibrias and Taviani 1985; Allouc 1987; Taviani and Remia 2001; Remia and Taviani 2004; Taviani et al. 2005); the species is also known from submerged Holocene skeletal assemblages in the eastern Atlantic and Mediterranean (Allen and Wells 1962; Delibrias and Taviani 1985).

The Mediterranean specimen was recovered from *Madrepora*-dominated mounds at 370-410 m in the NE Tyrrhenian Sea (Remia and Taviani 2004), and the Australian specimen was trawled off the Great Australian Bight at c. 1000 m, included within a gorgonian *Keratosis*.

Methods

Coral samples were ultrasonically cleaned with distilled/deionised water, impregnated with epoxy resin and sawed with a diamond blade along the maximum growth axis. Unlike traditional methods (e.g., thermal ionisation mass spectrometry, solution ICP-MS) which are very time consuming, the laser ablation ICP-MS has the great advantage of rapid multi-element *in situ* analysis, without time consuming sample dissolution. In addition, the use of a small laser slit provides high spatial resolution, enabling narrow structures (10-250 μm) to be analysed. The laser beam was masked using a rectangular slit 20 μm wide by 220 μm long, enabling the careful sampling of coralline portions only, thus avoiding any potential region contaminated by foreign sediment. The use of the high spatial resolution LA ICP-MS has permitted detailed transects along specific coralline internal structures (septa). The LA ICP-MS system at the Research School of Earth Sciences (Australian National University) uses an ArF excimer laser with a wavelength of 193 nm coupled to a modified VG PQ2+ with enhanced sensitivity. Ablation occurs in a sealed chamber under a helium atmosphere, and ablated material is then entrained in an Ar gas stream. The laser was pulsed at 5 Hz using 50 MJ energy and the coral samples were scanned continually at a speed of 20 μm/sec.

In order to correct for any long-term machine drift, standards (NIST 612 and a *Porites* pressed powder disc) were analysed before and after the analysis of the corals samples together with backgrounds (gas blanks), collected before and after sample analysis. The LA ICP-MS analysis protocol is similar to that reported by Sinclair et al. (1998) and Fallon et al. (1999).

Before acquisition of data, any possible surface contamination was removed by a sequence of two pre-ablation scans. Under the analytical conditions used, a layer of a few microns of aragonite was removed at each passage.

[84]Sr, [25]Mg, [238]U, [11]B, ^{31}P, [138]Ba and [55]Mn, normalized to [43]Ca, the major constituent of the coral, have been measured within the mid-plane of the S1 septum for each sample (Fig. 2). This region of the septum consists of aragonite fibers arranged in fasciculi which grow out at low angle from a central calcifying region (trabecular center).

A 6.6 and a 9.9 mm length of the Mediterranean and the Pacific coral respectively was tracked, starting from the upper portion of the coral (calyx) and going towards the base. These transects taken along the mid-plane of the septum should comprise a complete series of sequentially deposited aragonite (Lazier et al. 1999).

Two replicate analyses of the same track A'-B' of *D. dianthus* from the Australian sample have been used to monitor the long-term reproducibility, as a secondary standard check. They were acquired during separate analytical sessions a week apart and the analytical parameters used were the same for each replicate.

Results and discussion

The analytical error between the two replicates is within 5 %, indicating that this technique is reproducible. Some of the variability may be related to inaccurate realigning of the laser tracks, which are not easily visible on the septa.

Most of the trace and minor elements show significant correlations (Table 1; Figs. 3 and 4), indicating that coherent geochemical factors are controlling partitioning between seawater and coral aragonite. Surprisingly no significant correlations were found between the main water-temperature sensitive proxies Sr and U. This, together with the large trace element range, clearly indicate that the forcing function of these elements is not the very small bottom water temperature variations but must be related to vital or kinetic effects. In particular, Sr/Ca variations range between 9 mmol/mol and 10.5 mmol/mol for both the corals, implying a bottom temperature

Table 1 Correlation coefficients between elements in *D. dianthus* for both the Mediterranean Sea (upper right part) and the Great Australian Bight (lower left part). Bold type represents p-value significant at 0.1 % *a*-level. Italic type represents p-value significant at 5 % -level

	B/Ca	Mg/Ca	P/Ca	Mn/Ca	Sr/Ca	Ba/Ca	U/Ca
B/Ca	□	0.04	**-0.62**	**-0.61**	-0.06	**-0.59**	*-0.21*
Mg/Ca	-0.14	□	**0.54**	**0.47**	0.13	**0.54**	**-0.52**
P/Ca	**-0.57**	**0.49**	□	**0.87**	0.08	**0.86**	*-0.21*
Mn/Ca	**-0.54**	**0.51**	**0.90**	□	0.05	**0.79**	*-0.25*
Sr/Ca	-0.17	**0.36**	**0.66**	**0.62**	□	*0.24*	*0.35*
Ba/Ca	**-0.53**	**0.45**	**0.98**	**0.89**	**0.71**	□	-0.05
U/Ca	0.13	**-0.76**	**-0.70**	**-0.68**	*-0.39*	**-0.69**	□

Fig. 3 Trace and minor element ratios plotted against distance in mm from the apex of the coral for the Mediterranean sample. The grey line represents unsmoothed data, the solid line the same data set smoothed by a 10 adjacent average smoothing

Figure caption: 10 point Adjacent Average Smoothing. Plots of Mg/Ca (mmol/mol), U/Ca (µmol/mol), B/Ca (mmol/mol), Ba/Ca (µmol/mol), P/Ca (mmol/mol), and Mn/Ca (µmol/mol) versus Distance from apex of coral (mm).
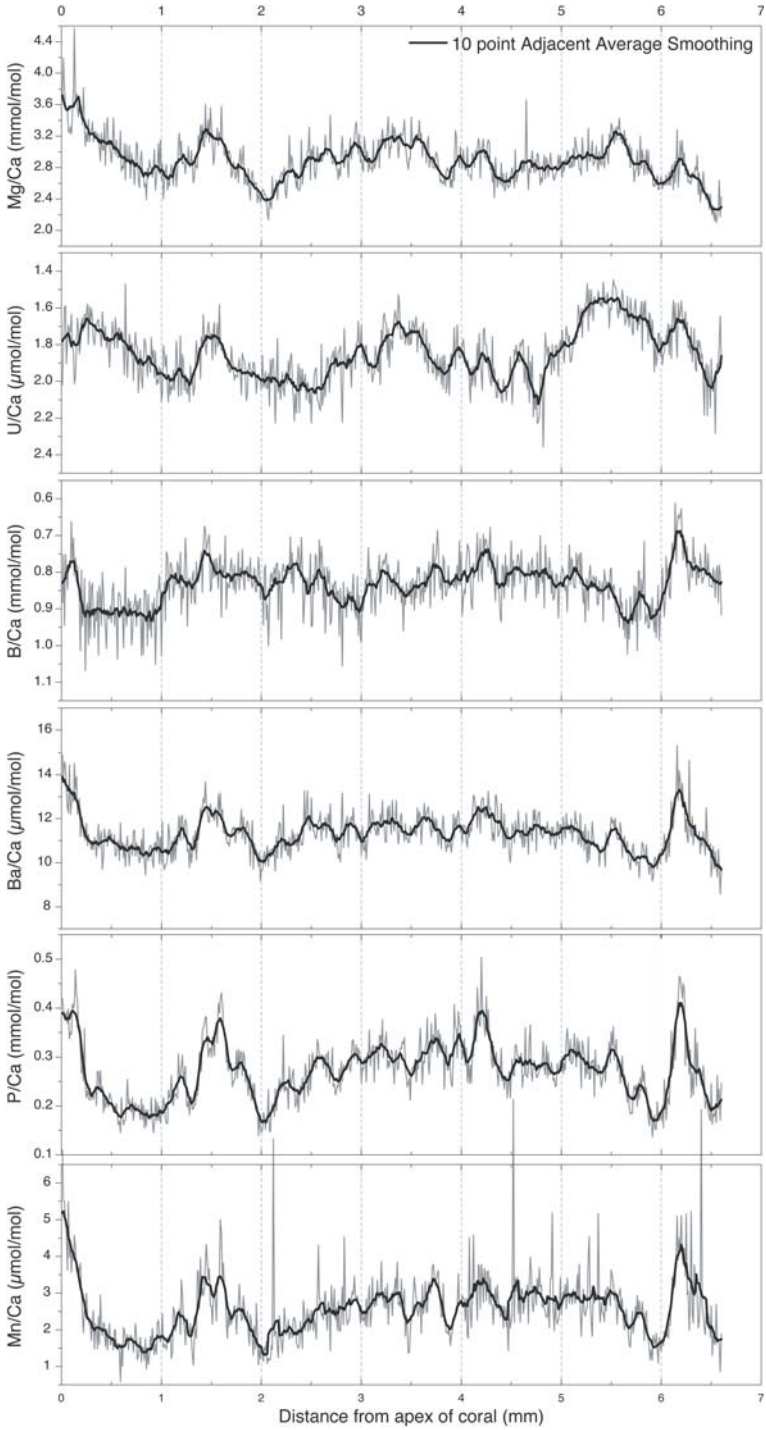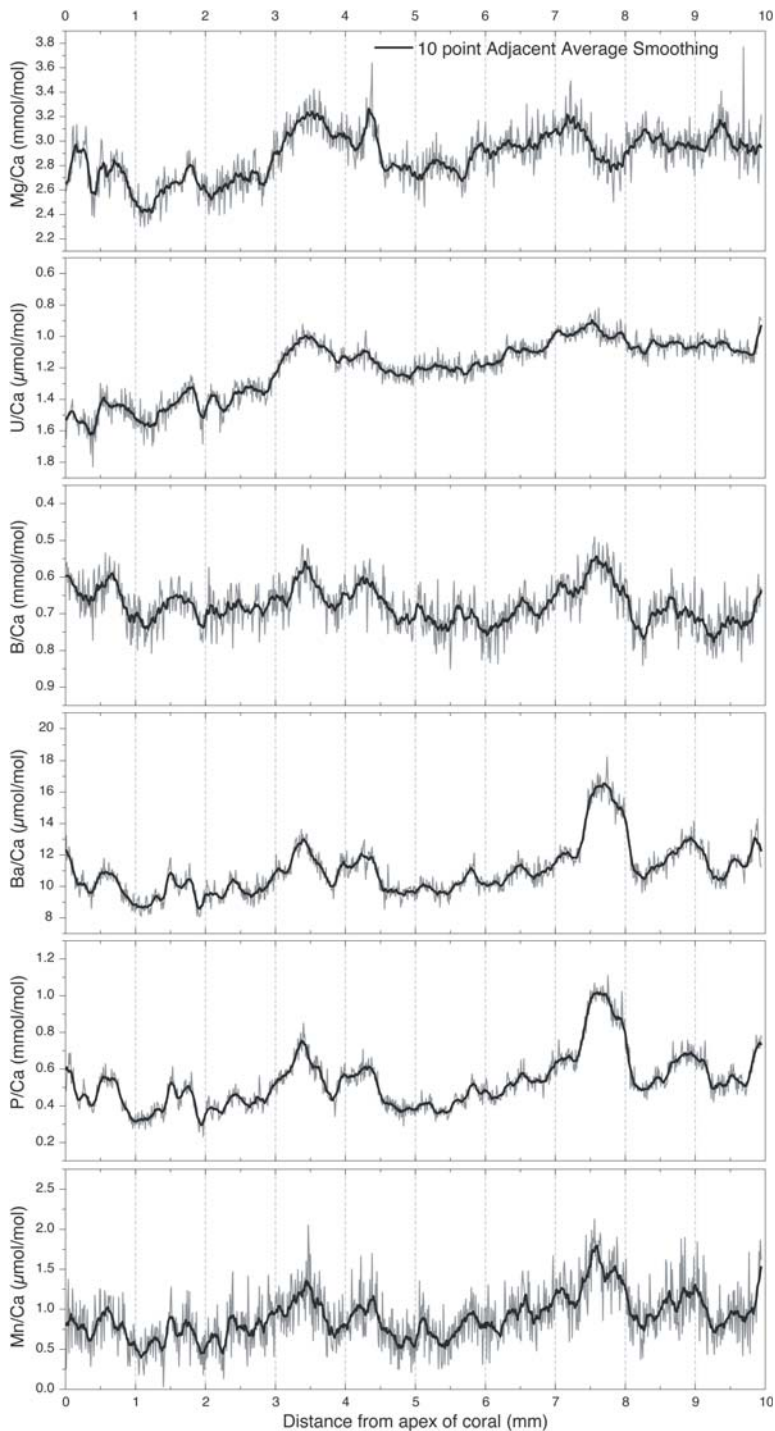
change of 29°C (using the Sr/Ca-SST calibration of Schrag 1999) or 19°C (using the Sr/Ca-SST equation of de Villiers et al. 1994). Clearly, the bottom temperature is not the driving force for the Sr/Ca changes.

Although the growth rate for this scleractinian coral species is uncertain (Cheng et al. 2000), the Mediterranean and Australian geochemical tracks are estimated to correspond to ~70 and ~100 years of coral growth respectively. This implies that some of the element concentrations exhibit approximate "seasonal" patterns, probably related to specific environmental parameters (e.g., water chemistry) or a combination of other parameters, such as growth rate, pH, carbonate ion concentration, and/or biologically induced "vital effect". The timing of these latter correlations however remains to be verified by independent determinations of coral growth rate.

The typical water-temperature sensitive elements are the subject of ongoing research which will be reported elsewhere, thus the next part of the paper will focus on P, Ba and Mn variations.

In fact, an interesting observation, which may have potentially important implications for paleoproductivity studies, is the strong positive correlations observed between the key nutrient elements P, Ba, and Mn (Table 1; Figs. 3 and 4).

Ba/Ca, P/Ca and Mn/Ca ratios exhibit large variations in both corals, and some spikes are significantly greater than the background. Most of them are spread over 0.3-0.8 mm in the extension direction, suggesting that they are real and not related to analytical problems.

Phosphorus is a major bio-limiting nutrient as nitrate and silicate and, similar to Ba, displays a nutrient type distribution within the water column, exhibiting surface depletion and enrichment at depth. This is a result of the involvement of the element in the biogeochemical cycle of fixation into organic tissues of phytoplankton and subsequent regeneration *via* oxidative processes. In fact, once in the sediment, a variety of diagenetic processes begin to affect the organic matter and this results in an increased concentration of dissolved phosphate in the porewater (Howarth et al. 1995). Phosphate dissolved in porewater also diffuses along a concentration gradient toward the sediment surface, and in some cases, is released from the sediment back to the overlying water (Howarth et al. 1995).

Mn is a micronutrient trace element with a distribution characterized by a surface enrichment and depletion at depth. It is normally scavenged throughout the water column on a time scale of roughly 10-100 years and is regenerated only under sub-oxic or anoxic conditions (Bruland 1983).

Under suboxic conditions in sediments, solid-phase manganese is reduced, and Mn^{2+} is released into the pore waters (Froelich et al. 1979). This is a diagenetic release at the seawater-sediment interface as a result of reducing conditions induced by decaying organic matter. Depending on the redox conditions or on the rate of

Fig. 4 Trace and minor element ratios plotted against distance in mm from the apex of the coral for the Pacific sample. The grey line represents unsmoothed data, the solid line the same data set smoothed by a 10 adjacent average smoothing

organic burial, the Mn^{2+} can migrate upwards into the sediment very fast, on the order of 10 cm in only a year (Froelich et al. 1979).

Reichart et al. (2003) analyzed trace element concentrations in benthic Foraminifera, using a LA ICP-MS, concluding that measurement of Mn in carbonate of Foraminifera has a great potential for reconstructing past pore-water redox gradients.

It is important to note that nutrients are quickly utilized by marine phytoplankton at the surface and returned to depth as biogenic particles. The most crucial effect of this process is the removal of CO_2 dissolved in surface waters and the transport of carbon to depth. It has been suggested, for example, that changes in Southern Ocean nutrient utilization may have play an important role in absorbing CO_2 during glacial cycles (Sigman and Boyle 2000).

Thus, assessing past changes in the export of biological production is a key issue, not only to understand past changes in atmospheric CO_2, but also to help predict how the ocean may buffer future increases in global CO_2.

Until now, measures of paleo-nutrient concentrations have been hampered by the complexity of foraminiferian/seawater fractionation factors. For instance, the proxies most commonly used for this purpose, namely carbon isotopes ($\delta^{13}C$) and Cd/Ca ratios (with a very similar oceanic behavior to phosphate) in foraminiferan tests, appear to respond to a range of environmental factors including nutrient concentration, carbonate ions, $\delta^{13}C$ of foraminiferan diet, and seawater temperature (Spero et al. 1997; Rickaby and Enderfield 1999).

Similar to phosphorus, dissolved Ba in the ocean displays bio-intermediate nutrient-like vertical and horizontal distribution (Bernat et al. 1972; Chan et al. 1977; Collier and Edmond 1984). Ba is removed from the surface and the major carrier of the vertical particulate flux of Ba is believed to be marine barite ($BaSO_4$) (Dehairs et al. 1980; Bishop 1988). Subsequently, this barite is partially released again at the seafloor (Chan et al. 1977).

The accumulation rate of Ba in marine sediments is thought to be a tracer of variations in marine biological productivity through time (Dymond et al. 1992) but its use as a paleoproductivity proxy is dependent upon the preservation in the sediment record (McManus et al. 1998).

In addition, Ba has been used to predict the alkalinity of past oceans from Ba/Ca ratios in benthic Foraminifera (Lea and Boyle 1989; Lea 1993). They concluded that Ba content of Foraminifera shells reflects ambient dissolved Ba concentration.

The remarkable correlations exhibited for the three elements P, Ba and Mn within the aragonite skeleton of *D. dianthus* suggest an unique forcing function or a combination of linked factors.

At this point, an understanding of the mechanisms of incorporation of P, Ba and Mn into the coral skeleton is fundamental in order to provide possible explanations for the covariant element variations.

Alibert et al. (2003) carried out coral leaching experiments on *Porites* species from the Great Barrier Reef and they concluded that a significant portion of P may be adsorbed on surface rather than substituting for major cations in the aragonite crystals. The fact that P is discriminated against in the coral lattice is due to the

different structure of phosphate. In addition they suggested that some peaks of P observed in the coral in early summer may reflect minute amounts of organic matter incorporated into the coral skeleton.

In corals the Mn is believed to be mostly lattice bound (Shen et al. 1991; Delaney et al. 1993) even if it appears to be discriminated against in the coral lattice relative to Ca, with a distribution coefficient of 0.1-0.5 (Shen et al. 1991). Another mechanism of incorporation may be the adsorption or occlusion within aragonite as an oxide or in some organic phase (Shen et al. 1991).

Ba should substitute for Ca into the lattice of coral skeleton due to the orthorhombic structure of aragonite and this incorporation should reflect seawater-dissolved Ba, with a partition coefficient about 1 (Lea et al. 1989). As shown by Allison and Tudhope (1993), Tudhope et al. (1996) and Alibert et al. (2003), Ba can exist in a contaminant phase. By using SEM examination and ion probe technique, Tudhope et al. (1996) observed small (<1 mm) lozenge-shaped, barite crystals, and an elevated Ba levels associated with sub-micron pores. They also hypothesized that Ba is associated with organic matter, as noted by Alibert et al. (2003) as well. Finally, there are some evidences that Ba may be adsorbed on coral surface (Pingitore et al. 1989).

It is important to emphasize that the laser tracks were obtained along the mid-plane of the septum, which comprises a chain of calcification centers. Calcification centers in shallow and deep-water corals have been described to have specifically secreted organic mineralizing matrices (Cuif and Dauphin 1998; Cuif et al. 2003), which are known to control both crystallization pattern and minor element concentration (Cuif and Dauphin 1998). In addition, calcification centers are sites characterized by an enrichment of minor organic matter compared to fibrous aragonite (Allison and Tudhope 1993; Tudhope et al. 1996).

Recently, Montagna et al. (2004b) studied the laser ablation trace element systematics in *D. dianthus* samples, showing significant differences between calcification centers and fibrous aragonite.

Despite the intricacies in the understanding of the different mechanisms involved in trace element uptake during calcification of fibrous aragonite and calcification centers during the biomineralization processes, we propose two possible explanations for the Ba, P and Mn variations observed in the samples studied. The first hypothesis concerns with the increase biological productivity and the second one involves the growth rate dependence of trace element uptake.

The most crucial effect of an increase in the supply of marine and/or terrestrial organic matter (e.g., from surface productivity) on the ocean floor is a decrease in bottom water oxygen concentration (Froelich et al. 1979). Consequently, the diagenesis of organic matter would proceed by MnO_2 reduction, releasing dissolved Mn^{2+} to the pore water and eventually, if the oxygen conditions are low enough, to the bottom water.

We speculate that this process might account for this strong correlation between P, Ba and Mn. In particular, Ba and P variations could reflect either changes in minute amounts of marine organic matter or changes of element adsorption during organic matter diagenesis. Both the mechanisms of incorporation should be enhanced along

the chain of calcification centers due either to the metal binding capability of the organic matrix produced by the coral tissue or the higher degree of microporosity compared to the surrounding areas.

Mn variations may reflect changes in Mn (lattice bound) during different redox conditions (in this case different organic matter supply), thus giving hints on paleoproductivity.

In both corals we found a similar slope for the regressions Ba *vs*. P (0.044), suggesting that these two elements may be incorporated in coral skeleton following the same mechanism.

However, a number of issues relating to the understanding of the factors which exactly control the uptake of these elements in the skeleton of this species remain to be studied in more detail. This requires a direct comparison between the elemental composition of modern coral skeletons and the chemistry of ambient seawater in which they grew. Further research is thus necessary to prove the applicability of extracting productivity proxies from deep-water scleractinian corals and to ascertain rapid changes in deep-sea nutrient chemistry from strategic locations.

An alternative explanation assumes the role of kinetic processes during calcification.

Adkins et al. (2003) and Rollion-Bard et al. (2003a, b), studying the mechanism of $\delta^{18}O$ and $\delta^{13}C$ fractionation into corals, concluded that the calcification centers represent coral portions characterized by a faster calcification rate compared to the fibrous aragonite. As expected from the growth rate dependence of trace element uptake (Lorens 1981; Tesoriero and Pankow 1996; Watson 2004), the element concentration on crystal surface depends upon the growth rate and the mobility of atoms in the near-surface region. Even though these experiments were carried out for calcite, the major conclusions should be applicable for biogenic aragonite as well, but this is an assumption. Following this model based on the growth rate variations, the two domains (calcification centers and fibrous aragonite) should uptake different element concentrations.

The chain of calcification centers in the mid-plane of the septum is not parallel to the septal surface but it moves zigzaggy inside the septum. This implies that in some parts the laser track includes both the calcification centers and fibrous aragonite and in others it includes the fibrous aragonite alone. The enrichments of element concentration should correspond to greater portions of calcification centers ablated and *vice versa*.

These uncertainties in the interpretation of the trace element underline the need for detailed investigations both on the correlation between corals and chemistry of ambient seawater and the trace element uptake in deep-water corals.

Conclusions

Although preliminary, data presented here clearly demonstrate that corals calcifying below the photic zone display cyclical and generally highly correlated patterns of covariation, in particular U/Ca *vs*. Mg/Ca, B/Ca *vs*. Ba/Ca, and P/Ca *vs*. Mn/Ca. The recognition of correlated chemical signals in deep-water scleractinian

corals, therefore, provides an important new approach to help unravel climatic variability with respect to the temporal evolution of the chemical composition of intermediate and deep waters.

Trace element uptake in the aragonite skeletons of shallow-water corals is to first order controlled by sea surface temperature. The application for example of Sr/Ca and Mg/Ca as paleothermometers in shallow-water corals is however limited by modulation or distortion of these ratios by algal symbionts, a vital-effect disadvantage not present within corals living below the photic zone which do not contain such light-dependent symbionts. In deep-water scleractinian corals the temperature proxy elements U and Sr, do not exhibit correlations indicating that other factors are dominant. The chemical variation of productivity controlled elements of P, Mn, Ba (and perhaps B) although complex, is highly coherent reflecting changes in seawater concentrations rather than being governed by temperature. In particular we have suggested two possible explanations for the P, Mn and Ba variations, involving either changes in the supply of organic matter on the ocean floor or the growth rate dependence of trace element uptake. The regular minor and trace element systematics obtained using the pulsed laser ablation microsampling indicated that *D. dianthus* has the potential to become a powerful archive of deep-water chemistry.

Acknowledgments

References

Adkins JF, Boyle EA (1999) Age screening of deep-sea corals and the deep ocean record of climate change at 15.4 ka. In: Abrantes F, Mix A (eds) Reconstructing Ocean History: A Window into the Future. Plenum, New York, pp 103-120

Adkins JF, Boyle EA, Cheng H, Edwards RL, Druffel ERM (1995) Paleo-ventilation ages from paired C-14 and Th-230 dates of deep-sea corals. AGU Fall Meeting, pp 292

Adkins JF, Cheng H, Boyle EA, Druffel ERM Edwards RL (1998) Deep-sea coral evidence for rapid change in ventilation of the deep North Atlantic 15,400 years ago. Science 280: 725-728

Adkins JF, Boyle EA, Curry WB, Lutringer A (2003) Stable isotopes in deep-sea corals and a new mechanism for "vital effects". Geochim Cosmochim Acta 67: 1129-1143

Aharon P (1985) Carbon isotope record of late Quaternary coral reefs: possible index of sea surface paleoproductivity. AGU Geophys Monogr 32: 343-355

Aharon P, Chappell J (1983) Carbon and oxygen isotope probes of reef environment histories. In: DJ Barnes (ed) Perspectives on Coral Reefs. Austral Inst Mar Sci, Townsville, pp 1-15

Alibert C, McCulloch MT (1997) Strontium/calcium ratios in modern *Porites* corals from the Great Barrier Reef as a proxy for sea surface temperature: calibration of the thermometry and monitoring of ENSO. Paleoceanography 12: 345-363

Alibert C, Kinsley L, Fallon S, McCulloch MT, Berkelmans R, McAllister F (2003) Source of trace element variability in Great Barrier Reef corals affected by the Burdekin flood plumes. Geochim Cosmochim Acta 67: 231-246

Allen JRL, Wells JW (1962) Holocene coral banks and subsidence in the Niger Delta. J Geol 70: 381-397

Allison N, Tudhope AW (1993) Nature and significance of geochemical variations in coral skeletons as determined by ion microprobe analysis. Proc 7th Int Coral Reef Symp, Guam, pp 173-178

Allouc J (1987) Les paléocommunautés profondes sur fond rocheux du Pléistocène méditerranéen. Description et essai d'interprétation paléoécologique. Géobios 20: 241-263

Amiel AJ, Friedman GM, Miller DS (1973) Distribution and nature of incorporation of trace elements in modern aragonite corals. Sedimentology 20: 47-64

Beck JW, Edwards RL, Ito E, Taylor F, Récy J, Rougerie F, Joannot P, Henin C (1992) Sea-surface temperature from coral skeleton strontium/calcium ratios. Science 257: 644-657

Beck JW, Récy J, Taylor F, Edwards RL, Cabioch G (1997) Abrupt changes in the early Holocene tropical sea surface temperature derived form coral records. Nature 385: 705-707

Bernat M, Church T, Allegre C (1972) Barium and strontium concentrations in Pacific and Mediterranean sea water profiles by direct isotope dilution mass spectrometry. Earth Planet Sci Lett 16: 75-80

Bishop JKB (1988) The barite-opal-organic carbon association in oceanic particulate matter. Nature 332: 341-343

Bruland KW (1983) Trace element in sea-water. Chem Oceanogr 8: 157-220

Cairns SD, Parker SA (1992) Review of the Recent Scleractinia of South Australia, Victoria, and Tasmania. Rec South Austral Mus Monogr Ser 3: 82 pp

Cairns SD, Stanley GD (1981) Ahermatypic coral banks: living and fossil counterparts. Proc 4th Int Coral Reef Symp, Manila 1: 611-618

Carriquiry JD, Risk MJ, Schwarcz HP (1994) Stable isotope geochemistry of corals from Costa Rica as proxy indicator of the El Niño/Southern Oscillation (ENSO). Geochim Cosmochim Acta 58: 335-351

Chan LH, Drummond D, Edmond JM, Grant B (1977) On the barium data from the Atlantic GEOSECS expedition. Deep-Sea Res 24: 613-649

Cheng H, Adkins JF, Edwards RL, Boyle EA (1995) [230]Th dating of deep-sea solitary corals. AGU Fall Meeting: F292

Cheng H, Adkins JF, Edwards RL, Boyle EA (2000) [230]Th dating of deep-sea corals. Geochim Cosmochim Acta 64: 2401-2416

Cita MB, Benelli F, Biggiogero B, Chezar H, Colombo A, Fantini Sestini N, Freeman-Lynde R, Iaccarino S, Jadoul F, Legnani R, Malinverno A, Massiotta P, Paggi L, Premoli-Silva I (1980) Contribution to the geological exploration of the Malta Escarpment (eastern Mediterranean). Riv Ital Paleont 86: 317-356

Cobb KM, Charles CD, Cheng H, Kastner M, Edwards RL (2003) U/Th-dating of young fossil corals from the central tropical Pacific. Earth Planet Sci Lett 210: 91-103

Cole JE (1994) Reconstructing and predicting climate variability. Geotimes Nov 1994: 12-15

Cole JE, Fairbanks RG, Shen GT (1993) Recent variability in the Southern Oscillation isotopic results from the Tarawana Atoll coral. Science 260: 1790-1793

Collier R, Edmond LM (1984) The trace element geochemistry of marine biogenic particulate matter. Progr Oceanogr 13: 113-119

Cuif JP, Dauphin Y (1998) Microstructural and physico-chemical characterization of "centers of calcification" in septa of some Recent scleractinian corals. Paläont Z 72: 257-270

Cuif JP, Dauphin Y, Doucet J, Salome M, Susini J (2003) XANES mapping of organic sulfate in three scleractinian coral skeletons. Geochim Cosmochim Acta 67: 75-83

Dehairs F, Chesselet R, Jedwab J (1980) Discrete suspended particles of barite and the barium cycle in the open ocean. Earth Planet Sci Lett 49: 528-550

Delaney ML, Linn LJ, Druffel ERL (1993) Seasonal cycles of manganese and cadmium in coral from the Galapagos Islands. Geochim Cosmochim Acta 57: 347-354

Delibrias G, Taviani M (1985) Dating the death of Mediterranean deep-sea scleractinian corals. Mar Geol 62: 175-180

De Villiers S, Shen GT, Nelson BK (1994) The Sr/Ca-temperature relationship in coralline aragonite: influence of variability in (Sr/Ca) seawater and skeletal growth parameters. Geochim Cosmochim Acta 58: 197-208

Di Geronimo I (1995) Benthic assemblage of the Plio-Quaternary soft and hard substrata in the Straits of Messina area. In: Guglielmo L, Manganaro A, De Domenico E (eds) The Straits of Messina Ecosystem. Proc Symp, Messina, 4-6 April 1991, pp 105-118

Dunbar RB, Cole J (1993) Coral records of the ocean-atmosphere variability. NOAA Climate Global Change Program Spec Rep 10

Dunbar RB, Wellington GM (1981) Stable isotopes in a branching coral monitor seasonal temperature variation. Nature 293: 453-455

Dunbar RB, Linsley BK, Wellington GM (1996) Eastern Pacific corals monitor El Niño/Southern Oscillation, precipitation and sea surface temperature variability over the past 3 centuries. In: Jones PD, Bradley RS, Jouzel J (eds) Climatic fluctuations and forcing mechanisms of the last 2000 years. Springer, Berlin Heidelberg, pp 375-407

Dymond J, Suess E, Lyle M (1992) Barium in deep-sea sediment: a geochemical proxy for paleoproductivity. Paleoceanography 7: 163-181

Esat T, McCulloch MT, Chappell J, Pillans B, Omura A (1999) Rapid fluctuations in sea level recorded at Huon Peninsula during the Penultimate Interglacial. Science 283: 197-201

Fallon SJ, McCulloch MT, Van Woesik R, Sinclair DJ (1999) Corals at their latitudinal limits: laser ablation trace element systematics in *Porites* from Shirigai Bay, Japan. Earth Planet Sci Lett 172: 221-238

Fosshagen A, Høisæter T (1992) The second Norwegian record of the deep-water coral, *Desmophyllum cristagalli* Milne-Edwards and Haime, 1848 (Cnidaria: Scleractinia). Sarsia 77: 291-292

Freiwald A (2002) Reef-forming cold-water corals. In: Wefer G, Billett D, Hebbeln D, Jørgensen BB, Schlüter M, van Weering T (eds) Ocean Margin Systems. Springer, Berlin Heidelberg, pp 365-385

Freiwald A, Fosså JH, Grehan AJ, Koslow JA, Roberts M (2004) Cold-water coral reefs. UNEP-WCMC Rep, Biodiversity Ser 22: 1-84

Froelich PN, Klinkhammer GP, Bender M., Luedtke NA, Heath GR, Cullen D, Dauphin P, Hammond D, Hartman B, Maynard V (1979) Early oxidation of organic matter in pelagic sediments of the eastern equatorial Atlantic: suboxic diagenesis. Geochim Cosmochim Acta 43: 1075-1090

Goldstein SJ, Lea DW, Chakraborty S, Kashgarian M, Murrell MT (2001) Uranium-series and radiocarbon geochronology of deep-sea corals: implications for Southern Ocean ventilation rates and the oceanic carbon cycle. Earth Planet Sci Lett 193: 167-182

Grottoli AG (1999) Variability of stable isotopes and maximum linear extension in reef-coral skeletons at Kaneohe Bay, Hawaii. Mar Biol 135: 437-449

Hart SR, Cohen AL (1996) An ion probe study of annual cycles of Sr/Ca and other trace elements in corals. Geochim Cosmochim Acta 60: 3075-3084

Heiss GA, Camoin GF, Eisenhauer A, Wischow D, Dullo W-Chr, Hansen B (1997) Stable isotopes and Sr/Ca - signals in corals from the Indian Ocean. Proc 8th Int Coral Reef Symp, Panama, pp 1713-1718

Howarth RW, Jensen HS, Marino R, Postma H (1995) Transport to and processing of P in near-shore and oceanic water. In: Tiessen H (ed) Phosphorus in the global environment. John Wiley and Sons, pp 323-356

Lazier AV, Smith JE, Risk MJ, Schwarcz P (1999) The skeletal structure of *Desmophyllum cristagalli*: the use of deep-water corals in sclerochronology. Lethaia 32: 119-130

Lea D (1993) Constrains on the alkalinity and circulation of glacial circumpolar deep water from benthic foraminiferal barium. Global Biogeochem Cycles 7: 695-710

Lea D, Boyle E (1989) Barium content of benthic foraminifera controlled by bottom-water composition. Nature 338: 751-753

Linn LJ, Delaney ML, Druffel ERM (1990) Trace metals in contemporary and seventeenth-century Galapagos coral: records of seasonal and annual variations. Geochim Cosmochim Acta 54: 387-394

Lorens RB (1981) Sr, Cd, Mn and Co distribution coefficients in calcite as a function of calcite precipitation rate. Geochim Cosmochim Acta 45: 553-561

Marshall AT (1996) Calcification in hermatypic and ahermatypic corals. Science 271: 637-639

Marshall JF, McCulloch M (2002) An assessment of the Sr/Ca ratio in shallow water hermatypic corals as a proxy for sea surface temperature. Geochim Cosmochim Acta 66: 3263-3280

McCulloch MT, Gagan MK, Mortimer GE, Chivas AR, Isdale PJ (1994) A high-resolution Sr/Ca and $\delta^{18}O$ coral record from the Great Barrier Reef, Australia, and the 1982-1983 El Niño. Geochim Cosmochim Acta 58: 2747-2754

McCulloch M, Mortimer G, Esat T, Xianhua L, Pillans B, Chappell J (1996) High-resolution windows into early Holocene climate: Sr/Ca coral records from the Huon Peninsula. Earth Planet Sci Lett 138: 169-178

McCulloch M, Fallon S, Wyndham T, Hendy E, Lough J, Barnes D (2003) Coral record of increased sediment flux to the inner Great Barrier Reef since European settlement. Nature 421: 727-730

McManus J, Berelson WM, Klinkhammer GP, Johnson KS, Coale KH, Anderson RF, Kumar N, Burdige DJ, Hammond DE, Brumsack HJ, McCorkle DC, Rushdi A (1998) Geochemistry of barium in marine sediments: implications for its use as a paleoproxy. Geochim Cosmochim Acta 62: 3453-3473

Mitsuguschi T, Matsumoto E, Abe O, Uchida T, Isdale PJ (1996) Ma/Ca thermometry in coral skeletons. Science 274: 961-963

Montagna P, McCulloch M, Mazzoli C, Silenzi S (2004a) B/Ca, Sr/Ca, U/Ca and Mg/Ca ratios of a non-tropical coral (*Cladocora caespitosa*) from the Northern Adriatic Sea (Mediterranean Sea) and their relationship to sea surface temperature. 10th Int Coral Reef Symp, June 28-July 2, Okinawa, Japan, pp 269

Montagna P, McCulloch M, Taviani M, Remia A, Mazzoli C (2004b) Laser ablation trace element systematics in deep-water corals (*Desmophyllum dianthus*) from the Mediterranean Sea and the Pacific Ocean. 8th Int Conf Paleoceanogr, Sept 5-10 2004, Biarritz, France, pp 184

Mullins HT, Newton CR, Heath K, Vanburen HM (1981) Modern deep-water coral mounds north of Little Bahama Bank: criteria for recognition of deep-water coral bioherms in the rock record. J Sediment Petrol 51: 999-1013

Newton CR, Mullins HT, Gardulski AF (1997) Coral mounds on the Western Florida Slope: unanswered questions regarding the development of deep-water banks. Palaios 2: 359-367

Pingitore NE, Rangel Y, Kwarting A (1989) Barium variations in *Acropora palmata* and *Montastrea annularis*. Coral Reefs 8: 31-36

Reichart G-H, Jorissen F, Anschutz P, Mason PRD (2003) Single foraminiferal test chemistry records the marine environment. Geology 31: 355-358

Remia A, Taviani M (2004) Shallow-buried Pleistocene *Madrepora*-coral mounds on a muddy continental slope, Tuscan Archipelago, NE Tyrrhenian Sea. Facies 50, DOI 10.1007/s10347-004-0029-2

Rickaby REM, Elderfield H (1999) Planktonic foraminiferal Cd/Ca: paleonutrients or paleotemperature? Paleoceanography 14: 293-303

Rollion-Bard C, Blamart D, Cuif JP, Juillet-Leclerc A (2003a) Microanalysis of C and O isotopes of azooxanthellate and zooxanthellate corals by ion microprobe. Coral Reefs 22: 405-415

Rollion-Bard C, Chaussidon M, France-Lanord C (2003b) pH control on oxygen isotopic composition of symbiotic corals. Earth Planet Sci Lett 215: 275-288

Schrag DP (1999) Rapid determination of high-precision Sr/Ca ratios in corals and other marine carbonates. Paleoceanography 14: 97-102

Schröder-Ritzrau A, Mangini A, Lomitschka M (2003) Deep-sea corals evidence periodic reduced ventilation in the North Atlantic during the LMG/Holocene transition. Earth Planet Sci Lett 216: 399-410

Seguenza G (1864) Disquisizioni paleontologiche intorno ai Corallarii fossili delle rocce terziarie del distretto di Messina. Mem R Acc Sci Torino (ser 2) 21: 399-560

Shen GT, Dunbar RB (1995) Environmental controls on uranium in reef corals. Geochim Cosmochim Acta 59: 2009-2024

Shen GT, Campbell TM, Dunbar RB, Wellington GM, Colgan MW, Glynn PW (1991) Paleochemistry of manganese in corals from the Galapagos Islands. Coral Reefs 10: 91-100

Sigman DM, Boyle EA (2000) Glacial/interglacial variations in atmospheric carbon dioxide. Nature 407: 859-869

Sinclair DJ, Kinsley LPJ, McCulloch M (1998) High-resolution analysis of trace elements in corals by laser ablation ICP-MS. Geochim Cosmochim Acta 62: 1889-1901

Smith SV, Buddemeier RW, Redalje RC, Houck JE (1979) Strontium-calcium thermometry in coral skeletons. Science 204: 404-406

Smith JE, Risk MJ, Schwarcz HP, McConnaughey T (1997) Rapid climate change in the North Atlantic during the Younger Dryas recorded by deep-sea corals. Nature 386: 818-820

Smith JE, Schwarcz HP, Risk MJ, McConnaughey T, Keller N (2000) Paleotemperatures from deep-sea corals: overcoming "vital effects". Palaios 15: 25-32

Sorauf JE, Jell JS (1977) Structure and incremental growth in the ahermatypic coral *Desmophyllum cristagalli* from the North Atlantic. Paleontology 20: 1-9

Spero HJ, Bijma J, Lea DW, Bemis BE (1997) Effect of seawater carbonate concentration in foraminiferal carbon and oxygen isotopes. Nature 390: 497-500

Squires DF (1965) Deep-water coral structure on the Campbell Plateau, New Zealand. Deep-Sea Res 12: 785-788

Stanley GD, Cairns SD (1988) Constructional azooxanthellate coral communities: an overview with implications for the fossil record. Palaios 3: 233-242

Taviani M, Colantoni P (1979) Thanatocoenoses würmiennes associées aux coraux blancs. Rapp Comm Int Mer Médit 25/26: 141-142

Taviani M, Colantoni P (1984) Paléobiocenoses profondes a scléractiniaires sur l'escarpement de Malte-Syracuse (Mer Méditerranée): leur structure, leur âge et leur signification. Rev Inst Franc Pétr 39: 547-552

Taviani M, Remia A (2001) I coralli del buio: archivi climatici degli oceani passati. Ricerca Futuro 18: 28-30

Taviani M, Freiwald A, Zibrowius H (2005) Deep coral growth in the Mediterranean Sea: an overview. In: Freiwald A, Roberts JM (eds) Deep-water Corals and Ecosystems. Springer, Berlin Heidelberg, pp 137-156

Tesoriero AJ, Pankow JF (1996) Solid solution partitioning of Sr^{2+}, Ba^{2+} and Cd^{2+} to calcite. Geochim Cosmochim Acta 60: 1053-1063

Tudhope AW, Lea D, Shimmield GB, Chilcott CP, Head S (1996) Monsoon climate and Arabian Sea coastal upwelling recorded in massive corals from Southern Oman. Palaios 11: 347-361

Tursi A, Mastrototaro F, Matarrese A, Maiorano P, D'Onghia G (2004) Biodiversity of the white coral reefs in the Ionian Sea (Central Mediterranean). Chem Ecol 20 (Suppl 1): S107-S116

Veron JEN (1995). Corals in space and time. Southwood Press, 321 pp

Vertino A (2003) Sclerattiniari Plio-Pleistocenici ed attuali del Mediterraneo (Sistematica, Biostratinomia e Paleoecologia). Unpubl PhD thesis, Univ Messina, 306 pp

Watson EB (2004) A conceptual model for near-surface kinetic controls on the trace-element and stable isotope composition of abiogenic calcite crystals. Geochim Cosmochim Acta 68: 1473-1488

Weber JN (1973) Deep-sea ahermatypic scleractinian corals: isotopic composition of the skeleton. Deep-Sea Res 20: 901-909

Wellington GM, Dunbar RB (1995) Stable isotope signatures of ENSO in eastern Pacific (Panama) corals. Coral Reefs 14: 5-25

Zibrowius H (1977) Taxonomy in ahermatypic scleractinian corals. Palaeont Amer 54: 80-85

Zibrowius H (1980) Les Scléractiniaires de la Méditerranée et de l'Atlantique nord-oriental. Mém Inst Océanogr Monaco 11: 284 pp

Zibrowius H (1981) Thanatocoenose pléistocène profonde à spongiaires et scléractiniaires dans la fosse Hellénique. J Étud Syst Évol Biogéogr Médit Cagliari, 13-14 octobre 1980, CIESM Monaco, pp 133-136

Zibrowius H (1987) Scléractiniaires et Polychètes Serpulidae des faunes bathyales actuelle et plio-pléistocène de Méditerranée. Doc Trav IGAL 11: 255-257

VIII

Conservation

Chapter content

Identifying critical information needs and developing institutional partnerships to further the understanding of Atlantic deep-sea coral ecosystems

Kimberly A. Puglise, Robert J. Brock, John J. McDonough III

U.S. National Oceanic and Atmospheric Administration, Silver Springs, MD 20910, USA
(kimberly.puglise@noaa.gov)

Abstract. The deep-sea (>200 m) represents the largest portion of the ocean, but it is probably the least understood because of the technological challenges and financial resources required to explore and research this environment. With the advancement of underwater technology, astonishing images of deep-sea corals living at depths from the surface to greater than 1000 m are now becoming available to both policy makers and the public. More specifically, in the North Atlantic Ocean, these images have led many countries to begin to assess the distribution, status, health, and potential threats faced by these important ecosystems, which appear to be connected by the uniting influence of the Gulf Stream and its associated currents. Since deep-sea coral ecosystems extend beyond national boundaries and encounter similar threats, it was determined that a cooperative effort on both sides of the Atlantic could be beneficial to maximize available resources, share expertise, and exchange data to rapidly increase scientific understanding of deep-sea coral ecosystems. Thus, an international *Deep-Sea Corals Workshop* was held to identify critical information needs related to: locating and mapping deep-sea corals; understanding more about coral biology and ecology; and using specific deep-sea coral species as indicators of climate change. Priority information needs identified at the workshop were the need to: (1) conduct both low- and high-resolution mapping to locate and characterize deep-sea coral habitats; (2) conduct research on factors that influence deep-sea coral life history patterns; (3) examine how they function as habitat for fish and invertebrate species; (4) develop a comprehensive inventory of deep-sea coral species; and (5) further efforts to analyze past climate changes and to improve climate forecasting models. Described herein are: the results of the *Deep-Sea Corals Workshop*; other events with a focus on deep-sea corals; and potential pathways to increase U.S.-international collaborative partnerships.

Keywords. Deep-sea coral, institutional partnerships, North Atlantic

Introduction

In the United States, deep-sea corals are emerging as a highly visible marine policy issue. Although initially described over two centuries ago in Norwegian waters (Pontoppidan 1755) and over a century ago in North American waters (Verrill 1862), it wasn't until the past twenty years that deep-sea corals began to draw interest from the marine policy community. This growing political interest in deep-sea corals stems from an increase in the documentation of: (1) their association with high abundances of rich and diverse fish and invertebrate communities, including some commercial species (Jensen and Frederiksen 1992; Husebø et al. 2002; Reed 2002); and (2) impacts from anthropogenic and natural processes on deep-sea corals and the species that depend on them (Koenig et al. 2000; Fosså et al. 2002; Hall-Spencer et al. 2002; NRC 2002).

Habitat-forming deep-sea corals have been shown to be associated with both fish and invertebrate species (Jensen and Frederiksen 1992; Krieger and Wing 2002; Reed 2002). *Lophelia pertusa*, a reef forming deep-sea coral, was described as being closely associated with ca. 298 species (Jensen and Frederiksen 1992); and *Oculina varicosa*, the ivory tree coral, located off the coast of Florida was found to be associated with commercially and recreationally important fish species, including the gag (*Mycteroperca microlepis*) and scamp (*Mycteroperca phenax*), groupers, the greater amberjack (*Seriola dumerili*), and snappers (Koenig et al. 2000; Koenig 2001; Reed 2002). Deep-sea corals appear to offer species critical complex habitat in areas that lack defined topography. Fishermen have observed that more fish are located in coral areas than adjacent areas that lack high relief, complex habitat. In Norwegian waters, Husebø et al. (2002) noted that redfish (*Sebastes marinus*), ling (*Molva molva*), and tusk (*Brosme brosme*) were larger and more abundant around deep-sea corals than compared to non-coral habitats. A similar relationship between fish and corals has also been documented in Alaska's Aleutian Island Chain, where rockfish (*Sebastes* spp. and *Sebastolobus alascanus*), Atka mackerel (*Pleurogrammus monopterygius*), flatfish (Bothidae and Pleuronctidae), and a gadid (*Theragra chalcogramma*) were observed to be associated with gorgonian and octocoral habitat (Heifetz 2002; Krieger and Wing 2002).

Deep-sea corals are long-lived, slow growing, fragile, and are facing an uncertain future in all ocean basins (Andrews et al. 2002; Risk et al. 2002). Assessments of deep-sea corals have shown that damage to deep-sea coral habitats in many areas has occurred or may occur from fishing associated bottom trawling, bottom-set fishing gears (e.g. bottom long-lines and gill nets), oil and gas exploration and drill cuttings, mineral mining, cable laying, dredging, and sedimentation (Butler and Gass 2001). Of the known impacts, fishing associated damage from bottom trawling appears to have the largest impact on deep-sea coral ecosystems (Koenig et al. 2000; Fosså et al. 2002; Hall-Spencer et al. 2002; NRC 2002); resulting in several countries establishing area closures to bottom trawl fisheries (EC 2003, 2004; DFO 2003; pers. communication with J.H. Fosså, 16 Mar 2004).

The purpose of this paper is to document recent activities to further the understanding of deep-sea corals in policy and scientific forums, including

international meetings containing deep-sea coral subject matter that detail critical information needs for deep-sea corals, as well as current management strategies. Additionally, the need to develop an integrated, Atlantic-wide approach to locate, study, and manage deep-sea coral habitats influenced by the Gulf Stream (Fig. 1) is discussed and encouraged.

Fig. 1 The Gulf Stream current originates in the Gulf of Mexico and carries a current of warmer water through the North Atlantic Ocean, where it terminates

Recent events focusing on deep-sea corals

Deep-sea corals, unlike shallow-water tropical corals, have suffered from the "out-of-sight and out-of-mind" syndrome because they are not easily accessible by scuba diving. However, interest has increased considerably in recent years with the production of high quality images and videos of deep-sea coral communities. For example, in the late 1990's, public interest sparked by video images of Sula Reef in Norway, the largest known reef of *Lophelia pertusa* at that time, ultimately led to closure of the reef to all fishing gears (per communication with J.H. Fosså, 2004).

As international interest and information on deep-sea corals continued to expand, it became clear that the United States needed to assess the importance of deep-sea corals within its jurisdiction. Subsequently, the U.S. National Oceanic and Atmospheric Administration (NOAA), the agency responsible for managing marine living resources in the United States, scheduled a "meet and greet" session for deep-sea coral scientists attending the *Symposium on Effects of Fishing Activities on Benthic Habitats* (Tampa, FL: November 12-14, 2002) to become acquainted with the international community of deep-sea coral researchers, assess the types of research being conducted, and establish potential areas for international collaboration. During the two-hour *Deep-Sea Corals Collaboration Planning Meeting* (Tampa, FL: November 14, 2002) five common research themes surfaced and were identified as: (1) mapping the distribution of deep-sea corals; (2)

ecology of organisms associated with deep-sea corals; (3) physiology of deep-sea corals – indicators and responses to change; (4) taxonomic studies; and (5) paleo-retrospective analyses. The overwhelming interest of the participants in establishing more formal collaborations and assessing deep-sea coral research for information gaps led to the development of a workshop on deep-sea corals.

The *Deep-Sea Corals Workshop* (Galway, Ireland: January 16-17, 2003) was hosted by the Irish Marine Institute and organized by NOAA and the National University of Ireland, Galway, in response to the *Deep-Sea Corals Collaboration Planning Meeting* (McDonough and Puglise 2003). The workshop brought together an international group of researchers from the United States, Canada, Ireland, the United Kingdom, Belgium, Germany, Sweden, and Norway. The objectives of the workshop were to further identify and assess the critical information needs associated with the common themes developed at the *Deep-Sea Corals Collaboration Planning Meeting* and to identify current and future research projects or forums to advance international collaboration particularly in the Atlantic.

Critical information needs

The five common deep-sea corals research themes defined at the *Deep-Sea Corals Collaboration Planning Meeting* were further refined into three categories of critical information needed to enable a better understanding and management of deep-sea coral ecosystems (McDonough and Puglise 2003). The three critical information categories were:

Locating and mapping deep-sea corals. As a first step in building an information base, deep-sea coral habitats need to be located, charted, and characterized in terms of their distribution, diversity, and abundance. In addition, a comparison must be made between deep-sea coral habitat locations and commercial fishing areas to assess potential impacts. Two levels of mapping are required: (1) low-resolution (>10 m pixels) large-scale mapping for broad areas where no information currently exists; and (2) high-resolution (<10 m pixels) mapping in key areas where deep-sea coral habitats may be threatened. Priority low-resolution mapping areas identified by the workshop participants included Pulley Ridge (Gulf of Mexico, U.S.), the *Lophelia pertusa* banks (southeastern U.S.), the Grand Banks and George's Bank (northeastern U.S. and southeastern Canada), Skagerrak (Sweden), and the canyon heads off France. High-resolution mapping is needed in areas such as Stellwagen Bank (northeastern U.S.), the Northeast Passage (Canada), Rockall Bank (Ireland), and the Røst Reef (Norway).

Understanding deep-sea coral biology and ecology. Several fundamental questions regarding the physiology of deep-sea corals, their ecological role, geographic distribution, and genetic differences have yet to be answered. Priority information needs were those identified as critical to developing a better understanding of the: (1) ecological role of the corals, including their functioning as

habitat for fish and invertebrate species; (2) abiotic and biotic factors that influence deep-sea coral growth, reproduction, and distribution; and (3) food web and species interactions, including estimating deep-sea coral and fish stock abundances. In addition, a comprehensive species inventory is needed to establish a baseline for future deep-sea coral characterization efforts. Researchers agreed that although this work could be carried out anywhere that deep-sea corals are known to exist, it would be helpful to conduct it in coordination with the mapping efforts described above, as well as in areas that are currently closed to fishing.

Using specific deep-sea corals as indicators of climate change. Paleo-retrospective and prospective analysis may be a tool to separate natural oscillations from anthropogenic effects. Information derived from paleontological studies may also assist resource managers in determining whether changes seen in fish stock assessments are likely the result of natural variations in climate, oceanographic conditions, and/or anthropogenic stressors. Deep-sea corals may provide a unique record of temperature changes and serve as a good climate change proxy because they: (1) have a worldwide distribution from shallow waters to the abyssal depths (>6000 m) and from polar to equatorial latitudes; (2) appear suitable for disequilibria dating; and (3) contain relatively stable skeletal growth rates over a period of decades to centuries (Smith et al. 1996, 2000). Priority information needs to further efforts to analyze past climate changes and to improve forecasting models are to: (1) collect high-quality oceanographic data along the Gulf Stream and associated currents to better understand existing conditions as related to climate and corals; (2) collect deep-sea coral samples for paleoclimate analysis from discrete areas along the Gulf Stream and associated currents to better understand the relationship between past oceanographic currents and the growth rate of corals; and (3) conduct controlled growth experiments to calibrate geochemical signals and relevant water mass properties.

Additional information needs not identified at the *Deep-Sea Corals Workshop*, but of particular concern as deep-sea coral related activities expand are:

Defining the difference between deep-sea corals and shallow-water corals. As interest in deep-sea corals increases within the marine policy community and with the public, it has become apparent that a clear and concise definition is needed to differentiate deep-sea corals from their tropical counterparts (i.e., shallow-water corals) due to differing management strategies and requirements. A simple way to artificially separate cold, deep-sea corals from tropical, shallow water corals is by temperature and/or depth. Although the term "deep-sea corals" is commonly used, the term "cold-water corals" is actually more precise because some deep-sea corals can be found in "cold," but shallow waters. However, within the U.S., where both shallow-water corals and deep-water corals exist, the term "deep-sea corals" is commonly used to signify the fact that these corals live predominately in deeper waters, "out-of-sight and out-of-mind" of those responsible for managing

them. Thus, a suggested definition for deep-sea coral ecosystems for future policy development is:

> *Deep-sea coral ecosystems occur deeper than 50 m, often consisting of both reef-like structures and/or thickets, and other species of organisms associated with these deep-sea coral habitats, and the nonliving environmental factors that directly affect deep-sea corals, that together function as an ecological unit in nature.*

Understanding the vulnerability and resilience of deep coral habitats to various anthropogenic threats. As anthropogenic activities expand into deeper waters, it is critical to document the effects on seafloor habitats, as this information is the foundation for developing sound policy and making wise management decisions.

Obtaining access to state-of-the-art advanced underwater technologies. Deep-sea coral habitats, unlike their shallow water counterparts, require specialized types of underwater technologies (e.g. remotely operated vehicles, human occupied submersibles, autonomous underwater vehicles, and advanced technical diving) to identify, map, understand, and manage them. As a result, building institutional capacities in advanced underwater technologies will be necessary to expand exploration and research activities related to deep-sea coral ecosystems.

Current and future collaborations

Recognizing the importance of developing an integrated approach to implement exploration, research, management, and education and outreach strategies for deep-sea corals, and build on existing regional initiatives, such as the European Fifth Framework Programme's *Atlantic Coral Ecosystem Study* (Freiwald et al. 2000; Grehan et al. 2001), participants of the *Deep-Sea Corals Workshop* identified future key events where deep-sea coral issues could be discussed and formal collaborations established. Table 1 lists events occurring since the *Deep-Sea Corals Collaboration Planning Meeting* that included significant discussions on deep-sea corals. Highlights from the events list are: (1) a presentation to the United States House of Representatives Oceans Caucus (Washington, D.C.: 14 March 2003), which provided an opportunity for international and U.S. scientists to make a case for continued support for exploration, research, and management related to deep-sea corals; (2) the United Nations Open-ended Informal Consultative Process on Oceans and the Law of the Sea (New York City, NY: June 2003), which focused discussions around threats to vulnerable marine ecosystems (e.g., seamounts and deep-sea coral areas) and governance issues of high seas marine protected areas; and (3) the *Second International Symposium on Deep-Sea Corals* (Erlangen, Germany: 9-12 September 2003) in which researchers presented results of their work on deep-sea corals and continued discussions of upcoming opportunities for collaborative efforts.

Table 1 Events from November 2002 to September 2003 that included significant discussions on deep-sea coral ecosystems

Date	Meeting	Location
Nov 2002	Deep-Sea Corals Collaboration Planning Meeting	Tampa, FL, U.S.A.
Jan 2003	Deep-Sea Corals Workshop	Galway, Ireland
Mar 2003	U.S. House of Representatives Oceans Caucus Luncheon	Washington, DC, U.S.A.
Jun 2003	United Nations Open-ended Informal Consultative Process on Oceans and the Law of the Sea and Discussions on Threats to Vulnerable Marine Ecosystems	New York City, NY, U.S.A.
Jun 2003	Workshops on High Seas Biodiversity Conservation and Ecosystem-Based Management	Cairns, Australia
Aug 2003	10th Deep-Sea Biology Symposium	Coos Bay, OR, U.S.A.
Sep 2003	World Parks Congress	Durban, South Africa
Sep 2003	Second International Symposium on Deep-Sea Corals	Erlangen, Germany
Sep 2003	Ocean Margins Deep-Water Research Consortium Meeting	Paris, France

Management strategies

Within the United States, the principal legislation governing the management of fisheries is the *Magnuson-Stevens Fishery Conservation and Management Act* (Magnuson-Stevens Act 1996). In 1996, the Magnuson-Stevens Act was amended to include legislation to protect ecologically important fisheries habitat or essential fish habitat (EFH). This amendment known as the *Sustainable Fisheries Act* stipulated that waters and substrate necessary to a fish species for spawning, breeding, feeding and growth to maturity should receive increased protections (Sustainable Fisheries Act 1996). The amended Magnuson-Stevens Act requires federal agencies to identify EFH for managed species and document measures that will conserve and enhance the habitat necessary for fish to carry out their life cycles (Fluharty 2000). The U.S. through its Regional Fisheries Management Councils have used the Magnuson-Stevens Act to prohibit destructive fishing gears in areas that possess vulnerable and ecologically important deep-sea coral habitat (e.g., the *Oculina Habitat Area of Particular Concern*). The 315 km^2 (92 nmi^2) *Oculina Habitat Area of Particular Concern* (HAPC) was closed beginning in 1984 to mobile trawling gear. In 1994, this ban was expanded to all mechanically disruptive bottom gear (i.e., bottom trawls, long-lining, dredging, and traps) to protect *Oculina varicosa*, an

azooxanthellate coral known to exist only in this particular location (South Atlantic EEZ 2003). In 2000, legislation was enacted that expanded the *Oculina* HAPC to 1029 km^2 or 300 nmi^2 (Reed 2002).

In response to documented trawling damages to deep-sea corals, Canada, Norway, and the European Union also recently established area closures that prohibit bottom trawling in areas known to contain deep-sea corals. In 2002, Canada designated the Northeast Channel Coral Conservation Area off Nova Scotia (Williams and Meyers 2002). This 424 km^2 deep-sea coral area prohibits all bottom trawling in order to protect deep-sea corals and associated groundfish species (Fenton et al. 2002). Canada has also used the provisions in the Oceans Act (Canada 1996) to put forth a proposal to designate another deep-sea coral area off Nova Scotia, the Sable Gully, as a marine protected area (DFO 2003). In 2003, the Norwegian Ministry of Fisheries issued prohibitions on bottom trawling along the Røst Reef off the Norwegian coast. These regulations protect the world's largest known (35 km long x 3 km wide) deep-sea coral reef of *Lophelia pertusa* (per communication with J.H. Fosså, 2004). In August 2003, the European Union banned deep-water trawling for a six-month period in an area off Scotland known as the Darwin Mounds (EC 2003). The deep-water trawling ban for Darwin Mounds was extended in February 2004 (EC 2004) for an additional six months to allow time for a more permanent protection of the habitat by amending Council Regulation (EC) No 850/98.

Institutional partnerships

A considerable amount of progress has been made toward establishing United States-international collaborative partnerships. In Spring 2002, NOAA and the Irish Marine Institute added deep-sea corals to a list of priority collaborative efforts as part of the Joint Statement of Understanding to establish and guide collaborative efforts related to marine research entered into in 1995. This decision led to the development of both the *Deep-Sea Corals Collaboration Planning Meeting* and the *Deep-Sea Corals Workshop* (McDonough and Puglise 2003), and continues to serve as the basis for developing future collaborative efforts.

In order to take advantage of the increased interest in establishing international collaborative partnerships, researchers and resource managers involved in the development and refinement of the critical information needs described herein have discussed and identified four potential pathways of international collaboration: (1) developing a *State of the Deep-Sea Corals Report* to organize existing knowledge on deep-sea coral habitats, the perceived threats they currently face, and elucidate on the critical information required for making management decisions; (2) identifying current and future exploration, research, and education projects with potential for international collaboration; (3) developing an *International Deep-Sea Corals Action Plan* to provide a blueprint for participating nations to collaborate on exploration, mapping, research, public awareness, and management of deep-sea corals in international waters; and (4) conducting an *International Transatlantic Expedition* to explore and research deep-sea coral habitats.

As currently conceived, the primary goal of the *International Transatlantic Expedition* would be to explore and research deep-sea coral habitats along the path of the Gulf Stream and associated currents. This includes both the reef-building type corals such as *Oculina varicosa* and *Lophelia pertusa* that are found along the continental shelf break and slope, as well as the soft corals that are often found in association with seamounts. The *International Transatlantic Expedition* would focus on the following at-sea objectives: (1) conducting multibeam and side-scan sonar surveys; (2) developing real-time maps and 3-D computer simulations; (3) conducting oceanographic observations; (4) collecting rock and sediment samples; (5) conducting visual surveys using digital still and video cameras; (6) collecting discrete samples of specific deep-sea coral species; (7) collecting samples of associated fish and invertebrates; (8) deploying a suite of *in situ* instruments to monitor conditions over time; and (9) conducting targeted research projects to answer hypothesis-driven questions relating to deep-sea coral ecosystems.

By using a consistent approach to gather, organize, and process these data, post-expedition progress could be made on conducting studies and developing products such as peer-reviewed publications, data atlases, integrated web-based databases, and other products that meet the goal of characterizing and understanding deep-sea coral habitats in terms of biogeographical changes, recruitment patterns and transport of larvae, habitat function (associated species abundance, diversity, and interaction), and natural and anthropogenic impacts. The collection of these data in a consistent manner will also provide an unprecedented opportunity to further efforts to use deep-sea corals to determine how past changes in ocean currents influence global climate change, and to use this information for refining climate change projection models.

Planning of this expedition has not been formalized as of yet. However, preliminary discussions have occurred among representatives from the United States, Canada, Norway, and the member countries of the European Union that have an active interest in deep-sea coral issues.

Conclusions

Scientists in Europe, Canada, and the U.S. continue to discover, characterize, and research deep-sea coral ecosystems. The workshops, policy, and research forums described herein provide a foundation for guiding future exploration, research, and management efforts. In order to maintain the momentum that has been established, to make progress in a consistent and collaborative manner, and to capitalize on international partnerships, it is critical that the dialogue continues to expand. As human activities spread offshore into areas inhabited by deep-sea corals, and public and political interest continues to grow, efforts such as developing a *State of the Deep-Sea Corals Report* and conducting an *International Transatlantic Expedition* will be critical for answering questions regarding their global distribution, abundance, biology, and ecological role as refugia for fish and invertebrates to spawn, feed, and grow to maturity. Furthermore, the development of an *International Deep-*

Sea Corals Action Plan could provide a blueprint for countries to collaborate on exploration, mapping, research, public awareness, and management of deep-sea corals in the international waters of the North Atlantic Ocean.

Acknowledgements

The views presented in this paper are the opinions of the authors and not necessarily those of the U.S. National Oceanic and Atmospheric Administration.

References

Andrews AH, Cordes EE, Mahoney MM, Munk K, Coale KH, Cailliet GM, Heifetz J (2002) Age, growth, and radiometric age validation of a deep-sea, habitat-forming gorgonian (*Primnoa resedaeformis*) from the Gulf of Alaska. Hydrobiologia 471: 101-110

Butler M, Gass S (2001) How to protect corals in Atlantic Canada. In: Willison JHM, Hall J, Gass SE, Kenchington ELR, Butler M, Doherty P (eds) Proceedings of the First International Symposium on Deep-Sea Corals. Ecology Action Centre, Nova Scotia Museum, Halifax, Nova Scotia, pp 156-165

Canada. Oceans Act, S.C. (1996), c. 31

Department of Fisheries and Oceans [DFO], Canada (2003) Gully Marine Protected Area regulations: regulatory impact analysis statement. Canada Gaz Part I 137: 3882-3905

European Commission [EC] (2003) Commission Regulation (EC) No 1475/2003 of 20 August 2003 on the protection of deep-water coral reefs from the effects of trawling in an area north west of Scotland. Off J Eur Union L 211: 14–15

European Commission [EC] (2004) Commission Regulation (EC) No 263/2004 of 16 February 2004 extending for six months the application of Regulation (EC) No 1475/2003 on the protection of deep-water coral reefs from the effects of trawling in an area north-west of Scotland. Off J Eur Union L 46: 11

Fenton DG, Macnab PA, Rutherford RJ (2002) The Sable Gully Marine Protected Area Initiative: history and current efforts. In: Munro NWP (ed) Managing Protected Areas in a Changing World. Proc Sci Manage Protected Areas IV Univ Waterloo, Wolfville, Canada, May 14-19, 2000

Fluharty D (2000) Habitat protection, ecological issues, and implementation of the Sustainable Fisheries Act. Ecol Appl 10: 325-337

Fosså JH, Mortensen PB, Furevik DM (2002) The deepwater coral *Lophelia pertusa* in Norwegian waters: distribution and fishing impacts. Hydrobiologia 471: 1-12

Freiwald A, ACES party (2000) The Atlantic Coral Ecosystem Study (ACES): a margin-wide assessment of corals and their environmental sensitivities in Europe's deep waters. EurOCEAN 2000 Project Synopses. Marine Processes, Ecosystems and Interactions. 1: 312-317

Grehan AJ, Freiwald A, ACES Consortium (2001) The Atlantic Coral Ecosystem Study (ACES): forcing a new partnership between scientists and principal stakeholders. In: Willison JHM, Hall J, Gass SE, Kenchington ELR, Butler M, Doherty P (eds) Proceedings of the First International Symposium on Deep-Sea Corals. Ecology Action Centre, Nova Scotia Museum, Halifax, Nova Scotia, pp 95-105

Hall-Spencer J, Allain V, Fosså JH (2002) Trawling damage to NE Atlantic ancient coral reefs. Proc R Soc London 269: 507-511

Heifetz J (2002) Coral in Alaska: distribution, abundance, and species associations. Hydrobiologia 471: 19-28

Husebø A, Nøttestad L, Fosså JH, Furevik DM, Jørgensen SB (2002) Distribution and abundance of fish in deep-sea coral habitats. Hydrobiologia 471: 91-99

Jensen A, Frederiksen R (1992) The fauna associated with the bank-forming deepwater coral *Lophelia pertusa* (Scleractinia) on the Faroe shelf. Sarsia 77: 53-69

Koenig CC (2001) *Oculina* Banks: habitat, fish populations, restoration, and enforcement. Rep South Atlantic Fish Manage Council, 24 pp

Koenig CC, Coleman FC, Grimes CB, Fitzhugh GR, Scanlon KM, Gledhill CT, Grace M (2000) Protection of fish spawning habitat for the conservation of warm-temperature reef-fish fisheries of shelf-edge reefs of Florida. Bull Mar Sci 66: 593-616

Krieger KJ, Wing BL (2002) Megafauna associations with deepwater corals (*Primnoa* spp.) in the Gulf of Alaska. Hydrobiologia 471: 83-90

Magnuson-Stevens Conservation and Management Act (1996) Public Law 94-265, 16 U.S.C. §1801 *et seq*

McDonough JJ, Puglise KA (2003) Summary: Deep-Sea Corals Workshop. International Planning and Collaboration Workshop for the Gulf of Mexico and the North Atlantic Ocean. Galway, Ireland, January 16-17, 2003. U.S. Dep. Commerce, NOAA Tech. Memo. NMFS-F/SPO-60, 51 pp. Available from: NOAA's Undersea Research Program, NOAA's Office of Ocean Exploration and/or NOAA Fisheries Office of Science and Technology

National Research Council [NRC] (2002) Effects of trawling and dredging on seafloor habitat. National Academy of Sciences, Washington DC, 126 pp

Pontoppidan E (1755) The natural history of Norway. Linde, London

Reed JK (2002) Deep-water *Oculina* coral reefs of Florida: biology, impacts, and management. Hydrobiologia 471: 43-55

Risk MJ, Heikoop JM, Snow MG, Beukens R (2002) Lifespans and growth patterns of two deep-sea corals: *Primnoa resedaeformis* and *Desmophyllum cristagalli*. Hydrobiologia 471: 125-131

Smith JE, Risk MJ, Schwarcz HP, McConnaughey TA (1996) Rapid climate change in the North Atlantic during the Younger Dryas recorded by deep-sea corals. Nature 386: 818-820

Smith JE, Schwarcz HP, Risk MJ, McConnaughey TA, Keller N (2000) Paleotemperatures from deep-sea corals: overcoming 'vital effects'. Palaios 15: 25-32

South Atlantic EEZ (2003) South Atlantic EEZ seasonal and/or area closures. 50 C.F.R. §622.35c

Sustainable Fisheries Act (1996) Public Law 104-297, 110 STAT, 3559

Verrill AE (1862) Notes of a *Primnoa* from Georges Bank. Proc Essex Inst, Salem MA, 3: 127-129

Williams W, Meyers C (2002) Deep-sea coral research and conservation in offshore Nova Scotia. Backgrounder: B-MAR-02-(5E). Available at: http://www.mar.dfo-mpo.gc.ca/communications/maritimes/back02e/B-MAR-02-%285E%29.html

Oceana's efforts to protect deep-sea coral in the United States

Michael F. Hirshfield, Santi Roberts, David L. Allison

Oceana, 2501 M Street NW #300,Washington DC 20037,USA
 (mhirshfield@oceana.org)

Abstract. As awareness of deep-sea corals increases, global efforts to conserve them are increasing as well. Oceana, a non-governmental conservation organization that merged with the American Oceans Campaign in 2002, is focusing significant attention and resources on the conservation of deep-sea coral communities in United States' waters. Oceana is carrying out a number of activities as part of its deep-sea coral campaign. These include:

- Working to pass legislation that would ban the use of particularly destructive bottom trawls in all U.S. waters in collaboration with the Marine Conservation Biology Institute;
- Working to pass legislation that would specifically protect known deep-sea coral and sponge areas and establish a process for future protections;
- Working to protect deep-sea coral and sponge habitats in the U.S. through the regional fishery management councils;
- Developing educational materials for decision-makers, the media, and the general public;
- Developing a petition to achieve threatened or endangered species status for *Oculina varicosa*.

The goal of Oceana's deep-sea coral protection activities is to ban bottom trawling in all U.S. waters containing significant amounts of deep-sea corals and sponges by the end of 2006. The purpose of this paper is to discuss the activities that Oceana is engaged in to achieve this goal. As Oceana's capacity develops in other parts of the world, its efforts to protect coral in other regions (especially Europe and South America) will increase as well.

Keywords. Conservation organization, United States, protection, communication, public awareness

Introduction

Founded in mid-2001, Oceana is a non-profit international advocacy organization dedicated to protecting and restoring the health of the world's oceans. Oceana's diverse professional staff is comprised of marine scientists and economists, policy experts, lawyers, and communications professionals - all dedicated to protecting the global marine environment. Headquartered in Washington DC, Oceana has U.S. staff from Alaska to California and New England and international offices in South America (Santiago, Chile) and the European Union (Madrid, Spain). Oceana has over 100,000 members and activists from all over the world who enjoy, depend on and seek to protect and restore the world's oceans. In 2002, to further its effectiveness and influence, Oceana merged with American Oceans Campaign, a nonprofit environmental organization founded by actor and ocean activist Ted Danson in 1987.

Oceana was created to address the root causes of problems affecting life in the sea, with a particular emphasis on overfishing, habitat destruction and pollution. Oceana works at the local and national level to promote solutions to these problems, and is currently engaged in three national campaigns aimed at solving particular problems that exist in the United States and in many other parts of the world.

1)   The *Stop Dirty Fishing* campaign is focused on reducing the vast amounts of marine life including fish, sea birds, and marine mammals that are caught inadvertently each year by fishing vessels and thrown overboard either dead or dying.

2)   The *Cruise Pollution* campaign is designed to ensure that cruise ships do not continue to pollute some of the world's most pristine ocean waters with human sewage and toxic chemicals.

3)   The purpose of the *Stop Destructive Trawling* campaign is to restrict or eliminate the most destructive types of bottom trawling from sensitive seafloor habitat in U.S. waters. The campaign is focused on protecting deep-sea corals and sponges and associated species.

Oceana has developed an overarching approach to protect deep-sea coral and sponge habitats from bottom trawling, which it is pursuing at both the national and regional levels in the United States. It includes the following elements:

1.   Identify all areas not fished within the past three years with bottom trawls, and close such areas to bottom trawling;

2.   Identify, map, and list all known areas containing high concentrations of deep-sea coral and sponge habitat;

3.   Designate all known areas containing high concentrations of deep-sea coral and sponge habitat both as "Essential Fish Habitat" (EFH) and "Habitat Areas of Particular Concern" (HAPC), and close these HAPC to bottom trawling;

4. Monitor bycatch to identify areas of deep-sea coral and sponge habitat that are currently being fished, establish appropriate limits or caps on bycatch of deep-sea coral and sponge habitat, and immediately close areas to bottom trawling where these limits or caps are reached until such time as the areas can be mapped, identified as EFH and HAPC, and permanently protected;

5. Establish a program to identify new areas containing high concentrations of deep-sea coral and sponge habitat through bycatch monitoring, surveys, and other methods, designate these newly discovered areas as EFH and HAPC, and close them to bottom trawling;

6. Enhance monitoring infrastructure, including observer coverage, vessel monitoring systems, and electronic logbooks for vessels fishing in areas where they might encounter high concentrations of deep-sea coral and sponge habitat (including encountering HAPC);

7. Increase enforcement and penalties to prevent deliberate destruction of deep-sea coral and sponge habitat and illegal fishing in already closed areas; and

8. Fund and initiate research to further identify, map, and protect deep-sea coral and sponge habitat, and restore it where damage has already occurred.

Oceana national activities

Existing statutes

Oceana has submitted a petition in which we request the National Marine Fisheries Service (NMFS), the agency that has responsibility for managing fisheries in the United States, to carry out the eight activities described above.

Under United States law, the Magnuson-Stevens Fishery Conservation and Management Act (MSA), 16 U.S.C. §§1801 *et seq.*, requires fishery management plans prepared by the Secretary of Commerce (the head of the Department containing NMFS) or Fishery Management Councils (which are regional fisheries management bodies) to identify "Essential Fish Habitat" (EFH) and "habitat areas of particular concern" (HAPC) (Fig. 1).

EFH are "waters and substrate necessary to fish for spawning, breeding, feeding or growth to maturity." HAPC are areas that: (1) provide important ecological functions; (2) are sensitive to human-induced environmental degradation; (3) are stressed by development activities; or (4) are a rare habitat type.

Through the petition, Oceana argues that deep-sea coral and sponge communities are not being protected adequately under existing fishery management plans (FMPs), that pending legislation does not take into account the most recent scientific data, and that ongoing efforts to designate essential fish habitat (EFH) are proceeding so slowly that without immediate protection, many of these sensitive habitats will suffer irreparable harm. Oceana further argues that existing law requires the Secretary of Commerce to take strong steps to protect these habitats from destructive fishing practices, and specifically to establish rules that will achieve the Oceana approach described above.
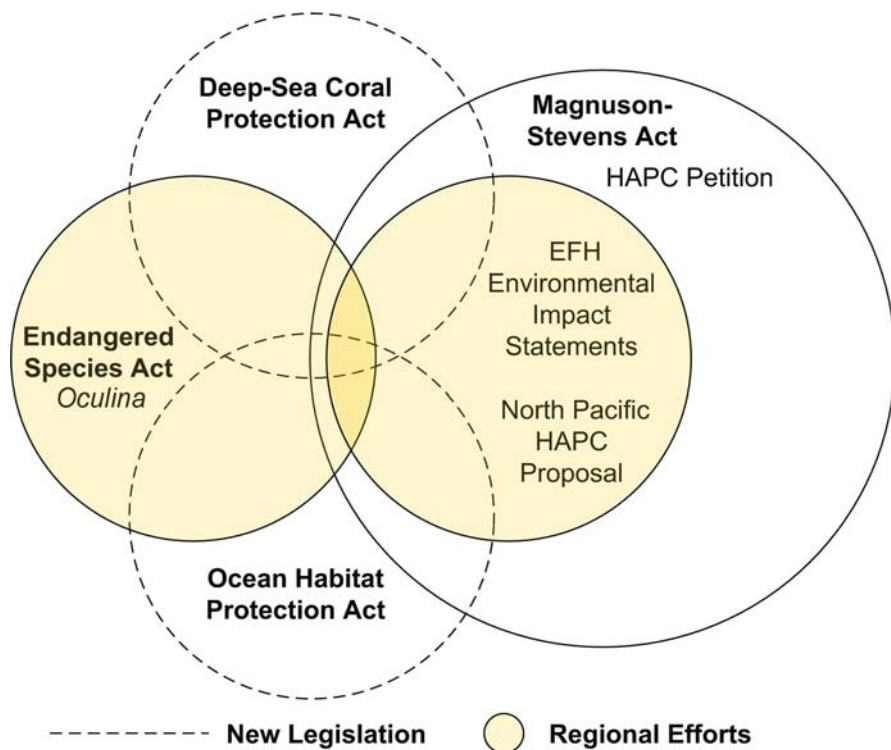
Fig. 1 Oceana is working through several different avenues to build or improve protections for deep-sea coral and sponge habitats in U.S. waters. There is considerable overlap between activities, such that the education and outreach undertaken for one activity supports the others

New legislation

In addition to pressing for protections for deep-sea corals and sponges under existing law, Oceana is working to pass legislation that would specifically act to restrict trawling and protect deep-sea coral communities. Oceana is working with a number of United States conservation and fishing organizations on these efforts, and in particular its close partner, the Marine Conservation Biology Institute. Two pieces of legislation have been introduced in the current United States Congress as a direct result of Oceana's work.

The first of these is the Ocean Habitat Protection Act of 2003 (HR 1690). This piece of legislation, introduced into the United States House of Representatives by Congressman Hefley of Colorado, would:

- Ban all rockhoppers, which are non-rotating devices used only to access the most structurally complex habitats;
- Restrict rollers to an 8 inch diameter;
- Allow for larger rollers to be used in exempted areas to reduce bycatch

of managed species. These areas would be declared by the Secretary of Commerce based on evidence submitted by the regional fishery management councils that the bottom habitat is predominately sand or mud;

- Provide $100 million over ten years for a habitat mapping program so we have more information on the locations of structurally complex habitats;
- Provide for three types of economic incentives and assistance to fishermen affected by the gear changes:
- Up to $4000 to retrofit gear from rockhoppers or large rollers to 8 inch or smaller rollers;
- Up to $10,000 to switch out of trawling and into fixed gears (hook and line or fish pots or traps);
- Up to 2 years of economic assistance and job training to leave fishing entirely and engage in a different profession.

The second piece of legislation is the Deep-Sea Coral Protection Act (S 1953), introduced into the United States Senate by Senator Lautenberg of New Jersey. It includes the following statement of policy:

> *It is the policy of the United States to protect deep-sea corals and sponges, including protecting such organisms that are found in the continental margins, canyons, seamounts, and ridges of the world's oceans, and the habitats of such organisms from damage from gear and equipment used in commercial fishing, particularly mobile bottom-tending gear.*

This piece of legislation incorporates many of the elements of the Oceana approach, including closing of areas where trawling has not occurred recently, establishing areas for long term closure to bottom trawling, and establishing a process for finding, mapping, and protecting newly discovered coral communities. It also authorizes funding for these activities as well as additional exploration and research. The legislation specifically designates several known and mapped deep-sea coral and sponge locations as Coral Management Areas (areas closed to trawling). They are the Coral Gardens in the Aleutian Islands, Oceanographer Canyon, Lydonia Canyon, the *Oculina* reefs off Florida, the *Lophelia/Enallopsammia* reefs off the East Coast, and the Bear Seamount (Fig. 2). Oceana and its partners will continue to gather support for these pieces of legislation in both chambers of Congress.

Education

Oceana's advocacy efforts have included a significant public education component. In 2003, Oceana published *"Deep-Sea Corals: Out of Sight, but No Longer Out of Mind"*, a colorfully-illustrated and jargon-free description of deep-sea corals and the threats to their persistence. A paper of the same name was also published in the journal Frontiers in Ecology and the Environment in 2004 (Roberts and Hirshfield 2004). In addition, Oceana has produced a variety of fact sheets,

Fig. 2 Broad scale map showing approximate locations of the areas specifically identified for designation as Coral Management Areas under the Deep-Sea Coral Protection Act. A - Oceanographer Canyon, Lydonia Canyon, and Bear Seamount. B - *Lophelia / Enallopsammia* reefs. C - *Oculina* reefs. D - Coral Gardens

CDs, and other materials in support of its efforts, most of which can be found at its websites http://www.Oceana.org and http://www.SaveCorals.com. The latter site focuses primarily on corals off the United States Pacific Coast but also includes much general material.

Oceana regional activities

The 1996 amendments to the MSA required federal fisheries managers to adopt regulations to protect EFH from the impacts of fishing and fishing gear. The managers failed to enact such rules in all of the regional fishery councils.

North Pacific

Oceana won a court decision requiring the North Pacific Fishery Management Council (NPFMC) (and four other Councils) to prepare adequate and comprehensive Environmental Impact Statements (EIS) on EFH, including the impacts of fishing operations on habitat. The settlement of the litigation includes a provision that the EIS include a range of proposed alternative actions to minimize the impacts of fishing and fishing gear on fish habitat.

In the North Pacific, Oceana has proposed an alternative for inclusion in the

EIS process that would close a very large portion of the ocean floor off the coast of Alaska to bottom trawling, in particular areas with a high incidence of deep-sea corals and sponges and a comparatively low value for bottom trawl fisheries. That alternative, which would implement most elements of the Oceana overall approach in the North Pacific region, was accepted for review and analysis by the NPFMC but not chosen as its preferred alternative. Oceana is working to change that tentative decision, including pursuing a Freedom of Information Act request for the information used in making the decision. In accordance with the Council's approach (although not accepting it as valid), Oceana is also recommending specific locations for designation as HAPC in the North Pacific. Oceana is engaged in a similar effort in the Pacific Fishery Management Council, although the process is at an earlier stage of development. Oceana has also prepared a variety of materials focused on the effort in the North Pacific and Pacific regions, which can be found at http://www.SaveCorals.com.

In late 2003, Senator Stevens (R-AK), chairman of the Senate Appropriations Committee introduced a legislative "rider" on the Appropriations bill for the Commerce Department that would have undermined Oceana's work in the North Pacific aimed at protecting ocean bottom habitat and deep-sea corals in particular. Specifically, Senator Steven's Rider would have prevented spending any federal funds on researching or protecting deep-sea coral and sponge habitat in the North Pacific. Oceana successfully led an effort to get Senator Stevens to remove his Rider, an outcome many publicly doubted could be achieved. In carrying out that effort, Oceana and its partners carried out the following activities:

- Wrote a sign-on letter and secured 21 signatures of prominent scientists in opposition to the Rider;
- Wrote two sign-on letters and, working with other groups, secured 63 recreational and commercial fishing groups, conservation groups and others to sign;
- Sent out three alerts to Oceana Wavemakers asking them to contact their Congressman or Senator;
- Successfully labeled the effort with a slogan, "Sink the Stevens Fish Rider" brochure and advertisements and buttons in Congress;
- Developed and distributed a "Sink the Stevens Fish Rider" brochure;
- Made more than 500 phone calls to the House to help convince 59 Congressmen to sign a letter opposing the Rider;
- Wrote and placed three Oceana signed op-eds in the Anchorage Daily News, the San Francisco Chronicle and the Portsmouth Herald;
- Generated 18 newspaper editorials against the Stevens Rider, including the New York Times, Washington Post, Boston Globe, Tampa Tribune, Seattle Times, Seattle Post-Intelligencer, Newsday, and Portland Herald Press.

One extremely important side benefit of the effort to fight the Stevens rider was the opportunity to educate newspaper reporters and editorial writers on the importance of deep-sea corals and the threats from bottom trawling. This education

should prove helpful as the campaign to protect deep-sea coral through legislation proceeds.

South Atlantic

Oceana's efforts in the South Atlantic Region of the United States are focused on the protection of the unique deep-sea form of *Oculina varicosa*. The only known reefs of any *Oculina* species are found off the Atlantic coast of Florida, and they are believed to exist nowhere else in the world. These reefs, known as the *Oculina* Banks, are comprised of the stony coral *O. varicosa*. The unique, incredibly productive nature of the reefs, combined with their fragility and sensitivity to mechanical disturbance, has resulted in protections being put into place that close the area to bottom fishing of all types. Protections have expanded and increased since first implemented in 1984, but recent surveys indicate a loss of 90-99 % of the *Oculina* within the protected areas, and illegal trawling still continues due to poor enforcement (Koenig et al. in press). For these reasons, Oceana intends to petition NMFS to list *O. varicosa* as endangered under the Endangered Species Act (ESA). 16 U.S.C. § 1533.

The ESA defines an endangered species as "any species which is in danger of extinction throughout all or a significant portion of its range." A threatened species is "any species which is likely to become an endangered species within the foreseeable future throughout all or a significant portion of its range." Under section 4(b) of the ESA and implementing regulations, the NMFS shall list a species as endangered or threatened, based solely on the best scientific and commercial data available after conducting a review of the species' status, if any one or a combination of the following factors exist:

(1)   The present or threatened destruction, modification, or curtailment of its habitat or range;
(2)   Over-utilization for commercial, recreational, scientific, or educational purposes;
(3)   Disease or predation;
(4)   The inadequacy of existing regulatory mechanisms; or
(5)   Other natural or manmade factors affecting its continued existence.

Oceana believes that, because the first, fourth, and fifth factors exist, *O. varicosa* should be listed as endangered.

Conclusions

Although scientific understanding of deep-sea corals and sponges has increased in recent years, too little of this habitat is protected from damage and destruction from bottom trawls. Public pressure is an essential part of the effort to convince government bodies to act. Oceana and its partners in the conservation movement in the United States are working to educate the public about deep-sea corals and

sponges, and are working hard in a number of efforts to convince both national and regional decision-making bodies to protect deep-sea corals and sponges. Although the challenges remain significant, we are confident that ultimately we will succeed.

Acknowledgements

References

Koenig CC, Shepard AN, Reed JK, Coleman FC, Brooke SD, Brusher J, Scanlon KM (in press) A deep-water *Oculina* coral ecosystem in the western Atlantic: habitat fish populations restoration and enforcement. Amer Fish Soc Spec Publ, Bethesda, MD
Roberts S, Hirshfield M (2004) Deep-sea corals: out of sight, but no longer out of mind. Frontiers Ecol Environ 3: 123-130

A cost effective approach to protecting deep-sea coral and sponge ecosystems with an application to Alaska's Aleutian Islands region

Geoff Shester[1], Jim Ayers[2]

[1] Interdisciplinary Program in Environment and Resources, Stanford University, USA
  (gshester@stanford.edu)
[2] Oceana, Pacific Office, 175 S. Franklin St., Ste 418, Juneau, AK 99801, USA

Abstract. There is much debate about how to protect deep-sea coral and sponge ecosystems using the data currently available. The Aleutian Islands in Alaska contain some of the most abundant, diverse, and pristine deep-sea coral and sponge ecosystems on Earth. From 1990 to 2002, U.S. federal fishery observer data indicates approximately 2,176,648 kg of coral and sponge bycatch occurred in the Aleutian Islands, equaling 52 % of all coral and sponge bycatch in Alaska. Coral and sponge bycatch rates in the Aleutians were over 12 times the rate in the Bering Sea or Gulf of Alaska. The National Marine Fisheries Service (NMFS) estimates that 87 % of coral bycatch and 91 % of sponge bycatch is caused by bottom trawling in the Bering Sea/Aleutian Islands management areas. The conservation organization Oceana developed an interdisciplinary fishery management approach to mitigating adverse impacts of fishing on deep-sea coral and sponge ecosystems, which has been used by NMFS to formulate a habitat protection alternative for the Aleutian Islands that is being considered in an Environmental Impact Statement. The Oceana Approach is offered as a cost effective model for reducing the adverse effects of fishing on deep-sea coral and sponge ecosystems. The approach uses observer data to identify areas of high coral and sponge bycatch rates to develop a comprehensive management policy that allows bottom trawling only in specific designated areas with high fish harvest and low habitat impacts. All areas not specified as open would be closed to bottom trawling. To prevent effort displacement, bottom trawl effort is reduced by the amount that historically occurred in areas that would become closed. The Oceana Approach also includes coral and sponge bycatch limits and a plan for comprehensive seafloor research, mapping, and monitoring. An enforcement strategy for these management measures is developed based on agency capabilities, and includes increased observer coverage, vessel monitoring systems, and electronic logbooks. This approach allows for continued catch of target species with minimal adverse impacts on coral and sponge habitat. Successful implementation of the Oceana Approach will protect areas of high known trawl impacts to deep-sea coral

and sponge ecosystems and prevent trawl effort from moving into new, unexplored areas. The methodology is recommended for application to other regions and should be adjusted based on the available fishery and biological data for each region.

Keywords. Aleutian Islands, essential fish habitat, biogenic, deep-sea corals, conservation, bottom trawling

Introduction

Advances in technology have enabled fishermen to harvest biomass from the ocean more effectively than ever before. The world's demand for fish has created economic incentives for fishermen to build bigger boats with higher horsepower and use fishing gears that can be used in deeper and harder to reach areas, catching high quantities of fish very quickly. Industrial bottom trawling is one such gear type that has enabled more effective harvest of fish stocks by towing large nets and cables over the seafloor. However, these hard on bottom fishing activities can alter and damage seafloor ecosystems, which may impose serious adverse impacts on the features of the ocean that make it so productive. These incidental externalities of increased harvesting ability have prompted serious concerns in the scientific and conservation communities about the effects of bottom trawling on seafloor habitat (Dayton et al. 1995; Watling and Norse 1998; NRC 2002; Roberts and Hirshfield 2003). Deep-sea corals and sponges are living animals that can provide three-dimensional structures that form habitat for commercial groundfish, shellfish, and other marine life (Heifetz 2002; Husebø et al. 2002; Krieger and Wing 2002; Malecha et al. 2002). They are found at depths from 30 m to over 3000 m (Krieger and Wing 2002). Because these long-lived filter feeders are attached to the seafloor, they may be important indicators of areas in the ocean that have consistently favorable ecological conditions worth protecting for other reasons as well.

Bottom trawling is known to decrease the quality of these habitats because they are vulnerable to damage and may take decades to centuries to recover (Cimberg et al. 1981; Freese et al. 1999; Freese 2001; Hall-Spencer et al. 2001; Krieger 2001; Andrews et al. 2002; Fosså et al. 2002; NRC 2002). Figure 1 shows that the rate of coral and sponge bycatch per metric ton (mt) of total catch is roughly four times greater for bottom trawls than for longline or pot gear types in Alaska. Because of their importance as habitat and vulnerability to human impacts, all corals and sponges have already been designated as Habitat Areas of Particular Concern (HAPCs) deserving of special protection by the National Marine Fisheries Service (NMFS) and the North Pacific Fishery Management Council (NPFMC 1998; Hogarth, Assistant Administrator for Fisheries pers. comm.). HAPCs are a subset of Essential Fish Habitat (EFH) defined in U.S. law that are especially vulnerable to fishing (NMFS 2002a). Under the Magnuson-Stevens Fishery Conservation and Management Act of 1996 which governs federal fishery management in the U.S., NMFS is required to take actions that minimize the adverse impacts of fishing on EFH to the extent practicable (16 U.S.C. 1863(a)(7)). However, no additional management measures have been implemented to date to protect these HAPCs.
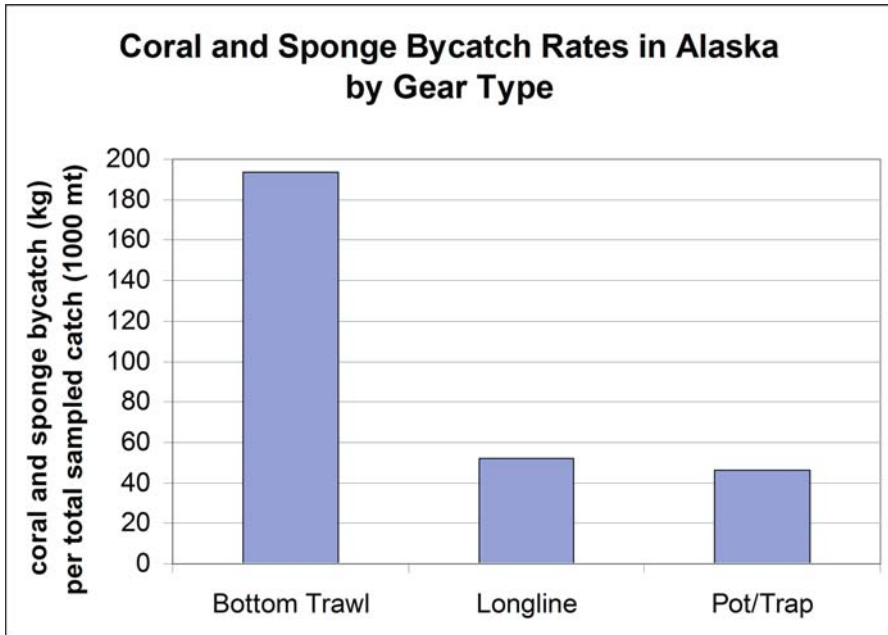
Fig. 1 Bycatch rates for groundfish fishing gears in Alaska, based on data from 1990-2002. Bycatch rates are defined as the weight of reported bycatch divided by the weight of total sampled catch. These rates may not reflect actual damage to seafloor since fishing gears may not retain all corals and sponges that are impacted. Data source: NMFS (2002b)

The Aleutian Islands contain some of the most abundant, diverse, and pristine deep-sea coral and sponge ecosystems known on Earth. Stone (pers. comm.) estimates that this region easily contains over 100 species of corals and sponges. Table 1 shows observer bycatch data for corals and sponges and total catch data

Table 1 Summary of coral and sponge bycatch data for Alaska groundfish fisheries from 1990-2002 as of 9/25/02. Official total catch values are listed in the extrapolated rows in the total catch column. Sampled data represents the amounts reported by observers. Extrapolated data represents the sampled bycatch multiplied by the ratio of Official Total Catch to total sampled catch. Bycatch values are in kilograms (kg); total catch values are in metric tons (mt). "Coral Bycatch" includes bryozoans. Confidential data excluded. Data source: NMFS (2002b)

	Coral Bycatch (kg)	Sponge Bycatch (kg)	Coral & Sponge Bycatch (kg)	Total Catch (mt)
Aleutian Islands (sampled)	201,472	1,376,074	1,577,546	1,307,144
Aleutian Islands (extrapolated)	277,985 (52 % of Alaska)	1,898,663 (52 % of Alaska)	2,176,648 (52 % of Alaska)	1,803,556 (8 % of Alaska)
All Alaska (sampled)	388,627	2,628,855	3,017,482	16,460,425
All Alaska (extrapolated)	537,063	3,632,945	4,170,008	22,747,477

for the Aleutian Islands as well as Alaska-wide totals. The spatial distribution of this bycatch is depicted in Figure 2. Observer bycatch records are perhaps the best indicators of damage to deep-sea coral and sponge ecosystems because they reflect the spatial heterogeneity of coral and sponge distribution and they directly measure relative removals of these habitat features from different areas. However, bycatch figures underestimate total damage because they do not count damaged corals and sponges that remain on the seafloor (trawl gear is not designed to retain corals and sponges). Total coral and sponge bycatch in the Aleutian Islands region accounts for 52 % of all coral and sponge bycatch in Alaska, despite the fact that only 8 % of Alaska's groundfish catch occurs in this region (NMFS 2002b). Coral and sponge bycatch rates in the Aleutian Islands were over 12 times the rate in the Bering Sea or Gulf of Alaska (NMFS 2002b). Though much damage is not reflected in reported bycatch, these numbers provide quantitative evidence of adverse impacts to habitats currently designated as HAPCs. NMFS (2002b) estimates that 87 % of coral bycatch and 91 % of sponge bycatch in the Bering Sea /Aleution Islands managment areas is caused by bottom trawling. Legally, NMFS is required to take action if the adverse impacts of fishing on EFH are more than minimal and not temporary (NMFS 2002a).
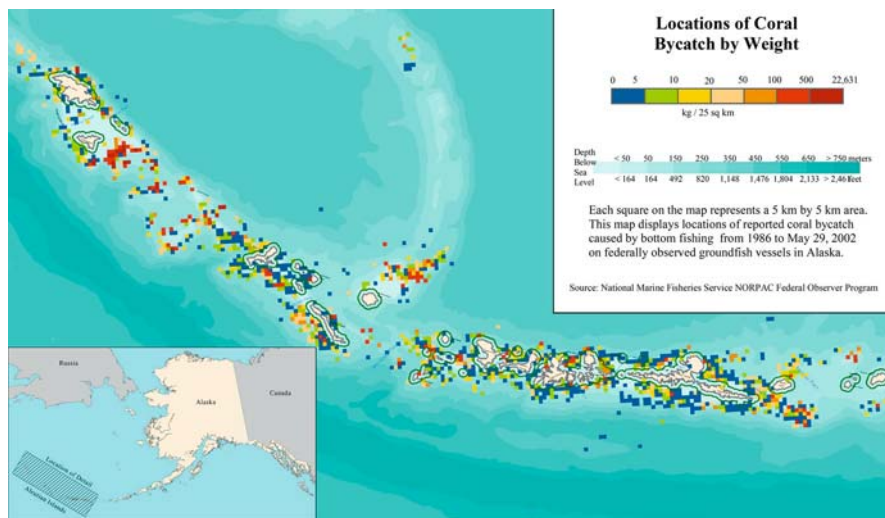
Fig. 2 Coral bycatch in the Aleutian Islands reported by weight aggregated from 1986-2002. Data provided by NMFS NORPAC Federal Observer Program. Map produced by Conservation GIS Support Center, Anchorage, AK

The three major trawl fisheries in the Aleutian Islands target Atka mackerel, Pacific cod, and rockfish (including Pacific Ocean perch, northern rockfish, and other rockfish). Estimated gross product revenue for trawl fisheries in the Aleutian Islands was $51.9 million in 2000 (J. Terry, NMFS economist, pers. comm.). The Aleutian Islands are split into three management areas roughly equivalent in size (Areas 541, 542, and 543) and totaling 1,004,130 km^2. In Alaska, the following species are

known to associate with corals and sponges: rougheye rockfish, redbanded rockfish, shortraker rockfish, sharpchin rockfish, Pacific Ocean perch, dusky rockfish, yelloweye rockfish, northern rockfish, shortspine thornyhead, several species of flatfish, Atka mackerel, golden king crab, shrimp, Pacific cod, walleye pollock, greenling, Greenland turbot, sablefish, and various non-commercial marine species (Heifetz 1999; Freese 2000; Else et al. 2002; Heifetz 2002; Krieger and Wing 2002). Deep-sea corals are known to provide protection from predators, shelter, feeding areas, spawning habitat, and breeding areas (Krieger and Wing 2002). Most corals caught in the Aleutian Islands region are gorgonian corals and hydrocorals, some of which are known to live for hundreds of years (Andrews et al. 2002; Heifetz 2002; R. Stone pers. comm.).

It is well documented that the first pass of a trawl over sensitive habitat does far greater damage than subsequent passes (Moran and Stephenson 2000; NMFS 2004a). Trawl industry representatives have asserted that current trawl effort is very patchy, and thus has a low impact on habitat because the same areas are trawled repeatedly. If this is indeed true, management measures that reduce the 'footprint' of trawl effort by maintaining the same patchy distribution over time may be an effective way to prevent further damage to sensitive areas that have not yet been trawled. Therefore, management measures that identify specific open areas to trawling while closing other areas to trawling have the potential to maintain profitable fishing opportunities while protecting remaining pristine coral and sponge ecosystems. This 'open area' spatial management strategy for bottom trawling attains a high level of precaution when the complete distribution of coral and sponge ecosystems is not yet known, as is the case in most areas of the world. Figure 2 indicates that high amounts of coral and sponge bycatch in discrete areas (see areas in red and orange). In many cases, these 'bycatch hotspots' do not occur in areas with high groundfish catch, indicating spatial heterogeneity in coral and sponge bycatch rates. These differences in bycatch rates are the basis for our hypothesis that it is possible to greatly reduce coral and sponge bycatch (and hence mitigate adverse effects on EFH) without major reductions in groundfish catch. The differences in bycatch rates between different areas likely reflect the heterogeneity in the spatial distribution of seafloor habitat types as well as commercial fish population densities.

The NMFS Alaska Region is currently in the process of completing an Environmental Impact Statement on Essential Fish Habitat Identification and Conservation in Alaska. This process, which is scheduled to be completed in 2006, will result in a document (EIS) containing a range of several alternatives, or policy options, for identifying EFH and HAPCs and minimizing adverse effects of fishing on EFH as required by law. The preliminary steps of the process included several stakeholder meetings and opportunities for public comment, with participation from the fishing industry, scientists, fishery managers, and conservation organizations including Oceana. Through an iterative process of acquiring data on trawl impacts and the known information about coral and sponge ecosystems in Alaska, Oceana advanced a policy proposal for protecting coral and sponge ecosystems from bottom trawling in the Aleutian Islands. The policy proposal model was developed

with input from other scientists, fishing industry representatives, agency staff, and conservation organizations throughout the Essential Fish Habitat stakeholder process. We refer to the Oceana Approach as the principles and concepts contained in this proposal.

One of the alternatives being considered in the document (EFH mitigation Alternative 5B) incorporated the principles of the Oceana Approach in developing management measures for the Aleutian Islands. While the specific application of the Oceana Approach to this region was ultimately developed by NMFS, the authors believe it is an example of model habitat protection policy. By developing a habitat protection model for such a biologically exceptional area, we hope to provide a model for protecting ocean habitat throughout the world. The Oceana Approach is offered as a general methodology for minimizing adverse impacts of fishing on EFH to the extent practicable, while Alternative 5B is a concrete example of how the Oceana Approach can be applied to a region that is currently experiencing major habitat impacts from bottom trawling.

Management components of the Oceana Approach

The Oceana Approach shifts fishery management to better reflect and coincide with the productive ecosystems that produce commercial fisheries. The approach is considered a first step in an effort to protect vulnerable EFH, such as deep-sea coral and sponge ecosystems in the Aleutian Islands, from fishing gears known to be destructive to structural habitat features. The goal of the Oceana Approach is to protect as much deep-sea coral and sponge habitat as possible at the lowest cost to the fishing industry, including locations of these habitats that have not been discovered yet. Using available data to identify areas of high coral and sponge bycatch, Oceana developed a comprehensive management policy for deep-sea coral and sponge protection. The Oceana Approach is a methodology for developing a comprehensive suite of management measures that reduce adverse impacts to EFH while maintaining vibrant fisheries. The five components of the Oceana Approach are:

1.   Designated open areas to bottom trawling;
2.   Trawl effort reduction to prevent increased trawl effort in remaining open areas;
3.   Coral and sponge bycatch limits;
4.   Additional monitoring and enforcement requirements including vessel monitoring systems (VMS), increased observer coverage, and electronic logbooks; and
5.   A comprehensive research and mapping program to inform adaptive management efforts.

Detailed descriptions and methodologies of each policy component can be found below. While Oceana developed the concept for this approach, the details contained

in the methodology used to formulate Alternative 5B were developed by NMFS (2004b) as noted.

1. Designated open areas to bottom trawling

The objective of the spatial management components of the Oceana Approach is to mitigate adverse impacts on EFH by permitting destructive fishing practices only in designated open areas with high target species catch where bottom contact will do the least damage to habitat.

Identifying the potential capabilities of enforcement agencies are an essential first step in the process of considering the options for spatial management. If enforcement capabilities are strong and can be done at small spatial scales, it is possible to design management measures that reflect the resolution of spatial heterogeneity of seafloor habitats. However, if enforcement cannot be done at small spatial scales, it is necessary to design open and closed areas to different fishing gears with larger grid cells. There is a tradeoff in this policy choice. Enforcement of a complex system of small-scale open and closed areas may be very expensive, but may be better able to protect sensitive areas without major impacts on fishing opportunities. However, enforcement of broad-scale open and closed areas is easier and less costly, but removes many potential opportunities to protect sensitive habitat without closing major fishing grounds. We considered these costs and benefits and took into account the specific enforcement situation in the Aleutian Islands. Ultimately, the resolution of the spatial components of Alternative 5B was selected based on advice from the US Coast Guard, which recommended a Latitude/Longitude grid based on 3 minutes of latitude by 6 minutes of longitude (NPFMC 2003). This aligns with and subdivides existing 1/2 by 1 degree Alaska Department of Fish & Game statistical areas in the geo-reference system familiar to the fishing fleets, and is roughly equivalent to a 5 by 5 km block. This resolution is a compromise between cost of enforcement and the ability to capitalize on the spatial heterogeneity of seafloor habitat features.

The first objective of analysis is to identify areas of high and low relative economic importance to the trawl fleet. Two methods for identifying these areas are to determine the gross dollar value of fish caught annually and total number of tows over the period being analyzed. We obtained data on historic trawl effort from the Aleutian Islands to identify all grid blocks with less than a specified threshold level of fishing effort. The choice of years to use for the analysis should be broad enough to predict where the fleet is likely to be in the future and incorporate variation in fish locations over time. This increases the likelihood that the resulting policy will be successful even if the fish move. Figure 3 shows an example map of trawl effort data for the Aleutian Islands region from 1999-2001 at a resolution of 5 by 5 km blocks. In areas where fishing locations are relatively static, such as continental slope areas, a shorter time series is likely encompass this variation, while on shelf habitats where fish may move over greater distances, a longer time series is more appropriate. However, it is important to note that more recent data may better reflect current fishing activity and areas where habitat interaction is greatest. Once the
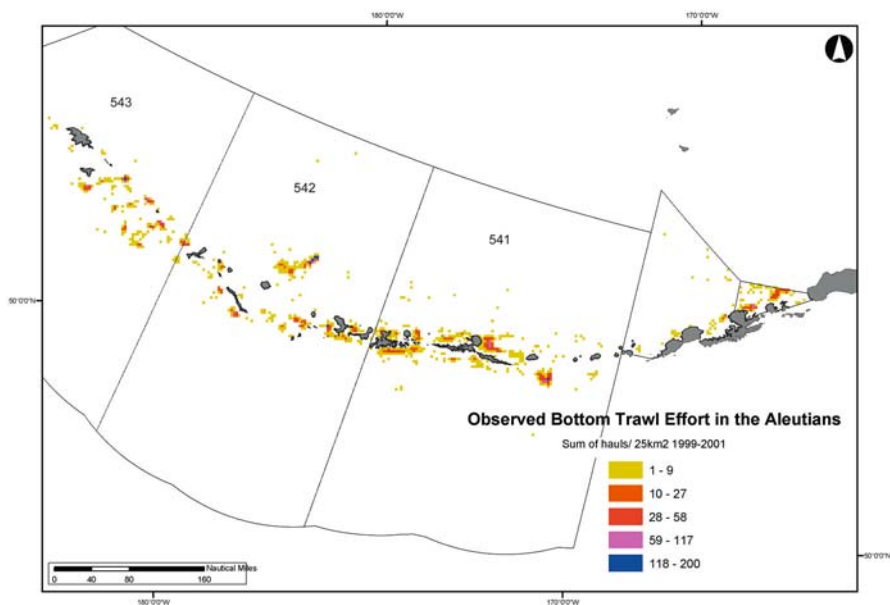
Fig. 3 Observed bottom trawl effort in the Aleutian Islands management region from 1999-2001. Map provided by C. Coon, North Pacific Fishery Management Council

fishing effort time series has been selected and obtained, a threshold effort level must be selected.

This threshold specifies the level of effort in the block that is considered low enough that there will be minimal impact on the trawl fleet if the block is closed. For example, this threshold might be selected so that if closed may represent less than 1 % of the historic effort, depending on what is considered minimal. Since the complete distribution of coral and sponge habitats in the Aleutian Islands and most other locations are not yet known, these areas are closed to bottom trawling in the Oceana Approach on the precautionary basis that they may contain important and sensitive habitat without representing a major loss to the trawl fleet. Some of these areas may be reopened in the future as additional research and mapping identifies areas that are not sensitive to trawl impacts (see Component 5 below). This approach will close extensive areas for fisheries that occur in specific concentrated locations, while it will close less area in fisheries that are prosecuted over a more widespread area. In the creation of Alternative 5B, NMFS kept all areas open that had greater than 10 trawl tows per grid cell over the years 1990-2001 and attempted to make these areas as linear as possible (least number of sides) (NMFS 2004b). Note that this threshold level chosen can dramatically influence the extent of closures and the associated reductions in groundfish catch. For a detailed description of the analysis and results of the spatial management components used in Alternative 5B, refer to NMFS (2004b). See Figure 4 for the version of a map of the resulting open and closed areas to bottom trawling being analyzed in Alternative 5B (NMFS 2004b).
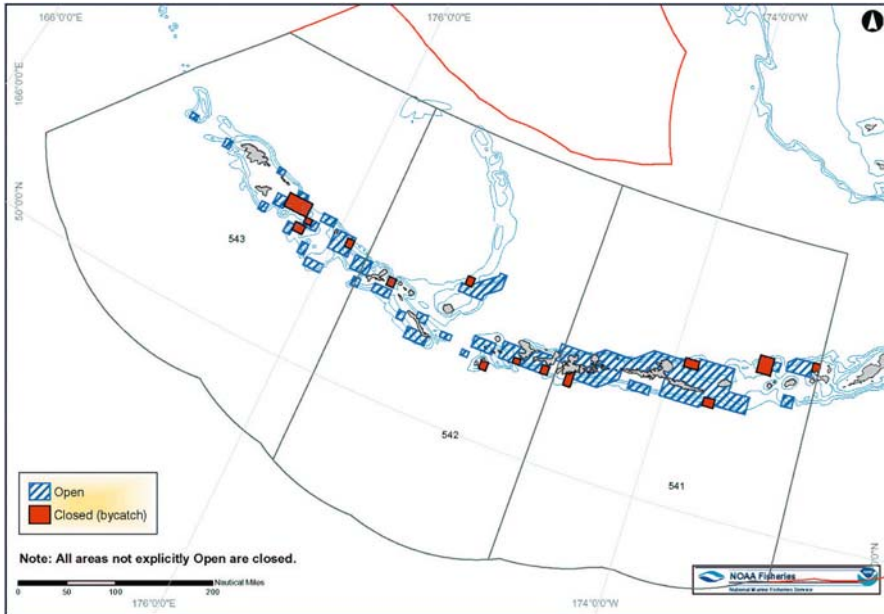
Fig. 4 Map of proposed open and closed areas to bottom trawling in the Aleutian Islands management areas in Alternative 5B, which was developed by NMFS using the Oceana Approach. Areas in white would be closed to bottom trawling on the precautionary basis that they contain less than one trawl tow per year, while potentially containing pristine deep-sea coral and sponge ecosystems. Red areas would be closed to bottom trawling on the basis that the rate of coral or sponge bycatch per metric ton of groundfish catch exceeds a threshold set by NMFS. Blue striped areas would remain open to bottom trawling on the basis that they have coral and sponge bycatch rates below the threshold set by NMFS, while incorporating most of the historic trawl effort in the region. Figure from January 2004 Draft Environmental Impact Statement for Essential Fish Habitat Identification and Conservation in Alaska, NMFS. Figure 2-50, Chapter 2

Careful examination of the differences in bycatch rates allows an informed selection of area closures that will provides the greatest mitigation of coral and sponge bycatch with the lowest impacts on trawl catch. To accomplish this objective, we developed two indices of habitat impact rates for each block that remains open. The first was the ratio of observed coral bycatch to observed total groundfish catch from 1990-2001. The second was the ratio of observed sponge bycatch to observed total groundfish catch from 1990-2001. These ratios represent a way to measure how much impact to EFH is caused per economic benefit gained by fishing. NMFS (2004b) used natural breaks in the data to determine a threshold value for each of the two indices. Note that the method employed by NMFS may be considered arbitrary since a desired level of bycatch reduction was not selected as a basis for the threshold. Ideally, threshold values should be selected based on a thorough examination of the costs and benefits associated with different threshold values. Blocks with an impact rate above the threshold for either index become closed to bottom trawling under

this approach to ensure that bycatch reduction is cost effective. These closures are considered to be the areas where the adverse impacts of bottom trawling on EFH are mitigated. These areas are represented as the solid red areas in Figure 4. Note that the threshold level chosen can dramatically influence the extent of closures and the associated reductions in groundfish catch. The selection of this threshold value should reflect the extent to which mitigation is warranted as well as different economic costs associated with different potential threshold values. The essence of this approach is that for any specific level of bycatch reduction desired, this approach minimizes the necessary reduction in groundfish catch.

All remaining grid blocks (those that contained more than a minimum level of historic fishing effort and were below the threshold value for the coral and sponge impact indices) remain open to bottom trawling. These areas are represented by the striped blue areas in Figure 4. It is important to note that the open areas encompass areas where some coral and sponge bycatch has occurred. Ultimately, catching targeted species without contacting these habitats is the only way to protect the remaining deep-sea coral and sponge ecosystems. The coral and sponge bycatch limits described below provide a mechanism to protect corals and sponges in remaining open areas. All existing closures and management measures remain in effect and should not be altered by this methodology.

2. Effort reduction

It is well established that area closures to protect habitat must be paired with effort reduction to offset the effects of displaced effort into the areas that remain open (NRC 2002). This objective can be accomplished in several ways, such as reducing the Total Allowable Catch (TAC) allocated to the bottom trawl fleet and/or by reallocating a percentage of the bottom trawl quota to less destructive gear types. Due to the controversial nature of the latter option, we recommended reducing bottom trawl effort in the Aleutian Islands through reductions in Total Allowable Catch (TAC) equal to the proportion of total catch that occurred in areas that would become closed to bottom trawling. For a detailed description of the analysis and results of the TAC reductions used in Alternative 5B, refer to NMFS (2004b). In summary, observer data from 1998-2002 were queried to estimate the percent of bottom trawl target species catch taken from areas that would be closed to bottom trawling under Alternative 5B. For each trawl fishery in the Aleutian Islands, trawl allocation of TACs was reduced proportionally to the historic catch that was caught in areas that would become closed.

This was straightforward for the Atka mackerel and rockfish fisheries, which have TACs specifically allocated in the Aleutian Islands. However, for Pacific cod, the TAC is currently allocated for the Bering Sea and Aleutian Islands areas combined. For this reason, we recommended splitting the TAC into two separate allocations (one for Bering Sea management areas and one for the Aleutian Islands management areas) and implementing the TAC reduction in the Aleutian Islands only. To meet the objective of preventing increased trawl effort in areas that remain open, TAC reductions are necessary only in regions where closures encompass historic fishing

effort. Therefore, for TAC reductions to be cost effective, TACs must be allocated at the same regional scale to which the Oceana Approach is applied.

3. Coral and sponge bycatch limits

Currently there are no limits on the bycatch of corals and sponges anywhere in North America. As of May 2002, observer bycatch records from Alaska documented 535 instances since 1990 where an observer reported bycatch of over one metric ton of corals or sponges from a single trawl tow (J. Heifetz pers. comm. 2002). Since there are no bycatch limits or penalties for this bycatch, there is currently little economic incentive to avoid this unreasonably high bycatch particularly if the catch per unit effort of target species is relatively high. Though coral and sponge bycatch limits may appear to continue destruction of habitat, we offer this tool as one component of the first step in a comprehensive strategy to reduce and eventually eliminate damage to deep-sea coral and sponge ecosystems while maintaining fisheries. The three main objectives of coral and sponge bycatch limits are to:

I.   Create an incentive for trawlers to avoid setting their nets in coral and sponge habitat;
II.   Ensure that the bycatch mitigated through area closures does not simply shift to areas that remain open; and
III.   Provide a mechanism for future habitat protection and controls on habitat impacts by fishery managers through further reductions in bycatch limits in remaining open areas.

Essentially, bycatch limits set an incidental catch allowance while fishermen pursue commercial target species. In Alaska, groundfish fishery management already uses bycatch limits for other valuable species such as halibut, salmon, and crabs. Therefore, this management component of the Oceana Approach is an extension of a management tool already in place. In general, bycatch limits can be applied at a fleetwide, sector, co-operative, or individual vessel basis, and result in in-season and/or post-season consequences depending on observer coverage and enforcement capabilities.

Without estimates of the total biomass of corals and sponges or the amount of actual damage reflected in observed bycatch, it may be necessary to establish the limits based on historical bycatch data. We assumed that the bycatch that occurred in areas that would become closed (red areas in Figure 4) would be mitigated by the closures. Therefore, we recommend that only bycatch that historically occurred in remaining open areas should be used to determine initial bycatch limits.

For a detailed account of the development and results of the coral and sponge bycatch limits developed by NMFS in Alternative 5B, see NMFS (2004b). In the development of Alternative 5B, NMFS determined the limits by counting all historic coral and sponge bycatch, which results in substantially higher limits than if they were determined solely from areas that remain open (NMFS 2004b). Observed bycatch numbers were expanded relative to the proportion of observed to

unobserved hauls to account for unobserved bycatch. Bycatch limits were set at or near the upper end of the observed annual bycatch levels. In some cases, the bycatch limits were reduced if there appeared to be outliers, defined as an annual bycatch estimate over 2 metric tons that was more than twice the amount estimated for any of the other years examined (NMFS 2004b).

One of the most important components of a successful bycatch limit strategy for corals and sponges is determining appropriate consequences for exceeding the cap, or incentives to keep bycatch below the cap. We considered in-season area or fishery closures, further TAC reductions in subsequent fishing seasons, and/or fines on individual vessels. Consequences applied at an individual vessel level may require 100 % observer coverage and be more difficult to enforce, but ensure individual accountability. Conversely, fleetwide or sectorwide consequences may not provide proper incentives. NMFS (2004b) analyzed Alternative 5B by applying the bycatch limits by fishery and management area, using in-season closures of management areas to trawl fisheries that exceed the bycatch limit for either corals or sponges.

One potential unintended consequence of coral and sponge bycatch caps is that they may create an incentive for gear modifications that retain less bycatch without reducing habitat impacts (e.g., increased roller sizes that crush corals rather than catch them in trawl nets). For this reason, it is necessary to impose gear restrictions that prevent these types of modifications and consider gear conversion to off-bottom fishing. In summary, the application of bycatch limits should be tailored to the particular circumstances of each fishery.

4. Monitoring and enforcement

Obtaining data on interactions with corals and sponges is essential to designing effective management measures, evaluating those measures, and improving the system over time. We recommend increasing observer coverage to the extent practicable, particularly for fisheries with high gear interactions with habitat. Increased observer coverage also has wide ranging benefits for overall fisheries and ecosystem-based management, particularly because it provides higher statistical power in catch and bycatch estimates so managers have a better idea of what is actually happening in the water. Current requirements for observer coverage are based on vessel size, where 100 % is required for vessels over 125 feet, 30 % is required for vessels 60-125 feet, and 0 % is required for vessels less than 60 feet (in addition, some fisheries are required to carry two observers due to Steller sea lion protection measures, which is considered 200 % coverage). In Alternative 5B, observer coverage is increased to at least 100 % for all trawl fisheries. Because it may be more costly for smaller vessels to carry observers, some compensation to vessels affected by this management measure should be considered.

Vessel monitoring systems (VMS) are a new technology that tracks the location and speed of fishing vessels over time. Requiring this technology for fishing fleets that interact with habitat serves two purposes. First, it provides another mechanism for enforcing open and closed areas by displaying the real time locations of vessels and whether the vessels have deployed their gear based on their speed. Second,

it enables fishery managers to observe the precise tow locations fishermen are using. Combined with observer coverage, these data can show which tows are most successful for catching target species and the average level of coral and sponge bycatch associated with each tow. These data will also be invaluable for the adaptive management component described below.

Electronic logbooks can be used to augment observer and VMS data. It allows fishing captains to display the activities and catch associated with each location in real time, allowing more accurate monitoring and enforcement. This technology also provides data with greater spatial resolution, so managers can see more detailed trawl tow paths.

Use of these three management tools are key components of a comprehensive approach to habitat management and the benefits of their implementation are widespread to all components of fishery and oceans management. Strong monitoring and enforcement capabilities are crucial to the success of all other components of the Oceana Approach.

5. Research, seafloor mapping, and adaptive management

Research and mapping play an integral role in the Oceana Approach and provide a mechanism for the management measures to become more cost effective over time. It is imperative that we invest in research and mapping if we are to maintain and restore the health of ocean ecosystems. Several specific information-gathering objectives will increase the efficacy of the Oceana Approach in each application. Seafloor mapping that identifies living substrate habitat types is critical. This type of mapping may be conducted with sidescan sonar and multibeam scanning (see several other papers in this volume). Combined with ground-truthing activities such as submersible or remotely operated vehicle dives, this technology can reveal areas on the seafloor that may warrant additional protections as well as areas where bottom trawling may have less destructive impacts.

Examining habitat-specific gear impacts and potential gear modifications to mitigate these impacts will provide cost-effective solutions to the problem of habitat destruction. Understanding the impacts, severity, and effectiveness of various gear types may identify preferred gear types for each fishery and habitat type. Though the Oceana Approach is focused on reducing the impacts of bottom trawling on coral and sponge ecosystems, the principles can also be applied to other gear types if they are found to be destructive to seafloor habitat. Research may also inform decisions regarding the level of mitigation necessary for applying the Oceana Approach to other gear types in the future.

Research should also explore the community ecology of coral and sponge habitats, particularly the production functions between these biogenic habitat features and commercial fish species. Once the relationship between the productive capacity of commercial fisheries and the quality and quantity of vulnerable habitat features is better understood, management measures can be better designed to maintain and potentially enhance fisheries productivity. Basic biology and life history information is lacking for many deep-sea coral and sponge species. Understanding

growth rates, reproduction, dispersal, and ages of deep-sea corals and sponges will provide estimates of recovery time for different habitat types. In summary, the Oceana Approach includes research and mapping on coral and sponge ecosystems that is focused on where it is, what it does, what damages it, and how long it takes to grow back.

In the long term, an adaptive management approach will improve the cost effectiveness of management measures described thus far. Adaptive management is the concept that management measures should be designed using whatever data are available and improved over time by collecting data to address remaining policy questions and scientific uncertainties (see Holling 1978; Walters 1986). The monitoring and enforcement components described above can be used to identify areas where bycatch rates are highest within areas that remain open. Additionally, they may also reveal more spatially explicit information on which areas have more and less relative effort. These data should be used to develop additional closed areas based on areas of higher bycatch rates and areas that become not as important to the fishery. Research and mapping components may be used to identify coral and sponge gardens within open areas that should become closed. As enforcement and monitoring capabilities improve with technological innovations, the scale of management, or the size of the grid blocks, should decrease so that management can take place at a resolution that better fits the patchiness of the seafloor habitat types and the spatial resolution of fishing effort.

In addition, the research and mapping components can be designed to provide opportunity for re-opening areas previously closed. Criteria for opening areas could be that they have either been mapped or thoroughly observed *in situ* and do not contain sensitive habitats such as corals and sponges. When research identifies gear modifications that reduce impacts on habitats while still catching fish, these modifications can be incorporated into the management regime.

Expected results of implementing the Oceana Approach

NMFS (2004c) conducted significant analysis of Alternative 5B, which they developed based on the Oceana Approach described above. In addition, specific numerical statistics regarding the analysis were provided to the authors (J. Kurland, Director, NMFS Alaska Region Habitat Conservation Division pers. comm.). While these numbers may change with additional analysis, they provide an example of the results that can be expected of a habitat protection policy formulated using the Oceana Approach.

Alternative 5B would reduce the impact of bottom trawling over 82,023 km^2 of Aleutian Island seafloor habitat or 77.9 % of the current fishable area of 105,243 km^2 (NMFS 2004c). If implemented, Alternative 5B would significantly reduce coral and sponge bycatch in trawl fisheries in the Aleutian Islands. NMFS estimates that 36 % of the historic coral bycatch and 24 % of the historic sponge bycatch from 1990-2001 occurred in areas that would become closed to bottom trawling under this alternative (J. Kurland, Director, Habitat Division, NMFS Alaska Region pers.

comm.). Since these areas as well as previously untrawled areas would become closed, these values represent the minimum level of bycatch reduction can be expected if this alternative is implemented. Bycatch caps based on historical levels from remaining open areas will provide insurance that this mitigation will actually occur. NMFS (2004b) calculated that the TAC reductions based on the average percentage of catch that occurred in closed areas from 1998 to 2001 would be:

- 6.0 % for the Atka mackerel trawl fishery,
- 10.0 % for the Pacific cod trawl fishery, and
- 12.0 % for the rockfish trawl fisheries.

Therefore, the scale of coral and sponge bycatch reduction accomplished through the Aleutian Islands model is roughly three-fold greater than the reductions in groundfish catch imposed on the bottom trawl industry. The above results confirm our hypothesis that it is possible to design cost effective habitat protection measures by taking advantage of the fact that bycatch rates are spatially heterogeneous. This shows that it is possible to substantially mitigate the adverse impacts of fishing on Essential Fish Habitat while maintaining vibrant fisheries, assuming all other things being equal. These results would be expected to further improve through the adaptive management strategy described above.

Discussion

The Oceana Approach effectively reduces adverse impacts of bottom trawling on EFH at minimum cost to the bottom trawl industry, but is only a first step. As mentioned, some areas known to contain corals and sponges remain open to bottom trawling under this approach. To maintain the full productive capacity of fish habitat, fishermen must continue to reduce the ecosystem impacts of harvesting fish. Several scientists and managers have commented that it may be more appropriate to consider total coral and sponge bycatch rather than bycatch rates. While this may afford substantial protection to deep-sea coral and sponge ecosystems, this will necessitate a greater reduction in TAC than would be necessary for the same reduction in bycatch using a rate threshold.

This approach contrasts approaches that apply random closures or closures in areas of highest trawl effort, while leaving all remaining areas open. For random closures, such as strip closures across depth strata, it is most likely that the percentage of TAC reduction and bycatch reduction are roughly equivalent to the percentage of area closed. For closures in areas of high trawl effort, it is likely that the economic costs will be high with small habitat benefit and possibly increased habitat impacts in remaining open areas if fishing effort is not reduced.

In contrast to the status quo fishing regime in the Aleutian Islands, Alternative 5B embodies a more precautionary approach that errs on the side of conservation particularly with regard to rare species and habitat types. Due to the patchiness of deep-sea coral and sponge habitats and the high species richness observed at

many sites, these ecosystems likely contain rare or endemic species that may be found no where else in the world. The recent discovery of several new species and even a new genus of corals from recent submersible expeditions in the Aleutian Islands shows this is not merely postulation (R. Stone pers. comm.). Many of these species may also produce valuable cures to human diseases, climate change data, and genetic information (Witherell and Coon 2000). There also may be unique assemblages of deep-sea coral and sponge species resulting in rare habitat types yet to be discovered. Protecting these unexplored, untrawled sites ensures that these unique, undiscovered species and habitat types will exist for the benefit of future generations. With recovery times in the hundreds to thousands of years, damage to these habitats is for all practical purposes irreversible on a management time scale. Therefore, although the full value to society of protecting coral and sponge ecosystems is not yet understood, the option value of protecting these vulnerable ecosystems may be far greater than the short-term costs imposed on the industry. If a less precautionary approach is taken, such as the status quo, it is likely that many of these rare habitats and unique ecological linkages will be gone before they are discovered.

Successful implementation of the Oceana Approach requires an investment in better fisheries management. Enforcement must be able to enforce open and closed areas at a high level of spatial resolution. Observer coverage must increase and training must include identification of invertebrates. Managers and fishermen must use the latest technologies, including vessel monitoring systems, electronic logbooks, and state of the art sounders. Incentives must be enforceable and significant. Management must be flexible enough to incorporate new information to improve the various policy components. There must be a commitment to research and seafloor mapping to guide the adaptive management process. This investment will ensure that we have productive fisheries and healthy ocean ecosystems for generations to come.

The Oceana Approach is recommended for application to other regions and should be adjusted based on available fishery and biological data for each region. For example, thresholds selected for defining open areas should be selected relative to the data for each region, rather than a specific number. It is useful to view the results using different threshold values to compare the costs and benefits. The essence of this threshold rate approach is that it optimizes bycatch reduction subject to any chosen economic cost constraint. In other words, for any level of economic costs fishery managers are willing to impose on the trawl industry, it is possible to maximize the protection of deep-sea coral ecosystems.

Management measures designed using the Oceana Approach will be most effective in regions with accurate spatial records of coral and sponge bycatch, but the approach can also be applied at a coarser scale based on any level of available data. For example, if observer data are not available, trawl survey data may be used to determine the relative ratio of coral and sponge concentration to target species catch per unit effort. The approach works best in areas where fishery locations are relatively static, but can be tailored to more dynamic fisheries by incorporating

longer time series in the determination of open areas. The methodologies described above could also potentially be applied to any gear type that may have adverse impacts to EFH. It can also be applied to other habitat features that are vulnerable to fishing activities. To do this, it is necessary to determine which features of EFH are vulnerable to disturbance, and the extent to which each gear type affects these features.

If there is indeed a positive functional relationship between deep-sea coral and sponge ecosystems and commercial fish populations as suggested by the documented species associations, it is clear that the adverse impacts from bottom trawling are continuing to reduce the productivity of their own fisheries as well as fisheries prosecuted with other gear types. In the end, a sustainable groundfish fishery in the Aleutian Islands will require developing new fishing techniques that effectively harvest the fish without destroying the habitat the fish need to survive, reproduce, and grow to maturity. Considering the current political strength of the trawl industry in Alaska's fishery management context, the only way to stop bottom trawling on corals, sponges and seamounts may be to simply buy out the capacity. As in other resource conflicts such as groundfish collapses on the U.S. west coast and New England, federal buyouts are often the inevitable results of unsustainable resource management. The paradox is that while there may be economic incentives encouraging bottom trawling in deep-sea coral and sponge habitats, the irreversible consequences of this destructive activity will ultimately hurt the economy. A truly sustainable human existence on this planet requires that we actively develop new policy approaches and technologies that provide opportunities to maintain the economy and catch fish without destroying natural habitats and ecosystems.

Acknowledgements

References

Andrews AH, Cordes E, Mahoney MM, Munk K, Coale KH, Cailliet GM, Heifetz J (2002) Age and growth and radiometric age validation of a deep-sea habitat-forming gorgonian (*Primnoa resedaeformis*) from the Gulf of Alaska. Hydrobiologia 471: 101-110

Cimberg RL, Gerrodette T, Muzik K (1981) Habitat requirements and expected distribution of Alaska coral. Final Rep, Res Unit 601, VTN Oregon, Inc, US Dept Commerce, NOAA, OCSEAP Final Rep 54 (1987), pp 207-308

Dayton PK, Thrush S, Agardy TM, Hofman RJ (1995) Environmental effects of marine fishing: aquatic conservation. Mar Freshw Ecol 5: 205-232

Else P, Haldorson L, Krieger KJ (2002) Shortspine thornyhead (*Sebastolobus alascanus*) abundance and habitat associations in the Gulf of Alaska. Fish Bull 100: 193-199

Fosså JH, Mortensen PB, Furevik DM (2002) The deep-water coral *Lophelia pertusa* in Norwegian waters: distribution and fishery impacts. Hydrobiologia 471: 1-12

Freese JL (2000) Cruise report survey of a potential habitat area of particular concern. Auke Bay Lab, Alaska Fish Sci Cent, NMFS

Freese JL (2001) Trawl-induced damage to sponges observed from a research submersible. Mar Fish Rev 63: 7-13

Freese L, Auster PJ, Heifetz J, Wing BL (1999) Effects of trawling on seafloor habitat and associated invertebrate taxa in the Gulf of Alaska. Mar Ecol Progr Ser 182: 119-126

Hall-Spencer J, Allain V, Fosså JH (2001) Trawling damage to Northeast Atlantic ancient coral reefs. Proc R Soc London B 269: 507-511

Heifetz J (1999) Effects of fishing gear on sea floor habitat. Progr Rep FY1999. Auke Bay Lab, Alaska Fish Sci Cent, NMFS

Heifetz J (2002) Coral in Alaska: distribution, abundance, and species associations. Hydrobiologia 471: 19-28

Holling CS (1978) Adaptive environmental assessment and management. John Wiley and Sons, New York

Husebø A, Nøttestad L, Fosså JH, Furevik DM, Jørgensen SB (2002) Distribution and abundance of fish in deep-sea coral habitats. Hydrobiologia 471: 91-99

Krieger KJ (2001) Coral (*Primnoa*) impacted by fishing gear in the Gulf of Alaska. In: Willison JHM, Hall J, Gass SE, Kenchington ELR, Butler M, Doherty P (eds) Proceedings of the First International Symposium on Deep-Sea Corals. Ecology Action Centre, Nova Scotia Museum, Halifax, pp 106-116

Krieger KJ, Wing BL (2002) Megafauna associations with deepwater corals (*Primnoa* spp.) in the Gulf of Alaska. Hydrobiologia 471: 83-90

Malecha PW, Stone RJ, Heifetz J (2002) Living substrate in Alaska: distribution, abundance, and species associations. Symp Effects Fish Activities Benthic Habitats, Tampa, Florida, November 12-14, 2002

Moran MJ, Stephenson PC (2000) Effects of otter trawling on macrobenthos and management of demersal scalefish fisheries on the continental shelf of north-western Australia. ICES J Mar Sci 57: 510-516

National Marine Fisheries Service (NMFS) (2002a) Essential Fish Habitat final rule, 50 C.F.R. 600.815(a)(2)

National Marine Fisheries Service (NMFS) (2002b) Summary of North Pacific groundfish fisheries observer data provided to Oceana by Dr. James Balsiger, Alaska Regional Administrator, on October 17, 2002

National Marine Fisheries Service (NMFS) (2004a) Draft Environmental Impact Statement for Essential Fish Habitat Identification and Conservation in Alaska. NOAA Fish: Append B

National Marine Fisheries Service (NMFS) (2004b) Draft Environmental Impact Statement for Essential Fish Habitat Identification and Conservation in Alaska. NOAA Fish: Append H

National Marine Fisheries Service (NMFS) (2004c) Draft Environmental Impact Statement for Essential Fish Habitat Identification and Conservation in Alaska. NOAA Fish: chapter 4: Environmental Consequences of the Alternatives

North Pacific Fishery Management Council (NPFMC) (1998) Amendment 55/55 to BSAI and GOA Fishery Management Plans. North Pacific Fish Manage Counc

North Pacific Fishery Management Council (NPFMC) (2003) Council Motion on Essential Fish Habitat, dated February 3, 2003. North Pacific Fish Manage Counc

National Research Council (NRC) (2002) Effects of trawling and dredging on seafloor habitat. Committee on Ecosystem Effects of Fishing: Phase I - Effects of bottom trawling on seafloor habitats. Natl Res Counc, Washington, DC

Roberts S, Hirshfield M (2003) Deep sea corals: out of sight, but no longer out of mind. Oceana, Washington, DC, 16 pp

Walters CJ (1986) Adaptive management of renewable resources. MacMillan, New York

Watling L, Norse EA (1998) Disturbance of the seabed by mobile fishing gear: a comparison to forest clearcutting. Conserv Biol 12: 1180-1197

Witherell D, Coon C (2000) Protecting gorgonian corals off Alaska from fishing impacts. Report to NPFMC. In: Willison JHM, Hall J, Gass SE, Kenchington ELR, Butler M, Doherty P (eds) Proceedings of the First International Symposium on Deep-Sea Corals. Ecology Action Centre, Nova Scotia Museum, Halifax, pp 117-125

Conservation and management implications of deep-sea coral and fishing effort distributions in the Northeast Pacific Ocean

Lance E. Morgan[1], Peter Etnoyer[2], Astrid J. Scholz[3], Mike Mertens[3], Mark Powell[4]

[1] Marine Conservation Biology Institute, 4878 Warm Springs Rd., Glen Ellen, CA 95442, USA
 (lance@mcbi.org)
[2] Aquanautix Consulting, 3777 Griffith View Drive, Los Angeles, CA 90039, USA
[3] Ecotrust, 721 NW Ninth Avenue, Portland, OR 97209, USA
[4] The Ocean Conservancy, 2479 Soundview Dr. NE, Bainbridge Island, WA 98110, USA

Abstract. The conservation of deep-sea corals is of growing interest in the United States. A range of issues including biodiversity protection, conservation of seafloor habitats, and the role of deep-sea corals as essential fish habitat places greater significance on understanding the distributions of these corals and fishing activities. At the same time overfishing of some groundfish populations highlights the need for ecosystem-based management. Here we present records of habitat-forming deep-sea corals from the United States Pacific Fishery Management Council region that we analyze in relation to differential ecological impacts of demersal fishing gears. We use an ecological footprint approach combining groundfish catch by gear type with a previously published ecological severity ranking of fishing gears.

Deep-sea corals in the Isididae, Paragorgiidae, Primnoidae, Antipathidae and Stylasteriidae families are widespread throughout their depth ranges in the Northeast Pacific, although the scleractinian families Oculinidae and Caryophylliidae are relatively rare. In this qualitative analysis, we highlight areas of relatively high coral concentration such as the West Coast continental shelf break and Monterey submarine canyon, areas that are presently relatively lightly fished but where corals are recorded. Bottom trawling gear has far and away the region's largest ecological footprint. Other gears with smaller footprints include bottom longline, pot/trap and hook and line gear. Most of these impacts seem to have occurred in areas where deep-sea corals are relatively scarce, but fishing closures to protect rockfish implemented in 2002 may have the unfortunate effect of redistributing fishing effort to areas of deep-sea coral aggregations. An ecosystem-based management approach would detect and prevent such unintended consequences of redistributing fishing effort and placing deep-sea corals in harm's way.

Keywords. Conservation, management, Octocorallia, fishing gear impact

Introduction

Deep-sea corals are a paraphyletic assemblage of organisms belonging to the phylum Cnidaria. Some corals are more closely related to sea anemones than other "corals" such as hydrocorals. Moreover, some species usually considered deep-sea corals can be found in shallow waters (<200 m). Following Etnoyer and Morgan (2003) we use the term deep-sea coral to refer to a variety of hexacoral, octocoral, and hydrocoral families living in temperate waters.

In general, deep-sea corals are a poorly documented group that are increasingly at the center of conservation concern because they are considered important habitat for commercially important fishes, as well as a wide variety of other fishes and invertebrates. On the Atlantic Coast of the United States deep-sea corals occur from Georges Bank (e.g., *Paragorgia arborea*), to *Lophelia* reefs such as the Agassiz coral hills on the Blake Plateau in the mid-latitudes of North Carolina (George 2002), to the *Oculina* (*Oculina varicosa*) banks off Florida (Reed 2002). Deep-sea coral records in the Northeast Pacific date to the late 19th century (Dall 1884), but contemporary concerns such as biodiversity conservation, commercial fishery sustainability, benthic impacts of commercial fishing gears and essential fish habitat (EFH) are revitalizing interest in the distribution and abundance of habitat-forming deep-sea corals (e.g., Witherell and Coon 2001; Etnoyer and Morgan 2003).

In 1996, the United States Congress revised the Magnuson-Stevens Fishery Conservation and Management Act (MSFCMA) to include changes in the way fisheries are managed. Key additions include reducing bycatch, avoiding overfishing and identifying EFH. These measures also provide an option for decision-makers to designate habitat areas of particular concern (HAPC), as in the case of *Oculina* Banks off Florida - a spawning area for commercially important snappers and groupers - from trawling and other forms of fishing (Reed 2002). Proposals to protect corals with similar HAPC designations are being developed in other areas of the US Exclusive Economic Zone (EEZ). Interest in Pacific deep-sea corals is driven by declining catches of groundfish, (Ralston 1998; PMCC 1999; Fig. 1), which may rely on coral habitats at various life stages.

In January 2000, the US Secretary of Commerce declared the West Coast groundfish fisheries a federal disaster. Groundfish is a general term used for 83 species of demersal fishes that are managed by the Pacific Fishery Management Council (PFMC), which includes the Federal and state waters off California, Oregon and Washington. These species are targeted by fishermen using trawl nets, bottom longlines, pots/traps, and hook and line gears. A substantial number of managed groundfish are rockfishes in the genus *Sebastes*. Approximately 55 species of rockfishes are targeted by fishermen and marketed under the generic term 'red snapper' (PMCC 1999). Currently nine of the 83 managed west coast groundfish species are listed as "overfished" by NOAA Fisheries, the federal agency responsible for managing fisheries in US federal waters.

Recent management action to protect declining groundfish has closed areas along a restricted depth interval of the continental shelf from Mexico to Canada beginning in the 2002 season. Under the provisions of MSFCMA, fisheries managers are
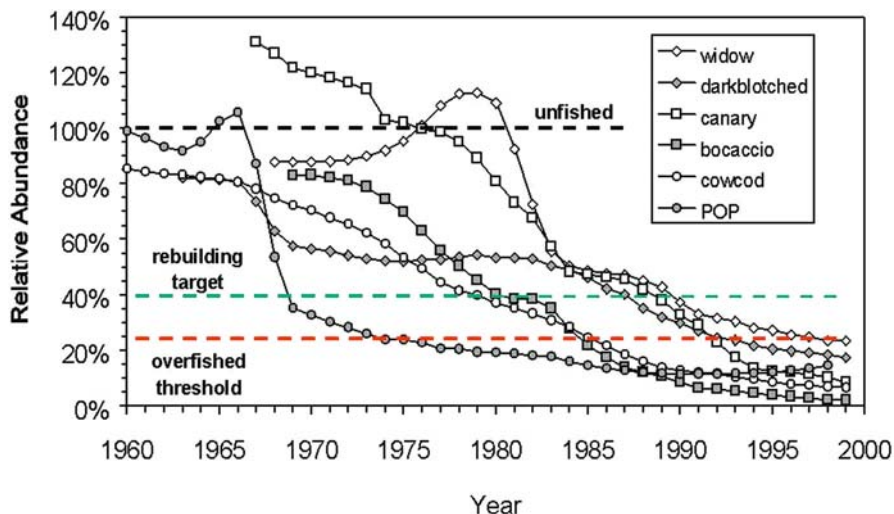
Fig. 1 Decline of six species of west coast rockfish and management thresholds (from S. Ralston pers. comm., NOAA Fisheries, based on Stock Assessments of NOAA Fisheries)

required to adopt the precautionary approach when scientific data are unavailable. In essence this means that wherever fishing poses a threat to the resource and/or the surrounding environment, precautionary measures must be taken even if the scientific results are not yet established. However, in practice the case for protection of corals from destructive fishing methods and their role as important seafloor habitat has typically been left as a "case to be made" and little precautionary action has been taken to protect them from fishing threats.

Habitat value of deep-sea corals

Several studies document that the diversity, quality and extent of bottom habitats are vital determinants of rockfish diversity, distribution and abundance (Pearcy et al. 1989; Carr 1991; O'Connell and Carlisle 1993; Nasby-Lucas et al. 2002). Additionally species richness and community composition over smaller scales also correlate with three-dimensional structure (Love et al. 1991; Krieger 1993; Yoklavich et al. 2000). Corals create extensive three-dimensional habitat that fishes use for shelter, feeding, spawning and as nursery areas for post-settlement individuals. Studies document diverse faunal associations with deep-sea corals (Heifetz 2002; Krieger and Wing 2002). Gorgonians such as red-tree coral (*Primnoa* spp.), which can grow as large as 7 m and form discrete aggregations, are now widely acknowledged as important fish habitats, and are considered EFH by the North Pacific Fishery Management Council[1] (Witherell and Coon 2001). Likewise organisms that provide three-dimensional structure, such as sponge beds, are also important fish habitats (Freese 2003).

---

[1] North Pacific FMC region includes federal waters seaward of Alaska state waters.

Several studies suggest commercially important fish species are found in association with deep-sea corals, such as Atka mackerel, *Pleurogrammus monopterygius,* and shortspine thornyhead, *Sebastolobus alascanus,* in Alaska (Heifetz 2002). Krieger and Wing (2002) report rockfishes as well as several other megafaunal assemblages associated with *Primnoa* corals in the Gulf of Alaska, and highlighted the importance of *Primnoa* to deep-water ecosystems. Rockfishes in Alaska, which have similar life histories to those in the PFMC region, are found in association with the same corals occurring in PFMC waters (Krieger and Wing 2002). Likewise Fosså et al. (2002) present results indicating a dense aggregation of *Sebastes* sp. associated with *Lophelia* corals off the coast of Norway. Husebø et al. (2002) found that fish in coral habitat tended to be larger than in non-coral habitat.

Impact of fishing on deep-sea corals

Deep-sea corals are considered valuable fishing areas. Historically, damage to corals from fishing was likely light to moderate as less robust gear and smaller vessels limited damage. This has changed dramatically with larger, more powerful vessels, much stronger synthetic fibers and the advent of roller and rockhopper trawl gears. With increased technology and aids to navigation including fish finders, precision depth profilers, and inexpensive geo-positioning electronics, it is much easier to target specific areas. Longlines and gillnets damage *Lophelia* reefs in Norway (Fosså et al. 2002). Hook and line, pot/trap and longline methods occur in and near coral areas and can lead to snagging and breaking of corals as well (Dall 1884; Breeze et al. 1997; Fosså et al. 2002). Additionally, the setting of traps on corals damages or crushes corals, and traps in set-lines are particularly damaging (Barnette 2001), especially when hauled with hydraulic winches. These modifications allow fishermen to recover gear and catch in areas that previously would have been off-limits to fishing and therefore served as natural refugia.

There is a strong emerging scientific consensus that destructive fishing is having alarming and increasing impacts on seafloors (Watling and Norse 1998; Auster and Langton 1999; Thrush et al. 2001; Dayton et al. 2002; NRC 2002; Thrush and Dayton 2002; Pew Oceans Commission 2003). Physical damage occurs to living seafloor structures (e.g., corals, sponges, seagrasses) as well as the geologic structures (e.g., boulders, cobbles, gravel, sand, mud) that serve as nursery areas, refuges, and homes for fishes and organisms living in, on or near the seafloor. The impact of mobile demersal gear, especially bottom trawling, on European deep-sea coral is a major concern (Rogers 1999; Duncan 2001). Hall-Spencer et al. (2002) document widespread trawling damage to deep-sea coral reefs at 840-1300 m depth along the West Ireland continental shelf break and at 200 m off West Norway. Trawling also damages deep-sea coral reefs off Norway and Tasmania (Koslow et al. 2000, 2001; Fosså et al. 2002).

In US waters, few studies evaluate the actual impacts of fishing gear on corals. *Oculina* coral reefs are believed to have been damaged by benthic fishing gears as long ago as the 1970's though this is not well-documented (Reed 2002). Shrimp

trawlers have been caught illegally fishing in the reserve since its designation in 1984, and the reef is now nearly totally destroyed (Reed et al. 2005). Scleractinians are not the only vulnerable corals; Krieger and Wing (2002) document bycatch and damage to *Primnoa* from bottom trawls and longline gear in Alaska.

Evaluating the differential impacts of bycatch and habitat damage, and the severity of these impacts among different gear types, is a challenging task. A recent report by Morgan and Chuenpagdee (2003) reviewed over 170 documents on the bycatch and habitat impacts of ten fishing gears and provided a ranking of the ecological impacts of these gears. This report includes an experts' rating of fishing gear impacts to physical and biological habitats and five bycatch groups (i.e., shellfish and crabs, finfish, sharks, marine mammals, and seabirds and sea turtles). These ratings provided the basis for a survey of the ecological severity of the gear impacts sent to another group of experts using the 'damage schedule' approach developed by Chuenpagdee et al. (2001a, b). Their responses were combined in one overall ecological severity scale. The fishery experts considered the ecological impacts caused by bottom trawls, bottom gillnets, dredges, and midwater gillnets to be the highest, followed by moderately impacting gears: pots and traps, pelagic and bottom longlines. Finally, gears causing relatively low impacts are midwater trawls, purse seines and hook and line methods.

In this report we compare the distribution of deep-sea coral records along the West Coast of the USA, and the distribution of groundfish landings in 2000 to determine areas of potential conflict. Next we review deep-sea coral distributions in the context of recent management actions in the Pacific FMC to alleviate overfishing of groundfish. We then use the Morgan and Chuenpagdee (2003) ranking of fishing gears to develop an ecological footprint (ecological severity of gear multiplied by landings) for each gear involved in the groundfish fleet to highlight the nature of fishing threats to deep-sea corals. Finally we conclude with suggestions of appropriate policy responses.

Methods

Coral occurrences

Deep-sea coral records along the Pacific coast of the US compiled by Etnoyer and Morgan (2003) are used to examine deep-sea coral distributions (Fig. 2). These records include members of eight cnidarian families recorded in the literature and in institutional databases. Institutions include the NMFS RACEBase, California Academy of Sciences, Scripps Institution of Oceanography, Smithsonian Institution, Monterey Bay Research Institute, Santa Barbara Museum of Natural History, NOAA-Office of Exploration and one previous report (Cimberg et al. 1981). The 8 families (Caryophylliidae, Oculinidae, Antipathidae, Primnoidae, Paragorgiidae, Isididae, Coralliidae, Stylasteriidae) were chosen based on their ability to grow large enough to provide habitat for commercially important groundfish. It did not include solitary sclearactinian cup-corals, nor was it exhaustive, thus certain families such as the Paramuricidae are excluded.
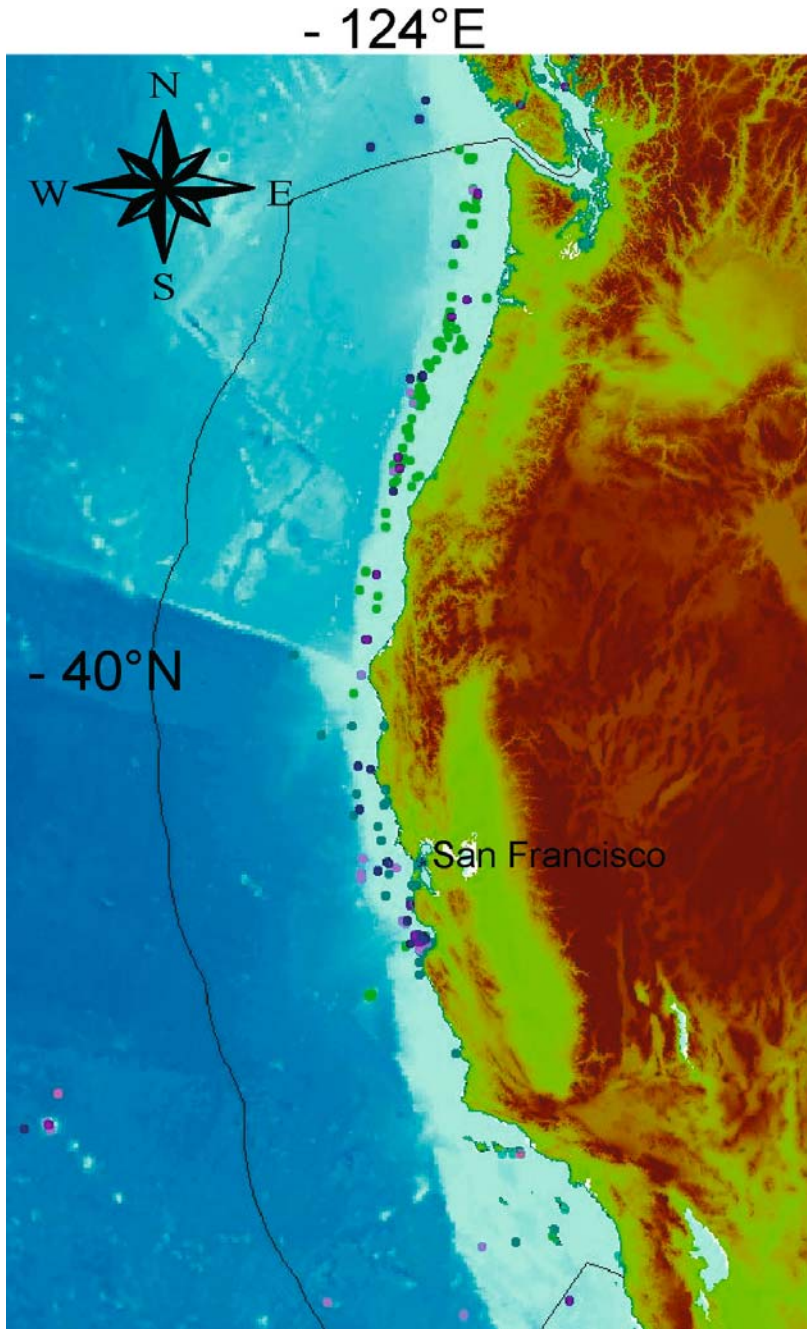
Fig. 2 Deep-sea coral records from Etnoyer and Morgan (2003). Teal - Stylasteriidae, Pink - Isididae, Purple - Paragorgiidae, Blue - Primnoidae, Green - Antipathidae. Other families are rare in the database for the U.S. West Coast

Fishing gear impacts

A recent study ranking the differential impacts of fishing gears (Chuenpagdee et al. 2003; Morgan and Chuenpagdee 2003) is used here to establish the ecological footprint of different fishing gears used in the Pacific coast groundfish fleet (Scholz 2003; Scholz et al. 2003).

Using information from NOAA Fisheries for the year 2000, summarized by Scholz et al. (2003), we plot the distribution of four fishing gears used in the groundfish fleet (bottom trawls, bottom longlines, pots and traps and hook and line) in 9 x 9 km blocks. These gears range over the three impacts levels (low, moderate and high) in Morgan and Chuenpagdee (2003) and illustrate the level of catch by these gears throughout the PFMC region. For each gear class we multiplied landings in each 9 x 9 km cell by 1, 2 or 3 (1 = low, 2 = moderate or 3 = high impact) to develop a scale of relative ecological impact. Landings by block were arbitrarily split into 5 classes: no landings, 1-100,000 lbs; 100,001-200,000 lbs; 200,001-300,000 lbs; and over 300,000 lbs. Together this information (impact level and landings) gives us an estimate of the ecological footprint of each of these gears for use in policy development to protect deep-sea corals and associated seafloor habitats.

Results

Antipatharian, octocorallian and hydrocorallian records are much more common than scleractinian records in the NE Pacific region. The shelf break along the coast of Washington, Oregon and northern California, and the Monterey submarine canyon edge are the areas with the largest number of records. The largest area of localized richness appears to be the Monterey Canyon. Records for Stylasteriidae tend to be the nearest to the shore, but there are also records in deeper waters. The California hydrocoral, *Stylaster californicus*, is common to rocky reefs and banks in California, especially banks off southern California, while other Stylasteriidae species are recorded from deeper waters. The Pacific region in general has not been extensively explored for deep-sea corals and new explorations will undoubtedly document new records and perhaps even new species. DeVogelaere et al. (2005) recently recorded *Corallium* sp. from Davidson Seamount, a species entirely absent from the Etnoyer and Morgan (2003) database along the US West Coast.

Plotting the deep-sea coral occurrences with the 2000 landings data in the groundfish fishery (as compiled by Scholz 2003; Scholz et al. 2003) shows that there appears to be little overlap with the groundfish fishery (Fig. 3). Areas of high coral diversity and abundance do not conflict with recent landings in the groundfish fishery. One notable exception is Monterey Canyon, where there is substantial overlap (Fig 3). In general fishing occurs on the shelf while coral records occur in deeper waters near the shelf break.

Plotting the 2002 groundfish closures (implemented by the PFMC in order to assist in the recovery of overfished rockfish populations) with coral records (Fig. 4) suggests these closures, which are restricted to the shelf, do not overlap many of the known coral occurrence records. This is true along the length of the three Pacific Coast states, with few exceptions.

Finally by plotting fish landings (9 x 9 km blocks) scaled by the gear ranking (Chuenpagdee et al. 2003; Morgan and Chuenpagdee 2003) we develop an ecological footprint for each of the 4 gears in use in the groundfish fleet in 2000 (Scholz 2003; Scholz et al. 2003). This plot by fishing gear (Fig. 5) shows the relative difference
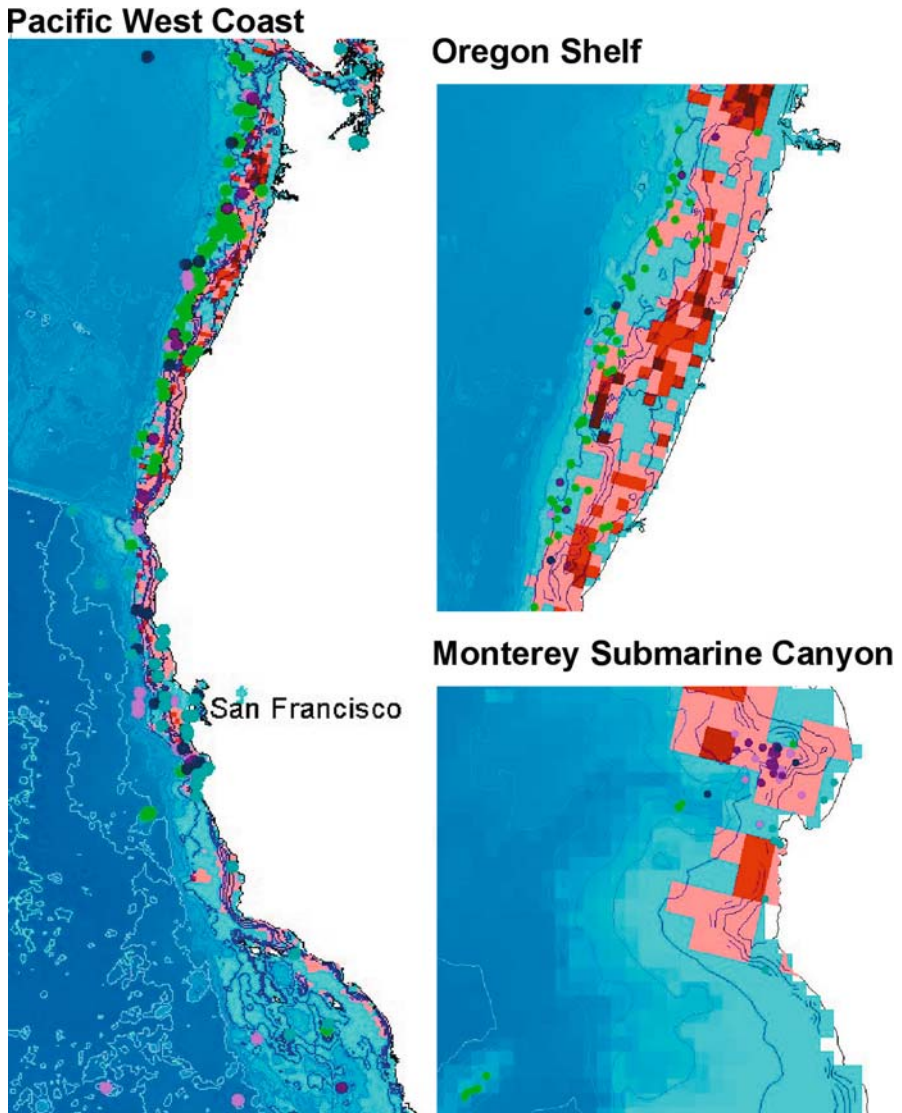
Fig. 3 Occurrences of cold-water corals and groundfish fleet catch along the Pacific west coast (left) (darker red indicates larger landings. Color code of coral records; light green - Antipathidae, teal - Stylasteriidae, pink - Isididae, purple - Paragorgiidae, dark blue - Primnoidae. Oregon shelf showing abundant records along the shelf break (upper right). Monterey Canyon showing abundant and diverse records at the canyon break (lower right)

in gear usage, as well as a severity scale (green: light impact to black: heavy impact) by the different gear types. Bottom trawl gear is the most widely used gear as well as the most ecologically severe, therefore having the largest ecological footprint.
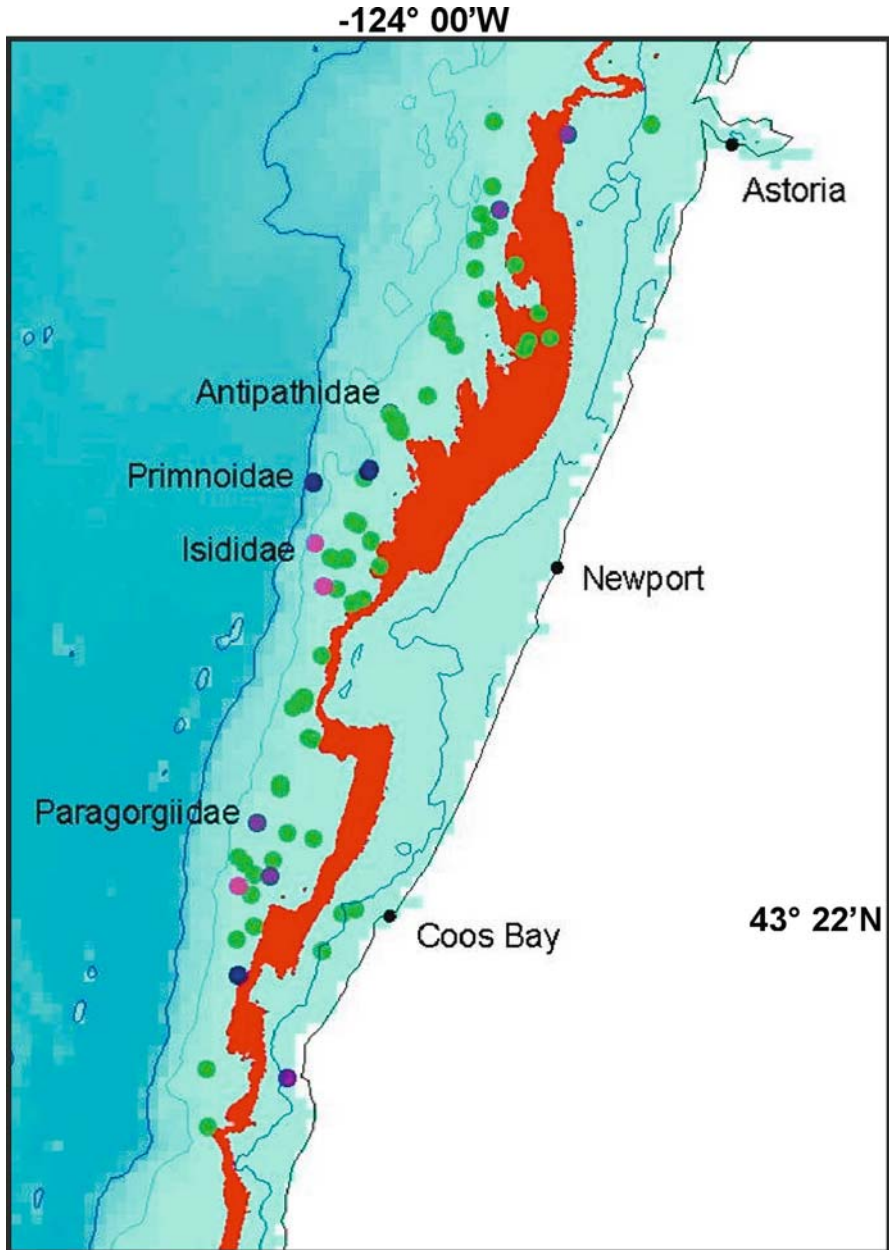
Fig. 4 Groundfish closures (red) as implemented by PFMC to protect rockfish populations. Deep-sea coral occurrences offshore of Oregon (Etnoyer and Morgan 2003)
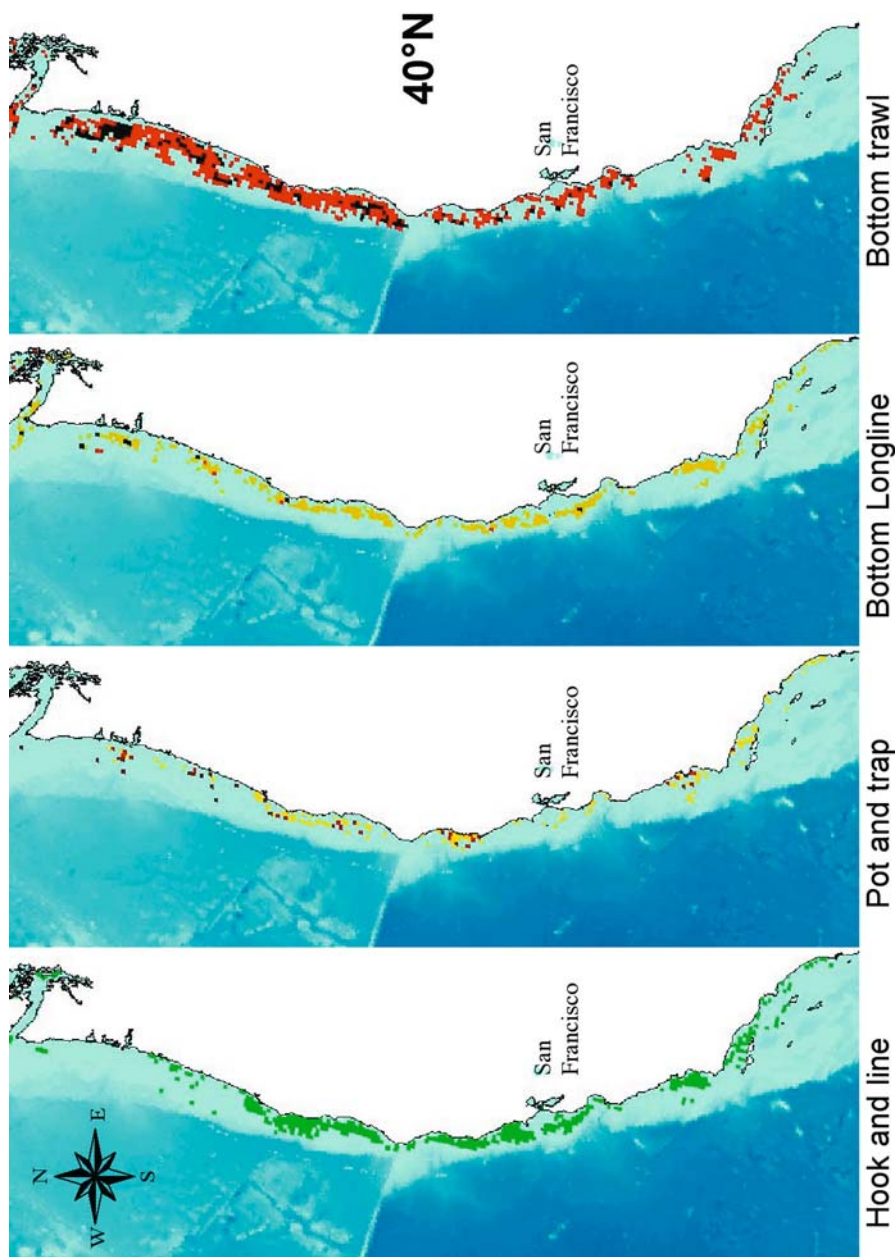
Fig. 5 Ecological footprint (landings x gear ranking) for four gear types used in the Pacific Fishery Management Council region to land groundfish. Impact scale: green - light, yellow - moderate, red - heavy, black - very heavy. Landings from year 2000 see Scholz et al. (2003), gear ranking from Morgan and Chuenpagdee (2003)

The other gears are used extensively throughout the PFMC region, but have smaller footprints.

Discussion

Our qualitative analysis of deep-sea corals shows that five of the eight coral families are widely distributed along the Pacific Coast of North America. The area of highest occurrence is the shelf break, an area of high bathymetric relief. Plots of landings in the groundfish fleet and deep-sea coral occurrences in the region managed by the Pacific Fishery Management Council show interesting patterns that may be difficult to interpret. Groundfish landings in 2000 are mostly confined to the shelf, while deep-sea coral occurrences are greatest along the continental shelf break and Monterey submarine canyon. While it is conceivable that these records reflect greater sampling intensity, especially in the Monterey Bay region, it is not likely that the shelf break has been better sampled than the shelf region. This pattern suggests that either there is limited overlap between fishery operations and deep-sea corals, or that fishing has already had a substantial negative impact on coral occurrences. Since our records do not reflect historic coral distribution, it is difficult to know the impacts of past fishing.

As early as 1873, Dall reports that *Stylaster* corals from the Farallones Islands in northern California were entangled in fishermen's hooks and brought to the surface. Pauly (1995) refers to the erosion of our knowledge of abundance, range and distribution of species resulting from human impacts as a shifting baseline. That is, we view incremental loss as insignificant because we have no memory of the full magnitude of our impact over time frames larger than our individual history. It is possible that over 100 years of fishing and at least 30 years of trawling have impacted corals to the degree that we are no longer have an accurate picture of their distribution and abundance. Anecdotal information from fishermen in the Canadian Maritimes suggests that long-time fishermen have been well aware of these corals and have witnessed a notable decline (records from the 1800s, see Gass 2002). Given the potential ages of gorgonians - 100's to 1000's of years (Druffel et al. 1995; Andrews et al. 2002; Risk et al. 2002; Roark et al. 2003) - these species might be irrevocably harmed by a single trawl pass, and may not recover.

Fishing closures implemented in 2002 to help depleted rockfishes may have the unintended consequence of redirecting fishing effort into areas with deep-sea corals as fishermen move further offshore in search of groundfish. Further examination of this question is needed based on current data, but conventional management that is focused on maximizing catch of a few species is all too likely to make such unintended errors. Without a holistic approach such as ecosystem-based management, fishery managers will continue to witness consequences to non-target species which they are unable to predict and which results in the overall degradation of the system (see Springer et al. 2003).

Bottom trawling has the largest ecological footprint in this study (landings x severity of impact; Fig. 5), and is likely to move deeper in pursuit of fish (Roberts

2002). Bottom longlines cause moderate impacts, but have a rather small overall ecological footprint because of their much more limited use in the PFMC region. Pots and traps and hook and line methods are similarly limited in impact and use in this region. Bottom longlines can damage corals (Gass 2002; Krieger and Wing 2002); longlines, like trawl nets, frequently remove coral trees from the rocks and boulders they grow upon (Krieger and Wing 2002). But bottom trawling is the most ecologically damaging method of fishing (Morgan and Chuenpagdee 2003). The benthic impacts of this mobile fishing gear has been compared to clear-cutting techniques in old growth forests (Watling and Norse 1998).

The groundfish closures on the shelf left the continental slope open to fishing, increasing the chances that fishermen might harm corals. The shelf break is important habitat for deep-sea corals (Leverette and Metaxas 2005) and fishing along the shelf break will likely have a large impact on corals. Research on rockfishes and their habitat relationships is ongoing in this region (Yoklavich et al. 2000; Nasby-Lucas et al. 2002), but there has been little research conducted on the associations of rockfishes and corals. The Northeast Pacific has far more species of rockfishes than elsewhere (e.g., 96 species *vs.* 4 species in the North Atlantic), making it likely that at least some of these species are habitat specialists. Knowledge of habitat relationships of rockfish is increasing, but we may never understand the degree to which habitat degradation has occurred, or its impact on depleted populations. More research on these types of relationships for the various rockfish species is needed. Likewise better documentation by submersibles and ROVs is needed in areas of high rockfish catch.

Management implications

Ecosystem-based management (EBM) is our best hope for maintaining all interacting components of an ecosystem (Dayton et al. 1995; Pitcher and Pauly 1998). Conventional management goals targeting maximum sustainable yield are ill-equipped to account for deep-sea corals, as well as other seafloor habitats, in the absence of a directed fishery. Provisions for EFH and marine protected areas (MPAs) are important steps in the process of moving towards EBM, but are not sufficient. Ecosystem-based management will progress only by acknowledging differential impacts of fishing gears and by restricting certain gears to protect not just target species, but their habitats and associated species as well (i.e., deep-sea corals, other invertebrates and non-target fish species).

There is urgent need for appropriate policy responses to minimize fishing gear impacts on seafloor habitats. The severity ranking of the ten commonly used gears in the US provides a basis for formulating fisheries policies aimed at protecting corals (Chuenpagdee et al. 2003; Morgan and Chuenpagdee 2003). Fishery policies should encourage a shift from gears with higher impacts to gears with lower impacts for Pacific groundfish among the four gear types used by the groundfish fleet (Scholz 2003; Scholz et al. 2003; see Fig. 5). A good example of this "shifting gears" is the California spot prawn (*Pandalus platyceros*) fishery, where rockfish bycatch is

being greatly reduced by shifting from bottom trawls to traps (Reilly and Geibel 2002). Reduced use of bottom trawls not only benefits overfished rockfish stocks, but also lessens damage to benthic habitat on which spot prawns, rockfishes and deep-sea coral species rely. Prawns caught in traps also have a higher market value because they are less damaged by fishing gear. Clearly, shifting gears pays off in the long run, as fishers can maintain high economic returns, without long-term damage to groundfish habitats. However this gear shift is initially an expensive proposition for fishermen, and incentives are one way to encourage fishers to voluntarily shift gears that is worth exploring.

Throughout the USA, fishery management councils are required to address the impacts of fishing through the National Environmental Protection Act (NEPA) by developing Environmental Impact Reports (EIR) to address the multiple impacts of fishing. Furthermore the US Magnuson-Stevens Fishery Conservation and Management Act, as reauthorized and amended in 1996 by the Sustainable Fisheries Act, mandates more attention to habitat protection, including designation of EFH and consideration of actions to conserve such habitat (Section 110). A number of actions have been taken in the USA to address habitat impacts of fishing. For example, measures to reduce habitat damage include banning of bottom trawls throughout the 1.5 million square miles of the Western Pacific Fishery Management Council (Code of Federal Regulations 2002) and closed areas for the groundfish fishery on Georges Bank in New England (Collie et al. 1997). Moreover, areas closed to trawls to reduce bycatch, such as closures aimed at reducing bycatch of red king crabs (*Paralithodes camtschaticus*) in federal waters off Alaska, might also have substantial benefits for other benthic species.

Proactive closures, such as MPAs aimed at the most destructive gears in the most sensitive habitats offers a robust means to protect both habitat and fishermen without the need for draconian measures such as the massive closures from Canada to Mexico as implemented in 2002 by the PFMC. Effective implementation of MPAs depends largely on the acceptance of user groups and others affected by it. Thus a fair, transparent and inclusive process in the design can facilitate implementation and can be achieved by incorporating the differences in the ways fishing gears impact marine ecosystems. The most destructive gears should be managed using appropriately stringent policies, for example, complete prohibition of use in ecologically sensitive areas, such as concentrations of deep-sea corals. One useful management measure is banning the use of roller and rockhopper gear on bottom trawls that allow fishing in these coral habitats. This is the approach taken in the Ocean Habitat Protection Act (HR 1690) legislation introduced in the 108th U.S. Congress.

At the same time fishery management councils can provide incentives through additional catch allocations to fishermen using less destructive gears and technologies. In the Pacific Fishery Management Council's groundfish fishery, a matrix of habitat sensitivity and gear impact is one way forward in addressing catch allocation among the four groundfish gear types. The severity ranking of fishing gears suggests the need for policies that encourage shifting from high-impact gears

to low-impact gears. Regardless of the gear, where impacts occur to threatened or endangered species or sensitive habitats, their management should be considered high priority. In cases where habitat impacts cannot be addressed by alternative fishing gears and practices, implementing closed areas will protect healthy ocean ecosystems and species (Collie et al. 1997; NRC 2002).

Of course, scientific research is essential to intelligent fishery management. We recommend more mapping research on deep-sea coral distribution and abundance and determining the degree to which coral aggregations provide EFH for groundfish in the PFMC region and beyond. Managers must also move to a more holistic appreciation of the impacts of fishing, looking not only at impacts to target species such as rockfish, but the collateral impacts to the ecosystems that support them.

Acknowledgments

References

Andrews AH, Cordes E, Mahoney MM, Munk K, Coale KH, Cailliet GM, Heifetz J (2002) Age and growth and radiometric age validation of a deep-sea, habitat-forming gorgonian (*Primnoa resedaeformis*) from the Gulf of Alaska. Hydrobiologia 471: 101-110

Auster PJ, Langton RW (1999) The effects of fishing on fish habitat. In: Benaka LR (ed) Fish Habitat: Essential Fish Habitat and Rehabilitation. Amer Fish Soc Symp 20: 150-187

Barnette MC (2001) Review of fishing gear utilized within the Southeast Region and their potential impacts on essential fish habitat. NMFS-SEFSC-449. US Dept Commerce, NOAA, St. Petersburg

Breeze H, Davis DS, Butler M (1997) Distribution and status of deep sea corals off Nova Scotia. Marine Issues Comm Spec Publ 1, Ecology Action Center, Halifax

Carr MH (1991) Habitat selection and recruitment of an assemblage of temperate marine reef fishes. J Exp Mar Biol Ecol 146: 113-137

Chuenpagdee R, Knetsch JL, Brown TC (2001a) Coastal management using public judgments, importance scales, and predetermined schedule. Coast Manage 29: 253-270

Chuenpagdee R, Knetsch JL, Brown TC (2001b) Environmental damage schedule: community judgments of importance and assessments of losses. Land Econ 77: 1-11

Chuenpagdee R, Morgan LE, Maxwell S, Norse EA, Pauly D (2003) Shifting gears: addressing the collateral impacts of fishing methods in US waters. Front Ecol Environ 9: 517-524

Cimberg RL, Gerrodette T, Muzik K (1981) Habitat requirements and expected distribution of Alaskan coral. Final Rep Res Unit 601, VTN Oregon, Inc, Rep Off Marine Poll Assess, Alaska Off, US Dept Commerce, NOAA, OCSEAP Final Rep 54: 207-308

Code of Federal Regulations (2002) Fisheries off West Coast States and in the Western Pacific: gear restrictions. Code Fed Regul 50: 461-556

Collie JS, Escanero GA, Valentine PC (1997) Effects of bottom fishing on the benthic megafauna of Georges Bank. Mar Ecol Progr Ser 35: 159-172

Dall WA (1884) On some Hydrocorallinae from Alaska and California. Proc Biol Soc Washington 2: 111-115

Dayton PK, Thrush SF, Agardy MT, Hofman RJ (1995) Environmental effects of marine fishing. Aquat Conserv 5: 205-232

Dayton PK, Thrush SF, Coleman FC (2002) Ecological effects of fishing in marine ecosystems of the United States. Arlington, VA, Pew Oceans Comm

DeVogelaere AP, Burton EJ, Trejo T, King CE, Clague DA, Tamburri MN, Caillet GM, Kochevar RE, Douros WJ (2005) Deep-sea corals and resource protection at the Davidson Seamount, California, U.S.A. In: Freiwald A, Roberts JM (eds) Cold-water Corals and Ecosystems. Springer, Berlin Heidelberg, pp 1189-1198

Duncan C (2001) Offshore marine conservation, 'Darwin Mounds' and beyond. Mar Conserv 5: 14-15

Druffel ERM, Griffin S, Witter A, Nelson E, Southon J, Kashgarian M, Vogel J (1995) *Gerardia*: Bristlecone pine of the deep-sea? Geochim Cosmochim Acta 59: 5031-5036

Etnoyer P, Morgan LE (2003) Occurrences of habitat-forming, deep-sea corals in the Northeast Pacific. Final Rept NOAA Off Protected Resour

Fosså JH, Mortensen PB, Furevik DM (2002) The deep-water coral *Lophelia pertusa* in Norwegian waters: distribution and fishery impacts. Hydrobiologia 471: 1-12

Freese JL (2003) Trawl-induced damage to sponges observed from a research submersible. Mar Fish Rev 63: 7-13

Gass SE (2002) An assessment of the distribution and status of deep sea corals in Atlantic Canada by using both scientific and local forms of knowledge. MSc thesis, Dalhousie Univ, Halifax, Nova Scotia

George RY (2002) Ben Franklin temperate reef and deep-sea 'Agassiz Coral Hills' in the Blake Plateau off North Carolina. Hydrobiologia 471: 70-81

Hall-Spencer J, Allain V, Fosså JH (2002) Trawling damage to Northeast Atlantic ancient coral reefs. Proc R Soc London B 269: 507-511

Heifetz J (2002) Coral in Alaska: distribution, abundance, and species associations. Hydrobiologia 471: 19-28

Husebø A, Nøttestad L, Fosså JH, Furevik DM, Jørgensen SB (2002) Distribution and abundance of fish in deep-sea coral habitats. Hydrobiologia 471: 91-99

Koslow JA, Boehlert GW, Gordon JDM, Haedrich RL, Lorance P, Parin N (2000) Continental slope and deep-sea fisheries: implications for a fragile ecosystem. ICES J Mar Sci 57: 548-577

Koslow JA, Gowlet-Holmes K, Lowry JK, O'Hara T, Poore GCB, Williams A (2001) Seamount benthic macro-fauna off southern Tasmania: community structure and impacts of trawling. Mar Ecol Progr Ser 213: 111-125

Krieger KJ (1993) Distribution and abundance of rockfish determined from a submersible and by bottom trawling. Fish Bull 91: 87-96

Krieger KJ, Wing BL (2002) Megafauna associations with deepwater corals (*Primnoa* spp.) in the Gulf of Alaska. Hydrobiologia 471: 82-90

Leverette T, Metaxas A (2005) Predicting habitat for two species of deep-water coral on the Canadian Atlantic continental shelf and slope. In: Freiwald A, Roberts JM (eds) Cold-water Corals and Ecosystems. Springer, Berlin Heidelberg, pp 467-479

Love MS, Carr MH, Haldorson LJ (1991) The ecology of substrate-associated juveniles of the genus *Sebastes*. Environ Biol Fish 30: 225-243

Morgan LE, Chuenpagdee R (2003) Shifting gears: addressing the collateral impacts of fishing methods in US waters. Pew Science Ser, Washington DC

Nasby-Lucas NM, Embley BW, Hixon MA, Merle SG, Tissot BN, Wright DJ (2002) Integration of submersible transect data and high-resolution multibeam sonar imagery for a habitat-based groundfish assessment of Heceta Bank, Oregon. Fish Bull 100: 739-751

National Research Council (NRC) (2002) Effects of Trawling and Dredging on Seafloor Habitat. National Academy Press, Washington DC

O'Connell VM, Carlilse CW (1993) Habitat-specific density of adult yelloweye rockfish *Sebastes ruberrimus* in the eastern Gulf of Alaska. Fish Bull 91: 304-309

Pacific Marine Conservation Council (1999) Rockfish Report: The Status of West Coast Rockfish. http://www.pmcc.org/rockfishreport.html, Astoria, Oregon

Pauly D (1995) Anecdotes and the shifting baseline syndrome of fisheries. Trends Ecol Evol 10: pp 430

Pauly D, Christensen V, Dalsgaard J, Froese R, Torres F (2002) Towards sustainability in world fisheries. Nature 418: 689-695

Pearcy WG, Stein DL, Hixon MA, Pikitch EK, Barss WH, Starr RM (1989) Submersible observations of deep-reef fishes of Heceta Bank, Oregon. Fish Bull 87: 955-965

Pew Oceans Commission (2003) America's living oceans: charting a course for sea change. A report to the nation - recommendations for a new ocean policy. Pew Oceans Comm, Washington DC

Pitcher TJ, Pauly D (1998) Rebuilding ecosystems, not sustainability, as the proper goal of fisheries management. In: Pitcher TJ, Hart PJB, Pauly D (eds) Reinventing Fisheries Management. Chapman and Hall, London, pp 311-329

Ralston S (1998) The status of federally managed rockfish on the U.S. West Coast. In: Yoklavich M (ed) Marine harvest refugia for West Coast rockfish: a workshop. NOAA Tech Memo, NMFS-SWFSC-255

Reed J (2002) Deep-water *Oculina* coral reefs of Florida: biology, impacts, and management. Hydrobiologia 471: 43-55

Reed J, Shephard AN, Koenig CC, Scanlon KM, Gilmore RG (2005) Mapping, habitat characterization, and fish surveys of the deep-water *Oculina* coral reef Marine Protected Area: a review of historical and current research. In: Freiwald A, Roberts JM (eds) Cold-water Corals and Ecosystems. Springer, Berlin Heidelberg, pp 443-465

Reilly PN, Geibel J (2002) Results of California Department of Fish and Game Spot Prawn Trawl and Trap Fisheries Bycatch Observer Program, 2000-2001. California Dept Fish Game, Belmont

Risk MJ, Heikoop JM, Snow MG, Beukens R (2002) Lifespans and growth patterns of two deep-sea corals: *Primnoa resedaeformis* and *Desmophyllum cristagalli*. Hydrobiologia 471: 125-131

Roark EB, Guilderson T, Flood-Page S, Dunbar RB, Ingram BL (2003) Radiocarbon based age and growth rates estimates on deep-sea corals from the Pacific. Erlanger Geol Abh Sonderbd 4: 71

Roberts CM (2002) Deep impact: the rising toll of fishing in the deep-sea. Trends Ecol Evol 17: 242-245

Rogers AD (1999) The biology of *Lophelia pertusa* and other deep-water reef forming corals and impacts from human activities. Int Rev Hydrobiol 84: 315-406

Scholz AJ (2003) Groundfish fleet restructuring information and analysis project: Final Report. March 23, 2003. Pacific Marine Conserv Counc/Ecotrust. http://www.ecotrust.org/gfr

Scholz AJ, Mertens M, Sohm D, Steinback C, Bellman M (2003) Place matters: spatial tools for assessing the socioeconomic implications of marine management measures on the Pacific Coast of the United States. In: Barnes PW, Thomas J (eds) Benthic habitats and the effects of fishing. Amer Fish Soc, Symp 2002, Bethesda

Springer AM, Estes JA, van Vliet GB, Williams TM, Doak DF, Danner EM, Forney KA, Pfister B (2003) Sequential megafaunal collapse in the North Pacific Ocean: an ongoing legacy of industrial whaling? Proc Nat Acad Sci 100: 12223-12228

Thrush SF, Dayton PK (2002) Disturbance to marine benthic habitats by trawling and dredging: implications for marine biodiversity. Ann Rev Ecol Syst 33: 449-73

Thrush SF, Hewitt JE, Funnell GA, Cummings VJ, Ellis J, Schultz D, Talley D, Norkko A (2001) Fishing disturbance and marine biodiversity: the role of habitat structure in simple soft-sediment systems. Mar Ecol Progr Ser 223: 277-286

Watling L, Norse EA (1998) Disturbance of the seabed by mobile fishing gear: a comparison with forest clear-cutting. Conserv Biol 12: 1189-1197

Witherell D, Coon C (2000) Protecting gorgonian corals off Alaska from fishing impacts. Report to NPFMC. In: Willison JHM, Hall J, Gass SE, Kenchington ELR, Butler M, Doherty P (eds) Proceedings of the First International Symposium on Deep-Sea Corals. Ecology Action Centre, Nova Scotia Museum, Halifax, pp 117-125

Yoklavich MM, Greene HG, Caillet GM, Sullivan DE, Lee RN, Love MS (2000) Habitat associations of deep-water rockfishes in a submarine canyon: an example of a natural refuge. Fish Bull 98: 625-641

Deep-sea corals and resource protection at the Davidson Seamount, California, U.S.A.

Andrew P. DeVogelaere[1], Erica J. Burton[1], Tonatiuh Trejo[2], Chad E. King[3], David A. Clague[4], Mario N. Tamburri[5], Gregor M. Cailliet[2], Randall E. Kochevar[6], William J. Douros[1]

[1] Monterey Bay National Marine Sanctuary, 299 Foam Street, Monterey, CA 93940, USA
 (andrew.devogelaere@noaa.gov)
[2] Moss Landing Marine Laboratories, 8272 Moss Landing Road, Moss Landing, CA 95039, USA
[3] Sanctuary Integrated Monitoring Network, Monterey Bay National Marine Sanctuary, 299 Foam Street, Monterey, CA 93940, USA
[4] Monterey Bay Aquarium Research Institute, 7700 Sandholdt Road, Moss Landing, CA 95039, USA
[5] Chesapeake Biological Laboratory, University of Maryland, P.O. Box 38, Solomons, MD 20688, USA
[6] Monterey Bay Aquarium, 886 Cannery Row, Monterey, CA 93940, USA

Abstract. The Davidson Seamount is located 120 km to the southwest of Monterey, along the California coast, USA. It is 2,400 m tall; yet, it is still 1,250 m below the sea surface. In May 2002, 90 hours of digital video was recorded from all depths of the Davidson Seamount, using a remotely operated vehicle, and deep-sea coral specimens were collected. Preliminary analyses indicate that 20 coral taxa were found, and they were almost exclusively located in high relief, ridge areas. Other species were noted on or adjacent to the corals. Because of its pristine nature, as well as human threats and great potential for education, the Davidson Seamount is under consideration for protection as part of the Monterey Bay National Marine Sanctuary.

Keywords: Davidson Seamount, resource protection, coral distribution, habitat, education, *Paragorgia*

Introduction

With recent advances in technology, the description of deep-sea coral communities is a growing subject (Genin et al. 1986; Malakoff 2003). In addition, a sense of urgency has developed for this work because of human impacts to these corals [e.g., from deep sea fisheries (Koslow et al. 2000; Roberts and Hirshfield 2003)] and their

slow recovery rates (Andrews et al. 2002). Moreover, these corals may provide essential fish habitat and a structural base for some deep-sea species assemblages (e.g., Husebø et al. 2002). Seamounts are one important habitat for deep-sea corals, and they also have a high degree of endemism of all species associated with them (de Forges et al. 2000). The taxonomy of deep-sea corals is challenging, as there are still relatively few scientific collections or high quality, *in situ* images of the corals. The body of literature on deep-sea coral ecology is growing, and the natural cause of some distribution patterns has been related to substratum type and currents (e.g., Genin et al. 1986). Our interest was in the deep-sea corals of the Davidson Seamount, including the assessment of: the distribution and abundance of species, a description of their associated fauna, and the need for resource protection. A related project, not addressed here, was to involve the public, through a range of outreach techniques and education materials, in a multidisciplinary exploration of the Davidson Seamount (NOAA 2002; DeVogelaere et al. in press).

Methods

Study site

Davidson Seamount is located 120 km to the southwest of Monterey and is one of the largest known seamounts along the Western United States (Fig. 1). It is 42 km long and 13.5 km wide. From base to crest, Davidson Seamount is 2,400 m tall; yet, it is still 1,250 m below the sea surface. Davidson Seamount has an atypical seamount shape, having northeast-trending ridges created by a type of volcanism only recently described (Davis et al. 2002); it last erupted about 12 million years ago. Davidson Seamount was first surveyed in 1933 by the United States Coast and Geodectic Survey (a forerunner of the National Ocean Service of the National Oceanic and Atmospheric Administration). This large geographic feature was the first to be characterized as a "seamount" in 1938 by the United States Board on Geographic Names, and was named in honor of the United States Coast and Geodectic Survey scientist George Davidson (1825-1911), a leader in charting the waters of the west coast (Davidson Seamount 1990).

Transects and collections

It is only with recent technological advances that we can effectively access the Davidson Seamount. The Monterey Bay Aquarium Research Institute (MBARI) has developed innovative remotely operated vehicle (ROV) technology to record images and collect organisms from the deep sea. In May 2002, we used the unmanned ROV, *Tiburon*, a state-of-the-art platform for exploring the deep sea to depths of 4,000 meters. The vehicle is equipped with cameras, lights, manipulator arms, accurate positioning systems, and *in situ* pressure, temperature, dissolved oxygen, and conductivity sensors. ROV dives were selected to include all depths and habitats (base, flank, and crest) of the seamount with the available ship time. Six full-day dives were completed: two dives were conducted from base to crest on either side of the seamount (to include all depths and representative habitats); and four dives

were conducted at the seamount crest, along ridges, or at deeper cones (to focus on the most diverse and interesting habitats relative to corals). To document habitat
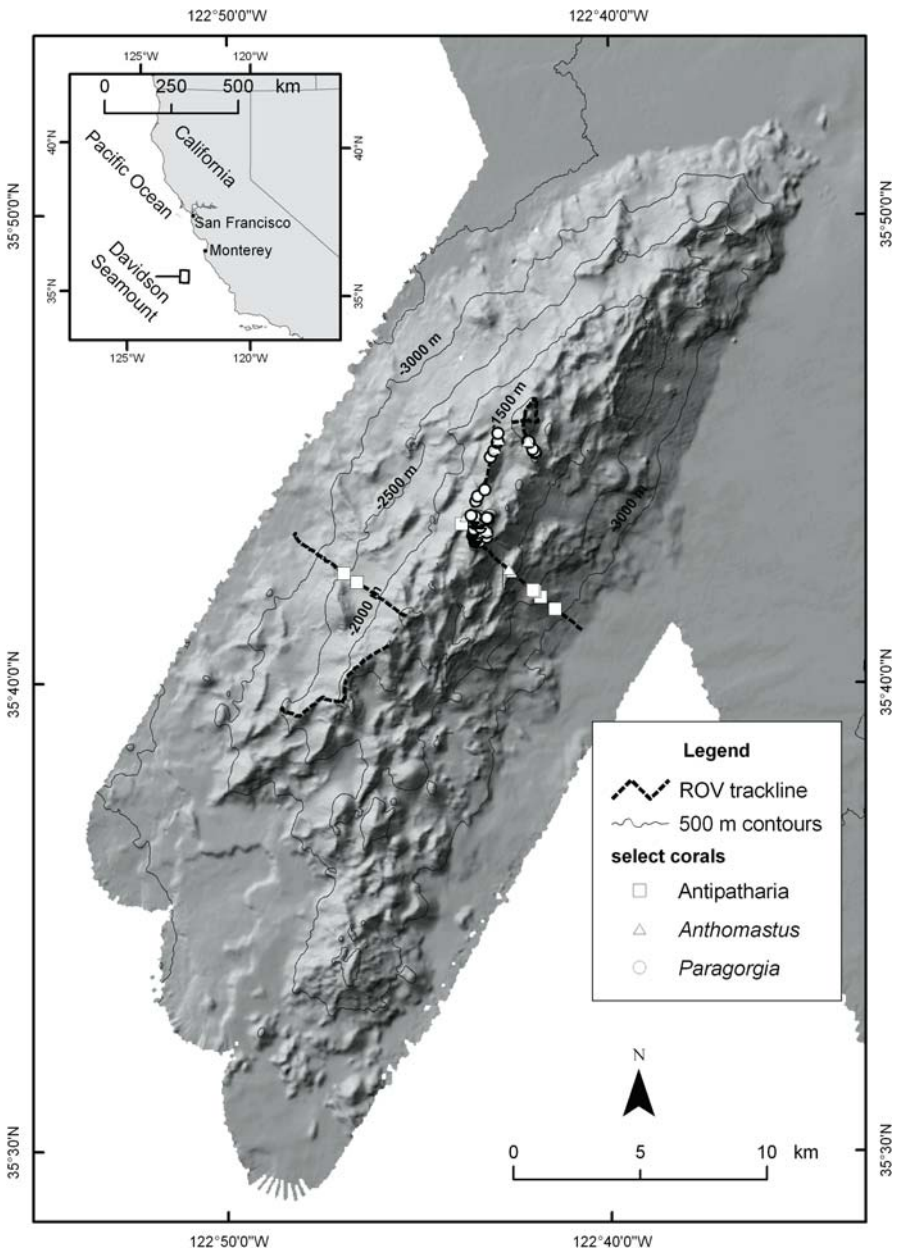
Fig. 1 Observed distribution of three corals during May 2002 Davidson Seamount Exploration using ROV *Tiburon*. Bathymetric data derived from Monterey Bay Multibeam Survey (MBARI 2000)

and species occurrence at the Davidson Seamount, 90 hours of digital video was continuously recorded from all seamount depths (Fig. 1), supplemented by high-quality digital still images during periods of intense observation. Moreover, during each ROV dive, video frame grabs were recorded and annotated on-board using MBARI's computer video annotation program. Following the cruise, preliminary frame grab annotations were refined and edited at MBARI's Video Lab. Animals captured on the videotapes were identified as accurately as possible, although it was often the case that species names were not known. In some cases, images (and tissue samples, if collected) of the unknown animals were provided to taxonomic experts to determine whether the animals could be identified or described. Cup coral (Scleractinia) were observed, but not counted in this analysis.

Analyses

All corals were classified into taxa and given a descriptive name. The frequency of each taxon, excluding cup corals, was estimated by reviewing 2,507 digital frame grabs taken throughout the cruise, selecting those which were annotated as having coral species present, and subtracting frame grabs with multiple images of the same individual. This estimate of coral frequency using frame grabs is an underestimate, because not all corals seen throughout the dive transects received a frame grab, especially if they were small and very numerous in one location. Moreover, there were many individuals of some coral taxa in a single frame grab. The depth at which each frame grab was taken was used to develop an observed depth range for each taxon. Finally, to determine species associations with corals, each frame grab was analyzed for the presence of species either on or adjacent to the corals.

Topographic Position Index (TPI) was used to characterize ROV transects and the entire Davidson Seamount "landscape" into categories of ridges, valleys, and slopes. TPI is a quantification of how deep a given location is, relative to its surrounding area. The TPI algorithm used in this study was adapted from Weiss (2002). Multibeam sonar data were used in the TPI analyses (MBARI 2000; 40 x 40 m resolution). TPI was calculated by subtracting the mean depth of an area of 25 x 25 cells (1 km^2) from the depth of the cell in the center of that area. This process was automated for all 280,613 cells of bathymetric data surrounding the Davidson Seamount. This neighborhood size was chosen arbitrarily as optimal for resolution of valleys and ridges. There is no quantitative guide for neighborhood size selection; a larger neighborhood will not reveal ridges and valleys on the seamount, while a smaller neighborhood tends to mask overall morphological features of the seamount. Resulting negative values represent areas below the average depth of the surrounding areas (valleys), while positive values represent areas above (ridges). Flat plains and slopes are values around zero. In our graphic representation of the seamount "landscape" (Fig. 2), we classified a TPI range to three topographic layers, based on the Jenks optimization method (Minami 2000) to represent valleys (-130 to -29), slopes and flat areas (-30 to 49), and ridges (50 to 196). TPI analyses were performed with GIS software (ArcMap 8.1 and Spatial Analyst, copyright Environmental Systems Research Institute). Position data from ROV transects and

from each coral sighting were assigned a geospatially corresponding TPI value and mapped (Figure 2).
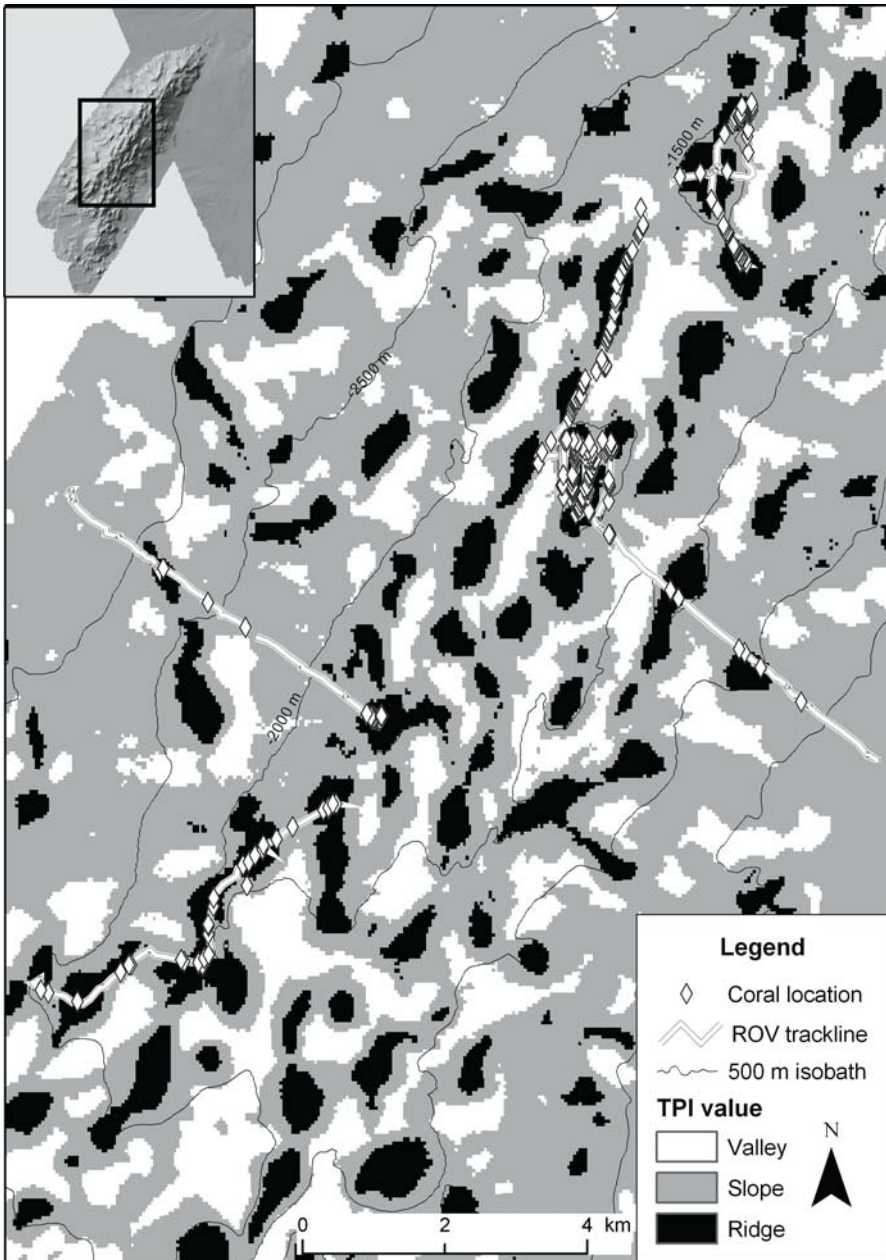
Fig. 2 Topographic Position Index (TPI) characterizing ROV transects and coral distribution at the Davidson Seamount

Results

A total of 20 deep-sea coral taxa were seen during 90 hrs of diving on the Davidson Seamount (Table 1; Fig. 3). During the 6 dives, the ROV traversed a bottom distance of 43,537 linear meters. Of the total distance traveled, 56 % of the distance was traversed on ridges, 41 % on slope and flat areas, and 3 % in valleys. While many of the corals have yet to be conclusively identified, we have specimen collections of 12 taxa and high-resolution images of all of them. The depth range of the corals was from 2,846 m to the top of the seamount at 1,248 m. Frequently observed *Paragorgia* sp. were the most dramatic coral in their size (>2 x 2 meters in height and width) and their extensive "forests" along several ridges at the top of the

Table 1 Corals of the Davidson Seamount, with frequency of framegrabs with taxa present (F), depth range observed, and topographic position index (TPI). The cup coral was not analyzed (NA) because it was not originally identified as a coral

Order / Genus	Descriptive Name	F	Depth (m)	Mean TPI (± SE)
*Unknown	White Coral 1	89	1296-1935	99 ± 33
*Alcyonacea / *Paragorgia*	Bubblegum Coral	79	1248-1743	94 ± 6
*Alcyonacea / *Corallium* [a]	Small Pink Coral 1	58	1357-2447	89 ± 7
*Unknown	Orange Bottlebrush Coral	35	1345-2254	74 ± 9
*Alcyonacea / *Keratoisis* [b]	Bamboo Coral	28	1374-1707	66 ± 6
Alcyonacea / *Anthomastus*	Mushroom Soft Coral	23	1307-1927	77 ± 12
*Unknown	Gold Coral	21	1374-2073	71 ± 7
Unknown	White Coral 2	14	1496-1690	44 ± 15
Unknown	Small Yellow Coral	11	1325-1840	100 ± 13
Unknown	Orange Bottle-bushy Coral	8	1880-2056	105 ± 21
*Unknown	Orange Bushy Coral	7	1953-2320	83 ± 14
*Antipatharia / unknown	Black Coral	7	1336-2846	38 ± 16
*Unknown	Big White Coral	6	1374-1904	38 ± 23
*Unknown	Small Red Coral	2	1346-1352	84 ± 10
Unknown	Small Pink Coral 2	2	1493-1524	79 ± 4
Unknown	Carpet Coral	2	1511-1779	126 ± 2
Unknown	Leaning Tower of Coral	2	1950-1973	88 ± 13
Unknown	White Coral 3	1	2710	78 ± 0
*Unknown	Glassy Coral	1	2486	61 ± 0
*Scleractinia / unknown	Cup Coral	NA	NA	NA

* Specimen collected
[a] One collection identified as *Corallium*
[b] One collection identified as *Keratoisis*

Fig. 3 Several coral taxa observed at the Davidson Seamount. **A** White coral 1. **B** Bubblegum coral (*Paragorgia* sp.). **C** Mushroom soft coral (*Anthomastus* sp.). **D** Small pink coral 1 (*Corallium* sp.). **E** Gold coral. **F** Black coral (Antipatharian). **G** Bamboo coral (*Keratoisis* sp.). Scale bar = 15 cm
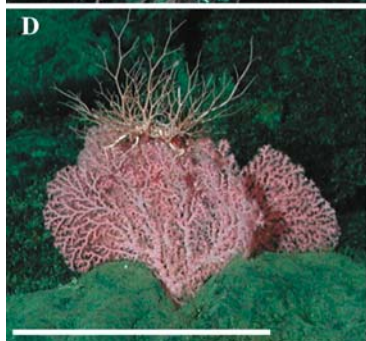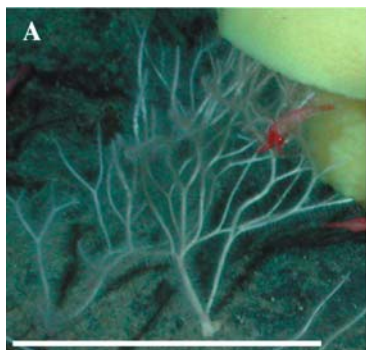
seamount, but other species were also abundant. While regular observations of trash (bottles, cans, fabric, paper, etc.) were made on the seamount, the area appeared pristine as there was no damage to large fragile corals and no indication of direct human disturbance from trawling or other collecting.

A clear pattern in the distribution of the corals was that they were almost exclusively on ridge areas (Table 1; Fig. 2). Some genera were found exclusively on ridges at the top of the seamount (e.g., *Paragorgia*), while others (e.g., *Anthomastus*) were found on shallow and deeper water ridges developed from promontories along the sides of the seamount (Fig. 1). Black coral, order Antipatharia, had one of the lowest TPI values, but its positive value still indicates association to areas with topographic relief.

With the exception of *Anthomastus*, all of the deep-sea corals had other obvious megafauna associated with them. Living on the corals were polychaete worms, isopods, shrimps, crabs, basket stars, crinoids, brittle stars, and anemones. Present adjacent to corals were rattails (*Coryphaenoides* sp.), thornyheads (*Sebastolobus* sp.), sponges, other corals, seastars, clams, sea cucumbers, and octopi (*Graneledone* sp.). Invariably, as the ROV transects reached the highest crests of the seamount, diversity of corals and associated species increased dramatically. The organisms were often visibly oriented to maximize surface area towards the current.

Discussion

The Davidson Seamount is populated by a diversity of deep-sea corals, most of which have other species associated with them. *Paragorgia* sp. was abundant, forming dense and expansive patches. An unidentified blue polychaete (scale worm) was present in large numbers on almost all of the *Paragorgia* sp. corals. Similar associations were observed on seamounts in the Gulf of Alaska (pers. comm. Amy Baco, Woods Hole Oceanographic Institute). While most of the corals were found at the highest peak areas of the seamount, others were found deeper, and still, almost exclusively on ridge formations. The cause of this pattern is possibly higher current velocities and less sediment deposition, enhancing food availability and minimizing the smothering of new recruits (e.g., Genin et al. 1986).

The Davidson Seamount is a relatively pristine area with coral abundance and diversity. However, many of the species are large and fragile to physical disturbance, and some individuals may be hundreds of years old (Andrews et al. 2005). Trawling has been achieved at depths as deep as the Davidson Seamount (Koslow et al. 2000; Koslow et al. 2001), and there is potential for bioprospecting for medicinal chemistry of these corals. The high degree of endemism on seamounts argues for regional protection of this type of habitat. For these reasons, and the great potential for public education on seamounts and deep-sea corals, the Monterey Bay National Marine Sanctuary (MBNMS) is formally assessing the option of providing National Marine Sanctuary status to the Davidson Seamount. In August 2003, the MBNMS Sanctuary Advisory Council unanimously voted to agree with a working group initial finding that the Davidson Seamount meets Sanctuary designation standards. This opinion was developed by scientists, educators, marine policy experts,

marine resource managers, conservation interests, and fishermen; however, fishing organizations currently oppose designation because it may lead to future regulations on fishing. Sanctuary designation documents are currently being drafted and will include proposed: limited collection deeper than 915 m (currently all commercial fishing occurs at depths shallower than 50 m in this area); increased physical and biological characterization of the area; development of a monitoring program for the seamount; resource protection and regulation plans; and development of education materials at local and national levels. Currently, there are no government education programs broadly focusing on seamount biology and conservation in the United States. A draft management plan for the Davidson Seamount, and the entire MBNMS, will be available for public comment in mid 2005, with a final decision expected in 2006 (NOAA 2002).

Acknowledgements

References

Andrews AH, Cordes EE, Mahoney MM, Munk K, Coale KH,Cailliet GM, Heifetz J (2002) Age, growth and radiometric age validation of a deep-sea, habitat-forming gorgonian (*Primnoa resedaeformis*) from the Gulf of Alaska. Hydrobiologia 471: 101-110

Andrews AH, Cailliet GM, Kerr LA, Coale KH, Lundstrom C, DeVogelaere A (2005) Investigations of age and growth for three deep-sea corals from the Davidson Seamount off central California. In: Freiwald A, Roberts JM (eds) Cold-water Corals and Ecosystems. Springer, Berlin Heidelberg, pp 1021-1038

Davidson Seamount (1990) United States Board on General Names Centennial: 1890-1990 A Century of Service [bathymetric map]. Washington, DC. US Dept Commerce, NOAA, Natl Ocean Serv

Davis AS, Clague DA, Bohrson WA, Dalrymple GB, Greene, HG (2002) Seamounts at the continental margin of California: a different kind of oceanic intraplate volcanism. Geol Soc Amer Bull 114: 316-333

De Forges BR, Koslow JA, Poore GC (2000) Diversity and endemism of the benthic seamount fauna in the southwest Pacific. Nature 944-947

DeVogelaere AP, Kochevar R, Tamburri M, Cailliet G, Burton, EJ, Benson S, Douros WJ (in press) Exploring the Davidson Seamount: combining science, public outreach, and resource management. In: Magoon OT, Converse H, Baird B, Miller-Henderson M (eds) California and the World Ocean 2003. Santa Barbara, CA

Genin, A, Dayton PK, Lonsdale PF, Spiess FN (1986) Corals on seamount peaks provide evidence of current acceleration over deep-sea topography. Nature 322: 59-61

Husebø A, Nøttestad L, Fosså JH, Furevik DM, Jørgensen SB (2002) Distribution and abundance of fish in deep-sea coral habitats. Hydrobiologia 471: 101-110

Koslow JA, Boehlert GW, Gordon JDM, Haedrich RL, Lorance P, Parin N (2000) Continental slope and deep-sea fisheries: implications for a fragile ecosystem. ICES J Mar Sci 57: 548-557

Koslow JA, Gowlett-Holmes K, Lowry JK, O'Hara T, Poore GCB, Williams A (2001) Seamount benthic macrofauna off southern Tasmania: community structure and impacts of trawling. Mar Ecol Progr Ser 213: 111-125

Malakoff D (2003) Cool corals become hot topic. Science 299: 195

Minami, M (2000) Using ArcMap. Environ Syst Res Inst, Inc, Redlands, CA, p 146

Monterey Bay Aquarium Research Instititute (2000) Monterey Bay Multibeam Survey. CD-ROM, Digital Data Ser 3

National Oceanic and Atmospheric Administration (2002) NOAA Explorer web site: http://oceanexplorer.noaa.gov/explorations/02davidson/davidson.html

Roberts S, Hirshfield M (2003) Deep sea corals: out of sight, but no longer out of mind. Oceana Rep, Washington DC, 16 pp

Weiss A (2002) Topographic position and landforms analysis. ESRI User Conf, San Diego, CA

Conserving corals in Atlantic Canada: a historical perspective

Mark Butler

Ecology Action Centre, 1568 Argyle Street, Halifax, Nova Scotia, B3J 2B3,
  Canada
  (ar427@chebucto.ns.ca)

Abstract. Trawling or dragging was introduced into Atlantic Canadian fisheries in the 1950's and soon became the dominant method of fishing for groundfish in the region. Since its introduction, fishermen warned about its negative impacts on habitat and the productivity of the fishery. In the last decade considerable research has been conducted on the impacts of bottom tending mobile gear on habitat, including major reviews by large scientific agencies. The International Council for the Exploration of the Seas and the U.S. National Research Council both formulated similar conclusions on how to minimize impacts: 1) reduce fishing effort; 2) close areas; and 3) modify and substitute gear. Following the stock collapses and closures of many fisheries in the early 1990's the Canadian government took steps to reduce fishing effort. In recent years, partly in response to growing concern about the impacts of dragging, the government has embarked on a program to identify and establish marine protected areas. However, the Canadian government has taken no steps to implement the third recommendation: gear substitution or modification. Public and scientific interest in deep-water corals has been a major factor in advancing efforts to investigate and conserve benthic habitat in Atlantic Canada, including the establishment of three marine protected areas (MPAs). Alongside effort reduction and MPAs, gear measures should be an equal and concurrent component of efforts to conserve benthic biodiversity and restore fisheries as the conservation benefits extend to all areas where fishing occurs.

Keywords. Conservation, Atlantic Canada, marine protected areas, fisheries management, gear substitution, traditional ecological knowledge

Introduction

The Canadian government, industry, and conservation groups have begun to address the impacts of trawling (or dragging, as it is referred to in the region,) on benthic habitats in Atlantic Canada. Public and scientific interest in deep-water corals has been a major factor in advancing efforts to investigate and conserve benthic habitat in general in Atlantic Canada.

The government, supported to varying degrees by conservation groups and industry, is relying on marine protected areas (MPAs) as the primary tool to conserve corals. This approach generates a number of questions. What human activities, if any, should we allow in these areas? Should we allow fishing in these areas? If so, which fisheries or gear types? Are we going to conserve corals outside of protected areas? If so, how, and how much? What other benthic fauna or features (e.g., maerl) do we want to protect from bottom damaging activities? What about other options to protect habitat such as using more environmentally friendly fishing gear or ocean zoning?

Agardy et al. (2003) observe that "MPAs are often implemented without a firm understanding of the conservation science - both ecological and socio-economic - underlying marine protection". The science of MPAs is being scrutinized and there are calls for more and better studies of the design and benefits of MPAs (Gell and Roberts 2003; Willis et al. 2003). Agardy et al. (2003) encourage a re-examination of targets for MPAs, whether no-take MPAs are the only good MPAs, and the need to employ a range of tools to protect the oceans, including multi-use MPAs and wider seascape level ocean governance.

The 'rediscovery' by scientists of the existence of deep-sea corals in Atlantic Canada began when hook and line fishermen, concerned about the impact that dragging was having on corals, brought their concerns to conservation groups, scientists and the public in the mid-1990's. Breeze et al. (1997) collected all available information, much of it coming from fishermen, on the status and distribution of deep-sea corals off Nova Scotia, with a focus on southern Nova Scotia (Fig. 1). Fishermen reported three areas of high coral concentration along the edge of the Scotian Shelf: 1) the Stone Fence, 2) the Sable Island Gully, and 3) the Northeast Channel. Gass (2002) and Gass and Willison (2005) identified the same three hotspots. There are also reports or records of corals from a number of locations on and along the Scotian Shelf and into the Bay of Fundy, particularly if the soft corals, sea pens, and smaller gorgonians and scleractinians are included (MacIssac et al. 2001; Gass and Willison 2005).

Subsequent scientific exploration of the three areas listed above has confirmed the presence of corals and also tends to confirm fishermen's observations about the condition or status of these corals (MacIssac et al. 2001; Gass 2002). For example, fishermen reported that the Stone Fence had hosted high concentrations of gorgonians and the scleractinian *Lophelia pertusa*, but that beginning in the 1950s dragging badly damaged and removed much of the corals (Breeze et al. 1997). In September 2003 scientists on a research vessel cruise (Hud 2003-059) discovered and documented live *Lophelia* and *Lophelia* rubble (Pål Mortensen pers. comm.).

It is this author's impression that fishermen played a crucial role in locating corals in Atlantic Canada and that information provided by them largely matches the information obtained by scientists through research and cruises (MacIssac et al. 2001; Gass 2002). At the same time it is important to remember the limitations of information from fishermen:
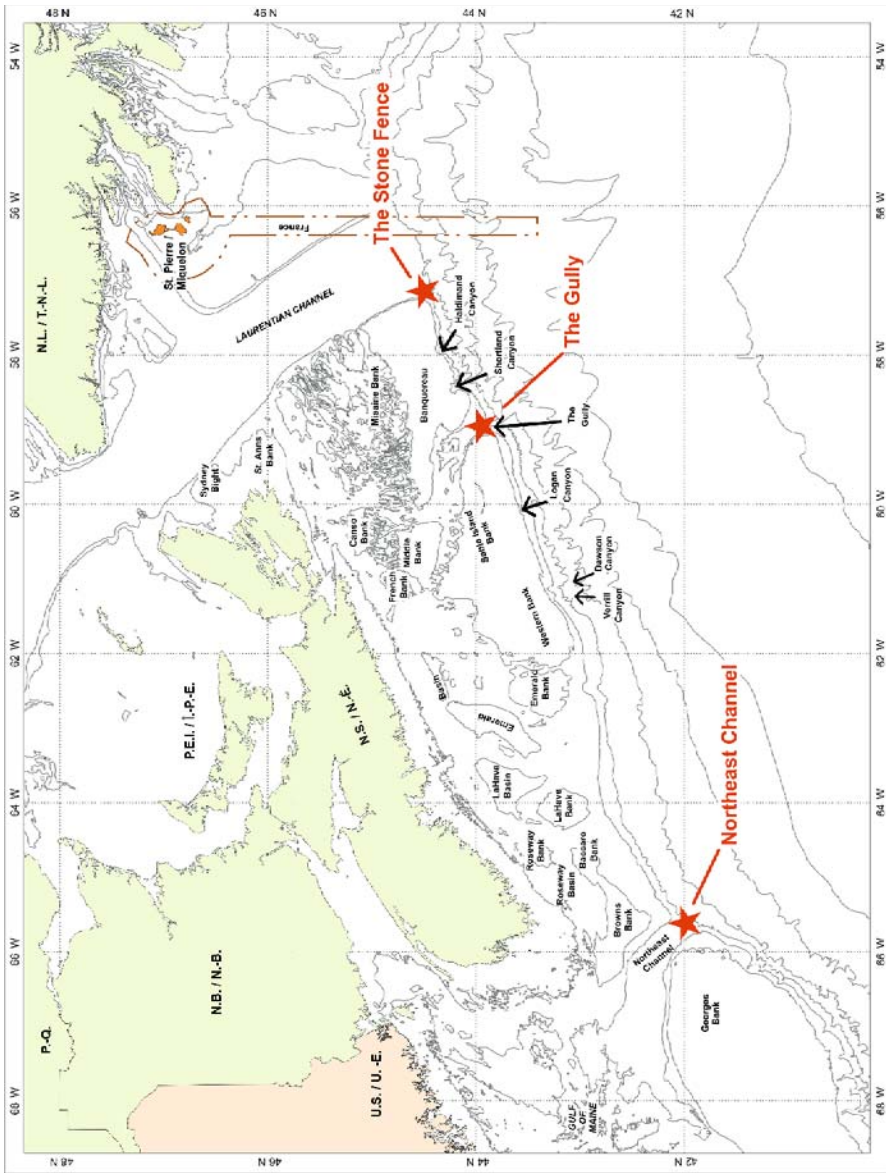
Fig. 1 The three hotspots or areas of confirmed concentration of corals on the Scotian Shelf are the Northeast Channel, the Gully and the Stone Fence. All three areas have protected area status (modified from Fisheries and Oceans Canada)

- It is biased toward where fishing occurs (although if there is a correlation between corals and fish this source of information may be quite comprehensive).
- Depending on the memory and age of fishermen interviewed, it may or not give us a picture of where corals used to occur before the impacts of fishing.
- Most fishing (and research) has occurred in less than 500 metres of water.

Impacts

Fishing, hydrocarbon activities, cable laying, and dumping of munitions are human activities that have an impact on the ocean floor and have occurred or are occurring in areas of known coral distribution (Butler and Gass 2001). Human activities that could have an impact on deep-sea corals, but are not yet occurring in Canadian waters include aggregate and mineral extraction and harvesting of corals for bio-medical or other use. As is reflected across the literature, and for almost every region or nation for which we have information, fishing, specifically trawling or dragging, has had and continues to have the biggest impact on corals (Koslow and Gowlett-Holmes 1998; Krieger 2001; Fosså et al. 2002; Gass and Willison 2005). Fixed gears such as gillnets, traps, and longlines also damage coral, but to a much lesser extent. For a review of the impacts of all gears on corals in Atlantic Canada, see Butler and Gass (2001).

In Atlantic Canada, draggers have been active in areas of known coral concentration since the 1950's (Breeze et al. 1997). Until recently, no institution collected data on interactions between fisheries and corals; all the information came from fishermen (Gass 2002). Canadian fishermen active from the 1950's to 1990's, report nets coming up full of coral (Breeze et al. 1997). Given the nature of otter trawl gear and how it interacts with the ocean floor (Krieger 2001), it is likely that relatively fragile, long-lived, upright organisms such as corals would have been badly damaged and indeed removed in the early days of the fishery. Corals are no longer likely to be found in areas where there has been a sustained dragger fishery; clues to their former presence will have to come only from an analysis of environmental conditions, the memories of fishermen, or collection records.

The Canadian Department of Fisheries and Oceans (DFO) has only recently begun to calculate the area of the ocean floor affected by dragging. Kulka and Pitcher (2001) estimate the spatial extent of the continental shelf in Atlantic Canada affected by dragging for the years 1980-2000 ranges from a low of 8 % to a high of 38 %. These estimates are preliminary and probably underestimate the area affected, at least in part, because the activities of some fleets are not captured in the review.

Three tools for conservation

The impacts of dragging and dredging on a range of benthic habitats, including stable biogenic habitats, are increasingly well documented (Dayton et al. 1995; Auster and Langton 1999; Collie et al. 2000; Thrush and Dayton 2002). Responding

to growing concern about the severe and widespread impact that dragging has on the seafloor, fishery managers at the National Marine Fisheries Service in the United States and their counterparts at the European Commission requested advice from scientists on how to address the impact of trawl and dredge fisheries on the seafloor. The National Research Council and the International Council for the Exploration of the Seas issued reports (ICES 2000; NRC 2001) which contained three major and similar recommendations: 1) fishing effort reduction, 2) closed areas, and 3) gear substitution or modification.

1. Effort reduction

In adopting a 200-mile limit in 1977, the Canadian government also encouraged and supported the expansion of the country's fishing fleet, in particular the construction of new trawlers (Parsons 1993; Blades 1995). Often with the help of financial incentives, individuals and companies bought new and larger vessels. During the 1980's Canadian catches reached record levels. In the early 1990's stocks collapsed and the government closed fisheries completely or severely reduced the quotas. Canada followed up these closures with programs to buy fishing enterprises and reduce capacity.

The Fisheries Resource Conservation Council considers that the buy-back programs did little or nothing to reduce capacity (FRCC 1996). Much of the capacity was redirected to other fisheries, including bottom trawl fisheries, such as shrimp, which also damage corals. In addition, the Canadian government made no distinction between gear types when purchasing back licences and did not see this as an opportunity to retire destructive gear types and promote more environmentally friendly fishing methods.

Closures resulted in reduced effort and a reduction in impacts on the seafloor and corals, but unfortunately this was not the consequence of a policy change, but rather of circumstance - fisheries were closed or quotas greatly reduced in response to bleak stock assessments. If the fishery returns, so will the effort and the damage to the bottom, unless less destructive methods of fishing are encouraged.

2. Closed areas or Marine Protected Areas

Marine protected areas have been used as a tool to conserve biodiversity and enhance fisheries, as well as offer opportunities for scientific research, education, recreation and sustainable economic development (Ballantine 1995; Agardy 1997). The Canadian government can use the Fisheries Act, the Oceans Act, and the recently approved Canada National Marine Conservation Areas Act to close areas. It can employ the Fisheries Act to meet fishery management objectives, and the Oceans Act and Conservation Areas Act to meet broader conservation purposes. To date, the government has protected three of the prime areas with legislation.

Northeast Channel

Three gorgonian species are known to occur in the Northeast Channel (Fig. 1), which lies between Georges Bank and Browns Bank (Breeze et al. 1997; Mortensen et al. in press). The DFO closed an area of 424 km^2 in the Northeast Channel in

2002 under the Fisheries Act. Government scientists and managers selected the area because of its high abundance of corals. The DFO closed 90 % of it to all bottom fishing (longline, gillnet, and trawl) and allowed longlining in the remaining 10 %.

A review of groundfish catches (1997-2001) reveals that longlining has been the predominant method of fishing in the closed area and overlaps heavily with coral distribution (Fig. 2). Mortensen et al. (in press) notes that the Northeast Channel has supported an active fishery since the early 1800's which up until the 1950s would solely have been a longline fishery. From the catch data, dragging was restricted to a small portion of the area now closed, and there was little overlap with coral distribution. It is likely that draggers did not fish here because of the rough seafloor conditions.
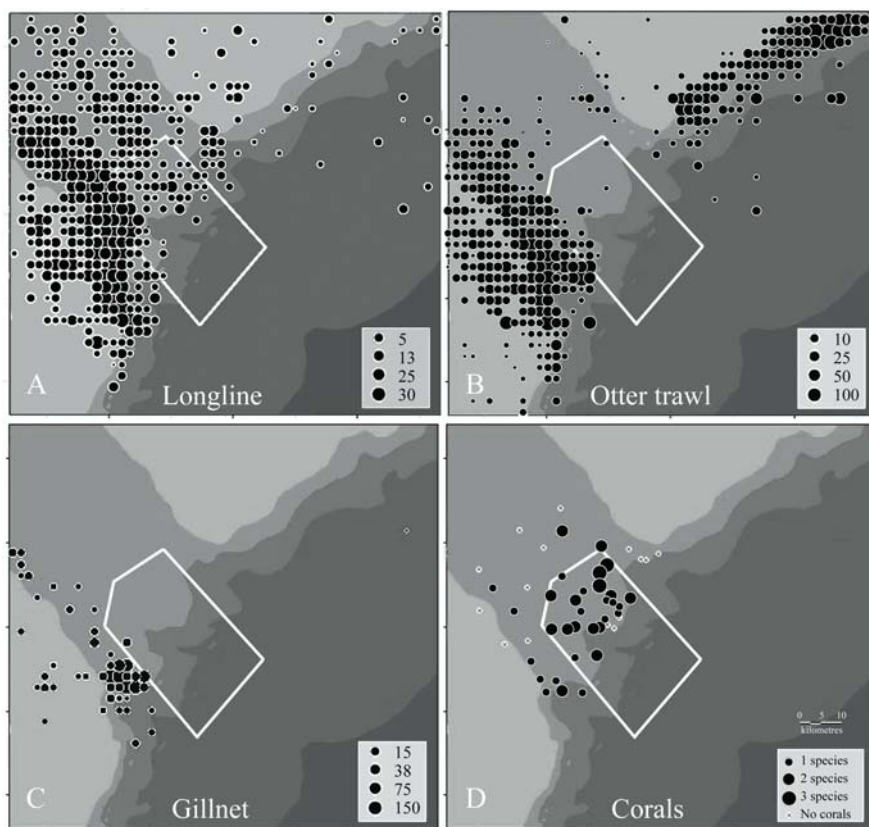
Fig. 2 Distribution of groundfish catches (1997-2001 (**A-C**) and coral (**D**) in the general region of the Northeast Channel (Mortensen et al. in press). The size of the circles represents aggregated catches given in metric tonnes. Also plotted on the same scale is the distribution of corals revealed from video surveys in 2000 and 2001. The boundary of the coral conservation area is indicated by the white line. The latitude and longitude for northern- and southern-most points of the coral box is 42°37'N and 65°34'W and 43°50' N and 65°34'W

Mortensen et al. (in press) conducted a video survey of the coral colonies in the closed area and found evidence of damage to corals from longline gear, but observed little or no evidence of damage from dragging. These findings conform with the fishing data. Damaged corals (broken or tilted) were observed on 29 % of the transects and four percent of the coral colonies observed were damaged. Parted off or broken longline gear was observed on 37 % of the transects.

Of interest here is that the area has been fished using longline gear since the 1800's, yet DFO describes it as having a high concentration of corals and video transects reveal a relatively low level of damage - four percent of observed colonies affected.

Sable Island Gully

The Sable Island Gully (Fig. 1) is the largest submarine canyon on the southeastern Canadian continental margin (Fader 2003). The Gully, as it is usually called, is situated adjacent to the most active area of petroleum exploration and development on the Scotian Shelf and the petroleum industry considers it to have some hydrocarbon potential. Upon urging from conservation groups, including World Wildlife Fund, in 1998 the Canadian government designated the Gully an Area of Interest under the Oceans Act. The Gully is home to a vulnerable population of northern bottlenose whales and other marine mammals. The initial and prime motivation for protecting the Gully was to protect the whales (Fenton et al. 2002). At the same time, Breeze et al. (1997) identified it as an area of high coral concentration, both of gorgonians and scleractinians, and documented damage to corals from fishing. Further research by Breeze (2000) has shown that the Gully has experienced high levels of fishing in the past. As interest in deep-sea corals grew following the release of the Breeze report in 1997, corals joined whales as another important reason for protecting the Gully and designating it an MPA.

The present plan is to divide the Gully into three zones, with mineral and hydrocarbon extraction excluded from all zones, and limited fishing, excluding bottom dragging, allowed in the outer two zones.

Stone Fence

Breeze et al. (1997), through interviews with fishermen, and Gass (2002) through interviews with fishermen and collection of fisheries data, identified the Stone Fence as an area containing high concentrations of corals, including *Lophelia*. At the same time fishermen reported that it was the hotspot most extensively damaged by fishing activities beginning in the 1950s and 60s. "Draggers have got all that stuff tore up…Russian draggers cleaned out the Stone Fence. 70 or 80 boats, dragging back and forth over the same line" (Breeze et al. 1997: 26).

In 2002, government scientists on a research cruise to the Stone Fence obtained the first footage of live *Lophelia* in Canadian waters (Pål Mortensen pers. comm.). In September 2003 scientists on a second research cruise (Hud 2003-059) returned to the area and obtained footage of a badly damaged reef composed of live coral and large amounts of rubble.

Just prior to the discovery of the rubble reef in September 2003, an environmental organization, Canadian Parks and Wilderness Society-Nova Scotia Chapter, made a

request to DFO to close an area of the Stone Fence to all fishing. In August 2004 the Canadian government closed an area of 15 km^2 to bottom fishing.

3. Gear modification or substitution

The reasoning behind gear modification or substitution is that some gear types, or modification of that gear type, are less destructive than others. Therefore, if you can encourage the use of less destructive gear types you can advance conservation and allow fishing to continue. While all gears have impacts, it is now widely accepted that gears can be ranked as to their impact on the ocean floor (ICES 2000; NRC 2001; Morgan and Chuenpagdee 2003). For bottom groundfish fisheries, the ranking, from most destructive to least destructive, is usually as follows:

Trawling and dredging
Gillnetting
Longlining
Handlining or hook and line

There is ample evidence that bottom longlining catches and damages corals. Longlines will tangle with any large organism, like coral, that sticks up from the ocean floor. However, the level of damage is much less than if an area were dragged. Despite an active and long-established longline fishery in the Northeast Channel, the area was considered the best candidate for protected area status.

Along with gear substitution, gear can also be modified. For example, rockhopper gear, which allows draggers to fish on rough and rocky bottom, can be removed from the foot rope of dragger gear. This modification would prevent draggers from fishing on rough bottom where gorgonian corals and other emergent epifauna are often present.

The DFO has taken almost no initiatives to encourage the modification of bottom trawling gear or the substitution of that gear for less destructive gear, such as bottom longline gear in order to reduce habitat damage (McCallum 2001). This is in contrast to its efforts to increase the selectivity of gear to reduce bycatch of non-target commercial species (DFO 1999).

Gear modification or substitution is feasible in nearly every respect. Many, but not all groundfish species can be caught with a hook. There is already a commercially viable bottom hook and line fleet in Atlantic Canada. It is technologically feasible to convert a dragger to a longliner (E.Y.E. Marine Consultants 1991). The principal obstacle is political will. However, if decision makers will not consider gear substitution, MPAs will obviously be more attractive to those seeking action from government.

Discussion

We need to employ a range of tools, including no-take MPAs to conserve the ocean. Nonetheless, the caution from Agardy et al. (2003) that we should think carefully about MPA design and not forget other approaches is timely.

In efforts to protect corals and other benthic habitats by closing areas to one or all gears, consideration needs to be given to displacement of effort. If an area is closed, and the quota remains the same, then the displaced boats will have to fish elsewhere, possibly on equally important or sensitive habitat. Any management measure, including a MPA proposal, should consider displacement of effort.

Those designing MPAs should also pay attention to socio-economic considerations. The message sent to the fishing industry by the closure of the Northeast Channel was, in part, that if you fish in a relatively sustainable manner and leave the habitat relatively intact, your fishing grounds will be a candidate for a closed area. However, if your fishery degrades the ocean floor, removes all emergent epifauna and prominent physical features, and leaves little of value to conservationists, your fishing grounds will not be targeted for closure.

While there is considerable resistance to gear substitution within parts of the fishing industry, it offers a number of benefits:

- It allows for protection of corals in unknown locations.
- It allows for re-colonization of areas by corals.
- It protects a wide range of habitats and species.
- It is not an information-intensive process, e.g., no area needs to be surveyed or delineated before a program is put in place.
- It rewards better fishing practices.
- There can be other ecological and social benefits of using more benign gear.

Shester and Ayers (2005) discuss the impacts of dragging on corals and sponges in Alaskan waters and propose a management approach which attempts to minimize the impact on these species and maximize the catch of target fish species. The approach is quantitative and involves calculation of area trawled, volume of coral and sponge bycatch, and catch of target fish species. Minimizing impacts on the benthos and maximizing catch are objectives by which we might want to measure other conservation measures such as closed areas or gear substitution or modification.

Conclusions

If we want to conserve corals and the rest of the ocean floor from the impacts of fishing and return to a healthy ocean and fishery we need:

- MPAs, including no-take areas;
- to think carefully about MPA design and consider displacement of effort and the 'fairness' of any proposed area;
- gear modification and substitution; and
- to implement MPAs and gear substitution and modification at the same time.

Acknowledgements

Thanks to Glen Hebert, Pål Mortensen, Susan Gass and Heather Breeze for information and assistance. Thanks to June Hall, Gretchen Fitzgerald, Penny Doherty, Susanna Fuller, and Julia Baum for guidance. A special thank you to Walter Jaap for the time he took to review the manuscript as well as to an anonymous reviewer.

References

Agardy TS (1997) Marine Protected Areas and Ocean Conservation. R.E. Landes Press, Austin, TX, 224 pp

Agardy T, Bridgewater P, Crosby MP, Day J, Dayton PK, Kenchington R, Laffoley D, McConney P, Murray PA, Parks JE, Peau L (2003) Dangerous targets? Unresolved issues and ideological clashes around Marine Protected Areas. Aquat Conserv 13: 353-367

Auster PJ, Langton RW (1999) The effects of fishing on fish habitat. In: Beneka L (ed) Fish Habitat: Essential Fish Habitat and Rehabilitation. Amer Fish Soc, Bethesda, MD

Ballantine WJ (1995) Networks of 'no-take" marine reserves are practical and necessary. In: Shackell NL, Willison JHM (eds) Marine Protected Areas and Sustainable Fisheries. Wolfville, N.S. Canada, pp 13-20

Blades K (1995) Net destruction: the death of Atlantic Canada's fishery. Nimbus Publ Ltd, Halifax, Nova Scotia

Breeze H (2000) Commercial fisheries of the Sable Gully and surrounding region: historical and present activities. Canad Manuscr Rep Fish Aquatic Sci 2612, Fish Oceans Canada, Dartmouth, Nova Scotia

Breeze H, Davis D, Butler M, Kostylev V (1997) Distribution and status of deep sea corals off Nova Scotia. Marine Issues Comm Spec Publ 1, Ecology Action Centre, Halifax, NS

Butler M, Gass SE (2001) How to protect corals in Atlantic Canada. In: Willison JHM, Hall J, Gass SE, Kenchington ERL, Butler M, Doherty P (eds) Proceedings of the First International Symposium on Deep-Sea Corals. Ecology Action Centre, Halifax, Nova Scotia, pp 156-165

Collie JS, Hall SJ, Kaiser MJ, Poiner IR (2000) A quantitative analysis of fishing impacts on shelf-sea benthos. J Anim Ecol 69: 785-798

Dayton PK, Thrush SF, Agardy TS, Hofman RJ (1995) Environmental effects of marine fishing. Aquat Conserv 5 205-232

Department of Fisheries and Oceans Canada (1999) An assessment of trawling technology in Canada. Fish Manage, Fish Oceans Canada. Ottawa, Canada

E.Y.E. Marine Consultants (1991) Study on the conversion of trawlers to longliners. Fish Oceans Canada. Halifax, N.S., Canada

Fader G (2003) The mineral potential of The Gully Marine Protected Area, a submarine canyon of the outer Scotian Shelf. Geol Surv Canada, Open File 1634

Fenton DG, Macnab PA, Rutherford RJ (2002) The Sable Gully Marine Protected Area Initiative: history and current efforts. In: Bondrup-Nielsen S, Munro NWP, Nelson G, Willison JHM, Herman TB, Eagles P (eds) Managing Protected Areas in a Changing World. SAMPAA, Wolfville, pp 1343-1355

Fisheries Resource Conservation Council (FRCC) (1996) Building the bridge: 1997 Conservation Requirements for Atlantic Groundfish. Rep Minister Fish Oceans, FRCC.96.R.2, Ottawa, Canada

Fosså JH, Mortensen PB, Furevik DM (2002) The deep-water coral *Lophelia pertusa* in Norwegian waters: distribution and fishery impacts. Hydrobiologia 471: 1-12

Gass SE (2002) An assessment of deep sea corals in Atlantic Canada using both scientific and local forms of knowledge. MES thesis, Dalhousie Univ, Halifax, NS

Gass SE, Willison JHM (2005) An assessment of the distribution of deep-sea corals in Atlantic Canada by using both scientific and local forms of knowledge. In: Freiwald A, Roberts JM (eds) Cold-water Corals and Ecosystems. Springer, Berlin Heidelberg, pp 223-245

Gell F, Roberts C (2004) Difficulties involved in studying marine reserves. MPA News 5(6): 4

International Council for the Exploration of the Sea (ICES) (2000) Extract from the 2000 Report of the Advisory Committee on the Marine Environment: Effects of different types of fisheries on North Sea and Irish Sea benthic ecosystems - Review of the IMPACT II Report to the European Commission Directorate-General Fisheries. Int Counc Explor Sea, Copenhagen

Koslow JA, Gowlett-Holmes K (1998) The seamount fauna off southern Tasmania: benthic communities, their conservation and impacts of trawling. Final Rep Environ Australia and Fish Res Develop Corp, Doc, FRDC Proj 95/058

Krieger KJ (2001) Coral (*Primnoa*) impacted by fishing gear in the Gulf of Alaska. In: Willison JHM, Hall J, Gass SE, Kenchington ELR, Butler M, Doherty P (eds) Proceedings of the First International Symposium on Deep-Sea Corals. Ecology Action Centre, Nova Scotia Museum, Halifax, pp 106-116

Kulka DW, Pitcher DA (2001) Spatial and temporal patterns in trawling activity in the Canadian Atlantic and Pacific. ICES CM 2001/R:02, 55 pp

McCallum B (2001) The impact of mobile fishing gear on benthic habitat and the implications for fisheries management. Master Marine Stud, Fish Marine Inst Mem Univ Newfoundland. St. John's, Newfoundland

MacIssac K, Bourbonnais C, Kenchington E, Gordon D, Gass S (2001) Observations on the occurrence and habitat preference of corals in Atlantic Canada. In: Willison JHM, Hall J, Gass SE, Kenchington ELR, Butler M, Doherty P (eds) Proceedings of the First International Symposium on Deep-Sea Corals. Ecology Action Centre, Nova Scotia Museum, Halifax, pp 58-75

Morgan L, Chuenpagdee R (2003) Shifting gears: addressing the collateral impacts of fishing methods in U.S. waters. Pew Science Ser, Island Press, Washington, DC

Mortensen PB, Buhl-Mortensen L, Gordon DC, Fader GBJ, McKeown DL, Fenton DG (in press). Effects of fisheries on deep-water gorgonian corals in the Northeast Channel, Nova Scotia (Canada). In: Thomas J, Barnes P (eds) Effects of Fishing Activities on Benthic Habitats: Linking Geology, Biology, Socioeconomics, and Management. Amer Fish Soc Symp, November 12-14, 2002 Tampa, Florida

National Research Council (NRC) (2001) Effects of trawling and dredging on seafloor habitat. National Academy Press. Washington, DC

Parsons LS (1993) Management of marine fisheries in Canada. Canad Bull Fish Aquat Sci 225, 784 pp

Shester G, Ayers J (2005) A cost effective approach to protecting deep-sea coral and sponge ecosystems with an application to Alaska's Aleutian Islands region. In: Freiwald A, Roberts JM (eds) Cold-water Corals and Ecosystems. Springer, Berlin Heidelberg, pp 1151-1169

Thrush SF, Dayton PK (2002) Disturbance to marine benthic habitats by trawling and dredging: implications for marine biodiversity. Ann Rev Ecol Syst 33: 449-473

Willis T, Millar R, Babcock R, Tolimieri N (2004) The science of marine reserves: how much of it is science? MPA News. 5(6): 3-4

Index

A